

# EuropaCat 2019

AACHEN · GERMANY · 18 – 23 AUGUST

## 14<sup>th</sup> EuropaCat – European Congress on Catalysis

“Catalysis without Borders”

A joint event from the catalysis communities of  
Germany, the Netherlands and Belgium



Follow us on Twitter  
[#europacat2019](#)

## Book of Abstracts (poster)

# Particle Size Effects for Carbon-Supported Cu and CuZnO<sub>x</sub> Catalysts in Methanol Synthesis

*Rolf Beerthuis,\* C. E. Pompe, Krijn P. de Jong and Petra E. de Jongh, Debye Institute for Nanomaterials Science, Utrecht University, Utrecht, The Netherlands.*

*\*) R.Beerthuis@uu.nl, www.inorganic-chemistry-and-catalysis.eu.*

Methanol is essential to produce chemicals such as acetic acid, alkyl acrylates and various olefins. Over 65 million metric tons of methanol are produced each year by Cu(ZnO<sub>x</sub>)-catalyzed hydrogenation of CO and CO<sub>2</sub>. However, fundamentals such as the nature of the active site, the effect of particle size, and the origin of the ZnO<sub>x</sub> promoter effect are still being debated.<sup>[1-3]</sup> Recently, a DFT study predicted a strong decrease in activity for particle sizes below 20 nm, due to loss of effectiveness of the ZnO<sub>x</sub> promotion.<sup>[2]</sup> Our group was the first to publish experimental results on the dependency of turn-over frequency (TOF) on particle size, showing decreasing activities for particles below 8 nm.<sup>[3]</sup> Although structure sensitivity was postulated as an underlying cause, the results for unpromoted Cu particles were inconclusive, leaving space for an alternative explanation *via* the effectiveness of the ZnO<sub>x</sub> promoter. These previous studies employed different supports, mostly metal oxides, to allow variation of the particle size. However, the nature of the support may affect the efficiency of Cu and ZnO<sub>x</sub>, thus obscuring intrinsic particle size effects. In this study, we utilized carbon as an inert catalyst support to elucidate the particle size effects for both Cu and CuZnO<sub>x</sub>.

The carbon-supported Cu particle size was tuned between 3–13 nm, both in absence and presence of ZnO<sub>x</sub>, which was achieved by systematic variation of the synthesis parameters, including fine-tuning of the Cu loading, carbon surface functionalization and the final heat treatment temperature. Transmission electron micrographs for two typical carbon-supported Cu (Cu/C) catalysts are displayed in Fig. 1a,b. The catalytic performance for the full set of Cu/C catalysts was evaluated under industrially relevant conditions. The surface-specific activity was strongly dependent on the Cu size, corroborating earlier results. Interestingly, the Cu-based activity was consistently higher for the SiO<sub>2</sub>-supported catalysts compared to carbon, for the same Cu size (Fig. 1c). In presence of ZnO<sub>x</sub>, the particle size effects still existed, yet



the activity was dominated by the strong promoter effect. Using carbon as an inert support unequivocally proved that structure sensitivity contributes significantly to the particle size dependence of methanol synthesis, using Cu and CuZnO<sub>x</sub> nanoparticulate catalysts with sizes between 3–10 nm. Moreover, we revealed the pivotal role of the support on the Cu and CuZnO<sub>x</sub> particle size-activity relationships in methanol synthesis. These findings may assist in the rational design of more efficient industrial catalysts and ultimately lead to conserving energy and material resources.

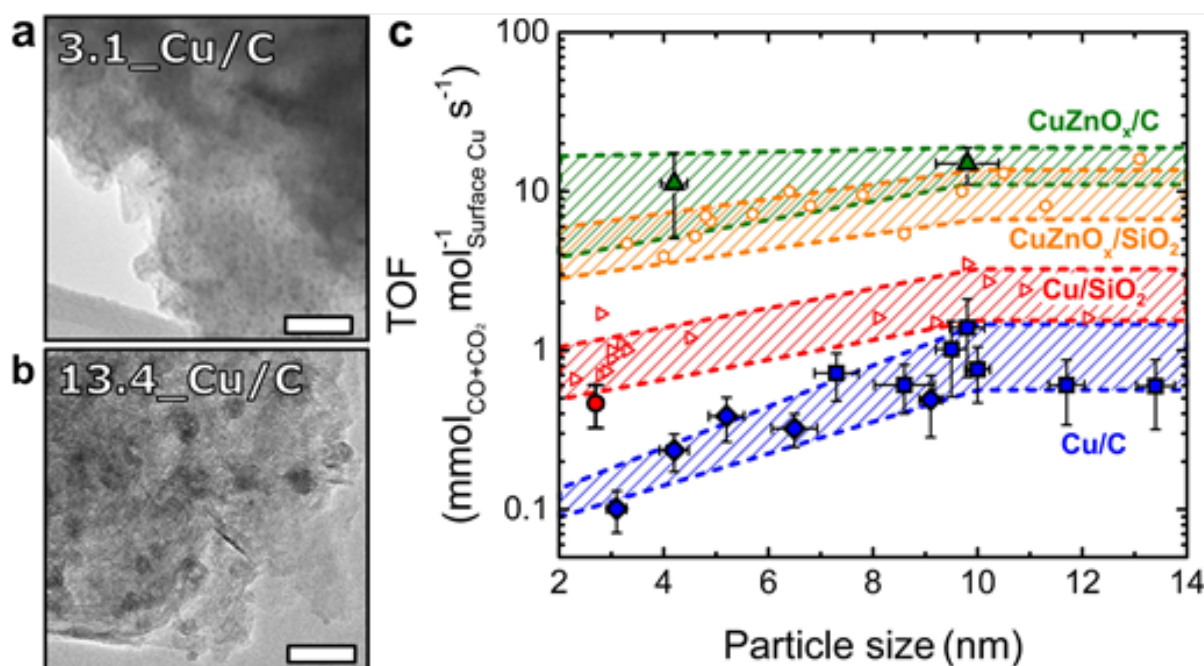


**Fig. 1:** **a)** Micrograph of 3.1 nm Cu/C catalyst; **b)** Micrograph of 13.4 nm Cu/C catalyst, white scale bars measure 50 nm; **c)** Activity versus surface-averaged particle size for Cu/C (blue squares), CuZnO<sub>x</sub>/C (green triangles) and Cu/SiO<sub>2</sub> (red circle) catalysts during methanol synthesis from CO<sub>2</sub>-enriched synthesis gas. The TOF results for Cu/SiO<sub>2</sub> (empty triangles) and CuZnO<sub>x</sub>/SiO<sub>2</sub> (empty hexagons)<sup>[3]</sup> were incorporated for direct comparison under the same reaction conditions: H<sub>2</sub>:CO:He:CO<sub>2</sub> = 60:23:10:7 vol%, 260 °C and 40 bar(g), GHSV 1,000–7,000 h<sup>-1</sup>.

## References

- [1] M. Behrends, F. Studt, I. Kasatkin, S. Kühl, M. Hävecker, F. Abild-Pedersen, S. Zander, F. Girgsdies, P. Kurr, B.-L. Kniep, M. Tovar, R. W. Fischer, J. K. Nørskov, R. Schlögl Science, 2012, 336, 893.
- [2] S. Kuld, M. Thorhauge, H. Falsig, C. F. Elkjær, S. Helveg, I. Chorkendorff, J. Sehested, Science 2016, 352, 969.
- [3] R. van den Berg, G. Prieto, G. Korpershoek, L. I. van der Wal, A. J. van Bunningen, S. Lægsgaard-Jørgensen, P. E. de Jongh, K. P. de Jong, Nat. Comm., 2016, 7, 13057.

# Selectivity-determining factors in non-oxidative propane dehydrogenation over ZrO<sub>2</sub>-based catalysts

*Anna Perechodjuk<sup>1)</sup>, Yaoyuan Zhang<sup>2)</sup>, Guiyuan Jiang<sup>2)</sup>, Evgenii V. Kondratenko<sup>1)\*</sup>*

*<sup>1)</sup>Leibniz-Institut für Katalyse e.V. an der Universität Rostock, Albert-Einstein-Str. 29a, Rostock, 18059, Germany. <sup>2)</sup> State Key Laboratory of Heavy Oil Processing, China University of Petroleum Beijing, Beijing, 102249, China.*

## Introduction

Owing to the multipurpose applications of propene, the demand for this olefin is continuously increasing but cannot be fully covered by oil-based steam and fluid catalytic cracking. To close the propene gap, non-oxidative propane dehydrogenation to propene (PDH) over Pt- or CrO<sub>x</sub>-based catalysts has been developed. Although the catalysts are active and selective, they have drawbacks related to cost or environmental impact. Recently we have introduced non-toxic and low-cost ZrO<sub>2</sub>-based catalysts [1]. Two coordinatively unsaturated Zr cations (Zr<sub>cus</sub>) were suggested to participate in propene formation [2]. The purpose of this study was to identify the active sites and the factors affecting both desired selectivity as well as formation of coke, which is the main undesired product. In particular, we focused on the role of (i) ZrO<sub>2</sub> phase composition, (ii) the size of crystallites, (iii) the kind of promoter (Y<sub>2</sub>O<sub>3</sub> or La<sub>2</sub>O<sub>3</sub>) for ZrO<sub>2</sub> and (iv) supported metal (Ir, Pt, Ru or Rh) in PDH.

## Results and Discussion

The catalysts were prepared through support impregnation with an ethanol solution of metal nanoparticles (NP) of about 1 nm. For all catalyst, the use of metal NP positively affected the rate of propene formation. The supported metals can be ordered in terms of their positive effect on the activity as follows Rh>Ru>Ir>Pt. Importantly, SiO<sub>2</sub>-supported metals showed negligible activity thus suggesting that there is a synergy effect between the ZrO<sub>2</sub>-based supports and the supported metals.

To derive insights into reaction pathways of product formation in the course of PDH, catalytic tests were carried out at different degrees of propane conversion to construct selectivity-conversion relationship. Figure 1 exemplary shows such dependences to illustrate how Rh loading, reaction temperature and the size of crystallite of bare monoclinic ZrO<sub>2</sub> affect the selectivity to propene and coke with the latter being the main undesired product. For all materials, the selectivity to propene

decreases with rising propane conversion, while the selectivity to coke increases with exception for  $\text{ZrO}_2$  with 9.1 nm crystallites, where the latter selectivity did not

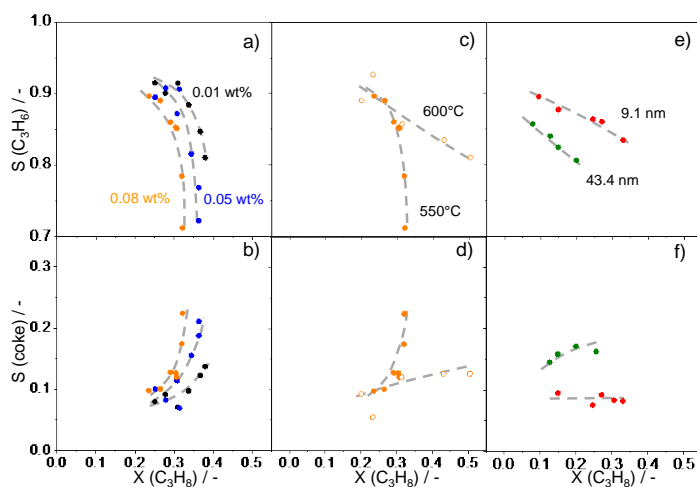


**Figure 1.** The selectivity to (a, c, e) propene and (b, d, f) coke as a function of propane conversion over (a-d)  $\text{YZrO}_x$  catalysts with (a, b) 0.01 wt% (●), 0.05 wt% (●) or 0.08 wt% (●) Rh and over (e, f) monoclinic  $\text{ZrO}_2$  with 9.1 and 43.4 nm crystallites. Reaction conditions: 550°C (filled symbols) or 600°C (open symbols), 40 vol% propane in  $\text{N}_2$ .

significantly depend on the conversion. It is obvious that the higher the Rh loading, the stronger the negative effect of propane conversion on the selectivity to propene is. A similar dependence was also established for all  $\text{ZrO}_2$ -based catalysts with Ru, Pt or Ir NP. The metals can be ordered in terms of their undesired effect as follows  $\text{Pt} > \text{Ru} \sim \text{Rh} > \text{Ir}$ .

When the PDH reaction was performed at 600°C, the selectivity to propene increased, while the selectivity to coke decreased (Figure 1 c, d). This is probably due to increased propene desorption. Another selectivity-affecting factor is the crystallites size of bare monoclinic  $\text{ZrO}_2$  [2]. The smaller the crystallites, the higher the propene selectivity is (Figure 1 e, f). Phase composition of zirconia is also important. The selectivity to coke over monoclinic  $\text{ZrO}_2$  was also lower than over tetragonal  $\text{ZrO}_2$ . According to operando UV-vis analysis, the phase composition and the size of crystallites affect the rate of conversion of coke precursors (seeds) into higher oligomerized species.

## Summary

The obtained results provide fundamentals for controlling activity and particularly selectivity of  $\text{ZrO}_2$ -based catalysts in the non-oxidative dehydrogenation of propane to propene. The catalyst performance can be tuned through changing the size of crystallites and phase composition of  $\text{ZrO}_2$ , the kind of promoter for  $\text{ZrO}_2$  and the kind of supported metal. The knowledge derived may be used for designing other alternative-type catalysts on the basis of non-reducible metal oxides.

## References

- [1] T. Otroshchenko, S. Sokolov, M. Stoyanova, V. A. Kondratenko, U. Rodemerck, D. Linke, E. V. Kondratenko, *Angewandte Chemie International Edition* **2015**, *54*, 15880.
- [2] Y. Zhang, Y. Zhao, T. Otroshchenko, H. Lund, M.-M. Pohl, U. Rodemerck, D. Linke, H. Jiao, G. Jiang, E. V. Kondratenko, *Nature Communications* 2018, *9*, 3794.

# Supported Cu Catalysts with a Carbon–Nitrogen Matrix Derived from MOFs for Selective Oxy-carbonylation of Methanol to DMC<sup>‡</sup>

*Jinping Zhang, Xiaoying Liu, Weikun Chen, Huihuang Fang, and Youzhu Yuan\**  
State Key Lab of Physical Chemistry of Solid Surfaces, National Engineering Lab for Green Chemical Productions of Alcohols–Ethers–Esters, iChEM, College of Chemistry and Chemical Engineering, Xiamen University, Xiamen 361005, PR China  
\*Corresponding author: +86 592 2181659, [zyuan@xmu.edu.cn](mailto:zyuan@xmu.edu.cn)

## 1. Introduction

Nitrogen-containing carbons (NCs) have been used in a wide variety of fields. However, it is still under debate on the nature of active N sites, mainly pyrrolic, pyridinic and graphitic N, due to the blending and inhomogeneity of different N types in NCs. Zeolitic imidazolate frameworks (ZIFs), a subfamily of metal-organic frameworks (MOFs), are ideal candidates to prepare NCs with exceptional chemical and thermal stability by pyrolysis. Different from other MOFs, the ZIFs promise an increase of active site density and a more uniform distribution of N species. Supported Cu catalysts have been widely used in oxy-carbonylation of methanol to dimethyl carbonate (DMC). To this end, NCs are considered as a class of novel catalyst carriers for the oxy-carbonylation reaction. However, the in-depth investigation on the functions of active N sites is sporadic. Here, we employ ZIF-7 and ZIF-8 to prepare NCs and then supported Cu catalysts for the oxy-carbonylation of methanol. The results indicate that the Cu/NCs with proper N content and pyrrolic/pyridinic N ratio can markedly enhance the performance and stability.

## 2. Experimental

ZIFs and *Pm*PDA-C samples were synthesized according to the previous works [1,2]. The NCs were then obtained by pyrolysis under an Ar atmosphere, being denoted as NCs-*T*, NCs-*T*-wet-*t*, NCs-*T*<sup>\*</sup>, and NCs-P-*T* (*T* represents the calcination temperature, P represents the polymerization, *t* represents the time of vapor treatment). The supported Cu catalysts were prepared by using different NCs as the carrier and copper salts as the precursor with a conventional impregnation method, labeling as Cu/NCs-*T*, Cu/NCs-*T*-wet-*t*, Cu/NCs-*T*<sup>\*</sup>, Cu/NCs-P-*T*. The oxy-carbonylation of

---

<sup>‡</sup> This work is supported by the National Key R&D Program of China (2017YFA0206801).



methanol was evaluated in a fixed-bed reactor system. The catalyst structure was characterized by a series of spectroscopic techniques.

### 3. Results and discussion

Fig. 1a shows the TEM image of Cu/NCs-1000, indicating its morphology is similar to ZIFs. Fig. 1b depicts a preliminary correlation of DMC yield and pyrrolic/pyridinic N ratio. When the ratio is among 1.3–2.0, the DMC yield is above 30.0%. The yield does not change much when the pyrrolic/pyridinic N ratio is further increased to 5. Fig. 1c displays a comparison of performance over different catalysts as a function of TOS. The Cu/NCs-1000, Cu/NCs-P-1000 and Cu/NCs-1000\* catalysts show better catalytic activity compared with Cu/XC-72. On the other hand, all catalysts show deactivation, but the deactivation rate is different. The deactivation rate during 20 h are 19%, 15%, 20% and 50% for Cu/NCs-1000, Cu/NCs-P-1000, Cu/NCs-1000\* and Cu/XC-72, respectively. The reasons are essentially due to the agglomeration of Cu particles and the structure changes of N species.

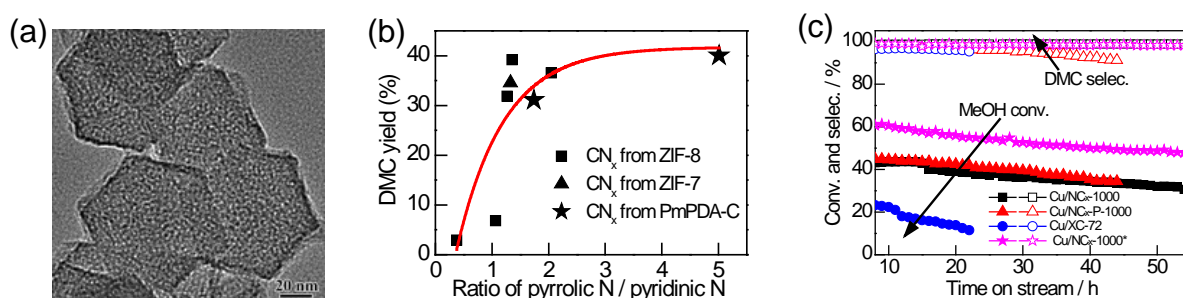


**Fig. 1.** (a) TEM image of Cu/NCs-1000; (b) Correlation of DMC yield and pyrrolic/pyridinic N ratio; (c) Performance of Cu/NCs catalysts as a function of TOS.

### 4. Conclusions

The NCs can inherit the octahedral structure of ZIFs. The Cu catalysts with NCs containing pyrrolic/pyridinic N ratio around 1.3–2.0 outperform Cu/XC-72 and other Cu/NCs catalysts for the selective oxy-carbonylation of methanol to DMC. The preliminary correlation between DMC yield and pyrrolic/pyridinic N ratio may further rationalize the catalyst design for such reaction and provide a new thought on better understanding the catalysis by using NCs as support.

### References

1. Lee, S.; Kim, J.; Kim, J.; et al., *Chem. Mater.* **2018**, 30, 447-455.
2. Zhang, J.P.; Nagamatsu, S.; Du, J.M.; et al., *J. Catal.* **2018**, 367, 16-26.

# **The effect of pressure on methane aromatization over Mo/HZSM-5 catalyst in a micro fluidized bed reactor**

*Yang Song, Koji Kuramoto and Zhanguo Zhang*

*National Institute of Advanced Industrial Science and Technology, Tsukuba, Japan*

*z.zhang@aist.go.jp*

## **Introduction**

For the Mo/HZSM-5 catalyzed methane dehydroaromatization reaction, increasing the operating pressure enable to improve the heat and mass transfer efficiency of the catalyst bed, suppress coke formation, and increase catalytic stability [1], whereas leading to a decrease in CH<sub>4</sub> conversion due to equilibrium limitations. Thus there should exist an optimum operating pressure to maximize the reactor performance. In this study we performed the reaction in a micro fluidized bed reactor at 5 different pressures (1-5 atm) and 1073 K. We aimed at collecting the catalytic performance of a spherically-shaped, binder-free Mo/HZSM-5 at these pressures so that a data-based evaluation on the pressure-affected bed performance becomes possible.

## **Experimental**

A spherically-shaped binder-free 6wt%Mo/HZSM-5 catalyst was used. Its catalytic tests were carried out in a micro fluidized bed reactor (15 mm ID) at 1073 K and pressures from 1 to 5 atm for 100-150 min. The amount of the catalyst sample and the feed rate of methane used in each test were proportionally increased with increasing the operating pressure to have a fixed superficial gas velocity (about 7.5 cm/s) and hence to form a similar uniform bubble fluidized bed. During the reaction period at 1073 K a small amount of the reacted effluent was depressurized and introduced into a 10 port-valve sampler held at 503 K, and on-line analyzed by two gas chromatographs. Over the whole test period the pressure was monitored by a pressure sensor and confirmed to remain stable.

## **Results and Discussion**

At all test operating pressures and bed heights from 13 to 95 mm CH<sub>4</sub> conversion reached the highest level at the first sampling time point (5 min after the 10%Ar/CH<sub>4</sub>

make-up was introduced into the reactor at 1073K) and then began to decrease, first at a small rate and last at an increased rate. As expected, due to the equilibrium limitations, the maximum CH<sub>4</sub> conversion was indeed decreased with increasing the operating pressure. On the other hand, the benzene formation rate, in most of the tests, reached its maximum at the second sampling time point (15 min) or a delayed timing due to the suppressive effect of H<sub>2</sub> produced via CH<sub>4</sub> pyrolysis on reduced Mo species [2]. Only in a few cases where the gas hourly space velocities reached very high, the benzene formation rate attained the maximum at the first sampling. With respect to the effect of the operating pressure, the benzene formation rate always remained higher at a raised pressure. This confirms that increasing the CH<sub>4</sub> partial pressure does increase rather than decrease the overall benzene formation rate. In addition, the time-dependences of both CH<sub>4</sub> conversion and benzene formation rate suggested that continuous deactivation does occur over the whole reaction course at all test pressures. At the same time, however, the product selectivity to benzene obtained in all the cases remained stable and high at the levels 65-70% over the first 50-100 min, and then dropped rapidly to the levels of 10-20% in 20-40 min. This suggests that the narrowing of the openings of the zeolite channels by coke accumulation through the benzene selectivity-stable period might dominate the deactivation process of Mo/HZSM-5 catalyst [3]. Moreover, lowering the gas hourly space velocity by increasing the amount of catalyst packed in the bed enabled to improve the catalytic stability of the bed for benzene production, although the benzene yield itself was decreased with raising the operating pressure of the reactor.

## Conclusions

A constant benzene selectivity of 65-70% was achieved at all test pressures. The CH<sub>4</sub> conversion obtained decreased and the maximum benzene formation rate increased with increasing the operating pressure of the catalyst bed.

## References

- [1] Shu et al., J. Catal., 206, 134-142 (2002)
- [2] Xu et al., Appl. Catal. A: Gen. , 168, 390-402 (2011)
- [2] Song et al., Appl. Catal. A: Gen. , **530**, 12-20 (2017)

# The study of self-oscillations during CH<sub>4</sub> oxidation over Ni by the pulse method

*Bychkov Victor, Tulenin Yuriy, Slinko Marina, Korchak Vladimir, Semenov Institute of Chemical Physics, Moscow, Russia, bychkov@chph.ras.ru*

## Introduction

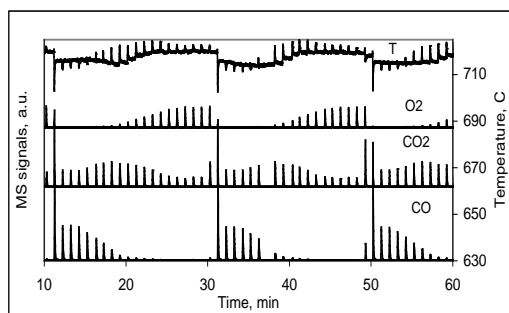
Self-oscillations of catalytic reaction rate is an interesting kinetic phenomenon that allows to reveal in more details a mechanism of the reaction. It was believed that self-oscillations could be observed only for open systems with continuous supply of reactants. We assumed that self-oscillations during some heterogeneous catalytic reaction could be also detected with pulse supply of reagents and the results would give an additional information about the reaction mechanism. Methane oxidation over Ni was selected for the investigation because of well-known self-oscillations under the continuous supply mode.

## Materials and methods

Ni foil sample (4x3x0.5 mm) with an internal thermocouple was prepared from a Ni capillary. Catalytic experiments were carried out in a tubular quartz flow-through reactor. A quadrupole mass-spectrometer (Pfeiffer, OmniStar GSD 301) was employed to analyze the composition of the outlet gas flow.

## Results and discussion

Periodic variations of MS signals related to reagents and products in series of 7.3%O<sub>2</sub>-40.8%CH<sub>4</sub>-He pulses were observed in the range of the Ni foil temperature from 650 to 800°C [1]. The waveform of the periodic variations (Fig.) reminds one of a well-known effect whereby a high-frequency oscillation signal becomes modulated by a low-frequency oscillation signal. Therefore, this phenomenon will be henceforth referred to as “modulated” oscillations with the period equal to the number of pulses



between the repetitive responses.

The Ni temperature curve demonstrates that there are at least two types of temperature effects. Temperature effects of the first type are caused by heat evolution during the gas pulse contact with the catalyst. These effects were exothermic or endothermic depending on



a selectivity of CH<sub>4</sub> transformation in every pulse. Effects of the second type led to the step-wise changes in the temperature of the Ni foil when in He flow between the reaction mixture pulses. Such step-wise changes were related to changes in heat transfer between the Ni foil and the surrounding furnace because they occurred when Ni foil changed its color between light metallic Ni and dark NiO.

The pulse experiments allowed more accurate measurements of O- and C-containing gas components and calculations of O and C balances in every pulse. Positive or negative O disbalances in some pulses have proved NiO reduction or Ni oxidation correspondingly in different stages of the oscillation cycle. Similarly, C disbalances revealed the stages with carbon accumulation or removal. The observed selectivities of CH<sub>4</sub> transformation (total oxidation to CO<sub>2</sub> and H<sub>2</sub>O, partial oxidation to CO and H<sub>2</sub>, decomposition to C and H<sub>2</sub>) depended on the oxidation and carbonization degrees in each pulse.

### **Conclusions**

For the first time it has been shown that the self-oscillatory behavior during heterogeneous catalytic reactions can be studied by the pulse method. The pulse method allows to eliminate the influence of heat and mass-transfer effects on the reaction rate and to reveal the role of reactor dynamics in the origin of the self-oscillations. The complicated waveform of the temperature variations during the "modulated" oscillations allowed to distinguish the heat effects from the chemical reaction proper as well as from the heat transfer processes in the reactor-furnace system. The application of the pulse method can "freeze" some of the states of the catalyst during the fast stages of the self-oscillations revealing the fine structure of the oscillation cycle. The detailed structure of the self-oscillation cycle can be described as a sequence of at least five reaction stages. The role of the accumulated carbon and oxygen in the mechanism of methane oxidation over Ni has been revealed. The new results allow to fill in some of the gaps in our knowledge about the mechanism of self-oscillations during methane oxidation thus enabling further mathematical modelling of the process.

### **Acknowledgments**

This work was supported by the Russian Science Foundation (grant N 17-13-01057).

### **References**

[1] Bychkov V.Yu., Tulenin Yu.P., Slinko M.M. *et al.*, *Cat. Lett.* 147:2664-2673, 2017

# Catalytic upgrading of biorenewables: palladium-catalyzed aerobic oxidation of *cis*-jasmone

*Maíra S. Costa; Amanda C. Faria; Elena V. Gusevskaya\**

*Departamento de Química, Universidade Federal de Minas Gerais, 31270-901, Belo Horizonte, MG, Brazil,*

*\* elena@ufmg.br*

## 1. Scope

Oxidation reactions enable the catalytic upgrading of renewable feedstocks through the incorporation of a functional group, resulting in compounds potentially useful in cosmetic and pharmaceutical applications. An economically attractive and environmentally friendly approach is the use of molecular oxygen as the final oxidant for these transformations [1].

Palladium salts are highly efficient and versatile catalysts in homogeneous organic oxidations [2]. In order to maintain the catalytic cycle, auxiliary reversible co-catalysts, such as *p*-benzoquinone (BQ), are usually required for the regeneration of palladium(II) active species. BQ readily re-oxidizes zerovalent palladium and can be regenerated under superatmospheric oxygen pressure, or under atmospheric pressure in the presence of an electron transfer mediator (e.g. Cu(OAc)<sub>2</sub>). Both approaches have been successfully applied in the palladium-catalyzed oxidation of several naturally occurring alkenes [3-6].

In the present communication, we focused on our recent results on the palladium-catalyzed homogeneous oxidation of *cis*-jasmone, a fragrance ingredient used in many scent mixtures, found in cosmetics, perfumes and other products [7]. The catalytic functionalization of the abundant, naturally occurring *cis*-jasmone represents an attractive entry to new fragrant compounds.

## 2. Results and discussion

We found that the exocyclic double bond in the *cis*-jasmone (**1**) molecule can be successfully oxidized by molecular oxygen as final oxidant using the Pd(OAc)<sub>2</sub>/BQ catalytic system. The reaction was performed under atmospheric pressure in the presence of catalytic amounts of Cu(OAc)<sub>2</sub> as an electron transfer mediator for the effective regeneration of BQ during the catalytic cycle. Alternatively, a more

environmental friendly oxidation process in the absence of any co-catalyst was performed at superatmospheric pressures (up to 10 atm).

After the optimization of the reaction variables, combined selectivity of 90% for the allylic oxidation products was achieved at nearly complete substrate conversion. Allylic acetate **2** shown in Figure 1 was the major reaction product, responsible for 80% of the mass balance in most of runs.

Initial reaction rates were strongly dependent on the BQ concentration, suggesting that the re-oxidation of hydroquinone was the rate-determining step in the process. Temperatures higher than 80 °C should be avoided in order to prevent the loss in selectivity due to the substrate decomposition and over-oxidation of the primarily formed products to give high boiling compounds.

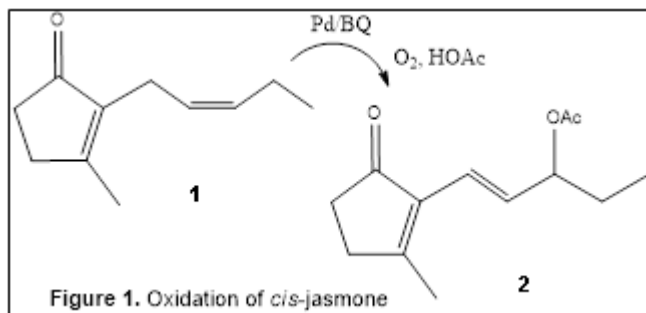


Figure 1. Oxidation of *cis*-jasmone

### 3. Conclusion

A novel selective Pd<sup>2+</sup>/BQ catalyzed oxidation of *cis*-jasmone, a naturally occurring substrate, by molecular oxygen has been developed. Catalytic systems and reaction conditions were selected to allow high yields for the major allylic ester, a novel compound, under mild conditions. The functionalized product is potentially useful as component of synthetic perfumes, cosmetics and pharmaceuticals.

### Acknowledgements

We acknowledge CNPq, FAPEMIG, and INCT-Catálise (Brazil) for the financial support.

### References

- [1] W. Wu, H. Jiang, *Accounts of Chemical Research*. 2012, 45, 1736 – 1748.
- [2] S. Manna, L. Benhamoub, T. Sheppard. *Synthesis*. 2015, 47, 3079-3117.
- [3] L. A. Parreira, L. Menini, E. V. Gusevskaya, *Catal. Sci. Technol.* 2014, 4, 2016 -2022.
- [4] M. S. Costa, A. L. P. de Meireles, E. V. Gusevskaya. *Asian J. Org. Chem.* 2017, 6, 1628 -1634.
- [5] A. C. Faria, T. A. S. W., E. E. Alberto, E. V. Gusevskaya, *App. Catal. A*. 2017, 548, 33-38.
- [6] L. A. Parreira, Ana. F. Azevedo, L. Menini, E. V. Gusevskaya. *J. Mol. Catal. A*, 2017, 426, 429-434.
- [7] J. Scognamiglio, L. Jones, C. S. Letizia, A. M. Api. *Fd Chem. Toxic.* 2012, 50, 613–618.

# Hydrogenation of succinic acid over supported molybdenum carbide

Marwa Abou Hamdan, Catherine Pinel, Noémie Perret, IRCELYON, UMR CNRS 5256, Villeurbanne, France; Mohamad Jahjah, LCIO, Université Libanaise, Beyrouth, Liban

## Scope

The development of new catalytic systems for the conversion of biomass-derived molecules into valuable chemicals and fuels has attracted the attention of many research studies. Succinic acid is a C4 platform chemical which can easily be obtained by bacterial fermentation of glucose. The hydrogenation of succinic acid over heterogeneous catalysts can generate value added chemicals such as  $\gamma$ -butyrolactone, butyric acid and 1,4-butanediol (Figure 1). This reaction has principally been studied over noble metal supported catalysts in aqueous phase where  $\gamma$ -butyrolactone is predominantly obtained over monometallic (e.g. Pd/C [1]) catalysts; the incorporation of a second metal switch the selectivity towards 1,4-butanediol (e.g. Pd-Re/TiO<sub>2</sub> [2]).

Transition metal carbides are potential substitutes for the conventional noble metal catalysts usually used for such reactions; their catalytic activity is comparable to noble metals but with unique pathways and distinct products selectivity [3]. In this work, Mo carbide were used for the first time for the hydrogenation of succinic acid. We prepared novel molybdenum carbide supported on TiO<sub>2</sub>, ZrO<sub>2</sub> and C. The effects of the preparation conditions on the catalyst composition and its corresponding catalytic response were investigated.

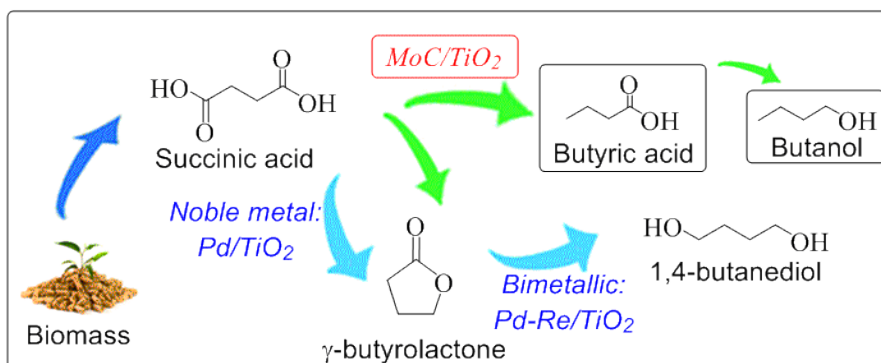


Figure 1: Hydrogenation of succinic acid



## Results

A range of supported-molybdenum carbides were synthesized by impregnation followed by temperature programmed reduction carburization.  $\text{TiO}_2$ ,  $\text{ZrO}_2$  and C were used as support. For the carburization, the effect of nature of the carbon source ( $\text{CH}_4$ ,  $\text{C}_2\text{H}_6$ ), the gas composition (5-40% v/v  $\text{C}_x\text{H}_y/\text{H}_2$ ), the gas hourly space velocity ( $\text{GHSV} = 1000\text{-}7600 \text{ h}^{-1}$ ), and the final temperature (600-800°C) were investigated.

The catalysts were characterized by XRD, ICP, STEM, TEM and XPS. All the catalysts exhibited well dispersed particles (< 5nm) of cubic MoC (Figure 2). The method of preparation was shown to affect the degree of carburization and the amount of free carbon on the surface.

Succinic acid reactions were conducted in a batch reactor, at 160-240°C and under high  $\text{H}_2$  pressure (90-150 bars). Periodical samples were analyzed by GC and HPLC.

In the presence of supported MoC catalysts, full conversion of SA were obtained after 24 h at 240 °C and 150 bars in water. After 24 h, the main products obtained were butyrolactone and butyric acid. After 48 h, these intermediates were converted to butanol, THF, and 1,4-butanediol. Among the 3 supports,  $\text{MoC}/\text{TiO}_2$  was the most active. Changing the nature of the carbon source during carburization did not affect the catalytic results. However when increasing the carburization temperature, the hydrocarbon content or GHSV, higher selectivity towards butyric acid were obtained.

For the first time, yield up to 70% of butyric acid was obtained during the hydrogenation of succinic acid. Performing this reaction in absence of noble metals is a step towards the development of a sustainable economy, since molybdenum is more abundant and less expensive than noble metals catalysts usually used.

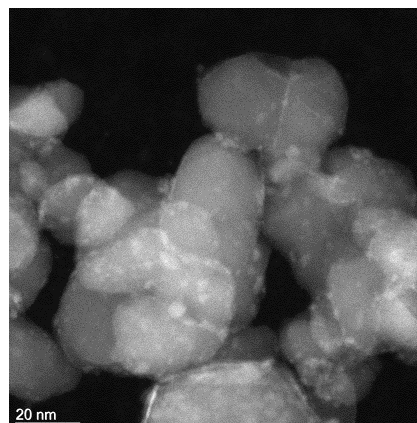


Figure 2: STEM of  $\text{MoC}/\text{TiO}_2$

## References

- [1] B.Tapin, F.Epron, C.Especel, B. Khanh Ly, C.Pinel, M.Besson, *ACS Catalysis*, **2013**, 3, 2327-2335.
- [2] B. Khan Ly et al., *ChemCatChem*, **2015**, 7, 2161–2178.
- [3] 2. S.T. Oyama, *The Chemistry of Transition Metal Carbides and Nitrides*, **1996**, 311.

# **In-situ synchrotron radiation photoionization mass spectrometry (SR-PIMS) for the detection of gas-phase catalytic products**

*Wu Wen, Minggao Xu, Shengsheng Yu, Jiuzhong Yang, and Yang Pan\**

*(E-mail: panyang@ustc.edu.cn)*

*National Synchrotron Radiation Laboratory, University of Science and Technology of China, Hefei, Anhui 230029, P. R. China*

The gas-phase mechanism in catalytic reaction mainly involves the reaction kinetics process of gas-phase intermediates desorbed from the surface of catalysts. Thus, in-situ observation of active intermediates, especially free radicals is of great significance for the establishment of reaction mechanism.<sup>[1, 2]</sup>

In this work, a spatially-resolved catalytic reactor combined with *in-situ* synchrotron photoionization mass spectrometry (SR-PIMS) was developed to investigate the nascent gaseous products during solid-gas catalytic reactions. In comparison with former used methods, this apparatus can obtain stable and short-lived species at varied temperature (up to 800 °C), space distance (2 to 55 mm from the catalyst surface), and a wider pressure range (0.1 to 360 Torr) in real time. Oxidative coupling of methane (OCM) with Li/MgO as model catalyst was adopted to evaluate the performance of this reactor coupled with SR-PIMS. Key intermediate  $\cdot\text{CH}_3$  was observed with high sensitivity. All the products were found to be greatly affected by temperature, distance and reaction pressure. These findings can provide deep insights about the primary heterogeneous reaction and subsequent secondary gas-phase reactions network, which can depict the whole picture of solid-gas catalytic reactions with known surface mechanisms.

## **References**

- [1] L. Luo, X. Tang, W. Wang, Y. Wang, S. Sun, F. Qi, W. Huang, *Sci. Rep.* **2013**, 3, 1625.
- [2] Y. Li, F. Qi, *Accounts of Chemical Research* **2010**, 43, 68-78.

# **In-situ synchrotron radiation photoionization mass spectrometry (SR-PIMS) equipped with a high-pressure catalytic reactor**

*Shengsheng Yu, Wu Wen, Jiuzhong Yang, and Yang Pan\**

*(E-mail: panyang@ustc.edu.cn)*

*National Synchrotron Radiation Laboratory, University of Science and Technology of China, Hefei, Anhui 230029, P. R. China*

In-situ observation of the gas-phase catalytic products under ambient and high pressure atmosphere is crucial for the elucidation of reaction mechanisms. In this work, a high pressure catalytic reactor was designed and combined with in-situ synchrotron radiation ultraviolet photoionization mass spectrometry (SR-PIMS) <sup>[1]</sup>. The reactor was connected to the ionization chamber ( $\sim 10^{-3}$  Pa) through a differential-pumping system, and the working pressure of this reactor could be adjusted from atmospheric pressure to around 4MPa.

Fischer-Tropsch reaction with Co/SiO<sub>2</sub> as the model catalyst was selected to evaluate the performance characteristics of the reactor. Main products ranging from C<sub>1</sub> to C<sub>11</sub> were detected in real time <sup>[2]</sup>. The amounts of reaction products showed a significant pressure-dependant trend. This device could be used to detect and depict more precise processes during medium or high pressure heterogeneous catalytic reactions.

## References

[1] Jiao F, Li J, Pan X, et al. Selective conversion of syngas to light olefins[J]. Science, 2016, 351(6277): 1065-1068.

[2] Navarro V, van Spronsen M A, Frenken J W M. In situ observation of self-assembled hydrocarbon Fischer-Tropsch products on a cobalt catalyst[J]. Nature chemistry, 2016, 8(10): 929.

# Binary Alkoxide Ionic Liquids for Catalysis

*P. McNeice; A. C. Marr and P. C. Marr.*

*School of Chemistry and Chemical Engineering, and QUILL, Queen's University  
Belfast, Belfast, Northern Ireland.*

We address here the dual problems of ionic liquid instability under basic conditions, and the lack of versatile basic ionic liquids. Ionic liquids are materials which are composed entirely of ions, and are often hailed as “Green Solvents”.<sup>[1]</sup> Exchanging one ion for another allows the properties of ionic liquids to be tuned, which has led to the concept of “functionalised ionic liquids” (previously known as task-specific ionic liquids).<sup>[2]</sup> However, there are relatively few examples of base-catalysed reactions being performed in ionic liquids, probably because of the lacuna of basic ionic liquids, resulting from the instability of many ionic liquids under basic conditions.

We have prepared binary mixtures of ionic liquids containing alkoxide anions to produce highly basic ionic liquids (Figure 1).<sup>[3]</sup> The basicity of these materials is higher than many traditional bases such as Et<sub>3</sub>N, pyridine and even KOH. These novel materials have been proven to be homogeneous basic catalysts for Knoevenagel condensations and Aldol reactions. We are working towards heterogenising the system *via* sol-gel process and immobilisation upon mineral supports.

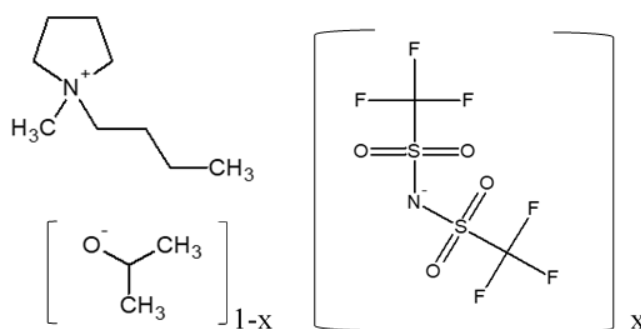


**Fig. 1 Binary alkoxide ionic liquids**

## References

- <sup>1</sup> M. Freemantle, *An Introduction to Ionic Liquids*, RSC Publications, Cambridge, UK, 2010.
- <sup>2</sup> E.D. Bates, R.D. Mayton, I. Ntai and J.H. Davis Jr., *J. Am. Chem. Soc.*, 2002, **124**, 926-927.
- <sup>3</sup> P. McNeice, A. C. Marr, P. C. Marr, M. J. Earle, K. R. Seddon, Binary Alkoxide Ionic Liquids, *ACS Sustainable Chem. Eng.*, 2018, **6**, 13676-13680.



# Hydrodeoxygenation of sorbitol into bio-alkanes and -alcohols over phosphated ruthenium molybdenum catalysts

*Yujing Weng and Yulong Zhang\**

*Henan Polytechnic University, Jiaozuo, Henan, 454000 (China)*

Increasing issues on environmental pollution and rapid consumption of fossil resources promote interests to explore sustainable production of chemicals and fuels from renewable resources. Herein, carbon supported phosphated ruthenium-molybdenum (RuMoP) catalysts were employed in a continuous trickle-bed reactor for biomass sorbitol into renewable alkanes and higher alcohols. Sorbitol was chosen for its higher thermal stability and natural hydrophilicity due to its high oxygen content than carbohydrates and readily available from degradation/hydrogenation of glucose or cellulose. The result showed that AC supported RuMoP presented complete sorbitol conversion and high yields of gasoline- and diesel-range alkanes and alcohols. Subsequently, RuMoP/CNT catalyst was prepared and studied in detail for comparison. RuMoP/CNT displayed a less C-C cracking activity with much lower content of C1-C4 products and higher content of C6 species both in gas- and oil-phases. The surface morphology, surface area, compositions and acidity of the catalysts were studied by XRD, XPS, BET, TEM, NH<sub>3</sub>-TPD and Py-IR.

## Materials and Methods

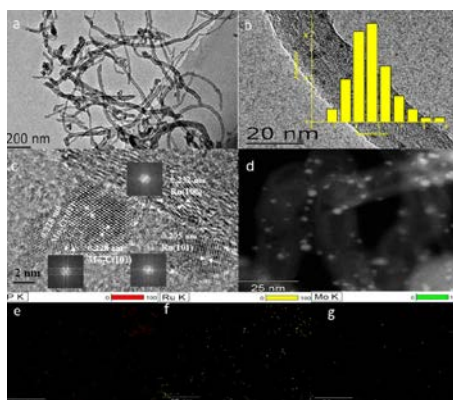


**Figure 1.** Typical TEM and HRTEM images (a, b, c, d), and corresponding EDX elemental mapping of P, Ru and Mo atoms (e, f, g) of RuMoP/CNT spent sample.

Phosphated ruthenium molybdenum carbon catalysts (RuMoP/C and RuMoP/CNT) were prepared by sequential impregnation with 1.5 wt.% Ru loading amount and molar ratio of Ru/Mo=1. HDO reaction was carried out in a tubular stainless-steel trickle-bed reactor (inner diameter of 10 mm; length of 350 mm) at 4 MPa H<sub>2</sub> pressure. During reaction, the sorbitol aqueous solution (20 wt.%) was pumped into

the trickle-bed reactor at different flow rates by a high-pressure liquid pump (HPLP). H<sub>2</sub> flow (150 cm<sup>3</sup> min<sup>-1</sup>) was purged into the reactor at the same time. The reactor set-up kept H<sub>2</sub> pressure at 4 MPa with the use of pre- and rear-pressure controller and operated in the co-current-flow of liquid and hydrogen from top to bottom.

## Results and Discussion

As reported, the HDO reaction is a catalytic process whereby the total or partial removal of oxygen from biomass derivatives.<sup>[1]</sup> Obviously, the results of sorbitol test indicated that the mono-alcohol products were key intermediates in the HDO reaction of sorbitol into alkanes and could be changed by adjusting the space velocity of the sorbitol solution. Generally, the increase of reactant space velocity could decrease the contact time, which would lead to oxygenated intermediates such as mono-alcohol. Therefore, the low C-C cracking property of metal catalyst would enhance the yield and selectivity to higher alcohols. Herein, the RuMoP catalyst presented a lower C-C cracking property with higher C5-C6 products in gas- and oil-phase. The subsequent characterizations over relevant catalysts (RuMoP/C and RuMoP/CNT) suggested that Ru and partial reduced MoO<sub>x</sub> were highly dispersed on the support with intimate contact, which would suppress the cracking property of metal Ru. Additionally, the adsorbed phosphate groups would be Bronsted acid sites and would work in concert with metal sites in HDO reaction according to literature.<sup>[2]</sup> Among the catalysts, RuMoP/CNT exhibited excellent HDO performance with high selectivity to C6 products in gas-phase (C6 alkane, 74.7%) and oil-phase (C6 alkane and alcohols, 87.8%). Detailed characterization studies suggested that RuMoP/CNT presented nice dispersion of nanoparticles on outer surface of carbon-nanotubes, which significantly increased the contact surface between the reactants and active sites, and greatly minimize the diffusion limitation<sup>[3]</sup>.

## References

- [1] Y. T. Kim, J. A. Dumesic, G. W. Huber, *J. Catal.* **2013**, *304*, 72-85.
- [2] aJ. Wang, H. Liu, S. Yang, J. Zhang, C. Zhang, H. Wu, *Appl. Surf. Sci.* **2014**, *316*, 443-450; bO. A. Rusu, W. F. Hoelderich, H. Wyart, M. Ibert, *Applied Catalysis B: Environmental* **2015**, *176-177*, 139-149; cN. Li, G. A. Tompsett, G. W. Huber, *ChemSusChem* **2010**, *3*, 1154-1157.
- [3] Y. Weng, T. Wang, C. Wang, Q. Liu, Y. Zhang, P. Duan, L. Wang, H. Yin, S. Liu, L. Ma, *ChemCatChem* **2018**.

# Higher activity of Ni/Al<sub>2</sub>O<sub>3</sub> over Fe/ and Ru/Al<sub>2</sub>O<sub>3</sub> for catalytic NH<sub>3</sub> synthesis in non-thermal atmospheric-pressure plasma of N<sub>2</sub> and H<sub>2</sub>

*Masakazu Iwamoto, Keigo Aihara, Ryu Hashimoto, Masataka Horikoshi,  
Tomiko Sawaguchi, Masahiko Matsukata  
Research Institute for Science and Engineering, Waseda University,  
3-4-1 Okubo, Sinjuku-ku, Tokyo 169-8555, Japan.*

Developing a novel ammonia synthesis process from N<sub>2</sub> and H<sub>2</sub> is of interest to the catalysis and hydrogen research communities [1]. Nickel-supported alumina ( $\gamma$ -Al<sub>2</sub>O<sub>3</sub>: Strem Chemicals Inc., USA (SC) or Kanto Chemical Co., Japan (KC)) was determined capable of serving as an efficient catalyst for ammonia synthesis using non-thermal plasma under atmospheric pressure without heating. The activity of Ni/Al<sub>2</sub>O<sub>3</sub> was quantitatively compared with that of Fe/Al<sub>2</sub>O<sub>3</sub> and Ru/Al<sub>2</sub>O<sub>3</sub>, which contained active metals for the conventional Haber-Bosch process. The activity sequence was Ni/Al<sub>2</sub>O<sub>3</sub> > Al<sub>2</sub>O<sub>3</sub> > Fe/Al<sub>2</sub>O<sub>3</sub> > no additive > Ru/Al<sub>2</sub>O<sub>3</sub>, surprisingly indicating that the loading of Fe and Ru decreased the activity of Al<sub>2</sub>O<sub>3</sub>, as shown in Figure 1. The catalytic activity of Ni/Al<sub>2</sub>O<sub>3</sub> was dependent on the calcination temperature and the reaction time. That of Ni/Al<sub>2</sub>O<sub>3</sub> calcined at 773 K decreased gradually with the reaction time and became stabilized after 2 h, while that of Ni/Al<sub>2</sub>O<sub>3</sub> calcined at 1073 K increased during the first 30 min and was stable after that. XRD, visual, and XPS observations of the catalysts before and after the plasma reaction indicated the generation of NiO, NiAl<sub>2</sub>O<sub>4</sub>, and Ni (metal) on Al<sub>2</sub>O<sub>3</sub>. The NiO species was readily reduced to Ni in the plasma reaction, whereas the NiAl<sub>2</sub>O<sub>4</sub> species, generated upon high-temperature calcination, was difficult to reduce. The catalytic behavior could be attributed to the production of small Ni particles that served as active sites. The N<sub>2</sub>/H<sub>2</sub> ratio dependence and rate constants of formation and decomposition of ammonia were determined for Al<sub>2</sub>O<sub>3</sub> and Ni/Al<sub>2</sub>O<sub>3</sub>, and summarized in Figure 2. The ammonia yields were 3.0 and 6.3 % for the catalysts at a residence time of reactant gases of 0.12 min and H<sub>2</sub>/N<sub>2</sub>=1. The results provide new insights into ammonia synthesis that will be significant for the future hydrogen economy.

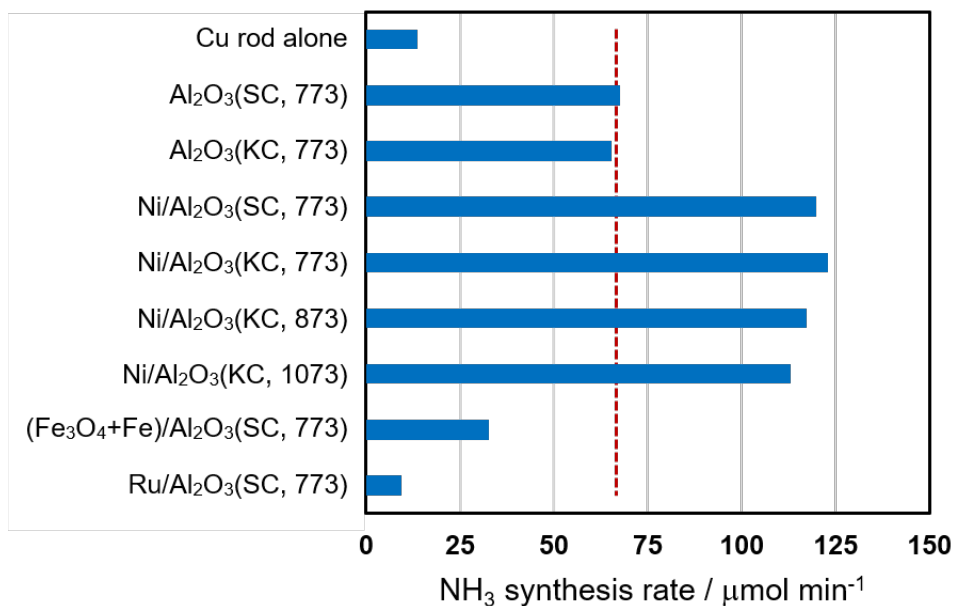


Figure 1. Comparison of activities of Ni-, Fe-, and Ru-supported  $\gamma$ -Al<sub>2</sub>O<sub>3</sub> catalysts. The broken red line indicates the average activity of Al<sub>2</sub>O<sub>3</sub> (SC) and Al<sub>2</sub>O<sub>3</sub> (KC). Reaction conditions: applied voltage, 6 kV; frequency, 50 kHz; electrode length, 150 mm; total flow rate, 100 mL min<sup>-1</sup>; and H<sub>2</sub>/N<sub>2</sub>=1.

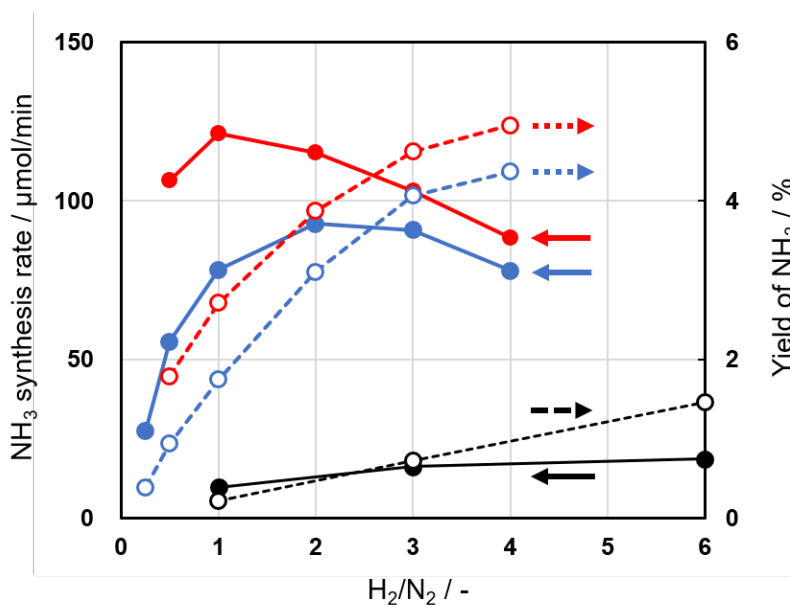


Figure 2. Change in the synthesis rate (closed) and yield (open) of ammonia as a function of the N<sub>2</sub>/H<sub>2</sub> ratio using Al<sub>2</sub>O<sub>3</sub>(KC) (blue) and Ni/Al<sub>2</sub>O<sub>3</sub>(KC, 773) (red) catalysts. The results of the blank experiment (black) are also shown for comparison. Reaction conditions: applied voltage, 6 kV; frequency, 50 kHz; electrode length, 150 mm; total flow rate, and 100 mL min<sup>-1</sup>.

## Rhodium-Catalyzed Hydroformylation promoted by Cyclodextrins: Scale-up approach into a Continuous Process

*K.U. Künnemann; D. Vogt, J.M. Dreimann, TU Dortmund, Dortmund, Germany*

Sustainability and efficiency are highly important in chemical industry. Considering the principles of Green Chemistry the development of novel, efficient production processes and the use of green solvents is needed. Therefore, the rhodium-catalyzed hydroformylation in an aqueous/organic two-phase system is considered as an economical and safe approach for the production of linear and/or branched aldehydes (Figure 1).

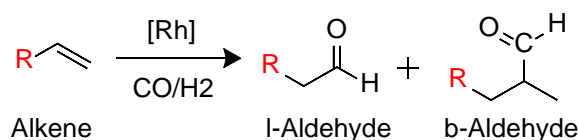


Figure 1: Rhodium catalysed hydroformylation of olefins

A biphasic system allows the recovery of the catalyst by simple phase separation, since the catalyst is dissolved in the polar aqueous phase and the organic substances represent the apolar phase. The Ruhrchemie-Rhône Poulenc process for the hydroformylation of propene, using an aqueous biphasic system is successfully applied on a large scale. Unfortunately, this rhodium-based hydroformylation process has only shown potential for the conversion of lower alkenes up to butene.<sup>[1]</sup> The solubility of higher alkenes in water is generally too low to achieve industrial important conversion rates. For the hydroformylation of longer chain alkenes is often carried out with cobalt-based catalysts at higher temperature and pressure while giving lower selectivity to the linear aldehydes.<sup>[2]</sup>

In order to use a highly efficient rhodium catalyst and water as solvent it has been reported that cyclodextrins increase reaction rates at mild reaction conditions. With their shape of a conical cylinder, with a hydrophobic inner surface and a hydrophilic outer surface, the cyclic oligosaccharides constituted of multiple D-glucopyranose units, act as mass transfer promoters between the aqueous and organic phase.<sup>[3]</sup>

Several investigations have been reported on small-scale batch experiments (10-20 ml) for the conversion of long-chained alkenes such as 1-octene or 1-decene.<sup>[4]</sup>

Therefore, this research examines the scale-up of the cyclodextrin-promoted hydroformylation into a 1-liter pressure autoclave, which is subsequently connected to a phase separator to enable a flow process by continuously recycling the catalyst (Figure 2).

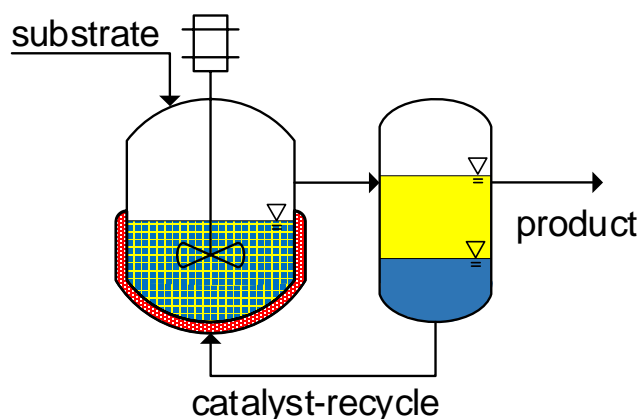


Figure 2: General flow chart of the continuous process consisting of a CSTR and a phase separator

The long-term stability of the catalyst and the cyclodextrin will be shown for this process with regard to the reaction indicators such as regioselectivity and substrate conversion. In addition, different obstacles like foam formation and their influence on the reaction performances will be discussed.

#### Reference

- [1] C. W. Kohlpaintner, R. W. Fischer, B. Cornils, *Applied Catalysis A: General* **2001**, 221, 219.
- [2] A. Behr, *Angewandte homogene Katalyse*, WILEY-VCH, Weinheim, **2008**.
- [3] H. Dodziuk, *Cyclodextrins and their complexes. Chemistry, analytical methods, applications*, WILEY-VCH, Weinheim, **2006**.
- [4] a) L. Leclercq, F. Hapiot, S. Tilloy, K. Ramkisoensing, J. N. H. Reek, P. W. N. M. van Leeuwen, E. Monflier, *Organometallics* **2005**, 24, 2070; b) E. Monflier, G. Fremy, Y. Castanet, A. Mortreux, *Angew. Chem.* **1995**, 107, 2450.

# Catalytic Hydrogenation of Sunflower Oil Over a Supported Platinum Catalyst

*K. Toshtay<sup>1</sup>, A.B. Auyezov<sup>1</sup>, Zh.A. Bizhanov<sup>1</sup>,  
S.K. Toktasinov<sup>1</sup>, Nurakyshev A<sup>1</sup>, Korkembay Zh<sup>1</sup>.*

*<sup>1</sup>Science&Technology Park, Al-Farabi Kazakh National University, Almaty,  
Kazakhstan*

*E-mail: kainaubek.toshtay@kaznu.kz*

## 1. Introduction

Catalytic hydrogenation of edible oils is most commonly used process for the food industry, during partially hydrogenated oil, mainly trans-fatty acids (TFA) are formed due to cis/trans isomerization [1]. Modern studies have shown that trans isomer adverse effects for human health. High intake of TFA has been associated with increased risk of coronary heart disease, diabetes mellitus and linked in cholesterol and promotes inflammation [2, 3]. The main challenge is now to develop more active and selective catalysts for the hydrogenation of edible oils and to reduce the trans content of hydrogenated fat products that conform to international standards. The present work concerns the synthesis, characterization and the activity of platinum supported on  $\gamma$ -Al<sub>2</sub>O<sub>3</sub>. The catalytic performance of 1.0%Pt/ $\gamma$ -Al<sub>2</sub>O<sub>3</sub> was investigated in selective hydrogenation of sunflower oil.

## 2 Experimental/methodology

1.0% Pt/ $\gamma$ -Al<sub>2</sub>O<sub>3</sub> catalyst was prepared by the colloid adsorption method. The catalyst was characterized by BET, XRD, TEM, H<sub>2</sub>-TPR and NH<sub>3</sub>-TPD. The hydrogenation tests were carried out in a batch microreactor of 100 ml. Analysis fatty acids composition and trans-isomer were determined by using a capillary gas chromatograph (CP-Sil 88, 100 m x 0.25 mm i.d., 0.2  $\mu$ m film) equipped with a flame ionization detector according to the ISO 52677 standard method.

## 3 Results and discussion

Hydrogenation of sunflower oil tests were carried out in the presence of the 1.0% Pt/ $\gamma$ -Al<sub>2</sub>O<sub>3</sub> catalyst, at three different temperatures: 90,110 and 130°C. under 0.5 MPa hydrogen pressure and stirring rate of 800 rpm. Using 0.06g catalyst per 60ml oil were loaded into the reactor.

Table 1 shows the changes of fatty acids composition and physical properties in hydrogenated sunflower oil.

Table 1. Fatty acid composition of initial and hydrogenated sunflower oil

Fatty acids (wt%)	Initial sunflower oil	1.0% Pt/ $\gamma$ -Al <sub>2</sub> O <sub>3</sub>		
		90 °C	110 °C	130 °C
C14:0 - Myristic acid	0.11	0.07	0.08	0.07
C16:0 - Palmitic acid	6.90	6.33	6.42	6.51
C18:0 - Stearic acid	4.00	17.76	18.92	19.11
C18:1 Cis -oleic acid	21.16	41.09	40.92	41.39
C18:1 Trans -oleic acid	0.21	4.08	6.15	7.10
C18:2 Cis - linoleic acid	65.71	23.24	22.23	20.75
C18:2 Trans - linoleic acid	0.83	0.44	0.56	0.71
C20:0 - Arachidic acid	0.24	0.30	0.14	0.30
C22:0 - Behenic acid	0.58	0.71	0.72	0.72
Total <i>trans isomer</i>	1.04	4.52	6.71	7.81
Iodine value	133.68	80.7	80.5	80.1
Refractive index	1.4645	1.4582	1.4582	1.4582
Melting point (°C)	-16.3	36.4	37.0	38.09

Table 1 showed 1.0% Pt/ $\gamma$ -Al<sub>2</sub>O<sub>3</sub> the best performance in activity and selectivity during the selective hydrogenation of sunflower oil. The formation of trans isomer was dramatically reduced in the hydrogenated sunflower oil. At an iodine value 80.7 the platinum catalyst formed 4.52% trans, at temperature 90°C. And trans isomer content of hydrogenated products is found to be 7.81%, at temperature 130°C.

#### 4 Conclusions

Pt catalyst was found to be active and formed to low levels of trans isomer for hydrogenation of sunflower oil and the reduced hydrogenation temperatures produces hydrogenated fat of low saturated stearic acid content.

#### Acknowledgements

The authors acknowledge the financial support of the Ministry of Agriculture of the Republic of Kazakhstan through Research program BR06249228.

#### References

1. G.R. List, J.W. King. Hydrogenation of fats and oils: theory and practice. AOCS Press, 2011. –P. 420
2. K.W.J. Wahle, W.P.T. James, Eur. J. Clin. Nutr. 1993, 47, 828-839.
3. D. Mozaffarian, B. Martijn, and et all, N. Engl. J. Med. 2006, 354,1601-1613.



# On the influence of promoters on the reduction behavior and activity of wuestite-based iron catalysts for ammonia synthesis

*R. Eckert,<sup>3</sup> J. Folke,<sup>1</sup> H. Song<sup>1</sup>, K. Kähler,<sup>1</sup> K. Dembele,<sup>2</sup> T. Lunkenbein,<sup>2</sup> B. Kniep,<sup>3</sup> S.J. Reitmeier,<sup>3</sup> A. Reitzmann,<sup>3</sup> H. Ruland,<sup>1</sup> R. Schlögl<sup>1,2</sup>*

<sup>1</sup> *MPI for Chemical Energy Conversion, Mülheim an der Ruhr, Germany*

<sup>2</sup> *Fritz Haber Institute of the Max Planck Society, Berlin, Germany*

<sup>3</sup> *Clariant Produkte (Deutschland) GmbH, Heufeld, Germany*

## Introduction

Ammonia synthesis over Fe-based catalysts is one of the most important processes in the chemical industry (Haber-Bosch process) [1]. Its usage in fertilizer production is essential for feeding today's world population. Although the Haber-Bosch process has been applied for more than 100 years already, further optimization is still ongoing with particular focus on process efficiency and energy saving [2]. The Fe-catalyzed NH<sub>3</sub> synthesis is a highly structure-sensitive reaction and even for industrial catalysts some studies estimate that less than 5 % of the Fe surface is actually covered with catalytically active centers [2].

The conventional Fe catalyst of the Haber-Bosch process is derived by reduction of a magnetite (Fe<sub>3</sub>O<sub>4</sub>) precursor with incorporation of small amounts of wuestite (Fe<sub>1-x</sub>O), α-Fe and several promoters. This was the only industrially applied Fe-based catalyst system until the discovery of a catalyst originated from a multi-promoted wuestite precursor in 1986 [3]. Compared to a magnetite-based catalyst, a wuestite-based one is easier to reduce and exhibits a higher catalytic activity [2,3]. However, further investigations are necessary for a better understanding of its superior performance. This work focuses on the influence of the main promoters (K, Al, Ca) on the properties of wuestite-based NH<sub>3</sub> synthesis catalysts (as a catalyst model system) by studying different laboratory samples prepared by the industrially applied melting process. Especially the effect of promoters on e.g., catalytic activity, reduction behavior and nanostructure is investigated.

## Experimental

Three different laboratory samples of FeO-based catalysts were tested and compared to a multi-promoted industrial FeO-based catalyst. The laboratory samples differ in their degree of promotion: besides the unpromoted wuestite sample, one catalyst precursor was promoted with K and Al and a third sample with Ca in

addition. The ammonia synthesis tests were performed in a flow set-up equipped with a guard and a synthesis reactor as well as an online IR-detector for quantitative gas analysis. 1 - 3 g of catalyst precursor were activated in a synthesis gas flow (75 % H<sub>2</sub>, 25 % N<sub>2</sub>) by reducing it to  $\alpha$ -Fe applying heating rates from 1.2 K/min to 0.2 K/min up to 500 °C and at 30 barg. The catalytic tests were performed at 400-500 °C and 90 barg.

## Results

The catalytic activity for the investigated catalyst series is shown normalized to the activity of a wuestite-based industrial catalyst at 400 °C in Figure 1. The intermediate steps at 500 °C serve as stress test, where the NH<sub>3</sub> formation is thermodynamically limited. Comparing the activity at 400 °C, an increasing activity with increasing promotion is observed. Furthermore, all samples show stable activity. In addition, the promoters have a strong influence on the reduction behavior of FeO (see Figure 2). Due to thermal disproportionation of FeO into Fe<sub>3</sub>O<sub>4</sub> and  $\alpha$ -Fe, several reduction peaks are observed for the less promoted samples; with increasing promotion the disproportionation of FeO is suppressed. Further investigations are performed to clarify the correlation between reduction behavior and activity.

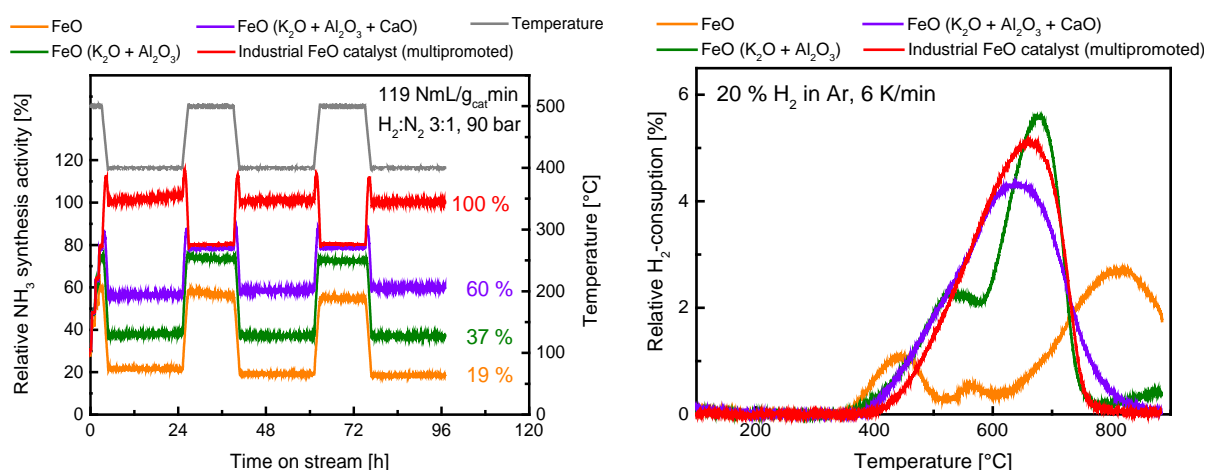


**Figure 1:** Relative NH<sub>3</sub> synthesis activity of the FeO-based samples at 400 and 500 °C.

**Figure 2:** Temperature-programmed reduction of the FeO samples.

## References

- [1] M. Appl, *Ammonia, 2. Production*, Ullmann's Encyclopedia of Industrial Chemistry (2012).
- [2] R. Schlögl, in *Handbook of Heterogeneous Catalysis*, G. Ertl, H. Knötzinger, F. Schüth, J. Weitkamp (Eds.), Wiley-VCH 2nd edition (2008).
- [3] H. Liu, W. Han, *Catalysis Today*, 297(2017) 276-291

# **Polymer-derived carbons as active and selective catalysts in the oxidative dehydrogenation of ethanol to acetaldehyde**

*Stefan Prosch, Felix Herold, Niklas Oefner, Patrick Schmatz, Alfons Drochner,*

*Bastian J.M. Etzold*

*Ernst-Berl-Institut für Makromolekulare und Technische Chemie,*

*Technische Universität Darmstadt, Alarich-Weiss-Str. 8, 64287 Darmstadt, Germany*

## **Introduction**

Solely carbon materials are known to be active catalysts for the oxidative dehydrogenation (ODH) of organic substrates like ethylbenzene [1], alkanes [2], or alcohols [3]. Especially nano-carbons were widely investigated and showed attractive yields and selectivity. Nevertheless, for an application as industrial catalysts such nano-materials keep some drawbacks with regard to the scale up of their synthesis, the pressure drop induced by a fixed bed of nano-materials and unclear health risks. Recently, the excellent catalytic properties of mesoporous graphitic carbide-derived carbons (CDC) was demonstrated, giving potential alternatives to nano-carbons [4]. Nevertheless, CDCs need to be prepared from expensive carbides and employing chlorine at temperatures above 1000 °C. With this contribution we expand the alternatives to polymer-derived carbons (PDC), which can be produced in a more economical and ecological manner. The application of these PDC materials as catalysts in the ODH of ethanol was studied.

## **Methods**

Polymer-derived carbon was synthesized by polymerization of phloroglucinol and formaldehyde in presence of the structure directing agent Pluronic F127 [5]. The resulting polymer was mixed with chloroacetic acid to increase the ion-exchange capacity and loaded afterwards with Ni as graphitization catalyst via ion exchange. Subsequent, the Ni-loaded polymer particles are submitted to carbonization between 700 and 1500 °C. The graphitization catalyst is removed by acid leaching. The kinetic investigations were performed in a fixed bed reactor with MS online analytic. A feed of 4.3 vol.-% ethanol and 10 vol.-% O<sub>2</sub> was employed at ambient pressure. Textural changes of the catalysts were analysed by N<sub>2</sub>-physisorption and Raman-spectroscopy prior and after reactions.

## Results

Spherical carbon particles with an average size of 100  $\mu\text{m}$  resulted from the synthesis. Depending on pyrolysis temperature the texture of the PDCs varied. However, in all cases mesoporous materials with BET-surfaces in the range of 80 – 570  $\text{m}^2 \text{g}^{-1}$  were obtained.

Pristine material didn't show catalytic activity. After pre-treatment with oxygen (20 %, 5 h, 300 °C) activity towards acetaldehyde as main product resulted. However, strong changes in activity and selectivity during time on stream were observed in long term runs and steady state could only be achieved after several hours (e.g. 100 h). Characterization of the catalyst after this "induction period" revealed 1) a loss of catalyst mass, 2) a formation of macropores and 3) a predominant removal of amorphous parts, while parts with higher degree of crystallinity seem to remain. Most probably during the "induction period" the active, selective and stable phase of the catalyst is formed by burning the amorphous parts. Determining activities and selectivity only after these "induction" time is crucial.

It was found that the "induction time" is strongly influenced by the pyrolysis temperature during PDC synthesis, which most likely results in a different hybrid of amorphous and crystalline carbon. Furthermore, conversion and selectivity depend strongly on the pyrolysis temperature. Exemplarily, PDC1200 shows a conversion of 61 % and a selectivity to acetaldehyde of 67 % while PDC1500 shows a conversion of 30 % and a selectivity to the aldehyde of 82 %. In addition to kinetic investigations mechanistic studies were also performed. By-products are only combustion products and ethyl acetate, acetic acid is not observed. In the presence of additionally fed water (2.5 and 5.0 vol.-%) the formation of ethyl acetate vanishes and acetic acid is detectable while the conversion of ethanol and the selectivity to acetaldehyde remains unaffected. The preferred pathway to form the ester seems to be the reaction of ethanol and acetic acid, because a co-feed with both compounds shows a strongly increase of ethyl acetate formation.

## References

- [1] N. V. Qui, P. Scholz, T. F. Keller, K. Pollok, B. Ondruschka *Chem. Eng. Tech.* 2013, 36, 300-306.
- [2] J. Zhang, X. Liu, R. Blume, A. Zhang, R. Schlögl, D. S. Su *Science* 2008, 322, 73-77.
- [3] Y. N. Zhitnev, E. A. Tveritinova, S. A. Chernyak, S. V. Savirov, V. V. Lunin *Russ. J. Phys. Chem. A* 2016, 90, 1128-1131.
- [4] J. Gläsel, J. Diao, Z. Feng, M. Hilgart, T. Wolker, D. S. Su, B. J. M. Etzold *Chem. Mater.* 2015, 27, 5719-5725.
- [5] S.-H. Chai, J. Y. Howe, X. Wang, M. Kidder, V. Schwartz, M. L. Golden, S. H. Overbury, S. Dai, D.-E. Jiang, *Carbon* 2012, 50, 1574-1582.

# Highly Selective Dehydrogenation of Bioethanol to Acetaldehyde using Copper Catalyst Supported on Mesoporous Carbon

*Rouzana Pulikkal Thumbayil; David Benjamin Christensen; Jerrick Jørgen Mielby; Søren Kegnæs, DTU Chemistry, Technical University of Denmark, Lyngby, Denmark*

## Introduction

Current dependency on non-renewable resources as energy bases are causing environmental issues like global warming, climate change and urban smog. Biomass, often called as molecular platform, could be a powerful candidate for the utilization of renewable resources for producing intermediated materials for the industry [1][2]. Acetaldehyde is an important intermediate in many of fine and bulk chemical industrial process. Today's industrial production of acetaldehyde involves oxidation of non-renewable ethylene using  $\text{PdCl}_2$  and  $\text{CuCl}_2$  in a strong acidic and corrosive solution [3]. Other methods including oxidative dehydrogenation of ethanol using gold, palladium and copper on metal oxides employed suffers from formation of highly oxidized side products, acetic acid,  $\text{CO}_2$  and  $\text{CO}$  are few among them [4]. Catalytic dehydrogenation of ethanol to acetaldehyde (DHEA) provides an inexpensive pathway for the conversion of bioethanol to acetaldehyde [5]. Here we investigate different copper catalyst supported on mesoporous carbon for the selective DHEA reaction with high conversion rate and stability with improved energy efficient process [6].

## Experimental

Various mesoporous carbon supports were synthesized typically based on a surfactant F127, resorcinol and hexamethylene tetraamine. Catalysts are synthesized by impregnating different copper precursors on mesoporous carbon support followed by reduction in pure hydrogen to obtain copper nanoparticles on mesoporous carbon support. Catalyst was loaded in a flow reactor, which is set with 10% ethanol/water mixture at atmospheric pressure and reactor outlet connected to an online GC for the timely analysis of products after regular intervals.

## Results and Discussion

Various parameters like metal loading, nature of supporting carbon, temperature etc. are tested for DHEA reaction. The role of particles distribution of nanoparticles is analysed by transmission electron microscopy (TEM) and the image is shown in Figure 1(a). The conversion results analysed using product distribution curve in Figure 1(b) over a temperature range from 210 to 350°C shows an increase in acetaldehyde production with conversion nearly 85% at 350°C, with no side products.

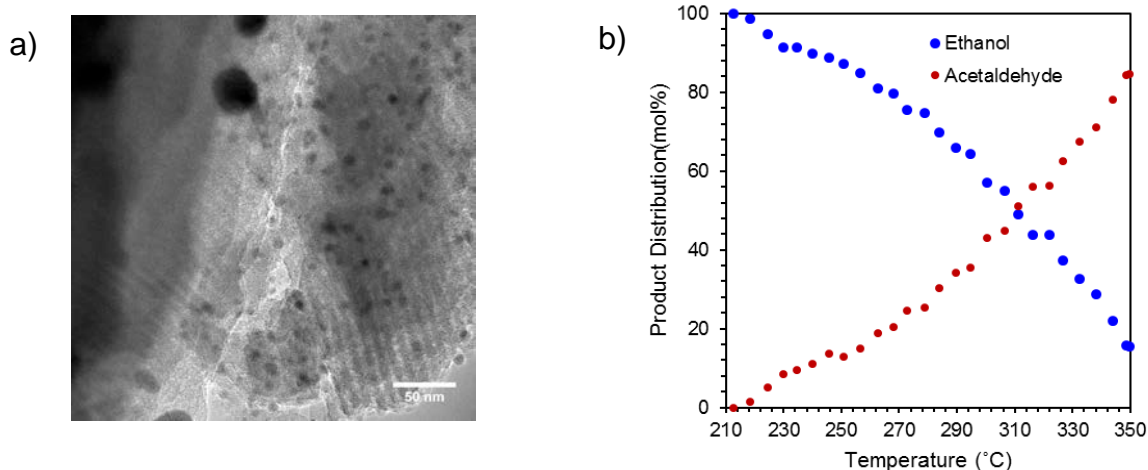


Figure 1: a) TEM image of Cu/Meso carbon b) Product distribution curve

## Conclusions

In conclusion, we report copper catalyst supported on mesoporous carbon for dehydrogenation of ethanol to acetaldehyde. The reaction is found to be highly selective. Additionally, sintering stable nature of the copper nanoparticles is confirmed by particle size analysis after the reaction via TEM. The effect of nitrogen on the reaction are also studied by altering the mesoporous carbon support by nitrogen doping.

## References

- [1] Serrano-Ruiz, J. C., Luque, R. & Sepúlveda-Escribano, A. *Chem. Soc. Rev.* **40**, 5266–5281 (2011).
- [2] Thumbayil, R. P. *et al*, *Topic Catal*, 2019, accepted
- [3] Mielby, J. Abildstrøm J. O, Wang F., Kasama T., Weidenthaler C., and Kegnæs S., *Angew. Chemie - Int. Ed.* **53**, 12513–12516 (2014).
- [4] Zhang, P. *et al*. *ChemCatChem* **9**, 505–510 (2017).
- [5] Wang, Q. N. *et al*. *Catal. Sci. Technol.* **8**, 472–479 (2018).
- [6] Thumbayil, R. P. *et al*, 2019, submitted

# Role of Base Catalyst in the Synthesis of Porous Phenol-Formaldehyde Carbons

*Inchan Yang, Jihoon Yoo, Suna An, Ji Chul Jung\*, Department of Chemical Engineering, Myongji University, Yongin, 17058, Republic of Korea*

## Introduction

In 1989, R. W. Pekala successfully synthesized porous resorcinol-formaldehyde carbons (RF carbons) from poly-condensation using base catalysts [1]. Subsequently, several studies have been conducted [2-4]. Particularly, studies on properties of porous RF carbons by controlling the type and amount of catalysts have been actively performed because different application fields require various physical properties (*e.g.*, surface area, pore size, and pore volume) [3,4]. In addition, many attempts have been conducted to replace resorcinol, which is a relatively high-cost starting material, to other inexpensive starting materials. As a starting material for porous carbons, phenol has been used due to its relatively low-cost and similar chemical formation with resorcinol. However, the reactivity of such phenol with formaldehyde is relatively low. In this study, thus, we attempted to synthesize porous phenol-formaldehyde carbons (PF carbons) using an appropriate amount of catalysts.

## Experimental

To prepare PF carbons with different physical properties, phenol and formaldehyde were poly-condensed using sodium carbonate as the base catalyst. The molar ratio of phenol and formaldehyde was kept as 1:2, and the molar ratio of phenol to catalyst (P/C) was controlled from 30 to 150. We termed the prepared porous carbons as PF\_X (X = P/C). Successful preparations of porous PF\_Xs were strongly supported by characterizations.

## Results and discussion

In the nitrogen adsorption-desorption isotherms (Fig. 1), we confirmed that all synthesized PF carbons were microporous carbon materials, and PF\_50 showed the highest micropore volume. To clearly confirm the physical properties of the prepared PF\_Xs, we calculated the values of physical properties (Table 1). All prepared PF carbons showed considerable specific surface area. Particularly, PF\_50 showed the

highest specific surface area. Consequently, we successfully prepared porous carbons with high surface area using phenol and formaldehyde under base catalyst conditions.

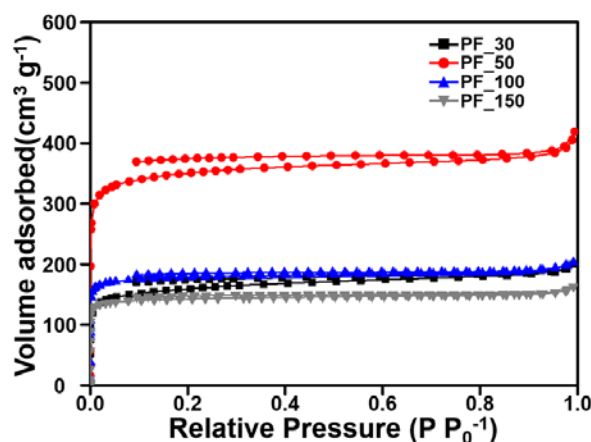


**Fig. 1.** Nitrogen adsorption-desorption isotherms of the prepared carbon materials.

**Table 1.** Physical properties of the prepared porous carbon materials.

Sample	Specific surface area [m <sup>2</sup> g <sup>-1</sup> ]	Mean pore diameter [nm]	Total pore volume [cm <sup>3</sup> g <sup>-1</sup> ]
PF_30	596.5	2.1	0.31
PF_50	1373.3	1.9	0.63
PF_100	709.4	1.8	0.31
PF_150	571.3	1.7	0.25

## Conclusions

In this study, phenol and formaldehyde were poly-condensed using sodium carbonate as the base catalyst to synthesis of porous PF carbons. In the results of nitrogen adsorption-desorption isotherms, we confirmed all PF carbons were microporous, and PF\_50 showed the highest surface area owing to abundant micropores. Finally, we successfully prepared PF carbons with high surface area under base catalyst conditions. In addition, physical properties of PF carbons well-controlled by controlling the amount of catalyst.

## References

- [1] R.W. Pekala, J. Mater. Sci., 24 (1989) 3221.
- [2] Y.J. Lee *et al.*, Curr. Appl. Phys., 10 (2010) 682.
- [3] S.J. Taylor *et al.*, Langmuir, 30 (2014) 10231.
- [4] I. Yang *et al.*, Electrochim. Acta, 223 (2017) 21.



# Progress in homogeneously catalyzed oxidation reactions – sustainability through catalyst recycling

*Johanna Vondran, Dieter Vogt, Thomas Seidensticker, Laboratory of industrial chemistry, Technical University, Dortmund, Germany*

## Abstract

Due to the change of mindset in terms of sustainability in the 21<sup>st</sup> century, the conversion of renewable resources to valuable products gains in importance in the chemical industry. An indispensable tool for walking along energy-saving reaction routes is the application of catalysis. Especially homogeneous transition metal catalysis offers formidable advantages of mild reaction conditions, high catalyst activities and high selectivities. Nevertheless, catalyst separation and recycling are challenging and often the pivotal reason for the chemical industry to decide upon heterogeneous catalysts for chemical process development due to cost-efficiency and pureness of products.

Amongst homogeneous catalysis, oxidation reactions have the highest worldwide capacity of 18 million tons per year.<sup>[1]</sup> The present challenge is the use of “green” oxidants that meet the requirements of sustainability. In particular, the prevention of waste has come to the fore. Oxidants like potassium permanganate or chromium trioxide are expensive and often result in the formation of undesired co-products, whereas with economic oxidants like oxygen (from air) or hydrogen peroxide only water is formed.<sup>[1]</sup>

To name two types of homogeneously catalyzed oxidations as model reactions, the Wacker-Tsuji oxidation and the oxidative cleavage of higher olefins are interesting subjects of research opening up a plethora of valuable products, including methyl ketones, aldehydes and (di-)carboxylic acids.<sup>[2,3]</sup> In the present work, recycling studies for the two model reactions are focused on two main concepts, i.e. thermomorphic multiphase systems (TMS) and membrane technique (Figure 1).

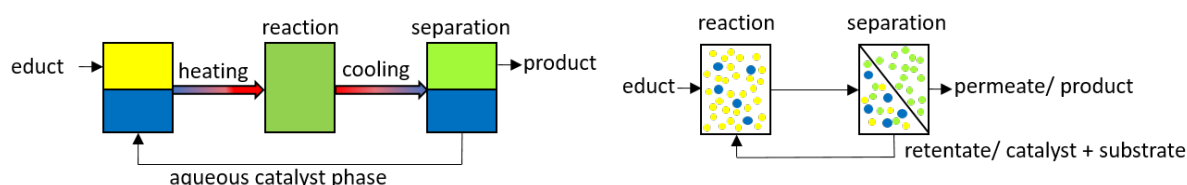


**Figure 1: catalyst separation and recycling via TMS (left) or membrane technique (right)**

Homogeneously catalyzed oxidative cleavage of higher olefins like oleic acid provides an alternative to the energy-demanding industrial ozonolysis resulting in pelargonic acid and azelaic acid, both of industrial relevance. This ruthenium-catalyzed reaction makes use of hydrogen peroxide as oxidant and is performed under relatively mild reaction conditions. Dipicolinic acid has been reported as most active ligand, nevertheless, in terms of developing a suitable TMS, the catalyst should be preferably soluble in the aqueous phase. Additionally, acetonitrile is used as a solvent, so that the mixture is homogeneous at any temperature.<sup>[4]</sup> In conclusion, for implementation of catalyst recycling *via* TMS, an investigation towards water-soluble ligands and the reduction of acetonitrile as solvent are of need.

Another approach for recycling is based on replacing the ruthenium catalyst by polyoxometalates like phosphotungstic acid, which exhibit a high molecular weight and solubility in polar solvents, so that a membrane separation is conceivable as well as the development of a TMS (Figure 2).

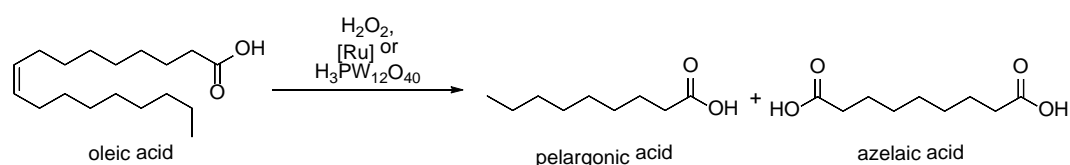


**Figure 2: homogeneous transition metal catalyzed oxidative cleavage of oleic acid**

In the Palladium-catalyzed Markownikow-selective Wacker-Tsuji oxidation of terminal alkenes to methyl ketones, a broad variation of reactants has been reported, although a recycling of the homogeneous catalyst has not been investigated so far. Green oxidants like hydrogen peroxide are of special interest for regeneration of the (co-)catalyst. Feasible recycling of the catalytic system could be implemented in a TMS, since aqueous solvents are applied for the conversion to organic products. From the state of research, the lack of homogeneous catalyst recycling in the oxidative cleavage of fatty acids and the Wacker-Tsuji oxidation of olefins as exemplaries for industrially relevant sustainable oxidations becomes apparent. In this work, we report TMS and membrane technique as promising approaches for process development.

## References

- [1] A. Behr, *Angewandte Homogene Katalyse*, Wiley-VCH Verlag GmbH & Co. KGaA, Weinheim, **2008**.
- [2] A. E. Kerenkan, F. Béland, T.-O. Do, *Catal. Sci. Technol.* **2016**, *6*, 971–987.
- [3] T. Veetil, E. Gravel, E. Doris, I. N. N. Namboothiri, *Tetrahedron Lett.* **2016**, *57*, 3993–4000.
- [4] N. Tenhumberg, *Katalytische Oxidative Spaltung Des Ölsäuremethylesters*, Verlag Dr. Hut, München, **2013**.

# **One-pot synthesis of vanadium-containing silica SBA-3 materials and their catalytic activity for propene epoxidation**

*Ewa Janiszewska, Agnieszka Held, Jolanta Kowalska-Kuś, Aldona Jankowska, Krystyna Nowińska, Stanisław Kowalak, Adam Mickiewicz University, Faculty of Chemistry, 61-614 Poznań, Poland*

Vanadium species supported on mesoporous silica materials such as MCM-41, SBA-15, HMS or MCF are known to be effective catalysts in oxidative dehydrogenation (ODH) of alkanes, partial oxidation of methane or methanol oxidation to formaldehyde. Recently, it was shown that all silica mesoporous materials of SBA-3 structure modified with vanadium by means of impregnation method are active catalyst in propene epoxidation with  $N_2O$  as an oxidant [1]. However, there are some literature reports showing that vanadium containing mesoporous materials obtained by the direct synthesis show better catalytic performance than their vanadium supported counterparts. Their high performance has been attributed to the wide dispersion of highly reducible vanadium-isolated species with tetrahedral coordination.

Our studies presents synthesis, characterization and catalytic activity of novel promising vanadium-containing SBA-3 catalysts. In the presented study V-SBA-3 mesoporous catalysts were prepared by means of one-pot hydrothermal procedure using different vanadium precursors ( $NH_4VO_3$  or  $VOSO_4$ ) and under various pH of the reaction mixture (pH<1, 2.2 or 3.1). The combined usage of various physicochemical methods (DR UV-vis, FTIR, EPR,  $H_2$ -TPR) allowed to determine the nature of vanadium species in the studied samples. The catalytic activity of the samples was tested in propene epoxidation with  $N_2O$  as an oxidant.

It was evidenced that silica SBA-3 molecular sieves with incorporated vanadium can be successfully prepared in acidic medium using  $VOSO_4$  or  $NH_4VO_3$  as V precursors. The nature of precursor as well as pH of the synthesis mixture influence the properties of the resulting products and their catalytic activity. Using of  $VOSO_4$  allowed to introduce only small amount of vanadium (< 1 wt. %) regardless of the pH of the synthesis mixture, whereas in the presence of  $NH_4VO_3$  and at higher pH value the high V content samples (~5 wt. %) have been obtained (Table 1). All the investigated samples show highly dispersed, isolated tetrahedrally coordinated  $VO_x$

species including both monomeric  $\text{VO}_4$  vanadyl and oligomeric  $\text{VO}_x$  species, regardless of vanadium content.

Table 1 Chemical and structural properties of samples

Sample	V source	pH	Si/V <sup>a</sup>	S <sub>BET</sub> <sup>b</sup> [m <sup>2</sup> g <sup>-1</sup> ]
Vs <sub>1</sub> -SBA-3	VOSO <sub>4</sub>	<1	165	1411
Vs <sub>2</sub> -SBA-3	VOSO <sub>4</sub>	2.2	140	1275
Vs <sub>3</sub> -SBA-3	VOSO <sub>4</sub>	3.1	162	1327
Vm <sub>1</sub> -SBA-3	NH <sub>4</sub> VO <sub>3</sub>	<1	354	1370
Vm <sub>2</sub> -SBA-3	NH <sub>4</sub> VO <sub>3</sub>	2.2	14	1020
Vm <sub>3</sub> -SBA-3	NH <sub>4</sub> VO <sub>3</sub>	3.1	12	965

<sup>a</sup> the molar ratio of Si/V calculated from the ICP results, <sup>b</sup> BET specific surface area

Catalyst have been tested in direct propene epoxidation in the presence of  $\text{N}_2\text{O}$  as an oxidant in the temperature of 380 and 400°C. We have evidenced that vanadium modified SBA-3 materials show noticeable activity in the formation of epoxide. The activity is significantly affected by vanadium content resulting from the usage of different pH of the synthesis and, even more, from vanadium precursor.

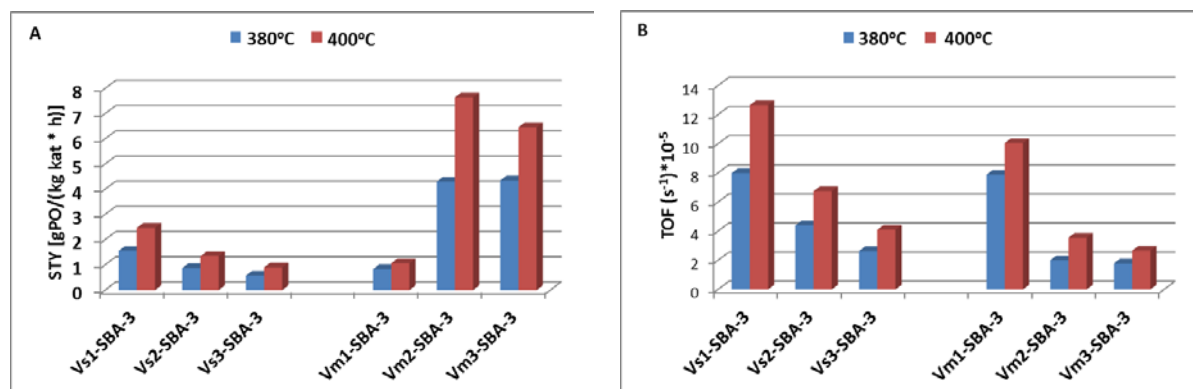


Figure 1. Comparison of specific activity expressed as space time yield (STY) (A) and turn over frequency (TOF) (B) for propene epoxidation toward propene oxide on V-SBA-3 at different reaction temperatures: at 380 °C and 400 °C (V<sub>s</sub>-SBA-3 series obtained with VOSO<sub>4</sub>, V<sub>m</sub>-SBA-3 series obtained with NH<sub>4</sub>VO<sub>3</sub>).

Although the highest propene oxide (PO) productivity was achieved over V-SBA-3 samples with high vanadium content (> 5 wt. %), the comparison of TOF values evidenced that some vanadium species do not show activity towards mild electrophilic oxygen species generation enable the formation of PO (Figure 1).

## References

[1] A. Held, J. Kowalska-Kuś, K. Nowińska, Catal. Commun. 17 (2012) 108-113.

## Acknowledgements

This work was supported by National Science Centre (grant no. 2016/23/B/ST5/00615).

## **Epoxidation of propane and propene with nitrous oxide and/or oxygen on silica-supported vanadium catalysts**

*Agnieszka Held, Justyna Czerepińska, Ewa Janiszewska, Jolanta Kowalska-Kuś,  
Krystyna Nowińska, Adam Mickiewicz University, Faculty of Chemistry,  
61-614 Poznań, Poland*

Propylene oxide (PO) is a very important intermediate applied for the production of many various consumer goods such as polypropylene glycol, polyether polyols and many others. Despite the development of new methods of PO production, more than 40% of world production is still conducted by means of the chlorhydrine method [1]. Recently, we have evidenced that propene [2] and also propane [3] can be directly processed to propylene oxide with  $N_2O$  over vanadium-containing mesoporous materials. Nevertheless, the activity of the vanadium supported catalysts decreased noticeable with time on stream, especially when propane was used as a substrate. We have found that the reduction of vanadium was mainly responsible for the rapid deactivation of the V-containing system in propane oxidation [3]. Propane oxydehydrogenation occurs according to Mars van Krevelen mechanism, while reoxidation of vanadium in the presence of  $N_2O$  is much slower when compared to molecular oxygen [4]. Therefore, in the presented studies the effect of oxidant ( $N_2O$  or oxygen or the mixture of both oxidants) on catalysts performance in propene and propane epoxidation has been searched. Synergy effect of oxygen and nitrous oxide in propane oxidative dehydrogenation has been already reported in literature [5].

In the presented studies supported vanadium catalysts have been prepared by wet impregnation of vanadium compounds solution over various mesoporous silica supports (SBA-15, MCF, MCM-41, SBA-3). The nature of vanadium species in the studied catalysts was investigated by different physicochemical methods (DR UV-vis, FTIR, Raman,  $H_2$ -TPR). Catalytic activity was measured in glass flow reactor in the temperature range of 673 to 743 K under atmospheric pressure. Composition of reagents and products mixtures was estimated from GC analysis using two chromatographs equipped with TCD and FID detectors. Typically, a total flow rate was  $28.5 \text{ cm}^3/\text{min}$  and the feed composition was 1 vol.% of propene/propane and 15 vol.% of  $N_2O$  or 1 vol.% of  $O_2$  + 13 vol.% of  $N_2O$  in helium.

Both oxidation activity and product distribution recorded as an effect of propene or propane oxidation in the presence of N<sub>2</sub>O or with the mixture of N<sub>2</sub>O and O<sub>2</sub> differ significantly. Propane oxidation requires higher reaction temperature (703 – 773 K), while propene epoxidation occurred already at 673 K, regardless of the applied oxidant. We have found that during the oxidation both propane and propene in the presence of O<sub>2</sub> (both alone oxygen and in the mixture with N<sub>2</sub>O) the selectivity to CO<sub>x</sub> markedly increases. When exclusively N<sub>2</sub>O was used as an oxidant in propene epoxidation, besides PO we have observed the oxygen-bearing products such as propionaldehyde, acrolein and acetone. Addition of O<sub>2</sub> into the reaction mixture resulted in growing selectivity to acrolein at the expense of propionaldehyde and acetone.

The contribution of oxygen in the mixture with N<sub>2</sub>O in direct propane epoxidation resulted in much lesser decrease in hydrocarbon conversion with time on stream. It confirms our previous suggestions about the crucial role of vanadium reoxidation in direct propane epoxidation. On the basis of spectroscopic measurements and the catalytic data the possible mechanism of propane and propene oxidation with nitrous oxide or O<sub>2</sub> and N<sub>2</sub>O mixture has been proposed.

#### **References**

- [1] T. A. Nijhuis, M. Makkee, J. A. Moulijn, B. M. Weckhuysen, *Ind. Eng. Chem. Res.* 45 (2006) 3447-3459.
- [2] A. Held, J. Kowalska-Kuś, K. Nowińska, *Catal. Commun.* 17 (2012) 108-113.
- [3] A. Held, J. Kowalska-Kuś, K. Nowińska, *J. Catal.* 336 (2016) 23-32.
- [4] E. V. Kondratenko, M. Cherian, M. Baerns, D. Su, R. Schlögl, X. Wang, I. E. Wachs, *J. Catal.* 234 (2005) 131–142.
- [5] R. Bulánek, B. Wichterlová, K. Novoveská, V. Kreibich, *App. Catal. A: Gen.* 264 (2004) 13–22.

#### **Acknowledgements**

This work was supported by National Science Centre (grant no. 2016/23/B/ST5/00615).

# Encapsulation of Metal Nanoparticle Catalysts in Porous Silica-based Shells

*Simone Louise Zacho, Technical University of Denmark, Kgs. Lyngby, Denmark;*

*Jerrik Mielby, Technical University of Denmark, Kgs. Lyngby, Denmark;*

*Søren Kegnæs, Technical University of Denmark, Kgs. Lyngby, Denmark*

## Introduction

A pronounced focus in the field of supported metal nanoparticle catalysts is the synthesis of small metal nanoparticles encapsulated in shells to enhance catalytic efficiency. The synthesis of conventional nanoparticle catalysts often suffer from poor control of nanoparticle size distribution and their deactivation by sintering at high temperatures [1]. However, highly sinter-stable catalysts have recently been achieved by encapsulation of individual nanoparticles in porous materials [2-4].

Here we present the use of different zeolite and silica-based shells to encapsulate metal nanoparticles to enhance the control of the metal loading, metal nanoparticle size distribution and leaching, among other things. An example is the use of Metal-Organic Frameworks (MOFs) as templates and self-sacrificing precursors to obtain various high surface area catalysts with encapsulated metal nanoparticles. These catalysts show promising activity and excellent stability as catalysts for several reactions including CO oxidation [5].

## Experimental

All prepared materials were synthesized from commercially available chemicals. The MOFs were prepared by mixing metal nitrates with 2-methylimidazole in methanol. The metal oxide shells were synthesized by adding a surfactant and a metal oxide precursor. All syntheses included a final heating step in either Ar and/or air to yield the final catalysts.

The catalysts were characterized with TEM, SEM, STEM, XRD, XPS, XRF and N<sub>2</sub> physisorption.

## Results and discussion

We have proved that it is possible to obtain a better control and higher stability by encapsulating catalysts in porous silica-based shells. One example demonstrated

the ability to synthesize nanorattle catalysts of different metal loadings, nanoparticle size distributions and nanorattle particle sizes from MOFs. Moreover, it was possible to control the 3D distribution of the encapsulated metal nanoparticles by simple changes in the heating steps [6]. The synthesis route had a large effect on the catalytic activity, which as a proof of concept was shown in CO oxidation. Here, the best activity was achieved with a nanorattle catalyst comprised of Co nanoparticles in a mesoporous SiO<sub>2</sub> shell. Figure 1. presents the synthesis route to obtain the encapsulated nanoparticle catalysts (nanorattles) with different characteristics. Other work has been conducted on encapsulation of polyoxometalates and FeMo-based catalysts in zeolites and SiO<sub>2</sub> shells.

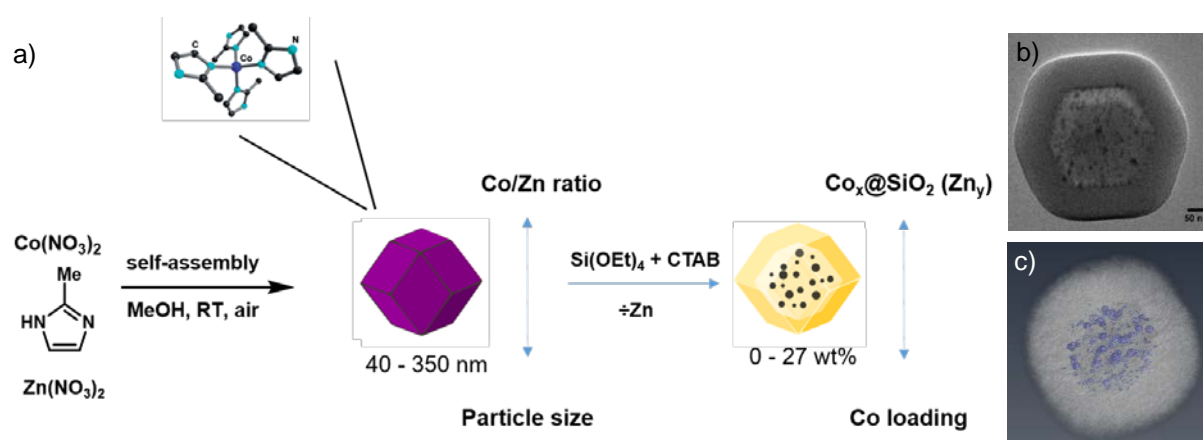


**Figure 1.** a) Illustration of catalyst synthesis pathway. b) TEM image of Co nanorattle catalyst and c) tomographic reconstruction of Co nanoparticles inside a mesoporous SiO<sub>2</sub> nanorattle catalyst, entitled Co<sub>x</sub>@SiO<sub>2</sub> (Zn<sub>y</sub>) where x and y are variables.

## Conclusions

These results illustrates a simple way to prepare various encapsulated metal nanoparticles catalysts in porous silica-based shells, which can be used to develop efficient and more sinter-stable catalysts.

## References

- [1] T. W. Hansen, A. T. DeLaRiva, S. R. Challa and A. K. Datya, *Acc. Chem. Res.* **2013**, 46, 125.
- [2] P. M. Arnal, M. Comotti and F. Schüth, *Angew. Chem. Int. Ed.* **2006**, 45, 8224.
- [3] B. Chen, Z. Yang, Y. Zhu and Y. Xia, *Journal of Materials Chemistry a.* **2014**, 2(40), 16811-16831.
- [4] K. Shen, X. Chen, J. Chen and Y. Li, *ACS Catalysis.* **2016**, 6(9), 5887-5903.
- [5] S. L. Zacho, J. Mielby and S. Kegnaes, *Topics in Catalysis.* **2019**, accepted.
- [6] S. L. Zacho, J. Æ. Hyllested, T. Kasama and J. Mielby, *Catalysis Communications.* **2019**, accepted.



# **Structure effects of supported silver catalysts prepared via melt infiltration in the selective hydrogenation of cinnamaldehyde**

*Petra H. Keijzer, Lee J. Durndell, Baira Donoeva, Jovana Zečević,*

*Petra E. de Jongh, Krijn P. de Jong, Inorganic Chemistry and Catalysis, Debye Institute for Nanomaterials Science, Utrecht University, Utrecht, The Netherlands*

## **Introduction**

Silver catalysts are industrially used amongst others to produce formaldehyde from methanol, and to selectively oxidize ethylene to ethylene oxide [1]. Moreover, silver has promising catalytic properties for the selective hydrogenation of  $\alpha,\beta$ -unsaturated aldehydes [2]. Supported silver catalysts are generally synthesized using precipitation or impregnation routes. As an alternative technique we explore melt infiltration: we heat a physical mixture of silver nitrate and a porous silica support, in this case SBA-15, above the melting point of silver nitrate, which then enters the pores as a result of capillary forces. Advantages are that catalysts with high metal loadings can be obtained and dissolution of the precursor salt is not needed [3], but challenges arise regarding control over the particle size and distribution of the silver. We show the synthesis of either supported silver nanowires or spherical particles, and their application in the hydrogenation of cinnamaldehyde.

## **Results**

The narrow pore size distribution of the chosen ordered mesoporous silica support, SBA-15, allowed us to study the infiltration process using differential scanning calorimetry, by measuring the heat loss or gain during phase transitions. We found that >90% of the silver nitrate infiltrated into the pores of the SBA-15 after heating the material to 250 °C for 20 h. Subsequently, the silver nitrate was decomposed to obtain supported silver nanoparticles or nanowires. The well-defined pore structure, and hence absence of support irregularities, allowed direct control over silver size and shape. Both transmission electron microscopy and in-situ X-ray diffraction were used to follow the decomposition process. By varying the decomposition conditions (temperature and gas atmosphere), either long silver nanowires (Figure, left) or spherical silver particles (Figure, right) inside the mesopores of the SBA-15 were obtained, while few large silver particles were

present on the external surface area in all cases (see Figure). Silver nanowires inside the SBA-15 pores were obtained when the composite was heated slowly to 130 °C in a 10% hydrogen in nitrogen flow, while spherical particles were obtained by starting the reduction at 250 °C following prior heating in nitrogen flow.

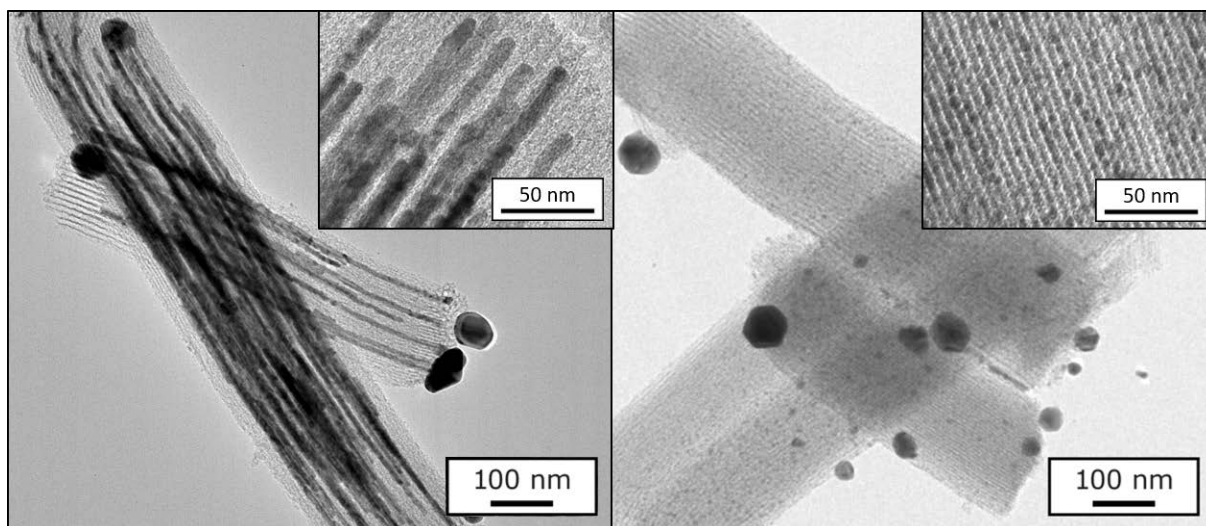


Figure: Transmission electron microscopy images of Ag/SBA-15 composites obtained after reduction of silver nitrate in hydrogen.

Subsequently, we investigated the influence of Ag morphology and size when used as a catalyst for the liquid phase hydrogenation of cinnamaldehyde. In this reaction, both the C=O and the C=C bond of this  $\alpha,\beta$ -unsaturated aldehyde can be hydrogenated. We found that the silver wires were more selective towards C=O bond hydrogenation (75% at 35% conversion), which gives the desired cinnamyl alcohol, than spherical silver particles (52% at 35% conversion). Claus et al. reported silver particle size effects in the hydrogenation of another  $\alpha,\beta$ -unsaturated aldehyde, crotonaldehyde, in the gas phase [2]. Building on their findings, we propose that also in liquid phase catalysis, the higher selectivity towards C=O bond hydrogenation for the silver wires can be ascribed to the greater exposure of Ag(111) facets, while spherical particles have more edge and corner sites.

#### References

- [1] M. O. Ozbek, I. Onal, R. A. van Santen, *J. Catal.*, 284, 230–235 (2011)
- [2] P. Claus, H. Hofmeister, *J. Phys. Chem. B*, 103, 2766–2775 (1999)
- [3] P. E. de Jongh, T. M. Eggenhuisen, *Adv. Mater.*, 25, 6672–6690 (2013)

# Heterogeneous Transition Metal-Catalysed Amination of Alcohols: A Computational Study

*Julien Engel, Alberto Roldan*

*School of Chemistry, Cardiff University, Cardiff, Wales, United Kingdom*

Amines are probably the most important group of organonitrogen compounds as they are among the basic building blocks of all living organism and are used in chemical industry as agrochemicals, drugs, polymers, and reactive intermediates in the production of a large variety of fine and bulk chemicals.<sup>[1]</sup> Therefore, cheap and sustainable methodologies for the formation of amines and the introduction of new C–N bonds are of particular interest.

Alcohols are readily available substrates and their direct conversion to amines is highly atom economic. Due to the relative unreactive nature of the alcohols, they have to be converted to more reactive derivatives such as aldehydes or ketones. To avoid an expensive and inefficient step-wise process using oxidation and reducing agents and potentially multiple purification steps, efficient catalysts are required to promote all of the reaction steps: the oxidation to the carbonyl compound, the imination, as well as the reduction of the imine intermediate (cf. Figure 1).<sup>[2]</sup> This reaction mechanism is often called “*borrowing hydrogen concept*”, since the hydrogen produced in the oxidation step is retained and used for the reduction step.

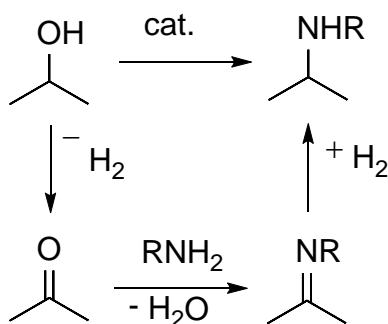


**Figure 1: Amination of alcohols following a borrowing hydrogen mechanism.**

In recent years, several effective transition metal-based heterogeneous catalysts for the amination of alcohols through a *borrowing hydrogen mechanism* have been developed.<sup>[3]</sup> However, many of these systems require the use of additives like Brønsted bases, Lewis acids or hydrogen gas, which dramatically reduces the atom economy of the reaction. The need for these additives indicates weak performance of the catalysts in some of the reaction steps.

In this study, the amination of alcohols with heterogeneous group VIII-X transition metal catalysts is investigated using density functional theory calculations. Theoretical calculations give the unique possibility to investigate the intrinsic performance of the catalysts in each step of the amination process to identify properties and parameters giving high catalytic performance. This valuable information can be used for a rational design of new materials with optimised catalytic efficiency and without the need for additives.

## References

[1] S. A. Lawrence, *Amines: Synthesis, Properties, and Applications*, Cambridge University Press, Cambridge, **2004**.

[2] K. Shimizu, *Catal. Sci. Technol.* **2015**, *5*, 1412.

[3] For examples see: a) R. Pfützenreuter, M. Rose, *ChemCatChem* **2016**, *8*, 251; b) K. I. Shimizu, K. Kon, W. Onodera, H. Yamazaki, J. N. Kondo, *ACS Catal.* **2013**, *3*, 112; c) A. Corma, T. Ródenas, M. J. Sabater, *Chem. - A Eur. J.* **2010**, *16*, 254; d) K. Shimizu, K. Shimura, M. Nishimura, A. Satsuma, *RSC Adv.* **2011**, *1*, 1310; e) H. Liu, G. K. Chuah, S. Jaenicke, *J. Catal.* **2012**, *292*, 130; f) L. He, X. B. Lou, J. Ni, Y. M. Liu, Y. Cao, H. Y. He, K. N. Fan, *Chem. - A Eur. J.* **2010**, *16*, 13965.

# **Pt on activated carbon for carbohydrate oxidation: effect of particle size and support surface chemistry**

*Marlene Führer, Tomas van Haasterecht and Harry Bitter,  
Biobased Chemistry and Technology Laboratory, Wageningen University,  
harry.bitter@wur.nl*

## **Introduction**

Oxidized starch is considered to be a promising renewable replacement for polyacrylates and polyacrylamides because of its efficient absorbing properties [1]. In particular, the paper and textile industry have a major interest in oxidized starch. However, the current production routes of oxidized starch utilize hazardous bleaching agents, such as halogens and peroxides. Hence, this study aims at employing a heterogeneous catalyst for the oxidation of starch, using air as a sustainable and environmentally friendly oxidant.

Platinum on activated carbon (Pt/AC), has previously been shown to be suitable for the selective oxidation of carbohydrates [2, 3]. Here, we will also consider the oxidation of glucose and later starch. The focus of this study will be to investigate the effect of particle size and support surface chemistry on the catalytic performance of Pt/AC.

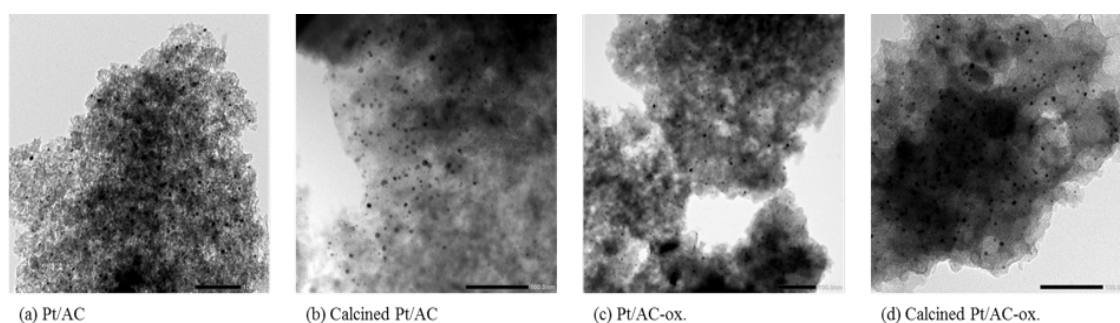
## **Materials/methods**

Two different methods for modifying the Pt were used: 1) calcination of the catalyst before catalyst activation (reduction) or 2) introduction of oxygen groups on the surface of the support. It is hypothesized that both procedures reduce the Pt particle size and enhance the dispersion of Pt on the support. In addition to the direct influence of particle size on activity by making available more reactive surface area the oxygen groups could also influence the catalytic activity either by modifying the adsorption of the reactants or via an electronic effect on the Pt.

## **Results and Discussion**

Figure 1 summarizes the obtained particle sizes from different characterization techniques and the Turnover Frequency (TOF) of the glucose oxidation reactions. As

the catalyst was calcined (b & d), the particle size becomes smaller compared to the non-calcined catalyst (a & c), while the oxidation treatment of the support seems not to have an effect on the catalyst preparation (a & b compared to c & d). Based on the TOF, a slightly higher catalytic activity for the calcined catalyst (b & d) can be seen which might be explained by a particle size effect. However, the calcined Pt catalyst on an oxidized support (d) exhibited the highest catalytic activity (2.8 s<sup>-1</sup>). Apparently only the combination of oxidizing the support and calcining the precursor lead to a high activity. This cannot be explained by a particle size effect or adsorption effect of reactants. Therefore we tentatively explain this by an electronic modification of the Pt after these treatments. A more detailed investigation with a.o., XPS and XAFS is



Samples	Particle Size (nm)			TOF <sup>a</sup> (s <sup>-1</sup> )
	TEM	XRD	Chemisorption	
(a) Pt/AC	4.9	1.5	2.5	1.2
(b) Calcined Pt/AC	4.6	0.9	1.9	1.9
(c) Pt/AC-ox.	4.9	2.2	3.2	0.6
(d) Calcined Pt/AC-ox.	4.0	1.3	1.7	2.8

currently carried out.

**Figure 1.** Preliminary Pt particle size and glucose oxidation degree (TOF) of the Pt/AC catalyst either thermal pre-treated and supported on different AC

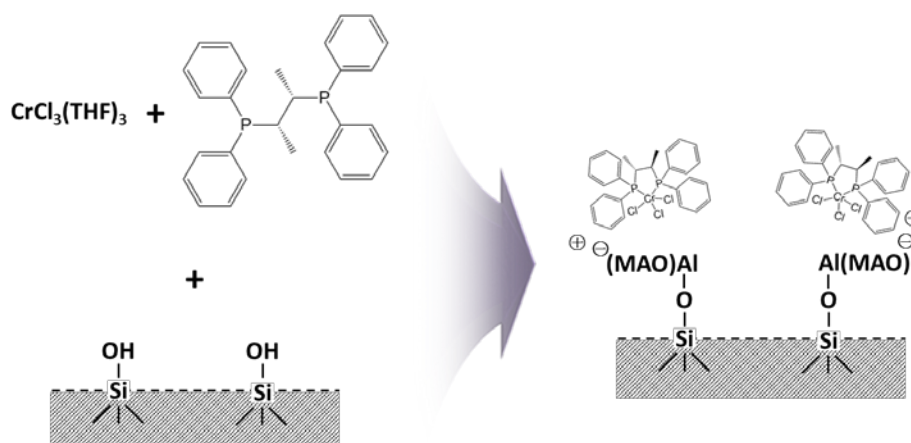
## References

1. Chen, Xiaoli, et al. "Effect of Cs content on Cs x H 5- x PMo 10 V 2 O 40 properties and oxidative catalytic activity on starch oxidation by H 2 O 2." *RSC Advances* 4.22 (2014).
2. Besson, Michèle, Pierre Gallezot, and Catherine Pinel. "Conversion of biomass into chemicals over metal catalysts." *Chemical Reviews* 114.3 (2013).
3. Lee, Jechan, Basudeb Saha, and Dionisios G. Vlachos. "Pt catalysts for efficient aerobic oxidation of glucose to glucaric acid in water." *Green Chemistry* 18.13 (2016).

## The selective oligomerization of ethylene using silica supported chromium-phosphide catalysts

*Min Suk Choi, Department of Chemical and Biomolecular Engineering, Korea Advanced Institute of Science and Technology, Daejeon 34141, South Korea; Hyunjoo Lee\*, Department of Chemical and Biomolecular Engineering, Korea Advanced Institute of Science and Technology, Daejeon 34141, South Korea;*

Linear alpha-olefins, such as 1-hexene and 1-octene, are used primarily as comonomer for the synthesis of linear low-density polyethylene (LLDPE), plasticizers and synthetic lubricants [1-4]. Most of the ethylene tri-/tetramerization catalyst system based on homogeneous chromium catalyst [5-9]. However, even the most ethylene oligomerization catalysts usually produce polyethylene as a side product leads to reactor fouling and clogging of lines in laboratory scale batch reactions. Also, this catalytic system must be avoided from impurities because they are very vulnerable to air and moisture. One possible solution is heterogeneous catalytic system. In this study, Cr/PCCP catalyst was supported on various silica supports such as fumed silica, silica nanopowder and mesoporous silica for ethylene oligomerization reaction. Mesoporous silica supported Cr/PCCP catalyst presented comparable oligomerization activity with homogeneous catalyst. Also, improved selectivity of polyethylene and 1-octene were observed with mesoporous silica supported Cr/PCCP. Interestingly, heterogeneous catalysts have better resistance to impurity than homogeneous catalysts. Heterogeneous catalyst which was treated with air and moisture showed similar activity and selectivity to as-made sample.



## References

1. Bollmann, A.; Blann, K.; Dixon, J. T.; Hess, F. M.; Killian, E.; Maumela, H.; McGuinness, D. S.; Morgan, D. H.; Neveling, A.; Otto, S.; Overett, M.; Slawin, A. M. Z.; Wasserscheid, P.; Kuhlmann, S., Ethylene tetramerization: A new route to produce 1-octene in exceptionally high selectivities. *J Am Chem Soc* 2004, 126 (45), 14712-14713.
2. Skupinska, J., Oligomerization of Alpha-Olefins to Higher Oligomers. *Chem Rev* 1991, 91 (4), 613-648.
3. Tullo, A. H., Single-site catalysts - New tailor-made plastics with superior properties are scoring big with film producers as polyolefin makers vie to get in the game. *Chem Eng News* 2000, 78 (32), 35-+.
4. Morse, P. M., Downturn for petrochemicals. *Chem Eng News* 1999, 77 (11), 19-24.
5. Agapie, T.; Schofer, S. J.; Labinger, J. A.; Bercaw, J. E., Mechanistic studies of the ethylene trimerization reaction with chromium-diphosphine catalysts: Experimental evidence for a mechanism involving metallacyclic intermediates. *J Am Chem Soc* 2004, 126 (5), 1304-1305.
6. Overett, M. J.; Blann, K.; Bollmann, A.; Dixon, J. T.; Haasbroek, D.; Killian, E.; Maumela, H.; McGuinness, D. S.; Morgan, D. H., Mechanistic investigations of the ethylene tetramerisation reaction. *J Am Chem Soc* 2005, 127 (30), 10723-10730.
7. Jiang, T.; Zhang, S.; Jiang, X. L.; Yang, C. F.; Niu, B.; Ning, Y. N., The effect of N-aryl bisphosphineamine ligands on the selective ethylene tetramerization. *J Mol Catal a-Chem* 2008, 279 (1), 90-93.
8. Blann, K.; Bollmann, A.; de Bod, H.; Dixon, J. T.; Killian, E.; Nongodlwana, P.; Maumela, M. C.; Maumela, H.; McConnell, A. E.; Morgan, D. H.; Overett, M. J.; Pretorius, M.; Kuhlmann, S.; Wasserscheid, P., Ethylene tetramerisation: Subtle effects exhibited by N-substituted diphosphinoamine ligands. *J Catal* 2007, 249 (2), 244-249.
9. Jiang, T.; Ning, Y. N.; Zhang, B. J.; Li, J. Z.; Wang, G.; Yi, J. J.; Huang, Q., Preparation of 1-octene by the selective tetramerization of ethylene. *J Mol Catal a-Chem* 2006, 259 (1-2), 161-165



# Tuning Porosity of Boron Nitride for Oxidative Dehydrogenation Reactions

*Patrick Schmatz, Isabel Moritz, Kai Brunnengräber, Alfons Drochner,  
Bastian J. M. Etzold,*

*Ernst-Berl-Institut für Technische und Makromolekulare Chemie, Technische  
Universität Darmstadt, Alarich-Weiss-Straße 8, D-64287, Darmstadt, Germany*

## Introduction

Recently, the availability of shale gas and natural gas resources, which contain considerable amounts of light alkanes ( $C_2$ - $C_4$ ), has been growing. Therefore, gas based dehydrogenation routes to olefins are of high interest. Nevertheless, conversion of direct dehydrogenation reactions suffers from thermodynamic limitations and a continuous catalyst deactivation by coking takes place. Oxidative dehydrogenation reactions (ODH) are an attractive alternative because they are thermodynamically not limited and deactivation by coking is negligible. However, the combustion of light alkanes to CO or  $CO_2$  is the main drawback of ODH reactions. In 2016, Grant *et. al.* discovered that the oxidation of propane to propylene is catalyzed by boron nitrides (BN).<sup>[1]</sup> Further, it is shown that the use of BN in the ODH of ethane and butane achieves a remarkable selectivity to olefins in comparison to metal oxide catalyst systems, like  $Cr_2O_3$  or  $VO_x$  on  $Al_2O_3$ .<sup>[2,3]</sup> Since the postulated mechanism suggests active sites on the edge of the boron nitride structure, a rational catalyst design aims to increase such active sites. In this work, the synthesis of high surface area porous boron nitride is studied, while the boron- and nitrogen-source, the pyrolysis conditions as also the post purification treatment were varied.

## Experimental and results

With a template-free synthesis strategy, starting with boron oxide or boric acid as boron (B)-precursor and urea or melamine as nitrogen (N)-precursor, boron nitride is gained in four synthesis steps (Figure 1). Initially, the precursors are suspended and a nearly homogeneous solid mixture is obtained by a controlled precipitation subsequently (1.). The mixture is pyrolyzed to boron nitride at temperatures between 600 °C and 1000 °C in presence of nitrogen (2.).

Unreacted boron oxide is extracted by guanidine hydrochloride in methanol (3.). Carbon residues are removed by a post oxidation treatment at 600 °C in air (4.).

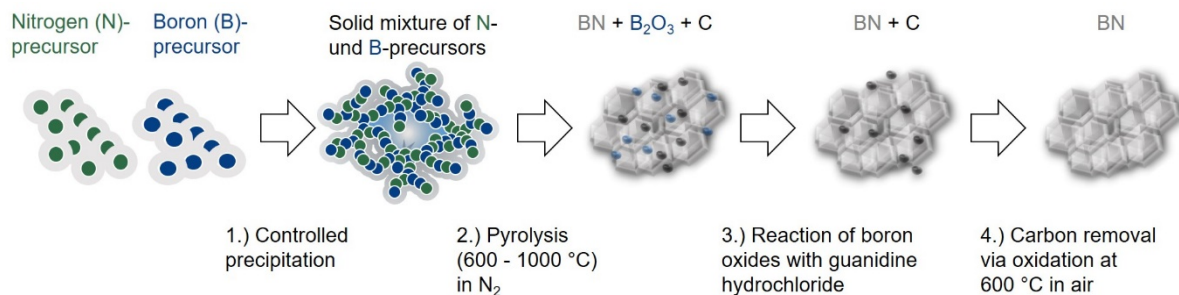


**Figure 1:** Synthesis of porous boron nitride.

The stoichiometric ratio between nitrogen and boron as well as the kind of N-precursor have significant influence on the boron nitride yield. With Melamine as N-precursor, the yield of boron nitride increases. The cleaning procedure with guanidine hydrochloride leads to a higher mesopore volume. In comparison to commercial boron nitride, the surface area is increased from 20 to approximately 200 m<sup>2</sup> g<sup>-1</sup>. The synthesized material is stable against oxidation up to 800 °C.

## Conclusion

A simple method with low-cost precursors (boric acid / boron oxide and urea / melamine) and a new cleaning procedure were developed for the synthesis of mesoporous boron nitride with only small amounts of micropores. The porosity and the high oxidation stability are predestined properties for a catalytic application in oxidative dehydrogenation reactions.

## References

- [1] J. T. Grant, C. A. Carrero, F. Goeltl, J. Venegas, P. Mueller, S. P. Burt, S. E. Specht, W. P. McDermott, A. Chiericato, I. Hermans, *Science* **2016**, *354*, 1570.
- [2] R. Huang, B. Zhang, J. Wang, K.-H. Wu, W. Shi, Y. Zhang, Y. Liu, A. Zheng, R. Schlögl, D. S. Su, *ChemCatChem* **2017**, *9*, 3293.
- [3] J. M. Venegas, J. T. Grant, W. P. McDermott, S. P. Burt, J. Micka, C. A. Carrero, I. Hermans, *ChemCatChem* **2017**, *9*, 2118.

## TEM Characterization of Ionic Liquid modified Catalysts

Kai Brunnengräber, TU Darmstadt, Darmstadt, Germany;

Gui-Rong Zhang, TU Darmstadt, Darmstadt, Germany;

Bastian JM Etzold, TU Darmstadt, Darmstadt, Germany

Ionic Liquids (ILs) are due to their extremely low vapor pressure in combination with widely variable chemical properties interesting in catalysis [1-3]. Despite the use as solvent, where huge amounts of IL would be needed, porous solids coated with a minor amount of IL are attractive and widely studied. Conceptually, these thin film systems can be divided into two main variants: *Supported Ionic Liquid Phase* (SILP) for immobilizing homogeneous catalysts and *Solid Catalyst with Ionic Layer* (SCILL) for modifying heterogeneous catalysts [1]. Performance of these catalysts typically shows a volcano-plot dependency on IL loading [1,4], highlighting the beneficial and detrimental effect of an IL coating. Consequently, the interaction between support and confined IL has attracted much attention [1,4,5]. However, the distribution of IL within a SCILL/SILP catalyst is poorly understood, despite its impact on performance. To study the IL distribution, most researcher use gas sorption measurements to examine changes to bulk texture as a result of IL modification [5].

Our current work is therefore focused on the development of a method to enable a meaningful determination of the IL distribution on a SCILL PEMFC (Polymer Electrolyte Membrane Fuel Cell) catalysts via EDS spectral imaging at the scale of the local environment of catalyst particles.

### Method Outline

EDS was chosen over EELS mapping because it offers a superior energy range for analysis. This wide range is necessary to determine the typically lighter elements of support and IL as well as the usually heavy metal catalysts. On the other side, EDS maps suffer from poor efficiency for light elements, amplified by the usually low IL loading of SCILL catalysts. Another problem is a very heterogeneous background, which is neglected by most researchers, leading to biased results. In our approach these problems are overcome by applying multivariate statistical analysis (MSA) methods and fitting of a sophisticated background model.

## Results and Discussion

Figure 1 shows EDS-maps of a tri-metallic PEMFC catalyst supported on carbon black (PtNiCo/C), used in an ongoing project of our workgroup. The catalyst is loaded with [MTBD][beti] ( $C_{12}H_{16}F_{10}N_4O_4S_2$ ), a highly hydrophobic IL.

To demonstrate the capabilities of our method, sulphur element maps were selected, as shown in Figure 1a-c. Figure 1a shows the as measured elemental map of sulphur, exhibiting unsatisfactory contrast. After pre-processing (Figure 1b), a significant improvement is achieved. After correcting for the background bremsstrahlung (shown in Figure 1c), a meaningful elemental map for sulphur is derived (Figure 1d). Since the carbon support contains no detectable amounts of sulphur, any sulphur on the sample can be assigned to the IL. Figure 1e shows a compositional phase of the material, derived via machine learning assisted, model-free principle component analysis. Based on its sum-spectrum, this phase can be identified as IL. The phase-map is consistent with the previous result. In conclusion it can be seen that evaluating only the raw data from the detector, most of the potential information is lost. It was further shown that neglecting bremsstrahlung leads to significant bias in the resulting elemental map. Derivation of an IL phase-map was also demonstrated.

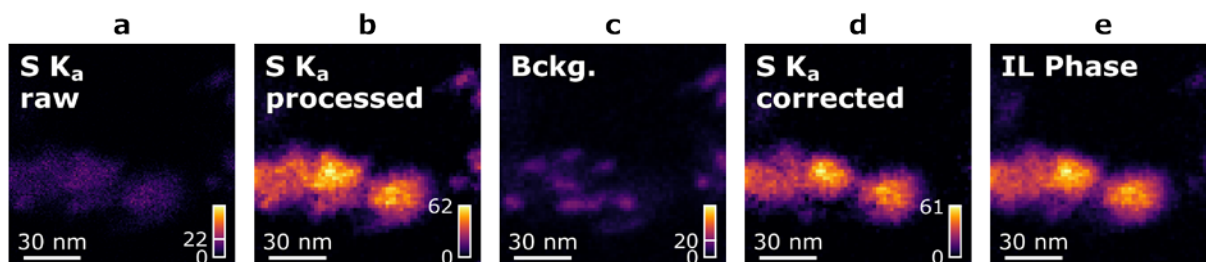


Figure 1: a-c) Sulphur element maps at different stages in the processing pipeline: a) as measured, b) after preprocessing and c) after correcting for background and overlap with Pt  $M_g$  line. d) shows the background removed from the Sulphur map. e) shows a principle component derived via NNMF, which incorporates all lines of the ionic liquid: N  $K_a$ , F  $K_a$  and S  $K_a$ .

## References

- [1] Steintrück et al., *Catal. Letters*, **2015**, 145, 380–397
- [2] Babucci, M. et al., *J. Phys. Chem. C*, **2016**, 120, 20089–20102
- [3] Sobhani, S. et al., *ACS Sustain. Chem. Eng.*, **2017**, 5, 4598–4606
- [4] Zhang, S. et al., *Chem. Rev.*, **2017**, 117, 6755–6833
- [5] Heinze, M. T. et al., *Phys. Chem. Chem. Phys.*, **2014**, 16, 24359–24372

# Providing experimental data to validate CFD-simulation of NH<sub>3</sub>-oxidation on platinum based catalysts

*M. Schöpp<sup>1</sup>, P. Reif<sup>1</sup>, D. Born<sup>2</sup>, M. Votsmeier<sup>1,2</sup>, A. Drochner<sup>1</sup>, B.J.M. Etzold<sup>1</sup>*

*<sup>1</sup>Technische Universität Darmstadt, Ernst-Berl-Institut für Technische und  
Makromolekulare Chemie, Alarich-Weiss-Straße 8, D-64287 Darmstadt*

*<sup>2</sup>Umicore AG & Co. KG, Rodenbacher Chaussee 4, D-63457 Hanau-Wolfgang*

## Introduction

With a production capacity of about 80 million tons per year<sup>[1]</sup> the NH<sub>3</sub>-oxidation via the Ostwald process represents the most relevant way of producing nitric acid. At the same time, this process and its products are one of the main sources of anthropogenic emissions of the high potential greenhouse gas N<sub>2</sub>O<sup>[2]</sup>. With regard to global warming it is a goal to abate these N<sub>2</sub>O emissions in nitric acid production.

A fundamental understanding of the surface mechanism under realistic conditions is needed to reach that aim. Furthermore, harsh reaction conditions (hazardous and corrosive media, temperatures up to 900 °C) and mass transport limitation of the reaction<sup>[3]</sup> increase the degree of complexity to investigate kinetic steps and influencing factors of the Pt catalysed NH<sub>3</sub>-oxidation.

A lab-scale setup, engineered to process mechanism investigations under these obstacle conditions, is presented in this contribution.

## Methods

By this means, the lab-scale setup for investigating the Pt catalysed NH<sub>3</sub>-oxidation was developed and engineered to work at different conditions - including industrial ones (volume flow of about 4560 L h<sup>-1</sup> (STP), NH<sub>3</sub> volume fraction of 10,5 % (L L<sup>-1</sup>) in air, 900-1000 °C and up to 5 atm). The setup consists of three modules (gas supply, reactor/analytics and exhaust after-treatment). The gas supply offers the opportunity to not just feed the reactants (NH<sub>3</sub> and air), but also product gases such as N<sub>2</sub>O or NO. The reactant gas mixture is feeded into the reactor after it is heated up in three steps up to 450 °C. The tubular reactor itself has an inner diameter of 30 mm in which the catalyst gauzes fit in a special cartridge. This makes it possible to quickly change the gauzes and also investigate other types of Pt catalyst geometries. An online quadrupole mass spectrometer (MS) is used for analytics. It allows to determine the volume fractions of all the occurring species time resolved. The

sampling of the MS is realised via a silica capillary. This capillary is implemented into the reactor and offers the possibility to sample directly at the catalyst.

## Results and discussions

Experiments with the lab-scale setup show that there is the possibility to investigate the Pt catalysed  $\text{NH}_3$ -oxidation under industrial conditions. The use of an inert silica cartridge prevents the detection of side reactions taking place in the high temperature area around the catalyst. Additionally, with the sampling via a silica capillary, it is possible to determine selectivities resulting from catalytic reactions on Pt only.

The main advantage results in screening different types of gauzes (woven, knitted) and investigations on model catalysts. These are necessary for validating and improving the surface mechanism. With their simplified flow field, they are well amenable for CFD simulations. Together with experimental data from the lab-scale setup the simulation can help to improve reaction mechanisms.

First tests with a Pt disc as a model catalyst (OD: 24.0 mm, 0.5 mm thick) show the reactivity of the catalyst in the presented system (figure1).

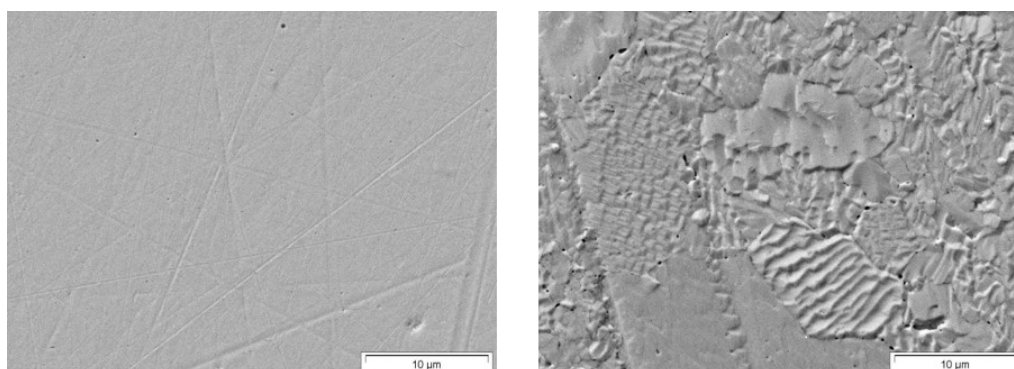


Figure 1: SEM images of fresh Pt disc (left) and Pt disc after 5 h reaction time (right).

In the future, these investigations spend a learning outcome, which can be used to investigate the catalytic mechanism concerning elementary kinetic steps as well as mass transport phenomena. The realistic reaction conditions can help to bridge the upscaling gap to rationally design Pt-geometries or optimise experimental conditions in order to reduce the  $\text{N}_2\text{O}$  emission.

## References

- [1] M. Bertau, A. Müller, P. Fröhlich, M. Katzberg, *Industrielle Anorganische Chemie*, 4. Auflage, Wiley-VCH, Weinheim **2013**.
- [2] J. Pérez-Ramirez, F. Kaptejin, K. Schöffel, J. Moulijn, *Applied Catalysis B: Environmental*, **2003**, *44*, 117-151.
- [3] R. Imbihl, A. Scheibe, Y. F. Zeng, S. Gunther, R. Kraehnert, V. A. Kondratenko, M. Baerns, W. K. Offermans, A. P. J. Janse, R. A. van Santen, *Phys. Chem. Chem. Phys.*, **2007**, *9*, 3522-3540.

# Gold on cerium oxycarbonate for allyl alcohol oxidation

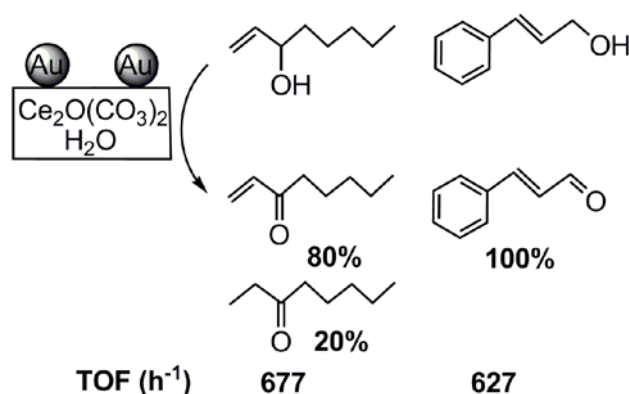
*Werner Oberhauser, CNR-ICCOM, Sesto Fiorentino, Italy; Claudio Evangelisti, CNR-ISTM, Milano, Italy; Cinzia Cepek, CNR-IOM, Laboratorio TASC, Basovizza, Italy*

## 1. Scope

The selective oxidation of allyl alcohols to the corresponding unsaturated carbonyl compounds is an important organic transformation, [1] which should apply heterogeneous catalysts and oxygen or air as hydrogen acceptor in order to be considered a sustainable process. Promising heterogeneous catalysts are Pd [2], Ru [3] and Au [4]-based. Particularly, Au-based heterogeneous catalysts show good chemoselectivity in alcohol oxidation reactions, but exhibit only a sluggish activity in the absence of a Brønsted base, which aids the generation of the alcoholate intermediate. Hence the close proximity of a suitable Brønsted base site and Au-nanoparticles (NPs) is a requisite for a fast alcohol dehydrogenation reaction.

## 2. Results and discussion

We used cerium oxycarbonate monohydrate ( $\text{Ce}_2\text{O}(\text{CO}_3)_2 \cdot \text{H}_2\text{O}$ ) as support for Au-NPs, which were generated by the metal vapor synthesis (MVS) approach (Scheme 1). [5] For comparison reason, Au-NPs on  $\text{CeO}_2$  (nano-powder from Aldrich) were synthesized.



Catalytic conditions: Au(0.5 wt%), toluene, 120 °C, p(air)= 20 bar, t= 20 h  
substrate/catalyst molar ratio= 5790

**Scheme 1.** Catalytic conversion of selected allyl alcohols by Au@( $\text{Ce}_2\text{O}(\text{CO}_3)_2 \cdot \text{H}_2\text{O}$ ).

TEM and XPS measurements carried out on both latter catalysts confirmed important differences: (i) The NPs' size of Au@Ce<sub>2</sub>O(CO<sub>3</sub>)<sub>2</sub>·H<sub>2</sub>O was significantly larger compared to that of Au@CeO<sub>2</sub> (*i.e.* 4.0 vs 2.0 nm); (ii) The oxidation state of Au in Au@Ce<sub>2</sub>O(CO<sub>3</sub>)<sub>2</sub>·H<sub>2</sub>O was exclusively 0, while Au@CeO<sub>2</sub> showed, as reported, oxidized Au species.[4] The application of both catalyst for the aerobic allyl alcohol oxidation to the corresponding carbonyl compounds conducted in toluene (Scheme 1) gave for Au@Ce<sub>2</sub>O(CO<sub>3</sub>)<sub>2</sub>·H<sub>2</sub>O a threefold higher catalytic activity compared to Au@CeO<sub>2</sub>. This beneficial solvent effect is absent, when methanol is used as reaction medium, due to its strong interactions with surface carbonate groups.[6]

### 3. Conclusions

Au@Ce<sub>2</sub>O(CO<sub>3</sub>)<sub>2</sub>·H<sub>2</sub>O outperformed Au@CeO<sub>2</sub> in the catalytic aerobic allyl alcohol oxidation in terms of activity, if toluene was used as reaction medium. The carbonate unit in close proximity to the Au-NPs accelerated the generation of the alcoholate, which is the key species in the Au-mediated dehydrogenation reaction. The catalyst is completely recyclable for several catalytic runs in air atmosphere. Neither the Au-NPs' size nor the support structure experienced any significant alteration.

### References

- [1] M. Hudlucky, *Oxidations in Organic Chemistry*, ACS Monograph Series, American Chemical Society, Washington, **1990**.
- [2] K. Mori, T. Hara, T. Mizugaki, K. Ebitani, K. Kaneda, *J. Am. Chem. Soc.* **2004**, 126, 10657-10666.
- [3] K. Yamaguchi, N. Mizuno, *Angew. Chem. Int. Ed.* **2002**, 41, 4538-4542.
- [4] A. Abad, P. Concepción, A. Corma, H. García, *Angew. Chem. Int. Ed.* **2005**, 44, 4066-4069.
- [5] G. Vitulli, C. Evangelisti, A. M. Caporusso, P. Pertici, N. Panziera, S. Bertozzi, P. Salvadori, Metal Nanoclusters in Catalysis and Material Science: The Issue of Size Control, in: B. Corain, G. Schmid, N. Toshima (Eds.), Elsevier, Amsterdam, **2008**, pp.437-451.
- [6] N. Bovet, M. Yang, M. S. Javadi, S. L. S. Stipp, *Phys. Chem. Chem. Phys.* **2015**, 17, 3490-3496.



# Single Atom Catalysis – Theoretical investigation of heterogeneous hydroformylation

*Jonas Amsler, Philipp N. Plessow, Felix Studt,*

*Institute of Catalysis Research and Technology (IKFT), Karlsruhe, Germany*

## Introduction

Despite a cost-intensive and cumbersome recycling procedure, the hydroformylation process emerged as one of the most relevant homogeneously catalyzed reactions. [1] However, heterogeneous catalysts are generally preferred in industrial applications due to facile separation of the catalyst from the reaction mixture and subsequent reuse. Still, a heterogeneous catalyst with sufficient activity, selectivity and stability has yet to be found for the hydroformylation process.

Amongst some attempts to synthesize heterogeneous catalysts via immobilization or phosphine-functionalized polymers, Single Atom Catalysts (SACs) are a promising alternative. [2,3,4] Consisting of dispersed single metal atoms on a heterogeneous support, these materials feature isolated reaction sites and utilize the precious metal efficiently – similar to homogeneous catalysts but with the benefits of heterogeneous catalysts. Our research is motivated by the goal to find a heterogeneous catalyst for the hydroformylation process and to systematically investigate SACs based on (ab initio) quantum chemistry calculations.

## Methods and Outline

The challenge is not only to predict stabilities and activities across the catalytic reaction cycle in Fig. 1 but further to understand electronic effects of a bulk surface in the role of a ligand. Strong adsorption of the active rhodium complexes on the surface relative to the gas phase is essential for a stable heterogeneous catalyst. Hence, we employ DFT calculations with periodic boundary conditions to compute adsorption energies of RhH-carbonyl complexes on flat and stepped surfaces of different support materials (MgO, ZnO, CeO<sub>2</sub>). Inspired by mechanistic studies on homogeneous catalysts, [5] we predict reaction free energies and transition states of heterogeneous SACs along the reaction coordinates corrected by DLPNO-CCSD(T) calculations. The catalytic activity of adsorbed rhodium complexes will be discussed for the most relevant surfaces and compared to homogeneous catalysts.

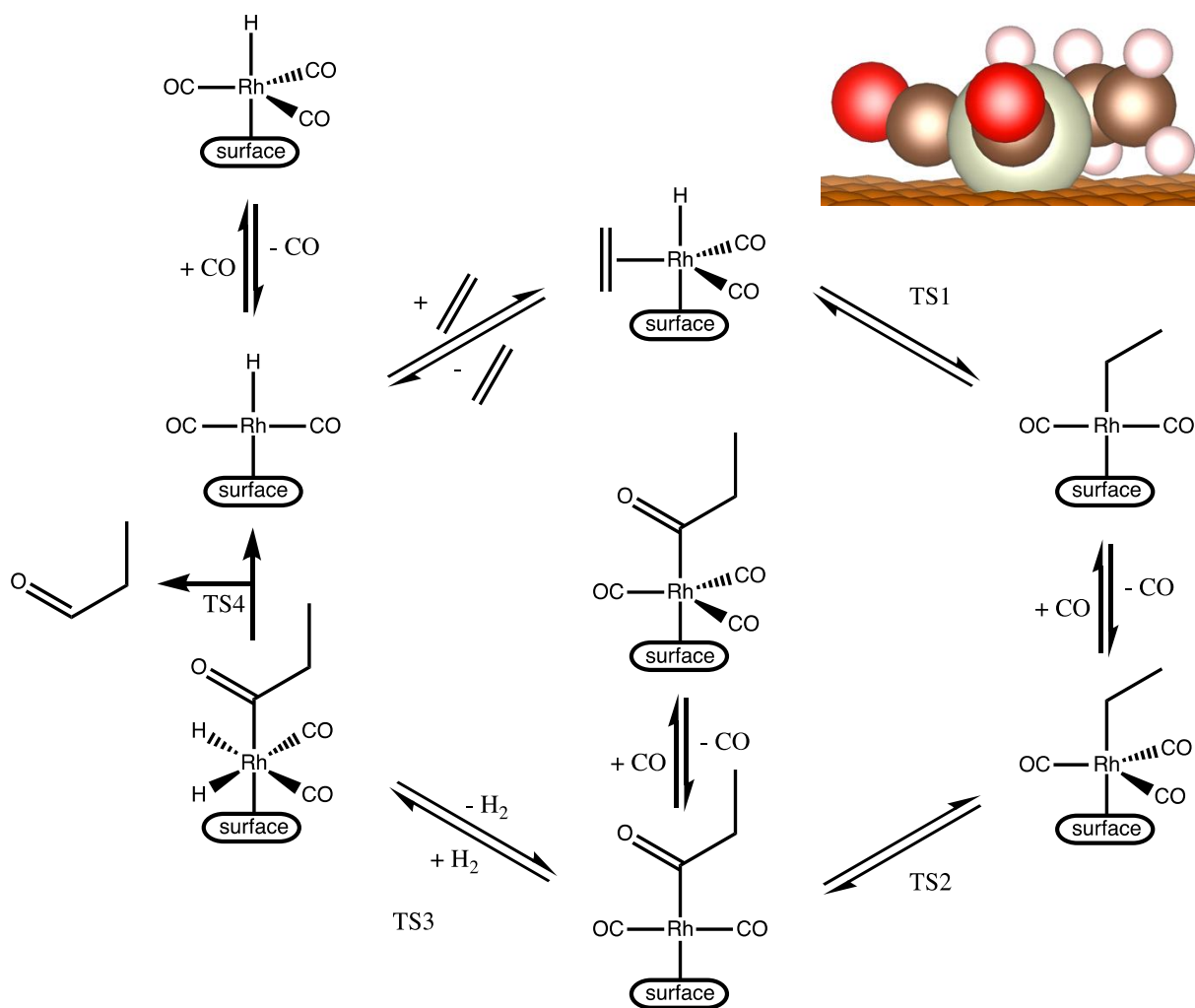


Figure 1: The catalytic reaction cycle of the hydroformylation with a heterogeneous SAC was inspired by mechanistic studies on the homogeneously catalyzed Heck and Breslow mechanism. [5,6,7] Each step comprises varying ligands at a single rhodium atom situated on the surface of a support material (MgO, ZnO, CeO<sub>2</sub>). There are four transition states (TS1-4).

## References

- [1] Franke, R.; Selent, D.; Börner, A.; *Chem. Rev.* **2012**, *112*, 5675–732.
- [2] Lang, R.; Li, T.; Matsumura, D.; Miao, S.; Ren, Y.; Cui, Y.-T.; Tan, Y.; Qiao, B.; Li, L.; Wang, A.; Wang, X.; Zhang, T.; *Angew. Chem. Int. Ed.* **2016**, *55*, 16054–16058.
- [3] Wang, L.; Zhang, W.; Wang, S.; Gao, Z.; Luo, Z.; Wang, X.; Zeng, R.; Li, A.; Li, H.; Wang, M.; Zheng, X.; Zhu, J.; Zhang, W.; Ma, C.; Si, R.; Zeng, J.; *Nat. Commun.* **2016**, *7*, 14036.
- [4] Sun, Q.; Dai, Z.; Liu, X.; Sheng, N.; Deng, F.; Meng, X.; Xiao, F.-S.; *J. Am. Chem. Soc.* **2015**, *137*, 5204–5209.
- [5] Sparta, M.; Børve, K. J.; Jensen, V. R.; *J. Am. Chem. Soc.* **2007**, *129*, 8487–8499.
- [6] Breslow, D. S.; Heck, R. F.; *Chem. Ind. (London, U. K.)* **1960**, 467.
- [7] Heck, R. F.; Breslow, D. S.; *J. Am. Chem. Soc.* **1961**, *83*, 4023–4027.

# Selective oxidation of 2-propanol over unsupported cobalt-based spinel nanoparticles

*Sven Anke, Tobias Falk, Martin Muhler*

*Laboratory of Industrial Chemistry, Ruhr-University Bochum, Bochum, Germany*

*Georg Bendt, Stephan Schulz*

*Inorganic Chemistry, Universität Duisburg-Essen and Cenide, Essen, Germany*

## Introduction

Unlike oxidation catalysts containing noble metals, mixed-metal oxides are less expensive and exhibit higher resistance to poisoning and high thermal stability. Especially cobalt-based spinels are considered promising in replacing commonly used oxidation catalysts in industrial applications like the oxidation of CO or volatile organic compounds (VOCs).<sup>[2,3]</sup> They offer a great tunability of the catalyst composition and related properties due to the presence of octahedral and tetrahedral sites within the oxygen lattice, while the structure remains stable. Nevertheless,  $\text{Co}_3\text{O}_4$  or  $\text{CoFe}_2\text{O}_4$  catalysts can also deactivate during oxidation reactions due to coking.<sup>[4,5]</sup> Gaining insight in deactivation is of crucial importance for the understanding of the reaction mechanism and the design of superior catalysts. The selective oxidation of 2-propanol is applied as probe reaction for the redox and acid-base properties of the spinels.

## Experimental

Cobalt oxide and cobalt ferrite were synthesized by using a colloidal one-pot method by decomposition of  $\text{M}(\text{acac})_2$  in the presence of oleyl amine followed by calcination at 573 K.<sup>[5]</sup> The  $\text{Co}_3\text{O}_4$  and  $\text{CoFe}_2\text{O}_4$  nanoparticles were tested in the selective 2-propanol oxidation in a microreactor set-up with a fixed-bed reactor and a calibrated quadrupole mass spectrometer. The catalysts were oxidatively pretreated (TPO) in 10%  $\text{O}_2/\text{He}$  at 573 K prior to the oxidation reaction. Using a feed of 0.18% 2-propanol / 0.18%  $\text{O}_2 / \text{He}$  (100 sccm), the catalysts (100 mg) were heated to 573 K with a heating rate of  $0.5 \text{ K min}^{-1}$  under quasi steady-state conditions. DRIFT spectra were acquired with oxidatively pretreated  $\text{CoFe}_2\text{O}_4$  diluted with diamond powder (1:2) during  $(\text{CH}_3)_2\text{CHOH}$  dehydrogenation at 503 K for 30 min with subsequent desorption in inert gas.

## Results

The results of the catalytic 2-propanol oxidation conversion over  $\text{Co}_3\text{O}_4$  and  $\text{CoFe}_2\text{O}_4$  (Figure 1 A,B) reveal that both cobalt based oxides are highly active and selective in the oxidative dehydrogenation of 2-propanol yielding acetone. Up to 573 K the selectivity only drops slightly due to the formation of the total oxidation product  $\text{CO}_2$ . Especially  $\text{Co}_3\text{O}_4$  showed remarkable results reaching almost full conversion with 100% selectivity to acetone at 430 K, but only during the first oxidation run.<sup>[6]</sup> Various transient kinetic experiments indicate the selective character of involved surface lattice oxygen.

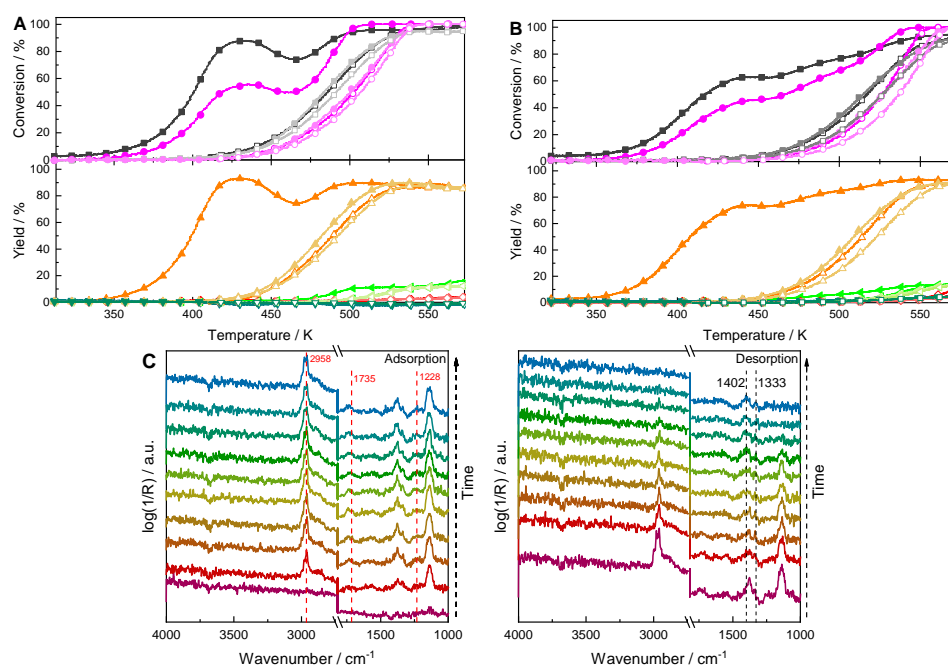


Figure 1: Conversion of  $(\text{CH}_3)_2\text{CHOH}$  (■) and  $\text{O}_2$  (●) as well as yields of  $(\text{CH}_3)_2\text{CO}$  (▲),  $\text{CH}_2=\text{CHCH}_3$  (▼),  $\text{H}_2$  (◆) and  $\text{CO}_2$  (◄) during the first and subsequent second (brighter colors) 2-propanol oxidation over  $\text{Co}_3\text{O}_4$  (A) and  $\text{CoFe}_2\text{O}_4$  (B). Traces with full symbols were obtained during heating and traces with hollow symbols during cooling of the catalyst. Additional DRIFTS investigation of 2-propanol dehydrogenation at 503 K over  $\text{CoFe}_2\text{O}_4$  (C).

According to the DRIFT spectra of 2-propanol dehydrogenation shown in Figure 1 C supported by acetic acid adsorption experiments, inhibition of the low-temperature reaction pathway is caused by acetate species formed during unselective oxidation.<sup>[7]</sup> Carbonates are found to be spectators, whereas TPO and XPS studies of the spent catalyst reveal additional carbon deposition causing further deactivation.

## References

- [1] X. Xie, Y. Li, Z.-Q. Liu, M. Haruta, W. Shen, *Nature* **2009**, *458*, 746.
- [2] S. Zafeiratos, T. Dintzer, D. Teschner, R. Blume, M. Hävecker, A. Knop-Gericke, R. Schlögl, *J. Catal.* **2010**, *269*, 309.
- [3] O. Vozniuk, C. Bazzo, S. Albonetti, N. Tanchoux, F. Bosselet, J.-M. M. Millet, F. Di Renzo, F. Cavani, *ChemCatChem* **2017**, *9*, 2219.
- [4] L. Lukashuk, N. Yigit, R. Rameshan, E. Kolar, D. Teschner, M. Hävecker, A. Knop-Gericke, R.

- Schlögl, K. Föttinger, G. Rupprechter, *ACS Catal.* **2018**, *6*, 8630.
- [5] K. Chakrapani, G. Bendt, H. Hajiyani, I. Schwarzrock, T. Lunkenbein, S. Salamon, J. Landers, H. Wende, R. Schlögl, R. Pentcheva, M. Behrens, S. Schulz, *ChemCatChem.* **2017**, *9*, 2988.
- [6] S. Anke, G. Bendt, I. Sinev, H. Hajiyani, H. Antoni, I. Zegkinoglou, H. Jeon, R. Pentcheva, B. Roldan Cuenya, S. Schulz, M. Muhler, submitted to *ACS Catal.*
- [7] S. Anke, T. Falk, G. Bendt, I. Sinev, I. Zegkinoglou, H. Jeon, B. Roldan Cuenya, S. Schulz, M. Muhler, submitted to *J. Catal.*

# Selective CO<sub>2</sub> hydrogenation over supported Rh catalysts

*Junpei Suzuki,<sup>a</sup> Hiroki Miura,<sup>a,b,d</sup> Tetsuya Shishido,<sup>a,b,c,d</sup>*

<sup>a</sup> Department of Applied Chemistry, Graduate School of Urban Environmental Sciences, Tokyo Metropolitan University, 1-1 Minami-Osawa, Hachioji, Tokyo 192-0397, Japan

<sup>b</sup> Research Center for Hydrogen Energy-Based Society, Tokyo Metropolitan University, 1-1 Minami-Osawa, Hachioji, Tokyo 192-0397, Japan

<sup>c</sup> Research Center for Gold Chemistry, Tokyo Metropolitan University, 1-1 Minami-Osawa, Hachioji, Tokyo 192-0397, Japan

<sup>d</sup> Elements Strategy Initiative for Catalysts & Batteries, Kyoto University, Katsura, Nishikyoku, Kyoto 615-8520, Japan

## Introduction

CO<sub>2</sub> fixation has attracted much interest in achieving a low carbon society. Both Sabatier reaction ( $\text{CO}_2 + 4\text{H}_2 \rightarrow \text{CH}_4 + 2\text{H}_2\text{O}$ ) and reverse water gas shift reaction ( $\text{CO}_2 + \text{H}_2 \rightarrow \text{CO} + \text{H}_2\text{O}$ ) have been recognized as attractive and important reactions in CO<sub>2</sub> utilization and these reactions proceed competitively. To achieve the selective formation of CH<sub>4</sub> or CO, it is necessary to reveal the dominant factor for changing the selectivity in CO<sub>2</sub> hydrogenation. We found that the selectivity in CO<sub>2</sub> hydrogenation was drastically changed by support of Rh catalysts. Based on DRIFT spectra, the effect of support on reaction mechanism was discussed.

## Experimental

Supported Rh catalysts (Rh loading amount: 1wt%) were prepared by an impregnation method. The reaction (CO<sub>2</sub>:H<sub>2</sub> = 1:4) was carried out in a fixed bed flow reactor. The adsorbed species on the catalyst surface was characterized by using DRIFT spectra.

## Results and Discussion

Fig.1 shows the yield of the products in CO<sub>2</sub> hydrogenation. On Rh/Nb<sub>2</sub>O<sub>5</sub>, CH<sub>4</sub> was mainly formed, whereas selective formation of CO was observed on

Rh/NbOPO<sub>4</sub>. As is the case for Nb-based materials, metal oxide-supported Rh catalysts (TiO<sub>2</sub>, Y<sub>2</sub>O<sub>3</sub>, ZrO<sub>2</sub>, CeO<sub>2</sub>) shows high CH<sub>4</sub> selectivity, and CO was selectively formed on Rh/phosphates (TiPO<sub>4</sub>, YPO<sub>4</sub>, ZrP<sub>2</sub>O<sub>7</sub>, CePO<sub>4</sub>) regardless of temperature.

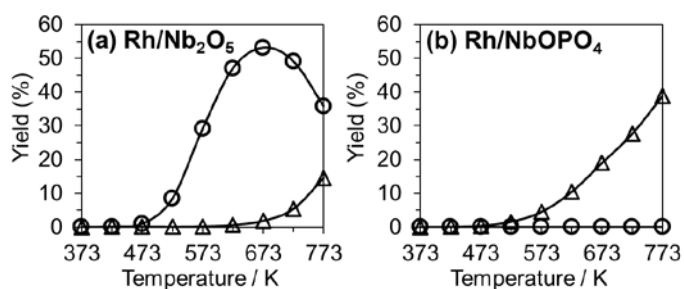


Fig.1 Yield of products in CO<sub>2</sub> hydrogenation over (a) Rh/Nb<sub>2</sub>O<sub>5</sub> and (b) Rh/NbOPO<sub>4</sub>. (○) CH<sub>4</sub>, (△) CO

*In situ* DRIFT spectra (Fig.2) indicate that methanation of CO<sub>2</sub> proceeded through hydrogenation of adsorbed CO species on Rh and formate species [2]. For Rh/metal oxide, positive  $\Delta x$  value (the difference in peak position due to linear carbonyl species at 373 and 673 K) was observed, and CH<sub>4</sub> was selectively formed. The positive  $\Delta x$  value may be due to coexistence of CO and H on Rh (absorption bands (3)). On the other hand, for Rh/phosphate,  $\Delta x$  was almost zero, and CO was selectively formed. These results suggest that CO hydrogenation to CH<sub>4</sub> did not proceed on Rh supported on phosphate because H was not coexistent with CO.

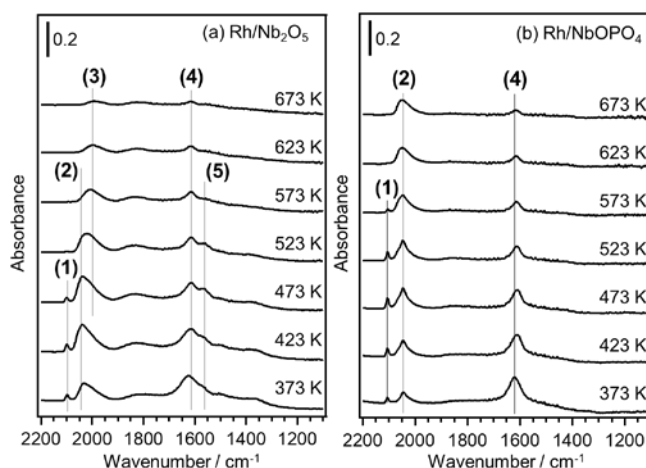
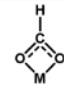
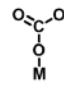
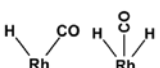
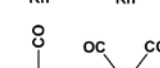



Fig.2 *In situ* DRIFT spectra of adsorbed species on (a) Rh/Nb<sub>2</sub>O<sub>5</sub> and (b) Rh/NbOPO<sub>4</sub> in CO<sub>2</sub>/H<sub>2</sub> gas.

Table.1 Assignment of absorption bands of *in situ* DRIFT spectra

No.	Peak frequency	Assignment	Surface species
(5)	1570	$\nu_a(\text{CO}_2)$ Bidentate	Formate 
(4)	1625	$\nu_a(\text{CO}_3)$	Bicarbonate 
(3)	2020 ~ 2030		Rh-H, CO 
(2)	2050	$\nu(\text{CO})$	Rh-CO 
(1)	2100, 2050		Rh-(CO) <sub>2</sub> 

From CO-DRIFTS and Rh 3d XPS, it was revealed that electron deficient Rh was dispersed on phosphates. This is caused by the electron withdrawing effect of the PO<sub>4</sub> units [2]. This electron deficient Rh suppressed adsorption and activation of adsorbed CO species on Rh (Table.1)

## Conclusion

We found that selectivity in CO<sub>2</sub> hydrogenation (CH<sub>4</sub> or CO) could be controlled by support (metal oxides or phosphate) of Rh catalysts. The electronic state of Rh and adsorbed species on Rh were affected by support, resulting in the change in selectivity.

## References

- [1] D. Heyl, U. Rodemerck, U. Bentrup, *ACS Catal.* **2016**, 6, 6275-6284.  
 [2] M. Machida et al. *J. Phys. Chem. C*, **2015**, 119, 373-380.

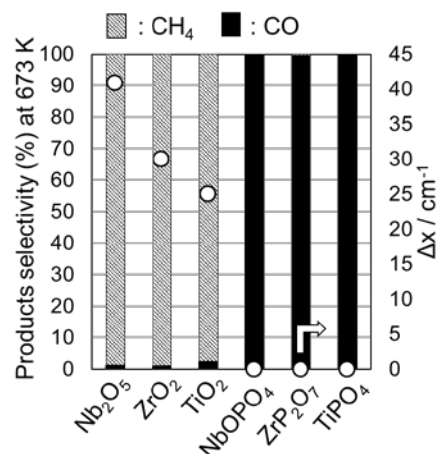


Fig.3 Selectivity in CO<sub>2</sub> hydrogenation and  $\Delta x$  (the difference in peak position due to linear carbonyl species at 373 and 673 K).

# Selective Oxidation of Methanol to Formaldehyde – Performance of Alkali Earth Metal Molybdates

Joachim Thrane<sup>1\*</sup>, Martin Høj<sup>1</sup>, Max Thorhauge<sup>2</sup>, Uffe Vie Mentzel<sup>2</sup> and Anker Degn Jensen<sup>1\*</sup>

<sup>1</sup>*Technical University of Denmark, Kgs. Lyngby, Denmark*

<sup>2</sup>*Haldor Topsøe A/S, Kgs. Lyngby, Denmark*

\*joathr@kt.dtu.dk or aj@kt.dtu.dk

In this work alkali earth metal molybdate catalysts with Mo:M = 1.0 and 1.1 stoichiometry have been synthesized and tested for the selective oxidation of methanol to formaldehyde in a lab scale fixed bed reactor setup. Excess Mo gave better initial activity and selectivity but a higher rate of deactivation during 100 h on stream.

## Background

Formaldehyde is the most significant aldehyde commercially available as it is an irreplaceable C<sub>1</sub> building block for higher-valued products [1]. The annual global production of formaldehyde is expected to increase with 4.8-5.8% per year and reach 36.6 million tons by 2026 [2,3]. Formaldehyde is mainly produced through either the silver process (Silver catalyst) or the Formox process (metal oxide catalyst) [1].

In the Formox process, methanol is selectively oxidized over an iron molybdate catalyst (MoO<sub>3</sub>/Fe<sub>2</sub>(MoO<sub>4</sub>)<sub>3</sub>), which achieve high selectivities >92 % at conversions larger than 99% [1]. The catalyst is however not stable under reaction conditions due to formation of volatile molybdenum compounds [4]. The alkali earth metal molybdates were reported to have high thermal stability [5], with expected lower volatility of Mo in MeOH atmosphere, and their properties as catalysts for selective oxidation of methanol are scarcely investigated in the literature.

## Results and Discussion

M<sub>2</sub>MoO<sub>4</sub> (M = Mg, Ca, Sr, Ba) catalyst samples with stoichiometric amounts and 10 mol% excess Mo were synthesized by a sol-gel method. The samples with excess Mo had superior selectivity compared to the samples with stoichiometric Mo content (Figure 1a, the Sr and Ba catalysts were far less active and are not shown here). Furthermore, it can be seen that the Mo:Ca = 1.1 and Mo:Mg = 1.1 samples have the same selectivity as function of conversion, both close to the industrial reference. The activity of the catalysts with excess Mo was superior to stoichiometric catalysts. This shows that the excess Mo has a significant role w.r.t. the activity and selectivity for



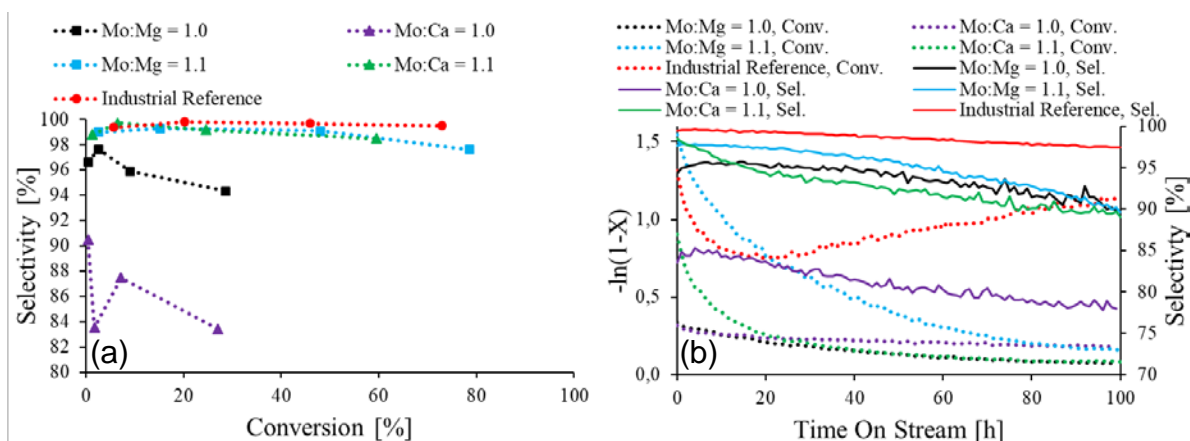


**Figure 1.** (a): Reversible products corrected selectivity (DME = 2 MeOH, DMM = 2 MeOH + CH<sub>2</sub>O, MF = CO + MeOH) towards formaldehyde vs. the conversion of methanol achieved at 250 °C, 300 °C, 350 °C and 400 °C. (b):  $-\ln(1-X)$  vs. time on stream at 400 °C for 100 h. Conditions: Catalyst loading: 25 mg 150-250 μm particles, SiC for dilution 150 mg. Feed: ~5 % MeOH in 127.5 NmL/min of N<sub>2</sub> and 15 NmL/min of O<sub>2</sub>.

the oxidation of methanol to formaldehyde. The importance of excess Mo has also been reported for the industrial iron molybdate catalyst [7].

Stability tests for 100 h on stream (Figure 1b) showed that the first order rate constant for methanol oxidation decreased faster for the M:Mo = 1.1 samples, than the M:Mo = 1.0 samples. This is probably due to the initial vaporization of the excess Mo. This is also indicated by the selectivity of the Mo:Mg = 1.1 being equal to the selectivity of Mo:Mg = 1.0 after 100 h. None of the alkali metal molybdate catalysts showed the reactivation behavior observed for the industrial reference, as discussed in [8], and none of the catalysts had activity comparable with the industrial reference after 100 h on stream (ranged 6-16% of industrial reference after 100 h compared to 24-118% initially). Furthermore, it was found that the stoichiometric CaMoO<sub>4</sub> catalyst was significantly more stable than the stoichiometric MgMoO<sub>4</sub> catalyst, which might be related to the thermal stability, which is reported higher for CaMoO<sub>4</sub> than for MgMoO<sub>4</sub> [5].

## References

1. A. W. Franz et al., Formaldehyde, Ullmann's enc. of ind. chem., 2016.
2. [prnewswire.com/news-releases/global-formaldehyde-market-2018-2022-300633054.html](https://www.prnewswire.com/news-releases/global-formaldehyde-market-2018-2022-300633054.html), Accessed: 10.11.2018
3. [transparencymarketresearch.com/formaldehyde-market.html](https://www.transparencymarketresearch.com/formaldehyde-market.html), Accessed: 10.11.2018
4. B. I. Popov, V. N. Bibin, B. K. Boreskov, Kin. i Kat. 17 (1976), p. 371
5. Gmelin Handbook of Inorganic and Organometallic Chemistry, Molybdän, 1935.
6. M. Høj, A. D. Jensen, J.-D. Grunwaldt, Appl. Cat. A: Gen. 451 (2013), p.207
7. C. Brookes, M. Bowker, P. Wells, Catalysts 6 (2016), p. 92
8. K. V. Raun, L. F. Lundegaard, J. Chevallier, P. Beato, C. C. Appel, K. Nielsen, M. Thorhauge, A. D. Jensen, M. Høj, Catal. Sci. Technol. 8 (2018), p.4626

# A multi-wavelength Raman spectroscopy for operando catalysis research

Yuanqing Wang<sup>1,2</sup>, Oliver Rohm<sup>3</sup>, Frank Rosowski<sup>2,4</sup>, Robert Schlögl<sup>1,5</sup>, Annette Trunschke<sup>1</sup>

<sup>1</sup>Department of Inorganic Chemistry, Fritz-Haber-Institut der Max-Planck-Gesellschaft, Faradayweg 4-6, 14195 Berlin, Germany

<sup>2</sup>BasCat - UniCat BASF JointLab, Technische Universität Berlin, Sekr. EW K 01, Hardenbergstraße 36, 10623 Berlin, Germany

<sup>3</sup>S&I Spectroscopy & Imaging GmbH, Boerdestraße 1, 59581 Warstein, Germany

<sup>4</sup>BASF SE, Process Research and Chemical Engineering, Heterogeneous Catalysis, Carl-Bosch-Straße 38, 67056 Ludwigshafen, Germany

<sup>5</sup>Department of Heterogeneous Reactions, Max-Planck-Institut für Chemische Energiewandlung, Stiftstraße 34-36, 45470 Mülheim an der Ruhr, Germany

## Introduction

Raman spectroscopy can be a powerful tool for characterizing structural information of studied material by analyzing the vibrational mode whose position is directly related to the reduced mass and bond strength of the oscillator. However, owing to intrinsic property of sample (e.g., fluorescence, low scattering cross section) and efficiencies of optics and detector, Raman bands are sometimes not quite pronounced and resolved under specific laser excitation. Alternatively, a Raman band can be selectively enhanced if the excitation laser frequency is close to the frequency of an electronic band, which is called resonance Raman (RR). In particular, it would be of great interest if the enhanced Raman band is related to active site of a catalyst.<sup>1-2</sup> To correlate structure with performance directly, an operando implementation of resonance Raman spectroscopy is preferred. For these purposes, we describe here a customized multi-wavelength Raman spectroscopy setup with an integrated laser source covering from deep ultraviolet (UV) light to near infrared (NIR) range. It is easily tunable and highly compatible with operando study.

## Description of the setup

As shown in Figure 1, a triple-spectrograph system (TriVista 557, Princeton Instruments) combining 9 lasers was adopted. Gratings from 150 to 3600 grooves/mm suitable for various light ranges were installed. Higher resolution or low frequency Stokes/anti-Stokes Raman spectrum is available with additive or subtractive mode. The light path in Figure 1 shows the case of using mono-stage grating. Scattered light signals are monitored by back-illuminated CCD detectors

(PyLoN:2K and PyLoN:100 from Princeton Instruments). The former detector with 2048 x 512 imaging array and 13.5  $\mu\text{m}$  x 13.5  $\mu\text{m}$  pixels is highly sensitive both in UV and visible range (quantum efficiency (QE): 50 % - 70%). The latter one with 1340 x 100 imaging array and 20  $\mu\text{m}$  x 20  $\mu\text{m}$  pixels is highly sensitive both in visible and NIR range (QE > 80%). A reactor sitting below the microscope is coupled with mass spectrometer and micro-GC to allow products analysis.

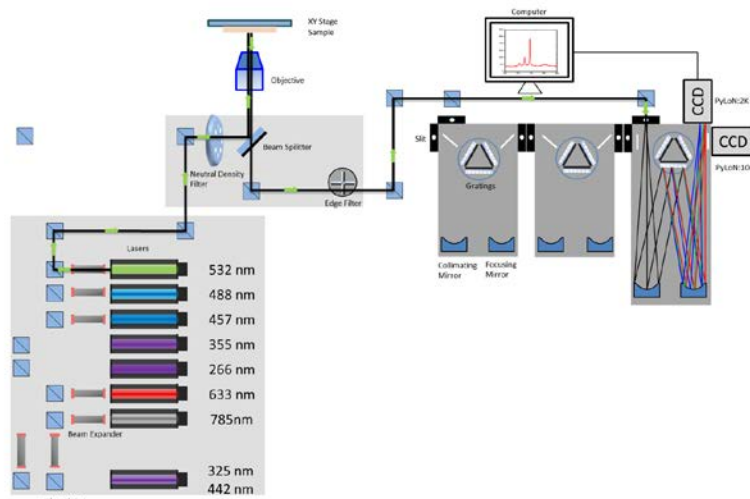


Figure 1. Schematic diagram of the multi-wavelength Raman spectroscopy setup.

## Results

As shown in Figure 2, Raman spectra of Si wafer as a standard were obtained with decent signal counts by the built multi-wavelength Raman spectroscopy. The largest deviation of band position as compared to 520.0  $\text{cm}^{-1}$  is 3 pixels ( $\sim 1.5 \text{ cm}^{-1}$ ) in the case of 355 nm laser excitation with 2400 grooves/mm grating. At present, pulse experiments performed on real catalysts (vanadium based oxides) were on-going.

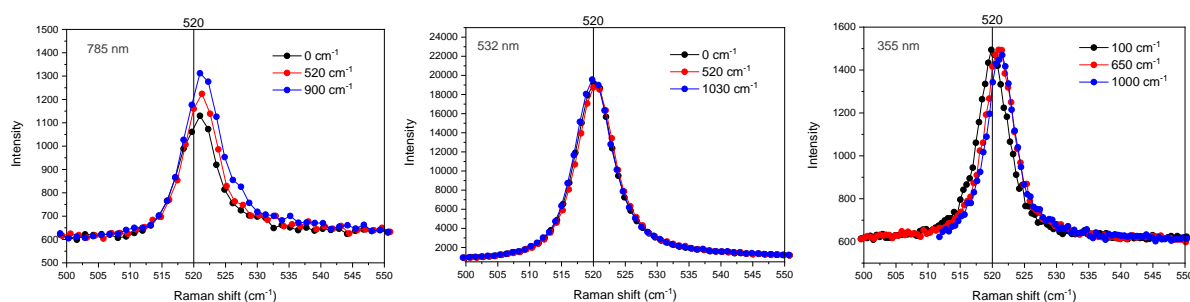


Figure 2. Selected Raman spectra recorded on Si wafer from multi-wavelength excitation. The numbers in the legend represent light wavenumber in the central CCD chips. A power of 2.3 mW for 785 nm, 13.0 mW for 532 nm and 0.9 mW for 355 nm laser was used. Acquisition time was set at 1 second for 785 nm and 532 nm laser excitation and 10 seconds for 355 nm laser excitation.

## References

- [1] Woertink, J. S.; Smeets, P. J.; Groothaert, M. H.; Vance, M. A.; Sels, B. F.; Schoonheydt, R. A.; Solomon, E. I., *Proc Natl Acad Sci U. S. A.* **2009**, 106 (45), 18908-13.
- [2] Wu, Z.; Dai, S.; Overbury, S. H., *The Journal of Physical Chemistry C* **2010**, 114 (1), 412-422.

## **Regeneration of supported catalytically active liquid metal solutions (SCALMS) for dehydrogenation of light alkanes**

*Moritz Wolf, Narayanan Raman, Nicola Taccardi, Marco Haumann, Lehrstuhl für Chemische Reaktionstechnik, Friedrich-Alexander-Universität Erlangen-Nürnberg (FAU), Erlangen, Germany; Peter Wasserscheid, Lehrstuhl für Chemische Reaktionstechnik, Friedrich-Alexander-Universität Erlangen-Nürnberg (FAU), Erlangen, Helmholtz-Institut Erlangen-Nürnberg für Erneuerbare Energien (IEK-11), Forschungszentrum Jülich, Germany*

Supported catalytically active liquid metal solutions (SCALMS) offer the potential for new and unusual catalytic reactivity in alkane dehydrogenation. SCALMS are composed of catalytically active liquid alloy droplets on a porous support [1]. In contrast to conventional supported liquid phase catalysis, the catalytic reaction in SCALMS occurs only at the highly dynamic liquid metal/gas interface, as the liquid metal does not provide any relevant reactant solubility. Recently, we reported the use of Ga-rich Ga/Pd mixtures (atomic Ga/Pd ratio >10) on porous glass in the highly endothermic n-butane dehydrogenation [1]. The liquid nature of the supported alloy droplet under the reaction conditions was confirmed through a combination of XRD, SEM, XPS, and ab initio dynamics calculations. Most remarkably, these SCALMS materials outperform commercial dehydrogenation catalysts (Pt/Al<sub>2</sub>O<sub>3</sub>, Cr<sub>2</sub>O<sub>3</sub>/Al<sub>2</sub>O<sub>3</sub>) without any material or process optimisation. The most remarkable finding, however, is that coking, the typical deactivation mechanism for this type of high temperature hydrocarbon chemistry under reductive conditions [2-4], is largely suppressed with SCALMS systems. As explanation for this unexpected behaviour molecular dynamics calculations suggest that the topmost layer of the Ga-rich Ga/Pd alloy is depleted in Pd, but the layer directly underneath is enriched [1].

In our current study, the scope of SCALMS was extended to Al<sub>2</sub>O<sub>3</sub> supported Ga-rich Ga/Rh catalysts for propane dehydrogenation. The unique properties of the SCALMS approach resulted in a remarkable activity and selectivity towards propene, which is in contrast to literature reporting a poor performance of Rh based catalysts in alkane dehydrogenation [5,6]. Once again, the formation of carbon was limited by the highly dynamic liquid/gas interface of the supported liquid alloy. Nevertheless, observed deactivation may be related to the formation of coke. Hence, spent catalysts were

regenerated via temperature programmed oxidation (TPO) in 21% O<sub>2</sub>/He. The TPO was monitored by means of thermogravimetry in a XEMIS sorption analyser (Hiden Isochema) equipped with a mass spectrometer (MS) to identify different types of carbonaceous species. Furthermore, performance data during dehydrogenation are compared to the amount of formed coke. In addition, in situ dehydrogenation-regeneration cycles were conducted allowing for direct monitoring of the formation of coke while deactivation can be validated using the MS. Lastly, the kinetic of coke oxidation by O<sub>2</sub> during catalyst regeneration has been analysed by isoconversional methods providing insight into the reactivity of the formed coke.

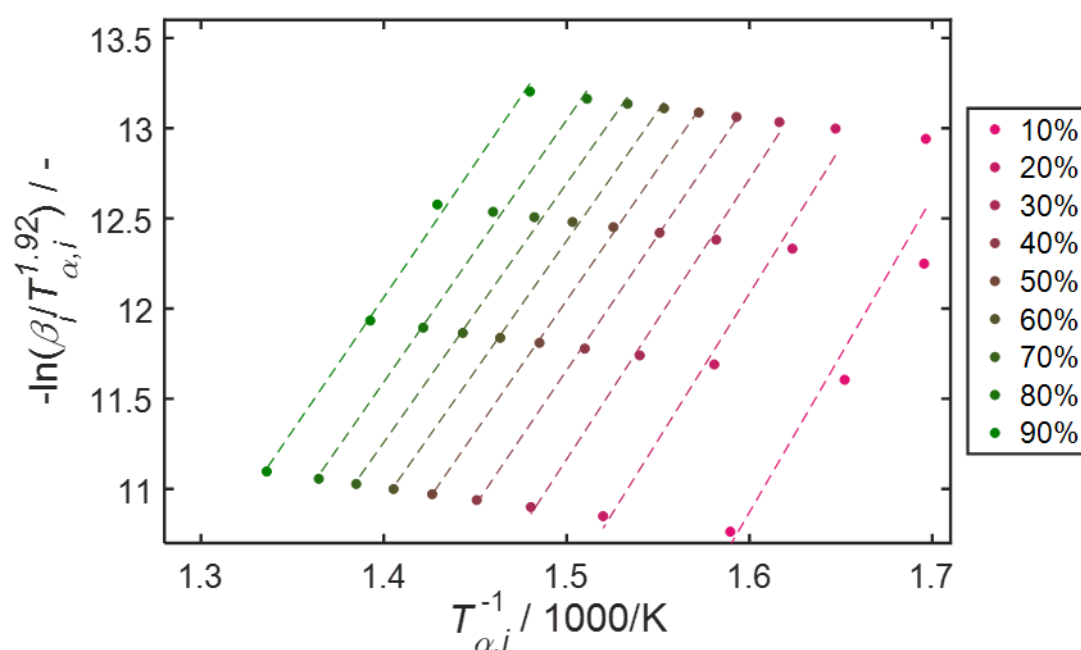


**Figure 1** Comparison of various conversion levels of coke ( $\alpha_i$ ) in the Arrhenius plot according to the isoconversional method by Starink [7] during temperature programmed oxidation in 21% O<sub>2</sub>/He at different heating rates ( $\beta_i$ ) for a spent Ga/Rh SCALMS catalyst applied in propane dehydrogenation.

## References

- [1] N. Taccardi, M. Grabau, J. Debuschewitz, M. Distaso, M. Brandl, R. Hock, F. Maier, C. Papp, J. Erhard, C. Neiss, W. Peukert, A. Görling, H.P. Steinrück, P. Wasserscheid, *Nat. Chem.* **9** (2017) 862.
- [2] J.R. Rostrup-Nielsen, *J. Catal.* **85**, (1984) 31.
- [3] V.L. Kuznetsov, A.N. Usol'tseva, Y.V. Butenko, *Kin. Catal.* **44** (2003) 726.
- [4] J.J.H.B. Sattler, J. Ruiz-Martinez, E. Santillan-Jimenez, B.M. Weckhuysen, *Chem. Rev.* **114** (2014) 10613.
- [5] D.E. Resasco, G.L. Haller, *J. Phys. Chem.* **88** (1984) 4552.
- [6] F. Solymosi, P. Tomalcsov, K. Kedves, *J. Catal.* **216** (2003) 377.
- [7] M.J. Starink, *Thermochim Acta* **404** (2003) 163.

# Elucidating the effect of hydrophobicity of methyl-functionalized titania-silica mixed oxides in the catalytic epoxidation of olefins

*Lucia E. Manangon-Perugach<sup>a</sup>, Alvise Vivian<sup>b</sup>, Pierre Eloy<sup>a</sup>, Damien P. Debecker<sup>a</sup>, Carmela Aprile<sup>b</sup> and Eric M. Gaigneaux<sup>a\*</sup>*

*<sup>a</sup>Institute of Condensed Matter and Nanosciences, Université catholique de Louvain, Louvain-la-Neuve, Belgium; <sup>b</sup>Unit of Nanomaterial Chemistry, Department of Chemistry, University of Namur, Namur, Belgium*

Titania-silica (TiO<sub>2</sub>-SiO<sub>2</sub>) mixed oxides are often considered as catalysts for the epoxidation of olefins. The catalyst active sites, isolated framework-Ti [1], are obtained only at low Ti loadings, which limits their number and thus the overall catalytic performance. Thus the need to search other approaches to boost the latter. We have hypothesized that increasing the catalyst hydrophobicity by promoting the presence of organic moieties on the catalyst surface could improve the catalytic performance by favoring both adsorption of the hydrophobic olefins and desorption of the less hydrophobic epoxides. Some previous studies have already correlated superior performance of catalysts with increasing hydrophobicity [2], but other studies found a negative or negligible effect of hydrophobization on the epoxidation of olefins [3], demonstrating that more understanding should still be gained.

In this work, hydrophobic TiO<sub>2</sub>-SiO<sub>2</sub> mixed oxides were prepared through one-pot sol-gel procedure. Hydrophobization was achieved by partial substitution of tetraethoxy silane (TEOS) by methyl triethoxy silane (MTES). Titanium butoxide (TiBut) was used as the Ti precursor to reach a nominal Ti molar fraction (Ti/(Si+Ti)) of 0.025. Additionally, the corresponding totally inorganic TiO<sub>2</sub>-SiO<sub>2</sub> catalyst was synthesized as reference material. The samples were dried under vacuum at 140 °C and calcined at 500 °C. The calcined samples were characterized by Solid-State <sup>29</sup>Si DE-MAS NMR, TGA-MS, ICP-AES, FTIR, DRUV, XPS, N<sub>2</sub> physisorption, and water vapor sorption. The catalytic activity was tested in the epoxidation of cyclooctene with hydrogen peroxide (H<sub>2</sub>O<sub>2</sub>).

Our TiO<sub>2</sub>-SiO<sub>2</sub> samples exhibited four degrees of methylation: 0%, 1%, 5%, and 14%, determined from direct excitation NMR experiments. They are noted as TS-x%Me, where x represents the effective percentage of methyl-functionalization. The characterization of the Ti species, performed by FTIR, DRUV and XPS, confirmed the presence of significant amount of the active framework-Ti (FW-Ti) (Table 1).

Table 1. Ti molar ratios quantified by ICP-AES and XPS

Sample	bulk Ti/(Si+Ti) molar ratio (ICP-AES)	Ti/(Si+Ti) molar ratio (XPS)	FW-Ti/(Si+Ti) molar ratio (XPS)
TS-0% Me	0.025	0.020	0.014
TS-1% Me	0.029	0.018	0.013
TS-5% Me	0.031	0.017	0.011
TS-14% Me	0.023	0.011	0.009

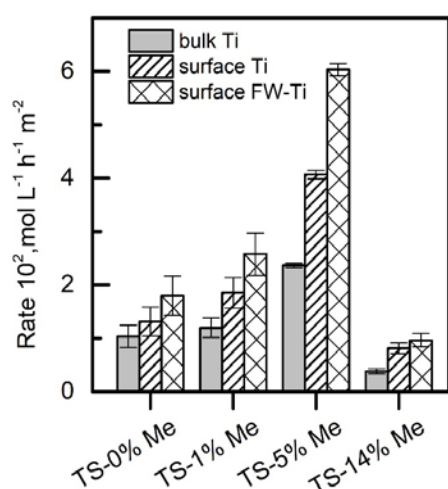


**Figure 1** Initial reaction rates normalized to the corresponding specific surface area and to the Ti molar fractions Ti/(Si+Ti): bulk Ti, surface Ti and surface FW-Ti.

Figure 1 shows that the initial rate was the highest for the 5% methyl content whatever the normalization, which indicates that there is an optimal methylation degree that improves the catalytic performance. An excessive methylation degree is detrimental to the catalytic activity, not only due to the lower FW-Ti content it induces but also due to the too high hydrophobic character it brings. Indeed, the water vapor sorption isotherm of TS-14%Me showed a very reduced affinity for water, likely decreasing its affinity for H<sub>2</sub>O<sub>2</sub> and preventing the oxygen atom transfer from H<sub>2</sub>O<sub>2</sub> to the FW-Ti site required for the olefin epoxidation.

## Conclusions

The synthesis of methyl-functionalized TiO<sub>2</sub>-SiO<sub>2</sub> catalysts by one-pot sol-gel procedure was successful at incorporating a significant amount of the active FW-Ti species and different degrees of hydrophobicity. Isolating the hydrophobic effect on the catalytic epoxidation performance was possible. Hydrophobic TiO<sub>2</sub>-SiO<sub>2</sub> performed much better than inorganic more hydrophilic TiO<sub>2</sub>-SiO<sub>2</sub>. However, a too high degree of methylation and thus hydrophobicity led to diminished catalyst performance, likely due to a too low affinity between the too hydrophobic catalyst surface and H<sub>2</sub>O<sub>2</sub>.

## References

1. M. G. Clerici and O. A. Kholdeeva, Liquid phase oxidation via heterogeneous catalysis: organic synthesis and industrial applications, *John Wiley & Sons*, **2013**.
2. H. Kochkar, F. Figueras, *J. Catal.* **1997**, *171*, 420-430; V. Smeets, L. Ben Mustapha, J. Schnee, E. M. Gaigneaux and D. P. Debecker, *Molecular Catalysis*, **2018**, *452*, 123-128.
3. C.A. Müller, M. Maciejewski, T. Mallat, A. Baiker, *J. Catal.* **1999**, *184*, 280-293; J. M. Fraile, J. I. García, J. A. Mayoral and E. Vispe, *J. Catal.* **2001**, *204*, 146-156.

# **Towards combining electro-catalytic and bio-electro-catalytic CO<sub>2</sub> reduction: microbial growth-medium electrolyte enhances electro-catalytic conversion of CO<sub>2</sub> to formate**

*K. Chatzipanagiotou<sup>1</sup>; V. Soekhoe<sup>1,2</sup>; dr. D.P.B.T.B. Strik<sup>2</sup>; prof. dr. C.J.N. Buisman<sup>2</sup>; prof. dr. J.H. Bitter<sup>1</sup>. 1: Biobased Chemistry & Technology, Wageningen University and Research, Wageningen, the Netherlands; 2: Environmental Technology, Wageningen University and Research, Wageningen, the Netherlands*

## **Background**

Globally, there is ongoing effort to recycle CO<sub>2</sub> emissions into fuels and commodity chemicals. With the expected future availability of cheap renewable energy, electricity-driven conversions could be a viable approach. Non-noble metal catalysts, like copper, are able to electro-catalytically reduce CO<sub>2</sub> in aqueous electrolytes, to products such as hydrogen, carbon monoxide, methane, formate, ethylene and ethanol. On the other hand, microorganisms can also catalyse CO<sub>2</sub> electro-reduction in aqueous electrolytes, via Microbial Electro-Synthesis (MES), with acetate and methane as the main products. These bio-electro-catalysts can directly utilize electrons from the electrode, as well as electro-chemically produced electron equivalents (e.g. formate or hydrogen).

Interestingly, formate is an intermediate product of CO<sub>2</sub> conversion for both types of electro-catalysts (metal and microbial). Therefore, a "metabolic cooperation" between (metal-) electro-catalytic and bio-electro-catalytic CO<sub>2</sub> reduction could be envisioned. However, in order to use formate as a metabolic intermediate between electro-catalysts and MES, both catalytic processes should ideally take place in the same aqueous electrolyte, as extraction would be challenging due to high solubility. Here, we investigate the feasibility of electro-catalytic formate production with copper electro-catalysts in microbial growth-medium electrolyte, as the first step in assessing the feasibility of metabolic cooperation.

## **Results & Discussion**

CO<sub>2</sub> electro-reduction has been typically performed using a bicarbonate-based electrolyte [1]. In contrast, when using microorganisms, the electrolyte has a different composition, mainly phosphates (Na<sub>2</sub>HPO<sub>4</sub> - KH<sub>2</sub>PO<sub>4</sub> buffer), growth nutrients



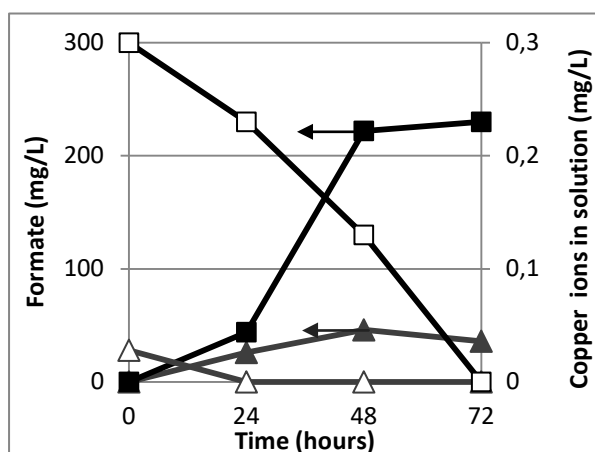


**Fig.1: Formate production (left axis, ■ microbial medium, ▲ bicarbonate) and dissolved copper (right axis, □ microbial medium, △ bicarbonate) over time. Cathode potential: -1 V vs. SHE, T= 298 K, pH= 6.7; CO<sub>2</sub> flushing rate in electrolyte = 50 ml/min.**

(NH<sub>4</sub><sup>+</sup>, Cl<sup>-</sup>, Mg<sup>2+</sup>, Ca<sup>2+</sup>), and trace elements (ions of Fe, B, Cu, I, Mn, Mo, Zn, Co, Ni). This medium was found to enhance formate production (pure Cu-electrode, Fig. 1), likely due to trace elements contained in the microbial medium [1]. Thus, the medium needed for microbial growth can also enhance the activity of copper electro-catalysts. Initially, Cu-ions leached from the electrode, but within 24 h (in bicarbonate) or 72 h (microbial medium), Cu-ion

concentration in solution decreased to zero (Fig. 1). This is due to re-deposition of the metal on the electrode, as a result of the negative cathode potential applied. Compared to bicarbonate electrolyte, leaching of Cu-ions in solution is enhanced, and re-deposition is delayed in microbial growth-medium, likely due to chelating agents contained in the medium, which stabilize the dissolved species. Overall, these results show that microbial growth-medium is a suitable electrolyte for metal-catalysed CO<sub>2</sub> electro-reduction.

## Outlook

We show that MES electrolyte not only allows the electro-catalytic conversion of CO<sub>2</sub> to formate, but in fact enhances the catalytic activity of copper electrodes. Therefore, there is great potential for combining metal- and bio-electro-catalytic CO<sub>2</sub> conversion in microbial growth-medium electrolytes. We are further investigating this combination, by combining both catalytic processes *in situ*, as well as in sequential reactions. This could improve the kinetics of both reactions, as it would increase the concentration of substrate (formate) for MES, while decreasing the concentration of products for the metal catalyst (i.e. formate consumption via MES). This could also enable the production of different final products, if a metabolic intermediate is introduced that changes the overall reaction pathway. Similar combinations can be envisioned for reactions that do not share a common substrate (i.e. CO<sub>2</sub> in this study), as long as the right metabolic intermediates are identified.

## References

1. R. Kortlever, K.H. Tan, Y. Kwon, M.T.M. Koper, *J Solid State Electrochem* 17 (2013) 1843.

## The Structure-Function Correlations of $\alpha$ -Fe(II)/ $\alpha$ -O Sites

*M.L. Bols<sup>1</sup>, B.E.R. Snyder<sup>2</sup>, S.D. Hallaert<sup>1</sup>, D. Plessers<sup>1</sup>, H.M. Rhoda<sup>3</sup>, K. Pierloot<sup>1</sup>, R.A. Schoonheydt<sup>1</sup>, E. I. Solomon<sup>3</sup>, B.F. Sels<sup>1</sup>*

<sup>1</sup> KU Leuven, Leuven, Belgium <sup>2</sup> University of Berkeley, Berkeley CA, U.S.A. <sup>3</sup> Stanford University, CA U.S.A

### Introduction

Highly reactive  $\alpha$ -O sites, capable of the low temperature activation of CH<sub>4</sub> and C<sub>6</sub>H<sub>6</sub> were recently defined as a high spin (S=2) square pyramidal Fe(IV)=O species.[1] The  $\alpha$ -O site can be formed by oxygen atom abstraction from N<sub>2</sub>O by the  $\alpha$ -Fe(II) precursor, which is hosted in extra-framework cation exchange sites of 6MR containing zeolites with specific positioning of aluminum-substituted T-atoms.[2]

### Tuning the $\alpha$ -Fe(II) sites by manipulating the coordination environment

The high-spin  $\alpha$ -Fe(II) precursor preferentially adopts a square planar coordination and is highly stable relative to spectator species.[3] Not every zeolite structure provides an optimal coordination environment for  $\alpha$ -Fe(II) binding. Still, various zeolite topologies with varying 6MR symmetries can be used to host  $\alpha$ -Fe(II) sites with very comparable reactive properties. A balance is struck between deformation of the host 6MR (strain energy on the lattice) and deviation from square planar coordination and ideal Fe-O<sub>FW</sub> bond length (strain on the Fe(II) coordination).[4] An exemplary case is given by  $\alpha$ -Fe(II) sites in Fe-\*BEA and Fe-CHA. The BEA-6MR is narrower and of lower symmetry (C<sub>2</sub>) than the wider CHA-6MR with C<sub>3v</sub> symmetry, resulting in predictive changes in electronic structure and spectroscopic parameters. The case illustrates the opportunity of tuning the active site function through adjusting structure. This can be achieved by modifying the host matrix structure and flexibility.

### The entatic state in N<sub>2</sub>O activation and $\alpha$ -O reactivity

The distorted coordination environment of  $\alpha$ -Fe(II) has implications for reactivity. Work submitted for publication indicates that N<sub>2</sub>O binding and activation to form the  $\alpha$ -O site is contingent on slight deformations of the most favorable Fe(II) ligand field environment enforced by the rigid zeolite matrix.

Moreover, for the reactive  $\alpha$ -O site, an entatic state was defined, tuning up the reactivity towards HAA from CH<sub>4</sub> – again reflecting the importance of the zeolite 6MR host. The square pyramidal  $\alpha$ -O structure is disfavoured in absence of lattice

constraints, relaxing to a structure with a trans axial O ligand. This instability versus reaction product creates a driving force introducing high reactivity, even at room temperature. The underlying reason is the exceptionally high electrophilic character of the  $\alpha$ -O Fe  $d_{z^2}$  derived LUMO. The same characteristic tunes down the barrier of C-O formation on benzene with  $\alpha$ -O.[5]

### Selecting the zeolite to match application

From the foregoing, the zeolite host selection could be optimized to match application. A wide variety of zeolite matrices is available from synthesis and zeolite tuning is increasingly becoming common practice. Firstly, aluminum distribution must be tailored to application. Secondly, the pore structure must be selected to match the reaction system's components. Thirdly, the coordination environment of the active site can be used to specifically stabilize certain intermediates over others, as demonstrated by the previous examples. It is, for example, not the CH<sub>4</sub> HAA step which is limiting in the methane to methanol reaction cycle with currently employed Fe-zeolites. Rather it is the activation of N<sub>2</sub>O forming the highly reactive  $\alpha$ -O. Our results suggest that it is possible to tune down the entatic effect on the  $\alpha$ -O site and simultaneously to destabilize the  $\alpha$ -Fe(II) precursor versus the transition state and  $\alpha$ -O by introducing elevated distortion on the host 6MR. This comes at a penalty in  $\alpha$ -O electrophilicity, which is not problematic given its excessively high reactivity.

### References

1. B.E.R. Snyder, P. Vanelderen, M.L. Bols, S.D. Hallaert, L.H. Böttger, L. Ungur, K. Pierloot, R.A. Schoonheydt, B.F. Sels, E.I. Solomon. *Nature* **2016**, *536*, 317-321.
2. B.E.R. Snyder, L.H. Böttger, M.L. Bols, R.A. Schoonheydt, B.F. Sels, E.I. Solomon et al. *PNAS* **2018**, *115*, 4565-4570.
3. S.D. Hallaert, M.L. Bols, P. Vanelderen, R.A. Schoonheydt, B.F. Sels, K. Pierloot. *Inorg. Chem.* **2017**, *56*, 10681-10690.
4. M.L. Bols, S.D. Hallaert, B.E.R. Snyder, J. Devos, D. Plessers, H.M. Rhoda, M. Dusselier, R.A. Schoonheydt, K. Pierloot, E.I. Solomon, B.F. Sels. *JACS* **2018**, *140*, 12021-12032.
5. B.E.R. Snyder, M.L. Bols, H.M. Rhoda, R.A. Schoonheydt, B.F. Sels, E.I. Solomon et al. *PNAS*, **2018**, *115*, 12124-12129.

# Hydrophobic hybrids constructed from Keggin phosphotungstic acid and bipyridine as heterogeneous epoxidation catalysts

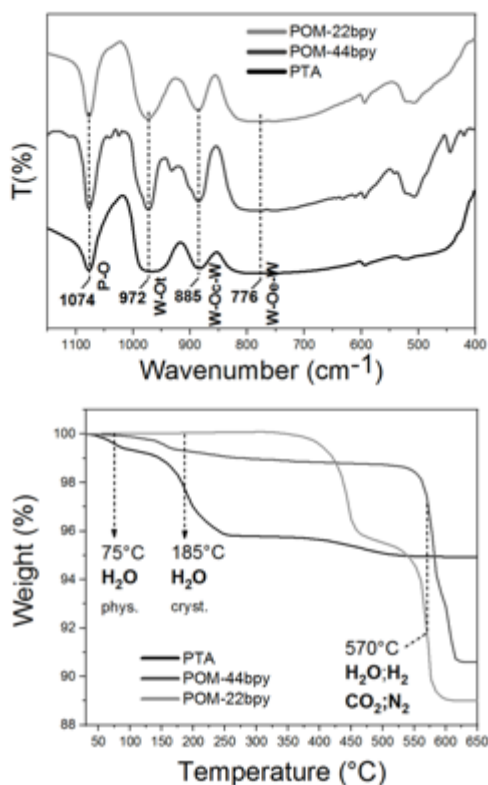
*Gabriel Hidalgo, M. Devillers and Eric M. Gaigneaux*

*Institute de la matière condensée et des nanosciences (IMCN), Université catholique de Louvain, Place Louis Pasteur 1, L4.01.09, Louvain-La-Neuve, Belgium.*

Among the diverse types of polyoxometalates (POMs) used in catalysis, Keggin heteropolyacids constitute one of the most promising structures adopted by POMs [1]. However, one of the main drawbacks related to heterogeneous catalysis is their high solubility in polar solvents which makes them prone to leach [2]. One efficient strategy to overcome this problem is the hybridization of POMs with nitrogen-containing heterocycles [3]. Precisely, this research aims to study the heterogenization of a hydrophilic phosphotungstic acid  $H_3PW_{12}O_{40}$  (PTA), with hydrophobic bipyridine (bpy) ligands (2,2'-bpy and 4,4'-bpy), for the catalytic epoxidation of cyclooctene (C.O) with  $H_2O_2$ .

The great availability, low cost and environmentally friendly  $H_2O_2$  makes this oxidising agent attractive for catalytic epoxidation reactions. However, the fact that  $H_2O$  is produced as the main by-product, presents a number of consequences for several catalysts. Indeed, water can affect sensitive functions of the catalyst operation by trying to compete effectively for binding at the hydrophilic POM active sites and, consequently, inactivating and rendering the catalyst less selective. Therefore, in this study we hypothesize that the hydrophilic nature of the POM in PTA can be mitigated by introducing hydrophobic bipyridine molecules through a simple ionic exchange between the moieties. The overall hydrophobicity of the solid catalyst would accelerate the desorption of water produced, by expelling the latter from the hydrophilic POM active sites and thereby, this would facilitate a new adsorption of reagent at the catalyst surface, initiating a new successive catalytic cycle.

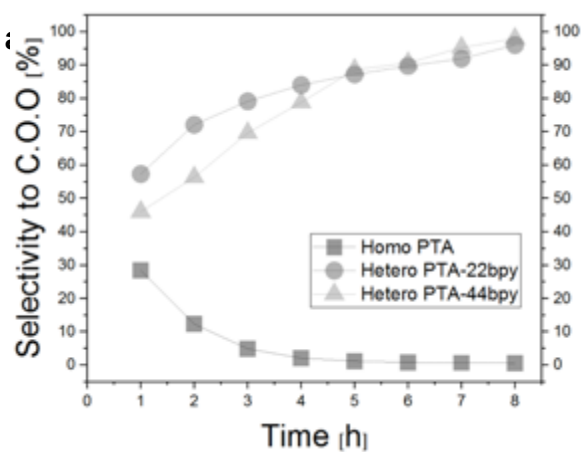
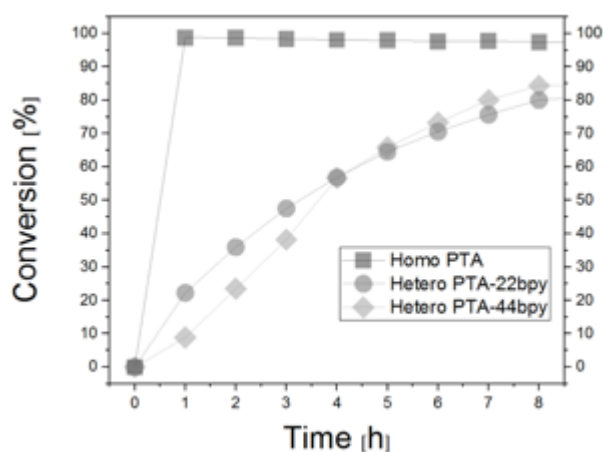
To achieve the targeted sort of hybrids, a rigorous control and monitoring on their synthesis is needed. We will show that keeping the intrinsic properties of the POM anion after the hybridization, can be achieved through non-covalent interactions between the moieties via a simple hydrothermal synthesis. (Fig.1).



FTIR confirms that after hybridization the POM anion integrity is preserved. Moreover, a TGA-MS analysis reveals the almost total absence of water after hybridization, confirming the hydrophobic properties of the constructed solids. Additional Raman and NMR data will be provided demonstrating the structure of the hybrids; besides TPD-NH<sub>3</sub> and DR-UV-Vis reveal respectively that the hybrids do not have remaining acidity and still display a marked oxidative potential, which makes them promising for epoxidation catalysis.

The two insoluble solid hybrids indeed present excellent catalytic activities and selectivities toward the epoxide (Fig. 2). The heterogeneous reaction proved to be more selective than its homogeneous counterpart (pristine PTA), since the opening

The two insoluble solid hybrids indeed present excellent catalytic activities and selectivities toward the epoxide (Fig. 2). The heterogeneous reaction proved to be more selective than its homogeneous counterpart (pristine PTA), since the opening



epoxide ring was prevented.

**Figure 2.** Evolution of (a) conversion and (b) selectivity to cyclo-octene-oxide for the epoxidation of cyclo-octene with H<sub>2</sub>O<sub>2</sub> in acetonitrile. Note that the PTA operates in homogeneous phase.

## References

1. Pope M.T. *Heteropoly and Isopoly oxometalates*; **1983**.
2. Rafiee, E.; Eavani; S. RSC adv. **2016**, vol. 6 (52), 46433-46466
3. Song, Y.; Tsunashima, R. Chem. Soc. Rev., **2012**, vol. 41 (22), 7384-7402

# Insights into potassium promoter effects in $\text{CuCl}_2/\gamma\text{-alumina}$ catalyzed ethylene oxychlorination

*Y. Qi, Norwegian University of Science and Technology(NTNU), Trondheim, Norway; E. Fenes, NTNU, Trondheim, Norway; H. Ma, NTNU, Trondheim, Norway; KR. Rout, SINTEF, Trondheim, Norway; T. Fuglerud, INOVYN, Herøya Industrial Park, Norway; D Chen, NTNU, Trondheim, Norway*

## Introduction

Ethylene oxychlorination is an important step in the industrial production of vinyl chloride monomer (VCM), which is needed for polyvinyl chloride (PVC) production.  $\text{CuCl}_2/\gamma\text{-Al}_2\text{O}_3$  based catalysts are effective to catalyze ethylene, HCl and oxygen to produce 1,2-dichloroethane (EDC) in this process [1-2]. The promoter, K, is widely used in the industrial catalysts to achieve optimum performance. Many researches are devoted to studying the effect of K [3-4], however, the underlying nature of the promoter effects is not fully understood yet. Herein, we employed density functional theory to study the role of potassium in the reaction.

## Method and Model

We performed DFT calculations by using VASP5.3.2. We used Bayesian error estimation functional with van der Waals correlation (BEEF-vdW) functional[5] and the projected augmented wave (PAW) method[6] combined with the plane-wave expansion at a kinetic energy cutoff of 400 eV. The Brillouin zone integration was performed with a  $4 \times 4 \times 1$  k-point grid. The ground-state atomic geometries of bulk and surface were obtained when the total energy difference between two steps of the SCF loop was below  $1 \times 10^{-4}$  eV, and residual forces on atoms were converged when below 0.03 eV/Å. The surfaces are simulated using a slab model with eight atomic layers for the dehydrated  $\gamma\text{-Al}_2\text{O}_3$  (110) surface. A vacuum of 15 Å is set between two periodic repeated slabs.

## Results and Discussion

The interaction between support and copper plays an important role in the reaction and thus we built a model with three  $\text{CuCl}_2$  molecules supported on  $\gamma\text{-Al}_2\text{O}_3$  (110). KCl was co-adsorbed on the surface to represent the K-promoted catalysts. The co-adsorbed KCl significantly changed the structure of  $\text{CuCl}_2$  and decreased the adsorption strength of  $\text{CuCl}_2$ . The results revealed that both the reduction and

oxidation rates depend on the Cl/Cu ratios, where different numbers of Cl atoms were removed to represent different Cl/Cu ratios.

The effect of the co-adsorption of KCl in  $\text{CuCl}_2$  on ethylene adsorption depends on the Cl/Cu ratio. Co-adsorbed KCl in  $\text{CuCl}_2$  weakened ethylene adsorption heat and thus increased the reduction barrier at a high Cl/Cu ratio (i.e. Cl/Cu = 2), while it had a negligible effect on the adsorption energy of ethylene at relatively low Cl/Cu ratios (i.e. Cl/Cu = 1.33 and 1.67). Moreover, it is found that co-adsorbed KCl increased the adsorption strength of oxygen at various Cl/Cu ratios and decreased the barrier of oxygen dissociation by 0.36 eV compared to the neat  $\text{Cu}^+$  catalysts (i.e.,  $3\text{CuCl}_2\text{-}3\text{Cl}/\gamma\text{-Al}_2\text{O}_3$ ). The electronic properties such as charge density of Cu and Cl and band gap have been analyzed to unravel the underlying nature of potassium promoter effects.

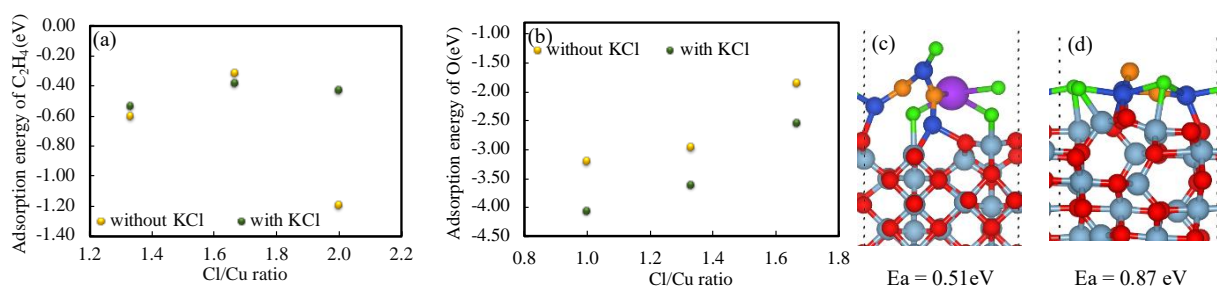


Figure 1. Adsorption energy of ethylene(a) and oxygen (b) on the surface with various Cl/Cu ratios, the transition states and activation barrier of oxygen dissociation on the surface with KCl (c) and without KCl (d). Red balls represent O in alumina, gray balls are Al, green balls are Cl, blue balls are Cu, the purple ball is K, and yellow balls are dissociated O.

## Conclusion

DFT study provides a better understanding of the catalytic cycle of ethylene oxychlorination on Cu based catalysts. The co-adsorbed KCl enhances the oxygen adsorption and thus facilitates its dissociation and improves significantly  $\text{Cu}^+$  oxidation, which is typically the rate-determining step of Cu catalysts. In addition, the co-adsorbed KCl weakens the ethylene adsorption heat and increases the reduction barrier.

## References

1. Leofanti G, Marsella A, Cremaschi B, Garilli M, Zecchina A, Spoto G, Bordiga S, Fiscaro P, Prestipino C, Villain F, Lamberti C (2002) *J. Catal.* 205: 375-381
2. Rout KR, Fenes E, Baidoo MF, Abdollahi R, Fuglerud T, Chen D (2016) *ACS Catal.* 6: 7030-7039
3. Rout KR, Baidoo MF, Fenes E, Zhu J, Fuglerud T, Chen D (2017) *J. Catal.* (2017) 352: 218-228
4. Muddada NB, Olsbye U, Fuglerud T, Vidotto S, Marsella A, Bordiga S, Gianolia D, Leofanti G, Lamberti C (2011) *J. Catal.* (2011) 236-246
5. Wellendorff J, Lundgaard KT, Mogelhoj A, Petzold V, Landis DD, Norskov JK, Bligaard T, Jacobsen KW (2012) *Phys. Rev. B* 85: 235149
6. resse G, Joubert D (1999) *Phys. Rev. B* 59: 1758-1775

# Formation of metathesis active sites in $\text{WO}_x/\text{SiO}_2$ catalyst: a DFT study

*Jarosław Handzlik\**, Maciej Gierada, Kamil Kurlito

*Faculty of Chemical Engineering and Technology, Cracow University of Technology,  
ul. Warszawska 24, 31-155 Krakow, Poland*

## Introduction

$\text{WO}_x/\text{SiO}_2$  system is an industrial catalyst for large-scale metathesis of light alkenes [1-3]. Tungsten alkylidene sites, required for alkene metathesis, are generated *in situ* from the surface tungsten oxide species upon contact with alkene [2-6]. The structure and oxidation state of the tungsten oxide precursors are not exactly known. The mechanism of the transformation of the surface metal oxide species into the active sites is also not well recognised, although several routes for this initiation stage of alkene metathesis were proposed [2,4-8].

In this computational study we have examined potential initiation mechanisms for olefin metathesis catalysed by the  $\text{WO}_x/\text{SiO}_2$  system, using density functional theory (PBE0-D3) and the cluster approach.

## Results and discussion

Surface W(VI), W(V) and W(IV) oxide species are considered as the active site precursors. A number of potential pathways for their transformations into tungsten alkylidene species have been calculated to understand the initiation stage of olefin metathesis.

At first, the pseudo-Wittig mechanism involving the formation of oxatungstacyclobutane intermediate from W(VI), W(V) and W(IV) oxide precursors is discussed. The reactivity of ethene towards dioxo W(VI) species is predicted to be significantly lower, compared to propene and 2-butene, in accordance with the reported experimental results [4]. The calculated activation barrier for the formation of W(VI) mono(alkylidene) species is reasonable, taking into account the moderate or high temperature of the process. On the other hand, the recently suggested [4] formation of W(VI) bis(alkylidene) species does not seem to be kinetically and thermodynamically accessible. According to the calculations, the W(V) and W(IV) oxide species are less likely as the active site precursors than the dioxo W(VI) species. Transformation of the monooxo W(VI) species into W(VI) alkylidene centre



is shown to be highly improbable, in general agreement with the recent experimental findings [6].

We have also calculated the pathway for reduction of the dioxo W(VI) species to W(IV) site by propene, with participation of the neighbouring silanol group, analogous to the initiation mechanism recently proposed for MoO<sub>x</sub>/SBA-15 system [8]. Although the overall reduction process is found to be less preferred kinetically and thermodynamically than the pseudo-Wittig mechanism, the first step is exergonic and kinetically favoured.

Finally, 1,2-hydrogen shift and formation of tungstacyclopentane intermediate, followed by 1,4-hydrogen shift, are considered as other potential initiation mechanisms for the W(IV) oxide species. Although both pathways cannot be excluded, generation of tungstacyclopentane species is strongly favoured kinetically and thermodynamically.

## Conclusions

At higher temperatures, the W(VI) species can be activated according to the pseudo-Wittig mechanism or reduced to W(IV) sites. The W(V) oxide precursors should be less reactive than the W(VI) species. For W(IV) oxide precursors, tungstacyclopentane formation, followed by 1,4-hydrogen shift, seems to be the most likely initiation mechanism.

Acknowledgments: This work has been supported by the National Science Centre, Poland, Project No. 2015/19/B/ST4/01836 and by the PL-Grid Infrastructure.

## References

1. J.C. Mol, *J. Mol. Catal. A: Chem.* 213 (2004) 39-45.
2. S. Lwin, I.E. Wachs, *ACS Catal.* 4 (2014) 2505-2520.
3. S. Lwin, Y. Li, A.I. Frenkel, I.E. Wachs, *ACS Catal.* 6 (2016) 3061-3071.
4. S. Lwin, I.E. Wachs, *ACS Catal.* 7 (2017) 573-580.
5. K. Ding, A. Gulec, A.M. Johnson, T.L. Drake, W. Wu, Y. Lin, E. Weitz, L.D. Marks, P.C. Stair, *ACS Catal.* 6 (2016) 5740-5746.
6. J.G. Howell, Y.-P. Li, A.T. Bell, *ACS Catal.* 6 (2016) 7728-7738.
7. K. Amakawa, S. Wrabetz, J. Kröhnert, G. Tzolova-Müller, R. Schlögl, A. Trunschke, *J. Am. Chem. Soc.* 134 (2012) 11462-11473.
8. K. Amakawa, J. Kröhnert, S. Wrabetz, B. Frank, F. Hemmann, C. Jäger, R. Schlögl, A. Trunschke, *ChemCatChem* 7 (2015) 4059-4065.

# Unveiling the active phase of highly active supported ZnO/TiO<sub>2</sub> - SAPO-34 hybrid catalysts in syngas to olefins process

*Alexey V. Kirilin<sup>1\*</sup>, Adam Chojecki<sup>1</sup>, David F. Yancey<sup>2</sup>, Vera Santos<sup>1</sup>, Kyle Andrews<sup>2</sup>, Joseph F. DeWilde<sup>2</sup>, Davy Nieskens<sup>1</sup>, Ewa Tocha<sup>1</sup>, Brian Dickie<sup>1</sup> and Andrzej Malek<sup>2</sup>*

<sup>1</sup>The Dow Chemical Company Herbert H. Dowweg 5, Building 443 (BBB), 4252 NM, Hoek, the Netherlands; <sup>2</sup>The Dow Chemical Company, Building 1776, Midland, Michigan 48674, United States, [akirilin@dow.com](mailto:akirilin@dow.com)

## Introduction

Recently a direct route to olefins from syngas employing mixed oxide (MMO) -zeolite catalysts was proposed over ZnCrOx – SAPO-34 [1] and Zn/ZrO<sub>2</sub> – SAPO-34 [2] systems. The reaction proceeds via CO hydrogenation to an oxygenated intermediates which are simultaneously converted to olefins over SAPO-34 [1,2]. Despite a high peak selectivity to olefins [1], challenges in olefin yield and stability remain due to apparent catalyst transformations over time. Literature on Zn-Cr catalysts teaches that an inversed ZnCr<sub>2</sub>O<sub>4</sub> spinel with Zn occupying octahedral coordination sites is an active phase in methanol synthesis [4]. Unfortunately, the structural stability of the non-stoichiometric Zn-Cr phase under syngas is limited. Our hypothesis was to employ a structurally similar (i.e., Zn in octahedral coordination) but more stable inversed Zn-containing spinel based on titania (Zn<sub>2</sub>TiO<sub>4</sub>) [4].

In the present study, we evaluated a series of different titanium oxides as supports for Zn to form active mixed metal oxide components for hybrid catalysts with SAPO-34.

## Materials and Methods

Commercially available TiO<sub>2</sub> was used: 100% anatase, 100% rutile and anatase-rutile mixed phase. Supports were crushed and sieved to 60-80 mesh. ZnO/TiO<sub>2</sub> catalysts were prepared by incipient wetness impregnation using aq. zinc nitrate solution. The catalysts were dried and calcined on air, and were characterized by XRF, XRD, TPR, XPS, XANES and TEM methods. SAPO-34 was prepared following standard literature procedures and characterized by XRD, SEM, BET and NH<sub>3</sub>-TPD. Prior to use SAPO-34 was calcined to remove template (600°C/4h) and compacted to 60-80 mesh size. Syngas conversion testing was performed in a stainless steel fixed-bed tubular reactor (i.d. 3 mm). Hybrid catalysts were prepared by mixing ZnO/TiO<sub>2</sub> with SAPO-34. The experiments spanned the following condition ranges:

390-400°C, 20-40 bar, H<sub>2</sub>/CO feed ratio=2 and GHSV: 900-3000 h<sup>-1</sup>. Data was collected for at least 100 h on stream and the reported values (Cmol%) are at steady state. Reaction components and products were analyzed by online GC and the carbon balance in experiments was 95-105%.

## Results and Discussion

Syngas conversion over ZnO/TiO<sub>2</sub>-SAPO-34 was in the range of 20-35%; selectivity to C<sub>2</sub>-C<sub>5</sub> olefins selectivity reached 35% at moderate paraffin (<25%) and low methane made (<5%). Among the phase composition tested, we found that high surface area anatase supports are preferred over mix phases and pure rutile materials. Supported ZnO/TiO<sub>2</sub> catalysts demonstrate better stability of olefin make with time than bulk Zn/Cr materials (Figure 1a).

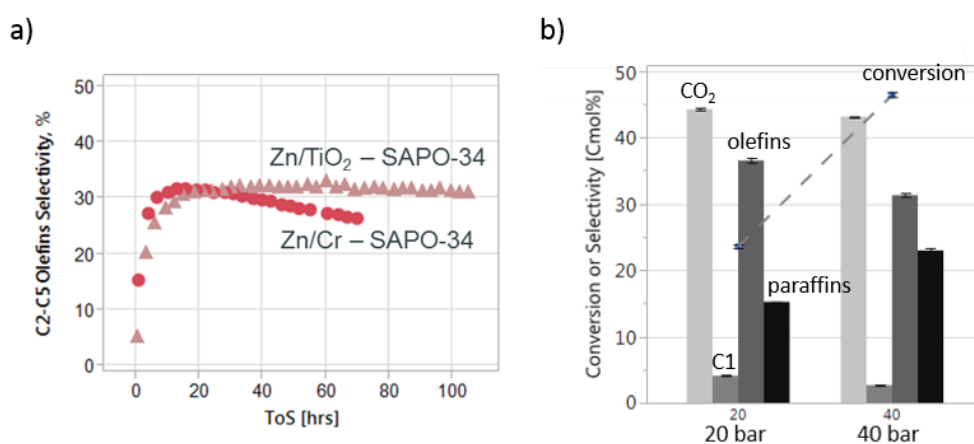


**Figure 1.** a) Selectivity to olefins over ZnO/TiO<sub>2</sub> and bulk Zn-Cr containing hybrid catalysts vs time (20 bar, 390°C) and b) steady state data for ZnO/TiO<sub>2</sub>-SAPO-34 (CO<sub>2</sub>, C<sub>2</sub>-C<sub>5</sub> olefins, C<sub>2</sub>-C<sub>5</sub> paraffins, C<sub>1</sub> (methane) selectivities and syngas conversion) at 20 and 40 bar, respectively. Data collected at H<sub>2</sub>/CO=2, GHSV=1200 h<sup>-1</sup>.

Active and stable ZnO/TiO<sub>2</sub> catalysts advance catalyst development in the direct syngas to olefins conversion over hybrid catalysts and outperform existing bulk Zn-Cr oxides reported in literature [1,5]. Detailed analysis of the catalyst structure by XRD, XANES and TEM has enabled identification of the active phase in ZnO/TiO<sub>2</sub> system under reaction conditions.

## References

1. Jiao, F., Li, J., Pan, X., Xiao, J., Li, H., Ma, H., Wei, M., Pan, Y., Zhou, Z., Li, M., Miao, S., Li, J., Zhu, Y., Xiao, D., He, T., Yang, J., Qi, F., Fu, Q., Bao, X. *Science* 351, 1065 (2016).
2. Cheng, K., Gu, B., Liu, X., Kang, J., Zhang, Q., Wang, Y. *Angew. Chem. Int. Ed.* 55, 1 (2016).
3. Del Piero, G., Trifiro, F., Vaccari, A. *J. Chem. Soc. Chem. Comm.* 0, 656 (1984).
4. Villa, P., Delpiero, G., Lietti, L., Garagiola, F., Mologni, G., Tronconi, E., Pasquon, I. *Appl. Catal.* 35, 47 (1987).
5. Kirilin, A. V., Dewilde, J. F., Santos, V., Chojecki, A., Scieranka, K., Malek, A. *Ind. Eng. Chem. Res.* 56(45), 13392 (2017)

# In Situ XAS Study of Supported Palladium in the Direct Synthesis of Hydrogen Peroxide in Ethanol-Based Solvents Using a Continuous-Flow High-Pressure Setup

*B.J. Deschner, D.E. Doronkin, T.L. Sheppard, J.-D. Grunwaldt, R. Dittmeyer,  
Karlsruhe Institute of Technology, Karlsruhe, Germany*

## Introduction

Hydrogen peroxide is a very attractive commodity from the point of view of industrial single-oxygen transfer reactions. Following molecular oxygen, it is the most efficient oxidizing agent [1] and is also environmentally friendly because its decomposition reaction only produces water as a by-product. The current standard for industrial production is the anthraquinone process, which impedes cost-effective production due to the high number of process stages and the limited recyclability of the organic anthraquinone [1].

In contrast, the liquid-phase catalyzed direct synthesis of hydrogen peroxide is an attractive synthesis route which involves contacting both molecular hydrogen and oxygen using a heterogeneous catalyst in a single reaction. In recent years, intensive research has been carried out into the understanding of the reaction mechanism in order to achieve a knowledge-based increase in selectivity, which currently impedes industrial implementation. In particular, the structural elucidation by X-ray absorption spectroscopy (XAS) has contributed to a considerable increase in knowledge [2-4]. In this contribution, we show the evolution from our low-pressure XAS study with aqueous solvent [3] to a continuous-flow high pressure setup. This setup enables *in situ* X-ray absorption spectroscopy to reveal structure-activity relationships at technically relevant conditions, i.e. elevated pressure and alcohol-containing reaction media. We disclose an experimental design that allows XAS studies under the boundary conditions of synchrotron facilities at pressures up to 100 bar.

## Experimental Details

We investigated a 1%Pd/TiO<sub>2</sub> catalyst in a fixed bed continuous flow of an ethanol-based solvent at 40 bar system pressure. The setup and the cell (Fig. 1) made mainly of passivated stainless steel allow safe H<sub>2</sub> and O<sub>2</sub> dosing and dissolution in separate liquid streams. In this way variation of many experimental parameters such as pressure, H<sub>2</sub>:O<sub>2</sub> ratios, flow rate and residence times etc. on the structure and activity of catalysts can be studied. X-ray absorption data at Pd K-edge were

recorded at the CAT-ACT beamline at KIT synchrotron whereas the corresponding catalyst productivity was linked to  $\text{H}_2\text{O}_2$  concentrations determined by subsequent manual  $\text{Ce}(\text{SO}_4)_2$  titration. We studied the effect of the liquid phase  $\text{H}_2:\text{O}_2$  ratios over a broad range as well as the effect of adding  $\text{H}_2\text{SO}_4$  and  $\text{Br}^-$  promoters.

## Results and Discussion

Analysis of XAS spectra points out that even below stoichiometric  $\text{H}_2:\text{O}_2$  ratios Pd lattice expansion occurs. The Pd-Pd distance gradually increases with increasing  $\text{H}_2:\text{O}_2$  ratio, whereas some lattice expansion is visible already at a  $\text{H}_2:\text{O}_2$  ratio of 0.67, opposite to our findings in water [3]. Moreover, no sign of surface-chemisorbed oxygen could be identified in the XANES spectra, even in  $\text{O}_2$ -saturated ethanol.

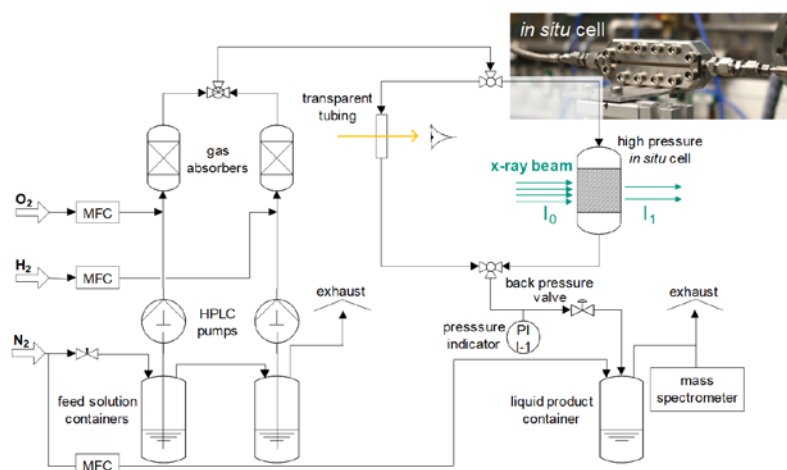


**Fig. 1.** Scheme of the experimental setup for operando X-ray studies during continuous  $\text{H}_2\text{O}_2$  synthesis at high pressures.

## Conclusions

In conclusion, a platform for *operando* studies of  $\text{H}_2\text{O}_2$  synthesis catalysts under technically relevant conditions is developed and the first results on the structure and catalytic performance of 1%Pd/TiO<sub>2</sub> in ethanol are presented in comparison with the results of previous studies in aqueous solution [3]. Effects of  $\text{H}_2\text{SO}_4$  and NaBr addition on the structure and performance of Pd species were also evaluated. The setup can be used directly or with small modifications to expand the characterization portfolio to other techniques such as XRD or Raman spectroscopy.

## References

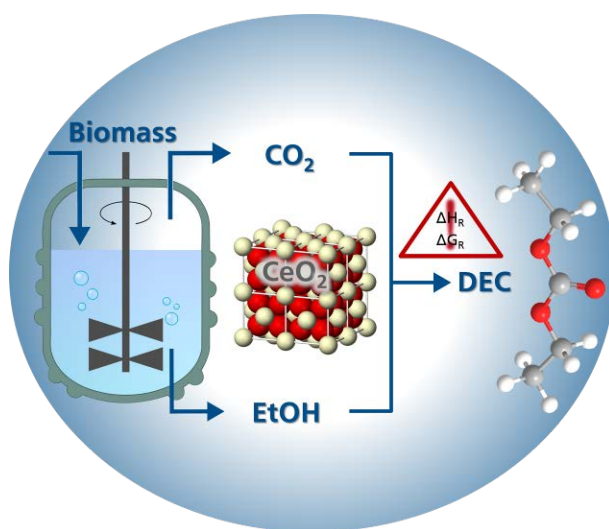
- [1] C. Samanta, Appl. Catal., A, 350 (2008) 133.
- [2] P. Centomo, et al., ChemCatChem 7 (2015) 3712.
- [3] M. Selinsek et al., ACS Catal. 8 (2018) 2546.
- [4] S. Kanungo et al., J. Catal. 370 (2019) 200.

# **Cerium oxide-catalyzed formation of diethyl carbonate from carbon dioxide and ethanol**

*Marco Buchmann, Martin Lucas, Marcus Rose  
Ernst-Berl-Institut für Technische und Makromolekulare Chemie,  
TU Darmstadt, Germany.*

Diethyl carbonate (DEC) has great potential to be used as solvent, alkylation agent, fuel additive and electrolyte for lithium ion batteries. Furthermore it is a volatile, non-toxic and bio-degradable chemical.<sup>[1]</sup> It can be produced by direct conversion of carbon dioxide and bio-ethanol as both reactants are obtained simultaneously by fermentation. The main challenge of the formation of DEC is the thermodynamic limitation due to the formation of water. From literature it is well known that cerium oxide catalysts are good catalysts for the direct reaction of carbon dioxide and ethanol.<sup>[2]</sup> In our work we synthesized various pure cerium oxide catalysts by precipitation with different basic agents from an aqueous solution.<sup>[3]</sup> The precipitation and calcination temperature were varied to identify the optimal conditions and elucidate property-activity-relations. Furthermore, different basic precipitation agents and defined pH values were applied under well-defined and automatized precipitation conditions. The catalysts were characterized by various techniques such as nitrogen physisorption, XRD, SEM as well as ammonia and carbon dioxide temperature-programmed desorption (TPD). The ammonia TPD experiments show one broad peak which decreases by increasing the calcination temperature. In contrast, the carbon dioxide TPD shows two peaks at low calcination temperatures and only one decreasing peak with increasing the calcination temperature indicating several different basic surface sites. Accompanied by the vanishing of one peak the catalytic activity of the catalysts rises. As shown by XRD measurements the crystallinity of the cerium oxides increases with increasing calcination temperature. All observed reflexes in the diffraction pattern could be assigned to phase pure cerium oxide. By comparing the different precipitation agents and conditions, cerium oxide catalysts, which were prepared by using an aqueous ammonia solution at a pH value of 10 and 50 °C, showed the by far best results for the catalytic activity. The increase in catalytic activity can be assigned to smaller crystallites and a slightly higher BET surface area compared to the urea precipitated catalyst. Concurrently, the ammonia uptake increases significantly with nearly the same carbon dioxide uptake. This

indicates a higher activation towards ethanol and no loss of activity towards carbon dioxide.<sup>[5]</sup> The catalytic activity of cerium oxide is mainly caused by defects in the crystal structure. In this case two phenomena are often discussed in literature, the oxygen storage capacity (OSC) and the oxygen vacancy defects (OVD).<sup>[4]</sup> Especially OVDs can increase the adsorption and activation of carbon dioxide. Both the synthesis of OVDs and their exact characterization are very demanding. In a first approach we investigated the introduction of these defects by partial reduction of the cerium oxide surface under a pure hydrogen stream at different temperatures. First results showed a slightly higher activity and, interestingly, no formation of diethyl ether as a byproduct. In summary, with optimized cerium oxide catalysts we obtained a very good performance and an understanding of property-activity relations regarding the influence of crucial synthesis parameters. In future work, the main task is to overcome thermodynamic limitations that arise from the formation of water by combining the reaction with *in situ* water removal.



## References

- [1] B. Schöffner, F. Schöffner, S. P. Verevkin, A. Börner, *Chem. Rev.* **2010**, *110*, 4554-4581.
- [2] E. Leino, P. Mäki-Arvela, K. Eränen, M. Tenho, D. Y. Murzin, T. Salmi, J.-P. Mikkola, *Chem. Eng. J.* **2011**, *176-177*, 124-133.
- [3] M. Buchmann, M. Lucas, M. Rose, *manuscript in preparation*.
- [4] C. Zhang, A. Michaelides, D. A. King, S. J. Jenkins, *Phys. Rev. B* **2009**, *79*, 075433.
- [5] K. Tomishige, Y. Ikeda, T. Sakaihorii, K. Fujimoto, *J. Catal.* **2000**, *192*, 355-362.

# Tuning catalytic performance of MoC<sub>x</sub>/C by controlling the carburization degree

*J. Zhu, N.A. Kosinov, E.J.M. Hensen,*

*Laboratory of Inorganic Materials and Catalysis, Eindhoven University of Technology,  
Eindhoven, Netherlands*

Since the pioneering work of Levy and Boudart [1], transition metal carbides (TMCs) are widely investigated as a cheap alternative to noble metal catalysts due to their promising catalytic properties. Among all the explored TMCs, molybdenum carbide is of particular interest and has been applied to various reactions in which hydrogen activation plays a role, such as CO<sub>x</sub> hydrogenation, the water-gas shift reaction, and biomass hydrodeoxygenation (HDO). One of the central questions regarding molybdenum carbide catalysts is the relation between catalytic performance and carbide surface structure, in particular the inclusion of heteroatoms of reactants in the metal carbide surface under working conditions. Bhan et al. showed that about 0.29 monolayers of oxygen was incorporated during transient anisole HDO experiments [2]. Another related aspect is that in many studies a passivation step in preparation is used because of the pyrophoric nature of metal carbides. The resulting passivated catalyst often needs to be reactivated before catalytic test, yet its performance is influenced by the way how it is passivated and reactivated (activation gas, activation temperature *etc.*).

In this work, we prepared MoC<sub>x</sub>/C catalysts by carburization of ammonium heptamolybdate (NH<sub>4</sub>)<sub>6</sub>Mo<sub>7</sub>O<sub>24</sub> (AHM), impregnated on activated carbon. We evaluated the catalytic performance of these catalysts without a passivation step in CO<sub>2</sub> hydrogenation and anisole HDO. Firstly, a combination of *in situ* XANES and TPR-MS was employed to trace the stepwise carburization process (AHM → MoO<sub>3</sub> → MoO<sub>2</sub> → MoO<sub>x</sub>C<sub>y</sub> → MoC<sub>x</sub>). Based on the aforementioned data, four carburization temperatures were selected to prepare MoC<sub>x</sub>/C catalysts with different carburization degrees and the resulting catalysts were further carefully characterized (XRD, XPS, EXAFS *etc.*) and tested without exposure to ambient conditions. The results show that both activity and selectivity depend strongly on the catalyst carburization degree: CO<sub>2</sub> and anisole conversion increased with increasing carburization temperature. The main products during anisole HDO shifted from



benzene and phenol to only benzene (>90%) as the carburization temperature was increased from 600 °C to 700 °C. Such observations indicate that pure molybdenum carbide is more efficient than molybdenum oxycarbide for H<sub>2</sub> activation and oxygen removal reactions. Moreover, there was a stronger deactivation observed during anisole HDO than CO<sub>2</sub> hydrogenation. XPS on spent catalysts for both reactions and in situ XANES on catalysts under anisole HDO condition were employed to study the possible catalyst structure and compositional changes. These obtained results showed that no significant catalyst oxidation occurred for both reactions, indicating that coke formation may be the main reason for deactivation in these cases.

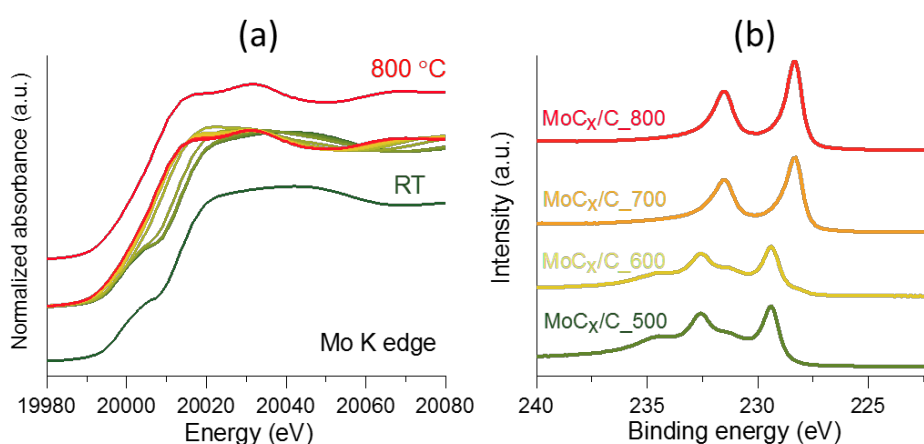


**Fig. 1.** (a) In situ XANES spectra during carburization ramping to 800 °C (b) XPS spectra of MoC<sub>x</sub>/C catalysts prepared at different temperature

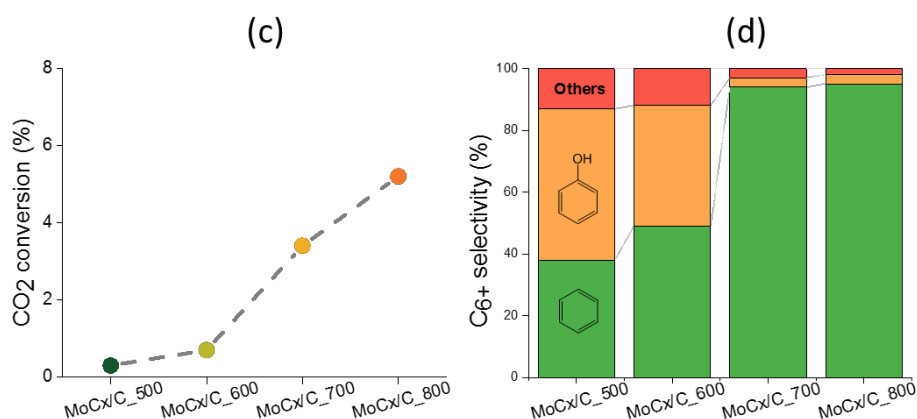


**Fig. 2.** (c) CO<sub>2</sub> conversion for CO<sub>2</sub> hydrogenation and (d) C<sub>6+</sub> product selectivity for anisole HDO of MoC<sub>x</sub>/C catalysts prepared at different temperature

## References

- [1] M. Boudart, R. B. Levy, *Science*, 191 (1973), 547.
- [2] W.-S. Lee, A. Kumar, Z. Wang, A. Bhan, *ACS Catal.* 5 (2015). 4104.

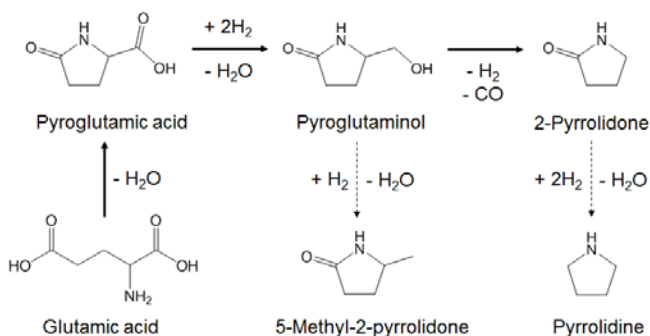
# Synthesis of 2-pyrrolidone from glutamic acid on Ru catalyst

*Satoshi Suganuma; Akihiro Otani; Shota Joka; Etsushi Tsuji; Naonobu Katada*

*Center for Research on Green Sustainable Chemistry, Tottori University, Tottori, Japan*

## 1. Introduction

Nitrogen-containing organic compounds have been produced through the insertion of ammonia into organic matrix at high pressure and temperature. In place of these processes consuming energy and resources, conversion of a natural nitrogen-containing compound such as amino acid in moderate conditions is promising to produce the valuable compounds. Glutamic acid is commercially produced through fermentation of saccharides extracted from sugarcane, corn, cassava, etc.<sup>[1]</sup> Therefore, it has potential as a raw material of nitrogen-containing organic compounds. Herein, we report the synthesis of 2-pyrrolidone from pyroglutaminol and then glutamic acid under high pressure of hydrogen at 433 K (Scheme 1). 2-Pyrrolidone has been utilized as a solvent, feedstock of polymer and pharmaceutical medicine. The activities of noble metal catalysts were compared.



**Scheme 1.** Proposed reaction pathways in conversion of pyroglutamic acid into 2-pyrrolidone

## 2. Experimental

Noble metal catalysts loaded on Al<sub>2</sub>O<sub>3</sub> (metal loading: 5 wt%) were purchased and then treated at 673 K for 3 h in H<sub>2</sub> flow to obtain Ru/Al<sub>2</sub>O<sub>3</sub>, Pt/Al<sub>2</sub>O<sub>3</sub>, Rh/Al<sub>2</sub>O<sub>3</sub>, and Pd/Al<sub>2</sub>O<sub>3</sub>. In the reactions, an aqueous solution of a reactant (pyroglutaminol, pyroglutamic acid or glutamic acid; 0.026 mol L<sup>-1</sup>, 50 mL) and catalyst (0.2 g) were charged into a batch autoclave reactor (120 mL). The atmosphere was set at desired pressure of H<sub>2</sub>. After designated time at 423 K, the resulting solution was analyzed using a gas chromatograph with a flame ionization detector.

### 3. Results and Discussion

Figure 1 compares the yield of products in the conversion of pyroglutaminol for 1 h in 1 MPa of H<sub>2</sub>. Ru/Al<sub>2</sub>O<sub>3</sub> exhibited extremely high activity for the formation of 2-pyrrolidone, while the other catalysts had little activity. It is noteworthy that the turnover frequency on Ru/Al<sub>2</sub>O<sub>3</sub> was more than 200 times larger than those on the other catalysts. Such by-products as pyrrolidine and 5-methyl-2-pyrrolidone, predicted as Scheme 1, were not significantly observed in the liquid products.

Reactions of pyroglutamic acid and glutamic acid on Ru/Al<sub>2</sub>O<sub>3</sub> were examined for 2 h in 2 MPa of H<sub>2</sub> (Figure 2). Apparently high yield of 2-pyrrolidone was found in both reactions. Pyroglutaminol, an intermediate on the pathway from pyroglutamic acid to 2-pyrrolidone, was also observed, but the yields of the by-products were small. No significant influence due to the difference of reactants between pyroglutamic acid and glutamic acid was observed.

### 4. Conclusions

Ru/Al<sub>2</sub>O<sub>3</sub> exhibited remarkably high activity for the formation of 2-pyrrolidone from pyroglutaminol. Pyroglutamic acid and glutamic acid were also converted into 2-pyrrolidone over Ru/Al<sub>2</sub>O<sub>3</sub>.

#### Reference

[1] W. Leuchtenberger, K. Huthmacher, K. Drauz, *Appl. Microbiol. Biotechnol.* **2005**, 69, 1.

#### Acknowledgements

A part of this study was funded by JSPS KAKENHI Grant Number 18K14261.

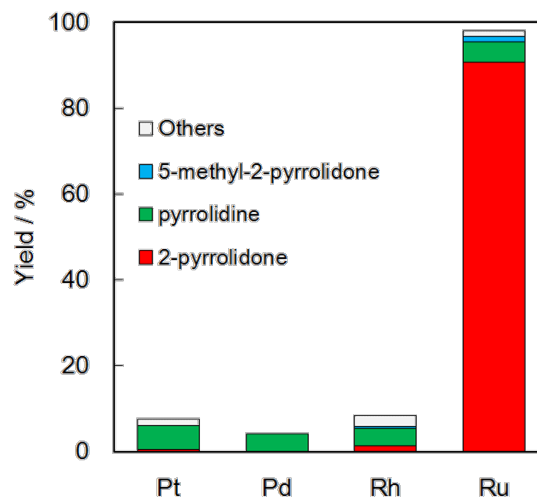


**Figure 1.** Yield of products in the conversion of pyroglutaminol using supported metal catalysts for 1 h in 1 MPa of H<sub>2</sub>.

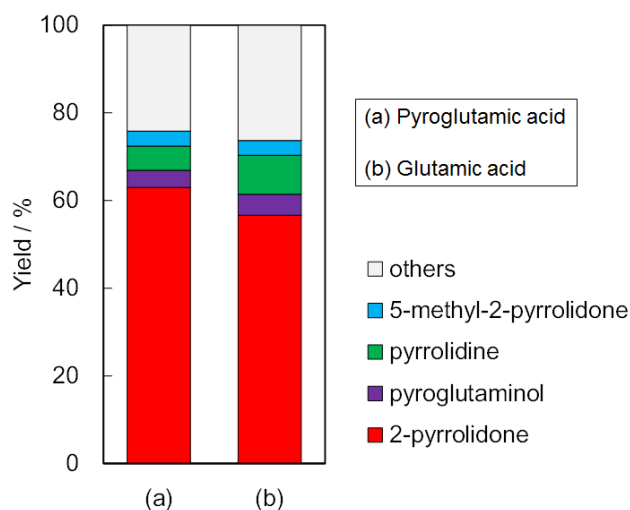


**Figure 2.** Yield of products in the conversion of pyroglutamic acid and glutamic acid with Ru/Al<sub>2</sub>O<sub>3</sub> for 2 h in 2 MPa of H<sub>2</sub>.

# Synthesis and Properties of Silica-Coated Nanocrystalline TiO<sub>2</sub> and ZrO<sub>2</sub> with High Thermal Stability

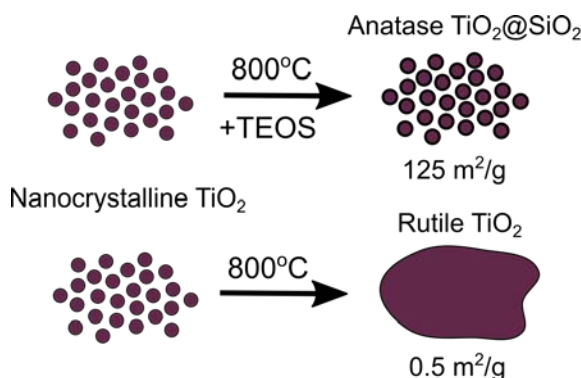
*Ekaterina Shuvarakova, Alexander Bedilo, Alexander Volodin*

*Boreskov Institute of Catalysis, Novosibirsk, Russia*

Titanium dioxide with the anatase crystalline structure is widely used for many practical applications, primarily as a photocatalyst for oxidation of various organic impurities in air and water and as a support for heterogeneous catalysts. However, the anatase TiO<sub>2</sub> modification is converted to rutile as the temperature is increased above 600–700 °C. This phase transformation results in a substantial decrease of the particle dispersity and surface area significantly worsening the TiO<sub>2</sub> catalytic properties. A similar effect is known for ZrO<sub>2</sub>: during the heat treatment it undergoes conversion from initially formed tetragonal phase to monoclinic.

Anatase particle size is an important factor affecting the temperature of the anatase phase transformation to rutile. We have recently demonstrated that its thermal stability can be improved by depositing of an intelligent carbon or SiO<sub>2</sub> coating on its surface [1, 2]. In this report we shall present our recent results on the synthesis and properties of TiO<sub>2</sub>@SiO<sub>2</sub> and ZrO<sub>2</sub>@SiO<sub>2</sub> nanocrystalline core-shell materials with low SiO<sub>2</sub> concentrations featuring improved thermal stability.

Deposition of the silica shell on nanocrystalline xerogel TiO<sub>2</sub> results in significant improvement of its thermal stability. As low as 0.5% Si was sufficient to preserve the small anatase crystallite size after calcination at 600 °C. Meanwhile, such treatment led to considerable sintering of TiO<sub>2</sub> nanocrystals without the silica shell with the average particle size growth from 9 to 50 nm, surface area decrease from 135 to 22 m<sup>2</sup>/g and partial anatase conversion to rutile. The temperature range where the phase composition, crystalline size, and surface area of 5%Si-TiO<sub>2</sub> samples were largely preserved was extended till at least 800 °C.



Substantial improvement of the thermal stability after deposition of the silica shell was also observed for nanocrystalline  $\text{ZrO}_2$ . The 12% $\text{SiO}_2$ - $\text{ZrO}_2$  sample remained in the tetragonal phase with the average crystallite size 8 nm and surface area 67  $\text{m}^2/\text{g}$  after calcination at 900 °C. Meanwhile, without the  $\text{SiO}_2$  shell  $\text{ZrO}_2$  nanocrystals after the same treatment grew to 17.5 nm, were converted to monoclinic phase, and the surface area of the sample was as low as 23  $\text{m}^2/\text{g}$ .

Typical EPR spectrum of perylene radical cations was observed after perylene adsorption on all  $\text{TiO}_2@ \text{SiO}_2$  samples with anatase crystalline structure and all  $\text{ZrO}_2@ \text{SiO}_2$  samples. This means that electron-acceptor sites capable of ionizing perylene are present on their surface. So, the silica shell formation improves the thermal stability  $\text{TiO}_2$  and  $\text{ZrO}_2$  without limiting access to the surface active sites. Recently it was suggested that such electron-acceptor sites could be the sites accounting for the activity of nanocrystalline  $\text{MgO}$  and other metal oxides in destructive sorption of halocarbons [3] and catalytic dehydrochlorination reactions [4]. Our latest data suggest that nanocrystalline  $\text{TiO}_2$  and  $\text{ZrO}_2$  samples have higher activity in these reactions than  $\text{MgO}$  aerogels.

The presence of active sites on the surface of  $\text{TiO}_2@ \text{SiO}_2$  and  $\text{ZrO}_2@ \text{SiO}_2$  core-shell structures with high thermal stability implies that these materials are very promising for various catalytic and adsorption applications where  $\text{TiO}_2$  or  $\text{ZrO}_2$  have promising properties but insufficient thermal stability. Furthermore, deposition of the silica shell can be suggested as a universal approach to improve the thermal stability of various nanocrystalline oxides operating in the oxidizing atmosphere.

## References

1. A. M. Volodin, A. F. Bedilo, I. V. Mishakov, V. I. Zaikovskii, A. A. Vedyagin, R. M. Kenzhin, V. O. Stoyanovskii, K. S. Golohvast. "Carbon nanoreactor for the synthesis of nanocrystalline high-temperature oxide materials", *Nanotechnologies in Russia*, 9 (2014) 700-706.
2. A.F. Bedilo, E.I. Shuvarakova, A.M. Volodin. "Silica-coated nanocrystalline  $\text{TiO}_2$  with improved thermal stability", *Ceramics International*, 45 (2019) 3547-3553.
3. A. F. Bedilo, E. I. Shuvarakova, A. M. Volodin, E. V. Ilyina, I. V. Mishakov, A. A. Vedyagin, V. V. Chesnokov, D. S. Heroux, K. J. Klabunde, "Effect of modification with vanadium or carbon on destructive sorption of halocarbons over nanocrystalline  $\text{MgO}$ : The role of active sites in initiation of the solid-state reaction", *J. Phys. Chem. C*, 118 (2014) 13715-13725.
4. E.I. Shuvarakova, A.F. Bedilo, V.V. Chesnokov, R.M. Kenzhin. "Dehydrochlorination of 1-chlorobutane over nanocrystalline  $\text{MgO}$ : The role of electron-acceptor sites", *Top. Catal.*, 61 (2018) 2065-2041.

# Renewable short-chain olefin production through dehydration reactions over nano-HZSM-5/ $\gamma$ -Al<sub>2</sub>O<sub>3</sub> hybrid catalysts

A. de Reviere<sup>a,b</sup>, M.K. Sabbe<sup>a,b</sup>, A. Verberckmoes<sup>a</sup>

<sup>a</sup>Industrial Catalysis and Adsorption Technology, Ghent, Belgium

<sup>b</sup>Laboratory for Chemical Technology, Ghent, Belgium

## Scope

The recent shale gas boom, has oversaturated the petrochemical market with ethylene due to the cheap availability of ethane as a cracking feedstock, this disrupted the European petrochemical market, which is highly dependent on the more expensive naphtha as cracking feedstock [1] to produce the highly demanded short-chain olefins, such as propylene and butenes. Simultaneously with the market disruption, the bio-based economy has been gaining importance, as illustrated by the increasing number of European biorefineries [2]. It is in this context that the sustainable production of bio-olefins through acid catalyzed alcohol dehydration reactions is interesting. The obtained olefins could act as a *drop-in* for classic fossil-based olefins. Bio-derived alcohols are generally obtained as mixtures, therefore novel hybrid catalysts (i) having a broad acid strength distribution, to reduce the difference in alcohol reactivity and (ii) that are able to improve the catalyst stability are necessary. The hybrid catalysts consist of HZSM-5, which is an important zeolite catalyst already used within classic refineries [3] and dehydration reactions [4], and  $\gamma$ -Al<sub>2</sub>O<sub>3</sub> which is typically used as a catalyst support [5].

## Results and discussion

First hexagonal shaped nano-sized HZSM-5 (n-HZSM-5) catalysts were synthesized following a clear solution method [6], see XRD and SEM image in Figure 1.

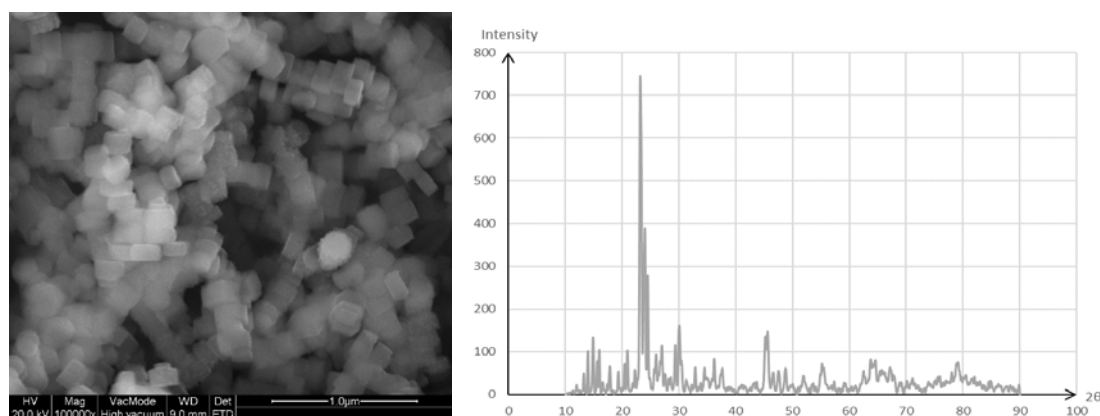


Figure 1: SEM-image (left) and XRD pattern (right) of the nano-sized ZSM-5 crystals

Following, nano-HZSM-5/ $\gamma$ -Al<sub>2</sub>O<sub>3</sub> hybrid catalysts, were synthesized upon hydrothermal synthesis by preparing nano-HZSM-5 zeolites [6] in the presence of commercial alumina. To obtain the hybrid materials, first the aluminum source is dissolved in TPAOH to obtain a clear solution, this is followed by adding adequate amounts of NaOH, H<sub>2</sub>O and TEOS, the mixture is stirred at room temperature during 24 hours and before crystallization,  $\gamma$ -Al<sub>2</sub>O<sub>3</sub> is added to the mixture. The novel hybrid catalysts as well as the nano-HZSM-5 zeolites and alumina catalyst were characterized using XRD, N<sub>2</sub> adsorption, SEM and NH<sub>3</sub>-TPD. The catalysts were tested in a high throughput set-up at temperatures ranging from 453 K to 523 K and alcohol partial pressures of 10-30 kPa to analyze the conversion-selectivity profiles and evaluate the deactivation of the catalyst. The hybrid systems are compared with the separate components from which it consists, i.e., (1) nano-HZSM-5 zeolites and (2) alumina, as well as with a commercial HZSM-5 (c-HZSM-5) with comparable Si/Al ratio, see Table 1 for the properties of the different catalysts.

**Table 1: Properties of the different catalyst materials**

Code	S <sub>BET</sub> (m <sup>2</sup> /g)	Acid site density (mol/kg)	Crystal size (nm)	Si/Al through EDX
n-HZSM-5	330	329	80-200	29.4
c-HZSM-5	394	430	300-500	28.1
$\gamma$ -Al <sub>2</sub> O <sub>3</sub>	198	n.a.	n.a.	0

The combined catalyst synthesis and high-throughput testing approach results in an efficient route to explore the most important hybrid catalyst properties and optimal dehydration reaction conditions. This allows to fasten the sustainable development and potential upscaling and commercialization of the emerging bio-based olefins.

#### References

1. A. Horncastle, J.G., F. Ozeir, S. Singh, 2014, Strategy& Consortium, B.-b.I., *Biorefineries in Europe 2017*. 2017.
2. Argauer, R.J. and G.R. Landolt, 1972, Mobil Oil Corp, US 3702886 A.
3. Gunst, D., et al., *Appl. Catal., A*, 2017. **539**: p. 1-12.
4. Euzen, P., et al., in *Handbook of Porous Solids*. 2008.
5. Song, W., et al., *Langmuir*, 2004. **20**(19): p. 8301-8306.

# Synthesis and Characterization of Nanocrystalline Calcium Aluminate with Mayenite Crystal Structure C12A7

*Alexander Bedilo, Alexander Volodin, Ekaterina Shuvarakova, Ekaterina Ilyina*

*Boreskov Institute of Catalysis, Novosibirsk, Russia*

Unique properties of calcium aluminate with  $12\text{CaO}\cdot 7\text{Al}_2\text{O}_3$  stoichiometry (usually labeled as C12A7) were discovered and investigated by H. Hosono et al. [1-3]. These materials possess a stable cation framework  $[\text{Ca}_{24}\text{Al}_{28}\text{O}_{64}]^{4+}$  and changeable anion sublattice  $4\text{X}^-$ . Chemical and electrophysical properties of these materials can be easily varied in a wide range by substitution of  $\text{X}^-$  anions. Particularly interesting are materials with  $\text{X}^- = \text{O}^-$  that supply reactive radical anions in chemical and catalytic oxidation reactions [2] and electriles ( $\text{X}^- = \text{e}^-$ ) that can behave as electron donors in organic reactions or as superbasic supports for heterogeneous catalysts [3].

Ceramic method was usually used for synthesis of C12A7 materials leading to materials with low surface area that are not well suited for catalytic applications. Recently we demonstrated that nanocrystalline C12A7 electriles could be prepared in a carbon shell starting with a mixture of nanocrystalline aluminum and calcium hydroxides [4]. In the current presentation we shall explore the methods of synthesis and properties of nanocrystalline C12A7 materials.

For synthesis of nanocrystalline C12A7 materials in aqueous solution, a mixture of aluminum and calcium hydroxides with required stoichiometry was used as the precursor. The mixture was thoroughly stirred in distilled water for 10 h, filtered and dried at 110 °C. Then it was calcined in air at 600 °C for 6 h. The obtained sample with mayenite (C12A7) crystallite structure, crystallite size about 15 nm and the surface area about 80 m<sup>2</sup>/g was used as the starting material for synthesis of other high-temperature materials based on C12A7.

Nanocrystalline oxide aerogels are materials with very small particle sizes, high surface areas and pore volumes prepared by sol-gel method usually in an alcohol solution followed by drying in an autoclave under supercritical conditions avoiding collapse of the pore structure. In this study C12A7 aerogels were prepared for the first time starting from a mixture of calcium methoxide prepared by dissolving calcium metal in methanol and aluminum isopropoxide in isopropanol taken in the appropriate ratio. The surface area of amorphous hydroxide obtained after hydrolysis



with stoichiometric amount of water, gelation overnight and drying under supercritical conditions was about 450 m<sup>2</sup>/g. Detailed information on the effect of its treatment at high temperatures in air and in the argon flow will be reported.

One of possible application areas of finely dispersed C12A7 materials is their use in catalytic technologies. Therefore, it was important to study various active sites on their surface. After treatment at elevated temperatures in the oxygen-containing atmosphere mayenite samples are known to undergo partial substitution of dielectric oxide or hydroxide anions for O<sup>-</sup> and/or O<sub>2</sub><sup>-</sup> radical anions.

Electron-acceptor and electron-donor sites are very active surface species observed by EPR using the formation of radical cations and radical anions after adsorption of appropriate probe molecules [5]. We observed that sites of both types were present on the surface of C12A7-600 sample. In particular, the concentration of electron-acceptor sites tested using phenothiazine as the probe proved to be as high as on the surface of Al<sub>2</sub>O<sub>3</sub> sample with 2.5 times higher surface area.

Remarkable results were obtained after diphenylamine adsorption on C12A7-600. The observed EPR spectrum can be attributed to adsorbed diphenyloxy nitroxyl radicals. These radicals are formed from diphenylamine in solution in the presence of peroxides due to reaction with hydroxyl radicals. Apparently, the surface of nanocrystalline C12A7 activated in air has a significant concentration of active OH or O<sup>-</sup> radicals. It seems to be a specific feature of this material related to its unique structure that merits further investigation as we did not observe similar signals on any other oxide material. So, C12A7 is likely to have unusual properties in various oxidation catalytic reactions related to the presence of active radicals on its surface.

This study was supported by RFBR, Project 19-03-00834.

## References

1. K. Hayashi, S. Matsuishi, T. Kamiya, M. Hirano, H. Hosono, "Light-induced conversion of an insulating refractory oxide into a persistent electronic conductor", *Nature*, 419 (2002) 462-465.
2. S.W. Yang, J. N. Kondo, K. Hayashi, M. Hirano, K. Domen, H. Hosono, "Partial oxidation of methane to syngas over promoted C12A7", *Appl. Catal. A.*, 277 (2004) 239-246.
3. M. Kitano, Y. Inoue, Y. Yamazaki, F. Hayashi, S. Kanbara, S. Matsuishi, T. Yokoyama, S.W. Kim, M. Hara, H. Hosono, "Ammonia synthesis using a stable electride as an electron donor and reversible hydrogen store", *Nature Chemistry*, 4 (2012) 934-940.
4. A. M. Volodin, V.I. Zaikovskii, R.M. Kenzhin, A.F. Bedilo, I. V. Mishakov, A. A. Vedyagin, "Synthesis of nanocrystalline calcium aluminate C12A7 under carbon nanoreactor conditions", *Mater. Lett.*, 189 (2017) 210-212.
5. A.F. Bedilo, E.I. Shuvarakova, A.A. Rybinskaya, D.A. Medvedev, "Characterization of electron-donor and electron-acceptor sites on the surface of sulfated alumina using spin probes", *J. Phys. Chem. C*, 118 (2014) 15779-15794.

# Catalytic Hydrogenation of CO<sub>2</sub>-based Ionic Liquids into Methanol – Process Intensification and Optimization

*Roger Marti, Ennio Vanoli, Pauline Sanglard, Institute ChemTech, Haute école  
d'ingénierie et d'architecture Fribourg, HES-SO, 1700 Fribourg, Switzerland*

Methanol is recognized today as an important and valuable energy carrier with a high potential in replacing fossil resources [1]. A sustainable and carbon-neutral approach to produce methanol is by hydrogenation of carbon dioxide by using hydrogen from solar water splitting. The challenge of this reaction is that CO<sub>2</sub> is a rather inert molecule and typically, high pressure and temperature and the use of expensive catalysts with loadings are needed [2]. Further, a CO<sub>2</sub>-capture system is needed if one wants to use CO<sub>2</sub> from the environment. As shown in Figure 1, we developed a capture method using amines to form CO<sub>2</sub>-based ionic liquids that can then be further hydrogenated to methanol.

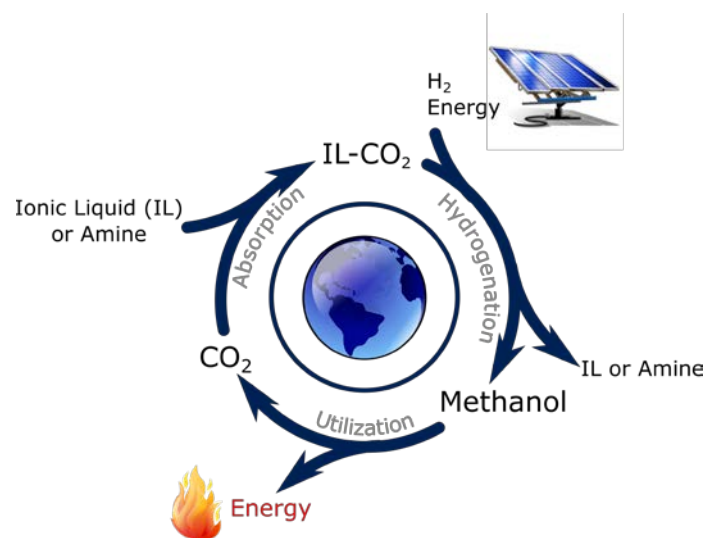


Figure 1: Concept of CO<sub>2</sub>, IL-based CO<sub>2</sub> to Methanol Process

Here, we present our work on the process intensification and optimization of the hydrogenation steps of CO<sub>2</sub>-based ionic liquids. We discuss our DoE studies on the influence of reaction parameters, optimization of the work-up and isolation of the methanol, and of the scale-up.

## References

- [1] A. Goeppert, M. Czaun, J.-P. J., G. K. Surya Prakash, G. A. Olah, *Chem. Soc. Rev.*, **2014**, *43*, 7995.
- [2] Q.-W. Song, Z.-H. Zhou, L.-N. He, *Green Chem.*, **2017**, *19*, 3707.

# Acceptor and Donor number as an efficient tool for the selection of solvents in acid-base heterogeneous catalysis

Vijaykumar S. Marakatti,<sup>1</sup> Eric M. Gaigneaux<sup>1</sup>

<sup>1</sup>*Institute of Condensed Matter and Nanosciences, Université catholique de Louvain, Louvain-La-Neuve, Belgium*

[Vijaykumar.marakatti@uclouvain.be](mailto:Vijaykumar.marakatti@uclouvain.be), [eric.gaigneaux@uclouvain.be](mailto:eric.gaigneaux@uclouvain.be)

Solvents are extensively used in all the steps of a catalytic process, including the synthesis of the catalyst, the catalytic test and finally the product purification. Specifically, during the catalytic reaction, the role of the solvent is critical in determining the rate, conversion, and selectivity of products. However, so far, very little attention has been paid in understanding the role of solvent in heterogeneous catalysis. The reasons could be 1) the difficulty in selecting the appropriate solvents from the large bunch of solvents with different physicochemical properties, and 2) the existence of a complex solid-liquid and solid-gas interfaces, making the investigation of boundary interactions difficult. In reality, there is no rule of thumbs in selecting a solvent for a specific reaction.

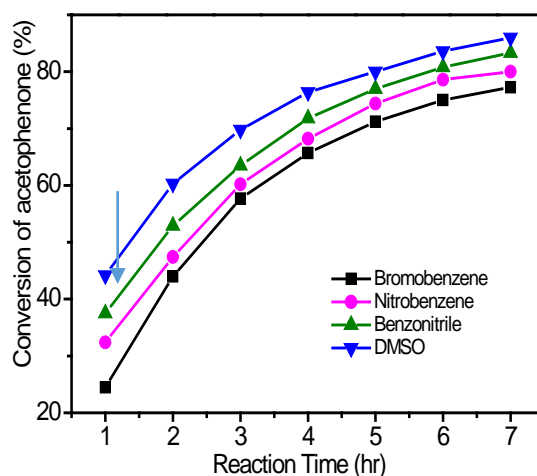
Therefore, we tried to rationalize different properties of a solvent as dielectric constant, boiling point, polarity and protic/aprotic nature, with the observed catalytic activity first in several acid catalyzed reactions, such as Prins condensation of  $\beta$ -Pinene to nopol (catalyst: Zn-beta), Prins cyclization of styrene to dioxane (Sulfated zirconia), acylation of butanol (H-beta), and Friedel-Craft butylation of resorcinol (H-Y zeolite). None of these properties helped in direct correlation with the activity/selectivity. Therefore, we came up with other properties in the form of numbers as given by Gutman *et.al*, i.e. Acceptor (AN) and Donor (DN) numbers of solvent, which somehow measure the Lewis acidic and basic properties of the solvent, respectively. [1] We found that increasing the AN of the solvent used from cyclohexane to 1,2-dichloroethane increases the activity in the probed acid catalyzed reactions; at the same time increasing the DN of solvent used from nitrobenzene to Dimethyl sulfoxide decreases the activity of the catalysts for these same reactions. [2-3] A good correlation exists between these numbers and catalytic activity in all these catalytic reactions (Table 1).

**Table.1. Influence of Acceptor and Donor number in acid catalyzed reactions.**

solvents	Catalytic activity				
			Prins condensation	Acylation reaction	Alkylation reaction
	AN	DN	Conversion of $\beta$ -pinene	Conversion of butanol	Conversion of resorcinol
cyclohexane	0	0	94.0	46.2	44.8
Benzene	8.2	0	99.6	56.2	50.9
1,2-dichloroethane	16.7	0	100	69.7	59.3
Nitrobenzene	14.8	4.4	99.0	52.1	42.2
Benzonitrile	15.5	11.9	76.4	38.5	35.8
Dioxane	10.3	14.3	*69.5	34.3	30.5
Dimethyl formamide	16.0	26.6	5.0	29.6	0

\*acetonitrile (AN=18.9, DN= 14.1)

These interesting trends observed in acid catalysis drive our curiosity to look at base catalyzed reactions assuming the trends will be reversed. In order to test this hypothesis, Knoevenagel and Claisen-Schmidt condensation reactions were carried over hydrotalcite catalyst. As an example, in Claisen-Schmidt condensation, the catalytic activity was completely inverse in trend compared to acid catalysis (Figure: Claisen-Schmidt condensation reaction, T=140 °C, Acetophenone: Benzaldehyde = 1:1.5, catalyst = 0.2, Solvent = 3ml). The highest DN solvent (DMSO) indeed exhibits highest acetophenone conversion compared to the high AN solvents (Bromobenzene).



The mechanism of AN and DN of solvents in these reactions were understood by spectroscopic (FTIR, UV, TGA-MAS) and adsorption techniques. The molecular interaction of solvents with the reactants elucidates hydrogen bonding and stabilization of intermediate carbocations/anions in the reaction. Furthermore, the adsorption of solvent on the catalyst surface was also a crucial factor in dictating the observed trend. In summary, high AN and DN are excellent solvents in acid and base catalyzed reactions, respectively. The present finding provides a rationale tool for selecting an appropriate solvent in any acid-base catalysis.

#### References

1. V. Gutmann, *Coord. Chem. Rev.* 18 (1976) 225–255.
2. V. S. Marakatti, G. V. Shanbhag, A.B. Halgeri, *Appl. Catal. A: Gen.* 2013, 451, 71
3. V. S. Marakatti, G. V. Shanbhag, A.B. Halgeri, *Catal. Sci. Technol.*, 2014, 4, 4065.

# Highly Efficient CO<sub>2</sub> Hydrogenation to Aromatics via a Consecutive Olefination–Aromatization Route

Tijun Wu, Shunwu Wang, Yushan Ji, Minghua Qiao\*

*Department of Chemistry and Shanghai Key Laboratory of Molecular Catalysis and Innovative Materials, Fudan University, Shanghai 200438, P. R. China*

## Introduction

The aromatics occupy about one-third of the market for commodity petrochemicals [1]. Recently, it was reported that on ZnAlO<sub>x</sub>&HZSM-5 [2] and ZnZrO/HZSM-5 [3], high aromatics selectivities of about 73% could be obtained in CO<sub>2</sub> hydrogenation. However, the aromatics productivities over these catalysts based on the concept of methanol synthesis–aromatization are low due to the poor intrinsic hydrogenation activity of the metal oxide components. Herein, we report that a bifunctional catalyst constituted by honeycomb-structured graphene (HSG) supported FeK1.5 (FeK1.5/HSG) and HZSM-5 designed based on the concept of consecutive olefination–aromatization can convert CO<sub>2</sub> to the aromatics in high efficiency. The effect of the zeolite type was also investigated and discussed.

## Results and discussion

HSG was fabricated by reacting Li<sub>2</sub>O with CO. Iron and potassium with nominal loadings of 20 wt% and 1.5 wt%, respectively, were loaded successively on HSG. In CO<sub>2</sub> hydrogenation under the reaction conditions of 613 K, H<sub>2</sub>/CO<sub>2</sub> ratio of 3, 2.0 MPa, and SV of 26 L h<sup>-1</sup> g<sup>-1</sup>, FeK1.5/HSG alone afforded the CH<sub>4</sub> selectivity of 26%, C<sub>2</sub>–C<sub>4</sub> selectivity of 70% (C<sub>2</sub><sup>=</sup>–C<sub>4</sub><sup>=</sup> of 59%), and C<sub>5+</sub> selectivity of 4.1% (Fig. 1).

When HZSM-5 was packed downstream of FeK1.5/HSG, the high carbon-number products, including the aromatics, were boosted at the expense of the light olefins, clearly evidencing the occurrence of the olefination–aromatization pathway. The aromatics selectivity was 68%, only 5.9% lower than the best value reported so far [2]. Ethylbenzene (36%), xylenes (18%), toluene (10%), and ethyltoluenes (10%) are the major aromatics. Benefited from the outstanding hydrogenation activity of FeK1.5/HSG, the aromatics productivity amounted to 131 μmol<sub>CO<sub>2</sub></sub> g<sub>Fe</sub><sup>-1</sup> s<sup>-1</sup>, which is about two orders of magnitude higher than the literature values.

When FeK1.5/HSG was combined with SAPO-34, HY, Hβ, and HMCM-22, the

hydrocarbon distribution varied with the zeolite type. SAPO-34 with the smallest pore size gave the lowest aromatics selectivity, as its pore is too small even for ethylene with kinetic diameter of 3.9 Å to facilitate access to the acid sites inside. Although both HY and H $\beta$  have 12-member large pores, H $\beta$  has an additional 12-member small pore of 5.6 Å  $\times$  5.6 Å. It is known that benzene has a kinetic diameter of 5.85 Å. The kinetic diameters of toluene and *p*-xylene are about the same [4]. Hence, H $\beta$  displays better shape-selectivity to the aromatics than HY. HMCM-22, similar to ZSM-5, has two sets of 10-member pores of 4.0 Å  $\times$  5.5 Å and 4.1 Å  $\times$  5.1 Å, but they are slightly smaller than those of ZSM-5 (5.1 Å  $\times$  5.5 Å and 5.3 Å  $\times$  5.6 Å), thus giving the aromatics selectivity second to ZSM-5.

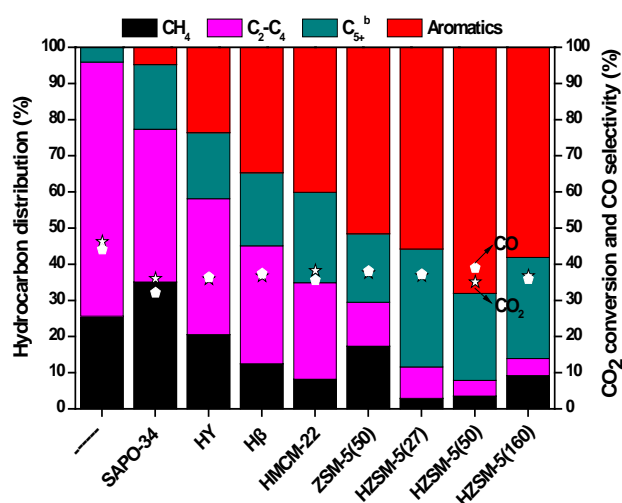


**Fig. 1** Effect of zeolite type on CO<sub>2</sub> conversion and product selectivity over the FeK1.5/HSG and zeolite composite catalysts; reaction conditions: 0.15 g FeK1.5/HSG and 0.15 g zeolite, packed in dual layer, 613 K, H<sub>2</sub>/CO<sub>2</sub> = 3, 2.0 MPa, SV = 26 L g<sup>-1</sup> h<sup>-1</sup>, and TOS = 24 h; <sup>b</sup> exclusive of the aromatics..

## Conclusions

We demonstrate for the first time that the direct and efficient hydrogenation of CO<sub>2</sub> to the aromatics can be achieved on a catalyst designed based on the concept of consecutive olefination–aromatization. Using FeK1.5/HSG as the olefination component, the aromatics selectivity is mainly determined by the pore size of the zeolite, and the optimal pore diameter is around 5 Å.

## Acknowledgements

This work was supported by the State Key Research and Development Project of China (2018YFB0604501) and the National Natural Science Foundation of China (21872035).

## References

- [1] A. M. Niziolek, O. Onel, C. A. Floudas, *AIChE J.* **2016**, 62, 1531–1556.
- [2] Y. M. Ni, Z. Y. Chen, Y. Fu, Y. Liu, W. L. Zhu, Z. M. Liu, *Nat. Commun.* **2018**, 9, 3457.
- [3] Z. L. Li, Y. Z. Qu, J. J. Wang, H. L. Liu, M. R. Li, S. Miao, C. Li, *Joule* **2019**, 3, 1–14.
- [4] D. B. Shah, C. J. Guo, D. T. Hayhurst, Effect of Structural Heterogeneity on the Diffusion of Aromatic Hydrocarbons in Large Silicalite Crystals, in *Fundamentals of Adsorption*, M. Suzuki (ed.), Elsevier, **1993**, pp. 575–582.

# Theoretical Investigations of Propane Dehydrogenation Over Palladium Surfaces

*Eduard Araujo-Lopez*, † *Bart D. Vandegehuchte*, § *Lennart Joos*, § *Dmitry Sharapa*, † and *Felix Studt*\*, †, ‡

† Institute of Catalysis Research and Technology, Karlsruhe Institute of Technology, Hermann-von-Helmholtz Platz 1, 76344 Eggenstein-Leopoldshafen, Germany

§ Total Research & Technology Feluy, Zone Industrielle Feluy C, B-7181, Seneffe, Belgium

‡ Institute for Chemical Technology and Polymer Chemistry, Karlsruhe Institute of Technology, Engesserstrasse 18, 76131 Karlsruhe, Germany

The uses of propylene derivatives have grown rapidly over the last years and are likely to continue doing so. There is a large demand for short alkenes and the on-purpose propylene technologies (OPP) are called to fill the supply gap of the global demand. The propane dehydrogenation (PDH) process is the most widely used OPP technology, which is a simple approach to generate propylene by elimination of two hydrogen atoms from propane. Another option is the oxidative dehydrogenation of propane using CO<sub>2</sub> as a soft oxidant (CO<sub>2</sub>-ODHP) to produce additionally water and carbon monoxide. [1]

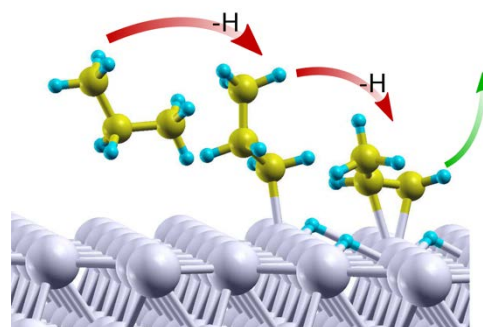
While Palladium-based catalyst have not been extensively studied in the past for these processes, they have been coming more into focus in recent years [2-4]. These catalysts are particularly interesting for the oxidative dehydrogenation using CO<sub>2</sub> as a soft oxidant. [3] In this contribution we aim at shedding light on the reaction mechanism of this soft oxidative dehydrogenation of propane over Pd-ceria catalysts employing density functional theory (DFT) calculations.

## Computational Methods

All DFT calculations were performed using the VASP program [5] employing the BEEF-vdW functional [6] that has shown promising results for transition metal catalysis. [7,8] Pd (111) and (211) surfaces were modelled using a 3x3x4 supercell where the two topmost layers were allowed to relax and the two bottom layers fixed at the bulk position. An energy cut-off of 450 eV and a k-point sampling of 4x4x1 have been used.

## Results and Discussion

The dehydrogenation of propane to propylene has been investigated on both Pd(111) and Pd(211) surfaces. In order to investigate the influence of the soft oxidant CO<sub>2</sub> the reaction pathway was investigated using surface oxygen and hydroxyl where the hydrogen can be abstracted producing hydroxyl and adsorbed water, respectively. Correspondingly, CO<sub>2</sub> activation producing CO and adsorbed oxygen has been investigated on both the metal and the ceria support. Finally, we compare the effect of oxygen on the dehydrogenation pathway on propylene on these two different surfaces.



## References

- [1] J. J. H. B. Sattler et al. *Chem. Rev.* 2014, 114 (20), 10613–10653.
- [2] C. Yang et al. *Catal. Today* 2019, 323, 123–128.
- [3] E. Nowicka et al. *ACS Catal.* 2018, 8 (4), 3454–3468.
- [4] Z. Wu, Z. et al. *Catal. Sci. Technol.* 2016, 6 (18), 6965–6976.
- [5] G. Kresse and J. Furthmüller. *Phys. Rev. B* **1996**, 54, 11169.
- [6] J. Wellendorff et al. *Phys. Rev. B* **2012**, 85, 235149.
- [7] J. Wellendorff, et al., *Surf. Sci.* **2015**, 640, 36.
- [8] S. M. Sharada et al., *J. Phys. Chem. C* **2017**, 121, 19807.



# **Dehydrogenation and oxidative dehydrogenation of medium and short chain paraffins over confined NiNbAl nanorod composites using air and CO<sub>2</sub> as oxidants**

*Holger B. Friedrich, University of KwaZulu-Natal, Durban, South Africa; Majid D. Farahani, University of KwaZulu-Natal, Durban, South Africa; Itegbeyogene P. Ezekiel, University of KwaZulu-Natal, Durban, South Africa; Thomas Moyo, University of KwaZulu-Natal, Durban, South Africa*

The transformation of gas, coal and biomass to liquid fuel created a large pool of intermediate-length straight-chain alkanes. The dehydrogenation (DH) of paraffins and their transformation to olefins is a commercially established technique. This reaction has the advantage of high selectivity towards the olefins. However, drawbacks of this process are it being endothermic, coke formation and the low equilibrium conversion. Therefore, high operating temperatures and frequent catalyst regenerations are required to have a constant production output in time on line process. The need for an efficient replacement for the DH process has motivated researchers in the field to conduct a wide spectrum of investigations on the oxidative dehydrogenation (ODH) of paraffins [1].

ODH using air is an exothermic reaction, which makes it operable at lower temperatures than DH [2]. Coke formation usually is minimal in ODH reactions, and the reverse water gas shift reaction (RWGS) decreases the limiting role of the equilibrium conversion in DH [2]. However, the major disadvantage of this reaction is a high production of carbon-containing greenhouse gases such as CO<sub>2</sub>, CO and CH<sub>4</sub>, which prevents it from achieving commercialisation.[2]

CO<sub>2</sub> as a soft oxidant has received considerable attention over the past years. The use of this greenhouse gas for the ODH of paraffins can completely suppress the combustion reaction while minimising the contribution of equilibrium conversion that was observed during the DH of paraffins via reverse water gas shift (RWGS) reaction. The use of CO<sub>2</sub> has also been found to inhibit the accelerated catalyst deactivation via coke deposition. Also, this oxidant is seldomly reported to maintain the applied metals in their oxide forms during the DH reaction [3].

Doped or supported nickel oxide based catalysts are amongst the most studied catalysts for activation of ethane. Doped NiO with Nb was found to have a better Mars-van Krevelen mechanism (MvK) (redox mechanism where nucleophilic oxygen

species are involved) with a minimised formation of electrophilic oxygen species (responsible for CO<sub>x</sub> formation) [4]. Both factors resulted in a significant improvement in efficiency of NiO in the ODH of ethane. Considering the high stability of ethene in comparison to ethane, the theory mentioned above has been challenged by many researchers [5].

To examine all discussed theories involving NiO in the ODH of paraffins, NiNbAl composites with different Ni/Nb ratios, but unified structures were synthesised using glycol-thermal techniques. They were tested for activation of medium chain paraffins (*n*-octane as a model in this study) and examining the sensitivity of the products formed against different possible oxygen species. In addition, the ODH of propane was also carried out as reference. These two series of catalytic data, as well as the applied characterisation techniques such as XPS, in situ XRD, H<sub>2</sub>-TPR and O<sub>2</sub>-TPO, revealed some new science behind these materials. Our study showed that the release of a high concentration of nucleophilic oxygen species with possibly high entropy resulted in the combustion of the *n*-octane and the primary formed products. However, this is not the case for ethane and ethene which have greater stabilities, that can be selectively activated possibly using electrophilic oxygen species or even radical mechanisms.

Furthermore, this study introduces the CO<sub>2</sub>-ODH of *n*-octane over NiO based catalysts for the first time. Obtained characterisation data and the comparison of the catalytic data to the dehydrogenation results showed that the distance between Ni and Nb is a pivotal parameter to activate the CO<sub>2</sub> over these catalysts. The formed oxygen species were found to enhance the RWGS reaction and participate *in* coke removal from the surface of the catalyst, which allowed for enhanced longevity of the catalyst under time on line conditions.

## References

- [1] J.J.H.B. Sattler, J. Ruiz-Martinez, E. Santillan-Jimenez, B.M. Weckhuysen, Catalytic Dehydrogenation of Light Alkanes on Metals and Metal Oxides, *Chem. Rev.*, 114 (2014) 10613-10653.
- [2] C.A. Gärtner, A.C. van Veen, J.A. Lercher, Oxidative Dehydrogenation of Ethane: Common Principles and Mechanistic Aspects, *ChemCatChem*, 5 (2013) 3196-3217.
- [3] R. Koirala, R. Buechel, F. Krumeich, S.E. Pratsinis, A. Baiker, Oxidative Dehydrogenation of Ethane with CO<sub>2</sub> over Flame-Made Ga-Loaded TiO<sub>2</sub>, *ACS Catal.*, 5 (2015) 690-702.
- [4] E. Heracleous, A.A. Lemonidou, Ni–Nb–O mixed oxides as highly active and selective catalysts for ethene production via ethane oxidative dehydrogenation. Part I: Characterization and catalytic performance, *J. Catal.*, 237 (2006) 162-174.
- [5] H. Zhu, D.C. Rosenfeld, M. Harb, D.H. Anjum, M.N. Hedhili, S. Ould-Chikh, J.-M. Basset, Ni–M–O (M = Sn, Ti, W) Catalysts Prepared by a Dry Mixing Method for Oxidative Dehydrogenation of Ethane, *ACS Catal.*, 6 (2016) 2852-2866.

# **The Consortium for Operando and Advanced Catalyst Characterization via Electronic Spectroscopy and Structure (Co-ACCESS) at SSRL**

*Simon R. Bare, Adam S. Hoffman, Alexey Boubnov, Sunjay Melkote, and Oliver  
Müller*

*SSRL, SLAC National Accelerator Lab, Menlo Park, CA 94025 (USA)*

## **Introduction**

The use of synchrotrons for in-situ and in-operando characterization of catalysts has proven to be essential for linking structural information to the performance of the working catalyst. The diverse techniques available at such user facilities, e.g. X-ray absorption spectroscopy, small- and wide-angle x-ray scattering, x-ray microscopy, and ambient pressure X-ray photoelectron spectroscopy, provide crucial information that cannot be obtained by other means. At Stanford Synchrotron Radiation Lightsource (SSRL) at SLAC National Accelerator Laboratory we have initiated a new methodology, the Consortium for Operando and Advanced Catalyst Characterization via Electronic Spectroscopy and Structure (Co-ACCESS). The goal of Co-ACCESS is to enable any catalysis researcher (whether they study heterogeneous, homogeneous, electro- or photo-catalysis) with an interest in using X-ray methods for in-situ/in-operando catalyst characterization, to be able to pursue those interests in an expedient manner, with minimal barrier to conducting the research. This program builds on the proven success of the Synchrotron Catalysis Consortium at NSLS [1].

## **Materials and Methods**

We are creating a holistic suite of integrated in-situ and operando synchrotron-based catalytic reactors by: (i) fabricating a suite of user-accessible in-situ cells, (i) constructing automated feed delivery systems, (iii) coupled with on-line analytics. These experimental facilities are enhanced by investments and developments at SSRL, e.g. in data collection methods, and new beamlines, coupled with access to a wet chemistry laboratory, designed for catalysis studies, to allow the synthesis, proper handling, and activation of catalysts on-site. All of these activities are assisted by experienced staff.

## **Results and Discussion**

This presentation will focus on the capability development, with details provided on the infrastructure that is now available at SSRL for catalysis studies and a look

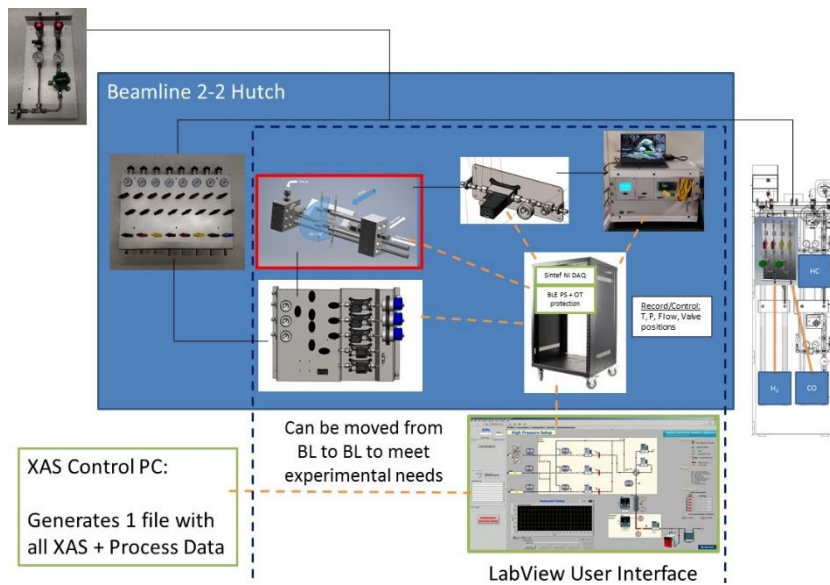


Figure 1. Schematic of the gas delivery system and analytics for in-situ catalysis studies at SSRL

forward to some of the new capabilities under development. These capabilities will be illustrated by research that have been collaboratively conducted:

(i) The development of safe and routine operations at high

pressure, facilitating research in syngas

chemistry for higher alcohol synthesis and Fisher-Tropsch catalysis [2]. (ii) The application of high-energy resolution fluorescence detection methods for determining the active site complex [3][4], (iii) The development of time-resolved studies via continuous scanning of the monochromator, and (iv) The use of multi-modal methods, including XRD/XAS and XAS/TXM in order to extract more information for a given system [4].

## Summary

SSRL offers a growing suite of techniques and methodologies for *in-situ/operando* advanced catalyst characterization. These techniques are driving new catalyst discoveries by determining the structure responsible for the activity, and vice-versa, the need to understand catalyst activity is also driving new experiments at SSRL.

Co-ACCESS, is supported by the U.S. Department of Energy, Office of Science, Office of Basic Energy Sciences.

## References

1. SCC website, <https://you.stonybrook.edu/scc2/>, last accessed 23-Oct-2018.
2. Hoffman, A.S., Singh, J.A., Bent, S.F., and Bare, S.R. J. Synchr. Rad. (2018) 25 <https://doi.org/10.1107/S1600577518013942>
3. Hoffman, A.S., Sokaras, D., Zhang, S., Debeve, L.M., Fang, C.-Y., Gallo, A., Kroll, T., Dixon, D.A., Bare, S.R., Gates, B.C., Chemistry -A European Journal 23 1-10 (2017).
4. Hoffman, A.S., Azzam, S., Zhang, K., Xu, Y., Liu, Y., Bare, S.R., Simonetti, D.A., Reaction Chemistry & Engineering (2018) 3 668 – 675.

# The reason of high stability of Ni/CeO<sub>x</sub> in Dry Reforming: the promotion of interfacial oxygen on CO\* production and desorption

*Zan Lian, Dang Sheng Su, Bo Li\**

*Institute of Metal Research, Chinese Academy of Sciences, Shenyang, People's  
Republic of China*

*\*e-mail : boli@imr.ac.cn*

## Introduction

Dry reforming (DRM) is an environment-friendly reaction, which consumes two greenhouse gases, CO<sub>2</sub> and CH<sub>4</sub>, and produces syngas[1]. Because of the cheap price and high activity, Nickel based catalysts have been studied widely[2, 3], while the stability of Ni based catalyst is unfavorable comparing with noble metals. Changing of support is an effective strategy to improve the stability of Ni based catalyst. Lanthanide oxide supporting Ni catalysts show highest stability in several supported catalysts, and the “bi-functional” mechanism was proposed[4]. Recently, A literature reports that only the metal atoms at perimeter have high coke resistance ability, in contrast, non-perimeter Ni is deactivated rapidly[5]. Besides, the oxygen vacancies are supposed to be another reason of high stability, and the “step-wise redox” mechanism was proposed[6]. Therefore, it is necessary to discuss the mechanism of DRM on lanthanide oxide supporting Ni catalyst.

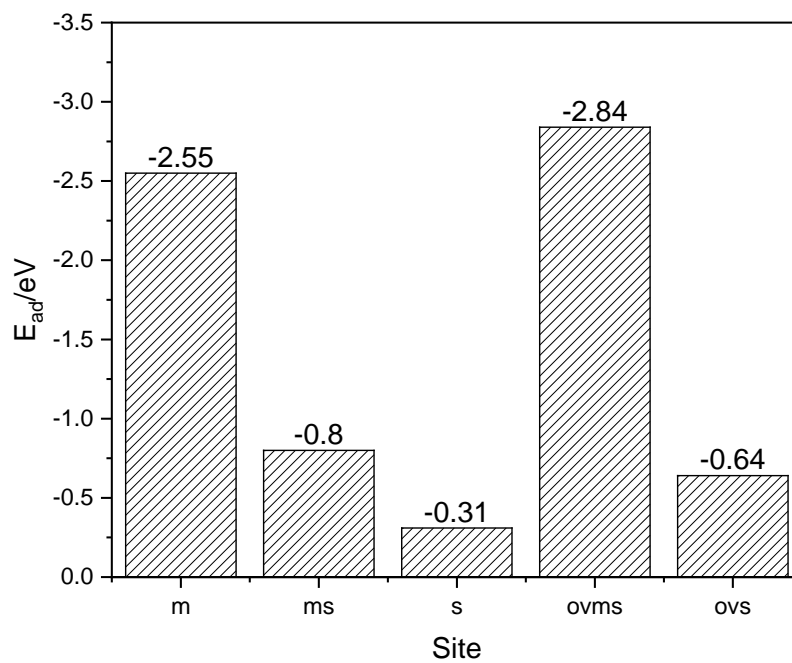
## Calculation Detail

The calculations reported here were performed using periodic density functional theory as implemented in the form of Vienna ab initio simulation package(VASP)[7-9]. Five different sites from three models of Ni/CeO<sub>x</sub> are investigated in this work. Which are surface of metal nanoparticle (**m**), surface of support (**s**), interface of metal nanoparticle and support (**ms**), oxygen vacancy at interface (**ovms**) and oxygen vacancy at support (**ovs**).

## Results and Conclusions

Oxygen vacancy contained interface (**ovms**) shows the highest activity for both of CO<sub>2</sub>, CH<sub>4</sub> activation and CO\* production, and oxygen vacancy contained surface of support (**ovs**) is also high activity for CO<sub>2</sub> activation. However, the oxygen vacancies are easily filled and are hardly regenerated. When neglect the exist of oxygen vacancies, surface of nanoparticle (**m**) shows the highest activity for both of CO<sub>2</sub> and

CH<sub>4</sub> activation, and interface containing interfacial oxygen (**ms**) is highest activity for CO\* production. While only **ms** is favorable for CO\* desorption because of the existence of interfacial oxygen. Therefore, **m** is blocked easily and **ms** is the site for adsorbate transform to CO\* and CO\* desorption. Therefore, the interfacial oxygen is the key for the high stability of CeO<sub>x</sub> supported Ni based catalyst.



The adsorption energy of CO\* on different site

#### References

1. Subramani, V. and S.K. Gangwal, Energy & Fuels, 2008. **22**(2): 814-839.
2. Becerra, A., et al., Granular Matter, 2001. **3**(1-2): 79-81.
3. Daza, C.E., et al., Catalysis Today, 2008. **133**: 357-366.
4. Slagtern, A., et al., Journal of Catalysis, 1997. **172**(1): 118-126.
5. Lou, Y., et al., Journal of Catalysis, 2017. **356**: 147-156.
6. Makri, M.M., et al., Catalysis Today, 2015. **259**: 150-164.
7. Kresse, G. and J. Hafner, Physical Review B, 1993. **47**(1): 558-561.
8. Kresse, G. and J. Furthmuller, Computational Materials Science, 1996. **6**(1): 15-50.
9. Kresse, G. and J. Furthmuller, Physical Review B, 1996. **54**(16): 11169-11186.

# Atom Economic Synthesis of Amines from Alkenes with Recycling of the Homogeneous Catalyst in Thermomorphic Solvent Systems

*Jonas Bianga, Alexander Kühn, Lisa Goclik, Dieter Vogt\*, Thomas Seidensticker\*,  
TU Dortmund, Dortmund, Germany*

## Introduction

Homogeneous catalysis bears enormous potential in the direct synthesis of amines from alkenes for example by the hydroaminomethylation (HAM). This tandem catalytic reaction consists of an initial alkene hydroformylation, followed by the reductive amination of the intermediate aldehyde to the desired amine. In comparison to most industrially established processes, there is no need to resort to already functionalized starting materials.<sup>[1]</sup> Overall there is a large potential for an improvement in terms of the selectivities and reduction of byproducts and waste.

For the development of efficient and sustainable homogeneously catalyzed processes, the reuse of the catalyst might be necessary. Among the various concepts for catalyst recycling, the use of thermomorphic multiphase systems (TMS) is very promising. These systems are characterized by a homogeneous reaction followed by a phase separation, induced by a temperature switch. Advantages of these systems are the general use of standard solvents and commercially available catalyst systems. Especially in the HAM of alkenes the use of TMS brings a big advantage. Non-polar alkenes can be brought into a single-phase reaction with partially strongly polar amines.

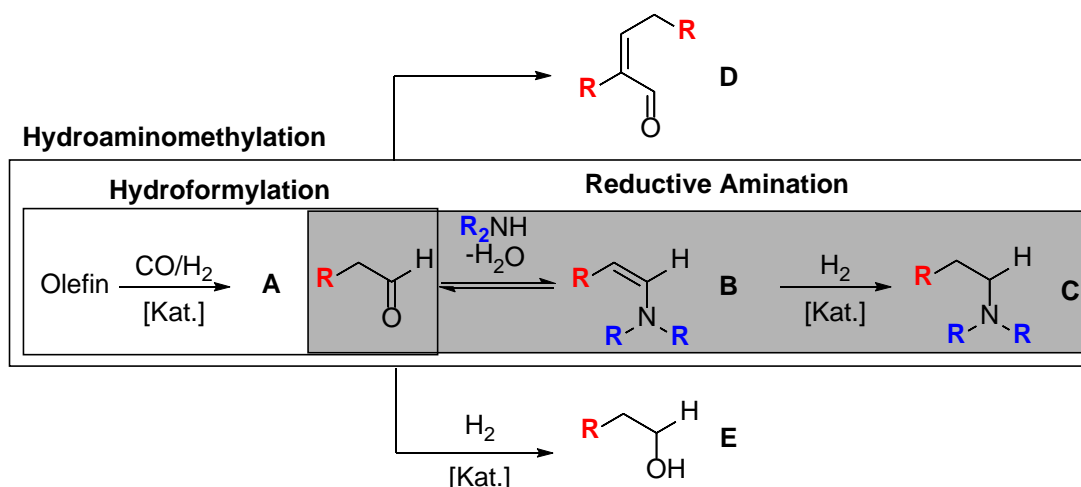


Figure 1: Reaction network of the hydroaminomethylation.

HAM reactions with various substrates in different TMS are already reported in literature.<sup>[2-6]</sup> Up to now a continuous HAM process has not been created. Especially high catalyst leaching into the product phase limited the approach of TMS in most cases.

We will present our work within the research cluster “InPrompt, SFB Transregio 63” on the development of a continuous process for the HAM of 1-decene and diethylamine in a TMS. To this end a systematic investigation of different solvent systems is carried out to identify the most appropriate solvents. Starting from a catalytic system published in 2008 by *Vogt et al.* the influence of different solvents on the reaction and the catalyst, as well as on product separation was investigated. These and other results on the way to establish more efficient industrial processes for the homogeneously catalyzed synthesis of amines from readily available starting materials will be presented in detail.

#### References

- [1] K. S. Hayes, *Appl. Catal., A*, **2001**, 221, 187–195.
- [2] A. Behr, R. Roll, *J. Mol. Catal. A: Chem.* **2005**, 239(1-2), 180–184.
- [3] A. Behr, A. J. Vorholt, N. Rentmeister, *Chem. Eng. Sci.* **2013**, 99, 38–43.
- [4] A. J. Vorholt, P. Neubert, A. Behr, *Chem. Ing. Tech.* **2013**, 85(10), 1540–1547.
- [5] A. Behr, T. Seidensticker, A. J. Vorholt, *Eur. J. Lipid Sci. Technol.* **2014**, 116(4), 477–485.
- [6] A. J. Vorholt, S. Immohr, K. A. Ostrowski, S. Fuchs, A. Behr, *Eur. J. Lipid Sci. Technol.* **2017**, 119(5), 1600211.
- [7] B. Hamers, P.S. Bäuerlein, C. Müller, D. Vogt, *Adv. Synth. Catal.* **2008**, 350, 332 – 342.

#### Corresponding authors:

Dr. Thomas Seidensticker, Prof. Dr. Dieter Vogt

Company: Laboratory of Industrial Chemistry, TU Dortmund University,

Address: Emil-Figge-Str. 66, 44227 Dortmund,

Email: Thomas.Seidensticker@tu-dortmund.de

Dieter.Vogt@tu-dortmund.de



## **Synthesis and Physicochemical Characterization of Vanadium-containing BEA zeolite for Oxidative Dehydrogenation (ODH) of Light Alkanes**

*M. Smoliński, Jerzy Haber Institute of Catalysis and Surface Chemistry, PAS, 30-239 Krakow, Poland; K. Samson, Jerzy Haber Institute of Catalysis and Surface Chemistry, PAS, 30-239 Krakow, Poland; J. Podobiński, Jerzy Haber Institute of Catalysis and Surface Chemistry, PAS, 30-239 Krakow, Poland; M. Ruggiero-Mikołajczyk, Jerzy Haber Institute of Catalysis and Surface Chemistry, PAS, 30-239 Krakow, Poland; A. Drzewiecka-Matuszek, Jerzy Haber Institute of Catalysis and Surface Chemistry, PAS, 30-239 Krakow, Poland; D. Rutkowska-Zbik, Jerzy Haber Institute of Catalysis and Surface Chemistry, PAS, 30-239 Krakow, Poland*

*L. Valentin, Laboratoire de Réactivité de Surface, Sorbonne Université, UMR 7197, 75005 Paris, France; F. Averseng, Laboratoire de Réactivité de Surface, Sorbonne Université UMR 7197, 75005 Paris, France; Y. Millot, Laboratoire de Réactivité de Surface, Sorbonne Université, UMR 7197, 75005 Paris, France; S. Dzwigaj, Laboratoire de Réactivité de Surface, Sorbonne Université-CNRS, UMR 7197, 75005 Paris, France;*

Production of light alkenes via oxidative dehydrogenation (ODH) of alkanes is becoming an alternative to olefin extraction by conventional methods, such as catalytic cracking or conventional dehydrogenation, and is associated with lower energy consumption and less catalyst coking compared to conventional dehydrogenation of alkanes [1]. Vanadium based systems are the important class of ODH catalysts, but their performance depends strongly on vanadium dispersion [2] and there is a lack of clear indication which types of vanadium centers are active in ODH: isolated vanadium centers in tetrahedral or octahedral coordination or polymeric V-O-V chains. Microporous materials, such as zeolites, may serve as support for vanadium, offering the possibility to introduce it in a well-defined environment controlling its dispersion and speciation.

Our aim was to design series of vanadium-containing materials in which varying location of V centers results in their different geometry and electronic properties, leading to distinct reactivity in ODH of propane.

The non-modified BEA zeolite (Si/Al = 17), its partially dealuminated form, and fully dealuminated form were chosen as a support for vanadium. The samples were synthesized using  $\text{NH}_4\text{VO}_3$  as vanadium precursor, at pH equal to 2.5 and 7.0 by the following methods: two-step postsynthesis method [3], traditional impregnation, and ion exchange. V content varied from 0.1 to 7.0 V wt %.

The chemical composition of the samples was confirmed with XRF, phase composition by XRD, BET provided surface area and porosity. Reducibility was measured with  $\text{H}_2$ -TPR method, while  $\text{NH}_3$ -TPD gave information on the type and strength of acid centres. The nature of the introduced vanadium species was probed by DR UV-vis,  $^{51}\text{V}$  MAS NMR, and EPR. The active sites present in the samples are characterized by DFT calculations (PBE/def2-TZVP). The catalysts are submitted to catalytic tests in ODH of 7.1 %vol. propane in air at temperature 420 – 520 °C in gas-flow fixed-bed reactor coupled to GC.

In fully dealuminated samples, the presence of vanadium(V) of tetrahedral coordination incorporated in the structure of the dealuminated BEA zeolite was demonstrated by DR UV-vis bands at 260 and 340 nm and  $^{51}\text{V}$  MAS NMR peaks at -590 and -620 ppm at lower loadings. At higher loadings octahedral sites appear. In samples prepared with parent zeolite, vanadium is present mainly as extra-framework octahedral V(V) species as evidenced by a broad DR UV-vis band at around 430 nm and the  $^{51}\text{V}$  MAS NMR peak at -730 ppm. At lower loadings, it forms tetrahedral sites, whereas at higher loadings octahedral sites appear. DFT calculations suggest that vanadium can substitute T atoms in all available crystallographic positions in BEA, but preferably is present as V=O center in T2 and/or T3, exhibiting pseudo-tetrahedral coordination. The preliminary catalytic tests show that tetrahedral vanadium sites are responsible for selective ODH reaction, while octahedral vanadium sites are responsible for total combustion.

Acknowledgments: This work was supported by the National Science Centre, Poland within project no 2016/23/B/ST4/02854.

#### References:

- [1] A. Kubacka, E. Włoch, B. Sulikowski, R.X. Valenzuel, V. Cortés Corberán, *Catal. Today* 61 (2000) 343
- [2] B. Schimmoeller, Y. Jiang, S.E. Pratsinis, A. Baiker, *J. Catal.* 274 (2010) 64
- [3] S. Dzwigaj, P. Massiani, A. Davidson, M. Che, *J. Mol. Catal. A* 155 (2000) 169

# Butane dry reforming catalysed by a $Ti_2AlC$ MAX Phase

*Maria Ronda-Lloret, University of Amsterdam, Amsterdam, The Netherlands;*

*Noë I. Watson, University of Amsterdam, Amsterdam, The Netherlands;*

*Willem G. Sloof, Delft University of Technology, Delft, The Netherlands;*

*Gadi Rothenberg, University of Amsterdam, Amsterdam, The Netherlands;*

*N. Raveendran Shiju, University of Amsterdam, Amsterdam, The Netherlands.*

## Introduction

MAX phases are layered ternary carbides or nitrides featuring both ceramic and metallic properties. Their name reflects their chemical build-up: M is an early transition metal, A is typically a group 13 or 14 element, and X is either carbon or nitrogen.<sup>[1]</sup>  $Ti_2AlC$  is one of the most stable MAX phases (Figure 1a), with an oxidation resistance up to 1100 °C.<sup>[2]</sup> MAX phases are well known in electrical, thermal and mechanical applications, yet few studies focus on their catalytic potential.<sup>[3,4]</sup>

We are interested in the catalytic conversion of  $CO_2$  into high value chemicals.  $CO_2$  activation requires high temperature, so co-reactants of higher energy are often used to lower the thermodynamic penalty of the reaction. The dry reforming of butane (DRB) is especially interesting as it can run at relatively low temperatures (500–600 °C). Moreover, butane is widely available from shale gas and from crude oil cracking. Therefore, DRB can be a practical solution for using  $CO_2$ . Here we study the catalytic properties and stability of  $Ti_2AlC$ -based materials in the DRB reaction. We use  $Ti_2AlC$  as a support for  $Co_3O_4/CoO$  species (represented hereafter as  $CoO_x$ ), and compare it to the more conventional supports  $\gamma-Al_2O_3$ ,  $TiO_2$  and  $TiC$ .

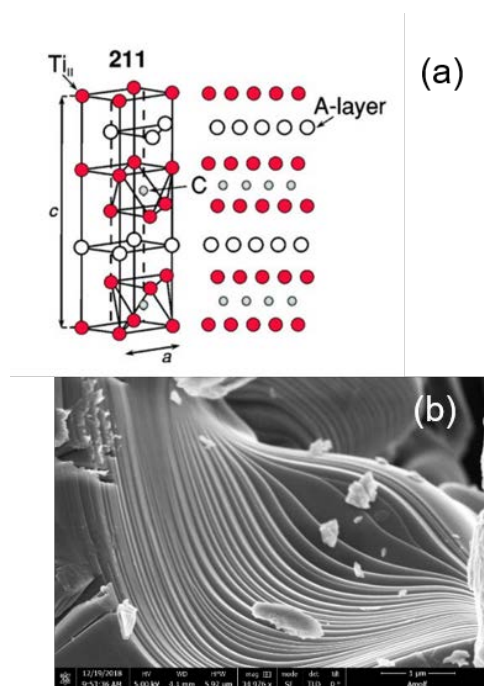


**Figure 1.** (a) Hexagonal crystal structure of  $Ti_2AlC$ . There is one Al layer for every second layer of Ti. The  $Ti_{II}$  atoms have chemical bonds to both C and Al.<sup>[2]</sup> (b) Scanning Electron Microscopy (SEM) image of  $Ti_2AlC$ , showing its layered structure.

## Catalytic results

The  $\text{Ti}_2\text{AlC}$  MAX phase was synthesized by mixing powders of Ti, Al and TiC and heating the mixture to 1350 °C for 2 h under pressure.<sup>[5]</sup> Supported 5 wt.%  $\text{CoO}_x$  samples were prepared by wet impregnation followed by calcination at 450 °C. In catalytic tests at 650 °C (Figure 2a), we see that  $\text{CoO}_x/\text{Ti}_2\text{AlC}$  catalyst converts 20% of  $\text{CO}_2$  and is stable for at least 18 h on stream. The  $\text{CoO}_x/\text{Al}_2\text{O}_3$  catalyst has higher activity, but is less stable over time. Butane conversion values are similar to the  $\text{CO}_2$  ones, and both catalysts show similar selectivity towards CO (64%) and  $\text{H}_2$  (34%).

Overall, we prove that  $\text{CoO}_x/\text{Ti}_2\text{AlC}$  is an active and stable material during DRB. Furthermore, the MAX phase support incurs less coking compared to alumina (Figure 2b). The low amount of coke increases the stability of the catalyst and with it the efficiency of the reaction. In the lecture, we will show how the structure and the textural properties of the  $\text{Ti}_2\text{AlC}$  MAX phase affects the catalysis and the resistance to coking side reactions.

## References

- [1] M. W. Barsoum, T. El-Raghy, *Am. Sci.* **2001**, 89, 334.
- [2] M. Magnuson, O. Wilhelmsson, J. P. Palmquist, U. Jansson, M. Mattesini, S. Li, R. Ahuja, O. Eriksson, *Phys. Rev. B* **2006**, 74, 1–8.
- [3] W. H. K. Ng, E. S. Gnanakumar, E. Batyrev, S. K. Sharma, P. K. Pujari, H. F. Greer, W. Zhou, R. Sakidja, G. Rothenberg, M. W. Barsoum, N.R. Shiju, *Angew. Chem. Int. Ed.* **2018**, 1485–1490.
- [4] X. Xie, Y. Xue, L. Li, S. Chen, Y. Nie, W. Ding, Z. Wei, *Nanoscale* **2014**, 6, 11035–11040.
- [5] L. Boatemaa, M. Bosch, A. S. Farle, G. P. Bei, S. van der Zwaag, W. G. Sloof, *J. Am. Ceram. Soc.* **2018**, 101, 5684–5693.

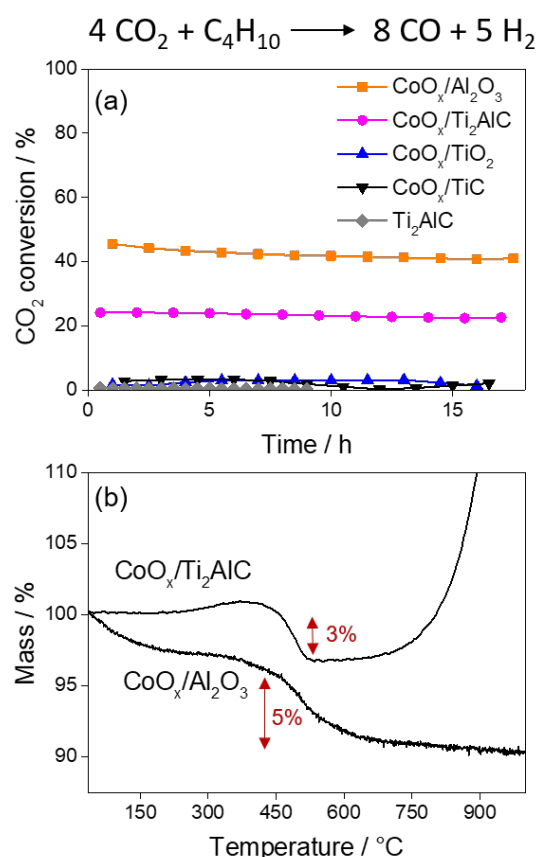


**Figure 2.** (a)  $\text{CO}_2$  conversion over time of the 5 wt.%  $\text{CoO}_x$  catalysts. Reaction conditions: 100–50 mg catalyst,  $\text{CO}_2:\text{C}_4\text{H}_{10} = 4:1$ , total flow  $20 \text{ mL}\cdot\text{min}^{-1}$ , atmospheric pressure, 650 °C. (b) TGA profiles of the used catalysts. The mass loss at 450–600 °C corresponds to the oxidation of carbon nanotubes formed during reaction.

# Degree of Mass Transfer Control and CFD analysis of NH<sub>3</sub> oxidation catalyst: A tool for investigating mass transfer limited catalytic processes

*Michael Haas<sup>1</sup>, Dirk Born<sup>2</sup>, Alfons Drochner<sup>1</sup>, Bastian Etzold<sup>2</sup>, Martin Votsmeier<sup>1,2</sup>*

*<sup>1</sup>Technische Universität Darmstadt, Ernst-Berl-Institut für Technische und Makromolekulare Chemie, Alarich-Weiss-Straße 8, 64287 Darmstadt (Germany)*

*<sup>2</sup>Umicore, Rodenbacher Chaussee 4, 63457 Hanau-Wolfgang (Germany)*

## Introduction

The mechanistic understanding of chemical surface processes in heterogeneous catalysis is constantly improving, with many detailed surface mechanistic and kinetic models for a variety of heterogeneously catalyzed processes having been published in the literature [1]. As lot of these processes underlie mass transfer limitations, a detailed knowledge of the interaction between external mass transfer and the chemical reactions occurring on the surface of the catalyst are essential for the understanding of the catalytic process as such, for the rational design of catalysts and for the adjustment of process parameters in order to achieve optimal performance.

Rapid improvement and increasing availability of powerful computational hardware, as well as more and more efficient mathematical algorithms have opened the window to the direct investigation of even very large surface kinetic models all the way to the coupling of those models to detailed CFD simulations of resolved complex geometries and systems [2, 3].

In this contribution, we present a new combined approach of CFD simulation and sensitivity analysis of a micro kinetic model with coupled mass transfer in order to investigate the interaction between flow, mass transfer and surface chemistry of a heterogeneously catalyzed system. Industrial NH<sub>3</sub> oxidation on platinum gauze catalysts, which is a prominent example for a mass transfer limited process, is utilized as a test case.

## Methods

Based on the “Degree of Rate Control” (DoRC) analysis, published by Campbell et al. [4], we extended the concept by explicit incorporation of external mass transfer to the network of elementary step surface processes. We introduce this concept as

“Degree of Mass Transfer Control” and applied it to a mean field micro-kinetic model for  $\text{NH}_3$  oxidation [5]. In order to obtain local mass transfer coefficients, laminar CFD simulations of a resolved catalyst gauze model with coupled surface chemistry were carried out using the commercial package Fluent.

## Results and Discussion

The distribution of the local  $\text{NH}_3$  mass transfer coefficient on the catalyst (Figure 1a) reveals areas of different mass transfer intensity due to the geometry and the flow field throughout the catalyst. The effects of inhomogeneity in mass transfer on the chemistry is described by a “Degree of Mass Transfer Control” analysis, identifying elementary steps that are governed by mass transfer and predicting the sensitivity of product selectivities to perturbations in external mass transfer (Figure 1b). A combination of these two approaches reveals catalyst zones of different selectivity towards certain product species (e.g. unwanted side products like  $\text{N}_2\text{O}$  or  $\text{N}_2$ ) and therefore providing insights and understanding of mechanisms governing the performance of a catalyst in a mass transfer limited process on one hand and aiding in developing more efficient catalysts on the other (for instance by tuning the catalysts geometry). This method offers great potential for *in silico* catalyst design, as it can be applied to any mass transfer limited process for which a detailed surface kinetic model is at hand.

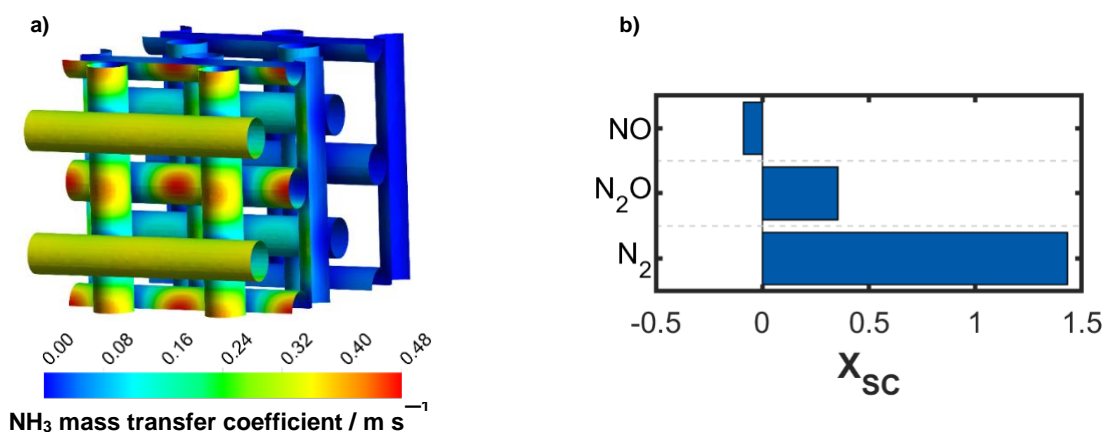


**Figure 1.** (a) Local mass transfer coefficient on the catalyst and (b) Degree of selectivity control for the three product species NO,  $\text{N}_2\text{O}$  and  $\text{N}_2$ .

## References

1. Kraehnert R. and Baerns M., *Chem. Eng. J.*, 137, 361-375 (2008).
2. Partopour B. and Dixon A.G., *Comput. Chem. Eng.*, 88, 126-134 (2016).
3. Klingenberger M., Hirsch O. and Votsmeier M., *Comput. Chem. Eng.*, 98, 21-30 (2017).
4. Campbell C.T., *ACS Catal*, 7, 2770-2779 (2017).
5. Traversac, X. “Experimental and Microkinetic Modelling Study of Ammonia Oxidation over Platinum”, *PhD thesis*, Sydney (2007).

## **Molecular level-based study on the formation of aromatics in zeolites starting from polyenes**

*Delphine De Saegher, Ghent University-Center for Molecular Modeling, Ghent, Belgium; Simon Bailleul, Ghent University-Center for Molecular Modeling, Ghent, Belgium; Julianna Hajek Ghent University-Center for Molecular Modeling, Ghent, Belgium; Veronique Van Speybroeck, Ghent University-Center for Molecular Modeling, Ghent, Belgium*

### **Role of polyenes in the formation of aromatics within zeolites**

Aromatics are omnipresent within hydrocarbon chemistry in zeolites. In fluid catalytic cracking aromatics are known to be the precursors for cokes which deactivate the zeolitic catalyst. Furthermore, in the zeolite-catalyzed methanol-to-olefins (MTO) process aromatics appear not only as deactivating species, but also play an active role in the aromatic cycle of the hydrocarbon pool (HP) mechanism, which is known to govern the methanol conversion in this process [1]. However, the formation of aromatics in zeolites is still not well understood on the molecular level. Recently, indisputable experimental evidences were given for the presence of polyenes in the reaction system which might suggest their intermediate role in aromatics formation [2-5]. Despite many experimental efforts in this field the mechanism of aromatics formation from polyenes in zeolites is still not disclosed.

### **Possible mechanisms of aromatics formation from polyenes**

Within this contribution, a combination of state-of-the-art static and dynamic periodic DFT calculations are used to obtain insight into the formation mechanism of aromatics starting from polyenes within the small pore zeolite H-SSZ-13. This catalyst is characterized by cages interconnected by 8-ring windows, which may further influence the formation and growth of aromatics from polyenes. To this end different reaction mechanisms, such as the intramolecular rearrangement, dimerization and cyclization, Diels-Alder reaction and electrophilic aromatic substitution are studied using both static and dynamics based molecular simulations to unravel the nature and stability of intermediate species at operating conditions. Heptatriene, for which the resonance-stabilized carbocation is depicted in Figure 1, is chosen as a model compound for polyenes and a starting point for this study. Exemplary aromatic products from the intramolecular arrangement and electrophilic

aromatic substitution of heptatriene over the zeolite are shown in Figure 1. The obtained free energy profiles of the different pathways will be compared to assess the relative importance and hence unravel the most feasible reaction mechanism for aromatics formation in zeolites starting from polyenes. The insights are obtained by using molecular dynamics based methods that allow to simulate reaction pathways and intermediates at operating conditions, taking into account the flexibility of the material, effect of temperature and pressure. The obtained insight gives crucial insights into the formation of aromatics and possible deactivating routes for important processes such as alcohol conversion, catalytic cracking reactions. Such knowledge is mandatory to propose valuable design guidelines for the next generation of catalysts, optimizing product selectivity and catalyst lifetime.

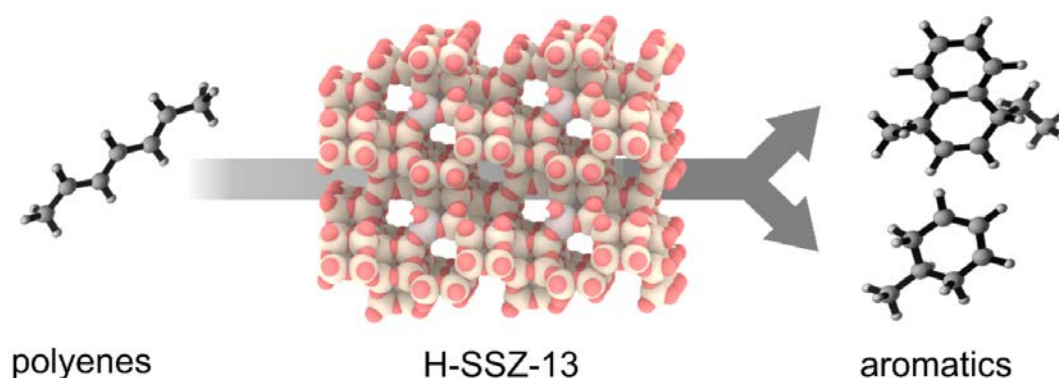


Figure 1: Protonated heptatriene reacts over a chabazite-type zeolite to various aromatics.

## References

- [1] U. Olsbye, S. Svelle, K. P. Lillerud, Z. H. Wei, Y. Y. Chen, J. F. Li, J. G. Wang, W. B. Fan, The formation and degradation of active species during methanol conversion over protonated zeotype catalysts, *Chemical Society Reviews*, 44 (2015) 7155-7176.
- [2] A. Hwang, M. Kumar, J. D. Rimer, and A. Bhan, Implications of methanol disproportionation on catalyst lifetime for methanol-to-olefins conversion by HSSZ-13, *Journal of Catalysis*, 346 (2017) 154-160.
- [3] J. S. Martinez-Espin, K. De Wispelaere, T. V. W. Janssens, S. Svelle, K. P. Lillerud, P. Beato, V. Van Speybroeck, U. Olsbye, Hydrogen Transfer versus Methylation: On the Genesis of Aromatics Formation in the Methanol-To-Hydrocarbons Reaction over H-ZSM-5, *ACS Catalysis*, 7 (2017) 5773-5780.
- [4] A. D. Chowdhury, A. L. Paioni, K. Houben, G. T. Whiting, M. Baldus, and B. M. Weckhuysen, Bridging the Gap between the Direct and Hydrocarbon Pool Mechanisms of the Methanol-to-Hydrocarbons Process, *Angewandte Chemie*, 57 (2018) 8095-8099.
- [5] Y. T. Chua and P. C. Stair, An ultraviolet Raman spectroscopic study of coke formation in methanol to hydrocarbons conversion over zeolite H-MFI, *Journal of Catalysis*, 213 (2003) 39-46.



## **ROMEO - A major step toward more sustainable hydroformylation processes**

*Marco Haumann<sup>a</sup>, Markus Schörner<sup>a</sup>, Jennifer Hasselberg<sup>b</sup>, Robert Franke<sup>c,d</sup>, Frank Stenger<sup>e</sup>, Morten Logemann<sup>f</sup>, Jakob Marinkovic<sup>g</sup>, Anders Riisager<sup>g</sup>*

*<sup>a</sup> Friedrich-Alexander-Universität Erlangen-Nürnberg (FAU), Lehrstuhl für Chemische Reaktionstechnik (CRT), Egerlandstr. 3, 91058 Erlangen, Germany, E-mail: markus.schoerner@fau.de, <sup>b</sup> Evonik Technology & Infrastructure GmbH, Paul-Baumann-Str. 1, 45772 Marl, Germany, <sup>c</sup> Evonik Performance Materials GmbH, Paul-Baumann-Str. 1, 45772 Marl, Germany, <sup>d</sup> Ruhr-Universität Bochum, Lehrstuhl für Theoretische Chemie, Universitätsstr. 150, 44780 Bochum, Germany. <sup>e</sup> Evonik Technology & Infrastructure GmbH, Rodenbacher Chaussee 4, 63457 Hanau-Wolfgang, <sup>f</sup> Rheinisch-Westfälische Technische Hochschule Aachen (RWTH), Lehrstuhl für chemische Verfahrenstechnik, Forckenbeckerstraße 51, 52074 Aachen, <sup>g</sup> Technical University of Denmark (DTU), Department of Chemistry, Kemitorvet, Building 207, DK-2800 Kgs. Lyngby*

One of the most prominent industrially applied reactions is alkene hydroformylation. More than 10 million tons of chemical products rely on this reaction step every year; thus, a permanent improvement of this homogeneously catalyzed reaction is of utmost interest for many chemical companies worldwide<sup>[1]</sup>.

Here we present the latest results of the developments in the field of hydroformylation within the currently running EU funded project ROMEO (Reactor Optimization by Membrane Enhanced Operation)<sup>[2]</sup>. This project aims at the combination of a catalyzed reaction with the separation step on a single support structure<sup>[3]</sup>. This combination in an innovative “2-in-1” reactor opens the possibility to omit or at least significantly downsize the separation units. This concept allows increasing the efficiency of catalytic reactions by immediately removing the desired products from the reaction zone and thereby reducing consecutive reactions.

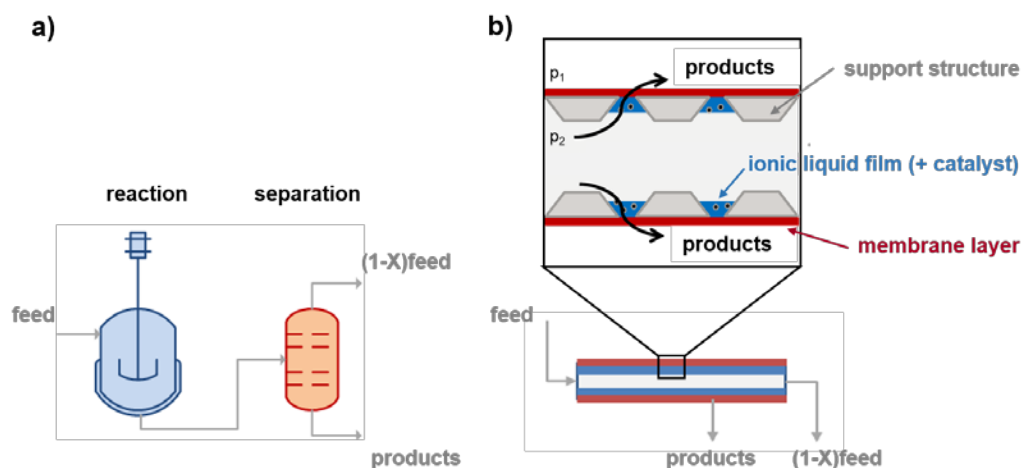


Figure 1. Schematic representation of the ROMEO approach for reaction and separation of homogeneously catalyzed reactions.

ROMEO's approach is to use and combine existing or only slightly modified building blocks such as supports, coatings and catalysts. The consortium further focuses on the development of a new reactor methodology. In addition to the actual technical developments, a universal modelling tool will be implemented in order to allow the accurate prediction of ROMEO's benefit for other homogeneously catalyzed reactions. The European Commission is providing financial backing to the project and its nine academic and industrial partners through the Horizon 2020 research program (<http://www.romeo-h2020.eu/>). In the wide range of tasks within the project, this work focuses on the experimental investigation of the developed reactor module.

## References

- [1] Robert Franke, Detlef Selent, Armin Börner „Applied Hydroformylation“ in *Chem. Rev.*, **2012**, 112 5675-5732, DOI: 10.1021/cr3001803
- [2] <http://www.romeo-h2020.eu/>, (last visited 10th January 2019)
- [3] Jakob Marinkovic, Anders Riisager, Robert Franke, Peter Wasserscheid, Marco Haumann. „Fifteen Years of Supported Ionic Liquid Phase-Catalyzed Hydroformylation: Material and Process Developments“ in *Ind. Eng. Chem. Res.*, to be published, DOI: 10.1021/acs.iecr.8b04010

# Investigation of the active sites of MoS<sub>2</sub> based hydrotreating catalysts by modulated excitation X-ray absorption spectroscopy

*A. Gaur<sup>1,2</sup>, T. M. Hartmann Dabros<sup>3</sup>, M. Høj, A. Boubnov<sup>2</sup>, T. Prüssmann<sup>1</sup>, J. Jelic<sup>1</sup>,  
F. Studt<sup>1,2</sup>, A.D. Jensen<sup>3</sup>, J.-D. Grunwaldt<sup>1,2</sup>*

*<sup>1</sup>Institute of Catalysis Research and Technology, Karlsruhe Institute of Technology (KIT), Karlsruhe, Germany, <sup>2</sup>Institute for Chemical Technology and Polymer Chemistry, KIT, Karlsruhe, Germany, <sup>3</sup>DTU Chemical Engineering, Technical University of Denmark (DTU), Kgs. Lyngby, Denmark*

## Introduction

Due to ever increasing environmental regulations and the shift towards more sulfur containing feedstocks, there is continued interest in improved MoS<sub>2</sub> based hydrotreating catalysts for hydrodesulfurization of crude oil [1, 2]. Such catalysts are also relevant for the hydrodeoxygenation of feedstocks derived from biomass, e.g., bio-oil derived via fast pyrolysis [3, 4]. The atomic-scale structure and morphology of MoS<sub>2</sub>, Co-MoS<sub>2</sub> and Ni-MoS<sub>2</sub> catalysts have been widely studied using density functional theory (DFT) along with transmission electronic microscopy (TEM) and scanning tunneling microscopy. DFT studies indicate that exposure of MoS<sub>2</sub> to water vapor can lead to exchange of S with O at the edge of MoS<sub>2</sub> and that promotion stabilizes the catalyst [5]. The active sites of Co-MoS<sub>2</sub> and Ni-MoS<sub>2</sub> catalysts are probably located at the edges and corners of MoS<sub>2</sub> and thus only constitute a small fraction. Modulation excitation spectroscopy (MES) [6] coupled X-ray absorption spectroscopy (XAS) is an excellent tool to elucidate the structural changes of such minute amounts of active sites as function of the concentration of water and sulfur containing species. In the present study, we demonstrate how XAS coupled with MES supported by DFT calculations can help in identifying the active sites of MoS<sub>2</sub>, Co-MoS<sub>2</sub> and Ni-MoS<sub>2</sub> based catalyst as a function of the applied reaction conditions.

## Results and Discussion

Figure 1 shows the overview of the procedure employed for the MES experiments [7]. MES studies were performed by cycling between H<sub>2</sub>O/H<sub>2</sub> and H<sub>2</sub>S/H<sub>2</sub> gas conditions with a total period of 360 seconds. Time-resolved quick-scanning EXAFS (QEXAFS) spectra were collected at a frequency of 20 Hz for all samples at the Mo

K-edge and for the NiMo sample additionally at the Ni K-edge at the SuperXAS beamline (SLS, Villigen, Switzerland). By employing MES coupled XAS for unpromoted as well as Co- and Ni-promoted  $\text{MoS}_2$

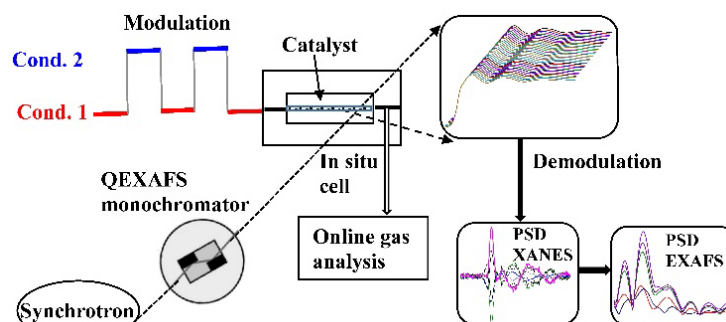


Fig. 1: Experimental procedure employed for the MES

catalysts, it has been shown that upon cycling between  $\text{H}_2\text{O}/\text{H}_2$  and  $\text{H}_2\text{S}/\text{H}_2$  conditions, O atoms replace S atoms at the edges of  $\text{MoS}_2$ , an insight which is not accessible by conventional XAS. As compared to Mo, the lower amplitude of the demodulated spectra observed for CoMo and NiMo strongly suggests a

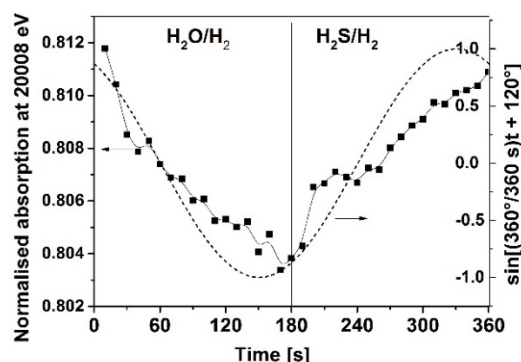


Fig. 2. Kinetics of the phase transition of Mo observed as function of time.

decrease in S-O exchange upon promotion. In the case of the Ni- $\text{MoS}_2$ , MES-XAS at the Ni K-edge revealed fast oxidation of the Ni while the S-O exchange at the Mo-edge is rather slow. The kinetics of the reaction occurring at the time scale of the MES measurements can also be probed as shown in Figure 2 [7]. Theoretical calculations based on DFT also suggest that the thermodynamics of the S/O exchange become more favorable in the order Ni > Mo > Co edge atoms. In conclusion, we have demonstrated that by employing well-designed experiments MES is able to probe changes on catalyst surfaces at the atomic-scale as a function of variation in the chemical environment. This approach is also of general interest for investigating the mechanism of heterogeneous catalysts.

## References

- [1] H. Wang, J. Male, Y. Wang, Y. *ACS Catal.* **2013**, *3*, 1047-1070.
- [2] E. Furimsky, *Catal. Today* **2013**, *217*, 13-56.
- [3] P. M. Mortensen et al., *Appl. Catal. A* **2011**, *407*, 1-19.
- [4] T. M. H. Dabros et al., *Prog. Energy Combust. Sci.* **2018**, *68*, 268-309.
- [5] T. M. H. Dabros et al., *Appl. Catal. A* **2018**, *551*, 106-121.
- [6] A. Urakawa, T. Bürgi, A. Baiker, *Chem. Phys.* **2006**, *324*, 653-658.
- [7] A. Gaur et al., *ACS Catal.*, submitted for publication.

# ***P*-Xylene Production By Tandem Green and Direct Flow Process from Cellulosic Biomass-Derived 2,5-dimethylfuran and Acrylic Acid over Zeolite**

Jose A. Mendoza Mesa, Markus Antonietti, Majd Al-Naji\*

Max Planck Institute of Colloid and Interfaces, Department of Colloid Chemistry, Am Mühlenberg 1, 14476 Potsdam, Germany

In 2015, around 37 million metric tons of *p*-xylene was consumed in wide range of chemical industries [1]. In general, xylenes, *i.e.*, *o*, *m* and *p*-xylene, is simply produced from the purified petroleum reformat with 20% yield [1]. The environmental concern motivate researchers to develop alternative and eco-friendly route for production of poly(ethylene terephthalate) (PET) from renewable resources, *i.e.*, cellulosic biomass. In the last decades, *p*-xylene were synthesized from Diels-Alder reaction using cellulosic biomass-derived 2,5-dimethylfuran (DMF) in the presence of ethylene over zeolite catalysts through the intermediate 1,4 dimethyl-7-oxabicyclo[2.2.1] hept-2-ene. This approach always required batch system and high temperature (~ 573 K), ethylene pressure (> 5.0 MPa) and long reaction time (~24 h) [2,3]. Alternatively, Ni *et al.* [4] reported on the 2 step batch synthesis of *p*-xylene from DMF in the presence of acrylic acid (AA) as green and safer replacement of ethylene using metal triflates in ionic liquid as a solvent.

In this work we report for the first time on a green and direct liquid-phase tandem flow-process for DMF upgrading to *p*-xylene in the presence of AA over different zeolite catalyst (Scheme 1), *i.e.*, ZSM-5, Beta and Y. Furthermore, the influence of zeolite porosity modification, acid site density, space time, reaction temperature and DMF/AA molar ratio will be introduced.



**Scheme 1:** Synthesis of *p*-xylene from cellulosic biomass-derived DMF and AA over different zeolite catalyst.

Over all tested catalyst above 90% of DMF conversion was observed at short residence time (15 min) and reaction temperature 423 K, 473 K and 523 K. In this approach, only *p*-xylene (dominant product) and 2,5-dimethylbenzoic acid (2,5-DMBA) were produced. Among the tested catalyst, Beta zeolite exhibits the highest yield of *p*-xylene (81%) at 473 K with carbon balanced of 99.6% (Fig. 1). Furthermore, as expected increasing the reaction temperature from 234 K to 473 K resulted in higher *p*-xylene and 2,5-DMBA yields (Fig. 1). However, higher reaction temperature, *i.e.*, 523 K, led to slight decrease in *p*-xylene yield and higher 2,5-DMBA yield (Fig. 1).

In conclusions, *p*-xylene was selectively synthesized (81%) via and direct and eco-friendly and alternative heterogeneously-catalyzed route in flow system. These findings will envisage the pave for sustainable production PET from renewable resource.

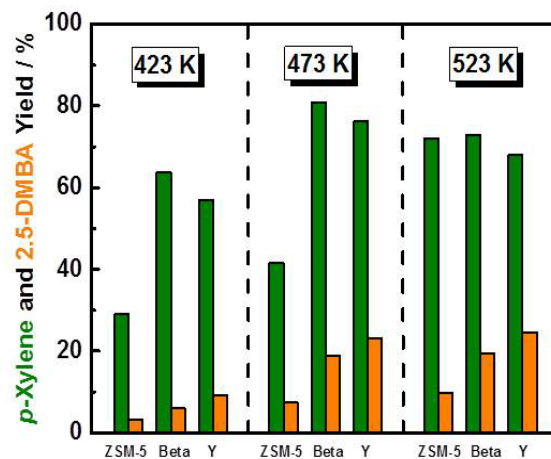


**Fig. 1:** *p*-xylene and 2,5-DMBA yield over ZSM-5, Beta and Y zeolites at different reaction temperatures (423 K, 473 K and 523 K); reaction condition:  $m_{\text{DMF}} = 2.5$  g,  $m_{\text{AA}} = 12.5$  g,  $Q_{\text{reactant}} = 0.3$  cm<sup>3</sup> min<sup>-1</sup>,  $t_{\text{residence}} = 15$  min.

## References

- [1] A.E. Settle, L. Berstis, N.A. Rorrer, Y. Roman-Leshkóv, Green Chem. 19 (2017) 3468-3492.
- [2] I.F. Teixeira, B.T.W. Lo, P. Kostetsky, M. Stamatakis, L. Ye, C.C. Tang, G. Mpourmpakis, S.C. Tsang, Angew. Chem. Int. Ed. 55 (2016) 13061-13066.
- [3] C.L. Williams, C.C Chang, P. Do, N. Nikbin, S. Caratzoulas, D.G. Vlachos, R.F. Lobo, W. Fan, P.J. Dauenhauer, ACS Catal. 2 (2012) 935-939.
- [4] L. Ni, J. Xin, H. Dong, X. Lu, X. Liu, S. Zhang, ChemSusChem 10 (2017) 2394-2401.

## Propane Dehydrogenation using various Ga-M Supported Catalytically Active Liquid Metal Solutions (SCALMS) catalysts

*Narayanan Raman, Moritz Wolf, Nicola Taccardi, Marco Haumann, FAU Erlangen–Nürnberg, Erlangen, Germany; Peter Wasserscheid, FAU Erlangen–Nürnberg, Erlangen, Germany, Helmholtz-Institute Erlangen-Nürnberg for Renewable Energy (IEK-11), Forschungszentrum Jülich, Erlangen, Germany*

Single atom catalysis (SAC) has recently become one of the most active frontiers of heterogeneous catalyst research [1]. The SAC approach has shown to boost the catalytic performance of a metal over their corresponding bulk metal counterpart. Facilitated by the advances in material synthesis, various strategies have been employed to achieve atomic dispersion and stabilization of metal on a solid support.

One innovative strategy developed in our institute is the *Supported Catalytic Active Liquid Metal Solutions (SCALMS)* concept, where a solution of an active metal (e.g. Pd, Pt, Rh etc.) in a low melting metal, e.g. Ga, is deposited on a porous support (Figure 1) [2]. The concept was successfully demonstrated for butane dehydrogenation with a Pd-Ga liquid metal solution. The use of liquid metal overcomes any temperature limitation, which is the major drawback in the case of other supported liquid phase catalyst concepts.

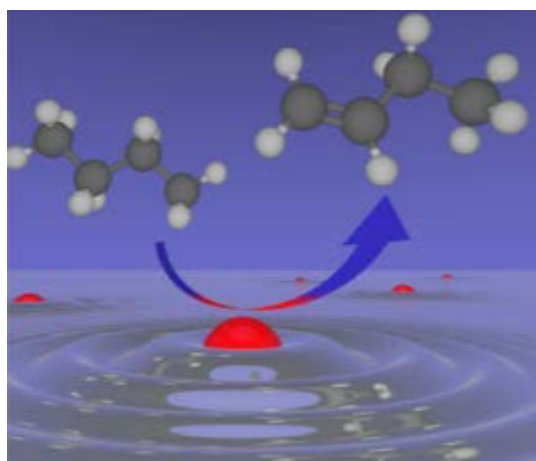


Figure 1: Illustration of the *Supported Catalytic Active Liquid Metal Solutions (SCALMS)* concept [2]

Moreover, since the reaction occurs only at the highly dynamic gas/liquid metal interphase, the catalyst showed higher resistance to deactivation by coking. As a

natural extension of this work, we have been testing the concept for different metals. Of particular interest is the performance of RhGa-SCALMS catalyst for propane dehydrogenation (PDH). Very few examples for Rh as an active dehydrogenation catalyst have been reported, mostly with very poor activity and selectivity [3,4]. Indeed, pure rhodium supported on aluminium oxide (Rh/Alox) showed negligible conversion and low selectivity while the RhGa/Alox SCALMS catalyst showed activity and selectivity comparable to state of the art catalyst for PDH (See Figure 2). Additionally, analysis of the spent catalyst showed that Rh/Alox showed excessive coking.

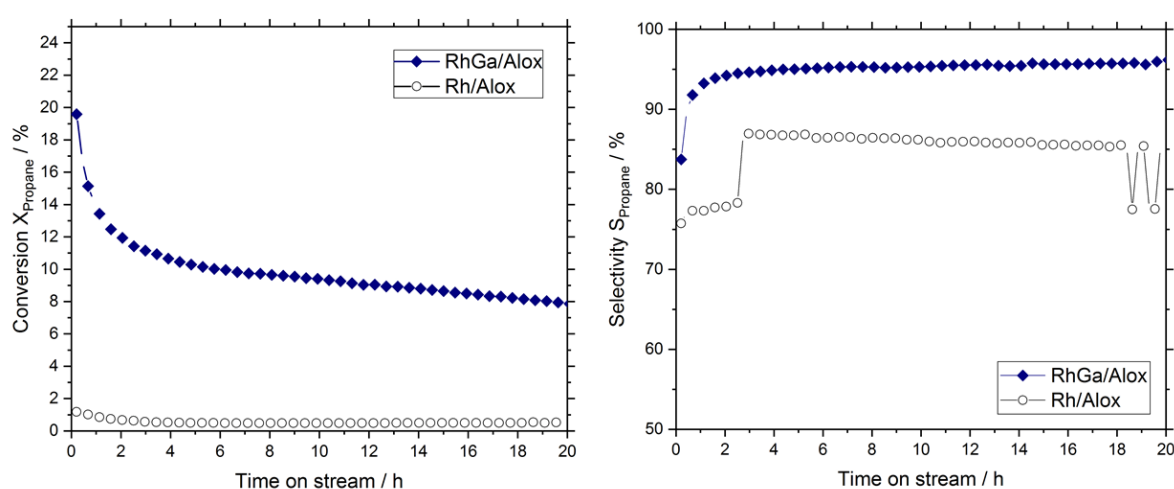


Figure 2: Conversion (a) and Selectivity(b) of Rh supported on Alox (circle) and RhGa SCALMS catalyst supported on Alox (diamond).

The nature of SCALMS material has also been probed using XPS, DRIFTS and TEM. Furthermore, in order to understand the role of the dynamic liquid surface towards coking, highly sensitive gravimetric analysis paired with mass spectroscopy under reaction conditions was performed.

## References

- [1] Mitchell, S. et al. *Catal. Sci. Technol.*, 7, 4248–4249 (2017)
- [2] Taccardi, N. et al. *Nat. Chem.*, 9, 862–867 (2017)
- [3] Resasco, D.E. et al. *J. Phys. Chem.*, 88, 4552–4556 (1984)
- [4] Solymosi, F. et al. *J. Catal.*, 216, 377–385 (2003)



# The Low Temperature Oxidation of Cyclohexanediol to Adipic Acid Using Vanadium Bronzes and Pt/C with Molecular Oxygen

*O. Rogers,<sup>1</sup> S. Pattison,<sup>1</sup> R. V. Engel,<sup>1</sup> K. Whiston,<sup>2</sup> S. H. Taylor<sup>1</sup> and G. J. Hutchings<sup>1</sup>*

<sup>1</sup>Cardiff Catalysis Institute, School of Chemistry, Cardiff University, Main Building, Park Place, Cardiff, CF10 3AT.

<sup>2</sup>INVISTA Performance Technologies. The Wilton Centre, Wilton, Redcar, TS10 4RF.

## Introduction

Adipic acid is predominantly used as a co-monomer in the production of nylon-6,6 alongside hexamethylenediamine. Annually, it is produced on a scale of around 2.5 million metric tonnes worldwide as of 2012. The industrial production of adipic acid historically relies on the aerobic oxidation of cyclohexane. However, the possibility of using cyclohexene as a feedstock has become an option due to the recent improvements in the partial hydrogenation of benzene in the Asahi process.[1] The higher reactivity of cyclohexene allows it to be oxidised by less environmentally harmful oxidants such as O<sub>2</sub> and H<sub>2</sub>O<sub>2</sub>. Cyclohexanediol would offer an intermediate in this reaction route to adipic acid, therefore its aerobic oxidation in air is of continuing research interest.

Previous work in the group of Obara *et al.* has shown that a one-pot synthesis of adipic acid from cyclohexanediol can be achieved by using a combination of Pt/C and vanadium oxide. The Pt/C catalyst aids this reaction by catalysing the conversion of cyclohexane diol to 2-hydroxycyclohexanone (2-HCO) while the vanadium oxide then directs this towards adipic acid with high selectivity [2] as shown in Figure 1.

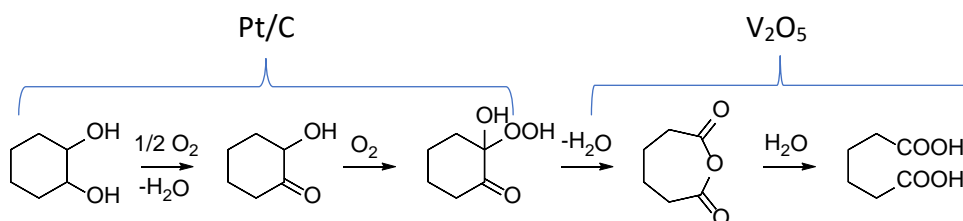


**Figure 1** Oxidation of cyclohexanediol to adipic acid using Pt/C and vanadium catalysts.

## Results and discussion

In this work we investigate the use of vanadium bronzes in this reaction as a substitute for the homogeneous  $\text{V}_2\text{O}_5$  catalyst used in the study by Obara *et al.* Leaching in aqueous media is a particular concern for vanadium catalysts, however

stabilisation as a truly heterogeneous catalyst would increase the industrial viability of this system. Incorporating metals such as silver or copper into the vanadium oxide lattice under a hydrothermal procedure we aim to stabilise this material against leaching.

Table 1 shows in entry 1 that a Pt/C catalyst exhibits an appreciable conversion of 47.6 %, however 90.2% of its selectivity is directed towards 2-HCO. Although NaV<sub>6</sub>O<sub>15</sub> shows only low activity on its own, its use as a co-catalyst with Pt/C enables both high conversion and selectivity towards adipic acid. Furthermore, this is achieved with a relatively low catalyst loading. However, leaching data for this reaction analysed *via* MP-AES revealed high levels of vanadium in the reaction solution, suggesting a large contribution from homogeneous vanadium. This was further confirmed by study of a reaction spiked with the leached solution from the bronze. Interestingly, when we switch to a CuV<sub>2</sub>O<sub>6</sub> bronze (entry 5) we sacrifice some activity, however selectivity is still strongly directed towards adipic acid. This CuV<sub>2</sub>O<sub>6</sub> bronze also exhibits much lower leaching compared to the NaV<sub>6</sub>O<sub>15</sub> analogue, dropping from 36.8 % vanadium leaching to only 2.5 % in CuV<sub>2</sub>O<sub>6</sub>.

**Table 1** Oxidation of *trans*-1,2-cyclohexanediol over vanadium bronzes and Pt/C utilising molecular oxygen

Entry	Catalyst	Conversion / %	Selectivity / %					Vanadium leaching / %
			Adipic acid	2-HCO	Glutaric acid	Succinic acid	Unknowns	
1	Blank	0	0	0	0	0	0	0
2	Pt/C	47.6	3.1	90.2	2.7	1.3	3.8	0
3	NaV <sub>6</sub> O <sub>15</sub>	3.0	0	0	0	0	100	47.6
4	NaV <sub>6</sub> O <sub>15</sub> + Pt/C	40.9	70	2.1	0	1.4	26.8	36.8
5	CuV <sub>2</sub> O <sub>6</sub> + Pt/C	27.2	60.4	9	0	0	30.6	2.5
6	AgVO <sub>3</sub> + Pt/C	18.4	41.6	21.3	0	2.1	35	2.9

Reaction conditions: 80 °C, 3 bar O<sub>2</sub>, 10 000 ppm cyclohexanediol in water (5 mL), 4 hr, 10 mg 5% Pt/C, 4mg vanadium bronze

## Conclusion

Vanadium bronzes, when combined with Pt/C, are effective catalysts for the selective cleavage of vicinal diols in cyclohexanediol. These catalysts are hindered by the level of leaching observed, however this can be lowered by the incorporation of copper or silver into the bronze structure, while still maintaining good selectivity and activity. This represents progress towards a truly heterogeneous catalyst for this reaction.

## References

- 1 H. Nagahara, M. Ono, M. Konishi and Y. Fukuoka, *Appl. Surf. Sci.*, 1997, **121**, 448–451.
- 2 N. Obara, S. Hirasawa, M. Tamura and Y. Nakagawa, *ChemCatChem*, 2016, **8**, 1732–1738.

# Elucidating Cu species by *operando* XAS – UV-Vis of CuCl<sub>2</sub> Oxychlorination Catalysts

Samuel K. Regli<sup>1</sup>, Endre Fenes<sup>1</sup>, Hongfei Ma<sup>1</sup>, Kumar R. Rout<sup>2</sup>, Terje Fuglerud<sup>3</sup>, De  
Chen<sup>1</sup>, Magnus Rønning<sup>1</sup>

<sup>1</sup>Department of Chemical Engineering, Norwegian University of Science and Technology (NTNU),  
Trondheim, Norway; <sup>2</sup>SINTEF Materials and Chemistry, Oil and Gas Process Technology, Trondheim,  
Norway; <sup>3</sup>INOVYN, Porsgrunn, Norway

## Introduction

Oxychlorination is an important industrial process to produce ethylene dichloride (EDC), a precursor of the vinyl chloride monomer (VCM) for polyvinylchloride (PVC) plastic with a wide range of applications [1]. During oxychlorination, ethylene, hydrogen chloride and oxygen react over supported copper chloride catalyst (CuCl<sub>2</sub>) in temperature range of 200-550 °C to form EDC and water [2]. The oxychlorination reaction is assumed to proceed in three steps; (I) chlorination of ethylene where the chlorinating agent is the catalyst and it reduces from CuCl<sub>2</sub> to CuCl, (II) oxidation of CuCl to form oxy-chloride and (III) re-chlorination of the oxy-chloride using HCl to form CuCl<sub>2</sub> and H<sub>2</sub>O. Although CuCl<sub>2</sub> oxychlorination catalysts are already applied in commercial plants around the world, several problems related to industrial operation still exist. One of the main challenges of this process is that the Cu<sup>1+</sup> formed during the reaction aggregates and leads to a loss of Cu active material due to its low melting point and volatility.

## Materials and Methods

*Operando* X-ray absorption spectroscopy (XAS), powder X-ray diffraction (PXRD) and UV-Vis spectroscopy were carried out at the Swiss-Norwegian Beamlines at the European Synchrotron Radiation Facility for a better understanding of catalyst composition during reaction, and the impact of alkaline metal dopants. The goal of this study was to find a strategy to optimize the reaction conditions and catalyst composition to reduce the amount of Cu<sup>1+</sup> in the catalyst during reaction.

*Operando* studies were performed on 5 wt% CuCl<sub>2</sub> on  $\gamma$ -Al<sub>2</sub>O<sub>3</sub> prepared by impregnation for transient and steady-state reaction conditions, as reported by our earlier publications [3-5]. Cu K-edge XAS data was collected to extract Cu<sup>1+</sup> and Cu<sup>2+</sup> fractions. UV-Vis spectra were collected simultaneously with a UV-Vis probe. PXRD

was collected at the beginning and end of transients to detect the different crystalline phases formed *in situ* when doping with alkaline metals. Reaction products were monitored with an on-line mass spectrometer.

## Results and Discussion

The linearly combined near edge XAS data presented in figure 1 shows the evolution of the Cu species present during reduction (I) and oxidation (II) as well as during the oxychlorination reaction of a potassium doped catalyst. The fraction of  $\text{Cu}^{1+}$  and  $\text{Cu}^{2+}$  obtained by UV-Vis spectroscopy was found to be in agreement with the fractions obtained by XAS.

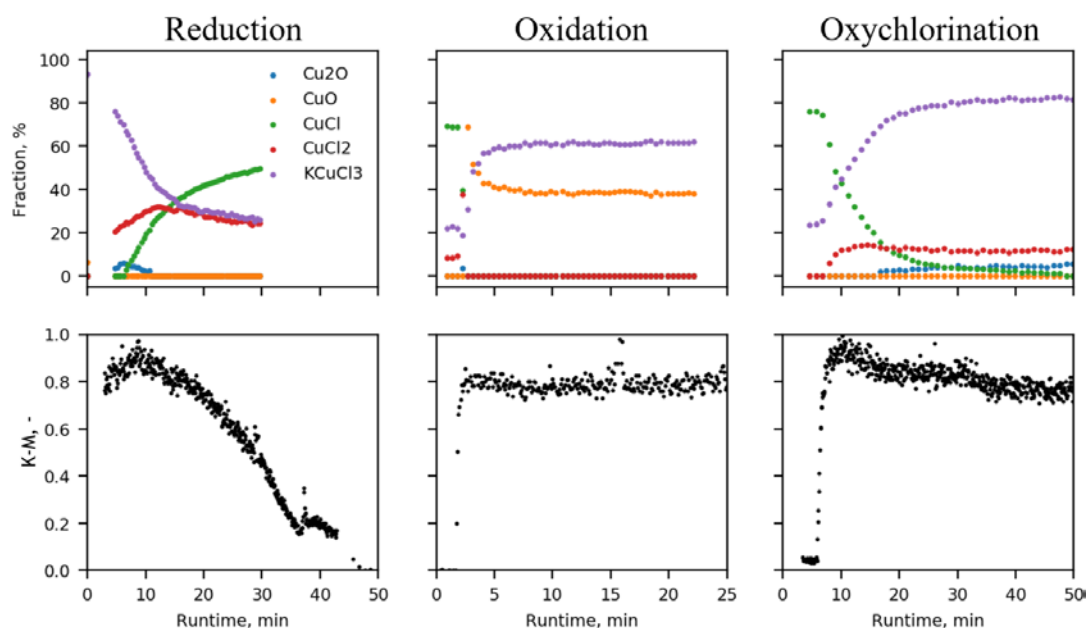


**Figure 1.** Transients of the reduction and oxidation of 0.4 K/Cu mol/mol 5 wt% Cu on  $\gamma\text{-Al}_2\text{O}_3$ , as well as the oxychlorination reaction followed operando by XAS and UV-Vis spectroscopy. Top row: Fraction of the Cu species determined by linear combination fitting of the near edge X-ray absorption spectra. Bottom row: Normalized Kubelka-Munk function of the UV-Vis signal at 796 nm. The fractions obtained via UV-Vis spectroscopy are in agreement with the XAS data.

## References

1. Magistro AJ, Cowfer JA. *J. Chem. Educ.* **1986**,63:1056-1058.
2. Lamberti C, Prestipino C, Bonino F, Capello L, Bordiga S, Spoto G, Zecchina A, Moreno SD, Cremaschi B, Garilli M, Marsella A, Carmello D, Vidotto S, Leofanti G. *Angew. Chem. Int. Ed.* **2002**,41:2341-2344.
3. Rout KR, Fenes E, Baidoo MF, Abdollahi R, Fuglerud T, Chen D. *ACS Catal.* **2016**,6:7030-7039.
4. Rout KR, Baidoo MF, Fenes E, Zhu J, Fuglerud T, Chen D. *J. Catal.* **2017**,352:218-228.
5. Baidoo, MF, Fenes E, Rout KR, Fuglerud T, Chen D. *Catal. Today.* **2018**,299:164-171.

# **Shell-protected core hierarchical zeolite for selective catalysis**

*Kristoffer Hauberg Rasmussen, Technical University of Denmark, Kongens Lyngby, Denmark; Farnoosh Goodarzi, Technical University of Denmark, Kongens Lyngby, Denmark; Jerrik Mielby, Technical University of Denmark, Kongens Lyngby, Denmark; Søren Keghnæs, Technical University of Denmark, Kongens Lyngby, Denmark*

## **Introduction**

Zeolites are extensively used in the chemical industry as both catalytic supports and as catalysts. Encapsulation of metal particles in microporous zeolites provide a shape and size selectivity for the reactions, however, limited diffusion in the microporous channels can result in lower yields and deactivation by coking. Hierarchical zeolites can be used to enhance the diffusion of the molecules which results in higher yields and lower rate of deactivation.<sup>[1-3]</sup> Metals supported in mesopores will benefit from a higher diffusion, however, it may reduce the selectivity of the reactions. Core-shell materials provides a way for introducing the shape selectivity of a microporous shell while still having the metal supported in a mesoporous core.<sup>[4]</sup>

Here, we present a new method for growing a microporous shell around a hierarchical silicalite-1 zeolite containing metals nanoparticles. The effect of the shell was evaluated based on hydrogenation reaction with substrates varying in size.

## **Experimental**

A hierarchical silicalite-1 zeolite was prepared by use of carbon as hard template during steam assisted synthesis conditions. Metal particles were supported on the hierarchical zeolite by incipient wetness impregnation. Finally, a protective silicalite-1 shell was grown around the metal containing hierarchical zeolite.

The materials were characterized using X-ray powder diffraction, N<sub>2</sub> physisorption, X-ray photoelectron spectroscopy, transmission and scanning electron microscopy. To evaluate the effect of the protective shell, the materials were tested in different hydrogenation reactions.

## Results and discussion

The transmission electron microscope image (Figure 1 left) shows a shell formed around a porous metal containing interior. The encapsulation of mesopores inside a microporous shell is also supported by the physisorption isotherms of hierarchical zeolite and hierarchical core zeolite with shell (Figure 1 right).

Catalytic tests show that the microporous shell provide the materials with a selectivity for the molecules that can enter the microporous shell and reach the reactive core.

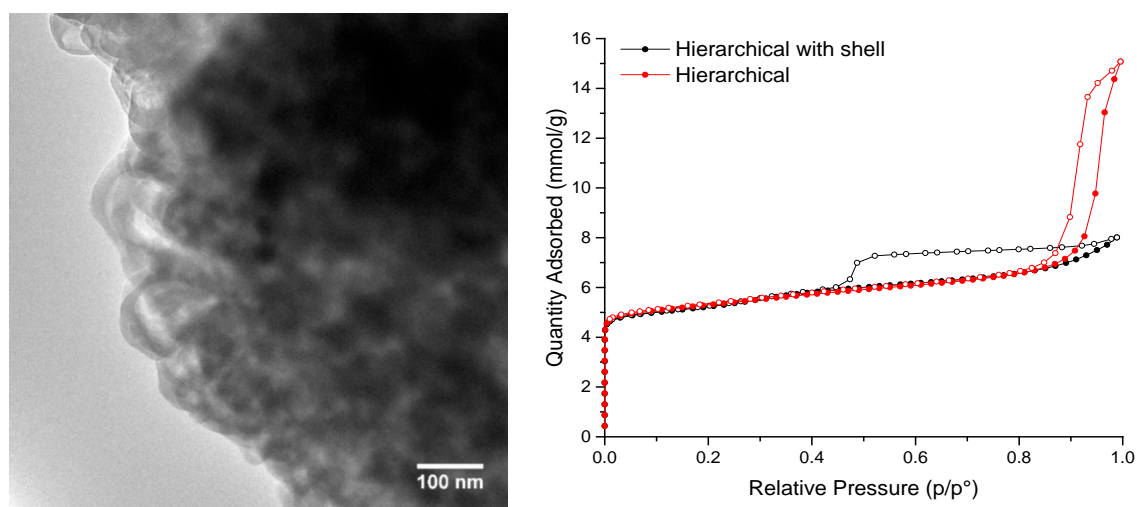


Figure 1: Left: TEM image of hierarchical zeolite with shell, Right: physisorption isotherms of hierarchical zeolite and a hierarchical core zeolite with microporous shell.

## Conclusion

We developed a new method to protect and encapsulate metal particles supported on a hierarchical zeolite with a microporous shell. The shell induced a selectivity for the molecules that could diffuse and react in the catalytically active interior.

## References

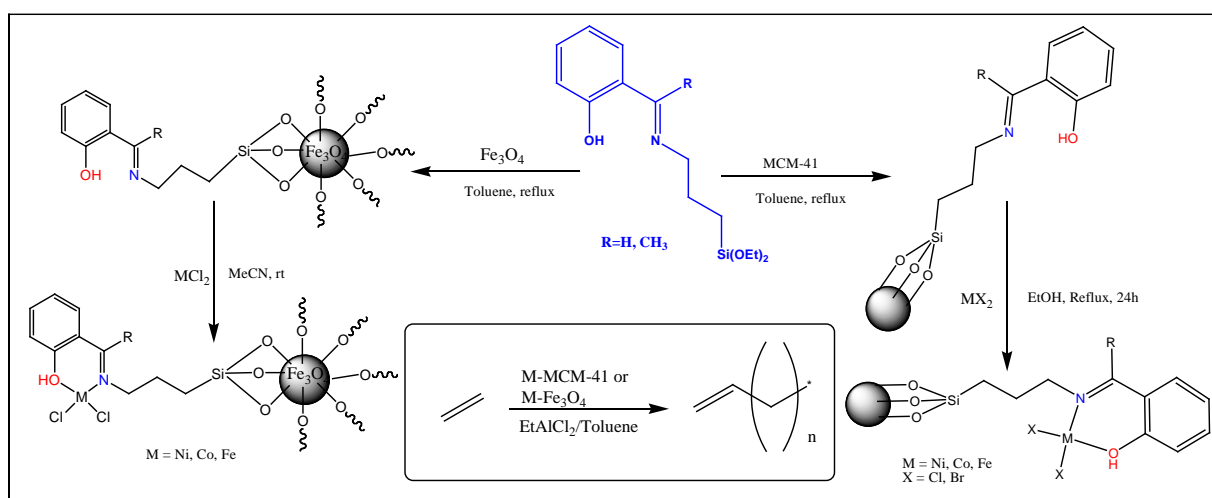
- [1] T. Prasomsri, W. Jiao, S. Z. Weng, J. Garcia Martinez, *Chem. Commun.* **2015**, 51, 8900–8911.
- [2] I. I. Ivanova, E. E. Knyazeva, *Chem. Soc. Rev.* **2013**, 42, 3671–3688.
- [3] J. O. Abildstrøm, M. Kegnæs, G. Hytoft, J. Mielby, S. Kegnæs, *Microporous Mesoporous Mater.* **2016**, 225, 232–237.
- [4] D. Farrusseng, A. Tuel, *New J. Chem.* **2016**, 40, 3933–3949.

# Preparation of immobilized supported N<sup>^</sup>O donor Ni(II), Co(II) and Fe(II) complexes for ethylene oligomerization reactions

Stephen O. Ojwach, Supervisor, Pietermaritzburg, South Africa; Makhosonke Ngcobo, Student, Pietermaritzburg, South Africa

## Catalysis

Homogeneous and heterogeneous catalysts both can efficiently catalyze ethylene oligomerization reactions.[1, 2] However, there are some major drawbacks associated with each of these catalysis processes. Therefore, the aim of this research project is to bridge the lacuna between homogeneous and heterogeneous catalysis by immobilizing the homogeneous catalysts on silica support and iron magnetic nanoparticles in order to develop a separable single-site catalyst.[3, 4] The immobilized complexes have been successfully synthesized using the sequential approach according to Scheme 1. Characterization of the compounds using NMR, infrared spectroscopy, SEM, TEM, EDX, TGA and ICP-OES confirmed the formation, stability, morphology and metal contents of the immobilized pre-catalysts for ethylene oligomerization reactions.



**Scheme 1** Synthesis of MCM-41 and Fe<sub>3</sub>O<sub>4</sub> nanoparticles supported Co(II), Ni(II) and Fe(II) N<sup>^</sup>O donor complexes for ethylene oligomerization reactions.

## References

1. Finiels, A., Fajula, F., Hulea, V., *Catal. Sci. Technol.*, **2014**, *4*: p. 2412-2426.
2. Hajjami, M., Tahmasbi, B., *Rsc. Adv.*, **2015**, *5*: p. 59194-59200.
3. Keypour, H., Saremi, S. G., Noroozi, M., Veisi, H., *Appl. Organometal. Chem.*, **2017**, *31*: p. 1-7.
4. Rezaei, S., Ghorbani-Choghamarani, A., Badri, R., *Appl. Organometal. Chem.*, **2016**, *30*: p. 985-990.

# Mechanochemical method: a key way in the insertion of large cations in the LDH-type structure

*O.D. Pavel<sup>1,\*</sup>, B. Cojocaru<sup>1</sup>, R. Birjega<sup>2</sup>, R. Zăvoianu<sup>1</sup>, V.I. Pârvulescu<sup>1</sup>*

*<sup>1</sup>University of Bucharest, Faculty of Chemistry, Department of Organic Chemistry, Biochemistry and Catalysis, Bucharest, Romania*

*<sup>2</sup>National Institute for Lasers, Plasma and Radiation Physics, Măgurele, Romania*

*\*Tel/fax: (+4) 0214100241, e-mail: [octavian.pavel@chimie.unibuc.ro](mailto:octavian.pavel@chimie.unibuc.ro)*

## Introduction

There is a growing interest focused on the synthesis and properties of layered double hydroxides as part of the anionic clays materials [1]. The main method of preparation of LDH is still the co-precipitation by contacting an aqueous solution of the salts containing the target cations with an alkaline solution [1]. However, it involves some disadvantages as the inability to insert large cations into the octahedral network, multiple synthesis steps, high energy consumption, use of specific vessels in each stage of the process. Accordingly, the mechanochemical method resulted as an alternative to co-precipitation involving only one step mixing in a mortar of all the reactants followed by washing and drying [2]. The aim of this study was to perform a comparative analysis of the physico-chemical properties and catalytic activity of hydrotalcite with La<sup>3+</sup>;Y<sup>3+</sup>-modified hydrotalcites (Mg<sup>2+</sup>/Al<sup>3+</sup>+La<sup>3+</sup>(Y<sup>3+</sup>)=3) prepared by co-precipitation, hydrothermal and mechanochemical routes. These catalysts were investigated in the liquid-phase oxidation of cyclohexene towards the corresponding epoxides.

## Experimental

The hydrotalcite (Mg/Al = 3 molar ratio) was obtained at pH 10 by co-precipitation of nitrates of the corresponding cations and basic solution under low supersaturation [3]. The modified hydrotalcite was prepared by adding La or Y nitrate to the initial nitrate solution. In the mechanochemical method, all metal nitrates were mechanically mixed with Na<sub>2</sub>CO<sub>3</sub> and NaOH in the desired ratio for 1h [4]. For the hydrothermal route the oxides of Mg, Al and La(Y) were placed in an autoclave filled with bi-distilled water and kept at 120 °C for 1,3,5, or 10 days. All samples were washed until neutral pH, dried at 120°C, and calcined in air atmosphere at 460°C.



The resulted mixed oxides were then rehydrated in order to reconstruct the layered structure. The characterisation of samples has been carried out by chemical analysis, XRD, DRIFT, BET, irreversible adsorption of organic acids of different  $pK_a$  values. The cyclohexene oxidation was performed with  $H_2O_2$  in presence of acetonitrile at 60 °C or molecular oxygen in presence of iso-butyraldehyde at room temperature.

## Results and discussion

Hydrothermal synthesis provides the hydrotalcite-type structure confirmed by the corresponding diffraction lines of  $Mg(OH)_2$  (001, 101, 102, 110, 111) and LDH-3R2-polytype phase (014, 017, 01.10, 01.11). Co-precipitation is also confirmed as effective by the XRD typical pattern of Mg,Al-LDH structure (JCPDS card 00-054-1029) incorporating a large amount of  $CO_3^{2-}$  anion than  $OH^-$  in the interlayer space. The insertion of La or Y was not demonstrated. These cations exist in conjunction with Mg-Al hydrotalcite as hydroxides or hydroxycarbonates. Very different, the mechanochemical method allows the formation of the LDH structure via solid-solid reactions occurring in the presence of the hydration water of nitrates. It incorporates more  $OH^-$  groups than  $CO_3^{2-}$  thus providing more basic materials. Only Y ( $Mg^{2+}/Al^{3+} + Y^{3+}=3$  and  $Al^{3+}/Y^{3+}=1$ ) led to an isomorphous substitution of Al from octahedral positions modifying the “a” parameter in the XRD patterns. Mechanochemical method, for hydrotalcite, led to a smaller surface area ( $85\text{ m}^2\cdot\text{g}^{-1}$ ) compared to the co-precipitation route ( $122\text{ m}^2\cdot\text{g}^{-1}$ ). The catalytic tests showed a linear correlation between the yields to cyclohexene-oxide and the population of medium and weak base sites. Mechanochemical route provided hydrotalcites which after calcination generated mixed oxides affording yields of 65% after 5 h ( $H_2O_2$ /acetonitrile/60°C system) compared to 52% for samples produced via co-precipitation. The same behavior resulted for  $O_2$ /isobutyraldehyde yield of 61.5% for mechanochemical route compared to 50.2% for co-precipitation.

**Acknowledgements** This work was supported by a grant of the Romanian Ministry of Research and Innovation, CCCDI – UEFISCDI, project number PN-III-P1-1.2-PCCDI-2017-0387/ 80PCCDI, within PNCDI III and PN-III-P1-1.1-TE-2016-0562 TE10/2018.

## References

- [1] F. Cavani, F. Trifiro, A. Vaccari, *Catal. Today* 11 (1991) 173.
- [2] J. Qu, Q. Zhang, X. Li, X. He, S. Song, *Appl. Clay Sci.* 119 (2016) 185.
- [3] O.D. Pavel, R. Zăvoianu, R. Bîrjega, E. Angelescu, *Catal. Commun.* 12 (2011) 845.
- [4] O.D. Pavel, R. Zăvoianu, R. Bîrjega, E. Angelescu, V.I. Pârvulescu, *Appl. Catal. A*, 542 (2017) 10.

# The catalytic oxidation of benzyl alcohol via the *in-situ* production of H<sub>2</sub>O<sub>2</sub> – exploring Pd non-precious metal catalysts.

Caitlin M. Crombie, Cardiff University, Cardiff, UK; Richard J. Lewis, Cardiff University, Cardiff, UK; Martin Skov Skjøth-Rasmussen, Haldor Topsoe, Kongens Lyngby, Denmark; Graham J. Hutchings, Cardiff University, Cardiff, UK.

## 1. Introduction.

Hydrogen peroxide (H<sub>2</sub>O<sub>2</sub>) is considered a powerful and efficient and green oxidant, due to its high active oxygen content and producing only water as the by-product. [1] The use of H<sub>2</sub>O<sub>2</sub> in the production of fine and commodity chemicals has seen growing interest in recent years with the production of benzaldehyde, an important substrate in the flavor and fragrances sector a pertinent example. However the use of *ex-situ* generated H<sub>2</sub>O<sub>2</sub> has significant drawbacks, including the need for high molar excess for oxidation transformations, its high energy intensive production from the sequential hydrogenation and oxidation of anthraquinone, this also requires the transportation of highly concentrated solutions of H<sub>2</sub>O<sub>2</sub> which does not come without it's risks. It has already been shown that by combining knowledge of AuPd based catalysts which are well known to produce H<sub>2</sub>O<sub>2</sub> directly from H<sub>2</sub> and O<sub>2</sub> with the oxidation reaction can lead to an increase in selectivity towards the aldehyde and acid products under milder conditions. [2]

## 2. Experimental.

1 wt. % XPd (where X is Au, Cu, Fe, Co, Mn and Ce) supported catalysts with X:Pd 1:1 were synthesised following a modified impregnation preparation procedure. [2] Aqueous PdCl<sub>2</sub> (0.58M HCl) and solid chloride X precursor were supported onto TiO<sub>2</sub> before being dried and reduced (500 °C, 4 hrs, 5 % H<sub>2</sub>/Ar). Catalytic activity for the oxidation of benzyl alcohol, via the *in-situ* production of H<sub>2</sub>O<sub>2</sub>, was investigated at 50 °C for 30 minutes in a 50 ml Parr Instruments stainless steel autoclave. Catalyst (0.01g), methanol (7.1 g) and benzyl alcohol (1.04 g, 9.6 mmol) were all added to the reactor before the reactor was filled with a mixture of 5 % H<sub>2</sub>/CO<sub>2</sub> and 25 % O<sub>2</sub>/CO<sub>2</sub>, before heating and reaction commenced. Oxidation products were evaluated and quantified using a Varian 3200 GC.

## 3. Results and Discussion.

Typically the oxidation of benzyl alcohol is carried out with molecular O<sub>2</sub> at 100–120 °C and though high conversions can be observed the addition of H<sub>2</sub> to the reaction

can activate oxygen at lower temperatures and via the production of H<sub>2</sub>O<sub>2</sub> and hydroperoxy radical intermediates. [3] The oxidation of benzyl alcohol is believed to proceed via a radical process involving hydroperoxy intermediate where normally high temperatures are utilised to produce these intermediates. [3] The oxidation of benzyl alcohol via the *in-situ* production of H<sub>2</sub>O<sub>2</sub> has previously been shown with a 5% AuPd/TiO<sub>2</sub> and these have shown to generate H<sub>2</sub>O<sub>2</sub> and its hydroperoxy intermediate, which was believed to aid the oxidation of benzyl alcohol at lower temperatures and potentially higher selectivities. [2] This series of catalysts will explore the use of novel Pd non-precious supported catalysts.

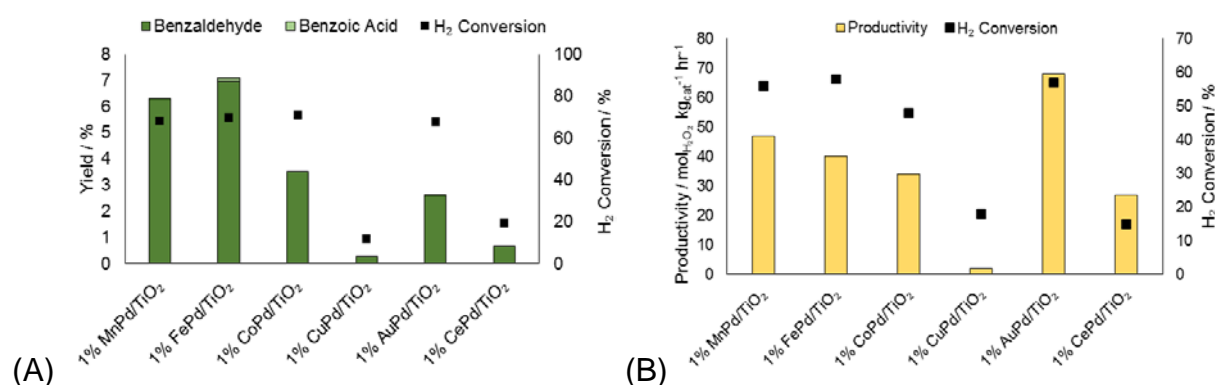


**Figure 1. (A) Catalytic activity of 1 wt. % XPd catalysts towards the oxidation of benzyl alcohol. 0.01 g catalyst, 1.05 g benzyl alcohol, 7.1 g methanol, 29 bar 5 % H<sub>2</sub>/CO<sub>2</sub> and 11 bar 25 % O<sub>2</sub>/CO<sub>2</sub>, 1200 RPM, 50 °C, 30 minutes. (B) Synthesis of H<sub>2</sub>O<sub>2</sub>, 0.01 g catalyst, 2.9 g water, 5.6 g methanol, 29 bar 5 % H<sub>2</sub>/CO<sub>2</sub> and 11 bar 25 % O<sub>2</sub>/CO<sub>2</sub>, 1200 RPM, 30 minutes, room temperature.**

It has been shown that the combination of Pd with low cost non-noble metals such as Mn and Fe can produce higher yields of benzaldehyde compared to the conventional AuPd catalyst. It is postulated that this is due to these catalysts being superior at producing hydroperoxy and hydroxyl radicals *in-situ*.

#### 4. Conclusion.

A combination of base-metal supported catalysts have been synthesised and have been shown to be active for the oxidation of benzyl alcohol, with a high selectivity towards benzaldehyde. The non-noble Pd supported catalysts have proven more active than previously well studied analogous AuPd catalysts.

#### 5. References.

- [1] C. Samanta, *Appl Catal A: Gen*, **2008**, 350, 133–149.
- [2] M. Santonastaso *et al.*, *Org. Process Res. Dev.*, **2014**, 18, 1455–1460.
- [3] D. I. Enache *et al.*, *Science*, **2006**, 311, 362.

# New Chemoenzymatic Reaction Sequence for the Fatty Alcohol Synthesis

*K. E. Schlipkötter<sup>1</sup>, T. Betke<sup>2</sup>, J. Kleber<sup>1</sup>, A. Stöbener<sup>1</sup>, H. Gröger<sup>2</sup>, A. Liese<sup>1</sup>*

<sup>1</sup>*Institute of Technical Biocatalysis, Hamburg University of Technology, Germany*

<sup>2</sup>*Chair of Organic Chemistry 1, Bielefeld University, Germany*

Fatty alcohols are important intermediates in the cosmetic industry for the production of emulsifiers and surfactants. They can be obtained out of petrochemical or renewable raw materials. In 2005, the production capacity was estimated to be 2.5 million t/a [1]. One of the currently applied industrial processes to produce fatty alcohols requires high temperatures and pressures about 100 bar as well as long reaction times [2]. Our aim is the significant reduction of the energy input in terms of temperature and pressure by using a combination of heterogeneous biocatalysts with

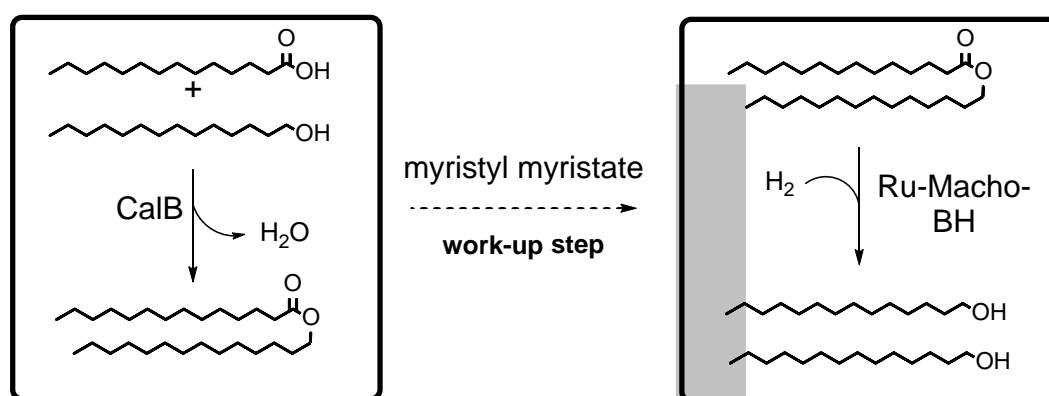


**Figure 1: Reaction sequence of a biocatalyzed esterification by lipase B of *Candida antarctica* (CalB) and a chemocatalyzed hydrogenation by Ru-Macho-BH for the synthesis of myristyl alcohol**

homogeneous chemocatalysts.

This two-step reaction sequence (Figure 1) focusses on the conversion of fatty acids to the corresponding fatty alcohols. We chose myristic acid for our investigations.

Esterification as first step is catalyzed by immobilized lipase B from *Candida antarctica* (CalB) in a bubble column reactor, which was successfully implemented at industrial scale [3, 4]. This reactor type demonstrates two major advantages: firstly, the removal of formed reaction water, secondly, the low energy input by bubble aeration to agitate sensitively the reaction medium. The second step is the

hydrogenation of myristyl myristate using homogeneously soluble chemocatalyst (Ru-Macho-BH) in an autoclave.

For continuous operation, both reaction steps get connected via simple filtration to separate the CalB particles.

In the case of the solvent-free esterification, we investigated the kinetics for different substrate ratios of myristyl alcohol to myristic acid as well as for the temperature range of 60 up to 90 °C. This analysis revealed a decreasing reaction rate with increasing myristyl alcohol mass fraction and a temperature optimum of 75 °C. Due to the acid sensitivity of the chemocatalyst Ru-Macho-BH, full conversion of the acid in the first step is required to realize a direct connection between both steps without additional downstream processes besides filtration. Consequently, a slight excess of the alcohol should be favoured to convert all myristic acid in the esterification step.

In the case of the hydrogenation step, we investigated the pressure dependency and a possible recycling method for the chemocatalyst. Complete conversion of myristyl myristate was achieved in 18 hours at a hydrogen pressure of 30 bar. To achieve solvent-free conditions in the hydrogenation, a specific amount of myristyl alcohol has to be added to solve the homogeneous Ru-Macho-BH in the substrate myristyl myristate, enabling a simple downstream processing.

In summary, a convenient new method for the synthesis of fatty alcohols in comparison to currently applied industrial processes is demonstrated, utilizing a two-step sequential chemoenzymatic reaction sequence at low pressure, temperature and short reaction time.

## References

- [1] K. Noweck, W. Grafahrend, Fatty alcohols, Ullmann's Encyclopedia of Industrial Chemistry, Wiley-VCH Verlag GmbH & Co. KGaA, Weinheim, **2012**
- [2] M.A. Sánchez, G. C. Torres, V.A. Mazzieri, C. L. Pieck, J. Chem. Technol. Biotechnol. **2017**, 92, 27.
- [3] J. Müller, M. Neumann, P. Scholl, L. Hilterhaus, M. Eckstein, O. Thum, A. Liese, Anal. Chem. **2010**, 82, 6008.
- [4] L. Hilterhaus, O. Thum, A. Liese, Org. Proc. Res. Dev. **2008**, 12, 618.

# Supported Liquid Phase Catalysts for Oxidative Dehydrogenation of Propane

**Ezgi Erdem<sup>a,b,\*</sup>, Pierre Kube<sup>b</sup>, Andrey Tarasov<sup>b</sup>, Frank Rosowski,<sup>a,c</sup> Robert Schlögl,<sup>a,b</sup> Annette Trunschke<sup>b,\*</sup>**

<sup>a</sup>*BasCat - UniCat BASF Joint Lab, Technische Universität Berlin, Germany.*

<sup>b</sup>*Department of Inorganic Chemistry, Fritz-Haber-Institut der Max-Planck-Gesellschaft, Berlin, Germany.*

<sup>c</sup>*Process Research and Chemical Engineering, Process Catalysis Research, BASF SE, Ludwigshafen, Germany.*

*\*Corresponding authors: erdem@fhi-berlin.mpg.de and trunschke@fhi-berlin.mpg.de*

## Introduction

Introducing additives to supported vanadia catalysts has been intensively studied with the aim to improve the catalyst performance in oxidative dehydrogenation of propane (ODP).<sup>[1-3]</sup> Alkali metal additives such as Li-, K-, and Rb- on supported V<sub>2</sub>O<sub>5</sub> decrease the activity while increases the selectivity to propylene due to modification of the redox and acid-base properties.<sup>[1-4]</sup> Possibly formed alkali vanadates (for example K<sub>3</sub>V<sub>5</sub>O<sub>14</sub>) have melting points that range from ~ 390°C to ~ 510°C, which are in the reaction temperature range for ODP. The objective of the present work is the investigation of the effect of liquefaction on the propane oxidation kinetics by measuring the catalyst performance for three different alkali (A: K, Cs, and Rb) added to V<sub>2</sub>O<sub>5</sub>/SiO<sub>2</sub> with different ratios of A:V.

## Experimental

A physical mixture of alkali carbonates (K<sub>2</sub>CO<sub>3</sub>, Cs<sub>2</sub>CO<sub>3</sub> and Rb<sub>2</sub>CO<sub>3</sub>) and V<sub>2</sub>O<sub>5</sub> (10 wt.% as total of alkali carbonates and V<sub>2</sub>O<sub>5</sub>) have been deposited on SiO<sub>2</sub> (Aerosil 300) and calcined at 620°C for 16 hours in air. Physical and chemical properties of the materials have been analyzed using DSC, XRF, BET and XRD. The samples have been tested in the ODP reaction in a 1:1 feed of propane and oxygen (i.e. C<sub>3</sub>H<sub>8</sub>:O<sub>2</sub>:N<sub>2</sub>= 7.5/7.5/85 vol.%) in an 8-fold parallel reactor set-up and an operando-DSC.

## Results and Discussions

By varying the composition of alkali in between 20-40 mole %, supported alkali vanadate phases were successfully synthesized. For K-added V<sub>2</sub>O<sub>5</sub>/SiO<sub>2</sub> samples,

different alkali vanadates are formed at the surface of the support such as  $K_3V_5O_{14}$ ,  $K_2V_6O_{16} \cdot 1.5H_2O$  and mixtures of both phases. The sample with a 37 mole% of K-loading was found as phase pure  $K_3V_5O_{14}$  which melts at  $410^\circ C$ . On the other hand, in case of Cs addition,  $CsV_2O_5$  was the only crystalline phase detected in all samples. Specifically for the 28 mole %-loaded Cs-sample, melting in the range  $430 - 446^\circ C$  was observed. Similarity with K, Rb addition leads to formation of the mixtures of  $Rb_2V_4O_{11}$  and  $Rb_3V_5O_{14}$  phases whose melting points are in between  $390-438^\circ C$ . Both, catalytic test in a fixed bed reactor as well as operando DSC reveal that activity drastically decreases when reaching the melting point (Fig.1). In case of the K- and Rb-containing catalyst, the selectivity is rapidly increased after melting, which is not the case for the Cs-containing catalysts perhaps due to the broad temperature range of melting. At higher temperatures the selectivity of the two catalysts approaches similar values. Changes in specific surface area or loss of oxygen can be excluded as reason for the drop in activity. The results will be discussed based on spectroscopic investigation of the materials and comparison with Li- and Na-catalysts.

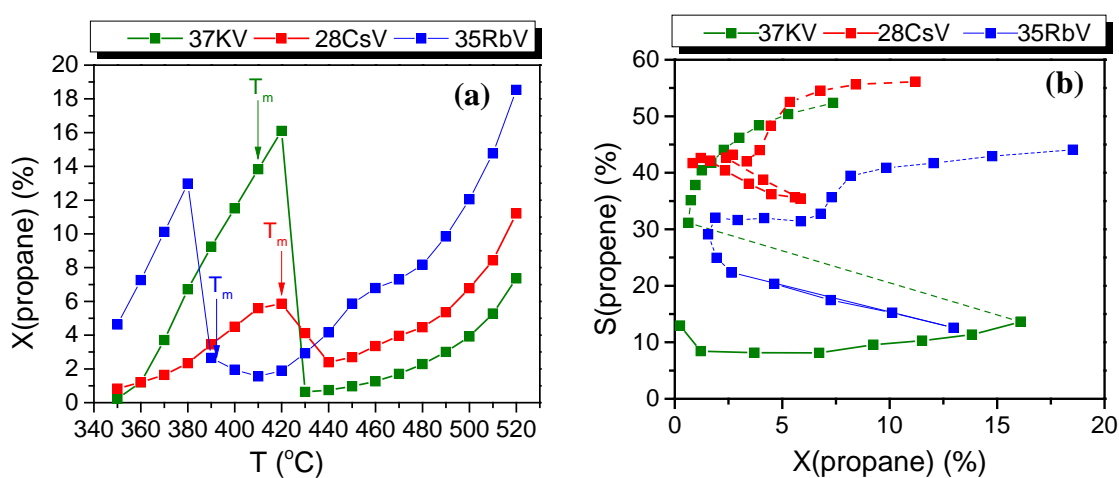


Fig 1. (a) Conversion of propane in the oxidative dehydrogenation of propane with increasing temperature, and; (b) propylene selectivity as a function of propane conversion ( $T = 350-520^\circ C$ ;  $C_3H_8/O_2/N_2 = 7.5/7.5/85$  vol.%;  $W/F (K) = 1.8$  g s ml<sup>-1</sup>;  $W/F (Cs) = 0.67$  g s ml<sup>-1</sup>;  $W/F (Rb) = 1.8$  g s ml<sup>-1</sup>)

1)

## References

- [1] G. G. Cortez, J. L. G. Fierro, M. A. Banares, *Catalysis Today* **2003**, *78*, 219-228.
- [2] D. Courcot, A. Ponchel, B. Grzybowska, Y. Barboux, M. Rigole, M. Guelton, J. P. Bonnelle, *Catalysis Today* **1997**, *33*, 109-118.
- [3] A. A. Lemonidou, L. Nalbandian, I. A. Vasalos, *Catalysis Today* **2000**, *61*, 333-341.
- [4] R. Grabowski, B. Grzybowska, K. Samson, J. Słoczyński, J. Stoch, K. Wcisło, *Applied Catalysis A: General* **1995**, *125*, 129-144.

## Selective Oxidation: Kinetic Investigations under Reaction Conditions using a Lab-Scale Profile Reactor

*Rhea Christodoulou<sup>a</sup>, Michael Geske<sup>a</sup>,  
Raimund Horn<sup>c</sup> and Frank Rosowski<sup>a,d</sup>*

<sup>a</sup> *BasCat, UniCat BASF JointLab, Technische Universität Berlin,  
Hardenbergstraße 36, 10623 Berlin, Germany*

<sup>c</sup> *Institute of Chemical Reaction Engineering, Hamburg University of Technology,  
Eißendorfer Str. 38, D-21073 Hamburg, Germany*

<sup>d</sup> *BASF SE, Chemicals Research and Engineering  
Carl-Bosch-Straße 38, D-67056 Ludwigshafen, Germany*

In-situ studies are irreplaceable to gain a deep understanding of a catalytic process. Fix-bed reactors are particularly relevant because of their wide use in industrial applications. A powerful in-situ set-up should provide various methods for analysing simultaneously state of catalyst, temperature and gas phase composition. Especially, tracking of intermediates along catalytic bed would help to study chemical reaction networks in detail. Traditional tube measurements accomplish this with the measurements of different catalyst masses at constant gas flow or increasing gas velocity. Drawbacks of these measurements are the high time and catalyst material consumption (8 points – 8 reactors) or changed reaction conditions. [1;2;3].

One main challenge is the correct analysis in the very low product concentration regime, caused by low conversions of already low reactant concentrations in the feed. Those conditions are essential in order to stay close to industrial conditions and to respect explosion limits. With Profile Reactors for spatially resolved high-resolution profiles of species we are able to study kinetics in an alternative way. With one profile many kinetic data are available without changing temperature or gas velocity. Those big data sets can be used to verify or to feed kinetic simulations. [4] The size of the reactor was chosen to fit to typical amounts from lab scale catalyst synthesis, normally < 1g. The lab scale profile reactor consists of a quartz tube with an inner diameter of 4 mm. The chosen catalyst bed length is 40 mm.

Focus of this study is the selective oxidation of *n*-butane to maleic anhydride (MAN) over vanadyl pyrophosphate (VPP). First kinetic results of oxidation of *n*-butane to maleic anhydride measured by GC are shown at Fig. 1. Implementing a methanizer in GC improved detection limits of CO<sub>2</sub> and CO below 5 ppm and product formation under 0.02 vol.-% are visible. Furthermore, temperature profile shows a nearly isothermal behavior ( $\Delta T < 2$  K) within catalytic bed.



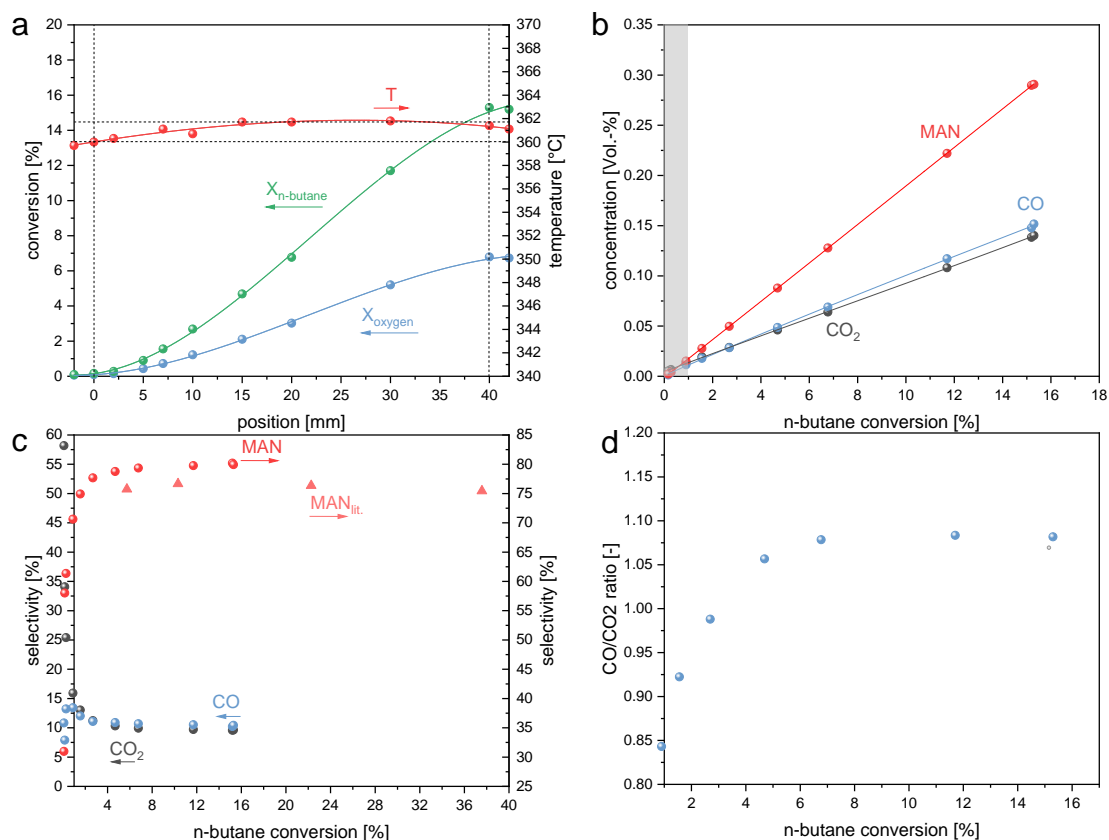


**Figure 1:** Selective oxidation of *n*-butane at GHSV: 2000 1/h, oxygen/*n*-butane/water/helium: 20/2.4/3/74.6 vol.-%,  $T_{\text{heating block}}$ : 366 °C. **a:** Conversion of reactants and temperature over length of catalytic bed. **b:** Concentrations of main products as function of *n*-butane conversion. **c:** Comparison between Selectivities of main products as function of *n*-butane conversion and MAN selectivity of conventional kinetic studies [5] (isothermes of 360 °C at 2000, 4000, 8000, and 16000 h<sup>-1</sup>) of selective oxidation of *n*-butane over VPP. **d:** CO to CO<sub>2</sub> ratio as a function of *n*-butane conversion.

At a *n*-butane conversion between 6 % and 17 % selectivities remain on a constant level. At lower conversion (1-6 %) MAN selectivity decreases by 10 %. Comparing to previous work in parallel reactors [5] the unknown selectivity gap at conversions under 6 % could be successfully closed. Below a *n*-butane conversion of 1 % concentration of products are very close and low that a valid selectivity statement is not possible. Lower selectivities of MAN at low *n*-butane conversion could be caused by initially higher MAN consumption rate or by an initially formation of MAN intermediates. In addition, a decrease of MAN selectivity goes along with a decrease of CO/CO<sub>2</sub> ratio.

#### References

- [1] Alfred Hagemeyer, Peter Strasser and Anthony F. Volpe, Jr., Wiley-VCH, High-Throughput Screening in Chemical Catalysis: Technologies, Strategies and Applications, 2006.
- [2] Ib Chorkendorff and J. W. Niemantsverdriet. Concepts of modern catalysis and kinetics. Wiley-VCH, Weinheim, 2., rev. and enl. ed. edition (2007).
- [3] M.V. Sargent, F.M. Dean, in: A.R. Katritzky, C.W. Rees (Eds.), Comprehensive Heterocyclic Chemistry, Pergamon Press, Oxford, 1977, p. 599.
- [4] Ying Dong, Michael Geske, Oliver Korup, Nils Ellenfeld, Frank Rosowski, Cornelia Dobner, Raimund Horn Chemical Engineering Journal. ISSN: 1385-8947, Vol: 350, Page: 799-811 (2018).
- [5] Christian Schulz, Felix Pohl, Matthias Driess, Robert Glaum, Frank Rosowski, and Benjamin Frank, Industrial & Engineering Chemistry Research, Article ASAP, (2018)

## Methane to Chloromethane by Mechanochemical Activation

*Marius Bilke, Pit Losch, Olena Vozniuk, Alexander Bodach and Ferdi Schüth*  
*Max-Planck-Institut für Kohlenforschung, Mülheim an der Ruhr, Germany*

Chloromethane ( $\text{CH}_3\text{Cl}$ ) is an important intermediate for a large variety of bulk chemicals. [1] Existing methods for direct chlorination of methane suffer from low product selectivities and harsh operating conditions. These rely on the use of corrosive reagents and typically yield multiply chlorinated products. [2]

This study describes an alternative strategy to mechanochemically convert methane into chloromethane at overall mild conditions. Trichloroisocyanuric acid (TCCA), a commonly used disinfecting and bleaching agent, is considered as a cheap, non-toxic and non-corrosive solid chlorinating agent. [3] Besides being a safe chlorinating compound it exhibits an exceptionally high active chlorine content of 46 wt.% (comparable to  $\text{Cl}_2$  (g) with 50 wt.%). This molecule is stable under ambient conditions and thermally decomposes only above 200 °C. For these reasons we chose TCCA as a chlorine source for this work. Our idea was to use TCCA at low temperatures, releasing active chlorine species upon milling to functionalize methane (**Figure 1**).

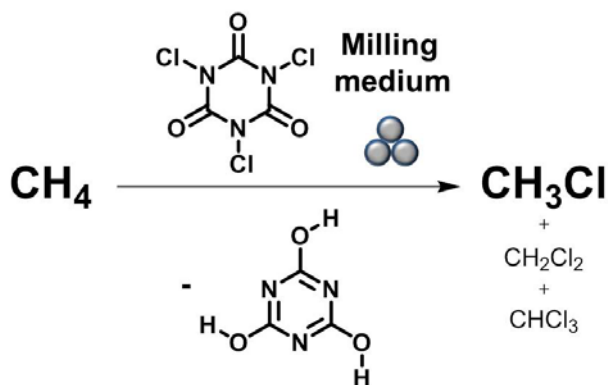


**Figure 1.** Conceptual scheme for mechanochemical chlorination of methane.

We adapted an available ball milling set up that has been designed in our group for the use in gas flow reactions. [4] Screening different materials unveiled a strong structure-activity relationship (**Figure 2**). Basic  $\text{MgO}$  was compared to redox active  $\text{Fe}_2\text{O}_3$ , weakly acidic  $\text{SiO}_2$ , Brønsted acidic zeolite H-USY (Si/Al = 6), non-reducible ( $\gamma\text{-Al}_2\text{O}_3$ ), and reducible Lewis acids ( $\text{TiO}_2$  and  $\text{CeO}_2$ ) and to the milling jar material

WC. **Figure 2A** shows the respective reaction rates in  $\mu\text{mol}(\text{CH}_4_{\text{conv}})\cdot(\text{g}\cdot\text{s})^{-1}$  over a reaction of 40 minutes. The Lewis acidic materials result as the most promising for the given transformation.

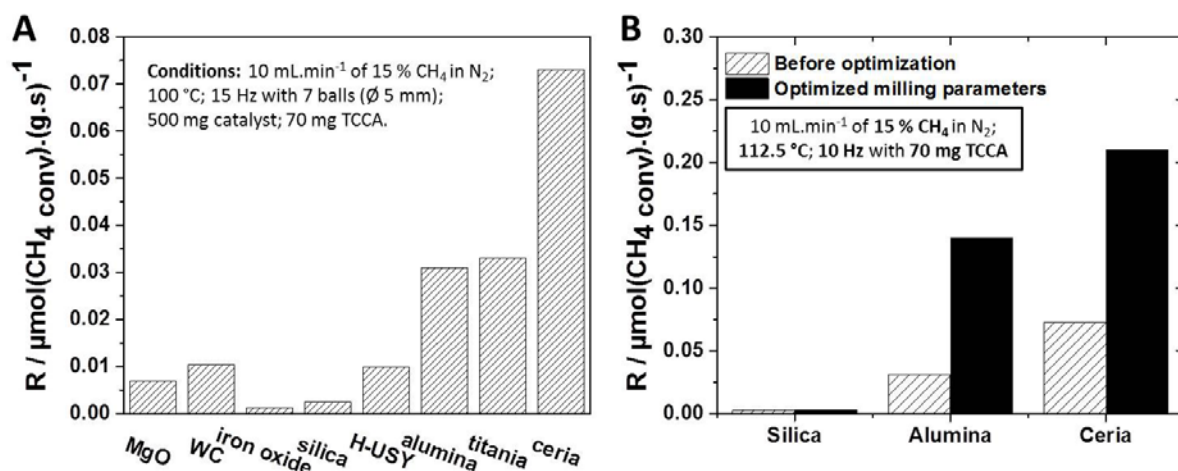


**Figure 2.** A) Reaction rate (R) integrated over 40 min for different materials under identical milling conditions. In all the reactions only  $\text{CH}_3\text{Cl}$  was detected. B) Reaction rates for three different materials after multi-parametric optimization.

The benefit of our setup is the possibility to screen catalytically relevant parameters in a systematic manner. Temperature (from RT to 150 °C), contact time (i.e. composition and rate of gas flow) and the transfer of kinetic energy or momentum (by varying the shaking frequency) were studied. Thereby a thorough milling parameter optimization could be performed. As a result of this optimization the loading of the chlorinating agent as well as the shaking frequency emerged as key parameters. **Figure 2B** displays reaction rates for ceria, alumina and silica before and after the optimization. The reaction rates for ceria and alumina were increased by a factor of 3-4. In contrast, silica still showed no detectable activity. Intriguingly, we reached a maximum methane chlorination rate of  $0.8 \mu\text{mol}(\text{CH}_4_{\text{conv}})\cdot(\text{g}\cdot\text{s})^{-1}$ , which is comparable to state-of-the-art chlorination processes. [1]

## References

- [1] Zichittella, G.; Paunović, V.; Amrute, A. P.; Pérez-Ramírez, J., *ACS Catalysis* **2017**, 7, 1805-1817.
- [2] Rossberg, M.; Lendle, W.; Pfeleiderer, G.; Tögel, A.; Torkelson, T. R.; Beutel, K. K. (2011). Chloromethanes. In *Ullmann's Encyclopedia of Industrial Chemistry*, (Ed.).
- [3] a) Ziegler, K.; Spath, A.; Schaaf, E.; Schumann, W.; Winkelmann, E., *Anal. Chem.* **1942**, 551, 80. b) Tilstam, U.; Weinmann, H., *Organic Process Research & Development* **2002**, 6, 384-393.
- [4] a) Immohr, S.; Felderhoff, M.; Weidenthaler, C.; Schüth, F. *Angewandte Chemie International Edition* **2013**, 52, 12688-12691; b) Eckert, R.; Felderhoff, M.; Schüth, F. *Angewandte Chemie International Edition* **2017**, 56, 2445-2448; c) Schreyer, H.; Immohr, S.; Schüth, F. *Journal of Materials Science* **2017**, 52, 12021-12030.

# Sol-gel auto-combustion synthesis of Fe modified $\text{MgAl}_2\text{O}_4$ for oxidative dehydrogenation of *n*-octane with $\text{CO}_2$

DS Adam, MD Farahani, AS Mahomed, MD Bala and HB Friedrich

Email: 217081346@stu.ukzn.ac.za

School of Chemistry and Physics, University of KwaZulu-Natal, Westville,  
Durban 4000, South Africa

## **Abstract**

The ease of oxygen vacancy formation is often used as a primary descriptor for the catalytic activity of metal oxides in oxidation processes taking place by the Mars and van Krevelen mechanism. We, therefore, hypothesized that doping  $\text{MgAl}_2\text{O}_4$  with Fe will create a disturbance in the spinel lattice, increase lattice oxygen mobility and lower the energy requirement for surface oxygen vacancy formation, thereby increasing the rate of *n*-octane and  $\text{CO}_2$  conversion.

Here in we report a low cost self-sustaining synthesis of four (4) Fe modified  $\text{MgAl}_2\text{O}_4$  nano-catalysts with nominal composition  $\text{MgFe}_x\text{Al}_{2-x}\text{O}_4$  ( $x = 0, 0.02, 0.04$  and  $0.06$ ) represented as SP-Fe(0), SP-Fe(2), SP-Fe(4) and SP-Fe(6) respectively. In each case, aqueous solutions of appropriate amounts of the corresponding metal nitrates and urea were mixed, gelled and combusted at 673K, and calcined at 1073K under the flow of air. The catalysts were characterized using PXRD, FT-IR, BET, SEM & SEM-EDX, TEM, elemental mapping (HR-TEM) and ICP-OES. The PXRD results showed only spinel peaks (at  $2\theta = 18.95^\circ, 31.21^\circ, 36.78^\circ, 44.73^\circ, 59.26^\circ, 65.14^\circ$  and  $82.49^\circ$ ) with no phase contamination, while the FT-IR spectra of the materials showed two distinct peaks at around 675 and  $495\text{ cm}^{-1}$  attributed to tetrahedral Mg-O and octahedral  $\text{AlO}_6$  or  $(\text{FeAl})\text{O}_6$  stretching vibrations respectively. These observations indicated the formation of the normal spinel. BET surface area of the materials were in the range of  $60 \pm 6\text{ m}^2/\text{g}$  with pore diameters in the mesoporous range (4.4 - 4.9 nm). SEM images showed particles with sheet-like morphology that are stacked together in layered form while SEM-EDX results qualitatively indicated the incorporation of Fe into the spinel. This observation was quantitatively confirmed by ICP-OES. TEM images showed particles of different sizes owing to agglomeration resulting from high temperature treatment. The average particle sizes obtained from XRD using the Scherrer equation fell in the range 4.0- 7.0 nm. HR-TEM elemental

mapping of the materials, however, showed that Fe is poorly dispersed with some clustering/ aggregation at higher Fe loading. To further confirm the incorporation of Fe into the spinel lattice, Mossbauer spectroscopy and X-ray photoelectron luminescence (XPS) studies were carried out. H<sub>2</sub>-TPR and CO<sub>2</sub>-TPD results revealed the effect of Fe doping on the redox and acid-base properties of the materials respectively. These catalysts were tested for CO<sub>2</sub>-ODH of *n*-octane in a continuous flow fixed bed reactor at temperatures between 723 and 823 K. The catalytic results, including the mechanism of action of the catalysts, as well as effect of temperature and GHSV on CO<sub>2</sub> conversion and olefin selectivity will be presented and discussed at the conference.

**Table 1:** Chemical composition and texture parameters of SP-Fe(x) nanocatalysts

Catalyst	Fe (wt%) <sup>a</sup>	S <sub>BET</sub> (m <sup>2</sup> g <sup>-1</sup> ) <sup>b</sup>	V <sub>p</sub> (cm <sup>3</sup> g <sup>-1</sup> ) <sup>c</sup>	D <sub>p</sub> (nm) <sup>d</sup>	D (nm) <sup>e</sup>
SP-Fe(0)	-	62	0.09	4.4	5.82
SP-Fe(2)	1.67	64	0.09	4.5	5.79
SP-Fe(4)	4.2	66	0.09	4.9	5.12
SP-Fe(6)	5.82	55	0.08	4.7	6.71

<sup>a</sup> Weight percentage of Fe obtained from ICP-OES analysis

<sup>b</sup> Specific surface area calculated by applying the BET method

<sup>c</sup> Total pore volume (BJH desorption method)

<sup>d</sup> Average pore diameter calculated from the BJH method

<sup>e</sup> Average crystallite size calculated from XRD data (Debye Scherrer method)

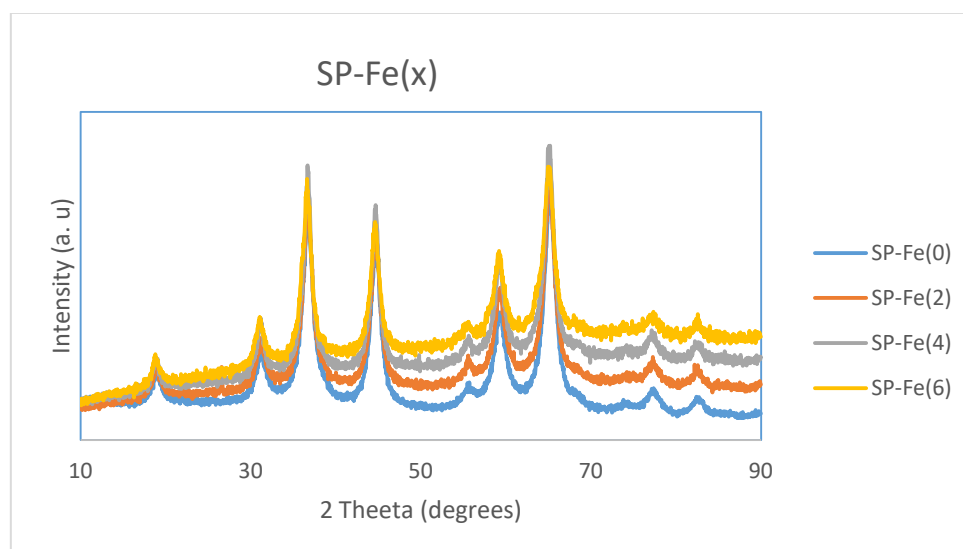


**Figure 1:** Powder XRD spectra of SP-Fe(x) nanocatalysts

# Acetaldehyde from ethanol over copper on self-supported ordered mesoporous zirconia

Özgül Aqbaba Sener, Wolfgang Schmidt, Ferdi Schüth

Max-Planck-Institut für Kohlenforschung, Mülheim an der Ruhr, Germany

Acetaldehyde is a very important bulk chemical which is widely used as precursor for the synthesis of acetic acid, acetic anhydride, ethyl acetate and many more largely produced chemicals with a worldwide production exceeding 1 million tons/year [1-3]. As a green chemistry alternative to the petroleum-based Wacker process, acetaldehyde can also be produced from bio-based ethanol via two routes, either by oxidative or non-oxidative dehydrogenation of ethanol [2-3]. Only few studies have been reported on the non-oxidative dehydrogenation of ethanol to acetaldehyde so far, and in those Cu-based catalysts were successfully used. However, acetaldehyde selectivity was typically limited due to the formation of side products, such as ethyl acetate, 1-butanol and 2-butanone, as well as short life-time of the catalyst caused mostly by the agglomeration of copper nanoparticles.

Our previous studies have shown that copper particles have a good interaction with nanostructured zirconia supports which reduces the agglomeration tendency of copper on the surface of the support material [4]. More specifically, zirconia nanotube arrays prepared from a hard template, such as SBA-15, could be an excellent support for the impregnation of copper particles. For this purpose self-supported ordered mesoporous zirconia was synthesized via hard templating using SBA-15 and KIT-6. After removing the templates, these materials were used as support and Cu was impregnated on them. Furthermore, for comparison, commercial zirconia with two different structures was also used as support materials.

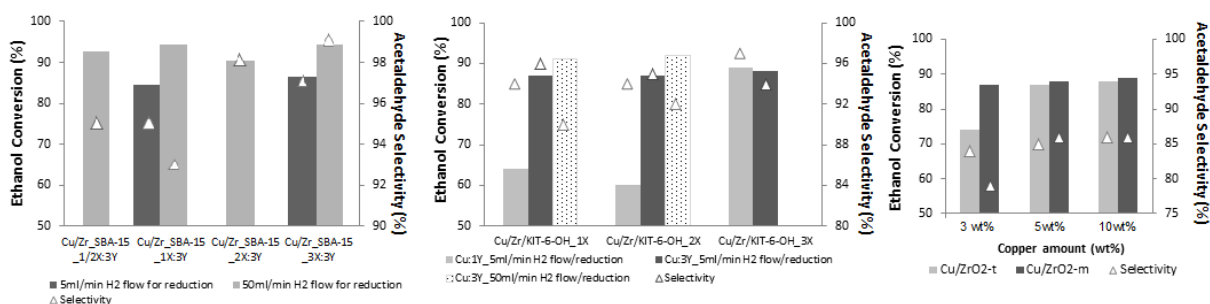


**Figure 1:** Ethanol conversion and acetaldehyde selectivity for *Left:* different Zr loadings (keeping the Cu amounts similar) on catalysts templated from SBA-15-OH; *Middle:* different Zr loadings (varying Cu amounts) on catalysts templated from KIT-6-OH; *Right:* catalysts supported on commercial zirconia with different copper loadings.

The performance of the catalysts was evaluated in a continuous flow, fixed-bed tubular reactor at 250 °C and atmospheric pressure. Regardless of the amount of zirconium, all catalysts showed very high conversions (90-94%) and acetaldehyde selectivities (93-99%). Overall, catalysts comprising of Cu supported on nanostructured self-supported zirconia revealed superior conversion and selectivity to catalysts obtained by impregnating Cu on commercial zirconia supports as well as to catalysts reported in literature for non-oxidative dehydrogenation of ethanol so far. Furthermore, the reaction temperature can be kept lower than usual. This study allows the development of new methods for the precise design of composite supports with multi-interfaces, adjusted surface structure, and enhanced dispersibility as well as stability of active nanoparticles.

### References

- [1] Rass-Hansen, J.; Falsig, H. Jorgensen, B.; Christensen, C. H., Bioethanol: fuel or feedstock? *Journal of Chemical Technology and Biotechnology*, 2007, 82(4): p. 329-333.
- [2] Caro, C.; Thirunavukkarasu, K.; Anilkumar, M.; Shiju, N. R.; Rothenberg, G., Selective Autooxidation of Ethanol over Titania-Supported Molybdenum Oxide Catalysts: Structure and Reactivity. *Advanced Synthesis and Catalysis* 2012, 354 (7): p.1327-1336.
- [3] Marc Eckert, G.F., Reinhard Jira, Hermann M. Bolt, Klaus Golka, Acetaldehyde, in *Ullmann's Encyclopedia of Industrial Chemistry*. 2007, Wiley-VCH: Weinheim.
- [4] Gu, D. Schmidt, W.; Pichler, C. M.; Bongard, H. J.; Spliethoff, B.; Asahina, S.; Cao, Z. W.; Terasaki, O.; Schuth, F., Surface-Casting Synthesis of Mesoporous Zirconia with a CMK-5-Like Structure and High Surface Area. *Angewandte Chemie-International Edition*, 2017. 56(37): p. 11222-11225.

# Catalytic Gas-Phase Cyclization of alpha-hydroxy Esters: A Novel process Toward PLA and Glycolide-Based Bioplastics

*De Clercq Rik, Makshina Ekaterina, Sels Bert, Dusselier Michiel*

*Centre for Surface Chemistry and Catalysis, KU Leuven, Leuven, Belgium*

## Abstract

A catalytic method to obtain cyclic di-lactones from alpha-hydroxy esters in the gas phase based on Ti-catalysis is presented. One such prominent di-lactone, lactide, is the cyclic dimer of lactic acid, a key monomer for the production of bioplastic PLA (polylactic acid). The novel catalytic process is based on the gas-phase transesterification of alkyl lactates over TiO<sub>2</sub>/SiO<sub>2</sub> catalysts. These provide an excellent selectivity to lactide of up to 90%. Furthermore, the process is also amenable to produce glycolide, the cyclic monomer for polyglycolic acid, given some kinetic and thermodynamic considerations. Structure-activity relations for Ti-Si oxides in this process were unearthed. [1, 2 and 3].

## Experimental

Catalytic reactions with methyl glycolate and methyl lactate were performed in a custom-built plug-flow fixed-bed reactor equipped with 6 parallel quartz reactors. Feed solutions typically consisted of 95 vol%  $\alpha$ -hydroxy ester and 5 vol% o-xylene (non-interfering internal standard, similar boiling point). The solution was fed to an evaporation chamber and mixed there with a N<sub>2</sub> flow (typically 20 ml min<sup>-1</sup>) yielding a molar composition of 5.6/0.2/94.2 of the gas mixture ( $\alpha$ -hydroxy ester/o-xylene/N<sub>2</sub>). Changes in molar composition of the vapor fraction (e.g. higher concentration of esters) were realized by simultaneously changing the feed mixture and N<sub>2</sub> to ensure the same total molar amount of gas was used. The diluted feed gas was then passed to the reactor (220-300°C) and over the catalyst bed, prior to online GC analysis. Supported TiO<sub>2</sub>/SiO<sub>2</sub> catalysts (5 and 0.4 wt% TiO<sub>2</sub> loading) were prepared by incipient wetness impregnation of an amorphous, large-pore SiO<sub>2</sub>-gel with a suitable amount of Ti-isopropoxide dissolved in 2-propanol. Experimental details are found in ref [1, 2 and 3].

## Results and conclusion

Lactide and glycolide are the key building block of the biodegradable plastics polylactic acid and polyglycolic acid. Instead of the current industrial two-step route, which involves the polycondensation of GA (glycolic acid) or LA (lactic acid) followed by the depolymerization of the polymer, a direct route based on the gas-phase transesterification of methyl glycolate (MGA) or methyl lactate (MLA) over a fixed catalyst bed is presented. (Fig. 1 for PLA). The catalytic performance of the active TiO<sub>2</sub> phase



was found to be completely modified by interaction with the SiO<sub>2</sub> support. The specific catalytic activity of TiO<sub>2</sub> was strongly correlated to its geometric features and the corresponding band gap energies derived from DR UV-VIS spectroscopy.

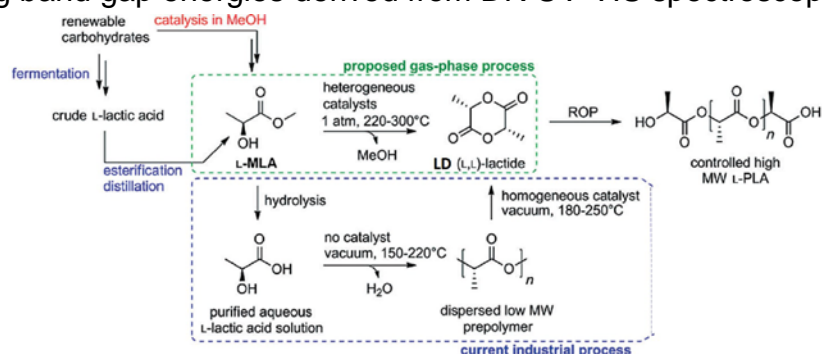


**Fig. 1.** Proposed new process in the gas phase starting from esters, based on Ti-Si-oxides, and transesterification. Current process needs two steps, starting from the acid.

For glycolide, with specific supported TiO<sub>2</sub> catalysts, a high selectivity of 75-78% can be achieved at the thermodynamically-limited equilibrium conversion of MGA (54% at 300°C, 5.6vol% MGA, 1 atm). The absence of a methyl substitution on the alpha-carbon seems to lead to faster cyclization kinetics of MGA when compared to MLA or the double-substituted methyl-2-hydroxy-isobutyrate. Contrarily, glycolide production is less favored thermodynamically compared to lactide. The absence of glycolide decomposition at temperatures up to 300°C however allows to increase equilibrium conversion by taking the endergonic reaction to higher temperatures (Fig. 2, e.g. 300 °C). A thermodynamic analysis is also presented.

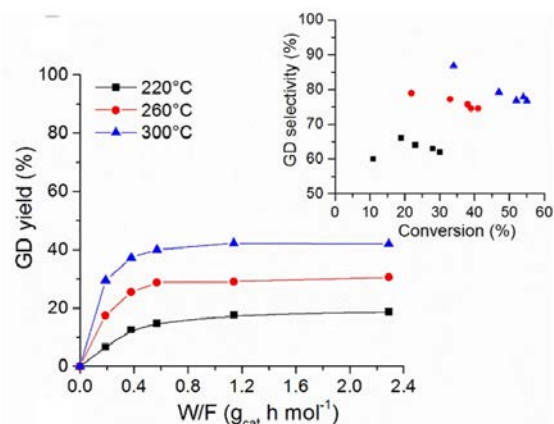


**Fig. 2** Kinetic plots of glycolide formation from MGA at different temperatures.

## References

- [1] R. De Clercq, M. Dusselier, E. Makshina, B. F. Sels, *Angew. Chem. Int. Ed.* **2018**, *57*, 3074-3078
- [2] R. De Clercq, M. Dusselier, C. Poleunis, D. P. Debecker, L. Giebeler, S. Oswald, E. Makshina, B. F. Sels, *ACS Catal.* **2018**; *8* (9), pp 8130-8139
- [3] R. De Clercq, E. Makshina, B. F. Sels, M. Dusselier, *ChemCatChem* **2018**, *10*, 5649-5655.

# **The impact of silica to alumina ratio on the methane formation and product distribution of light naphtha cracking measured at initial activity of the catalyst**

*Wojciech Supronowicz, Khalid Ali Almajnouni Sabic Technology Centre, Riyadh, Saudi Arabia*

Fluid catalytic cracking (FCC) continues to be one of the major conversion processes in most of the refineries. Recent developments on the field of FCC including catalyst modification (application of mesoporous zeolite Y- Rive Technology [1]), new process concept (dual riser FCC process [2], high severity FCC and DCC) to maximize propylene, and using new feed that is light [3] underline the importance of FCC process in the future and its potential to response to challenges of fast changing chemicals market.

FCC traditionally processes heavy feedstock such as vacuum gas oil and residual gas oil. In addition, it is used for olefinic light feedstock as in the case of KBR superflex, now K-COT [4]. For light naphtha feedstock, steam cracking is well developed to process such a feed. Recently KBR announced K-COT commercialization for naphtha feed. Fundamental understanding of the conversion of the feed to desirable products at the commercial conditions to optimize the process further is required.

This work will highlight the kinetics study of a model component representing light naphtha using riser simulator. The Impeller, in the riser simulator, induced circulation of gases through the catalyst basket fluidize the catalyst bed, which allows to operate at conditions closer to the FCC units (Figure 1).The product distribution reflects the initial catalyst activities, fresh catalyst, unlike fixed bed study where the measured products distribution does not reflect the initial rates. Moreover, the reactor is connected to a vacuumed chamber. After reaching the desired feed-catalyst contact time, the connection is opened automatically and the reaction products and unreacted feed is rapidly transferred to the vacuumed chamber, which terminates the reaction and allows to precisely control the contact time.

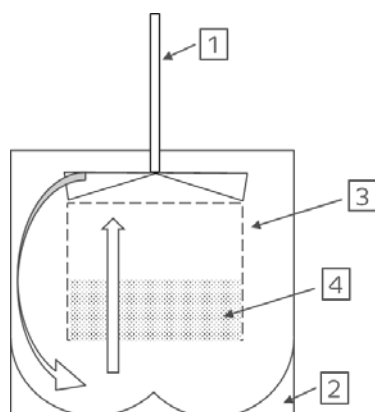


**Figure 1.** Simplified reactor scheme showing principle of gas circulation through the catalyst bed. 1) Impeller; 2) Reactor body; 3) Catalyst basket; 4) Catalyst bed

Two topics of industrial importance will be covered in this presentation; 1) the methane formation and how it can be minimized; 2) and the impact of different silica to alumina ratio on the product distribution with the focus on light olefins. The finding is supported with kinetics study to determine the activation barrier difference between different pathways.

Applying the above mentioned system, series of tests of hexane cracking at simulated riser conditions were conducted. Various feed-catalyst contact time (5-9s) and temperatures (460 – 520°C) were tested. To further mimic the industrial conditions, the tested H-ZSM5 samples were mixed with kaolin and colloidal silica (, calcined (550°C) and crushed to obtain uniformed size of particles.

#### References

- [1] J. Garcia-Martinez, K. Li, G. Krishnaiah, Chem. Commun., 2012, 48, 11841–11843
- [2] P. K. Niccum, E. A. Gbordzoe, US Patent 7,611,622 B2
- [3] M. J. Tallman, C. Santner, R. B. Miller, US Patent 7,128,827 B2
- [4] S. Mukherjee, KBR Olefins Technology – Technology options to meet uncertain market conditions, 4th Petrochem Conclave, Delhi, 12th February 2015

# Bimetallic Oriented ( $\text{Au}/\text{Cu}_2\text{O}$ ) vs. monometallic 1.1.1 Au (0) or 2.0.0 $\text{Cu}_2\text{O}$ Graphene-Supported Nanoplatelets as Very Efficient Catalysts for Henry Addition

N. Candu<sup>1</sup>, A. Simion<sup>1</sup>, S.M. Coman<sup>1</sup>, V.I. Parvulescu<sup>1</sup>, A. Primo<sup>2</sup>, H. Garcia<sup>2</sup>

<sup>1</sup>- *University of Bucharest 4-12 Regina Elisabeta Blv, Bucharest, Romania,*  
*natalia.candu@chimie.unibuc.ro*

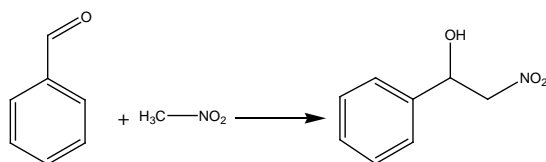
<sup>2</sup>- *Universidad Politecnica de Valencia, Avda. de los Naranjos, Valencia, Spain*

## Introduction

Graphene, an allotrope of carbon, is considered as an excellent suitable catalytic support due to its high carrier mobility, high electrical and thermal conductivity, high surface area (theoretical value of 2630 m<sup>2</sup>/g), unique two-dimensional (2D) honeycomb lattice, high electron mobility, strong metal-support interactions and easy surface functionalization [1,2]. In addition, doping graphene-nanosheets with heteroatoms became an attractive method of tuning its electronic and catalytic properties [3]. On the other side, graphene supported metal nanoparticles (MNPs) have already shown very active and selective properties for various organic transformations such as: oxidations,[4] reductions[5] or coupling reactions [6]. Henry coupling is a classic carbon–carbon bond formation reaction, consisting in the addition of a nucleophilic anion derived from nitroalkane to an electrophilic aldehyde or ketone [7]. Under classical conditions, this reaction is generally catalyzed by many organic bases, including carbonates, bicarbonates, alkali metal hydroxides, alkoxides, and organic nitrogen bases in the presence of organic solvents, and long reaction times, which may lead to environmentally hazardous residues and undesirable by-products [8]. In order to prove the versatility of the graphene supported MNPs in coupling reactions in this study we extended the investigation of these materials from the monometallic to bimetallic  $\text{Au}/\text{Cu}_2\text{O}/f\text{-G}$  (*f* meaning few layers structures; *G* meaning defective graphene) films looking for a synergistic effect in the Henry coupling (Scheme 1).

## Experimental

The catalysts were prepared using a reported procedure [6] and exhaustively characterized by powder XRD, CO<sub>2</sub>-TPD, Raman spectroscopy, XPS and HRTEM.



Scheme 1. Henry coupling of benzaldehyde with nitromethane

The activity tests were carried out using 0.5mmoles of benzaldehyde and 10mmoles of nitromethane in 3mL of isopropanol, as solvent, at 50°C for 24h and 1×1 cm<sup>2</sup> plate of *Au*/fl-G, *Cu<sub>2</sub>O*/fl-G or *Au*/*Cu<sub>2</sub>O*/fl-G film as catalysts. The products were analyzed and identified by using GC-MS and a Bruker Advance III UltraShield 500 MHz spectrometer.

## Results and discussion

The concentration of the basic sites decreased in the order *Au*/*Cu<sub>2</sub>O*/fl-G > *Cu<sub>2</sub>O*/fl-G > *Au*/fl-G while the strength of these sites, appreciated from the CO<sub>2</sub> desorbed at around 350°C, in the *Au*/*Cu<sub>2</sub>O*/fl-G > *Au*/fl-G > *Cu<sub>2</sub>O*/fl-G order. These results parallel the catalytic data showing TON values of 1×10<sup>7</sup> for *Au*/*Cu<sub>2</sub>O*/fl-G, 2.7×10<sup>5</sup> for *Cu<sub>2</sub>O*/fl-G and 1.2×10<sup>5</sup> for *Au*/fl-G respectively. They also correlate to the catalysts characterization by XPS and HRTEM confirming the increase of the activity of the bicomponent Cu<sub>2</sub>O-Au/graphene catalyst as a the result of the direct interaction of Au with Cu<sub>2</sub>O.

## Conclusions

The new catalytic approach provides a facile, economic, and environmentally friendly method for the synthesis of nitroaldol products with high yields, up to 94.2%. The *Au*/*Cu<sub>2</sub>O*/fl-G provide a remarkable catalytic activity affording the coupling reaction in the absence of any extrinsic inorganic base. In addition, the catalyst fits the green chemistry demands being easily recoverable and recyclable.

**Acknowledgements.** The authors kindly acknowledge UEFISCDI (project PN-III-P4-ID-PCE-2016-0146, nr. 121/2017) for the financial support.

## References

1. S. Park, R. S. Ruoff, *Nat. Nanotechnol.* 2009, 4, 217–224.
2. G. Bottari, M. A. Herranz, L. Wibmer, M. Volland, L. Rodriguez-Perez, D. M. Guldi, A. Hirsch, N. Martin, F. D'Souza, T. Torres, *Chem. Soc. Rev.* 2017, 46, 4464–4500.
3. A. Bostwick, F. Speck, T. Seyller, K. Horn, M. Polini, R. Asgari, *Science* 2010, 328, 999-1002.
4. M. D. Esrafilii, P. Nematollahi, R. Nurazar, *Superlattices Microstruct.* 2016, 92, 60-67.
5. H. Woo, J. W. Kim, M. Kim, S. Park, K. H. Park, *RSC Adv.* 2015, 5, 7554-7558.
6. A. Primo, I. Esteve-Adell, S. M. Coman, N. Candu, V. I. Parvulescu, H. Garcia, *Angew. Chem. Int. Ed.* 2016, 55, 607-612.
7. A. Roucoux, J. Schulz, H. Patin, *Chem. Rev.*, 102 (2002) 3757.
8. C. Xu, X. Wang, J. Zhu, *J. Phys. Chem. C*, 112 (2008) 19841.

# Single-atom Catalysis on a Silica Support: A DFT study

*Xavier Deraet, Jan Turek, Mercedes Alonso, Frederik Tielens, Frank De Proft*

Eenheid Algemene Chemie (ALGC), Vrije Universiteit Brussel, Pleinlaan 2, 1050  
Brussels, Belgium

## Introduction

Despite the fact that metal-based catalysts have been used for decades, scientists are still seeking for those catalysts delivering the largest atomic efficiency. This concept is based on the evidence that the availability of most of the 3d, 4d and 5d metals used in catalytic processes is rather low and continuously diminishing as well as on the awareness that most of these processes occur at the metal surface, meaning that any atom that could not be approached by reactant molecules is wasted. These observations together with the aim of developing greener catalytic processes has led to the systematic reduction in size of the cluster to the most extreme situation where only single metal atoms are dispersed on a support, a so-called single-atom catalyst (SAC). However, the stability and catalytic activity of such a SAC are still highly debated. Therefore, we are aiming to systematically reduce the number of metal atoms on an amorphous silica support and analyse changes in catalytic activity and chemical reactivity within the framework of conceptual and periodic density functional theory (DFT).

## Computational details and model description

The computational model was built using a previously constructed hydroxylated amorphous silica slab.<sup>[1]</sup> Single atoms of Fe, Ni and Cu were placed above various siloxane ring systems of the silica slab containing 4, 5 and 6 Si-atoms to form a catalytic complex. The DFT calculations have been performed using the Vienna Ab initio Simulation Package (VASP).<sup>[2]</sup> The electron-ion interactions were described using the projector augmented plane wave (PAW) method<sup>[3]</sup> with a cutoff energy of 400 eV. The Perdew Burke Ernzerhof (PBE) functional<sup>[4]</sup> was employed.

## Results and discussion

We observed that the highest adsorption energy for Fe, Ni and Cu was always obtained at the same siloxane ring containing five Si atoms, which is in line with the

obtained Molecular Electrostatic Potential (MEP). Nevertheless, the interaction between the transition metal and the surface is highly dependent on the investigated system. Therefore, the adsorption and corresponding Bader charges of the remaining group 8 (Ru, Os), group 10 (Pd, Pt) and group 11 (Ag, Au) as well as group 9 (Co, Rh, Ir) metals were scrutinized. This leads to a conclusion that the adsorption of the metals on the silica surface increases across a period and within a group with the exception of Pd and the inert metals of group 11. The corresponding Bader charges appeared to decrease when moving down and across the rows from group 8 to group 10 elements, after which they converged to a quasi-zero charge for the inert metals. Furthermore, only for the Pt and Ir-atom a negative Bader charge was obtained, which could also be expected since these elements are characterized by an electron affinity that is higher than that of oxygen.

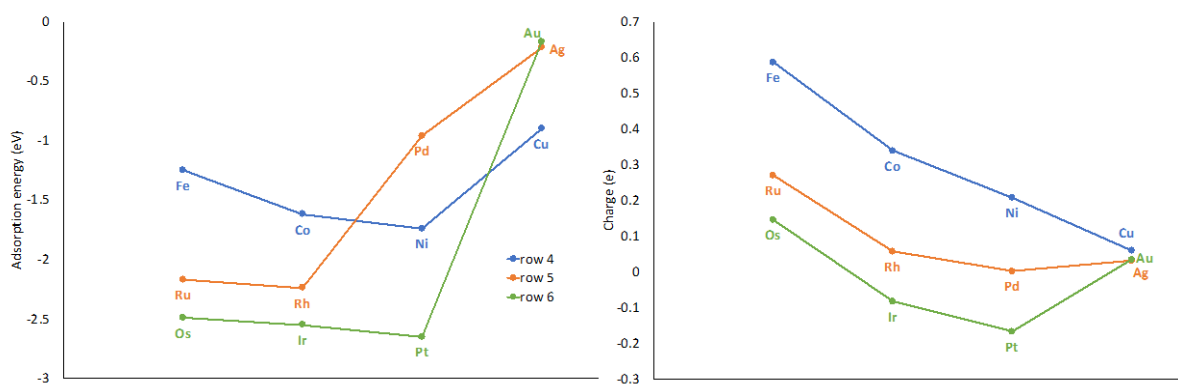


Figure 1: Adsorption energy (left) and corresponding Bader charges (right) of a single transition metal (group 8-11) interacting with an amorphous, hydrated silica slab.

In general, the observed trends for Bader charges are, with the exception of Pd, in good agreement with the electron affinity trends for transition metals of group 8 until group 11. Current research consists of calculating conceptual DFT reactivity indices such as the Fukui functions, which are related to the local density of states, and the dual descriptor. These indices should provide us with a picture of the reactivity of the surfaces for processes where charge transfer is dominant.

## References

- [1] Tielens, F.; Gervais, C.; Lambert, J.F.; Mauri, F.; Costa, D., *Chem. Mater.*, **2008**, 20 (10), 3336-3344.
- [2] Kresse, G.; Hafner, J.; *Phys. Rev. B*, **1993**, 47 (1), 558-561.
- [3] Kresse, G., Joubert, D., *Phys. Rev. B*, **1999**, 59 (3), 1758-1775.
- [4] Perdew, J.P.; Burke, K.; Ernzerhof, M., *Phys. Rev. Lett.*, **1996**, 77 (18), 3865-3868.

# **In Silico Catalyst Design for Urethane Cleavage Reactions based on Quantum Chemical Methods**

*Christoph Gertig, Institute of Technical Thermodynamics, RWTH Aachen University,  
Aachen, Germany;*

*Janik Hense, Institute of Technical Thermodynamics, RWTH Aachen University,  
Aachen, Germany;*

*Lorenz Fleitmann, Institute of Technical Thermodynamics, RWTH Aachen University,  
Aachen, Germany;*

*André Bardow, Institute of Technical Thermodynamics, RWTH Aachen University,  
Aachen, Germany and Institute of Energy and Climate Research (IEK-10),  
Forschungszentrum Jülich, Jülich, Germany;*

*Kai Leonhard, Institute of Technical Thermodynamics, RWTH Aachen University,  
Aachen, Germany*

The identification of powerful catalysts is key to efficient and economic production of chemicals. Usually, catalysts are developed based on experiments, which can be expensive, time-consuming and therefore often limited in scope. In silico studies with quantum chemical methods already offer an alternative to experiments for many applications in chemistry and chemical engineering. However, the fully computational design of catalysts is still regarded as one of the “Holy Grails in Chemistry” [1] and the development of in silico catalyst design methods is still in its infancy.

To enable a reliable in silico design of catalysts, prediction methods are required that yield accurate results in acceptable computation time. Even then, the results of quantum chemical calculations alone are usually insufficient since we need to assess the performance of the designed catalysts in the overall chemical process.

In this work, we propose an approach to in silico catalyst design integrating predictions based on advanced quantum chemical methods with chemical process simulations. In this approach, catalyst structures are mutated using a library of molecular fragments. Reaction rate constants achieved with the obtained catalysts are calculated based on transition state theory. The transition states are identified using the density functional theory method B3LYP-D3. Electronic energies are computed with the accurate yet efficient DLPNO-CCSD(T) method [2]. The rigid rotor harmonic oscillator approximation is used to calculate partition functions. Solvation



effects are accounted for with the advanced solvation model COSMO-RS [3]. The performance of designed catalysts is evaluated by process simulations, which are directly integrated into the design.

The proposed design approach is demonstrated for urethane cleavage reactions, which are part of a possible production route to industrially important isocyanates [4]. Urethane cleavage has been shown to be catalysed by organic acids [5]. By mutations of the catalyst structure, the barriers in Gibbs free energy along the reaction path are reduced significantly, as shown in Figure 1 below.

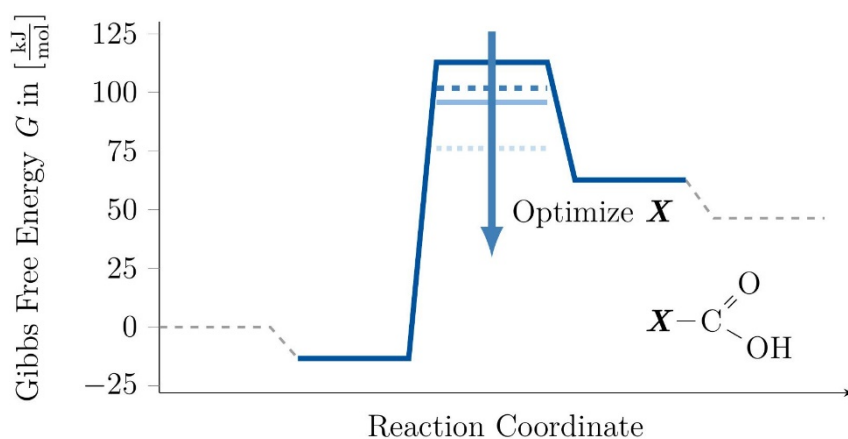


Figure 1: Reduction of the barrier in  $G$  along reaction path by optimization of catalyst.

Besides the impact on the free energy barrier and thus on the reaction rates, mutations of the catalyst structure also affect the catalyst holdup in the reactor, which is accounted for by the process simulations in our approach. Thereby, we successfully identify catalysts with a better process performance in urethane cleavage.

The proposed design approach is generally applicable to a variety of reactions. Moreover, the catalyst design approach can be fully automated. Thereby, we can further reduce effort and eliminate human bias in the exploration of large design spaces.

## References

- [1] C. Poree and F. Schoenebeck, 2017. A Holy Grail in Chemistry: Computational Catalyst Design: Feasible or Fiction?. *Accounts of Chemical Research* 50 (3), 605-608.
- [2] F. Neese, 2018. Software update: the ORCA program system, version 4.0. *WIREs Computational Molecular Science* 8, e1327.
- [3] F. Eckert and A. Klamt, 2002. Fast solvent screening via quantum chemistry: COSMO-RS approach. *AIChE Journal* 48 (2), 369-385.
- [4] C. Six and F. Richter, 2000. Isocyanates, organic. *Ullmann's Encyclopedia of Industrial Chemistry*.
- [5] D. P. N. Satchell and R. S. Satchell, 1975. Acylation by ketens and isocyanates. A mechanistic comparison. *Chemical Society Reviews* 4 (2), 231-250.

# Effect of Support Acidity on Ammonia Synthesis Reaction over Supported Ru Catalysts

M.Y. Aslan<sup>1</sup>, S. Akbayrak<sup>2</sup>, K. Sac<sup>1</sup>, S. Ozkar<sup>2</sup> and D. Uner<sup>1,\*</sup>,  
<sup>1</sup>Chemical Engineering, and <sup>2</sup>Chemistry Middle East Technical University, Ankara, Turkey

\*uner@metu.edu.tr

When Ru is supported on basic materials, the observed rates of NH<sub>3</sub> synthesis were higher [1,2]. On the other hand, an intensified NH<sub>3</sub> synthesis process using an acidic absorbent -such as MgCl<sub>2</sub>- in the reactor, maintained a low partial pressure of ammonia in the gas phase, and the reaction equilibrium shifted to right [3]. Along these lines, the effect of surface acidity of the hydroxyapatite (HAp), zeolite-Y and carbon (Vulcan XC72R) supports on the NH<sub>3</sub> synthesis rate over Ru is reported in this study.

## Experimental

NH<sub>3</sub> synthesis experiments were carried out at 300-400 °C, 1 atm, and under flow of 100 mL/min (H<sub>2</sub>:N<sub>2</sub>:Ar=3:1:2) gas flow over 4 wt% Ru/HAp, 1.37 wt% Ru/Zeolite-Y and 1 wt% Ru/Carbon catalysts. The reaction rate of ammonia synthesis was determined following the change of conductivity of 0.00108 M H<sub>2</sub>SO<sub>4</sub> solution with respect to time at 25 °C and 1 atm. After NH<sub>3</sub> synthesis reaction test is completed, the total adsorbed NH<sub>3</sub> during the reaction was quantified after desorption under 100 ml/min pure Ar flow at reaction temperature. Dispersion measurements were conducted at room temperature in a home built static chemisorption system [4]. The surface acidity of the support materials are determined with an approximate method using a heat flow calorimetry (Tian Calvet Seteram C80). The heat released upon dosing 0.01 M NH<sub>3</sub> solution at 100 °C and 1 atm was used to rank the acidity of the support.

## Results and Discussions

NH<sub>3</sub> synthesis reaction rates reported in Table 1 exhibited an increasing trend with increasing temperatures indicating that the reaction is well away from equilibrium. The highest activity was measured over Ru/zeolite-Y catalyst at 400 °C. Activation energies were calculated as 63.7, 28.9, and 22.4 kJ/mol for Ru/HAp, Ru/Zeolite-Y and Ru/Carbon catalysts, respectively. In Table 2, desorbed amount of NH<sub>3</sub> after the reaction tests were reported. Significant amounts of NH<sub>3</sub> desorbed from all catalysts and temperatures. The lowest amount of ammonia desorption was measured at 300 °C over Ru/Hap as expected.

Structural characterization results are reported in Table 3. Zeolite Y has the highest BET surface area, while all of the catalysts have similar Ru dispersions as measured by volumetric hydrogen chemisorption.

Table 1. Initial NH<sub>3</sub> synthesis reaction rates

	Reaction Rates, $\mu\text{mol NH}_3/\text{g}_{\text{cat}}\text{-h}$		
	Ru/HAp	Ru/Zeolite-Y	Ru/Vulcan
573 K	103	304	249
598 K	127	323	250
623 K	304	308	316
648 K	321	332	349
673 K	329	468	422

Table 2. NH<sub>3</sub> desorption after the reaction tests

	Total amount of desorbed NH <sub>3</sub> , $\mu\text{mol}/\text{g}_{\text{cat}}$		
	Ru/HAp	Ru/Zeolite-Y	Ru/Vulcan
573 K	35	150	145
598 K	65	155	95
623 K	155	100	80
648 K	120	115	75
673 K	90	100	100

Table 3. Surface characteristics of support materials and catalysts

	BET surface area, $\text{m}^2/\text{g}$	Ru metal dispersion, %	Effective activation energy, $\text{kJ}/\text{mol}$	Acidity
HAp	13	30	63.7	Weak base
Zeolite-Y	744	36	28.9	Strong acid
Vulcan	222	28	22.4	To be determined

Activation energies reported for NH<sub>3</sub> synthesis over Ru catalysts are in the range of 60-110 kJ/mol [5,6]. The activation energy determined over Ru/HAp is in agreement with literature values. The discrepancy between the activation energies obtained over acidic and basic supports indicate large quantities of ammonia adsorption over the support surface. The effective activation energies measured in this work agree very well with the heat of vaporization of ammonia (~23.4 kJ/mol at 25 °C, 1 atm). In other words, the dominant component during the rate measurements seems to be the desorption of ammonia from the adsorbed ammonia multilayers, but not the true kinetics, especially from the supports exhibiting acidic nature. A microkinetic model [4] is presently modified to demonstrate the role of ammonia retained on the support on the reaction rates.

## Acknowledgement

The financial support from METU GAP-304-2018-2707 project is gratefully acknowledged.

## References

- [1] Z. You, K. Inazu, K.-I. Aika, T. Baba, *Journal of Catalysis*, 251 (2007), 321–331
- [2] Z. Wang, J. Lin, R. Wang, K. Wei, *Catalysis Communications*, 32 (2013), 11-12
- [3] M.S. Huberty, A.L. Wagner, A. McCormick, E. Cussler, *AIChE Journal*, 58 (2012), 3526-3532
- [4] D. Uner and M.Y. Aslan, *Catalysis Today*, 272 (2016), 49-57
- [5] Y. Kadowaki and K.I. Aika, *Journal of Catalysis*, 161 (1996), 178-185
- [6] S.E. Siporin and R.J. Davis, *Journal of Catalysis*, 225 (2004), 359-368

# On the catalytic hotspots in Fischer Tropsch Synthesis

Zoya Nayyer<sup>1</sup>, Bilal Rizwan<sup>1</sup>, Daniyal Shaukat<sup>1</sup>, Ertugrul Erkoç<sup>2</sup>, Deniz Uner<sup>1\*</sup>

<sup>1</sup>Chemical Engineering, Middle East Technical University, Ankara 06800 Turkey

<sup>2</sup>Chemical Engineering, Bursa Technical University, Bursa Turkey

\*uner@metu.edu.tr

## Introduction

The effect of cobalt loading on the local hot spots leading to changes in activities and selectivities of exothermic Fischer Tropsch reaction was investigated experimentally and through mathematical modeling.

## Catalyst Preparation and Characterization

3 wt % and 21 wt % Co//Al<sub>2</sub>O<sub>3</sub> catalysts were prepared by incipient wetness technique starting from a cobalt nitrate precursor (Matheson Coleman & Bell) and Al<sub>2</sub>O<sub>3</sub> (Riedel De Haen). 3 wt % catalyst was prepared by differential dosing of a very dilute cobalt nitrate solution to ensure a good metal support interaction. After each layer, the slurry was dried and the subsequent dose was impregnated until 3 wt % was obtained. The prepared catalysts were dried in an oven at 70 °C overnight and calcined in the oven at 450°C for 45 minutes. The catalysts were characterized by SEM (Tescan, Vega 3) for particle sizes and EDS analyses were performed for the coating uniformity. In order to develop the catalyst coating methodology over an aluminum microfluidic substrate, a thorough study was conducted to select etching parameters and coating strategy. Hierarchical micro-porosity was induced into the aluminum plates through etching, using a mixture of acetic acid, nitric acid, phosphoric acid and distilled water while thoroughly maintaining the surface cleanliness of the aluminum plates prior to the etching (by cleaning with ethanol and acetone). A masking agent was used to protect the non-reactive domains. The results of etching were monitored using SEM. TPR on these samples was performed using the Micromeritics Chemisorb 2720 instrument under the flow of 25 ml/min argon containing 2% H<sub>2</sub> and a heating rate of 5 °C/min.

## Experimental results

The etched layers of aluminum exhibited hierarchical porosity observed from SEM results. The EDAX analysis results shown in Figure 1 belong to the powdered

catalysts with Co loading, which clearly demonstrates the dispersion quality of low loading catalyst (Figure 1a) in comparison to the high loading catalyst (Figure 1b).

Element	Weight %	Atomic %	Error %
O K	49.07	67.44	7.12
NaK	1.22	1.16	15.48
BrL	13.92	3.83	3.48
AlK	31.79	25.91	4.27
ClK	0.68	0.42	22.83
CoK	3.33	1.24	12.58

Element	Weight %	Atomic %	Error %
C K	5.49	11.41	13.43
O K	30.32	47.36	8.10
NaK	0.20	0.22	32.51
BrL	9.81	3.07	4.35
AlK	35.54	32.92	4.92
ClK	0.84	0.60	12.79
CoK	6.45	2.74	7.90
ErL	11.34	1.69	21.11

Figure 1a

Figure 1b

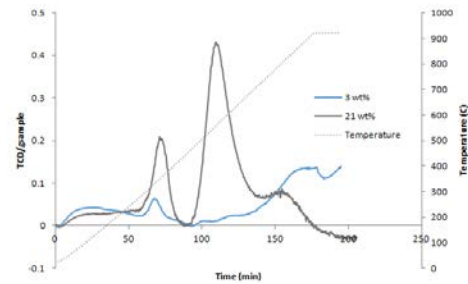


Figure 2

The reduction characteristics of powdered catalyst were determined using TPR, as shown in Figure 2. Normally, Co exhibits two distinct peaks, a high temperature peak and a low temperature peak which each correspond to the reduction of  $\text{Co}_3\text{O}_4$  to  $\text{CoO}$  and then  $\text{CoO}$  to  $\text{Co}$ . However, for the case of 3%  $\text{Co}/\text{Al}_2\text{O}_3$ , the high temperature peak was not observed, signaling that  $\text{CoO}$  was not reduced to  $\text{Co}$ . Co spreads on alumina like a uniform monolayer for the lower metal loading, whereas clumps of Co are observed on higher metal loadings. When clumps are present, they can be fully reduced to the metallic state of Co. When the monolayer is present, it interacts strongly with the alumina and does not get fully reduced. As metal loadings are altered, particle size also changes. Thus, an experimental excursion is in progress to determine an optimum range of metal loading and metallic dispersion

### Mathematical Model

Using COMSOL, it was demonstrated that during the reaction the temperatures on the catalyst particles were immediately equilibrated indicating that the heat of reaction being dissipated very quickly on the metal particles. However, the dissipation of heat between the metal and the support is not as rapid. A series of calculations carried out for two extremities: one, where all the heat of reaction is absorbed by the catalyst, and the other, where the gases are continuously in contact with the catalyst surface. The temperatures calculated by the two extremes were very different; one was in the order of  $10^{20}$  whereas the other was very slightly higher than the operating temperature of the reactor, which is around 573K. Further modeling analysis is in progress elucidating the selectivity of the reaction as a function of local temperatures.

# Hydrogen Adsorption over Pd/CeO<sub>2</sub> monitored by in situ <sup>1</sup>H NMR using a benchtop spectrometer

Deniz Uner and Ecem Volkan

Chemical Engineering, Middle East Technical University, 06800 Ankara, Turkey

uner@metu.edu.tr

Interaction of hydrogen with palladium below subcritical temperatures and pressures of PdH give rise to two distinct hydride phases known as  $\alpha$ -PdH and  $\beta$ -PdH. These phases are identified with distinct chemical shift values by *in situ* solid state NMR spectroscopy reveal two chemically distinct environments[1] assigned to alpha and beta hydrides. We report here using a compact NMR spectrometer to obtain <sup>1</sup>H NMR data of hydrogen adsorbed over Pd/CeO<sub>2</sub> under fast exchange conditions.

## Experimental

1 gram 1.66 wt% Pd/CeO<sub>2</sub> was used to collect NMR spectra over a benchtop unit (MAGRITEK Spinsolve 42.5 MHz) connected to a vacuum manifold described elsewhere [2]. Prior to the NMR measurements, the catalyst was exposed to several cycles of hydrogen for in situ reduction at room temperature, sufficient for the reduction of the catalyst as was previously demonstrated [2]. The NMR spectra and the adsorption isotherms were simultaneously collected at different pressures up to 700 mm Hg.

## Results and Discussion

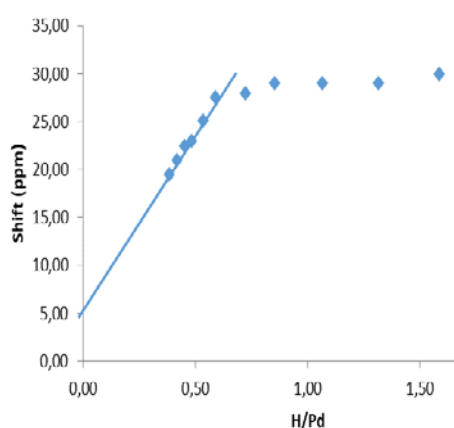
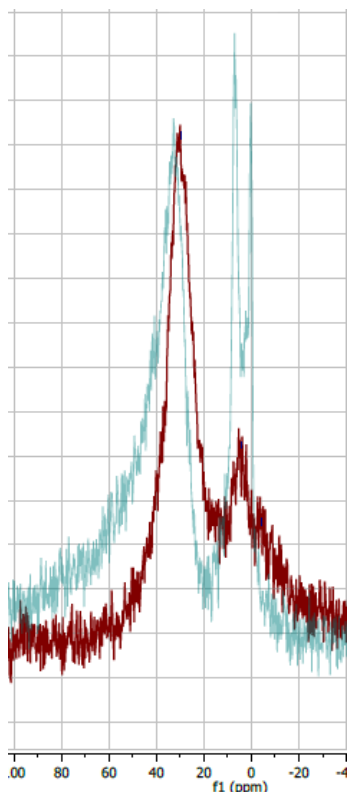


Figure 1. Chemical shift as a function of H/Pd ratio

NMR spectra of Pd/CeO<sub>2</sub> gives rise to two distinct and broad peaks: one is attributed to OH groups originating from CeO<sub>2</sub>, and the second one was assigned to  $\beta$ -PdH, in the light of the previous reports in the literature. The chemical shift of the  $\beta$ -PdH peak obtained from NMR versus H/Pd ratio determined in situ volumetrically are plotted in Figure 1. Two distinct domains were identified: The domain below H/Pd<0.60 had a strong dependency of the chemical shift on H/Pd ratio. At H/Pd ratios higher than 0.60, chemical shift values were independent of the absorbed hydrogen amounts. It is well known that for H/Pd<0.60,  $\alpha$  and  $\beta$  phases of PdH coexist. Whether there is a fast exchange between the spin states of  $\alpha$  and  $\beta$

phases of PdH, the equation of the straight line shown in Figure 1 is determined as  $\sigma = 37.5 (H/Pd) + 5.3$ . In other words, in the diminishing limit of the spin populations of the  $\beta$  phase of PdH, another peak -most probably  $\alpha$  phase- with a chemical shift of 5.3 ppm existed.



The direct evidence for this state came from a measurement of the spectrum at the highest pressure (~700 mm Hg), when the NMR spectrum of the sample was recorded after immersing the sample in liquid nitrogen and then collecting the spectrum. Spectrum collected as such (green) was compared to the spectrum from the same sample recorded at room temperature (brown) in Figure 2 clearly indicate two distinct sharp peaks one at 7 ppm and another at around 0 ppm. 0 ppm peak was attributed to gas phase hydrogen while 7 ppm peak was assigned to the missing  $\alpha$  peak during the room temperature measurement.

Figure 2. *in situ*  $^1\text{H}$  NMR spectra of hydrides of Pd under ~700 mm Hg hydrogen pressure. Brown: room temperature, green: after being immersed in liquid nitrogen.

These results indicate that at pressures greater than 5 mm Hg, both  $\alpha$  and  $\beta$  hydride of Pd have enough mobility as well as long enough T2 to exhibit liquid like behavior even at room temperature and below. The ability to make such measurements *in situ* using a benchtop spectrometer has already opened the possibility of facile NMR spectroscopy of the adsorbed species *in operando*, revealing not only the identity of the surface species but also the dynamics as can be measured by a plethora of multidimensional NMR spectroscopic techniques.

### Acknowledgement

Members of TETRA (MAGRITEK representative in Turkey) team are kindly acknowledged.

### References

1. Dekura et al. *Angew. Chem. Int. Ed.* 57 (2018) 9823-9827.
2. Kaya et al. *Catal. Today.* 323(2019) 143-127.

# Benefits of precursor phase purity on the activity of iron-based layered double hydroxide derived ammonia decomposition and synthesis catalysts

D. Rein<sup>1,2</sup>; K. Friedel Ortega<sup>1</sup>; M. Behrens<sup>1</sup>; J. Folke<sup>2</sup>; H. Ruland<sup>2</sup>; R. Schlögl<sup>2</sup>

<sup>1</sup> Max Planck Institute CEC, Mülheim an der Ruhr, Germany

<sup>2</sup> University of Duisburg-Essen, Essen, Germany

## Introduction

The usage of layered double hydroxides (LDHs) as precursor materials for the synthesis of heterogeneous Fe-based catalysts is one promising approach. Since iron has two accessible oxidation states in aqueous solution, it is possible to obtain nanostructured spinels by calcination of co-precipitated LDHs that contain Fe<sup>2+</sup> and Fe<sup>3+</sup> ions in the proper stoichiometry.<sup>[1]</sup> However, controlling the formation of by-phases besides the target LDH structure is a challenging task. *In situ* XRD analysis in combination with H<sub>2</sub>-TPR experiments revealed that the reduction behavior of the oxide precursor is strongly affected by the presence of undesired by-phases formed already in the precursor stage.<sup>[2]</sup> Ageing time has a huge impact on these critical aspects so to further investigate this matter, LDHs with equimolar amounts of Mg<sup>2+</sup>:Fe<sup>2+</sup>:Fe<sup>3+</sup> and Mg<sup>2+</sup>:Co<sup>2+</sup>:Fe<sup>3+</sup> were respectively synthesized using different anionic species of the corresponding metal salts for two ageing times at constant pH. Upon calcination and reduction, the thoroughly characterized samples were systematically investigated at 1 atm in the ammonia decomposition and at 90 bar in the ammonia synthesis.

## Results and discussion

Via co-precipitation in an automated laboratory reactor system (OptiMax, Mettler Toledo) mesoporous Mg<sup>2+</sup>:Fe<sup>2+</sup>:Fe<sup>3+</sup> and Mg<sup>2+</sup>:Co<sup>2+</sup>:Fe<sup>3+</sup> hydrotalcite-like compounds were obtained. Powder XRD analysis showed that during the synthesis of Mg<sup>2+</sup>:Fe<sup>2+</sup>:Fe<sup>3+</sup>-LDHs magnetite forms, which is generally evidenced after calcination in the form of hematite. This by-phase formation is favored in the presence of nitrates for an ageing time of 1 h. Despite lowering the LDH fraction in favor of the co-precipitated spinel phase, the formation of magnetite is fully suppressed if the ageing time is increased to 24 h. This results in a crystallographic phase pure



magnesioferrite after calcination. A further improvement is achieved by substituting the metal nitrates with the corresponding chlorides. In view of the absent oxidizing power of the former, a kinetically controlled formation of the LDH phase is favored during the prolonged ageing period of 24 h, since the chloride-derived LDH shows a considerably lower amount of magnesioferrite by-phase. Similar experiments using  $\text{Co}^{2+}$  instead of  $\text{Fe}^{2+}$  cations show that the former are less sensitive to the chemical environment. This is observed in the higher degree of phase purity of the corresponding

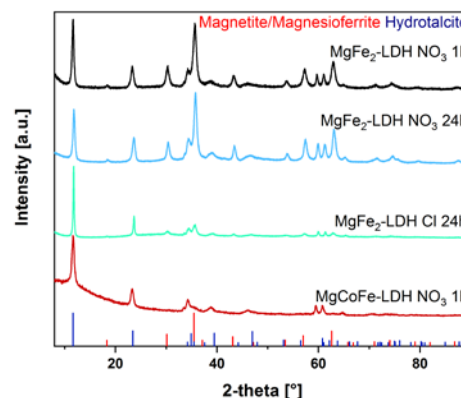


**Figure 1:** PXRD of freshly synthesized LDH precursor materials.

LDH precursors (Figure 1). Interestingly, this aspect has a strong impact on the catalytic activity (Figure 2). Both reactions are substantially enhanced in the absence of hematite. A further increase is observed in the  $\text{NH}_3$  decomposition for the  $\text{MgFe}_2\text{O}_4$  activated catalyst derived from a crystallographically phase pure spinel. Changes in the slopes reveal that the nature of the promoting Co effect is substantially different than the one achieved by the anisotropic effect of the otherwise structurally identical  $\text{MgFe}_2\text{O}_4$ . These experiments reveal that the extent of by-phase formation is highly sensitive to the chemical environment, which in turn controls the kinetics of the solids formed in the liquid phase.

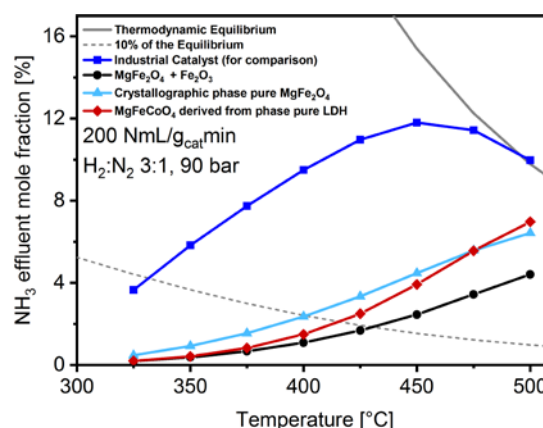
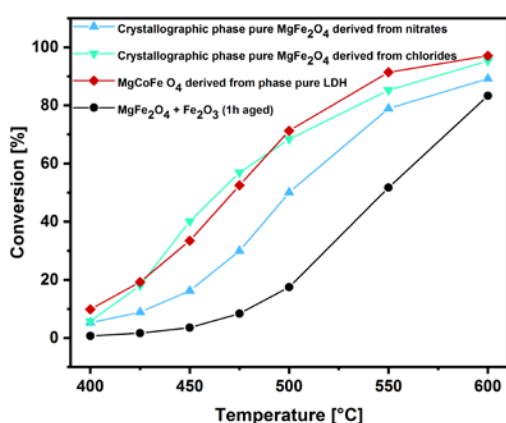


**Figure 2:** Temperature dependent  $\text{NH}_3$  conversion (a) and synthesis (b) over reduced pure and Co-modified magnesioferrites derived from LDH precursors with different fractions of spinel by-phases.

## References

- [1] K. Friedel, D. Rein, C. Lüttmann, J. Heese, F. Özcan, M. Heidelmann, J. Folke, K. Kähler, R. Schlögl, M. Behrens, *ChemCatChem*. **2017**, 9, 659-671.
- [2] D. Rein, K. Friedel, C. Weidenthaler, E. Bill, M. Behrens, *Appl. Catal. A* **2017**, 548, 52-61.

# Cyclohexane Dehydrogenation over $\text{MoO}_3/\gamma\text{-Al}_2\text{O}_3$ , $\text{V}_2\text{O}_5/\gamma\text{-Al}_2\text{O}_3$ and $\text{Cr}_2\text{O}_3/\gamma\text{-Al}_2\text{O}_3$ Catalysts: Effects of the Support Surface Coverage by Transition Metal Oxides

*I.Y. Petrov<sup>1</sup>, B.G. Tryasunov<sup>2</sup>*

<sup>1</sup>*Federal Research Center of Coal & Coal Chemistry SB RAS, Kemerovo, Russia*

<sup>2</sup>*Kuzbass State Technical University, Kemerovo, Russia*

## Introduction

$\gamma$ -Alumina supported chromia, vanadia and molybdena systems are considered to be highly efficient catalysts for oxidative and non-oxidative dehydrogenation of hydrocarbons [1]. In this work we tried to compare dehydrogenation activities of these catalysts depending on concentrations of the supported transition metal oxides in combination with characterization of these samples by potentiometry, XRD and DRS techniques.

## Experimental

$\text{MoO}_3/\gamma\text{-Al}_2\text{O}_3$ ,  $\text{Cr}_2\text{O}_3/\gamma\text{-Al}_2\text{O}_3$  and  $\text{V}_2\text{O}_5/\gamma\text{-Al}_2\text{O}_3$  catalysts containing 0-25 wt.% of supported transition metal oxides were prepared by sequential impregnation of commercial  $\gamma\text{-Al}_2\text{O}_3$  (200 m<sup>2</sup>/g) with aqueous solutions of corresponding amounts of the precursor salts [(NH<sub>4</sub>)<sub>2</sub>Mo<sub>2</sub>O<sub>7</sub>, (NH<sub>4</sub>)<sub>2</sub>Cr<sub>2</sub>O<sub>7</sub> and NH<sub>4</sub>VO<sub>3</sub>], followed by drying (120°C, 4 h) and calcining (600°C, 6 h) in air of the impregnates after each component deposition. Apparent monolayer surface coverages in the supported systems were estimated by pH measurements of suspensions of catalysts in aqueous solutions of KCl (0.1 M) [2]. Specific surface areas of the catalysts were determined by low temperature adsorption of Ar at -196°C. The supported samples were also characterized by XRD and UV/VIS-DRS techniques. Their catalytic activities in cyclohexane dehydrogenation were tested using a conventional pulse chromatographic method (T=620°C;  $\tau_c$ = 1s; P=0.1 MPa).

## Results

According to the XRD data of these materials, bulk phases of  $\text{Al}_2(\text{MoO}_4)_3$ ,  $\text{AlVO}_4$  and  $\alpha\text{-Cr}_2\text{O}_3$  appear in  $\text{MoO}_3/\gamma\text{-Al}_2\text{O}_3$ ,  $\text{Cr}_2\text{O}_3/\gamma\text{-Al}_2\text{O}_3$  and  $\text{V}_2\text{O}_5/\gamma\text{-Al}_2\text{O}_3$  catalysts, respectively, at the supported transition metal oxide concentrations exceeding

monolayer coverages of  $\gamma$ -alumina support. Concentration dependences of the catalyst activities and suspension pH values are presented in Fig. 1 (a-c).

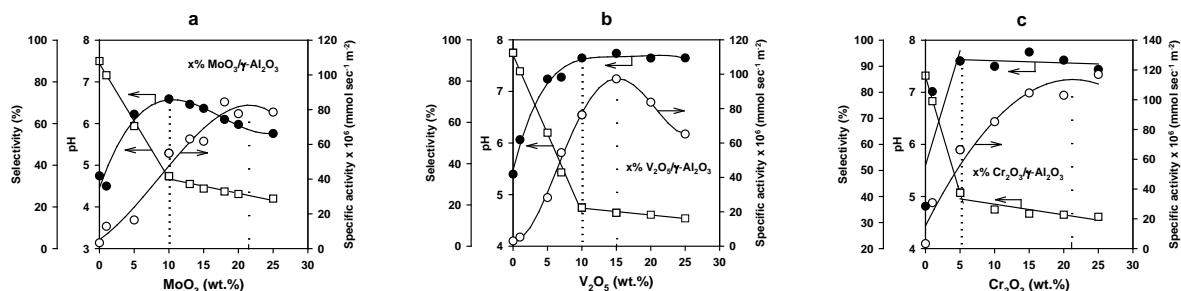


Fig. 1. Suspension pH values ( $\square$ ), specific dehydrogenation activities (O) and selectivities to benzene ( $\bullet$ ) for MoO<sub>3</sub>/ $\gamma$ -Al<sub>2</sub>O<sub>3</sub> (a), V<sub>2</sub>O<sub>5</sub>/ $\gamma$ -Al<sub>2</sub>O<sub>3</sub> (b) and Cr<sub>2</sub>O<sub>3</sub>/ $\gamma$ -Al<sub>2</sub>O<sub>3</sub> (c) catalysts as functions of the supported transition metal oxides contents

Maximal selectivities of MoO<sub>3</sub>/ $\gamma$ -Al<sub>2</sub>O<sub>3</sub>, Cr<sub>2</sub>O<sub>3</sub>/ $\gamma$ -Al<sub>2</sub>O<sub>3</sub> and V<sub>2</sub>O<sub>5</sub>/ $\gamma$ -Al<sub>2</sub>O<sub>3</sub> systems to benzene seem to be correlated with the amounts of monolayer structures of molybdate, vanadate and chromate species on the surfaces of oxidized catalysts. However, maximal specific dehydrogenation activities of these catalysts are observed at transition metal concentration levels corresponding to “full monolayer” coverages of  $\gamma$ -Al<sub>2</sub>O<sub>3</sub> by transition metal oxides, with additional formation of multilayered metalates and, partly, bulk phases of Al<sub>2</sub>(MoO<sub>4</sub>)<sub>3</sub>, AlVO<sub>4</sub> and  $\alpha$ -Cr<sub>2</sub>O<sub>3</sub>, respectively.

## Conclusions

Catalytic activities and selectivities to benzene for MoO<sub>3</sub>/ $\gamma$ -Al<sub>2</sub>O<sub>3</sub>, V<sub>2</sub>O<sub>5</sub>/ $\gamma$ -Al<sub>2</sub>O<sub>3</sub> and Cr<sub>2</sub>O<sub>3</sub>/ $\gamma$ -Al<sub>2</sub>O<sub>3</sub> systems in cyclohexane dehydrogenation have been investigated. It is supposed that the differences in concentration levels corresponding to maximal specific activities and selectivities of these catalysts for cyclohexane dehydrogenation could be related to different degrees of  $\gamma$ -alumina coverages by monomeric and polymeric forms of transition metal ions.

## References

1. J.J.H.B. Sattler, J. Ruiz-Martinez, E. Santillan-Jimenez, B.M. Weckhuysen, *Chem. Rev.*, **114**, 10613 (2014).
2. S.A. Moya, M. Escudey, *J. Chem. Soc. Chem. Commun.*, **16**, 1829 (1994).

# Ammonia synthesis activity of copper- and iron-substituted $\text{Ni}_2\text{Mo}_3\text{N}$

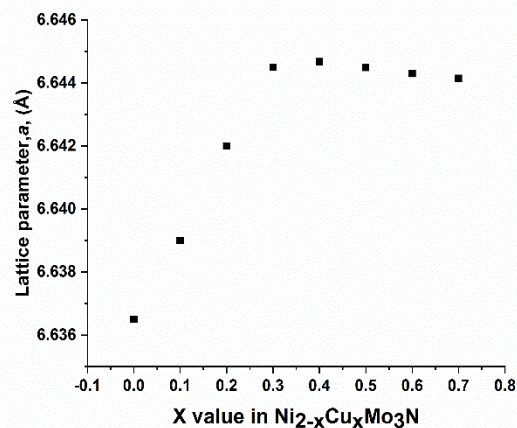
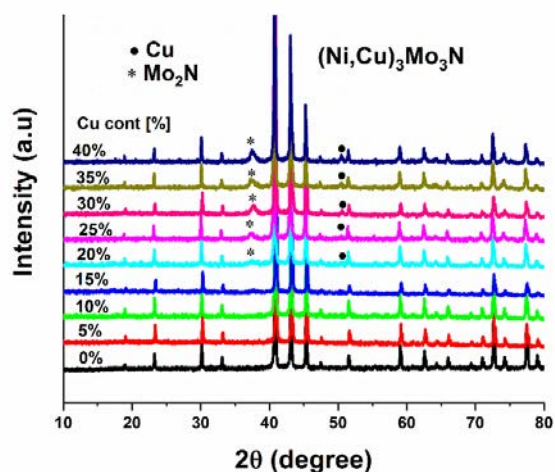
*Samia Al Sobhi, University of Southampton, UK; Justin S. J. Hargreaves, University of Glasgow, UK; Andrew L. Hector, University of Southampton, UK; Said Laassiri, University of Glasgow, UK*

## Introduction

Metal nitride materials have attracted attention as catalysts for a variety of heterogeneous catalytic processes [1] and some materials have shown a significant activity of for ammonia synthesis [2, 3]. There is a significant literature of ternary materials including  $\text{Co}_3\text{Mo}_3\text{N}$  and  $\text{Ni}_2\text{Mo}_3\text{N}$  but few studies exist of varying the electronic structure of these materials by substitution. In this work we have produced solid solutions of the form  $(\text{Ni},\text{M})_2\text{Mo}_3\text{N}$  ( $\text{M} = \text{Cu}$  or  $\text{Fe}$ ) and investigated their ammonia synthesis activity.

## Results and Discussion

A citrate-gel route was used to make intimate mixtures of oxide materials that were fired in ammonia at 900 °C to produce the quaternary metal nitrides. The lattice parameters of  $\text{Ni}_{2-x}\text{Cu}_x\text{Mo}_3\text{N}$  initially increase in an almost a linear trend with increasing contents of copper in the compositions up to  $x = 0.3$ , but with further Cu additions impurity levels increase and the lattice parameter no longer changes (Figure 1). This appears to be the solubility limit of Cu in  $\text{Ni}_2\text{Mo}_3\text{N}$  under these synthesis conditions. Addition of iron resulted in a linear increasing lattice parameter



in the compositions up to  $x = 1.2$  with impurities produced when doping beyond this limit.

Figure 1: XRD patterns (left) and refined lattice parameters (right) of  $\text{Ni}_{2-x}\text{Cu}_x\text{Mo}_3\text{N}$ . Ammonia synthesis from 75%  $\text{H}_2$  and 25%  $\text{N}_2$  was carried out at ambient pressure. All of the materials were found to be highly active at 500 °C, while only limited amounts of ammonia was generated at 400 °C. The catalytic ammonia synthesis results revealed that doping  $\text{Ni}_2\text{Mo}_3\text{N}$  with iron metal increases its catalytic activity. In contrast, the addition of copper to the  $\text{Ni}_2\text{Mo}_3\text{N}$  lattice resulted in decreased performance (Fig. 2).

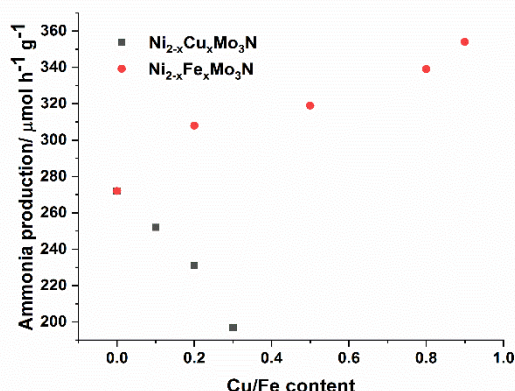


Table 1: Ammonia synthesis rates for  $\text{Ni}_{2-x}\text{Cu}_x\text{Mo}_3\text{N}$

$\text{Ni}_{2-x}\text{Fe}_x\text{Mo}_3\text{N}$  systems at 500 °C for 5 hr

$\text{Ni}_{2-x}\text{Cu}_x\text{Mo}_3\text{N}$ (x)	Ammonia rate μ mole of $\text{NH}_3$ $\text{h}^{-1}\text{g}^{-1}$	$\text{Ni}_{2-x}\text{Fe}_x\text{Mo}_3\text{N}$ (x)	Ammonia rate μ mole of $\text{NH}_3$ $\text{h}^{-1}\text{g}^{-1}$
0	272	0	272
0.1	252	0.2	308
0.2	231	0.5	319
0.3	197	0.8	339
		0.9	354

Figure 2: Ammonia synthesis rates for  $\text{Ni}_{2-x}\text{Cu}_x\text{Mo}_3\text{N}$  and  $\text{Ni}_{2-x}\text{Fe}_x\text{Mo}_3\text{N}$  systems at 500 °C for 5 hr

## Conclusion

- $\text{Ni}_{2-x}\text{Cu}_x\text{Mo}_3\text{N}$  systems were successfully developed up to  $x=0.3$
- Doping process over  $\text{Ni}_2\text{Mo}_3\text{N}$  using transition metals such as iron has been demonstrated to be an effective way in improving the efficiency of ammonia synthesis process.

## References

- 1 S. T. Oyama, *Catal. Today*, 1992, **15**, 179–200.
- 2 R. Kojima and K. I. Aika, *Appl. Catal. A Gen.*, 2001, **219**, 141–147.
- 3 N. Bion, F. Can, J. Cook, J. S. J. Hargreaves, A. L. Hector, W. Levason, A. R. McFarlane, M. Richard and K. Sardar, *Appl. Catal. A Gen.*, 2015, **504**, 44–50.

# **Effect of thermal vapor treatment of support material on catalytic performance of NaWMn/SiO<sub>2</sub> in oxidative coupling of methane**

*Ponomareva E.A., Gordienko Yu.A., Sinev M. Yu., Semenov Institute of Chemical Physics, Russian Academy of Sciences, Moscow, Russian Federation;  
Ivakin Yu.D., Lomonosov Moscow State University, Moscow, Russian Federation*

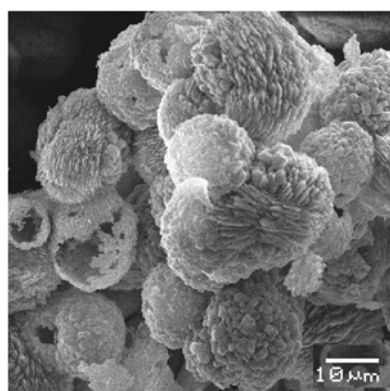
Mixed NaWMn-oxide supported on SiO<sub>2</sub> is the most efficient catalyst for the highly attractive one-step conversion of methane into ethylene (oxidative coupling of methane – OCM) and, at the same time, the most mysterious in terms of its operation mechanism [1]. It is already well established that the presence and interaction of all the components, including the SiO<sub>2</sub> support ( $\alpha$ -cristobalite), are crucial for the high activity and selectivity of this system. In this regard, the research interest is focused on the preparation techniques and/or silica support variation [2,3]. It should be noted that usually the starting silica is X-ray amorphous. Its phase transformation into  $\alpha$ -cristobalite occurs at the calcination step (> 650°C) in the presence of alkali metal (sodium). Without it, crystallization of amorphous silica starts at temperatures above 1000°C; it is accompanied by annealing and collapse of the initial porous structure. The treatment of silica with water vapor at temperatures close to the critical point of water (374°C, 22,1 MPa) makes it possible to convert amorphous phase into crystalline at lower temperatures and gives unique opportunity to directly control both the crystallinity and morphology of the resulted material [4]. In this work we studied the effect of the preliminary thermal vapor treatment (TVT) of the silica support onto the catalytic performance of the NaWMn/SiO<sub>2</sub> samples of the same composition in the OCM reaction.

## **Experimental**

The TVT of amorphous silica (SiO<sub>2</sub>, particle size of 200-300  $\mu$ m, Davisil, Aldrich) was performed at 300, 340, and 370°C and equilibrium pressure of saturated water vapor. XRD and SEM techniques served to characterize structure and morphology of the obtained materials which further were used as supports. The catalysts containing (in wt. %): 0.8 Na, 3.2 W, 2 Mn, were prepared by the incipient wetness impregnation. Catalytic experiments were carried out in a flow type quartz reactor at 800°C and atmospheric pressure.

## Results

Being treated at 370°C, the granulated SiO<sub>2</sub> turned into powder, while the particles remained granulated at lower temperatures. As seen at Fig. 1, a single particle of SiO<sub>2</sub>-340 consists of stuck silica globules of 10-20 μm in diameter; two morphologies of SiO<sub>2</sub> – thin plate-like and rounded crystallites – are well distinguished. According to the XRD data, α-cristoballite dominated in SiO<sub>2</sub>-300, while α-quartz – in SiO<sub>2</sub>-370 sample; the intensities of α-cristoballite and koezite reflexes were nearly the same for the sample treated at 340°C. Based on their morphology and crystalline structure, SiO<sub>2</sub>-300 and SiO<sub>2</sub>-340 were chosen for the preparation of NaWMn/SiO<sub>2</sub> catalysts.



ig.1 SEM images of TVT-treated SiO<sub>2</sub> at 340°C

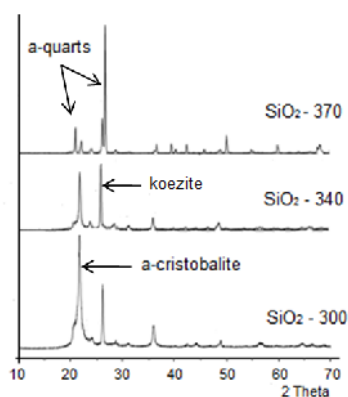


Fig.2 XRD pattern of TV-treated silica

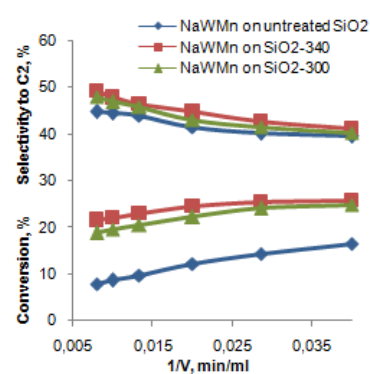


Fig.3 Methane conversion and selectivity to C<sub>2</sub>-products versus reverse flow rate

The activity of the catalysts based on the TV-treated silica was nearly twice higher and their selectivity towards C<sub>2</sub>-products was also higher (Fig.3). Taking into account that chemical compositions and specific surface areas of all three catalysts were equal, the differences in their catalytic performance were attributed to the morphological features of the support and its interaction with the deposited mixed oxides [1]. All in all, it was shown that the catalytic performance of the NaWMn-oxide deposited on silica can be improved by the preliminary thermal vapor treatment of the support that allows one to vary its phase composition and morphology.

This work was financially supported by the RFBR (Project No. 18-29-06055)

## References

1. Sinev M., Ponomareva E., Sinev I. *et al. Cat. Today., in press*, DOI 10.1016/j.cattod.2018.06.028 (2018).
2. Uzunoglu, C., Leba, A. & Yildirim, R. *Appl. Catal. A Gen.* 547, 22–29 (2017).
3. Yildiz, M., Aksu Y., Simon U., *et al. Appl. Catal. A Gen.* 525, 168–179 (2016).
4. M. Danchevskaya, S. Torbin, Yu. Ivakin, *et al. J. Supercritical Fluids* 42, 419-424(2007).

# Microkinetic Modeling of Olefin Cracking and Methanol-to-Olefins (MTO) over ZSM-5

*Sebastian Standl; Tobias Kühlewind; Felix M. Kirchberger; Johannes A. Lercher;*

*Olaf Hinrichsen*

*Technical University of Munich, Department of Chemistry, Lichtenbergstraße 4,  
85748 Garching near Munich, Germany;*

*Technical University of Munich, Catalysis Research Center, Ernst-Otto-Fischer-  
Straße 1, 85748 Garching near Munich, Germany;*

*Markus Tonigold*

*Clariant Produkte (Deutschland) GmbH, Waldheimer Straße 13, 83052 Bruckmühl,  
Germany*

## Introduction

Alternative concepts for producing lower olefins on demand gain in importance. Using shape-selective acid zeolites like ZSM-5, catalytic cracking of higher olefins as well as methanol-to-olefins (MTO) [1] can be exploited to satisfy growing propene demands. For these processes, the reaction networks are extremely complex due to the consideration of thousands of elementary steps, which complicates their theoretical description. On the other hand, lumping is not an option when the model should allow extrapolation out of the experimentally covered regime [2]. In this work, it is shown how the flexibility of a microkinetic model for 1-pentene cracking [3] can be enhanced [4]. Subsequently, this model can be transferred to MTO through introducing the methanol related reactions. Finally, an industrial multi-stage recycle reactor according to the methanol-to-propylene (MTP) concept is simulated.

## Methods

Microkinetics are applied here as these are helpful not only to describe the reactor output, but also to obtain insight into intermediates and preferred reaction pathways. The single-event methodology is used to keep the number of estimated fitting parameters within a reasonable range [5]. The application range of the cracking model is increased by strictly separating between kinetic and catalyst descriptors which includes an analysis of sorption processes. For the creation of the MTO model, the reactions between methanol, DME and water have to be implemented as well as the olefin methylation reactions both via methanol and DME. In addition, the formation of side products is incorporated according to the pathway postulated in [6].



## Results

The validity of the cracking model over broad reaction conditions and catalyst properties can be proven [4]. Consequently, it is suitable to be transferred to MTO. The updated reaction network contains over 4000 steps, but only twelve

estimated parameters are necessary to achieve a reasonable description of all species, see Figures 1 and 2. It can be shown that fast methylation rates and subsequent cracking of higher olefins are the crucial pathways for maximum propene

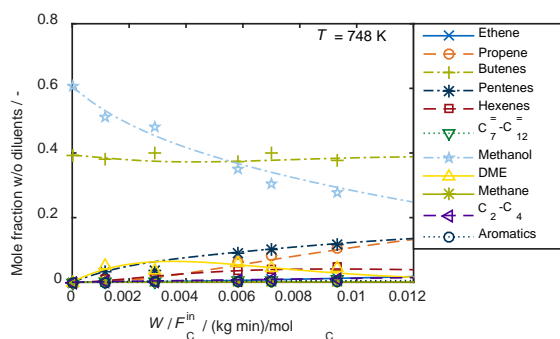


**Figure 2:** Comparison between kinetic data (symbols) and microkinetic model (lines).

## Conclusions

Through microkinetic modeling, vast insight into reactivity can be obtained. This concept is applied to describe the complex hydrocarbon conversion over ZSM-5 on a fundamental level. Such

information about preferred reaction pathways is indispensable to optimize the industrial recycle reactor with the aim of maximum propene production.

## References

- [1] U. Olsbye *et al.*, *Angew. Chem. Int. Ed.* **2012**, *51*, 5810–5831.
- [2] S. Standl and O. Hinrichsen, *Catalysts* **2018**, *8*, 626.
- [3] T. von Aretin *et al.*, *Ind. Eng. Chem. Res.* **2015**, *54*, 11792–11803.
- [4] S. Standl *et al.*, *Ind. Eng. Chem. Res.* **2017**, *56*, 13096–13108.
- [5] J.W. Thybaut and G.B. Marin, *J. Catal.* **2013**, *308*, 352–362.
- [6] S. Müller *et al.*, *J. Am. Chem. Soc.* **2017**, *7*, 5773–5780.

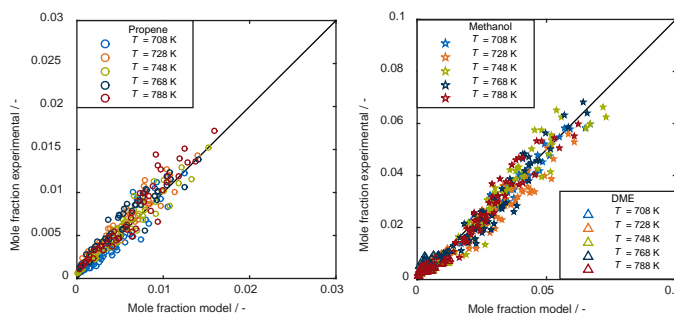


**Figure 1:** Parity plots for propene (left) and oxygenates (right).

yields. This insight is exploited in a following step where the industrial MTP reactor is simulated. Figure 3 shows propene as main product; however, the propene-to-ethene ratio should be further increased by optimizing process conditions.

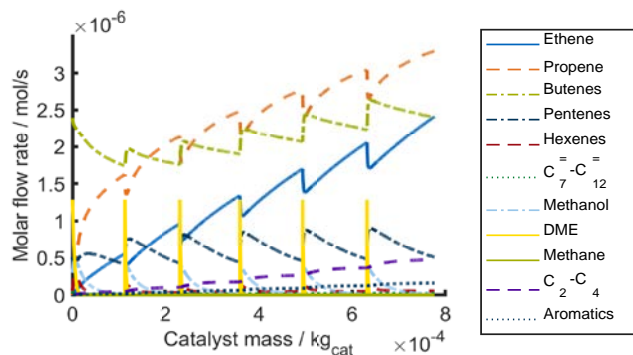


**Figure 3:** MTP reactor model with six catalyst beds at  $T = 748$  K.

# Oxidative Dehydrogenation of Ethane over MoVTeNb Mixed Metal Oxides: Kinetic Investigation and Modeling

*Philipp Donaubauer, Daniel Melzer, Maricruz Sanchez-Sanchez,*

*Johannes A. Lercher and Olaf Hinrichsen*

*Technical University of Munich, Department of Chemistry,*

*Lichtenbergstr. 4, 85748 Garching near Munich, Germany*

*Technical University of Munich, Catalysis Research Center,*

*Ernst-Otto-Fischer-Str. 1, 85748 Garching near Munich, Germany*

*Klaus Wanninger, Gerhard Mestl*

*Clariant Produkte (Deutschland) GmbH,*

*Waldheimer Str. 13, 83052 Bruckmühl, Germany*

## Introduction

Oxidative dehydrogenation (ODH) of ethane is a promising route towards selective production of ethene. One of the most promising catalytic materials is the M1 phase of MoVTeNb mixed metal oxides (cf. Fig. 1) being highly active at mild temperatures around 300 to 350 °C [1]. Hence, a high ethane selectivity and yield can be achieved by suppressing side reactions to carbon oxides or oxygenates like acetic acid (cf. Fig. 1). Formation of the latter is dependent on the water partial pressure [2]. In this study, we investigate the kinetic behavior of a MoVTeNbO<sub>x</sub> catalyst.

## Methods

The MoVTeNbO<sub>x</sub> catalyst was synthesized following the metal oxide based procedure developed by Mestl *et al.* [3] with a metal molar ratio of 1:0.30:0.05:0.05. Measurements were performed in PFR setup with SiC-diluted catalyst bed. Reactor effluents were analyzed using a modified Shimadzu GC2014 equipped with TCD and FID detector capable of quantifying C<sub>2</sub> hydrocarbons and oxygenates, CO, CO<sub>2</sub>, O<sub>2</sub> as well as N<sub>2</sub> (used as internal standard). Bed temperatures were recorded and used for the kinetic model. Inter- and intraparticle transport effects could be excluded.

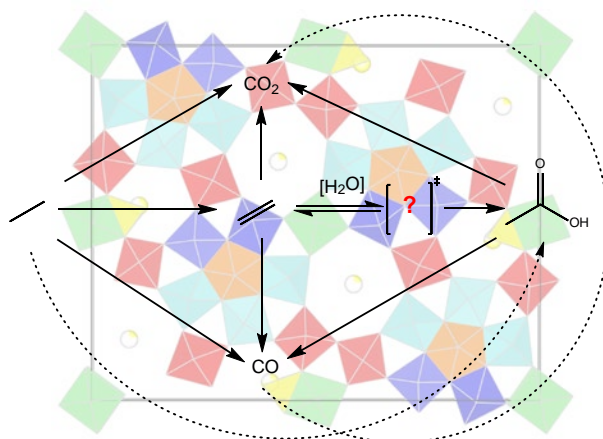


**Fig 1:** Reaction scheme for ODH of ethane and the 2D unit cell of the M1 phase along the 001 axis.

Temperature was varied between 290 and 370 °C. Inlet partial pressures of C<sub>2</sub>–species and O<sub>2</sub> ranged from 0.025 to 0.65 mbar and 0.05 to 0.25 mbar, respectively. Model discrimination is performed for five responses resulting in more than 600 degrees of freedom during optimization. A multitude of kinetic models is derived and tested by statistical methods.

## Results and Discussion

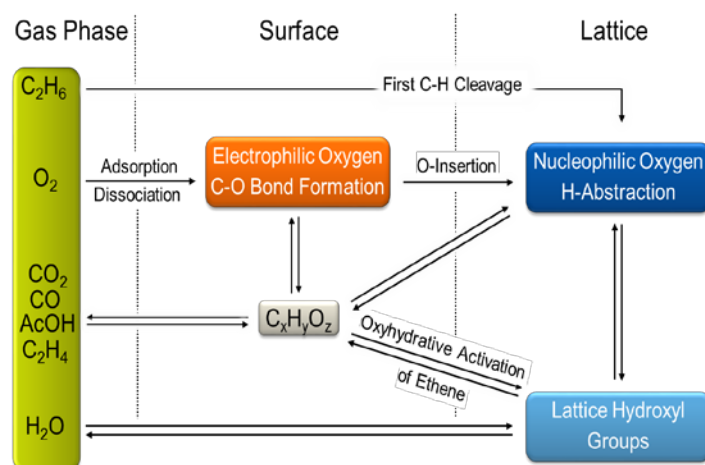


**Fig 2:** Schematic illustration of possible reaction pathways in ODH of ethane over MoVTenb mixed metal oxides.

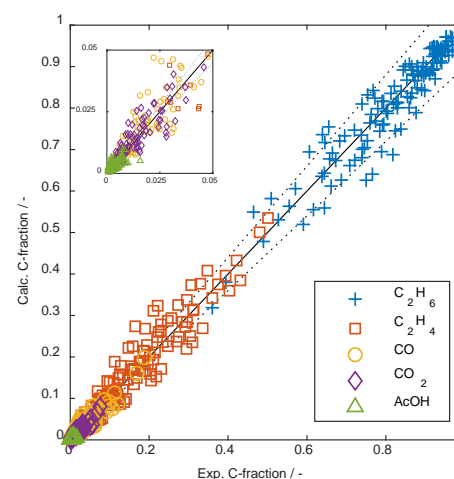


**Fig 3:** Parity plot of carbon fractions comparing kinetic model and experiments.

Reaction pathways of ODH over MoVTenb mixed metal oxide are currently highly under debate. The origin and nature of the active oxygen species, responsible for the first C-H bond cleavage, is one of the crucial aspects during model development [4, 5]. In addition, the role of hydroxyl groups and the formation of oxygenates have to be evaluated, to build a sophisticated kinetic model. The scheme in Fig. 2 displays the interactions between the species in the gas phase, on the surface and in the surface-near oxide lattice. First results indicate that multiple active oxygen species are necessary to adequately account for the different surface reactions, which is in accordance to a kinetic description developed for selective propane oxidation [6]. Experimental and numerically predicted values for the carbon fractions in the product stream are compared to the model predictions in Fig. 3.

## References

- [1] Gärtner, C.A. *et al.*, *ChemCatChem* **2013**, 5, 3196.
- [2] Li, X., Iglesia, E., *J. Phys. Chem. C* **2008**, 112, 15001.
- [3] Mestl, G. *et al.*, German Patent DE 102017000861 (A1), 2017.
- [4] Zhu, Y. *et al.*, *J. Am. Chem. Soc.* **2017**, 139, 12342.
- [5] Cheng, M.-J. and Goddard, W. A. (III), *Top. Catal.* **2016**, 59, 1506.
- [6] Sprung, C. *et al.*, *Catalysts* **2018**, 8, 330.

# **M1-MoVTenb metal oxide catalysts with high intrinsic activity in ethane oxidative dehydrogenation**

*Daniel Melzer<sup>1</sup>, Gerhard Mestl<sup>2</sup>, Klaus Wanninger<sup>2</sup>, Yuanyuan Zhu<sup>3</sup>, Maricruz Sanchez-Sanchez<sup>1</sup>, Johannes Lercher<sup>1,3</sup>,*

*<sup>1</sup>Department of Chemistry and Catalysis Research Center, Technische Universität München, Garching, Germany, <sup>2</sup>Clariant Produkte (Deutschland) GmbH, Bruckmühl, Germany, <sup>3</sup>Institute for Integrated Catalysis, and Fundamental and Computational Science Directorate, Pacific Northwest National Laboratory, Richland (WA), USA*

## **Introduction**

The M1 crystalline phase of Mo-V-Te-Nb mixed metal oxides is an exceptionally active and selective catalyst for selective oxidation of lower alkanes.[1, 2] However, the activity in oxidative dehydrogenation (ODH) of ethane of M1 catalysts must be increased in order to compete with the established production of ethene in large steam crackers. Here, we investigate the chemistry involved in the formation and crystalline growth of complex MoVTenb oxides, with the objective of maximizing the surface concentration of active sites.

## **Experimental**

A series of MoV(Te,Nb) mixed metal oxides was prepared by hydrothermal synthesis. Samples extracted during the synthesis were characterized by electron microscopy, XRD, N<sub>2</sub> adsorption, UV/VIS spectroscopy and ICP-OES. Catalytic activity in ethane ODH was tested in the range of 330 – 420 °C in a plug flow reactor.

## **Results and Discussion**

We have developed a new synthesis method of MoVTenb oxides [3] that yielded catalysts one order of magnitude more active in ODH of ethane (Figure 1, a). Controlling the metal stoichiometry and the concentration of ions in solution allowed the direct formation of crystalline M1 phase at temperatures ca. 400 °C lower than previous methods.

Analysis of HAADF-STEM images with atomic resolution (Figure 1, b) revealed that the superior catalytic performance of M1 oxides formed at low temperatures is related to the preferential formation of crystal terminations that expose active facets [4].

We also investigated the effect of metal composition on the catalytic performance of these new M1-MoVTeNb oxides. Limiting the concentrations of Te and Nb to values below 5 mol % significantly promoted the activity in ethane ODH and maintained a high selectivity towards ethylene.

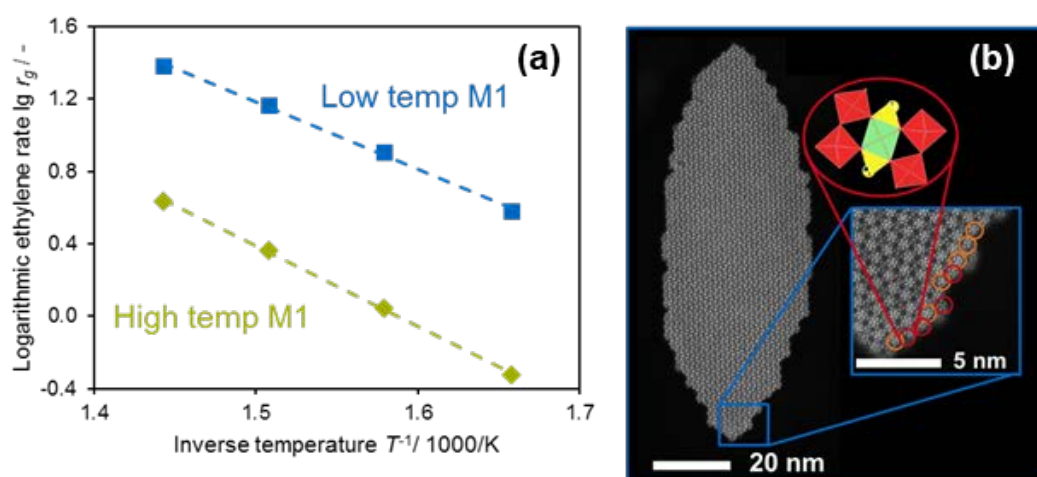


**Figure 1.** a) Arrhenius type plot of ODH activity for M1 materials prepared at high (600 °C) and low (190 °C) temperatures.  $C_2H_6/O_2/He$  mixtures of 9/9/82 mol,  $p = 1$  bar(a),  $WHSV = 6.8-14.5 h^{-1}$ . b) HAADF-STEM image of a M1-MoVTeNb oxide crystal formed at low temperatures. The inset shows crystal lateral termination exposing metal lattice positions where active vanadyl species are located.

## Conclusions

A better understanding of the chemical processes involved in the formation of crystals and the location of active sites on their surface has led to improvement of the catalytic performance of M1-MoVTeNb metal oxides.

## References

- [1] C.A. Gärtner, A. C. Van Veen, J. A. Lercher. *ChemCatChem* 5, 3196 (2013).
- [2] P. Kube, B. Frank, S. Wrabetz, J. Kröhnert, M. Hävecker, J. Velasco-Vélez, J. Noack, R. Schlögl, A. Trunschke. *ChemCatChem* 9, 573 (2017).
- [3] G. Mestl, K. Wanninger, D. Melzer, M. Sanchez-Sanchez, J. Tseglakova, J. A. Lercher. WO 2018/141652 A1, WO 2018/141653 A1, WO 2018/141654 A1
- [4] D. Melzer, P. Xu, D. Hartmann, Y. Zhu, N. D. Browning, M. Sanchez-Sanchez, J. A. Lercher. *Angew. Chem. Int. Ed.* 55, 8873 (2016)

# **Re- and Cs-copromoted silver catalysts for ethylene epoxidation: A theoretical study**

*M.A. Salaev, Tomsk State University, Tomsk, Russia; A.A. Salaeva, Tomsk State University, Tomsk, Russia; O.V. Vodyankina  
Tomsk State University, Tomsk, Russia*

Ethylene oxide is a well-known valuable chemical building block used in various branches of industry. The promoted silver catalysts supported on  $\alpha$ -alumina are employed in industrial ethylene epoxidation. The catalyst performance is significantly boosted by the application of various promoters and modifiers, including Cs, Cl, etc. [1,2]. Among the latter, Re occupies a special place and enhances the catalyst selectivity towards ethylene oxide. Despite the importance of rhenium and detailed experimental investigations, there are only rare data on its surface state and the mechanism of its involvement in the processes [3], while the role of Re is still a debating issue. In the present work we focus on new insights on the nature and mechanism of the synergistic effects in Re- and Cs-promoted Ag catalysts for ethylene epoxidation obtained using the density functional theory approach.

Multiple systems containing silver slabs and/or ethylene and/or promoter (Re or/and Cs) were calculated using the OpenMX software package [4] installed at SKIF "Cyberia" supercomputer of Tomsk State University. The models of active sites for Re- or/and Cs-promoted catalysts were developed, and various oxygen species were considered. The GGA approximation and PBE functional with the periodic boundary conditions were employed. A periodic model of silver surface was proposed, where the silver layers were separated by a layer of vacuum sufficient to prevent the interaction between the adjacent layers. The surface model was tested to obtain the constant surface energy. A set of k-points of  $5 \times 5 \times 1$  and the cutoff energy of 400 eV were used. The geometries of all obtained structures were fully optimized. The predicted change in energy of less than  $-1.0 \times 10^{-8}$  was taken as a convergence criterion.

The nature and peculiarities of the promoting action of Re oxyanion are proposed and discussed. The roles of oxygen species bound to silver and Re are proposed. Re and Cs are shown to exhibit a synergistic action in a cooperation with silver. Cs is shown to stabilize Re oxyanion that enhances the catalyst performance. Re is

proposed to alter the electronic density distribution, with oxygen atoms of Re oxyanion compensating the oxygen vacancies and covering the non-selective sites over silver.

### **Acknowledgements**

This work was supported by the Russian Science Foundation (grant No. 18-73-00296).

### **References**

- [1] S. Linic, M.A. Barteau. *J. Am. Chem. Soc.* 126 (2004) 8086.
- [2] M.O. Özbek, I. Önal, R.A. van Santen. *ChemCatChem* 5 (2013) 443.
- [3] W. Diao, C.D. Di Giulio, M.T. Schaal, S. Ma, J.R. Monnier. *J. Catal.* 322 (2015) 14.
- [4] T. Ozaki, *Phys. Rev. B.* 67, 155108, (2003).

# Hydrodeoxygenation of glycerol to propylene over Mo-based catalysts: Effect of dopant and support nature

V.-L. Yfanti<sup>1</sup>, E. Tsarouchi<sup>1</sup>, V. Zacharopoulou<sup>1</sup>, A.A. Lemonidou<sup>1,2</sup>

<sup>1</sup>*Department of Chemical Engineering, Aristotle University of Thessaloniki, University campus, Thessaloniki, 54124, Greece*

<sup>2</sup>*Chemical Process Engineering Research Institute, Thessaloniki, 57001, Greece*

## 1. Introduction

Over the last decades the demand for olefins is constantly raising as they are key building blocks in the chemical industry. However, their production is limited by economic and environmental concerns related to the use of fossil resources as feedstock. [1] Thus the need for alternative and sustainable routes for olefin production is imperative. Biomass derived intermediates, such glycerol, can serve as feedstock for olefin production, following alternative reaction pathways. This study refers to one-step bio-propylene production via complete glycerol de-oxygenation, over Mo-based catalysts, a novel research subject that has not yet been thoroughly explored in the open literature. Typically, glycerol de-oxygenation takes place in liquid phase, at 300°C, for 2hr and under 8.0MPa H<sub>2</sub>, using water as a solvent [2]. This work focusses on the effect of dopants (Pd, Ir, Ni) and supports (black carbon, ZrO<sub>2</sub>, CeO<sub>2</sub>-ZrO<sub>2</sub>, HZSM-5) on the performance of Mo-based catalysts in hydrodeoxygenation of glycerol to propylene.

## 2. Results and discussion

Up to now Mo/C catalyst have showed very promising results obtaining 70% selectivity to C<sub>3</sub>H<sub>6</sub> at 68% glycerol conversion for 2h reaction time [2]. The addition of Fe has a negative effect on Mo/C acidity leading to lower glycerol conversion values (48.9%). However, Fe-Mo/C performance increases after 6hr reaction time, showing 89% and 76.1% conversion and selectivity to C<sub>3</sub>H<sub>6</sub>, respectively [2]. In both cases, C<sub>3</sub>H<sub>6</sub> is the main product formed and the only one in gas phase, while 2-propenol and propylene-glycol are the main products in the liquid phase (though with significantly lower selectivity, 4-8%), maintaining at the same time the 3C atoms on



the glycerol molecule. Increased temperature and especially H<sub>2</sub> pressure favor glycerol conversion towards C<sub>3</sub>H<sub>6</sub>, suppressing the formation of partially de-oxygenated products [2]. C<sub>3</sub>H<sub>6</sub> is mainly formed via glycerol conversion to 2-propenol and subsequent conversion of the latter to C<sub>3</sub>H<sub>6</sub>. However, the low contribution to propylene formation of a secondary route which involves the successive hydrodeoxygenations of glycerol to 1,2-propanediol and 2-propanol and the dehydration of the latter, could not be excluded [3]. The presence of H<sub>2</sub> is a key parameter as it suppresses the 2-propenol to propanal isomerization, leading to increased concentration of 2-propenol, thus enabling its subsequent conversion to C<sub>3</sub>H<sub>6</sub>. The reduced states of MoO<sub>3</sub>, Mo<sup>+4</sup> and Mo<sup>+5</sup> are considered as the active sites for the selective conversion of glycerol to C<sub>3</sub>H<sub>6</sub>, as indicated by XRD and XPS measurements. Most likely, the formation of Mo<sup>+4</sup> and Mo<sup>+5</sup> species drives the reaction to the desired product formation through two consecutive reverse Mars–van Krevelen mechanistic cycles [3].

In order to improve the catalytic performance (increase catalyst acidity as well as hydrogenation rate), bifunctional catalysts with both metal and medium to strong acids sites are to be prepared. Apart from black carbon other materials with varying acidity like ZrO<sub>2</sub>, CeO<sub>2</sub>-ZrO<sub>2</sub>, sulfated ZrO<sub>2</sub> and H-ZSM-5 will be used as supports for Mo catalysts or added mechanically mixed as co-catalysts. Efforts will be also devoted to strengthen the metallic function of Mo species by adding Pd, Ir, or Ni. The preparation of the catalysts and their evaluation in the selective de-oxygenation of glycerol to propylene is in progress.

#### **Acknowledgements**

*This research has been co-financed by the European Union and Greek national funds through the Operational Program Competitiveness, Entrepreneurship and Innovation, under the call RESEARCH–CREATE–INNOVATE(projectcode:T1EDK-02864)*

#### **References**

- [1] Z. Y. Zakaria, N.A.S. Amin, J. Linnekoski, Biomass Bioenerg. 55 (2013) 370-385.
- [2] V. Zacharopoulou, E. Vasiliadou, A.A. Lemonidou, Green Chem. 17 (2015) 903-912.
- [3] V. Zacharopoulou, E. Vasiliadou, A.A. Lemonidou, ChemSusChem 11 (2018) 264-275.

# Revealing the structural and chemical state of platinum nanoparticles during oxidation of NO to NO<sub>2</sub> at nitric acid plant conditions

Ata ul Rauf Salman<sup>1</sup>; Samuel K. Regli<sup>1</sup>; Bjørn Christian Enger<sup>2</sup>; Rune Lødeng<sup>2</sup>; David Waller<sup>3</sup> and Magnus Rønning<sup>1</sup>.

<sup>1</sup> Department of Chemical Engineering, Norwegian University of Science and Technology (NTNU), Sem Sælands vei 4, NO-7491 Trondheim, Norway

<sup>2</sup> SINTEF Industry, Kinetic and Catalysis group, P.O. Box 4760, Torgarden, NO-7465 Trondheim, Norway

<sup>3</sup> YARA Technology Center, Herøya Forskningspark, Bygg 92, Hydrovegen 67, NO-3936 Porsgrunn, Norway

## Introduction

Nitric acid is an important commodity chemical produced industrially via the Ostwald process. Oxidation of NO is an important chemical step in the process, carried out as a gas phase homogenous reaction in a series of heat exchangers [1]. Process intensification can be achieved by using a catalyst for NO oxidation, which can potentially speed up the process, enable significant heat recovery and reduce capital expenditure (CAPEX). Typical gas composition at the outlet of the NH<sub>3</sub> combustor is 10% NO, 6% O<sub>2</sub> and 15% H<sub>2</sub>O [1], which defines the boundary limits for the catalytic process. Platinum catalysts supported on alumina have shown excellent activity towards oxidation of NO at nitric acid plant conditions [2]. High steam content is an integral component of the feed but the effect of water on the activity of the catalyst is not fully understood.

Here we report operando studies on the impact of water on the structural and chemical state of platinum during oxidation of NO at simulated nitric acid plant conditions using X-ray diffraction (XRD) and X-ray absorption spectroscopy (XAS).

## Materials and Methods

A 5wt.% Pt/γ-Al<sub>2</sub>O<sub>3</sub> was prepared by incipient wetness impregnation. Operando studies were performed at the European Synchrotron Radiation Facility (BM31, ESRF France). An *in situ* cell based on a quartz capillary reactor (O.D = 1mm) was used. Collection of XAS data was performed in transmission mode. X-ray diffraction patterns were collected and effluent gas was analyzed using a mass spectrometer. The effect of water was investigated by performing four sequential temperature ramp experiments in absence and presence of 15% water in an artificial feed stream (10% NO, 6% O<sub>2</sub>) at 1 bar simulating nitric acid plant conditions.

## Results and Discussion

The blank run shows the contribution from gas phase reactions, NO conversion decreasing with increasing temperatures as shown in Fig.1(a), which is in accordance with the negative activation energy for NO oxidation [3]. For the first temperature ramp carried out in dry feed, catalytic activity starts at 200°C and increases gradually until it becomes thermodynamically limited close to 400°C. Addition of water in the feed in the subsequent temperature ramp does not affect the onset temperature of catalytic activity. However, a slight inhibition effect is observed in the range 270-375°C. A significant increase in conversion is observed in the subsequent ramp in absence of water. Succeeding temperature ramps in wet feed show a more pronounced inhibition effect compared to the second ramp.

Analysis of the acquired in situ Pt-L<sub>3</sub> edge EXAFS spectra shows that after reduction, the Pt/ $\gamma$ -Al<sub>2</sub>O<sub>3</sub> catalysts resembles the Pt foil spectrum, indicating a complete reduction of Pt. However, on exposure to NO & O<sub>2</sub> during the first ramp, partial oxidation of platinum occurs as seen in Fig.1(b). Upon exposure to water, sintering of platinum occurs indicated by significantly higher contribution from the Pt-Pt path length and increase in Pt-Pt coordination number as shown in Fig.1(c). XRD patterns confirmed sintering of platinum with an increase in crystallite size from 2.5 nm to 8 nm. NO Oxidation over Pt is structure sensitive with larger particles favoring the reaction [4]. This explains the higher conversion in the third ramp while the inhibition effect of water is attributed to the competitive adsorption of water on active sites.

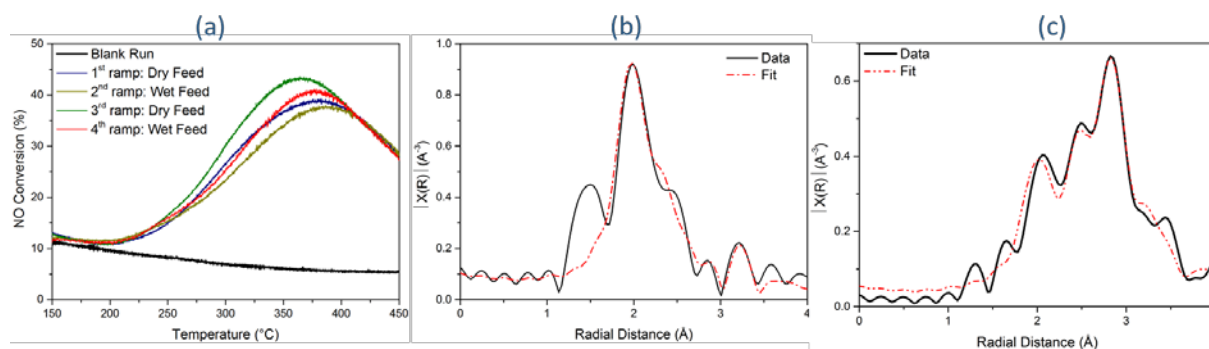


**Figure 1** (a) Conversion of NO to NO<sub>2</sub> as a function of temperature for feed composition: 10% NO and 6% O<sub>2</sub> (15% H<sub>2</sub>O if present) in Ar. k<sup>2</sup>-weighted Fourier transformed Pt-L<sub>3</sub> edge EXAFS spectra (r-space) in (b) dry feed (c) wet feed.

## References

1. Honti, Akademiai Kiado, 1976, pp. 400-413.
2. A. u. R. Salman, B. C. Enger, X. Auvray, R. Lødeng, M. Menon, D. Waller and M. Rønning, *App. Catal. A: General*, 564, 142 (2018).
3. D. Baulch, D. Drysdale and D. Horne, CRC Press, 1973, pp. 285–300.
4. E. Xue, K. Seshan and J. R. H. Ross, *Appl. Catal. B: Environ.*, 1996, **11**, 65-79.

# IR Operando Study of Ethanol Dehydration over MFI Zeolites

*Shashikant A. Kadam, Mariya V. Shamzhy*

*Department of Physical and Macromolecular Chemistry, Faculty of Science, Charles University in Prague, Hlavova 2030, 12840, Prague 2, Czech Republic*

## 1. Scope

Recent advances in the synthesis of layered (2D) zeolites have a major impact on the continuous improvement of zeolites as tailor-made catalysts. Despite high prospect for application of layered zeolites in catalysis, there are very few studies describing the intrinsic reactivity of the acid sites in 2D zeolites [1].

The catalytic dehydration of alcohols has the potential for the production of valuable chemicals. Insights in the reaction mechanism, such as the effect of acid strength and confinement on the formation of targeted products are essential for the process design. Recent kinetic studies of Iglesia et al. on methanol-to-DME dehydration allowed to relate the values of both zero- and first-order rate constants to the strength of acid sites in zeolites [2] and revealed a crucial influence of confinement on the first-order rate constant [3].

In this work, we firstly apply *operando* FTIR spectroscopy to address intrinsic reactivity of 2D and conventional 3D MFI zeolites using ethanol-to-DEE dehydration as a model reaction. Simultaneous examination of turnover rates and Brønsted acid sites coverage in 2D and 3D MFI allowed direct assessment of the kinetic (i.e. first-order and zero-order rate constants) and adsorption thermodynamic ( $\Delta H_{\text{ads}}$ ,  $\Delta S_{\text{ads}}$ ) parameters of the most abundant surface species (MASS) with further interpretation of structure–function relationship.

## 2. Experimental part

3D MFI zeolite (Si/Al = 20) was purchased from the Institute for Oil and Hydrocarbon Gases (Slovak Republic), while 2D MFI (Si/Al = 43) was synthesized according to Ref. [4]. The catalysts were characterized using XRD,  $\text{N}_2$  ad-desorption, SEM, FTIR spectroscopy of adsorbed pyridine. Steady-state ethanol dehydration was carried out under atmospheric pressure and various ethanol partial pressures using a transmission *operando* IR reactor-cell as described in Ref. [5].

## 3. Results and discussion

The measured ethanol-to-DEE dehydration turnover rates ( $R_{\text{DEE}}$ ) followed first-order kinetics at  $P_{\text{EtOH}} < 24\text{mbar}$  and zero-order kinetics at  $P_{\text{EtOH}} > 24\text{mbar}$  for both zeolite

catalysts. Such  $R_{\text{DEE}}$  vs.  $P_{\text{EtOH}}$  dependence expressed by Associative dehydration mechanism [6] was subjected to nonlinear regression to extract the first-order and zero-order rate constants and activation energies ( $E_{\text{first}}$ ,  $E_{\text{zero}}$ , Fig. 1). Intensity of the band at  $3604\text{ cm}^{-1}$  in FTIR spectra of “working” catalysts was used to determine the total Brønsted acid coverage and to evaluate the adsorption enthalpies/entropies of ethanol monomeric and dimeric species ( $\Delta H_{\text{ads-M or D}}$ ,  $\Delta S_{\text{ads-M or D}}$ , Fig. 1).

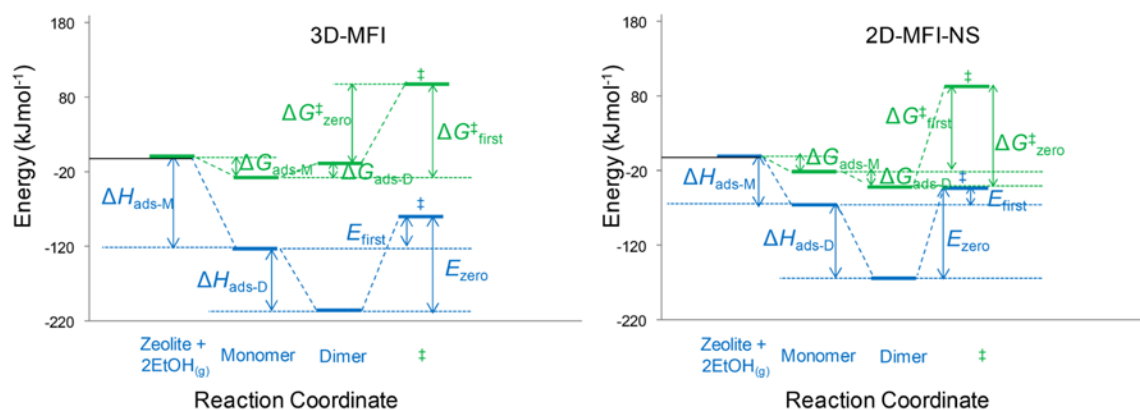


**Figure 1. Reaction coordinate diagram for ethanol-to-DEE dehydration followed Associative mechanism over 3D- and 2D MFI zeolites at  $T = 448\text{ K}$ .**

#### 4. Conclusions

The catalytic results showed smaller first-order activation energy for 2D MFI ( $E_{\text{first}} = 16 \pm 4\text{ kJ mol}^{-1}$ ) vs. 3D MFI ( $E_{\text{first}} = 41 \pm 1\text{ kJ mol}^{-1}$ ) and similar zero-order activation energies ( $E_{\text{zero}} = 117 - 124\text{ kJ mol}^{-1}$ ) for both catalysts. Correlating the kinetic and thermodynamic parameters revealed that the difference in stabilization of adsorbed ethanol monomers and dimers is the origin behind the differences in the intrinsic activities of 2D and 3D MFI zeolites which is reflected in the corresponding zero-order activation entropies ( $\Delta S_{\text{zero}}^{\ddagger} = -24$  and  $15\text{ J K}^{-1}\text{ mol}^{-1}$  for 2D and 3D MFI, respectively).

#### References

- [1] Sauer, J. Faraday Discuss. 2016, 188, 227–234.
- [2] Jones, A. J.; Carr, R. T.; Zones, S. I.; Iglesia, E. J. Catal. 2014, 312, 58–68.
- [3] Jones, A. J.; Zones, S. I.; Iglesia, E. J. Phys. Chem. C 2014, 118, 17787–17800.
- [4] Choi, M.; Na, K.; Kim, J.; Sakamoto, Y.; Terasaki, O.; Ryoo, R. Nature 2009, 461, 246.
- [5] Kadam S.A.; Shamzhy M. J. Phys. Chem. C 2018, 122, 24055–24067.
- [6] Alexopoulos, K.; John, M.; Van der Borght, K.; Galvita, V.; Reyniers, M.-F.; Marin, G. B. J. Catal. 2016, 339, 173–185.

# A greener preparation route of Cu/ZnO catalyst for hydrogenation of carbon dioxide to methanol

*Nat Phongprueksathat, Institute of Chemical Research of Catalonia (ICIQ), Tarragona, Spain; Atsushi Urakawa, Institute of Chemical Research of Catalonia (ICIQ), Tarragona, Spain, Barcelona Institute of Science and Technology (BIST), Barcelona, Spain,*

Utilizing fossil-fuels-derived carbon dioxide by its hydrogenation to methanol is a promising strategy for reducing greenhouse gas emission and producing a renewable chemical feedstock, fuel, and energy carrier [1]. This process commonly employs conventional Cu/ZnO/Al<sub>2</sub>O<sub>3</sub> catalyst due to the high catalytic performance originated from Cu-ZnO synergy [2,3]. However, the preparation method by co-precipitation is not an eco-friendly process due to the production of toxic wastewater containing Na<sup>+</sup> and NO<sub>3</sub><sup>-</sup>, and many alternative precursors have been reported [4–6].

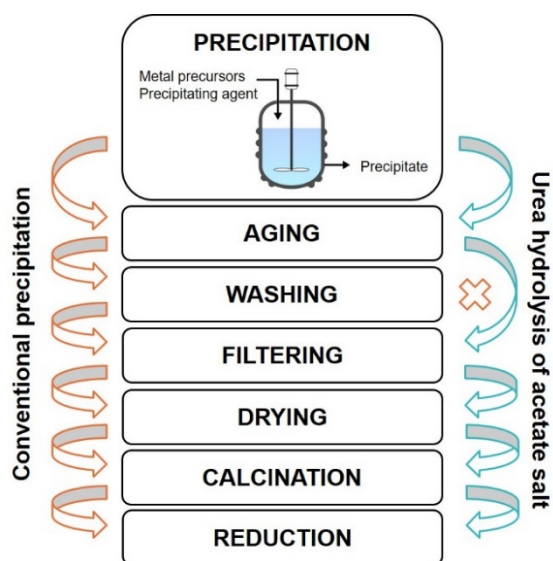


**Fig. 1.** Simplified preparation procedure of Cu/ZnO catalyst from each method.

In this study, a homogeneous precipitation method via urea hydrolysis of acetate salts was developed to prepare 50 wt% Cu-ZnO catalysts. This method was able to intrinsically eliminate not only the catalyst-poisoning components, such as Na<sup>+</sup> and NO<sub>3</sub><sup>-</sup>, but also the washing step, minimizing the amount of wastewater (Fig. 1.). The catalysts were also compared with the one derived from common nitrate salts at the same condition.

XRD characterization of as-precipitated copper zinc hydroxyl carbonate showed that only aurichalcite phase was obtained from acetate salts, while mixed aurichalcite and rosasite phases were obtained from nitrate salts due to the formation of difference meta-stable phase during synthesis confirmed by pH evolution profiles.

Washing step essential for conventional co-precipitation method is also important for urea hydrolysis in case the nitrate salts are used since  $\text{NO}_3^-$  promotes Cu agglomeration during calcination, resulting in larger CuO crystallite size from 8.1 to 18.7 nm (if not washed). On the other hand, the catalyst prepared with the acetate salts gave a comparable CuO crystallite size of 8.1 nm without the washing step.

The performance of the catalysts in high-pressure  $\text{CO}_2$  hydrogenation at 331 bar is shown in Fig. 2. The Cu/ZnO catalyst prepared by urea hydrolysis of nitrate or acetate salts with the washing step exhibited a comparable  $\text{CO}_2$  conversion and methanol selectivity to the commercial Cu/ZnO/ $\text{Al}_2\text{O}_3$  catalyst. Consistent with CuO crystallite size, the unwashed-nitrate catalyst showed very low catalytic activity due to the loss of active Cu surface area, while the unwashed-acetate catalyst showed almost the same catalytic activity as the washed catalyst. This finding allows the designing of a new highly active catalyst synthesis process that produces less amount of wastewater since the washing step can be skipped completely.

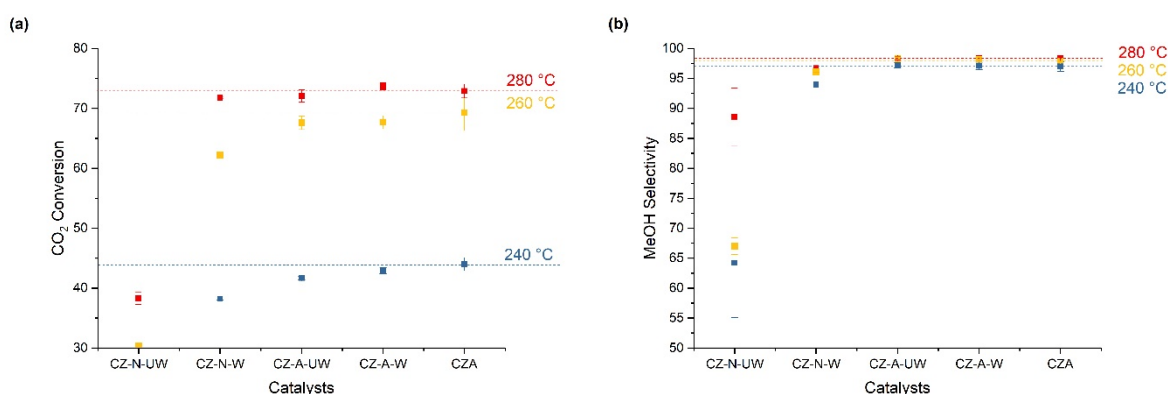


**Fig. 2.**  $\text{CO}_2$  conversion and methanol selectivity in stoichiometric  $\text{CO}_2$  hydrogenation over Cu-ZnO catalyst (CZ) prepared via urea hydrolysis of nitrate (N) and acetate (A) salts with washing (W) and without washing (UW). The commercial Cu/ZnO/ $\text{Al}_2\text{O}_3$  methanol synthesis catalyst (CZA, Alfa Aesar #45776) was used as the benchmark. Conditions:  $\text{H}_2/\text{CO}_2 = 3$ ,  $T = 240\text{--}280$  °C,  $P = 331$  bar,  $\text{SV} = 5$   $\text{NL/g} \cdot \text{h}$  ( $\text{GHSV} = 8500 \text{ h}^{-1}$ ) at  $\text{TOS} = 3$  h.

## References

- [1] G.A. Olah, A. Goepfert, G.K.S. Prakash, *Beyond Oil and Gas: The Methanol Economy: Second Edition*, 2009.
- [2] G.A. Olah, *Angew. Chemie - Int. Ed.* 52 (2013) 104–107.
- [3] A. Goepfert, M. Czaun, J.P. Jones, G.K. Surya Prakash, G.A. Olah, *Chem. Soc. Rev.* 43 (2014) 7995–8048.
- [4] G. Prieto, K.P. de Jong, P.E. de Jongh, *Catal. Today* 215 (2013) 142–151.
- [5] M. Behrens, S. Kißner, F. Girsgdies, I. Kasatkin, F. Hermerschmidt, K. Mette, H. Ruland, M. Muhler, R. Schlögl, *Chem. Commun.* 47 (2011) 1701.
- [6] P.J. Smith, S.A. Kondrat, P.A. Chater, B.R. Yeo, G.M. Shaw, L. Lu, J.K. Bartley, S.H. Taylor, M.S. Spencer, C.J. Kiely, G.J. Kelly, C.W. Park, G.J. Hutchings, *Chem. Sci.* 8 (2017) 2436–2447.

# Ga-promoted pathways in catalytic conversion of methanol and dimethyl ether to aromatics over H-MFI zeolite

Felix M. Kirchberger,<sup>a</sup> Yue Liu,<sup>a</sup> Markus Tonigold,<sup>b</sup> Maricruz Sanchez-Sanchez,<sup>a</sup>  
Johannes A. Lercher<sup>a,\*</sup>

<sup>a</sup> Department of Chemistry and Catalysis Research Center, Technische Universität München, Garching, 85747, Germany

<sup>b</sup> Clariant Produkte (Deutschland) GmbH, Bruckmühl 83052, Germany

\*Corresponding author: johannes.lercher@ch.tum.de

## 1. Scope

Conversion of methanol and dimethyl ether into hydrocarbons has gained more and more attention since its first report in the 1970s.<sup>[1]</sup> Increasing specification over the following decades lead to the development of processes driven by the desired products such as methanol to olefins (MTO), methanol to gasoline (MTG) or methanol to aromatics (MTA). Especially the conversion to aromatics has created scientific attention over the last years.<sup>[2]</sup> Several optimized catalysts, i.e. Ga-MFI, Zn-MFI, have been reported to achieve a high aromatic yield up to 69%.<sup>[3]</sup> In this work we investigated the pathways for the formation of aromatics in different sections of the catalytic bed and their dependence on the active sites in the catalyst.

## 2. Results and discussion

Three types of catalysts were prepared, an H-MFI, a Ga-impregnated H-MFI with (GaMFI-H<sub>2</sub>) and without H<sub>2</sub> treatment (GaMFI) before catalytic testing. The samples were tested under MTA conditions showing an increased aromatics formation in the cases the zeolite contained gallium and a further increase of aromatics yield if the sample was reduced beforehand (Figure 1). Under MTA conditions aromatics can be formed by three main pathways: (1) hydrogen transfer (HT) between olefins, (2) dehydrogenation of hydrocarbon

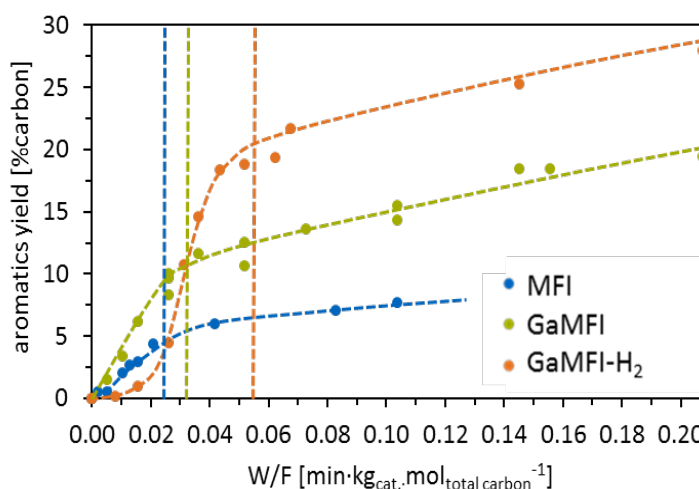


**Figure 1:** Yield (in %carbon) of aromatics versus the contact time.

Dashed lines indicate the contact time when full conversion is reached. (Reaction conditions: DME 90 mbar in N<sub>2</sub>, 475 °C)



products, (3) formaldehyde intermediated pathway. Evaluation of the different pathways along the catalyst bed showed that the increased aromatics selectivity of GaMFI catalysts is based on their dehydrogenation functionality and the increased HCHO formation rate from DME and methanol. The benefit of H<sub>2</sub> treatment of the GaMFI catalyst is mainly the formation of Ga<sup>+</sup>-species replacing one BAS and forming Ga<sup>+</sup>-BAS pair with an adjacent BAS.<sup>[4]</sup> The formation of these modified sites lead to a decrease of the methylation rate because of BAS loss while increasing the dehydrogenation activity resulting in a larger ratio of HT+dehydrogenation rates to methylation rate. However, these sites are not stable in the presence of water produced as a byproduct in MTA. Consequently in later sections of the catalyst bed after a large fraction of DME is converted the GaMFI-H<sub>2</sub> as the same activity as GaMFI.

### 3. Conclusions

The presence of Ga in an H-MFI zeolite increases the aromatics yield significantly due to dehydrogenation of beforehand formed olefins and an increase of HCHO formation from methanol and DME while HT reactions remain unchanged. Pre-reaction treatment with hydrogen of the catalyst makes more active Ga<sup>+</sup>-BAS pairs but the water formed during the DME conversion reverses the formation of such site pairs. The qualitative and quantitative understanding of these reaction steps and their respective sites will help to improve catalyst design as well as reaction conditions in order to maximize aromatics yield at minimum amounts of unwanted byproducts.

### References

- [1] S. Meisel, *CHEMTECH;(United States)* **1976**, 6.
- [2] a) M. Conte, J. A. Lopez-Sanchez, Q. He, D. J. Morgan, Y. Ryabenkova, J. K. Bartley, A. F. Carley, S. H. Taylor, C. J. Kiely, K. Khalid, *Catalysis Science & Technology* **2012**, 2, 105-112; b) P. Gao, J. Xu, G. Qi, C. Wang, Q. Wang, Y. Zhao, Y. Zhang, N. Feng, X. Zhao, J. Li, F. Deng, *ACS Catalysis* **2018**; c) P. Gao, Q. Wang, J. Xu, G. Qi, C. Wang, X. Zhou, X. Zhao, N. Feng, X. Liu, F. Deng, *ACS Catalysis* **2018**, 8, 69-74.
- [3] H. Zaidi, K. Pant, *Catalysis Today* **2004**, 96, 155-160.
- [4] M. W. Schreiber, C. P. Plaisance, M. Baumgärtl, K. Reuter, A. Jentys, R. Bermejo-Deval, J. A. Lercher, *Journal of the American Chemical Society* **2018**, 140, 4849-4859.

# Effect of boron promotion on coke formation during propane dehydrogenation over Pt/ $\gamma$ -Al<sub>2</sub>O<sub>3</sub> catalysts

*Mostafa Aly, Ghent University, Ghent, Belgium; Esteban Fornero, Ghent University, Ghent, Belgium; Jenoff De Vrieze, Ghent University, Ghent, Belgium; Vladimir Galvita, Ghent University, Ghent, Belgium; Mark Saeys, Ghent University, Ghent, Belgium*

## Introduction

Propylene is an important building block for a variety of bulk chemicals and polymers [1]. The shift in steam cracking feedstock from naphtha to more abundant shale gas, as well as the growth in propylene demand, have motivated a switch to “on-purpose” propylene production processes such as catalytic propane dehydrogenation (PDH). While many research efforts have addressed deactivation of Pt-based catalysts during PDH [1], coke formation continues to be a challenge. Boron promotion drastically reduces coke formation on Ni [2] during steam reforming, and on Co [3] during Fischer-Tropsch synthesis. DFT calculations indicate that boron atoms selectively block step and/or subsurface sites, thus preventing the nucleation and growth of deactivating carbon [2, 3]. The nature of boron, either as alloy or an amorphous oxide, depends on the catalytic system and reaction conditions.

## Experimental

### Preparation

B-Al<sub>2</sub>O<sub>3</sub> support materials were prepared via wet impregnation of aqueous H<sub>3</sub>BO<sub>3</sub> onto commercial  $\gamma$ -Al<sub>2</sub>O<sub>3</sub>. The mixture was stirred continuously at 50 °C until total evaporation of the solvent, then calcined in stagnant air at 650 °C for 4 hr. Pt/XB-Al<sub>2</sub>O<sub>3</sub> (X = 0.5, 1.0, 1.5, 5.6 wt.%) catalysts were prepared via wet impregnation of aqueous H<sub>2</sub>PtCl<sub>6</sub> onto XB-Al<sub>2</sub>O<sub>3</sub> support materials, followed by solvent evaporation and calcination. Similarly, Pt/Al<sub>2</sub>O<sub>3</sub> was prepared as a reference. In order to evaluate the effect of the impregnation sequence, 1B/Pt-Al<sub>2</sub>O<sub>3</sub> was prepared via inverse sequential wet impregnation of aqueous H<sub>3</sub>BO<sub>3</sub> onto Pt/Al<sub>2</sub>O<sub>3</sub>. Finally, Pt-B-Al<sub>2</sub>O<sub>3</sub> was prepared by co-impregnation of boron and Pt. The Pt loading was fixed at 3 wt.%.

## Results

The effect of the boron loading and impregnation sequence was investigated using 20 min PDH experiments at 600 °C and a  $C_3H_8/H_2$  ratio of 1/1 in a quartz reactor. The sequential impregnation of Pt onto B- $Al_2O_3$  support materials was found to be the most promising. The Pt/1B- $Al_2O_3$  catalyst showed only a minor reduction in activity during the short experiment, but a 2.6-fold reduction in the amount of deposited carbon for an optimal boron loading of 1 wt%.

12 hr experiments confirmed the improved stability and selectivity of Pt/1B- $Al_2O_3$  (Fig 1a). The enhanced selectivity suggests that boron modifies the active sites. Boron promotion removes the low temperature TPO peak (Fig 1b) and reduces the high temperature peak. Propylene decomposition experiments on pure and boron modified  $\gamma$ - $Al_2O_3$  show that the low temperature peak is related to carbon deposited on the support.

$NH_3$ -TPD experiments indicate that boron modifies the number and the strength of the support acid sites. In-situ XRD patterns under  $H_2$  at 600 °C do not show the formation of a Pt-B alloy. TEM-EDS analysis shows a uniform distribution of boron. Thermodynamic DFT calculations support the formation of boron oxide, rather than a Pt-B alloy. Clearly, the promoting effect of boron is more complex than often assumed [4].

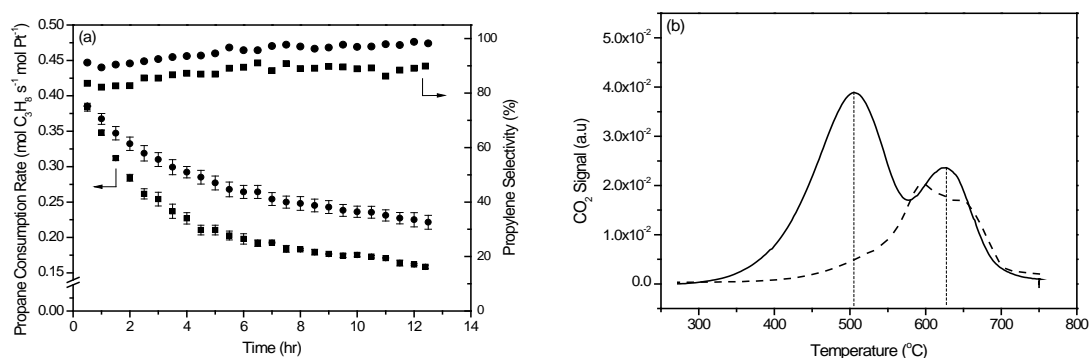


**Figure 1: (a) Effect of boron promotion on the activity and selectivity: Pt/ $Al_2O_3$  (■) and Pt/1B- $Al_2O_3$  (●) (b) TPO profiles for Pt/ $Al_2O_3$  (—) and Pt/1B- $Al_2O_3$  (---) after 12 hr of propane dehydrogenation performed at 600 °C, 1 bar,  $C_3H_8/H_2/Ar$  ratio of 1/1/3,  $W/F_{C_3H_8} = 3.0 \text{ kg}_{cat}\cdot\text{s}/\text{mol}_{C_3H_8}$ , and  $X_{C_3H_8} = 18\%$ .**

## References

- [1] J.J.H.B. Sattler, J. Ruiz-Martinez, E. Santillan-Jimenez, B.M. Weckhuysen, *Chem. Rev.*, 114 (2014) 10613.
- [2] J. Xu, L. Chen, K.F. Tan, A. Borgna, M. Saeys, *J. Catal.*, 261 (2009) 158.
- [3] K.F. Tan, J. Chang, A. Borgna, M. Saeys, *J. Catal.*, 280 (2011) 50.
- [4] M.-A. Ha, E.T. Baxter, A.C. Cass, S.L. Anderson, A.N. Alexandrova, *JACS*, 139 (2017) 11568.

# Co-precipitated Ga-Ni Metal Catalysts for CO<sub>2</sub> Conversion

*F. Özcan, B. Mockenhaupt, K. Friedel Ortega, M. Behrens, Inorganic Chemistry,  
University of Duisburg-Essen, Essen Germany;*

*F. Özcan, Max-Planck-Institute for Chemical Energy Conversion, Mülheim an der  
Ruhr, Germany*

## Introduction

In the need of replacing diminishing fossil sources and integrating renewable energy into the value chain of chemical industries and the energy sector, a growing interest in and demand for materials working as suited catalysts at the key processes is observed.<sup>[1]</sup> Especially in the context of recently passing the threshold of 400 ppm of CO<sub>2</sub> in the atmosphere,<sup>[2]</sup> research in this area has been intensified over the last years. Theoretical studies and first experimental confirmation show the potential of GaNi intermetallic phases as promising CO<sub>2</sub> conversion catalysts.<sup>[3]</sup>

In the present work, co-precipitated gallium/nickel containing catalysts are investigated in the conversion reaction of CO<sub>2</sub> synthesis gas. The catalysts are prepared via the co-precipitation route resulting in gallium and nickel containing layered double hydroxides (LDH) as a catalyst precursor class giving rise to a controlled and reproducible way of synthesis. This procedure enables a systematic study on structure-activity correlations in the targeted catalytic application. Hence, for reasons of comparison GaOOH<sup>[4]</sup> based bimetallic catalysts are added to the investigation.

## Experimental

Co-precipitation synthesis was conducted in an automated laboratory reactor system (OptiMax, Mettler Toledo). The characterization of the resulting precursors and their processing products along catalyst activation involved various techniques, e.g. (P)XRD, TEM, TGA, N<sub>2</sub> physisorption etc. H<sub>2</sub>-TPR studies gave insight into the reduction process and the active state formation of the investigated catalysts. Dynamic CO<sub>2</sub> conversion experiments were conducted in a 3:1 H<sub>2</sub>/CO<sub>2</sub> gas stream. Both H<sub>2</sub>-TPR and catalyst testing were conducted in a commercial catalyst analyzer (BELCAT-B, MicrotracBEL Corp., Japan).

## Results and discussion

XRD analysis confirms the presence of the LDH precursor in a single phase for the precursor series with different gallium to nickel ratios.

Detailed TEM analysis of the hydrogen activated phases prior to catalytic testing indicate that  $\text{Ga}^{3+}$  species are partially reduced, which is indicative for the bimetallic character of the Ga-Ni phases.  $\text{H}_2$ -TPR experiments support these results, as a higher  $\text{H}_2$  consumption is observed compared to the expected amount derived from the available cationic Ni species. Yet, by means of XRD and available TEM data the resulting intermetallic phases after catalyst activation are rather inconclusive with regards to the complex gallium-nickel phase diagram.

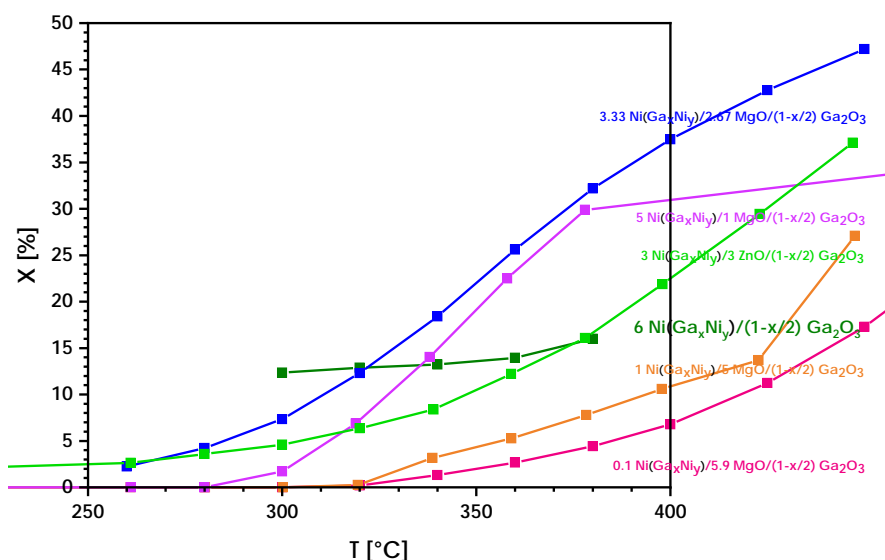


**Fig. 1:** Steady state  $\text{CO}_2$  conversions for selected catalysts within the systematic series obtained at 1 atm.

The application in the hydrogenation of  $\text{CO}_2$  (Fig. 1) reveals interesting conversion rates depending on composition variation in the precursor structure and the resulting phases in the activated catalyst state.

While reaction conditions at ambient pressure settings favor  $\text{CO}$  over  $\text{CH}_4$  both obtained as the main products, a first qualitative assessment in a high-pressure setup indicates only  $\text{CH}_4$  as main product with very low amounts of ethane and ethene as further hydrogenation products.

## References

- [1] Centi, G., Quadrelli, E. A., Perathoner, S. *Energy Environ. Sci.* **6**, 1711 (2013).
- [2] Betts, R. A., Jones, C. D., Knight, J. R., Keeling, R. F., Kennedy, J. J. *Nature Clim. Change* **6**, 806–810 (2016).
- [3] Studt, F., Sharafutdinov, I., Abild-Pedersen, F., Elkjær, C. F., Hummelshøj, J. S., Dahl, S., Chorkendorff, I., and Nørskov, J. K. *Nat Chem* **6**(4), 320 – 324 (2014).
- [4] Li, L., Wei, W., Behrens, M. *Solid State Sciences* **14**, 971-981 (2012).

# Insertion of Carbon Dioxide into Pd<sup>II</sup>-Aryl Bonds

Gregor Voit<sup>b</sup>, Markus Hölscher<sup>b</sup>, Sangeth Jenthra<sup>b</sup> and Walter Leitner<sup>a,b</sup>

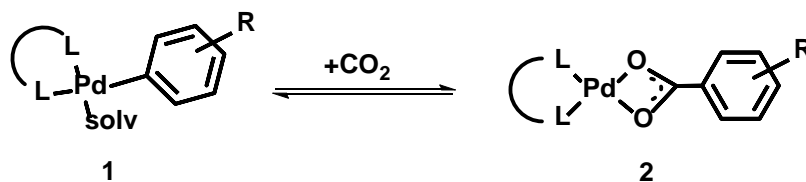
<sup>a</sup>Max-Planck-Institute for Chemical Energy Conversion, Stiftstraße 34-36, 45470  
Mülheim an der Ruhr, Germany

<sup>b</sup>Institut für Technische und Makromolekulare Chemie, RWTH Aachen University,  
Worringerweg 2, 52074 Aachen, Germany

email: [voit@itmc.rwth-aachen.de](mailto:voit@itmc.rwth-aachen.de)

In view of increasing anthropogenic carbon dioxide emissions and the corresponding impact on the environment, the chemical utilization of CO<sub>2</sub> is a topic of huge societal relevance. Among other molecules aromatic carboxylic acids are very desirable target compounds for carboxylation reactions with CO<sub>2</sub> as a building block, due to their wide application in pharmaceuticals and other high value compounds. To achieve a high atom efficiency the direct catalytic carboxylation of arenes, which are not preactivated is very desirable and a topic of a wide range of investigations<sup>[1, 2]</sup>. Our research has been aiming for the implementation of catalytic cycles that enable the direct carboxylation of arenes without the need for stoichiometric additives by the use of DFT calculations and rational design of late transition metal complexes<sup>[3]</sup>. A crucial step of these cycles is the activation of the relatively inert CO<sub>2</sub> molecule to facilitate an insertion into a previously formed metal-aryl bond.

Herein we report on the insertion behavior of carbon dioxide into different palladium-aryl bonds to form the corresponding palladium carboxylato complexes (**2**). In dependency on the substitution pattern of the aromatic compound, we could either observe insertion of CO<sub>2</sub>, or catalytic decarboxylation of aromatic carboxylic acids under formation of Pd<sup>II</sup> aryl complexes (**1**).



Scheme 1: Insertion of Carbon Dioxide into Pd<sup>II</sup>-aryl bonds.

## References

[1] a) I. I. Boogaerts, S. P. Nolan, *J. Am. Chem. Soc.* **2010**, *132*, 8858-8859. b) L. Zhang, J. Cheng, T. Ohishi, Z. Hou, *Angew. Chem.* **2010**, *122*, 8852-8855. [2] a) H. Mizuno, J. Takaya, N. Iwasawa, *J. Am. Chem. Soc.* **2010**, *133*, 1251-1253. b) T. Suga, H. Mizuno, J. Takaya, N. Iwasawa, *Chem. Commun.* **2014**, *50*, 14360-14363. [3] A. Uhe, M. Hölscher, W. Leitner, *Chem. Eur. J.* **2012**, *18*, 170-177.

# Methylformate from CO<sub>2</sub> via an Integrated Process

Martin Scott<sup>a</sup>, Christian Westhues<sup>a</sup>, Janine Baums<sup>a</sup>, Teresa Kaiser<sup>b</sup>, Andreas Jupke<sup>b</sup>,  
Giancarlo Franciò<sup>a</sup>, Walter Leitner<sup>a,c</sup>

<sup>a</sup>Institut für Technische und Makromolekulare Chemie, RWTH Aachen, Germany

<sup>b</sup>Lehrstuhl für Fluidverfahrenstechnik, RWTH Aachen, Germany

<sup>c</sup>Max Planck Institut für Chemische Energiekonversion, Mülheim an der Ruhr, Germany

A major challenge for the efficient production of formic acid (FA) and its derivatives from CO<sub>2</sub> is an effective integration of the hydrogenation step with the catalyst reutilization and product isolation.<sup>[1]</sup> One option for facilitating the isolation of FA consists in its derivatization with methanol to methyl formate (MF) in one pot or in a subsequent step.<sup>[2]</sup> We describe here a biphasic catalytic system comprising methanol (MeOH) as the product phase, *n*-decane as the catalyst phase, a tailored-Ru catalyst and an amine as a stabilizing agent for FA (Figure 1).

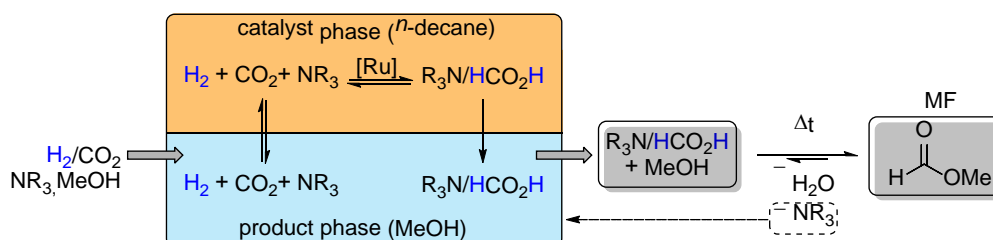


**Figure 1:** Envisioned process for integrating the hydrogenation of CO<sub>2</sub> and the subsequent conversion to methyl formate.

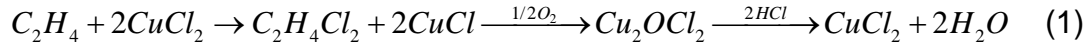
The resulting methanolic solution of the formate-amine adduct was investigated as a feed for the synthesis of MF via a subsequent reactive distillation step. The selection of a suitable amine was crucial for achieving a good compromise between the hydrogenation and the esterification step. High productivities, effective catalyst retention and recycling were obtained in the hydrogenation step using a largely automated reactor set-up, while the isolation of pure MF was verified using a 900 mL scale distillation apparatus.<sup>[3]</sup>

- [1] a) J. Klankermayer, S. Wesselbaum, K. Beydoun, W. Leitner, *Angew. Chem. Int. Ed.* **2016**, *55*, 7296-7343; b) J. Artz, T. E. Muller, K. Thenert, J. Kleinekorte, R. Meys, A. Sternberg, A. Bardow, W. Leitner, *Chem. Rev.* **2018**, *118*, 434-504.
- [2] a) S. Kar, R. Sen, A. Goeppert, G. K. S. Prakash, *J. Am. Chem. Soc.* **2018**, *140*, 1580-1583; b) T. Schaub, D. M. Fries, R. Paciello, K.-D. Mohl, M. Schäfer, S. Rittinger, D. Schneider, *United States Patent* **2014**, US, 8791297.
- [3] M. Scott, C. Westhues, J. Baums, T. Kaiser, A. Jupke, G. Franciò, W. Leitner, *manuscript in preparation* **2019**.

# Alkali Metal Doping of Ethylene Oxychlorination Catalysts: Chemistry, Kinetics and Descriptors.

E. Fenes, NTNU<sup>1</sup>, Trondheim, Norway, H. Ma<sup>1</sup>, Y. Qi<sup>1</sup>, K. R. Rout, SINTEF Industry, Trondheim, Norway, T. Fuglerud, INOVYN Norway, Porsgrunn, Norway, D. Chen<sup>1</sup>

Ethylene oxychlorination (Eq.1) over CuCl<sub>2</sub>/γ-Al<sub>2</sub>O<sub>3</sub> based catalysts, producing 1,2-ethandichloride (EDC) is an important step in poly vinyl chloride (PVC) production. [1]



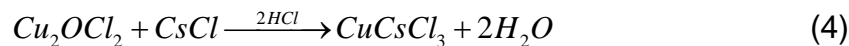
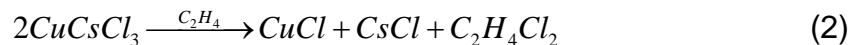
Although oxychlorination is a commercial process, several key factors are still not fully understood. With an operando approach, we are beginning to understand the effects of Cu-dopant salt formation, cluster size and Cu-support interactions on catalyst performance and correlate to the catalyst electronic properties.

## Methods

Incipient wetness impregnation of CuCl<sub>2</sub> and the respective alkali metal (A) chloride salt on γ-Al<sub>2</sub>O<sub>3</sub> yielded catalysts containing 5wt% Cu with a 1:0.4 Cu:dopant ratio. Catalyst characterization was done with *ex-situ* XPS, TPR (P<sub>C<sub>2</sub>H<sub>4</sub></sub>=0.2, 2 K/min), *in situ* XRD and operando UV-Vis spectroscopy. [2] The dynamic changes in chemistry and active sites in catalytic cycle were studied by combined operando XRD, UV-Vis and XANES at the Swiss-Norwegian beamline at ESRF.

## Results

The catalytic process of oxychlorination is highly dynamic involving reduction, oxidation and hydrochlorination steps [2]. The operando study for the first time [3] identified existence of CuA<sub>x</sub>Cl<sub>2+x</sub> (A=K, Cs, Rb) double salt as well as the dynamic change in the phase with a function of Cl concentration on the surface of a working oxychlorination catalyst. XRD profiles on Figure 1a indicate part of CuCsCl<sub>3</sub> reduced (Eq. 2) in the reduction step where the phase separated with lower Cl concentrations on the surface revealed by operando XANS study. However, after oxidation (Eq. 3) and hydrochlorination (Eq. 4) the phase recombined back to the initial state. The chemistry of the catalytic cycle can be described in Eqs. 2-4.



Transient kinetic study of individual steps as shown in Eqs. 2-4 and steady state



reactions were performed to systematically study the effect of alkaline metal promoters. The initial  $\text{Cu}^{2+}$  reduction rates and  $\text{Cu}^+$  oxidation rates depend linearly on the band gap energy of  $\text{CuCl}_2$  and  $\text{Cu}_2\text{OCl}_2$ , as shown in Figure 1 b and c, respectively. The catalyst band gap ( $E_g$ ) reflects electronic properties and its redox potentials, found to be linearly correlated to the first ionization energy of the alkali metal. The catalyst band gap energy can be utilized as a descriptor for the catalyst performance. DFT calculations were performed to get a better understanding of the catalyst electronic properties, Cu and alumina interaction, active sites and their dynamic nature. DFT study provided detailed structure of  $\text{CuK}_x\text{Cl}_{2+x}$ , and the interaction with alumina surfaces. The results clearly suggest a heterogeneous reactivity of Cl in the catalyst. The promoters and surface Cl concentrations and interaction with the support unambiguously alter the catalyst electronic properties and thus the activity, where the electronic properties can be unified to the Cl charge. The relationship between  $E_g$  and the Cl charge will be discussed.

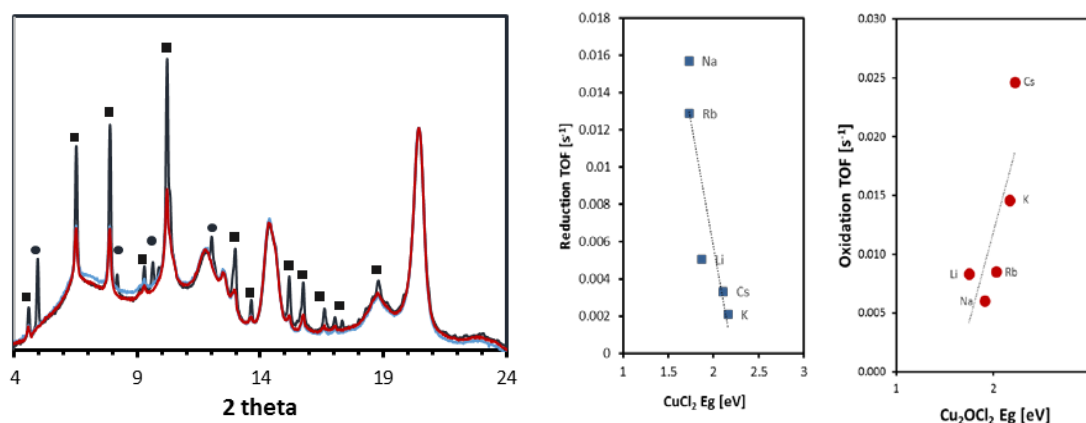


**Figure 1:** a) *In situ* XRD profiles of the active (black), reduced (blue) and oxidized (red) Cs doped catalyst. ( $\text{CuA}_x\text{Cl}_{2+x}$  ■,  $\text{Cu}_2(\text{OH})_3\text{Cl}$  ●) b) Reduction TOF. ( $P_{\text{C}_2\text{H}_4}=0.1$ ,  $T=230^\circ\text{C}$ ) c) Oxidation TOF. ( $P_{\text{O}_2}=0.2$ ,  $T=230^\circ\text{C}$ )

A kinetic model has been developed to well describe the dynamic evolution of gas phase composition and active sites. Hence, from a multidisciplinary approach, we are now beginning to understand the chemistry of A:Cu interaction, the electronic effects controlling catalyst activity and have developed a kinetic model to describe the observed phenomenon.

## References

- [1] G. Leofanti et.al. J. Catal. **205**, 375–381 (2002)
- [2] K. R. Rout et.al. J. Catal. **352**, 218-228 (2017)
- [3] Gmelin Handbuch der anorganischen chemie, 8. auflage, Kupfer: Teil B-Lieferung 3. (1963)

## Multifunctional $\text{Fe}_3\text{O}_4@\text{Nb}_2\text{O}_5@\text{Co}@\text{Re}$ catalysts for lignin fragmentation

*Madalina Tudorache, University of Bucharest, Bucharest, Romania; Cristina Opris, University of Bucharest, Bucharest, Romania; Bogdan Cojocaru, University of Bucharest, Bucharest, Romania; Simona Coman, University of Bucharest, Bucharest, Romania; Nicoleta Gheorghe, National Institute of Materials Physics, Magurele, Romania; Bahir Duraki, ETH, Zurich, Switzerland; Jeroen A. van Bokhoven, ETH, Zurich, Switzerland; Vasile I. Parvulescu, University of Bucharest, Bucharest, Romania*

In the past decade lignin receives special interest, firstly because is one of the most-abundant biomass components, and secondly because its conversion is expected as a potential route for the production of a large variety of products (e.g. aromatic hydrocarbons and their oxygenated derivatives) [1-3]. One of the current trends to accomplish the lignin valorization is to combine the hydrogenolysis of the C-O bonds with the hydrogenation of the resulted fragments.

The aim of this study was to determine the role of rhenium as promoter for lignin fragmentation reaction over  $\text{Fe}_3\text{O}_4@\text{Nb}_2\text{O}_5@\text{Co}$  catalysts having magnetite as a magnetic core.  $\text{Fe}_3\text{O}_4@\text{Nb}_2\text{O}_5@\text{Co}$  are designed as effective catalysts for the fragmentation of lignin following a concerted hydrolysis/hydrogenolysis mechanism.

Multifunctional  $\text{Fe}_3\text{O}_4@\text{Nb}_2\text{O}_5@\text{Co}@\text{Re}$  catalysts with metal loadings in the range from 2 to 7 wt% were prepared in a multistep process [2]. Magnetic nanoparticles prepared by co-precipitation were covered with a niobia shell followed by the deposition of cobalt using a deposition/precipitation procedure. Finally, rhenium has been deposited based on three different routes: i) impregnation, ii) deposition/precipitation of rhenium chloride (ImC and PP, respectively) and iii) impregnation with ammonium perrhenate (ImA). The characterization of these catalysts was carried out by XRD, Raman,  $\text{H}_2$ -TPD and  $\text{NH}_3$ -TPD, XPS, and TEM showing the influence of the preparation procedure, reduction and cooperation Re/Co upon the dispersion and reduction degree. ImC and ImA routes led to more reduced catalysts, and the decrease of the cobalt content corresponded to more reduced rhenium. An inverse relation between the acidity and the reduction degree has been evidenced.

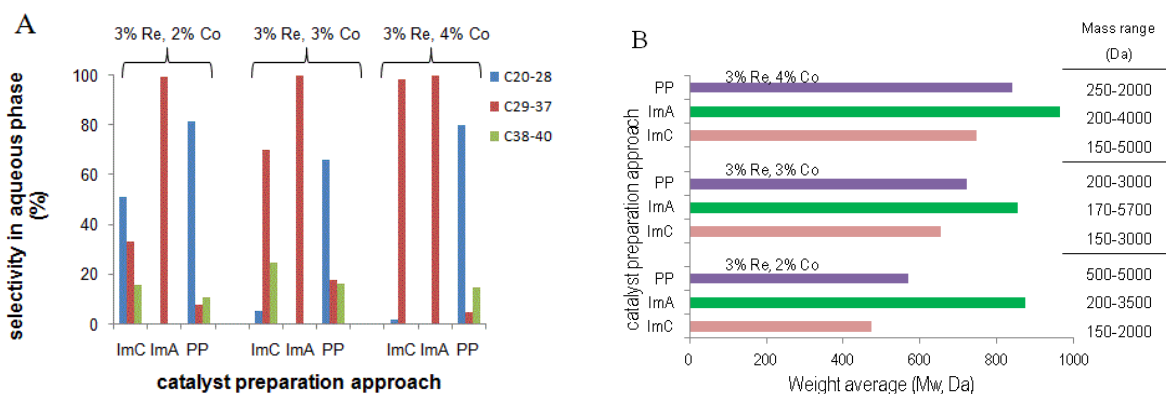


Figure 1. Influence of the catalyst preparation method on the mass distribution of water soluble (A) and insoluble (B) fragments. (A) represents the mass distribution for C<sub>20</sub>-C<sub>28</sub> (blue), C<sub>29</sub>-C<sub>37</sub> (red) and C<sub>38</sub>-C<sub>40</sub> (green). (B) represents the mass distribution of lignin fragments correlated with the catalyst composition.

Figure 1, A & B presents an evaluation of the mass fragments composition for both phases. The ImA catalyst showed high selectivity for the fragments C<sub>29</sub>-C<sub>37</sub>. For ImC series, small fragments (C<sub>20</sub>-C<sub>28</sub>) dominated the liquid phase for a metal loading of 3 wt% Re and 2 wt%Co. Further increase of the cobalt content from 2 wt% to 4 wt% catalyst led to a decrease of the selectivity in the favor of C<sub>29</sub>-C<sub>37</sub> fragments (Figure 1, A). Very important, the PP catalysts yielded a more advanced fragmentation in which the dominants were the C<sub>20</sub>-C<sub>28</sub> fragments. Irrespective of the preparation route, the solid phase was composed by entities with masses in the range 400-1000 Da (Figure 1, B).

The deposition of rhenium and cobalt onto Fe<sub>3</sub>O<sub>4</sub>@Nb<sub>2</sub>O<sub>5</sub> led to multifunctional catalysts in which Fe<sub>3</sub>O<sub>4</sub> ensured the total recoverability of the samples at the end of the reaction. Niobium and rhenium provided the acidity required for the disruption of the etheric groups, while cobalt and rhenium cooperated for the hydrogenolysis of the C-O bonds and hydrocracking of the C-C bonds. A very important feature of these catalysts, they were totally recovered by application of a magnetic field, and after a simple washing with water they were recycled for six times without any loss in the activity and selectivity.

## References

1. C. Opris, B. Cojocaru, N. Gheorghe, M. Tudorache, S.M. Coman, V.I. Parvulescu, B. Duraki, F. Krumeich, J.A. Van Bokhoven, *Journal of Catalysis*, **2016**, 339, 209-227.
2. C. Opris, B. Cojocaru, N. Gheorghe, M. Tudorache, S.M. Coman, V.I. Parvulescu, B. Duraki, F. Krumeich, J.A. Van Bokhoven, *ACS Catalysis*, **2017**, 7, 3257-3267.
3. M. Tudorache, C. Opris, B. Cojocaru, N.G. Apostol, A. Tirsoaga, S.M. Coman, V.I. Parvulescu, B. Duraki, F. Krumeich, J.A. Van Bokhoven, *ACS Sustainable Chemistry and Engineering*, **2018**, 6(8), 9606-9618.

# Mechanocatalytic Nitrogen Fixation

Karoline Lena Heibisch,<sup>1,2</sup> Andrew W. Tricker,<sup>1</sup> George Samaras,<sup>1</sup> Marta Hatzell,<sup>1</sup>  
Matthew Realf, <sup>1</sup> Carsten Sievers<sup>1\*</sup>

<sup>1</sup> Georgia Institute of Technology, Atlanta, GA, U.S.A.

<sup>2</sup> Technische Universität Darmstadt, Darmstadt, Germany

## Introduction

Ammonia (NH<sub>3</sub>) is one of the most important bulk chemicals and critical for fertilizer production. Industrial world-scale Haber-Bosch plants for NH<sub>3</sub> production operate under harsh reaction conditions (typically 400-500 °C, 150-250 bar). Finding a novel approach for sustainable, low cost, and scalable ammonia production is an important research direction [1]. Mechanocatalysis offers multiple advantages over traditional chemical production: unique reactive domains and surface chemistry as well as minimal infrastructure demands and investment costs. The approach of mechanocatalysis is to utilize mechanical forces to drive reactions. The resulting high stress environment generates thermal hot spots and transient surface sites, which can both enable reactions that would need high temperature and pressure in conventional reactors [2]. This contribution illustrates that mechanocatalytic ammonia synthesis over reducible metal oxide catalysts is possible under nominally ambient reaction conditions.

## Results and Discussion

To understand energy transfer during mechanical collisions and the resulting generation of transient reactive environments, the decomposition of CaCO<sub>3</sub> to CaO and CO<sub>2</sub> was studied in a Retsch MM400 ball mill that was continuously purged with an argon stream. The rate of CO<sub>2</sub> formation was measured by MS analysis of the effluent and compared to thermal reactions (Figure 1). Milling frequencies between 22 and 30 Hz resulted in rates of CO<sub>2</sub> formation that would require the entire amount of CaCO<sub>3</sub> to reach 850-885 K. The actual temperatures of reactive environments must be even higher because mechanical collisions impart transient hot spots that decay rapidly by thermal conduction. Estimations of the temperatures of hot spots and their rates of decay will be discussed based on modeling studies. Regardless of the exact nature of the transient temperature profile, it is safe to conclude that the

mechanical forces in the ball mill generate hot spots with temperatures that are equal to or higher than the operating conditions of the Haber-Bosch process.

Mechanochemical nitrogen fixation was investigated using  $\text{TiO}_2$  as catalyst. The mechanochemical formation of oxygen vacancies in  $\text{TiO}_2$  in the presence of  $\text{H}_2$  was shown based on isotopic labeling studies. After ball milling  $\text{TiO}_2$  with a continuous feed of  $\text{N}_2$  and  $\text{H}_2$ , ToF-SIMS analysis of the catalyst showed pronounced increases in several mass peaks that are characteristic for the formation of surface nitride and nitrous oxide species. This suggests the formation of nitrogen-based surface species as key intermediates in nitrogen fixation reactions. After reaction, the samples were washed with water and the resulting solution was analyzed for  $\text{NH}_3$  by ion chromatography (Figure 2). After subtracting the background signal from the fresh catalyst, an approximately linear increase of the amount of formed  $\text{NH}_3$  was observed with regards to milling time. Thus, it is proposed that milling of  $\text{TiO}_2$  in the presence of  $\text{N}_2$  and  $\text{H}_2$  leads to the formation of oxygen vacancies that are cable to forming nitrogen-based surface species and that the latter can be hydrogenated to form  $\text{NH}_3$ .

To identify descriptors for the observed catalytic performance, various fresh and spent  $\text{TiO}_2$  catalysts were characterized. TEM indicated a size reduction and the formation of rounder interfaces, while XRD and XANES showed phase transitions due to the mechanochemical process. The nature of active sites and paths for their formation will be discussed based on these and other characterization experiments.

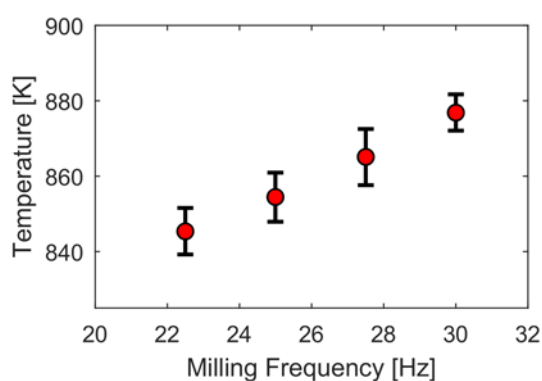


**Figure 1:** Apparent temperature that would be required to form  $\text{CO}_2$  from  $\text{CaCO}_3$  at the observed rate in a thermal reaction.

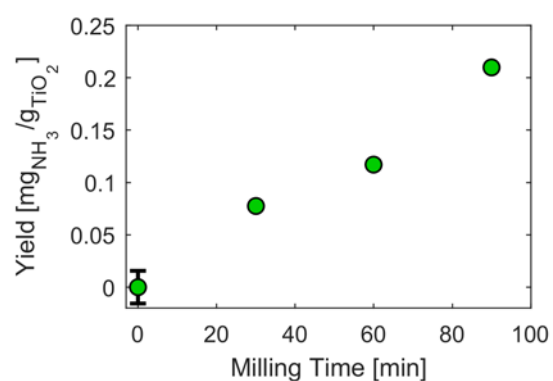


**Figure 2:**  $\text{NH}_3$  yield after milling  $\text{TiO}_2$  anatase for 30, 60 and 90 min in a reactive atmosphere (5 sccm  $\text{H}_2$ , 25 sccm  $\text{N}_2$ ), 2.0 g  $\text{TiO}_2$ , one 20 mm  $\varnothing$  grinding ball, 25 Hz.

## References

1. Patil, B.S., et al., *Nitrogen Fixation*. Ullmann's Encyclopedia of Industrial Chemistry, 2017.
2. James, S.L. at al., *Chem. Soc. Rev.*, 2012, **41**, 413-447.

**A meta-analysis tool for heterogeneous catalysis:  
Property-performance correlations extracted from literature data  
for the oxidative coupling of methane**

*R. Schmack<sup>1</sup>, A. Friedrich<sup>2</sup>, E. V. Kondratenko<sup>3</sup>, A. Werwatz<sup>2</sup>, R. Kraehnert<sup>1,\*</sup>*

*1 Institut für Chemie, Technische Universität Berlin, Germany*

*2 Fachgebiet Ökonometrie und Wirtschaftsstatistik, Technischen Universität Berlin,  
Germany*

*3 Leibniz Institute for Catalysis (LIKAT Rostock), Rostock, Germany*

*\* ralph.kraehnert@tu-berlin.de*

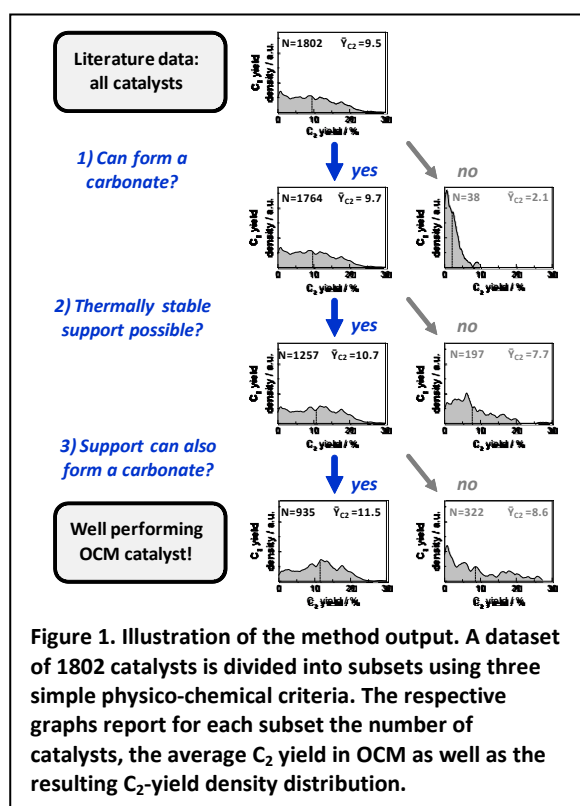
For many reactions in heterogeneous catalysis several thousand literature reports exist. Each report provides experimental performance data for few selected catalysts. However, extracting general knowledge from this data has been an unsolved challenge for many decades.

Meta-analysis is a powerful tool to rigorously assess the findings of published research. Successful meta-analysis studies were reported in research fields where quantitative analysis of independently conducted experiments is prevalent. Particularly in medical research, meta-analysis is used to aggregate individual studies aiming at the same treatment effect and employing the same research design. In this case, the main goal and benefit is to obtain a more precise and robust effect estimate than any individual study can deliver.

Despite the existence of a vast amount of well-documented experimental research also in heterogeneous catalysis, only few respective meta-analyses have been reported. A major reason is the heterogeneity among the reported reaction conditions, the rather small datasets (typically less than 400 data points), and challenges in finding appropriate descriptor variables. Hence, neither did these studies identify structure-activity relationships nor could they provide simple chemical explanations for the observed statistical effects.

Zavyalova, Holena, Schloegl and Baerns collected the first data set in heterogeneous catalysis that is sufficiently large for a comprehensive statistical evaluation [1]. The data was extracted from 421 publications and contained 1866 distinct catalyst compositions and respective catalytic performance data for the OCM reaction, the oxidative coupling of methane.

We report the first meta-analysis in heterogeneous catalysis that can identify chemically meaningful and statistically significant correlations between physico-chemical catalyst properties and their performance in a particular reaction. The method combines physico-chemical properties inferred from catalyst composition and well-known elemental reference data to formulate a working hypothesis that divides the dataset into subsets. Differences in the catalytic performance between these subsets are then tested for statistical significance against the pooled literature data. An iterative hypothesis refinement yields a statistical model that represent probable property-performance relationships. Figure 1 illustrates exemplarily how the method is used to structure the data into meaningful subsets.



We demonstrate the method exemplarily for the OCM, performing a comprehensive and novel re-analysis of the data compiled by Zavyalova et al. [1]. In the final model four simple hypotheses suffice to sort 1802 catalysts into 10 groups of distinct OCM performance. Numerous tests confirm the statistical robustness of the final model. The model suggests that only well-performing catalysts provide two independent functionalities, i.e. a thermodynamically stable carbonate and a thermally stable oxide support, at the respective temperatures of OCM testing.

The method is applicable also to other reactions. Using the method, researchers can easily test if their interpretation of a catalytic effect is likely to explain the data reported in literature. The derived model can guide the design of new catalysts as well as new experiments, spectroscopic studies and quantum chemical calculations.

## References

[1] U. Zavyalova, M. Holena, R. Schlögl and M. Baerns, ChemCatChem 2011, 3, 1935-1947

# **Cu-Co/ZnO/Al<sub>2</sub>O<sub>3</sub> Catalysts for CO Conversion to Higher Alcohols synthesized from co-precipitated LDH precursors**

*B. Mockenhaupt, F. Özcan, T. Machowski, K. Friedel Ortega, M. Behrens, Inorganic Chemistry, University of Duisburg-Essen, Essen Germany;*

*F. Özcan, Max-Planck-Institute for Chemical Energy Conversion, Mülheim an der Ruhr, Germany*

## **Introduction**

Fischer-Tropsch synthesis (FTS) is an established process technology with a high potential towards the reduction of the CO<sub>2</sub> footprint derived from fossil fuels. Beside natural gas biomass and biogas are typical sources of CO synthesis gas for greener Fischer-Tropsch synthesis.<sup>[1-2]</sup> Advantages of this process lie in the possibility to tune the octane/cetane number of fuels and to synthesize higher alcohols.<sup>[3]</sup>

Cobalt on alumina is a typical low temperature FT catalyst.<sup>[4]</sup> Introducing copper to this system can increase the selectivity to alcohols,<sup>[5]</sup> primarily to methanol and isobutanol, caused by the associative adsorption and insertion of CO and the H<sub>2</sub> spillover at a copper site in contrast to the dissociative adsorption and CO activation of a typical Fischer-Tropsch metal.<sup>[1, 3, 6-7]</sup>

In the present work we combined Cu/ZnO and Co/Al<sub>2</sub>O<sub>3</sub> in co-precipitated Cu-Co/ZnO/Al<sub>2</sub>O<sub>3</sub> catalysts with different Cu:Co ratios. These catalysts are investigated in the CO synthesis gas conversion. The catalysts are prepared via the co-precipitation route resulting in cobalt and copper containing layered double hydroxides (LDH) as a catalyst precursor class giving rise to a controlled and reproducible way of synthesis. Prepared such way, they enable a systematic study on structure- and composition-activity correlations in the targeted catalytic application.

## **Experimental**

Co-precipitation synthesis was conducted in an automated laboratory reactor system (OptiMax, Mettler Toledo). The characterization of the resulting precursors and their processed products along catalyst activation involved various techniques, e.g. (P)XRD, TEM, TGA, N<sub>2</sub> physisorption. H<sub>2</sub>-TPR studies in a commercial catalyst analyzer (BELCAT-B, MicrotracBEL Corp., Japan) enabled to assess the reduction process and the active state formation of the investigated catalysts.



## Results and discussion

Characterization of the as-synthesized precursors via XRD analysis confirms the presence of the LDH precursor in a single phase in each sample within the series (Fig. 1). Table 1 summarizes the targeted compositions of the precursors. Calcination as a processing step along the activation procedure of the catalysts leads to an increase

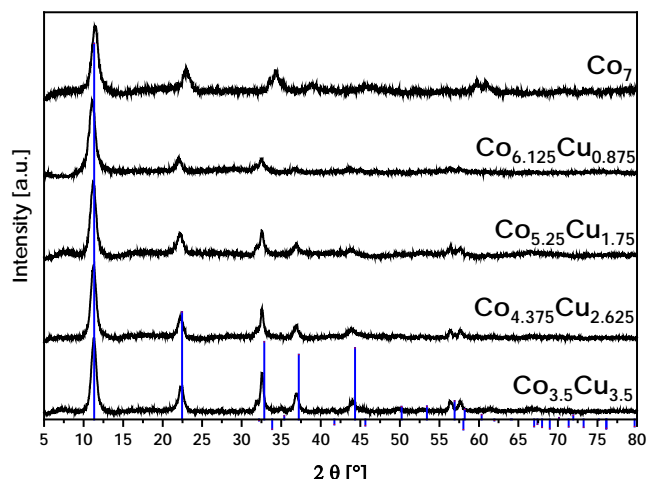


**Fig. 1:** Diffractograms of the LDH precursors compared to the reference of  $[\text{Co}_4\text{Al}_2(\text{OH})_{12}]\text{CO}_3 \cdot 3\text{H}_2\text{O}$  (—) (ICSD Coll. Code 172995).

in BET surface area in the range of 25 -100 % starting at an  $S_{\text{BET}}$  of  $\sim 80 \text{ m}^2/\text{g}$  for the pristine samples.  $\text{H}_2$ -TPR data indicate that the Cu species is reduced below  $200 \text{ }^\circ\text{C}$  while Co needs higher temperatures for reduction with its increasing content.

**Table 1:** Nominal compositions of the investigated catalyst series.

sample label	targeted compositions	Cu:Co ratio
$\text{Co}_7$	$[\text{Co}_7\text{ZnAl}_2(\text{OH})_{20}]\text{CO}_3 \cdot m \text{H}_2\text{O}$	100 % Co, 0 % Cu
$\text{Co}_{6.125}\text{Cu}_{0.875}$	$[\text{Co}_{6.125}\text{Cu}_{0.875}\text{ZnAl}_2(\text{OH})_{20}]\text{CO}_3 \cdot m \text{H}_2\text{O}$	87.5 % Co, 12.5 % Cu
$\text{Co}_{5.25}\text{Cu}_{1.75}$	$[\text{Co}_{5.25}\text{Cu}_{1.75}\text{ZnAl}_2(\text{OH})_{20}]\text{CO}_3 \cdot m \text{H}_2\text{O}$	75 % Co, 25 % Cu
$\text{Co}_{4.375}\text{Cu}_{2.625}$	$[\text{Co}_{4.375}\text{Cu}_{2.625}\text{ZnAl}_2(\text{OH})_{20}]\text{CO}_3 \cdot m \text{H}_2\text{O}$	62.5 % Co, 37.5 % Cu
$\text{Co}_{3.5}\text{Cu}_{3.5}$	$[\text{Co}_{3.5}\text{Cu}_{3.5}\text{ZnAl}_2(\text{OH})_{20}]\text{CO}_3 \cdot m \text{H}_2\text{O}$	50 % Co, 50 % Cu

A first qualitative assessment of the catalysts in the conversion of a  $\text{CO}/\text{H}_2$  feed in a high-pressure setup confirms the expected Fischer-Tropsch activity of the system. The beneficial impact of Cu substitution becomes evident with higher selectivities towards higher alcohols with an increasing amount of this transition metal. This study demonstrates the potential of generating a LDH-based Cu/Co catalyst system for the higher alcohol synthesis containing Zn and Al as promoters.

## References

- [1] V. Garcilaso, J. Barrientos, L. F. Bobadilla, O. H. Laguna, M. Boutonnet, M. A. Centeno, J. A. Odriozola, *Renewable Energy* **2019**, *132*, 1141-1150.
- [2] V. R. Calderone, N. R. Shiju, D. C. Ferré, G. Rothenberg, *Green Chemistry* **2011**, *13*, 1950-1959.
- [3] K. Fang, D. Li, M. Lin, M. Xiang, W. Wei, Y. Sun, *Catalysis Today* **2009**, *147*, 133-138.
- [4] M. E. Dry, *Catalysis Today* **2002**, *71*, 227-241.
- [5] G. Prieto, S. Beijer, M. L. Smith, M. He, Y. Au, Z. Wang, D. A. Bruce, K. P. de Jong, J. J. Spivey, P. E. de Jongh, *Angew Chem Int Ed Engl* **2014**, *53*, 6397-6401.
- [6] K. Xiao, X. Qi, Z. Bao, X. Wang, L. Zhong, K. Fang, M. Lin, Y. Sun, *Catalysis Science & Technology* **2013**, *3*, 1591-1602.
- [7] J. Anton, J. Nebel, C. Göbel, T. Gabrysch, H. Song, C. Froese, H. Ruland, M. Muhler, S. Kaluza, *Topics in Catalysis* **2016**, *59*, 1361-1370.

# Controlling Catalytic Hydrogenation via Organic Modification of Oxide-Supported Metals

*J. Will Medlin, University of Colorado, Boulder, CO, USA*

Organic ligands are widely employed as surfactants for the controlled synthesis of metal nanoparticles used in catalysis. Several recent studies have shown that leaving these ligands in place can often have beneficial effects for catalyst performance, especially related to selectivity.[1] This observation suggests that it might be useful to add organic ligands even to uncoated metal nanoparticles on supported catalysts, and it has indeed been found that this strategy can lead to the ability to control selectivity in many reactions.[2] Because the ligands are generally bound to metal active sites, gains in catalyst selectivity are often accompanied by significant losses in activity, though several exceptions to this general trend have been demonstrated.

Rather than depositing ligands on the metal nanoparticles, a related strategy is to deposit them on the support. Support modification potentially avoids excessive blocking of precious metal sites, but can hypothetically still provide the ability to control catalyst selectivity, especially for reactions in which rates are controlled by sites at the metal – support interface. By varying the structure and chemical functionality of the organic ligands, there are possibilities to improve catalyst activity, selectivity, and stability in reactions requiring bifunctional sites present at the interfaces between metals and metal oxides. These reactions include hydrodeoxygenation (HDO) of biomass-derived oxygenates and CO<sub>2</sub> hydrogenation carried out in both the gas and liquid phase.

We deposited PAs on a variety of metal-support combinations, such as Pd/Al<sub>2</sub>O<sub>3</sub>, Pt/TiO<sub>2</sub>, and Ni/Al<sub>2</sub>O<sub>3</sub>. When Pt was used as the active metal, PA deposition appeared to be confined to the oxide support; for other metals, some deposition on metal sites was also observed.[3-7] On the other hand, relatively well-ordered SAMs were produced for all oxide supports investigated in this study. Infrared spectroscopy showed that the designed functional groups could be tethered to the catalyst via the PA chemistry.[3,4] Pyridine adsorption demonstrated that the PA ligands retained

Brønsted acidity, and in fact that the acidity could be adjusted by changing the organic ligands (Fig. 1). Alternatively, CO<sub>2</sub> adsorption studies indicated that basic sites could also be introduced in a controlled way using the ligand strategy.

PA-modified catalysts were studied for several reaction chemistries, focusing on selective hydrogenation of biomass-derived oxygenates and CO<sub>2</sub>. Kinetic results and control experiments indicated that adjusting the properties of the organic tail functions could improve activity via introduction of acidic cooperative sites, basic sites, or via electronic modification of metal sites and the metal-support interface. Moreover, the sensitivity of catalytic activity and selectivity to ligand structure suggested that organic monolayer composition could provide a new tunable parameter for designing improved catalysts.

## References

- [1] G.M. Lari, B. Puértolas, M. Shahrokhi, N. López, and J. Pérez-Ramírez, *Angew. Chemie - Int. Ed.* **56** (2017) 1775.
- [2] C.A. Schoenbaum, D.K. Schwartz, and J.W. Medlin, *Acc. Chem. Res.* **47** (2014) 1438.
- [3] J. Zhang, L.D. Ellis, B. Wang, M.J. Dzara, S. Pylypenko, E. Nikolla, and J.W. Medlin, *Nat. Catal.* **1** (2018) 148.
- [4] P.D. Coan, L.D. Ellis, M.B. Griffin, D.K. Schwartz, and J.W. Medlin, *J. Phys. Chem. C* **122** (2018) 6637.
- [5] P. Hao, D.K. Schwartz, and J.W. Medlin, *Appl. Catal. A Gen.* **561** (2018) 1.
- [6] T. Van Cleve, D. Underhill, M. Veiga Rodrigues, C. Sievers, and J.W. Medlin, *Langmuir* **34** (2018) 3619.
- [7] P. Hao, D.K. Schwartz, and J.W. Medlin, *ACS Catal.* **8** (2018) 11165.

# A Solid Molecular Catalyst for Hydroformylation: Phosphine Organic Frameworks as Porous Macroligand

*Sara Lena Nophut, Martin Lucas, Marcus Rose*

*TU Darmstadt, Ernst-Berl-Institut für Technische und Makromolekulare Chemie,  
Darmstadt, D-64289 (Germany)*

Hydroformylation of propene is one of the most important reactions in industrial scale giving the aldehyde butanal, a common additive and bulk chemical [1]. The process is catalysed homogeneously although in general, heterogeneous catalysts are preferred to facilitate product separation and catalyst recycling. Classical supported catalysts have the drawback of slower reaction rates compared to the homogeneous equivalents. Also, the immobilization of molecular metal complexes typically gives unstable catalysts that are prone to metal leaching. Hence, the “holy grail” for the immobilization of single site metal complexes to be active in catalytic cycles is to find the ideal support material. In recent years, nanoporous organic frameworks have evolved with great opportunities in catalyst development [2]. Among this class of materials, polyphosphanes with permanent porosity have been reported [3,4].

In our work we investigated these polyphosphanes as macroligands to immobilize Wilkinson’s catalyst ( $\text{Rh}(\text{PPh}_3)_3\text{Cl}$ ), typically used for homogeneous hydroformylation. The porous polyphosphane was synthesised by a one-step organolithium route yielding a white solid with permanent porosity and specific surface area of up to  $670 \text{ m}^2\text{g}^{-1}$ . The existence and durability of triphenylphosphane units as building blocks in the frameworks was proven by  $^{31}\text{P}$  MAS NMR. The rhodium complex was immobilised on the polyphosphane by ligand exchange from solution. Catalytic experiments for the gas phase hydroformylation of propene to butyraldehyde were carried out successfully in a continuously operated plug flow reactor that proves the concept of a heterogenized molecular catalyst for hydroformylation reaction. In future work, a kinetic study of this catalyst using a BERTY-type differential loop reactor developed for gas phase reactions is carried out.

## References

- [1] R. Franke, D. Selent, A. Börner, *Chem. Rev.* **2012**, 112, 5675–5732.
- [2] M. Rose, *ChemCatChem* **2014**, 6, 1166–1182.
- [3] J. Fritsch, F. Drache, G. Nickerl, W. Böhlmann, S. Kaskel, *Micropor. Mesopor. Mater.* **2013**, 172, 167–173.
- [4] P. J. C. Hausoul, T. M. Eggenhuisen, D. Nand, M. Baldus, B. M. Weckhuysen, R. J. M. Klein Gebbink, P. C. A. Bruijninx, *Catal. Sci. Technol.* **2013**, 3, 2571–2579.

# Enhanced catalytic stability in strongly exothermal reactions by improving heat conductivity

*Yi Zuo, Tonghui Li, Min Liu, Xinwen Guo, State Key Laboratory of Fine Chemicals, School of Chemical Engineering, Dalian University of Technology, Dalian, China; Junbo Xu, Chao Yang, Key Laboratory of Green Process and Engineering, State Key Laboratory of Biochemical Engineering, Institute of Process Engineering, Chinese Academy of Sciences, Beijing, China*

The epoxidation of alkenes over titanium silicalite-1 (TS-1) is strongly exothermal, which leads to the rapid deactivation of the catalyst. The enhanced heat conductivity benefits the prolonging of catalytic lifetime. From this point of view, the monolithic catalyst and high heat-conductive substances doped extruded catalyst were prepared for improving the stability of alkene epoxidation.

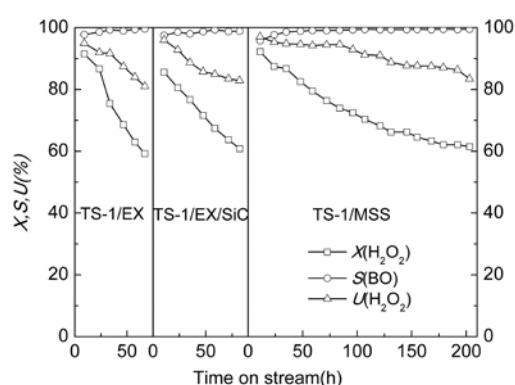
## 1. Introduction

TS-1 was first hydrothermally synthesized by Taramasso et al. in 1983 [1]. In the past three decades, the synthesis and applications of TS-1 attract much attention, because of the excellent catalytic performances of TS-1 with  $\text{H}_2\text{O}_2$  for selective oxidation reactions and the environmentally friendly routes. The epoxidation of alkenes catalyzed by TS-1 often occurs in a fixed-bed reactor [2], the catalysts of which should be shaped. Extrusion is one of the most commonly used shaping methods. Having a large amount of active component is the advantage of the method. However, the heat conductivity property of the extrudates are not satisfactory, especially for strongly exothermal reactions such as epoxidation of alkenes. Therefore, we tried to improve the catalytic performance of TS-1 extrudates by promoting the removing of exotherm. Two kinds of the TS-1 catalysts with high heat conductivity were prepared, which were the monolithic catalyst and extruded catalyst. Furthermore, the reasons for the improvement were studied by the characterization and simulation of temperature distribution in the reactor.

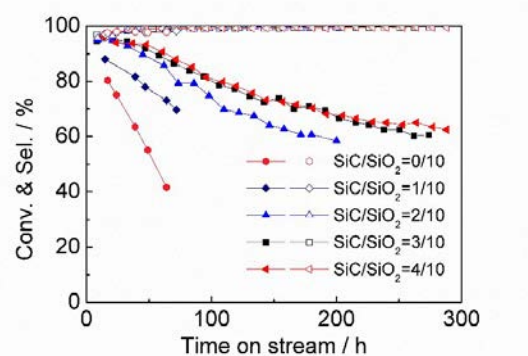
## 2. Results and discussion

Figure 1 shows the catalytic performances of 1-butene epoxidation over the traditional extruded TS-1 (TS-1/EX) and monolithic TS-1 (TS-1/MSS). The time that the  $\text{H}_2\text{O}_2$  conversion ( $X(\text{H}_2\text{O}_2)$ ) decreases to 60% is much longer over TS-1/MSS

than that over TS-1/EX. The stability can also be slightly improved, when mixing some SiC in the extruded TS-1 (TS-1/EX/SiC). Enlightened by this result, we introduced some substances with high heat conductivity to the extruded TS-1 during the extrusion process. The catalytic activity and stability of the samples containing SiC are enhanced significantly (Fig. 2). The addition of metals, such as copper and iron, can also improve the heat conductivity rate of the extruded TS-1. The temperature distribution in the reactor was simulated. It shows that the highest temperature in monolithic catalyst bed is obviously lower than that in traditional extruded catalyst bed.



**Figure 1.** Catalytic performances of the 1-butene epoxidation over different TS-1 catalysts.



**Figure 2.** Catalytic performances of the 1-butene epoxidation over the TS-1 catalysts with different SiC content.

### 3. Conclusions

The catalytic stability of TS-1 was improved by preparing the catalysts with high heat conductivity. These methods are probably helpful for the applications of TS-1 on the epoxidation of alkenes with long carbon chain, and for other strongly exothermic reactions.

### References

- [1] M. Taramasso, G. Perego, B. Notari, U.S. Pat. 4410501 (1983).
- [2] Y. Zuo, M. Wang, W. Song, X. Wang, X. Guo, Ind. Eng. Chem. Res. 51, 10586-10594 (2012).

# Catalytic Hydrogenation of Levulinic Acid to $\gamma$ -Valerolactone in Batch and Continuous-flow: Insights into the Influence of Feed Impurities on Catalyst Performance

Homer C. Genuino,<sup>1,2</sup> Henk H. van de Bovenkamp,<sup>1</sup> Erwin Wilbers,<sup>1</sup> Andrey Goryachev,<sup>3</sup> Jan P. Hofmann,<sup>3</sup> Emiel J. M. Hensen,<sup>3</sup> Pieter C. A. Bruijninx,<sup>2</sup> Bert M. Weckhuysen,<sup>2</sup> Hero J. Heeres<sup>1</sup>

<sup>1</sup>Engineering and Technology institute Groningen (ENTEG), Department of Chemical Engineering, University of Groningen, Groningen, The Netherlands; <sup>2</sup>Inorganic Chemistry and Catalysis, Debye Institute for Nanomaterials Science, Utrecht University, Utrecht, The Netherlands; <sup>3</sup>Department of Chemical Engineering, Eindhoven University of Technology, Eindhoven, The Netherlands

$\gamma$ -Valerolactone (GVL) is readily obtained by the hydrogenation of levulinic acid (LA) and is considered a sustainable platform chemical for the production of bio-based chemicals [1-2]. Herein the performance and particularly the long-term stability of Ru-based catalysts (1 wt.% Ru) supported on TiO<sub>2</sub> and ZrO<sub>2</sub> for LA hydrogenation to GVL [3] was investigated in the liquid phase in batch and continuous-flow reactors, and the influence of biogenic and process-derived impurities on LA hydrogenation dioxane and water was determined. Benchmark continuous-flow experiments at extended time-on-stream (i.e., 190 h; 10 wt.% LA, 50 bar H<sub>2</sub>, 150 °C in dioxane, 90 °C in water, WSHV of 2.4 g<sub>feed</sub> g<sub>cat</sub><sup>-1</sup>h<sup>-1</sup> in dioxane, 3.6 g<sub>feed</sub> g<sub>cat</sub><sup>-1</sup>h<sup>-1</sup> in water) showed that the Ru/ZrO<sub>2</sub> catalyst is more stable than Ru/TiO<sub>2</sub>. Characterization studies of spent catalysts after the long-term stability runs showed that the deactivation of Ru/TiO<sub>2</sub> is strongly linked to reduction of the TiO<sub>2</sub> support and a reduction of the specific surface area. Ru/ZrO<sub>2</sub> showed no signs of support reduction and displayed morphological and structural stability, though some deposition of carbonaceous material was observed. The effect of the presence of impurities in the LA feed such as formic acid (HCOOH), sulfuric acid (H<sub>2</sub>SO<sub>4</sub>), furfural (FFR), 5-hydroxymethylfurfural (HMF), industrial humins (higher molecular weight condensation products between sugars and intermediates), and S-containing amino acids (i.e., thiols, thioether, disulfides) on catalyst performance and long-term stability was also investigated in batch and continuous-flow reactors. HCOOH addition to LA

leads to rapid catalyst deactivation and that reactivation of the catalysts is possible. The loss of activity is possibly attributed to preferential adsorption of HCOOH instead of LA on Ru sites and CO poisoning. A more gradual drop in activity was found when co-feeding FFR, HMF, and humins for both solvents. H<sub>2</sub>SO<sub>4</sub>, cysteine, cystine, and methionine all result in irreversible deactivation of the Ru catalysts. The results obtained provide additional insights into the (in)sensitivity of Ru-based hydrogenation catalysts to potential impurities in LA feeds.

### References

- [1] J.-P. Lange, R. Price, P. Ayoub, J. Louis, L. Petrus, L. Clarke, H. Gosselink, *Angew. Chem. Int. Ed.* **2010**, *49*, 4479-4483.
- [2] A. S. Piskun, J. E. de Haan, E. Wilbers, H. H. van de Bovenkamp, Z. Tang, H. J. Heeres, *ACS Sustainable Chem. Eng.* **2016**, *4*, 2939-2950.
- [3] J. Ftouni, A. Muñoz-Murillo, A. Goryachev, J.-P. Hofmann, E. J. M. Hensen, L. Lu, C. J. Kiely, P. C. A. Bruijninx, B. M. Weckhuysen, *ACS Catal.*, **2016**, *6*, 5462-5472.

### Acknowledgements

The authors gratefully acknowledge the Smart Mix Program of the Netherlands Ministry of Economic Affairs and the Netherlands Ministry of Education, Culture and Science within the framework of the Dutch CatchBio Program. The authors also thank Avantium Chemicals B.V., The Netherlands for providing the industrial humins samples.



# Silver-catalyzed selective hydrogenation of CO<sub>2</sub> into formic acid

Gaetano Calvaruso,<sup>a,b</sup> Nils Theyssen,<sup>a</sup> Walter Leitner<sup>b,c</sup>

<sup>a</sup>Max-Planck-Institut für Kohlenforschung, Mülheim an der Ruhr, Germany

<sup>b</sup>Institut für Technische und Makromolekulare Chemie, Lehrstuhl für Technische Chemie und Petrochemie, RWTH Aachen, Aachen, Germany

<sup>c</sup>Max Planck Institute for Chemical Energy Conversion,  
Mülheim an der Ruhr, Germany

CO<sub>2</sub> has gained increasing attention as a precursor of C-1 chemicals, which can be obtained via reductive routes.<sup>[1]</sup> Stepwise hydrogenation of CO<sub>2</sub> leads to the formation of formic acid, which may be further hydrogenated to MeOH and methane. Hydrogenation of CO<sub>2</sub> into MeOH and methane are exergonic reactions with a  $\Delta G$  of -9.5 and -165.0 kJ mol<sup>-1</sup>, respectively.<sup>[2]</sup> Conversely, gas-phase hydrogenation of CO<sub>2</sub> into formic acid presents a positive  $\Delta G$  (+32.9 kJ mol<sup>-1</sup>).<sup>[3]</sup>

However, it has been demonstrated that liquid-phase hydrogenation of CO<sub>2</sub> into formic acid is possible if bases or certain solvents are utilized. Many authors reported the homogeneous catalyzed hydrogenation of CO<sub>2</sub> into formic acid and various noble and base metal complexes are known to be active. Mori et al. have shown that hydrogenation of CO<sub>2</sub> into formic acid is possible in a heterogeneous system composed of ruthenium supported on a layered double hydroxide without utilizing bases.<sup>[4]</sup> Selective hydrogenation of CO<sub>2</sub> into formic acid, although in poor yields, is also obtained using a carbon nanotube-graphene supported PdNi alloy catalysts.<sup>[5]</sup> Hence, there is a need for understanding and developing solid catalysts for the mentioned reaction.

Several metals supported on metal oxides have been used for hydrogenation reactions. Silver has been less investigated because of its low affinity towards H<sub>2</sub>, due to the filled d-band as well as the position of the d-band centered relative to the Fermi level.<sup>[6]</sup> Notable exceptions are selective hydrogenations of aldehydes and nitroaromatics.<sup>[7]</sup> Moreover, silver supported on different metal oxides has been reported to be active in the hydrogenation of CO<sub>2</sub> into methanol.<sup>[8]</sup>

Therefore, it is interesting to evaluate the suitability of silver as a cheaper alternative to other noble metals towards CO<sub>2</sub> hydrogenation. Herein, we report preliminary results on CO<sub>2</sub> hydrogenation, carried out in the liquid phase and using alumina-

supported silver and other noble metals (i.e., ruthenium, copper and palladium) as catalysts. No bases were utilized in this work to highlight the role of the metals. The catalysts were prepared via wet impregnation of  $\gamma$ -alumina, followed by drying and calcination at 600 °C. Table 1 shows that silver is a preferred hydrogenating catalyst for the conversion of CO<sub>2</sub> into formic acid. High selectivities are obtained for both Ag, Pd and copper under the applied reaction conditions. The effect of temperature, support, co-solvents and other reaction parameters are investigated. Silver catalysts were also characterized via TEM (Fig. 1), XPS, BET and H<sub>2</sub>-TPR to get information regarding the catalyst structure. Compared to the above-mentioned solid catalysts, the alumina-supported silver catalyst has practical advantage in recycling.

**Table 1.** Comparison of alumina-supported Ag, Pd, Cu and Ru catalysts for CO<sub>2</sub> hydrogenation to formic acid

Entry	Catalyst	n Metal (mol)	Temperature (°C)	c (HCOOH) (mol L <sup>-1</sup> )	TON	TOF
1	1 wt.% Ru/ $\gamma$ -Al <sub>2</sub> O <sub>3</sub>	$8.9 \times 10^{-7}$	100	0	0	0
2	1 wt.% Cu/ $\gamma$ -Al <sub>2</sub> O <sub>3</sub>	$1.4 \times 10^{-6}$	100	$2.93 \times 10^{-3}$	16.8	$2.1 \times 10^{-4} \text{ s}^{-1}$
3	1 wt.% Pd/ $\gamma$ -Al <sub>2</sub> O <sub>3</sub>	$9.4 \times 10^{-7}$	100	$1.52 \times 10^{-3}$	19.5	$2.7 \times 10^{-4} \text{ s}^{-1}$
4	1 wt.% Ag/ $\gamma$ -Al <sub>2</sub> O <sub>3</sub>	$8.3 \times 10^{-7}$	100	$3.70 \times 10^{-3}$	36.6	$5.1 \times 10^{-4} \text{ s}^{-1}$

Reaction conditions: 10 mg catalyst, 10 mL 1,4-dioxane, 100°C, 20 h, 110 bar (80 bar H<sub>2</sub>; 30 bar CO<sub>2</sub>).

## References

- [1] J. Klankermayer, S. Wesselbaum, K. Beydoun, W. Leitner, *Angew. Chem. Int. Ed.* **2016**, *55*, 7296-7343.
- [2] a) W.-H. Wang, Y. Himeda, J. T. Muckerman, G. F. Manbeck, E. Fujita, *Chem. Rev.* **2015**, *115*, 12936-12973; b) J. Gao, Y. Wang, Y. Ping, D. Hu, G. Xu, F. Gu, F. Su, *RSC Advances* **2012**, *2*, 2358-2368.
- [3] W. Leitner, *Angewandte Chemie International Edition in English* **1995**, *34*, 2207-2221.
- [4] K. Mori, T. Taga, H. Yamashita, *ACS Catal.* **2017**, *7*, 3147-3151.
- [5] L. T. M. Nguyen, H. Park, M. Banu, J. Y. Kim, D. H. Youn, G. Magesh, W. Y. Kim, J. S. Lee, *RSC Advances* **2015**, *5*, 105560-105566.
- [6] C. Fröhlich, R. A. Köppel, A. Baiker, M. Kilo, A. Wokaun, *Appl. Catal., A* **1993**, *106*, 275-293.
- [7] a) Z. Jia, F. Zhou, M. Liu, X. Li, A. S. C. Chan, C.-J. Li, *Angew. Chem. Int. Ed.* **2013**, *52*, 11871-11874; b) R. Poreddy, E. J. Garcia-Suarez, A. Riisager, S. Kegnaes, *Dalton Transactions* **2014**, *43*, 4255-4259.
- [8] S. Sugawa, K. Sayama, K. Okabe, H. Arakawa, *Energy Conversion and Management* **1995**, *36*, 665-668.

---

## Synthesis and characterization of barium and cesium promoted ruthenium catalysts supported on KL zeolite for the ammonia synthesis.

M.P., Nery<sup>1</sup>, L.F.F.P.G. Bragança<sup>2</sup>, M.I.P. da Silva<sup>\*,1</sup>

<sup>1</sup> Departamento de Química, Pontifícia Universidade Católica do Rio de Janeiro, Rio de Janeiro, Brazil, 22451-900. \* isapais@puc-rio.br

<sup>2</sup> Departamento de Engenharia Química e Petróleo, Universidade Federal Fluminense, Niterói, Rio de Janeiro, Brazil, 24210-240.

---

Keywords: KL zeolite, ammonia synthesis, ruthenium catalysts.

---

### 1 Introduction

The main advantage of Ru-based catalysts for ammonia synthesis is the higher resistance to ammonia poisoning than Fe-based catalysts [1]. Also, it has been reported the use of KL zeolite as support for many applications [2]. The aim of this work was to evaluate ruthenium catalysts supported on KL zeolite promoted by basic cations for ammonia synthesis reaction. The influence of barium introduction order was examined.

### 2 Experimental/methodology

The KL zeolite was provided by TOYO SODA. For ionic exchange with cesium, 50 mL of CsNO<sub>3</sub> 1M solution (MERCK) were added dropwise to the zeolitic support at 90°C under stirring. Then it was centrifuged and heated to 120 °C (2°C/min) and then to 300°C for 4 h. After the support was washed and centrifuged successively for removal residual nitrate and dried at 80°C for 16 h. For ionic exchange with barium a solution of Ba(NO<sub>3</sub>)<sub>2</sub> 0.3M (MERCK) was used in a similar procedure described above. For ruthenium introduction by ionic exchange, a solution of Ru(NH<sub>3</sub>)<sub>6</sub>Cl<sub>2</sub> 0.1M (ALDRICH) was added dropwise at 90°C under magnetic stirring. The resulting catalysts were washed and centrifuged to remove the residual chloride and then were dried at 80°C for 24 h. The amount of incorporated metal was analysed by Atomic Absorption Spectrometry. Nitrogen isotherms for the support and promoted catalysts were measured at liquid nitrogen temperature using a Micromeritics ASAP2010 apparatus. The X-ray diffraction (XRD) measurements were performed in a Siemens D5000 diffractometer. Hydrogen chemisorption was used to verify the degree of metallic dispersion using a Micromeritics ASAP 2010C instrument. The catalytic performance in NH<sub>3</sub> synthesis for both catalysts were evaluated at three different temperatures: 300°C, 400°C and 500°C.

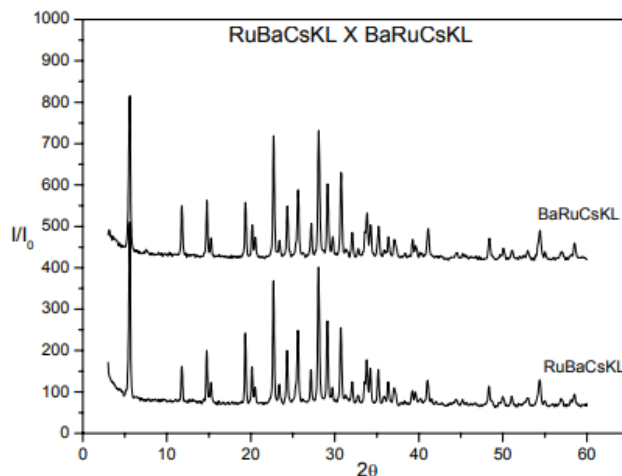
### 3 Results and discussion

The chemical composition and the textural properties of KL support and catalysts are listed in Table 1. The structural properties showed higher specific area and pore volume values for BaRuCsKL sample. The XRD patterns of both catalysts are shown in Fig. 1. Both catalysts showed similar diffractograms, indicating that the order of barium and ruthenium introduction did not affect the crystallinity of zeolite KL. The BaRuCsKL sample presented a greater dispersion (69%) than RuBaCsKL (42%). The relative conversions for NH<sub>3</sub> synthesis are summarized in Table 1. According to the data obtained a higher conversion was obtained for RuBaCsKL. The subsequent introduction of Ba to Ru probably resulted in a displacement of the Ru ions to more internal positions of the zeolite improving its dispersion but making access to the metallic sites more difficult.

**Table 1.** Chemical composition, textural properties and NH<sub>3</sub> relative conversion for both catalysts.

Samples	%Ru	%Ba	%Cs	BET area (m <sup>2</sup> /g)	TPV* (cm <sup>3</sup> /g)	% conversion		
						300°C	400°C	500°C
KL	-	-	-	346	0.14	-	-	-
RuBaCsKL	3.3	4.0	6.0	276	0.11	6.1	14.2	8.3
BaRuCsKL	3.3	5.8	4.3	318	0.13	5.8	9.2	5.4

\*TPV = Total Pore Volume



#### 4 Conclusion

The addition of ruthenium after barium by ionic exchange to the KL support led to more active catalysts for ammonia synthesis.

#### References

- [1] P. Stolze, Phys. Sci. 36, 824 (1987).
- [2] J.F. da Silva, L F.F.P.G. Bragança, M I P. da Silva, Reaction, Mechan, and Catal. 124,563 (2018).

# Oxidative coupling of methane over TiO<sub>2</sub>/ZSM-5 composite catalyst with the assistance of electric field

Qiao Han<sup>1</sup>, Shunsuke Morimoto<sup>1</sup>, Atsuhiko Tanaka<sup>1</sup>, Yoshihiro Kubota<sup>1</sup>, Satoshi Inagaki<sup>1,2</sup>

<sup>1</sup>Yokohama National University, Yokohama, Japan

<sup>2</sup>JST, PRESTO, Kawaguchi, Japan

## Introduction

Oxidative coupling of methane (OCM) is one of the most attractive reactions that directly convert methane to C<sub>2</sub> hydrocarbons. This reaction is thermodynamically favorable because it is an exothermic reaction. Nevertheless, most catalytic reactions need a high temperature over 700°C and the yield of C<sub>2</sub> hydrocarbons is low due to the over-oxidation of reaction intermediates into CO and CO<sub>2</sub> [1]. As an alternative approach, the electric-field-assisted reaction system catalyzed by semiconductive solids has been developed [2-4]. Recently, Ogo and co-workers have suggested that the cerium-tungstate-modified CeO<sub>2</sub> catalyst efficiently work for OCM in electric field to achieve relatively high C<sub>2</sub> selectivity [3,4]. We expected that the combination of this catalytic reaction system and the ethylene-to-propylene reaction catalyzed by H-ZSM-5 zeolite [5] would give propylene and higher olefins continuously. Therefore, we attempted to prepare the core-shell-type catalyst particles, which consists of H-ZSM-5 core and TiO<sub>2</sub> shell, to utilize for OCM and ETP reactions in electric field.

## Experimental

TiO<sub>2</sub> nanoparticles (7.0 g) and H-ZSM-5 (Si/Al = 16, 7.0 g) were treated using a powder composer to prepare the core-shell-type particles, which is designated as TiO<sub>2</sub>/ZSM-5. Then, TiO<sub>2</sub>/ZSM-5 and TiO<sub>2</sub> were thermally treated at 800°C for 12 h; the treated samples are designated as TiO<sub>2</sub>/ZSM-5\_800 and TiO<sub>2</sub>\_800, respectively. The prepared samples were characterized by powder X-ray diffraction (XRD) and field-emission scanning electron microscopy (FE-SEM). Catalytic reaction was performed using a fixed bed continuous-flow reactor equipped with a quartz tube. The catalyst powder (100 mg), sieved into 355–500 μm, was charged in the reactor. Two stainless-steel electrodes were separately set in the reactor with no contact each other; one electrode contacts with the upper end of the catalyst bed, and the other contacts with the lower end. The electric field was controlled using a constant current with a DC power supply. The furnace temperature was maintained at 150°C during the reaction in electric field. The reactants were fed into the reactor (CH<sub>4</sub>: O<sub>2</sub>: Ar = 25: 15:

60 cm<sup>3</sup> (SATP) min<sup>-1</sup>, W/F of CH<sub>4</sub> = 1.6 g-cat. h mol<sup>-1</sup>). The products were analyzed using GC-FID and GC-TCD.

## Result and Discussion

Table 1 shows the typical catalytic results of TiO<sub>2</sub>/ZSM-5\_800. In the reaction over simple TiO<sub>2</sub> catalyst, extremely low conversion of CH<sub>4</sub> in OCM was observed both under electric field (150°C) and with only thermal heating at 600°C. In contrast, the use of TiO<sub>2</sub>/ZSM-5 composite catalyst resulted in high CH<sub>4</sub> conversion (11.3 %) under electric field (1.1 kV, 6.0 mA), while this type of catalyst did not work under thermal heating at 600°C. This indicates that the interface between TiO<sub>2</sub> and ZSM-5 particles might efficiently work for O<sub>2</sub> and CH<sub>4</sub> activation assisted by electric field. In terms of the product selectivity, the single use of TiO<sub>2</sub> afforded only CO and CO<sub>2</sub> even at the lower CH<sub>4</sub> conversion. With electric field, TiO<sub>2</sub>/ZSM-5 composite catalyst showed relatively high selectivities to C<sub>2</sub>H<sub>6</sub> and C<sub>2</sub>H<sub>4</sub> (13.6 and 15.1%, respectively). Moreover, TiO<sub>2</sub>/ZSM-5 can produce a meaningful amount of propylene in electric field, due to the Brønsted acidity in ZSM-5 to promote the ETP reaction. The reaction with simple thermal heating at 600–900°C gave only CO and CO<sub>2</sub>.

We found that the active oxygen species was adsorbed on the TiO<sub>2</sub> surface of TiO<sub>2</sub>/ZSM-5 in electric field and O<sub>2</sub> flow, which can be desorbed slowly after shut-off the constant current. Such oxygen species on TiO<sub>2</sub> in electric field could activate CH<sub>4</sub> into CH<sub>3</sub> radical followed by ethane/ethylene formation.

Table 1: Influence of electric field on the catalytic properties of TiO<sub>2</sub>/ZSM-5\_800

EF (kV)	Input current (mA)	Furnace temp. (°C)	Temp. of catalyst bed (°C)	CH <sub>4</sub> conv. (C-%)	Selectivity (C-%)						Yield (C-%)	
					CO	CO <sub>2</sub>	C <sub>2</sub> H <sub>6</sub>	C <sub>2</sub> H <sub>4</sub>	C <sub>2</sub> H <sub>2</sub>	C <sub>3</sub> H <sub>6</sub>	C <sub>2</sub>	C <sub>3</sub> H <sub>6</sub>
1.1	6.0	150	417	11.3	58.4	2.7	13.6	15.1	7.8	2.5	4.1	0.3
		600	612	0.2	93.0	7.0	0.0	0.0	0.0	0.0	0.0	0.0
		750	758	2.4	91.0	7.7	1.1	0.2	0.0	0.0	0.0	0.0
0.0	0.0	900	901	16.9	84.9	11.0	1.5	2.5	0.0	0.0	0.7	0.0

## References

- [1] U. Zavyalova, M. Holena, R. Schlogl, M. Baerns, *ChemCatChem*, 3 (2011) 1935.
- [2] K. Tanaka, Y. Sekine, K. Oshima, Y. Tanaka, M. Matsukata, E. Kikuchi, *Chem. Lett.*, 41 (2012) 351.
- [3] S. Ogo, K. Iwasaki, K. Sugiura, A. Sato, T. Yabe, Y. Sekine, *Catal. Today*, 299 (2018) 80.
- [4] S. Ogo, H. Nakatsubo, K. Iwasaki, A. Sato, K. Murakami, T. Yabe, A. Ishikawa, H. Nakai, Y. Sekine, *J. Phys. Chem. C*, 122 (2018) 2089.
- [5] e.g., B.M. Lin, Q.H. Zhang, Y. Wang, *Ind. Eng. Chem. Res.*, 48 (2009) 10788.

# Assessing the Structure of Defective Ti in TS-1 by Experiments and Theory

Matteo Signorile<sup>1</sup>, Valentina Crocellà<sup>1</sup>, Luca Braglia<sup>2</sup>, Alessandro Damin<sup>1</sup>, Carlo Lamberti,<sup>3</sup> Silvia Bordiga<sup>1</sup> and Francesca Bonino<sup>1</sup>

<sup>1</sup> Department of Chemistry, NIS and INSTM Reference Centre, Università di Torino, Via G. Quarello 15, I-10135 and Via P. Giuria 7, I-10125, Torino, Italy

<sup>2</sup> IOM-CNR, APE-HE beamline, S.S. 14 km 163.5, Basovizza, I-34149 Trieste, Italy

<sup>3</sup> Department of Chemistry, NIS, INSTM Reference Centre and CrisDi, Università di Torino, Via P. Giuria 1, I-10125, Torino, Italy and IRC "Smart Materials", Southern Federal University, Zorge street 5, 344090 Rostov-on-Don, Russia

Titanium Silicalite-1 (TS-1) is a well-known and deeply characterized catalyst for partial oxidation reactions [1]. Nowadays, many studies concerning TS-1 deal with the defective Ti sites often found in poor quality/high Ti loading materials. Still, both their structure(s) and their effect on the catalytic performances are not univocally assessed [2-4]. Our work aims to improve the understanding on these peculiar Ti sites, by combining several characterization techniques with state of the art computational methods.

On the experimental side, we compared two catalysts, TS-1A (a perfect material, i.e. containing only tetrahedral framework Ti sites) and TS-1B (a defective material, where some defective sites are present together with tetrahedral ones). A thoroughly characterization of these catalysts has been recently reported and correlated to their catalytic performances in the HPPO reaction [4]. On the basis of these data and by including more recent results, we obtained a multifaceted view on the nature of the sites.

All the techniques applied point out that the defective Ti are most probably characterized by higher coordination number in the first shell, i.e. 15000 cm<sup>-1</sup> red-shift of the LMCT, new features in the NEXAFS spectra typical of coordination higher than tetrahedral and peculiar resonant fingerprint in Raman.

On the basis of these experimental insights and previous reports [2,3], we hypothesized possible defective structures and we simulated their spectroscopic fingerprint through quantum chemistry methods. In detail, the structural models were constructed with a periodic approach, in order to retain the framework effect on the localized Ti site [5]. Thus, large clusters calculations were adopted to simulate the associated spectroscopic features. All the calculations were performed at the

B3LYP/DZ computational level. Some relevant models, together with the reference perfect tetrahedral Ti site, are shown in Figure 1.

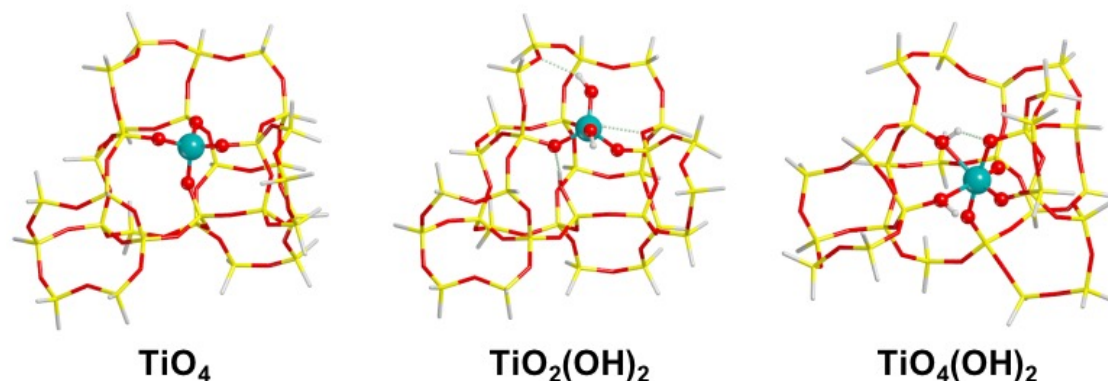


Figure 1. Models (cluster) for perfect and defective Ti.

Preliminary results show as the  $\text{TiO}_4(\text{OH})_2$  model properly reproduces some of the experimental features, including a resonantly enhanced Raman peak at  $\sim 690 \text{ cm}^{-1}$  and a red-shift of  $\sim 15000 \text{ cm}^{-1}$  for the LMCT electronic transition. Further simulation over different models are ongoing, in order to finally shed light on the complex nature of the defective Ti sites in TS-1.

#### References

- [1] Notari, B.; Perego, G.; Taramasso, M.; US4410501 A, 1983.
- [2] Guo, Q.; Sun, K.; Feng, Z.; Li, G.; Guo, M.; Fan, F.; Li, C.; Chem. Eur. J. 2012, 18, 13854–13860.
- [3] Zuo, Y.; Liu, M.; Zhang, T.; Hong, L.; Guo, X.; Song, C.; Chen, Y.; Zhu, P.; Jaye, C.; Fischer, D.; Rsc Adv. 2015, 5, 17897–17904.
- [4] Signorile, M.; Crocellà, V.; Damin, A.; Rossi, B.; Lamberti, C.; Bonino, F.; Bordiga, S.; J. Phys. Chem. C 2018, 122, 9021–9034.
- [5] Signorile, M.; Damin, A.; Bonino, F.; Crocellà, V.; Ricchiardi, G.; Lamberti, C.; Bordiga, S.; J. Phys. Chem. C 2018, 122, 1612–1621.



# **Zn-doped ZrO<sub>2</sub>-based catalysts prepared by different methods for the direct dehydrogenation of isobutane to isobutene**

*Zhiping Zhao*<sup>1</sup>, *China University of Petroleum-Beijing*<sup>1</sup>, *Beijing*<sup>1</sup>, *China*<sup>1</sup>; *Yang Liu*, *China University of Petroleum-Beijing*<sup>2</sup>, *Beijing*<sup>2</sup>, *China*<sup>2</sup>; *Ming Ke*<sup>3</sup>, *China University of Petroleum-Beijing*<sup>3</sup>, *Beijing*<sup>3</sup>, *China*<sup>3</sup>

## **Author list**

1 Zhiping Zhao: zhao920604@163.com

2 Yang Liu: mwyl123@sina.com

3 Ming Ke: keming@cup.edu.cn, or keming\_cup@126.com

## **Note**

DECHEMA will not make any changes or correctiv action regarding the author information.

## **Abstract**

Isobutene is an important “member” of chemical raw materials, which is widely utilized in the production of various industry chemicals with high-added value. With the increasing requirement for isobutene around the world, the resources of fossil fuels, which are applied in the traditional methods for producing isobutene, have been obviously dwindled. However, it’s more economical that a large volume of shale gas as well as nature gas has been gradually exploited with the development of exploration in recent years. The above factors make isobutane catalytic dehydrogenation become an efficient alternative technique for the production of isobutene.

In our previous works, a series of Zn-doped mixed oxides catalysts (ZnZrO-x) for isobutane direct dehydrngenation were prepared by the hard-template method. The physicochemical properties, active sites, and reaction mechanism of ZnZrO-x were also studied.<sup>[1]</sup> In this thesis, we further researched the effect of the preparation method on the physicochemical properties of the catalysts. Specially, we respectively prepared three Zn-doped ZrO<sub>2</sub>-based catalysts with Zr/Zn=5 using hard-template (ZnZrO-5<sup>H</sup>), incipient-wetness impregnation (ZnZrO-5<sup>I</sup>), and coprecipitation method

(ZnZrO-5<sup>c</sup>). Moreover, the physical structures, acid-base properties, and the formation of active sites for each sample were studied by a series of characterizations (including N<sub>2</sub> adsorption-desorption isotherms, XRD, TEM, XPS, and Py-IR) and activity evaluations.

#### **References**

[1] Yang Liu, Chenjie Xia, Qi Wang, Lei Zhang, Ao Huang, Ming Ke, Zhaozheng Song. Direct dehydrogenation of isobutane to isobutene over Zn-doped ZrO<sub>2</sub> metal oxide heterogeneous catalysts. *Catalysis Science & Technology*, 2018, 8(19): 4916-4924.

# Bottom-up design of heterogeneous gold catalysts for the oxidative coupling of methanol

*Cansunur Demirci, Department of Nanochemistry - Istituto Italiano di Tecnologia, Genoa, Italy; Massimo Colombo, Department of Nanochemistry - Istituto Italiano di Tecnologia, Genoa, Italy; Liberato Manna, Department of Nanochemistry - Istituto Italiano di Tecnologia, Genoa, Italy*

## Introduction

In the last decades, nanoporous gold (NPG) structures gained more and more interest in the field of heterogeneous catalysis.[1, 2] This kind of structures, usually synthesized by a top-bottom approach, are showing high activities and selectivity for different reactions, exhibiting catalytic properties that are not displayed by the corresponding supported catalysts.[3] According to the currently employed synthesis method, the pure miscible metals like gold, silver, copper or aluminum are alloyed and afterwards the less noble metal is selectively etched by chemical or electrochemical methods.[1] In many works, the enhancing effect of the metal traces on catalytic activity was claimed.[4] Despite these fascinating catalytic functions, the synthesis method of these materials has many drawbacks, like the limitation of the chemical composition of the final product.[5] Yet, there is no possibility to synthesize pure nanoporous gold without residuals of metals after the dealloying step, leaving the role of the metal traces still under discussion. For this reason, the development of a new method for the synthesis of nanoporous structures is desirable. In our work, we chose a bottom up approach, based on the self-assembly of nanoscale units, i.e. metallic nanoparticles (NPs), through the cryogelation method to build 3D disordered porous structures (i.e. cryogels).[6, 7] The cryogelation of Au NPs enabled us to synthesize pure, self-standing, porous gold gels, without the presence of any residual metal trace. This allowed us to study the role of metal traces in NPG catalysis and to overcome the compositional restrictions of gold alloys.

## Methods and Results

The aqueous Au NPs were prepared by a citrate reduction approach at room temperature and subsequently concentrated to the required volume ratio of 0.1% prior to undergo the cryogelation step, so to obtain gold cryogels.[7] The concentrated solution was injected in liquid N<sub>2</sub> and subsequently freeze-dried to remove the ice templates and obtain a 3D self-standing nanoporous structures of

gold. The oxidative coupling of methanol was performed on fresh samples, washed samples and on samples dropcasted with different sodium salts to further investigate the influence of metal traces on the activity. The macroscopic images in Figure 1 are showing the self-supported monoliths of assembled Au NPs ( $3.8 \pm 1.1$  nm determined by transmission electron microscopy). The scanning electron microscopy images in Figure 1 give us insights into highly porous, non-ordered and interconnected networks of sheets and wires revealing a specific surface area of  $\sim 1$  m<sup>2</sup>/g confirmed by krypton physisorption. The microscopic change of the gels after high temperature catalytic tests (exposure for 1 h at 300°C in 10% O<sub>2</sub> v/v atmosphere balanced with He) could be monitored by X-ray diffraction using the SCHERRER-equation, disclosing the increase of the crystallite domains from 6 to 20 nm. By using X-ray photoelectron spectroscopy the presence and absence of sodium impurities on the catalyst surface could be quantified and correlated with the catalytic activity in the methanol coupling reaction. The pure gold sample resulted to be inactive in this reaction. Even considering the different synthetic approach, we believe that the results of the present work can be extended to nanoporous gold structures obtained via a dealloying process.

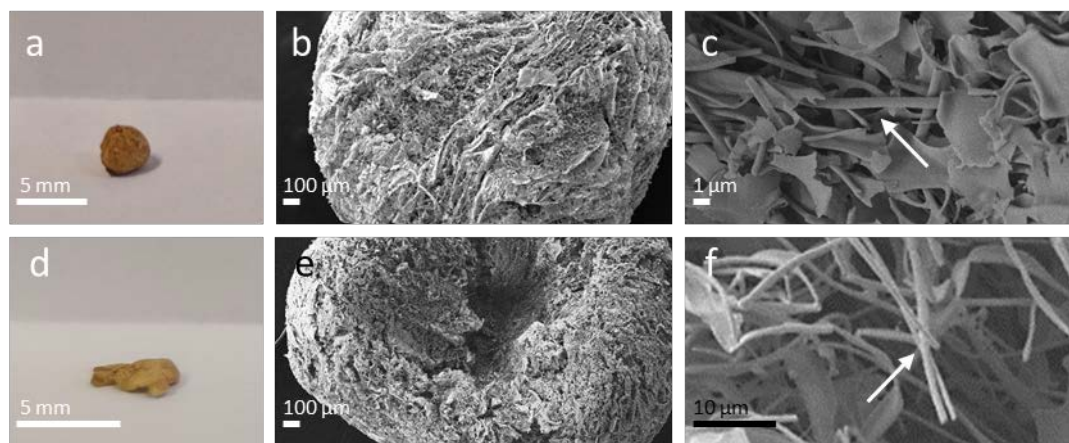


Figure 1 Macroscopic (a, d) and microscopic (b-c, e-f) images of gels before (a-c) and after (d-f) exposure to catalytic conditions.

## References

- [1] Qiu, H. J., et al., *Nanoscale* **2015**, 7 (2), 386-400.
- [2] Erlebacher, J., et al., *Nature* **2001**, 410 (6827), 450-453.
- [3] Kameoka, S.; Tsai, A. P., *Catalysis Letters* **2007**, 121 (3-4), 337-341.
- [4] Wittstock, A., et al., *Science* **2010**, 327 (5963), 319-322.
- [5] Rugolo, J., et al., *Nature materials* **2006**, 5, 946.
- [6] Liu, W., et al., *Accounts of chemical research* **2015**, 48 (2), 154-162.
- [7] Freytag, A., et al., *Angew. Chem. Int. Ed.* **2016**, 55 (3), 1200-1203.

# Dehydration vs. dehydrogenation of ethanol on Co, Ga-doped LaAlO<sub>3</sub> perovskites

*Quang Nguyen Tran*<sup>1,2</sup>, *Nathalie Tanchoux*<sup>1</sup>, *Monica Ceretti*<sup>1</sup>, *Stefania Albonetti*<sup>3</sup>,  
*Werner Paulus*<sup>1</sup>, *Barbara Bonelli*<sup>2</sup>, *Francesco Di Renzo*<sup>1</sup>

<sup>1</sup>*Institut Charles Gerhardt, Montpellier, France;* <sup>2</sup>*DISAT, Politecnico di Torino, Italy;*

<sup>3</sup>*Dpt Industrial Chemistry Toso Montanari, University of Bologna, Italy*

## Scope

If perovskites are well-known as photoelectrocatalysts or redox catalysts [1], the exploitation of their acid-base properties in catalysis has received very limited attention [2,3]. Fine tuning of acid-base and redox activity of catalysts is required in the chemical valorisation of bioethanol [4]. Sol-gel synthesis methods, providing materials with larger surface area, can create the conditions for investigating the potential of perovskites for processes implying a competition between reactions of dehydration and dehydrogenation.

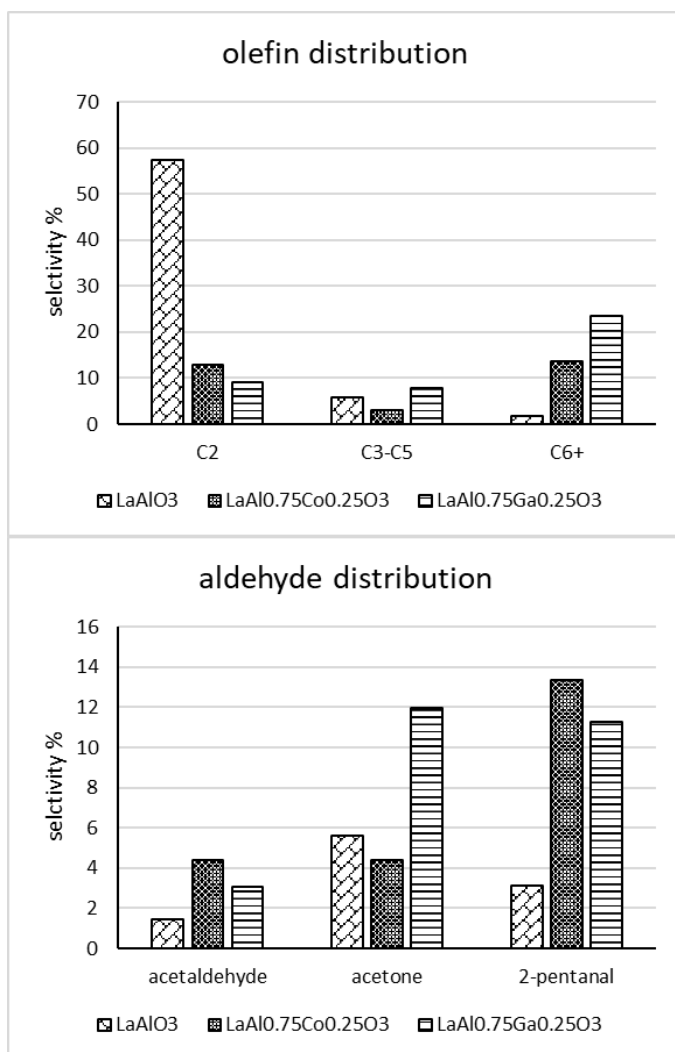
## Experimental

Series of perovskite oxides LaAl<sub>1-x</sub>Co<sub>x</sub>O<sub>3</sub> (x = 0;0.25;0.5;0.75 and 1) and LaAl<sub>1-x</sub>Ga<sub>x</sub>O<sub>3</sub> (x = 0.1; 0.15; 0.20 and 0.25) were prepared by citric acid method and calcination at 700°C. Catalysts were characterized by XRD, H<sub>2</sub> TPR, CO<sub>2</sub>/NO and NH<sub>3</sub> TPD, N<sub>2</sub> sorption and FT-IR. Ethanol conversion was carried out in glass flow reactors in the temperature range 300-400°C with WHSV 0.23-0.92 h<sup>-1</sup>.

## Results

All catalysts featured a monophasic perovskite structure with surface areas between 11 and 15 m<sup>2</sup> g<sup>-1</sup>. At 400°C, ethanol conversion was higher than 95% for LaAlO<sub>3</sub> and the Ga-substituted samples, whereas the lower redox stability of the Co-substituted samples lowered the conversion to about 85%. The competition between dehydration and dehydrogenation reactions was completely controlled by the composition of the catalysts. The olefin/aldehyde ratios in the products was higher than 6 for LaAlO<sub>3</sub> and was between 1.3 and 1.5 for the Co- and Ga-substituted catalysts.

The relative rates of reactions consecutive to the formation of the primary products, ethylene and acetaldehyde, was also controlled by the composition of the catalysts. On LaAlO<sub>3</sub>, acetaldehyde represented more than 85% of the aldehydes formed. The



introduction of weak acid sites by the incorporation of cobalt and - much more- of gallium induced the formation of heavier olefins by cascade reactions of dehydration-dimerization-metathesis.

The distribution of aldehydes was also heavily modified by the introduction of acid sites. Easier decarboxylation favoured the cascade of Tischenko reaction and ketonisation to acetone [5]. Further condensation of acetone and acetaldehyde, leading to 2-pentanal by hydrodeoxygenation, was especially favoured on the more reducible sites of the Co-substituted perovskite.

It can be observed that crotonaldehyde was just a minor

product, the distribution of acid and basic sites being not favourable to Guerbet coupling of acetaldehyde.

## Conclusions

Perovskite catalyst feature a significant activity in ethanol conversion despite their relatively high temperature of preparation. The easy modification of the solid composition and the marked variations of reaction selectivity with moderate levels of substitution make them an ideal testing ground for the study of the modification of surface active sites.

## References

- [1] J. Wang et al. Science 2017,358,751-756
- [2] G.S. Foo et al. ACS Catal. 2017, 7, 4423-4434
- [3] F. Polo-Garzon, Z. Wu. J. Mater. Chem. A 2018, 6, 2877–2894.
- [4] J. Sun, Y. Wang. ACS Catal. 2014, 4, 1078-1090
- [5] S. Tosoni, G. Pacchioni, J. Catal. 2016, 344, 465-473

## Synthesis of nano [B]-ZSM-5 for Methanol to Propylene Reaction

*Busra Karakaya, Middle East Technical University, Department of Chemical Engineering, Ankara, Turkey; Bahar Ipek, Middle East Technical University, Department of Chemical Engineering, Ankara, Turkey*

The growing gap between the propene demand and production, which is currently produced via steam cracking process, is sought to be closed by alternative processes such as methanol to hydrocarbon routes. Methanol-to-propylene (MTP) route is carried under the atmospheric pressure and temperatures of 723–753 K using H-ZSM-5 with typical propylene selectivity values of 40–50 %. The propylene selectivity is desired to be increased using different approaches. Using lower concentrations of Brønsted acid sites or higher Si/Al ratios [1,2], substitution of Al for Fe (to decrease the acid strength and aromatic and paraffin production) [3,4] or higher reaction temperatures, which results in decreased catalyst lifetime. The catalyst deactivation in methanol to olefins is a commonly observed phenomena resulting from formation of carbonaceous deposits such as polymethylbenzenes and polycyclic aromatics. Polymethylbenzenes are also products of the hydrocarbon pool mechanism that is suggested to be one of the dual mechanisms playing role in olefin formation [5]. Produced polycyclic aromatics are suggested to deposit both inside the pores of the zeolite and at the outer surface of the crystals, both of which results in blocking of individual acid sites responsible for activity [6]. Enhanced diffusion of the reaction products as well as carbonaceous species via mesopores [7,8] or shorter diffusion path lengths as in the case of nanosized crystals [3,9] are considered to increase the lifetime of the catalyst as well as increasing the propylene selectivity. In addition to mesopores and altered acidity, B incorporated ZSM-5 catalysts are reported to enhance the catalyst lifetime significantly due to weak acid sites associated with B [10,11].

In this study, boron containing nano and mesoporous ZSM-5 crystals are synthesized with mesopore volumes ranging from 0.11 to 0.14 cm<sup>3</sup>/g (with preserved microporosity: 0.11-0.14 cm<sup>3</sup>/g) and Si/B ratios ranging from 38 to 112 using CTABr as the crystal growth inhibitor. These zeolites are designed for post synthesis partial deboronation and Fe substitution to be tested for MTP reaction at 480 °C, aiming to achieve longer catalyst lifetimes and higher propylene selectivity values.

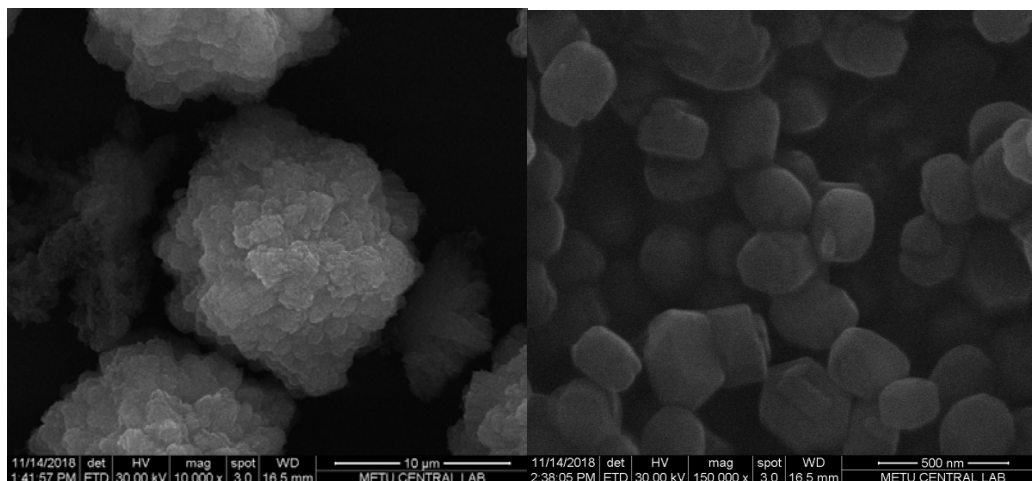


Figure 1. SEM images of a) mesoporous and b) nano [B]-ZSM-5 samples

## References

- [1] Prinz D, Riekert L. Formation of ethene and propene from methanol on zeolite ZSM-5: I. Investigation of Rate and Selectivity in a Batch Reactor. *Appl Catal* 1988;37:139–54.
- [2] Liu J, Zhang C, Shen Z, Hua W, Tang Y, Shen W, et al. Methanol to propylene: Effect of phosphorus on a high silica HZSM-5 catalyst. *Catal Commun* 2009;10:1506–9. doi:10.1016/j.catcom.2009.04.004.
- [3] Taniguchi T, Yoneta K, Nakaoka S, Nakasaka Y, Yokoi T, Tago T, et al. Methanol Conversion Reaction over MFI Ferroaluminosilicate Nano Crystal. *Catal Letters* 2016;146:442–51. doi:10.1007/s10562-015-1650-0.
- [4] Jiang X, Su X, Bai X, Li Y, Yang L, Zhang K, et al. Conversion of methanol to light olefins over nanosized [Fe,Al]ZSM-5 zeolites: Influence of Fe incorporated into the framework on the acidity and catalytic performance. *Microporous Mesoporous Mater* 2018;263:243–50. doi:10.1016/j.micromeso.2017.12.029.
- [5] Olsbye U, Svelle S, Bjrgen M, Beato P, Janssens TVW, Joensen F, et al. Conversion of methanol to hydrocarbons: How zeolite cavity and pore size controls product selectivity. *Angew Chemie - Int Ed* 2012;51:5810–31. doi:10.1002/anie.201103657.
- [6] Müller S, Liu Y, Vishnuvarthan M, Sun X, Van Veen AC, Haller GL, et al. Coke formation and deactivation pathways on H-ZSM-5 in the conversion of methanol to olefins. *J Catal* 2015;325:48–59. doi:10.1016/j.jcat.2015.02.013.
- [7] Mei C, Wen P, Liu Z, Liu H, Wang Y, Yang W, et al. Selective production of propylene from methanol: Mesoporosity development in high silica HZSM-5. *J Catal* 2008;258:243–9. doi:10.1016/j.jcat.2008.06.019.
- [8] Rownaghi AA, Hedlund J. Methanol to gasoline-range hydrocarbons: Influence of nanocrystal size and mesoporosity on catalytic performance and product distribution of ZSM-5. *Ind Eng Chem Res* 2011;50:11872–8. doi:10.1021/ie201549j.
- [9] Palčić A, Ordonsky V V., Qin Z, Georgieva V, Valtchev V. Tuning Zeolite Properties for a Highly Efficient Synthesis of Propylene from Methanol. *Chem - A Eur J* 2018;24:13136–49. doi:10.1002/chem.201803136.
- [10] Hu Z, Zhang H, Wang L, Zhang H, Zhang Y, Xu H, et al. Highly stable boron-modified hierarchical nanocrystalline ZSM-5 zeolite for the methanol to propylene reaction. *Catal Sci Technol* 2014;4:2891–5. doi:10.1039/c4cy00376d.
- [11] Yaripour F, Shariatnia Z, Sahebdehfar S, Irandoukht A. Effect of boron incorporation on the structure, products selectivities and lifetime of H-ZSM-5 nanocatalyst designed for application in methanol-to-olefins (MTO) reaction. *Microporous Mesoporous Mater* 2015;203:41–53. doi:10.1016/j.micromeso.2014.10.024.



# Aerobic and anaerobic methanol transformation on W-Ti-O hexagonal tungsten bronze materials

*D. Delgado*<sup>1</sup>, *B. Solsona*<sup>2</sup>, *S. Zamora*<sup>1</sup>, *M. D. Soriano*<sup>1</sup>, *P. Concepción*<sup>1</sup>, *J.M. López Nieto*<sup>1</sup>

<sup>1</sup> *Instituto de Tecnología Química, UPV-CSIC, Valencia, Spain*

<sup>2</sup> *Chemical Engineering Department, University of Valencia, Valencia, Spain*

## 1. Introduction

Tungsten oxide bronze-related materials present highly adaptive compositional and structural features, what makes this structural types suitable for functional properties modulation [1-2]. In this work, we have studied the incorporation of titanium within the hexagonal tungsten oxide bronze (HTB) framework, and its effect on its acid and redox properties. For this purpose, we have characterized the titled materials by a wide variety of physicochemical techniques (XRD, XPS, HRTEM, SEM, Raman spectroscopy, XAS, TPD-NH<sub>3</sub> and methanol sorption FTIR) and evaluated their catalytic performance in methanol transformation in both aerobic and anaerobic conditions. The results are discussed in terms of the available surface active sites present in each case.

## 2. Experimental

W-Ti-O catalysts with HTB structure have been synthesized by a hydrothermal methodology (175 °C for 48 h) by using ammonium metatungstate and titanium (IV) ethoxide (Ti/(W+Ti) at. ratios in the range 0-0.50). Obtained solids were filtered off, dried at 100°C for 16h, and subsequently heat-treated at 500 °C in N<sub>2</sub> for 2h. The aerobic and anaerobic transformation of methanol was carried out in a fixed bed reactor at atmospheric pressure (T= 200-400 °C, at a total flow of 100 mL min<sup>-1</sup>) using methanol/oxygen/nitrogen ratios of 6/13/81 and 6/0/94, respectively.

## 3. Results and discussion

Figure 1A shows the XRD diagram of Ti-doped HTB and its corresponding BF-STEM image with its XEDS mapping (Ti/(W+Ti) at. ratio = 0.17). A homogeneous distribution of Ti on every single W-Ti oxide nanorod in the samples is observed. Moreover, XPS and EXAFS analyses suggest the isomorphic substitution of Ti<sup>4+</sup> for W<sup>5+</sup> in the HTB framework, what leads to a progressive increase in the acid strength

of surface acid sites. Effective  $\text{Ti}^{4+}$  incorporation in the framework of HTB is observed for samples with Ti/W ratio from 0.10 to 0.50, although  $\text{TiO}_2$  is observed as minority, for samples with Ti/W atomic ratio higher than 0.3.

The catalytic results presented in Figure 1B show the appearance of oxidation reaction, in addition to acid catalysis, for Ti-free sample. However, this is not observed in the case of Ti-containing catalysts, in which the formation of formaldehyde is no longer observed, likely due to the absence of  $\text{W}^{5+}$  in doped materials. In the absence of oxygen, a decrease in the catalytic activity and a drop of formaldehyde selectivity is observed in all the catalysts.

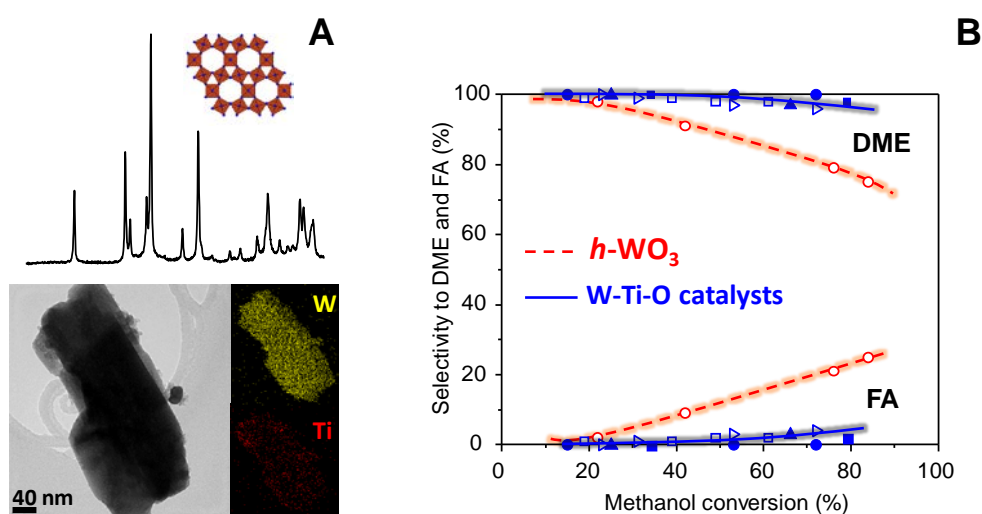


**Figure 1.** A) XRD and BF-STEM image with the corresponding XEDS map of a Ti-doped HTB (Ti/W ratio of 0.17). B) Variation of selectivity to dimethyl ether (DME) and formaldehyde (FA) with methanol conversion (contact time =  $0.073 \text{ g}_{\text{CAT}} \text{ min mL}^{-1}$ )

#### 4. Conclusions

The catalytic behavior in the presence and absence of  $\text{O}_2$ , and the specific features observed in FTIR spectra during methanol adsorption show that both methanol activation and redox activity are favored when  $\text{O}_2$  is present in the feed. Thereby, considering the dynamic nature of lattice oxygen in tungsten bronze-based materials, it can be tentatively proposed that the different catalytic behavior observed in the transformation of methanol under anaerobic conditions can be due to: i) a decrease in the number of surface sites for methanol activation and; ii) the depletion of  $\text{O}^{2-}$  redox surface sites for the partial oxidation of methanol and/or dimethyl ether.

#### References

- [1] A. Chiericato et al., ChemSusChem (2015), 8, 398 – 406.
- [2] D. Delgado et al., Eur. J. Inorg. Chem. (2018), 2018, 1204 – 1211.

# Hydrogenation of Dimethyl Oxalate to Ethylene Glycol by Cu/SiO<sub>2</sub> catalysts, role of tin as promoter

Gianfranco Giorgianni<sup>†</sup>, Salvatore Abate<sup>†</sup>, Siglinda Perathoner<sup>†</sup>, Gabriele Centi<sup>†</sup>

<sup>†</sup> Depts. MIFT and ChimBioFarAM (Industrial Chemistry), University of Messina, ERIC aisbl and INSTM/CASPE, V.le F. Stagno D'Alcontres 31, 98166 Messina, Italy.

## Introduction

The catalytic hydrogenation of biomass-derived oxalates to ethylene glycol is one of the most interesting route for replacing the current production scenario, based on the hydration of petroleum derive ethylene oxide. Cu/SiO<sub>2</sub> catalysts prepared by the ammonia evaporation (AE) method show a high productivity to EG. Such a high productivity was related to a partial oxidation of the Cu surface, presenting both metallic sites showing a mild hydrogenation activity and Cu<sup>+</sup> Lewis sites, that improve the adsorption of DMO [1,2]. Moreover, the low concentration of acidic/basic sites on the support minimize unwanted reactions leading to ethanol or to the formation of superior alcohols. However, deactivation of these catalysts by sintering and the delicate Cu<sup>+</sup>/Cu balance, very sensitive to the operating conditions, limits their industrial application. To improve the productivity and durability of Cu/SiO<sub>2</sub> catalysts, we studied the effect of Tin as a promoter.

We show that the introduction of Tin as a promoter improves both the productivity and stability of the catalysts by increasing the adsorption of both DMO/methyl glycolate and by hindering the migration of Cu on the surface of the support.

## Methods, Results and Discussion

A set of two catalysts were prepared according to the AE method [1,3], by using a 40% wt colloidal silica dispersion in water by Alfa Aesar (43110-A1) to achieve a final Cu loading of 18%. At the end of the procedure, the solid was dried at 110°C for 1h and calcined at 450°C, with a ramp 5°C/min for 4h (CAT-1). The second catalyst, CAT-2, was prepared by impregnating a SnSO<sub>4</sub> solution on previous catalyst.

All the prepared catalysts were studied by temperature programmed reduction, N<sub>2</sub> physisorption and atomic adsorption spectroscopy.

Both catalysts were pelletized at 16-25 mesh, in situ reduced at 200°C in pure H<sub>2</sub> and tested in the vapor phase at 25 barg and 200°C by using a Microactivity Effi apparatus (PID Eng & Tech.), equipped with two parallel fixed bed reactors and liquid/vapor separators. The performance of the reaction monitored by using a GC-FID (Trace GC, Thermo), equipped with a split injector and a SPB-624 column (30m, 0.25mm 1.40 μm).

To optimize the experimental conditions, CAT-1 was tested at different H<sub>2</sub>/DMO ratios (10-50) and GHSV (500-4500 h<sup>-1</sup>). Finally, we compared the catalytic performance of CAT-1 and CAT-2 and their stability in long run experiments.

The Sn promoted Cu/SiO<sub>2</sub> (CAT-2) catalyst has shown superior productivity and durability with respect to CAT-1. Its improved performance were mainly attributed to the presence of a larger concentration of Lewis sites on the catalyst surface, while, the improved stability was attributed to the hindering of Cu nanoparticles, preventing Cu sintering.

### **Acknowledgement**

This project has received funding from the European Union's Horizon 2020 research and innovation program under grant agreement No 767798 (OCEAN)

### **References**

- [1] L. Chen, P. Guo, M. Qiao, S. Yan, H. Li, W. Shen, H. Xu, K. Fan, Cu/SiO<sub>2</sub> catalysts prepared by the ammonia-evaporation method: Texture, structure, and catalytic performance in hydrogenation of dimethyl oxalate to ethylene glycol, *J. Catal.* 257 (2008) 172–180.
- [2] A. Yin, X. Guo, W.-L. Dai, K. Fan, The Nature of Active Copper Species in Cu-HMS Catalyst for Hydrogenation of Dimethyl Oxalate to Ethylene Glycol: New Insights on the Synergetic Effect between Cu<sup>0</sup> and Cu<sup>+</sup>, *J. Phys. Chem. C.* 113 (2009) 11003–11013.
- [3] S. Li, Y. Wang, J. Zhang, S. Wang, Y. Xu, Y. Zhao, X. Ma, Kinetics Study of Hydrogenation of Dimethyl Oxalate over Cu/SiO<sub>2</sub> Catalyst, *Ind. Eng. Chem. Res.* 54 (2015) 1243–1250.

# DFT and experimental study of palladium nitrosyl carboxylate complexes as catalysts for oxidative C-C coupling of arenes

O.N. Shishilov, MIREA – Russian Technological University, M.V. Lomonosov Institute of Fine Chemical Technologies, Moscow, Russia;

R.S. Shamsiev, MIREA – Russian Technological University, M.V. Lomonosov Institute of Fine Chemical Technologies, Moscow, Russia;

N.S. Akhmadullina, A.A. Baikov Institute of Metallurgy and Material Science, Russian Academy of Sciences, Moscow, Russia;

V.R. Flid, MIREA – Russian Technological University, M.V. Lomonosov Institute of Fine Chemical Technologies, Moscow, Russia

Nitrosyl complexes of transition metals are expected to be effective catalysts for oxidative processes due to high affinity of NO groups to oxygen. As a result, NO<sub>2</sub>/NO redox couple is highly effective in both transfer of oxygen and reoxidation of metal centers. Many examples can be given for activity of molybdenum, tungsten, iron and rhenium nitrosyl complexes in dehydrogenation and hydrogen transfer processes as well as in transfer of carbenes and [3+2]-cycloaddition [1]. However, palladium nitrosyl complexes are of rather limited use, although palladium compounds in general are among the most widely used catalysts for oxidation reactions. Palladium nitrosyls are quite difficult to prepare and to study, since most of them are polynuclear compounds formed under specific conditions.

Recently we have started our investigation of palladium nitrosyl carboxylates Pd<sub>3</sub>(NO)<sub>2</sub>(μ-CX<sub>3</sub>CO<sub>2</sub>)<sub>4</sub>(ArH)<sub>2</sub> (X = F, Ar = Tol; X = Cl, Ar = Ph) as potential catalysts for C-C coupling of arenes (fig. 1). The complexes already contain coordinated molecules of arenes, which makes them also convenient models for mechanistic studies. Moreover, it was found that thermolysis of the complexes in the presence of benzene or toluene leads to formation of corresponding biarenes [2].

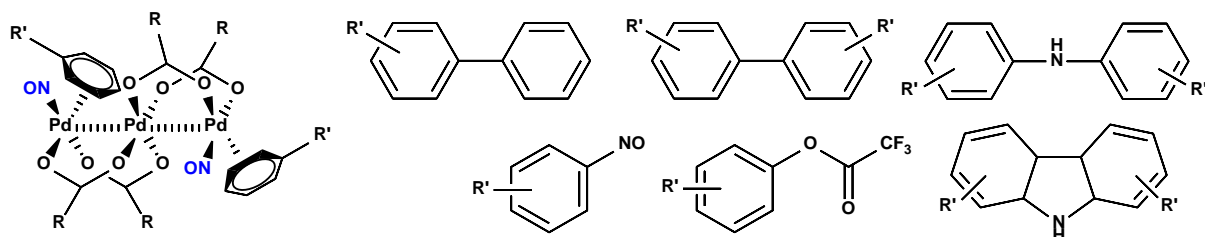


**Figure 1.** Pd<sub>3</sub>(NO)<sub>2</sub>(μ-CX<sub>3</sub>CO<sub>2</sub>)<sub>4</sub>(ArH)<sub>2</sub> and products of their thermolysis in benzene/toluene media.

We carried out preliminary study of catalytic activity of  $\text{Pd}_3(\text{NO})_2(\mu\text{-CF}_3\text{CO}_2)_4(\text{ToIH})_2$  in C-C coupling of toluene. It was found that reaction can proceed under relatively mild conditions ( $80^\circ\text{C}$ , 1 bar of air), TON and TOF was found to be ca. 8 and  $5\text{ h}^{-1}$  respectively. At the same time, we started DFT-study of possible mechanism of this reaction (scalar-relativistic approximation of DFT method, Priroda program [3], functional PBE + all electron L11 basis set). We considered the first key step, which is a hydrogen transfer from coordinated arene and formation of  $\text{Pd-C}_{\text{arene}}$  bond (figure 2).

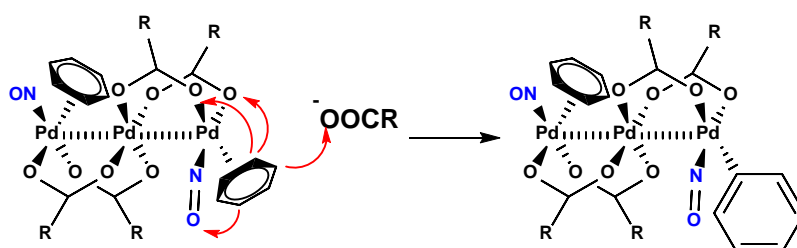


**Figure 2.** Possible pathways of hydrogen transfer and formation of  $\text{Pd-C}_{\text{arene}}$  bond. It was found that activation barriers exceed 25 kcal/mole for all intramolecular processes, while the corresponding barrier for transfer of hydrogen to free carboxylate ion is just ca. 12 kcal/mole (see fig. 3). So, we can conclude, that activation of arene in coordination sphere of 3-nuclear palladium nitrosyl trifluoroacetate requires an outer base, which was confirmed by experiments on C-C coupling in the presence of sodium trifluoroacetate.

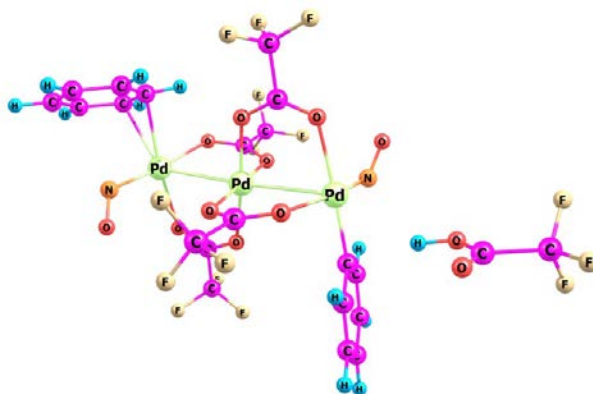


**Figure 3.** Structure of molecular complex  $[\text{Pd}_3(\text{NO})_2(\text{CF}_3\text{CO}_2)_4(\text{Ph})(\text{PhH}) + \text{HOCCF}_3]$ .

We are grateful for support to Russian Science Foundation (project № 18-13-00415).

#### References

- [1] Y. Jiang and H. Berke, Nitrosyl complexes in homogeneous catalysis in Nitrosyl complexes in inorganic chemistry, biochemistry and medicine I, Ed. D.M.P. Mingos, Springer, 2014, P. 167–228.
- [2] R.E. Podobedov et.al. // Russ. Chem. Bull.: Chem., 2010, V. 59, P. 473-475.
- [3] D.N. Laikov, Yu.A. Ustynyuk // Russ. Chem. Bull.: Int. Ed., 2005, V. 54, P. 820–826.

# Cellulose transformation to glucose and 5-HMF over solid acid carbon catalyst. Kinetics study and mechanistic insights

*Taran O.P.*<sup>1,2,3</sup>, *Gromov N.V.*<sup>2,4,5</sup> *Aymonier C.*<sup>4</sup>

<sup>1</sup>*Institute of Chemistry and Chemical Technology SB RAS, FRC KSC SB RAS, Krasnoyarsk, Russia,* <sup>2</sup>*Boreskov Institute of Catalysis, Novosibirsk, Russia,* <sup>3</sup>*Siberian Federal University, Krasnoyarsk, Russia,* <sup>4</sup>*CNRS, Universite Bordeaux, ICMCB UPR 9048, Pessac, France*

## Introduction

Glucose and 5-HMF are valuable chemicals. They seem to be promising for wide-application in chemical industry (plastics and pharmaceuticals) and fuel production [1]. Utilization of inedible cellulose as an alternative raw material, non-corrosive solid acid catalysts and one-pot design of the process could glucose and 5-HMF to be produced and the drawbacks of traditional cellulose hydrolysis methods to be overcome. The carbon materials seem to be promising catalysts for cellulose depolymerization into valuable chemicals like glucose and 5-HMF [2, 3].

This work was focused on the kinetic studies of cellulose hydrolysis-dehydration which is a multiple-route process including a lot of chemical paths and intermediates.

## Results and discussion

The Sibunit carbon catalyst was made via the sulfonation in H<sub>2</sub>SO<sub>4</sub> at 200 °C. The catalyst was characterized by N<sub>2</sub> absorption, XPS, TEM, XRF and titration with NaOH. Tests in the one-pot hydrolysis-dehydration of a mechanically activated cellulose and the process intermediates were made under hydrothermal conditions at 180 and 200 °C. The product yields were measured by HPLC.

The amount of acidic groups determined by titration on the surface of sulfonated carbon was 10 times higher than for the initial non-treated Sibunit. Catalytic tests showed high activity of sulfonated carbon catalysts in the cellulose hydrolysis-dehydration process. While pure untreated carbon was inactive. HPLC analysis revealed glucose and 5-HMF as the main products. The highest glucose and 5-HMF yields were shown 74.0% and 21.5% in flow and batch reactors, respectively.

For elucidation of the mechanism of catalysis the experiments with such intermediates as cellobiose, glucose, fructose and 5-HMF were carried out over the carbon and in the presence of diluted H<sub>2</sub>SO<sub>4</sub> as a catalyst. Based on these experiments, the process scheme which includes all the intermediates detected was

proposed. Based on the results obtained, the kinetic model was updated by adding side reactions of sugar decomposition and glucose conversion to mannose. The heterogeneous mechanism of the cellulose depolymerization was supposed base on the results of these experiments. A system of ten differential equations was derived and solved using the computer software. Inspection of the kinetic curves of the transformations led to conclude about the first orders of the reactions, kinetic constants of most of main process stages being of the order of  $10^{-2}$ – $10^{-3}$  that agreed with the literature data. The dissolution of cellulose appeared to be a limiting step of the process while hydrolysis was the fast reaction. Rearrangement of glucose to fructose was also slow reaction. The irreversible dehydration of fructose was the most rapid step. Moreover there were different ways of glucose transformations (except  $\text{glucose} \leftrightarrow \text{fructose} \rightarrow 5\text{-HMF}$ ). On the basis of the kinetic curves carried out from the kinetic experiments, the kinetic modeling was made for the cellulose hydrolysis-dehydration process and the kinetic parameters as the reaction rate constants and the orders of the reactions were evaluated. The model developed adequately described the experimental kinetics. To our knowledge, such an intricate process scheme was used for the first time for computer modeling of hydrolysis-dehydration of cellulose.

### **Conclusions**

The kinetic model of the process of hydrolysis-dehydration of cellulose in the presence of a solid sulfonated carbon catalyst was developed. The model was based on experimental data on hydrolysis-dehydration of cellulose and the main intermediates obtained using static and flow reactors. A complex multiple-route scheme was suggested, kinetic parameters of the reactions were determined. Cellulose dissolution and glucose isomerization to fructose were found to be the limiting stages. The model describes well the observed experimental results.

### **Acknowledgements**

The financial support of the work by RFBR, as well as by the Russian-French GDRI “Biomass” is gratefully acknowledged.

### **References**

1. I. Delidovich, K. Leonhard, R. Palkovits, *Energy Env. Sci.*, 2014, 7, 2803-2830.
2. J. Pang, A. Wang, M. Zheng, et. al, *Chem. Comm.*, 2010, 46, 6935-6937.
3. F. Yang, Q. Liu, X. Bai, et. al. *Bioresour. Technol.*, 2011, 102, 3424-3429.



# Can hydrogen transfer improve the valorisation of lignin from organosolv pulping?

*Author1, affiliation1, City1, Country1; presenting author, affiliation2, City2, Country2; author3, affiliation3, City3, Country3*

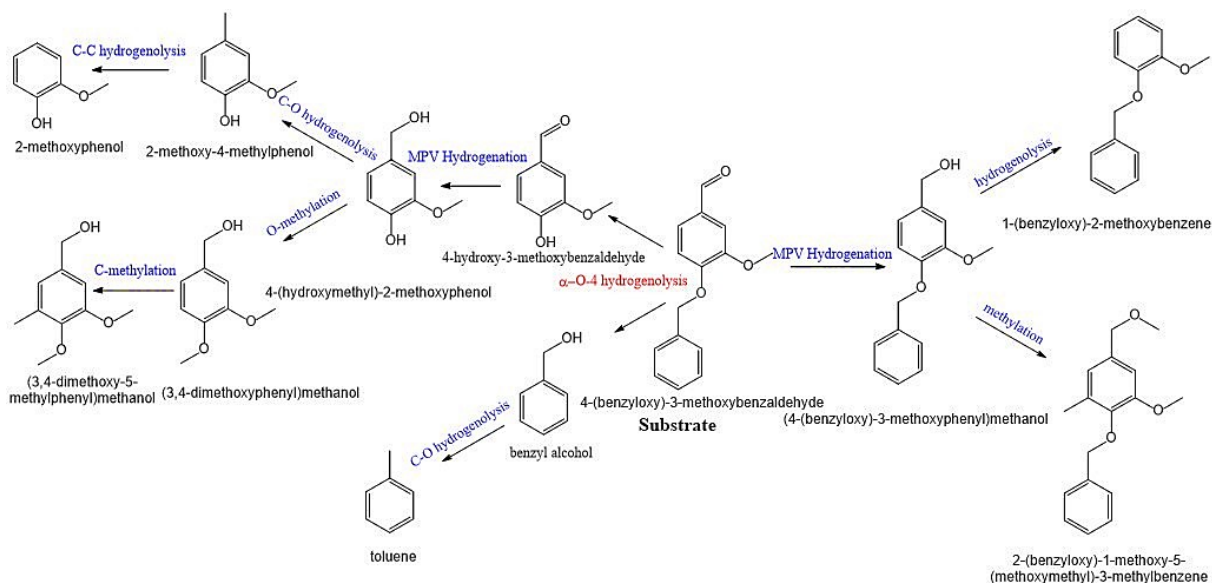
*Iqra Zubair Awan<sup>1,2</sup>, Olinda Gimello<sup>2</sup>, Thomas Cacciaguerra<sup>2</sup>, Nathalie Tanchoux<sup>2</sup>, Stefania Albonetti<sup>1</sup>, Fabrizio Cavani<sup>1</sup>, Francesco Di Renzo<sup>2</sup>*

*<sup>1</sup>Dpt Industrial Chemistry Toso Montanari, University of Bologna, Italy*

*<sup>2</sup>Institut Charles Gerhardt, Montpellier, France*

Organosolv pulping is finding a new revival in second generation ethanol refineries. Most interest in the conditions of pulping has been addressed to acid hydrolysis and solvation effects. The role of hydrogen-donor effects in pulping is just starting to receive proper attention. The increase of the H/C and decrease of O/C ratios can open new markets for lignin products. However, many questions have to be answered to assess the economics of implementing proper conditions, catalysts and processes to boost oxydehydrogenation in lignocellulose pulping. Does the increased added-value of lignin products compensate the lower energy recovery? How the oxidation of solvent fractions affects inventory and recycling of the pulping solution? Can heterogeneous catalysts allow to overcome the rentability threshold of organosolv pulping?

More data about H-transfer on substituted phenolic moieties in realistic conditions are needed to evaluate possible options. In this communication, we propose experimental data on the action of several solvents on model lignin systems in the presence of non-noble metals heterogeneous catalysts. Mixed oxides in the Ni-Cu-Fe and Ni-Cu-Al systems, designed for magnetic separation of catalysts, have been prepared from layered double oxide precursors. Relative rates of MPV reaction, O-H and C-C bonds hydrogenation and ether bonds hydrogenolysis have been determined and allowed to define which catalysts are more effective in deep dehydrogenation or in control of the polymerisation degree of lignin-derived products. Oxides obtained by thermal decomposition of LDH precursors are effective catalysts for H-transfer reactions to lignin model molecules, also in absence of the basic properties induced by Mg<sup>2+</sup> cations in the most usual catalysts ex hydrotalcites. In the case of the mixed Cu-Ni-Fe oxide catalysts, the conversion was always higher than



for the single-component oxides but the reactivity was enormously influenced by the Cu/Ni ratio in the catalyst. If benzyloxymethoxybenzaldehyde model dimer was converted at nearly 30% on the Ni-Fe catalyst in methanol at 200°C, the conversion rapidly rose to nearly 100% for Cu/divalents ratio of 0.4 or higher. With the increase of the conversion, formation of volatile products became relevant. Deeper hydrogenation was reached at the increase of the copper content. For catalysts with low copper content, the main product was benzyloxymethoxybenzyl alcohol, viz. the first MPV hydrogenation product of the substrate. At increasing copper content, the main product became benzyloxymethoxybenzene, the product of successive C-O hydrogenolysis of the alcohol group of benzyloxymethoxybenzyl alcohol and C-C hydrogenolysis of the intermediate product. When the Cu/divalent ratio approaches 0.5, the presence of nickel oxide accelerated the  $\alpha$ -O-4 hydrogenolysis, as observed also on the single-component oxides, and the main products became methoxycresol and toluene, respectively the C-O and C-C reduction products of the vanillic and benzylic moieties of the parent substrate. The relevance of benzyloxymethoxybenzene among the products clearly indicates that also aliphatic C-C bonds are hydrogenated. No products of hydrogenation of the aromatic ring were observed. The doping of CuO and NiO by iron undoubtedly affects the activity of the catalysts. Interestingly, the relative effectiveness of MPV hydrogenation and hydrogenolysis of phenylether bonds can orient the choice of the catalyst in a lignin organosolv environment towards the obtention of products with different molecular weight and level of functionalisation.

## **Direct non-oxidative coupling of methane over Fe@SiO<sub>2</sub>, an investigation into the characteristics of the reactor design**

*Rolf S Postma, University of Twente, Enschede, The Netherlands; L. Lefferts, University of Twente, Enschede, The Netherlands*

Methane is estimated to be the most abundant hydrocarbon on the planet and will be a major chemical feedstock of the 21st century [1, 2]. Methane will first need to be converted into a less stable molecule, e.g. methanol or ethylene, to become an easy to employ base chemical. The most common way to valorise methane is through a twostep process involving firstly syngas production followed by e.g. methanol- or Fischer-Tropsch-synthesis, which is costly and requires many process steps.

A way to directly valorise methane is through oxidative coupling of methane to higher hydrocarbons, such as ethane and ethylene. Since the 1980s oxidative methane coupling has been a rigorously studied subject, so far not yielding a satisfying process [3, 4].

In 2014 the group of Bao published an article in which they claim to have found a catalyst that is able to couple methane to higher hydrocarbons, non-oxidatively, without any coke formation at temperatures between 950-1100 °C [5]. Above ~650 °C methane becomes thermodynamically unstable and will readily be activated and couple to form both higher hydrocarbons as well as a significant amount of coke. This shows the importance of finely tuning the temperature profile as well as the fluid-dynamics of the reactor.

The poster will show the effects of tuning the temperature profile as well as the pre and post catalytic hot-volume. The results will be analysed based on homolytic coupling of methane as well as coke-deposition before, on and after the catalyst bed. This will be used as a framework to determine an optimal reactor-setup to be employed in research concerning catalytic methane coupling.

## References

1. Horn, R. and R. Schlögl, Methane Activation by Heterogeneous Catalysis. *Catalysis Letters*, 2014. 145: p. 23-39.
2. Taifan, W. and J. Baltrusaitis, CH<sub>4</sub> conversion to value added products: Potential, limitations and extensions of a single step heterogeneous catalysis. *Applied Catalysis B: Environmental*, 2016. 198: p. 525–547.
3. Naito, S., Methane conversion by various metal, metal oxide and metal carbide catalysts. *Catalysis Surveys from Japan*, 2000. 4: p. 3-15.
4. Tang, P., et al., Methane activation: the past and future. *Energy & Environmental Science*, 2014. 7: p. 2580-2591.
5. Guo, X., et al., Direct, Nonoxidative Conversion of Methane to Ethylene, Aromatics, and Hydrogen. *Science*, 2014. 344(6184): p. 616-619.
6. Guéret, C., M. Daroux, and F. Billaud, Methane pyrolysis: thermodynamics. *Chemical Engineering Science*, 1997. 52(5): p. 815-827.

---

## The influence of cationic promoters on the ruthenium catalysts activity in the ammonia synthesis reaction.

M.P., Nery<sup>1</sup>, L.F.F.P.G. Bragança<sup>2</sup>, M.I.P. da Silva<sup>\*,1</sup>

<sup>1</sup> *Departamento de Engenharia Química e de Materiais, Pontifícia Universidade Católica do Rio de Janeiro, Rio de Janeiro, Brazil, 22451-900. \* isapais@puc-rio.br*

<sup>2</sup> *Departamento de Engenharia Química e Petróleo, Universidade Federal Fluminense, Niterói, Rio de Janeiro, Brazil, 24210-240.*

---

Keywords: KL zeolite, ammonia synthesis, ruthenium catalysts.

---

### 1 Introduction

The main advantage of Ru-based catalysts is that they are less sensitive to poisoning by ammonia than Fe-based catalysts [1]. Also, it has been reported the use of KL zeolite as support for many general applications [2]. The objective of this work was to investigate the addition of promoter cations (Ba and Cs) in the activity of ruthenium catalysts supported on KL zeolite for the ammonia synthesis reaction.

### 2 Experimental/methodology

The KL zeolite was provided by TOYO SODA. For ionic exchange with cesium, 50 mL of CsNO<sub>3</sub> 1M solution (MERCK) were added dropwise to the zeolitic support at 90°C under stirring. Then it was centrifuged and heated to 120 °C (2°C/min) and then to 300°C for 4 h. After the support was washed and centrifuged successively for removal residual nitrate and dried at 80°C for 16 h. For ionic exchange with barium a solution of Ba(NO<sub>3</sub>)<sub>2</sub> 0.3M (MERCK) was used in a similar procedure described previously. For ruthenium introduction by ionic exchange, a solution of Ru(NH<sub>3</sub>)<sub>6</sub>Cl<sub>2</sub> 0.1M (ALDRICH) was added dropwise at 90°C under magnetic stirring. The resulting catalysts were washed and centrifuged to remove the residual chloride and then were dried at 80°C for 24 h. The analysed samples were designated as: RuKL, RuCsKL and RuBaCsKL. The amount of incorporated cations and RuI was studied by Atomic Absorption Spectrometry. Nitrogen isotherms at 77 K for the support and promoted catalysts were measured using a Micromeritics ASAP2010 instrument. Hydrogen chemisorption was used to verify the degree of metallic dispersion of the uncalcined catalysts using a Micromeritics ASAP 2010C apparatus. The morphological properties of the catalysts were examined using transmission electron microscopy (JEOL-JEM-2010 instrument). The catalytic performance in NH<sub>3</sub> synthesis of the catalysts were evaluated at three different temperatures: 300°C, 400°C and 500°C.

### 3 Results and discussion

The chemical composition and the textural properties of KL support and catalysts are listed in Table 1. The structural properties showed higher specific area and pore volume values for RuKL sample. The RuCsKL catalyst presented a higher dispersion (82%) compared to RuKL (75%) and RuBaCsKL (42%). TEM images of different Ru based catalysts supported on KL zeolite are shown in Fig.1. The RuBaCsKL catalyst directly reduced with the reactants gas mixture ( $H_2/N_2 = 3:1$ ) showed defined ruthenium particles with an average size of around 8 nm. Similarly, the RuCsKL catalyst showed a high dispersion with Ru particle size around 1.5 nm. The conversions for  $NH_3$  synthesis are summarized in Table 1. The promoted catalysts presented higher conversion percentages than the pure Ru catalyst supported on the KL zeolite. The RuBaCsKL was the most effective for all reaction temperatures. The results showed that the barium has a greater effect on the activity of the catalyst. When both are present, the conversion was greater than when only cesium was used as a promoter, although its presence led to lower Ru dispersion on zeolite KL.

**Table 1.** Chemical composition, textural properties and  $NH_3$  relative conversion for both catalysts.

Samples	%Ru	%Ba	%Cs	BET area ( $m^2/g$ )	TPV* ( $cm^3/g$ )	% conversion		
						300°C	400°C	500°C
KL	-	-	-	346	0.14	-	-	-
RuKL	3.0			326	0.13	5.7	7.1	5.4
RuCsKL	3.3		9.8	292	0.12	5.6	11.1	7.4
RuBaCsKL	3.3	4	6	276	0.11	6.1	14.2	8.3

\*TPV = Total Pore Volume

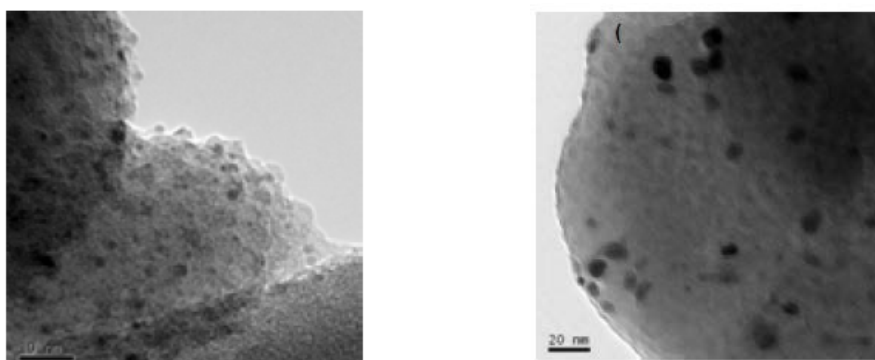


**Fig. 1.** TEM images of RuCsKL and RuBaCsKL

## 4 Conclusion

The barium plus cesium showed to be more effective on the synthesis of ammonia than only cesium as promoter.

## Reference

- [1] P. Stolze, Phys. Sci. 36, 824 (1987).
- [2] J.F. da Silva, L F.F.P.G. Bragança, M I P. da Silva, Reaction, Mechan, and Catal. 124,563 (2018).

# Stable Cu/C catalysts for selective hydrogenation of hydroxyacetone to 1,2-propanediol

*Martina Cazzolaro<sup>1</sup>, Rik de Clercq<sup>2</sup>, Jørgen Svendby<sup>1</sup>, Jia Yang<sup>1</sup>, Esben Taarning<sup>2</sup>,*

*De Chen<sup>1\*</sup>*

*1. Department of chemical engineering NTNU, Trondheim, Norway*

*2. Haldor Topsøe A/S, Haldor Topsøes Allé 1, 2800 Kgs. Lyngby, Denmark*

## **Introduction**

Various biomass-based processes lead to the production of hydroxyacetone (HA), i.e. biomass pyrolysis [1], sugar hydrogenolysis [2], glycerol dehydration [3]. Via selective hydrogenation of HA, a major commodity chemical as 1,2-propanediol (PD) can be produced [4]. Cu-based catalysts showed good activity in hydro-deoxygenation of bio-oil from biomass pyrolysis, but coke formation resulted in shortened catalyst lifetime [5]. High activity was also observed in hydrogenolysis of glycerol to PD, having HA as dehydration intermediate: Cu particle size, dispersion and active area were reported to be of great importance for high activity and stability; particles agglomeration and formation of irregularly shaped clusters were suggested as deactivation causes [6]. Carbon nanofibers (CNF) are attractive catalyst supports having high surface area [7] and large number of edges, exploitable as metals anchoring sites [8]. Moreover, surface oxidation, foreign-ion doping or confinement effect [9] can be used to adjust CNF surface properties. This project aims to develop a stable Cu-based catalyst for selective gas-phase hydrogenation of HA to PD, by tuning the carbon support properties.

## **Materials and methods**

Platelet carbon nanofibers (PCNF) were prepared via CVD of CO and H<sub>2</sub> at 600°C according to Yu et al. [10] over Fe powdered nanoparticles, prepared according to Kang et al. [11]. PCNF were characterized with TGA, N<sub>2</sub> physisorption, H<sub>2</sub>-TPR and TEM. 9 catalysts with 5wt% Cu loading were prepared via IWI of PCNF with 3 Cu precursors (nitrate, acetate and basic carbonate) and 3 solvents (water, ethanol, propanol). Other 9 catalysts supported on silica gel were prepared as non-carbonaceous reference. The catalysts were analyzed with TGA, N<sub>2</sub> physisorption and H<sub>2</sub>-TPR. A screening of the catalysts will be performed for gas-phase hydrogenation of hydroxyacetone at 240°C and 5bar; the products will be analysed with an online GC.

## Results and discussion

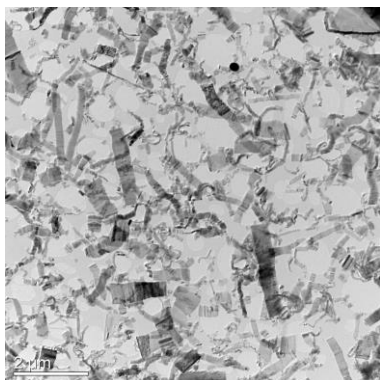


**Figure 1** TEM image of prepared PCNF

The platelet structure of the prepared CNF was observed with TEM (**Figure 1**). The PCNF-supported catalysts showed a decrease of surface area up to 1/3 after IWI with Cu nitrate (from 141.6 to 57.18, 46, 54.64 m<sup>2</sup>/g with water, ethanol, propanol respectively) indicating probable large Cu particles and suggesting need of improving the impregnation technique. The non-carbonaceous reference catalysts were tested in HA hydrogenation to

PD, showing good activity (conversion and selectivity up to around 80%). 21% yield loss was observed over a test of 48 hours indicating deactivation.

## Conclusions

The reference catalysts deactivated fast in the hydrogenation of HA to PD, highlighting the need of a more stable catalyst. Activity tests and characterization of PCNF-supported catalysts will follow and surface treatment of CNF will be explored. Additional characterization techniques (TEM, N<sub>2</sub>O chemisorption and XRD) will be exploited to get insights on the properties controlling the catalyst performance.

## References

- [1] P. Fu, X.Y. Bai, Z.H. Li, W.M. Yi, Y.J. Li, Y.C. Zhang, Fast pyrolysis of corn stovers with ceramic ball heat carriers in a novel dual concentric rotary cylinder reactor, *Bioresource Technol*, 263 (2018) 467-474.
- [2] Y. Hirano, K. Sagata, Y. Kita, Selective transformation of glucose into propylene glycol on Ru/C catalysts combined with ZnO under low hydrogen pressures, *Appl Catal a-Gen*, 502 (2015) 1-7.
- [3] T. Deng, H.J.G.C. Liu, Promoting effect of SnO<sub>x</sub> on selective conversion of cellulose to polyols over bimetallic Pt–SnO<sub>x</sub>/Al<sub>2</sub>O<sub>3</sub> catalysts, 15 (2013) 116-124.
- [4] R.V. Sharma, P. Kumar, A.K.J.A.C.A.G. Dalai, Selective hydrogenolysis of glycerol to propylene glycol by using Cu: Zn: Cr: Zr mixed metal oxides catalyst, 477 (2014) 147-156.
- [5] S. Cheng, L. Wei, X. Zhao, J.J.C. Julson, Application, deactivation, and regeneration of heterogeneous catalysts in bio-oil upgrading, 6 (2016) 195.
- [6] S. Zhu, X. Gao, Y. Zhu, Y. Zhu, H. Zheng, Y.J.J.o.c. Li, Promoting effect of boron oxide on Cu/SiO<sub>2</sub> catalyst for glycerol hydrogenolysis to 1, 2-propanediol, 303 (2013) 70-79.
- [7] J. Zhu, A. Holmen, D.J.C. Chen, Carbon nanomaterials in catalysis: proton affinity, chemical and electronic properties, and their catalytic consequences, 5 (2013) 378-401.
- [8] Z. Yu, D. Chen, B. Tøtdal, A.J.T.J.o.P.C.B. Holmen, Effect of support and reactant on the yield and structure of carbon growth by chemical vapor deposition, 109 (2005) 6096-6102.
- [9] X. Pan, X.J.A.o.c.r. Bao, The effects of confinement inside carbon nanotubes on catalysis, 44 (2011) 553-562.
- [10] Z. Yu, D. Chen, B. Tøtdal, A. Holmen, Effect of Support and Reactant on the Yield and Structure of Carbon Growth by Chemical Vapor Deposition, *The Journal of Physical Chemistry B*, 109 (2005) 6096-6102.
- [11] Y.S. Kang, S. Risbud, J.F. Rabolt, P. Stroeve, Synthesis and characterization of nanometer-size Fe<sub>3</sub>O<sub>4</sub> and gamma-Fe<sub>2</sub>O<sub>3</sub> particles, *Chem Mater*, 8 (1996) 2209-&.



# Synthesis, Characterization and Catalytic Applications of a Novel Iron(III) Silicate with a 2D-Nanosheet Morphology

*Yunxiang Qiao,<sup>a,b</sup> Bernd Spliethoff,<sup>a</sup> Nils Theyssen,<sup>a</sup> Thomas Lunkenbein,<sup>c</sup> Jan Folke,<sup>b</sup> Claudia Weidenthaler,<sup>a</sup> Wolfgang Schmidt,<sup>a</sup> Gonzalo Prieto,<sup>a</sup> Cristina Ochoa,<sup>a</sup> Eckhard Bill,<sup>a,b</sup> Shengfa Ye,<sup>a,b</sup> Yanhang Ma,<sup>d</sup> Osamu Terasaki,<sup>d</sup> Holger Ruland,<sup>b</sup> Ferdi Schüth,<sup>a</sup> Robert Schlögl,<sup>b,c</sup> Walter Leitner<sup>b,e</sup>*

<sup>a</sup>*Max-Planck-Institut für Kohlenforschung, Mülheim an der Ruhr, Germany*

<sup>b</sup>*Max-Planck-Institute for Chemical Energy Conversion, Mülheim an der Ruhr, Germany*

<sup>c</sup>*Fritz-Haber Institut der Max-Planck-Gesellschaft, Berlin, Germany*

<sup>d</sup>*Department of Materials and Environmental Chemistry, Stockholm University, Sweden*

<sup>e</sup>*Institut für Technische und Makromolekulare Chemie, Lehrstuhl für Technische Chemie und Petrochemie, RWTH Aachen, Aachen, Germany*

The most prominent iron silicate mineral existing in nature is Fayalite, an orthosilicate which has the chemical composition of  $\text{Fe}_2\text{SiO}_4$ . A literature known procedure for its production starts from an equimolar mixture of  $\text{SiO}_2$  and  $\text{Fe}_2\text{O}_3$ , which is heated to 1,100 °C for eight hours in an oxygen atmosphere.<sup>[1]</sup>  $\text{Fe}_2\text{SiO}_3$ , a spinel-type mineral, is also known.<sup>[2]</sup> Furthermore, the single chain silicate ferrosilite ( $\text{FeSiO}_3$ ) is existing in pure form, which is part of the pyroxene group. The synthesis was first described by *Lindsley* in 1965. Very high pressures of 2 GPa and temperatures exceeding 800 °C are needed to produce this material, which is not stable at any temperatures at atmospheric pressure.<sup>[3]</sup> Another known iron silicate is named iscorite with a molecular formula of  $\text{Fe(II)}_5\text{Fe(III)}_2\text{SiO}_{10}$ . It was reported by *Steyn* in 1969 and found in slags of a steel plants, which were normally kept at a temperature of about 1,300 °C.<sup>[4]</sup> Furthermore an iron silicate named Greenalite was reported by *Leith* in the beginning of last century. The rare magnesium free variant is best formulated as  $(\text{Fe(II)}, \text{Fe(III)})_{-6}[\text{Si}_4\text{O}_{10}](\text{OH})_8$  and was found in Minnesota<sup>[5]</sup> as well as in meteorites<sup>[6]</sup>.

In contrast to the rather severe reaction conditions reported for the production of these known iron silicates, we discovered the formation of an iron silicate material under very mild conditions. Initial observation was made by serendipity carrying out catalytic reactions with SBA-15 material in aqueous media in steel reactors. Based on this initial finding, a reproducible synthetic protocol was developed comprising the reaction of different silica sources and Fe powder in water as a solvent at 100 °C under air (Figure 1).

This iron(III) silicate with a silicon-to-iron-ratio of two to one appears as ultrathin two-dimensional (2D) nanosheets resulting in a relatively high surface area of around  $273 \text{ m}^2 \text{ g}^{-1}$ . Results from electron microscopy imaging with various methods and in combination with EDX analysis at various scales, elemental analysis, Mößbauer spectroscopy and pair distribution function (PDF) analysis make the presence of a sheet silicate with  $[\text{Si}_4\text{O}_{10}]^{4-}$  entities likely. The material is temperature stable up to  $800 \text{ }^\circ\text{C}$  under air, up to  $650 \text{ }^\circ\text{C}$  under nitrogen and up to  $550 \text{ }^\circ\text{C}$  under a reducing atmosphere ( $10\% \text{ H}_2$ ,  $90\% \text{ N}_2$ ) according to temperature-dependent X-ray diffraction (XRD) measurements. Moreover, it shows decent  $\text{CO}_2$  adsorption ability, has a remarkable activity in ammonia synthesis and is a promising catalyst support material.

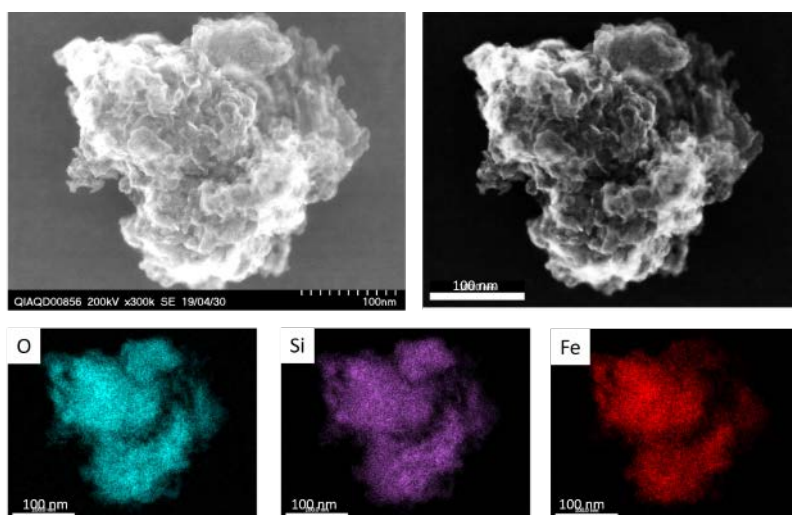


**Figure 1.** STEM-EDX mapping of the synthetic iron silicate nanosheets.

## References

- [1] J. Myers, H. P. Eugster, *Contrib. Mineral. Petrol.* **1983**, *82*, 75-90.
- [2] F. C. Pignatale, S. T. Maddison, V. Taquet, G. Brooks, K. Liftman. *Mon. Not. R. Astron. Soc.* **2011**, *414*(3), 2386-2405.
- [3] a) D. H. Lindley, I. D. MacGregor, B.T.C. Davis. *Synthesis and Stability of Ferrosilite in Carnegie Inst. Wash. Year Book* **1964**, *63*, 174-176; b) S. Sueno, M. Cameron, C. T. Prewitt. *Am. Mineral.* **1976**, *61*, 38-53; c) D. Zhrebetsky, G. Amthauer, M. Grodzicki, *Phys. Chem. Minerals* **2010**, *37*, 455–464.
- [4] a) J. Smuts, J. G. D. Steyn. *Acta Cryst.* **1969**, *B25*, 1251-1255; b) P. A. Van Aken, G. Mieke, A. B. Woodland, R. J. Angel, *Eur. J. Mineral.* **2005**, *17*, 723-731.
- [5] F. W. Clarke, *Monogr. U.S. Geol. Survey* **1903**, *43*, 243-247.
- [6] a) L. G. Kwasha, *Meteoritika* **1976**, *35*, 136-138; b) G. D. Price, A. Putnis, S. O. Agrell, D. G. W. Smith, *Can. Mineralogist* **1983**, *21*, 29-35.

# Atomically Precise Gold Cluster Catalysts for Enhanced Propylene Epoxidation

*Nidhi Kapi<sup>1</sup>, Michael M. Nigra<sup>2</sup>, Marc-Olivier Coppens<sup>1\*</sup>*

<sup>1</sup> *Centre for Nature Inspired Engineering and Department of Chemical Engineering, University College London, London, United Kingdom*

<sup>2</sup> *Department of Chemical Engineering, University of Utah, Salt Lake City, UT 84112, USA*

*\*Corresponding author: m.coppens@ucl.ac.uk*

The conversion of propylene to propylene epoxide (PO) is a reaction of great industrial importance, as PO is used to synthesize propylene glycol and polyether polyols, which is further applied in polyurethane foams, as well as in adhesives, paints, coatings, etc. Currently, PO is commercially produced using the chlorohydrin process or the hydroperoxide process, which has many limitations and drawbacks. Since Haruta's discovery of the catalytic activity of gold nanoparticles, the direct gas phase epoxidation of propylene to form PO using H<sub>2</sub> and O<sub>2</sub> has gained attention as a simple, environmentally benign route, using supported gold catalysts [1]. Numerous techniques to synthesize monodisperse gold nanoparticles have been reported so far, using a variety of stabilizers (mainly organic ligands, ionic liquids and surface active agents) to prevent them from agglomeration [2]. Catalytic activity of these nanoparticles is predominantly governed by geometric and electronic factors. Geometric effects arise due to the orientation of Au atoms in space, and electronic effects originate from metal-ligand interactions or quantum size effects [3]. Therefore, the catalytic properties can be tuned by varying the electronic, geometric and steric factors.

Here, we report a simple, one-pot route to synthesize very stable, atomically precise gold clusters (< 2nm core size) using triphenylphosphine as a stabilizing ligand. In addition to the batch synthesis, a microfluidic continuous flow system has also been developed to synthesize these particles. The continuous flow system exhibits several advantages over the batch system, such as controlled mixing and a narrow residence time distribution. Different gold (I) precursors of varying steric hindrance are employed to tune the final size of the gold clusters and to understand the role of bound phosphine ligands. Optical spectroscopy (UV/Vis) and electron microscopy (HAADF-STEM) are used as tools to calculate the final particle size. Our studies

reveal a correlation between the degree of steric hindrance around the gold nanoparticles and their final size, as shown in Figure 1. Furthermore, the pre-synthesized gold clusters have been successfully immobilized onto different metal oxide supports, such as TiO<sub>2</sub>, SBA-15 and titanosilicalite-1 (TS-1), without any change in the final size of the dispersed gold clusters. The catalytic activity of these supported gold clusters in the conversion of propylene to propylene epoxide using H<sub>2</sub> and O<sub>2</sub> will be presented. The effect of the different ligands and the support materials on the catalytic activity of these small gold clusters will also be demonstrated.

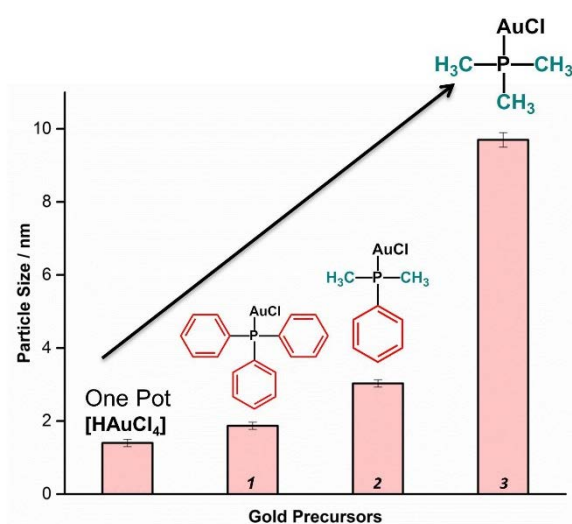


Figure 1. Dependence of gold nanoparticle size as a function of the steric hindrance around the Au(I) phosphine precursor.

## References

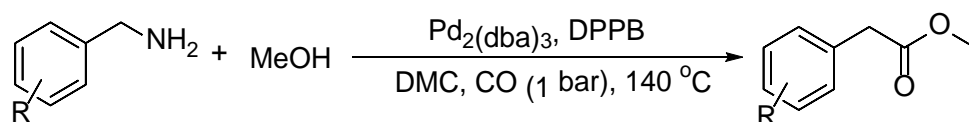
- [1] Hayashi, T., Tanaka, K. and Haruta, M., 1998. Selective vapor-phase epoxidation of propylene over Au/TiO<sub>2</sub> catalysts in the presence of oxygen and hydrogen. *Journal of Catalysis*, **178**(2), pp.566-575
- [2] Lu, Y. and Chen, W., 2012. Sub-nanometre sized metal clusters: from synthetic challenges to the unique property discoveries. *Chemical Society Reviews*, **41**(9), pp.3594-3623.
- [3] Jin, R., Zeng, C., Zhou, M. and Chen, Y., 2016. Atomically precise colloidal metal nanoclusters and nanoparticles: fundamentals and opportunities. *Chemical reviews*, **116**(18), pp.10346-10413.

# Carbonylative formation and transformation benzyl amines

Xiao-Feng Wu

Leibniz-Institut für Katalyse e.V. an der Universität Rostock, Albert-Einstein-Strasse 29a,  
18059 Rostock, Germany  
E-mail xiao-feng.wu@catalysis.de

In our recently work, we achieved a new procedure for the direct carbonylative transformation of benzyl amines.<sup>1</sup> Using dimethyl carbonate as the solvent, methyl 2-arylacetates can be produced in good to excellent yields from the corresponding primary, secondary and tertiary benzyl amines with palladium as the catalyst. Notably, no base or any other additive is required here. Additionally, our procedure can also be applied in the preparation of methylphenidate, which is a marketing drug and used in the treatment of attention deficit hyperactivity disorder (ADHD) and narcolepsy. More interestingly, benzyl amines can be produced from carbonylation procedure as well.<sup>2</sup>



## References:

1. Y. Li, Z. Wang, X.-F. Wu, *ACS Catal.* **2018**, *8*, 738-741.
2. X.-F. Wu, Submitted.

## **Towards chemoenzymatic one-pot reaction in tandem: co-encapsulation of chemo- and biocatalysts in biopolymer hydrogels**

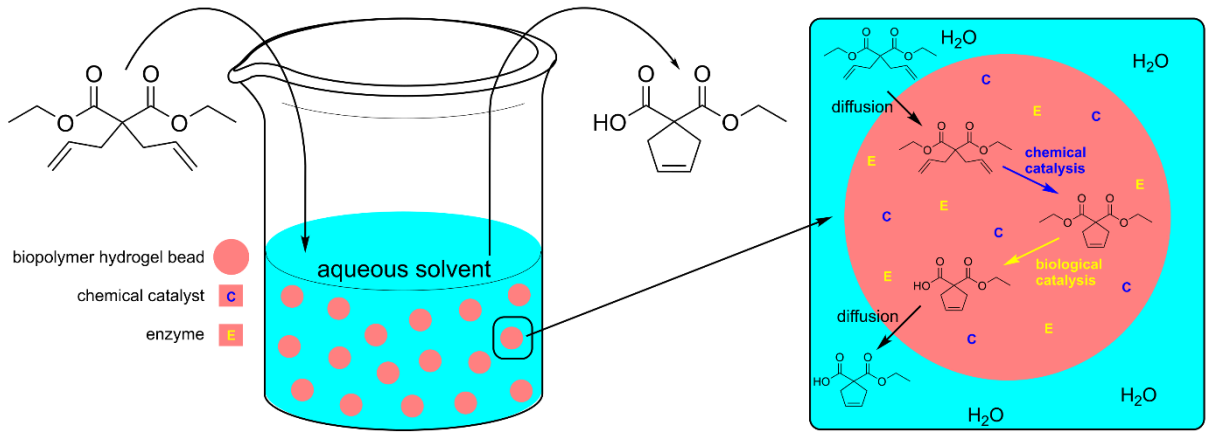
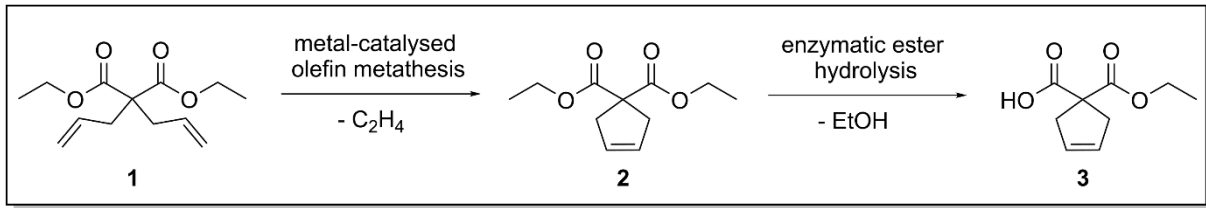
*Jan Pauly, Bielefeld University of Applied Sciences / Bielefeld University, Bielefeld, Germany; Harald Gröger, Bielefeld University, Bielefeld, Germany; Anant Patel, Bielefeld University of Applied Sciences, Bielefeld, Germany*

Several combinations of chemo- and biocatalysts for chemo-enzymatic one-pot syntheses have been investigated. This work is related to previous work<sup>[1]</sup> on a ring closing metathesis reaction followed by an enzymatic ester hydrolysis in water. For continuous processes, problems like catalyst separation, recycling and stability can be addressed by encapsulation. In our previous studies, we investigated the encapsulation of pig liver esterase (PLE) and Grubbs' catalyst (2<sup>nd</sup> generation) separately.<sup>[2]</sup> These immobilisates were successfully applied in a sequential chemoenzymatic one-pot reaction and research on using both immobilisates *in tandem* is currently ongoing. In this study, we investigated the co-encapsulation of PLE together with the Grubbs' catalyst in several biopolymer hydrogel beads. First, different beads made of a single core material with both catalysts encapsulated herein were created. After the tandem reactions were completed, we measured quantitative conversions. However, HPLC analysis revealed that a large amount of by-product was created because PLE can also hydrolyse diester **1** instead of diester **2**, leading to the corresponding by-product. Creating immobilisates with catalysts located in different compartments is one approach to a solution. Currently, we are addressing this by building multilayer beads with catalysts encapsulated in these different layers. In addition, more experiments on the bead matrix, bead size, encapsulation efficiency, leaching, recyclability and overall reaction rate are currently ongoing. This work will lay the scientific-technical foundation for the gentle co-immobilisation of other biological and chemical catalysts in biopolymer hydrogels and their application in aqueous media to merge the worlds of bio- and chemocatalysis.

### **References**

- [1] K. Tenbrink, M. Seßler, J. Schatz, H. Gröger, *Adv. Synth. Catal.* **2011**, 353, 2363.
- [2] a) J. Pauly, H. Gröger, A. V. Patel, *J. Biotechnol.* **2018**, 280, 42; b) J. Pauly, H. Gröger, A. V. Patel, *Green Chem.* **2018**, 20, 5179.

### Model reaction cascade with co-encapsulated bio- and chemocatalyst



## Mild and controlled photocatalytic oxidation of graphite to graphite oxide

*Niels Ostyn, Barbara Thijs, Julian Steele, Maarten Roeffaers and Johan Martens;  
Centre for Surface Chemistry and Catalysis, KU Leuven, 3001 Heverlee, Belgium*

Graphene, graphene oxide and graphite oxide (GO) are extraordinary carbon materials with superb physical and chemical properties like tensile strength, thermal and electrical conductivity and biocompatibility. These carbons are often described as the wonder materials of the 21<sup>st</sup> century. Supercapacitors, gas sensors and drug delivery systems are examples of high-end technological applications, and the field is expanding rapidly. Chemical oxidation of graphite is the most prominent route towards GO. The popular Hummers method and its derivatives involve the use of strong mineral oxidants like permanganate, and strong mineral acids. These state-of-the-art wet chemical oxidation methods are hazardous, produce lots of waste and do not allow handy control over the oxidation process and the physico-chemical properties of the GO product. Graphene oxide and graphene are obtained from the GO through exfoliation and chemical reduction, respectively. There is a manifested need for a more sustainable partial oxidation process enabling better control over the oxidation reaction, with spatial and temporal control, for fine tuning of the GO product. We propose a vapour phase photocatalytic process for oxidation of graphite (Figure 1) presenting these advantages. Graphite is photocatalytically oxidized at 100°C using a TiO<sub>2</sub> photocatalyst, UV light and a gas mixture consisting of molecular oxygen and water vapour (Figure 1).

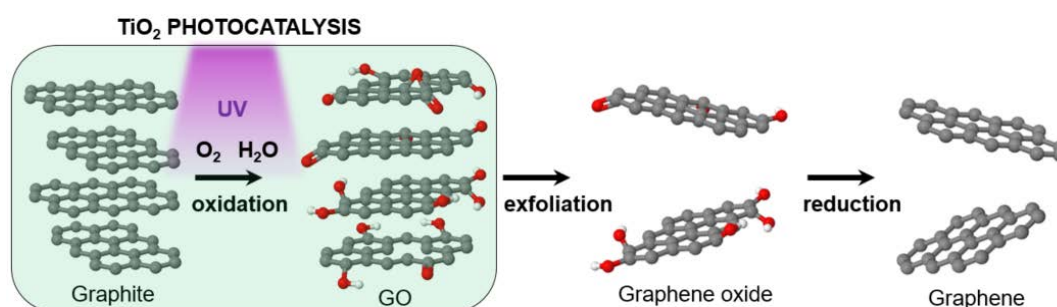


**Figure 1.** Photocatalytic conversion of graphite to graphite oxide (GO), an intermediate to graphene oxide and graphene.

In the photoreactor, the photocatalyst particles can be deposited on the graphite surface to be oxidized (contact oxidation mode), or even better, mounted on a



separate support positioned in front of the layer of graphite to be partially oxidized (remote oxidation mode). In this oxidation setup, the photocatalyst generates gaseous reactive oxidizing species that react with the graphite surfaces.

The physico-chemical properties of photocatalytically oxidized graphite are similar to those observed for GO materials obtained via liquid-phase chemical oxidation of graphite. Scanning electron microscopy images reveal the surface modification and the characteristic formation of surface blisters on natural graphite after contact photo-oxidation (Figure 2a) and synthetic graphite after remote photo-oxidation (Figure 2b).

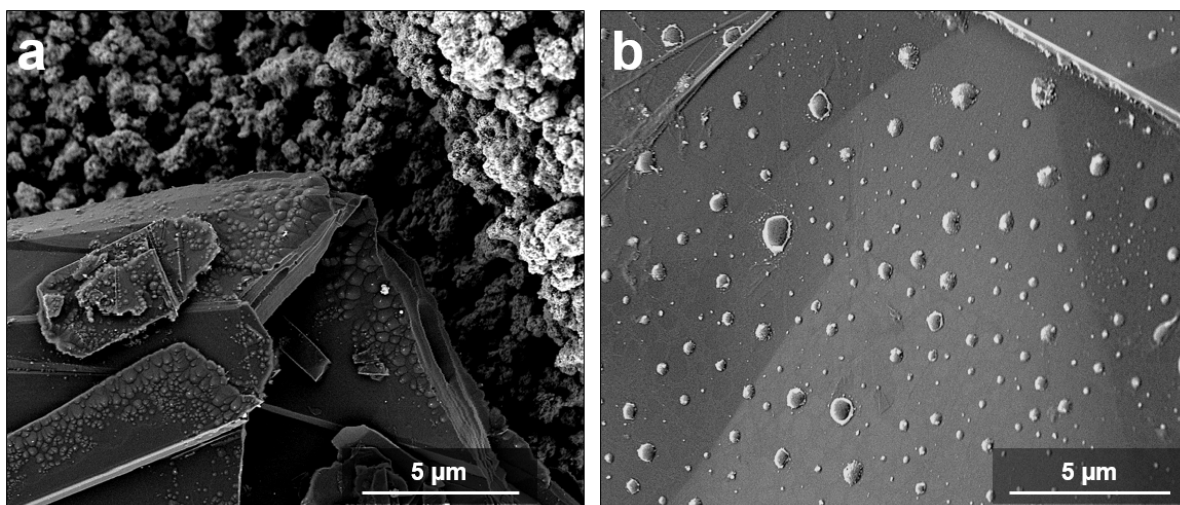


**Figure 2.** Scanning electron microscopy images of photocatalytically oxidized (a) natural graphite in contact mode and (b) highly ordered pyrolytic graphite in remote mode.

The photocatalytic oxidative modification of the graphite surface changing the carbon orbital hybridization from planar  $sp^2$  into  $sp^3$  is confirmed by Raman spectroscopy.

The remote photocatalytic oxidation process has potential technological advantages such as spatial control. Covering the graphite surface with a mask enables photocatalytic patterning and the formation of spatially resolved GO areas on graphite. Such patterning has potential applications in electronic devices.

In the paper, the contact and remote oxidation processes are presented and the GO materials characterized using nano-SEM, Raman, NMR, and AFM. The oxidation mechanism and the impact of reaction conditions ( $O_2$  and  $H_2O$  partial pressure and temperature) are discussed.

# **Synthesis of Styrene by The C-H Activation of Benzene over Palladium based Catalyst**

Kalpana Avasthi\*, Ashish Bohre, Blaž Likozar

Department of Catalysis and Chemical Reaction Engineering, National Institute of Chemistry,

Hajdrihova 19, 1000 Ljubljana, Slovenia

\*Presenter contact details: kalpana.avasthi@ki.si. +386-14760 504

## **Abstract**

Styrene is an important aromatic compound, which is applied in polystyrene plastic materials, polyesters, various protective coatings, resins, rubbers and other common copolymers. Currently, the majority of styrene is industrially produced by multiple-step and energy-intensive chemical processes from petroleum-derived ethylbenzene precursor. Beside the use of a non-renewable feedstock itself, these synthesis processes produce styrene with a low conversion selectivity. Thus, there is a need to develop novel sustainable processes for styrene building-block production from renewable carbon-containing resources, such as biomass-derived lignin residues. The current bio-refinery processes draw value from carbohydrates, leaving lignin as a waste. However, lignin represents a potentially valuable source of renewable aromatic/phenolic compounds for diverse chemical industries. We herein reported a cost effective catalytic route for the synthesis of styrene by oxidative coupling of benzene with styrene over palladium based catalyst.

*Effect of using MoO<sub>3</sub>, B<sub>2</sub>O<sub>3</sub>, ZrO<sub>2</sub> and WO<sub>3</sub> as modifier to  $\gamma$ -Al<sub>2</sub>O<sub>3</sub> support for dry reforming of methane using Ni catalyst*

*Ahmed Sadeq Al-Fatesh<sup>\*1</sup>, Ahmed Aidid Ibrahim<sup>1</sup>, Samsudeen Olajide Kasim<sup>1</sup>, Ahmed Elhag Abasaeed<sup>1</sup> Rasheed Arasheed<sup>2</sup>, Abdulaziz Bagabas<sup>2</sup> Biswajit Chowdhury<sup>3</sup>, Anis Hamza Fakeeha<sup>1</sup>*

<sup>1</sup>*Chemical Engineering Department, College of Engineering, King Saud University, P. O. Box 800, Riyadh 11421, Saudi Arabia*

<sup>2</sup>*National Petrochemical Technology Center (NPTC), Materials Science Research Institute (MSRI), King Abdulaziz City for Science and Technology, P.O. Box 6086, Riyadh 11442, Saudi Arabia*

<sup>3</sup>*Department of Applied Chemistry, Indian Institute of Technology (Indian School of Mines), Dhanbad, India.*

**Introduction:** The dry reforming of methane reaction to valuable synthesis gas (H<sub>2</sub> and CO), is a potential method for tackling the declining energy resources and global warming challenges at the same time [1]. Synthesis gas is the building block for petrochemical industry [2]. It is observed that reforming reactions are affected by side reactions [3] in which best stability of the catalyst with least carbon formation is a great challenge.

**Experimental:** Dry reforming of CH<sub>4</sub> experiments over Ni-based catalysts, calcined at 600 °C for 3 h, were performed at 700°C for 420 min and at atmospheric pressure in a vertical stainless steel fixed-bed tubular reactor (9.1 mm i.d. and 0.3 m long). Catalysts were activated with H<sub>2</sub> for 1 h at 800°C. An incipient wet impregnation method was used to prepare Ni catalyst supported on modified  $\gamma$ -Al<sub>2</sub>O<sub>3</sub>. The modifiers chosen were MoO<sub>3</sub>, B<sub>2</sub>O<sub>3</sub>, ZrO<sub>2</sub> and WO<sub>3</sub>. Feed gases (CH<sub>4</sub>, CO<sub>2</sub>, and N<sub>2</sub>) at the ratio of 6/6/1 and the overall gas flow rate of 65ml/min (space velocity: 39000 ml (/h.g<sub>cat.</sub>)<sup>-1</sup>) were used.

**Results:** **Fig. 1A** shows the N<sub>2</sub> adsorption and desorption isotherms. The isotherms of the materials can be classified as type IV, which is characteristic of mesoporous solids. The TPR profiles of different catalysts are shown in **Fig. 1B**. The catalysts display multiple peaks, where at lower temperature, it is related to the reduction of NiO with lower interaction with the support, while the large peaks at higher temperature exhibit the strong interaction of Ni with the support. The basic properties of the catalysts were

estimated by CO<sub>2</sub>-TPD techniques, which indicate the strength of the basic sites. All the catalysts possess basic sites of weak and medium strength. The catalyst synthesized using WO<sub>3</sub> as support's modifier gave the highest CH<sub>4</sub> and CO<sub>2</sub> conversions (66 and 75%) respectively as shown in **Fig1 (D,E)** and syngas ratio **Fig1F** of about 0.95. The same catalyst presents the best stability and least carbon formation for 420 min. time on stream. **In Fig1G**, the catalysts with support's modifiers Mo and B oxides exhibit similar performance profile but with lower activity and stability.

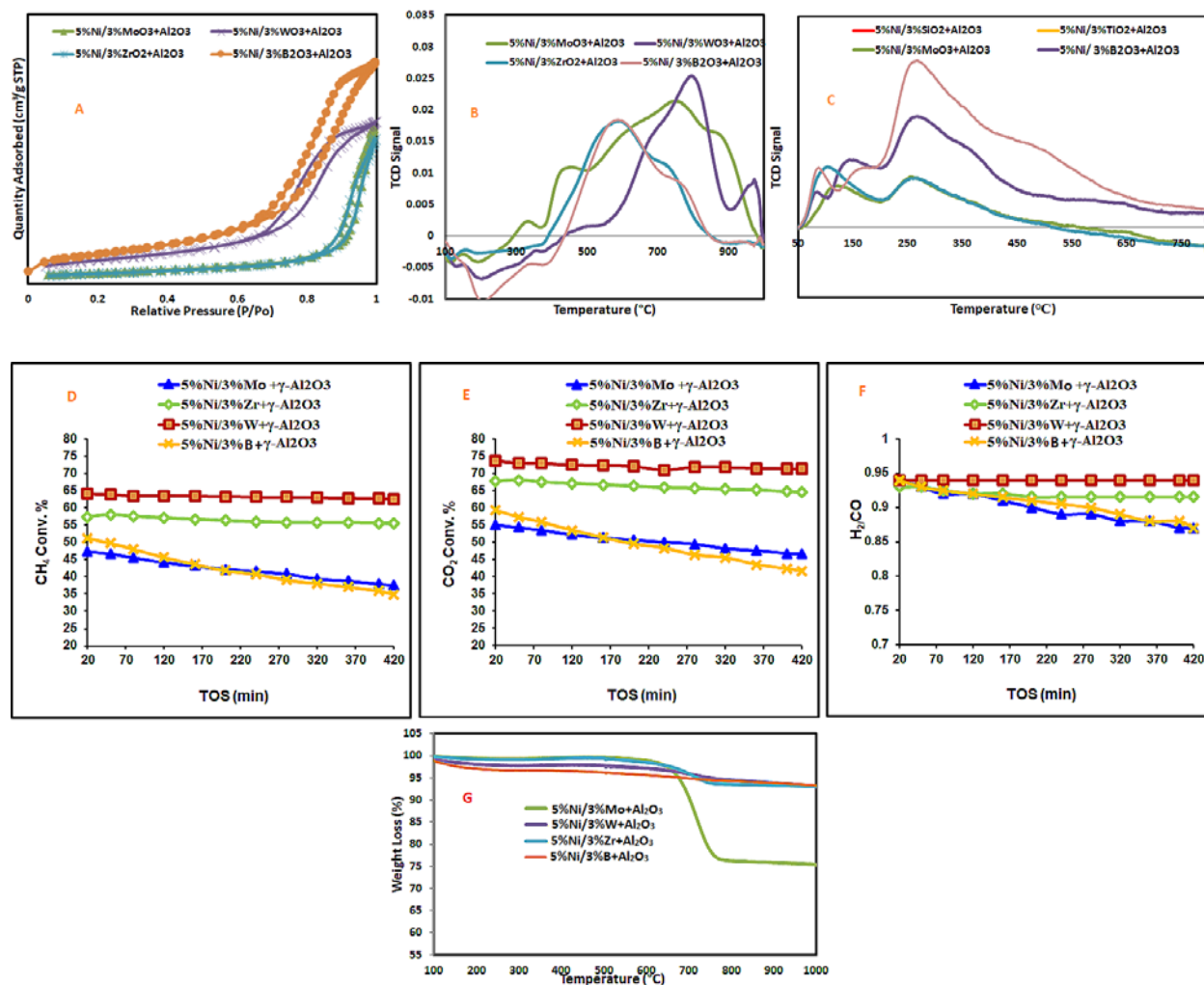


Fig 1 Activity & characterization of Ni prompted supported catalysts

#### References:

- [1] Maoshuai Li, André C. van Veen, Tuning the catalytic performance of Ni-catalysed dry reforming of methane and carbon deposition via Ni-CeO<sub>2</sub>-x interaction, *Applied Catalysis B: Environmental*, 237, 2018: 641-648
- [2] R. Y. Chein, W. H. Hsu, C. T. Yu, Parametric study of catalytic dry reforming of methane for syngas production at elevated pressures, *International Journal of Hydrogen Energy*, 42, 2017: 14485-14500
- [3] Jianwei Li, Jun Li, Qingshan Zhu, Carbon deposition and catalytic deactivation during CO<sub>2</sub> reforming of CH<sub>4</sub> over Co/MgO catalyst, *Chinese Journal of Chemical Engineering*, 26, 2018: 2344-2350.

# Direct conversion of heavy crude oil into light olefins over modified HZSM-5

Mohammed F. Alotibi<sup>a</sup>, Sergio González-Cortés, Peter P. Edwards<sup>b</sup>

<sup>a</sup>Material science Research Institute, King Abdulaziz City for Science and Technology (KACST), prince Turkey street 52 , 11442 Riyadh, Saudi Arabia, [mfalotaibi@kacst.edu.sa](mailto:mfalotaibi@kacst.edu.sa)

<sup>b</sup>KACST Centre of Excellence in Petrochemicals, Inorganic Chemistry Laboratory, University of Oxford, South Parks Road, Oxford, OX1 3QR, UK.

## Introduction

Petroleum oil continues to be major energy source up to 2040. As of 2014, the total primary energy supply was 273.9 million barrels of oil equivalent per day (mboe/d). On a global level, total primary energy demand is forecast to increase by 40% in the period to 2040 to reach 382 (mboe/d) according to OPEC's World Oil Outlook 2016 [1]. Due to the limited amount and depletion of traditional light petroleum resources, low quality heavy oils and or residues, which are subsequently obtained by processing heavy crudes, are considered as alternate suitable source for transportation fuels, energy and petrochemicals to fulfill the requirements of rapid population and civilization growth. Moreover, many statistical studies have showed that reservoirs of heavy crude are much larger than those of conventional crude, which made the appropriate deep upgrading of heavy crude, for both, refining and petrochemicals, more interesting and is attracting more and more attention from scientists and engineers [2,3].

Light olefins such as ethylene, propylene, and butylene are the key building blocks in the petrochemical industry and are widely used to synthesize downstream products, such as polymers, paints and solvents [4]. However, production of light olefins by using conventional cracking is challenging due to the low olefins selectivity in this process [5]. This is well established that pyrolysis of naphtha in the presence of zeolite catalyst is an effective process for the olefins production [6].

## Materials and Methods

All catalytic tests were performed on modified H-ZSM-5 zeolites at 500 °C and ambient pressure in a fixed bed reactor, The recants and products were analyzed by a gas chromatograph.**Results and dissections** In this study, numbers of modification methods have been applied for improving ZSM-5 performance in heavy crude oil (atmospheric residue) catalytic cracking process to increase the yield of light

olefins. High yield of total light olefins (ethylene, propylene and butylene) was achieved over hierarchical mesoporous ZSM-5 zeolite having Si/Al molar ratio=80. More than 55 wt. % of light olefins yield was obtained (Fig.1) which is much more than the light olefins yield obtained over the conventional ZSM-5 zeolite (about 32 wt.%). ZSM-5 with hierarchical mesoporous structure is necessary to improve the accessibility of the catalyst, lowering hydrogen transfer that reduce olefins yields and lowering coke formation.

### Significance

Direct conversion of the cheap and universally available heavy crude oil feedstock to petrochemicals is very attractive strategy to fulfill the increasing market demand and producer's needs. As far we know, our new catalyst showed very high olefins yield comparing to the obtained yield in the similar studies [7, 8].

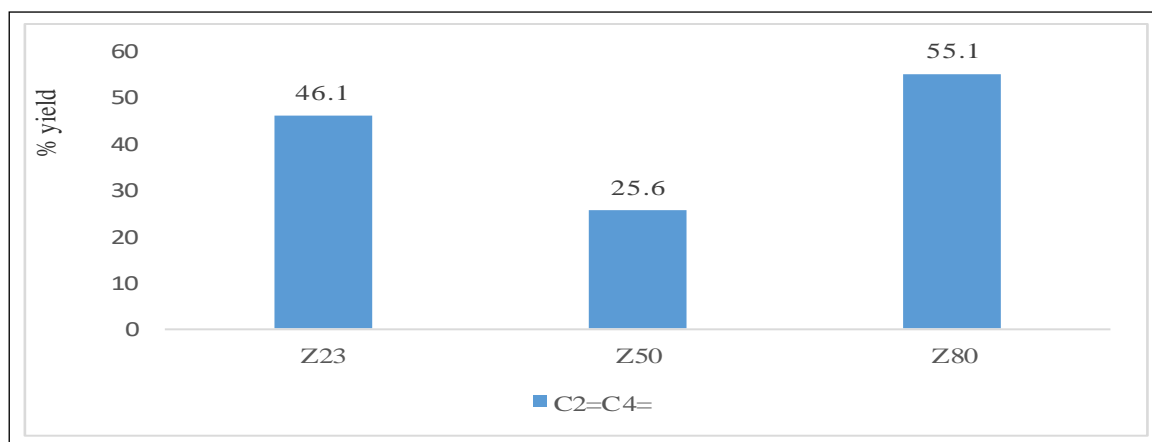


**Fig.1.**Total olefins yield over different modified ZSM-5 on heavy crude oil (atmospheric residue) catalytic cracking. Reaction conditions: feed flow rate 0.2 ml/min, reaction temperature 500 °C, catalyst load 1 g, pressure 1 am

### References

- [1] World Oil Outlook 2016.
- [2] Corma, A., E. Corresa, Y. Mathieu, L. Sauvanaud, S. Al-Bogami, M. S. Al-Ghrami, and A. Bourane. *Catalysis Science & Technology* 7, no. 1 (2017): 12-46.
- [3] Xieqing, Wang, Xie Chaogang, Li Zaiting, and Zhu Genquan.(2006): 149-168.
- [4] Chauvel A, Lefebvre G (1987) *Petrochemical Processes* 1:117. [5] W. Vermeiren, J.P. Gilson, *Topics in Catalysis* 52 (2009) 1131–1161.
- [6] H. Abrevaya, *Studies in Surface Science and Catalysis* 170 (2007) 1244–1251.
- [7] A.I. Hussain , A.M. Aitani , Martin Kubu° , Jirří Cějka , S. Al-Khattaf, *Fuel* 167 (2016) 226–23.
- [8] Iker Torre, Jose´ M. Arandes, Miren J. Azkoiti, Marti´n Olazar, and Javier Bilbao, *Energy & Fuels* 2007, 21, 11-1

# Sustainable and efficient bio-chemical catalytic cascade conversion of residual biomass to high quality biopolymers

Heracleous E.<sup>\*</sup>, Pachatouridou E., Lappas A.A.

Chemical Process & Energy Resources Institute (CPERI), Centre for Research and Technology Hellas (CERTH), 57001 Thessaloniki, Greece

\*[eheracl@cperi.certh.gr](mailto:eheracl@cperi.certh.gr)

## Introduction

Within the context of sustainability and the global efforts for CO<sub>2</sub> emission reduction, the investigation of routes for biomass conversion to fuels and chemicals has received tremendous attention. **BioCatPolymers** is a 3-year (Jan 2018 – Dec 2020) European project funded by the Horizon 2020 research and innovation programme, with the main objective to demonstrate a cost-effective, sustainable and efficient cascade technological route for the conversion of low-value, low-quality residual biomass to bio-polymers with equal or better performance than their fossil-based counterparts.

**BioCatPolymers** is specifically aiming at the efficient and economic production of isoprene and 3-methyl-1,5-pentanediol (3MPD), two monomers with very large markets that can be further processed in the existing infrastructure for fossil-based polymers for the production of elastomers and polyurethanes, respectively. The **BioCatPolymers** consortium consists of the Chemical Process and Energy Resources Institute of the Centre for Research & Technology Hellas (Greece) – coordinator, SEKAB E-Technology AB (Sweden), Visolis B.V. (Netherlands), Bioprocess Pilot Facility B.V. (Netherlands), Process Design Center (Netherlands), Quantis (Switzerland) and Covestro Deutschland AG (Germany).

## Concept, methodology and objectives

**BioCatPolymers** aims at demonstrating an integrated feedstock-flexible, economic and efficient technological route to convert low-cost, abundant and residual lignocellulosic biomass to high added value monomers that are converted to biopolymers via well-established manufacturing processes. In the framework of the project, a novel approach is being studied, which surpasses the impediments of traditional solely bio-based approaches by combining efficient hydrolysis of

lignocellulosic material to sugars which can be fermented with high yields to mevalonolactone (MVL), with highly efficient and selective thermochemical catalytic processes to the desired products, i.e. isoprene and 3MPD. The aim is to produce bio-isoprene at 50% cost reduction and 3MPD at 70% cost reduction compared to average market prices. This ambitious target will be attained by optimizing and demonstrating the entire value chain, starting from the pre-treatment of low quality biomass to biological fermentation to MVL, separation of MVL from the fermentation broth, selective catalytic conversion to the targeted monomer, purification to polymer grade quality and polymerization to the final polymer product, as shown in Figure 1. The optimization of the platform cell factories and all downstream processes and the efficient integration of the process modules are expected to increase the competitiveness of biological processes in terms of economics.

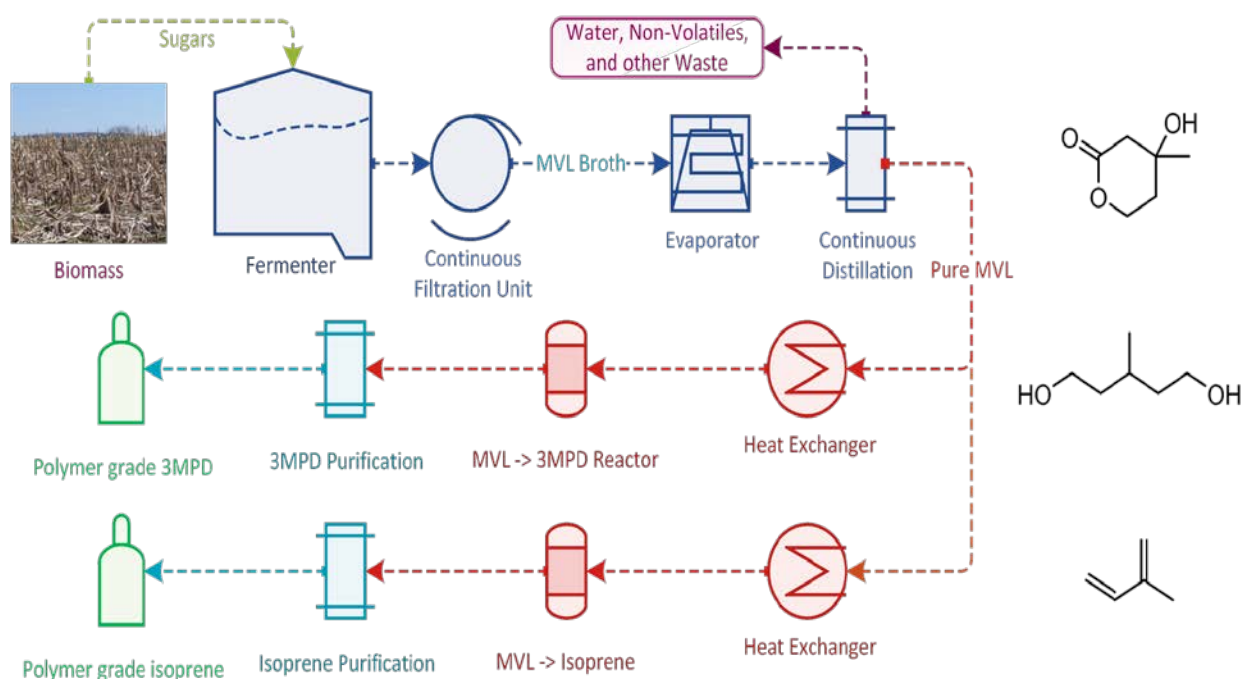


**Figure 1.** Overall concept of the Biocatpolymers project.

## Acknowledgments

This project has received funding from the EU Horizon 2020 research and innovation programme, under grant agreement No: 760802.



# MICROWAVE-ASSISTED CONVERSION OF HEAVY OILS TO LIGHT OLEFINS

Faisal M. Alotaibi<sup>a</sup>, Mohammed F. Alotibi<sup>a</sup>

<sup>a</sup>National Center for Petrochemicals Technology, King Abdulazeez City for Science & Technology, (KACST), P.O. Box 6086, Riyadh, 11442, Saudi Arabia

## ABSTRACT

Olefins, such as ethylene and propylene are important commodity petrochemicals useful in a variety of processes for making plastics and other chemical compounds. For many years now the primary process used for the production of the lighter olefins (ethylene and propylene) has been steam cracking of light hydrocarbons which is a highly energy intensive technology. Therefore, there is strong interest in development of more efficient and improved unconventional processing methods. The utilization of microwave irradiation for efficient chemical activation for the processing of petroleum to useful products has demonstrated that the selective and targeted dissipation of microwave energy has great potential to deliver shorter reaction times compared to conventional cracking processes driven by thermal energy.

The aim of this study is to develop new petrochemical approaches based on microwave-dielectric heating and rational designed catalysts based on ZSM-5 catalysts, whose duality can efficiently transform the crude oil and heavy naphtha to high-value chemicals. These innovations will be used for the selective cracking and dehydrogenation of crude oil into valuable light olefins for the petrochemical industry *via* new “unconventional process technologies.”

**Keywords:** Microwave-assisted conversion, Ethylene and propylene, Heavy crude oil upgrading, Fluid catalytic cracking, ZSM-5 zeolites

# In-situ generation of Brønsted acidity in the Pd-I bifunctional catalysts for selective reductive etherification

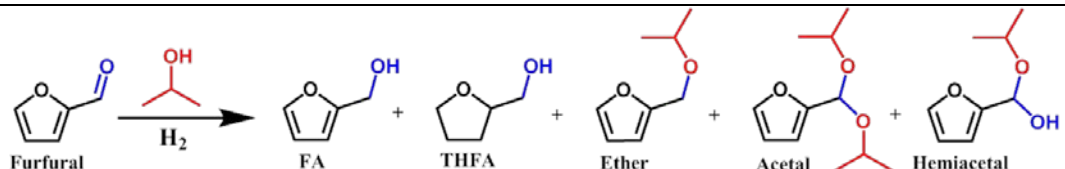
*Dan Wu, Unité de Catalyse et Chimie du Solide (UCCS), Lille, France; Willinton Y. Hernández, Eco-Efficient Products and Processes Laboratory (E2P2L), Shanghai, China; Andrei Y. Khodakov, UCCS, Lille, France; Vitaly V. Ordonsky, E2P2L, Shanghai, China.*

## Introduction

Ethers and its derivatives are widely used as solvents, surfactants, pharmaceuticals, polymers and liquid fuels. Traditional routes for the synthesis of ethers involve dehydration of alcohols and Williamson ether synthesis, which always need acidic catalyst at elevated temperatures (>150 °C) or environmentally harmful halides as intermediates <sup>[1]</sup>. Reductive etherification is an alternative sustainable way to valorize biomass feedstock <sup>[2]</sup>. The reaction requires a bifunctional catalyst and proceeds via intermediate acetalization of carbonyl groups over acid sites with subsequent hydrogenolysis to ethers over metal sites. Herein, we develop an extremely efficient bifunctional Pd-I catalyst for reductive etherification. The catalyst is prepared by “in situ” modification of a commercially available Pd-supported catalyst with organic iodide compounds. The Brønsted acidity for the reaction is reversibly generated in the presence of hydrogen in gaseous phase.

## Key Results and Discussion

**Table 1:** Etherification reaction of furfural over Pd catalysts treated and non-treated by iodine (T=60 °C, 20 bar H<sub>2</sub>, 0.1 g furfural, 2 g isopropanol, 15 mg organic iodide if needed, 50 mg catalyst, 1h)



Entry	Catalytic system	Conversion, %	Selectivity, %					
			FA	THFA	Ether	Acetal	Hemiacetal	Others
1	Pd/Al <sub>2</sub> O <sub>3</sub>	87	0	99	0	0	0	1
2	Pd/Al <sub>2</sub> O <sub>3</sub> + EtI	72	4	0	91	1	2	1
3	I-Pd/Al <sub>2</sub> O <sub>3</sub>	35	0	0	83	12	1	4

Commercial 5 wt% Pd/Al<sub>2</sub>O<sub>3</sub> has demonstrated high activity with formation of THFA as the main product. Addition of traces of ethyl iodide (EtI) or pre-treatment with EtI (I-Pd/Al<sub>2</sub>O<sub>3</sub>) leads to total change of the reaction route, causing favored formation of ether (2-(isopropoxymethyl)furan) as the main product (91 % and 83% selectivity). In addition, analysis of the products from Pd/Al<sub>2</sub>O<sub>3</sub> promoted with EtI showed the

presence of ethane. Thus, the modification of the catalyst might be explained by the Etl reaction with hydrogen on the surface of Pd with intermediate formation of atomic iodine on the surface.

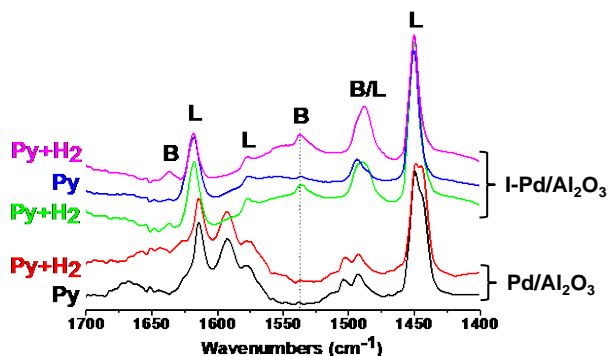


**Figure 1:** In-situ pyridine-FTIR analysis for I-Pd/Al<sub>2</sub>O<sub>3</sub> and Pd/Al<sub>2</sub>O<sub>3</sub>

exposure to H<sub>2</sub> and disappeared after removal of H<sub>2</sub> from the cell. Interestingly, the acidity could be recovered by dosing again hydrogen. This result indicates that the Brönsted acidity generation on the Pd-I catalysts is reversible and depends on partial pressure of hydrogen. A feasible reaction pathway was proposed. First, Brönsted acid sites (H<sup>+</sup>) are generated on the Pd-I sites via hydrogen dissociation. Then, the acetal intermediates are produced on the Brönsted acid sites followed by hydrogenolysis to ether over neighbored bare-Pd.

## Conclusion

In-situ generated Brönsted acidity in Pd-I catalyst is responsible of its enhanced catalytic performance in reductive etherification. This strategy can be extended to other reactions between various carbonyl compounds and alcohols requiring bifunctional catalysts.

## References

- [1] O. C. Dermer, *Chem. Rev.* **1934**, 14, 385.
- [2] Y. Wang, Q. Cui, Y. Guan, P. Wu, *Green Chem.* **2018**, 20, 2110.

Acetalization of carbonyl groups is usually considered as an acid catalyzed reaction, which takes place in the presence of Brönsted acid sites. Pyridine-IR analysis was carried out on Pd/Al<sub>2</sub>O<sub>3</sub> and I-Pd/Al<sub>2</sub>O<sub>3</sub> to verify the generation of acidity (Figure 1). A peak at 1540 cm<sup>-1</sup> assigned to Brönsted acid sites in I-Pd/Al<sub>2</sub>O<sub>3</sub> appeared after

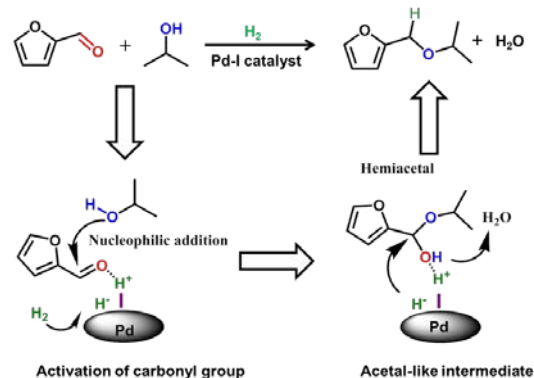
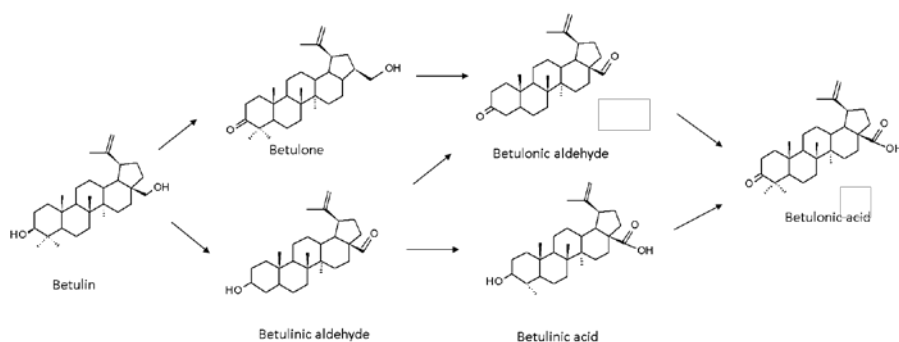


**Figure 2:** Scheme of the synthesis of ether by in situ acid generation in the presence of hydrogen over heterogeneous Pd-I catalyst

# Kinetics of Betulin Oxidation over Gold Supported Heterogeneous Catalysts for Production of Pharmaceuticals

*Päivi Mäki-Arvela<sup>1</sup>, Jarl Hemming<sup>1</sup>, Kari Eränen<sup>1</sup>, Dmitry Yu. Murzin<sup>1</sup>, <sup>1</sup>Johan Gadolin Process Chemistry Centre, Åbo Akademi University, Turku/Åbo, Finland; Ekaterina Kolobova<sup>2</sup>, Anna Buachidze<sup>2</sup>, Alexey Pestryakov<sup>2</sup>, <sup>2</sup>Research School of Chemistry & Applied Biomedical Sciences, Tomsk Polytechnic University, Tomsk, Russia*

Oxidation products of betulin, which is a wood extractive, are biologically active and exhibit several anticarcinogenic as well as antimicrobial properties [1]. Conventionally betulin has been oxidized with chromium containing catalysts, which are poisonous being also difficult to reuse. Heterogeneous silver supported catalysts [2] have been



used in betulin oxidation (Fig. 1). Kinetics of betulin oxidation has been very scarcely investigated. In this work kinetics of betulin oxidation over gold

Fig. 1. Reaction scheme.

supported catalysts was elucidated for the first time.

The catalysts were prepared by deposition precipitation method and characterized by nitrogen adsorption, XPS, CO<sub>2</sub> temperature programmed desorption and TEM. The kinetic experiments were performed in a glass reactor in mesitylene as a solvent at 140°C under atmospheric flow of synthetic air. In a typical experiment the initial betulin concentration was 4.5 mmol/l and the amounts of the catalyst and the liquid phase were 0.2 g and 100 ml. Small catalyst particles (< 63 μm) and high stirring rate of 450 rpm were used to suppress the internal and external mass transfer limitations. The samples were periodically taken from the reactor, silylated, analyzed in GC. The products were confirmed by GC-MS.

The initial TOF was the highest with 0.5 wt% Au/LT treated with O<sub>2</sub> (Au/LT= Au/La<sub>2</sub>O<sub>3</sub>/TiO<sub>2</sub>) containing the smallest gold particles. 4 wt% Au/TiO<sub>2</sub> with slightly

larger Au particles which deactivated very rapidly after 30 min giving only 25 % conversion of betulin in 6 h. On the other hand, 4 wt% Au/LT catalyst treated with hydrogen and containing 19 % gold as ions according to XPS, transformed betulin initially with a relatively high rate. The oxidation rate over this catalyst, however, declined after 30 min (betulin transformation rate decreases due to a competing reaction - transformation of betulone to betulonic aldehyde). When betulin was oxidized using a mixture of 4 wt% Au/LT and hydrotalcite (HT), the initial TOF was higher than in the absence of HT. Addition of HT, however, retained the catalyst mixture more active after prolonged reaction times giving conversion of 70%.

The liquid phase mass balance closure (the sum of the masses of reactant and products visible in GC) in betulin oxidation was high with Au/TiO<sub>2</sub> having the lowest concentration of medium and strong acid sites. The incomplete mass balance closure related to the amount of catalyst and its acidity, namely, the concentration of medium and strong acid sites is probably due to strong adsorption of the reactant and/or products on the catalyst surface. The main product was betulonic aldehyde with the yield of 54% over 0.5 wt% Au/LT containing 35% gold ions according to XPS (Fig. 2). The ratio between the initial rates for formation of betulonic aldehyde to betulone decreased as follows: 4 wt% Au/TiO<sub>2</sub> > 4wt% Au/LT > 4 wt% Au/LT+HT > 0.5 wt% Au/LT+HT i.e. being the highest with the largest Au particles. The final work will present kinetic analysis of betulin oxidation and correlate properties of catalysts with their performance.

#### References:

- [1] Tolstikova, T. G., Sorokina, I. V., Tolstikov, G. A., Flekhter, O. B., Russ. J. Bioorg. Chem. 32 (2006) 37-49.  
 [2] Kolobova, E., Kotolevich, Y., Pakrieva, E., Mamontov, G., Farias, M. H., Cortés, Corberán, V., Bogdanchikova, N., Hemming, J., Smeds, A., Mäki-Arvela, P., Murzin, D., Pestryakov, A., Fuel, 238 (2018) 110-119.

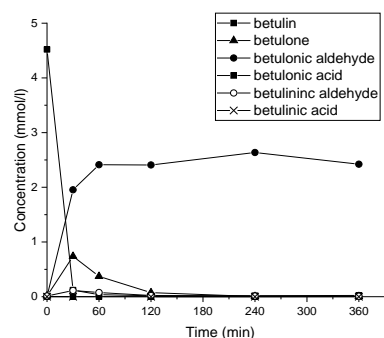


Fig. 2. Concentration profile for betulin oxidation. Conditions: 1.6 g catalyst, 0.5 wt % of Au, Au/La<sub>2</sub>O<sub>3</sub>/TiO<sub>2</sub> + 0.2 g hydrotalcite, c<sub>0,bet.</sub>=4.5 mmol/l, at 140°C, with synthetic air.

## **Extra-Small Porous Gallosilicate Materials as Heterogeneous Catalysts for the Conversion of Glycerol to Solketal**

*Michel Devillers, Institute of Condensed Matter and Nanosciences - Molecular Chemistry, Materials and Catalysis (IMCN/MOST), Université catholique de Louvain, Place Louis Pasteur 1/L4.01.03, Louvain-La-Neuve 1348, Belgium; Hussein Hussein, Université catholique de Louvain, Place Louis Pasteur L4.01.06, Louvain-La-Neuve 1348, Belgium; Carmela Aprile, Unit of Nanomaterials Chemistry (CNANO), University of Namur, Department of Chemistry, 5000 Namur, Belgium*

The development of eco-friendly, environmentally compatible, and recyclable heterogeneous catalysts with improved performances in the production of fine chemicals as well as in the conversion of renewables is a field in continuous evolution. The catalysts design may involve different strategies, going from the identification of new active species to the tailored design of structural and morphological features of the catalytic support [1].

Mesoporous solids bearing a metal element inserted as single sites in the silica matrix represent one of the most used class of heterogeneous catalysts that can find applications for different reactions including epoxidations, alkyl lactate production and glycerol conversion. The insertion of a metal center in the silica structure can be achieved *via* co-synthesis procedure or post-functionalization through wet or incipient wet impregnation [2]. The last strategy involves the use of a pre-formed solid with the desired features which is used as support for the active species. The advantage of this procedure is represented by the fact that all active species are located at the external surface of the solid support and are accessible to the reactants.

Here, we report the synthesis of novel catalysts synthesized *via* wet impregnation of an extra small (XS) MCM-41 material followed by calcination of the final solids. Two different precursors (the neutral gallium lactate  $\text{Ga}(\text{C}_3\text{H}_5\text{O}_3)_3 \cdot \text{H}_2\text{O}$  and the anionic gallium citrate complex  $(\text{NH}_4)_5[\text{Ga}(\text{C}_6\text{H}_4\text{O}_7)_2] \cdot 2\text{H}_2\text{O}$ ) were used as Ga sources. The different nature of the selected Ga-precursors will determine a different interaction with the support which could influence the overall catalytic activity of the final

materials. The two solids (XS-GaLac-MCM-41) and (XS-GaCit-MCM-41) were extensively characterized *via* powder X-ray diffraction, nitrogen physisorption, transmission electron microscopy and ammonia temperature programmed desorption (NH<sub>3</sub>-TPD), and then used as catalysts in the acetalization of glycerol with acetone to produce solketal (2,2-dimethyl-1,3-dioxolane-4-methanol) [3] with excellent results (Table 1). The outstanding catalytic behavior of the catalysts prepared via impregnation can be attributed to the good dispersion of gallium as well as to the higher accessibility of the active sites (all distributed at the surface).

**Table 1.** Catalytic performance of the XS-GaLac-MCM-41 and XS-GaCit-MCM-41 materials.

Entry	Catalyst	Si/Ga <sup>b</sup>	Temperature (°C)	Solketal yield (%)	TON <sup>c</sup>	Reference
1	XS-GaLac-MCM-41 <sup>a</sup>	118	50	53	3838	This work
2	XS-GaLac-MCM-41 <sup>a</sup>	118	80	65	4682	This work
3	XS-GaLac-MCM-41 <sup>d</sup>	118	80	29	840	This work
4	XS-GaCit-MCM-41 <sup>a</sup>	130	50	42	3355	This work
5	XS-GaCit-MCM-41 <sup>a</sup>	130	80	53	4229	This work
6	XS-GaCit-MCM-41 <sup>d</sup>	130	80	23	736	This work
7	XS-Ga-MCM-41-H <sup>d</sup>	15 <sup>e</sup>	80	28	125	X.Collard et al
8	XS-Ga-MCM-41-L <sup>d</sup>	44 <sup>e</sup>	80	25	361	X.Collard et al

<sup>a</sup> Reaction conditions: 10 mg of catalyst, 0.01 mol glycerol, 2.32 g acetone, 6 h. <sup>b</sup> Determined from ICP-OES analysis. <sup>c</sup> TON (Turnover number) defined as mol of glycerol converted/mol of Ga atoms.

<sup>d</sup> Reaction conditions: 25 mg of catalyst, glycerol (10 mmol), acetone (10 mmol), tert-butanol (1.48 g), 6 h.

<sup>e</sup> Si/Ga ratio determined by EDX.

In addition, the influence of reaction conditions such as reaction time, catalyst amount, and acetone/glycerol molar ratio was studied. Both catalysts achieved excellent turnover numbers higher than other Ga-based catalysts reported in literature. In order to prove the true heterogeneous nature of the materials recycling experiments were performed as well. The best catalyst (XS-GaLac-MCM-41) was used in multiple catalytic cycles without decrease in glycerol conversion. Moreover, a hot-filtration test allowed excluding the leaching of small amount of active species in solution.

## References

[1] Collard, X., Li, L., Sels, B. F., Bertrand, A., Aprile, C., Pescarmona, P. P., *J. Catal.* 314 (2014) 56-65.

[2] S.P.S. Andrew; *CHEMTECH* 9 (1979) 180.

[3] Da Silva, G. P.; Mack, M.; Contiero, J. *Biotechnol. Adv.* 27(1) (2009) 30-39.

# Cyclodextrin-assisted low-metal Ni-Pd/Al<sub>2</sub>O<sub>3</sub> bimetallic catalysts for the direct amination of aliphatic alcohols

Ajay Tomer,<sup>a,b</sup> Bright T. Kusema,<sup>b</sup> Cédric Przybylski,<sup>c</sup> Jean-François Paul,<sup>a</sup> Eric Monflier,<sup>a</sup> Marc Pera-Titus,<sup>b</sup> Anne Ponchel<sup>a</sup>

<sup>a</sup>Univ. Artois, CNRS Centrale Lille, ENSCL, Univ. Lille, UMR 8181, Unité de Catalyse et de Chimie du Solide (UCCS), F-62300 Lens, France.

<sup>b</sup>Eco-Efficient Products and Process Laboratory (E2P2L), UMR 3464 CNRS-Solvay, Shanghai, 201108 (PR China).

<sup>c</sup>Sorbonne Universités, Université Pierre et Marie Curie, IPCM-CNRS UMR 8232, Paris, 75252, France.

## Introduction

Amines are N-containing intermediates with a broad variety of applications in the chemical industry as solvents, agrochemicals, pharmaceuticals, detergents and fabric softeners. The direct amination of alcohols *via* the hydrogen borrowing mechanism is a promising strategy for preparing amines, since no external hydrogen supply is required and water is generated as main by-product. The present catalytic systems (Ni & Cu) suffer from poor selectivity and high metal loading (>10 wt%). In this work, we report a series of low-Ni based bimetallic catalysts synthesized by six different methods using  $\beta$ -CD as pre-shaping agent (Fig. 1) and their characterization in aqueous solution, dried, calcined and reduced states. The catalytic performance of the as-prepared formulations was assessed in the amination of 1-octanol (OL) with NH<sub>3</sub> (7 bar) and 55 mg catalyst at 160 °C for 4 h.

## Results

The primary Ni-Pd- $\beta$ -CD interaction was inspected by marrying ESI-MS experiments with DFT calculations. The results revealed a higher affinity of the Ni(II) nitrate precursor for  $\beta$ -CD to form a molecular complex compared to the Pd(II) precursor. This complex conditioned to an important extent the catalyst architecture in the further thermal treatment steps (drying, calcination, reduction), as inferred by combining H<sub>2</sub>-TPR, XPS, CO-pulse chemisorption and STEM-EDX-SDD. By optimizing the preparation protocol, 90% OL conversion and 79% selectivity to the primary amine (i.e. 1-octylamine) (TON = 93) could be achieved on a formulation



based on 5 wt%Ni and 0.5 wt%Pd prepared by pre-adsorbing  $\beta$ -CD on  $\text{Al}_2\text{O}_3$  before impregnating the Ni(II) and Pd(II) salts (Fig. 2). This results places this catalyst among the most active and selective Ni catalysts reported in the literature for the synthesis of primary amines from aliphatic alcohols.

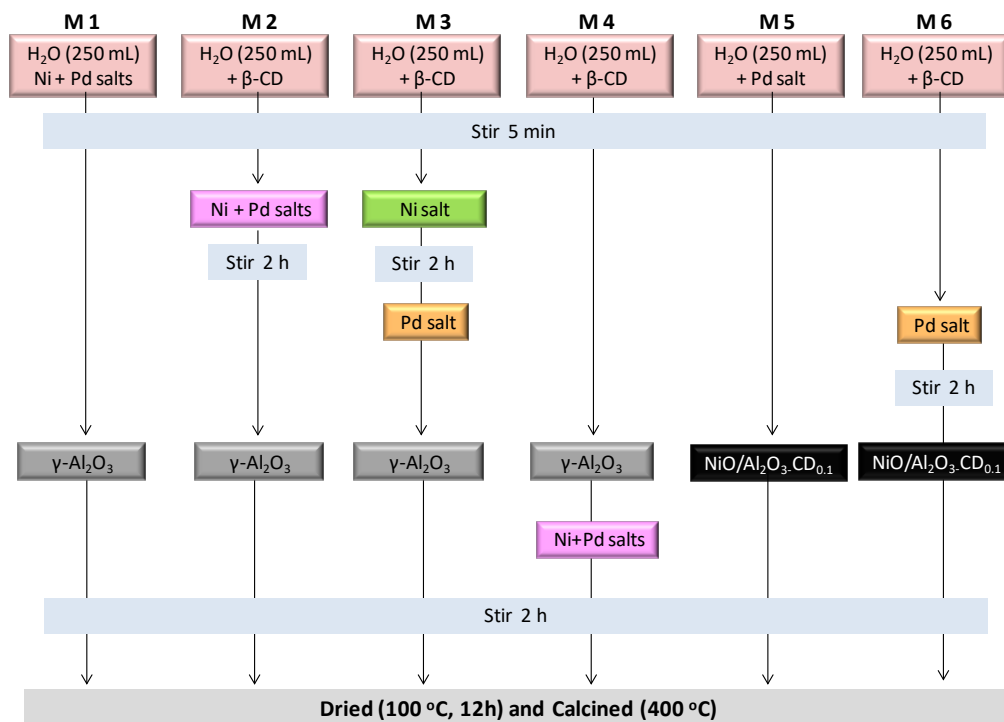


Fig. 1 Six different methods (M1-M6) used for the preparation of Ni-Pd/Al catalysts by wet impregnation.

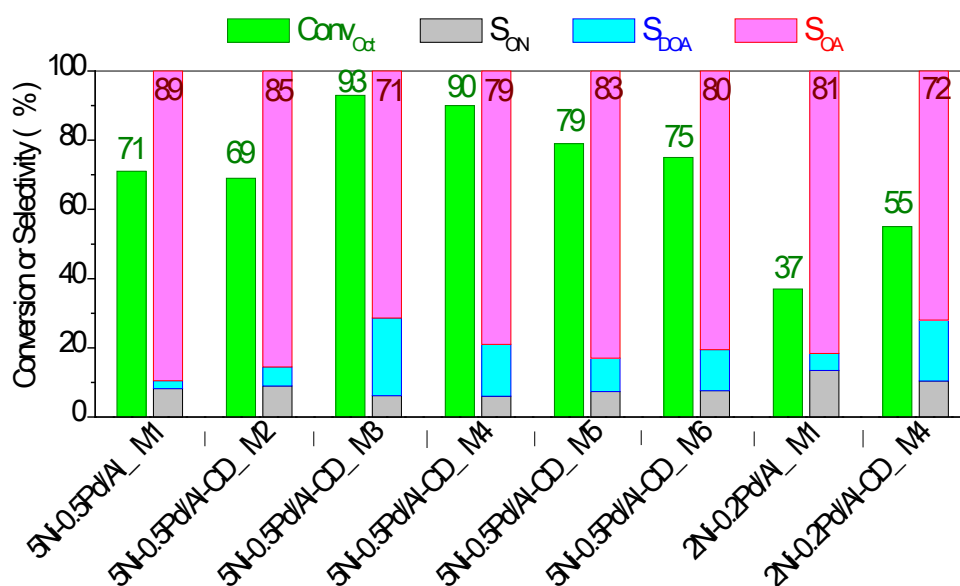


Fig. 2 Catalytic performances of the catalysts in the direct amination of 1-octanol.

# Relationship between structure and activity of $ABO_3$ perovskite catalysts in the oxidative coupling of methane

*Yujin Sim, Dahye Kwon, Inchan Yang, Ji Chul Jung\*, Department of Chemical Engineering, Myongji University, Yongin, 17058, Republic of Korea*

## Introduction

The oxidative coupling of methane (OCM) to  $C_2$  hydrocarbons is becoming one of the hottest issues in the research area of heterogeneous catalysis. The  $Na_2WO_4/Mn/SiO_2$  catalyst that is regarded as the best catalyst for OCM at present achieves a  $C_2$  yield as high as ca. 25%. However, because of the complex composition and structure of the  $Na_2WO_4/Mn/SiO_2$  catalyst, a great deal of ambiguity on the identity and nature of its active sites remains, leading to a difficulty in commercial applications. To overcome these drawbacks, it is necessary to perform a fundamental study to clarify the catalytic active sites for the OCM reaction. Therefore, we have intensively studied  $ABO_3$  perovskite catalysts having clear and simple structures. In this study, we investigated the relationship between structure and activity of  $ABO_3$  perovskite catalysts in the OCM. Particularly, we focused on tolerance factor ( $T_F$ ) and specific free volume ( $V_{SF}$ ) among various structure factors, because these factors are well known to control the oxygen ion conductivity, which has a strong influence on the catalytic activity in the OCM [1].

## Experimental

Various of  $ABO_3$  perovskite catalysts with different components ( $A=La, Pr, Nd, Sm, \text{ or } Gd, B=Al, Ga, \text{ or } In$ ) were prepared by a citrate sol-gel method. The crystal structures of the prepared catalysts were confirmed by powder X-ray diffraction (XRD). A continuous-flow fixed-bed reactor having a continuous-flow quartz reactor was used to perform the OCM reaction. The tolerance factor and specific free volume were calculated from literature data.

## Results and discussion

The successful formation of various  $ABO_3$  perovskite catalysts was confirmed by XRD measurements. The prepared catalysts show their characteristic peaks, as identified with JCPDS cards.  $T_F$  is a measure of the stability and distortion of the crystal structure and is calculated as follows:  $T_F = (r_A + r_O) / 2 (r_B + r_O)$ , where  $r_A, r_B$  and  $r_O$  are the mean ionic radii for A, B and O sites. When  $T_F = 1$ , the most

symmetrical cubic symmetric perovskite structure is formed. If  $T_F$  is far from 1, the structure is distorted and the anisotropy of the oxygen site is increased. High anisotropy of oxygen site interferes with oxygen transfer leading to low oxygen ion conductivity [1,2].  $V_{SF}$  is a function of the empty space in the unit cell and is calculated as follows:  $V_{SF} = (V - \text{total volume of the constituent ions})/V$ , where  $V$  is the unit cell volume. The larger the  $V_{SF}$ , the more oxygen ions can move to provide more space to induce high oxygen ion conductivity [3].

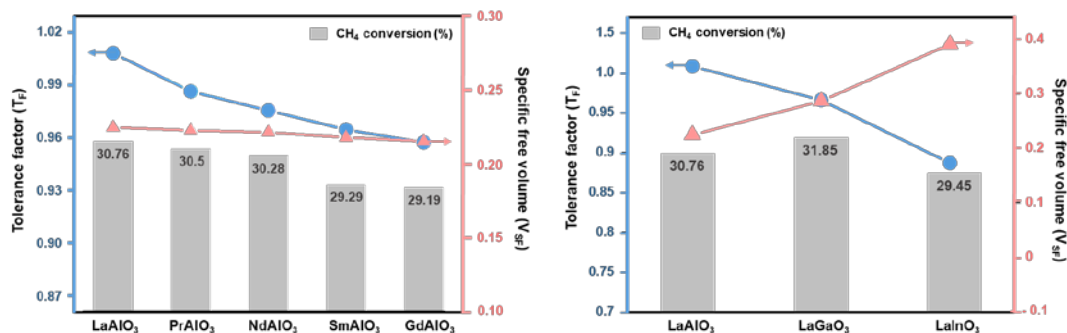


**Fig. 1.** Tolerance factor, specific free volume and catalytic activities of  $ABO_3$  catalysts (A = La, Pr, Nd, Sm or Gd, B = Al, Ga or In ) in the OCM.

Fig. 1 shows the calculated  $T_F$ ,  $V_{SF}$  and  $CH_4$  conversion of various  $ABO_3$  perovskite catalysts. Interestingly, methane conversion showed a similar trend as  $T_F$  when the  $V_{SF}$  is constant. In addition,  $LaGaO_3$  catalysts with appropriate  $T_F$  and  $V_{SF}$  are known to have the highest oxygen ion conductivities and showed the highest methane conversion in the OCM. From these results, we could infer that structural factors of  $ABO_3$  perovskite catalysts such as  $T_F$  and  $V_{SF}$  is closely related to their catalytic activity in the OCM.

## Conclusions

Oxidation coupling of methane over  $ABO_3$  perovskite (A = La, Pr, Nd, Sm or Gd, B = Al, Ga or In) catalysts were performed to produce  $C_2$  hydrocarbons from methane. The structural factors of perovskite catalysts such as  $T_F$  and  $V_{SF}$  have a strong influence on their oxygen ion conductivity, and thus, catalytic activity in the OCM. We concluded that structural factor can play a key role in systematically designing a high-performance perovskite catalyst for the OCM.

## References

- [1] R.L. Cook, Solid State Ionics, 45 (1991) 311.
- [2] Hayashi H, Solid State Ionics, 122 (1999) 1.
- [3] Richter, J., Monatsh. Chem., 140 (2009) 985.

# The effect of water on the efficiency of MPTMS anchoring and its stability in mesoporous silica SBA-15

*Katarzyna Stawicka<sup>1</sup>, Julia Gajewska<sup>1</sup>, Maciej Gierada<sup>2</sup>, Christina Siakat<sup>2</sup>,  
Frederik Tielens<sup>2</sup>, Maria Ziolk<sup>1</sup>*

<sup>1</sup>*Adam Mickiewicz University in Poznań, Faculty of Chemistry, Umultowska 89b, 61-614 Poznań, Poland*

<sup>2</sup>*Vrije Universiteit Brussel (Free University Brussels-VUB), General Chemistry (ALGC), Pleinlaan 2, 1050 Brussel, Belgium*

## Introduction

Organosilanes with different functional groups (e.g. amine, thiol) are often used for functionalization of ordered mesoporous silica in order to obtain hybrid catalysts or supports for noble metals. For both purposes the efficiency of organosilane anchoring and the stability of modifiers are very important in the application of the final materials as catalysts. Thus the knowledge of the role of the surface species on mesoporous silica supports in organosilica anchoring is crucial. The surface species on silica strongly depend on the hydration level. The important role of water in anchoring of bio-organic compounds has been already mentioned in [1]. The effect of water on silica surface on the efficiency and stability of organosilane anchoring has not been considered in literature in details, which has prompted us to consider these issues.

## Experimental

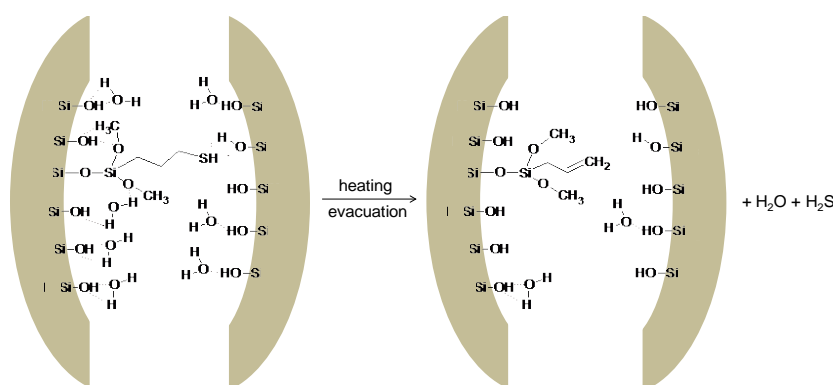
SBA-15 was fully hydrated and next dehydrated (calcined) at different temperatures (50°C, 100°C, 150°C, 200°C and 400°C). In this way the samples with different number of layers of water were obtained. 3-thiolpropyltrimethoxysilane (MPTMS) was anchored on the samples of different coverage with water. The materials were studied with N<sub>2</sub> ads./des., elemental analysis, XPS, TGA, FTIR after evacuation at different temperatures. The experimental results were supported by periodic DFT calculations. Hydroxylated and hydrated amorphous silica slab models were used comparable to those used in our previous study on silica ligand anchoring.[1]

## Results and Discussion

After heating of hydrated SBA-15 at different temperatures the samples were modified with MPTMS. The number of water layers at silica surface decreased from

7.6 layers in hydrated SBA-15 to 0.6 monolayer in the material calcined at 400°C. The efficiency of MPTMS anchoring decreased with the reduced amount of water on the silica support surface. The samples covered by ca one monolayer of water (MP/SBA-15 heated at 100°C, 150°C, 200°C) were found to contain a similar amount of anchored organosilane - ca. 0.46 mmol/g. If the number of layers increased up to 1.5 (heating at 50°C) the efficiency of MPTMS anchoring increased to 0.56 mmol/g, while if SBA-15 was covered by 0.6 water monolayer (heating at 400°C) it decreased to 0.39 mmol/g.

The stability of MPTMS anchored was estimated on the basis of TG analysis and FTIR spectra recorded after evacuation of MP/SBA-15 samples at different temperatures. With the decrease in the amount of water on MP/SBA-15 surface, the temperature of MPTMS decomposition decreased indicating a decrease in the stability of MPTMS. FTIR study allowed the evaluation of changes in MPTMS anchored upon the temperature of evacuation (Fig. 1). The intensity of the IR bands assigned to SiOH increased in line with the growth in the evacuation temperature. It



was correlated with the breaking of hydrogen bonds between SiOH and water molecules, or -OCH<sub>3</sub> or -SH species. In contrast, the decrease in the intensity of the band

due to -SH was caused by desorption of H<sub>2</sub>S, while the increase in the intensity of the band originating from methoxy species was caused by the breaking of hydrogen bond between -OCH<sub>3</sub> and water and/or SiOH. The breaking of hydrogen bond was evidenced by a significant decrease in the intensity of the FTIR band. The experimental results will be discussed in detail in relation to those of DFT calculations.

#### Acknowledgements

We are grateful to National Science Center in Poland (project N<sup>o</sup> UMO-2018/29/B/ST5/00137) for the financial support.

#### References

1. F. Tielens, N. Folliet, L. Bondaz, S. Etemovic, F. Babonneau, Ch. Gervais, T. Azaïs J.Phys.Chem.C, 121, 17339 (2017).

# Production of Valuable Chemicals from Cellulose, Hemicellulose, and Lignin in Lignocellulosic Biomass

*Aritomo Yamaguchi*<sup>1</sup>; *Naoki Mimura*<sup>1</sup>; *Osamu Sato*<sup>1</sup>

<sup>1</sup>*Research Institute for Chemical Process Technology, National Institute of Advanced Industrial Science and Technology (AIST), Sendai 983-8551, Japan*

## Introduction

Conversion and utilization of inedible lignocellulosic biomass, which mainly consists of cellulose, hemicellulose and lignin, have greatly attracted attention to reduce carbon dioxide emission and to establish the sustainable society. Cellulose and hemicellulose are polysaccharides, which can be converted into valuable products and fuels. Lignin is a three-dimensional polymer of aromatic compounds with cross-linking via C–O–C ether bonds and C–C bonds, which can be converted into aromatic products by depolymerization. Heterogeneous catalysts play a major role in the conversion of lignocellulosic biomass because the reaction rates are high and the catalysts are relatively stable and reusable compared with enzymes and homogeneous catalysts. Heterogeneous catalysts can convert cellulose and hemicellulose into useful chemicals; however, contamination of the catalysts by lignin after the reaction causes catalyst deactivation. We have reported that the cellulose and hemicellulose in lignocellulose can be directly converted into sugar alcohols such as sorbitol, mannitol, and xylitol without delignification by using supported metal catalysts with hydrogen gas [1, 2]. The lignin remains as a solid after the reaction. In that case, separation of the solid lignin from the supported metal catalysts in the solid residue is required. We have also reported cleavage of the C–O–C ether bonds in lignin model compounds using supported metal catalysts in supercritical water without adding hydrogen gas and without causing hydrogenation of the aromatic rings [3]. We therefore applied this technique to separation of the solid lignin from the supported metal catalysts by depolymerizing the lignin into soluble aromatic chemicals. Here, we show a cascade utilization of lignocellulose: conversion of cellulose and hemicellulose, followed by conversion of lignin into soluble aromatics at higher temperature. We also found that the supported metal catalyst was reusable.

## Results and Discussion

The conversion of cellulose and hemicellulose in the bagasse was carried out in a batch reactor at 463 K for 16 h using Pt/C with 5 MPa H<sub>2</sub> [1, 2]. The amounts of products, sorbitol, mannitol, xylitol, and arabitol were 0.25, 0.044, 0.14, and 0.065 g per gram of dry bagasse, respectively. The yield of total sugar alcohols was 64.0% based on the total moles of sugar in the reactant bagasse. This result indicated that the cellulose and hemicellulose in the bagasse could be converted into sugar alcohols by Pt/C with H<sub>2</sub> in water. The solid residue remaining after the reaction and the aqueous solution were separated by filtration.

The wet, solid residue from the first reaction, which was composed of mainly lignin and Pt/C, was treated at 673 K for 1 h with water (0.5 g cm<sup>-3</sup>) to depolymerize the lignin into aromatic compounds and to recover the Pt/C catalyst. The lignin was successfully depolymerized, and the weight of the solid residue after treatment at 673 K was only 1.9% of the weight of the reactant bagasse. The yields of benzene, toluene, ethylbenzene, and propylbenzene were 2.5%, 4.8%, 16.7%, and 11.9%, respectively. The total yield of aromatic compounds was 40.3%.

The Pt/C catalyst recovered after lignin depolymerization at 673 K was reused to convert the cellulose and hemicellulose in fresh bagasse in a batch reactor at 463 K for 16 h with H<sub>2</sub>. The amounts of sorbitol, mannitol, xylitol, and arabitol in the products were 0.29, 0.037, 0.19, and 0.038 g per gram of dry bagasse, respectively. The 70.5% yield of total sugar alcohols indicated that the catalyst kept its activity for the hydrogenolysis of cellulose and hemicellulose in bagasse. The wet, solid residue obtained after the reaction was then treated with water at 673 K for 1 h. The yields of benzene, toluene, ethylbenzene, and propylbenzene were 2.9%, 3.9%, 15.6%, and 10.4%, respectively, and the total yield of 40.7% was almost the same as the yield of 40.3% from the first run, indicating that the catalyst could be used repeatedly to convert all three components of lignocellulosic biomass into corresponding chemicals.

## References

- [1] Yamaguchi, A., Sato, O., Mimura, N., Hirotsuki, Y., Kobayashi, H., Fukuoka, A., and Shirai, M. *Catal. Commun.* 54, 22 (2014).
- [2] Yamaguchi, A., Sato, O., Mimura, N., and Shirai, M. *Catal. Today* 265, 199 (2016).
- [3] Yamaguchi, A., Mimura, N., Shirai, M., and Sato, O. *Scientific Reports* 7, 46172 (2017).

# Pickering Emulsions as Compartmentalized Reaction Media for Catalysis

*Carolien M. Vis, Inorganic Chemistry and Catalysis, Debye Institute for Nanomaterials Science, Utrecht University, Utrecht, The Netherlands; Luc C.J. Smulders, Inorganic Chemistry and Catalysis, Debye Institute for Nanomaterials Science, Utrecht University, Utrecht, The Netherlands; Pierre-François Vittoz, Inorganic Chemistry and Catalysis, Debye Institute for Nanomaterials Science, Utrecht University, Utrecht, The Netherlands; Anne-Eva Nieuwelink, Inorganic Chemistry and Catalysis, Debye Institute for Nanomaterials Science, Utrecht University, Utrecht, The Netherlands; Bert M. Weckhuysen, Inorganic Chemistry and Catalysis, Debye Institute for Nanomaterials Science, Utrecht University, Utrecht, The Netherlands; Pieter. C.A. Bruijnincx, Organic Chemistry and Catalysis, Debye Institute for Nanomaterials Science, Utrecht University, Utrecht, The Netherlands.*

Compartmentalization, the physical separation of conflicting substances in one system, is an effective method to deal with chemical complexity. Nature, for instance, uses cell membranes to compartmentalize chemically incompatible reagents to perform multiple reactions simultaneously. Here, we report the use of Pickering emulsions (PEs), emulsions stabilized by solid particles, for the synthetic compartmentalization of (antagonistic) catalysts and explore the properties of these emulsions for catalysis. This strategy offers opportunities for process intensification and a more efficient and greener conversion of renewables. As most of the few reported applications of PE in catalysis typically involve very mild reaction conditions and do not focus on stability of the PE under reaction conditions, their broader applicability remains to be established.

We report for the first time the formation of water-in-oil PEs formulated with three different lignin-derived organic solvents, *i.e.* 2-isopropylphenol (IPP), 4-propylguaiaicol (PG) and 2-sec-butylphenol (SBP), and hydrophobic fumed silica. The stability of these emulsions and hence the window of operation for catalytic conversion was studied as function of temperature, salt and acid concentrations, to mimic typical conditions of, for example, biorefinery operations. The PG based emulsions proved most stable, tolerating salt (NaCl) concentrations up to 30 wt% and a pH of 1.3 for over a month. This PE can also withstand temperatures of up to 100



°C, the boiling point of the dispersed phase, for more than 1 hour. An increase of interfacial area and the ability for compartmentalization with a physical boundary between the two phases, are two of the benefits that PEs possess over traditional biphasic systems which can be useful in catalysis. For instance, we use these advantages to show that PEs can serve as reaction media for tandem reactions with antagonistic catalysts. This is highlighted for tandem acid-base catalysis using the deacetalization-Knoevenagel probe reaction. In this case, the acid and base catalysts are compartmentalized in the water and organic phases of the PE, respectively, avoiding the immediate quenching of the acid and base catalysts that would otherwise occur (figure 1a).

The benefit of the increased interfacial area can also be used in biomass upgrading reactions. We show by kinetic studies that the lignin-derived PEs show good potential for the extraction of HMF (figure 1b) generated in the acid catalyzed dehydration of fructose, a reaction for which rapid extraction from the water phase is required to obtain good yields.

Finally, we show that confining a catalyst in the dispersed phase and substrates and products in the continuous phase of a PE offers the potential of heterogenization of homogeneous catalyst and continuous flow, using a microfluidics approach as well as the equivalent of a fixed bed reactor used in heterogeneous catalysis. Together the results show that PE can be attractive media for catalysis and the more sustainable production of chemical building blocks.

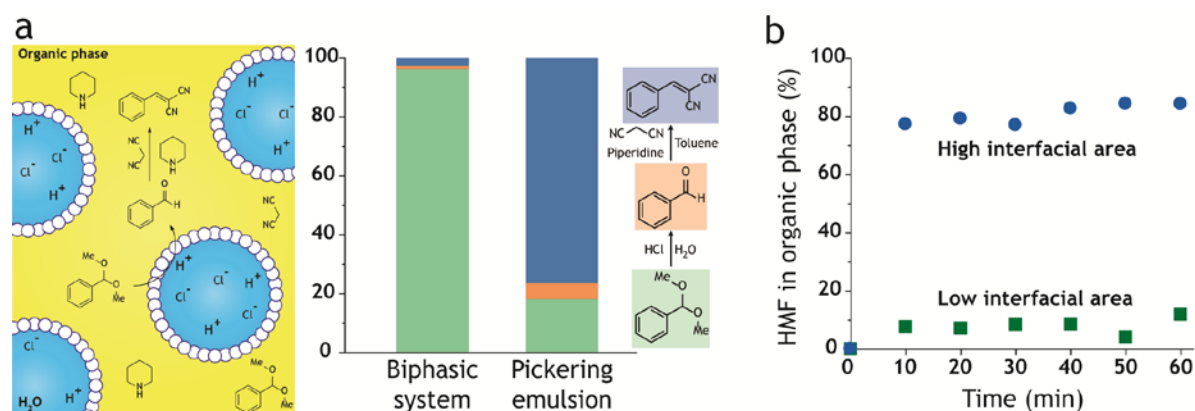


**Figure 1** a) Schematic representation of the deacetalization-Knoevenagel tandem reaction in a PE and product distribution of reaction mixtures in a traditional biphasic system and PE for this reaction. b) Influence of interfacial area of biphasic systems on the extraction of HMF from water to the lignin-derived organic solvents.

## **Obtaining enantiopure aliphatic amines by dynamic kinetic resolution utilizing ruthenium racemization catalysts.**

*Adriaensen K., Centre for Surface Chemistry and Catalysis, KU Leuven, Belgium;*  
*Vercammen J., Centre for Surface Chemistry and Catalysis, KU Leuven, Belgium; De*  
*Vos D.E., Centre for Surface Chemistry and Catalysis, KU Leuven, Belgium*

### **Introduction**

A large part of active pharmaceutical ingredients and agricultural components are best applied as their enantiopure forms, especially since other forms can cause undesired or even toxic (side) effects.[1] Obtaining enantiopure chemicals can be a difficult task, from synthesis to purification, due to the nearly identical physical properties of enantiomers. Separation is currently achievable by interaction with other chiral molecules (to form diastereomers) or with enantioselective catalysis.[2] An example of the latter is kinetic resolution, where a chiral catalyst (often an enzyme) selectively catalyses the conversion of one enantiomer to a product which can be easily separated by conventional methods such as precipitation, distillation or extraction. However, the main drawback of kinetic resolution and other separation methods is often that for every desired (isolated) enantiomer, the same amount of an undesired enantiomer is left over.[2-3]

The addition of a racemization catalyst in kinetic resolution systems has led to the conversion of the undesired enantiomer towards functionalized, desired product. The enzyme selectively functionalizes one enantiomer, while at the same time racemization assures that the ratio of unreacted enantiomers remains the same. As a result, the concentration of the undesired enantiomer decreases, while the desired form can be functionalized to a stable and separable product.

Many dynamic kinetic resolution systems exist for a wide array of substrates.[2-5] However, the dynamic kinetic resolution for aliphatic amines remains an unresolved challenge. Some systems for benzylic amines have had some moderate success on aliphatic substrates; but suffer from long reaction times, enzyme incompatibility, high catalyst loadings (> 5 mol%) and limited substrate scope.[6-8]

Hereby, we wish to present our initial results on a novel dynamic kinetic resolution system for aliphatic amines; studying racemization and kinetic resolution separately and in combination.

## Results and discussion

First, a suitable racemization catalyst was identified for the consecutive dehydrogenation/hydrogenation of an enantiopure substrate (*S*-2-aminooctane) – over an (short-lived) imine intermediate – by monitoring the enantiomeric excess (ee).[9] Starting with commercial ruthenium on carbon, a significant drop in ee was noted at high catalyst loadings (15 mol%). Further development of self-prepared ruthenium catalysts showed improved activity by dispersion of metallic Ru on alkaline spinel supports, in particular, magnesium aluminate. However, the Ru/spinel catalysts still required high catalyst loading. More success was found with zeolite supports. A wide array of zeolite topologies, both with Ru(III) and Ru(0), were screened. Surprisingly, the ionic ruthenium zeolites resulted in higher catalyst activities and thus lower enantiomeric excess.

Next, the kinetic resolution of aliphatic amines with enzymes was evaluated utilizing *Candida Antarctica* lipase B, a thermostable enzyme. Different resolution agents were investigated, such as esters and carbonates. Smaller, less hindered agents caused uncatalyzed, unselective conversion and alkylation, while larger resolution agents resulted in a highly selective turnover with minimal side-products.

Combination of both the racemization and the kinetic resolution system resulted in a selective dynamic kinetic resolution exceeding the kinetic resolution limit of 50%. Reaction conditions will be optimized to achieve the best results, at which point a wide substrate scope will be tested.

## References:

- [1]: Montalbetti, C. A. G. N.; Falque, V. *Tetrahedron* **2005**, *61*, 10827–10852
- [2]: Rachwalski, M.; Vermue, N.; Rutjes, F. P. J. T. *Chem. Soc. Rev.* **2013**, *42* (24), 9268–9282.
- [3]: Parvulescu, A.; Janssens, J.; Vanderleyden, J.; De Vos, D. *Top. Catal.* **2010**, *53* (13–14), 931–941.
- [4]: Verho, O.; Bäckvall, J. E. *J. Am. Chem. Soc.* **2015**, *137* (12), 3996–4009.
- [5]: Xiong, Z.; Pei, C.; Xue, peng; Lv, H.; Zhang, X. *Chem. Commun.* **2018**.
- [6]: Paetzold, J.; Bäckvall, J. E. *J. Am. Chem. Soc.* **2005**, *127* (50), 17620–17621.
- [7]: Parvulescu, A. N.; Jacobs, P. A.; De Vos, D. E. *Adv. Synth. Catal.* **2008**, *350* (1), 113–121.
- [8]: Kim, M.-J.; Kim, W.-H.; Han, K.; Choi, Y. K.; Park, J. *Org. Lett.* **2007**, *9* (6), 1157–1159.
- [9]: Parvulescu, A.; Vos, D. De; Jacobs, P. *Chem. Commun.* **2005**, No. 42, 5307.

# Influence of the Porosity of Carbon Supports on Catalytic Activity of Supported Gold Nanoparticles for Glucose Oxidation Reaction

*Milena Perovic<sup>1</sup>; Martin Oschatz<sup>1</sup>; Markus Antonietti<sup>1</sup>,*

*<sup>1</sup>Max Planck Institute of Colloids and Interfaces, Colloid Chemistry, 14476 Potsdam, Germany*

## Introduction

High surface area support materials play a crucial role in heterogeneous catalysis as they disperse and stabilize the catalytically active nanoparticles. Thus, they can have a significant influence on the activity and stability of the latter. Porous carbon materials are a versatile class of supports due to their high surface area, tailorable pore structure, and high chemical stability.[1] Precise control over their pore structure is crucial in order to tailor the sizes and distances of the deposited nanoparticles.[2] Gold nanoparticles (AuNPs) with size below 10 nm display exceptional catalytic activity, especially in selective oxidation reactions. One example where carbon-supported AuNPs show remarkable catalytic activity is the selective oxidation of D-glucose to D-gluconic acid in aqueous solution, using molecular oxygen.[3] Despite the large number of studies on such catalytic systems, profound understanding of the influence of the carbon porosity on the properties of gold catalysts for such reactions is still rare. A systematic study of the effect of the mesoporosity of chemically identical support materials on the catalysts' ability for conversion of glucose to gluconic acid will be reported.

## Results and Discussion

A series of salt-templated carbon materials (STCs) with tunable pore structure and high surface areas was synthesized by employing the salt template  $\text{ZnCl}_2$  as porogen and sucrose as a renewable carbon precursor (**Figure 1 a**).[4] Nitrogen adsorption isotherms display increasing amount of mesopores with increasing ratio of salt template, that is, from STC-1 to STC-8. Since the rather hydrophobic surface atomic structure of carbonaceous support materials has proven to stabilize smaller gold nanoparticles, all of the STCs were treated under reducing atmosphere for 2 h on 600 °C.[5] Colloidal AuNPs obtained by chemical reduction of tetrachloroauric acid in the presence of sodium citrate as a stabilizing agent were subsequently deposited on the STC supports.

Transmission electron microscopy shows that the size of AuNPs is comparable for the entire series of catalysts, with the average particle size in the range between 4.4 nm and 5.2 nm (**Figure 1 b**). The results of catalytic glucose oxidation suggest that the increasing amount of mesopores promotes the catalytic activity of AuNPs, leading to higher glucose conversion (**Figure 1 c**). As the average particle sizes do not seem to be dependent on the presence and the amount of mesopores, it is assumed that the available surface provided by mesopores leads to a better dispersion of AuNPs. This, in turn, affects the interaction with reactants and may slow down particle growth leading to faster conversion of glucose and enhanced stability of the catalysts.

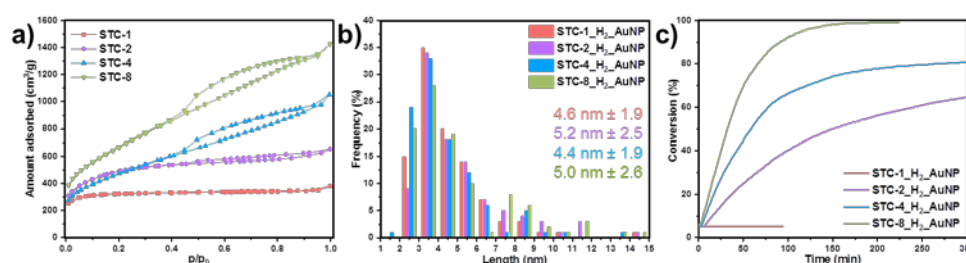


**Figure 1:** N<sub>2</sub> physisorption isotherms (at -196 °C) of STCs (a), particle size distributions of the catalysts together with the average particle sizes (b), and conversion vs. time diagram for glucose oxidation using the STC-supported catalysts (c).

## Conclusion

A series of AuNP catalysts supported on carbons of varying porosity and identical surface chemistry was presented. The increasing mesopore content lead to a higher catalytic activity, which can be ascribed to a better dispersion of the catalytically active phase. These results underline the importance of precise tailoring of porosity of a catalytic support.

## References

- [1] Serp, P., *Carbon Materials for Catalysis* **2009**, Hoboken, New Jersey: John Wiley & Sons, Inc.
- [2] Rodríguez-Reinoso, F., *Carbon* **1998**, 36, 3, 159-175.
- [3] Dimitratos, N., Lopez-Sanchez, J.A., and Hutchings, G.J., *Chemical Science* **2012**, 3, 1, 20-44.
- [4] Yan, R., Antonietti, M., and Oschatz, M., *Advanced Energy Materials* **2018**, 8, 1800026.
- [5] Lama, S. M. G., Schmidt, J., Malik, A., Walczak, R., Silva, D. V., Völkel, A., Oschatz, M., *ChemCatChem* **2018**, 10, 2458.

# Synergism of Au-Pd Bimetallic Nanoparticles for Nitrile Hydration and Nitrophenol Reduction

Podma Pollov Sarmah, Post Doctoral Fellow, Dibrugarh, India; Gauravijoti Dutta Kalita\*, Research Fellow, Dibrugarh, India; Pankaj Das, Professor, Dibrugarh, India  
Department of Chemistry, Dibrugarh University, Dibrugarh, Assam – 786004, India

\*E-mail: [chemgaurav10@gmail.com](mailto:chemgaurav10@gmail.com)

## Synergism in bimetallic nanoparticles

Bimetallic nanoparticles (BNPs) have witnessed an explosion of interests in recent years because of advances in synthesis and the unique chemical, mechanical, optoelectronic and catalytic properties of these materials. The potential applications of core-shell bimetallic nanoparticles (BNPs) are truly impressive, including computational technology [1], spectroscopic sensing [2], alternative energy [3], and the biological sciences [4]. The significant advantages of BNPs are a direct consequence of their distinctive surface properties arising from the phenomenon of synergistic effect.

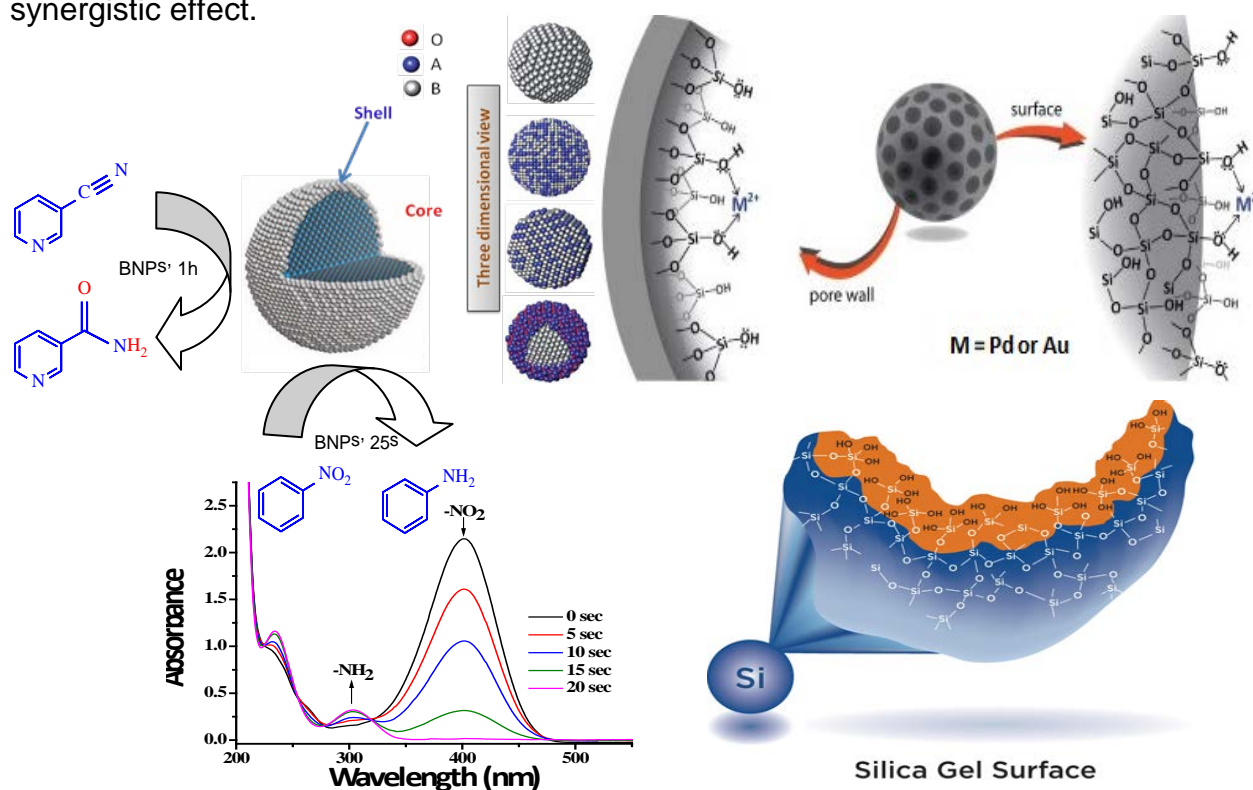


**Fig. 1** Figurative representation of bimetallic nanoparticles (BNPs) and their anchorage onto functionalized silica gel surface through the pore walls; catalytic applications in nitrile hydration and nitrophenol reduction

Immobilization of these BNPs into appropriate supporting material can greatly enhance their structural stability, surface active site count and thereby improve the catalytic efficiency. In the present work, Au-Pd BNPs supported on 2-diphenylphosphinoethyl (2-DPPE) functionalized silica gel support were synthesized via a suitable wet-impregnated galvanic replacement reaction followed by successive reduction at room temperature in water. The as synthesized bimetallic core-shell nanoparticles, viz. DPPE@Au@Pd were calcined at 400<sup>0</sup>C and characterized using PXRD, HAADF-STEM, FESEM-EDS, Single-atom trace imaging and XPS analysis. The material was screened for the catalytic hydration of nitriles to amides with *i*-PrOH: Water (3:1) as solvent and Cs<sub>2</sub>CO<sub>3</sub> as base at 50<sup>0</sup>C for 1h. The texture and activity of the material was compared with its monometallic counterparts i.e., DPPE@Pd, DPPE@Au and also the non-calcined material, DPPE@Au@PdNPs synthesized under similar experimental protocols. The reactivity order directly emulates from the 'synergistic effect' of the Pd core embedded within the Au shell: DPPE@Au@Pd(C) > DPPE@Au@Pd > DPPE@Pd > DPPE@Au. The bimetallic catalyst was recycled several times and was found to be active without any significant loss of efficiency. The synergism as speculated was also evident for the reduction of 4-nitrophenol (4-NP) to 4-aminophenol (4-AP) in water at room temperature and a range of nitrophenols and other nitroarenes were converted to corresponding amines.

## References

- [1] S. J. Mejia-Rosales, C. Fernandez-Navarro, E. Perez-Tijerina, D. A. Blom, L. F. Allard, M. Jose-Yacaman *J. Phys. Chem. C* **2007**, *111*, 1256-1260
- [2] N. Li, A. Tittl, S. Yue, H. Giessen, C. Song, B. Ding, N. Liu, *Nature* **1997**, *389*, 364
- [3] M. Oezaslan, F. Hasché, P. Strasser, *J. Phys. Chem. Lett.* **2013**, *4*, 3273–3291
- [4] K. Jagajjanani Rao and S. Paria, *ACS Appl. Mater. Interfaces* **2015**, *7*, 14018–14025

# Selective Silylation of Aryl halides by Supported Palladium-Gold Alloy Catalysts

*Yosuke Masaki<sup>1</sup>; Hiroki Miura<sup>1,2,4</sup>; Tetsuya Shishido<sup>1,2,3,4</sup>*

*<sup>1</sup>Department of Applied Chemistry for Environment, Graduate School of Urban Environmental Sciences, Tokyo Metropolitan University, Hachioji, Tokyo, Japan*

*<sup>2</sup>Research Center for Hydrogen Energy-based Society, Tokyo Metropolitan University, Hachioji, Tokyo, Japan*

*<sup>3</sup>Research Center for Gold Chemistry, Tokyo Metropolitan University, Hachioji, Tokyo, Japan*

*<sup>4</sup>Elements Strategy Initiative for Catalysts & Batteries, Kyoto University, Kyoto, Japan*

## Introduction

Arylsilane is widely used as raw materials for functional materials and intermediates for various organic reactions. The traditional method for preparing arylsilanes is nucleophilic substitution of chlorosilanes with organolithium or Grignard reagents. However, there remain some problems such as preparation of organometallic reagents and the limitation of substrates. In contrast, silylation of aryl halides with hydrosilane by Pd[1] or Rh[2] complex catalysts is an excellent method for synthesizing arylsilanes without using organometallic reagents. Although iodides and bromides are mainly employed as a substrate, few reports for the application of aryl chlorides have been appeared. On the other hand, it is important to apply heterogeneous catalyst which is easy to separate from reaction solution and can be reuse in terms of environmental chemistry. In this study, we found that selective silylation of aryl chlorides with hydrosilane proceeded efficiently by supported Pd-Au alloy catalysts.

## Results and Discussion

A series of supported Pd-Au alloy catalysts was prepared through sol-immobilization method[3]. The reactions of aryl halide (**1**) with 5 equiv. of triethylsilane (**2a**) in the presence of supported Pd-Au alloy catalysts with different metal ratios were investigated (Table 1). Au/C showed no catalytic activity for the reaction of chlorobenzene (entry 1). The reduction of substrate mainly proceeded to give



benzene (**4a**) in the presence of Pd/C (entry 4). In contrast, supported Pd-Au alloy catalysts gave the corresponding arylsilane **3aa** selectively, and the selectivity for **3aa** increased with decreasing Pd/Au atomic ratio (entries 2 and 3). Interestingly, arylsilanes were obtained selectively from chlorobenzene, while the reactions of bromo- and iodobenzene by 1Pd6Au/C resulted in low selectivities for arylsilane (entries 5 and 6). Among the supports for Pd-Au alloy tested, ZrO<sub>2</sub> supported catalysts showed the highest activity (entry 7). Under the optimized reaction conditions, the reactions of a variety of aryl chlorides with hydrosilanes were investigated (Table 2). 1Pd6Au/ZrO<sub>2</sub> showed high catalytic activity for silylation of various aryl chlorides with hydrosilanes to give the corresponding arylsilanes in good to high yields (entries 2-6). In addition, the present Pd-Au catalyst was also applicable to the silylation of heteroaromatic chlorides (entry 7).

Table 1. Silylation of aryl halides

Entry	Catalyst	X	Yield [%] <sup>a</sup>		Selec. [%] <sup>b</sup>
			<b>3aa</b>	<b>4a</b>	<b>3aa</b>
1	Au/C	Cl	0	0	0
2 <sup>c</sup>	1Pd6Au/C	Cl	19 (66)	4 (19)	84 (77)
3	1Pd1Au/C	Cl	40	56	42
4	Pd/C	Cl	11	82	12
5	1Pd6Au/C	Br	37	32	54
6	1Pd6Au/C	I	1	39	2
7	1Pd6Au/ZrO <sub>2</sub>	Cl	56	16	78

<sup>a</sup> GC yield, <sup>b</sup> (**3aa**)/(**3aa**+**4a**).

<sup>c</sup> In parentheses, GC yield and selectivity after 5 h.

Table 2. Scope of substrates

Entry	Aryl chloride	Hydrosilane	Products	Yield [%] <sup>a</sup>
1	<b>(1a)</b>	HSiEt <sub>3</sub> ( <b>2a</b> )	<b>(3aa)</b>	77
2	<b>(1a)</b>	HSi( <i>i</i> Pr) <sub>3</sub> ( <b>2b</b> )	<b>(3ab)</b>	34 <sup>b</sup>
3	<b>(1b)</b>	HSiEt <sub>3</sub> ( <b>2a</b> )	<b>(3ba)</b>	61
4	<b>(1c)</b>	HSiEt <sub>3</sub> ( <b>2a</b> )	<b>(3ca)</b>	63
5	<b>(1d)</b>	HSiEt <sub>3</sub> ( <b>2a</b> )	<b>(3da)</b>	61
6	<b>(1e)</b>	HSiEt <sub>3</sub> ( <b>2a</b> )	<b>(3ea)</b>	70
7	<b>(1f)</b>	HSiEt <sub>3</sub> ( <b>2a</b> )	<b>(3fa)</b>	80 <sup>b</sup>

<sup>a</sup> GC yield, <sup>b</sup> Isolated yield

## References

- [1] A. S. Manoso, P. D. Shong, *J. Org. Chem.* **2001**, *66*, 7449-7455.
- [2] M. Murata, M. Ishikura, M. Nagata, S. Watanabe, Y. Masuda, *Org. Lett.* **2002**, *11*, 1843-1845.
- [3] H. Miura, K. Endo, R. Ogawa, T. Shishido, *ACS Catal.* **2017**, *7*, 1543-1553.

# **An amberlite anion-exchange resin as a metal-free heterogeneous catalyst for the conversion of CO<sub>2</sub> with epoxides into cyclic carbonates**

*Yasser Alassmy and Paolo P. Pescarmona*

Chemical Engineering Group, University of Groningen, Nijenborgh 4, 9747 AG,  
Groningen, The Netherlands

[y.alassmy@rug.nl](mailto:y.alassmy@rug.nl)

Carbon dioxide has been recognised as an environmentally friendly C<sub>1</sub> building block because of its low-toxicity, availability, low cost and renewability. On the other hand, CO<sub>2</sub> has a high thermodynamic stability that makes its conversion quite challenging. To overcome this issue, carbon dioxide could be reacted with high free energy substrates such as H<sub>2</sub>, amines, and epoxides.<sup>[1,2]</sup> Among these options, the reaction of CO<sub>2</sub> with epoxides to produce cyclic carbonate has been receiving growing attention (Figure 1, A), because the cyclic carbonates are important compounds in organic chemistry, and they have relevant applications as intermediates for the preparation of fine chemicals and polymers, as green aprotic polar solvent, and as electrolytes in Li-ion batteries.<sup>[3,4]</sup>

Herein, we present an efficient, easily recyclable and readily-available metal-free heterogeneous catalyst for the reaction of CO<sub>2</sub> with epoxides to produce cyclic carbonates under mild conditions (80 °C, 10 bar of CO<sub>2</sub>, 18h). This catalytic system consists of amberlite ion-exchange resins in beads form with different functional groups such as trimethyl ammonium halide (IRA 900) and dimethyl ethanol ammonium halide (IRA 910) that act as active sites (Figure 1, B). Additionally, the presence of water as a hydrogen bond donor co-catalyst (HBD) was investigated. The beads form allow to recover the catalyst easily by simple filtration. These commercially available ion-exchange resins in chloride form were simply converted into iodide form by one step-ion exchange reaction with potassium iodide, since iodide anion typically exhibits high catalytic activity in the presence of water. Then, we tested the influence of different parameters such as the amount of water, CO<sub>2</sub> pressure and temperature on the catalytic system activity. The results demonstrated that by tuning the amount of water and using a lower pressure of CO<sub>2</sub>, we could

enhance the catalytic system activity, leading to achieve the conversion of CO<sub>2</sub> into several cyclic carbonates in high yield with an excellent selectivity under mild conditions. The highest catalyst activity was found with Amberlite IRA 910 due to its structure which contains an OH group and this OH group along with water play an important role on activating the oxygen atom of epoxide through hydrogen bonding interaction, thus promoting the nucleophilic attack by the halide leading to the ring opening of the epoxide easily.<sup>[3]</sup> Because of its OH group, this catalyst also showed high activity even in the absence of water, allowing to achieve high yield of styrene and propylene carbonates (57 % and 84 % respectively) with ≥ 99 % selectivity. The resins bead catalysts could be reused without losing their catalytic activities.

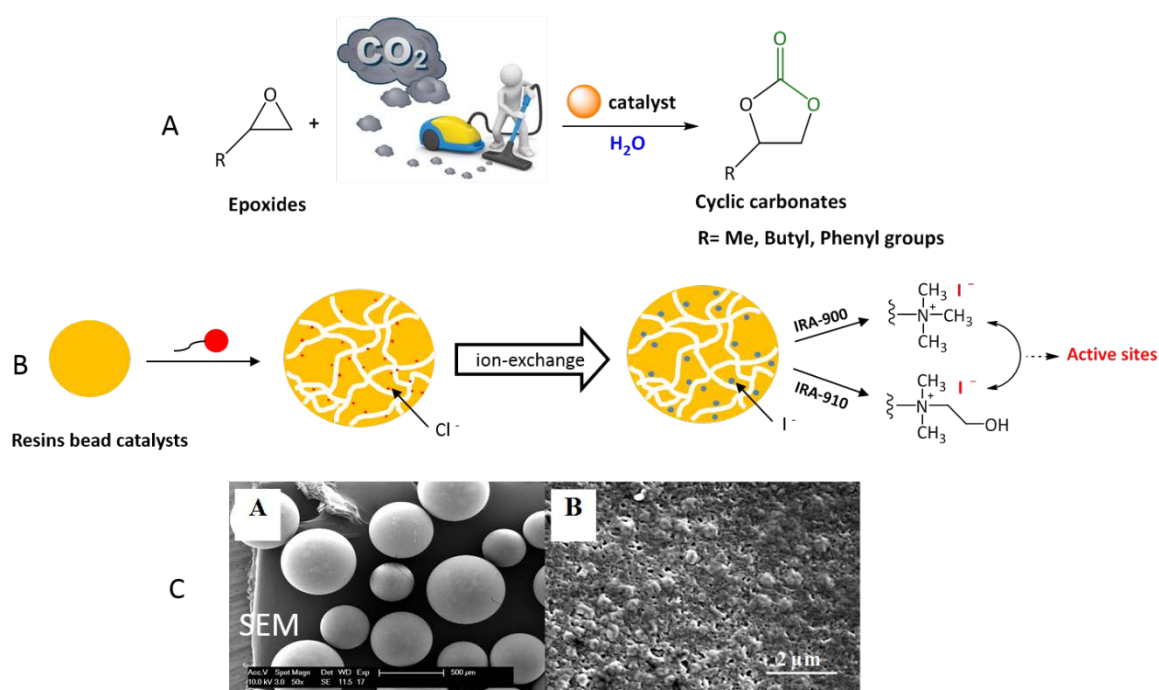


**Figure 1. A)** the synthesis of cyclic carbonates from CO<sub>2</sub> and epoxides using amberlites as metal-free heterogeneous catalysts. **B)** ion exchange resins bead reaction for amberlite IRA 900 and 910. **C)** SEM image of polymeric resin bead,(left image) and surface morphology,(right image) for Amberlite® IRA-900 chloride form.

#### References:

- [1] M. Alves, B. Grignard, R. Mereau, C. Jerome, T. Tassaing, C. Detrembleur, *Catal. Sci. Technol.* **2017**, 7, 2651–2684.
- [2] P. P. Pescarmona, M. Taherimehr, *Catal. Sci. Technol.* **2012**, 2, 2169.
- [3] M. Cokoja, M. E. Wilhelm, M. H. Anthofer, W. A. Herrmann, F. E. K??hn, *ChemSusChem* **2015**, 8, 2436–2454.
- [4] Y. Du, F. Cai, D. L. Kong, L. N. He, *Green Chem.* **2005**, 7, 518–523.

# CuZn catalysts activity dependence on calcination temperature

*Violetta Pospelova<sup>1</sup>, Jaroslav Aubrecht<sup>1</sup>, Oleg Kikhtyanin<sup>2</sup>, David Kubička<sup>1,2</sup>*

<sup>1</sup>*University of Chemistry and Technology, Prague, Czech Republic;*

<sup>2</sup>*Technopark UCT, Kralupy nad Vltavou, Czech Republic;*

## Introduction

A replacement of  $\text{CuCr}_2\text{O}_4$  catalysts for ester hydrogenolysis is sought intensively [1] to reduce the environmental risks of chromium-containing waste production. CuZn-based catalysts have shown a good activity in ester hydrogenolysis [1, 2]. However, there is a lack of studies devoted to optimization of their activity in ester hydrogenolysis. One of the optimization parameters is calcination temperature. It has been found that the CuZn catalyst activity was dependent on the CuO and ZnO particle sizes that were influenced by the calcination temperature [3]. Thus, we have investigated the effect of calcination temperature of a CuZn catalyst on its activity in ester hydrogenolysis using a batch reactor.

## Experimental

A single CuZn (Cu/Zn=1.5) precursor was prepared by co-precipitation. It was calcined in static air atmosphere at a broad range of temperatures: 220, 250, 300, 350, 400, and 450 °C and then reduced in hydrogen atmosphere at 220 °C. The catalysts were characterized by XRD. Then, the catalysts were tested at 220 °C and hydrogen pressure of 10 MPa in a batch reactor in dimethyl adipate hydrogenolysis (Figure 1).

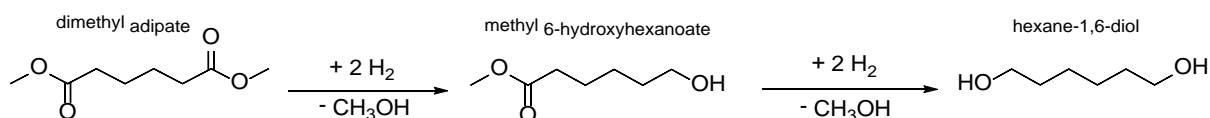


Figure 1. Overall reaction of dimethyl adipate hydrogenolysis

## Results and discussion

The as-prepared, calcined and spent catalysts were characterized by XRD. The as-prepared catalyst consisted of a mixture of aurichalcite and zincian malachite phases. After the calcination, the hydroxycarbonates phases were decomposed gradually with the increasing temperature. As the temperature increased, the crystallite size of ZnO and CuO increased as well. As seen in Figure 2A, the influence of temperature on the dimethyl adipate conversion was significant. The

samples calcined at the highest temperature showed the lowest conversion that could be explained by the large size of crystallites (Figure 2B). Non-calcined catalyst had conversion comparable to the samples calcined at low temperature. In terms of selectivity to the main product, there was the same trend for all samples and the selectivity was dependent on conversion as previously described [4].

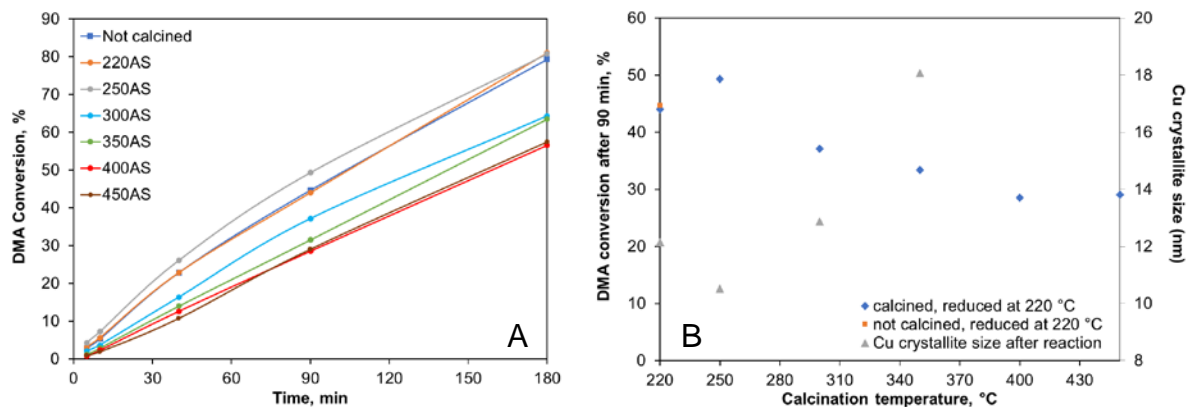


Figure 2A. Conversion of dimethyl adipate (DMA) for samples calcined at different temperatures in air  
Figure 2B. DMA conversion dependence on Cu crystallite size after reaction and calcination temperature

## Conclusion

In this study, we describe the effect of calcination temperature on activity of CuZn catalyst. It was confirmed that a complete decomposition of hydroxycarbonates occurred over 325 °C. However, the samples calcined at temperature under 325 °C showed the highest conversion with similar selectivity to the main product. It could be suggested that residual hydroxycarbonates that were found by XRD have a beneficial effect on activity.

## References

1. Yuan, P., et al., *Highly efficient Cu–Zn–Al catalyst for the hydrogenation of dimethyl adipate to 1,6-hexanediol: influence of calcination temperature*. Reaction Kinetics Mechanisms and Catalysis, 2010. **100**: p. 427-439.
2. Kikhtyanin, O., et al., *Effect of Calcination Atmosphere and Temperature on the Hydrogenolysis Activity and Selectivity of Copper-Zinc Catalysts*. Catalysts, 2018. **8**(10): p. 446.
3. Fujita, S.-i., et al., *Preparation of a coprecipitated Cu/ZnO catalyst for the methanol synthesis from CO<sub>2</sub> — effects of the calcination and reduction conditions on the catalytic performance*. Applied Catalysis A: General, 2001. **207**(1): p. 121-128.
4. Kubička, D., et al., *On the importance of transesterification by-products during hydrogenolysis of dimethyl adipate to hexanediol*. Catalysis Communications, 2018. **111**: p. 16-20.

# Dimethyl Adipate Hydrogenolysis as Another Application of CuZnAl Catalysts

Jaroslav Aubrecht<sup>1</sup>, Violetta Pospelova<sup>1</sup>, Oleg Kikhtyanin<sup>2</sup> and David Kubička<sup>1,2</sup>

<sup>1</sup>University of Chemistry and Technology, Prague, Czech Republic;

<sup>2</sup>Technopark UCT, Kralupy nad Vltavou, Czech Republic;

## Introduction

Catalysts containing copper, zinc and aluminium have been extensively used in methanol production from synthesis gas or water-gas shift reaction for several decades [1, 2]. However, they have a much broader application potential. Here we report their use in dimethyl adipate hydrogenolysis. Although in this industrial process copper-chromium-based catalysts called “Adkins catalysts” are widely used [3], the industry faces a demanding disposal of waste solution containing chromium from catalyst production and the European ban of chromium-containing catalysts.

## Experimental

For this purpose, two series of CuZnAl catalysts with different copper, zinc and aluminium content were prepared by co-precipitation. During the preparation two different pH values were used, namely pH = 7 (precipitation by Na<sub>2</sub>CO<sub>3</sub>) and pH = 9 (precipitation by KOH with K<sub>2</sub>CO<sub>3</sub>), to observe influence of the pH on the catalyst structure. These precipitates were then calcined in air at 350 °C and reduced in hydrogen at 220 °C. The catalysts were characterized prior and after each treatment by different methods (e.g. XRD, H<sub>2</sub>-TPR, nitrogen physisorption or TGA-MS).

All reduced catalysts were tested in a fixed-bed reactor in dimethyl adipate hydrogenolysis to yield hexane-1,6-diol. In this study, a temperature range of 160–205 °C and a pressure range of 80-160 bar were tested.

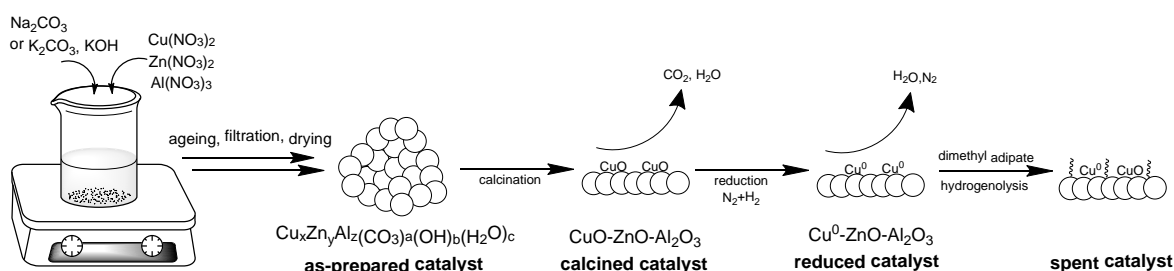
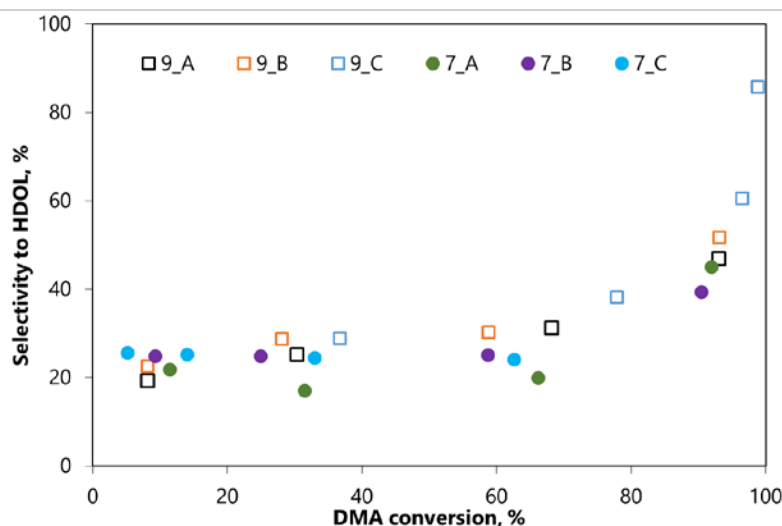


Figure 1. Preparation of the catalyst

## Results and discussion

The XRD study revealed that the hydrotalcite-like structure  $\text{Zn}_{0.66}\text{Al}_{0.34}(\text{OH})_2 \cdot (\text{CO}_3)_{0.17}(\text{H}_2\text{O})_{0.7}$  was the main phase in all as-prepared catalysts. Moreover, the catalysts precipitated by  $\text{Na}_2\text{CO}_3$  contained other copper-zinc hydroxyl-carbonates while CuO and ZnO were found in catalysts precipitated by KOH with  $\text{K}_2\text{CO}_3$ . The calcination at 350 °C converted these catalyst precursors to mixed oxides with only CuO being a crystalline phase in the first case and into a mixture of CuO and ZnO in the second case. The TPR results indicated that only 50-60% of copper was reduced. At the dimethyl adipate conversion under 80 % the selectivity to the hexane-1,6-diol reached only 30 %, then the yield of hexane-1,6-diol steeply increased (Fig. 2). The comparison of both catalyst groups clearly shows that over catalysts prepared at pH 9 higher DMA conversion was reached.



**Figure 2.** Comparison of selectivity to HDOL development for all tested catalysts. HDOL – hexane-1,6-diol, DMA – dimethyl adipate

## Conclusion

An increase in pH from 7 to 9 limited the formation of hydroxycarbonates and led to CuO and ZnO formation. As a result, DMA conversion was higher over catalysts prepared by pH 9.

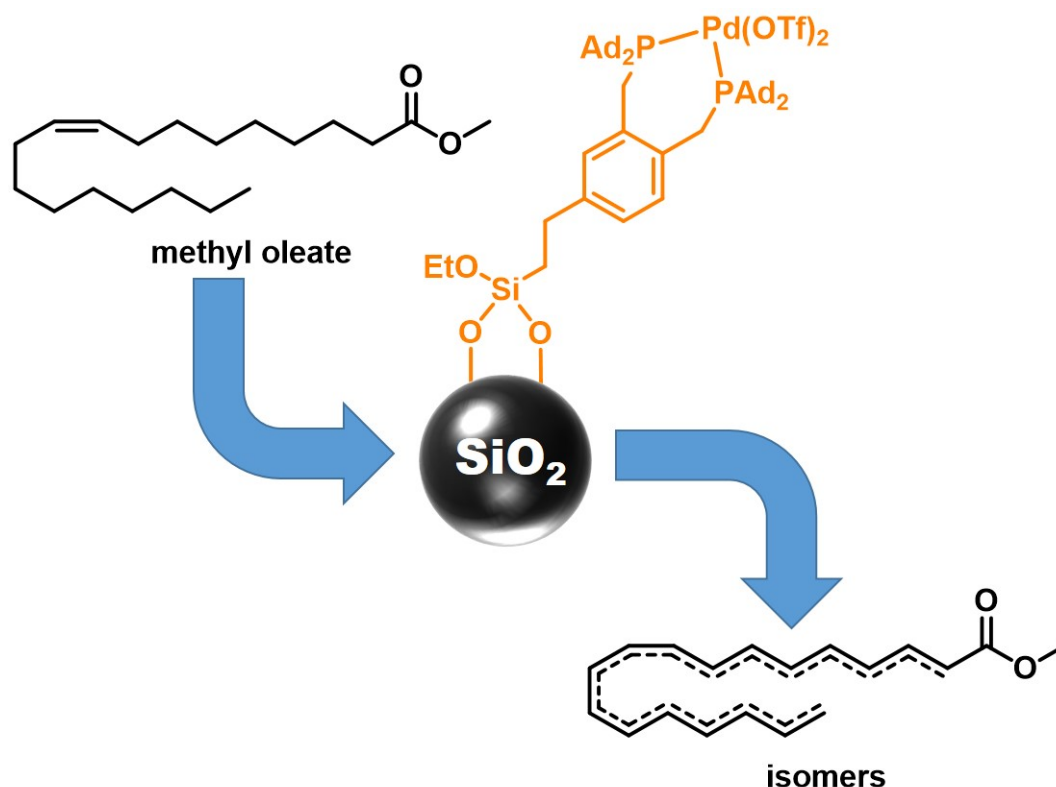
## References

1. Behrens, M. and R. Schloegl, *How to Prepare a Good Cu/ZnO Catalyst or the Role of Solid State Chemistry for the Synthesis of Nanostructured Catalysts*. *Zeitschrift Fur Anorganische Und Allgemeine Chemie*, 2013. **639**(15): p. 2683-2695.
2. Stone, F.S. and D. Waller, *Cu-ZnO and Cu-ZnO/Al<sub>2</sub>O<sub>3</sub> Catalysts for the Reverse Water-Gas Shift Reaction. The Effect of the Cu/Zn Ratio on Precursor Characteristics and on the Activity of the Derived Catalysts*. *Topics in Catalysis*, 2003. **22**(3): p. 305-318.
3. Turek, T. and D.L. Trimm, *The catalytic hydrogenolysis of esters to alcohols*. *Catalysis Reviews-Science and Engineering*, 1994. **36**(4): p. 645-683.

## Immobilized Molecular Catalysts for Lipid Isomerization

*Felix Einsiedler, Stefan Mecking, Chair of Chemical Material Science University of Konstanz, Konstanz, Germany.*

Fatty acids, as a renewable raw material, comprise long methylene sequences which can serve as a source of (functionalized) hydrocarbons. [1] In detail, the double bond functionality of unsaturated fatty acids can be used synthetically to obtain mid-chain olefinic compounds via alkenolysis. [2] In this context, prior isomerization of the internal double bond can drastically increase the number of accessible product chain lengths. One particular class of catalysts showing high activity in this isomerization are palladium (II) compounds bearing chelating diphosphine ligands. [3] However, these have commonly been used as soluble homogeneous catalysts. In order to enable continuous-flow approaches, heterogenized versions of these molecular catalysts are necessary. [4] We report on the successful immobilization of the bis(diadamantyl phosphino)-*o*-xylene palladium (II) triflate catalyst on mesoporous silica and its use in the isomerization of methyl oleate under mild conditions.



### References

1. Biermann, U.; Bornscheuer, U.; Meier, M. A. R.; Metzger, J. O.; Schäfer, H. J., *Angew. Chem. Int. Ed.* **2011**, *50* (17), 3854-3871.
2. Ohlmann, D. M.; Tschauer, N.; Stockis, J.-P.; Gooßen, K.; Dierker, M.; Gooßen, L. J., *J. Am. Chem. Soc.* **2012**, *134* (33), 13716-13729.
3. Roesle, P.; Caporaso, L.; Schütte, M.; Goldbach, V.; Cavallo, L.; Mecking, S., *J. Am. Chem. Soc.* **2014**, *136* (48), 16871-16881.
4. Cozzi, F., *Adv. Synth. Catal.* **2006**, *348* (12-13), 1367-1390.



# **Analysis of decisive structural parameters of zeolites for alkylation of benzene with ethylene**

*Somayeh F. Rastegar, Galina Sadovska, Jaroslava Moravkova, Radim Pilar, Petr Sazama*

*J. Heyrovsky Institute of Physical Chemistry, Academy of Sciences of the Czech Republic, Dolejskova 3, 182 23 Prague, Czech Republic*

## **1. Introduction**

The alkylation of benzene with light hydrocarbons over acidic catalysts for production of alkylaromatics is a process of industrial significance [1]. Zeolites have been proven to have superior catalytic performance for the liquid phase alkylation of benzene with ethylene without disadvantages of other acidic catalysts (e.g.; contamination of the alkyl aromatic products with chlorinated compounds). This report describes analysis of the effect of the zeolite structure, number of acid sites, and reaction conditions on the activity and selectivity in complex reactions of benzene alkylation with ethylene.

## **2. Experimental**

Al-rich beta zeolite with Si/Al ratio 4.5, denoted as BEA/4.5, was hydrothermally synthesized by an organotemplate-free synthesis [2]. The USY/6 and MOR/5 zeolites and high-silica beta zeolites BEA/12.5 and BEA/18 were kindly supplied by Zeolyst International. All the materials were characterised by XRD, N<sub>2</sub> adsorption at -196 °C, SEM, <sup>27</sup>Al and <sup>29</sup>Si MAS NMR, XPS and FTIR spectroscopy. The alkylation of benzene with ethylene was performed for 3 hours at temperature of 180° C and the constant pressure of 40 bar with continuous adding of ethylene.

## **3. Results and discussions**

Conversion, yield and selectivity were analysed over faujasite (FAU/6), beta (BEA/4.5) and mordenite (MOR/5) zeolites with comparable concentrations of acid sites to understand the role of the channel structures in the alkylation of benzene with ethylene (Fig. 1). The results indicate that the geometry and dimensionality of the channel system of zeolites play a decisive role in the activity and selectivity. The higher activity and selectivity of BEA relative to other zeolites is related to well accessible acid sites in the shape-selective environment of the three-dimensional channel system with 12-member ring openings. The lack of the shape-selectivity in the supercages of FAU zeolite increased the yield of by-products in expense of EB.

The accessibility of acid sites in 8-ring and mono-dimensional 12-ring channels in MOR are diffusion restricted and the efficiency of the catalytic process is strongly limited by mass transfer effects.

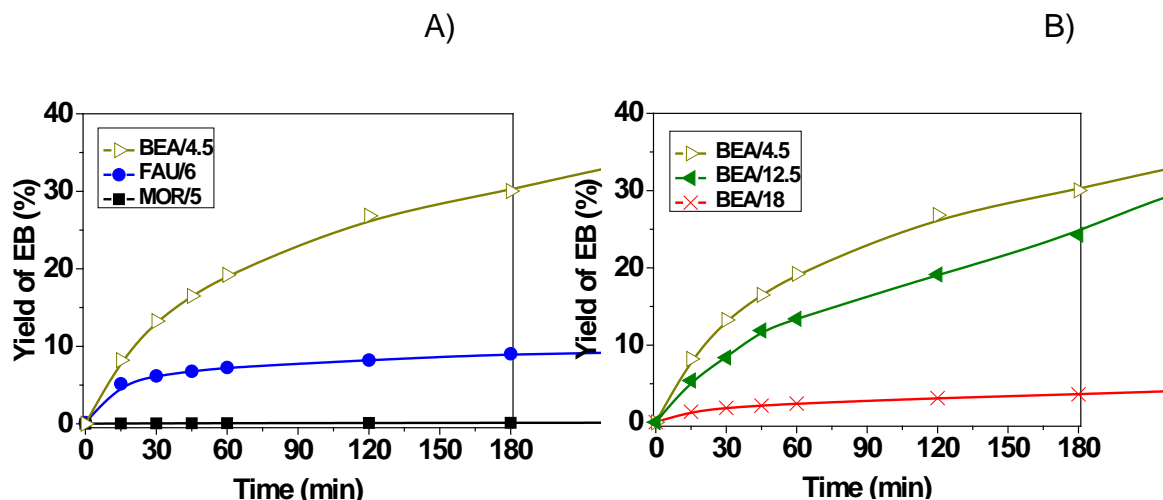


Figure 1. A) The effect of zeolite structure and B) concentration of acid sites on the EB yield in the alkylation of benzene with ethylene.

The strength and concentration of Brønsted acidic sites in the zeolite are assumed to be responsible for activity in the alkylation reaction. We analysed the effect of an increase in the density of the acidic protons in the Al-rich beta zeolites on the activity and selectivity. A high density of OH groups in the Al-rich H-\*BEA zeolite (Si/Al ~ 4) results in a significant increase in the EB yield due to higher activity and selectivity compared to the hitherto most active Si-rich zeolite catalysts.

#### 4. Conclusions

Well accessible acid sites in the shape-selective environment of the three-dimensional channel system with 12-member ring openings in BEA zeolites provide high activity and selectivity in alkylation of benzene with ethylene. The high concentration of Brønsted acidic sites in the highly regular structure of Al-rich beta zeolite are directly manifested in enhanced activity compared with conventional Si-rich beta zeolite.

#### References

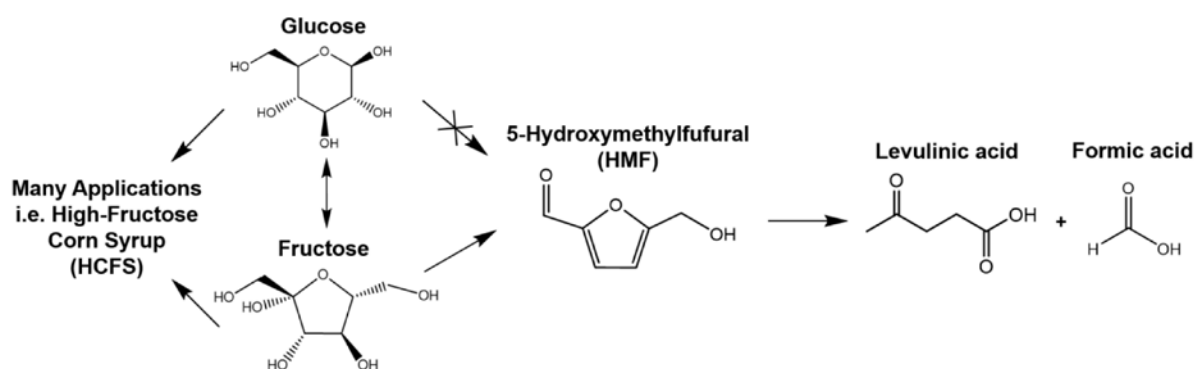
1. Sazama, P.; Wichterlova, B.; Sklenak, S.; Parvulescu, V. I.; Candu, N.; Sadovska, G.; Dedecek, J. et al. *J. Catal.* 2014, 318, 22.
2. Sazama, P.; Kaucky, D.; Moravkova, J.; Pilar, R.; Klein, P.; Pastvova, J. et al. *Appl. Catal. A: General* 2017, 533, 28.

# Novel and highly efficient Ga doped zeolite catalysts for the isomerisation of glucose to fructose: a new route to platform chemicals from sugars

*Marco Conte\**, Dedi Sutarma, Philippa James, University of Sheffield, Sheffield, UK; Naoko Sano, Nara Women's University, Nara, Japan; Xi Liu, State Key Laboratory of Coal Conversion, Institute of Coal Chemistry, Taiyuan, PR China.

## Introduction

The conversion of glucose into fructose for the production of high-fructose corn syrups is among the largest biocatalytic process worldwide, and it also represents a crucial intermediate step for the conversion of biomass to fuels and platform chemicals [1] and Scheme 1.



**Scheme 1:** isomerization of glucose to fructose as and further evolution to platform chemicals.

This reaction is typically catalysed by immobilized enzymes, a process which, however has high manufacturing costs, and requires the use of buffering solutions within a narrow operating temperature and in turn low productivity. In this context, and to tackle these drawbacks, it would be extremely beneficial to have a heterogeneous catalyst capable to catalyse this reaction. Current state of the art shows that Sn doped zeolites, and especially Sn/BEA zeolites, are highly active materials for the isomerization of glucose to fructose. Herein, we propose Ga doped zeolites [2] and by using commercially available zeolite Y as support, as a powerful alternative to currently employed Sn based catalysts, which currently represent the gold standard in this area [3].

## Materials and method

Metal doped zeolites were prepared by using a straightforward wetness impregnation protocol, and by subjecting the impregnated zeolites from Ga and Sn metal salt precursors, to an array of calcination steps from 120 °C to 550 °C. Catalytic activity

tests were performed in a customised batch reactor using CH<sub>3</sub>OH and CH<sub>3</sub>OH/H<sub>2</sub>O mixtures, in a temperature range from 80 °C to 110 °C, and a M: S (Metal: Substrate) ratio of 1:100. Characterization of the reaction mixtures was carried out by HPLC and H NMR. The catalysts were characterised by using an array of advanced techniques including: HR-TEM, XPS, NH<sub>3</sub> chemisorption as well as SS-NMR by analysing the dynamic of the sugars inside the pores of the zeolites.

## Results and discussion

Ga/Y zeolites were capable to show a similar activity to currently used Sn/Y zeolites (figure 1), and if Ga and Sn were simultaneously present, these were presenting a synergistic effect when bimetallic catalysts were used. Furthermore a striking feature of our materials was that whereas in Sn/Y catalyst, Sn (present as SnO<sub>2</sub>) was mainly distributed outside the pores of the zeolites, Ga (present as Ga<sub>2</sub>O<sub>3</sub>) was mainly distributed inside the pores of the zeolites (figure 2)

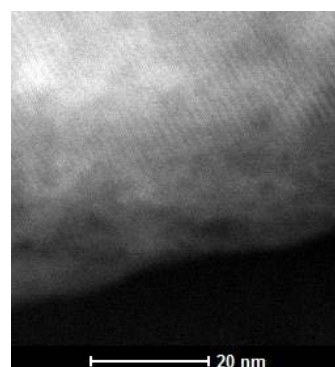
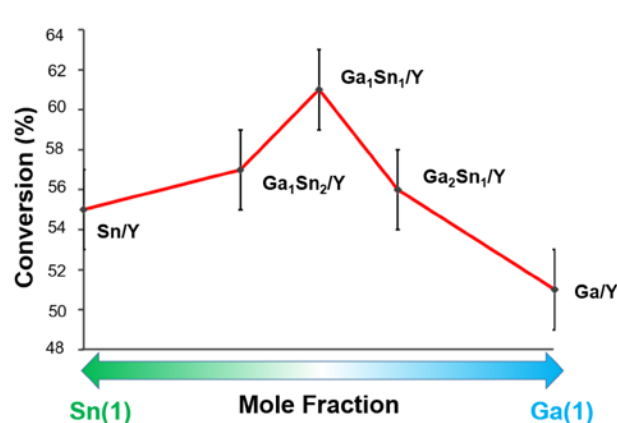


**Figure 1:** glucose conversion to fructose for CH<sub>3</sub>OH/H<sub>2</sub>O reaction mixtures, by using a M:S 1:100 a reaction temperature of 100 °C and endogenous pressure.

**Figure 2:** HR-TEM of a Ga/Y zeolite used for the catalytic tests reported in figure 1.

## Conclusions

It was possible to obtain highly active Ga/Y catalysts for the isomerization of glucose to fructose by using a straightforward preparation method and mild reaction conditions. This for a material capable to display catalytic performances of the same entity of established Sn-catalysts. We believe this work has a great potential, and will strongly contribute to the synthesis of platform chemicals from sugars.

## References

- [1] Y. Román-Leshkov, M. Moliner, J.A. Labinger and M.E. Davis, *Angew. Chem. Int. Ed.*, 2010, **49**, 8954–8957.
- [2] D. Sutarma, P. James, N. Sano, X. Liu and M. Conte, *in preparation*.
- [3] I. Delidovich and R. Palkovits, *ChemSusChem*, 2016, **9**, 547–561.

## Evolution of active metal sites in Pt- and Pd- functionalized metal-organic frameworks

A.L. Bugaev, A.A. Skorynina, A.V. Soldatov, *The Smart Materials Research Institute, Southern Federal University, Rostov-on-Don, Russia;*

A. Lazzarini, U. Olsbye, K. P. Lillerud, *University of Oslo, Oslo, Norway;*

C. Lamberti, *Department of Physics, University of Turin, Turin, Italy*

Using noble metals to functionalize metal-organic frameworks (MOFs) is a promising way for constructing new materials for catalytic application [1, 2]. Although numerous successful synthesis of MOFs functionalized by metal ions and metal nanoparticles were reported, the exact mechanisms of structural evolution of the metal sites in many cases is still unknown. Determination of these mechanisms as well as investigation of the intermediate active sites formed during the synthesis is important for tailoring the specific catalytic properties of materials. In this work, we investigate structural changes in UiO-67 functionalized by Pd and Pt depending on the activation conditions by a combination of theoretical and experimental techniques.

Functionalization of UiO-67 by Pd and Pt was achieved via substitution of 10% standard biphenyl dicarboxylate linkers by  $MCl_2$ -2,2-bipyridine-5,5-dicarboxylic acid ( $MCl_2$ bpydc,  $M = Pd, Pt$ ) [3, 4]. The obtained materials were further activated by heating to 300 °C in inert (He) and reducing ( $H_2/He$ ) atmospheres. Evolution of the atomic and electronic structure was monitored by *in situ* extended X-ray absorption fine structure (EXAFS), X-ray absorption near edge structure (XANES) spectroscopies and X-ray powder diffraction (XRPD). All spectroscopic data for Pd  $K$ - and Pt  $L_3$ -edges were analyzed simultaneously by MCR-ALS approach [5] to determine the number of pure species formed during the activation and their spectra.

To interpret the experimental data, we have performed DFT-calculations and XANES simulation by FDMNES code for different potential intermediates. The atomic models included the initial  $MCl_2$ bpydc linker (d) and a number of possible reaction pathways in presence of  $H_2$ : substitution of both chlorine atoms by hydrogen atoms with formation of  $Cl_2$  molecule, substitution of one chlorine by hydrogen atom with formation of HCl molecule (a); detachment of two chlorines with formation of two HCl molecules, detachment of  $MCl_2$  fragment from the linker with its substitution by two hydrogens bonded to nitrogen atoms of the linker (c); and simulating inert conditions:

simple detachment of  $MCl_2$  fragment, detachment of chlorines with formation of  $Cl_2$  molecule (b). All reaction pathways were ranged according to the calculated reaction enthalpies and XANES spectra were calculated for the most probable ones (Fig. 1). The calculated energy differences show that for UiO-67-Pd detachment of  $PdCl_2$  is the most probable pathway in both inert and  $H_2$  atmospheres which correlate with experimental results. For UiO-67-Pt, four different structures, including two intermediates were determined (Fig. 1, e). Formation of bare Pt-sites occurs from 200 to 300 °C in the inert flow. While in presence of  $H_2$ , substitution of Cl by H atoms occurs first, and formation of Pt NPs starts above 200 °C. Thus, the calculated XANES spectra allowed verifying and describing transitional experimental spectra.

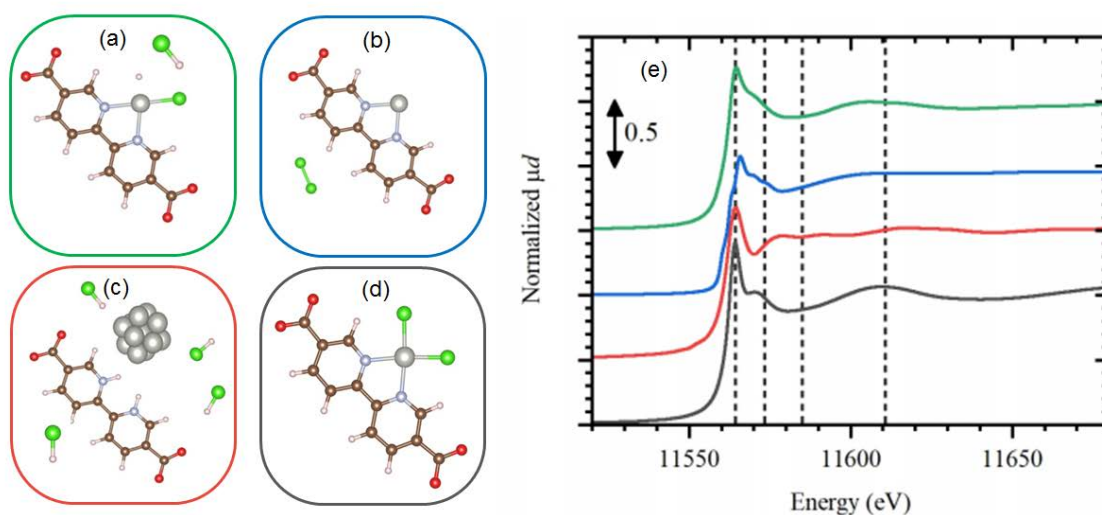


**Fig.1** Atomic structures (a-d) used for Pt  $L_3$ -edge XANES calculation (e). Atoms color code: Pt (gray), Cl (green), C (brown), H (white), O (red).

## References

1. Tanabe K. K., Cohen S. M. Postsynthetic modification of metal-organic frameworks--a progress report // *Chem Soc Rev.* – 2011. – T. 40, № 2. – C. 498-519.
2. Wang Z., Cohen S. M. Postsynthetic modification of metal-organic frameworks // *Chem Soc Rev.* – 2009. – T. 38, № 5. – C. 1315-29.
3. Braglia L., Borfecchia E., Martini A., Bugaev A. L., Soldatov A. V., Oien-Odegaard S., Lonstad-Bleken B. T., Olsbye U., Lillerud K. P., Lomachenko K. A., Agostini G., Manzoli M., Lamberti C. The duality of UiO-67-Pt MOFs: connecting treatment conditions and encapsulated Pt species by operando XAS // *Phys Chem Chem Phys.* – 2017. – T. 19, № 40. – C. 27489-27507.
4. Bugaev A. L., Usoltsev O. A., Guda A. A., Lomachenko K. A., Pankin I. A., Rusalev Y. V., Emerich H., Groppo E., Pellegrini R., Soldatov A. V., van Bokhoven J. A., Lamberti C. Palladium carbide and hydride formation in the bulk and at the surface of palladium nanoparticles // *The Journal of Physical Chemistry C.* – 2018. – T. 122, № 22. – C. 12029–12037.
5. Jaumot J., de Juan A., Tauler R. MCR-ALS GUI 2.0: New features and applications // *Chemometrics and Intelligent Laboratory Systems.* – 2015. – T. 140. – C. 1-12.

# Catalytic Synthesis of Anisotropic Conjugated Polymer Nanoparticles

*Annika Sickinger, Julian D. Ruiz Perez, Stefan Mecking,*

*Chair of Chemical Material Science, University of Konstanz, Konstanz, Germany.*

Materials based on anisotropic particles enable shape-dependent assembly and directional properties. As opposed to inorganic nanocrystals the introduction and control of anisotropy remains a largely unresolved problem for polymer nanoparticles, especially for conjugated polymers. Recently, a reliable protocol for the preparation of ellipsoidal polyfluorene particles by heterophase Suzuki-Miyaura polycondensation has been reported.<sup>[1]</sup> Studies on the origin of particle anisotropy suggest a concerted mechanism, including intersegmental chain packing concurrent with ongoing step-growth polymerization.

Further insight about the polymer chain conformation can be gained from electron paramagnetic resonance spectroscopy (ESR).<sup>[2]</sup> For this purpose, double spin labeled precise oligomers are prepared and incorporated into the nanoparticle structure. Measurement of the distance distributions between the paramagnetic centers offer the opportunity to study how individual polymer chains adopt their conformation in the particles.

Beyond internal structure, the particles surface chemistry and colloidal behavior can be altered by introduction of surface charge via tailored surfactants.<sup>[3]</sup> The resulting charged, fluorescent nanoparticles provide promising starting material to self-assemble, forming superstructures with directional properties.<sup>[4]</sup>

## References

- [1] Ruiz Perez, J. D.; Mecking, S. Anisotropic Polymer Nanoparticles with Tunable Emission Wavelengths by Intersegmental Chain Packing. *Angew. Chem. Int. Ed.* **2017**, *56*, 6147–6151.
- [2] Hintze, C.; Schütze, F.; Drescher, M.; Mecking, S. Probing of Chain Conformations in Conjugated Polymer Nanoparticles by Electron Spin Resonance Spectroscopy. *Phys. Chem. Chem. Phys.* **2015**, *17*, 32289–32296.
- [3] Harris, J. M. Laboratory Synthesis of Polyethylene glycol Derivatives. *J. Macromol. Sci. Polymer Rev.* **1985**, *25*, 325–373.
- [4] Odriozola, G. Revisiting the Phase Diagram of Hard Ellipsoids. *J. Chem. Phys.* **2012**, *136*, 134505.

# Controlling thermal stability of ZnO-based catalysts for improved durability in propane dehydrogenation

*Dan Zhao*<sup>1,2</sup>; *Ke Guo*<sup>1</sup>; *Shanlei Han*<sup>1,2</sup>; *Guiyuan Jiang*<sup>1\*</sup>; *Yuming Li*<sup>1</sup>, *Yajun Wang*<sup>1</sup>, *Zhen Zhao*<sup>1</sup>, *Chunming Xu*<sup>1</sup>,  
*Evgenii V. Kondratenko*<sup>2\*</sup>

<sup>1</sup> State Key Laboratory of Heavy Oil Processing, China University of Petroleum, Beijing, Beijing 102249, P. R. China;

<sup>2</sup> Leibniz-Institut für Katalyse e.V. an der Universität Rostock, Albert-Einstein-Strasse 29a, D-18059 Rostock, Germany

## Introduction

ZnO is one of the most often-used materials in heterogeneous catalysis. Its applicability under reducing conditions is, however, limited to lower temperatures, since metallic Zn can be formed, which melts at about 420°C thus resulting in material loss through evaporation. For non-oxidative propane dehydrogenation (PDH) requiring temperature above 550°C, catalysts possessing ZnO nanoparticles (NPs) were proved to show high activity<sup>[1, 2]</sup>, but irreversibly deactivate due to Zn loss. Herein, we demonstrate that thermal stability of supported ZnO NP can be improved through catalyst promoting with MgO. So designed catalysts showed high activity, on stream stability and durability in the PDH reaction.

## Experimental

Typically<sup>[3]</sup>, required amount of deionized water,  $\text{Zn}(\text{NO}_3)_2 \cdot 6\text{H}_2\text{O}$ ,  $\text{Mg}(\text{NO}_3)_2 \cdot 6\text{H}_2\text{O}$ , ethylenediamine, colloidal silica and tetrapropylammonium hydroxide were mixed and stirred for 6 h at 35°C. Hereafter, the resulting mixture was placed in 200 ml Teflon stainless-steel autoclaves at 150°C for 3 days. The solid product was collected after filtration, drying and calcination at 550°C for 6 h. The samples are denoted as 6%ZnO/S-1(xMg), x means the mole ratio of Mg and Zn.

## Results and Discussion

For the Mg modified ZnO-based catalysts, no apparent negative effect of Mg loading on the rate of propene formation was established, while zinc loss could be significantly inhibited. For example, an average rate of Zn removal estimated from ICP data of fresh and spent materials was 0.35%ZnO/h and 1.09%ZnO/h for the 6%ZnO/S-1(1.0Mg) and 6%ZnO/S-1(0.0Mg) catalysts, respectively. As seen in Fig. 1 (A, B), propane conversion over the latter catalyst decreases dramatically after several PDH/regeneration cycles. In contrast, the 6%ZnO/S-1(1.0Mg) catalyst fully recovered its activity for the last 3 cycles. In order to explain such excellent regeneration behavior, all catalysts were characterized by XPS, IR spectroscopy and CO-TPR. In comparison with MgO-free 6%ZnO/S-1, a shift in the binding energy of Zn 2p<sub>3/2</sub> to higher energy was obtained in 6%ZnO/S-1(0.0 Mg) thus that the promoter changes electronic properties of ZnO. The IR spectra shown in Fig. 1 (C) reveal a



blue-shift in the Mg modified ZnO sample, which is mainly caused by the dopant with smaller ion radius of  $\text{Mg}^{2+}$  (0.57 Å) than that of  $\text{Zn}^{2+}$  (0.60 Å)<sup>[4]</sup>. Thus, both XPS and IR data suggest that MgO strongly interacts with ZnO. Furthermore, as proven by CO-TPR, redox properties of ZnO change in the presence of MgO. The temperature of maximal CO consumption ( $T_{\text{max}}$ ) shifted to higher temperatures with an increase in Mg loading (Fig. 1(D)). The amount of consumed CO decreased with increasing Mg content. On the basis of all characterization data, we can conclude that promoting of ZnO with MgO results in inhibiting formation of metallic Zn under reducing conditions. As a consequence, Zn loss is reduced and durability of MgO-promoted samples in PDH is improved.

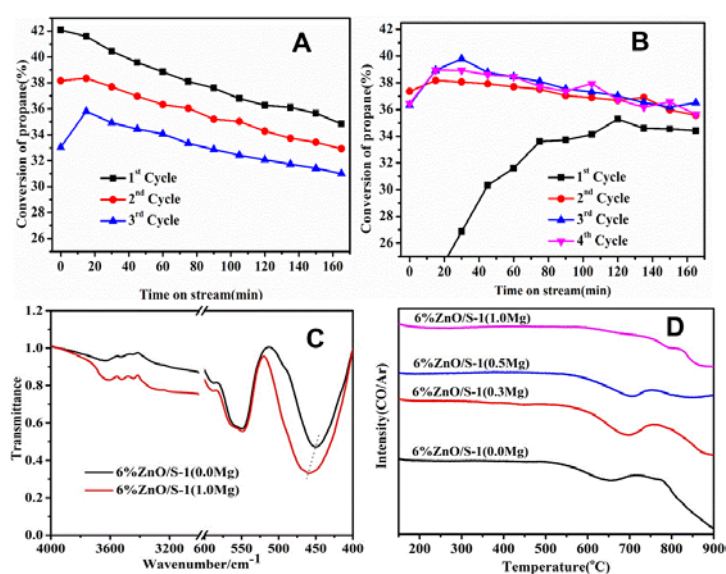


Fig. 1 (A), (B) The catalytic performances of 6%ZnO/S-1(0.0Mg) and 6%ZnO/S-1(1.0Mg), respectively, reaction conditions: 550°C,  $V(\text{N}_2):V(\text{C}_3\text{H}_8)=5:1$ ,  $\text{C}_3\text{H}_8$  flow rate is 1.5 ml/min; regeneration conditions: 500°C,  $V(\text{air})=9$  ml/min, 30 min for regeneration; (B) the XPS profiles; (C) the IR spectra; (D) the CO-TPR patterns.

## Summary

We presented a method to prevent ZnO loss under reducing conditions above the melting point of metallic Zn. It includes promoting ZnO with MgO. Owing to strong interaction between ZnO and MgO, reducibility of ZnO is suppressed thus minimizing formation of metallic Zn in the presence of propane at 550°C. Importantly, promoting with MgO did not negatively affect the rate of propane formation. So designed catalysts showed excellent regeneration behavior and stability in PDH.

## References

- [1] Chen C., Hu Z. Pan, Ren, J. T *et al.*, *ChemCatChem*, 2019, 11, 1-11.
- [2] Zhao D, Li Y. M., Han S. L. *et al.*, *accepted by iScience*, 2018.
- [3] Otto T., Zones S. I., Hong Y.C., *et al.*, *J. Catal.*, 2017, 356 173–185
- [4] Etacheri V., Roshan R., Kumar V., *ACS Appl. Mater. Interfaces*, 2012, 4, 2717–2725

## **Influence catalyst size on UHMwPE polymerization performance**

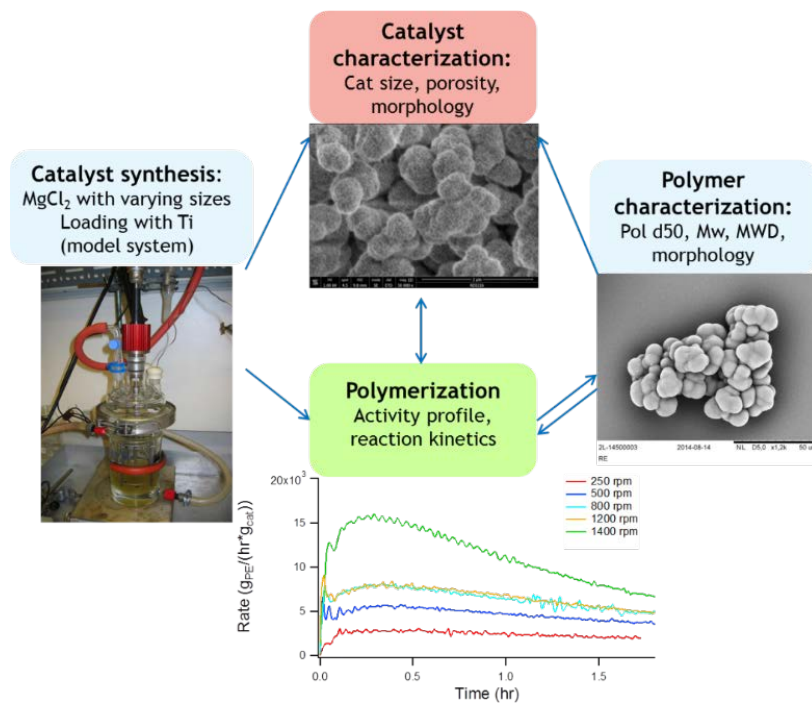
*An Philippaerts<sup>1</sup>, John Severn, Gert De Cremer<sup>1</sup>, Celine Fellay<sup>1</sup>, Tigran Margossian<sup>1</sup>,  
Richard Ensink<sup>1</sup>*

*1 DSM Material Science Center, Urmonderbaan 22, 6167RD Geleen,  
an.philippaerts@dsm.com*

The goal of this investigation was to study the influence of the size of the catalysts' support on the catalyst structure, the Ultra High Molecular Weight Polyethylene (UHMWPE) polymerization performance and the final polymer properties. Therefore MgCl<sub>2</sub> supports with varying particle sizes were prepared by varying the stirring speed during the synthesis, enabling us to study the effect on mass transfer and polymer morphology. Finally, the obtained supports were loaded with a Ti complex and the catalysts thus obtained were evaluated in homo- and co-polymerization reactions.

The catalyst platform obtained, allowed us to study:

- The link between the stirring speed during the support synthesis and the final catalyst morphology (size, surface texture, globular structure, porosity).
- The link between catalyst size and activity (activity profile, kinetics, mass transfer issues).
- The link between catalyst size and polymer properties (bulk density, Mw, MW distribution, polymer morphology)



## References

Philippaerts *et al.*, Journal of Polymer Science, Part A: Polymer Chemistry 2017, 55, 2679 - 2690

# Halogenation of Aromatic Hydrocarbons by Halide Anion Oxidation with Poly(heptazine imide) Photocatalysis

*Yevheniia Markushyna, Aleksandr Savateev and Markus Antonietti*  
Max-Planck Institute of Colloids and Interfaces, Department of Colloid Chemistry,  
Research Campus Golm, 14424 Potsdam, Germany  
E-mail: [Yevheniia.Markushyna@mpikg.mpg.de](mailto:Yevheniia.Markushyna@mpikg.mpg.de)

Chlorinated and brominated hydrocarbons are a pivot of the chemical industry – they are important reagents and solvents. Oxidative halogenation is probably the least harmful method to synthesize halogenated hydrocarbons.[1]

Polymeric carbon nitride, a visible light heterogeneous photocatalyst, possesses exceptionally high chemical and thermal stability that are a mandatory requirement if a conversion is performed in a highly oxidative medium.[2]

Recently, we also presented an improved modification of polymeric carbon nitrides, potassium poly(heptazine imide)s (K-PHI),[3-4] which shows a remarkably improved oxidation strength with a potential of valence band +2.54 V vs RHE (Fig. 1).[5]

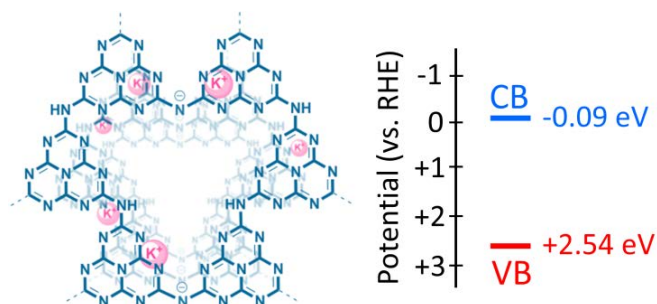
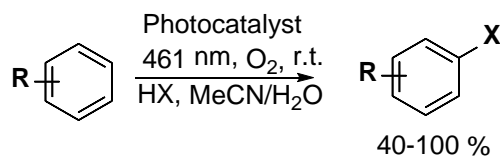


**Fig. 1.** Chemical structure (left) and band structure (right) of K-PHI.

Because of highly positive valence band potential of K-PHI,  $\text{Cl}^-$  can be theoretically oxidized to “ $\text{Cl}^+$ ” via a two electron process ( $E^0 = +1.36$  V) by the photocatalyst.

Indeed we found that using simple reaction conditions with HCl as chlorine source and electron donor and oxygen as electron acceptor with K-PHI photocatalyst, chlorination of electronically rich aromatic hydrocarbons could be reached with excellent yields. An important point of our approach is that  $\text{H}_2\text{O}_2$  is generated in situ in micro quantities right before consumption and is potentially surface-bound, and therefore substrate over-chlorination or over-oxidation is minimized.



X = Cl, Br.

R =  $\text{OCH}_3$ ,  $\text{N}(\text{CH}_3)_2$ ,  $\text{NHC}(\text{O})\text{CH}_3$ , etc.

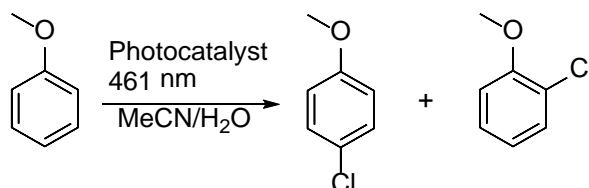
Further this simple approach was extended for brominating of aromatic compounds which goes smoothly as well.

Among studying the mechanism of the proposed reaction we found that this reaction could go by two different mechanisms independently

- 1)  $\text{Hal}^-$  two electron oxidation, then quenching of  $\text{Hal}^+$  by water;
- 2)  $\text{O}_2$  reduction to  $\text{H}_2\text{O}_2$  and subsequent reaction with  $\text{HCl}$ .

Both ways result in formation of electrophilic "HOCl" species, reacting in electrophilic halogenation of electron rich aromatic compounds.

Another abundant source of  $\text{Cl}^-$  could be found on Earth. Seawater is usually not considered as a reaction medium for fine chemistry. But in our work we showed that solution of  $\text{NaCl}$  could work in such reaction. However an acidic medium and a solvent stabilized  $\text{Cl}^+$  are essential to close the reaction.



For comparison purposes, different forms of carbon nitrides were studied. K-PHI gave chloroanisoles in 99% yield, Na-PHI in 35% yield, H-PHI produced chloroanisoles with 43% yield. Similarly graphitic carbon nitride (g-CN) gave chloroanisoles with 42% yield. Among the investigated homogenous catalysts, only  $\text{Ru}(\text{bpy})_3$  works in this reaction, but recovery of this photocatalyst is still challenging.

As a result of our investigation we propose a new simple way of photocatalytic halogenation of electron rich hydrocarbons promoted by K-PHI.

## References:

1. A. Podgoršek, M. Zupan, J. Iskra, Oxidative Halogenation with "Green" Oxidants: Oxygen and Hydrogen Peroxide, *Angew. Chem. Int. Ed.*, 48 (2009) 8424-8450.
2. A. Savateev, S. Pronkin, J.D. Epping, M.G. Willinger, M. Antonietti, D. Dontsova, Synthesis of an electronically modified carbon nitride from a processable semiconductor, 3-amino-1,2,4-triazole oligomer, via a topotactic-like phase transition., *J. Mater. Chem. A*, 5 (2017) 8394-8401.
3. A. Savateev, Z.P. Chen, D. Dontsova, Baking 'crumbly' carbon nitrides with improved photocatalytic properties using ammonium chloride, *RSC Adv.*, 6 (2016) 2910-2913.
4. D. Dontsova, S. Pronkin, M. Wehle, Z. Chen, C. Fettkenhauer, G. Clavel, M. Antonietti, Triazoles: A New Class of Precursors for the Synthesis of Negatively Charged Carbon Nitride Derivatives, *Chem. Mater.*, 27 (2015) 5170-5179.
5. A. Savateev, S. Pronkin, J.D. Epping, M. Willinger, C. Wolff, D. Neher, M. Antonietti, D. Dontsova, Potassium Poly(heptazine imides) from Aminotetrazoles: Shifting Band Gaps of Carbon Nitride-like Materials by 0.7 V for More Efficient Solar Hydrogen and Oxygen Evolution, *ChemCatChem*, (2017) 167-174.

# High throughput in silico reaction screening for tailored catalytic reactivity and selectivity

*Jacob L. Gavartin, Schrödinger, Cambridge, Cambridgeshire CB1 2JD, UK; Thomas J. L. Mustard, Schrödinger, Portland, OR 97204, USA; Thomas F. Hughes, Schrödinger, New York, NY 10036, USA; Art D. Bochevarov, Schrödinger, New York, NY 10036, USA; Leif D. Jacobson, Schrödinger, New York, NY 10036, USA; H. Shaun Kwak, Schrödinger, Cambridge, MA 02142, USA; Tsuguo Morisato, Schrödinger K.K., Chiyoda-ku, Tokyo 100-0005, Japan; Sudharsan Pandiyan, Schrödinger, Mahalakshmpuram, Bangalore 560 086, India; and Mathew D. Halls, Schrödinger, San Diego, CA 92121, USA*

## Introduction

Empirical reaction tuning is a laborious and expensive process. In contrast, reliable and efficient first-principles workflows can be employed in a high-throughput fashion to survey chemical design space and inform experiment. Systematic evaluation of steric and electronic contributions provides an unprecedented fundamental understanding of factors controlling a target reaction. With these structure-property relationships, one can re-design a reaction or catalyst to achieve desired activity. Paired with automated high throughput screening the rate of discovery and understanding is accelerated. In this work, a computational design methodology for the enhancement of reactivity and selectivity through an atomistic fundamental understanding is demonstrated.

## Methods and Tools

Fundamental understanding of the chemical system is the framework behind catalyst design. Using chemical knowledge, a set of catalyst derivatives are generated to test the underlying factors controlling reactivity and selectivity. This set of derivatives is dynamically updated as new information is obtained. Fortunately, the transition state geometries do not change drastically between catalysts of the same family. [1] Therefore, new catalysts can be mapped onto existing ground and transition state geometries. This drastically enhances throughput with automated tools.

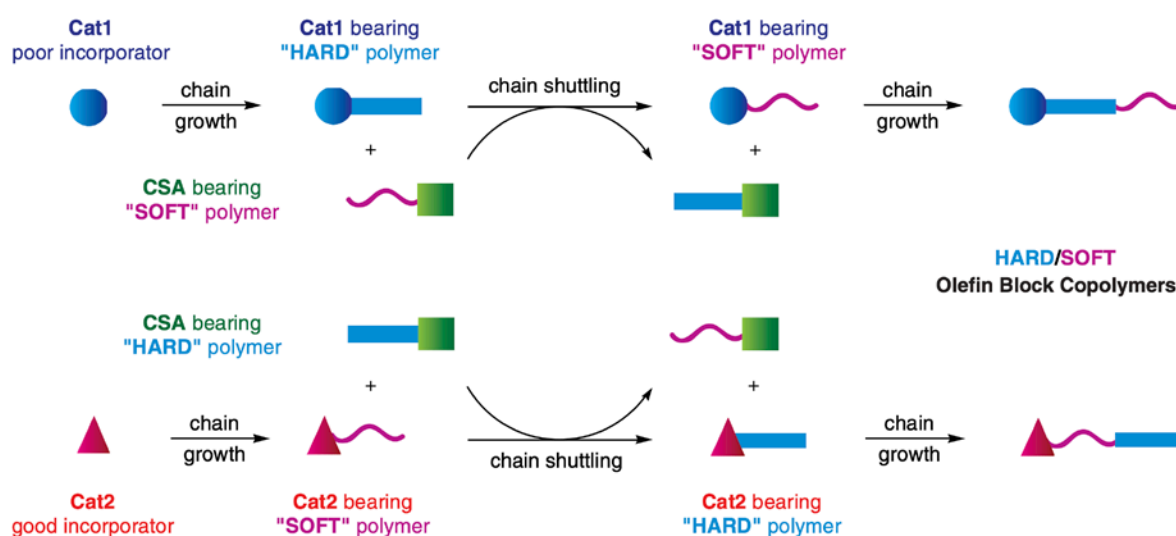
To fully study the relevant chemical space for a given catalyst design project, one must generate a library of catalyst derivatives that exhibit the underlying factors governing reactivity and selectivity. Utilizing the Reaction Workflow a novel catalyst scaffold can: (1) undergo R-Group enumeration, (2) mapped onto the known reaction coordinate, (3) undergo a conformational search for each reaction step, (4) *ab initio*

computations of each ground state and transition state geometry, and (5) calculate reaction energetics and structural properties. The enumeration and calculated structural properties define the inputs of QSAR/QSPR free energy relationships.

### Block Copolymer Comonomer Selectivity

Production of alkene-based polymer products has surpassed 100 million tons. Block copolymers have unique properties that include high strength, flexibility, and melting temperature. These physical properties are directly influenced by the polymer block length and distribution. The block size and distribution is determined by the kinetic comonomer selectivity and chain shuttling agent activity (Figure 1). Industrially, a combination of an ethene selective Zr catalyst, a propene selective Hf catalyst, and the chain shuttling agent ZnEt<sub>2</sub> are used to produce a block copolymer with high strength, high melting point ( $T_m$ ), and low density.[2] To fundamentally understand the comonomer selectivity, several catalyst derivatives were tested.

**Figure 1.** Proposed chain shuttling block copolymer mechanism.



### References

1. Mustard, T. J. L.; Wender, P. A.; Cheong, P. H.-Y. *ACS Catal.* **2015**, *5*, 1758–1763.
2. Arriola, D. J.; Carnahan, E. M.; Hustad, P. D.; Kuhlman, R. L.; Wenzel, T. T. *Science* **2006**, *312*, 714–719.

## The way of gold location on pillars in MCM-36 zeolite

*Iveta Kaskow; Anna Wojtaszek-Gurdak; Izabela Sobczak*

*Adam Mickiewicz University, Faculty of Chemistry, Poznan, Poland*

Layered zeolites with MWW (M-tWenty-tWo) topology are an important group of new materials that offer a lot of adsorptive and catalytic possibilities [1]. The layered MCM-22P precursor consisting of zeolite monolayers can be transformed, by swelling and pillaring, into MCM-36 zeolite, which is a relatively novel large pore pillared material containing interlamellar mesopores in addition to the layer microporosity. Nowadays, much attention has been paid to improvement of MCM-36 catalytic activity by its modification with various metals, among them with gold [e.g. 2]. One of the main challenges in the synthesis of Au-MCM-36 is the location of gold particles on the pillars of zeolite which allows the further construction of bifunctional catalyst containing separated oxidizing and acidic centres.

The aim of this work was to study the effect of zinc in MCM-36 on the location and surface properties of gold. ZnO was dispersed on zeolite surface and played the role of a support dopant. MCM-36 without zinc was used as the reference support. MCM-36 and Zn/MCM-36 (10 wt. % of Zn introduced by impregnation) catalysts were prepared according to [3] by the modification of functionalized support (MCM-36 and Zn/MCM-36 grafted with MPTMS - (3-Mercaptopropyl)trimethoxysilane) with Au (2 wt.%). The materials obtained were reduced with NaBH<sub>4</sub> and next calcined at 773 K. The physicochemical properties of catalysts were fully characterized by: N<sub>2</sub> adsorption/desorption isotherms, XRD, UV-vis, XPS and TEM. The surface acidity of samples was measured by pyridine adsorption combined with FTIR studies.

FTIR study after pyridine adsorption and XRD data indicated that zinc was incorporated into Zn/MCM-36 in the form of extra framework zeolite cations and in the form of zinc oxide. In the XRD pattern of Zn/MCM-36 peaks characteristic of bulk zinc oxide phase were identified. The FTIR spectrum of MCM-36 after pyridine adsorption showed the presence of Brønsted and Lewis (extra framework aluminium species and sodium cations) acid sites on the catalyst surface. Significant changes in acidity were observed after modification of MCM-36 with zinc. The number of BAS significantly decreased (Table 1) and LAS in the form of sodium cations disappeared as a result of zinc loading on the support surface. It means that zinc cations



exchanged protons from zeolite acidic OH groups and sodium cations. As  $\text{Zn}^{2+}$  replaced protons, the functionalization of Zn/MCM-36 with MPTMS occurred mainly on silica pillars. In contrast, functionalization in MCM-36 occurred on both, the zeolite surface (with participation of BAS) and on silanols in silica pillars. Therefore gold was located at both sites – zeolite surface and silica pillars in MCM-36 and mostly on silica pillars in the case of Zn/MCM-36.

Table 1. Number of Brønsted acid sites in MCM-36 zeolites ( $\text{BAS } \varepsilon(\text{B})=0.044 \text{ cm}^2 \mu\text{mol}^{-1}$ )

Catalyst	Number of BAS* [ $\mu\text{mol g}^{-1}$ ] $\times 10^{21}$ after evacuation at 423 K	Number of BAS* [ $\mu\text{mol g}^{-1}$ ] $\times 10^{21}$ after evacuation at 523 K
	MCM-36	2.91
Au-MCM-36	1.38	1.03
Zn/MCM-36	0.40	0.00
Au-Zn/MCM-36	0.26	0.25

XRD, TEM, UV-vis and XPS results showed that metallic gold dominated on the surface of Au-MCM-36 and Au-Zn/MCM-36 catalysts and that the introduction of zinc led to the generation of  $(\text{Au}^0)^{\delta-}$  species with negative charge on gold. ZnO in Au-Zn/MCM-36 played the role of a structural promoter reducing the size of gold particles (from 4.1 nm to 3.6 nm for Au-MCM-36 and Au-Zn/MCM-36, respectively).

In summary, modification of MCM-36 zeolite with zinc oxide resulted in a new support for gold in which zinc dopant played the role of structural (by reducing the size of gold particles) and electronic (by generating negatively charged metallic gold crystallites) promoter. Such a modification with zinc species before gold loading allowed location of gold mainly in mesopores on pillars.

### Acknowledgements

National Science Centre in Poland (project N<sup>o</sup> UMO-2018/29/B/ST5/00137) is acknowledged for the financial support.

### References

- [1] W. J. Roth, P. Nachtigall, R. E. Morris, J. Čejka, Chem. Rev. 114 (2014) 4807–4837
- [2] A. Wojtaszek-Gurdak, I. Sobczak, K. Grzelak, M. Ziolk, U. Hartfelder, J. A. van Bokhoven Mater. Res. Bull. 76 (2016) 169–178
- [3] X. Liu, A. Wang, X. Yang, T. Zhang, Ch-Y. Mou, D-S. Su, J. Li, Chem. Mater. 21 (2009) 410–418

# $\alpha$ -Alkylation of Ketones with Alcohol Electrophiles using Palladium on Carbon as Catalyst: Scope and Mechanism

*N. R. Bennedsen, DTU Chemistry, Lyngby, Denmark; S. Kramer, DTU Chemistry, Lyngby, Denmark; R. Mortensen, DTU Chemistry, Lyngby, Denmark; and S. Kegnæs, DTU Chemistry, Lyngby, Denmark.*

## Abstract

Formation of new carbon-carbon bonds is crucial for the synthesis of organic compounds for pharmaceuticals, agrochemicals, and functional materials.[1-2] The  $\alpha$ -alkylation reaction facilitates the formation of new  $C(sp^3)$ - $C(sp^3)$  bonds on the  $\alpha$ -carbon to a carbonyl and has received great attention over the years.[3-4] Conventional  $\alpha$ -alkylation methods have problems with undesired waste from the use of alkyl halides as electrophiles. However, using alcohols as a masked electrophile have attracted much attention as a green alternative as the only formed byproduct is water.[5-6]

Both homogeneous and heterogeneous catalysts are active in the  $\alpha$ -alkylation between a ketone and an alcohol. The reaction pathway is only well-studied for homogeneous systems with the general agreement that the pathway occurs through a hydrogen-borrowing pathway as illustrated in Figure 1. In the case of heterogeneous catalysis, only sparse kinetic studies has been performed on Pd/C catalysis in the  $\alpha$ -alkylation between ketones and alcohols.

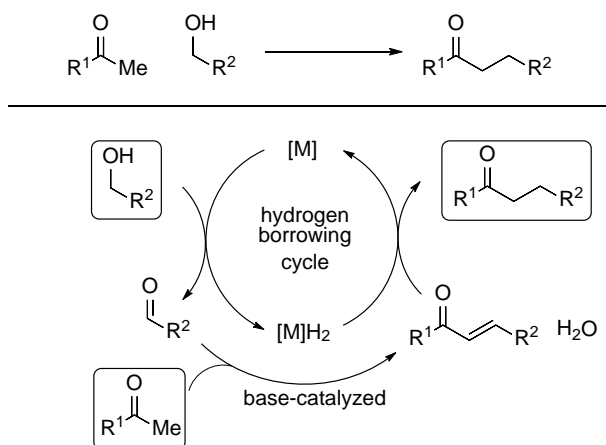


**Figure 1:** Hydrogen-borrowing pathway for the  $\alpha$ -alkylation between ketone and alcohol.

In our work,  $\alpha$ -alkylation between acetophenone and benzyl alcohol with commercially available Pd/C has been studied and optimized as a model reaction.[7] The excellent activity and selectivity of the catalysts have been showcased for a variety of different ketones and alcohols. Stoichiometric experiments and *in-situ* IR have provided crucial information about the reaction pathway for our heterogeneous system with an example of a reaction profile obtained by our IR-setup shown in Figure 2. With these results in hand, we have assessed the reaction pathway for our heterogeneous system in comparison to a homogeneous system and optimized the reaction conditions based on our kinetic results.

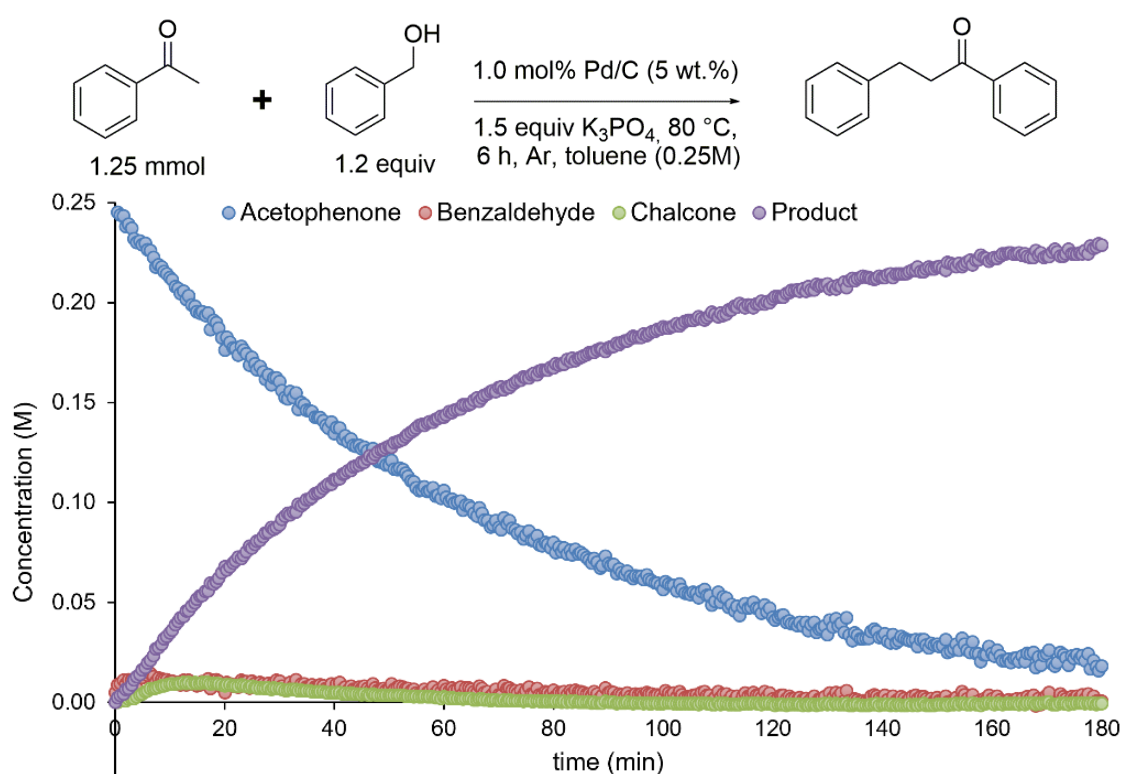


**Figure 2:** Reaction profile between acetophenone and benzyl alcohol with Pd/C as catalyst.

## References

- [1] Wang, F.; Mielby, J.; Richter, F. H.; Wang, G.; Prieto, G.; Kasama, T.; Weidenthaler, C.; Bongard, H.-J.; Kegnæs, S.; Fürstner, A.; Schüth F. *Angew. Chem. Int. Ed.* **2014**, *53*, 1-5.
- [2] Trnka, T. M.; Grubbs, R. H. *Acc. Chem. Res.* **2001**, *34*, 18–29.
- [3] Cano, R.; Zakarian, A.; McGlacken, G. P. *Angew. Chem. Int. Ed.* **2017**, *56*, 9278–9290.
- [4] Nicewicz, D. A.; MacMillan, D. W. C. *Science* **2008**, *322*, 77–90.
- [5] Corma, A.; Navas, J.; Sabater, M. J. *Chem. Rev.* **2018**, *118*, 1410–1459.
- [6] Huang, F.; Liu, Z.; Yu, Z. *Angew. Chem. Int. Ed.* **2016**, *55*, 862–875.
- [7] Bennedsen, N.; Kramer, S.; Mortensen, R.; Kegnæs, S. 2019, *Submitted*.

# Mechanistic insights into base-catalyzed isomerization of glucose into fructose

*Irina Delidovich, Matthias Fischer, Maria S. Gyngazova, Bianca Gieraths,  
Institut für Technische und Makromolekulare Chemie, RWTH Aachen, Germany*

Isomerization of glucose into fructose presents an important industrial process to produce sweet syrups for food industry [1]. Moreover, this reaction has been recently indicated as a key step for valorization of cellulosic biomass into fuels and chemicals [2]. The isomerization of glucose into fructose is an equilibrium reaction that takes place in the presence of a catalyst. Lobry de Bruyn and Alberda van Ekenstein discovered that the isomerization can be catalyzed by soluble bases as long ago as in 1885 [3]. Simple alkalis, such as KOH or NaOH, enable the isomerization. Nevertheless, the reaction is hampered by numerous side processes leading to a low selectivity for fructose (60% at 30% glucose conversion) [4]. We have recently uncovered that soluble phosphates  $\text{NaH}_2\text{PO}_4 + \text{Na}_2\text{HPO}_4$  at pH 7.5 enable the isomerization with quite a high selectivity for fructose (78% at 30% glucose conversion). The first results indicated that the reaction presents a specific-base-catalyzed isomerization proceeds via the formation of an enediol anion [5]. Later, we found a high efficiency of the phosphates for isomerization of pentoses ribose and lyxose into corresponding ketoses [6]. Interestingly, Yang et al. have recently reported an increasement of the reaction rate of glucose-fructose isomerization in the presence of salts, such as NaCl, NaBr, or NaI, using amines as base catalysts [7]. Nevertheless, the molecular mechanism of salt influence on the base-catalyzed isomerization has not been explained yet.

This work aims at understanding the reasons for improved reaction rates and/or selectivity for fructose in the presence of salts. Our current study focuses on developing a kinetic model to comprehend an influence of salt nature, salt concentration, and pH value on the kinetic parameters. At the same time, *operando* NMR studies utilizing partially deuterated carbohydrates are planned to get further insight into the reaction mechanism.

## Acknowledgements

We acknowledge financial support from the DFG (DE 2748/3-1).

## References

1. L. M. Hanover and J. S. White, *Am. J. Clin. Nutr.*, 1993, 58, 724S.
2. Y. Román-Leshkov, J. N. Chheda and J. A. Dumesic, *Science*, 2006, 312, 1933; Y. Román-Leshkov, C. J. Barret, Z. Y. Liu and J. A. Dumesic, *Nature*, 2007, 447, 982.
3. S. J. Angyal, The Lobry de Bruyn-Alberda van Ekenstein Transformation and Related Reactions. In *Glycoscience*, Springer Berlin, Heidelberg, 2001, vol. 215, p. 1.
4. I. Delidovich and R. Palkovits, *Catal. Sci. Technol.*, 2014, 4, 4322.
5. I. Delidovich and R. Palkovits, *Green Chem.*, 2016, 18, 5822.
6. I. Delidovich, M.S. Gyngazova, N. Sánchez-Bastardo, J.P. Wohland, C. Hoppe and P. Drabo, *Green Chem.*, 2018, 20, 724.
7. Q. Yang, W. Lan and T. Runge, *ACS Sus. Chem. Eng.*, 2016, 4, 4850.

# Hydrogenolysis of lactic acid to 1,2-propanediol over Cu/SiO<sub>2</sub> in the presence of Mg(OH)<sub>2</sub>

*Xinde Wang, Institut für Technische und Makromolekulare Chemie, RWTH Aachen University, Aachen, Germany; Anna Katharina Beine, Institut für Technische und Makromolekulare Chemie, Peter J.C. Hausoul, Institut für Technische und Makromolekulare Chemie, RWTH Aachen University, Aachen, Germany; Regina Palkovits, Institut für Technische und Makromolekulare Chemie, RWTH Aachen University, Aachen, Germany*

## Abstract

The limited availability and the environmental impact of fossil resources have motivated the exploration of alternative sustainable resources. In this respect, the production of 1,2-propanediol (1,2-PDO) from the sustainable biomass derived building block lactic acid has been increasingly meaningful.<sup>[1,2]</sup> Herein, a series of non-noble metal (Fe, Co, Ni, Cu and Zn) supported on SiO<sub>2</sub> catalysts were prepared. These catalysts were tested in the conversion of lactic acid to 1,2-PDO in the presence of base under aqueous conditions.<sup>[3]</sup> The results of HPLC displayed that Cu/SiO<sub>2</sub> outperformed the others especially in terms of selectivity to 1,2-PDO. Various bases were screened and Mg(OH)<sub>2</sub> was observed to improve the conversion of lactic acid significantly. Indeed 98% conversion of lactic acid with 95% selectivity to 1,2-PDO was obtained over Cu/SiO<sub>2</sub> in the presence of Mg(OH)<sub>2</sub> at 513 K, 5 MPa H<sub>2</sub> in 24h. The conversion of magnesium lactate was investigated over Cu/SiO<sub>2</sub> in the absence of base. Interestingly, magnesium lactate possesses a much higher rate of conversion than lactic acid in the presence of Mg(OH)<sub>2</sub>. Moreover, Mg(OH)<sub>2</sub> was recovered after the reaction. This model test indicates that magnesium lactate is a key important intermediate formed in the conversion of lactic acid in the presence of Mg(OH)<sub>2</sub>.

DFT calculation was employed to achieve deeper insights into the reaction mechanism. It discloses that the energetic span (determined based on the TOF-determining intermediate and TOF-determining transition state) of lactic acid conversion is decreased from 46.6 kcal/mol in the presence of OH<sup>-</sup> to 44.7 kcal/mol in the presence Mg(OH)<sub>2</sub>.

This is the first report on the conversion of lactic acid to 1,2-PDO with promising yield over a Cu catalyst under aqueous condition.

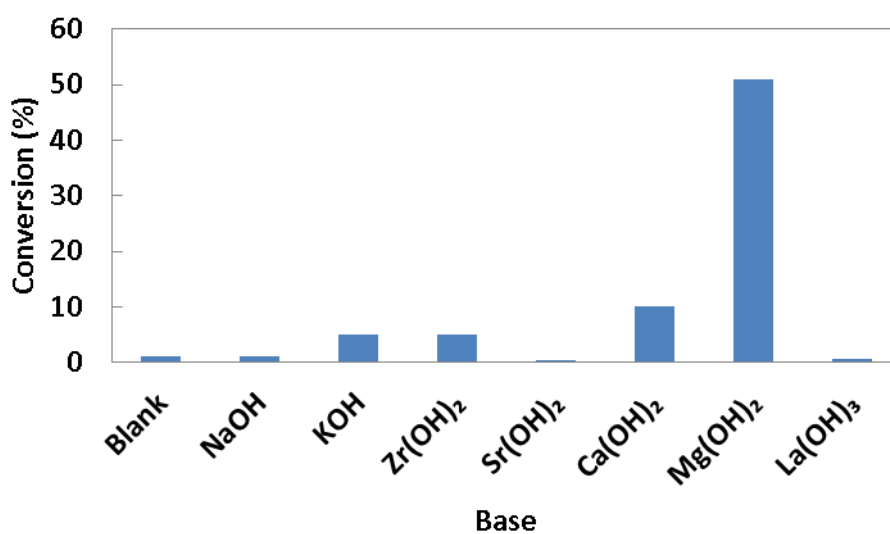


**Figure 1.** Conversion of lactic acid over 25%Cu/SiO<sub>2</sub> in the presence of different bases (the amounts of OH<sup>-</sup> charged are identical). Reaction conditions: 0.1g 25%Cu/SiO<sub>2</sub>, 0.5g LA, 0.0685M OH<sup>-</sup>, 20ml H<sub>2</sub>O, 513K, 5MPa H<sub>2</sub>, 4h.

### Acknowledgement

We acknowledge financial support of the Chinese Scholarship Council

### References

- [1] A. M. Ruppert, K. Weinberg, R. Palkovits, *Angew. Chem. Int. Ed.* 51 (2012) 11, 2564–2601;
- [2] K. Tajvidi, K. Pupovac, M. Kükrek, R. Palkovits, *ChemSusChem.* 5 (2012) 2139–2142;
- [3] K. Tajvidi, P. J. C. Hausoul, R. Palkovits, *ChemSusChem.* 7 (2014) 5, 1311–1317;
- [4] X. Wang, A. K. Beine, P. Hausoul, R. Palkovits, under preparation.

# Support Engineering of Catalytic Performance of Single Pt atom in Direct Propane Dehydrogenation

XiaoYing Sun and Zhen Zhao\*

sunxiaoying78@163.com

College of Chemistry and Chemical Engineering, Shenyang Normal University,  
Shenyang 110034, China

Platinum is the conventional catalyst for direct propane dehydrogenation<sup>[1]</sup>. In this study, the catalytic properties and performance of supported single Pt on doped graphene<sup>[2]</sup> and boron nitride sheet are investigated by DFT simulation. The nitrogen on the graphene support withdraws electrons from Pt, but boron donates electrons to Pt. Consequently, the d-band center of Pt atom is modified by either nitrogen or boron doping. The nitrogen doping shifts the d-band center of Pt atom closer to the Fermi level compared with the boron doping and the pristine ones. On the other hand, the d-band center has a significant influence on the C-H bond dissociation energy and reaction barrier. Therefore, better reactivity of Pt is found on the support with more nitrogen dopants as the d-band center is closer to the Fermi level. Also the calculated dissociation energy and the first C-H bond activation barrier obey the BEP rule. The different ratios between nitrogen and boron on the codoped graphene can continuously adjust the electronic structure of supported Pt and deliver the dissociation energy and reaction barrier in between the pure nitrogen- and boron-doped cases. Among various investigated supports, the graphene doped by pyridine nitrogen is predicted to be the most effective for enhancing Pt catalytic performance. On boron nitride sheet, single Pt supported on vacancies sites. Moreover, the relation between EMSI and the performance of Pt in propane direct dehydrogenation is carefully determined. The charge state and partial density of states of single Pt show distinct features on different anchoring positions which are boron (Bvac) and nitrogen (Nvac) vacancies respectively. Single Pt become positive and negative charged respective on boron or nitrogen vacancies. Therefore, the electronic structure of Pt can be adjusted by rational deposition on the support. Moreover, Pt with the different charge state has been shown to have diverse catalytic abilities. DFT calculations reveal that Pt-Bvac has much better reactivity towards the reactant/products adsorption and C-H bond activation than the counterpart supported on Nvac with larger adsorption energy and lower barrier along the reaction pathway. However, the



high reactivity of Pt-Bvac also cause the difficulty for the propene desorption which could lead unwanted deep dehydrogenation. Therefore, it is suggested that a balanced reactivity for C-H activation in propane and propene desorption is required which will give optimum yields. Based on this descriptor, the single Pt on nitrogen vacancy is considered to be an effective catalyst for PDH. Furthermore, the deep dehydrogenation of formed propene is much suppressed due to large barrier on Pt-Nvac.

### References

- [1] Sattler, Jesper J. H. B.; Ruiz-Martinez, Javier; Santillan-Jimenez, Eduardo; Weckhuysen, Bert M., *Chemical Reviews* **2014**, *114*, 10613-10653.  
[2] Sun, X.; Han, P.; Li, B.; Zhao, Z., *Journal of Physical Chemistry C* **2018**, *3*, 1570-1576

### References

List and number all bibliographical references at the end of the paper. When referenced within the text, enclose the citation number in square brackets, i.e. [1]

# **Oxidative dehydrogenation of short alkanes on the nanostructured carbon catalysts: a computational study**

*Bo Li*

*boli@imr.ac.cn*

*Institute of Metal Research, Chinese Academy of Science, ShenYang 110016 China*

The nanostructured carbon catalysts such as carbon nanotube and graphene have been achieved tremendous developments in recent years<sup>[1]</sup>. In particular, the oxidative dehydrogenation (ODH) of hydrocarbons is one of the most successful applications of the nanostructured carbon catalysts. For example, the surface modified carbon nanotube catalyst applied in ODH of butane gives a two-times selectivity of butadiene than the best contemporary metal oxide catalyst<sup>[2]</sup>. Furthermore, the ODH of ethane, propane, butane and ethylbenzene all have been extensively investigated by using the nanostructured carbon catalysts. The further improvements of the carbon catalysts in ODH rely on the accurate description of the active site and reaction mechanism which can provide the optimization strategy.

The numerous experimental works indicate the significant role of the oxygen functional group in ODH reaction on the carbon catalyst. It is very important to quantitatively evaluate the chemical reactivity of the various functional groups before the identification of the active site. The Fukui function calculations are carried to understand the nucleophilicity of the oxygen functional groups at both armchair and zigzag edges<sup>[3,4]</sup>. As shown in Figure 1a, the calculations reveal that the diketone and quinone groups are the most nucleophilic ones among the investigated groups which indicate their potential to be the active site as the electrophilic groups will favor the combustion in ODH. Furthermore, the quinone and diketone groups are more reactive than the others by examining the dissociation energy of the ethane molecule. Therefore, the reaction path of ODH of ethane is explored at the diketone site and the results are shown in Figure 1b<sup>[5]</sup>. The barrier of the first C-H breaking is the largest one along the reaction path which implies it is the rate-limit step. On the other hand, the reaction intermediate, ethoxide, is very stable and detrimental to the selectivity. The calculations suggest that the radical pathway (RR in Figure 1b) is likely to be the favorable reaction process of the ODH reaction. The active sites evolve into the phenol groups after reaction and the regeneration of the active site is

required to fulfill a catalytic cycle. The calculations uncover that the phenol groups are oxidized into  $\text{H}_2\text{O}_2$  by the oxygen molecule to regenerate the diketone groups. It is noted that the mechanism of the regeneration is different from the metal oxide catalysts in ODH which has a formation of water to recover the active sites. Not only the quinone or diketone but also the ketone group which has only one  $\text{C}=\text{O}$  can also activate the  $\text{C}-\text{H}$  bond in propane. In previous studies, it is a pre-requisite that two neighboring carbonyl groups are needed for ODH reaction on the carbon catalyst as each of them abstracts a hydrogen atom. However the DFT calculations reveal that the single ketone group has the similar barrier and dissociation energy compared with quinone and diketone for the propane activation as shown in Figure 1c<sup>[6-8]</sup>. The carbon atom, which is bonded with oxygen in ketone group, participates into the  $\text{C}-\text{H}$  bond activation together with the oxygen. The Bader charge analysis reveals that the most charges go to the carbon rather than oxygen in ketone group during the propane activation. The complete catalytic cycle from the calculations verifies the possibility of ODH at the single ketone site. Furthermore, the rate and TOF of ODH of ethane is calculated under the reaction condition by microkinetic modeling. Five elementary steps in ODH are identified. The free energy, equilibrium constant, and prefactor are calculated. In the end, TOF under reaction condition is obtained and shown in Figure 1d.

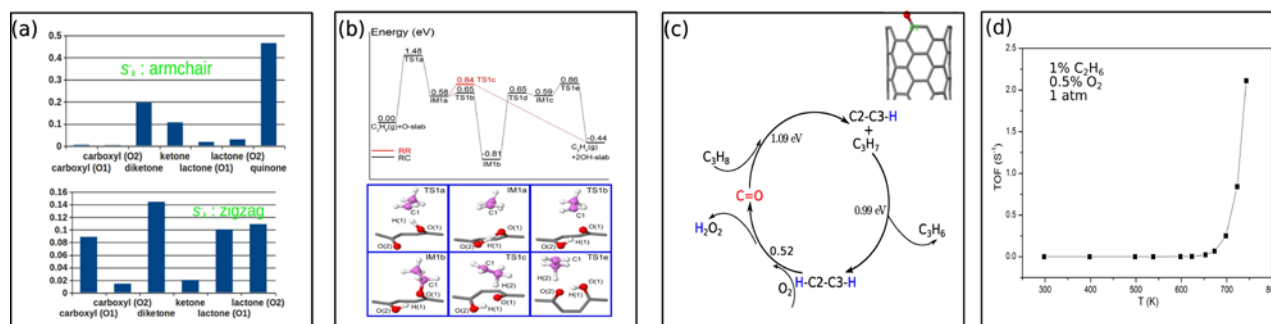


Figure 1. (a) The nucleophilicity of the oxygen functional groups from Fukui function calculations. (b) The reaction pathway and the important structures of ODH of ethane at diketone site. (c) The complete catalytic cycle of ODH at the single ketone site. (d) TOF of ODH of ethane from the DFT calculations.

## References

- [1] D. S. Su, S. Perathoner, G. Centi, *Chem. Rev.* 113 (2013), 5782-5816.
- [2] J. Zhang, X. Liu, R. Blume, A. Zhang, R. Schlögl, D. S. Su, *Science* 322 (2008), 73-77.
- [3] B. Li, D. S. Su, *Chem. Eur. J.* 20 (2014), 7890-7894.
- [4] B. Li, D. S. Su, *Phys. Chem. Chem. Phys.* 17 (2015), 6691-6694.
- [5] S. Mao, B. Li, D. S. Su, *J. Mater. Chem. A* 2 (2014), 5287-5294.
- [6] X. Y. Sun, B. Li, D. S. Su, *Chem. Commun.* 50 (2014), 11016-11019.
- [7] B. Li, D. S. Su, *Chem. Asian J.* 8 (2013), 2605-2608.
- [8] S. Mao, X. Y. Sun, B. Li, D. S. Su, *Nanoscale*, 7 (2015), 16597-16600.

# Conversion of biomass derived 5-hydroxymethylfurfural over supported bimetallic iridium based-catalysts

R.J.Chimentão<sup>1</sup>, H.Oliva<sup>1</sup>, K. Morales<sup>1</sup>, D.Y. Murzin<sup>2</sup>, P. Mäki-Arvela<sup>2</sup>, J.L.G. Fierro<sup>3</sup>,  
D. Ruiz<sup>1,\*</sup>

<sup>1</sup> Faculty of Chemistry, Universidad de Concepción, Concepción, Chile

<sup>2</sup> Åbo Akademi University, Turku, Finland

<sup>3</sup>Instituto de Catálisis y Petroleoquímica (CSIC), Cantoblanco, Madrid, Spain

Sustainable production of chemicals from biomass depends on the development of new technologies in the transformation of available bioresources [1]. HMF conversion (Fig. 1) can produce a variety of commodity chemicals [2].

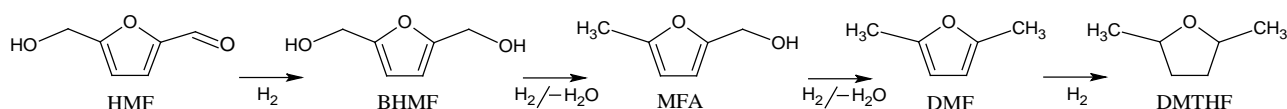


**Figure 1.** Overall reaction pathways for conversion of HMF.

Development of stable catalysts is a challenging task. A typical method to improve the performance of catalysts is the addition of a secondary metal to the active metal [3-5]. Here, the conversion of HMF to valuable chemicals such as BHMF and DMF was studied. The effect of the addition of a second metal (Ni, Co and Ru) on Ir catalyst in selectivity and stability was pursued. Assistance of formic acid (FA) and/or H<sub>2</sub>SO<sub>4</sub> as a strategy to improve the HMF conversion was examined.

In this work catalysts were synthesized by sequential impregnation method with loadings of 3 wt.% Ru and 5 wt.% of Ni or Co over 1 wt.%Ir/SiO<sub>2</sub>. Reactions were performed at 60 °C, in THF, 10 bar-H<sub>2</sub> and 100 mg of catalyst. Additional tests included the presence of FA and H<sub>2</sub>SO<sub>4</sub> acids together with the Ir based catalysts.

In the absence of catalyst no conversion of HMF occurred. Total selectivity to 2,5-bis-(hydroxymethyl)furan (BHMF) was observed for all catalysts in reactions without acid (FA and/or H<sub>2</sub>SO<sub>4</sub>) assistance. At this condition, the effect of a second metal on Ir based-catalysts was reflected on the apparent kinetic constant values of k<sup>a1</sup> (Table1). These kinetic constants (k<sup>a1</sup>) for Ir-Ni/SiO<sub>2</sub> and Ir-Co/SiO<sub>2</sub> were respectively 15.1 and 3.6 fold higher than that observed for Ir-Ru system. XPS surface atomic ratio Ir/Si increased from 0.0011 for Ir/SiO<sub>2</sub> to 0.0038 for Ir-Co/SiO<sub>2</sub>. This was reflected in the quantity of chemisorbed hydrogen (Table 1). Interaction between Ru -Ir could be reasonably expected to differ between Ir-Co and Ir-Ni.

Apparent kinetic constant values of  $k_{FA}^{a2}$  (Table1) were the lowest ones for all samples in the reactions assisted only by FA. At this condition catalyst deactivation and concomitant CO production from dehydration of FA are generally reported [6, 7]. Over-hydrogenolysis products such as DMTHF (2,5-dimethyltetrahydrofuran) were observed in the reactions assisted only by  $H_2SO_4$  and the apparent kinetic constant  $k_{SA}^{a3}$  values were enhanced when compared with the correspondent  $k^{a1}$  ones. The simultaneous assistance of FA and  $H_2SO_4$  promoted esterification of HMF to 5-formyloxy-methylfurfural (FMF) and one-step conversion of HMF to DMF was achieved. The apparent kinetic constant values  $k_{FA-SA}^{a4}$  were the highest ones.

**Table 1.** Kinetic parameters in the hydrogenation of HMF and physical chemical properties of iridium based-catalysts

Parameter	Catalyst	Ir/SiO <sub>2</sub>	Ir-Ni/SiO <sub>2</sub>	Ir-Co/SiO <sub>2</sub>	Ir-Ru/SiO <sub>2</sub>
$k^a \times 10^{-4}$ (min <sup>-1</sup> )	$k^{a1}$	24	166	40	11
	$k_{FA}^{a2}$	4	2	10	11
	$k_{SA}^{a3}$	27	44	81	36
	$k_{FA-SA}^{a4}$	55	40	98	52
<b>Conversion<sup>b</sup>, %</b>		78	68	91	69
<b>Selectivity<sup>c</sup>, %</b>		52 <sup>c1</sup> , 20 <sup>c2</sup>	15 <sup>c1</sup> , 13 <sup>c2</sup>	11 <sup>c1</sup> , 10 <sup>c2</sup>	30 <sup>c1</sup> , 34 <sup>c2</sup>
<b>(Ir/Si)<sub>at</sub> ratio<sup>d</sup></b>		0.0011	0.0010	0.0038	0.0009
<b>Chemisorbed H<sub>2</sub> (μmol × g<sub>cat</sub><sup>-1</sup>)<sup>e</sup></b>		13.1	17.5	22.2	37.5
<b>NH<sub>3</sub>-TPD (μmol × g<sub>cat</sub><sup>-1</sup>)</b>		94.1	134.7	249.7	202.5

$k^a$  Apparent kinetic constant determined by fitting from HMF hydrogenation experiments <sup>a1</sup> without assistance of acids. <sup>a2</sup> assisted by formic acid (FA). <sup>a3</sup> assisted by  $H_2SO_4$ . <sup>a4</sup> assisted by FA and  $H_2SO_4$ . <sup>b</sup> Conversion at 300 min of reaction assisted by FA and  $H_2SO_4$ . <sup>c</sup> Selectivity at 45% of conversion in the HMF hydrogenation assisted by FA and  $H_2SO_4$ , <sup>c1</sup> to DMF and <sup>c2</sup> to BHMF. <sup>d</sup> Surface atomic ratio determined by XPS. <sup>e</sup> Determined by chemisorption of  $H_2$ .

## References

- [1] J. N: Chheda, Y. Roman-Leshkov, J.A. Dumesic, Green Chem. 9 (2007) 342-350.
- [2] J. W. Medlin, ACS Catal. 1 (2011) 1284-1297.
- [3] V. Ponc, Appl. Catal. A 149 (1997) 27-48.
- [4] P. Mäki-Arvela, J. Hájek, T. Salmi, D. Y. Murzin, Appl. Catal. A, 292 (2005) 1-49.
- [5] J. Lee, Y. T. Kim, G. W. Huber, Green Chem. 16 (2014) 708- 718.
- [6] T. Thananathanachon, T. B. Rauchfuss, Angew. Chem. Int. Ed. 49 (2010) 6616 – 6618.
- [7] F. L. Grasset, B. Katryniok, S. Paul, V. N. Rataj, M. P. Titus, J. M. Clacens, F. D. Campo, F. Dumeignil, RSC Advances 3 (2013) 9942-9948.

# The influence of Zr residues in short channel SBA-15 on state and activity of metallic modifiers (Ag, Au, Cu, Fe)

Joanna Wisniewska<sup>a,b\*</sup>, Kalina Grzelak<sup>a,b</sup>, Shao-Peng Huang<sup>a,b</sup>, Izabela Sobczak<sup>a</sup>,  
Chia-Min Yang<sup>b</sup>, Maria Ziolek<sup>a</sup>

<sup>a</sup> Adam Mickiewicz University in Poznań, Faculty of Chemistry, Umultowska 89b, 61-614 Poznan, Poland

<sup>b</sup> Department of Chemistry, National Tsing Hua University, Hsinchu 30013, Taiwan

The morphology of SBA-15 can be changed by adding either co-surfactant, co-solvent, electrolytes, or organosilanes into the synthesis solutions. One of the methods is based on adding proper amounts of Zr(IV) ions in the conventional synthesis solution as these ions have the ability to accelerate the self-assembly of P123 micelles and TEOS [1,2]. The goal of this study was to get a deep insight into the role of residual zirconium species (involved in the preparation procedure of short channel SBA-15) on the surface properties of ordered mesoporous silica modified with different metals (Ag, Au, Cu, Fe). The main focus was on the interaction of zirconium cations with metallic modifiers and on subsequent modification of acid-base properties of the catalysts.

SBA-15 supports with short channels were prepared according to the procedure described in [1,3]. The molar composition of the reaction mixture was 1 TMOS: 0.017 P123 : 5.9 HCl : 193 H<sub>2</sub>O : 0.05 ZrOCl<sub>2</sub>. In the first approach, H<sub>2</sub>SO<sub>4</sub> (98%) was used in synthesis procedure to remove zirconium ions from supports (SBA-S1, SBA-S2), whereas in the second approach, this step was omitted (SBA-S3). Supports SBA-S1 and SBA-S2 differed by calcination conditions: 773 K for 4 h and 623 K for 9 h, respectively. Metallic catalysts (Ag, Au, Cu, Fe) were prepared by grafting of metal species on organosilane functionalized supports. Silver (Ag) was supported on SBA-S1, gold and copper (Au, Cu) – on SBA-S2, whereas for modification with iron (Fe) SBA-S3 was used as a support. Standard long channel SBA-15 (noted as SBA-L) modified with Ag, Au, Cu and Fe were prepared as reference materials.

Different preparation routes of the supports (with or without sulfuric acid) resulted in different contents of zirconium remained in silica structure or on its surface. Although 98.5 % of the initial amount of zirconium was leached thanks to the use of sulfuric acid, still 0.3-0.4 wt.% of zirconium was present in final metallic material. In SBA-S3, prepared without addition of sulfuric acid, the final amount of remained Zr was much higher (4.7 wt.%) than in the other supports. The remaining zirconium formed strong Lewis acid sites, which considerably influenced the surface properties of metallic materials. Characterization of metal-modified samples (XRD, UV-Vis and XP spectroscopy) allowed determination of the state of metallic modifiers:  $\text{Ag}^0$  and  $\text{Ag}_2\text{O}$  in Ag/SBA-S1,  $\text{Au}^0$  in Au/SBA-S2, CuO in Cu/SBA-S2 and  $\text{Fe}^{3+}$  in Fe/SBA-S3. Also some interactions between the metal modifier species and zirconium ( $\text{Zr}^{4+}$  in silica structure and  $\text{ZrO}_2$ ) was evidenced. Important information about zirconium residue in short channel SBA-15 supports has been estimated from the XPS study of O 1s and Zr 3d regions. It was concluded that iron, copper, and gold modifiers interact on the one hand via oxygen from zirconium oxide and with silica species on the other hand. The interaction between zirconium and silver species ( $\text{Ag}^0$ ,  $\text{Ag}_2\text{O}$ ) was of different nature than that between zirconium and copper, gold or iron. One of the possible reasons for this difference is the bigger size of  $\text{ZrO}_2$  crystallites which caused the exclusively interaction of silver species with zirconium oxide. Interactions between strong acidic zirconium species and metallic modifiers significantly affected the acidic/basic properties of metal catalysts as shown by the results of 2-propanol decomposition and pyridine adsorption combined with FTIR spectroscopy.

Thus, if the short channel SBA-15 is used as a support for metal species one should remember that it displays strong acidic properties by itself, which can significantly affect the properties of final materials.

#### **Acknowledgement**

*National Science Centre in Poland (Project N<sup>o</sup> UMO-2018/29/B/ST5/00137) is acknowledged for the financial support.*

#### **References**

- [1] S.Y. Chen, L.Y. Jang, S. Cheng, Chem. Mater. 16 (2004) 4174–4180. doi:10.1021/cm049247b.
- [2] S.Y. Chen, C.Y. Tang, W.T. Chuang, J.J. Lee, Y.L. Tsai, J.C. Chan, C.Y. Lin, Y.C. Liu, S. Cheng, Chem. Mater. 20 (2008) 3906–3916. doi:10.1021/cm703500c.
- [3] C.H. Liu, C.Y. Lin, J.L. Chen, N.C. Lai, C.M. Yang, J.M. Chen, K.T. Lu, J. Catal. 336 (2016) 49–57. doi:10.1016/j.jcat.2016.01.004.

# Physico-chemical, acid-base and catalytic properties of vanadium based catalysts in oxidative dehydrogenation of n-butane

Samira Slyemi<sup>1</sup>, Akila Barama<sup>1\*</sup>, Hassiba Messaoud<sup>1</sup>, Siham Barama<sup>1</sup> and Juliette Blanchard<sup>2</sup>

(\*email: [a\\_barama@yahoo.fr](mailto:a_barama@yahoo.fr))

<sup>1</sup>Laboratoire des Matériaux Catalytiques et Catalyse en Chimie Organique, Faculté de Chimie, Université des Sciences et de la Technologie Houari Boumediene (USTHB), BP 32, El Alia, Bab Ezzouar, Alger, Algérie.

<sup>2</sup>Sorbonne Universités, UPMC Université Paris 06, CNRS, Laboratoire de Réactivité de Surface, UMR 7197, 4 place Jussieu, F-75005 Paris, France.

Vanadium oxide based catalysts are very active and selective materials in the oxidative dehydrogenation of short hydrocarbons to their corresponding olefins [1]. Their catalytic performances are strongly affected by the environment and the dispersion of vanadium species on the catalyst surface [1,2]. In this work, three series of vanadium-based oxides  $V_2O_5$ -MgO,  $V_2O_5$ -SiO<sub>2</sub> and  $V_2O_5$ -MgO-SiO<sub>2</sub> with the following compositions: 30% $V_2O_5$ -70%MgO, 30% $V_2O_5$ -70%SiO<sub>2</sub> and 30% $V_2O_5$ -40%MgO-30%SiO<sub>2</sub> were prepared by the wet impregnation method and calcined at 550 °C. Their physico-chemical properties were investigated by the aid of different analysis techniques (XRD, Raman, BET, NH<sub>3</sub>-TPD, MET-EDX). Their catalytic performances were evaluated in two reactions: (i) the decomposition of isopropanol to determine their surface acid-base character and (ii) the oxidative dehydrogenation (ODH) of n-butane in order to evaluate their dehydrogenating properties.

XRD and Raman analyses revealed for all samples the formation of a mixture of phases: (i) (MgO, Mg<sub>3</sub>V<sub>2</sub>O<sub>8</sub>) for  $V_2O_5$ -MgO, (ii) (MgO, Mg<sub>3</sub>V<sub>2</sub>O<sub>8</sub>, Mg<sub>2</sub>SiO<sub>4</sub>) for  $V_2O_5$ -MgO-SiO<sub>2</sub> and (iii) ( $V_2O_5$ , amorphous SiO<sub>2</sub>) for  $V_2O_5$ -SiO<sub>2</sub>. The formation of mixed oxides was only observed in the case of MgO based systems because of the strong acid-base interactions between magnesium oxide (basic- character) and  $V_2O_5$  or silica (acidic character). While, in the case of  $V_2O_5$ -SiO<sub>2</sub> system, no formation of mixed oxide was observed due to the weak interactions between vanadium oxide and silica because of their acidic nature.



MET analysis showed that the better surface homogeneity and particles distribution on the catalyst surface were obtained for the  $V_2O_5$ -MgO catalyst. In contrast, larger particles and portions of amorphous forms of vanadium and silica were detected for the  $V_2O_5$ -SiO<sub>2</sub> and  $V_2O_5$ -MgO-SiO<sub>2</sub> oxides. Acidity measurements, using ammonia adsorption, have shown that all the catalysts have a low surface acidity. The acidic character is essentially associated with the presence of vanadium which generates Lewis acid sites ( $V^{5+}$  cations: electron acceptors) and Bronsted acid sites (V-O-H) obtained by hydroxylation of the surface. The lowest amount of adsorbed ammonia was found for the  $V_2O_5$ -MgO sample while the highest was obtained with the  $V_2O_5$ -SiO<sub>2</sub> formulation containing free  $V_2O_5$  oxide.

Results of isopropanol decomposition under nitrogen ( $T_r = 200^\circ\text{C}$ ) revealed that a major formation of propene (dehydration product) was observed on  $V_2O_5$ -SiO<sub>2</sub> and  $V_2O_5$ -MgO-SiO<sub>2</sub> samples confirming their very pronounced acidic character that we could associate with  $V_2O_5$  and  $Mg_2SiO_4$  phases. Whereas, a high production of acetone (dehydrogenation product) was obtained with  $V_2O_5$ -MgO catalyst indicating a dominant basic properties.

Catalytic activity for ODH of n-butane was measured at  $500^\circ\text{C}$  with air/n-butane ratio=5. For all samples, the catalytic tests showed the formation of butenes, cracking products and COx with a low butane conversion (not exceeding 16%). The selectivity to butenes (dehydrogenation products) varies as the following order:  $V_2O_5$ -MgO >  $V_2O_5$ -MgO-SiO<sub>2</sub> >  $V_2O_5$ -SiO<sub>2</sub>. Both  $V_2O_5$ -SiO<sub>2</sub> and  $V_2O_5$ -MgO-SiO<sub>2</sub> catalysts promote the total oxidation of n-butane (formation of COx) while  $V_2O_5$ -MgO sample favors the ODH of n-butane (up to 45% of butenes selectivity). These results are in good agreement with the surface acid-base properties of the catalysts. So, the higher the basicity of the surface, the higher the selectivity to butenes. The good butenes selectivity of  $V_2O_5$ -MgO catalyst, could be also correlated with its smaller crystallites size, better surface homogeneity and the presence of the magnesium orthovanadate phase ( $Mg_3V_2O_8$ ) in which, the mobility of lattice oxygen  $O^{2-}$  (basic species) could be responsible of the activation of the C-H bond and the formation of butenes..

## References

- [1] E.A. Mamedov and V. Cortés Corberán, Applied Catalysis A: General 127, no. 1 (June 22, 1995): 1-40.
- [2] H.H. Kung and M.C. Kung, Applied Catalysis A: General 157, no.1 (September 11, 1997): 105-116.

# MOF-derived metal oxide clusters in porous aluminosilicates: a new catalyst design for the synthesis of bioactive aza-heterocycles

*Nuria Martín, Michiel Dusselier, Dirk E. De Vos and Francisco G. Cirujano*

*Centre for Surface Chemistry and Catalysis, KU Leuven, Belgium.*

Alternative strategies to selectively modify important bio-active scaffolds in a clean and efficient manner, avoiding the waste generated during the steps of purification of pharmaceutically interesting compounds, are required. The new general heterogeneous catalytic methodology presented here is based on the solvent-free grinding and co-calcination of catalytic amounts of MOFs (HKUST-1 or MOF-5) with aluminosilicates (USY or MCM-41). This solid-state synthesis allows to generate MOF derived non-precious metal oxide nanoparticles as catalysts in C-C (alkynylation, alkylation, aldol condensation, hetero-Diels-Alder) and C-N (amination) bond formations to make propargylamine, (spiro)(ox)indole and quinoline derivatives (Fig. 1, bottom), with the highest TOFs ever reported for simple  $H^+/Zn/CuO$  active sites.

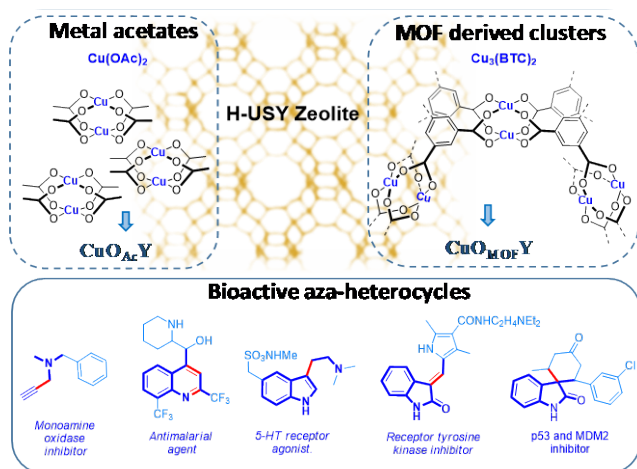


**Figure 1.** Pharmaceutically interesting scaffolds obtained using well-dispersed MOF derived metal oxides within porous H-USY.

metal oxide species since the microporous volume of the starting zeolite decreases after calcining the MOFs in the presence of the H-USY support.

The solids were used as active and stable heterogeneous catalysts for a range of C-C (compounds 1-5) and C-N (compounds 1 and 2) bond formations in N-heterocyclic scaffolds, resulting in substituted propargylamines (1), quinolines (2), indoles (3), oxindoles (4) and spirooxindoles (5), outperforming state-of-the-art Cu and Zn supported catalysts and MOF benchmarks. The higher availability of this metal oxide

sites.

On the one hand, X-ray diffraction (XRD) patterns of the starting HY zeolite and mixed hybrid  $CuO_{MOF}@HY$  and  $ZnO_{MOF}@HY$ , indicate that the zeolite structure is maintained after its co-calcination with the MOF while new peaks appear corresponding to the CuO or ZnO phases.  $N_2$  physisorption suggests some decrease of the H-USY porosity due to MOF derived

sites when they are dispersed within the porous matrix with respect to bulk metal-oxide or metal-organic framework, results in a better activity (TOFs up to two orders of magnitude higher) and reusability (by simple calcination), compared to the pure MOF (see Figure 2).

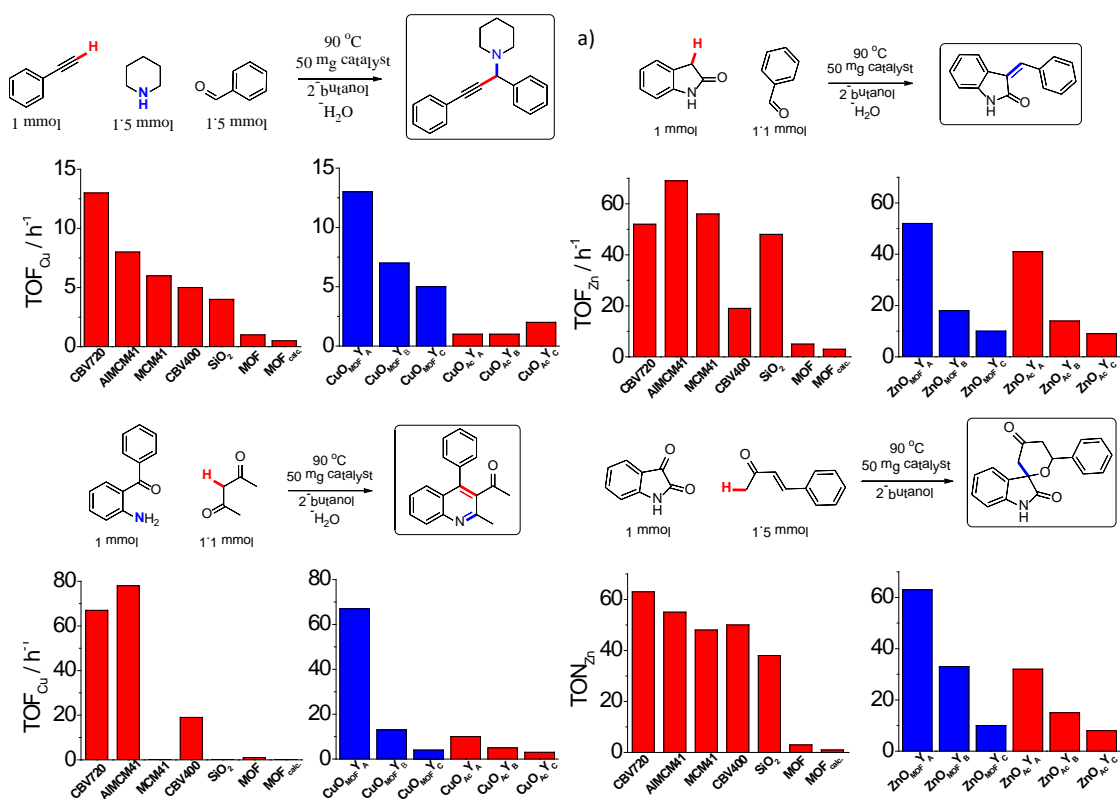


**Figure 2.** Catalytic performance of CuO (left) or ZnO (right) containing aluminosilicates and MOFs in the synthesis of propargylamine 1 (a) and quinoline 2 (b), substituted oxindoles 4 (a) or spirooxindoles 5 (b) at increasing metal loadings (A < B < C) on H-USY.

## References

List and number all bibliographical references at the end of the paper. When referenced within the text, enclose the citation number in square brackets, i.e. [1]

# **The ligand free heterogeneous Sonogashira cross-coupling reaction over an in situ organoiodine capsulized palladium anchored to perovskite catalyst**

*Saba Alapour, University of KwaZulu-Natal, Durban, South Africa; Majid D. Farahani, University of KwaZulu-Natal, Durban, South Africa; Deresh Ramjugernath, University of KwaZulu-Natal, Durban, South Africa; Neil A. Koorbanally, University of KwaZulu-Natal, Durban, South Africa; Holger B. Friedrich, University of KwaZulu-Natal, Durban, South Africa*

The Sonogashira cross-coupling reaction is an industrially important protocol since many electronic materials, pharmaceutical ingredients and liquid crystal materials are prepared via this reaction [1-5].

The use of Pd-based heterogeneous catalysts for cross-coupling reactions has gained considerable attention in recent years. Several studies on Pd based catalysts have shown that leaching can be reduced using suitable strategies to anchor Pd species to the surfaces of heterogeneous materials [6-8].

In this study,  $\text{LaCo}_{0.90}\text{Ni}_{0.05}\text{Pd}_{0.05}\text{O}_3$  perovskite based catalyst provided a high TOF of  $900 \text{ h}^{-1}$  via mainly a heterogeneous mechanism in an environmentally friendly azeotrope medium of water and acetonitrile. This material offered improved surface basicity, high hydrophobicity and also maintained its performance for six recovery cycles and no sign of deactivation was observed. Secondly, DMF and NMP were replaced with water-acetonitrile as a green azeotrope medium in this study. This change in the reaction medium was found to favour the catalytic reaction. Finally, and for the first time, the material perspective of Pd perovskite-based catalysts was investigated in detail and based on the key findings of this study a reaction mechanism that explains a nominal (at most) amount of leaching (stable for six consecutive recovery cycles) and the high reaction rate observed for this catalyst is also discussed.

Nano-sized Pd(0) sites were anchored to the surface of perovskite using an in situ formed colloidal agent. This capsulizing agent was found to consist of organic compounds containing iodine atoms that interacted strongly with basic sites of the

hydrophobic perovskite carrier using adsorption forces. This study illustrates a unique and strong principle for designing green heterogeneous catalysts for common valuable organic reactions.

A mechanism was also proposed where this *in situ* formed colloidal layer acts as an anchoring agent by capsulizing the migrated Pd(0) on the surface, preventing it from leaching to the reaction medium (Fig 1).

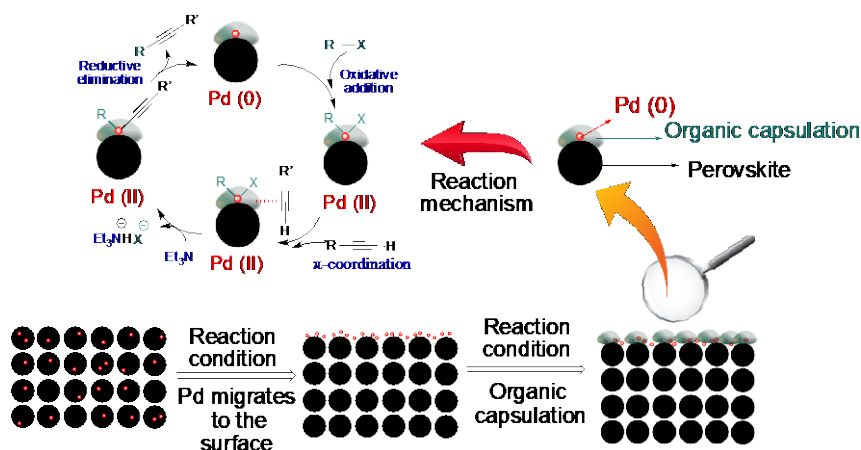


**Fig 1.** Proposed mechanism for heterogenous Sonogashira cross-coupling reaction over under study perovskite

## References

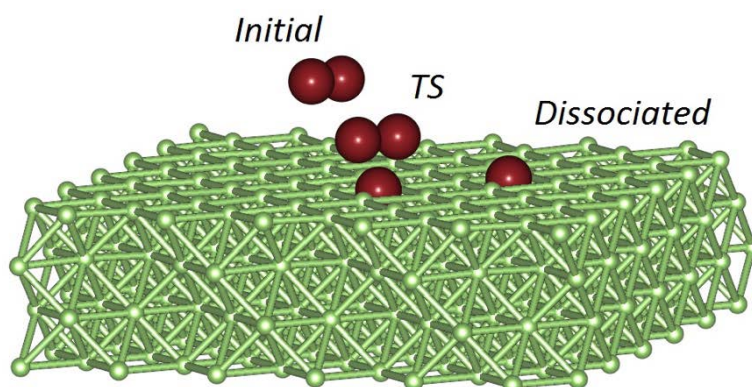
- [1] K.C. Nicolaou, P.G. Bulger, D. Sarlah, Palladium-Catalyzed Cross-Coupling Reactions in Total Synthesis, *Angewandte Chemie International Edition*, 44 (2005) 4442-4489.
- [2] W. Zhang, J.S. Moore, Shape-Persistent Macrocycles: Structures and Synthetic Approaches from Arylene and Ethynylene Building Blocks, *Angewandte Chemie International Edition*, 45 (2006) 4416-4439.
- [3] A. Hamajima, M. Isobe, Convergent Synthesis of the Right-Hand Segment of Ciguatoxin, *Organic Letters*, 8 (2006) 1205-1208.
- [4] P. Siemsen, R.C. Livingston, F. Diederich, Acetylenic Coupling: A Powerful Tool in Molecular Construction, *Angewandte Chemie International Edition*, 39 (2000) 2632-2657.
- [5] S. Alapour, S.J. Zamisa, J.R.A. Silva, C.N. Alves, B. Omondi, D. Ramjugernath, N.A. Koorbanally, Investigations into the flexibility of the 3D structure and rigid backbone of quinoline by fluorine addition to enhance its blue emission, *CrystEngComm*, 20 (2018) 2316-2323.
- [6] N. Huang, Y. Xu, D. Jiang, High-performance heterogeneous catalysis with surface-exposed stable metal nanoparticles, *Sci. Rep.*, 4 (2014) 7228.
- [7] M. Tukhani, F. Panahi, A. Khalafi-Nezhad, Supported Palladium on Magnetic Nanoparticles–Starch Substrate (Pd-MNPSS): Highly Efficient Magnetic Reusable Catalyst for C–C Coupling Reactions in Water, *ACS Sustainable Chemistry & Engineering*, 6 (2018) 1456-1467.
- [8] V. Kozell, M. McLaughlin, G. Strappaveccia, S. Santoro, L.A. Bivona, C. Aprile, M. Gruttadauria, L. Vaccaro, Sustainable Approach to Waste-Minimized Sonogashira Cross-Coupling Reaction Based on Recoverable/Reusable Heterogeneous Catalytic/Base System and Acetonitrile Azeotrope, *ACS Sustainable Chemistry & Engineering*, 4 (2016) 7209-7216.

## Computational Study of O-O dissociation on Palladium Surfaces

*Dmitry Sharapa,<sup>†</sup> and Felix Studt\*,<sup>†,‡</sup>*

<sup>†</sup> Institute of Catalysis Research and Technology, Karlsruhe Institute of Technology, Hermann-von-Helmholtz Platz 1, 76344 Eggenstein-Leopoldshafen, Germany

<sup>‡</sup> Institute for Chemical Technology and Polymer Chemistry, Karlsruhe Institute of Technology, Engesserstrasse 18, 76131 Karlsruhe, Germany



Dissociative chemisorption of  $O_2$  on metal surface, as well as of OOH and HOOH particles, plays crucial role in synthesis of hydrogen peroxide as well as in many other heterogeneously catalysed oxidative processes. Instability of palladium and its alloy catalysts under potential cycling is known issue[1] and growth of structural distortion of highly ordered particles of noble metals with the number of oxygen reduction reaction (ORR) steps is described [2], inspiring investigation of not only the primitive initial shapes of pure metals but also more advanced (e.g. edges), as well as hydrides (that might be easily formed in presence of  $H_2$  in reaction mixture), alloys without regular structure (instead of just intermetallides) and promoters. While Pd(111) shape (that corresponds to perfectly octahedral particles) was well studied computationally, other possible facets of palladium nanoparticles are quite often ignored. That is unreasonable while such surfaces observed experimentally and having much lower dissociation barriers (that might be favourable for some oxidation reactions or to be unwanted parasitic process which has to be suppressed in case of direct  $H_2O_2$  synthesis). We focused this study on dissociative adsorption of  $O_2$ , OOH and  $H_2O_2$  on Pd(100) surface, comparing results with Pd(111), Pd(110) and Pd(211), investigating effect of bromide and sulphate ions (experimentally known to promote direct hydrogen synthesis) as well as coverage effects and effect of In and Sn atoms in the topmost surface and the near-surface layers.

## Computational details

All calculations were performed with the Vienna ab initio simulation package (VASP), using the BEEF-vdW functional and a kinetic cut-off energy of 450 eV. Palladium slabs were constructed with four atomic layers from Pd-bulk preoptimised in the same functional. Unitcell height (perpendicular to the slab surface) was taken equal to 30Å.

## Results and discussion

On each investigated surface strong correlation was found between reaction energy and activation energy, in accordance with Bell–Evans–Polanyi principle. Reaction barriers found on Pd(100) surface appears to be much lower than on Pd(111). Simultaneously, high loading of the surface significantly suppress the dissociation process. Thus in case of O<sub>2</sub> dissociation on Pd(100) presence of any substituent on any of 8 nearest four-fold sites drastically increases reaction energies.

Pd/Sn and Pd/In in case of same conditions (O<sub>2</sub> dissociation on 100 surface) showed twice higher reaction barriers in comparison to pure Pd. This results correlates with experimentally observed grows of selectivity in case of alloys being used as catalysts.

[1] R.K. Singh, R. Rahul, M. Neergat, Stability issues in Pd-based catalysts: the role of surface Pt in improving the stability and oxygen reduction reaction (ORR) activity, *Phys Chem Chem Phys*, 15 (2013) 13044-13051.

[2] R. Chattot, O. Le Bacq, V. Beermann, S. Kühl, J. Herranz, S. Henning, L. Kühn, T. Asset, L. Guétaz, G. Renou, J. Drnec, P. Bordet, A. Pasturel, A. Eychmüller, T.J. Schmidt, P. Strasser, L. Dubau, F. Maillard, Surface distortion as a unifying concept and descriptor in oxygen reduction reaction electrocatalysis, *Nature Materials*, 17 (2018) 827-833.

# Porous silica coated Rh-Co bimetallic nanoparticles as selective catalyst for nitroarenes hydrogenation

*Tatiana M. Bustamante, Cristian H. Campos, Gina Pecchi; Universidad de Concepción, Facultad de Ciencias Químicas, Departamento de Fisicoquímica, Edmundo Larenas 129, Concepción, Chile.*

Porous silica coated Rh-Co bimetallic nanoparticles with Rh loading (0, 0.5, 1.0 and 3.0% by mass with respect to Co) were prepared by a solvothermal synthesis, with a ionic exchange for the incorporation of the noble metal, and a Stöber modified method for the mesoporous silica coated process. The synthesized nanoparticles characterized by TEM, H<sub>2</sub>-TPR, XRD, XPS, VSM and specific area were used as catalysts for the selective hydrogenation of nitroarenes to their respective aromatic aniline [1]. With special highlighted the selective hydrogenation of 4-nitrophenyl-morpholine (4-NFM) to 4-morpholino-aniline (4-MAN) as reaction test is evaluated. Even though different Pd, Pt, Rh, Ir and Au catalysts has been reported as active and selective catalysts for this reaction [2], but the high cost of the noble metals maintains the challenge to develop active, selective and operationally stable based on non-noble catalytic phases as principle phase. A new heterogeneous catalytic system in a core-shell structure [3] formed by a metallic Co core doped with lower Rh content, covered by a porous silica shell in a single unit formed by multifunctional components with large mechanical and catalytic stability is proposed.

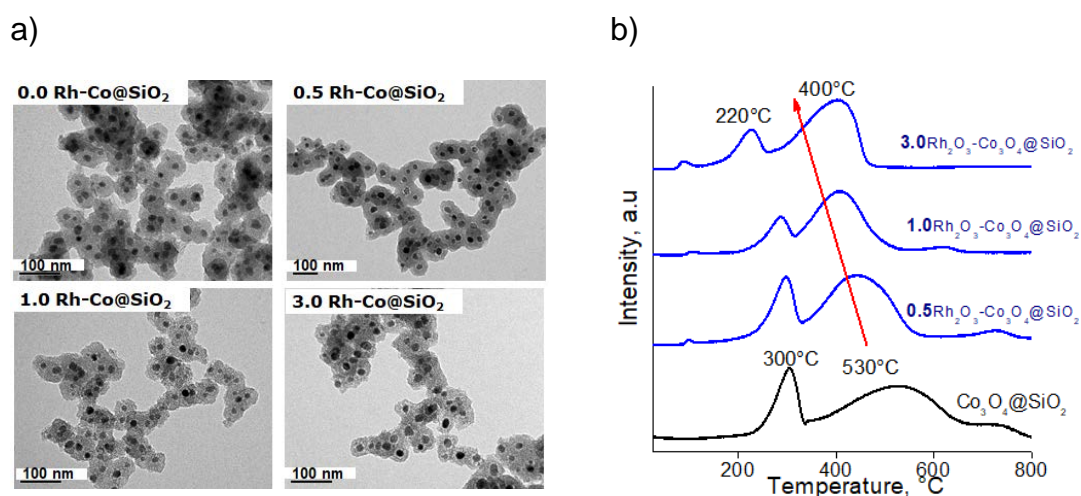


**Figure 1.** a) TEM images for the reduced Rh-Co@SiO<sub>2</sub> catalysts, b) H<sub>2</sub>-TPR profile for Rh<sub>2</sub>O<sub>3</sub>-Co<sub>3</sub>O<sub>4</sub>@SiO<sub>2</sub> precursors structures



The TEM micrographs shown in Fig 1.a) confirm the well-defined core-shell structure formation with a uniform size of 90 nm. To a better known of the reducibility properties of the bimetallic structures TPR profiles were carried out in hydrogen atmosphere. The two stages of reduction from  $\text{Co}^{+2,+3}$  up to  $\text{Co}^0$  for the monometallic cobalt structure that became well-defined and shifted towards lower temperature in the Rh content structures (Fig 1.b) indicate the positive effect of the noble metal in the cobalt reduction. The catalytic performance of the catalysts in the hydrogenation of 4-NFM is shown in Table 1. The large 4-NFM conversion in the Rh content catalysts, largest for the 0.5%Rh content indicate that only for this Rh-Co content improved the catalytic performance in compares with pristine Co and 1.0% and 3.0% Rh-Co core-shell catalyst. The further decrease in the conversion level for larger Rh content could be attributed to the different Rh-Co interaction. At 0.5%Rh content was evaluated the effect of the nature of the nitroarene, 4-NFM-F (4-(2-fluoro-4-nitrophenyl)-morpholine) and 4-NFM-Ona (4-Nitrophenyl)-3-morpholinone) molecules. This catalyst is also active for the 4-NFM-f and 4-NFM-Ona molecules with large selectivity towards the corresponding aromatic aniline.

**Table 1.** Catalytic performance of the Rh-Co@SiO<sub>2</sub> catalysts in nitroarene hydrogenation\*

Entry	Nitroarene	Catalyst	Conversion of the nitroarene (%)	Selectivity aromatic aniline (%)
1	4-NFM	0.0%Rh-Co@SiO <sub>2</sub>	71	99
2	4-NFM	0.5%Rh-Co@SiO <sub>2</sub>	98	99
3	4-NFM	1.0%Rh-Co@SiO <sub>2</sub>	86	99
4	4-NFM	3.0%Rh-Co@SiO <sub>2</sub>	80	99
5	4-NFM-Ona	0.5%Rh-Co@SiO <sub>2</sub>	99	99
6	4-NFM-F	0.5%Rh-Co@SiO <sub>2</sub>	90	97

\*Reaction conditions: Parr® Reactor; 30mg catalyst;  $\text{mol}_{\text{nitroarene}}/\text{mol}_{\text{cat}}:100$ ; P: 20 bar; T: 100°C; solvent:30mL ethyl acetate at 5 h of reaction.

### Acknowledgements

The authors acknowledge Fondecyt 1170083 (Chile), Fondecyt Initiation 11170095 (Chile). TMB thanks to Universidad de Concepción (Chile) for the postgraduate scholarship.

### References

- [1] A.S. Travis, *Manufacture and Uses of the Anilines: A Vast Array of Processes and Products*, 2009.
- [2] K.K.C. Liu, S.M. Sakya, C.J. O'Donnell, J. Li, *Mini-Reviews Med. Chem.* 9 (2009) 1655.
- [3] R.G. Chaudhuri, S. Paria, *Chem. Rev.* 112 (2012) 2373.

# Rapid and direct visualization of organic compounds/reactions/catalytic properties by near infrared imaging spectroscopy

*Kenji Wada, Kagawa University, Kagawa, Japan; Tsubasa Saito, Kagawa University, Kagawa, Japan; Hideya Taniguchi, Aoi Electronics Co.Ltd., Kagawa, Japan; Ichiro Ishimaru Kagawa University, Kagawa, Japan*

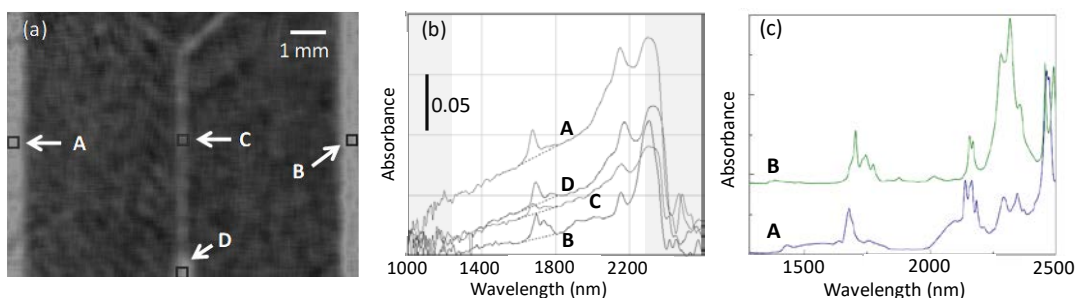
Near infrared (NIR) spectroscopy has developed as an extremely useful method of analysis in many fields. Recently, Takeuchi and co-workers applied this technique to the investigation of adsorbed ammonia of the acidic sites of zeolite-based catalysts [1], indicating utility of this method in catalyst research. However, analysis of two-dimensional (2D) composition distribution by the conventional spectroscopic imaging technology is generally slow and often takes several minutes or more. Ishimaru and co-workers of Kagawa University proposed a novel two-dimensional Fourier-transformed spectroscopic apparatus that is the phase-shift interferometry between the objective lights. This enables the 2D spectral image measurements within several seconds [2]. Because of its simple optical configuration, the palmtop-size portable apparatus (Fig. 1) has the strong robustness for mechanical vibrations. In the present study, rapid and direct analysis of compositional distribution of organic components in a reactor and two dimensional characterization of solid catalysts were examined by this technology.



Figure 1. Our apparatus

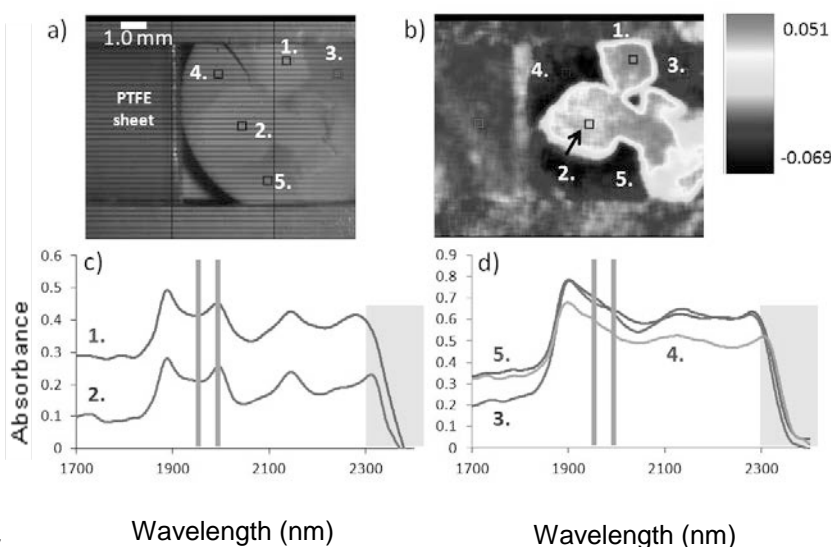
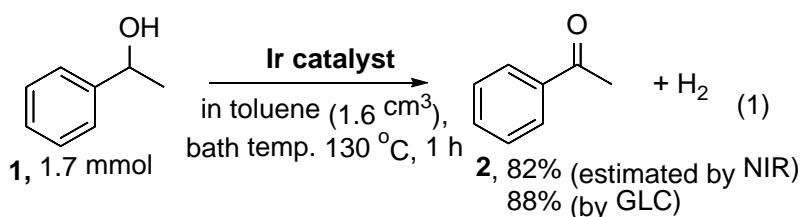
Near infrared imaging spectroscopic analysis was performed under the following conditions: Wavelength range from 1200 to 2300 nm, wavelength resolution 7.93 nm, usual acquisition time 5.625 sec/image. PLSR (Partial Least Squares Regression) analysis was performed using the Unscrambler X 10.5 on the merged spectrum of 11 × 11 pixels.

Fig. 2 show hyperspectral images of the Y-shaped glass mixer (YMC), which clearly shows the distribution of benzyl alcohol and mesitylene. The results of cross-validation of two- and three-component mixtures indicate excellent consistency between NIR-estimated and original data ( $R^2 > 0.99$ ).



**Figure 2.** (a) FTNIR mapping image (4 scans, peak areas at around 1700 nm) of benzyl alcohol and mesitylene in a Y-type mixer. (b) spectra of benzyl alcohol (A), mesitylene (B), and a mixture of them (C), (D). (c) Spectra of A and B obtained by a commercial FTNIR spectrometer.

Interpolation of the spectra by zero-filling greatly shorten the acquisition time (e.g. from 5.625 to 1.250 sec/image) without significant degradation of data quality. The quantitative analysis of the mixture after the catalytic runs [3,4] could rapidly estimate the yields of desired products, as shown in eq.1.



**Figure 3.** (a) NIR image and (b) mapping image of absorbance differences (1950 to 1990 nm) of the composite catalyst. FTNIR spectra at (c) points 1 and 2 ( $\text{Cu}^{2+}/\text{Na}^+/\text{ZSM-5}$ ) and (d) at points 3 to 5 ( $\text{JRC-Z-HY5.5}$ ). 16 scans.

The present technology has been applied for the 2D-characterization of the solid materials. For example, the analysis of adsorbed  $\text{NH}_3$  and  $\text{NH}_4^+$  species on the composite catalyst of  $\text{Cu}/\text{ZSM-5}$  and HY clearly visualized the distribution of  $\text{NH}_3$  adsorbed on  $\text{Cu}^{2+}$  species (Fig.3).

## References

- [1] Takeuchi M.; Tsukamoto, T.; Kondo, A.; Matsuoka, M., *Catal. Sci. Technol.* **5**, 4587 (2015).
- [2] For example, Qi, W.; Wada, K.; Ishimaru, I. et al., *Applied Optics*, **54**, 6254 (2015).
- [3] Wada, K. et al., *Catal. Today*, **303**, 235 (2018).
- [4] Kawahara, R.; Fujita, K. et al, *Angew. Chem. Int. Ed.*, **51**, 12790 (2012).

# Pt nanoparticles encapsulated in hierarchical zeolite framework as an efficient catalyst for oxidation of benzyl alcohol to benzaldehyde

*Piraya Wetchasat, Wannaruedee Wannapakdee, Duangkamon Suttipat,*

*Marisa Ketkaew, Chularat Wattanakit\**

*School of Energy Science and Engineering, Vidyasirimedhi Institute of Science and Technology (VISTEC), Rayong 21210, Thailand*

Zeolites are widely used as catalysts, especially in the field of fine-chemical and petrochemical industries. Typically, they contain well-defined porous structures in molecular dimensions. Moreover, the acidic property makes them highly active in various potential catalytic reactions. Unfortunately, conventional zeolites composing of microporous structures affect directly the diffusion limitation. In order to circumvent this problem, the hierarchical zeolites containing both micro- and mesoporous networks are suggested [1]. In the present study, we report the direct synthesis of Pt nanoparticles encapsulated in hierarchical zeolite framework using a simple one-pot hydrothermal synthesis with various Pt loadings. The ethylenediaminetetraacetic acid, EDTA solution [2] was used to control the size of Pt nanoparticles. As for the conventional zeolite, Pt nanoparticles are preferable deposited on external surfaces. This disadvantage also makes the disadvantage for the oxidation of alcohols. In strong contrast to this, the designed Pt nanoparticles encapsulated in hierarchical zeolite can greatly improve the higher conversion of reactant up to four times compared with the conventional zeolite with the similar Pt loading due to the well-dispersion of metal nanoparticles in zeolite frameworks.

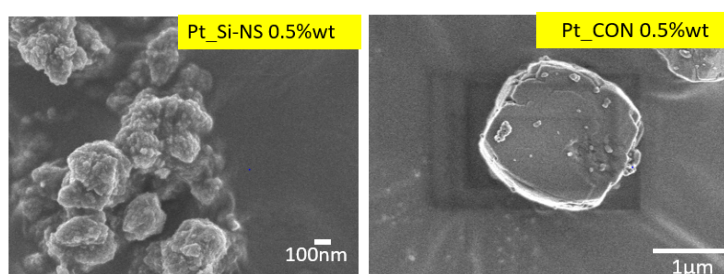


**Fig. 1** SEM images to illustrate the morphology of synthesized Pt-hierarchical zeolite catalysts

## Reference

- [1] W.Wannapakdee, C.Wattanakit, V.Paluka, T. Yutthalekha, and J. Limtrakul, *RSC Advances*, 2016, 6, 2875-2881.
- [2] S.Qiming, N.Wang, Q. Bing, R. Si, J. Liu, R. Bai, P. Zhang, M. Jia, and J. Yu, *Chem*, 2017, 3, 477-493.

# Direct Production of Aromatics from CO<sub>2</sub> and H<sub>2</sub> Achieved by Bulk Molybdenum Phosphide Catalysts #

*Xinping Duan*,\* *Yanting Huang*, *Wei Zhao*, *Linmin Ye*, *Xuelian Liang*, *Youzhu Yuan*\*

*State Key Laboratory of Physical Chemistry of Solid Surfaces, National Engineering Laboratory for Green Chemical Production of Alcohols-Ethers-Esters, College of Chemistry and Chemical Engineering, Xiamen University, Xiamen, 361005, China.*

\*Corresponding author: [zyyuan@xmu.edu.cn](mailto:zyyuan@xmu.edu.cn); [xpduan@xmu.edu.cn](mailto:xpduan@xmu.edu.cn)

## Introduction

Continuously increasing the emissions of greenhouse gas CO<sub>2</sub> is threatening our living environment.[1] To date, C<sub>1</sub> chemicals such as methanol, dimethyl ether, formic acid, etc. have been selectively synthesized.[2] However, production of C<sub>2+</sub> hydrocarbons from CO<sub>2</sub> are not easy because of high kinetic barriers for C–C coupling. More recently, high selective olefins or gasoline has been achieved from CO<sub>2</sub> hydrogenation via utilization of oxide-zeolite bifunctional catalysts.[3] Still, it is challenging to directly synthesize aromatics. Up to now, there are no reports on the highly selective conversion of CO<sub>2</sub> and H<sub>2</sub> into aromatics by one-step process. Here, we report the MoP-based catalysts made by simple H<sub>2</sub> reduction method, which exhibits 75.7% aromatics selectivity among the carbon products without CO in CO<sub>2</sub> hydrogenation reaction. Reverse water-gas shift (RWGS) reaction is completely inhibited by intercalating copper into bulk MoP catalysts.

## Experimental

The bulk oxide precursors were prepared by co-precipitation and bulk phosphide catalysts is obtained via in-situ reduction method. The obtained MoP-based samples, bulk or supported, were evaluated in CO<sub>2</sub> hydrogenation and characterized accordingly.

## Results and discussion

As described, the XRD patterns in Fig. 1a confirms the successful synthesis of MoP and Cu@MoP catalysts, indicative of the characteristic peaks of 28.0, 32.2, 43.2, 57.3°. The size of MoP NPs increases due to the addition of Cu (Fig. 1a). The TEM images of MoP and Cu@MoP validate that the MoP gives relative smaller NPs than that of the Cu@MoP NPs (Figs. 1b and c). Meanwhile, the intercalated Cu is well distributed through the whole MoP crystalline Cu is well distributed through the whole MoP crystalline, as evidenced by EDX-mapping in the right in Fig. 1c. Furthermore, the HRTEM image of Cu@MoP yields d-spacing 2.15 nm for the (100) crystallographic planes of Cu@MoP.

---

# This work is supported by the National Key R&D Program of China (2017YFA0206801).

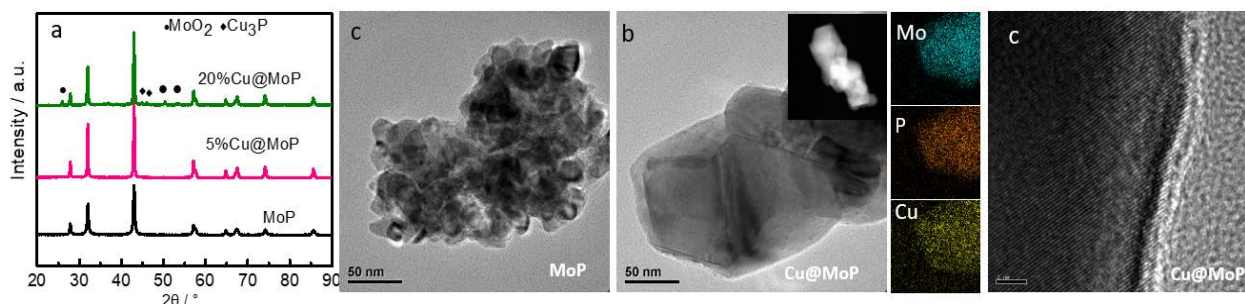


**Fig. 1** Physico-chemical property of bulk and Cu intercalated MoP catalysts. (a) XRD patterns of obtained bulk MoP-based catalysts; (b and c) TEM images of MoP and Cu@MoP catalysts, associated with the EDX-mapping; (c) HRTEM image of Cu@MoP sample.

As indicated in Table 1, copper-based (30 wt%) catalysts produce C1 products ( $\text{CH}_3\text{OH}$ ,  $\text{CH}_4$ , and  $\text{CO}$ ) in  $\text{CO}_2$  hydrogenation, regardless of reaction temperature. Whereas, MoP exhibits the aromatics formation with selectivity of 37.8%, indicating that the C-C bond coupling

Table 1 catalytic performance of various catalysts

Catalyst	Temp. °C	Conv. %	Selec. (CO)	Hydrocarbons Selec. %		
				$\text{CH}_4$	$\text{CH}_3\text{OH}$	Aromatics
CuZnAl	220	17.9	33.2	0.2	99.8	0
CuZnAl	320	24.5	41.5	35.6	64.4	0
Cu-SiO <sub>2</sub>	220	29.3	16	0.4	99.6	0
Cu-ZSM5-SiO <sub>2</sub>	320	25.5	3	39.7	66.2	0
MoP	320	4.8	71.3	52.4	9.6	37.8
20%Cu@MoP	320	7.6	0	15.6	8.6	75.7
20%Cu@MoP	340	9.4	0	30.4	10.9	58.6
Cu@MoP/SiO <sub>2</sub>	320	12.6	96.1	96.5	10.4	2.1

occurred over the MoP surface accompanying  $\text{CO}$  and  $\text{CH}_4$  presence owing to the RWGS. The Cu@MoP shows enhanced  $\text{CO}_2$  conversion and selectivity towards to aromatics with optimum value of 75.7%. Interestingly, no product  $\text{CO}$  was observed with the presence of Cu in MoP phase. To address the reason of aromatics formation over bulk phosphide, the noble metallic properties and moderate acid functions is responsible. Nonetheless, the supported counterpart shows negligible aromatics products due to the acid sites on the support surface.

## Conclusion

In summary, MoP-based catalysts (like Cu@MoP) exhibit an excellent performance for  $\text{CO}_2$  hydrogenation to aromatics. The selectivity of aromatics (excluding  $\text{CO}$ ) reaches as high as 75.7% with 9.4%  $\text{CO}_2$  conversion, coupling with the inhibition of RWGS effect. The tailoring of the external Brønsted acid of MoP by Cu species is beneficial to aromatization.

## References

- [1] Y. Ni, Z. Chen, et al., Nat. Commun. 9 (2018) 3457–3463.
- [2] O. Martin, A.J. Martín, et al., Angew. Chem. Inter. Ed. 55 (2016) 6261–6265.
- [3] F. Jiao, J. Li, et al., Science 351 (2016) 1065–1068.

# A mechanistic study of the dehydrogenation of propane over vanadia-titania catalysts

V.V. Kaichev, Yu.A. Chesalov, A.A. Saraev

*Boreskov Institute of Catalysis, Novosibirsk, Russia*

Propylene is an important starting product employed in the production of polypropylene, propylene oxide, acrylic acid, cumene, etc. The main part of propylene manufactures as a byproduct of oil refining and natural gas processing and only a small part of propylene produces by the catalytic propane dehydrogenation (PDH). Nowadays, CrO<sub>x</sub>- and Pt-based catalysts are mainly used in commercial dehydrogenation of propane. However, these catalysts fast deactivate under reaction conditions due to coke formation and sintering of the metal phase. Moreover, the high cost of platinum and serious pollution issues caused by chromium restrict the further development of the PDH industry. Supported V-based catalysts can be considered as one potential alternative due to their reasonable cost and environmental friendliness. Some vanadium oxide-based catalysts demonstrate the catalytic performance in PDH even better than the chromium oxide-based catalysts [1]. Certainly, the determination of the reaction mechanism and of the nature of the active species in each step of the propane dehydrogenation over V-based catalysts is of high interest. Herein we present first our results of the mechanistic study of the propane dehydrogenation. The oxidative and non-oxidative dehydrogenation of propane over a monolayer V<sub>2</sub>O<sub>5</sub>/TiO<sub>2</sub> catalyst were examined using *in situ* Fourier-transform infrared spectroscopy (FTIR) and *pseudo in situ* X-ray photoelectron spectroscopy (XPS). The combination of these methods allowed us to identify the main reaction intermediates adsorbed on the catalyst surface, the main products in the gas phase as well as the chemical state of vanadium cations under reaction conditions. Synthesis and characterization of the catalyst used are described in detail elsewhere [2,3].

It was found that vanadium on the surface of calcined catalyst is in the V<sup>5+</sup> state, however, the reduction of V<sup>5+</sup> to V<sup>3+</sup> occurs under a propane flow. Simultaneously, the formation of Ti–O–H groups, removing the vanadyl oxygen species and accumulation of carbonaceous deposits were detected by FTIR. Besides, XPS data indicate that the reduction of catalyst is accompanied by reversible destruction of the



vanadia monolayer and formation of 3D clusters or nanoparticles on the titania surface that leads to catalyst deactivation because a significant part of vanadium cations are inaccessible for interaction with propane. The accumulation of carbonaceous deposits and the destruction of the vanadia monolayer were not observed in the presence of O<sub>2</sub> in the gas phase. The V<sup>5+</sup> cations partially reduce to V<sup>4+</sup> under a propane/oxygen mixture. Isopropoxide, acetone, formate, acetate, and carbonate species were detected on the catalyst surface.

We suggest that the oxidative dehydrogenation of propane to propylene over vanadia oxide-based catalysts proceeds via the redox mechanism, where the oxidized catalyst surface oxidizes the propane and is reoxidized by gas-phase oxygen. The active sites contain the V<sup>5+</sup> cations. The C–H activation of propane occurs on the vanadyl oxygen species mainly. The key intermediate is isopropoxide which can dehydrogenate to propylene or acetone. Adsorbed acetone is unstable and can oxidize further to formate and acetate species which can oxidize to CO and CO<sub>2</sub>. The non-oxidative dehydrogenation of propane proceeds over the reduced catalyst. The active sites contain the coordinatively unsaturated V<sup>3+</sup> cations. The C–H activation of propane occurs on a V–O pair via a heterolytic dissociation mechanism. In this process the proton of propane and the negatively charged propyl fragment C<sub>3</sub>H<sub>7</sub><sup>δ-</sup> form bonds with the oxygen and metal ions, respectively. The bridging V–O–Ti oxygen species participate in the C–H activation. The Ti–O–H groups which are the key intermediates are detected by FTIR.

The mechanism of oxidative and non-oxidative dehydrogenation of propane over a monolayer V<sub>2</sub>O<sub>5</sub>/TiO<sub>2</sub> catalyst is discussed in detail.

### Acknowledgements

This work was partially supported by Budget Project No. AAAA-A17-117041710078-1 for Boreskov Institute of Catalysis. The authors thank G.Ya. Popova and E.V. Danilevich for synthesis of the vanadia-titania catalyst.

### References

- [1] S. Sokolov, M. Stoyanova, U. Rodemerck, D. Linke, E.V. Kondratenko, J. Catal. 293 (2012) 67-75.
- [2] V.V. Kaichev, G.Ya. Popova, Yu.A. Chesalov, A.A. Saraev, D.Y. Zemlyanov, S.A. Beloshapkin, A. Knop-Gericke, R. Schlögl, T.V. Andrushkevich, V.I. Bukhtiyarov, J. Catal. 311 (2014) 59-70.
- [3] V.V. Kaichev, Y.A. Chesalov, A.A. Saraev, A.Yu. Klyushin, A. Knop-Gericke, T.V. Andrushkevich, V.I. Bukhtiyarov, J. Catal. 338 (2016) 82-93.



# Deformylation pathway for catalytic synthesis of furfural from hexose sugars

Miyuki Asakawa<sup>1, 2</sup>, Abhijit Shrotri<sup>1</sup>, Atsushi Fukuoka<sup>1, \*</sup>

<sup>1</sup>Institute for Catalysis, Hokkaido University, Sapporo, 001-0021, Japan

<sup>2</sup>Graduate School of Chemical Science and Engineering, Hokkaido University, Sapporo, 060-8628, Japan  
fukuoka@cat.hokudai.ac.jp

## Introduction

Furfural is a versatile chemical precursor used for the synthesis of furan resins, fuels, and plastics. It is industrially produced by dehydration of xylose derived from hemicellulose. Conversion of sugars derived from cellulose to make furfural would produce a single product from the polysaccharide content of biomass, resulting in higher yield and better efficiency of the process. However, cellulose derived hexoses such as glucose and fructose are converted to 5-hydroxymethylfurfural. Furfural is mostly obtained as minor byproduct (<5%) in hexose degradation reaction. In addition, the underlying mechanism of its formation by removal of a carbon atom is unknown. In this work, we have developed a single step reaction for the synthesis of furfural in high yield from glucose and fructose using a combination of heterogeneous and homogeneous catalysts and describe the proposed reaction mechanism.

## Results and discussion

Synthesis of furfural from hexoses was solvent dependent (Fig. 1). Reaction of fructose in the presence of sulfolane (160 °C 2h) resulted in 42 % yield of furfural and 7 % 5-HMF. Comparable results were obtained in the presence of 3-methyl sulfolane and diethyl sulfone. However, in the presence of dimethyl sulfoxide, the selectivity was reversed and 5-HMF was obtained the major product (38 %). Addition of small amount of H<sub>3</sub>PO<sub>4</sub> (0.01 mmol) increased the rate of reaction and the yield of furfural (52 % in sulfolane) and 5-HMF (47% in DMSO) without effecting their selectivity. This suggested that the initial dehydration of fructose prior to removal of carbon atom was the rate limiting step in both cases.

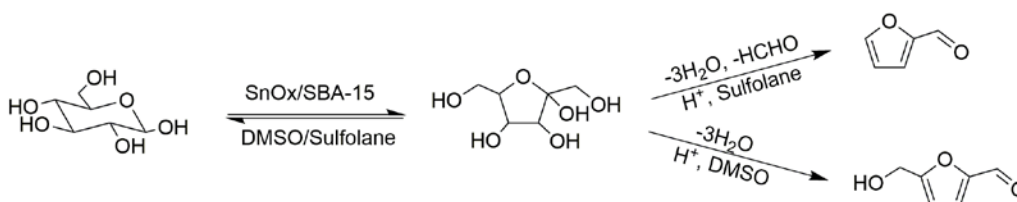


Fig.1: Solvent effect on synthesis of furfural and 5-HMF from hexoses.

For conversion of glucose to furfural, an SnO<sub>x</sub>/SBA-15 catalyst was used as a Lewis acid catalyst. Formation of fructose as the intermediate was confirmed by using <sup>13</sup>C-1 labelled glucose and observing the presence of fructose in <sup>13</sup>C NMR spectrum. The characterization of SnO<sub>x</sub>/SBA-15 catalyst using EXAFS, XRD, TEM and UV-Vis revealed active sites as highly dispersed clusters of tetrahedrally coordinated SnO<sub>2</sub> species for the isomerization reaction. Furfural yield of up to 35% (sulfolane, 160 °C, 2h) was obtained from glucose without H<sub>3</sub>PO<sub>4</sub>.

The elimination of carbon occurred by deformylation of the C6 carbon atom from glucose/fructose. This was confirmed by using <sup>13</sup>C-1-glucose and <sup>13</sup>C-6-glucose and analyzing using GC-MS

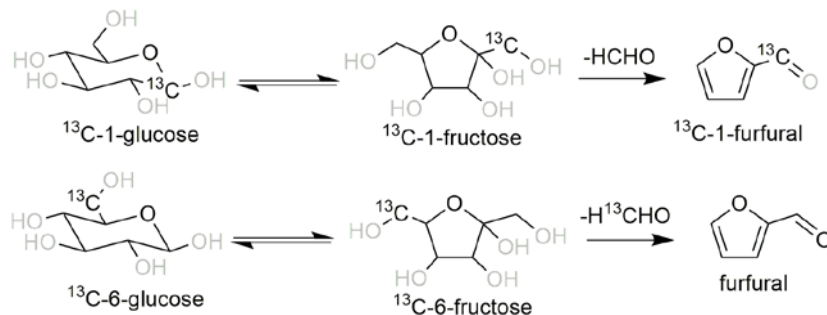


Fig. 2: Elimination of C6 carbon atom as formaldehyde confirmed by GC-MS and <sup>13</sup>C NMR of products obtained from <sup>13</sup>C labelled glucose.

(Fig 2). <sup>13</sup>C was detected at C1 position of furfural when <sup>13</sup>C-1 labelled glucose was used, and it was absent in furfural when <sup>13</sup>C-6-glucose was used. In addition, the <sup>13</sup>C NMR spectrum showed a peak at 84.1 ppm indicating the formation of formaldehyde. Based on these results we propose a mechanism where formation of the intermediate shown in Fig 3 is crucial for determining the selectivity of product. Deformylation proceeds with the abstraction of proton from the hydroxymethyl group and formation of stable furan ring with elimination of formaldehyde. The low basicity of sulfone group was crucial for furfural formation as it is unable to abstract the proton at C5 position which leads to formation of 5-HMF in DMSO.

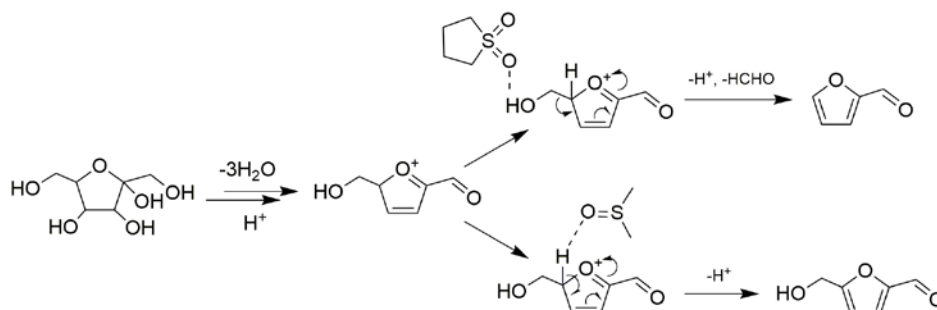


Fig. 3: Proposed mechanism of furfural formation in sulfolane and 5-HMF formation in DMSO

## References

- [1] J. Lange, E. Van Der Heide, J. Van Buijtenen, R. Price, *ChemSusChem*. 2012, 5, 150-166
- [2] A. Shrotri, H. Kobayashi, A. Fukuoka, *Acc Chem. Res.* 2018, 51, 761-768

## Layered Materials as Catalysts in Various Reaction Types

*Gábor Varga<sup>1</sup>, Marianna Kocsis<sup>1</sup>, Rebeka Mészáros<sup>2</sup>, Sándor B. Ötvös<sup>2</sup>, Ferenc Fülöp<sup>2</sup>, Pál Sipos<sup>3</sup>, István Pálinkó<sup>1</sup>*

*<sup>1</sup>Department of Organic Chemistry, University of Szeged, Szeged, Hungary*

*<sup>2</sup>MTA-SZTE Stereochemistry Research Group, Hungarian Academy of Sciences, Szeged, Hungary*

*<sup>3</sup>Department of Inorganic and Analytical Chemistry, University of Szeged, Szeged, Hungary*

Layered materials are promising materials as catalysts in various reaction types leading to the production of fine chemicals [1]. In this contribution, an account is given on the applications of Cu(II)Fe(III)-layered double hydroxide as catalyst in 1,3-dipolar cycloaddition and oxidative coupling reactions as well as that of a novel beyerite-like layered silver substance in the direct synthesis of terminal acetylenes to nitriles.

### **1,3-dipolar cycloaddition and oxidative dimerization reactions**

Cu(II)Fe(III)-layered double hydroxide (CuFe-LDH) is shown to efficiently catalyze 1,3-dipolar cycloadditions of organic azides to alkynes leading to valuable 1,2,3-triazoles as well as oxidative dimerizations of aromatic amines and acetylenes without the need for any auxiliary substances. In most cases, the dimerization reactions need the use of extraneous bases and ligands bearing significant disadvantages as far as environmental impacts and process costs are concerned. In this work, the inherent basic character of a copper-containing layered double hydroxide to facilitate the catalytic reaction was exploited. The reactions were studied in a continuous-flow system to achieve extended parameter spaces for chemical intensification, and to avoid undesired reaction pathways by means of strategic control over the residence time. Other benefits are the safe production as well as scalability. Valuable 1,2,3-triazoles, 1,4-disubstituted 1,3-diynes and diversely substituted aromatic azo compounds were achieved with high chemoselectivity in excellent yields and in short process times even on preparative scales.

The freshly prepared as well as the used CuFe-LDH samples were characterized by a range of state-of-the art instrumental methods (X-ray powder

diffraction, infrared, inductively coupled plasma atomic emission, energy dispersive X-ray and X-ray photoelectron spectroscopies, scanning and transmission electron microscopies and thermal methods). It was established that the catalytic activity of the as-prepared material could be derived from in situ reduction of Cu(II), generating lattice defects containing the catalytically active Cu(I) species. It was verified that oxidative homocoupling of the alkyne component was responsible for the conversion of Cu(II) to Cu(I), but a cooperation of certain structural items of the hydrotalcite-like material could also contribute to the outstanding catalytic efficiency. After successful gram-scale syntheses under high-pressure/high-temperature conditions, no destruction of the catalyst structure was found suggesting that the layered double hydroxide acted as a highly robust catalytic system.

### **Direct synthesis of nitriles from terminal acetylenes**

The synthesis and characterization of a silver-containing hybrid material is also reported as a novel heterogeneous noble metal catalyst. In order to eliminate the need for traditional immobilization techniques, and to create a solid material with structurally-bound silver catalytic centres, the layered structure of a naturally occurring mineral served as the basis of the initial catalyst design. The novel material was prepared by means of the urea-mediated homogeneous precipitation of the corresponding metal nitrates, and was fully characterized by means of diverse instrumental techniques (X-ray diffraction, Raman, IR, UV-Vis, EPR, X-ray photoelectron spectroscopies, thermal methods as well as atomic force, scanning and transmission electron microscopies). The as-prepared material exhibited outstanding activity in silver-catalysed carbon-carbon triple bond activation to yield organic nitriles directly from terminal alkynes with less environmental concerns as compared to the classical synthesis methods. The effects of the reaction time, the temperature, as well as the role of various solvents, nitrogen sources and additives were carefully scrutinized in order to achieve high-yielding and selective nitrile formation. The heterogeneous nature of the reaction was verified and the solid catalyst was recycled and reused numerous times without loss of its activity or degradation of its structure, thereby offering a sustainable synthetic methodology.

### **Reference**

[1] Ötvös, S.B., Pálincó, I., Fülöp, F.: Catalytic use of layered materials – catalytic transformations with the layered structure, *Catal. Sci. Technol.* **9**, 47–60 (2019).

# Photocatalytic reduction of furfural to furfuryl alcohol over titanium dioxide modified with organic compounds under visible light irradiation

*Yuhei Yamamoto, Graduate School of Science and Engineering, Kindai University, Higashiosaka, Japan; Makoto Fukui, Graduate School of Science and Engineering, Kindai University, Higashiosaka, Japan; Atsuhiko Tanaka, Department of Applied Chemistry, Kindai University, Higashiosaka, Japan; Hiroshi Kominami, Department of Applied Chemistry, Kindai University, Higashiosaka, Japan*

## Introduction

Development of visible-light-responding photocatalysts is an important topic for chemical syntheses using solar energy in the future. We have found that reduction of aromatic nitro compounds occurs over titanium dioxide ( $\text{TiO}_2$ ) modified with various organic compounds as visible light-responding photocatalyst<sup>1-3</sup>). However, the effect of modulator on activity has been still unclear. This effect is important in order to develop  $\text{TiO}_2$  photocatalysts modified with various organic compounds.

Furfural (FAL) is one of the important biomass to solve an environmental problem and resource depletion. Furfuryl alcohol (FOL) is an important compound as the raw material of resins and adhesives, and it can be produced from FAL.

In this study, we examined effects of various organic modulators for  $\text{TiO}_2$  on the reduction of FAL to FOL under irradiation of visible light. We found that FAL was almost quantitatively converted to FOL over binaphthol-modified  $\text{TiO}_2$  and that the rate of the FOL formation was dependent on the amount of FAL adsorbed on  $\text{TiO}_2$  modified with various organic compounds.

## Experimental

Methanol containing 1,1'-bi-2-naphthol (BINOL) ( $4 \text{ cm}^3$ ) was added to  $\text{TiO}_2$  powder in an evaporating dish and then methanol was evaporated by stirring with magnetic stirrer at room temperature. The resultant yellow powder was dried for 30 min in vacuo.

$\text{TiO}_2$  modified with BINOL (BINOL/ $\text{TiO}_2$ ) (50 mg) was suspended in  $5 \text{ cm}^3$  of acetonitrile containing FAL (50  $\mu\text{mol}$ ) and triethanolamine (TEOA, 150  $\mu\text{mol}$ ) as a hole scavenger in a test tube, which was sealed with a rubber septum and photoirradiated with a blue LED (115, 110  $\text{mW cm}^{-2}$ ) under Ar with magnetic stirring at room temperature.

## Results and discussion

Fig. 1 shows the time courses of photocatalytic reduction of FAL to FOL over 2.0 wt%BINOL/TiO<sub>2</sub> under irradiation of visible light from blue LED. The amount of FAL monotonously decreased with photoirradiation time and FAL was almost completely consumed after 12 h, while FOL was stoichiometrically obtained. The values of material balance close to unity and the high yield of FOL indicate that only reduction of the aldehyde group to a hydroxy group occurred and that no decomposition of FAL and FOL occurred.

As shown in Fig. 2(a) and (b), the plot of AQE calculated from the ratio of twice the amount of FAL formed and the number of photons irradiated showed a tendency similar to the absorption spectrum of BINOL/TiO<sub>2</sub>. Therefore, we concluded that reduction reaction of FAL in an acetonitrile suspension was induced by photoabsorption of BINOL/TiO<sub>2</sub>.

## Conclusions

We succeeded in novel metal-free and H<sub>2</sub>-free effective reduction of FAL to FOL over BINOL/TiO<sub>2</sub> photocatalyst under visible light irradiation.

## References

- [1] Ikeda *et al.*, *J. Photochem. Photobiol. A*, **2013**, 160, 61-67.
- [2] Fukui *et al.*, *Chem. Commun.*, **2017**, 53, 4215-4218.
- [3] Yamamoto *et al.*, *Catal. Sci. Technol.*, in press.

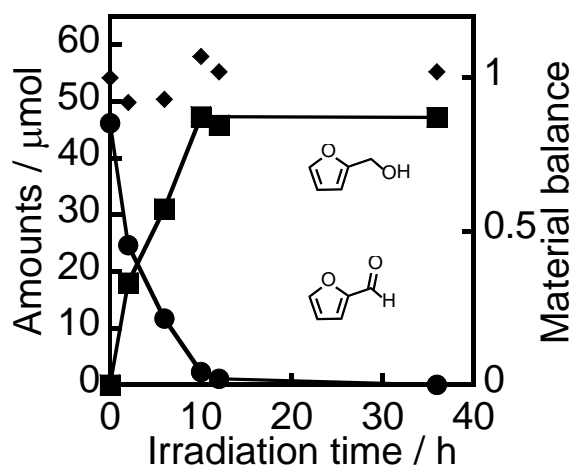


Fig. 1 Time courses of reduction of FAL to FOL in an acetonitrile suspension of BINOL/TiO<sub>2</sub> under irradiation of visible light from blue LEDs.

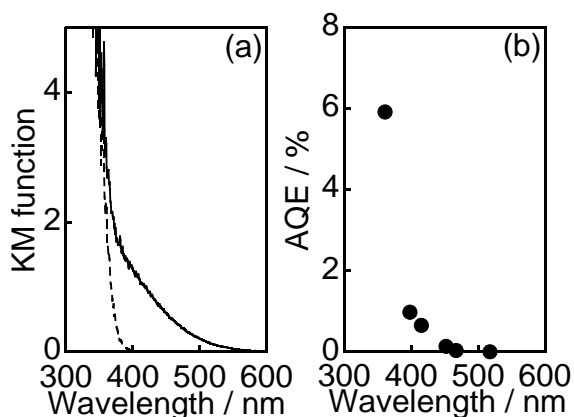


Fig. 2 (a) Absorption spectra of TiO<sub>2</sub> (dashed line) and BiNA/TiO<sub>2</sub> (solid line) and (b) action spectrum in the reduction of FAL to FOL over BINOL/TiO<sub>2</sub>.

**Titanium(IV) oxide having a copper co-catalyst:  
a new type of semihydrogenation photocatalyst working efficiently  
at an elevated temperature under hydrogen-free condition**

*Hiroshi Kominami, Misaki Shiba, Akimi Hashimoto, Shota Imai, Kousuke Nakanishi,  
Atsuhiko Tanaka, Keiji Hashimoto, Kazuya Imamura, Kindai University, Higashiosaka,  
Japan*

**Introduction**

Applications of photocatalytic reduction (hydrogenation) have been less frequently reported because the reduction potential of many organic compounds is more negative than the reduction potential of the conduction band of TiO<sub>2</sub>. Recently, we found that alkynes were successfully hydrogenated to corresponding *cis*-alkenes in alcohol suspensions of Cu-TiO<sub>2</sub> under an H<sub>2</sub>-free condition [1]. The excellence of Cu-TiO<sub>2</sub> is that the photocatalyst showed complete chemoselectivity, *i.e.*, no subsequent hydrogenation of alkenes to alkanes occurred over Cu-TiO<sub>2</sub>. This photocatalytic hydrogenation consists of two processes: 1) formation of an active hydrogen species over Cu particles loaded on TiO<sub>2</sub> under light irradiation and 2) hydrogenation of alkynes over Cu particles. In these processes, process 2) is not a photocatalytic process but a catalytic process. If process 1) is the rate determining step, the overall reaction rate can be increased by decreasing electron-hole recombination and increasing carrier trapping, which could be achieved by preparation of photocatalysts having high crystallinity and a large surface area. On the other hand, if process 2) is the rate determining step, acceleration of process 2) would be more effective than acceleration of process 1). In this study, we focused on the hydrogenation of alkynes in an alcohol suspension of a Cu-TiO<sub>2</sub> photocatalyst because we think that the latter hydrogenation process is the rate determining step. Here we show that the overall reaction rate can be greatly increased by acceleration of the catalytic (thermal) process at an elevated temperature.

**Experimental**

By using the photodeposition method, Cu as a co-catalyst was loaded on TiO<sub>2</sub> (P 25 supplied by Nippon Aerosil Co., Ltd.). In a typical run, Cu-TiO<sub>2</sub> (50 mg) was suspended in 5 cm<sup>3</sup> of methanol containing 50 μmol of 4-octyne in a test tube, which was sealed with a rubber septum and then photoirradiated under Ar with a xenon

lamp in a water bath. The temperature of the water bath was changed to evaluate the effects of reaction temperature on the rate, product selectivity and chemoselectivity of the photocatalytic reaction.

## Results and Discussion

Figure 1(a) shows the time course of photocatalytic conversion of 4-octyne at 298 K. 4-Octyne was consumed along with photoirradiation, while *cis*-4-octene was produced instead, indicating that 4-octyne was hydrogenated by active hydrogen species that were formed over Cu by reduction of protons by photogenerated electrons. Figure 1(b) shows the time course of the same reaction operated at 323 K. The reaction rate for semihydrogenation drastically increased at 323 K, and 4-octyne was almost completely consumed at 1 h and 40 min with chemoselectivity and diastereoselectivity being preserved as they were at 298 K, *i.e.*, 4-octyne was almost quantitatively hydrogenated to *cis*-4-octene within a short time. We noted that the formation of H<sub>2</sub> was completely suppressed during the production of *cis*-4-octene and that H<sub>2</sub> evolved only after consumption of 4-octyne. The results of photocatalytic reaction at 323 K were in contrast to those of the reaction at 298 K shown in Figure 1(a). After consumption of 4-octyne, no *cis*-4-octene was consumed, indicating that Cu-TiO<sub>2</sub> possessed complete chemoselectivity for semihydrogenation of 4-octyne, *i.e.*, no *cis*-4-octene was hydrogenated and isomerized to *trans*-4-octene over Cu-TiO<sub>2</sub> even at 323 K.

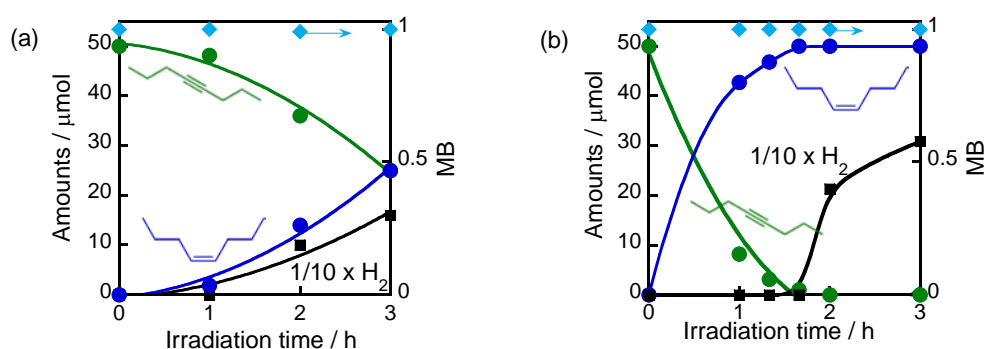


**Figure 1.** Time courses of the amounts of 4-octyne, *cis*-4-octene and H<sub>2</sub> and the material balance (MB) in a methanolic suspension of 0.5 wt% Cu-TiO<sub>2</sub> photocatalyst under deaerated conditions at (a) 298 K and (b) 323 K.

## References

[1] H. Kominami, M. Higa, T. Nojima, T. Ito, K. Nakanishi, K. Hashimoto, K. Imamura, *ChemCatChem*, **8**, 2019 (2016).



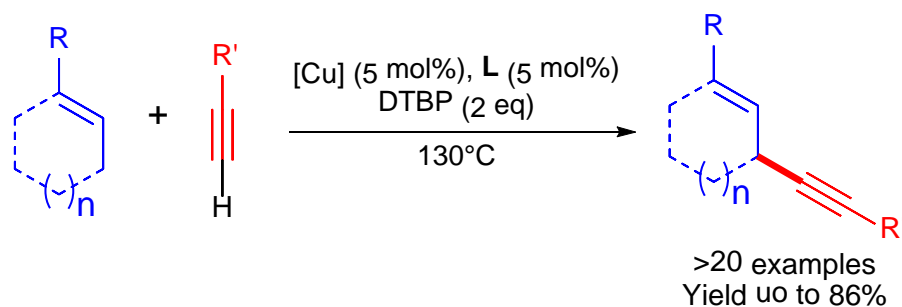
# Copper Catalyst for Direct Allylic-Alkynylation *via* Cross Dehydrogenative Coupling Reaction

Ahmad A. Almasalma, Dr. Esteban Mejía

Leibniz Institute für Katalyse e.V, Albert-Einstein Straße 29a, 18059 Rostock

C-C bonds are in numerous compounds and essential components of organic compounds' skeleton. For that, improvement of C-C bond formation reactions *via* efficient and direct approach is a highly attractive research area.<sup>1</sup> Cross dehydrogenative coupling reactions (CDC) are considered as the state of the art for C-C bond formation in organic synthesis. Direct using of the reactants without prefunctionalization, shorting the rout synthesis and minimizing the waste by products specially the metal salts, but temperature is still required to generate the radical, which will initiate the reaction.<sup>2</sup> At high temperatures the radical is very reactive increasing the possibility of byproducts formation and limiting the scope of reactants and the types of solvents. No doubt, running the reaction at ambient temperatures will overcome these limitations and increase the synthetic applications of CDC reactions. Direct functionalization of Csp<sup>3</sup>-H bond is still a challenging reaction due to similar highly reactive Csp<sup>3</sup>-H bonds in the molecule.<sup>3</sup> One of these important sp<sup>3</sup> carbons is allylic, its functionalization produces a new chiral carbon and controlling the chirality<sup>4</sup> obviously is very important in the pharmaceutical and medicinal chemistry.<sup>5</sup> Since radical is required an alternative way to generate could be using light *via* single electron transfer (SET), but still until now prefunctionalized reactants are required with using photo catalysts.<sup>6</sup> Recently, we were able to alkylate allylic carbon under oxidative conditions, but high temperature is unavoidable.<sup>7</sup> Combination between the advantages of CDC reactions and photo catalyst reactions to functionalize ubiquitous Csp<sup>3</sup>-H bonds is highly demand approach with using earth-abundant elements like Copper instead of precious elements. In our current contribution, we report for the first time in situ prepared copper complex photocatalyst to synthesis synthesize 1,4-enyne compounds directly from alkene and terminal alkyne at ambient temperatures (Figure 1).

our previous work; allylic alkynylation under thermal conditions



this work; allylic alkynylation at ambient temperature

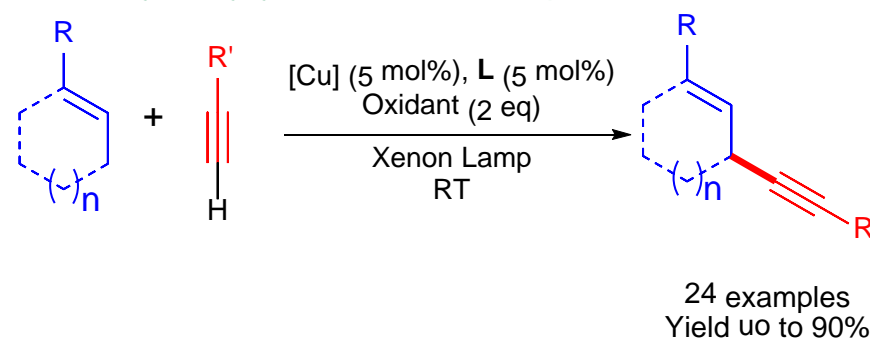


Figure 1: Allylic Alkynylation either at elevated or ambient temperature.

Under the optimized reaction conditions, wide scope of coupling compounds are convenient to furnish the desired products in good to excellent yield. In the mechanistic study we found the reaction does not follow radical path way comparing with the thermal conditions and the SET from the photo-catalyst excited state to the oxidant initiates the reaction. Furthermore we tried to control the stereo selectivity of the products by designing convenient ligands and we got some promising results. In our work we report new generation types of copper photocatalysts complexes, which could be optimized for more reactions and applications. We are trying to pave the way for more transformation from the classical reaction to modern ones using sustainable source of energy to achieve the increasing demand of fine chemical products.

## References

- (1) Yi, H.; Zhang, G.; Wang, H.; Huang, Z.; Wang, J.; Singh, A. K.; Lei, A. *Chem Rev* **2017**, *117*, 9016.
- (2) Varun, B. V.; Dhineshkumar, J.; Bettadapur, K. R.; Siddaraju, Y.; Alagiri, K.; Prabhu, K. R. *Tetrahedron Letters* **2017**, *58*, 803.
- (3) Gini, A.; Brandhofer, T.; Mancheno, O. G. *Organic & Biomolecular Chemistry* **2017**, *15*, 1294.
- (4) Cui, X. Y.; Ge, Y.; Tan, S. M.; Jiang, H.; Tan, D.; Lu, Y.; Lee, R.; Tan, C. H. *J Am Chem Soc* **2018**, *140*, 8448.
- (5) Li, Y.-X.; Xuan, Q.-Q.; Liu, L.; Wang, D.; Chen, Y.-J.; Li, C.-J. *J. Am. Chem. Soc.* **2013**, *135*, 12536.
- (6) Roslin, S.; Odell, L. R. *European Journal of Organic Chemistry* **2017**, *2017*, 1993.
- (7) Almasalma, A. A.; Mejia, E. *Chemistry* **2018**, *24*, 12269.

## **Nanocatalysis: A Powerful Instrument for Wastewater Valorization**

*Mariana Rocha, REQUIMTE/LAQV, Department of Chemistry and Biochemistry, Porto, Portugal; Clara Pereira, REQUIMTE/LAQV, Department of Chemistry and Biochemistry, Porto, Portugal; Cristina Freire, REQUIMTE/LAQV, Department of Chemistry and Biochemistry, Porto, Portugal*

The environmental concern about water pollution by toxic compounds has been increasing exponentially. [1] So, the design of efficient catalysts for the transformation of harmful organic pollutants found in water and wastewater into compounds with high added-value and lower toxicity has raised. [2] Nitroarene compounds, such as 4-nitrophenol (4-NP) and 4-nitroaniline (4-NA), are highly toxic and environmentally hazardous. [3] However, the respective reduction products, 4-aminophenol (4-AP) and 4-aminoaniline (4-AA), are useful compounds for many chemical industries, namely, to produce rubber, antioxidants, pharmaceuticals, dyes and agrochemicals. [4] Thence, significant research has been focused on the development of efficient and eco-friendly metal catalysts to be applied in the conversion of nitroarenes into the corresponding amine derivatives. However, metallic nanoparticles are difficult to remove from the reaction media and tend to aggregate in solution due to their high surface energy which decreases their catalytic activity. [5] The strategy to overcome this problem is to anchor the nanoparticles onto solid supports, such as titanium dioxide nanoparticles (TiO<sub>2</sub> NPs). TiO<sub>2</sub> is one of the best supports for metal NPs due to its thermal and chemical stability, non-toxicity, relative low cost and semiconducting properties. [6] In this work were synthesized Au/TiO<sub>2</sub> and Ag/TiO<sub>2</sub> nanocomposites through the adsorption of the metal salt precursors onto TiO<sub>2</sub> surface and posterior reduction of Au<sup>3+</sup> and Ag<sup>+</sup> to metal Au<sup>0</sup> and Ag<sup>0</sup>, using various reducing agents in this reduction step: citric acid, sodium borohydride or light source to promote the reduction ( $\lambda = 340$  nm). The influence of the type of reducing agent and its concentration on the Au and Ag NPs formation, loading, oxidation state and type of bond established with the TiO<sub>2</sub> solid support was investigated. Moreover, the effect of the type of immobilized NPs on the catalytic performance, Au *versus* Ag, was assessed. The performance of the prepared nanocomposites was evaluated in the heterogeneous catalytic reduction of two

model substrates (4-NP and 4-NA) in aqueous solution in the presence of sodium borohydride as the reducing agent.

Both Au- and Ag-based catalysts led to a total conversion of 4-NP within 260 and 40 s, respectively. The reaction followed a pseudo-first-order kinetic with rate constants of  $19.1 \times 10^{-3}$  and  $94.2 \times 10^{-3} \text{ s}^{-1}$ , respectively, demonstrating the higher catalytic performance of the Ag-based material. For the 4-NA reduction, the highest catalytic performance was observed with the Au-based material, achieving total conversion within 90 s with a rate constant of  $29.4 \times 10^{-3} \text{ s}^{-1}$ , while the Ag-based material achieved total conversion within 120 s. After catalysis, the Au nanoparticles retained their metallic state, whereas the Ag nanoparticles were partially oxidized, which is detrimental for their subsequent catalytic activity. The Au and Ag-based  $\text{TiO}_2$  catalysts could be reused for ten consecutive cycles without any treatment, with the Au-based catalysts showing the highest stability and robustness.

#### References

- [1] T. Bora, J. Dutta, J. Nanosci. and Nanotechno. 14 (2014) 613-626.
- [2] X. Le, Z. Dong, Y. Liu, Z. Jin, T.-D. Huy, M. Le, J. Ma, J. Mater. Chem. A 2 (2014) 19696-19706.
- [3] M. Kulkarni, A. Chaudhari, J. Environ. Manag. 85 (2007) 496-512.
- [4] I. Ibrahim, I.O. Ali, T.M. Salama, A.A. Bahgat, M.M. Mohamed, Appl. Catal. B-Environ. 181 (2016) 389-402.
- [5] X. Wang, F. Tan, W. Wang, X. Qiao, X. Qiu, J. Chen, Chemosphere 172 (2017) 147-154.
- [6] A.A. Ismail, A. Hakki, D.W. Bahnemann, J. Mol. Catal. A-Chem. 358 (2012) 145-151.

# ***Nonoxidative synthesis of dimethoxymethane by the gas-phase methanol dehydrogenation over bifunctional copper catalysts***

*Ruiyan Sun, RWTH Aachen, Aachen, Germany;*

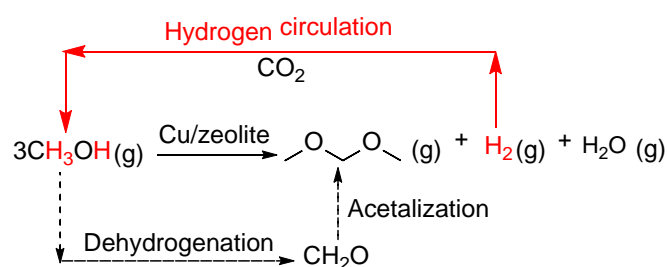
*Regina Palkovits\*, RWTH Aachen, Aachen, Germany*

The adverse effect of vehicle exhaust on human health and ecosystem has been increasingly recognized in the past decades, in addition to its considerable contributions to the greenhouse gas emission. As a result, many efforts have been devoted to seek powerful technical solutions to meet the stringent emission standards. Upgrading and sophisticating the exhaust after-treatment systems were in the focus;<sup>[1]</sup> however, these approaches increase costs, and more importantly, they are inherently limited in reducing the carbon footprint of the entire mobility sector. In this regard, a transition from conventional fossil fuels towards more renewable alternative fuels presents a highly promising strategy to address the issues resulting from the transportation sector. Specifically, for diesel-type fuels, a desirable substitute fuel should present a clean combustion property with reduced soot and NO<sub>x</sub> formation and be potentially synthesized in a sustainable approach based on CO<sub>2</sub>/H<sub>2</sub>. In addition, it would be a huge advantage if such substitute diesel can be directly used as a drop-in fuel without major modifications to the current transportation system. Numerous oxygen-containing compounds such as methanol, dimethyl ether and oxymethylene ethers, have been suggested as potential diesel fuel additives. Especially, oxymethylene ethers (OME) with medium chain length have attracted intense interests in recent years, owing to their excellent ability in reducing soot formation and good compatibility with diesel engines.<sup>[2]</sup> Dimethoxymethane (DMM) is the simplest compound of the oxymethylene ether homologues. Importantly, it can function as a platform chemical for longer chain OME synthesis and find applications in fine chemical industries.<sup>[3]</sup>

The current DMM production primarily relies on an oxidative reaction scheme, wherein methanol is either first oxidized to formaldehyde (FA) in the presence of oxygen followed by an acetalization of FA with methanol to yield DMM in two steps, or directly oxidized to DMM in one step. Hydrogen atoms in methanol are concurrently oxidized by O<sub>2</sub> to form water, thereby leading to low hydrogen efficiency and high energy inputs for water separation. To avoid these inefficient oxygen-involved pathways, a novel synthetic strategy via non-oxidative methanol

dehydrogenation to DMM with the formation of H<sub>2</sub> instead of H<sub>2</sub>O appears to be highly attractive. Within this new route, a closed H<sub>2</sub> circulation can be realized between methanol and DMM synthesis, thus improving the overall exergy efficiency of this process chain.

Herein, we report the first example of DMM synthesis following this novel strategy, enabled by bifunctional Cu/zeolite catalysts in gas-phase. Cu was fixed as metallic site for the dehydrogenation reaction. The variations in zeolite type and SiO<sub>2</sub>/Al<sub>2</sub>O<sub>3</sub> ratio as well as the proximity effect were investigated to optimize the synergy between zeolites and Cu, which needed to be spatial close in order to maximize DMM formation. Among the examined catalysts, 1% Cu/Hβ with a SiO<sub>2</sub>/Al<sub>2</sub>O<sub>3</sub> ratio of 650 presented the highest activity and selectivity toward DMM. 80% selectivity was achieved at a methanol conversion of 3.6% at GHSV of 14369 ml h<sup>-1</sup> g<sub>cat</sub><sup>-1</sup>, atmospheric pressure, and 200 °C in a continuous fixed-bed reactor. Interestingly, an induction period featuring a remarkable rise in DMM selectivity from 20 to 80% with time on stream was observed on this catalyst. The ongoing studies are expected to reveal the underlying phenomenon.



Scheme 1. New approach to synthesize DMM through gas-phase methanol dehydrogenation

*This work was funded by the German Federal Ministry of Education and Research (BMBF) within the Kopernikus Project P2X: Flexible use of renewable resources exploration, validation and implementation.*

## References

- [1] M. V. Twigg, Progress and future challenges in controlling automotive exhaust gas emissions. *Appl. Catal., B* **2007**, 70, 2-15.
- [2] C. J. Baranowski, A. M. Bahmanpour, O. Kröcher, Catalytic Synthesis of Polyoxymethylene Dimethyl Ethers (OME): A Review. *Appl. Catal., B* **2017**, 217, 407-420.
- [3] R. Sun, I. Delidovich, R. Palkovits, Dimethoxymethane as a Cleaner Synthetic Fuel: Synthetic Methods, Catalysts, and Reaction Mechanism. *ACS Catal.* **2019**, DOI: 10.1021/acscatal.8b04441.

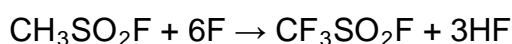
# The reactor design and operation for Simons electrochemical fluorination at pilot scale for synthesis of $\text{CF}_3\text{SO}_2\text{F}$

WANG Yaqiong, WANG Dawei, DING Yuanqiong, SHAO Qing, XU Wenlin  
(Coll. of Chem. & Chem. Eng., Yangzhou Uni., Yangzhou 225002, Jiangsu, China)

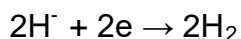
## 1. Principle of Electrochemical preparation of fluoride $\text{CF}_3\text{SO}_2\text{F}$

Electrochemical fluorination preparation of  $\text{CF}_3\text{SO}_2\text{F}$  is carried in HF solution and  $\text{CH}_3\text{SO}_2\text{F}$  as raw material, nickel as an anode by Simons electrochemical fluorination synthesis technology<sup>[1-4]</sup>.

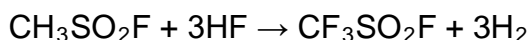
The reaction on anode reaction is:



Cathodic reaction:



Total reaction:



## 2. Process analysis in the Electrochemical fluorination preparation of $\text{CF}_3\text{SO}_2\text{F}$

Based on recent developments, the nickel fluorinating agent mediated mechanism in the Simons electrochemical fluorination of  $\text{CH}_3\text{SO}_2\text{F}$  to  $\text{CF}_3\text{SO}_2\text{F}$  is proposed. It is shown that the yield and current efficiency of the product mainly depend on the operating current density and the mass transport rate. Thus useful rules to optimize the process of electrochemical fluorination in anhydrous hydrogen fluoride (HF) for reactor design and operation for the Simons fluorination of  $\text{CH}_3\text{SO}_2\text{F}$  are formulated for the solid-liquid heterogeneous reaction system.

In order to improve the yield and current efficiency as well as reduce the produce rate of the free fluorine ( $\text{F}_2$ ), an effective method is proposed to improve the mass transfer and reduce operating current density. A three-dimensional electrode electrochemical reactor is designed with a large specific surface area, which can significantly reduce the operating intrinsic current density, and effectively improve mass transfer with a large specific surface area, increase the concentrations of  $\text{CH}_3\text{SO}_2\text{F}$  on the reaction surface of the anode. The three-dimensional electrode electrochemical reactors fundamentally reduces the likelihood of fluoride chemical reaction, and raises the production efficiency of electrochemical reactor.

### 3. The designed reactor used in the Electrochemical fluorination preparation of $\text{CF}_3\text{SO}_2\text{F}$

Based on methyl sulfonyl fluoride electrochemical fluorination process characteristics of electrochemical fluorination process for the reaction kinetics control process, in order to reduce the cell voltage, improve current efficiency and product yield. Therefore, this paper adopts three-dimensional electrode electrochemical reactor design and operation, improve the production ability of the reactor, current efficiency and reaction yield.

The designed reactor and operation results for an electrochemical fluorination process at 1kg/h  $\text{CF}_3\text{SO}_2\text{F}$  are as follows:

(1) A three-dimensional electrode anodet is designed packed 20-mesh nickel wire mesh as anode, iron as cathode, PTFE as membrane. The tank of the electrochemical reactor is a seamless steel tube with a volume of 120L and an internal surface area of  $1.55\text{m}^2$ . The geometric surface area of the nickel wire mesh is  $20\text{m}^2$ , the usable area of the anode is about  $15\text{m}^2$ , and the designed operating current is 1200A.

(2) The experiments was carried out in the electrochemical reactor with 80 L of HF and 12 kg  $\text{CH}_3\text{SO}_2\text{F}$ , operating temperature was  $5\text{ }^\circ\text{C}$  -  $12\text{ }^\circ\text{C}$ , at a operating current 1200A – 1500A. The results is that the yield of the product is more than 85%, current efficiency is over 95% , the operating cell voltage from 6.2 V to 6.8 V. At the generation rate of 1 kg/h $\text{CF}_3\text{SO}_2\text{F}$ .

(3) The electrochemical fluorination reaction of organics Simons using a three-dimensional electrode electrochemical reactor has many outstanding advantages. The electrochemical fluorination of organics by Simons electrochemical fluorination in three dimensional electrode electrochemical reactor is feasible and economical.

#### References

- [1] XU Wenlin, WANG Yaqiong, CUI Yaoxing. Progress of Simons electrochemical fluorination of organic compounds. *Chemical Industry and Engineering progress*, 2011, 30(8):1670-1675
- [2] Simons J H. *Fluorine Chemistry* Vol. 1.[M]. New York: Academic Press, 1950
- [3] Kirk K L. Fluorination in medicinal chemistry: Methods, strategies, and recent developments[J]. *Organic Process Research & Development*, 2008, 12(2):305-321
- [4] Conte L, Gambaretto Gian Paolo. Electrochemical fluorination: State of the art and future tendency[J]. *Journal of Fluorine Chemistry*, 2004, 125(2):139-144



# Bimetallic Nanocrystal-Based Catalysts for the Direct Synthesis of $\text{H}_2\text{O}_2$

*S. Wang, D. E. Doronkin, A. Zimina, S. Behrens, Karlsruhe Institute of Technology (KIT), Karlsruhe, Germany*

## Introduction

Hydrogen peroxide ( $\text{H}_2\text{O}_2$ ) is an important chemical with valuable application in industries, such as the paper and pulp, textile, as well as for waste water treatment or chemical oxidation reactions [1]. At an industrial scale,  $\text{H}_2\text{O}_2$  is produced by sequential oxidation and hydrogenation of anthraquinone, i.e. a multistep process that generates a large amount of waste and consumes extensive energy [2]. Due to the high capital investment and operating costs of this indirect process, its direct synthesis from  $\text{H}_2$  and  $\text{O}_2$  is highly desirable [3]. However,  $\text{H}_2\text{O}_2$  is a reactive intermediate that further decomposes or hydrogenates to water and the design of novel catalysts with improved selectivity and productivity of  $\text{H}_2\text{O}_2$  has remained of great interest.

To overcome the problem of poor  $\text{H}_2\text{O}_2$  selectivity, Pd catalysts have been alloyed with various elements (e.g., Au, Ag or Sn, etc.). Conventional impregnation and (co)precipitation methods often yield poorly defined particles with size, shape and compositional inhomogeneities. Here, colloidal nanocrystals (NCs) may provide well defined building units for model catalysts which allow independently and systematically addressing the influencing catalyst parameters of the NCs (size, shape, composition) and the metal oxide support [4, 5].

Herein, we present the synthesis of a Pd-based NC library with controlled size and a wide variety of compositions (PdM, M = Ni, Zn, Ga, Sn, In, Pb) which were successively immobilized on a support and used as catalysts in direct  $\text{H}_2\text{O}_2$  synthesis.

## Materials and Methods

Colloidal Pd and PdM NCs were synthesized from the metal acetylacetonate or metal acetate precursors in oleylamine and trioctylphosphine and successively supported on  $\text{TiO}_2$  (pretreated with  $\text{H}_2\text{SO}_4$ ). The structure, size and composition of the NCs and catalysts were characterized by X-ray diffraction (XRD), electron microscopy together with energy-dispersive X-ray analysis, atomic emission spectroscopy (ICP-AES) and

*ex situ* X-ray absorption spectroscopy (XAS). Catalytic tests were carried out in a semi-continuous batch reactor in ethanol with H<sub>2</sub>SO<sub>4</sub> promotor (40 bar, 30 °C, H<sub>2</sub>/O<sub>2</sub> ratio 0.24, diluted with 76% N<sub>2</sub>). The gas composition and H<sub>2</sub>O<sub>2</sub> concentration was analyzed by micro GC and UV-Vis spectrometry, respectively.

## Results and Discussion

Bimetallic PdM-based NCs were synthesized with uniform sizes in the range of 3.7 to 6.7 nm, controlled elemental composition (PdNi, PdZn, PdGa, PdIn, PdSn, PdPb) and different Pd/M ratio. Most bimetallic NCs (PdNi, PdZn, PdGa, and PdIn) were of random alloy-type structure, only PdSn and PdPb NCs revealed an ordered intermetallic composition. Pd NCs were used as a reference. The supported NCs revealed high productivities and selectivities towards H<sub>2</sub>O<sub>2</sub> of up to 80%. The catalytic tests showed that the type of alloyed promotor (M) and the Pd/M ratio influenced catalytic properties.

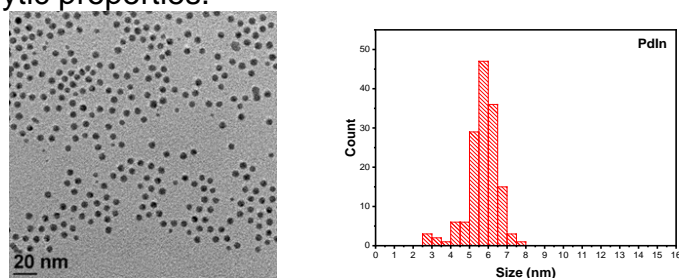


**Figure 1.** TEM image and particle size distribution of PdIn NCs.

## Conclusions

The library of PdM NCs has been successfully synthesized and characterized by XRD, XAS, TEM. Such NC-derived catalyst libraries provide well-defined model systems for systematically exploring ensemble and electronic effects in the direct synthesis of hydrogen peroxide, a step towards the future goal of rational catalyst design.

- [1] S.J. Freakley, Q. He, J.H. Harry, L. Lu, D.A. Crole, D.J. Morgan, E.N. Ntainjua, J.K. Edwards, A.F. Carley, A.Y. Borisevich, Palladium-tin catalysts for the direct synthesis of H<sub>2</sub>O<sub>2</sub> with high selectivity, *Science*, 351 (2016) 965-968.
- [2] D.A. Crole, S.J. Freakley, J.K. Edwards, G.J. Hutchings, Direct synthesis of hydrogen peroxide in water at ambient temperature, *Proc Math Phys Eng Sci*, 472 (2016) 20160156.
- [3] N.M. Wilson, D.T. Bregante, P. Priyadarshini, D.W. Flaherty, Production and use of H<sub>2</sub>O<sub>2</sub> for atom-efficient functionalization of hydrocarbons and small molecules, 29 (2017) 122-212.
- [4] M. Gentzen, D.E. Doronkin, T.L. Sheppard, J.-D. Grunwaldt, J. Sauer, S. Behrens, An intermetallic Pd<sub>2</sub>Ga nanoparticle catalyst for the single-step conversion of CO-rich synthesis gas to dimethyl ether, *Applied Catalysis A: General*, 562 (2018) 206-214.
- [5] P.D. Burton, D. Lavenson, M. Johnson, D. Gorm, A.M. Karim, T. Conant, A.K. Datye, B.A. Hernandez-Sanchez, T.J. Boyle, Synthesis and Activity of Heterogeneous Pd/Al<sub>2</sub>O<sub>3</sub> and Pd/ZnO Catalysts Prepared from Colloidal Palladium Nanoparticles, *Topics in Catalysis*, 49 (2008) 227-232.

# Aqueous-Phase Hydrogenation of Algae-Derived Glycolic Acid with Tunable Selectivity towards Ethylene Glycol or Acetic Acid

*F. M. Harth<sup>1</sup>, A. Tauber<sup>2</sup>, M. Goepel<sup>1</sup>, C. Wilhelm<sup>2</sup>, R. Gläser<sup>1</sup>*

<sup>1</sup>*Institute of Chemical Technology, Universität Leipzig, 04103 Leipzig, Germany*

<sup>2</sup>*Institute of Biology, Universität Leipzig, 04103 Leipzig, Germany*

## Introduction

Glycolic acid (GA) is the smallest  $\alpha$ -hydroxycarboxylic acid and has the potential to serve as a platform chemical, i.e., an intermediate in the synthesis of value-added products. Recent research is focused on renewable approaches to produce GA, e.g., via fermentation from biomass [1]. Wilhelm and coworkers [2] developed an approach named “New Green Chemistry” based on algae biomass as a route towards GA. The product is excreted into the medium and conventional harvesting of the algae is not required. This enables continuous production of diluted aqueous GA solutions. One promising upgrading pathway of GA is the selective hydrogenation to ethylene glycol (EG) and/or acetic acid (AA) which are versatile bulk chemicals for polymer production. Hydrogenation of GA can be achieved by conversion with  $H_2$  over supported Ru metal catalysts [3] (Fig. 1). In this study, Ru-based catalysts using a series of different supports were prepared, characterized and applied in the aqueous-phase hydrogenation of GA. Special focus was placed on the influence of support acidity, metal dispersion and metal-support interactions on the catalytic behavior. Furthermore, the influence of reaction conditions, especially regarding their influence on selectivity for EG and AA was investigated.

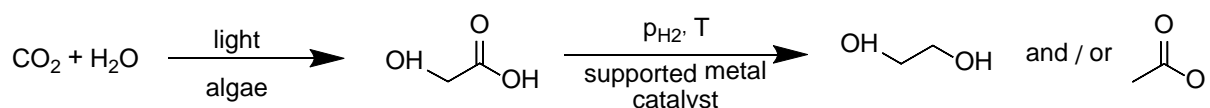


**Fig. 1:** Hydrogenation of algae-derived GA solutions over supported metal catalysts to EG and/or AA.

## Experimental Part

All catalysts were prepared by incipient wetness impregnation of the respective dried support material, i.e., activated carbon (AC),  $ZrO_2$ ,  $TiO_2$ ,  $SiO_2$ ,  $Al_2O_3$  and zeolite H-Y, using  $RuCl_3$  with a targeted Ru loading of 5 wt.-%. For the catalytic experiments, 150 mg of pre-reduced catalyst and 80 cm<sup>3</sup> 0.07 M aqueous GA solution were heated to 423 K in a PTFE-coated steel autoclave.  $H_2$  pressure was applied to start the

hydrogenation. Liquid-phase samples were quantitatively analyzed by HPLC and GC. A commercial catalyst (5Ru/C) was investigated as a reference.

## Results and Discussion

Over Ru on various supports clearly different activity and selectivity was observed in the aqueous-phase hydrogenation of GA (Fig. 2, left). For commercial 5Ru/C and Ru supported on TiO<sub>2</sub> and SiO<sub>2</sub>, the main liquid-phase product was EG with a selectivity of 30 - 40 %. Using 5Ru/AC up to 70 % EG selectivity at a GA conversion of 22 % was achieved. Ru supported on ZrO<sub>2</sub> or Al<sub>2</sub>O<sub>3</sub> showed a tendency towards formation of AA with a molar ratio of  $n_{AA}/n_{EG} \approx 2$ . Comparing 5Ru/TiO<sub>2</sub> and 5Ru/ZrO<sub>2</sub>, the main liquid-phase product can be tailored towards either EG or AA by choice of support material. In addition, reaction conditions also considerably affect the product selectivity. While the yields of EG and AA are comparable over commercial 5Ru/C at H<sub>2</sub> pressure of 10 bar, the selectivity is shifted towards liquid-phase products and especially EG at higher pressure (Fig.2, right). This can be explained by the higher amount of H<sub>2</sub> required to reduce GA to EG compared to AA. Therefore, differences in H<sub>2</sub> availability at the catalytically active site could be an important selectivity-directing factor. These results indicate that a tunable heterogeneously catalyzed upgrading of aqueous GA to different value-added products is feasible.

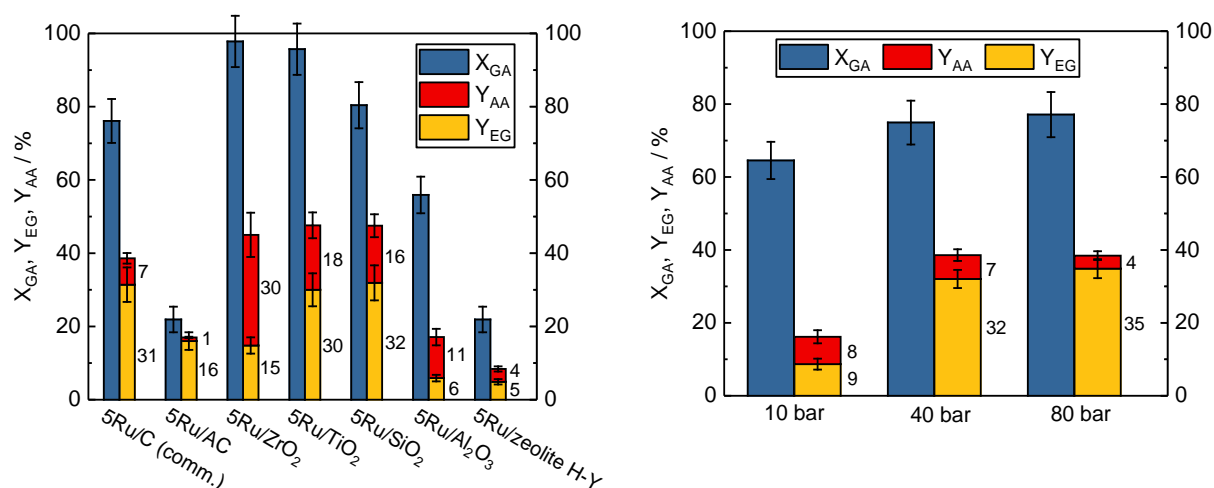


**Fig. 2:** Product yields of EG (Y<sub>EG</sub>) and AA (Y<sub>AA</sub>) as well as GA conversion (X<sub>GA</sub>) obtained for Ru (5 wt.%) on different supports in the aqueous-phase hydrogenation of GA (left) and over a commercial 5Ru/C applying different H<sub>2</sub> pressure (right) ( $m_{cat.} = 150$  mg,  $V = 80$  cm<sup>3</sup>,  $C_{GA} = 0.07$  M (H<sub>2</sub>O),  $T = 423$  K,  $p_{H_2} = 4.0$  MPa,  $t = 4$  h,  $n = 1000$  min<sup>-1</sup>).

## References

- [1] J. Becker, A. Lange, J. Fabarius, C. Wittmann, *Curr. Opin. Biotechnol.* 36 (2015) 168-175.
- [2] M. Fresewinkel, R. Rosello, C. Wilhelm, O. Kruse, B. Hankamer, C. Posten, *Eng. Life Sci.* 14 (2014) 560-573.
- [3] Y. Takeda, T. Shoji, H. Watanabe, M. Tamura, Y. Nakagawa, K. Okumura, K. Tomishige, *ChemSusChem* 8 (2015) 1170-1178.

## **Designing artificial lignin-based composites using enzyme catalysis for monolignols oxi-(co)polymerization**

*Madalina Tudorache, University of Bucharest, Bucharest, Romania; Sabina Ion, University of Bucharest, Bucharest, Romania; Cristina Lite, University of Bucharest, Bucharest, Romania; Irina Zgura, National Institute of Materials Physics, Magurele, Romania; Aurelian C. Galca, National Institute of Materials Physics, Magurele, Romania; Adina Bodescu, "Aurel Vlaicu" University, Arad, Romania; Madalin Enache, Institute of Biology Bucharest of the Romanian Academy, Bucharest, Romania; Gabriel-Mihai Maria, Institute of Biology Bucharest of the Romanian Academy, Bucharest, Romania; Vasile I. Parvulescu, University of Bucharest, Bucharest, Romania*

Lignin is one of the most abundant green polymer in the world together with the cellulose and hemicellulose. Beside the natural sources exploited up to maximum limit today, the pulp-paper as well as bio-refining industries are generous providers of lignin resources. As a consequence, new perspectives of lignin valorization are absolutely required.

We studied the construction of lignin-composites using monolignol fractions (e.g. sinapyl alcohol, SA or coniferyl alcohol, CA) based on the fact that lignin can be efficiently converted into a mixture of mono-/oligo-mers [1-3] with the ability to be recombined into artificial lignin [4,5]. A novel and practical one-pot system was developed for artificial lignin-composites production. Monolignols (SA/CA) were linked together with caffeic acid (CafAc) in a polymeric net similar with natural lignin based on oxi-(co)polymerization process with  $H_2O_2$  as oxidation reagent and peroxidase enzyme as biocatalyst.

Oxi-copolymerization process has been developed in a heterogeneous system, i.e. SA/CA dissolved in liquid phase, while CafAc was attached on acrylic particles ( $S_{C2}/S_{C6}$ -CafAc).  $S_{C2}/S_{C6}$ -CafAc- $L_1$  bio-composite was produced from CA, while SA oxi-copolymerization led to  $S_{C2}/S_{C6}$ -CafAc- $L_2$ . Different conversions were achieved for both functionalized supports demonstrating that the solid support together with type of monolignol affected the co-polymerization process (maximum conversion of 71.1 % and 49.8 %, for SA and CA).

Designed composites were investigated using different characterization techniques, e.g. FTIR, TPD-NH<sub>3</sub>, TGA, contact angle and SEM. FTIR spectra offered clear evidence of the artificial lignin deposition on the beads, while TPD-NH<sub>3</sub> analysis allowed to evaluate the bio-composite acidity. The acidity for SA-based bio-composite was higher than for CA-based bio-composite. Also, the artificial lignin attachment improved the thermo-stability of the composites compared to original/functionalized support.

Investigation of surface hydrophobicity for the new bio-composites was performed using contact angle measurements of distilled water drop on prepared surfaces. The contact angle of the bio-composites reached to 63° for CA-based polymer or 18° for SA-based polymer. Obviously, the results indicated an enhancement of the hydrophobicity for the oxi-copolymer belonged to CA monolignol. Similar hydrophobicity was reported in the literature for natural lignin attached on silica surfaces [5]. Moreover, it has to be mentioned that the artificial lignin prepared by oxi-copolymerization is more hydrophobic than some natural lignins (e.g. soda lignin from *Triticum sp* and *Saccharum officinarum* with 35° contact angle) [5].

Beside of an innovative system for bio-composite preparation with green chemical aspects, this work gives a new alternative for valorization of lignin residues. Versatility as well as green aspects of the polymeric structure on the bio-composite surface allow easy adjustment of proposed bio-composites to different applications. In this direction, we can mention the use of bio-composites as support or carrier for biomolecules (e.g. enzymes and whole cell) when specific properties of support/carrier are requested.

#### References

1. C. Opris, B. Cojocaru, N. Gheorghe, M. Tudorache, S.M. Coman, V.I. Parvulescu, B. Duraki, F. Krumeich, J.A. Van Bokhoven, *Journal of Catalysis*, 339 (2016) 209-227.
2. C. Opris, B. Cojocaru, N. Gheorghe, M. Tudorache, S.M. Coman, V.I. Parvulescu, B. Duraki, F. Krumeich, J.A. Van Bokhoven, *ACS Catalysis*, 7 (2017) 3257-3267.
3. M. Tudorache, C. Opris, B. Cojocaru, N.G. Apostol, A. Tirsoaga, S.M. Coman, V.I. Parvulescu, B. Duraki, F. Krumeich, J.A. Van Bokhoven, *ACS Sustainable Chemistry and Engineering*, **2018**, 6(8), 9606-9618.
4. C. Opris, N. Amanov, V.I. Parvulescu, M. Tudorache\*, *Comptes Rendus Chimie*, (2017).
5. S. Ion, C. Opris, . Cojocaru, M. Tudorache\*, I. Zgura, A.C. Galca, A.M. Bodescu, M. Enache, G.-M. Maria, V.I. Parvulescu, *Frontiers in Chemistry*, **2018**, 6, article 124, page 1-9.

# ***Ni-based catalyst for HDO by in-situ hydrogen generation from water splitting process***

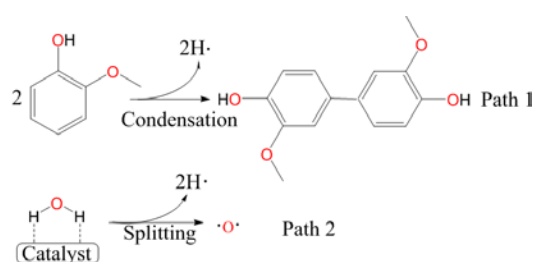
*Jin Wei, University of Surrey, Guildford, UK; Pastor-Perez Laura, University of Alicante, Spain; Juan J. Villora-Picó, Universidad de Alicante, Alicante, Spain; Gu Sai University of Surrey, Guildford, UK; Sepúlveda-Escribano A., University of Alicante, Spain; Ramirez Reina Tomas, University of Surrey, Guildford, UK*

## **Introduction**

Deteriorated properties of bio-oil derived from pyrolysis processes resulting from the high oxygen content (between 20 and 55 wt%) limits the direct application of bio-oil as transportation fuel or high-valued chemicals [1]. Catalytic hydrodeoxygenation (HDO) is the state of the art technology to upgrade bio-oil by removing the oxygen in the form of water with the participation of high pressure H<sub>2</sub> [2].

Recently, novel strategies (including catalytic transfer hydrogenation, reforming&HDO, metal oxidation with water&HDO and non-thermal plasma) are being developing for bio-oil upgrading in which other hydrogen sources are used, considering the cost of H<sub>2</sub> production and potential risk in terms of transportation and storage [3]. However, few studies have investigated the *in-situ* HDO of bio-oil or model compounds by using water as hydrogen source.

Being more precise, hydrogen required for HDO can be produced from the condensation of guaiacol (Path 1, Scheme 1), an undesired route or in contrast, water can act as the hydrogen source (Path 2, Scheme 1).



Scheme 1. Hydrogen production pathway in HDO reaction.

We propose a novel HDO method to carry out the *in-situ* HDO reaction suppressing the supply of external H<sub>2</sub>. It is speculated that water can undergo splitting on the surface of a metal catalyst to produce hydrogen. Hydrogen can further participate in the HDO of bio-oil, producing the oxygen removal purpose. A series of Ni-based catalysts supported on CeO<sub>2</sub>-C have been prepared, characterized and studied in the guaiacol HDO in a high-pressure batch reactor. In this process, the effect of support materials and the addition of promoter (Mo) were investigated. This novel

method is an interesting alternative that opens new research possibilities to further develop viable bio-oil upgrading process.

## Materials and methods

CeO<sub>2</sub> support was prepared by a precipitation method. Five different catalysts, namely Ni/CeO<sub>2</sub>, NiMo/CeO<sub>2</sub>, Ni/C, Ni/CeO<sub>2</sub>-C and NiMo/CeO<sub>2</sub>-C (15%Ni and 2% Mo) were synthesised by the wet impregnation method.

Catalytic activity tests were performed in a high pressure batch reactor. 0.2 g catalyst and 10 wt.% of guaiacol in water were used in each reaction. The reactor was held at 250 °C for 4 h at 50 bar under inert atmosphere. After the reaction, the catalyst was collected by filtration and organic products were extracted with ethyl acetate and further analysed by GC/MS and GC/FID.

## Results and discussions

Carbon-supported catalysts showed high activity in terms of guaiacol conversion (Figure 1). For example, the conversion of guaiacol in HDO over Ni/CeO<sub>2</sub>-C was twice compared to that of blank reaction. A reaction pathway of guaiacol HDO over Ni-based catalysts is proposed (Scheme 2). Besides, the selectivity to partially deoxygenated compounds (e.g. phenol and cresol) was enhanced when Mo was added in the formulation of catalysts. Some physicochemical characterisation of the catalysts was carried out before and after reaction to clarify this behaviour.

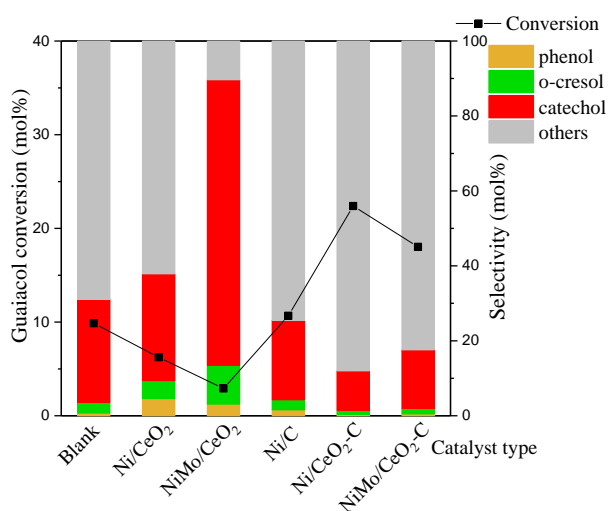
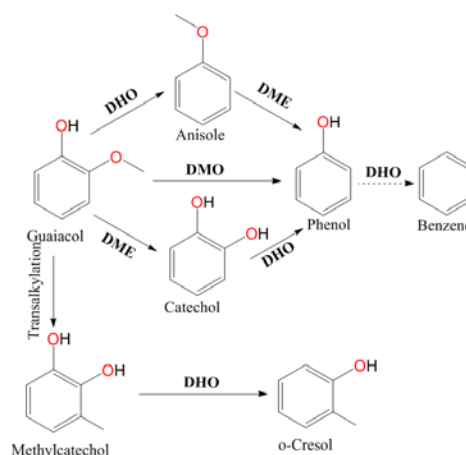


Figure 1. Activity of Ni-based catalysts in guaiacol in-situ HDO process.



Scheme 2. Proposed reaction pathway of guaiacol HDO over Ni-based catalysts (DMO: Demethoxylation; DME: Demethylation; DHO: Dehydroxylation)

## References

- [1] Y. Romero, F. Richard, S. Brunet, *Appl. Catal., B* **2010**, 98, 213-223.
- [2] A.M. Robinson, J.E. Hensley, J.W. Medlin, *ACS Catal.* **2016**, 6, 5026.
- [3] W. Jin, L. Pastor-Perez, D.K. Shen, et.al, *ChemCatChem* **2018**.

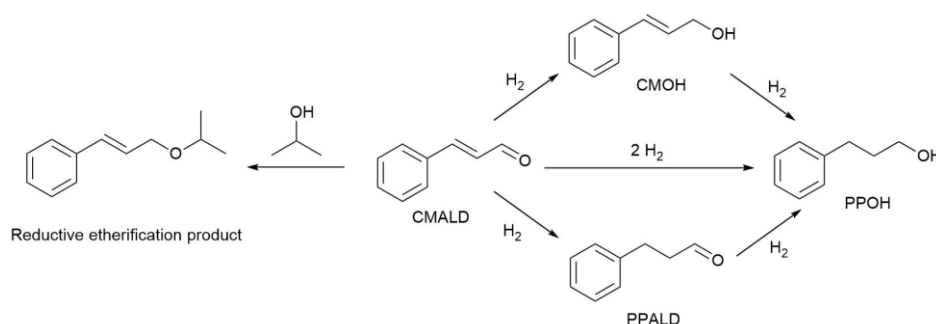


# Hydrogenation of cinnamaldehyde to phenylpropanal over Pd supported catalysts under mild conditions

*Matthew Conway, Mark Douthwaite, Rebecca V. Engel, Graham J. Hutchings, Cardiff Catalysis Institute, Cardiff University, Park Place, Cardiff, CF10 3AT, UK*

## Introduction

The selective reduction of  $\alpha,\beta$ -unsaturated aldehydes, such as cinnamaldehyde (Scheme 1), has received significant attention for fundamental and industrial reasons. Achieving high selectivity to a partially reduced product is challenging, C=C reduction is thermodynamically favoured over hydrogen addition to the C=O moiety; however, obtaining high selectivity to the saturated aldehyde remains problematic. Selective reduction of the alkene is typically performed at high temperature and/or high pressure.<sup>1</sup> Examples under more mild conditions require complex catalysts.<sup>1,2</sup> Phenylpropanal has applications in the flavours/fragrances industry and is a precursor for pharmaceuticals used to treat HIV.<sup>1</sup> In this study, the importance of catalyst support is studied with the principal aim of designing a catalyst that is simple to prepare and can produce phenylpropanal in high yields under mild conditions.



**Scheme 1** Relevant reaction pathways for cinnamaldehyde. CMALD: Cinnamaldehyde, CMOH: Cinnamyl alcohol, PPALD: Phenylpropanal, PPOH: Phenylpropanol

## Results and discussion

A series of palladium catalysts (1.8 wt.% Pd loading) supported on graphite (C<sub>G</sub>), activated carbon (C<sub>A</sub>), carbon black (C<sub>CB</sub>), graphene nanoplatelets (C<sub>GNP</sub>), or boron nitride (BN) were prepared by a modified impregnation method<sup>3</sup> and characterized by X-ray diffraction (XRD) (Figure 1). The XRD patterns for Pd/C<sub>A</sub>, Pd/C<sub>CB</sub>, Pd/C<sub>GNP</sub> were largely amorphous and no crystallites of Pd or PdO were observed. Contrarily, ordered phases of the support and Pd crystallites were visible for Pd/BN and Pd/C<sub>G</sub> catalysts, indicating larger metal nanoparticles.

The performance of these catalysts was evaluated (Figure 2) and the most selective catalyst was found to be Pd/BN, achieving a selectivity towards phenylpropanal of 55% at 80% conversion. The higher selectivity of the Pd/BN catalyst was not attributed to a particle size effect as poor selectivity was observed for Pd/C<sub>G</sub>. For butyraldehyde production from crotonaldehyde on a Pt/BN catalyst, the selectivity was attributed to the repulsion of the C=O group by the hydrophobic support and the weak metal-support interaction between Pt and BN.<sup>4</sup> The major side product for Pd/BN was identified by GCMS as the reductive etherification product of isopropyl alcohol and cinnamaldehyde (Scheme 1) and not the fully reduced product. No reaction was observed when BN was used without Pd. The use of other solvents to prevent this pathway has not yet been explored. Cinnamyl alcohol selectivity was 2% at 63% conversion for Pd/C<sub>GNP</sub> but was not observed in other experiments.

### Significance

A preliminary study revealed that good yields of phenylpropanal are achievable when using a 1.8 wt.% Pd/BN catalyst, potentially attributable to the high hydrophobicity of the support and a weak metal-support interaction. The selectivity was hindered by reductive etherification and not overreduction. This work is one of the only studies to investigate this reaction under mild conditions (30 °C, 3 bar H<sub>2</sub>) with a facile catalyst preparation method.

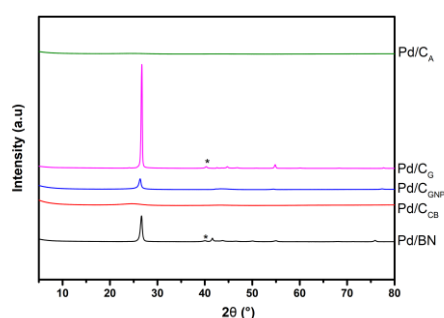


**Figure 1** XRD patterns for tested catalysts.  
\* Denotes Pd crystallite

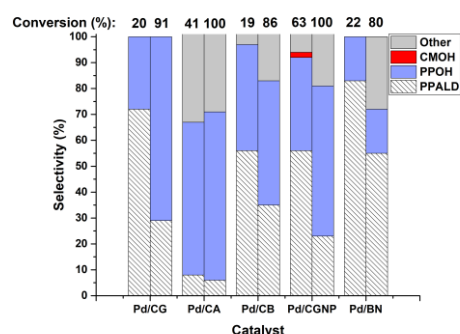


**Figure 2** Selectivities and conversions for catalysts after 2 and 8 hours. *Conditions:* 3 bar H<sub>2</sub>, 30 °C, 10 wt% solution of cinnamaldehyde in isopropyl alcohol

### References

- 1 A. S. Nagpure, L. Gurralla, P. Gogoi and S. V Chilukuri, *RSC Adv.*, 2016, **6**, 44333–44340.
- 2 S. Doherty, J. G. Knight, T. Backhouse, E. Abood, H. Alshaikh, I. J. S. Fairlamb, R. A. Bourne, T. W. Chamberlain and R. Stones, *Green Chem.*, 2017, **19**, 1635–1641.
- 3 M. Sankar, Q. He, M. Morad, J. Pritchard, S. J. Freakley, J. K. Edwards, S. H. Taylor, D. J. Morgan, A. F. Carley, D. W. Knight, C. J. Kiely and G. J. Hutchings, *ACS Nano*, 2012, **6**, 6600–6613.
- 4 J. C. S. Wu, C. Y. Chen and S. D. Lin, *Catal. Letters*, 2005, **102**, 223–227.

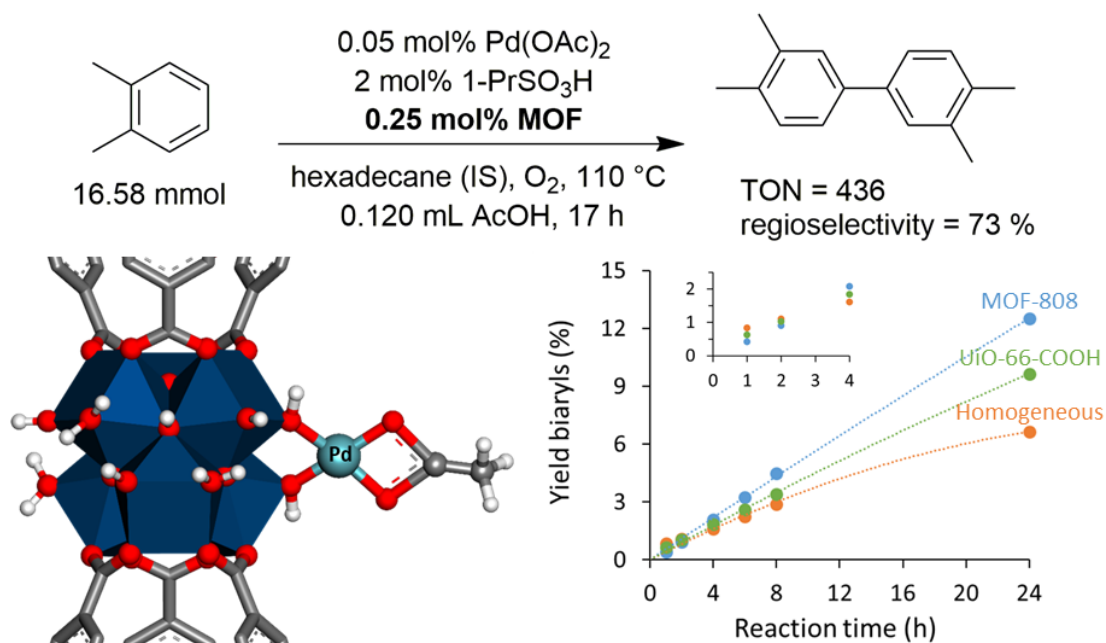
# Single-Site Metal-Organic Framework Catalysts for the Oxidative Coupling of Arenes via C-H/C-H activation

*Niels Van Velthoven, KU Leuven, Leuven, Belgium; Steve Waitschat, Christian-Albrechts University Kiel, Kiel, Germany; Sachin M. Chavan, University of Oslo, Oslo, Norway; Simon Smolders, KU Leuven, Leuven, Belgium; Jannick Vercammen, KU Leuven, Leuven, Belgium; Bart Bueken, KU Leuven, Leuven, Belgium; Karl Petter Lillerud, University of Oslo, Oslo, Norway; Norbert Stock, Christian-Albrechts University Kiel, Kiel, Germany; and Dirk E. De Vos, KU Leuven, Leuven, Belgium*

The synthesis of biaryls has attracted much attention over the past decades since these motives are abundantly present in pharmaceuticals, natural products, agrochemicals, specialty monomers and other fine chemicals. Typically, these compounds are synthesized via traditional coupling reactions, such as the Suzuki reaction, which require pre-functionalized substrates and produce stoichiometric amounts of salt waste. In recent years, formation of biaryls via palladium catalyzed cross-dehydrogenative coupling (CDC) reactions has been proposed as a more cost-efficient and environmentally benign alternative, since simple arenes can be used as substrate and water is the only byproduct if O<sub>2</sub> is used as the oxidant.[1] Given the relatively low turnover numbers (TONs) generally associated with CDC reactions compared to traditional coupling reactions, efficient recovery and recycling of the precious homogeneous palladium catalyst is a key aspect in the eventual implementation of this new synthetic strategy.[2] Moreover, since the valence state of palladium changes between Pd(0) and Pd(II) in the catalytic cycle, formation of Pd(0) aggregates is commonly recognized as an important deactivation pathway, highlighting the need for solid catalysts with stable, well-defined single-atom active sites.[3] Nevertheless, only very few heterogeneous catalysts for the oxidative coupling of arenes via C-H/C-H activation have been reported so far.

In this work, palladium-loaded metal-organic frameworks (MOFs) were tested as single-site catalysts for the oxidative coupling of arenes (e.g. *o*-xylene) via C-H/C-H activation. MOFs with various anchoring sites were screened and the heterogeneity of these solid catalysts was studied by recycling tests and metals analysis of the reaction solution. Notably, a threefold higher TON could be achieved for palladium-loaded MOF-808 ( $[\text{Zr}_6(\mu_3\text{-O})_4(\mu_3\text{-OH})_4(\text{btc})_2(\text{CH}_3\text{COO})_6]$ ,  $\text{btc}^{3-} = 1,3,5$ -

benzenetricarboxylate) and Pd leaching was minimized to 2%. The activity of the MOF-based catalyst could be retained over consecutive runs, resulting in a cumulative TON of 1218, which is well beyond the state-of-the-art.[4,5] In identical homogeneous reaction conditions, the Pd catalyst is irreversibly lost after only 151 turnovers. Analysis of the reaction kinetics revealed that the superior TONs at high reaction temperatures result from isolation of the active sites on the MOF material, which prolongs catalyst lifetime. Furthermore, the isolated palladium single-atom active sites on MOF-808 were successfully identified by FTIR and EXAFS spectroscopy. In conclusion, these results show that the TON of palladium in C-H activation reactions can be significantly increased by developing stable heterogeneous single-site catalysts.



## References

- [1] Y. Izawa, S. S. Stahl, *Adv. Synth. Catal.* 2010, 352, 3223.
- [2] Y. Álvarez-Casao, et al., *ChemCatChem.* 2018, 10, 1.
- [3] H. Duan, et al., *ACS Catal.* 2015, 5, 3752.
- [4] D. Wang and S. S. Stahl, *J. Am. Chem. Soc.*, 2017, 139, 5704–5707.
- [5] Y. Liu, et al., *Appl. Catal. B Environ.*, 2017, 209, 679–688..

# **Ruthenium and palladium bimetallic system achieving functional parity with a rhodium co-catalyst for TiO<sub>2</sub>-photocatalyzed ring hydrogenation of benzoic acid**

*Sakae Araki, Kindai University, Osaka, Japan; Kousuke Nakanishi, Kindai University, Osaka, Japan; Atsuhiko Tanaka, Kindai University, Osaka, Japan; Hiroshi Kominami, Kindai University, Osaka, Japan;*

## **Background**

Ring hydrogenation of benzoic acid (BA) generally requires the addition of an excess amount of H<sub>2</sub> gas at high temperature. On the other hand, safe and "green" reaction systems can be constructed by using TiO<sub>2</sub> photocatalyst, because photocatalytic reactions proceed at a room temperature under an atmospheric pressure. In the previous study, we found that Rh/TiO<sub>2</sub> photocatalyst shows a high activity for ring hydrogenation of BA to cyclohexane carboxylic acid (CCA) [1]. Since Rh is expensive, ring hydrogenation of BA without the use Rh co-catalyst has an impact at the viewpoint of element strategy. In this study, we investigated H<sub>2</sub>-free ring hydrogenation over an Rh-free photocatalyst and found that ruthenium and palladium bimetallic system achieved functional parity with a rhodium co-catalyst for TiO<sub>2</sub>-photocatalyzed ring hydrogenation of BA.

## **Experimental methods**

### **Preparation of photocatalyst**

Pd/TiO<sub>2</sub> was prepared by photodeposition method. TiO<sub>2</sub> (P 25) powder was suspended in 10 cm<sup>3</sup> of an aqueous solution of methanol (50 vol%) containing a PdCl<sub>2</sub> in a test tube. The test tube was photoirradiated with a mercury arc ( $\lambda > 300$  nm) under argon (Ar). The resulting powder was washed repeatedly with distilled water and dried in vacuo. Similarly, Ru was post-supported to prepare Ru-Pd/TiO<sub>2</sub>.

### **Photocatalytic ring-hydrogenation of BA**

Pd-Ru/TiO<sub>2</sub> (50 mg) was suspended in an aqueous solution (5 cm<sup>3</sup>) containing BA and oxalic acid (OA) as a hole scavenger in a test tube. The test tube was photoirradiated with a mercury arc ( $\lambda > 300$  nm) under Ar. The gas phase and the liquid phase after the reaction were determined with a gas chromatograph.

## Results and discussion

Ring hydrogenation of BA did not proceed when Pd/TiO<sub>2</sub> and Ru/TiO<sub>2</sub> were used under the same conditions. Fig. 1 shows the effect of hydrochloric acid (HCl) concentration during photodeposition of Ru on Pd/TiO<sub>2</sub> on yields of CCA and H<sub>2</sub>. Very interestingly, ring hydrogenation of BA occurred over bimetallic system, Rh-free Pd-Ru/TiO<sub>2</sub> and the CCA yield increased with the increase in the concentration of HCl during the Ru photodeposition process. In addition, formation of H<sub>2</sub> (2H<sup>+</sup> + 2e<sup>-</sup> → H<sub>2</sub>) was suppressed, indicating that the efficiency of electron utilization was improved. In order to elucidate this reason, adsorption experiment of Ru ion on TiO<sub>2</sub> was carried out. We found that adsorption of Ru ion on the TiO<sub>2</sub> surface was suppressed in the presence of HCl, resulting in the selective deposition of Ru on the Pd particles.

Fig. 2 shows the time course of ring hydrogenation of BA over Pd-Ru/TiO<sub>2</sub> under irradiation of UV light. BA was almost completely consumed after irradiation for 60 min, and CCA was almost quantitatively produced for 80 min. This means that the Rh-free ring hydrogenation of BA to CCA proceeded over Pd-Ru/TiO<sub>2</sub> photocatalyst without a side reaction. Structure of Pd-Ru/TiO<sub>2</sub> photocatalyst and electronic state of Pd and Ru loaded on TiO<sub>2</sub> were also investigated.

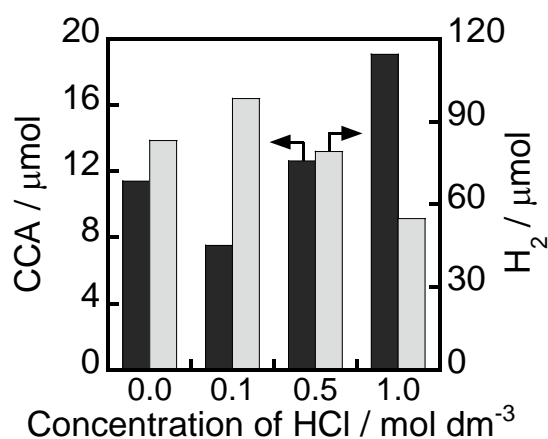


Fig. 1 Effect of HCl concentration during Ru photodeposition on yields of CCA and H<sub>2</sub> in an aqueous suspension of Pd-Ru/TiO<sub>2</sub> photocatalyst under irradiation of UV light for 30 min (BA: 50 μmol, OA: 300 μmol).

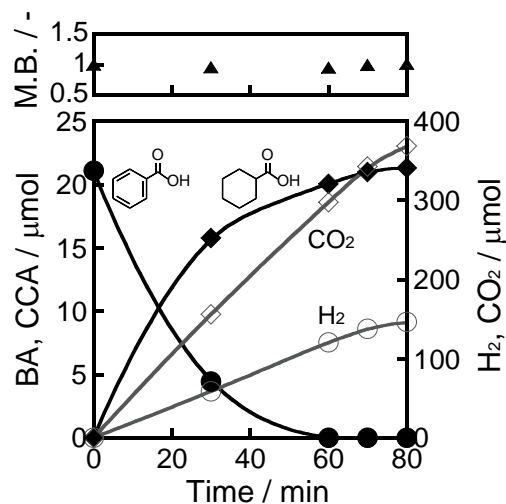


Fig. 2 Time courses of amounts of BA(●), CCA(◆), H<sub>2</sub>(○), and CO<sub>2</sub>(◇) in an aqueous suspension of Pd-Ru/TiO<sub>2</sub> under irradiation of UV light (BA: 21 μmol, OA: 300 μmol).

## References

- [1] Nakanishi *et al.*, *Catal. Sci. Technol.*, **8**, 139 (2018).

## **Effect of solid additive nature on the catalytic behavior of Au supported catalysts in betulin liquid-phase oxidation**

*Ekaterina Pakrieva<sup>1</sup>, Ekaterina Kolobova<sup>1</sup>, Anna Buachidze<sup>1</sup>, Alexey Pestryakov<sup>1</sup>, Research School of Chemistry & Applied Biomedical Sciences, Tomsk Polytechnic University, Tomsk, Russia<sup>1</sup>; Päivi Mäki-Arvela<sup>2</sup>, Jarl Hemming<sup>2</sup>, Kari Eränen<sup>2</sup>, Dmitry Yu. Murzin<sup>2</sup>, Johan Gadolin Process Chemistry Centre, Åbo Akademi University, Turku/Åbo, Finland<sup>2</sup>; Janne Peltonen<sup>3</sup>, Laboratory of Industrial Physics, Department of Physics and Astronomy, University of Turku, Turku/Åbo, Finland<sup>3</sup>; Sónia Alexandra Correia Carabineiro<sup>4</sup>, Centro de Química Estrutural, Instituto Superior Técnico, Universidade de Lisboa, Av. Rovisco Pais, Lisboa, Portugal<sup>4</sup>*

Betulin, and especially its oxo-derivatives (betulone, betulinic and betulonic aldehydes, betulinic and betulonic acids) have valuable biologically active properties (antiinflammatory, antiparasitic, anti-HIV activities, etc.) and are of exceptional interest for the pharmaceutical, cosmetic and food industries [1]. Nowadays, the main method for obtaining oxo-derivatives of betulin is its oxidation using Cr(VI) compounds in a strongly acidic medium, for example, the Jones's reagent. However, production of oxo-derivatives by Cr(VI) compounds is rather complex and challenging being characterized by a low yield of the target products, complexity of toxic Cr(III) utilization and very toxic residual of Cr(VI), etc. The most promising way to solve this problem is the development of new heterogeneous catalytic methods for obtaining of betulin oxo- derivatives. Thereby, the aim of the present study is to evaluate perspective of gold-based catalysts in liquid phase selective oxidation of betulin, to estimate influence of solid additives nature with aimed to improve performance of Au catalysts.

The catalysts (Au/TiO<sub>2</sub> – AT, Au/La<sub>2</sub>O<sub>3</sub>/TiO<sub>2</sub> – ALT, Au/CeO<sub>2</sub>/TiO<sub>2</sub> – ACT; the nominal Au loading was 4 wt%.) were prepared by deposition precipitation method with urea and characterized by BET, XRD, XPS, TEM, TPD NH<sub>3</sub> and CO<sub>2</sub>. CaO, SrO, MgO, Hydrotalcite (Ht), ZnO, ZrO<sub>2</sub> and  $\gamma$ -Al<sub>2</sub>O<sub>3</sub> were used as solid additives and characterized by BET, XRD, TPD NH<sub>3</sub> and CO<sub>2</sub>. Catalytic properties in betulin oxidation were studied in a glass reactor in mesitylene (100 ml) as a solvent at 140 °C under atmospheric flow of synthetic air. In a typical experiment the initial betulin concentration was 4.5 mmol/l and the amounts of the catalysts and solid additives

were 0.2 g. The samples were periodically taken from the reactor, silylated, analyzed in GC. The products were confirmed by GC-MS.

The modification of titanium oxide with transition metal oxides, in particular lanthanum oxide allowed to the greatest surface concentration of the stable active sites (singly charged gold ions) on support surface, and as a consequence to achieve the best catalytic results. Conversion of betulin over ALT catalyst reached 61% after 6 hours (for AT and ACT conversion of betulin was 17 and 29% respectively for the same time) with the selectivity towards betulone – 41%, the second largest reaction product was betulonic aldehyde (32%).

In the present study with aimed to improve performance of ALT, along with the catalyst, solid oxides of various in nature were added to the reaction mixture (Table 1). The best results were achieved with  $\gamma$ -Al<sub>2</sub>O<sub>3</sub>. The conversion of betulin in 6 hours for the system (ALT+ $\gamma$ -Al<sub>2</sub>O<sub>3</sub>) was 100% with selectivity for betulone and betulonic aldehyde of 14 and 86%, respectively. It was found that oxide additives with medium basicity have a positive effect on performance of ALT (MgO, Hydrotalcite and  $\gamma$ -Al<sub>2</sub>O<sub>3</sub>). In contrast, strongly basic oxides (CaO and SrO) reduce the catalytic activity of ALT by an average of 30%, and oxides with the lowest basicity (ZnO and ZrO<sub>2</sub>) lead to a drop in activity of 60%. The final work will present kinetic analysis of betulin oxidation and correlate properties of catalysts and solid additives with their performance.

Table 1. Catalytic behaviour of ALT in betulin oxidation depending on solid additive nature

Catalyst	X (%)	Selectivity (%)					Yield (%)		
		S <sub>1</sub>	S <sub>2</sub>	S <sub>3</sub>	S <sub>4</sub>	S <sub>5</sub>	Y <sub>1</sub>	Y <sub>2</sub>	Y <sub>3</sub>
ALT	61	41	32	tr.	27	0	25	19	16
ALT+SrO	46	48	20	tr.	32	0	22	10	14
ALT+MgO	62	42	28	tr.	30	0	26	17	18
ALT+CaO	40	56	15	tr.	29	0	22	6	11
ALT+Ht	65	54	25	0	21	0	33	17	14
ALT+ZnO	23	58	16	0	36	0	13	3	7
ALT+ZrO <sub>2</sub>	25	53	14	0	33	0	13	4	8
ALT+ $\gamma$ -Al <sub>2</sub> O <sub>3</sub>	100	14	86	0	0	0	14	86	0
$\gamma$ -Al <sub>2</sub> O <sub>3</sub>	22	87	2	tr.	11	0	19	tr.	2

X – conversion of betulin after 6 h (%); S<sub>1</sub> – selectivity to betulone (%); S<sub>2</sub> – selectivity to betulonic aldehyde (%); S<sub>3</sub> – selectivity to betulonic acid (%); S<sub>4</sub> – selectivity to betulonic aldehyde (%); S<sub>5</sub> – selectivity to betulonic acid (%); Y<sub>1</sub> – yield of betulone (%); Y<sub>2</sub> - yield of betulonic aldehyde (%); Y<sub>3</sub> - yield of betulonic aldehyde (%); tr. - traces

#### Reference:

[1] Tolstikova, T. G., Sorokina, I. V., Tolstikov, G. A., Flekhter, O. B., Russ. J. Bioorg. Chem. 32 (2006) 37-49.



# Silica-supported iron-molybdenum catalysts for selective oxidation of propylene glycol to methylglyoxal

*D.Yu. Savenko, N. Yu. Velieva, O.V. Vodyankina, Tomsk State University, Tomsk, Russia*

## Introduction

Methylglyoxal (pyruvaldehyde) is a key intermediate chemical that has wide applications in the fields of pharmacy, biochemistry, food industry, manufacturing of pesticides, textiles and other valuable products. Methylglyoxal can be produced from propylene glycol, which is a cheap chemical and renewable natural source, because it can be produced via the processing of biomass, biodiesel and by-products of these processes [1]. Noble metals have been actively studied as catalysts for selective oxidations of propylene glycol [2]. Along with the noble metals, the catalysts based on transition metals (Ti, Co, Ni, etc.), in particular, Fe- and Mo-based composites, are actively studied. The Fe–Mo–O catalysts find application in many processes [3, 4]. The aim of the present work is to synthesize the supported Mo–Fe–O/SiO<sub>2</sub> catalysts with different Mo/Fe ratio and to study the influence of the preparation method on the phase composition and catalytic properties of the obtained catalysts in propylene glycol oxidation to methylglyoxal.

## Experimental

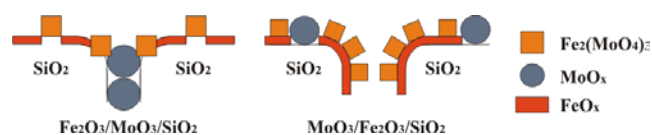
The Mo–Fe–O/SiO<sub>2</sub> catalysts were synthesized by sequential and joint incipient wetness impregnation methods. Silica (KSKG, LLC "Salavat Catalyst Plant", with a surface area of 300 m<sup>2</sup>/g) was used as a carrier. A series of Mo–Fe–O/SiO<sub>2</sub> catalysts was synthesized by the co-impregnation method with a citrate solution containing both ammonium paramolybdate and ferric nitrate in the corresponding concentrations. The Mo/Fe molar ratio varied from 0.5 to 3. The resulting samples were dried at 120 °C and calcined in the air flow at 550 °C. For the series of MoO<sub>3</sub>/Fe<sub>2</sub>O<sub>3</sub>/SiO<sub>2</sub> and Fe<sub>2</sub>O<sub>3</sub>/MoO<sub>3</sub>/SiO<sub>2</sub> catalysts prepared by sequential impregnation by varying the order of introduction of the components, the Mo/Fe molar ratio was 3. The resulting samples were dried at 120 °C and calcined in the air flow at 550 °C after each impregnation step.

The catalysts were characterized by XRD, UV-vis, IR and Raman spectroscopy, pulse NH<sub>3</sub> adsorption, low-temperature N<sub>2</sub> adsorption and TPR methods. The catalytic properties of the Mo–Fe–O/SiO<sub>2</sub> catalysts were studied in the gas-phase

propylene glycol oxidation to methylglyoxal at the temperature of 350°C (mixture composition: 3% C<sub>3</sub>H<sub>6</sub>(OH)<sub>2</sub>, 3.7% O<sub>2</sub>, 62% N<sub>2</sub>, 30% H<sub>2</sub>O). The major reaction products were methylglyoxal, formaldehyde, and hydroxyacetone.

## Results

The obtained UV-vis, Raman and TPR-H<sub>2</sub> results show the dependence of the catalyst surface composition from the order of component introduction, when the sequential impregnation is used. For the samples prepared by the direct order of component introduction (Mo-containing component is used at the first stage of impregnation, and Fe-containing component is used at the second stage of impregnation) the supported Fe<sup>III</sup>O<sub>x</sub> sites are found over the Mo-free regions of the SiO<sub>2</sub> surface along with Fe<sub>2</sub>(MoO<sub>4</sub>)<sub>3</sub>. Moreover, the interaction of SiOH groups of the silica surface with polymolybdate ions results in the localization of the adsorbed Mo<sub>7</sub>O<sub>24</sub><sup>4-</sup> anions preliminary in the outlets of pores and is accompanied by their partial blocking and a reduction of the specific surface area of the samples and a decreasing of the total concentration of acid sites (Scheme, left part).



For the catalysts prepared by the reverse method, the introduction of the Fe-containing component at the first stage of sequential impregnation to yield the adsorbed FeO<sub>x</sub> species during the interaction with the SiOH groups of the support determines the subsequent distribution of the Mo-containing species and facilitates the formation of highly dispersed Fe<sub>2</sub>(MoO<sub>4</sub>)<sub>3</sub> nanoparticles and MoO<sub>x</sub> species that are strongly bound with the SiO<sub>2</sub> surface (Scheme, right part). Thus, the 3MoO<sub>3</sub>/Fe<sub>2</sub>O<sub>3</sub>/SiO<sub>2</sub> catalyst prepared by a sequential impregnation with the introduction of the Mo-containing component on the support precovered by the adsorbed FeO<sub>x</sub> species (Mo/Fe=3) allows achieving the highest selectivity toward methylglyoxal at the alcohol conversion as high as 15 %.

## References

1. M. R. Monteiro, C. L. Kugelmeier, R. S. Pinheiro, M. O. Batalha, A. da Silva César, *Renewable and Sustainable Energy Reviews* 88 (2018) 109.
2. C.R. Ayre, R.J. Madix, *Surf. Sci.* 303 (1994) 279.
3. B.R. Yeo, G.J.F. Pudge, K.G. Bugler, A.V. Rushby, S. Kondrat, J. Bartley, S. Golunski, S.H. Taylor, E. Gibson, P.P. Wells, C. Brookes, M. Bowker, G.J. Hutchings, *Surface Science* 648 (2016) 163.P.
4. D.Yu. Ebert, N.V. Dorofeeva, A.S. Savel'eva, T.S. Kharlamova, M.A. Salaev, V.A. Svetlichnyi, O.V. Magaev, O.V. Vodyankina, *Catalysis Today* (2018), accepted in press.

# Synthesis of multi-functional materials as catalysts for carbon dioxide conversion

*Adrien Comès, Carmela Aprile, Unit of Nanomaterials Chemistry (CNANO),  
Department of Chemistry, University of Namur, Belgium*

## Introduction

During the past years, there was a rising interest of the scientific community towards the conversion of carbon dioxide into valuable compounds. This small molecule can be efficiently used as renewable C1 building block to synthesize a broad range of chemicals such as urea and urethanes derivatives, isocyanates, carboxylic acids, (poly)carbonates.[1-3] However, its elevated thermodynamic stability makes of the CO<sub>2</sub> transformation a still challenging topic, requiring high-energy starting materials as well as an efficient catalyst.

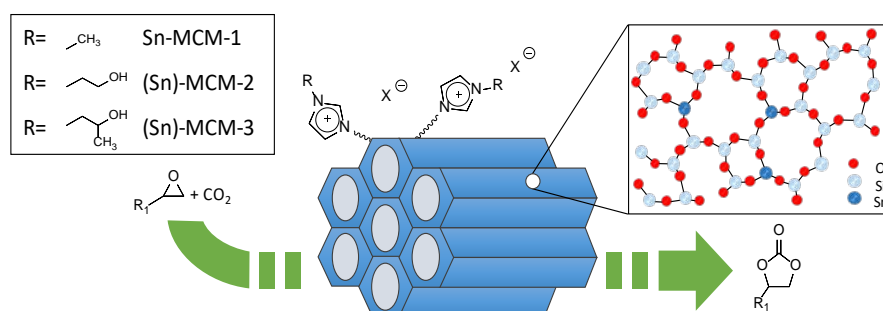
Imidazolium salts emerged as one of the most active catalysts for the conversion of CO<sub>2</sub> and epoxides into corresponding five-membered cyclic carbonates.[4-7] This process is a sustainable alternative to the use of phosgene and implies a 100 % atom economy.[8] However, when a catalyst such as an ammonium or imidazolium salt is used in the absence of a co-catalyst, high temperatures (usually higher than 125 °C) are needed.[3, 5] The high-energy input required for the transformation of carbon dioxide can be further reduced employing species able to activate the 3-member ring via coordination of the oxygen with a metal centre acting as Lewis acid or through formation of hydrogen bond.[3, 5, 9]

## Scientific strategy and key results

Herein, the design of novel heterogeneous multi-functional catalysts is presented. The synthesis procedure involves the initial preparation of a porous silica support bearing Sn inserted as single sites within the silica architecture (Sn-MCM) [10] followed by the grafting of imidazolium salts (Sn-MCM-Imi) [11] as depicted on Scheme 1. Various materials in which the imidazolium moieties are functionalized with a methyl group (Sn-MCM-Imi1), a primary (Sn-MCM-Imi2) or a secondary alcohol (Sn-MCM-Imi3) are presented. For comparison, analogous silica solids without Sn inserted as single site in structure were prepared as well (MCM-Imi-x, where x is 2 or 3 depending on the imidazolium salt used)

All the catalysts were compared selecting the challenging synthesis of cyclohexene carbonate as target reaction (Figure 1). As can be observed in Figure 1 the solids

bearing Sn inserted in the structure display higher TON than the corresponding all-silica based materials (compare entries 2 and 4 with 3 and 5 respectively). Moreover, the role of the functionalities on the imidazolium salts was also proved (compare entries 1, 2 and 4). The best catalyst was the one bearing imidazolium salts functionalized with a secondary alcohol (Sn-MCM-Imi3).[11] Various counter-anions ( $X^- = Cl^-; Br^-; I^-$ ) were also tested. Furthermore, the best solid (Sn-MCM-Imi3) was used in consecutive cycles (Figure 2) without relevant loss in the catalytic performances.



Scheme 1: Representation of porous silica materials embedding Sn in the network and grafted with various imidazolium salts

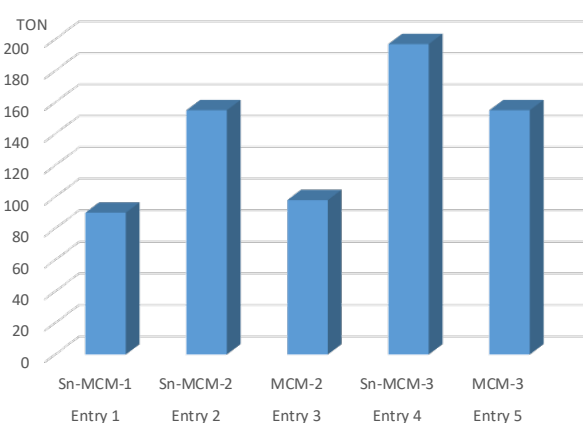


Figure 1: Turn-over number (TON defined as moles of carbonate formed/ moles of imidazolium moieties) of various materials for the conversion of cyclohexene oxide

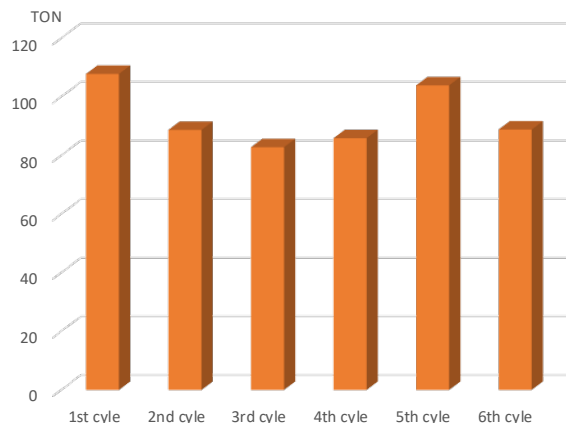


Figure 2: Recycling tests of Sn-MCM-3 for the conversion of styrene oxide.

## References

- [1] Maeda, C., Y. Miyazaki, and T. Ema, *Catalysis Science & Technology*, 2014. **4**(6): p. 1482-1497.
- [2] Fiorani, G., W. Guo, and A.W. Kleij, *Green Chemistry*, 2015. **17**(3): p. 1375-1389.
- [3] Sakakura, T., J.C. Choi, and H. Yasuda, *Chem Rev*, 2007. **107**(6): p. 2365-87.
- [4] Darensbourg, D., *Coordination Chemistry Reviews*, 1996. **153**: p. 155-174.
- [5] North, M., R. Pasquale, and C. Young, *Green Chemistry*, 2010. **12**(9): p. 1514-1539.
- [6] Jutz, F., J.M. Anderson, and A. Baiker, *Chem Rev*, 2011. **111**(2): p. 322-53.
- [7] Bobbink, F.D. and P.J. Dyson, *Journal of Catalysis*, 2016. **343**: p. 52-61.
- [8] Fukuoka, S., et al., *Green Chem.*, 2003. **5**(5): p. 497-507.
- [9] Bivona, L.A., et al., *Catalysis Science & Technology*, 2015. **5**(11): p. 5000-5007.
- [10] Godard, N., et al., *Applied Catalysis A: General*, 2018. **556**: p. 73-80.
- [11] Comès, A., et al., *RSC Advances*, 2018. **8**(45): p. 25342-25350.

# **The Design of Magnetically Recoverable Biocatalysts Based on Mono- and Bi-Enzyme**

*A.M. Sulman, Tver State Technical University, Tver, Russia; E.P. Golikova, Tver State Technical University, Tver, Russia; N.V. Lakina, Tver State Technical University, Tver, Russia; L.M. Bronstein, Indiana University, Bloomington, Indiana, United States; E.M. Sulman, Tver State Technical University, Tver, Russia; V.G. Matveeva, Tver State Technical University, Tver, Russia, Tver State University, Tver, Russia*

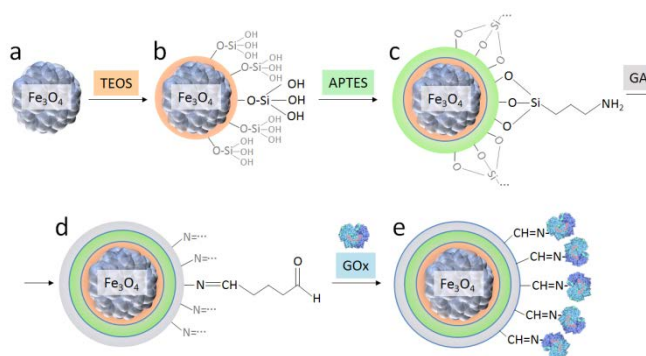
Immobilized enzymes are widely employed in syntheses of various complex drugs and drug intermediates under mild conditions without producing toxic side products. They are used in remediation of polluted water, air, and soil by efficient removal of persistent organic pollutants, in disease diagnosis, and in the correction of various genetic diseases due to the absence of metabolic enzymes [1].

To improve biologically active compounds synthesis processes the fundamental scientific basis for kinetic regularities, oxidation mechanisms of aromatic compounds and saccharides using new biocatalytic systems including magnetically separable ones will be laid. In the past decade, a significant growth of researchers' interest in magnetic nanoparticles (MNPs) and their derived materials is observed. The main field of magnetic materials application which has recently been of great interest is the development of magnetically separable catalysts. In this case, MNPs are functionalized and serve as a support for catalytic complexes formation. Such catalytic MNPs have unique catalytic properties through the high surface area and consequently the increase of active sites number [2].

The immobilization of enzymes on magnetic nanoparticles is an upcoming trend because these nanoparticles have a high surface area and provide easy separation from the reaction mixture. In magnetic nanoparticles obtained by  $\text{Fe}^{+2}$  and  $\text{Fe}^{+3}$  coprecipitation method in a basic medium were used for horseradish peroxidase (HRP, an enzyme of oxidoreductase group EC 1.11.1.7) immobilization. But unfortunately, magnetic nanoparticles obtained by the coprecipitation method have low aggregative stability and high polydispersity. Glucose oxidase (GOx, an enzyme of oxidoreductase group EC 1.1.3.4) is known to be used in D-glucose selective oxidation. Nowadays biocatalysts are widely studied to estimate the influence of (i)

nature of support, modifier and linking agent; (ii) introduction of the second enzyme; (iii) conditions of enzymes immobilization and oxidation reaction with them on the catalytic process. But according to the literature data, D-glucose oxidation to gluconic acid using glucose oxidase immobilized on magnetic nanoparticles was not investigated.

The current investigation is focused on the design of magnetically recoverable biocatalysts based on mono- and bi-enzyme. Scheme 1 represents of the mono-enzyme biocatalyst synthesis via the GOx immobilization on the magnetite nanoparticles [3].



Scheme 1. Schematic representation of the of the mono-enzyme biocatalyst synthesis via the GOx immobilization on the magnetite nanoparticles.

The development of bi-enzyme catalyst consisting of two types of enzymes can alleviate the problems of GOx caused by the  $\text{H}_2\text{O}_2$ . As the appropriate GOx partner for the bi-enzyme catalyst, horseradish peroxidase (HRP) can be designated because the enzyme catalyzes the toxic  $\text{H}_2\text{O}_2$  into  $\text{H}_2\text{O}$  by  $\text{H}_2\text{O}_2$  reduction reaction [4].

### Acknowledgment

The research leading to these results has received funding from the Russian Science Foundation (project 17-19-01408). Authors thank the Russian Foundation for Basic Research (grants 18-08-00468 and 18-38-00159).

### References

1. Dwevedi, A., *Enzyme Immobilization. Advances in Industry, Agriculture, Medicine, and the Environment*. Springer International Publishing Switzerland: Cham, Switzerland, **2016**.
2. Wang, D.; Astruc, D. *Chem. Rev.* 2014, 114 (14), 6949–6985.
3. B.P. Lawson, E.P. Golikova, A.M. Sulman, Barry D. Stein, D.G. Morgan, N.V. Lakina, A.Yu. Karpenkov, E.M. Sulman, V.G. Matveeva, L.M. Bronstein. *ACS Sustainable Chem. Eng.* 2018, 6, 9845–9853.
4. Y. Chung et al. / *Journal of Power Sources* 360 (2017) 172-179

# Biocatalytic Synthesis of Indigoid Pigments

Mikas Sadauskas, Roberta Statkevičiūtė, Justas Vaitekūnas, Renata Gasparavičiūtė,

Rita Meškienė, Nina Urbelienė, Rolandas Meškys

Department of Molecular Microbiology and Biotechnology, Institute of Biochemistry,

Life Sciences Center, Vilnius University, Vilnius, Lithuania

## Introduction

Indigo is one of the oldest pigments used in the dyeing industry. With the rise of modern sciences, we gained the ability to modify the indigo molecule and create new pigments with novel applications, including biological activities [1,2]. In order to overcome the hazardous effects of chemical indigo modifications, enzymatic synthesis was used to obtain novel variants of indigo [3,4]. Nevertheless, the selection of indigoids with desirable chemical modifications as well as enzymes capable of producing such pigments is still insufficient.

## Methods

Metagenomic DNA was extracted from different soil samples and used for the construction of metagenomic libraries. These libraries were screened in *Escherichia coli* for the ability to convert different indole molecules to corresponding indigoid pigments. Target genes were cloned to expression plasmids and the substrate specificity of recombinant enzymes was analyzed by TLC and HPLC/MS.

## Results

Among the selected metagenomic clones capable of converting indole derivatives to corresponding indigoids, a single clone was able to convert indole methanols (indole-4-methanol, indole-5-methanol, indole-6-methanol and indole-7-methanol) as well as indole carboxaldehydes (indole-4-carboxaldehyde, indole-5-carboxaldehyde, indole-6-carboxaldehyde and indole-7-carboxaldehyde) to corresponding indigo methanols and indigo carboxaldehydes. A gene responsible for this activity was identified, encoding for a 495 aa long NAD(P)/FAD-dependent monooxygenase from *Aminobacter* sp. In addition, indole methanols were enzymatically esterified using vinyl acetate and vinyl butyrate. The corresponding indole esters were also tested as substrates of the screened monooxygenase.

## Conclusions

In this work, production of novel indigoid pigments is described by enzymatic oxidation of indole derivatives. A NAD(P)/FAD-dependent monooxygenase, selected from metagenome, was demonstrated to oxidize indole methanols and indole carboxaldehydes to corresponding indigoid pigments. To our knowledge, production of such pigments was not reported neither by chemical nor enzymatic methods to date.

## References

- [1] Beauchard A, Laborie H, Rouillard H, Lozach H, Ferandin Y, Le Guevel R, Guguen-Guillouzo C, Meijer L, Besson T, Thiery V. Synthesis and kinase inhibitory activity of novel substituted indigoids. 2009, *Bioorganic Medicinal Chemistry*, 17:6257-6263.
- [2] Dodou HV, de Morais Batista AH, Sales GWP, de Medeiros SC, Rodrigues ML, Nogueira PCN, Silveira ER, Nogueira NAP. Violacein antimicrobial activity on *Staphylococcus epidermidis* and synergistic effect on commercially available antibiotics. 2017, *J Appl Microbiol*, 123:853-860.
- [3] Frabel S, Wagner B, Krischke M, Schmidts V, Thiele CM, Staniek A, Warzecha H. Engineering of new-to-nature halogenated indigo precursors in plants. 2018, *Metab Engineering*, 46:20-27.
- [4] Namgung S, Park HA, Kim J, Lee PG, Kim BG, Yang YH, Choi KY. Ecofriendly one-pot biosynthesis of indigo derivative dyes using CYP102G4 and PrnA halogenase. 2019, *Dyes and Pigments*, 162:80-88.



# Tandem reaction catalyzed by N-doped Graphene@ Nanodiamond Hybrid

**Qingqing Gu, Yuefeng Liu, Dang Sheng Su**

*DNL, Dalian Institute of Chemical Physics, CAS, Dalian 116023, China*

Developing efficient and reusable catalysts for multistep chemical reactions under environmentally benign conditions is an overarching goal in catalytic sciences. Nanocarbon have been reported to catalyze various types of reactions efficiently due to their multiple active sites endowed by surface functional groups or doped heteroatoms [1]. Graphene@nanodiamond, a core-shell  $sp^2@sp^3$  hybrid material, in which a diamond core is enclosed by few fullerene-like shells, have several unique properties since they not only benefit from the remarkable surface properties of graphene layers but also combine the intrinsic characters of a diamond core.

In this work, we selected nanodiamond as the base material and used ammonium carbonate to introduce nitrogen sites at 900 °C for preparing N-doped graphene@nanodiamond hybrid, namely, N-G@ND-900. Figure 1 illustrates the synthesis process of N-G@ND-900. According to the HR-TEM, the nanoparticle consists of a shell of graphitic layers ( $d_{002} = 3.56 \text{ \AA}$ ) and a diamond core ( $d_{111}=2.04 \text{ \AA}$ ). The N-G@ND-900 showed remarkable catalytic performance over aerobic synthesis of 2-substituted benzoxazoles, which is a tandem reaction consisted of the condensation of aminophenol and aldehyde and the following annulation of Schiff base. We proposed the acid oxygen functional groups and nitrogen sites are the active sites for condensation and annulation reactions, respectively.

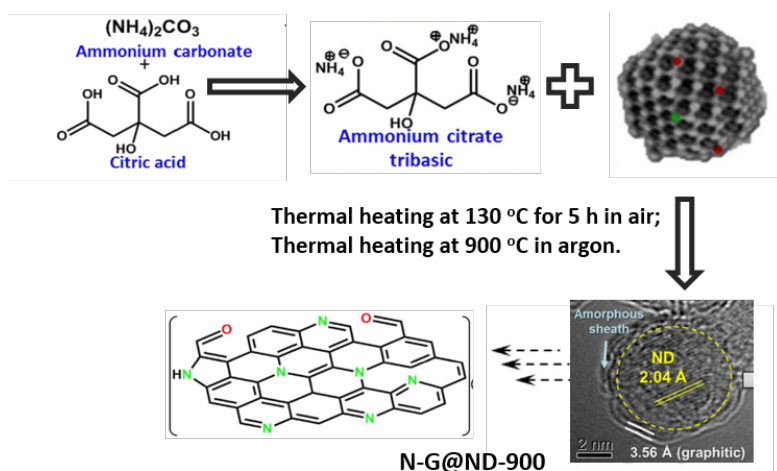


**Figure 1.** Schematic illustration for the fabrication of the N-doped graphene@nanodiamond.

## References

- [1] D. S. Su, G. D. Wen, S. C. Wu, et. al., *Angew. Chem., Int. Ed.* 56 (2017) 936–964.

# **Ru-containing Magnetically Recoverable Catalysts for the Conversion of Inulin to Mannitol**

*Manaenkov O., Ratkevich E., Kislitsa O., Matveeva V., Sulman M., Sulman E. Tver State Technical University, Tver, Russia*

## **Introduction**

Polyols are important materials which are widely used in various fields. Mannitol is employed in the pharmaceutical, chemical, and food industry as well as in biotechnology [1]. These applications determine the high demand for mannitol. There are several methods for mannitol syntheses. One of such methods is the hydrolytic hydrogenation of inulin [2], which is present in significant amounts in such plants as *Helianthus tuberosus* and *Cichorium intybus*. The inulin hydrolytic hydrogenation can be carried out as a one-pot procedure in the presence of heterogeneous catalysts containing various precious metals. Because inulin hydrolysis in subcritical water is fast, the hydrolytic hydrogenation efficiency is mainly determined by the activity of the most active in hydrolytic hydrogenation and hydrogenolysis. Magnetically separable catalysts received considerable attention due to easy magnetic separation from reaction mixtures, facilitating the catalyst repeated use. Magnetically separable catalysts have shown good results in cellulose conversion [3]. It is noteworthy that when the biomass conversion is incomplete, the magnetic separation is especially valuable for the catalyst recovery and the process optimization. In our preceding work, we developed a Ru-containing magnetically separable catalyst based on magnetic silica ( $\text{Fe}_3\text{O}_4\text{-SiO}_2$ ), where magnetite and Ru nanoparticles are formed in the silica pores.

## **Methods**

The catalyst synthesis was carried out according to the procedure published elsewhere [4]. Our tests were conducted in a 50-cm<sup>3</sup> high-pressure steel reactor equipped with a PARR 4843 controller and a propeller stirrer. After each test, the catalyst was separated from the reaction mass using a neodymium magnet.

## **Results and discussion**

We studied the behavior of the Ru-containing magnetically separable catalyst in the conversion of inulin to mannitol, exploring different reaction conditions. In the

hydrolytic hydrogenation of inulin the maximum selectivity to mannitol of 44.3% was obtained at 150 °C, P(H<sub>2</sub>) 60 bar, 0.1167 mmol of Ru per 1 g of inulin for 45 min with the catalytic activity of 2.53 h<sup>-1</sup>. Under these conditions, the inulin conversion reached 100%.

The results presented in Table 1 show that the selectivity of mannitol and the productivity of the catalyst remained virtually the same, testifying to the catalyst's stability in the hydrolytic hydrogenation of inulin.

**Table 1.** Mannitol selectivity (S) and catalyst productivity (A<sub>k</sub>) in consecutive cycles.

Cycle	S, %	A <sub>k</sub> , h <sup>-1</sup>
1	44.3	2.53
2	43.7	2.50
3	43.6	2.49

0.1167 mmol of Ru per gram of inulin; 0.3 g of inulin; 0.07 g of 5 % Ru- Fe<sub>3</sub>O<sub>4</sub>-SiO<sub>2</sub>; 30 mL of H<sub>2</sub>O; 150 °C; H<sub>2</sub> 60 bar; 45 min.

These factors and the excellent catalyst stability under hydrothermal conditions as well as easy magnetic separation make 5 % Ru-Fe<sub>3</sub>O<sub>4</sub>-SiO<sub>2</sub> the catalyst of choice for practical applications in biomass conversion.

### Acknowledgments

The authors thank L.M. Bronstein at the Nesmeyanov Institute of Organoelement Compounds, RAS, for her assistance in our research. This work was supported by the Russian Foundation for Basic Research, project nos. 19-08-00414, 18-08-00404; and by the Russian Science Foundation, project no. 18-19-00240.

### References

- [1] Ohrem HL, Schornick E, Kalivoda A, Ognibene R. Why is mannitol becoming more and more popular as a pharmaceutical excipient in solid dosage forms? *Pharmaceut Dev Technol* 2014;19(3):257-62.
- [2] Heinen AW, Peters JA, van Bekkum H. The combined hydrolysis and hydrogenation of inulin catalyzed by bifunctional Ru/C. *Carbohydr Res* 2001;330:381-90.
- [3] Zhang J, Wu S, Liu Y. Direct conversion of cellulose into sorbitol over a magnetic catalyst in an extremely low concentration acid system. *Energy Fuels* 2014;28:4240-6.
- [4] Manaenkov OV, Mann JJ, Kislitza OV, Losovyj Y, Stein BD, Morgan DG, Pink M, Lependina OL, Shifrina ZB, Matveeva VG, Sulman EM, Bronstein LM. Ru-containing magnetically recoverable catalysts: a sustainable pathway from cellulose to ethylene and propylene glycols. *ACS Appl Mater Interfaces* 2016;8(33):21285-93.

## Water enhanced activity in benzyl alcohol oxidation over platinum-based catalysts

*Avela Kunene,; Tracey van Heerden; Thobani Gambu; Eric van Steen*

*Catalysis Institute, Department of Chemical University of Cape Town, Cape Town  
South Africa*

Early studies of heterogeneous catalysis provided evidence that water in various processes can be more than just as a solvent [1]. The presence of water in alcohol oxidation in particular has been shown to enhance catalytic activity [2,3]. It has been observed that increasing water content in the system increases benzyl alcohol conversion, which is thought to assist in the initial H-abstraction. Moreover, it has been suggested that one of the main functions of water in selective oxidations is to promote oxygen adsorption and activation [1] through the formation of OOH intermediate over the catalyst [4].

The benzyl alcohol oxidation was investigated over Pt/TiO<sub>2</sub> prepared by impregnation of P25 using platinumic acid in a semi-batch reactor operating at 90°C and 5 bar. The effect of water on the rate of reaction was investigated by varying the initial benzyl alcohol to water ratio. The presence of OOH-intermediates was probed by the addition of oxygen centred radical scavengers (i.e. 0.25 mol-% hydroquinone) to the reaction mixture. Various liquid systems, i.e. benzyl alcohol (**B**), benzyl alcohol-hydroquinone (**BH**), benzyl alcohol-water-hydroquinone (**BWH**) and benzyl alcohol-water system (**BW**) were investigated for benzyl alcohol oxidation.

The benzyl alcohol conversion increased significantly upon addition of water reaching a conversion of ca. 37 mol-% after 5 hours. The addition of the oxygen scavenger hydroquinone to the benzyl alcohol water system (**BWH**) resulted in a strong decrease in the benzyl alcohol conversion (from 37 mol-% to 3 mol-%). Hydroquinone may also act as a simple inhibitor for the benzyl alcohol oxidation. However, the comparable level of benzyl alcohol conversion between **B** and **BH** suggests that it does not affect the oxidation reaction in the absence of water. This may indicate that hydroquinone in **BWH** system reacts with the *in-situ* formed hydroperoxyl species, thereby reducing benzyl alcohol conversion.

DFT analysis shows that H<sub>2</sub>O is beneficial to the dissociation of O<sub>2</sub> over Pt(111) in two ways. The adsorption of O<sub>2</sub> is stabilized by the presence of co-adsorbed H<sub>2</sub>O. At a constant O<sub>2</sub> coverage of 0.11 ML, increasing the coverage of H<sub>2</sub>O reduces the adsorption energy from  $E_{\text{ads}} = -0.64$  (at 0 ML H<sub>2</sub>O) to  $E_{\text{ads}} = -3.52$  eV (at 0.67 ML H<sub>2</sub>O). This is accompanied by a stretching of the O-O bond of adsorbed O<sub>2</sub> from 1.36 Å to 1.44 Å. This contributes to a reduced barrier for the dissociation of O<sub>2</sub> when H<sub>2</sub>O is present on the surface. The addition of 0.11 ML H<sub>2</sub>O reduces the barrier of O<sub>2</sub> dissociation from 0.41 eV to 0.19 eV (see Figure 1).

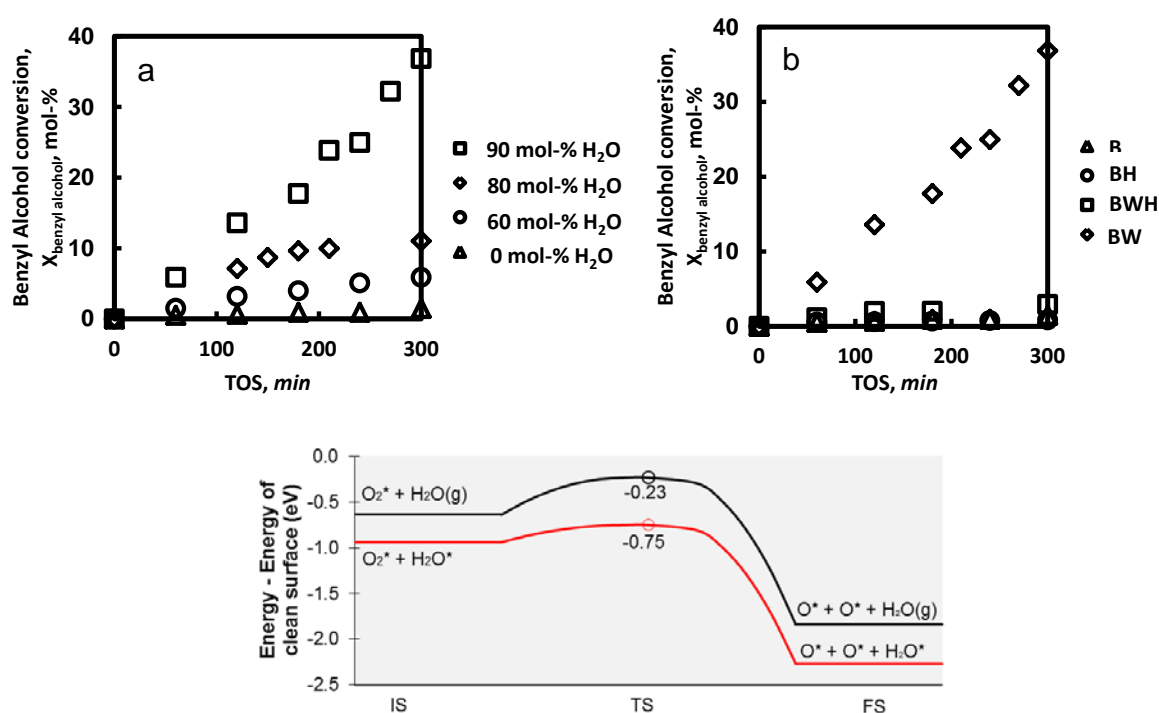


Figure 1: **(Top)** Benzyl alcohol oxidation over on Pt/TiO<sub>2</sub> (P25) as a function of time. Reaction conditions:  $V_{\text{Liquid}} = 70$  mL, 0.5 g catalyst, 90 °C,  $p_{\text{total}} = 5$  bar,  $V_{\text{air}} = 100$  mL<sub>n</sub>/min. **(bottom)** PES of dissociation of O<sub>2</sub> on Pt(111)-p(3x3) in the presence of 0.11 ML adsorbed H<sub>2</sub>O (red) and 0 ML of adsorbed H<sub>2</sub>O (black)..

## References

- [1] Davies, P. (2016). *Top. Catal.* **5**, 1.
- [2] Frassoldati A., Pinel C, Besson M. (2011). *Catal. Today* **173**, 81.
- [3] Donze C., Korovchenko P., Gallezot P., Besson M. (2007). *Appl. Catal. B: Environ.* **70**, 621.
- [4] Chang, C., Yang, X., Long, B. Li, J. (2013). *ACS Catal.* **3**, 1693.

# D-glucose Hydrocondensation Using Ni Impregnated Hypercrosslinked Polystyrene for N-methylglucoseamine Synthesis

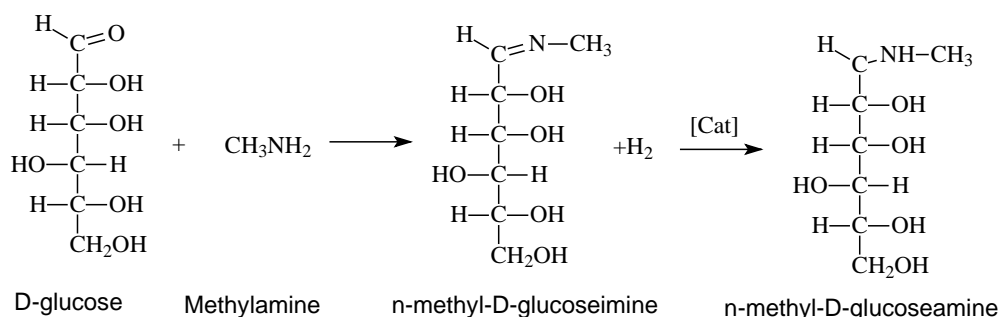
S. Mikhailov, V. Matveeva, V. Doluda, E. Sulman, M. Sulman

Department of biotechnology and chemistry, Tver State Technical University; Tver

Nab. A. Nikitina 22, 170023, Russia

## Introduction

D-glucose simultaneous catalytic hydro condensation with methylamine can be considered a promising way of methylglucosamine synthesis[1,2]. The reaction for the production of N-methylglucamine by reductive amination proceeds in one or two steps [1-2]:



## Methods

Methanol, glucose and methylamine solution in methanol was feed to the 4540 Parr instrument reactor and heated up to 85 °C one hour. After n-methyl-D-glucosimine synthesis, the reactor was flushed with nitrogen for methylamine evacuation followed by catalyst input into the reactor, reactor flashing with hydrogen. The hydrogen pressure was maintained 70 Bar all over the reaction, the hydrogenation was provided for two hours.

## Results and discussion

During the experiments n-methyl-d-glucosimine, n-methyl-D-glucosamine were found in reaction media and can be considered as main products, sorbitol was found as a main side product. Investigation of temperature influence on n-methyl-d-glucosimine and n-methyl-D-glucosamine yield showed appropriate increasing in n-methyl-d-glucosimine and n-methyl-D-glucosamine yield in case of temperature increase up to 120°C. Determined specific activation energies were found to be 39±7 kJ/mol and 30±9 kJ/mol for n-methylamine-D-glucosimine and n-methyl-D-glucosamine

synthesis process. Influence The investigation of the catalysts long term stability showed that after 10 reaction cycles of 2 hours hydrogenation the HPS-Ni catalyst was ground by a reactor mixer, therefore, catalysts particles diameter becomes smaller than 0.01-0.07 mm compare to initial. Besides the catalysts mechanical losses were calculated to be 78%, the catalyst weight losses can be attributed to the catalysts particles grinding and losses during the centrifugation and separation. The catalysts activity after 10 cycles of D-glucose transformation showed a little slowdown and was calculated to be for  $1.1 \text{ kg(Glu)/(kg(Cat)*h)}$  at 99.4-99.5% D-glucose conversion. Some losses of catalysts activity can be attributed to metal leaching. However, some increase in Ni dispersion is noticed that can be also explained by the catalyst particles grinding and particles transformation during the reaction. The oxidation state of an active metal according to XPS data remains +2 and Ni is mainly presented in the oxide form. It should be noted that D-glucose hydrogenation in the reactor equipped with impeller mixer results in high mechanical losses, therefore, the catalysts overall time on steam was only 20 h, that is insufficient for the study of metal leaching, posing, and nanoparticles transformation.

## Conclusions

D-glucose simultaneous catalytic hydro condensation with methylamine can be considered a promising way of methylglucosamine synthesis. Catalysts initial activity of Ni impregnated in hypercrosslinked polystyrene was found to be  $1.3 \text{ kg(Glu)/(kg(Cat)*h)}$  at 99.3-99.6% D-glucose conversion. Process selectivity to N-methyl-d-glucosamine was 97.6-97.8%.

## Acknowledgments

This study was funded by the Russian Foundation for Basic Research (grant 18-08-00489) and the Russian Science Foundation (grant 18-19-00240).

## References

1. WO 92/08687/ Process for preparing N-alkyl polyhydroxy amines in amine and amine/water solvents and fatty acid amides therefrom. Shumate P.R., Burdsall D., Scheibel J.J., Connor D. Pub. 29.05.1992.
2. Pat. WO 92/06984. Process for preparing N-alkyl polyhydroxy amines and fatty acid amides therefrom in hydroxy solvents. Scheibel J.J., Connor D., Shumate P.R., Laurent J. Pub. 30.04.1992.

# Structure-activity relationship for layered MCM-56 zeolite in Friedel-Crafts alkylation of bulky molecules

*Katarzyna Kałahurska, Aleksandra Korzeniowska, Barbara Gil, Wiesław J. Roth*

*Faculty of Chemistry, Jagiellonian University, Kraków, Poland*

## Introduction

Zeolites are large group of natural and synthetic microporous aluminosilicates. They are widely used as sorbents and catalysts. MCM-56 zeolite is composed of single layers with MWW topology, 2.5 nm thick, stacked disorderly and without inter-layer linking except for incidental cross-linking, thus may be considered as a delaminated zeolite generated by direct synthesis. It is an intermediate that transforms into the 3D framework material MCM-49 [1] but it was recently shown that this process may be suppressed in the presence of aniline as a structure promoting agent [2]. Potential high catalytic activity of MCM-56 in some important industrial processes has already been demonstrated [3]. This work focuses on understanding the effect on catalytic activity of the most important structure-related parameters of MCM-56: concentration and location of the acid sites and their accessibility to bulky reactant molecules.

## Experimental

MCM-56/-49 zeolites were synthesized using Aerosil as a silica source ( $\text{Si}/\text{Al}_{\text{gel}} = 10$ ), hexamethyleneimine as a structure-directing agent and optionally aniline as a structure promoting agent at 143°C for 48, 60, 83, 120, and 176 h (only the latter with aniline). Samples were characterized using  $\text{N}_2$  adsorption, XRD, quantitative FTIR (pyridine and pivalonitrile sorption). Catalytic tests were carried out in batch reactor for 6 h in a liquid phase at 80°C. Products were analyzed by gas chromatography.

## Results and discussion

Increased synthesis time resulted in transformation of layered MCM-56 zeolites into 3-D MCM-49, which is detected in XRD patterns showing initially a broad band between 8 and 10° 2 $\theta$ , without a dip (MCM-56) and then with the emerging valley in the middle (MCM-49), Fig. 1A. At the same time, the concentration of the Brønsted acid sites (BAS) and microporous volume of the materials increased with increased crystallinity of samples. Condensation of the layers (increasing MCM-49) caused decrease in the values of the external areas and lowered concentration of the acid



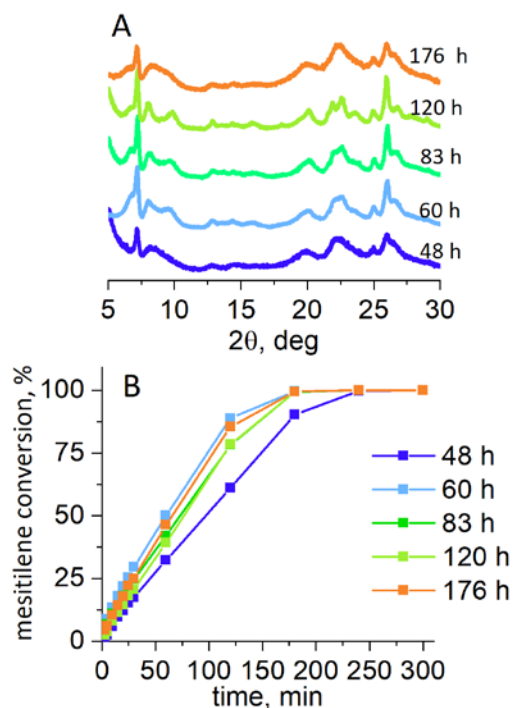
centers located at the external surfaces of the layers/crystals. The latter was investigated by the quantitative adsorption of pivalonitrile, which cannot pass through 10-rings opening of the MWW channels.

TABLE. Physicochemical properties of MCM-56/-49 samples under study.

sample	BAS, $\mu\text{mol/g}$	LAS, $\mu\text{mol/g}$	BAS <sub>ext</sub> , $\mu\text{mol/g}$	S <sub>BET</sub> , $\text{m}^2/\text{g}$	S <sub>ext</sub> , $\text{m}^2/\text{g}$	V <sub>micro</sub> , $\text{cm}^3/\text{g}$
48h	535	129	455	328	158	0.030
60h	792	99	447	359	138	0.061
83h	892	74	387	434	112	0.105
120h	942	156	404	463	107	0.112
175h	913	91	477	436	146	0.030

In catalytic tests between mesitylene and benzyl alcohol two reactions were observed, alkylation and etherification, with 1,3,5-trimethyl-2-benzylbenzene being the favored product (over 90% selectivity), Fig. 1B.

The alkylation, due to the presence of the bulky product, proceeds solely at the surfaces and thus may be correlated with the concentration of the acid sites determined by pivalonitrile adsorption. It can be seen that conversion of mesitylene for all MCM-56/-49 samples is similar, as concentrations of the external BAS do not differ significantly (380-480  $\mu\text{mol/g}$ ), while the total concentration of BAS vary considerably (530-950  $\mu\text{mol/g}$ ). Aniline as a structure promoting agent leads to the formation of high quality MCM-56 improved activity, as the final, not an intermediate product.



**Figure 1** XRD patterns and conversion of mesitylene over MCM-56/-49 zeolites.

## References

1. W.J. Roth, Stud. Surf. Sci. Catal. 158A and B (2005) 19-26.
2. J.C. Cheng, A.D. Fung, D.J. Klocke, S.L. Lawton, D.N. Lissy, W.J. Roth, C.M. Smith, D.E. Walsh, U.S. Patent, Mobil Oil Corp., USA (1995)
3. E. Xing, X. Gao, W. Xie, F. Zhang, X. Mu, X. Shu, RSC Adv. 4 (2014) 24893-24899.

## Acknowledgments

Katarzyna Kałahurska has been partly supported by the EU Project POWR.03.02.00-00-1004/16

# Selective Hydrogenation of Aliphatic Acyclic Primary Amides to Primary Amines with Recyclable Heterogeneous Ru-W Catalysts

*R. Coeck, D. E. De Vos, Centre for Surface Chemistry and Catalysis, KU Leuven, Leuven, Belgium*

## Introduction

The hydrogenation of amides is a challenging reaction, because of the high stability of amides. Traditionally amide reduction is achieved with an excess of hydride reagents such as  $\text{LiAlH}_4$  or  $\text{NaBH}_4$ , resulting in large quantities of inorganic chemical waste.<sup>[1]</sup> Over the last years, progress has been made with the development of heterogeneous bimetallic catalysts for amide hydrogenation. These catalysts typically contain a platinum group metal (Pt, Pd, Rh or Ru) promoted by a group 5, 6 or 7 metal oxide (V, Mo or Re).<sup>[2]</sup> However, several issues still need to be addressed. First, the hydrogenation of aliphatic, acyclic primary amides has been rarely investigated with these new bimetallic catalysts; most reports use cyclic or more activated amides as reactants. Secondly, in as far as aliphatic acyclic primary amides are considered, they are usually converted to the alcohol instead of to the amine. Finally, these catalysts have only been validated in a rather limited range of (toxic) solvents e.g. 1,2-dimethoxyethane, hexane and 1,4-dioxane. Here, we report the use of a new ruthenium-tungsten bimetallic catalyst for the hydrogenation of aliphatic acyclic primary amides, such as hexanamide, in the green and benign cyclopentyl methyl ether (CPME).<sup>[3]</sup> Besides the effect of the Lewis acid promotor,  $\text{NH}_3$  partial pressure is identified as the key parameter leading to high primary amine yields.

## Materials and Methods

Ru-W catalysts were prepared by mixing  $\text{RuCl}_3$ ,  $(\text{NH}_4)_{10}\text{H}_2(\text{W}_2\text{O}_7)_6$ , and a high surface area support ( $\text{SiO}_2$  or a spinel) in water, followed by water evaporation, drying and activation at  $450^\circ\text{C}$  under  $\text{H}_2$ . Catalytic experiments, with hexanamide as a test substrate, were performed in a 50 mL Parr autoclave, which can be loaded with controlled pressures of  $\text{H}_2$  and  $\text{NH}_3$ .

## Results and discussion

Preliminary experiments revealed that two side reactions are dominant when reducing aliphatic acyclic primary amides with a bimetallic catalyst. First, beside C-O cleavage, C-N cleavage can occur (Fig 1). We found this side reaction to be

promoted (in comparison with amine formation) at lower temperatures. Secondly, the initial alcohol and amine products can condensate to form secondary amines (Fig 2).

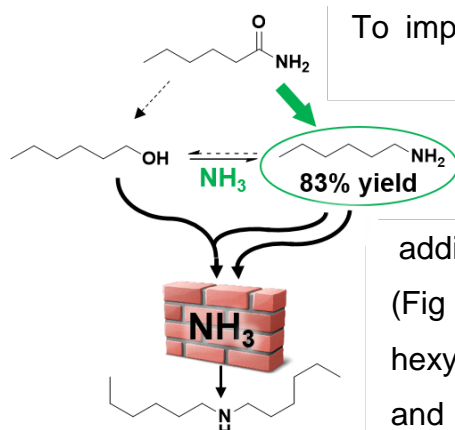


Figure 1 – Simplified reaction scheme for the hydrogenation of hexanamide

To improve the primary amine selectivity, we explored the use of a strongly basic support (e.g. a spinel), and the use of higher  $\text{NH}_3$  pressures; the latter option is most effective. At high  $\text{NH}_3$  pressures, the additional effect of a basic support is rather negligible (Fig 3). After a further optimization, a yield of up to 83% of hexylamine could be obtained at  $200^\circ\text{C}$ , with 50 bar  $\text{H}_2$  and 6 bar  $\text{NH}_3$  (= 2.5 M of ammonia) in CPME. Recyclability tests showed that the  $\text{RuWO}_x/\text{SiO}_2$  catalyst is

very robust, with an essentially unchanged activity after 4 runs (Fig 4). Summarizing, we found a relatively cheap and green amide hydrogenation system, that could potentially also be used for other applications, e.g. one pot synthesis of decamethylenediamine out of sebacic acid (in the polyamide industry).

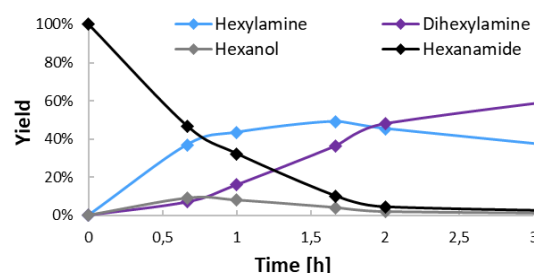


Figure 2 – Time profile of hexanamide hydrogenation with  $\text{RuWO}_x/\text{SiO}_2$  (5 mol% Ru) at  $200^\circ\text{C}$ , 50 bar  $\text{H}_2$ ; 0.5 bar  $\text{NH}_3$ .

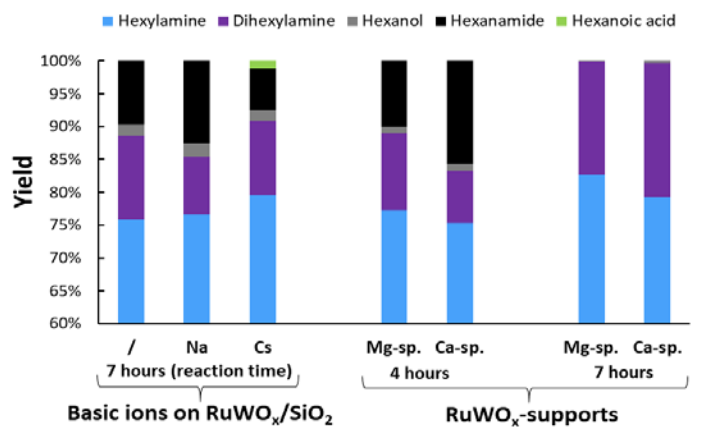


Figure 3 – Catalytic screening of  $\text{RuWO}_x$  on various supports: (left)  $\text{SiO}_2$  vs Na- & Cs-loaded  $\text{SiO}_2$  (7h); (right) Mg- vs Ca-spinel (4h & 7h). All reactions were performed with 7 mol% Ru at  $200^\circ\text{C}$ , 50 bar  $\text{H}_2$ ; 6 bar  $\text{NH}_3$ .

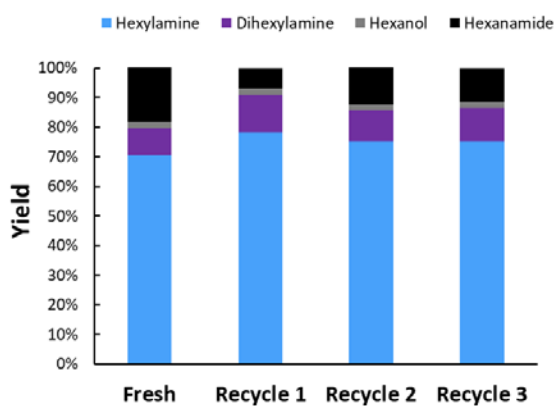


Figure 4 – Recyclability test of  $\text{RuWO}_x/\text{SiO}_2$  (7 mol% Ru) at  $200^\circ\text{C}$ , 50 bar  $\text{H}_2$ ; 6 bar  $\text{NH}_3$  for 7h.

## References

- [1] Smith, E. L. *et al. Chemical Reviews* **114**, 11060–11082 (2004)
- [2] (a) Hirose, C. *et al. Tetrahedron Letters* **37**, 6749–6752 (1996). (b) Beamson, G. *et al. J. of Catal.* **269**, 93–102 (2010). (c) Beamson, G. *et al. J. of Catal.* **278**, 228–238 (2011). (d) Mitsudome T. *et al. Angew. Chem. Int. Ed.* **56**, 9381–9385 (2017).
- [3] Watanabe, K. *et al. Org. Process Res. Dev.* **11**, 251–258 (2007)

# SILICA SUPPORTED EARLY-LATE TANTALUM-RHODIUM HETEROBIMETALLIC COMPLEX

*Ravi Srivastava,<sup>a</sup> Elsje Alessandra Quadrelli,<sup>a</sup> Clement Camp<sup>a,\*</sup> Université Lyon 1, ESCPE Lyon, 43 Bd du 11 Novembre 1918, F-69616 Villeurbanne, France*

Early-Late heterobimetallic transition metal complexes have unique ability to activate substrates because of the bifunctionality of the metal atoms involved. Although these homogeneous complexes are active and selective independently; they tend to decompose due to intermolecular interactions. One way to increase their lifetime and performance is to immobilize the complexes on a solid support. Recently the synergistic effect of bimetallic complexes grafted over silica has been studied but it involves only early transition metal complexes.<sup>[1]</sup> Herein we report a unique well-defined silica supported Tantalum-Rhodium (Early-Late) heterobimetallic complex. A bifunctional NHC with hydroxyl group tethered in one arm was used to assemble the oxophilic hard Tantalum center and nucleophilic soft Rhodium center.<sup>[2]</sup> <sup>13</sup>C labelled NHC was also synthesized to gain insight into the structure of the complex. Polyhedral Oligosilsequioxane (POSS) based homogenous molecular model of silica was developed to explore the various synthetic routes possible for grafting the bimetallic system. Based on our findings over POSS, the Tantalum-Rhodium bimetallic complex was successfully incorporated over silica (SBA<sub>15-700</sub>). Detailed characterization of these unique surface organometallic species via state of the art techniques and their catalytic activity to activate dinitrogen will be presented.

## Acknowledgements

I acknowledge the SINCEM program for funding this work. SINCEM is a Joint Doctorate programme selected under the Erasmus+ Action 1 Programme (FPA2013-0037).

## References

1. Samantaray, Manoja K.; Dey, Raju; Kavitate, Santosh; Hamad, Abou-Edy; Sedjerari, Bendjeriou-Anissa; Hamieh, Ali; Basset, J.M. *J. Am. Chem. Soc.*, **2016**, *138*, 8595.
2. Srivastava, Ravi; Moneuse, Raphael; Petit, Julien; Pavard, Alexis-Paul; Dardun, Vincent; Rivat, Madleen; Schiltz, Pauline; Solari, Marius; Jeanneau, Erwann; Veyre, Laurent; Thieuleux, Chloe; Quadrelli, Alessandra Elsje; Camp, Clement *Chem. Eur. J.*, **2018**, *24*, 1-11.

# **“H<sub>2</sub>-free” hydrodeoxygenation of guaiacol over Pt supported on N-doped carbon catalysts**

*Wei Jin, University of Surrey, Guildford, UK; Laura Pastor-Pérez, Universidad de Alicante, Alicante, Spain ; Juan J. Villora-Picó, Universidad de Alicante, Alicante, Spain; Antonio Sepúlveda-Escribano, Universidad de Alicante, Alicante, Spain; Tomas R. Reina, University of Surrey, Guildford, UK*

## **Introduction**

Catalytic hydrodeoxygenation (HDO) is a fundamental technology to upgrade bio-oil or oxygenated compounds in which hydrogen is consumed to remove the oxygen in the form of H<sub>2</sub>O [1]. The implementation of traditional HDO for large scale applications is hampered by the supply of expensive H<sub>2</sub> from the economic efficiency and sustainability perspective [2]. Researchers were encouraged to develop novel approaches to realize HDO suppressing external H<sub>2</sub> supply. Indeed, an attractive method for *in-situ* HDO is using H<sub>2</sub>O as hydrogen source. Cheng and co-workers [3] proposed a process for bio-oil upgrading in which H<sub>2</sub> produced *in-situ* from metal oxidation with water is utilised for HDO of bio-oil. However, limitations related to the high energy input in the metal regeneration process need to be further overcome.

In this work, we propose a novel method for bio-oil upgrading, in which hydrogen is generated by H<sub>2</sub>O splitting over the surface of metal catalysts, and further participate in the guaiacol HDO process. Pt supported on activated carbon (AC) and N-doped carbons (NC) were employed in the guaiacol HDO process. Carbon materials have a large number of applications in heterogeneous catalysis, either as supports for the active phases or as catalysts by themselves due to the redox-active functional groups that are located at the surface. Doping these carbons with nitrogen could increase their stability, oxidation resistance and modify their electronic properties, what can affect the catalytic activity of active phases supported on them. It is reported that the Pt-N interaction provokes an exchange of electrons from Pt into the N-doped system that increases the electron density of the material. Also, N-groups can act as nucleation centres for Pt nanoparticles, what favours Pt dispersion. Moreover, mesoporous carbons favour the transport of the reactants and the products to and from the active centres [4]. This innovative strategy based on simultaneous H<sub>2</sub>O splitting and HDO opens the horizons for the further development in bio-oil upgrading technologies.

## Materials and Methods

Three types of NC support (labelled, Mel, PPy and PANI) were prepared by using melamine, aniline and pyrrole as N source precursors. 1%Pt supported on AC (RGC-30) and NC materials were prepared by wet impregnation.

The catalytic activity tests were performed in a high pressure batch reactor (Parr 5500). 0.2 g catalyst and 10 wt.% of guaiacol in water were used in each reaction. The reactor was held at 250 °C for 4 h under inert atmosphere. After the reaction the catalyst was collected by filtration, and organic products were extracted with ethyl acetate and further analysed by GC/MS and GC/FID.

## Results and Discussion

An estimation of the surface chemistry of the N-doped carbon supports was obtained by XPS, where four nitrogen species including pyridinic, pyrrolic, amide and quaternary type were identified in the spectra (Figure 1). The electronic differences of the carbon species upon N introduction may tune the catalytic properties of prepared materials. Catalytic performance is reported in Figure 2. Interestingly the unpromoted catalyst, Pt/AC, is the most active sample, which can achieve around 45% conversion and around 80% selectivity towards typical aromatic products including phenol, cresol and catechol. Besides, Pt/PANI greatly promoted the selectivity of partial de-oxygenated compounds, such as phenol.

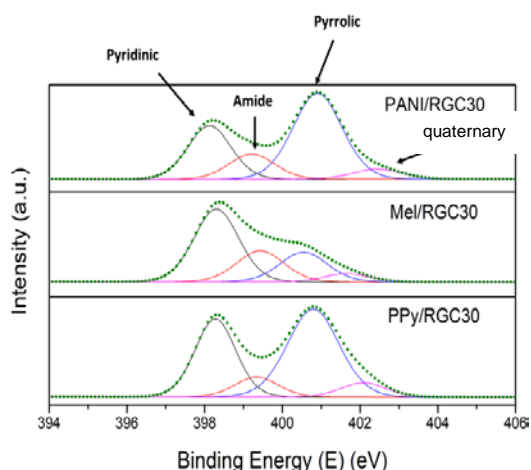


**Figure 1.** XPS N 1s spectra for the NC support (Mel/AC with 7%N, PPy/AC with 3.25%N, PANI/AC with 3.75%N).

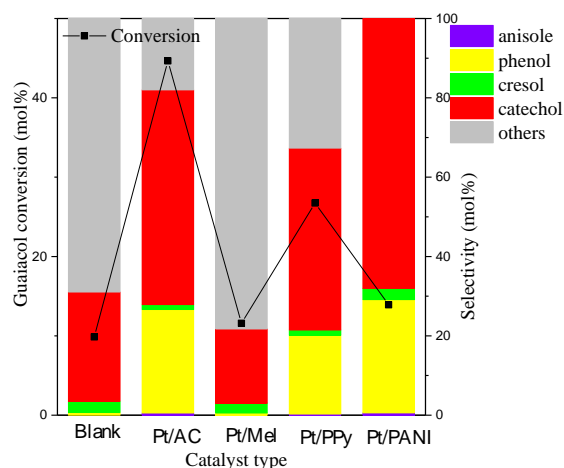


**Figure 2.** Catalytic activity of all catalysts in H<sub>2</sub>O without external H<sub>2</sub> supply.

## References

- [1] A.M. Robinson, J.E. Hensley, J.W. Medlin, *ACS Catal.* **2016**, 6(8), 5026.
- [2] D. Zhang, F. Ye, T. Xue, Y. Guan, Y.M. Wang, *Catal. Today* **2014** 234, 133.
- [3] S. Cheng, L. Wei, M.R. Alsowij, et. al, *J. Energy Inst.* **2018**, 91,163.
- [4] J. Melke et al. *ACS Appl. Mater. Interfaces* **2016**, 8.

# Preparation and catalytic properties of reduced Pd doped NiTiO<sub>3</sub> ilmenites for selective liquid-phase hydrogenation of nitroarenes

*Daniela González-Vera, Paula Osorio-Vargas, Escuela de Química, Facultad de Tecnología, Universidad Tecnológica de Pereira, Pereira, Colombia; Cecilia C. Torres, Facultad de Ciencias Exactas, Universidad Andres Bello, Sede Concepción, Talcahuano, Chile; Tatiana M. Bustamante, Robinson Dinamarca, Gina Pecchi, Cristian H. Campos, Facultad de Ciencias Químicas, Universidad de Concepción, Concepción, Chile.*

Catalytic hydrogenation of nitro-compounds (-NO<sub>2</sub>) is one of the most important organic reactions for preparation of amines (-NH<sub>2</sub>), which are used for synthesis of agrochemicals, pharmaceuticals, dyes, rubbers and pigments [1]. All the efforts are focused in the production of catalysts based on non-noble metals because noble metals possess scarce natural abundance and ensuing high cost. Among non-noble metals, nickel (Ni) has been reported as low cost benign alternative. The aim of this work was to synthesize and characterize Ni<sub>1-x</sub>Pd<sub>x</sub>TiO<sub>3</sub> catalysts with different amount of palladium to be used as reduced Pd doped NiTiO<sub>3</sub> (Pd-NTO) as selective catalysts in the hydrogenation of nitrobenzene (NB) to produce aniline (AN)) as test reaction.

The XRD characterization of reduced materials is shown in Figure 1.a). All samples exhibit a similar characteristics diffraction profile matched with database in JCPDS, No 98-016-2279 and 98-005-3808 for TiO<sub>2</sub> rutile and metallic Ni, respectively.

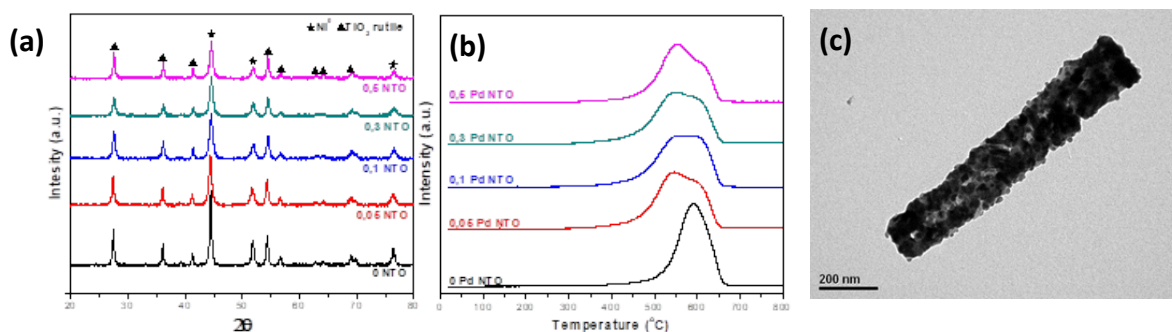


**Figure 1.** a) X-ray diffraction patterns of reduced catalysts. b) H<sub>2</sub>-TPR profiles. c) TEM images of 0,05% Pd NTO reduced ilmenite.

The TPR-H<sub>2</sub> profiles shown in Figure 1.b) indicates one well defined peak at ~600°C attributed to Ni<sup>2+</sup> reduction to metallic Ni, the addition of palladium decreases reduction temperature. In Figure 1.c) is shown the TEM micrograph of 0,05% Pd NTO reduced ilmenite, where the morphology is confirmed and the metallic particles are easily seen.

The catalytic activity results in the selective hydrogenation of NB are shown in Table 1. It can be observed at lower Pd content a slight decrease in the catalytic activity was detected. At nominal Pd 0.10wt% the maximum in the catalytic activity was detected. Finally the increase in the Pd loading (> 0.10 wt%) affords a decrease in the catalytic activity.

**Table 1.** Catalytic activity for NB hydrogenation on reduced Pd doped NiTiO<sub>3</sub> catalysts. Reaction conditions: Parr<sup>®</sup> Reactor; 20mg catalyst; mol<sub>NB</sub>/mol<sub>Ni</sub>: 60; P: 20 bar; T: 80°C; solvent: 50mL ethyl acetate at 3 h of reaction.

Reduced Pd-NiTiO <sub>3</sub> (wt% Pd)	X (%)	S <sub>AN</sub> (%)
0,00	82,0	99,0
0,05	73,5	99,3
0,10	100	100
0,30	64,5	99,3
0,50	51,0	99,2

<sup>a</sup>nitrosobenzene and N-(phenyl)-hydroxylamine was detected as intermediaries product.

The incorporation of Pd into NiTiO<sub>3</sub> ilmenite structure provides changes in the electronic environment of Ni as active phase. At nominal Pd 0.10wt% the presence of Pd promotes both activity and selectivity in the production of AN but a higher dopant content the catalytic activity decrease mainly attributed to an decrease in the hydrogenation capacity by formation of intermetallic Pd-Ni compounds with less catalytic activity than monometallic Ni and that reduced catalysts doped at < 0.10 Pd wt%.

#### Acknowledgements

The authors acknowledge CONICYT FONDECYT 1170083 and FONDECYT Initiation 11170095.

#### References:

[1] C.C. Torres, V.A. Jiménez, C.H. Campos et al, Molecular Catalysis 447 (2018) 21-27.



## Selective cinnamaldehyde hydrogenation on low-loaded Pt catalysts.

*Kseniia Vikanova, IOC RAS, Moscow, Russia; Elena Redina, IOC RAS, Moscow, Russia; Leonid Kustov. IOC RAS, Moscow, Russia.*

Selective hydrogenation of  $\alpha,\beta$ -unsaturated aldehydes such as cinnamaldehyde (CAL) allows to obtain compounds that are widely used as flavors, fragrances, intermediates for pharmaceutical manufacture and organic synthesis, but the successful obtaining of  $\alpha,\beta$ -unsaturated alcohol is complicated by the simultaneous hydrogenation of C=C bond, which is thermodynamically more favorable [1]. In this regard, the hydrogenation of cinnamaldehyde is interesting from fundamental and practical points of view.

Ceria-zirconia mixed oxide was chosen as a support due ability to impart metal-support interactions to enhance catalytic performances by generation of active centres at the interface between metal [2] and was synthesized by precursors co-precipitation method (Table 1). Monometallic catalysts with a Pt content of 0.025-1% mass were prepared by pH-controlled precursor precipitation method, followed by drying and reduction of the dry sample in a stream of hydrogen.

Table 1. Textural properties of the synthesized support

Support	Ce/Zr ratio	$D_{XRD}$ , nm	$D_{SEM}$ , nm	$S_{BET}$ , m <sup>2</sup> /g
CZ	4 : 1	6	5-7	103

The supported catalysts were investigated in the cinnamaldehyde hydrogenation reaction at different reaction conditions. At room temperature and atmospheric pressure cinnamyl alcohol (COL) yield > 80% was achieved (Table 2). After a slight increase in temperature and pressure, the yield of the desired product > 70% was obtained on a catalyst containing only 0.1% mass of platinum. The obvious advantage of the CZ carrier has been shown in comparison with catalysts supported on individual CeO<sub>2</sub>

Table 2. Cinnamaldehyde hydrogenation at different reaction conditions

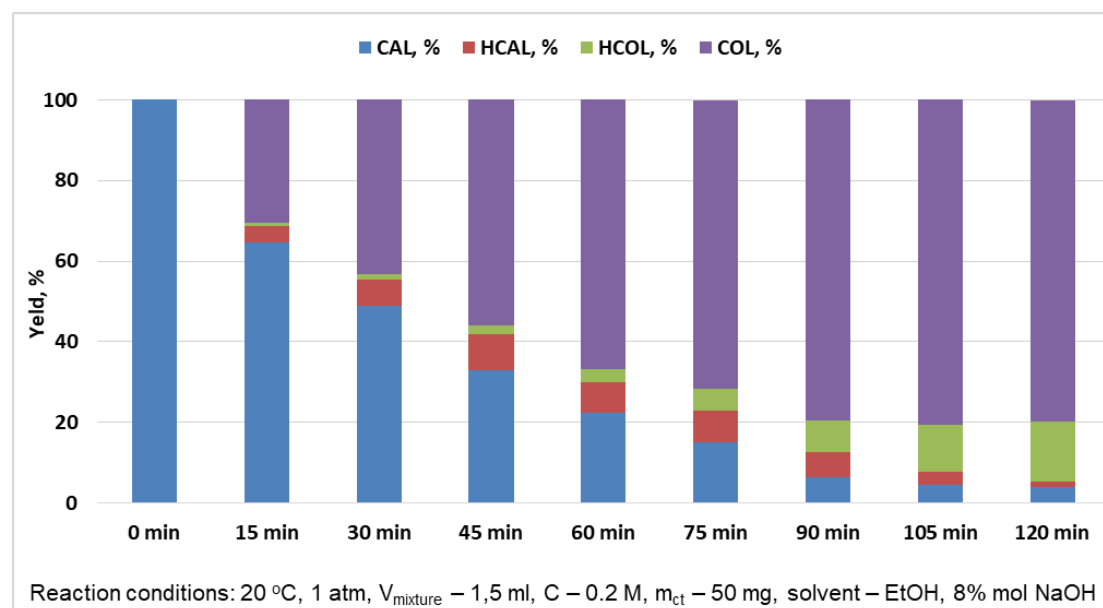
20 °C, 1 atm *			70 °C, 5 atm *		
Catalyst	Conversion, %	COL selectivity, %	Catalyst	Conversion, %	COL selectivity, %
1%Pt/CZ	96	83	0.1% Pt/CZ	88	83
0.5%Pt/CZ	85	80	0.05%Pt/CZ	45	84

0.1%Pt/CZ	15	71	0.025%Pt/CZ	9	65
1%Pt/CeO <sub>2</sub>	65	89	0.1%Pt/CeO <sub>2</sub>	19	23

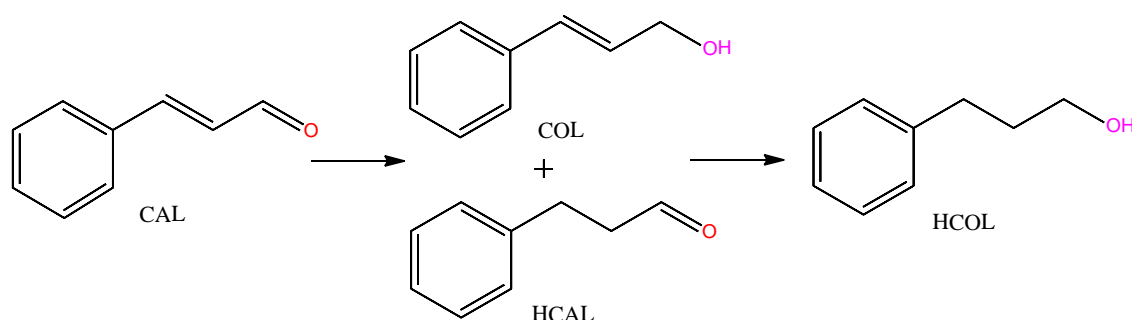
\*Other reaction conditions:  $V_{\text{mixture}} = 1,5$  ml,  $C = 0.2$  M, time – 2h,  $m_{\text{ct}} = 50$  mg, solvent – EtOH; 8% mol NaOH.

Also the dependence of the products composition on time at ambient conditions was obtained (fig. 1).

Fig. 1. Products accumulation diagram



The diagram shows that up to 90 minutes of the reaction, the two products of the hydrogenation, COL and HCAL, are formed in parallel, but then the process of sequential hydrogenation of the formed compounds into the product of complete hydrogenation, HCOL, begins to dominate. Based on the above, we can assume the following reaction scheme:



**Acknowledgement:** This work was supported by the Russian Science Foundation, grant 17-73-20282

#### References

1. K.V. Vikanova, E.A. Redina. Russian Journal of Physical Chemistry A, 2018, Vol. 92 (12), pp. 2355–2358.
2. S. Damyanova, B. Pawelec, K. Arishtirova, M.V. Martinez Huerta, J.L.G. Fierro. Applied Catalysis A: General 337 (2008) 86–96

# Metal complex catalysts for the production of alkyl lactates from the depolymerization of polylactic acid

*Luis A. Román-Ramírez<sup>1</sup>, Paul McKeown<sup>2</sup>, Matthew D. Jones<sup>2</sup> and Joseph Wood<sup>1</sup>*

<sup>1</sup> *School of Chemical Engineering, University of Birmingham, Edgbaston, Birmingham B15 2TT, United Kingdom.*

<sup>2</sup> *Department of Chemistry, University of Bath, Claverton Down, Bath BA2 7AY, United Kingdom.*

## Abstract

Alkyl lactates have been branded as *green solvents* due to their low toxicity and biodegradability. The alkyl lactate market is estimated at USD 16,800 million per annum and are seen as substitutes to oil-derived solvents with applications in polymer manufacture, biochemicals, pharmaceuticals, agricultural chemicals among many others applications.[1, 2] A recent study by our group [3] has shown that it is possible to obtain methyl lactate from the transesterification reaction of poly(lactic) acid (PLA) by means of a Zn(II) complex catalyst. In the present work, we report the use of two new complexes for the formation of methyl lactate and ethyl lactate from PLA. The ligands were prepared in one simple imine condensation step and complexed to Zn(II) to form the homoleptic complexes Zn(**A**)<sub>2</sub> and Zn(**B**)<sub>2</sub>. The new catalysts show stability under atmospheric condition in the solid state and were fully characterized by X-ray crystallography, multi-nuclear NMR spectroscopy and elemental analysis. Catalysts are compared based on PLA conversion, alkyl lactate yield and selectivity. Reaction conditions involved samples of PLA covering a wide range of molecular weights and industrial applications, and temperatures ranging from 50 to 110 °C. The progress of the reactions were followed by taking samples and different time intervals with further analysis by GC-FID, GPC and <sup>1</sup>H NMR.

The new catalysts showed higher activity compared with Zn(**1**)<sub>2</sub> for the PLA degradation, reducing in more than 40% the required degradation time. Higher lactate yields were also obtained with the new catalysts (Figure 1). A kinetic model based on the previous work was utilized to explain the differences between the catalysts. Kinetic constants and activation energies calculated from the model are presented.

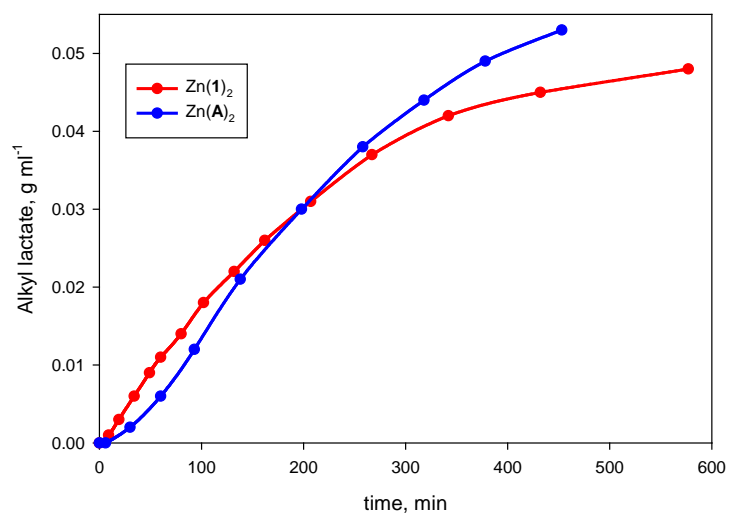


Figure 1. Alkyl lactate concentration profiles by two different Zn(II) catalysts.

## References

1. Calvo-Flores, F.G., et al., *Green and Bio-Based Solvents*. Topics in Current Chemistry, 2018. **376**(3).
2. NREL, *Chemicals from Biomass: A Market Assessment of Bioproducts with Near-Term Potential*, M.J. Bidy, C. Scarlata, and C. Kinchin, Editors. 2016, National Renewable Energy Laboratory.
3. Román-Ramírez, L.A., et al., *Poly(lactic acid) degradation into methyl lactate catalyzed by a well-defined Zn(II) complex*. ACS Catalysis, 2019. **1**: p. 409-416.

# The high activity of aerosol-made Ga-silicate catalysts for solketal synthesis explained by a deep structural investigation

Alvise Vivian,<sup>1</sup> Loraine Soumoy,<sup>1</sup> Luca Fusaro,<sup>1</sup> Damien P. Debecker<sup>2,\*</sup> and Carmela Aprile<sup>1,\*</sup>

[1] Unit of Nanomaterials Chemistry (CNANO), Department of Chemistry, University of Namur, 5000 Namur, Belgium, [2] Institute of Condensed Matter and Nanosciences - UCLouvain., 1348 Louvain-la-Neuve, Belgium

During the last decade, considerable attention has been devoted to the development of biofuels, above all biodiesel. The transesterification reaction yields as by-product an amount of glycerol that represents approximately 10wt% of the total biodiesel manufacture. With the increasing biodiesel production, glycerol is now considered as a waste and its efficient valorization have become a challenge for the scientific community. A promising route is represented by the condensation of glycerol with acetone to produce solketal, an added-value product with many applications.[1] A sustainable way to perform this reaction envisages the use of heterogeneous catalysts displaying both Brønsted and Lewis acid sites. Porous silicates presenting a metal inserted as single site in the framework can be active and selective catalysts for this reaction. In particular, it has been already reported that Ga-MCM-41 nanoparticles are one of the most efficient catalysts in the conversion of glycerol into solketal.[2] As reviewed recently,[3] aerosol processes have already been applied for the production of several metallosilicate materials exhibiting excellent catalytic performance in various chemical reactions.[4] The advantages of this process include: a limited number of steps, a limited waste generation and low environmental impact. Moreover, the catalyst preparation process can be scaled up easily and can be run in a continuous mode, making it industrially attractive. Here, the aerosol assisted sol-gel process was used as a powerful tool to synthesize silica-based solids with Ga inserted as single-site in the structure. The influence of different parameters on both morphological properties and catalytic activity were studied. Three different materials bearing a Si/Ga ratio of 34, 74 and 148 were synthesized and extensively characterized via N<sub>2</sub> physisorption, XRD, TEM, ICP-OES spectroscopy and <sup>71</sup>Ga solid state NMR among others. All materials displayed promising features for catalytic applications such as high surface area, controlled mesoporosity and narrow particles size distribution (see Figure 1). To investigate the

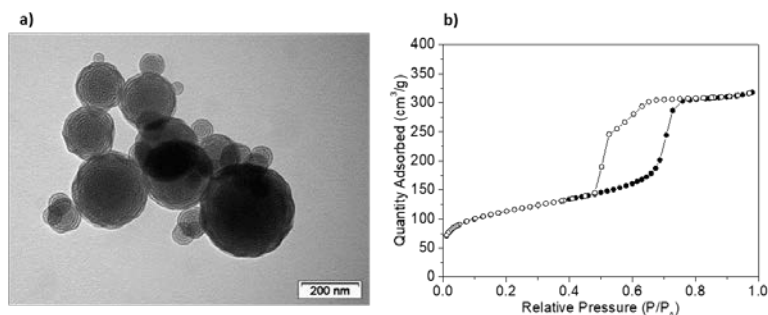


Figure 1. a) TEM micrograph and b) N<sub>2</sub> adsorption/desorption isotherm of Ga-74 material

coordination number/geometry of the metal center inserted within the silica matrix, a deep investigation was performed via solid state NMR of <sup>71</sup>Ga. The challenging study of quadrupolar <sup>71</sup>Ga allowed to observe a signal with a maximum at around 140 ppm that can be assigned to a predominant contribution of tetrahedral gallium present as single site in the silica framework. These aerosol-made mesoporous Ga-silicates showed excellent catalytic performance in the conversion of glycerol into solketal under solventless conditions and the best catalyst displayed high turnover number and high selectivity. Moreover, the best gallium silicate prepared via the aerosol process, Ga-74, outcompete in terms of TON other reference Ga-based catalysts already reported in the literature (compare entries 5 and 6 in Table 1). In order to further prove the stability of the solid under the selected reaction conditions, hot filtration tests were performed, demonstrating the absence of leaching of active sites. Moreover, the most active catalyst was successfully reused in multiple catalytic cycles thus proving its stability under the selected reaction conditions.

Table 1. Catalytic activity of Ga-silicates in the conversion of glycerol to solketal

Entry	Material	Si/Ga	Yield (%)	Sel. (%)	TON
1	Ga-37	38	30	85	721
2	Ga-74	79	28	85	1353
3	Ga-148	160	10	79	974
4	Ga-74*	79	25	95	596
5	XS-Ga-MCM-41* [2]	44	31	99	361

Si/Ga ratios determined by ICP-OES analysis; TON =  $n_{\text{solketal}}/n_{\text{Ga}}$ ; Glycerol: Acetone = 1: 4 (mol), \* Reaction conditions: 6h, 80°C, 25 mg of catalyst, glycerol (0,01 mol), acetone (0,01 mol), tert-butanol (0,02 mol)

[1] Nanda, M. R.; Zhang, Y.; Yuan, Z.; Qin, W.; Ghaziaskar, H. S.; Charles, C. *Renew. Sustain. Energy Rev.* **2016**, *56*, 1022–1031.

[2] Collard, X.; Li, L.; Lueangchaichaweng, W.; Bertrand, A.; Aprile, C.; Pescarmona, P. P. *Catal. Today* **2014**, *235*, 184–192.

[3] Debecker, D. P.; Le Bras, S.; Boissière, C.; Chaumonnot, A.; Sanchez, C. *Chem. Soc. Rev.* **2018**, *47*, 4112–4155.

[4] Vivian, A.; Fusaro, L.; Debecker D. P.; Aprile, C. *ACS Sustainable Chem. Eng.*, **2018**, *6*, 14095–14103

## Influence of synthesis method of $ZrO_2$ -supported Au-Pt catalysts in aerobic base-free oxidation of glucose towards glucaric acid

*Natalia Potrzebowska* 1, *Elie Derrien* 2, *Philippe Marion* 2, *Noémie Perret* 1,

*Catherine Pinel* 1, *Michèle Besson* 1,

1 *Univ Lyon, CNRS, IRCELYON, 69626 Villeurbanne Cédex, France*

2 *Solvay Research and Innovation Center of Lyon, 69192 Saint Fons, France*

Glucaric acid is a top value-added chemical from biomass. Its potential applications are numerous such as detergents, food ingredients, corrosion inhibitors and medication.<sup>[1]</sup> In place of the conventional production route by oxidation of glucose using nitric acid, glucaric acid could be produced using air and supported (bi)metallic catalysts.<sup>[1-3]</sup> The aerobic oxidation of glucose to gluconic acid has been well investigated. On the other hand, the much slower consecutive oxidation of the primary alcohol to yield glucaric acid gives rise to a variety of overoxidation products resulting in poor yield of glucaric acid (Figure 1).

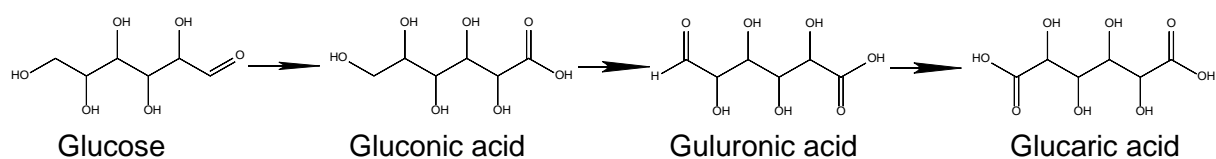


*Figure 1 Reaction pathway associated with the base-free oxidation of glucose to glucaric acid over Au-Pt/ $ZrO_2$  catalysts.*

In this work, different methods of preparation of  $ZrO_2$  supported Au-Pt catalysts were studied: wet impregnation (WI) and reduction by  $NaBH_4$ ,<sup>[3]</sup> colloidal method (Colloid) with PVA as AuNPs stabilizer,<sup>[4]</sup> and deposition precipitation (D-P) with urea.<sup>[5]</sup> The Colloid and D-P methods were studied in 1 and 2 steps. The actual loading of both metals was determined by ICP-OES, the formation or not of a Au-Pt alloy was verified by XRD and TEM-EDX analysis. The catalysts were tested in batch reactor (glucose/metal molar ratio 80) or in trickle-bed reactor (100°C, 40 bar air, 0.25 M glucose). Substrate and products were analyzed by ion-chromatography.

*Table 1. Characterization of Au-Pt/ $ZrO_2$  catalysts prepared by different methods and maximum yield of glucaric acid.*

Entry	Catalyst	method	Au/Pt mol ratio	alloy size (XRD) [nm]	max yield glucaric acid	reduction mode
1	2.7%Au-2.7%Pt	D-P 2 steps	1.02	7	4%	H <sub>2</sub>
2	2.3%Au-2.2%Pt	D-P 1 step	1.04	9	25%	H <sub>2</sub>
3	0.4%Au-2.8%Pt	Colloid 2 steps	0.14	-	15%	1 <sup>st</sup> step $NaBH_4$ ; 2 <sup>nd</sup> step H <sub>2</sub>
4	0.7%Au-0.8%Pt	Colloid 1 step	0.81	10	50%	$NaBH_4$
5	3.1%Au-2.8%Pt	WI	1.10	8	63%	$NaBH_4$
6	3.8%Au-3.4%Pt	WI-US	1.11	9	<b>84%</b>	$NaBH_4$

Table 1 summarizes some characterization data and the maximum yield of glucaric acid obtained in batch experiments. The metal deposition efficiency was dependent on the method of preparation. XRD patterns of most of the bimetallic catalysts exhibited a main (111) diffraction peak between  $2\theta = 38.2^\circ$  ( $\text{Au}^0$ ) and  $39.7^\circ$  ( $\text{Pt}^0$ ) due to the formation of an alloy. The absence of alloy (entry 3) gave poor yield of glucaric acid, whereas the catalysts containing Au-Pt alloy exhibited different performances. The catalysts prepared by WI gave the most promising results therefore different Au/Pt ratio were investigated.

Figure 2 shows the maximum yield of glucaric acid as a function of Au/Pt ratio for catalysts prepared by WI method. The Au/Pt molar ratio was essential. A 63% yield of glucaric acid at optimum Au/Pt molar ratio of 1.1 was achieved.

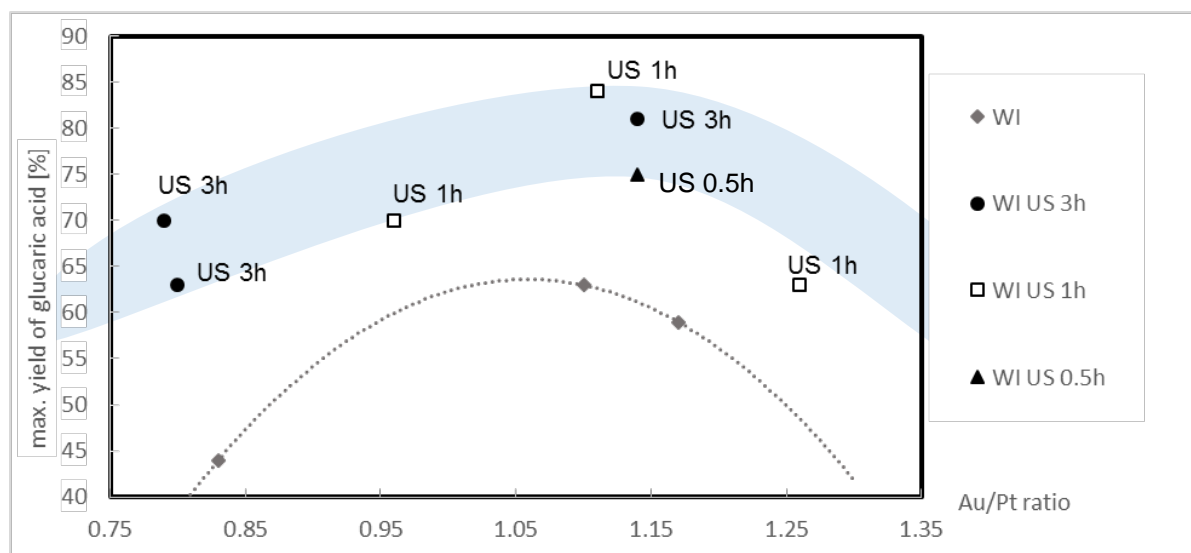


Figure 2 Effect of Au/Pt ratio and time of sonication during the catalyst synthesis on the yield of glucaric acid

Addition of a sonication step in an ultrasonic bath at 37 kHz during impregnation (WI-US) improved yield of glucaric acid up to 84%. Different times of sonication were investigated (Figure 2) and 1 h of treatment was sufficient.

Recycling of powder catalysts and tests in continuous reactor over pelleted catalysts demonstrated the stability of these catalysts.

## References

- [1] S. Li, W. Deng, S. Wang, P. Wang, D. An, Y. Li, Q. Zhang, Y. Wang, *ChemSusChem*, 2018, 11, 1995-2028
- [2] E. Derrien, P. Marion, C. Pinel, M. Besson, *Org. Process. Res. Dev.* 2016, 20, 1266-1275.
- [3] E. Derrien, M. Mounquengui-Diallo, N. Perret, P. Marion, C. Pinel, M. Besson, *Ind. Eng. Chem. Res.* 2017, 56, 13175-13189
- [4] A. Villa, D. Wang, D. Sheng Su, L. Prati, *ChemCatChem* 2009, 1, 510-514
- [5] A. Hugon, L. Delannoy, J. Krafft, C. Louis, *J. Phys. Chem. C* 2010, 114, 10823-108351.



# A Pt-Mo Hybrid Catalyst for Furfural Transformation.

*S. Cattaneo, Università degli studi di Milano, Milano, Italy; M. Stucchi, Università degli studi di Milano, Milano, Italy; S. Capelli, Università degli studi di Milano, Milano, Italy; A. Villa, Università degli studi di Milano, Milano, Italy; L. Prati, Università degli studi di Milano, Milano, Italy.*

## Introduction

Furfural is a high-value chemical, being the precursor of even more valuable compounds such as furfuryl alcohol and tetrahydrofurfuryl alcohol. Pt is known as active for furfural hydrogenation, but the high price limits its exploitation and imposes the search for alternatives [1,2]. Many papers reported that the introduction of transition metal into noble-metals based catalysts can have a significant influence on the catalytic activity and selectivity [3,4]. Here, we investigated the behavior of Mo and Pt/Mo supported on activated carbon (AC) derived from birch wood in furfural hydrogenation.

## Materials and methods

40% wt Mo-supported AC was firstly prepared by incipient-wetness impregnation method, using  $(\text{NH}_4)_6\text{Mo}_7\text{O}_{24} \cdot 4\text{H}_2\text{O}$  as precursor. The Mo-AC sample have been subsequently impregnated with pre-formed Pt NPs, prepared from a  $\text{Na}_2\text{PtCl}_4$  solution, PVA and  $\text{NaBH}_4$  (1%wt). Surface area and porosity distribution were obtained from  $\text{N}_2$  adsorption/desorption isotherms; samples were fully characterized by XPS, XRD and HR-TEM. Furfural hydrogenation reactions was carried out in a batch autoclave at 50 °C and 3 bar of  $\text{H}_2$ . Catalyst (substrate/metal ratio=500, mol/mol) was suspended in 10 ml of furfural solution (0.3 M in EtOH).

## Results and discussion

TEM and HR-TEM characterization on the 40% Mo-AC showed big and well contrasted Mo-containing agglomerates embedded in the carbon matrix. At higher magnification, such crystals display diffraction fringes with spacing typical of  $\text{Mo}_4\text{O}_{11}$  in the orthorhombic phase, in agreement with XRD. TEM analyses on Pt on bare AC showed the formation of small agglomerates whereas 1% Pt/40% Mo-AC showed highly dispersed Pt nanoparticles. Following the reaction profiles we can observed the 40%Mo-AC showed a pretty good activity even presenting a lower initial rate compared to the Pt containing analogues (1% Pt/AC and 1%Pt/40% Mo-AC).

Moreover, 40% Mo-AC appeared the most stable catalyst. A marked deactivation was observed in the case of 1%Pt/AC, and present even in a lesser extent also for 1%Pt/40%Mo-AC system. However, we found a strong different products distribution being the 40% Mo-AC fully selective to ethyl furfuryl ether (FEE), deriving from the reaction between furfuryl alcohol and the solvent, i.e. EtOH [5]. The 1% Pt/AC and 1%Pt/40% Mo-AC catalysts depressed bit the ethers formation and converted furfural also to furfuryl alcohol (21 %, 23 % respectively). A negligible amount of tetrahydrofurfuryl alcohol was detected in both cases. A strong metal-support interaction between the Pt and  $\text{Mo}_4\text{O}_{11}$  has been already reported in the literature [6] and it possibly promote hydrogen spillover and improve the poisoning tolerance. Thus, the presence of the  $\text{Mo}_4\text{O}_{11}$  orthorhombic phase could play a fundamental role in determining the increased catalytic activity of Pt/Mo-AC due to improving both Pt NPs dispersion and stability of the catalyst.

On the basis of these results, Mo-supported on activated carbon is a promising material, either as precious metal free-catalyst, or as support, improving Pt nanoparticles dispersion and the final catalytic activity in furfural hydrogenation.

## References

- [1] Sun, Y., Cheng, J. *Bioresour. Technol.* 2002, 83, 1– 11
- [2] Li, X., Pei, J., Wang, T. *ACS Catal.* 2016, 6(11), pp 7621–7640.
- [3] Gallezot, P. *Chem. Soc. Rev.* 2012, 41, 1538–1558.
- [4] Villa, A., Campisi, S., Giordano, C., Otte, K., Prati, L. *ACS Catal.* 2012, 2, 1377–1380.
- [5] D. Padovan, A. Al-Nayili, C. Hammond, *Green Chem.* 19 (2017) 2846.
- [6] F. Yang, F. Li, Y. Wang, X. Chen, D. Xia, J. Liu, *J. Mol. Catal. A: Chem.* 400 (2015) 7–13.

# A layered Zn-Co double metal cyanide with improved catalytic performance

*Carlos Marquez,<sup>1</sup> Arkadiy Simonov,<sup>2</sup> Michael T. Wharmby,<sup>3</sup> Bart Bueken,<sup>1</sup> Dirk De Vos,<sup>1</sup> and Trees De Baerdemaeker<sup>1</sup>*

<sup>1</sup> *Centre for Surface Chemistry and Catalysis, KU Leuven, Leuven, Belgium.*

<sup>2</sup> *Inorganic Chemistry Laboratory, University of Oxford, Oxford, United Kingdom.*

<sup>3</sup> *Deutsches Elektronen-Synchrotron (DESY), Hamburg, Germany.*

Double metal cyanides (DMCs) are cyanide bridged transition metal coordination polymers with the general formula  $M^1_u[M^2(CN)_n]_v \cdot xH_2O$  (hereafter abbreviated as “M<sup>1</sup>-M<sup>2</sup> DMC”). They have been used industrially as solid catalysts for ring opening polymerization reactions since the 1960s. Recently, their potential as catalysts for other organic reactions has been uncovered, with Zn-Co DMCs showing the best performance [1]. However, one of the drawbacks of these catalysts is that, as microporous materials, the pores are usually too small to allow diffusion of reactants and products, resulting in reactions taking place on the external surface. In this sense, several strategies have been suggested in order to increase the availability of active sites in the DMCs [2]. Herein, we report the synthesis, structure and catalytic activity of a new Zn-Co DMC phase, consisting of positively charged DMC layers linked by acetate anions. To the best of our knowledge, such a cationic, layered DMC (L-DMC) structure has not yet been reported in literature. Moreover, the advantages of L-DMC over the benchmark DMC catalyst (DMC-PTMEG) are demonstrated for two important catalytic applications of DMCs: hydroamination of phenylacetylene and 4-isopropylaniline, and epoxide polymerization of 1,2-epoxyhexane [3,4].

Single crystals of L-DMC were synthesized by slow diffusion in a silica gel and the structure was solved by single crystal X-ray diffraction. Through further synthesis optimization, we were able to obtain a phase pure microcrystalline powder of the L-DMC. Synchrotron powder diffraction data were collected and successfully refined by the Rietveld method. The structure crystallizes in the monoclinic space group  $P2_1/m$  and is shown in Fig. 1. The asymmetric unit consists of two symmetry independent Zn atoms and one Co atom, four cyanide groups, acetate and three water molecules (represented as isolated O atoms).

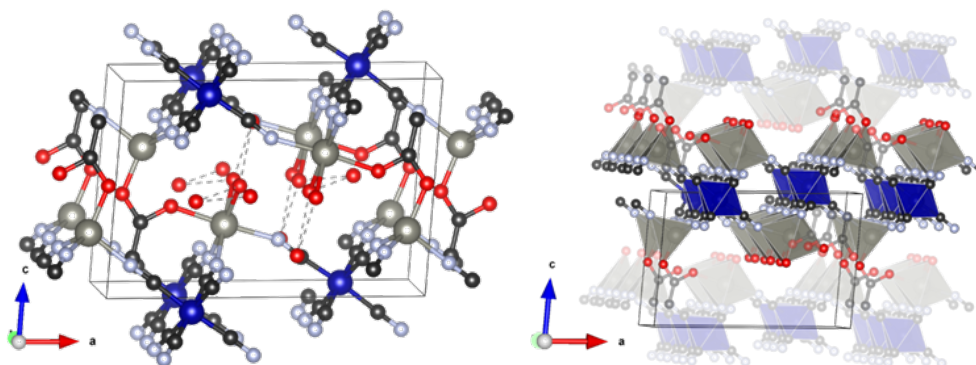
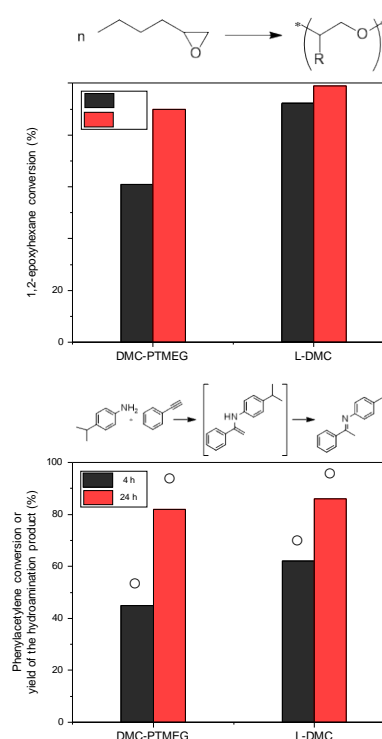


Fig. 1. Crystal structure of L-DMC (left) and polyhedral view showing the stacking of the layers in L-DMC (right). Grey, dark blue, light grey, black and red spheres represent Zn, Co, N, C and O atoms, respectively. H atoms were omitted for clarity.

For the ring opening polymerization, a significant increase in the 1,2-epoxyhexane conversion is observed when L-DMC is employed as catalyst (Fig. 2, top). Furthermore, the initial TOF (mol epoxyhexane consumed per mol of Zn per hour) obtained with L-DMC is 1.5 higher than the one obtained with DMC-PTMEG. For the hydroamination reaction, L-DMC also outperforms DMC-PTMEG (Fig. 2, bottom). The higher catalytic activity of L-DMC can be attributed to a combination of the easier accessibility of the catalytic sites and the changed coordination environment of the Zn atoms in the structure. As observed in both catalytic activity tests, the differences in activity exhibited by the DMCs highlight the advantages of L-DMC as an excellent catalyst.



## References

- [1] P. Valvekens and D. De Vos, in *New Materials for Catalytic Applications*, Elsevier, Amsterdam, 2016, pp. 1-12.
- [2] C. Marquez, M. Rivera-Torrente, P. P. Paalanen, B. M. Weckhuysen, F. G. Cirujano, D. De Vos and T. De Baerdemaeker, *J. Catal.*, 2017, 354, 92-99.
- [3] S. Lee, S. T. Baek, K. Anas, C-S. Ha, D-W. Park, J. W. Lee and I. Kim, *Polymer*, 2007, 48, 4361-4367.
- [4] A. Peeters, P. Valvekens, R. Ameloot, G. Sankar, C. E. A. Kirschhock and D. E. De Vos, *ACS Catal.*, 2013, 3, 597-607.

# On the Structure and Catalytic Properties of Thiolate-protected Au Nanoclusters in CO Oxidation

*Daria Pichugina, Nadezhda Nikitina, Nikolay Kuz'menko*

*Moscow State University, Department of chemistry, Moscow, Russian Federation*

Protected gold clusters are promising to produce heterogeneous catalysts with size-selected metal nanoparticles [1]. Gold clusters protected by thiolate or phosphine ligands have been studied extensively, but some aspects remain unclear:

- (i) modification of cluster's structure and charge after deposition on support;
- (ii) mechanism of small molecules activation on protected clusters or their fragments;
- (iii) ligand effect on the cluster activity and stability on support.

To reveal the questions, we performed quantum chemical study of catalytic properties of  $\text{Au}_{20}(\text{SCH}_3)_{18}$  including calculation of the cluster's structure in gas phase or on  $\text{CeO}_2$  surface, thermodynamic and kinetic data of the reactions of the cluster and  $\text{O}_2$ ,  $\text{CO}$  molecules, as well as simulation of further  $\text{CO}$  oxidation. Spin-polarized DFT/PBE level in the scalar-relativistic approach was used for cluster calculation. The calculation method has been tested in details in respect to predict structure and electronic properties of thiolate-protected gold nanoclusters [2]. The periodic calculation was performed at the GGA-level with spin-polarized DFT/PBE method using VASP program code. The orbital cutoff range was 5.0 Å.  $\text{CeO}_2$  was described with a  $5 \times 5$   $\text{CeO}_2$  (111) slab with 5 atomic layers and 20 Å of vacuum.

The structure and energies of five different  $\text{Au}_{20}(\text{SCH}_3)_{16}$  isomers have been calculated. The most stable one corresponds to structure predicted by X-ray analysis. The  $\text{Au}_7$  cluster's core consists of two tetrahedrons united by a common vertex; it is protected by an octameric ring, one triple and two monomeric staple  $\text{SR}(\text{AuSR})_x$  motifs (Fig. 1). Removal of ligand from the cluster was simulated through subsequent elimination of one, two, and three  $\text{SCH}_3$  groups.

The reaction of  $\text{O}_2$  and  $\text{Au}_{20}(\text{SCH}_3)_{16}$ ,  $\text{Au}_{20}(\text{SCH}_3)_{16-x}$ , staple  $\text{SR}(\text{AuSR})_x$  motifs, and octameric ring were studied. The cluster reacts with  $\text{O}_2$ , but the process requires pre-activation of  $\text{O}_2$  to singlet electronic state. From different cluster fragments the largest adsorption energy of  $\text{O}_2$  are calculated for  $\text{SRAuSR}$  monomeric staple fragment. The modification of the cluster under heating was simulated by

removing of one, two, and three  $\text{SCH}_3$  groups. Special  $\text{Au}_3$  fragment is created, which is active in  $\text{O}_2$  and  $\text{CO}$  activation.

The  $\text{O}_2$  and  $\text{CO}$  activation on  $\text{Au}_{20}(\text{SCH}_3)_{16-x}/\text{CeO}_2$  was simulated. According to calculation, oxygen can dissociate on  $\text{Au}_{20}(\text{SCH}_3)_{14}/\text{CeO}$ , in which two  $\text{SCH}_3$  were removed. Various scenarios of  $\text{CO}$  oxidation on supported Au cluster are considered. According to calculation cluster can be a catalyst of  $\text{CO}$  oxidation. It should be mentioned that the calculated activation energies of the corresponding steps of  $\text{CO}$  oxidation on the cluster's fragments ( $\text{Au}_2(\text{SR})_3$ ,  $(\text{AuSR})_4$ ,  $\text{Au}(\text{AuSR})_4$ ) are less than on the clusters. So, the fragments of the ligand-protected gold clusters can be involved in catalytic reactions.

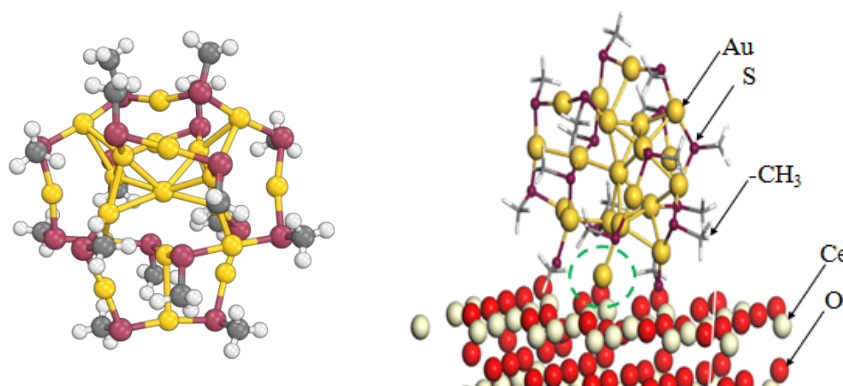


Figure 1. The calculated structure of  $\text{Au}_{20}(\text{SR})_{16}$  (left) and  $\text{Au}_{20}(\text{SR})_{16}/\text{CeO}_2$  (right).

**Acknowledgments.** The present work was supported by RFBR Grant N 17-03-00962. The research is carried out using the equipment of the shared research facilities of HPC computing resources at Lomonosov Moscow State University.

## References

- [1] D.A. Pichugina, N.E. Kuz'menko, A.F. Shestakov, *Rus. Chem. Rev.* 84 (2015) 1114.
- [2] N.N. Nikitina, D.A. Pichugina, A.V. Oleynichenko, O.N. Ryzhova, K.E. Kopylov, V.V. Krotov, N.E. Kuzmenko. *Supercomputing Frontiers and Innovations.* 5 (2018) 83.

# Composites of Graphene-like Carbon and 3D-metals or Their Oxides in Catalytic Hydrogenation of (Iso)Quinolines

*Asaula V.N.<sup>1</sup>, Buryanov V.V.<sup>2</sup>, Pariiska O.O.<sup>1</sup>, Ryabukhin S.V.<sup>2,3</sup>, Volochnyuk D.M.<sup>2,4</sup>,  
Kolotilov S.V.<sup>1</sup>*

<sup>1</sup>*L.V. Pisarzhevskii Institute of Physical Chemistry of the National Academy of Sciences of Ukraine, Kyiv, Ukraine;*

<sup>2</sup>*Enamine Ltd, Kyiv, Ukraine;*

<sup>3</sup>*National Taras Shevchenko University of Kyiv, Kyiv, Ukraine;*

<sup>4</sup>*Institute of Organic Chemistry, National Academy of Sciences of Ukraine, Kyiv, Ukraine;*

Reactions of catalytic hydrogenation are widely used in modern organic chemistry and industry for synthesis of active pharmaceutical ingredients, effective substances for plant protection etc. These processes are usually performed with catalysts based on platinum, palladium and other precious metals. Development of noble-metal-free materials, possessing high catalytic activity in the process of organic compounds hydrogenation, is actual task.

The aim of this work was to study the influence of the composition and structure of composites of graphene-like carbon and nanosized 3d-metals or their oxides deposited on the different carriers on their catalytic activity in quinoline hydrogenation.

The nanocomposites were prepared by pyrolysis Co(II), Ni(II), Zn(II) complexes with N-containing organic ligands (phenantroline, melamine, o-phenylenediamine) on aerosil (highly disperse SiO<sub>2</sub>), ZrO<sub>2</sub>, Al<sub>2</sub>O<sub>3</sub>, activated carbon. It was shown by transmission electronic microscopy that the nanocomposites contained carbon species with size of separate particles ca. 10-50 nm. Analysis of the Raman spectral data (Fig. 1) allowed to conclude that the graphene-like particles had more than 8 carbon monolayers. The size of carbonaceous particles, separated from the carrier, was in range from 80 to 120 nm according to the results of dynamic lights scattering in suspension.

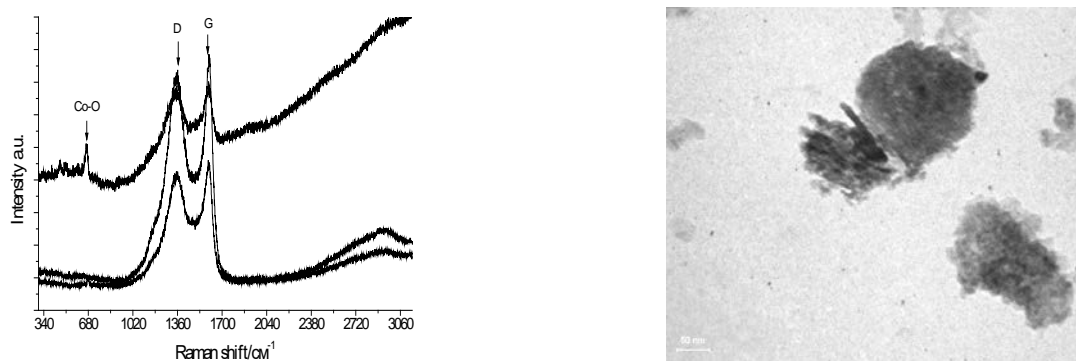


**Figure 1.** Raman spectra of the composites (left) and TEM image of the Co/C/Al<sub>2</sub>O<sub>3</sub> nanocomposite (right).

The obtained nanocomposites were catalytically active in hydrogenation of quinolines and isoquinolines to 1,2,3,4-tetrahydroderivatives 2a,b (Fig. 2). Under 100 atm pressure and 100°C temperature the yield of tetrahydro(iso)quinoline varied from 40 to almost 100 % depending on the composite. The tolerance to functional groups was also researched and discussed. Catalytic activity essentially depended on synthetic conditions (mainly pyrolysis rate) and the nature of the carriers. The Co-containing composites deposited on aerosil or ZrO<sub>2</sub> were the most active. Catalytic activity essentially increased at decreasing pyrolysis rate, as well as at increase of Co content.

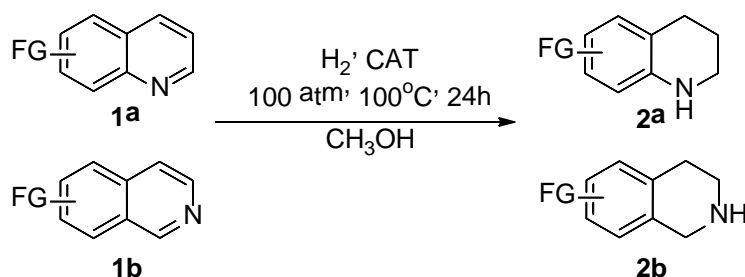


**Figure 2.** Using nanocomposites for hydrogenation.



## Cu-Catalyzed Pyridine Annulation via Oxidative Reaction of Cyclic Ketones with Propargyl Amine

Sotnik S.A.,<sup>1</sup> Subota A. I.,<sup>1</sup> Ryabukhin S. V.,<sup>1,2</sup> Volochnyuk D. M.,<sup>1,3</sup> Kolotilov S. V.<sup>4</sup>

<sup>1</sup>*Enamine Ltd., Kyiv, Ukraine;*

<sup>2</sup>*National Taras Shevchenko University of Kyiv, Kyiv, Ukraine;*

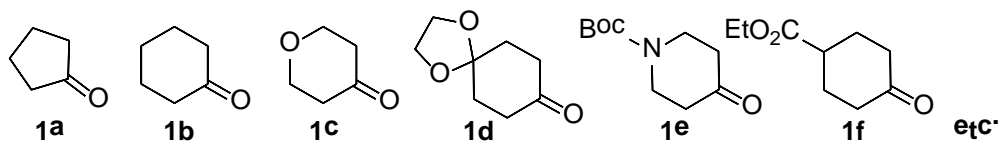
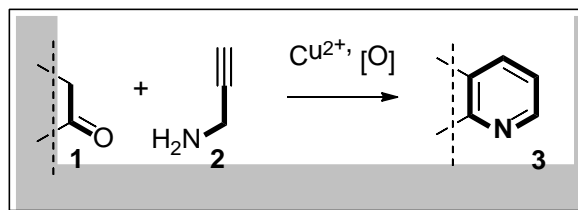
<sup>3</sup>*Institute of Organic Chemistry, National Academy of Sciences of Ukraine, Kyiv, Ukraine;*

<sup>4</sup>*L.V. Pisarzhevskii Institute of Physical Chemistry of the National Academy of Sciences of Ukraine, Kyiv, Ukraine;*

Since the discovery of gold-catalyzed one-step amination/annulation/aromatization reaction of carbonyl compounds and propargylamine by Abbiati et. al in 2003 [1] this reaction has been widely used for synthesis of functionalized pyridines, which are hardly accessible by other synthetic routes. At present, the dominating majority of reported reactions of this type were performed at presence of Au(III) compounds or Au nanoparticles. Moreover, recently the  $\text{Cu}_3(\text{btc})_2$  (where  $\text{btc}^{3-}$  is 1,3,5-benzenetricarboxylate) catalyzed version of the transformation was described [2]. The reaction proceeds in moderate yields during 21 h at 75°C.

In this study using a series of cyclic ketones **1** the influence of Cu(II) source ( $\text{CuCl}_2$ ,  $\text{Cu}(\text{NO}_3)_2$ ,  $\text{Cu}_3(\text{btc})_2$ , etc), solvents, presence of additional oxidants and time of the reaction were studied at ambient pressure of air.

The reaction mixtures were analyzed by HPCL and GC, while the products were identified by NMR and HPLC. It was found that  $\text{CuCl}_2$  and  $\text{Cu}(\text{NO}_3)_2$  as catalysts led to comparable results, while performance of  $\text{Cu}_3(\text{btc})_2$  was lower. In all cases aromatization of presumable dihydropyridine intermediate occurred due to reaction with air oxygen. The reaction time in some cases using the  $\text{CuCl}_2$  in alcohol media was less than 30 min. The method proposed allowed to achieve 50-70 % yield of the pyridines **3**. Gram-scale synthesis of ethyl 6-carboxy-5,6,7,8-tetrahydroquinoline **3f** was performed using the proposed Cu-catalyzed reaction.



1 G. Abbiati, A. Arcadi, G. Bianchi, S. Di Giuseppe, F. Marinelli, E. Rossi *J. Org. Chem.*, **2003**, 68(18), 6959–6966.

2 Y.Y. Meng, W.F. Kang, X.J. Si, Y.Y. Song, Y.J. Li, F. Xu, *Chem. Select.*, **2018**, 3, 8793.

# G3 and G4 Buchwald Precatalysts: Scale up, QC and application for the semi-automated parallel synthesis

Sotnik S.A.,<sup>1</sup> Kolotilov S. V.,<sup>2</sup> Radchenko D. S.,<sup>1</sup> Ryabukhin S. V.,<sup>1,3</sup>

Volochnyuk D. M.<sup>1,4</sup>

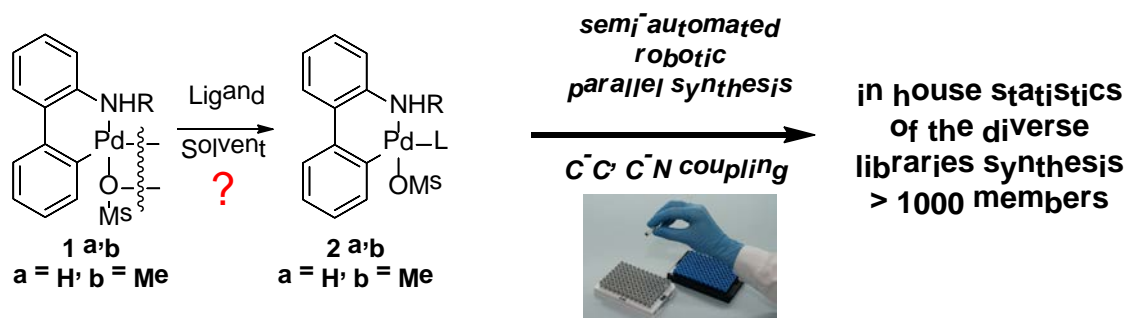
<sup>1</sup>Enamine Ltd., Kyiv, Ukraine;

<sup>2</sup>L.V. Pisarzhevskii Institute of Physical Chemistry of the National Academy of Sciences of Ukraine, Kyiv, Ukraine;

<sup>3</sup>National Taras Shevchenko University of Kyiv, Kyiv, Ukraine;

<sup>4</sup>Institute of Organic Chemistry, National Academy of Sciences of Ukraine, Kyiv, Ukraine;

In spite of numerous published examples of the application of the G3 and G4 Buchwald Precatalysts in organic synthesis, their laboratory scale up (up to 50 g from one synthetic run), routine quality control (QC), different possible solvate forms and their influence on catalytic properties are still remanding. In many cases, the solvate composition was not analyzed, but for some synthetic tasks, it appears to be critical. The commonly used solvent for the dimer **1** transformation to the precatalyst **2** is CH<sub>2</sub>Cl<sub>2</sub> (DCM), which leads to formation of the DCM solvates. It was found, that in large batches the DCM could not be removed from the solvate by vacuum drying without decomposition of the precatalyst. In the present report the multi gram laboratory synthesis of G3 and G4 Buchwald precatalysts (XphosPd G3, XantPhosPd G4, XantPhosPd G3, RuPhosPd G4, SphosPd G3, BrettPhos G3), their QC by commonly used NMR/LC MS methods and specific features of such catalyts preparation with innocent solvate molecules will be discussed. It was shown, that the use of THF as solvent led to precatalysts formation with high yields without the need of additional solvent exchange/removal from the solid samples.



The advantages of the use of such catalyts for the semi-automated parallel synthesis of large libraries of small molecules (more than 1000 members) *via* C-C and C-N coupling will be presented. It was found, that in many cases “traditional” catalyts did not provide satisfactory results compared to G3 and G4 ones.

# Quick evaluation of catalytic activity of hydrogenation catalysts by UV spectra using imidazo[1,5-a]pyridines as probes

Lytvynenko A.S.,<sup>1</sup> Ivanitsa N.A.,<sup>1,2</sup> Sotnik S.A.,<sup>2</sup> Tverdiy D.O.,<sup>3</sup> S. V. Ryabukhin,<sup>2,4</sup>  
D. M. Volochnyuk,<sup>2,5</sup> S. V. Kolotilov<sup>1</sup>

<sup>1</sup>L.V. Pisarzhevskii Institute of Physical Chemistry of the National Academy of Sciences of Ukraine, Kyiv, Ukraine;

<sup>2</sup>Enamine Ltd., Kyiv, Ukraine;

<sup>3</sup>Institute of Molecular Biology and Genetics National Academy of Sciences of Ukraine, Kyiv, Ukraine;

<sup>4</sup>National Taras Shevchenko University of Kyiv, Kyiv, Ukraine;

<sup>5</sup>Institute of Organic Chemistry, National Academy of Sciences of Ukraine, Kyiv, Ukraine;

Hydrogenation catalysts are widely used in modern organic synthesis and pharmacy for preparation of various compounds. The properties of such catalyst usually significantly depend on the details of preparation procedure and can vary even between different batches of one supplier. Quick quality control (QC) is important task for such catalysts application.

The aim of this work was to develop a method for hydrogenation catalysts QC in mild conditions, which does not require complicated products isolation and analysis.

It was found that hydrogenation of readily available substituted imidazo[1,5-a]pyridines by gaseous H<sub>2</sub> at 20–40 °C and 1 atm led to formation of two different products (Fig. 1), which significantly differed by their UV spectra. The advantage of this system was that the absorption bands of the products of partial or complete hydrogenation did not overlap. Formation of various products in certain time periods depended on the activity of the catalyst, such dependency allowed to make conclusion regarding catalytic activity of the sample.

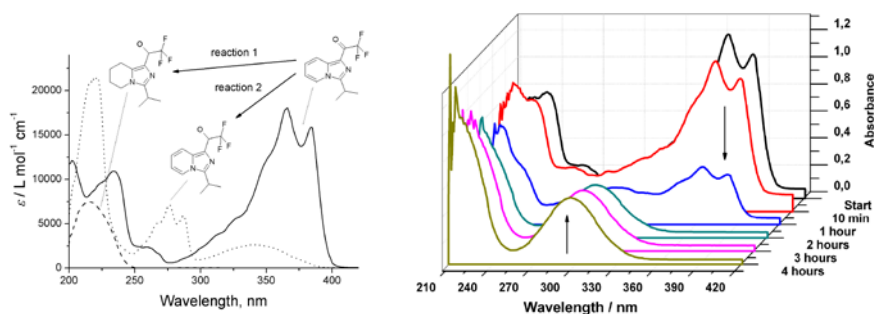


**Figure 1:** Reagent, product and their UV spectra depending on the reaction time (one example)

# Isorecticular UTL-derived zeolites as model materials for probing pore size-activity relationship

*M. Opanasenko, Y. Zhou, M. Shamzhy, S. A. Kadam, J. Čejka*

*Department of Physical and Macromolecular Chemistry, Faculty of Science, Charles University in Prague, Hlavova 8, 128 43 Prague, Czech Republic*

Isorecticular Al-IPC-n aluminosilicate zeolites with similar concentration of both Brønsted and Lewis acid sites, but gradually reduced channel size from 14- to 8-ring (9.5×7.1 Å, 8.5×5.5 Å, 6.6×6.2 Å, 5.4×5.3 Å, and 4.5×3.6 Å) have been firstly synthesized using ADOR (Assembly-Disassembly-Organization-Reassembly) strategy [1] combined with alumination of UTL germanosilicate [2]. Distribution of acid sites among the pores of different size was exhaustively characterized using FTIR spectroscopy of adsorbed probe molecules of variable size (d3-acetonitrile, quinoline, Fig. 1) and ethanol-to-diethyl ether kinetic study. Catalytic activity of Al-IPC-n zeolites in tetrahydropyranlation of alcohols of different size (ethanol, 1-hexanol, 1-decanol, Fig. 1) was related to the amount of acid centers sited in the pores of different size.

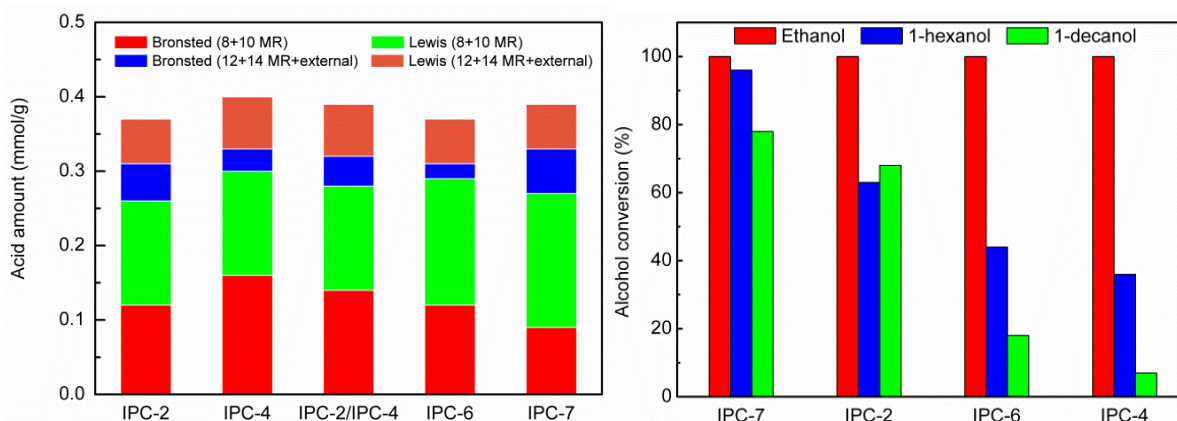


Fig. 1. Acid sites distribution of Al-IPC zeolites (left) and alcohol conversion for the tetrahydropyranlation of ethanol, 1-hexanol, 1-decanol for 24 h with dihydropyran over Al-IPC catalysts (right). Reaction conditions: catalyst, 50 mg; alcohol, 4.5 mmol; dihydropyran, 5 ml; mesitylene, 0.25 g; temperature, 333 K.

The results of chemical analysis,  $^{27}\text{Al}$  NMR and FTIR spectroscopy evidence similarity of isorecticular Al-IPC zeolites with respect to the content and coordination state of Al, type and total amount of acid sites, while distribution of acid sites between

the micropores and external surface of the catalysts' crystals slightly varies reflecting difference in their size. At the same time, isorecticular IPC zeolites possess micropores of remarkably different size, ranging from the ones restricted with 8- to 14-ring channels, which is reflected in decreasing micropore volume in the following sequence: AI-IPC-7 > AI-IPC-2 > AI-IPC-6 > AI-IPC-4. The catalytic activity in tetrahydropyranlation of either 1-hexanol or 1-decanol (Fig. 1) decreases with the micropore size/volume in the following sequence: IPC-7 > IPC-2 > IPC-6 > IPC-4. These results suggest that due to the diffusion limitation, the internal active sites in the IPC zeolites channels has limited accessibility for bulky reagents with IPC-4 with the lowest porosity being affected by diffusion limitations the most.

Obtained results reveal AI-IPC-n being excellent model materials for analysing the effect of micropore structure of zeolites on their catalytic activity. The use of AI-IPC-n as model catalysts in important acid-catalyzed reactions can shed a light on the fundamental structure-activity relationship and help to improve/optimize existing catalytic processes.

## References

1. Eliášová, P.; Opanasenko, M.; Wheatley, P. S.; Shamzhy, M.; Mazur, M.; Nachtigall, P.; Roth, W. J.; Morris, R. E.; Čejka, J. *Chem. Soc. Rev.* 2015, 44, 7177-7206
2. Shamzhy, M. V.; Eliasova, P.; Vitvarova, D.; Opanasenko, M. V.; Firth, D. S.; Morris, R. E. *Chem. Eur. J.* 2016, 22, 17377-17386

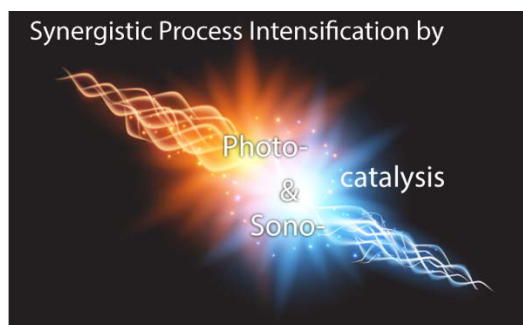
# Ultrasounds assisted process intensification of biomass derived model compounds' photocatalytic valorization by novel nanocomposites

*Dimitrios A. Giannakoudakis<sup>1</sup>; Bartosz Zawadzki<sup>1</sup>; Dariusz Łomot<sup>1</sup>; Juan Carlos Colmenares<sup>\*1</sup>*

<sup>1</sup> Institute of Physical Chemistry, Polish Academy of Sciences, Warsaw, Poland

\*Corresponding author's email: [jcarloscolmenares@ichf.edu.pl](mailto:jcarloscolmenares@ichf.edu.pl)

Heterogeneous photocatalysis is an important and favorable alternative to conventional organic synthetic chemistry. The main drawback of photochemistry is that it is a “nonselective” process in many cases, especially in aqueous media [1,2]. In the last few decades, the research effort is focused on the process intensification of the photocatalytic transformations by various methods. In addition, ultrasonication utilization has also revealed to be a promising candidate in synthetic chemistry due to the cavitation phenomena. The growth and implosion of acoustic cavitation can act as localized hotspots, since the temperature and the pressure can reach up to 5000 °C and 1000 bars, respectively [3]. Mechanical effects, such as elevated mass transfer, de-passivation effect, de-aggregating of the catalyst, and chemical effects, like advance oxidation processes by formed reactive oxygen species and radicals, are also vital factors under ultrasounds appliance [4]. Lately, a continuous growing research field is the generation of industrial valuable bio-chemicals from a widely available natural and renewable resource; the lignocellulosic biomass. And the ultimate goal is to achieve complete valorization of the biomass and its derivatives following green-chemistry oriented approaches, by avoiding usage of precious noble and/or rare-earth metals-based catalyst, addition of hazardous and non-reusable chemicals, as well as harsh experimental conditions. The combination of ultrasound and light irradiation in heterogeneous catalysis, known as sonophotocatalysis, is a very innovative approach



that gathers a continual increase of attention, since it can positively promote the valorization reactions via a cost-effective and environmental-friendly manner [5].

The effort of our research is focused on the utilization of sonophotocatalysis for the selective transformation of lignin-based model molecules by using novel nanocomposites as catalyst. The synthesis of the latter is based on the unique effect of the cavitation phenomena [6], as ultrasounds was irradiated during the formation of the nanocatalyst. The main phase of the catalyst consists of nanostructured metal oxides ( $\text{TiO}_2$ ,  $\text{Mn}_x\text{O}_y$ ,  $\text{Fe}_2\text{O}_3$  or  $\text{Co}_3\text{O}_4$ ), while as fillers nano-scaled graphite or graphitic carbon nitride, unmodified or oxidized, were used. The synergistic effect during the composite formation led to unique structural, morphological, physical, optical, and surface chemistry heterogeneity features, resulting to enhanced reactivities [7,8]. The coupling of sonocatalysis with photocatalysis is found to have a beneficial effect on the lignin-model compounds transformation, since the combination led to improvement in the conversion and selectivity. A plethora of factors/parameters that affect the cavitation phenomena and as a result the potential of sonochemistry were investigated, like the acoustic frequency, power, and pulse protocol, the solvent's nature and temperature, the purged gas, and even the sonoreactor's geometry. Various important aspects of the photocatalysis such as the wavelength and intensity of the irradiated light, photocatalyst loading, type of solvent, mixture of solvents, and solution pH were also optimized. Special focus was given on understanding the synergistic effects upon light and ultrasounds irradiation during the reactions from a mechanistic point of view.

#### **ACKNOWLEDGEMENTS**

The authors are very grateful for the support from the National Science Centre in Poland within OPUS-13 project nr 2017/25/B/ST8/01592. (<http://photo-catalysis.org>)

#### **BIBLIOGRAPHY**

- [1] J.C. Colmenares, R. Luque, *Chem. Soc. Rev.*, 43 (2014) 765.
- [2] T. Zhou, X. Wu, J. Mao, Y. Zhang, T.-T. Lim, *Appl. Catal. B Environ.*, 160 (2014) 325.
- [3] J.C. Colmenares Q., *J. Nanosci. Nanotechnol.* 13 (2013) 4787.
- [4] A. Magdziarz, J.C. Colmenares, *Molecules*, 22 (2017) E216.
- [5] G. Chatel, S. Valange, R. Behling, J.C. Colmenares, *ChemCatChem*, 9 (2017) 2615.
- [6] J.C. Yu, J. Yu, W. Ho, L. Zhang, *Chem. Commun.*, 0 (2001) 1942.
- [7] D.A. Giannakoudakis, N.A. Travlou, J. Secor, T.J. Bandosz, *Small*, 13 (2017) 1601758.
- [8] D.A. Giannakoudakis, J.A. Arcibar-Orozco, T.J. Bandosz, *Appl. Catal. B Environ.*, 183 (2016) 37.



# Speciation and siting of divalent transition metal ions in silicon rich zeolites. A FTIR study

Mariia Lemishka<sup>1,2</sup>, Edyta Tabor<sup>1</sup>, Kinga Mlekodaj<sup>1</sup>, Alena Vondrova<sup>1</sup>, Zdenek Sobalik<sup>1</sup>, Stepan Sklenak<sup>1</sup>, Jiri Dedecek<sup>1</sup>

<sup>1</sup>*J. Heyrovský Institute of Physical Chemistry of the Czech Academy of Sciences, Dolejškova 2155/3, CZ-182 23 Prague 8, Czech Republic*

<sup>2</sup>*University of Pardubice, Pardubice, Czech Republic*

*e-mail: \*mariia.lemishka@jh-inst.cas.cz\**

Zeolites represent the key materials of the chemical production (heterogeneous catalysis, gas separation and purification). They are used as catalysts in a wide range of acid-catalyzed reactions for the transformations of hydrocarbons in the petrochemical industry and synthesis of fine chemicals [1]. Metal containing zeolites represents redox catalysts for NO/NO<sub>x</sub> elimination from diesel exhausts and N<sub>2</sub>O abatement. Bare cations of transition metal ions in zeolites are proposed to be the active sites in redox catalyzed reactions [2]. The aim of this study was the siting and distribution of bare Me<sup>2+</sup> (Co<sup>2+</sup>, Ni<sup>2+</sup> and Mn<sup>2+</sup>) ions in the ferrierites with maximum loading of Me<sup>2+</sup> ions as crucial for the formation of binuclear Me<sup>2+</sup> cationic structures unique for ferrierite, and suggested as highly active sites in redox reactions.

Commercially supplied ferrierite Si/Al 8.5 were further exchanged to obtain Co<sup>2+</sup>, Ni<sup>2+</sup> and Mn<sup>2+</sup> forms with various metal loading. Co-FER were prepared by ion exchange at RT. Low loading of the Me<sup>2+</sup> bare cations of Mn-FER and Ni-FER were prepared by ion exchange as well at 60°C or 80 °C. To obtain higher content of Ni<sup>2+</sup> and Mn<sup>2+</sup> in ferrierite, dry impregnation method was involved [3].

Number of bare cations and concentration of Me<sup>2+</sup> cations in these extra-framework sites were analyzed by FTIR spectroscopy of dehydrated Me-samples in the region of anti-symmetric T-O-T vibrations of the zeolite. FTIR spectra in the region 960 – 860 cm<sup>-1</sup> exhibited three bands (see Table 1) in α, β and γ cationic positions [4, 5].

The exclusive presence of bare cations in samples with Me/Al < 0.15 allows estimation of extinction coefficients of cations in individual cationic sites serving for

the quantitative analysis of  $\text{Me}^{2+}$  siting in the zeolite. The extinction coefficients obtained from the linear regression of the concentration dependence of the intensity of T-O-T vibration on metal loading in the concentration region below  $\text{Me}/\text{Al}$  0.15 are presented in the Table 1.

Table 1. Wavenumbers of T-O-T vibrations reflecting cations in the  $\alpha$ -,  $\beta$ - and  $\gamma$ - sites for Co-, Ni- and Mn- ferrierites [4].

	$\alpha$ $\text{cm}^{-1}$	$\beta$	$\gamma$	Extinction coefficient $\text{cm } \mu\text{mol}^{-1}$
Mn	953	928	902	30.4
Co	942	918	885	38.5
Ni	940	918	879	35.8

FTIR spectroscopy of perturbed antisymmetric T-O-T vibrations represents powerful tool for the (semi)quantitative analysis of the bare  $\text{Me}^{2+}$  ions, their siting, and distribution in the dehydrated metallozeolites. Co-, Ni-, and Mn-ferrierites with maximum possible loading of bare  $\text{Co}^{2+}$ ,  $\text{Ni}^{2+}$  and  $\text{Mn}^{2+}$  ions in cationic sites were successfully prepared by ion exchange or impregnation method. Such samples guarantee not only high concentration of bare  $\text{Me}^{2+}$  ions as active sites in ferrierite catalysts, but also formation of specific type of ferrierite active sites – pairs of bare  $\text{Me}^{2+}$  ions.

#### References

- [1] A. Corma, Chem. Rev. 95, **1995**, 559-614.  
 [2] A.M. Beale, F. Gao, I. Lezcano-Gonzalez, C.H.F. Peden, J. Szanyi, Chem. Soc. Rev. 44, **2015**, 7371-7405.  
 [3] D.P. Gamliel, B.P. Baillie, E. Augustine, J. Hall, G.M. Bollas, J.A. Valla, Microporous Mesoporous Mater. 261, **2018**, 18-28.  
 [4] Z. Sobalik, Z. Tvaruzkova, B. Wichterlova, J. Phys. Chem., 102, **1998**, 1077-1085.  
 [5] J. Dědeček, Z. Sobalík, B. Wichterlová, Catal rew, 54, **2012**, 135-223.

# **Bimetallic AuAg catalysts supported on MgO, ZnO and Nb<sub>2</sub>O<sub>5</sub> for n-octanol oxidation: the effect of support and preactivation**

*Iveta Kaskow<sup>1,2</sup>; Izabela Sobczak<sup>1</sup>; Maria Ziolk<sup>1</sup>; Vicente Cortés Corberán<sup>2</sup>*

*<sup>1</sup>Adam Mickiewicz University, Poznan, Poland*

*<sup>2</sup>Institute of Catalysis and Petroleumchemistry (ICP), CSIC, Madrid, Spain*

Selective oxidation of alcohols plays a key role in industry [1]. Many valuable chemicals as aldehydes, esters and acids can be produced from them. Catalysts containing gold are in the center of the research interest because they show high catalytic activity and selectivity in aerobic oxidation of long-chain alcohols performed in the liquid-phase and under mild conditions such as low reaction temperatures (below 140°C) and atmospheric pressure [e.g., 1, 2].

The aim of this work was to study the effect of the support nature and the preactivation conditions on the surface and catalytic properties of AuAg catalysts. Three metal oxides (MgO, ZnO, Nb<sub>2</sub>O<sub>5</sub>) representative of different types of properties (basic, amphoteric and acidic, respectively) were used as supports for gold and silver. The catalysts were prepared according to a two-step process [3] by the addition of 2 wt.% Au and 1 wt.% Ag, and characterized by N<sub>2</sub> adsorption/desorption isotherms, XRD, Uv-Vis, XPS, and TEM. Monometallic gold samples were also studied for comparison. All catalyst samples were tested in n-octanol oxidation after thermal treatment in O<sub>2</sub> or H<sub>2</sub> (10 mL/min, 1 h, 400°C) and are denoted hereinafter by the corresponding suffix. Then, their catalytic activity was tested in the liquid phase oxidation of n-octanol with oxygen under atmospheric pressure at 80°C for 6 h.

XRD, TEM, UV-vis and XPS results indicated the presence of both metallic gold and silver in bimetallic catalysts. Moreover, UV-Vis analysis indicated formation of AuAg-alloy on the surface of AuAg-MgO (the band was blue shifted from 528 nm for Au-MgO to 506 nm for AuAg-MgO). Thermal treatment of bimetallic catalysts in hydrogen flow led to alloy formation or silver enrichment of the alloy.

The most active catalyst was AuAg-MgO-H<sub>2</sub> (Table 1). This is in line with previous results obtained for Au/Mg/TiO<sub>2</sub>-H<sub>2</sub> modified with an electron-donor additive (MgO) [2]. The same composition but pretreated in oxygen, AuAg-MgO-O<sub>2</sub>, showed lower activity. The increase in alcohol conversion with silver addition revealed the influence of alloy on the activity. The main reaction product over AuAg-MgO was the

Table 1. Activity and selectivity of catalysts in n-octanol oxidation at 80°C (after 6 h)

Catalyst	Conversion, %	Selectivity, %		
		aldehyde	ester	acid
Au-MgO-H <sub>2</sub>	26	33	49	18
Au-MgO-O <sub>2</sub>	50	45	26	29
AuAg-MgO-H <sub>2</sub>	62	30	62	8
AuAg-MgO-O <sub>2</sub>	38	20	67	13
Au-ZnO-H <sub>2</sub>	38	18	82	0
Au-ZnO-O <sub>2</sub>	48	12	88	0
AuAg-ZnO-H <sub>2</sub>	21	88	12	0
AuAg-ZnO-O <sub>2</sub>	10	94	6	0
Au-Nb <sub>2</sub> O <sub>5</sub> -H <sub>2</sub>	6	46	54	0
Au-Nb <sub>2</sub> O <sub>5</sub> -O <sub>2</sub>	11	52	48	0
AuAg-Nb <sub>2</sub> O <sub>5</sub> - H <sub>2</sub>	3	100	0	0
AuAg-Nb <sub>2</sub> O <sub>5</sub> - O <sub>2</sub>	12	61	39	0

ester. The effect of the thermal treatment on activity for AuAg-MgO was similar to that for AuAg-ZnO, but activity of AuAg-ZnO-H<sub>2</sub> and AuAg-ZnO-O<sub>2</sub> was much lower. However, very high selectivity to octanal was obtained. Catalysts supported on Nb<sub>2</sub>O<sub>5</sub> showed the lowest activity, which can be related to the acidic character of the support. The bare supports (MgO, ZnO, Nb<sub>2</sub>O<sub>5</sub>) were not active in the reaction. The relationships between surface properties of the metallic catalysts and their catalytic activity and selectivity will be discussed in detail.

In summary, one may conclude that the changes in catalytic performance of bimetallic AuAg catalysts in n-octanol oxidation upon different thermal treatments (in oxygen or hydrogen) strongly depend on the surface properties of the metal oxide supports. High selectivity to the aldehyde or the ester can be reached by combining the proper choice of the support and the atmosphere of the pretreatment (O<sub>2</sub> or H<sub>2</sub>).

### Acknowledgements

Funding by National Science Centre in Poland (project N° UMO-2018/29/B/ST5/00137), Erasmus+ exchange programme and MINECO in Spain (project CTQ2017-86170-R) is acknowledged

### References

- [1] S. Martínez-González, A. Gómez-Avilés, O. Martynyuk, A. Pestryakov, N. Bogdanchikova, V. Cortés Corberán, *Catal. Today* 227 (2014) 65-70
- [2] Y. Kotolevich, E. Kolobova, G. Mamontov, E. Khramov, J.E. Cabrera Ortega, H. Tiznado, M.H. Farías, N. Bogdanchikova, Ya. Zubavichus, J.D. Mota-Morales, V. Cortés Corberán, R. Zanella, A. Pestryakov, *Catal. Today* 278 (2016) 104-112
- [3] X. Liu, A. Wang, X. Yang, T. Zhang, Ch-Y. Mou, D-S. Su, J. Li, *Chem. Mater.* 21 (2009) 410–418

# Alumina: discriminative analysis using 3D correlation of solid-state NMR parameters

*C. Vinod Chandran<sup>1</sup>, Christine E. A. Kirschhock<sup>1</sup>, Sambhu Radhakrishnan<sup>1</sup>, Francis Taulelle<sup>1</sup>, Johan A. Martens<sup>1</sup>, Eric Breynaert<sup>1,\*</sup>*

*<sup>1</sup>KU Leuven, COK-KAT, Leuven, Belgium. \*eric.breynaert@kuleuven.be*

Synthetic transition alumina's ( $\chi$ ,  $\kappa$ ,  $\theta$ ,  $\gamma$ ,  $\delta$ ,  $\eta$ ,  $\rho$ ) exhibit unique adsorptive and catalytic properties leading to numerous practical applications. They are good Al sources for manufacturing aluminium metal through the Bayer process. Gamma, theta and eta alumina are popular in catalytic applications such as dehydration of alcohols, isomerisation of olefins, production of sulphur from H<sub>2</sub>S, etc.[1] Other important alumina-catalysed reactions include chlorination of methanol, dehydrofluorination of organic fluorides, alkylation of phenols, de-oxygenation of bio-oils and decomposition of triglycerides. Large scale applications as catalyst support for metals include hydrodesulfurization in petroleum refinery using cobalt and nickel promoted molybdenum sulfide, NO<sub>x</sub> reduction, and CO and hydrocarbon oxidation reactions on supported noble metals. Wash coated monolithic exhaust gas purification catalysts are further examples.[1]

Generated by thermal transformation of aluminium (oxy)hydroxides, structural differences between transition alumina's arise from the variability of aluminium coordination numbers and degree of dehydroxylation. For some time they were considered as highly disordered or even completely amorphous.[2] Clear assignment of structural models to the different phases severely was, and still is hampered by the occurrence of complex phase assemblies along the calcination path in combination with their typical micro and nanocrystalline nature. Whereas the latter is a direct consequence of their formation by the release of structural water and consequent, densification, it results in broadening of the X-ray diffraction lines, rendering PXRD patterns very difficult or impossible to analyse.

Quadrupolar interactions of <sup>27</sup>Al nuclei, highly sensitive to each site symmetry, render advanced <sup>27</sup>Al solid-state NMR a unique spectroscopic tool to fingerprint and identify the different phases.[3], [4] <sup>27</sup>Al NMR spectroscopic data on alumina reported in literature represents a comprehensive library. Analyzing this dataset using a new 3D correlative method of NMR parameters enabling fingerprinting and identification of

these phases. Providing a gold standard from crystalline samples, this approach demonstrates that any sort of crystalline, ill crystallized or amorphous, mixed periodic or aperiodically ordered transition alumina can now be assessed beyond the current limitations of characterisation. Adopting the presented approach as a standard characterisation of alumina samples will readily reveal NMR parameter–structure–property relations suitable to develop new or improved applications of alumina. Methodological guidance is provided to assist consistent implementation of this characterisation throughout the fields involved.

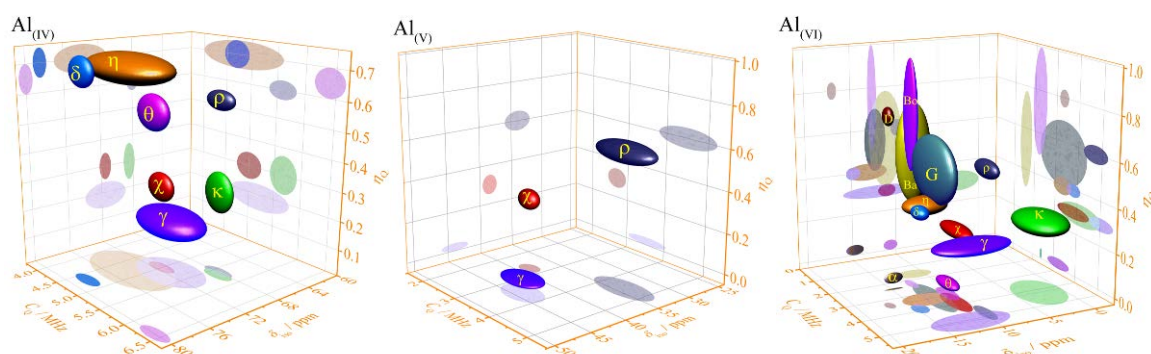


**Figure 1.** Plots of  $^{27}\text{Al}$  NMR parameters ( $d_{iso}$ ,  $C_Q$  and  $h_Q$ ) of four-, five- and the six Al-O coordinations in transition alumina phases ( $\alpha$ ,  $\chi$ ,  $\kappa$ ,  $\theta$ ,  $\gamma$ ,  $\delta$ ,  $\eta$ ,  $\rho$ ) and their precursors (Bayerite (Ba), Boehmite (Bo) Gibbsite (G) and Diaspore (D)).

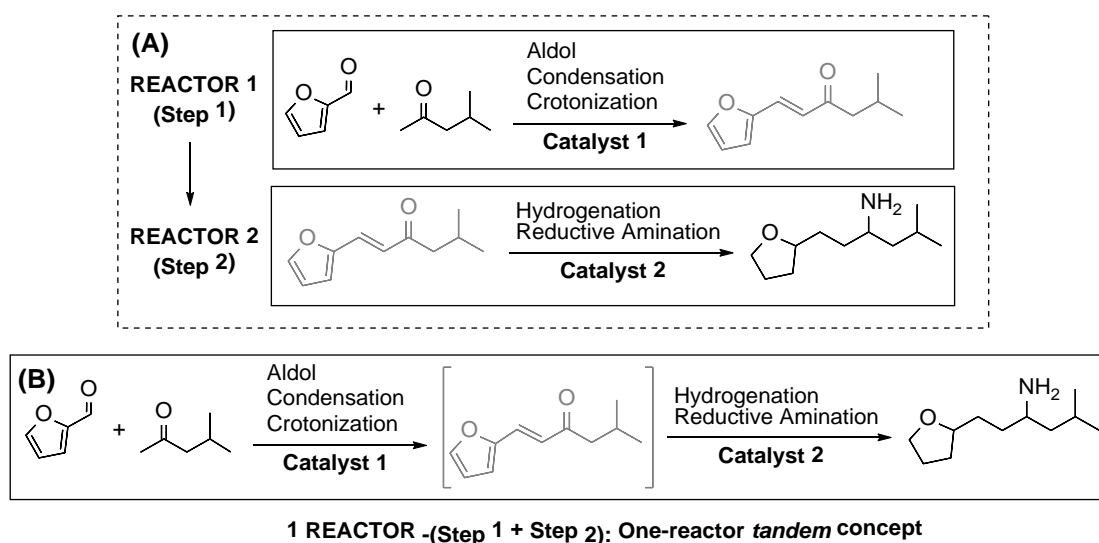
## References

- [1] G. Busca, *Structural, Surface, and Catalytic Properties of Aluminas*, 1st ed., vol. 57. Elsevier Inc., 2014.
- [2] P. S. Santos, H. S. Santos, and S. P. Toledo, "Standard transition aluminas. Electron microscopy studies," *Mater. Res.*, vol. 3, no. 4, pp. 104–114, 2000.
- [3] C. V. Chandran, C. E. A. Kirschhock, S. Radhakrishnan, F. Taulelle, J. A. Martens, and E. Breynaert, "Alumina: discriminative analysis using 3D correlation of solid-state NMR parameters," *Chem. Soc. Rev.*, vol. 48, no. 1, pp. 134–156, 2019.
- [4] E. Breynaert and C. V. Chandran, "3D Correlation of Solid-State NMR Parameters for Alumina - 3D interactive chart." Harvard Dataverse, 2018.

# Synthesis of THF-derived Amines by Transformation of Bio-derived Furfural

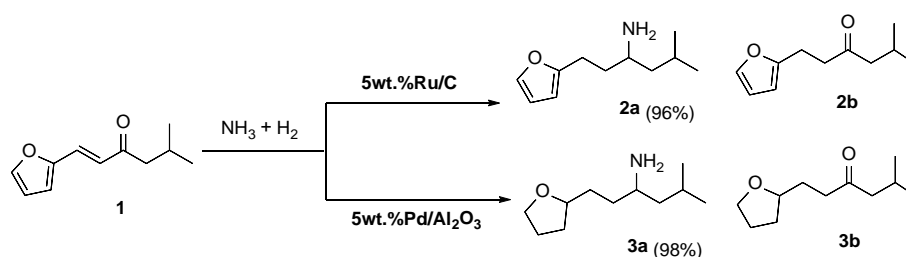
Shi Jiang, *Marc Pera-Titus*, E2P2L UMI 3464 CNRS-Solvay, 201108 Shanghai, China; Eric Muller, Research & Innovation Center Lyon, 69192 Saint Fons, France; François Jérôme, Karine De Oliveira Vigier, IC2MP, UMR 7285 CNRS-Université de Poitiers, 86073 Poitiers, France

The transformation of biomass into valuable amines is highly desirable in view of the synthesis of biosolvents and biosurfactants. As of today, only few amination studies have been reported on biobased substrates, targeting mainly the reductive amination of small platform molecules issued directly from biomass. For instance, furfural, derived from the hydrolysis of xylose, can be selectively converted into furfurylamine over supported ruthenium catalysts [1,2]. To increase the molecular complexity and diversity of biobased amines, it is necessary to develop catalytic processes combining C-C and C-N coupling reactions. One option could be the combination of the aldol condensation/crotonization reaction of furfural with ketones with variable chain length and ramification degree (e.g., methyl isobutyl ketone or MIBK), followed by reductive amination (Scheme 1 – route A). The aldol condensation of furanic compounds has been reported so far, but targeting mainly the production of liquid alkanes [3].



Scheme 1. (A) Two-reactor process for the synthesis of furfural- and THF-derived amines by combining aldol condensation (C-C) and reductive amination (C-N); (B) one-reactor tandem concept.

Herein we report the preparation of a new family of furan- and THF-derived amines with high selectivity, starting from bio-derived ketones issued from the aldol condensation of furfural with MIBK, using  $\text{NH}_3$  or amines as a nitrogen source and  $\text{H}_2$  as reducing agent. By combining the basic Amberlyst-26 (catalyst 1) with 5wt.%Ru/C or 5wt.%Pd/ $\text{Al}_2\text{O}_3$  (catalyst 2), functionalized furanic and THF-amines could be directly accessed from furfural in a single reactor (one-reactor *tandem* concept) without need of isolating the aldol intermediate (Scheme 1 – route B). The reaction conditions were optimized for both catalysts to maximize the yield of the final amine product (Scheme 2 and Figure 1). In these tests, the aldol intermediate was first generated *in situ* after 4 h reaction and subsequently  $\text{NH}_3$  and  $\text{H}_2$  were introduced. A yield up to 70% and 74% towards the furan- and THF-derived amines was achieved.



Scheme 2. Main products obtained in the reductive amination of the aldolization product (1) over 5wt.%Ru/C and 5wt.%Pd/ $\text{Al}_2\text{O}_3$  and corresponding yields after 14 h and 20 h reaction time. Detailed results and experimental conditions can be found in the caption of Figure 1.

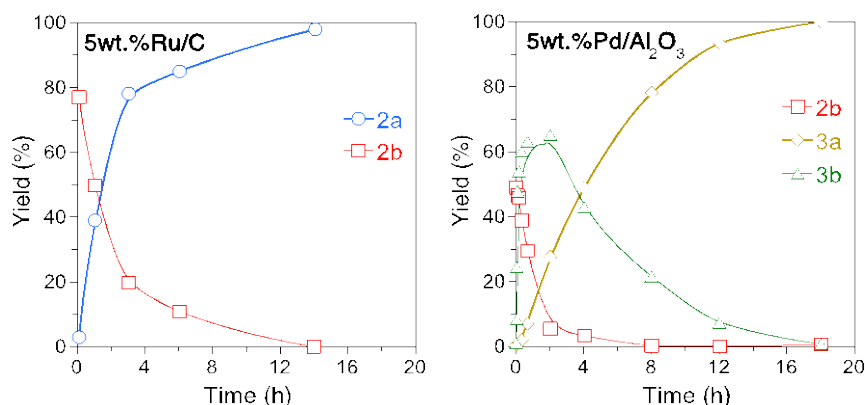


Figure 1. Time-evolution of the yield of the observed products in the reductive amination of the aldolization product (1) over 5wt.%Ru/C (left) and 5wt.%Pd/ $\text{Al}_2\text{O}_3$  (right) in a batch reactor. Reaction conditions (Ru/C): 1.7 mmol (1), 5 bar  $\text{NH}_3$ , 15 bar  $\text{H}_2$ , 0.87 mol% Ru, 1.3 mL ethanol, 100 °C; Reaction conditions (Pd/ $\text{Al}_2\text{O}_3$ ): 1.1 mmol (1), 5 bar  $\text{NH}_3$ , 20 bar  $\text{H}_2$ , 0.42 mol% Pd, 2.5 mL ethanol, 120 °C.

## References

- [1] S. Nishimura, K. Mizuhori, K. Ebitani, *Res. Chem. Int.* **206**, 42, 19.
- [2] T. Komanoya, T. Kinemura, Y. Kita, K. Kamata, M. Hara, *J. Am. Chem. Soc.* **2017**, 139, 11493.
- [3] J. Q. Bond, D. M. Alonso, D. Wang, R. M. West, J. A. Dumesic, *Science* **2010**, 327, 1110.



# The role of metal-support interaction in Ag-CeO<sub>2</sub> catalysts for room-temperature nitrophenol reduction to aminophenol

M. Sadlivskaya<sup>1</sup>, N. Mikheeva<sup>1</sup>, V.I. Zaikovskii<sup>2</sup>, G.V. Mamontov<sup>1</sup>

1 – Tomsk State University, Tomsk, Russia

2 – Boreskov Institute of Catalysis, Novosibirsk, Russia

## Introduction

Being an environmentally safe and highly effective method, the catalytic hydrogenation of nitroarenes into amines is of great scientific and practical interest, since the amines are the important precursors in the chemical industry. The Ag-based catalysts are the most promising composites because they are cheaper as compared to other noble-metal-based materials and possess high chemical activity.

The metal-support interaction was found to play an important role in the Ag/CeO<sub>2</sub> catalysts [1]. The interest to CeO<sub>2</sub> support is connected with both its unique redox properties and the phenomena of strong metal-support interaction (SMSI). In the present work we focus on the controlling of the MSI in the Ag/CeO<sub>2</sub> catalysts by applying different preparation techniques, namely, impregnation, co-precipitation, and impregnation of the prereduced ceria. The aim of the work is to study the influence of the MSI on the catalytic activity of Ag-CeO<sub>2</sub> catalyst in the reduction of p-nitrophenol into p-aminophenol in the presence of NaBH<sub>4</sub> under mild conditions (room temperature, atmospheric pressure).

## Experimental

Ceria and Ag-CeO<sub>2</sub> catalysts (Ag loading varied from 1 to 15 wt.%) were prepared by precipitation and impregnation techniques. The new approach for Ag/CeO<sub>2</sub> catalyst preparation was developed: prior to the impregnation the ceria support was pre-reduced at 500 °C to generate the surface Ce<sup>3+</sup> species, and their redox reactions with Ag<sup>+</sup> ions led to the strong Ag-CeO<sub>2</sub> interfacial interaction [2]. The catalysts were characterized by the low-temperature N<sub>2</sub> adsorption, XRD, HR-TEM and TPR-H<sub>2</sub> methods and tested in the reduction of p-nitrophenol into p-aminophenol with NaBH<sub>4</sub> at room temperature and atmospheric pressure.

## Results and discussion

The preparation method (co-precipitation and impregnation) is shown to affect the structures of the resulting Ag/CeO<sub>2</sub> catalysts. Small silver clusters (0.5-3 nm) are

observed by the HR-TEM on the CeO<sub>2</sub> surface in the catalysts prepared by the impregnation technique (Fig. 1a). The spherical agglomerates with a diameter of ~300 nm are formed in the Ag-CeO<sub>2</sub> catalyst prepared by co-precipitation. The SMSI is revealed for the Ag/CeO<sub>2</sub> catalysts prepared during the redox reaction between Ce<sup>3+</sup> and Ag<sup>+</sup> during the co-precipitation or impregnation of the pre-reduced ceria support.

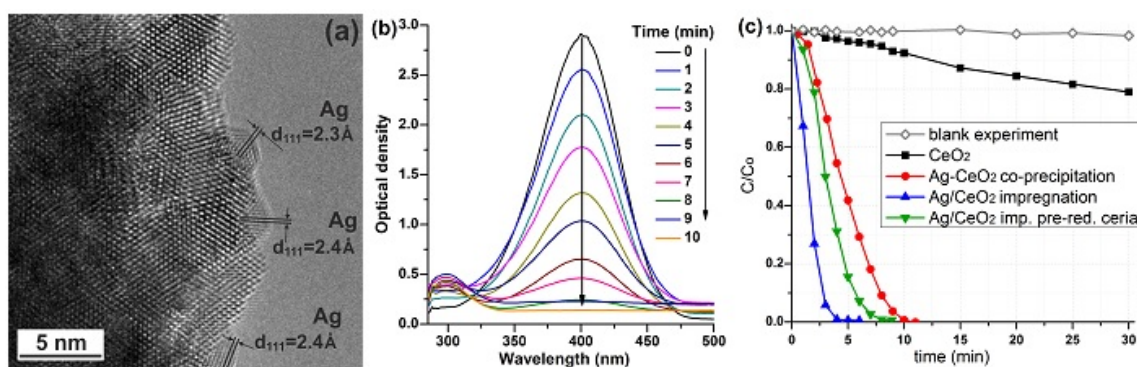


Fig. 1. The HR-TEM image of Ag/CeO<sub>2</sub> (impregnation) catalyst (a), UV-Visible spectra of aqueous solutions of p-nitrophenol in the presence of NaBH<sub>4</sub> and Ag/CeO<sub>2</sub> catalyst (b), and kinetic curves of p-nitrophenol reduction (c).

Fig. 1b shows the UV-vis spectra of p-nitrophenol ( $\lambda=400$  nm) reduction into p-aminophenol ( $\lambda\approx 300$  nm) in the presence of NaBH<sub>4</sub> and Ag/CeO<sub>2</sub> catalyst at room temperature (25 °C) and atmospheric pressure. As can be seen from the kinetic curves (Fig. 1c), CeO<sub>2</sub> does not catalyze the reduction of 4-nitrophenol under these conditions. The introduction of silver into the catalyst facilitates the reaction, and the total conversion of p-nitrophenol is achieved in 5-10 minutes. The catalysts prepared by impregnation are more active in this reaction due to the localization of silver predominantly on the surface of the ceria support. The catalyst prepared by co-precipitation is characterized by the silver localization both on the surface and in the bulk of the Ag-CeO<sub>2</sub> agglomerates and lower catalytic activity.

### Acknowledgements

This work was supported by Russian Science Foundation (Grant № 18-73-10109).

### References

- [1] Grabchenko M, Mikheeva N, Mamontov G, Salaev M, Liotta L, Vodyankina O (2018) *Catalysts* 8(7): 285.
- [2] Grabchenko M, Mamontov G, Zaikovskii V, La Parola V, Liotta L, Vodyankina O (2018) *Catalysis Today* (in press) DOI: 10.1016/j.cattod.2018.05.014.

# **MCM-56 zeolites synthesized using aniline as structure promoting agent – the influence of post synthetic modifications on their catalytic properties**

*Karolina Grzybowska, Aleksandra Korzeniowska, Barbara Gil, Wacław Makowski*

*Faculty of Chemistry, Jagiellonian University, ul. Gronostajowa 2, 30-387 Kraków, Poland*

The aim of this work was to investigate the catalytic properties of modified MCM-56 zeolites (MWW type) in alkylation of mesitylene (1,3,5-trimethylbenzene) with benzyl alcohol. The Friedel-Crafts alkylation represent an important group of organic chemistry reactions, which are widely used in various industry segments. Acidic zeolites are regarded as an eco-friendly alternative to homogenous catalysts that are being used in the alkylation processes. As conventional zeolites show low activity in the studied reaction due limited accessibility of the active centers, post-synthetic modifications aimed at increasing the number of accessible acid sites are extensively studied. This work focuses on exploring the unique benefits of MWW zeolites with layers containing acid centers to design new, active catalysts by modifying spatial arrangement of the layers by swelling, pillaring or desilication [1].

MWW zeolites have been synthesized with hexamethyleneimine and aniline. Aniline was introduced as the structure promoting agent (SPA) to couple with HMI as the structure directing agent (SDA) to achieve temperature-controlled phase-transfer hydrothermal synthesis of MCM-56 [2]. It has been reported that the MCM-56 zeolite synthesized via this route is not transformed into further derivatives. Post synthetic modifications comprised swelling with the use of cationic surfactant (CTAB – cetyltrimethylammonium hydroxide/chloride) and pillaring with tetraethylortosilicate (TEOS), followed by calcination.

Structure of the obtained materials was characterized by X-ray diffraction (XRD). Elemental composition was examined by XRF. Infrared spectroscopy of adsorbed probe molecules was applied for studying acidity. Porosity was assessed by low temperature N<sub>2</sub> adsorption and quasi-equilibrated temperature programmed desorption and adsorption (QE-TPDA) [3]. SEM imaging was used for morphology

characterization. Liquid phase alkylation of mesitylene with benzyl alcohol was used as a catalytic test reaction.

XRD patterns of the parent and modified zeolites confirm presence of the MWW structure (Fig. 1, left). The modified zeolites exhibit considerably higher activity in alkylation of mesitylene (Fig. 1, right). However, IR data on pyridine adsorption reveal decreased number of acid sites upon pillaring (by ca 30%). Despite this, better catalytic performance of the modified zeolites was attributed to the increased accessibility of the acid sites. This was corroborated by the increased selectivity of the bulky alkylation product which may be formed only on the active sites exposed to the surface. Molecules of the other main product (dibenzyl ether) are much smaller and may be formed on the sites located within the framework.

The preliminary results confirm that post synthetic swelling and pillaring of MCM-56 zeolites synthesized using aniline may result in obtaining acidic zeolites containing large numbers of active sites accessible for large molecules. Further research aimed at better understanding of this findings and exploring other modification methods is underway.

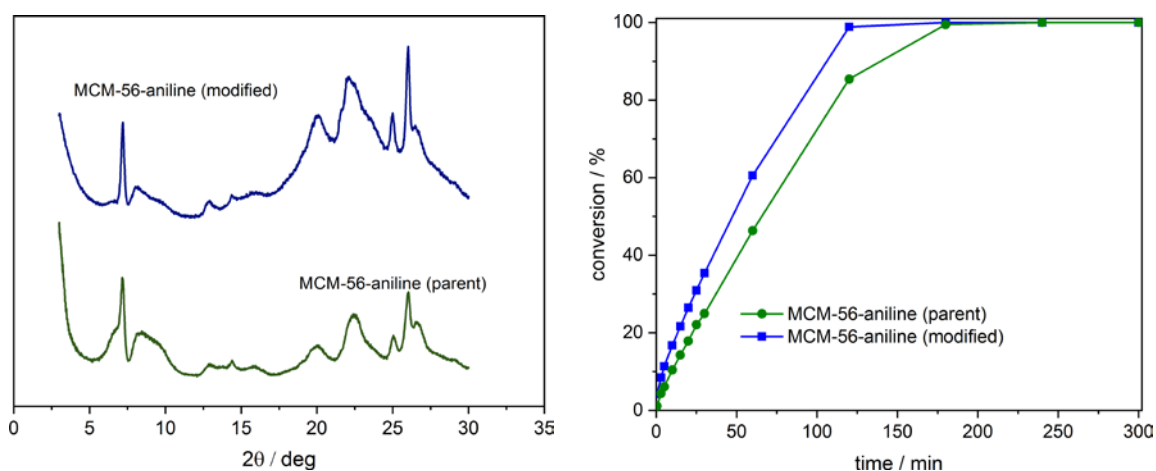


Figure 1. Comparison of XRD patterns and catalytic data observed for MCM-56 zeolites.

## References

- [1] Roth, W.J., Chlubná, P., Kubů, M., and Vitvarová, D. Swelling of MCM-56 and MCM-22P with a new medium - Surfactant- tetramethylammonium hydroxide mixtures. *Catal. Today*. 204 (2013) 8-14
- [2] Xing, E., Shi, Y., Xie, W., Zhang, F., Mu, X., and Shu, X. Synthesis, characterization and application of MCM-22 zeolites via a conventional HMI route and temperature-controlled phase transfer hydrothermal synthesis. *RSC Adv.* 5 (2015,) 8514-8522
- [3] Makowski, W., Gil, B., Majda, D., Characterization of acidity and porosity of zeolite catalysts by the equilibrated thermodesorption of n-hexane and n-nonane, *Catal. Lett.* 120 (2008) 154-160

## Supported CrO<sub>x</sub> catalysts for non-oxidative and oxidative dehydrogenation of light alkanes

*T. Bugrova<sup>1</sup>, V. Dutov<sup>1</sup>, V. Svetlichnyi<sup>1</sup>, V. Cortés Corberán<sup>2</sup>, G. Mamontov<sup>1</sup>*

*<sup>1</sup> Tomsk State University, Tomsk, Russia;*

*<sup>2</sup> Institute of Catalysis and Petroleumchemistry, CSIC, Madrid, Spain*

A growing demand in high-purity olefins requires new technologies of their production in addition to traditional steam and catalytic cracking methods. Olefins are widely used in chemical and pharmaceutical industry to produce a wide range of valuable chemicals. For these purposes the catalytic non-oxidative (DH) and oxidative (ODH) direct dehydrogenation of alkanes into olefins represent a wide scientific interest. The DH of alkanes is a promising method due to high selectivity towards olefins. In turn, the ODH with CO<sub>2</sub> as a mild oxidant is also of interest due to the opportunity of shifting of the dehydrogenation reaction equilibrium and CO<sub>2</sub> utilization. Both DH and ODH pathways strongly depend on redox properties of support and active component. To date, different types of mixed oxides [1, 2] have been studied as catalysts for these processes. In spite of toxicity of chromium compounds, the Cr-containing catalysts remain one of the most active among the DH catalysts. The use of CrO<sub>x</sub> as an alumina-supported active component is caused by the ability towards multiple and reversible oxidation-reduction (Cr<sup>V/VI</sup>↔Cr<sup>III/IV</sup>). The supported Cr-containing catalysts also show high activity in ODH-CO<sub>2</sub> of propane and isobutane. However, the use of oxide supports for Cr catalysts with the active oxygen and redox properties is preferable for higher activity and stable operation of the catalyst. Alumina shows poor redox ability, while ZrO<sub>2</sub>, CeO<sub>2</sub> and mixed ceria–zirconia oxides are the best candidates as supports for ODH catalysts due to their unique redox properties. Thereby, the purpose of the present work is to compare the activity of the Cr-containing systems on different supports in nonoxidative and oxidative dehydrogenation of alkanes.

γ-Al<sub>2</sub>O<sub>3</sub>, CeO<sub>2</sub>, ZrO<sub>2</sub>, Ce<sub>x</sub>Zr<sub>(1-x)</sub>O<sub>2</sub> were used as supports. Cr-containing catalysts with Cr loading corresponding to a monolayer (5 at<sub>Cr</sub>/nm<sup>2</sup>) were prepared by incipient wetness impregnation of the supports using aqueous solution of H<sub>2</sub>CrO<sub>4</sub>. The catalysts were dried at 80 °C for 12 h and calcined at 600 °C for 4 h. The catalysts

were characterized by low-temperature N<sub>2</sub> sorption, XRD, TPR, DRS, RS and tested in the DH of isobutane and ODH-CO<sub>2</sub> of ethane.

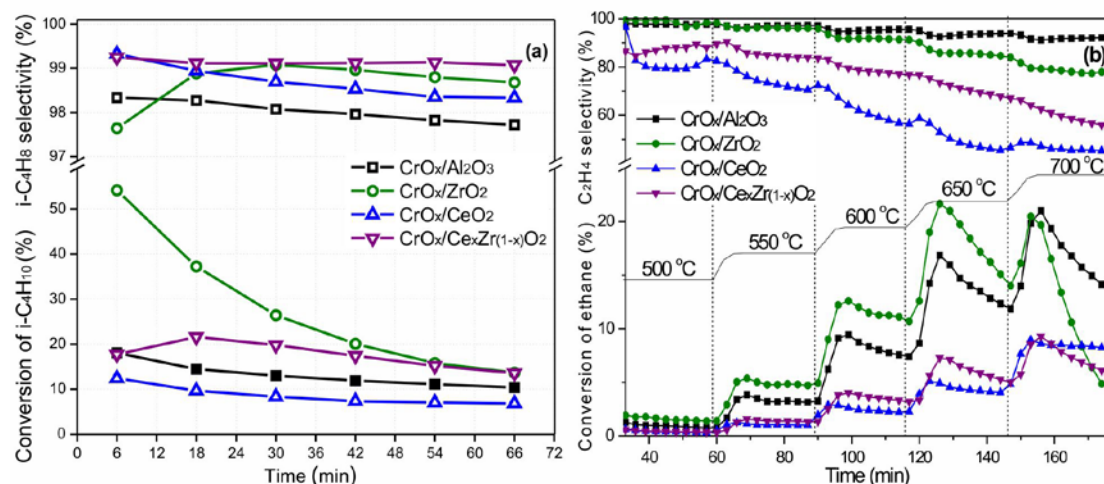


Fig. 1. (a) i-C<sub>4</sub>H<sub>10</sub> conversion and i-C<sub>4</sub>H<sub>8</sub> selectivity; (b) ethane conversion and C<sub>2</sub>H<sub>4</sub> selectivity

According to the results obtained, the state of Cr on the surface is different over different supports. The formation of  $\alpha$ -Cr<sub>2</sub>O<sub>3</sub> particles was observed only for the CrO<sub>x</sub>/CeO<sub>2</sub> catalyst. Several chromium states were identified by the DRS method. The activity of CrO<sub>x</sub>/ $\gamma$ -Al<sub>2</sub>O<sub>3</sub> was slightly higher than the one of CrO<sub>x</sub>/CeO<sub>2</sub> (Fig. 1(a)). TPR-H<sub>2</sub> results showed that the CrO<sub>x</sub>/ZrO<sub>2</sub> and CrO<sub>x</sub>/Ce<sub>x</sub>Zr<sub>(1-x)</sub>O<sub>2</sub> contain the highest amount of redox Cr<sup>5+/6+</sup> species. These catalysts are the most active in the i-C<sub>4</sub>H<sub>10</sub> dehydrogenation. Thus, the chromium state mainly affects the catalyst activity in the DH of isobutane. However, in the case of ODH-CO<sub>2</sub> of ethane the reaction pathway, activity and stability of the catalyst depend on both chromium state and support features (acid-base and redox properties) (Fig. 1(b)). The CrO<sub>x</sub>/ $\gamma$ -Al<sub>2</sub>O<sub>3</sub> and CrO<sub>x</sub>/ZrO<sub>2</sub> catalysts exhibited the highest ethylene formation rates, but the reaction followed different pathways. For CrO<sub>x</sub>/ $\gamma$ -Al<sub>2</sub>O<sub>3</sub> catalyst, ethylene is formed via the DH of ethane accompanied by the reverse water–gas shift reaction, while for the CrO<sub>x</sub>/ZrO<sub>2</sub> catalyst ethylene is formed via the selective ODH, while non-selective and/or dry reforming reactions take place on CrO<sub>x</sub>/CeO<sub>2</sub>.

This work was supported by Tomsk State University competitiveness improvement program.

## References

1. Sattler, J.J.H.B.; Ruiz-Martinez, J.; Santillan-Jimenez, E.; Weckhuysen, B.M. Chem. Rev. 2014, 114, 10613-10653.
2. Gartner, C.A.; van Veen, A.C.; Lercher, J. A. ChemCatChem 2013, 5, 3196-3217.

## Methane oxidation over bimetallic centres in zeolites

Edyta Tabor<sup>1</sup>, Kinga Mlekodaj<sup>1</sup>, Mariia Lemishka<sup>1,2</sup>, Zdenek Sobalik<sup>1</sup>,  
Alena Vondrová<sup>1</sup>, Jiri Dedecek<sup>1</sup>, Stepan Sklenak<sup>1</sup>

<sup>1</sup> J. Heyrovský Institute of Physical Chemistry of the CAS, Dolejškova 3/2155, 182 23 Prague, Czech Republic

<sup>2</sup> Faculty of Chemical Technology, University of Pardubice, Studentská 573, 532 10 Pardubice, Czech Republic

\*e-mail: edyta.tabor@jh-inst.cas.cz

Selective oxidation of methane represents a promising way of the transformation of natural and shale gases into more valuable key chemical feed stocks with an enormous possible economic impact [1]. Due to, high C-H bond strength (439 kJ mol<sup>-1</sup>), low polarizability, weak acidity and low electron and proton affinity methane molecule is relatively inert and for its oxidation active oxygen form is necessary. Zeolites offer the matrix for stabilization of transition metal ions (Me = Fe, Ni, or Co), which would provide selective oxidation of hydrocarbons over Me centres. It was confirmed that Fe-\*BEA effectively stabilizes oxygen originating from N<sub>2</sub>O and uses this oxygen to oxidize methane to methanol [1]. Ferrierite (FER) structure offer a special arrangement for the stabilization of Fe ions as binuclear centres across the zeolite channel [2]. Over this binuclear structure, N<sub>2</sub>O was effectively dissociated and active oxygen form was stabilized on Fe(II). The aim of this work was targeted at synthesis preparation of binuclear Co- Ni-, and Fe- species in FER and analysis of their redox properties in selective oxidation of methane by N<sub>2</sub>O to methanol using *in situ* FTIR and Mössbauer spectroscopy. The products of methane oxidation over Me-FER by N<sub>2</sub>O were monitored by mass spectrometry.

The highest concentration of binuclear metal centers in FER is observed when Me/Al ratio reaches 0.33 (this value represents the total exchange capacity of FER). The series of Me-FER (Me = Co, Fe, and Ni) with Me/Al ~ 0.3 were prepared. In the FTIR spectrum of dehydrated samples all prepared Me-FER exhibited the band with maximum intensity at 915 cm<sup>-1</sup>, which characterizes the Me(II) species in 6MRs (Fig. 1A). Interaction of dehydrated Me-FER with N<sub>2</sub>O at 220 °C resulted in the shift of the band describing Me(II) from 915 to 887 cm<sup>-1</sup> (Fig. 1B). The new band at 887 cm<sup>-1</sup> was assigned to active oxygen originating from N<sub>2</sub>O stabilized on metal cations (Co, Fe,

and Ni) in cationic positions. The introduction of CH<sub>4</sub> at 220 °C to Me-FER containing active oxygen species (formed after exposure to N<sub>2</sub>O) resulted in a full shift of the band from 887 cm<sup>-1</sup> to 915 cm<sup>-1</sup> (reduced form of cation) (Fig. 1C). This result clearly confirms the complete reduction of the [Me(III)-O]<sup>2+</sup> species by CH<sub>4</sub>. In the FTIR spectra after CH<sub>4</sub> treatment the new bands at 2920 and 2832 cm<sup>-1</sup> (Fe-OCH<sub>3</sub>) and the bands at 2979 and 1371cm<sup>-1</sup> (CH<sub>3</sub>OH vibrations) were observed. Speciation of iron in Fe-FER analyzed by Mössbauer spectroscopy revealed that majority (~ 80 %) of iron is present as Fe(II) located in 6MRs in T<sub>d</sub> coordination, with the rest of the iron being Fe-oxo species in O<sub>h</sub> coordination. Mössbauer *in situ* studies of Fe-FER revealed a total transformation of Fe(II) to Fe(III) after N<sub>2</sub>O treatment at 220 °C. The Mössbauer spectrum of Fe-FER recorded after interaction with methane at 220 °C over N<sub>2</sub>O-oxidized Fe-FER corresponded exclusively to Fe(II) species,

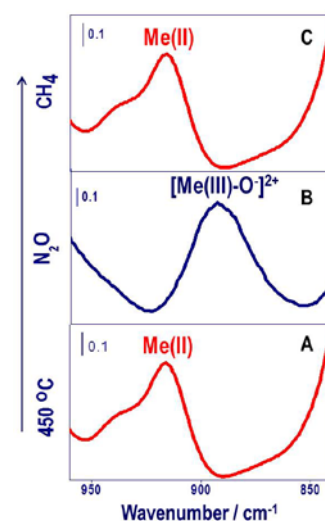


Fig. 1. FTIR spectra of Fe-FER after: A) dehydration at 450 °C, B) interaction with N<sub>2</sub>O at 220 °C, and C) interaction with CH<sub>4</sub> at 220 °C preceded by Fe-

which confirmed a reduction of Fe(III) to Fe(II) using CH<sub>4</sub>. Oxidation of methane by N<sub>2</sub>O at 220°C over Me-FER monitored by a quadrupole mass spectrometer confirmed the formation of methanol (m/z = 31) and formaldehyde (m/z = 29). The methanol production related to the Me cation did not exceed 0.5 mol<sub>CH<sub>3</sub>OH</sub>/mol<sub>Me</sub>, which confirms that the active sites for the formation of the α-oxygen and methanol oxidation represent two cooperating Me cations.

FTIR and Mössbauer *in situ* studies confirmed what was previously predicted by DFT calculations, i.e. that binuclear transition metal (Fe, Mn, Co, and Ni) species in FER can split N<sub>2</sub>O. This interaction results in the stabilization of active oxygen on the metal cation in FER cationic positions and N<sub>2</sub> formation. For the first time, we showed that the active oxygen form N<sub>2</sub>O stabilized on metal cations (Co, Fe, and Ni) easily oxidizes methane to methanol at 220 °C. The oxidation properties strongly depend on the transition metal ion embedded to FER structure. Among studied Me-FER, the Ni-FER was the most active in oxidation of methane to methanol.

#### References:

1. Snyder, B. E. R.; Vanelderren, P.; Bols, M. L.; Hallaert, S. D.; Böttger, L. H.; Ungur, L.; Pierloot, K.; Schoonheydt, R. A.; Sels, B. F.; Solomon, E. I., *Nature* 536 (7616), 317-321, 2016.
2. Sklenák, S.; Andrikopoulos, P. C.; Boekfa, B.; Jansang, B.; Nováková, J.; Benco, L.; Bucko, T.; Hafner, J.; Dědeček, J.; Sobalík, Z., *J. Catal.* 272 (2), 262-274, 2010.



# SINGLE STEP SELECTIVE SYNTHESIS OF CYCLOHEXYLPHENOL FROM PHENOL OVER CoP/BETA ZEOLITE CATALYSTS

Santiago Gutiérrez-Rubio<sup>1</sup>, Inés Moreno<sup>1, 2</sup>, Juan M. Coronado<sup>3</sup>, David P. Serrano<sup>1,2</sup>

<sup>1</sup>IMDEA Energy Institute, Móstoles, Spain; <sup>2</sup> Rey Juan Carlos University, Móstoles, Spain; <sup>3</sup>Institute of Catalysis and Petrochemistry, CSIC, Madrid, Spain.

## Scope

Cyclohexylphenol is a high added-value chemical, extensively used for the synthesis of dyes, resins and biocides. [1] This molecule is currently synthesized by alkylation reaction using phenol and cyclohexene/cyclohexanol as reactants and high-polluting and toxic Brønsted acids such as H<sub>2</sub>SO<sub>4</sub> or H<sub>3</sub>PO<sub>4</sub> as catalysts. [2] As an alternative, the present contribution investigates the production of cyclohexylphenol, using a one-pot greener route, which involves the partial phenol hydrodeoxygenation (HDO), leading to cyclohexene, followed by an alkylation step, which promotes C-C bonding between phenol and the in-situ produced cyclohexene. This process requires a catalyst with an adequate balance of acidic and hydrogenation sites, so they can operate cooperatively to promote these coupled reactions. Furthermore, phenol is one of the most abundant aromatic compounds presents in pyrolysis bio-oils obtained from lignocellulosic biomass. The use of this renewable feedstock could increase the environmental value of this alternative synthesis route. As catalyst, cobalt phosphide loaded on different amounts (1.5, 2.5, 5 and 10 % wt. Co) over a commercial Beta zeolite were used (Clariant) ([Si/Al]<sub>MOL</sub> = 13). Catalytic reaction tests were carried out in a stirred batch reactor at 240 °C, using 40 bar of H<sub>2</sub> and 3.3 % wt. of phenol in decaline.

## Results and discussion

XRD analyses (Fig. 1, A) revealed that, after metal phosphide loading, the zeolitic structure was preserved with high crystallinity degree, although some contribution of AlPO<sub>4</sub> was also observed for the samples with higher cobalt content. Likewise, reflections corresponding to the metal rich phosphide phase (Co<sub>2</sub>P) were detected in high loaded samples (10-CoP/Beta and 5-CoP/Beta). [3] However, for samples with low loading (2.5-CoP/Beta and 1.25-CoP/Beta) only the zeolite peaks appear in the XRD, suggesting high dispersion of this phase. In the case of 1.25-CoP/Beta the low

temperature feature of the H<sub>2</sub>-TPR profile indicate the formation a Co<sup>0</sup> rather than phosphide. Acidity of the catalysts decreased with regards to parent zeolite with increasing active phase loading, surely due to acid sites coverage. Figure 1 (B) shows phenol conversion, as well as the product distribution obtained using catalysts with different CoP content. In these conditions, as expected, when CoP loading decreases, lower conversions were obtained. In particular, it is worth highlighting the very little activity observed in the case of 1.25-CoP/Beta, due to the fact that no CoP is present. Same tendency was observed in HDO activity, being 10-CoP/Beta catalyst the most active in that reaction, showing a cyclohexane selectivity of 48 %. However, cyclohexylphenol selectivity presents a maximum on the catalysts with cobalt loading in the 2.5 - 5 % wt. range. Those results confirm that an equilibrated proportion of active sites for both hydrodeoxygenation (needed for cyclohexene production) and alkylation reaction is required. Since alkylation activity shows an opposite trend with CoP loading than HDO, due to the blocking of active acidic sites, the most beneficial balance is achieved for that intermediate loading range.

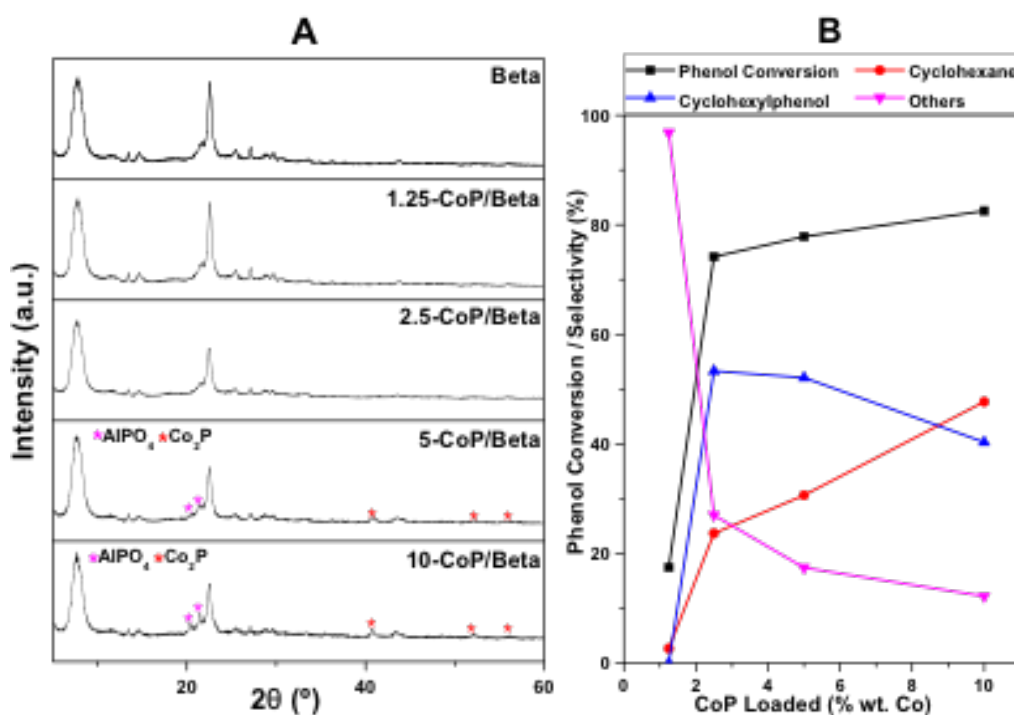


**Figure 1.** XRD patterns of parent zeolite and loaded catalysts (A) and phenol conversion and liquid product distribution (B)

## References

- [1] G. D. Yadav and P. Kumar, *Appl. Catal., A*, 2005, 286, 61.
- [2] A.R. Abdurasuleva, T.P. Royand S.A. Hutchinson, *Zh. Org. Khim.* 1972, 8(1), 134.
- [3] Cecilia, J. A., Infantes-Molina, A., Rodríguez-Castellón, E., & Jiménez-López, A, *J. Hazard. Mater.* 2013, 260, 167-175.

# Catalytic Hydroboration of Carbon dioxide and Organic Carbonates using Manganese Pincer Complex

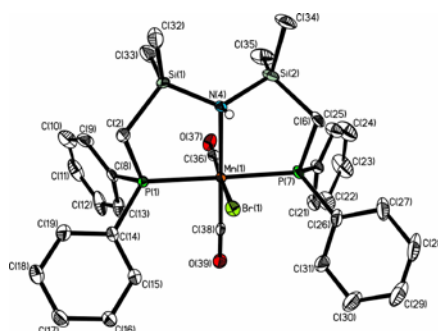
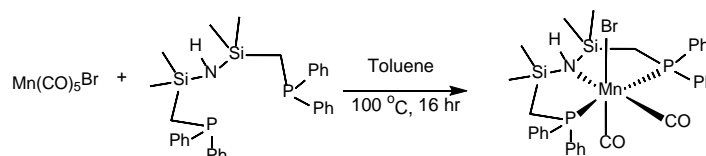
Akash Kaitha<sup>1</sup>, Suman Sen<sup>1</sup>, Christina Erken<sup>1,2</sup>, Thomas Weyhermüller<sup>2</sup>, Markus Hölscher<sup>1</sup>, Christophe Werlé<sup>2</sup> & Walter Leitner<sup>1,2</sup>

<sup>1</sup>Lehrstuhl für Technische Chemie und Petrolchemie  
RWTH Aachen University  
Worringer Weg 2, 52074 Aachen  
[akash.kaithal@gmail.com](mailto:akash.kaithal@gmail.com)

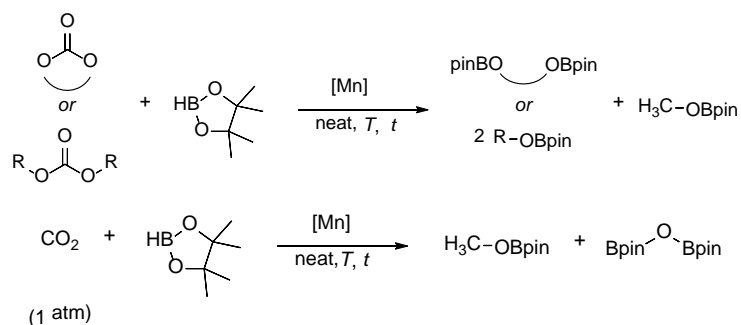
<sup>2</sup>Max-Planck-Institute for Chemical Energy Conversion, Stiftstraße 34-36, 45470  
Mülheim an der Ruhr, Germany

Functional reduction of the C=O unit in carbonic acid derivatives, and in carbon dioxide is a challenging process of key importance for the synthesis of value-added chemicals.<sup>[1-2]</sup> It can enable novel synthetic pathways such as preparation of fine chemicals and pharmaceutical synthesis through manipulation of functional groups in agreement with the principles of Green Chemistry. In particular, these transformations are important in the utilization of alternative feedstocks derived from biomass or from carbon dioxide.<sup>[3-6]</sup> Catalysts based on earth-abundant, cheap, and benign metals would greatly contribute to the development of sustainable synthetic processes derived from this concept.<sup>[6]</sup>

Herein, we report the reduction of a broad range of organic carbonates, and CO<sub>2</sub> using a new manganese pincer complex [Mn(Ph<sub>2</sub>PCH<sub>2</sub>SiMe<sub>2</sub>)<sub>2</sub>NH(CO)<sub>2</sub>Br] and pinacolborane as reducing agent.



Reactions occur at mild conditions (80-120°C), low catalyst loadings (0.036 – 0.1 mol%) and run under solvent-less conditions which enables catalytic reductive functionalization for a wide range of structurally diverse substrates through hydroboration of cyclic five- and six-membered carbonates, linear carbonates, and even carbon dioxide.



Mechanistic studies confirmed that the B-H activation of pinacolborane is facilitated *via* metal ligand cooperation including crystallographic characterization of a borane adduct at the pincer complex.

## References

1. Erythropel, H. C. *et al. Green. Chem.* **2018**, *20*, 1929–1961.
2. Bryan, M. C. *et al. Org. Process Res. Dev.* **2017**, *21*, 1464–1477.
3. Balaraman, E., Gunanathan, C., Zhang, J., Shimon, L. J., Milstein, D. *Nat. Chem.* **2011**, *3*, 609–614.
4. Kaithal, A., Sen, S., Erken, C., Weyhermüller, T., Hölscher, M., Werlé, C., Leitner, W. *Nat. Commun.* **2018**, *9*, 4521.
5. Chakraborty, S., Zhang, J., Krause, J. A., Guan, H. *J. Am. Chem. Soc.* **2010**, *132*, 8872–8873.
6. Kaithal, A., Hölscher, M., Leitner, W. *Angew. Chem. Int. Ed.* **2018**, *130*, 13637–13641.

## **Bimetallic catalysts supported on carbon xerogels for PEMFC cathode**

Aleksandra Grzelak<sup>1\*</sup>, Anthony Zubiaur<sup>1</sup>, Nathalie Job<sup>1</sup>

<sup>1</sup>*Université de Liège, Department of Chemical Engineering –Nanomaterials, Catalysis, Electrochemistry (NCE), Building B6a, Sart-Tilman, B-4000 Liège*

A fuel cell is an electrochemical device that converts the chemical energy of a fuel (e.g. hydrogen, methanol) directly into electrical energy following the principle is shown in Figure 1. The main advantages of fuel cells are: (i) they produce zero or very low emissions, especially greenhouse gases, (ii) they produce electrical energy with a very high yield (up to 60%), (iii) they can be used for combined heat and power purposes, further increasing the efficiency of energy production and (iv) they are entirely silent.

One of the types of fuel cell is Proton Exchange Membrane Fuel Cells (PEMFCs). They work at low temperature (< 100°C), uses a proton-exchange membrane, *i.e.* Nafion® as an electrolyte. The most frequent catalysts used in PEMFCs are platinum nanoparticles deposited on carbon (Pt/C). The major hurdle is stability: the platinum nanoparticles can dissolve, coalesce, grow, and the carbon support may oxidise, which leads to nanoparticle detachment, a decrease of electrochemically surface. Also, due to the sluggish Oxygen Reduction Reaction (ORR), large amounts of Pt are used, which makes the fuel cell manufacturing expensive. In the exploration of alternative catalysts, researchers have looked at several other types of materials, one of the ideas is to decrease the amount of needed precious metal by the partial substitution of Pt with potential candidates such as cobalt [1].

Among the various possible structures, hollow particles are considered. Hollow particles have void space in their body, are presently attracting great attention due to their unique properties such as high surface-to-volume ratio, and excellent chemical and thermal stabilities. They display higher activity and are more stable than usual Pt nanoparticles [2]. The PtCo alloys are much more active than pure Pt due to the strain-ligand effect on the Pt lattice obtained by introducing cobalt atoms. Synthesis of PtCo hollow nanoparticles on carbon xerogels was previously performed [2]. The obtained catalysts showed high activity and resistance to degradation. However, the synthesis method is

complex, and the next step is to optimise the procedure and simplify it while reaching larger platinum loading (> 20 wt.%). Synthesised catalysts will be investigated by various physicochemical and electrochemical techniques.

a)

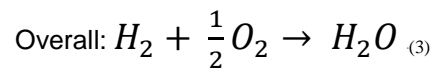
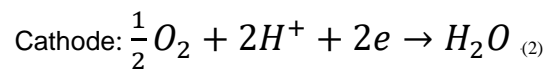
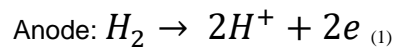


Figure 1 Summary reactions are occurring in PEMFC.

## References

1. A. Hamnett *Handbook of Fuel Cells. Handbook of Fuel Cells - Introduction to fuel cells types*, Vol 3, p.1-10, John Wiley & Sons, Ltd (2010).
2. Zubiaur, A, *Development of new catalysts for proton exchange membrane fuel cells (PEMFCs)*, University of Liège, PhD thesis (2017)

# Adamantyl-BINOL-based chiral porous polymers for heterogeneous catalysis

Cristina Monterde,<sup>1,2</sup> Antonio Valverde,<sup>2</sup> Rodrigo Navarro,<sup>3</sup> Marta Iglesias, Félix Sánchez<sup>1</sup>.

<sup>1</sup>Instituto de Química Orgánica General. C.S.I.C. Madrid, 28006, Spain; <sup>2</sup>Instituto de Ciencia de Materiales de Madrid. C.S.I.C., Madrid, 28049, Spain; <sup>3</sup>Instituto de Ciencia y Tecnología de Polímeros. C.S.I.C., Madrid, 28006, Spain.

We report the synthesis of adamantyl-BINOL-based chiral porous aromatic polymers (Ad-BINOL-PAFs) for heterogeneous catalysis.

## Introduction

Porous organic polymers (POPs) as covalent organic frameworks (COFs), hypercross-linked polymers (HCPs), conjugated microporous polymers (CMPs), polymers of intrinsic microporosity (PIMs), have been prepared from different building blocks and have been applied for gas storage, catalysis, sensors and organic optoelectronics [1]. The “bottom-up” approach is a more effective strategy to heterogenize molecular catalysts in comparison with the classical supported catalysts and the resulting porous polymers catalysts possess the catalytic centers more accessible and homogeneously distributed.

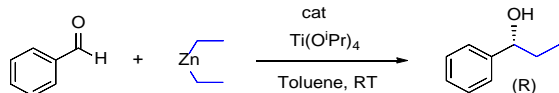
## Results and discussion

The synthesis of chiral polymer Ad-BINOL-OH-PAFs and their soluble counterpart Ad-BINOL-OH is outlined in Scheme 1. The precursor (B) was easily done from commercially available (*R*)-BINOL and 1-adamantanol. Robust BINOL-frameworks (BINOL-PAFs) were prepared via palladium-catalyzed Suzuki or Sonogashira cross-coupling reaction (under microwave heating) of (*R*)-4,4'-dibromo-2,2'-diethoxy-6,6'-adamantyl (B) with a boronic acid or an alkyne structural building block and deprotection with BBr<sub>3</sub>. The solid materials were characterized by FTIR, <sup>13</sup>C CP/MAS NMR and the porous properties measured by nitrogen adsorption/desorption isotherms at 77 K indicated that Ad-BINOL-OH-PAFs are porous with BET surface area of 365.5 - 455 m<sup>2</sup>.g<sup>-1</sup>.

Ad-BINOL-OH-PAFs were used as heterogenized BINOL ligand for the formation of chiral catalysts by treating with excess Ti(OiPr)<sub>4</sub>. Resulting Ti-catalysts were applied

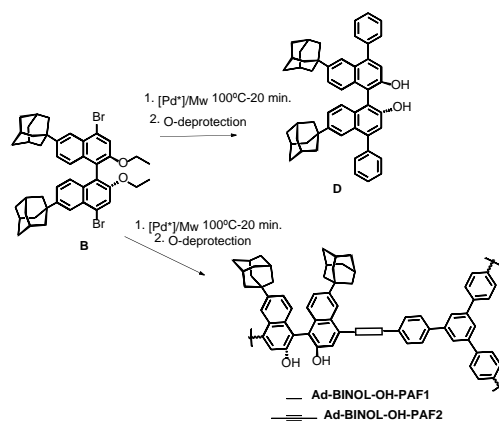
for the addition of diethylzinc to benzaldehyde and compared with that obtained from the corresponding soluble D-[Ti]-catalyst (Table 1).

Table 1. Asymmetric ethylation of benzaldehyde-



Entry	Catalyst	Conv (%) <sup>b</sup> (h)	ee (%) <sup>c,d</sup>
1	D-[Ti] <sup>a</sup>	91 (1)	87.0
2	Ad-BINOL-O[Ti]-PAF1 <sup>b</sup>	100 (3)	88.0
3	Ad-BINOL-O[Ti]-PAF2 <sup>b</sup>	100 (3)	78.0
5	7run	90 (3)	50.0

<sup>a</sup>D/[Ti]/Aldehyde/[Zn] (0.1/1/1.0/3.0), 1h; <sup>b</sup>cat./Aldehyde/[Zn] (20mg/10/7.0/ 20), 3h; <sup>c,d</sup>GC using (CP-Chirasil-Dex).



Scheme 1. Preparation of BINOL-PAF.

When soluble and heterogenized Ad-BINOLs were treated with  $\text{Ti}(\text{O}i\text{Pr})_4$  are a highly active catalytic system in the addition of diethylzinc to benzaldehyde to afford (*R*)-1-phenylpropan-1-ol. The reactions are quantitative and selective for the secondary alcohol. The enantiomeric excess for the heterogenized catalyst was 88% (from at least three batch) similar to that obtained with the corresponding soluble D-[Ti].

The recovered catalyst (after washing) was able to perform diethylzinc addition to benzaldehyde for seven cycles without loss of conversion although the enantioselectivity decreases due to the rest of zinc oxides or unreactive titanium compounds

## Conclusions

We have incorporated chiral adamantyl-BINOLs into porous polymeric frameworks giving solid recyclable catalysts for ethylation of aldehydes.

## References

[1] A. I. Cooper, Adv. Mater., 2009, 21, 1291.

Authors acknowledge to MINECO of Spain (Project MAT2017-82288-C2-2-P) for financial support. AGV thanks for FPU fellowship.



# Rhodium Based Heterogeneous Catalyst Towards Direct Addition of Ethylene Across Amines

*Manideepa Sengupta<sup>†‡</sup>, Ankur Bordoloi<sup>†</sup>*

*† Conversions & Catalysis Division, CSIR-Indian Institute of Petroleum, Dehradun, Uttarakhand-248005, India.*

*‡ Department of Chemistry, University of Kalyani, West Bengal-741235, India.*

## Introduction

Catalytic hydroamination or the direct addition of N-H bond across unsaturated C-C bond in presence of catalyst is of considerable interest in the pharmaceutical and chemical industries, since such addition led to the formation of organo-nitrogen compounds with 100 % atom efficiency, which are present as important building blocks in the areas of natural products (which afford pharmaceutical and biological activities) fine chemicals, polymers, agrochemicals, dyes and surfactants. Though hydroamination is thermodynamically achievable, however, the presence of a considerable kinetic barrier makes the decision for using of a catalyst. [1] Even though numerous catalysts have been explored under both homogeneous and heterogeneous system, with aromatic and activated C-C multiple bonds, [1-4] however, there are few reports of hydroamination with ethylene, where D. R. Coulson first reported the catalytic addition of secondary amines to ethylene over various rhodium and iridium compounds, [5] and hydroamination of ethylene by aniline with platinum salts as reported by R. Poli *et al.*[6] Although homogeneous systems provide outstanding yields, however, unlike heterogeneous system it requires tedious methods in the separation of the catalyst, low recyclability. In this context, highly uniform rhodium oxide nanoparticles have been embedded within the mesochannels of mesoporous silica and efficiently utilized as catalyst towards direct addition of amines to ethylene.

## Material and Methods

Rh oxide nanoparticles have been decorated on mesoporous silica by organic matrix decomposition method. Hydroamination has been carried out within Teflon-lined stainless-steel autoclave using Schlenk technique at 170-180 °C and the products were analysed by Gas Chromatograph (GC, Agilent 7890) connected with an HP5

capillary column (30 m length, 0.28 mmid, 0.5  $\mu\text{m}$  film thickness) and flame ionization detector (FID) and identified from GC-MS.

## Results and Discussion

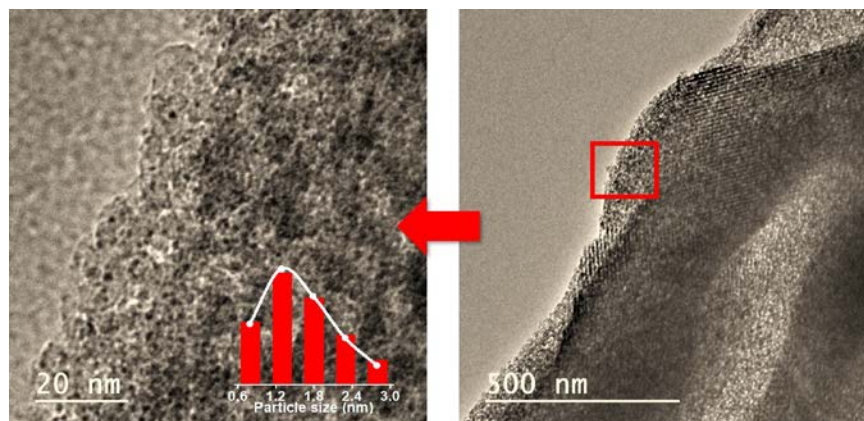


**Figure-1.** HRTEM images with particle size distribution (inset) of Rh@SiO<sub>2</sub>

The HRTEM images reveal uniform distribution of (1-2 nm) rhodium oxide nanoparticles within the mesochannels of silica and exhibits 25-30 % conversion and > 98 % selectivity towards direct addition of piperidine to ethylene with remarkable recyclability up to five cycles.

## Conclusion

Uniform Rh oxide nanoparticles have been grafted on mesoporous silica and efficiently utilized as catalyst for the direct addition of secondary amines to ethylene with constant activity and remarkable recyclability.

## References

1. T.E. Müller, M. Beller, *Chem. Rev.* 1998, 98, 675-704.
2. J. Seayad, A. Tillack, C.G. Hartung, M. Beller, Base-Catalyzed Hydroamination of Olefins: An Environmentally Friendly Route to Amines, *Advanced Synthesis & Catalysis*, 344 (2002) 795-813.
3. T. Joseph, G. Shanbhag, D. Sawant, S. Halligudi, Chemoselective anti-Markovnikov hydroamination of  $\alpha$ ,  $\beta$ -ethylenic compounds with amines using montmorillonite clay, *Journal of Molecular Catalysis A: Chemical*, 250 (2006) 210-217
4. M. Sengupta, S. Das, A. Bordoloi, Cu/Cu<sub>2</sub>O nanoparticle interface: Rational designing of a heterogeneous catalyst system for selective hydroamination, *Molecular Catalysis*, 440 (2017) 57-65.
5. D. R. Coulson, Catalytic Addition of Secondary Amines to Ethylene, *Tetrahedron Letters* No. 5 (1971) 429-430.
6. P. A. Dub, M. R. Zubiri, C. Baudequin, R. Poli, Hydroamination of Ethylene by Aniline: Catalysis in Water, *Green Chemistry*, 12 (2010) 1392-1396.

# A strategy for heterogeneously catalysed amination of simple arenes

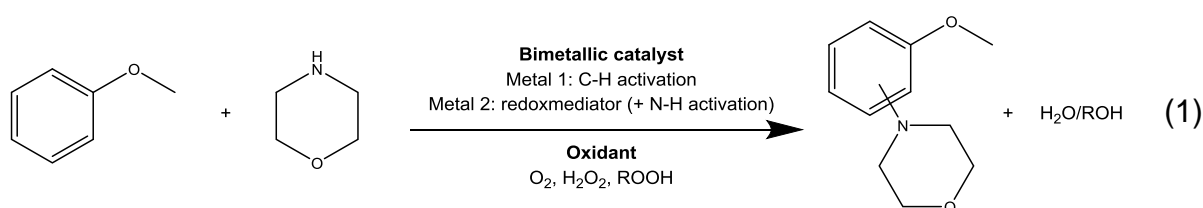
*Lisa Van Emelen, Dirk De Vos, KU Leuven, Leuven, Belgium*

N-substituted arylamines constitute indispensable intermediates in the synthesis of various high-value chemicals, such as pharmaceutical compounds, polymer precursors and dyes [1]. Ideally, they could be synthesized directly from the corresponding amine and aromatic compound. However, due to the nucleophilic character of both amine and aryl coupling partner; and the fact that a strong C-H and N-H bond must be replaced with a substantially weaker C-N bond, industry currently employs prefunctionalized substrates, in which the C-H bond is replaced by a more reactive group, such as C-X (with X = Cl, Br, I) [2, 3]. The well-known palladium-catalyzed Buchwald-Hartwig amination for example [4] enables the coupling of an aryl halide and an amine. Owing to its reliability and broad substrate scope, Buchwald-Hartwig amination has become widespread practice. Nevertheless, it also suffers from some serious drawbacks [2, 5]. Firstly, the use of prefunctionalized substrates increases the number of steps and shifts the problem of C-H functionalization to an earlier stage in the synthesis. The associated regioselectivity issue is relocated to previous steps as well. Furthermore, the formation of stoichiometric amounts of (halide salt) waste negatively affects the atom economy. Therefore, a method for direct coupling of non-prefunctionalized amines and arenes is highly desirable [2, 3, 5].

The goal of this research is to achieve C-N coupling with simple arenes, through cross-dehydrogenative coupling (CDC) [2] with an external, clean oxidant such as O<sub>2</sub> or (hydrogen) peroxide to thermodynamically drive the reaction. The efficient catalytic systems that are identified, are in a next step heterogenized on a solid support, viz. a zeolite. This will facilitate catalyst recycling and product purification.

For CDC, palladium and ruthenium are used to activate the C-H bond and generate the C-N bond. As reoxidation of the metal must be efficient, we will also demonstrate the use of a second metal such as Cu<sup>II</sup> or Ag<sup>I</sup> that acts as a redox mediator. This second metal may also be involved in activation of the N-H bond. Both are immobilised in the pores of the support (zeolite Y or beta). O<sub>2</sub>, H<sub>2</sub>O<sub>2</sub> or organic peroxides are employed as terminal oxidant, yielding only water or alcohols as waste

products. As a model reaction, the coupling of morpholine and simple aromatics like anisole is studied (reaction 1). The effect of the solvent (e.g., a non-polar like toluene versus polar non-protic like DMSO), type of oxidant, temperature, catalyst loading and additives (acids, bases...), are being investigated to determine reaction conditions under which the coupling products are observed. Besides, variation of the substituents on the arene (e.g., 1,3-dimethoxybenzene as a more electron-rich coupling partner) allows us to study electronic effects. For the heterogeneous system, the loading and dispersion of the two metals on the porous support, as well as its acidity and the cations present, are to be taken into account too.



Finally, we will show our efforts towards regioselective coupling by exploiting the sterically constrained environment of the zeolite pores. To this aim, zeolites with different topologies (e.g., ZSM-5 (10 membered ring channels) or zeolite Y (cages with 12 membered rings)) are tested in combination with substrates of variable size.

## References

- [1] Vogt, P. F. and Grafahrend, J. J. (2012). *Amines, aromatic*, in *Ullmann's Encyclopedia of Industrial Chemistry*, 699-718.
- [2] Park, Y., Kim, Y. and Chang, S. (2017). *Chem. Rev.*, 117, 9247-9301.
- [3] Louillat, M.-L. and Patureau, F. W. (2014). *Chem. Soc. Rev.*, 43, 901-910.
- [4] Hartwig, J. F. (1998). *Angew. Chem. Int. Ed.*, 37, 2046-2067.
- [5] Jia, J., Murakami, K. and Itami, K. (2016). *ACS Catal.*, 6, 610-633.

# Bimetallic Nanoparticles-SILP for Selective Benzylideneacetone Hydrogenation

*Sheetal Sisodiya<sup>1</sup>, Simon Rengshausen<sup>1,2</sup>, Alexis Bordet<sup>1</sup>, Walter Leitner<sup>1,2</sup>*

<sup>1</sup> *Max-Planck-Institut für Chemische EnergieKonversion, Stiftstraße 34-36, 45470, Mülheim an der Ruhr (Germany).*

<sup>2</sup> *Institut für Technische und Makromolekulare Chemie RWTH, Aachen University, 52074 Aachen (Germany)*

## Abstract

The catalytic hydrogenation of aromatic compounds containing carbonyl functionalities has widespread applications in the chemical industry.[1] However, a major challenge lies in the design and the development of catalysts possessing high activity, stability, and tunable selectivity.

In this context, the synthesis of metal nanoparticles (NPs) in Supported Ionic Liquid Phases (SILP) produces NPs@SILP materials which are highly tunable and combine the advantages of NPs in ionic liquid catalysts with those of conventional supported catalysts.[2] As a result, NPs@SILP catalysts have been proven to possess superior catalytic properties for a variety of transformations, as evidenced in recent studies.[3]

In particular, our group has recently shown that the dilution of Ru with Fe to produce Fe<sub>25</sub>Ru<sub>75</sub>@SILP bimetallic catalysts results in enhanced catalytic activity and selectivity in the hydrogenation of aromatic ketones.[4] However, while the formation of 3d metal/noble metal NPs alloys appears as an efficient tool to tune the activity and selectivity of catalysts, systematic studies on the influence of the ratio and the nature of the 3d metal on the resulting properties of bimetallic catalysts are scarce.

Hence, in this study we report the synthesis of bimetallic M<sub>x</sub>Ru<sub>1-x</sub>@SILP (M = Fe, Co, Ni) with tunable metal ratios through an organometallic approach. Electron microscopy evidenced the formation of small and well dispersed NPs in all cases, and their bimetallic nature was confirmed by STEM-EDX elemental mapping. (Figure 1)

The catalytic properties of the materials obtained were systematically investigated for the hydrogenation of benzylideneacetone as a model substrate. Interestingly, the catalysts' selectivity is highly dependent on the ratio between M/Ru. While monometallic Ru NPs lead to the formation of the completely saturated product, increasing contents of Fe, Co or Ni results in a change of selectivity, in particular an

enhanced C=O hydrogenation rate and no aromatic ring hydrogenation. (Figure 1) The selective hydrogenation of C=O bonds in aromatic compounds is challenging to achieve with heterogeneous catalysts, and is a critical step in the synthesis of various fine chemicals (e.g., in flavor, fragrance, or pharmaceutical chemistry) In addition, the M/Ru ratio for which this selectivity switch is observed (full hydrogenation Vs conservation of the aromatic ring) depends on the 3d metal considered. These results show that the dilution of noble metals with 3d metals can not only reduce the amount of noble metal used, but also produce catalysts with catalytic properties that are not accessible using the pure metals.

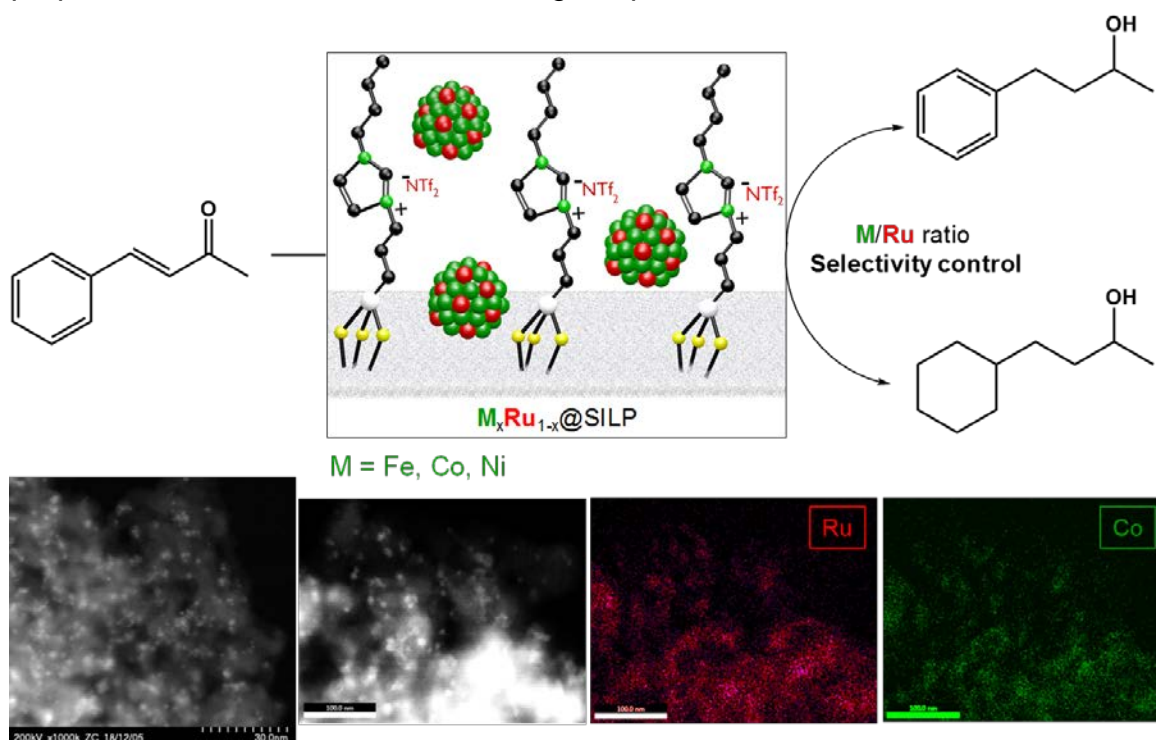


**Figure 1.** Selective hydrogenation of benzilideneacetone using bimetallic  $M_xRu_{1-x}@SILP$  catalysts. Top: illustration of the catalysts and catalytic transformations considered. Bottom: characterization of the catalyst using STEM-HAADF-EDX elemental mapping, example with  $Co_{75}Ru_{25}@SILP$ .

## References

- [1] W. Leitner, J. Klankermayer, S. Pischinger, H. Pitsch, K. Kohse-Höinghaus, *Angew. Chem. Int. Ed.* 2017, 56, 5412-5452.
- [2] A. Riisagera, R. Fehrmanna, M. Haumannb, P. Wasserscheid, *Top. Catal.*, 2006, 40, 91-102.
- [3] a) K. L. Luska, P. Migowski, W. Leitner, *Green Chem.*, 2015, 17, 3195–3206. b) K. L. Luska, P. Migowski, S. El Sayed, W. Leitner, *Angew. Chem., Int. Ed.* 2015, 54, 15750–15755.
- [4] K. L. Luska, A. Bordet, S. Tricard, I. Sinev, W. Grunert, B. Chaudret, W. Leitner, *ACS Catal.* 2016, 6, 3719-3726.

# Alkylation of Cyclododecanone with Allyl Acetate in Presence of CuO as Radical Initiator

*Hanan Atia<sup>1</sup>, Angela Köckritz<sup>1</sup>, Reinhard Eckelt<sup>1</sup>, Oskar Koch<sup>2</sup>, Peter Esser<sup>2</sup>,  
Johannes Panter<sup>2</sup>, Wolfgang Baumann<sup>1</sup>*

*<sup>1</sup>Leibniz-Institut für Katalyse, Rostock, Germany;*

*<sup>2</sup> Symrise AG, Holzminden, Germany*

## Introduction

The synthesis of 2-[3-(hydroxy)propyl] cyclododecanone (CDDPOH) can be carried out by alkylation of cyclododecanone (CDD) with allyl alcohol (AIOH) in the presence of DTBP as initiator [1]. CDDPOH is the first intermediate for producing the musky fragrance Globalide. A problem occurring with AIOH is its tendency to polymerize. Therefore, an excess amount of CDD is used in order to achieve complete conversion of AIOH and to minimize undesired CDD side products. In this work, allylacetate (AIAC) was applied for the alkylation of CDD instead of allyl alcohol to obtain CDDPA [2]. The processing was carried out by continuous dosing of AIAC over time in such a manner, that always a relatively low local concentration of AIOH was present in the reaction mixture. This method has two advantages: the AIAC concentration was always low over the whole experiment which minimized the formation of unwanted by-products. Furthermore, it was possible to work at higher reaction temperatures with increased reaction rates. CuO was found to be active, stable at high temperatures, cheap and also re-oxidizable by air, therefore, it was selected for the experiments.

## Experimental

CuO initiators were prepared from two different precursors, Cu(OH)<sub>2</sub> and CuCO<sub>3</sub> and calcined at different temperatures (400 °C and 650 °C). The CuO was labelled as CuO-400 (C), in which 400 indicates the calcination temperature and (C) or (H) the carbonate or hydroxide precursor used. The reaction was done at atmospheric pressure in a 3-necked round bottom flask (250 ml) .182 g of CDD was placed in the flask and the system was heated up to 180 °. Then the CuO initiator was added. The initial concentration for all the experiments was kept constant by feeding 2 mL of the required amount of AIAC with a rate of 1 mL/min. The remaining amount of AIAC was added over 6 hours with a rate of 67 µL/min (final ratio CDD/AIAC=4:1).

## Results and discussion

The surface areas of the prepared CuO (C) calcined at 400 and 650 °C were found to be 10.5 and 3.9 m<sup>2</sup>/g, respectively. The TPR profiles of CuO-400 (C), CuO-600 (C) and CuO-650 (H) (see Fig.1) demonstrated that the calcination at higher temperatures led to the formation of larger particles which required higher reduction temperatures. SEM pictures showed that the surface of CuO-400 (C) is finely structured (see Fig.2a), while larger CuO crystallites are formed on calcination at 650 °C (see Fig.2b).

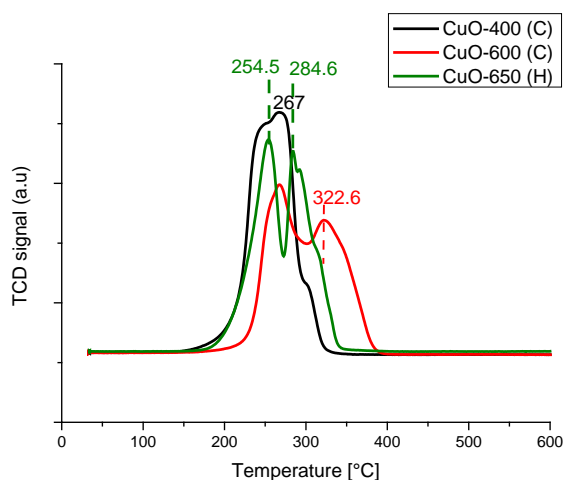


Fig.1: TPR profiles of CuO calcined at different temperatures

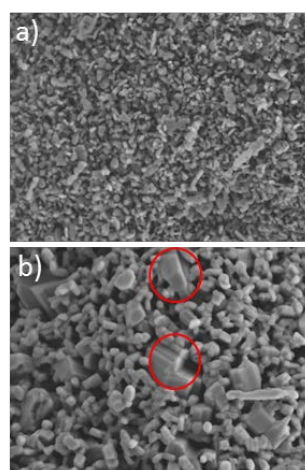
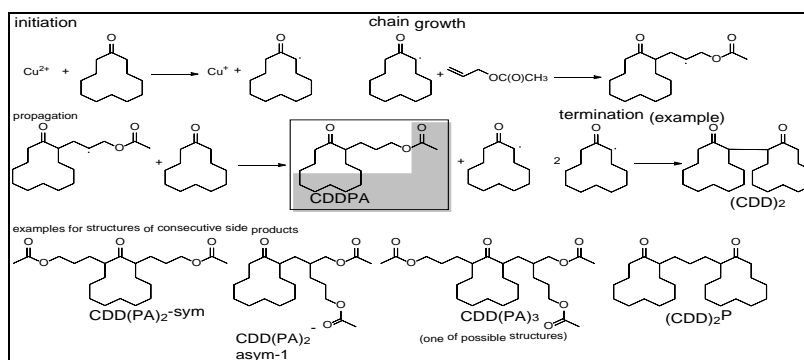


Fig.2: SEM images (20.000x) of CuO prepared from copper carbonate calcined at a) 400 and b) 650 °C

The possible steps for CDDPA formation and by products are shown in Scheme 1. The best result with 76% selectivity to CDDPA and 21% CDD conversion was obtained using CuO-400 (C) with the highest available surface of the prepared copper oxides. Optimal amount of CuO determined by its surface area, CDD:AlAc ratio, and feeding rate of AlAc are crucial parameters to achieve high yields of CDDPA.



Scheme 1: Cu<sup>2+</sup>-initiated radical reaction of CDD and AlAc, reaction steps and product spectrum.

## References

- [1] A. Krempel, O. Koch, H. Erfurt, EP 0926122 (10/12/1998).
- [2] A. Köckritz et al., Eur. J. Inorg. Chem. 2018, 2776.



# Aminotriazole Mn (I) Complexes as Cheap and Efficient Catalyst for Reducing Reactions

Oriol Martínez-Ferraté,<sup>1,2</sup> Giancarlo Franciò,<sup>2</sup> Christophe Werlé,<sup>1</sup> Walter Leitner<sup>1,2</sup>

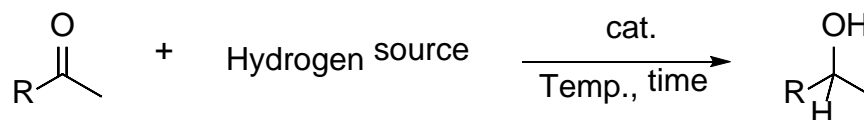
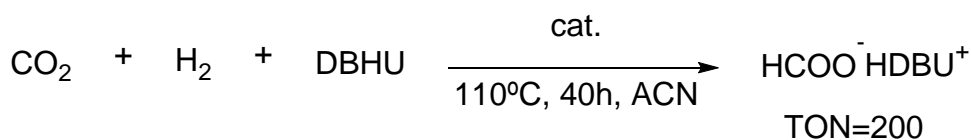
<sup>1</sup> Institute of Technical and Macromolecular Chemistry, RWTH Aachen University,  
Worringerweg 1, 52074 Aachen, Germany

<sup>2</sup> Max-Planck-Institute for Chemical Energy Conversion, Stiftstraße 34-36, 45470  
Mülheim an der Ruhr, Germany

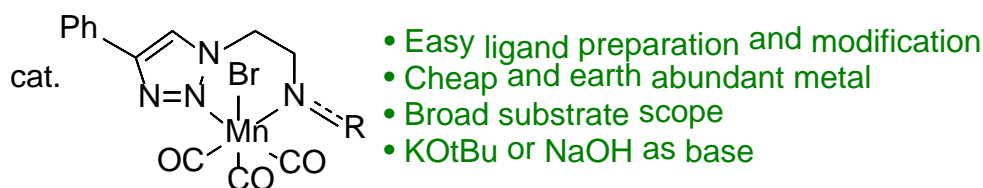
The efficient use of environmentally friendly catalysts to promote new chemical transformations certainly follows some aspect of green chemistry and thus is highly desirable.[1] Hence, the usage of manganese is beneficial. Recently, Mn complexes demonstrated the aptitude to catalyze a wide range of reactions (i.e., transfer hydrogenation, hydrogenation of carbon dioxide or N-alkylation of amines with alcohols) in good yields.[2] Therefore, the improvement of catalytic activity constitutes an important challenge. The development of new triazole-based ligands through click-chemistry constitutes a promising way to enhance the catalytic activity as a whole because of the high tunability, and flexibility of the synthetic route.[3]

Herein, we present the synthesis and catalytic performance of a series of aminotriazole Mn-based complexes with different ligand denticity and donor atoms (NN, NNO, NNP) toward carbonyl and CO<sub>2</sub> reduction.

The obtained results show the aptitude of these complexes to reduce CO<sub>2</sub> to formate in the presence of DBU with turnover numbers up to 200 without further additives. Furthermore, these complexes reduced a wide range of ketones to the corresponding alcohols by transfer hydrogenation or hydrosilylation. For both catalytic systems, alcohols were obtained in moderate to high yields under mild conditions (transfer hydrogenation: 80°C, 20h, and 3% catalyst loading, hydrosilylation: 80°C, 1h, and 0.25% of catalyst loading). Interestingly, the catalytic system shows good functional group tolerance for both reducing methods.



Hydrogen source = *i*PrOH, PhSiH<sub>3</sub>



## References

List and number all bibliographical references at the end of the paper. When referenced within the text, enclose the citation number in square brackets, i.e. [1]

[1] (a) P. T. Anastas and M. M. Kirchhoff, *Acc. Chem. Res.*, 2002, **35**, 686-694. (b) J. A. Linthorst, *Found. Chem.*, 2009, **12**, 55-68. (c) P. Anastas and N. Eghbali, *Chem. Soc. Rev.*, 2010, **39**, 301-312.

[2] (a) A. Dubey, L. Nencini, R. R. Fayzullin, C. Nervi and J. R. Khusnutdinova, *ACS Catal.*, 2017, **7**, 3864-3868. (b) J. R. Carney, B. R. Dillon and S. P. Thomas, *Eur. J. Org. Chem.*, 2016, **2016**, 3912-3929. (c) M. Garbe, K. Junge and M. Beller, *Eur. J. Org. Chem.*, 2017, **2017**, 4344-4362.

[3] (a) R. J. Detz, S. A. Heras, R. de Gelder, P. W. N. M. van Leeuwen, H. Hiemstra, J. N. H. Reek and J. H. van Maarseveen, *Org. Lett.*, 2006, **8**, 3227-3230. (b) E. M. Schuster, M. Botoshansky and M. Gandelman, *Organometallics*, 2009, **28**, 7001-7005. (c) M. E. Garner, W. Niu, X. Chen, I. Ghiviriga, K. A. Abboud, W. Tan and A. S. Veige, *Dalton Trans.*, 2015, **44**, 1914-1923. (d) M. Valencia, H. Muller-Bunz, R. A. Gossage and M. Albrecht, *Chem. Commun.*, 2016, **52**, 3344-3347.

# Temperature switchable Rh@SILP catalyst for the selective hydro(deoxy)genation of aromatic ketones

Gilles Moos,<sup>[a]</sup> Alexis Bordet,<sup>[a]</sup> Walter Leitner<sup>[a,b]</sup>

[a] Max Planck Institute for Chemical Energy Conversion, Mülheim an der Ruhr,  
Germany;

[b] Institute for Technical and Macromolecular Chemistry, Aachen, Germany

Hydrodeoxygenation reactions were identified as key transformations in the production of fine chemicals, and during the process of converting renewable resources to value added chemicals and tailor-made biofuels.<sup>[1]</sup>

To efficiently catalyze the consecutive hydrogenation and deoxygenation steps, the combination of a metal catalyst and an acid catalyst is typically required. Our group has recently shown that metal nanoparticles – especially ruthenium and iron-ruthenium nanoparticles – immobilized on acid functionalized supported ionic liquid phases (SILP) are efficient catalysts for this transformation.<sup>[2-4]</sup> Besides the well-known benefits of SILP supports, the above mentioned catalytic systems possess the advantage of bringing the metal sites and the acid sites (sulfonic acid functionalized imidazolium ionic liquid) in close proximity on a single support, which was demonstrated to be the key to high hydrodeoxygenation activities.<sup>[3,4]</sup>

Herein, we report the synthesis of rhodium nanoparticles on a triphenylphosphonium-based SILP (Rh@SILP(Ph<sub>3</sub>-P-NTf<sub>2</sub>), see Figure 1), and were initially aiming for the deep hydrogenation of aromatic ketones. Phosphonium-based ILs and SILPs indeed represent an interesting alternative to imidazolium-based systems, due to their comparatively low production costs, and their high thermal and chemical stabilities (lack of acidic proton). Interestingly, besides the expected hydrogenation activity, the resulting Rh@SILP(Ph<sub>3</sub>-P-NTf<sub>2</sub>) catalyst was also found to possess excellent activity for the hydrodeoxygenation of aromatic ketones under mild reaction conditions although no acid was added and no residues from reduction agents were present.<sup>[5]</sup> In addition, we show that the product selectivity can be easily switched between the hydrogenated and the hydrodeoxygenated products by modifying the reaction

conditions. Control experiments evidenced that neither RhNPs stabilized on imidazolium-based SILPs nor Ru@SILP(Ph<sub>3</sub>-P-NTf<sub>2</sub>) displayed a significant hydrodeoxygenation activity even at high temperatures. These results suggest that a specific interaction between the RhNPs and the phosphonium-based SILP is giving rise to this unexpected reactivity. The Rh@SILP(Ph<sub>3</sub>-P-NTf<sub>2</sub>) catalyst could be reused at least six times without any loss of activity and was applied to the hydrogenation/hydrodeoxygenation of a range of substituted benzylic and non-benzylic aromatic ketones.

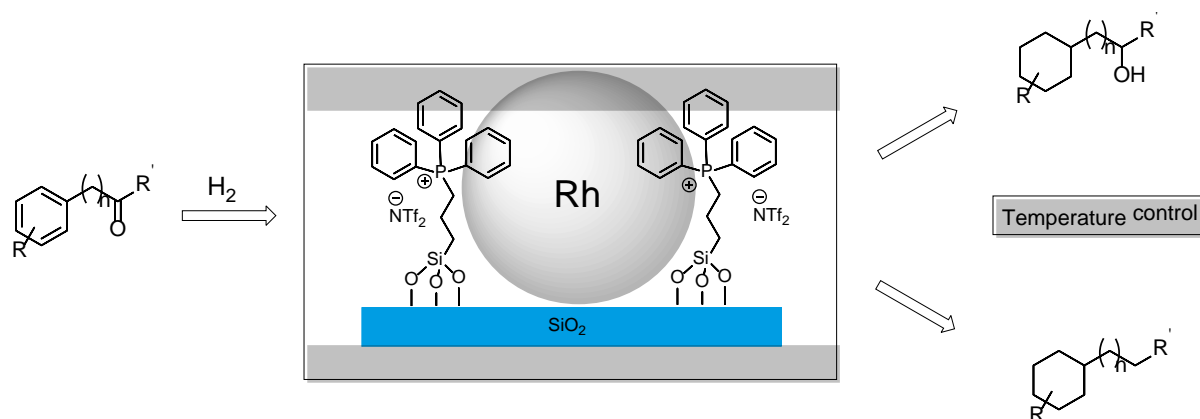


**Figure 1:** Catalytic hydro(deoxy)genation using rhodium nanoparticles stabilized on a triphenylphosphonium-based supported ionic liquid phase (Rh@SILP(Ph<sub>3</sub>-P-NTf<sub>2</sub>)).

## References

- [1] Y. Nakagawa, S. Liu, M. Tamura, K. Tomishige, *ChemSusChem*. **2015**, *8*, 1114.
- [2] K. L. Luska, J. Julis, E. Stavitski, D. N. Zakharov, A. Adams, W. Leitner, *Chem. Sci*. **2014**, *5*, 4895.
- [3] K. L. Luska, P. Migowski, S. El Sayed, W. Leitner, *Angew. Chem. Int. Ed*. **2015**, *54*, 15750.
- [4] L. Offner-Marko, A. Bordet, G. Moos, S. Tricard, S. Rengshausen, B. Chaudret, K. L. Luska, W. Leitner, *Angew. Chem. Int. Ed*. **2018**, *57*, 12721.
- [5] A. Banerjee, R. W. J. Scott, *Green Chem.*, **2015**, *17*, 1597.

# Direct conversion of bio renewable limonene into a fragrance acetal via tandem hydroformylation/acetalization

*Gabriel M. Vieira\**, Amanda C. Monteiro, Elena V. Gusevskaya, Eduardo N. dos Santos

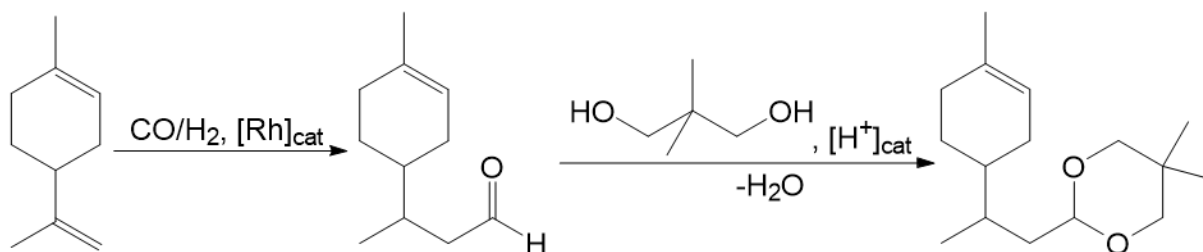
*Universidade Federal de Minas Gerais, Belo Horizonte, Brazil*

*\*gabrielmatosvieira@yahoo.com.br*

## 1. Introduction

Aldehydes are a versatile class of compounds that can be used as synthetic precursors of numerous useful derivatives. An efficient way of obtaining aldehydes is the rhodium catalyzed olefin hydroformylation, which can be associated in sequential reactions (tandem catalysis) resulting in aldehyde derivatives in a single operation [1]. If optimized, tandem catalysis can improve the yields of the desired products with no need of purification steps between the two transformations [2-3].

In this work, we present the tandem sequence hydroformylation/cyclic acetalization of the naturally occurring limonene with the commodity diol neopentyl glycol, to obtain a cyclic acetal (Scheme 1). The product is useful as fragrance [4].



Scheme 1

## 2. Results and Discussion

The catalytic system employed was [Rh(cod)(OMe)]<sub>2</sub> / PPh<sub>3</sub> / pyridinium p-toluenesulfonate. The reaction parameters studied were: temperature, acid catalyst concentration and diol:olefin molar ratio (Table 1). Increasing the temperature from 80 °C to 120 °C resulted in a higher conversion of the substrate into the aldehyde, and also improved the formation of acetal. Increasing the acid:Rh molar ratio from 5 to 10 resulted in a much higher yield of acetal. Surprisingly, it also improved the hydroformylation step, with a higher substrate conversion after 24 h. A further

increase in the molar ratio to 20 did not improve the yield. Decreasing the limonene:diol to 1:1 resulted in a strong decrease in the acetalization. In a molar ratio of 2:1, however, almost all the aldehyde was converted into acetal. Surprisingly, the yield was better than for the ratio 3:1 (c.f. entry 1), probably due to the deceleration of the hydroformylation step in higher concentrations of diol.

Table 1 - Hydroformylation/acetalization of limonene with neopentyl glycol<sup>a</sup>

Entry	T /°C	PyH <sup>+</sup> :Rh	diol:limonene	%Conv.	% Yield		acetal: aldehyde.
					Aldehydes	Acetals	
1	80	5	3	79	31	46	1.5
2	100	5	3	94	11	83	7.5
3	120	5	3	99	2	97	48.5
4	80	10	3	91	0	91	-
5	80	20	3	89	0	89	-
6	80	5	1	87	79	8	0.10
7	80	5	2	91	2	89	44.5

<sup>a</sup>limonene (10 mmol), [Rh(cod)(OMe)]<sub>2</sub> (0.005 mmol), PPh<sub>3</sub> (0.1 mmol), PyH<sup>+</sup>TsO<sup>-</sup>, THF (17.5 mL), 40 bar (1 CO:1 H<sub>2</sub>), 24 h.

### 3. Conclusion

The fragrance acetal derived from neopentyl glycol and limonene can be obtained via tandem hydroformylation/acetalization in good yields. The optimization of the reaction parameters is not straightforward and this work enlightened some of its aspects.

### Acknowledgements

CNPq, INCT Catalysis for financial support.

### References

- [1] R. Franke et al. Applied Hydroformylation, 2012, 112 (11), p. 5675.
- [2] S.R. Khan, B. M. Bhanage. Tetrahedron Letters, 2013, 54 (45), p. 5998.
- [3] J. Mormul et al. ACS Catalysis, 2016, 6 (5), p. 169.
- [4] P.D. Lappe, et al. European Patent EP1316553A1, 2005.

## **Conversion of ethanol over copper based catalytic systems.**

*G. Pampararo, G. Garbarino, P. Riani, E. Finocchio, G. Busca, DCCI, DICCA and DIFAR, University of Genova, Italy; M. Villa García, V. Sanchez Escribano, Departamento de Química Inorgánica, Universidad de Salamanca, Spain.*

### **Introduction**

Ethanol produced by fermentation of lignocellulosics is expected to become a primary intermediate in the new industrial organic chemistry based on renewables. Many efforts are in progress for obtaining new nano-structured catalysts. In particular, many studies are dealing with the manufacture of acetic acid, ethylacetate, acetone, 1-butanol, butadiene, isobutene, by single step processes starting from (bio)ethanol. Among the secondary intermediates, (bio)acetaldehyde may play a relevant role since it has been recognised as one of the main intermediate for the production of several industrial chemicals [1]. For the dehydrogenation of alcohols into carbonyl compounds, systems such as Cu-ZnO, Cu-SiO<sub>2</sub>, Cu-Al<sub>2</sub>O<sub>3</sub>, Cu-ZnO-Al<sub>2</sub>O<sub>3</sub>, Cu-MgAl<sub>2</sub>O<sub>4</sub> have often been studied. For instance, zinc aluminate spinel is an active catalyst for converting ethanol, but it lacks selectivity, achieving only an acetaldehyde yield near 50% [2]. Calcined Mg-based hydrotalcite revealed some selectivity to acetaldehyde but also the production of acetone and other ketones [3]. Recently, our group worked on Cu-ZnO-Al<sub>2</sub>O<sub>3</sub> and tested the performances to obtain selectively acetaldehyde [4]. Cu- based catalysts can be applied as catalysts converting ethanol into different categories of chemicals as certainly aldehyde. By tailoring support-metal interaction, acido-basic properties, metal clusters size and metal-support interaction and possibly with the addition of promoters, it would be possible produce also C<sub>4</sub> oxygenates molecules, aromatics and/or hydrocarbons fractions usable into gasoline. The aim of this work is to develop new Cu-based supported catalysts for (bio)ethanol conversion into high added value chemicals.

### **Experimental**

Copper-based catalysts with different Cu loadings (10%, 30%, 50% as  $\text{wt}_{\text{CuO}} \cdot 100 / \text{wt}_{\text{support}}$ ) were prepared by conventional wet impregnation method by using  $\text{Cu}(\text{NO}_3)_2 \cdot 3\text{H}_2\text{O}$  aqueous solution and different support, i.e. ZnAl<sub>2</sub>O<sub>4</sub>, Mg-hydrotalcite and Al<sub>2</sub>O<sub>3</sub>. The synthesized catalyst has been dried for 5 h at 363 K under magnetic stirring and then have been calcined in static air at 773 K for 2 hours.

The fresh catalysts were characterized by XRD, ICP-OES, IR and DR-UV-Vis spectroscopies, FE-SEM microscopy, BET and pore volume measurements. The catalysts have been tested in a fixed bed tubular quartz flow reactor at different ethanol partial pressures and by varying contact time and temperatures [4]. The spent catalysts were characterized by XRD, FE-SEM and DR-UV-Vis. In some cases, in order to evaluate an increase yield in the desired intermediate, dual catalytic bed were used.

### **Results and discussion**

In Figure 1, the microphotographs of the calcined catalysts, acquired with a solid-state detector for backscattered electrons, are reported. It is possible to detect that in all cases copper is both dispersed on the support and partially agglomerated on the surface. Cu/ZnAl<sub>2</sub>O<sub>4</sub> system results to be highly efficient in ethanol dehydrogenation to acetaldehyde with selectivities exceeding 95% at low conversion and lowered at 90% at higher temperatures (88% on 30CuZA). Copper-based catalysts are easily reduced in the reactive atmosphere during ethanol conversion giving rise to the most active species that according to our data are Cu metal nanoparticles supported on Zn-poor sub-stoichiometric spinel particles. Preliminary results on dual catalytic reactors show that a remarkable acetone yield (27%) at intermediate temperature (i.e. 623 K) can be obtained by coupling 30%CuZA with a Mg-based catalyst. Selectivities to C3 and C4 molecules depend on reaction conditions, in particular contact time and reaction temperature, as well as on catalyst composition.



Figure 1: A) Cu/ZnAl<sub>2</sub>O<sub>4</sub>, B) Cu/MgAl<sub>2</sub>O<sub>4</sub>, C) Cu/Al<sub>2</sub>O<sub>3</sub> systems

### **References**

- [1] Sun J., Wang Y., ACS Catalysis 4 (2014) 1078-1090.
- [2] Garbarino G., Riani P., Villa Garcia M., Finocchio E., Escrivano VS, Busca G., Reac Kinet Mech Cat (2018) 124:503–522.
- [3] Phung T.K., Hernández P.L., Busca G., Applied Catalysis A: General 489 (2015) 180–187.
- [4] Garbarino G, Riani P, Villa Garcia M, Finocchio E, Escrivano VS, Busca G, Catalysis Today (2019).



# Mechanisms of Palladium Leaching from Solid Catalysts and Correlation with Reaction Kinetics of Heck Reactions

*C. Gnad, K. Köhler,*

*Technical University of Munich, Department of Chemistry, Lichtenbergstr. 4, 85748 Garching, Germany*

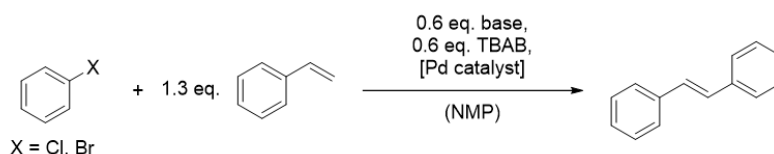
*Technical University of Munich, Catalysis Research Center, Ernst-Otto-Fischer-Straße 1, 85748 Garching, Germany*

## Introduction

Palladium leaching in Heck and Suzuki-reactions with solid catalysts has been a highly discussed topic for more than a decade by now. Initially, effort was put into (and still is) the endeavor to create highly stable and efficient non-leaching catalysts consisting of immobilized Pd species. Very soon, the leaching phenomenon itself became a research issue as e.g. in the early studies by Arai et al.<sup>[1]</sup> and Köhler et al.<sup>[2]</sup> While leaching of palladium into solution (and re-deposition) has been definitively been proven in many experiments, the mechanisms of leaching remain largely unclear in detail. In order to understand the relevant steps of dissolution and re-deposition of palladium during the reaction, the present investigation focused on the correlation of the amount of dissolved Pd species with the conversion of the educt and the yield of the product. Very detailed conclusions became accessible by variation of all relevant parameters. Thus, we applied very different catalysts, from supported palladium oxide particles to isolated structurally well-defined supported palladium complexes prepared by grafting of organometallic precursors.<sup>[3]</sup> In particular, aryl bromides as well as demanding aryl chlorides have been converted in Heck reactions in such a mechanistic study for the first time. The latter allowed investigations spanning very different time scales of few minutes to several hours of reaction time and highly interesting new mechanistic insights.

## Experimental

Different dimethylpalladium(II)-complexes with various backbone ligands were grafted on high-vacuum pretreated SiO<sub>2</sub>. The successful synthesis was confirmed by inert IR spectroscopy and MAS NMR spectroscopy. The synthesized materials were applied in the Heck coupling reaction of bromo- and chlorobenzene with styrene:



The results were compared with classical supported Pd oxide particles. The amount of Pd dissolved into solution was determined parallel to substrate conversion as a function of time varying a number of parameters.

## Results and Discussion

The active species is generated *in situ* by dissolving palladium off the solid catalyst. Kinetic investigations and simultaneous detection of palladium leaching during the coupling reactions revealed different dissolution and reduction mechanisms depending on the applied (pre)catalyst.

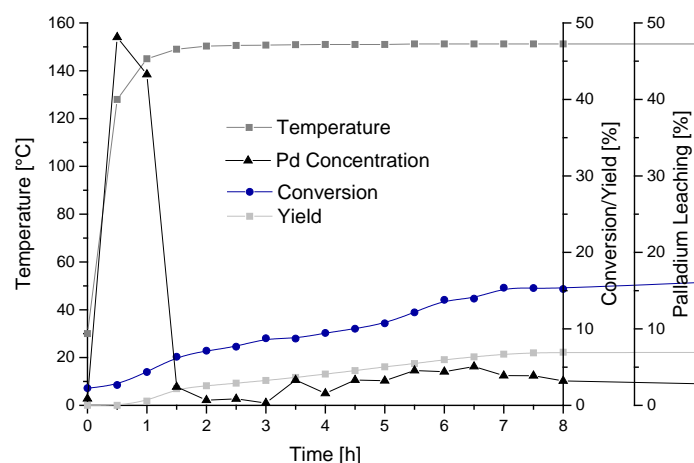


**Figure 1:** Correlation between the amount of dissolved palladium and the conversion of chlorobenzene at 160 °C catalyzed by PdMe<sub>2</sub>(tmeda)/SiO<sub>2</sub> (cut-out of measurements over 30 hours).

The course of the palladium concentration in solution for the grafted catalyst suggests that palladium is dissolved prior to its reduction (Figure 1), whereas for palladium oxide particles the dissolution is directly linked to the start of the reaction. The longer time scale with chlorobenzene as substrate allowed the resolution of different leaching mechanisms during an initial period and the following hours.

## References

- [1] F. Zhao, K. Murakami, M. Shirai, M. Arai, J. Catal. 194 (2000) 479-483; [2] K. Köhler, W. Kleist, S. S. Pröckl, *Inorg. Chem.* **2007**, 46, 1876; [3] C. Copéret, M. Chabanas, R. Petroff Saint-Arroman, J.-M. Basset, *Angew. Chem. Int. Ed.* **2003**, 42, 156.

# Control of Selectivity in the Phenol Oxidation with H<sub>2</sub>O<sub>2</sub> over Multi-dimensional Large-pore Titanosilicates

*Satoshi Inagaki,<sup>1</sup> Mei Takeyama,<sup>1</sup> Ryo Ishizuka,<sup>1</sup> Kai Asanuma,<sup>1</sup> Yoshihiro Kubota<sup>1</sup>*

<sup>1</sup>*Yokohama National University, Yokohama, Japan*

## Introduction

It is well documented that titanosilicates, which contain isolated tetrahedral Ti species in the zeolite framework, are highly efficient catalysts for the selective oxidation of a wide range of organic substrates using hydrogen peroxide as an oxidant [1]. Ti-MCM-68 (**MSE** topology) has been developed as phenol oxidation catalyst showing high activity and selectivity toward *para*-isomer, hydroquinone [2, 3]. In contrast, Ti-beta (**\*BEA** topology) showed almost no conversion of phenol in neat conditions [2]. In this work, we investigated various preparation techniques of \*BEA-type titanosilicates as well as their catalytic properties for the phenol oxidation with H<sub>2</sub>O<sub>2</sub> in the presence of cosolvent.

## Experimental

[Ti]-beta catalysts were obtained by the post-synthetic modification of framework Al of Al-beta into Ti via the acid treatment (dealumination) and the following vapor-phase TiCl<sub>4</sub> treatment. The hydrothermal synthesis of Al-beta was performed with [4, 5] or without [6] the aid of tetraethylammonium (TEA) cations; the former and the latter are designated as Al-beta\_TEA and Al-beta OSDAF, respectively. On only Al-beta OSDAF, steaming at 500°C was performed before acid treatment in order to stabilize the framework [6]. The prepared Al-beta samples were treated with 13.4 mol L<sup>-1</sup> HNO<sub>3</sub> solution under reflux conditions to give dealuminated samples. For Ti-insertion, each sample was exposed to a flow of argon (30 mL min<sup>-1</sup>) bubbled through a vessel containing TiCl<sub>4</sub> maintained at room temperature. And then, TiCl<sub>4</sub> flow was continued for 1 h at 600°C. The Ti-modified samples were further calcined at 650°C for 4 h ([Ti]-beta\_TEA, and [Ti]-beta OSDAF).

## Results and Discussion

All the as-synthesized products possessed \*BEA framework without any impure phases, as confirmed by powder X-ray diffraction. After calcination and subsequent dealumination treatments, the framework structures remained unchanged. UV-vis spectra of Ti-beta samples showed a sharp peak at ca. 210 nm (due to tetra-

coordinated Ti) with broad shoulder peaks at 250–290 nm (assignable to penta- and/or hexa-coordinated Ti species). This means that most of Ti atoms can be incorporated into the \*BEA framework via vapor-phase TiCl<sub>4</sub> treatment at 600°C.

Table 1 lists the results of phenol oxidation with H<sub>2</sub>O<sub>2</sub> over titanasilicate catalysts prepared in this work. The total yields in the reaction over [Ti]-beta catalysts prepared via post-synthetic TiCl<sub>4</sub> treatments were significantly greater than that over conventional Ti-beta. All [Ti]-beta catalysts exhibited greater *ortho*-selectivity compared with TS-1. Table 1 also lists typical results for phenol oxidation over titanasilicate catalysts in the presence of ethanol (EtOH) as a cosolvent. For example, the use of EtOH in the [Ti]-beta\_OSDAF system resulted in 77.5 % of *para*-selectivity. This improvement may be caused by lower opportunity of *ortho*-hydroxylation on the external tetrahedral Ti sites of [Ti]-beta due to coverage by alcohols. As another factor, [Ti]-beta could allow interaction between EtOH and Si-OH on the surface of micropores within the catalysts, leading to enhancement of steric restriction within 12-ring micropores. These factors can make shape-selective reactions more likely to occur over the [Ti]-beta catalysts.

Table 1: Phenol oxidation over titanasilicate catalysts with the addition of ethanol as a cosolvent

Catalyst	Ti content (mmol/g)	Cosolvent	TON <sup>a</sup>	Yield (%)				<i>p</i> -Sel. (%) <sup>b</sup>	H <sub>2</sub> O <sub>2</sub>	
				Total	HQ	CL	<i>p</i> -BQ		Conv. (%)	Eff. (%) <sup>c</sup>
[Ti]-beta_OSDAF	0.272	Neat	68	8.1	1.4	5.0	1.7	38.1	22.9	34.4
[Ti]-beta_OSDAF	0.272	EtOH	36	4.5	1.1	1.0	2.4	77.5	8.3	53.2
[Ti]-beta_TEA	0.286	Neat	64	8.4	1.4	4.4	2.6	47.9	34.7	23.4
[Ti]-beta_TEA	0.286	EtOH	22	3.0	0.7	0.7	1.5	75.2	15.8	18.1
TS-1	0.373	Neat	90	15.2	8.6	6.6	<0.1	56.8	–	–
TS-1	0.373	EtOH	27	4.8	3.5	1.4	<0.1	71.9	–	–

a. Turnover number, (HQ + CL + *p*-BQ)-mol/Ti-mol.

b. *para* Selectivity = (HQ+*p*-BQ)-mol/(HQ+CL+*p*-BQ)-mol.

c. H<sub>2</sub>O<sub>2</sub> efficiency = (HQ+CL+*p*-BQ)-mol/(H<sub>2</sub>O<sub>2</sub> converted)-mol.

Reaction conditions: catalyst, 20 mg; phenol, 21.25 mmol; H<sub>2</sub>O<sub>2</sub>, 4.25 mmol; EtOH (cosolvent), 4.0 g; temperature, 70°C; time, 60 min.

## References

- [1] (a) B. Notari, *Adv. Catal.*, 41 (1996) 253; (b) P. Wu, T. Tatsumi, *Catal. Surv. Asia*, 8 (2004) 137.
- [2] Y. Kubota, Y. Koyama, T. Yamada, S. Inagaki, T. Tatsumi, *Chem. Commun.* (2008) 6224.
- [3] S. Inagaki, Y. Tsuboi, M. Sasaki, K. Mamiya, S. Park, Y. Kubota, *Green Chem.*, 18 (2016) 735.
- [4] R. Nakao, Y. Kubota, N. Katada, N. Nishiyama, K. Kunimori, K. Tomishige, *Appl. Catal. A*, 273 (2004) 63.
- [5] F. Vaudry, F. D. Renzo, P. Espiau, F. Fajula, *Zeolites*, 19 (1997) 253.
- [6] Y. Kubota, K. Itabashi, S. Inagaki, Y. Nishita, R. Komatsu, Y. Tsuboi, S. Shinoda, T. Okubo, *Chem. Mater.*, 26 (2014) 1250.

# ODH of ethane on Orthorhombic MoV-based catalysts: the key aspect is the control of the olefin overoxidation

A. de Arriba<sup>1</sup>, R. Sanchis<sup>2</sup>, D. Delgado<sup>1</sup>, B. Solsona<sup>2</sup>, J.M. López Nieto<sup>1</sup>

<sup>1</sup>*Instituto de Tecnología Química, UPV-CSIC, Valencia, Spain*

<sup>2</sup>*Department of Chemical Engineering, Universitat de Valencia, Valencia, Spain*

## Introduction

With the declining use of oil derivatives as fuels, Petrochemistry is expected to grow in importance. Currently, ethylene is the main feedstock in Petrochemistry but is produced through “steam cracking”, a very energy consuming process [1]. Oxidative dehydrogenation of ethane into ethylene is a promising alternative much more efficient in the energetic aspect. Most promising catalysts for this reaction contain MoVTeNbO oxides with an orthorhombic phase, named as M1 [2] whereas standard bimetallic MoV catalysts present poor performance [3]. In this work, it is seen that bimetallic Mo-V-oxide catalyst can drastically improve the selectivity to ethylene if an orthorhombic structure is synthesized. In addition, the influence of the composition and surface characteristics of MoVO, MoVTeO and MoVTeNbO catalysts, presenting M1 crystalline phase, on catalytic performance is discussed.

## Experimental

Catalysts, i.e. *MoV-nc*, *MoV(M1)*, *MoVTe(M1)* and *MoVTeNb(M1)*, have been synthesized by the hydrothermal method [2]. They have been characterized by XRD, H<sub>2</sub>-TPR, Raman, FT-IR, TEM and N<sub>2</sub> adsorption. Ethane (5%), oxygen (5%) and helium (90%) have been fed to a fixed bed reactor filled with different amounts of catalysts. The flow used varied from 25 to 100 ml/min (0.300 g of catalyst). The reaction temperature studied ranges from 325 to 400°C.

## Results and discussion

Although there are differences among the catalysts regarding both the angle and the intensity of some diffraction peaks, the XRD patterns of *MoV(M1)*, *MoVTe(M1)* and *MoVTeNb(M1)* catalysts evidence in all cases the presence of an orthorhombic structure, whereas *MoV-nc* sample presents low crystallinity (Fig. 1A), with changes in Raman spectra (1B).

The no-crystalline *MoV-nc* sample presents lower selectivity to ethylene, whereas the M1-based samples have shown a high selectivity to ethylene in the ODH of ethane. The differences among the catalysts presenting M1 phase are mainly observed at high conversion, in which MoVTeNb(M1) catalyst presents the highest values; i.e. the selectivity to ethylene still exceeds 90% at ethane conversion of 70% (Fig. 1C). These catalytic results confirm that multicomponent MoVTeNbO catalysts have a very low capacity for activating ethylene (this way avoiding the overoxidation). Interestingly, the catalytic performance of the catalysts tested is mainly due to the better or worse control of the olefin overoxidation, which seems to be the key aspect.

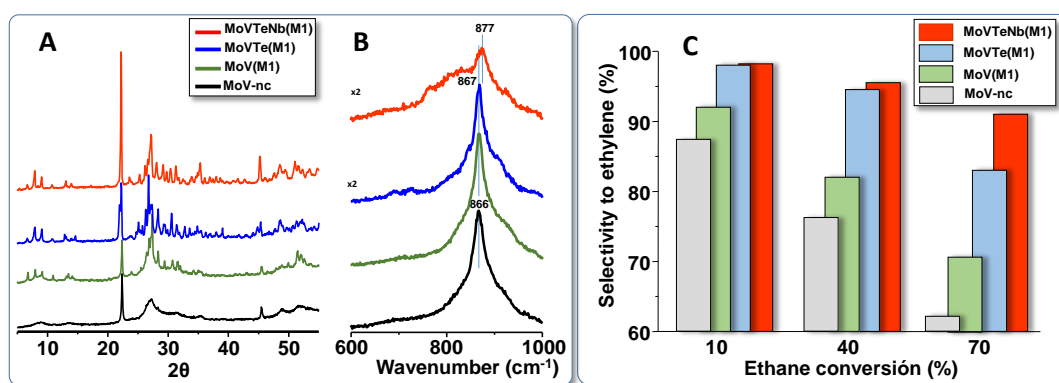


Figure 1. XRD (A) and Raman (A) results of MoV-AM, MoV-M1, MoVTe-M1 and MoVTeNb-M1 catalysts. C) Selectivity to ethylene at different ethane conversions for MoV-based catalysts. Reaction conditions: T= 350-400°C.

We must mention that the orthorhombic *MoV(M1)* catalyst synthesized in this work presents a catalytic performance much better than a standard *MoV* sample with the same composition prepared by co-precipitation as the catalytic activity is ca. 10 times higher and the selectivity to ethylene at isoconversion is ca. 30 points higher.

## Conclusions

MoVO, MoVTeO and MoVTeNbO catalysts with an orthorhombic structure (the so-called M1 phase) are highly selective to ethylene in the ODH of ethane, although MoVTeNbO is the most efficient catalyst (yields > 70%). This is mainly due to its low capacity for activating/decomposing ethylene.

## References

- [1] T. Ren, M.K. Patel, K. Blok, *Energy* 33 (2008) 817.
- [2] J.M. López Nieto, P. Botella, M.I. Vázquez, A. Dejoz, *Chem. Commun.* 17 (2002) 1906.
- [3] B. Solsona, M.I. Vázquez, F. Ivars, A. Dejoz, P. Concepción, J.M. López Nieto, *J. Catal.* 252 (2007) 271.

# Effects of calcium exchanged sites in zeolites KL, NaY and NaX as active sites in ethanol conversion

*J. Alvarez-Rodríguez<sup>1,2</sup>, A. Maroto-Valiente<sup>1,2</sup>, A. Guerrero-Ruiz<sup>1,2</sup>*

*Dpto. de Química Inorgánica y Química Técnica, Facultad de Ciencias, UNED,  
Ciudad Universitaria, 28040 Madrid, España*

*Grupo de Diseño y Aplicación de Catalizadores Heterogéneos, UNED-ICP(CSIC)*

## Introduction

For at least ten years the global capacity of ethanol production is increasing, reached 27 billion gallons at 2017 (Alternative Fuel Data Center, USA). This production capacity may be an opportunity to revalue bioethanol, as this wide commercial availability, as an alternative chemical platform for the synthesis of industrial commodities of greater commercial value such as ethylene, acetaldehyde, diethyl ether, long chain olefins and some aromatic compounds. Among them, forecast for diethyl ether demand is estimated to witness a robust growth, in parallel to pharmaceutical, fragrance and cellulose industry in spite of the fact that a scarce number of works with zeolites as catalytic materials have been reported [1,2]. In this sense, as a part of our research program to explore bioethanol valorisation in zeolite catalytic process [3,4], we present our finding about the effect of calcium in zeolites NaY, NaX and KL on the reaction of bioethanol.

## Experimental

Union Carbide commercial zeolites and prepared by ion exchanged method with calcium of K-L (SK-45), Na-Y (LZY-52) and Na-X (13X) have been used as catalysts. Ion exchanged zeolite were prepared with calcium chloride aqueous solutions. All these samples, parent and exchanged zeolites were dried in air at 388 K for 12h and calcined at 673K for 3 h before their use. All the samples were characterized by chemical analysis (XRF), specific surface area (BET), X-ray diffraction (XRD) and thermal programmed desorption of chemisorbed probe molecule (TPD-CO<sub>2</sub>). A conventional tubular reactor and a mixed gas flux with diluted ethanol (96% Sigma-Aldrich) in helium (99.999% pure, Carbueros Metálicos) were used in the catalytic performance reaction. All the reaction products were characterized in-line by gas chromatography (GC).

## Results and discussion

The chemical analysis by XRF of the exchanged zeolites shows that the calcium exchange degree reached for all the samples is high, expressed as Ca/Al atom ratio has been around 50% in the Ca-KL and close to 90% in the FAU type zeolites. These values evidence a great efficacy of the procedure followed in the exchange treatment. The crystallinity of the parent and exchanged zeolites was verified by XRD diffraction patterns and shows the main diffraction lines of the KL zeolite at  $2\theta = 5.5^\circ$ ,  $19.3^\circ$ ,  $22.6^\circ$ ,  $28.0^\circ$  and  $30.7^\circ$ , NaY at  $2\theta = 9.2^\circ$ ,  $12'6^\circ$ ,  $16'5^\circ$ ,  $24'2^\circ$  and  $27'8^\circ$  and those of the NaX at  $2\theta = 9'92^\circ$ ,  $11'6^\circ$ ,  $15'7^\circ$ ,  $22'4^\circ$  and  $30'0^\circ$ . Regarding to the large calcium amount incorporated to FAU framework by ion exchange method it should be expected an extensive occupancy at the three crystallographic sites (SI', SII, and SIII), while the lower ion exchange degree achieved in Ca-KL zeolite should be related to C and D are the only open countercations positions. These hypothesis for calcium location was reinforce by surface area reduction close to 20% in Ca-exchanged from parents KL and faujasite zeolites.

The catalytic performance results in the conversion of ethanol at 600 K showed as the initial activity of the catalysts decays along time, remained similar of the original zeolites with that of the Ca-exchanged. The main reaction products were in all cases ethylene, acetaldehyde and diethyl ether and the main effect observed on the calcium exchanged samples is an increase in selectivity towards diethyl ether with decrease of selectivity towards ethylene, while that of acetaldehyde is not affected.

## Conclusions

The effect catalytic activity is studied for the chemical revalorization of bioethanol on NaX, NaY and KL and that of calcium exchanged showed ethylene as the main reaction product for all the zeolites, while an increase of selectivity towards diethyl ether is obtained with calcium exchanged ones.

## Funding

Ministerio de Economía, Industria y Competitividad, CTQ2017-89443-C3-1-R.

## References

- [1] Alharbi, W.; Brown, E.; Kozhevnikova, E.F.;Kozhevnikov, I.V.. J. Catal. 2014, 319, 174-181.
- [3] Phung, T. K.; Busca, G.. Chemical Engineering J., 2015, 272, 92-101
- [3] Almohalla, M.; Gallegos-Suarez, E.; Arcoya, A.; Álvarez-Rodríguez, J.; Rodríguez-Ramos, I.; Guerrero-Ruiz, A.. Applied Catalysis A: General, 2017, 535, 61–68.
- [4] Álvarez-Rodríguez, J.; Maroto-Valiente, A.; Guerrero-Ruiz, A.; Arcoya, A.. Catalysts, 2019, submitted.



# GLUCOSE DEHYDRATION TO VALUABLE CHEMICALS OVER FUNCTIONALIZED CARBON CATALYSTS PROMOTED BY CALCIUM CHLORIDE.

Ch. Bounoukta<sup>1,2</sup>, S. Ivanova<sup>1</sup>, F. Ammar<sup>2</sup>, M. A. Centeno<sup>1</sup>, J.A. Odriozola<sup>1</sup>

<sup>1</sup>*Departamento de Química Inorgánica Universidad de Sevilla e Instituto de Ciencia de Materiales de Sevilla, CSIC-US, Avd. Americo Vesputio 49, 41092 Sevilla, Spain*

<sup>2</sup>*LGPC, Department of chemical process engineering, Ferhat-Abbas Sétif-1 University, 19000 Sétif, Algeria*

## INTRODUCTION

Glucose as the monomer of cellulose is the most abundant and low-cost six-carbon monosaccharide that can be used for Biorefinery concepts [1]. With its five hydroxyl and one aldehyde group glucose molecule appears ideal feedstock to synthesize various chemicals and fuels such as furfural, hydroxymethylfurfural (HMF), formic acid (FA), and levulinic acid (LA) [2]. LA synthesis process includes firstly glucose dehydration to HMF as intermediate product, rapidly rehydrated to LA and FA in the presence of acidic catalyst at relatively high temperature. This process also suffers formation of by-products, such humins and other soluble/insoluble polymers, which decrease the reaction yield and provoke catalyst deactivation [3]. So the main challenge in this reaction is to find very selective catalysts unable to form undesired products maintaining high selectivity to LA.

In this study a series of catalysts based on activated commercial carbon DARCO (AC) were developed via functionalization with different agents containing sulfonic group (Brønsted acidic sites) such as sulfuric, sulfalinic and p-toluenesulfonic acid (PTSA) (ACS, ACS-B, AC-PTSA samples respectively). Those samples were used as catalysts for glucose dehydration at 175°C temperature using methyl isobutylketone (MIBK) as organic co-solvents in water/organics phase and calcium chloride as inorganic salt. The later helps to increase the partition coefficient of the  $\alpha$ , D-glucopyranose anomere to  $\beta$ , D-glucopyranose form in aqueous media in order to achieve higher yield of the valuable products [4].

### Catalysts textural properties

Data analysis of the N<sub>2</sub> adsorption/desorption isotherm (shown in table 1) presents the effect of the sulfonation method on the solid's textural properties. According to IUPAC, solids with average pores size > 2nm are classified as mesoporous

materials. In general, an increase the pore size is observed after the functionalization. However the use of sulfalinic and p-toluenesulfonic acid provokes important changes, loss of specific surface and total pore volume. If we compare the size of the introduced functional groups, in the case of ACS-B and AC-PTSA samples two voluminous groups are found  $-C_6H_4-SO_3H$  and  $CH_3-C_6H_4-SO_3H$  whereas for the ACS sample only the  $SO_3H$  group should be present. The difference of the functional groups size can explain the difference observed in the specific area of samples referring to a possible pores blocking by the bulky molecules.

**Table 1: Surface properties of activated and functionalized activated carbon catalysts.**

Samples	Porous Volume ( $cm^3/g$ )	BET surface area( $m^2/g$ )	Average pore size (nm)
AC	0,368	928	4,6
ACS	0,577	959	6,4
ACS-B	0,320	532	6,7
AC-PTSA	0,125	79	14,7

### Catalytic dehydration of glucose to levulinic acid:

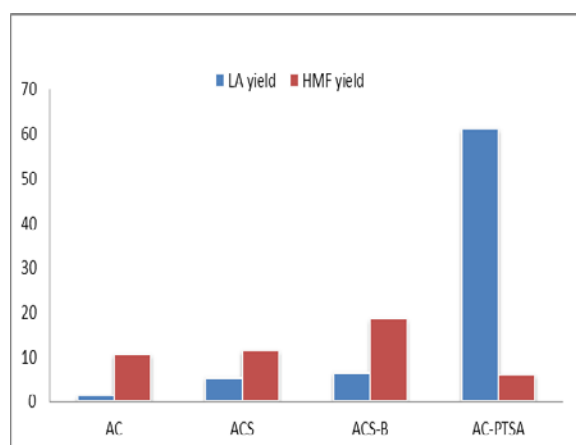


Fig 1. LA and HMF yield for the functionalized carbons in the presence of  $CaCl_2$  (175°C, 2h)

Within the series of functionalized carbons, AC-PTSA sample shows the best selectivity in LA when  $CaCl_2$  is used as Lewis acid sites additive. However the variation of LA yield on the functionalized materials can be considered also a consequence of the porosity difference and Brønsted acid sites number and force. The poor yield of LA for the initial AC catalyst could be explained by the small pores size and  $SO_3H$  groups' absence. Actually

greater the pore size greater the LA yield.

### Conclusion

The introduction of Brønsted acidity improves the glucose dehydration towards LA over the initial materials and a forward addition of Lewis acids like  $CaCl_2$  triples the LA yield. Important influence of pore size is also observed.

### References:

- [1] G P. Perez, A. Mukherjee, M-J Dumont. Journal of Industrial and Engineering Chemistry 70 (2019), P 1-34.
- [2] H. Xin, T. Zhang, W. Li, M. Su, S Li, Q Shao, L. Ma. RSC Adv., 7 (2017), p 41546–41551.
- [3] W. Weiqi, W. Shubin. Fuel 225 (2018), p 311–321
- [4] C. García-Sancho, I. Fúnez-Núñez, R. MorenoTost, J. Santamaría-González, E. Pérez-Inestros, J.L.G. Fierro, P. Maireles-Torres. Applied Catalysis B: Environmental 206 (2017), p 617–625.

# Moving the Mechanism of C-C Coupling Reactions Catalyzed by Palladium Species from the Surface of the Nanoparticles to Homogeneous Species Depending of the Aryl Halide

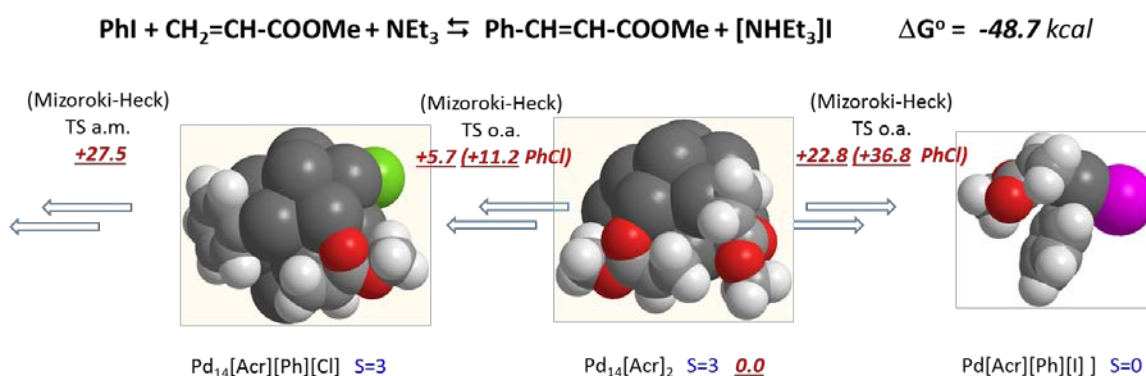
*V. Martinez-Merino, A. Cornejo*

*Dpt. of Sciences - INAMAT, Public University of Navarre, 31006, Pamplona, Spain.  
merino@unavarra.es*

## Abstract

Many C-C coupling reactions catalyzed by homogeneous palladium species have been incorporated in the pharmaceutical industry during the last decades.<sup>1</sup> Using palladium nanoparticles (PdNPs) as catalysts in C-C cross coupling reactions is an exciting new area in industry because of their higher activity and recyclability.<sup>2</sup> However, the nature of the active Pd catalysts in heterogeneous catalysis is still controversial because the reaction could be catalyzed either by solid Pd surface or by leached Pd species whose characterization is a very difficult task.<sup>3</sup> In this context, DFT calculations can shed light on that problem, but all reported mechanistic studies up to date have been performed on homogeneous species including only one or two Pd atoms.<sup>4</sup> Here we present the first DFT study where Pd(0)<sub>14</sub> clusters and Pd(0) leached species are competing as Mizoroki-Heck catalysts.

*Figure:  $\Delta\Delta G^\circ$  (kcal) from B2-PLYP-D including BSSE in DMF*



We have calculated all TS and intermediate structures for the complete catalytic cycles in the Mizoroki-Heck cross-coupling of iodo or chlorobenzene and methyl acrylate (figure), catalyzed both on the surface of a Pd(0)<sub>14</sub> cluster (figure, on the left)

and by Pd(0) leached species (figure, on the right). Structures were optimized at mPW1PW91/Pd(CEP-121G):6-31G(d) level in gas phase at the appropriate spin state and their solvation energies were estimated at the same level by means of SMD method in DMF. Additional single point calculations, at B2PLYP-D high level of theory, were performed including basis set superposition errors. The rate determining step (RDS) in the Mizoroki-Heck cycle was very different in the studied systems. Thus, the RDS was the aryl migration to alkene on surface of Pd(0)<sub>14</sub> cluster (on the left, typical for aryl chlorides), and oxidative addition of PhX to Pd(0) species from leachates (on the right, typical for aryl iodides). It is worth noting that solvation processes in high permittivity solvents favored homogeneous catalysis.

### Acknowledgements

We thank Fundación Caja Navarra-‘La Caixa’, UNED and UPNA for financial support.

### References

- [1] N. Hazari, P. R. Melvin, M. M. Beromi, *Nat. Rev. Chem.* 2017, 1, 0025.
- [2] J. Magano, J. R. Dunetz, *Chem. Rev.* 2011, 111, 2177.
- [3] A. J. Reay, I. J. S. Fairlamb, *Chem. Commun.* 2015, 51, 16289.
- [4] P. Veerakumar, P. Thanasekaran, K.-L. Lu, K.-C. Lin, S. Rajagopal, *ACS Sustainable Chem. Eng.* 2017, 5, 8475.

# Methane and Methanol catalytic oxidation over metal oxides catalysts supported on silica

William Giovanni Cortés-Ortiz<sup>1,2</sup>, José Manuel López Nieto<sup>2</sup>, Benjamin Solsona<sup>3</sup>,  
Carlos Alberto Guerrero-Fajardo<sup>1</sup>

<sup>1</sup> Aprovechamiento Energético de Recursos Naturales; Facultad de Ciencias,  
Universidad Nacional de Colombia, Bogotá, Colombia.

<sup>2</sup> Instituto de Tecnología Química, UPV-CSIC, Valencia, Spain

<sup>3</sup> Department of Chemical Engineering, Universitat de Valencia, Valencia, Spain

## Introduction

Partial oxidation of methane to methanol/formaldehyde in a single catalytic step is one of the most challenging catalytic reactions [1], [2]. However, at the moment low yields to formaldehyde has been reported, although Fe-containing catalysts seems to be the most selective ones [1]–[3]. In this work, silica-supported V and Fe oxides catalysts have been synthesized, characterized and studied in the partial oxidation of methane and methanol to formaldehyde. The catalytic results are discussed in terms of extension of parallel and consecutive reactions.

## Experimental

Catalytic materials of VO<sub>x</sub>, VFeO<sub>x</sub>, VMoO<sub>x</sub>, and VFeMoO<sub>x</sub> oxides supported over silica (with metal charges of 0.5 and 1.5 wt%) were prepared by wet impregnation of ethanolic solutions using amorphous silica as support. The resulting materials were dried and finally calcined at 750 °C for 6 hours. The catalysts were named xV-Si in which *x* indicates the content in wt% of metal or metals. The catalysts characterized by X-ray diffraction (XRD), Raman spectroscopy, UV-Vis spectroscopy, temperature programmed desorption (H<sub>2</sub>-TPR), and SEM-EDX and tested for the partial oxidation of methane and methanol.

## Results and discussion

XRD patterns of the samples indicate a non-crystalline structure in which a broad peak at  $2\theta = 23.0^\circ$  can be seen for all samples. This broad peak at  $2\theta = 23.0^\circ$  corresponds to amorphous silica (JCPDS: 00-002-0242) [1]. However, sample 1.5 VFe-Si showed peaks at  $33.2^\circ$ ,  $35.5^\circ$ ,  $49.6^\circ$ ,  $54.0^\circ$ ,  $62.6^\circ$ , and  $63.9^\circ$  which correspond to iron species, Fe<sub>2</sub>O<sub>3</sub> PDF Card No. 01-072-0469 (JCPDS: 01-072-0469) [4]. However, no crystalline phases were observed in the rest of catalysts,

Raman spectra of catalysts (Fig. 1A) confirm also the absence of crystalline metal oxides, except in the case of 1,5VFe-Si, suggesting the presence of isolated metal oxides species on the surface of the support.

H<sub>2</sub>-TPR results are shown in Figure 1B. It can be seen that peaks at around ca. 480 °C can be related to V-species [5], [6]. In addition, the incorporation of iron favors a shift of the peak at ca. 450 °C assignable to the reduction of Fe<sub>2</sub>O<sub>3</sub> → Fe<sub>3</sub>O<sub>4</sub> or Fe<sub>3</sub>O<sub>4</sub> → FeO [4]. However, the incorporation of Mo shifts the reduction peak to higher temperature.

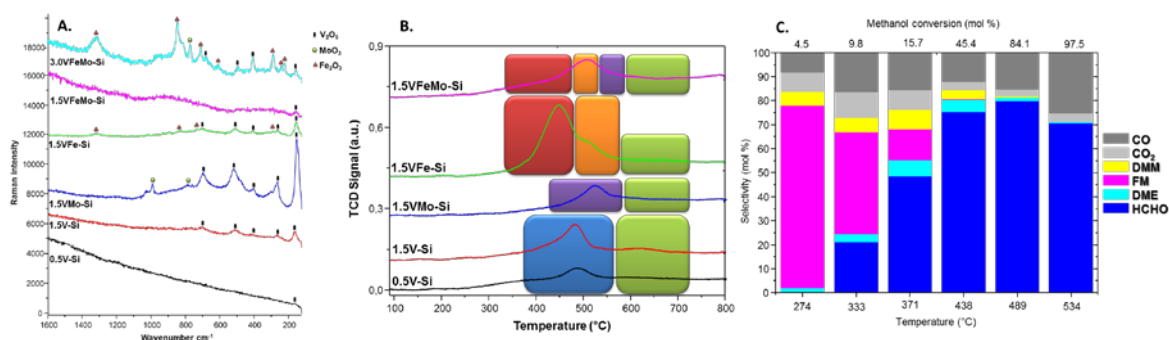


Figure 1. Raman spectra (A), H<sub>2</sub>-TPR profiles (B) of SiO<sub>2</sub> supported catalysts: 0.5V-Si, 1.5V-Si, 1.5VMo-Si, 1.5VFe-Si and 1.5 VFeMo-Si and catalytic results of 1.5 VFeMo-Si (C) (HCHO: formaldehyde, DME: Dimethyl eter, FM: Methyl formate, and DMM: Dimetoxy methane)

Catalytic results for methane partial oxidation suggest the formation of formaldehyde at low methane conversion, but the selectivity decreases when increasing the methane conversion levels. However, in the case of methanol oxidation (Fig. 1C) all the catalysts presented selectivity to formaldehyde higher than those observed for methane oxidation. On the other hand, it has been observed a parallelism between selectivity to formaldehyde from methane and from methanol, suggesting that the reaction rate for formaldehyde formation and formaldehyde combustion during methane oxidation strongly depend on the characteristics of catalysts.

According to these catalytic results the activity for methane oxidation strongly depend on the presence of vanadium and iron species whereas the selectivity to formaldehyde was favored when Fe cations rather than Fe<sub>2</sub>O<sub>3</sub> were incorporated in the catalyst formulation due to their redox properties.

## References

- [1] Q. Zhang, Y. Li, D. An, and Y. Wang, "Catalytic behavior and kinetic features of FeOx/SBA-15 catalyst for selective oxidation of methane by oxygen," *Appl. Catal. A Gen.*, vol. 356, no. 1, pp. 103–111, Mar. 2009.

- [2] C. A. Guerrero-Fajardo, D. Niznansky, Y. N'Guyen, C. Courson, and A.-C. Roger, "Methane selective oxidation to formaldehyde with Fe-catalysts supported on silica or incorporated into the support," *Catal. Commun.*, vol. 9, no. 5, pp. 864–869, 2008.
- [3] W. G. Cortés Ortiz and C. A. Guerrero Fajardo, "Selective catalytic oxidation for methane conversion to methanol: A review," *Cienc. e Ing. Neogranadina*, vol. 28, pp. 45–71, 2018.
- [4] Y. K. Chow, N. F. Dummer, J. H. Carter, C. Williams, G. Shaw, D. J. Willock, S. H. Taylor, S. Yacob, R. J. Meyer, M. M. Bhasin, and G. J. Hutchings, "Investigating the influence of acid sites in continuous methane oxidation with N<sub>2</sub>O over Fe/MFI zeolites," *Catal. Sci. Technol.*, 2017.
- [5] L. Nguyen, S. Loidant, H. Launay, A. Pigamo, J. Dubois, and J. Millet, "Study of new catalysts based on vanadium oxide supported on mesoporous silica for the partial oxidation of methane to formaldehyde: Catalytic properties and reaction mechanism," *J. Catal.*, vol. 237, no. 1, pp. 38–48, 2006.
- [6] I. E. Wachs and B. M. Weckhuysen, "Structure and reactivity of surface vanadium oxide species on oxide supports," *Appl. Catal. A Gen.*, vol. 157, no. 1–2, pp. 67–90, Sep. 1997.

# GOLD CATALYSTS SCREENING FOR REVERSE WATER GAS SHIFT REACTION

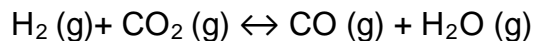
*L. Blandon, S. Ivanova, M.A. Centeno, J.A. Odriozola*

*Departamento de Química Inorgánica Universidad de Sevilla e Instituto de Ciencia de Materiales de Sevilla, CSIC-US, Avd. Américo Vespucio 49, 41092 Sevilla, Spain*

## **Introduction**

With the industrial revolution, the average global carbon dioxide atmospheric concentration and related average temperature increased causing climate changes and arising continuous environmental concerns. In 2013, 32,19 Gt of CO<sub>2</sub> have been emitted in the atmosphere a value expected to increase by the year 2040 to 45Gt [1]. This prognostic urges the research for viable solution and one of the proposed approaches is the use of captured atmospheric carbon dioxide for the production of high added value chemical compounds. Reverse water gas shift (RWGS) reaction is one of the possible routes for CO<sub>2</sub> valorization.

RWGS is an equilibrium limited reaction favored at high temperatures due to its endothermic nature



Usually, supported metals such as Cu, Pt and Rh are used as catalysts for CO<sub>2</sub> hydrogenation [1, 2]. Cu and Pt usually work at low temperature for the gas phase hydrogenation meanwhile Rh is widely used in the homogeneous CO<sub>2</sub> hydrogenation. Few studies consider the use of gold for this reaction, even being one of the metals with great potential for the direct water gas shift reaction [3, 4].

That is why, this work is devoted to the preparation of a series of gold titania supported catalyst with different promoters and the screening of their performance in the RWGS reaction.

## ***Synthesis and characterization of the catalysts***

The commercial TiO<sub>2</sub> (Degussa P25) was used as received or doped with 2 wt% K, Na and Y. Over the support material, 2 wt% gold was deposited using direct anionic exchange method assisted by ammonia [5].

The XRD profiles of the studied solids do not show structural changes of titania phase with the addition of the dopants, and gold signals are absent. The later suggests important dispersion of the gold nanoparticles within the nanometer size as confirmed also by TEM microscopy. However slight influence over the particle size is



observed with the addition of dopants. The presence of sodium increases the mean gold particle size being thus the size fluctuation within the series of catalyst between 2 and 5 nm.

### Catalytic activity

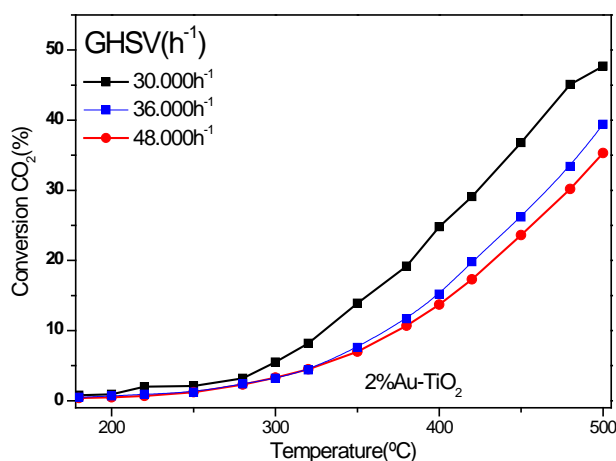
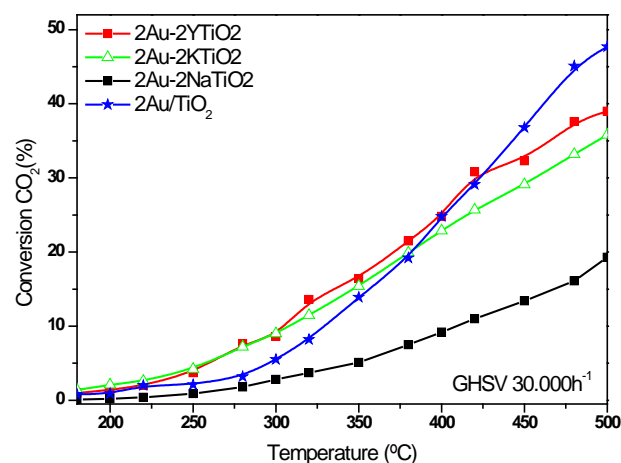


Figure 1. Gold catalyst screening in RWGS reaction CO<sub>2</sub>:H<sub>2</sub> 1:4 and N<sub>2</sub> as balance

Gold metal loading does not influence significantly catalysts behaviour but the presence of dopants and reaction space velocities changes seems to affect it in a great extent (Fig 1.). The presence of K and Y provokes a decrease of gold particle size which reflect in higher activity at low temperature on the contrary to effect provoke by Na.

As for the space velocities, an optimal value of conversion is obtained at gas hour space velocity (GHSV) of 30 000 h<sup>-1</sup>.

### Conclusions

One of the main conclusion of this study is the presence of dopants is beneficial for the gold particles size decrease and reflects in improved catalytic behaviour in the RWGS reaction.

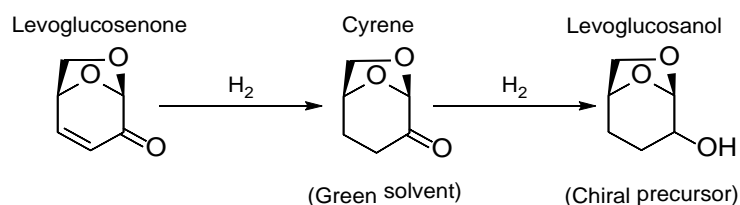
### References:

- [1] Daza, Y.A. and J.N. Kuhn, RSC Advances, 2016. **6** 49675-49691.
- [2] Ronda-Lloret, M; Rico-Frances, S; Sepulveda-Escribano, A; Ramos-Fernandez, E , Appl. Cat. A: General, 2018, 562,28-36
- [3] Bobadilla, LF, Santos, JL, Ivanova, S; Odriozola, JA, Urakawa, A , ACS Catalysis, 2018, 8, 7455-7467.
- [4] Kyriakou, V , Vourros, A , Garagounis, I, Carabineiro, SAC, Maldonado-Hodar, FJ , Mamellos, GE , Konsolakis, M, Cat. Comm., 2017, 98, 52-56
- [5] Ivanova, S., C. Petit, and V. Pitchon, Appl. Cat. A: General, 2004. 267, 191-201.

# Tuning Metal Supported on Zirconia Catalysts for the Selective One-pot Step Hydrogenations of Levoglucosenone

Jaime Mazarío, ITQ (UPV-CSIC), Valencia, Spain; Miriam Parreño, ITQ (UPV-CSIC), Valencia, Spain; Marvin Chávez-Sifontes, ITQ (UPV-CSIC), Valencia, Spain; Rolando Spanevello, IQUIR (UNR-CONICET), Rosario, Argentine; María B. Comba, IQUIR (UNR-CONICET), Rosario, Argentine; Alejandra Suárez, IQUIR (UNR-CONICET), Rosario, Argentine; Marcelo Domine\*, ITQ (UPV-CSIC), Valencia, Spain

Nowadays, lignocellulosic biomass stands out as the only renewable alternative to produce organic chemicals[1]. In this sense, levoglucosenone (Scheme 1) is a cellulose derived chiral synthon widely used in organic synthesis[2]. More recently, the Furacell™ technology, a continuous process to convert cellulosic biomass into levoglucosenone[3], opened the possibility of producing, not only fine, but also commodity chemicals starting from this molecule. Following this idea, Huber and co-workers[4] offered an insight into how to transform this molecule into high added value products such as  $\alpha,\omega$ -diols, monomers of polyesters and polyurethanes. They reported the use of Pd on carbon,  $\text{Al}_2\text{O}_3$  and  $\text{SiO}_2\text{-Al}_2\text{O}_3$  to obtain interesting products via hydrogenation, such as dihydrolevoglucosenone (Cyrene) and levoglucosanol. However, high hydrogen pressures and catalyst loadings, organic solvents, as well as catalytic deactivation remain as disadvantages for these catalytic processes. In this work the adequate combination of the specific metallic species (Pd, Pt) with the adequate support ( $\text{SiO}_2$ ,  $\text{Al}_2\text{O}_3$ ,  $\text{TiO}_2$ ,  $\text{ZrO}_2$ ) is studied to carry out the selective hydrogenation of levoglucosenone to either Cyrene or levoglucosanol (Scheme 1), avoiding the aforementioned drawbacks, while understanding the required physicochemical properties to produce the desired hydrogenated product in highly selective one-pot processes.



Scheme 1. Levoglucosenone and its simplest hydrogenated derivatives.

## Results and Discussion

After screening of different metal supported on metallic oxides catalysts, the results showed that it is possible to carry out the hydrogenation of levoglucosenone to

dihydrolevoglucosenone (Cyrene) in a more efficient and selective way with Pd-based catalysts. Particularly, the Pd/*t*-ZrO<sub>2</sub> (tetragonal zirconia) catalyst was capable to achieve near 95% yield to Cyrene by working under mild reaction conditions (80 °C and P<sub>H<sub>2</sub></sub> = 10 bar), with low catalyst loadings (≈3wt%) and using water as solvent. In addition, the Pd/*t*-ZrO<sub>2</sub> system could be reused after the adequate washing with ethanol/water mixture, achieving almost the same Cyrene yields (≥90%, Fig. 1a).

On the other hand, complete hydrogenation of levoglucosenone to levoglucosanol was attained for the first time in a one-pot process with a Pt-based heterogeneous catalyst (Pt/ZrO<sub>2</sub>-mix, tetragonal/monoclinic zirconia mixture) with high yield (≈90%). This catalytic process becomes a very interesting option to produce this levoglucosenone derivative, due to the low temperatures (45 °C) and mild pressures (P<sub>H<sub>2</sub></sub> = 18 bar) here used (Fig. 1b). The comparison of the results attained with other Pt-supported metallic oxides (TiO<sub>2</sub>, Al<sub>2</sub>O<sub>3</sub>, SiO<sub>2</sub>) let us to conclude that, although not observed for the hydrogenation of levoglucosenone to Cyrene, the Lewis acidity of the catalysts played an important role during the hydrogenation process to give selectively levoglucosanol. Moreover, although Pt/ZrO<sub>2</sub>-mix catalyst clearly deactivated after the first catalytic cycle (due to carbon deposition on catalyst surface), this fact is again totally solved by washing the catalyst with an ethanol/water mixture, thus showing the possible application and scale-up of this catalytic system.

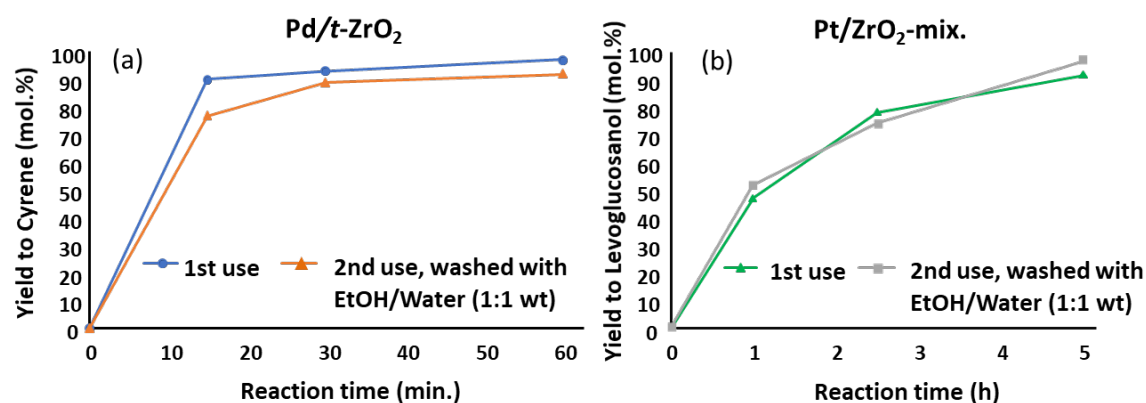


**Figure 1.** Levoglucosenone hydrogenations with (a) Pd/*t*-ZrO<sub>2</sub> and (b) Pt/ZrO<sub>2</sub>-mix. Reaction conditions: (a) 0.13 g levoglucosenone, 0.50 g water, 3.0wt% Pd/*t*-ZrO<sub>2</sub> at 80 °C and P<sub>H<sub>2</sub></sub> = 10 bar, during 60 min. (b) 0.13 g levoglucosenone, 0.50 g water, 25wt% of Pt/ZrO<sub>2</sub>-mix at 45 °C and P<sub>H<sub>2</sub></sub> = 18 bar, during 5 h.

## References

- [1] A. Corma, S. Iborra, A. Velty, *Chem Rev.*, 2007, 107, 2411.
- [2] A.M. Sarotti, M.M. Zanardi, R.A. Spanevello, A.G. Suarez, *Curr. Org. Synth.*, 2012, 9, 439.
- [3] CIRCA GROUP Pty Ltd, US Pat. 0 111 714, 2016.
- [4] J. He, K. Huang, K.J. Barnett, S.H. Krishna, D.M. Alonso, Z.J. Brentzel, S.P. Burt, T. Walker, W.F. Banholzer, C.T. Maravelias, I. Hermans, J.A. Dumesica, G.W. Huber. *Faraday Discuss.*, 2017, 202, 247.

# Identification of active species in graphitic oxide for the initiator and metal free epoxidation of dec-1-ene.

*Samuel Pattisson, David J. Morgan, Graham J. Hutchings*

*Cardiff Catalysis Institute, Cardiff University, Cardiff, United Kingdom*

## Introduction

The selective epoxidation of linear alkenes is of major interest both in academia and industrial synthesis. We have previously shown that graphitic oxide is active for this reaction in the absence of metal or commonly required radical initiators. [1] However, this carbocatalyst demonstrated large fluctuations in activity depending on the amount and type of oxidant used (fig 1a and b). Inactivity was previously thought to be dictated by the presence of both inorganic and covalently bound sulfur species (fig 1c). While the former remains true, the latter appears to be a spectator in this reaction and an artefact of the oxidation. In this study we show that careful removal of all sulfur species allows activity to be correlated with specific oxygen functionality. Over oxidation of this species leads to a lower activity in highly oxidised catalysts.

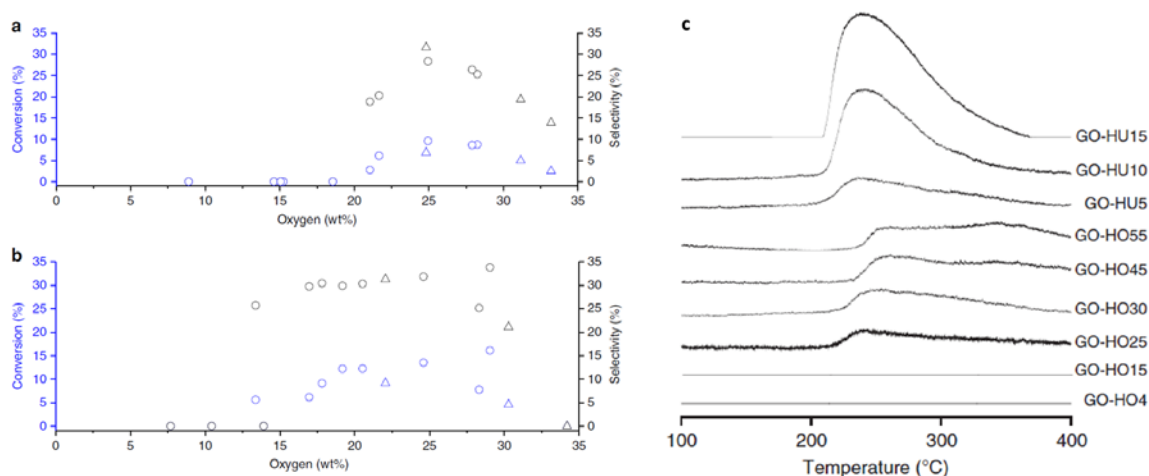


**Figure 1. Activity of graphitic oxide catalysts (a) before and (b) after water washing for epoxidation of dec-1-ene. (90 °C, 48 h, dec-1-ene 10 ml, GO 0.1 g) and (c) TGA-MS m/z 64 (SO<sub>2</sub>)**

## Results and Discussion

As previously described, the activity of these catalysts was found to be influenced by amount and type of oxidant. The optimum catalyst was found to be prepared *via* a modified Hofmann method using 30 g of oxidant per 5 g graphite. In order to assess whether the higher oxidised catalysts were poisoned with organosulfate, catalysts were subjected to a series of washings. After washing in NaOH (0.1 M) the highly oxidised Hummers catalyst remained inactive (table 1). Due to the amount of sodium introduced via this method it was necessary to subsequently wash using a pH

switching method between NaOH and HCl. These catalysts remained inactive despite being free of all sulfur and sodium species. To assess the potential detrimental effect of NaOH on any active species,  $\text{NH}_3\text{OH}$  was also used to completely remove sulfur from both Hummers and Hofmann catalysts. In this case, the Hummers catalyst remained completely inactive. The optimum Hofmann catalyst showed no change in activity before and after removal of organosulfate. This suggests that the organosulfate does not play a role in deactivation of the catalyst and that activity is dictated by the presence of a specific oxygen functionality. In order to investigate this theory a number of experiments were conducted. Firstly, a range of the synthesised carbons were washed with ammonium hydroxide to completely remove the organosulfate, which was confirmed by TGA-MS and XPS. The catalysts were then tested, and activity was correlated with various oxygen functionality according to XPS C1s region. The results suggest that activity is dictated by specific oxygen functionality rather than an overall oxygen abundance as previously suggested. Although low oxidised catalysts are poisoned by inorganic sulfate, it appears that organosulfate on highly oxidised materials does not act as a poison. Inactivity is rather linked to the over oxidation of the surface and changes to the abundance of an active functionality.

**Table 1 Activity of graphitic oxide catalysts before and after various base washings for epoxidation of dec-1-ene. (90 °C, 48 h, dec-1-ene 10 ml, GO 0.1 g)**

	HU15	HU15 NaOH	HU15 NaOH, HCl	HU15 $\text{NH}_3\text{OH}$	HO30	HO30 $\text{NH}_3\text{OH}$
Conversion (%)	0	0	0	0	10.5	10.4
Selectivity (%)	0	0	0	0	27.3	27.5

## Conclusion

The results presented in this study suggest that the commonly used methods for production of graphitic and graphene oxide are not suitable for all applications. For catalytic purposes, specific oxygen functionality should be targeted rather than overall level of oxidation of the surface. The development of new selective oxidation methods is desirable for the production of highly active carbocatalysts for this important reaction.

## References

1. S. Pattison, E. Nowicka, U. N. Gupta, G. Shaw, R. L. Jenkins, D. J. Morgan, D. W. Knight & G. J. Hutchings, Nat. Commun.(2016), 7, 1-9.

# Molecular Catalysts based on Well-defined Metallic Cores as Building Blocks of Catalytic Materials

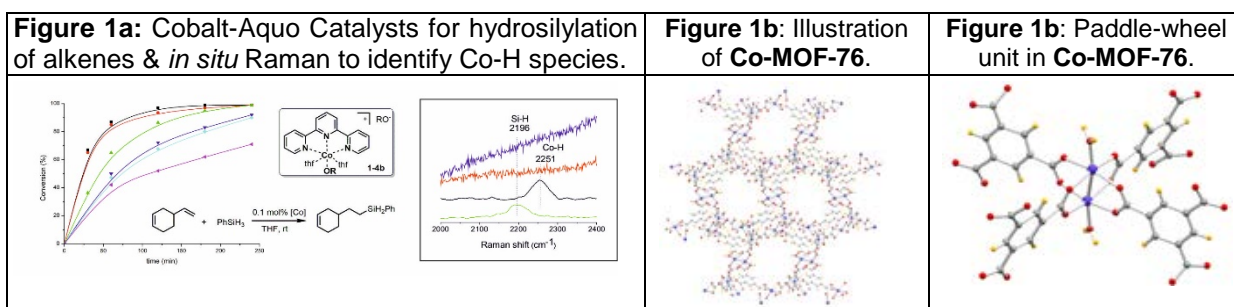
Silvia Gutiérrez-Tarriño,<sup>1</sup> Patricia Concepción,<sup>1</sup> and Pascual Oña-Burgos<sup>1</sup>

<sup>1</sup> Instituto de Tecnología Química, Universitat Politècnica de Valencia Consejo Superior de Investigaciones Científicas, Valencia, 46022, Spain

First, air stable aquo-cobalt catalysts for anti-Markovnikov alkene hydrosilylation have been developed that can be used under aerobic conditions without dry solvents or additives (Figure 1a). These catalysts can be generated from low-cost commercially available precursors. In addition, these catalysts possess good catalytic ability for both hydrosilanes and hydroalcoxysilanes. Finally, a mechanistic study demonstrates the silane and the catalyst generates a Co-H species in the course of the reaction, which has been observed by in-situ Raman spectroscopy.[1]

Secondly, mono-nuclear cobalt complexes have been employed to promote sub-nanometric clusters over activated carbon, which has shown a high efficiency and selectivity to hydrogenation of nitroarenes.[2]

Finally, tetra-nuclear cobalt clusters have been studied as building block of **Co-MOF-76** (Figure 1b), which has analogous structure that Cu-HKUST-1,[3] where Co<sup>2+</sup> ions form dimmers with the well-known paddle-wheel structure (Figure 1c). To the best of our knowledge there is not precedent related to this core structure in MOF based on cobalt. Moreover, **Co-MOF-76** has been evaluated in gas storage and as electrocatalyst in the O<sub>2</sub> evolution reaction (OER).[2]



## References

- [1] Gutiérrez-Tarriño, S.; Concepción, P.; Oña-Burgos, P. *Eur. J. Inorg. Chem.* **2018**, 4867-4874.
- [2] Gutiérrez-Tarriño, S.; Concepción, P.; Oña-Burgos, P. *Paper to submit*.
- [3] Moellmer, J.; Moeller, A.; Dreisbach, F.; Glaeser, R.; Staudt, R., *Microporous and Mesoporous Materials*, **2011**, 138, 140-148.

# **Production of 2-ethyl-1,3-dioxolane-4-methanol by hydrogenolysis of glycerol on molybdenum and iron-molybdenum supported catalysts**

*Camila G. Silva, Fabio B. Passos. Departamento de Engenharia Química e de Petróleo, Universidade Federal Fluminense, Niterói, Brazil.*

## **1- Introduction**

The growth of biodiesel production has resulted in a significant drop in the price of glycerol, which makes it more attractive as a raw material for the chemical industry [1]. The catalytic hydrogenolysis of glycerol to glycols is one of the most attractive route to convert glycerol into high added value products. Some of these products are 1,2-propanediol (1,2-PDO), 1,3-propanediol (1,3-PDO) and ethylene glycol (EG). All are often used as antifreeze, in paints, functional fluids, humectants, and polyester resins and are currently produced from petrochemical resources [2].

In this work, a series of Fe–Mo bimetallic catalysts supported in  $\text{Al}_2\text{O}_3$ ,  $\text{SiO}_2$  and HZSM-5 were prepared and evaluated for the hydroconversion of glycerol.

## **2. Experimental methods**

Mo and Fe catalysts were prepared supported on  $\gamma\text{-Al}_2\text{O}_3$ ,  $\text{SiO}_2$  and HZSM-5 SAR Si/Al 23. Mo catalysts were prepared by the wet impregnation method using  $((\text{NH}_4)_6[\text{Mo}_7\text{O}_{24}]\cdot 4\text{H}_2\text{O})$ . The obtained mixtures were oven dried at 100 °C overnight. The catalysts generated, Mo/ $\gamma\text{-Al}_2\text{O}_3$ , Mo/HZSM-5 and Mo/ $\text{SiO}_2$  were calcined at 500 °C for 2h at a rate of 5 °C/min. FeMo/ $\gamma\text{-Al}_2\text{O}_3$ , FeMo/HZSM-5 and FeMo/ $\text{SiO}_2$  catalysts were prepared from the Mo/ $\gamma\text{-Al}_2\text{O}_3$ , Mo/HZSM-5 and Mo/ $\text{SiO}_2$  catalysts by incipient wetness impregnation method. An iron nitrate precursor mass  $\text{Fe}(\text{NO}_3)_3\cdot 9\text{H}_2\text{O}$  was used sufficient to obtain 2% by weight of Fe in the catalyst. The solutions were impregnated into the respective Mo catalysts. After drying at 100 °C for 12 h, the solids obtained were calcined at 450 °C for 4h at a rate of 5 °C/min.

X-ray diffraction (XRD), Diffuse Reflectance Infra-red Fourier Transform Spectroscopy (DRIFTS) and X-ray photoelectron spectroscopy (XPS) were used to characterize the metal components of the catalysts. Catalytic tests were performed in a 300 mL autoclave reactor (Parr Instrument Co.) The reactor was charged 30 g of glycerol in 120 g of water and 1 g of reduced passivated catalyst at 365 psi  $\text{H}_2$  and 250 °C.

### 3. Results and discussion

Figure 5 shows the conversion and yield for the major liquid products generated in the reaction: propanal, 1,2-propanediol, 2-ethyl-1,3-dioxolane-4-methanol and acetaldehyde after 12 hours of reaction for all catalysts. The conversion was calculated considering both the liquid phase and the gas phase products.

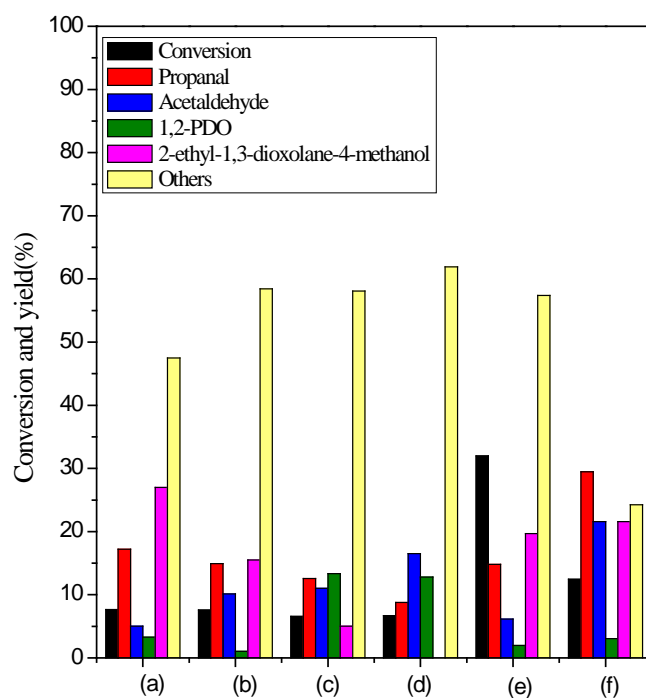


**Figure 1. Comparison of conversion and yield of the main products of the liquid phase: propanal, 1,2-PDO and 2-ethyl-1,3-dioxolane-4-methanol in the hydrogenolysis reaction of glycerol at 250 °C after 12 h of reaction under the catalysts (a) Mo/ $\gamma$ -Al<sub>2</sub>O<sub>3</sub>, (b) FeMo/ $\gamma$ -Al<sub>2</sub>O<sub>3</sub>, (c) Mo/SiO<sub>2</sub>, (d) FeMo/SiO<sub>2</sub>, (e) Mo/HZSM-5 and (f) FeMo/HZSM-5.**

The conversion of glycerol based on the supports increased in the order HZSM-5 >  $\gamma$ -Al<sub>2</sub>O<sub>3</sub> > SiO<sub>2</sub>, which reinforces the fact that hydrogenolysis depends on the presence of OH species on the surface of the catalyst, which may be related to the acidity of the support. 2-ethyl-1,3-dioxolane-4-methanol was one of the main products generated in the reactions, mainly for the catalysts supported in zeolite. This product has higher added value compared to crude glycerol

### References

- [1] A.J. Pamphile-Adrián, P.P. Florez-Rodriguez, M.H.M. Pires, G. Perez, F.B. Passos, *Catal. Today* 289 (2017) 302–308.
- [2] A. Von Held Soares, H. Atia, U. Armbruster, F.B. Passos, A. Martin, *Appl. Catal. A Gen.* 548 (2017) 179–190.



# Conversion of C1 – C2 alcohols into hydrocarbons catalyzed by zeolites

*Zilacleide S. B. Sousa, DPQ/IQ/UERJ, Rio de Janeiro, Brazil; Cristiane A. Henriques, PPGEQ/IQ/UERJ, Rio de Janeiro, Brazil; Victor Teixeira da Silva, PEQ/COPPE/UFRJ, Rio de Janeiro, Brazil.*

Methanol and ethanol are converted into hydrocarbons over zeolites with different pore structure and acid properties at 500 °C and atmospheric pressure. The product distribution and the stability of the catalyst were significantly influenced by the alcohol studied. It can be suggested that these results reflect the difference in the mechanism for hydrocarbons formation.

## 1. Scope

Methanol (MeOH) and ethanol (EtOH) can be converted into hydrocarbons using zeolites as acid catalysts. Zeolites have been widely studied as catalysts for these reactions not only due to their porous structure but also due to their density and strength of acid sites. Both are important factors for the activity, stability, and selectivity of the catalysts. In this work, the conversion of methanol and ethanol into hydrocarbons was studied over zeolites with different pore structure and acid properties.

## 2. Results and Discussion

Table 1 compares MeOH and EtOH conversion and product distribution obtained after 5, 137, and 273 min on stream. It can be observed that under the studied conditions both alcohols are completely converted at the beginning of the reaction. As the reaction proceeds, the catalytic activity of HZSM-5, HMCM-22, and HITQ-2 for MeOH conversion decreases continuously whereas a complete conversion (100 %) of EtOH is observed for the three zeolites during the reaction. Table 1 also shows that the product distribution with time-on-stream is substantially different depending on the alcohol. Comparison of the distribution of the products formed from EtOH over HZSM-5 and HMCM-22 indicates that both C2-C4 olefins and C6+ formation were favored by HZSM-5, while HMCM-22 was highly selective to ethylene (> 90 %). For these two materials, consideration should be given not only to the differences in their acidic properties but also to those related to textural and structural properties to explain the observed differences in the product distribution.

Table 1: Influence of TOS on MeOH and EtOH conversion and product distribution

TOS (min)	Methanol									Ethanol		
	HZSM-5			HMCM-22			HITQ-2			HZSM-5		
	5	137	273	5	137	273	5	137	273	5	137	273
Conv. (% molar)	100	49	41	100	92	80	100	85	61	100	100	100
C <sub>1</sub> -C <sub>4</sub>	11	8	4	14	10	9	27	24	12	8	12	12
C <sub>2</sub> <sup>=</sup>	30	8	1	18	13	9	20	11	8	56	52	51
C <sub>3</sub> <sup>=</sup>	27	4	0	26	17	10	21	11	6	24	23	23
C <sub>4</sub> <sup>=</sup>	15	1	0	18	9	8	6	8	1	6	6	6
C <sub>5</sub> <sup>=</sup> +C <sub>5</sub>	6	1	0	12	13	9	12	13	7	2	1	1
DME/DEE	0	21	36	0	1	6	0	2	19	0	0	0
C <sub>6</sub> <sup>+</sup>	12	3	0	13	25	29	14	20	11	4	5	6

As to the porous structure, HZSM-5 and HMCM-22 are both medium-pore zeolites but have quite different pore systems. Regarding the HITQ-2 zeolite, ethylene was virtually the unique product formed from ethanol under the studied conditions (> 95 %). These results were similar to those reported for HMCM-22. For MeOH, C<sub>2</sub>-C<sub>3</sub> olefins and C<sub>6</sub><sup>+</sup> are the main products at the beginning of the reaction (TOS = 5 min). As the reaction proceeds the formation of hydrocarbons gradually decreases (except for HMCM-2) while DME (dimethyl ether) increases along the reaction. It is currently accepted that its transformation into light olefins (ethylene and propylene) occurs through the hydrocarbon pool mechanism which involves the large polymethylbenzenes species as intermediates [3]. Over HZSM-5 the high density of strong acid sites favors the formation of coke inside the pore structure causing its deactivation. On the other hand, to HMCM-22, it can be inferred that there is enough space into the larger supercages to accommodate not only the polymethyl benzene species but also the coke molecules.

### 3. Conclusions

The influence of TOS on catalytic activity and product distribution reflects the different susceptibilities of the studied zeolites to the formation of coke inside its porous structure.

### References

- [1] A. Corma, C. Corel, J. Perez-Pariente, *Zeolites*, 15 (1995) 2-8.
- [2] A. Corma et al., *Microporous and Mesoporous Materials*, 38 (2000) 301-309.
- [3] U. Olsbye et al., *Angew. Chem. Int. Ed.* 51 (2012) 5810

# Ruthenium isomorphous substitution into a $\alpha$ - $\text{MnO}_2$ structure. Study of its physicochemical properties and catalytic activity

*Ferran Sabaté; María José Sabater; José Luis Jordà; Avelino Corma,*

*Instituto de Tecnología Química – Universitat Politècnica de València (CSIC – UPV),  
46022, València, Spain*

## Introduction

Manganese oxides ( $\text{MnO}_2$ ) are present in a wide number of geological deposits as ocean floors (nodules) or bottoms of water lakes. This type of oxides present a high grade of polymorphism, so different phases ( $\alpha$ ,  $\beta$ ,  $\gamma$ , ...) can be described [1]. They have numerous applications [2]; *i.e.* in heterogeneous catalytic systems, as supercapacitors, batteries, environmental control, medical applications, etc...

Metal doping processes have been widely used to improve their properties [3]. In our study, ruthenium (Ru) has been incorporated into the framework of  $\alpha$ - $\text{MnO}_2$  through an easy synthetic route. Ruthenium cations can be incorporated into the octahedral lattice of  $\alpha$ - $\text{MnO}_2$  by replacing  $\text{Mn}^{3+}$  and  $\text{Mn}^{4+}$  ions. That changes its properties due to the electronic environment modification.

## Results and Discussion

The incorporation of Ru into the structure has been proved by means of IR, Raman and XPS spectroscopies, XRD, as well as HR-TEM and SEM microscopy. In this context, it has been proved by XRD that  $\alpha$ - $\text{MnO}_2$  does not present any appreciable structural change after the Ru-doping process (Figure 1).

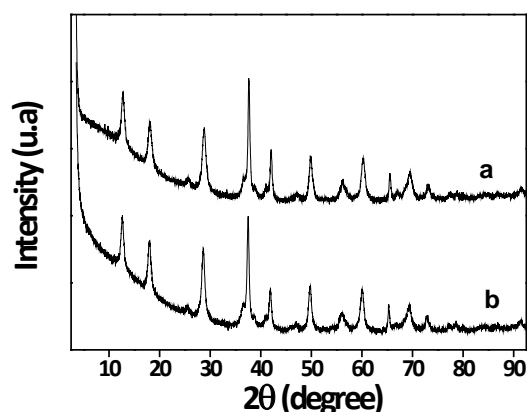


**Figure 1:** a) XRD pattern for the  $\alpha$ - $\text{MnO}_2$  (a) and  $[\text{Ru}]\text{-}\alpha\text{-MnO}_2$  (b)

In this study, the oxidation of benzyl alcohol to benzaldehyde has been used as model reaction in order to find out a correlation between the new physicochemical

Pd catalyst decreases with the addition of quinoline and further decreases when quinoline is used in a combination with Pb.

The strongly adsorbing alkene adsorption sites may act as over-hydrogenation reaction centres and decrease the catalyst selectivity. In this respect, the observed decrease in the relative alkene to alkyne capacities shows an excellent correlation with the observed catalyst selectivity.

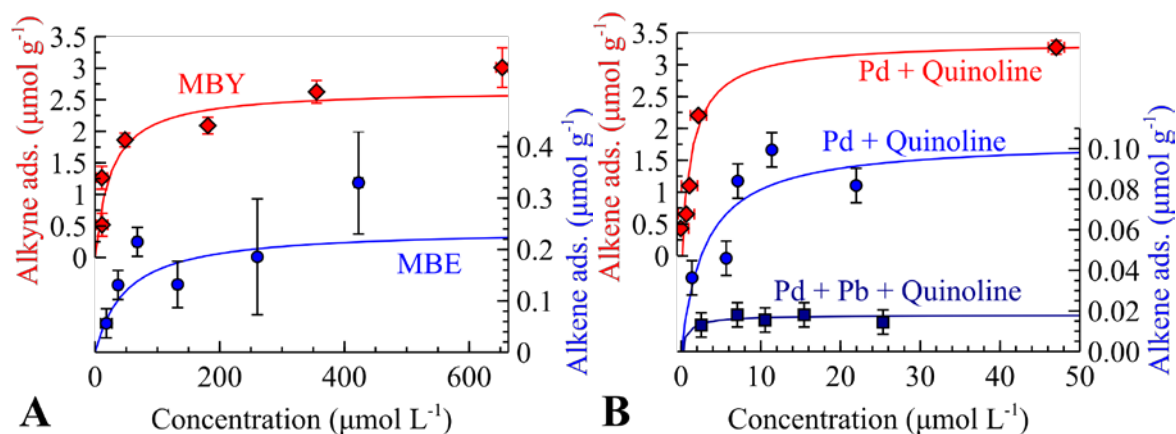


Fig. 1. Liquid phase adsorption isotherms of individual species: 2-methyl-3-butyn-2-ol (alkyne) and 2-methyl-3-butene-2-ol (alkene) over the (A) original 2 wt% Pd/CaCO<sub>3</sub> and (B) Pd catalyst poisoned with Pb and 40 μM quinoline.

## Conclusions

The data indicate that the conventional thermodynamic-focused explanation of high alkyne hydrogenation selectivity over the Pd catalysts is important, but not determinant because the experimental adsorption constants for alkyne and alkene are close. It seems that there are non-selective sites that strongly adsorb and hydrogenate alkene molecules and result in over-hydrogenation. A comparison with the literature data indicates that these sites may be low-coordination edge and near-edge Pd sites. Poisoning of these sites with Pb and quinoline results in a higher alkene selectivity of Lindlar catalysts.

## References

- García-Mota M.; Gómez-Díaz J.; Novell-Leruth G.; Vargas-Fuentes C.; Bellarosa L.; Bridier B.; Pérez-Ramírez J.; López N. *Theor. Chem. Acc.* 2011, 128, 663
- Cherkasov N.; Bai Y.; Exposito A.; Rebrov E. V. *React. Chem. Eng.* 2018, article ASAP. DOI: 10.1039/C8RE00046H.

# Hydrogenation of Bio-derived Compounds Using Ru Incorporated in Zeolites

*Kai Gao, Technical University of Denmark, 2800 Kgs. Lyngby, Denmark; Kristoffer Hauberg Rasmussen, Technical University of Denmark, 2800 Kgs. Lyngby, Denmark; Farnoosh Goodarzi, Technical University of Denmark, 2800 Kgs. Lyngby, Denmark; Søren Kegnæs, Technical University of Denmark, 2800 Kgs. Lyngby, Denmark*

## Introduction

High-value added chemicals such as 2,5-dimethyl furfural are mainly obtained from bio-derived compounds like 5-hydroxymethylfurfural (HMF). However, the selectivities of desired products are not high enough due to the side-reactions of the substrates, which causes the difficulties for downstream separation and purification processes. Recently, one of the methods to overcome this challenge has been applying mesoporous zeolite as the hydrogenation catalyst because of its relative big pore size and surface area. However, the selectivity of desired product is strongly limited due to the small pore diameter of microporous zeolite, which causes several side reactions. Mesoporous zeolite is in its advantage of abundant exposed activate sites in ZSM-5 with open mesopores. Many Pd-, Ni- and Pt-based zeolites are reported to convert HMF to valuable chemicals.<sup>[1-3]</sup> Compared with the above noble metal elements, Ru is found to be more efficient for hydrogenation of biomass derived compounds such as glucose and sorbitol.<sup>[4]</sup> Therefore, in our research, a novel catalyst is designed in which Ru is supported on the mesoporous zeolite to combine both advantages.

Here we report a novel Ru mesoporous zeolite supported Ru as high efficient and selectivity catalyst for the hydrogenation of bio-derived alcohols and aldehydes including compounds like HMF. Ruthenium was employed as the hydrogenation catalyst, which was competitive enough with the commercial carbon supported Ru catalyst. The Ru nanoparticle mesoporous zeolite is very active for the hydrogenation of bio-derived compounds and demonstrates excellent selectivity.

## Experimental

The Ru on mesoporous zeolite catalyst was prepared through impregnation of mesoporous ZSM-5 with a Ru metal precursor. The prepared ZSM-5 supported Ru catalyst is employed in the hydrogenation of different bio-derived compounds including HMF, which are performed in an autoclave and hydrogen pressure for a

certain reaction time. The conversion and selectivity were determined using GC-MS analysis.

### **Results and discussions**

The alcohol conversions reached to 85% and 100% after 6 and 12 hours after reaction in the presence of mesoporous ZSM-5 supported Ru catalyst, respectively. Mesoporous ZSM-5 supported Ru showed to be an excellent catalyst in hydrogenation of choice alcohol.

### **Conclusion**

In summary, our research discloses that mesoporous ZSM-5 supported Ru catalyst exhibits high catalytic activity, excellent selectivity for converting of alcohols. The excellent catalytic properties are mainly based on the open mesopores, which has accessible activate sites exposed to bulky molecules.<sup>[5]</sup>

### **References**

- [1] Xuan Xu, Yi Li, Yutong Gong. *et al.* J. Am. Chem. Soc. 2012, 134, 16987-16990
- [2] Hidetoshi Ohta, Hirokazu Kobayashi, Kenji Hara. *et al.* Chem. Commun. 2011, 47, 12209-12211
- [3] Jean-Philippe Tessonier, Alberto Villa, Olivier Majoulet. *et al.* Angew. Chem. Int. Ed. 2009, 48, 6543–6546.
- [4] Arturo Azua, Matthew Finn, Hannah Yi. *et al.* ACS Sustainable Chem. Eng. 2017, 5, 5, 3963-3972
- [5] Liang Wang, Jian Zhang, Xianfeng Yi. *et al.* ACS Catal. 2015, 5, 2727-2734

# In-situ ATR Spectroscopy CO chemisorption on bio-inspired catalysts in liquid environments

*Maria João Enes da Silva, University of Twente, Enschede, The Netherlands, Jimmy Faria, University of Twente, Enschede, The Netherlands*

There has been an increasing interest in tailoring catalysts with stimuli-responsive polymers to improve their selectivity, stability, and recyclability in liquid environments[1,2]. In these systems the external surface of the catalyst is functionalized with polymer brushes that can undergo reversible conformational transitions from solvated to insoluble or “collapse” state depending on the conditions of the reaction environment (e.g. pH, temperature, solvent polarity). In the solvated state the catalytic active sites are easily accessible to molecules in the liquid and as a result the reaction can take place. Upon conformational transition to the “collapse” state the polymers form a dense layer at the surface of the catalyst that limits molecular diffusion of reactants to the active site [3]. These transitions allow us to remotely turn “on” and “off” the catalyst during reaction. Many of the existing reports are focused on the utilization of this strategy to control the dispersability of nano-catalysts in liquid environments. However, very little efforts have been done in understanding the interaction of polymer functionalities with surface reaction intermediates. In this work, we investigate the interplay between the stimulus-responsive polymeric brushes covalently attached to the catalyst and chemisorbed molecules in liquid environments. For that purpose, we employed poly(*n*-isopropylacrylamine) PNIPAm, a typical thermoresponsive polymer that exhibits a sharp change in solubility at temperatures above 32 °C, to create a coating on Pd-Al<sub>2</sub>O<sub>3</sub> catalyst. The isothermal chemisorption of CO was studied as a function of temperature using in-situ attenuated total reflectance (ATR) infrared spectroscopy in aqueous environments. These results will be instrumental in the development of new mechanisms that could operate at higher temperatures and pressures for the remote control of catalytic activity.

## References

- [1] D. Díaz Díaz, D. Kühbeck, R.J. Koopmans, Chem. Soc. Rev. 40 (2011) 427–448.
- [2] X. He, M. Aizenberg, O. Kuksenok, L.D. Zarzar, A. Shastri, A.C. Balazs, J. Aizenberg, Nature 487 (2012) 214–218.
- [3] G. Prieto, H. Tüysüz, N. Duyckaerts, J. Knossalla, G.H. Wang, F. Schüth, Chem. Rev. 116 (2016) 14056–14119.

# Gold and Palladium Based Catalysts Prepared Batch and Semi-Continuous Colloidal Methods for the Selective Oxidation of 5-hydroxymethyl-2-furfural

Takudzwa Bere<sup>a</sup>, Stefano Cattaneo<sup>a</sup>, Manuel S. Grasiña<sup>a</sup>, Nikolaos Dimitratos<sup>a</sup>, Danilo Bonincontro<sup>b</sup> and Stefania Albonetti<sup>b</sup>

<sup>a</sup>Cardiff Catalysis Institute, Cardiff University, Main Building, Park Place, Cardiff CF10 3AT, U.K.

<sup>b</sup>Dipartimento di Chimica Industriale "Toso Montanari", Università di Bologna, Viale del Risorgimento, 4, 40136 Bologna BO, Italy

## 1. Scope

Supported Au-Pd alloys exhibit high activity for a number of oxidation reactions such as the selective oxidation of alcohols and the synthesis of H<sub>2</sub>O<sub>2</sub> from H<sub>2</sub> and O<sub>2</sub>.<sup>1</sup> The selective oxidation of 5-hydroxymethyl-2-furfural (HMF) yields a sustainable biomass-derived intermediate, 2,5-furandicarboxylic acid (FDCA); a monomer for the production of Polyethylene 2,5-furandicarboxylate (PEF).<sup>2</sup> The activity of mono and bimetallic catalysts for the selective oxidation of HMF is size, shape and morphology dependent; all of which can be altered by the synthetic strategy. Previous studies report the dependence of the activity on the preparation method, reaction pressure and temperature, substrate-to-catalyst ratio, catalyst support, amount and nature of base used. Catalyst composition also previously showed mechanistic differences when segregation of Pd or Au atoms occurs.<sup>3</sup> The current work aims to report a detailed study of the oxidation of HMF with varying catalyst compositions prepared via the batch and semi-continuous colloidal method. Catalysts with different Au:Pd atomic ratios were synthesized to investigate the effect on the catalytic activity and product selectivity (Figure 1). For a proper comparison, we prepared monometallic Au and Pd using the same methodologies.

## 2. Results and Discussion

We found that Pd/TiO<sub>2</sub> catalysts exhibited the lowest activity due to deactivation caused by poisoning by dioxygen.<sup>4</sup> The contrary was observed for Au/TiO<sub>2</sub> XPS data suggested catalytically active surface Au<sup>0</sup> species. In both cases the ratio 0.75Au:Pd was the most selective to FDCA. Moreover, the semi-continuous catalyst showed better activity than the batch which was due to the formation of a more uniform alloy. An increase in Au content corresponded to an increase in FDCA selectivity. XPS and XRD results suggested an alloyed structure with surface PdO species and TEM suggested a size dependency to activity. Reusability studies revealed the increased stability of the 0.75Au:Pd semi-continuous catalyst. Further heat



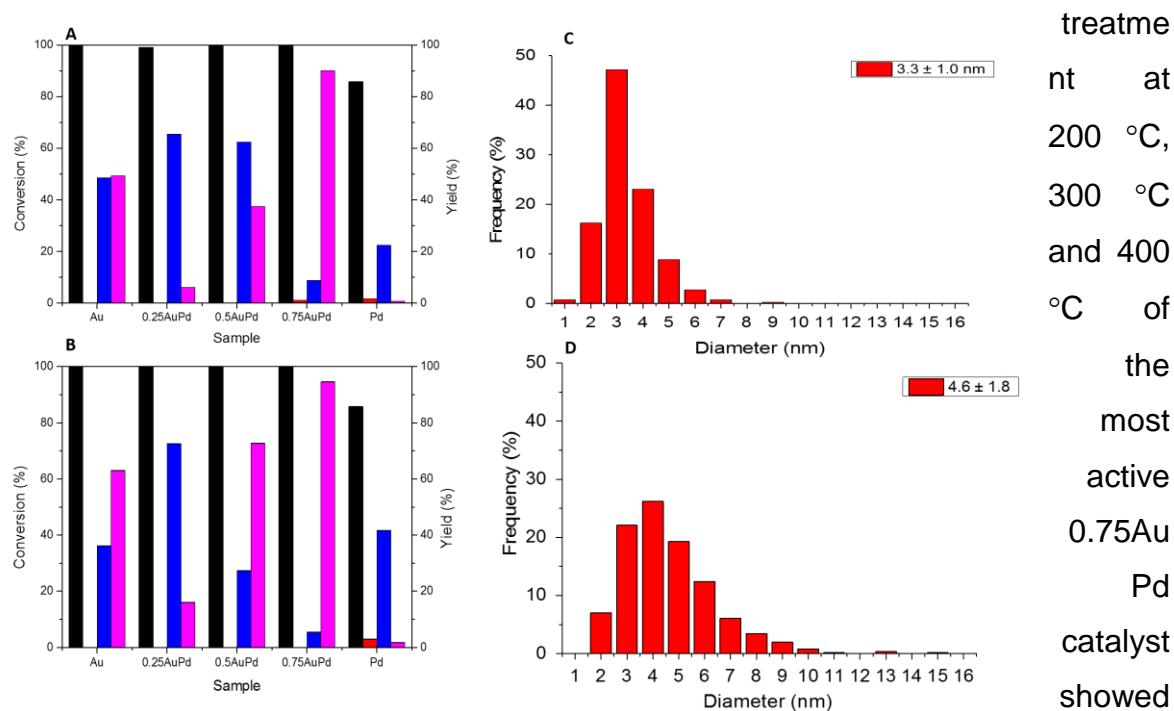


**Figure 1.** Catalytic data for (A) semi-continuous and (B) batch 1 wt % catalysts with different composition showing HMF conversion (black), FFCA yield (red), HMFCFA yield (violet) and FDCA yield (blue). Particle size distribution of 0.75Au:Pd semi-continuous (C) fresh and (~D) spent, after 4 runs, at 200 °C

that both 200 °C and 300 °C treatments achieved 100% FDCA yield. However, reusing the 200 °C catalyst a decrease in FDCA yield to 86% after 4 runs due to an increase in the particle size as shown by TEM (Figure 2). A possible rationale was the removal of the PVA that protects against particle agglomeration.

### 3. Conclusions

We have shown that the semi-continuous method improved the catalytic system, increasing selectivity and yield toward, FDCA. TEM images suggested a monodisperse, homogeneous distribution with a narrow particle size distribution, forming a proposed single-phase alloy as suggested by XPS and XRD. The results suggest the semi-continuous method formed a more uniform alloy with smaller particle size and distribution.

### References

1. Lopez-Sanchez, J. A. *et al.* Reactivity studies of Au–Pd supported nanoparticles for catalytic applications. *Appl. Catal. Gen.* **391**, 400–406 (2011). 2. de Jong, E., Dam, M. A., Sipos, L. & Gruter, G.-J. M. Furandicarboxylic Acid (FDCA), A Versatile Building Block for a Very Interesting Class of Polyesters. in *Biobased Monomers, Polymers, and Materials* **1105**, 1–13 (American Chemical Society, 2012). 3. Loli, A. *et al.* Insights into the reaction mechanism for 5-hydroxymethylfurfural oxidation to FDCA on bimetallic Pd–Au nanoparticles. *Appl. Catal. Gen.* **504**, 408–419 (2015). 4. Mallat, T. & Baiker, A. Oxidation of Alcohols with Molecular Oxygen on Solid Catalysts. *Chem. Rev.* **104**, 3037–3058 (2004).

treatme  
nt at  
200 °C,  
300 °C  
and 400  
°C of  
the  
most  
active  
0.75Au  
Pd  
catalyst  
showed

# Ultrafast and Continuous-Flow Synthesis of Aluminosilicate Zeolites

Andrei-Nicolae Parvulescu<sup>1\*</sup>, Hannah Schreyer<sup>1</sup>, Zhendong Liu<sup>2</sup>, Kenta Iyoki<sup>2</sup>, Shoko Miyagi<sup>2</sup>, Chokkalin-gam Anand<sup>2</sup>, Ulrich Müller<sup>1</sup>, Tatsuya Okubo<sup>2</sup>, and Toru Wakihara<sup>2\*</sup>

<sup>1</sup>BASF-SE 67056 Ludwigshafen, Germany

<sup>2</sup>Department of Chemical System Engineering, The University of Tokyo, Tokyo 113-8656, Japan

\*E-mail: andrei-nicolae.parvulescu@basf.com, wakihara@chemsys.t.u-tokyo.ac.jp

Synthesis of zeolites is typically conducted in a batch reactor, which has several drawbacks such as low energy efficiency as well as time-consuming start-up and shut-down operations. Given ever-increasing demands for zeolites arising from several new applications over the last decade such as emission control or on-purpose olefin production, rethinking the concepts of mass production of zeolites at a larger scale must be conducted. One of the possible production routes is continuous-flow synthesis of zeolites. To realize this, zeolites must be obtained in short synthesis time, within residence time for the practical flow reactors. Very recently, using a tubular reactor with rapid heating Okubo–Wakihara group has demonstrated the continuous-flow synthesis of several zeolites with diverse chemical compositions at a laboratory scale [2–8] (**Figure 1**).

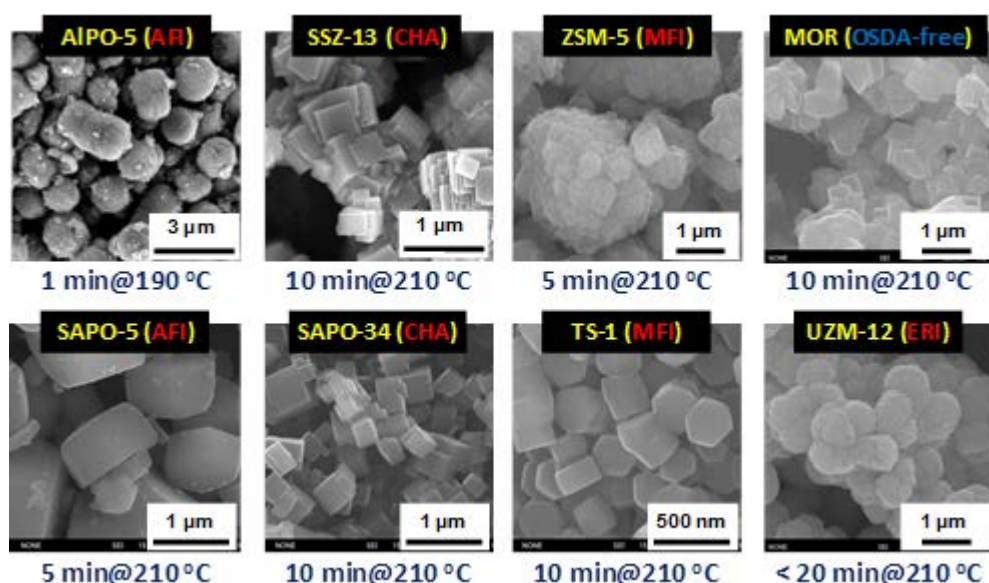


**Figure 1.** Zeolite structure obtained through ultrafast synthesis

Small-pore zeolites defined as the zeolites with the pore openings limited by 8 tetrahedral atoms (8-ring, 8r) have received increasing attention recently because they have shown promising performance in several important applications, for example, as catalysts for methanol-to-olefin (MTO) reactions and selective catalytic reduction of nitrogen oxides (deNO<sub>x</sub>) [9]. Among several small-pore zeolites, CHA- and AEI type zeolites having large cage cavities with 8r openings are intensively studied, particularly for MTO and deNO<sub>x</sub> MTO applications. We will address in this contribution the status and recent results in the ultrafast zeolite synthesis and the main factors that influence the zeolite crystallization and enablers for the ultrafast synthesis (**Figure 2**). For CHA for example 10 min crystallization [4] could be achieved and the impact of different organo-templates on the zeolite crystallization kinetics will be addressed as well.

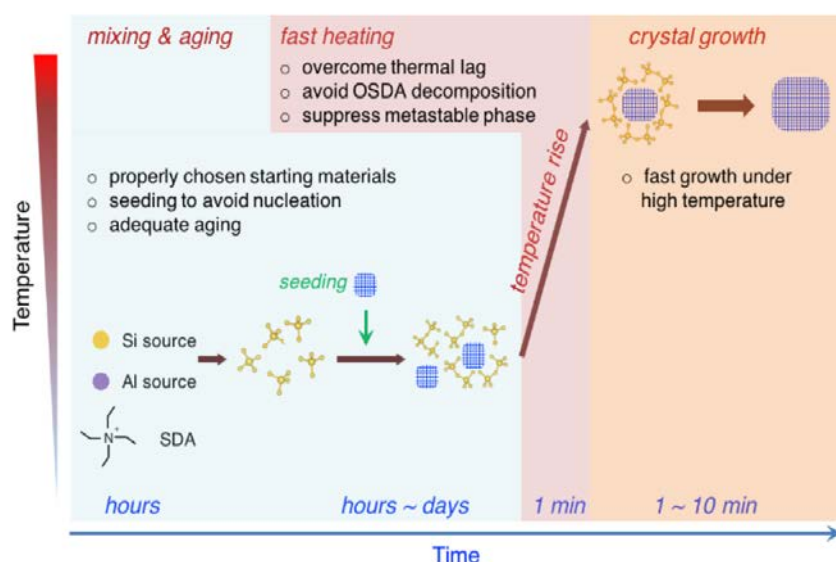


**Figure 2.** Generalized scheme for Ultrafast Synthesis of Zeolites

#### Reference:

- [1] W. Chaikittisilp, T. Okubo, in Handbook of Solid State Chemistry, Vol. 4 (Eds.: R. Dronskowski, S. Kikkawa, A. Stein), Wiley-VCH Verlag GmbH & Co. KGaA, Weinheim, 2017, pp. 97–119.
- [2] Z. Liu, T. Wakihara, D. Nishioka, K. Oshima, T. Takewaki, T. Okubo, Chem. Commun., 50 (2014) 2526.
- [3] Z. Liu, T. Wakihara, D. Nishioka, K. Oshima, T. Takewaki, T. Okubo, Chem. Mater. 26 (2014) 2327.
- [4] Z. Liu, T. Wakihara, K. Oshima, D. Nishioka, Y. Hotta, S. P. Elangovan, Y. Yanaba, T. Yoshikawa, W. Chaikittisilp, T. Matsuo, T. Takewaki, T. Okubo, Angew. Chem. Int. Ed., 54 (2015) 5683.
- [5] Z. Liu, T. Wakihara, C. Anand, S. H. Keoh, D. Nishioka, Y. Hotta, T. Matsuo, T. Takewaki, T. Okubo, Microporous Mesoporous Mater., 223 (2016) 140.
- [6] Z. Liu, T. Wakihara, N. Nomura, T. Matsuo, C. Anand, S. P. Elangovan, Y. Yanaba, T. Yoshikawa, T. Okubo, Chem. Mater. 28 (2016) 4840.
- [7] J. Zhu, Z. Liu, A. Endo, Y. Yanaba, T. Yoshikawa, T. Wakihara, T. Okubo, CrystEngComm, 19 (2017) 632.
- [8] J. Zhu, Z. Liu, K. Iyoki, C. Anand, K. Yoshida, Y. Sasaki, S. Sukenaga, M. Ando, H. Shibata, T. Okubo, T. Wakihara, Chem. Commun., 53 (2017) 6796.
- [9] M. Moliner, C. Martínez, A. Corma, Chem. Mater., 26 (2014) 246.

# Water-Stable Metal-Organic Frameworks as Heterogeneous Catalysts for Conversion of Biomass-Derived Sugars

*Thomas W. Chamberlain, University of Warwick, Coventry, UK; Ryan Oozeerally, University of Warwick, Coventry, UK; David L. Burnett, University of Warwick, Coventry, UK; Richard I. Walton, University of Warwick, Coventry, UK; Volkan Degirmenci, University of Warwick, Coventry, UK*

Heterogeneous catalysts are desired for the conversion of biomass derived glucose, but the current benchmark catalysts require extended, multi-step syntheses using environmentally hazardous solvents.

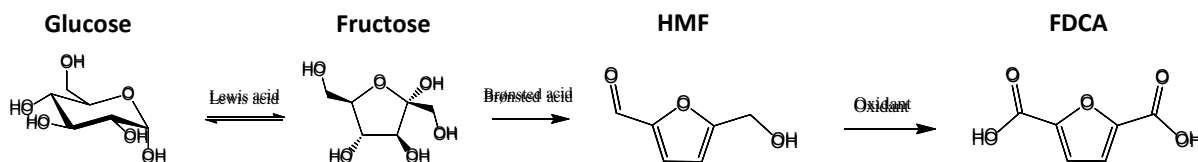


*Figure 1:* Schematic of conversion of biomass into glucose, acid catalysed dehydration of glucose into HMF and finally oxidation of HMF into the useful monomer FDCA.

Here, we describe the efficient and benign syntheses and interconversion of a family of novel ytterbium based metal organic frameworks (MOFs) and investigate their feasibility as Lewis acidic heterogeneous catalysts in the conversion of glucose to 5-hydroxymethyl furfural (HMF) in water. We recently reported the solvothermal synthesis of three related ytterbium dicarboxylate frameworks formed simply by altering solvent ratios and synthesis temperature.<sup>[1]</sup> A new dense coordination polymer  $\text{Yb}_2(\text{BDC})_3$  is formed under aqueous conditions, while the hydrothermal treatment of  $\text{Yb}_2(\text{BDC})_3(\text{DMF})_2(\text{H}_2\text{O})_2$  at 200 °C with an excess of  $\text{YbCl}_3$  yields the MOF  $[\text{Yb}_6\text{BDC})_7(\text{OH})_4(\text{H}_2\text{O})_4].2\text{H}_2\text{O}$ . The latter is a porous coordination polymer with hexanuclear clusters of ytterbium and loosely bound water as shown in Figure 1. The catalytic properties of this highly water stable material are assessed for glucose conversion in water and results are compared to homogeneous  $\text{YbCl}_3$  catalysts. The material is shown to have moderate activity, good selectivity, and is recyclable.

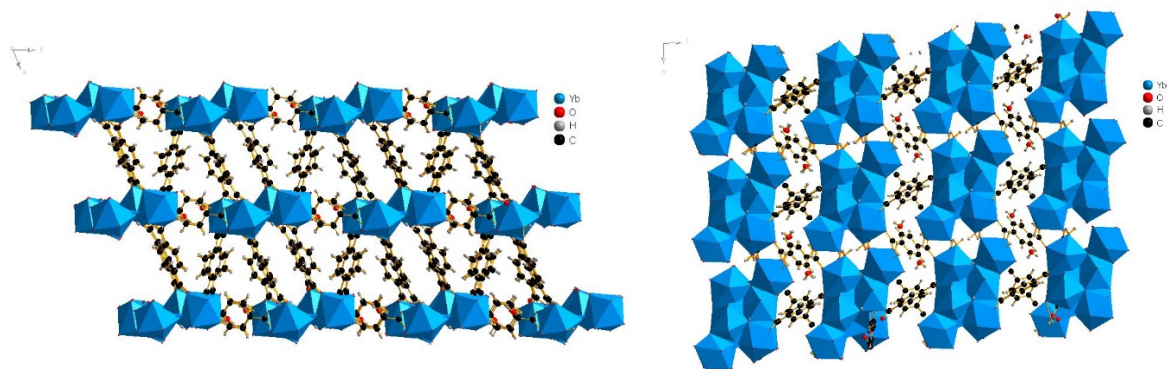


*Figure 2:* Two views of the hydrothermally stable MOF  $[\text{Yb}_6\text{BDC})_7(\text{OH})_4(\text{H}_2\text{O})_4].2\text{H}_2\text{O}$ .

MIL-100 (Fe) is a well-known water stable MOF, synthesised under relatively mild hydrothermal conditions. It contains trimers of Fe(III) connected by trimesic acid forming two distinct cage structures, a small cage (25 Å) and a large cage (29 Å). Uncoordinated Fe(III) sites may be accessible to substrates within the pores and on the surface of the material, allowing the Fe sites to act as redox active catalysts. We report the water based synthesis of MIL-100, investigate its stability to oxidising aqueous conditions and evaluate its potential use as a heterogeneous redox catalyst in the oxidation of HMF into the useful monomer 2,5-furan dicarboxylic (FDCA) acid in water.

#### References

[1] M. I. Breeze, T. W. Chamberlain, G. J. Clarkson, R. P. de Camargo, Y. Wu, J. F. de Lima, F. Millange, O. A. Serra, D. O'Hare, R. I. Walton, *CrystEngComm*, 2017, 19, 2424-2433.

# Triple hydrogen bonds (thio)urea organocatalyst for ring-opening polymerization of cyclic esters

*Lei Zhang, zhanglei1994@njtech.edu.cn, Nanjing, China; Kai Guo, kaiguo@njtech.edu.cn, Nanjing, China; Zhenjiang Li, zjli@njtech.edu.cn, Nanjing, China*

Aliphatic polyesters attract great interest for their notable advantages of biocompatibility, biodegradability, and relatively low toxicity. Aliphatic polyesters can be synthesized by the method of ring-opening polymerization (ROP) in cyclic esters. H-bonding organocatalysis using (thio)urea/amine achieved massive success in field of polymerization. The strength of H-bonding can be improved by increasing number of H-bond donor and ionized hydrogen bonds. Here a triple hydrogen bonds organocatalyst, the most acidic one of triple hydrogen bonds combined with organic base as an ionic H-bond donor (IHBD), promoted fast ring-opening polymerization (ROP). A negatively charged IHBD (thio)urea exhibits exceptional activating ability to initiator, and other two hydrogen bonds show reasonable activating effect to monomers. Several of triple hydrogen bonds organocatalysts were synthesized in this work. These organocatalysts' partnership with DBU demonstrate excellent IHBA-HBA binary catalysis in ROP of L-lactide (L-LA), trimethylene carbonate (TMC),  $\delta$ -valerolactone ( $\delta$ -VL) and  $\epsilon$ -caprolactone ( $\epsilon$ -CL). NMR measurements, kinetics investigations, and chain extension experiments indicated that the catalytic system of triple hydrogen bonds organocatalysts and DBU were controlled/living nature. Untreated PLA, PTMC, PVL, PCL were tested by an MTT assay using the HepaRG cell line for certificating the safety of polymers. The results demonstrated the polymers by ROP with the triple hydrogen bonds organocatalysts have a good prospect for potential biomedical applications.

**Keyword:** (Thio)urea organocatalyst; Triple hydrogen bonds; Ring-opening polymerization; Ionic H-bonding; Potential biomedical application

## **Combining chemo- and biocatalysis to convert xylan into xylitol**

*Mick Miro Ayubi<sup>1</sup>, Susanne Steudler<sup>2</sup>, Anett Werner<sup>2</sup>, Thomas Bley<sup>2</sup>,  
Thomas Walther<sup>2</sup>, Rüdiger Lange<sup>1</sup>, Gerd Hilpmann<sup>1</sup> 1...Chair of Chemical  
Engineering and Process Plants, Institute of Process Engineering and Environmental  
Technology, 2...Chair of Bioprocess Engineering, Institute of Natural Materials  
Technology, Technische Universität Dresden/ 01062 Dresden*

In times of climate change, substituting petroleum-based processes is a high research priority for the preservation of our future economic strength and our environment. The concept of the biorefinery envisages the separation and refinement of biomass for the sustainable production of intermediate products and products such as energy, fuels, materials and chemicals using all material flows. Lignocellulose is a promising platform for a future biorefinery that does not compete with food production. Lignocellulose consists of the three fractions cellulose, lignin and hemicellulose. The cellulose contained in lignocellulose is already used, for example, in the paper or building materials industry. For the efficiency of such a lignocellulose biorefinery it is of great importance to which refinement the lignin and hemicellulose fractions are added. The splitting of hemicelluloses into their sugar monomers, which is required for their refinement, is usually realized in industry by the use of strong acids under high energy use (re-use acids).

The focus of this work is the simultaneous use of chemical and biological catalysts and the combination of their advantages for the eco-friendly conversion of the hemicellulose xylan (beechwood) to the sugar alcohol xylitol. The process was carried out at low temperatures and pressures. The first step of xylan conversion (hydrolysis) was realized with the help of different commercially available enzyme complexes. The subsequent hydrogenation was carried out with the aid of a Ru/C catalyst. The reaction can be optimized by a suitable process control. The process was realized through different process management concepts which involves a classical one-pot and a new two-step process. The experiments were performed in a batch reactor (Parr Inst., 300...500 ml). The analysis was carried out by HPLC using a Na and a Pb column. The highest xylitol yield of over 70 % was achieved by

applying a two-stage reaction control. In contrast, single-stage constant conditions gave comparatively low xylitol yields.

Parts of the presented results are contributions to the European research project “CrossCat”. Funding via EFRE (ERA-IB ID 100271549) is gratefully acknowledged.

### **References**

[1] Hilpmann, G., Steudler, S., Ayubi, M.M., Pospiech, A., Walther, T., Bley, T. Lange, R.: Combining Chemical and Biological Catalysis for the Conversion of Hemicelluloses: Hydrolytic Hydrogenation of Xylan to Xylitol. *Catal Lett* (2019),149:69-76. <https://doi.org/10.1007/s10562-018-2598-7>



# Hydrogenation of Bio-Derived Succinic Acid to 1,4-Butanediol using Supported Bimetallic Catalysts

*Son Dinh Le, Shun Nishimura\**

*Graduate School of Advanced Science and Technology, Japan Advanced Institute of  
Science and Technology (JAIST), 1-1 Asahidai, Nomi, Ishikawa 923-1292, Japan.*

*Email: s\_nishim@jaist.ac.jp*

1,4-butanediol (BDO) is an important chemical which is widely used as a starting material for the synthesis of polymers [1]. The hydrogenation of succinic acid (SA) to BDO is typically carried out under high pressure of hydrogen using both supported monometallic [2,3] and bimetallic catalysts [4,5] which consist of precious metallic centers. The construction of bimetallic active centers is much attractive approach since the additional element could result in a significant improvement on the catalytic performance [6]. In this research, supported Cu-based bimetallic catalysts are studied for direct hydrogenation of SA to BDO. The use of Cu is promising because it is not only reported as active sites for effective hydrogenations of molecules containing C=O double bonds [7,8] but also used to minimize the heavy dependence on noble metals.

First, various Cu-based catalysts were evaluated their activities in dioxane solvent. In which, a hydroxyapatite-supported Cu-Pd (denoted as Cu-Pd/HAP) was found to be a potential catalyst for the production of BDO with high selectivity, while other Cu-M/HAP catalysts produce  $\gamma$ -butyrolactone (GBL) as the main product. Optimization on the Cu/Pd mixing ratio was implemented while the total loading was fixed at 10 wt.%. The results show that the monometallic Cu or Pd catalysts were unable to produce BDO, while in the case of bimetallic catalysts, the formation of BDO via ring-opening step of GBL is favorable rather than the hydrogenation of GBL to butyric acid (BA). Particularly, as the increase of Cu content, the yield of BDO increases, affording 82% over the Cu(8wt%)-Pd(2wt%)/HAP catalyst (**Fig. 1A**).

The powder X-ray diffraction (XRD) showed the peak shifts at Pd<sup>0</sup>(111) position towards higher  $2\theta$  value together with the increase of Cu content in the Cu-Pd/HAP catalysts, indicating the incorporation of Cu into the Pd system to form Cu-Pd alloy [9]. Results from the temperature programmed reduction (H<sub>2</sub>-TPR) also supported that the active surface of Pd was altered by alloying with Cu contents, leading to the

shifts in H<sub>2</sub>-TPR profiles from lower to higher temperature [10]. The extended X-ray absorption fine structure (EXAFS) analyses conducted at BL07 in Saga-LS, Japan (Proposal No. 1901136T), shows that the localized Pd structure was obviously changed due to the introduction of Cu with different concentrations, confirming the alloy structures in the examined bimetallic catalysts (**Fig. 1B**).

In conclusion, Cu-Pd/HAP catalysts are developed as efficient catalysts for hydrogenation of bio-derived SA in which BDO can be selectively tunable by adjusting the metal ratio. The alloy structure is supposed crucial for controlling the formation BDO via ring-opening step of the intermediate GBL.

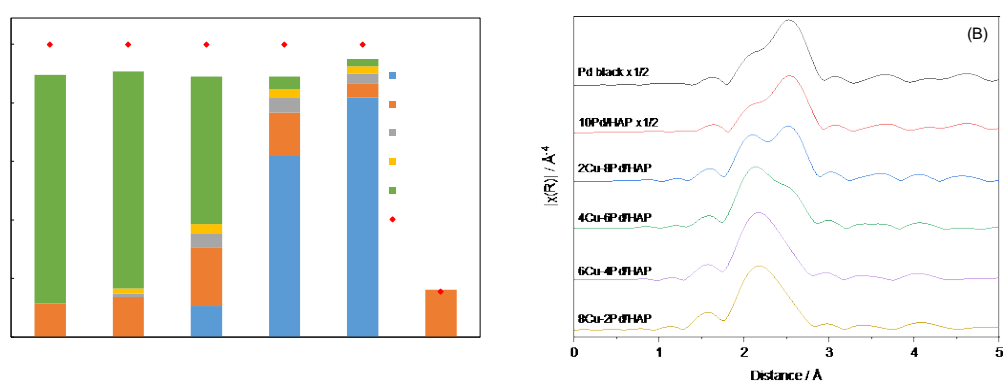


**Fig. 1** (A) Hydrogenation of SA over Cu-Pd/HAP catalysts<sup>a</sup>, (B) the Fourier transform (FT) of the  $k^3$ -weighted at Pd K-edge<sup>b</sup>.

<sup>a</sup>Reaction conditions: SA (0.1 g), 1,4-dioxane (10 mL), temperature (200 °C), catalyst (0.1 g), H<sub>2</sub> pressure (8 MPa), time (96h). <sup>b</sup>The data analyses were performed in the range of 2.5-12 Å<sup>-1</sup> by using Athena and Artemis software (ver. 0.9.26).

## References

- [1] D. Sun, S. Sato, W. Ueda, A. Primo, H. Garcia, A. Corma, *Green Chem.* **2016**, *18*, 2579–2597.
- [2] R. Luque, J. H. Clark, K. Yoshida, P. L. Gai, *Chem. Commun.* **2009**, *0*, 5305.
- [3] U. G. Hong, H. W. Park, J. Lee, S. Hwang, J. Yi, I. K. Song, *Appl. Catal. A Gen.* **2012**, *415–416*, 141–148.
- [4] Y. Takeda, M. Tamura, Y. Nakagawa, K. Okumura, K. Tomishige, *Catal. Sci. Technol.* **2016**, *6*, 5668–5683.
- [5] X. Di, C. Li, B. Zhang, J. Qi, W. Li, D. Su, C. Liang, *Ind. Eng. Chem. Res.* **2017**, *56*, 4672–4683.
- [6] C. Delhomme, D. Weuster-Botz, F. E. Kühn, *Green Chem.* **2009**, *11*, 13–26.
- [7] Y. Zhu, X. Kong, X. Li, G. Ding, Y. Zhu, Y.-W. Li, *ACS Catal.* **2014**, *4*, 3612–3620.
- [8] Y. Wang, Y. Shen, Y. Zhao, J. Lv, S. Wang, X. Ma, *ACS Catal.* **2015**, *5*, 6200–6208.
- [9] L. Di, W. Xu, Z. Zhan, X. Zhang, *RSC Adv.* **2015**, *5*, 71854–71858.
- [10] S. Hamid, S. Bae, W. Lee, *Chem. Eng. J.* **2018**, *348*, 877–887.

## **Synthesis and application of N-doped porous carbons and carbon nitride as catalysts and supports for base catalyzed reactions**

*N.D. Shcherban, L.V. Pisarzhevsky Institute of Physical Chemistry, National Academy of Sciences of Ukraine, Kyiv, Ukraine; P. Mäki-Arvela, Johan Gadolin Process Chemistry Centre, Åbo Akademi University, Turku, Finland; E.A. Diyuk, Institute for Sorption and Problems of Endoecology, National Academy of Sciences of Ukraine, Kyiv, Ukraine; D.Yu. Murzin, Johan Gadolin Process Chemistry Centre, Åbo Akademi University, Turku, Finland*

Condensation reactions with formation of C–C bonds such as aldol, Knoevenagel condensations, etc. as well as oxidation processes are ubiquitous reactions in organic chemistry spanning a broad range of potential applications from the syntheses of small molecules to preparation of intermediates for pharmaceuticals. These condensation reactions are generally catalyzed by weak bases like primary, secondary and tertiary amines, ammonium or ammonium salts under homogeneous conditions, while oxidation requires presence of metal nanoparticles deposited mainly on inert or almost inert supports. Solid catalysts are more preferable for this purpose because they provide operational simplicity and higher selectivity with a possibility of reusability [1]. Solid base catalysts are receiving an increased attention recently as they facilitate a variety of organic reactions taking place via carbanionic intermediates.

The aim of this work was to prepare solid base catalysts possessing different porosity and basicity as well as to investigate catalytic activity of metal-free catalysts along with supported metals nanoparticles in several catalytic processes (Knoevenagel condensation, alcohols (betulin, sugars, ethanol) oxidation). N-doped porous carbons and carbon nitride ( $C_3N_4$ ) were used as catalysts and supports.

The catalytic activity of melamine-derived g- $C_3N_4$  in the Knoevenagel condensation between benzaldehyde and ethylcyanoacetate with formation of ethyl- $\alpha$ -cyanocinnamate (Fig. 1), a precursor for synthesis of potentially biologically active compounds was demonstrated, exhibiting conversion of benzaldehyde up to 100% with the yield up to 51%. The presence of weak basic sites assigned as C-N=C species contributes to an increase of selectivity towards the desired product [2].

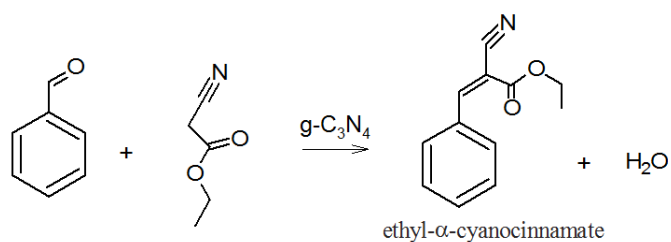


Fig. 1. Scheme of the Knoevenagel condensation of benzaldehyde with ethylcyanoacetate using graphitic carbon nitride as a catalyst [2].

Ru supported catalysts based on graphitic carbon nitride or N-doped carbon prepared via a mild reduction of the initial Ru precursor with hydrazine were studied in catalytic oxidation of betulin. Ru/carbon nitride demonstrated higher catalytic activity in betulin oxidation than Ru/N-doped carbon elevating the conversion level of betulin to ca. 70% from 30%, respectively. Selectivity to different oxidation products was dependent on the support properties [3].

Application of carbon nitride or doped carbons, in particular, nitrogen-containing ones, as supports of metal nanoparticles significantly affects their catalytic properties increasing activity and selectivity due to the stabilizing effect of such functional groups on deposited nanoparticles.

Application of carbon nitrides and N-doped carbons was explored in other oxidation reactions. Several materials based on carbon nitride including nonstoichiometric one and N-doped carbon varying in porosity (micro-, micro-meso- and mesoporosity) and basicity (type and quantity of basic sites) were investigated in oxidation reactions, in particular, sugars and ethanol. Dehydrogenation of ethanol was possible over metal-free N-doped carbons giving mainly acetaldehyde formation, while for oxidation of sugars presence of gold nanoparticles was required.

Summarizing it can be concluded that promising results in condensation and oxidation reactions were obtained with the catalysts on the basis of N-doped porous carbons and carbon nitride containing high concentration of basic sites and accessible porous structure. The catalyst properties will be correlated in the final work with their performance.

## References

- [1] S.H.Y.S. Abdullah, N.H.M. Hanapi, A. Azid, R. Umar, H. Juahir, H. Khatoon, A. Endut, *Renew. Sust. Energy Rev.*, 2017, 70, 1040.
- [2] N.D. Shcherban, P. Mäki-Arvela, A. Aho, S.A. Sergiienko, P.S. Yaremov, K. Eränen, D.Yu. Murzin, *Catal. Sci. Technol.*, 2018, 8, 2928.
- [3] N.D. Shcherban, P. Mäki-Arvela, A. Aho, S.A. Sergiienko, M.A. Skoryk, E. Kolobova, I.L. Simakova, K. Eränen, A. Smeds, J. Hemming, D.Yu. Murzin, *Catal. Lett.*, 2019, 1.

# Encapsulation of Pd nanoparticles within MWW via transformation of 2D to 3D zeolite for shape-selective hydrogenation of nitroarenes

Yuyan Zhang<sup>1</sup>, Michal Mazur<sup>1</sup>, Jiří Čejka<sup>1</sup> Department of Physical and Macromolecular Chemistry, Faculty of Science, Charles University, Hlavova 2030/8, 128 43, Prague, Czech Republic, [yuyan.zhang@natur.cuni.cz](mailto:yuyan.zhang@natur.cuni.cz),

[michal.mazur@natur.cuni.cz](mailto:michal.mazur@natur.cuni.cz), [cejkaji@natur.cuni.cz](mailto:cejkaji@natur.cuni.cz)

Martin Kubů<sup>2</sup>, J. Heyrovský Institute of Physical Chemistry of the Czech Academy of Sciences, Dolejškova 2155/3, 182 23, Prague, Czech Republic

[martin.kubu@jh-inst.cas.cz](mailto:martin.kubu@jh-inst.cas.cz)

Katarina Fulajtarova<sup>3</sup>, Milan Hronec<sup>3</sup> Department of Organic Technology, Slovak University of Technology, Radlinskeho 9, 812 37 Bratislava, Slovakia

[katarina.fulajtarova@stuba.sk](mailto:katarina.fulajtarova@stuba.sk), [milan.hronec@stuba.sk](mailto:milan.hronec@stuba.sk)

Zeolites with encapsulated metal nanoparticles (NPs) attract much attention due to the catalytic activity, stability and shape-selective properties of such materials in heterogeneous catalysis [1-2]. One of the methods for introduction of metal NPs into the zeolite system is based on use of two dimensional (2D) layered precursors that are loaded with metal source and consecutively transformed to three dimensional (3D) zeolites [3-4].

Here we report a synthesis strategy for the encapsulation of Pd NPs inside MWW zeolite. During the swelling process at ambient temperature diethylenediamine palladium(II) acetate ( $\text{Pd}(\text{en})_2(\text{Ac})_2$ ) is introduced into interlayer space of layered zeolite. Pd@MCM-22 catalyst was formed during the transformation from 2D to 3D zeolite by calcination. The material was investigated by XRD, nitrogen sorption, ICP-OES, and electron microscopy methods. Structural and textural analysis proved no significant changes after the Pd NPs were encapsulated when compared with the parent sample. The Pd loading was 0.79 wt% with a uniform distribution of Pd NPs of about 1.5 nm.

The Pd@MCM-22 catalyst exhibits distinct shape-selective properties in hydrogenation of nitroarenes to anilines; showing very high hydrogenation activity for 3-nitrotoluene and almost no activity for 1-nitronaphthalene. Further, the general application and chemo-selectivity of nitroarenes will also be tested.

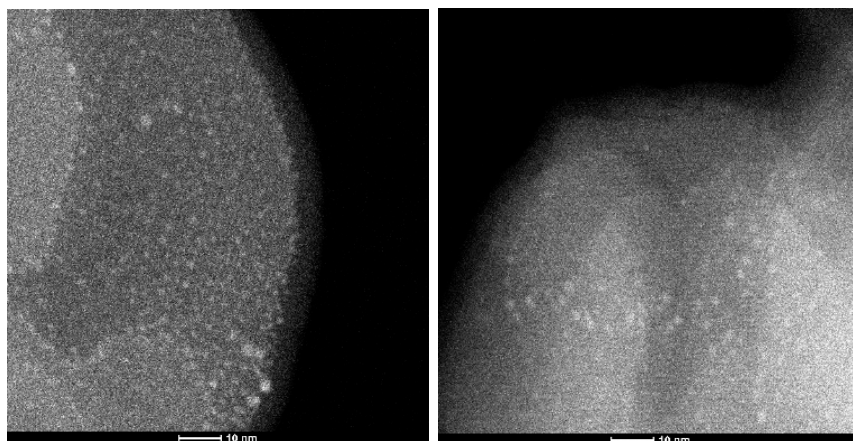


**Fig.1** STEM images of Pd@MCM-22.

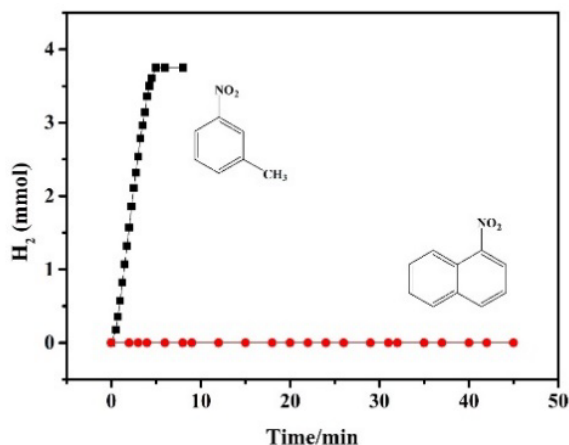


**Fig.2** Hydrogenation reaction kinetic profiles over Pd@MCM-22 catalyst.

#### References

- [1] M.D. Marcinkowski et al., ACS Catal. 2016, 7, 413-420.
- [2] L. Nie et al., Science 2017, 358, 1419-1423.
- [3] Y. Zhang, M. Kubů, M. Mazur, J. Čejka, Catal. Today 2018, doi.org/10.1016/j.cattod.2018.07.015.
- [4] A. Corma et al., Nat. Commun. 2018, 9, Art.-Nr 574.

# **Balancing activity and stability for the production of light paraffins from syngas using a hybrid catalyst: Compositional optimization of MeOH synthesis catalyst function**

*Glenn Pollefeyt<sup>1</sup>, Davy Nieskens<sup>1</sup>, Mark McAdon<sup>2</sup>, Alexey Kirilin<sup>1</sup>, Adam Chojecki<sup>1</sup>, David Yancey<sup>2</sup>, Ewa Tocha<sup>1</sup>, Vera Santos<sup>1</sup>, Andre Malek<sup>2</sup>.*

*<sup>1</sup>Dow Benelux B.V., Herbert H. Dowweg 5, 4542 NM Hoek, The Netherlands*

*<sup>2</sup>The Dow Chemical Company, 1776 Building, Midland MI 48674, U.S.A.*

*\*Corresponding author: GPollefeyt@dow.com*

## **Introduction**

The need to reduce the global carbon footprint and our dependency on oil has directed research towards the development of alternative feedstocks and processes to produce chemicals. Synthesis gas, a mixture of CO and H<sub>2</sub>, is the most practical option for utilization of carbon containing feedstocks such as methane, biomass and waste plastics. Over the last years, the development of polyfunctional tandem catalysts, using oxygenates as a chemical intermediate, has gained attention for the direct conversion of syngas to light hydrocarbons.[1, 2] In such a hybrid catalyst, a methanol synthesis component (typically a mixed metal oxide) is coupled with a methanol conversion component (typically a molecular sieve). For the production of light paraffins (suitable as cracker or dehydrogenation feedstock) from syngas, typically a copper-based methanol synthesis catalyst is used. However, because of the high temperature (> 380 °C) at which this process is operated, the catalysts are particularly prone to deactivation. This presentation will focus on the development of a highly active and high temperature resistant CuCrZnAl-based MeOH synthesis component through a design of experiment approach. Within this design, the influence of both synthesis parameters and compositional space on the catalyst activity and stability were screened, revealing various structure-activity-stability relationships.

## **Experimental**

Over 50 different CuCrZnAl mixed metal oxides were prepared by co-precipitation synthesis at 50 °C and pH=7, using either ammonium- or sodium carbonate as precipitating agent. After drying and calcination, the microstructural and physicochemical properties of the catalysts were characterized by XRF, XRD, TPR, XPS, XAS and TEM. SAPO-34 was prepared according to the procedure described

by Lok *et al.*[3] The hybrid catalyst was prepared by mixing the desired amounts of mixed metal oxide and SAPO-34 sieve fractions (40-80 mesh). Syngas conversion was performed in a stainless steel fixed-bed reactor system (*i.d.* 7.7 mm) at 50 bar and  $H_2/CO = 3$ , WHSV ranging from 1.4 to 5.5  $h^{-1}$  in a fixed testing protocol. The outlet gas composition was measured using an online Maxum process GC.

## Results

As can be observed from Figure 1, hybrid catalysts consisting of SAPO-34 and a CuCrZnAl-based mixed metal oxide showed a significantly higher catalytic activity over conventional high temperature CrZn-based catalysts and a better stability compared to the industrially employed CuZnAl-based methanol synthesis catalysts. Through statistical modelling, a compositional space for optimal hydrocarbon productivity could be described by a combination Cu, Zn, Cr and Al atomic ratios:  $0.25 < Cu/Zn < 1.5$ ;  $0 < Cr/Zn < 1$  and  $(Al + Cr)/(Cu+Zn+Cr+Al) < 0.4$  (Figure 1b).

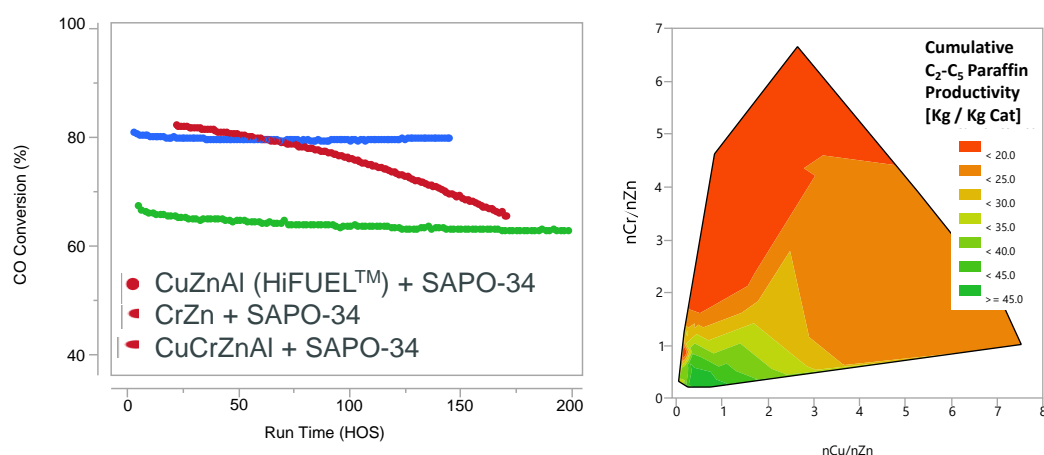


**Figure 1: a) CO conversion as function of time on stream and b) Composition - C<sub>2</sub>-C<sub>5</sub> Productivity relationship for Hybrid catalysts comprising CuCrZn(Al) mixed metal oxides.**

Detailed characterization revealed that within this compositional range, the as-prepared catalysts consist of a nano-crystalline mixture of highly dispersed CuO on ZnO and Zn-containing spinel phases. This in turn leads to the **high activity** in combination with **increased stability** as compared to commercial Cu-based methanol catalysts.

## References

- [1] D.L.S. Nieskens, A. Ciftci, P.E. Groenendijk, M.F. Wielemaker, A. Malek, Production of Light Hydrocarbons from Syngas Using a Hybrid Catalyst, *Industrial & Engineering Chemistry Research*, 56 (2017) 2722-2732.
- [2] F. Jiao, J. Li, X. Pan, J. Xiao, H. Li, H. Ma, M. Wei, Y. Pan, Z. Zhou, M. Li, S. Miao, J. Li, Y. Zhu, D. Xiao, T. He, J. Yang, F. Qi, Q. Fu, X. Bao, Selective conversion of syngas to light olefins, *Science*, 351 (2016) 1065-1068.
- [3] B.M. Lok, *Crystalline silicoaluminophosphates*, US4440871A, 1984.



# Stabilization of homogeneous Mo catalysts by bulky $\beta$ -diketonates in deoxydehydration reactions

*Maxime Stalpaert; Dirk De Vos, KU Leuven, Leuven, Belgium*

The global use of fossil feedstocks as the main resource for the production of energy, chemicals and materials results in several issues, most importantly global warming. While for energy needs several alternatives are available, biomass is likely the only realistic option for the sustainable production of chemicals. However, the components of biomass generally have a high oxygen functionalization degree compared to common industrial chemicals and, as a result, deoxygenation reactions are required. An interesting deoxygenation reaction is deoxydehydration (DODH), which involves the reductive removal of two vicinal hydroxy groups, resulting in formation of a double bond.<sup>[1-4]</sup> Earth abundant Mo and V have been reported as active catalysts; however, yields and activities are much lower than with the more active, but expensive, Re catalysts. Furthermore, for Mo, the effect of ligands on the metal catalyst has barely been investigated. Therefore, we have examined the effect of several  $\beta$ -diketonate ligands on a Mo catalyst. We have demonstrated the positive effect of 2,2,6,6-tetramethyl-3,5-heptanedionate (TMHD) as ligand in the DODH reaction.<sup>[5]</sup>

In our screening of  $\beta$ -diketonate ligands, both an electronic and steric effect were observed, however, the latter was dominant. The bulky electron donating  $\beta$ -diketonate 2,2,6,6-tetramethyl-3,5-heptanedionate (TMHD) had the most positive effect, resulting in up to a ten-fold increase in yield and turn-over frequency (TOF) for the desired DODH product. The positive effect of TMHD can be explained by its coordination to Mo, which results in a steric barrier that hampers the formation of oligonuclear Mo oxo-clusters. If this clustering is allowed to continue unimpeded, it results in precipitation and, hence, deactivation of the catalyst. The stabilization of the homogeneous catalyst was demonstrated by filtration experiments and electrospray ionization mass spectroscopy (ESI-MS). Using the latter method, oligonuclear Mo species and even mononuclear  $\text{MoO}(\text{TMHD})_2$  were detected after reaction in the presence of TMHD. On the other hand, in the absence of TMHD, barely any Mo remained in solution after reaction. The precipitation of the Mo catalyst

is a known problem in DODH literature.<sup>[6]</sup> This work represents the first time the cause of this issue is examined. Furthermore, we demonstrate that an appropriate ligand can be chosen to avoid precipitation. Finally, we have shown that the positive effect of TMHD is present for several different substrates and reductants.

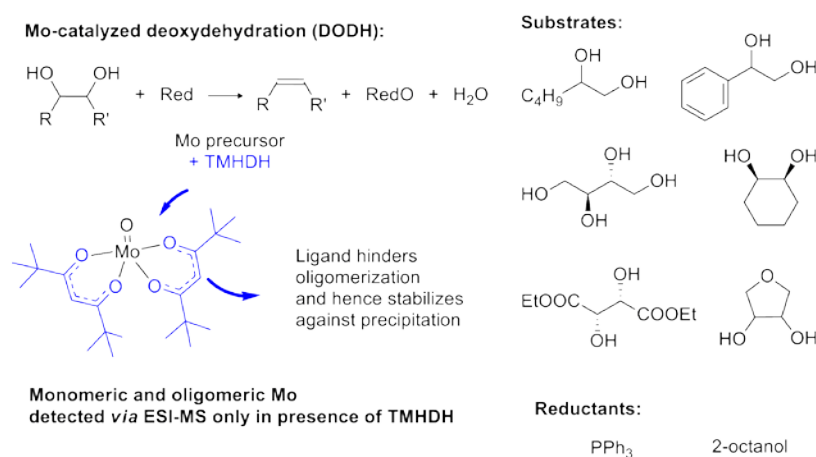


Figure 1: Graphical abstract

## References

- [1] J. R. Dethlefsen, P. Fristrup, *ChemSusChem* **2014**, *8*, 767–775.
- [2] A. R. Petersen, P. Fristrup, *Chem. - A Eur. J.* **2017**, *23*, 10235–10243.
- [3] C. Boucher-Jacobs, K. M. Nicholas, in *Sel. Catal. Renew. Feed. Chem.* (Ed.: K.M. Nicholas), Springer-Verlag, Berlin, Germany, **2014**, pp. 163–184.
- [4] S. Raju, M.-E. Moret, R. J. M. Klein Gebbink, *ACS Catal.* **2015**, *5*, 281–300.
- [5] M. Stalpaert, D. De Vos, *ACS Sustain. Chem. Eng.* **2018**, *6*, 12197–12204.
- [6] J. R. Dethlefsen, D. Lupp, A. Teshome, L. B. Nielsen, P. Fristrup, *ACS Catal.* **2015**, *5*, 3638–3647.

# In-situ Quick-XAS following of CoMoP/Alumina catalyst precursors sulfidation – Effect of organic compounds

*B. GUICHARD<sup>1</sup>, C. LEGENS<sup>1</sup>, V. BRIOIS<sup>2</sup>, O. DELPOUX<sup>1</sup>*

<sup>1</sup> IFP Energies nouvelles, Rond-point de l'échangeur de Solaize BP3, 69360 Solaize, France ; <sup>2</sup> Synchrotron SOLEIL L'orme des Merisiers, 91192 Gif-sur-Yvette Cedex, France

## Introduction

The “CoMoS” active phase used for middle distillates hydrotreating (HDT) consists in well-dispersed MoS<sub>2</sub> nanocrystallites decorated by cobalt and obtained by sulfidation of the oxide precursors. The use of additive-impregnated catalysts led to a new generation of industrial HDT catalysts [1,2]. Nevertheless, the origins of the activity enhancement remain controversial : (i) the additives may act as low temperature sulfidation inhibitors [1]; (ii) but the presence of the organic compounds also hinders the interaction between the active phase precursors and alumina and enhances the dispersion of metallic species [3,4]. For instance, glycol molecules have been proposed as suitable compounds, leading to significant gains in hydrodesulfurization activity [5]. To identify more precisely the improvement mechanisms of activity gains due to the use of organic compounds, an Quick-XAS in-situ sulfidation of additive-impregnated and their counterpart without additive was performed at the ROCK beam-line in SOLEIL Synchrotron. Two kinds of additive were selected to do so : citric acid (CA) and Tri-Ethylene-Glycol (TEG).

## Experimental work

X-ray Absorption Spectroscopy (XAS) has been performed on crushed catalysts. The sulfidation is carried out in a dedicated cell with H<sub>2</sub>S/H<sub>2</sub> (15:85 v/v) from room temperature to 400°C at 2°C/min before a 2 hours step. Mo(Co)-K-edge spectra are recorded during 45s leading to one average spectrum every 5.3°C. CoMoP catalyst were prepared by incipient wetness impregnation of a  $\gamma$ -alumina and only drying. Citric acid was introduced into the same impregnating solution as metal and TEG was introduced by a consecutive impregnation of dried CoMoP. The data were analysed by Principal Component Analysis (PCA) and Multivariate Curve Resolution by Alternating Least Square (MCR-ALS) minimization in order to determine the concentration profiles of the species involved during activation and the XAS spectra of these pure species [6]. To complete the characterization, Raman spectroscopy was performed on oxide catalysts and XPS at the end of the sulfidation step.

## Results

The PCA of normalized EXAFS spectra evolution at Mo(Co)-K-edge suggest the use of 4(3) components to describe the system evolution whatever the CoMoP catalyst. The MCR-ALS was used to describe the components and the evolution of their relative concentration (Figure 1).

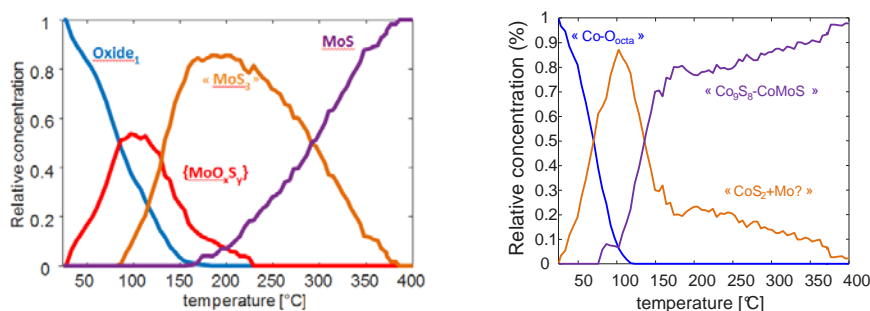


Figure 1 : Evolution of relative concentration of Co and Mo components with temperature for additive free CoMoP revealed by MCR-ALS

The additives modify the nature of the oxide and of the first intermediate species, whereas the final species look similar from a local structure point of view.

We did not evidence any sulfidation delay of Mo and Co when citric acid was added, compared to catalyst without additives. In presence of TEG, the MoS<sub>2</sub> phase was formed at lower temperature, and a complete sulfidation of cobalt was achieved around 300°C instead of ~380°C for the dried catalyst (Figure 2).

Those result can be discussed regarding catalytic activity and respective roles of additives.

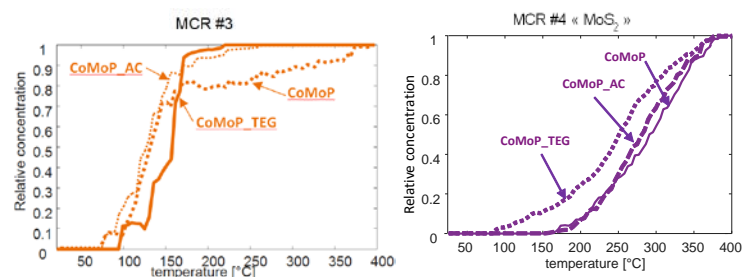


Figure 2 : Comparison of relative concentration of the final MCR components at Mo- and Co K-edges in function of sulfidation temperature

## References

- [1] P. Mazoyer-Galliou et al., Oil&Gas Sci. Tech.- Rev. IFP 2005, 60(5), 791-799
- [2] D. Nicosia et al., J. Catal. 2005, 229, 424-438
- [3] J. Escobar et al., Appl. Catal. B 2009, 88, 564-575
- [4] V. Costa et al., Catal. Today 2008, 130(1), 69-74
- [5] Patent EP0601722A1 (1994).
- [6] Rochet et al., J. Phys. Chem. C 2017 , 121, 18544-18556

# **The inhibition of hydrogen and oxygen recombination over Pt-TiO<sub>2</sub> and enhancement of photocatalytic over-all water splitting**

*Gongxuan Lu, Lanzhou Institute of Chemical Physics, Chinese Academy of Sciences, Lanzhou, China*

Semiconductor photocatalysts for overall water splitting into H<sub>2</sub> and O<sub>2</sub> require metal cocatalyst, such as Pt, to catalyze H<sub>2</sub> evolution efficiently. However, these metal cocatalysts can also catalyze hydrogen and oxygen recombination to form water. In this work, we found that the pre-adsorbed halogen atom catalyst could inhibit the reverse reaction of water formation from H<sub>2</sub> and O<sub>2</sub> due to the decrease of adsorption energies of H<sub>2</sub> and O<sub>2</sub> on Pt. The adsorption energy decrease of H<sub>2</sub> and O<sub>2</sub> followed the order of F/Pt < Cl/Pt < I/Pt < Br/Pt. H<sub>2</sub>-TPD results exhibited similar dependence. This inhibition was achieved via the occupation of halogen atom on the Pt surface sites, and thereby the adsorption and activation of hydrogen and oxygen molecules were decreased. The occupation difference of halogen atoms are determined by radius of halogen ions, which further leads the different activity for H<sub>2</sub> and O<sub>2</sub> recombination. By inhibition of water formation reverse reaction, the over-all water splitting over Pt/TiO<sub>2</sub> photocatalysts has been achieved. Isotope experiments with D<sub>2</sub>O and H<sub>2</sub><sup>18</sup>O confirmed the over-all water splitting to H<sub>2</sub> and O<sub>2</sub>. This study may help scientist to develop high-efficient photocatalyst for overall water splitting.

# An Unified Algorithms Based eNRTL Model for Aqueous Sulfuric Acid System

Shailesh Pathak, Department of Chemical Engineering, IIT Delhi, New Delhi-110016, India

Sreedevi Upadhyayula, Department of Chemical Engineering, IIT Delhi, New Delhi-110016, India

Damaraju Parvatalu, ONGC Energy Center, India

Bharat Bhargava, ONGC Energy Center, India

## Introduction

In closed loop Iodine-Sulfur (I-S) process for hydrogen production, sulfuric acid is formed at 70 wt.% in Bunsen reaction at about 353-393 K which needs to concentrate up to 92 wt.% before decomposing to sulfur trioxide [1]. This concentration and reaction involves many ionic species whose thermodynamic properties including phase behavior, speciation, heat capacity of this complex sulfuric acid system in the temperature ranges (up to 1173 K) need to be determined. However, this task still a vital challenge to researcher due to chemical speciation, non-ideal azeotrope formation above 92 wt.% concentration and thermal dissociation of sulfuric acid [2–6]. Henceforth, this work is an attempt to develop algorithm based eNRTL model to predict the thermodynamic behavior including chemical speciation, phase equilibria and enthalpy of the sulfuric acid system.

## Model development and methodology

### 1) Vapor Liquid Equilibrium

At equilibrium, in the multicomponent system, fugacity of molecular species in liquid phase is equal to the vapor phase fugacity.

$$Py_i\varphi_i = x_i\gamma_i f_i^o \quad (1)$$

where,  $P$  = System pressure,  $y_i$  = Mole fraction (Vapor phase) of component  $i$ ,  $\varphi_i$  = Fugacity coefficient (Vapor Phase) of component  $i$ ,  $x_i$  =

Mole fraction (Liquid Phase) of component  $i$ .  $\gamma_i$  = Activity coefficient (Liquid phase) for component  $i$ ,  $f_i^o$  = Liquid phase fugacity of pure component  $i$ .

### 2) Activity coefficient model

$$\ln \gamma_i = \ln \gamma_i^{SR} + \ln \gamma_i^{LR} \quad i, j = m, c, a \quad (2)$$

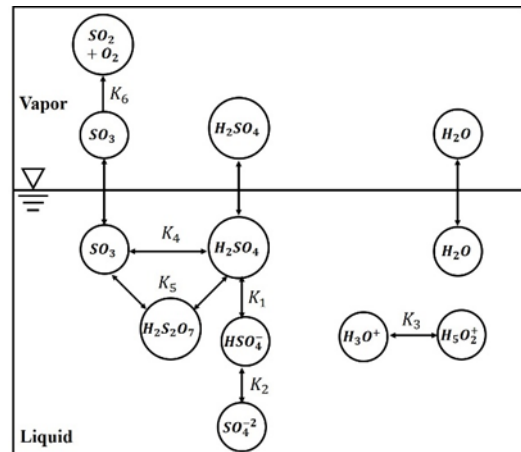


Figure 1 Chemical speciation in sulfuric acid solution

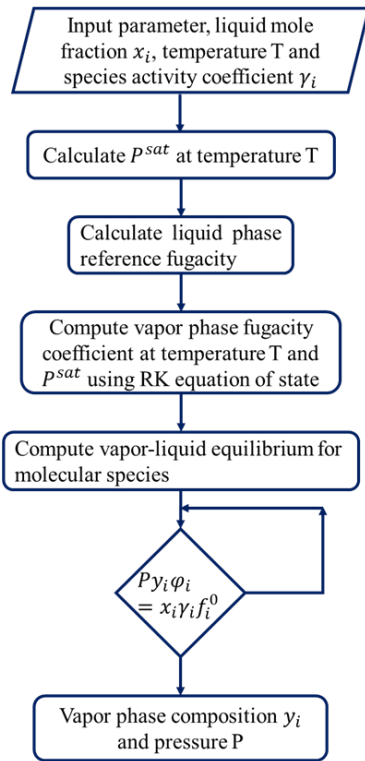


Figure 2 Algorithm for pressure calculation

## Conclusion

In this work, we have developed a rigorous model to estimate the thermodynamic properties for sulfuric acid system in I-S for hydrogen production. The model involved the chemical speciation computational optimization framework to estimate the thermodynamic properties and showed good consistent with the experimental data. eNRTL model explicitly accounting for “extent of dissociation” and consistent results in the whole concentration range even at extremely high temperature.

Model results are consistent with reference to the experimental data sets reported in literature. This study will be extremely useful for further development and process of sulfuric acid system in I-S process for hydrogen production.

## Acknowledgement

The authors are thankful to ONGC Energy Center Trust (OECT), India for financial support.

Where,  $\gamma_i^{SR}$  and  $\gamma_i^{LR}$  are short range and long range activity coefficient from NRTL modeling.

The sulfuric acid in aqueous solution follow the chemical speciation as shown in figure 2. The equilibrium constant of these reactions can be written in terms of mole fraction and activity coefficient. The equilibrium constant for the second speciation reaction can be as per equation 3.

$$K'_2 = \frac{x_{H^+} x_{SO_4^{2-}}}{x_{HSO_4^-}} \left( \frac{\gamma_{H^+} \gamma_{SO_4^{2-}}}{\gamma_{HSO_4^-}} \right) \quad (3)$$

Algorithm for pressure calculation is shown in figure 2, similar algorithms for the equilibrium rate and activity coefficient can be written. First step methodology is the initial guess estimation of the speciation in the aqueous solution and solve iteratively till specific conditions (convergence criterion) of equilibrium constant estimation as shown in equation 3 is satisfied.

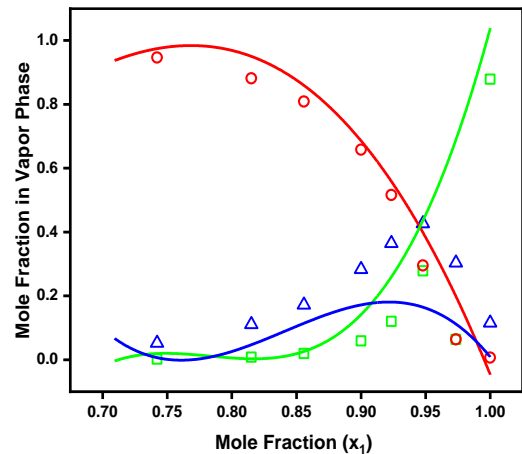


Figure 3 Component distribution in vapor phase as functions of  $H_2SO_4$  concentration in aq. solution at 483.15 K. — Model results ( $H_2O$ ),  $\circ$  Perry et al. [7] ( $H_2O$ ), — Model results ( $H_2SO_4$ ),  $\triangle$  Perry et al. [7] ( $H_2SO_4$ ), — Model results ( $SO_3$ ),  $\square$  Perry et al. [7] ( $SO_3$ )

## References

- [1] Y. Shin, K. Lee, Y. Kim, J. Chang, W. Cho, K. Bae, A sulfur-iodine flowsheet using precipitation, electro dialysis, and membrane separation to produce hydrogen, *Int. J. Hydrogen Energy*. 37 (2012) 16604–16614. doi:10.1016/j.ijhydene.2012.02.082.
- [2] J.I. Gmitro, T. Vermeulen, Vapor-Liquid Equilibria for Aqueous Sulfuric Acid, *Aiche J.* 10 (1964) 740–746.
- [3] D. O'Keefe, C. Allen, G. Besenbruch, L. Brown, J. Norman, R. Sharp, K. McCorkle, Preliminary results from bench-scale testing of a sulfur-iodine thermochemical water-splitting cycle, *Int. J. Hydrogen Energy*. 7 (1982) 381–392. doi:10.1016/0360-3199(82)90048-9.
- [4] S.L. Clegg, P. Brimblecombe, Equilibrium partial pressures and mean activity and osmotic coefficients of 0-100% nitric acid as a function of temperature, *J. Phys. Chem.* 94 (1990) 5369–5380. doi:10.1021/j100376a038.
- [5] P. Bolsaitis, J.F. Elliott, Thermodynamic Activities and Equilibrium Partial Pressures for Aqueous Sulfuric Acid Solutions, *J. Chem. Eng. Data*. 35 (1990) 69–85. doi:10.1021/je00059a022.
- [6] E.M. Collins, The Partial Pressure of Water in Equilibrium with Aqueous Solutions of Sulfuric Acid., *J. Phys. Chem.* 37 (1932) 1191–1203. doi:10.1021/j150351a009.
- [7] R.H. Perry, D.W. Green, J.O. Maloney, *Perry's Chemical Engineers' Handbook*, Seventh, 1997. doi:10.1021/ed027p533.1.



# Plasmon and Cocatalyst-Mediated Photoanodes Enhance Photoelectrochemical Water Oxidation Efficiency

Ruirui Wang, Lan Luo, Xu Xiang\*

State Key Laboratory of Chemical Resource Engineering, Beijing University of Chemical Technology,

Beijing, 100029 China

E-mail: [xiangxu@mail.buct.edu.cn](mailto:xiangxu@mail.buct.edu.cn)

Generation of hydrogen from photoelectrochemical (PEC) water splitting is one of the most promising pathways to boost clean energy economy.[1,2] It is highly desirable to improve the efficiency of the photoelectrochemical (PEC) anodes because the water oxidation at the anodes is a thermodynamic unfavorable and dynamics sluggish reaction.[3,4] The common way to improve PEC efficiency is to modify photoanodes with water oxidation catalysts (WOCs). We designed a sandwich structure photoanode i.e., LDHs/Au@SiO<sub>2</sub>/BiVO<sub>4</sub>, where LDHs acted as water oxidation cocatalyst and the localized surface plasmon resonance (LSPR) effect of Au@SiO<sub>2</sub> was utilized. The Au@SiO<sub>2</sub>/LDHs/ BiVO<sub>4</sub> was prepared as a control, where the LDHs were firstly grown on the BiVO<sub>4</sub>. The LDHs/Au@SiO<sub>2</sub>/BiVO<sub>4</sub> achieved a photocurrent density of 1.92 mA·cm<sup>-2</sup> (1.23 V vs. RHE), a 52% enhancement compared to the Au@SiO<sub>2</sub>/LDHs/BiVO<sub>4</sub> (1.26 mA·cm<sup>-2</sup>). The oxidation efficiency of LDHs/Au@SiO<sub>2</sub>/BiVO<sub>4</sub> was around 69% (1.23 V vs RHE), 1.3 times higher than that of Au@SiO<sub>2</sub>/LDHs/BiVO<sub>4</sub>. The findings verified that the BiVO<sub>4</sub> mainly contributes to charge separation and the LSPR effect of Au is strongly position-dependent. LDHs acted as a cocatalyst to accumulate photo-generated holes and accelerate water oxidation.[5,6] The combination of catalysis and plasmon effect enables the enhanced water oxidation performance.

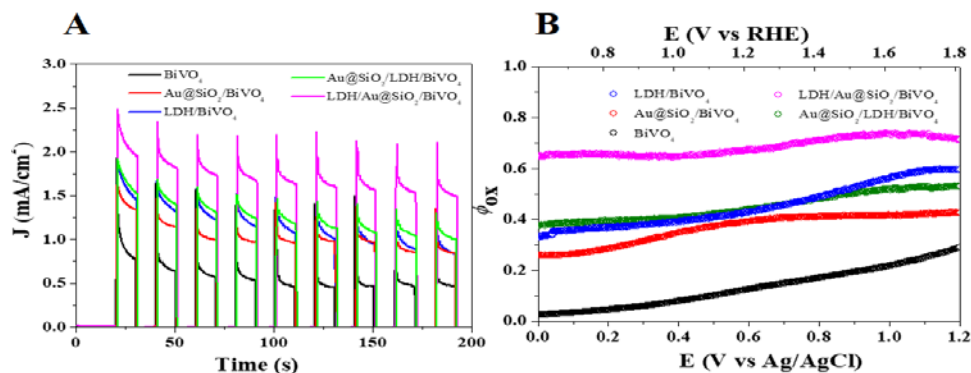


Figure 1 Chopped photocurrent-time curves under AM1.5G light irradiation (A),  
oxidation efficiency of surface-reaching holes (B).

#### References

- [1] Yu, Z.; Li, F.; Sun, L. *Energy Environ. Sci.*, 2015, 8, 760-775.
- [2] He, W.; Yang, Y.; Wang, L.; Xiang, X. et al., *ChemSusChem.*, 2015, 8, 1568-1576.
- [3] Tang, Y.; Fang, X.; Zhang, X. et al., *ACS Appl. Mater. Interfaces* 2017, 9, 36762-36771.
- [4] Tang, Y.; Wang, R.; Yang, Y. et al., *ACS Appl. Mater. Interfaces* 2016, 8, 19446-19455.
- [5] Li, Y.; Zhang, L.; Xiang, X. et al., *J. Mater. Chem. A*, 2014, 2, 13250-13258.
- [6] He, W.; Wang, R. Zhang, L.; Xiang, X. et al., *J. Mater. Chem. A*, 2015, 3, 17977-17982.

# Catalysis of hydrodeoxygenation of octanoic acid parallel with hydrodesulfurization of benzothiophene by NiMo sulfides: Support effect

*L. Kaluža, J. Karban, J. Moravčík, D. Gulková*

*Institute of Chemical Process Fundamentals of CAS, v. v. i., Rozvojová 135, CZ-16502 Prague 6; Czech Republic*

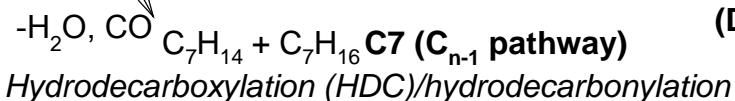
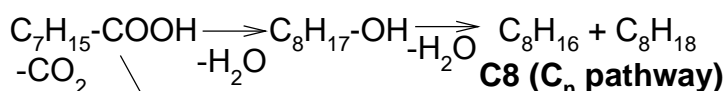
Among variety of synthetic crudes (originated from plastic or biomass waste), only the biomass derived crude satisfy the need of renewable hydrocarbon resource. Specifically, vegetable oils (high fatty acid content) are the cheapest raw material in the bio-oil market with high energy density. For this reason, they have been already utilized as fatty acid methyl esters (FAME) in diesel fuel. Despite that, stability of FAME remains problematic due to the presence of reactive C=C double bonds and carboxylic group. Furthermore, the utilization of waste (high content of free fatty acids and other contaminants) or non-edible triglycerides call for hydrotreating reaction over sulfidic catalysts instead of transesterification reaction in order to produce high quality bio-fuels. Advantages of the simultaneous hydrodeoxygenation (HDO)/hydrodesulfurization (HDS) also lays in keeping catalysts in sulfidic form by sulfur containing compound and in the use of existing refinery hydrotreating infrastructure. Therefore, we have compared MgO (300 m<sup>2</sup>g<sup>-1</sup>), C (225 m<sup>2</sup>g<sup>-1</sup>), ZrO<sub>2</sub> (108 m<sup>2</sup>g<sup>-1</sup>), Al<sub>2</sub>O<sub>3</sub>, (262 m<sup>2</sup>g<sup>-1</sup>), TiO<sub>2</sub>, (140 m<sup>2</sup>g<sup>-1</sup>), SiO<sub>2</sub>-Al<sub>2</sub>O<sub>3</sub> (480 m<sup>2</sup>g<sup>-1</sup>), supports for deposition of NiMo sulfides in order: i) To determine the catalysts activity in HDO reaction of octanoic acid, which was run together with HDS reaction of 1-benzothiophene; ii) To determine the influence of the supports on promotion effect of Ni on HDO/HDS activity of Mo sulfide; and iii) To analyze simple reaction progress kinetic (RPKA) of the HDO reaction over the most active catalysts giving insight into selectivity hydrogenolysis (HYG)/ hydrodecarboxylation (HDC) and selectivity of formation of olefins during HDO. The catalysts were prepared by conventional impregnation of supports to achieve the loadings of Mo with surface density of 3.5 metal atoms per nm<sup>2</sup> (the modified surface area was used for the microporous carbon support; SiO<sub>2</sub>-Al<sub>2</sub>O<sub>3</sub> was loaded with surface density 1.0 metal atoms per nm<sup>2</sup>). Ni loadings corresponded to atomic ratio Ni/(Ni + Mo) of 0.3. C-supported

catalysts were not calcined and MgO supported catalysts were prepared by non-aqueous impregnation.

330 °C and 1.6 MPa

### Hydrogeoxygenation (HDO)

*Hydrogenolysis (HYG)/dehydration*



### Hydrodesulfurization (HDS)

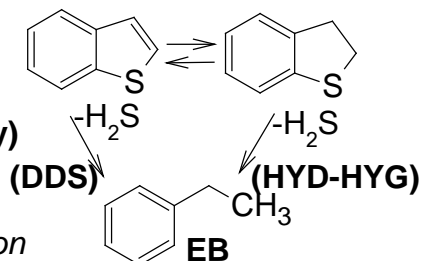


Figure 1. Scheme of HDO of octanoic acid and HDS of 1-benzothiophene.

It was ascertained that the parallel reactions of HDO of octanoic acid and HDS of 1-benzothiophene revealed that the support type influenced the activity and selectivity of the studied NiMo sulfides. Unsupported NiMo sulfide, prepared for the matter of comparison, resulted in the lowest HDO and HDS activities due to its low surface area of 33 m<sup>2</sup>g<sup>-1</sup>. Also the basic and amphoteric oxides MgO and Al<sub>2</sub>O<sub>3</sub>, ZrO<sub>2</sub> do not lead to highly active NiMo catalysts presumably due to low hydrothermal stability during HDO. The most active catalysts represented NiMo sulfides supported on TiO<sub>2</sub> and C, which yielded exclusively linear hydrocarbons by the HDO reaction. Decrease of point of zero charge of the support, i.e. an increase of acidity, increased selectivity HDO/HDS of the deposited NiMo phase. Deposition of the Ni promoter, however, shifted the selectivity towards product of hydrodecarboxylation reaction, i.e. heptanes (C<sub>n-1</sub> pathway), almost independently on the support type. Nevertheless, the most active NiMo/TiO<sub>2</sub> in HDO was the most selective catalyst from the studied NiMo phases to n-octane, the product of octanoic acid hydrogenolysis (C<sub>n</sub> pathway). Pronounced isomerization and cracking activity during HDO was observed over NiMo/SiO<sub>2</sub>-Al<sub>2</sub>O<sub>3</sub> catalyst.

### Acknowledgement

Special thanks to doctors Z. Vít and M. Zdražil, who helped with SiO<sub>2</sub>-Al<sub>2</sub>O<sub>3</sub> synthesis and RPKAs, respectively. Czech Science Foundation (grant No. 17-22490S) is gratefully acknowledged for the financial support.

### References

[1] L. Kaluža, J. Karban, D. Gulková (2018): The effect of support type on promotion of activity and selectivity of Mo, CoMo, and NiMo sulfides in parallel hydrodeoxygenation and hydrodesulfurization (in preparation).

# Machine Learning for Statistical Analysis and Design of Heterogeneous Catalysis

*Takashi Toyao<sup>1,2</sup>, Satoru Takakusagi<sup>1</sup>, Ichigaku Takigawa<sup>3</sup>, Ken-ichi Shimizu<sup>1,2</sup>*

*<sup>1</sup>Institute for Catalysis, Hokkaido University, N-21, W-10, Sapporo 001-0021, Japan*

*<sup>2</sup>Elements Strategy Initiative for Catalysis and Batteries, Kyoto University, Katsura, Kyoto 615-8520, Japan*

*<sup>3</sup>Graduate School of Information Science and Technology, Hokkaido University, N-14, W-9, Sapporo 060-0814, Japan*

## Introduction

Machine learning (ML) methods have gained much attention among the molecular and materials science communities for use in the prediction of various kinds of physical and chemical properties. ML methods could serve as a fast and high-precision alternative to the first-principles modelling. Several successful examples are already available for predictions and discoveries of organic chemistry reactions including ones that use homogeneous catalysts. However, targets of ML predictions for heterogeneous catalysis have been limited. Our group has been trying to contribute to establishing “Catalysis Informatics” by utilizing ML.<sup>1-3</sup> Herein, we propose a ML approach that considers elemental features as input representation instead of considering catalyst compositions themselves. This novel ML method could lead to catalysts discovery even for catalytic reactions having less information and less catalyst composition diversity. Oxidative coupling of methane (OCM) was chosen as an example to confirm effectiveness of the proposed method and were analyzed by several the-state-of-the-art ML methods.

## Methodology

We employ widely used implementations of scikit-learn (version 0.19) for all ML models except XGB, and for XGB the original implementation of XGBoost is used. The key hyperparameters of each model are best tuned in an exhaustive way (i.e. grid search) within the specified ranges. The quantitative evaluations of prediction accuracy are based on the root mean squared errors (RMSEs) calculated by 10-fold cross validation, the most widely used method for estimating prediction error.

## Results and discussion

We evaluate the prediction performance of the proposed approach with 7 different ML methods, as shown in Figure 1. All evaluations were carried out by the 10-fold cross validation and the root mean square error (RMSE) of the difference between predicted value and ground truth, and their standard deviations are also calculated. Figure 1 shows the prediction error (RMSEs) for C<sub>2</sub> yield prediction of OCM catalysts. Non-linear methods perform better than linear methods, and in particular, tree ensemble methods (RFR, XGB, ETR) result in small training and test error. The best prediction performance (by XGB) is RMSE of 0.525 (training error) and 4.111 (test error) for predicting C<sub>2</sub> yield (%).

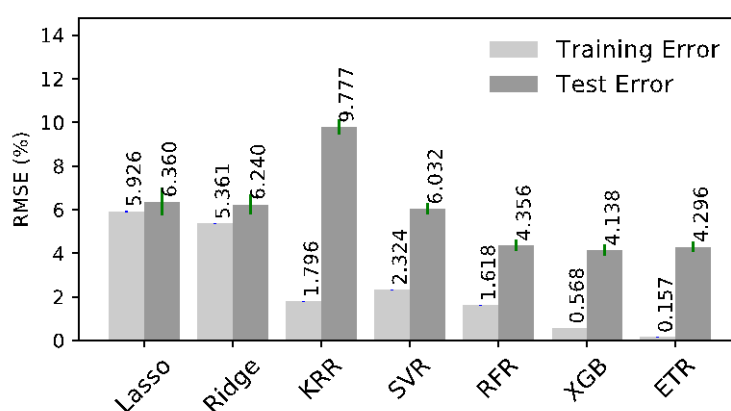


Figure 1. The prediction-error comparisons for catalyst performance (C<sub>2</sub> yield) for OCM. The proposed approach is tested with 7 the-state-of-the-art machine learning methods. The evaluations are done with respect to RMSEs estimated by 10-fold cross validation.

## Conclusions

A novel machine learning (ML) approach that deals with elemental features as input representation instead of catalyst compositions themselves was proposed and demonstrated by employing the previous experimental catalytic data on oxidative coupling of methane (OCM).

## References

- (1) I. Takigawa, K. Shimizu, K. Tsuda, S. Takakusagi "Machine-learning prediction of the d-band center for metals and bimetals" *RSC Advances*, **2016**, 6, 52587-52595.
- (2) T. Toyao, K. Suzuki, S. Kikuchi, S. Takakusagi, K. Shimizu, I. Takigawa "Toward effective utilization of methane: machine learning prediction of adsorption energies on metal alloys" *The Journal of Physical Chemistry C*, **2018**, 122, 8315–8326.
- (3) K. Suzuki, T. Toyao, Z. Maeno S. Takakusagi, K. Shimizu, I. Takigawa "Statistical analysis and discovery of heterogeneous catalysts based on machine learning from diverse published data" submitted.

## **Enhancing hydrothermal stability of framework Al in ZSM-5: a mechanism study on the interaction between P and Al species**

*Lei Han, Research Institute of Petroleum Processing, Sinopec, Beijing, China; Ying Ouyang, Research Institute of Petroleum Processing, Sinopec, Beijing, China; Enhui Xing, Research Institute of Petroleum Processing, Sinopec, Beijing, China; Yibin Luo, Research Institute of Petroleum Processing, Sinopec, Beijing, China; Zhijian Da, Research Institute of Petroleum Processing, Sinopec, Beijing, China*

Catalytic cracking over acid zeolites is an important hydrocarbon upgrading process to produce transportation fuel and petro-chemicals. For FCC process, it is effective to burn off coke deposits on catalysts at high temperatures, however it also promotes dealumination, gradual but permanent deactivation of the catalyst, which would also occur in high-temperature reactions with H<sub>2</sub>O as a by-product<sup>[1,2]</sup>. Therefore promoting the hydrothermal stability for zeolites have been extensively proved important to decrease the zeolite consumption, equal to promoting the recyclability and sustainability of zeolites<sup>[3]</sup>. Phosphorus modification has been extensively proven effective to improve hydrothermal stability of zeolites, with modification on acidity and shape selectivity of zeolites.

However, phosphorus species mainly as condensed polyphosphate species blocked the micropore severely during phosphorus modification. The diffusion resistance on phosphorus is the main reason to reduce the stabilization efficiency on framework aluminum. H<sub>2</sub>O molecules diffused more easily than phosphorus into channels of ZSM-5, resulting in the dealumination and monoclinic/orthorhombic transition during the steam activation. Therefore, tetrahedrally coordinated framework aluminum (TFAI) should be stabilized as much as possible before the steam activation. The interaction between phosphorus and aluminum has been systemically studied with dealumination, alkali treatment, phosphorus modification and the steam treatment on ZSM-5. <sup>29</sup>Si/<sup>27</sup>Al/<sup>31</sup>P MAS NMR was performed to verify the changes of Si, Al and P atoms during phosphorus modification. It turned out that the NaOH treatment was most effective to form mesopore to improve the P/Al ratio, the retention of micropores, and the relative crystallinity. More importantly, it also reduced the diffusion resistance on phosphorus to penetrate the zeolite channel to access framework aluminum for better interaction between phosphorus and aluminum.

Meanwhile, the TFAL-P species had been formed before steam activation with suitable mesopores. The key physicochemical index measuring efficiency of phosphorus modification was set as the sharp signal at 39 ppm with good symmetry in  $^{27}\text{Al}$  MAS NMR before steam activation (Fig. 1). Mesopores within ZSM-5 could not only improve the retention of acidity by phosphorus, but also enhanced accessibility of acid sites by cracking reactants especially ethylcyclohexane. A possible mechanism of the interaction between phosphorus and aluminum is proposed (Fig. 2). In ideal cases, TFAL should be stabilized as much as possible before the steam treatment. It would benefit the sustainable utilization of zeolites. After NaOH treatment, the proper mesopores could promote the diffusion of phosphorus to approach, access and stabilize TFAL, and then strengthen the interaction between phosphorus and aluminum to form the TFAL-P (39 ppm in  $^{27}\text{Al}$  MAS NMR) before steam activation.

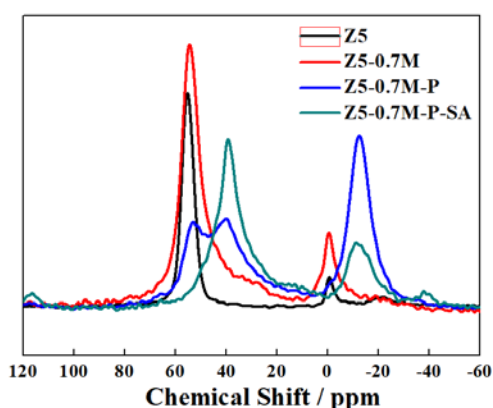


Fig.1  $^{27}\text{Al}$  MAS NMR spectra of Z5-0.7M-P-SA

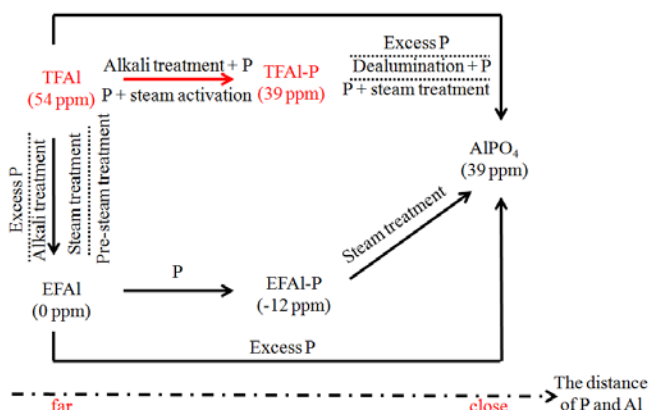


Fig. 2 Proposed mechanism of the interaction between phosphorus and aluminum

## References

- [1] W.W. Keating, C. Chu, L.B. Young, S.A. Butter, *Journal of Catalysis*, 12 (1981) 392-398.
- [2] W.W. Kaeding, L.B. Young, C.C. Chu, *Chemischer Informationsdienst*, 89 (1985) 267-273.
- [3] E.T. Vogt, B.M. Weckhuysen, *Chemical Society Reviews*, 44 (2015) 7342.



# **H<sub>2</sub> Production from Photocatalytic Reforming of Cellulose Using TiO<sub>2</sub> Supported Catalysts**

*Xiaolei Fan, University of Manchester, Manchester, UK; Lan Lan, University of Manchester, Manchester, UK; Christopher Hardacre, University of Manchester, Manchester, UK*

## **Introduction**

Light-driven hydrogen production by photoreforming of an aqueous solution containing either biomass or bio-derived chemicals is a promising way to generate sustainable energy with reduced carbon footprint. The photoreforming process can improve the photocatalytic water-splitting process by using the organic components as the hole-scavenger [1], suppressing the electron/hole recombination. Herein, in order to develop an efficient photocatalytic process for H<sub>2</sub> generation, we suppose to study the photocatalytic generation of H<sub>2</sub> via photoreforming of cellulose by using Pt loaded TiO<sub>2</sub> with two types of titania supports (anatase and P25).

## **Materials and Methods**

Catalysts used in the photoreforming reaction were prepared by the wet impregnation of TiO<sub>2</sub> supports with the H<sub>2</sub>PtCl<sub>6</sub> solution followed by drying at 150°C and calcination at 500°C. Prior to activity testing, the catalysts were reduced in pure H<sub>2</sub> at 200°C. The synthesized catalysts were characterized by X-ray diffraction, BET analysis, transmission electron microscope and UV-Vis spectroscopy.

Catalytic activity tests were performed in a flat-bottomed glass flask with a jacket outside. During the reaction, the circulating bath was applied into the jacket for controlling the reaction temperature. For a typical photoreforming reaction experiment, 75 mg of catalyst and 100 ml of distilled water were placed in the reaction set-up, together with a 0.1 g of cellulose (microcrystalline cellulose). The mixture was stirred for 30 min at room temperature and then purged with Ar for 1.5 h to remove the dissolved oxygen. After purging, the reactor was sealed and irradiated by a UV-A lamp for 5 h. Gas samples were taken after reaction and analysed in a gas chromatography (GC).

## Results and Discussion

The morphology and light absorptive property of catalysts were investigated by XRD, BET and UV-Vis spectroscopy. After the wet impregnation process, the morphologies of both anatase and P25 titanias were not changed. The absorption increased with Pt loading in visible region and showed an optimum absorption with regard to Pt loading in UV region.

Figure 1 shows the comparison result of H<sub>2</sub> generation from photoreforming of cellulose when using P25 and anatase as supports. H<sub>2</sub> and CO<sub>2</sub> are the main gas products in the photoreforming reaction of cellulose. Pt/P25 shows an optimum Pt loading at 0.16% while Pt/Anatase shows an optimum Pt loading at 0.5%. This is because Pt could act as electron sinks to trap the photo-generated electrons and therefore improve the separation of electrons and holes. However, when excess Pt are generated on the surface of TiO<sub>2</sub> supports, the light becomes hard to reach to titania and the separation of electrons and holes will decrease. A higher performance in producing H<sub>2</sub> can also be observed in anatase supported catalyst which could be due to the higher anatase content in Pt/Anatase than that of Pt/P25.

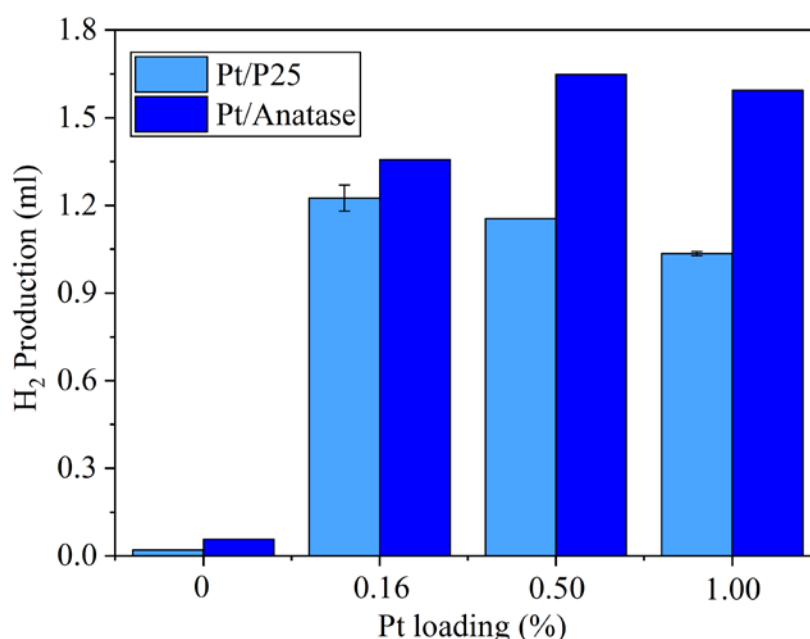


Figure 1. H<sub>2</sub> production from photoreforming of cellulose using Pt/P25 and Pt/Anatase with different Pt loading amounts.

## References

- [1] Caravaca, A.; Jones, W.; Hardacre, C. *Proc. R. Soc. A* **2016**, *472*:20160054.

# **Novel hybrid ZnO material as free-noble metal catalyst support for selective hydrogenolysis of glycerol into 1,2-PDO**

*Lama OMAR, Noémie PERRET, Stéphane DANIELE*

*IRCELYON, UMR CNRS 5256, 2 avenue Albert Einstein, 69626 Villeurbanne Cedex, France.*

## **Introduction**

The exponential growth in the demand for fossil fuels have motivated researchers to explore alternative bio-resources and bio-technologies for fuels and chemicals. In this context, biomass conversion into biofuel leads to the production of ~1 735 540 <sup>[1]</sup> tons a year of glycerol, a nontoxic molecule that can be transformed into more valuable products. In our case, we focused on the hydrogenolysis of glycerol into 1,2 propanediol (1,2-PDO), for large industrial applications (pharmacology, biochemistry, cosmetics...) <sup>[2]</sup> The aim of our study is to develop efficient and selective copper-based catalysts (Cu, Cu-Al, Cu-Ni) supported on novel self-assembly mesospheres hybrid ZnO/PAA support (PAA = Poly Acrylic Acid).

## **Results and discussion**

Synthesis of the hybrid ZnO/PAA (fig.1) was reported via a sol-gel method while changing some synthesis parameters in order to modify the size of the aggregates and to increase the specific surface area. <sup>[3]</sup> This led to mesospheric self-assembly hybrid ZnO-PAA nanomaterials that can be used as novel ZnO catalytic supports with rare high specific surface area ( $>100 \text{ m}^2.\text{g}^{-1}$ ) compared to conventional or commercial ones (around  $10\text{-}20 \text{ m}^2.\text{g}^{-1}$ ).

In our presentation, we will address the importance of the synthetical pathway of the hybrid support and the copper deposition process onto the performances for the catalytic hydrogenolysis of glycerol into 1,2-PDO. We will present results about the influence (i) of the metal percentage deposition (5-40 % wt.), (ii) of the catalyst weight, (iii) of the dispersion of the metallic phase, (iv) of the transformation of the support during the reaction and (v) of the reusability of our catalysts on the

conversion (up to 65 %) and selectivity (up to 99 %). Benchmarking study with commercial ZnO was also conducted in order to compare the effect of this innovative hierarchical nanostructured ZnO support.

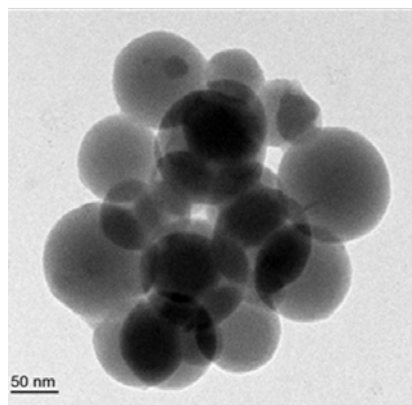


Figure 1: TEM ZnO/PAA NPs

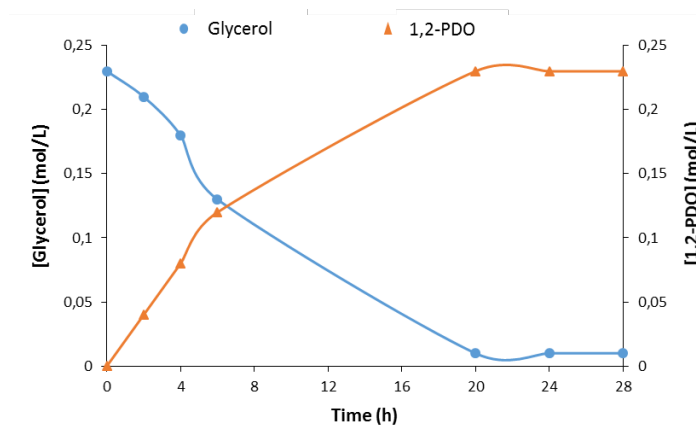


Figure 2: Evolution of the concentrations in glycerol and 1,2-PDO over Cu-Zn-Al catalyst. (T= 200°C, P<sub>H2</sub> = 30 bar)

Incorporation of aluminum in our Cu-ZnO system was also achieved through a one-pot synthesis and has demonstrated a remarkable increase of the conversion up to 96% while maintaining an outstanding selectivity of 99% (fig.2). This was not always the case for different studies made with Cu or with other catalytic systems.<sup>[4-6]</sup> In this part, we will also highlight the importance of the presence of the spinel phase ZnAl<sub>2</sub>O<sub>4</sub> on the high stability of our Cu-Zn-Al catalyst during the reaction.

## References

- [1] C. J. A. Mota, B. Peres Pinto, and A. L. de Lima, "Glycerol," *Cham: Springer International Publishing*, 2017.
- [2] A. M. Ruppert, K. Weinberg, and R. Palkovits, "Hydrogenolysis Goes Bio: From Carbohydrates and Sugar Alcohols to Platform Chemicals," *Angew. Chem. Int. Ed.*, 51, 11, 2564–2601, 2012.
- [3] S. Daniele, T. Cornier, and A. Valette, Patent PCT 2015/1458575
- [4] Y. Yan, Y. Zhang, T. Jiang, T. Xiao, P. P. Edwards, and F. Cao, "Glycerol hydrogenolysis over a Pt–Ni bimetallic catalyst with hydrogen generated in situ," *RSC Adv.*, 7, 61, 38251–38256, 2017.
- [5] D. W. Kim *et al.*, "Hydrogenolysis of Glycerol to Propylene Glycol on Nanosized Cu–Zn–Al Catalysts Prepared Using Microwave Process," *J. Nanosci. Nanotechnol.*, 15, 1, 656–659, 2015.
- [6] T. Gabrysch, B. Peng, S. Bunea, G. Dyker, and M. Muhler, "The Role of Metallic Copper in the Selective Hydrodeoxygenation of Glycerol to 1,2-Propanediol over Cu/ZrO<sub>2</sub>," *ChemCatChem*, 10, 6, 1344–1350, 2018.

# Catalytic Pyrolysis of Xylan over Alkali Metal Salts with Synchrotron Photoionization Mass Spectrometry

*Yamin Li, Minggao Xu, Jiuzhong Yang, and Yang Pan\**

(E-mail: panyang@ustc.edu.cn)

*National Synchrotron Radiation Laboratory, University of Science and Technology of China, Hefei, Anhui 230029, P. R. China*

As the inherent inorganic materials found in biomass, alkali metals show profound catalytic effect on biomass pyrolysis.<sup>[1]</sup> In this study, the catalytic pyrolysis of xylan, the primary hemicellulose polysaccharide presented in biomass, was investigated over different concentrations of Na<sub>2</sub>CO<sub>3</sub> and K<sub>2</sub>CO<sub>3</sub> by using a homemade tubular furnace at 300 °C. As a result of on-line sampling and the use of tunable synchrotron vacuum ultraviolet photoionization mass spectrometry (SVUV-PIMS)<sup>[2]</sup>, the evolution of unstable products, such as 4-hydroxy-5,6-dihydro-pyran-2-one (*m/z* 114), could be monitored in real time. The obtained photoionization mass spectra were interpreted by statistical analysis and the mechanisms of xylan pyrolysis with alkali metal salts were further discussed. The differences in thermogravimetry curves, photoionization mass spectra and time-evolved profiles revealed the important effects of alkali metal ions on both the decomposition temperature and reaction rates during xylan pyrolysis. Furthermore, we showed that alkali metal ions can promote the formation of char and lighter compounds. This work can provide guidance on the better utilization of hemicellulose resources with the help of alkali metal salts.

## References

- [1] A.V. Bridgwater, Review of Fast Pyrolysis of Biomass and Product Upgrading. *Biomass Bioenergy* 38(2012) 68-94.
- [2] Y. Wang, Q. Huang, Z. Zhou, J. Yang, F. Qi, and Y. Pan, Online Study on the Pyrolysis of Polypropylene over the HZSM-5 Zeolite with Photoionization Time-of-Flight Mass Spectrometry. *Energy Fuels* 29(2015) 1090-1098.

# Microwave Catalytic Synthesis of Ammonia for Energy Storage and Transformation

Jianli Hu, West Virginia University, USA

Dushyant Shekhawat, Christina Wildfire, National Energy Technology Laboratory, USA

Robert Dagle, Pacific Northwest National Laboratory, USA

*Al Stiegman, Florida State University, USA*

Hydrogen production from renewable energy (solar and wind) has been practiced at fairly large scale<sup>1</sup>. However, hydrogen is not a choice of energy carrier due to incompressibility and low volumetric energy density. In contrast, liquid ammonia possesses all the physicochemical properties of an energy-dense carrier to store and transport renewable energy<sup>2-4</sup>. In addition, the production of ammonia from renewable source can reduce dependence on fossil energy<sup>5</sup> and it serves as an effective hydrogen source (17.6 wt% hydrogen) for fuel cell industry<sup>6</sup>. Using air and water as feedstock to economically produce ammonia is a challenge, especially when renewable energy installations are not at a large scale.

This paper presents an innovative approach of producing carbon neutral energy-dense liquid ammonia. The approach synergistically integrates microwave reaction chemistry with novel heterogeneous catalysis that decouples N<sub>2</sub> activation from high temperature and high pressure reaction, altering reaction pathways and lowering activation energy. Results have shown that ammonia synthesis can be carried out at 280°C and ambient pressure to achieve ~1.8% ammonia concentration over supported Ru catalyst systems. Adding promoters of K, Ce and Ba has significantly improved the ammonia production rate over Ru-based catalysts attributing to enhanced electromagnetic sensitivity of the catalysts under microwave irradiation. We have discovered that under microwave catalytic conditions, ammonia concentration higher than corresponding thermal equilibrium can be obtained using either Fe or Ru catalyst. This study also illustrates the advantages of an innovative variable-frequency microwave reactor for ambient pressure ammonia synthesis. It is the first reporting of variable frequency microwave catalytic reaction. Overall, microwave catalytic ammonia synthesis is fundamentally different from commercial Haber-Bosch process, having cost advantages at small scale that is comparable with commercial ammonia process of 10-20 times larger. It can be tolerant to intermittent renewable energy supply, therefore effectively operated at variable rates of production.

Electromagnetic radiation in the form of microwaves has become a focus for chemical synthesis in recent years due to the increased selectivity and decrease in reaction times and temperatures. Microwaves have the unique ability to selectively activate active sites on the surface of heterogeneous catalyst. One of the microwave relaxation processes in the catalytic materials is the dipolar or Debye processes which involve the coupling of the microwave irradiation with dipoles in the solid material. These dipoles can be defect sites (i.e. atomic vacancies) in the materials or dangling bonds on the surface. The coupling of the microwave irradiation will result in selective heating of the dipole. From the standpoint of catalysis, dipoles on the surface can be reactant or products that would be susceptible to selective heating effects, which in turn can affect reaction rates. Microwaves have been shown to decrease the activation energy needed for the reaction. Microwave can also selectively heat metals on catalyst surface, especially in the presence of promoters, facilitating electron transfer between catalyst and reaction intermediates. Taking advantages of “state-of-the art” non-equilibrium microwave technology, catalytic ammonia synthesis undergoes a new reaction pathway where the barrier for the initial dissociation of the dinitrogen is decoupled from the bonding energy of the intermediates.

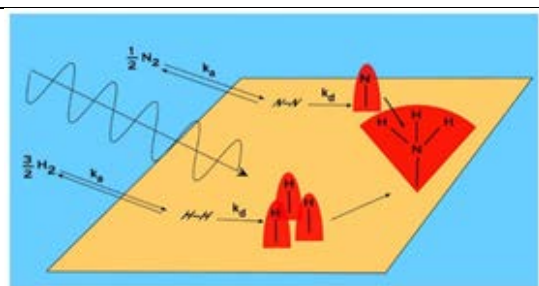


Figure 1. Illustration of microwave catalytic synthesis of ammonia

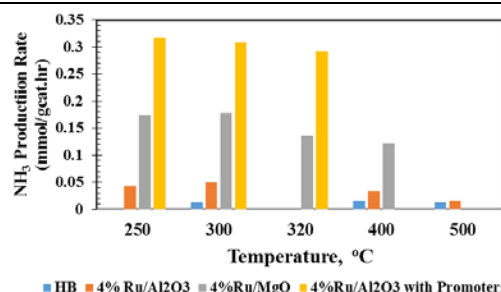


Figure 2. Effect of promoters on the performance of microwave catalytic synthesis of ammonia

## References

- [1] Renewable Electrolysis, NREL, <https://www.nrel.gov/hydrogen/renewable-electrolysis.html>
- [2] J. Norskov, J.G. Chen, sustainable ammonia synthesis (DOE Roundtable Report, 2016)
- [3] C. Philibert, Renewable energy for industry: from green energy to green materials and fuels (IEA Report, 2017)
- [4] J. Guo, P. Chen, Catalyst: NH<sub>3</sub> as an energy carrier, Chem 3, 709-712 (2017)
- [5] J. Chen, R. Crooks, L.C. Seefeldt, K.L. Bren, R. M. Bullock, M.Y. Darensbourg, P.L. Holland, B. Hoffman, M.J. Janik, A. K. Jones, M.G. Knatzidis, P. King, K. M. Lancaster, S.V. Lymar, P. Pfromm, W.F. Schneider, R. R. Schrock, Beyond fossil fuel-Driven nitrogen transformations, Science, 2018, 360, 873-880.
- [6] D. Cheddle, Ammonia as Hydrogen source for fuel cells, A review. Open peer-reviewed book. <http://dx.doi.org/10.5772/47759>.

## Monitoring inorganic catalysts during ammonia decomposition by *in situ* diffraction experiments

Claudia Weidenthaler, Max-Planck-Institut für Kohlenforschung, Mülheim an der Ruhr, Germany, Jo-Chi Tseng, Deutsches Elektronen-Synchrotron DESY, Hamburg, Germany

Ammonia is discussed for on-site generation of hydrogen for fuel cells or its direct use in ammonia-fed solid oxide fuels cells.<sup>[1-4]</sup> The decomposition of ammonia requires temperatures above 400 °C. Therefore, highly active catalysts which guarantee high-temperature stability and long lifetime need to be developed. Several metals, alloys, and noble metals have been tested for ammonia decomposition. High costs and limited availability of conventional noble metal catalysts are limiting factors for large scale applications and force development of alternative catalysts. Different transition metal-based compounds, with or without support, have been discussed as potential catalysts. Previous studies showed that different catalysts used for ammonia decomposition may behave significantly different with respect to the chemical composition and the active components formed during reaction.<sup>[5-7]</sup>

In this study, *in situ* synchrotron and laboratory diffraction studies on different transition metal based catalysts under working conditions will be presented. Changes of the crystal structures, phase transformation processes and compositional changes under reaction conditions will be discussed. Furthermore, the structural properties are related to the catalytic performances of the catalysts (Figure 1).

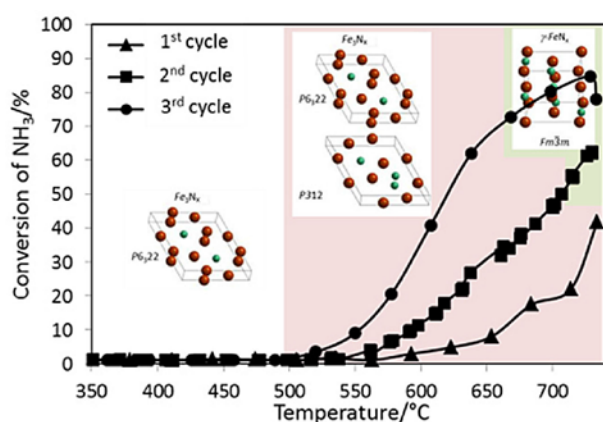


Figure 1: Structural and compositional changes of Fe-based catalyst observed *in situ* during ammonia decomposition.<sup>[7]</sup>



## References

- [1] S. F. Yin, B. Q. Xu, X. P. Zhou, C. T. Au, *Appl. Catal.* (2004) A 277, 1.
- [2] A. S. Chellappa, C. M. Fischer, W. J. Thomson, *Appl. Catal.* (2002) A 227, 231.
- [3] Q. Ma, R. R. Peng, L. Z. Tian, and G. Y. Meng, *Electrochem. Commun.* (2006) 8, 1791.
- [4] W. Zheng, T. P. Cotter, P. Kaghazchi, T. Jacob, B. Frank, K. Schlichte, W. Zhang, D. S. Su, F. Schüth, and R. Schlögl, *J. Am. Chem. Soc.* (2013) 135, 3458.
- [5] V. Tagliazucca, M. Leoni, C. Weidenthaler, *Phys.Chem.Chem.Phys.* (2014) 16, 6182.
- [6] Y.Q. Gu, X.P. Fu, P.P. Du, D. Gu, Z. Jin, Y.Y. Huang, R. Si, L.Q. Zheng, Q.S. Song, C.J. Jia, C. Weidenthaler, *J. Phys. Chem.C.* (2015) 119(30), 17102.
- [7] J.C. Tseng, D. Gu, C. Pistidda, C. Horstmann, M. Dornheim, J. Ternieden, C. Weidenthaler, *ChemCatChem.* (2018) 10, 4465.

# Physico-chemical and catalytic properties of industrial slag catalysts synthesized using different types of organic surfactants

<sup>1</sup>Ekaterina Kholkina, <sup>1</sup>Narendra Kumar, <sup>2</sup>Taina Ohra-aho, <sup>2</sup>Juha Lehtonen, <sup>2</sup>Christian Lindfors, <sup>3</sup>Markus Perula, <sup>4</sup>Janne Peltonen, <sup>4</sup>Jarno Salonen, <sup>1</sup>Kari Eränen, <sup>1</sup>Dmitry Yu. Murzin

<sup>1</sup>Åbo Akademi University, Laboratory of Industrial Chemistry and Reaction Engineering, <sup>2</sup>VTT Technical Research Centre of Finland Ltd, FI-02150, Espoo, Finland, <sup>3</sup>University of Turku, Institute of Biomedicine, Faculty of Medicine, Turku, Finland, <sup>4</sup>University of Turku, Laboratory of Industrial Physics, FI-20014, Turku, Finland

## Introduction

Efficient and rational utilization of industrial solid residual from chemical, petrochemical, metallurgical, iron and steel industry is significant from the green process technology, sustainable development of society and effective utilization of limited natural resources. Proper utilization of natural resources is important from the point of view of mitigation of climate change, saving planet earth, human health and development of environmental friendly technology for the present and future generations. In this research main aim was synthesis and characterization of catalytic materials from industrial slags obtained from iron and steel industry.

## Experimental

The organic surfactants selected for the studies were: Cetyl tetramethyl ammonium bromide  $(\text{CH}_3)_4\text{N}(\text{Br})$ , Tetra ethylammonium bromide  $(\text{C}_2\text{H}_5)_3\text{N}(\text{Br})\text{CH}_3$ , tetramethyl ammonium hydroxide  $(\text{CH}_3)_4\text{N}(\text{OH})$ , tetra ethylammonium hydroxide  $(\text{C}_2\text{H}_5)_4\text{N}(\text{OH})$ , Tetradecyl trimethyl ammonium bromide  $(\text{C}_{16}\text{H}_{33}\text{N}(\text{Br})(\text{CH}_3)_3)$ , Tetra ethyl ammonium bromide  $(\text{C}_{14}\text{H}_{29}\text{N}(\text{Br})(\text{CH}_3)_3)$ , hexa-decyltrimethyl ammonium chloride  $(\text{C}_{16}\text{H}_{33}\text{N}(\text{Cl})(\text{CH}_3)_3)$  and tetrabutyl ammonium bromide  $(\text{C}_4\text{H}_9)_4\text{N}(\text{Br})$ . *Mikseri kuona* industrial slag was ball milled and fraction  $< 90 \mu\text{m}$  was pretreated with 0.6 M NaOH. The 0.6 M NaOH pretreated *mikseri kuona* was added to the 0.1 M surfactant, and synthesis was performed at ambient temperature. After the synthesis, surfactant pretreated material was filtered and washed with distilled water, followed by drying at  $100^\circ\text{C}$  and thermal treatment in a muffle oven using step calcination procedure. Similar procedure was used for pretreatment of 0.6 M NaOH pretreated slag with all the above surfactants. The characterization of the surfactant pretreated *mikseri*

*kuona* was carried out using X-ray powder diffraction for structural identifications, scanning electron microscopy for morphological studies and energy dispersive X-ray micro analyses for measurement elemental composition. Transmission electron microscopy was applied for the determination of structure, porosity and periodicity of pores and metal oxide particle size distributions. Nitrogen physisorption was performed to measure the surface area and pore volume.

## Results and discussion

The highest surface area ( $38 \text{ m}^2/\text{g}$ ) and pore volume ( $0.0134 \text{ cm}^3/\text{g}$ ) was measured for the slag catalyst synthesized with pretreatment of 0.1 M tetraethyl ammonium hydroxide. The surface area ( $19 \text{ m}^2/\text{g}$ ) and pore volume ( $0.0069 \text{ cm}^3/\text{g}$ ) was measured for the untreated *mikseri kuona*. Hence, it was concluded that the surfactant pretreatment resulted in the enhancement of surface area and pore volume. It was also observed that surface area and pore volume of the pretreated slag catalysts depended on the type of surfactants. The surfactant 0.1 M tetramethyl ammonium bromide pretreated slag catalyst exhibited surface area ( $29 \text{ m}^2/\text{g}$ ) and pore volume ( $0.0134 \text{ cm}^3/\text{g}$ ). The slag material pretreated with EDTA, followed by subsequent pretreatment with 0.6 M NaOH-0.1M TEAH resulted in the surface area ( $79 \text{ m}^2/\text{g}$ ) and micropore volume  $0.0282 \text{ cm}^3/\text{g}$ . Transmission electron microscopy exhibited the presence of formation of internal porosity for the surfactant pretreated slag catalytic materials. 0.6 M NaOH-0.1 M TEAH for 4 h at  $65 \text{ }^\circ\text{C}$  slag catalytic material exhibited the presence of average channel size (4.1 nm). The 0.6 M NaOH-0.1 M TEAH EDTA pretreated at  $25 \text{ }^\circ\text{C}$  for 4 h slag catalyst with highest surface area ( $79 \text{ m}^2/\text{g}$ ) showed the average internal channel size (1.1 nm). The hydrothermal synthesis of 0.6 M NaOH-0.1 M TEAH at  $150 \text{ }^\circ\text{C}$  for 4 h, exhibited presence of spherical shape crystals with average crystal size 140.5 nm. It is noteworthy to mention, that transmission electron microscopy also showed the presence of external mesopores with average size (70 nm). The energy dispersive X-ray micro-analyses exhibited presence of FeO,  $\text{TiO}_2$ , CaO, S,  $\text{SiO}_2$ ,  $\text{Al}_2\text{O}_3$ , MgO,  $\text{Na}_2\text{O}$  for the 0.6 M NaOH-0.1M TEAH slag catalytic material. The 0.1 M TEAH-0.6 M NaOH surfactant pretreated slag catalyst exhibited significant catalytic activity in analytical fast pyrolysis of pine sawdust. The in-depth physico-chemical characterization of the slag catalytic materials together with the correlation of the catalytic activity results will be presented during the conference.

# The photocatalytic study of TiO<sub>2</sub> microspheres in benzene removal and H<sub>2</sub> production

*Xin Liu, Hajime Hojo, Hisahiro Einaga,*

*Faculty of Engineering Sciences, Kyushu University, Kasuga, Fukuoka, Japan*

TiO<sub>2</sub> is an important functional material, which has been widely studied due to its high photoactivity and stability<sup>1</sup>. To improve the efficiency of TiO<sub>2</sub>-catalyzed photocatalytic reaction, the suppression of electron-hole recombination and the increase of TiO<sub>2</sub> surface area are effective methods. Recently, much attention has been focused on shape-controlled TiO<sub>2</sub> because catalytic properties can be improved by changing the morphology of materials<sup>2</sup>. In this study, we synthesized the high surface area TiO<sub>2</sub> and Pt/TiO<sub>2</sub> microspheres. According to the experiment results, the high surface area TiO<sub>2</sub> and Pt/TiO<sub>2</sub> manifest higher photocatalytic activity in benzene removal and H<sub>2</sub> production, respectively. Especially, the samples (TiO<sub>2</sub> and Pt/TiO<sub>2</sub>) that were heated at 300 °C exhibited the highest benzene degradation conversion (11.17%) and H<sub>2</sub> production rate (50.03 μmol h<sup>-1</sup>), while the P25 and Pt/P25 just displayed 1.98% conversion and 39.12 μmol h<sup>-1</sup> H<sub>2</sub> production rate, respectively.

XRD patterns of TiO<sub>2</sub> calcined at different temperatures are displayed in Fig. 1a. All of the diffraction patterns can be indexed to anatase TiO<sub>2</sub> that are consistent with the previous report<sup>3</sup>. Meanwhile, all the samples' diffraction peaks do not change significantly. SEM images of TiO<sub>2</sub>-MS samples depicted in Fig. 1b show that all the samples consisted of uniform microspheres with the diameter was ~200-300 nm.

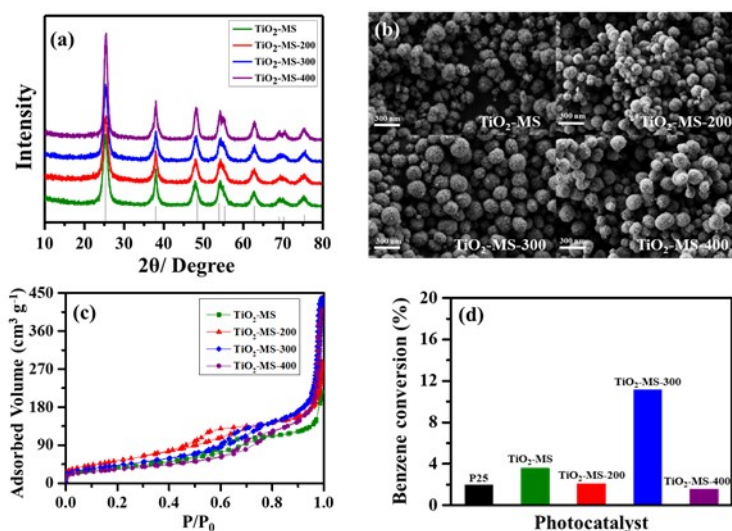


Fig. 1 (a) XRD patterns, (b) SEM images, (c) N<sub>2</sub> adsorption-desorption isotherms of microspheres at different temperatures. (d) Photocatalytic degradation ratio of TiO<sub>2</sub> microspheres at different temperatures and P25 after 150 minutes irradiation.

Both XRD and SEM images indicate that the TiO<sub>2</sub> microspheres have good thermal stability. N<sub>2</sub> adsorption-desorption isotherms of TiO<sub>2</sub>-MS samples (Fig. 1c) shows the surface areas are 137, 204, 159.23 and 119.72 m<sup>2</sup> g<sup>-1</sup>, respectively. Fig.1d shows the photocatalytic degradation activity of TiO<sub>2</sub> samples and commercial P25 nanoparticles for comparison. Under the lighting irradiation in the period of 150 minutes, the TiO<sub>2</sub>-MS-300 sample is able to degrade over 11.17% of the original benzene, while value for P25 is 1.98%.

Besides, the Pt/ TiO<sub>2</sub> microspheres were used to test the activity of H<sub>2</sub> production. After loading Pt, it can be found that the phase of TiO<sub>2</sub>-MS-300-1% Pt is still anatase (Fig. 2a), as the same as the original TiO<sub>2</sub> microspheres. The morphology of TiO<sub>2</sub>-MS-300-1% Pt is also not changed (Fig. 2b). This means the Pt deposition cannot affect the structure and morphology of these TiO<sub>2</sub> microspheres. Fig. 2c shows that the H<sub>2</sub> production rate of TiO<sub>2</sub>-MS-300-1%Pt (50.03 μmol h<sup>-1</sup>) is higher than P25-1%Pt (39.12 μmol h<sup>-1</sup>). This also proved that change the morphology of TiO<sub>2</sub> could improve the photocatalytic activity.

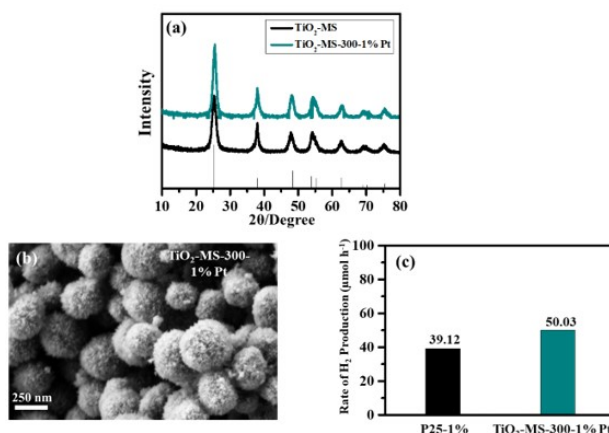


Fig. 2 (a) XRD patterns, (b) SEM image of TiO<sub>2</sub>-MS-300-1%Pt. (c) Photocatalytic H<sub>2</sub> evolution rate of P25-1%Pt and TiO<sub>2</sub>-MS-300-1%Pt (solution: ethanol=2 ml and H<sub>2</sub>O= 8 ml).

In conclusion, we studied basic properties of the TiO<sub>2</sub> and Pt/TiO<sub>2</sub> microspheres, and found these microspheres have good photocatalytic activity in benzene degradation and H<sub>2</sub> production, especially TiO<sub>2</sub>-MS-300 and TiO<sub>2</sub>-MS-300-1%Pt with high surface area, stable structure, shown much higher activity than other samples in both benzene removal (11.17%) and H<sub>2</sub> evolution rate (50.03 μmol h<sup>-1</sup>). Finally, this work can help others to start deeper research in shape-controlled TiO<sub>2</sub> in the future.

## References

- [1] Kazuya Nakata, Akira Fujishima. *J. Photoch. Photobio. C: Photochemistry Reviews*. 13 (2012) 169.
- [2] Z. Sun, J. H. Kim, Y. Zhao, F. Bijarbooneh, V. Malgras, Y. Lee, Y.-M. Kang and S. X. Dou, *J. Am. Chem. Soc.* 133 (2011) 19314.
- [3] Y. B. Liu, T. B. Lan, W. F. Zhang, X. K. Ding and M. D. Wei, *J. Mater. Chem. A*, 2 (2014) 20133.

# Inducing Cooperative Catalytic Interactions Using Titanium and Tin-Chitosan Hybrids

*Christine Khoury; Oz M. Gazit, Chemical Engineering, Technion-Israel Institute of Technology, Haifa, Israel*

## Introduction

Obtaining acid-base cooperative interactions between metal and organic active sites in a heterogeneous synthetic system is a challenging task. The key is to develop a synthetic control over the proximity and orientation between mild active sites.<sup>[1]</sup> If this can be achieved, the catalyst can be active under mild reaction conditions and also allow tuning of the reaction selectivity.<sup>[2]</sup> An important example where such a catalyst can be highly beneficial is the aldol condensation reaction, which is extensively used in the synthesis of fine chemicals and also in the transformation of biomass-derived molecules to fuels.

Previous reports on cooperative heterogeneous catalysts, focused on developing active site cooperativity by grafting amines to a rigid support such as silica. However, in such cases the rigidity of the support limits the catalyst tunability. Recently, the use of a flexible polymer-based system to induce cooperative interactions was shown to have a high potential.<sup>[3]</sup> Polymeric systems can self-assemble to adjust proximity and orientation of the active sites, which are more challenging to obtain in a rigid solid system. However, this high degree of flexibility is limiting in terms of keeping a constant distance between the acid and base sites. In this work we combine between a rigid and a flexible system by grafting titanium (Ti) or tin (Sn) sites to the backbone of an amine contain polymer (chitosan, CS).

## Material Preparation and Methods

The preparation of the grafted hybrid materials was obtained by the reacting Ti or Sn precursors with the hydroxyl groups on CS. Tuning of the synthesis conditions allowed us to produce three configurations (see **Figure 1.**) 1) Ti/Sn grafted on CS with protonated amines (G-Ti-NH<sub>3</sub><sup>+</sup> and G-Sn-NH<sub>3</sub><sup>+</sup>+NPs), 2) Ti/Sn grafted on CS with primary amines (G-Ti-NH<sub>2</sub> and G-Sn-NH<sub>2</sub>+NPs), and 3) inter-grafted Ti/Sn sites on CS with primary amines (IntG-Ti-NH<sub>2</sub> and IntG-Sn-NH<sub>2</sub>+NPs). To study these unique hybrids, the materials were characterized by FTIR, XRD, N<sub>2</sub>-physisorption, HRTEM and XPS.

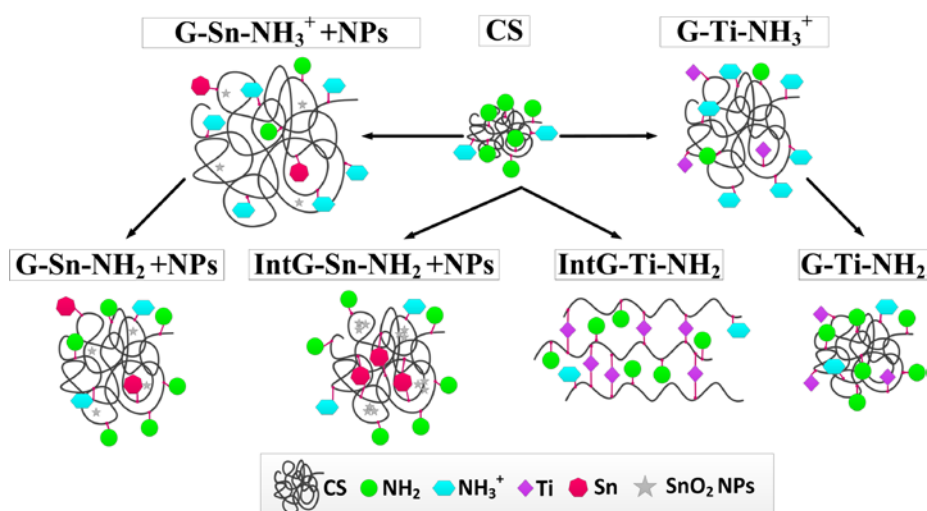


**Figure 1.** Schematic representation of the various configurations of the Ti and Sn-CS Hybrids.

## Results

The synthetic approach produced high surface area Ti-CS-hybrid materials (up to  $130 \text{ m}^2\text{g}^{-1}$ ) and Sn-CS-hybrid materials (up to  $190 \text{ m}^2\text{g}^{-1}$ ) without the need for special drying methods. It was found that while in the IntG-Ti-NH<sub>2</sub> the CS is able to self-organize into a sub-nanometer organized pattern, in the case of the IntG-Sn-NH<sub>2</sub>+NPs, the Sn precursor forms SnO<sub>2</sub> nanoparticles that prevent the self-assembly of CS. The high surface was found to be stable up to  $110 \text{ }^\circ\text{C}$  under vacuum.

Testing the obtained hybrid materials as catalysts for the nitro-aldol condensation showed cooperativity between the incorporated metal site and the pendant primary amine site on CS. This cooperativity was translated into a reduction of  $\sim 25\%$  in the apparent reaction activation energy and a distinct correlation to selectivity. No difference between Ti and Sn in terms of catalytic activity was found. However, significant differences were measured between the catalytic performance of the grafted and inter-grafted material configurations. The sum of these results allowed us to identify the active site and sketch a proposed mechanism.

## Significance

The development of active site cooperativity provides access to more energy efficient catalytic materials. In this work we present a new approach for the synthesis of hybrid organic-inorganic solid catalysts that can self-assemble into a specific structure that promotes acid-base cooperativity.

## References

- [1] N. A. Brunelli, C. W. Jones, *J. Catal.* **2013**, 308, 60.
- [2] C. Khoury, O. M. Gazit, *ChemNanoMat* **2018**, DOI 10.1002/cnma.201700358.
- [3] C. B. Hoyt, L. C. Lee, A. E. Cohen, M. Weck, C. W. Jones, *ChemCatChem* **2017**, 9, 137.

# Explaining redox activity of V-substituted heteropoly acid catalysts in biomass oxidation through liquid core waveguide membrane microreactor studies

Sebastian Ponce<sup>1</sup>, Jakob Albert<sup>2</sup>, Alfons Drochner<sup>1</sup>, Bastian J.M. Etzold<sup>1</sup>; <sup>1</sup>Ernst-Berl-Institute for Technical and Macromolecular Chemistry, Technische Universität Darmstadt, 64287 Darmstadt, Germany; <sup>2</sup>Lehrstuhl für Chemische Reaktionstechnik, Universität Erlangen-Nürnberg, 91058 Erlangen, Germany

Catalytic partial oxidation employing molecular oxygen is one important pillar of today's industrial chemistry and future sustainable scenarios. Partial oxidation is e.g. studied for conversion of biomass into valuable energy carrier molecules, platform chemicals, and other bio-based products [1]. Among others, the use of heteropolyacid (HPA-n) catalysts ( $H_x[PV_nMo_zO_{40}]$ ) has emerged as a promising method for the selective transformation of biomass into formic acid and  $CO_2$ , as recently demonstrated by Albert et al., in the so-called OxFA process [2]. While vanadium substitution is known to show an influence on the overall activity, experimental observations show a contrasting behavior. Thus, further studies how V-substitution influences the redox cycle are necessary. HPA-n catalysts present characteristic UV/Vis absorption spectra in their oxidized and reduced forms. Thus, reduction and reoxidation rates under anaerobic and aerobic conditions could be studied. Recently, we reported a liquid core waveguide membrane microreactor (LCWM), based on a Teflon AF tube (Fig. 1), which allows *in situ* UV/Vis spectra of liquid phases while complete gas/liquid saturation is achieved [3]. In this study, the novel concept of a LCWM microreactor is used to carry out spectrometric studies of the redox kinetics of different HPA-n catalysts during the OxFA process.

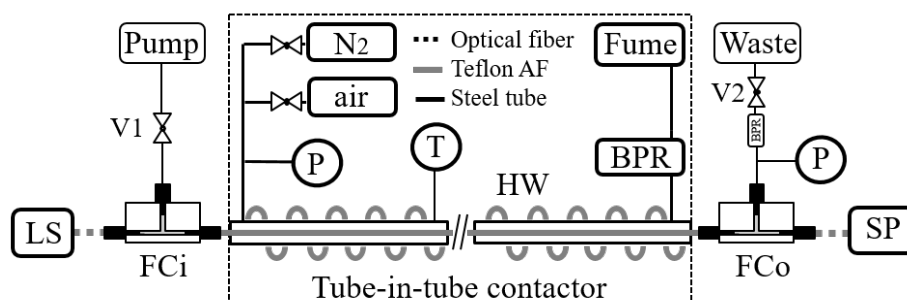


**Figure 1:** Scheme of LCWM setup., LS: light source, FC: fluidic cells, P: pressure sensor, T: temperature control, HW: heating wire, BPR: backpressure regulator, SP: spectrometer, V: two-way valve.



## Results

While high V-substituted (HPA-5) catalysts showed the fastest reduction kinetics, no direct linear correlation of the substitution degree to the reduction kinetics was obtained. Combining the kinetic results with Cyclovoltammetry (Fig. 2 left) and EPR characterization indicates, that two competing active sites influence the reduction kinetics. On the one hand, dissolved  $V^{5+}$ , and on the other hand the heteropolyanion itself. While the activity of the heteropolyanions as active site itself seem to slow down with higher V-substitution degree, the amount of highly active  $V^{5+}$  dissolved increases with higher substitution. The detrimental effect of V-substitution on activity and number of active sites explains the observed reduction activity trend as also selectivity patterns reported in literature [1]. Moreover, for reoxidation experiments, the degree of V-substitution played again a determinant role. HPA-0 and HPA-1 catalysts are only reoxidized above 100 °C (Fig. 2 right) and due to the decomposition of formic acid at high temperatures not suitable for this reaction. In contrary, HPA-2 and HPA-5 showed suitable reoxidation below 80 °C, while HPA-5 shows a 10 times higher reoxidation compared to HPA-2. All in all, this study shows, that the recently introduced LCWM microreactor concept suits very well for fast and reliable *in situ* UV/Vis kinetic studies on gas-liquid systems.

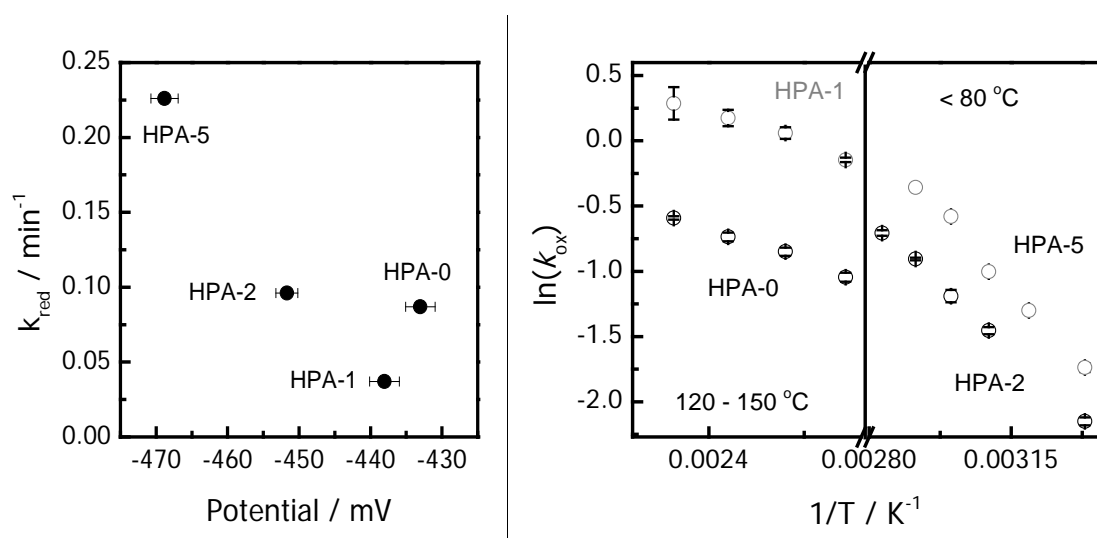


**Figure 2:** Left: Correlation between reduction rate constants and reduction potential of the HPA-n catalysts, and right: Arrhenius plot for reoxidation of HPA-n catalysts.

## References

- [1] J. Albert, *Faraday discussions* **2017**, 202, 99-109.
- [2] J. Albert, R. Wölfel, A. Bösmann, P. Wasserscheid, *Energy & Environmental Science* **2012**, 5 (7), 7956-7962.
- [3] S. Ponce, H. Christians, A. Drochner, B. J. M. Etzold, *Chemie Ingenieur Technik* **2018**, (90), 1-10.

## **The Catalytic Upgrade of Acetone, Butanol and Ethanol (ABE) to Added Value Products**

*Elham Ketabchi, University of Surrey, Guildford, UK; Laura Pastor-Perez, University of Surrey, Guildford, UK; Tomas Ramirez Reina, University of Surrey, Guildford, UK; Harvey Arellano-Garcia, University of Surrey, Guildford, UK*

The history of many sectors of manufacturing and production has shown that they inevitably go through significant changes that should be addressed. Hence, many operational systems that were successful in the past may no longer be so in the future. One of the main industries that is no exception to this change, is oil refining; being a crucial industry in our day to day lives. Nonetheless, financial and environmental issues have led to the search for alternatives such as biomass based processes in order to reduce the dependency on crude oil. Bio-refinery processes, fed by biomass, produce high value chemicals and materials with the advantage of having reduced environmental drawbacks such as CO<sub>2</sub> emissions when compared to the conventional refinery.

In this work, we have carried out a complex reaction network towards upgrading Acetone, Butanol and Ethanol (ABE), a biomass based mixture, aiming to produce valuable products while utilising economically viable catalysts in comparison to the expensive catalytic materials used in the vast majority of similar research. The reactants of this process, ABE, are the products of sugar fermentation via bacterial species that are obtained and separated via various distillation units that are quite costly and energy intensive[1]. Therefore, the upgrading process following that should be economically favourable to decrease the cost burden. This has led to the use of catalysts that are affordable and readily available as well as producing chemicals that are of added value. The vast majority of research carried out in this area have proceeded with expensive catalysts, i.e. noble metals, but nevertheless have obtained promising results[2][3]. Furthermore, our research has omitted the necessity of noble metals leading to a significant cost decrease while also producing outstanding results.

The catalysts required for this process were synthesised successfully through the wet incipient method and characterised by XRD, Raman, BET, TPR and N<sub>2</sub> Isotherm.

These materials performed favourably towards producing the intended chemicals after being activated in an H<sub>2</sub> flow at 700 °C.

The reaction consists of the self-condensation and cross condensation of the alcohols and acetone, respectively, using a variety of active metals on basic supports as catalysts at high temperatures and pressure in a batch reactor.

The results have shown exceptional performance for the catalysts in terms of conversion and selectivity, having conversions as high as 90%. The catalysts have also proven to yield valuable products identified to be of need in the chemical industry. In conclusion, this route has shown promising results in terms of providing valuable C<sub>3</sub>-C<sub>15</sub> products, useful for both the petrochemical industry and the transportation industry while using economically favourable catalysts in comparison with previous studies. These products, the presence of which was confirmed with GC-MS, are proven to have a considerably higher market value than the simple alcohol reactants.

#### References

- [1] I. Patraşcu, C. S. Bîldea, and A. A. Kiss, "Eco-efficient butanol separation in the ABE fermentation process," *Sep. Purif. Technol.*, vol. 177, pp. 49–61, 2017.
- [2] G. Onyestyák, G. Novodárszki, R. Barthos, S. Klébert, Á. F. Wellisch, and A. Pilbáth, "Acetone alkylation with ethanol over multifunctional catalysts by a borrowing hydrogen strategy," *RSC Adv.*, vol. 5, no. 120, pp. 99502–99509, 2015.
- [3] K. A. Goulas *et al.*, "ABE Condensation over Monometallic Catalysts: Catalyst Characterization and Kinetics," *ChemCatChem*, vol. 9, no. 4, pp. 677–684, 2017.

## **CO adsorption on iron carbide thin films supported on Cu(100) as a Fischer-Tropsch synthesis model catalyst**

*Daniel García, DIFFER, Eindhoven, The Netherlands; Jose Gracia, Magnetocat S.L., Alicante, Spain; J.W. Niemantsverdriet, SynCat@DIFFER, Eindhoven, The Netherlands; C.J. Weststrate, SynCat@DIFFER, Eindhoven, The Netherlands*

Although technologically well-developed, the Fischer-Tropsch synthesis (FTS) reaction can be ranked among the most complex reaction mechanisms in the chemical industry. In order to obtain meaningful molecular level insight into the mechanism by which synthesis gas ( $\text{CO} + \text{H}_2$ ) reacts on the surface of the iron-based catalyst to produce the desired hydrocarbon products, the complexity of the real catalyst needs to be reduced to a well-defined flat surface. Since single crystal surfaces of iron carbide are not available we instead aim to produce thin iron carbide films supported on a single crystal of copper to obtain a relevant  $\text{FeC}_x$  model system. Iron carbide is the active phase in the iron-based catalyst used for FTS. [1]

Growth of ultrathin films (via evaporation in an UHV) of Fe on Cu(100) was studied with Low Energy Electron Diffraction (LEED). At an iron coverage of around 2 ML new spots appear in the LEED pattern with a (4x1) periodicity, indicating that at least one of the iron layers must be reconstructed [2]. This shows that Fe does not grow epitaxially on the Cu(100) substrate but instead forms complex overlayer structures with a structure that depends on the thickness of the iron layer. Using DFT calculations we found that the structure giving rise to the (4x1) pattern in LEED is indeed more stable than a structure where iron follows the registry of the Cu(100) substrate. We dose ethylene onto our iron thin films to transform the Fe films into an iron carbide. AES was used to determine how the iron to carbon ratio depends on the preparation procedure used. The shape of the C(KLL) peak at 272 eV is characteristic for carbidic carbon (Fig1.) [3]. The LEED picture taken afterwards shows a  $p4g(2 \times 2)$ , called "clock" reconstruction. This pattern has been found previously on a Ni(100) surface as a result of a carbon-induced surface reconstruction [4].

Temperature programmed desorption (TPD) have been done to study the adsorption and desorption of CO and H<sub>2</sub> on the thus prepared FeC<sub>x</sub> layers. CO was adsorbed at 100K and it desorbs again when heated, at 225K and 325K. DFT calculations done elsewhere show CO dissociation on Fe<sub>5</sub>C<sub>2</sub> (010) [5], and in our most recent experiments, we have indications of CO dissociation. H<sub>2</sub>, on the contrary, doesn't adsorb at UHV conditions on FeC<sub>x</sub> surfaces, which means that H<sub>2</sub> has a very low sticking coefficient and high pressures are needed to make it adsorb on the surface.

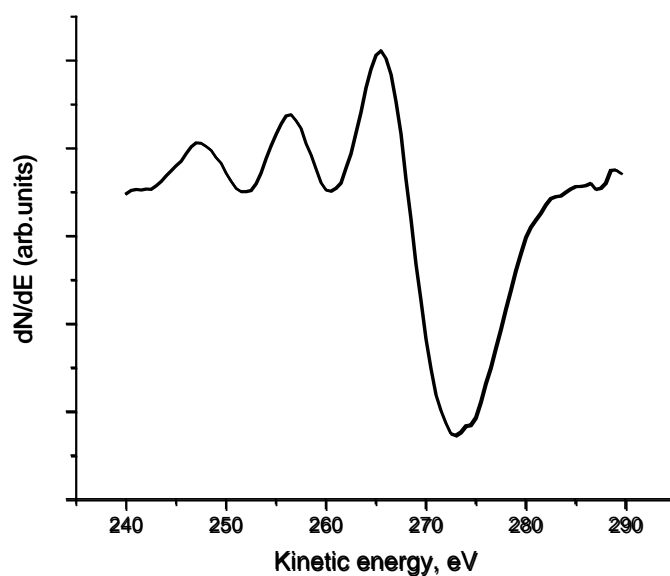


**Figure 1** The carbon KLL Auger spectra. Shows the carbide shape on the iron carbide structure.

#### References

1. De Smit, E.; Weckhuysen, B. The renaissance of iron-based Fischer-Tropsch synthesis: on the multifaceted catalyst deactivation behaviour. *Chem. Soc. Rev.* **2008**. 37, 2758-2781.
2. Heinz, K.; Muller, S.; Bayer, P. Iron Multilayers on Cu(100) – a case of complex reconstruction investigated by quantitative LEED. *Surf.Sci.* **1996**. 352-354, 942-950.
3. Lesiak, B.; Mrozek, P.; Jablonski, A. Analysis of the Auger KLL spectra of Carbon by the Pattern Recognition Method. *Surf.Interface Anal.* **1986**. 8, 121-126.
4. Gauthier, Y.; Baudoing-Savois, R.; Heinz, K.; Landskron, H. Structure determination of p4g Ni (100)-(2x2)C by LEED. *Surf.Sci.* **1986**. 251, 493-497.
5. Petersen, M.; Van Rensburg, W. CO dissociation at vacancy sites on Hagg iron carbide: Direct versus hydrogen-assisted routes investigated with DFT. *Top Catal.* **2015**. 58, 665-674.

# Validation of In-situ Microwave-assisted Catalytic Upgrading of Heavy Oil

*Mohamed Adam, University of Nottingham, Nottingham, UK; Abarasi Hart, University of Birmingham, Birmingham, UK; Joseph Wood, University of Birmingham, Birmingham, UK; John P. Robinson, University of Nottingham, Nottingham, UK; Sean P. Rigby, University of Nottingham, Nottingham, UK*

## Introduction

Despite the encouraging growth in sustainable energy sources, oil and gas are projected as needing to satisfy up to 55% of the world's energy demand in 2040 [1]. With the decline in light oil reserves, attention has been shifting towards unconventional oil, such as heavy oils and bitumen. Toe-to-Heel Air Injection (THAI) with its catalytic add-on (CAPRI, CAlytic upgrading PRocess in-situ) is considered one of the most promising technologies for simultaneous recovery and in-situ upgrading of heavy oils. Previous studies showed that a temperature of about 425°C is needed for successful catalytic upgrading [2]. However, further studies suggested that the actual temperature of the oil passing through catalyst packing around the horizontal well in the THAI process does not exceed 300°C [3]. Microwave heating has been proposed as a possible strategy to overcome this deficiency and provide the requisite additional heating to increase the temperature at the catalyst packing and/or the oil in its immediate vicinity to the required 425 °C or more. Crude oils, in general, are considered to be poor microwave absorbers, and heating them may require adding microwave susceptors. However, we have recently [4] shown that, at high temperatures, which is the case in THAI-CAPRI, heavy oils are, themselves, more susceptible to being heated directly with microwaves. The aim of the current study was to develop a lab-scale microwave-heated reactor and use it to examine if heavy oils can be heated directly with microwaves up to 425°C to achieve catalytic upgrading, with each API point of upgrading estimated to be worth ~\$1.2 per barrel.

## Results and Discussion

Figure 1 is a schematic of the microwave heating system which was built to investigate the catalytic upgrading of the heavy oils. It involves a flanged 30 mm i.d quartz tube inside a single-mode microwave applicator. The heavy oil used in this study was supplied by Touchstone Exploration Inc. Canada, and was produced

through THAI technology. It has an API gravity of 14.3°, a viscosity of 1.36 Pa.s and a sulphur content of 3.2%. During the experiments, typically 15 g oil was mixed with 1.0 g solid catalyst in the quartz reactor. The catalyst used was a commercially available CoMo/Al<sub>2</sub>O<sub>3</sub>. The

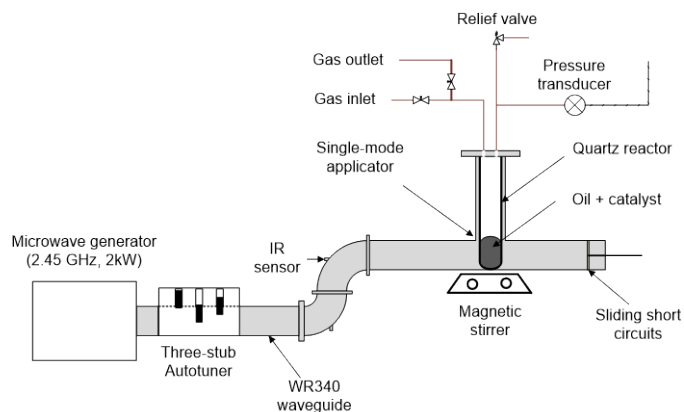


**Figure 1: Schematic of the microwave heating system**

The microwave power was used to control the oil temperature. It was possible to heat the oil up to 425°C with no need for a microwave susceptor. An increase in the API specific gravity of up to 2.8° was achieved after 15 minutes heating at 425°C. Table 1 compares the performance of the metal catalyst (CoMo/Al<sub>2</sub>O<sub>3</sub>) to that of two control cases; one is with Al<sub>2</sub>O<sub>3</sub> and the other is with only oil. The higher increase in the API when CoMo/Al<sub>2</sub>O<sub>3</sub> was used reflects its catalytic contribution. The increase in the specific gravity seen in other two cases can be attributed to thermal cracking.

**Table 1: Effect of the catalyst on the specific gravity of THAI oil**

Type of solid/catalyst	CoMo/Al <sub>2</sub> O <sub>3</sub>	Al <sub>2</sub> O <sub>3</sub>	None
Increase in the specific gravity (°API)	2.8 ± 0.1	2.2 ± 0.2	2.1 ± 0.1

## Conclusions

This study demonstrated that heavy oils can be heated directly with microwaves to 425°C which is the temperature needed for a successful CAPRI process. Upgrading with an increase in the API of up to 2.8° was achieved.

**Acknowledgements:** This research was supported by the Engineering and Physical Sciences Research Council [grant number EP/N032985/1].

## References

1. EIA, *International Energy Outlook 2017*. 2017, U.S. Department of Energy, Energy Information Administration
2. Shah, A., et al., *Experimental Optimization of Catalytic Process In Situ for Heavy-Oil and Bitumen Upgrading*. J Can Petrol Technol, 2011. **50**(11-12): p. 33-47.
3. Rabiou Ado, M., M. Greaves, and S.P. Rigby, *Dynamic Simulation of the Toe-to-Heel Air Injection Heavy Oil Recovery Process*. Energy & Fuels, 2017. **31**(2): p. 1276-1284.
4. Zhang, Y., et al., *Impact of Oil Composition on Microwave Heating Behavior of Heavy Oils*. Energy & Fuels, 2018. **32**(2): p. 1592-1599.

# The effect of rhenium in the conversion of glycerol to mono-alcohols over nickel catalysts under continuous flow conditions

*Mzamo L. Shozi<sup>1</sup>, Venkata D.B.C. Dasireddy<sup>1,2</sup>, Sooboo Singh<sup>1</sup>, Alisa Govender<sup>3</sup>, Pheladi Mohlala<sup>3</sup> and Holger B. Friedrich<sup>1</sup>*

<sup>1</sup>*School of Chemistry and Physics, University of KwaZulu-Natal, Durban, South Africa*

<sup>2</sup>*Department of Catalysis and Chemical Reaction Engineering, National Institute of Chemistry, Hajdrihova 19, Ljubljana, Slovenia*

<sup>3</sup>*Group Technology, Sasol South Africa, Sasolburg, South Africa*

## Introduction

Glycerol is a major by-product of the biodiesel production process and its availability will increase due to the remarkable growth of biodiesel production worldwide. Since the existing supply and demand market cannot accommodate the excess amounts of glycerol generated, the conversion of glycerol to value-added products has become important. One of the processes that converts glycerol to value-added products is hydrogenolysis, where glycerol is converted to lower alcohols [1]. Lower alcohols such as ethanol and 1-propanol are important, as ethanol is used as fuel and a fuel additive and 1-propanol is used as a multipurpose solvent and chemical feedstock for organic compounds. Propylene glycol (1,2-propanediol) and ethylene glycol, which are also formed during this process, have important uses as antifreeze liquids and additives in liquid detergents [2, 3]. The use of rhenium as a catalyst promoter in the hydrogenolysis of glycerol has received much attention over the years [4, 5]. All catalytic testing reported in these studies was by batch process in an autoclave. When rhenium is used as a promoter on supported platinum group metal catalysts such as Ir/SiO<sub>2</sub>, Ru/Al<sub>2</sub>O<sub>3</sub> and Rh/SiO<sub>2</sub>, the catalysts have been found to be more selective towards 1,3-propanediol and 1-propanol under various conditions [6]. We now report on the use of supported nickel catalysts and the effect of rhenium on their activity in the hydrogenolysis of glycerol in a continuous flow process for the first time.



## Materials and Methods

The supported Ni catalysts were prepared by impregnating the supports,  $\gamma$ -Al<sub>2</sub>O<sub>3</sub> and SiO<sub>2</sub> with an aqueous solution of Ni(NO<sub>3</sub>)<sub>2</sub>·6H<sub>2</sub>O to obtain a nominal loading of 30 wt% NiO. After impregnation, the catalysts were dried at 110 °C for 12 hours, followed by calcination in air at 550 °C for 3 hours. Re-Ni catalysts were prepared by impregnating the calcined supported Ni catalysts with an aqueous solution of NH<sub>4</sub>ReO<sub>4</sub> to obtain a nominal loading amount of 1 wt% Re. The catalysts were characterized using XRD, TPR, TPD, TEM, SEM and BET surface area. These catalysts were evaluated in the hydrogenolysis of glycerol in a continuous flow fixed bed reactor in a temperature range of 250 – 325 °C and a H<sub>2</sub> pressure of 60 bar.

## Results and Discussion

Rhenium-promoted nickel catalysts are effective in the continuous flow hydrogenolysis of glycerol to mono-alcohols due to the increase in Brønsted acidity of the catalyst. An increase in temperature led to an increase in the conversion of glycerol. The alumina catalysts were found to be more active than the silica catalysts as they exhibited higher metallic surface areas and more Brønsted acid sites aiding in the dehydration of glycerol to 1,2-propanediol. An increase in temperature favoured the formation of mono-alcohols (methanol, ethanol and 1-propanol). The silica catalysts were found to favour C–C bond cleavage with respect to the yield of methanol and ethylene glycol. The effect of pressure and H<sub>2</sub>:glycerol ratio had a positive effect in terms of the catalyst activity and yield of mono-alcohols. The presence of Re in the catalyst influences the activity positively even at a glycerol concentration as high as 60 wt%.

## References

1. H. W. Tan, A. R. Abdul Aziz and M. K. Aroua, *Renew. Sust. Energ. Rev.* 27, 118 (2013)
2. Y. Wang, J. Zhou and X. Guo, *RSC Adv.* 5, 74611 (2015)
3. P. Gallezot, *Chem. Soc. Rev.* 41, 1538 (2012)
4. L. Ma, Y. Li and D. He, *Chin. J. Catal.* 32, 872 (2011)
5. Y. Li, H. Liu, L. Ma and D. He, *RSC Adv.* 4, 5503 (2014)
6. L. Ma and D. He, *Catal. Today* 149, 148 (2010)

# **“Making cheaper bio-oil” via hydrogen free HDO reactions using noble metal based catalysts supported on activated carbon**

*J.L. Santos<sup>1</sup>, J. Weř<sup>2</sup>, L. Pastor-Perez<sup>2</sup>, M. A. Centeno<sup>1</sup> and T. R. Reina<sup>2</sup>*

*<sup>1</sup>Departamento de Química Inorgánica, Universidad de Sevilla, Instituto de Ciencias de Materiales de Sevilla Centro mixto US-CSIC Avda. Américo Vespucio 49, 41092 Seville, Spain*

*<sup>2</sup>Department of Chemical and Process Engineering, Faculty of Engineering and Physical Sciences, University of Surrey, Guildford, UK*

## ***Introduction***

The production of hydrocarbon fuels from biomass is a major challenge in the effort to develop advanced biofuels for a low carbon society. In order to produce petroleum-like hydrocarbon fuels, the oxygen atoms in bio-oils must be removed, which is typically achieved by catalytic hydrodeoxygenation (HDO) a standard and promising route. Nevertheless, the “Achilles Heel” of this approach is the supply of H<sub>2</sub>-an expensive resource which imposes a tremendous economic limitation to the implementation of HDO in large scale production units <sup>[1]</sup>. In order to overcome this restriction, in this work water was used as a hydrogen source thus improving the overall economic efficiency for the bio-oil upgrading process. Hydrogen free guaiacol hydrodeoxygenation was investigated using different noble metal (Ru, Rh, Pd, Au)-based catalysts tested at 250 °C. Both fresh and spent catalysts were comprehensively characterized.

## ***Experimental***

A charcoal powder DARCO® used as carbon support. Catalysts were prepared by wetness impregnation with acetone and aqueous solutions of metal precursors. Because of a difficulty of obtaining small gold particle sizes by wetness impregnation, the gold catalyst was prepared by colloidal synthesis. In all cases, the catalysts were synthesized with a nominal value of 2% (wt.%) of the reduced metal.

All solids were characterized by means of S<sub>BET</sub>, XRD, SEM and HR-TEM microscopies, ICP, Elemental analysis, TPD and DRIFTS.

The HDO catalytic activity was tested in a Parr reactor at 50 bar pressure and 250°C during 4 h. The experiments were carried out under the following conditions: 50 mL

of a 0,01 mg/mL guaiacol solution and 200 mg of catalyst. Guaiacol and possible products concentrations were determined by gas chromatograph-flame ionisation detector (GC/FID) and the activity expressed in terms of products conversion were represented.

### Results and discussions

The synthesized noble metal catalyst present particle size below than 10 nm, **figure 1** in all cases with a metal loading close to nominal value (2%) indicating the suitability of the preparation method for all metals. Dispersion of the active phase was taken from TEM data, assuming cuboctahedra particles and the experimental active phase charge measured by ICP analysis. All the noble metal catalyst was slightly acidic and the metal dispersion decreased in following order: Ru/C>Pd/C>Au/C>Rh/C, **table 1**.

**Table 1.** Catalyst characterization.

Metal	TEM particle size (nm)	% Metal [ICP]	Calculated Dispersion (%)	Acidity (pH)
Au	5.95	1.96	22.2	6.5
Pd	3.92	2.94	33.5	6.47
Rh	6.96	1.39	20.1	6.38
Ru	2.61	2.05	48.2	6.74

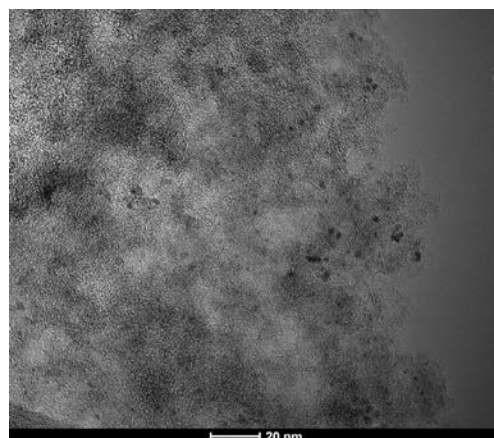


**Figure 1.** Ru/C<sub>darco</sub> TEM micrograph.

The highest selectivity to deoxygenated products, 9% selectivity at 25% guaiacol conversion after 4 h was obtained in guaiacol hydrodeoxygenation in hydrogen free conditions with Ru/C catalyst, **figure 2**.

Both demethoxylation and/or dihydroxylation were promoted by Ru/C, which exhibited rather high dispersion.

No sintering process was found in spent Ru/C catalyst, showing similar dispersion and metal particle size after reaction.

### References

[1] W. Jin, L.Pastor- Pérez, D. Shen, A. Sepúlveda-Escribano, S. Gu, T. R.Reina Catalytic upgrading of biomass model compounds: Novel approaches and lessons learnt from traditional hydrodeoxygenation – a review ChemCatChem DOI 10.1002/cctc.201801722.

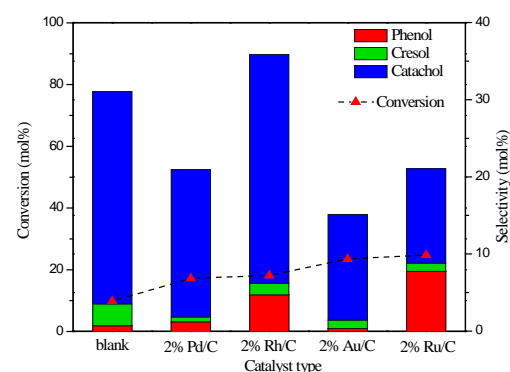


**Figure 2.** Activity of noble catalysts in in-situ HDO process.

# Hierarchical zeolites as catalysts for glycerol with acetone ketalization in a continuous flow system

*J. Kowalska-Kuś, A. Held, K. Nowińska, Faculty of Chemistry, Adam Mickiewicz University, 61-614 Poznan, Umultowska 89b, Poland*

Biofuels are produced from vegetable oils or animal fats by means of catalytic transesterification reaction with methanol. Besides the main product, a biodiesel, also by-product called a waste glycerol phase is formed with the amount of about 10%. In a consequence of the increasing biodiesel production, the amount of a glycerol phase is growing. Therefore, a lot of interest has been devoted to the glycerol processing into valuable chemicals by various catalytic procedures. One of the important glycerol derivative is solketal (2,2-dimethyl 1,3-dioxalane-4-methanol), a product of glycerol with acetone reaction. This compound can be used as an intermediate for the production of a number of commodities as well as a fuel additive [1, 2].

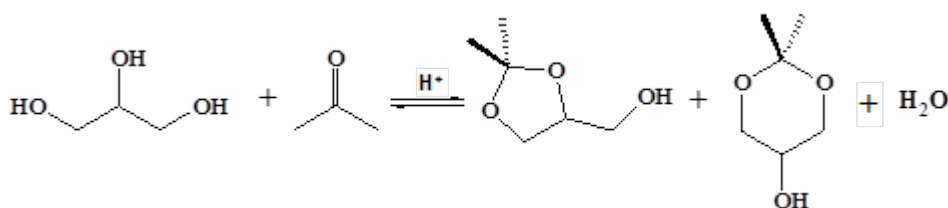


Fig. 1. Ketalization reaction of glycerol with acetone

Conventionally, the ketalization reaction is catalyzed by liquid mineral acids, which results in the formation of unaccepted liquid wastes. Considering that, different solid materials of acidic character [3, 4] were tested in ketalization reaction. Among them hierarchical zeolites (micro-mesoporous system) have attracted much attention, because they could overcome the drawbacks related to hamper mass transfer and limited accessibility of acidic sites of conventional zeolites [5]. Taking this into account, we have applied the hierarchical zeolites of ZSM-5, mordenite and Beta structure as catalysts for glycerol with acetone ketalization.

Micro-mesoporous zeolites were prepared by means of alkaline treatment (using 0.2 M aqueous NaOH at 353 K for 2 h) with the following washing, filtration and ionic

exchange with  $\text{NH}_4\text{NO}_3$  (0.5 M  $\text{NH}_4\text{NO}_3$  aqueous solution at 308 K for 24 h) and a subsequent treatment with citric acid (0.5 M citric acid (CA) solution at 353 K for 3 h). The synthesis of solketal was carried out in a continuous down-flow reactor operating under atmospheric pressure. The feed containing acetone, glycerol and methanol as a solvent was pumped continuously at room temperature into the reactor heated to 323 K. The product was collected every 0.5 h and analyzed by GC.

The hierarchical zeolites preserved an original crystallinity (XRD) after desilication process and only small decrease in XRD reflection intensity has been recorded. The applied modification of commercial zeolites resulted in an increased surface area and in a considerable growth of total porosity due to the contribution of formed mesopores. The Si/Al ratio of modified zeolites estimated by F-AAS analysis was lower than that of the microporous catalyst. The acidity measured on the basis of IR spectra of adsorbed pyridine indicated an increase in the number of Lewis acid sites and a decrease in the number of Brønsted acid sites as a result of alkaline treatment with following ionic exchange with aqueous solution of  $\text{NH}_4\text{NO}_3$ . A subsequent treatment with citric acid resulted in some decrease in a number of Lewis acids (as an effect of Al-rich debris removal [5]).

Hierarchical zeolites of ZSM-5, mordenite, and Beta structure showed a very high and stable activity for glycerol acetalization (during 24 hours). The conversion of glycerol over hierarchical zeolites showed almost 94 %, while selectivity to solketal achieved 98 %, which results in solketal yield of about 91 %. Catalytic activity of hierarchical ZSM-5, mordenite and Beta zeolites demonstrates its superior performance in the reaction of glycerol with acetone ketalization carried out in a flow-system at low temperature and under atmospheric pressure.

## References

1. J. Kowalska-Kuś, A. Held, M. Frankowski, K. Nowińska J. Mol. Catal. A: Chem. 426 (2017) 205
2. K. Stawicka, A.E. Díaz-Álvarez, V. Calvino-Casilda, M. Trejda, M.A. Bañares, M. Ziolek J. Phys. Chem. C, 120 (30) (2016) 16699
3. A. Talebian-Kiakalaieh, N.A.S. Amin, N. Najaafi, S. Tarighi, Front. Chem. 6 (2018) 573
4. M.R. Nanda, Z. Yuan, W. Qin, H.S. Ghaziaskar, M.-A. Poirier, C. Xu, Appl. Energy, 123 (2014) 75
5. D. Verboekend, S. Mitchell, M. Milina, J.C. Groen, J. Pérez-Ramírez, J. Phys. Chem. C, 115 (2011) 14193

## **Utilization of crude glycerol by means of ketalization process performed over zeolites of different structure**

*J.Kowalska-Kuś, A.Held, K. Nowińska, Adam Mickiewicz University, Faculty of  
Chemistry, 61-614 Poznan, Umultowska 89b, Poland*

Biodiesel production performed by transesterification of biological oils with methanol under base catalysis conditions results not only in desirable material but also in waste glycerol phase constituting 10% of the final product. Glycerol phase, besides glycerol (50 - 60%) comprises various impurities such as unreacted methanol, fatty acids, soaps, and alkaline catalysts residue. The increasing demand for biodiesel causes a glycerol oversupply. Purification of waste glycerol is expensive and it results in the growing prices both of biodiesel and glycerol [1]. Considering that, application of crude glycerol for direct transformation to valuable products seems to be very actual and important task. One of these attempts is the use of waste glycerol for production of acetals or ketals, which may be applied as potential gasoline additives [2].

Our study presents the application of hierarchical zeolites of different structures such as ZSM-5, Beta, mordenite, and also USY zeolite as catalysts for ketalization of crude glycerol with acetone. Hierarchical zeolites were prepared according to the procedure described earlier [3], while crude glycerol was delivered by ADM Malbork Company. Prior to the catalytic experiments all the catalysts were calcined at 823 K for 3 h. The synthesis of solketal was carried out in a continuous down-flow reactor. The feed containing acetone and glycerol (molar ratio of 3:1) as well as methanol as a solvent was pumped continuously at room temperature into the reactor heated to 323 K. The product was collected every 0.5h and analyzed by GC.

All hierarchical zeolites showed considerable activity in glycerol ketalization reaction for the first 3 h. Modified ZSM-5 and Beta and also USY zeolites indicated the highest value of glycerol conversion (about 90 % after the first hour and 50 % after the third hour on stream). However the longer exploitation resulted in the further deactivation of catalysts. On the other hand, the selectivity to solketal was high (more than 90 % after the first hour on stream) and did not diminish below 70 % during eight hours on stream. Considering our earlier results, when glycerol deprived of sodium impurities has been used (catalysts showed a high and stable activity), we

can suggest that mainly sodium cations are responsible for a decrease in the activity of zeolites with time on stream. Sodium cations can migrate from the liquid phase to the pores of the catalyst, neutralizing their acid centers. In addition, the presence of water might facilitate the above process [5]. Fortunately, regeneration of spent catalysts by means of calcination with following treatment with citric acid restores the initial activity of the applied catalysts.

#### References

1. M. Ayoub, A. Z. Abdullah *Renew. Sust. Energ.* 16 (2012) 2671
2. P. Ferreira, I.M. Fonseca, A.M. Ramos, J. Vital, J.E. Castanheiro, *Appl. Catal. B: Environ.* 98 (2010) 94
3. J. Kowalska-Kuś, A. Held, M. Frankowski, K. Nowińska *J. Mol. Catal. A: Chem.* 426 (2017) 205
4. C.-Y. HSU, P.E. Ellis, United State Patent 4,775,447
5. C.X.A. da Silva, C.J.A. Mota, *Biomass Bioenerg.* 35 (2011) 3547

# Ammonia Synthesis using Cobalt Rhenium Catalysts Supported on Magnesium Oxide

*Justin S. J. Hargreaves, School of Chemistry, Joseph Black Building, University of Glasgow, Glasgow G12 8QQ, U.K.; Yalinu Poya, School of Chemistry, Joseph Black Building, University of Glasgow, Glasgow G12 8QQ, U.K.*

## Introduction

The Haber–Bosch Process which was developed in the early 1900's, was a landmark achievement of the 20th Century. Currently, the process produces over 180 million tonnes of ammonia annually, establishing an accessible route for the production of over 450 million tonnes of synthetic fertilizer. In itself this sustains food production for 40% of the global population [1]. The Haber–Bosch Process involves combining pure H<sub>2</sub> and N<sub>2</sub> feed streams directly over a promoted iron catalyst at temperatures of around 400°C and reaction pressures of over 100 atmospheres. The reaction is exothermic and is equilibrium limited, thus it is thermodynamically favoured at lower reaction temperatures. Despite this, the temperature of operation is dictated by the requirement to achieve acceptable process kinetics [2].

Due to the reaction conditions involved in the process at a global scale, including the generation of feedstock, the operation of the Haber–Bosch Process currently consumes 2% of the world's energy demand and produces 1.6% of man-made CO<sub>2</sub> emissions [2]. To reduce these harmful effects and yield massive rewards both in terms of economic and environmental benefits, there is great interest in the development of small scale local ammonia production plants based on renewable hydrogen generated from water via electrolysis and powered by sustainable electricity sources such as wind energy. In such a context, which would facilitate the production of ammonia on a localised scale close to its point of use such as on a farm, it is necessary to develop novel ammonia synthesis catalysts which are active under less severe operational conditions appropriate to smaller scale reactors.

It is notable that a number of active ammonia synthesis catalysts comprise of cobalt in addition to or promoters [3] [4] other active metals [5] [6] – a combination of cobalt and rhenium as a bimetallic catalyst shows high ammonia synthesis activity despite its low surface area [7]. Accordingly, the development of a more highly dispersed catalytically active phase is highly desirable. Magnesium oxide is a support of interest



which as well as potentially possessing high surface area also could act as a chemical promoter in the reaction, due to its inherent basicity. Consequently, in this study a series of novel magnesium oxide supported cobalt rhenium catalysts prepared and applied to ammonia synthesis have been observed to exhibit interesting activity.

## Materials and Results

Cobalt rhenium supported on magnesium oxide was prepared by incipient wetness impregnation of  $\text{Co}(\text{NO}_3)_2 \cdot 6\text{H}_2\text{O}$  and  $\text{NH}_4\text{ReO}_4$  onto magnesium oxide (MgO) to give a CoRe 10% wt. metal loading. The material was dried at 125°C for 12 hours, calcined in air at 700°C for 3 hours, and then pre-treated at 600°C under  $\text{N}_2/\text{H}_2$  (1:3) gas mixture for 2 hours prior to ammonia synthesis. Techniques such as powder XRD, Raman, BET Surface Area, CHN, TGA and SEM/EDX were used to characterise the material before and after reaction. Using 0.5g of catalyst ambient pressure ammonia synthesis rates of  $98 \mu\text{molh}^{-1}\text{g}^{-1}$  and  $317 \mu\text{molh}^{-1}\text{g}^{-1}$  were obtained at reaction temperatures of 400°C and 500°C respectively and these results will be discussed in the context of known high activity catalysts.

## Conclusion

The use of cobalt rhenium supported on magnesium oxide catalysts in ammonia synthesis represents a novel approach which is a potential route to high dispersion and inclusion of promoter species leading to the potential development of catalysts of high performance.

## References

1. Smil, V., *Nitrogen and Food Production: Proteins for Human Diets*. AMBIO: A Journal of the Human Environment, 2002. **31**(2): p. 126-131.
2. Smil, V., *Enriching the earth: Fritz Haber, Carl Bosch, and the transformation of world food production*. 2004: MIT press.
3. Hagen, S., et al., *New efficient catalyst for ammonia synthesis: barium-promoted cobalt on carbon*. Chemical Communications, 2002(11): p. 1206-1207.
4. Magdalena, Z., et al., *Properties and activity of the cobalt catalysts for  $\text{NH}_3$  synthesis obtained by co-precipitation – the effect of lanthanum addition*. Polish Journal of Chemical Technology, 2015. **17**(1): p. 138-143.
5. Hunter, S.M., et al., *A Study of  $^{15}\text{N}/^{14}\text{N}$  Isotopic Exchange over Cobalt Molybdenum Nitrides*. ACS Catalysis, 2013. **3**(8): p. 1719-1725.
6. AlShibane, I., et al., *The Role of Composition for Cobalt Molybdenum Carbide in Ammonia Synthesis*. ACS Sustainable Chemistry & Engineering, 2017. **5**(10): p. 9214-9222.
7. Mathisen, K., et al., *An In Situ XAS Study of the Cobalt Rhenium Catalyst for Ammonia Synthesis*. Topics in Catalysis, 2018. **61**(3): p. 225-239.

## Fischer-Tropsch synthesis on *hcp*-Co nanowires grown on carbon nanotubes and copper powder.

Amel Cydric Ghogia<sup>1,2,3</sup>, Simon Cayez<sup>2</sup>, Ange Nzihou<sup>1</sup>, Philippe Serp<sup>3</sup>, Katerina Soulantica<sup>2</sup>, Doan Pham Minh<sup>1</sup>

<sup>1</sup>Université de Toulouse, IMT Mines Albi, UMR CNRS 5302, Centre RAPSODEE, Campus Jarlard, F-81013 Albi, cedex 09, France. aghogia@mines-albi.fr

<sup>2</sup>LPCNO, Université de Toulouse, CNRS, INSA, UPS, Toulouse.

<sup>3</sup>LCC, CNRS-UPR 8241, ENSIACET, Université de Toulouse, France.

Fischer-Tropsch Synthesis (FTS) is a catalytic process, which converts CO and H<sub>2</sub> obtained from natural gas (GTL process), coal (CTL process) or biomass (BTL process) into a mixture of linear gaseous, liquid and solid hydrocarbons[1]. Previous works claimed that Co with a hexagonal-close-packed (Co-*hcp*) structure possesses a higher catalytic activity in comparison to face-centered cubic cobalt (Co-*fcc*)[2,3]. Recently, Harmel *et al.* have successfully grown cobalt nanowires (NW) exhibiting the *hcp* structure on a Co/Al<sub>2</sub>O<sub>3</sub>-SiO<sub>2</sub> catalyst[4]. The as-obtained catalysts have shown high stability in FTS in slurry reactor compared to a reference catalyst[4]. Multi-tubular fixed bed and slurry bubble column reactors are currently used on industrial scale. The fixed bed reactor is widely used for FTS, because it offers many advantages especially when the catalyst used is cobalt-based[5]. However, the fixed-bed reactor is subjected to local overheating of the catalyst surface that may lead to a fast deactivation and to higher production of methane [6]. Developments of novel FTS catalysts with high thermal conductivity for efficient heat management is one of the key challenges of research into FTS. In order to manage the strong exothermicity of the FTS reaction, Harmel *et al.* have also used Cu metallic foam as conductive support, on which they have grown Co-*hcp* NW[7]. This catalyst exhibited outstanding catalytic activity and high stability in fixed bed reactor[7].

In this work, two conductive supports, carbon nanotubes and copper powder with different thermal conductivity (CNT, 17 W.m<sup>-1</sup>.K<sup>-1</sup> and Cu, 485 W.m<sup>-1</sup>.K<sup>-1</sup>) have been used. The catalysts were prepared by a colloidal approach. Co-*hcp* NW were grown on copper powder by epitaxial growth (Figure 1a), directly from a solution containing

a coordination compound of cobalt and stabilizing ligands[7]. Concerning *Co-hcp*/CNT, firstly, *Co-fcc* nanoparticles were deposited on the surface of CNT as seeds for cobalt NW growth. Then, *Co-hcp* NW were grown on the surface of *Co-fcc*/CNT (Figure 1b). Finally, the performances of the catalysts were evaluated in FTS using a fixed-bed reactor (Figure 1c). The impact of thermal conductivity of catalyst supports and Co structure on their catalytic performances will be discussed.

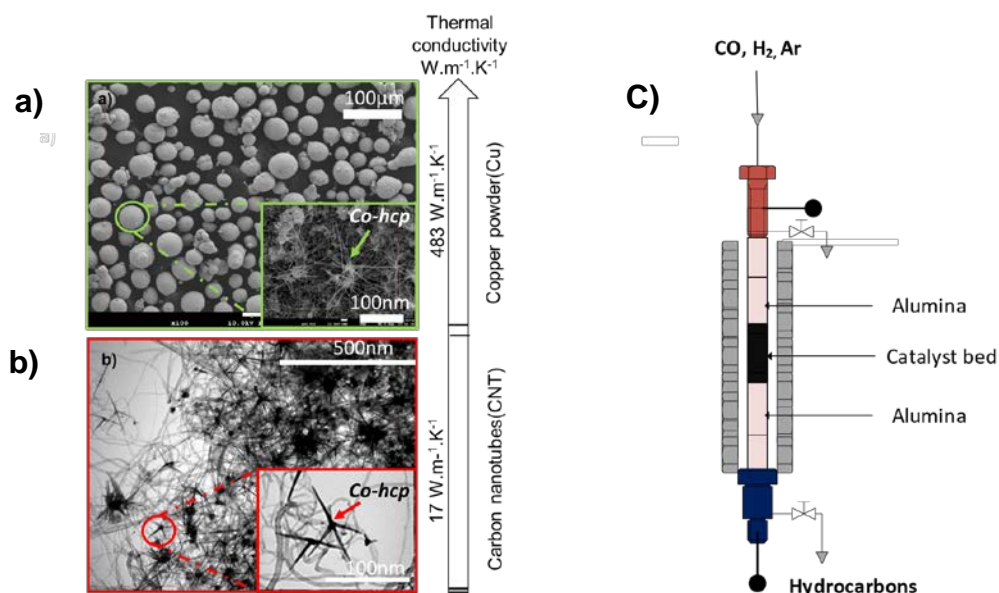


Fig.1. News catalysts: a) SEM image of *Co-hcp*/Cu and b) TEM image of *Co-hcp*@*Co-fcc*/CNT; and c) Catalyst loading in the fixed bed FTS reactor

## References

- [1] R. Philippe, M. Lacroix, L. Dreibine, C. Pham-Huu, D. Edouard, S. Savin, F. Luck, D. Schweich, *Catal. Today.* (2009) S305–S312.
- [2] J.X. Liu, H.Y. Su, D.P. Sun, B.Y. Zhang, W.X. Li, FCC, *J. Am. Chem. Soc.* 135 (2013) 16284–16287.
- [3] S. Lyu, L. Wang, J. Zhang, C. Liu, J. Sun, B. Peng, Y. Wang, K.G. Rappé, Y. Zhang, J. Li, L. Nie, *ACS Catal.* 8 (2018) 7787–7798.
- [4] J. Harmel, A. Berliet, K. Dembélé, C. Marcelot, A.-S. Gay, O. Ersen, S. Maury, A. Fécant, B. Chaudret, P. Serp, K. Soulantica, *ChemCatChem.* 10 (2018) 1614–1619.
- [5] X. Zhu, X. Lu, X. Liu, D. Hildebrandt, D. Glasser, *Chem. Eng. J.* 247 (2014) 75–84.
- [6] S. Chambreyra, P. Fongarlanda, H. Karacaa, S. Pichéa, A. Griboval-Constanta, D. Schweichb, F. Luckc, S. Savinc, A.Y. Khodakov, *Catal. Today.* 171 (2011) 201–206.
- [7] J. Harmel, L. Peres, M. Estrader, A. Berliet, S. Maury, A. Fécant, B. Chaudret, P. Serp, K. Soulantica, *Angew. Chem.* 57 (2018) 10579–10583.

# Equilibrium Modelling Insights to Process Tolerance and Operational Capabilities of Waste Plasma Gasification as Power-to-X Concept

Maximilian Hungsberg<sup>1</sup>, Christian Dreiser<sup>2</sup>, Stefan Brand<sup>2</sup>, Alfons Drochner<sup>1</sup>,  
Bastian JM Etzold<sup>1</sup>

<sup>1</sup>Technische Universität Darmstadt, Darmstadt/Germany;

<sup>2</sup>CLARIANT, Group Process Technology, Frankfurt/Germany

## Introduction

An increasing supply of fluctuating renewable energies results in a rising need for highly flexible electricity-driven processes [1,2]. The gasification of organic waste material by using electricity-based plasma as an energy supply opens up the possibility of a demand-side utilization of renewables. In addition, plasma gasification can contribute to the realization of a Circular Economy in connecting the ends of a linear (take-make-use-dispose) economy by converting waste as alternative feedstock and renewable energy into synthesis gas [3]. Through this material cycle, variations in feed stream composition are highly probable, which makes up the demand for tolerant processes. In this sense, plasma gasification is a promising technology, not only capable to handle these feedstock variations but also power fluctuations.

## Results

To study the capability of waste plasma gasification in Power-to-X concepts, a non-stoichiometric equilibrium model was employed. As feedstocks, representing low to highly functionalized materials, coal ( $\text{CH}_{0.6}\text{O}_{0.02}$ ), lignin ( $\text{CH}_{1.1}\text{O}_{0.4}$ ), and cellulose ( $\text{CH}_{1.65}\text{O}_{0.8}$ ) were chosen. Furthermore, the addition of oxygen, hydrogen and steam as gasification agents and also pre-drying of the feedstock was studied. The changed composition, resulting after these steps, is named *operational composition* and is represented by overall O:C- and H:C-ratios. For these compositional variations and temperatures from 800 to 1800 K the equilibrium product gas composition is calculated. In difference to waste to energy concepts, not the caloric value of the product stream, but the achievable total amount of syngas ( $\text{H}_2+\text{CO}$ ), the syngas ratio ( $\text{H}_2/\text{CO}$ ) and also the amount of solid carbon formed is in focus. Solid carbon not only represents unused feedstock, but high solid carbon

contents give also rise to difficulties in the handling of the gasification process and product gas purification. It can be observed that for temperatures above 1400 K a plateau is reached, where variations in temperature only slightly affect the molar amount of syngas and the syngas ratio, which is an important prerequisite for a tolerant process. If a certain product gas composition is needed, the present model can be used to determine the optimal route to the target specification, while accounting for given constrains. This could be for example the aimed syngas ratio, minimal amounts of total syngas produced and maximum amount of solid carbon. From the thermodynamic calculations borderlines for each constrain can be drawn within the van Krevelen plot. Subsequently, the region of O:C- and H:C-ratios fulfilling all criteria can be identified (Figure 1, white area). Furthermore, this van Krevelen plot allows to identify which, use of gasification agents or a pre-drying of the feedstock, allows to operate within this window, as exemplarily illustrated in Figure 1 for moist, ash-free lignin.

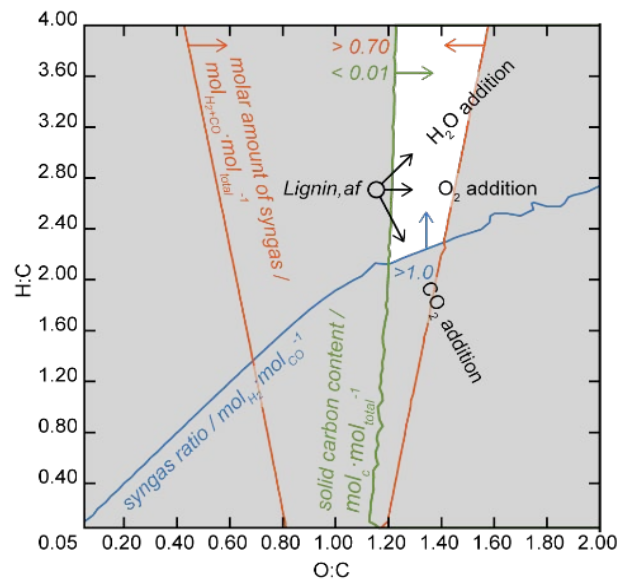


Figure 1: van Krevelen plot with overlaying borderlines for the aimed product gas gives the proper area of the operational composition (white). Lignin (af) is the moist, ash-free feedstock composition. The arrows represent possible shifts by adding the labelled gasification agent.

## Conclusion

The thermodynamic study reveals that the high temperatures during plasma gasification and the use of gasification agents, gives rise to a process being highly tolerant to various or fluctuating feedstocks – a key element for the implementation of closed material cycles.

## References

- [1] Ausfelder, F.; Beilmann, C.; Bertau, M.; Bräuninger, S.; Heinzl, A.; Hoer, R.; Koch, W.; Mahlendorf, F.; Metzelthin, A.; Peuckert, M., *CHEM-ING-TECH.* **2015**, *87*, 17–89.
- [2] Moseley, P. T.; Garche, J. *Electrochemical Energy Storage for Renewable Sources and Grid Balancing*; Elsevier Science: Burlington, **2014**.
- [3] Lieder, M.; Rashid, A., *J. Clean Prod.* **2016**, *115*, 36–51.

# Study on CO<sub>2</sub> reduction activity of Ga<sub>2</sub>O<sub>3</sub> supported with various metal oxides

Ryota Ito<sup>1</sup>, Masato Akatuka<sup>1</sup>, Akiyo Ozawa<sup>1</sup>, Muneaki Yamamoto<sup>2</sup>, Tetsuo Tanabe<sup>2</sup>,  
Tomoko Yoshida<sup>2</sup>

<sup>1</sup>*Applied Chemistry and Bioengineering Graduate School of Engineering, Osaka City University, Osaka, Japan.*

<sup>2</sup>*Advanced Research Institute for National Science and Technology, Osaka City University, Osaka, Japan.*

## Introduction

Recently Ga<sub>2</sub>O<sub>3</sub> has attracted a lot of interests as a photocatalyst for water splitting and CO<sub>2</sub> reduction with water, and various efforts have been paid to improve its photocatalytic activity [1]. However, its photocatalytic activity for CO<sub>2</sub> reduction remains still low. In order to improve the photocatalytic activity of Ga<sub>2</sub>O<sub>3</sub>, in our previous study, we succeeded in improvement of the photocatalytic activity by loading of Ga<sub>2</sub>O<sub>3</sub> on Al<sub>2</sub>O<sub>3</sub>. For the further improvement, in the present study, we compared CO<sub>2</sub> reduction activity of Ga<sub>2</sub>O<sub>3</sub> supported with various metal oxide.

## Experimental

Samples were prepared by impregnation of metal oxides (La<sub>2</sub>O<sub>3</sub>, Al<sub>2</sub>O<sub>3</sub>, Yb<sub>2</sub>O<sub>3</sub>, Y<sub>2</sub>O<sub>3</sub>, Nd<sub>2</sub>O<sub>3</sub>, ZSM-5, ZrO, TiO<sub>2</sub>, ZnO, CeO<sub>2</sub>, MgO) with aqueous solution of gallium nitrate followed by dry and calcination in air at 823 K for 4 h. The loading amount of Ga<sub>2</sub>O<sub>3</sub> was decided as 40 wt% because 40 wt% Al<sub>2</sub>O<sub>3</sub> supported Ga<sub>2</sub>O<sub>3</sub> (Ga<sub>2</sub>O<sub>3</sub>/Al<sub>2</sub>O<sub>3</sub>) showed the highest activity for CO<sub>2</sub> reduction with water in our previous study. The photocatalytic CO<sub>2</sub> reduction with water was carried out for all prepared samples. Each prepared sample (0.1 g) was dispersed in an aqueous solution of NaHCO<sub>3</sub> (1.0 M) in the fixed-bed flow reactor cell under CO<sub>2</sub> gas with a flow rate at 3.0 mL/min and irradiated by UV-light (Xe lamp). The reaction products (CO, H<sub>2</sub> and O<sub>2</sub>) were analyzed with gas chromatography.

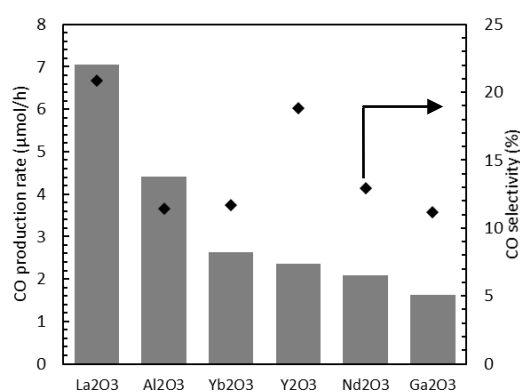
## Result and discussion

Fig.1 compares CO production rate and CO selectivity for all prepared samples. Ga<sub>2</sub>O<sub>3</sub> supported with La<sub>2</sub>O<sub>3</sub> and Al<sub>2</sub>O<sub>3</sub> had much higher CO production rate than a bare Ga<sub>2</sub>O<sub>3</sub>. However, Ga<sub>2</sub>O<sub>3</sub> supported with other metal oxides had lower activity

than a bare Ga<sub>2</sub>O<sub>3</sub>. In particular, Ga<sub>2</sub>O<sub>3</sub> supported with ZSM-5 showed low activity, although ZSM-5 has the largest specific surface area among the metal oxide supports used in this study. It is considered that the photocatalytic activity for CO production is not directly connected with the specific surface area of a metal oxide support.

We focused on Ga<sub>2</sub>O<sub>3</sub> supported with Al<sub>2</sub>O<sub>3</sub> or La<sub>2</sub>O<sub>3</sub> which showed high activity for photocatalytic CO<sub>2</sub> reduction. In our previous work, it was revealed that the supporting of Ga<sub>2</sub>O<sub>3</sub> with Al<sub>2</sub>O<sub>3</sub> has improved the photocatalytic activity for CO<sub>2</sub> reduction due to highly dispersion of Ga<sub>2</sub>O<sub>3</sub> with the mixed structure of α and γ phases. As for Ga<sub>2</sub>O<sub>3</sub> supported with La<sub>2</sub>O<sub>3</sub> (Ga<sub>2</sub>O<sub>3</sub>/La<sub>2</sub>O<sub>3</sub>), it was confirmed that CO<sub>2</sub> reduction to CO does not proceed over La<sub>2</sub>O<sub>3</sub>. Fig.3 shows XRD patterns of Ga<sub>2</sub>O<sub>3</sub>/La<sub>2</sub>O<sub>3</sub> before and after the reaction. The crystal structure of La<sub>2</sub>O<sub>3</sub> supported Ga<sub>2</sub>O<sub>3</sub> sample had remarkably changed after the reaction, while the crystal structure did not greatly differ when flowing CO<sub>2</sub> and when flowing He. After the reaction, XRD diffraction peaks attributed to NaLa(CO<sub>3</sub>)<sub>2</sub> were observed, suggesting that the change in crystal structure derived from the reaction of La<sub>2</sub>O<sub>3</sub> with NaHCO<sub>3</sub> aqueous solution. Therefore, the Ga<sub>2</sub>O<sub>3</sub> supported with NaLa(CO<sub>3</sub>)<sub>2</sub> would promote CO<sub>2</sub> reduction.

The details will be discussed in the conference.



**Fig.1** CO production rate after 5h reaction for samples showing higher activity than Ga<sub>2</sub>O<sub>3</sub>

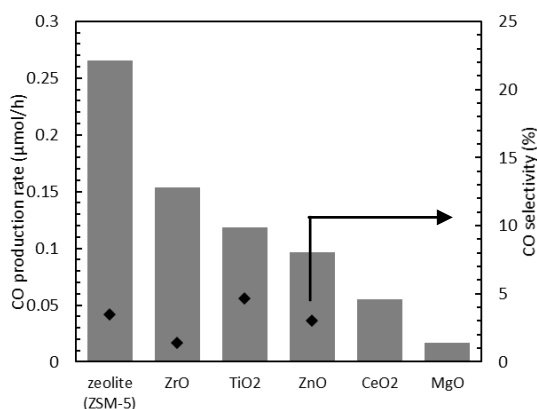


**Fig.2** CO production rate after 5h reaction for samples showing lower activity than Ga<sub>2</sub>O<sub>3</sub>

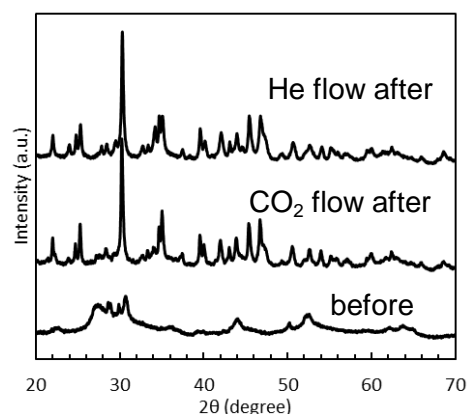


**Fig.3** XRD patterns of 40 wt% Ga<sub>2</sub>O<sub>3</sub>/La<sub>2</sub>O<sub>3</sub> before and after the reaction

## References

[1] N. Yamamoto, T. Yoshida, S. Yagi, et al., e-J Surf. Sci. Nanotech., Vol. 12 (2014) 263-268.

## **One Dimensional Symmetric and Asymmetric Heterostructures with Improved Charge Separation for Water Splitting**

*Xinheng Li,\* State Key Laboratory for Oxo Synthesis and Selective Oxidation and Suzhou Research Institute of LICP, Lanzhou Institute of Chemical Physics (LICP), Chinese Academy of Sciences, Suzhou 215123, China; Xianmei Xiang, State Key Laboratory for Oxo Synthesis and Selective Oxidation and Suzhou Research Institute of LICP, Lanzhou Institute of Chemical Physics (LICP), Chinese Academy of Sciences, Suzhou 215123, China; Denghui Jiang, Centre for Mineral Materials, School of Minerals Processing and Bioengineering, Central South University, Changsha 410083, China.*

Solar energy as a clean renewable alternative energy has attracted great attentions with potential applications for photocatalysis. But, its conversion efficiency has been a severe crucial problem largely because of extremely low efficiency of charge carriers separation i.e. rapid recombination rates of electrons and holes [1,2,3]. Herein, we report our recent progress on improving charge carriers separation efficiency for water splitting. We design and synthesize symmetric and asymmetric nanoheterojunctions of one dimensional colloidal nanorods respectively, featuring that electrons and holes are able to be guided to separate along the linear nanorod driven by internal built-up electric field.

We prepared symmetric heterojunctions, i.e. AuPd - CdS nanorod - AuPd and PdS - CdS nanorod - PdS, respectively by solvent pyrolysis and cation exchange methods. The UV-vis absorption spectra and fluorescent spectra of the above-mentioned samples have demonstrated that the fluorescence of the CdS nanorods was strongly quenched after being selective deposition of metals and semiconductors on the ends. Moreover, it was found that as for the AuPd - CdS nanorod - AuPd samples, excited electrons were transferred to double ends of the nanorods. But, as for the PdS - CdS nanorod - PdS sample, holes were transferred to double ends [4, 5]. Therefore, we proved that transport directions of electrons/holes were able to be guided by the designed heterostructures with improved charge separation efficiency.



Furthermore, we prepared asymmetric heterojunctions of one dimensional colloidal nanorods by combining solvent pyrolysis with cation exchange methods, i.e. PdS - CdS nanorod - Au [1]. It was found that excited electrons were transferred to Au end while holes were transferred to the opposite end i.e. PdS. The asymmetric nanoheterostructures demonstrated excellent photocatalytic activity for water splitting, ca. 2 orders increase for H<sub>2</sub> production. In the meanwhile, the as-obtained samples have improved photostability. The enhance water splitting performance was mainly attributed to excellent charge separation. It is hypothesized that asymmetric heterostructures had superposition of two internal electric fields benefiting better charge separation.

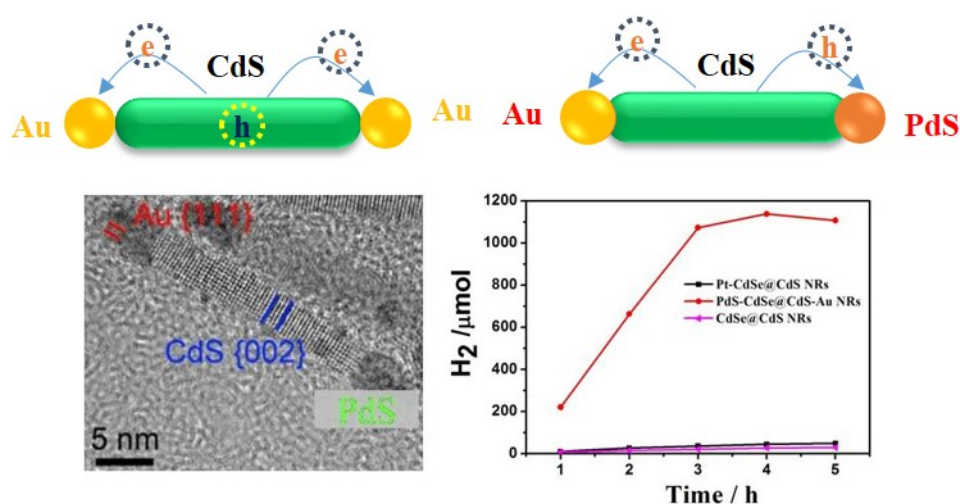


**Fig. 1** (Upper) Schematic of symmetric and asymmetric nanoheterostructures of CdSe@CdS nanorods; (Bottom left) TEM image of PdS - CdSe@CdS - Au nanorods, (Bottom right) water splitting as a function of visible light irradiation time. [1]

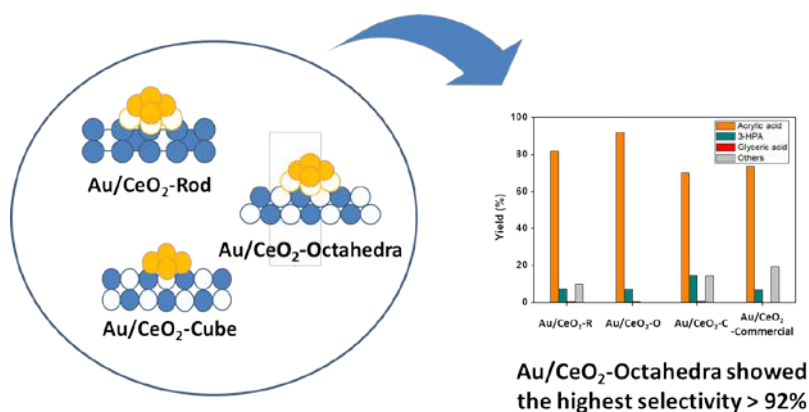
#### References:

1. Xianmei Xiang, Lingjun Chou, Xinheng Li, *Chin. J. Catal.*, 2019, 39,407.
2. Denghui Jiang, Jianbin Xue, Liqiong Wu, Weizhou, Yuegang Zhang, Xinheng Li, *Appl. Catal. B* 2017, 211, 199.
3. Denghui Jiang, Yuegang Zhang, Xinheng Li, *Nanoscale* 2017, 9, 12348.
4. Xianmei Xiang, Lingjun Chou, Xinheng Li, *Phys. Chem. Chem. Phys.* 2013, 15, 19545.
5. Xinheng Li, Jie Lian, Ming Lin, and YinThai Chan, *J. Am. Chem. Soc.* 2011, 133, 672.

# Highly Selective Production of Acrylic Acid from Glycerol via Two-step Pathway

*Minsu Kim, Department of Chemical and Biomolecular Engineering, Korea Advanced Institute of Science and Technology, Daejeon, Republic of Korea; Hyunjoo Lee, Department of Chemical and Biomolecular Engineering, Korea Advanced Institute of Science and Technology, Daejeon, Republic of Korea*

High value chemical production is important for a sustainable development in chemical industry. Biomass-derived glycerol has recently been considered as a novel platform to produce C3 chemicals.[1] Among various approaches to utilize excessive glycerol, a pathway for the production of acrylic acid has attracted attention.[2] In this work, glycerol was selectively converted to 87 % yield of acrylic acid by two-step pathway; glycerol was converted to allyl alcohol by formic acid-mediated deoxydehydration (DODH), then the glycerol-derived allyl alcohol was oxidized into 92% yield of acrylic acid at room temperature in a basic aqueous solution using Au/CeO<sub>2</sub> catalysts. The gold catalysts enabled the highly selective production of acrylic acid from glycerol-derived allyl alcohol. From a hydrothermal method, rods, octahedra, and cubes CeO<sub>2</sub> were prepared, and deposition-precipitation method generated a highly active gold species on the surface of CeO<sub>2</sub>. Octahedral CeO<sub>2</sub> provided high surface area and reducibility for the oxidation of allyl alcohol. Therefore, highly selective and stable production of acrylic acid from glycerol was achieved up to 5 cycles of conversion using gold on octahedral CeO<sub>2</sub>. [3]



## References

- [1] *Eur. J. Lipid Sci. Technol.* 2014, 116, 1432–1439
- [2] *Green Chem.* 2017, 19 3186–3213
- [2] *ACS Sustainable Chem. Eng.* 2017, 5, 12, 11371-11376

# Turning a Deactivated Phase into Valuable Catalyst Precursor – A Case Study on Cobalt based CO<sub>2</sub> Methanation

*Tanja Franken, Andre Heel*

*IMPE – Institute of Materials and Process Engineering, ZHAW - Zurich University of Applied Sciences, CH-8401 Winterthur, Switzerland.*

[Tanja.franken@zhaw.ch](mailto:Tanja.franken@zhaw.ch)

A promising technology for a successful energy transition from fossil to renewable energy carriers is hydration of CO<sub>2</sub> with renewable hydrogen towards e.g. methane among other energy carrier. Even though strong progress has been made a highly active, selective, stable as well as cheap catalyst still needs to be explored as economically attractive business case.

Besides Ni also Co based catalysts show substantial activity for the CO<sub>2</sub> hydrogenation at low temperatures. Co based catalysts usually suffer from low CH<sub>4</sub> selectivity in CO<sub>2</sub> methanation and thus create large amounts of undesired CO as by-product. An additional challenge of commonly used Co/Al<sub>2</sub>O<sub>3</sub> catalysts is the formation of a spinel-type CoAl<sub>2</sub>O<sub>4</sub> as secondary phase causing catalyst deactivation due to decrease of the active metal surface area under reaction conditions that results in even lower CH<sub>4</sub> yield. In our approach, exactly this disadvantageous phase was reactivated by tailoring its low temperature reducibility by a compositional modification towards CoAl<sub>2-x</sub>Mn<sub>x</sub>O<sub>4</sub> to use it as a catalyst precursor. For the investigation CO<sub>2</sub> methanation is used as a model reaction to elucidate the influence of catalyst precursor composition on the catalytic activity as well as selectivity.

It is shown, that formation of the undesired CoAl<sub>2</sub>O<sub>4</sub> phase is avoided under reductive reaction conditions and highly dispersed as well as active Co-particles grew on the catalyst surface upon activation. The tailored spinel based CoAl<sub>2-x</sub>Mn<sub>x</sub>O<sub>4</sub> catalyst shows highly improved activity and selectivity compared to the CoAl<sub>2</sub>O<sub>4</sub>-based catalyst (c.f. Figure 1). With the tailored catalyst composition high CO<sub>2</sub> conversion up to 80 % at 350 °C is obtained at high GHSV of 16800 h<sup>-1</sup> and stoichiometric CO<sub>2</sub>/H<sub>2</sub> ratio of 1/4, surprisingly without detectable site formation of CO. Arrhenius-plots indicate a decrease of activation energy from 94 kJ/mol for the CoAl<sub>2</sub>O<sub>4</sub> precursor down to 56 kJ/mol for the manganese tailored catalyst precursor and thus indicate a shift of reaction mechanism.

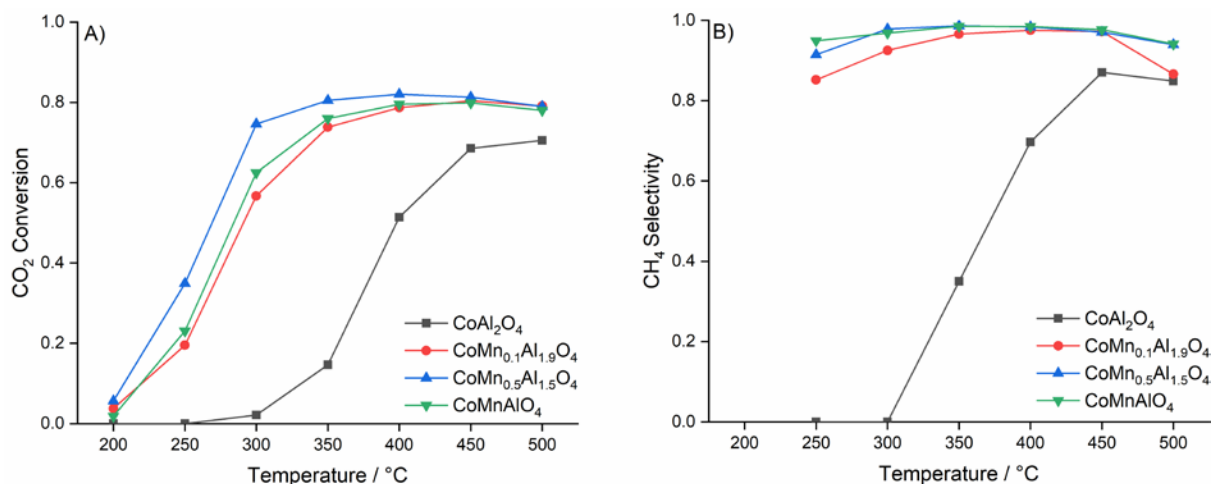


**Figure 1: Performance of activated Co based catalyst precursor in the methanation of CO<sub>2</sub> towards methane. A) CO<sub>2</sub> conversion & B) CH<sub>4</sub> selectivity. (Activation conditions: 50% H<sub>2</sub> in Ar 500 °C 30 min, Methanation conditions: CO<sub>2</sub>/H<sub>2</sub> = 1/4, GHSV = 16800cm<sup>-1</sup>).**

Due to careful characterization with XRD, TPR, CO<sub>2</sub>-TPD, CO<sub>2</sub>-DRIFTS, CO pulse titration and N<sub>2</sub>-physisorption it is concluded that the pronounced change in reactivity is caused on the one hand by the improved reducibility of the spinel type precursor phase and continuous re-reduction of Co under reductive reaction conditions. On the other hand, after catalyst activation the compositional changes in the spinel precursor phase induce an altered surface basicity compared to the unmodified CoAl<sub>2</sub>O<sub>4</sub> precursor. By correlating the structural and surface characterizations with *operando* DRIFTS methanation experiments it will be shown, that these altered redox and surface properties lead to a shift in reaction mechanism, wherein the intermediate production of CO by dissociative CO<sub>2</sub> adsorption is suppressed and direct hydration of adsorbed CO<sub>2</sub> to formate species takes place instead. This is identified as the main reason for the highly improved CH<sub>4</sub> selectivity of the Mn-modified catalysts.

In conclusion, use of Mn tailored Co based catalysts in CO<sub>2</sub> methanation as a model reaction, strategies are presented on how to tailor an undesired secondary phase with minimal modification, that it becomes a valuable catalyst precursor with enhanced activity, selectivity and stability. In general, the presented results recommend an uncommon and innovative strategy of catalyst optimization for systems wherein the formation of secondary phases are the main reason for catalyst deactivation.

# Activation of the bulk-type mechanism for the 1-butanol dehydration on Keggin-type ammonium salts

*Charlotte Lang<sup>1</sup>, François Devred<sup>1</sup>, Josefina Schnee<sup>2</sup>, Eric M. Gaigneaux<sup>1</sup>*

*<sup>1</sup>Université catholique de Louvain, IMCN, Louvain-La-Neuve, Belgium*

*<sup>2</sup>Normandie Université, ENSICAEN, UNICAEN, CNRS, LCS, Caen, France*

## Introduction

In the current energetic transition context, it is important to replace oil derivatives like fuels, polymers and other fine chemicals by more sustainable resources coming from new routes such as biomass valorisation. In this context, it is possible to produce some alcohols by biomass fermentation, which can then be transformed through a dehydration route to molecules that can finally be used to replace oil derivatives [1].

We focus here on 1-butanol dehydration that can lead to useful butene isomers and dibutylether (DBE). This reaction can be performed over the hetero-polyacid (HPA) catalyst  $H_3PW_{12}O_{40}$  that is known to have a very strong acidity and was demonstrated in the dehydration of methanol to work along a bulk-type mechanism after a specific activation procedure (dehydration in inert gas 1h/320 °C, cooling down to 25 °C in inert, exposure to alcohol at 25 °C, and then only heating to the reaction temperature) [2]. With methanol, the bulk-type mechanism led to increase the activity by allowing the access to all the acid sites located in the bulk. Unfortunately, the larger size of 1-butanol and its higher hydrophobicity hinder the bulk-type mechanism. This is why we synthesized ammonium hetero-polyoxometalates Keggin salts from  $H_3PW_{12}O_{40}$  (hereafter H3PW), in order to modify the structure and hydrophilic properties of the latter, and thus to facilitate the access of 1-butanol to the bulk during the activation step.

## Preparation and characterizations

$(NH_4)_xH_{3-x}PW_{12}O_{40}$  catalysts (hereafter  $(NH_4)_xPW$ ) are prepared by adding drop by drop a  $NH_4HCO_3$  aqueous solution ( $0.025 \text{ mol.L}^{-1}$ ) (room temperature, under stirring) to a  $H_3PW_{12}O_{40}$  aqueous solution ( $0.055 \text{ mol.L}^{-1}$ ) in adequate proportions to obtain the desired  $x$  [3] ( $x = 0.5, 1, 1.5, 2, 2.5$  and  $3$ ). After the precipitation and ageing for 1 night (ambient temperature, ambient air in a covered flask), the suspension is slowly dried at 50 °C under vacuum in a rotary evaporator. A thermal treatment (150 °C for 8h under air) then allowed to homogenize the different species [4].

Characterization by XRD shows the homogeneity of the catalysts with  $x \geq 2$ , and a decrease in the lattice parameter when  $x$  increases, going in parallel to the loss of structural water (observed by TGA, comparing the  $(\text{NH}_4)_x\text{PW}$  with the pristine H3PW). Accordingly, the smaller amount of structural water present in the  $(\text{NH}_4)_x\text{PW}$  catalysts allows hypothesizing that these catalysts are less hydrophilic than H3PW, which might lead to a better interaction with 1-butanol and a possible bulk activation. Besides, ammonia TPD profiles confirm the preserved strong acidity (similar to H3PW) of the  $(\text{NH}_4)_x\text{PW}$  catalysts with  $x \leq 2$ , whereas when  $x \geq 2.5$  only a weak acidity remains.

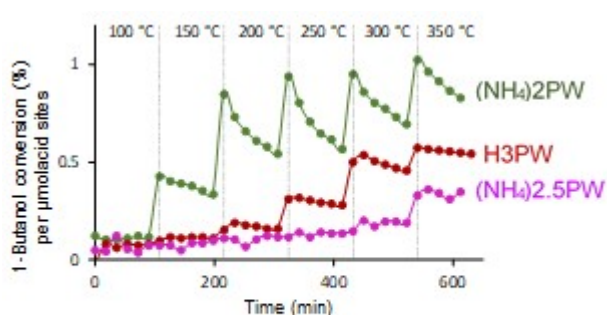


Figure 1: 1-butanol conversion per  $\mu\text{mol}$  of acid sites as a function of time and temperature.

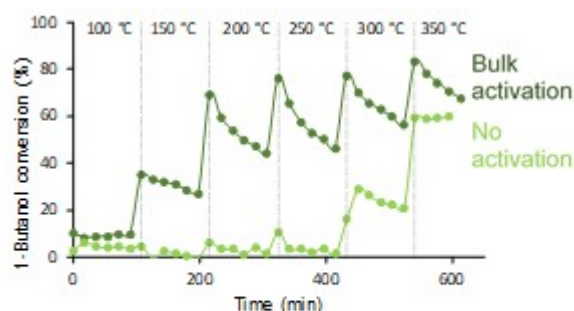


Figure 2: 1-butanol conversion as a function of time and temperature for  $(\text{NH}_4)_2\text{PW}$  catalyst with and without bulk activation procedure.

### Catalytic tests

The catalytic activities of  $(\text{NH}_4)_2\text{PW}$  and  $(\text{NH}_4)_2.5\text{PW}$  were compared to that of  $\text{H}_3\text{PW}$  by taking into account the number of acid sites in the reactor (figure 1) and after the bulk activation procedure. In all cases DBE selectivity is high at low temperature, while butene selectivity increases with the temperature. Furthermore, the carbon balance decreases (coke formation) when the temperature increases highlighting the interest to operate at a low reaction temperature. The low activity of  $(\text{NH}_4)_2.5\text{PW}$  compared to  $\text{H}_3\text{PW}$  can be explained by its weaker acidity revealed by ammonia TPD. Otherwise, it clearly appears that  $(\text{NH}_4)_2\text{PW}$  has a higher activity per acid site in comparison to the other catalysts. It can be related to the fact that the bulk is accessible after activation, that is to say a higher number of acid sites are accessible for the reaction. Indeed, a large difference in activity is observed for  $(\text{NH}_4)_2\text{PW}$  catalyst with and without the bulk activation procedure (figure 2), confirming that this procedure is now also effective in this case of 1-butanol.

#### References

[1] D. Zhang, S. A. I. Barri, and D. Chadwick, *Appl. Catal. A Gen.* 2011, vol. 403, no. 1–2, 1–11. [2] J. Schnee and E. M. Gaigneaux, *Catal. Sci. Technol.* 2017, vol. 7, no. 4, 817–830. [3] T. Ito, K. Inumaru, and M. Misono, *J. Phys. Chem. B* 1997, vol. 101, no. 48, 9958–9963. [4] M. Misono, *Chem. Commun.* 2001, no. 13, 1141–1152.

# Aromatization of bio-derivable isobutyraldehyde over zeolite catalysts

*Jeff Deischer, Kai Schute, Regina Palkovits*

*Institute of Technical and Macromolecular Chemistry, RWTH Aachen University,  
Germany*

## Heterogeneously catalyzed upgrading to bio-aromatics

Aromatic hydrocarbons such as benzene, toluene, ethylbenzene and xylene isomers (referred as BTX) play a very important role for the petrochemical and fine chemical industry. Currently, BTX is mainly obtained from catalytic cracking and catalytic reforming processes of petroleum.[1] Renewable and sustainable alternatives for accessing Bio-BTX, however, remain challenging. In view with the world-wide search for bio-derivable energy carriers, oxygen-containing hydrocarbons e.g. acetone or isobutanol, which are accessible *via* biomass fermentation, have been considered for the production of aromatics.[2] Besides the more common candidates such as ketones and alcohols, also aldehydes like isobutyraldehyde (IBA) are promising starting materials. Their production fulfills the criteria of sustainable chemistry as they can be readily obtained either from glucose in a bio-catalytic pathway or by the direct photosynthetic recycling of carbon dioxide.[3] Herein, we report a novel heterogeneously catalyzed aromatization process of isobutyraldehyde over HZSM-5 zeolites in a continuous fixed bed reactor (Figure 1).[4,5]

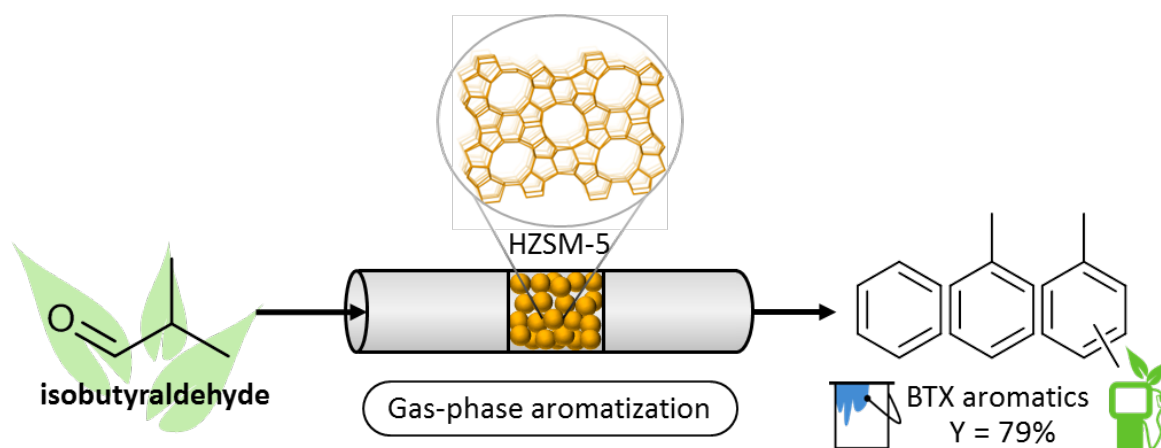


**Figure 1:** Continuous gas-phase aromatization process of isobutyraldehyde to aromatic hydrocarbons.



The effect of catalyst properties, in particular the Si/Al ratio of the zeolite material, as well as the reaction parameters weight hourly space velocity (WHSV) and temperature were carefully studied. The utilized zeolite catalysts were characterized using XRD, NH<sub>3</sub>-TPD, N<sub>2</sub>-physisorption, and ICP-OES. Moreover, long term stability and successful catalyst recycling through *in situ* calcination were demonstrated as similar results over several reaction cycles could be achieved.

#### References

- [1] G. Ertl, H. Knözinger, F. Schüth, J. Weitkamp, *Handbook of Heterogeneous Catalysis. 2nd Edition*, Wiley-VCH.
- [2] S. Setiadi, N. M. Slamet, *Int. J. Eng. Technol* **2011**, 11, 72-79.
- [3] S. Atsumi, W. Higashide, J. C. Liao, *Nat. Biotechnol.* **2009**, 27, 1177.
- [4] J. Deischter, K. Schute, R. Palkovits, *DE Patent Application Pending, No. 10 2018 114 979.4* **2018**.
- [5] J. Deischter, K. Schute, R. Palkovits, *under preparation*

## **Acetalization of glycerol with acetone on acidic silicalite-1**

*E. Janiszewska<sup>1</sup>, J. Kowalska-Kuś<sup>1</sup>, K. Nowińska<sup>1</sup>, S. Kowalak<sup>1</sup>, Adam Mickiewicz*

*University, Faculty of Chemistry, Umultowska 89b, 61-614 Poznan, Poland,*

*K. Góra-Marek<sup>2</sup>, Jagiellonian University, Faculty of Chemistry, Gronostajowa 2, 30-*

*387 Krakow, Poland*

Large-scale production of biodiesel from biological oils results in formation of copious amounts of glycerol as a waste product. Therefore, an utilization of glycerol has become very urgent and challenging problem. One of the attempts consists in its acetalization with aldehydes or ketones to form the products employed as fuel additives. They improve a viscosity, oxidation stability and fulfill requirements for flash point.

The aim of the present study was catalytic ketalization of glycerol with acetone in order to obtain the cyclic ketal known as solketal (2,2-dimethyl-1,3-dioxolan-4-methanol). Conventionally, the condensation of glycerol with acetone is carried out in the presence of strong mineral acids, which is environmentally unfriendly. The above drawbacks can be overcome by the use of heterogenous, acidic catalysts. The role of the number and strength as well as the nature of the acid sites (Lewis/Brønsted) in acetalization of glycerol has been discussed in many papers [1].

We applied silicalite-1 (MFI) modified with aqueous solutions of ammonium compounds ( $\text{NH}_4\text{F}$ ,  $\text{NH}_4\text{Cl}$ ,  $\text{NH}_4\text{NO}_3$ ,  $\text{NH}_4\text{OH}$ ) without any supplement of alkaline agents. Then the samples were thermally treated to generate the acidic sites in silicalite-1. The obtained samples were characterized by XRD,  $\text{NH}_3$ -TPD,  $\text{N}_2$  adsorption/desorption measurements, FTIR with pyridine (Py) and pivalonitrile (Pn) as a base probe, and SEM analysis. Their catalytic activity in ketalization of glycerol with acetone was conducted in closed vials at 347 K for 1 h with magnetic stirring. The reaction products were analyzed by GC and mass spectroscopy.

XRD analysis indicates that MFI structure with high crystallinity was maintained upon the used modification procedure. Scanning electron micrographs (SEM) show the similar morphologies of the pristine Sil-1 and the modified samples. The treatment of silicalite-1 with ammonium compounds change its textural properties. Except the sample modified with  $\text{NH}_4\text{NO}_3$ , the others show higher surface area, pore volume and average pore size in comparison to unmodified silicalite-1. The total pore volume

( $V_t$ ) for modified samples increased, regardless of unchanged volume of micropores ( $V_{\text{micro}}$ ), which implies a generation of new mesopores during the modification procedure. This is confirmed by the measured enhanced mesopore area ( $S_{\text{ext}}$ ). The most conspicuous changes shows the sample modified with  $\text{NH}_4\text{OH}$ . They could be caused by a partial leaching of silicon from silicalite-1 framework upon treatment with slightly alkaline solution. A treatment with solution of ammonium agents results in the formation of network's defects. IR spectra indicate the formation of internal isolated OH groups ( $3730\text{ cm}^{-1}$ ), significant number of hydrogen-bonded or vicinal hydroxyl groups ( $3685\text{ cm}^{-1}$ ) as well as the silanol nests ( $3600\text{-}3300\text{ cm}^{-1}$ ).

The  $\text{NH}_3$ -TPD and FTIR analysis with adsorbed pyridine indicate the generation of acid sites of both Lewis and Brønsted type during the modification with the predominance of the Lewis sites. The number and strength of generated acid sites depend on the nature of modifying ammonium compound. The samples modified with the  $\text{NH}_4\text{F}$  and  $\text{NH}_4\text{Cl}$  solutions show the highest total acidity and the highest contribution of strong acid sites. The samples treated with  $\text{NH}_4\text{NO}_3$  and  $\text{NH}_4\text{OH}$  indicate the presence of almost exclusively weak acid sites.

All the modified silicalites show considerable activity for glycerol acetalization with acetone and high selectivity towards solketal. The activity correlates with acidity of the samples. The highest activity for glycerol acetalization shows sample modified with  $\text{NH}_4\text{F}$  (Sil-1\_F), that exhibits the highest number of strong Lewis acids sites and some amount of Brønsted acid sites. Although, the accessibility of internal acid sites is higher for the sample modified with  $\text{NH}_4\text{OH}$ , the accessible centres are much weaker compared to these presented in Sil-1\_F and Sil-1\_Cl and it turns to its lower activity. The proposed reaction mechanism considers a combined contribution of both Lewis and very weak Brønsted acid sites.

### **Acknowledgements**

FTIR studies were financed by Grant No. 2015/18/E/ST4/00191 from the National Science Centre, Poland.

### **References**

[1] A. Talebian-Kiakalaieh, N.A.S. Amin, N. Najaafi, S. Tarighi, *Front. Chem.* 6 (2018) 573.

# Characterisation of Novel Doped Perovskite Catalysts by XRD, XPS and SEM – Tailored Exsolution of Metal Nanoparticles

*L. Lindenthal<sup>1</sup>, J. Popovic<sup>1</sup>, J. Raschhofer<sup>1</sup>, R. Rameshan<sup>1</sup>, A. Nenning<sup>2</sup>, A.K. Opitz<sup>2</sup>,  
C. Rameshan<sup>1</sup>*

*1 Technische Universität Wien, Institute of Materials Chemistry, Vienna, Austria*

*2 Technische Universität Wien, Institute of Chemical Technologies and Analytics,  
Vienna, Austria*

Perovskite-type oxides are a large class of materials with many interesting properties, including piezo- and pyroelectricity, mixed ionic-electronic conductivity and high catalytic activity. Thus, there is a wide range of applications, for example the use as sensors or as electrode materials in solid oxide fuel cells. Their general chemical formula is  $ABO_3$ , with two different cations A (bigger) and B (smaller). The ideal structure is cubic, but it is often distorted as can be seen for  $La_{0.9}Ca_{0.1}FeO_3$  (figure 1). The high versatility of the material class is due to the possibility of adjusting the properties by choosing different elements for the cations. Doping either one or both of the cation sites opens up an even larger matrix for materials design.

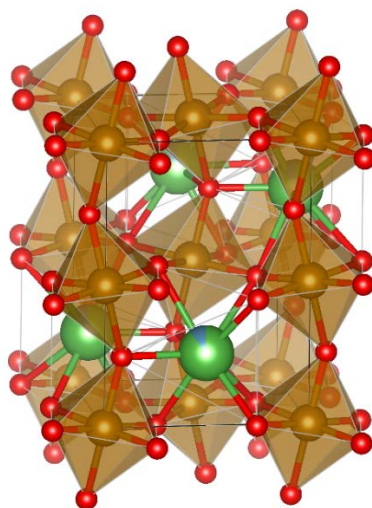


Figure 1: Distorted perovskite structure of  $La_{0.9}Ca_{0.1}FeO_3$ , data from XRD measurement (La/Ca-green/blue, Fe-brown, O-red).

In terms of catalysis, another recently shown outstanding property of perovskites is the exsolution of metal nanoparticles under reducing conditions. This surface modification (by migration of cations to the surface) can change the catalytic activity

and selectivity of the perovskite surface completely and is the core topic of our ERC project.

Several perovskite-type oxides (e.g.  $\text{La}_x\text{Ca}_{1-x}\text{FeO}_3$  or  $\text{Nd}_x\text{Ca}_{1-x}\text{FeO}_3$ ), that are promising catalyst materials, have been synthesised and subsequently characterised. These perovskites are promising catalyst materials for several energy related reactions, such as the (reverse) water gas shift reaction. Using different reducing conditions, the stability and reducibility of the synthesized perovskites were investigated. X-ray diffraction (XRD) allowed structural determination, while X-ray photoelectron spectroscopy (XPS) gave additional chemical information on the surface state. These characterisations have been complemented by additional analytical methods (e.g. SEM). It was possible to show the reversible exsolution of metal nanoparticles in an ideal metastable window (figure 2).

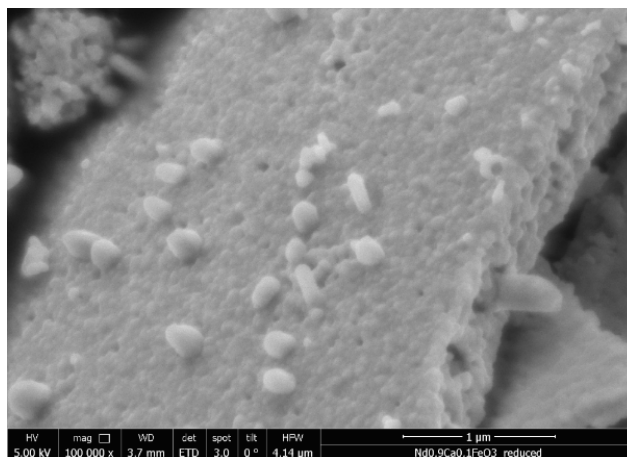


Figure 2: SEM picture of exsolved nanoparticles on  $\text{Nd}_{0.9}\text{Ca}_{0.1}\text{FeO}_3$ .

Following the basic characterisation, further experiments were conducted with a new lab-based Near-Ambient-Pressure XPS system (NAP-XPS). This was designed and set up in cooperation with SPECS, specifically for the investigation of electrode materials (e.g. for the use in solid oxide fuel cells). With this setup, it is possible to combine catalytic experiments, NAP-XPS and electrochemical measurements at the same time, thereby correlating catalytic activity of the material with its surface state and its electrochemistry. Thus, it directly gives access to information as to how exsolution changes the catalytic properties of a perovskite material.

### **Acknowledgement**

This project has received funding from the European Research Council (ERC) under the European Union's Horizon 2020 research and innovation programme (grant agreement n° 755744 / ERC - Starting Grant TUCAS)

## **A photoluminescence study of Zn-containing Ferrierite**

*Joanna E. Piotrowska<sup>1,2</sup>, Maria Lemishka<sup>1,3</sup>, Kinga Mlekodaj<sup>1</sup>, Edyta Tabor<sup>1</sup>, Milan Bernauer<sup>1</sup>, Alena Vondrová<sup>1</sup>, Pavel Kubát<sup>1</sup>, Štěpán Sklenák<sup>1</sup>, Jiří Dědeček<sup>1</sup>*

<sup>1</sup> *J. Heyrovský Institute of Physical Chemistry, CAS, Prague, Czech Republic*

<sup>2</sup> *J. Haber Institute of Catalysis and Surface Chemistry, PAS, Kraków, Poland*

<sup>3</sup> *University of Pardubice, Pardubice, Czech Republic*

Zeolite materials are well-known to accommodate various metal ions and metal oxo species, due to negative charge of the silica-alumina framework [1]. The properties of such metal ion centers, especially those of transition metals, differ substantially from the corresponding ones in bulk oxides. Introducing metal centers into the zeolite structure stands for a useful replacement for highly selective, but economically unfavorable enzyme-mimetic structures containing Co, Ni, Zn and Cu as active sites [2,3]. This gives rise to a vast catalytic potential of the metal-zeolite structures, reflected in their high activity in the variety of important redox reactions.

Recently, Zn-containing zeolites has attracted much attention, due to their activity in activation of methane [4], a highly desirable chemical route staying in agreement with green chemistry postulates. Moreover, applications encompassing dehydrogenation of other light alkanes, aromatization of hydrocarbons, hydration of acetylene and deNO<sub>x</sub> reactions [5] make those Zn-doped hydrated aluminosilicates a useful tool for hydrocarbon processing industry.

Extending the knowledge about the nature of active sites and the effect of their distribution is of key importance for understanding, predicting and even designing properties of catalytic materials in order to maximize their potential performance. Some efforts have been devoted to clarifying the nature and form of Zn species embedded in the zeolite matrix [6]. Nevertheless, it is still not fully resolved, mainly in Si-rich zeolite matrices. To obtain a deeper insight into the siting and redox behavior of metal Zn centers, the photoluminescence study of metal-containing zeolitic structures should be suggested as an powerful tool, analogously as was already reported for Cu-zeolites [7,8]. In this paper, we report the first attempt to analyze the nature, location and arrangement of Zn ion species by the laser induced kinetic emission spectroscopy combined with DFT calculations and FTIR spectroscopy.

For this purpose a set of Zn-ferrierites (Si/Al 8.5) with various Zn was prepared by ion exchange to the parent NH<sup>+</sup>-ferrierite. Kinetic emission spectra of evacuated samples (450 C) were collected after excitation by a laser pulse at 308 nm at RT. The Zn<sup>2+</sup> emission spectra were compared with the FTIR spectra of evacuated samples recorded in the region of anti-symmetric T-O-T vibrations of the zeolite framework. The experimental data were compared with DFT prediction of Zn<sup>2+</sup> siting and coordination and of energy of emitted photons.

Zn<sup>2+</sup> kinetic emission spectroscopy represents a powerful and promising tool for the study of Zn speciation in zeolites. Analysis of the emission decay allows easy to differentiate bare Zn<sup>2+</sup> ions in cationic sites and other Zn species. In the case of ferrierite, three cationic  $\alpha$ -,  $\beta$ - and  $\gamma$ -sites of bare cations are occupied by Zn<sup>2+</sup> cations and emission at 545, 480, and 425 nm was attributed to these sites.

## References

- [1] Sobalík, Z., Dědeček, J., Ikonnikov, I., Wichterlová, B., *Microporous Mesoporous Mater.* **1998**, 21, 525-532
- [2] Rubio-Cervilla, J., González, E., Pomposo, J. A., *Nanomaterials* **2017**, 7, 341-361
- [3] He, W., Wamer, W., Xia, Q., Yin, J., Fu, P. P., *J. Environ. Sci. Health, Part C* **2014**, 32, 186–211
- [4] Oda, A., Torigoe, H., Itadani, A., Ohkubo, T., Yumura, T., Kobayashi, H., Kuroda, Y., *J. Phys. Chem. C* **2013**, 117, 19252-19534
- [5] Wang, L., Sang, S., Meng, S., Zhang, Y., Qi, Y., Liu, Z., *Mater. Lett.* **2007**, 61, 1675-1678
- [6] Yakovlev, A. L., Schubin, A. A., Zhidomirov, G. M., van Santen, R. A., *Catal. Lett.* **2000**, 70, 175-181
- [7] Wichterlová, B., Dědeček, J., Sobalík, Z., Vondrová, A., Klier, K., *J. Catal.* **1997**, 169, 194-202
- [8] Dědeček, J., Wichterlová, B., *J. Phys. Chem.* **1994**, 98, 5721-5727

# **Comparative study of N,O with O functional groups over graphene nanosheets supported cobalt catalyst in Fischer-Tropsch synthesis**

*Somayeh Taghavi, CATMAT Lab, Department of Molecular Sciences and Nanosystems, Ca' Foscari University Venice and INSTM Consortium, RU of Venice, Via Torino 155, 30172 Venezia Mestre, Italy; Ahmad Tavasoli, School of Chemistry, College of Science, University of Tehran, Tehran, Iran; Michela Signoretto, Federica Menegazzo, CATMAT Lab, Department of Molecular Sciences and Nanosystems, Ca' Foscari University Venice and INSTM Consortium, RU of Venice, Via Torino 155, 30172 Venezia Mestre, Italy; Alireza Asghari, Department of Chemistry, Semnan University, Semnan, Iran*

## **1. Scope**

Fischer–Tropsch synthesis (FTS) is one of the most important achievements of the chemical industries in the 20th century. The dwindling resources of oil in conjunction with the increased costs of crude oil over the last decade yielded an opportunity for the synthesis of transportation fuels from other carbon-containing resources, such as natural gas, biomass, coal, or oil residue [1]. Among all catalysts, Co-catalysts are widely used because of their economically high activity and selectivity. In graphene nano sheet (GNS)-supported cobalt catalyst, the strong metal-support interactions reduce to a large extent. Functionalization of the supports immobilizes the metal particles preventing them from excessive sintering upon heating and also play an important role in the dispersion of active metal on the GNS [2]. In the present work, GNS were functionalized with O and N,O functional groups before loading of cobalt precursors. Catalysts were prepared with 15 wt% cobalt loading and characterized by ICP, XRD, TPR. The catalysts were assessed in FTS in a fixed bed microreactor at 220 °C and 1.8 Mpa during 240 h continues synthesis.

## **2. Results and discussion**

Table 1 shows XRD data and catalytic performance of calcined catalysts at steady state condition. As shown, FTS reaction rate (g CH/g cat./h) of Co/O-GNS catalyst is Higher than Co/N,O-GNS. According to fig.2, the whole TPR profiles of cobalt nano crystallite on the O-GNS is slightly shifted towards lower temperatures compared with catalyst prepared on N,O-GNS, indicating that cobalt oxide nanoparticles supported on O-GNS are reduced faster than those supported on N,O-GNS. In addition, O-functional groups decreased the average cobalt particle sizes more than N,O functional groups (fig.1, table1). All these



effects can be evidenced for increasing the number of surface active cobalt sites and as a result increasing the FTS reaction rate [3]. As shown in table 1, the methane selectivity is increased and The C5+ selectivity is decreased for functionalized O-GNS supported catalysts. This trend can be justified by the presence of more functional groups which increases the amount of hydrogen adsorbed on the catalyst surface and then promote the termination reactions to paraffin instead of chain growth to heavier hydrocarbons. One of the major reasons for catalyst deactivation is sintering which occurred during FT synthesis. As can be seen in fig.3, after 240 hrs of FTS, Co/O-GNS catalyst was more stable than Co/N,O-GNS against Co sintering because of the higher amounts of functional groups and defects on support surface combined with the preserved integrity of GNS [4].

### 3. Conclusions

In conclusion, O-GNS showed better performance than N,O-GNS with shifting the reduction peaks to a lower temperature, improving the catalyst activity, increasing metal–support interaction, decreasing the sintering of cobalt nano particles and increasing the stability of catalyst.

Table 1. XRD data and Catalytic performance of calcined catalysts (T = 220 °C, H<sub>2</sub>/CO ratio = 2, P = 1.8 MPa)

Catalyst	dXRD (nm)	CO conversion (%)	O/P	FTS rate (gCH/(gcat · h))	%CO <sub>2</sub> Selectivity	% CH <sub>4</sub> Selectivity	%C <sub>5</sub> <sup>+</sup> Selectivity
Co/O-GNS	10.6	73.3	1.08	0.341	0.69	14.53	84.01
Co/N,O-GNS	11.1	71.1	1.12	0.332	0.73	12.91	85.06

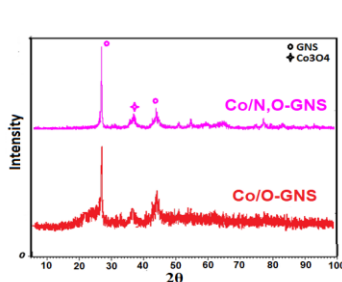


Fig.1. XRD pattern

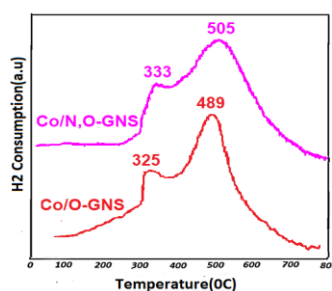


Fig.2. TPR

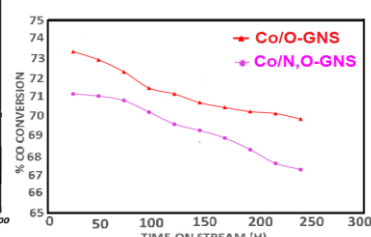


Fig. 3. %CO conversion variations with time on stream

### References

- [1] H. Sajjad, H.H. Masjuki, M. Varman, M.A. Kalam, M.I. Arbab, S. Imtenan, S.M.A. Rahman, *Renew. Sustain. Energy Rev.* 30 (2014) 961–986.
- [2] S. Taghavi, A. Asghari, A. Tavasoli, *Chem. Eng. Res. Des.* 119 (2017) 198–208.
- [3] M. Trépanier, A. Tavasoli, A.K. Dalai, N. Abatzoglou, *Fuel Process. Technol.* 90 (2009) 367–374.
- [4] S.A. Chernyak, E.V. Suslova, A.S. Ivanov, A.V. Egorov, K.I. Maslakov, S.V. Savilov, V.V. Lunin, *Appl. Catal. A Gen.* 523 (2016) 221–229.

## **Rapid Scan IR spectroscopy supported by 2D COS Analysis as an efficient tool for intermediates searching**

*Kinga Gołabek, Kinga Góra-Marek, Karolina Tarach, Kamila Pyra, Faculty of Chemistry, Jagiellonian University in Kraków, Kraków, Poland;*

*Edyta Tabor, Veronika Pashkova, Jiri Dedecek, J. Heyrovský Institute of Physical Chemistry, Prague, Czech Republic.*

Description of the site-reagent interaction in real-time allows inferring about the nature of the complex formed, transition states or short-living intermediate entities. However, in this matter an indispensable factor influencing the accuracy of the results gained on the diffusion and adsorption processes as well as on the transformation of substrates into intermediate and final products is the time scale of the respective phenomena.

Restricted transition state selectivity, as well as reagent diffusional limitations, are most vital in the bulky molecules transformations in 10-ring zeolites (ZSM-5, IM-5, TNU-9, TNU-10). Xylene isomerization in the 10-ring zeolites with different pore topology was followed by rapid scan IR spectroscopy, received 1D spectra were subjected to two-dimensional correlation analysis. The 2DCOS IR spectra supported the hypothesis on the partial loss of the aromatic character of xylene molecules upon the adsorption, and their further transformation in the methylbenzenium ions  $\text{CH}_3\text{-C}_6\text{H}_5^+\text{-CH}_3$  and diphenyl methane derivatives. It is identified as the restricted rotation of the methyl groups on an aromatic ring around the C-CH<sub>3</sub> bond.

However, stabilization of the transition state by the van der Waals interactions from the zeolite framework cannot be neglected also for the small molecules conversions. The importance of the confinement effects arising from van der Waals interactions and the framework geometry effect was proved for ethanol dehydration on ZSM-5 with on-purpose tuned Al distribution within the framework. The presence of Al-pairs in ZSM-5 was responsible for the formation of the ethanol dimeric entities of high stability preventing them from decomposition in monomeric moieties at temperatures below 130 °C. Aluminum atoms homogenously distributed in the form of isolated Si(OH)Al groups within the zeolitic framework bonded ethanol molecules in the form of monomeric species. This adsorption adducts differentiation resulted in diverse

paths of ethanol to diethyl ether and ethene transformation. Single Al atoms ZSM-5 provided the protonic sites that were restored simultaneously when ethene molecule was released. The presence of Al-pairs in zeolite structure effectively inhibited the ethane formation yielding diethyl ether exclusively. What is more, the intermolecular dehydration to ether and ether dehydration to ethylene was established as controlling step in the ethanol transformation in zeolite hosting Al-pairs. Conversely, the presence of isolated species advantaged single-molecule elimination reaction where very reactive carbenium ions formed by reaction with the Brønsted acid sites yielded linear olefins and aromatic intermediate species (tropylium and/or cyclopentadienyl ions) similar to those found during xylene isomerization in 10-ring zeolites of different pore architecture (ZSM-5, IM-5, TUN-9, TNU-10). Our studies on ethanol sorption in TNU-10 demonstrated also the rapid transformation of alcohol substrate into intermediate not providing the interference of the spectra by Fermi resonance. It demonstrates that IR spectroscopy is powerful tool to discussing the difference in the activity between zeolites resulting from the adsorption phenomena linked to the confinement effects.

### **Acknowledgement**

The work was financed by the Grant No. 2015/18/E/ST4/00191 from the National Science Centre, Poland.

# Zeolite Features Forced Loss of Aromaticity of Methylated Benzenes

*Kinga Góra-Marek, Paweł Kozyra, Witold Piskorz, Kinga Gołębek, Karolina Tarach  
Faculty of Chemistry, Jagiellonian University, Kraków, Poland;*

The unique shape-selective characteristic of 10-ring zeolites is their paraselectivity in isomerization, alkylation and disproportionation of alkyl aromatics. Additionally, the zeolites with the small internal cages along the channels (TNU-10, ZSM-5) are particularly resistant to the formation of carbonaceous species. Restricted transition state selectivity, as well as reagent diffusional limitations, are the most vital in the isomerization of xylenes. It is commonly known that the adsorption of xylene molecules is related to the loss of the aromatic character due to the proton addition and transformation in the methylbenzenium ions  $\text{CH}_3\text{-C}_6\text{H}_5^+\text{-CH}_3$ .

The *m*- and *o*-xylene isomerisation, as well as the secondary disproportionation reactions, over the 12-, 10-, and 8-ring zeolites with different pore topology were studied by 2D COS IR spectroscopy and DFT modeling. The analysis of 2DCOS maps allows for concluding that the adsorption of xylene molecules and their further transformation in the methylbenzenium ions  $\text{CH}_3\text{-C}_6\text{H}_5^+\text{-CH}_3$  leads to the partial loss of the aromatic character. It is identified as the restricted rotation of the methyl groups on an aromatic ring around the C-CH<sub>3</sub> bond, confirmed in the experiments carried out for deuterated zeolites especially. The steric hindrance of CH<sub>3</sub> rotation is more vital for *o*-xylene than for *m*-xylene, thus the out-of-phase CH<sub>3</sub> stretch bands are more intensively perturbed by the additional hindrance delivered zeolite channels upon *o*-xylene adsorption and protonation. However, the deformation of the xylene molecules forced by the size and geometry of the channels is an additional factor ruling the loss of aromaticity of methylated benzenes. This effect is more pronounced for the zeolites of the smaller pores.

Total of 14 possible structures of protonated xylenes embedded in four zeolites (ca. 60 systems) were modeled while searching for intermediate formed from methylbenzenium ions. Overall, the studied structures are generally more stable in small-pore zeolites indeed, namely in CHA. They are less stable in MFI and eventually in BEA or MOR. However, according to the calculation, only one structure (2,6-dimethylbicyclo[3.1.0]hexane, labelled C5o) is stabilized in respect gaseous *o*-

xylene. The amount of protonated intermediate is experimentally indicated based on the IR band (at  $1485\text{ cm}^{-1}$ ). Calculated adsorption energy agrees with the IR measurements – the amounts decreases in the sequence of CHA, MFI, BEA. Finally, the vibrational analysis shows that only C5o structure, independently on zeolite, gives the band ca.  $1485\text{ cm}^{-1}$  in calculated spectrum what supports the assumption of C5o structure as an intermediate in xylene isomerization process (see Figure 1.).

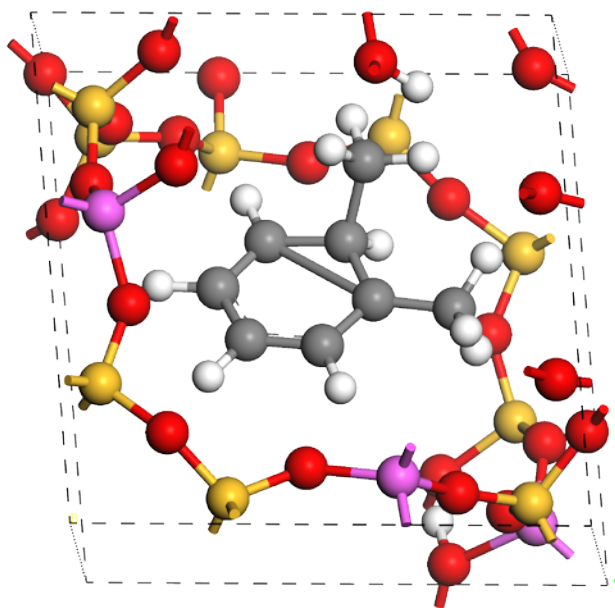


Figure 1. Selected structure of protonated o-xylene intermediate in the CHA (Si/Al = 3) cage.

### Acknowledgment

IR studies were financed by the Grant No. 2015/18/E/ST4/00191 from the National Science Centre, Poland. Quantum-chemical calculations were funded by the National Science Centre, Poland, grant no. 2016/23/B/ST4/00088.

## Optimized Biodiesel production through heterogeneous catalysts

*Graça Rocha, University of Aveiro, Aveiro, Portugal; Mariana Almeida, University of Aveiro, Aveiro, Portugal; André Francisco, University of Aveiro, Aveiro, Portugal*

The world of today is facing tremendous danger from human activity that is severely jeopardizing precious resources for future generations. One direct consequence of this negligence is the global warming caused by the abundance of CO<sub>2</sub> in the atmosphere. As such, the search for renewable and safer resources for unlimited usage and less environmental impact is now mandatory if we want to secure our health. An alternative fuel must be technically feasible, economically competitive, environmentally acceptable and readily available<sup>1,2</sup>.

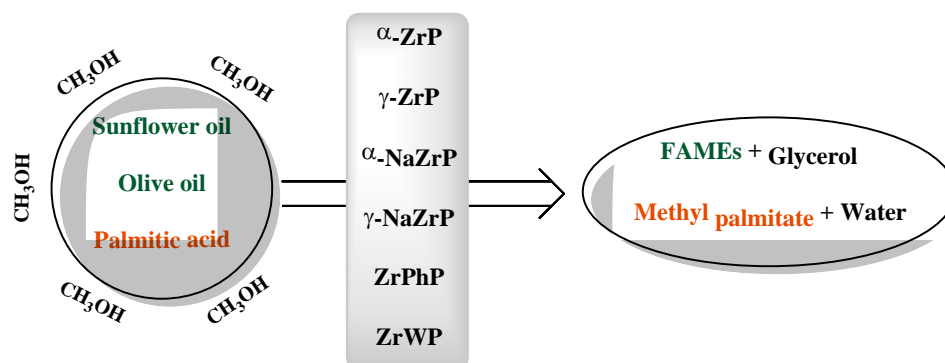
Biodiesel includes these conditions. From the environmental point of view, it is free of aromatic compounds and sulphur, biodegradable and obtained from renewable sources. However, the production of biodiesel is also a controversial issue because it is based on intensive crops causing deforestation and high water consumption.

Biodiesel production can be performed in the presence of acidic, basic and enzymatic catalysts. Homogeneous alkaline catalysts are the widely used because they allow high conversions, in relatively short reaction times. However, the disadvantages associated with its use, namely, in the biodiesel/catalyst separation processes, encouraged the use of **heterogeneous catalysts** in the last decades<sup>3,4</sup>.

In this perspective, the structural features of the **tetravalent metal phosphates and phosphonates** are fundamental to act as efficient solid catalysts<sup>5</sup>. We are not aware of any reference in the literature concerning the use of tetravalent metal phosphates and phosphonates in the biodiesel production.

Our experimental work started with the synthesis, characterization and catalytic evaluation of the  $\alpha$ - and  $\gamma$ -zirconium phosphates ( $\alpha$ - and  $\gamma$ -ZrP) and the sodium exchanged  $\alpha$ - and  $\gamma$ -zirconium phosphates ( $\alpha$ -NaZrP and  $\gamma$ -NaZrP) in the transesterification reactions of **sunflower oil**. The fatty acid methyl esters (FAMES) formed with  $\alpha$ -NaZrP and  $\gamma$ -NaZrP were identified by GC-MS and quantified by GC. The best yields were obtained after varying sequentially the molar ratio methanol:oil, temperature, mass ratio catalyst:oil and reaction time (green rows in the Table). Then, the former best reaction conditions achieved with the sunflower oil were tested in the transesterification reactions of **olive oil** (green rows in the Table). No FAMES

were observed with  $\alpha$ - and  $\gamma$ -ZrP or in the “blank” reaction either with the sunflower or with the olive oils.



In a parallel study, the  $\alpha$ - and  $\gamma$ -ZrP, zirconium phenylphosphonate (ZrPhP) and zirconium tungstate phosphate (ZrWP) were tested in the esterification reaction of **palmitic acid**. The quantification of methyl palmitate was done by HPLC. After the initial studies, the best yield was reached with  $\gamma$ -ZrP (45.0%). Following this result, the reaction conditions were optimized by varying sequentially the amount of  $\gamma$ -ZrP, molar ratio palmitic acid:methanol and temperature. With the best conditions a yield of 86% was reached. A “blank” reaction was also performed (20.0%).

Catalysts	Sunflower oil	Olive oil	Palmitic acid
“Blank”	—	—	20.0 %
$\alpha$ -NaZrP	76.4 %	28.5 %	—
$\gamma$ -NaZrP	86.3 %	42.8 %	—
$\gamma$ -ZrP	—	—	45.0 %
$\gamma$ -ZrP	—	—	86.0 %

As predictable, the best yields of FAMES were obtained with  $\alpha$ -NaZrP and  $\gamma$ -NaZrP since the mechanism involved in the transesterification reactions is simpler in basic conditions. On the other hand, since the esterification reactions are favoured in acid conditions, the best yield of methyl palmitate was achieved with  $\gamma$ -ZrP.

The interlayer distance of the  $\gamma$ -NaZrP and  $\gamma$ -ZrP is another important issue since it contributes to facilitate the approach of the triglycerides and the palmitic acid to the active sites of the catalysts followed by the reaction with methanol and the formation of the corresponding FAMES and methyl palmitate.

The structure of the catalysts and the optimization of the reaction conditions will be discussed during the presentation with detail.

#### References

- [1] Mittelbach M., *Eur. J. Lipid Sci. Tech.* 2015, 117, 1832-1846.
- [2] Chuah L. F., Klemeš, Yusup S., Bokhari A., Akbar M. M., *J. Clean Prod.* 2017, 146, 181-193.
- [3] Diamantopoulos N., Panagiotaras D., Nikolopoulos D., *J. Thermodyn. Catal.* 2015, 6(1), 1-8.
- [4] Avhad M. R., Marchetti J. M., *Renew. Sust. Energ. Rev.* 2015, 50, 696-718.
- [5] Pica M., *Catalysts* 2017, 7, 190-207.

# Dehydrogenation of Methylcyclohexane over Noble Metal Catalysts for Hydrogen Delivery Applications

*Ye Song, Research Institute of Petroleum Processing, Sinopec, Beijing, China; Wei Lin, Research Institute of Petroleum Processing, Sinopec, Beijing, China; Xue Yang, Research Institute of Petroleum Processing, Sinopec, Beijing, China; Lei Wang, Research Institute of Petroleum Processing, Sinopec, Beijing, China; Jun Liu, Research Institute of Petroleum Processing, Sinopec, Beijing, China*

In the present work, we employed density functional theory (DFT) calculation to investigate methylcyclohexane (MCH) dehydrogenation reaction chemistry on Pt. Comparing the reaction energy barrier of the rate-determining step of the MCH dehydrogenation on different noble metals, such as Pt, Pd, Rh, and Ir. The results indicate that the dehydrogenation activity of noble metals can be rationally characterized by the molecular structure characteristic parameters of the lowest unoccupied orbital energy  $E_{LUMO}$ . In other words, the lower  $E_{LUMO}$  of transition metal, the stronger electron capture capability. Furthermore, it also can be acquired that the more delocalized density of state around the Fermi level, which can accept electrons easier, and if the d-band center of noble metals closer to the Fermi level, it may have a better catalytic dehydrogenation activity and selectivity of MCH. On the basis of DFT study results, selective dehydrogenation of MCH to toluene over Pt, Pd, Rh and Ir supported on  $\gamma\text{-Al}_2\text{O}_3$  was studied in the context of the hydrogen storage using MCH-toluene-hydrogen cycle. The catalysts were characterized by variety of techniques such as X-ray fluorescence spectrometry, X-ray diffraction (XRD),  $\text{N}_2$  adsorption-desorption isotherms, temperature-programmed reduction of  $\text{H}_2$  ( $\text{H}_2\text{-TPR}$ ), CO-chemisorption metal analysis, transmission electron microscopy (TEM) and Raman spectroscopic techniques. Under steady-state conditions, the initial activity of the catalysts followed the order:  $\text{Pt}/\gamma\text{-Al}_2\text{O}_3 > \text{Rh}/\gamma\text{-Al}_2\text{O}_3 > \text{Pd}/\gamma\text{-Al}_2\text{O}_3 > \text{Ir}/\gamma\text{-Al}_2\text{O}_3$ . The reduced  $\text{Pt}/\gamma\text{-Al}_2\text{O}_3$  catalyst exhibited higher activity and selectivity toward toluene (>95%) than its Rh, Pd and Ir-based counterparts. From the combined CO-chemisorption metal analysis and TEM analysis, the enhancement of activity and selectivity of the  $\text{Pt}/\gamma\text{-Al}_2\text{O}_3$  sample was ascribed to moderate metal-support interaction leading to formation of moderate Pt particles having lower amount of hydrogenolysis sites (kink sites) and the higher dispersion of Pt.



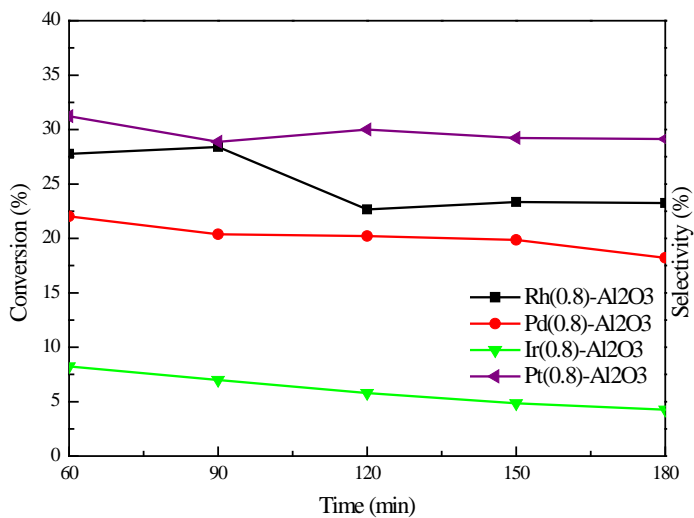


Fig.1 MCH conversion over M/ $\gamma$ -Al<sub>2</sub>O<sub>3</sub> (M=Pt,Rh,Pd,Ir)  
Al<sub>2</sub>O<sub>3</sub> (M=Pt,Rh,Pd,Ir)

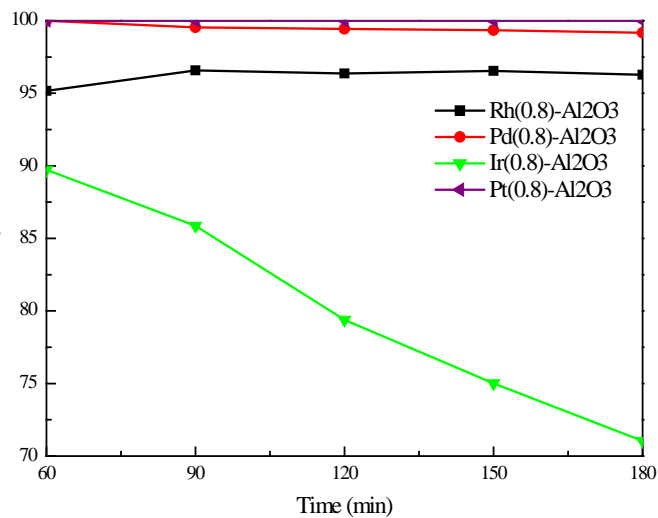


Fig.2 Toluene selectivity over M/ $\gamma$ -Al<sub>2</sub>O<sub>3</sub> (M=Pt,Rh,Pd,Ir)

# Mechanism of Methane Activation on Zn-modified Zeolites

## Investigated by Solid-State NMR In Situ

*A.G. Stepanov, Boreskov Institute of Catalysis, Novosibirsk, Russia; A.A. Gabrienko, Boreskov Institute of Catalysis, Novosibirsk, Russia; S.S. Arzumanov, Boreskov Institute of Catalysis, Novosibirsk, Russia; V.N. Parmon, Boreskov Institute of Catalysis, Novosibirsk, Russia; D. Freude, Leipzig University, Leipzig, Germany*

### Introduction

Methane activation is one of the important steps in various industrially relevant processes such as conversion of methane to higher hydrocarbons and methanol [1, 2]. Recent claims on methane coaromatization with  $C_{2+}$  alkanes on Zn and Ga-containing zeolites [3,4] stimulated our interest to understanding particular mechanisms of methane C–H bond activation on Zn-modified zeolite catalysts. To understand the mechanisms of methane C–H bond activation, we need to identify reaction intermediates, to clarify the role of various active sites: different in nature metal-containing species and Brønsted acid sites (BAS), to establish the role of possible impurities which could be present in methane flow and might be in charge of the formation of important intermediates providing involvement methane in  $C_{2+}$  alkane aromatization reaction. Motivated by this goal, we have monitored the transformation of methane on zeolites BEA and ZSM-5 modified with zinc using in situ magic-angle-spinning (MAS) NMR under conditions of static reactor.

### Results and Discussion

We have identified different in nature intermediates [5], primarily and secondarily formed from methane, clarified the role of different Zn-species ( $Zn^{2+}$  cations and small ZnO clusters located inside the zeolite pores) in the formation of detected intermediates [6], analyze H/D hydrogen exchange between BAS and methane molecule for Zn-modified zeolite in comparison to pure acid form zeolite [7], elucidate the mechanism of methane and propane co-aromatization on zeolite Zn/H-BEA [5, 8].

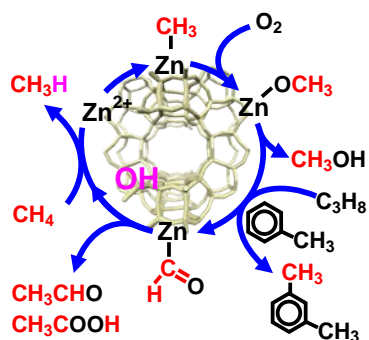
First, we identify Zn-methyl species [5], the primary stable intermediate formed at interaction of methane with zeolite and the secondary intermediate, Zn-methoxy species, which forms by oxidation of Zn-methyl with molecular oxygen presented in methane adsorbed on zeolite as impurity [9]. Finally we investigate the mechanism of

methane and propane co-aromatization, which is established to occur by alkylation with methane of aromatic molecules formed directly from propane, Zn-methoxy species being the key intermediate in this reaction [5,8] (Scheme 1).

We examine the H/D exchange between methane and BAS and show the synergy of BAS and Zn-species in activation of methane C–H bond. Synergy is displayed as a dramatic acceleration of the exchange when zeolite becomes modified with zinc [7,10]. Both  $Zn^{2+}$  cations and ZnO species provide synergy of Zn-species and BAS in activation of methane C-H bonds [6].

Based on our experimental results, we also discuss the role of both different Zn-species and impurities of oxygen in methane flow on the performance of methane and propane co-aromatization on Zn-modified zeolites [6, 9].

The detected ease of oxidation of Zn-methyl intermediate to Zn-methoxy with molecular oxygen invites further investigations of direct methane oxidation with molecular oxygen to methanol and other oxygenates on zinc modified zeolite catalysts under mild conditions.



**Scheme 1.** Primary and secondary intermediates detected by solid-state NMR and their successive transformation to the aromatic and oxygenate products formed at methane activation on Zn-modified zeolite.

## References

- [1] A.I. Olivos-Suarez, A. Szecsenyi, E.J.M. Hensen, J. Ruiz-Martinez, E.A. Pidko, and J. Gascon, *ACS Catal.* 6 (2016) 2965.
- [2] P. Schwach, X.L. Pan, and X.H. Bao, *Chem. Rev.* 117 (2017) 8497.
- [3] O.A. Anunziata, G.V.G. Mercado, and L.B. Pierella, *Catal. Lett.* 87 (2003) 167.
- [4] V.R. Choudhary, A.K. Kinage, and T.V. Choudhary, *Science* 275 (1997) 1286–1288.
- [5] M.V. Luzgin, V.A. Rogov, S.S. Arzumanov, A.V. Toktarev, A.G. Stepanov, and V.N. Parmon, *Angew. Chem. Int. Edit.* 47 (2008) 4559.
- [6] A.A. Gabrienko, S.S. Arzumanov, A.V. Toktarev, I.G. Danilova, I.P. Prosvirin, V.V. Kriventsov, V.I. Zaikovskii, D. Freude, and A.G. Stepanov, *ACS Catal.* 7 (2017) 1818.
- [7] A.G. Stepanov, S.S. Arzumanov, A.A. Gabrienko, A.V. Toktarev, V.N. Parmon, and D. Freude, *J. Catal.* 253 (2008) 11.
- [8] M.V. Luzgin, V.A. Rogov, S.S. Arzumanov, A.V. Toktarev, A.G. Stepanov, and V.N. Parmon, *Catal. Today* 144 (2009) 265.
- [9] A.A. Gabrienko, S.S. Arzumanov, M.V. Luzgin, A.G. Stepanov, and V.N. Parmon, *J. Phys. Chem. C* 119 (2015) 24910.
- [10] A.G. Stepanov, S.S. Arzumanov, A.A. Gabrienko, V.N. Parmon, I.I. Ivanova, and D. Freude, *ChemPhysChem* 9 (2008) 2559.

# **Zeolite Brønsted Acidity: Direct Quantitative Assessment by FTIR Spectroscopy and Solid-State $^1\text{H}$ MAS NMR**

*A.A. Gabrienko, Boreskov Institute of Catalysis, Novosibirsk, Russia; I.G. Danilova, Boreskov Institute of Catalysis, Novosibirsk, Russia; A.G. Stepanov, Boreskov Institute of Catalysis, Novosibirsk, Russia*

## **Introduction**

Zeolites are applied for numerous commercial applications. These crystalline materials, having unique microporous nature and strong Brønsted acidity, find broad usage in heterogeneous catalysis [1, 2]. Zeolite Brønsted acidity, caused by the presence of bridging Si–O(H)–Al or silanol Si–OH groups [3], attracts much attention since it determines the activity and selectivity of zeolite-based catalysts for acid-governed reactions. For adequate prediction of zeolite catalytic properties, it is crucial to have a reliable and feasible approach to measure the quantity of different hydroxyl O–H groups or Brønsted acid sites (BAS).

Fourier transform infrared (FTIR) spectroscopy is broadly applied nowadays for probing the concentration and strength of acid sites in zeolite catalysts [4, 5]. FTIR spectroscopy is able to measure zeolite Brønsted acidity directly by the observation of the absorption bands corresponding to different O–H groups or BAS. However, the accuracy of direct assessment of the quantity of different O–H groups by FTIR method suffers from uncertainty of the integrated molar absorption coefficients,  $\epsilon$ . The  $\epsilon$  values reported by different authors might differ by an order of magnitude [6].

## **Scope of the work**

This paper aims to demonstrate an elegant approach for reliable determination of the integrated molar absorption coefficients [7]. The approach is based on joint work of  $^1\text{H}$  MAS NMR and FTIR spectroscopy techniques. The feasibility and accuracy of the proposed methodology have been verified on a series of zeolite samples.

The concentration of different O–H groups for H-ZSM-5 and H-ZSM-23 zeolite samples with different Si/Al ratio has been reliably established with  $^1\text{H}$  MAS NMR, using methane and benzene as internal standards. Further, same zeolite samples have been analyzed with FTIR spectroscopy to obtain the integrated absorbance of the IR bands related to the O–H groups. As the result, the information on the values of the integrated molar absorption coefficients has been derived by comparing H

MAS NMR and FTIR data. The  $\epsilon$  coefficients have been reliably determined to be  $3.06 \pm 0.04$  and  $1.50 \pm 0.06 \text{ cm}^2\mu\text{mol}^{-1}$  for the IR bands at  $3605\text{--}3615$  and  $3740\text{--}3747 \text{ cm}^{-1}$ , respectively. Interestingly, the  $\epsilon$  values are similar for both HZSM-5 and H-ZSM-23 zeolites. It is also established that the  $\epsilon$  values are constant with respect to the concentration of O–H groups for H-ZSM-5 and H-ZSM-23 zeolites. The determined  $\epsilon$  coefficients can be further used for reliable quantitative assessment of zeolite Brønsted acidity with the aid of the widely available and relatively simple methodology of FTIR spectroscopy.

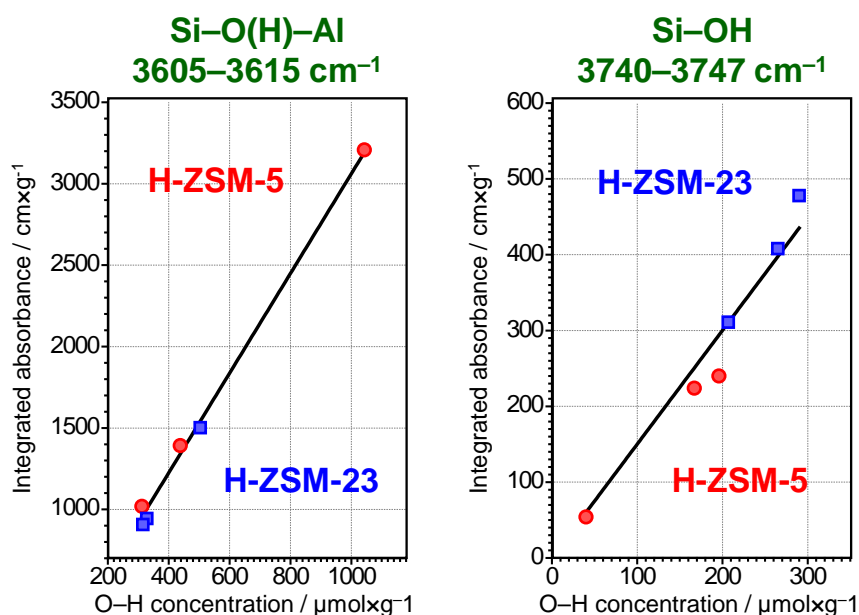


**Figure 1.** Integrated intensity of the IR band versus the concentration of O–H groups for H-ZSM-5 and H-ZSM-23 zeolites.

## Acknowledgments

This work was supported by Russian Foundation for Basic Research (grant no. 18-03-00189).

## References

- Vogt, E.T.C., Weckhuysen, B.M. // *Chem. Soc. Rev.*, 2015, Vol. 44(20), P. 7342–7370.
- Schwach, P., Pan, X.L., Bao, X.H. // *Chem. Rev.*, 2017, Vol. 117(13), P. 8497–8520.
- Gabrienko, A.A., Danilova, I.G., Arzumanov, S.S., Toktarev, A.V., Freude, D., Stepanov, A.G. // *Microporous Mesoporous Mater.*, 2010, Vol. 131(1–3), P. 210–216.
- Corma, A. // *Chemical Reviews*, 1995, Vol. 95(3), P. 559–614.
- Farneth, W.E., Gorte, R.J. // *Chemical Reviews*, 1995, Vol. 95(3), P. 615–635.
- Hadjiivanov, K.I., Vayssilov, G.N., Eds. *Characterization of oxide surfaces and zeolites by carbon monoxide as an IR probe molecule. Advances in Catalysis*, Vol 47. 2002, San Diego, Elsevier Academic Press Inc.
- Gabrienko, A.A., Danilova, I.G., Arzumanov, S.S., Pirutko, L.V., Freude, D., Stepanov, A.G. // *The Journal of Physical Chemistry C*, 2018, Vol. 122(44), P. 25386–25395.

# The evaluation of the photocatalysis of silver loaded Ga<sub>2</sub>O<sub>3</sub> nanosheets made with graphene oxide as a template

*Kenta Sonoda<sup>1</sup>, Muneaki Yamamoto<sup>2</sup>, Tetsuo Tanabe<sup>2</sup>, Tomoko Yoshida<sup>2</sup>*

*<sup>1</sup>Department of Engineering, Osaka City University, Osaka, Japan*

*<sup>2</sup>Advanced Research Institute for Natural Science and Technology, Osaka City University, Osaka, Japan*

## Introduction

Ga<sub>2</sub>O<sub>3</sub> is one of the photocatalyst to show the relatively high activity for water splitting as well as carbon dioxide reduction when by loading silver as a co-catalyst. In our research, it was suggested that the reaction proceeds at the interface between the silver clusters and the Ga<sub>2</sub>O<sub>3</sub> photocatalyst [1]. Therefore, if we develop a nanomaterial having a large amount of the interface between silver clusters and Ga<sub>2</sub>O<sub>3</sub> photocatalyst, further photocatalytic activity improvement is expected.

Recently, it was reported that metal oxide nanosheets with a thickness of several nm was formed by the slight growth of metal oxide on two-dimensional graphene oxide (GO) [2,3]. Thereafter, burning off the GO in the presence of oxygen, isolated metal oxide nanosheets can be obtained. It was also reported that metal oxide nanosheets including metal nanoparticles was obtained by fixing metal nanoparticles on GO firstly and growing metal oxide upon them [4]. The nanomaterials would be expected to have a large amount of the interface between metal oxide and metal nanoparticles. To develop a photocatalyst promoting the reduction of carbon dioxide efficiently, in the present study, we fabricated a silver loaded Ga<sub>2</sub>O<sub>3</sub> nanosheets photocatalyst using GO as a template.

## Preparation of Ga<sub>2</sub>O<sub>3</sub> nanosheets

GO was prepared by a Hummers method using graphite as a starting material. The GO and gallium tri-n-butoxide were stirred in a cyclohexane solvent overnight, followed by a centrifugation. The residue was dispersed in cyclohexane again and then autoclaved at 453 K for 6 hours. After washing by centrifugation, the residue of the suspension was dried in vacuum. Thus, the composite of Ga<sub>2</sub>O<sub>3</sub> precursor and GO (Ga<sub>2</sub>O<sub>3</sub> precursor/GO) was synthesized by the above procedures. The composite was calcined at a given temperature of 823 – 1123 K, and Ga<sub>2</sub>O<sub>3</sub> nanosheets were obtained (Fig. 1).

## Preparation of Ag/Ga<sub>2</sub>O<sub>3</sub> nanosheets

Ag/Ga<sub>2</sub>O<sub>3</sub> nanosheets were fabricated by photodeposition of colloidal silver nanoparticles on Ga<sub>2</sub>O<sub>3</sub> precursor/GO followed by calcination at 1123K for 5 hour.

## Results and discussion

TEM images of the obtained Ga<sub>2</sub>O<sub>3</sub> nanosheets are shown in Fig. 1. As is evident from these TEM images, the samples calcined at 823 – 1123 K formed nanosheets. The crystal structures of the nanosheet samples were analysed by XRD measurements (Fig.2) as follows; the samples calcined at 823 K and 1123 K were assigned to  $\gamma$ -Ga<sub>2</sub>O<sub>3</sub> phase and  $\beta$ -Ga<sub>2</sub>O<sub>3</sub> phase, respectively, while those calcined at 923 K and 1023 K were consisted of mixed-phases of  $\beta$ - and  $\gamma$ - Ga<sub>2</sub>O<sub>3</sub>. The TEM image of Ag/Ga<sub>2</sub>O<sub>3</sub> nanosheets (Fig. 3) shows that Ag nanoparticles are highly dispersed and loaded on Ga<sub>2</sub>O<sub>3</sub> nanosheets. At the conference, we will discuss the reaction activities of Ag/Ga<sub>2</sub>O<sub>3</sub> nanosheets for photocatalytic carbon dioxide reduction.

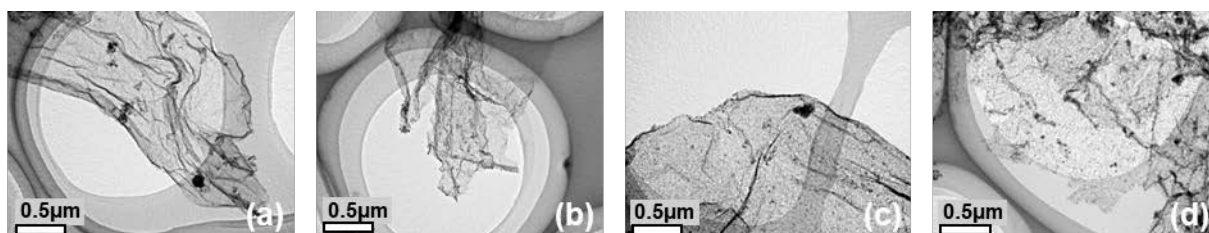


**Figure 1.** TEM images of Ga<sub>2</sub>O<sub>3</sub> nanosheets calcined at 823 K (a), 923 K (b), 1023 K (c) and 1123 K (d).

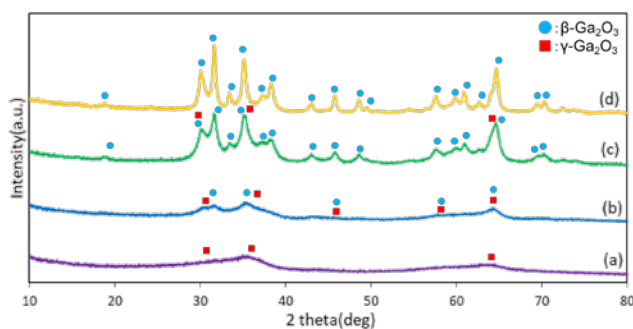


**Figure 2.** XRD patterns of Ga<sub>2</sub>O<sub>3</sub> nanosheets calcined at 823 K (a), 923 K (b), 1023 K (c) and 1123 K (d).

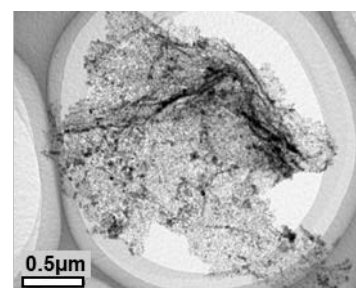


**Figure 3.** TEM image of Ag/Ga<sub>2</sub>O<sub>3</sub> nanosheets.

## References

- [1] M. Yamamoto *et al.*, *J. Mater. Chem. A* **2015**, 3, 16810-16816.
- [2] G. Zhao *et al.*, *Chem. Sci.* **2012**, 3, 433-437.
- [3] S. Takenaka *et al.*, *J. Phys. Chem. C* **2015**, 119, 12445-12454.
- [4] S. Takenaka *et al.*, *Appl. Catal. A* **2018**, 566, 52-59.

# Methane Interaction with Cu<sup>2+</sup> Sites of Cu/H-ZSM-5 Zeolite: EPR, UV-Vis, FTIR and NMR Spectroscopic Investigation

*A.A. Gabrienko, Boreskov Institute of Catalysis, Novosibirsk, Russia; A.M. Sheveleva, International Tomography Center, Novosibirsk, Russia; S.A. Yashnik, Boreskov Institute of Catalysis, Novosibirsk, Russia; M.V. Fedin, International Tomography Center, Novosibirsk, Russia; A.G. Stepanov, Boreskov Institute of Catalysis, Novosibirsk, Russia*

## Introduction

Nowadays, zeolites loaded with copper attract much attention as potential catalysts for methane processing to valuable chemicals via selective oxidation to methanol [1, 2]. Performed fundamental and applied studies admit a crucial role of Cu<sup>2+</sup> and/or Cu<sup>+</sup> cationic species present in the zeolites for methane activation [3-6]. Though, possible involvement of Brønsted acid sites (BAS) of a zeolite in methane activation can be also supposed.

Hence, both Cu<sup>2+</sup> sites and BAS can be responsible for methane activation and conversion on Cu-containing zeolites. Therefore, it is an interesting problem to investigate the interaction of methane with these sites in order to inquire into the mechanism of methane-to-methanol transformation. Such problem could be addressed with the help of different spectroscopic techniques. In particular, the data to be obtained by FTIR, UV-vis, NMR, and EPR methods can provide valuable molecular-level details on the possible interactions of methane and Cu<sup>2+</sup> species and BAS.

## Scope of the work

A set of the spectroscopic methods, namely, DRIFTS, UV-vis. DRS, solid-state <sup>1</sup>H and <sup>13</sup>C MAS NMR, and pulse EPR, has been applied in this work aiming to obtain valuable information on the peculiarities of methane interaction with the surface sites of Cu-loaded acid-form zeolite of ZSM-5 type.

The initial state of Cu<sup>2+</sup> species as well as its perturbation caused by the interaction with adsorbed methane has been investigated with the application of UV-vis. DRS method. Methane adsorption on Cu<sup>2+</sup> sites has been studied with DRIFTS technique to reveal formation of specific molecular complex characterized by polarized C–H bond which might be responsible for efficient methane C–H bond activation by BAS



[7]. EPR method has offered the detailed description on the structure of this molecular complex with the certain C–Cu and H–Cu distances being determined.  $^1\text{H}$  MAS NMR approach, being applied to monitor the kinetics of the H/D exchange between methane- $d_4$  and BAS *in situ*, has confirmed promoting effect of  $\text{Cu}^{2+}$  sites on the activation of methane C–H bond by BAS. Finally,  $^{13}\text{C}$  MAS NMR spectroscopy has revealed that C–H bond activation assisted by both  $\text{Cu}^{2+}$  sites and BAS has led to the formation of surface methoxy species which is considered to be an intermediate towards methanol formation.

### Acknowledgments

This work was supported by Russian Scientific Foundation (grant no. 18-73-00016).

### References

1. Alayon, E.M.C., Nachtegaal, M., Ranocchiari, M., van Bokhoven, J.A. // CHIMIA International Journal for Chemistry, 2012, Vol. 66(9), P. 668–674.
2. Vanelderen, P., Hadt, R.G., Smeets, P.J., Solomon, E.I., Schoonheydt, R.A., Sels, B.F. // Journal of Catalysis, 2011, Vol. 284(2), P. 157–164.
3. Li, G., Vassilev, P., Sanchez-Sanchez, M., Lercher, J.A., Hensen, E.J.M., Pidko, E.A. // Journal of Catalysis, 2016, Vol. 338, P. 305–312.
4. Grundner, S., Markovits, M.A.C., Li, G., Tromp, M., Pidko, E.A., Hensen, E.J.M., Jentys, A., Sanchez-Sanchez, M., Lercher, J.A. // Nature Communications, 2015, Vol. 6, P. 7546.
5. Tomkins, P., Mansouri, A., Bozbag, S.E., Krumeich, F., Park, M.B., Alayon, E.M.C., Ranocchiari, M., van Bokhoven, J.A. // Angewandte Chemie, 2016, Vol. 128(18), P. 5557–5561.
6. Bozbag, S.E., Alayon, E.M.C., Pecháček, J., Nachtegaal, M., Ranocchiari, M., van Bokhoven, J.A. // Catalysis Science & Technology, 2016, Vol. 6(13), P. 5011–5022.
7. Gabrienko, A.A., Arzumanov, S.S., Toktarev, A.V., Danilova, I.G., Prosvirin, I.P., Kriventsov, V.V., Zaikovskii, V.I., Freude, D., Stepanov, A.G. // ACS Catalysis, 2017, Vol. 7(3), P. 1818–1830.

# Measuring diffuse reflectance UV-Vis spectra of silver loaded gallium oxide photocatalyst under in-situ conditions

*Daiki Kitajima<sup>1</sup>, Muneaki Yamamoto<sup>2</sup>, Tetsuo Tanabe<sup>2</sup>, Tomoko Yoshida<sup>2</sup>*

*<sup>1</sup>Department of Engineering, Osaka City University, Osaka, Japan*

*<sup>2</sup>Advanced Research Institute for Natural Science and Technology, Osaka City University, Osaka, Japan*

## Introduction

It has been reported that many photocatalysts loading silver as a co-catalyst are highly active for the carbon dioxide reduction with water to carbon monoxide. Here, the silver co-catalyst is considered as a reaction site of the carbon dioxide reduction. On the other hand, silver particles change to larger particles during the reaction, resulting in the decrease of the photocatalytic activity [1]. We attempted a real time observation of the redox state as well as the change in particle size of silver co-catalyst over gallium oxide photocatalyst by monitoring silver localized surface plasmon resonance (LSPR) absorption during the reaction.

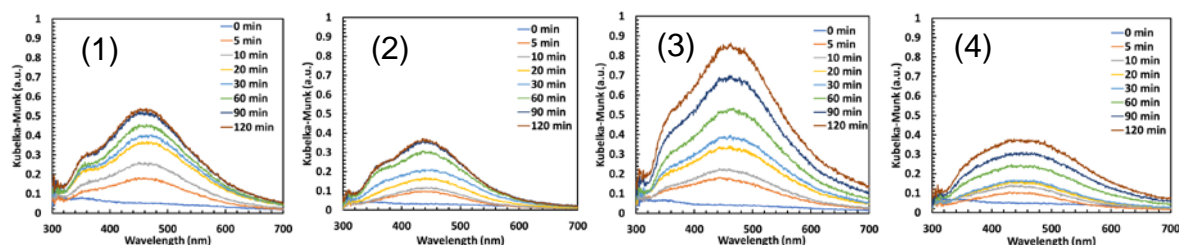
## Experimental

Silver loaded gallium oxide ( $\text{Ag}/\text{Ga}_2\text{O}_3$ ) sample was prepared by impregnation of  $\text{Ga}_2\text{O}_3$  with an  $\text{AgNO}_3$  solution, followed by drying and calcination in air at 623 K for 2 h. The Ag loading amount was 0.5 wt%. In-situ measurements of UV-Vis spectra were conducted with a self-made optical system equipped with an in-situ diffuse reflectance cell. Light from a xenon lamp was collimated and introduced to the sample set in this cell, and the diffuse reflected light was detected by a multi channel analyser. The in-situ diffuse reflectance spectra of  $\text{Ag}/\text{Ga}_2\text{O}_3$  were measured under Ar or  $\text{CO}_2$  gas with/without bubbling into water with a flow rate at 100 mL/min. The xenon lamp was also used for the reaction inducing light for  $\text{Ag}/\text{Ga}_2\text{O}_3$  samples.

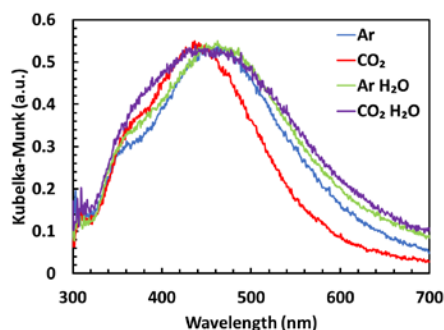
## Results and discussion

Fig. 1 shows time courses of the UV-Vis spectra of  $\text{Ag}/\text{Ga}_2\text{O}_3$  under light irradiation with different conditions. The absorption band ranging from 350 to 650 nm is attributed to LSPR absorption of Ag metal nanoparticles. Although LSPR absorption is not observed before light irradiation, LSPR absorption peak appeared as light irradiation started and grew with the time. The peak top intensity of LSPR

absorption gradually increased and saturated. Not only the increase in the peak top intensity, but also the peak shape differed by the conditions. Note that the peak top intensity increased even after 120 min when water vapor was introduced. Here, the spectra measured at 120 min were normalized by their peak top intensities. Fig. 2 compares the normalized spectra for different conditions. The peak at 350 nm is assignable to Ag small clusters and the other peaks around 450 nm and 600 nm are attributed to a localized surface plasmon resonance of Ag nanoparticles and larger Ag nanoparticles, respectively. Under CO<sub>2</sub> flow, the peak intensity at 600 nm was low compared with other conditions. This result indicates that the size increase of the silver particles is remarkably suppressed by the adsorption of CO<sub>2</sub> molecules on the surface of Ga<sub>2</sub>O<sub>3</sub> and/or the Ag particles. The peak top intensity of LSPR absorption at 450 nm is plotted against the light irradiation time (Fig. 3). When the peak intensity for Ag/Ga<sub>2</sub>O<sub>3</sub> under CO<sub>2</sub> and H<sub>2</sub>O flow is doubled, its time course profile is almost the same as that under Ar and H<sub>2</sub>O flow. This suggests that the mechanism of the Ag particle growth is basically the same and the growth rate only changes. At the conference, we will also present the results of the experiments carried out by controlling the wavelength (energy) of irradiated light.



**Fig.1** Time courses of the UV-Vis spectra of silver loaded gallium oxide under light irradiation with different conditions (1) Ar flow (2) CO<sub>2</sub> flow (3) Ar and H<sub>2</sub>O flow (4) CO<sub>2</sub> and H<sub>2</sub>O flow



**Fig.2** Normalized spectra of Ag/Ga<sub>2</sub>O<sub>3</sub> measured at 120 min with different conditions.

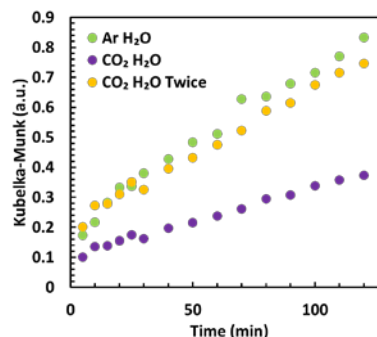


**Fig.3** Time courses of the intensity of LSPR absorption at 450 nm.

## References

[1] M. Yamamoto, T. Yoshida, N. Yamamoto, T. Nomoto, Y. Yamamoto, S. Yagi and H. Yoshida, J. Mater. Chem. A, 2015, 3, 16810.

# In Operando Spectroscopy of CO<sub>2</sub> Reduction Reactions at Pt/Ionic Liquid Interfaces

*Andre Kemna, Björn Ratschmeier, Björn Braunschweig, Institut für Physikalische  
Chemie, Westfälische Wilhelms-Universität Münster, Corrensstraße 28/30, 48149  
Münster, Germany*

CO<sub>2</sub> reduction reactions (CO<sub>2</sub>RR) at Pt(poly)/electrolyte interfaces were studied with cyclic voltammetry and in operando with IR absorption (IRAS) as well as sum frequency generation (SFG) spectroscopy. The combination of IRAS and SFG is a powerful tool to study mechanistic details in bulk solutions and at interfaces. Using [BMIM][BF<sub>4</sub>] and [EMIM][BF<sub>4</sub>] room-temperature ionic liquids (RTIL) as electrolytes, we have investigated the influence of H<sub>2</sub>O co-reactants and the chemical identity of the RTIL as co-catalyst on the activity of Pt electrodes for CO<sub>2</sub>RR.

Cycling the potential from 0.1 V to -1.4 V vs SHE, IRAS revealed a vibrational band centered at 1670 cm<sup>-1</sup>, which arises at an onset potential of -0.65 V. We attribute this band to the carbonyl stretching mode of zwitterionic imidazolium carboxylates, which is generated via a carbene intermediate as evidenced by IRAS.

During the potential sweep from -1.4 V to 2.4 V in [BMIM][BF<sub>4</sub>], CO<sub>2</sub>RR products are formed and give rise to vibrational bands at 1730 and 1750 cm<sup>-1</sup>. This is accompanied by a decrease of the imidazolium carboxylate band at 1670 cm<sup>-1</sup>. We assign the former vibrational modes to C=O vibrations of formic acid, which is produced at an onset potential of 1.4 V. This indicates that electrolysis of CO<sub>2</sub> to formic acid may be possible in a two-step reaction process.

In operando SFG spectra revealed the formation of surface adsorbed CO. The CO adsorbate layer poisons the Pt catalyst, and leads to a deactivation over many potential cycles. From our spectroscopic analysis, we provide evidence for two main products of CO<sub>2</sub> reduction reactions - CO and formic acid - which may be used in power-to-X applications.

## References

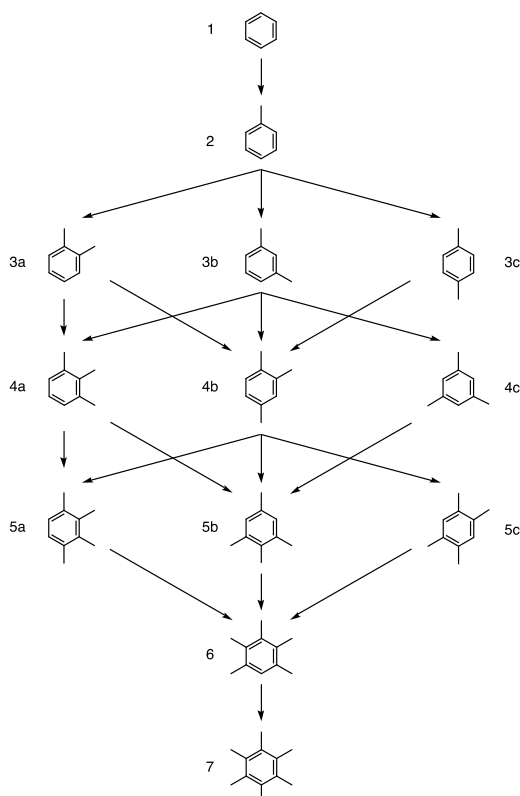
- B. A. Rosen, J. L. Haan, P. Mukherjee, B. Braunschweig, W. Zhu, A. Salehi-Khojin, D. D. Dlott, R. I. Masel, *J. Phys. Chem C.*, 2012, 116, 15307-15312. [1]  
B. Braunschweig, P. Mukherjee, J. L. Haan, D. D. Dlott, *J. Electroanal. Chem.*, 2017, 800, 144-150. [2]

# Aromatics in Methanol-to-hydrocarbons Conversion

*Michal Fečík, Karlsruhe Institute of Technology, Eggenstein-Leopoldshafen, Germany; Philipp Pleßow, Karlsruhe Institute of Technology, Eggenstein-Leopoldshafen, Germany; Felix Studt, Karlsruhe Institute of Technology, Eggenstein-Leopoldshafen, Germany*

## Motivation

Methanol-to-hydrocarbons (MTH) conversion, carried out over acidic catalysts such as various zeotypes, represents a promising way to renewable chemicals and fuels.[1] It allows the use of biomass or other alternative sources (such as natural gas or coal) as a feedstock for the synthesis of hydrocarbons in the methanol-to-olefins (MTO) and methanol-to-gasoline (MTG) processes and can thus play an important role in post-oil society. The aromatic cycle of the hydrocarbon pool (HCP)[2] has been found to be important for a number of catalysts, for example SAPO-34[3-5] and H-BEA[6-9]. The aromatic cycle consists of a number of reactions among which we will systematically investigate the methylation of polymethylbenzenes (polyMBs). Better understanding of the reactivity of polyMBs will bring more insight into MTO reactions involving these intermediates.



## Results and Discussion

We systematically study consecutive methylation of benzene to hexamethylbenzene while investigating all possible pathways as well as geometries for stepwise and concerted mechanisms. For the latter, we also investigate methylation through use of methanol (MeOH) as well as dimethyl ether (DME). Our aim is to determine and understand trends for activation barriers. Afterwards, we will study the side-chain methylation mechanism in which polyMBs act as intermediates. We aim to determine activation barriers of methanol-to-ethylene and methanol-to-propylene reactions

while we vary methylation level of used intermediates. We also focus on uncovering any trends in activation barriers that would transpire due to these changes.

We investigate the H-SSZ-13 zeolite using periodic density functional theory (DFT) calculations at the PBE-D3 level of theory along with MP2/def2-TZVPP- and DLPNO-calculations on cluster models of the zeolite. These cluster models capture the entire pore of the CHA structure where the reactants are located.

Our results show that contributions coming from van der Waals (vdW) interactions scale linearly with increasing total number of atoms of the studied polyMBs for all three studied pathways. Obtained slopes of these trends are comparable with previous reports for MeOH adsorption and olefin methylation in H-SSZ-13[10-11]. Observed deviations are originating mainly from steric confinement of the zeolite framework. This is in accordance with our previous studies on CHA and MFI zeotypes[11-12], where we showed that steric demand and mesomeric stabilization can cause a reactant to deviate from trends otherwise valid for similar group of reactants.

## References

1. Olsbye, U.; Svelle, S.; Bjorgen, M.; Beato, P.; Janssens, T. V.; Joensen, F.; Bordiga, S.; Lillerud, K. P., Conversion of methanol to hydrocarbons: how zeolite cavity and pore size controls product selectivity. *Angew. Chem., Int. Ed. Engl.* **2012**, *51* (24), 5810-31.
2. Dahl, I. M.; Kolboe, S., On the reaction mechanism for propene formation in the MTO reaction over SAPO-34. *Catal. Lett.* **1993**, *20* (3), 329-336.
3. Song, W.; Haw, J. F.; Nicholas, J. B.; Heneghan, C. S., Methylbenzenes Are the Organic Reaction Centers for Methanol-to-Olefin Catalysis on HSAPO-34. *J. Am. Chem. Soc.* **2000**, *122* (43), 10726-10727.
4. Arstad, B.; Kolboe, S., Methanol-to-hydrocarbons reaction over SAPO-34. Molecules confined in the catalyst cavities at short time on stream. *Catal. Lett.* **2001**, *71* (3), 209-212.
5. Arstad, B.; Kolboe, S., The Reactivity of Molecules Trapped within the SAPO-34 Cavities in the Methanol-to-Hydrocarbons Reaction. *J. Am. Chem. Soc.* **2001**, *123* (33), 8137-8138.
6. Sassi, A.; Wildman, M. A.; Ahn, H. J.; Prasad, P.; Nicholas, J. B.; Haw, J. F., Methylbenzene Chemistry on Zeolite HBeta: Multiple Insights into Methanol-to-Olefin Catalysis. *J. Phys. Chem. B* **2002**, *106* (9), 2294-2303.
7. Bjørgen, M.; Bonino, F.; Kolboe, S.; Lillerud, K.-P.; Zecchina, A.; Bordiga, S., Spectroscopic Evidence for a Persistent Benzenium Cation in Zeolite H-Beta. *J. Am. Chem. Soc.* **2003**, *125* (51), 15863-15868.
8. Bjørgen, M.; Olsbye, U.; Petersen, D.; Kolboe, S., The methanol-to-hydrocarbons reaction: insight into the reaction mechanism from [12C]benzene and [13C]methanol coreactions over zeolite H-beta. *J. Catal.* **2004**, *221* (1), 1-10.
9. Bjørgen, M.; Olsbye, U.; Svelle, S.; Kolboe, S., Conversion of Methanol to Hydrocarbons: The Reactions of the Heptamethylbenzenium Cation over Zeolite H-Beta. *Catal. Lett.* **2004**, *93* (1), 37-40.
10. Wang, C.-M.; Brogaard, R. Y.; Xie, Z.-K.; Studt, F., Transition-state scaling relations in zeolite catalysis: influence of framework topology and acid-site reactivity. *Catal. Sci. Technol.* **2015**, *5* (5), 2814-2820.
11. Plessow, P. N.; Studt, F., Olefin methylation and cracking reactions in H-SSZ-13 investigated with ab initio and DFT calculations. *Catal. Sci. Technol.* **2018**, *8* (17), 4420-4429.
12. Fečík, M.; Plessow, P. N.; Studt, F., Simple Scheme to Predict Transition-State Energies of Dehydration Reactions in Zeolites with Relevance to Biomass Conversion. *J. Phys. Chem. C* **2018**, *122* (40), 23062-23067.

# COx free hydrogen generation from photocatalytic NH<sub>3</sub> decomposition

*Venkata D. B. C. Dasireddy and Blaz Likozar*

*Department of Catalysis and Chemical Engineering, National Institute of Chemistry,  
Hajrihova ulica 19, Ljubljana, Slovenia. E-mail: [Dasireddy@ki.si](mailto:Dasireddy@ki.si)*

## Introduction

Ammonia is a second most widely produced chemical in the world (after sulphuric acid), with over 100 million tons per year being transported [1-3]. It is promising hydrogen (H<sub>2</sub>) carrier because of many advantages. The main reason is the high H<sub>2</sub> content of 17.8 mass% in NH<sub>3</sub> [4]. Different supported metal catalyst systems have been examined for ammonia decomposition including a variety of supports such as Al<sub>2</sub>O<sub>3</sub>, SiO<sub>2</sub>, TiO<sub>2</sub>, ZrO<sub>2</sub>, mesoporous and microporous materials, activated carbon, multi-walled carbon nanotubes (MWCNTs) etc [1, 2, 5]. In this study, we present a novel synthesis route of a Cu-Ti/MWCNT catalyst. Cu-Ti based materials are highly conductive, have a high specific surface area, and are promising in ammonia decomposition reaction for H<sub>2</sub> production. MWCNT is low-cost semi-conducting material as well and there is no published study on Cu-Ti/MWCNT mixed oxides as a promising alternative to replace expensive catalysts and high-temperature process for a real scale application of hydrogen generation.

## Methods

Cu-Ti mixed metal oxide alloy was prepared using the sol-gel method and citrate methods and then impregnated on the MWCNT supports. The characterisation of catalysts was carried out by N<sub>2</sub> physisorption, XRD, H<sub>2</sub>-TPR, N<sub>2</sub>O chemisorption, NH<sub>3</sub>-TPD, CO<sub>2</sub>-TPD, H<sub>2</sub>-TPD, XPS and TEM. The photocatalytic decomposition of ammonia was carried out at a GHSV of 15,000 h<sup>-1</sup> with varying flow rates and stability of the catalysts was examined for 24 h.

## Results and discussion

In the present study, the performance of copper, titanium dioxide and carbon nanotube catalysts in the photocatalytic decomposition of NH<sub>3</sub> with a combination of Cu/MWCNT, Ti /MWCNT and Cu-Ti/MWCNT were evaluated. The NH<sub>3</sub> conversions over the synthesized catalysts remarkably increased with the combination of Cu and

Ti with MWCNT. Both bare supports showed a lower conversion and hydrogen formation rate. All the catalysts containing copper showed a high conversion and hydrogen formation rate. With ammonia decomposition being an apparent first-order reaction, the effective activation energy ( $E_a$ ) of  $132 \pm 1$  kJ/mol was estimated for Cu-Ti/MWCNT, which is in good agreement with the similar values, pertinent to other catalysts, employed for the same process [1, 2, 5]. Furthermore, hydrogen formation rate was lower over the catalysts, prepared via the sol-gel method with regard to the citrate method. Additionally, both alumina-supported catalysts were also characterized by the slightly higher activation energy for ammonia decomposition. This could be due to a highly basic character of the surface of these materials.

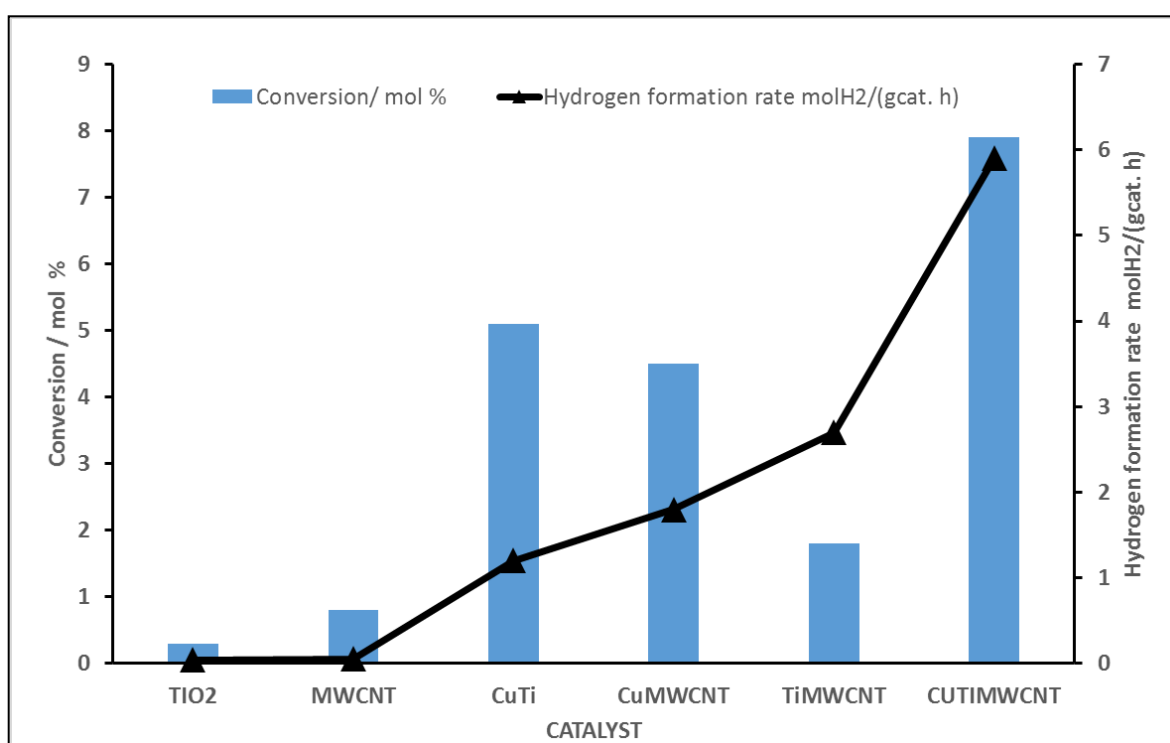


**Figure 1** Photocatalytic conversion of ammonia over Cu, Ti, MWCNT based catalysts and hydrogen formation rate during the reaction

## References

- [1] Š. Hajduk, V.D.B.C. Dasireddy, B. Likozar, G. Dražić, Z.C. Orel, *Appl. Catal., B*, 211 (2017) 57-67.
- [2] V.D.B.C. Dasireddy, B. Likozar, *Fuel* 196 (2017) 325-335.
- [3] H. Inokawa, T. Ichikawa, H. Miyaoka, *Appl. Catal., A* 491 (2015) 184-188.
- [4] S. Podila, S.F. Zaman, H. Driss, Y.A. Alhamed, A.A. Al-Zahrani, L.A. Petrov, *Catal. Sci. Tech.* 6 (2016) 1496-1506.
- [5] X. Duan, G. Qian, X. Zhou, Z. Sui, D. Chen, W. Yuan, *Appl. Catal., B*, 101 (2011) 189-196.



# Vapor-Phase Dehydrogenation of Formic Acid using Nitrogen-doped Ordered Mesoporous Carbon

*David B. Christensen, Technical University of Denmark, Kgs. Lyngby, Denmark;*

*Jerrick Mielby, Technical University of Denmark, Kgs. Lyngby, Denmark;*

*Søren Kegnæs, Technical University of Denmark, Kgs. Lyngby, Denmark*

## Introduction

Hydrogen (H<sub>2</sub>) as an energy source is one of the most promising alternatives to fossil fuels, but transporting it in pressurized or cryogenic containers present weight and safety issues [1-2]. Storing H<sub>2</sub> as liquid formic acid makes transport and delivery both easier and safer. In addition, biomass can be converted into formic acid, it has a high hydrogen density (53 g H<sub>2</sub>/L [3]), can be released at low temperature (T < 80°C have been reported [4]) and high pressure (P = 750 bar [5]). The challenge with the use of formic acid is its ability to selectively undergo dehydrogenation into H<sub>2</sub> + CO<sub>2</sub> and avoid dehydration into H<sub>2</sub>O + CO (a common poison for H<sub>2</sub> fuel cells). Our work focuses on synthesis and characterization of different nitrogen-doped and nitrogen-free ordered mesoporous carbon catalysts for the dehydrogenation of formic acid to H<sub>2</sub> in the vapor phase using a continuous setup.

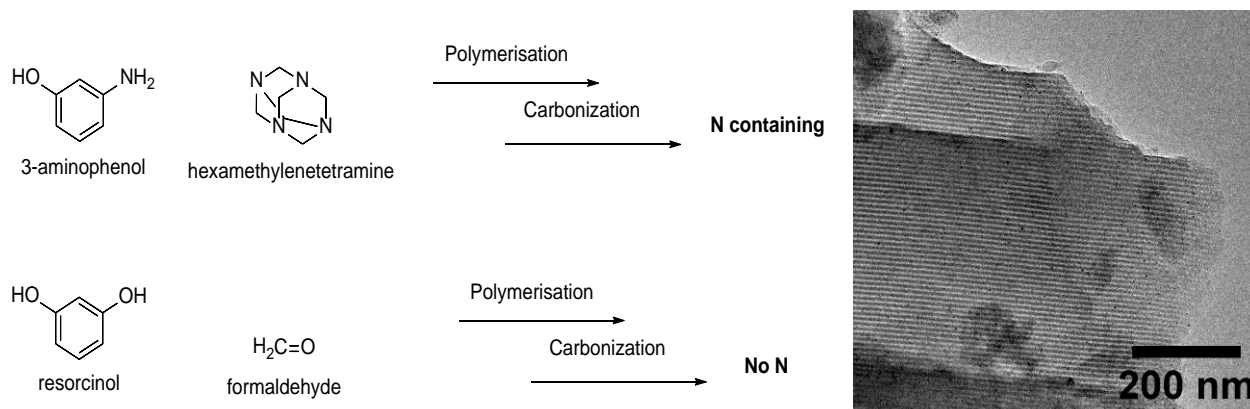
## Experimental

The catalytic supports were synthesized by growing a polymer based on either 3-aminophenol/hexamethylenetetramine or resorcinol/formaldehyde in an aqueous solution containing a surfactant. The grown polymers were carbonized to generate the carbon support and to burn off the surfactant, leaving a mesoporous and ordered structure. The active metals were added afterwards either by incipient-wetness impregnation or metalation. The metals tested include Ag, Au, Pd, Pt, Ru, Ir and an Au/Pd alloy.

## Results and Discussion

The resulting structure was examined using a range of different techniques including N<sub>2</sub>-physisorption, TEM, SEM, XPS, XRD, TGA and ICP. Particular focus was put on the influence of having nitrogen-doped versus a nitrogen-free carbon support. Parameters of interest include dispersion, stability and efficiency for the targeted

process. Dehydrogenation was carried out in the vapour phase with a nitrogen flow of 50 mL/min containing 10% formic acid.



Continuous production of  $H_2$  could be achieved with no detectable amount of CO by-product at temperatures of  $120^\circ\text{C}$ , achieving full conversion at around  $180^\circ\text{C}$ . TEM images show a fine dispersion of particles  $<5\text{ nm}$  were achieved for most of the prepared catalysts regardless of the presence of nitrogen. Sintering effects were studied afterwards using TEM on the used catalysts, showing varying increases in particle size.

## Conclusion

Ordered Mesoporous Carbon with and without nitrogen have proven capable of continuously producing pure  $H_2$  under mild conditions. The influence of nitrogen on the stability and efficiency was examined in detail.

## References

- [1] M. Navlani-García, K. Mori, Y. Kuwahara, and H. Yamashita, "Recent strategies targeting efficient hydrogen production from chemical hydrogen storage materials over carbon-supported catalysts," *NPG Asia Mater.*, vol. 10, no. 4, pp. 277–292, 2018.
- [2] T. Sinigaglia, F. Lewiski, M. E. Santos Martins, and J. C. Mairesse Siluk, "Production, storage, fuel stations of hydrogen and its utilization in automotive applications-a review," *Int. J. Hydrogen Energy*, vol. 42, no. 39, pp. 24597–24611, 2017.
- [3] K. Müller, K. Brooks, and T. Autrey, "Hydrogen Storage in Formic Acid: A Comparison of Process Options," *Energy and Fuels*, vol. 31, no. 11, pp. 12603–12611, 2017.
- [4] Y. Zhao *et al.*, "Selective decomposition of formic acid over immobilized catalysts," *Energy and Fuels*, vol. 25, no. 8, pp. 3693–3697, 2011.
- [5] C. Fellay, P. J. Dyson, and G. Laurency, "A viable hydrogen-storage system based on selective formic acid decomposition with a ruthenium catalyst," *Angew. Chemie - Int. Ed.*, vol. 47, no. 21, pp. 3966–3968, 2008.

# **Steam cracking of heavy oil in the presence of dispersed catalysts based on various metals**

*G.A. Sosnin, Boreskov Institute of Catalysis and Novosibirsk State University, Novosibirsk, Russia; P.M. Yeletsky, Boreskov Institute of Catalysis, Novosibirsk, Russia; O.O. Zaikina, Boreskov Institute of Catalysis and Novosibirsk State University, Novosibirsk, Russia; V.A. Yakovlev, Boreskov Institute of Catalysis and Novosibirsk State University, Novosibirsk, Russia*

## **Introduction**

With the constant development of technology and the growth of energy consumption, the demand of liquid products with a low boiling point is constantly increasing. As a result, the involvement of heavy oil feedstocks (heavy oil, bitumen, atmospheric and vacuum residues, etc.) in the infrastructure of oil refining is inevitable. The depth-increasing problem of extracted heavy oil feedstock upgrading to produce a maximum possible amount of light distillate fractions (gasoline and diesel) obtained is to be solved. All the approaches to heavy oil upgrading can be divided into carbon rejection, or hydrogen addition [1]. The basis of the approaches mentioned above is the thermal treatment to obtain low-viscous upgraded oil. On the one hand, carbon rejection based processes are the simplest in industrial implementation, have minimal economic expenses, but on the other hand, this approach is characterized by a low yield of light fractions, as well as a significant amount of obtained by-products (gaseous products and coke) [2]. To reduce the coke yields and to increase the selectivity towards light fractions, molecular hydrogen is used [3]. The main disadvantage of hydrogen addition a high cost and the use of high hydrogen pressures [4]. Recently, processes combining the advantages of two approaches, for example, thermal catalytic processes using water (in gas, sub- and supercritical phase states), have been actively developing [5].

## **Results and discussion**

This work is aimed at the investigation of steam cracking process in a 1000 ml batch reactor at 425 and 450 °C, weight ratio of water to feed 0.3 : 1, and stirring rate of 1000 rpm. The process was catalysed using the dispersed catalysts based on such

metals as Mo, Ni etc. High-sulphuric heavy oil from Rep. of Tatarstan (Russia) was chosen as the substrate in the experiments.

Catalytic steam cracking, thermal cracking, steam cracking, catalytic cracking in the absence of water, and hydrocracking were carried out to establish the effect of water, a catalyst and other process conditions on a composition and properties of the produced upgraded oil. Efficacy was evaluated in terms of the yields of light fractions (b.t. < 350 °C), synthetic oil (b.t. < 500 °C), upgraded oil (total liquid product), coke and gaseous products. In addition, the H : C atomic ratio, sulphur content, density and viscosity of the upgraded oils were estimated. Catalysts were investigated by a wide range of methods (XRD, TEM, etc.). It was shown that the type of the metal used could significantly change the route of desulphurization as well as yield of the products.

The work is supported by Ministry of Higher Education and Science of Russian Federation: project No 14.607.21.0172, identification number RFMEFI60717X0172

#### References

1. A review of recent advances in catalytic hydrocracking of heavy residues / R. Sahu, B.J. Song, J.S. Im, Y.P. Jeon, C.W. Lee // *Journal of Industrial and Engineering Chemistry*. – 2015. – V. 27. – P. 12–24.
2. Castañeda L.C., Muñoz J.A.D., Ancheyta J. Current situation of emerging technologies for upgrading of heavy oils // *Catalysis Today*. – 2014. – V. 220–222. – P. 248–273.
3. Ancheyta J., Speight J.G. *Hydroprocessing of heavy oils and residua*. – London: CRC Press, 2007. – 376 p.
4. Fathi M.M., Pereira-Almao P. Catalytic aquaprocessing of arab light vacuum residue via short space times // *Energy and Fuels*. – 2011. – V. 25. – № 11. – P. 4867–4877.
5. Catalytic Steam Cracking of Heavy Oil Feedstocks: a Review / P.M. Eletsii, O.O. Mironenko, R.G. Kukushkin, G.A. Sosnin, V.A. Yakovlev // *Catalysis in Industry*. – 2018. – V. 10. – № 3. – P. 185–201.

# Photocatalytic reduction of CO<sub>2</sub> with water including methanol over Ga<sub>2</sub>O<sub>3</sub> with Ag co-catalyst

*Kokoro Yoshioka<sup>1</sup>; Muneaki Yamamoto<sup>2</sup>; Akiyo Ozawa<sup>1</sup>; Tetsuo Tanebe<sup>2</sup>;*

*Tomoko Yoshida<sup>2</sup>*

*<sup>1</sup>Applied Chemistry and Bioengineering, Graduate School of Engineering, Osaka City University, Osaka, Japan <sup>2</sup>Advanced Research Institute for Natural and Technology, Osaka City University, Osaka, Japan*

## 1. Introduction

Ga<sub>2</sub>O<sub>3</sub> (Gallium oxide) photocatalyst is known to promote CO<sub>2</sub> reduction with water to produce CO, H<sub>2</sub> and O<sub>2</sub> under UV light irradiation. In previous works [1, 2], it has been reported that Ag loading on Ga<sub>2</sub>O<sub>3</sub> as co-catalyst significantly improves the photocatalytic activity for CO<sub>2</sub> reduction to CO. However, the role of Ag co-catalyst is unclear. In order to clarify the role of Ag, it is necessary to control and to know chemical and physical characters of Ag loaded Ga<sub>2</sub>O<sub>3</sub> (Ag/Ga<sub>2</sub>O<sub>3</sub>). In preliminary work, we have found that the aggregation and dissolution of Ag were suppressed with using reducing agent of methanol solution. In this study, we have investigated the effect of methanol addition in water on photocatalytic CO<sub>2</sub> reduction with water over Ga<sub>2</sub>O<sub>3</sub> with Ag co-catalyst.

## 2. Experimental

Ag as co-catalyst was loaded on Ga<sub>2</sub>O<sub>3</sub> by an impregnation method (calcination; 2 h, in air, at 723 K). The loading amount of Ag was 1.0 wt%. In the photocatalytic reduction tests, the prepared sample (0.1 g) was dispersed into either “1 M NaHCO<sub>3</sub>” or “1 M NaHCO<sub>3</sub>+ 20 vol% methanol” aqueous solution (10 mL) under CO<sub>2</sub> gas flow (3.0 mL/min) and irradiated with photons given by a 300 W Xe lamp. Reaction products dominated with CO, H<sub>2</sub> and O<sub>2</sub> were analyzed by GC-TCD. The loading state of Ag nanoparticles were investigated by UV-vis DR measurements and SEM.

## 3. Results and discussion

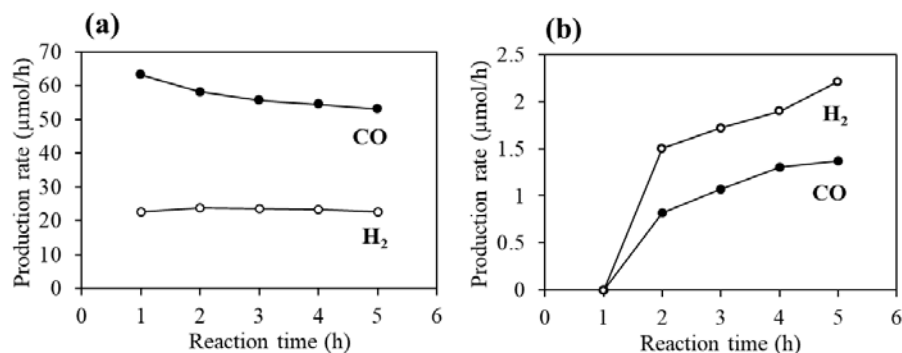
Fig. 1 compares results of photocatalytic CO<sub>2</sub> reduction tests, (a) with or (b) without methanol. One can clearly see that the addition of methanol significantly increased the production rates of CO and H<sub>2</sub> with stable rates. Without methanol, the production rates were very small, though they were gradually increasing.

Fig. 2 compares UV-vis DR spectra of Ag/Ga<sub>2</sub>O<sub>3</sub> sample before and after 5 hours' reaction. Strong absorption below 290 nm and broad

peak around 430 nm were assigned to band gap transition of Ga<sub>2</sub>O<sub>3</sub> and localized surface plasmon resonance (LSPR) of Ag nanoparticles, respectively. Before the reaction test, no peak corresponding to LSPR of Ag appeared, indicating loaded Ag by the impregnation method on Ga<sub>2</sub>O<sub>3</sub> was not likely metallic but probably existing as a composite oxide with Ga [3]. After the reaction with methanol, the LSPR peak became larger. This suggests that the addition of methanol enhanced reduction of Ag to make metallic nanoparticles and also inhibited elution of Ag. It should be mentioned that UV-vis spectra for Ag/Ga<sub>2</sub>O<sub>3</sub> samples in "1 M NaHCO<sub>3</sub>+ 20 vol% methanol" aqueous solution rapidly changed to that given in Fig.2 (b) and afterward no appreciable change appeared. Without methanol, reduction of the composite oxide with Ga or formation of Ag nanoparticles was suppressed as seen in Fig. 2(c). Still the reduction seems continuing to increase the photocatalytic activity during the reduction test. Thus, we have tentatively concluded that methanol assists the reduction of Ag deposited on Ga<sub>2</sub>O<sub>3</sub>, enhancing Ag nanoparticles formation and suppressing their aggregation or dissolution. The intensity of LSPR can be correlated to the photocatalytic activity, which should be studied quantitatively.

## References

- [1] K. Iizuka, T. Wato, Y. Misaki, K. Saito and A. Kudo, *J. Am. Chem. Soc.*, 2011, 133, 20863-20868
- [2] N. Yamamoto, T. Yoshida, S. Yagi, Z. Like, T. Mizutani, S. Ogawa, H. Nameki and H. Yoshida, *e-j. Surf Sci. Nanotech.*, 2014, 12, 263-268
- [3] M. Yamamoto, T. Yoshida, N. Yamamoto, Y. Yamamoto, S. Yagi and H. Yoshida, *J. Mater. Chem. A*, 2015, 3, 16810-16816



**Fig. 1** Production rates of CO and H<sub>2</sub> in photocatalytic CO<sub>2</sub> reduction tests for 5 hours. (a)with in 20 vol% methanol and (b)without methanol

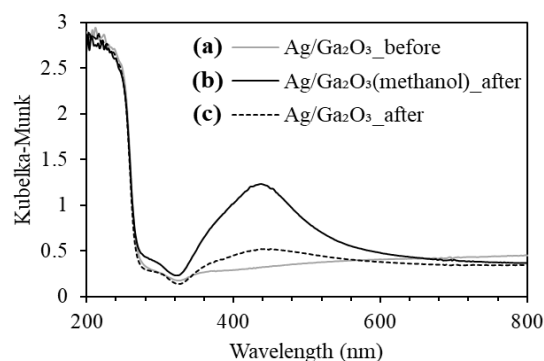


**Fig. 2** UV-vis DR spectra of Ag/Ga<sub>2</sub>O<sub>3</sub> sample, (a) before the reduction test, and after 5 hours reduction tests (b)with and (c)without methanol.

# Revealing Optimized Pure Platinum Shapes and Sizes for Enhanced Oxygen Electroreduction Efficiency

Marlon Rück<sup>\*, a</sup> & Alessio Gagliardi<sup>a</sup>

<sup>a</sup> Department of Electrical and Computer Engineering, Technical University of Munich,  
80333 Munich, Germany.

Reducing the Platinum loading, which is required for the oxygen reduction reaction (ORR), constitutes a huge obstacle toward economically viable commercialization of polymer electrolyte membrane fuel cells (PEMFCs). Tailored pure Pt nanostructured electrocatalysts harbor great potential to enhance the ORR activity [1], while keeping the high stability of state-of-the-art Pt/C commercial electrocatalysts [2]. Following the Sabatier principle, it is widely accepted that the ORR activity is decisively controlled by the adsorption energies of the reaction intermediates. Weakening the \*OH adsorption energy by  $\sim 0.1$ - $0.15$  eV with respect to Pt(111) improves the ORR activity, which has been shown by various experimental [3] and theoretical [1] studies.

Exposing that adsorption energies of ORR intermediates can be fine-tuned in unstrained pure Pt nanostructured electrocatalysts, Calle-Vallejo et al. have extended the geometrical concept of coordination numbers to second nearest neighbors [4]. The generalized coordination number (GCN) reveals fundamental design principles on how to tailor active single sites in pure Pt electrocatalysts. The large effects from atom coordination highlight that the interplay between shapes and sizes tunes the adsorption energies and, therefore, shapes and sizes rule the ORR activity.

In our present work, we combine site-specific design principles from theory with experimental studies to develop a computational model [4], which rapidly predicts ORR mass activities of nanostructured pure Pt electrocatalysts in precise agreement with experiments. Rapid prediction of mass activity is highly essential to identify optimal Pt nanostructures for efficient oxygen electroreduction.

Herein, we identify not only optimal nanoparticle sizes, but also shapes, for the oxygen electroreduction on PEMFCs with respect to high mass activity, controllable size distribution, and appropriate mechanical stability. Various kinds of symmetric

shapes are created mathematically by a continuously spanned parameter space. The Pt nanostructures are carefully optimized in shape and size toward highest mass activity by Particle Swarm Optimization. Theoretical single-atom-resolved size effect studies, which are performed for the most promising nanostructures, provide chemical routes for experimental synthesis (see Figure). Our computational screening of thousands of shapes and sizes predicts tailored Pt electrocatalyst shapes with high mass activities up to 3.86 A/mgPt, which corresponds to an enhancement of 700% over Tanaka commercial Pt/C electrocatalysts.

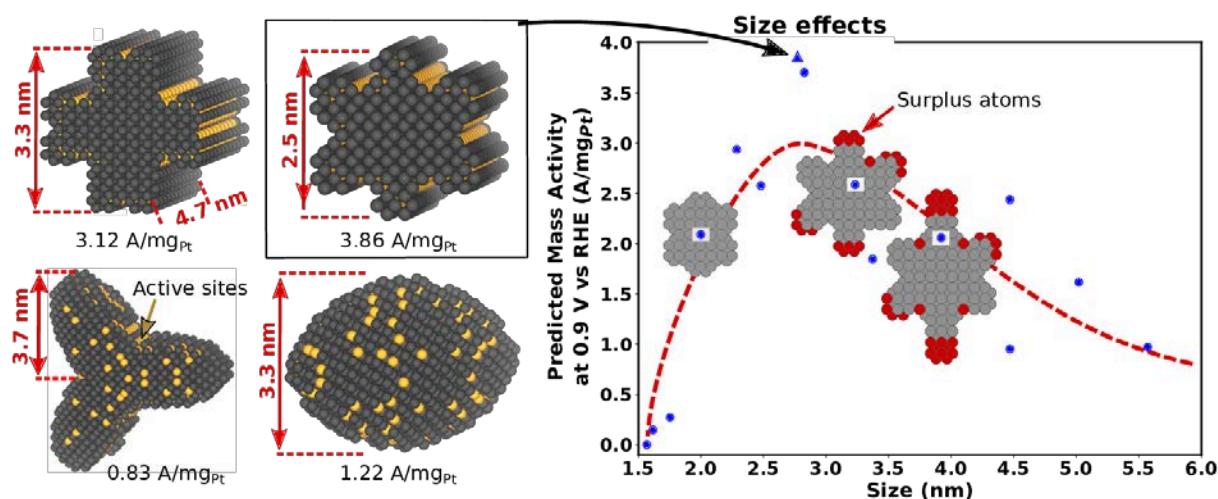


Figure: Optimized nanostructured Pt electrocatalysts (left). Size effects on the catalytic activity for the most active shape (right).

## References

- [1] F. Calle-Vallejo, J. Tymoczko, V. Čolić, Q.H. Vu, M.D. Pohl, K. Morgenstern, D. Loffreda, P. Sautet, W. Schuhmann & A.S. Bandarenka, *Science* (2015), 350, 6257.
- [2] B. Garlyyev, K. Kratzl, M. Rück, A.S. Bandarenka, A. Gagliardi, R. Fischer et al. (submitted).
- [3] V. Čolić, A.S. Bandarenka, *ACS Catalysis* (2016), 6, 8.
- [4] M. Rück, A. Bandarenka, F. Calle-Vallejo, A. Gagliardi, *J. Phys. Chem. Lett.* (2018), 9.



# Cracking of Hexane and Pentane over high density acid sites

## Al-rich BEA zeolites

*Dalibor Kaucký, Jaroslava Morávková, Jana Pastvová, Radim Pilař, Petr Sazama,  
J. Heyrovský Institute of Physical Chemistry, AS ČR, Prague, Czech Republic;*

### Introduction & Aim

The cracking and hydrocracking of linear alkanes into various low-molecular fragments/products represents an essential process during production of present gasoline fuels. Such cracking reactions carried out over zeolites represent alternative way to application of older bulk-based catalysts. The BEA zeolite is traditionally used in this field. This contribution is oriented to demonstrate the perspective of Al-rich BEA zeolites compared to conventional BEA zeolites and to enlarge understanding of the relation between location/concentration of active acid sites in these zeolites with their specific activity in cracking reactions.

### Experimental & Preparation Part

The classical BEA and Al-rich BEA zeolites (with molar Si/Al ratio ranging in 4-11), were synthesized using a hydrothermal method, using sodium aluminate as Al-source and fumed silica as Si-source; with or without organic template [1]. The synthesized materials were characterized by XRD, acidity analysis using FTIR, surface measurement and  $^{27}\text{Al}$  and  $^{29}\text{Si}$  MAS NMR analysis. The BEA materials were then subjected to catalytic cracking: in their mere acidic forms (i.e. without any further modification); prior to the reaction the activation preceded: in  $\text{O}_2$  and then in  $\text{H}_2+\text{N}_2$ ; the n-hexane and/or n-pentane cracking was then carried out in concentration 1mol% and nearly atmospheric pressure; all the products were analysed by on-line GC.

### Results

Broad range of cracking products was formed, with overall yield which decreased with time-on-stream, on scale of several hours. The cracking activity of Al-rich BEA exceeded the conventional BEA zeolites. The (TOF) catalytic activity was evaluated from time-of-stream measurements, by using extrapolated initial values of conversion. The series of time-of-stream measurements at temperature range 250-450°C were then used for an assessment of Activation energies. The corresponding

Arrhenius plots are depicted in the Fig. 1, where Al-rich BEA with conventional BEA is compared.

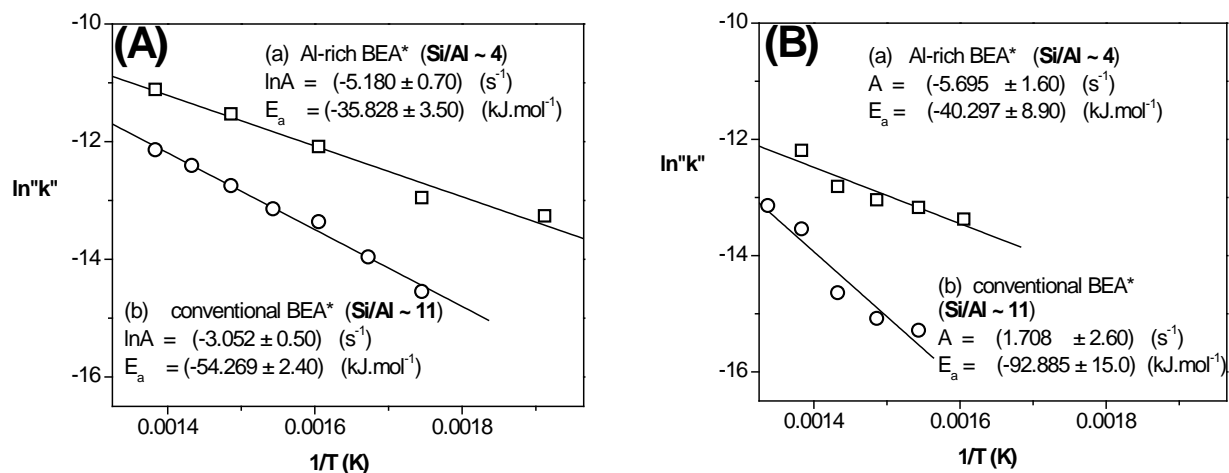


Figure 1. The Arrhenius plots of overall cracking rate, over Al-rich (Si/Al 4) BEA (a) compared with conventional Si/Al 11 BEA (b); in cracking of n-hexane (A) and cracking of n-pentane (B).

The activation energy for  $C_6$  cracking was cca  $-35 \text{ kJ.mol}^{-1}$  over Al-rich BEA and cca  $-55 \text{ kJ.mol}^{-1}$  over conventional BEA; the activation energy for  $C_5$  cracking was cca  $-40 \text{ kJ.mol}^{-1}$  over Al-rich BEA and cca  $-90 \text{ kJ.mol}^{-1}$  over conventional BEA (Fig. 1).

## Conclusion

The cracking activity of the Al-rich BEA was superior to the conventional BEA zeolites. The cracking activity was related to the acid sites in Al-rich BEA zeolites and represents the important key factor for their application as new active catalytic materials.

*Acknowledgement:* This work was supported by the Grant Agency of the Czech Republic under the Project No. 18-20303S and Technology Agency of the Czech Republic, grant Project No.TH03020184.

## References

[1] P. Sazama, B. Wichterlova, S. Sklenak, V.I. Parvulescu, N. Candu, G. Sadovska, J.Dedecek, P. Klein, V. Pashkova, P. Stastny, J. Catal. 318 (2014) 22–33.

# Stability in the catalytic performance of the sour water-gas shift

## Mo, W and Re supported catalysts

*D. Nikolova<sup>1</sup>, R. Edreva-Kardjieva<sup>1</sup>, M. Gabrovska<sup>1</sup>*

*Institute of Catalysis<sup>1</sup>, Bulgarian Academy of Sciences<sup>1</sup>, Sofia<sup>1</sup>, Bulgaria<sup>1</sup>;*

### Introduction

Sour water-gas shift catalyst design and development is expected to help increasing the versatility of the fuel production process. It has been shown in our previous findings that Mo-, W- and Re-based catalysts promoted with Ni, Co, and K are considered a promising catalyst for WGS reaction with S-containing feed [1-4].

In order to evaluate the stability in the catalytic performance the catalytic tests were proceeded at the reaction temperature 400°C in the S-free feed in order to enable a quick check of the effect of oxidizing agents as H<sub>2</sub>O vapour or CO<sub>2</sub> on the primarily formed active sulphide species, which directly reflects on the activity of the catalysts.

Single-component Mo, W and Re samples were prepared by incipient wetness impregnation of  $\gamma$ -Al<sub>2</sub>O<sub>3</sub> support. Their oxide weight content corresponds to a surface density of 2 atoms metal/nm<sup>2</sup> support, aiming formation of one and the same type of surface oxide species. Nickel or cobalt was added as a second component while potassium was introduced either as a second or third component in concentrations, namely 3 wt.% NiO or CoO and 5 wt.% K<sub>2</sub>O. The samples were pre-sulphided *in situ* through simultaneous sulphidation/reduction at atmospheric pressure with 6 vol.% H<sub>2</sub>S in H<sub>2</sub> at 400°C for 2 h at a gas hour space velocity (GHSV) of 2000 h<sup>-1</sup>. The reaction temperature of 400°C is chosen to take advantage of kinetics for greater reaction rate. The reaction was carried out in H<sub>2</sub>S absence feed at 400°C and steam/gas ratio 0.3, by varying the GHSV: 2000 h<sup>-1</sup> for 3 h; four-fold higher space velocity 8000 h<sup>-1</sup> for 2 h; returning to lower 2000 h<sup>-1</sup> for 1 h.

### Results and discussion

The general observation of the figures shows that the tri-component Mo-, W- and Re-based catalysts are most active. The potassium presence affected their reducibility.

Main results for the different systems are:

– KNiMo shows a trend toward a higher activity than KCoMo, however, the constant conversion value of KCoMo at the returning to 2000 h<sup>-1</sup> indicates more stability of the

active forms on the surface (Fig. 1). The simplest explanation is related to a higher instability of the Ni sulfide species in KNiMo;

– KCoRe shows higher activity than the KNiRe. The degree of conversion is preserved almost constant during the reaction and it is high till the end of the test (72%) (Fig. 2). It should be noted that the reason is the stability of the active forms on H<sub>2</sub>O vapour or CO<sub>2</sub> oxidation.

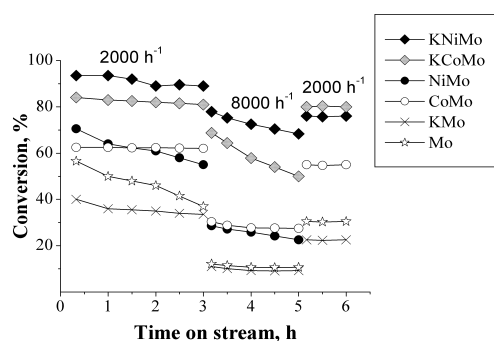


Fig. 1. Catalytic activity of the Mo-based samples

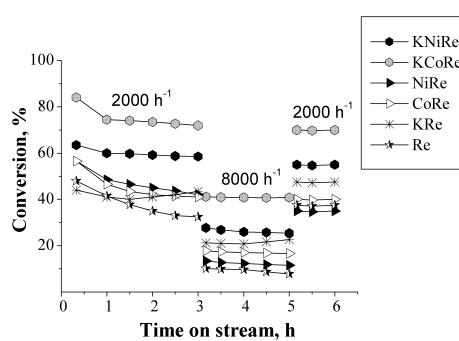


Fig. 2. Catalytic activity of the Re-based samples

– KCoW and KNiW rapidly lose initial activity (65–75%) and the conversion is quite low at the end of the test, about 20% (Fig. 3). Decrease in the degree of conversion evidences the partial oxidation of the primary formed sulfide species;

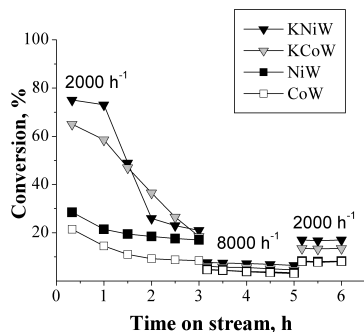


Fig. 3. Catalytic activity of the W-based samples

All the catalysts gained their initial activity after repeating the activation procedure (sulphidation/reduction step) thus demonstrating that catalyst deactivation is reversible.

## Conclusion

In conclusion, the reported results disclose that KCoMo and KCoRe catalysts are more stable and they possess the reproducible activity, which is an indication that no considerable physicochemical changes occurred in the active forms on the catalysts surface during reaction.

## References

- [1] D. Nikolova, R. Edreva-Kardjieva, G. Gouliev, T. Grozeva, P. Tzvetkov, *Appl Catal A General* 297 (2006) 135-144.
- [2] D. Nikolova, T. Grozeva, R. Edreva-Kardjieva, E. Serwicka. *Proceedings of the 9th Int. Conference on Fundamental and Applied Aspects of Physical Chemistry*, A. Antić-Jovanović (Ed.), Belgrade, Serbia, 2008, pp. 163-165.
- [3] D. Nikolova, R. Edreva-Kardjieva, T. Grozeva, *React. Kinet. Mech. Catal.* 103 (2011) 71-86.
- [4] D. Nikolova, R. Edreva-Kardjieva, E. Serwicka, R. Dula, T. Grozeva, *Appl. Catal. A: General* 480 (2014) 108-119.

# Co-based Fischer–Tropsch Catalysts with Different Heat Conductive Additives

*Sineva L.V., Kulchakovskaya E.V., Asalieva E.Yu., Gryaznov K.O., Mordkovich V.Z.,  
all — Technological Institute for Superhard and Novel Carbon Materials, Troitsk,  
Moscow, Russian Federation*

## Introduction

Fischer–Tropsch synthesis (FTS) is a highly exothermal process with 146–176 kJ released per a mole of carbon monoxide [1]. Although FTS is a key stage of some existing XTL technologies, the intra-catalyst heat transfer difficulties are still an obstacle for further progress in practical applications. In order to facilitate heat

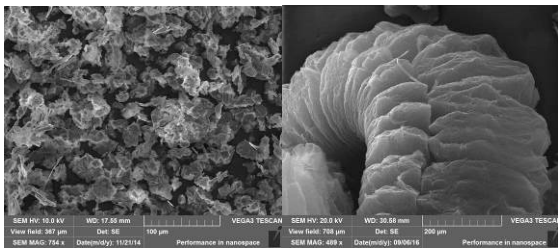


**Fig 1. SEM of thermally conductive additives: left — aluminum, right — graphite**

transfer one can introduce thermally conductive additives into a catalyst [2].

This work presents an experimental comparison of two different thermally conductive additives: aluminum metal and exfoliated graphite (Fig. 1). Aluminum metal was used as a powder comprising flakes of appr.  $20 \times 30 \times 1 \mu\text{m}^3$  size, while exfoliated

graphite particles were bigger, i.e. appr.  $150 \times 300 \times 160 \mu\text{m}^3$ .

## Experimental

A thermally conductive additive was introduced into a catalyst during preparation of paste for extrusion. The extrudates were calcined and then impregnated by aqueous solution of cobalt nitrate for getting 20% weight of Co in the ready catalyst. SEM

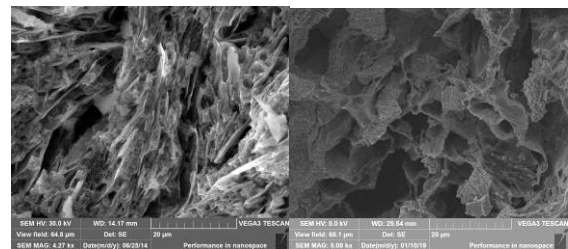


**Fig 2. SEM of catalysts surface: left — aluminum, right — graphite**

images of fractures of the ready catalysts show that the thermally conductive additives reveal their flaky structure (Fig. 2). The values of thermal conductivity were similar despite difference in the additive content as shown in Tab. 1.

**Table 1. Catalysts composition as prepared and its heat conductivity**

Catalysts	Composition, wt.%				Heat conductivity, W/(m·K)	
	Co	Zeolite	Binder	HT additive	Along the axis	Across the axis
AHB	20	24	16	40	6.8	3.6
GHB	20	34	23	23	7.9	3.6

## Results

**Table 2. Fischer–Tropsch synthesis rates (236°C, 20 MPa, GHSV — 4000 hr<sup>-1</sup>)**

Catalyst	CO conv., %	Selectivity, mol.%				Productivity, gC <sub>5+</sub> /(kgCat·hr)	Activity, mkmolCO/(s·gCo)
		CH <sub>4</sub>	C <sub>2</sub> –C <sub>4</sub>	C <sub>5+</sub>	CO <sub>2</sub>		
AHB	64	19	13	66	2	363	55
GHB	82	22	13	61	4	505	83

Tab. 2 summarizes some catalytic properties of the synthesized catalysts. It is obvious that graphite shows advantages in CO conversion, activity and productivity

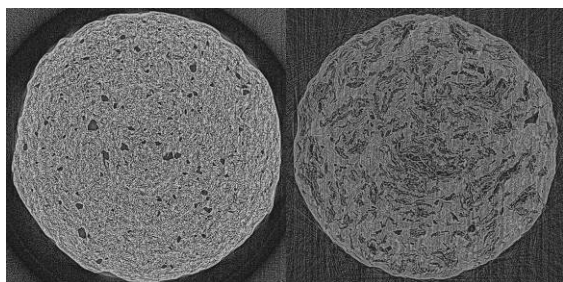


**Fig 3. X-ray tomography of catalysts surface: left — aluminum, right — graphite**

without significant selectivity loss. Supposedly it is explained by different macropore structure as revealed by Fig. 3, where X-ray tomography technique helped in identification of interesting slit pores in graphite-based catalysts. The slit pores of GHB provide better conditions for both heat- and mass-transfer in the catalyst.

Another interesting observation is lower contribution of olefins, iso-paraffins and C<sub>5</sub>–C<sub>10</sub> hydrocarbons into liquid FTS product in case of GHB. It maybe a circumstantial evidence of better heat removal as the mentioned hydrocarbons are the product of temperature-induced secondary transformations. (Tab. 3).

**Table 3. C<sub>5+</sub> composition, wt.% (236°C, 20 MPa, GHSV — 4000 hr<sup>-1</sup>)**

Catalyst	C <sub>n</sub> H <sub>2n</sub>	n-C <sub>n</sub> H <sub>2n+2</sub>	i-C <sub>n</sub> H <sub>2n+2</sub>	C <sub>5</sub> –C <sub>10</sub>	C <sub>11</sub> –C <sub>18</sub>	C <sub>19+</sub>
AHB	36	33	31	84	16	0
GHB	30	46	24	78	21	1

## Conclusions

The comparative investigation of FTS catalysts with different heat conductive additives revealed advantages in performance of exfoliated graphite-based catalysts due to high thermal conductivity and extended slit macropore system.

## References

- [1] Steynberg A.P. Fischer–Tropsch Technology / A.P. Steynberg, M.E. Dry Elsevier Science & Technology. **2004**. — 722 p.
- [2] Asalieva E., Gryaznov K., Kulchakovskaya E., Ermolaev I., Sineva L., Mordkovich V. // Appl Cat A, 2015, v. 505, p.260-266

# Oxygenate Formation over K/ $\beta$ -Mo<sub>2</sub>C Catalysts

## Role of Preparation and Promotion

Wijnand Marquart<sup>1</sup>, David J. Morgan<sup>2</sup>, Graham J. Hutchings<sup>2</sup>, Michael Claeys<sup>1</sup>,

Nico Fischer<sup>1</sup>

<sup>1</sup>DST-NRF Centre of Excellence in Catalysis c\*change and Department of Chemical Engineering, University of Cape Town, Cape Town, South Africa

<sup>2</sup>Cardiff Catalysis Institute, School of Chemistry, Cardiff University, Cardiff, UK

### Introduction

The Fischer-Tropsch synthesis (FTS), producing long chained waxes and transportation fuels, is competing directly with fuels derived from crude oil, and its profitability is therefore dependent on the global crude price [1]. However, increasing the value of synthesized products could render the profitability of the FTS independent of the volatility of the oil market. Oxygenates have been identified as target species as they are platform chemicals which can be converted to industrial chemicals or polymers. While they are a typical by-product of the FTS, selectivity limitations of the commonly employed catalysts do not support commercial FTS based technologies producing oxygenates at a significant yield [2].

Typically, transition metals such as Fe, Co, Rh and Ni are active for the FT synthesis. Depending on reaction conditions employed, commercial Fe and Co based catalysts have been shown to produce between 6 and 12 C% oxygenates [3]. Rh has been demonstrated to have a higher oxygenate selectivity, but the associated high raw material cost becomes prohibitive for use as a commercial FTS catalyst [4]. Catalysts other than the traditionally known active compounds have also shown promising results. Transition metal carbides such as Mo<sub>2</sub>C, were investigated under CO hydrogenation conditions. While the bare carbide produces mainly methane and other hydrocarbons, upon promotion with potassium the selectivity is reported to shift towards oxygenates [5].

### Results and Discussions

$\beta$ -Mo<sub>2</sub>C was obtained via carburization of MoO<sub>3</sub> in a mixture of methane and hydrogen at different temperatures. It could be confirmed by TEM, Raman and detailed XPS analysis, that the formation of carbon deposits increases with

increasing temperature. In the absence of the carbon layer, samples re-oxidized to MoO<sub>2</sub> upon exposure to air at room temperature. A mild passivation treatment in 1% O<sub>2</sub> in N<sub>2</sub> prevented the bulk re-oxidation. Selected carbides were subsequently promoted with up to 6.2 wt.-% potassium through impregnation.

Compared to pristine β-Mo<sub>2</sub>C, the CO conversion of passivated & subsequently reactivated and of the carbon coated catalysts is significantly lower. Interestingly, at iso-conversion, the passivated sample showed an eight times higher oxygenate content in the organic product while at the same time displaying a higher CO<sub>2</sub> selectivity and a lower methane selectivity. The composition of the oxygenate fraction remained relatively constant with 74-79 C% MeOH. This change in selectivity is possibly linked to the introduced oxidic Mo species evidenced by Raman, supporting a different mechanistic pathway. Upon promotion with K, the CO conversion of the catalyst decreased in parallel to an increase in CO<sub>2</sub> and a decrease in CH<sub>4</sub> selectivity. The amount of potassium added did not influence the performance within the studied range (1.9 to 6.2 wt.-%). The oxygenate fraction in the organic product also increased upon promotion. The composition of the oxygenate fraction changes drastically. While still dominated by the alcohols, ethanol is now the most prominent product with significant amounts of aldehydes detected at lower conversion levels.

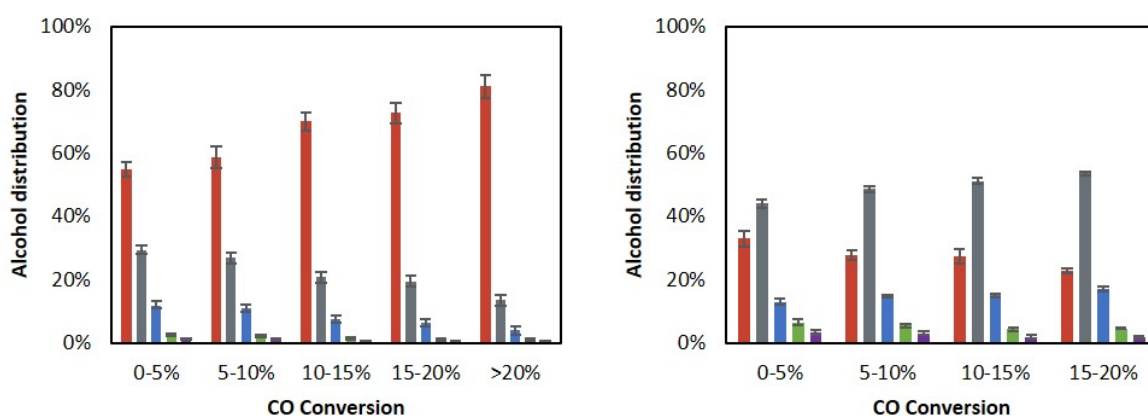


**Figure 1.** Alcohol distribution over the unpromoted samples (left) and the promoted samples (right) as a function of the CO conversion. From left to right per series methanol (red, #1), ethanol (grey, #2), propanol (blue, #3), C4 alcohols (green, #4) and C5+ alcohols (purple, #5).

## References

1. Dry, M.E., *Catal. Tod.*, 227, 71 (2002).
2. Klimkiewicz, R., *Chem. Central J.*, 77, 8 (2014).
3. Klerk, A.d., *Energy & Env. Sci.*, 1177, 4 (2011).
4. Forzatti, P., Tronconi, E., and Pasquon I., *Catal. Rev.*, 109, 33 (1991).
5. Woo, H.C., et al., *Appl. Catal.*, 267, 75 (1991).



# Hydrocracking of perhydrophenanthrene over Pt-modified zeolite catalysts : products distribution and reaction pathways

*L. Brito, G. Pirngruber, E. Guillon, F. Albrieux, IFP Energies Nouvelles, Solaize, France; J. Martens, KU Leuven, Leuven, Belgium*

Hydrocracking is used for the conversion of heavy oil cuts into lighter fractions, for instance, the processing of Vacuum Gas Oil into middle distillates. Vacuum Gas Oil is in large majority composed of cyclic molecules (aromatics and naphthenes) and paraffins. The latter have been extensively studied in literature. Regarding naphthenes, their hydrocracking reactions, as in the case of alkanes, follow the rules of carbenium ion chemistry. Several works have studied the hydroconversion of bicyclic structures, in particular decalin and its isomers [1]. Polycyclic naphthenes undergo isomerization and endocyclic cracking, i.e. opening of a cycle, but the last naphthenic ring is mainly kept intact, due to orbital constraints. As a consequence of this steric effect, substituted naphthenes with at least 10 carbon atoms go through what is called Paring reactions: the alkyl chain isomerizes until a favored configuration for exocyclic cracking is achieved, producing a smaller naphthene and a paraffin. In contrast, scarce literature is provided for hydrocracking of tricyclic naphthenes, and their reaction pathways are even more complex. This work aims to study the hydrocracking of polycyclic naphthenes over Pt-modified zeolites shaped with alumina.

Catalytic tests were performed in a continuous fixed bed reactor, under high hydrogen pressure, by using perhydrophenanthrene ( $C_{14}H_{24}$ ) as a model feedstock. The saturated molecule was obtained after the *in situ* hydrogenation of the parent aromatic compound, phenanthrene ( $C_{14}H_{10}$ ). Two large pore acid zeolite catalysts, USY (CBV720) and Beta (CP814e), with hydrogenating function provided by Pt, were compared in the hydrocracking of perhydrophenanthrene. The reaction generates up to 300 compounds and their precise identification is essential to constitute the reaction pathways involved in this complex network. This was achieved thanks to an analytic method specially conceived for this application, based on coupling GCxGC to FID and MS detections.

An important step after a thorough analysis of each product consists in the lumping in families (figure 1). The main families observed in the hydroconversion of perhydrophenanthrene were composed of alkyladamantanes, the most stable isomers of perhydrophenanthrene [2] and rarely reported in bifunctional catalysis; ring-opening products (ROP, i.e. products with two rings and 14 carbon atoms); and cracked naphthenes presenting 12 or less carbon atoms. At high conversion, a small production of isoparaffins ( $nC \leq 6$ ) was also noticed.

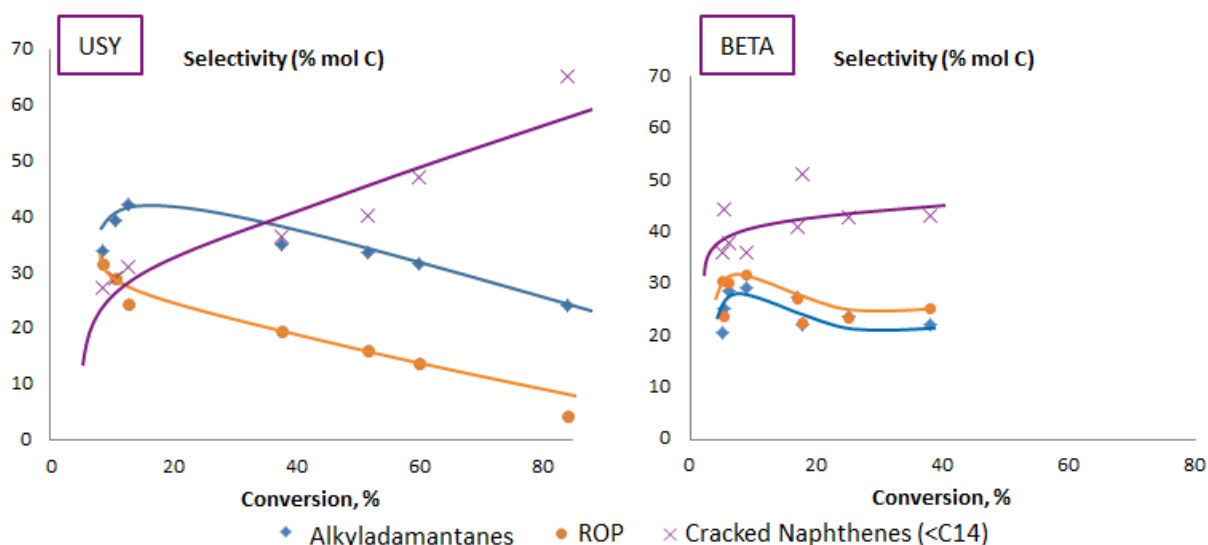


**Figure 1.** Selectivity as a function of conversion for USY and Beta catalysts.

Primary products consisted of alkyladamantanes and ring-opening compounds on both zeolites. A higher selectivity to the former was observed on USY-based catalysts. This has been attributed in literature to the larger pores of USY [3], which could better accommodate the tricyclic structure. Regarding ring-opening products, different intermediates were observed on USY and Beta catalysts, which could explain the different product distribution obtained for each zeolite. In fact, cracking distribution on Beta is mainly centered on C7 while USY generates a broader carbon number distribution. The results clearly show that the zeolite pore structure has a huge impact on reactivity and product distribution.

These aspects as well as a comparison between Pt and sulfide-based catalysts on hydrocracking of perhydrophenanthrene will be presented at the meeting.

## References

- [1] Kubička D et al., *J. Catal.* 2004, 227 (2), 313-327.
- [2] Schneider A, Warren RW, Janoski EJ, *J. Org. Chem* 1966, 31, 1617–1625.
- [3] Wang L, Chen Y, Jin S, Chen X, Liang C, *Energy & Fuels* 2016, 30, 4, 3403-3412

# CO<sub>2</sub> hydrogenation on Cu and Pd monometallic and bimetallic nanoparticles supported on ZnO

*Klaus Dobrezberger, Julian Stropp, Julie Neuhauser; Anna Aspalter; Martin Huber; Karin Föttinger; Günther Rupprechter*

*Technische Universität Wien / Institute of Materials Chemistry, Vienna, Austria*

Cu/ZnO and Pd/ZnO nanoparticle catalysts have been widely studied for hydrogenations. In this work, ZnO supported Cu and Pd nanoparticle catalysts are used for CO<sub>2</sub> hydrogenation and the dependence on parameters such as temperature, pressure and reduction temperature were analyzed. Palladium is more active than copper and forms a PdZn phase at higher reaction temperatures. Alloying cannot be observed with copper. Sintering effects were observed by electron microscopy. Palladium initially has smaller particles than copper, but they sinter strongly. The long-term stability was also investigated and it was concluded that all catalysts have relatively good stability over the reaction time. At atmospheric pressure mainly CO was formed, whereas at a pressure of 20 bar also methane and traces of methanol were produced.

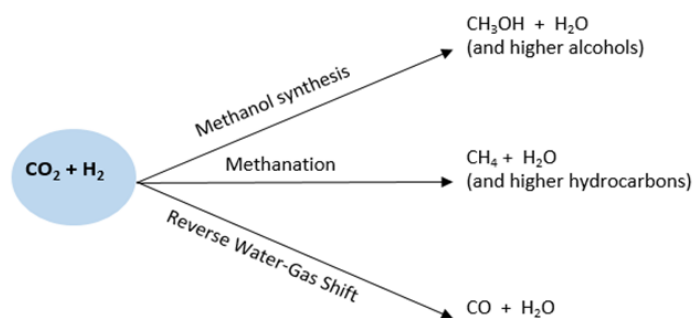


**Fig. 1** Main pathways for the hydrogenation of CO<sub>2</sub>.

These pathways are related to temperature, pressure and

## 1. Introduction and summary

The increased use of CO<sub>2</sub> to produce higher quality chemicals may be a future approach for recycling CO<sub>2</sub>. Cu and Pd particles on different supports (oxides) can serve for this purpose, with ZnO being frequently used. Cu is often commercially applied but has the disadvantage that it oxidizes and is less catalytically active than palladium. Palladium, on the other hand, is expensive. Therefore, a way should be found to combine the positive aspects of both metals and to minimize their disadvantages. For this purpose, besides monometallic catalysts (Cu/ZnO, Pd/ZnO), bimetallic PdCu catalysts, in particular, were produced, characterized and kinetic tests were performed for the hydrogenation of CO<sub>2</sub> to various products [1], [2]. The selectivity of the reaction depended on the reaction temperature, the pressure and

the respective catalyst. Since  $\text{CO}_2$  is a thermodynamically stable molecule, high temperatures but also the oxide are required for activation. The formation of PdZn alloys, which form in Pd/ZnO catalysts, also plays a role for the catalytic activity [3], [4].

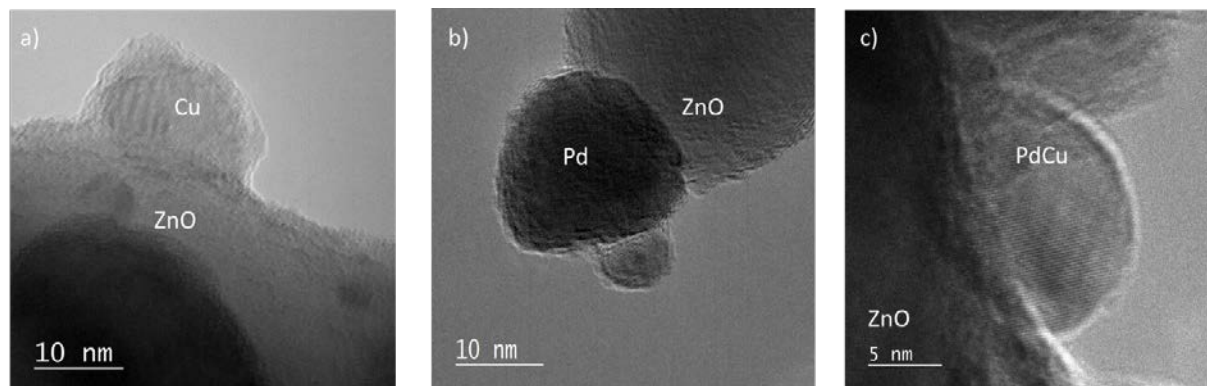


**Fig. 2** HR-TEM images of Cu/ZnO (a), Pd/ZnO (b) and PdCu/ZnO (c) nanoparticle catalysts

In bimetallic (PdCu) systems a different selectivity of  $\text{CO}_2$  hydrogenation to CO or  $\text{CH}_4$  can be often observed [5]. In order to better describe the dependence on pressure and (reaction and reduction) temperature, type of support and metal, various methods were tested in the context of this work, including HR-TEM, STEM-HAADF, TPD, TPR and XRD.

**Acknowledgments:** Supported by the Austrian Science Fund (FWF) via Doctorate School Solids4Fun (W1243) and SFB FOXSI (F4502-N16).

## References

- [1] X. Jiang, N. Koizumi, X. Guo, and C. Song, "Bimetallic Pd-Cu catalysts for selective  $\text{CO}_2$  hydrogenation to methanol," *Appl. Catal. B Environ.*, vol. 170–171, pp. 173–185, 2015.
- [2] J. Díez-Ramírez, J. A. Díaz, P. Sánchez, and F. Dorado, "Optimization of the Pd/Cu ratio in Pd-Cu-Zn/SiC catalysts for the  $\text{CO}_2$  hydrogenation to methanol at atmospheric pressure," *J. CO<sub>2</sub> Util.*, vol. 22, no. September, pp. 71–80, 2017.
- [3] H. H. Holzapfel, A. Wolfbeisser, C. Rameshan, C. Weilach, and G. Rupprechter, "PdZn surface alloys as models of methanol steam reforming catalysts: Molecular studies by LEED, XPS, TPD and PM-IRAS," *Top. Catal.*, vol. 57, no. 14, pp. 1218–1228, 2014.
- [4] K. Föttinger and G. Rupprechter, "In situ spectroscopy of complex surface reactions on supported Pd-Zn, Pd-Ga, and Pd(Pt)-Cu nanoparticles," *Acc. Chem. Res.*, vol. 47, no. 10, pp. 3071–3079, 2014.
- [5] W. Zhu *et al.*, "Morphological and Compositional Design of Pd-Cu Bimetallic Nanocatalysts with Controllable Product Selectivity toward  $\text{CO}_2$  Electroreduction," *Small*, vol. 14, no. 7, pp. 1–7, 2018.

# A Computational investigation of OME-synthesis through homogeneous acid catalysis

*Tiago Gonçalves, Karlsruhe Institute of Technology, Karlsruhe, Germany; Felix Studt, Karlsruhe Institute of Technology, Germany; Philipp Pleßow, Karlsruhe Institute of Technology, Germany*

Oxymethylene Dimethyl Ethers (OMEs) are promising candidates as diesel fuel additives since they lead to lower soot and NO<sub>x</sub> emissions.[1-3] OMEs are made from methanol and formaldehyde, both of which intermediates that can be based on renewable feedstocks. The most common route for the synthesis of OMEs is via polymerization of formaldehyde derivatives in the presence of methanol[4].

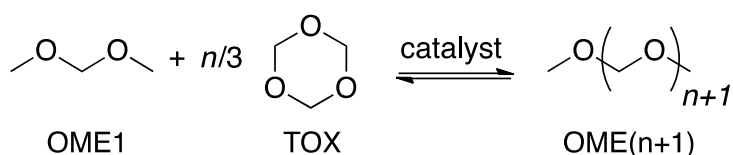


**Figure 1:** OME(n+1) synthesis from TOX and OME1

Different catalysts, such as acidic zeolites, homogeneous acids such as sulfuric acid as well as ion exchanged sieves have been explored. Ab initio and density functional theory (DFT) calculations will be performed to shed light on the reaction mechanism of the synthesis of OMEs from TOX and OME1 and the influence of the presence and the strength of a Brønsted acid.

## Computational Methods

All structures considered use MP2/def2-TZVPP//PBE0-D3/dhf-SV(P) energies, with the RI approximation. Geometry optimization, singlepoints, transition state scan using the TRIMM algorithm and a thermodynamic analysis at T=300K were performed using the TURBOMOLE program package. Whereas for the Free energy correction in solution, the GAMESS-US program package using the SMD solvation model was employed with a reference concentration of 1 mol/L, using the M06 functional and the cc-pVTZ basis-set. Additional calculations with PBC were performed using ASE with the VASP program package, the PAW method and the PBE-D3 functional.

## Current Results and Discussion

In our investigation, we assume that a Brønsted acid (HA) acting as precatalyst is able to protonate the reactant OME1, thus creating OME1-H<sup>+</sup> and that the corresponding base (A<sup>-</sup>) is not exerting a significant influence. With this assumption, acids differ only in their ability to protonate OME1. We can therefore discuss the reaction mechanism starting from OME1-H<sup>+</sup> and study the influence of acid strengths on the reaction mechanism through variation in HA. Figure 2 shows the computed free energy diagram for the initial reaction of OME1 with TOX to OME4. This reaction starts from A11 (OME1) with an additional CH<sub>2</sub>-OMe cation bound to one of its oxygens. The free energies are referenced to A11 (G=0). Additionally, various potential precatalysts, such as the Brønsted acids HCl and H-BEA and methylated DME (trimethyl oxonium cation) are shown. The free energies of these precatalysts are related to A11 and X1 through the reaction shown.

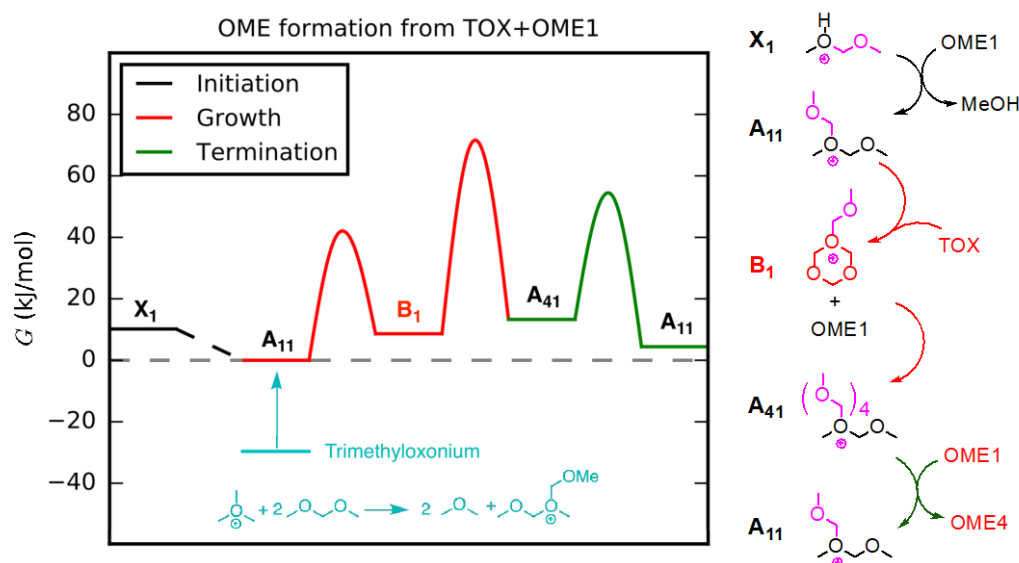


**Figure 2:** Gibbs free energy diagram at  $T = 300$  K, using MP2 with def2-TZVPP basis-set, for the catalytic formation of OME4.

## References

1. Lautenschütz, L., et al., *Physico-chemical properties and fuel characteristics of oxymethylene dialkyl ethers*. *Fuel*, 2016. **173**: p. 129-137.
2. Burger, J., et al., *Poly(oxymethylene) dimethyl ethers as components of tailored diesel fuel: Properties, synthesis and purification concepts*. *Fuel*, 2010. **89**(11): p. 3315-3319.
3. Haltenort, P., et al., *Heterogeneously catalyzed synthesis of oxymethylene dimethyl ethers (OME) from dimethyl ether and trioxane*. *Catalysis Communications*, 2018. **109**: p. 80-84.
4. Goncalves, T.J., et al., *Theoretical Investigation of the Acid Catalyzed Formation of Oxymethylene Dimethyl Ethers from Trioxane and Dimethoxymethane*. *ACS Catalysis*, 2017. **7**(5): p. 3615-3621.

# Facile preparation of CoO<sub>x</sub>@graphene composite as efficient electrocatalysts for hydrogen evolution reactions

*Xinyue Liu, Sun Yat-sen University, Guangzhou 510275, Guangdong, P. R. China; Guowei Yang, Sun Yat-sen University, Guangzhou 510275, Guangdong, P. R. China.*

Hydrogen evolution reaction (HER) is an appropriate candidate for converting renewable energy to clean hydrogen fuel<sup>[1]</sup>. Exploring highly efficient, stable and cost-effective electrocatalysts with high performances for sustainable HER is still a big challenge<sup>[2]</sup>. Herein, a facile and novel strategy is developed to synthesize amorphous cobalt oxides and graphene composite (CoO<sub>x</sub>@Gr) on carbon cloth. The composite electrocatalyst was prepared using a room-temperature chemical gel deposition and photochemical method. UV light irradiation caused condensation and densification of cobalt oxides film by photochemical activation at room temperature. The synergistic effect of the CoO<sub>x</sub> and graphene provided higher electrochemical activity<sup>[3][4]</sup>. The resulting CoO<sub>x</sub>@Gr composite electrocatalyst exhibits significantly outstanding catalytic activity, with an overpotential of 104.4 mV to deliver a current density of 10 mA/cm<sup>2</sup> in 0.1 KOH electrolyte. Further, the electrocatalyst displays good stability for 20000 cycles. These findings make amorphous transition metal oxides and graphene composite as promising electrocatalytic materials for HER, thus opening the perspective to design other efficient amorphous transition metal oxides used as electrocatalysts.

**Keywords** hydrogen evolution; CoO<sub>x</sub>@Gr composite; photochemical method; electrocatalyst



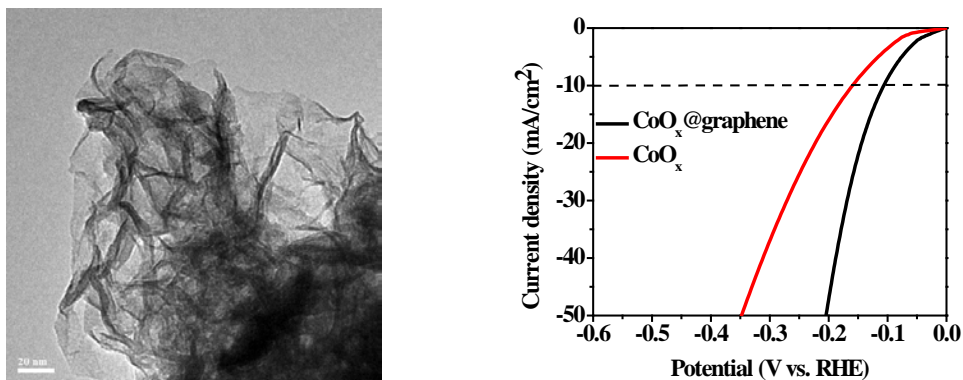


Figure 1 (a) TEM image of  $\text{CoO}_x$  sample. (b) Linear sweep voltammetry curves of  $\text{CoO}_x@\text{Gr}$  and  $\text{CoO}_x$  samples at 10 mV/s in 0.1 M KOH.

## Acknowledgements

The National Basic Research Program of China (2014CB931700), Guangdong province (20170918) and State Key Laboratory of Optoelectronic Materials and Technologies supported this work.

## References

- [1] Seh, Z. W.; Kibsgaard, J.; Dickens, C. F.; Chorkendorff, I.; Norskov, J. K.; Jaramillo, T. F. Combining theory and experiment in electrocatalysis: insights into materials design. *Science* 2017, 355, 146-148.
- [2] Dias, P.; Schreier, M.; Tilley, S. D.; Luo, J.; Azevedo, J.; Andrade, L.; Bi, D.; Hagfeldt, A.; Mendes, A.; Grätzel, M. Transparent cuprous oxide photocathode enabling a stacked tandem cell for unbiased water splitting. *Adv. Energy Mater.* 2016, 5, 1501537.
- [3] Yan, X.; Tian, L.; He, M.; Chen, X. Three-dimensional crystalline/amorphous  $\text{Co}/\text{Co}_3\text{O}_4$  core/shell nanosheets as efficient electrocatalysts for the hydrogen evolution reaction. *Nano Lett.* 2015, 15, 6015-6021.
- [4] Wei, Z.; Wang, J.; Mao, S.; Su, D.; Jin, H.; Wang, Y.; Xu, F.; Li, H.; Wang, Y. In situ generated  $\text{CoO}-\text{Co}_3\text{O}_4/\text{N}$ -doped carbon nanotubes hybrids as efficient and chemoselective catalysts for hydrogenation of nitroarenes, *ACS Catal.* 2015, 5, 4783–4789.

# Diffusion of symmetric molecules through H-SSZ-13 and H-ZSM5

*Ashley Smith, Philipp N. Plessow, Felix Studt*

*Institute of Catalysis Research and Technology (IKFT), Karlsruhe, Germany*

## Introduction

Our society depends heavily on crude oil as chemical feedstock and for use as a transportation fuel. With crude oil being both finite and its combustion environmentally detrimental, renewable alternatives need to be found. The methanol-to-hydrocarbons (MTH) process is a promising approach to produce fuels from methanol, which itself can be synthesized from biogas via syngas. Acidic zeolites such as H-SSZ-13 can be used as catalyst for the MTH process. While the reaction kinetics at the active site [1] are one important part of the kinetics, diffusion limitations impose another constraint leading to so-called shape selectivity. While it may be obvious for very small or very large molecules that they can diffuse very easily or not at all through the pores of a given zeolite, things are less clear for intermediate cases. Here, explicit calculation of diffusion barriers can help to determine the mobility of these species.

## Methods

The diffusion [2] of straight chain branched and aromatic molecules through the rings of both H-SSZ-13 [3] and H-ZSM5 is investigated using periodic density functional theory calculations at the PBE-D3 level of theory. The dimer method, NEB and constrained optimizations are employed to obtain transition states. The molecules are chosen to have incrementally increasing Van der Waals diameters.

## Results and Discussion

When large molecule pass through the pore, the zeolite needs to distort significantly and often a high-energy intermediate is found, where the diffusing species is stuck inside the pore with two transitions state leading towards stable minima within the two adjacent cavities.

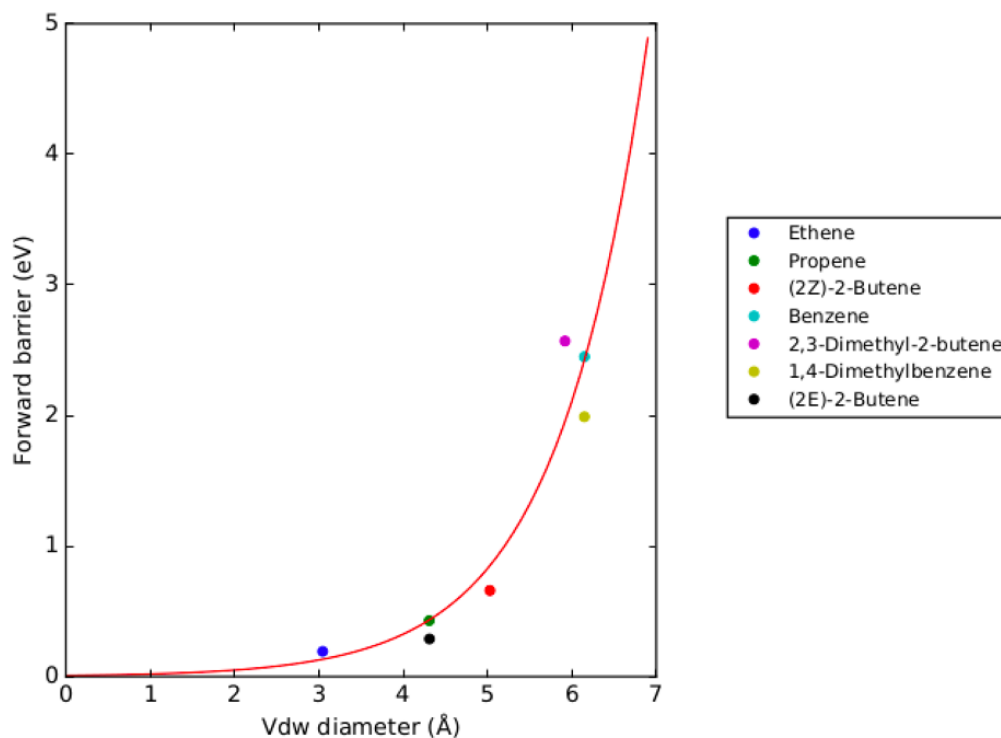


Figure 1: The relationship between Van der Waals diameter and diffusion barrier in H-SSZ-13 for a selection of symmetric molecules involved in the MTO process

An exponential correlation between the diffusion barrier and the molecular size is found.

$$E(r) = a * e^{br} \quad (1)$$

In the H-SSZ-13 system molecules with a Van der Waals diameter larger or equal to 6 Å are extremely unlikely to pass through the pores.

### References

- [1] Philipp N. Plessow ; Felix Studt, ACS Catalysis, **2017**, 7 (11), 7987-7994
- [2] J. Kärger, S. Vasenkov, Microporous and Mesoporous Materials, **2005**, 85 (3), 195-206
- [3] Wang, C. M.; Wang, Y. D.; Du, Y. J.; Yang, G.; Xie, Z. K., Catal. Sci. Technol, **2015**, 5, 4354-4364

# Water-Gas Shift activity of Gold-containing Layered Double Hydroxides

*M. Gabrovska<sup>1</sup>, T. Tabakova<sup>1</sup>, I. Ivanov<sup>1</sup>, Institute of Catalysis<sup>1</sup>, Bulgarian Academy of Sciences<sup>1</sup>, Sofia<sup>1</sup>, Bulgaria<sup>1</sup>;*

*D. Kovacheva<sup>2</sup>, Institute of General and Inorganic Chemistry<sup>2</sup>, Bulgarian Academy of Sciences<sup>2</sup>, Sofia<sup>2</sup>, Bulgaria<sup>2</sup>*

## Introduction

The water-gas shift reaction (WGSR,  $\text{CO} + \text{H}_2\text{O} \leftrightarrow \text{CO}_2 + \text{H}_2$ ) is a classical industrial catalytic process traditionally used for hydrogen generation by conversion of CO in H<sub>2</sub>-rich gas streams. The development of fuel-cell processors and the need of high-purity hydrogen stimulated a great activity in the design of novel, highly active and stable WGS catalysts. A very recent review summarized the recent advances in the application of Au-based catalysts for WGSR at low temperatures [1]. It was also established that co-precipitated NiAl layered double hydroxides (LDH) with takovite-like (TKI) structure, alone or promoted by Mg were active catalysts for medium-temperature WGSR [2].

The aim of this work was to combine the favorable features of LDH and supported gold nanoparticles in design of novel catalytic systems of improved efficiency for WGSR. The catalytic behavior and structure of the co-precipitated NiMgAl ( $(\text{Ni}^{2+} + \text{Mg}^{2+})/\text{Al}^{3+} = 2.5$ ) and Mg-free NiAl ( $\text{Ni}^{2+}/\text{Al}^{3+} = 2.5$ ) were compared with those of the same Au-promoted materials. The samples were characterized by Powder X-ray diffraction (PXRD) technique before and after WGSR.

## Results and discussion

The CO conversion over the studied catalysts as a function of the temperature during WGSR is represented in Fig. 1. The comparison of the activity discloses that NiAl catalyst shows 98.8% CO conversion at 260 °C, while NiMgAl demonstrates lower CO conversion of 30.8 % at the same temperature. The deposition of Au over NiMgAl markedly improves the WGS activity, namely 86% CO conversion is achieved over Au-NiMgAl at 260 °C. Nevertheless, the promoting effect of Au is clearly presented by Mg-free Au-NiAl catalyst which displays CO conversion of 97.6 % at 240 °C, a value almost equal to the CO equilibrium conversion degree. PXRD patterns of the fresh samples comprise reflections of the takovite structure (Fig. 2a). The presence of Mg in NiMgAl sample provokes partial amorphization of the TKI structure

evidenced by the mean crystallite sizes of the TKI phase: 11 nm for NiAl and 8.7 nm for NiMgAl, respectively. The deposition of Au on both samples prompts appearance of additional reflections of Au<sup>0</sup> phase.

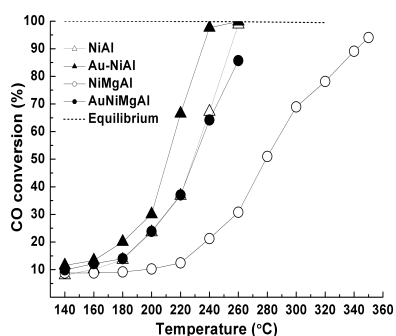


**Fig. 1.** WGS activity.

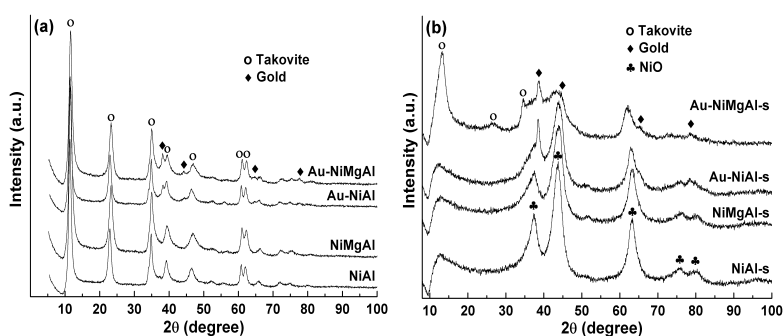


**Fig. 2.** PXRD patterns of the fresh (a) and spent (b) samples.

PXRD patterns of the spent catalysts (Fig. 2b) display reflections of cubic NiO phase, better pronounced in NiAl-s as well as Au<sup>0</sup> phase in Au-containing catalysts. A collapse of the layered structure occurred accompanied by the appearance of NiO phase during the WGS tests. The large amount of water vapor in the reaction mixture causes partial hydroxylation of the NiO surface leading to formation of Ni(OH)<sub>2</sub> and NiOOH structures, containing Ni<sup>2+</sup> and Ni<sup>3+</sup> cations, respectively. Participation of these structures in the redox WGS is associated with occurrence of a reversible redox transition between the active nickel species (Ni<sup>2+</sup> ↔ Ni<sup>3+</sup>). The appearance of some diffraction lines of TKI phase in Au-NiMgAl-s catalyst is due to the property of the mixed oxides generated from LDHs to regenerate the initial layered structure in the presence of H<sub>2</sub>O and CO<sub>2</sub>. The lesser amount of Ni<sup>2+</sup> ions on the catalyst surface may explain the lower activity of Au-NiMgAl catalyst. Additional textural and surface analyses are in progress in order to clarify the parameters governing the WGS activity.

## Conclusion

The WGS activity is strongly affected by the amount of nickel in the catalysts. An optimal surface Ni<sup>2+</sup>/Ni<sup>3+</sup> ratio as well as the adsorption and activation of CO molecule on the gold particles contributed to improved WGS performance.

**Acknowledgements** This work was supported by the Bulgarian Ministry of Education and Science under the National Research Programme E+: Low Carbon Energy for the Transport and Households, Grant agreement D01-214/2018.

## References

- [1] J.H. Carter, G.J. Hutchings, *Catalysts*, 8 (2018) 627-642.
- [2] M. Gabrovska, R. Edreva-Kardjieva, V. Idakiev, B. Kunev, *Bulg. Chem. Commun.*, 34(3/4) (2002) 395-404.

# CO<sub>2</sub> hydrogenation to methanol under dynamic conditions

*Holger Ruland, Kevin Kähler, Robert Schlögl*

*Max Planck Institute for Chemical Energy Conversion, Mülheim a.d. Ruhr, Germany*

## Introduction

Depleting fossil resources and a rising greenhouse effect due to CO<sub>2</sub> emissions require alternative processes to provide a sustainable feedstock for future utilization.<sup>1</sup> A promising route seems to be the optimization of common industrial processes with respect to the altered requirements. Because of the still growing world-wide demand for methanol as fuel as well as bulk chemical, a combination of the usage of CO<sub>2</sub>-rich exhaust gases, e.g. from steel mills, with hydrogen from renewable energy sources for the synthesis of methanol bears good prospects for an economical application.<sup>2,3</sup> Nevertheless, the incorporation of renewable resources within this process chain will cause dynamic changes of synthesis conditions. Their impact on the commercial ternary Cu-based catalyst is not sufficiently investigated. Therefore, to optimize the overall process with respect to the altered requirements coming along with the implementation of renewable energies, their impact on the performance and stability of the catalyst has to be worked out.

## Experimental

In the present work the influence of dynamic changes of reaction parameters on an industrial Cu/ZnO/Al<sub>2</sub>O<sub>3</sub> catalyst in CO<sub>2</sub> hydrogenation was investigated. Catalyst testing was performed in a flow set-up with a fixed bed reactor. The products are condensed at 5 °C and reaction pressure for subsequent offline analysis by GC-MS. Time-on-stream measurements were performed up to 1000 h with frequent switches between defined reaction parameters. Switches usually were carried out every 24 h. The parameters considered for these variations were mainly temperature, pressure, residence time as well as the partial pressures of CO<sub>2</sub> and H<sub>2</sub>. For comparison a measurement at constant reaction conditions was performed. In addition to switches from one day to another, also fast switches every 15 minutes were applied for the variation of the H<sub>2</sub> partial pressure. Here, the switching experiment was monitored by an IR detector, while at reference conditions the products were condensed and analyzed offline.

## Results

In Figure 1 the results obtained at reference conditions for several switching experiments are shown. After a strong deactivation in the beginning of CO<sub>2</sub> hydrogenation, most likely because of sintering of the Cu particles, the methanol production rate at 30 bar and 250 °C reaches a nearly steady state in the end of the investigated period. Comparing the methanol productivity at reference conditions derived from the switching experiments to the reference test, similar productivities for methanol were observed. As a conclusion, dynamic switches in the investigated regimes during CO<sub>2</sub> hydrogenation to methanol do not accelerate the deactivation of an industrial Cu/ZnO/Al<sub>2</sub>O<sub>3</sub> catalyst independent of the time period modified conditions were applied.

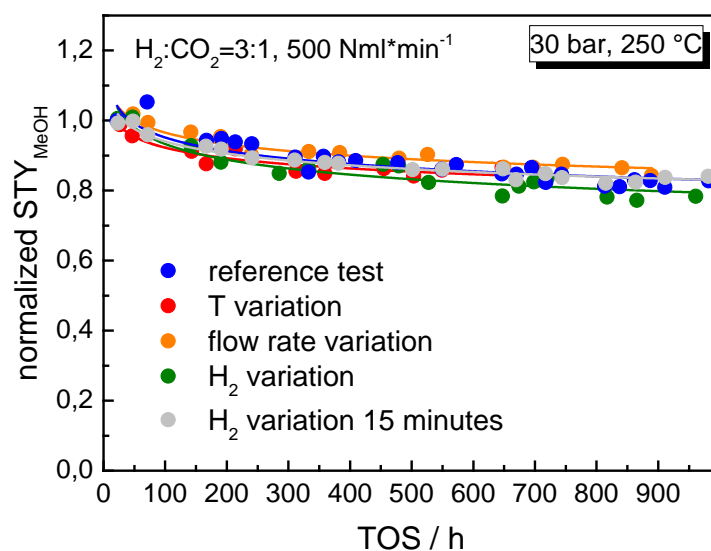


**Figure 1:** Normalized space-time yields for methanol over Cu/ZnO/Al<sub>2</sub>O<sub>3</sub> catalyst at reference conditions for several switching experiments.

## Acknowledgement

Carbon2Chem is funded by the Federal Ministry of Education and Research (Bundesministerium für Bildung und Forschung, BMBF). Support code: 03EK3039D.

## References

1. C. Song, *Catal. Today* **2006**, *115*, 2-32.
2. G.A. Olah, *Angew. Chem. Int. Ed.* **2005**, *44*, 2636-2639.
3. M. Kauw, R.M.J. Benders, C. Visser, *Energy* **2015**, *90*, 208-217.

# Reaction Intensification through Layer Management

Heiner Schwarz, Sebastian Werner, Stephan J. Reitmeier, Stefan Gebert, Andreas Reitzmann: Clariant, Heufeld/Munich, Germany;

Nga Thi Quynh Do, Stephane Haag, Veronika Gronemann, Timm Schuhmann, Tobias Oelmann, Martin Gorny: Air Liquide, Frankfurt a.M., Germany

## Increasing MeOH reactor performance by loading optimized catalyst schemes

The methanol synthesis from synthesis gas over CuO/ZnO/Al<sub>2</sub>O<sub>3</sub> catalysts is a process of prominent industrial relevance. Clariant (CL, formerly Süd-Chemie) and Air Liquide (AL) have been collaborating in this field for many years and have successfully investigated together the possibility of improving performance of an industrial methanol catalyst and reactor, e.g. increasing space time yield, catalyst lifetime, conversion and selectivity. CL also offers high performance catalyst solutions for selective oxidations, i.e. the PhthaliMax<sup>®</sup> product series for production of phthalic anhydride and the FAMAX<sup>®</sup> product series for the production of formaldehyde for which layer management (LM) concepts as technology are successfully applied [1,2,3]. The know-how gathered from this technology is transferred to the methanol production process by tailoring the catalyst layers according to the changing process conditions over the reaction path.

The AL E&C's reactor systems (water- and gas-cooled reactor) are already the benchmark for per pass conversion and heat management but are typically loaded with a single catalyst type only. The utilization of those reactors can be further intensified by applying the LM technology while improving the reaction rates over the reaction path thus optimizing temperature profile and selectivity. The potential of the LM approach has been confirmed in studies [4,5] and test campaigns in dedicated pilot plants of AL.

At first glance, this concept is attractive for methanol producers who are interested in a catalyst lifetime and/or methanol capacity extension as a simple refill solution for an existing plant. Furthermore, it has a game-changing potential for stand-alone plants in future. This application is another example of successful cross-market technology transfer and joint-development between an engineering company and a catalyst provider working in close collaboration.

## References

- [1] Robert Marx, 2012, doctoral thesis, Clausthal University of Technology, *Kinetics of the Selective Oxidation of o-Xylene to Phthalic Anhydride*
- [2] C. Gueckel, H. Dialer, M. Estenfelder, W. Pitschi, WO 2006/092305 A1, *Method for producing a multi-layer catalyst for obtaining phthalic anhydride*; C. Gueckel, M. Niedermeier, M. Estenfelder, WO 2006/125468 A1, *Multi-layered catalyst for producing phthalic anhydride*
- [3] M. Estenfelder, R. Zaino, WO 2010/076246 A1, *Improved process for oxidation on fixed catalytic bed of methanol to formaldehyde*
- [4] H. Schlichting, P.M. Hackel, T. Wurzel, WO 2011/101081 A1, *Process for preparing methanol*
- [5] HJ. Freund, R. Frind, T. Henkel, M. Kaiser, T. Schuhmann, W. Seuffert, S. Werner, WO 2018/149811 A1, *Reactor and Method for Maximizing Methanol Yield by Using Catalyst Layers*



# Effects of preparation conditions on the catalytic activity of chicken eggshell catalysts for the transesterification of oils to biodiesel

***Stefan Pavlović<sup>1\*</sup>, Dalibor Marinković<sup>1</sup>, Biljana Milovanović<sup>2</sup>, Milan Kostić<sup>3</sup>,  
Margarita Gabrovska<sup>4</sup>, Dimitrinka Nikolova<sup>4</sup>, Miroslav Stanković<sup>1</sup>***

<sup>1</sup>University of Belgrade, Institute of Chemistry, Technology and Metallurgy, Njegoševa 12, 11000 Belgrade, Serbia

<sup>2</sup>Alumina Ltd., Zvornik, Bosnia and Herzegovina

<sup>3</sup>University of Niš, Faculty of Technology, Bulevar oslobođenja 124, 16000 Leskovac, Serbia

<sup>4</sup>Institute of Catalysis, Bulgarian Academy of Sciences, Acad. G Bonchev 11, 1113 Sofia, Bulgaria

\*Corresponding author: [stefan.pavlovic@ihm.bg.ac.rs](mailto:stefan.pavlovic@ihm.bg.ac.rs)

*Eggshell based catalysts were synthesized by calcination (600 and 900 °C, 4 h) of raw and re-hydration (RH) modified (RH-temperature of 80 °C, S/L ratio of 1/5, and RH-time of 6 h) eggshell. After RH-treatment, the sample underwent calcination at 600 °C, 4 h. Obtained catalysts were characterized by XRD, SEM, N<sub>2</sub>-physisorption, and Hg-porosimetry, whereas the catalytic activity was analyzed in a batch reactor (reaction temperature of 60 °C, sunflower oil/methanol molar ratio of 1/12, and catalyst concentration of 4 wt.%). The concentration of fatty acid methyl esters (FAMES) was determined by HPLC. The reaction has reached equilibrium (FAME > 97%) with re-hydrated catalyst for 1.5 h, whereas with catalyst calcined at 900 °C for 4 h.*

## 1. Scope

CaO-based catalysts are known as highly active, easily accessible and low price catalytic materials and are widely used for the transesterification of vegetable oils to biodiesel [1]. Catalysts, derived from biological resources as raw waste materials such as egg, oyster or clam shells may be suitable sources of calcium, which can be easily converted into CaO. The catalytic activity of such materials generally depends on the catalyst preparation conditions [2, 3]. In the present study, the influence of thermal activation by calcination and re-hydration involving calcination-hydration-dehydration-calcination steps on the activity of the catalysts derived from the raw chicken eggshell (ESR) in the transesterification of the sunflower oil to biodiesel were studied.

## 2. Results and discussion

XRD patterns showed (Fig. 1) that the ESR is converted into active form at 900 °C, whereas modified calcined form is converted at 600 °C. The hysteresis loop

corresponds to type III (Fig. 2), characteristic for the non-rigid aggregate of plate-like structure (SEM micrograph). Textural properties and catalyst activity of prepared catalysts presented in Table 1 show that thermal and re-hydration treatment lead to significant improvement in the porous structure (specific surface and pore diameter).

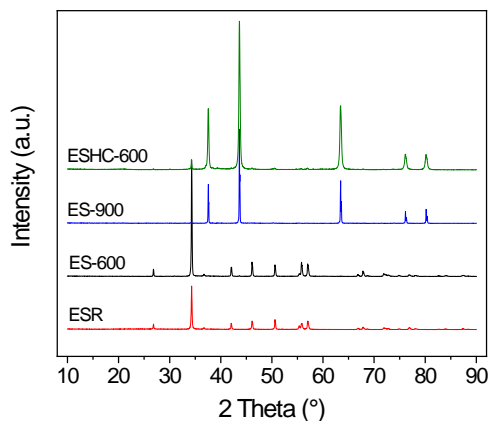


Figure 1. XRD patterns of synthesized catalysts

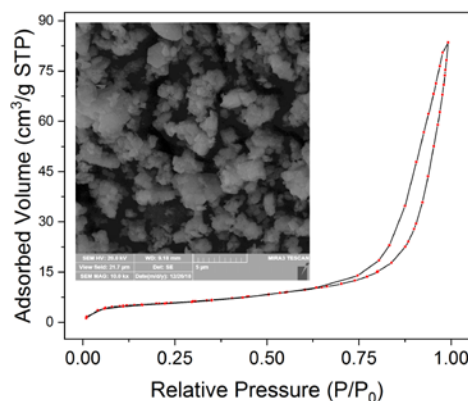


Figure 2. BET adsorption-desorption isotherms and SEM micrographs of ESHC-600

Table 1. Textural properties and activity of prepared catalysts from chicken eggshell

Sample	ESR	<sup>a</sup> ES-600	<sup>b</sup> ES-900	<sup>c</sup> ESHC-600
<i>Textural properties</i>				
<sup>d</sup> S <sub>BET</sub> (m <sup>2</sup> /g)	<1	-	<1	<b>19.3</b>
<sup>e</sup> D <sub>p,av,BJH</sub> (nm)	8.7	-	28.0	<b>17.0</b>
<sup>f</sup> V <sub>p,BJH</sub> (mm <sup>3</sup> /g)	0.9	-	0.7	<b>121.2</b>
<sup>g</sup> P (vol.%)	29.8	27.0	55.2	<b>73.6</b>
<i>Catalytic activity</i>				
<sup>h</sup> FAME (%)	0.0	0.0	46.5	<b>97.4</b>

<sup>a,b</sup>ES-t-eggshell calcined at 600 and 900 °C; <sup>c</sup>ESHC-600-eggshell calcined at 900 °C-re-hydrated-calcined at 600 °C; <sup>d</sup>S<sub>BET</sub>-specific surface; <sup>e</sup>D<sub>p,av,BJH</sub>-average pore diameter; <sup>f</sup>V<sub>p,BJH</sub>-pore volume; <sup>g</sup>P-porosity; <sup>h</sup>FAME (%) after 1.5h.

### 3. Conclusions

Non-active carbonate form obtained from eggshell can be converted to the active oxide form by means of a thermal treatment. However, thermal treatment combined with re-hydration leads to catalysts with more favourable structural and morphological properties and with a significant improvement in the catalytic activity. The high FAME concentration (>97%) is achieved with ES-900 and ESHC-600 catalysts for different reaction time, 4 and 1.5 h, respectively.

### Acknowledgements

This work was supported by the Ministry of Education, Science and Technological Development of the Republic of Serbia within the framework of the project III 45001.

### References

- [1] D.M. Marinković, M.V. Stanković, A.V. Veličković, J.M. Avramović, M.R. Miladinović, O.O. Stamenković, V.B. Veljković, D.M. Jovanović, *Renew. Sust. Energ. Rev.* **2016**, *56*, 1387-1408.
- [2] R. Risso, P. Ferraz, S. Meireles, I. Fonseca, J. Vital, *Appl. Catal. A-Gen.* **2018**, *56*, 56-64.
- [3] S. Niju, K.M. Meera, S. Begum, N. Anantharaman, *J. Saudi. Chem. Soc.* **2014**, *18(5)*, 702-706.

# **Alloy stability and its role in the enhanced oxygen resistance of a Ni<sub>3</sub>Fe/Al<sub>2</sub>O<sub>3</sub> catalyst during dynamic CO<sub>2</sub> methanation**

M.-A. Serrer<sup>1,2</sup>, K. F. Kalz<sup>1,2</sup>, E. Saraçlı<sup>1,2</sup>, H. Lichtenberg<sup>1,2</sup>, J.-D. Grunwaldt<sup>1,2</sup>

<sup>1</sup>Institute for Chemical Technology and Polymer Chemistry, <sup>2</sup>Institute of Catalysis Research and Technology, both Karlsruhe Institute of Technology (KIT), Germany

## **Introduction**

Future energy supply concepts with stronger contributions from renewable sources call for long-term storage systems for excess renewable energy [1]. In this context power-to-X (P2X) concepts have recently attracted growing attention. One solution is to store the excess energy in methane, as a chemical energy carrier (“power-to-gas” concept). Renewable H<sub>2</sub> from electrochemical water splitting, and CO<sub>2</sub>, e.g. from industrial exhaust gases, can be used as reactants in this catalytic process, for which Ni-based catalysts have been extensively studied [2]. Recently it was reported that catalysts based on a bimetallic Ni-Fe alloy displayed enhanced long-term stability and higher conversion under stationary reaction conditions compared to monometallic Ni-based catalysts [3, 4]. In the present study, we investigated the stability of a Ni<sub>3</sub>Fe alloy and its influence on the oxygen resistance in comparison to a Ni/Al<sub>2</sub>O<sub>3</sub> catalyst under dynamically operated methanation conditions by using combined *operando* X-ray absorption spectroscopy (XAS) and X-ray diffraction (XRD).

## **Results and Discussion**

Structural changes in the Ni<sub>3</sub>Fe alloy during *operando* XAS and XRD studies at atmospheric pressure between 250 °C and 450 °C are displayed in Figure 1. The Fe-K edge X-Ray absorption near edge structure (XANES) spectra clearly show a correlation between increasing temperature and the relative concentration of oxidized Fe<sup>2+</sup> species in the sample. The shift of the Ni (200) reflection in the XRD data from 2 $\Theta$  = 16.02° to 2 $\Theta$  = 16.05° upon an increase in temperature from 250 °C to 450 °C proves, according to Vegard’s law, that the formation of the Fe<sup>2+</sup> species is accompanied by dealloying (Figure 1, right). Surprisingly, no change in the catalytic activity was observed upon depletion of Fe in the Ni-Fe alloy, although Ni<sub>3</sub>Fe is assumed to be very active for CO dissociation [5]. Thus, an enhanced dissociation of CO and CO<sub>2</sub> on the Ni<sub>3</sub>Fe surface might not be the only reason for the overall better performance.

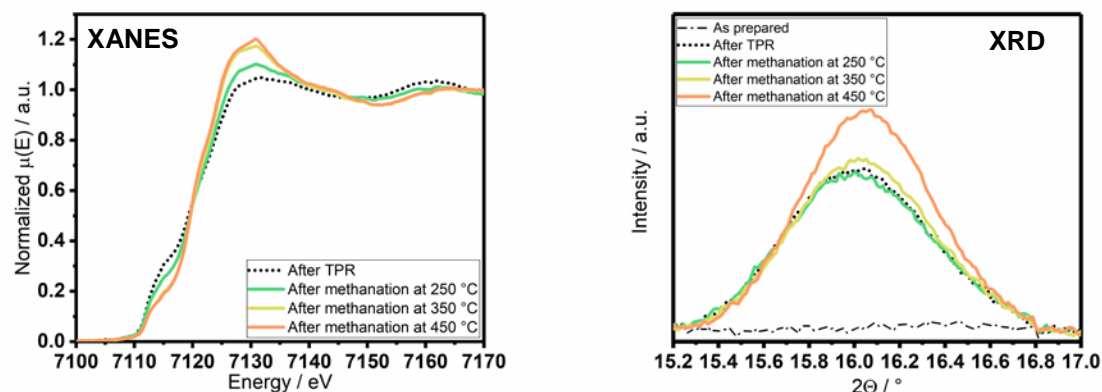


Figure 1. *Operando* Fe-K edge XANES spectra (left) and XRD data (right) of the Ni<sub>3</sub>Fe/Al<sub>2</sub>O<sub>3</sub> catalyst during methanation of CO<sub>2</sub> at 250 °C, 350 °C and 450 °C at atmospheric pressure.

To gain a deeper insight into the mechanism of dealloying and the overall catalyst stability under dynamic conditions, we performed combined XAS- and XRD-experiments during H<sub>2</sub> dropouts using technical grade gases (CO<sub>2</sub>: O<sub>2</sub> < 0.5 ppm; N<sub>2</sub>: O<sub>2</sub> < 10 ppb), as well as O<sub>2</sub>-purified gases (O<sub>2</sub> < 0.1 ppm, O<sub>2</sub>-trap by *Restek*). Using technical grade CO<sub>2</sub>, the reduced Ni species in the Ni-Fe alloy were more stable and less prone to oxidation than the corresponding Ni species in the monometallic Ni catalyst during H<sub>2</sub> dropout. In the Ni<sub>3</sub>Fe/Al<sub>2</sub>O<sub>3</sub> catalyst the initial Ni oxidation state and performance was retained during the methanation cycle following to the H<sub>2</sub> dropout.

We can conclude that during methanation of CO<sub>2</sub>, as well as under H<sub>2</sub> dropout conditions, Fe migration to the surface occurs along with Fe<sup>2+</sup> formation, resulting in dealloying of Ni<sub>3</sub>Fe. The fact that we did not observe any loss of activity indicates that the Fe-rich surface protects the active Ni-species from deactivation by oxidation. This results in an overall better performance and stability of the Ni<sub>3</sub>Fe/Al<sub>2</sub>O<sub>3</sub> catalyst during dynamically operated methanation of CO<sub>2</sub>, which not only makes it an attractive system for P2X applications but also sheds new light on the mechanism.

## References

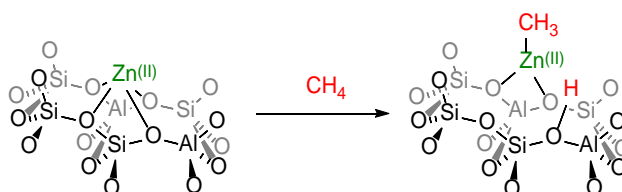
- [1] K. F. Kalz, R. Kraehnert, M. Dvoyashkin, R. Dittmeyer, R. Gläser, U. Krewer, K. Reuter, J.-D. Grunwaldt, *ChemCatChem* **2017**, *9*, 17-29.
- [2] B. Mutz, H. W. P. Carvalho, S. Mangold, W. Kleist, J.-D. Grunwaldt, *J. Catal.* **2015**, *327*, 48-53.
- [3] B. Mutz, M. Belimov, W. Wang, P. Sprenger, M.-A. Serrer, D. Wang, P. Pfeifer, W. Kleist, J.-D. Grunwaldt, *ACS Catal.* **2017**, *7*, 6802-6814.
- [4] C. Mebrahtu, F. Krebs, K. Simeonov, S. Abate, S. Perathoner, G. Centi, R. Palkovits, *Chem. Ing. Tech.* **2016**, *88*, 1261-1261.
- [5] M. P. Andersson, T. Bligaard, A. Kustov, K. E. Larsen, J. Greeley, T. Johannessen, C. H. Christensen, J. K. Nørskov, *J. Catal.* **2006**, *239*, 501-506.

# METHANE ACTIVATION AND FUNCTIONALISATION IN ZEOLITES

*Meera Shah, Durham University, Durham, UK; Russell Taylor, \* Durham University, Durham, UK*

The direct and efficient conversion of hydrocarbon resources to higher value products remains a major goal, both academically and industrially. While catalysts for the conversion of methane and light alkanes to aromatics using metal impregnated zeolites are well known,<sup>[1,2]</sup> developing zeolite catalysts that can effectively convert methane and light alkanes to oxygenated hydrocarbons such as alcohols remains a major challenge.<sup>[3]</sup> Recently, the first low temperature, catalytic, direct conversion of methane to methanol in the presence of oxygen has been reported to occur over a Cu-H-ZSM-5 catalyst. The process demonstrated good selectivity for methanol formation (70%), but a low turnover – 1.6 turnovers in 300 hours.<sup>[4]</sup> This highlights the success of CuO in zeolites functionalising C-H bonds catalytically, but indicates the need for further improvement in these processes.

To date, the development of a direct, catalytic conversion of methane to methanol has not been achieved over Zn/ZSM-5. However, extraframework Zn(II) cations within the micropores of ZSM-5 have been reported to activate methane at room temperature and the resulting  $[\text{Zn-CH}_3]^+$  species (shown in Scheme 1).<sup>[5]</sup> This species has been shown to undergo subsequent functionalisation, as monitored by solid-state NMR spectroscopy.<sup>[6]</sup>



**Scheme 1: Activation of methane over extra framework Zn(II) forming  $[\text{Zn-CH}_3]^+$  and a new Brønsted acid site.**

Methane activation on zinc modified ZSM-5, prepared by both zinc vapour deposition (VD) and ion exchange (IE), has been previously explored.<sup>[7,8]</sup> However, to date, no studies have been reported to elucidate the role of the zeolite framework in the activation and functionalisation of methane by Zn(II) cations. Using <sup>13</sup>C CP MAS NMR spectroscopy studies, we have shown activation of the C-H bond of methane within zinc exchanged FER and MOR zeolite frameworks alongside ZSM-5. The  $[\text{Zn-CH}_3]^+$  species was observed through a distinctive -19 ppm signal in the NMR

spectrum (Figure 1). This  $[\text{Zn-CH}_3]^+$  species also shows differing reactivity, depending on the framework, when subsequently exposed to  $\text{O}_2$ .

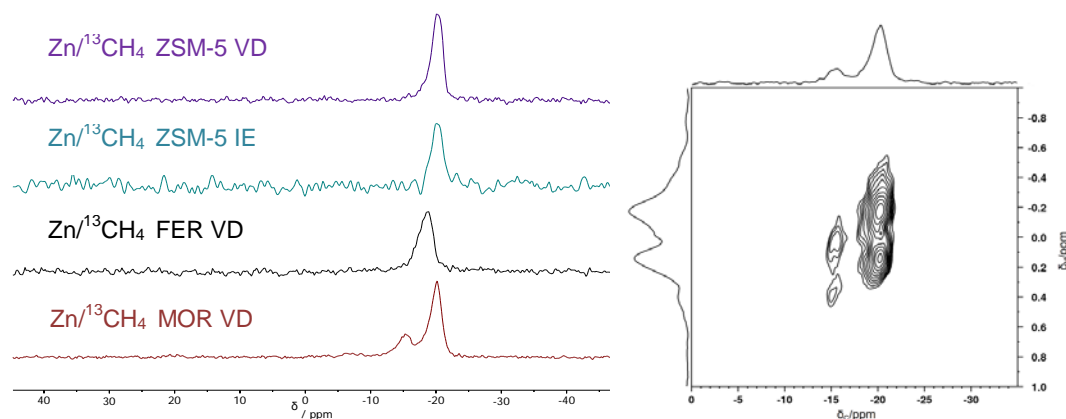


**Figure 1:** Left:  $^{13}\text{C}$  CP MAS NMR spectra showing a characteristic peak at around -19 ppm for the  $[\text{Zn-CH}_3]^+$  species for ZSM-5, MOR and FER. Right:  $^1\text{H}$ - $^{13}\text{C}$  heteronuclear correlation (HETCOR) MAS NMR spectrum for Zn/ $^{13}\text{CH}_4$  MOR indicating two distinct  $[\text{Zn-CH}_3]^+$  environments.

Additionally, a second signal was observed in the  $[\text{Zn-CH}_3]^+$  range at -15 ppm for Zn/MOR. Evidence from further NMR studies (Figure 1) highly suggest that the two peaks observed in the  $^{13}\text{C}$  NMR spectrum of MOR correspond to  $[\text{Zn-CH}_3]^+$  species contained within the two different framework environments of MOR, the 12MR channel and the 8MR side pocket. These two distinctive  $[\text{Zn-CH}_3]^+$  species demonstrate differing rates of reaction with small molecules due to confinement effects of the different environments within the zeolite framework.

Catalysis of methane using these zinc modified zeolites for the production of aromatics in flow was tested both with and without the addition of small molecules such as acetone. These results from methane activation and functionalisation studies illustrate critical properties of zinc based zeolite catalysts.

## References

- [1] C. Coperet Chem. Rev. 2010, 110, 656
- [2] A. I. Olivos-Suarez *et al.*, J. ACS Catalysis 2016, 6, 2965.
- [3] P. Tomkins *et al.*, Angew. Chem. Int. Ed., 2016, 55, 5476
- [4] K. Narsimhan *et al.*, ACS Cent. Sci., 2016, 2, 424
- [5] J. Xu *et al.*, Chem. Sci. 2012, 3, 2932
- [6] J. Wu *et al.*, Chem. Eur. J. 2010, 16, 14016
- [7] A. Gabrienko *et al.*, J. Phys. Chem. C. 2015, 119, 24910
- [8] A. Oda *et al.*, J. Phys. Chem. C. 2013, 117, 19525

# Effect of the Crystallographic Phase of Ruthenium Nanosponges on Arene and Substituted-Arene Hydrogenation Activity

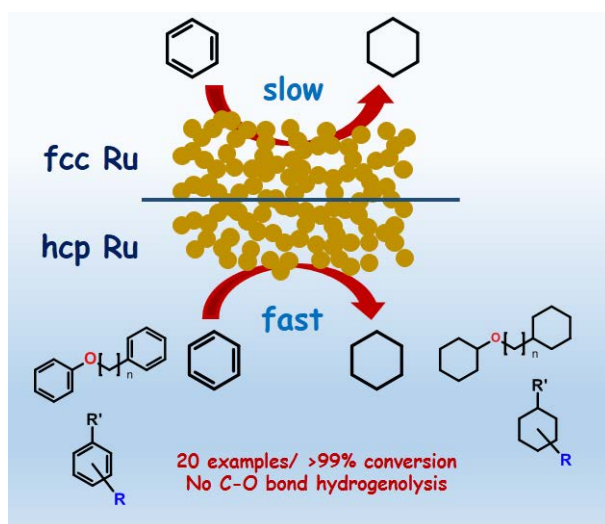
*Sourav Ghosh, IPC Department, Indian Institute of Science, Bangalore, Karnataka-560012, India; Balaji R. Jagirdar, IPC Department, Indian Institute of Science, Bangalore, Karnataka-560012, India.*

## Abstract

In heterogeneous catalysis, the catalytic activity is governed by many parameters, such as, active phase composition, particle size, crystal structure, morphology, and supports. In case of self-supported metals, namely, metal nanosponges, the effect of the support can be eliminated. Therefore, for a particular morphology of the material, the activity solely depends on the crystal structure of the metal. Additionally, porous structures of metal further enhance the substrate diffusion and expose more numbers of surface active sites for catalysis [1]. Over the decades, identifying the crystal structure sensitivity of catalysts in chemical reactions to accomplish the maximum productivity remains one of the most significant yet challenging issues in heterogeneous catalysis [2]. Selective hydrogenation of substituted arenes and aryl ethers to their respective alicyclic derivatives is one of the most important reactions carried out in the industry for generation of various intermediates that are important precursors to produce polymers, dyes, and fine chemicals. Principally, selective hydrogenation of aromatic cores of oxygenated aromatics to the respective alicyclic ethers are rather unusual transformation. This is because of low C–O bond dissociation energy, which causes mostly C–O bond hydrogenolysis products [3]. In case of metal based arene hydrogenation catalysts, ruthenium catalysts are preferred over other precious metal catalysts, such as, rhodium, iridium, and platinum, because of its moderate cost and high catalytic activity. Herein, we have investigated the effects of crystal phase of ruthenium towards hydrogenation of benzene [4].

In this work, one step template-less chemical reduction method was used for the synthesis of self-supported mesoporous ruthenium nanosponges. It was found that, reduction of ruthenium chloride using ammonia borane (AB) and tert-butylamine borane (TBAB) as reducing agents result in ruthenium nanosponge in its *hcp* phase. On the other hand, use of sodium borohydride (SB) led to the formation of *fcc* phase

ruthenium nanosponge. The as prepared *hcp* ruthenium nanosponge was found to be catalytically more active as compared to the as prepared *fcc* ruthenium nanosponge for hydrogenation of benzene. The *hcp* ruthenium nanosponge was also found to be thermally more stable than the *fcc* phase and recyclable over several cycles of benzene hydrogenation. Moreover, this self-supported *hcp* ruthenium nanosponge shows excellent catalytic activity towards hydrogenation of various substituted benzenes. The ruthenium nanosponge catalyst was also found to bring about selective hydrogenation of aromatic cores of phenols and aryl ethers to the respective alicyclic products without hydrogenolysis of the C–O bond. The catalytic activity of these nanosponge catalysts opens new opportunities for the valorization of lignin derived aromatic compounds under mild conditions in a green and sustainable manner. The result of these studies will be presented.



## References

1. D. R. Rolison, *Science* **2003**, 299, 1698.
2. J. X. Liu, W. X. Li, *WIREs Comput. Mol. Sci.* **2016**, 6, 571.
3. X. Cui, A. E. Surkus, K. Junge, C. Topf, J. Radnik, C. Kreyenschulte, M. Beller, *Nat. Commun.* **2016**, 7, 11326.
4. S. Ghosh, B. R. Jagirdar, *ChemCatChem* **2018**, 10, 3086.

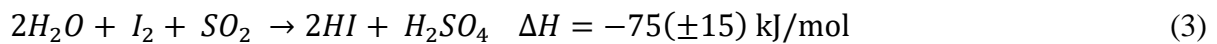
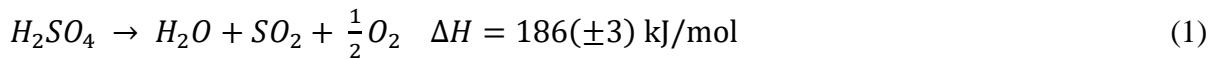


# Sulfuric acid decomposition over supported $\text{CuFe}_2\text{O}_4$ catalysts

Sachin Tomar, Department of Chemical Engineering, IIT Delhi, New Delhi, India;  
Satyam Gangwar, Department of Chemical Engineering, IIT Delhi, New Delhi, India;  
Kishore Kondamudi, Department of Chemical Engineering, IIT Delhi, New Delhi,  
India; Sreedevi Upadhyayula, Department of Chemical Engineering, IIT Delhi, New  
Delhi, India; Damaraju Parvatalu, ONGC Energy Centre, Mumbai, India

## Introduction

Sulfur-Iodine (S-I) cycle is considered as one of the feasible processes for hydrogen production on large scale. This cycle consists of the following reactions [1]:

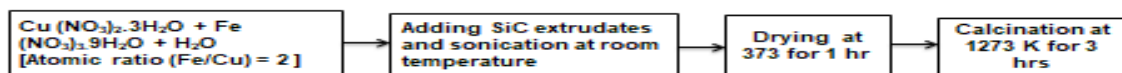


In the above reactions sulfuric acid decomposition is the most endothermic step. In this work  $\text{CuFe}_2\text{O}_4$  catalysts over  $\beta\text{-SiC}$  and  $\text{SiO}_2$  supports were prepared and tested for the decomposition of sulfuric acid.

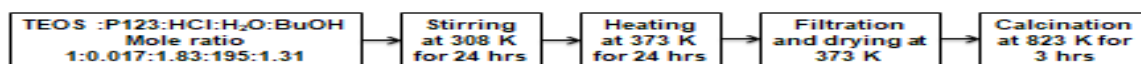
## Experimental

### Catalyst preparation

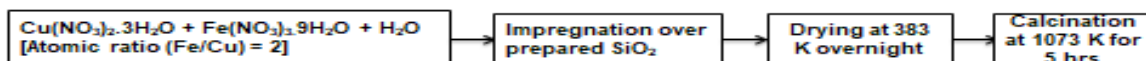
#### Synthesis of 10 wt % $\text{CuFe}_2\text{O}_4/\beta\text{-SiC}$ [2]



#### Synthesis of mesoporous silica ( $\text{SiO}_2$ ) support [3]



#### Synthesis of 10 wt % $\text{CuFe}_2\text{O}_4/\text{SiO}_2$



### Catalyst activity testing

The reactions were carried out at five different temperatures, K, 1073, 1098, 1123, 1148 and 1173 and at wide range of weight hour space velocity (WHSV,  $\text{h}^{-1}$ ), 2.22, 5.16, 8.1, 11.04, and 13.98.

## Results and Discussion

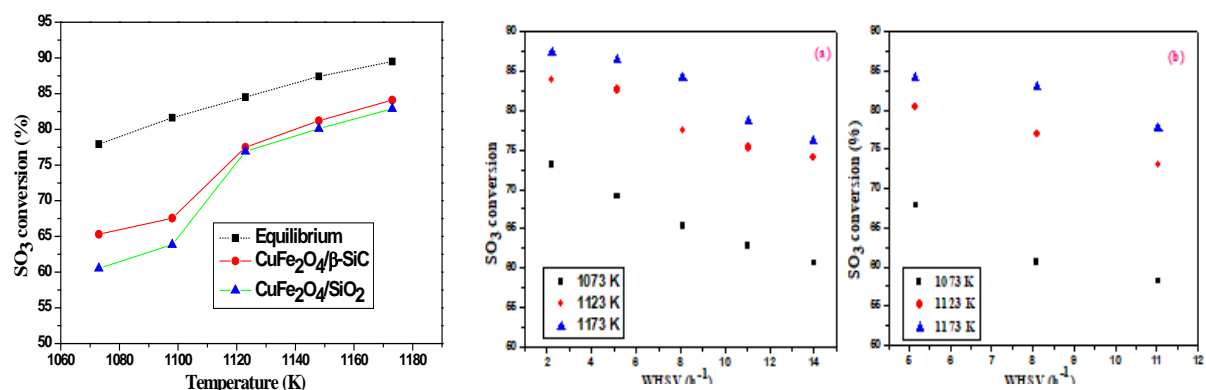


Fig. 1 SO<sub>3</sub> conversion with temperature. Fig.2 SO<sub>3</sub> conversion with WHSV for (a) CuFe<sub>2</sub>O<sub>4</sub>/β-SiC (b)

CuFe<sub>2</sub>O<sub>4</sub>/SiO<sub>2</sub> catalyst.

The SO<sub>3</sub> conversion increased with increase in temperature and decreased with increase in WHSV. The maximum SO<sub>3</sub> conversion was achieved at 1173 K.

## Conclusion

In the present work, catalytic decomposition of sulfuric acid over CuFe<sub>2</sub>O<sub>4</sub>/SiO<sub>2</sub> and CuFe<sub>2</sub>O<sub>4</sub>/β-SiC catalysts was investigated experimentally. CuFe<sub>2</sub>O<sub>4</sub>/β-SiC showed the promising activity for the reaction.

## Acknowledgement

The authors are thankful to ONGC Energy Centre Trust (OECT), India for the financial support.

## References

- [1] A. Giaconia, R. Grena, M. Lanchi, R. Liberatore, P. Tarquini, Hydrogen/methanol production by sulfur-iodine thermochemical cycle powered by combined solar/fossil energy, *Int. J. Hydrogen Energy*. 32 (2007) 469–481.
- [2] S. Upadhyayula, A. Bhaskarwar, K. Kondamudi, P. Damraju, B. Bhargava, S. Bannerjee, Catalyst composition for conversion of sulfur trioxide and hydrogen production process, (2017) PCT/IN2017/050151.
- [3] F. Kleitz, S.H. Choi, R. Ryoo, Cubic Ia3d large mesoporous silica: synthesis and replication to platinum nanowires, carbon nanorods and carbon nanotubes, *Chem Commun.* (2003) 2136–2137.

# Modified Ni/ $\gamma$ -Al<sub>2</sub>O<sub>3</sub>-based catalysts for partial oxidation of methane to synthesis gas

*Abbas Khaleel; Sheik Jobe, Department of Chemistry; Sulaiman Al-Zuhair, Department of Chemical and Petroleum Engineering, United Arab Emirates University, Al-Ain, UAE*

## Introduction

Abundant natural gas, if efficiently utilized, is a potential source of more cost-effective and environmentally friendly energy and chemicals than petroleum oil. Disadvantages of natural gas as a direct fuel include its low energy density by volume, and high cost of transportation, which resulted in its underutilization as an alternative energy source [1]. Therefore, the conversion of methane to more easily-handled and value-added products is becoming a promising route for natural gas utilization. Compared to steam reforming of methane to syngas, which is the most commercially applied route, partial oxidation is a more cost-effective promising route. While noble metals have been the most active catalysts, Ni-based catalysts are widely studied due to their lower costs. One of the drawbacks of such catalysts is their deactivation due, mainly, to carbon deposition and structural instability during reactions. Therefore, developing modified Ni-based catalysts to overcome these problems is becoming an important and promising area of research. In the present work, the effect of the alumina support pre-treatment, and the effect of selected metal dopants on the Ni-support interaction, coke formation, and catalytic activity was studied.

## Experimental methods and results

High-surface-area powders of Ni/ $\gamma$ -Al<sub>2</sub>O<sub>3</sub>-based catalysts were prepared in different Ni concentrations using wet impregnation. The catalysts were characterized by powder XRD, TEM, N<sub>2</sub> sorption, H<sub>2</sub>-TPR, and CO adsorption. The catalytic activity was studied using a continuous flow fixe-bed quartz reactor (9 mm ID) at temperatures in the range of 600-900 °C under atmospheric pressure using a feed gas composed of CH<sub>4</sub> and air in a CH<sub>4</sub>/O<sub>2</sub> ratio of 2. The gaseous products were evaluated using a gas chromatograph equipped with a TCD detector. The catalyst composition and coke formation after reactions were studied by XRD, TEM, and temperature programmed oxidation.

The temperature of the pre-treatment of  $\gamma$ - $\text{Al}_2\text{O}_3$  showed a significant effect on the dispersion and crystallinity of the NiO particles on the surface as shown by the XRD patterns in Figure 1. NiO crystallites were noticeably larger on the support calcined at 500 °C compared with that calcined at 750 °C. At a calcination temperature of 950 °C,  $\gamma$ - $\text{Al}_2\text{O}_3$  converted to  $\theta$ - $\text{Al}_2\text{O}_3$  and similar behavior was observed. This behavior could be referred to the fact that  $\gamma$ - $\text{Al}_2\text{O}_3$  is a metastable phase which sinters considerably upon heat-treatment. The results indicate that sintering of the support enhances the active phase sintering resulting in larger metal particles. Therefore, calcination of the support at higher temperatures before introducing the active phase is desired. This high-temperature pre-treatment leads to a more texturally stable support and hence a more stable and better dispersed active phase on the surface, despite the considerable decrease in the surface area. Interestingly the coke formation was also suppressed and the catalytic activity was improved when the support was pre-calcined at elevated temperatures, which can be referred, in part, to the active phase smaller particle size. As shown in Figure 1, the catalysts of which the support was calcined at 750 °C and 950 °C, showed higher conversion of methane and higher selectivity to CO on the account of coke formation with a  $[\text{H}_2]/[\text{CO}]$  ratio in the range of 1.95-2.05. This study is still undergoing and preliminary results showed that doping with other selected metals, including Cr, resulted in suppression of coke formation.

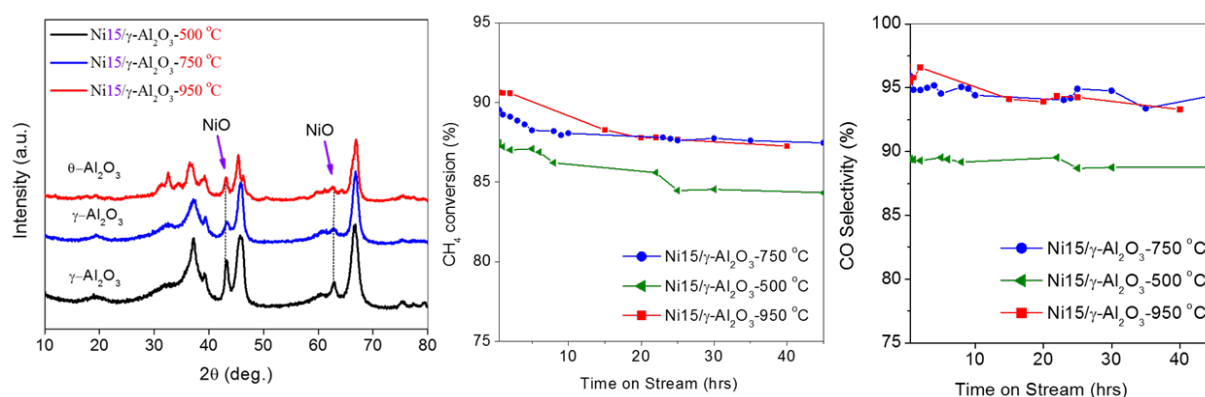


**Figure 1.** XPR patter,  $\text{CH}_4$  conversion, and CO selectivity over Ni15/ $\gamma$ - $\text{Al}_2\text{O}_3$  with support calcined at different temperatures.

## References

- [1] M. Lehner, R. Tichler, H. Steinmüller, M. Koppe, Power-to-Gas: Technology and Business Models, Springer, 2014.
- [2] N.A.K. Aramouni, J.G. Touma, B.A. Tarboush, J. Zeaiter, M.N. Ahmed, Renewable Sustainable Energy Rev. 82 (2018) 2570-2585.

# PHOTOCATALYTIC HYDROGEN PRODUCTION ON CHEMICALLY ETCHED STRONTIUM TITANATE SURFACES

*Ramazan YILDIRIM, Burcu ORAL, Dilara SAADETNEJAD,*

*Department of Chemical Engineering, Boğaziçi University, İstanbul, Turkey*

## **Introduction**

Photocatalytic water splitting is a hydrogen production method which utilizes water, catalyst and light. Metal oxide semiconductors are suitable for water splitting when they are irradiated by photons but their efficiencies are limited [1]. For an efficient water splitting, the semiconductor should have narrow band gap in order to be visible light active. Anion and/or cation doping, dye sensitization and surface modifications are some of the methods that can be applied to increase the photocatalytic activity of a photocatalyst. Wet chemical etching is also used to remove some atoms from the materials; by etching, it is possible to change the surface area of a catalyst. When a semiconductor has high crystallinity, the surface area increases as well as surface adsorption and active sites in addition the possibility of recombination of charges is decreased [2,3]. Strontium titanate is a titanate based semiconductor which is frequently used as photocatalyst even though it has band gap of 3.2 eV; its stability and corrosion property makes it attractive for photocatalytic applications [4]. SrTiO<sub>3</sub> has SrO and TiO<sub>2</sub> atomic layers in its structure, where SrO is basic oxide and TiO<sub>2</sub> is acidic [5]. Therefore, finding a solution that dissolves one layer but not the other is important for changing the surface structure of SrTiO<sub>3</sub>.

## **Experimental Work**

In this work, wet chemical etching is performed on strontium titanate (SrTiO<sub>3</sub>) and the photocatalytic performance of the etched catalyst is investigated. As co-catalyst, 1wt. % Pt is impregnated on SrTiO<sub>3</sub>. SrTiO<sub>3</sub> catalyst is prepared by solid state reaction and for Pt deposition incipient-to-wetness impregnation is used. For etching, 1 M and 4 M of citric acid and hydrochloric acid solutions are used. 5 grams of catalyst is mixed with acid solution and they are filtrated under vacuum. In addition, post treatment after etching is also investigated, etched catalysts are washed with distilled water and/or annealed at elevated temperatures. Photocatalytic hydrogen production occurred at room temperature and 1 bar under solar light simulated by 300W Xe lamp. Catalysts are characterized by SEM, FTIR, XRD and UV-VIS. Photoelectrochemical characterization of the catalyst are done in a

photoelectrochemical cell. Mass spectrometer is used for analysis of product gases and produced hydrogen and oxygen amounts are calculated.

## Results

From XRD results it is seen that by solid state reaction it is possible to obtain cubic strontium titanate. It is observed that acid etching increased hydrogen production. Citric acid etching increased the hydrogen production amount more than hydrochloric acid etching and washing the samples after etching decreased the photocatalytic activity (Figure 1).

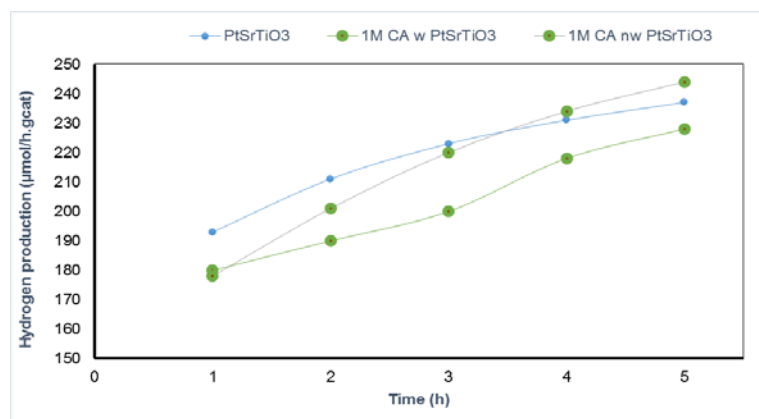


Figure 1. Comparison of hydrogen production on etched and not etched SrTiO<sub>3</sub>

## Acknowledgement:

This work is economically funded by Boğaziçi University Research Fund, through Project No: 14002

## References

1. Van de Krol, R., Liang, Y., Schoonman, J., Krol, R. Van De, Liang, Y., & Schoonman, J. (2008). Solar hydrogen production with nanostructured metal oxides. *Journal of Materials Chemistry*, 18(20), 2311. <http://doi.org/10.1039/b718969a>
2. Luca Chiarello, G., & Selli, E. (2010). Photocatalytic Hydrogen Production. *Recent Patents on Engineering*, 4, 155–169. <http://doi.org/10.2174/187221210794578600>
3. Yu, H., Ouyang, S., Yan, S., Li, Z., Yu, T., & Zou, Z. (2011). Sol–gel hydrothermal synthesis of visible-light-driven Cr-doped SrTiO<sub>3</sub> for efficient hydrogen production. *Journal of Materials Chemistry*, 21(30), 11347. <http://doi.org/10.1039/c1jm11385b>
4. Bi Y., Ehsan M. F., Huang Y., Jin J., He T. (2015). Synthesis of Cr-doped SrTiO<sub>3</sub> photocatalyst and its application in visible-light-driven transformation of CO<sub>2</sub> into CH<sub>4</sub>. *Journal of CO<sub>2</sub> Utilization*, 12, 43–48. <https://doi.org/10.1016/j.jcou.2015.10.004>
5. Kawasaki, M., Maeda, T., Tsuchiya, R., & Koinuma, H. (1993). Atomic control of the SrTiO<sub>3</sub> Crystal Surface. *Science*, 266(5190), 1–3. <http://doi.org/10.1126/science.266.5190.1540>

# Enhancement of Photocatalytic Activity of TiO<sub>2</sub> for Oxygen Evolution by Brownmillerite-type Ca<sub>2</sub>FeCoO<sub>5</sub> Ultrafine Particles

*Etsushi Tsuji; Ryosuke Nanbu; Takeyuki Watanabe; Satoshi Suganuma; Naonobu*

*Katada*

*Center for Research on Green Sustainable Chemistry, Tottori University, Tottori,  
Japan*

Brownmillerite-type Ca<sub>2</sub>FeCoO<sub>5</sub> ultrafine particles with nano-metric dimension were synthesized by a reverse micelle method on TiO<sub>2</sub> nanoparticles. The photocatalytic activity of TiO<sub>2</sub> for oxygen evolution reaction was improved by loading of the Ca<sub>2</sub>FeCoO<sub>5</sub> ultrafine particles. The origin of improvement was the promotion of surface oxidation reaction, but not the suppression of excited carrier recombination.

## Introduction

The increasing demand of hydrogen fuel production has promoted the development of effective oxygen evolution reaction (OER) photocatalysts used for water splitting. Although noble metal oxides were used as cocatalysts active for OER, the lack of resources prohibits their large-scale uses. On the other hand, recently we found that brownmillerite-type Ca<sub>2</sub>FeCoO<sub>5</sub> (CFCO) showed higher OER activity than the noble metal oxides [1]. On this stage of study, CFCO was synthesized by a conventional sol-gel method, and the particle size was about several dozen nanometers, which is too large for a cocatalyst. In this study, we synthesized CFCO ultrafine particles with less than 10 nm diameters by a reverse micelle (RM) method on TiO<sub>2</sub> nanoparticles and investigated the photocatalytic activity.

## Experimental

An aqueous solution containing metal nitrates (Ca:Fe:Co=2:1:1) was mixed with cyclohexane and hexaethyleneglycol nonylphenyl ether (NP-6) as a surfactant at 10 °C to obtain a RM solution. Another RM solution was also prepared from cyclohexane, NP-6 and 10% tetramethylammonium hydroxide (TMAH) aqueous solution. These RM solutions were mixed and stirred at 10 °C for 1 h. Anatase TiO<sub>2</sub> powders (A-100, Ishihara Sangyo Kaisha, LTD.) dispersed in cyclohexane was added and excess ethanol was added to break the RM. The formed precipitates were collected, dried at 110 °C for overnight and calcined at 600 °C for 5 h in air.

The morphology, particle size and crystallinity of the composites were analyzed by a high resolution transmission electron microscope (HRTEM). The photocatalytic activity was evaluated under UV light irradiation ( $7.5 \text{ mW cm}^{-2}$ ) in an aqueous solution containing AgF as an electron scavenger after Ar bubbling for 30 min. The evolved oxygen gas was detected by a gas chromatograph with TCD.

## Results and Discussion

Fig. 1a shows HRTEM image of 0.5 wt% CFCO/TiO<sub>2</sub> nanocomposite particles. The half-spherical ultrafine particle (about 5 nm) was found on the TiO<sub>2</sub> surface, and the spacing of lattice fringes in it was 0.26 nm, corresponding to the (025) face of brownmillerite-type CFCO. The particle size of CFCO synthesized by the RM method without TiO<sub>2</sub> was about 30 nm, suggesting that presence of TiO<sub>2</sub> support played a role to get or keep the CFCO ultrafine particles, presumably during the calcination.

Fig. 1b,c show photocatalytic activity of the CFCO/TiO<sub>2</sub> for OER. The rate of OER increased up to 0.5 wt% CFCO loading and then decreased (Fig. 1b). Intensities of photoluminescence of CFCO/TiO<sub>2</sub> and bare TiO<sub>2</sub> were similar, indicating that the enhancement of activity was not due to the recombination of excited electrons and holes. Thus, the promotion of surface oxidation rate of water is suggested to induce the enhancement. The enhanced photocatalytic activity of the 0.5 wt% CFCO/TiO<sub>2</sub> for OER was close to that of 0.5 wt% RuO<sub>2</sub>/TiO<sub>2</sub> (Fig. 1c).

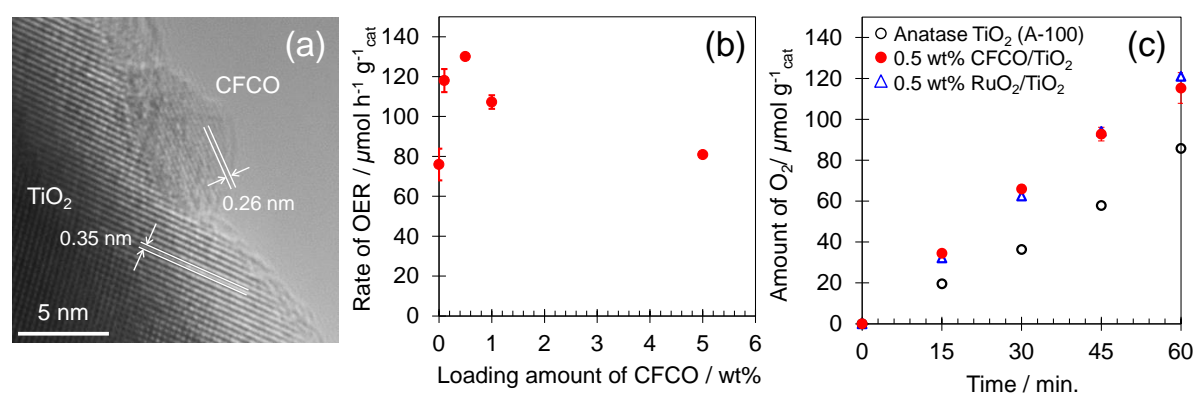


Fig. 1 (a) HRTEM image of 0.5 wt% CFCO/TiO<sub>2</sub>, (b) rate of oxygen evolution reaction over CFCO/TiO<sub>2</sub>, and (c) time courses of oxygen evolution over TiO<sub>2</sub>, 0.5 wt% CFCO/TiO<sub>2</sub> and 0.5 wt% RuO<sub>2</sub>/TiO<sub>2</sub>.

## References

- [1] E. Tsuji, T. Motohashi, H. Noda, D. Kowalski, Y. Aoki, H. Tanida, J. Niikura, Y. Koyama, M. Mori, H. Arai, T. Ioroi, N. Fujiwara, Y. Uchimoto, Z. Ogumi and H. Habazaki *ChemSusChem* **2017**, *10*, 2864.

## Acknowledgements

A part of this study was funded by JSPS KAKENHI Grant Number 18K2527500, a research granted from the Murata Science Foundation and ENEOS Hydrogen Trust Fund, Japan.



# **Effect of indium oxide as a promoter in catalysts based on Cu/CeO<sub>2</sub> nanocomposites for CO<sub>2</sub> hydrogenation to methanol.**

*Marco Aurélio Rossi, São Carlos Institute of Chemistry- University of São Paulo, São Carlos, Brazil; Marco Andre Fraga, National Institute of Technology, Rio de Janeiro, Brazil; José Mansur Assaf, São Carlos Federal University, São Carlos, Brazil; Elisabete Moreira Assaf, São Carlos Institute of Chemistry- University of São Paulo, São Carlos, Brazil.*

## **Introduction:**

The catalytic process of carbon dioxide hydrogenation with the aim to obtain products with higher added value, such as methanol, is one of the most promising strategies for the utilization of this atmospheric pollutant. The main catalysts used in this process are based on composites between copper (responsible for the H<sub>2</sub> adsorption and activation) and a metal oxide (responsible for CO<sub>2</sub> adsorption) [1]. Recent studies presented the impressive potential of indium oxide used as catalyst for methanol production with high selectivity, although, the conversions are lower than those observed for catalysts based on copper and higher pressures and amounts of hydrogen are needed [2,3]. Until the moment, the effect of indium oxide as a promoter in copper-based catalysts was not studied, so, the objective of this work was to investigate the effect of indium oxide as a promoter in Cu/CeO<sub>2</sub> catalysts for the CO<sub>2</sub> hydrogenation to methanol reaction.

## **Experimental Section:**

Cu/CeO<sub>2</sub> catalysts (50%/50% in molar content), without promoter and with 5% and 10% of indium oxide, in molar content, were synthesized by the co-precipitation method at constant pH assisted by the CTAB surfactant, followed by calcination in air. The materials were characterized by TGA-DSC, ex-situ and in-situ XRD, N<sub>2</sub>-physisorption (using the BET model), TEM-EDX, H<sub>2</sub>-TPR, CO<sub>2</sub>-TPD, N<sub>2</sub>O-chemisorption, XPS and XANES. The catalytic tests were performed in a continuous flow tubular fix-bed reactor (*PID Microactivity Effi* model) under pressure of 3 MPa, temperature of 250°C, CO<sub>2</sub>/H<sub>2</sub> ratio of 1:3 and GHSV of 6 L.g<sup>-1</sup>.h<sup>-1</sup>. Prior to the reactions, the catalysts were reduced under H<sub>2</sub> flow of 30mL.min<sup>-1</sup> for 1 hour at 230°C

## **Results and Discussion:**

The results in table 1 allowed to verify that the addition of indium oxide, even in the lowest content, considerably increased the selectivity to methanol, from 40% to more than 60%, and several factors contribute to this. The indium oxide optimizes the occurrence of the reaction mechanism by the formate route, being this, the most effective pathway to generate methanol with high selectivity, once it does not generate CO as intermediary, which could desorb as an unwanted by product, as occurs for copper materials [4]. Besides this, the XPS analyses revealed the existence of non-stoichiometric oxides contributions in the ceria and indium oxide structure due to the presence of oxygen vacancies, which are important as basic sites for the adsorption of CO<sub>2</sub> acid molecules. In fact, CO<sub>2</sub>-TPD analyses showed that the basicity slightly increased with indium oxide addition to the materials, probably, due to the occurrence of oxygen vacancies as a result of the differences in the oxidation states between cerium and indium ions [5]. A decrease in the CO<sub>2</sub> conversion was observed for the promoted catalysts. This can be explained by the particles aggregation and area loss that commonly occurs in materials containing indium oxide submitted to calcination process [2]. This is in agreement with results obtained from the N<sub>2</sub>-physisorption and N<sub>2</sub>O-chemisorption, that showed a decrease in the specific surface area and in the copper surface metallic area for the catalysts with indium oxide. Despite the decrease in conversion, the obtained values are still considerably higher than those from pure indium oxide and were obtained under significantly milder reaction conditions of pressure and hydrogen consume.

Table1: Catalytic performance for the catalysts unpromoted and promoted with indium oxide.

Catalysts	Xco <sub>2</sub> (%)	SCH <sub>3</sub> OH (%)	SCO (%)	SCH <sub>4</sub> (%)
Cu/CeO <sub>2</sub>	8	40	58.9	1.1
Cu/CeO <sub>2</sub> -5%In	5.5	67	31	2.0
Cu/CeO <sub>2</sub> -10%In	5.3	65	33	2.0

### Acknowledgements:

The authors gratefully acknowledge FAPESP for the financial support in processes 2015/06246-7 and 2017/10154-6.

### References:

- [1] GONG, J. et al. *Chemical Society Reviews*, v. 40, n. 7, p. 3703-27, 2011. ISSN 1460-4744
- [2] PÉREZ-RAMÍREZ, J. et al. *Angewandte Chemie International Edition*, v. 55, n. 21, p. 6261-5, 2016. ISSN 1521-3773
- [3] LIU, C. et al. *Journal of CO<sub>2</sub> Utilization*, v. 12, p. 1-6, 2015. ISSN 2212-9820.
- [4] LIU, P. et al. *Journal of the American Chemical Society*, v. 138, n. 38, p. 12440-50, 2016. ISSN 1520-5126
- [5] MCFARLAND, E. W.; METIU, H. *Chemical Reviews*, v. 113, n. 6, p. 4391-427, 2013. ISSN 1520-6890

## Preparation of isolated fcc cobalt nanoparticles employing exfoliated graphite as novel support material

*Moritz Wolf, Nico Fischer, Michael Claeys, Catalysis Institute and DST-NRF Centre of Excellence in Catalysis c\*change, University of Cape Town, South Africa*

For a long time, most support materials have been regarded as inert. The potential presence of metal-support interaction anchoring metallic nanoparticles on common metal oxide carriers such as  $\text{Al}_2\text{O}_3$  or  $\text{SiO}_2$  was established in literature in the 1980s [1,2]. More recently, such metal oxide carriers have been shown to exhibit a strong effect on the catalytic behaviour of supported metallic nanoparticles [3]. On the one hand, a strong interaction is desired as it increases the stability of the nanoparticles, e.g. against sintering, but on the other hand the interaction is typically associated with a loss in active phase. Pristine carbon does not exhibit such stabilising properties, but may be functionalised in order to increase interaction with and hence stabilisation of supported nanoparticles [4]. Carbon supports are seldom applied in industry due to their lower mechanical strength when compared to widely applied metal oxide carriers [5]. However, their inert character makes carbon supports the carrier of choice for fundamental studies on relatively isolated nanoparticles.

Herein, pristine graphite powder has been exfoliated *via* ultrasonication in 1-methyl-2-pyrrolidinone (NMP) followed by a size selection *via* centrifugation [6,7]. The BET surface area of the obtained exfoliated graphite (EG) is  $48 \text{ m}^2/\text{g}$  and double the surface area of the pristine powder. Most of the EG flakes have a thickness of 58-100 graphene layers as estimated from size analysis of the (002) reflex in the X-ray diffraction (XRD) pattern. An estimation of the mean in-plane crystallite size by means of Raman spectroscopy [8] results in 107 nm before and 66 nm after exfoliation. This inert support material was applied in a comparative *in situ* XRD study on the size-dependent reduction behaviour of cobalt oxide in  $\text{H}_2$ . Well-defined  $\text{Co}_3\text{O}_4$  nanoparticles were synthesised in a sol-gel approach *via* the benzyl alcohol route [9,10], re-dispersed in ethanol and supported on EG utilising ultrasonication [10]. Crystallites with average crystallite sizes of 3-8 nm were reduced at temperatures in the range of 330 to 370 °C (1 °C/min) for 5 h. Sintering of a significant fraction of nanoparticles was identified for a Co loading of 5 wt.% in three different catalysts during reduction to CoO and, more pronounced, in the second reduction step to fcc-Co. The little stabilisation provided by the rather inert EG support may allow for this

increase in size. Even though sintering induced a widening of the size distribution, a mild size-dependent reduction behaviour was identified. The absolute onset temperatures, as well as the temperature ranges of the reduction steps, increase with decreasing crystallite size (Figure 1a). Both indicators for the reducibility of a catalyst are significantly increased when compared to an unsupported sample. In particular the second reduction step from CoO to fcc-Co is delayed in the case of supported crystallites. Synchrotron radiation-based *in situ* XRD studies on the reduction behaviour of 1 wt.% Co/EG model catalysts revealed the absence of sintering. The significantly increased inter-particle distance may allow for the isolated reduction of nanoparticles preventing a significant increase in crystallite size, which was confirmed in post-run analyses *via* transmission electron microscopy (TEM; Figure 1b,c). Thus, the developed 1 wt.% Co/EG catalysts resemble ideal model catalysts for studying the effect of crystallite size on the catalytic performance or physicochemical properties of fcc-Co nanoparticles in the absence of strong interaction with the support material.

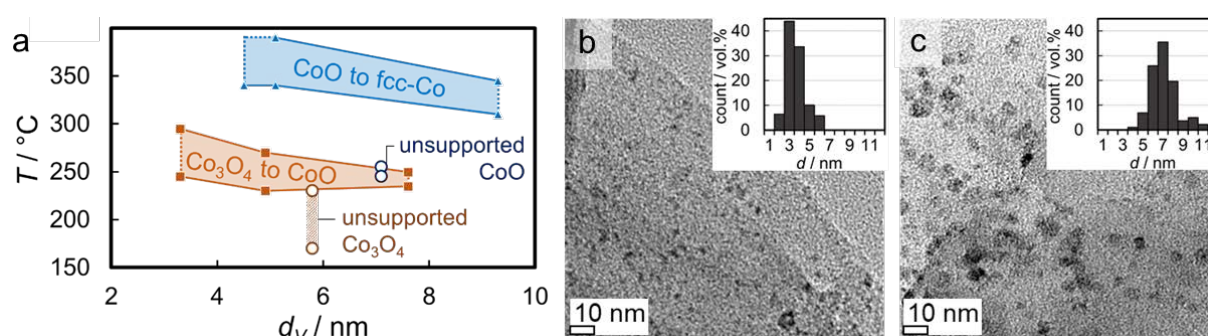


**Figure 1** (a) Temperature ranges of the reduction of supported (5 wt.% Co/EG) and unsupported Co<sub>3</sub>O<sub>4</sub> crystallites to CoO and fcc-Co in H<sub>2</sub> as observed *via in situ* XRD (1 °C/min) for various volume-mean crystallite sizes (Rietveld refinement), as well as micrographs of (b) 3.5 nm and (c) 7.6 nm Co<sub>3</sub>O<sub>4</sub> crystallites (1 wt.% Co/EG) after reduction in H<sub>2</sub> for 5 h at 350 and 330 °C (1 °C/min), respectively, with volume-mean particle size distributions as obtained *via* post-run TEM analysis of the passivated model catalysts.

## References

- [1] S.J. Tauster, S.C. Fung, R.T.K. Baker, J.A. Horsley, *Science* **21** (1981) 1121.
- [2] G.L. Haller, D.E. Resasco, *Adv. Catal.* **36** (1989) 173.
- [3] S. Lögdberg, M. Boutonnet, J.C. Walmsley, S. Järås, A. Holmen, E.A. Blekkan, *Appl. Catal. A Gen.* **393** (2011) 109.
- [4] J.L. Figueiredo, M.F.R. Pereira, M.M.A. Freitas, J.J.M. Órfão, *Carbon* **37** (1999) 1379.
- [5] J. van de Loosdrecht, M. Datt, J.L. Visagie, *Top. Catal.* **57** (2014) 430.
- [6] Y. Hernandez, V. Nicolosi, M. Lotya, F.M. Blighe, Z. Sun, S. De, I.T. McGovern, B. Holland, M. Byrne, Y.K. Gun'Ko, J.J. Boland, P. Niraj, G. Duesberg, S. Krishnamurthy, R. Goodhue, J. Hutchison, V. Scardaci, A.C. Ferrari, J.N. Coleman, *Nat. Nanotechnol.* **3** (2008) 563.
- [7] U. Khan, A. O'Neill, H. Porwal, P. May, K. Nawaz, J.N. Coleman, *Carbon* **50** (2012) 470.
- [8] L.G. Cançado, K. Takai, T. Enoki, M. Endo, Y.A. Kim, H. Mizusaki, A. Jorio, L.N. Coelho, R. Magalhães-Paniago, M.A. Pimenta, *Appl. Phys. Lett.* **88** (2006) 12.
- [9] N. Shi, W. Cheng, H. Zhou, T. Fan, M. Niederberger, *Chem. Commun.* **51** (2015) 1338.
- [10] M. Wolf, H. Kotzé, N. Fischer, M. Claeys, *Faraday Discuss.* **197** (2017) 243.

## Effect of SiO<sub>2</sub> addition on heat resistance of alumina carrier

*Akira Hasegawa, NIT Hachinohe College, Hachinohe, Japan; Shizuka Ogasawara, Renaissance Energy Research Co., Ltd., Osaka, Japan; Hiromi Nakamura, Renaissance Energy Research Co., Ltd., Osaka, Japan; Yoshihiro Kadoma, NIT Hachinohe College, Hachinohe, Japan; Osamu Okada, Renaissance Energy Research Co., Ltd., Osaka, Japan*

Alumina was prepared by adding Si(OC<sub>2</sub>H<sub>5</sub>)<sub>4</sub>, La(NO<sub>3</sub>)<sub>3</sub>, and Ba(NO<sub>3</sub>)<sub>2</sub> to an aqueous aluminum nitrate solution. The crystal structure, specific surface area, and NH<sub>3</sub>-TPD of the samples were determined. The addition of a small amount of SiO<sub>2</sub> was found to improve the heat resistance.

### 1. Scope

The carrier of the steam-reforming catalyst needs to maintain a high specific surface area under the high-temperature, high-pressure steam atmosphere and suppress the coking reaction. We have previously reported that SiO<sub>2</sub>-doped alumina prepared by coprecipitation exhibits extremely high heat resistance [1]. However, the addition of solid acidic SiO<sub>2</sub> may cause coking. Therefore, in this study, we prepared a heat-resistant alumina carrier, which suppressed the solid acidity.

### 2. Results and discussion

SiO<sub>2</sub>-, BaO-, and La<sub>2</sub>O<sub>3</sub>-added alumina samples were prepared by a precipitation method. Figure 1 shows the relationship between the specific surface area of these samples after calcination at 1200°C for 5 h and the amount of additive used. Samples with 5-10 mass% SiO<sub>2</sub> exhibited a specific surface area as high as 60 m<sup>2</sup>/g or more, while samples with La<sub>2</sub>O<sub>3</sub> or BaO had a maximum specific surface area of about 30 m<sup>2</sup>/g. SiO<sub>2</sub> addition was found to be the most effective for improving

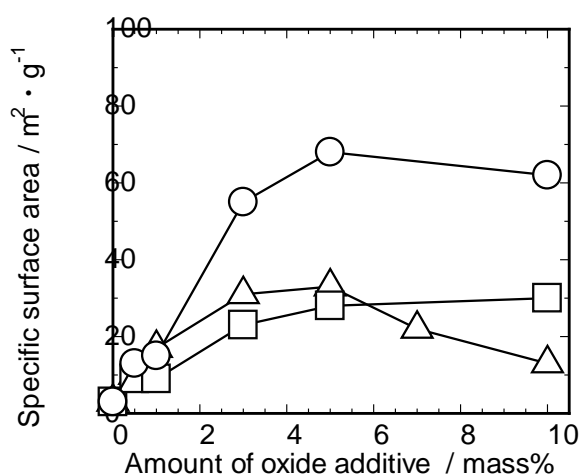


Figure 1. Dependence of specific surface area of calcined alumina on additive amount. ○: SiO<sub>2</sub>, △: BaO, □: La<sub>2</sub>O<sub>3</sub>.

the heat resistance of alumina. However, the addition of excess  $\text{SiO}_2$  causes coking during the steam-reforming reaction. Figure 2 shows the relationship between the amount of  $\text{SiO}_2$  added and  $\text{NH}_3$  desorption measured by  $\text{NH}_3$ -TPD. Solid acidity increased with addition of  $\text{SiO}_2$ . Figure 3 shows the relationship between calcination time and specific surface area at  $1200^\circ\text{C}$ . For the control sample containing no additives, the specific surface area decreased sharply very early on in the test. For samples with added  $\text{SiO}_2$ , the specific surface area initially decreased, but after 30 h, no large reductions in specific surface area were observed over long periods.  $\text{SiO}_2$ -added alumina calcined for 100 h showed a higher specific surface area than both the  $\text{La}_2\text{O}_3$ - and  $\text{BaO}$ -added samples.

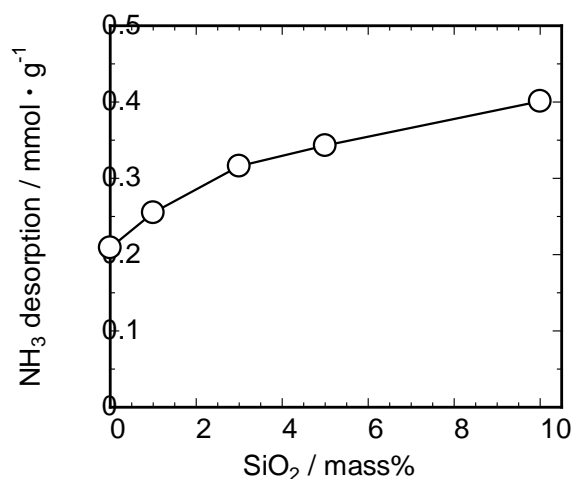


Figure 2. Variation in solid acidity with  $\text{SiO}_2$  addition.

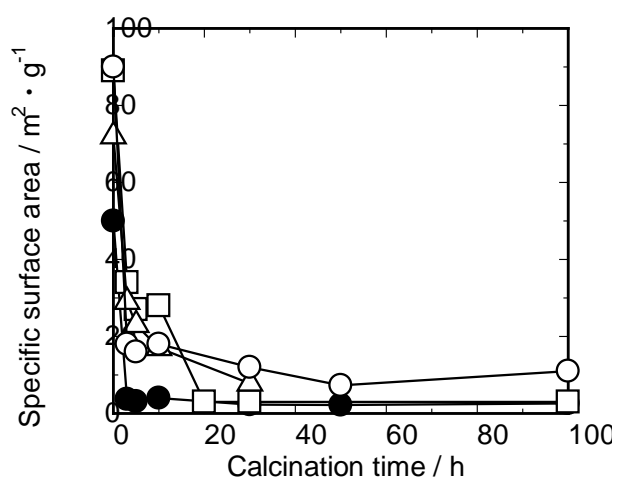


Figure 3. Relationship between specific surface area of heat-resistant alumina and calcination time at  $1200^\circ\text{C}$ .

○: 1 mass%  $\text{SiO}_2$ , △: 7 mass%  $\text{BaO}$ ,  
□: 3 mass%  $\text{La}_2\text{O}_3$ , ●: no additive.

### 3. Conclusion

Alumina containing a small amount of added  $\text{SiO}_2$  showed only a slight increase in solid acidity and an improved heat resistance. Furthermore,  $\text{SiO}_2$ -added alumina, calcined at  $1200^\circ\text{C}$  for 100 h, exhibited a specific surface area higher than both  $\text{La}_2\text{O}_3$ - and  $\text{BaO}$ -added samples. Since  $\text{SiO}_2$ -added alumina has high heat resistance and low acidity, it is expected to find application as a catalyst carrier for steam-reforming.

### References

- [1] A. Hasegawa, O. Okada, and C. Ito, U.S. Patent No. 9,440,222, 2016.

## **Synthesis of a novel two-dimensional metal-organic framework based on cyameluric nucleus derivative**

*Jingwen Sun, Nanjing University of Science and Technology, Nanjing, China;*

*Liming Dai, Nanjing University of Science and Technology, Nanjing, China;*

Two-dimensional (2D) nanostructure represent a family of materials with attractive property in various scopes like catalysis, gas separation and energy storage and exchange. Prospectively, 2D metal-organic framework with different metal-based nodes and multitopic organic ligands has been proved as a promising material in various functional devices for its high specific area and highly exposed active sites. <sup>[1-4]</sup> Herein, we introduce a novel two-dimensional metal-organic framework (MOF) based on cyameluric nucleus derivative. Specifically, this cyameluric nucleus derivative was a tri-s-triazine rings derivative  $C_6N_7(N_3H_3Na_3)$  which are cross-linked by N atoms. (Fig.1) And the probable structure of Mo-MOF was illustrated in the Fig.2, the crystal this Mo-MOF consists of alternating  $C_6N_7(N_3H_3)^{3-}$  group and metal ions Mo. The metal ions Mo are octahedrally coordinated and each Mo ions is coordinated with two N ions of  $C_6N_7(N_3H_3)^{3-}$  and four O ions of solvent, while the  $C_6N_7(N_3H_3)^{3-}$  was severed as the bridge to link three Mo ions.<sup>[5]</sup> The high potential of this type of Mo-MOF material was its ultrathin thin film and highly exposed Mo ions which probably could be used as the active sites of hydrogen-evolution reaction (HER). Further, the high content of N and C element of Mo-MOF could be served as C and N source in the annealing treatment to obtain nanostructured molybdenum carbide and molybdenum nitride. (Fig.3)

The organic ligands  $C_6N_7(N_3H_3Na_3)$  here was prepared by annealing treatment of the sodium (4,6-diamino-1,3,5-triazin-2-yl)amide for 4 h at 285°C under argon atmosphere which was synthesized by reaction of sodium hydrogen cyanamide and cyanoguanidine at 165°C for 24h. <sup>[6, 7]</sup> The Mo-MOF was prepared by mixing 20ml of 2.5mg/ml  $C_6N_7(N_3H_3Na_3)$  aqueous solution

and 12ml of 10mg/ml molybdenyl acetylacetonate DMF solution at 110°C for 2h, followed with stirring for 3h at room-temperature. After that, the resulted white solid was collected by centrifuge and wished with deionized water for three times.

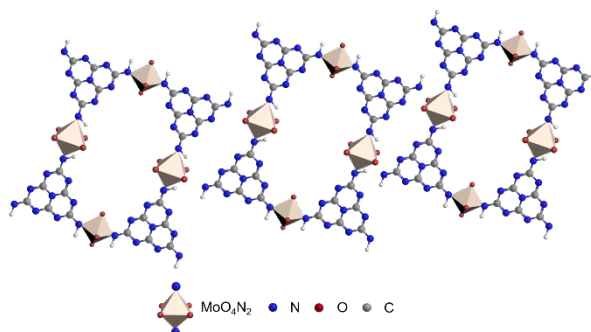
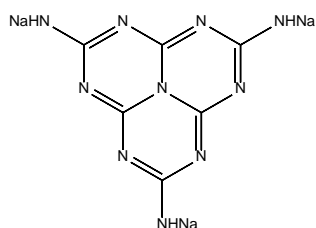


Fig.1 the structure of  $C_6N_7(N_3H_3Na_3)$ .

Fig.2 a probable crystal structure of Mo-MOF.

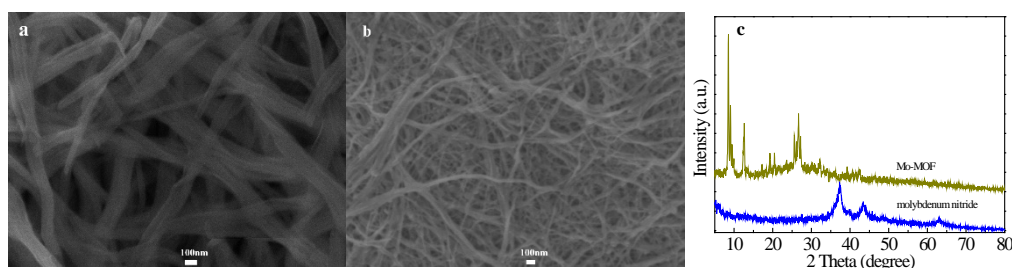


Fig.3 (a) the SEM image of Mo-MOF; (b) the SEM image of molybdenum nitride synthesized by annealing treatment of Mo-MOF; (c) the XRD analysis of Mo-MOF and molybdenum nitride.

- [1] J. Zhou, Y. Chen, K. Suenaga, et al, *Nature*, 556 (2018) 355.
- [2] J. Dong, K. Zhang, X. Li, et al, *Nat. Commun.*, 8 (2017) 1142.
- [3] W. Zhao, J. Peng, W. Wang, et al, *Coordin. Chem. Rev.*, 377 (2018) 44.
- [4] N. Lahiri, N. Lotfizadeh, R. Tsuchikawa, et al, *J. Am. Chem. Soc.*, 139 (2017) 19.
- [5] J. Duan, S. Chen, C. Zhao, et al, *Nat. Commun.*, 8 (2017) 15341.
- [6] R. Deans, G. Cooke, V. M. Rotello, *J. Org. Chem.*, 62 (1997) 4.
- [7] B. Jürgens, E. Irran, W. Schnick, et al, *J. Am. Chem. Soc.*, 125 (23) 10288.



# Half-unit-cell $\text{ZnIn}_2\text{S}_4$ monolayer with sulfur vacancies for photocatalytic hydrogen evolution

*Chun Du*<sup>1</sup>, *Guowei Yang*<sup>1</sup>

*1State Key Laboratory of Optoelectronic Materials and Technologies, Nanotechnology Research Center, School of Materials Science & Engineering, Sun Yat-sen University, Guangzhou 510275 Guangdong, China.*

*Presenting author email address: duch5@mail2.sysu.edu.cn*

Photocatalytic hydrogen evolution is an important potential method to produce clean energy by utilizing solar energy directly. However, it's still a major challenge to minimize the recombination of photo-generated electron-hole pairs for improving the photocatalytic efficiency.[1] Since the discovery of two-dimensional (2D) materials, they have been widely applied in photocatalysis due to the shorter diffusion length of charge carriers transfer to the surface which could effectively suppress the photo-generated electrons and holes.[2]  $\text{ZnIn}_2\text{S}_4$ , one of the layered ternary chalcogenide  $\text{AB}_2\text{X}_4$ , is dramatically attracting tremendous interests because of its narrow band gap for visible-light absorption, photo-stability and suitable energy band gap structure for photocatalytic hydrogen evolution.[3] Owing to the intrinsic bilayer structure in unit-cell with interlayer force, few-layer  $\text{ZnIn}_2\text{S}_4$  nanosheet has been reported. Although it generally performs better than the bulk in photocatalytic hydrogen production performance, the half-unit-cell  $\text{ZnIn}_2\text{S}_4$  monolayer has rarely been investigated.

Here, we for the first time demonstrate that half-unit-cell  $\text{ZnIn}_2\text{S}_4$  monolayer performs an excellent photocatalytic hydrogen evolution compared to the one-unit-cell bilayer because of its extended carrier lifetime. Additionally, the introduction of sulfur vacancies in the half-unit-cell  $\text{ZnIn}_2\text{S}_4$  monolayer can trap the photo-generated electrons for further prolonging the carrier lifetime. Benefiting from the dual purpose of separating the recombination, monolayer  $\text{ZnIn}_2\text{S}_4$  with sulfur vacancies has a superior photocatalytic hydrogen production rate up to 13.478 mmol/g/h under the visible light irradiation, improving by a factor of 7.8 by the introduction of sulfur vacancies which is

much higher than the available values reported of  $\text{ZnIn}_2\text{S}_4$  so far.

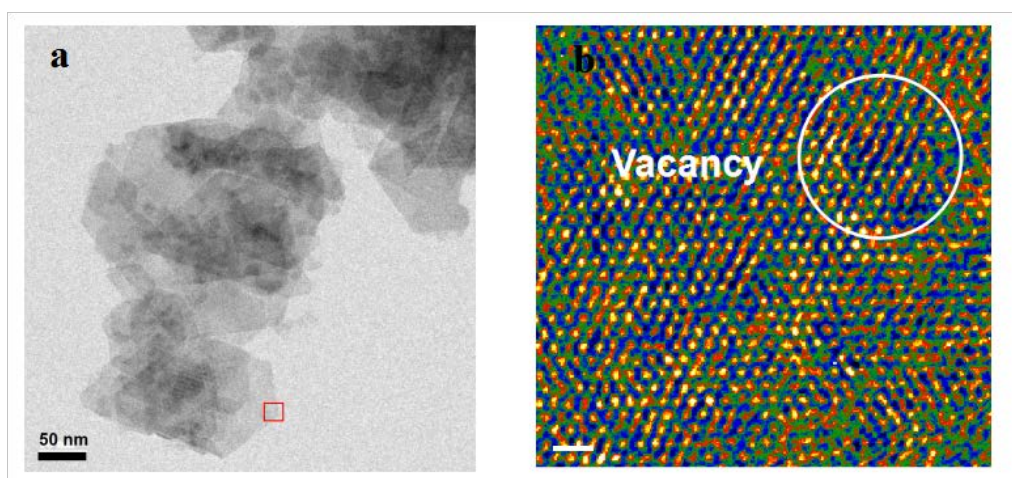


**Figure 1.** (a) TEM image of monolayer  $\text{ZnIn}_2\text{S}_4$  with S vacancies and (b) false-colour image of the HRTEM image of the region outlined in red in (a)

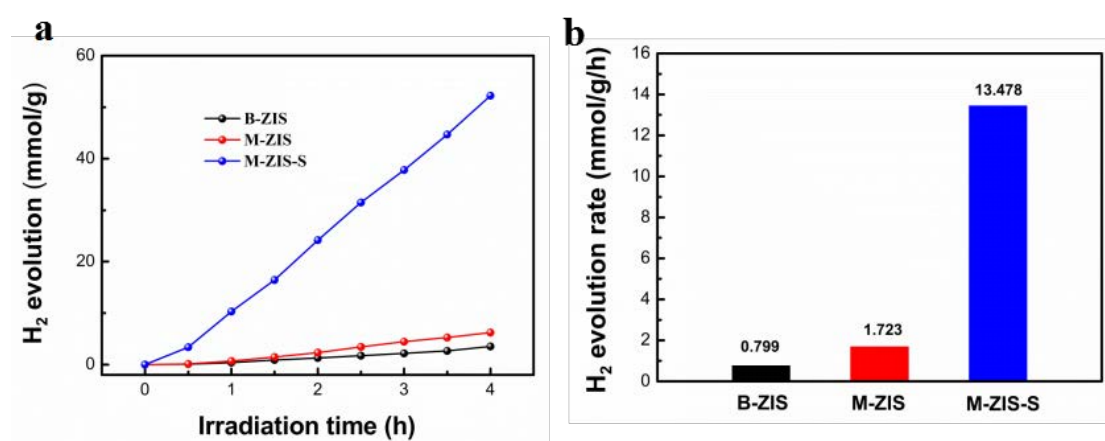


**Figure 2.** (a) Photocatalytic  $\text{H}_2$  evolution and (b)  $\text{H}_2$  evolution rates of B-ZIS (bilayer  $\text{ZnIn}_2\text{S}_4$ ), M-ZIS (monolayer  $\text{ZnIn}_2\text{S}_4$ ), and M-ZIS-S (monolayer  $\text{ZnIn}_2\text{S}_4$  with S vacancies).

## References

1. Maeda, K.; Domen, K., Photocatalytic Water Splitting: Recent Progress and Future Challenges. *J. Phys. Chem. Lett.* 2010, 1 (18), 2655-2661.
2. Zhou, M.; Lou, X. W.; Xie, Y., Two-dimensional nanosheets for photoelectrochemical water splitting: Possibilities and opportunities. *Nano Today* 2013, 8 (6), 598-618.
3. Li, W. J.; Lin, Z. Y.; Yang, G. W., A 2D self-assembled  $\text{MoS}_2/\text{ZnIn}_2\text{S}_4$  heterostructure for efficient photocatalytic hydrogen evolution. *Nanoscale* 2017, 9 (46), 18290-18298.

# Enhancing and stabilizing effect of the Au doping on PtCo/C nanoparticles for Proton exchange membrane fuel cell

*Juhyuk Choi, Hyunjoo Lee\**

*Department of Chemical and Biomolecular Engineering, Korea Advanced Institute of Science and Technology, Daejeon 34141, Republic of Korea*

Proton exchange membrane fuel cells (PEMFC) are considered as a renewable energy source for a future hydrogen energy society [1]. However, highly active and durable catalysts are required for the PEMFCs because of their high overpotential at the cathode and exposure under the acidic condition for oxygen reduction reaction (ORR) [2-6]. Many catalysts have been reported in efforts to enhance activity and durability for the ORR. However, most of them have complicated synthetic procedures which cannot be scaled-up, and have mainly been tested in a half-cell system. High activity in a half-cell test does not guarantee better performance in a single-cell system. In this work, we synthesized an Au-doped PtCo/C catalyst using a simple method of gas-phase reduction and galvanic replacement, and its activity and durability were tested in a both half-cell and single-cell. When current densities were compared at 0.6 V after a durability test of 30,000 cycles in 0.6 – 1.0 V, the values were 1.40, 0.81, and 0.63 A cm<sup>-2</sup> for the Au-doped PtCo/C, acid-treated PtCo/C, and commercial Pt/C catalysts, respectively. This facile method can provide a more realistic strategy to design better ORR catalysts for PEMFC application. Density functional theory (DFT) calculations confirmed that surface oxygen species bound more weakly at the catalyst surface and migration of a Co atom (Co segregation) to the surface was suppressed in the presence of Au. This facile method can provide a more realistic strategy to design better ORR catalysts for PEMFC application.

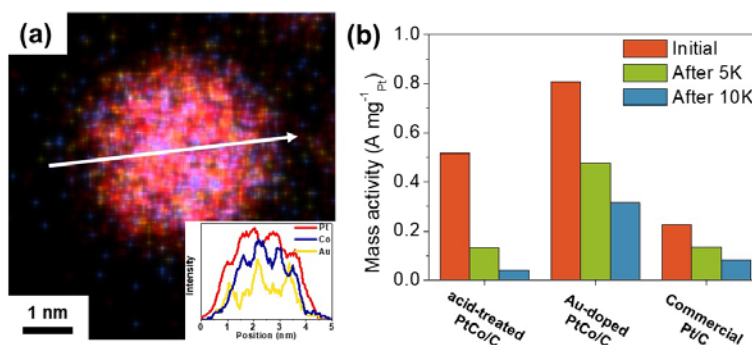


**Figure 1.** (a) EDS mapping images (inset: elemental line-scanning images) for Au-doped PtCo/C, (b) A photograph of the Au-doped PtCo/C catalyst synthesized in one batch, (c) The changes of mass activity after the durability tests.

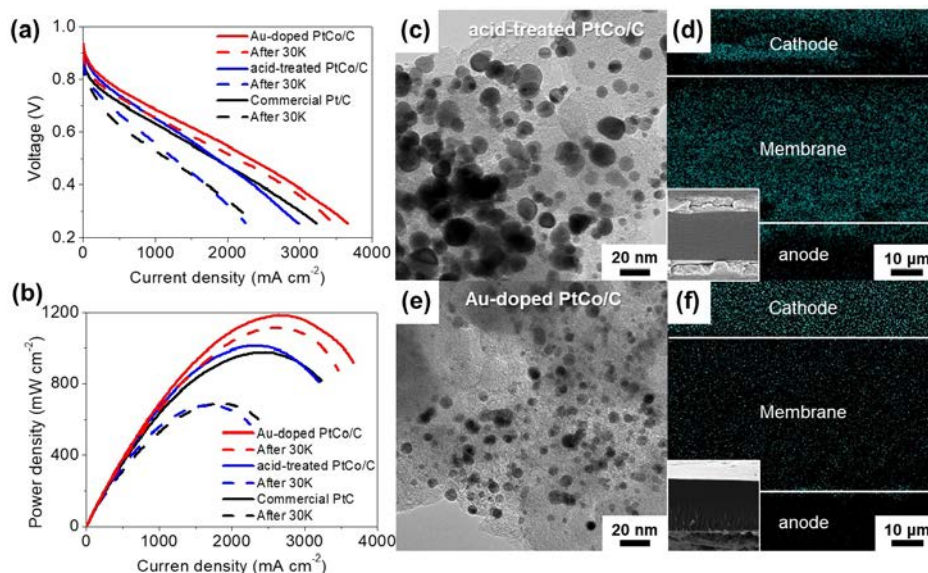


**Figure 2.** (a, b) I-V polarization curves of single-cells catalysts. (c, e) TEM images of the catalysts and (d, f) cross-sectional SEM-EDS mapping images of the MEAs (blue: Co) for the acid-treated PtCo/C and the Au-doped PtCo/C after 30,000 cycles of the durability tests.

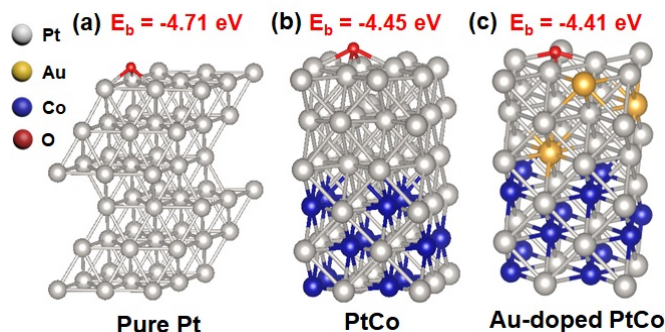


**Figure 3.** DFT calculation unit cell models for the (a) pure Pt, (b) as-made PtCo, (c) PtCo@PtAu, and the calculated oxygen binding energies (Pt: grey, Au: yellow, Co: blue, O: red).

## References

- [1] M. K. Debe, *Nature*, 486 (2012) 43.
- [2] N. M. Markovic, T. J. Schmidt, V. Stamenkovic, P. N. Ross, *Fuel Cells*, 1 (2001) 105.
- [3] J. Choi, Y. Lee, J. Kim, H. Lee, *J. Power Sources*, 307 (2016) 883.
- [4] J. Zhang, H. Yang, J. Fang, S. Zou, *Nano Lett.* 10 (2010) 638.
- [5] C. Cui, L. Gan, H.H. Li, S.H. Yu, M. Heggen, P. Strasser, *Nano Lett.* 12 (2012) 5885.
- [6] J. Wu, L. Qi, H. You, A. Gross, J. Li, H. Yang, *J. Am. Chem. Soc.* 134 (2012) 11880.

# Direct Production of Synthetic Natural Gas from CO<sub>2</sub> and H<sub>2</sub>O by Integrated Solid Oxide Electrolysis and Syngas Methanation

*Dr. Chalachew Mebrahtu, Institut für Technische und Makromolekulare Chemie (ITMC), RWTH Aachen University, Aachen, Germany; Prof. Dr. Rüdiger-A. Eichel, Institute of Energy and Climate Research, Fundamental Electrochemistry (IEK-9), Forschungszentrum Jülich GmbH, Jülich, Germany; Prof. Dr. Regina Palkovits, Institut für Technische und Makromolekulare Chemie (ITMC), RWTH Aachen University, Aachen, Germany*

## Introduction

The conversion of CO<sub>2</sub> into synthetic fuels and value added chemicals is currently of great interest in a rapidly expanding area of research tackling problems related to CO<sub>2</sub> emissions and renewable energy storage [1]. Among the CO<sub>2</sub> conversion methodologies, co-electrolysis with subsequent syngas methanation bears a high potential as a future element for sustainable energy generation and storage. High temperature co-electrolysis - i.e. the simultaneous CO<sub>2</sub> activation and water splitting process by means of electrolysis - integrated with adaptive syngas methanation enables the design of novel power-to-gas technologies. The special advantage of high-temperature co-electrolysis is the possibility to produce tailor-made synthesis gas compositions without further downstream process steps [2].

## Approach

The present work targets optimization of the methane selectivity, design aspects, and dynamic responds of the integrated setup. Prior to the integration into a single setup, both reactions are optimizing individually. Thus, syngas methanation was performed in a fixed-bed reactor using a hydrotalcite derived Ni-based (i.e. 20%Ni-2%Fe/(Mg, Al)O<sub>x</sub>) and a commercial Ni/Al<sub>2</sub>O<sub>3</sub> (CRG-F) methanation catalyst as selected materials. CO, CO<sub>2</sub>, H<sub>2</sub> and H<sub>2</sub>O fractions were varied in the feed mixture in order to simulate potential feeds provided by co-electrolysis.

## Results: catalyst characterizations and syngas methanation

20%Ni-2%Fe/(Mg, Al)O<sub>x</sub> was characterized using different techniques (**Figure 1**). From the XRD patterns, reflexes of hydrotalcites (dried) and NiO (calcined) were observed. TEM image of the reduced sample also proved a good metallic dispersion and a small average particle diameter (9 nm).



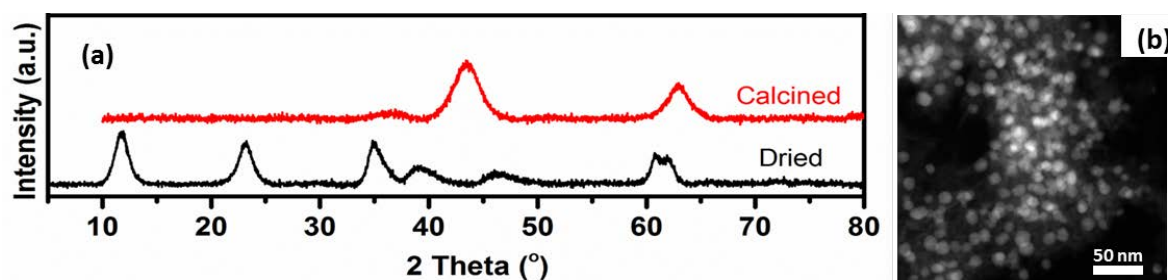


**Figure 1:** (a) XRD and (b) TEM image of the 20%Ni-2%Fe/(Mg, Al)O<sub>x</sub> catalyst.

The syngas conversion rate rises as the CO fraction increases. Substitution of H<sub>2</sub> by water (10%, 30%, and 50%) decreases the activity of both catalysts potentially caused by oxidation of the metallic Ni. As shown in **Figure 2**, a higher rate of CO<sub>x</sub> conversion was reached for the 20%Ni-2%Fe/(Mg, Al)O<sub>x</sub> catalyst, which can be assigned to the optimized amount of basic sites and superior metal dispersion.

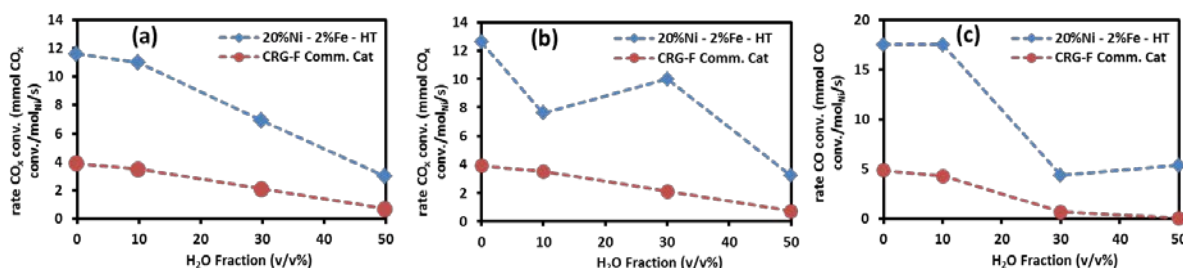


**Figure 2:** The catalytic syngas methanation under different CO and H<sub>2</sub>O fractions: (a) 5%CO, (b) 10%CO, and (c) 20%CO.

## Conclusion

A fixed bed reactor was built and syngas methanation was performed with different feed mixtures to optimize the catalytic performance under harsh reaction conditions (higher H<sub>2</sub>O fraction for example). An acceptable rate of syngas conversion was obtained with H<sub>2</sub>O contents up to 30% and was found to decrease significantly with 50% H<sub>2</sub>O in the feed. The next step will be coupling of the individually optimized reactors into a single setup for the direct generation of methane from CO<sub>2</sub> and H<sub>2</sub>O.

## Acknowledgment

We thank JARA Energy funded by the Excellence Initiative by the German federal and state governments to promote science and research at German universities.

## References

- [1] C. Mebrahtu, F. Krebs, S. Perathoner, S. Abate, G. Centi, R. Palkovits, *Catal Sci & Technol* **2018**, *8*, 1016.
- [2] S.R. Foit, I.C. Vinke, L.G.J. de Haart, R.-A. Eichel, *Angew. Chem.Int. Ed.* **2017**, *56*, 5402.

# Characterization of Particle Size and Distribution of Noble Metal Catalysts by Ultrathin Sectioning and TEM

*W. Y. YANG, Fushun Research Institute of Petroleum and Petrochemicals, Fushun, China; F. X. LING, Fushun Research Institute of Petroleum and Petrochemicals, Fushun, China; H.C. ZHANG, Fushun Research Institute of Petroleum and Petrochemicals, Fushun, China; S. J. WANG, Fushun Research Institute of Petroleum and Petrochemicals, Fushun, China*

Metal nanoparticle size and size distribution of supported precious metal catalysts have an extremely important influence on catalyst performance[1].

For Transmission Electron Microscopy(TEM), it usually has higher resolution, which can easily distinguish metal nanoparticles and perform particle size measurement and size distribution statistics. However, for some supported precious metal catalysts, the metal nanoparticles can not effectively distinguish between metal nanoparticles and catalyst carriers, because of its small size resulting in very weak mass thickness contrast.

In this paper, ultra-thin sectioning technology was used to deal with Pd/Al<sub>2</sub>O<sub>3</sub> catalyst, then the size and distribution of Pd particles were easily measured by TEM. Figure 1 (a) is a TEM image of the sample with a section thickness of 100nm. It can be seen that a relatively flat large-area thin region, approximately 0.5×1.0μm<sup>2</sup>, can be obtained, and the original texture structure of the catalyst can be retained without being destroyed. Figure 1(b) shows the TEM image of the ultrathin section of the catalyst with a thickness of 10nm. It can be seen that the texture of the catalyst remains intact and transparent at a thin thickness. Even if the size of the nanoparticles is very small, a significant contrast image can still be formed and the Pd particles can be easily distinguished.

Obviously, this particle size distribution obtained from a large number of particle size measurement data can better reflect the true state of the catalyst, and it is more convincing to modulate the performance of the catalyst according to metal nanoparticle size and size distribution

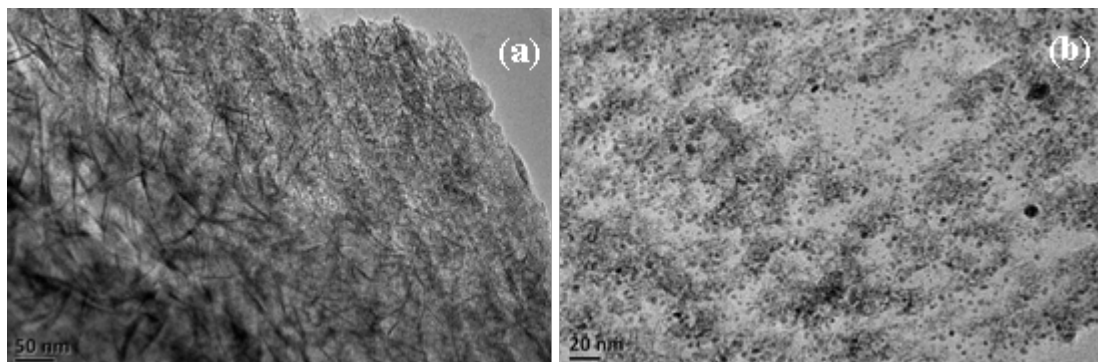


Figure 1 : TEM image of ultrathin section of catalyst. (a) Section thickness 100nm; (b) Slice thickness 10nm

## References

- [1] J. Xie, J. Yang, A. I. Dugulan, et al. Size and Promoter Effects in Supported Iron Fischer–Tropsch Catalysts: Insights from Experiment and Theory [J]. *ACS Catalysis*, 2016,6(5): 3147-3157.



# Ni-Ru/complex oxide nanocomposites supported on ordered mesoporous MgAl<sub>2</sub>O<sub>4</sub> as catalysts for methane and biofuels reforming

Pavlova S.<sup>1</sup>, Fedorova Y.<sup>1</sup>, Ishchenko A.<sup>1,2</sup>, Melgunov M.<sup>1,2</sup>, Simonov M.<sup>1</sup>, Bobin A.<sup>1</sup>, Rogov V.<sup>1,2</sup>, Krieger T.<sup>1</sup>, Glazneva T.<sup>1,2</sup>, Sadykov V.<sup>1,2</sup>, Lukashevich A.<sup>1</sup>, Roger A.-C.<sup>3</sup>

<sup>1</sup>Boriskov Institute of Catalysis, Russian Federation, [sadykov@catalysis.ru](mailto:sadykov@catalysis.ru);

<sup>2</sup>Novosibirsk State University, Russian Federation; <sup>3</sup> University of Strasbourg, France

## 1. Scope

Design of efficient, inexpensive and stable to coking catalysts for transformation of methane and biofuels into syngas and hydrogen is an urgent problem of sustainable and renewable energy field including hydrogen production, synfuels synthesis, internal reforming in solid oxide fuel cells, etc. In this study, for the first time, the results on synthesis, structural and redox properties of Ni-Ru/complex oxide nanocomposite catalysts loaded on ordered mesoporous MgAl<sub>2</sub>O<sub>4</sub> support are presented. Their activity in methane dry reforming (MDR), ethanol steam reforming and partial oxidation, ethyl acetate and glycerol autothermal reforming was estimated and discussed in relation to their physical-chemical properties.

## 2. Experimental

As a support the ordered mesoporous MgAl<sub>2</sub>O<sub>4</sub> prepared by the one-pot evaporation induced self-assembly (EISA) method [1] has been used. Nanocomposite active components containing 20%PrNi<sub>0.9</sub>Ru<sub>0.1</sub>O<sub>3</sub>(PNR), 2%wtNi+2%wtRu+10%MnCr<sub>2</sub>O<sub>4</sub>(NRM) or 5%wtNi+1%wtRu+10%Ce<sub>0.35</sub>Zr<sub>0.35</sub>Pr<sub>0.3</sub>O<sub>2</sub> (NRC) were loaded on the support by the incipient impregnation with corresponding solutions, and, for NRC, with addition of acetylacetone as a complexing agent. MgAl<sub>2</sub>O<sub>4</sub> support and catalysts were calcined under air at 700°C. The textural, structural, surface properties of samples and their reactivity have been characterized by N<sub>2</sub> adsorption-desorption analysis, BET, XRD, TEM with EDX, XPS, FTIRS of CO test molecule, H<sub>2</sub> and EtOH TPR. The catalytic properties of samples in methane dry reforming (MDR), ethanol partial oxidation and steam reforming, ethyl acetate and glycerol autothermal reforming were tested using tubular plug-flow reactors at short contact times following procedures earlier described in details [2, 3].

### 3. Results and discussion

According to low angles XRD,  $\text{MgAl}_2\text{O}_4$  has the ordered mesoporous structure confirmed by the  $\text{N}_2$  adsorption-desorption data showing IV type isotherm with H1 shaped hysteresis loop associated with 2D hexagonal cylindrical-like pores. TEM images show this ordering of pores (Fig.1), and EDX data confirm the spinel formation.  $\text{MgAl}_2\text{O}_4$  has SSA  $290 \text{ m}^2/\text{g}$ , pore volume  $0.63 \text{ cm}^3/\text{g}$  and a narrow pore size distribution with the mean size 12 nm. The catalysts retained mesoporous structure though their SSA decreased to  $100\text{-}210 \text{ m}^2/\text{g}$ . In XRD patterns reflections corresponding to supported oxide phases were weak and broaden (NRC) or not revealed (PNR, NRM) indicating their high dispersion and strong interaction with support, which agrees with XPS data. FTIRS spectra of adsorbed CO demonstrated suppression of support acidity and a high dispersion of Ni-Ru nanoparticles even in reduced catalysts with broad variation of the density of accessible metal sites and the ratio of terminal/bridging carbonyl bands intensity reflecting population of isolated/clustered sites [2].  $\text{H}_2$  and EtOH TPR data revealed a high reactivity of all catalysts substantially exceeding that of Ni-loaded mesoporous  $\text{MgAl}_2\text{O}_4$ . In all studied reactions developed catalysts demonstrated a high and stable performance exceeding that for those on Mg-doped  $\gamma\text{-Al}_2\text{O}_3$  [2, 3] due to a higher dispersion of the active component, higher reactivity and hampering of  $\text{C}_2\text{H}_4$  generation/coking due to suppressed acidity. Specific catalytic activity correlates with the number of metal surface sites estimated by FTIRS of adsorbed CO. At  $\sim 750 \text{ }^\circ\text{C}$  syngas yield approaches the equilibrium level even at ms contact times (Fig. 2).

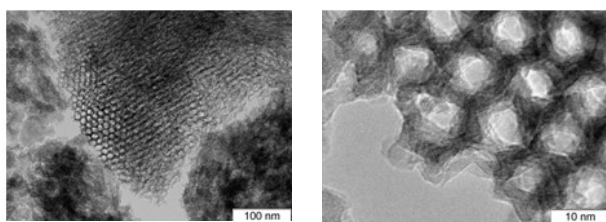


Fig. 1. TEM image of  $\text{MgAl}_2\text{O}_4$

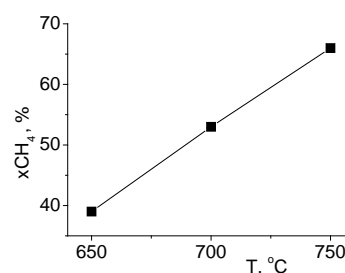


Fig. 2.  $x\text{CH}_4$  vs. T for PNR/ $\text{MgAl}_2\text{O}_4$  catalyst in MDR, 15%  $\text{CH}_4$  + 15%  $\text{CO}_2$  +  $\text{N}_2$ ,  $\tau$ 14 ms

Support by RFBR-CNRS 18-58-16007\_a Project is gratefully acknowledged.

### References.

- [1] Morris S.M., Fulvio P.F., Jaroniec M.M., J. Am. Chem. Soc., 2008, 130, 15210–15216.
- [2] Sadykov V., Pavlova S., Roger A.-C., et al, Catal. Today 2017, 293-294, 176–185.
- [3] Sadykov V., Mezentseva N., Simonov M., Pavlova S., Roger A.-C., et al, Int. J. Hydrogen Energy 2015, 40, 7511-7522.

# Analysis of photocatalytic water splitting over perovskites literature using data mining tools

Ramazan Yıldırım, Elif Can,

*Bogazici University, Department of Chemical Engineering, Istanbul, Turkey*

## Introduction

H<sub>2</sub> is considered as a promising energy carrier due to its high energy density, abundance in nature and cleanness. Semiconductor based photocatalytic water splitting (PWS) have been extensively studied in recent years because it is clean, renewable, and free of charge. Perovskites have also gained significant attention in recent years because they can be not only synthesized in numerous formulations and structures, but also easily modified by various methods. Existence of numerous options for materials and methods constitutes a large domain for PWS research. The machine learning and data mining tools, which were developed to extract non-trivial, previously unknown, and potentially useful knowledge from that large data domain can be used.

In this work, a database having 540 data points from 151 published papers on PWS over perovskites was constructed and analyzed using association rule mining (ARM) to determine the most important factors, decision tree (DT) to develop heuristics for the future studies and random forest (RF) regression to build predictive models [1].

## Methods

The database was constructed from 151 experimental papers on PWS over perovskites published in 2005-2017; online sources including Elsevier, Wiley Online Library, American Chemical Society and Royal Society of Chemistry were reviewed. All models were developed in RStudio; *apriori* algorithm in *arules* [2] package was used for association rule mining while *rpart* [3] and *randomForest* [4] were used for classification trees and random forest, respectively.

## Results

The analysis revealed that the most common perovskites in PWS are tantalates followed by titanates, niobates and In-perovskites; NaTaOs are the most frequently studied tantalates, and they are especially effective under UV light. About

half (48%) of perovskites in database are doped to A-site (31%) and/or B-site (27%). The effect of doping on band gap is observable; however, only some portion of doped catalysts had better PWS activity than plain perovskites. The doping also improved stability in some cases.

Solid-state reaction, hydrothermal synthesis, polymerized-complex and sol-gel are the most common methods for perovskite preparation; their average performances are similar for UV tests. As can be seen from Figure 1a. effects of preparation method on surface area, band gap and crystal structure are also observable; the last two partially explain the hydrogen production rates as well. Approximately 80% of cases contain co-catalyst (Pt is the most common). There are various successful applications; however, in overall, only some fraction of co-catalyst results in higher performance than the bare perovskites.

DT analysis provides some simple and easy to follow selection rules for both H<sub>2</sub> production (Figure 1b.) and band gap. RF models for H<sub>2</sub> production (especially for visible light) are quite successful in predicting the data not seen before; the same is true for band gap prediction (Figure 1c.).

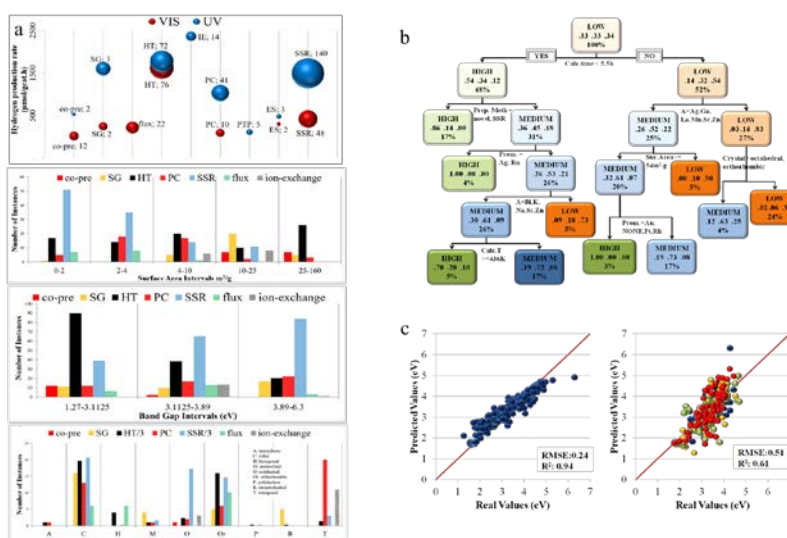


Fig 1. (a) Effects of preparation method on H<sub>2</sub> production, surface area, band gap and crystal structure. (b) The optimal decision tree for visible light data (c) Results of the random forest analysis of band gaps

## Acknowledgement

This work is financially supported by Bogazici University through project BAP-18A05D2.

## References

- [1] E. Can and R. Yildirim, 2019, Applied Catalysis B: Environmental, Vol.242, pp. 267-283.
- [2] M. Hahsler, C. Buchta, B. Gruen, A. Michael, C. Buchta, B. Gruen, K. Hornik, I. Johnson, 2018, Package 'arules'.
- [3] T. Therneau, B. Atkinson, B. Ripley, 2018, Package 'rpart'.
- [4] A. Liaw, M. Wiener, 2018, Package 'randomForest'.

# Study on the mechanism of photocatalytic reduction of CO<sub>2</sub> over the Ga<sub>2</sub>O<sub>3</sub> photocatalyst without Ag co-catalyst

*Masato Akatsuka, Yu Kawaguchi, Ryota Ito, Akiyo Ozawa, Muneaki Yamamoto, Tetsuo Tanabe, Tomoko Yoshida, Osaka City University, Osaka, Japan*

## Introduction

Gallium oxide (Ga<sub>2</sub>O<sub>3</sub>) is attracting attention as a photocatalyst because Ag loaded Ga<sub>2</sub>O<sub>3</sub> photocatalysts can reduce CO<sub>2</sub> with H<sub>2</sub>O to produce CO [1], although the reaction rate of CO production is not high enough for practical use. In our previous work [2], Ga<sub>2</sub>O<sub>3</sub> photocatalyst obtained by calcining Ga(NO<sub>3</sub>)<sub>3</sub> · 8H<sub>2</sub>O around 823 K in air showed very high CO production rate without Ag co-catalyst. It is noteworthy that this Ga<sub>2</sub>O<sub>3</sub> photocatalyst did not need Ag co-catalyst which was essential to reduce CO<sub>2</sub> to CO. In this study, we carried out various characterizations and photocatalytic CO<sub>2</sub> reduction tests to discuss the reason why the photocatalytic CO<sub>2</sub> reduction with H<sub>2</sub>O was enhanced over Ga<sub>2</sub>O<sub>3</sub> without Ag co-catalyst.

## Experimental

Ga<sub>2</sub>O<sub>3</sub> photocatalyst samples were prepared by calcination of Ga(NO<sub>3</sub>)<sub>3</sub>·8H<sub>2</sub>O powder in air at given temperatures (673 - 1173 K) for 4 h. Prepared samples are denoted as T-Ga<sub>2</sub>O<sub>3</sub> with T, calcination temperature. Ga<sub>2</sub>O<sub>3</sub> surface area was evaluated by BET method. XRD and XAFS spectra were obtained to investigate the structure of Ga<sub>2</sub>O<sub>3</sub>. We carried out in-situ FT-IR measurement to investigate the chemical state of adsorbed molecules on the Ga<sub>2</sub>O<sub>3</sub> surface during CO<sub>2</sub> reduction with water.

## Result and discussion

Ga<sub>2</sub>O<sub>3</sub> samples calcined at lower temperature showed larger surface areas. We carried out photocatalytic CO<sub>2</sub> reduction with H<sub>2</sub>O over all prepared Ga<sub>2</sub>O<sub>3</sub> samples and Fig.1 shows CO and H<sub>2</sub> production rates plotted to the surface area for each Ga<sub>2</sub>O<sub>3</sub> sample. It was found that the H<sub>2</sub> production rate increases with the surface area of the sample. As for CO production, Ga<sub>2</sub>O<sub>3</sub> prepared by calcination at 823 K (823-Ga<sub>2</sub>O<sub>3</sub>) showed a specifically high activity, although the H<sub>2</sub> production rate for this sample was comparable with those for 673, 773, 873-Ga<sub>2</sub>O<sub>3</sub>. The CO production rate of 823-Ga<sub>2</sub>O<sub>3</sub> was about 5 times higher than a highly active Ag loaded Ga<sub>2</sub>O<sub>3</sub>. If photo absorbance or electron and hole transfers to Ga<sub>2</sub>O<sub>3</sub> surface are improved in

823-Ga<sub>2</sub>O<sub>3</sub>, not only CO production rate but also H<sub>2</sub> production rate should be specifically high. H<sub>2</sub> production rates in the reaction tests with and without CO<sub>2</sub> flow were almost the same, suggesting that H<sub>2</sub> production site and CO production site are independence in 823-Ga<sub>2</sub>O<sub>3</sub>.

XRD and XAFS measurements revealed that  $\beta$ -phase Ga<sub>2</sub>O<sub>3</sub> increased in  $\gamma$ -phase Ga<sub>2</sub>O<sub>3</sub> as the calcination temperature rose. As is evident from the XRD pattern of 823-Ga<sub>2</sub>O<sub>3</sub>, this sample consisted of  $\beta$ ,  $\gamma$ -mixed phase Ga<sub>2</sub>O<sub>3</sub> with the lowest crystallinity (Fig. 2). In-situ FT-IR measurements suggested that 823-Ga<sub>2</sub>O<sub>3</sub>, which showed the highest photocatalytic activity can adsorb larger amount of CO<sub>2</sub> molecules as monodentate bicarbonate species even under water vapor atmosphere

while the inactive Ga<sub>2</sub>O<sub>3</sub> sample cannot remain adsorbed this species. The enhancement of CO<sub>2</sub> adsorption might be caused at the  $\beta$ ,  $\gamma$ -Ga<sub>2</sub>O<sub>3</sub> interface in 823-Ga<sub>2</sub>O<sub>3</sub>, in other words, such a hetero structure would provide high activity for CO<sub>2</sub> reduction without Ag co-catalyst.

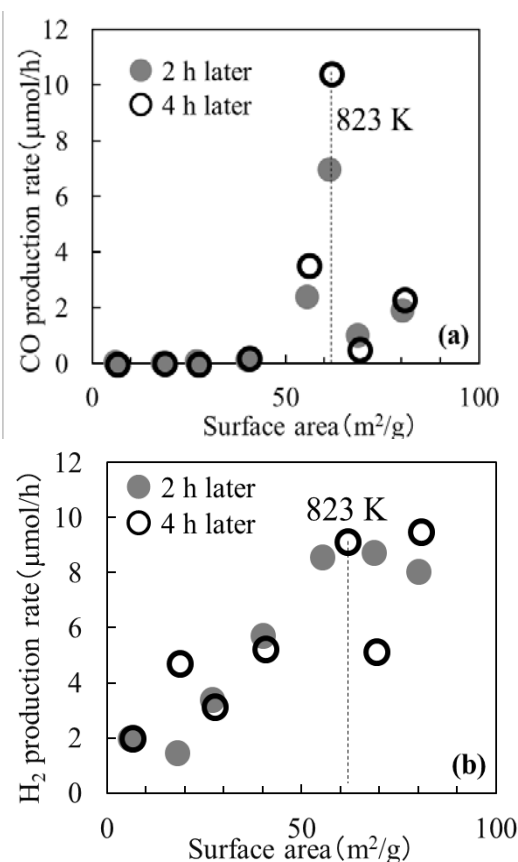


**Fig. 1** (a) CO and (b) H<sub>2</sub> production rates plotted to surface area of Ga<sub>2</sub>O<sub>3</sub> samples

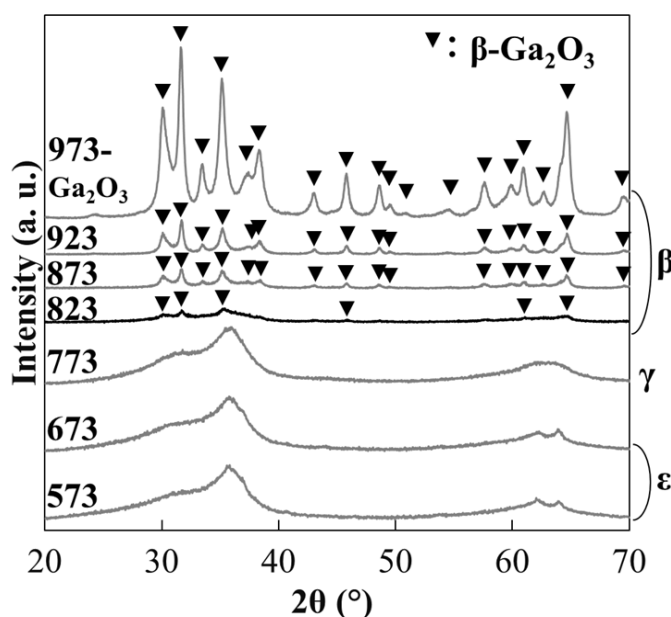


**Fig. 2** XRD patterns of the prepared Ga<sub>2</sub>O<sub>3</sub>

## References

- [1] M. Yamamoto, T. Yoshida, N. Yamamoto, H. Yoshida and S. Yagi, 2014, In-situ FT-IR study on the mechanism of CO<sub>2</sub> reduction with water over metal (Ag or Au) loaded Ga<sub>2</sub>O<sub>3</sub> photocatalysts, *J Surf. Sci. Nanotech.*, 12, 299-303.
- [2] Y. Kawaguchi, M. Akatsuka, M. Yamamoto, K. Yoshioka, A. Ozawa, Y. Kato, T. Yoshida, 2018, Preparation of gallium oxide photocatalysts and their silver loading effects on the carbon dioxide reduction with water, *J. Photochem. Photobiol. A: Chem.*, 358, 459-464.

# Synthesis of mixed alcohols with enhanced C3+ alcohol production by CO hydrogenation over potassium promoted molybdenum sulfide

*Feng Zeng<sup>‡</sup>, Chair of Heterogeneous Catalysis and Chemical Technology, ITMC, RWTH Aachen University, Aachen, Germany; Xiaoying Xi<sup>†</sup>, Green Chemical Reaction Engineering, Engineering and Technology Institute Groningen, University of Groningen, Groningen, Netherlands; Huatang Cao, Department of Advanced Production Engineering, Engineering and Technology Institute Groningen, University of Groningen, Groningen, Netherlands; Yutao Pei, Department of Advanced Production Engineering, Engineering and Technology Institute Groningen, University of Groningen, Groningen, Netherlands; Hero Jan Heeres<sup>\*</sup>, Green Chemical Reaction Engineering, Engineering and Technology Institute Groningen, University of Groningen, Groningen, Netherlands; Regina Palkovits<sup>\*</sup>, Chair of Heterogeneous Catalysis and Chemical Technology, ITMC, RWTH Aachen University, Aachen, Germany; <sup>‡</sup> These authors have contributed equally to this work; <sup>\*</sup> Corresponding authors: [h.j.heeres@rug.nl](mailto:h.j.heeres@rug.nl); [palkovits@itmc.rwth-aachen.de](mailto:palkovits@itmc.rwth-aachen.de)*

## Abstract

Since world's crude oil reserves are quickly consumed, alternatives for gasoline like alcohols, natural gas, and hydrogen are indispensable for a sustainable society. Alcohols including methanol and ethanol have been intensively studied and used as gasoline blend components. However, methanol and ethanol hold low energy density, high vapor pressure, and high affinity to water leaving room for further improvement. Compared with methanol and ethanol, C3+ alcohols generally possess higher energy density and lower vapor pressure, and C3+ alcohols like butanol exhibit a lower affinity to water. Thus alcohol mixtures with high C3+ alcohol content may have better performance as a gasoline blend component than lower alcohols. Sulfur-resistant potassium promoted molybdenum sulfide (K-MoS<sub>2</sub>) catalysts enable the synthesis of mixed alcohols through CO hydrogenation. However, the liquid oxygenate selectivity and yield of K-MoS<sub>2</sub> catalysts are usually low, and the alcohols follow the Anderson-Schulz-Flory (ASF) distribution, which means methanol and ethanol are the main liquid oxygenates. To achieve high liquid oxygenate selectivity and yield enhancing C3+ alcohol production, we designed multilayer K-MoS<sub>2</sub>

catalysts possessing well-contacted MoS<sub>2</sub> and KMoS<sub>2</sub> phases. The reduced rim site exposure and the MoS<sub>2</sub>-KMoS<sub>2</sub> dual sites induced by the multilayer structure enhance the chain growth through CH<sub>x</sub> β-addition and CO insertion (Figure 1). Accordingly, the observed higher alcohol composition deviates from the ASF distribution. By tailoring the K/Mo ratio, catalysts with varying composition of MoS<sub>2</sub> and KMoS<sub>2</sub> phases were obtained to suppress the formation of hydrocarbons and CO<sub>2</sub> effectively. An optimized production of liquid oxygenates with enhanced C<sub>3</sub>+ alcohol production under appropriate reaction temperature became possible. The optimized catalysts show liquid oxygenate selectivities and yields of 29.1-32.7% and 7.9-10.6%, respectively, yet with good stability. C<sub>3</sub>+ alcohols take up more than 46% (carbon atom fraction) in the liquid oxygenate and the C<sub>3</sub>+ alcohol yield reaches 3.6-5.1% [1].

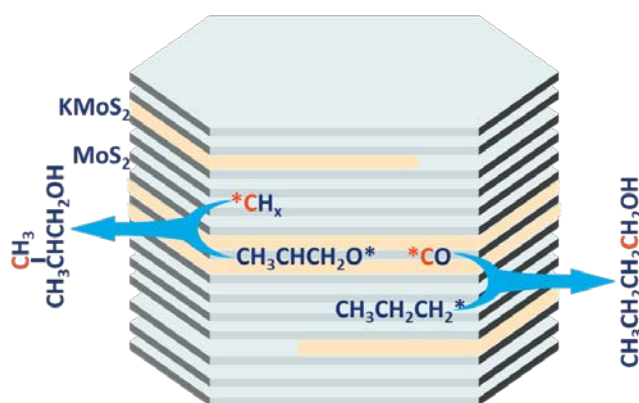


Figure 1. Schematic representation of the formation of linear primary alcohols through CO insertion and branched alcohols through CH<sub>x</sub> β-addition over K-MoS<sub>2</sub>.

### Acknowledgement

Feng Zeng and Xiaoying Xi acknowledge China Scholarship Council (CSC) for financial support. Regina Palkovits acknowledges the project house P2F (Competence Center Power to Fuel) of RWTH Aachen University financed by the Excellence Initiative of the German federal and state governments to promote science and research at German universities.

### References

[1] Synthesis of mixed alcohols with enhanced C<sub>3</sub>+ alcohol production by CO hydrogenation over potassium promoted molybdenum sulfide, Feng Zeng, Xiaoying Xi, Huatang Cao, Yutao Pei, Hero Jan Heeres, Regina Palkovits, *submitted*



# Progress in 1D and 3D Nanocrystal Zeolites for Hydrocarbon Cracking for Naphtha Reforming

Emad N. Al-Shafei<sup>1\*</sup>, Oki Muraza<sup>2</sup>, Mohammed A. Sanhoob<sup>2</sup>, Anas K. Jamil<sup>2</sup>,  
Mohammad Al-Bahhar<sup>1</sup>, Ali N. Al-Jishi<sup>1</sup>, Ki-Hyouk Choi<sup>1</sup>, Mohamed A. Abdullah<sup>1</sup>, and  
Ali S. Alnaser<sup>1</sup>

<sup>1</sup> Research and Development Center, Saudi Aramco, Dhahran 31311, Saudi Arabia

<sup>2</sup> Center of Excellence in Nanotechnology and Chemical Engineering, King Fahd  
University of Petroleum & Minerals (KFUPM), Dhahran 31261, Saudi Arabia.

## Abstract:

Zeolites are one of the major components of catalysts in refinery and petrochemical industry. In spite of well established protocols for using zeolite in commercial application, there are still several challenges that limit its performance with regards to selectivity and life-time. Activity of zeolite is generally deteriorated by coking and structural change during reaction. This study aimed to develop nano-structural zeolite having better stability for hydrocarbon conversion reaction [1]. In the study, zeolite crystal size was reduced to nanoscale to shorten the diffusion path length for improving the accessibility of molecules and hence accelerating the reaction rate. On the other hand, vulnerability of zeolite framework in hydrothermal condition was believed to open new windows to effectively modify and even to synthesize new zeolites [2]. The study investigated the effect of synthesis parameters on the catalyst activity and hydrothermal stability of nano-structured MFI and TON zeolites (Figure 1) having nano-sized one-dimensional and three-dimensional pores.

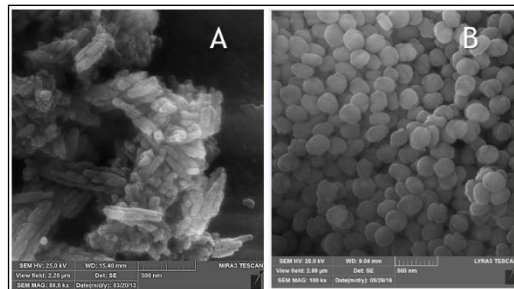


Figure 1. Nano-structures zeolite of TON (A) and MFI (B)

The primary and secondary cracking of product yield strongly depended on the stable framework and zeolite dimensional pores structure. Nano-structured MFI zeolite showed much higher and stable conversion in hydrocarbon cracking over time than that of conventional micro MFI as shown in Figure 2. This study also investigated the kinetics and reaction pathway of hydrocarbon cracking, cyclisation and isomerization to optimize the yield of reformate naphtha product. It was concluded that short diffusion path and 3D structural pores of nano zeolite were significant factor.

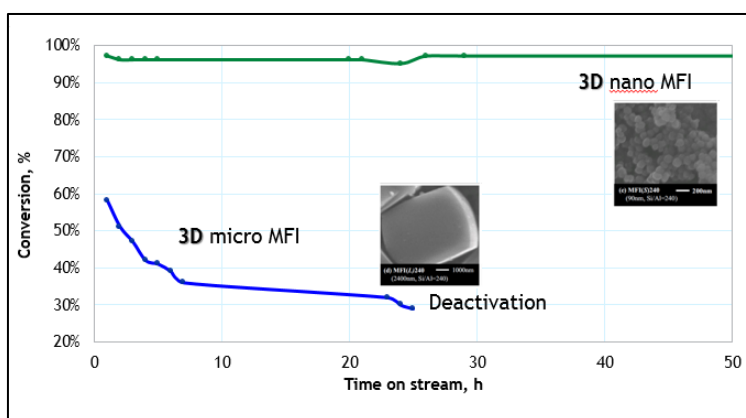


Figure 2. Conversion of hydrocarbon over conventional of micro-size MFI and nano-structured MFI zeolites.

### Reference:

1. Anas K. Jamil, Oki Muraza, Ryota Osuga, Emad N. Shafei, Ki-Hyouk Choi, Zain H. Yamani, Ali Somali, and Toshiyuki Yokoi (2016), Hydrothermal stability of one-dimensional pore ZSM-22 zeolite in hot water, *J. Phys. Chem.* 120, 40
2. Eliášová, P.; Opanasenko, M.; Wheatley, P. S.; Shamzhy, M.; Mazur, M.; Nachtigall, P.; Roth, W. J.; Morris, R. E.; Čejka, J. (2015), The Ador Mechanism for the Synthesis of New Zeolites. *Chem Soc Rev*, 44, 7177-7206.

# Support Effects in Catalytic Methanol Synthesis

*Jakob M. Christensen, Niels D. Nielsen, Anker D. Jensen*  
*Technical University of Denmark, Kgs. Lyngby, Denmark*

## Introduction

Methanol synthesis is a large-scale process, where  $H_2$  and  $CO_2$  react over a Cu/ZnO/Al<sub>2</sub>O<sub>3</sub> (CZnA) catalyst and form methanol. Despite more than 50 years of research, the origin of CZnA's active sites is still intensely debated. Several studies report a linear relation between the methanol rate ( $g_{MeOH}/g_{cat}/h$ ) and the specific Cu surface area ( $m^2 Cu/g_{cat}$ ) for different Cu-oxide catalysts [1,2]. The ratio between the rate and surface area corresponds to the turnover frequency (TOF: rate per Cu surface atom), which depends strongly on the support. Mechanistic investigations indicate, that the methanol synthesis proceeds via formate (HCOO) on the metal surface [3]. Consequently, it is of great interest to quantify the coverage of formate ( $\theta_{HCOO}$ ) at working conditions. This work seeks to evaluate  $\theta_{HCOO}$  on supported Cu catalysts and examine potential support effects on  $\theta_{HCOO}$ . The evaluation of  $\theta_{HCOO}$  involves development of methods for quantifying  $\theta_{HCOO}$  on catalysts operating at the high-pressure working conditions as well as spectroscopic investigations of metal-support interactions, which can modify the coverage of adsorbate species on the metallic surface of the working catalyst.

## Materials and Methods

Oxide-supported Cu catalysts are characterized by various methods after pre-reduction. Cu surface areas are obtained by surface oxidation using dilute  $N_2O$ , and the results enable the methanol TOF at reaction conditions ( $H_2/CO/CO_2 = 68/29/3$  at 250°C, 50 bar) to be measured by gas chromatography (GC) with subsequent quantification of  $\theta_{HCOO}$  by temperature programmed desorption (TPD) and mass spectrometry (MS). Characteristic IR frequencies of HCOO during desorption from Cu and the stretching frequency of CO bonded to Cu ( $\nu_{CO}$ ) are evaluated by Diffuse Reflectance IR Fourier Transform Spectroscopy (DRIFTS).

## Results and Discussion

Quantification of  $\theta_{HCOO}$  on the Cu surface of Cu/oxide catalysts after methanol synthesis at high temperature and pressure conditions is based on the amount of desorbed  $CO_2$  in a TPD experiment after quenching at reaction conditions. First, the methanol TOF at reaction conditions is measured and followed by rapid cooling with liquid  $N_2$  to preserve  $\theta_{HCOO}$  obtained at reaction conditions. Integrating the amount of

desorbed  $\text{CO}_2$  and  $\text{H}_2$  in a subsequent TPD experiment is a way to quantify  $\theta_{\text{HCOO}}$ . Significant  $\text{H}_2$  desorption from the oxide necessitates the use of desorbed  $\text{CO}_2$  for quantifying  $\theta_{\text{HCOO}}$ . The characteristic desorption temperature for HCOO bonded to Cu is around  $140^\circ\text{C}$  [4]. Raney Cu and Cu/ZnO catalysts yield relatively sharp  $\text{CO}_2$  desorption profiles, and Figure 1 shows, how these catalysts indicate a relation between the apparent  $\theta_{\text{HCOO}}$  and the TOF.

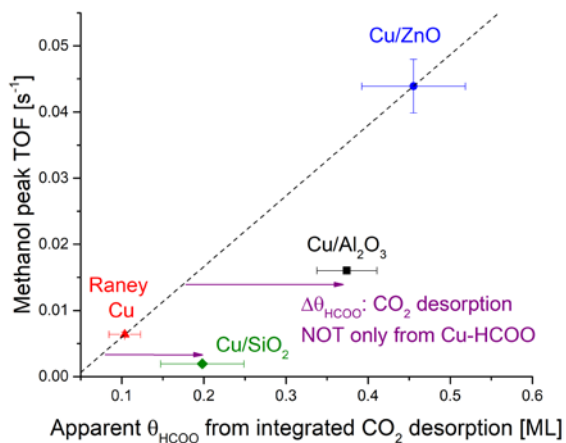


**Figure 1:** Methanol TOF ( $250^\circ\text{C}$ , 50 bar in syngas) as function of apparent  $\theta_{\text{HCOO}}$  based on integration of desorbed  $\text{CO}_2$  post methanol synthesis.

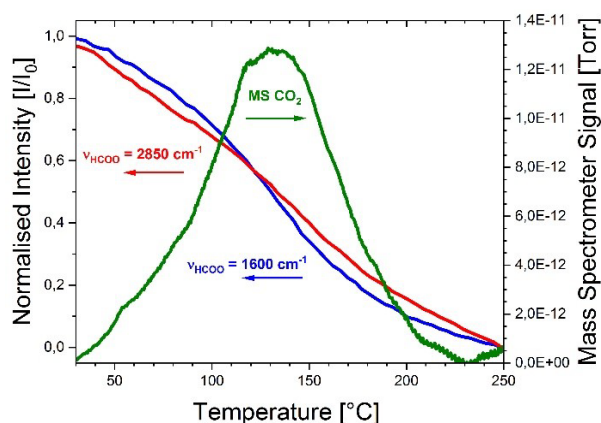


**Figure 2:** Combined MS and DRIFTS during TPD on Cu/ZnO with a partially HCOO-covered surface demonstrate concurrent  $\text{CO}_2$  and HCOO desorption and decreasing  $\nu_{\text{Cu-HCOO}}$ .

DRIFTS provides validation for the method of relating desorbed  $\text{CO}_2$  to  $\theta_{\text{HCOO}}$  by performing a TPD experiment after HCOO synthesis in syngas at  $100^\circ\text{C}$  (1 atm.). Figure 2 shows, for a Cu/ZnO catalyst, how the relative intensity ( $I/I_0$ ) of characteristic frequencies for HCOO on Cu ( $\nu_{\text{Cu-HCOO}}$ ) at 1600 and  $2850\text{ cm}^{-1}$  [4,5] (blue and red curves) and evolution of  $\text{CO}_2$  (green curve) vary, as  $\theta_{\text{HCOO}}$  desorbs upon heating. Concurrent  $\text{CO}_2$  and decreasing  $\nu_{\text{Cu-HCOO}}$  at around  $140^\circ\text{C}$  validates the quantitative method of integrating the  $\text{CO}_2$  desorption. However, other catalysts (Cu/ $\text{Al}_2\text{O}_3$  and Cu/ $\text{SiO}_2$ ) yield ill-defined  $\text{CO}_2$  desorption profiles and higher than expected  $\theta_{\text{HCOO}}$ 's ( $\Delta\theta_{\text{HCOO}}$ ) as shown in Figure 1.  $\text{CO}_2$  desorbed from oxide(s) and other surface species may explain  $\Delta\theta_{\text{HCOO}}$  and ongoing work is designed to examine this further.

Further work includes CO adsorption by IR to evaluate the electron donor ability.

## References

1. C. Baltes et al., *J. Catal.* 258, 334 (2008)
2. M. Kurtz et al., *Cat. Lett.* 86, 77 (2003)
3. S. Fujita, et al., *J. Catal.* 157, 403 (1995)
4. S. Neophytides et al., *App. Cat.*, 86, 45 (1992)
5. D. Clarke et al., *J. Catal.* 154, 314 (1995)

# **Biomass derivatives aldol condensation in continuous flow reactor: activity and stability studies**

*Jennifer Cueto; Laura Faba; Eva Díaz; Salvador Ordóñez, Department of Chemical and Environmental Engineering, Oviedo, Spain*

## **Introduction**

The replacement of fossil fuels involves a high effort to obtain not only alternative liquid fuels, but also new chemical processes to produce thousands of oil-derived chemicals. In this context, the upgrade of waste lignocellulosic biomass is a requirement. Aldol condensation is the key step in one of the most promising approaches, obtaining larger compounds from platform molecules such as furfural (FFL), acetone, cyclopentanone (CPO), etc. In this context, relevant advances are published in batch configuration. However, the scale-up requires a continuous configuration. Up to now, only one paper deals with this point, with promising results but conditioned by a strong deactivation after low time-on-stream (TOS) because of the presence of permanent adsorption [1]. In this work, we propose the use of CPO instead of acetone, obtaining faster reaction and larger compounds. Based on our previous results in batch configuration, an ethanol-water mixture is used as solvent to enhance the solubility, trying to prevent deactivation [2].

## **Materials and methods**

Reactions were carried out in a stainless-steel fixed-bed reactor with ½" i.d. and 6 cm length, at 323 K. The reactor was packed with 0.5 g of MgZr and glass balls. 1 mL·min<sup>-1</sup> is fed, with a 5 wt.% of FFL and CPO in a mixture of ethanol/water (2:1 volume ratio). Samples after different TOS were analyzed by GC-FID.

## **Results**

First experiments were carried out considering different ratios FFL:CPO, involving 10:1, 5:1, 1:1, 1:5, 1:10 and 1:15. Despite the conditions, a high conversion of the limiting reactant (higher than 40 %) is obtained during the first two hours, with a clear decreasing trend to a complete deactivation in less than 4 h, except in the case of 1:10, with a stable C10 yield of 4 % after more than 8 h. Even at the first 120 min, no C15 was observed, at any condition tested. Spent catalysts were recovered and analyzed with the aim of identifying the deactivation cause. Catalytic lixiviation was discarded, whereas XPS results suggest a relevant decrease of free Mg on the surface. Desorption analyses at programmed temperature were carried out under

inert and oxidizing conditions, comparing those results with profiles of pure C10 and C15. Results indicate two different causes of deactivation, being always related to the permanent deposition of heavy compounds. C15 and oligomers containing high amount of furfural when working at 10:1 and 5:1, as it was observed in batch conditions. However, working at stoichiometric or CPO excess, these oligomers indicate a high reactivity to CPO self-condensation. This result was not previously obtained in batch conditions, suggesting a different adsorption mode as function of hydrodynamic conditions (no so preferential to furfural in continuous mode, whereas the CPO adsorption in batch was demonstrated as negligible in comparison to the furfural one) [2]. This hypothesis was corroborated by thermogravimetric analyses and is congruent with the evolution of the carbon balance during the reaction.

With this premise, the role of pH was tested. Different reactions were carried out from the natural pH of the feed (4.75) to pH = 9. In order to analyze if the salt has any role, these pHs were obtained by adding NaOH or NaHCO<sub>3</sub>. Results with NaOH do not show any improvement, whereas in the case of NaHCO<sub>3</sub>, deactivation is slowed down for all the cases conditioned by CPO oligomers. Highlighting results were obtained at pH 8 (isoelectric point of Mg-Zr) and using 1:10, obtaining a stable C10 yield of 17 % for more than 16 h, with 2 % of C15, with a carbon balance closure higher than 95 %.

## Conclusions

Two different permanent adsorptions are identified, involving CPO or FFL as function of the conditions. Deactivation due to FFL cannot be prevented, but the one involving CPO is strongly reduced with the synergic effect of working at the isoelectric point (8) and with bicarbonate in the medium. This produces an optimum charge equilibrium on MgZr surface, introducing extra anchoring points. CPO oligomers are attracted by them, being adsorbed on them, keeping free the required ones for the reaction.

## References

- [1] O. Kikhtyanin, L. Hora, D. Kubicka, Catal. Commun. 58 (2015) 89-92.
- [2] J. Cueto, L. Faba, E. Díaz, S. Ordóñez, ChemCatChem 9 (2017) 1765-1770.

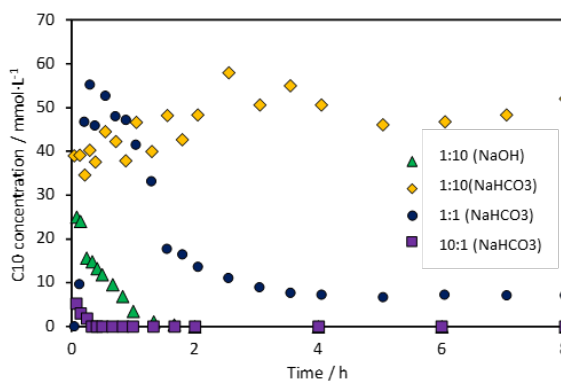


Figure 1. Evolution of C10 with the TOS working at pH 8

# Theoretical studies on the influence of size and metal-support interactions of copper catalysts for CO<sub>2</sub> hydrogenation to methanol

*Amir H. Hakimioun<sup>†</sup>, Bart D. Vandegehuchte,<sup>§</sup> Lennart Joos,<sup>§</sup> Philipp N. Plessow<sup>†</sup>,  
Felix Studt<sup>†‡</sup>*

*<sup>†</sup>Institute of Catalysis Research and Technology (IKFT), Hermann-von-Helmholtz-  
Platz 1, D-76344 Eggenstein-Leopoldshafen, Germany*

*<sup>§</sup>Total Research & Technology Feluy, Zone Industrielle Feluy C, B-7181 Seneffe,  
Belgium*

*<sup>‡</sup>Institute for Chemical Technology and Polymer Chemistry, Karlsruhe Institute of  
Technology, Karlsruhe 76131, Germany*

The conversion of CO<sub>2</sub> to methanol has attracted widespread attention as a possibility to mitigate the CO<sub>2</sub> problem while making chemicals and fuels. Industrially, methanol is produced from synthesis gas mixtures containing both CO<sub>2</sub> and CO at elevated pressures (up to 100 bar) and temperatures (200 – 300 °C) employing a Cu/ZnO/Al<sub>2</sub>O<sub>3</sub> catalyst. The reaction mechanism and the nature of the active site are still vividly debated and model catalysts are commonly employed in order to shed light on mechanistic details. The influence of metal-support interaction and the metal particle size on the catalytic activity of methanol synthesis have not been well understood to date. At industrially relevant conditions of methanol synthesis, for instance, it has been found that the catalytic activity of Cu nanoparticles can change by a factor of three by varying their sizes from 2 to 8 nm.<sup>[1]</sup>

Herein, we aim at disentangling the particle size and support effects and shed light on how the electronic structure influences the CO<sub>2</sub> hydrogenation activity for copper catalysts using density functional theory calculations. Copper particles up to ~ 3 nm in diameter have been investigated with a special focus on their interaction with the support.

## Computational Methods

All DFT calculations were performed using the VASP program<sup>[2]</sup> employing the BEEF-vdW functional<sup>[3]</sup> that has shown promising results for transition metal catalysis.<sup>[4,5]</sup> The particles were modeled using closed-shell cuboctahedra<sup>[6]</sup> in the range 1-3 nm supported on a single layer of graphene.

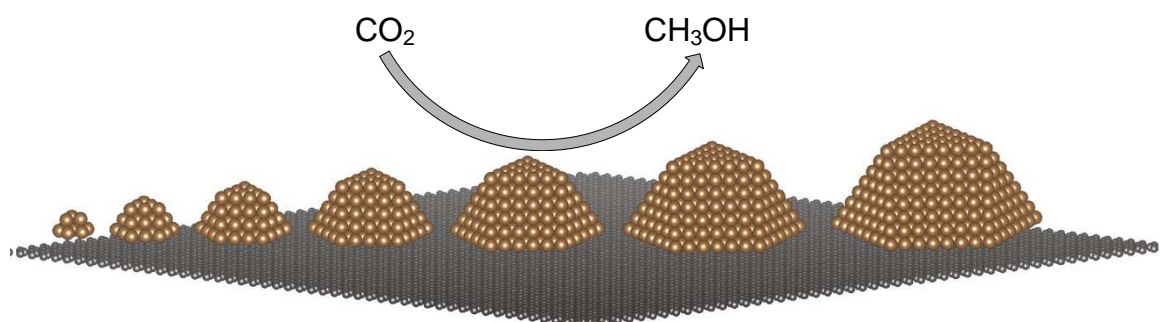


**Figure 1.** Schematic presentation of  $\text{CO}_2$  hydrogenation over copper particles of different sizes.

## Results and Discussion

The influence of particle size and support interactions on the  $\text{CO}_2$  hydrogenation activity were investigated by probing the variance in energy of a few adsorbates that are pinpointing to the overall observed activity. The electronic effect of the support has been investigated employing graphene with and without modifications of its electronic structure. Furthermore, correlations in adsorption strength between various adsorbates as a function of particle size and shape have been investigated.

## References

- [1] R. van den Berg, et al., *Nature Commun.* **2016**, 7, 13057.
- [2] Kresse, G.; Furthmüller, J., *Phys. Rev. B* **1996**, 54, 11169.
- [3] Wellendorff, J.; Lundgaard, K. T.; Møgelhøj, A.; Petzold, V.; Landis, D. D.; Nørskov, J. K.; Bligaard, T.; Jacobsen, K. W., *Phys. Rev. B* **2012**, 85, 235149.
- [4] J. Wellendorff, et al., *Surf. Sci.* **2015**, 640, 36.
- [5] S. M. Sharada et al., *J. Phys. Chem. C* **2017**, 121, 19807.
- [6] J. Kleis, et al., *Catal. Lett.* **2011**, 141, 1067.



# Catalytic hydrogenation of greenhouse gas CO<sub>2</sub> to methanol at atmospheric pressure: experimental study and kinetic modelling

Kaisar Ahmad, Sreedevi Upadhyayula\*

Department of chemical engineering, Indian institute of Technology Delhi, India.

\*presenting author

## Abstract

The methanol production from CO<sub>2</sub> hydrogenation is seen as a potential alternative source of fuel and chemicals, while at the same time it aids in the mitigation of CO<sub>2</sub> concentration in atmosphere. The CO<sub>2</sub> hydrogenation to methanol reaction over Ni-Ga catalyst was optimized in a plug flow fixed bed reactor at atmospheric pressure. The reaction mechanism study and kinetic modelling was performed using reaction route analysis and Langmuir-Hinshelwood-Hougen-Watson (LHHW) method respectively.

## Introduction

Methanol from CO<sub>2</sub> hydrogenation acts as a liquid H<sub>2</sub> carrier at ambient conditions which can be readily stored, transported, and distributed using essentially existing infrastructure [1]. The Ni-Ga is a new catalyst for the field of low-pressure methanol synthesis from direct hydrogenation of CO<sub>2</sub> in small scale discrete units. The objective of this study is to do study the reaction mechanism, derivation of kinetic model for the methanol synthesis ( $\text{CO}_2 + 3\text{H}_2 \leftrightarrow \text{CH}_3\text{OH} + \text{H}_2\text{O}$ ,  $\text{CO}_2 + \text{H}_2 \leftrightarrow \text{CO} + \text{H}_2\text{O}$ ) and parameter estimation.

## Methods

Catalyst preparation and characterization was followed by activity test in differential plug flow reactor at atmospheric pressure. The reaction parameters were optimized and kinetic data was obtained in kinetic regime. The reaction mechanism was investigated by reaction route analysis [2]. Two rate equation for methanol formation rate and reverse water gas shift reaction (RWGS) were derived based on LHHW method. Parameter estimation and curve fitting was performed for the derived model.

## Results and Discussion

The catalyst characterization revealed the formation of particular phase and desired particle size distribution in the final form. Effect of catalyst preparation method and influence of temperature, CO<sub>2</sub>/H<sub>2</sub> ratio, weight hourly space velocity, and time on

stream on CO<sub>2</sub> conversion, methanol selectivity, and formation rate was studied. The results in the form of figures are given as under.

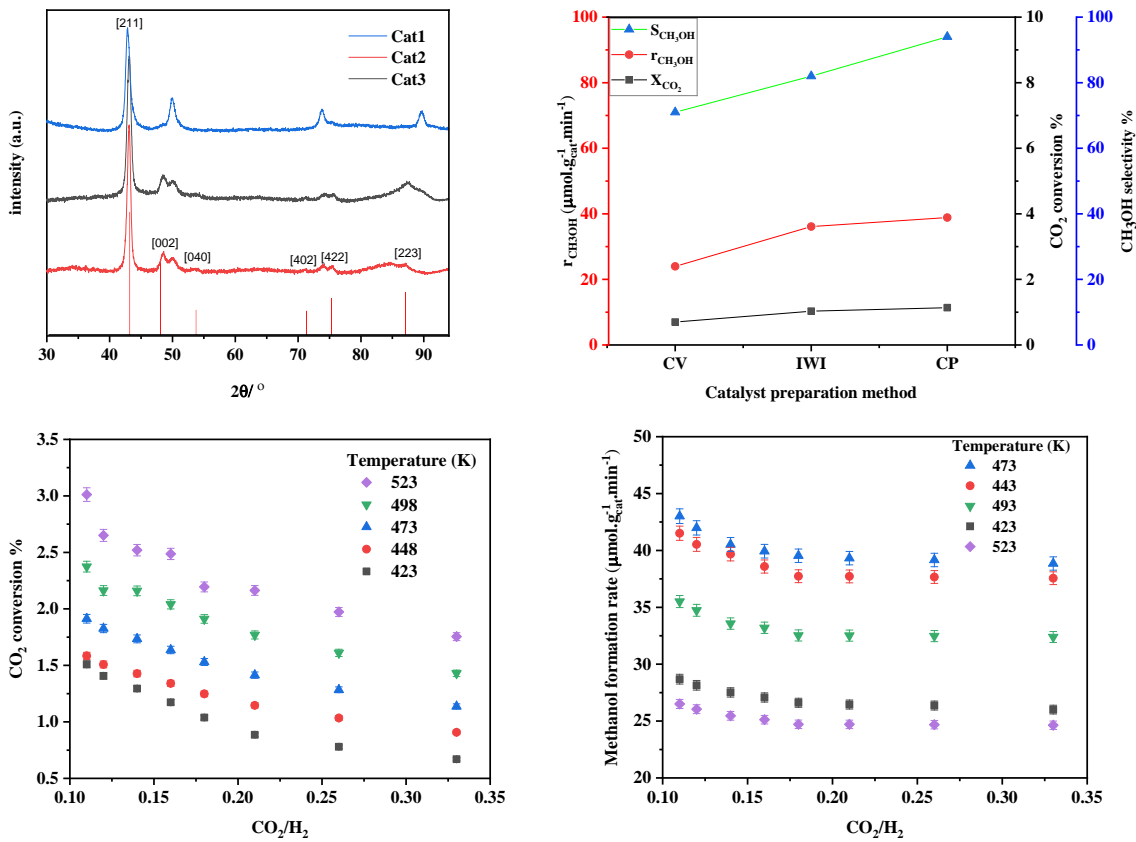


**Fig.1.** XRD and activity results of lab synthesized Ni-Ga catalysts.

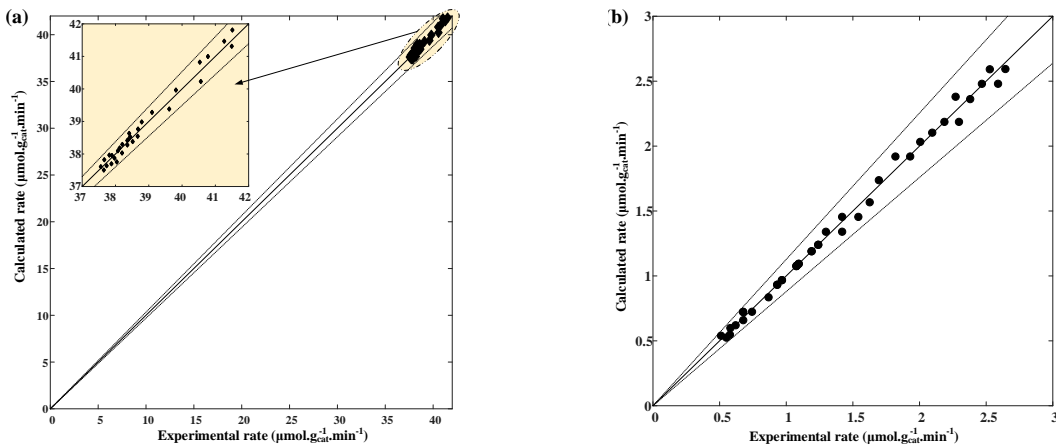


**Fig. 2** Parity plot: competitive adsorption model (a) methanol synthesis, (b) CO formation.

## References

- [1] M.D. Porosoff, B. Yan, J.G. Chen, Catalytic reduction of CO<sub>2</sub> by H<sub>2</sub> for synthesis of CO, methanol and hydrocarbons: challenges and opportunities, *Energy Environ. Sci.* 9 (2016) 62–73.
- [2] Ilie Fishtik, Caitlin A. Callaghan, and Ravindra Datta, Reaction Route Graphs. I. Theory and Algorithm, *The J. of Ph. Ch. B*, 108(2004) 5671-5682.

# Palladium-Oxo Clusters as Molecular Precursors for Heterogeneous Hydrogenation Catalysts

Ali S. Mougharbel and Ulrich Kortz\*

Jacobs University, Department of Life Sciences and Chemistry, Campus Ring 1,  
28759 Bremen, Germany. [u.kortz@jacobs-university.de](mailto:u.kortz@jacobs-university.de)

Polyoxometalates (POMs) constitute a large class of discrete metal-oxo anions of early *d*-block elements in high oxidation states (e.g. V<sup>V</sup>, Mo<sup>VI</sup>, W<sup>VI</sup>). POMs exhibit tunable shapes, sizes and compositions resulting in a large range of physicochemical properties which are of interest in catalysis, energy, medicine, and material science [1].

In 2008, our group discovered the first POM comprising exclusively palladium(II) ions as addenda [2]. Polyoxopalladates (POPs) represent molecular palladium(II)-oxo clusters based on square-planar coordinated Pd<sup>II</sup> ions. The family of POPs has witnessed an impressive development in the last 10 years, resulting in >70 structures with a fascinating variety of shape, size, composition, and properties [3].

Here we report on the use of discrete POPs of the {MPd<sup>II</sup><sub>12</sub>X<sub>8</sub>} nanocube and {Pd<sup>II</sup><sub>15</sub>X<sub>10</sub>} nanostar types (M = guest metal ion, X = capping group) as precursors for the formation of metallic Pd nanoparticles which were supported on a mesoporous silica support (apts-SBA-15). The catalytic activity of these unprecedented materials was investigated in the hydrogenation of aromatic compounds. We discovered that the catalytic activity strongly depends on the calcination temperature. In addition, we systematically varied the central metal ion guests and capping groups of the POP nanocubes {MPd<sup>II</sup><sub>12</sub>X<sub>8</sub>} (M = Mn<sup>II</sup>, Fe<sup>III</sup>, Co<sup>II</sup>, Ni<sup>II</sup>, Cu<sup>II</sup>, Zn<sup>II</sup>, Pd<sup>II</sup>; X = Se, PhAs, P) and observed important phenomena in the resulting catalytic activity.

## References

- [1] M. T. Pope, *Heteropoly and Isopoly Oxometalates*, Springer, 1983.
- [2] Chubarova, E. V.; Dickman, M. H.; Keita, B.; Nadjo, L.; Miserque, F.; Mifsud, M.; Arends, I. W. C. E.; Kortz, U. Self-Assembly of a Heteropolyoxopalladate Nanocube: [Pd<sub>13</sub>As<sub>8</sub>O<sub>34</sub>(OH)<sub>6</sub>]<sup>8-</sup>. *Angew. Chem. Int. Ed.* **2008**, *47*, 9542–9546.
- [3] Discovery and Evolution of Polyoxopalladates. Yang, P.; Kortz, U. *Acc. Chem. Res.* **2018**, *51*, 1599–1608.

## References

List and number all bibliographical references at the end of the paper. When referenced within the text, enclose the citation number in square brackets, i.e. [1]

# The Redox Property of Copper Nanoparticles Mediated by Cerium

*Bolun Wang,<sup>1</sup> Liqun Kang,<sup>1</sup> Luke Keenan,<sup>2</sup> Sotiris E. Pratsinis,<sup>3</sup> Feng Ryan Wang<sup>1\*</sup>*

<sup>1</sup> *Department of Chemical Engineering, University College London, London, UK.*

<sup>2</sup> *Beam Line I20, Diamond Light Source Ltd, Didcot, UK.*

<sup>3</sup> *Particle Technology Laboratory, ETH Zürich, Zürich, Switzerland.*

## Introduction

Cu based catalysts are capable of activating small molecules such as CO, H<sub>2</sub>, H<sub>2</sub>O and NH<sub>3</sub> in reactions including CO oxidation, methanol synthesis from syngas, water gas shift (WGS) and selective catalytic reduction (SCR) of NO<sub>x</sub> gas in the engine exhaust. To promote selective conversion of specific chemical species, different active Cu species are required. Metallic Cu, Cu<sub>2</sub>O/CuO clusters, Cu<sup>2+</sup> dimers and single site play distinct roles in the existing industrial catalysts. Under certain reductive atmosphere (CO, H<sub>2</sub>, NH<sub>3</sub>), oxidative atmosphere (O<sub>2</sub>, H<sub>2</sub>O) or their mixture, the oxidation states of Cu species are crucial in determining their catalytic behaviours. It was reported that the rate of CO oxidation decreased with increasing Copper oxidation state.<sup>[1]</sup> The strong electron-withdrawing effect of Cerium to Copper can efficiently modify its redox property and change the stable oxidation state of Copper under certain atmosphere and temperature. Based on Energy Dispersive X-ray Absorption Near Edge Structure (XANES), the valence state of Cu can be studied under reaction atmosphere with second-scale time resolution. The interaction between Copper and Cerium can thus be resolved by comparing the redox properties of Cu species with different content of Cerium. Pure CuO and CuO on neutral support SiO<sub>2</sub> have also been investigated under the same conditions as references.

## Materials and Methods

Pure CuO, CuO-CeO<sub>2</sub> and CuO-SiO<sub>2</sub> composites were synthesized by flame spray pyrolysis (FSP) method. The precursor solutions were prepared by mixing copper 2-ethylhexanoate with cerium 2-ethylhexanoate or hexamethyldisiloxane in a solution of acetic acid, methanol, and xylene (volume ratio 1:1:2). These precursor solutions were sprayed at 5 mL/min, dispersed with 5 L/min O<sub>2</sub>, and ignited by a premixed CH<sub>4</sub>/O<sub>2</sub> (flow rates 1 and 2 L/min, respectively) ring-shaped flamelet. XANES analysis of the Cu K edge (8.979 keV) was performed at 3.0 GeV on the Beamline B18 and I20 in the Diamond Light Source (UK).

## Results and Discussion

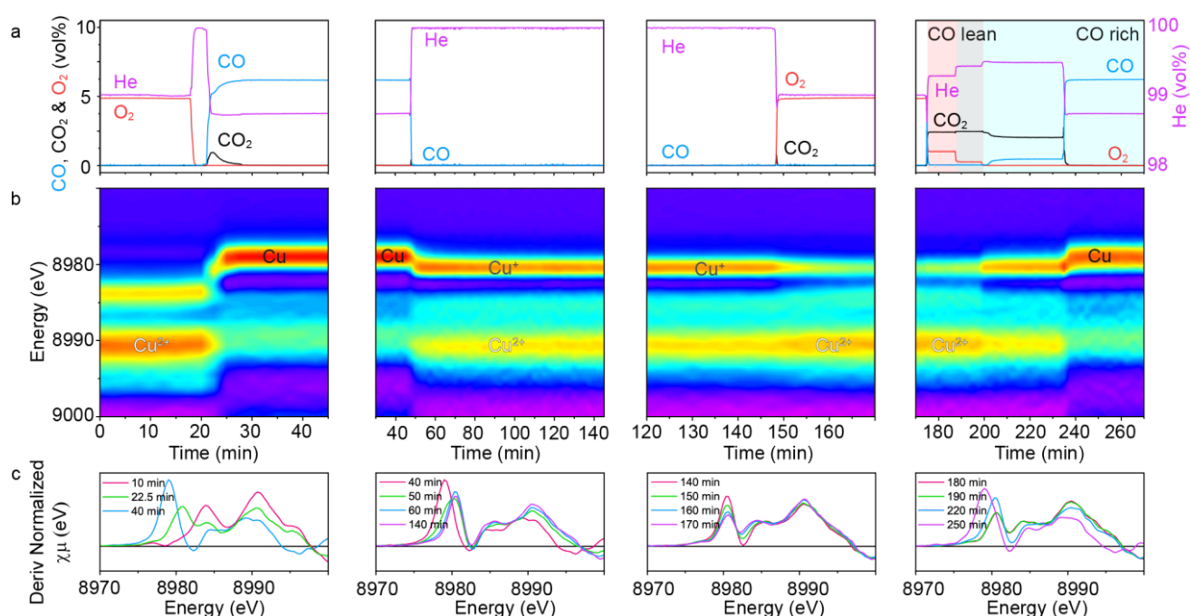


**Figure 1 Operando XANES study at Cu K edge of 20 wt% CuO-CeO<sub>2</sub>.** **a.** The gas concentration at the outlet of the *operando* reactor as the function of time. **b.** Contour map of the first derivative XANES spectra. **c.** Selection of first derivative XANES spectra at chosen time slot.

Based on our *operando* XANES study in B18 (Fig. 1), the 20 wt% CuO on CeO<sub>2</sub> is almost fully reduced to metallic Cu at 180 °C in 5% CO. As a comparison, Cu(II) species in pure CuO and 20 wt% CuO-SiO<sub>2</sub> are partly reduced to Cu(I) at 200 °C in 10% CO (recent data from I20, will be presented in the conference). Even with only 10% CeO<sub>2</sub> in 90 wt% CuO-CeO<sub>2</sub>, Cerium still can efficiently promote Cu(II) to be reduced to metallic Cu at 200 °C in 10% CO. The electron transfer between Cu and Ce is further validated by the phenomenon that metallic Cu in both 20 wt% and 90 wt% CuO-CeO<sub>2</sub> are quickly re-oxidized into Cu(I) by Ce<sup>4+</sup> in ultrapure He, which is in agreement with our previous publication.<sup>[2]</sup> An interesting chemical oscillation reflected by the rate of CO oxidation triggered by a pulse of CO is observed when the 90 wt% CuO-CeO<sub>2</sub> is tested for CO oxidation. Cu(II) species is partly reduced to Cu(I) under the co-existence of CO and O<sub>2</sub> (ratio 1:1 to 4:1). The higher activity of Cu(I) species towards CO oxidation results in lower concentration of CO and pushes the balance of oxidation state towards Cu(II). With more Cu(II), the CO concentration recovers and pushes the balance of oxidation state back to Cu(I). This oscillation can last for several circles until it completely decays.

## References

- [1] G. G. Jernigan, G. A. Somorjai, *J. Catal.* **1994**, *147*, 567–577.
- [2] F. Wang, R. Büchel, A. Savitsky, M. Zalibera, D. Widmann, S. E. Pratsinis, W. Lubitz, F. Schüth, *ACS Catal.* **2016**, *6*, 3520–3530.

# Direct hydrodeoxygenation of sugarcane residues over Mo<sub>2</sub>C catalyst in *Organosolv* system

Gleicielle T. Wurzler<sup>1</sup>, Ayla S. da Silva<sup>2</sup>, Débora A. Azevedo<sup>3</sup>, Victor T. da Silva<sup>1</sup>;  
Fábio B. Noronha<sup>2\*</sup>

<sup>1</sup> Chemical Engineering Program, Federal University of Rio de Janeiro, Rio de Janeiro, Brazil

<sup>2</sup> Catalysis Division, National Institute of Technology, Rio de Janeiro, Brazil

<sup>3</sup> Chemistry Institute, Federal University of Rio de Janeiro, Rio de Janeiro, Brazil

## Introduction

The fractionation of lignocellulosic biomass produces the bio-oil that can be converted into liquid fuel by catalytic hydrodeoxygenation (HDO). This is a multi-step process that involves: biomass residue treatment [1], lignin/bio-oil depolymerization [2], and enzymatic hydrolysis [3]. This makes the final product costly, since there is a need for product separations. Xia *et al.* [4] proposed a one-pot process involving the direct hydrogenation of the wood using a Pt/NbOPO<sub>4</sub> catalyst and cyclohexane at 190 °C and 5MPa H<sub>2</sub> for 20 h. They obtained liquid alkanes with mass yields up to 28.1 wt% in a single reaction. Few works investigated integrated strategies for lignin valorization via direct hydrodeoxygenation of biomass. Therefore, this work compares the products obtained by *Organosolv* fractionation process with the direct HDO of the biomass.

## Materials and Methods

20 wt% Mo<sub>2</sub>C/AC catalyst was prepared by incipient wetness impregnation of the support, activated carbon (AC – Merck), with an aqueous solution of (NH<sub>4</sub>)<sub>6</sub>Mo<sub>7</sub>O<sub>24</sub>·4H<sub>2</sub>O (Merck). After impregnation, the materials were dried at 100 °C for 12 h. Then, the sample was heated under a 20 % CH<sub>4</sub>/H<sub>2</sub> (v/v) mixture (200 mL min<sup>-1</sup> g<sub>oxide</sub><sup>-1</sup>) at 2.5 °C min<sup>-1</sup> up to 650 °C, remaining at this temperature for 2 h. The delignification of sugarcane bagasse was performed through the *Organosolv* treatment using 140 mL of solvent (iPrOH:H<sub>2</sub>O = 7:3, v/v), 3.5 g of the Mo<sub>2</sub>C/AC, 7 g of sugarcane bagasse. The reaction was conducted in a 300 mL autoclave at 180 °C for 3 h and 500 rpm. For the direct HDO of bagasse and sugarcane straw reaction, the *Organosolv* method was carried out in the presence of 50 bar of H<sub>2</sub>.

The analyses of the chemical composition of biomass were performed following National Renewable Energy Laboratory (NREL) analytical protocols. The bio-oils

were analysed via GCxGC-TOFMS, according to methodology described by Silva *et al.* (2017) [5]. For the enzymatic hydrolysis of solid residues, glucose concentration released was measured using a biochemical analyzer. A mixture of commercial enzymes (Celluclast 1.5L and Novozyme 188 at FPU:BGU ratio of 1:3) was used as source of cellulases and beta-glucosidase, respectively. The vials were sealed and packed in a rotary incubator maintained at 50 °C and 200 rpm for 72 h.

## Results and Discussion

The *Organosolv* treatment of the sugar cane bagasse produced low delignification (14 %) and glucose retention in the residue (31 %). The incorporation of H<sub>2</sub> favored the delignification, which increased from 14 to 69 % and there was considerable retention of cellulose in the solid residue (75 %). Similar results were obtained on the direct HDO of straw, with 77 % delignification and 80 % glucose retention.

For the enzymatic hydrolysis, the solid residue of bagasse *Organosolv* reaction led to the highest glucose yield (~67 %) and concentration of glucose (13.7 g L<sup>-1</sup>). However, the glucose concentration released on the hydrolysis of HDO bagasse (13.2 g L<sup>-1</sup>) and HDO straw (13.1 g L<sup>-1</sup>) residues is very close to that one for the *Organosolv* reaction, even with lower glucose yields (~37 and 43 %, respectively). This happens because most of glucose was hydrolysed in *Organosolv* reaction, while the HDO reaction retained glucose in the solid residue.

The incorporation of H<sub>2</sub> favored the delignification, the solid residue glucose retention and, consequently, a high glucose concentration was obtained on the enzymatic hydrolysis, indicating that the direct HDO of the biomass by using the *Organosolv* method in the presence of a catalyst has great potential for the production of fuels. The semi-quantification of the bio-oil is still being processed in order to evaluate and compare the species present in each bio-oil and these results will be presented at the congress.

## References

- [1] S. Van den Bosch, *et al*, *Green Chem.* 19 (2017) 3313.
- [2] R. Shu, *et al*, *Biores. Tech.* 179 (2015) 84.
- [3] A.S'A. da Silva, *et al*, *Proc. Biochem.* 51 (2016) 1561.
- [4] Q. Xia, *et al*, *Nature Comm.* 7 (2016) 11162.
- [5] R.V.S. Silva, *et al*, *Talanta* 164 (2017) 626.

# Catalytic activity of multi-wall carbon nanotubes in the hydrogenation/dehydrogenation of C2 hydrocarbons

*Igor Bychko, L. V. Pisarzhevsky Institute of Physical Chemistry of the National Academy of Sciences of Ukraine, Kyiv, Ukraine; Peter Strizhak, L. V. Pisarzhevsky Institute of Physical Chemistry of the National Academy of Sciences of Ukraine, Kyiv, Ukraine*

## Intriduction

The carbon-based nanomaterials such as multi-walled carbon nanotubes (CNTs) used in heterogeneous catalysis attract a growing interest due to their nanoscale tubular morphology that can offer a unique combination of the low porosity and a readily accessible surface.

Recently, several studies dedicated to the carbon materials catalytic activity in the hydrogenation reactions have been reported. Particularly the catalytic activity of graphenes has been demonstrated in the gas-phase hydrogenation of acetylene and alkenes. According to the high stability of carbon materials to the carbonization, a development of novel carbon materials for hydrogenation and dehydrogenation is of great interest.

The main problem of metal-based dehydrogenation catalysts is carbonaceous species that inevitably deposits on the surface of catalysts and cause a sharp loss of activity. The generally accepted view is perspective of metal-free catalysts, such as catalysts based on nanocarbon based materials, in particular CNT, which are perspective candidates due to their high stability toward deactivation by carbonization.

## Experimental

The CNT was synthesized by the catalytic decomposition of ethylene on Ni/CaO catalyst (20% Ni) with the following purification from the catalyst and amorphous carbon by treatment with nitric acid. The morphology of the CNT was characterized by SEM, TEM, XRD and Raman spectroscopy. Surface functionalities were determined by FTIR, XPS and Boehm titration. Surface area was determined by BET based on Nitrogen adsorption-desorption. The catalytic reactions were carried out in a stainless steel continuous flow reactor.



## Results

Catalytic activity of CNT was determined in the ethylene and acetylene hydrogenation and ethane dehydrogenation. Results shows, than the ethylene hydrogenation rate increases from  $2.5 \cdot 10^{-9} \text{ mol} \cdot \text{s}^{-1} \cdot \text{m}^{-2}$  at 100 °C to  $2.1 \cdot 10^{-7} \text{ mol} \cdot \text{s}^{-1} \cdot \text{m}^{-2}$  at 300 °C respectively. The acetylene hydrogenation rate increases from  $4,7 \cdot 10^{-8} \text{ mol} \cdot \text{s}^{-1} \cdot \text{m}^{-2}$  at 80°C to  $1,4 \cdot 10^{-6} \text{ mol} \cdot \text{s}^{-1} \cdot \text{m}^{-2}$  at 350°C. In both cases further temperature increase leads to the conversion decrease. At temperatures higher that 400 °C ethylene and acetylene decomposes in reactor, probably with the formation of oligomerisated compounds on the CNT surface. In the acetylene hydrogenation the selectivity to ethylene increase with temperature increase and reaches 90% at 400°C.

In the ethane dehydrogenation reaction during experiment the reaction products are  $\text{C}_2\text{H}_4$  and  $\text{CH}_4$ . The reaction occurs at temperatures  $\geq 550$  °C and ethane conversion increases from 0.1% at 550 °C to 50.7% at 800 °C. Resulting reaction products mixture at 800 °C contains 53%  $\text{C}_2\text{H}_4$ , 47%  $\text{CH}_4$ .

The structure of catalytic active sites on the surface of the carbon nanomaterials in the hydrogenation reaction is still an open problem. Particularly, it was shown that  $\text{H}_2$  activation can take place at the carbon atom vacancies [1]. A possibility of  $\text{H}_2$  activation by frustrated Lewis pairs on the carbons surface has been also discussed [2]. Recently, it has been indicated an activation via the  $\pi$ - $\pi$  interaction for aromatic compounds [3].

Our experiments indicate a fairly high stability of CNT in a comparison with the typical hydrogenation catalysts in both, hydrogen-rich and ethylene-rich, atmospheres. This offers new opportunities for the CNT-based catalysts application in the hydrogenation reaction at high temperatures, in particular, under conditions when the metal-containing catalysts deactivate due to the carbonaceous deposits formation.

## References

1. G. Sastre, A. Forneli, V. Almasan, V.I. Parvulescu, H. Garcia, Appl. Catal. A. 547 (2017) 52-59.
2. A. Primo, F. Neatu, M. Florea, V. Parvulescu, H. Garcia, Nat. Comm. 5 (2014) 5291.
3. R. Liu, F. Li, C. Chen, Q. Song, N. Zhao, F. Xiao, Catal. Sci. Technol., 7 (2017) 1217-1226.

# **Rational design of Cu based bimetallic catalysts for higher alcohols synthesis by combined micro-kinetic modeling and experiments**

*Weixin Qian, Department of chemical engineering, NTNU, Trondheim, Norway; East China University of Science and Technology, Shanghai, China; Yalan Wang, Xiaoli Yang, Jia Yang, De Chen, Anders Holmen, Department of chemical engineering, NTNU, Trondheim, Norway; Yanbo Xu, Yian Zhu, Weiyong Ying, East China University of Science and Technology, Shanghai, China*

## **Scope**

Fischer-Tropsch synthesis, a process that converting syngas from coal, natural gas and biomass into liquid fuels and other chemicals, is considered as an important way to maintain the sustainable development of energy [1]. Among the products, higher alcohols are attracting increasing attentions recently due to its potential applications as gasoline additives and high value-added chemical materials. The development of catalysts is one of the most critical parts of regulating the catalysts reactivity and selectivity of higher alcohols. However, there are still many difficulties in it because of the lack of a clear understanding of reaction mechanisms of higher alcohols synthesis (HAS) in Fischer-Tropsch synthesis.

The obtained adsorption energies and the reaction rate volcano plot by combining the DFT calculation and an improved UBI-QEP+BEP in a model-aided catalyst prediction (micro-kinetic modeling) could effectively help us understand the reaction mechanisms, design catalysts rationally and do preliminary catalyst screening, avoiding aimless searching [2]. Here we designed series of Cu based bimetallic catalysts for HAS based on the micro-kinetic modeling, aiming at improving the selectivity of higher alcohols by regulating the metallic elements of Cu based bimetallic catalysts and their ratios to make the catalyst locate in the region with high ethanol reactivity and relatively low methanol reactivity in the volcano plot and optimize the reaction performance of catalysts.

## **Experiment**

Cu based bimetallic catalysts are prepared by liquid reduction method, with carbon nanotube as a support and some specific elements like Mn as the promoters. NaBH<sub>4</sub> is used as the reducing agent. The catalyst precursors are dried in a tubular reactor under N<sub>2</sub> as a protective gas and then be passivated by 1%O<sub>2</sub>/Ar (V) for 12 hours

before using. The reaction performance evaluation of catalysts is carried out in a tubular fixed-bed reactor under conditions of 533 K, 30 bar,  $H_2/CO=2$ .

## Results and Discussions

The micro-kinetic modeling results imply that the 15 kinds of bimetallic catalysts with yellow stars labeled in Fig.1 are with relatively high ratio of ethanol to methanol reactivity. Considering the attainability and economic factors,  $Cu_3Al$  seems like a potential bimetallic catalyst for HAS under conditions of 533 K, 30 bar and  $H_2/CO=2$ .

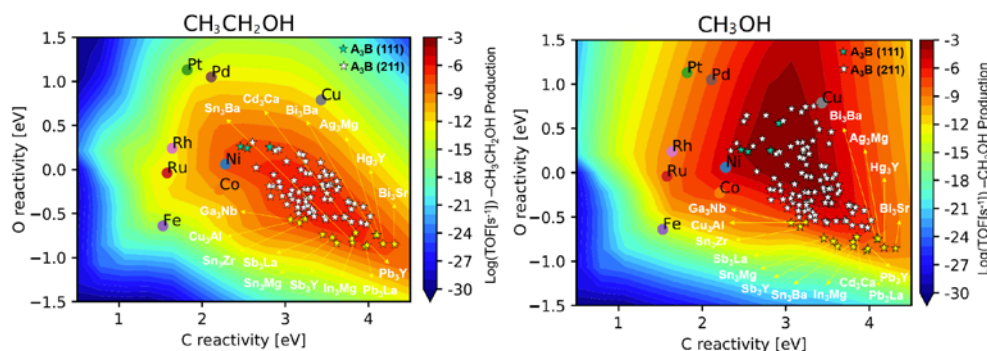


**Fig.1** Simulated reactivity for  $CH_3CH_2OH$  and  $CH_3OH$  production over different metallic elements bimetallic catalysts in FTS. Reaction condition:  $T=533$  K,  $P=30$  bar,  $H_2/CO=2$ .

Fig.1 also rationalizes the Cu-Fe catalysts often reported for HAS in FTS. Based on the segregation and mixing energy [3], Cu-Fe catalysts preferably has a subsurface of Fe under the Cu surface, alerting the C and O binding energy of Cu and making Cu more active. A series of Cu-Fe catalysts with different molar ratios of Cu to Fe was prepared by a liquid reduction method and the reaction performance are summarized in table 1. The lower Cu/Fe ratio resulted in a higher CO conversion, but lower selectivity to alcohols. The  $C_{2+}OH/C_1OH$  ratio increased with decreasing Cu/Fe ratio. The catalytic performance of CuAl and other predicted catalysts will be compared to Cu-Fe catalysts. The catalytic performance will be discussed and correlated to the adsorption properties and more fundamentally to the electronic properties of the catalysts.

**Table 1** Reaction performance of catalysts with different molar ratio of Fe and Cu at conditions of 533 K, 30 bar,  $P_{CO}=18$  bar,  $P_{H_2}=9$  bar,  $2000 h^{-1}$

Catalyst	$x_{CO}$ (%)	Alcohols selectivity (%)	$C_{2+}OH/C_1OH$
1Cu7Fe/CNTs	44.90	20.24	3.77
1Cu3Fe/CNTs	43.71	20.35	3.91
1Cu1Fe/CNTs	43.77	21.58	3.82
3Cu1Fe/CNTs	26.10	22.61	2.79

## References

- [1] J. Goldemberg. Science, 2007, 315(5813): 808-810.
- [2] A. J. Medford, C. Shi, M. J. Hoffmann, et al. Catalysis Letters, 2015, 145, 794-807.
- [3] A. Christensen, A. V. Ruban, P. Stoltze, et al. Physical Review B, 1997, 56, 5822-5834.

## Bimetallic Complexes for Oxygen Activation

*Maya Singer Hobbs, Ulrich Hintermair, Centre for Sustainable Chemical Technologies, University of Bath, Bath, UK*

Harnessing the reactivity of dioxygen for useful chemical processes, such as aerobic oxidations or the oxygen reduction reaction for fuel cell technologies, is a challenge that synthetic chemists have yet to fully tackle. The design of oxidatively robust, and catalytically active complexes, is therefore of interest.

### Background

A series of complexes designed by Lobet and Meyer [1] based on the bis pyridine pyrazole ligand (Figure 1a) show high activity for water oxidation, and have been briefly investigated for the oxygen reduction reaction using a model system.[2] The resting state of the dicobalt system shows a molecule of O<sub>2</sub> bound between the two metal centres (Figure 1b), suggesting the bimetallic nature of these molecules is key to their reactivity.

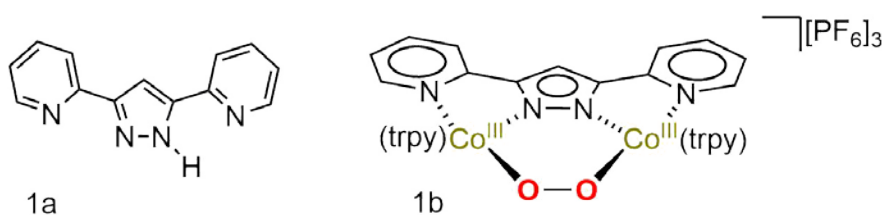


**Figure 1a** 3,5-bis(pyridine-2-yl)-pyrazole ligand (Hbpp). **1b** Bis-cobalt(III) (bpp)(trpy)μ-O-O complex showing the dioxygen bound between the two cobalt centres.

### Ligand Variation

In order to investigate the role of steric and electronic factors in the reactivity of these systems, a series of substituted ligands, and corresponding complexes, have been made (Figure 2).

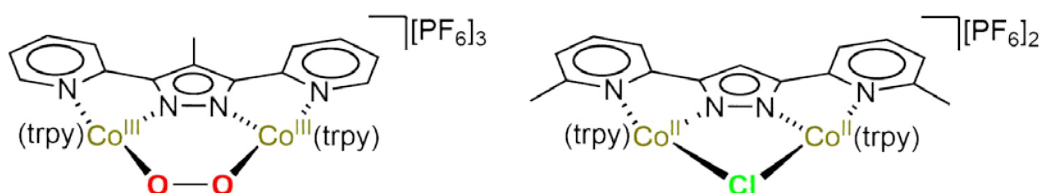


**Figure 2.** Dicobalt complexes with methyl substituents on the pyrazole backbone and ortho position of the Hbpp ligand.

Initial investigations into these systems suggest that the inclusion of steric bulk in the *ortho* position of the ligand reduces the rate of ORR. In addition, the inclusion of a methyl group on the backbone of the pyrazole also results in a depression in the rate, although to a lesser extent than that of the *ortho* methyl substituents.

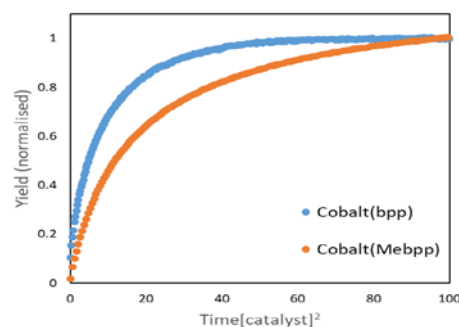


**Figure 3.** Variable Time Normalisation Analysis showing decreased activity of methylated cobalt analogue.

The potential electronic effect of the methyl substituent on the backbone on the rate of reaction will be further investigated by incorporating an electron withdrawing substituent in the same position. A series of further functionalised ligand systems have been synthesised (Figure 4) and their corresponding cobalt complexes

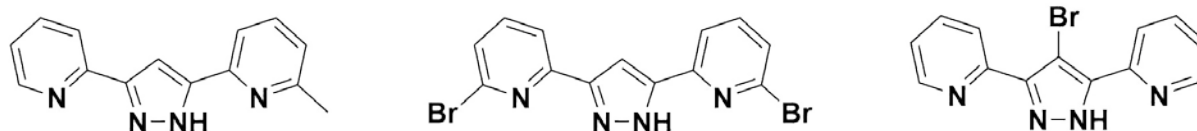


**Figure 4.** Further substituted ligand variants on the Hbpp system, incorporating unsymmetrical systems and electron withdrawing substituents.

## Conclusion

Initial studies show that changing substituents on the ligand backbone have an effect on the rate of oxygen reduction, using a model system. The activity of these systems will further be investigated by changing the electron donating methyl group for a bromo-substituent. The reactivity of these complexes towards aerobic oxidations will also be investigated.

The possibility of incorporating other metal centres into these systems, or the synthesis of heterobimetallic systems also opens scope for further unusual reactivities.

## References

- 1 F. Bozoglian, S. Romain, M. Z. Ertem, T. K. Todorova, C. Sens, J. Mola, M. Rodríguez, I. Romero, J. Benet-Buchholz, X. Fontrodona, C. J. Cramer, L. Gagliardi and A. Llobet, *J. Am. Chem. Soc.*, 2009, **131**, 15176–15187.
- 2 S. Fukuzumi, S. Mandal, K. Mase, K. Ohkubo, H. Park, J. Benet-Buchholz, W. Nam and A. Llobet, *J. Am. Chem. Soc.*, 2012, **134**, 9906–9909.

# On the Cooperative Synthesis of ZSM-5 Zeolite Nanosheets

*Xiaochun Zhu* \*, Jian Guo, Miaomiao Li, Yu Gao

*State Key Laboratory of Heavy Oil Processing; The Key Laboratory of Catalysis of CNPC; College of Chemical Engineering and Environment; China University of Petroleum, Beijing, 102249, PR China*

*\* corresponding author: xzhu@cup.edu.cn*

## Introduction

Porous material with MFI topology has been widely used as acid catalysts in the petrochemical and oil refining industry. Whereas the location of the acid sites embedded in zeolite crystals with dimensions of several microns may result in mass transport limitations during catalytic reactions. Considerable attention has been given to the strategies which could overcome these limitations by introducing additional mesoporosity in zeolite crystals. The approach of Ryoo and co-workers to use diquaternary ammonium surfactants to synthesize ZSM-5 nanosheets was a breakthrough<sup>[1]</sup>. However, such surfactants are expensive and require multiple preparation steps. The attempt to obtain MFI nanosheets with 2.5 nm thickness by minimizing the use of surfactant via the add of less expensive Na<sup>+</sup> or TPA<sup>+</sup> ended up as a failure<sup>[2]</sup>. The thickness of MFI nanosheets increased as the amount of surfactant decreased in the synthesis gel.

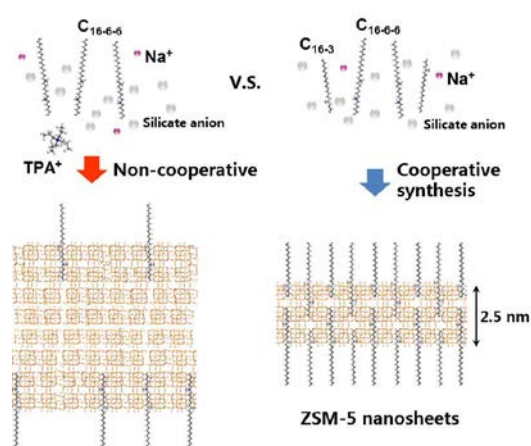
In this study, ZSM-5 zeolite nanosheets was cooperatively synthesized by combining diquaternary ammonium surfactant and less expensive mono-quaternary ammonium surfactant in the synthesis gel. The mono-quaternary ammonium surfactant serves as filler in the surfactant micelles, thus helps to stabilize the micelles and limit the growth of zeolite nanosheets when only a small amount of diquaternary ammonium surfactant was used in the synthesis.

## Experimental/methodology

Diquaternary ammonium surfactant [C<sub>16</sub>H<sub>33</sub>-N<sup>+</sup>(CH<sub>3</sub>)<sub>2</sub>-C<sub>6</sub>H<sub>12</sub>-N<sup>+</sup>(CH<sub>3</sub>)<sub>2</sub>-C<sub>6</sub>H<sub>13</sub>] Br<sub>2</sub> (denoted by C<sub>16-6-6</sub>) and mono-quaternary ammonium surfactant [C<sub>16</sub>H<sub>33</sub>-N<sup>+</sup>(CH<sub>3</sub>)<sub>2</sub>-C<sub>3</sub>H<sub>7</sub>] Br (denoted by C<sub>16-3</sub>) were synthesized according to our previous work. TEOS, Al(OH)<sub>3</sub>, NaOH, C<sub>16-6-6</sub>, C<sub>16-3</sub>, and distilled water were mixed to obtain a gel composition of 100SiO<sub>2</sub>/1Al<sub>2</sub>O<sub>3</sub>/mC<sub>16-6-6</sub>/nC<sub>16-3</sub>/11Na<sub>2</sub>O/6000H<sub>2</sub>O, the obtained samples were named as ZSM-5(m, n).

## Results and discussion

Scheme 1 shows the zeolite crystal growth in the non-cooperative or cooperative manner. The structure-directing action of  $\text{Na}^+$  or  $\text{TPA}^+$  are too slow or too fast for the cooperative structure direction with the surfactant  $\text{C}_{16-6-6}$ , generating zeolite crystals with sizes larger than 2.5 nm. On the contrary, the surfactants  $\text{C}_{16-6-6}$  and  $\text{C}_{16-3}$  can be used in a concerted manner, the growth of the nanosheets would be limited. The electron microscopy images in Fig. 1 show substantial differences in the morphology among the various samples. The thickness of the zeolite sheets increased from 2.5 nm to 50 nm as the amount of  $\text{C}_{16-6-6}$  continually decreased in the synthesis gel.



Compared with the sample ZSM-5(1, 0), the adding of small amount of  $\text{C}_{16-3}$  can largely limited the growth of zeolite nanosheets (Fig. 1e, j), indicating that the surfactant  $\text{C}_{16-3}$  could work in a concerted manner with  $\text{C}_{16-6-6}$ . For comparison, bulk ZSM-5 zeolite with micron-sized crystals (Fig. 1d, i) was obtained when only  $\text{C}_{16-3}$  presents in the synthesis gel.

**Scheme 1.** Formation of ZSM-5 nanosheets by cooperative synthesis of  $\text{C}_{16-6-6}$  and  $\text{C}_{16-3}$ .

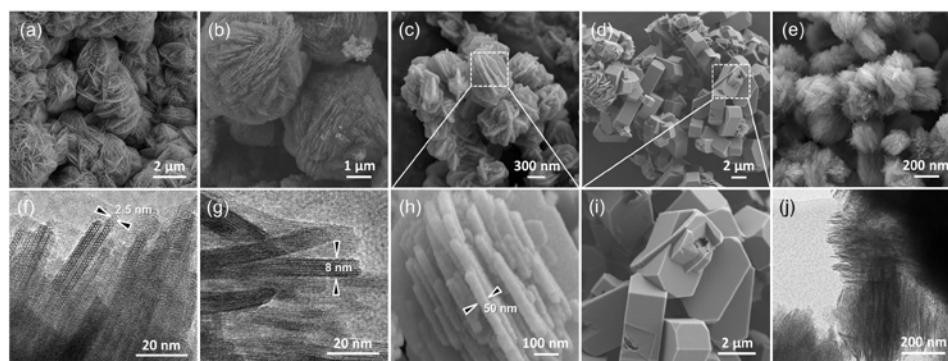


**Fig. 1.** SEM and TEM images of ZSM-5 zeolites. (a,f) ZSM-5(7.5, 0), (b,g) ZSM-5(2.5, 0), (c,h) ZSM-5(1, 0), (d,i) ZSM-5(0, 1), (e,j) ZSM-5(1, 1).

## Conclusions

Cost-effective ZSM-5 nanosheets has been cooperatively synthesized by combining a small amount of diquaternary ammonium-type surfactant and a less expensive mono-quaternary ammonium surfactant, the latter could stabilize the surfactant micelles and limit the growth of ZSM-5 zeolite nanosheets.

## References

- [1] M. Choi, K. Na, J. Kim, Y. Sakamoto, O. Terasaki, R. Ryoo, *Nature* 461 (2009) 246.
- [2] Y. Kim, K. Kim, R. Ryoo, *Chemistry of Materials* 29 (2017) 1752.

# Modified Fe<sub>2</sub>O<sub>3</sub> and Cu<sub>2</sub>O photoelectrodes for photoelectrochemical water splitting

Yongdan Li<sup>1,2,3\*</sup>

<sup>1</sup> School of Chemical Engineering and Technology, Tianjin University, Tianjin, 300072, China

<sup>2</sup> Collaborative Innovation Center of Chemical Science and Engineering (Tianjin), Tianjin, 300072, China

<sup>3</sup> Department of Chemical and Metallurgical Engineering, Aalto University, Aalto, FI-00076, Finland

E-mail addresses: yongdan.li@aalto.fi, ydli@tju.edu.cn

Photoelectrochemical water splitting has been regarded as a promising strategy to obtain hydrogen and thus solves the energy concerns related to the sustainable development of the humankind. However, the low efficiency seriously impedes its commercialization progress. Fe<sub>2</sub>O<sub>3</sub> (hematite) and Cu<sub>2</sub>O are among the most widely studied photoanode and photocathode, respectively, whereas the former suffering from poor electrical conductivity, short lifetime of the carriers, and sluggish water oxidation kinetics [1] whilst the latter photocorrosion in aqueous solution. We focus on developing various approaches including composition tuning, morphology control, and heterojunction preparation, and cocatalyst incorporation, to solve these issues.

For Fe<sub>2</sub>O<sub>3</sub> photoanode, proper amount doping of Ge can improve the density of the charge carriers [2]. Incorporating CuO as a sacrificial template agent removed by NaCl treatment can tune the Fe<sub>2</sub>O<sub>3</sub> morphologies by increasing the surface area [3]. Besides, rapid cooling from 800 °C during fabrication can reduce the nanosize of Fe<sub>2</sub>O<sub>3</sub> which can promote the carrier diffusion from bulk to surface [4]. Furthermore, loading an amorphous FeCoW oxy-hydroxide nanolayer on Fe<sub>2</sub>O<sub>3</sub> film significantly improves the performance [5]. The FeCoW layer can store the photogenerated holes from the Fe<sub>2</sub>O<sub>3</sub> film thus inhibiting surface recombination, and the layer can also shift the surface state to higher location which allows for a lowered onset voltage ( $V_{on}$ ). The  $V_{on}$  is 0.67 V vs. RHE and the applied bias photo-to-current efficiency of the composite is 2.7 times higher than that of the bare Fe<sub>2</sub>O<sub>3</sub>.

For Cu<sub>2</sub>O photocathode, we found that the photo-corrosion is strongly dependent on the facet. The {100} and {110} crystal facets are selectively corroded by the photo-



generated holes whereas the facet {111} is comparatively stable [6]. By preparing core/shell structured Cu/Cu<sub>2</sub>O photocathode on Cu mesh with a simple thermal conversion process, the photocurrent density can be further improved by carbon coating, which is enhanced from -1.5 to -2.75 mA/cm<sup>2</sup> at 0 V vs. RHE. However, the deposition of carbon films on Cu<sub>2</sub>O has little effect on improving the stability[7].

#### References

- [1] K. Sivula, et al. *ChemsusChem*, 2011, **4**, 432-449.
- [2] L. Zhao, et al. *Int. J. Hydrogen Energy*, 2018, **43**, 12646-12652.
- [3] Y. Li, et al. *ACS Appl. Mater. Inter.*, 2015, **7**, 16999-17007.
- [4] J. Xiao, et al. *J. Catal*, 2017, **350**, 48-55.
- [5] J. Xiao, et al. *Appl. Catal. B-Environ.*, 2017, **212**, 89-96.
- [6] Y. Li, et al. *Phys. Chem. Chem. Phys.*, 2016, **18**, 7023-7026.
- [7] Y. Li, et al. *Catal. Commun.*, 2016, **66**, 1-5.

# Mechanochemically-Assisted Preparation of Mo-Incorporated MFI Zeolite and Its Catalytic Activity on Oxidative Coupling of Methane

*Mizuho Yabushita,<sup>1</sup> Mami Horie,<sup>1</sup> Fumiya Muto,<sup>1</sup> Motohiro Yoshida,<sup>1</sup> Sachiko Maki,<sup>1</sup> Kiyoshi Kanie,<sup>1</sup> Toshiyuki Yokoi,<sup>2,3</sup> Atsushi Muramatsu<sup>1,4</sup>*

*<sup>1</sup>Institute of Multidisciplinary Research for Advanced Materials, Tohoku University, Sendai, Japan; <sup>2</sup>Institute of Innovative Research, Tokyo Institute of Technology, Yokohama, Japan; <sup>3</sup>JST-PRESTO, Tokyo, Japan; <sup>4</sup>JST-CREST, Tokyo, Japan.*

## 1. Introduction

The oxidative coupling of methane (OCM) is a fascinating reaction, since this reaction converts methane, a main component of natural gas, to C<sub>2</sub> compounds (*i.e.*, ethane and ethylene), which are platform chemicals in chemical industry. In this context, heterogeneous catalysts that synthesize C<sub>2</sub> compounds in both high yield and selectivity and also suppress side reactions need to be devised. To hamper side reactions, methyl radical, an intermediate of the OCM, should not be released into gas phase from catalyst surface, because it readily reacts with other gaseous species to be CO<sub>2</sub>. Considering the confinement of methyl radical into/onto catalysts, microporous zeolites containing active sites are expected to be good catalysts for the OCM reaction.

This idea motivated us to incorporate active species into zeolite framework. We previously prepared [Ti]- and [Sn]-MFI zeolites via our novel two-step method consisting of mechanochemical reaction of two solid materials (SiO<sub>2</sub> and heteroatom source) and subsequent hydrothermal synthesis [1,2]. In this work, we applied this method to preparation of [Mo]-MFI, and investigated its catalytic activity in the OCM.

## 2. Experimental

SiO<sub>2</sub> and MoO<sub>3</sub> were milled together at 600 rpm for 24 h with planetary ball-mill. As-prepared sample was characterized by XRD, UV-vis, FT-IR, and TEM-EDS. This prepared sample, SiO<sub>2</sub>, (*n*-C<sub>3</sub>H<sub>7</sub>)<sub>4</sub>NOH aq., 2 M KCl aq., and H<sub>2</sub>O were charged into an autoclave, and then the mixture was stirred at 160 °C for 120 h. The precipitate was washed, dried, calcined at 550 °C for 12 h, and treated in 2 M NH<sub>4</sub>NO<sub>3</sub> at 80 °C for 3 h. After calcination at 550 °C for 12 h, [Mo]-MFI was obtained.

The OCM reaction was conducted by using a fixed-bed flow reactor. 100 mg of [Mo]-MFI was charged into a quartz tube, and mixed gas of CH<sub>4</sub>, O<sub>2</sub>, and Ar (their flow rates were 8.0, 2.0, and 2.5 mL min<sup>-1</sup>, respectively) was flowed through the

catalyst bed at 600 °C. The reacted gas mixture was analyzed by both GC-TCD and GC-FID.

### 3. Results and Discussion

After the milling, any diffraction peaks derived from  $\text{MoO}_3$  were not observed, indicating no crystalline phase of either  $\text{SiO}_2$  or  $\text{MoO}_3$ . UV-vis and FT-IR spectroscopy showed the presence of tetrahedral Mo species with Si–O–Mo bonding. The TEM-EDS image suggested that the sample has a core-shell structure, where core and shell consist of Si and Mo, respectively (Figs. 1A and 1B). These data indicate that during the milling, mechanochemical reaction occurs at the interface of  $\text{SiO}_2$  and  $\text{MoO}_3$ , to form Si–

O–Mo bonding. In contrast to the reported mechanical alloying process [3], the blending of two oxides forms such Si–O–Mo bonding, which leads to the amorphization.

The hydrothermal treatment of amorphous precursor and  $\text{SiO}_2$  successfully prepared [Mo]-MFI, where the addition of  $\text{SiO}_2$  is a key to the formation of crystalline zeolite framework, since the dilution of Mo species in solids allows the material to be crystalline. Another key is the use of amorphous precursor, from which Si–O–Mo-bond-containing complexes were once dissolved and then were reprecipitated as [Mo]-MFI; as a result, Si–O–Mo bonding originally present in the precursor was maintained and Mo species were dispersed well in the whole [Mo]-MFI particles (Figs. 1C and 1D).

Thus prepared [Mo]-MFI was tested as catalyst for the OCM reaction. It should be noted that we observed the production of  $\text{C}_2$  compounds over [Mo]-MFI even at the reaction temperature of as low as 500 °C. At 600 °C, [Mo]-MFI produced 0.0093% yield of  $\text{C}_2$  compounds with 0.22% yield of  $\text{CO}_2$ , while 1 wt%  $\text{MoO}_x/\text{MFI}$  produced the same degree of  $\text{C}_2$  compounds with 15-fold larger amount of  $\text{CO}_2$ . This comparison suggests that the Mo species in the zeolite framework work as more

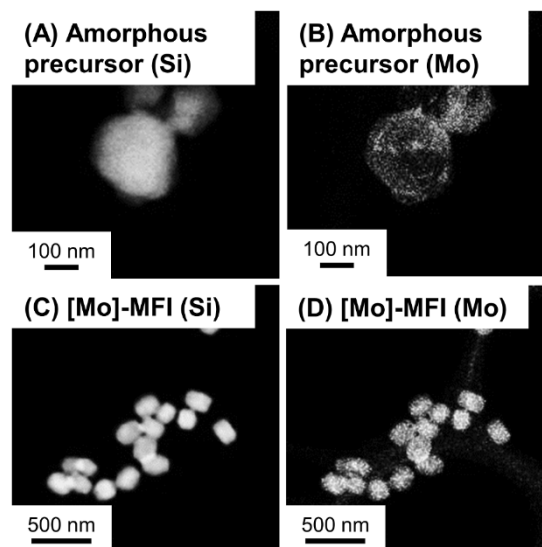


**Fig. 1** TEM-EDS images of amorphous precursor and [Mo]-MFI.

active and selective sites for the OCM reaction than ones simply deposited on the zeolite surface.

### References

- [1] K. Yamamoto, S. E. B. Garcia, F. Saito, A. Muramatsu, *Chem. Lett.* **2006**, 35, 570–571.
- [2] K. Kanie, M. Sakaguchi, F. Muto, M. Horie, M. Nakaya, T. Yokoi, A. Muramatsu, *Sci. Technol. Adv. Mater.* **2018**, 19, 545–553.
- [3] C. Suryanarayana, *Prog. Mater. Sci.* **2001**, 46, 1-184.

# Aqueous-phase reforming of alcohols over alumina-supported ruthenium and platinum catalysts

*Run Xu, Kai Xu, Chaopeng Hou, Guofu Xia, Zhihai Hu, Hong Nie*

*Research Institute of Petroleum Processing, SINOPEC, Beijing, 100083, China*

## 1 Introduction

Hydrogen is a very important element for needs of chemical industry, oil and biorefinery, and also has a perspective to be used as a clean energy carrier [1]. Aqueous-phase reforming (APR) is a promising technology which allows the formation of H<sub>2</sub> directly from aqueous solutions of various organic compounds [2]. Generation of H<sub>2</sub> by liquid phase reforming at low temperatures is accompanied by selectivity challenges because the reaction of H<sub>2</sub>, CO or CO<sub>2</sub> to form alkanes is highly favorable at these low temperatures [3]. The H<sub>2</sub> selectivity is dependent on the type of metals, the nature of the support, the feed reactant molecules, and the reaction conditions. Pt, Ru, Pd, Ni and Rh metals have been reported to have a catalytic activity for APR reaction [4]. Among these metals, Ru and Pt were considered as high efficient catalysts. In the present study, the effects of reaction conditions on the APR reaction of methanol and ethanol over Ru/Al<sub>2</sub>O<sub>3</sub> and Pt/Al<sub>2</sub>O<sub>3</sub> catalysts were investigated.

## 2 Results and discussion

The Ru/Al<sub>2</sub>O<sub>3</sub> and Pt/Al<sub>2</sub>O<sub>3</sub> catalysts were prepared using a conventional impregnation method. The catalysts were characterized by X-ray powder diffraction, transmission electron microscopy, N<sub>2</sub> sorption, and CO chemisorption techniques. The performance of the catalysts was tested in a continuously operated tubular stainless steel reactor. In the APR reaction of methanol over Ru/Al<sub>2</sub>O<sub>3</sub>, H<sub>2</sub>, CH<sub>4</sub> and CO<sub>2</sub> were the major products in the gas phase. Minute amount of CO was detected during the reaction that indicated the water-gas shift reaction to form CO<sub>2</sub> was expected to occur very rapidly under aqueous phase reaction conditions. The selectivity of CH<sub>4</sub> increased obviously while the selectivity of H<sub>2</sub> decreased during the increase of reaction temperature due to the strong ability of Ru for CO and CO<sub>2</sub> hydrogenation. The selectivity of H<sub>2</sub> and CO<sub>2</sub> increased from 20.7% and 34.5% to 67.2% and 58.3% as the feed flow rate increased from 1h<sup>-1</sup> to 10h<sup>-1</sup> (as shown in

Figure 1). In the APR reaction of ethanol over Ru/Al<sub>2</sub>O<sub>3</sub>, H<sub>2</sub>, CH<sub>4</sub> and CO<sub>2</sub> were the main products in the gas phase. Very low levels C<sub>2</sub>H<sub>6</sub> and CO were detected. The selectivity of H<sub>2</sub> was constant during the increase of reaction temperature. The ratio of CH<sub>4</sub> and CO<sub>2</sub> was 1:1 at 210°C and shifted to 1.5:1 at 230°C. The selectivity and products distribution in APR of methanol and ethanol were compared in different reaction temperature and feed flow rate. In the APR reaction of methanol over Pt/Al<sub>2</sub>O<sub>3</sub>, H<sub>2</sub>, and CO<sub>2</sub> were the major products in the gas phase. None CO was detected during the reaction. The activity of methanol reforming increased sharply during the increase of reaction temperature, while the selectivity of H<sub>2</sub> kept over 98%. In the APR reaction of ethanol over Pt/Al<sub>2</sub>O<sub>3</sub>, H<sub>2</sub>, CH<sub>4</sub> and CO<sub>2</sub> were the main products in the gas phase, which indicated the Pt/Al<sub>2</sub>O<sub>3</sub> have high activity of cleavage of C-C bond. The possible reaction pathways were discussed.

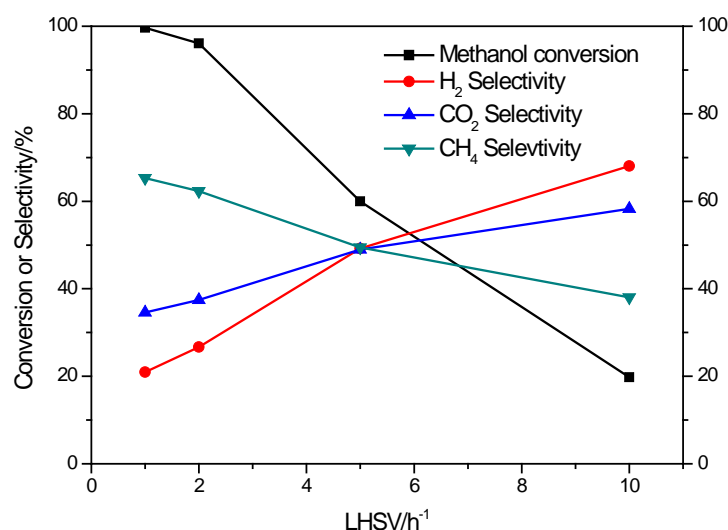


Figure 1. The performance of Ru/Al<sub>2</sub>O<sub>3</sub> for methanol APR under different LHSV

## References

- [1] R.D. Cortright, R.R. Davda and J.A. Dumesic, *Nature*, 2002, 418, 964–967.
- [2] G.W. Huber, S. Iborra and A. Corma, *Chem. Rev.*, 2006, 106, 4044–4098.
- [3] B. Roy, U. Martine, K. Loganathan, A.K. Datye and C.A. Leclerc, *International Journal of Hydrogen Energy*, 2012, 37, 8143-8153.
- [4] T. Nozawa, Y. Mizukoshi, A. Yoshida and S. Naito, *Appl. Catal. B*, 2014, 146, 221-226.

# Optimization of the composition of the Pt/MgAlO<sub>x</sub> catalyst and the conditions of the reaction of propane dehydrogenation

*Liudmila Stepanova, Institute of Hydrocarbons Processing SB RAS, Omsk, Russia;*

*Olga Belskaya, Institute of Hydrocarbons Processing SB RAS, Omsk State Technical University, Omsk, Russia; Vladimir Likholobov, Institute of Hydrocarbons Processing*

*SB RAS, Omsk, Russia*

## Introduction

Pt/MgAlO<sub>x</sub> are promising catalytic systems for their use in the reactions of dehydrogenation of light and higher alkanes. Supports for these catalysts are mixed oxides MgAlO<sub>x</sub>, made by calcination of layered double hydroxides (LDH) at temperatures. Mixed oxides possess moderate basicity and high specific surface areas, and their properties can be easily regulated by changing the composition of their precursors, i.e., LDH. Platinum catalysts are more active and selective compared with the systems based on chromium oxides. But platinum based catalysts are rapidly deactivated. Moreover, composition of Pt/MgAlO<sub>x</sub>, as well as conditions of reaction of propane hydrogenation when this type of catalyst is used are still not optimized.

Therefore the aim of these work was synthesis of the Pt/MgAlO<sub>x</sub> catalysts with different platinum active sites localization and support basicity (different Mg/Al ratio), and investigation of the catalytic properties of the catalysts in propane dehydrogenation at different conditions and studying their deactivation processes.

## Experimental

MgAl-LDH-CO<sub>3</sub> (with CO<sub>3</sub><sup>2-</sup> anions into interlayer space) were synthesized by coprecipitation method by adding of magnesium and aluminum nitrates to sodium carbonate at constant pH = 10 and temperature = 60 °C. «Activated» LDH with preferential content of OH<sup>-</sup> anions in interlayer space (MgAl-LDH-OH) were made by calcination of MgAl-LDH-CO<sub>3</sub> at 550 °C and subsequent rehydration in distilled water. The platinum anchoring on selected supports was carried out by using of excess of H<sub>2</sub>[PtCl<sub>6</sub>] solution. The concentration of metals in catalysts (after dissolution) was estimated by inductively coupled plasma atomic emission spectroscopy on a Varian 710-ES system. The catalytic properties of the systems

were investigated in propane dehydrogenation (sample loading 0.5 g., the molar ratio  $H_2/C_3H_8 = 0$  or 0.25, atmospheric pressure, feed space velocity of  $8 \text{ g h}^{-1}$ ). The reaction temperature was 550, 590 и 620 °C. Before each experiment the samples were oxidized and reduced at 620 °C. Thermal analysis of deactivated samples was carried out at STA-449C Jupiter (Netzch) instrument. Platinum dispersion in catalysts was estimated by hydrogen chemisorption on AutoChem II 2920 («Micromeritics») device with thermal conductivity detector (TCD).

## Results and discussion

For the Pt/MgAlO<sub>x</sub> catalysts prepared by using of OH-containing support precursors, decrease of propane conversion during the reaction occurred. Herewith the greatest propane conversion and propylene selectivity (more than 97 %) without significant coke deposits on the surface (according to thermal analysis data) were at 590 °C. The Pt/MgAlO<sub>x</sub> catalysts obtained using carbonate-containing support precursors, were characterized by lesser activity at 550 и 590 °C compared with the catalysts prepared from OH-containing precursors. Propane conversion at 620 °C rose with time as a result of increasing the contribution of non-target C – C bond hydrogenolysis reactions. Higher activity of Pt/MgAl-OH catalysts, made by using of MgAl-OH-LDH, was explained by more platinum dispersion and larger amount of metallic platinum in the catalysts. The resulting kinetic curves were described by a model that takes into account deactivation by the formation of coke (the main source of coke is propylene), which is accompanied by the self-regeneration of the catalyst under the action of hydrogen.

*Characterization of the catalysts was performed using equipment of the Omsk Regional Center of Collective Usage, Siberian Branch of the Russian Academy of Sciences. The work was financially supported by the Ministry of Science and Higher Education of the Russian Federation in accordance with the Program of fundamental scientific research of the State Academy of Sciences for 2013-2020 in direction V.46, project V.46.2.4. (project registration number AAAAA17-117021450095-1).*



## **Biogas upgrading with CO<sub>2</sub> hydrogenation**

*Vissanu Meeyoo, Noppadol Panchan, Centre for Advanced Materials and Environmental Research, Mahanakorn University of Technology, Bangkok 10530 Thailand and Chunshan Li, Beijing Key Laboratory of Ionic Liquids Clean Process, State Key Laboratory of Multiphase Complex System, Institute of Process Engineering, Chinese Academy of Sciences, Beijing 100190, PR China*

### **Introduction**

Methanation of CO<sub>2</sub> has drawn a considerable attention due to its potential for the production of substitute syngas, demanding for the storage of excess electricity. This reaction occurs competitively with a reverse water gas shift reaction and CO methanation. With the exothermic nature of the reaction, the CO<sub>2</sub> conversion is not favorable at a high temperature operation. To overcome this problem, highly active catalysts at low temperatures are required. Ni catalysts are commonly chosen due to their low cost and high activity. The nature of the support was also found to affect the reaction. It was reported [1] that Ce-Zr oxides have demonstrated as a good potential for the catalyst support for methanation due to its advantages, including good redox properties, high thermal stability, resistance to sintering and coke formation. In this work, we prepared high Ni loading over Ce-Zr catalysts via one-pot hydrothermal synthesis

### **Experimental**

Ni<sub>1-x</sub>Ce<sub>0.75x</sub>Zr<sub>0.25x</sub>O<sub>δ</sub> catalysts were prepared via one-pot hydrothermal synthesis adopted from what reported elsewhere [2]. Typically, 0.1 M of metal salt solutions were premixed to the desired ratio of Ni/Ce/Zr. The resultant solution was then mixed with 0.4 M of urea solution at the metal to urea ratio of 2:1. Then, the solution was transferred to teflon lining autoclave and kept at 105°C for 50 hrs. CO<sub>2</sub> methanation was carried out in a packed bed reactor (i.d. 0.6 mm) placed in a tubular furnace equipped with temperature controllers. The products were analyzed using Shimadzu GC14B gas chromatograph equipped with TCD and Alltech CTR I and Supelco Carboxen columns.

### **Results and discussion**

The XRD patterns of the catalysts showed a typical cubic fluorite structure of CeO<sub>2</sub> indices at 2θ = 28°, 33°, 48° and 58°. The additional of Ni at a low loading (below 15 wt%) was not found significantly to affect the XRD patterns indicating a dissolution of Ni in Ce-Zr structure. However, at a higher loading, the separation peaks at 37°, 43°, 63° and 75° attributed to NiO. The presence of Ni also influenced the lattice parameter of pure mixed oxides. This might be due to the incorporation of nickel ions into the Ce-Zr structure, as their ionic radius is smaller than zirconium ions radius [3]. BET surface areas the catalysts are in the range of ca. 140-190 m<sup>2</sup>/g.

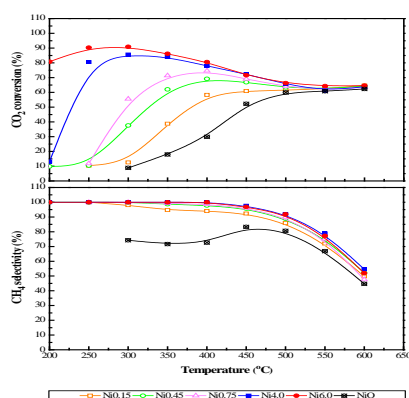


**Fig. 1** Results of catalytic performances (a) CO<sub>2</sub>-Conversion and (b) CH<sub>4</sub>-yield.

As shown in Fig. 1, the Ni<sub>1-x</sub>Ce<sub>0.75x</sub>Zr<sub>0.25x</sub>O<sub>δ</sub> catalysts were superior to a bare Ni catalyst. The CO<sub>2</sub> conversion is quite close to the equilibrium even at 200 °C. Ni6.0 catalyst was found to be the most active with the Ni loading of up to 71.5 wt%. At above 450°C, methane selectivity was decreased as a reverse water gas shift reaction starts to contribute to the overall reactions.

## Conclusions

It can be concluded that high Ni loading: Ni<sub>1-x</sub>Ce<sub>0.75x</sub>Zr<sub>0.25x</sub>O<sub>δ</sub> catalysts can be prepared via hydrothermal synthesis, resulted with high surface area catalysts. Ni6.0 catalyst was reported to be the most active catalyst showing a good activity even at low temperature.

## References

- [1] M. A. A. Aziz, A. A. Jalil, S. Triwahyono, A. Ahmad, *Green Chemistry*, **2017**, 17, 2647-2663.
- [2] R. Wang, S. I. Mutinda, M. Fang, *RSC Advances*, **2013**, 3, 19508-19514.
- [3] F. Ocampo, B. Louis, L. Kiwi-Minsker, A. Roger, *Applied Catalysis A: General*, **2011**, 392, 36-44.

# **Methanol Assisted Methane Conversion into Hydrocarbons over Mo-Ga loaded MCM-22**

*Anushree<sup>1</sup>, Bhanumurthy S.<sup>1</sup>, Pradeep Kumar Budde<sup>1</sup>, Sreedevi Upadhyayula<sup>1\*</sup>*

*Department of Chemical Engineering, Indian Institute of Technology Delhi, Hauz Khas, New Delhi, India, 110016*

\*Corresponding Author:

Email: [sreedevi@chemical.iitd.ac.in](mailto:sreedevi@chemical.iitd.ac.in), Contact number: 01126591083

Natural gas is an abundant source of energy. However, it is an underutilized feedstock for the production of liquid transportation fuels. Methane is the main component of natural gas (80%-95% by volume). Therefore, conversion of abundant methane to fuel range hydrocarbons has attracted significant attention, which can offer many advantages like high energy density, safer storage and less transportation cost.

Direct conversion of methane is very economical and environmentally friendly, but it is challenging due to the symmetrical tetrahedral structure of methane with high C-H bond strength of 435 kJ/mol [1]. Methane activation in presence of gaseous oxygen has been widely investigated, but the irreversible deep oxidation of hydrocarbons presents the low aromatic selectivity. The non-oxidative catalytic route is a potentially attractive option, where methane is directly converted to aromatic compounds in absence of gaseous oxygen. But, high deactivation caused by coking of catalyst at high operating temperature is the major obstacle to industrial adoption of this technique. The presence of soft oxidant as a co-reactant with CH<sub>4</sub> can manipulate the incompatible side reactions and suppress the coke formation, due to activation of methane molecule at low temperature [2].

Present work was undertaken to investigate the conversion of methane over bifunctional zeolite catalyst, i.e., Mo-Ga/MCM-22. Due to difficulty in direct activation of methane, methanol was used as an oxygenate co-reactant. MCM-22 (SAR=30) was prepared by hydrothermal method and it was modified with Mo and Ga using ion-exchange techniques. The prepared catalysts were characterized by XRD, FT-IR, BET surface area and FE-SEM techniques. The catalyst activity was tested in a fixed bed quartz tube reactor at 565°C under atmospheric pressure.

The effect of metal loading over MCM-22 zeolite was studied for its activity in methane dehydroaromatization reaction (MDA). 2 wt% Mo and 2 wt% Ga metal loading over the MCM-22 support exhibited the maximum methane conversion of 26%, with 88% selectivity to aromatics at a gas hourly space velocity of  $1200 \text{ cm}^3 \text{ gm}^{-1} \text{ h}^{-1}$  and methane to methanol mole ratio of 6. The TGA analysis revealed low coke weight loss from deactivated catalyst in the presence of methanol as a co-reactant. No structural collapse was observed at high temperature, which indicated the stability of catalyst during reaction.

The acidity and shape selectivity of MCM-22 zeolite support towards higher hydrocarbons was a key factor for effective methane conversion [3]. The modification of MCM-22 with Mo and Ga was appropriate for proper tuning of acidic and metallic sites of catalyst [4].

#### References

- [1] Karakaya C, Robert J. Kee, Progress in the direct catalytic conversion of methane to fuels and chemicals, *Progress in Energy and Combustion Science*, 55 (2016) 60–97.
- [2] Bijani PM, Sohrabi M, Sahebdehfar S. Nonoxidative aromatization of  $\text{CH}_4$  using  $\text{C}_3\text{H}_8$  as a coreactant: thermodynamic and experimental analysis. *Industrial Engineering and Chemical Research*, 53 (2014) 572–581.
- [3] Mishra S, Balyan S, Pant KK, Haider MA, Non-oxidative conversion of methane into higher hydrocarbons over Mo/MCM-22 catalyst, *Journal of Chemical Science*, 129 (2017) 1705–1711.
- [4] Ma D, Zhu QJ, Wu ZL, Zhou DH, Shu YY, Xin Q, The synergic effect between Mo species and acid sites in Mo/HMCM-22 catalysts for methane aromatization. *Journal of Physical Chemistry and Chemical Physics*, 7 (2005) 3102–3109.

# Synthesis and Characterization of Core-shell Beta/MCM-22 Composite Zeolites

*W. Y. YANG, Fushun Research Institute of Petroleum and Petrochemicals, Fushun, China; F. X. LING, Fushun Research Institute of Petroleum and Petrochemicals, Fushun, China; Z. Q. Sheng, Fushun Research Institute of Petroleum and Petrochemicals, Fushun, China; H. C. ZHANG, Fushun Research Institute of Petroleum and Petrochemicals, Fushun, China; Fushun Research Institute of Petroleum and Petrochemicals, Fushun, China, China*

Alkylation of benzene with propylene is an industrially important reaction for the production of isopropylbenzene, an intermediate for the production of acetone and phenol. Beta and MCM-22 zeolites as solid acid catalyst, have been successfully applied in the processes of alkylating benzene with propylene to form isopropylbenzene[1,2].

In this paper, a briefly study to obtain core-shell Beta/MCM-22 micro-microporous composite zeolites is reported. We expect it will have advanced physical structure and exhibit higher activity and selectivity in the reaction of alkylation of benzene with propylene.

Beta/MCM-22 composites were produced by conventional hydrothermal process. Chemical materials, silicasol,  $\text{NaAlO}_2$ ,  $\text{NaOH}$ , HMI and Beta zeolites were purchased. Beta calcined in air at 300C for 3h, were pretreated through a  $\text{Ar-H}_2$  plasma (50W,  $\text{H}_2/\text{Ar}=1.25$ , 70mTorr) at room temperature using Gatan 950 plasma system[3]. The typical batch composition in terms of molar ratio was:  $\text{SiO}_2$ :  $\text{Al}_2\text{O}_3$ :  $\text{OH}^-$ : HMI:  $\text{H}_2\text{O}=1$ : 0.033: 0.10: 0.35: 25, Beta excluded here. The As-synthesized powders calcined at 550°C in air for 5h in a muffle furnace to remove organics, were characted via various methods such as XRD, SEM and TEM.

The XRD patterns of Beta, plasma-pretreated Beta, MCM-22, and Beta/MCM-22 are shown in Fig. 1. The patterns of both Beta zeolites are in good agreement with those reported previously, indicating plasma treating does not damage the crystalline structure of Beta. The patterns of Beta/MCM-22 are very complex. The peaks at 7.7°, 21.7°, 22.4°, 25.4°, 26.8° and 29.6° were assigned to the diffraction of Beta- rays, while these peaks at 7.1°, 7.2°, 8.1°, 10.0°, 14.2°, 26.1° and 28.1° can be assigned to MCM-22.

SEM and TEM results as shown in Fig. 2. The images of the composite with uniform morphology are obviously different from the Beta zeolites which look smooth (Fig. 2b). The surface morphology of the composite shows flakes similar to MCM-22 in Fig. 2c and 2d. The results of EM exhibit the Beta/MCM-22 composite core-shell structure instead of physical mixture.

The reasons for our uniform Beta/MCM-22 composite zeolites attribute to the surface energy, Si-OH groups and surficial positive charges of Beta zeolites, which pre-treated by Ar-H<sub>2</sub> plasma.

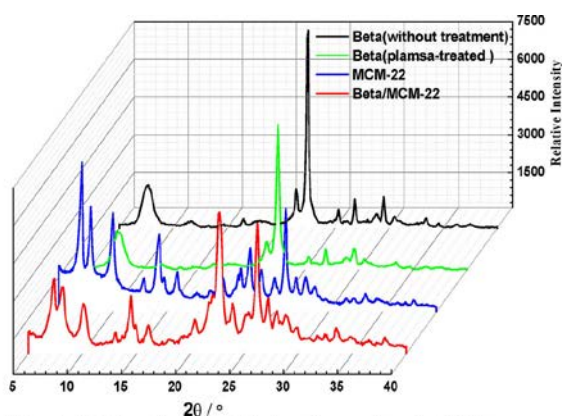


Fig. 1. XRD patterns of Beta, plasma-treated Beta, MCM-22, and Beta/MCM-22 zeolites

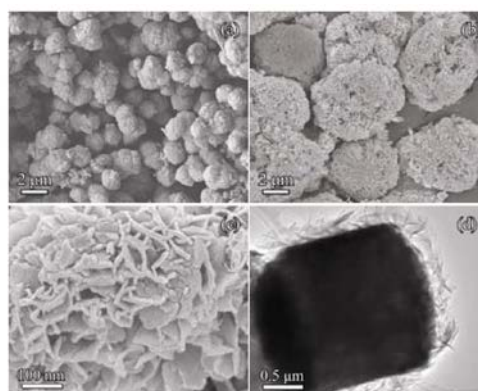


Fig. 2. SEM and TEM images of Beta (a) and Beta/MCM-22 zeolites (b, c, and d)

## References

- [1] Han, M, S. Lin, et al. Applied Catalysis A: General (2003), 243(1): 175
- [2] Fu, J., C. Ding. Catalysis Communications (2005), 6(12): 770
- [3] Kameoka, S., M. Kuroda, et al. Applied Surface Science (1997), 121-122: 351

## **Towards a bio-circular economy: Catalysis for humins valorisation**

*Layla Filiciotto<sup>1</sup>, Universidad de Cordoba<sup>1</sup>, Cordoba<sup>1</sup>, Spain<sup>1</sup>; Alina M. Balu<sup>2</sup>, Universidad de Cordoba<sup>2</sup>, Cordoba<sup>2</sup>, Spain<sup>2</sup>; Antonio A. Romeo<sup>3</sup>, Universidad de Cordoba<sup>3</sup>, Cordoba<sup>3</sup>, Spain<sup>3</sup>; Jagdeep Singh<sup>4</sup>, Avantium<sup>4</sup>, Amsterdam<sup>4</sup>, The Netherlands<sup>4</sup>; Ed de Jong<sup>5</sup>, Avantium<sup>5</sup>, Amsterdam<sup>5</sup>, The Netherlands<sup>5</sup>; Jan C. van der Waal<sup>6</sup>, TNO<sup>6</sup>, Delft<sup>6</sup>, The Netherlands<sup>6</sup>; Rafael Luque<sup>7</sup>, Universidad de Cordoba<sup>7</sup>, Cordoba<sup>7</sup>, Spain<sup>7</sup>.*

### **Biomass by-product valorisation through catalytic approaches**

Production of chemicals (e.g. plastics) from biomass is taking hold as a valid renewable alternative to the traditional and polluting petroleum-based chemistry [1]. In particular, the acid-catalysed hydrolysis of lignocellulosic biomass would give an economic and easily-implemented process for a variety of platform chemicals (e.g. furanics, levulinates) that possess a wide application potential [2]. However, when (hemi)cellulosic sugars are in the presence of heat and an acid catalyst (being either homogeneous or heterogeneous), a dark and insoluble product is formed known as humin by-products [3]. Also known simply as humins, these by-products could have high yields being the thermodynamic favoured product [4], thus close to being inevitable. Few minimization studies can achieve low humins yields, although employing expensive measures (e.g. ionic liquids [5]) whose industrialisation would not be able to compete with the current petroleum-based market.

Also, new sustainability approaches call for the implementation of a circular economy (i.e. make, use, reuse), where the concept of waste becomes obsolete and everything finds value and application [6]. Along these lines, valorisation of humins becomes crucial to the development of an economically viable bio-industry. Some valorisation routes of these by-products to syngas [7], aromatics [8], adhesives [9], and composites [10] are being explored in the scientific community.

Catalysis as a broad concept can become an ally to humins valorisation, as well as the understanding of their nature and structure. In fact, herein we propose the use of catalysis as a basis for structural identification of humins by means of catalytic (transfer) hydrogenolysis and analysis of decomposition products. The information obtained from the classes of products identified and their reactivity (e.g. Diels-Alder rearrangement to aromatics) can then be employed to further develop humins

applications, such as (photo)catalytic transformations to valuable products (e.g. organic acids) or the use of humins as carbon-sources for catalytic nanocomposites active in selective oxidations. In particular, batch [11] and continuous flow oxidation of isoeugenol (*i.e.* potentially lignin-derived molecule) to high added value flavouring agent vanillin has been explored.

Overall, catalysis has the potential to further upgrade biorefineries' by-products, thus improving the economical competitiveness of bio-based industries as opposed to the traditional petroleum market.

## References

- [1] Filiciotto, L.; Luque, R. Biomass promises: A bumpy road to a renewable economy. *Current Green Chem.*, **2018**, *5*, 47-59.
- [2] Kang, S.; Fu, J.; Zhang, G. From lignocellulosic biomass to levulinic acid: A review on acid-catalyzed hydrolysis. *Renew. Sust. Energ. Rev.*, **2018**, *94*, 340-362.
- [3] van Zandvoort, I. Towards the valorization of humin by-products. Ph.D. Thesis, Utrecht University, **2015**.
- [4] Sumerskii, I.V.; Krutov, S.M.; Zarubin, M.Ya. Humin-like substances formed under the conditions of industrial hydrolysis of wood. *Russ. J. Appl. Chem.*, **2010**, *83*(2), 320-327.
- [5] Eminov, S.; Wilton-Ely, J.D.E.T.; Hallet, J.P. The highly selective and near-quantitative conversion of fructose to 5-hydroxymethylfurfural using mildly acidic ionic liquids. *ACS Sustain. Chem. Eng.*, **2014**, *2*(4), 978-981.
- [6] What is a circular economy? <https://www.ellenmacarthurfoundation.org/circular-economy/concept> (accessed Dec 30, 2018)
- [7] Hoang, T.M.C.; Lefferts, L.; Seshan, K. Humin-based by-products from biomass processing as a potential carbonaceous source for synthesis gas production. *Green Chem.*, **2015**, *17*(2), 959-972.
- [8] Agarwal, S.; van Es, D.; Heeres, H.J. Catalytic pyrolysis of recalcitrant, insoluble humin byproducts from C6 sugar biorefineries, *J. Anal. Appl. Pyrolysis*, **2017**, *123*, 134-143.
- [9] Kang, S.; Fu, J.; Zhang, G.; Zhang, W.; Yin, H.; Xu, Y. Synthesis of Humin-Phenol-Formaldehyde Adhesive, *Polymers*, **2017**, *9*, 373-382.
- [10] Pin, J.M.; Guigo, N.; Mija, A.I Vincent, L.; Sbirrazzuoli, N.; van der Waal, J.C.; de Jong, E. Valorization of biorefinery side-stream products: Combination of humins with polyfurfuryl alcohol for composite elaboration. *ACS Sustain. Chem. Eng.*, **2014**, *2*(9), 2182-2190.
- [11] Filiciotto, L.; Balu, A.M.; Romero, A.A.; Rodríguez-Castellón, E.; van der Waal, J.C.; Luque, R. Benign-by-design preparation of humin-based iron oxide catalytic nanocomposites. *Green Chem.*, **2017**, *19*(18), 4423-4434.



# Integrated TiC-SiC Supported Co Catalysts with Enhanced Active Phase Dispersion in Fischer–Tropsch Synthesis

*Qian Jiang<sup>1</sup>, Yuefeng Liu<sup>1</sup>, Dangsheng Su<sup>1</sup>*

*1 DNL, Dalian Institute of Chemical Physics, Chinese Academy of Sciences, Dalian 116023, China*

Silicon carbide ( $\beta$ -SiC) has been reported as an efficient support for Fischer-Tropsch synthesis (FTS) reaction with good stability and high C5+ selectivity due to the physical properties with high mechanical strength, high thermal conductivity, high oxidative resistance and meso- and macroporous structure [1, 2]. While the chemical inertness of this support resulting in the low metal-support interaction of  $\beta$ -SiC support cobalt based catalyst thus leading to the relatively low CO hydrogenation performance. In this work, titanium carbide-decorated silicon carbide (TiC-SiC) supported catalyst with improved metal-support interactions were synthesized and tested in FTS reaction. Additionally, Pt promoter was also considered for the further improvement of the catalytic performance.

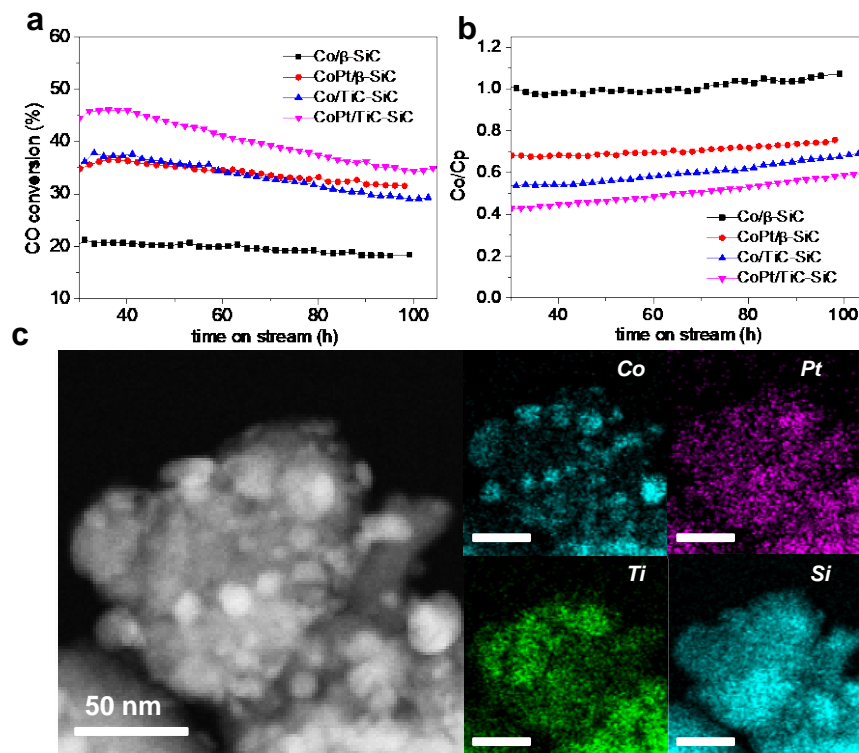


Figure 1 CO conversion (a) and C2-C5 olefin/paraffin ratios (b) as a function of time

on stream of Co/ $\beta$ -SiC, CoPt/ $\beta$ -SiC, Co/TiC-SiC and CoPt/TiC-SiC catalysts. HAADF-STEM images and EDS elemental mapping (c, scale bar 50 nm) after reduction for CoPt/TiC-SiC by in-situ STEM

It can be apparently seen that the incorporation of TiC in the support as well as the introduction of Pt promoter both benefit the FTS performance (Figure 1) with the C5+ productivity of 123 g/kg cat/h, 260 g/kg cat/h, 302 g/kg cat/h and 390 g/kg cat/h for Co/ $\beta$ -SiC, CoPt/ $\beta$ -SiC, Co/TiC-SiC and CoPt/TiC-SiC, respectively. Small particles were observed when TiC-SiC was used as the support or Pt was introduced (see STEM images) with the metallic cobalt surface area (see H<sub>2</sub> chemisorption results) of 3.30 m<sup>2</sup>/g<sub>cobalt</sub>, 5.74 m<sup>2</sup>/g<sub>cobalt</sub>, 6.04 m<sup>2</sup>/g<sub>cobalt</sub> and 7.33 m<sup>2</sup>/g<sub>cobalt</sub>, respectively, meaning that active sites were better dispersed. Metallic cobalt also provides the active sites for H<sub>2</sub> dissociation thus the catalyst with bigger metallic cobalt surface area presents lower olefin/ paraffin ratio (C2-C5) in the products. Co/TiC-SiC shows lower CO hydrogenation temperature than Co/ $\beta$ -SiC in CO-TPSR.

## References

- [1] Y.F. Liu, B. de Tymowski, F. Vigneron, I. Florea, O. Ersen, C. Meny, P. Nguyen, C. Pham, F. Luck, C. Pham-Huu, ACS Catal 3 (2013) 393-404.
- [2] Y.F. Liu, I. Florea, O. Ersen, C. Pham-Huu, C. Meny, Chem Commun 51 (2015) 145-148.

## Acknowledgement

Hiroaki Matsumoto is gratefully acknowledged for conducting in-situ STEM on HITACHI HF5000 microscopy. Cuong Pham-Huu is gratefully acknowledged for meaningful discussions. SICAT company is acknowledged for providing silicon carbide materials.

# Potentials of Zeolite-catalyzed Transacetalization Reactions of Oxymethylene Dialkyl Ethers

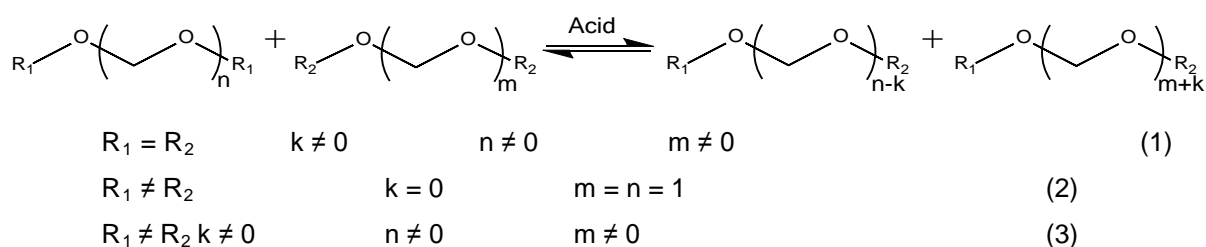
*Philipp Haltenort, Ulrich Arnold, Jörg Sauer,*

*Karlsruhe Institute of Technology (KIT),*

*Institute of Catalysis Research and Technology (IKFT),*

*Hermann-von-Helmholtz-Platz 1, 76344 Eggenstein-Leopoldshafen, Germany*

Oligomeric oxymethylene dialkyl ethers are acetals of the type  $R_1O(CH_2O)_nR_2$ . Their molecular structure exhibit high oxygen contents and in case of oxymethylene dimethyl ethers (OMDME<sub>n</sub>,  $CH_3(CH_2O)_nCH_3$ ) they provide a complete absence of carbon-carbon bonds. OMDMEs caught interest due to their high compatibility with self-ignition engines in recent years [1,2]. Their application as fuel or fuel additive leads to a tremendous reduction of soot and NO<sub>x</sub> emissions from internal combustion machines [3]. Transacetalizations are a unique type of acid-catalyzed reactions of acetal compounds (Scheme 1) and enable the exchange of CH<sub>2</sub>O units (1) and end-capping groups (2). Furthermore, both outlined modifications could appear simultaneously (3). Previous work on OMDMEs showed that transacetalization reactions according to (1) equilibrate oligomeric compounds according to a Schulz-Flory distribution [4].



**Scheme 1. Transacetalization reactions of oxymethylene dialkyl ethers for the exchange of CH<sub>2</sub>O units (1), exchange of end-capping groups (2) and their simultaneous appearance (3).**

The presented work describes an experimental study on the potential of heterogeneously catalyzed transacetalization reactions, employing highly acidic large pore zeolites. Results regarding product modification and exchange of end-capping groups are shown in Figure 1. The transacetalization of OMDME<sub>1</sub> and OMDME<sub>3</sub> (Figure 1 - A) tends to a Schulz-Flory product distribution of OMDME<sub>1-5</sub>. The reaction proceeds within a few minutes, under mild conditions, at low catalyst loading and

would therefore be easily applicable on technical scale. A feasible application of this concept would be an efficient upgrading of long-chain OMDMEs ( $\text{OMDME}_{>6}$ ) with  $\text{OMDME}_1$  to oligomers for solvent ( $\text{OMDME}_2$ ) and fuel ( $\text{OMDME}_{3-5}$ ) applications.

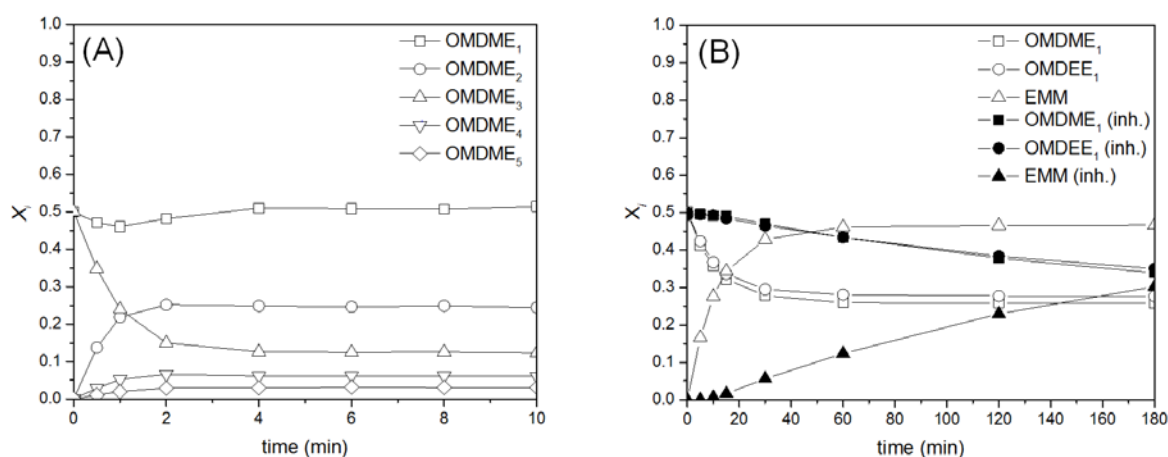


**Figure 1: Mole fraction  $X_i$  over time for the transacetalization reactions of (A) 0.05 mol  $\text{OMDME}_1$  and 0.05 mol  $\text{OMDME}_3$  ( $0.3 \text{ g}_{\text{BEA25}}/\text{mol}_{\text{reactants}}$ , 25 °C, 1 atm, 800 rpm) and (B) 0.17 mol  $\text{OMDME}_1$  and 0.17 mol  $\text{OMDEE}_1$  ( $0.6 \text{ g}_{\text{BEA25}}/\text{mol}_{\text{reactants}}$ , 30 °C, 1 atm, 800 rpm) with catalyst inhibition (inh.) by addition of  $0.18 \text{ g}_{\text{H}_2\text{O}}/\text{mol}_{\text{reactants}}$ .**

The exchange of end-capping groups between  $\text{OMDME}_1$  and  $\text{OMDEE}_1$  (Figure 1 - B) leads to the formation of ethoxy methoxy methane (EMM) and indicates the potential for the synthesis of well-defined acetal compounds by this strategy. Due to their manageable efforts on analytics, mild reaction conditions and the possibility of kinetic tuning, reactions according to (2) have a promising potential as model reactions for catalyst and reactor characterization. The kinetic modification of zeolite catalyzed reactions by water was identified previously [4] and investigated in detail for the large pore zeolites BEA25 (Figure 1 - B) and Y30 within this study. Our work therefore contributes to a better understanding of transacetalization reactions, their interaction with zeolite catalysts and outlines related applications for technical and modelling purposes.

## References

- [1] D. Deutsch, D. Oestreich, L. Lautenschütz, P. Haltenort, U. Arnold, J. Sauer, *Chemie Ingenieur Technik* **2017**, 89 (4), 486–489.
- [2] C. J. Baranowski, A. M. Bahmanpour, O. Kröcher, *Applied Catalysis B: Environmental* **2017**, 217, 407–420.
- [3] M. Härtl, K. Gaukel, D. Pélerin, G. Wachtmeister, *MTZ Worldwide* **2017**, 78 (2), 52–59.
- [4] L. Lautenschütz, D. Oestreich, P. Haltenort, U. Arnold, E. Dinjus, J. Sauer, *Fuel Processing Technology* **2017**, 165, 27–33.

# Catalytic hydropyrolysis – Effect of CoMo loading and support acidity

*M.Z. Stummann, Technical University of Denmark (DTU), Kgs. Lyngby, Denmark; A.B. Hansen, Haldor Topsøe A/S, Kgs. Lyngby, Denmark; J. Gabrielsen, Haldor Topsøe A/S, Kgs. Lyngby, Denmark; P.A. Jensen, DTU, Kgs. Lyngby, Denmark; M. Høj, DTU, Kgs. Lyngby, Denmark; A.D. Jensen, DTU, Kgs. Lyngby, Denmark*

## 1. Intro

Recent research has shown that catalytic hydropyrolysis of biomass is an efficient process for the production of renewable liquid fuels [1,2]. In this process fast pyrolysis and hydrodeoxygenation (HDO) is combined, ensuring that the reactive oxygenates formed during the pyrolysis, which may participate in polymerization reactions [3], are hydrogenated immediately, thus leading to a stable product with a low oxygen content compared to pyrolysis oil [4]. However, despite being a very promising process, there is very limited information in the open literature regarding the effect of the catalyst in the fluid bed reactor.

In this work we have investigated the effect of the CoMo loading and the support acidity on the product distribution and composition. The catalysts were tested in their sulfided form. The oxide catalyst precursors were characterized with BET, ICP-OES, NH<sub>3</sub>-TPD, and Raman spectroscopy, and the spent catalysts were studied with SEM and STEM. The organic phase was analyzed with GCxGC-MS/FID, GC-AED, and the S, H, and O concentrations were measured.

## 2. Results and discussion

Catalytic hydropyrolysis of beech wood was conducted in a fluid bed reactor at 450 °C and 26 bar pressure. Using MgAl<sub>2</sub>O<sub>4</sub> (MgAl) as support the CoMo loading was varied between 4 and 12 wt.% with a Co/Mo atomic ratio of 0.3. The effect of the support acidity was tested by maintaining a CoMo loading of 4 wt.% and testing two supports consisting of zeolite (H-ZSM-5) mixed with alumina, denoted at CoMoZA#1 and CoMoZA#2. CoMoZA#2 contained 44 % more zeolite than CoMoZA#1.

Increasing the CoMo loading from 4 to 12 wt.% decreased the condensable organic yield from 25.2 to 22.7 wt.% dry ash free basis (daf) while increasing the C<sub>1</sub>-C<sub>3</sub> yield from 10.3 to 14.0 wt.% daf, as shown in Figure 1. Using CoMoZA#1 and CoMoZA#2 decreased the condensable organic yield to 24.4 and 23.9 wt.% daf, respectively.

The C<sub>1</sub>-C<sub>3</sub> gas yield also increased to 13.0 wt.% daf for CoMoZA#1 and 13.9 wt.% daf for CoMoZA#2 mainly due to an increase in the C<sub>2</sub>-C<sub>3</sub> yield.

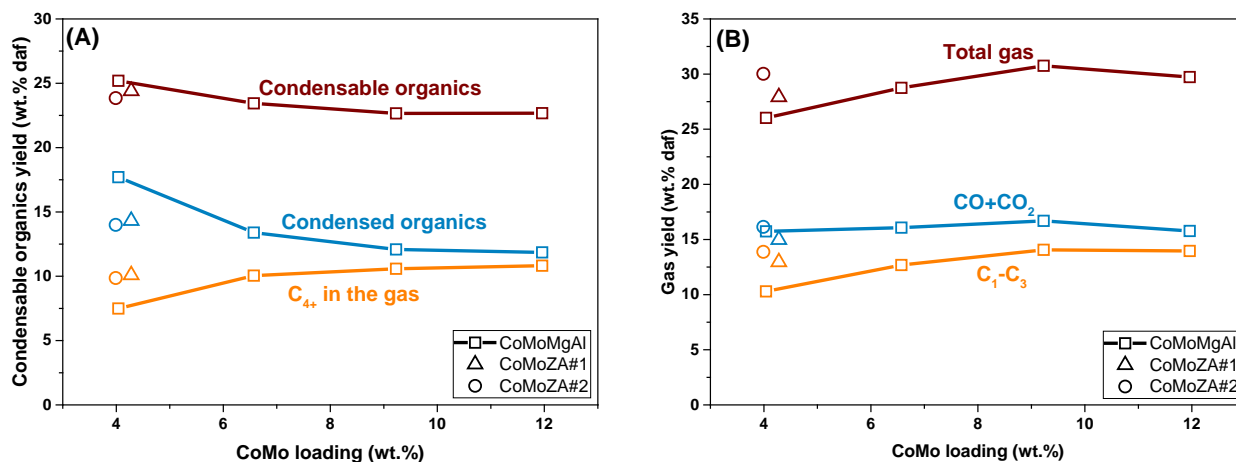


**Figure 1** Effect of the CoMo loading and support acidity on the condensable organic yield (A), and gas yield (B).

Analysis of the condensed organic phase showed that the concentration of monoaromatics and naphthenes increased with increasing CoMo loading, while the concentration oxygenates decreased, see Figure 2. Using CoMoZA#1 and CoMoZA#2 efficiently removed the oxygenated aliphatics, and increased the concentration of aromatics.

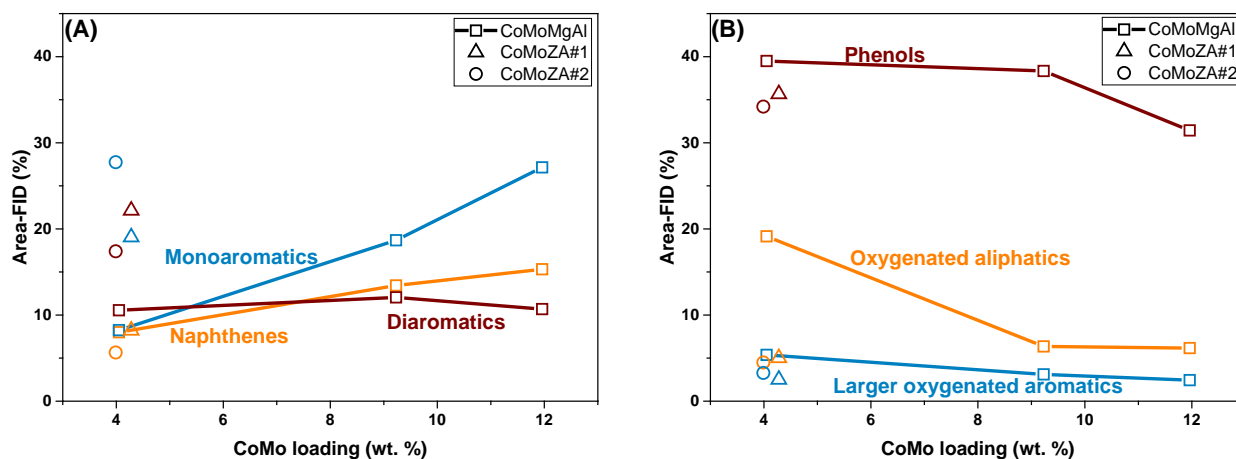


**Figure 2** Effect of the CoMo loading and support acidity on the concentration of naphthenes, mono and diaromatics (A), and oxygenates (B).

## References

1. Stummann, M.Z., Høj, M., Schandel, C.B, Hansen, A.B., Wiwel, P., Jensen, P.A., and Jensen, A.D. *Biomass Bioenergy* 115, 97 (2018)
2. Marker, T.L, Felix, L.G., Linck, M.B., and Roberts, M.J. *Environ. Prog. Sustain. Energy.* 31, 31 (2011)
3. Hurt, M.R., Degenstein, J.C., Gawecki, P., Borton II, D.J., Vinueza, N.R., Yang, L., Agrawal, R., Delgass, W.N., Ribeiro, F.H., and Kenttämaa, H.I. *Anal. Chem.* 85, 10927 (2013)
4. Dayton, D.C., Carpenter, J., Farmer, J., Turk, B., and Gupta, R. *Energy Fuels* 27, 3778 (2014)

# HYDROPROCESSING OF GASOLINE AND DIESEL FRACTIONS ON MODIFIED Ni(Co)-Mo-Al<sub>2</sub>O<sub>3</sub> CATALYSTS

**B.T.Tuktin, A.C.Tenizbaeva, Zh.A.Sailau**

*D.V. Sokolsky Institute of Fuel, Catalysis and Electrochemistry.050010, Kunaev st.  
142, Almaty, Kazakhstan.e-mail: [tuktin\\_balga@mail.ru](mailto:tuktin_balga@mail.ru)*

In connection with the involvement in the processing of high-sulfur fuel oil and the deepening of its processing, the requirements for catalysts for hydropurification gasoline and diesel fractions of oil have increased. Due to the need to deepen oil refining, the proportion of secondary processes increases, including thermal and catalytic cracking. In gasoline secondary processes there are large amounts of olefins, sulfur and nitrogen which reduce their stability. These gasoline fractions are not stable during storage, the olefin hydrocarbons contained in them, due to oxidation and polymerization which lead to the decrease of their commercial qualities. In the process of hydropurification of catalytic cracking and coking gasoline, hydrogenation of olefin hydrocarbons also occurs along with the hydrogenation reaction of organic sulfur compounds, which usually leads to a decrease of the octane number.

Modified zeolite catalysts for hydropurification and hydroisomerization of gasoline and diesel fractions were developed and prepared: KGO-18 (CoO-MoO<sub>3</sub>-REE-P-Al<sub>2</sub>O<sub>3</sub>-ZSM), KGO-6 (NiO-MoO<sub>3</sub>-REE-P-Al<sub>2</sub>O<sub>3</sub>-ZSM) and KGO-16 (CoO-MoO<sub>3</sub>-REE-P<sub>2</sub>O<sub>5</sub>-Al<sub>2</sub>O<sub>3</sub>-ZSM-HY). The catalysts were prepared by impregnating a mixture of aluminum hydroxide and ZSM, HY zeolites with aqueous solutions of nickel, cobalt, molybdenum, and the introduction of modifying additives (REE (Rare Earth Elements), P). Hydroprocessing of gasoline and diesel fractions were carried out in a flow-through installation with a stationary catalyst bed at temperatures of 320-400°C, raw material flow rate 2 hours<sup>-1</sup>, pressure 4.0 MPa.

The results obtained by hydroprocessing of various gasoline fractions show that the KGO-18 catalyst has the highest hydrodesulfurization activity. The sulfur content of catalyzate during hydroprocessing of straight-run gasoline at a temperature of 400°C is less than 0.001%. On the KGO-6 catalyst, the octane number after hydroprocessing of straight-run gasoline rises to 94.9, which is significantly higher than on other catalysts, and this is mainly due to its high hydroisomerizing activity.

When hydroprocessing of catalytic cracking gasoline on the KGO-18 catalyst at 320-350°C, the content of isoalkanes increases from 25.4 to 42.6-48.1% comparing to the initial one. The content of aromatic and naphthenic hydrocarbons varies from 30.1 to 36.1%, from 7.0 to 10.4%, respectively. The amount of olefin hydrocarbons under these conditions decreases sharply from 31.2 to 4.3-3.3%. The octane number of the gasoline produced practically does not change. It should be noted that catalytic cracking gasoline hydrated on the KGO-18 catalyst at 320°C has a sulfur content of 0.0033% (in the original 0.0134%), which indicates a rather high hydrodesulfurization activity of this catalyst.

Tests of KGO-18, KGO-16 and KGO-6 catalysts were carried out in the process of hydroprocessing of the diesel fraction of oil. With an increase in the process temperature to 400°C, the sulfur content on the KGO-18 catalyst decreases to 0.0683%, on KGO-16 to 0.0429%, respectively. The highest hydrodesulfurization activity in the processing of diesel fraction has the catalyst KGO-6. The residual sulfur content in the reaction products of the hydrodesulfurization of the diesel fraction on this catalyst under optimal conditions is 0.0013% and there is a significant decrease in temperature and freeze point, due to the high hydroisomerizing activity of these catalysts.

By the TPD method of ammonia it has been established that the catalysts are characterized by the presence of mainly acid sites with an ammonia desorption temperature of 195-220°C. The highest concentration of acid sites with an average binding energy (desorption temperature  $T_{\max} = 210^\circ\text{C}$ ) is characteristic of the KGO-6 catalyst, which determines its high hydroisomerizing activity in the hydroprocessing of gasoline and diesel fractions. According to the results of electron microscopy and TPD of ammonia, on the surface of these catalysts, acid sites coexist with metal ones: the presence of acidic,  $M^0$  - or  $M^{n+}$  - metal and mixed centers are characteristic. The composition of acid centers can include metals in various degrees of oxidation, fixed both inside the zeolite cavities and on their outer side. Their simultaneous presence ensures the multifunctionality of the catalytic system.

Thus, multifunctional modified zeolite-containing catalysts for hydroprocessing gasoline and diesel fractions have been developed, which are capable of simultaneously performing hydropurification, hydroisomerization and hydrocracking in one stage and allow to obtain environmentally clean high-octane gasoline and low-sulfur of low-condensation diesel fuel that conform to international standards.



# Density Functional Theory-Based Microkinetic Analysis of Oxidative Coupling of Methane Catalyzed by Pure and Lithium-Doped Magnesium Oxide

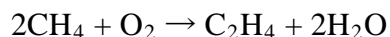
*Atsushi Ishikawa, Japan Science and Technology Agency (JST), Saitama, Japan*  
*Yoshitaka Tateyama, National Institute for Materials Science (NIMS), Tsukuba, Japan*

## 1. Introduction

The oxidative coupling of methane (OCM) has long been studied because it is an effective approach to make higher hydrocarbons from natural gas. The reaction mechanism is complicated because it involves both gas-phase and surface-mediated reactions. For the full understanding on the reaction mechanism, theoretical study, especially from atomic or molecular level is helpful. At the same time, macroscopic scale simulation is also important from practical aspect because estimation of activity such as CH<sub>4</sub> conversion and selectivity of target C<sub>2</sub> compounds is needed to discover new catalyst systems. To this aim, we carried out density functional theory (DFT) combined with microkinetics and chemical reactor modeling, as this approach enables the activity and selectivity prediction from atomic or molecular level simulations.

## 2. Theoretical method

We investigated the OCM reaction



catalyzed by Li-doped MgO, found by Lansford et al.[1] The reaction model includes 109 gas-phase and 54 surface reactions. Using DFT, reaction energy ( $\Delta E$ ) was calculated and activation barrier ( $E_a$ ) were evaluated using Polanyi rule. For the DFT calculation, VASP 5.4 program package was used. We used spin polarized DFT method using RPBE functional. From  $\Delta E$  and  $E_a$  values, we evaluate the reaction rate constants and constructed reaction rate equations. Reaction rate equations were solved numerically using MATLAB. Composition of inlet and outlet gas was calculated using the transient continuously stirred tank model (CSTR). The conversion of reactants and product selectivity was evaluated from composition of the inlet and outlet gas.

## 3. Results and Discussions

In Table 1, results of the microkinetic and reactor analysis were summarized; the CH<sub>4</sub> conversion, O<sub>2</sub> conversion, C<sub>2</sub> selectivity, and CO<sub>x</sub> (CO and CO<sub>2</sub>) selectivity were shown.

Table 1. CH<sub>4</sub> and O<sub>2</sub> conversions and C<sub>2</sub> and CO<sub>x</sub> (CO and CO<sub>2</sub>) selectivities calculated by microkinetic and reactor simulations. Reaction temperature was 700 °C, and total pressure was set to 1 bar.

	without catalyst		CH <sub>4</sub> : O <sub>2</sub> = 2 : 1		CH <sub>4</sub> : O <sub>2</sub> = 10 : 1	
	Exptl.	Calc.	Exptl.	Calc.	Exptl.	Calc.
CH <sub>4</sub> conversion (%)	4.1	1.7	12.2	11.1	7.2	10.0
O <sub>2</sub> conversion (%)	28.2	9.1	N/A	11.5	N/A	26.8
C <sub>2</sub> selectivity (%)	51.1	63.8	48.8	41.9	74.0	64.8
CO <sub>x</sub> selectivity (%)	48.8	36.0	N/A	57.3	N/A	34.8

Experimental values were taken from Refs [1] and [2]. Our calculation reproduced experimental tendency i.e. both CH<sub>4</sub> conversion and C<sub>2</sub> selectivities were improved in the presence of catalyst, and C<sub>2</sub> selectivity was higher when the partial pressure of CH<sub>4</sub> is high.

The temperature dependence of the conversion and selectivity was also analyzed; we changed temperature from 700 to 1000 °C. In Figure 3, the CH<sub>4</sub> conversion and composition of carbon-containing compounds were shown. With the increase of temperature, the CH<sub>4</sub> conversion becomes higher but C<sub>2</sub> compounds decrease, which agrees with experimental tendency. Thus, our study has successfully shown that the DFT combined with microkinetics and reactor simulation correctly reproduces the activity and selectivity tendency of the OCM catalyst.

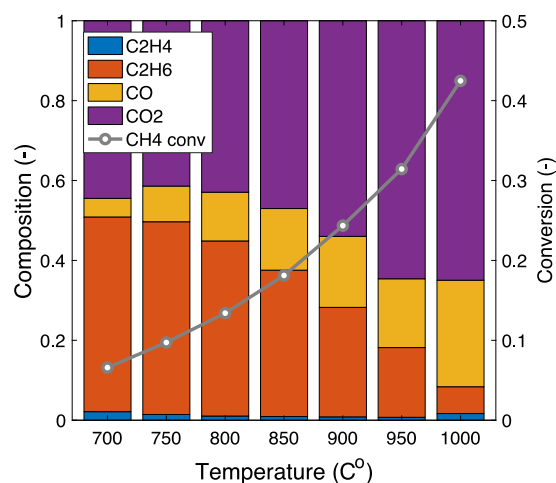


Figure 1. The CH<sub>4</sub> conversion and the composition of carbon containing compounds at 700-1000 °C.

## References

- [1] T. Ito, J. H. Lunsford et al., *J. Am. Chem. Soc.*, 107, 5062 (1985)
- [2] Shi, C.; Lunsford, J. H.; et al., *Catal. Today*, 13, 191-199 (1992)
- [3] Geerts, J. W. M. H.; et al., *Catal. Today*, 6, 519-52 (1990)

# Effect of carbon chain length in the hydroisomerization of paraffins on Pt/SAPO-11

*Karakoulia S.A.<sup>1\*</sup>, Heracleous E.<sup>1,2</sup>, Lappas A.A.<sup>1</sup>*

<sup>1</sup> *Chemical Process & Energy Resources Institute/Centre for Research and  
Technology Hellas (CPERI/CERTH), Thessaloniki, Greece*

<sup>2</sup> *School of Science & Technology, International Hellenic University (IHU),  
Thessaloniki, Greece*

*\*matoula@cperi.certh.gr*

## Introduction

Hydroisomerization is catalyzed by bifunctional catalysts that provide the necessary functionalities for the reaction to occur: metal sites for dehydrogenation /hydrogenation and acid sites for the skeletal re-arrangement of the carbon chain. The structure and pore size of the support can guide the process either to the selective hydroisomerization of the paraffin or its further cracking to lighter products. In this study, we use a 0.5 %wt Pt catalyst supported on a micro/mesoporous SAPO-11 zeolite with SiO<sub>2</sub>/Al<sub>2</sub>O<sub>3</sub> ratio 0.3 to investigate the effect of the hydrocarbon chain length using n-C<sub>8</sub> and n-C<sub>16</sub> as feedstock. The ultimate goal is to use this catalyst to improve the octane number and cold flow properties of kerosene and diesel-range fuels under mild operating conditions.

## Experimental

Silicoaluminophosphate (SAPO-11) was synthesized hydrothermally using a structure directing agent. Tetraethoxysilane (TEOS), orthophosphoric acid (85%), pseudoboehmite (Catapal B) and di-*n*-propylamine (DPA) were used as starting materials. After appropriate stirring, the gel consisting in molar ratio of 1.2 DPA:1.0Al<sub>2</sub>O<sub>3</sub>:1.0P<sub>2</sub>O<sub>5</sub>:0.3SiO<sub>2</sub>:120H<sub>2</sub>O was transferred into a Teflon-lined stainless steel autoclave and was hydrothermally crystallized at 185°C for 48h. The mixture was filtered, washed, dried at 110°C overnight and then calcined at 650°C for 5h in air. Pt (0.5 wt%) was deposited on the support via wet impregnation with chloroplatinic acid followed by calcination at 400°C for 3h in air. The catalyst was characterized with ICP, XRD, N<sub>2</sub> adsorption/desorption and pyridine-FTIR. Catalytic performance was investigated in a high-pressure fixed bed reactor unit at constant

conditions (WHSV 4 h<sup>-1</sup>, T 300°C, P 30 bar and H<sub>2</sub>/n-C<sub>8</sub> or C<sub>16</sub> molar ratio 15). The catalyst was pre-reduced in situ in H<sub>2</sub> at 300°C.

## Results/Discussion

SAPO-11 presents the characteristic diffraction peaks of  $2\theta$ : 8.1°, 9.4°, 13.1°, 15.6°, 20.3° and 21.1-23.2°, indicating the typical crystal phase with AEL structure. N<sub>2</sub> adsorption/desorption isotherms (Fig.1) are typical of a microporous zeolitic structure with generated secondary mesoporosity with average pore diameter of 6.5-7 nm. The acidity is mild, with 78 μmol/g Brønsted and 33 μmol/g Lewis acid sites, with equal distribution in acid site strength ranging from very weak to strong.

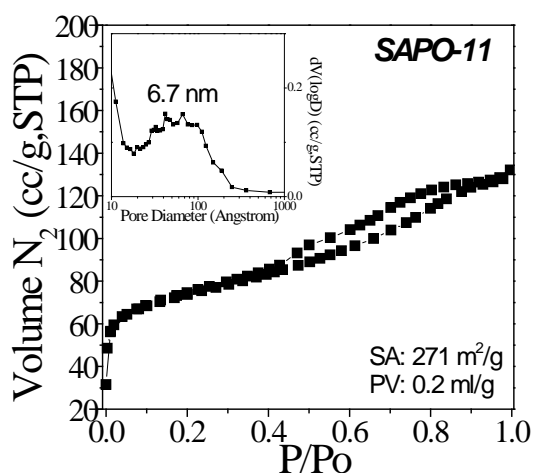


**Figure 1.** N<sub>2</sub> adsorption/desorption isotherms of SAPO-11 support

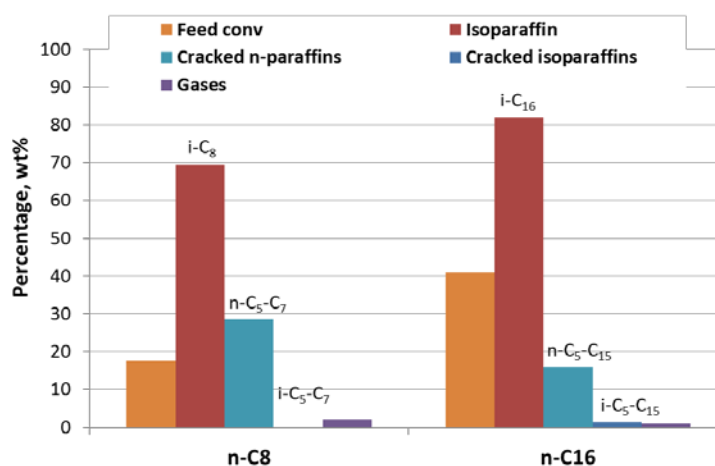


**Figure 2.** Conversion and product selectivity in the hydroisomerization of n-C<sub>8</sub> and n-C<sub>16</sub>

Testing of the 0.5 wt% Pt/SAPO-11 catalyst in hydroisomerization reaction confirmed that the hydrocarbon chain length can influence both the activity and the selectivity of the reaction. Higher activity is obtained with n-C<sub>16</sub>, which is converted by 40 wt% compared to 18 wt% for the n-C<sub>8</sub> (Fig. 2). This is consistent with the tendency of large chain hydrocarbons to be more reactive. The major product obtained in both cases is the isomerized paraffin with very high selectivity. Selectivity to i-C<sub>16</sub> is higher than that of i-C<sub>8</sub>, suggesting that the acidity and porous structure of SAPO-11 favors the isomerization of longer chain molecules. With both feedstocks, the major by-products are cracked linear alkanes, with extremely low formation of gases (C<sub>1</sub>-C<sub>4</sub>).

**Acknowledgments:** This research has been co-financed by the European Union and Greek national funds through the Operational Program Competitiveness, Entrepreneurship and Innovation, under the call RESEARCH – CREATE – INNOVATE (project code:T1EDK-03057)

## **Advances in CO<sub>2</sub> photoreduction: ZnO as photocatalytic adsorbent**

*Danny Zanardo, Federica Menegazzo, Michela Signoretto, Dipartimento di Scienze Molecolari e Nanosistemi, CATMAT lab, Università Ca' Foscari Venezia, Venezia, Italy*

*Giuseppe Cruciani, Dipartimento di Fisica e Scienze della Terra, Università di Ferrara, Ferrara, Italy*

The requirement of a more sustainable society can be claimed as the emergency of the XXI century. Increasing the uses of renewable energy and reducing the emission of pollutant gases, carbon dioxide (CO<sub>2</sub>) in particular, are two of the main challenges in the sustainability scenario. CO<sub>2</sub> photocatalytic reduction with water is an appealing technology to fulfill both goals: a waste gas can be converted into useful compounds by using directly sunlight [1]. One of the important issue of photocatalytic system is the requirement of a CO<sub>2</sub>-rich reaction medium, due to the competitive water adsorption on catalyst's surface [2]. An appealing way to overcome the former problem and allow the uses of diluted sources of CO<sub>2</sub>, relies on a bifunctional material, able to adsorb CO<sub>2</sub> in dark and then convert it, in presence of water, upon irradiation [3]. In this study, we focused our attention on zinc oxide (ZnO), a semiconductor material able to drive photocatalytic reactions [4]. The photocatalyst was prepared by an easy and cheap technique, namely precipitation from aqueous solution. The as-prepared material was then annealed in air at 673 K, yielding ZnO. We also prepared a nanocomposite by introducing 1% mol of titanium dioxide (TiO<sub>2</sub>) on ZnO surface. These materials were tested in gas-phase photoreduction of CO<sub>2</sub> rig, using conditions previously optimized in our research group [5]. We observed the selective formation of methane (CH<sub>4</sub>) and oxygen (O<sub>2</sub>) as the only reduction products and the amount of O<sub>2</sub>, fairly exceeding the stoichiometric value for photoreduction, was halved by using the nanocomposite. This suggests an improvement in catalysts photostability, a known issues for ZnO [6]. X-ray diffraction (XRD) and nitrogen physisorption analyses showed no difference in crystal structure, size and surface areas on both samples, suggesting that improved photostability arises from other effects (i.e. suppression of surface defects by TiO<sub>2</sub>). Focusing on the TiO<sub>2</sub>-ZnO nanocomposite, we run a blank test using water vapor only. We surprisingly observed that CH<sub>4</sub> was still produced, along with some CO<sub>2</sub>: the yielded CH<sub>4</sub> was likely to arise from naturally air-adsorbed CO<sub>2</sub> by ZnO surface. We finally assessed

the photocatalytic-adsorbent properties of this material by running the reaction with water only, then letting the catalysts under a diluted flow of CO<sub>2</sub> in dark and repeating again the photoreduction with water. We observed that methane was still formed with neither activity nor selectivity losses, fulfilling the hypothesized bifunctional behavior. Concluding, we were able to synthesize ZnO photocatalysts through an easy and cheap method that was capable to selectively photoreduce CO<sub>2</sub> to CH<sub>4</sub>. Despite the very low activity, namely 0.0023% solar-to-fuel efficiency, the material was capable to adsorb CO<sub>2</sub> from a diluted source and then converting it upon irradiation, thus avoiding the requirement of a CO<sub>2</sub>-rich system.

### References

- [1] P. Usubharatana, D. McMartin, A. Veawab, P. Tontiwachwuthikul. Photocatalytic Process for CO<sub>2</sub> Emission Reduction from Industrial Flue Gas Streams. *Ind. Eng. Chem. Res.* **2006**, *45*, 2558-2568
- [2] A. Olivo, D. Zanardo, E. Ghedini, F. Menegazzo, M. Signoretto. Solar Fuels by Heterogeneous Photocatalysis: From Understanding Chemical Bases to Process Development. *ChemEngineering* **2018**, *2*, 42
- [3] L. Liu, C. Zhao, J. Xu, Y. Li. Integrated CO<sub>2</sub> capture and photocatalytic conversion by a hybrid adsorbent/photocatalyst material. *Appl. Env. B* **2015**, *179*, 489-499
- [4] S. Girish Kumar, K. S. R. Koteswara Rao. Zinc oxide based photocatalysis: tailoring surface- bulk structure and related interfacial charge carrier dynamics for better environmental applications. *RCS Adv.* **2015**, *5*, 3306-3351
- [5] A. Olivo, E. Ghedini, P. Pascalicchio, M. Manzoli, G. Cruciani, M. Signoretto. Sustainable Carbon Dioxide Photoreduction by a Cooperative Effect of Reactor Design and Titania Metal Promotion. *Catalysts* **2018**, *8*, 41
- [6] Y. Li, W. Xie, X. Hu, G. Shen, X. Zhou, Y. Xiang, X. Zhao, P. Fang. Comparison of Dye Photodegradation and its Coupling with Light-to-Electricity Conversion over TiO<sub>2</sub> and ZnO. *Langmuir* **2010**, *26(1)*, 591-597

# Exceptionally Active and Stable Catalysts for CO<sub>2</sub> Reforming of Glycerol to Syngas

Selin Bac, Department of Chemical Engineering, Bogazici University, Bebek 34342, Istanbul, Turkey, Zafer Say, Department of Chemistry, Bilkent University, 06800, Ankara, Turkey, Department of Physics, Chalmers University of Technology, 41296, Göteborg, Sweden, *Didem Dede*, Department of Chemical Engineering, Bogazici University, Bebek 34342, Istanbul, Turkey, Pelinsu Bulutoglu, Department of Chemical Engineering, Bogazici University, Bebek 34342, Istanbul, Turkey, Yusuf Koçak, Department of Chemistry, Bilkent University, 06800, Ankara, Turkey, Ahmet K. Avci, Department of Chemical Engineering, Bogazici University, Bebek 34342, Istanbul, Turkey, *Emrah Ozensoy*, Department of Chemistry, Bilkent University, 06800, Ankara, Turkey, UNAM-National Nanotechnology Center, Bilkent University, 06800, Ankara, Turkey,  
Corresponding Authors: *Emrah Ozensoy*; e-mail: [ozensoy@fen.bilkent.edu.tr](mailto:ozensoy@fen.bilkent.edu.tr); Ahmet K. Avci; e-mail: [avciahme@boun.edu.tr](mailto:avciahme@boun.edu.tr)

## Introduction

Biodiesel is conventionally synthesized by the trans-esterification of animal-based or vegetable oils in the presence of methanol or ethanol, yielding glycerol as a side product which typically accounts ~10% by mass of the resulting mixture. This fraction, however, causes a notable surplus of glycerol when the scale of biodiesel production is considered. By the year 2020, cumulative global glycerol supply is forecasted to be about 6 times greater than the global glycerol demand (*i.e.*  $3 \times 10^6$  ton, vs.  $5 \times 10^5$  ton, respectively). Unless valorized into useful products, surplus glycerol will elevate the cost of biodiesel synthesis. Among several options of valorization, catalytic transformation of glycerol to synthesis gas (*i.e.* syngas) receives increasing interest as it contributes to the sustainability of commercially important processes such as Fischer-Tropsch (FT), methanol and dimethyl ether syntheses, all of which start from syngas. Glycerol-to syngas conversion is carried out typically by catalytic steam reforming. Steam reforming of methane favors syngas with  $H_2/CO > 2$ , which is suitable for hydrogen production, but is not aligned with the preferred composition ( $H_2/CO \sim 1$ ) needed for long-chain hydrocarbon production *via* FT synthesis. The required specification, however, can be obtained by reforming glycerol with CO<sub>2</sub> which can give a theoretical syngas composition of 0.75. Moreover, glycerol dry reforming (GDR) has a characteristic benefit of making syngas, a valuable product, through a carbon-negative path, *i.e.* by consuming CO<sub>2</sub> (*i.e.* a greenhouse gas) and glycerol (*i.e.* waste of biodiesel synthesis).

## Materials and Methods

**Catalyst Preparation.** Rh/ZrO<sub>2</sub> [1], Rh/CeO<sub>2</sub> [1], Rh/Al<sub>2</sub>O<sub>3</sub>-ZrO<sub>2</sub>-TiO<sub>2</sub>(AZT) [2], Ni/AZT [2], and Co/AZT [1] catalysts were prepared using incipient wetness impregnation of the active sites on the support materials. CeO<sub>2</sub> support material was prepared from Ce(NO<sub>3</sub>)<sub>3</sub>·6H<sub>2</sub>O (Sigma) *via* calcination at 800 °C, while ZrO<sub>2</sub> support was commercially acquired from Alfa Aesar. AZT support was prepared using a sol-gel procedure described in our former reports [3-4]. For the active site loading, 1 wt.% was used for Rh catalysts, whereas 5 wt.% loading was used for Ni and Co catalysts. **Ex-situ Characterization measurements (XRD, BET, TEM, EDX, Raman Spectroscopy, XPS)** were performed in order to reveal structure and functionality relationships for fresh and spent catalysts. **In-situ Fourier Transform Infrared (FTIR) experiments** were also carried out to probe the nature of the active sites using CO as a probe molecule. **Catalytic performance experiments** were carried out in a down flow, quartz tubular packed bed reactor. Experiments were performed by varying reaction temperature, CO<sub>2</sub>/Glycerol ratio and residence time within 600-750 °C, 0-4 and 0.5-5.5

mg.min/Nml, respectively. In addition to the regular 5 h activity tests, additional 72 h stability tests were also performed.

## Results and Discussion

Rh/ZrO<sub>2</sub> and Rh/CeO<sub>2</sub> catalysts revealed increased glycerol conversions with increasing temperature, where the magnitude of response became particularly notable above 650 and 700 °C on, respectively. Syngas was obtained at H<sub>2</sub>/CO ~0.8, very close to the ideal composition for FT synthesis, and C formation was minimized with increasing temperature. Glycerol (G) conversion decreased monotonically, whereas, after an initial increase, CO<sub>2</sub> conversion remained constant upon increasing CO<sub>2</sub>/G from 1 to 4. Due to the higher specific surface area of and smaller average Rh-particle size on ZrO<sub>2</sub>, Rh/ZrO<sub>2</sub> exhibited higher conversions and syngas yields than that of Rh/CeO<sub>2</sub>. Characterization studies indicated that Rh/CeO<sub>2</sub> revealed strong metal-support interaction, through which CeO<sub>2</sub> seemed to encapsulate Rh nanoparticles and partially suppressed the catalytic activity. However, such interactions also seemed to improve the stability of Rh/CeO<sub>2</sub>, rendering its activity loss to stay below that of Rh/ZrO<sub>2</sub> after 72 h stability tests. Enhanced stability of CeO<sub>2</sub> was associated with the inhibition of coking of the catalyst surface by the mobile oxygen species and creation of oxygen vacancies on ceria domains. Deactivation of Rh/ZrO<sub>2</sub> was attributed to the sintering of Rh nanoparticles and carbon formation. In order to enhance the performance and stability of the ZrO<sub>2</sub> support, AZT supports were utilized in Rh/AZT, Ni/AZT and Co/AZT formulations. Catalytic activity, quantified by glycerol and CO<sub>2</sub> conversions, follows the decreasing order of Rh/AZT > Ni/AZT > Co/AZT. Rh/AZT functions exceptionally at 750 °C and CO<sub>2</sub>/G=2–4 where conversions of glycerol and CO<sub>2</sub> exceeds 90% of their pertinent thermodynamic counterparts with a 0.5 mg<sub>cat</sub>.min.Nml<sup>-1</sup> of residence time. Increasing residence time above 1.25 mg<sub>cat</sub>.min.Nml<sup>-1</sup> further boosts the activity of Ni/AZT to ~95% of the theoretical CO<sub>2</sub> conversion at 750 °C and CO<sub>2</sub>/G=4. A minor loss in CO<sub>2</sub> conversion was detected during the 72 h longevity tests confirming stability and activity of Rh/AZT and Ni/AZT catalysts which significantly outperform their counterparts reported in the literature.

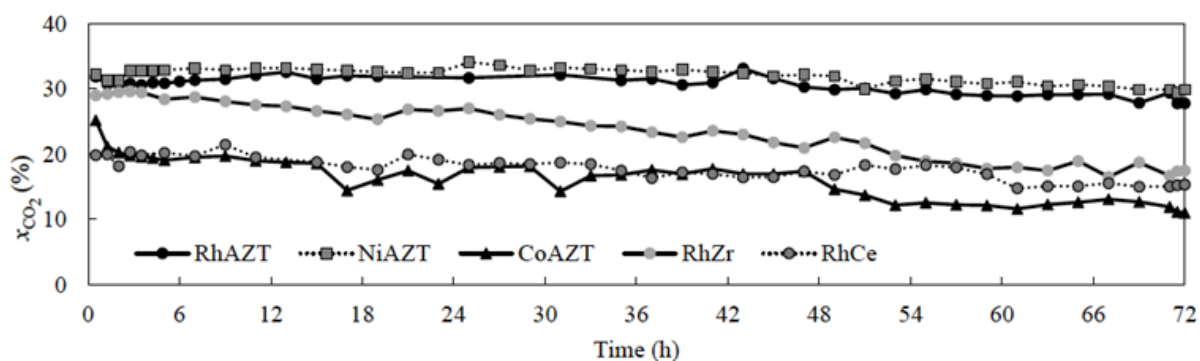


**Figure 1.** CO<sub>2</sub> conversions obtained in the stability tests carried out for 72 h (T=750 °C, CO<sub>2</sub>/G=4, residence time=3.75 mg<sub>cat</sub>.min.Nml<sup>-1</sup>).

## References

- [1] Bulutoglu, P. S.; Say, Z.; Bac, S.; Ozensoy, E.; Avci, A. K. *Applied Catal. A*, 564,157–171 (2018).
- [2] Bac, S.; Say, Z.; Bulutoglu, P. S.; Kocak, Y.; Ozensoy, E.; Avci, A. K. submitted (2018).
- [3] Say, Z.; Mihai, O.; Kurt, M.; Olsson, L.; Ozensoy, E. *Catal. Today*. 320, 152-164 (2019).
- [4] Say, Z.; Mihai, O.; Tohumeken, M.; Ercan, K. E.; Olsson, L.; Ozensoy, E. *Catal. Sci. Tech.* 7, 133-144 (2017).



# Methanolysis of ammonia borane over supported Pd-Au alloy catalysts

Tetsuya Shishido,<sup>a,b,c,d</sup> Hiroki Miura,<sup>a,b,d</sup> Mitsuhiro Tominaga<sup>a</sup>

<sup>a</sup> Department of Applied Chemistry for Environment, Graduate School of Urban Environmental Sciences, Tokyo Metropolitan University, 1-1 Minami-Osawa, Hachioji, Tokyo 192-0397, Japan

<sup>b</sup> Research Center for Hydrogen Energy-Based Society, Tokyo Metropolitan University, 1-1 Minami-Osawa, Hachioji, Tokyo 192-0397, Japan

<sup>c</sup> Research Center for Gold Chemistry, Tokyo Metropolitan University, 1-1 Minami-Osawa, Hachioji, Tokyo 192-0397, Japan

<sup>d</sup> Elements Strategy Initiative for Catalysts & Batteries, Kyoto University, Katsura, Nishikyo-ku, Kyoto 615-8520, Japan

## Introduction

Hydrogen is considered to be alternative energy carriers to oil because it is high gravimetric energy density and environmental friendly. On the other hand, hydrogen is low volumetric energy density and flammable. Therefore, the development of efficient and safe system for hydrogen storage and transportation is highly demanded. Ammonia borane ( $\text{NH}_3\text{-BH}_3\text{:AB}$ ) has attracted attention as a promising hydrogen carriers due to its high hydrogen content (19.6 %) and  $\text{H}_2$  release at ambient conditions.<sup>[1]</sup> In this study, the correlation between the catalytic activity toward methanolysis of AB and the state of supported AuPd alloy NPs was investigated in detail.

## Results and Discussion

Figure 1 shows catalytic activity and  $\text{H}_2$  production rate for methanolysis of AB over AuPd alloy catalysts with various molar ratio.  $x\text{Au}y\text{Pd}/\text{AC}$  showed higher  $\text{H}_2$  production rate than  $\text{Pd}/\text{AC}$ , whereas  $\text{Au}/\text{AC}$  exhibited no activity, implying that Pd is active species. Among  $x\text{Au}y\text{Pd}/\text{AC}$  tested, 1Au1Pd/AC exhibited the highest activity per unit weight of catalyst. The TOF

value normalized amount of adsorbed CO was increased with decreasing Pd/Au ratio and 10Au1Pd/AC showed the highest TOF. Au  $\text{L}_3$  edge XANES spectra and XPS of the catalysts indicated the charge transfer from Pd to Au atoms. Curve-fitting analysis of EXAFS and XRD patterns elucidated the formation of random AuPd alloy NPs. As

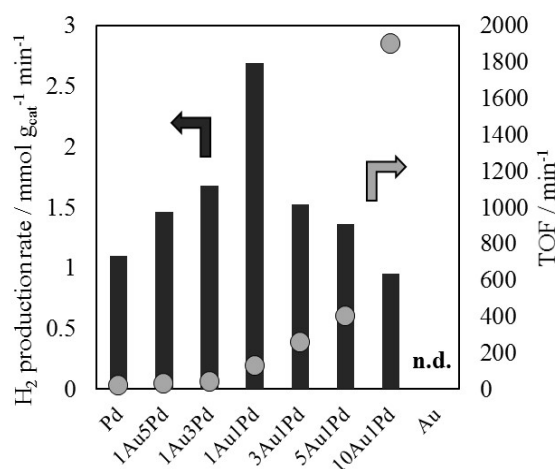


**Fig. 1**  $\text{H}_2$  production rate and TOF value of Pd/AC, AuPd/AC and Au/AC at 298 K.

for the catalyst with a low Pd/Au ratio, it seems that electron-deficient and isolated single Pd atoms surrounded by Au atoms were formed on the catalysts.

On the basis of kinetics, a possible reaction mechanism of methanolysis of AB over 10Au1Pd/AC is proposed (Fig. 2). AB is adsorbed on catalyst surface and B-H bond in AB is cleaved over Pd atom (step (i)). B-N bond in AB is cleaved and amine group adsorbs on Au atoms which work as Lewis acid (step (ii)). Then, unoccupied orbitals of boron atom is formed and oxygen atom in methanol that has lone pairs is coordinated to the boron atom, resulting in dissociation of methanol to proton (step (iii)). KIE measurement

indicated step (iii) is rate-determining step. H<sub>2</sub> molecule is formed by coupling proton and hydride on Pd atom derived from hydrogen atom in B-H bond. Boron species and amine group is recombined to form B-N bond and resulting product desorbs on catalyst surface (step (iv)).

Therefore, we proposed that electron-deficient Pd atom surrounded by Au atoms in random

AuPd alloy NPs promotes cleavage of methanol to form proton, in other word, stabilize conjugate base of methanol, resulting in acceleration of formation of H<sub>2</sub> molecules.

## Conclusion

Supported AuPd alloy catalysts showed higher activity than supported monometallic catalysts toward methanolysis of AB. Their catalytic activity remarkably depended on Pd/Au ratio. Based on structural characterization and kinetic analysis of methanolysis of amine boranes, we conclude that electron-deficient Pd atom surrounded by Au atoms in random AuPd alloy NPs work as active sites.

## References

[1] P.V. Ramachandran, P.D. Gagare, *Inorg. Chem.*, **2007**, 46, 7810.

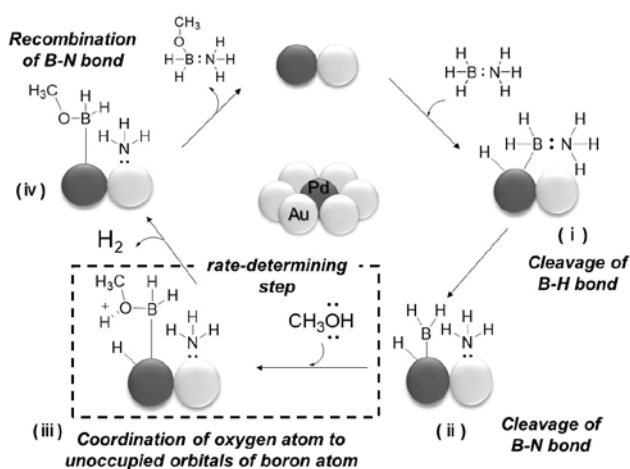


**Fig. 2** Proposed reaction mechanism of methanolysis of AB

## Three metallic catalysts for ethanol valorization

*Jaroslav Kocík, Zdeněk Tišler, Jiří Kolena*

*Unipetrol Centre for Research and Education, Záluží-Litvínov, Czech Republic*

Bioethanol is one of the primary bio-based chemicals. It is the aim of the European Union that 27 % of energy consumption will be produced from bio-based resources in the future. Bioethanol produced by fermentation is used in large quantities as a gasoline component. Its world production has been increasing in recent years, reaching 27 billion gallons in 2017. Bioethanol has also attracted attention as starting material for producing chemicals, e.g. branched higher alcohols. The branched alcohols are currently produced mainly from propylene and butane. However, they can also be synthesized from ethanol by the Guerbet reaction. The Guerbet reaction mechanism consists of 4 subsequent reaction steps i.e. dehydrogenation of alcohol to carbonyl compound, aldol-condensation, dehydration of aldol and hydrogenation of unsaturated alcohol [1]. Generally, aldol-condensation is catalyzed by a base catalyst. The hydrogenation and dehydrogenation steps are catalyzed by a redox catalyst. However, the dehydrogenation steps could also be catalyzed by base catalysts at high temperature. The reaction conditions of the mentioned reaction steps are different. Dehydrogenation should be carried out at high temperature and hydrogenation, as well as aldol-condensation, typically require low temperature. Therefore, the choice of suitable reaction conditions and effective catalyst is a key problem of this process. Many heterogeneous catalysts, e.g. MgO, hydroxyapatite, hydrotalcite etc [2] have been described in the literature as being suitable for Guerbet reaction.

It was the aim of our research to study three types of mixed metallic oxides with redox and acid-base properties and verified their effectiveness in the Guerbet condensation of ethanol. The mixed oxides were prepared by calcination of synthetic hydrotalcites in which Mg and Al, typical for natural hydrotalcites, were substituted with another bivalent or trivalent metals respectively. The acid-based properties as well as the redox properties were controlled by MII/MIII molar ratio and the metal type choice. Mg-Al mixed oxides are typical acid-base catalysts with variable acid-based properties. For this reason, they were used as catalysts for Guerbet reaction in the first stage of our research. The Mg-Fe mixed oxide was further used with the aim to

increase the catalyst redox properties. The redox properties of the mixed oxides were also modified by incorporation of another transition metal like Cu, Cr, Mn or Co into the catalyst structure. The structure of the hydrotalcites and the mixed oxides derived from them was verified by XRD. The influence of the transition metal type on the selectivity to 2-butanol in Guerbet reaction was studied. The transition metal ion increased the reaction rate of dehydrogenation and hydrogenation steps, which had a positive effect on the total reaction rate of the Guerbet reaction and the selectivity to main alcohols. Following methods were used for the catalysts characterization and for the explanation of the testing results. The acid-base and redox properties were measured by TPD-CO<sub>2</sub>, -NH<sub>3</sub> and TPR-H<sub>2</sub>. The pore distribution was measured by N<sub>2</sub>-adsorption and Hg-porosity. The catalytic tests were performed in a stainless steel flow microreactor. The catalytic tests were carried out at identical reaction conditions for the representative comparison of the catalytic properties of individual catalysts.

## References

[1] Sun Z., Vasconcelos A. C., Bottari G., Stuart M. C. A., Bonura G., Cannilla C., Frusteri F., Barta K.: Efficient Catalytic Conversion of Ethanol to 1-Butanol via the Guerbet reaction over Copper and Nickel-Doped Porous

[2] Gabriëls, D., Hernández, W. Y., Sels B., Voort, P. V. D., Verberckmoes, A.: Review of catalytic systems and thermodynamics for the Guerbet condensation reaction and challenges for biomass valorization, *Catalyses Science and Technology*, 1, 2013, 1-100

## Acknowledgement

This work was supported by the Czech Science Foundation, Project No. 19-00669S. The work has been integrated into the National Sustainability Programme I of the Ministry of Education, Youth and Sports of the Czech Republic (MEYS) through the project Development of the UniCRE Centre (LO1606). The work was achieved using the infrastructure included in the project Efficient Use of Energy Resources Using Catalytic Processes (LM2015039) which has been financially supported by MEYS within the targeted support of large infrastructures.

# Ultrasound assisted oxidative desulfurization of marine fuels using alumina supported molybdenum catalysts.

S. HOUDA<sup>1,2\*</sup>, C. LANCELOT<sup>1</sup>, P. BLANCHARD<sup>1</sup>, L. POINEL<sup>2</sup>, C. LAMONIER<sup>1</sup>

1- Université Lille, CNRS, Centrale Lille, ENSCL, Université Artois, UMR 8181 UCCS- Unité de Catalyse et Chimie du Solide, F-59000 Lille, France.

2- SEGULA Technologies, 71 Rue Henri Gautier, 44450 Montoir de Bretagne, France.  
Email address: sara.houda.etu@univ-lille.fr

Nowadays, maximum sulfur content permitted in marine fuels in designated emission control areas is 0.1 wt.%S. For ships operating outside these areas, the current limit for sulfur content in ships fuel oil is 3.5 wt.%S but will be decreased to only 0.5 wt.%S in 2020, as imposed by the International Maritime Organization in the MARPOL convention. Meeting these new specifications is a challenge. While light fractions are conventionally upgraded in refineries by hydrodesulfurization, the treatment of heavy fuels implies higher operating costs due to the severe conditions needed [1]. Alternative methods have thus been considered [2], among which oxidative desulfurization (ODS) has attracted much attention. Indeed, it operates under mild conditions (low temperature and under atmospheric pressure) and avoids the use of costly hydrogen. It is a two-step process: the sulfur containing compounds are first oxidized to the corresponding sulfones in the presence of an oxidant; then, a purification step is carried out in which oxidized sulfur compounds are separated mainly using extraction or adsorption methods. However most of the studies on oxidative desulfurization are dedicated to the treatment of model molecules and diesel fractions. The ODS technology for heavy fractions is still immature.

In this work, oxidative desulfurization of 3 intermediate fuel oils (IFO) with various viscosities of 380, 500 and 700 cSt and sulfur contents of 0.6, 3.2 and 2.9 wt.%S has been performed. Composition of the fuels has been determined regarding sulfur/nitrogen (SSD, NCD) containing molecules by gas phase chromatography with sulfur/nitrogen specific detectors, and regarding aromatic hydrocarbon compounds using HPLC.

Oxidative desulfurization of the IFO samples was conducted using hydrogen peroxide as oxidizing reagent and MoO<sub>3</sub>/Al<sub>2</sub>O<sub>3</sub> as catalyst at 80°C and under atmospheric pressure.

Chromatograms of the reaction mixture before and after oxidation are presented in figure 1, showing after ODS a decrease in intensity of peaks corresponding to sulfides and the appearance of new peaks corresponding to formed sulfones.

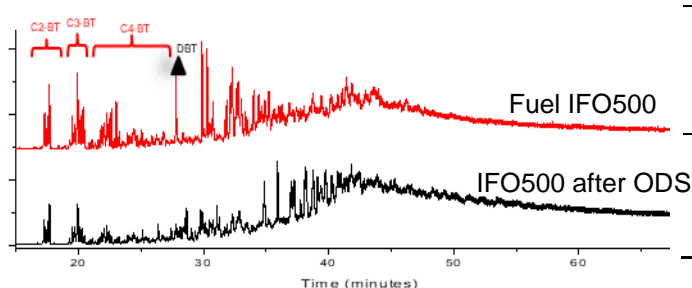


Figure 1: Chromatograms using specific sulfur detector: marine fuel before and after oxidation.

Fuels	BTs conversion(%)	DBT conversion (%)
IFO500	35	61
IFO380	57	75
HSFO700	25	60

Table 1: conversion of sulfur compounds in ODS of different fuels.

As usually in the literature, ODS catalytic performance has been expressed as a total sulfur removal, after extraction by dimethylformamide. Moreover, owing to SSD chromatography, we have been able to monitor the conversion of the alkyl benzothiophene compounds as well as that of dibenzothiophene molecule. Results of ODS reactions on different fuels after centrifugation are presented in table 1. ODS appears to be less effective on the fuels with increasing viscosity and sulfur content.

The effects of  $\text{MoO}_3$  loading (10 to 25%), reaction time and the oxidant to sulfur molar ratio  $\text{Ox/S}$  were investigated for one particular marine fuel (IFO500). The catalyst with 20% loading showed the best activity in ODS. The conversion of BTs and DBT molecule after one-hour reaction using  $\text{Ox/S}=3$  reached respectively 35% and 61% with a total S removal of 56% after extraction. The activity of sulfur compounds in fuel slightly increased to 55 and 65% with the increase of  $\text{Ox/S}$  from 3 to 25 due to phase transfer problems related to hydrogen peroxide. The application of ultrasound in the oxidative desulfurization of marine fuel was also successfully explored. With  $\text{Ox/S}=25$ , conversion of BTs and DBT was 71 and 80% when ultrasound was used, thus highlighting the beneficial use of ultrasonic irradiation.

## References

1. Rana, M.S.; Sámano, V.; Ancheyta, J.; Diaz, J.A.I. A review of recent advances on process technologies for upgrading of heavy oils and residua. *Fuel* **2007**, *86*, 1216–1231.
2. Aitani, A.M.; Ali, M.F.; Al-Ali, H.H. A Review of Non-Conventional Methods for the Desulfurization of Residual Fuel Oil. *Petroleum Science and Technology* **2000**, *18*, 537–553.

# Exploring the potential of hierarchical Mo/HZSM5 in reactive adsorption desulfurization of liquids from tire pyrolysis

*E. Kantarelis; S. Somsri; K. Engvall,*

*Department of Chemical Engineering, KTH Royal Institute of Technology, Stockholm, Sweden*

## **Abstract**

Around 3.3 Mtons of scrap tires are generated each year in EU [1]. A promising route for their treatment is pyrolysis, where tires are heated in the absence of oxygen and converted into a valuable carbonaceous solid material, as well as steel, gas, and oil. Of particular interest is the oil fraction of the process, which can potentially be used as a fuel or a feedstock for chemicals production [2]. Upgrading of the liquid product is required due to its high sulfur content limiting its adaption to the market. In the present study, the reactive adsorptive desulfurization at 320°C using desilicated Mo/HZSM5 catalysts was investigated. Experimental results showed that development of mesoporosity is important for removal of bulkier sulfur compounds, while Mo introduction improves deoxygenation and denitrogenation efficiencies significantly.

## **Materials and methods**

The parent zeolite was provided by Süd Chemie (TZP-302) in ammonium form. Desilication of the zeolite was carried out by treatment of the calcined zeolite (HZSM5) in a NaOH solution. Mo incorporation was performed by means of incipient wetness impregnation. The desilicated catalysts are designated as Ds-HZSM5, and Mo/Ds-HZSM5.

The experimental facility consisted of a stainless-steel reactor, heated by a 3 zone electrically heated furnace. The liquid was injected through a gas-liquid atomization nozzle. All experimental runs were carried out at LHSV of 45-50 h<sup>-1</sup> for ~45 min at a temperature of 320°C.

## **Results and discussion**

Reactive adsorption resulted in changes of the obtained liquids' specific gravity. The use of catalyst results in slightly lighter liquid products due to increased cracking activity, as well as a strong sorption and conversion of heavier molecules on the acid sites of the catalyst. Desilicated zeolites reduced the coking tendency of the liquids

as expressed by the micro-carbon residue determination. Incorporation of Mo improves the effective hydrogen index, indicating a removal of undesired heteroatoms(S, N, and O) and preservation of hydrogen in the liquid. The desulfurization (DeS) is enhanced by the larger pores in the zeolite, while Mo incorporation does not have any major impact. The desilication also enhances the denitrogenation (DeN) performance. Introduction of Mo into the zeolite promotes the deoxygenation (DeO) significantly (Fig. 1). The effect of pore size is also indicated by the improved conversion of the bulky dibenzothiophene as determined by GC/MS.

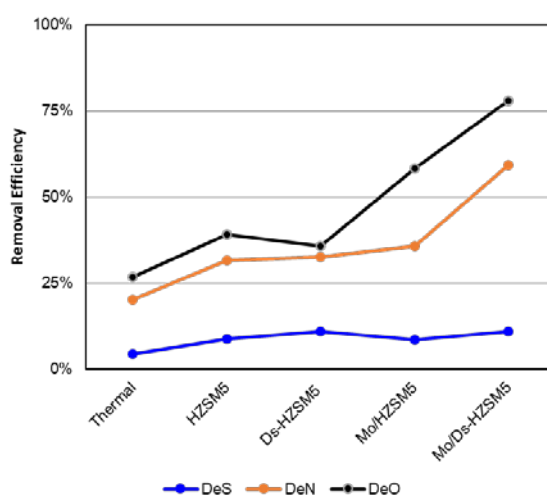


**Fig. 1 Desulfurization, denitrogenation and deoxygenation activity of catalysts used**

## Conclusions

In the present work, the reactive adsorptive desulfurization of tire pyrolysis oil, using Mo modified desilicated HZSM5 zeolites, was investigated. The results under specific experimental conditions (high LHSV), indicate a mild desulfurization (~10%) with mesopores being more important than Mo modification. Moreover, addition of Mo both to parent as well as desilicated HZSM5 zeolites, increased the DeO activity, while the combination of mesoporosity and Mo modification, significantly increases the DeN of the oil. The availability of larger pores in the zeolite results in an improvement of the desulfurization efficiency. This is also shown by the higher conversion of bulky dibenzothiophene, compared to non-desilicated counter parts. The above results indicate that Mo-modified and pore-tailored HZSM5 catalysts have a potential use in upgrading of tire pyrolysis oil.

## References

- [1] P. T. Williams, Waste Management, 33, 1714–1728, 2013.
- [2] A. Quek, R. Balasubramanian, Journal of Analytical and Applied Pyrolysis, 101, 1–16, 2013.



# Accessing Bio-Based Pyrrolidones by Supported Metal Catalysts

*Yannik Louven, Moritz O. Haus, Regina Palkovits*

*Institute for Technical and Macromolecular Chemistry (ITMC), RWTH Aachen University, Germany*

To date, the lack of efficient conversion strategies for bio-based platform chemicals, such as succinic, itaconic and levulinic acid, hampers the necessary replacement of fossil resources as feedstock of the chemical industries. This is mostly due to the inapplicability of traditional catalytic routes, established in oil-chemicals processing, to the upgrading of oxygen-rich, biomass-derived moieties.<sup>[1]</sup> In this context, strategies for the introduction of nitrogen functionalities are especially sought-after. Consequently, the manufacture of pyrrolidones from carboxylic acids has been described in several articles, dealing mostly with the production of N-substituted pyrrolidones as pharmaceutical intermediates or solvents.<sup>[2]</sup>

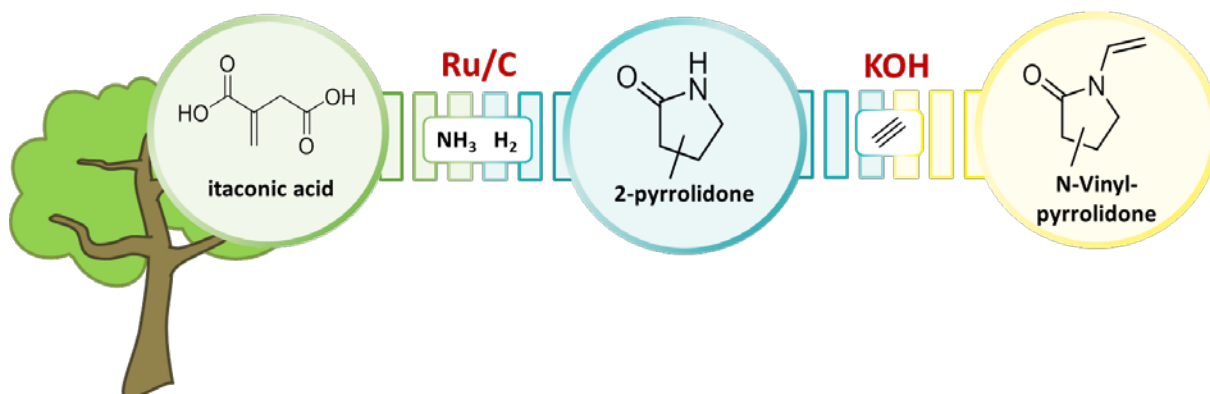


**Figure 1: Proposed route to access methyl-N-vinyl-2-pyrrolidones from itaconic acid.**

In contrast, our research focuses on the conversion of carboxylic acids towards N-vinyl-2-pyrrolidone (NVP), which may be polymerized to polyvinylpyrrolidone, a water-soluble, non-toxic polymer with numerous applications in the pharma, cosmetic and food industry. While reducing the need for fossil resources, the envisioned valorization chain also has economic potential due to the steadily expanding NVP demand, which leaves room for new producers and production strategies.<sup>[3]</sup>

In this context, we have intensively investigated the exemplary conversion of itaconic acid and ammonia to an isomeric mixture of 3- and 4-methyl-2-pyrrolidone (**Figure 1**), including analysis of the reaction network, process conditions and catalytic materials.<sup>[4]</sup> A supported ruthenium catalyst provided high activity and

selectivity together with excellent stability upon recycling reaching yields up to 90 %. The purification of produced pyrrolidones and their further conversion to methyl-substituted NVP through Reppe vinylation (**Figure 1**) was likewise successful.

### **Acknowledgement**

We thank the German Federal Ministry of Education and Research (BMBF) for funding of the project Bio-PVP (FKZ 031B0487A) in the framework "Neue Produkte für die Bioökonomie".

### **References**

- [1] T. A. Werpy, J. E. Holladay, J. F. White, *Top Value Added Chemicals From Biomass. I. Results of Screening for Potential Candidates from Sugars and Synthesis Gas*, **2004**.
- [2] X.-L. Du, L. He, S. Zhao, Y.-M. Liu, Y. Cao, H.-Y. He, K.-N. Fan, *Angew Chem Int Ed* **2011**, *50*, 7815.
- [3] Grand View Research Inc., "Polyvinylpyrrolidone (PVP) Market Worth \$2.75 Billion By 2024", **2016**.
- [4] Y. Louven, K. Schute, R. Palkovits, *ChemCatChem* **2018**, *6*, 74.

# Elucidating the structure of supported vanadia catalysts during ethanol and propane ODH using *operando* UV Raman spectroscopy

Simone Rogg, Moritz Mathes, Philipp Waleska<sup>1</sup>, Christian Hess

Eduard-Zintl-Institut für Anorganische und Physikalische Chemie, TU Darmstadt,  
Darmstadt, Germany

<sup>1</sup>*h.a.l.m. elektronik gmbh, Frankfurt/Main, Germany*

Supported vanadia catalysts have attracted much attention owing to their unique catalytic properties for a variety of reactions such as the oxidative dehydrogenation (ODH) of alcohols and alkanes. Despite previous work, a detailed understanding of the mode of operation of supported vanadia catalysts is still missing. Recently, we have shown that UV Raman spectroscopy can provide new insights into the vanadia structure by exploiting resonance effects.[1,2] In this contribution, we address the structural dynamics of silica supported vanadia catalysts during the ODH of ethanol in comparison to propane ODH by using *operando* UV Raman spectroscopy. Based on these results, we highlight the added value of our approach for the detailed understanding of the reaction mechanisms of ethanol and propane ODH.

As support material silica SBA-15 was employed ( $\sim 700 \text{ m}^2\text{g}^{-1}$ ). Catalysts were prepared via incipient wetness impregnation of vanadium isopropoxide.[1,2] Raman experiments were performed by using laser excitation at 256.7 nm. For product analysis the gas-phase composition at the outlet of the *operando* Raman cell was measured via FTIR spectroscopy for ethanol ODH and gas chromatography for propane ODH. In addition, the Raman cell was used in fluidized bed mode to minimize temperature gradients at higher temperatures ( $>200^\circ\text{C}$ ) and to avoid photodecomposition during UV irradiation.

Figure 1 depicts *operando* Raman spectra of a  $\text{VO}_x/\text{SiO}_2$  catalyst ( $0.5 \text{ Vnm}^{-2}$ ) during a) ethanol ODH at  $128^\circ\text{C}$  (conversion: 1.8%, selectivity (acetaldehyde): 98.5%), and b) propane ODH at  $500^\circ\text{C}$  (conversion: 9%, selectivity (propene): 49.5%). In case of ethanol, structural changes of the catalyst are observed at  $\sim 520$  and  $1031 \text{ cm}^{-1}$  when switching from oxidative (20%  $\text{O}_2$ , 80%  $\text{N}_2$ ) to reaction conditions (1%  $\text{C}_2\text{H}_5\text{OH}$ , 8%  $\text{O}_2$ , 91%  $\text{N}_2$ ) indicating the conversion of V-O-V bonds and the reduction of vanadium (V).[3] The three bands at  $\sim 922$ ,  $1056$ , and  $1095 \text{ cm}^{-1}$  are adsorbate related and have

recently been assigned to C-C, C-O stretching and CH<sub>3</sub> rocking modes of chemisorbed ethoxy species.[3] In contrast, only minor structural changes are visible for propane upon switching from oxidative conditions (12.5 % O<sub>2</sub>, 87.5 % He) to reaction conditions (12.5 % C<sub>3</sub>H<sub>8</sub>, 12.5 % O<sub>2</sub>, 75 % He). Raman features appear at ~867 and 1057 cm<sup>-1</sup>, which can be attributed to C-C vibrations of adsorbed propoxy species. Additional C-H stretching features of gas-phase propane are detected at 2900 and 2940 cm<sup>-1</sup>.

The comparison of the two ODH reactions indicates a strong dependence of the structure of the working vanadia catalyst on the substrate, which has not been reported in the literature yet.

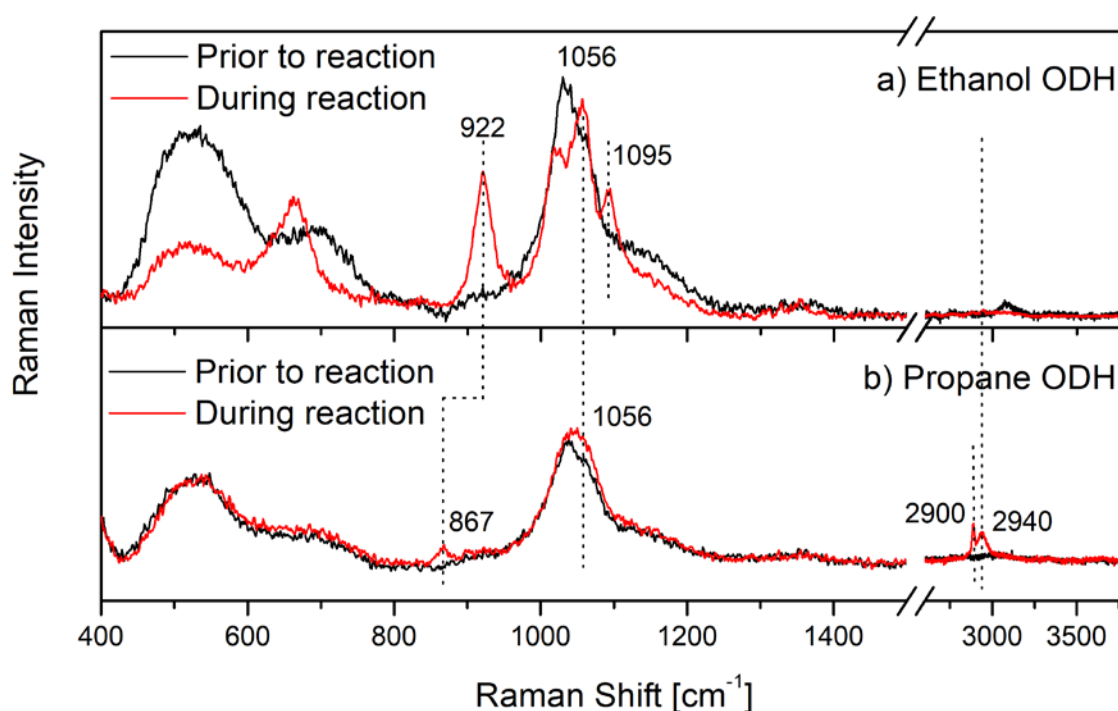


**Figure 1** *Operando* UV Raman spectra of VO<sub>x</sub>/SiO<sub>2</sub> (0.5 Vnm<sup>-2</sup>) for ethanol and propane ODH taken a) during oxidative (O<sub>2</sub>/N<sub>2</sub>) and reaction conditions (C<sub>2</sub>H<sub>5</sub>OH/O<sub>2</sub>/N<sub>2</sub>) at 128°C (50 ml<sub>r</sub>/min), and b) during oxidative (O<sub>2</sub>/He) and reaction conditions (C<sub>3</sub>H<sub>8</sub>/O<sub>2</sub>/He) at 500°C (40 ml<sub>r</sub>/min).

In conclusion, the potential of *operando* UV Raman spectroscopy to gain new insights into the structure of vanadia catalysts during ODH reactions is demonstrated, thereby highlighting a strong dependence on the substrate.

## References

- [1] D. Nitsche, C. Hess, *J. Phys. Chem. C* **2016**, *120*, 1025-1037.
- [2] P. Waleska, C. Hess, *J. Phys. Chem. C* **2016**, *120*, 18510-18519.
- [3] P. Waleska, S. Rupp, C. Hess, *J. Phys. Chem. C* **2018**, *122*, 3386.

# Dry reforming of methane for hydrogen production over CeO<sub>2</sub>-Ni embedded catalyst

André L. A. Marinho<sup>1,2</sup>, Fabio S. Toniolo<sup>1</sup>, Nicolas Bion<sup>2</sup>, Florence Epron<sup>2</sup>, Fabio B. Noronha<sup>3</sup>

<sup>1</sup> Federal University of Rio de Janeiro, Rio de Janeiro, Brazil

<sup>2</sup> University of Poitiers, Poitiers, France

<sup>3</sup> National Institute of Technology, Rio de Janeiro, Brazil

## 1. Introduction

The production of hydrogen from dry reforming of methane (DRM) is a promising technology to convert biogas into high value-added products [1]. Ni-based catalysts have been extensively studied for DRM due to its low cost and high activity but this metal is prone to coking [2]. Recently, the use of confined metals has been reported to avoid the carbon formation [3]. The use of ceria-based materials and its doping with Zr improves catalyst stability during DRM due to their high reducibility and oxygen storage capacity [4]. Therefore, the aim of this work is to study the performance of nickel embedded in ceria and ceria-zirconia for the hydrogen production by DRM.

The embedded catalysts were prepared by sol-gel method [5], with pure CeO<sub>2</sub> or a Ce/Zr molar ratio equal to 4.0 and 10 wt% of Ni (Ni@CeO<sub>2</sub> and Ni@CeZrO<sub>2</sub>). A catalyst was also prepared by incipient-wetness impregnation for comparison (Ni/CeO<sub>2</sub>). The catalysts were characterized by in-situ X-ray diffraction (XRD) and isotopic oxygen exchange at 400 °C and the post-reaction samples by thermogravimetric (TG) analysis. DRM was carried out at 800 °C and atmospheric pressure, using a CH<sub>4</sub>:CO<sub>2</sub> molar ratio equal to 1.0.

## 2. Results and discussion

The diffractograms before reduction of Ni@CeO<sub>2</sub> and Ni@CeZrO<sub>2</sub> exhibited only the characteristics lines of CeO<sub>2</sub> cubic phase, with slightly shift to higher 2θ for the sample Ni@CeZrO<sub>2</sub>, indicating the formation of Ce-Zr solid solution [6]. Ni/CeO<sub>2</sub> also shows a line corresponding to NiO phase. The Ni nanoparticle of Ni@CeO<sub>2</sub> and Ni@CeZrO<sub>2</sub> reduces at higher temperature and its crystallite size is lower than that of the Ni/CeO<sub>2</sub> (Figure 1). Furthermore, the Ni@CeZrO<sub>2</sub> catalyst showed the highest thermal stability with the lowest Ni crystallite size after reduction at 800 °C.

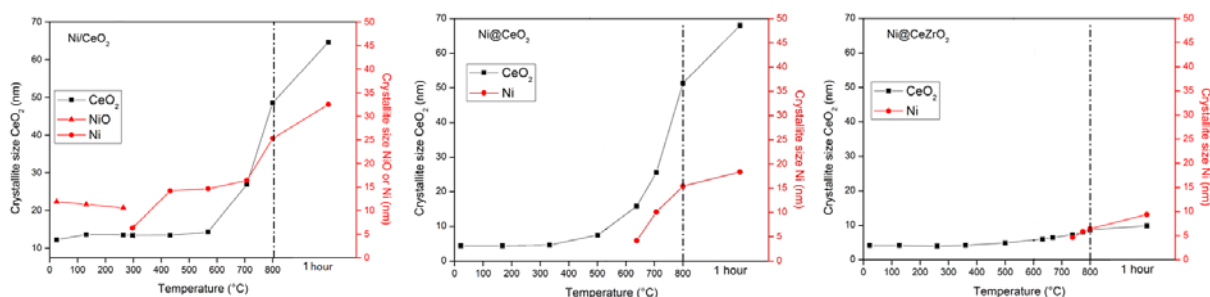


**Figure 1.** Ni crystallite size during reduction process.

Analyzing the isotopic oxygen exchange results, the initial rate of exchange for the Ni@CeO<sub>2</sub> catalyst ( $150 \times 10^{17} \text{ at.g}^{-1}.\text{s}^{-1}$ ) is higher than that for the Ni/CeO<sub>2</sub> catalyst ( $48.5 \times 10^{17} \text{ at.g}^{-1}.\text{s}^{-1}$ ), which is due to the strong interaction in the embedded structure. The presence of Zr increased the O atoms exchanged percentage (Table 1) because of the highest mobility of O atoms from the bulk phase [7]. The catalysts were tested for the DRM, showing similar initial conversions and H<sub>2</sub>/CO molar ratio (~70 % CO<sub>2</sub>, ~59 % CH<sub>4</sub> and ~0.8 H<sub>2</sub>/CO) and stable activity during 24 h. The Ni@CeZrO<sub>2</sub> catalyst did not show carbon formation during the DRM reaction (Table 1), which is likely due to the deeper O mobility and lower Ni crystallite size.

**Table 1.** Oxygen isotopic exchange results and rate of carbon formation during DRM.

Catalyst	O atoms exchanged at 400 °C (%)	Rate of carbon formation (mgC.g <sub>cat</sub> <sup>-1</sup> .h <sup>-1</sup> )
Ni/CeO <sub>2</sub>	46.4	9.7
Ni@CeO <sub>2</sub>	48.7	1.6
Ni@CeZrO <sub>2</sub>	54.7	0.0

### 3. Conclusions

Ni@CeZrO<sub>2</sub> is a promising catalyst for the conversion of biogas to hydrogen, showing high activity and stability. The embedded Ni nanoparticles into the support as well as the doping with Zr promotes higher oxygen mobility and thermal stability, which avoid carbon formation and promotes the stability during DRM.

### References

- [1] L. Yang, X. Ge, C. Wan, F. Yu, Y. Li, *Renewable and Sustainable Energy Reviews*. **2014**, 40, 1133.
- [2] J.R. Rostrup Nielsen, J.H. Bak Hansen, *Journal of Catalysis*. **1993**, 144, 38.
- [3] F. Wang, B. Hang, L. Zhang, L. Xu, H. Yu, W. Shi, *Applied Catalysis B: Environmental*. **2018**, 235, 26.
- [4] S.M. Stagg-Williams, F.B. Noronha, G. Fendley, D.E. Resasco, *Journal of Catalysis*. **2000**, 194, 240.
- [5] Y. Wang, Y. Zhao, J. Lv, X. Ma, *ChemCatChem*. **2017**, 9, 2085.
- [6] A. Kozlov, H. Do, A. Yezerets, P. Andersen, H. Kung, M. Kung, *Journal of Catalysis*. **2002**, 209, 417.
- [7] Y. Madier, C. Descorme, A. Le Govic, D. Duprez, *The Journal of Physical Chemistry B*. **1999**, 103, 10999.

# Epoxides Hydration Catalyzed by the Highly Cross-Linked Poly(ionic liquid)s

*Dawei Shang, Shanghai Research Institute of Petrochemical Technology, Shanghai, China; Wenjun He, Shanghai Research Institute of Petrochemical Technology, Shanghai, China*

Ethylene glycol (EG) is an important raw material for the production of polyester, which is in high demand around the world. At present, the production of EG in the industry mainly adopts the method of ethylene oxide (EO) hydration without catalysis and suffers from the low EG selectivity, high water ratio and energy consumption. Researchers from both academic and industrial fields have concentrated on the development of EO catalytic hydration and focused on the designing of highly effective catalysts, including metals, metal oxides, organic amine salt, Co<sup>III</sup>(Salen), ion exchange resin and so on [1-3]. However, there are still no commercial catalysts applied in industry until now.

Ionic liquids (ILs) are composed of cations and anions that are liquid at room temperature, which have low vapor pressure, good thermal stability and flexible structure adjustment. For example, Su designed series of carboxyl-functionalized ILs for the hydration of EO and obtained the yield of EG over 99%[4]. Although the ILs showed good catalytic performance in the EO hydration reaction, it was difficult for the ILs to be separated from the products as homogeneous catalysts. Therefore, the development of heterogeneous catalysts based ILs have attracted more and more attention. Poly(ionic liquid)s (PILs) comprise a polymeric backbone and an IL species in monomer repeating units [5] and are the promising heterogeneous catalysts for the epoxides hydration. Liu *et al.* synthesized IL functionalized mesoporous polymer PDVB-[C<sub>1</sub>vim][SO<sub>3</sub>CF<sub>3</sub>] and showed over 99.9% conversion of the propylene oxide (PO) [6].

Inspired by the above results, we designed kinds of acidic and basic poly(ionic liquid)s, such as the protic PILs, for the catalysis of epoxides hydration. The initial results show that the PO hydration catalyzed by protic PILs could achieve over 95% conversion of PO (at the condition of 333K and H<sub>2</sub>O/PO molar ratio of 5) and the PILs behaved good recyclability.

## References

- [1] Y. Li, S. Yan, B. Yue, W. Yang, Z. Xie, Q. Chen, H. He, Selective catalytic hydration of ethylene oxide over niobium oxide supported on  $\alpha$ -alumina, *Applied Catalysis A: General* 272 (2004) 305-310.
- [2] M. Zhong, Y. Zhao, Q. Yang, C. Li, Epoxides hydration on CoIII(salen)-OTs encapsulated in silica nanocages modified with prehydrolyzed TMOS, *Journal of Catalysis* 338 (2016) 184-191.
- [3] F. Yu, H. Cai, W. He, W. Yang, Z. Xie, Synthesis and characterization of a polymer/multiwalled carbon nanotube composite and its application in the hydration of ethylene oxide, *Journal of Applied Polymer Science* 115 (2010) 2946-2954.
- [4] Q. Su, *Ionic Liquids Modifying Porous Materials for Synergistic Synthesis of Diols [D]*, Institute of Process Engineering, Chinese Academy of Sciences, 2018.
- [5] W. Qian, J. Texter, F. Yan, *Frontiers in poly(ionic liquid)s: syntheses and applications*, *Chem Soc Rev* 46 (2017) 1124-1159.
- [6] F. Liu, L. Wang, Q. Sun, L. Zhu, X. Meng, F.-S. Xiao, Transesterification Catalyzed by Ionic Liquids on Superhydrophobic Mesoporous Polymers: Heterogeneous Catalysts That Are Faster than Homogeneous Catalysts, *Journal of the American Chemical Society* 134 (2012) 16948-16950.



# Comparative effect of silicon source on the synthesis of IM-5 molecular sieve

C.Y. Yang\*, F. X. Ling, H.C. Zhang and S.J. Wang

<sup>1</sup> Fushun Research Institute of Petroleum and Petrochemicals, China

\*Corresponding author: [yangchunyan.fshy@sinopec.com](mailto:yangchunyan.fshy@sinopec.com) Dandong Road 31, Wanghua District, Fushun City, Liaoning Province, China

## 1. Introduction

IM-5 molecular sieve has unique crystal structure and physicochemical properties, and has good application prospects in petrochemical industry[1,2]. As an important component in the hydrothermal synthesis of molecular sieves, silicon source has an important influence on the structure and physicochemical properties of molecular sieve products[2]. Although there are many studies on the synthesis of IM-5 molecular sieves, there are relatively few studies on the effects of silicon sources on the synthesis and properties of the molecular sieves.

## 2. Experimental

The typical synthesis procedure is as follows: a clear solution was prepared by 1,5-bis(methylpyrrolidinium)pentane bromide, Silicon source, NaOH, NaAlO<sub>2</sub> and H<sub>2</sub>O under vigorous stirring. The final molar composition of synthesized gel was 30 SiO<sub>2</sub>: 0.75 Al<sub>2</sub>O<sub>3</sub>: x Na<sub>2</sub>O: 4.5 SDA: 32H<sub>2</sub>O, where 0.1 ≤ x ≤ 0.5. Once homogenous gel formed, the mixture was then transferred to a 100 mL Teflon-lined autoclave, crystallized at 443 K for 7days. The solid products were recovered by filtration, washed with distill water, dried at 393 K overnight. All as-synthesized products were calcined at 823 K for 6 h in the air in order to remove the organic species.

## 3. Results and Discussion

The effects of different silicon sources (silicic acid, silica gel, silica sol, fumed silica) on the synthesis of synthetic IM-5 molecular sieves were investigated by dynamic hydrothermal synthesis. The above silicon source can obtain IM-5 molecular sieve in the basic substance.

The product synthesized by silica gel as silicon source contains a large amount of ZSM-12 mesoporous molecular sieve; the fumed silica as a silicon source, the obtained IM-5 molecular sieve has a relatively high specific surface area and a large pore volume; The samples of IM-5 molecular sieve using silica sol as silicon source, have a relatively high crystallinity and relatively high proportion of medium strong acid and B acid, and a large value of SiO<sub>2</sub>/Al<sub>2</sub>O<sub>3</sub>. Silica sol is a preferred source of silicon.

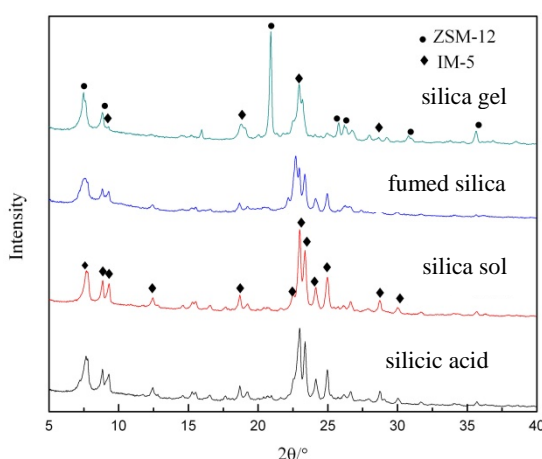


**Figure 1.** XRD patterns of zeolites by different source  
**Table 1.** FT-IR Acidity of zeolites BY different silicon source

Acid intensity distribution	silicic acid		silica sol		fumed silica	
	%	$C_B/C_L$	%	$C_B/C_L$	%	$C_B/C_L$
Total acidity (mmol/g)	0.61 5	0.89	0.8 78	3.82	1.0 14	0.39
160-250°C	31%	0.42	16 %	2.18	26 %	0.03
250-450°C	26%	2.36	26 %	5.53	28 %	0.81
450°C-	43%	0.19	58 %	2.82	46 %	0.31

#### 4. Conclusions

Silica sol is inexpensive and the size of prepared IM-5 is uniform. In general, silica sol is a preferred source of silicon.

#### References

1. Z D Wang, Y M Liu, J G Jiang, et al. Journal of Materials Chemistry, 20(2010) 10193-10199.
2. X D Wang, W L Yang, Y. Tang, et al. Chemical. Communications,21(2000) 2161-2162.

# **Hydrotreatment of atmospheric gasoil and co-processing of rapeseed oil on supported carbide and nitride bimetallic catalysts**

*H. de Paz Carmona, J. Horáček, Z. Tišler, U. Akhmetzyanova. Unipetrol Centre for Research and Education, Litvínov-Záluží, Czech Republic*

## **Abstract**

In order to improve the security of fuels supply and reduce the greenhouse gas emissions, the European Union (EU) Council agreed in 2014 the 2030 framework of strategy for climate and energy, which sets out the target of 27% as the share of renewable energy consumed in 2030 in the EU. According with this framework, the Directives 2009/28/EC and 2009/30/EC promote the development of new and more efficient biofuels.

The most common way to produce biofuels is the triglycerides transesterification into fatty acid methyl esters (FAME) [1]. However, the catalytic hydrotreatment of vegetable oils at high temperatures and pressures (300-400 °C and 50-70 bar), is a very interesting way to produce advanced biofuels, due to its realtime application in petroleum industry, in the form of co-hydroprocessing with atmospheric gas oils (AGO) in hydrodesulfurization (HDS) units [2].

This catalytic co-processing involves the removal of sulfur and nitrogen content from the petroleum feedstocks, as well as the oxygen removal by hydrodeoxygenation (HDO) and/or decarboxylation/decarbonylation (HDC/HDCn) from the triglycerides. During this process, the triglycerides are mainly converted in linear paraffins with 15-18 carbon atoms, which is commonly called hydrogenated vegetable oil (HVO). Other by-products of triglycerides co-processing are water or light gases such as: CO<sub>2</sub>, CO, C<sub>3</sub>H<sub>8</sub> or CH<sub>4</sub>. [3]

The commercial catalyst for HDS are generally composed by NiMo or CoMo over alumina supports, and can be used during the catalytic co-processing of gasoil with vegetable oils [4]. However, in order to avoid the sulfur leaching of the catalyst during the co-processing, a small concentration of vegetable oil is used (5-10 wt.%). In this sense, sulfur free catalysts such as the supported carbide and nitride bimetallic (NiMo and CoMo) catalysts, could represent an interesting alternative to conventional catalysts to resolve these problems [5].

This work shows a study of the catalytic activity of sulfur free alumina supported NiMo/CoMo carbide and nitride catalysts (NiMoC<sub>x</sub>, NiMoN<sub>x</sub>, CoMoC<sub>x</sub> and CoMoN<sub>x</sub>) during AGO hydrotreatment and its co-processing with rapeseed oil (5-10-25 wt.%), at typical industrial operating conditions (330 – 350 °C and 5.5 MPa). Preliminary results showed high catalyst activity, up to 75 % HDS, as well as an improvement in gasoil properties during vegetable oil co-processing, particularly significant in product density, due to the increase of linear paraffins (mainly nC<sub>15</sub> – nC<sub>18</sub>).

### **Acknowledgement**

The work is result of the project Development of the UniCRE Centre (Project Code LO1606), which has been financially supported by the Ministry of Education Youth and Sports of the Czech Republic under the National Sustainability Programme I.

The results was achieved using the infrastructure of the project Efficient Use of Energy Resources Using Catalytic Processes (LM2015039) which has been financially supported by MEYS within the targeted support of large infrastructures.

### **References**

1. Bezergianni S, Dimitriadis A. Comparison between different types of renewable diesel. *Renew Sust Energy Rev.*, 2013;21:110-16.
2. Al-Sabawi M, Chen J. Hydroprocessing of Biomass-Derived Oils and Their Blends with Petroleum Feedstocks: A Review. *Energ Fuel*, 2012;26:5373-99.
3. Kim SK, Han JY, Lee H, Yum T, Kim Y, Kim J. Production of renewable diesel via catalytic deoxygenation of natural triglycerides: Comprehensive understanding of reaction intermediates and hydrocarbons. *Appl. Energ.*, 2014;116:199-205.
4. De Paz Carmona H, Horáček J, Brito Alayón A, Macías Hernández JJ. Suitability of used frying oil for co-processing with atmospheric gas oil. *Fuel* 2018;214:165-173.
5. Diaz B, Sawhill SJ, Bale DH, Main R, Phillips DC, Korlann S, Self R, Bussell ME. Hydrodesulfurization over supported monometallic, bimetallic and promoted carbide and nitride catalysts. *Appl. Catal. A-Gen.* 2003;86:191-209.

# Synthesis of the Cd<sub>1-x</sub>Zn<sub>x</sub>S Photocatalysts for the Gas-Phase CO<sub>2</sub> Reduction under Visible Light

*Ekaterina A. Kozlova<sup>1,2</sup>, Mikhail N. Lyulyukin<sup>1,2</sup>, Dina V. Markovskaya<sup>1,2</sup>, Dmitry S.*

*Selishchev<sup>1,2</sup>, Svetlana V. Cherepanova<sup>1,2</sup>, Denis V. Kozlov<sup>1,2</sup>*

*<sup>1</sup>Boreskov Institute of Catalysis, Novosibirsk, Russia*

*<sup>2</sup>Novosibirsk State University, Novosibirsk, Russia*

The chemical binding of CO<sub>2</sub> is an urgent problem not only from the standpoint of its use as a carbon source but also as a method to reduce its concentration in the atmosphere. Carbon dioxide is regarded as a source for production of useful organic compounds [1]. However, CO<sub>2</sub> is the thermodynamically and kinetically stable molecule, and carbon dioxide has a limit application in the chemical industry. Thus, conversion of CO<sub>2</sub> into useful organic compounds can be achieved only under intensive physical exposure. One of the promising techniques is photocatalytic reduction of CO<sub>2</sub>. Among the various photocatalysts used for photocatalytic reduction of CO<sub>2</sub>, metal sulfides (e.g., CdS) have attracted considerable attention as the photocatalysts for CO<sub>2</sub> reduction under visible light due to their appropriate band gaps and catalytic functions. A solid solution of Cd and Zn, Cd<sub>1-x</sub>Zn<sub>x</sub>S, with a controllable bandgap and band edge positions is known to be efficient photocatalysts for H<sub>2</sub> production from water solutions of electron donors under visible light. The ratio of cadmium to zinc in a solid solution of sulfides has previously shown to strongly affect both the rate of CO<sub>2</sub> reduction and the distribution of reduction products [2]. This study was aimed at the synthesis of Cd<sub>1-x</sub>Zn<sub>x</sub>S solid solutions for the photocatalytic reduction of carbon dioxide under visible light ( $\lambda = 450$  nm). We investigated the influence of cadmium to zinc ratio in Cd<sub>1-x</sub>Zn<sub>x</sub>S on the photocatalyst activity and the distribution of reduction products.

The Cd<sub>1-x</sub>Zn<sub>x</sub>S (x = 0; 0.2; 0.4; 0.6; 0.8; 1.0) nanocomposite photocatalysts were prepared via a simple two-stage synthesis including the stage of metal hydroxides formation [3]. The samples are referred to as **Cd0.0**, **Cd0.2** etc., where number denotes the mole fraction of cadmium embedded in the synthesis. The activity of synthesized photocatalysts was evaluated in the gas-phase photocatalytic reduction of carbon dioxide under visible light ( $\lambda = 450$  nm). All the synthesized Cd<sub>1-x</sub>Zn<sub>x</sub>S solid solutions are capable of providing chemical transformations under the conditions

considered (Fig. 1). Carbon monoxide was the major product (up to 88%) in the CO<sub>2</sub> reduction while methane was the minor product (up to 7%).

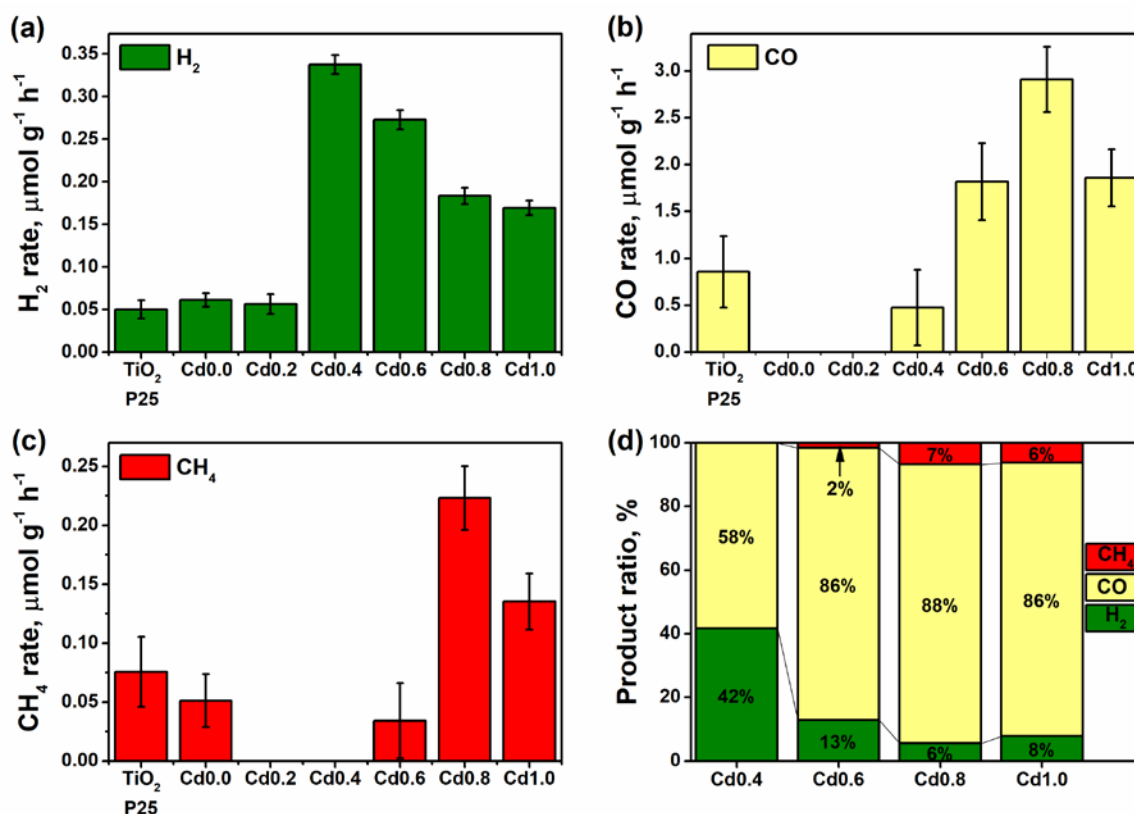


**Figure 1.** The rates of the hydrogen (a), carbon monoxide (b), and methane (c) formation over the samples Cd<sub>0.0</sub>-Cd<sub>1.0</sub>; the distribution of carbon dioxide and water reduction products over Cd<sub>0.4</sub>-Cd<sub>1.0</sub> photocatalysts (d). Conditions: 285 mW/cm<sup>2</sup>, 1 atm CO<sub>2</sub> with saturated water vapor, T=25 °C

The formation of hydrogen resulted from the photocatalytic water splitting was also observed during the process. It was shown that the actual cadmium to zinc ratio affected the activity of samples and product distribution. The activity was increased as the cadmium molar fraction was increased due to an increase in the absorption of visible light. The Cd<sub>0.94</sub>Zn<sub>0.06</sub>S photocatalyst had the highest activity, 2.9  $\mu\text{mol CO} + 0.22 \mu\text{mol CH}_4$  per gram per hour, and selectivity, 95%, which exceed the corresponding values for CdS alone. The achieved values are very high for CO<sub>2</sub> reduction over the sulfide-based photocatalysts under visible light.

This work was supported by RFBR grant 18-03-00775.

## References

- [1] T. Sakakura, J.C. Choi, H. Yasuda, Chem. Rev. 107 (2007) 2365–2387.
- [2] E.A. Kozlova, V.N. Parmon, Russ. Chem. Rev. 86 (2017), 870-906.
- [3] E.A. Kozlova, M.N. Lyulyukin, D.V. Markovskaya, D.S. Selishchev, S.V. Cherepanova, D.V. Kozlov, Photochem. Photobiol. Sci. (2019) Advance Article, doi: 10.1039/C8PP00332G

# **Synthesis gas processing over ultrafine catalysts based on composite material**

*M.V. Kulikova, A.L. Maximov*

*A.V.Topchiev Institute of Petrochemical Synthesis, RAS, 29, Leninsky prospekt,  
Moscow, 119991, Russian Federation  
m\_kulikova@ips.ac.ru*

Ability to control the structure and properties of nanocomposites makes these systems are very promising for use as catalysts for petrochemical processes based on the synthesis gas (mix of CO and H<sub>2</sub>): Fischer-Tropsch synthesis, methanol synthesis, dimethyl ether synthesis and other [1]. The original approach to the synthesis of composite materials with high activity in reactions based on CO and H<sub>2</sub> was created in A.V.Topchiev Institute of Petrochemical Synthesis (Russia) [2,3]. Using as active component metal-polymeric composite particles leads to formation of fundamentally new catalytic active particles with unique properties. The selectivity and activity of composites in reactions based on H<sub>2</sub> and CO can be controlled by the polymer nature, polymer concentration and a method of introducing a polymer composition in the composite material. Synthesized composites were characterized by complex phys-chemical methods: magnetometry in situ, IR- spectroscopy, dynamic light scattering, transmission electron microscopy. Nanoheterogeneous contacts distributed in solid organic matrix were synthesized by method of polymercontaining composite materials. Initial organic matrixes represent polyconjugated systems decomposing to carbon during formation of the catalyst. These particles of 10-20 nm in size metal formed from salts immobilized on polymers. The polymers flexibility and its effect on coils formation was determined by molecular modeling method. [4] Analyzing of the polymers folding into coils and comparative study of their geometry revealed significant differences of the final structure of the polymer molecules forming a complex metal-containing particle - polymer structure.

The work was carried out with the financial support of the Ministry of Education and Science of the Russian Federation (Agreement No. 14.607.21.0168, unique identifier of applied scientific research RFMEFI60717X0168)

## References

- [1] M.V. Kulikova, M. I. Ivantsov, L. M. Zemtsov, G. P. Karpacheva, S.N. Khadzhiev. XII international conference on Nanostructured Materials (NANO 2014) . p. 1038.
- [2] Chudakova M.V., Kulikova M.V., Ivantsov M.I., Bondarenko G.N., Efimov M.N., Vasil'ev A.A., Zemtsov L.M., Karpacheva G.P., Khadzhiev S.N.// Petroleum Chemistry. 2017. V. 57. №8. P. 694-699.
- [3] Ivantsov M.I., Kulikova M.V., Gubanov M.A., Dement'eva O.S., Chudakova M.V., Bondarenko G.N., Khadzhiev S.N.// Petroleum Chemistry. 2017. V.57. №7. P. 571-575
- [4] Tsvetkov V.B.,\_Kulikova M.V., Khadzhiev S.N.// Petroleum Chemistry. 2017. V. 57. №7. P. 600-607.



## **Polymer-assisted synthesis of catalysts for hydrotreatment reactions**

*Valentin Hetier, Institut Charles Gerhardt Montpellier UMR 5253 CNRS, Université de Montpellier, Montpellier, France ; Laurence Courthéoux, Institut Charles Gerhardt Montpellier UMR 5253 CNRS, Université de Montpellier, Montpellier, France ; Julien Pinaud, Institut Charles Gerhardt Montpellier UMR 5253 CNRS, Université de Montpellier, Montpellier, France ; Patrick Lacroix-Desmazes, Institut Charles Gerhardt Montpellier UMR 5253 CNRS, Université de Montpellier, Montpellier, France ; Annie Pradel, Institut Charles Gerhardt Montpellier UMR 5253 CNRS, Université de Montpellier, Montpellier, France ; Etienne Girard, IFP Energies Nouvelles, Solaize, France ; Denis Uzio, IFP Energies Nouvelles, Solaize, France ; Diego Pena, Institut de Chimie des Milieux et Matériaux de Poitiers UMR CNRS 7285, Université de Poitiers, Poitiers, France ; Sylvette Brunet, Institut de Chimie des Milieux et Matériaux de Poitiers UMR CNRS 7285, Université de Poitiers, Poitiers, France*

Worldwide growth of the global mobility of people and merchandises, along with industrial activity have resulted in a severe increase in airborne pollutants concentration in the last decades. The production of cleaner fuels has been imposed to refiners and has stimulated research and innovations in hydrotreatment processes and heterogeneous catalysts. Conventional hydrotreating catalysts are based on transition metal sulphides ( $\text{MoS}_2$ ) usually promoted by nickel or cobalt. Active sites are located at the edges of the slabs. Improvements could be achieved by a better control of the physico-chemical properties of the active phase such as the size /shape, assembly of the  $\text{MoS}_2$  slabs, electronic properties or surface composition...

This study aimed at addressing these challenges by combining thiomolybdate soft chemistry reactions in presence of polymers in an original synthesis route of NiMoS catalysts. Commercial and homemade polymers with controlled architectures have been used to play the role of steric stabilizers of sulphides nanoparticles or to interact specifically and at the molecular level with metallic precursors in solution. The performances of these various materials in hydrotreatment reactions have been assessed with different model molecules – 3methylthiophene (3MT) and benzothiophene (BT) mixed with C5 olefin – representative of those present in real

feedstocks under operating conditions close to industrial processes. This kinetic study allowed to determine activity and selectivity. Competition effects have also been evaluated.

The catalysts have been synthesized by mixing the precursors of molybdenum and nickel in water in presence of a polymer at ambient temperature. After washing and drying, a thermal treatment leads to the catalytic active phase called NiMoS. The XRD analyses on the obtained solids reveal the presence of the MoS<sub>2</sub> phase. The introduction of Pluronic® P123 as polymer during the synthesis allowed to decrease the stacking of the MoS<sub>2</sub> to two or three layers, as shown in figure 1. Furthermore, the specific surface area increased from 31 to 120 m<sup>2</sup>.g<sup>-1</sup> in the presence of Pluronic® P123. Regarding the transformation of the 3-methylthiophene and the benzothiophene, as well as mixtures, significant differences of activities and selectivities were observed. A complete set of results including physico-chemical characterization (XPS, XRD, HRTEM) and kinetic study with a modelling approach provided comprehensive information and will be presented.

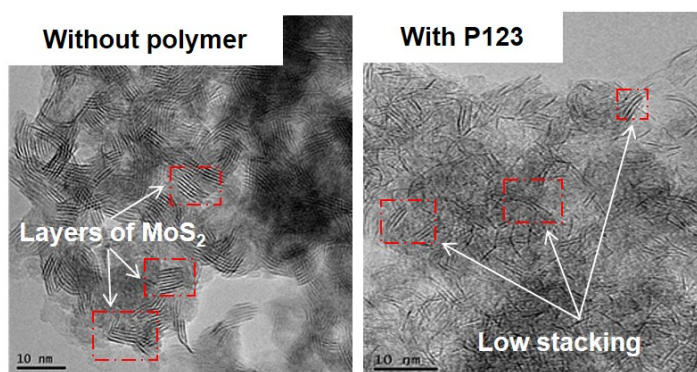


**Figure 1: TEM images of the catalysts prepared without and with Pluronic® P123.**

# Photocatalytic selective oxidation of alcohols to corresponding carbonyl compounds by visible light responsive bismuth vanadate

*Kazuki Morishita, Kindai University, Osaka, Japan, Atsuhiko Tanaka, Kindai University, Osaka, Japan, Hiroshi Kominami, Kindai University, Osaka, Japan*

## Introduction

By using titanium oxide(IV) ( $\text{TiO}_2$ ) as a semiconductor photocatalyst, oxygen as an oxidizing agent, and water as a reducing agent, an environmentally harmonious reaction system can be constructed. However, in the photocatalytic reaction using  $\text{TiO}_2$ , oxygen are reduced by the photogenerated electrons, and oxygen radical species such as superoxide anion radicals ( $\text{O}_2^-$ ) and hydroperoxyl radicals ( $\cdot\text{OH}$ ) are generated. Since they show strong oxidizing power [1], the reaction selectivity decreases in the oxidation of organic compounds.[2] On the other hand, the potential of the conduction band of bismuth vanadate ( $\text{BiVO}_4$ , hereafter BVO) is lower than the reduction potential of  $\text{O}_2$  to  $\text{O}_2^-$  and  $\cdot\text{OH}$ . Therefore, selective oxidation of organic compounds over BVO is possible because these oxygen radical species are not generated. Recently, selective oxidation of benzyl alcohol (BAL) using BVO was reported.[3] However, there are many parts not clarified such as photocatalytic activity and selectivity. Selective oxidation using photocatalyst and  $\text{O}_2$  is expected as one of environmentally conscious processes. Since selective synthesis of aldehydes that are used as raw materials for food additives, pharmaceuticals and dyes is an important process in the chemical industry, investigation of photocatalytic oxidation over BVO provides useful information. Therefore, in this study, we examined effects of various parameters such as metal co-catalysts and solvents on oxidation of alcohols over BVO and physicochemical experiments to understand the photocatalytic performance of BVO.

## Experimental

BVO was synthesized by liquid phase method.[4] Loading of Pt nanoparticles (1.0 wt%) on BVO was performed by photodeposition (Pt-BVO). Pt-BVO (50 mg) was suspended in acetonitrile ( $5 \text{ cm}^3$ ) containing BAL (ca.  $15 \mu\text{mol}$ ) in a test tube. The test tube was irradiated with a blue LED ( $\lambda_{\text{max}} = 468 \text{ nm}$  and  $470 \text{ nm}$ ) under  $\text{O}_2$ . The amounts of BAL and benzaldehyde (BAD) in the liquid phase were determined with a gas chromatograph.

## Results and discussions

Fig. 1 shows the oxidation of BAL over  $\text{TiO}_2$  photocatalyst under irradiation of UV light, indicating that BAL was oxidized to BAD, benzoic acid and  $\text{CO}_2$ . Fig. 1 also shows the oxidation of BAL over Pt-BVO photocatalyst under irradiation of blue light, which shows that BAL was selectively converted to BAD. Fig. 2 shows the time course of the oxidation of BAL over Pt-BVO under irradiation of blue light. BAL was almost completely consumed after irradiation for 8 h, while productions of benzoic acid and  $\text{CO}_2$  were negligible during the photoirradiation. We noted that BAD was formed with a quite high selectivity (>98%) at >99% conversion of BAL and that a high material balance (>99%) was always preserved, indicating that BAL was almost quantitatively converted to BAD in the present photocatalytic reaction system under irradiation of blue light. In addition, adsorption experiments revealed that Pt-BVO possesses a high adsorption ability to BAL. To expand the applicability of Pt-BVO, selective oxidation of various alcohols was also examined under irradiation of blue light, revealing that Pt-BVO has a photocatalytic property suitable for the selective oxidation of various alcohols.

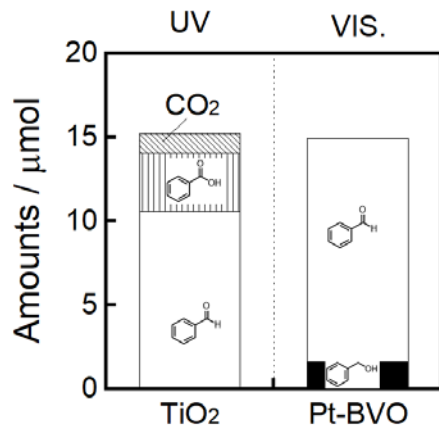


Fig. 1 Amounts of BAL, BAD,  $\text{CO}_2$  and benzoic acid in acetonitrile suspensions of  $\text{TiO}_2$  (P25) under irradiation of UV light or Pt-BVO under irradiation of visible light for 5 h.

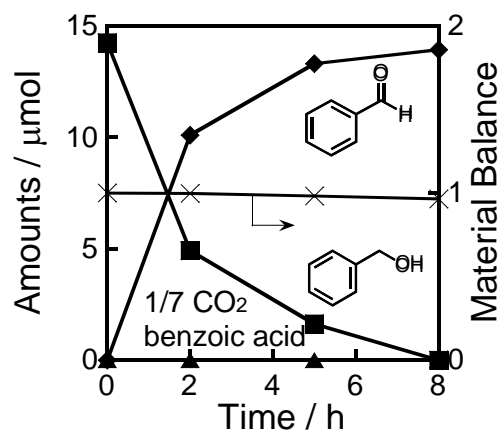


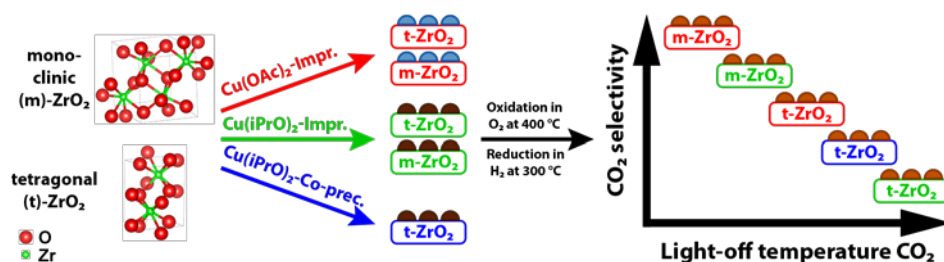
Fig. 2 Time course of amounts of BAL, BAD,  $\text{CO}_2$ , benzoic acid and material balance in acetonitrile suspensions of Pt-BVO under irradiation of visible light.

## References

- [1] R. Dietz *et al.*, *J. Chem. Soc. B*, 816 (1970). [2] A. Fujishima *et al.*, *J. Photochem. Photobiol.*, 1, 1 (2000). [3] E. Douthwaite *et al.*, *J. Catal.*, **354**, 152-159 (2017). [4] A. Kudo *et al.*, *J. Am. Chem. Soc.*, **121**, 11459 (1999).

# The Role of the ZrO<sub>2</sub> Polymorph in Cu-Based Catalysts in Methanol Steam Reforming

*Kevin Ploner, Maximilian Watschinger, Bernhard Klötzer, Simon Penner, Department of Physical Chemistry, University of Innsbruck, 6020 Innsbruck, Austria; Lukas Schlicker, Aleksander Gurlo, Chair of Advanced Ceramic Materials, Institut für Werkstoffwissenschaften und -technologien, Technische Universität Berlin, 10623 Berlin, Germany; Albert Gili, Andrew Doran, Advanced Light Source, Lawrence Berkeley National Laboratory, Berkeley, California 94720, USA; Lei Zhang, Marc Armbrüster, Institute of Chemistry, Materials for Innovative Energy Concepts, Chemnitz University of Technology, 09107 Chemnitz, Germany*



Methanol is considered to be one of the most promising candidates as a chemical storage medium for renewable energy due to its beneficial physicochemical properties. It is liquid at ambient conditions, which enables it to be stocked and distributed utilizing the currently available fuel infrastructure, and can be provided by conversion of CO<sub>2</sub> with H<sub>2</sub> or water. Recovery of the stocked energy can be achieved with a combination of methanol steam reforming (MSR), yielding H<sub>2</sub> and CO<sub>2</sub>, and generating electricity with a proton exchange membrane fuel cell (PEMFC). [1,2]

The industrially most commonly employed catalyst for MSR was initially developed for methanol synthesis and consists of Cu/ZnO/Al<sub>2</sub>O<sub>3</sub>. However, it forms too high amounts of CO, which acts as a poison for the PEMFC electrodes, and deactivates by copper particle sintering. [2] In order to avoid the introduction of additional purification steps for the reformat gas, the CO<sub>2</sub> selectivity has to be increased. In this respect, auspicious results have already been reported in the Cu/ZrO<sub>2</sub> system, where the influence of the support polymorph is still hotly debated. Cu on tetragonal zirconia (t-ZrO<sub>2</sub>) prepared by a polymer gel templating technique by Purnama et al.

[3] exhibited enhanced CO<sub>2</sub> selectivity, activity and long-term stability compared to the abovementioned industrial catalyst. Mayr et al. [4] synthesized an intermetallic Cu/Cu<sub>51</sub>Zr<sub>14</sub> sample, which was decomposed into a selective state consisting of Cu and predominantly t-ZrO<sub>2</sub> upon exposure to the MSR mixture. This activation leads to high activity and up to 100 % CO<sub>2</sub> selectivity in methanol steam reforming.

Our work focuses on the influence of the ZrO<sub>2</sub> polymorph as a support material for Cu on the CO<sub>2</sub> selectivity as the main performance indicator in MSR. Therefore, three different synthesis routines (aqueous impregnation with Cu(II) acetate, water-free impregnation with Cu(II) isopropoxide and co-precipitation of Zr(IV) isopropoxide and Cu(II) isopropoxide) were employed, yielding five different systems. After calcination and pre-reduction, two of them consist of metallic Cu on the thermodynamically stable monoclinic zirconia (m-ZrO<sub>2</sub>) and three of them of Cu(0) on t-ZrO<sub>2</sub>. *In situ* X-ray diffraction (XRD) enables direct correlation of the catalytic performance and the bulk crystal structure of the two constituents. The results reveal that the Cu precursor as well as the support polymorph impact the CO<sub>2</sub> selectivity in MSR, with the latter being more pronounced in catalysis. CO<sub>2</sub> selectivities below 55 % over the entire temperature range have been observed for the systems with t-ZrO<sub>2</sub>, whereas the m-ZrO<sub>2</sub> supported catalysts exhibit temperature regions without any detectable CO formation. Additionally, the catalysts prepared by impregnation with Cu(II) acetate display a more desirable performance in MSR on both ZrO<sub>2</sub> polymorphs considering the selectivity towards CO<sub>2</sub>. The crystal structure of ZrO<sub>2</sub> does not change during MSR in any of the systems, whereas the Cu oxidation state depends on both preparation and ZrO<sub>2</sub> polymorph. Only the catalyst obtained by Cu(II) acetate impregnation of m-ZrO<sub>2</sub> displays predominantly metallic Cu with traces of Cu<sub>2</sub>O in certain temperature regions, whereas the other four systems exhibit intermediary oxidation to CuO.

## References

- [1] G. A. Olah, A. Goepfert and G. K. S. Prakash. *Beyond Oil and Gas: The Methanol Economy*, WILEY-VCH Verlag GmbH & Co. KGaA (2009).
- [2] M. Behrens and M. Armbrüster. *Methanol Steam Reforming*. In *Catalysis for Alternative Energy Generation*; L. Guzzi and A. Erdöhelyi, Eds.; Springer: New York (2012).
- [3] H. Purnama, F. Girgsdies, T. Ressler, J. H. Schattka, R. A. Caruso, R. Schomäcker and R. Schlögl. *Catal. Lett.* **94** (2004), 61-68.
- [4] L. Mayr, B. Klötzer, D. Schmidmair, N. Köpfle, J. Bernardi, S. Schwarz, M. Armbrüster and S. Penner. *ChemCatChem* **8** (2016), 1778-1781.

# **The Electroelectrolytic Hydrogen Production with Low Energy Consumption Coupling with Oxidation of SO<sub>2</sub> by Redox Fe<sup>3+</sup>/Fe<sup>2+</sup>**

*XU Wenlin, DING Yuanqiong, SHAO Qing, WANG Yaqiong*

*(Coll. of Chem. & Chem. Eng., Yangzhou Uni., Yangzhou 225002, Jiangsu, China)*

## **1. The importance of the hydrogen energy and oxidation of SO<sub>2</sub> to SO<sub>3</sub>**

Hydrogen is viewed as the most potential energy carrier because it is clean, efficient and renewable. Hydrogen is widely used in chemistry, materials, metallurgy industry and other fields.

Of all the heavy industrial chemicals, sulfuric acid is perhaps the most fundamentally important, in that it has a number of large-scale uses not only within the chemical industry but in other industries as well. Sulfuric acid is manufactured from sulfur dioxide. The catalytic oxidation of SO<sub>2</sub> to SO<sub>3</sub> is an exothermic, reversible reaction and is the key reaction step in the process.

SO<sub>2</sub> is also a major pollutant of air. The gas creates problems for humans, such as acid rain. There are many processes to reduce SO<sub>2</sub> from the air. Among these methods, the process of removing SO<sub>2</sub> at low temperatures is important. These methods require less energy and equipment. The removal of SO<sub>2</sub> gas from industrial exhaust is important to reduce environmental pollution.

## **2. The existing production technology of water electrolysis and catalytic oxidation of SO<sub>2</sub>**

Among the various hydrogen production technologies, water electrolysis powered by renewable energy is the most mature and most promising method, and is the best way to the coming hydrogen economy. The existing technology for hydrogen production mainly includes alkaline water electrolysis and polymer electrolyte membrane water electrolysis.

The oxidation and conversion of SO<sub>2</sub> to SO<sub>3</sub> is the most important and a difficult reaction in the production of sulfuric acid and the removing SO<sub>2</sub> is important for the reaction is an exothermic, reversible one. The liberated heat must be dissipated under controlled conditions in such a way as to maintain optimum gas temperatures in the converter system and optimum acid temperatures in the dryer and absorber circuits, thereby ensuring that sulfur dioxide concentrations in the tail gas are minimized and sulfuric acid mist and sulfur trioxide at the stack outlet are avoided

insofar as possible. The systems for gas and acid cooling are therefore essential components of a sulfuric acid plant.

### 3. Problems in hydrogen production technology existing of electrolytic water

Only the half electrodes is effective use, for the target product hydrogen is generated only at cathode and the by-product oxygen is generated at anode, thus the production cost is higher in the existing water electrolysis technique. Due to the high potential of overpotential for oxygen evolution, the operating cell voltage of the electrolysis process is high and the energy consumption is high also.

The value of energy has risen so much that systems for maximum energy recovery are becoming increasingly economical despite the associated considerable increase in capital cost. This is especially true for the extremely large-capacity double-absorption sulfuric acid plants now in use for the conversion of  $\text{SO}_2$  to  $\text{SO}_3$ .

### 4. Developed hydrogen production technology

A novel technique of lower electricity consumption electrolysis producing  $\text{H}_2$  has been developed. The schematic diagram of the system is shown in Fig. 1. The system composed a two-reactor system of an oxidation reactor and an electrochemical reactor for production of hydrogen. In the oxidation reactor  $\text{SO}_2$  was oxidized by  $\text{Fe}^{3+}$  in acidic medium to  $\text{SO}_3$ , while ferric ion was reduced as  $\text{Fe}^{2+}$ . The  $\text{SO}_3$  is dissolved in the liquid and to produce  $\text{H}_2\text{SO}_4$ . The hydrogen production

technology by water electrolysis in the electrochemical reactor is a coupling technology mainly composed of the reduction  $\text{H}^+$  in an electrochemical reaction unit whin a cathodic chamber using sulfuric acid solution as an electrolyte, and the oxidation of  $\text{Fe}^{2+}$  to  $\text{Fe}^{3+}$  in an anodic chamber using sulfuric acid solution containing  $\text{Fe}^{2+}$  as an electrolyte. In electrochemical reactor  $\text{Fe}^{2+}$  was oxidized at

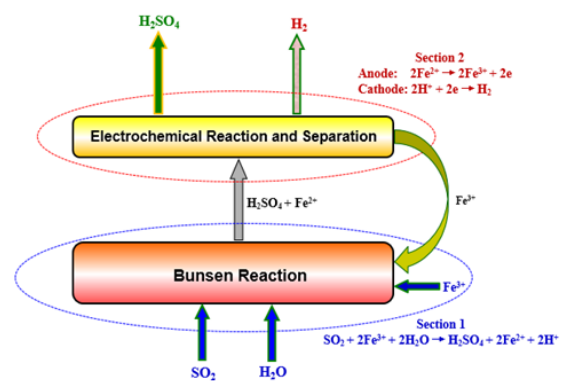


Fig. 1 Schematic diagram of a two-reactor system.

anode, pure hydrogen was produced at cathode and the Faradaic efficiency for hydrogen production was about 100%. The electrical voltage used is 1.2 V, only 1/3-1/2 electricity consumption of that used in conventional water electrolysis.

The results indicated that the cyclic process between the electrochemical reactor and the oxidation reactor can be carried out steadily.



# Mechanistic study of CO hydrogenation to C<sub>2</sub>-oxygenates over supported single-metallic Rh catalysts

*Max Schumann<sup>1</sup>, Jakob Munkholt Christensen<sup>1</sup>, Anker Degn Jensen<sup>1</sup>*

*<sup>1</sup>Technical University of Denmark, Department of Chemical Engineering, Lyngby, Denmark*

## Abstract

C<sub>2</sub>-oxygenate (C<sub>2</sub>-O) formation from CO/H<sub>2</sub> was studied over supported metallic Rh catalysts. Impregnation experiments with the target to unravel the different involved reaction intermediates were performed. Hereby, a 1% Rh/SiO<sub>2</sub> catalyst was populated with adsorbates that derived from impregnation with formic acid and CH<sub>2</sub>Cl<sub>2</sub>. Subjecting this model system to a temperature programmed hydrogenation (TPH) revealed the same MS signal-pattern for CH<sub>3</sub>CO-fragments as after a catalytic CO-H<sub>2</sub> reaction treatment. The similarity between the two TPH-patterns gives strong evidence that the formation of acetaldehyde (AcH) can occur via the reaction of formate and alkyl species.

## Introduction

Single-metal supported Rh catalysts are known for their ability to produce C<sub>2</sub>-oxygenate compounds [1] (mainly AcH and EtOH) from CO/H<sub>2</sub>. However, Rh based catalysts suffer from a low CO conversion range within which C<sub>2</sub>-O are formed in considerable yield (ca. 10-15 %). Expanding the basic knowledge of the involved reaction intermediates and their interplay with the different Rh sites and the applied supports is hoped to feed back into the development of better catalysts.

## Results and Discussion

Two different impregnation experiments were performed in order to unravel the reaction pattern for the CO hydrogenation on supported Rh catalysts. Different precursors were populated on the Rh surface. Subjecting those model systems to a TPH was used to verify, whether C<sub>2</sub>-O production is a feasible reaction from these intermediates. The TPH pattern from a catalyst that was treated in CO-H<sub>2</sub> atmosphere shows an AcH-formation peak around 220 °C and serves as reference (Figure 1, black line).

In a first experiment, it was tested whether AcH can be produced from CO insertion into alkyl species. A reduced 1% Rh/SiO<sub>2</sub> catalyst was preadsorbed with a CH<sub>2</sub>Cl<sub>2</sub> (DCM) loaded He gas flow at 50 °C. This temperature was assumed to be sufficient to decompose DCM into CH<sub>x</sub> alkyls species that would bind on the catalyst surface. Afterwards, 9.5% CO/Ar was adsorbed and a subsequent TPH showed a clear AcH formation peak at 213 °C (blue line in Figure 1) whereby no AcH was formed during the TPH when the catalyst was only preadsorbed with 9.5% CO/Ar (red line). In another experiment, the 1% Rh/SiO<sub>2</sub> catalyst was populated with precursors that are assumed to lead to CH<sub>2</sub> and HCOO- species on the surface by applying a flow of He loaded with DCM and HCOOH to the reduced catalyst. During the subsequent TPH the formed adsorbates react to C<sub>2</sub>-O and shows a peak in the TPH pattern of AcH around 190 °C (green line).

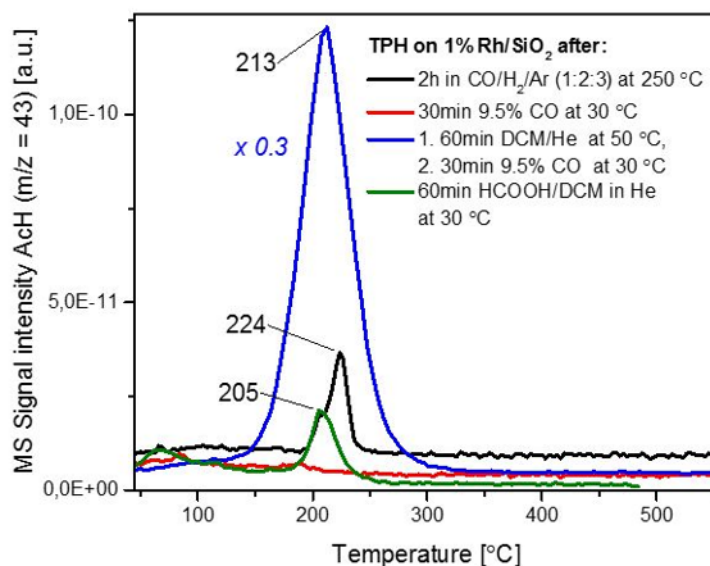


**Figure 1:** Comparison of MS signal patterns from TPH sequences. Catalyst was prepared via wet impregnation of Rh(NO<sub>3</sub>)<sub>3</sub>. TPH patterns from 1% Rh/SiO<sub>2</sub> after adsorption of CO, formic acid and or DCM in He.

The similarity between the MS signal-patterns from the TPH of a Rh catalyst that was populated with C<sub>2</sub>-O species under CO-H<sub>2</sub> reaction conditions and the TPH patterns derived from the model reactions provides strong evidence, that C<sub>2</sub>-O products can be produced from the reaction of alkyl and formate surface adsorbates.

## References

[1] M. Ichikawa, Bull. Chem. Soc. Jpn. 1978, 51, 2273 – 2277.

# Synthesis of Mg-Fe mixed oxides from various precursors and their influence on transesterification of oils

*Martin Hájek<sup>1</sup>, Aleš Vávra<sup>1</sup>, Karel Frolich<sup>1</sup>, Jaroslav Kocík<sup>2</sup>*

<sup>1</sup> *Faculty of Chemical Technology (department of Physical Chemistry), University of Pardubice, Pardubice, The Czech Republic;*

<sup>2</sup> *Unipetrol Centre for Research and Education, Litvínov-Záluží 1, The Czech Republic*

This work is focused on the use of heterogeneous catalyst for the biomass conversion, especially the transesterification of rapeseed oil by methanol and the aldol condensation of furfural. The Mg-Fe mixed oxides, which were synthesized from hydrotalcites (known also as hydrotalcites layered double hydroxides), were used as a heterogeneous catalyst. The aim of this study was describe and explain the influence of different precursors or their combinations on the various properties of hydrotalcites and especially mixed oxides and also they catalytically activity.

The mixed metal oxides are often used as a heterogeneous catalyst for acid-based reactions such as transesterification, glycerolysis or aldol condensation [1]. The mixed oxides can be synthesized from hydrotalcites by thermal pre-treatment (calcination). The general formula of hydrotalcites is  $[M_{1-x}^{2+}M_x^{3+}(OH)_2]^{x+}A_{x/n}^{n-} \cdot zH_2O$ , where M represents bivalent (Mg, Ca and Zn) or trivalent metallic cations (Al and Fe),  $A^{n-}$  is usually inorganic anion (such as carbonate, nitrate, chloride, bromide, etc.) and x is the molar ratio of  $M^{3+}$  [2]. The catalyst activity is influenced by the properties of mixed oxides, which depend on the type of metals, molar ratio of metals and also by the conditions of synthesis, such as type of precursors, temperature, time and intensity of stirring. The mixed oxides are usually synthesis only from chloride or nitrates precursors [3].

The formed mixed oxides were tested as an acid-base heterogeneous catalyst in two reactions in the batch reactor (transesterification of rapeseed oil to form of esters and aldol condensation of furfural). The influence of type of mixed oxides on reaction conversion and selectivity of these two reactions was also study. Therefore, the Mg-Fe hydrotalcites (called pyroaurite), with constant molar ratio (Mg/Fe 3:1), were synthesized from various precursors: chlorides, bromide, nitrates and sulfates of

magnesium and iron metals and their combinations. The hydrotalcites were thermally treated at constant temperature (500 °C) and so the mixed oxides were formed.

All synthesized materials were characterized by several techniques such as (i) XRD (the confirmation of structure and calculation of crystallite size), (ii) ICP-OES and XRF for determination of metals content, (iii) thermogravimetric analysis with a mass spectrometer for determination of temperature changes throughout calcination, (iv) N<sub>2</sub> adsorption for determination of specific surface area and pore size distribution, (v) TPD-CO<sub>2</sub> and TPD-NH<sub>3</sub> for the determination of basic and acid sites.

The different properties of synthesized hydrotalcites and also mixed oxides were found, such as different crystallite size, different TGA profiles and pore size distribution of mixed oxides. The mixed oxides, which were synthesized from sulfate precursors, had the lowest concentration of basic sites (31 μmol.g<sup>-1</sup>) and also the lowest total pore volume (0.21 cm<sup>3</sup>.g<sup>-1</sup>), which was in accordance with the lowest pores (maximum was in the range 6-8 nm). On the other hand, this mixed oxides had the largest surface area (152 m<sup>2</sup>.g<sup>-1</sup>). The highest basicity (115 μmol.g<sup>-1</sup>) and also pore size (maximum was in the approximately 30 nm) was determined for mixed oxides synthesized from chloride precursor. The ester yield was the highest for this type of mixed oxides.

### **Acknowledgements**

This work was supported by the Czech Science Foundation, Project No. 19-00669S. The authors gratefully thank to Ministry of Education, Youth and Sports of Czech Republic, project code LM2015039. The project has been integrated into National Sustainability Programme I: Development of UniCRE Centre, Project Code LO1606.

### **References**

- [1] Guerrero-Urbaneja, P., Garcia-Sancho, C., Moreno-Tost, R., Merida-Robles, J., Santamaria-Gonzalez, J., Jimenez-Lopez, A., Maireles-Torres, P., 2014. Glycerol valorization by etherification to polyglycerols by using metal oxides derived from MgFe hydrotalcites. *Appl Catal a-Gen* 470, 199-207
- [2] Takagaki, A., Iwatani, K., Nishimura, S., Ebitani, K., 2010. Synthesis of glycerol carbonate from glycerol and dialkyl carbonates using hydrotalcite as a reusable heterogeneous base catalyst. *Green Chem* 12, 578-581
- [3] Hájek, M., Tomášová, A., Kocík, J., Podzemná, V. 2018. Statistical evaluation of the mutual relations of properties of Mg/Fe hydrotalcites and mixed oxides as transesterification catalysts. *Applied Clay Science* 154, 28-35

# Steam Ethanol Reforming on promoted Co-Ni/Hydrotalcite structures: Catalyst optimization

*Nikolaos E. Tsakoumis, Yalan Wang, Mario Ernesto Casalegno Garduño, Edd A.*

*Blekkann, De Chen, Department of chemical engineering, NTNU, Trondheim, Norway;*

*Kumar Ranjan Rout, SINTEF Process Technology, Trondheim, Norway; Yian Zhu, State Key Laboratory of Chemical Engineering, East China University of Science and Technology, Shanghai, China.*

## Introduction

The transition towards more sustainable means of energy production, distribution and use is a key issue. Slowing down, or even reversing, the negative climatic effects from the utilization of fossil fuels is the ultimate goal. Utilization of hydrogen ( $H_2$ ) as an energy carrier can be a sustainable solution that will reduce the impact of human activities on the environment. Provided that  $H_2$  is produced in a sustainable way from renewable sources, such as water or biomass [1] it has the potential, through its use in fuel cells with favorable efficiencies, to cover energy needs with a significant reduction in greenhouse gas emissions.  $H_2$  production through steam reforming of hydrocarbons is a mature technology that can be extended to use ethanol as a feedstock. Bioethanol formed by fermentation processes has significant advances and appears to be a strong candidate as an energy vector suitable for  $H_2$  production.

The transportation sector consumes approx. 25% of the world's energy. Here we are targeting the reduction of the carbon footprint of the transportation sector by developing an integrated system, on board device, for mobile  $H_2$  production. The produced  $H_2$  can be fed into a fuel cell and provide the energy needed to propel a vehicle, using ethanol/water mixtures as the feedstock. The work deals with a thermodynamic feasibility study of the integral system comprising a steam ethanol reforming (SER) microreactor which is heat integrated with combustion of the effluent stream and delivers hydrogen to be used in a fuel cell. The study is assisted by microkinetic modelling for catalyst optimization.

## Materials and Methods

Catalysts are based on Co-Ni bimetallic nanoparticles supported on hydrotalcite-type structures and promoted by various elements depending on the reaction application. These materials have been tested experimentally, using co-precipitation as the preparation method [2]. The activity and stability have been examined in a tubular fixed-bed steel

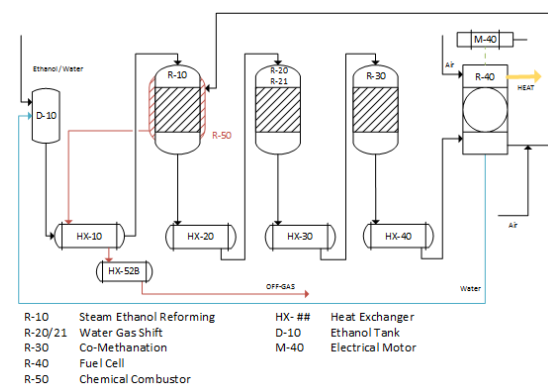


**Figure 1.** Simplified thermodynamic integration.

reactor at various conditions for obtaining intrinsic kinetic properties. The objective of future work is to test the system in a full-scale prototype that is under construction. Process simulation was built in the Aspen plus simulator version V10 (36.0.0).

The simulation includes a SER reactor (RGibbs) at different pressures and temperature conditions, two Water Gas Shift reactors (REquil), a CO-methanation reactor (RGibbs), a fuel cell (REquil) and a chemical combustor (RStoich). Theoretical DFT calculations were used to estimate adsorption and activation energies on dense surfaces of metals including Ni, Rh, Pt, Pd, Fe, Ru and Co. Then the CatMAP (Catalysis Microkinetic Analysis Package) was used for building a microkinetic model [3].

## Results and Discussion

Our basic thermodynamic calculations show that a 60 Lt tank (90%v Ethanol) can produce up to 6.9 kg of H<sub>2</sub> after water gas shift reaction converting CO to levels <10 ppm (700°C and 5 atm). With the current fuel cell technology this amount of H<sub>2</sub> produced [4] is sufficient to move a car up to 690 km at 100 km/h. The utilization of Ni-Co bimetallic supported nanoparticles will allow better selectivities towards H<sub>2</sub> to be achieved and have the potential to further enhance the system efficiency. Combination of DFT calculations with microkinetic modeling is an important tool for the prediction of catalyst performance. Results obtained solely on theoretical input appear to be in agreement with our former laboratory tests on Ni-Co mixtures [2] (Figure 2). In our approach, we use theory assisted design of catalysts in order to enhance catalyst performance through the addition of specific promoters.

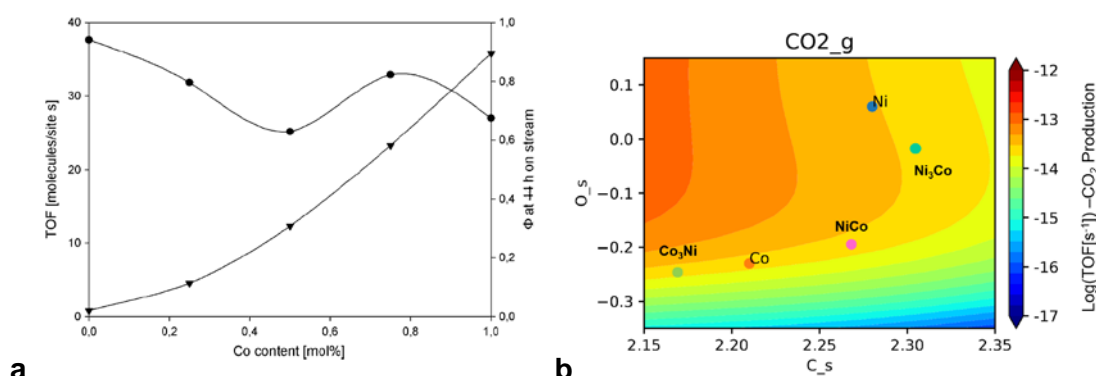


**Figure 2.** (a) Obtained performance versus Co–Ni composition. (b) Volcano plot of the theoretical estimation of TOF for CO<sub>2</sub> formation at different Co–Ni compositions.

Our future efforts will be focusing on improving the understanding of the catalysts functions through kinetic investigations that will be the basis for a further optimization and the demonstration of the viability of the described process scheme.

## References

- [1] G.A. Deluga, J.R. Salge, L.D. Schmidt, X.E. Verykios, Renewable Hydrogen from Ethanol by Autothermal Reforming, *Science* (80-. ). 303 (2004) 993–997. doi:10.1126/science.1093045.
- [2] L. He, H. Berntsen, E. Ochoa-Fernández, J.C. Walmsley, E.A. Blekkan, D. Chen, Co–Ni Catalysts Derived from Hydrotalcite-Like Materials for Hydrogen Production by Ethanol Steam Reforming, *Top. Catal.* 52 (2009) 206–217. doi:10.1007/s11244-008-9157-1.
- [3] A.J. Medford, C. Shi, M.J. Hoffmann, A.C. Lausche, S.R. Fitzgibbon, T. Bligaard, J.K. Nørskov, CatMAP: A Software Package for Descriptor-Based Microkinetic Mapping of Catalytic Trends, *Catal. Letters.* 145 (2015) 794–807. doi:10.1007/s10562-015-1495-6.
- [4] Honda Clarity <https://automobiles.honda.com/clarity-fuel-cell>

## The HT originated mixed oxides in aldolization reactions – analysis of the active catalytic sites

*Karel Frolich<sup>1</sup>, Martin Hájek<sup>1</sup>, Aleš Vávra<sup>1</sup>, Jaroslav Kocík<sup>2</sup>, Jan Šafář<sup>2</sup>*

*<sup>1</sup>Department of Physical Chemistry, Faculty of Chemical Technology, University of Pardubice, Studentská 573, 532 10 Pardubice, Czech Republic*

*<sup>2</sup>Unipetrol Centre for Research and Education, s r.o., Areál Chempark 2838, 436 70, Litvínov-Záluží 1, Czech Republic*

Lignocellulosic biomass has the potential to be converted into many chemicals and a variety of fuels. It consists of three main components: cellulose, hemicellulose and lignin. For the fuel production, hemicellulose represents the starting material involved in the production of xylitol, furfural and furfural derivatives [1-2]. Furfural can be used to produce alternative fuels. To produce long-chain hydrocarbons, aldol condensation of furfural and ketones can be exploited. In the case of aldol condensation of furfural with acetone, hydrocarbons of chain lengths up to 13 carbons are obtained [3]. These compounds can be used after further treatment as additives to fossil hydrocarbon fractions.

In general, aldol condensation can be performed via homogeneous catalysis using both acid and basic catalysts. To obtain the desired long-chain products, basic catalysis with aqueous hydroxide solutions was applied. The major drawbacks of this classical route are the difficulty of catalyst regeneration and corrosion of equipment. The alternative route is represented by heterogeneous catalysis using basic catalysts.

Mixed metal oxides prepared by the thermal decomposition of the hydrotalcite (HT) derived compounds show well dispersed  $\text{Me}^{3+}$  and  $\text{Me}^{2+}$  cations, variable surface acidity/basicity, and relatively high surface area. Due to large versatility, such oxides are exploited as heterogeneous catalysts in a number of catalyzed reactions. For the aldol condensation reaction, acid/basic feature(s) are tuned.

HT derived mixed oxides have sites with a broad distribution of their basic strength. Three different basic site groups are present on the surface: (i) weak basic sites attributed to  $\text{OH}^-$  groups, (ii) medium strength sites related to oxygen in both  $\text{Me}^{2+}\dots\text{O}$  and  $\text{Me}^{3+}\dots\text{O}$  pairs, and (iii) strong basic sites corresponding to isolated  $\text{O}^{2-}$  ions [4]. The Lewis acid sites are represented by unsaturated metal ions  $\text{Me}^{2+}$  and/or  $\text{Me}^{3+}$ .

As is well known, catalytic behavior in aldol condensation is determined by the structure of alkaline sites on the oxide surface. A wide-ranging discussion was performed on the kind of basic sites responsible for the conversion of reactants [3, 5-8]. In spite of that, there is insufficient detailed knowledge concerning the influence of site type on catalytic performance, and how to achieve significantly improved catalytic performance via tuning the population of alkaline species still remains a challenge.

In this contribution we show the catalytic performance of selected HT-derived mixed oxides in aldol condensation of furfural with acetone with the aim to provide insight on the role of individual basic sites on the conversion of furfural and the role of acid and basic sites on the composition of reaction mixture. Materials are studied with respect to their phase purity (XRD) and textural properties ( $N_2$ -BET). Acidobasic properties are studied using TPD and FTIR techniques. The series of samples differing in the total concentration of acid and basic sites and their distribution is exploited. Combined catalytic and statistical analysis was used for the description and explanation of mutual relationships among the material properties such as density of acid and basic sites, and the catalyst activity (conversion and selectivity).

### **Acknowledgement**

This work was supported by the Czech Science Foundation, Project No. 19-00669S. The work has been integrated into the National Sustainability Programme I of the Ministry of Education, Youth and Sports of the Czech Republic (MEYS) through the project Development of the UniCRE Centre (LO1606). The work was achieved using the infrastructure included in the project Efficient Use of Energy Resources Using Catalytic Processes (LM2015039) which has been financially supported by MEYS within the targeted support of large infrastructures.

### **References**

- [1] Mamman AS, Lee JM, Kim YC, Hwang IT, Park NJ, Hwang YK, Chang JS, Hwang JS, *Biofuel Bioprod Bior* 2:438-454 (2008).
- [2] Lange JP, van der Heide E, van Buijtenen J, Price R, *Chemsuschem* 5:150-166 (2012).
- [3] Ordonez S, Diaz E, Leon M, Faba L, *Catal Today* 167:71-76 (2011).
- [4] Debecker DP, Gaigneaux EM, Busca G, *Chem Eur J* 15:3920-3935 (2009).
- [5] Diez VK, Apesteguia CR, Di Cosimo JI, *J Catal* 240:235-244 (2006).
- [6] Kikhtyanin O, Capek L, Smolakova L, Tisler Z, Kadlec D, Lhotka M, Diblikova P, Kubicka D, *Ind Eng Chem Res* 56: 13411-13422 (2017).
- [7] Smolakova L, Frolich K, Kocik J, Kikhtyanin O, Capek L, *Ind Eng Chem Res* 56:4638-4648 (2017).
- [8] Kocik J, Frolich K, Perkova I, Horacek J, *J Chem Technol Biotechnol* 94: 435-445 (2019).



## **Ab initio modeling of the zeolite-catalyzed conversion of alkylphenols into phenol and olefins**

*Massimo Bocus, Center for Molecular Modeling, Ghent University, Belgium; Julianna Hajek, Center for Molecular Modeling, Ghent University, Belgium; Yuhe Liao, Center for Surface Chemistry and Catalysis, KU Leuven, Belgium; Bert F. Sels, Center for Surface Chemistry and Catalysis, KU Leuven, Belgium; Veronique Van Speybroeck, Center for Molecular Modeling, Ghent University, Belgium*

### **Importance of lignin-to-chemical processes**

Olefins are among the most valuable raw materials in the modern chemical industry, as they are used to produce a wide range of essential molecules and polymeric materials. The depletion of crude oil reservoirs all around the planet has then exacerbated the need of alternative routes to produce large amounts of olefins, possibly with an environmental friendly approach. An enticing opportunity is nowadays represented by the lignin-to-chemicals processes, that can be classified in the more general field of chemicals from renewable biomasses. Lignin is a polymeric molecule contained in the plant cells walls and it presents the larger concentration by weight of aromatic groups with respect to all the other natural polymers. A plethora of depolymerization techniques have been developed in the past few years to decompose lignin in simpler and valuable molecules. Typical products of those reactions are alkyl-substituted phenols, such as ethylphenols (EPs) and propylphenols (PPs) [1]. Alkylphenols themselves, however, are not remarkably useful in the chemical industry. Therefore, innovative processes are being devised to convert them in added-value chemicals like olefins. Recently, Sels and co-workers reported that the acidic zeolite H-ZSM-5 can selectively catalyze the dealkylation of both EPs and PPs to produce phenols and ethene or phenol and propene, respectively [2-4]. Interestingly, this new process exhibits some peculiarities in water steam presence. Firstly, water is required to prevent a rapid deactivation of the catalyst and, secondly, it has also been proved to have an active role in the reaction, lowering the temperature at which the maximal conversion is reached. Both those effects have still not been completely understood.

### **Mechanistic view on dealkylation**

Our main purpose is to unravel the mechanistic pathway of the dealkylation reaction within the acidic zeolite pores, to provide an explanation of the high selectivity towards phenol and olefins as well as to understand the dual role of water steam. The dealkylation of EPs and PPs can theoretically proceed through multiple routes and intermediates as already highlighted for a similar reaction, *i.e.* the zeolite-catalyzed ethylation of benzene with ethene [5]. To investigate the reaction mechanism, static and dynamic density functional theory calculations are performed. The effect on the selectivity imposed by the zeolite pores constrain is taken into account through periodic boundary conditions. Molecular dynamics simulations are used to deduce which intermediate species are stable within the zeolite framework at the reaction conditions. Complementary static calculations allow to energetically characterize the transition states that connect those intermediates and to identify the lowest energy pathways for the dealkylation reaction. The complete investigation of the reaction mechanism with multiple approaches will allow us to unravel its main unusual features and provide a contribution to the development of more efficient processes for the coveted production of chemicals from renewable biomasses.

#### Acknowledgement:

Financial support for this research was received from the EoS project BIOFACT and the European Union's Horizon 2020 research and innovation program (consolidator ERC grant agreement No. 647755 - DYNPOR (2015-2020)) and the Research Board of Ghent University.

#### References

- [1] W. Schutyser, T. Renders, S. Van den Bosch, S.-F. Koelewijn, G. T. Beckham and B. F. Sels, *Chem. Soc. Rev.*, 2018, **47**, 852-908.
- [2] D. Verboekend, Y. Liao, W. Schutyser and B. F. Sels, *Green Chem.*, 2016, **18**, 297-306.
- [3] Y. Liao, M. d'Halluin, E. Makshina, D. Verboekend and B. F. Sels, *Appl. Catal. B Environ.*, **234**, 2018, 117-129.
- [4] Y. Liao, R. Zhong, E. Makshina, M. d'Halluin, Y. van Limbergen, D. Verboekend and B. F. Sels, *ACS Catal.*, 2018, **8**, 7861-7878.
- [5] N. Hansen, T. Brüggemann, A. T. Bell and F. J. Keil, *J. Phys. Chem. C*, 2008, **112**, 15402-15411.

# **ALD Pt nanoparticles and thin-film coatings on silicon photocathodes for stable and efficient solar water splitting**

*Christos Trompoukis, KU Leuven, Center for Surface Chemistry and Catalysis, Celestijnenlaan 200F, Leuven and Ghent University, Photonics Research Group, iGent Technologiemark Zwijnaarde 126, Ghent, Belgium; Ji-Yu Feng, Ghent University, Department of Solid State Sciences, Krijgslaan 281/S1, Ghent, Belgium; Tom Bosserez, KU Leuven, Center for Surface Chemistry and Catalysis, Celestijnenlaan 200F, Leuven, Belgium; Jolien Dendooven, Ghent University, Department of Solid State Sciences, Krijgslaan 281/S1, Ghent, Belgium; Jan Rongé, KU Leuven, Center for Surface Chemistry and Catalysis, Celestijnenlaan 200F, Leuven, Belgium; Christophe Detavernier, Ghent University, Department of Solid State Sciences, Krijgslaan 281/S1, Ghent, Belgium; Roel Baets, Ghent University, Photonics Research Group, iGent Technologiemark Zwijnaarde 126, Ghent Belgium; Johan Martens, KU Leuven, Center for Surface Chemistry and Catalysis, Celestijnenlaan 200F, Leuven, Belgium*

## **Introduction**

Renewable fuels are indispensable for achieving a complete decarbonization of our energy systems. Fossil fuels can be substituted by hydrogen ( $H_2$ ), a versatile fuel which can be used not only in end applications which are difficult to electrify (seasonal storage or heavy-duty mobility) but also in sectors which have no renewable alternative (industrial fuels). For producing renewable  $H_2$ , photoelectrochemical solar water splitting is one of the most promising approaches. However, the instability of semiconductors in direct contact with aqueous electrolytes remains a challenge [1]. In this work, we use atomic layer deposition (ALD) to improve both the catalytic performance and stability of silicon (Si) photocathodes.

## **Results, discussion and perspectives**

Platinum (Pt) nanoparticles were deposited on  $pn^+$  Si photocathodes by ALD (topography shown in Fig. 1a) following two approaches: alternating exposures to the  $MeCpPtMe_3$  precursor and either  $N_2$  plasma (Pt- $N_2$ ) or  $O_2$  pulse (Pt- $O_2$ ) [2]. As shown in Fig. 1b, an insulating layer ( $SiO_2$ ) between the Pt nanoparticles and the  $pn^+$  photocathode resulted in a bad catalytic activity. The presence of  $SiO_2$ , either by a controlled deposition (grey curve) or during the  $O_2$  pulse (blue curve) deposited before the Pt nanoparticles resulted in lower onset potentials ( $V_{on}$ ) compared to the

bare pn+ Si photocathode (red curve). On the contrary, the Pt-N<sub>2</sub> had a better V<sub>on</sub> (purple curve) and when capped by a SiO<sub>2</sub> thin-film the V<sub>on</sub> reached 530 mV (black curve), a value which is among the highest obtained in literature [1].

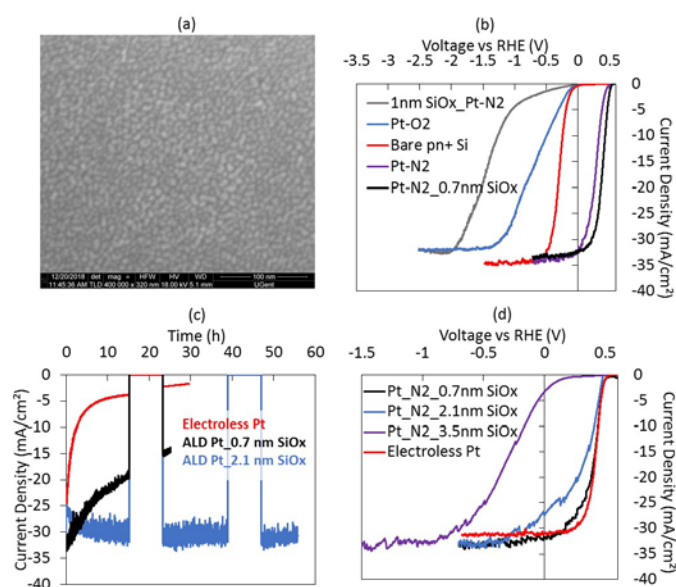


Figure 1: (a) SEM picture of ALD deposited Pt nanoparticles, (b) and (d) current density – voltage performance of various ALD coated photocathodes in 0.5M H<sub>2</sub>SO<sub>4</sub> and (c) chronoamperometry (@0V vs RHE) results in a day/night cycle operation.

The presence of the SiO<sub>2</sub> on top of the Pt nanoparticles acted as a capping layer and as a result their agglomeration was avoided [3]. Compared to the reference case used for benchmarking (pn+ Si photocathodes with Pt nanoparticles deposited electrolessly, red curve in Fig. 1d) where the catalytic activity rapidly degraded after a couple of hours because of the agglomeration of the nanoparticles (red curve in Fig. 1c), capping the Pt nanoparticles by a thin SiO<sub>2</sub> layer resulted in a stable operation for several 15h-day/8h-night cycles (blue curve in Fig. 1c). As for the capping oxide, a trade-off between stability and photoelectrochemical performance is present: a too thin oxide is not stable (black curve in Fig. 1c) while a too thick has bad photoelectrochemical behavior (purple curve in Fig. 1d).

Overall, such a combination of controlled Pt deposition with low loadings and a protective thin-film capping layer resulting in high V<sub>on</sub> and stable operation can enable low cost and efficient solar water splitting devices.

## References

- [1] J. W. Ager et al., Energy Environ. Sci. 8 (2015) 2811–2824.
- [2] J. Dendooven et al., Nature Communications 8 (2017) 1074
- [3] N. Y. Labrador et al., Nano Lett. 16 (2016) 6452 - 6459

## **Monitoring deactivation behavior of modified ZSM-5 zeolite catalysts in selective conversion of ethanol to small aromatics**

*Markus Seifert, Mathias S. Marschall, Torsten Gille, Oliver Busse, Wladimir Reschetilowski, Jan J. Weigand, Technische Universität Dresden, Dresden, Germany*

Conversion of ethanol to hydrocarbons over porous acidic zeolite H-ZSM-5 (ETH process) is considered according to the hydrocarbon pool mechanism in methanol-to-olefin catalysis (MTO process). An increase in durability and yield of small aromatics during the ethanol conversion are main challenges to improve industrial relevance for prospective application in refining. But this is prevented by a simultaneous increasing formation of undesired ethylene and as the consequence the pore-blocking by nano-sized coke molecules. [1]

The synthesis of ZSM-5 and its post-synthetic modification together with the adaption of process parameter in ethanol conversion aims to overcome challenges in long term stability of catalysts used. Moreover, it will give insights in the formation mechanism of ethanol towards small aromatics. Inside and outside the zeolite pores of ZSM-5 (0.52 – 0.56 nm). Special focus was directed to change typically applied methods for zeolite modification by new treatments including acid and base washing or steaming in combination with the variation of residence time and feed flow.

Trends of durability changes and yields of small aromatics are explained not only by developing an understanding of bicyclic hydrocarbon pool mechanism using mechanistic approaches. They are also described by molecular processes near active sites particularly with the constellation of special site multiplets.

Comparative discussion of catalytic results, solid-state properties (e.g. Si/Al) and imaginary experiments on catalytic active multiplet centers together with local conversion pathways from ethanol to products and coke give hints to distinct dominant multi-site formation pathways towards olefins, small aromatics and poly-aromatic coke precursors. Zeolite powder characterization of fresh and modified ZSM-5 by Clariant (structure (XRD), surface property and acidity (TPAD), elemental composition (ICP-OES), framework and extra-framework structure species (NMR), particle size analysis (REM, LDA)) is combined with the product analysis (GC, GC-MS) of catalytic test reactions in a fixed-bed reactor setup and discussed. By means

of the models for deactivation kinetics and center-controlled reactive intermediates (CRI) the obtained catalytic results are verified. [3]

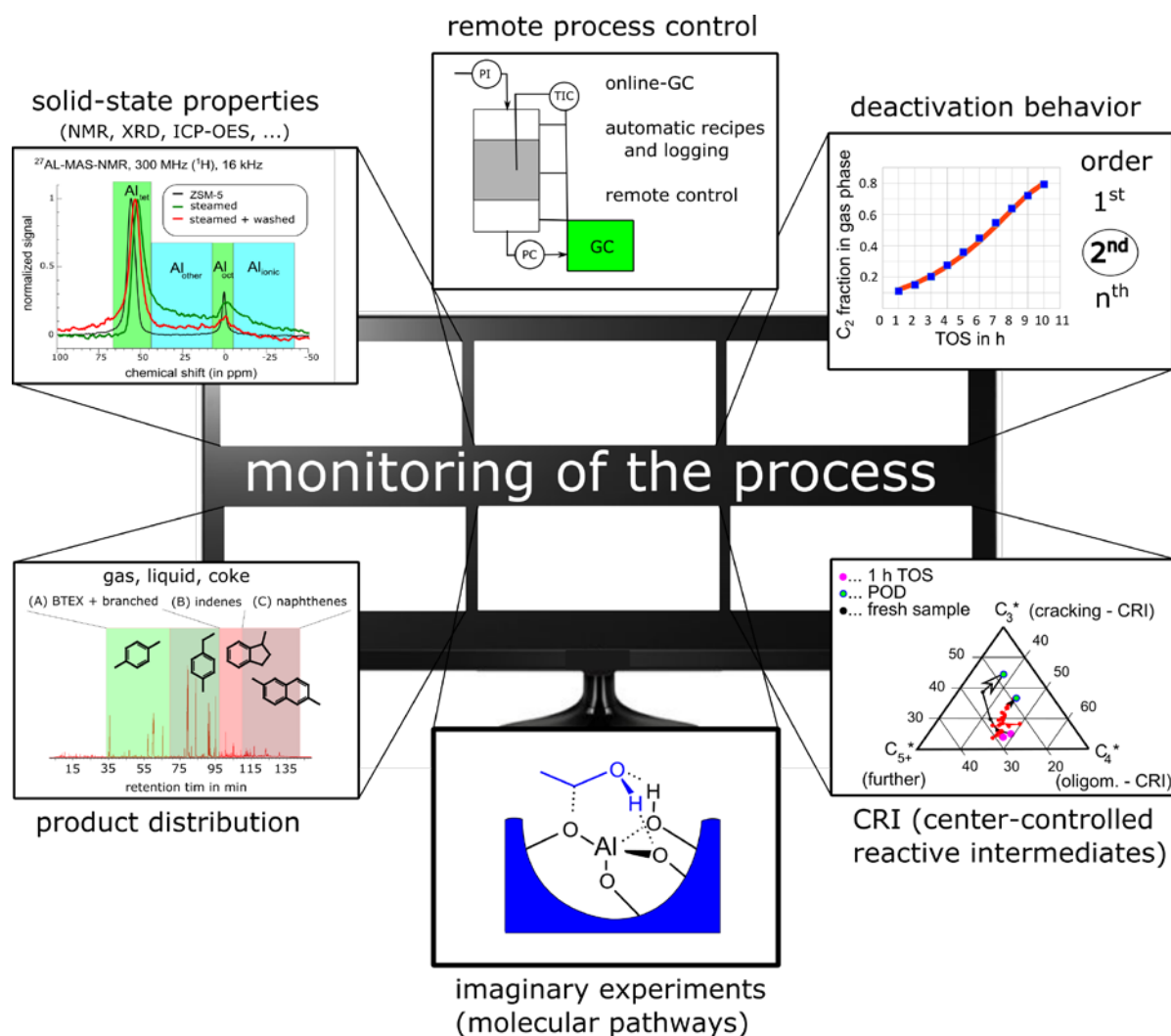


**Fig.** Scheme of different aspects of process and catalyst monitoring and control in combination with imaginary experiments to reach an extended level of mechanistic understanding

### Acknowledgement

The authors sincerely thank the German Research Foundation (DFG) for funding the research project RE 906/11-1.

### References

- [1] Däumer, D., Seifert, M., Reschetilowski W., *Micropor. Mesopor. Mat.*, **219**, 66 (2016).
- [2] Cumming, K.A., Wojciechowski, B.W., *Catal. Rev. – Sci. Eng.*, **38(1)**, 101 (1996).
- [3] Hamieh, S., Canaff, C., Tayeb, K.B., Tarighi, M., Maury, S., Vezin, H., Pouilloux, Y., Pinard, L., *Eur. Phys. J. Special Topics*, **224**, 1817 (2015).

# State of zinc counts: different efficiency of $Zn^{2+}$ cations and ZnO species in activation of propane on Zn-modified zeolite BEA

*S.S. Arzumanov, Boreskov Institute of Catalysis, Novosibirsk, Russia;*

*A.A. Gabrienko, Boreskov Institute of Catalysis, Novosibirsk, Russia; A.V. Toktarev,*

*Boreskov Institute of Catalysis, Novosibirsk, Russia; D. Freude, Leipzig University,*

*Leipzig, Germany; A.G. Stepanov, Boreskov Institute of Catalysis, Novosibirsk, Russia*

## Introduction

Zinc containing zeolites represent efficient catalysts for aromatization of  $C_{2+}$  alkanes. [1] The role of different zinc species as well as Brønsted acid sites (BAS) should be understood in details to unravel the successive stages of alkane transformation and improve technology for alkane aromatization. In this study, in situ MAS NMR spectroscopy was applied to clarify activation and conversion of propane on zinc-modified zeolite. Two zeolite catalysts, containing either  $Zn^{2+}$  cations or small ZnO clusters ( $Zn^{2+}/HBEA$  and  $ZnO/HBEA$  samples) were specially synthesized. Kinetics of H/D exchange of propane with BAS and propane conversion, was studied to explore peculiarities of propane interaction with zinc species of different nature.

## Results and Discussion

$Zn^{2+}/HBEA$  zeolite containing  $Zn^{2+}$  cations provides regioselective H/D exchange of BAS with methyl groups of propane. The rate is higher by one order of magnitude

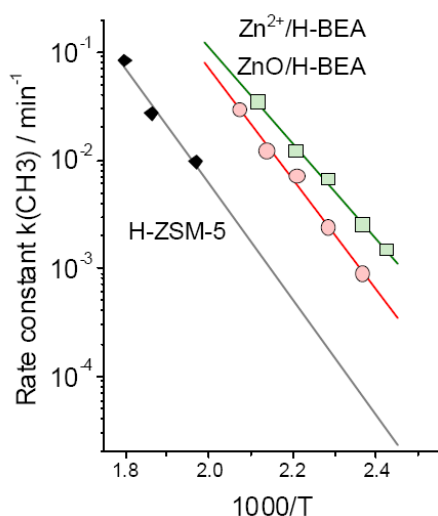


Fig. 1. Arrhenius plot for the H/D exchange in methyl groups of propane on H-ZSM-5,  $Zn^{2+}/H-BEA$ , and  $ZnO/H-BEA$  zeolites.

and activation energy is lower compared to the H/D exchange for propane on pure-acidic zeolite (Fig.1). Much slower rate was observed for H/D exchange in the  $CH_2$  group of propane on  $Zn^{2+}/HBEA$  (Fig.2) with the kinetic parameters similar to pure-acid form zeolite. It was suggested that  $Zn^{2+}$  cations form a transient complex [2] of BAS with C-H bond of methyl group of propane providing a significant promotion of the hydrogen exchange in propane methyl groups. The absence of accelerating effect of Zn on H/D exchange with the  $CH_2$

implied occurrence of the exchange of this group of propane with involvement of pentacoordinated carbonium ion as a transition state. [3]

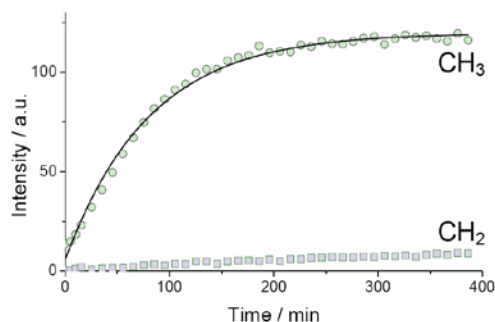


Fig.2. Kinetics of H/D exchange in propane-D<sub>8</sub> on Zn<sup>2+</sup>/H-BEA zeolite at 453K.

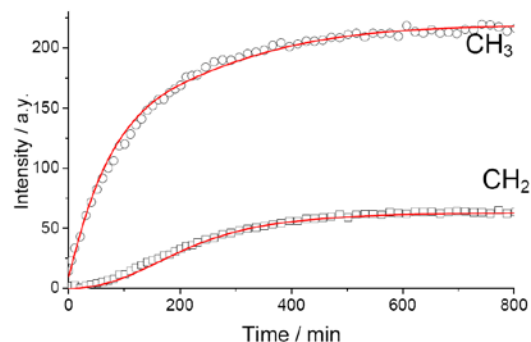


Fig.3. Kinetics of H/D exchange in propane-D<sub>8</sub> on ZnO/H-BEA zeolite at 453K.

Different kinetic behaviour for H/D exchange was observed for ZnO/HBEA zeolite. Both CH<sub>2</sub> and CH<sub>3</sub> groups of propane are involved in the H/D exchange with equal rates, but higher than for pure acid form zeolite. However, the CH<sub>2</sub> kinetics exhibits an induction period for ca. 100 min (Fig.3). Regioselective H/D exchange in the methyl groups during induction period is succeeded presumably by intramolecular process of hydrogen scrambling which can be provided by carbenium-ion species (isopropyl cation). This hypothesis is supported by <sup>13</sup>C MAS NMR data showing formation of small amounts of propylene on ZnO/HBEA zeolite at the end of induction period. Protonation of propane by BAS can provide isopropyl cation formation. Interestingly, Zn<sup>2+</sup>/H-BEA performs propane dehydrogenation easier, compared to ZnO/H-BEA. However, the formed propylene does not violate the regioselectivity of the H/D exchange in the methyl groups. The reason could be a higher stability of propylene complex with Zn<sup>2+</sup> cations, which does not allow protonation of propylene. Thus, different kinetic behaviour of H/D exchange for Zn<sup>2+</sup>/H-BEA and ZnO/H-BEA zeolites reflecting difference in activation of propane by these differently modified with Zn zeolites may be related with different stability of propene complex with Zn<sup>2+</sup> cations and ZnO species.

**Acknowledgement.** The research was supported by Russian Science Foundation (grant #19-43-04101) and DFG (grant #HA 1893/22-1).

## References

- [1] Y. Ono, Catal. Rev.-Sci. Eng. 34 (1992) 179-226.
- [2] S.S. Arzumanov, A.A. Gabrienko, D. Freude, A.G. Stepanov, Catal. Sci. Technol. 6 (2016) 6381–6388.
- [3] S.S. Arzumanov, S.I. Reshetnikov, A.G. Stepanov, V.N. Parmon, D. Freude, J. Phys. Chem. B 109 (2005) 19748–19757.



# Use of hierarchical H-Y zeolite for the Fluid Catalytic Cracking of bio-oil with Vacuum Gas Oil

*Y. Chapellière<sup>1\*</sup>, A. Tuel<sup>1</sup>, C. Mirodatos<sup>1</sup>, D. Farrusseng<sup>1</sup>, Y. Schuurman<sup>1</sup>*

*<sup>1</sup>IRCELYON, Université UCBL Lyon1, CNRS, UMR5256, Villeurbanne, France*

*\*yann.chapelliere@ircelyon.uni-lyon1.fr*

## Introduction

Fluid Catalytic Cracking (FCC) gasoline represents one third of the global gasoline pool. In order to meet objectives regarding increased renewable share in transportation fuels, production of a hybrid bio/fossil fuel by co-refining biomass pyrolysis liquids with crude oil fractions in a conventional oil refinery, is an achievable approach [1]. However, oxygenated molecules, typical for the bio-feedstock, are still present in pyrolytic liquids. For high oxygenated molecule content, co-refining may lead to severe changes in products quality, such as a higher aromaticity and residual oxygenates in the hybrid fuels that are produced. In order to adjust the reactivity of FCC catalysts, Y zeolites have been upgraded by creating an additional mesoporosity. The aim of this mesopore network is to improve the diffusion of the large lignocellulosic fragments throughout the catalytic cracking catalysts.

## Materials and Methods

Hierarchical H-Y zeolites were prepared according to post synthetic processes performed on commercial CBV720 from Zeolyst [2, 3]. Solid acid catalysts were characterized by XRD, TEM, IR spectroscopy of adsorbed pyridine, N<sub>2</sub> physisorption, <sup>27</sup>Al and <sup>29</sup>Si NMR. Co-processing of pyrolysis liquid with Vacuum Gas Oil (VGO) were carried out in a Micro Activity Test (MAT) unit that simulates FCC units. Both liquids were injected through the reactor using their own synchronized pump systems. The reactants were fed at different catalyst-to-oil (Cat/Oil) ratios from 0.3 to 1.8. Gas products were analyzed by a compact GC. Liquids products, collected in a cold trap, were characterized by simulated distillation and GC 2D. To determine the coke yield, the regeneration gases were analyzed by IR for their CO<sub>2</sub> content.

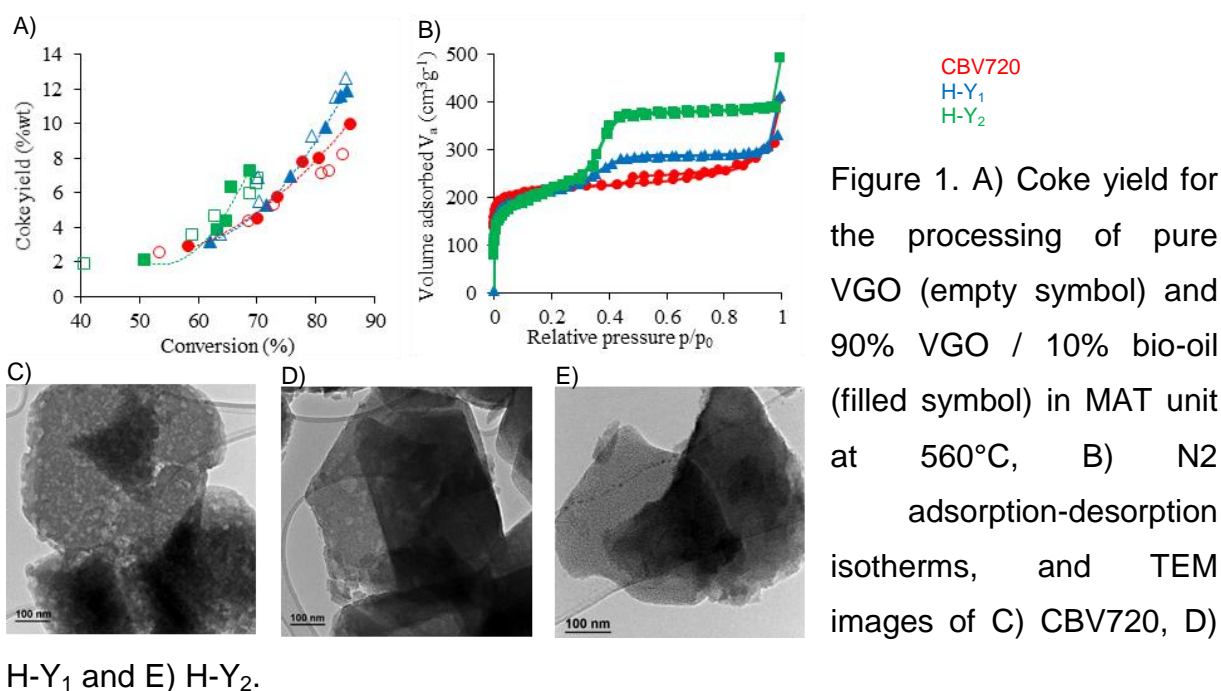
## Results and Discussion

The characterization results show that most of the hierarchical catalysts retained a high crystallinity. Si/Al ratio of 15 was found for all the materials prepared

from CBV720. As the pore structure was modified, the Brønsted acid sites concentration decreased whereas the Lewis acid sites increased.

Three catalysts with well distinct multilevel pore networks were tested on a MAT catalytic test bench. The addition of 10% of bio-oil to the VGO into the feed led to a small decrease of naphtha yield. Production of dry gas and Liquid Paraffin Gas (LPG) slightly increased. The analysis of liquid products by GC 2D revealed the presence of phenols as residual oxygenated components. Peaks of sugars and acids were not identified contrary to what had been seen for the analysis of bio-oil before the processing in the MAT test. The main difference of selectivity between the three materials was the coke yield (Figure 1.A). H-Y<sub>1</sub> and H-Y<sub>2</sub> were unexpected to achieve higher coke yield than CBV720 since higher mesopore volumes were found (Figure 1.B). However, the post synthetic modifications of CBV720 induced structure rearrangement [2]. The progressive disappearance of the large mesopore-macropores (Figure 1.C-E) explained the aforesaid coke production.

It is highlighted that the pore structure of the hierarchical zeolites plays a key role for the co-processing of bio-oil with VGO. Catalytic cracking of model molecules on the presented materials will be presented in order to identify the roles of oxygenates on catalytic performances.



## References

- [1] Schuurman Y., Fogassy G. and Mirodatos C. in *The Role of Catalysis for Sustainable Production of Bio-fuels and Bio-chemicals*, p. 321-349, Elsevier, 2013.
- [2] Garcia-Martinez J., Johnson M., Valla J., Li K. and Ying J. Y. *Catal. Sci. Technol.* 2, 987-994 (2012).
- [3] Chal R., Cacciaguerra T., van Donk S. and Gerardin C. *Chem. Com.* 46, 7840-7842 (2010).

# Synthesis of $Ce_{1-x}Zr_xO_{2-\delta}$ Complex Oxides In Supercritical Alcohols For Catalytic Hydrogen Production

*Y. Bepalko<sup>1\*</sup>, M. Simonov<sup>1,2</sup>, E. Smal<sup>1</sup>, V. Fedorova<sup>1</sup>, V. Sadykov<sup>1,2</sup>*

1 - Boreskov Institute of Catalysis, Novosibirsk, Russia

2 - Novosibirsk State University, Novosibirsk, Russia

\* - [bepalko@catalysis.ru](mailto:bepalko@catalysis.ru)

The nature of starting compounds of zirconium and supercritical media on the synthesis of ceria–zirconia mixed oxides by solvothermal method in a flow reactor was investigated. Addition of a complexing agent (acetylacetonone) allows to obtain a homogeneous solid solution.

Catalysts comprised of Ni supported on  $Ce_{1-x}Zr_xO_{2-\delta}$  oxides demonstrate a high yield of synthesis gas and stable performance in methane dry reforming.

## 1. Scope

Mixed  $Ce_{1-x}Zr_xO_{2-\delta}$  oxides are of permanent interest due to their intense use in catalysis, in particular, as catalysts supports for the reaction of methane dry reforming (MDR), which is one of the most promising reactions of green chemistry converting two greenhouse gases into syngas. Ceria–zirconia based solid solutions have been reported to ensure coking suppression due to their high oxygen mobility and reactivity [1,2]. In our work  $Ce_{1-x}Zr_xO_{2-\delta}$  were synthesized using supercritical fluid technology. This method is characterized by simplicity and a high performance, being environmentally friendly and practical when employed at a large scale.

## 2. Results and discussions

Solutions of  $Ce(NO_3)_3$  (0.25 M) and zirconium butoxide (0.117 M) in isopropanol were used as reagents for the synthesis of  $Ce_{1-x}Zr_xO_{2-\delta}$  systems. A 2-fold molar excess of acetylacetonone (AA) was added to the butoxide solution. Solutions were mixed to obtain the necessary ratio of Ce/Zr and supplied into the U-shaped reactor. Simultaneously, into the reactor at a rate of 8 ml/min was supplied isopropanol preheated to 150°C. The reaction of synthesis occurred at 400°C and a pressure of 120-130 atm. The products of synthesis were separated from the mother solution by decantation. The precipitates were dried and calcined at 600°C for 2 hours. The Ni/ $Ce_{1-x}Zr_xO_{2-\delta}$  catalysts were prepared by impregnating supports with required amount of aqueous solution of  $Ni(NO_3)_2 \cdot 6H_2O$  to yield a 5 wt% Ni.

All obtained materials were characterized using XRD, Raman spectroscopy, XPS and TPR techniques. The morphology and textural properties were studied by TEM and thermal desorption of nitrogen. The activities and resistance of Ni catalysts to coking in DRM were evaluated using 15 vol.% CH<sub>4</sub>+15 vol.% CO<sub>2</sub>+ 70 vol.% N<sub>2</sub> feed in the temperature range of 600–750 °C. Before testing, catalysts were reduced in the stream of 5% H<sub>2</sub> in He. To determine the extents of carbon formation, TEM analyses was performed for catalysts tested in the catalytic reaction.

Samples synthesized without AA were bi-phasic with reflections of cubic and tetragonal phases being observed in their XRD patterns. The most homogeneous phase composition was found for a sample which contained more than 90 wt.% of zirconium-enriched solid solution of Ce<sub>0.25</sub>Zr<sub>0.75</sub>O<sub>2</sub>. For samples prepared with addition of AA, according to XRD and Raman data, a homogeneous pseudocubic fluorite-type phase of Ce<sub>1-x</sub>Zr<sub>x</sub>O<sub>2-δ</sub> is formed with BET surface areas varying between 70-85 m<sup>2</sup> g<sup>-1</sup>. The resulting Ni-loaded catalysts were found to have surface areas ranging from 25 to 40 m<sup>2</sup> g<sup>-1</sup>. According to analyses of XPS and TPR data, they are characterized by strong metal- support interaction, with pronounced incorporation of Ni cations into the bulk of bi-phasic samples. For all catalysts prepared with AA addition, methane conversion is substantially higher (up to 60% at 650 °C) than for catalysts with bi-phasic supports (<20% at 650 °C). As a whole, at 650 °C for the best 5 wt% Ni/ Ce<sub>1-x</sub>Zr<sub>x</sub>O<sub>2-δ</sub> catalytic system CO<sub>2</sub> conversion of 84% is achieved with H<sub>2</sub> yield of 48% and H<sub>2</sub>/CO ratio of 0.81-0.86, coking being suppressed.

### 3. Conclusion

Ni/Ce<sub>1-x</sub>Zr<sub>x</sub>O<sub>2-δ</sub> catalysts with supports prepared in supercritical alcohols with addition of acetylacetonate as complexon and characterized by the homogeneous phase composition demonstrate a high and stable performance in the methane dry reforming due to a higher concentration of Ni in the near-surface layer along with a suppression of coking and resistance to sintering.

The work was supported by the Russian Science Foundation (Project 18-73-10167).

### References

[1] G. Vlaic, R. Di Monte, P. Fornasiero, E. Fonda, J. Kaspar, and M. Graziani, *J. Catal.* 182, 378 (1999).

[2] M.M. Makri, M.A. Vasiliades, K.C. Petalidou, A.M. Efstathiou, *Catalysis Today*. 259,150 (2015) .

# Plasma enhanced CaCO<sub>3</sub> hydrogenation for fuel production

*Guido Giammaria, University of Twente, Enschede, The Netherlands;*

*Leon Lefferts, University of Twente, Enschede, The Netherlands*

## Introduction

Plasma catalysis is receiving more attention in the last few years, since the interactions between plasma and catalyst surface may lead to synergistic effects [1]. Dielectric Barrier Discharge (DBD) plasma is a promising technique for plasma-catalytic conversion, since the non-equilibrium plasma has very high electron temperatures ( $10^5\text{K}$ ), and rather low rotational and translational temperatures ( $10^2\text{K}$ ), allowing application of a catalyst directly in the plasma generation zone without fast deactivation, maximizing the interaction between active species and catalytic phase.

This study assesses the potential of H<sub>2</sub> plasma to enhance CaCO<sub>3</sub> decomposition. CaCO<sub>3</sub> is a relevant material for CO<sub>2</sub> separation via Calcium Looping Cycle [2], consisting of carbonation of CaO for capturing, followed by calcination of CaCO<sub>3</sub> in order to recycle calcium oxide and to produce pure CO<sub>2</sub>. However, the calcination reaction requires temperatures of at least 950°C to achieve 1 bar 100% CO<sub>2</sub>, resulting in sintering and decreasing of CO<sub>2</sub> capture capacity when CaO is recycled. Using a DBD plasma during CaCO<sub>3</sub> decomposition might circumvent the need for such high temperatures, and CO<sub>2</sub> will be converted by plasma into CO, converting electrical energy into chemical energy. H<sub>2</sub> as a co-reactant leads to a decrease in the decomposition temperature of ca. 50°C and production of CO and H<sub>2</sub>O [3].

The decomposition in H<sub>2</sub> plasma is studied, distinguishing between thermal effects and plasma chemical effects on the reaction rate, based on the fact that plasma cannot exist in pores smaller than a few micrometers.

## Materials and Methods

CaCO<sub>3</sub> samples with 3 different surface areas and 3 particles sizes are synthesized, characterized by N<sub>2</sub> physisorption, XRD, XRF and SEM, and decomposed in a fixed bed reactor in 10% H<sub>2</sub> in Ar, temperature of 590-630°C and plasma power of 0-6 W.

## Results and Discussion

We observed that plasma induces an increase in the concentration of all the products, i.e. CO<sub>2</sub>, CO and H<sub>2</sub>O, as function of power. Figure 1 shows that the

increase in CO<sub>2</sub> concentration depends on the internal surface area of the CaCO<sub>3</sub> sample, which is not exposed to plasma, but is affected by temperature changes induced by the plasma. On the other hand, the CO<sub>2</sub> concentration appears independent of the external surface area, which is exposed to plasma. Thus, CO<sub>2</sub> formation is influenced only by the gas temperature, and no plasma-chemistry is contributing. Figure 1 shows also that the increase in CO formation is influenced by internal surface area at constant plasma power, implying that plasma chemistry is involved. Experiments performed in absence of plasma show that the formation of CO is hardly affected by the CO<sub>2</sub> concentration in the packed bed, suggesting that the CO is formed directly on the CaCO<sub>3</sub> surface rather than consecutive reaction in the gas phase. The temperature increase in the plasma, as estimated based on the kinetics of the CO<sub>2</sub> production (R<sub>1</sub>), is not enough to explain the significant increase of CO in presence of plasma, confirming the conclusion that plasma chemistry is involved. Ongoing experiment are going to discriminate whether plasma enhances surface- (R<sub>2</sub>) or gas phase- (R<sub>3</sub>) CO production.

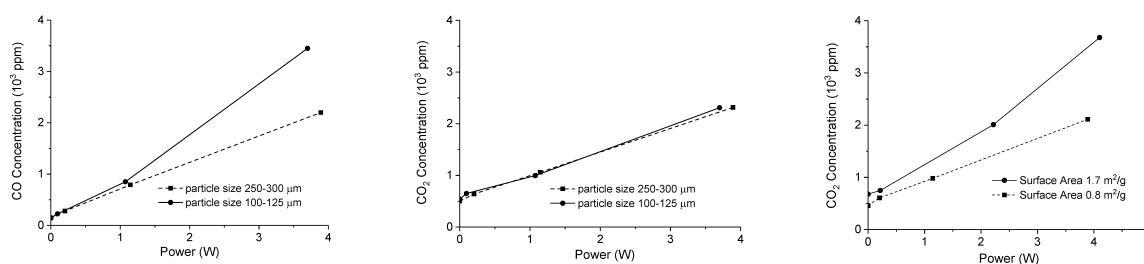
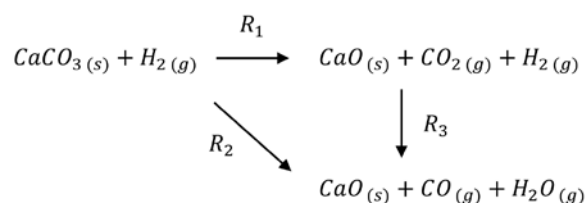


**Figure 1.** Concentration of CO (1a) and CO<sub>2</sub> (1b,c) during isothermal decomposition of CaCO<sub>3</sub> samples with different particle size (1a,b) and with different surface area (1c); flow rate is 30ml/min, gas composition is 10%H<sub>2</sub> in Ar, temperature is 590°C.



**Scheme 1**

## References

1. E. C. Neyts, K. Ostrikov, M. K. Sunkara, and A. Bogaerts, "Plasma Catalysis: Synergistic Effects at the Nanoscale," *Chem. Rev.*, vol. 115, no. 24, pp. 13408–13446, 2015.
2. J. Blamey, E. J. Anthony, J. Wang, and P. S. Fennell, "The calcium looping cycle for large-scale CO<sub>2</sub> capture," *Prog. Energy Combust. Sci.*, vol. 36, no. 2, pp. 260–279, 2010.
3. A. Reller, C. Padeste, P. Hug. "Formation of Organic Compounds from Metal Carbonates." *Nature* 329, pp. 527-529, 1987.

# Modifications on hierarchical ZSM-5 zeolites for methanol to hydrocarbons (MTH) process in a fluidized bed reactor

*D. Zapater; A. Sanz-Martínez; J. Lasobras; J. Soler; J. Herguido; M. Menéndez*

*Catalysis, Molecular Separations and Reactor Engineering Group (CREG) Aragon Institute of Engineering Research (I3A), University of Zaragoza, Zaragoza, 50018, Spain (dzapater@unizar.es)*

## Introduction

Production of hydrocarbons from alternative carbon sources includes as a promising process the reaction of methanol over zeolite catalysts in fixed bed reactors [1]. These reactors are common but have disadvantages such as hot spots and high-pressure drop; to avoid these problems a fluidized bed reactor is proposed. The catalysts used in MTH process are often zeolites like ZSM-5 or SAPO-34 [2], but their hardness and mechanical resistance must be improved to allow their use in a fluidized bed.

## Experimental Section

Two catalysts were synthesized by agglomeration of ZSM-5 (Zeolyst International), Boehmite (Sasol Germany) and  $\alpha$ -Al<sub>2</sub>O<sub>3</sub> (Alfa Aesar) with a mass ratio of 50/30/20 wt.%. Additionally, one of the samples was treated with a 0.2 M NaOH solution.

Catalytic tests were performed in a fluidized bed reactor loaded with 15 g of catalyst, at temperatures between 400°C and 500°C. Methanol and carrier gas (N<sub>2</sub>) were feed to operate at two times the minimum fluidization velocity, maintaining 90% vol. MeOH. To quantify C<sub>1</sub>-C<sub>4</sub> products, a Varian CP-3800 gas chromatograph was used, while C<sub>5+</sub> and BTX products were analyzed by a CG-MS (Shimadzu QP-2010).

## Results and Discussion

Table 1 shows the surface and porous characterization of the samples.

**Table 1. Surface and porous characterization of the samples.**

Sample	BET surface area (m <sup>2</sup> ·g <sup>-1</sup> )		Pore volume (cm <sup>3</sup> ·g <sup>-1</sup> )		Pore diameter (nm)	
	Total	Micro	Total	Micro	Total	Micro
HZSM-5	320	202	0.23	0.11	2.8	2.1
Boehmite	212	-	0.49	-	9.0	-
$\alpha$ -Al <sub>2</sub> O <sub>3</sub>	179	-	0.38	-	8.1	-
HZ+Boehmite	288	113	0.40	0.06	5.5	2.1
HZ+Boehmite+NaOH	296	114	0.47	0.05	6.3	1.8

On the one hand, agglomeration results in a physical mix of structures with weighted (50/30/20%) properties. The binder does not affect the microporous structure but the mean surface area is reduced. On the other hand, NaOH treatment modifies the structure of the zeolite by building new mesoporous channels.

Agglomeration allows operating with a fluidized bed reactor, as  $\text{Al}_2\text{O}_3$  improves mechanical resistance and Boehmite gives a bigger particle size (160 - 315  $\mu\text{m}$ ) to minimize the drag of the catalyst.

The effect of reaction temperature was studied for both catalysts. As an example, Figure 1 shows the product selectivity for both catalyst samples at 450°C. Methanol conversion was higher than 99.9% with both catalysts. The activity of the catalyst improves with the NaOH treatment as is shown in the reduction of DME selectivity. Product distribution was also modified, enhancing C<sub>1</sub>-C<sub>4</sub> (mainly ethylene and propylene) and BTX (mainly p-xylene) production at the expense of C<sub>5+</sub> hydrocarbons. Octane number was calculated as a weighted mean of the octane number of products. Table 2 shows the octane numbers of C<sub>5+</sub> + BTX produced with both catalysts and a comparison with commercial gasoline.

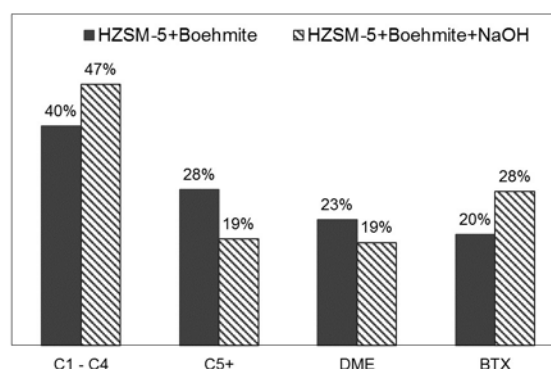


**Figure 1. Product selectivity for the agglomerated catalysts.**

**Table 2. Octane numbers of commercial and produced gasoline.**

Sample	Octane Number	Source
Exxon and Mobil Synergy™ Regular Gasoline	87	Exxon.com
Exxon and Mobil Synergy™ Extra Gasoline	89	Exxon.com
Exxon and Mobil Synergy SUPREME+™ Gasoline	91 - 93	Exxon.com
Cepsa Optima 98	98	Cepsa.es
Cepsa Star 95	95	Cepsa.es
HZSM-5 + Boehmite	108	-
HZSM-5 + Boehmite + NaOH	110	-

## References

- [1] Galadima, A., Muraza, O. Journal of Natural Gas Science and Engineering, Vol: 25, Page: 303-316 (2015).
- [2] Zhou, Y., Qi, L., Wei, Y., & Liu, Z. Molecular Catalysis, Vol. 433, Page: 20-27 (2017).



# Identification of Active Center for CO<sub>2</sub> Hydrogenation to Higher Alcohols by Neural-Network Enhanced Genetic Algorithm

*Shenjun Zha<sup>1</sup>; Dmitry, Sharapa<sup>1</sup>; Felix Studt<sup>\*1, 2</sup>*

*<sup>1</sup> Institute of Catalysis Research and Technology, Karlsruhe Institute of Technology, Hermann-von-Helmholtz Platz 1, 76344 Eggenstein-Leopoldshafen, Germany*

*<sup>2</sup> Institute for Chemical Technology and Polymer Chemistry, Karlsruhe Institute of Technology, Engesserstrasse 18, 76131 Karlsruhe, Germany*

## Abstract

Using CO (an intermediate of CO<sub>2</sub> hydrogenation) to synthesize higher alcohols stands out as a catalytic route of eminent interest. It has been generally accepted that the synergy between active centers with different functionality is necessary for this reaction.<sup>1</sup> Take CoCu catalyst for an example, the role of Co is to dissociate CO and subsequently hydrogenate and the role of Cu is to nondissociative adsorption of CO and insert CO.<sup>2</sup> However, the final structures of catalysts are still under debate. The structures of CoCu catalysts will segregate after dealing with different atmospheres.<sup>3</sup> Besides, the Co with a positive valence state can replace the role of Cu and the atmosphere and support may greatly change the charge state of Co.<sup>4</sup> Thus, an explicit catalyst model is extremely important for understanding the mechanism of this reaction.

Genetic algorithm can effectively local the global minimum, which means the finding of the most possible structure under reaction condition.<sup>5</sup> However, Utilizing DFT-based genetic algorithm is too time-consuming to simulate the supported CoCu catalysts. Therefore, neural-network based genetic algorithm is applied to boost the calculations.<sup>6</sup>

## Computational Details

DFT: VASP, 4x4x3 slab, CoCu cluster with 18 atoms, gamma point, energy cutoff: 300eV

Genetic Algorithm: ASE, an initial population of 20 candidates, about 1000 offsprings.

Neural Network: Amp, Gaussian descriptor (G2 and G4), Neural network (2 hidden layers, each with five nodes)

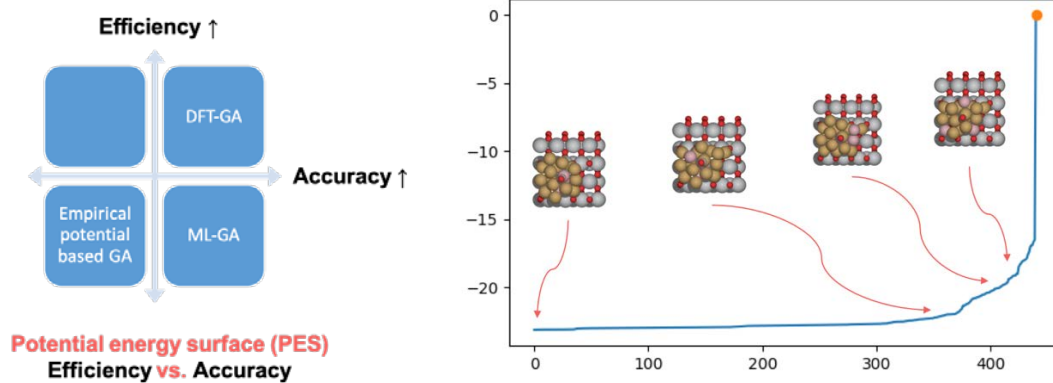


**Fig 1.** (left) The importance of machine learning based genetic algorithm; (right) The most possible structure of CoCu/TiO<sub>2</sub> with CO adsorbate.

## Keywords

CO Hydrogenation; Higher Alcohols; Neural Network; Genetic Algorithm

## References

1. Ao, M., Pham, G. H., Sunarso, J., Tade, M. O. & Liu, S. Active Centers of Catalysts for Higher Alcohol Synthesis from Syngas: A Review. *ACS Catal.* **8**, 7025–7050 (2018).
2. Luk, H. T., Mondelli, C., Ferré, D. C., Stewart, J. A. & Pérez-Ramírez, J. Status and prospects in higher alcohols synthesis from syngas. *Chem. Soc. Rev.* **46**, 1358–1426 (2017).
3. Xiang, Y., Barbosa, R. & Kruse, N. Higher Alcohols through CO Hydrogenation over CoCu Catalysts: Influence of Precursor Activation. *ACS Catal.* **4**, 2792–2800 (2014).
4. Alayoglu, S. *et al.* Surface Composition Changes of Redox Stabilized Bimetallic CoCu Nanoparticles Supported on Silica under H<sub>2</sub> and O<sub>2</sub> Atmospheres and During Reaction between CO<sub>2</sub> and H<sub>2</sub>: In Situ X-ray Spectroscopic Characterization. *J. Phys. Chem. C* **117**, 21803–21809 (2013).
5. Vilhelmsen, L. B. & Hammer, B. Systematic Study of Au<sub>6</sub> to Au<sub>12</sub> Gold Clusters on MgO(100) *F* Centers Using Density-Functional Theory. *Phys. Rev. Lett.* **108**, 126101 (2012).
6. Kolsbjerg, E. L., Peterson, A. A. & Hammer, B. Neural-network-enhanced evolutionary algorithm applied to supported metal nanoparticles. *Phys. Rev. B* **97**, 195424 (2018).

# Layered double hydroxide (LDH) derived multinary magnesio-ferrites as alternative precursors for ammonia synthesis catalysts

*J. Folke<sup>1</sup>, H. Song<sup>1</sup>, K. Kähler<sup>1</sup>, D. Rein<sup>2</sup>, K. Friedel Ortega<sup>2</sup>, H. Ruland<sup>1</sup>, M. Behrens<sup>2</sup>, R. Schlögl<sup>1</sup>*

<sup>1</sup> *MPI for Chemical Energy Conversion, Mülheim an der Ruhr, Germany*

<sup>2</sup> *University Duisburg-Essen, Essen, Germany*

## Introduction

One of the most important processes of the chemical industry is the NH<sub>3</sub>-synthesis over Fe-based catalysts (Haber-Bosch process) [1]. With its usage in fertilizer production NH<sub>3</sub> is essential for feeding today's world population. Due to the possible usage of NH<sub>3</sub> as a hydrogen carrier for the storage of renewable energies, it is likely that the importance of NH<sub>3</sub> will even increase in the future [2].

Although the Haber-Bosch process is already performed for more than 100 years, its further optimization is ongoing [3]. Due to thermodynamic and kinetic limitations the NH<sub>3</sub> synthesis needs to be performed at high pressures and temperatures. The Fe-catalyzed NH<sub>3</sub> synthesis is a highly structural sensitive reaction and even for the greatly optimized industrial catalyst some studies estimate that only less than ca. 5 % of the Fe surface is actually covered with catalytic active centers [3]. Countless studies were performed on the nature of the Fe-based ammonia synthesis catalyst. Most of the experimental methods can only be performed with idealized materials and/or at low pressures, which still leaves a "material" and a "pressure gap" to industrial application.

This work is focusing on model catalysts for NH<sub>3</sub> synthesis derived from LDH materials. Due to a broad variability of LDH materials in composition and structure it is possible to investigate the influence of promoters and the structural sensitivity of the reaction under industrial relevant conditions. Furthermore, the LDH-based precursors can be synthesized under relatively mild conditions (50 °C) compared to the very harsh fusion processes (> 1600 °C) of recent industrial catalysts [4].

## Experimental

For the catalytic test a commercial flow set-up was used equipped with a guard and a synthesis reactor as well as an online IR-detector (Emerson X-stream) for quantitative gas analysis of NH<sub>3</sub> and H<sub>2</sub>O. 1 g catalyst precursor was activated in a

synthesis gas flow (75 % H<sub>2</sub>, 25 % N<sub>2</sub>) by reducing it to  $\alpha$ -Fe applying a heating rate of 1 K/min up to 500 °C and at low pressures. The catalytic tests were performed at 325-500 °C and 90 bar.

## Results

The LDH-based materials exhibit already with only Mg as a structural promoter a clear catalytic activity, even compared to an optimized and multipromoted industrial catalyst. A further improvement of the activity could be obtained by optimizing the phase purity of the precursor and the addition of K as an additional promoter (Figure 1). The optimized phase purity is achieved by increasing the aging time from 1 to 24 h during the synthesis of the LDH phase.

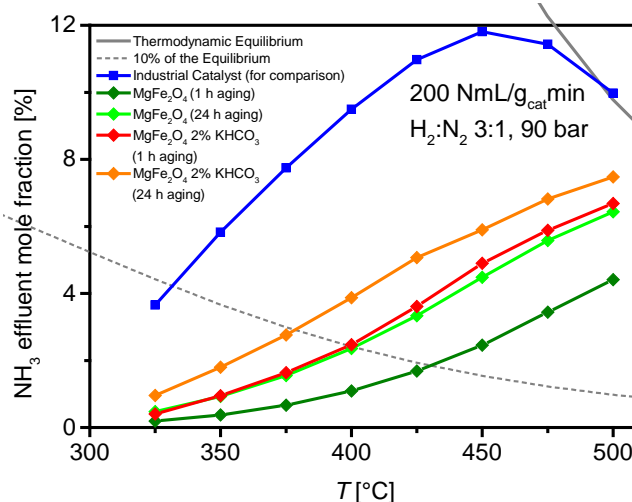


**Fig. 1:** NH<sub>3</sub> synthesis activity vs. temperature of MgFe<sub>2</sub>O<sub>4</sub> with and without K promotion.

Ex-situ characterization of the MgFe<sub>2</sub>O<sub>4</sub> materials shows a dissociation into agglomerates of nanoparticles (ca. 100 nm) with separated phases of  $\alpha$ -Fe and MgO (Figure 2). This specific nanostructure leads to a high specific iron surface area.

A further optimization of the catalysts can be achieved by the introduction of additional promoters like Co and Al as well as a variation of preparation and pretreatment conditions to influence the precursor phase and structure.

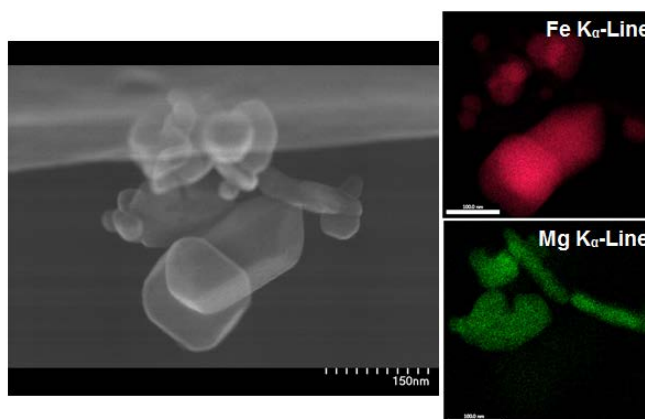


**Fig. 2:** SEM (left) and EDX mapping (right) of MgFe<sub>2</sub>O<sub>4</sub> after catalytic testing.

## References

- [1] M. Appl, *Ammonia, 2. Production*, Ullmann's Encyclopedia of Industrial Chemistry (2012).
- [2] J. O. Jensen, A. P. Vestbø, Q. Li, N.J.Bjerrum, *Journal of Alloys and Compounds*, 446-447(2007) 723-728.
- [3] R. Schlögl, in *Handbook of Heterogeneous Catalysis*, G. Ertl, H. Knötzinger, F. Schüth, J. Weitkamp (Eds.), Wiley-VCH 2nd edition (2008).
- [4] K. F. Ortega, D. Rein, C. Lüttmann, J. Heese, F. Özcan, M. Heidelmann, J. Folke, K. Kähler, R. Schlögl, M. Behrens, *ChemCatChem*, 9(2017) 659-671.

# Employing acid treatment to uncover the nature and quantity of active sites on bulk transition metal sulfides

*Hui Shi<sup>1</sup>, Manuel Wagenhofer<sup>1</sup>, Sylvia Albersberger<sup>1</sup>, Oliver Y. Gutiérrez<sup>1,2</sup>, Johannes A. Lercher<sup>1</sup>*

<sup>1</sup>*Technische Universität München, Department of Chemistry and Catalysis Research Center, Lichtenbergstraße 4, 85748 Garching, Germany*

<sup>2</sup>*Present address: Pacific Northwest National Laboratory, 902 Battelle Blvd, Richland, WA 99354, USA*

## Introduction

Industrial catalysts for hydrotreating crude petroleum feedstocks are comprised of Al<sub>2</sub>O<sub>3</sub>-supported or self-supported molybdenum and tungsten sulfides, promoted with cobalt or nickel. Key quests in fundamental and applied research are to decipher the structure of the active sites in such complex compositions and to maximize their catalytic activities for a number of H<sub>2</sub>-involving reactions removing heteroatoms and saturating aromatic rings.[1] Despite decades of research efforts, it has remained challenging to correlate, in a quantitative manner, the concentration and intrinsic properties of active sites in these complex catalysts with their activities, due mainly to the concomitant formation of Ni(Co) sulfide crystals along with the active Ni(Co)-incorporated Mo(W)S<sub>2</sub> phase.[2] The segregated Ni(Co) sulfide phases themselves are generally perceived to be hardly active in the various hydrotreating reactions of interest, thus adding inert mass and possibly also blocking active sites at the Mo(W)S<sub>2</sub> perimeter. To address these problems, we will present results showing that treatment of the sulfide materials, in their unsupported forms, in strongly acidic solutions enhances the catalytic activities of these materials and allows drawing structure-function relations for hydrodenitrogenation (HDN) and hydrodesulfurization (HDS) reactions.

## Materials and Methods

Typically, bimetallic (Ni-Mo, Ni-W) and trimetallic (Ni-Mo-W) oxide precursors were synthesized by co-precipitation or hydrothermal methods for unsupported catalysts, followed by drying in air and in-situ sulfidation in liquid-phase mixtures of H<sub>2</sub> and S-containing hydrocarbons at elevated temperatures and pressures. For post-

synthetic treatments, the obtained sulfides were suspended in concentrated hydrochloric acid (pH -1) to dissolve the inactive and site-blocking NiS<sub>x</sub> phases, assisted with heating in some cases. The catalytic performance of acid-treated materials was evaluated in a trickle bed down-flow reactor (where sulfidation was carried out) at varying space times, temperatures and H<sub>2</sub> pressures. X-ray absorption spectroscopy, pulsed NO experiments, H<sub>2</sub>/D<sub>2</sub> scrambling, as well as several routine techniques (e.g., XRD, TEM, N<sub>2</sub> adsorption), have been employed to characterize the nature and concentration of active sites on the sulfide surfaces.

## Results

Treating unsupported sulfide materials in strongly acidic HCl solutions barely affected the morphologies and atomic arrangements of the Mo(W)S<sub>2</sub> slabs while removing a substantial fraction of Ni. The mass-specific activities for a number of hydrotreating-relevant reactions were observed to increase after acid-treatment, with the product distribution and measured activation energies affected only to a minor extent. This clearly shows that the catalytic activities stem from the same type of active site that only differed in its concentration before and after the acid treatment. However, the effect of the acid is rather complex, beyond simply providing protons that react with excessive NiS<sub>x</sub> phases. Earlier works with Al<sub>2</sub>O<sub>3</sub>-supported sulfide catalysts, including ours [1], relied on IR spectroscopy of probe molecules such as NO and dimethylpyridine to quantify the surface exposure of coordinatively unsaturated sites (CUS) associated with Ni-substituted slab edge and sulfhydryl (SH) groups. However, this approach was met with significant challenges for unsupported catalysts whose IR beam transmission was poor. Therefore, pulsed NO uptakes and H<sub>2</sub>-D<sub>2</sub> exchange experiments were used to provide proxies of active site counts. By this means, we found on acid-treated catalysts robust linear relationships between the catalytic activity and the concentration of Ni-substituted CUS or SH at the slab edge; due to the excessive presence of NiS<sub>x</sub>, these linear relations were not seen on parent sulfide counterparts.

## References

- [1] W. Luo, H. Shi, E. Schachtl, O. Y. Gutiérrez, J. A. Lercher, *Angew. Chem. Int. Ed.* **2018**, 57, 14555.
- [2] J. Hein, O. Y. Gutiérrez, E. Schachtl, P. Xu, N. D. Browning, A. Jentys, J. A. Lercher, *ChemCatChem* **2015**, 7, 3692.

# A rapid synthesis of MFI zeolite nanosponges possessing uniform mesopores

*Evgeny R. Naranov<sup>1</sup>, Alexey A. Sadovnikov<sup>2</sup>, Anton L. Maximov<sup>1,3</sup>*

*naranov@ips.ac.ru*

<sup>1</sup> Topchiev Institute of Petrochemical Synthesis, Russian Academy of Sciences, Moscow, Russia;

<sup>2</sup> Kurnakov Institute of General and Inorganic Chemistry, Russian Academy of Sciences, Moscow, Russia

<sup>3</sup> Department of Chemistry, Moscow State University, Moscow, Russia

## Subheading

The research of secondary (mesoporous) structure in zeolite materials is an actual subject [1,2]. It was shown that double-templating synthesis of micro-mesoporous materials is an appropriate way to obtain composite materials [3,4]. Recently, ultrathin MFI zeolite nanosheets were synthesized using multi-ammonium surfactant molecules as the structure-directing agent (SDA) that could function in meso and micro length scales simultaneously. The pioneering work was done by Ryoo and co-workers who developed a strategy for designing bi-functional SDA (structure-directing agent) molecules acting as micropore- and mesopore-porogenic agents [5]. A main problem with the surfactant-directed zeolites nanosheets is the long hydrothermal reaction times required for synthesis.

In the present study we attempted to decrease the synthesis time by the microwave irradiation. The result was more rapid generation of MFI nanosheets. Even at high-content of Al in the gel the synthesis took much less than 11 days at 150 °C. The results from the TEM and XRD analyses confirm the formation of MFI nanosheets. Moreover, <sup>27</sup>Al MAS NMR measurements indicate that the framework of aluminum species in the samples is practically the same as in the bulk zeolite. The catalytic study shows that MFI zeolite nanosheets are excellent supports for the catalysts in the processes such as cracking and hydrogenation. We demonstrated that the mesopores of the MFI nanosheets are not as highly ordered as in mesoporous MCM-41 materials, but it has higher specific surface area and a very narrow distribution of mesopores, compared to micro-mesoporous materials obtained by classic double-templating hydrothermal synthesis.

## Acknowledgements

This work was performed as part of TIPS RAS State Plan.

## References

- [1] D.P. Serrano, J.M. Escola, P. Pizarro, *Chem. Soc. Rev.* 42 (2013) 4004–35.
- [2] W.J. Roth, B. Gil, W. Makowski, B. Marszalek, P. Eliášová, *Chem. Soc. Rev.* 45 (2016) 3400–3438.
- [3] E.R. Naranov, A.L. Maximov, *Catal. Today* (2018).
- [4] E.R. Naranov, A.A. Sadovnikov, A.L. Maximov, E.A. Karakhanov, *Microporous Mesoporous Mater.* 263 (2018) 150–157.
- [5] M. Choi, K. Na, J. Kim, Y. Sakamoto, O. Terasaki, R. Ryoo, *Nature* 461 (2009) 246–249.



# Operation of a Rh/Ce<sub>0.75</sub>Zr<sub>0.25</sub>O<sub>2-δ</sub>-η-Al<sub>2</sub>O<sub>3</sub>/FeCrAl wire mesh honeycomb catalytic module in diesel autothermal reforming

V.N. Rogozhnikov<sup>a</sup>, N.A. Kuzin<sup>b</sup>, P.V.Snytnikov<sup>a,b,c</sup>, D.I. Potemkin<sup>a,c</sup>,  
P.A. Simonov<sup>a</sup>, V.A. Shilov<sup>a,c</sup>, N.V.Ruban<sup>a,c</sup>, A.V. Kulikov<sup>a</sup>, V.A. Sobyenin<sup>a</sup>

<sup>a</sup>Boreskov Institute of Catalysis, Novosibirsk, Russia

<sup>b</sup>UNICAT Ltd, Novosibirsk, Russia

<sup>c</sup>Novosibirsk State University, Novosibirsk, Russia

Catalytic autothermal reforming is considered as one of the most effective methods of producing hydrogen from heavy hydrocarbon fuels for solid oxide fuel cells (SOFC). Diesel is an attractive fuel because of high energy density, wide applications and well - developed infrastructure. The catalysts supported on structured carriers (FeCrAl blocks) provide controlled reaction conditions throughout the reactor volume that favorably competes, for example, fixed bed reactors. The use of the structured catalysts provides efficient heat and mass transfer, low gas dynamic resistance, and high catalyst performance that allows reducing the catalyst quantity per unit volume of the reactor. The opportunity to perform the process under controlled optimum conditions allows to increase the selectivity and minimize undesirable side reactions, such as coke formation.

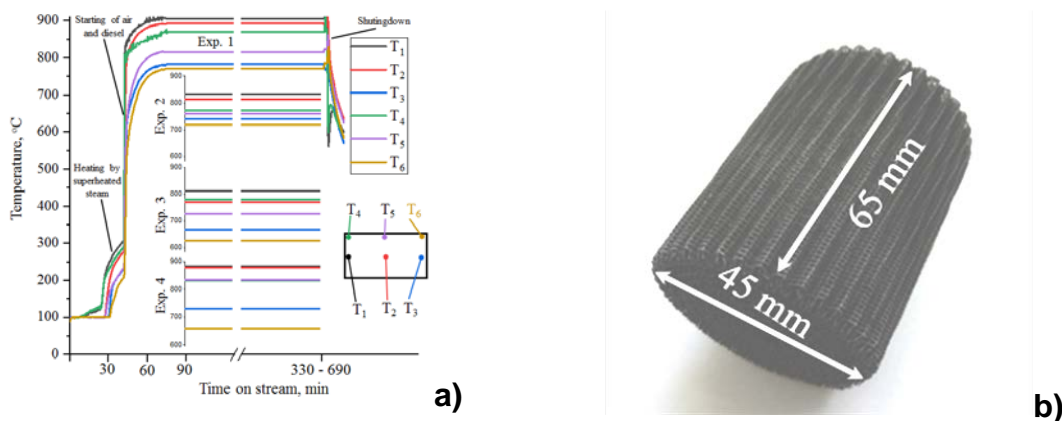


**Fig. 1.** Temperatures (°C) inside the catalytic module during typical experimental runs (a) and overview of catalytic module after tests (b).

Experimental conditions: Diesel fuel flow = 150 g / h; Water flow = 350 g / h;

Exp. 1: O<sub>2</sub>/C = 0.69; GHSV = 14600 h<sup>-1</sup>; Air flow = 784 l/h;

Exp. 2: O<sub>2</sub>/C = 0.59; GHSV = 13500 h<sup>-1</sup>; Air flow = 672 l/h;

Exp. 3: O<sub>2</sub>/C = 0.59; GHSV = 6750 h<sup>-1</sup>; Air flow = 672 l/h;

Exp. 4: O<sub>2</sub>/C = 0.69; GHSV = 7150 h<sup>-1</sup>; Air flow = 784 l/h;

In the present work, active component Rh/CZ was supported on FeCrAl metal meshes using Al<sub>2</sub>O<sub>3</sub> as a binding structural component. The obtained catalyst

Rh/CZ- $\eta$ -Al<sub>2</sub>O<sub>3</sub>/FeCrAl was tested in the laboratory and pilot scale reactors in the n-hexadecane and diesel autothermal reaction conditions (Fig.1). Winter grade diesel used in the experiments contained up to 30 % of aromatics. Operating conditions were found to provide a 100% conversion of n-hexadecane and diesel and stable catalyst activity for a long time-on-stream exposure.

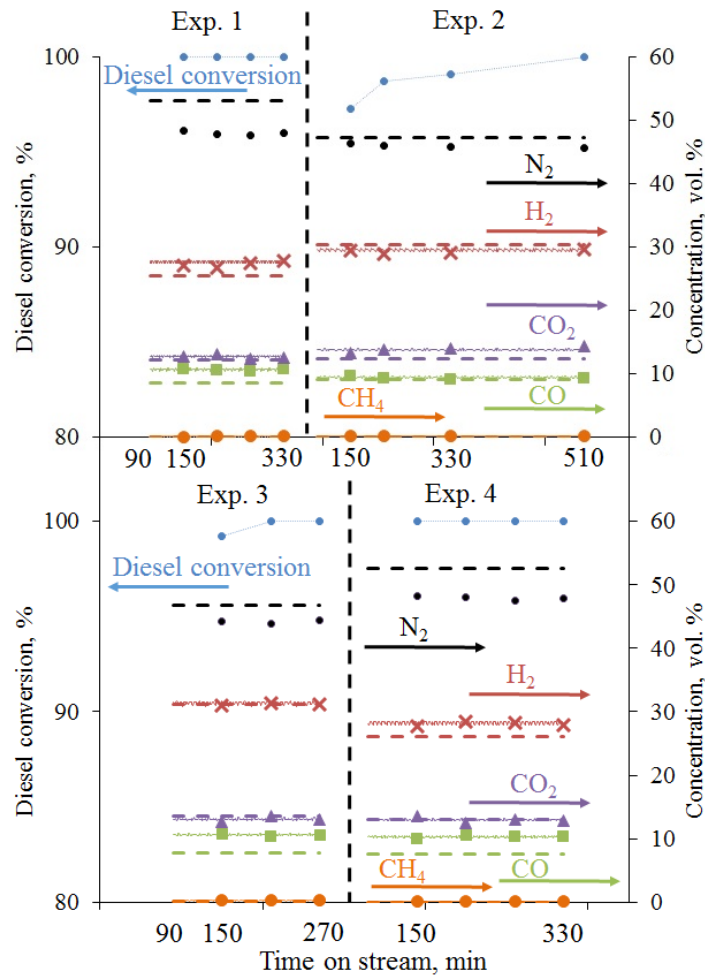


Fig. 1. Diesel conversion and reformate composition as a function of time on stream. Experimental conditions: as described at Fig 1.

It was shown that 0.24wt.%Rh/(12wt.%Zr<sub>0.25</sub>Ce<sub>0.75</sub>O<sub>2.5</sub>- $\eta$ -Al<sub>2</sub>O<sub>3</sub>)/FeCrAl catalyst provided complete n-hexadecane conversion with the maximum syngas (CO + H<sub>2</sub>) productivity of 6.2 m<sup>3</sup>Lcat<sup>-1</sup>h<sup>-1</sup> (STP) at GHSV of 13,300 h<sup>-1</sup>, while complete diesel conversion was observed at GHSV of ~7,000 h<sup>-1</sup> (Fig.2). The produced syngas can be supplied as a fuel for power generation units based on high-temperature solid oxide fuel cells.

## **Biogas reforming over Pt/doped-CeO<sub>2</sub>/Al<sub>2</sub>O<sub>3</sub> catalysts**

Renata O. Fonseca.<sup>1,2</sup>, Raimundo C. Rabelo-Neto.<sup>2</sup>, Rita C.C.<sup>3</sup>, Lisiane V. Mattos<sup>3</sup>  
Fabio B. Noronha<sup>1,2</sup>

<sup>1</sup>Military Institute of Engineering, Chemical Engineering Department, Rio de Janeiro, Brazil

<sup>2</sup>National Institute of Technology, Catalysis Division, Rio de Janeiro, Brazil

<sup>3</sup>Fluminense Federal University, Chemical Engineering Department, Niterói, Brazil

### **1- Scope**

The emission of biogas produced by the anaerobic digestion of organic matter to the atmosphere may contribute significantly to the greenhouse effect. Thus, the conversion of biogas into synthesis gas by dry reforming of methane (DRM) is a promising technology for energy generation through fuel cells since it can promote the sustainable use of natural resources as well as the reduction of greenhouse gases emissions [1]. However, one of the major problems of this process is the deactivation of the catalysts due to carbon [2]. Ceria based oxides exhibit a high oxygen exchange capacity that promotes the mechanism of carbon removal. Moreover, the addition of dopants promotes the oxygen mobility due to the formation of a solid solution, improving the carbon removal [1,3]. Furthermore, the deposition of ceria-mixed oxides over a high-surface area oxide such as alumina improves the metal dispersion that also avoids carbon deposition. Thus, the aim of this work is to investigate the performance of Pt supported on cerium oxide doped with Gd, Nb and Zr deposited on alumina for DRM reaction.

Ceria-doped oxides were prepared by co-impregnation of alumina with an aqueous solution of cerium (IV) ammonium nitrate and the dopant precursor salts. After calcination at 1073 K, the catalysts (1 wt.% Pt) were synthesized by incipient wetness impregnation of the supports with an aqueous solution of H<sub>2</sub>PtCl<sub>6</sub> and calcined at 673 K. The samples were characterized by N<sub>2</sub> adsorption, *in situ* X-ray diffraction (XRD), XANES at Ce L<sub>III</sub>-edge, dehydrogenation of cyclohexane and temperature-programmed oxidation (TPO). The DRM reaction was carried out at 1073 K, using CH<sub>4</sub>/CO<sub>2</sub> = 1.0.

### **2- Results and Discussion**

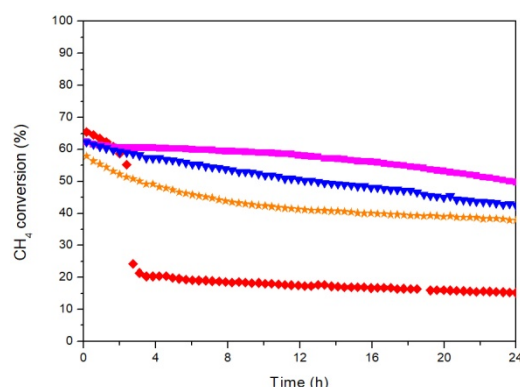
The diffractograms of calcined samples suggest the formation of solid solution for the samples containing Gd and Zr. *In situ* XRD patterns obtained during reduction showed that increasing the temperature led to a shift of the characteristic lines of

CeO<sub>2</sub> to lower 2θ positions and an increase in the lattice parameter. This could be attributed to the partial reduction of Ce<sup>4+</sup> to Ce<sup>3+</sup>. The XANES spectra revealed that the fraction of Ce<sup>3+</sup> was approximately the same for all samples. Before DRM, Pt/Al<sub>2</sub>O<sub>3</sub> exhibited the highest metal dispersion (Table 1). The lowest values of Pt dispersion were obtained for Pt/CeGd/Al<sub>2</sub>O<sub>3</sub> and Pt/CeZr/Al<sub>2</sub>O<sub>3</sub>. After DRM, a reduction in Pt dispersions was observed for all catalysts, mainly for Pt/Al<sub>2</sub>O<sub>3</sub> and Pt/CeNb/Al<sub>2</sub>O<sub>3</sub>. The CH<sub>4</sub> and CO<sub>2</sub> conversions strongly decreased during the reaction over Pt/Al<sub>2</sub>O<sub>3</sub> catalyst (Fig. 1). For the other samples, the deactivation was less pronounced. The amount of carbon formed during DRM (obtained by TPO analysis) showed that Pt/Al<sub>2</sub>O<sub>3</sub> exhibited the highest carbon formation. All other samples exhibited a very low carbon deposition, Thus, the deactivation of Pt/Al<sub>2</sub>O<sub>3</sub> could be attributed to Pt sintering as well as carbon deposition. In the case of the ceria doped samples, the lost of activity was likely due to Pt sintering.

**Table 1.** Pt dispersion of fresh and used catalysts and the amount of carbon deposited during the DRM for 24 h of TOS.

Catalyst	D (%)		mgC/g <sub>cat</sub> .h
	Fresh	Used	
Pt/Al <sub>2</sub> O <sub>3</sub>	42	29	0,45
Pt/CeGd/Al <sub>2</sub> O <sub>3</sub>	16	12	0,20
Pt/CeNb/Al <sub>2</sub> O <sub>3</sub>	24	15	0,07
Pt/CeZr/Al <sub>2</sub> O <sub>3</sub>	14	11	0,12

**Figure 1.** (a) CH<sub>4</sub> conversion versus TOS for: (♦) Pt/Al<sub>2</sub>O<sub>3</sub>, (■) Pt/CeGd/Al<sub>2</sub>O<sub>3</sub>, (✦) Pt/CeNb/Al<sub>2</sub>O<sub>3</sub>, (▼) Pt/CeZr/Al<sub>2</sub>O<sub>3</sub> during DRM at 1073K



### 3- Conclusion

The results revealed that the addition of ceria-mixed oxide suppressed the deposition of carbon on the surface of Pt particles. This is likely due to the mechanism of carbon removal promoted by the oxygen vacancies and Ce<sup>3+</sup> species created during the reduction. Moreover, Pt sintering is responsible for the deactivation of the doped ceria samples.

### References

1. Fonseca, R.O., Silva, A.A.A., Signorelli, M.R.M., Neto, R.C.R., Noronha, F.B., Colman, R.C., Mattos, L.V. *Journal of Brazilian chemical society* 25, 2356 (2014).
2. Seshan, K., Tenborge, H.W., Hally, W., Vankeulen, A.N.J., Boss, J.R.H. *Studies in surface science and catalysis* 81, 285 (1994).
3. Kaspar, J., Fornasiero, P., Graziani, M. *Catalysis Today* 50, 285 (1999).

# Activity Increase and Aging Behavior of Mn-doped Hydrotalcite-Derived Ni-Al Catalysts for the Methanation Reaction of CO<sub>2</sub>

*Thomas Burger, Philip Reuschl, Olaf Hinrichsen*

*Technical University of Munich, Department of Chemistry, Lichtenbergstr. 4, 85748 Garching near Munich, Germany, Technical University of Munich, Catalysis Research Center, Ernst-Otto-Fischer-Straße 1, 85748 Garching near Munich, Germany*

## Introduction

The highly exothermal character ( $\Delta H_R = -165 \text{ kJ mol}^{-1}$ ) of the CO<sub>2</sub> methanation reaction limits the maximum CH<sub>4</sub> yield at high temperature and therefore leads to a demand for highly active catalysts to achieve decent CH<sub>4</sub> yields at mild conditions. Recently, we brought up Mn as an efficient promoter to enhance the activity of co-precipitated hydrotalcite-derived Ni-Al (molar ratio Ni/Al = 1) catalysts.[1, 2] In this study, the deactivation behaviors of co-precipitated Ni-Mn-Al and Ni-Al catalysts, coupled with detailed characterization of fresh and spent catalyst samples, are compared to get further insights into the role of the Mn and its impact on kinetics.

## Experimental

The Ni-Al and Ni-Mn-Al catalysts were prepared via co-precipitation at constant pH of 9 and 30 °C, calcined at 450 °C, and reduced at 485 °C. Their initial catalytic activity was evaluated under differential conditions at 230 °C, 4 bar, and 600 NL g<sub>cat</sub><sup>-1</sup> h<sup>-1</sup> (Ar/H<sub>2</sub>/CO<sub>2</sub> = 75/4/1). Then, the catalysts were subjected to aging conditions at 450 °C and 8 bar at a reactant flow of 18 NL g<sub>cat</sub><sup>-1</sup> h<sup>-1</sup> (Ar/H<sub>2</sub>/CO<sub>2</sub> = 5/4/1) to simulate hotspot conditions. To track catalyst aging under differential conditions, the catalyst bed was periodically cooled down to 230 °C and the activity was re-evaluated under the conditions mentioned above. After 0 h, 6 h, 36 h, and 72 h, the catalysts were removed from the setup under inert conditions for material characterization.

## Results and Discussion

Fig. 1 illustrates the decrease of the weight time yield (WTY) of CH<sub>4</sub> over aging time. Ni-Al loses 28 % of its initial activity within the first 2 h of aging, and reaches a stable level after 36 h at 49 %. In contrast, Ni-Mn-Al, which initially features a 92 % higher

WTY than Ni-Al, loses 23 % of activity within the first 2 h of aging. In contrast to Ni-Al, the WTY decreases up to 72 h at a low deactivation rate. Table 1 shows that the apparent activation energy is slightly higher for Ni-Mn-Al, but that they do not change over aging time. Both the initial values as well as the decays of the Ni surface areas and the BET surface areas, attributed to sintering effects, are very similar, which highlights that the impact of Mn on the Ni surface area and the catalyst structure, including sintering effects, is rather low. Therefore, the improved methanation activity of the fresh Ni-Mn-Al catalyst is supposed to be caused by the increased CO<sub>2</sub> uptake capacity (+ 65 % compared to Ni-Al). CO<sub>2</sub>-TPD and *in situ* IR spectroscopy show a higher number of medium basic sites, which were reported to enhance CO<sub>2</sub> methanation activity,[3] on Ni-Mn-Al.[1] The crucial role of basic site density is in line with the further decrease of CO<sub>2</sub> uptake and WTY(CH<sub>4</sub>) for Ni-Mn-Al from 36 h to 72 h of aging, while all other relevant characterization data stay constant (*c.f.* Ni-Al).

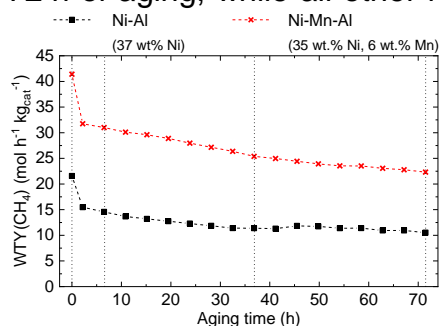


**Fig. 1:** WTY(CH<sub>4</sub>) for Ni-Al and Ni-Mn-Al as a function of aging time.

**Table 1:** Sorption data and activation energies as a function of aging time.

Catalyst	$t_a$ h	$S_{Ni}$ $m^2 g_{cat}^{-1}$	$D_c^a$ nm	$S_{BET}$ $m^2 g_{cat}^{-1}$	$U(CO_2)$ $\mu mol g_{cat}^{-1}$	$E_A$ $kJ mol^{-1}$
Ni-Al	0	30.1	3.2	293	199	74.1±2.1
	6	15.3	4.2	207	123	73.9±3.5
	36	12.2	4.8	131	84	75.1±1.7
	72	12.1	4.8	132	82	74.1±2.9
Ni-Mn-Al	0	29.4	3.3	294	328	78.9±0.4
	6	18.8	4.1	210	181	80.6±0.7
	36	12.7	4.5	135	148	80.6±1.1
	72	12.7	4.5	130	131	82.5±0.7

<sup>a</sup> crystallite size determined by XRD, Ni reflex at  $2\theta = 51.7^\circ$ .

## Conclusion

The data suggest that the improved methanation performance of Ni-Mn-Al is caused by an increased CO<sub>2</sub> uptake capacity caused by the introduction of Mn. Besides, an electron-donating effect of basic Mn oxides on the Ni centers cannot be excluded so far. CO<sub>2</sub>-TPD on spent catalyst samples may provide further insights into the nature and the decay of basic sites as a function of aging time. Comparison of the CO<sub>2</sub> methanation kinetics over Ni-Mn-Al to the kinetic model derived for Ni-Al [4] may help to derive descriptors for the improved methanation performance of Ni-Mn-Al.

## References

- [1] T. Burger, F. Koschany, O. Thomys, K. Köhler, O. Hinrichsen, *Appl. Catal. A*, 558 (2018) 44–54.
- [2] T. Burger, F. Koschany, A. Wenng, O. Thomys, K. Köhler, O. Hinrichsen, *Catal. Sci. Technol.*, 8 (2018) 5920–5932.
- [3] Q. Pan, J. Peng, T. Sun, S. Wang, S. Wang, *Catal. Commun.*, 45 (2014) 74–78.
- [4] F. Koschany, D. Schlereth, O. Hinrichsen, *Appl. Catal. B*, 181 (2016) 504–516.

# IN SITU STUDY OF Cu–Fe–Al COMPOSITE CATALYSTS IN REACTION OF CO OXIDATION IN THE PRESENCE OF H<sub>2</sub>O

*Z.S. Vinokurov*<sup>1,2</sup>; *A.A. Saraev*<sup>1,2</sup>; *O.A. Bulavchenko*<sup>1,2</sup>; *A.V. Fedorov*<sup>1</sup>;  
*V.V. Kaichev*<sup>1,2</sup>; *A.M. Tsapina*<sup>1</sup>

*1 Borekov Institute of Catalysis SB RAS, Novosibirsk, Russia*

*2 Novosibirsk State University, Novosibirsk, Russia*

In our recent work we studied the catalytic activity of Fe-Al and Cu-Fe-Al nanocomposite catalysts obtained from the melts of aluminium, iron, and copper salts in the oxidation of CO [1]. The Fe-Al composites has been shown to have moderate activity in the low-temperature CO oxidation with the optimal composition of 82%wt Fe<sub>2</sub>O<sub>3</sub> and 18%wt Al<sub>2</sub>O<sub>3</sub>. The promotion of this composition with Cu led to a significant increase in activity. The composition with 5%wt CuO was found to have the minimal activation energy of CO oxidation. The next step was the structural study of the Fe<sub>82</sub>Al<sub>18</sub> and Cu<sub>5</sub>Fe<sub>78</sub>Al<sub>17</sub> catalysts in reduction (1%CO) and redox (CO:O<sub>2</sub> = 2:1) conditions [2] to reveal the chemical state of copper and iron, phase composition of the catalyst during the reduction by CO and in the oxidation of CO. We observed the formation of highly dispersed CuO particles for Cu<sub>5</sub>Fe<sub>78</sub>Al<sub>17</sub> catalyst that could easily reduce to metal in CO flow even at low temperature and provide CO activation.

The catalytic oxidation of fuel in a fluidized bed suggests the presence of substantial amounts of water vapor, which in turn can affect the catalyst behavior [3]. In this work we continued our study of Cu-Fe-Al nanocomposite catalysts under close-to-real conditions.

## **Acknowledgement**

This work was supported by RSF (project No. 17-73-20157). The XRD experiments were carried out using the equipment of the shared research center (BINP, Novosibirsk, Russia).

## **References**

- [1] Fedorov, A.V., Tsapina, A.M., Bulavchenko, O.A., Saraev, A.A., Odegova, G.V., Ermakov, D.Y., Zubavichus, Y.V., Yakovlev, V.A., Kaichev, V.V., 2018. *Catal. Lett.* 148, 3715–3722. <https://doi.org/10.1007/s10562-018-2539-5>.
- [2] A.A. Saraev, A.M. Tsapina, A.V. Fedorov, A.L. Trigub, O.A. Bulavchenko, Z.S. Vinokurov, Y.V. Zubavichus, V.V. Kaichev, *Rad. Phys. Chem.* In press. <https://doi.org/10.1016/j.radphyschem.2018.11.025>.
- [3] Zhu M, Rocha TCR, Lunkenbein T, Knop-Gericke A, Schlögl R, Wachs IE, *ACS Catal.* 2016, 6, 2, 722-732. <https://doi.org/10.1021/acscatal.5b02594>.

# Nickel Nanoparticles Supported on Graphene Aerogels as Catalysts for Ammonia Decomposition Reaction

*Tolga Kocer, Dept. of Chemical & Biological Engineering, Koç University, Istanbul, Turkey; F. Eylul Sarac Oztuna, Dept. of Material Science and Engineering, Koç University, Istanbul, Turkey; Samira Kurtoglu, Dept. of Chemical & Biological Engineering, Koç University, Istanbul, Turkey; Alper Uzun\*, Dept. of Chemical & Biological Engineering, Koç University, Istanbul, Turkey; Ugur Unal\*, Dept. of Chemistry, Koç University, Istanbul, Turkey*

*\*Corresponding Authors, E-mail: auzun@ku.edu.tr, E-mail: ugunal@ku.edu.tr*

## Introduction

Due to inevitable depletion of fossil fuels, strong need is arisen for alternative and clean energy sources. Hydrogen is one of the most promising ones thanks to its high energy density and CO<sub>x</sub>-free combustion. Nevertheless, it requires very high pressures or very low temperatures for storage and transportation. To surpass this issue, storing it chemically in ammonia (NH<sub>3</sub>) has been proposed since it has low liquification pressure (8-10 bar) at room temperature, high hydrogen weight content (17.7 wt%), well-established infrastructure and most importantly, it does not cause any CO<sub>x</sub>-emission. [1] High performance catalysts for ammonia decomposition reaction are Ru-, Ni-, Co-, and Fe- based ones and among these metals, Ru is the most active one. However, because of the scarcity and high price of Ru, Ni is widely utilized. [2] As support materials, graphene aerogels (GAs) are very promising thanks to their very high specific surface area and electrical conductivity, which provide highly dispersed metal nanoparticles and improved electron transfer. [3]

## Methods

In this study, graphene oxide solution was synthesized via modified Hummer's method. [4] Then, GAs were prepared by hydrothermal treatment of graphene oxide solution. [3] After GA synthesis, different types of catalysts were produced via simple impregnation by using different nickel precursors. Ni/GA, Ni-Ac/GA and Ni-EA/GA were produced by immersing GA into Ni(NO<sub>3</sub>)<sub>2</sub>·6H<sub>2</sub>O, Ni(acac)<sub>2</sub>, and Ni-ethanolamine complex ethanolic solutions, respectively. Following impregnation, supercritical CO<sub>2</sub> drying was performed to preserve the porous structure of the aerogel. Before catalytic tests, all catalysts were reduced under H<sub>2</sub>/Ar mixture at 600 °C for 2 hours. Then, catalytic performance tests were performed in a tubular quartz



reactor in a split furnace under the flow of pure ammonia. The effluent stream was directly sent to a mass spectrometer, which had been calibrated for N<sub>2</sub>, H<sub>2</sub>, and NH<sub>3</sub> prior to catalytic measurements.

## Results & Discussion

Field emission scanning electron microscopy images of the catalysts revealed that nickel nanoparticles were uniformly dispersed on graphene aerogel with an average diameter of 10-20 nm. These results are also confirmed by X-ray diffraction analysis. Furthermore, nickel loadings of the catalysts can be tuned with the concentration of impregnation solutions, which were determined by thermogravimetric analysis. Accordingly, all the samples contain approximately 10 wt% Ni. After catalytic measurements, it has been seen that Ni-Ac/GA showed the best performance among others with 70.2% conversion at 600 °C and 30,000 mL NH<sub>3</sub> h<sup>-1</sup> g<sub>cat</sub><sup>-1</sup>, outperforming most of the similar catalysts in the literature. By comparison, reduced graphene oxide supported Ni (10 wt%) exhibited 55 % conversion at same temperature and space velocity. [5] This study illustrated that the catalytic performance can be tuned by simple modifications.

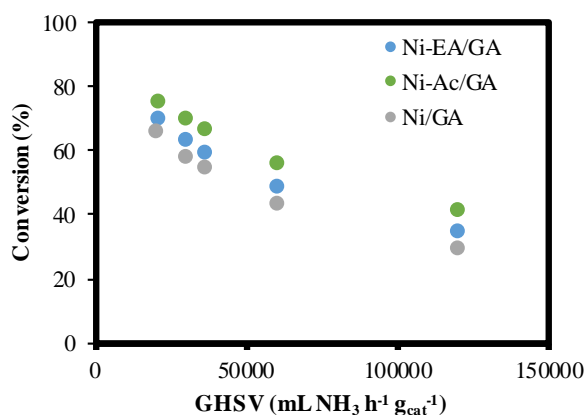


**Figure 1:** Change of ammonia conversion with space velocity on prepared nickel catalysts on graphene aerogel supports. Data recorded at 600 °C by varying the space velocity.

This project is funded by Tubitak with the project number of 117M153.

## References

- [1] F. Schüth, R. Palkovits, R. Schlögl, D.S. Su, *Energy Environ. Sci.* 5 (2012) 6278–6289.
- [2] T.E. Bell, L. Torrente-Murciano, *Top. Catal.* 59 (2016) 1438–1457.
- [3] F.E. Sarac Oztuna, S.B. Barim, S.E. Bozbag, H. Yu, M. Aindow, U. Unal, C. Erkey, *Electrochim. Acta.* 250 (2017) 174–184.
- [4] T. Beyazay, F.E. Sarac Oztuna, U. Unal, *Electrochim. Acta.* 296 (2019) 916–924.
- [5] T. Meng, Q.-Q.Q. Xu, Y.-T.T. Li, J.-L.L. Chang, T.-Z.Z. Ren, Z.-Y.Y. Yuan, *J. Ind. Eng. Chem.* 32 (2015) 373–379.

## **Effect of iridium presence on the properties of anode material for high-temperature fuel cells with solid oxides electrolyte**

*M. Ruggiero-Mikołajczyk, Jerzy Haber Institute of Catalysis and Surface Chemistry, Polish Academy of Sciences, Niezapominajek 8, 30-239 Cracow, Poland; G. Mordarski, Jerzy Haber Institute of Catalysis and Surface Chemistry, Polish Academy of Sciences, Niezapominajek 8, 30-239 Cracow, Poland; F. Rivadulla, Centro de Investigación en Química Biológica y Materiales Moleculares (CIQUS), c/Jenaro de la Fuente s/n, Campus Vida, Universidad de Santiago de Compostela, 15782-Santiago de Compostela, Spain; M. Śliwa, Jerzy Haber Institute of Catalysis and Surface Chemistry, Polish Academy of Sciences, Niezapominajek 8, 30-239 Cracow, Poland; K. Samson, Jerzy Haber Institute of Catalysis and Surface Chemistry, Polish Academy of Sciences, Niezapominajek 8, 30-239 Cracow, Poland; D. Rutkowska-Zbik, Jerzy Haber Institute of Catalysis and Surface Chemistry, Polish Academy of Sciences, Niezapominajek 8, 30-239 Cracow, Poland*

In view of the exhaustion of fossil fuel resources and the simultaneous increase in demand for energy, fuel cells deserve special attention as an alternative power generators. The aim of this study is to improve the functioning of anodic materials dedicated for use in high-temperature fuel cells based on electrolyte from solid oxides i.e. SOFC (*solid oxide fuel cell*). This modification mainly concerns the elimination of one of the still existing problems associated with the deposition of solid carbon during operation of a cell supplied with hydrocarbon fuel. The research objective includes modification of the surface of the anode by coating a thin cathodic layer on it, which prevents blocking active anode centres responsible for the correct course of electrochemical oxidation of hydrocarbon fuel.

To study the effect of iridium as an additive, catalytic activity studies on modified systems and electrochemical measurements were carried out, and their physico-chemical characteristics were also performed. Cathode materials such as:  $\text{La}_{0.6}\text{Sr}_{0.4}\text{Co}_{0.2}\text{Fe}_{0.8}\text{O}_3$  (LSCF) and  $\text{La}_{0.6}\text{Sr}_{0.4}\text{Co}_{0.2-x}\text{Ir}_x\text{Fe}_{0.8}\text{O}_3$  (LSCFIr) were tested for determination of their usefulness in a system that prevents the solid carbon deposition during the operation of the cell. A hydrocarbon conversion test was carried out for individual materials and their surface condition was checked after completion of the process. The comparison of the anodes with a thin cathode layers shows that the conversion of methane on the sample with iridium is higher than on the sample without this addition. Electrochemical impedance spectroscopy (EIS) measurements in controlled compositions of oxidizing atmosphere at four temperatures: 700, 750, 800, 850 °C were carried out. Analysis of the obtained results indicates that iridium doped LSCF exhibits better oxidizing properties than the LSCF without iridium.

Acknowledgements: We thank Dr Jan Wyrwa from AGH University of Science and Technology for technical support in implementation of the above study.

# Cascade production of alkyl levulinates from furfural

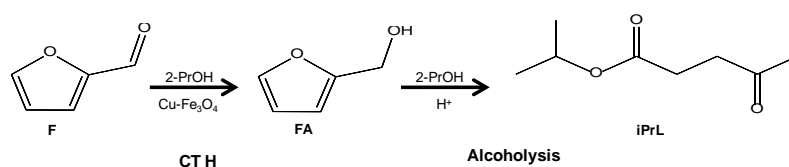
*Hilda Gómez Bernal*<sup>1\*</sup>, *Tiziana Funaioli*<sup>1</sup>, *Anna Maria Raspolli-Galletti*<sup>1</sup>.

<sup>1</sup>*Dipartimento di Chimica e Chimica Industriale, Università di Pisa. Via Giuseppe Moruzzi, 13, 56124 Pisa, Italy*

Alkyl levulinates are promising bio based molecules with several applications in strategic sectors, substituting current chemicals produced from petro-chemical routes. This work explores the production of isopropyl levulinate from furfural by a two-step microwave assisted cascade process using simply synthesized magnetically recoverable Cu-Fe<sub>3</sub>O<sub>4</sub> catalysts in the selective transfer hydrogenation of furfural to furfuryl alcohol and commercial sulfonic resins to catalyze FA rearrangement to isopropyl levulinate. The cascade process results quite promising allowing adequate tune up of reaction conditions in each catalytic step.

## Scope

New technologies for biofuel production involving biomass conversion are eagerly sought. In this context, alkyl levulinates possess outstanding properties as biofuels and fuel blends due to their ability to raise the oxygen content in fuels allowing a more complete combustion thus reducing the release of harmful gases [1]. Producing alkyl levulinates from abundant platforms such as furfural (F), readily obtained from hemicelluloses [2], is highly desirable. This process involves a first hydrogenation step to furfuryl alcohol (FA) and a subsequent acid-catalyzed ring opening of FA in alcoholic media. In this work, catalytic transfer hydrogenation (CTH) of F was performed with Cu-Fe<sub>3</sub>O<sub>4</sub> magnetic catalyst in presence of 2-propanol as solvent and H-donor. Afterwards, the alcoholysis of FA-rich CTH liquors to isopropyl levulinate (iPrL) is investigated using commercial sulfonic resins Amberlyst 70, as depicted in Scheme 1. Throughout the process, microwave dielectric heating was employed.



Scheme 1. Cascade process for furfural valorization to isopropyl levulinate.

## Results and discussion

Cu-Fe<sub>3</sub>O<sub>4</sub> catalyst, used in the CTH of F, was prepared by a green hydrothermal method consisting in the co-decomposition of iron(II) acetate and Cu carbamate

( $\text{Cu}_2(\text{O}_2\text{CNEt}_2)_4 \cdot 2\text{NHEt}_2$ ) in 96% aqueous ethanol through MW-irradiation. Ex-situ reduction of the obtained catalyst containing 3.9 wt% of copper was performed in 2-propanol with 50 atm  $\text{H}_2$  at 180°C for 5 h.

Transfer hydrogenation of F in 2-PrOH was tested at temperatures ranging from 140-190°C with the as-obtained and reduced  $\text{Cu-Fe}_3\text{O}_4$  catalyst. Results in Table 1 show that reduced copper species enhance both activity and selectivity of this catalyst probably by activating 2-PrOH through the metal hydride route, reaching the best FA yields at 185°C.

Table 1. Furfural CTH with  $\text{Cu-Fe}_3\text{O}_4$  at different conditions<sup>a</sup>

Run	Pre-treatment	T (°C)	t (h)	X (mol%)	$Y_{\text{FA}}$ (mol%)	$S_{\text{FA}}$ (mol%)
1	-	185	2	14	10	75
2	reduced	160	2	38	27	70
3	reduced	180	2	61	56	92
4	reduced	185	2	64	61	96
5 <sup>b</sup>	$\text{Fe}_3\text{O}_4$	185	2	25	14	54

<sup>a</sup> F/Cu molar ratio of 86 mol/mol. F/catalyst wt ratio of 5 wt/wt

<sup>b</sup> F/catalyst weight ratio of 5 wt/wt.

Increasing catalyst loading to 43 F/Cu molar ratio led to 71% FA yield. Moreover, the catalyst proved stable during three reaction cycles.

The subsequent alcoholysis of FA-rich CTH liquors to yield iPrL was performed using Amberlyst 70 sulfonic resin and takes place through the intermediate formation of furfuryl isopropyl ether (iPrFE) (Fig.1). Temperatures as low as 120°C enhance iPrL yields reducing degradation reactions such as diisopropyl ether formation and FA polymerization.

## Conclusions

The obtained results are quite promising since they demonstrate the possibility of reaching high iPrL yields from FA rich streams adopting simple commercial sulfonic resins, without the intermediate expensive FA isolation notwithstanding the presence of unreacted F.

## References

- [1] A. Demolis, N. Essayem, F. Rataboul, ACS Sustain. Chem. Eng., 2014, 2, 1338-1352.
- [2] H. Gómez Bernal, L. Bernazzani, A.M. Raspolli Galletti, Furfural from corn stover hemicelluloses. A mineral acid-free approach, Green Chem., 2014, 16, 3734-3740.

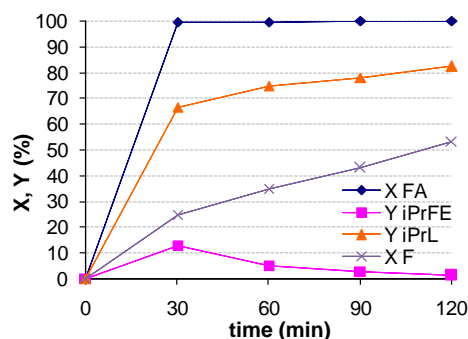


Figure 1. Alcoholysis of FA-rich CTH liquors using A70. Reaction conditions: FA (0.56 mmol) and F (0.2 mmol) in 2-prOH (1.5 ml), mmol FA/meq  $\text{H}^+$  = 6.9, T=120°C.

# Stability and reactivity of doped core-shell catalysts from *ab initio* calculations

*Jacob L. Gavartin, Schrödinger, Cambridge, UK; Caroline Krauter, Schrödinger, Mannheim, Germany; Thomas J. L. Mustard, Schrödinger, Portland, OR 97204 USA; Alexandr Fonari, Dave Giesen, Schrödinger, New York, USA; Tsuguo Morisato, Schrödinger K.K. Tokyo Japan; H. Shaun Kwak, Schrödinger, Cambridge, USA; Sudharsan Pandiyan, Schrödinger, Bangalore India; Alexander Goldberg, Mathew D. Halls, Schrödinger, San Diego, USA*

## Introduction

Novel core-shell catalysts containing non-noble metal core and a skin of just a few atomic layers of a noble metal attract significant research interest due to their reported high activity and selectivity and potential significant cost reduction [1]. However, properties of core-shell nanoparticles are found to be very sensitive to the manufacturing process. In particular, the catalyst often suffer from low durability and fast degradation through leaching or sintering. It is generally observed that skin surface stability can be enhanced by chemical modification of particle's core. However, general understanding of the mechanisms of such stabilization is lacking. In theoretical terms the surface stability is characterized by the near surface energy of mixing of base and noble metals. This energy may significantly deviate from the bulk value. It is also affected by the pH of the atmosphere above the surface (or electrolyte) and applied electrostatic potential. In this paper we discuss a general method of *ab initio* calculation of equilibrium surface composition and its application to the stability analysis of the core-shell alloys for oxygen reduction reaction (ORR) in electrocatalysis.

## Computational approach

We utilize plane wave density functional theory implemented in Quantum Espresso code [2] and combinatorial structure enumeration [3] to calculate energies for the ensembles of low Miller index metallic surfaces with varying distribution of Pt atoms and transition metals (M=Co, Ni, Ta) doped with nitrogen. Based on these calculations we evaluate equilibrium surface composition diagram as a function of composition, doping level and temperature [4]. Next, we calculate ORR activity

descriptors for the equilibrium models. O<sub>2</sub> adsorption and dissociation energies were used and compared with the d-band center analysis for the ORR activity.

The entire workflow including generation, calculations and analysis of hundreds of surface structures is implemented and executed within the Schrödinger Materials Science Suite [5].

## Discussion

Developed workflow allows simultaneous theoretical analysis of the stability and catalytic activity of the metallic structures. It is predicted that equilibrium surface may significantly deviate from the idealized core-shell structure. Base atoms of the core may significantly intermix with the noble atoms of the skin. Relative concentration of base atoms at the surface depends on the level and distribution of the N doping of the core. This concentration also vary with applied external potential, which is a likely source of the leaching observed experimentally. However equilibrium structure variations may be moderated by optimal distribution of N atoms, thus increasing surface durability.

Proposed theoretical approach helps to rationalize activity and stability of the core-shell systems towards the rational design of effective catalysts with improved stability.

## References

1. Na Tian, Bang-An Lu, Xiao-Dong Yang, *et al.* "Rational Design and Synthesis of Low-Temperature Fuel Cell Electrocatalysts", *Electrochemical Energy Reviews*, 1, 54-83 (2018).
2. P. Giannozzi, *et al.* "Advanced capabilities for materials modelling with Quantum ESPRESSO," *J. Phys.: Condens. Matter* 29 465901 (2017).
3. Gus L. W. Hart, Lance J. Nelson, and Rodney W. Forcade, "Generating derivative structures at a fixed concentration," *Comp. Mat. Sci.* 59 101-107 (2012).
4. J. L. Gavartin, M. Sarwar, D. C. Papageorgopoulos, *et al.* Exploring fuel cell cathode materials: A high throughput calculation approach. *Transactions of the Electrochemical Society* **25**(1) 1335-1344 (2009).
5. Materials Science Suite Version 3.2, Schrödinger, LLC, New York, NY, 2018.

# Steady-state kinetic analysis of CO oxidation over transition metal oxides

*Maik Dreyer, Stefanie Becker, Klaus Friedel Ortega, Malte Behrens,*

*Inorganic Chemistry, University of Duisburg-Essen, Essen*

## Introduction

Transition metal oxides (TMOs) are cost-effective materials with interesting properties for oxidation catalysis due to their wide range of accessible oxidation states. Insights into the nature of redox-active catalysts can be gained using CO oxidation as a probe reaction.<sup>[1]</sup> Several groups have shown a substantial impact of highly reactive surface oxygen species on the catalytic activity, especially for cobalt and nickel oxides studied under steady-state conditions.<sup>[2,3]</sup> In the transient regime, surface restructuring has been observed. Brittan *et al.*<sup>[4]</sup> developed a kinetic model for CO oxidation over hopcalite that includes the concentration of non-uniform surface oxygen sites to account for this particular observation. Strong indications for similar reconstruction processes have been encountered for bulk<sup>[5]</sup> and ultrathin manganese oxide films<sup>[6]</sup>. According to our kinetic data obtained under O<sub>2</sub>-rich conditions (CO:O<sub>2</sub>=1:2), manganese oxides with different initial oxidation states undergo similar surface reconstruction upon treatment in a reactive environment.

## Experimental

Manganese oxides in the forms of Bixbyite (Mn<sub>2</sub>O<sub>3</sub>), Hausmannite (Mn<sub>3</sub>O<sub>4</sub>), and Cryptomelane (K<sub>x</sub>Mn<sup>+IV</sup><sub>8-x</sub>Mn<sup>+III</sup><sub>x</sub>O<sub>16</sub>) were prepared by precipitation and subsequent calcination. For the former two, an amorphous precursor was isothermally prepared by precipitation of MnSO<sub>4</sub> and KOH at a constant pH of 11 and ageing for 1 h. Afterwards, Bixbyite was generated by subjecting the precursor to a thermal treatment at 800 °C in static air, while Hausmannite was prepared at 400 °C under otherwise similar conditions. Cryptomelane was synthesized *via* a synproportionation reaction of KMnO<sub>4</sub> and Mn(OAc)<sub>2</sub> under reflux conditions, followed by calcination at 330 °C. Characterization was performed using PXRD, N<sub>2</sub> physisorption, ATR-FTIR spectroscopy, Raman spectroscopy and XPS. Kinetic analyses of the CO oxidation reaction over the various manganese oxides were obtained in a catalyst analyzer (BELCAT-B, MicrotracBEL Corp., Japan) using a U-shaped quartz reactor containing the catalyst and silicon carbide (250-355 μm) in a 1:10 ratio.

## Results

Surface area normalized CO oxidation rates obtained under steady-state conditions in 3% CO and 6% O<sub>2</sub> decreased in the order Mn<sub>2</sub>O<sub>3</sub> > K<sub>x</sub>Mn<sup>+IV</sup><sub>8-x</sub>Mn<sup>+III</sup><sub>x</sub>O<sub>16</sub> > Mn<sub>3</sub>O<sub>4</sub>. Evidently, the initial oxidation state of manganese is insufficient to properly describe the encountered reactivity trend, which is most likely due to changes in the surface composition and structure during catalysis.<sup>[5]</sup> In addition, an initial deactivation at moderately elevated temperatures was generally observed. A similar deactivation was observed for CO oxidation experiments carried out over monolayer MnO<sub>x</sub> films grown on Pt(111) with a O<sub>2</sub>:CO ratio lower than 10.<sup>[6]</sup> However, this undesired phenomenon could be suppressed in the initial feed by a prolonged thermal treatment in a reactive environment at high conversions. These severe conditions seem to accelerate the surface reconstruction, yielding an active state that was stable for various chemical potentials of CO and oxygen (Figures 1a,b). Interestingly, the activation energies after catalyst preconditioning showed similar values in the range of 41-46 kJ mol<sup>-1</sup> for all manganese oxides (Figure 1c). However, major differences were observed in terms of the reaction orders of O<sub>2</sub>, covering a range from 0.42 to 1.12. Thus, a similar surface state is generated during reactive preconditioning, which exhibited different interactions with the gas phase oxygen depending on the initial oxidation state of manganese. Such dynamics of MnO<sub>x</sub> will be compared in our contribution to other TMOs such as CoFe<sub>2</sub>O<sub>4</sub> and LaFe<sub>1-x</sub>Co<sub>x</sub>O<sub>3</sub>.

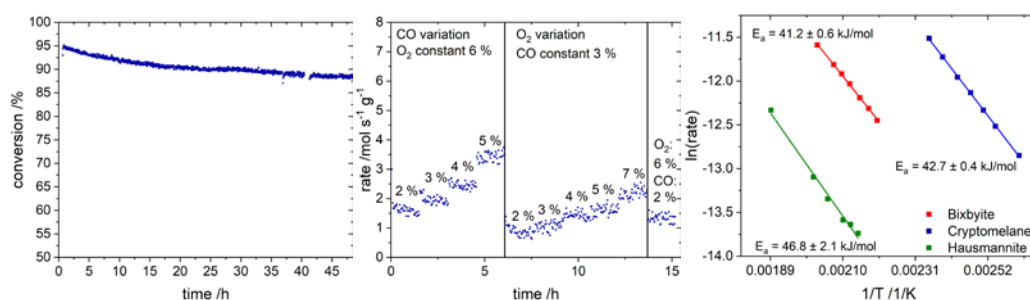


**Figure 1:** (a) CO conversion during 48 h reactive preconditioning and (b) rates at various chemical reactant potentials for Cryptomelane. (c) Arrhenius plots obtained for all catalysts after pretreatment. This research was funded by the Deutsche Forschungsgemeinschaft (DFG) within the CRC/TRR 247 "Heterogeneous Oxidation Catalysis in the Liquid Phase".

## References

- [1] H.-J. Freund, G. Meijer, M. Scheffler, R. Schlögl, M. Wolf, *Angew. Chem. Int. Ed.* **2011**, *50*, 10064.
- [2] G. A. El-Shobaky, M. M. Selim, I. F. Hewaidy, *Surf. Technol.* **1980**, *10*, 55.
- [3] G. Parravano, *J. Am. Chem. Soc.* **1953**, *75*, 1448.
- [4] M. I. Brittan, H. Bliss, C. A. Walker, *AIChE J.* **1970**, *16*, 305.
- [5] J. Xu, Y.-Q. Deng, Y. Luo, W. Mao, X.-J. Yang, Y.-F. Han, *J. Catal.* **2013**, *300*, 225-234.
- [6] Y. Martynova, M. Soldemo, J. Weissenrieder, S. Sachert, S. Polzin, W. Widdra, S. Shaikhutdinov, H.-J. Freund, *Catal. Lett.* **2013**, *143*, 1108-1115.



# Hydrogen production via steam reforming of LPG over supported metal catalysts

*Aliki Kokka and Paraskevi Panagiotopoulou*

*School of Environmental Engineering, Technical University of Crete, Chania, Greece*

## Introduction

The use of H<sub>2</sub>, in combination with fuel cells, is one of the most environmentally sound methods for the production of electrical energy [1]. Among various processes that have been proposed for H<sub>2</sub> production, steam reforming of Liquefied Petroleum Gas (LPG) is of special interest, especially in remote areas, where the existing power grids address serious problems [1]. LPG typically consists of propane (C<sub>3</sub>H<sub>8</sub>) and butane (C<sub>4</sub>H<sub>10</sub>) with various ratios depending on its source. In addition to H<sub>2</sub> and carbon oxides (CO and CO<sub>2</sub>), LPG can be converted to methane (CH<sub>4</sub>), ethane (C<sub>2</sub>H<sub>6</sub>) and ethylene (C<sub>2</sub>H<sub>4</sub>), via the reaction of CO or CO<sub>2</sub> methanation and the decomposition of C<sub>3</sub>H<sub>8</sub> and C<sub>4</sub>H<sub>10</sub>, respectively. The major issue of the LPG steam reforming reaction is carbon deposition due to decomposition of C<sub>2</sub>H<sub>6</sub>, C<sub>2</sub>H<sub>4</sub> and CH<sub>4</sub>, resulting in progressive catalyst deactivation. Thus, it is important to develop active and stable catalysts, able to convert LPG selectively to H<sub>2</sub>, suppressing the deposition of carbon on the catalyst surface. In the present study, the catalytic performance of supported metal catalysts for the title reaction is investigated with respect to the nature (Ni, Ru, Rh, Ir, Re, Pt) and loading (0-5 wt.%) of the metallic phase as well as the nature of the support (Al<sub>2</sub>O<sub>3</sub>, YSZ, CeO<sub>2</sub>, SiO<sub>2</sub>). The effects of crystallite size on the specific activity of the supported metal and of operational parameters (H<sub>2</sub>O/C<sub>3</sub>H<sub>8</sub> ratio) on the catalytic performance have been also examined.

## Experimental

Catalysts were prepared by the wet impregnation method and characterized employing nitrogen physisorption and selective chemisorption of H<sub>2</sub> (or CO). Since propane is the main component of LPG, preliminary catalytic performance tests were carried out in the temperature range of 400-800°C using a feed stream consisting of 4.5% C<sub>3</sub>H<sub>8</sub>, 0.15% Ar and 44% H<sub>2</sub>O (balance He).

## Results

Results showed that both catalytic activity and selectivity depends strongly on the nature of the dispersed metallic phase. Supported Rh catalyst exhibited superior

performance, which can be further improved with increasing Rh loading or crystallite size. Experiments conducted with the use of Rh catalysts of the same metal loading (0.5 wt.%) showed that the nature of the support affects significantly catalytic performance (Fig.1A). Propane conversion was found to be higher when Rh is supported on YSZ, compared to  $\text{Al}_2\text{O}_3$  and  $\text{SiO}_2$ , whereas  $\text{CeO}_2$ -supported catalyst presents lower activity. Typical results of product distribution obtained from 0.5%Rh/YSZ catalyst are presented in Fig. 1B. The main products detected are  $\text{H}_2$ ,  $\text{CO}$ ,  $\text{CO}_2$ ,  $\text{C}_3\text{H}_6$  and smaller amounts  $\text{CH}_4$ . Increasing temperature results in an increase of  $S_{\text{H}_2}$  from 89 to 96%. Selectivity toward  $\text{CO}_2$  decreases with increasing temperature, whereas the opposite is observed for  $\text{CO}$  selectivity. This implies production of  $\text{CO}$  at the expense of  $\text{CO}_2$  and is most possibly due to occurrence of the RWGS reaction. Methane production, via  $\text{CO}$  or  $\text{CO}_2$  hydrogenation, is low in the entire temperature range examined, whereas propylene production at low temperatures is most possibly related to  $\text{C}_3\text{H}_8$  dehydrogenation. Qualitatively similar results were obtained for all the investigated catalysts, with propylene production being higher for the less active samples. Catalytic performance can be significantly improved with increasing the molar ratio of  $\text{H}_2\text{O}/\text{C}_3\text{H}_8$  in the feed.

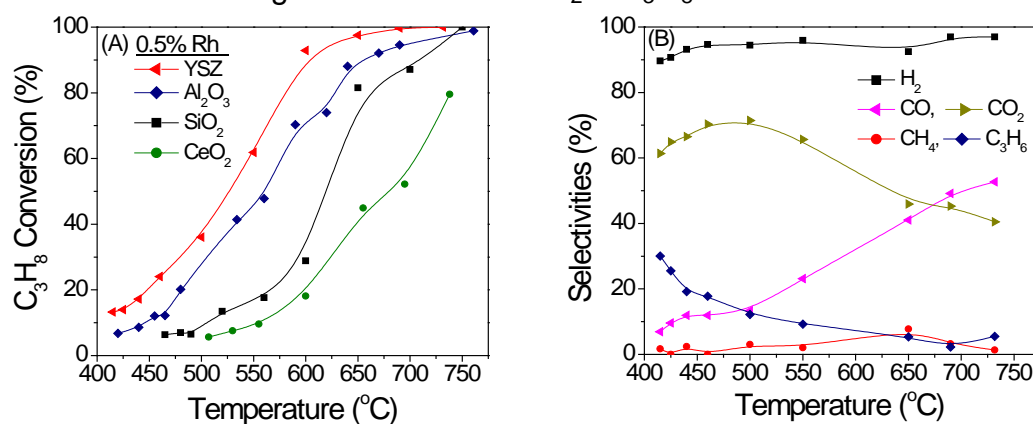


**Figure 1.** (A) Effect of the nature of support on  $\text{C}_3\text{H}_8$  conversion and (B) product selectivities over 0.5%Rh/YSZ catalyst as a function of reaction temperature.

## Acknowledgements



Co-financed by Greece and the European Union

This research has been co-financed by the European Union and Greek national funds

through the Operational Program Competitiveness, Entrepreneurship and Innovation, under the call RESEARCH – CREATE – INNOVATE (project code:T1EDK- 02442).

## References

- [1] E.C. Faria, R.C. Rabelo-Neto, R.C. Colman, R.A.R. Ferreira, C.E. Hori, F.B. Noronha, Catal. Letters. 146 (2016) 2229–2241

# Partial oxidation of dimethyl ether and dimethoxymethane to synthesis gas over noble metal catalysts

S.D. Badmaev<sup>a,b</sup>, N.O. Akhmetov<sup>a,b</sup>, T.B. Shoynkhorova<sup>a</sup>, P.A. Simonov<sup>a,b</sup>, V.D. Belyaev<sup>a</sup>, V.A. Sobyenin<sup>a,b,\*</sup>

<sup>a</sup>*Boriskov Institute of Catalysis, Novosibirsk, Russia*

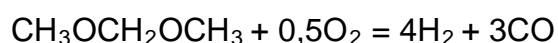
<sup>b</sup>*Novosibirsk State University, Novosibirsk, Russia*

\*Corresponding author: [sobyenin@catalysis.ru](mailto:sobyenin@catalysis.ru)

## 1. Introduction

Dimethyl ether (DME) and dimethoxymethane (DMM) are environmentally benign oxygenated compounds of C1 chemistry with a wide scope of applications. In particular, DME and DMM have been recognized as a promising feedstock for production of hydrogen for fuel cell feeding [1, 2]. Recently, we proposed efficient bifunctional catalysts CuO-CeO<sub>2</sub>/γ-Al<sub>2</sub>O<sub>3</sub> for DME and DMM steam reforming [1] reactions showing high promises for PEMFC applications. In the case of SOFC, steam reforming needs too much external heating to perform the endothermic process and the evaporation of water. Hydrogen production by partial oxidation (PO) reaction usually shows several advantages over steam reforming, including short response time, compactness, “water independence” and easy start-up of the SOFC-based power units.

Literature survey revealed no references devoted to PO DMM and respective catalysts. This reaction can be expressed as:



In our PO DMM experiments, we used noble-metal-based catalysts which are known for their high performance in PO DME [2].

Herein, we report the first example of the PO DMM. Using supported noble metal catalysts, the feasibility of synthesis gas production was shown. Comparative analysis of the catalysts behaviour in PO DMM and PO DME was performed.

## 2. Experimental

Pt-, Rh- and Ru-supported on Ce<sub>0.75</sub>Zr<sub>0.25</sub>O<sub>2-δ</sub> catalysts were prepared by sorption-hydrolytic deposition described in [3]. The catalysts were characterized by XRD, HRTEM, EDX and TPO. The partial oxidation of DME and DMM were performed in a fixed-bed quartz continuous flow reactor under ambient pressure, feed gas composition, vol. %: fuel/O<sub>2</sub>/N<sub>2</sub>=28.6/14.3/57.1 and GHSV=10000 h<sup>-1</sup>.

### 3. Results and discussion

Fig. 1 illustrates the effect of temperature on the DME/DMM conversions and the outlet product concentrations in PO DME and PO DMM over the Pt/Ce<sub>0.75</sub>Zr<sub>0.25</sub>O<sub>2-δ</sub> catalyst. It showed the highest activity among the studied catalysts. As is seen from Fig. 1, the DME and DMM conversions increase with temperature and reach ~100% at 400°C. However, the effect of temperature on the outlet concentrations in the PO DME and PO DMM reactions follows inverse trends. The most probable explanation for this observation is differences in mechanism of the reactions.

The obtained data (Fig.1) demonstrate that the Pt/Ce<sub>0.75</sub>Zr<sub>0.25</sub>O<sub>2-δ</sub> catalyst provides syngas production with nearly the same composition at a temperature of 400 and ~700 °C in, respectively, PO DME and PO DMM. Obviously, PO DMM is more effective for producing syngas than PO DME.

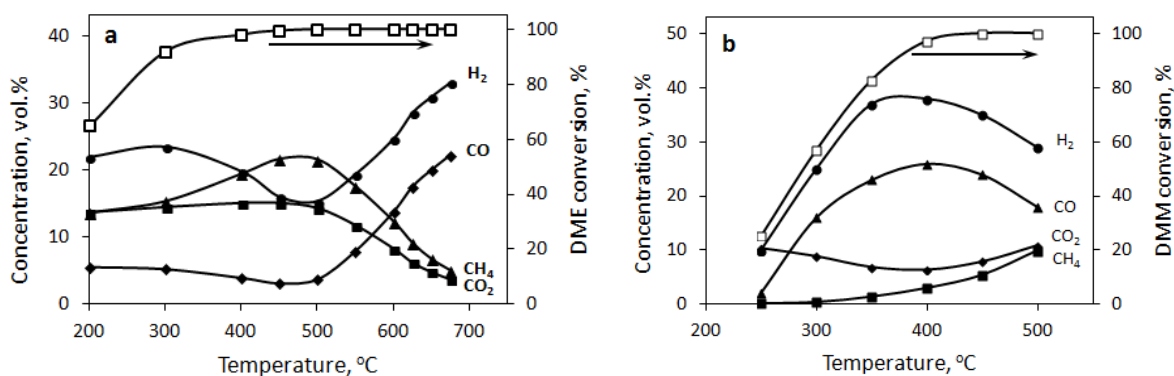


**Fig. 1.** Effect of temperature on DME and DMM conversions and H<sub>2</sub>, CO<sub>2</sub>, CO, CH<sub>4</sub> concentrations in DME (a) and DMM (b) partial oxidation over Pt/Ce<sub>0.75</sub>Zr<sub>0.25</sub>O<sub>2-δ</sub> catalyst.

### 4. Conclusion

Partial oxidation of DMM over noble metal catalysts at low temperature is highly feasible for syngas production. In particular, the Pt/Ce<sub>0.75</sub>Zr<sub>0.25</sub>O<sub>2-δ</sub> catalyst provides complete conversion of DMM with high syngas production rate at GHSV = 10000 h<sup>-1</sup> and T = 400 °C.

### Acknowledgements

This work was conducted within the framework of the budget project № AAAA-A17-117041710088-0 for Boreskov Institute of Catalysis.

### References

1. Pechenkin A., Badmaev S., Belyaev V., Sobyenin V. Appl. Catal. B. 2015. V. 166-167. P. 535.
2. Chen Y., Shao Z., Xu. N. J. Natural Gas Chem. 2008. V.17. P.75.
3. Shoykhorova T.B., Simonov P.A., Potemkin D.I., Snytnikov P.V., Belyaev V.D., Ishchenko A.V., Svintsitskiy D.A., Sobyenin V.A. . Appl. Catal. B. 2018. V. 237. P. 237.

# Supported catalysts based on heteropolyacid applied to bio-alcohol conversion

*Natalia Ogrodowicz, Anna Micek-Ilnicka*

*Jerzy Haber Institute of Catalysis and Surface Chemistry, Polish Academy of Sciences, Niezapominajek 8 PL-30239 Krakow, Poland*

The goal of this study is to investigate catalytic properties the heteropolyacid supported on oxides and nitrides in bio-alcohol dehydration. Heteropolyacids (HPAs) are crystalline solids used as catalysts because of their unique physico-chemical properties. Very high acidity and considerable thermal stability facilitates the use of HPAs as catalysts in those homo- and heterogeneous reactions which require strong acidic and/or redox active centres. Our recent researches focused on the measurements of catalytic properties of supported HPA dodecatungstophosphoric acid ( $\text{H}_3\text{PW}_{12}\text{O}_{40}$ , HPW). Heteropolyacids typically possess rather low specific surface area, therefore they need to be deposited on high surface area supports in order to enhance the availability of active centres. As supports have been chosen titanium dioxide ( $\text{TiO}_2$ ), boron nitride (BN) and silicon nitride ( $\text{Si}_3\text{N}_4$ ). Deposition of the active phase has been conducted using wet impregnation (i) and mechanical (m) methods. Catalytic activity of the prepared supported materials has been studied in the reaction of bio-butanol conversion, due to significant industrial usefulness of the obtained products. Dehydration of two butanol molecules on Brønsted acidic centres produces di-n-butyl ether (DNBE). In a parallel reaction, taking place also Brønsted acidic sites, dehydration of butanol leads to 1-butene, which can be further isomerised into trans- and cis-2-butene. In this study catalytic reaction has been carried in the gas phase under atmospheric pressure and in temperature range 100-300 °C. The catalytic activity of supported materials was compared to the unsupported HPW. The highest conversion of alcohol (100% in 230 °C) was achieved for the HPW/ $\text{TiO}_2$  catalyst whereas for the unsupported heteropolyacid, the maximal conversion had 58% at 110 °C. The hBN-supported catalysts reached the same level n-butanol conversion, independent of technique of their preparation. The sequence of n-butanol conversion was found to be:



It was also noticed that the synthesis method of HPW/hBN catalysts turned out to affect significantly their selectivity. The catalyst HPW/hBN(m) obtained by mechanical method showed the highest selectivity to trans-2-butene (Fig.1).

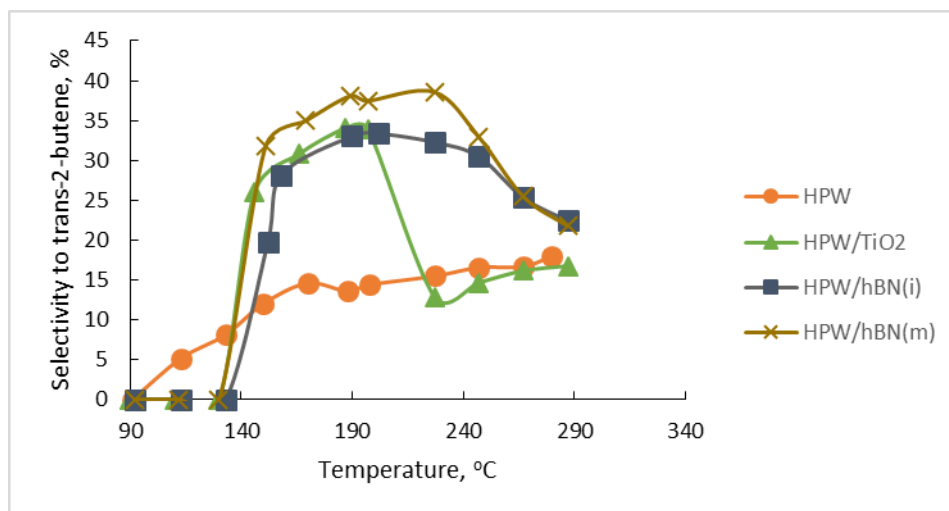


**Fig. 1. Selectivity to trans-2-butene vs, reaction temperature.**

It is worth to notice that the selectivity to cis-2-butene was higher than selectivity to trans-2-butene for others catalysts. The highest selectivity to di-n-butyl ether was reached for HPW/hBN(i) (32% at 150 °C), whereas for others catalysts this selectivity equals 20 %.

### **Acknowledge**

Authors acknowledge financial support of the statutory research fund of ICSC PAS and for dr. A. Kusior for synthesized TiO<sub>2</sub>.

# Interaction of Hydrogen with Co Surfaces: Insights from Temperature Programmed Desorption and Density Functional Theory Study

*Mehdi Mahmoodinia, Norwegian University of Science and Technology (NTNU), Trondheim, Norway; C.J. (Kees-Jan) Weststrate, SynCat@DIFFER, Eindhoven, The Netherlands; Mari Helene Farstad, Norwegian University of Science and Technology (NTNU), Trondheim, Norway; Ingeborg-Helene Svenum, SINTEF Industry, Trondheim, Norway; Marie D. Strømsheim, Norwegian University of Science and Technology (NTNU), Trondheim, Norway; J.W. (Hans) Niemantsverdriet, SynCat@Beijing, Beijing, China; Hilde J. Venvik, Norwegian University of Science and Technology (NTNU), Trondheim, Norway*

## Introduction

A fundamental understanding of the adsorbates on Co surfaces [1-3] and the elementary reaction steps involved [4-5] is an essential tool for catalyst design and optimization in the Fischer–Tropsch synthesis (FTS). One of the elementary reaction steps in the FTS process is the dissociative adsorption of H<sub>2</sub> on the Co surface, to enable the hydrogenation steps on the surface. One question is how the surface structure of cobalt catalysts affects the H<sub>2</sub> dissociation and the adsorption strength of atomic hydrogen, considering the fact that surface structure of supported Co particles is heterogeneous and exposes a variety of sites (corners, edges, steps, kinks, reconstructions). In this work, different single crystal terminations of Co have been applied to address this question.

## Materials and methods

Three different single crystal surfaces of cobalt were used in this study: Co(0001), Co(10-12) and Co(11-20). A combination of density functional theory (DFT) study, temperature programmed desorption (TPD) and low electron energy diffraction experiments have been used to gain insight into the structure of cobalt surfaces and study the adsorption strength of hydrogen atoms as a function of surface structure and surface coverage.

## Results and Discussion

Our results show that the influence of surface structure on the adsorption and dissociation of hydrogen is surprisingly large. The TPD data showed lower desorption

temperatures for hydrogen atoms on the more open surfaces. This is in agreement with the results from DFT calculations for both low and high coverages, finding that hydrogen adsorbs weaker on the corrugated (11-20) and (10-12) surfaces compared with the flat (0001) surface (see Figure). The insight into the lateral interactions between adsorbed hydrogens was also investigated using DFT calculations as we sequentially increased the surface hydrogen coverages. The results were qualitatively in line with the trend in the desorption temperatures observed in the TPD spectra for the three surfaces. In the context of hydrogenation of CO over supported Co particles, our study agrees with previous work suggesting that undercoordinated Co sites are important for efficient H<sub>2</sub> dissociation [2]. After dissociation, diffusion of hydrogen atoms to sites with higher adsorption strength on the flat terrace is facile, making it available for hydrogenation reactions.

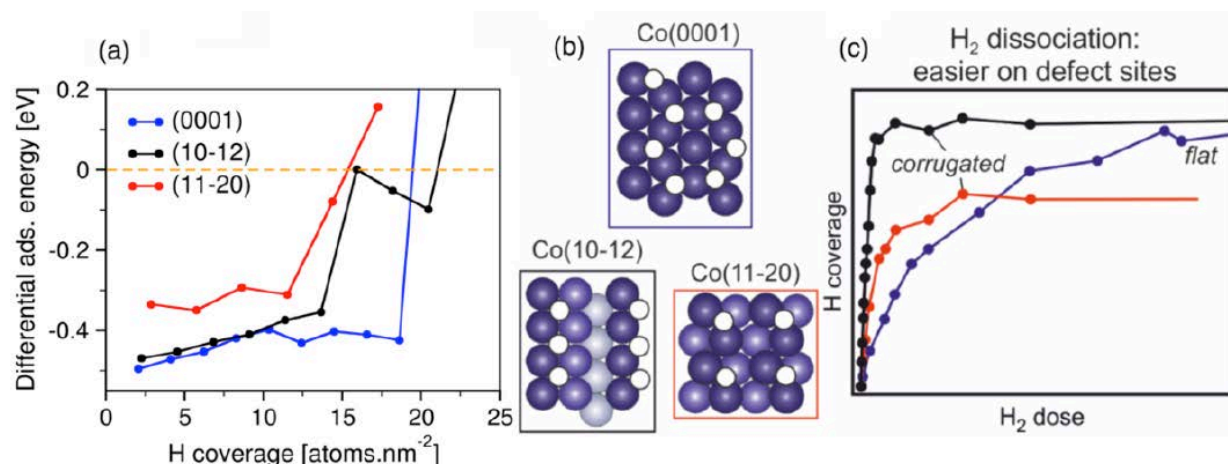


Figure: Hydrogen adsorption on the Co(0001), Co(10–12), and Co(11–20) surfaces. (a) Calculated differential adsorption energies of H atoms as a function of coverage. (b) Theoretically derived site populations for the experimentally determined saturation coverages. (c) Hydrogen coverage as a function of dose at 100 K as obtained from the TPD experiments.

## References

- [1] H.J. Venvik, C. Berg, A. Borg, Surf. Sci. 402–404 (1998) 57–61.
- [2] P. van Helden, J.-A. van den Berg, C.J. Weststrate, ACS Catal. 2 (2012) 1097–1107.
- [3] M.D. Strømsheim, I.H. Svenum, M.H. Farstad, Z. Li, L. Gavrilovic, X. Guo, S. Lervold, A. Borg, H.J. Venvik, Catal. Today 299 (2018) 37–46.
- [4] C.J. Weststrate, J.W. Niemantsverdriet, Faraday Discuss. 197 (2016) 101–116.
- [5] B. Sarup, B.W. Wojciechowski, Can. J. Chem. Eng. 67 (1989) 62-74.



# Catalytic hydrogenation of CO<sub>2</sub> from flue gas to valuable compounds on MoS<sub>2</sub>-based catalysts

*Gernot Pacholik, Ludwig Enzberger, Karin Föttinger*

*TU Wien / Institute of Materials Chemistry, Vienna, Austria*

## Introduction

CO<sub>2</sub> is a well known greenhouse gas and the amount in the atmosphere is still rising. The goal of this work was the utilization of carbon dioxide in flue gas by catalytic reduction. Flue gas contains about 10 – 15 vol.% CO<sub>2</sub>, oxygen, water and traces of sulfur containing substances like H<sub>2</sub>S. There are several ways to convert CO<sub>2</sub> into valuable compounds using different catalysts. For example: Ni based catalysts for CH<sub>4</sub> formation, Cu/ZnO/Al<sub>2</sub>O<sub>3</sub> for methanol production or MoS<sub>2</sub> based catalysts for alcohol synthesis. However, the sulfur contamination in the flue gas leads to deactivation of many catalysts. MoS<sub>2</sub> based catalysts should not be affected by sulfur containing feed gas. Co-Mo-S materials are known as hydrodesulfurization catalysts and are also active for CO<sub>2</sub> hydrogenation. [1] Therefore, in this work, we have studied Co-Mo-S catalysts in order to learn about correlations between synthesis and composition, structural and catalytic properties.

## Summary

In this work different formulations of Co-Mo-S catalysts were synthesized hydrothermally [2] and by precipitation [3] and compared to each other. Different supports (activated carbon and alumina) were used. Catalytic properties were tested in a plug flow reactor up to 20 bar. Products were mainly CO, methane and traces of methanol. Fig. 1 shows the yield of CO and CH<sub>4</sub> over different Co-Mo-S catalysts. Additionally, the effect of potassium as promoter was investigated. Catalysts with potassium promoter produced much less CH<sub>4</sub> and more CO under the given conditions. There was no dependence on the support. Reaction orders of the reactants and apparent activation energies of the product formation were calculated. A long-term test was done to ensure the stability of the catalyst.

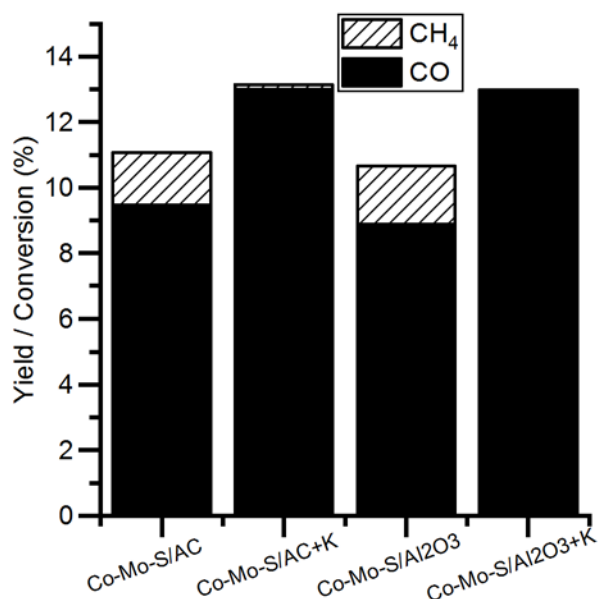


Fig. 1: Yield of CO and CH<sub>4</sub> at 330 °C, 21 bar, 3000 mlN/(g<sub>catalyst</sub> \*h)

The catalysts were characterized by TPD, TPR, TPO, XRD, UV-Vis and N<sub>2</sub> physisorption and the changes of the catalyst during the reaction were investigated. Furthermore, tests MoS<sub>2</sub> based catalyst were synthesized hydrothermal in different formulations with cobalt, nickel and potassium promoters. [4] These catalysts were compared with respect to their catalytic activity to the Co-Mo-S catalyst synthesized by precipitation.

Acknowledgements: We thank OMV for supporting this project

## References

- [1] M. D. Porosoff, B. Yan, and J. G. Chen, "Catalytic reduction of CO<sub>2</sub> by H<sub>2</sub> for synthesis of CO, methanol and hydrocarbons: challenges and opportunities," *Energy Environ. Sci.*, vol. 9, pp. 62–73, 2016.
- [2] H. Li et al., "Nanosheet-structured K–Co–MoS<sub>2</sub> catalyst for the higher alcohol synthesis from syngas: Synthesis and activation," *J. Energy Chem.*, 2018.
- [3] S. Liu, H. Zhou, Q. Song, and Z. Ma, "Synthesis of higher alcohols from CO<sub>2</sub> hydrogenation over Mo–Co–K sulfide-based catalysts," *J. Taiwan Inst. Chem. Eng.*, vol. 76, pp. 18–26, 2017.
- [4] D. Li et al., "The performances of higher alcohol synthesis over nickel modified K<sub>2</sub>CO<sub>3</sub>/MoS<sub>2</sub> catalyst," *Fuel Process. Technol.*, vol. 88, no. 2, pp. 125–127, 2007.

# Hybrid system of biocatalyst and semiconductor based photocatalyst for light-driven CO<sub>2</sub> reduction to formate

*Yutaka Amao, Osaka City University, Osaka, Japan; Tomoya Ishibashi Osaka City University, Osaka, Japan; Shigeru Ikeda, Konan University, Kobe Japan*

## Introduction

Light-driven CO<sub>2</sub> reduction to formate systems with the coupling the photoreduction of various 4,4'- or 2,2'-bipyridinium salts (4,4'- or 2,2'-BPs) with Ru(bpy)<sub>3</sub><sup>2+</sup> or water soluble zinc porphyrin and formate dehydrogenase (FDH) have been reported [1-3]. In this system, the single-electron reduced form of BPs acts as a co-enzyme for FDH instead of natural co-enzyme NADH. To develop the effective light-driven CO<sub>2</sub> reduction to formate systems with the coupling the photoreduction of BP with dye molecule and FDH, development and exploration of photocatalytic materials with highly photosensitizing function and highly tolerance against irradiation are necessary. Among various photocatalytic materials, metal oxide based semiconductor photocatalysts are widely used in the hydrogen production system due to the light-driven water splitting. In this report, we devoted to the semiconductor based photocatalyst TiO<sub>2</sub> nanoparticle as an effective photosensitizing material for CO<sub>2</sub> reduction to formate system with the coupling the photoreduction of MV<sup>2+</sup> and FDH in the presence of triethanolamine (TEOA) as an electron donor as shown in Figure 1.

In this paper, to develop the effective light-driven CO<sub>2</sub> reduction to formic acid, the hybrid system consisting of semiconductor based photocatalyst TiO<sub>2</sub> nanoparticle and biocatalyst FDH mediated MV<sup>2+</sup> photoreduction in the presence of TEOA was studied.

## Results and Discussion

A solution consisting of TEOA (300 mM), TiO<sub>2</sub> nanoparticle (6.8 mg•L<sup>-1</sup>) and MV<sup>2+</sup> (500 μM) and FDH (7.5 μM) in 5.0 ml of 10 mM sodium pyrophosphate buffer (pH

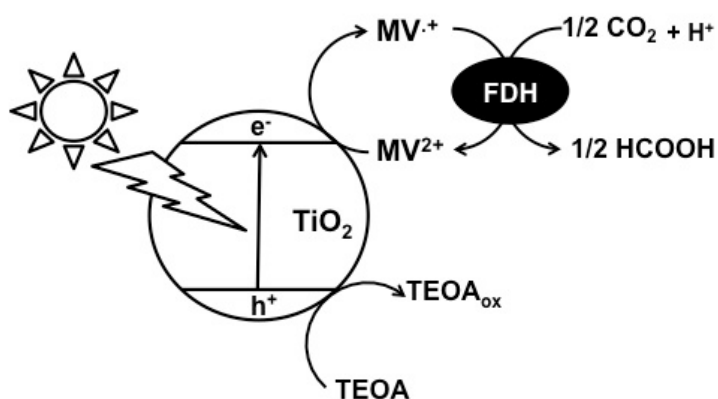


Figure 1. Light-driven CO<sub>2</sub> reduction to formate system consisting of TEOA as an electron donating molecule, TiO<sub>2</sub> nanoparticle, MV<sup>2+</sup> and FDH.

7.4) was deaerated by freeze-pump-thaw cycles repeated 5 times and the gas phase was replaced CO<sub>2</sub> gas. The sample solution was irradiated with a 400 W Xe lamp at a distance of 5.0 cm at 30 °C. To prevent direct reduction of MV<sup>2+</sup>, wavelengths of more than 300 nm of Xe lamp with a cut-off filter also were selected in the CO<sub>2</sub> reduction. The amount of formic acid was detected by an ion chromatography (Dionex ICS-1100; electrical conductivity detector) with an ion exclusion column (Thermo ICE AS1; column length: 9 x 150 mm; composed of a 7.5 μm cross-linked styrene/divinylbenzene resin with functionalized sulfonate groups). The 1.0 mM octane sulfonic acid and 5.0 mM tetrabutylammonium hydroxide were used as an eluent and a regenerant, respectively. Figure 2 shows the time dependence of CO<sub>2</sub> reduction to formate production with the systems of TEOA, TiO<sub>2</sub> nanoparticle, MV<sup>2+</sup> and FDH. After 120 min irradiation, 152 μM of formate was produced in the CO<sub>2</sub> saturated buffer solution containing TEOA, TiO<sub>2</sub> nanoparticle, MV<sup>2+</sup> and FDH. The turnover number of FDH in the system using TiO<sub>2</sub> nanoparticle was estimated to be 10.1 h<sup>-1</sup>. From these results, the effective light-driven CO<sub>2</sub> reduction to formic acid with FDH, the hybrid system consisting of photocatalyst TiO<sub>2</sub> nanoparticle, MV<sup>2+</sup> and FDH in the presence of TEOA was accomplished.

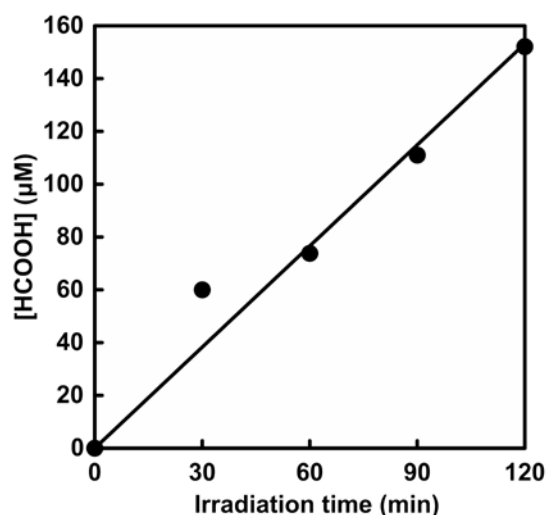


Figure 2. Time dependence of formic acid production in the solution consisting of TEOA, TiO<sub>2</sub> nanoparticle, MV<sup>2+</sup> and FDH

This work was partially supported by Grant-in-Aid for Scientific Research on Innovative Areas “Artificial Photosynthesis (2406)” and “Innovations for Light-Energy Conversion (4906)”.

#### References

- [1] Y. Amai, *Chemistry Letters* 46(2017) 780–788
- [2] Y. Amai, *Journal of CO<sub>2</sub> Utilization* 26 (2018) 623–641
- [3] Y. Amai, *Sustainable Energy Fuels*, 2 (2018)1928–1950

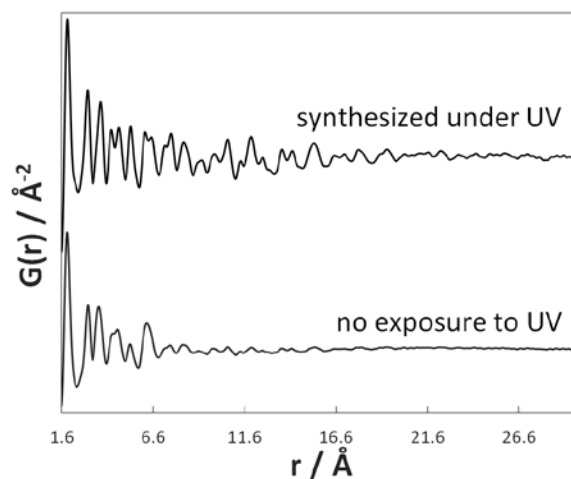
## **Total scattering experiments for the local structure analysis of amorphous photocatalytic materials**

*Ezgi Onur Şahin, Harun Tüysüz, Max-Planck-Institut für Kohlenforschung, Mülheim an der Ruhr, Germany; Candace K. Chan, Arizona State University, Tempe, USA; Wolfgang Schmidt, Claudia Weidenthaler, Max-Planck-Institut für Kohlenforschung, Mülheim an der Ruhr, Germany*

Amorphous materials have gained significant interest in catalysis research.[1] According to the studies on oxide photocatalysts carried out in our group, higher activities were obtained with amorphous catalysts compared to crystalline counterparts.[2,3] Besides benefiting from the high activities it is also important to understand the reasons behind this activity on the atomic level. In case of amorphous catalysts structural stability is a critical issue. Therefore examining the local structure is also helpful in keeping the structure under control. As local structures of non-crystalline materials are not accessible by conventional X-ray diffraction methods, local probes, such as total scattering techniques (Pair Distribution Function analysis, PDF) are required.

One exemplary study involves titanium oxides tested as a photocatalytic material for water splitting. Amorphous titanium oxide was synthesized and tested for ultraviolet (UV) light-induced water splitting. The amorphous samples yielded higher activities compared to commercial TiO<sub>2</sub> (P25) [2]. During the photocatalytic process the material was subjected to light illumination and several changes were observed. As hydrogen gas is generated a color change is observed. This is an indication of change of oxidation state of Ti. In this study, possible change in the local structure related to the change in the coordination environment of Ti was investigated using PDF analysis. After *in situ* and *ex situ* synchrotron total scattering experiments, PDF analysis was applied to scattering data of obtained from both samples in suspension and in dried powder form. PDFs did not show significant changes during or right after the photocatalytic reaction. It was concluded that observed color changes are only limited to surface of the titania particles. Another observation was the enhanced crystallization of the samples over time indicating that the amorphous state of the oxides is only metastable. However, illuminated samples were observed to crystallize faster than non-illuminated ones (see figure).

The state of the photocatalysts and the effects of these changes were further analysed by complementary characterization techniques including Raman spectroscopy and X-ray photoelectron spectroscopy.



### References

1. B R. Goldsmith, B. Peters, J. K. Johnson, B. C. Gates, S. L. Scott, *ACS Catal.* 2017, 7, 11, 7543-7557.
2. T. Grewe, H. Tüysüz, *ChemSusChem* (2015) 8, 3084.
3. D. Zywitzki, H. Jing, H. Tüysüz, C. K. Chan, *J. Mat. Chem. A* (2017) 5, 10957-10967.

# **Theoretical perspective on the water-induced dealumination in zeolite ZSM-5**

*Katarina Stanciakova, Inorganic Chemistry and Catalysis group, Debye Institute for Nanomaterials Science, Utrecht University, The Netherlands*

*Bernd Ensing, Van 't Hoff Institute for Molecular Sciences, University of Amsterdam, The Netherlands*

*Florian Goeltl, Department of Chemical and Biological Engineering, University of Wisconsin–Madison, USA*

*Rosa E.Bulo, Inorganic Chemistry and Catalysis group, Debye Institute for Nanomaterials Science, Utrecht University and Free University of Amsterdam, The Netherlands*

*Bert M. Weckhuysen, Inorganic Chemistry and Catalysis group, Debye Institute for Nanomaterials Science, Utrecht University, The Netherlands*

Environmental challenges make the development of alternative production routes for chemicals and fuels from renewable resources one of the most pressing priorities. The zeolite-catalysed production of green chemicals from oxygen abundant alternatives, such as biomass, ethanol or methanol, is an attractive option, but it is accompanied by water production, which is harmful to the active catalyst. A systematic improvement of catalyst performance and stability requires control over the water-induced zeolite deactivation and fundamental understanding of the underlying reactions. Based on the results from molecular simulations a rather comprehensive mechanism for the water-induced dealumination was proposed [1], involving a series of hydration steps, each catalysed by a single water molecule. In our work, we increase the complexity of this approach by modelling the initial dealumination steps in zeolite ZSM-5 in the presence of two water molecules for three different Al site locations.

We identify a set of four possible reaction pathways for the Al-O(H) bond breaking consisting of two different types of reactions. The first three proposed mechanisms follow the mechanism from the literature [1], where the first three Al-O bonds are broken after water adsorption and dissociation of at least one water molecule. The fourth mechanism is different and leads to a different reaction product bonded to three framework oxygen atoms and a water molecule, suggesting an

alternative follow-up mechanism towards the formation of free extra-framework Al species. In this the most energetically favourable situation, the Al-O(H) bond breaking is induced by non-dissociative adsorption of two water molecules. Each of the reaction mechanism is initiated from a different metastable adsorption mode (Fig. 1), therefore, water reorganization from the most stable and unreactive mode (Zundel ion [2]) needs to occur prior to hydrolysis of the Al-O(H) bond.

While a single water molecule model predicts the Al atoms located in the intersection is the most reactive towards the first Al-O(H) bond breaking, the first three mechanisms of two water molecule model suggest that the Al located in the sinusoidal channel is the most reactive. By including two explicit water molecules into our model, we show that micro-solvation alters the dealumination reaction landscape as well as its mechanism. We established a direct link between a water loading and the susceptibility of Al site towards dealumination. We identify that one of the main factors that determine Al site susceptibility towards the first Al-O(H) bond breaking is the Al accessibility that can be predicted from the coordination number of water molecules in the metastable adsorption modes. Based on these results, we suggest that pressure-controlled dealumination can be used as a post-synthetic treatment to synthesize hydrothermally stable and reactive zeolite catalysts.

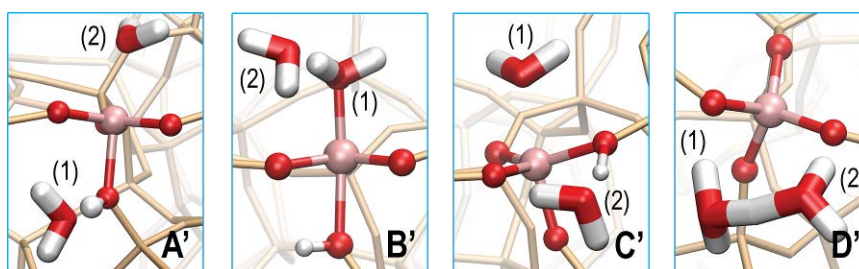


Figure 1: Four stable adsorption modes have been determined via which the initial interaction of two water molecules with zeolite can occur. Two water molecules coordinate simultaneously: to the Bronsted acid site (BAS) and to the Al atom in the *anti*-position to the BAS (A'); to the Al atom in the *anti*-position to the BAS (B'); to the Al atom in the *syn*-position to the BAS and on the BAS (C'); to the BAS to form an asymmetric Zundel ion<sup>2</sup>, which is the most stable, but unreactive configuration.

## References

- [1] M. C. Silaghi, C. Chizallet, E. Petracovschi, T. Kerber, J. Sauer, P. Raybaud, ACS Catal. 2015, 5, 11-15.
- [2] S. Jungstittiwong, J. Limtrakul, N. T. Truong, N.T. J. Phys. Chem. B. 2005, 109, 13342-13351.



## Comprehensive analysis of Fe-based FTS as function of temperature: 1D and 2D GC study

*Mohamed I. Fadlalla<sup>1</sup>, Nico Fischer<sup>1</sup>,<sup>1</sup>Catalysis Institute and C\*Change (DST-NRF Center of Excellence in Catalysis), Department of Chemical Engineering, University of Cape Town, Private Bog X3, Rondebosch 7701, Cape Town, South Africa. Hans (J.W) Niemantsverdriet<sup>2</sup>,<sup>2</sup>Syngaschem BV and Laboratory for Physical Chemistry of Surfaces, Eindhoven University of Technology, P.O. Box 513, Eindhoven 5600 MB, Eindhoven, The Netherlands. Michael Claeys<sup>\*1</sup>,<sup>1</sup>Catalysis Institute and C\*Change (DST-NRF Center of Excellence in Catalysis), Department of Chemical Engineering, University of Cape Town, Private Bog X3, Rondebosch 7701, Cape Town, South Africa.*

The Fischer-Tropsch (FTS) product spectrum is divided into major products (*i.e.* paraffins and olefins) and minor products (*i.e.* branched hydrocarbon, oxygenates and aromatics)[1]. The mechanistic pathway for the formation of major products is relatively understood, unlike minor products. The limited detailed analysis of minor products could be due to instrument limitations, thus pre-analysis treatment or liquid chromatography analysis is required [2]. Comprehensive analysis of minor products is required for better understanding of the FTS mechanism, which could result in the development of more efficient catalysts.

Comprehensive two-dimensional gas chromatography (2D GCxGC), is utilized for the analysis of complex product spectrums, such as petrochemicals and FTS samples [2]. Grobler *et al.* [2] demonstrated the superior qualitative and quantitative aspects of 2D GCxGC over conventional 1D GC for the analysis of the oxygenate fraction. Furthermore, 2D GCxGC requires no pre-analysis treatment, relatively short analysis time and provides high information output [3].

This study focuses on investigating the shifts in Fe- based FTS product spectrum (*i.e.* paraffins, olefins, aromatics and oxygenates) as a function of reaction temperature (*i.e.* 240, 275 and 350 °C) by comprehensive 2D GCxGC (Figure 1). The total selectivity to oxygenates (*e.g.* linear alcohols, branched alcohols, secondary alcohols, aldehydes and ketones) decreased at elevated reaction temperature, while, the selectivity to acids increased with increase in the reaction temperature. The aromatics (*i.e.* alkylbenzenes, alkenylbenzenes and *iso*-alkylbenzenes) selectivity is

low at all reaction temperatures, however, alkylbenzene selectivity increased, while alkenylbenzene selectivity decreased with increase in the reaction temperature.

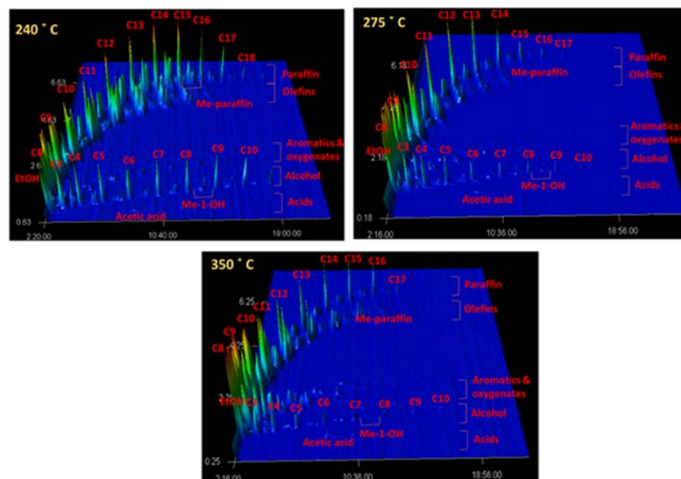


Figure 1: Online 2D GCxGC -MS analysis of FTS product spectrum over Fe-based catalyst as a function of reaction temperature (*i.e.* 240, 275 and 350 °C).

## References

- [1] Dry M. E, *Catal. Today*, 2002,71, 227-241
- [2] Grobler T, Claeys, M, van Steen, E, Janse van Vuuren, M. J, *Catal. Commun.*, 2009, 10, 1674-1680
- [3] Dallüge J, Beens J, Brinkman U. A. T, *J. Chromatogr. A*, 2003, 1000, 69-108.

# Chelating N-donor Complexes of First Row Earth Abundant Metals for Alkane Oxidation

*L. Soobramoney, University of KwaZulu-Natal, Durban, South Africa; D. O Ywaya, University of KwaZulu-Natal, Durban, South Africa; H. B. Friedrich, University of KwaZulu-Natal, Durban, South Africa*

Alkanes, also known as paraffins, are regarded as relatively inert compounds because they contain localised C–C and C–H bonds and also lack empty orbitals of low energy or filled orbitals of high energy required for the progression of chemical reactions [1]. These form major components of crude oil and natural gas and are therefore present in great quantity, particularly from petroleum industries. Most often, these hydrocarbons are exploited for energy production in combustion reactions, and although it is possible to convert them into more reactive products, usually harsh reaction conditions are required, including extremely elevated temperatures and pressures, subsequently leading to uncontrollable reactions and unwanted by-products [2]. For this reason systems have been, and are continually being, developed to activate and functionalize the inert alkanes to more valuable or reactive products that have wider applications at industrial level [2-4].

This work involves the development of economical and relatively ecological homogeneous catalysts for application in paraffin oxidation. Chelating N-donor ligands have been chosen to improve stability of the overall resulting complex, thereby potentially enhancing catalyst lifetime. More specifically, chelating imidazolyl based ligands have been selected because they are able to stabilize a wide range of metals at various oxidation states (Fig. 1).

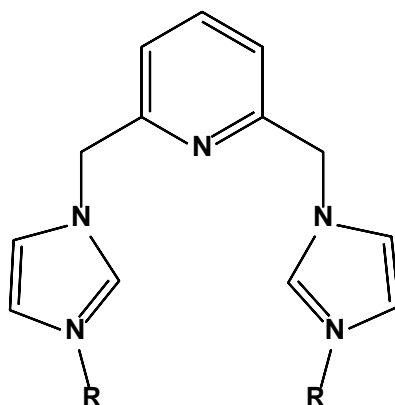


**Figure 1:** General structure of a chelating imidazolyl based ligand where the functional group (R) can be varied.

They also form strong bonds with the metals and thus limit ligand dissociation, a feature that is beneficial in catalysis.

By incorporating earth abundant, first row transition metals such as iron, cobalt, nickel and copper, a more cost effective approach is encouraged. Previous studies have shown promising results in the activation and functionalization of *n*-octane to corresponding oxygenates using chelating SNS ligands coordinated to Co(II), Ni(II) and Cu(II) metal centers (Fig. 2) [5-7].

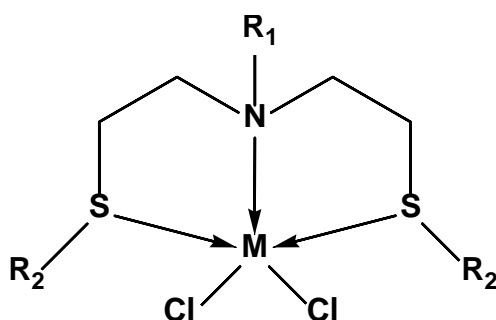


**Figure 2:** General representation of some of the SNS complexes used for paraffin oxidation, where M is Co, Ni or Cu; R<sub>1</sub> = H, CH<sub>3</sub> or C<sub>6</sub>H<sub>6</sub> and various substituents were R<sub>2</sub>.

Effectively, this work aims to develop simpler, more cost efficient processes capable of operating under mild reaction conditions, as opposed to other systems that utilize expensive metals with high temperatures and pressures in the catalytic reactions.

## References

- [1] Labinger, J. A.; Bercaw, J. E. *Nature* 2002, 417, 507.
- [2] Conley, B. L.; Tenn Iii, W. J.; Young, K. J. H.; Ganesh, S. K.; Meier, S. K.; Ziatdinov, V. R.; Mironov, O.; Oxgaard, J.; Gonzales, J.; Goddard Iii, W. A.; Periana, R. A. *Journal of Molecular Catalysis A: Chemical* 2006, 251, 8.
- [3] Shul'pin, G. B. *Journal of Molecular Catalysis A: Chemical* 2002, 189, 39.
- [4] Crabtree, R. H. J. *Organometallic Chemistry* 2004, 689, 4083.
- [5] Soobramoney, L.; Bala, M. D.; Friedrich, H. B. *Dalton Transactions* 2014, 43, 15968.
- [6] Soobramoney, L.; Bala, M. D.; Friedrich, H. B. *Inorganica Chimica Acta* 2018, 479, 97.
- [7] Soobramoney, L.; Bala, M. D.; Friedrich, H. B. *Polyhedron* 2019, in press.

# **Development of quaternary metal/metal oxide catalysts as micro-structured wall catalysts for “Power-to-Gas” applications through combinatorial High-Throughput Screening**

*Mirko Pfeifer, Chemnitz University of Technology, Chemnitz, Germany; Thomas Schwarz, Chemnitz University of Technology, Chemnitz, Germany; Klaus Stöwe, Chemnitz University of Technology, Chemnitz, Germany.*

The Sabatier reaction is an essential component of “Power-to-Gas” systems to reduce the greenhouse gas carbon dioxide using hydrogen to form methane. The reaction is very exothermic and liable to volume contraction. Therefore, low temperatures and high pressures are used in accordance with thermodynamic parameters [1].

To control the heat of reaction (at  $T = 520 - 670$  K;  $p = 15 - 30$  bar) micro-structured reactors were used. Typically, the specific dimensions of these reactor types are below one millimeter at least in one dimension. Thus, they have a huge surface-to-volume ratio. That leads to increased mass and heat transport processes. The heat transfer coefficients have values in the order of  $10 \text{ kW}\cdot\text{m}^{-2}\cdot\text{K}^{-1}$  which enables exact control of heat supply and dissipation. Therefore, it is possible in many cases to perform the reaction isothermally [2].

Syntheses of the quaternary metal/metal oxide catalysts were implemented with industrial established methods such as sol-gel, incipient wetness impregnation and wet impregnation. To obtain defined thickness of the layers on the micro-structured reactor high-volume low-pressure (HVLP) spray-coating was used [3]. The plates coated with the wall catalysts were tested with a custom-built 10-fold gas flow reactor as shown in Figure 1 with a defined gas flow channel between catalyst layer and reactor wall for catalyst screening – in view of conversion, selectivity and space-time yield. Objective was to find active catalysts with reduced coking behavior at low  $\text{H}_2:\text{CO}_2$  ratios at higher long-time stability compared to the nickel catalysts currently used. The best catalysts will be validated with micro parallel plate reactor – in view of aging and stability against catalyst poisoning.

Figure 2 shows the first qualitative results from the Primary Screening using the following reaction parameters:  $T = 573$  K;  $p = 15$  bar;  $\text{H}_2:\text{CO}_2 = 4:1$ , GHSV:  $50.000 \text{ h}^{-1}$ . Influences of the active metals, support materials and syntheses methods on the activity of the catalysts will be discussed. The screening shows that catalysts with the

same chemical composition but different synthesis methods of the supported catalyst materials show different activities. Therefore, it is interesting to find out whether the Sabatier reaction is structure-sensitive or insensitive considering different active metals as well as support materials [4].

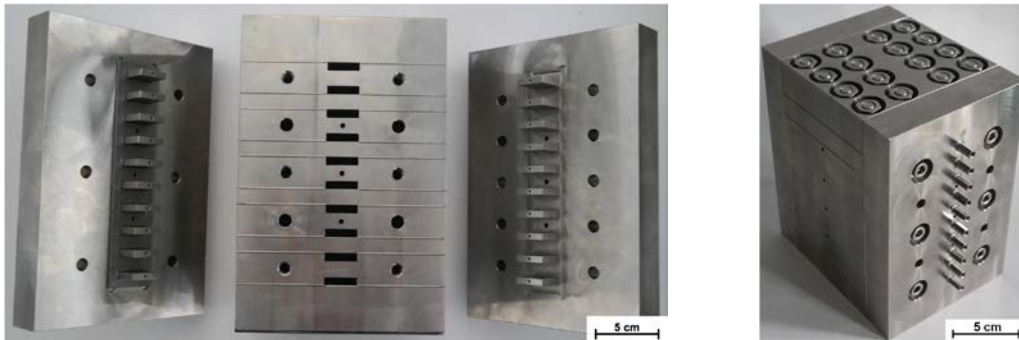


Figure 1: 10-fold gas flow reactor system with reactor body as well as gas inlet/outlet (left side) and assembled reactor unit (right side).

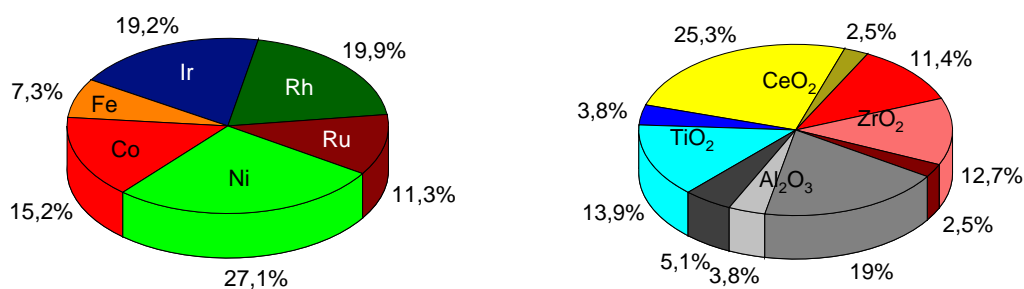


Figure 2: Qualitative catalyst primary screening results as percentage share of catalyst active metal components (left side) and colour coded support materials; grey: three different alumina, blue: two different titania, yellow-greenish: two different ceria, red: three different zirconia (right side).

## References

- [1] R. Myrstad, S. Eri, P. Pfeifer, E. Rytter, A. Holmen, *Cat. Today*, **2009**, 147S, S301 – S304.
- [2] G. Emig, E. Klemm, *Technische Chemie: Einführung in die chemische Reaktionstechnik*, 6. Auflage, Springer, Berlin, Heidelberg, 2017.
- [3] T. Schwarz, H. Döring, E. Klemm, S. Schirmeister, *CIT*, **2010**, 82, 921 – 928.
- [4] D. Beierlein, D. Häussermann, M. Pfeifer, T. Schwarz, K. Stöwe, Y. Traa, E. Klemm, *Appl. Catal. B*, accepted, <https://doi.org/10.1016/j.apcatb.2018.12.064>.

# Molecular adsorption and dissociation of CO on a defect-rich Co surface

*D. Sharma, Dutch Institute For Fundamental Energy Research, Eindhoven, The Netherlands; D. Garcia Rodriguez, Dutch Institute For Fundamental Energy Research, Eindhoven, The Netherlands; M.A. Gleeson, Dutch Institute For Fundamental Energy Research, Eindhoven, The Netherlands; J.W. Niemantsverdriet, Syngaschem BV, Eindhoven, The Netherlands; C.J. Weststrate, Syngaschem BV, Eindhoven, The Netherlands;*

## Introduction

Formation of hydrocarbons and water by Fischer Tropsch (FT) synthesis over a catalyst containing cobalt (Co) as an active component has been both academically and industrially interesting to study. A Co catalyst nanoparticle exposes various kinds of facets along with significant quantity of steps [1]. Literature suggests that the presence of defects lowers the barrier for CO dissociation [2]. We use a sputter-damaged defect rich Co(0001) surface to represent a highly stepped surface with smaller terraces. In the present work, the first elementary step of the complex FT mechanism which is CO adsorption subsequently followed by its dissociation, is studied in a comparative study between flat Co(0001) and sputtered Co(0001) surface.

## Results

Sincrotrone XPS was used to qualitatively determine the CO concentration on the surface after exposing it to CO at 90 K. A comparison of the C1s and O1s spectra measured on the annealed and sputtered surface after CO adsorption show that the amount of CO adsorbed on the sputtered surface is 84% of that adsorbed on the flat Co(0001) surface. Fig (1a) shows the O1s spectra of an annealed and sputtered surface. The C1s and O1s spectra also provide an insight on the sites occupied by CO. XPS results suggest that the first 0.33 ML of CO is adsorbed on the top site (285.5 eV) and the next 0.23 ML adsorb on the hollow sites (285 eV). There's no bridge site occupation as also shown in the infrared (IR) spectra Fig (1b). The RAIRS spectra shows hollow site ( $1880\text{ cm}^{-1}$ ) occupation at high coverages but negligible bridge site ( $1901\text{ cm}^{-1}$ ) occupation. Work-function measurements (WF) and Mass spectrometry (MS) techniques are also used to determine the amount of CO adsorbed and dissociated. Heating the CO saturated sputtered surface resulted into

CO dissociation which can be identified by separate peaks of atomic carbon (282.7 eV) and atomic oxygen (529.4 eV) around 450 K as shown in Fig (1c). It is observed that the amount of CO dissociated on heating the CO saturated sputtered surface presence of  $1 \times 10^{-7}$  mbar CO is more than that on heating it in vacuum. As the temperature is increased further to 670 K, the atomic oxygen and carbon peaks diminish in intensity suggesting recombination of CO as can be seen in the XPS results. The CO recombination peak can be observed in MS at 630 K.

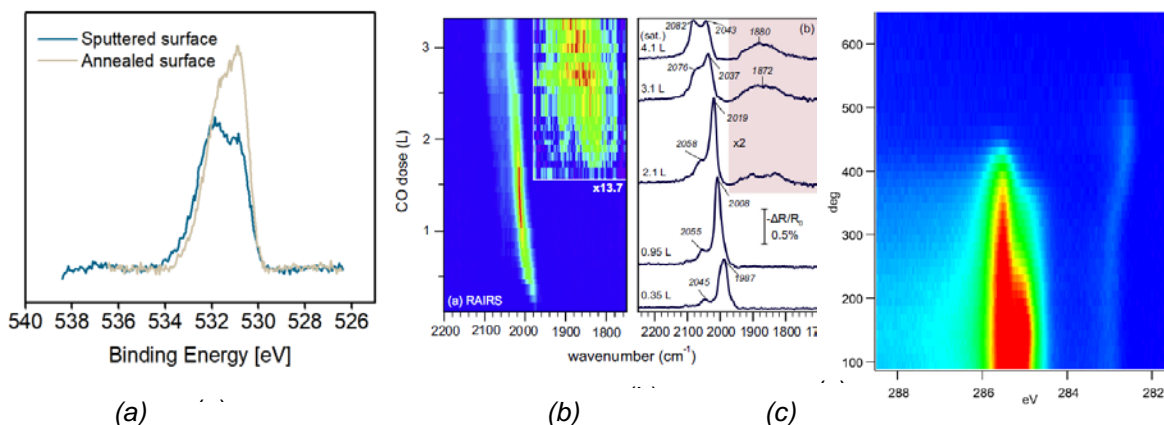


Figure 1: (a) O1s spectra comparing CO coverage on sputtered and annealed surface (b) CO adsorption on a defect-rich cobalt surface selected spectra for the CO doses (adapted from [2]) (c) C1s spectra of heating CO saturated sputtered surface

## Discussion and conclusions

As the experimental results show, the sputtered surface adsorbs less amount of CO as compared to the annealed flat surface. This can be a result of inability of the small terraces on the sputtered surface to form large ordered structures of CO at higher coverages. This argument is supported by the similarity of high coverage CO TPD spectra with broad peaks just like other stepped surfaces. The dissociation barrier for CO is too high for flat surface. Therefore, very minimal dissociation is seen on flat surface. Whereas on defect sites, CO dissociation occurs around the desorption temperature. Therefore, both dissociation and desorption are competitive at high temperature and pressure.

## References

- [1] van Helden, Pieter, Ionel M. Ciobîcă, and Roelof LJ Coetzer. *Catalysis Today* 261 (2016): 48-59.
- [2] Weststrate, C. J., J. van de Loosdrecht, and J. W. Niemantsverdriet. *Journal of Catalysis* 342 (2016): 1-16



## Direct Methane Reforming

### –Difference in shape of produced carbon by reaction conditions–

*Naruka Tamai, Fumitaka Kondo, Noriyasu Okazaki,  
Kitami institute of technology, Kitami, Hokkaido, Japan*

#### Introduction

Direct methane reforming (DMR:  $\text{CH}_4 \rightarrow \text{C} + 2\text{H}_2$ ) is a direct decomposition of methane to hydrogen and carbon. Then the formed carbon is nano carbon. We succeed in producing it in quantities by a short time in use of DMR[1]. Nano carbon can be applied as a functional carbon material because it has electrical and heat conduction property. And it is different in the use depending on its shapes. However, the shape control of nano carbon is difficult in the present situation. Therefore, in this study, we investigated how the difference in reaction conditions of DMR affects the diameter of nano carbon and tried control of it.

#### Experimental

We used iron-based catalyst physically mixed with  $\text{Fe}_2\text{O}_3$  and  $\text{Al}_2\text{O}_3$  and nickel-based catalyst physically mixed with  $\text{NiO}$  and  $\text{MgO}$ .

The reaction device used a fixed bed flow type reactor. The catalyst was put in the center of quartz tube (an inner diameter and length 2.5 and 100 cm, respectively). DMR was carried out using methane as a reaction gas at 30 to 180 ml/min. And the concentration of the reaction gas was set at 100%, 67% and 33%. The temperature of the reaction gas of nickel-based catalyst is 600 °C, and that of iron-based catalyst is 750 °C. Reaction time is 180 min, and catalyst weight is set to 0.1 g.

The composition of the outflow gas from the reactor was determined by GC (TCD). The catalysts of before and after reaction were analyzed with XRD.

#### Results and discussion

We compared the result of DMR which conducted under some reaction conditions. In the case of iron-based catalyst, order of the active of DMR was a 30 ml/min > 180 ml/min when the concentration of the reaction gas was constant in

100%. And it was a 30 ml/min > 90 ml/min > 180 ml/min, when the concentration of the reaction gas was constant in 33%. When the reaction gas is 30 ml/min, the activity of DMR showed high activity when the higher the concentration of the reaction gas (fig.1). On the other hand, in the case of nickel-based catalyst, showed highest activity, which is about 28%, when the concentration of the reaction gas is 100% and the flow rate is 30 ml/min. However, it showed little activity under other reaction conditions.

We observed formed carbon with SEM, and it was fibrous nano carbon. We measured a diameter of the nano carbon in each reaction conditions. In the case of iron-based catalyst, the concentration of reaction gas of 33% was more different in the diameter of nano carbons by different in flow rate of reaction gas than 100%. On the other hand, nickel-based catalyst was showed a large difference of that when the concentration of reaction gas of 100%. Therefore, it is considered that nano carbon produced by DMR is greatly affected by the concentration and flow rate of reaction gas, and indicated that the control of the diameter of nano carbon is possible by optimization of reaction conditions.

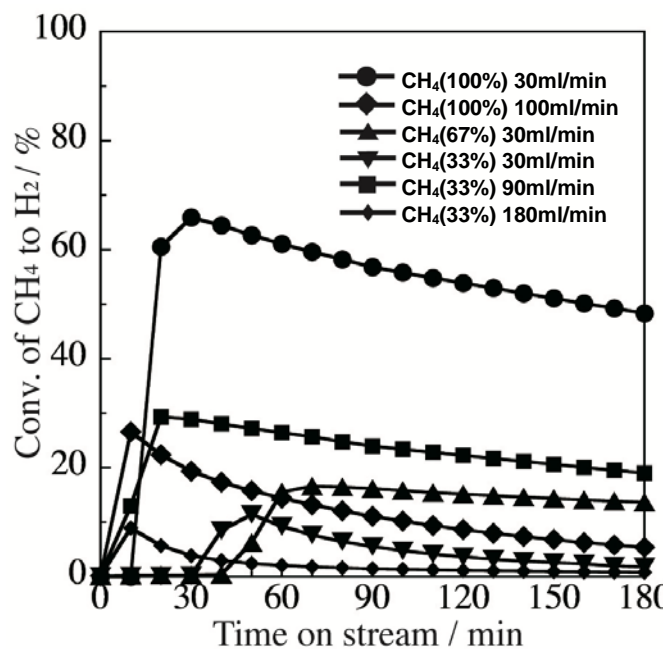


Fig.1 Activities of iron-based catalyst.

## References

- [1] A. Tada, T. Matsunaga, N. Okazaki, *Trans. of the MRS-J*, **33**[4] 1059 (2008).

# A Topological Model for the Adsorption of Polycyclic Aromatic Hydrocarbons on Late-Transition Metal Surfaces

*Zhao-Bin Ding<sup>1</sup>, Matteo Tommasini<sup>2</sup>, and Matteo Maestri<sup>1</sup>*

<sup>1</sup>*Laboratory of Catalysis and Catalytic Processes, Dipartimento di Energia, Politecnico di Milano, Via Lambruschini, 4, 20156 Milano (Italy)*

<sup>2</sup>*Dipartimento di Chimica, Materiali e Ingegneria Chimica "G. Natta", Politecnico di Milano, Piazza Leonardo da Vinci 32, 20133, Milano (Italy)*

## Introduction

Controlling the coke formation, one of the primary cause of catalyst deactivation, is an important aspect of improving catalyst performance. Understanding the general adsorption mechanism of polycyclic aromatic hydrocarbons (PAH) on metal surfaces is the first step to model the coking formation. Despite of such demand, a complete investigation of the adsorption of PAH is hindered by the broad variety of PAH structures and the adsorption configurations. Inspired by the dependency of the formation enthalpy of the metal-organic complexes to the number of metal-ligand bonds [1], in this work, we develop a topological model to facilitate the description of the adsorption of PAH on late-transition metal surfaces. We first assess the analogy between the adsorption mechanism of PAHs and the metal-organic ligand bonding in complexes through density functional theory calculations. Then a topological model is developed for predicting the adsorption energy of arbitrary PAH. Finally the analogy between the bonding mechanisms reflected by the model and the principles in the coordination chemistry is revealed.

## Methods

Benzene, naphthalene, tetracene, phenanthrene and pyrene adsorbed in different configurations on Ni(111), Rh(111), Pd(111) and Pt(111) surfaces are calculated using PBE functionals with Grimme D2 correction for the van der Waals interactions. All the calculations are performed using Quantum ESPRESSO.

## Results and Discussion

The charge difference upon adsorption is calculated to understand the bonding mechanism of PAH. Results, shown in Figure 1a, indicate that electron flows from the orbitals that is delocalized on the whole PAH ring to the M-C bonds. This binding mechanism is analogous to the back-donation interactions between metal atoms and the C=C bonds in metal-alkene complexes [2]. Based on such analogy, here we

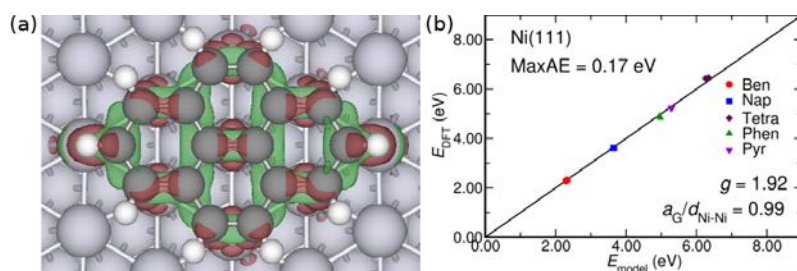


Figure 1. a) Charge density difference maps of pyrene on Rh(111) surface. Darker area shows electron gain, and brighter area shows electron depletion. b) Accuracy of adsorption energy on Ni(111) surface estimated by Eq.(1). Adapted from [3].

propose a model to relate the adsorption energy of PAHs to the topology of the PAH-metal bonding (namely the number of  $\eta^1$  coordinations ( $n_1$ ) and the number of  $\eta^2$  coordinations ( $n_2$ )) and PAH geometry (namely the number of rings on PAH,  $n_{ph}$ ) as:

$$E_{bind} = E_{ph}n_{ph} + E_{M-C}n_1 + gE_{M-C}n_2 \quad (1)$$

Figure 1b shows that this model well describes the adsorption energies of all the PAHs on metal (111) surfaces with the correlation coefficients all higher than 0.99. Furthermore, Figure 1b indicates that the ratio between the adsorption energy contributions from each  $\eta^2$  M-C bond and that from each  $\eta^1$  M-C bond,  $g$ , approaches to 2 when the lattice mismatch between the aromatic rings and the metal surface decreases. This ideal value of  $g$  factor reveals that the adsorption energy of PAH is only determined by the number of C bound with metal, which is analogous to the formation enthalpy of metal-organic complexes [1]. Therefore, these findings further approve the intrinsic connection between surface adsorption and the formation of metal-organic complexes.

## Conclusions

Our work reveals the essential analogy between the PAH adsorption and the formation of multidentate metal-organic complexes, and provide an accurate topological model to facilitate the description of PAH adsorption on metal surfaces. This work therefore paves the way to model the complex kinetics of the surface processes that involve carbonaceous species. Financial support from the European Research Council (G.A.677423) is gratefully acknowledged.

## References

1. Spike C. G., Parry R. W., J. Am. Chem. Soc., 1953, 75, 2726–2729
2. Avery, N. R., Surf. Sci., 1984, 146(2-3), 363–381.
3. Ding Z. -B., Tommasini M., Maestri M. React. Chem. Eng., DOI: 10.1039/C8RE00229K

# Unprecedented transesterification activity of CuZn and CuZnAl catalysts during hydrogenolysis of dimethyl adipate

*Oleg Kikhtyanin, Violetta Pospelova, Jaroslav Aubrecht and David Kubička,  
University of Chemistry and Technology Prague, Technická 5, 166 28 Prague Czech  
Republic; david.kubicka@vscht.cz*

## Introduction

CuZn and CuZnAl catalysts show a good activity in hydrogenolysis of dimethyladipate (DMA) to 1,6-hexanediol (HDOL) that outperforms the classical Adkins catalyst. The CuZn-based catalysts could, thus, become an environmentally friendly replacement of the Adkins catalyst containing harmful chromium. This, however, necessitates detailed understanding of the reaction pathway and its implications for the selectivity to HDOL, i.e. the desired product. Recently, we have reported the formation of various transesterification products during DMA hydrogenolysis [1] that resulted in decreased HDOL selectivity. Here, we elucidate on the role of these intermediates or by-products in DMA conversion.

## Experimental

CuZn and CuZnAl catalysts precursors were prepared by co-precipitation of the corresponding nitrates. The precursors were calcined in different atmospheres (air, nitrogen, hydrogen) over a broad range of temperatures 220 – 500°C and then reduced in hydrogen atmosphere at 220 °C. The catalysts were characterized by BET, XRD, N<sub>2</sub>O chemisorption, NH<sub>3</sub>-TPD and CO<sub>2</sub>-TPD to assess their key properties. Then, the catalysts were tested at 220 °C and hydrogen pressure of 10 MPa in a batch reactor in dimethyl adipate hydrogenolysis. Both, pure DMA and mixtures of DMA with HDOL were used as starting reactants.

## Results and Discussion

The experiments performed over catalysts obtained by calcination in different atmospheres showed that calcination in air at 350°C is the most preferable way of preparing an active hydrogenolysis catalyst with a good selectivity towards HDOL (at

30% DMA conversion ca. 8% yield of HDOL and ca. 12% of esters). On the other hand, calcination in hydrogen or nitrogen at 500°C led to an inactive catalyst (DMA conversion <2%) whereas by calcination in nitrogen at 350°C, the catalyst showed a pronounced transesterification activity and negligible hydrogenolysis activity (at 30% DMA conversion <1% yield of HDOL and ca. 28 % yield of esters). This clearly points to the different nature of active sites for both reactions. Detailed characterization work is still in progress as is a targeted preparation of new catalysts to indisputably correlate the catalytic performance with catalyst characterization data.

The experiments starting not from pure DMA, but rather from mixtures of DMA with HDOL showed that at a molar ratio of DMA to HDOL 9:1, esterification proceeded fast and in less than an hour the starting HDOL was completely consumed (under nitrogen atmosphere) yielding predominantly a product with 3 C<sub>6</sub> moieties (the alcohol groups in HDOL reacted with DMA ester groups, selectivity ca. 80%). In hydrogen, the scheme was more complex as the hydrogenolysis reaction proceeded simultaneously to the transesterification reaction. The experiments, nevertheless, indicated that the transesterification reaction is faster than the hydrogenolysis.

## Conclusion

The experimental results clearly indicate that the CuZn and CuZnAl catalysts possess distinct active sites responsible for transesterification and for hydrogenolysis. The results also suggest that under the investigated experimental conditions that rate of transesterification exceeds the rate of hydrogenolysis having salient implications for producing selectively HDOL.

## References

1. Kubička, D., et al., *On the importance of transesterification by-products during hydrogenolysis of dimethyl adipate to hexanediol*. Catalysis Communications, 2018. **111**: p. 16-20.

# Catalytic reforming of CH<sub>4</sub> with CO<sub>2</sub> over nanocrystalline Ni/ $\gamma$ -Al<sub>2</sub>O<sub>3</sub> bimodal pore catalyst in a fixed bed reactor: Kinetic evaluation and reactor simulation aspects

Mumtaj Shah<sup>1</sup>, Ankur Bordolo<sup>2</sup>, Aameya Kumar Nayak<sup>3</sup>, Prasenjit Mondal<sup>1\*</sup>

<sup>1</sup>Department of Chemical Engineering, Indian Institute of Technology Roorkee, India

<sup>2</sup>Refining Technology Division, CSIR-Indian Institute of Petroleum, Dehradun-248005

<sup>3</sup>Department of Mathematics, Indian Institute of Technology Roorkee, India

\*Corresponding author: [mondal2001@gmail.com](mailto:mondal2001@gmail.com); Tel: (+91)- 1332-285181

## Abstract

The kinetics of methane reforming with CO<sub>2</sub> has been performed over nanocrystalline Ni/ $\gamma$ -Al<sub>2</sub>O<sub>3</sub> (5 wt% Ni) bimodal pore catalyst as the function of temperature (500-700°C) and partial pressures of reactants and products. The bimodal pore structured  $\gamma$ -alumina support was prepared by the sol-gel method and the 5 wt.% Ni nanoparticles were synthesized by the urea deposition-precipitation method, as described in [1]. A fixed-bed reactor is setup to gather the kinetic data by eliminating the diffusional effects and the reaction conditions are setup according to the Froment and Bischoff (1990) [2]. A quartz tube reactor with OD of 3/8 in. was charged with 20mg and reduced in situ at 800°C with 10% H<sub>2</sub>/Ar before introducing the reactants in the reactor. The amount of water produced in reaction is measured through the trap of Na<sub>2</sub>SO<sub>4</sub>. The kinetic model is derived from a mechanistic model which is proposed on the basis of detailed study of reaction mechanism. A kinetic model was developed based on the Langmuir–Hinshelwood formulations, assuming the CH<sub>4</sub> dissociative adsorption of CH<sub>x</sub> and CO<sub>2</sub> as the rate-determining step. The kinetic parameters were estimated by applying a nonlinear least-square method. The derived parameters are thermodynamically consistent and statistically significant. The study showed that the enhancement in CH<sub>4</sub> consumption is resulted with the increase in partial pressure of CO<sub>2</sub> and the reverse water gas shift reaction is an essential feature of dry reforming reaction.

A steady state comprehensive two dimensional numerical model which contained axial dispersion term, was developed with incorporating the kinetic model and solved using the finite difference method. The numerical model consist of mass and energy balance equations as given below in Eqns (1) and (2) [3]. The

experimental data for the validation of simulation study was obtained on a bench scale reactor, operating between 500-800°C and 1-10 bar. The influence of several parameters including inlet space velocity, temperature and pressure on the syngas productivity, hydrogen yield and H<sub>2</sub>/CO was investigated [4].

$$D_{eff} \left[ \frac{\partial^2 C_i}{\partial r^2} + \frac{1}{r} \frac{\partial C_i}{\partial r} \right] + D_{eff} \frac{\partial^2 C_i}{\partial z^2} + \rho_B v_i r_j = u_z \frac{\partial C_i}{\partial z} \quad (1)$$

$$(\Delta H_j) \rho_B v_i r_j(r, z) + \lambda_{eff} \left[ \frac{\partial^2 T(r, z)}{\partial r^2} + \frac{1}{r} \frac{\partial T(r, z)}{\partial r} \right] + \lambda_{eff} \frac{\partial^2 T(r, z)}{\partial z^2} = \rho_B C_P u_z \frac{\partial T(r, z)}{\partial z} \quad (2)$$

With boundary conditions;

$$C_i(r, 0) = C_i^0, \quad T(r, 0) = T^0 \quad \text{at } z = 0 \text{ and } 0 \leq r \leq r_1,$$

$$\frac{\partial C_i}{\partial r}(0, z) = 0, \quad \frac{\partial T}{\partial r}(r_1, z) = 0 \quad \text{at } r = 0 \text{ and } 0 \leq z \leq L,$$

$$\frac{\partial C_i}{\partial r}(r_1, z) = 0, \quad \lambda_{eff} \frac{\partial T}{\partial r}(r_1, z) = -U_{tw}(T - T_0) \quad \text{at } r = r_1 \text{ and } 0 \leq z \leq L,$$

The results of simulation study showed that the developed kinetic model fits the experimental data very well, with a R<sup>2</sup> value above 0.96 and also predicts the fixed bed reactor performance satisfactorily.

## References

- [1] M. Shah, S. Das, A.K. Nayak, P. Mondal, A. Bordoloi, Smart designing of metal-support interface for imperishable dry reforming catalyst, *Appl. Catal. A Gen.* 556 (2018). doi:10.1016/j.apcata.2018.01.007.
- [2] G. Froment, K. Bischoff, J. De Wilde, *Chemical reactor analysis and design*, (1990). [https://scholar.google.com/scholar\\_lookup?title=Chemical Reactor Analysis and Design&author=G.F. Froment&publication\\_year=2011](https://scholar.google.com/scholar_lookup?title=Chemical+Reactor+Analysis+and+Design&author=G.F.+Froment&publication_year=2011) (accessed September 28, 2018).
- [3] E. Akpan, Y. Sun, P. Kumar, H. Ibrahim, A. Aboudheir, R. Idem, Kinetics, experimental and reactor modeling studies of the carbon dioxide reforming of methane (CDRM) over a new Ni/CeO<sub>2</sub>-ZrO<sub>2</sub> catalyst in a packed bed tubular reactor, *Chem. Eng. Sci.* 62 (2007) 4012–4024. doi:10.1016/J.CES.2007.04.044.
- [4] A. Aboudheir, A. Akande, R. Idem, A. Dalai, Experimental studies and comprehensive reactor modeling of hydrogen production by the catalytic reforming of crude ethanol in a packed bed tubular reactor over a Ni/Al<sub>2</sub>O<sub>3</sub> catalyst, *Int. J. Hydrogen Energy.* 31 (2006) 752–761. doi:10.1016/J.IJHYDENE.2005.06.020.



# Combined steam and dry reforming of methane over Ni/Al<sub>2</sub>O<sub>3</sub> based catalysts

*Mihaela D. Lazar, Monica Dan, Maria Mihet*

*National Institute for R&D of Isotopic and Molecular Technologies – INCDTIM, 67-103 Donat Street, 400293, Cluj-Napoca, Romania*

## Introduction

The biogas composition, after purification, consists mainly in methane, carbon dioxide and water vapors. Nowadays its main utilization is to produce electricity and/or heat. One possible way to add more economic value to the biogas would be its transformation in syngas, by reacting its components in dry reforming of methane catalytic process [1]. The main drawback of this reaction is the carbon formation, especially on nickel-based catalysts, its accumulation on the catalysts active sites leading to catalyst deactivation. In this paper two ways to diminish the carbon formation will be employed: (i) the addition of water in the reaction resulting the so-called combined steam and dry reforming of methane process (CSDRM); and (ii) the addition of MgO and La<sub>2</sub>O<sub>2</sub> oxides to the alumina support, being known the positive effect of these oxides on both steam reforming and CO<sub>2</sub> reforming of methane [2,3].

## Experimental

The catalysts were prepared by a modified co-precipitation method, followed by calcination in Ar at 450°C and reduction in H<sub>2</sub> at 650°C. The target concentration of both Ni and supplementary oxide was 10 wt.%. All catalysts were subjected to the following characterization methods: X-Ray diffraction (XRD) – to establish the crystallinity of the support and the size of Ni crystallites; N<sub>2</sub> adsorption-desorption isotherms – to calculate the surface area using BET method and the porosity using Dollimore-Heal model; temperature programmed reduction (TPR) – to estimate the strength of the metal-support interaction; electronic microscopy (STEM) – to analyze the size and dispersion of nickel nanoparticles; temperature programmed desorption (H<sub>2</sub>-TPD and CO<sub>2</sub>-TPD) to estimate the type and strength of catalytic active sites. The catalysts were tested using 0.5g catalyst at 600, 650 and 700°C, atmospheric pressure, CH<sub>4</sub>:CO<sub>2</sub>:H<sub>2</sub>O = 1:0.5:0.8 and GHSV=13647 h<sup>-1</sup>. The reaction products were analyzed on-line using a gas chromatograph.

## Results and Discussion

The catalysts structural parameters are given in Table 1.

Catalyst	$S_{tot}$ (m <sup>2</sup> /g)	$D_m$ (nm)	$D_{Ni}$ (nm)	$T_{red}$ (°C)
Ni/Al <sub>2</sub> O <sub>3</sub>	220	7.5 and 16	6	527
Ni/MgO/Al <sub>2</sub> O <sub>3</sub>	233	7.5 and 18	3.8	650
Ni/La <sub>2</sub> O <sub>3</sub> /Al <sub>2</sub> O <sub>3</sub>	209	7.5 and 16	2.5	420; 510

$S_{tot}$  – total surface area,  $D_m$  – pore medium diameter,  $D_{Ni}$  – nickel crystallite size,  $T_{red}$  – maximum TPR peak  
 It can be seen that the total surface area is not significantly changed by the addition of supplementary oxide. The bimodal porous structure is also unaffected by the existence of the second oxide. The Ni nanoparticle size and reduction temperature, instead, are influenced by MgO and La<sub>2</sub>O<sub>3</sub>. As previously reported the presence of La<sub>2</sub>O<sub>3</sub> contribute to better Ni dispersion and reducibility, and MgO also improve Ni dispersion, but decrease the reducibility of the catalyst precursor.

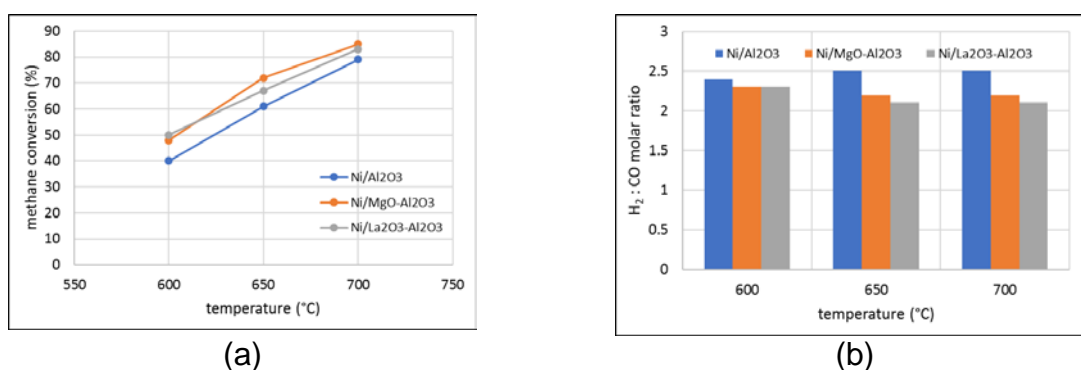


**Figure 1.** (a) methane conversion and (b) H<sub>2</sub>:CO ratio in CSDRM on Ni catalysts

The catalytic activity is expressed as methane conversion variation with temperature (Figure 1a). The addition of both MgO and La<sub>2</sub>O<sub>3</sub> contribute to a better methane conversion especially at low temperatures. At 700°C the methane conversion in the presence of Ni/MgO-Al<sub>2</sub>O<sub>3</sub> is almost 90%. Another important parameter is the ratio of H<sub>2</sub> and CO in the reaction products. By properly designing the reagents ratio, this parameter is obtained around 2 (Figure 1 b), the ideal value for further synthetic fuels preparation. The catalysts' stability was tested for 24h time on stream, proving no decrease of the catalytic performances. The characterization of used catalysts revealed the formation of filamentous carbon on the catalyst surface, which in the above mentioned conditions did not lead to catalyst deactivation

## References

- [1] D. Pakhare, J. Spivey, A review of dry (CO<sub>2</sub>) reforming of methane over noble metal catalysts, Chem. Soc. Rev., 43 (2014) 7813
- [2] M. Dan, M. Mihet, Z. Tasnadi-Asztalos, A. Imre-Lucaci, G. Katana, M. D. Lazar, Hydrogen production by ethanol steam reforming on nickel catalysts: Effect of support modification by CeO<sub>2</sub> and La<sub>2</sub>O<sub>3</sub>, Fuel, 147 (2015) 260-268
- [3] R. Yang, C. Xing, C. Lv, L. Shi, N. Tsubaki, Promotional effect of La<sub>2</sub>O<sub>3</sub> and CeO<sub>2</sub> on Ni/γ-Al<sub>2</sub>O<sub>3</sub> catalysts for CO<sub>2</sub> reforming of CH<sub>4</sub>, Appl. Catal. A: General, 385 (2010) 92-100

# Nanoscale Fe@SiO<sub>2</sub> Core-Shell Model Catalysts for Methanation of CO/CO<sub>2</sub> Mixtures

C. Zambrzycki, A. Straß-Eifert, R. Güttel

*Institute of Chemical Engineering, Ulm University, 89081 Ulm, Germany*

Iron based catalysts are widely used in Fischer-Tropsch synthesis and gained more and more attention for use in hydrogenation reactions in recent years [1,2]. One of the most prominent deactivation mechanisms in these catalytic reactions is the temperature driven sintering of metal nanoparticles associated with a loss of catalytic active surface [3]. In addition, it is well known that Fe based catalysts undergo complex structural changes during CO<sub>x</sub> hydrogenation, e.g. phase transformations, deposition of different carbon species and morphological changes [4]. Therefore, core-shell arrangements seem to be a promising possibility to manage both stabilization and deactivation issues properly [5]. A well controllable synthesis of these materials makes it possible to develop new strategies for the investigation of catalyst deactivation, which plays an important role in heterogeneous catalysis [4,6].

In this contribution the advantages of Fe based core-shell materials as stable model catalysts for studying catalyst deactivation during methanation of CO/CO<sub>2</sub> mixtures will be outlined. The systematic bottom-up synthesis strategy of the Fe based core-shell structures was achieved using a modified water-in-oil microemulsion system [7]. The physical-chemical properties of the material were investigated by X-ray diffraction, N<sub>2</sub> physisorption and transmission electron microscopy (Figure 1). Moreover, methanation activity of the core-shell catalysts was tested after H<sub>2</sub> activation at 1 bar and 260 to 400°C.

With defined variation of synthesis parameters Fe<sub>2</sub>O<sub>3</sub>@SiO<sub>2</sub> core-shell particles with core sizes < 10 nm, overall sizes of the composite particles < 30 nm and a broad range of metal loadings from 6 up to over 40 wt% (Fe based) can be obtained. The characterization of the samples after CO<sub>2</sub> methanation by TEM (Figure 1, left) revealed the thermal stability against sintering and that the most prominent reason for catalyst deactivation is not due to visible changes of the catalyst's structure. The catalytic test during CO<sub>2</sub> hydrogenation reveals an average reaction rate of  $1.32 \cdot 10^{-6}$  mol g<sub>Fe</sub><sup>-1</sup> s<sup>-1</sup> at 320 °C, 1 bar and at a stoichiometric H<sub>2</sub>/CO<sub>2</sub> ratio (Figure 1, right).

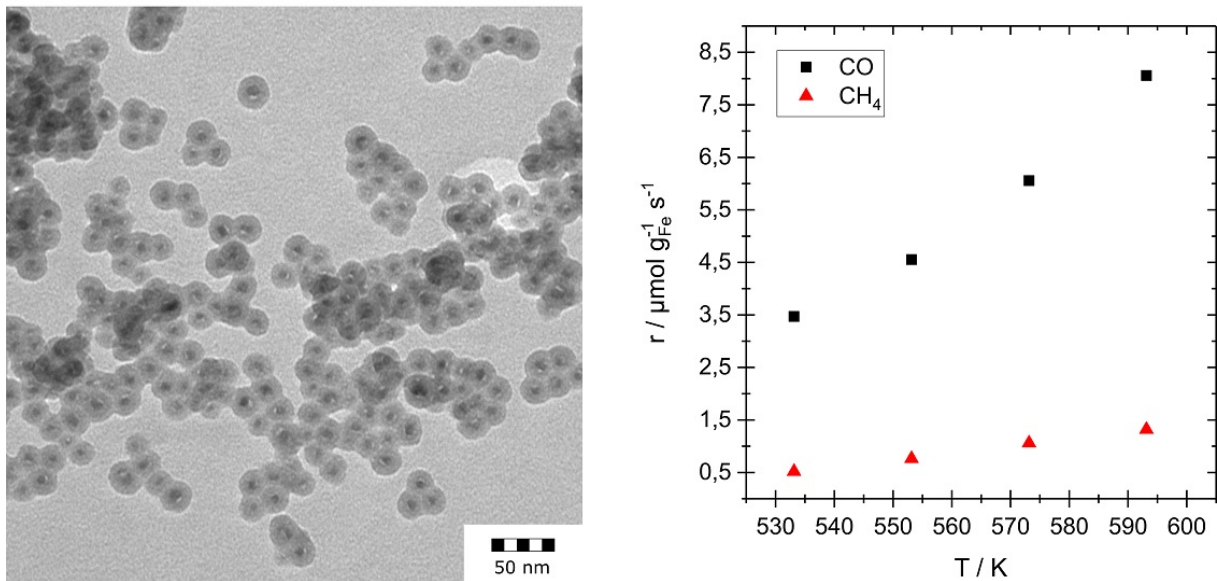


**Figure 1:** left: TEM micrograph of  $\text{Fe}_2\text{O}_3@\text{SiO}_2$  after 18h TOS (methanation at  $400^\circ\text{C}$ , 1 bar,  $\text{H}_2/\text{CO}_2 = 4/1$ ); right: temperature dependency of formation rates of CO and  $\text{CH}_4$  (methanation at  $260 - 320^\circ\text{C}$ , 1 bar,  $\text{H}_2/\text{CO}_2 = 4/1$ )

The variety of iron based core-shell catalysts regarding the size of the Fe core can help to study the size effect on intrinsic and transient kinetics, the reaction mechanism as well as deactivation processes (e.g. carbonization and reoxidation), as they offer a well-defined and easily accessible catalyst structure suitable for various characterization methods. Furthermore, Fe-based catalysts are also suitable to other catalytic processes besides methanation, which allow to transfer the methodology of the present contribution to other applications for exhaust treatment.

## References

- [1] M. Boutonnet, S. Lögberg, E. E. Svensson, *Curr. Opin. Colloid Interface Sci.* **2008**, *13*, 270-286.
- [2] J. Kirchner, J. K. Anolleck, H. Lösch, s. Kureti, *Appl. Catal. B: Environmental* **2018**, *223*, 47-59.
- [3] A. Cao, R. Lu, G. Veser, *Physical chemistry chemical physics: PCCP* **2010**, *12*, 13499-13510.
- [4] C. H. Bartholomew, *Applied Catalysis A: General* **2001**, *212*, 17-60.
- [5] F. Schüth, *Chem. Mater.* **2014**, *26*, 423-434.
- [6] J. A. Moulijn, A. E. van Diepen, F. Kapteijn, *Applied Catalysis A: General* **2001**, *212*, 3-16.
- [7] S. Takenaka, H. Umebayashi, E. Tanabe, H. Matsune, M. Kishida, *Journal of Catalysis* **2007**, *245*, 392-400.

# Catalytic oxidation of 5-hydroxymethylfurfural (HMF) to valuable dicarboxylic acids

Magdi El Fergani, Vasile I. Parvulescu, Simona M. Coman, Department of Organic Chemistry, Biochemistry and Catalysis, Faculty of Chemistry, University of Bucharest, Bucharest, Romania; Alina Tirsoaga, Catalysts and Catalytic Processes Research Center, Faculty of Chemistry, University of Bucharest, Bucharest, Romania

## 1. Scope

The catalytic transformation of biomass to high-value chemicals is one of the most attractive and challenging topics in heterogeneous catalysis. However, for such transformations an efficient separation of the catalyst through filtration or centrifugation encounters difficulties. To overcome this drawback, the use of magnetic solid catalysts, which can be efficiently separated by an external magnetic field without affecting the catalytic performances started to be considered as a potential economical approach. An enlightening example in this respect is the developed cationic Ru(III)-Fe<sub>3</sub>O<sub>4</sub>@SiO<sub>2</sub> magnetic catalyst able to transform different renewable raw materials into important platform molecules such as glucose, polyols, levulinic acid (LA) or succinic acid (SA) [1-3]. However, the high price of noble metals demands innovating cheap alternatives, where transition metal-based heterogeneous catalysts would be preferred. Thus, we focused our efforts for designing transition metal oxide (Mn, Co)-based Fe<sub>3</sub>O<sub>4</sub>@SiO<sub>2</sub> catalysts. The main purpose of the present study was, therefore, to compare the former Ru-Fe<sub>3</sub>O<sub>4</sub>@SiO<sub>2</sub> catalysts with the (Mn, Co)-based catalysts in terms of catalytic efficiency and stability in the HMF oxidation.

## 2. Results and discussion

In the presence of Ru-based catalysts, a selectivity to 2,5-furandicarboxylic acid (FDCA) of 64% was reached after 48h for total conversion of HMF (Figure 1A). *In-situ* modification of the catalyst with *n*-butylamine led to a slight decrease in HMF conversion but to a substantial increase of the selectivity to FDCA to 80.6% (Figure 1B). Replacing ruthenium with a transitional one and NaOH with *n*-butylamine ensured further advantages, such as the increase of HMF stability and the possibility to tune the selectivity for other valuable oxidation products. Thus, under similar reaction conditions, the Fe<sub>3</sub>O<sub>4</sub>@SiO<sub>2</sub>-CoO<sub>x</sub> catalyst provided selectivity to SA of 92.7% for a HMF conversion of 78.6%, and the Fe<sub>3</sub>O<sub>4</sub>@SiO<sub>2</sub>-MnO<sub>x</sub> catalyst led to

72% selectivity to MAc for HMF conversion of 5%. However, the performances in this reaction have been improved (85% selectivity to MAc for HMF conversion of 35.6%) working with a metal-free catalyst ( $\text{Fe}_3\text{O}_4@\text{SiO}_2\text{-NH}_2$ ), in which the  $\text{-NH}_2$  functionalization substituted the role of the homogeneous strong base. All the investigated catalysts showed very good stability.

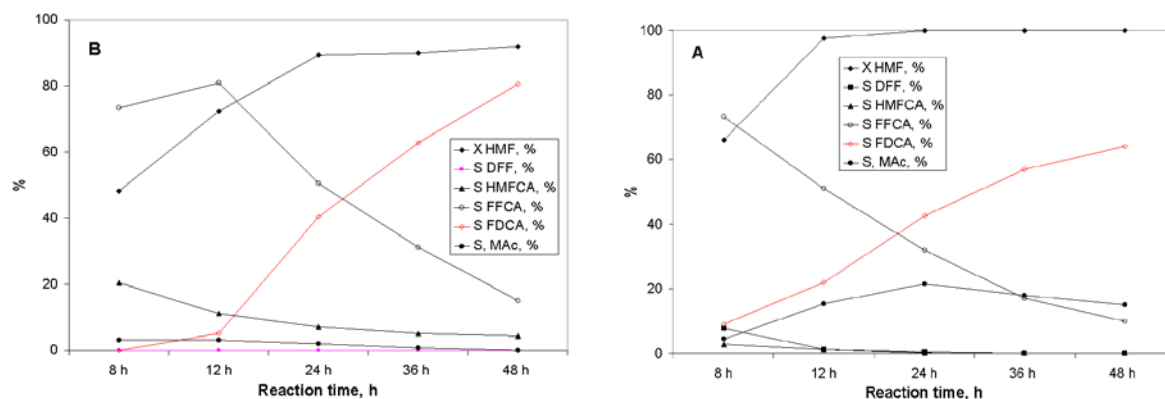


**Figure 1.** Time-evolution of the HMF oxidation in the presence of Ru (4wt%)- $\text{Fe}_3\text{O}_4@\text{SiO}_2$  (catalytic sites: cationic ruthenium (III) docked onto  $\text{-NH}_2$  groups) (A) and *bis*-amine modified Ru (4wt%)- $\text{Fe}_3\text{O}_4@\text{SiO}_2$  (B) catalysts (catalytic sites: Ru(IV)-*bis*-amine adducts).

### 3. Conclusions

In summary, Ru(IV)-*bis*-amine adducts afford an efficient catalytic system for the oxidation of HMF to FDCA. Under similar conditions, replacing Ru with Mn or Co tuned the selectivity in the sense of production of other valuable oxidation products, such as MAc or SA. The catalysts were magnetically separable, and showed no significant loss in catalytic activity during several recycling experiments. These newly developed catalytic systems are examples of sustainable alternatives for the selective valorization of biomass.

### 4. Acknowledgements

Prof. Simona M. Coman kindly acknowledges UEFISCDI for the financial support (project PN-III-P4-ID-PCE-2016-0533, Nr. 116/2017).

### References

- [1] Negoii, A.; Trotus, I.T.; Mamula Steiner, O.; Tudorache, M.; Kuncser, V.; Macovei, D.; Parvulescu, V.I.; Coman, S.M., *ChemSusChem* **2013**, *6*, 2090-2094
- [2] Podolean, I.; Kuncser, V.; Gheorghe, N.; Macovei, D.; Parvulescu, V. I.; Coman, S.M., *Green Chem.* **2013**, *15*, 3077-3082
- [3] Podolean, I.; Rizescu, C.; Bala, C.; Rotariu, L.; Parvulescu, V.I.; Coman, S.M.; Garcia, H., *ChemSusChem* **2016**, *9*, 2307-2311

## ***H<sub>2</sub> Thermo-Photo-Catalytic production over Ru co-catalyst TiO<sub>2</sub> materials***

*U. Caudillo-Flores,<sup>1</sup> G. Agostini,<sup>2</sup> C. Marini,<sup>2</sup> A. Kubacka,<sup>1</sup> M. Fernández-García,<sup>1</sup>*

*1) Instituto de Catálisis y Petroleoquímica, CSIC.C/Marie Curie 2, 28049-Madrid, Spain. [ucaudillo@gmail.com](mailto:ucaudillo@gmail.com);*

*2) Alba Synchrotron Light Source. Cerdanyola del Vallès, 08290 Barcelona, Spain*

Catalytic technologies to produce H<sub>2</sub> from bio-alcohols can use light or thermal energy and TiO<sub>2</sub> based materials. In the case of photocatalysis, the low reaction rates and consequently, low quantum efficiencies usually achieved have limited its industrial application. In the case of thermal catalysis, even though it can be an industrial technology, the reduction of the operation conditions (high temperature and pressure) of the process and the search of a good and stable catalyst appear as a key research activity for the future. Alternatively to both thermal or photon-based catalytic technologies, the combination of heat and light energy sources using the adequate catalytic material would drive to a convenient way to overcome most of the problems related to thermal or light alone based decontamination technologies [1]. Here we study the behavior of a series of Ru co-catalyst supported on TiO<sub>2</sub> support (this last, previously prepared by microwave and spray dryer, 70 m<sup>2</sup> g<sup>-1</sup>) materials in the thermo-photo-catalytic H<sub>2</sub> production using a methanol/water mixture, UV light and different temperature conditions in a gas phase reaction system.

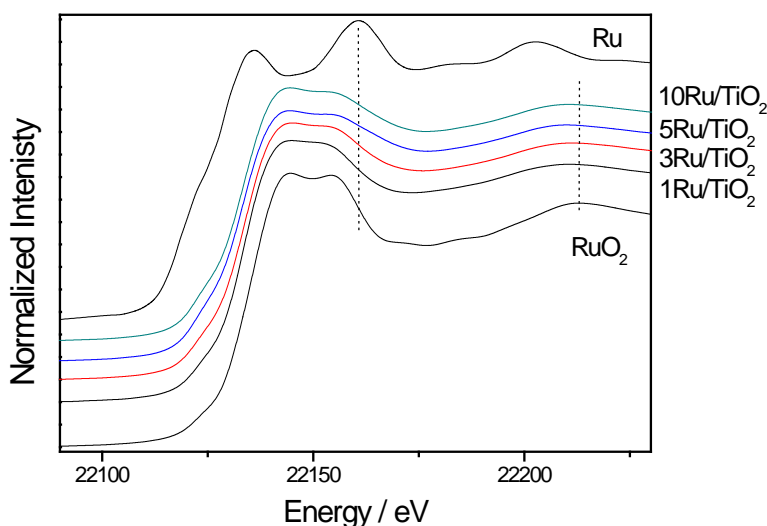


Figure 1. XANES of xRu/TiO<sub>2</sub> and reference materials.

The different xRu/TiO<sub>2</sub> materials prepared (x being the Ru weight %) were examined by X-ray absorption spectroscopy (XAS) in order to determine the oxidation nature of

the Ru species on the TiO<sub>2</sub> surface. The X-ray absorption near edge structure (XANES, Figure 1) indicate that all materials show a mixed state, ruthenium metallic and Ru(II) oxide, with the first increasing (from ca, 10 to 25 % of total Ru) with the ruthenium amount in the sample.

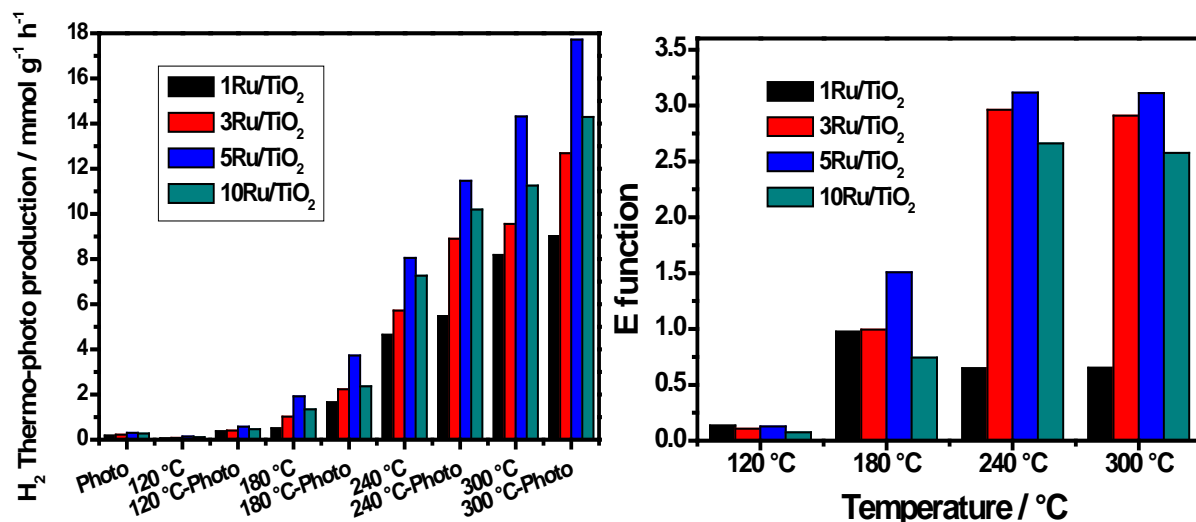


Figure 2. H<sub>2</sub> thermo-photo-catalytic production (Left) and Enhancement function (E function, described in eq. 1) vs Temperature (Right) for xRu/TiO<sub>2</sub> samples.

In Figure 2 (Left), it is observed that all Ru/TiO<sub>2</sub> materials are active under illumination conditions, having activity under heat at 120 °C. Comparing the results of both photo and thermal process, an enhancement in the H<sub>2</sub> production is appreciated in the combined use of the light and heat for all materials. To analyze the different process, in Fig. 2 (Right) we plot the enhancement function (E), measured as [1]:

$$E = \text{Rate (Thermo-photo)} - ((\text{Rate (photo)} + (\text{Rate (thermo)})) \quad (1)$$

It is observed that all xRu/TiO<sub>2</sub> materials show a favorable and clear synergic effect in the thermo-photo process with respect to the thermal or photo alone processes, which is more evident above 180 °C and reaches a plateau above 240 °C. The xRu/TiO<sub>2</sub> materials displays an improved performance under the combined (as well as the independent) use of the two energy sources that helps to increase in 5 times the H<sub>2</sub> production whit respect to precious metals, as Pt, Pd co-catalyst titania based materials [2]. This observation opens the opportunity of using Ru-titania co-catalyst systems as an interesting base material for thermo-photo catalytic processes. The physico-chemical basis of this process is analyzed using a multitechnique approach.

## References

- [1] M.J. Muñoz-Batista, et al., *Appl. Catal. B.* (2017) DOI: 10.1016/j.apcatb.2017.11.073  
 [2] U. Caudillo-Flores, et al., *Appl. Catal. B.* (2018); DOI: 10.1016/j.apcatb.2018.07.047



## Oriented MoS<sub>2</sub> Nanoplatelets Supported on few Layers Graphene as very active Catalysts for CO<sub>2</sub> Methanation

A. Primo,<sup>1</sup> J. He,<sup>1</sup> B. Jurca,<sup>2\*</sup> B. Cojocaru,<sup>2</sup> C. Bucur,<sup>2</sup> V.I. Parvulescu,<sup>2</sup> H. Garcia,<sup>2</sup>  
<sup>1</sup>University Bucharest, Romania, [bjurca@gmail.com](mailto:bjurca@gmail.com); <sup>2</sup>TUV Valencia, Spain

Recycling CO<sub>2</sub> emissions with the scope to produce fuels is envisaged as one of the ecologic alternatives [1]. Hydrogenation of CO<sub>2</sub> is a thermodynamically downhill transformation and, as an additional very important advantage, does not require noble metal catalysts. Adequate reaction rates can be achieved under reasonable conditions, also affording good selectivities [2]. Molybdenum oxides and chalcogenides have been proposed as alternative catalysts to platinum for a series of reactions, including hydrogen evolution in electrolysis, hydrodesulfuration and synthesis gas conversions [3]. Also, the use of graphene (G) as hydrogenation catalyst [4] and molybdenum disulfide supported on G for electrocatalytic hydrogen evolution have been considered a breakthrough [5]. Aimed at expanding the scope of MoS<sub>2</sub>/G as catalyst and considering the above-commented interest in CO<sub>2</sub> hydrogenation and reports on the molybdenum catalysts, the present contribution reports the catalytic activity of MoS<sub>2</sub>/G for CO<sub>2</sub> methanation, comparing the performance of MoS<sub>2</sub>/G with that of analogous MoO<sub>3</sub>/G, prepared by impregnation of preformed MoO<sub>3</sub> nanoparticles on G [6].

### Experimental section

*Samples* with loadings of MoS<sub>2</sub> in the range 0.9-12.7wt% were prepared by mixing (NH<sub>4</sub>)<sub>2</sub>MoS<sub>4</sub>, alginate acid and NH<sub>4</sub>OH in the right proportion. After evaporation, the solids were pyrolysed under argon flow at 250 °C for 2 h and, then, at 900 °C for 2 h and the powder was ground and exfoliated in water using a high intensity ultrasonic liquid processor. *Synthesis of MoO<sub>3</sub>/G samples* was made by sonication of different amounts of commercial MoO<sub>3</sub> with G in liquid suspensions. These samples were characterized Raman, XRD patterns, XPS, AFM, FESEM and HRTEM images. *Catalytic tests and kinetics* were performed with a Microactivity tester, PID Eng&Tech coupled on line at a chromatograf at temperatures between 300 and 500 °C. Kinetics was determined based on measured *diffusion coefficients* (Blanc's law), calculation of the Weisz-Prater criterion, rate constants and of the activation energies.

### Results and discussions

The *catalytic activity* of MoS<sub>2</sub>/G sharply contrasts with that of bulk MoS<sub>2</sub> for which CO is the major product and reflects the important role of graphene on the activity of

supported Mo species. However MoS<sub>2</sub> undergoes some desulfuration MoS<sub>2</sub> leading to an optimal MoO<sub>3</sub> that exhibits a remarkable activity and stability. Although less active than MoS<sub>2</sub>, the methanation was almost complete on MoO<sub>3</sub>/G. These results illustrate the potential of graphene as support of active molybdenum species in gas-phase hydrogenations. The particle size is a critical parameter controlling the catalytic activity. In the case of MoO<sub>3</sub> nanoparticles, their average particle size is not altered in the adsorption process and, consequently, higher loadings of 10 nm particles can be achieved, this resulting in an increasing catalytic activity. These results illustrate the potential of graphene as support of active molybdenum species in gas-phase hydrogenations.

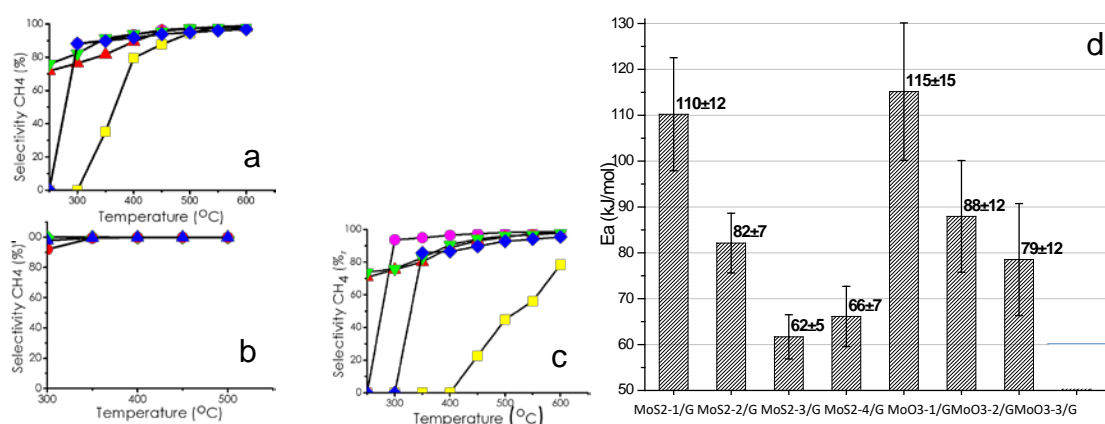


Figure 1. Selectivity methane (a, b and c) plots for CO<sub>2</sub> hydrogenation as a function of the temperature promoted by MoS<sub>2</sub>/G or MoO<sub>3</sub>/G catalysts and loading. Reaction conditions 20 mg catalyst amount: b) 15 bars; H<sub>2</sub>: 3 mL/min; CO<sub>2</sub>: 1 mL/min; c) 10 bars; H<sub>2</sub>: 3 mL/min; CO<sub>2</sub>: 1 mL/min; d) 10 bars, H<sub>2</sub>: 15 mL/min; CO<sub>2</sub>: 5 mL/min. ■) G; ●) MoS<sub>2</sub>-1/G; ▲) MoS<sub>2</sub>-2/G ▼) MoS<sub>2</sub>-3/G ◇) MoS<sub>2</sub>-4/G; and d) Comparison between the activation energy values for the methanation process in presence of the investigated graphene-based catalysts.

## Conclusions

MoS<sub>2</sub>/G is efficient in promoting the selective CO<sub>2</sub> methanation, but it undergoes a gradual deactivation attributable to the conversion of MoS<sub>2</sub> to MoO<sub>3</sub>. However, the methanation is almost complete on MoO<sub>3</sub>/G compared to MoS<sub>2</sub>/G on which part of the CO<sub>2</sub> is reduced only to CO. These results illustrate the potential of graphene as support of active molybdenum species in gas-phase hydrogenations.

## References

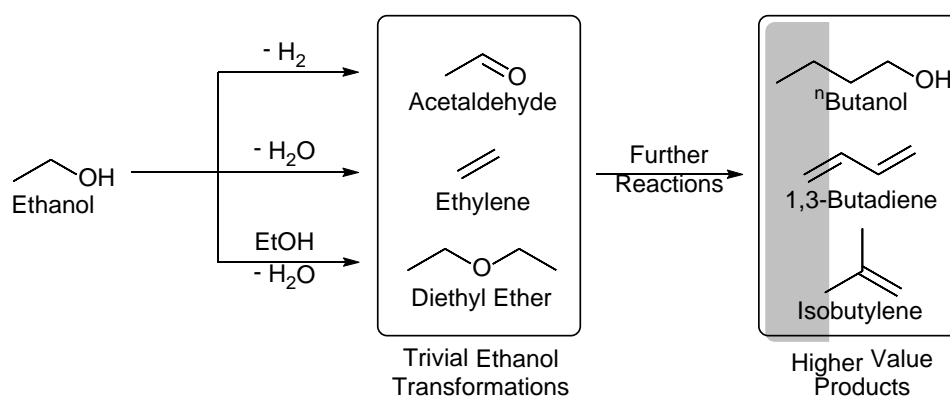
- [1] A. Corma, H. Garcia, *J. Catal.* **308** (2013) 168.
- [2] W. Wang, S. Wang, X. Ma, J. Gong, *Chem. Soc. Rev.* **40** (2011) 3703.
- [3] S. Zaman, K.J. Smith, *Catal. Rev.* **54** (2012) 41.
- [4] A. Primo, F. Neatu, M. Florea, V.I. Parvulescu, H. Garcia, *Nat. Commun.* **5** (2014) 5291.
- [5] F. Meng, J. Li, S.K. Cushing, M. Zhi, N. Wu, *JACS*, **135**, 2013, 10286.
- [6] A. Primo, J. He, B. Jurca, B. Cojocar, C. Bucur, V.I. Parvulescu, H. Garcia, *Appl. Catal. B: Environ.* **245** (2019) 351-359.

# Cascade Conversion of Bio-derived Platform Chemicals with Multifunctional Zeolitic Materials

*Samuel Raynes, Durham University, Durham, UK; Russell Taylor,\* Durham University, Durham, UK*

As of early 2017, more bio-derived ethanol is produced in the United States than demand for gasoline blending and exports exists.[1] Due to the wide array of reaction schemes that are accessible, ethanol is an extremely versatile platform molecule (Scheme 1).[2] Hence, excess bio-derived ethanol has the potential to be a cheap, convenient and renewable carbon source from which to produce high value chemicals that are typically derived from fossil fuels.

Zeolites, microporous aluminosilicate materials, are considered to be promising alternative materials to many current generation catalysts owing to their distinctive properties. Due to the multitude of potential modification techniques and their unique ability to confer shape-selectivity to reactions through channels and cages of molecular dimensions, catalysts can be attained that target production of small linear molecules such as <sup>n</sup>butanol and 1,3-butadiene. Zeolites have been suggested to perform these transformations in a single reaction process due to their ability to incorporate several disparate active centres into their frameworks and channel system.[3-5]



**Scheme 1: Trivial transformations and potential higher-value end products from the upgrading of bio-derived ethanol.**

In this work, the transformation of ethanol to acetaldehyde under flow conditions is effected over several framework morphologies, namely ZSM-5 (MFI), beta (BEA\*) and mordenite (MOR). It is shown by solution state <sup>1</sup>H NMR spectroscopy of the

liquid effluent that, whilst the former two frameworks produce large relative quantities of aromatics in both their protic and zinc-exchanged forms, MOR produces little to no aromatic products when compared to the desired acetaldehyde. Hence, we display that careful choice of framework morphology can lead to a significant decrease in liquid range side products within the liquid effluent of these transformations. Furthermore, the effect of parent zeolite form, be it H-MOR or Na-MOR, and modification method, either Zn exchange or impregnation, is shown to have a large effect on relative acetaldehyde production. Several other metal species (Fe, Co, Cu, etc.) have also been introduced into zeolites of interest and their reaction profiles monitored in a similar fashion. Further studies with on-line GC-MS analysis aim to better quantify these observations and from there allow calculation of total selectivity to the desired product, taking gaseous products into account also.

In addition to this, several Lewis basic species have been incorporated into zeolites and tested in a similar regime as above in order to probe the efficacy of aldol condensation of acetaldehyde to crotonaldehyde. Following discovery of a successful candidate, the two species are combined into the same zeolite sample and the new bifunctional catalysts tested for the total transformation of ethanol to crotonaldehyde. This process is repeated throughout the multistep synthesis in order to ascertain a multifunctional catalyst capable of the efficient and selective direct single-step transformation of ethanol to one of the previously specified higher value products.

## References

1. Administration, U.S.E.I. *U.S. fuel ethanol production continues to grow in 2017*. 2017 [cited 08/01/18; Available from: <https://www.eia.gov/todayinenergy/detail.php?id=32152>].
2. Sun, J. and Y. Wang, *Recent Advances in Catalytic Conversion of Ethanol to Chemicals*. ACS Catalysis, 2014. **4**(4): p. 1078-1090.
3. Kyriienko, P.I., et al., *Ethanol Conversion into 1,3-Butadiene by the Lebedev Method over MTaSiBEA Zeolites (M = Ag, Cu, Zn)*. ACS Sustainable Chemistry & Engineering, 2017. **5**(3): p. 2075-2083.
4. Dai, W.L., et al., *Zeolite Structural Confinement Effects Enhance One-Pot Catalytic Conversion of Ethanol to Butadiene*. ACS Catalysis, 2017. **7**(5): p. 3703-3706.
5. Ennaert, T., et al., *Potential and challenges of zeolite chemistry in the catalytic conversion of biomass*. Chemical Society Reviews, 2016. **45**(3): p. 584-611.

# In situ UV-vis characterization and activity testing of flat model catalysts in custom built micro reactors

*Hans O.A. Fredriksson, Syngaschem BV, Eindhoven, Netherlands;*

*J. W. (Hans) Niemantsverdriet, SynCat@DIFFER, Syngaschem BV, Eindhoven, Netherlands; SynCat@Beijing, Synfuels China Technology Co., Ltd, Huairou, PR China;*

## 1 Introduction

Catalysis research is complex and multidisciplinary in its nature. The performance of an industrially used catalyst is influenced by a multitude of factors, from material composition and oxidation state, support porosity, reactant and product distribution in the reactor as well as temperature gradients and local hot spots. Therefore, under “real” conditions, it is difficult to single out the most important properties of a catalyst. By preparing simplified model systems, it is possible to eliminate some of the variables. Applying in situ characterization to such model catalyst, during performance testing, allows us to learn about the dynamics of fundamental material properties under relevant conditions.

## 2 Experimental/methodology

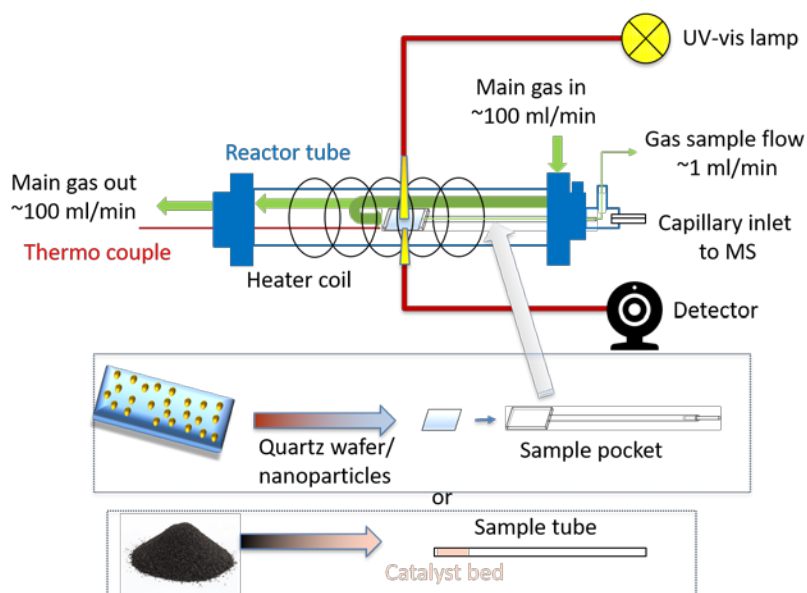


Figure 1 Custom made micro reactor for testing of flat model catalysts with in situ UV-vis spectroscopy and mass spectrometry. The design allows testing of catalysts with a total loading down to a few  $\mu\text{g}$ .

We prepare flat model catalysts, consisting of merely a few  $\mu\text{g}$  of catalytically active material and test them in a custom made micro reactor, equipped with in-situ mass

spectrometry and UV-vis spectroscopy as shown in figure 1. The same reactor can also be used to test industrial type powder catalysts. Several ex-situ techniques, such as TEM, XPS and XRD are also used to complement the in situ results.

### 3 Results and discussion

The flat model catalysts have the advantage that there are no hot spots or diffusion limitations in the gas phase that can obscure the findings and that all catalyst material is accessible to in-situ characterization. A range of model catalysts, from sub monolayer deposits of size selected nano clusters and thin particle films to nanoparticles supported on porous as well as non-porous 3D structures has been tested and various reactions such as Fischer-Tropsch synthesis, water-gas shift reaction, preferential oxidation of CO in H<sub>2</sub>, NH<sub>3</sub> decomposition and catalytic combustion of volatile organic compounds has been addressed[1–5]. A few examples will be presented, where the importance of the oxidation state of the active material and the interaction between catalyst, support and promoter is elucidated. Finally, we demonstrate that being able to perform measurements on both idealized, flat model catalysts and industrial grade catalysts in the same reactor, helps us confirm the relevance of the results in real applications.

### References

- [1] Y. Bu, S. Er, J.W. (Hans) Niemantsverdriet, H.O.A. Fredriksson, Preferential oxidation of CO in H<sub>2</sub> on Cu and Cu/CeO<sub>x</sub> catalysts studied by in situ UV-Vis and mass spectrometry and DFT, *J. Catal.* 357 (2018) 176–187.
- [2] Y. Bu, J.W. (Hans) Niemantsverdriet, H.O.A. Fredriksson, Cu model catalyst dynamics and CO-Oxidation kinetics studied by simultaneous in situ UV-Vis and mass spectroscopy, *ACS Catal.* 6 (2016) 2867–2876.
- [3] H.O.A. Fredriksson, E.M. Larsson Langhammer, J.W. Niemantsverdriet, Reduction of Cu-Promoted Fe model catalysts studied by in situ indirect nanoplasmonic sensing and X-ray photoelectron spectroscopy, *J. Phys. Chem. C.* 119 (2015) 4085–4094.
- [4] M. Dad, R.J. Lancee, M.J. van Vuuren, J. van de Loosdrecht, J.W.H. Niemantsverdriet, H.O.A. Fredriksson, SiO<sub>2</sub>-supported Fe & FeMn colloids—Fischer-Tropsch Synthesis on 3D model catalysts, *Appl. Catal. A Gen.* 537 (2017) 83–92.
- [5] Y. Bu, C.J. Weststrate, J.W. Niemantsverdriet, H.O.A. Fredriksson, Role of ZnO and CeO<sub>x</sub> in Cu-Based Model Catalysts in Activation of H<sub>2</sub>O and CO<sub>2</sub> Dynamics Studied by in Situ Ultraviolet-Visible and X-ray Photoelectron Spectroscopy, *ACS Catal.* 6 (2016) 7994–8003.

# Control of alumina textural properties by nanorods morphology and organization

Audrey Valette<sup>1,2</sup>, Christophe Vallée<sup>2</sup>, Mathieu Digne<sup>2</sup>, Séverine Humbert<sup>2</sup>, Olivier Durupthy<sup>1</sup>, Corinne Chanéac<sup>1</sup>

<sup>1</sup>*Sorbonne Université, CNRS, Collège de France, Laboratoire de Chimie de la Matière Condensée de Paris, 4 Place Jussieu, F-75005 Paris, France*

<sup>2</sup>*IFP Energies nouvelles, Rond-point de l'échangeur de Solaize, BP 3, 69360 Solaize, France*

**Key words:** Alumina, boehmite, nanorods, hydrothermal synthesis, catalysis, nanomaterial processing.

$\gamma$ -Al<sub>2</sub>O<sub>3</sub> is a porous material that is used as a support in heterogeneous catalysis, especially in petroleum chemistry[1]. Experimental and theoretical studies demonstrated that gamma alumina acid–base and catalytic properties are strongly related to particle morphology, through exposed crystalline faces[2]. The change of particles' morphology from isotropic to anisotropic has a direct impact on the exposed faces. They will be different, or the same but in different relative proportions and will lead to an improvement of catalytic properties. In addition, for anisotropic material such as nanorods, new textural properties with a strong increase of the pore volume[3] and diameter are achievable, which will lead to new diffusional properties. That is why anisotropic gamma alumina materials have been tested for different reactions like ethanol dehydration, ultra deep hydrodesulfurization and benzylic alcohol oxidation[4,5].

Gamma alumina is usually obtained through the topotactic transformation of boehmite  $\gamma$ -AlOOH above 450°C. The final product therefore is strongly related to the nature of the starting material. In this work, we have developed a simple and scalable synthesis for boehmite nanorods with well-controlled size in water and without any additives.

We present the rationalization of boehmite nanorods synthesis to get an aspect ratio higher than 10 and a section below 10 nm. We report the key experimental parameters that induce morphology change, from platelets to nanorods. Reaction temperature higher than 160 °C is mandatory to ensure rods formation in fair reaction time while Al(III) precursors' concentration and hydrolysis rates truly control the possibility to growth thin boehmite rods.

Coupled structural (XRD) and morphological (TEM) analyses to further characterize the nanorods and their formation steps allowed us to provide new insights on the formation mechanism. The nanorods are formed through oriented aggregation of primary nanoplatelets with a defined preferential growth direction. Then, the different exposed faces were identified by electron diffraction. The acid properties of these anisotropic materials have been compared to those of isotropic samples by means of IR spectroscopy (coupled with CO adsorption) and ethanol TPD.

Finally, we have processed boehmite nanorods into extrudates via kneading-extrusion and compared their textural properties to those obtained from nanoplatelets synthesis using the same protocol at lower temperature. Insights about the nanorods organization were obtained by SAXS and TEM analyses. Furthermore, we proved the increase of the pore volume when the anisotropic ratio increases (from  $0.51 \text{ cm}^3 \cdot \text{g}^{-1}$  for platelets to  $0.73 \text{ cm}^3 \cdot \text{g}^{-1}$  for nanorods) as expected by theoretical approach. The molecular transport properties of these nanorod-based extrudates were evaluated by pulsed field gradient NMR.

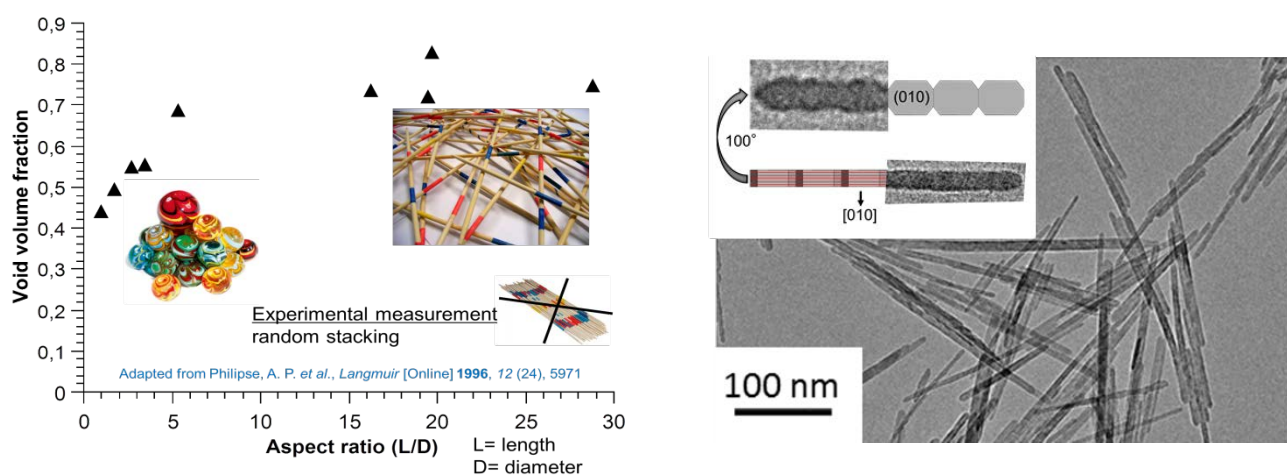


Figure 1 : Effect of the aspect ratio on the void volume fraction (left) and TEM image of boehmite nanorods with a diameter of 12 nm and 180 nm in length with an insert schematically representing the nanorods in 3D (right).

## References

- [1] P. Euzen *et al.*, Handbook of Porous Solids (2002) 1591–1677.
- [2] M. Digne *et al.*, Journal of Catalysis 226 (2004) 54–68.
- [3] A.P. Philipse, Langmuir 12 (1996) 5971.
- [4] L. Chen *et al.*, Microporous and Mesoporous Materials 266 (2018) 126–131.
- [5] J. N. Díaz de León *et al.*, Journal of Catalysis 321 (2015) 51–61.



## **Production of important fine chemicals by liquid phase catalytic hydrogenation of furfural**

*K.E. Salnikova, Tver Technical University, Tver, Russia, Tver State University, Tver, Russia; M.G. Sulman, Tver Technical University, Tver, Russia; Yurii V. Larichev, Boreskov Institute of Catalysis, Novosibirsk, Russia, Novosibirsk State University, Novosibirsk, Russia; S.P. Mikhailov, Tver State University, Tver, Russia; A.V. Bykov, Tver Technical University, Tver, Russia; V.G. Matveeva\*, Tver Technical University, Tver, Russia, Tver State University, Tver, Russia*

*\*Corresponding author: [matveeva@science.tver.ru](mailto:matveeva@science.tver.ru)*

The increasing interest to the biomass as a source of chemicals and energy has recently arisen due to the limited fossil fuel resources and the demand for new clean chemical processes [1]. The research on the development of alternative liquid transport fuels has considerably increased in recent years influenced by the implementation of legislation and directives on alternative energy. To achieve these aims in an ethical, environmental and economical manner the use of lignocellulosic biomass or agri-waste for the production of second generation biofuels is proposed [2]. Chemicals derived from biomass have recently attracted a considerable interest. The production of biofuels from hemicellulose requires acid hydrolysis to open the biomass structure giving large quantities of xylose. The synthesis of furfural (FF) as a by-product of this biofuel production process has developed an additional important research area. Furfural is one of the key derivatives which can be obtained from renewable biomass for the production of different important fine chemicals [3].

Selective hydrogenation of furfural has attracted much attention to the production of furfuryl alcohol (FA), methyl furan, tetrahydrofurfuryl alcohol and others. Furfuryl alcohol is widely used in chemical industry, mainly for the production of special resins, polymers and coatings on their basis, which are resistant to acids, alkalies and various solvents. In addition, furfuryl alcohol is employed as a diluent for epoxy resins and as a solvent for phenol formaldehyde resins and poorly soluble pigments. In the organic synthesis, furfuryl alcohol is a feedstock for the production of tetrahydrofurfuryl alcohol and 2,3-dihydropyran and an intermediate in the synthesis of lysine, vitamin C, various lubricants and plasticizers. There are two ways of producing furfuryl alcohol: through hydrogenation of furfural, gas phase

hydrogenation and liquid phase hydrogenation. In industry, furfuryl alcohol is obtained by catalytic hydrogenation of furfural in a liquid or vapor phase. The liquid-phase process is carried out with copper chromite systems as the catalysts. The main disadvantage of copper-chromite catalysts is their toxicity caused by the presence of chromium oxides, which allows considering such catalysts as environmental pollutants [2].

By varying the conditions of furfural hydrogenation (pressure, temperature, etc.), it is possible to regulate the selectivity to one or another product. In this paper, we want to demonstrate the use of hypercrosslinked polystyrene (HPS) as a stabilizer. HPS is the class of cross-linked polymers is characterized by the unique topology and unusual properties. HPS consists of nanosized rigid micro- and meso-cavities. This material can act as a nanostructured matrix, which governs the particles growth [4]. The nanoparticles of catalytically active metals such as Ru, Pt, Pd were successfully stabilized in the pores of the HPS matrix and showed high catalytic activity in the selective hydrogenation reactions [5, 6]. In addition, HPS is commercially available and produced on an industrial scale (PUROLATE International Ltd).

This research is devoted to the development of the catalytic system (namely, the choice of precursor) and to the determination of furfural hydrogenation conditions for achieving maximum selectivity to furfuryl alcohol.

## **Acknowledgements**

The research leading to these results has received funding from the Russian Science Foundation (project 18-19-00240) and from the Foundation for Assistance to the Development of Small Enterprises in the Scientific and Technical Sphere (program "Member of the youth science and innovation competition", grant 50098).

## **References**

- [1] A. Halilu, T.H. Ali, A.Y. Atta, P. Sudarsanam, S.K. Bhargava, S.B. Abd Hamid. *Energy Fuels*. 30 (2016) 2216–2226.
- [2] M. J. Taylor, L. J. Durndell, M. A. Isaacs, C. M. Parlett, A. K. Wilson, A. F. Lee, G. Kyriakou. *Appl. Catal. B*. 180 (2016) 580–585.
- [3] L. Hu, G. Zhao, W. Hao, X. Tang, Y. Sun, L. Lin, S. Liu. *RSC Adv*. 2 (2012) 11184–11206.
- [4] L.M. Bronstein, V.G. Matveeva, E.M. Sulman. *Nanoparticulate Catalysts Based on Nanostructured Polymers. Nanoparticles and Catalysis* Ed. Didier Astruc' Wiley-VCH , Weinheim, 2007, 640 pp.
- [5] V.N. Sapunov, M.Ye. Grigoryev, E.M. Sulman, M.B. Konyaeva, V.G. Matveeva. *J. Phys. Chem. A*. 117 (2013) 4073–4083.
- [6] V.G. Matveeva, E.M. Sulman, O.V. Manaenkov, A.E. Filatova, O.V. Kislitzka, A.I. Sidorov, V.Y. Doluda, M.G. Sulman, E.V. Rebrov. *Catalysis Today*. 280 (2017) 45-50.

# Kinetic Analysis of the Oxidative Dehydrogenation of Ethane over a NiSnO catalysts.

Carlos Alvarado C.<sup>1,2</sup>, Jeroen Poissonnie<sup>2</sup>, Joris W. Thybaut<sup>2</sup>, Carlos O. Castillo-Araiza<sup>1</sup>

<sup>1</sup> Autonomous Metropolitan University, Group of Processes of Transport and Reaction in Multiphase Systems, Mexico City, Mexico/

<sup>2</sup>Laboratory for Chemical Technology Ghent University, Ghent, Belgium.

## 1. Introduction

Oxidative dehydrogenation of ethane (ODH-C<sub>2</sub>) is a promising alternative reaction to produce ethylene since it overcomes main limitations in current conventional processes [1-3]. Nevertheless, its implementation at industrial scale critically depends on the rational design of a highly selective catalyst. Because of their high selectivity towards ethylene, nickel (Ni) and vanadium (V) based materials have been already rather widely investigated, the focus was mainly at the macroscopic level, i.e., less relevant for the rational optimization of this type of catalytic materials. This contribution aims at developing a kinetic analysis at microscopic level of ODH-C<sub>2</sub> over a Ni-Sn-O catalyst accounting for well-established experimental and theoretical stages.

## 2. Results and Discussion

Steady-state experiments were performed at total pressures from 1 to 5 bar, temperatures from 350 to 480 °C, an O<sub>2</sub> inlet concentration from 3 to 9 mol%, and space velocity from 2300 to 10260 hr<sup>-1</sup>. All the experiments were carried out in intrinsic regime, in a laboratory-scale micro-reaction unit (Micromeretics PID ENG&TECH model MA12216). To relate the reaction rates to the varying operating conditions via the corresponding reaction mechanisms taking place at the investigated operating conditions, five kinetic models based on Langmuir-Hinshelwood-Hougen-Watson (LHHW) and Mars-van Krevelen (MvK) formalisms were derived. Table 1 presents the main characteristics of these models. The MvK model (MvK-2) exhibited the best capacity to fit the observations, i.e., the F-value obtained for the MvK-2 model amounted to 1870, a value which exceeds those obtained for model MvK-1 (1277), LHHW-3 (1240), LHHW-2(924) and LHHW-1 (828), by a factor of 1.4, 1.5, 2.0 and 2.3, respectively. The obtained kinetic parameters indicated that: (i) ethylene formation has the lowest activation energy(see Table. 1); (ii) for all models the total oxidation of ethane relates to the highest activation energy (see Table. 1); (iii) the partial pressure of O<sub>2</sub> is the main variable influencing the selectivity towards ethylene; (iv) when oxygen adsorption is dissociative, the models exhibit to higher F values; (v) the fractional coverage of the surface at the outlet is the highest for water, ranging from 25.0% to 75.0% approximately, while the fractional coverage of ethane and oxygen oscillated

from 5.0% to 20.0% and from 0.0% to 10.0% respectively, and the fractional coverage of carbon oxides and ethylene never exceeded 5%. The latter observation shows that water, being one of the main reaction products in ODH-Et, is, the main component negatively impacting reaction rates.

Figure 1. a) Parity plot comparing experimental with calculated reactor outlet molar flow rates for MVK- model.

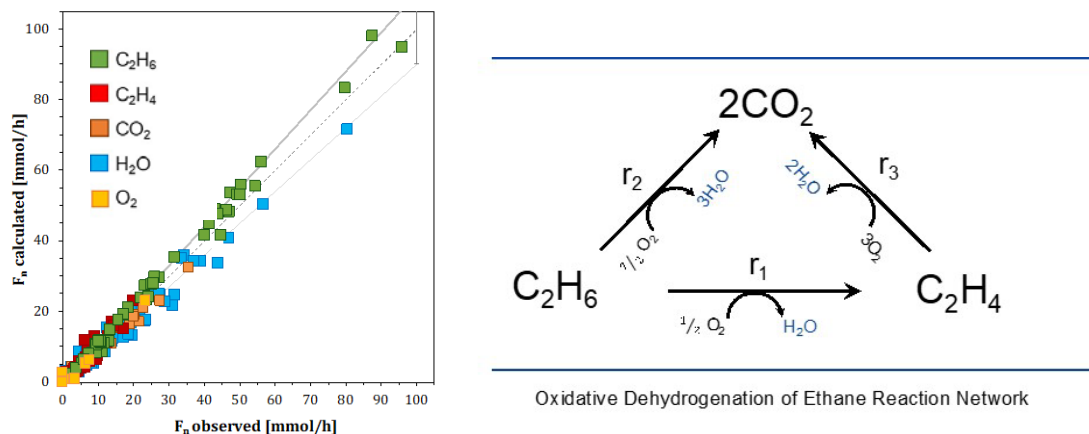


Table 1. Characteristics of the models

MODEL NAME	LHHW1	LHHW2	LHHW3	MVK1	MVK2
Oxygen adsorption and Rate Limiting Step	Dissociative RLS Reactions	Molecular RLS Reactions	Dissociative RLS Reactions	Catalyst reoxidation order n= 1.0 RLS Reactions	Catalyst reoxidation order n= 0.5 RLS Reactions
References construction model	Heynderickx <sup>d</sup>	Heynderickx <sup>d</sup>	Stegelman <sup>e</sup>	Heracleous <sup>e</sup>	Heynderickx <sup>d</sup>
No. Parameters	16	16	16	8	8
FVALUE	828	924	1240	1277	1870
Activation Energies KJ/mol	Ea <sub>1</sub> = 70 Ea <sub>2</sub> = 113 Ea <sub>3</sub> = 106	Ea <sub>1</sub> =78 Ea <sub>2</sub> =131 Ea <sub>3</sub> =115	Ea <sub>1</sub> =70 Ea <sub>2</sub> =103 Ea <sub>3</sub> =150	Ea <sub>1</sub> =77 Ea <sub>2</sub> =80 Ea <sub>3</sub> =83 Ea <sub>4</sub> = 167	Ea <sub>1</sub> = 78 Ea <sub>2</sub> = 81 Ea <sub>3</sub> = 84 Ea <sub>4</sub> = 137

## Conclusion

The ODH-C<sub>2</sub> kinetic analysis allows acquiring a better understanding of the corresponding the reaction mechanism over Ni-Sn-O catalyst. Both physicochemical and statistical criteria are employed to compare the performance of the constructed kinetic models and to define the most suitable one. Although the five models reported, in general, physical meaningful parameters and consistent statistics, the MVK-2 model is found to exhibit the best capacity to reproduce the referred experimental information.

## References

- [1] Che-Galicia, G., Quintana-Solórzano, R., Ruiz-Martínez, R. S., Valente, J. S. y Castillo-Araiza, C. O. Kinetic modeling of the oxidative dehydrogenation of ethane to ethylene over a MoVTaNbO catalytic system. *Chem. Eng. J.* 252, 75–88 (2014).
- [2] Solsona, B. López-Nieto, J. M., Agouram S., Soriano M. D., Dejoz A., Vazquez M. I. y Concepción P. Optimizing Both Catalyst Preparation and Catalytic Behaviour for the Oxidative Dehydrogenation of Ethane of Ni–Sn–O Catalysts. *Top. Catal.* 59, 1564–1572 (2016).
- [3] Heracleous, E. y Lemonidou, A. A. Ni-Me-O mixed metal oxides for the effective oxidative dehydrogenation of ethane to ethylene - Effect of promoting metal Me. *J. Catal.* 270, 67–75 (2010).
- [4] M.P. Heynderickx, J.W. Thybaut, H. Poelman, D. Poelman, G.B. Marin, Kinetic modeling of the total oxidation of propane over CuO–CeO<sub>2</sub>/c-Al<sub>2</sub>O<sub>3</sub>, *Appl. Catal. B: Environ.* 95 (2010) 26–38.
- [5] C. Stegelmann, N.C. Schiødt, C.T. Campbell, and P. Stoltze. Microkinetic modeling of ethylene oxidation over silver. *J. Catal.* 221 (2004) 630–649.

# Nanosize Effect of the Supported Fe Nanoparticles in the Hydrogenation Processes and Water Shift Gas Reaction

*Kalishyn Ye. Yu.*

*L. V. Pysarzhevsky Institute of the Physical Chemistry of the National Academy of Sciences of Ukraine; Prospect Nauky, 31; Kyiv-03028; Ukraine.*

[kalishyn.yevhen@gmail.com](mailto:kalishyn.yevhen@gmail.com)

The range of applications of heterogeneous catalysis covers chemical manufacturing, energy harvesting, conversion, and storage, to environmental technology. Many commercially important catalysts comprise catalytically active nanoparticles dispersed on supports various types. Such catalysts are typically highly complex multi-component materials that are optimized to work for millions of turnovers, at high reaction rates, and with high selectivity. The performance of metal particles in catalytic reactions is could governed by their size. One of the most used metals in heterogeneous catalysis is the iron. It can catalyze various processes, such as hydrogenation, oxidation, alkylation etc.

In this work, the structure sensitivity of various catalytic reactions that are catalyzed by supported Fe nanoparticles was shown. It was synthesized the series Fe containing catalysts in the range of the nanoparticles 2 – 15 nm. The structure and morphological properties of catalysts were studied in detail. We examined the structure sensitivity of the ethylene hydrogenation and water shift gas reaction processes catalyzed by Fe supported nanoparticles.

Fig. 1 indicates the dependence the rate reaction of the ethylene hydrogenation on the size of supported Fe nanoparticles in the Fe/CNT catalysts.

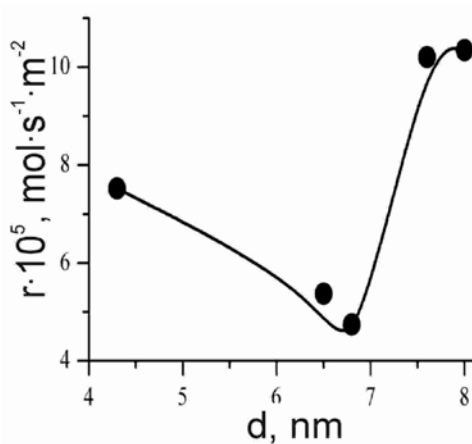


**Fig. 1.** The dependence of reaction rate of ethylene hydrogenation on size of supported Fe nanoparticles in Fe/CNT

Our experimental studies have shown that the reaction of ethylene hydrogenation in the certain conditions on the nanophase Fe/CNT is structural sensitive.

The mostly structure sensitivity of catalytic reaction is characterized by linear dependencies the rate of reaction on the size or volcano shape curve, whereas we first observed nonlinear dependence the rate of ethylene hydrogenation on the size of supported nanoparticles with the minimum.

# Selective Hydrogenation of Levulinic Acid over Polymer-Based Ruthenium Catalysts

*L.Zh. Nikoshvili, M.E. Grigorev, D.A. Abusuek, I.I. Protsenko, M.G. Sulman, E.M. Sulman, Tver Technical University, Tver, Russia*

The biofuels of the first generation are produced from sugars, starches and vegetable oils; however, the limited availability of starting materials (due to restricted amounts of fertile soils) and competition with food from feedstocks are limiting factors for their production [1]. The advanced biofuels of the second generation are mainly produced from lignocellulosic biomass, one of the most inexpensive and abundant raw materials. Levulinic acid (LA) is a substance, which can be obtained from cellulosic biomass via acid hydrolysis [2]. Hydrogenation of LA to gamma-valerolactone (GVL) is one of the most promising reactions in the field of biomass valorization to fine chemicals and liquid transportation fuels [3]. Potentially, GVL obtained from lignocellulosic biomass is a versatile intermediate for the production of fuel additives and chemicals. Due to high demand for GVL, its efficient production is currently a topic of intensive research. Investigations are mainly focused on hydrogenation of LA and its esters by molecular hydrogen in the presence of metal catalysts. Application of supported metal catalysts is especially advantageous, owing to simplicity of product recovery and catalyst recycling [4].

5%-Ru/C [5], 10%-Pd/C and Raney Ni [6] are the most widespread heterogeneous catalysts of the GVL synthesis from LA. Currently, the conventional catalyst of the LA hydrogenation is 5%-Ru/C [7], the use of which allows achieving high yields of GVL. In order to achieve high degrees of the LA conversion, the use of ruthenium nanoparticles (NPs) with high surface areas is important. It allows competing with and surpassing the traditional industrial catalysts such as Ru/C. However, for successful use of Ru NPs in the LA hydrogenation the former should be stabilized. A successful solution to this problem, i.e., providing control over the size and size distribution of catalytically active metal NPs, is possible via the use of stabilizing agents, the most promising among which are porous polymers. Highly-porous hyper-cross-linked polystyrene (HPS) based catalysts were successfully used in different oxidation and hydrogenation processes.

This work is devoted to the use of ruthenium-containing catalysts based on HPS in the hydrogenation of LA to GVL. Ru-containing NPs immobilized in HPS were synthesized

at the variation of Ru loading and type of HPS (functionalized or without functional groups). Hydrogenation of LA was carried out in Parr Series 5000 Multiple Reactor System in an aqueous medium at the variation of reaction temperature and hydrogen partial pressure. Samples of the reaction mixture were analyzed via HPLC method.

Synthesized catalysts were found to be highly active and selective in the hydrogenation of LA to GVL. For example, the use of HPS of MN100 type (functionalized with amino groups) as a support for the development of the catalysts allowed more than 99% yield of GVL for 120 min of reaction duration at mild reaction conditions (90°C, 2 MPa of hydrogen partial pressure) in an aqueous medium. It is noteworthy that NPs of hydrated RuO<sub>2</sub>, which were located on the surface of the polymeric matrix and in its pores as grape-like aggregates, was found to be an active phase of HPS-based Ru catalysts.

Moreover, for the most active HPS-based catalyst, main kinetic parameters (apparent activation energy, reaction orders) were calculated and formal kinetic modeling was carried out for deeper understanding of the observed kinetic behavior.

### **Acknowledgments**

This work was supported by the Russian Foundation for Basic Research (project 18-58-80008)

### **References**

1. D.M. Alonso, J.Q. Bond, J.A. Dumesic, *Green Chem.*, 12 (2010) 1493.
2. D. Sivasubramaniam, N.A.S. Amin, *Chem. Eng. Transactions*, 45 (2015) 907.
3. R.O.M.A. De Souza, L.S.M. Miranda, L. Rafael L., *Green Chem.*, 16 (2014) 2386.
4. M.G. Al-Shaal, M. Calin, I. Delidovich, R. Palkovits, *Catal. Commun.*, 75 (2016) 65.
5. A.M.R. Galletti, C. Antonetti, V. De Luise, M. Martinelli, *Green Chem.*, 14 (2012) 688.
6. Zh. Yan, L. Lin, Sh. Liu, *Energy & Fuels*, 23 (2009) 3853.
7. M. Selva, M. Gottardo, A. Perosa, *ACS Sustain. Chem. Eng.*, 1 (2013) 180.



# Computational Insights into Hydrodeoxygenation of Biomass-derived $\gamma$ -Valerolactone on Ru(0001) and Rh(111)

*Minttu Maria Kauppinen and Karoliina Honkala,*

*Department of Chemistry, NSC, FI-40014, University of Jyväskylä, Finland*

## Introduction

Lignocellulosic biomass is a potential renewable source of hydrocarbons suitable for transportation fuels, and in recent years a variety of valorisation processes have been investigated[1]. Levulinic acid (LA) is one of the top value added biomass derived chemicals. LA can be converted into C<sub>10</sub>-dimers via aldol condensation to increase chain length of products[2]. Recently,  $\gamma$ -nonalactone (GNL) has been used as a model compound to study the hydrodeoxygenation (HDO) of the LA dimers into C<sub>8</sub> and C<sub>9</sub> hydrocarbons over Ru/ZrO<sub>2</sub> and Rh/ZrO<sub>2</sub>, the latter being the more selective towards the desired hydrocarbons[3]. One suggested pathway is the direct conversion of GNL into alcohols which can be further hydrogenated to yield C<sub>8</sub> hydrocarbons (see Fig.1). However, undesirable ketones were also formed over both catalysts.

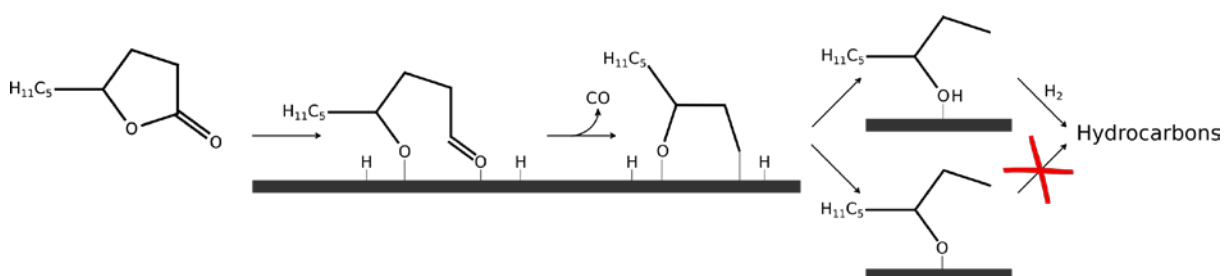


**Fig. 1:** Simplified reaction route for alcohol and ketone formation from GNL.

In this computational study, we will address the elementary reactions involved in the HDO reaction network using density-functional theory (DFT) in order to rationalise the differences in selectivity and activity between the two catalysts.

## Computational Methods & Models

The DFT calculations were carried out in the grid-based projector augmented wave (PAW) formalism using the GPAW software with BEEF-vdW density functional and PAW setups. A grid basis with a 0.19 Å maximum grid spacing was used in all calculations. Transition states were located using a climbing image automated nudged elastic band (CI-AutoNEB) method. The Rh and Ru catalysts were modeled with four layers thick 3x3 supercells of (111) and (0001) surface slabs, respectively.  $\gamma$ -Valerolactone (GVL) was used as a model compound for GNL.

## Results & Conclusions

The thermodynamics of adsorption of GVL and hydrogen and the ring-opening, decarbonylation, and hydrogenation steps were calculated on Rh(111) and Ru(0001)(see Fig. 2).

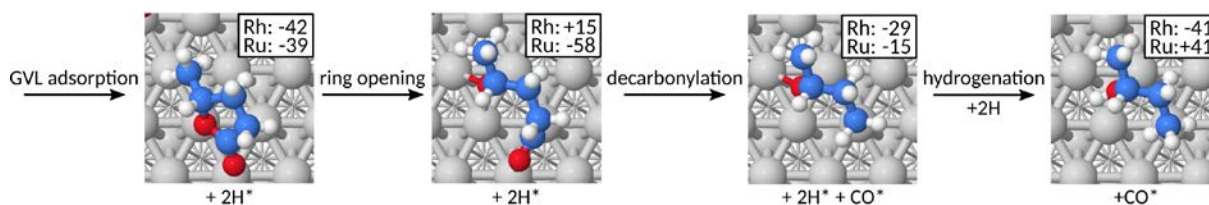


Fig. 2: Adsorption geometries of important intermediates on Rh(111). Rh, O, H, and C atoms are shown in grey, red, white, and blue, respectively. The reaction energy of each elementary step is reported in  $\text{kJ} / \text{mol}^{-1}$ .

GVL adsorbs on both surfaces equally exothermically with similar adsorption geometries. Dissociative hydrogen adsorption is exothermic by 53 and 78  $\text{kJ} / \text{mol}^{-1}$  on Rh and Ru, respectively. Ring opening is more thermodynamically favourable on Ru. The decarbonylation step is slightly more favourable on Rh than Ru, but is exothermic on both metals. Hydrogenation of the decarbonylated intermediate into the alcohol product is more favourable on Rh than Ru by 82  $\text{kJ} / \text{mol}^{-1}$ .

The Rh and Ru surfaces show clear differences in adsorption and reaction energies of the first steps of hydrodeoxygenation of  $\gamma$ -Valerolactone. These results together with additional calculations of elementary steps and kinetic barriers will help rationalise the different behavior observed experimentally for the two metal catalysts.

## References

- [1] Huber, G. W.; Cortright, R. D.; Dumesic, J. A. *Angew. Chem., Int. Ed.* 2004, 43, 1549. ;Corma, A.; Iborra, S.; Velty, A. *Chem. Rev.* 2007, 107, 2411. ; Vispute, T. P.; Zhang, H. Y.; Sanna, A.; Xiao, R.; Huber, G. W. *Science* 2010, 330, 1222.
- [2] Blessing, R. W.; Petrus, L. WO 2006/056591 A1, 2006. Kaldstrom, M.; Lindblad, M.; Lamminpaa, K.; Wallenius, S.; Toppinen, S. *Ind. Eng. Chem. Res.* 2017, 56, 13356.
- [3] Gonzalez Escobedo, J. L.; Makela, E.; Braunschweiler, A.; Lehtonen, J.; Lindblad, M.; Puurunen, R. L.; Karinen, R. Unpublished.

# Direct oxidation of methane to methanol over Cu-zeolites at mild conditions

*Mauro Álvarez; Pablo Marín; Salvador Ordóñez,*

*Dep. of Chemical and Environmental Engineering, University of Oviedo,*

*Facultad de Química, Julián Clavería 8, Oviedo, Spain*

## 1. Introduction

Methane is a powerful greenhouse gas (global warming potential 28 times higher than carbon dioxide) with increasing atmospheric concentration in the last decades. Therefore, its capture and harnessing is of great interest to fight against climate change [1]. Transforming it into a product with higher superior energy and easier to transport seem like a better solution than just flaring into the atmosphere.

Nowadays the commercially established technology for methane upgrading is steam reforming, which is a process that requires a lot of energy and a high capital investment. Finding a suitable technique capable of producing methanol by direct oxidation at mild reaction conditions is highly desirable.

The scope of this work is to produce methanol directly from methane at mild reaction conditions (less than 200°C), using different Cu-zeolites as heterogeneous catalysis [2, 3].

## 2. Experimental

The catalysts, Cu-MOR and Cu-ZSM5, were prepared by ion exchange using a copper acetate solution, followed by drying and calcination. The catalysts were characterized by ICP-MS, DRX and BET surface analysis.

The experiments were performed in a fixed bed isothermal reactor of 3/8" OD, charged with 3 g of catalyst (particle size 355-1000 µm). Pressure was maintained constant to 1 atm through all the tests. The catalyst was activated using a flow of pure oxygen with a ramp of 1°C/min up to 450°C for 4 h.

The reactor effluent was sent to a cold trap where condensable compounds (water, methanol, etc.) are recovered. The liquid samples were analyzed in a Shimadzu gas chromatograph GC-2010, equipped with a CP-Sil 8CB column and an FID detector. The reactor effluent can also be analyzed in an OmniStar GSD 301 mass spectrometer (MS).

### 3. Results and discussion

First, the adsorption of methane on the catalysts was tested at reaction conditions. A flow of pure methane was fed into the reactor at 200°C for 20 min. Then, pure oxygen was introduced and temperature was increased with a ramp of 10°C/min. The reactor effluent was analyzed by MS. Obtained result shows the CO<sub>2</sub> signal, generated by oxidation of the adsorbed methane when temperature increases. The presence of two peaks suggests there are two active sites on the catalyst surface of different strength. The same signal is obtained when the test is done in the absence of oxygen, so oxygen atoms from the catalyst can also oxidize adsorbed methane.

The methane to methanol reaction was accomplished in two steps: adsorption of methane and desorption of methanol in a gas flow of 2% H<sub>2</sub>O/N<sub>2</sub>. Different temperatures were tested for both steps, the optimal results being obtained performing the adsorption step at 200°C and the desorption steps at 150°C. To test the regeneration capacity of the catalysts, several reaction and activation cycles were repeated at these optimal conditions, obtaining a similar methanol value after every cycle. For the Cu-MOR zeolite, 12.35 μmol<sub>methanol</sub>/g<sub>cat</sub> was obtained in the fourth cycle.

It has been demonstrated that Cu-zeolites can successfully adsorb methane and catalyse its oxidation to methanol in cyclic processes at low temperature (200°C) and pressure (1 atm). This is an important advantage with respect to commercial processes based on wet reforming. Nevertheless, further research is needed to simplify and optimize the cyclic process.

#### Acknowledgments

This project was funded by the Research Found for Coal and Steel (UE-17-RFCS216-METHENERGY).

#### References

- [1] Ravi, M., M. Ranocchiari, and J.A. van Bokhoven. *Angewandte Chemie International Edition*, 2017. 56(52): p. 16464-16483.
- [2] Alayon, E.M., et al., *Chemical Communications*, 2012. 48(3): p. 404-406.
- [3] Narsimhan, K., et al. *Acs Central Science*, 2016. 2(6): p. 424-429.

## **Bifunctional Pt Modified Beta-Bentonite Extrudates for Hydroisomerization of Straight Chain Paraffinic Hydrocarbons**

*Zuzana Vajglová<sup>1</sup>, Narendra Kumar<sup>1</sup>, Markus Peurla<sup>2</sup>, Leena Hupa<sup>1</sup>, Kirill Semikin<sup>3</sup>, Dmitry A. Sladkovsky<sup>3</sup>, Dmitry Yu. Murzin<sup>1</sup>*

*<sup>1</sup>Åbo Akademi University, Johan Gadolin Process Chemistry Centre, Biskopsgatan 8, Turku/Åbo, Finland; <sup>2</sup>University of Turku, Turku, Finland; <sup>3</sup>St. Petersburg State Institute of Technology, St. Petersburg, Russia*

Hydroisomerization of straight chain paraffinic hydrocarbons C5–C6 is one of the cheapest ways to increase the production of high octane gasoline components with improved environmental characteristics. Linear alkanes such as n-hexane and n-heptane are characterized with low octane numbers, while the (hydro)isomerization increases the octane numbers substantially if multi-branched/di-branched isomers are obtained [1].

Isomerization of n-alkanes over bifunctional metal/acid catalysts involves dehydrogenation of alkanes, skeletal isomerization of olefins and hydrogenation of the latter. Hydrogenation and dehydrogenation happen on the metallic sites, while isomerization or cracking require acid sites, thus diffusion of the olefinic intermediates from metallic sites to acidic ones and back is important [1, 2]. From this description of bifunctional catalytic transformations, it seems obvious that the catalyst properties: activity, stability and selectivity, should depend on two main parameters: the characteristics of the metal and acid sites and those of the diffusion path of these intermediates, essentially the acidic component micropores [1]. In order to reduce the degree of complexity, usually studies on hydroisomerization catalysts are carried out over bifunctional zeolite-based catalysts in the powder form [3]. However, if a zeolite based catalyst is to be used at an industrial level, it is shaped into bodies such as granules, spheres, and extrudates.

This work aims at elaborating the synthesis parameters to be controlled during the scale-up of bifunctional catalysts from powder to shaped bodies. The focus was held both at the impact of shaping on the Beta zeolite properties and method of preparation with controlled deposition of platinum. Understanding of correlations between the physico-chemical (surface, structural, textural and morphological) and catalytic characteristics of shaped Pt-catalysts (Figure 1), could significantly

contribute to the design of “ideal” (highly active, stable and selective) bifunctional shaped catalysts indispensable to develop cleaner processes. As a model reaction isomerization of n-hexane containing 1% benzene was chosen.

Results of this study revealed that various ways of Pt deposition on the extrudates strongly effected the metal to acid sites ratio (from 0.07 to 1.12). This ratio is a key parameter for developing active and selective bifunctional shaped catalysis.

The best result was obtained over extrudates prepared via in-situ synthesis allowing controlled deposition of platinum on the zeolite. The extrudates prepared in this way have the highest metal to acid sites ratio and the closest proximity between them. Such extrudates resulted, however, in somewhat lower but still acceptable mechanical strength.

More details on the catalyst preparation, characterization and catalytic tests will be given in the final presentation.

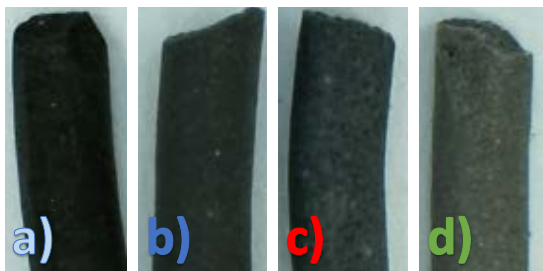


Figure 1. Pt-extrudates of Beta zeolite agglomerated with bentonite as a clay binder. The extrudates differ in the way Pt was introduced: a) after extrusion, or prior to extrusion on b) zeolite and binder, c) binder, d) zeolite

## References

1. Stojkovic, N., M. Vasic, M. Marinkovic, M. Randjelovic, M. Purenovic, P. Putanov, and A. Zarubica, *A comparative study of n-hexane isomerization over solid acid catalysts: sulfated and phosphated zirconia*. Chemical Industry & Chemical Engineering Quarterly, 2012, **18**, 209-220.
2. Zecevic, J., G. Vanbutsele, K.P. de Jong, and J.A. Martens, *Nanoscale intimacy in bifunctional catalysts for selective conversion of hydrocarbons*. Nature, 2015, **528**, 245-254.
3. Mendes, P.S.F., J.M. Silva, M.F. Ribeiro, A. Daudin, and C. Bouchy, *From powder to extrudate zeolite-based bifunctional hydroisomerization catalysts: on preserving zeolite integrity and optimizing Pt location*. Journal of Industrial and Engineering Chemistry, 2018, **62**, 72-83.

# Effects of oxygen impurities on the stability of Cu-based catalysts

*Julian Schittkowski, Holger Ruland, Robert Schlögl*

*Max Planck Institute for Chemical Energy Conversion, 45470 Mülheim an der Ruhr, Germany*

The mitigation of CO<sub>2</sub> emission is an essential topic in current research on energy conversion [1-2]. Within the cross-industry approach of Carbon2Chem<sup>®</sup>, one way to realize the utilization of CO<sub>x</sub> compounds may be the catalytic conversion of industrial waste or process gases from steel mills via hydrogenation into methanol [3]. While standard methanol synthesis as well as catalyst texture was highly investigated in the past, the utilization of exhaust gases is challenging due to fluctuating concentrations and availability as well as a high number of possible catalyst poisons, e.g. O<sub>2</sub> [4-5]. In case of a complete purification being too complex and expensive, there is only the possibility to develop a more robust catalyst or to validate the gas purification thresholds of known catalysts to maintain its stability.

For utilization of coke oven gas as possible hydrogen source, a removal of O<sub>2</sub> is mandatory. This can be conducted by established techniques as PSA, leaving minor residuals of O<sub>2</sub> in the gas. To obtain a complete removal of O<sub>2</sub> an additional deoxygenation step is required. Therefore, the focus was set on the maximum allowable concentration of O<sub>2</sub> in the feed gas and the impact of intermitting O<sub>2</sub> concentrations on the catalyst stability to verify if an additional deoxygenation step is necessary (Figure 1).

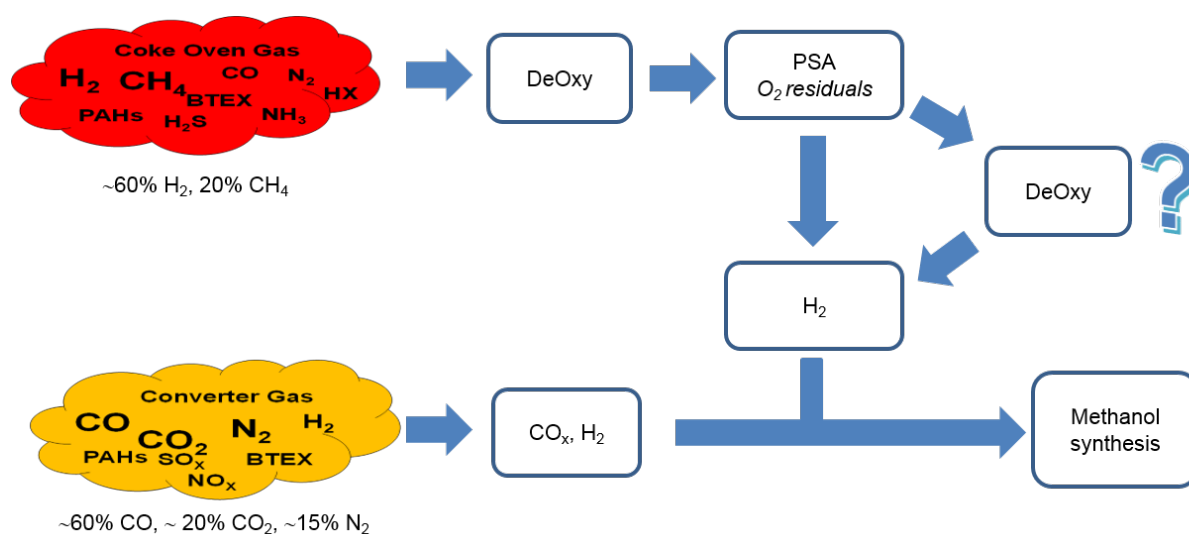


**Figure 1: Process scheme of the hydrogenation of CO<sub>x</sub> species from converter gas mixed with purified H<sub>2</sub> from coke oven gas via PSA to methanol.**

For this reason, the oxygen poisoning of a Cu/ZnO/Al<sub>2</sub>O<sub>3</sub> catalyst, which was previously reduced in diluted H<sub>2</sub>, was tested for methanol synthesis at temperatures of 220 °C to 260 °C and pressures in the range of ambient pressure to 50 bar with synthesis gas containing CO, CO<sub>2</sub> and H<sub>2</sub>.

For the investigation of the influence of oxygen impurities during methanol synthesis, a selected oxygen concentration in the range from 0 to 1000 ppm can be adjusted as long-term steady-state or transient measurements as well as the application as defined pulses that can be introduced into the feed gas.

Additionally, the changing surface morphology during oxygen exposure was investigated using temperature-programmed desorption of H<sub>2</sub>, which suits nicely for copper based surface [6] and can directly performed in-situ with the aged catalyst in between two activity measurements. Under this purpose, it gives insight in the poisoning character of oxygen at different reaction condition and structure-activity correlations can be established showing how large the impact of different oxygen concentration on activity as well as catalyst structure is.

### Acknowledgement

We gratefully appreciate the support received from the Federal Ministry of Education and Research (Bundesministerium für Bildung und Forschung, BMBF, Verbundvorhaben Carbon2Chem).

### References

- [1] G. A. Olah, *Angew. Chem. Int. Ed.* **2013**, *52*, 104-107.
- [2] J. Lundgren, T. Ekbom, C. Hulteberg, M. Larsson, C. E. Grip, L. Nilsson, P. Tunå, *Appl. Energ.* **2013**, *112*, 431-439.
- [3] M. Oles, W. Lüke, R. Kleinschmidt, K. Büker, H.-J. Weddige, P. Schmöle, R. Achatz, *Chem. Ing. Tech.* **2018**, *90*, 169-178.
- [4] J. Schittkowski, H. Ruland, D. Laudenschleger, K. Girod, K. Kähler, S. Kaluza, M. Muhler, R. Schloegl, *Chem. Ing. Tech.* **2018**, *90*, 1419-1429.
- [5] A. Zurbel, M. Kraft, S. Kavurucu-Schubert, M. Bertau, *Chem. Ing. Tech.* **2018**, *90*, 1-5.
- [6] J. Schittkowski, D. Buesen, K. Toelle, M. Muhler, *Catal. Lett.* **2016**, *146*, 1011-1017.



# DFT Study of CO<sub>2</sub> hydrogenation on Cd<sub>4</sub>/TiO<sub>2</sub> catalyst

*Jittima Meeprasert, Guanna Li, Evgeny Pidko,*

*Chemical Engineering Department, Delft University of Technology, Delft, The Netherlands*

## Introduction

The hydrogenation of CO<sub>2</sub> into valuable chemicals has received much attention in the recent years due to the environmental and energy issues caused by CO<sub>2</sub> emission [1]. Among various products generated from the CO<sub>2</sub> hydrogenation, CH<sub>3</sub>OH is highly desirable because it is an important fuel and starting feedstock for production of fine chemicals. Industrially, the commercialized catalyst for the production of CH<sub>3</sub>OH from CO<sub>2</sub> is Cu/ZnO/Al<sub>2</sub>O<sub>3</sub>. However, the disadvantages of low CH<sub>3</sub>OH selectivity and H<sub>2</sub>O induced catalyst deactivation motivate researchers developing new catalysts [2-3].

Recent experimental work has found that Cd nanoparticles supported on TiO<sub>2</sub> allows reducing CO<sub>2</sub> with H<sub>2</sub> and obtaining high CO<sub>2</sub> conversion along with exceptional methanol selectivity. However, the nature of the active site and the mechanism of the reaction process are unclear. This inspired us to carry out a computational study on the mechanism of CO<sub>2</sub> hydrogenation over a model Cd<sub>4</sub>/TiO<sub>2</sub> catalyst to unravel the key factors controlling the CO<sub>2</sub> reduction reactivity and methanol selectivity.

## Computational details

All calculations are performed using the Vienna Ab Initio Simulation package (VASP). The DFT calculations are carried out using PBE exchange and correlation functional. The energy cutoff and convergence criteria used are 400 eV, 10<sup>-5</sup> eV and 0.05 eV/Å for the electronic and ionic loops, respectively. Cd<sub>4</sub>/TiO<sub>2</sub> models containing a Cd<sub>4</sub> cluster supported on the (101) surface of the 1x3 and 2x4 supercells of anatase-TiO<sub>2</sub> are used for study the H<sub>2</sub> dissociation and CO<sub>2</sub> hydrogenation, respectively. The CI-NEB method was used to locate the transition states.

## Results and discussion

**1. H<sub>2</sub> dissociation:** All possible active sites of Cd<sub>4</sub>/TiO<sub>2</sub> and clean TiO<sub>2</sub> surface for the dissociation of H<sub>2</sub> have been evaluated computationally. The results indicate that H<sub>2</sub> cannot be dissociated on the clean TiO<sub>2</sub> surface. For the reaction on Cd<sub>4</sub>/TiO<sub>2</sub> catalyst, it is found that H<sub>2</sub> can be easily dissociated at the interface between Cd and

TiO<sub>2</sub> surface with an activation energy about 0.5 eV. However, H<sub>2</sub> dissociation reaction over the Cd<sub>4</sub> cluster is more difficult ( $E_a = 0.88$  eV). Therefore, it is proposed that the Cd-TiO<sub>2</sub> interface is the reaction center for activation of H<sub>2</sub> molecule.

**2. CO<sub>2</sub> hydrogenation:** Two main reaction pathways of CO<sub>2</sub> hydrogenation have been investigated: (1) the reversed water-gas shift (RWGS) pathway, and (2) the formate pathway. From the reaction profile (see Figure 1), it can be seen that the formate pathway dominates over the RWGS pathway since the conversion of HOCO\* intermediate to CO and subsequent CO hydrogenation steps are energetically less favorable compared to those involved in the formate reaction pathway. The formation of H<sub>2</sub>CO\* intermediate is the rate-determining step for the CO<sub>2</sub> hydrogenation to methanol via the formate pathway ( $E_a = 0.75$  eV). More importantly, it is found that all elementary steps take place at the interface of the catalyst, i.e., the boundary between Cd<sub>4</sub> and TiO<sub>2</sub> surface, except the formation HOCO\* and CO\* intermediates along the RWGS pathway, which can only take place at the TiO<sub>2</sub> site as a result of hydrogen spillover from the Cd-TiO<sub>2</sub> interface to the TiO<sub>2</sub> surface.

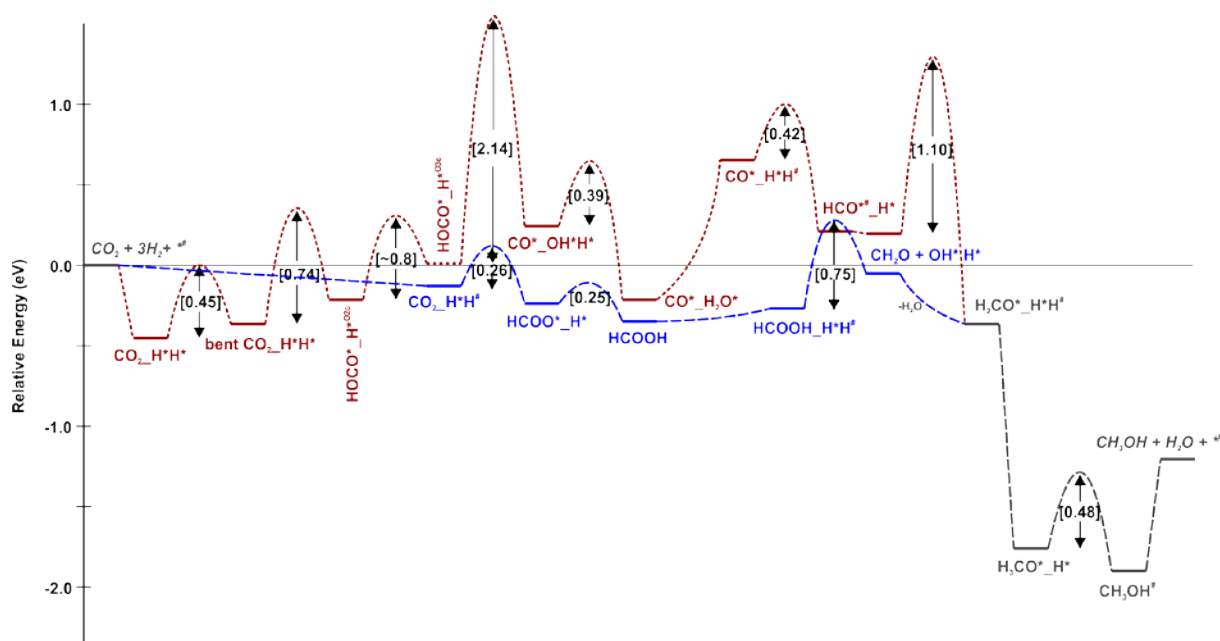


**Figure 1. Reaction diagram of CO<sub>2</sub> hydrogenation to CH<sub>3</sub>OH over the Cd<sub>4</sub>/TiO<sub>2</sub> catalyst (red line: RWGS pathway; blue line: formate pathway).**

## References

- [1] W. Wang, S. Wang, X. Ma, J. Gong. *Chem Soc Rev.* **2011**, 40 (7), 3703-27.
- [2] S. Kattel, P. J. Ramírez, J. G. Chen, J. A. Rodriguez, P. Liu. *SCIENCE.* **2017**, 355, 1296-1299
- [3] K. Larmier, W. C. Liao, S. Tada, E. Lam, R. Verel, A. Bansode, A. Urakawa, A. Comas-Vives, C. Coperet, *Angew. Chem. Int. Ed. Engl.* **2017**, 56 (9), 2318-2323

# The effect of platinum deposition order on the active surface of Pt-Co/SiO<sub>2</sub>

Sandeeran Govender<sup>1</sup>, Amélie C. Roche<sup>2</sup>, Santiago J.A. Figueroa<sup>2</sup>, Thobani G. Gambu<sup>1</sup>, Túlio C. R. Rocha<sup>2</sup> and Eric van Steen<sup>1</sup>

<sup>1</sup>Catalysis Institute, Department of Chemical Engineering, University of Cape Town, Cape Town, South Africa

<sup>2</sup>Laboratório Nacional de Luz Sincrotron-LNLS/CNPEM, Campinas, Brazil

## Introduction

Platinum is usually added to cobalt-based Fischer-Tropsch catalysts to increase the metallic cobalt surface area. The addition of platinum to the catalyst precursor can also lead to a higher turnover frequency or synergistic promotion in the Fischer-Tropsch synthesis [1]. A synergistic promotion is suggested as a result of intimate, bimetallic interaction of cobalt and noble metal particles on the support [2].

Recently, Cook *et al.* [3] reported a higher turnover frequency in the Fischer-Tropsch synthesis for an alumina supported catalyst prepared by co-deposition of platinum and cobalt compared to sequential-deposition [3], although the H<sub>2</sub>-TPR profiles were the same for both catalysts, and the extent of reduction was better for the catalyst prepared by sequential-deposition. It may be assumed that the preparation of the promoted catalyst influenced the electronic properties of the active surface resulting in enhanced catalytic performance. In this work, we study the active surface through reduction-oxidation treatments of Pt-Co<sub>3</sub>O<sub>4</sub>/SiO<sub>2</sub> prepared by sequential-deposition and co-deposition.

## Experimental

For a selective deposition [4] of platinum on Co<sub>3</sub>O<sub>4</sub>, aqueous H<sub>2</sub>PtCl<sub>6</sub>•6H<sub>2</sub>O was added to Co<sub>3</sub>O<sub>4</sub>/SiO<sub>2</sub> at pH=2. Aqueous (NH<sub>3</sub>)<sub>4</sub>PtCl<sub>2</sub> was added to Co<sub>3</sub>O<sub>4</sub>/SiO<sub>2</sub>, at pH=9, for a preferential deposition of platinum on SiO<sub>2</sub>. For the precursor prepared by co-deposition, an aqueous solution containing cobalt, and, platinum from H<sub>2</sub>PtCl<sub>6</sub>•6H<sub>2</sub>O, was deposited in one-step on SiO<sub>2</sub>. All precursors were dried at 60 °C for 16 hours and calcined at 350 °C for 6 hours. The metal content in the catalyst precursors was 10 wt.-% Co and 0.4-0.45 wt.-% Pt.

In-situ XAS studies were performed at the Pt L<sub>III</sub> edge. The precursors were reduced in pure H<sub>2</sub>, at 5 °C/min to 350 °C and held for 1 hour. Subsequently, the powders

were oxidized in air, from room temperature at 5 °C/min to 350 °C and held for 1 hour. After each reduction and oxidation, the powders were cooled to room temperature, respectively, and XAFS measurements were recorded.

## Results and discussion

After activation in pure H<sub>2</sub>, platinum was observed to be in its metallic state in all powders (Figure 1A). However, the XANES regions were significantly different to Pt foil, possibly due to more electron density in the d-band i.e. platinum being more electronegative than cobalt withdraws electrons when in intimate interaction. After oxidation (Figure 1B), platinum returns to its oxidic state in the catalyst powders prepared by sequential-deposition. On the other hand, co-deposition results in platinum remaining in its metallic state upon reduction-oxidation. We hypothesize that the sequential deposition of platinum leads to an active surface rich in platinum after H<sub>2</sub>-activation, whilst co-deposition results in a bulk Pt-Co alloy. Analysis of the XAFS regions should provide us with more information on the Pt-Co and Pt-Pt coordination numbers to support our hypothesis.

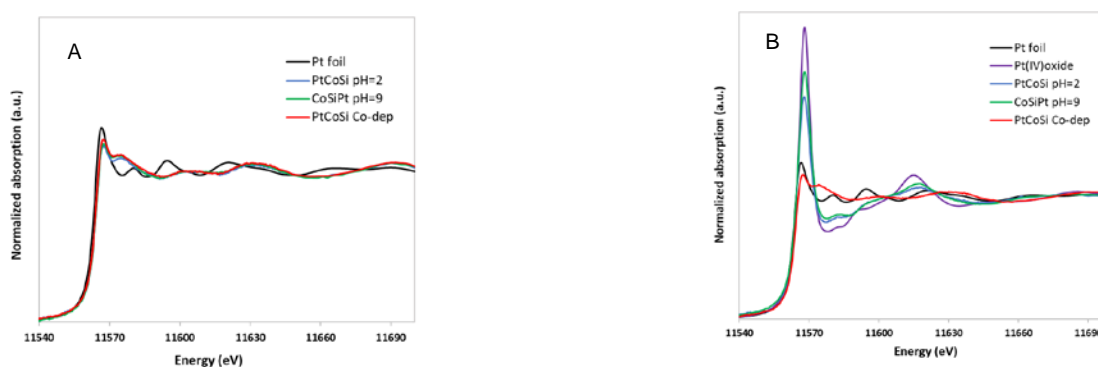


**Figure 1.** Normalized X-ray absorption spectra A) After reduction in H<sub>2</sub> B) After reduction in H<sub>2</sub> and oxidation in air

## References

- [1] Nabaho D., Niemantsverdriet J.W., Claeys M., van Steen E. (2016). *Catal. Today* **261**, 17.
- [2] Iglesia E., Soled S.L., Fiato R.A., Via G.H. (1993). *J. Catal.* **143**, 345.
- [3] Cook K.M., Perez H.D., Bartholomew C.H., Hecker, W.C. (2014). *Appl. Catal. A: Gen.* **482**, 275.
- [4] Feltes T.E., Espinosa-Alonso L., de Smit E., D'Souza L., Meyer R.J., Weckhuysen B.M. Regalbuto J.R. (2010). *J. Catal.* **270**, 95.

# CO<sub>2</sub> reduction to CH<sub>4</sub> using Ru on carbon nanostructures and on alumina coated monoliths

*Ainhoa Bustinza, Laura Roldán, Enrique García-Bordejé, Instituto de Carboquímica (ICB-CSIC), Miguel Luesma Castán 4, 50018, Zaragoza, Spain, jegarcia@icb.csic.es*

## 1. Introduction

Renewable energies are one of the energetic solutions for the future, due to the limitation and environmental risk of fossil fuels. Nevertheless, the production of energy from renewable sources does not match the time and location of the demand. Therefore, it is urgent developing ways for its storage and transport. A solution is the conversion of renewable energy in H<sub>2</sub> via electrolysis. When long time storage is needed, the conversion of H<sub>2</sub> to synthetic natural gas (CH<sub>4</sub>) by reaction with CO<sub>2</sub>, is a plausible solution, additionally entailing environmental benefit. The reaction between CO<sub>2</sub> con H<sub>2</sub> is known as Sabatier reaction and it was discovered a century ago [1]. Different transition metal and noble metal supported on different metallic oxides have been used as catalyst. Up to our knowledge, carbon nanomaterials have not been used as catalyst support in this reaction. In fact, there are some reports that CNT are inactive for this reaction, which is attributed to the inertness of the support to chemisorb CO<sub>2</sub> [2]. Another important aspect for the industrial deployment of this technology is the design of the catalytic reactor. The CO<sub>2</sub> hydrogenation to produce CH<sub>4</sub> reaction is highly exothermic ( $\Delta H_R^\circ = -165$  kJ/mol). Therefore, a proper heat management to avoid temperature rise is essential for CH<sub>4</sub> conversion and catalyst lifetime. To overcome this, different solutions have been used such as, fluidized bed, multi-tubular reactors externally cooled or staged reactors with intermediate cooling by heat exchangers [3]. Another option is washcoating the catalyst on the surface of heat-exchangers, hence integrating both reaction and cooling. In this context, the catalyst washcoat on monoliths has been also proposed as a model for catalyst wash-coat on heat exchangers for CO<sub>2</sub> methanation [4

Herein, we have supported Ru nanoparticles on carbon nanotubes (CNTs), carbon nanofibers (CNFs) and nitrogen-doped carbon nanofibers (N-CNF). The 5% Ru catalysts supported on CNF and N-CNF have been benchmarked against 5% Ru on CNT and on conventional alumina support (Ru/Al<sub>2</sub>O<sub>3</sub>). To study the structure-performance relationship, the catalysts have been exhaustively characterized by TEM and by transient techniques such as temperature programmed desorption

(TPD) and temperature programmed surface reaction (TPSR). In a second part, cordierite monoliths have been washcoated with alumina. Subsequently, Ni, Ru and bimetallic catalyst have been impregnated and tested in reaction.

## 2. Results and discussion

In previous paper [5], it was found that the selectivity is highly sensitive to the Ru loading. For the lower Ru loadings (0.5 y 2 wt% Ru), the main product is CO while for the highest Ru loading (5 wt%), the selectivity to CH<sub>4</sub> is ~ 97 % in all the temperature range. Ru on 5% Ru NCNF provided competitive CH<sub>4</sub> conversion and selectivity compared to commercial 5% Ru/Al<sub>2</sub>O<sub>3</sub> and 5% Ru/CNT, specially for higher conversions [6] (Figure 1). Contrary to the general belief about the inert nature of carbon supports, it is demonstrated that NCNF is a non-innocent spectator in CO<sub>2</sub> methanation due to its ability to store a high amount of CO<sub>ad</sub> reaction inter-mediate.

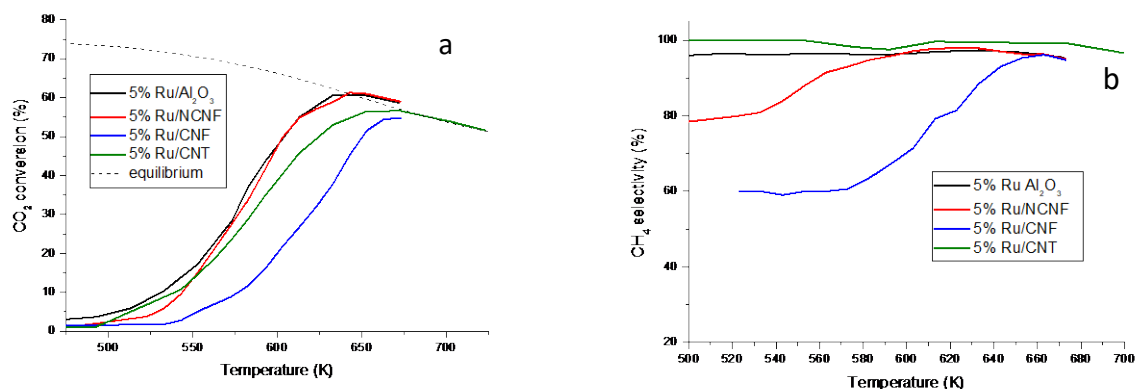


Figure 1. CO<sub>2</sub> conversion (a) and selectivity to CH<sub>4</sub> (b)

Finally, the feasibility of metal (Ni, Ru) on alumina coated monolith for CO<sub>2</sub> reduction is demonstrated. The use of Ni and bimetallic Ni-Ru catalyst affords a reduction in catalyst costs and enhanced catalytic performance than pure Ru catalyst.

## References

- [1] P. Sabatier. *Compt. Rend. Heb. Acad. Sci.* 134 (1902) 689.
- [2] J. H. Kwak, L. Kovarik, J. Szanyi. *ACS Catal.* 3 (2013), 2094.
- [3] J. Kopyscinski, T.J. Schildhauer, S.M.A. Biollaz, *Fuel*, 89 (2010) 1763-1783.
- [4] C. Janke, M.S. Duyar, M. Hoskins, R. Farrauto, *Appl. Catal. B: Environ*, 152-153 (2014) 184-191.
- [5] L. Roldán, Y. Marco, E. García-Bordejé, *ChemCatChem*, 7 (2015) 1347–1356
- [6] L. Roldán, Y. Marco, E. García-Bordejé, *ChemSusChem*, 10 (2017) 1139 –1144

Aknowledgements. The authors are indebted to the funding of European Commission (FREECATS project, grant agreement No. 280658), Financial support from Spanish Ministry MINECO (project ENE2016-79282-C5-1-R), Gobierno de Aragón (Grupo Reconocido DGA T03\_17R), and associated EU Regional Development Funds are gratefully acknowledged.

# How to convert ethanol to ethyl acetate in one step? Ethanol oxidation catalyzed by palladium supported on Keggin type heteropolyacids and compounds formed by their thermal decomposition

*Urszula Filek<sup>1</sup>, Robert P. Socha<sup>1</sup>, Dorota Duraczyńska<sup>1</sup>, Dariusz Mucha<sup>1</sup>, Michał Śliwa<sup>1</sup>, Karolina Tarach<sup>2</sup>, Kinga Góra-Marek<sup>2</sup>, Małgorzata Witko<sup>1</sup>*

*<sup>1</sup>Jerzy Haber Institute of Catalysis and Surface Chemistry Polish Academy of Sciences, Niezapominajek 8, 30-239 Krakow, Poland; <sup>2</sup>Faculty of Chemistry, Jagiellonian University in Kraków, Gronostajowa 2, 30-387 Kraków, Poland*

## Introduction

It is known that bioethanol is a cheap starting renewable source for the production of more complex chemicals. Depends on reaction and catalyst type different products can be obtained; bioethanol dehydration leads to formation of ethylene and diethyl ether while dehydrogenation or oxidation to acetaldehyde and/or acetic acid, ethyl acetate.

Ethyl acetate is an important chemical compound used as solvent for paints, adhesives, nitrocellulose, plastics, herbicides, oils, fats, organic synthetics, as a food flavoring additive and in the perfumery industry. Classic methods of obtaining ethyl acetate require the use of acetic acid or acetaldehyde known as hazardous substrates (corrosive, toxic). A promising alternative would be the one-step ethyl acetate synthesis from ethanol, which uses single raw material and one-step reactor, resulting in low production and investment costs. There are two ways of direct synthesis of ethyl acetate from ethanol: a dehydrogenation process [1] and an oxidation process. In the process of ethanol dehydrogenation, over palladium-based and copper catalysts, in addition to ethyl acetate and hydrogen, other by-products (such as butanone) are produced, which increase the cost of ethyl acetate purification. In the case of the oxidation process over PdO-based catalysts, the purification of ethyl acetate is easier. The main by-products of ethanol oxidation are acetaldehyde, acetic acid and CO<sub>2</sub>.

The possibility of obtaining ethyl acetate directly from ethanol by oxidation in the presence of palladium supported on heteropolyacids, such as H<sub>3</sub>PW<sub>12</sub>O<sub>40</sub> and

H<sub>3</sub>PMo<sub>12</sub>O<sub>40</sub>, and materials created by the thermal decomposition of polyoxometalates in air (its bronzes) is discussed.

## Experimental

The catalyst precursors were synthesized from palladium chloride and heteropolyacid, H<sub>3</sub>PW<sub>12</sub>O<sub>40</sub> or H<sub>3</sub>PMo<sub>12</sub>O<sub>40</sub>, then activated in mixture of ethanol and helium at 230 °C that led to Pd-H<sub>3</sub>PW<sub>12</sub>O<sub>40</sub> (PdPW\*) or Pd-H<sub>3</sub>PMo<sub>12</sub>O<sub>40</sub> (PdPMo\*) system. Further thermal decomposition of precursors resulted in PdO supported on phosphorus-tungsten and phosphorus-molybdenum bronzes formation. Synthesized materials were characterized using XRD, SEM/EDX, XPS, FT-IR, TPD NH<sub>3</sub> and thermal analysis. The catalytic activity of the obtained catalysts were investigated in oxidation of ethanol with air in fixed-bed flow reactor connected online to gas chromatograph. The catalytic tests were performed at the temperature range of 70-290 °C under ambient pressure at WHSV of 2.1 h<sup>-1</sup>. Additional tests were performed at 5.2 kPa and 8.6 kPa ethanol pressures with constant flow of air 35 ml/min. Moreover, the influence of water on catalysts activity was investigated at two ethanol concentrations of 96 wt.% and 82 wt.% at constant WHSV 2.1 h<sup>-1</sup>. Additionally, the possibility of synthesis of ethyl acetate from ethanol via dehydrogenation route was also studied.

## Results

The investigated materials show the relatively high activity for ethyl acetate. The catalysts exhibit the highest selectivity to ethyl acetate at 190-210 °C. The higher yield to ethyl acetate is obtained over catalysts containing the tungsten. The yield to ethyl acetate over PdPW\* catalyst was 40% (selectivity 61%) while over PdPW-bronze yield was 27% (selectivity 47%). The influence of ethanol partial pressure and water content in feedstock were also studied. Both catalysts show lack of decrease of catalytic activity to ethyl acetate with increasing water content in the feedstock. Unexpectedly, the yield to the ester increases to 38% for the conversion of 82 wt.% ethanol in the presence of bronze. The investigated materials are less efficient during synthesis of ethyl acetate from ethanol via dehydrogenation route than the via oxidation reaction. Synthesized materials are promising catalysts for the one-step synthesis of ethyl acetate from ethanol via oxidative route.

## References

[1] J.M.R. Gallo, J.M.C. Bueno, U. Schuchardt, J. Braz. Chem. Soc. 25(12) (2014) 2229



# Overall ORR activity over adjacent Pt(111) and Pt(001) facets: a micro-kinetic analysis

Thobani G. Gambu<sup>1</sup>; Melissa A. Petersen<sup>1</sup>; Glenn Jones<sup>2</sup>; Eric van Steen<sup>1</sup>

<sup>1</sup>Catalysis Institute, Department of Chemical Engineering, University of Cape Town, Private Bag X3, Rondebosch, 7701, South Africa; <sup>2</sup>Johnson Matthey Technology Center, Blount's Court, Sonning Common, Reading, RG4 9NH, United Kingdom

## Introduction

The oxygen reduction reaction (ORR), catalyzed by platinum-based materials, is known to be a rather slow reaction resulting in poor platinum utilization [1]. Understanding the reaction kinetics over various platinum surfaces is key to designing better ORR catalysts. Pt{111} and Pt{001} surfaces are expected to be the dominant terminations of Pt nanoparticles [3]. The elementary step over the Pt(111) and Pt(001) surfaces with the highest activation barrier is hydrogenation of  $O^*$  and  $OH^*$ , respectively [4]. Whilst a lot of effort has been put into understanding the ORR kinetics over single and isolated Pt(111) and Pt(001) surfaces [5], to our knowledge, no kinetic models have been presented on the overall ORR activity over kinetically connected Pt{111} and Pt{001} facets. Due to the surface sensitivity of the ORR, kinetic connectivity of the Pt{111} and Pt{001} may influence the overall ORR activity.

## Methodology

Density functional theory (DFT) calculations were conducted using the Vienna *Ab Initio* Simulation Package (VASP) [6] and the GGA-PBE exchange-correlation functional [7] together with the projector augmented wave (PAW) potential method. A comprehensive list of elementary reaction steps involved in the ORR was studied over both Pt(111)- $p(3 \times 3)$  and Pt(001)- $p(3 \times 3)$  supercell slabs each with 3 relaxed top layers. To account for species exchange between the Pt{111} and Pt{001} facets, diffusion of both  $O^*$  and  $OH^*$  over the edge. Furthermore, exchange of  $-H$  between terrace- and edge-bound  $OH^*$  and  $O^*$  species was considered. The elementary reaction steps were incorporated in a microkinetic model using mean-field approximations. The analysis focusses on the ORR activity at a Pt surface/gas interface with a gas composition of 37%  $O_2$  and 67%  $H_2$  and a total gas pressure of 1 bar.

## Results and discussion

Both  $O^*$  and  $OH^*$  adsorb rather strongly at edge sites resulting in a deep well in the potential energy surface. Our calculations show a rather low energy barrier for the exchange of  $-H$  between co-adsorbed, edge- and terrace-bound  $O^*$  and  $OH^*$  as an additional kinetic connectivity between adjacent terraces. At all temperatures below 650 K, our microkinetic analysis predicts a higher ORR activity over Pt(111) than over Pt(001) (see Fig. 1a). Connecting Pt{111} and Pt{001} terraces, we predict an increase in the rate of  $H_2O$  desorption over the Pt{001} facets at  $T < 650$  K and over the Pt{111} facets at  $T > 650$  K, compared to that predicted over the isolated Pt(001) and Pt(111) surfaces, respectively. Our simulations show that the Pt{001} facet has a high coverage with  $O^*$  at  $T < 650$  K and  $H_2$  adsorption is rate controlling. The connectivity between adjacent {111} and {001} facets aids the ORR over the {001} facet by via  $-H$  transfer from  $OH^*$  on the Pt{111} facets towards  $O^*$  on the Pt{001} facets. At  $T > 650$  K,  $O_2$  dissociation is the rate determining step over an isolated Pt(111) surface. Upon connecting the facets, over 90 % of the water produced from the Pt{111} facet at  $T > 650$  K, contains  $O^*$  originating from the {001} facet.

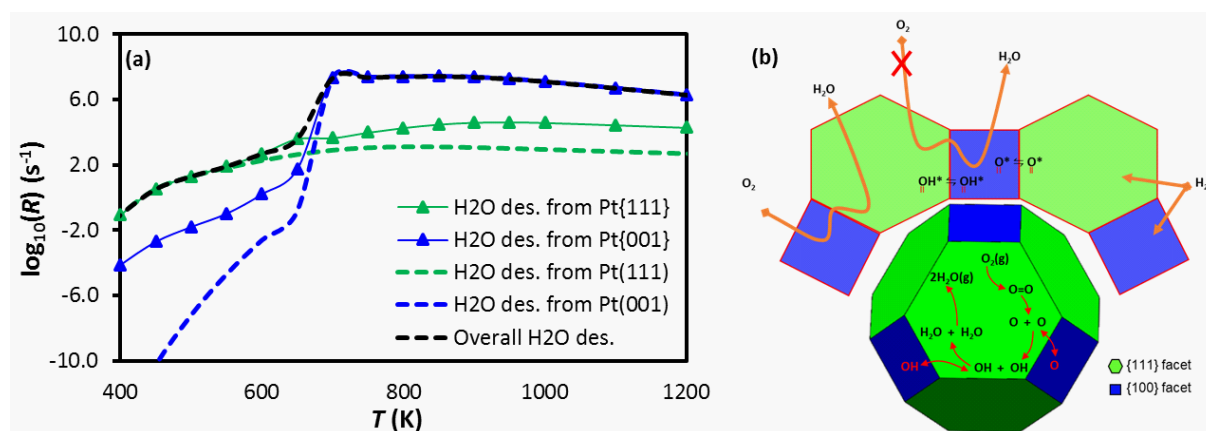


**Figure 1.** Effect of inter-facet connectivity of Pt{111} and Pt{001} on the ORR activity, a) comparison between  $H_2O$  production rates from different surfaces (dashed lines: no connectivity between facets; solid line: connectivity between facets), b) illustration of the ORR over nanoparticle with kinetically connected surfaces at  $T > 650$  K

## References

- [1] Gasteiger, H.A., Kocha, S.S., Sompalli, B., Wagner, F.T. (2005). *Appl. Catal. B Environ.* **56**, 9.
- [3] Vitos, L., Ruban, A.V., Skriver, H.L., Kollar, J. (1998). *Surf. Sci.* **411**, 186.
- [4] Li, K., Li, Y., Wang, Y., He, F., Jiao, M., Tang, H., Wu, Z. (2015). *J. Mater. Chem. A* **3**, 11444.
- [5] Tripković, V., Cerri, I., Bligaard, T., Rossmeisl, J. (2014). *Catal. Letters* **144**, 380.
- [6] Kresse, G., Furthmüller, J. (1996). *Phys. Rev. B* **54**, 11169.
- [7] Perdew, J.P., Burke, K., Ernzerhof, M. (1996). *Phys. Rev. Lett.* **77**, 3865.

# A Molecular Single-Source Precursor Approach to Well-Defined Rh-Based Catalysts for the Conversion of Syngas to Ethanol

*Phil Preikschas,<sup>a</sup> Julia Bauer,<sup>a</sup> Xing Huang,<sup>b,c</sup> Shenglai Yao,<sup>d</sup> Raoul Naumann d'Alnoncourt,<sup>a</sup> Ralph Kraehnert,<sup>a</sup> Annette Trunschke,<sup>c</sup> Frank Rosowski,<sup>a,e</sup> and Matthias Driess<sup>a,d</sup>*

<sup>a</sup> BasCat - UniCat BASF JointLab, Technische Universität Berlin, Berlin, Germany

<sup>b</sup> Scientific Center for Optical and Electron Microscopy, ETH Zürich, Zürich, Switzerland

<sup>c</sup> Department of Inorganic Chemistry, Fritz-Haber-Institut der Max-Planck-Gesellschaft, Berlin, Germany

<sup>d</sup> Technische Universität Berlin, Institut für Chemie, Berlin, Germany

<sup>e</sup> BASF SE, Process Research and Chemical Engineering, Ludwigshafen, Germany

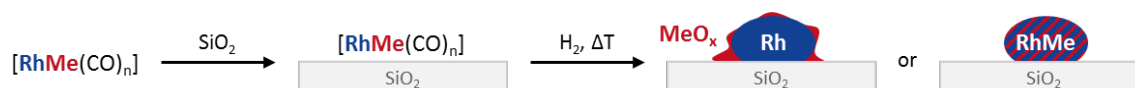
## Introduction

Depletion of fossil fuel resources and rising crude oil prices lead to one of the most important scientific challenges of the 21<sup>st</sup> century – finding a promising alternative to petroleum-derived fuels. The direct conversion of syngas (CO and H<sub>2</sub>) to ethanol (StE) might be this promising process utilizing coal, natural gas, or preferably biomass as carbon source for syngas generation. To make this process technically and commercially feasible, a selective and economic catalyst for the direct conversion is highly desirable.<sup>[1]</sup>

As supported rhodium is the only monometallic catalyst that has demonstrated a selectivity towards ethanol, a wide range of promoters were tested, e.g. Fe, Mn, Li, and even rare earth oxides.<sup>[2]</sup> In this manner, the addition of Fe or Mn leads to an enhanced oxygenate selectivity and a suppressed methane formation. However, the role of Mn and Fe as a modifier and the actual active site in Rh-based catalysts are still unclear.

## Results and Discussion

Herein, we present the molecular single-source precursor (SSP) approach to RhMnO<sub>x</sub>/SiO<sub>2</sub> and RhFe/SiO<sub>2</sub> catalysts (Scheme 1) leading to a better understanding of catalyst structure-function relationships.



**Scheme 1:** The molecular single-source precursor (SSP) approach: a suitable SSP with predefined Rh–Me (Me = Fe or Mn) bonds and highly volatile CO ligands is impregnated on an oxide support. The silica-supported [RhMe(CO)<sub>n</sub>] cluster is transformed into the final RhMeO<sub>x</sub>/SiO<sub>2</sub> or RhMe/SiO<sub>2</sub> catalyst by a thermal treatment in 10% H<sub>2</sub>/Ar and elevated temperature.

Since no suitable RhMn single-source precursor is known in literature as yet, we synthesized the first molecular carbonyl RhMn cluster Na<sub>2</sub>[Rh<sub>3</sub>Mn<sub>3</sub>(CO)<sub>18</sub>] **1** which acts as a molecular SSP for the low temperature preparation of nearly uniform RhMnO<sub>x</sub>/SiO<sub>2</sub> catalysts.<sup>[3]</sup>

Three SSP-derived RhMnO<sub>x</sub> catalysts **2–4** were tested for the direct conversion of StE and compared with reference as well as literature-reported examples. The selectivity towards ethanol could be substantially enhanced by a factor of 1.54 and is, to our knowledge, the highest reported ethanol selectivity (Fig. 1a). By investigating the fresh and spent catalyst with (HR)-TEM, STEM with EDX and EELS, and XPS, we reason that this enhancement in selectivity is due to a higher dispersion of Rh nanoparticles in a tightly surrounded MnO<sub>x</sub> matrix (Fig. 1b). This situation can increase the number of tilted CO adsorption sites which, in turn, facilitate the formation of ethanol.<sup>[4]</sup>

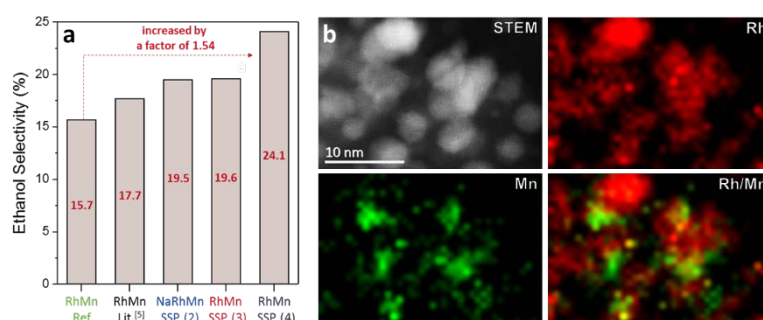


**Figure 1.** a) Ethanol selectivity at iso-conversion (11–16 %) for the reference catalyst, a literature example, and the SSP-derived RhMnO<sub>x</sub> catalysts **2–4**; b) composition analysis of the as-synthesized RhMnO<sub>x</sub>/SiO<sub>2</sub> catalyst **4**.

With the introduction of the molecular SSP approach as a useful method for solid catalysts design, we are able to gather information about the influence of promoters on Rh-based catalysts. Beside the study of RhMnO<sub>x</sub> catalysts, we investigated the structural transformation of RhFe catalysts during the reaction by using N(Et)<sub>4</sub>[RhFe<sub>2</sub>(CO)<sub>11</sub>] as molecular SSP. These investigations indicate the formation of a RhFe phase which might suppress the ability of Rh to facilitate C–C coupling, an important step for C<sub>2+</sub> oxygenate formation. Further analyses, such as Mössbauer spectroscopy, will be conducted to face the structural changes in RhFe/SiO<sub>2</sub> catalysts.

#### Experimental Details

Na<sub>2</sub>[Rh<sub>3</sub>Mn<sub>3</sub>(CO)<sub>18</sub>] was prepared by a salt metathesis reaction of RhCl<sub>3</sub> and Na[Mn(CO)<sub>5</sub>] in 49 % isolated yields and structurally characterized by CHN, FTIR, NMR (<sup>13</sup>C, <sup>55</sup>Mn), ESI-MS and single-crystal XRD. The SSP-derived catalysts were synthesized by a thermal treatment in 10 % H<sub>2</sub>/Ar at 260 °C, characterized before and after catalysis by XPS, XRD, (S)TEM, EDX, EELS, and ICP-OES. The reference catalysts were prepared by impregnation of metal nitrates and subsequent calcination. Catalytic tests were performed in a fixed-bed parallel test setup at common reaction conditions (GHSV = 3500 h<sup>-1</sup>, p = 54.0 bar, H<sub>2</sub>:CO = 3:1, T = 243–260 °C).

#### References

- [1] H. T. Luk, C. Mondelli, D. C. Ferré, J. A. Stewart, J. Pérez-Ramírez, *Chem. Soc. Rev.* **2017**, *46*, 1358–1426.
- [2] J. Hu, Y. Wang, C. Cao, D. C. Elliott, D. J. Stevens, J. F. White, *Catal. Today* **2007**, *120*, 90–95.
- [3] P. Preikschas, J. Bauer, X. Huang, S. Yao, R. Naumann d'Alnoncourt, R. Kreahnert, A. Trunschke, F. Rosowski, M. Driess, *ChemCatChem*, DOI 10.1002/cctc.201801978.
- [4] X. Pan, Z. Fan, W. Chen, Y. Ding, H. Luo, X. Bao, *Nat. Mater.* **2007**, *6*, 507–511.
- [5] W. Mao, J. Su, Z. Zhang, X.-C. Xu, W. Dai, D. Fu, J. Xu, X. Zhou, Y.-F. Han, *Chem. Eng. Sci.* **2015**, *135*, 312–322.

# Enhancement of C2 yields in oxidative conversion of methane by optimizing the component of zeolite framework

Toshiyuki Yokoi,<sup>1,2</sup> Keita Sago,<sup>1</sup> Yusuke Kunitake,<sup>1</sup> Ryota Osuga,<sup>1</sup> Junko N. Kondo,<sup>1</sup>  
Atsushi Muramatsu<sup>3,4</sup>

<sup>1</sup>*Institute of Innovative Research, Tokyo Institute of Technology, Yokohama, Japan;* <sup>2</sup>*JST-PRESTO, Tokyo, Japan;* <sup>3</sup>*Institute of Multidisciplinary Research for Advanced Materials, Tohoku University, Sendai, Japan;* <sup>4</sup>*JST-CREST, Tokyo, Japan.*

## 1. Introduction

Methane is a highly abundant and inexpensive source of fuel and chemicals. The development of novel technologies that can convert methane easily into chemicals has strongly been desired. However, its kinetic inertness and low reactivity limit the industrial utilization of methane.<sup>1</sup> Note that, in zeolite-based catalysts, aluminosilicates have been mostly used as zeolite, and the component of zeolite framework has not been optimized. Recently, it has been reported that Ni-supported zeolites are a promising catalyst for conversion of methane into methanol at low temperature; mono( $\mu$ -oxo)dinickel species (Ni-O-Ni) are active for the direct oxidation of methane.<sup>2</sup>

In this work, the effect of incorporation of boron into the CHA-type zeolite on the oxidative conversion of methane was investigated in detail. We first report a dramatic enhancement of C2 yields in oxidative conversion of methane by incorporation boron atoms into the framework.

## 2. Experimental

The CHA-type aluminosilicate and borosilicate zeolites were directly synthesized in the presence of *N,N,N*-trimethyl-1-adamantammonium cation (TMAda<sup>+</sup>), and Al<sub>2</sub>SO<sub>4</sub> and B(OH)<sub>3</sub> were used as Al and B sources, respectively. Introduction of 2 wt% Ni species was carried out by impregnation method using Ni(NO<sub>3</sub>)<sub>2</sub> aq. Thus prepared catalysts were designated as Ni/Al-CHA and Ni/B-CHA, respectively.

The catalytic reaction was performed in a fixed bed reactor. The flow rates of the reactants were CH<sub>4</sub>/O<sub>2</sub>/Ar = 16/4/5 (SCCM). The reaction temperature was varied ranging from 400 to 600 °C, and the reaction time at each temperature was 5 min.

The products including CO and CO<sub>2</sub> were analyzed by GC-TCD, and other hydrocarbon products were analyzed by GC-FID.

### 3. Results and Discussion

By the XRD patterns, both Ni/Al-CHA and Ni/B-CHA were identified as the CHA structure with a high crystallinity, and no peaks attributed to NiO species were observed. The Si/Al and Si/B ratios for Ni/Al-CHA and Ni/B-CHA were 11 and 22, respectively. Thus prepared catalysts were tested as catalyst for oxidative conversion of methane (Fig. 1). The conversion of methane over Ni/Al-CHA was higher than that over Ni/B-CHA. The yields of CO and CO<sub>2</sub> over Ni/Al-CHA were also higher than those over Ni/B-CHA. Focusing on the yields of C<sub>2</sub> products, ethane and ethylene, Ni/B-CHA gave clearly higher yields compared to Ni/Al-CHA at the reaction temperature over 550°C. These results indicate that the use of borosilicate retarded the complete oxidation of methane, and enhanced the formation of C<sub>2</sub> products. Note that the production of H<sub>2</sub> was only observed when Ni/Al-CHA was used as catalyst, implying that Ni/Al-CHA would enhance methane reforming.

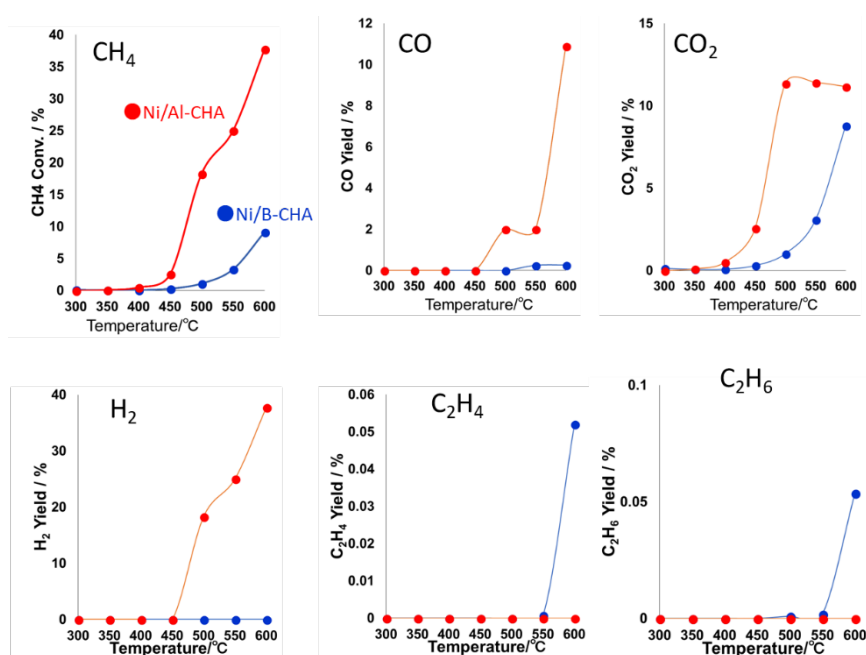


Fig. 1 Oxidative conversions of methane over Ni/Al-CHA and Ni/B-CHA.

### References

- [1] H. Schwarz, *Angew. Chem. Int. Ed.* **2011**, 50, 10096 – 10115
- [2] J. Shan, W. Huang, L. Nguyen, Y. Yu, S. Zhang, Y. Li, A. I. Frenkel, F. Tao, *Langmuir* **2014**, 30, 8558–8569.
- [2] Q. Zhu, M. Hinode, T. Yokoi, M. Yoshioka, J. N. Kondo, T. Tatsumi, *Catal. Comm.* **2009**, 10, 447–450.

# Selectivity enhancement by manganese promotion of Pt-Co/Al<sub>2</sub>O<sub>3</sub> for the once-through Fischer-Tropsch process

*Chelsea Tucker; Eric van Steen, Catalysis Institute, Department of Chemical Engineering, University of Cape Town, Rondebosch, South Africa*

## Introduction

The Fischer-Tropsch (FT) synthesis can be used to convert carbon containing feedstock, e.g. biomass, into liquid fuels in a carbon neutral manner [1]. The Fischer-Tropsch process is, however, highly capital-intensive [2]. The economic viability of small-scale, Fischer-Tropsch plants could be improved by removing the air separation unit and running the system in a simple once-through mode [3]. However, this requires a high conversion in the Fischer-Tropsch synthesis, and thus operation at a high partial pressure of H<sub>2</sub>O and low partial pressures of CO and H<sub>2</sub>. These conditions typically result higher methane and consequently low C<sub>5+</sub> selectivity. The addition of small amounts of Mn has been widely reported to increase CO conversion rate, C<sub>5+</sub> selectivity and decrease the selectivity towards methane for cobalt-based catalysts at low conversion [4–6]. This study reports on the effect of different levels of manganese promotion on the selectivity of a platinum-promoted cobalt catalyst between 30% and 97% CO conversion ( $X_{CO}$ ).

## Experimental

Platinum promoted cobalt on alumina (0.05Pt-22Co/Al<sub>2</sub>O<sub>3</sub>) was prepared via slurry impregnation with nitrate precursors. This catalyst was further impregnated with manganese (II) acetate in order to produce catalysts with Mn:Co mass ratios varying between 0 and 0.5. The catalysts were characterized using XRD, BET, H<sub>2</sub> chemisorption, XPS and TPR to assess differences in terms of surface morphology, crystallite size and reducibility. The catalysts were then tested in a slurry bed reactor at T=220°C, p=20 bara, N<sub>2</sub>:H<sub>2</sub>:CO=3:2:1 to mimic air-blown gasification. During the first 100 hours, each catalyst was monitored for online deactivation at a 30% conversion level. At 100 hours the conversion was increased to assess selectivity changes in CH<sub>4</sub>, CO<sub>2</sub> and C<sub>5+</sub>. Spent catalyst samples were measured for coke deposition using TPH.

## Results and discussion

Increasing Mn:Co ratios from 0-0.5 was found to change the reducibility and Co crystallite size of Mn-Pt-Co/Al<sub>2</sub>O<sub>3</sub> significantly.

The initial activity in the Fischer-Tropsch synthesis was improved by up to 20% upon Mn promotion, however deactivation in the first 100 hours was also accelerated. After 60 hours on-line, the activity dropped below the level of Pt-Co/Al<sub>2</sub>O<sub>3</sub>. In the conversion range of 15% to 97% the CH<sub>4</sub> and CO<sub>2</sub> selectivity was altered significantly by promotion of Mn. Un-promoted Pt-Co/Al<sub>2</sub>O<sub>3</sub> exhibited a decrease in the methane selectivity from 11% to 8.5% in the conversion regime  $X_{CO} < 75\%$ , whilst the methane selectivity obtained over Mn-Pt-Co/Al<sub>2</sub>O<sub>3</sub> with Mn:Co =0.125:1 was stable at  $5.0 \pm 0.3\%$ . Promotion with Mn did not completely eliminate the strong increase in CH<sub>4</sub> selectivity in the high conversion regime, its onset was delayed. The CO<sub>2</sub> selectivity increased slightly from 0.5-1.5% 1.5-2.5% for Pt-Co/Al<sub>2</sub>O<sub>3</sub> and Mn-Pt-Co/Al<sub>2</sub>O<sub>3</sub> respectively. Promotion with manganese results in a much lowered selectivity for CO<sub>2</sub> at high conversion. The obtained results are being discussed in relation to the increase in strength of CO-adsorption upon promoting the catalyst with Mn resulting in a higher surface coverage of with carbon even at low partial pressures of CO resulting in a more favourable selectivity at these conditions.

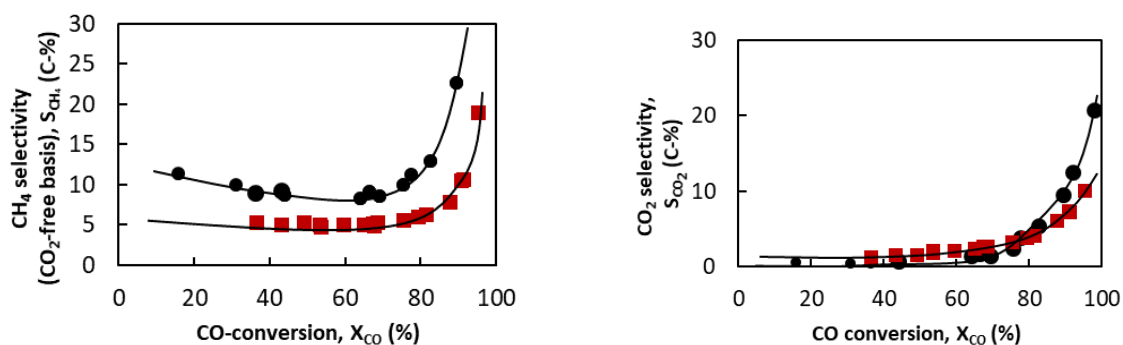


**Figure 1.** CH<sub>4</sub> and CO<sub>2</sub> selectivity for PtCo/Al<sub>2</sub>O<sub>3</sub> (●) and MnPtCo/Al<sub>2</sub>O<sub>3</sub> (■) with a Mn:Co of 0.125:1 in a slurry bed reactor at T=220°C, P=20 bara, N<sub>2</sub>:H<sub>2</sub>:CO=3:2:1.

## References

- [1] Liu G., Larson E.D., Williams R.H., Kreutz T.G., Guo, X. (2011). *Energy & Fuels* **25**, 415.
- [2] Zennaro R. (2013). in "Greener Fischer-Tropsch Processes". (P.M Maitlis, Ed), p. 149–169. Wiley-VCH, Weinheim.
- [3] Aasberg-Petersen K., Bak Hansen J.-H., Christensen T.S., Dybkjaer I., Seier Christensen P., Stub Nielsen C., Winter Madson S.E.L., Rostrop-Nielsen, J.R. (2001). *Appl. Catal. A: General* **221**, 379.
- [4] Zhang J.L., Rue J., Chen J.G., Yu-Han, S. (2002). *Acta Phys. Chim. Sin.* **18**, 260.
- [5] Dinse A., Aigner M., Ulbrich M., Johnson G.R., Bell A.T. (2012) *J Catal.* **288**, 104.
- [6] Bezemer G.L. Radstake P.B., Falke U., Oosterbeek H., Kuipers H.P.C.E., van Dillen A.J., de Jong, K.P. (2006). *J. Catal.* **237**, 152.



# Study of the gas-phase catalytic transfer hydrogenation of methyl levulinate with ethanol over ZrO<sub>2</sub>

*Blair Vasquez, P.<sup>1</sup>; Tabanelli, T.<sup>1</sup>; Monti, E.<sup>1</sup>; Dimitratos, N.<sup>1</sup>; Albonetti, S.<sup>1</sup>; Cavani, F.<sup>1</sup>*

*Dipartimento di Chimica Industriale "Toso Montanari", Università di Bologna, Bologna, Italy<sup>1</sup>*

Levulinic acid (LA) is a polyfunctional molecule that can be obtained from biomass. Because of its particular structure and reactivity, The United States Department of energy has classified LA as one of the top 12 building block chemicals [1]. Nowadays, the most common strategy for its valorization is the chemical reduction in order to obtain valuable chemicals such as fuel additives, solvents and other added-value chemicals such as  $\gamma$ -valerolactone (GVL). The most common approach is the hydrogenation with molecular hydrogen (H<sub>2</sub>) done typically in batch systems, with high H<sub>2</sub> pressures and with noble metal catalysts, making it expensive and less applicable due to the extreme conditions [2]. The need for an alternative approach has led to the study of catalytic transfer hydrogenation (CTH) through the Meerwein–Ponndorf–Verley (MPV). This approach uses organic molecules (e.g. alcohols) that are capable of acting as a hydride transfer agent (H-donor), in order to reduce a molecule containing a carbonyl group [3,4]. Studies have reported the batch liquid-phase CTH of levulinate esters with secondary alcohols which show higher reactivity given the stability of the carbocationic intermediate [5,6]. Some of the best results (in terms of GVL yield) have

been obtained over ZrO<sub>2</sub>, a catalyst containing both Lewis acid and basic sites [7–10]. However, there are no studies in the literature reporting the continuous gas-phase CTH of levulinate esters using primary alcohols. Hence, in this study

we have synthesized ZrO<sub>2</sub> with high surface area and tested it for the first time for the gas-phase CTH of methyl levulinate (ML) at different temperatures using ethanol

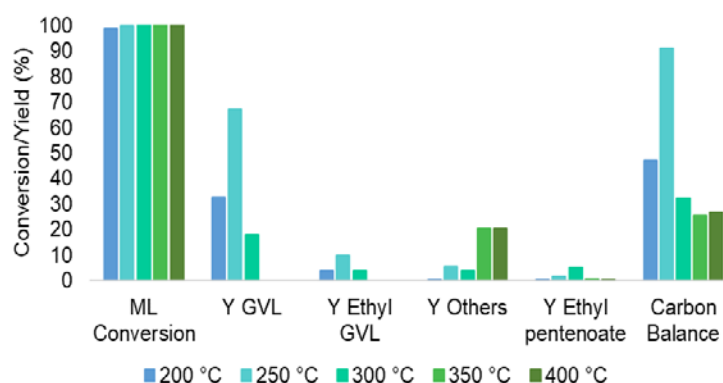


**Figure 1.** Conversion of ML and yield of main products, reaction time 240 min, EtOH:ML-10:1.

as H-donor and used ex situ and in situ techniques to performed characterization analysis. The highest GVL yield obtained was around 67% with an almost complete conversion of ML (~99%) at 250 °C after 240 min of reaction (figure 1). In addition, since ethanol can be easily obtained from biomass, tests using bio-ethanol as H-donor have been conducted. To determine reaction pathways and overall reaction network (figure 2), mechanistic studies were performed using the intermediates as

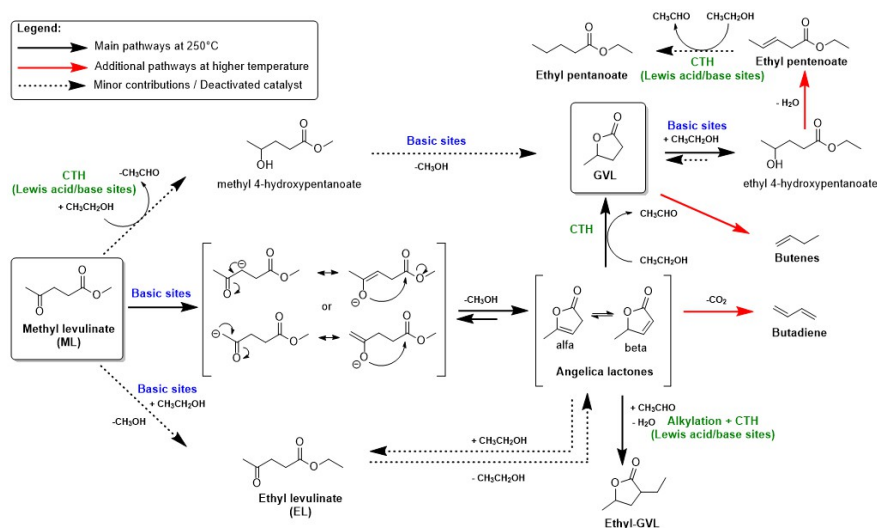


**Figure 2.** Proposed reaction mechanism for the CTH of ML with EtOH over ZrO<sub>2</sub>.

reactants. Moreover, long-term stability tests were carried out to evaluate the performance of ZrO<sub>2</sub> and deactivation of the catalysts was observed. To explore the reasons for deactivation we have carried out a series of experiments

(catalytic and spectroscopic studies) to identify the possible causes of deactivation. This presentation aims to discuss in detail structure-activity relationships, reaction pathways and to present for the first time an efficient continuous gas-phase process for the CTH of ML.

## References

- [1] Werpy, T. & Petersen, G. Top Value Added Chemicals from Biomass Volume I — Results of Screening for Potential Candidates from Sugars and Synthesis Gas. U.S. Dep. Energy (2004)
- [2] Rackemann, D. W. & Doherty, W. O. Biofuels, Bioprod. Biorefining 5, 198–214 (2011).
- [3] Chia, M. & Dumesic, J. A. Chem. Commun. 47, 12233 (2011).
- [4] Gilkey, M. J. & Xu, B. ACS Catal. 6, 1420–1436 (2016).
- [5] Kuwahara, Y., Kaburagi, W. & Fujitani, T. RSC Adv. 4, 45848–45855 (2014).
- [6] Yang, Z., Huang, Y.-B., Guo, Q.-X. & Fu, Y. Chem. Commun. 49, 5328 (2013).
- [7] He, J., Li, H., Lu, Y., Liu, Y., Wu, Z., Hu, D., Yang, S. Appl. Catal. A Gen. 510, 11–19 (2016).
- [8] Tang, X., Hua, L., Zhao, G., Hao, W., Lin, L. RSC Adv. 3, 10277 (2013).
- [9] Cirujano, F. G., Corma, A. & Llabrés i Xamena, F. X. Chem. Eng. Sci. 124, 52–60 (2015).
- [10] Li, F. et al. Appl. Catal. B Environ. 214, 67–77 (2017).

# **One-pot isomerized alkanes production from model esters over bifunctional Ni-based catalysts**

*P.M. Yeletsky, Boreskov Institute of Catalysis SB RAS, Novosibirsk, Russia;*

*R.G. Kukushkin, Boreskov Institute of Catalysis SB RAS, Novosibirsk, Russia and  
Novosibirsk State University, Novosibirsk, Russia;*

*V.A. Yakovlev, Boreskov Institute of Catalysis SB RAS, Novosibirsk, Russia and  
Novosibirsk State University, Novosibirsk, Russia*

## **Introduction**

Today, there is a great interest to development of approaches to conversion of various lipidic feedstocks (e.g. vegetable oils, microalgae lipids etc.) into biofuels similar to conventional diesel and jet fuel via hydrotreating and hydroisomerization [1]. Conventionally, hydrotreating (hydrodeoxygenation, hydrodecarboxylation, hydrodecarbonylation) and hydroisomerization are carried out sequentially, and now there exist examples of the implemented processes of isomerized alkanes production like Neste Renewable Diesel (Neste) and Ecofining<sup>TM</sup> (Honeywell UOP).

Such consecutive conducting of hydrotreating and isomerization processes in two separated stages is a significant disadvantage, which complicates the conversion of vegetable oils and microalgae lipids in the components of motor fuels, giving rise to increased cost and reduced yield of the target products. Thus, of interest is a merging of these steps into the one. Central point of this merging is the use of appropriate catalysts active in the both hydrotreating and isomerization [2]. They should have a non-sulfided nature, low cost, high activity to deoxygenation and selectivity to iso-alkanes of fuel purposes in comparison with the cracking products. Taking into account the above requirements, the most attractive are non-sulfided Ni-based catalysts, which are often modified with other 3d metals (e.g., Mo) as well as P [3,4]. However, there is a serious lack in research in the field of application of such catalysts for one-pot isomerized alkanes production from lipidic feedstocks.

Thence, the goal of this work is a development of modified non-sulfided Ni-based catalysts having bifunctional nature to produce isomerized fuel alkanes. At the first stage, as model compounds, a mixture of esters (methylpalmitate dissolved in ethylcaprate) has been used.

## Results

A series of nickel-based catalysts were synthesized by wet impregnation using alumina, silica and zeolites as supports. The catalysts were further promoted by Cu and/or Mo, W as well as by phosphorus. It was shown that the modification by different metals could significantly change activity and selectivity on liquid products. For example, promotion by copper decreases activity of the Ni-based catalysts in the esters hydrodeoxygenation and as a result – methane formation suppression was observed. Modification of Ni-based catalysts by Mo and W changes selectivity on products and enables to save the carbon skeleton of initial fatty acid.

The main difference in activity in hydrodeoxygenation of esters of the Ni-based catalysts supported by different supports, which have different acid-based properties was a selectivity to isomerized alkanes and alkanes formed through hydrocracking of longer C-C chain alkanes.

The catalysts were investigated by a wide range of techniques (XRD, XPS, TPR and FTIR). TPR study of the modified samples showed shifting of hydrogen uptake peaks to lower temperatures region in the case of Cu modified catalysts, and to higher temperatures region in the case of Mo and W modified catalysts. XRD showed that there exist changes in metallic Ni lattice after promotion by Cu and Mo.

*The work is supported by The Russian Science Foundation, Project № 18-43-08002.*

## References

1. Gaurav N. et al., *Renew. Sust. Energy Rev.*, 2017, 73, 205–214.
2. Galadima, A., Muraza, O. *Int. J. Energy Res.* 2015, 39, 741–759.
3. Liu, Y et al., *Appl. Catal. B: Environ.* 2015, 174–175, 504–514.
4. Chen, N. et al., *Appl. Catal. B: Environ.* 2015, 174–175, 253–263.

# **Ni/La<sub>2</sub>O<sub>3</sub> catalysts for dry reforming of methane: effect of synthesis conditions on the structural properties and catalytic performances**

G. Pantaleo<sup>1</sup>, M. Grabchenko<sup>2</sup>, F. Puleo<sup>1</sup>, O. Vodyankina<sup>2</sup>, L.F. Liotta<sup>1</sup>

*Institute for the Study of Nanostructured Materials<sup>1</sup>, Palermo, Italy;*

*Tomsk State University<sup>2</sup>, Tomsk, Russia*

## **Scope**

Dry reforming of methane (DRM) is an attractive way of utilizing biogas, a clean and environment friendly fuel that is produced typically from anaerobic degradation of biomass and mainly composed of CO<sub>2</sub> and CH<sub>4</sub>. DRM also eliminates two major greenhouse gases (CO<sub>2</sub> and CH<sub>4</sub>) simultaneously while producing valuable feedstock. DRM is highly endothermic ( $\Delta H^{\circ}_{25^{\circ}\text{C}} = 247 \text{ kJ/mol}$ ) and normally requires temperatures above 700 °C to attain good conversion levels [1]. Ni-based catalysts supported on the materials with high specific surface show high activity. Noble metals (Rh, Ru, Pt, Ir, Pd, etc.) are also used in the DRM process and show higher stability, but their cost exceeds the one of Ni-based catalysts [2]. The main drawback of Ni based catalysts is represented by the production of significant amount of carbon and by the sintering at the high temperatures of the reaction. Carbon deposits are formed when the rate of methane dissociation is faster than the oxidation of carbon by the surface oxygen species arising from CO<sub>2</sub> dissociation on the metal component or from carbonates formed at the metal support interface [3,4]. Until now, many studies have demonstrated that metal oxides such as CeO<sub>2</sub>, MgO, ZrO<sub>2</sub> have positive effects on catalytic activity, stability and carbon suppression of nickel catalysts for DRM [5]. In the present work the physical chemical properties, the related catalytic activity and the long-run stability of Ni-La<sub>2</sub>O<sub>3</sub> catalysts have been evaluated in DRM reaction. The aim was to investigate the effect of ammonia addition during the synthesis of La<sub>2</sub>O<sub>3</sub> oxide carried out by sol-gel method in presence of citric acid.

## **Results and discussion**

Ni(10%wt) was deposited by wetness impregnation over two La<sub>2</sub>O<sub>3</sub> oxides prepared with and without adding NH<sub>3</sub> solution during the synthesis, the corresponding catalysts were labelled as *Ni-La CA* and *Ni-La CA-NH<sub>3</sub>*, respectively. The so far prepared catalysts were characterized by BET, XRD and TPR techniques. The XRD patterns of the supports calcined at 800 °C showed that ammonia addition favors the

formation of  $\text{La}_2\text{O}_3$  phase with respect to  $\text{La}(\text{OH})_3$ .  $\text{La}_2\text{O}_3$  was the only lanthanum phase detected in the XRD pattern of *Ni-La CA-NH<sub>3</sub>*, after calcination at 600 °C and reduction treatment at 700 °C, moreover, weak features attributed to dispersed metallic Ni particles were found. While in the case of *Ni-La CA*, both phases,  $\text{La}_2\text{O}_3$  and  $\text{La}(\text{OH})_3$  were present along with well visible peaks of metallic Ni suggesting the presence of big clusters. DRM gradient catalytic test performed between 400 °C to 800 °C revealed higher catalytic activity of *Ni-La CA*, nevertheless long run test showed a better stability of *Ni-La CA-NH<sub>3</sub>* catalyst. The spent catalysts were characterized by XRD, TGA, Raman and TEM analyses. In both samples  $\text{La}_2\text{O}_2\text{CO}_3$  phase was formed together with C graphite peak of higher intensity in the case of *Ni-La CA* in agreement with greater weight loss revealed by TGA and stronger deactivation during long run with respect to *Ni-La CA-NH<sub>3</sub>*. The effect of the nature of the catalyst on the amount of carbon coke formed during DRM was also confirmed by Raman and TEM results.

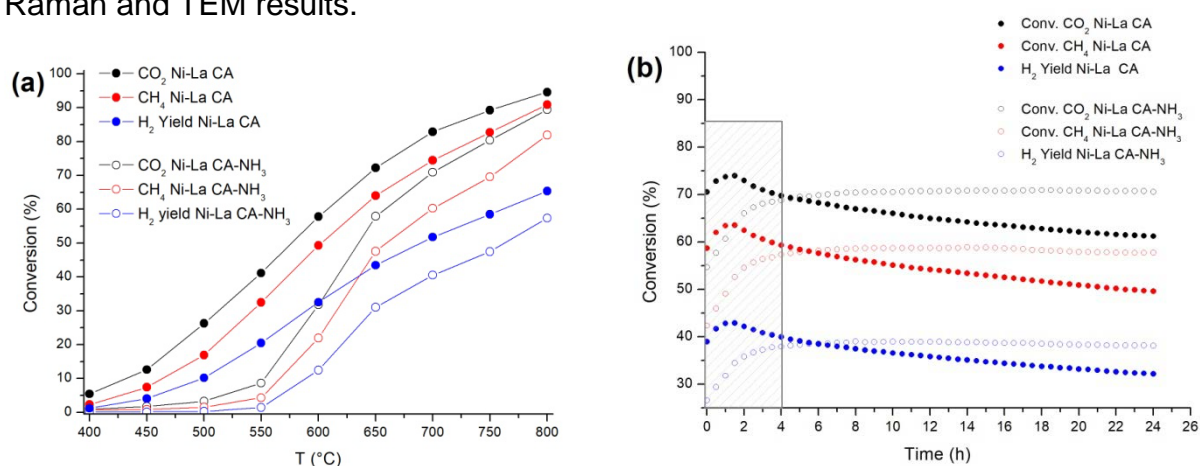


**Figure 1.** DRM gradient (a) and long run (650 °C during 24h) (b) tests of Ni/La<sub>2</sub>O<sub>3</sub> catalysts

## Conclusions

It was shown that  $\text{NH}_3$  generates a support of  $\text{La}_2\text{O}_3$  with increased specific surface area that favors the dispersion of the metallic Ni.  $\text{NH}_3$  produced a quite stable Ni- $\text{La}_2\text{O}_3$  catalyst in the conversion of  $\text{CH}_4$  and  $\text{CO}_2$  (long run 650 °C 24h) and able to limit the formation of carbonaceous residues and carbonates.

## References

1. Lavoie, J.M.; *Front Chem.* 2014, 11, 2-81.
2. Pakhare D. and Spivey J.; *Chem. Soc. Rev.*, 2014, 43, 7813-7837.
3. Jia, Z.; Kou, K.; Qin, M.; Wu, H.; Puleo, F.; Liotta, L.F.; *Catalysts* 2017, 7, 256-276.
4. Horváth A. Gucci L., Kocsonya A., Sáfrán G., La Parola V., Liotta L.F., Pantaleo G., Venezia, A.M.; *Applied Catalysis A: General* 2013, 468 250– 259.
5. Mesrar, F.; Kacimi, M.; Liotta, L.F.; Puleo, F.; Ziyad, M.; *Int J Hydrogen Energy* 2017, 42, 19458-19466

## **CO<sub>2</sub> Methanation on Highly Loaded Ni-Al<sub>2</sub>O<sub>3</sub> Catalysts – From the Microscopic to the Macroscopic Level**

<sup>1</sup>*Dennis Beierlein, Dorothea Häussermann, Yvonne Traa, Elias Klemm, University of Stuttgart, Institute of Chemical Technology, 70550 Stuttgart, Germany;*

<sup>2</sup>*Mirko Pfeifer, Thomas Schwarz, Klaus Stöwe, Institute of Chemistry, Chemnitz University of Technology, 09111 Chemnitz, Germany*

The „Power to Gas“ (PtG) process is a promising concept for energy storage, where surplus electricity is converted into „substitute natural gas“ (SNG) which can be used for chemical energy storage and afterwards again for power generation [1].

For an industrial application, catalysts with high selectivity, space time yield (STY) and stability are favored. We prepared catalysts with Ni mass fractions between 14 and 88wt% with four different methods, i.e., dry impregnation, wet impregnation, deposition precipitation and coprecipitation, and tried to understand the fundamental relationship between preparation method, Ni loading, particle size/dispersion and catalyst stability. By applying proven experimental conditions [2], we could show that, for supported Ni-Al<sub>2</sub>O<sub>3</sub> catalysts, the Ni particle size is independent of the Ni loading and similar to the pore size even at high Ni loadings, if the Ni is deposited in the mesopores of the support. During deposition precipitation, Ni can, via the formation of a hydrotalcite-like precursor, completely be deposited in the mesopores. During dry and wet impregnation, Ni is partially unsupported or located outside the mesopores on the external surface of the support. Thus, an increase in the Ni loading leads to an increase of the Ni surface, as long as the Ni is deposited in the mesopores of the support during the preparation of the catalyst. The Ni particle size of the coprecipitated catalysts is independent of the Ni loading, and thus, an increase of the Ni loading leads to a considerable increase of the Ni surface in this case. Therefore, deposition precipitation and coprecipitation are the best methods for the preparation of catalysts with high Ni surface areas.

Structure-activity relationships determine which catalyst properties have to be modified in order to increase the STY. Some authors assume that the activity depends on the nickel particle size and that the particle geometry has a significant influence (structure-sensitive reaction) [3-5], other results indicate that the activity

only depends on the Ni surface area [6]. Therefore, the aim of this work is to determine the structure-activity relationships of the CO<sub>2</sub> methanation.

Our catalytic investigation clearly shows that the CO<sub>2</sub> methanation on Ni-Al<sub>2</sub>O<sub>3</sub> catalysts is a structure-insensitive reaction and that the terrace atoms are the active sites (Fig. 1). Other parameters, such as metal-support interactions, the metal-support interface, AlO<sub>x</sub> particles or alkali metals do not have a significant influence on the activity. Thus, the activity seems to be a specific property of Ni, and the Ni surface area is the microscopic property which determines the CO<sub>2</sub> conversion.

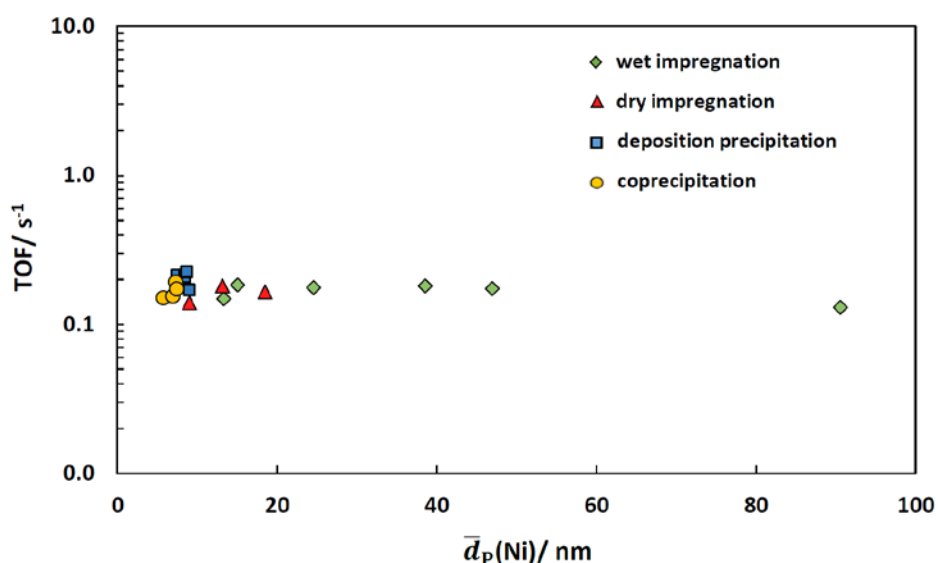


**Figure 1:** TOF determined over a period of 6 h at 300 °C, 200 kPa, X(CO<sub>2</sub>) = 30% plotted against the Ni particle size which is determined by static H chemisorption [7].

In measurements with a constant modified residence time, a linear correlation between the Ni surface area and the conversion can be observed. Therefore, the catalysts with the highest Ni surface areas achieve the highest weight time yields. Furthermore, with increasing mass fraction of the Na impurity, a linear increase of the selectivity to CO results.

**Acknowledgments:** The authors thank thyssenkrupp Industrial Solutions AG for financial support and Dr. Steffen Schirmer for valuable guidance.

## References

- [1] M. Götz, J. Lefebvre, F. Mörs, A.M. Koch, F. Graf, S. Bajohr, R. Reimert, T. Kolb, *Renew. Energy* 85 (2016) 1371.
- [2] D. Beierlein, S. Schirmer, Y. Traa, E. Klemm, *Reac. Kinet. Mech. Cat.* 125 (2018) 157.
- [3] S. He, C. Li, H. Chen, D. Su, B. Zhang, X. Cao, B. Wang, M. Wei, D.G. Evans, X. Duan, *Chem. Mater.* 25 (2013) 1040.
- [4] H.C. Wu, Y.C. Chang, J.H. Wu, J.H. Lin, I.K. Lin, C.S. Chen, *Catal. Sci. Technol.* 5 (2015) 4154.
- [5] J.K. Kesavan, I. Luisetto, S. Tuti, C. Meneghini, G. Iucci, C. Battocchio, S. Mobilio, S. Casciardi, R. Sisto, *J. of CO<sub>2</sub> Util.* 23 (2018) 200.
- [6] F. Koschany, D. Schlereth, O. Hinrichsen, *Appl. Catal. B* 181 (2016) 504.
- [7] D. Beierlein, D. Häussermann, M. Pfeifer, T. Schwarz, K. Stöwe, Y. Traa, E. Klemm, *Appl. Catal. B*, accepted, <https://doi.org/10.1016/j.apcatb.2018.12.064>.



# Surface Structure Characterization of Co-Ce/ZrO<sub>2</sub> Catalysts for Carbon Dioxide Reforming of Methane

*Aysun Ipek Paksoy, Department of Chemical Engineering, Boğaziçi University, 34342, Bebek, Istanbul, Turkey; Burcu Selen Caglayan, Advanced Technologies R&D Center, Boğaziçi University, 34342, Bebek, Istanbul, Turkey; Ahmet Erhan Aksoylu, Department of Chemical Engineering, Boğaziçi University, 34342, Bebek, Istanbul, Turkey*

## Abstract

This study aims to investigate surface structure and its change, *including the adsorption properties of the formed sites*, in Co-Ce/ZrO<sub>2</sub> catalyst system for Carbon Dioxide Reforming of Methane (CDRM) in response to the change in Co/Ce loading ratio via FTIR-DRIFTS. In this context, a comparative analysis of FTIR-DRIFTS spectra obtained upon CO adsorption on Co-Ce/ZrO<sub>2</sub> catalysts having different Co/Ce loading ratios was performed. The results underlined the significance of Co/Ce ratio on catalyst structure; such that CO adsorption becomes weaker with the increase in Co loading, and formation of various carbonate and formate surface species is dependent on Ce loading.

## Introduction

Syngas production via CDRM has attained attention as one of the routes to deal with global warming and attain alternative energy sources for fossil fuels owing to its environmental impact on mitigating the most abundant greenhouse gases, CH<sub>4</sub> and CO<sub>2</sub>. However, the details of performance and mechanistic features of CDRM need to be enlightened both for developing efficient catalysts having stable performance and for assessing its industrial applicability. In that manner, the aim of this study is to determine the surface properties of Co-Ce/ZrO<sub>2</sub> system for CDRM utilizing CO adsorption via FTIR-DRIFTS, and relate the findings with the pre-evaluated CDRM activity data [1-3].

## Results and Discussion

CO adsorption was conducted on catalysts with different Co/Ce loading ratios in order to determine surface structural properties of Co-Ce/ZrO<sub>2</sub> system.

The presence of bridge and linear-bonded CO adsorbed on Co metallic sites was verified for all tested samples [4,5]. However, it was clear that the peaks at adsorbed

CO region showed a sharper decrease after He flush for the catalysts with 10% Co loading; pointing out that CO adsorption is weaker on the surface of these catalysts.

At the region attributed to gas phase and adsorbed  $\text{CO}_2$  [5], a shift to higher wavenumbers at  $\text{CO}_2(\text{g})$  position was observed at the spectrum belonging to the analysis over 10%Co-2%Ce/ $\text{ZrO}_2$ , and the peak intensities were lower for that over 10%Co-3%Ce/ $\text{ZrO}_2$ .

For the catalysts having the same Co loading, the monodentate carbonate peak [5] was more pronounced at the spectra corresponding to those having higher Ce loading, hinting a relation between monodentate carbonate formation and ceria loading. It should be noted that enhanced formation of surface carbonates might decrease the oxygen mobility of the catalyst and therefore, reduces  $\text{CO}_2$  activation during CDRM [6].

Possible CO-catalyst surface interaction yielding OH-involving species was also addressed for all tested samples.

## Conclusions

This study underlined the impact of Co/Ce loading ratio on the surface properties of Co-Ce/ $\text{ZrO}_2$  system.

## Acknowledgement

The financial support was provided by TUBITAK through project 111M144, and by Republic of Turkey Ministry of Development through project 2016K121160.

## References

1. A.I. Paksoy, B.S. Caglayan, A.E. Aksoylu, *App Cat B: Environ.* **2015**, *168*, 164-174.
2. A.I. Paksoy, B.S. Caglayan, E. Ozensoy, A.N. Okte, A.E. Aksoylu, *Int J Hydrogen Energy.* **2018**, *43*, 4321-4334.
3. A.I. Paksoy, C. Yassı Akdag, B.S. Caglayan, A.E. Aksoylu, *Int J of Chem Kinet.* **2019**, *51*, 138-145.
4. D. Song, J. Li, *J Mol Catal A: Chem.* **2006**, *247*, 206–212.
5. B. Bachiller-Baeza, C. Mateos-Pedrero, M.A. Soria, A. Guerrero-Ruiz, U. Rodemerck, I. Rodríguez-Ramos, *App Cat B: Environ.* **2013**, *129*, 450–459.
6. P. Djinić, I.G.O. Crnivec, B. Erjavec, A. Pintar, *ChemCatChem*, **2014**, *6*, 1652–1663.

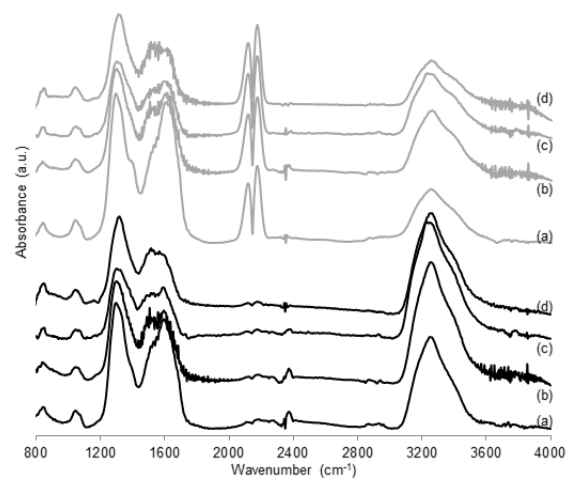


Figure 1. FTIR-DRIFTS spectra for 1% CO adsorption at room temperature on (a) 5%Co-2%Ce/ $\text{ZrO}_2$ , (b) 5%Co-3%Ce/ $\text{ZrO}_2$ , (c) 10%Co-2%Ce/ $\text{ZrO}_2$ , and (d) 10%Co-3%Ce/ $\text{ZrO}_2$  just after CO adsorption (grey spectra), and upon He flush (black spectra).

# Sum-Frequency Generation Spectroscopy of CO<sub>2</sub> Reduction Reactions at Au and Pt/[EMIM][DCA] Electrode/Electrolyte Interfaces

*Björn Ratschmeier, Andre Kemna, Björn Braunschweig*

*Institute of Physical Chemistry, Westfälische Wilhelms-University, Corrensstraße  
28/30, 48149 Münster, Germany*

Using potentiodynamic broadband sum-frequency generation (SFG) and cyclic voltammetry (CV), polycrystalline Pt and Au electrodes interfaces with 1-ethyl-3-methylimidazolium dicyanamide ([EMIM][DCA]) electrolytes were studied in situ. As an interface sensitive method, SFG spectroscopy can be used to follow the progress of CO<sub>2</sub> reduction reactions (CO<sub>2</sub>RR) through the detection of surface-adsorbed CO. In previous studies with different room-temperature ionic liquids (RTILs), it was already shown that the use of imidazolium-based RTILs leads to unprecedented low overpotentials for CO<sub>2</sub>RR [1,2]. In this contribution, we present new information on the use of [EMIM][DCA] for CO<sub>2</sub>RR, which is an interesting water-miscible electrolyte because of its low viscosity and excellent conductivity as well as CO<sub>2</sub> solubility.

CV of Au- and Pt interfaces in CO<sub>2</sub>-saturated [EMIM][DCA] indicates CO<sub>2</sub> reduction between -1.2 and +0.6 V vs SHE. CV also indicates a reduction of the onset potential for CO<sub>2</sub>RR, when water is present.

Furthermore, CO formation at Pt/[EMIM][DCA] interfaces is observed in situ with SFG spectroscopy. The intensity of the apparent CO band increases with the number of potential cycles (-1.2 to 0.6 V) and reaches a Stark shift of 24 cm<sup>-1</sup>/V after 20 cycles, while DCA related bands show only little changes with electrode potential. The latter Stark shift of the CO band is indicative for a closed-packed CO adlayer on the Pt surface. In fact, the formation of surface-adsorbed CO leads to a poisoning of the Pt surface and is accompanied by a significant reduction of CO<sub>2</sub> reduction currents.

## References

B. A. Rosen, J. L. Haan, P. Mukherjee, B. Braunschweig, W. Zhu, A. Salehi-Khojin, D. D. Dlott, R. I. Masel, *J. Phys. Chem C*. **2012**, *116*, 15307-15312. [1]

B. Braunschweig, P. Mukherjee, J.L. Haan, D.D. Dlott, *J. Electroanal. Chem.* **2017**, *800*, 144–150. [2]

# **Fundamental analysis of the effective thermal conductivity of cellular materials as catalyst supports for non-adiabatic processes**

*Mauro Bracconi, Matteo Ambrosetti, Matteo Maestri, Gianpiero Groppi and Enrico Tronconi*

*Laboratory of Catalysis and Catalytic Processes, Politecnico di Milano, Milano - Italy*

## **Introduction**

Conductive structured catalysts have been proposed as a suitable solution for strongly exo- and endothermic processes, being able to intensify heat transfer and thus solve heat management problems, a crucial feature of many industrial processes like methane steam reforming and Fischer-Tropsch synthesis. We focus on random (open-cell foams) and regular (periodic ordered cellular structures – POCS) reticulated interconnected solid structures, whose repeated open-cells are composed by solid struts and open windows. The totally interconnected solid matrix of these structures promotes the heat transfer rates, once conduction in the solid matrix becomes the main contribution to the heat transport. In this view, the analysis of the heat conduction mechanism is crucial to enable the rational design of these structures. In this work, a parametric analysis of the effect of the topological and geometrical properties of cellular materials on their effective thermal conductivity is carried out, providing design guidelines for these innovative substrates.

## **Methods**

The conductive heat transport in the solid matrix is analyzed by 3D numerical simulations on virtually reconstructed structures. Accurate reconstructions of the geometries [1] are employed for the generation of the computational domains. The simulations enable to compute the heat flux in the solid structure and, consequently, the effective heat conductivity for foams and for several different POCS.

## **Results and discussion**

The numerical method has been assessed by a comparison with literature data available for open-cell foams. A good agreement was obtained over the entire range of investigated porosities [2]. Then, a parametric analysis of the effect of the geometrical properties has been performed on both foams and POCS. Our results reveal that the cell size as well as the strut cross section shape have a negligible

effect on the effective thermal conductivity [3]. The heat transfer performances are governed by the solid volumetric fraction ( $1-\varepsilon$ ): an increment of the solid fraction at constant cell size increments more than linearly the normalized effective conductivity, as shown in Figure 1(a). POCS with different unit cells and foams show comparable performances at the same solid fraction. Hence, the effect of cell shape and topology on the effective thermal conductivity is negligible. The regular and ordered structures of POCS provide additional room for design. In this view, we have investigated the effect of local modifications of the structures on the heat conduction performances in view of promoting the radial conductivity. Along these lines, the cubic cell has been modified to present two different strut diameters along the different directions, as shown in Figure 1(b). By changing the ratio between the two strut diameters at constant porosity, it is possible to enhance, up to 50%, the effective thermal conductivity in the selected direction, revealing the potential of these structures for being tailored to the process requirements

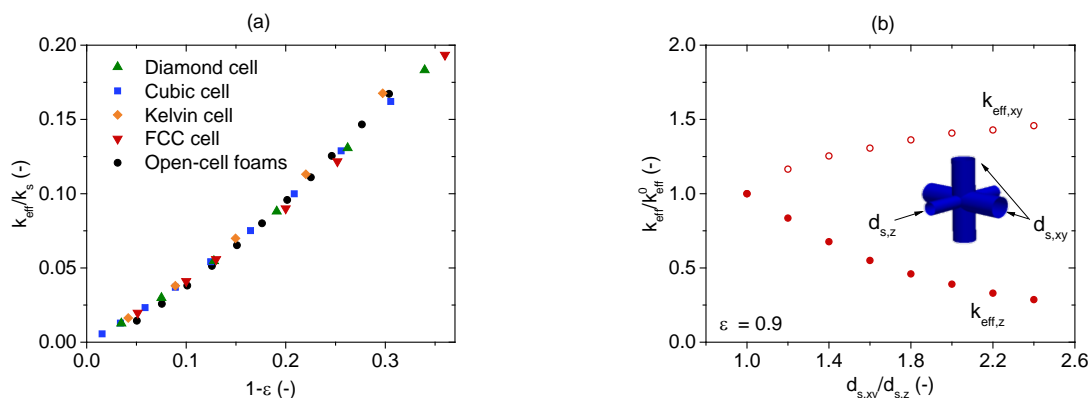


**Figure 1.** Effect of the solid volume fraction and cell size on the effective heat conductivity of cellular media (a) and effect of local anisotropy of the performance of cubic cells (b).

## Significance

We have systematically analyzed the effects of the geometrical properties on the effective thermal conductivity of catalyst substrates based on open-cell foams and POCS. Moreover, we demonstrate the potential of these structures to be designed according to the process needs by maximizing the heat transport in radial direction.

## Acknowledgements

This project has received funding from the European Research Council under Grant Agreement no. 694910 (INTENT).

## References

- [1] M. Bracconi, et al., Chem. Eng. J. 315 (2017) 608–620.
- [2] M. Bracconi, et al., Chem. Eng. Process. - Process Intensif. 129 (2018) 181–189.
- [3] E. Bianchi, et al., Adv. Eng. Mater. 18 (2016) 608-614.

# Controlling Tungsten Carbide Phase Composition: Designing Hydrogenation-Catalysts for Optimum Performance

*Patrick Bretzler, Michael Huber, Klaus Köhler*

*Department of Chemistry, Inorganic Chemistry, Lichtenbergstrasse 4 and Catalysis  
Research Center, Ernst-Otto-Fischer-Strasse 1, Technical University of Munich,  
85747 Garching, Germany*

## Introduction

Tungsten carbide possesses catalytic properties similar to those of Platinum<sup>[1]</sup>. This lead to its use in several fields of catalysis, most prominently electrocatalysis<sup>[2-3]</sup> and the upgrading of biomass<sup>[4]</sup>. Even though the material has been investigated for several decades, the preparation of a phase pure tungsten carbide without the use of a carbon support remains challenging. The carburization proceeds over the reduction of a tungsten precursor, over the metastable tungsten semicarbide ( $W_2C$ ) to the thermodynamically favored tungsten monocarbide (WC). The different properties of the crystal phases often remain unreported even though they play a crucial role in catalytic performance. Similarly, the influence of oxidic supports, especially on the carbide synthesis remains mostly unexplored. Herein we present a systematic approach to better understand tungsten carbide hydrogenation catalysts, control the carburization process and shed light on the role of silica as a stabilizer in this catalyst system. Additionally, we are able to show a clear relation between the tungsten semicarbide phase and catalytic activity for hydrogenation reactions.

## Experimental

Influence of several synthetic parameters on the carburization process and catalytic hydrogenation activity are investigated using a design of experiments approach. Tungsten carbide catalysts are prepared by an isothermal carburization reaction in a  $CH_4/H_2$ -mixture at temperatures between 650 °C and 800 °C. The process is monitored by online mass spectrometry of the exhaust gas stream. Silica modified tungsten(VI) oxide precursors are prepared by an incipient wetness impregnation method of ammonium metatungstate hydrate solution on silica and subsequent calcination. Catalytic activity is tested by the hydrogenation of butyraldehyde to 1-butanol in a heated stirring tank reactor at 200 °C and 65 bar hydrogen pressure. The catalytic reaction is monitored by intermediate sampling of the reaction mixture.

## Results and Discussion

Silica modification improves the catalytic activity of the implicated tungsten carbide sites but does not act as a classical support. According to our findings, the decisive role of silica is to be found in the tungsten carbide synthesis, stabilizing and thus favoring the formation of tungsten semicarbide. This stabilizing effect does not necessarily include the accessible surface area, as might be expected. The ratio of tungsten to silica is of major importance regarding the catalytic performance.

Phase composition for bulk, and silica modified tungsten carbide systems can be tuned to tungsten semicarbide contents between 15 wt.-% and 91 wt.-%, as determined by *Rietveld* analysis. Design of experiment evaluation results in a linear model that enables the targeted preparation of different phase compositions even outside of this range. Additionally, design of experiment confirms the extraordinary stabilizing effect of silica on the tungsten semicarbide phase.

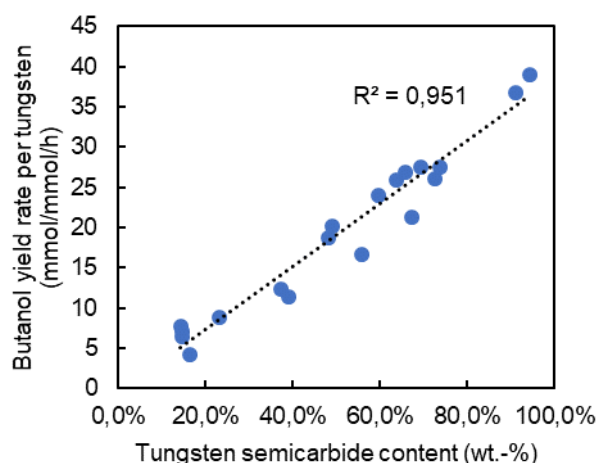


Figure 1: Tungsten semicarbide content vs. butyraldehyde hydrogenation rate for tungsten carbide catalysts prepared under varying conditions.

Catalysis tests on the hydrogenation of butyraldehyde show a direct relation between catalytic hydrogenation activity and the tungsten semicarbide content (Fig. 1). This distinct correlation strongly suggests the phase composition being the most important indicator for catalytic activity in this system. The obtained results allow the purposeful improvement of tungsten carbide hydrogenation catalysts, especially for the upgrading of biomass.

## References

- [1] R. B. Levy, M. Boudart, *Am Assoc Adv Sci Pub* **1973**, *181*, 547-549.
- [2] M. C. Weidman, D. V. Esposito, I. J. Hsu, J. G. Chen, *Journal of The Electrochemical Society* **2010**, *157*, F179.
- [3] S. Meyer, A. V. Nikiforov, I. M. Petrushina, K. Köhler, E. Christensen, J. O. Jensen, N. J. Bjerrum, *Int J Hydrogen Energy* **2015**, *40*, 2905-2911.
- [4] Z. Lin, R. Chen, Z. Qu, J. G. Chen, *Green Chem.* **2018**, *20*, 2679-2696.

# **The effect of fuel selection in combustion synthesised copper-ceria catalysts for methanol synthesis from carbon dioxide hydrogenation**

*Mahomed A.S., University of KwaZulu-Natal, Durban, South Africa; Xaba B.S., University of KwaZulu-Natal, Durban, South Africa; Friedrich H.B., University of KwaZulu-Natal, Durban, South Africa; Singh S., University of KwaZulu-Natal, Durban, South Africa*

## **Scope**

The exhaustion of fossil fuels in the future is the inevitability that cannot be ignored, therefore, there is a growing need to find an alternative fuel that has the capacity to be as effective as fossil fuels in electricity generation, as transportation fuel and in bulk chemical synthesis. Methanol has the versatility to be that alternative or replacement for fossil fuels in the foreseeable future as advocated by Olah and company.[1] The production of methanol from carbon dioxide hydrogenation is perceived as a sustainable chemical loop, given that hydrogen is produced from a self-sustaining pathway such as water electrolysis.[2] Industrially, the Cu/ZnO/Al<sub>2</sub>O<sub>3</sub> catalyst is utilized in methanol synthesis, however, studies have shown that the Cu/CeO<sub>2</sub> catalyst has comparable activity to the industrial catalyst.[3] This study is aimed at synthesising Cu-CeO<sub>2</sub> catalysts by the solution combustion method and investigating the role of various fuels in the prevailing physicochemical properties of the prepared catalysts. Three different fuels were applied in the synthesis namely urea (U), ethylene glycol (EG) and citric acid (CA). The prepared catalysts will be evaluated for methanol synthesis from carbon dioxide hydrogenation.

## **Results**

The P-XRD was performed for identification of the phases that are present in the prepared catalysts. A consistent presence of tenorite and cerianite was observed for all the catalysts as shown in **Figure 1**. The diffractograms for all the catalysts were dominated by the reflections of cerianite in comparison to the tenorite phase. This could be due to a higher content of ceria in the sample relative to copper oxide or it might be because of the encapsulation of copper oxide inside the lattice of ceria.



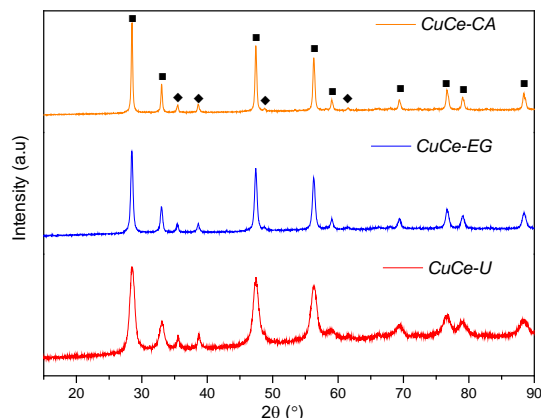


**Figure 1: XRD patterns of Cu-CeO<sub>2</sub> catalysts synthesised with different fuels, Symbols: (◆) CuO and (■) CeO<sub>2</sub>**

The reducibility of the catalysts was assessed by H<sub>2</sub>-TPR. The H<sub>2</sub>-TPR profiles showed a large peak at approximately 180 °C which was further deconvoluted to two Gaussian peaks as shown in **Figure 2**. The lower temperature peak is ascribed to the reduction of the surface copper oxide to metallic copper, while the higher temperature peak is due to the reduction of copper oxide that has been encapsulated in the ceria lattice to metallic copper. An observable small peak around 795 °C is attributed to the reduction of ceria from Ce<sup>4+</sup> to Ce<sup>3+</sup>.

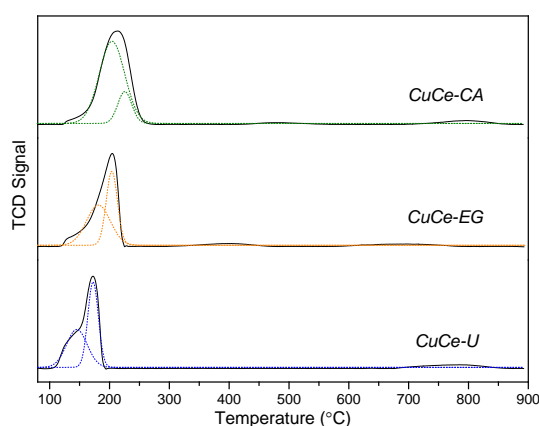


**Figure 2: H<sub>2</sub>-TPR profiles of Cu based catalysts**

## References

- G. A. Olah, A. Goepfert and G. K. S. Prakash, Beyond Oil and Gas: The Methanol Economy, Wiley, 2011. [1]
- A. Taheri Najafabadi, International Journal of Energy Research, 2013, 37, 485-499.[2]
- B. Ouyang, W. Tan and B. Liu, Catalysis Communications, 2017, 95, 36-39.[3]

# The glucose hydrogenation activity and stability of carbon-supported Fe-Ni alloy catalysts

*Yang Fu, Sophie Hermans*

*Université catholique de Louvain, IMCN Institute, Place L. Pasteur 1, 1348 Louvain-la-Neuve, Belgium*

## Introduction

Hydrogenation of D-glucose into D-sorbitol is a significant process for the industry, as sorbitol is a building block for various chemicals and is also applied as additive. Ipatieff was the first to reduce glucose to sorbitol by hydrogenation in the presence of nickel catalyst [1]. Although ruthenium is the most effective active phase, most commercial processes are still using Raney nickel given its economic price. More recently, the hydrogenation of glucose with nanoparticles, especially supported nickel nanoparticles, are widely studied in view of their higher number of catalytic sites [2].

The deactivation of (promoted) Raney-type or supported nickel is due to leaching of promoter and nickel or blocking of active sites by stronger adsorption of organics such as gluconic acid. However, the causes of Ni leaching are still unclear. Here, we study both the catalytic performance and leaching behavior of alloyed FeNi/carbon black (FeNi/CB) catalysts for the selective hydrogenation of glucose into sorbitol.

## Results and discussion

Carbon black (CB) supported Ni, Fe, or FeNi alloy were synthesized through wet-impregnation method. Fig. 1 gives the XRD patterns of the samples obtained. The position of the diffraction peaks for FeNi/CB agree with literature data for alloys in the Fe-Ni system [3]. XPS spectra for FeNi/CB catalyst (Fig. 2a) displays Ni 2p peaks at 853.3 eV and 855.8 eV, that are ascribed respectively to metallic nickel ( $\text{Ni}^0$ ) and oxidized nickel ( $\text{Ni}^{2+}$ ). By contrast, there is no metallic peak of  $\text{Ni}^0$  in monometallic nickel catalyst. Low amount of metallic Ni on the surface leads to uncompetitive catalytic properties. So even with 50 wt.% metal loading, its conversion (34.6 % within 2 hours) is much lower than the alloy with only 10 wt.% load of Ni and 10 wt.% of Fe (75.2 % conversion in 2h). Besides, the selectivity in sorbitol with the alloy catalyst shows fewer signs of subsiding in comparison to monometallic Ni catalyst. After glucose hydrogenation test, 10.8 % of Ni leached away in Ni/CB. In contrast, there is only 7.1 % of Ni lost in FeNi/CB. Since Fe is more electropositive, it can be positively charged and act as adsorption sites for the glucose aldehydic form via the

oxygen atom. So Fe could enhance the activity of Ni catalyst and reduce the leaching of Ni at the same time. After hydrogenation, there is no additional phase formed in the catalyst (FeNi/CB\_Spent) compared with starting FeNi/CB. Moreover, the average crystallite size calculated using Scherrer formula almost did not change after hydrogenation. The decrease of relative area for metallic nickel and increase for oxidized nickel (XPS, Fig. 2b) give the evidence that surface Ni was oxidized during the hydrogenation of glucose. In addition, the disappearance of metallic XPS peak for iron (707.2 eV) shown in Fig. 2d illustrates that metallic Fe was oxidized as well. After three recycle tests, the conversion of glucose is still 49% in 2 hours, which is 5 times higher than monometallic Ni in our conditions.

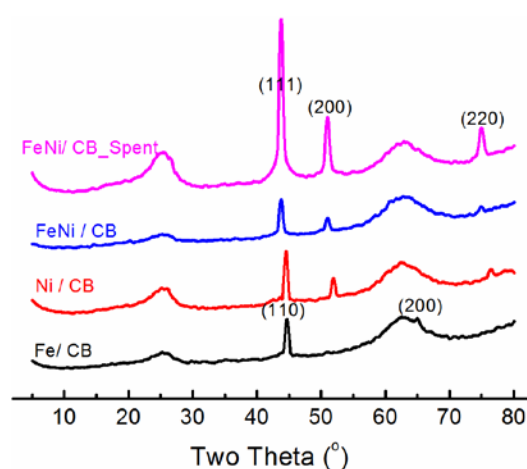


**Fig. 1** XRD patterns of the 10%Fe/CB, 10%Ni/CB, FeNi/CB, FeNi/CB\_Spent catalysts.

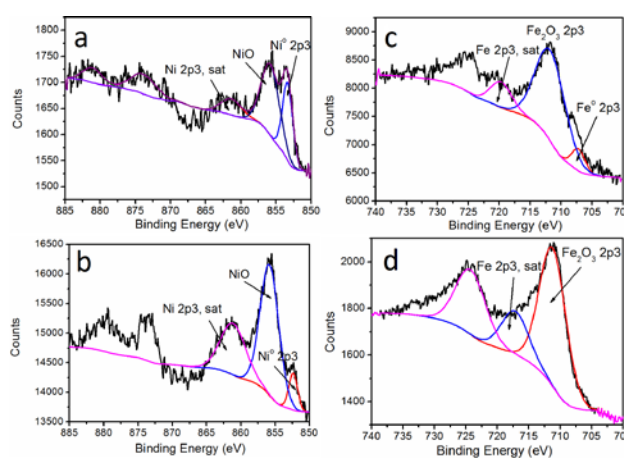


**Fig. 2** Ni 2p and Fe 2p XPS spectra of FeNi/CB catalyst before (a, c) and after (b, d) hydrogenation.

## Conclusion

We have prepared carbon black supported FeNi alloy catalyst. The metals oxidation and leaching are the main reasons for the deactivation of alloy catalysts. However, the presence of Fe enhances both activity and stability compared to monometallic counterparts. So it would be meaningful to investigate the relationship between leaching rate, conversion and selectivity with well-defined Fe<sub>3</sub>Ni/CB and FeNi<sub>3</sub>/CB catalysts.

## References

- 1 Abdel Akher, M., Ghali, J., Raouf, M.S., and Roushdi, M.: Starch - Stärke, 1974, 26, (9), 307-312
- 2 Singh, H., Rai, A., Yadav, R., and Sinha, A.K.: Molecular Catalysis, 2018, 451, 186-191
- 3 Wu, H.-Q., Cao, Y.-J., Yuan, P.-S., Xu, H.-Y., and Wei, X.-W.: Chemical Physics Letters, 2005, 406, (1), 148-153

# Catalytic Effect of Hydrogen Spillover in Nanorattle Catalysts Derived from Metal-Organic Frameworks

*Simone Zacho and Jerrik Mielby, DTU Chemistry, Technical University of Denmark,  
Kgs. Lyngby, Denmark*

## Introduction

Beside their high porosity, high surface area and low density, hollow nanomaterials offer a number of key advantages with respect to loading and functionalization of their hollow interior. Hollow nanostructured materials therefore hold great promise for new and emerging technologies in energy conversion and catalysis [1]. The synthesis of hollow nanomaterials are typically based on templating, using either soft or hard templates, or template-free methods, which rely on the Kirkendall effect [2], Ostwald ripening [3], selective dissolution [4] or recrystallization [5-6]. In general, these methods all have advantages and disadvantages, but usually suffer from complicated synthesis procedures, expensive additives, poor yield and non-uniform materials.

Here, we report a simple and efficient method to synthesize Co nanoparticles inside mesoporous nanorattle catalysts. In this method, the metal-organic framework ZIF-67 is exploited as structural template for the preparation of a mesoporous metal oxide shell as well as sacrificial precursor to form Co nanoparticles inside the shell. In a subsequent step, preformed Pt nanoparticles are supported on the external surface of the mesoporous shell by conventional impregnation. For the first time, the separation between the Co on the inside and Pt on the outside allow us to study the catalytic effect of spillover hydrogen migrating across a well-defined distance on the nanometer length scale. Depending on the reducibility of the metal oxide support, we show that small amounts of Pt have a significant effect on the reduction temperature of Co and, consequently, on the catalytic activity in CO<sub>2</sub> methanation.

## Experimental

In one example, small crystals of the metal-organic framework ZIF-67 were synthesized from cobalt nitrate and 2-methylimidazole in methanol. The ZIF-67 were then used as structural template for the synthesis of a mesoporous ZrO<sub>2</sub> shell using hexadecylamine as pore generating template. The ZIF-67@ZrO<sub>2</sub> composite material were dried and then calcined to remove the organic templates. Half of the sample were then impregnated with an aqueous dispersion 3 nm Pt nanoparticles. The

catalytic activity of the two samples were then compared in CO<sub>2</sub> methanation. Similar catalysts were made with mesoporous shells of TiO<sub>2</sub> and SiO<sub>2</sub>, respectively.

The prepared catalysts were characterized using a variety of techniques, including XRD, XRF, XPS, N<sub>2</sub> physisorption, TPR, DRIFTS, SEM, TEM, STEM and electron tomography. The catalytic tests were performed in a fixed bed reactor equipped with an online GC-FID/TCD or MS.

## Results and discussion

Figure 1a show a TEM image of a core-shell material comprised of ZIF-67 metal-organic framework core and a mesoporous ZrO<sub>2</sub> metal oxide shell prepared as described. Figure 1b show the TPR of the same material with and without Pt. The TPR show no significant decrease of the main reduction peak at around 345°C. Since ZrO<sub>2</sub> has a low reducibility, Pt and hydrogen spillover does not improve the catalytic activity of Co in this case.

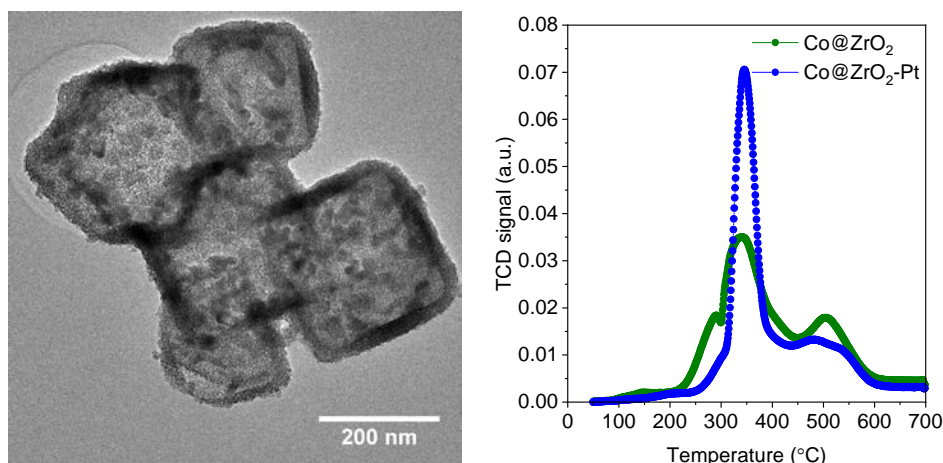


**Figure 1.** a) TEM image of Co@ZrO<sub>2</sub>. b) TPR of Co@ZrO<sub>2</sub> and Co@ZrO<sub>2</sub>-Pt, respectively.

## Conclusions

Exploiting metal-organic frameworks as both structural template and sacrificial precursor offers extraordinary control of size, shape and structure and opens up new exciting opportunities for designing advanced model catalysts. This may simplify catalytic interpretations and help untangle mechanistic information.

## References

- [1] G. Prieto, H. Tu, N. Duyckaerts, J. Knossalla, G. Wang, F. Schüth, *Chem. Rev.* 116 (2016) 14056.
- [2] W. Wang, M. Dahl, Y. Yin, *Chem. Mater.* 25 (2013) 1179.
- [3] C. C. Yec, H. C. Zeng, *J. Mater. Chem. A* 2 (2014) 4843.
- [4] X. Fang, C. Chen, Z. Liu, P. Liu, N. Zheng, *Nanoscale* 3 (2011) 1632.
- [5] J. Mielby, J. Abildstrøm, F. Wang, T. Kasama, C. Weidenthaler, S. Kegnæs, *Angew. Chem.* 46 (2014) 12513
- [6] F. Goodarzi, L. Kang, F. R. Wang, F. Joensen, S. Kegnæs, J. Mielby, *ChemCatChem*, 10 (2018)

# Catalytic reforming of model biomass-derived producer gas

*Lola Azancot, Luis F. Bobadilla, Miguel A. Centeno and José A. Odriozola*

*Departamento de Química Inorgánica and Instituto de Ciencia de Materiales de Sevilla, Centro mixto CSIC – Universidad de Sevilla, 49 Av. Américo Vespucio, 41092-Sevilla (Spain), e-mail: [lola.azancot@icmse.csic.es](mailto:lola.azancot@icmse.csic.es)*

## Introduction

The production of liquid fuels and chemicals from the syngas generated by biomass gasification is one of the most promising alternatives for replacing definitely the fossil fuels. The gaseous effluent produced from biomass gasification, designated as “producer gas”, contains significant concentrations of light hydrocarbons, including methane, and tars that must be reformed to clean-up the syngas. These tars are well known precursors of coke and can deactivate rapidly the reforming catalysts. This work includes a complete study of the reaction of reforming of a simulated producer gas stream using Ni-based catalysts doped with different loadings of potassium for enhancing the resistance to the coke formation.

## Experimental procedure

A support based on  $\text{MgAl}_2\text{O}_4$  spinel oxide was prepared by coprecipitation and calcined at 900 °C for 24 h to obtain a highly homogeneous solid. Then, a 10 wt. % of nickel was co-impregnated with different loadings of potassium (0, 1, 3 and 5 wt. %) on the support and calcined subsequently at 550 °C for 4 h. The prepared samples were fully characterized by XRD, XRF, XPS, Raman and UV-Vis spectroscopy, HRTEM,  $\text{N}_2$  physisorption, TPR, TPSR of methane and toluene, TPO, FTIR  $\text{CO}_2$  adsorption and FTIR CO adsorption at 77 K.

The catalytic reforming tests were performed in a lab-scale reaction system using a fixed-bed flow reactor consisting of a quartz tube (9 mm i.d.) containing 100 mg of non-diluted catalyst between plugs of quartz wool. Prior to testing, the catalysts were reduced in situ at 800 °C for 1 h passing a flow of 100 mL  $\text{min}^{-1}$  of 50 vol. %  $\text{H}_2/\text{N}_2$ . Toluene was selected as model of tar and the gas composition simulating a typical producer gas stream was 5 vol.%  $\text{CH}_4$ , 18 vol.%  $\text{CO}_2$  and 1 vol.% tar diluted in  $\text{N}_2$  with a total gas flow of 100 mL  $\text{min}^{-1}$ . The reaction was carried out at three temperatures (550, 650 and 750 °C) with a time-on-stream of 10 h at each temperature. The reactor effluent was on-line analyzed by gas chromatography using

a system equipped with three columns coupled with two TCD and one FID detectors enabling the quantification of the permanent gases and hydrocarbons, respectively.

## Results and discussion

Characterization details reveal that all catalysts presented metallic nickel particles with average size between 10 and 20 nm dispersed on  $\text{MgAl}_2\text{O}_4$  spinel oxide. Furthermore, it was observed that potassium species are partially covering the nickel particles and neutralizing the hydroxyls groups on the support. Figure 1 shows the catalytic performance in terms of conversion for the four prepared catalysts as function of the potassium loading at each temperature. As can be observed, the conversion of methane, tar, and  $\text{CO}_2$  are increased by increasing the reaction temperature in all samples. On the other hand, the conversion is improved with the potassium loading until reaching an optimal content of 3 wt. %. Additionally, post-reaction studies by TPO and Raman demonstrated that this catalyst presented the lower amount of formed coke and the lower stability of the carbonaceous species deposited.

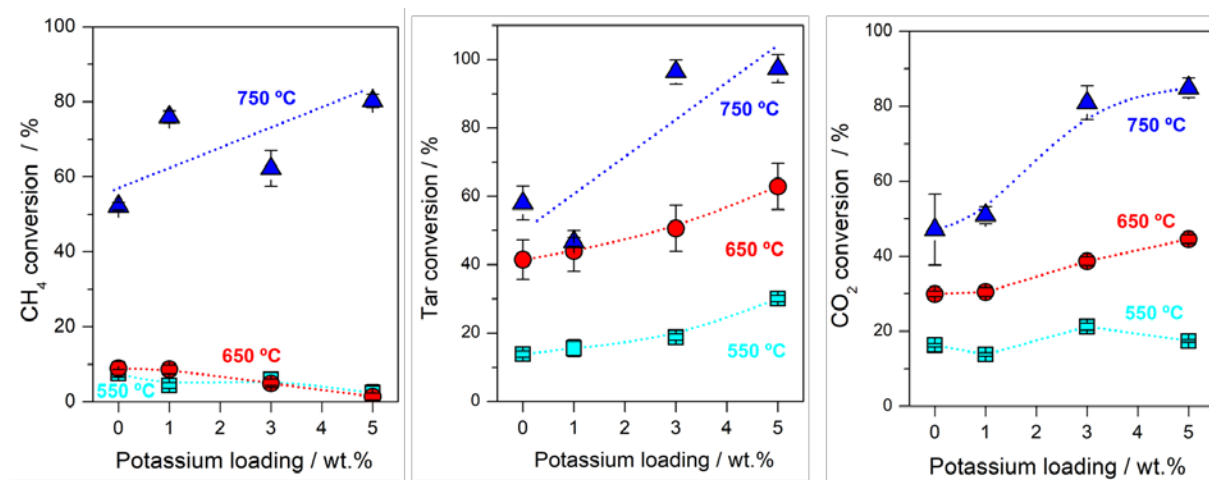


**Figure 1.** Methane, tar (toluene) and  $\text{CO}_2$  conversion as function of the potassium loading at 550, 650 and 750 °C

## Conclusions

This study demonstrated that exist an optimum of potassium content of 3 wt.% that minimizes the coke formation to achieve an efficient reforming process of producer gas and produce a clean-up syngas. To further understand the effect of potassium loading in the reaction mechanism and the role of potassium in the gasification of carbonaceous species, *operando* DRIFTS studies were performed under reaction conditions. These results will be further presented in the congress.

## CO-PROX reaction over $\text{Co}_3\text{O}_4/\text{Al}_2\text{O}_3$ catalysts

G. Grzybek<sup>1</sup>, K. Ciura<sup>1</sup>, J. Gryboś<sup>1</sup>, P. Indyka<sup>1</sup>, A. Davó-Quiñonero<sup>2</sup>,  
D. Lozano-Castelló<sup>2</sup>, A. Bueno-Lopez<sup>2</sup>, A. Kotarba<sup>1</sup>, Z. Sojka<sup>1</sup>

<sup>1</sup>Faculty of Chemistry, Jagiellonian University, Krakow, Poland

<sup>2</sup>Department of Inorganic Chemistry, University of Alicante, Alicante, Spain

*A series of  $\text{Co}_3\text{O}_4/\text{Al}_2\text{O}_3$  catalysts with various exposition of the spinel planes (100), (111) and (110) was prepared. The catalysts were thoroughly characterized by means of XRF, XRD, RS, STEM, TPR techniques. The CO-PROX catalytic activity of the samples was studied. A strong impact of the spinel nanograins morphology on the catalyst performance was observed, with the (100) termination found as the most active.*

### 1. Scope

The CO-PROX reaction is a catalytic route for selective oxidation of residual content of CO present in the  $\text{H}_2$ -rich flows. So far, many catalytic systems such as Pt/ $\text{Al}_2\text{O}_3$ , Pd/zeolites, Ru/ $\text{Al}_2\text{O}_3$  have been investigated in the CO-PROX process. The transition metals and metal oxides supported on oxide carriers ( $\text{CeO}_2$ ,  $\text{CeO}_2\text{-ZrO}_2$ ,  $\text{Al}_2\text{O}_3$ ) have been studied as potential CO-PROX catalysts as well. One of the most efficient systems is the benchmarking CuO/ $\text{CeO}_2$  catalyst, owing to the remarkable oxygen storing/releasing capacity of ceria [1]. Likewise,  $\text{Co}_3\text{O}_4$  spinel is a promising catalytic active phase for CO-PROX reaction. It has been found that  $\alpha\text{-Al}_2\text{O}_3$  support is the most suitable for  $\text{Co}_3\text{O}_4$  dispersion, and leads to development of well shaped spinel nanocrystal morphology [2]. Furthermore, modification of the spinel deposition method by glycerol addition results in a controlled exposition of the active facets [3]. The aim of the presented studies was to establish the most active termination of cobalt spinel active phase supported on  $\alpha$ -alumina in the CO-PROX process.

### 2. Results and discussion

The polyhedral shape of the nano-spinel active phase of obtained  $\alpha\text{-Al}_2\text{O}_3$  supported cobalt spinel catalysts was controlled via glycerol and/or Zn additions to the impregnation solution. The samples were characterized with respect to  $\text{Co}_3\text{O}_4$  loading (XRF), active spinel phase structure (XRD, Raman Spectroscopy) and morphology (SEM, TEM). The results of the elemental composition based on XRF analysis of the investigated samples confirmed that the content of the spinel active



phase of  $10\pm 1$  %wt. reflects well the desired loading. The phase analysis with XRD and RS confirmed the presence of a nanocrystalline cobalt spinel. The morphological analysis underlined the significant difference in the spinel nanograins shape and hence in the number and nature of the exposed cobalt sites ( $\text{Co}^{2+}$  and  $\text{Co}^{3+}$ ).

Therefore, the observed CO-PROX performance (Figure 1) was examined with respect to the relative abundance of the (100), (110) and (111) facets exposed by the polyhedral spinel nanograins of the catalysts. The abundance was revealed from analysis of calibrated STEM images using an inverse Wulff construction.

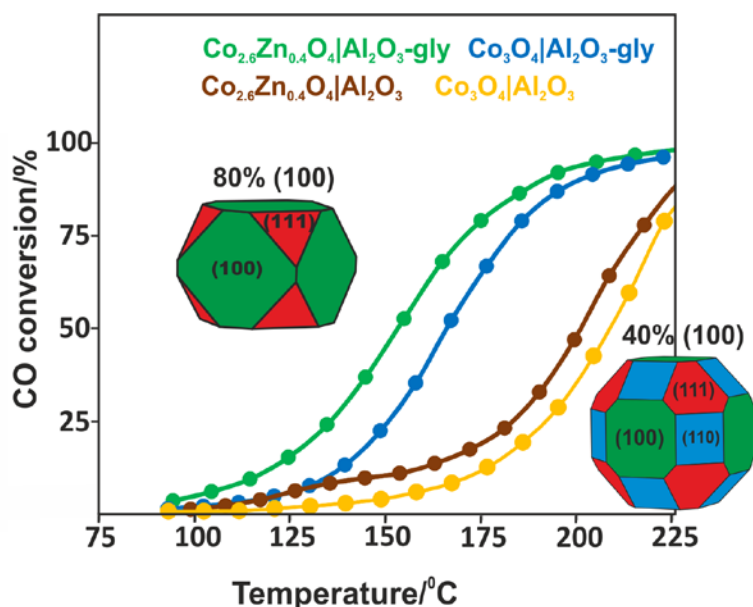


**Figure 1.** Catalytic performance of supported cobalt spinel in the CO-PROX reaction together with a predominant polyhedral shape of the nanocrystal for the most and the less active samples.

the content of the surface  $\text{Co}^{3+}$  cations and the CO oxidation yield confirms experimentally their key role as the reaction active sites.

The observed strong impact of the morphological factor on the CO-PROX catalytic activity of the investigated samples was associated with the exposition of the beneficial (100) facet (Figure 1). It can be explained by the fact that the (100) facets exhibit the highest areal concentration of the octahedral  $\text{Co}^{3+}$  cations, which are believed to act as PROX active sites.

A linear correlation between

### Acknowledgement

Authors would like to acknowledge the funding awarded by the Polish National Science Center (decision number 2017/27/B/ST4/01155).

### References

- [1] A. Davó-Quiñonero, et. al., ACS Catal., 2016, 6 (3), 1723–1731.
- [2] G. Grzybek, et. al., Catal. Sci. & Technology 7 (2017) 5723-5732.
- [3] S. Gudyka, et. al., Appl. Catal. B Environ. 2017, 201, 339–347.

# Making a Supported Nickel Catalyst Completely Selective for Partial Hydrogenation by Ionic Liquid Coatings

*Ahsan Jalal and Alper Uzun, Koç University, Istanbul, Turkey*

## Introduction

Ionic liquid (IL) coatings offer a tremendous potential for controlling the performance of supported metal catalysts. Their ligand and filter effects not only control the electronic environment on the active sites, but also adjust the effective concentrations of reactants, intermediates, and products. Here, we show that an ordinary supported nickel catalyst becomes completely selective for partial hydrogenation, when coated with an IL, providing the insights on the influence of IL on the catalytic performance.

## Results and Discussion

Data in Figure 1a show a selectivity higher than 95% for total butenes irrespective of conversion on 1-*n*-butyl-3-methylimidazolium tetrafluoroborate ([BMIM][BF<sub>4</sub>])-coated supported nickel catalyst (Ni65, 65 wt% Ni, Sigma-Aldrich) for 1,3-butadiene partial hydrogenation at 40 °C and at a molar ratio of 1,3-butadiene:H<sub>2</sub> = 1:2. These results illustrate that the IL coating makes the supported nickel catalyst more selective for partial hydrogenation. For probing the ligand effect, the XPS measurements were made on the uncoated and IL-coated Ni65. Data showed a decrease in binding energies of nickel sites upon coating the catalyst with [BMIM][BF<sub>4</sub>], indicating the presence of electron donation from IL to metal sites. Density functional theory (DFT) calculations complemented these results and showed that when there is an IL molecule presents next to a nickel cluster, the electron density on the nickel sites increases. Furthermore, DFT calculations further illustrated that such increase in electron density on the active sites influences the binding energies of adsorbates in the favor of high selectivity for partial hydrogenation. Accordingly, the binding energy differences between 1,3-butadiene and different olefin intermediates on nickel becomes much more significant in the presence of the IL molecule. Thus, when there is an IL-coating layer present, the intermediates formed at the end of the first hydrogenation step cannot compete with 1,3-butadiene and, desorb without finding another chance for hydrogenation. The filter effect was investigated by COSMO-RS calculations. Data indicated that 1,3-butadiene is not significantly more (approximately three-times) soluble than butenes in [BMIM][BF<sub>4</sub>]. Thus, we inferred

that the ligand effect is the dominant factor leading to high partial hydrogenation selectivity, while the filter effect helps to maintain the selectivity at all conversion levels.[1] For improving the selectivity even further, we then worked on optimizing the reaction conditions on the uncoated catalyst. Accordingly, at 145 °C and 1,3-butadiene and H<sub>2</sub> partial pressure of 0.16 and 0.32 bar, respectively, the Ni65 can provide approximately 95% total butene selectivity. Because, [BMIM][BF<sub>4</sub>] cannot withstand these conditions for long time periods, we considered another IL, tributyl(methyl)phosphonium methyl sulfate, [P<sub>4441</sub>][MeSO<sub>4</sub>]. [P<sub>4441</sub>][MeSO<sub>4</sub>]-coated Ni65 catalyst at these optimized conditions provides a complete selectivity towards butenes (Figure 1b). We infer that the ligand and filter effects of the IL help to reach the complete selectivity towards total butenes at these optimized conditions.[2]

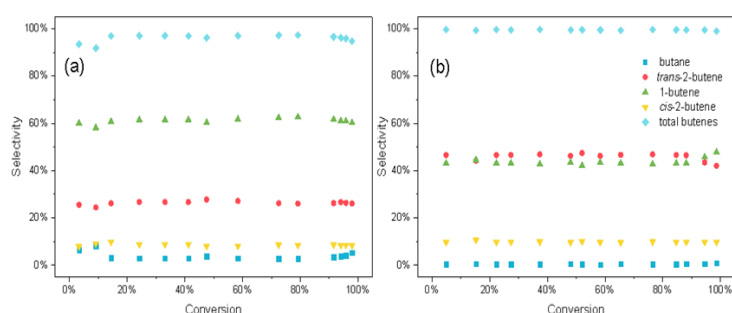


**Figure 1:** Product selectivity for partial hydrogenation of 1,3-butadiene over (a) [BMIM][BF<sub>4</sub>]-coated Ni65; (b) [P<sub>4441</sub>][MeSO<sub>4</sub>]-coated Ni65.

## Conclusions

The selectivity for partial hydrogenation of an ordinary supported nickel catalyst was improved by coating the catalyst with ILs. Data indicated electron donation from IL to metal sites. This effect works synergistically with the filter effect to offer a high partial hydrogenation selectivity. An IL with a high thermal stability offers opportunities for optimizing the reaction conditions to reach a complete partial hydrogenation selectivity. Considering that there is an infinite number of ILs with tunable properties, structure of these catalysts can be tuned for exceptional performance. Data presented here illustrate this broad potential and provide insights for rational design.

## Acknowledgments

We thank TUBITAK for funding (113M552). A.U. acknowledges TUBA-GEBIP award.

## References

- [1] Jalal, A., Uzun A. *J. Catal* 350, 86 (2017).
- [2] Jalal, A., Uzun A. *Appl. Catal. A: General* 189, 321 (2018).

## **Reinventing the MeOH synthesis by advanced quantum mechanical simulations**

*Marek P. Checinski, CreativeQuantum GmbH, Berlin, Germany; Pavel Ryabchuk, Leibniz Institut für Katalyse, Rostock, Germany; Matthias Beller, Leibniz Institut für Katalyse, Rostock, Germany*

Methanol is one of the most important high volume chemical produced by the chemical industry. It is produced at >100 Mt/a scale and is mostly used for production of formaldehyde, acetic acid, MTO/MTP, DME, MTBE, Fuel Blending, and Biodiesel.

Nowadays, the largely used process is based on a heterogeneous Cu/ZnO/Al<sub>2</sub>O<sub>3</sub> catalyst working at 240-260°C and 50-100 bar. Heating and compressing 100 Mt of substrates under these conditions makes it a very energy intense and expensive process with a high CO<sub>2</sub> footprint. Decreasing the temperature and especially the pressure significantly would have a big impact on the environment and on CAPEX and OPEX. This could lead to smaller and decentralized production sites.

This motivation leads us to think about new approaches from scratch, which were evaluated by intense and fast quantum mechanical simulations within a few weeks. After identifying that the possible rate limiting steps for some new approaches would be manageable below 200°C, a first virtual high throughput screening for promising catalysts was performed. After identifying the first few candidates, a literature study for these kinds of catalysts and single reaction steps was done, which resulted in the finding that these new catalysts and this new process should be practicable.

A following investigation of >100 catalysts by virtual high throughput screenings within two months revealed how a good catalyst should look like. These promising candidates were tested within one and a half months in the laboratory, and it was proven that the predicted good catalysts synthesized MeOH under very mild conditions while the bad ones did not.

The first unoptimized catalyst system for the proof-of-concept produced MeOH at <160°C and <50 bar pressure with a TON of >400.

# Hydrogen adsorption and CO<sub>2</sub> conversion into fuels and chemicals over transition metal carbides: A DFT study

*Fabrizio Silveri, Matthew G. Quesne, Alberto Roldan, Nora H. De Leeuw, C. Richard A. Catlow,*  
*Cardiff University, Department of Chemistry, Park Place, Cardiff, CF10 AT (UK)*

## Abstract

Transition metal carbides (TMCs) are a class of materials that combines low cost and high durability with interesting catalytic activity[1,2]. In this work, the bulk and surface properties of TiC, VC, ZrC and NbC have been put in relation with their activity over the hydrogen evolution reaction and carbon dioxide reduction, as part of a wider project investigating the conversion of CO<sub>2</sub> into fuels and chemicals. For each carbide, four low index surfaces were investigated, cut along the {001}, {011} and {111} atomic planes. The study was performed computationally using periodic DFT, as implemented in the VASP code[3].

## Results and Discussion

A preliminary study of the bulk and surface properties of several stoichiometric monocarbides has been performed, and 4 of these (TiC, VC, ZrC and NbC) have been selected on such basis for further studies on H<sub>2</sub> and CO<sub>2</sub> adsorption.

The adsorption of hydrogen was shown to be favourable on all investigated surfaces except for NbC (001), with a preference for C<sub>on top</sub> sites when available. Similarly, CO<sub>2</sub> adsorption was found to be favourable on all surfaces, and in both cases it was possible to derive the same surface reactivity sequence on all carbides, which is as follows:

$$(111)\text{-C} > (111)\text{-M} \approx (011) > (001)$$

this is in good agreement with the predictions made on the pristine surfaces based on surface energies, work functions ( $\Phi$ ) and d-band centre positions for each surface.

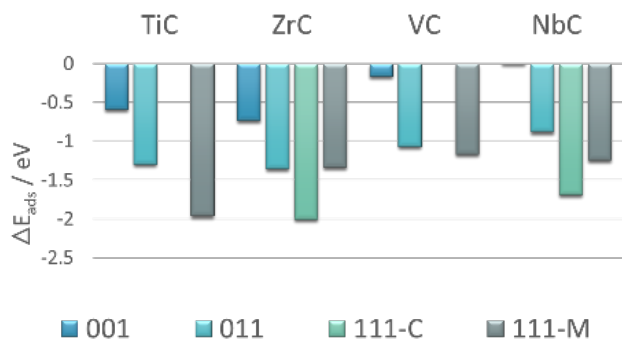
Similarly, on each surface the effect of the metal in the carbide can be shown to follow the series:

$$\text{TiC} \approx \text{ZrC} > \text{VC} \approx \text{NbC}$$

showing a clear effect of the group, again in good agreement with surface properties. The effect of the period is less marked, however it can be seen on (111)-C surfaces, which are unstable on TiC and VC in the presence of both H<sub>2</sub> and CO<sub>2</sub>, and in the longer bond distances found for the activated CO<sub>2</sub> on ZrC and NbC.

In the case of hydrogen, different loadings have been considered up to 1 ML: as the hydrogen loading is increased, a decrease in  $\Delta E_{\text{ads}}$  per atom is observed, matched by a similar decrease in  $\Phi$ . An analysis of the surface free energies has predicted the coverage state of each surface at zero potential in varying conditions of temperature and pressure, although significant variations are only found on (001) surfaces, which in turn are considered the most promising for hydrogen evolution reaction.

Lastly, the catalytic activity of the TMCs above over CO<sub>2</sub> reduction has been investigated following different paths. Direct hydrogenation of CO<sub>2</sub> was studied via the formation of both HCOO and COOH, and dissociation onto CO + O was also tested: the former are found to be significantly endothermic, but both the transition states and the products are found to be stabilized by the presence of water, while the latter are found to be exothermic, but with significantly high barriers, especially on TiC.



H<sub>2</sub> adsorption energies over all TMCs surfaces  
**Figure 1.** Adsorption energies per atom of H<sub>2</sub> on each surface and carbide, in eV.

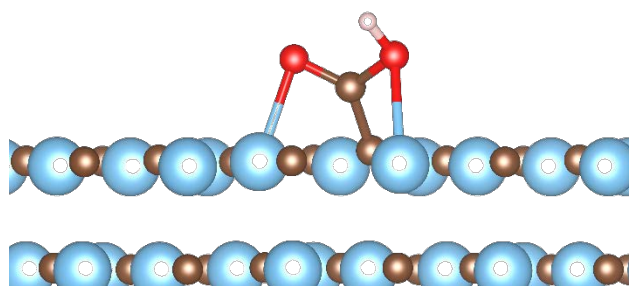


**Figure 2.** Activated COOH\* species on the TiC (001) surface.

## References

1. H. H. Hwu, J. G. Chen, Chem. Rev. 105 (2005) 185-212
2. W. Chen, J. T. Muckerman, E. Fujita, Chem. Commun. 49 (2013), 8896
3. G. Kresse, J. Furthmüller, Comp. Mat. Sci. 6, 1 (1996) 15-50

# WGS Performance of Pt-Re-Na Catalysts and Oxygen Storage Capacity (OSC) Effect on Performance

*B. Merve Eropak, Boğaziçi University, Department of Chemical Engineering, İstanbul, Turkey; B. Selen Çağlayan, Boğaziçi University, Advanced Technologies R&D Center, İstanbul, Turkey; A. Erhan Aksoylu\*, Boğaziçi University, Department of Chemical Engineering, İstanbul, Turkey*

The aim of this study was to design and develop alkali promoted Pt-based WGS catalysts which have promising activity and selectivity characteristics to be used in a fuel processor [1,2]. The metal loading, support type, feed composition and temperature were the parameters used in the catalyst design and testing studies. Highest activity was achieved over 1%Pt-1%Re-2%Na/CeO<sub>2</sub> at 400°C. The activity trend obtained at 350°C was found to be similar with the trend of effective Oxygen Storage Capacity (E-OSC) attained at the same temperature.

## Experimental

WGS reaction tests were performed under two types of feed, namely ideal (CO+H<sub>2</sub>O) and realistic (additionally including CO<sub>2</sub> and H<sub>2</sub>) feeds, each having two different H<sub>2</sub>O/CO ratios. Tests conducted under each feed composition were performed at 300°C, 350°C and 400°C. Each performance and OSC test was conducted over 75 mg *in-situ* reduced catalyst samples. OSC experiments involving the reaction test, were carried out under diluted forms of realistic feed flow and subsequent desorption process was performed up to 800°C.

## Results and Discussion

In view of the results obtained under realistic feed conditions, activities obtained at 350°C and 400°C under realistic feed #1 were determined to be higher than obtained under realistic feed #2. 51.5% CO conversion, which was attained over 1%Pt-1%Re-2%Na/CeO<sub>2</sub> under realistic feed #1 (H<sub>2</sub>O/CO=6.7) , was found to be the highest activity achieved. Another important indication of WGS activity and selectivity, i.e. net H<sub>2</sub> production percentages are presented with related CO conversion levels in Figure 1. In accordance with CO conversion results, maximum net H<sub>2</sub> production was observed as 11.3% at 400°C under realistic feed #1 over 1%Pt-1%Re-2%Na/CeO<sub>2</sub>. Increase in temperature had a positive effect on net H<sub>2</sub> production under realistic feed #1, however such a trend did not exist under realistic feed #2 (H<sub>2</sub>O/CO=16.2).

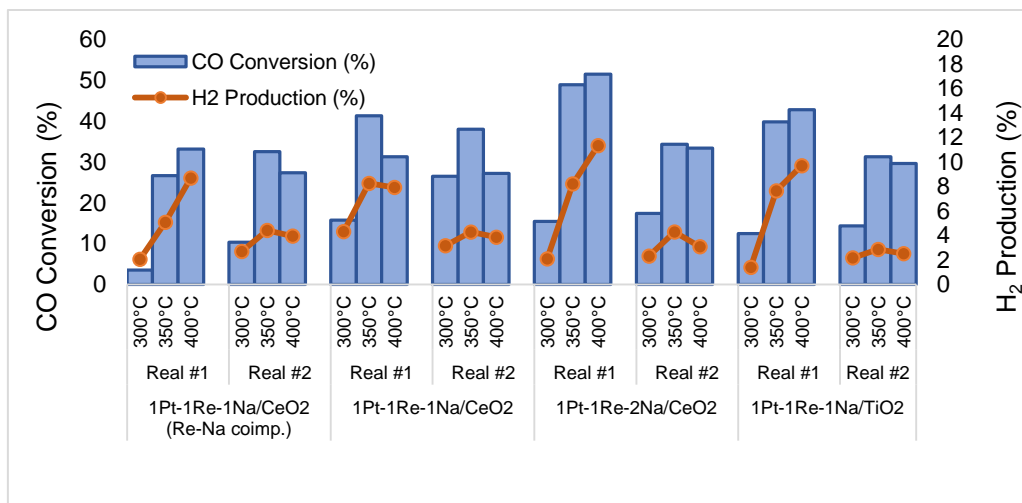


Figure 1. CO conversion and H<sub>2</sub> production percentages for each catalyst at different temperatures under realistic feed #1 and #2 conditions.

Our results strongly indicate that WGS performance is related with oxygen storage ability of the catalysts. Although coimpregnated 1%Pt-1%Re-1%Na/CeO<sub>2</sub> catalyst had a high total oxygen storage capacity (T-OSC) including structural oxygen, its relatively lower catalyst activity compared to those of sequentially impregnated ones was found related to its lower effective oxygen capacity (E-OSC), excluding structural oxygen. Higher E-OSCs and WGS activity were observed under realistic feed #1. Sequentially impregnated 1%Pt-1%Re-2%Na/CeO<sub>2</sub> was found to be the most promising one among all catalysts regarding its high activity and E-OSC.

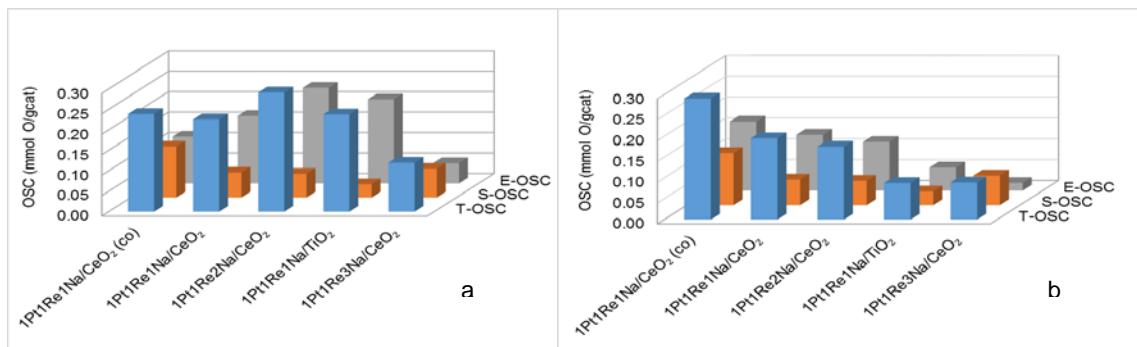


Figure 2. Oxygen storage capacities of catalysts at 350°C under a) diluted realistic feed #1 b) diluted realistic feed #2

## Acknowledgements

The financial support was provided by TÜBİTAK through project 214M170 and Turkish Ministry of Development through project 2016K121160.

## References

- [1] Pazmiño J.H., Shekhar M., Williams W.D., Akatay M.C., Miller J.T., Delgass W.N., Riberio F.H., *Journal of Catalysis* 286 (2012) 279-286.
- [2] Zhu X., Hoang T., Lobban L.L., Mallinson R.G., *Catalysis Letters* 129 (2009) 135-141.



**The effect of synthesis parameters on SCS (solution combustion synthesis) and in situ generated defect sites of VMgO catalysts for oxidative dehydrogenation of n-octane**

P Ntola, S Singh , H B Friedrich, A S Mahomed

<sup>a</sup> *School of Chemistry, University of Kwa Zulu Natal,, Private Bag X54001, Durban 4000, South Africa, E-mail: [217081870@stu.ukzn.ac.za](mailto:217081870@stu.ukzn.ac.za).*

Supported vanadia catalysts have received considerable attention due to their enhanced activity and selectivity in various oxidation reactions [1]. The aim of this study is to synthesize VMgO catalysts using solution combustion synthesis (SCS) and to evaluate the effects introduced by synthesis parameters during catalyst preparation, on their physical and chemical properties and defect sites formation for the oxidative dehydrogenation of n-octane. Amongst the various parameters, fuel plays an important role in determining the properties of the final SCS product. Defect sites, like oxygen vacancies, have been documented to have a direct impact on the electronic and geometric properties of a catalyst which in turn modifies the performances of the active sites [3]. Therefore, characterizing these sites is important to probe the structure activity relationship in order to improve catalytic performance. Defects sites are also reported to form during reactions, these may affect the activity of the catalyst, and hence, this work seeks to compare synthesis induced and in situ induced defect sites.

Five catalysts, synthesized by solution combustion synthesis were prepared using five different fuels. These have been characterized using XRD, FTIR, HR-TEM, TEM and BET. XRD and FTIR were used to identify different types of VO<sub>x</sub> species formed during the SCS of these catalysts. For four catalysts, MgO was the dominant phase followed by the formation of the magnesium orthovanadate phase. The orthovanadate phase has been reported to be the phase responsible for higher activity of the VMgO catalysts. The formation of these phases were confirmed by FTIR. EDX provided insights regarding the composition, as well as V dispersion in these catalysts. TEM analysis was conducted and the particle sizes of the catalyst

ranged from 11 nm- 54 nm. Further characterization will be done using EPR, XANES and XPS to characterize and quantify of formed defect sites in these catalysts. The latter analysis will give a more conclusive insight on the effect of the above mentioned parameters on the ODH of n-octane. This characterization will also be done on used catalysts to evaluate the formation of defect sites during a reaction. These catalysts have been tested on a fixed bed reactor. Catalytic data indicates that there may be differences in the synthesized catalysts introduced by the difference in the fuels used.

1. Li Y. , Wei Z. , Gao F., Kovarik L. , Baylon R. A. L. , Peden C.H.F. , Wang Y. *ACS Catal.* **2015** , 5, 3006-3012.
2. Kingsley J.J., Patil K.C. *Mater. Sci.*, **1988**, 6, 427
- 3 . Sun Y. , Gao, F. Lei, ., Xie.Y. *Chem. Soc. Rev.*, **2015**, 44, 623-636.

## **Novel TiO<sub>2</sub>-based supports for Fischer–Tropsch synthesis**

*Ralf Becker, Venator Germany GmbH, Duisburg, Germany; Carsten Knobloch, hte GmbH – The high throughput experimentation company, Heidelberg, Germany; Alfred Haas, hte GmbH – The high throughput experimentation company, Heidelberg, Germany;*

### **Introduction**

Fischer–Tropsch synthesis (FTS) converts natural gas, coal or biomass derived syngas to long chain hydrocarbons for chemicals and clean fuel production. Especially for fuel applications supported Co-based catalysts are used with high C<sub>5+</sub> productivity (chain growth probability), minimum C<sub>1-4</sub> selectivity at high once through CO conversion. One of the most prospective support materials is TiO<sub>2</sub> which is known to have strong Co metal support interaction [1]. FTS catalyst activity and selectivity is very much dependent on the dispersion of the reduced Co ensembles as well as on the accessibility of the active sites which is affected by the pore volume distribution, tortuosity and other properties of the support materials.

Four newly developed support materials were used as supports for Co-based FTS catalysts and tested under relevant industrial process conditions for the low-temperature FTS. The objective was to measure the relationship between the unique TiO<sub>2</sub> structure and Co–FTS performance. Catalysts have been tested in 32-fold parallel fixed bed reactor system (hte GmbH).

### **Materials and Methods**

TiO<sub>2</sub> powders (Table 1) were synthesized by proprietary synthesis routes based on the commercial large-scale sulphate production process and were modified by silica and zirconia [2, 3]. The 125 – 160 μm particle size fractions were treated with Co(NO<sub>3</sub>)<sub>2</sub> via conventional impregnation techniques to obtain concentrations of 10 or 20 wt.-% Co. The calcined catalysts were loaded without diluent into the isothermal zone of stainless steel reactors with 3.6 mm inner diameter. In the first reactor block the catalyst bed of 16 reactors contained 80 mg Co while in the second reactor block only 40 mg Co was used. Catalysts were activated in-situ at atmospheric pressure under pure Ar atmosphere at 120 °C for 2 h and 25 vol.-% H<sub>2</sub> in Ar at 350 °C for 24 h, respectively.

Support material		TiO <sub>2</sub> #07	TiO <sub>2</sub> #08	TiO <sub>2</sub> #09	TiO <sub>2</sub> #11
Polymorph	%	anatase > 98	anatase > 98	anatase > 98	anatase > 98
TiO <sub>2</sub>	wt.-%	91.5	94.6	81.1	79.8
SiO <sub>2</sub>	wt.-%	8.5	5.4	6.9	7.7
ZrO <sub>2</sub>	wt.-%	-	-	10.4	10.8
BET	m <sup>2</sup> /g	70	48	56	77
Pore volume	ml/g	0.56	0.24	0.17	0.32
Average pore size	nm	28	18	7	17

**Table 1:** Analytical data of TiO<sub>2</sub>-based supports for FTS.

## Results and Discussion

The FTS process conditions and obtained CO conversions are presented in Figure 1. The reactor temperature was increased stepwise at constant pressure, volume flow and gas composition from 150 °C up to 207.5 °C (heating block 1) and 220 °C (heating block 2), respectively. The data clearly show very high activity, low CH<sub>4</sub> selectivity and marginal decay for six catalysts (four different TiO<sub>2</sub> supports) which are described in detail in Table 2. Since all catalysts have been prepared and activated with the identical standard operating procedures, the performance differences can directly be correlated to the properties of the TiO<sub>2</sub> support materials. The highly active materials all comprise the pure anatase phase. At relevant process conditions no mass transfer limitation was observed. Activation energies were found to be in the range between 110 – 130 kJ/mol consistent with values reported in the literature [4]. All newly developed supports showed very promising results with high activities and C<sub>5+</sub> productivities at > 50 % CO conversion at very low time-on-stream deactivation. The activity, selectivity and decay have been studied in a broad parameter space of temperature, partial pressure and space velocity.

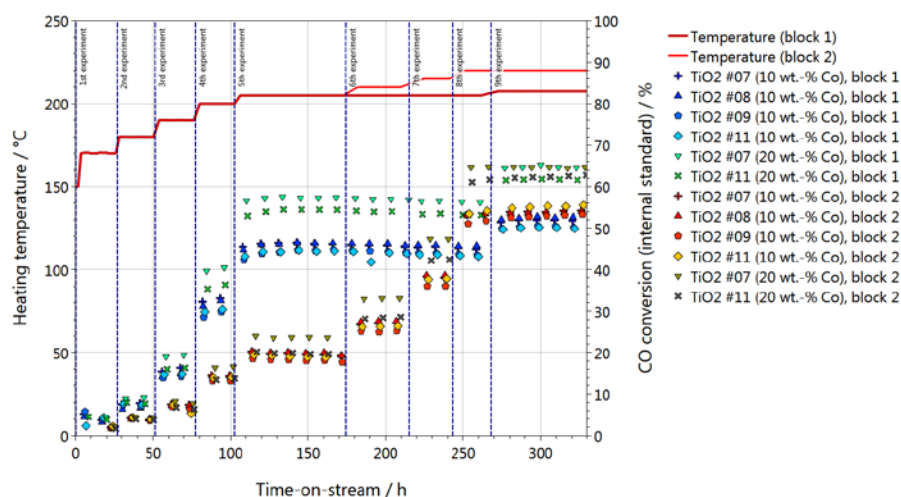


**Figure 1:** CO conversion for the experiments at 20 bar, 1.56 L/h feed per reactor, H<sub>2</sub>/CO ratio of 2, 220 °C, 10 % Ar in feed.

Catalyst	$X_{CO}$ %	$S_{CH_4}$ %	$P_{C_{5+}}$ $g_{C_{5+}}/(g_{CO}h)$	$S_{CO_2}$ %
TiO <sub>2</sub> #07 (10 wt.-% Co)	54.0	7.2	3.5	0.6
TiO <sub>2</sub> #08 (10 wt.-% Co)	53.8	7.2	3.4	0.6
TiO <sub>2</sub> #09 (10 wt.-% Co)	52.9	7.7	3.3	0.6
TiO <sub>2</sub> #11 (10 wt.-% Co)	55.2	7.8	3.4	0.7
TiO <sub>2</sub> #07 (20 wt.-% Co)	64.6	7.0	4.1	0.7
TiO <sub>2</sub> #11 (20 wt.-% Co)	62.4	7.8	3.9	0.7

**Table 2:** Catalyst characteristics and key parameters of experiment 9 (20 bar, 1.56 L/h feed per reactor, H<sub>2</sub>/CO ratio of 2, 220 °C, 10 % Ar in feed) for the best performing catalysts.

## Summary

The newly developed TiO<sub>2</sub> support materials have been synthesized using proprietary synthesis routes based on the large-scale sulphate production process. The results in Co-based FTS make these supports very attractive candidates for commercial applications.

## References

1. T. Eschemann, J. Bitter, K. de Jong, *Catalysis Today* 228 (2014).
2. WO2017211712
3. WO2017211710
4. M. Post et al., *AIChE Journal* 35 (1989)

## High Pore Volume TiO<sub>2</sub> for Hydrotreating Applications

*T. Thiede, VENATOR Germany GmbH, 47198 Duisburg, Germany;*

*R. Becker, VENATOR Germany GmbH, 47198 Duisburg, Germany;*

*A. Nennemann, VENATOR Germany GmbH, 47198 Duisburg, Germany*

For decades predominantly Al<sub>2</sub>O<sub>3</sub> has been used as catalytic support material for hydrotreating (HDT) applications due to its versatile and tunable properties such as pore size, pore volume and specific surface area (SSA). Despite the well-known benefits of TiO<sub>2</sub> for catalytic applications, standard TiO<sub>2</sub> has not been widely employed as catalytic support, predominantly due to low pore volumes (~ 0.3 ccm/g) and small pore sizes (~ 4 nm).

Herein, we report on a novel High Pore Volume (HPV) TiO<sub>2</sub> material that was developed and scaled up to industrial scale by VENATOR Germany GmbH. The novel HPV TiO<sub>2</sub> combines high pore volume (~ 0.8 ccm/g), high SSA (~ 350 m<sup>2</sup>/g) and large mesopores (see Figure 1). These characteristics are preserved even under harsh conditions like extrusion processing, thermal or acidic treatment. The robustness of VENATOR's HPV TiO<sub>2</sub> is achieved by implementation of different metal oxides (e.g. SiO<sub>2</sub>, Al<sub>2</sub>O<sub>3</sub>, ZrO<sub>2</sub>) as stabilizing agents.

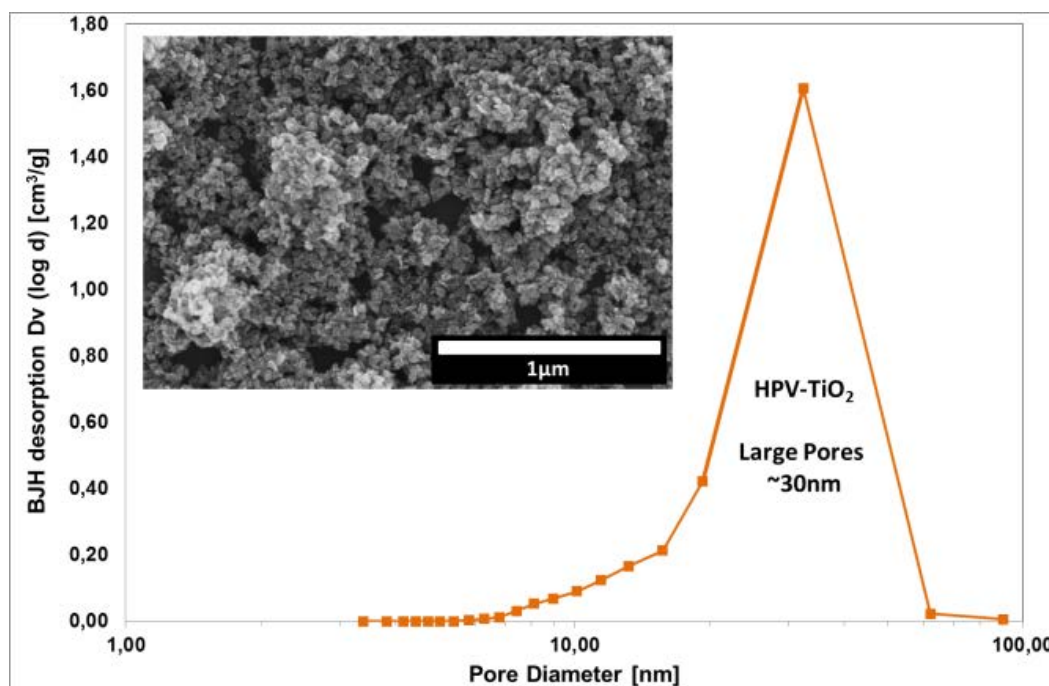


Figure 1. Pore size distribution of novel HPV TiO<sub>2</sub>. (Small figure: SEM analysis of HPV TiO<sub>2</sub>.)

To verify the applicability of novel HPV TiO<sub>2</sub> material for HDT applications and to prove the competitiveness of HPV TiO<sub>2</sub> material to state of the art Al<sub>2</sub>O<sub>3</sub> based catalysts, extensive hydrotreating performance tests were conducted. Therefore, a variety of different HPV TiO<sub>2</sub> materials were extruded, impregnated via incipient wetness impregnation (CoMo and NiMo), dried and finally calcined.

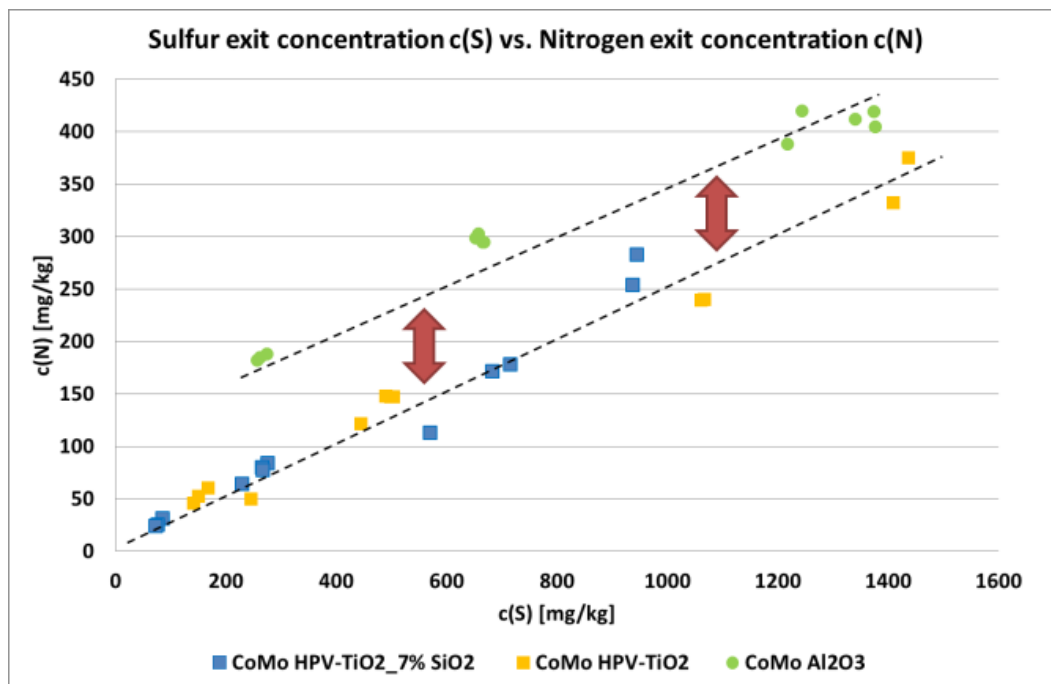


Figure 2. Absolute nitrogen concentration plotted against absolute sulfur concentration of hydrotreated VGO-feed using two different HPV TiO<sub>2</sub> based catalysts and one Al<sub>2</sub>O<sub>3</sub> based catalyst (green) measured under FCC-pretreatment conditions.

HDT performance tests were conducted in a fully automated 16-fold high throughput reactor system equipped with 16 reactors, each filled with ~ 4 ml catalyst extrudates diluted with inert SiC. The experiments were conducted under realistic conditions with a refinery vacuum distillation feed at temperatures ranging from 370 to 400 °C and pressures ranging from 80 to 120 bar. The tests revealed that HPV TiO<sub>2</sub> based catalysts show better HDS and HDN performance than state of the art Al<sub>2</sub>O<sub>3</sub> based catalysts. Most interestingly, HPV TiO<sub>2</sub> based CoMo catalysts showed significantly higher selectivity for HDN reaction, compared to state of the art Al<sub>2</sub>O<sub>3</sub> based CoMo catalyst (see Figure 2).

# Electrochemical Ammonia Synthesis in Molten Salt Systems

*Tim Sudmeier, Ian J. McPherson, S.C. Edman Tsang, Inorganic Chemistry  
Laboratory, Oxford, United Kingdom*

## Scope

Ammonia is one of the most important base chemicals in the world being a quintessential ingredient in most fertilizers. It is produced on the mega ton per year scale via the Haber-Bosch process using hydrogen and nitrogen at temperatures of around 400-500°C and pressures of up to 200 atmospheres leading to emissions of approximately 2% to global CO<sub>2</sub> exhaust.[1] A promising alternative for small scale applications is electrochemical ammonia production.[1] Such systems work at ambient pressure, moderate temperature and use renewable hydrogen sources like water potentially enabling small local production of ammonia as an energy storage vector.[2] Recently, a lot of progress has been made in the field, especially with aqueous systems though most systems still suffer from low rates, as well as current efficiencies due to the competing hydrogen evolution reaction.[1] An alternative approach involves the use of molten chloride electrolytes which permit the direct reduction of dinitrogen to the nitride ion (N<sup>3-</sup>) and potentially enable much higher ammonia production rates.[1]

We have previously investigated the redox chemistry in the molten alkali chlorides during nitrogen reduction over a Nickel catalysts.[2] Using insights from this analysis we have set up a novel protocol to test catalysts for electrochemical ammonia production in molten salts and conclusively show electrocatalytic nitrogen reduction. [2]

Other than Nickel, few materials have been evaluated as electrocatalysts for ammonia synthesis in molten salts.[1] Metal nitrides, in particular Co<sub>3</sub>Mo<sub>3</sub>N, have been shown to thermally form ammonia from dihydrogen and dinitrogen via a Mars-van-Krevelen-type mechanism.[3,4] More recently binary metal nitrides such as vanadium nitride have been shown computationally, as well as experimentally to work as nitrogen reduction electrocatalysts in aqueous systems, albeit with low current efficiencies. [1]



In this work we have synthesised several binary and ternary metal nitrides, including  $\text{Fe}_3\text{Mo}_3\text{N}$ ,  $\text{Mo}_2\text{N}$ ,  $\text{Co}_3\text{Mo}_3\text{N}$  and  $\text{Ni}_2\text{Mo}_3\text{N}$  using temperature-programmed nitridation of oxide precursors. The formed materials were characterised using powder XRD, XPS, TEM, SEM and TPR. The stability of the materials in the molten chloride media was assessed using cyclic voltammetry, as well as chronoamperometry under varying conditions. Finally, we supported our nitride materials on porous carbon foam using a novel electrodeposition protocol and tested said materials for continuous electrochemical ammonia synthesis followed by post-mortem analysis.

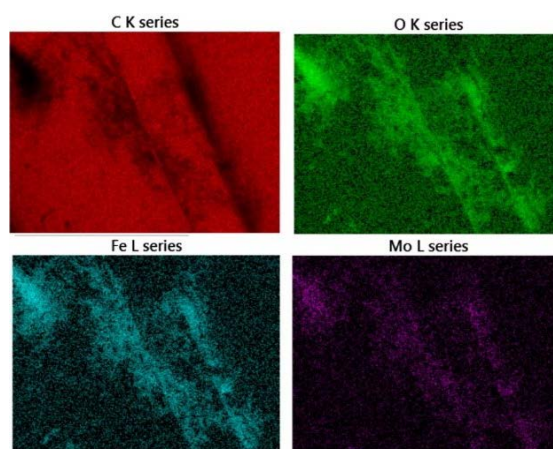


Figure 2. Electronmicrograph of  $\text{FeMoOx}$  on carbon felt with EDX mapping of the elements carbon (red), oxygen (green), iron (blue) and molybdenum (purple).

## References

- [1] McPherson, I. J., Sudmeier, T., Fellowes, J., & Tsang, S. C. E. (2019). Materials for electrochemical ammonia synthesis. *Dalton Transactions*.
- [2] McPherson, I. J., Sudmeier, T., Fellowes, J., & Tsang, S. C. E. (2019). To be published soon.
- [3] Abghoui, Y., Skúlasson, E. (2015) *Procedia Computer Science*, 51, 1897.
- [4] Howalt, J. G.; Vegge, T. (2013) *Phys. Chem. Chem. Phys.* 15, 48, 20957.

# Mesoporous Ni-Al<sub>2</sub>O<sub>3</sub> derived from metal organic framework: A promising catalyst for CO<sub>2</sub> methanation

*Leila Karam<sup>1,2</sup>, Julien Reboul<sup>1</sup>, M.C. Bacariza<sup>3</sup>, J.M. Lopes<sup>3</sup>, C. Henriques<sup>3</sup>, Nissrine El Hassan<sup>2</sup>, Pascale Massiani<sup>1</sup>*

<sup>1</sup> *Laboratoire de Réactivité de Surface, Sorbonne Université, Campus Pierre et Marie Curie, 4 Place Jussieu, 75005, Paris, France*

<sup>2</sup> *Department of Chemical Engineering, Faculty of Engineering, University of Balamand, P.O. Box 33, Amioun, El Koura, Lebanon*

<sup>3</sup> *Centro de Química Estrutural, Instituto Superior Técnico, Universidade de Lisboa, Av. Rovisco Pais, 1049-001 Lisboa, Portugal*

As the global climate threat is increasing gradually, the CO<sub>2</sub> emissions by the combustion of fossil fuels has reached around 82% of the anthropogenic greenhouse gases contributing to environmental problems such as rise of sea levels and melting in glaciers. On the bright side, CO<sub>2</sub> is considered as useful raw material for many chemical processes and specifically its conversion to low-carbon fuels (CH<sub>4</sub>) through catalytic hydrogenation. The CO<sub>2</sub> methanation reaction carries additional advantages: 1) It requires the use of H<sub>2</sub> as reactant to convert CO<sub>2</sub> to CH<sub>4</sub>, which is derived from sustainable sources such as biomass and water splitting, 2) the produced synthetic natural gas (CH<sub>4</sub>) can be easily injected and transported by the existing pipeline system and used as source of energy in manufacturing and transport, 3) the potential of obtaining natural gas at low temperature and at atmospheric pressure [1]. Ni has been extensively studied in this reaction and is considered as the most favorable non-expensive active phase able to replace noble metals. On the other hand, the Ni-based catalysts still face problems such as sintering inhibiting the full reduction of CO<sub>2</sub> to CH<sub>4</sub>. In this context, we recently demonstrated the benefit of intimately mixing the Ni species within an alumina matrix in order to synthesize highly active and stable catalysts based on Al<sub>2</sub>O<sub>3</sub>-supported Ni metal nanoparticles. To this end, we developed an innovative strategy consisting in incorporating the Ni source within the alumina synthesis medium: Ni salts (5-15 wt% Ni) are first impregnated within the highly porous MIL-53(Al) and subsequently calcined. After reduction under H<sub>2</sub> flow, the MOF route results in Ni-Al<sub>2</sub>O<sub>3</sub> samples made of two-dimensional  $\gamma$ -Al<sub>2</sub>O<sub>3</sub> sheets (figure 1a-d) with nickel particles very well

dispersed and embedded inside the walls of  $\text{Al}_2\text{O}_3$ . The obtained catalyst acquired a high surface area of  $225 \text{ m}^2\cdot\text{g}^{-1}$ .

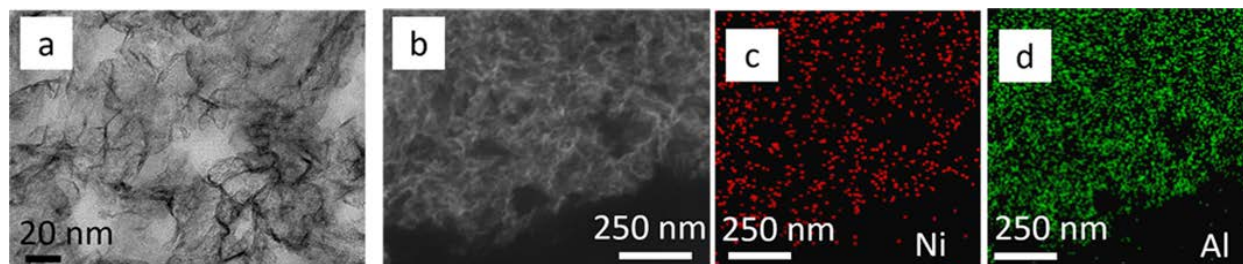


**Figure 1: (a) HR-TEM image of mesoporous  $5\text{Ni-Al}_2\text{O}_3\text{MIL-53}$  prepared by MOF route, and (b-d) STEM/EDX chemical mapping on the same MOF-derived sample confirming the superimposed Ni and Al distributions.**

The high reduction temperature ( $T = 800 \text{ }^\circ\text{C}$ ) indicated by TPR analysis, in addition to  $\text{NiAl}_2\text{O}_4$  spinel-like phases detected by XPS, stress on the high nickel-support interaction leading to remarkable catalytic activity and stability under  $\text{CO}_2$  methanation reaction conditions ( $T = 350 \text{ }^\circ\text{C}$ ,  $\text{TOS} = 20 \text{ h}$ ), preventing nickel sintering ( $\Phi = 8 \text{ nm}$ ) and providing more accessible Ni sites during reaction. The less performing catalysts (lower activity, figure 2) show lower reduction temperatures and larger Ni particle size ( $15\text{Ni}^\circ\text{-Al}_2\text{O}_3\text{One-pot}$  ( $\Phi_{\text{Ni}} = 9 \text{ nm}$ ), commercial catalyst ( $\Phi_{\text{Ni}} = 12 \text{ nm}$ ),  $15\text{Ni}^\circ\text{@USY}$  ( $\Phi_{\text{Ni}} = 40 \text{ nm}$ ),  $15\text{Ni}^\circ\text{@SBA-15}$  ( $\Phi_{\text{Ni}} = 17 \text{ nm}$ )).

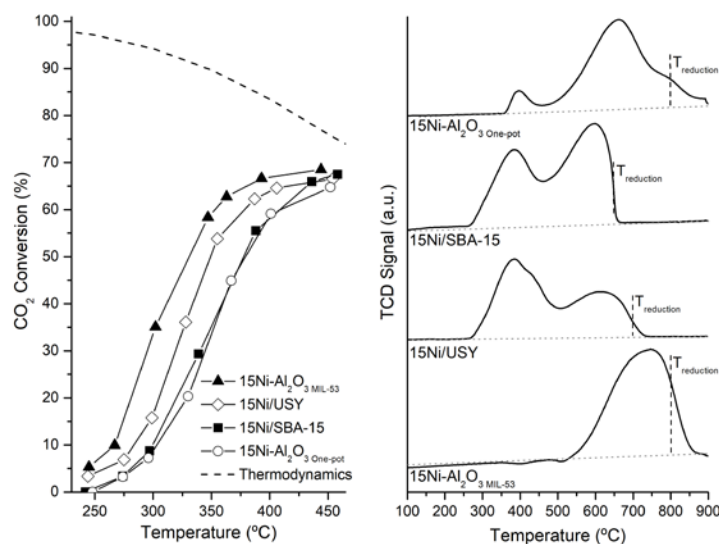


**Figure 2:  $\text{CO}_2$  conversion and TPR profiles of prepared catalysts**

## References

[1] W. Li, H. Wang, X. Jiang, J. Zhu, Z. Liu, X. Guo, C. Song, RSC Advances 8 (2018) 7651-7669.

## Thermal control of the defunctionalization of supported $\text{Au}_{25}(\text{glutathione})_{18}$ catalysts for liquid phase oxidation reactions

*Zahraa SHAHIN* 1, Institut de Recherches sur la Catalyse et l'Environnement de Lyon (IRCELYON), 2, avenue Albert Einstein – 69626, Villeurbanne, France; Hyewon JI 1; Rodica CHIRIAC 2, Laboratoire des Multimateriaux et Interfaces (LMI), 22, avenue Gaston Berger– 69622, Villeurbanne, France; Nadine ESSAYEM 1; Franck RATABOUL 1; Aude DEMESSENCE 1

Atomically well-defined gold nano-clusters (GNCs), due to their size related properties, are known to be active in oxidation catalysis at relatively low temperature [1]. Supported on metal oxides,  $\text{Au}_{25}(\text{SR})_{18}$  clusters are able to catalyze benzyl alcohol and CO oxidation reactions, styrene epoxidation in addition to nitrobenzene reduction. During these catalytic reactions, the gold thiolate clusters have been calcined to totally remove the thiolate molecules, in order to exhibit maximum activity [2-5]. Nevertheless, recently, Haruta showed that mild temperature calcination, that generates partially defunctionalized  $\text{Au}_{38}(\text{2-phenylethanethiolate})_{24}$  supported over activated carbon, can also provide a maximum catalytic activity toward glucose oxidation [6]. In this context, we successfully synthesized new composite materials,  $\text{Au}_{25}(\text{SG})_{18}$  (SG – glutathione) clusters deposited on  $\text{ZrO}_2$  nanoparticles, and calcined them at different temperatures to study the ligand and particle size effects in liquid phase oxidation reactions by using different substrates. Thermally treated at 300 °C, the partially defunctionalized  $\text{Au}_{25}(\text{SG})_{18}@\text{ZrO}_2$  catalyst loses 53 % of its ligands, resulting in well-dispersed 1.7 nm gold particle size. As a heterogeneous catalyst for oxidation reaction, it exhibited complete conversion of benzyl alcohol into benzaldehyde in toluene under mild conditions, with a great TOF = 261  $\text{h}^{-1}$  [7].

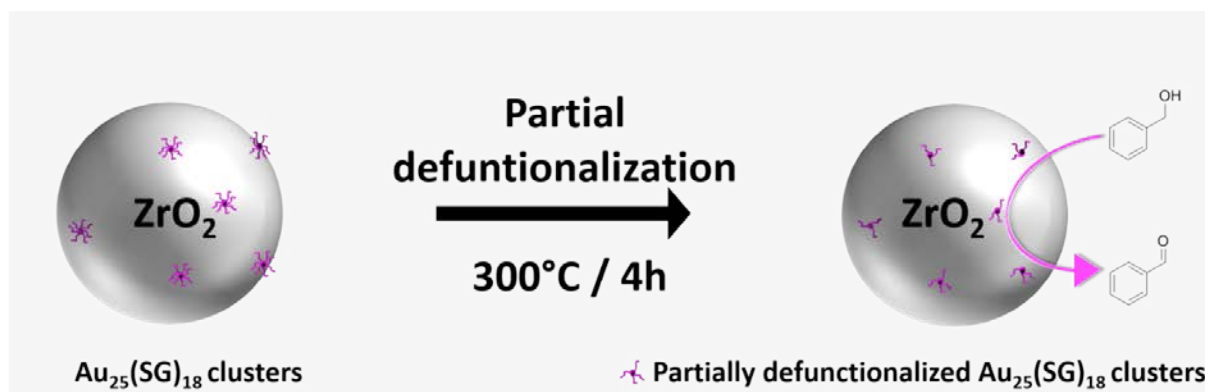


**Figure 1** Partially defunctionalized  $\text{Au}_{25}(\text{SG})_{18}@\text{ZrO}_2$  for benzyl alcohol oxidation

To valorize this composite material as a sustainable catalyst for biomass conversion, its catalytic activity was tested for the conversion of furfural in aqueous and different alcoholic media. Thus, furoic acid was selectively formed when the reaction was performed in water, and the corresponding esters were observed in the different alcoholic media. This clusters-based catalyst showed excellent activity in the transformation of a bio-based molecule, furfural, into sustainable alternatives of petroleum-based compounds, even without a base.

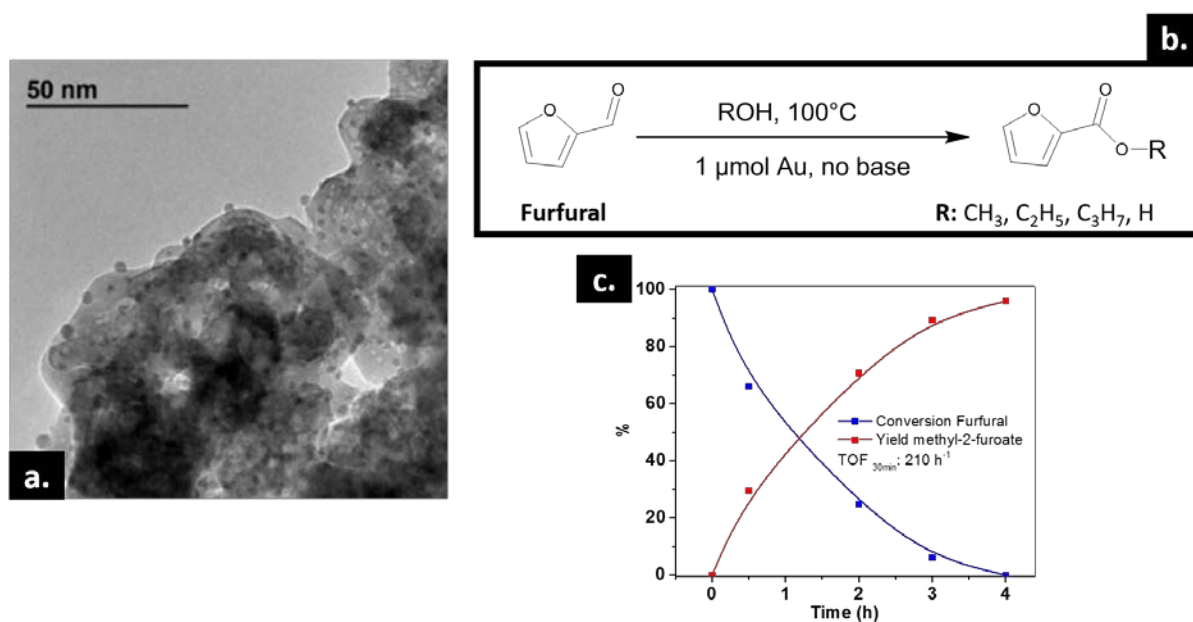


**Figure 2** TEM image of  $\text{Au}_{25}(\text{SG})_{18}@\text{ZrO}_2$  calcined at  $300^\circ\text{C}$ , 4h, air (a). Furfural oxidation reaction (e), conversion of Furfural (blue) and formation of Methyl-2-furoate (red) (f).

## References

- [1]. R. Jin, C. Zeng, M. Zhou, Y. Chen; Chem. Rev. **2016**, 116, 10346-10413.
- [2]. C. Lavenn, A. Demessence, A. Tuel ; J. Catal., **2015**, 322, 130-138.
- [3]. Z. Wu, D. E. Jiang, A. K. P. Mann, D. R. Mullins, Z. A. Qiao, L. F. Allard, C. Zeng, R. Jin, S. H. Overbury, J.Am.Chem.Soc., **2014**, 136, 6111-6122.
- [4]. P. Huang, G. Chen, Z. Jiang, R. Jin, Y. Zhu, Y. Sun, Nanoscale, **2013**, 5, 3668-3672.
- [5]. J. Fang, J. Li, B. Zhang, X. Yuan, H. Asakura, T. Tanaka, K. Teramura, J. Xie, N. Yan, Nanoscale, **2015**, 7, 6325-6333.
- [6]. C. Liu, J. Zhang, J. Huang, C. I. Zhang, F. Hong, Y. Zhou, G. Li and M. Haruta, ChemSusChem, **2017**, 10,1976–1980.
- [7]. Z. Shahin, H. Ji, R. Chiriac, N. Essayem, F. Rataboul, A. Demessence, Beilstein J. Nanotechnol, **2019**, Accepted.

## **The influence of oxide additives on the catalytic properties of nanoscale iron-containing catalysts of Fischer-Tropsch synthesis**

*Kulikova M.V., Dement'eva O.S., Chudakova M.V., A.V.Topchiev Institute of Petrochemical Synthesis, Moscow, Russian Federation*

The study of the catalytic properties of suspensions with additives as modifying agents  $\text{Al}_2\text{O}_3$ ,  $\text{ZrO}_2$  and  $\text{SiO}_2$  for the Fischer-Tropsch synthesis in a slurry reactor was carried out. The samples were prepared by thermal decomposition of solutions of metal precursors in the mix of paraffins ( $\text{C}_{19}\text{H}_{40}$ - $\text{C}_{32}\text{H}_{66}$ ) with the formation of contacts with the concentration of active Fe-containing phase 1% mass. for all samples. The particle size of the catalytic suspensions, determined by the method of dynamic light scattering, was 2-4 nm. The synthesis of hydrocarbons from CO and  $\text{H}_2$  was carried out in a slurry reactor in the presence pre-activated samples in the temperature range of 260–320 °C ( $P = 2$  MPa,  $\text{CO}:\text{H}_2 = 1:1$  mol., feed rate 10 l/h). Studying the series of samples with modifying additives 0.025% mass. of  $\text{Al}_2\text{O}_3$ ,  $\text{ZrO}_2$  and  $\text{SiO}_2$  was found that the nature of the additive caused a significant effect on the composition of the reaction products at the same values of feedstock conversion (fig.1, table 1). For all samples, a CO conversion of 69–71% was achieved and the yield of  $\text{C}_{5+}$  hydrocarbons increased in the range 59 ( $\text{ZrO}_2$ ) < 69 ( $\text{Al}_2\text{O}_3$ ) < 78 ( $\text{SiO}_2$ )  $\text{g}/\text{m}^3$  of the passed synthesis gas. It is interesting to note that in the same series an increase of gasoline fraction in the composition of liquid hydrocarbons was observed from 50 to 62% mass. The highest yield of oxygen-containing reaction products ( $\text{C}_1$ - $\text{C}_4$ -alcohols) in temperature range 280-320°C was recorded for the sample with the addition of  $\text{Al}_2\text{O}_3$ : it was 19-25  $\text{g}/\text{m}^3$  versus 6-19  $\text{g}/\text{m}^3$  for the sample modified with zirconium. In the presence of silicon in the composition of the sample, the formation of insignificant amounts of  $\text{C}_5$ - $\text{C}_6$ -alcohols was observed - their content in the aqueous phase was 0.15% by weight. with a total concentration of oxygen-containing products of 36.5%.

To optimize the composition of the catalytic system, catalytic suspensions were formed with different contents of the  $\text{Al}_2\text{O}_3$  as a modifying additive. The concentration of the additive was varied from 0.025 to 0.500% mass.

It was shown that modifying additive variation from 0.025 to 0.1% mass. led to decreasing in the degree of CO conversion from 69 to 62% with a simultaneous

increasing in the yield of liquid hydrocarbons from 69 to 101 g/m<sup>3</sup> of the passed synthesis gas. This effect was achieved by reducing the formation of C<sub>1</sub>-C<sub>4</sub> hydrocarbons and carbon dioxide: from 36 to 23 and from 221 to 67 g/m<sup>3</sup>, respectively. A further increasing of the additive concentration to 0.500% mass. led to reduction in CO conversion to 38-54% with a symbate increasing in the of gaseous hydrocarbons formation to 37-61 g/m<sup>3</sup>.

Thus, in the course of this study, it was established that the nature and concentration of the oxide modifying additive had a significant effect on the fractional and group composition of hydrocarbon and oxygen-containing products of Fischer-Tropsch synthesis in the gas-liquid-solid system.

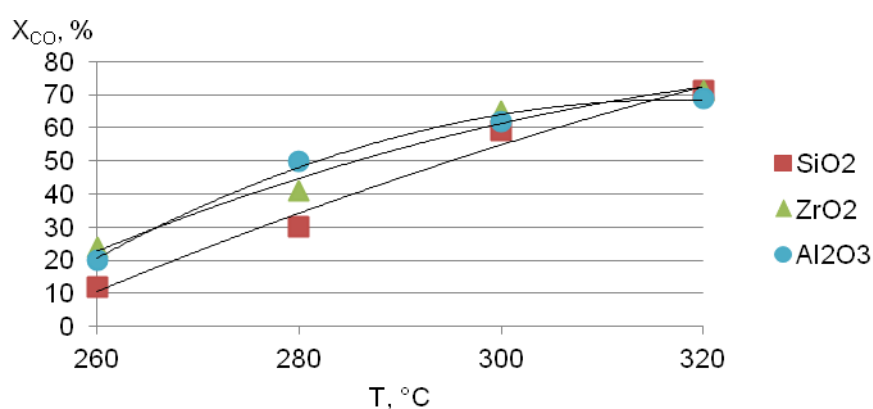


Fig. 1. The effect of process temperature on CO conversion in the presence of 1%Fe-0.025%additive-suspensions

Table 1. The composition of liquid hydrocarbons obtained in the presence of 1%Fe-0.025%additive-suspensions

Additive	T, °C	Fractional composition			Group composition		
		C <sub>5</sub> -C <sub>10</sub>	C <sub>11</sub> -C <sub>18</sub>	C <sub>19+</sub>	n.paraffins	iso-paraffins	olefins
ZrO <sub>2</sub>	280	42	37	21	44	40	16
	300	44	34	22	45	39	16
	320	50	33	17	39	39	22
Al <sub>2</sub> O <sub>3</sub>	280	48	31	21	33	36	32
	300	55	31	14	27	38	35
	320	61	32	7	21	46	33
SiO <sub>2</sub>	280	42	46	12	22	57	21
	300	58	36	6	31	56	13
	320	62	34	4	30	54	16

#### Acknowledgements

This study, supported by the Russian Science Foundation (project no. 17-73-30046), was conducted at the Topchiev Institute of Petrochemical Synthesis, Russian Academy of Sciences.

# Synthesis-structure-activity relations in Fe-CHA for C-H activation: interzeolite conversion allowing Al-distribution control<sup>[1]</sup>

*Julien Devos, Max Bols, Bert Sels, Michiel Dusselier*  
*KU Leuven, Leuven, Belgium*

## Abstract

The methane to methanol reaction is an important catalytic challenge in need of efforts on multiple fronts: in the synthesis of zeolite hosts, the identification of the active sites (e.g. Cu cations) and the engineering of the reaction. By using FAU-to-CHA interzeolite conversion (IZC) and single parameter variations many synthesis-structure-activity relations were revealed. We can now steer small pore zeolites to be more active, originating from both control over the structure of the zeolite and the active catalytic species. These insights shed light on the potential key role of Al during crystallization during IZC.

**Keywords:** CHA, methane to methanol, Al-pairing.

## 1. Introduction

Methane partial oxidation is one of the holy grails of catalysis. Methanol is an important chemical building block with huge volumes produced annually. Its low-temperature oxidative synthesis using transition-metal ions (TMI) incorporated into zeolite hosts is a topic under intense investigation.<sup>[2-5]</sup> The zeolite host plays a crucial role in allowing the right TMI active sites to form and operate.<sup>[4-5]</sup> Some 8MR-zeolites have a lot of benefits as a host for this reaction, i.e. stability, high pore volumes, internal cages, etc.<sup>[2,5]</sup> The influence of the Al-distribution in small-pore zeolites on the reaction is crucial.<sup>[6]</sup> Since synthetic variation can affect the latter, we set out to investigate if synthesis-structure-activity relations can be found.

## 2. Experimental

Small pore zeolites with the CHA-topology were made according to modified versions of standard recipes using N,N,N-trimethyl-adamantylammonium hydroxide as organic-structure directing agent (OSDA), graciously donated by SACHEM.<sup>[7-8]</sup> The Al-distribution was probed with Co-ion exchange, according to ref. 9 and related work. Fe cations were exchanged onto the materials according to ref. 3 and 6. Methane oxidation (one-pass) was performed after oxidation/activation of the active sites (1 turnover), and methanol was extracted from the material afterwards.



Characterization of the catalysts included elemental analysis, PXRD, DR-UV-VIS, N<sub>2</sub>-physisorption, Co-probing and TGA.

### 3. Results and discussion

SSZ-13 zeolites have been successfully reproduced using various single parameter variations of the synthetic recipe. By Co-probing of the calcined zeolite we noted that the synthetic route followed impacted the Al-distribution in unexpected ways. Briefly we could use different synthetic variations to modify the value of a numerical structure descriptor based on the Co-probing data, and directly link this numerical descriptor to the activity of the TMI-zeolite (methanol produced per gram, Si/Al more or less constant). The underlying hypothesis involves steering the number and nature of the active site TMI-species. The methanol-productivities per gram link well to the structural descriptor, which probes the presence and number of hosting arrangements in the framework of the desired active TMI species. The structural descriptor results suggests that the divalent cation capacity of the zeolite, based on Al siting, is controlled by both kinetic and thermodynamic contributions. These unprecedented synthesis-structure relations offer pieces to a puzzle that could lead to atomic length scale understanding of the crucial role of Al during zeolite synthesis.

### 4. Conclusions

A series of CHA-zeolites was made and their Al-distribution assessed with cobalt-probing. With a numerical descriptor based on these data, we were able to link synthesis and activity of the TMI-exchanged zeolite, through the structural properties of the zeolite host. Using this relation as a guide, one is able to create optimal synthetic recipes and attain high methanol productivities.

### References

1. Devos et al. Submitted, 2019
2. M. J. Wulfers, S. Teketel, B. Ipek and R. F. Lobo, *Chem. Commun.*, 2015, 51, 4447-4450.
3. B. E. R. Snyder, P. Vanelderen, M. L. Bols, S. D. Hallaert, L. H. Böttger, L. Ungur, K. Pierloot, R. A. Schoonheydt, B. F. Sels and E. I. Solomon, *Nature*, 2016, 536, 317-321.
4. B. E. R. Snyder, M. L. Bols, R. A. Schoonheydt, B. F. Sels and E. I. Solomon, *Chem. Rev.* 2018, 118, 718–2768.
5. D. K. Pappas, E. Borfecchia, M. Dyballa, I. Pankin, K. A. Lomachenko, A. Martini, M. Signorile, S. Teketel, B. Arstad, G. Berlier, C. Lamberti, S. Bordiga, U. Olsbye, K. P. Lillerud, S. Svelle and P. Beato, *J. Am. Chem. Soc.*, 2017, advance online.
6. M. L. Bols, S. D. Hallaert, B. E. R. Snyder, J. Devos, D. Plessers, H. M. Rhoda, M. Dusselier, R. A. Schoonheydt, K. Pierloot, E. I. Solomon and B. F. Sels, *J. Am. Chem. Soc.*, 2018, 140, 12021–12032
7. S.I. Zones and R.A. Van Nordstrand, *Zeolites*, 1988 , 8 (3), 166-174.
8. J. R. Di Iorio and R. Gounder, *Chem. Mater.*, 2016, 28, 2236-2247.
9. P. Sazama, E. Tabor, P. Klein, B. Wichterlova, S. Sklenak, L. Mokrzycki, V. Pashkova, M. Ogura and J. Dedecek, *J. Catal.*, 2016, 333, 102-114.

# Valorising CO<sub>2</sub> with plasma-catalyst discharges

*Sean Kelly, and James A Sullivan, UCD School of Chemistry, Belfield, Dublin 4, Ireland*

## Introduction

Higher global temperatures and more frequent extreme weather events have brought the environmental [1] and economic perils [2] of anthropogenic climate change to the fore recently. In order to limit the most severe destruction (e.g. coral eradication, melting of arctic summer sea ice) the Inter-governmental Panel on Climate Change (IPCC) has recently advised limitation of warming below 1.5 °C (above pre-industrial levels) by 2100 [3]. Realisation of such targets will require a 45 % reduction in greenhouse gases by 2030 with achievement of net zero emissions by 2050 [3]. Such efforts are raising the necessity for increased carbon taxation, carbon sequestration, carbon storage and ultimately carbon utilisation technologies to offset costs. In this context, plasma technology is garnering increasing research interest with renewed focus on plasma applications for CO<sub>2</sub> utilisation [4].

Thermal conversion of CO<sub>2</sub> requires very high temperatures. Conversion yields of ~60 % require temperatures in the region of ~3,500 K [4] which are practically difficult. Non-thermal plasma-based solutions present a promising alternative to thermal conversion [5]. Plasma generation in CO<sub>2</sub> results in CO and O<sub>2</sub> formation where the CO produced is a valuable chemical feed-stock [4]. Optimal routes for CO<sub>2</sub> dissociation in atmospheric non-thermal plasma have been identified as electron induced vibrational excitation pathways (costing ~5.5 eV for bond breaking) rather than dissociation via direct electronic excitation (~7 eV for bond breaking) [4,5].

## Reactor configuration

A spark discharge (SD) reactor (figure 1 a) consisting of cylindrical steel HV electrodes (separation 18 mm) inside a quartz tube is investigated. A well-studied configuration known as packed bed Dielectric barrier discharge (DBD) (figure 1 b) is investigated as a comparator configuration. The discharge is ignited here using a kHz High Voltage supply (up to 20 kV) in combination with power pulsing to limit streamer to arc transition which maintains the plasma's non-equilibrium character.

A range of heterogenous catalyst are incorporated into the plasma gas discharge volume. SiO<sub>2</sub> & Al<sub>2</sub>O<sub>3</sub> substrates are fabricated with meso & macro-porous features

and impregnated with transition metals (including Nickel and Cobalt) at a range of wt. %. The morphology of the catalyst packing materials is explored using coated spherical beads, coated wool and pelletised catalyst forms.

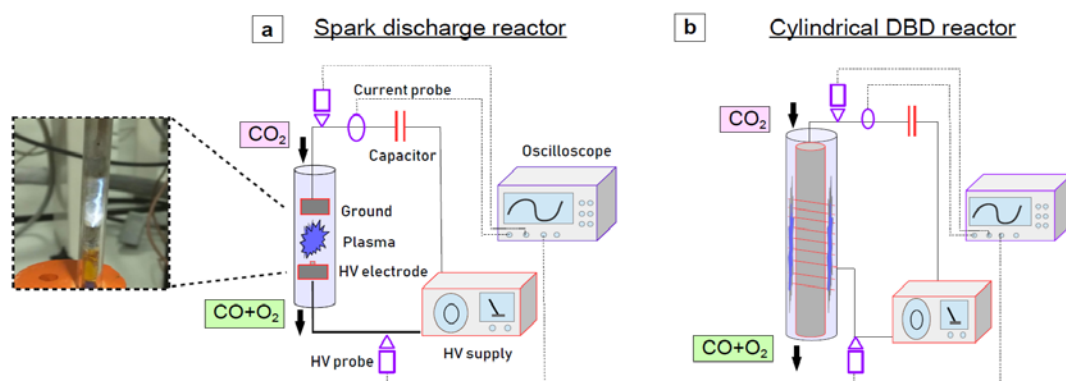


**Figure 1:** setup of spark plasma and Dielectric Barrier Discharge (DBD) reactors

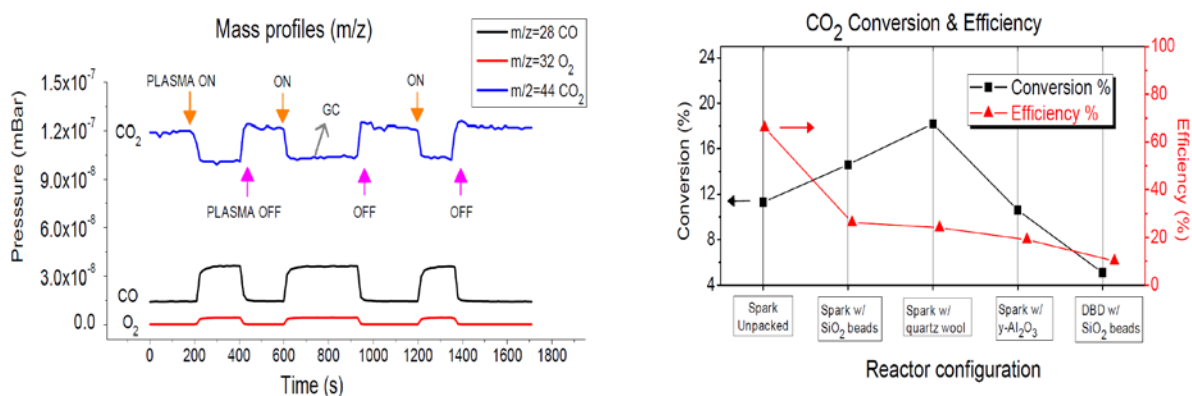


**Figure 2:** Left: CO/ O<sub>2</sub> / CO<sub>2</sub> levels (m/z) for three plasma ignitions over 25 minutes; Right: Conversion (%) from Gas Chromatography (GC) analysis and Efficiency (%).

## Conclusions

Packing of common catalyst materials is found to enhance CO<sub>2</sub> conversion although efficiency is found to decrease. The reactor is shown to be particularly amenable to powering via intermittent renewable electricity sources.

## Acknowledgements

The Irish Research Council are thanked for funding under GOIPD/2017/1000.

## References

- [1] W Steffen et al., PNAS August 14, 2018 115 (33) 8252-8259.
- [2] M Burke et al., Nature, 557(7706):549–553, 2018.
- [3] IPCC special report, 48th Session, Republic of Korea, 2018.
- [4] R Snoeckx et al. Chem. Soc. Rev., 46:5805–5863, 2017.
- [5] A Bogaerts et al. ACS Energy Letters, 3(4):1013–1027, 2018.

# Comparison of thermal- and plasma-promoted dry reforming of methane over Ni/Al<sub>2</sub>O<sub>3</sub> catalysts: Influence of support morphology.

*Kristy Stanley, Sean Kelly and James A Sullivan,  
UCD School of Chemistry, Belfield, Dublin 4, Ireland*

*Al<sub>2</sub>O<sub>3</sub> supported Ni catalysts were synthesized via sol-gel, hydrothermal and wet-impregnation methods. They were characterized using SEM/EDX, TEM, XRD, FTIR, Raman spectroscopy and TPR. Each catalyst was tested under thermal dry reforming (DRM) conditions at 500 °C, 700 °C and 900 °C then under plasma promoted DRM conditions and conversions were compared. Characterization was carried out (DFTIR, TGA/MS, SEM) to identify any material changes following reaction.*

## **Scope**

Anthropogenic climate change is a hugely important topic in current times, the release of greenhouse gasses into the atmosphere due to combustion of fossil fuels is the major contributor to this and CO<sub>2</sub> concentrations are currently over 400 ppm [1]. CH<sub>4</sub> extracted at remote oil exploration sites is considered too expensive and hazardous to store and transport and is oftentimes combusted at source. This is a waste of a valuable resource and contributes to rising atmospheric CO<sub>2</sub> levels.

The dry reforming process produces syngas (CO/H<sub>2</sub> mixtures) from CH<sub>4</sub> and CO<sub>2</sub> and syngas is a versatile feed stock for Fischer Tropsch and methanol synthesis [2]. If a simple, cost effective process can be found to produce syngas then the current attitude towards CH<sub>4</sub> would change.

## **Experimental**

The objective of this work was to synthesis a range of Al<sub>2</sub>O<sub>3</sub> supports with differing morphologies [3, 4] to analyse whether morphology affected performance. Along with  $\gamma$ -Al<sub>2</sub>O<sub>3</sub> pellets supplied by Jonhson Matthey, the supports were then wet-impregnated with Ni at 7 wt% and 14 wt%. After characterization by the above-mentioned techniques, thermal DRM reactions were performed at 500 °C, 700 °C and 900 °C. Each catalyst was then tested under plasma-promotion conditions. The reactivities were then compared to determine whether plasma promotion produces affects conversion or stability of the catalysts.

## Characterisations

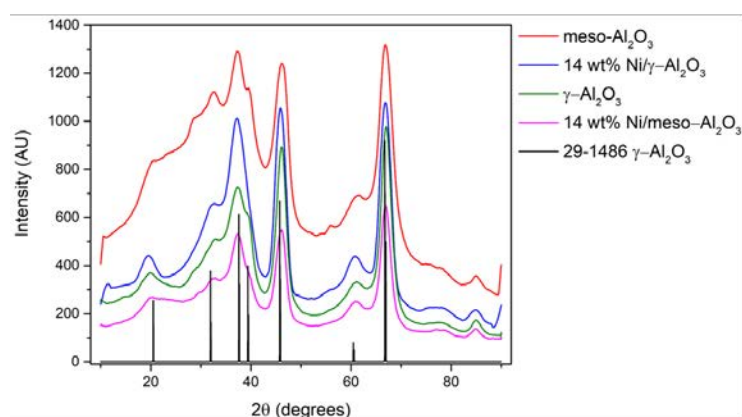


**Fig. 1** XRD patterns of mesoporous Al<sub>2</sub>O<sub>3</sub> and γ-Al<sub>2</sub>O<sub>3</sub> with and without Ni loading

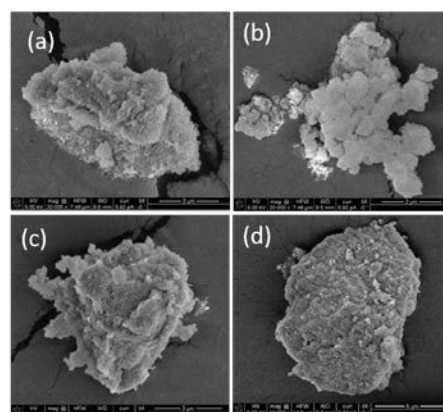


**Fig. 2** SEM images of (a) γ-Al<sub>2</sub>O<sub>3</sub> (b) meso-Al<sub>2</sub>O<sub>3</sub> (c) 14% Ni/γ-Al<sub>2</sub>O<sub>3</sub> (d) 14% Ni/meso-Al<sub>2</sub>O<sub>3</sub>

**Figure 1** shows XRD patterns for the synthesized mesoporous Al<sub>2</sub>O<sub>3</sub> and the γ-Al<sub>2</sub>O<sub>3</sub> pellets with and without 14 wt% Ni loading. These show a crystalline structure and match the profile for standard γ-Al<sub>2</sub>O<sub>3</sub> (JCPDS 29-1486).

No new peaks appear with the addition of Ni, indicating the particles are small and well dispersed throughout the support. **Figure 2** shows SEM images of the same materials, γ-Al<sub>2</sub>O<sub>3</sub> (a) and 14% Ni/γ-Al<sub>2</sub>O<sub>3</sub> (c) show similar 2D flake-like structures, with no significant change after Ni impregnation. Mesoporous Al<sub>2</sub>O<sub>3</sub> (b) shows 3D spheres constructed of 2D micro-flakes.

## Conclusions

Alumina catalysts with varying morphologies and Ni loadings were synthesised and characterised with a range of techniques. The effects of plasma promotion on the different catalyst's reactivity in the DRM reaction were analysed.

## Acknowledgements

This research has been funded by the Irish Research Council under the Government of Ireland Postgraduate Programme, grant number GOIPG/2018/2880.

## References

1. US Department of Commerce, N., Earth System Research Laboratory, *ESRL Global Monitoring Division - Global Greenhouse Gas Reference Network*. 2016.
2. Roddy, D.J., *A syngas network for reducing industrial carbon footprint and energy use*. Applied Thermal Engineering, 2013. **53**(2): p. 299-304.
3. Ray, J.C., et al., *Mesoporous alumina (I): Comparison of synthesis schemes using anionic, cationic, and non-ionic surfactants*. Microporous and Mesoporous Materials, 2007. **100**(1): p. 183-190.
4. Deng, W., M.W. Toepke, and B.H. Shanks, *Surfactant-assisted synthesis of alumina with hierarchical nanopores*. Advanced Functional Materials, 2003. **13**(1): p. 61-65.

## **Influence of experimental parameters on the electrochemical characterization of catalysts for the oxygen evolution reaction**

*Marc F. Tesch, Max Planck Institute for Chemical Energy Conversion, Stiftstr. 34-36, 45470 Mülheim an der Ruhr, Germany; Praveen V. Narangoda, Max Planck Institute for Chemical Energy Conversion, Stiftstr. 34-36, 45470 Mülheim an der Ruhr, Germany; Sabita Bhandari, Max Planck Institute for Chemical Energy Conversion, Stiftstr. 34-36, 45470 Mülheim an der Ruhr, Germany; Ioannis Spanos, Max Planck Institute for Chemical Energy Conversion, Stiftstr. 34-36, 45470 Mülheim an der Ruhr, Germany; Robert Schlögl, Max Planck Institute for Chemical Energy Conversion, Stiftstr. 34-36, 45470 Mülheim an der Ruhr, Germany; Anna K. Mechler, Max Planck Institute for Chemical Energy Conversion, Stiftstr. 34-36, 45470 Mülheim an der Ruhr, Germany*

The increased need in developing sustainable energy sources triggered tremendous efforts in the research on the production of hydrogen from water via electrolysis. It can subsequently act directly as fuel or as an intermediate for further reactions. While the cathodic hydrogen evolution half reaction is energetically more favorable, the sluggish oxygen evolution half reaction on the anode acts as the limiting factor in the overall process. Therefore, the development of catalysts materials facilitating the oxygen evolution reaction is of high importance for future applications of this technique.

A reliable and reproducible electrochemical characterization of the catalysts is of equal importance as the often reported determination of structure and reaction mechanism of the catalytic materials.<sup>[1]</sup> Several parameters that are not directly related to the catalyst material itself can drastically influence the electrochemical properties toward oxygen evolution. This means that deviations in the characterization protocol can make a comparison of results among different groups very challenging.

We will discuss a standardized protocol for OER catalysts in alkaline media<sup>[2]</sup> and present the influence of different experimental as well as well as preparation

parameters on the catalyst characterization. This comprises the use of binder materials (Figure 1), measurement techniques, ink compositions, electrolyte impurities, and catalyst/electrode pretreatment. It will be shown that a reliable characterization of catalysts is possible, but needs careful consideration of all these effects by external parameters.

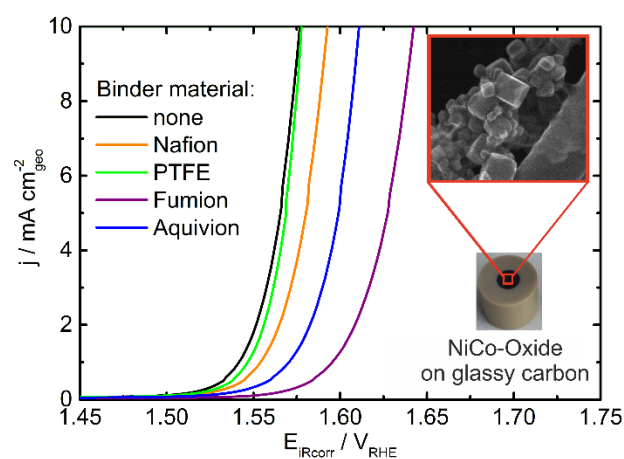


Fig. 1: Linear scan voltammetry of NiCo-oxide on glassy carbon for different binder materials. Experiments were performed with a rotational disc electrode in 1 M KOH.

## References

- [1] C. C. L. McCrory, S. Jung, I. M. Ferrer, et al., *J. Am. Chem. Soc.*, 2015, 137, 4347-4357
- [2] I. Spanos, A. A. Auer, S. Neugebauer, et al., *ACS Catal.*, 2017, 7, 3768-3778.

# Synthesis and Investigation of Ni Supported on Ceria-Zirconia Doped With Nb, Ti and Nb+Ti for Dry Reforming of Methane

*M. Simonov<sup>1,2</sup>, Y. Bepalko<sup>1</sup>, E. Smal<sup>1</sup>, V. Fedorova<sup>1</sup>, V. Sadykov<sup>1,2</sup>*

1 - Boreskov Institute of Catalysis, Novosibirsk, Russia

2 - Novosibirsk State University, Novosibirsk, Russia

## 1. Scope

Dry reforming of methane is a perspective way to transform two greenhouse gases as well as a model reaction for biofuels transformations. Ni-based catalysts have been widely investigated because of their good compromise between high activity and low price. The main weakness of such catalysts is the formation of carbon followed by deactivation due to the blocking of active centers. A way to solve this problem is to use oxides with high oxygen mobility as carriers for the gasification of coke precursors. Ceria is extensively studied in the literature, and the oxygen storage capacity of ceria can be increased through the insertion of various cations. In cases where the size of the dopant cations (Zr, Ti,) is smaller than that of cerium, this leads to the formation of longer or shorter bonds with the oxygen lattice, and, hence, to a greater oxygen mobility [1].

In our work ceria-zirconia mixed oxides doped with Nb and Ti were synthesized, characterized by physical-chemical methods and tested in dry reforming of methane reaction (MDR).

## 2. Results and discussion

$\text{Ce}_{0.75}\text{Zr}_{0.25}\text{O}_{2-\delta}$ ,  $\text{Ce}_{0.5}\text{Zr}_{0.5}\text{O}_{2-\delta}$ ,  $\text{Ce}_{0.75}\text{Nb}_{0.1}\text{Zr}_{0.15}\text{O}_{2-\delta}$  oxides were prepared by Pechini and  $\text{Ce}_{0.75}\text{Ti}_{0.1}\text{Zr}_{0.15}\text{O}_{2-\delta}$ ,  $\text{Ce}_{0.75}\text{Ti}_{0.05}\text{Nb}_{0.05}\text{Zr}_{0.15}\text{O}_{2-\delta}$  by citrate method. Organic precursors obtained by Pechini/citrate route were dried for 12 h and calcined at 700°C for 2h. The 5 wt% Ni/ Ni/Ce-Zr-(Nb/Ti)-O catalysts were prepared by impregnation of oxides with  $\text{Ni}(\text{NO}_3)_2 \cdot 6\text{H}_2\text{O}$ . The reaction of methane dry reforming was carried out in a tubular quartz plug flow reactor using the feed of 15%  $\text{CH}_4 + 15\% \text{CO}_2 + \text{N}_2$  balance at 550-750°C and contact time 7.5 ms. The supports and catalysts were characterized by XRD, FTIRS and Raman spectroscopy, BET, SEM and TEM with EDX, XPS,  $\text{H}_2$ -TPR.

According to XRD and Raman spectroscopy all samples are single phase mixed oxides with pseudocubic fluorite-like structure.



As can be seen from the figure, the catalysts are activated in the flow of the reaction mixture almost immediately, but in different ways. It is noticeable that short-term stability tests reveal that methane conversion on Ni/ceria-zirconia samples including Nb-doped (sample C) immediately reaches the maximum value, followed by subsequent decreasing. At the same time, samples doped with Ti (D) and Ti + Nb (E) are activated gradually, that may be due to the slow reduction of nickel due to the strong interaction with the carrier. The highest conversion is achieved on a catalyst doped with Nb, while the lowest deactivation rate is observed on a sample simultaneously doped with Ti + Nb (E). The introduction of titanium and niobium cations alters the electronic properties of oxides, contributing to the activation of an oxidizing agent and an increase in the stability of these catalysts even at relatively high concentrations of reagents.

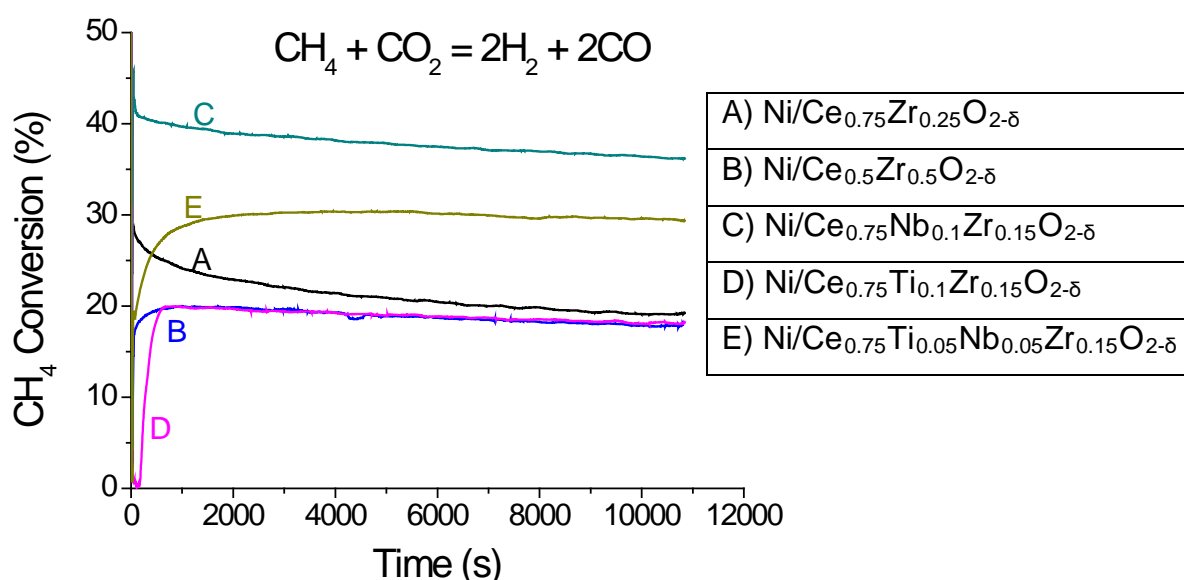


Figure 1. Methane conversion during catalytic DRM reaction over prepared samples. T=700 °C.

### 3. Conclusion

Single-phase samples of doped ceria-zirconia oxides were synthesized by modified Peccini and citrate methods. Doping of nickel-loaded ceria-zirconia with niobium and titanium has a positive effect on both activity and stability in MDR.

The work was supported by the Russian Science Foundation, Project 18-73-10167.

### References

- [1] Dutta, G., Waghmare, U.V., Baidya, T. et al. Catal Lett (2006) 108: 165. <https://doi.org/10.1007/s10562-006-0040-z>

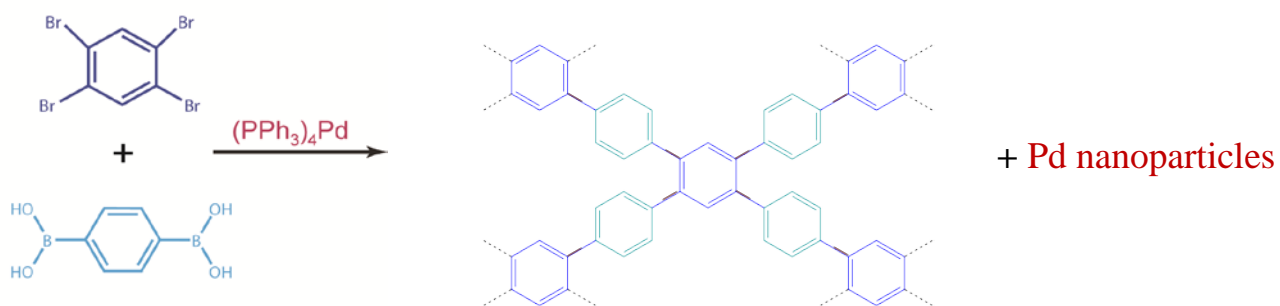
# Polyphenylene Supported Metal Catalyst for Hydrogenolysis of 5-hydroxymethylfurfural

*Qiming Wang<sup>1</sup>, Materials and Catalysis Laboratory, Department of Chemical Engineering, University College London<sup>1</sup>, London1, UK1; [Qiming Wang](#)*

The green conversion from nonedible biomass to renewable biofuel has attracted attention in last decades as it is provide alternative route for the production of transportation fuels and chemicals. It is a sustainable and cost-efficient route and because the production of vegetals from biomass consumes CO<sub>2</sub>, it is more environmentally friendly than the exploitation of conventional fossil fuel. 5-hydroxymethylfurfural (HMF) serves as a particular bridges connecting biomass raw materials to the biofuel, and heterogeneous catalysis plays a crucial role in this reaction route. The catalyst performances are highly depends on the nature of active site, the support-active site interaction and local coordination environment, and obviously on reaction conditions.

Polyphenylene (PPhen) [1] support is found to serves as an excellent platform for metal-catalyzed reactions, which can efficiently catalyze the reaction by providing a “solvent”-like reaction environment and easily to active metal particles. Here we described a polypheylene supported ruthenium (Ru/PPhen), cobalt (Co/PPhen) and nickel (Ni/PPhen) and bimetallic (RuNi/PPhen) catalysts for the conversion of 5-hydroxymethylfurfural (HMF) to 2,5-dimethylfuran (DMF). This support provides the  $\pi$ - $\pi$  stacking effect which helps to stabilized HMF and DMF on the surface, preventing over hydrogenation. In the Hydrogenolysis of HMF, 6mg of catalysts were examined respectively at operating pressure 10bar of hydrogen gas with 0.000213mmol of HMF added, notably, Ru/PPhen catalyst provided remarkably 92% DMF yield, with 98% of selectivity, which outperforms the best performing systems in the literature and provides an effective pathway for the conversion of biomass to fuel.

PPhen support was successfully synthesised by the cross coupling of 1,2,4,5-tetrabromobenzene and benzene-1,4-diboronic acid, catalysed by tetrakis (triphenylphosphine) palladium. The formed mixture was then heated at 100°C to obtain a palladium free polymer (pure PPhen).



*Scheme 1. Synthesis of the polyphenylene support shows that the Pd nanoparticles are formed from the catalyst and are weakly bonded at the surface of the polyphenylene. These are subsequently removed by leaching.*

10%Ru/PPhen catalyzes the reaction effectively and have the potential for further development into catalysts capable of large-scale applications. Considering the potential value of PPhen material, further possible research on the PPhen support includes looking into other metals or combinations of effective metals on the same polymer substrate and their synergy with this material.

## References

[1] Wang, F., Mielby, J., Richter, F.H., Wang, G., Prieto, G., Kasama, T., Weidenthaler, C., Bongard, H.J., Kegnæs, S., Fürstner, A. and Schüth, F., 2014. A polyphenylene support for Pd catalysts with exceptional catalytic activity. *Angewandte Chemie*, 126(33), pp.8789-8792

## 3D Spatial Distribution of Carbon Deposits in an Industrial Catalyst Particle Studied by Hard X-ray Spectro-Microscopy

*Martin Veselý, Inorganic Chemistry and Catalysis, Debye Institute for Nanomaterials Science, Utrecht University, Universiteitsweg 99, 3584 CG Utrecht, The Netherlands;*

*Roosbeh Valadian, Inorganic Chemistry and Catalysis, Debye Institute for Nanomaterials Science, Utrecht University, Universiteitsweg 99, 3584 CG Utrecht, The Netherlands; Mareike Toepperwien, Institute for X-ray Physics, University of Göttingen, 37077 Göttingen, Germany; Kathryn Spiers, Deutsches Elektronen-Synchrotron DESY, Notkestrasse 85, 22607 Hamburg, Germany; Jan Garrevoet, Deutsches Elektronen-Synchrotron DESY, Notkestrasse 85, 22607 Hamburg, Germany; Eelco T. C. Vogt, Inorganic Chemistry and Catalysis, Debye Institute for Nanomaterials Science, Utrecht University, Universiteitsweg 99, 3584 CG Utrecht, The Netherlands & Albemarle Catalysts Company BV, Research Center Amsterdam, PO box 37650, 1030 BE Amsterdam, The Netherlands; Tim Salditt, Institute for X-ray Physics, University of Göttingen, 37077 Göttingen, Germany; Bert M. Weckhuysen, Inorganic Chemistry and Catalysis, Debye Institute for Nanomaterials Science, Utrecht University, Universiteitsweg 99, 3584 CG Utrecht, The Netherlands; Florian Meirer, Inorganic Chemistry and Catalysis, Debye Institute for Nanomaterials Science, Utrecht University, Universiteitsweg 99, 3584 CG Utrecht, The Netherlands;*

Carbon deposits in a heterogeneous catalyst are an unwanted side product of any chemical reaction where hydrocarbons act as a reactant. The deposits can play different roles and can cover the active sites of the catalyst or limit mass-transport of reaction species to/from the active sites by pore-narrowing and pore-clogging.

In this work, we present a complex analytical approach, which is depicted and described in Figure 1, combining differential synchrotron-based hard X-ray holotomography (microscopy) and synchrotron-based X-ray fluorescence tomography (spectroscopy) of the same catalyst particle. As a showcase example we studied an individual Fluid Catalytic Cracking (FCC) catalyst particle, for which we determined the 3D distribution of the carbon deposits within tens of nanometers precision, imaged the macropore architecture of the catalyst body and correlated carbon deposits with the 3D spatial distribution of the catalyst's active sites as well as the distribution of metal deposits (iron and nickel).

The FCC catalyst particle contained 2.37 vol.% carbon deposits, which were located everywhere in the catalyst structure. The carbon deposits blocked the pore-mouths on the particle surface, plugged the pores in the particle, lengthened diffusion paths of the reaction species and caused a significantly reduced porosity in the center of

the particle. Lanthanum, used as a marker for rare earth exchanged USY zeolite domains, evinced the highest selectivity (spatial correlation) towards the carbon deposits. Domains of increased concentrations of Ni, which can act as a dehydrogenation catalyst, showed higher spatial correlation with carbon deposits than iron and much higher selectivity than the metal-free catalyst microstructure.

Correlative hard X-ray spectro-microscopy enables to quantify the pore-narrowing effect caused by carbon deposits in an individual catalyst particle and to pinpoint a relation between carbon deposits and complex catalyst microstructure.

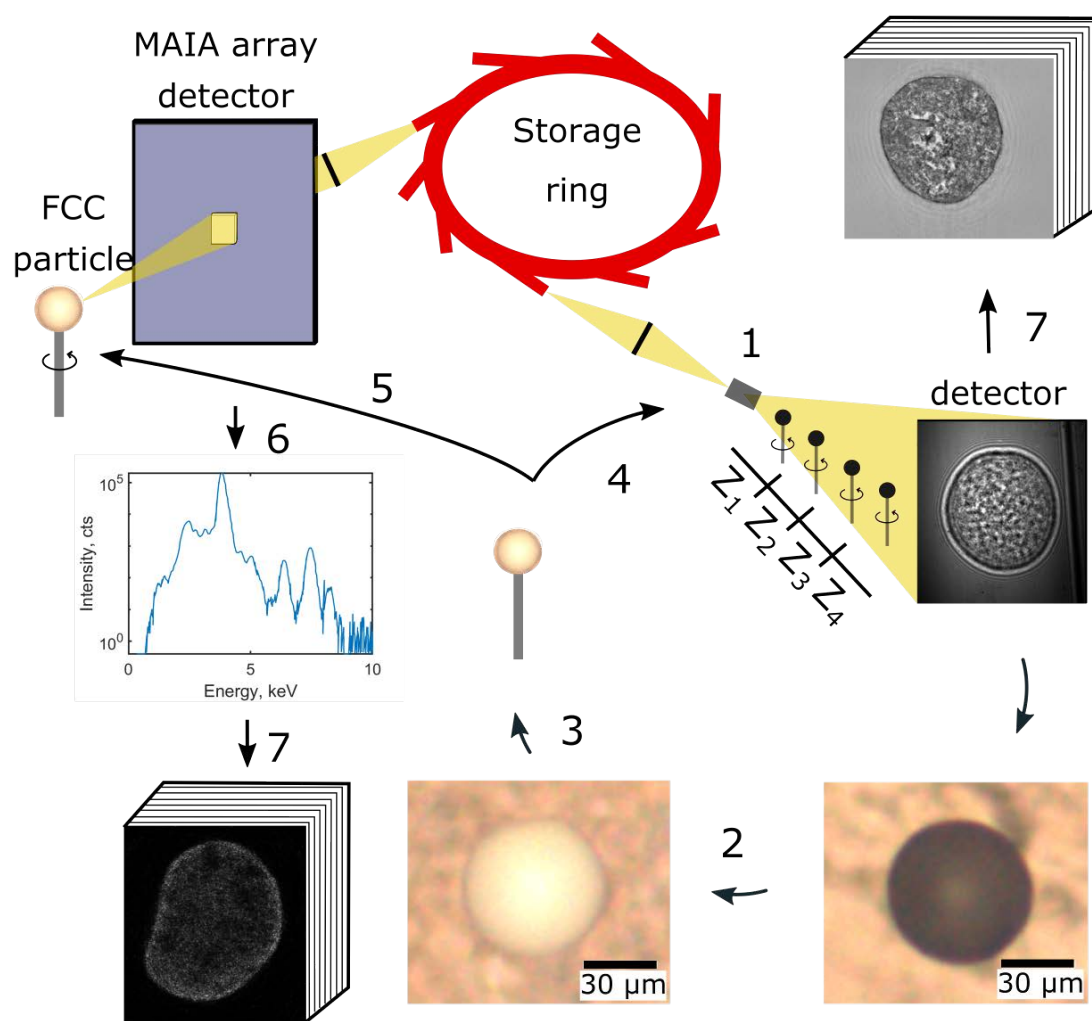


Figure 1: Experimental workflow: (1) X-ray Holotomography (GINIX, Göttingen Instrument for Nano-Imaging with X-Rays) installed at the P10 beamline (DESY, Hamburg, Germany) acquires a holotomography projections of the FCC catalyst particle mounted on a carbon tip. The acquisition was performed using 1000 projection angles covering  $180^\circ$  at four different distances between sample and detector. The transmitted signal was detected using a scintillator-based fiber-coupled sCMOS detector. (2) After the first holotomography acquisition, the particle was calcined to burn off coke deposits. During the calcination step the particle color changed from black to white evidencing the removal of the carbon deposits. (3) After coke removal, the catalyst particle was again mounted and measured using the same setup (4) for differential contrast imaging. After that the catalyst was imaged by XRF tomography (5) at the Po6 beamline (DESY, Hamburg, Germany), using a 200 nm focused X-ray beam and 120 projection angles covering  $360^\circ$ . The emitted XRF was detected by means of a Maia detector (6) and XRF spectra were fitted to quantify the relative concentrations of the detected elements in every single pixel and at each projection angle. (7) In the final step 3-D representations of the sample density as well as the 3-D distribution of coke deposits have been reconstructed from X-ray holotomography, and the 3-D distribution of specific elements of interest has been reconstructed from XRF tomography.

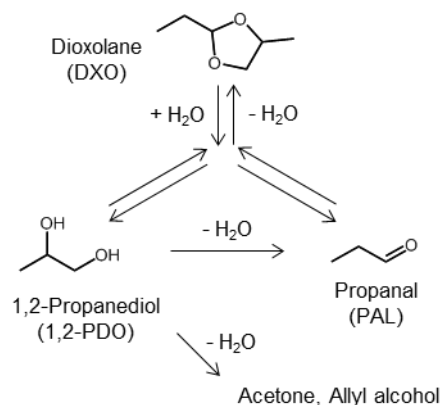
# Highly selective dehydration of 1,2-propanediol to propanal over boron phosphate catalyst in the presence of steam

*Ryoichi Otomo,<sup>1,\*</sup> Chiaki Yamaguchi,<sup>2</sup> Daiki Iwaisako,<sup>2</sup> Shun Oyamada,<sup>2</sup> Yuichi Kamiya<sup>1</sup>; <sup>1</sup>Faculty of Environmental Earth Science, <sup>2</sup>Graduate School of Environmental Science, Hokkaido University, Sapporo, Japan.*

*Corresponding author: Dr. R. Otomo, e-mail; otomo@ees.hokudai.ac.jp*

## Introduction

Since polyols can be produced in high yields through the hydrogenolysis of cellulose and glycerol [1], the selective conversion of polyols into value-added chemicals is desired toward the utilization of plant biomass. Dehydration of 1,2-propanediol (1,2-PDO) to propanal (PAL) has attracted research interest (Scheme 1), because PAL is a potential intermediate material to obtain bio-based chemicals. In the dehydration of 1,2-PDO, formation of by-products such as acetone, allyl alcohol and dioxolane (DXO) were inevitable but should be suppressed. Although various types of solid acid catalysts have been developed for the dehydration of 1,2-PDO, it is still difficult to produce PAL in a sufficiently high yield. Herein, we disclose that boron phosphate showed outstanding durable catalytic activity for the dehydration of 1,2-PDO and achieved a high yield of PAL >95% [2].



Scheme 1 Reaction pathways for dehydration of 1,2-PDO.

## Experimental

Boron, aluminum, iron, nickel and lanthanum phosphates (BP, AlP, FeP, NiP and LaP) were prepared by standard methods and calcined at 350 °C in air prior to use. Gas-phase dehydration of 1,2-PDO was conducted under atmospheric pressure using a vertical fixed-bed flow reactor.

## Results and discussion

Among various types of metal phosphate catalysts, BP exceptionally high catalytic activity for the dehydration of 1,2-PDO, even though BP has a small number of Brønsted acid sites (Table 1).

Upon increasing reaction temperature, BP showed higher yield of PAL and finally gave the yield of PAL reached 95% at 300 °C. It is noteworthy that BP produced only a negligible amount of other C3 products, while other metal phosphates produced 10 – 25% yield of acetone and allyl alcohol.

Unexpectedly, we found that the catalytic activity of boron phosphate was remarkably enhanced in the presence of the co-fed steam (Entries 2 and 3). This is because B-O-P bonds on BP was partially hydrolyzed to B-OH and P-OH groups by the steam during the reaction and the number of active Brønsted acid sites was increased. As a comparison, H<sub>3</sub>PO<sub>4</sub>/SiO<sub>2</sub> was prepared. In spite of its smaller number of Brønsted acid sites, BP showed much higher activity than H<sub>3</sub>PO<sub>4</sub>/SiO<sub>2</sub> for the dehydration, suggesting that B-OH and P-OH groups on BP cooperatively promoted the dehydration of 1,2-PDO. The co-fed steam also caused the hydrolytic decomposition of DXO to PAL, resulting in improvement in the yield of PAL.

Catalytic performance of BP was compared with those of ZSM-5, SiO<sub>2</sub>-Al<sub>2</sub>O<sub>3</sub>, and Nb<sub>2</sub>O<sub>5</sub> that have been reported to be highly active for the dehydration of 1,2-PDO (Figure 1). BP constantly gave 100% conversion of 1,2-PDO throughout 10 h. Initially the yield of PAL was >95%, but thereafter gradually decreased and became constant at ~70%. ZSM-5 initially gave 81% yield of PAL, but severely deactivated. SiO<sub>2</sub>-Al<sub>2</sub>O<sub>3</sub> and Nb<sub>2</sub>O<sub>5</sub> showed poor catalytic activity. Obviously, BP showed higher and more durable activity with higher selectivity to PAL than these conventional catalysts.

Table 1 Dehydration of 1,2-PDO over metal phosphate catalysts with/without co-fed steam.

Entry	Catalyst	Acid (mmol/g)	Conv. (%)	Yield (C-%)	
				PAL	DXO
1	BP	0.25	100	86	7
2	BP <sup>a</sup>		39	1	37
3	BP <sup>b</sup>		90	52	38
4	AiP	0.90	30	1	18
5	FeP	0.60	5	5	0
6	NiP	0.65	12	4	0
7	LaP	0.55	23	2	0
8	H <sub>3</sub> PO <sub>4</sub> /SiO <sub>2</sub>	0.60	30	2	27

Catalyst, 0.2 g; W/F 27 g·h/mol; 513 K, 0.5 h; Without steam. <sup>a</sup> 473 K; <sup>b</sup> 473 K, with 20 Vol.% steam.

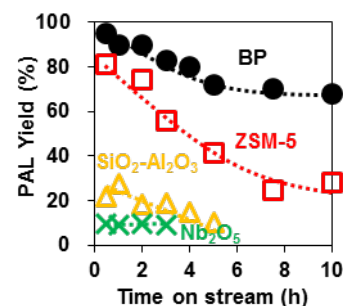


Figure 1 Dehydration of 1,2-PDO over BP and conventional catalysts. Catalyst, 0.2 g; W/F 27 g·h/mol; 513 K; With 20 Vol.% steam.

## References

- [1] C.-H. Zhou, X. Xia, C.-X. Lin, D.-S. Tong, J. Beltramini, *Chem. Soc. Rev.*, **2011**, *40*, 5588.
- [2] R. Otomo, C. Yamaguchi, D. Iwaisako, S. Oyamada, Y. Kamiya, *ACS Sustainable Chem. Eng.*, **2019**, *in press*.

## ***Operando Quick-XAS S on Cu /Cu oxide foam for CO<sub>2</sub>RR***

*Alexandra Dworzak, Mehtap Oezaslan, Carl von Ossietzky University, Oldenburg, Germany*

New and improved strategies to secure our global energy economy and chemical industry in the future are needed due to the strong dependence on limited fossil resources and the socio-environmental problems associated with increasing anthropogenic emissions of CO<sub>2</sub>. To counteract this problem and simultaneously to reduce the concentration of the CO<sub>2</sub> as well-known greenhouse gas, a very promising route is the electrochemical CO<sub>2</sub> reduction reaction (CO<sub>2</sub>RR) into hydrocarbons and alcohols. Different reaction mechanisms and kinetics for the CO<sub>2</sub>RR are postulated.[1-3] In particular, the role of Cu oxide during the C<sub>2</sub> formation like ethylene and ethanol is poorly understood to date. Further critical issues are addressed: (i) high overpotentials, (ii) broad product distribution, (iii) fast degradation by catalyst poisoning and (iv) competition reaction at high cathodic potentials, referred to as hydrogen evolution reaction.

Our work is focusing on the fundamental understanding about the mechanism and kinetics for the CO<sub>2</sub>RR on nano-porous copper (np-Cu) foams derived from the Cu oxide probed by Quick-XAS technique. The np-Cu foams prepared by dealloying of Cu-based alloys or by electrodeposition exhibit large surface area-to-volume ratios, improved catalytic performance and high C<sub>2</sub> selectivity compared to a flat Cu surface. The catalytic properties (activity and selectivity) can be controlled by the pore size and curvature of the ligaments of the np-Cu. By using operando Quick-X-ray absorption spectroscopy (XAS), we studied the various structures and oxidation states of the Cu species in np-Cu foams as function of the applied potential, kind of electrolyte and pH value during the CO<sub>2</sub>RR. In addition, we identified the potential range for the catalyst aging via coarsening and suggest strategies to stabilize the ligament structure and size of the Cu foams during the CO<sub>2</sub>RR.

Based on our *operando* XAS studies, we obtained a deeper insight to the mechanism and kinetics of the CO<sub>2</sub>RR on porous Cu foams and clarified the role of Cu oxides for the C<sub>2</sub> production.

### **References**

1. K. P. Kuhl , E. R. Cave, D. N. Abram, and T. F. Jaramillo, *Energy Environ. Sci.*, 5 (2012) p. 7050.
2. R. Reske, M. Duca, M. Oezaslan, K. J. P. Schouten, M. T. M. Koper, and P. Strasser, *J. Phys. Chem. Lett.*, 4 (2013) p. 2410.
3. A. Dutta, M. Rahaman, N. C. Luedi, M. Mohos, and P. Broekmann, *ACS Catal.*, 6 (2016) p. 2804.
4. B. Hecker, C. Dosche, M. Oezaslan, *The Journal of Physical Chemistry C*, 122 (2018) p. 26378.



# Nature of the electrophile in liquid-phase phenolics-alcohol alkylation over acidic zeolites

*Hui Shi<sup>1</sup>, Yuanshuai Liu<sup>1</sup>, Johannes A. Lercher<sup>1,2</sup>*

*<sup>1</sup>Technische Universität München, Department of Chemistry and Catalysis Research Center, Lichtenbergstraße 4, 85748 Garching, Germany*

*<sup>2</sup>Present address: Pacific Northwest National Laboratory, 902 Battelle Blvd, Richland, WA 99354, USA*

## Introduction

Biomass-derived phenolic oils, obtained from pyrolysis or hydrolysis of lignin, can be catalytically converted to fuels and chemicals. One important class of reaction is acid-catalyzed alkylation between bio-sourced phenols and alcohols, producing alkylated phenolics which can be used as specialty chemicals [1]. Meanwhile, the carbon number in these phenolics falls in the desirable range for fuels and can be further upgraded by deoxygenation catalysis on metal catalysts. This lecture aims to highlight our recent efforts at deciphering several previously unresolved mechanistic details of this old class of reaction within zeolite confines in the context of liquid-phase processing.

## Materials and Methods

A commercial BEA (Si/Al = 75, Clariant) zeolite in its protonic form was thermally activated before catalytic reactions or NMR measurements. All chemicals (>98% purity, or 99% <sup>13</sup>C-enriched 1-<sup>13</sup>C-labeled phenol and cyclohexanol in NMR experiments) were purchased from Sigma Aldrich and used without further purification. Alkylation reactions of phenol and cyclohexanol/cyclohexene were performed with decalin as solvent in a 300 ml, gradientless autoclave reactor (Parr) at 393–433 K while stirring at 700 rpm. Aliquots of liquid samples collected during reaction were analyzed on Shimadzu 2010 GC and GCMS (QP2010S). In situ NMR experiments were carried out on a Varian 500 MHz NMR spectrometer using a 7.5 mm HX MAS probe with a spinning rate of 3.1 kHz at a resonance frequency of 125.7 MHz.

## Results

Preliminary experiments showed that Lewis acid sites were much less active than Brønsted acid sites for the alkylation of phenol in decalin. With alcohol as the starting alkylating reagent, multiple routes can generate the electrophile: (1) alkoxonium ion from protonation of alcohol; (2) carbenium ion from alcohol-derived intermediates; (3) carbenium ion from olefin re-adsorption and protonation. Alkylation can also proceed via a concerted mechanism or ether rearrangement. For both ortho- and para-monoalkylation, the concentrations of 2-<sup>13</sup>C-cyclohexyl phenols were significantly higher than 1-<sup>13</sup>C-cyclohexyl phenols (Figure 1). These results are consistent with re-adsorption and protonation of 1- and 3-<sup>13</sup>C-cyclohexenes at the BAS that forms more 2-<sup>13</sup>C-cyclohexyl carbocations than 1-<sup>13</sup>C-cyclohexyl carbenium ions. If phenol reacted with the alkoxonium ion or carbenium ion directly generated from dehydration of 1-<sup>13</sup>C-cyclohexanol before significant hydride shift had occurred, most of the C-alkylation products should have contained 1-<sup>13</sup>C-cyclohexyl. Thus, electrophiles directly produced from cyclohexanol (cyclohexyl cation or cyclohexonium) are not able to account for the observed excess of 2-<sup>13</sup>C-cyclohexyl phenols. We will also discuss other valuable mechanistic information extracted from the <sup>13</sup>C isotope scrambling data (such as cyclohexene isotopomers).

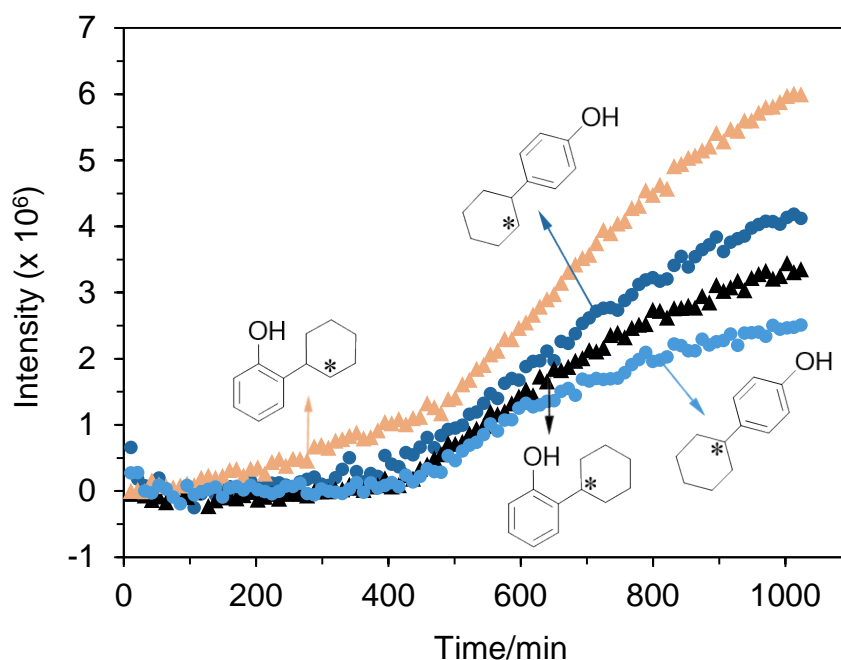


Figure 1. Evolution of <sup>13</sup>C labeled mono-alkylation products as a function of reaction time monitored in situ by NMR. Data have been published in Ref. [2].

## References

1. M.Á. González-Borja, D.E. Resasco, *AIChE J.* 61 (2015) 598.
2. Z. Zhao, H. Shi, C. Wan, M.Y. Hu, Y. Liu, D. Mei, D.M. Camaioni, J.Z. Hu, J.A. Lercher, *J. Am. Chem. Soc.* 139 (2017) 9178.

# Isolated Zr Surface Sites on Silica Promote Hydrogenation of CO<sub>2</sub> to CH<sub>3</sub>OH in Supported Cu Catalysts

*Erwin Lam, ETH Zurich, Zurich, Switzerland; Kim Larmier, ETH Zurich, Zurich, Switzerland; Patrick Wolf, ETH Zurich, Zurich, Switzerland; Shohei Tada, ETH Zurich, Zurich, Switzerland; Olga V. Safonova, PSI, Villigen, Switzerland; Christophe Copéret, ETH Zurich, Zurich, Switzerland*

The increasing amount of carbon dioxide (CO<sub>2</sub>) in the atmosphere has a direct impact on global warming and is a direct consequence of the use of fossil fuels as our main energy sources. One way to mitigate its increase is to incorporate CO<sub>2</sub> in a carbon-energy-cycle and to transform it into more valuable compounds such as methanol following the concept of the “methanol economy”. [1] The hydrogenation of CO<sub>2</sub> to methanol is possible with Cu-based catalysts. Promising catalytic efficacy (methanol activity and selectivity) can be reached by choosing specific metal oxide supports, such as zirconia, while silica as a support favors the competing reverse water-gas-shift reaction (RWGS), forming CO and H<sub>2</sub>O instead. [2] We have recently shown that the improved activity and selectivity in zirconia-supported Cu nanoparticles is due to the favored formation of CH<sub>3</sub>OH at the interface between copper and zirconia. [3] In particular, it has shown that the role of Zr Lewis acid sites at the surface of zirconia and in close proximity to the Cu nanoparticles, is to facilitate the formation of formate and their conversion into methoxy species.

We reasoned that it is possible to tailor the activity of CO<sub>2</sub> hydrogenation catalysts by selectively incorporating Zr(IV) species at the interface with the Cu particles. We thus used a surface organometallic chemistry (SOMC) combined with a thermolytic precursor (TMP) approach to generate first well-defined isolated Zr(IV) surface sites on silica and then grow small and narrowly distributed Cu nanoparticles by grafting a Cu molecular precursor followed by a treatment under H<sub>2</sub>. This material demonstrates promotional effect in CO<sub>2</sub> hydrogenation at 230 °C and 25 bars, providing increased activity and selectivity towards CH<sub>3</sub>OH formation in comparison to benchmark Cu/SiO<sub>2</sub> catalysts. In addition, thanks to the presence of isolated Zr(IV) surface sites, it is possible to monitor the coordination environment and oxidation state of zirconium using in-situ and ex-situ X-ray absorption, NMR and IR spectroscopy. This study allows rationalizing and understanding on a molecular level

the role of oxide supports in catalysis and provides guidelines to improve catalyst design. [4]

### References

- [1] Goeppert, A.; Czaun, M.; Jones, J.-P.; Prakash, G.K.S.; Olah, G. A., *Chem. Soc. Rev.*, **2014**, *43*, 7995.
- [2] Fisher, I.A.; Bell, A.T.; *J. Catal*, **1997**, *172*, 222.
- [3] Larmier, K, Liao, W.-C.; Tada, S.; Lam, E; Vérel, R.; Bansode, A.; Urakawa, A.; Comas-Vives, A.; Copéret, C., *Angew. Chem. Int. Ed.*, **2017**, *56*, 2318.
- [4] Lam, E.; Larmier, K.; Wolf, P.; Tada, S.; Safonova, O.V.; Copéret, C., *J. Am. Chem. Soc.*, **2018**, *140*, 10530.

# CO oxidation and CO-PROX on oxide-supported Au catalysts: Is the impact of the H<sub>2</sub> on the CO oxidation dependent on the nature of the support?

*Cruz, A.R.M.; Gomes, J.F.; Assaf, J.M., UFSCar, São Carlos, Brazil*

## Introduction

Metal oxide-supported Au catalysts have been widely investigated because of their good performances in low temperature CO oxidation reactions. The particle size as well as the morphology and thermal stability of the Au particles were shown to be dependent on the properties of the support <sup>[1]</sup> that, in turn, impacts on the catalytic activity of these materials. Despite the large number of published papers about the preferential oxidation of CO in H<sub>2</sub>-rich streams (CO-PROX) on Au catalysts, the impact of the H<sub>2</sub> on the oxidation of CO is still controversial <sup>[2,3]</sup>. In the present work, the oxidation of CO in absence and presence of H<sub>2</sub> on catalysts with nominally 1 wt.% of Au supported on CeO<sub>2</sub>, MnO<sub>2</sub>, SiO<sub>2</sub> and TiO<sub>2</sub> were evaluated.

## Experimental

CeO<sub>2</sub> support, synthesized by the precipitation method, and commercial MnO<sub>2</sub>, SiO<sub>2</sub>, TiO<sub>2</sub> supports were used. Au catalysts were prepared by a modified deposition-precipitation method based on that of Zanella et al. <sup>[4]</sup>. The materials were studied by XRF or ICP-OES, BET and, after applying the catalysts to the reactions, HRTEM using HAADF-STEM. The catalytic performances were evaluated using a fixed bed tubular reactor and a gas chromatograph Varian CP-3800.

## Results and Discussion

The Au/CeO<sub>2</sub> catalyst showed 1.0 wt.% of Au and 58 m<sup>2</sup>/g<sub>cat</sub> of surface area, as investigated by XRF and BET, respectively. It was not possible to evaluate the Au particle size by HAADF-STEM results due to the lack of contrast between Ce and Au atoms. The Au/MnO<sub>2</sub> catalyst presented 1.4 wt.% of Au and 6 m<sup>2</sup>/g<sub>cat</sub> of surface area. The TEM image showed highly dispersed AuNPs on the support with a mean Au particle size of about 6.2 ±1.7 nm. The Au/SiO<sub>2</sub> catalyst presented Au content of 0.25 wt.%, as investigated by ICP-OES, and a surface area of 265 m<sup>2</sup>/g<sub>cat</sub>. The TEM result showed a broad distribution of Au particle sizes, varying between 10 and 30 nm. The Au/TiO<sub>2</sub> catalyst exhibited 1.0 wt.% of Au and 107 m<sup>2</sup>/g<sub>cat</sub> of surface area. According to the TEM result, AuNPs were monodispersed on the support, with mean

particle size of  $2.31 \pm 0.44$  nm. Although the same conditions were applied in the synthesis of these catalysts, their properties varied significantly according to the support.

The catalytic results of the investigated materials are shown in Fig. 1. In general, the performance of the Au/CeO<sub>2</sub>, Au/MnO<sub>2</sub> and Au/TiO<sub>2</sub> in the oxidation of CO and CO-PROX were better than those of the corresponding pure supports. On the other hand, Au/SiO<sub>2</sub> as well as SiO<sub>2</sub> were inactive in both reactions. By comparing the catalytic behaviors of gold supported on MnO<sub>2</sub> and TiO<sub>2</sub> in the CO oxidation with those corresponding to the CO-PROX reaction, one observes that for these materials the CO conversion is generally lower in presence of H<sub>2</sub>. This is due to the fact that CO and H<sub>2</sub> compete for adsorption sites [2]. In contrast, for the Au/CeO<sub>2</sub> catalyst, the conversion of CO was improved in the presence of H<sub>2</sub>. This particular behavior is

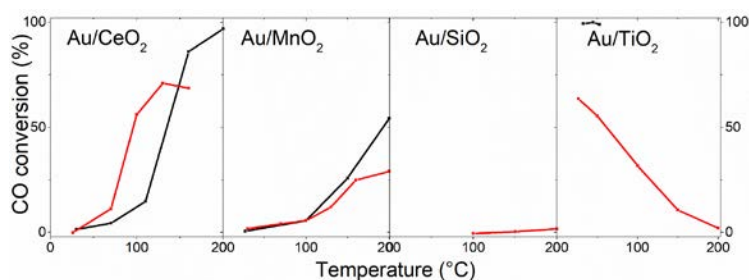


**Fig. 1.** CO conversion as a function of the temperature for CO oxidation (black curve) and CO-PROX reaction (red curve) on oxide-supported Au catalysts indicated in the figure. Reaction Conditions: 50 mg of catalyst; 1 atm; Flow: 50 mL/min: CO/O<sub>2</sub>/N<sub>2</sub> = 2/1/22 (%) for CO oxidation; H<sub>2</sub>/CO/O<sub>2</sub>/N<sub>2</sub> = 50/4/2/44 (%) for CO-PROX reaction.

consistent with the formation of a hydroperoxy (HO<sub>2</sub>) intermediate. This species may easily oxidize CO, preventing the catalyst deactivation by water from hydrogen oxidation and enhancing the CO oxidation rate [3].

## Conclusions

Au/CeO<sub>2</sub>, Au/MnO<sub>2</sub> and Au/TiO<sub>2</sub> were active in the oxidation of CO and CO-PROX in opposition to Au/SiO<sub>2</sub>. By comparing both reactions on each catalyst, we have demonstrated that the impact of the H<sub>2</sub> on the CO oxidation over Au-based materials depends on the support characteristics, although contributions of surface area, gold content and particle size to the observed performances can not be discarded. For MnO<sub>2</sub> and TiO<sub>2</sub>-supported Au materials, the CO conversion was generally lower in presence of H<sub>2</sub>. Differently, for Au/CeO<sub>2</sub>, the conversion of CO in the CO-PROX reaction was higher compared to that in the total oxidation of CO. Our results indicate a difference in the mechanism of the CO-PROX reaction on these materials.

The authors would like to thank CNPq, CAPES and RCGI (grant n. 2014/50279-4).

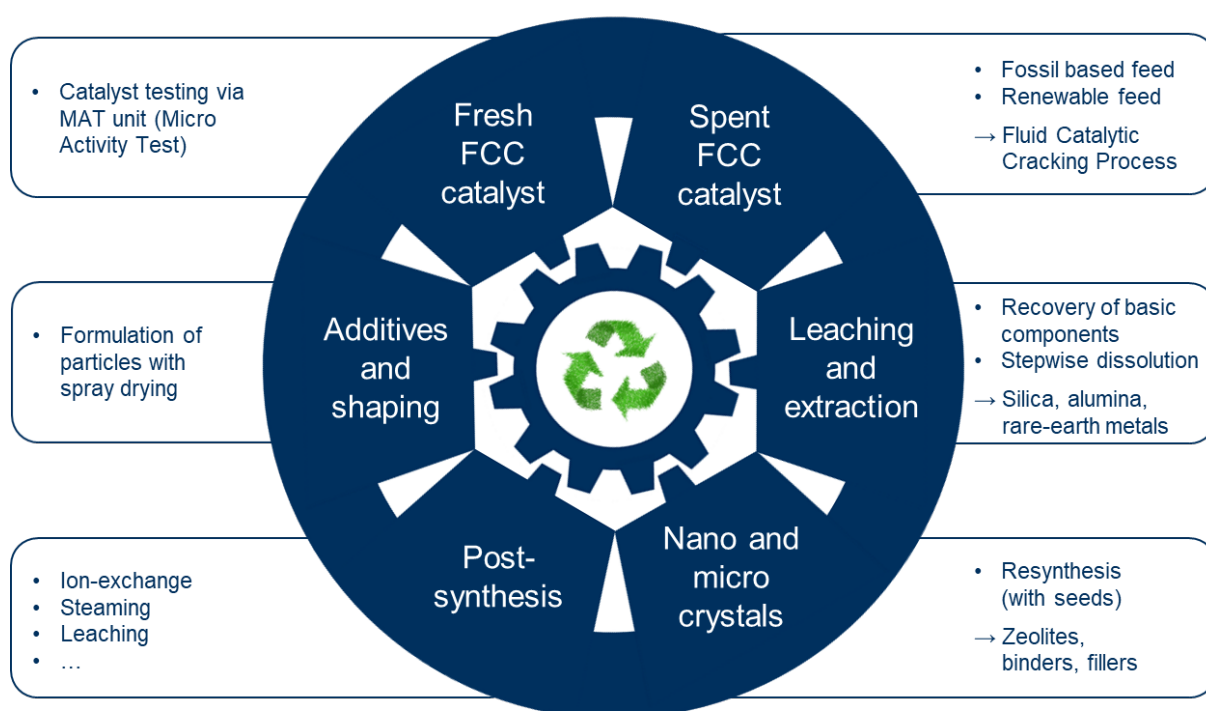
## References

- [1] M. C. Kung, R. J. Davis, H. H. Kung, *J. Phys. Chem. C* 2007, 111, 11767–11775.
- [2] Y. Hartadi, R. Behm, D. Widmann, *Catalysts* 2016, 6, 21.
- [3] M. Lomello-Tafin, A. A. Chaou, F. Morfin, V. Caps, J.-L. Rousset, *Chem. Commun.* 2005, 388.
- [4] R. Zanella, S. Giorgio, C. R. Henry, C. Louis, *J. Phys. Chem. B* 2002, 106, 7634–7642.
- [5] S. Carrettin, et. al., *Angew. Chemie - Int. Ed.* 2004, 43, 2538–2540.

## Recycling of spent FCC Catalysts – Dissolution, Recovery, Resynthesis

*Mathias S. Marschall, Malte Ritschel, Oliver Busse, Jan J. Weigand, Technische Universität Dresden, Chemistry and Food Chemistry, Dresden, Germany*

Nowadays, 2300 tons per day of spent catalyst in the **Fluid Catalytic Cracking (FCC)** process are generated worldwide for the production of fuels and basic chemicals.<sup>[1]</sup> As a result of the irreversible deactivation processes that takes place during the cracking process (such as poisoning, fouling, etc.)<sup>[2]</sup>, this material is up-to now considered useless for the further processes. The spent catalyst is currently either recycled as waste in cement processing or stored in landfills. Therefore, harmful pollutants leach into the environment and causes significant problems. So far spent **FCC** catalysts are mainly recycled with respect to recover rare-earth metals that are used as stabilizers.



An international research consortia teamed up to work on a project named ReCaLI (**Recycling of Catalysts Locally**). ReCaLI intends to develop recycling concepts in cooperation with a Vietnamese refinery group and other partners in order to further utilize the matrix of spent **FCC** catalyst beyond only the recovery of the rare-earth metals.<sup>[3]</sup> Thus, it is intended to either use the matrix for the synthesis of fresh **FCC** catalyst in order to close a recycling loop or to synthesize value added products.

## Acknowledgement

ReCaLI (**R**ecycling of **C**atalysts **L**ocally) project for international partnerships is funded by CLIENT II (BMBF, FONAS<sup>3</sup>), Funding Code: 033R188A.

## References

- [1] E.T.C. Vogt, B.M. Weckhuysen, *Chem. So. Rev.*, **44**, 7342 (2015).
- [2] M.D. Argyle, C.H. Bartholomew, *Catalyst*, **5**, 145 (2015).
- [3] M. Wenzel, K. Schnaars, N. Kelly, L. Götzke, S. Robles M., K. Kretschmer, Phuc Nguyen Le, Dang Thanh Tung, Nguyen Huu Luong, Nguyen Anh Duc, Dang Van Sy, K. Gloe, J.J. Weigand, Hydrometallurgical Recovery of Rare Earth Metals from Spent FCC Catalysts. In *Rare Metal Technology 2016*, S. Alam, H. Kim, N.R. Neelameggham, T. Ouchi, H. Oosterhof, Eds.; Springer Berlin Heidelberg, 2016; pp 37-45.



# Low Temperature Production of Oxymethylenethers (OME) catalyzed by Heteropoly acids

*Daniel Huth, Martin Lucas, Marcus Rose  
Ernst-Berl-Institut für Technische und Makromolekulare Chemie,  
TU Darmstadt, Germany.*

Oxymethylenethers (OME) are a promising solution to reduce soot and NO<sub>x</sub> emissions in Diesel engines.<sup>[1]</sup> These oligomeric hydrocarbons with a high oxygen content and the molecular formula CH<sub>3</sub>-O-(CH<sub>2</sub>-O)<sub>n</sub>-CH<sub>3</sub> show varying physicochemical properties that depend on the chain length n. OME<sub>1</sub> and OME<sub>2</sub> can be used as an additive which lowers the pollutant emission significantly. To meet the specifications of pure diesel, OME<sub>3-5</sub> are suitable.<sup>[2]</sup> OME can be produced by different routes that are all catalyzed by acids. Depending on the applied substrates water is typically formed, such as in the condensation of methanol and formaldehyde. Alternatively, OME<sub>1</sub> (methylal) is used and the chain growth is based on addition of formaldehyde units. A commercial production of OME in China is mainly based on acidic ion exchange resins as catalysts, while many other acidic catalysts have been proposed and investigated already.<sup>[3]</sup>

In our work, we carried out an initial catalyst screening for the OME formation in the water-free system of trioxane and methylal using various inorganic and organic solid acids. The best catalytic results were shown by the heteropoly acid phosphotungstic acid (H<sub>3</sub>PW<sub>12</sub>O<sub>40</sub>; HPW). We optimized reaction conditions and found high selectivities of OME<sub>3-5</sub> as well as high conversions of trioxane. The catalysts exhibited an outstanding activity with full conversion of trioxane at reaction conditions close to ambient temperature (30 °C) with catalytic amount of the active acid in less than 10 minutes.<sup>[4]</sup> A detailed investigation of the reaction kinetics was carried out and modelled accordingly. The Arrhenius parameters proved the exceptionally low activation barrier. Hence, a highly efficient OME synthesis beyond conventional zeolite and ion exchange resin-catalysis is enabled.

[1] A. Feiling, M. Münz, C. Beidl, *ATZextra worldwide* **2016**, 21, 16-21.

[2] S. Deutz, D. Bongartz, B. Heuser, A. Kätelhön, L. Schulze Langenhorst, A. Omari, M. Walters, J. Klankermayer, W. Leitner, A. Mitsos, S. Pischinger, A. Bardow, *Energy & Environmental Science* **2018**, 11, 331-343.

[3] K. Hackbarth, P. Haltenort, U. Arnold, J. Sauer, *Chemie Ingenieur Technik* **2018**, 90, 1520-1528.

[4] M. Rose, D. Huth, *Manuscript in preparation* **2019**.

# **Aqueous-phase alcohol dehydration on tungstated domains: effects of domain size and support**

*Niklas Pfriem<sup>1</sup>; Hui Shi<sup>1</sup>; Johannes A. Lercher<sup>1</sup>; Gary L. Haller<sup>2</sup>*

*<sup>1</sup>Technische Universität München, Department of Chemistry and Catalysis Research Center, Lichtenbergstraße 4, 85748 Garching, Germany;*

*<sup>2</sup>Yale University, Department of Chemical and Environmental Engineering, New Haven, CT 06520-8682, USA*

## **Introduction**

When processing biomass-derived feedstocks at elevated temperatures in water or in biphasic mixtures containing water, catalyst stability becomes an important factor. Compared to zeolites and silica which substantially dissolve in hot liquid water, structurally stable  $\text{WO}_3$  is seen to play an important role in the catalytic conversion of various biomass-derived feedstocks.[1] Despite its known strong acidity (comparable to zeolites) that allows it to catalyze alcohol dehydration with high turnover rates in the gas phase, the origin of its catalytic activity in aqueous phase is not fundamentally understood. In particular, this study addresses the effects of surface density and dispersion of  $\text{WO}_x$  domains on different supports, which are compared against observations reported for gas-phase alcohol dehydration reactions.[2]

## **Materials and Methods**

A series of tungstate-based catalysts was prepared by loading different amounts of  $\text{WO}_3$  on various supports. As another means, a commercial tungstated zirconium hydroxide (XZO1251/02 MEL Chemicals) was annealed at 600-900 °C in a static air muffle furnace.  $\text{NO}_x$ -TPD was performed to calculate the  $\text{WO}_x$ -surface densities from accessible  $\text{ZrO}_2$  surfaces.[3] The catalytic activity of these materials for cyclohexanol dehydration was evaluated in a 100 ml, gradientless batch reactor (Parr) under  $\text{N}_2$  atmosphere (40 bar, 473 K, 700 rpm). The active sites were determined by a proton exchange method established recently (unpublished results).

## **Results and Discussion**

We first report dehydration rates and corresponding turnover frequencies (TOFs) as a function of surface W density for a series of supported  $\text{WO}_x$  catalysts on  $\text{ZrO}_2$ . Increasing the surface density of  $\text{WO}_x$ -domains induced the agglomeration of mono-tungstate to larger  $\text{WO}_3$ -crystallites, as often reported. Maximum mass-specific

dehydration rates were found at monolayer coverage of the tungsten domain ( $\sim 5 \text{ W nm}^{-2}$ ), as shown in Figure 1. However, after normalizing to the concentration of exchangeable surface protons, a nearly constant TOF was observed over this series of catalysts, independent of the  $\text{WO}_x$  surface density. This site-normalized rate was significantly higher than that exhibited by the aqueous acids, indicating that the hydronium ion catalyzed dehydration on these solids is indeed mediated through the surface rather than catalyzed in a homogeneous fashion. In this contribution, we will also present results concerning the profound support effects on the ability of  $\text{WO}_x$  domains to generate surface protons that become hydronium ions in the presence of liquid water, as well as on the intrinsic catalytic activity of hydronium ion confined at the solid-water interface. Altogether, the protocols designed to measure active sites densities in the aqueous phase enabled a quantitative evaluation of catalytic activities as a function of surface agglomeration states of  $\text{WO}_x$ .

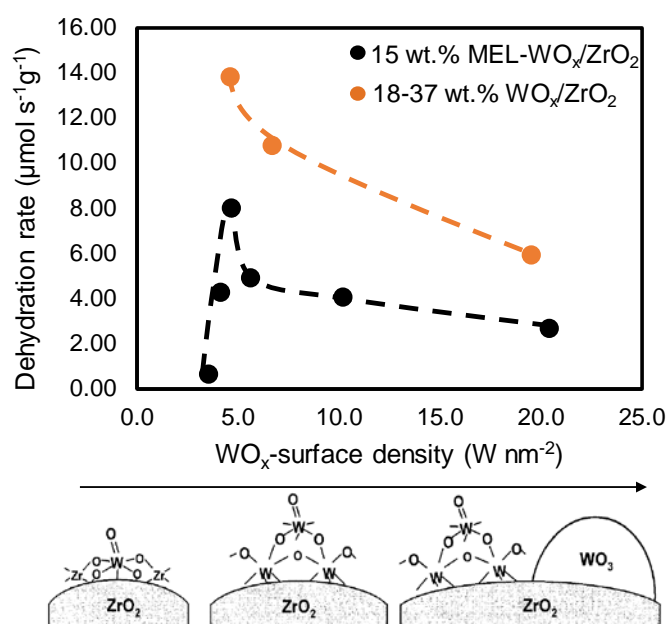


**Figure 1** Rate of cyclohexanol dehydration as a function of  $\text{WO}_x$  surface density for a series of tungstated zirconia catalysts in aqueous phase (0.33 M, 200 °C, 40 bar). A depiction of evolution of surface  $\text{WO}_x$  domains is also shown.

## Reference

- [1] Y. Liu, C. Luo, H. Liu, *Angew. Chem. Int. Ed* 124, 3303-3307 (2012).
- [2] J. Macht, C.D. Baertsch, M. May-Lozano, S.L. Soled, Y. Wang, E. Iglesia, *J. Catal.* 227, 479-491 (2004).
- [3] H.Y. Law, J. Blanchard, X. Carrier, C. Thomas, *J. Phys. Chem. C* 114, 9731-9738 (2010).

# The effect of Pt and dopant M (Pr<sup>3+</sup>, Ti<sup>4+</sup>) in the Ce<sub>1-x</sub>M<sub>x</sub>O<sub>2-δ</sub> – supported NiPt catalyst on the carbon pathways in the dry reforming of methane studied by transient and isotopic techniques

*M.A. Vasiliades, C.M. Damaskinos, K.K. Kyprianou, A.M. Efstathiou\**

*Heterogeneous Catalysis Lab, Chemistry Department, University of Cyprus, 2109, Nicosia, Cyprus*

## 1. Scope

Dry reforming of methane (DRM: CH<sub>4</sub> + CO<sub>2</sub> ↔ 2CO + 2H<sub>2</sub>) has reattracted much attention in the recent past mainly due to the progress made towards the design of catalysts with significant “carbon” resistance, and its benefits for utilizing natural gas rich in CO<sub>2</sub> or biogas towards the formation of liquid fuels and useful chemicals. Improving the understanding and quantifying the relative importance of each of the *inactive “carbon”* formation routes becomes therefore a very important task. Methane decomposition (CH<sub>4</sub> → C-s + 2H<sub>2</sub>) and the Boudouard reaction (2CO ↔ C-s + CO<sub>2</sub>) are considered as the main sources of inactive “carbon” formation. Recent studies [1,2] on Ce<sub>1-x</sub>M<sub>x</sub>O<sub>2-δ</sub> (M = Y<sup>3+</sup>, Zr<sup>4+</sup>, Pr<sup>3+</sup>) reducible metal oxides - supported Ni and bimetallic NiPt catalysts demonstrated the very small amounts of deposited carbon and its relevant deposition rates (< 0.07 mg g<sub>cat</sub><sup>-1</sup> h<sup>-1</sup>) for long time-on-stream (ca. 50 h). The aim of the present work was to investigate (i) the role of Pr<sup>3+</sup> or Ti<sup>4+</sup> dopant in the Ce<sub>1-x</sub>M<sub>x</sub>O<sub>2-δ</sub> (M = Pr<sup>3+</sup> or Ti<sup>4+</sup>) used as carrier of 5 wt% Ni, and (ii) the role of Pt used in the NiPt/Ce<sub>1-x</sub>M<sub>x</sub>O<sub>2-δ</sub> on the origin of carbon accumulation (CH<sub>4</sub> vs CO<sub>2</sub> activation), and the rates of “carbon” deposition (CH<sub>4</sub> decomposition, reverse Boudouard reaction and the combination of two) and “carbon” removal (via the participation of support's active mobile oxygen species) in DRM reaction conditions (T = 750 °C). The importance of an alternative path of CO<sub>2</sub> activation on support's surface oxygen vacant sites was also probed. These investigations concerned the use of a powerful suit of transient isothermal reaction experiments, including the use of <sup>18</sup>O<sub>2</sub> before DRM, and <sup>13</sup>CO<sub>2</sub> in the DRM, and temperature-programmed oxidation (TPO). HR-TEM and SEM studies were also employed to relate the effect of Ni and Pt on the morphological characteristics of inactive “carbon”.

## 2. Results and discussion

The CeO<sub>2</sub>-doped supports (solid solutions, PXRD) were prepared by the modified citrate sol-gel method, whereas deposition of 0.5 wt% Pt and/or 5 wt% Ni was made by the wet impregnation method. Four catalytic systems were prepared, named: (A) Ni/CeO<sub>2</sub>, (B) Ni/Ce<sub>0.8</sub>Pr<sub>0.2</sub>O<sub>2-δ</sub>, (C) NiPt/Ce<sub>0.8</sub>Pr<sub>0.2</sub>O<sub>2-δ</sub>, and (D) Ni/Ce<sub>0.8</sub>Ti<sub>0.2</sub>O<sub>2-δ</sub>. HRTEM and H<sub>2</sub>-TPDs suggested the formation of NiPt alloy. Fig. 1 reports the amount of inactive “carbon” accumulated after 12 h in DRM at 750 °C (20% CH<sub>4</sub>/20% CO<sub>2</sub>/He). It is illustrated that 5 wt%

Ni/CeO<sub>2</sub> shows significantly larger rates of “carbon” accumulation resulting in 80 mg C g<sub>cat</sub><sup>-1</sup> after 12 h on stream. The amount of deposited “carbon” drops by a factor of ~ 2 in the case of 20 atom-% Pr<sup>3+</sup> doped CeO<sub>2</sub> (41 mg C g<sub>cat</sub><sup>-1</sup>), and after the use of 0.5 wt% Pt led to the remarkable decrease of ~ 60 times (1.4 mg C g<sub>cat</sub><sup>-1</sup>). On the other hand, doping of CeO<sub>2</sub> with 20 atom-% Ti<sup>4+</sup> resulted in ~ 320 times less accumulated “carbon” (0.25 mg C g<sub>cat</sub><sup>-1</sup> or 0.021 mg C g<sub>cat</sub><sup>-1</sup> h<sup>-1</sup>), which is considered, to the best of our knowledge, as one of the lowest values ever reported, where at the same time, all other DRM performance parameters were improved towards desirable values (e.g. H<sub>2</sub>/CO ~ 1, increase of CH<sub>4</sub>-conversion and H<sub>2</sub>-yield). This extraordinary decrease in “carbon” accumulation was found to be due to: (i) the presence of a *large pool of active oxygen* in the support which participates to the gasification of “carbon” towards CO, and (ii) the presence of surface oxygen vacant sites in the support which participate in an alternative CO<sub>2</sub> dissociation route towards CO and lattice oxygen (O<sub>L</sub>).

Similar trend as that shown in Fig. 1 was obtained for longer times on stream (ca. 50 h).

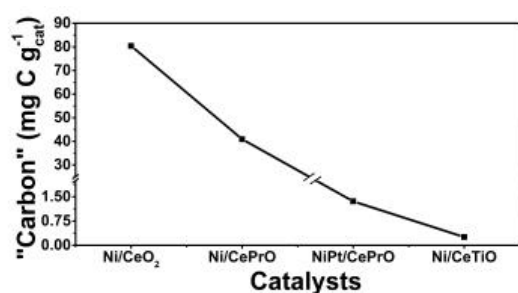


**Fig. 1.** Amount (mg C g<sub>cat</sub><sup>-1</sup>) of “carbon” formed after 12 h in DRM at 750 °C.

Fig. 2 shows the <sup>12</sup>CO<sub>2</sub> and <sup>13</sup>CO<sub>2</sub> transient response curves recorded during TPO (10% O<sub>2</sub>/He) after 30 min in DRM (5% <sup>13</sup>CO<sub>2</sub>/5%

<sup>12</sup>CH<sub>4</sub>/Ar) at 750 °C. The differences in the shape/position (kinetics of “carbon” oxidation), and the area (amount of “carbon”) of <sup>13</sup>CO<sub>2</sub> (oxidation of <sup>13</sup>C-“carbon”) and <sup>12</sup>CO<sub>2</sub> (oxidation of <sup>12</sup>C-“carbon”) traces among the catalysts are apparent. It is illustrated that “carbon” deposition via CH<sub>4</sub> decomposition is dominant on all catalytic systems but to a different extent. The introduction of Ti<sup>4+</sup> in the crystal lattice of CeO<sub>2</sub> which led to the remarkable decrease of “carbon” deposition was found to be derived almost exclusively via the CH<sub>4</sub> activation route, and only to a very minor extent via the CO disproportionation route.

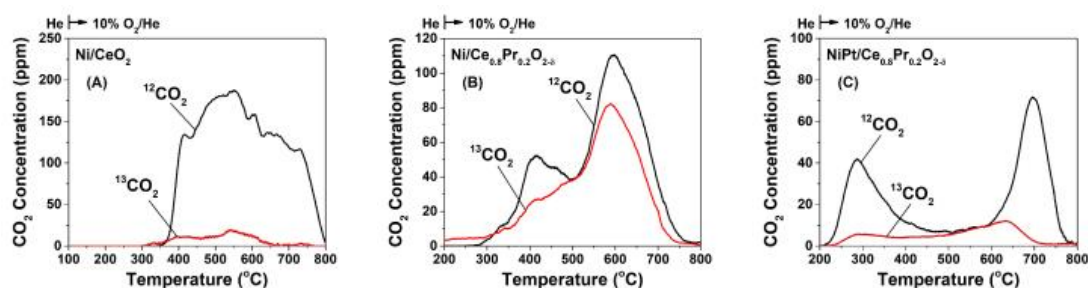


**Fig. 2.** <sup>12</sup>CO<sub>2</sub> and <sup>13</sup>CO<sub>2</sub> traces obtained during TPO of “carbon” formed after DRM (with labeled <sup>13</sup>CO<sub>2</sub>) at 750 °C over (A) Ni/CeO<sub>2</sub>, (B) Ni/CePrO, and (C) NiPt/CePrO catalysts.

## References

- [1] L. N. Bobrova, A. S. Bobin, N. V. Mezentseva, V. A. Sadykov, J. W. Thybaut, G. B. Marin, Appl. Catal. B Environ. 182 (2016) 513-524.
- [2] M. A. Vasiliades, M. M. Makri, P. Djinović, B. Erjavec, A. Pintar, A. M. Efstathiou, Appl. Catal. B Environ. 197 (2016) 168-183.

# The mono- and bimetallic Fe-Co BEA zeolite as novel active and selective catalysts for Fischer-Tropsch synthesis

*K.A. Chalupka,<sup>a,\*</sup> P. Mierczynski,<sup>a</sup> M. Lason-Rydel,<sup>b</sup> J. Rynkowski<sup>a</sup>, S. Dzwigaj<sup>c,\*</sup>*

<sup>a</sup>Lodz University of Technology, Institute of General and Ecological Chemistry, Zeromskiego 116, 90 924 Lodz (Poland), [\\*karolina.chalupka@p.lodz.pl](mailto:*karolina.chalupka@p.lodz.pl)

<sup>b</sup>Institute of Leather Industry, Laboratory of Environment, Zgierska 73, 91 – 462 Lodz, (Poland)

<sup>c</sup>Laboratoire de Réactivité de Surface, Sorbonne Université-CNRS, UMR 7197, F-75005, Paris (France), [\\*stanislaw.dzwigaj@upmc.fr](mailto:*stanislaw.dzwigaj@upmc.fr)

## Introduction

During Fischer-Tropsch synthesis (FTS) syngas is catalytically converted into wide spectrum of hydrocarbons chain [1]. Depending on the process conditions and the used catalysts, the reaction products spectrum can be shifted to alkenes and alcohols [2]. In recent years a considerable interest was focused on FT metal/zeolites catalysts because the presence of acid sites in zeolites could influence the activity and selectivity catalysts in CO hydrogenation [3]. In this work we have investigated the influence of the kind of used zeolite catalyst (monometallic CoSiBEA, FeSiBEA and bimetallic FeCoSiBEA systems) and the content of active phase (cobalt or iron) on the activity and selectivity towards liquid products in FTS.

## Experimental

Cobalt and iron zeolite catalysts were prepared by two-step postsynthesis method (Co<sub>x</sub>SiBEA and Fe<sub>x</sub>SiBEA). The bimetallic system iron-cobalt zeolite was prepared in the following way: in first step the CoSiBEA zeolite was prepared by two-step postsynthesis method and in the second step the prepared CoSiBEA zeolite was impregnated with aqueous solution of iron salt (Fe(NO<sub>3</sub>)<sub>3</sub>). The physicochemical properties of prepared catalysts were investigated by DR UV-vis, XRD, BET, H<sub>2</sub>-TPR, TPD – NH<sub>3</sub>, FTIR. The catalytic activity test of FTS was carried out in a fixed bed reactor using a gas mixture of CO and H<sub>2</sub> with a molar ratio 1:2 under pressure 30 atm and mass of catalyst 500 mg. The reagents were analyzed by gas chromatograph. Before the catalytic test the catalysts were reduced in situ in H<sub>2</sub> flow for 1 h. The catalytic tests were carried out for 24 h.

## Results and discussion

The catalytic investigation showed that the most active catalyst was Red-C-Co<sub>20</sub>SiBEA, with CO conversion of about 90 % and selectivity towards liquid products (saturated and unsaturated hydrocarbons C<sub>6</sub> – C<sub>18</sub>) of about 85 %. The carbon deposition was 10.8 - 12.4 %. Among of Red-C-Fe<sub>y</sub>SiBEA catalysts the highest activity showed Fe<sub>20</sub>SiBEA with CO conversion of 62 % and selectivity towards liquid products near 70 %. Among of liquid products the n-alkanes, isoalkanes, olefins and oxidative products (alcohols, aldehydes, ketones) were identified. The amount of carbon deposition on Fe<sub>y</sub>SiBEA was above 20.4 – 35.4 %. Among of bimetallic system the most active catalyst was Red-C-Fe<sub>10</sub>Co<sub>10</sub>SiBEA with CO conversion of 81 % and selectivity towards liquid products near 77 %. The amount of carbon deposition on this catalyst was above 15.3 - 15.6 %. It suggests that combination of iron (situated outside zeolite framework) and cobalt (placed into zeolite framework) in one bimetallic zeolite system links the advantages of cobalt and iron catalysts, while reducing their disadvantages (the selectivity towards CH<sub>4</sub> and CO<sub>2</sub> is 2 times lower for FeCoSiBEA systems than for monometallic CoSiBEA and the amount of carbon deposition on FeCoSiBEA is also much more (2.5 times) lower in comparison to monometallic FeSiBEA).

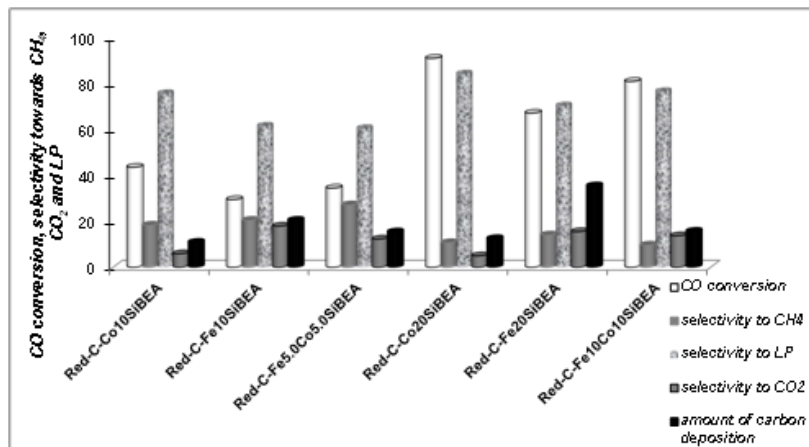


**Figure 1.** The comparison of activity of monometallic CoSiBEA and FeSiBEA catalysts and bimetallic FeCoSiBEA systems in Fischer-Tropsch synthesis.

#### ACKNOWLEDGMENTS

We acknowledge the financial support from Fund of Young Scientists of Chemical Department in Lodz University of Technology (grant of Chemical Department Dean for Young Researchers in 2014, 2015 and 2017).

#### REFERENCES

- [1] H. Ming, B.G. Baker, Appl. Catal. A 123 (1995) 23 – 36.
- [2] M. E. Dry, J. Chem. Technol. Biotechnol. 77 (2002) 43 – 50.
- [3] L. Gucci, I. Kiricsi, Appl. Catal. A 186 (1999) 375.

## Characterization of NiMoO<sub>4</sub>/Al<sub>2</sub>O<sub>3</sub> catalyst tailored for lignin depolymerization

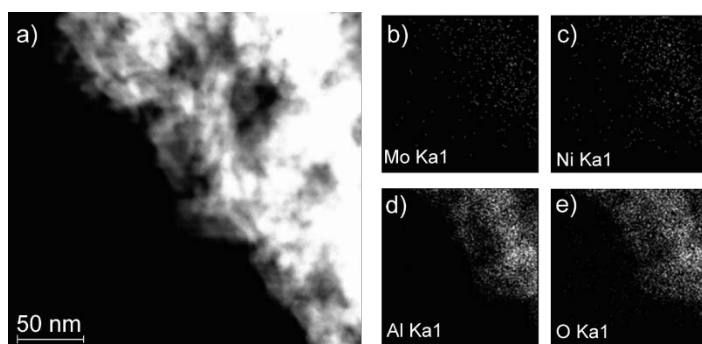
*Sara Blomberg, Chemical Engineering, Lund University, Sweden; Maria E. Messing, Solid state Physics, Lund University, Sweden; Niclas Johansson, MAX IV, Lund University, Sweden; Esko Kokkonen, MAX IV, Lund University, Sweden; Linnéa Kollberg, SunCarbon, Malmö, Sweden; Christian Hulteberg, Chemical Engineering, Lund University, Sweden;*

The depletion of fossil fuels as well as the increasing global warming confirms the importance of finding alternative fuels in the near future. An increased number of possible candidates for renewable resources has already been proposed over the last decades.

Conventional pulp and paper industries generate a large amount of lignin as a byproduct that is mainly used as low-quality fuel. Lignin is the second most abundant natural polymer, and because of that, it is suggested to have great potential to being used as a value-added chemical feedstock [1]. It is also the only natural source of aromatics.

Ni promoted MoS<sub>2</sub> catalysts are well-established hydrotreating catalysts in the conventional oil purification, but these bimetallic catalysts have also shown to be active in the depolymerization of lignin. To activate the hydrotreating NiMo catalysts, the NiMo oxide is reduced and replaced by an active sulfidic phase. The oxidic phase of the NiMo is therefore crucial for the sulfidation process and by that also the activity of the catalyst. The main difference between the two oxidic phases of the NiMoO<sub>4</sub> is the octahedral Mo<sup>6+</sup> species that are formed in the  $\alpha$ -phase while a tetrahedral Mo<sup>4+</sup> species is formed in the  $\beta$ -phase.

Herein we present the characterization of the tailored NiMo/Al<sub>2</sub>O<sub>3</sub> catalyst that successfully been used for the depolymerization process of lignin in the production of biofuel. The STEM HAADF image and the STEM XEDS Ni and Mo maps show an evenly dispersed Ni and Mo over the Al<sub>2</sub>O<sub>3</sub> substrate, ideal for optimizing the number



of active sites of the catalyst (Fig. 1a-e).

*Figure 1. The STEM HAADF image a) and the STEM XEDS Mo b) and Ni c)*



maps indicating a well-dispersed Ni and Mo over the  $\text{Al}_2\text{O}_3$  substrate d-e).

To achieve information about the Mo and Ni composition and structure, a combination of surface- as well as bulk sensitive techniques were used. The Temperature-Programmed Reduction performed on the  $\text{NiMo}/\text{Al}_2\text{O}_3$  showed a sharp reduction peak at 450 °C which is attributed to the partial reduction of the octahedral  $\text{Mo}^{6+}$ , indicating an  $\alpha$ -phase formation of the  $\text{NiMoO}_4$ [2] (Fig. 2a). The reduction of the  $\text{Mo}^{6+}$  in  $\text{MoO}_3/\text{Al}_2\text{O}_3$  was observed at approximately 100 °C higher temperature, suggesting that Ni is promoting the reducibility of the Mo. The formation of the  $\alpha$ - $\text{NiMoO}_4$  is also in good agreement with the X-ray Photoelectron Spectroscopy measurements, where a highly shifted Mo 3d peak is observed. The Mo 3d<sub>5/2</sub> peak was deconvoluted with two components where the main component at 233.5 eV is assigned to the  $\text{Mo}^{6+}$  in the  $\alpha$ - $\text{NiMoO}_4$ (Fig. 2 c)[3].

The identification of the oxide phase that is formed on the  $\text{NiMo}/\text{Al}_2\text{O}_3$  is important for optimization of the activation process of the catalyst.

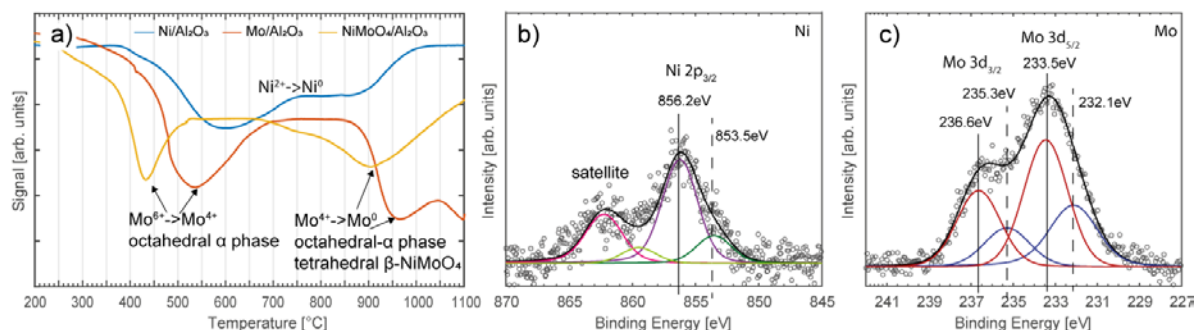


Figure 2 a)  $\text{H}_2$ -TPR of  $\text{NiO}/\text{Al}_2\text{O}_3$ ,  $\text{MoO}_3/\text{Al}_2\text{O}_3$  and  $\text{NiMoO}_4/\text{Al}_2\text{O}_3$  b) Ni 2p<sub>3/2</sub> and c) Mo 3d XPS spectra of  $\text{NiMoO}_4/\text{Al}_2\text{O}_3$  catalyst. Both the TPR and XPS results indicate of well-mixed Ni and Mo, forming  $\alpha$ - $\text{NiMoO}_4$  structure.

## References

1. Abdelaziz, O.Y., et al., *Biological valorization of low molecular weight lignin*. Biotechnology Advances, 2016. **34**(8): p. 1318-1346.
2. Qu, L.L., et al., *MAS NMR, TPR, and TEM studies of the interaction of NiMo with alumina and silica-alumina supports*. Journal of Catalysis, 2003. **215**(1): p. 7-13.
3. Ojagh, H., et al., *Effect of Thermal Treatment on Hydrogen Uptake and Characteristics of Ni-, Co-, and Mo-Containing Catalysts*. Industrial & Engineering Chemistry Research, 2015. **54**(46): p. 11511-11524.

# Possibility of processing plastic waste in the production of diesel fuel

*Aleš Vráblík, Nikola Bringlerová, Martin Pšenička Jose Hidalgo, Radek Černý  
Unipetrol Centre for Research and Education, a.s. (UNICRE), Litvínov, Czech  
Republic*

## Abstract

Fuel producers are forced to use a larger and larger amount of non-fossil sources because of bioenergy sustainability policy developed by the Council of European Union via directive 2009/28/EC. Nowadays biofuels of the first generation are the most used, typically fatty acids methyl esters in diesel production. However this way is not so perspective because of a reduction of indirect land use change (ILUC) for biofuels, possibly starting from 1. 1. 2021. In this context, one of the possibilities is to utilize the process of pyrolysis of waste plastics to produce a pyrolysis oil as an alternative non-fossil fuel. We tested a fraction of middle distillates, derived from pyrolysis of (I) sorted and (II) unsorted plastic waste. Two parallel tests were performed on a HDS pilot testing units in down-flow mode. The standard test conditions and a commercial catalyst (CoMo/Al<sub>2</sub>O<sub>3</sub>) were used in co-process with standard feedstock. The influence of addition of 5 wt% (I) and (II) on hydrotreating conditions was monitored, especially the differences in catalyst activity and changes in exotherm. The resulting qualitative parameters of the individual products were assessed and compared to each other. Significant differences in the co-processing of sorted and unsorted waste material is described.

## Acknowledgement

The publication is a result of a project which was carried out under the financial support of the Ministry of Industry and Trade of the Czech Republic with institutional support for the long-term conceptual development of a research organization. The project has been integrated into the National Sustainability Programme I of the Ministry of Education, Youth and Sports of the Czech Republic through the Development of the UniCRE Centre project, Project Code LO1606. The result was achieved using the infrastructure of the project Efficient Use of Energy Resources Using Catalytic Processes (LM2015039) which has been financially supported by MEYS within the targeted support of large infrastructures.

# CO clean-up of hydrogen–rich reformat by selective CO methanation for PEM FC application

M.V. Konishcheva<sup>1,2,3\*</sup>, D.I. Potemkin<sup>1,2,3</sup>, P.V. Snytnikov<sup>1,2,3</sup>, V.A. Sobyenin<sup>1</sup>

<sup>1</sup>*Boriskov Institute of Catalysis SB RAS, Novosibirsk, Russia*

<sup>2</sup>*Novosibirsk State University, Novosibirsk, Russia*

<sup>3</sup>*EFCOM LLC, Moscow, Russia*

\* *Corresponding author: [konischeva@catalysis.ru](mailto:konischeva@catalysis.ru)*

*The present report summarizes the results obtained during a systematic study of catalysts, their performances, fundamental principles of the selective CO methanation reaction and reactor concept design. The most attention is concentrated on chlorinated Ni/CeO<sub>2</sub> catalysts and the ability to transfer the properties of efficient powder catalysts to structured modules.*

Selective CO methanation is one of the promising methods for CO removal from hydrogen–rich gas mixtures (reformat). Recently we have shown [1-2] that powdered Ni/CeO<sub>2</sub> catalyst with chlorine addition showed the good performance and was the most selective. This phenomenon could be explained by ceria surface blocking by chlorine species and appropriate inhibition of CO<sub>2</sub> hydrogenation activity. The methanation reactions of carbon oxides are highly exothermic. Therefore, the design of the catalytic CO clean-up unit should provide sufficient heat removal from the reaction zone for preventing formation of hot spots and ensuring precise and reliable temperature control.

The use of a FeCrAl wire mesh with a  $\eta$ -Al<sub>2</sub>O<sub>3</sub> protective coating as a support of Cl-containing Ni/CeO<sub>2</sub> enabled production of a catalyst with the ability of high rates of heat removal, that is similar in performance to the most efficient powder catalysts. [3]. The catalysts were prepared by incipient wetness impregnation of the CeO<sub>2</sub> powder and  $\eta$ -Al<sub>2</sub>O<sub>3</sub>-FeCrAl wire mesh with an aqueous solution of ammonium chloride and aqueous solutions of Ce(NO<sub>2</sub>)<sub>3</sub> and a mixture of nickel salts (Ni(NO<sub>3</sub>)<sub>2</sub>:NiCl<sub>2</sub> = 4), respectively. The Ni loading in all samples was set to 10 wt.% with regard to CeO<sub>2</sub>. The CeO<sub>2</sub> loading was 10 wt.% with regards to  $\eta$ -Al<sub>2</sub>O<sub>3</sub>/FeCrAl weight. For simplicity, the Ni(Cl)/CeO<sub>2</sub>/ $\eta$ -Al<sub>2</sub>O<sub>3</sub>/FeCrAl wire mesh catalyst labeled as Ni/Ce/FCA.

The catalysts were characterized by BET, XRD, XPS, HAADF-STEM, EDX-mapping, SEM, TPR, TPD techniques, FTIR in situ and CO chemisorption techniques.

For correct comparison of the powdered and structured catalysts, all experiments were performed under similar conditions as described in [1-3]. The experiments were carried out in a U-shaped reactor at 1 atm in temperature interval 180 – 330 °C.

Fig. 1a illustrates the temperature dependencies of the outlet CO concentration and the CO selectivity of the CO selective methanation over powdered Ni/CeO<sub>2</sub>(Cl<sup>\*</sup>) and structured Ni/Ce/FCA catalysts. It is seen that the catalytic activity and selectivity of both nickel catalysts is similar. The Ni/Ce/FCA catalyst can reduce carbon monoxide concentration at temperature range from 230 to 290 °C to below 10 ppm with a selectivity as high as 70%. According to the TEM and SEM data (Fig. 1b,c) the surface structure of the structured Ni/Ce/FCA catalyst is like that of the powdered chlorinated nickel ceria catalysts [2,3].

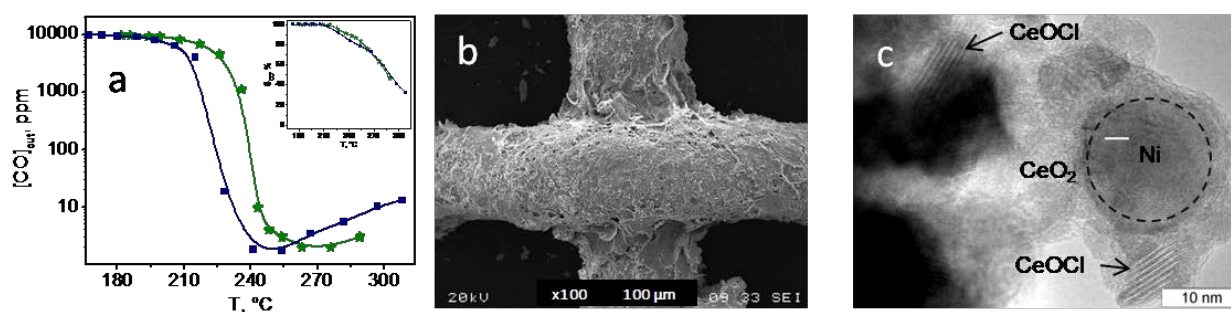


Fig. 1. The temperature dependence of the CO outlet concentration and CO selectivity (a) for the selective CO methanation over the (■) Ni/Ce/FCA and (★) Ni/CeO<sub>2</sub>(Cl<sup>\*</sup>) catalysts. Feed gas composition (vol%): 1.0 CO, 65 H<sub>2</sub>, 10 H<sub>2</sub>O, 20 CO<sub>2</sub> with He as balance gas; WHSV: 29 L g<sup>-1</sup> h<sup>-1</sup>. SEM (b) and TEM image (c) of the used Ni/Ce/FCA catalyst.

The microchannel wire mesh catalytic module based on Ni/Ce/FCA catalyst could be recommended for 1–100 W<sub>e</sub> PEM FC systems. According to our estimations, the structured Ni/Ce/FCA catalyst with the following parameters: volume 0.6 L, weight 480 g, and weight of catalytic coating 48 g, is capable to provide CO clean-up of reformate gas for feeding a 1 kW<sub>e</sub> PEM FC system.

In the part of preparation and catalytic properties study the work was conducted within the framework of budget project #AAAA-A17-117041710088-0 for Boreskov Institute of Catalysis. In the part of catalyst characterization the work was supported by RFBR project 18-33-00702 (M.V. Konishcheva).

## References

- [1] M.V. Konishcheva, D.I. Potemkin, P.V. Snytnikov, M.M. Zyryanova, V.P. Pakharukova, P.A. Simonov, V.A. Sobyenin, *Int. J. Hydrogen Energy*, 40 (2015), p. 14058.
- [2] M.V. Konishcheva, D.I. Potemkin, P.V. Snytnikov, O.A. Stonkus, V.D. Belyaev, V.A. Sobyenin, *Appl. Catal. B.*, 221 (2018), p. 413.
- [3] M. V. Konishcheva, P. V. Snytnikov, V. N. Rogozhnikov, A. N. Salanov, D. I. Potemkin, V. A. Sobyenin, *Cat. Com.*, 118 (2019). p. 25.

# CO and CO<sub>2</sub> hydrogenation over highly dispersed Ru-, Rh- and Pt/Ce<sub>0.75</sub>Zr<sub>0.25</sub>O<sub>2</sub> catalysts

M.V. Konishcheva<sup>1,2\*</sup>, D.I. Potemkin<sup>1,2</sup>, N.O. Akhmetov<sup>1,2</sup>, S.D. Pushkina<sup>1,2</sup>,

P.A. Simonov<sup>1,2</sup>, P.V. Snytnikov<sup>1,2</sup>, V.A. Sobyenin<sup>1</sup>

<sup>1</sup>*Boreskov Institute of Catalysis SB RAS, Novosibirsk, 630090, Russia*

<sup>2</sup>*Novosibirsk State University, Novosibirsk, 630090, Russia*

\*Corresponding author: [konischeva@catalysis.ru](mailto:konischeva@catalysis.ru)

This work is aimed at solving an actual problem related to the utilization of CO<sub>2</sub> and the involvement of CO<sub>2</sub> in chemical conversions for the synthesis of valuable chemical compounds, such as methane and light hydrocarbons [1]. The increase of CO<sub>2</sub> concentration in the atmosphere is considered as the main cause of the greenhouse effect on the planet leading to subsequent climate changes. At the same time, carbon dioxide (CO<sub>2</sub>) is a promising raw material for the chemical industry and energy. Thus, the hydrogenation reaction can solve both the environmental problem (the reduction of CO<sub>2</sub> emissions and its recycling) and the energy problem (the storage of hydrogen in methane and light hydrocarbons). Considering that CO<sub>2</sub> is thermodynamically stable molecule, it is necessary to develop and study catalysts for hydrogenation of carbon dioxide.

Thermally stable commercial Ce<sub>0.75</sub>Zr<sub>0.25</sub>O<sub>2</sub> (Ecoalliance. Ltd, Novouralsk, Russia) was selected as the support carrier. For simplicity, the Ce<sub>0.75</sub>Zr<sub>0.25</sub>O<sub>2</sub> support labeled as CZ. Catalysts were prepared by sorption-hydrolytic deposition as described in [2]. Catalysts contained Pt, Ru and Rh deposited on CZ particles in the amount of 0.1 mmol/g (1 wt.% Ru and Rh, 1.9 wt.% Pt) are further denoted as Ru/CZ, Rh/CZ and Pt/CZ, respectively. This preparation procedure allowed to obtain catalysts with high dispersion of metal particles.

The catalysts were characterized by BET, XRD, XPS, TEM, EDX-mapping and CO chemisorption techniques. According to CO chemisorption data, the average size of metal particles in the as-prepared Rh/CZ, Ru/CZ and Pt/CZ catalysts was 1.1, 1.2 and 1.8 nm, respectively.

Since the formation of CO is possible during the CO<sub>2</sub> hydrogenation, we also studied the regularities of the reaction of CO and CO<sub>2</sub>. The experiments were carried out in a U-shaped reactor at 1 atm in temperature interval 150 – 390 °C, at WHSV = 30 L·g<sup>-1</sup>·h<sup>-1</sup>.

$^1 \cdot h^{-1}$  and feed gas composition (vol.%): 1.0 CO, 65 H<sub>2</sub> and He-balance; 1.0 CO<sub>2</sub>, 65 H<sub>2</sub> and He-balance.

The Fig.1 shows the temperature dependence of the conversion of CO and CO<sub>2</sub> and TOF during the reaction of hydrogenation of carbon oxides. It is seen that the activity of the catalysts in the hydrogenation reaction of CO and CO<sub>2</sub> decreases in the series Ru/CZ > Rh/CZ > Pt/CZ. Hydrogenation of carbon oxides on the Ru/CZ catalyst begins at 160°C, the main product of the reaction is methane. The complete methanation of CO and CO<sub>2</sub> on the Ru/CZ catalyst occurs at a temperature of 250 °C and 240°C, respectively. The full methanation of carbon oxides on the Rh/CZ catalyst occurs at 260°C. The complete hydrogenation of CO on the Pt/CZ catalyst occurs at 370°C, with the formation of C<sub>2+</sub> hydrocarbons (0.22 vol.% at 280°C). Hydrogenation of CO<sub>2</sub> occurs at a higher temperature. When hydrogenating CO<sub>2</sub>, CO is formed (0.5 vol.% at 310°C), which is then hydrogenated to methane.

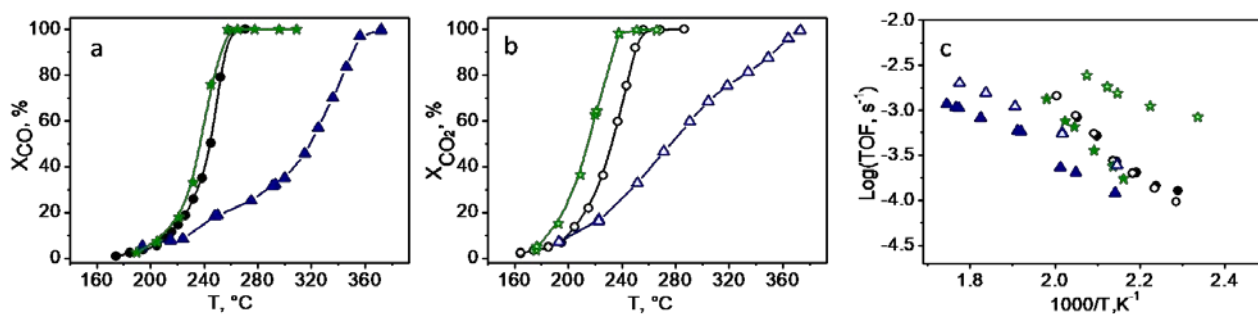


Figure 1. The temperature dependencies of the CO (a) and CO<sub>2</sub> (b) conversion and Arrhenius plots of turnover frequencies of metal surface atoms (TOF) (c) for the CO (filled symbols) and CO<sub>2</sub> (open symbols) methanation over Ru/CZ (★), Rh/CZ (●) and Pt/CZ (▲) catalysts. Feed gas composition (vol. %): 1.0 CO, 65 H<sub>2</sub> and He-balance; 1.0 CO<sub>2</sub>, 65 H<sub>2</sub> and He-balance. WHSV: 30 L·g<sup>-1</sup>·h<sup>-1</sup>.

Thus, Ru/CZ and Rh/CZ catalysts were the most active in the methanation reaction of CO<sub>2</sub>. However, further studies are needed to study the possibility of obtaining light hydrocarbons (C<sub>2+</sub>).

The work was supported by RFBR project 18-33-00702.

## References

- [1]. C.Song. Global challenges and strategies for control, conversion and utilization of CO<sub>2</sub> for sustainable development involving energy, catalysis, adsorption and chemical processing // *Catalysis today*-2006- 115 - P. 2-32.
- [2]. T.B. Shoykhorova, P.A. Simonov, D.I. Potemkin, P.V. Snytnikov, V.D. Belyaev, A.V. Ishchenko, D.A. Svintsitskiy, V.A. Sobyenin. Highly Dispersed Rh-, Pt-, Ru/Ce<sub>0.75</sub>Zr<sub>0.25</sub>O<sub>2</sub>- $\delta$  Catalysts Prepared by Sorption-Hydrolytic Deposition for Diesel Fuel Reforming to Syngas // *Applied Catalysis B: Environmental*. -2018- 237- P. 237-244.

# **Noble Synthetic Process of Alloy Nano Particles for Catalytic Application**

Heeyeon Kim, KIER, Daejeon, Korea(ROK); Guk-hyun Kwon, KIER, Daejeon, Korea(ROK) and Yonsei University, Wonju, Korea(ROK), Jang-won O, KIER, Daejeon, Korea(ROK) and Korea University, Seoul, Korea(ROK)

More than 85% of chemical processes are catalytic processes, where more than 85% of them use heterogeneous catalysts. In those chemical processes, the synthesis of the highest performance catalysts with lowest cost is still a major concern for catalyst researchers. Particularly, in a fuel cell (fuel cell) system or a hydrogen production process (hydrogen evolution reaction, HER), noble metals such as Pt, Pd, Rh, and Au exhibit excellent activity. In this study, we propose a process to synthesize alloy nanocatalyst of uniform size for the purpose of improving the activity of noble metal alloy catalyst with reduced manufacturing cost.

The wet impregnation method, which is most commonly used for catalyst production, is advantageous for synthesizing a large amount of catalyst at a low cost, but there is a limit in synthesizing a highly dispersed uniform nanocatalyst. In this study, the synthesis of alloy catalysts was controlled at atomic level by using chemical vapor deposition (CVD) method. As a result, a Pt-Co nano-alloy catalyst having a perfect Pt<sub>3</sub>Co structure was synthesized at a temperature of about 500 ° C., which is about 200 to 300°C lower than that of the conventional catalyst. In addition, NiP nanocatalysts, which are active in HER reaction, were synthesized by utilizing the ingredients contained in the natural plant materials themselves. Each of the catalysts was subjected to fuel cell electrode performance test and HER performance test, and the structure of the catalyst was analyzed by using TEM, STEM, EELS, XPS, XRD and the like.

## **References**

- [1] D. S. Choi et al., *Advanced Materials* (2018) 30, 1805023.
- [2] D. S. Choi et al., *Advanced Materials* (2016) 28, 7115.

# Design of a hybrid Ru and Ni based fixed bed Sabatier reactor

*Emanuele Moiola<sup>1,2</sup>, Noris Gallandat<sup>1,2</sup>, Andreas Züttel<sup>1,2</sup>*

<sup>1</sup> *Institute of Chemical Sciences and Engineering (ISIC), Basic Science Faculty (SB), École polytechnique fédérale de Lausanne (EPFL) Valais/Wallis, CH-1950 Sion, Switzerland*

<sup>2</sup> *Empa Materials Science & Technology, CH-8600 Dübendorf, Switzerland*

## Introduction

The Sabatier reaction is a promising solution for the storage of renewable energy into methane, a widely used energy carrier. Furthermore, the use of CO<sub>2</sub> coming from atmosphere or industrial emissions can ideally close the carbon balance of the energetic applications, allowing a more sustainable use of the energetic resources [1]. The application of the Sabatier reaction for production of energy carriers is affected by special requirements and constraints, related to the specifications required for the use of the products of the reaction. In particular, the content of hydrogen should be below a certain threshold (usually <2% mol/mol) and the heating value of the produced gas should be high enough to avoid problems in the burners used for combustion [2]. For this reason, the Sabatier reactor must be designed in high detail and the equipment must guarantee a high conversion value (above 99.5 %).

## Computational details

For the study the catalytic systems considered are Ru/Al<sub>2</sub>O<sub>3</sub> and Ni/MgAl<sub>2</sub>O<sub>4</sub> respectively. Kinetic models for the Sabatier reaction over these two catalysts are available in literature [3,4]. The reactor is simulated with a 1D heterogenous PFR model.

## Results

According to our calculations, the Sabatier reactor can be divided into three zones with different heat requirements: a first zone, where the reaction must be started by reaching the minimal temperature, a second zone, where the reaction rate is high and cooling is determinant to remove the reaction heat, and a third zone, where the heat removal and reaction rate must be adapted to reach high conversion [5]. The difference between the two catalysts changes according to the specific zone of the reactor (figure 1). In the first area the main difference is the diverse reaction activation temperature: the reaction over Ru activates at ca. 100 °C less than Ni. This



is in line with what experimentally observed [6]. However, the lower reaction rate on Ni allows an easier control of the reaction and the reach of the thermodynamic equilibrium at lower temperature and thus higher conversion value. In the second area, the trajectories in the space state coincide, because they follow the thermodynamic line and the reaction rate is controlled by cooling. This area corresponds to ca. 30 % of the residence time based on the Ru line. In the third area, the reaction rate on Ni is too low, so that the required conversion cannot be reached. In order to overcome this limitation, a more complex reactor (e.g. with intermediate condensation) must be employed. If a single reactor is used, only Ru can be employed to reach high conversion. In our presentation, we will outpoint the development of a reactor using a first Ni bed followed by a Ru section, which reaches the required conversion by limiting the catalyst cost.

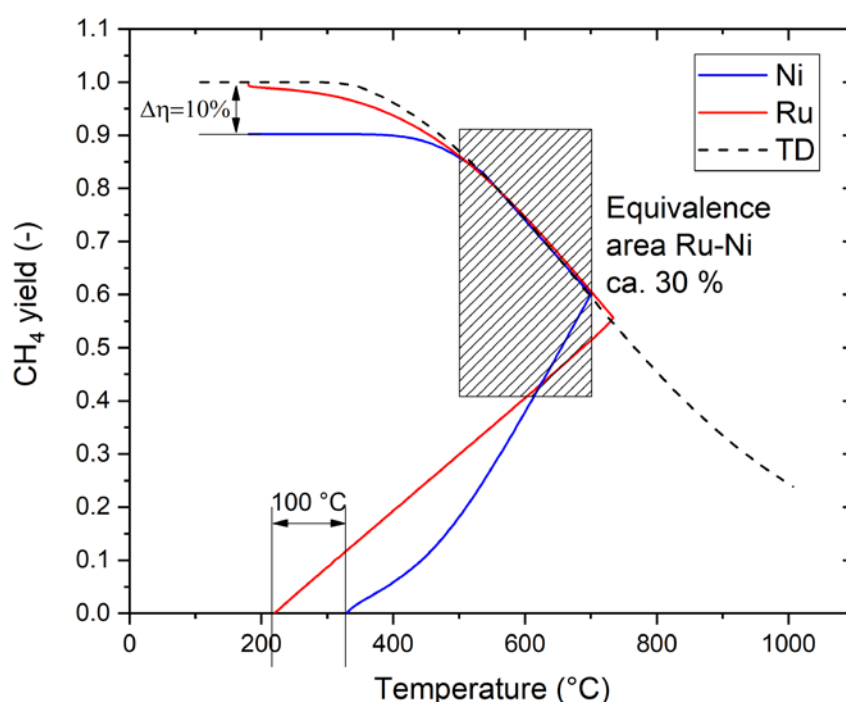


Figure 1 Comparison of the trajectory in state space for a Sabatier reactor working with a Ni or Ru catalyst

## References

- [1] A. Züttel et al., *Chim. Int. J. Chem.* 69 (2015) 264–268.
- [2] Schweizerischer Verein des Gas- und Wasserfaches SVGW/SSIGE, *Réglementation G18: Directive pour la qualité du gaz*, (2013). <http://www.svgw.ch/regelwerk>.
- [3] J.G. Xu, G.F. Froment, *Aiche J.* 35 (1989) 88–96.
- [4] L. Falbo et al., *Appl. Catal. B Environ.* 225 (2018) 354–363.
- [5] E. Moioli et al., *React. Chem. Eng.* 4 (2019) 100–111.
- [6] R. Mutschler et al., *J. Catal.* 366 (2018) 139–149.

# Mesoporous catalytic systems for contaminants removal from diesel fractions

**Golubev O.V.<sup>1</sup>, Naranov E.R.<sup>2</sup>, Maximov A.L.<sup>1,2</sup>, Karakhanov E.A.<sup>1</sup>**

<sup>1</sup> Chemistry Department of Lomonosov Moscow State University, Moscow, Russia,

<sup>2</sup> A.V.Topchiev Institute of Petrochemical Synthesis, RAS (TIPS RAS), Moscow, Russia

The prevention of catalyst poisoning in such processes of oil refining as hydrotreating, catalytic reforming etc. is a task of much interest. Catalysts are poisoned by very small amount of contaminants that can be found in crudes and distillates. For example, metals like Ni, V, Na, and Fe are well-known catalytic poisons and they are removed successfully. However, there are some non-obvious elements that also poison the catalyst. One of them is arsenic which cause serious damage to the hydrotreating catalysts. Arsenic is a true catalyst poison as it chemically reacts with active catalytic sites (nickel and cobalt sulfide) transforming them into NiAs or CoAs [1]. Thus it becomes obvious that special guard catalysts or even guard reactors are needed in order to treat poisonous arsenic. Current arsenic removal sorbents are comprised of Ni–Mo supported on Al<sub>2</sub>O<sub>3</sub> [2]. However, arsenic can remain in the guard reactor effluent either through incomplete sequestering of the arsenic in the guard reactor or by leaching of arsenic from the sorbent material.

In our work we have synthesized a number of guard layer catalysts that can remove arsenic from diesel fractions. We used mesoporous materials (SBA-15, Al-TUD and MCF) as a support for the catalyst to improve its sorption capacity and to reduce the diffusional limitations for bulky molecules. Arsenic removal process was carried out in a flow unit with fixed bed reactor. To simulate contaminated fuel, we added triphenylarsine into diesel fraction (5 ppmw As). It was shown that synthesized catalysts supported on mesoporous materials decrease arsenic content to level of 0.04 ppmw and can be applied in industrial hydrotreating units as a guard layer catalysts.

## References

[1] ART Catalagram®, 2010, 108, 9-13

[2] O.K. Bhan, US Patent 6759364, 2004.

# Microstructured reactor with Pt/La/HAP films for the WGS reaction: Design, activity and kinetic studies

*Zouhair Boukha, Juan R. González-Velasco, Miguel A. Gutiérrez-Ortiz*

Chemical Technologies for Environmental Sustainability Group, Department of Chemical Engineering, Faculty of Science and Technology, University of the Basque Country UPV/EHU, P.O. Box 644, E-48080 Bilbao, Spain

[zouhair.boukha@ehu.es](mailto:zouhair.boukha@ehu.es)

## Introduction

The design of new kinds of reactors for catalytic applications has attracted much attention in the last decade. Due to their high surface areas, the micro-structured reactors offer high heat/mass transfer coefficients and short contact time which results in a better control of the reaction conditions. These characteristics are essential for a precise control of the temperature and products distribution. Moreover, the metallic microreactors have supplementary advantages such as high thermal conductivity, high mechanical resistance and the possibility to adopt different geometry and configurations. The present work is concerned with the preparation, characterisation and activity of Pt/La/HAP films deposited onto stainless steel microgrids in the WGS reaction (in the presence of H<sub>2</sub> and CO<sub>2</sub>). Their characterisation involves BET, SEM, XRD, H<sub>2</sub>-TPR, CO-TPD, CO<sub>2</sub>-TPD, H<sub>2</sub>-TPD, UV-visible and XPS techniques.

## Experimental

In the present work the deposition of a hydroxyapatite film over stainless steel microgrids was carried out by using a modified version of the methods mentioned in the literature [1,2]. SEM microscopy and adhesion tests show that homogeneous and well adhered Pt/La/HAP films were deposited onto the used stainless steel microgrids (Fig. 1). Table 1 reports characterization and activity data corresponding to the investigated materials. A study on the promoting effect of lanthanum on the behaviour of the Pt/HAP system shows an eminent enhancement of its catalytic performance in the WGS reaction with the addition of La (Table 1). This improved performance is linked to suitable textural, structural and chemical properties, provided by La, which make the Pt active sites highly sintering-resistant. In accordance with a preliminary study, when deposited on the MG microreactor, the

Pt(1)/La(1)/HAP film demonstrated high stability and successfully withstand the shut-down/start-up conditions after three cycles operation (Fig. 2). Moreover, the investigated microreactor appears to be suitable for the determination of the kinetic parameters of the WGS reaction. The observed reaction rates fitted to an empirical power-law rate expression. According to the latter, the WGS reaction is 0.4, 1.0, -0.3, and -0.7 order with respect to CO, H<sub>2</sub>O, CO<sub>2</sub>, and H<sub>2</sub>, respectively.

Table 1. Characterization and activity data for the Pt/La(x)/HAP catalysts

Samples	Pt, wt. %	La, wt. %	S <sub>BET</sub> , m <sup>2</sup> g <sup>-1</sup>	V <sub>p</sub> , cm <sup>3</sup> g <sup>-1</sup>	d <sub>p</sub> , nm	X <sub>CO</sub> at 300 °C <sup>(a)</sup>
HAP	0	0	53	0.39	27	-
Pt(1)/HAP	0.85	0	49	0.37	27	17
Pt(1)/La(1)/HAP	0.84	1	53	0.38	28	35
Pt(1)/La(4)/HAP	0.87	3.5	51	0.37	25	37
Pt(1)/La(8)/HAP	0.85	6.7	53	0.35	24	25

<sup>(a)</sup> CO conversion in the WGS reaction (11.7%CO/28%H<sub>2</sub>O/44%H<sub>2</sub>/4.7%CO<sub>2</sub>, 4280 h<sup>-1</sup>)

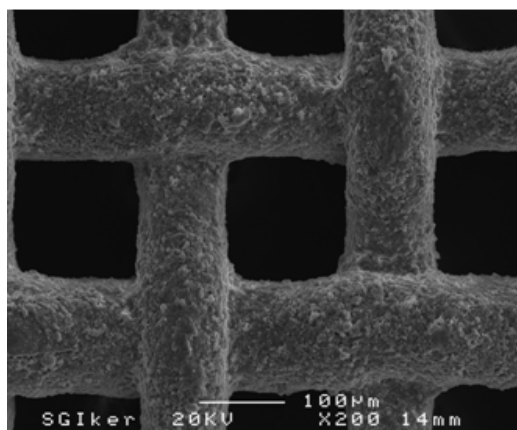


Fig. 1. SEM micrograph for Pt(1)/La(1)/HAP film deposited onto SS316 micro-grids

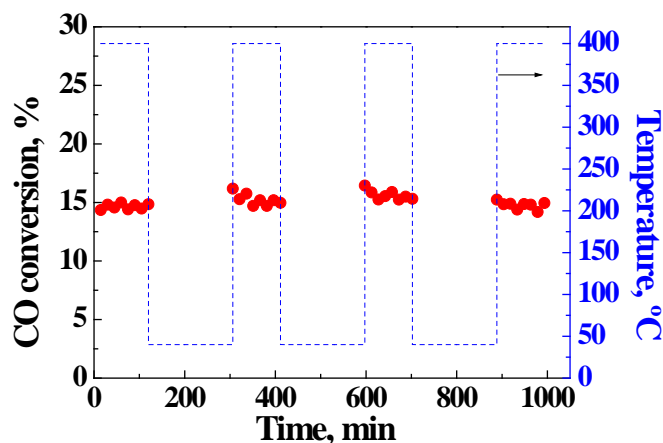


Fig. 2. Cyclic shut-down/start-up study over Pt(1)/La(1)/HAP-MG. (4%CO/23%H<sub>2</sub>O/8%CO<sub>2</sub>/38%H<sub>2</sub>/23%He) (GHSV = 3120 h<sup>-1</sup>, WHSV = 139000 ml g<sup>-1</sup> h<sup>-1</sup>).

## References

- [1] Z. Boukha, J.L. Ayastuy, A. Iglesias-González, B. Pereda-Ayo, M.A. Gutiérrez-Ortiz, J.R. González-Velasco, *Int. J. Hydrogen Energ.* 40 (2015) 7318-7328.
- [2] Z. Boukha, J.L. Ayastuy, A. Iglesias-González, B. Pereda-Ayo, M.A. Gutiérrez-Ortiz, J.R. González-Velasco, *Appl. Catal. B-Environ.* 160-161 (2014) 629-640.

## Acknowledgements

The financial support for this work provided by Ministerio de Economía y Competitividad (CTQ2015-73219-JIN (AEI/FEDER/UE), ENE2013-41187-R and ENE2016-74850-R) and Gobierno Vasco (GIC IT-657-13) is gratefully acknowledged.

# Effect of metal loading on activity in the dry reforming of methane over Ni-pyrochlore-perovskite catalysts

*Adriana P. Ramon<sup>1</sup>, Elisabete M. Assaf<sup>2</sup>, José M. Assaf<sup>1</sup>*

*1Federal University of São Carlos, Department of Chemical Engineering, São Carlos-SP, Brazil*

*2University of São Paulo, Institute of Chemistry of São Carlos, São Carlos-SP, Brazil*

*\*+55 16 3351 8266, mansur@ufscar.br*

## Introduction

Currently, due to the growing environmental concern over greenhouse gases, the dry reforming of methane (DRM) has attracted increasing attention in syngas production ( $\text{CO} + \text{H}_2$ ). The main problems in DRM are the large formation of carbon deposition over the catalyst and the metal sintering [1]. In an attempt to overcome these problems, different supports consisting of mixed oxides with stable structure such as pyrochlore ( $\text{A}_2\text{B}_2\text{O}_7$ ) and perovskite ( $\text{ABO}_3$ ) types have been developed [2,3]. The pyrochlore structure presents interesting properties such as the possibility of substitution of transition metals at the B site and the oxygen mobility due to the vacancies created during the synthesis [2] and the perovskite structure produces catalysts with very small and highly dispersed metal particles [3]. All these properties lead to a material with greater stability and resistance to the carbon formation [2,3].

In the present work the catalyst  $\text{La}_2\text{Ce}_{2-x}\text{Ni}_x\text{O}_{7-\lambda}$  was synthesized by sol-gel method [1] with 0, 1, 3 and 5 wt% of Ni, represented here by LCN<sub>x</sub>, where x is the amount of Ni. The samples were characterized by X-Ray diffraction (XRD), temperature-programmed reduction (TPR) and thermogravimetric analysis. The catalytic activity was tested at 850°C during 7 hours. The samples were reduced in situ at 750°C for 1 hour under  $\text{H}_2$  flow of 30 mL/min at a heating rate of 10°C/min. The catalytic tests were performed with 100 mg of catalyst, with continuously feeding of  $\text{CH}_4$  and  $\text{CO}_2$  at a flow rate of 15 mL/min for each gas.

## Results and Discussion

The XRD spectra of all freshly calcined samples showed typical diffraction peaks of the  $\text{La}_2\text{Ce}_2\text{O}_7$  structure (ICSD 188491). However, besides this phase, the addition of Ni led to the partial segregation of this metal with La in the  $\text{LaNiO}_3$  perovskite phase (ICSD 173477). Furthermore, two main reduction peaks with the profile characteristic of perovskite reduction were observed through the TPR analysis in all Ni-containing catalysts. Nevertheless, if the perovskite was the only phase in the samples with the possibility of reduction, the ratio between the intensities of the

second and the first peaks should be 2 [4]. However, this behavior is not observed, suggesting the presence of other reducing species along with the first stage of perovskite reduction. The extra consumption of H<sub>2</sub> could be related to the reduction of Ni in the pyrochlore structure or the reduction of well dispersed NiO, not detected by XRD, due to the resolution range of this equipment.

Figure 1 shows the conversion of the reactants as a function of time. The support LCN0 did not show any catalytic activity. The increase in the Ni load led to an increase in the conversion of the reactants as expected, and the LCN5 catalyst had the higher conversion as well as stoichiometric conversion, which was not observed in the LCN1 and LCN3. This suggests that the surface composition of these two catalysts tend to favor parallel reaction such as reverse water-gas shift, since the formation of water during reaction was observed only in these two catalysts. Furthermore, all materials did not show deactivation profile in both CH<sub>4</sub> and CO<sub>2</sub> conversion over time, differently from using pure LaNiO<sub>3</sub> perovskite that deactivates due to deposition of carbon on the surface of the catalyst [4]. After the test performed for 7 hours, the Temperature-Programmed Oxidation showed no significant amounts of deposited carbon (<2% in 7 h).

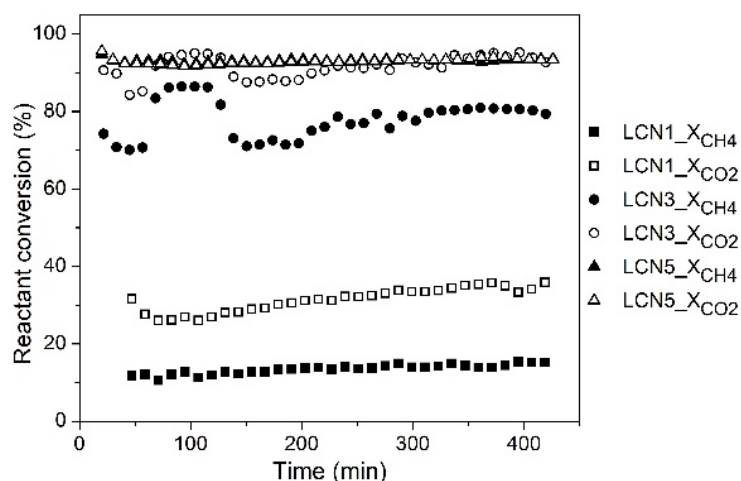


**Figure 1.** Conversion of the reactants as a function of time.

## Conclusions

The pyrochlore-perovskite system as far as known has not been applied to DRM. In this work, this system proved to be promising for application in this reaction, especially the catalyst LCN5, which presented good stability during 7 hours of analysis with high catalytic activity (~93%).

## References

1. Pakhare, D., Haynes, D., Shekhawat, D. and Spivey, J. Appl. Petrochem. Res. 2, 27 (2012).
2. Pakhare, D., et al. J. Catal. 316, 78 (2014).
3. Valderrama, G., et al. Catal. Today 107, 785 (2005).
4. de Lima, S. M., Peña, M. A., Fierro, J. L. G. and Assaf, J. M. Catal. Letters 124, 195 (2008).

The authors would like to thank CAPES and FAPESP (Proc. 2015/06246-7) for the sponsorship and APR thank FAPESP for the studentship Proc. 2016/16329-0.

# Highly selective PROX catalysis based on hydrophobic materials: the case of Pt/graphene

Loïc Michel, Cerise Robert, Sécou Sall, Valérie Caps

*Institut de Chimie et des Procédés pour l'Energie, l'Environnement et la Santé  
(ICPEES), UMR CNRS 7515, 25 rue Becquerel, 67087 Strasbourg, France.*

## Introduction

The selective oxidation of carbon monoxide in hydrogen-rich streams (PROX) is a key reaction of the future hydrogen economy based on proton-exchange membrane fuel cells. It indeed allows removing traces of CO present in the hydrocarbon-based hydrogen fuel before it enters the cell, thereby avoiding poisoning and deactivation of the electro-catalyst which compromises the fuel cell viability [1]. The overall efficiency of the process is however critically dependent on the selectivity of the reaction. Oxidation of the hydrogen fuel must be avoided. Conventional oxide-supported catalysts are poorly selective due to their inherent ability to oxidize hydrogen *via* the terminating hydroxyl functions of the support [2, 3]. We have been developing PROX catalysts supported on OH-free, hydrophobic materials for 10 years, overcoming key synthetic challenges regarding metal deposition efficiency and particle size control [4]. This has allowed us to show for example that commercially available methylated silica yields more selective and more durable gold catalysts for PROX [5, 6] and other reactions [7, 8]. Here we will present the specific features of graphene-based PROX catalysis using platinum nanoparticles (Pt NPs) [9].

## Experimental

A series of catalysts were prepared by NaBH<sub>4</sub> reduction of K<sub>2</sub>PtCl<sub>4</sub> in the presence of high purity natural graphite (Alfa Aesar, 99.9999%) in DMF, using a modified sonication method [4] and varying the Pt content from 0.2 to 11 wt.%. The catalysts were characterized by TEM, XRD, TPR, XPS, and tested for PROX in a fully automated fixed-bed flow reactor (i.d. 10 mm, 26 mg Pt/graphene composite, 1%CO/1%O<sub>2</sub>/24%H<sub>2</sub> in He, 100 mL min<sup>-1</sup>, 1 atm, GHSV ~ 15,000 h<sup>-1</sup>, from 20 to 300°C, 1°min<sup>-1</sup>) on-line connected to a Compact Gas Chromatograph (Interscience).

## Results and discussion

The as-dried composites exhibit a highly exfoliated graphitic structure essentially



made of bi-layer graphene (Figure 1a) and containing  $2.0 \pm 0.6$  nm Pt NPs, whatever the Pt loading. Pt NPs are essentially found at the edges of graphene sheets. It is consistent with the recently observed nucleation and growth of M NPs on “defective” terminating graphene sites [10]. It is explained by the absence of in-plane graphite functionalization. These composites exhibit an intrinsic activity for the overall PROX reaction, which is close to that of the silica-based EuroPt-1 benchmark. However, they exhibit a much higher selectivity towards the oxidation of CO (Figure 1b), which can be tuned by the O/Pt ratio of the composite, as determined by XPS.

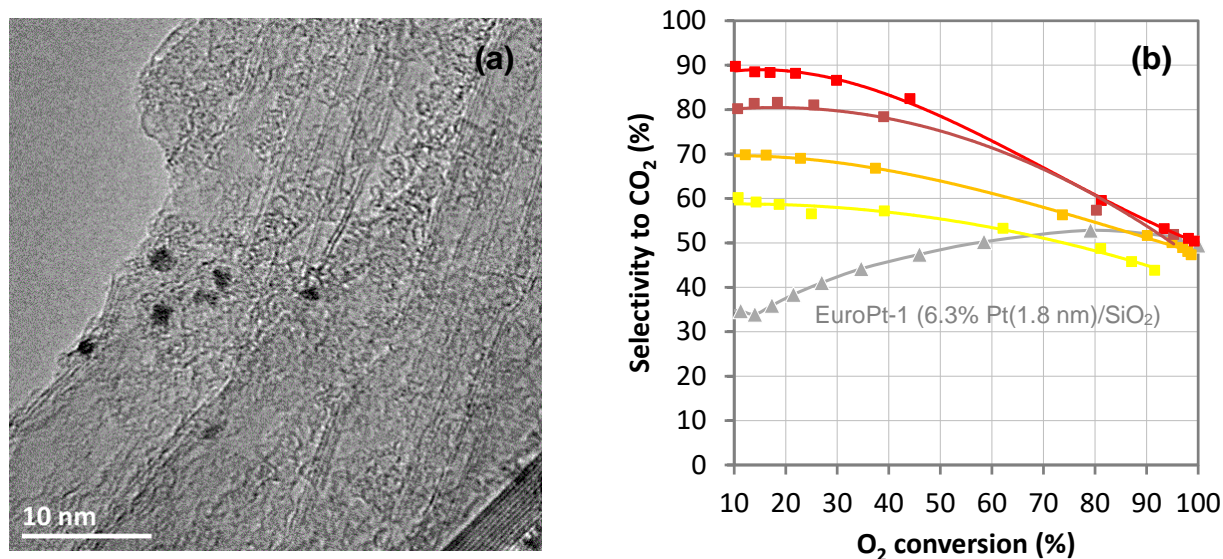


Figure 1: (a) TEM picture of 5.3wt.%Pt/graphene (b) Selectivity to CO<sub>2</sub> observed in PROX over Pt/graphene with 0.24 wt.% (■), 1.7 wt.% (■), 5.3 wt.% (■) and 11.0 wt.% (■) Pt.

## Conclusion

By tuning the Pt content, a state-of-the-art 80% selectivity for CO<sub>2</sub> at 50% O<sub>2</sub> conversion may be achieved by Pt/graphene in PROX, surpassing that of EuroPt-1.

## References

- [1] S. Ivanova, V. Pitchon, C. Petit, V. Caps, *ChemCatChem* 2 (2010) 556.
- [2] C. Pedrero, T. Waku, E. Iglesia, *J. Catal.* 233 (2005) 242.
- [3] K. Liu, A. Wang, T. Zhang, *ACS Catal.* 2 (2012) 1165.
- [4] F. Vigneron, A. Piquet, W. Baaziz, P. Ronot, A. Boos, I. Janowska, C. Pham-Huu, C. Petit, V. Caps, *Catal. Today* 235 (2014) 90.
- [5] D. Gajan, K. Guillois, P. Delichère, J.-M. Basset, J.-P. Candy, V. Caps, C. Copéret, A. Lesage, L. Emsley, *J. Am. Chem. Soc.* 131 (2009) 14667.
- [6] P. Laveille, K. Guillois, A. Tuel, C. Petit, J.-M. Basset, V. Caps, *Chem. Commun.* 52 (2016) 3179.
- [7] K. Guillois, L. Burel, A. Tuel, V. Caps, *Appl. Catal. A* 415-416 (2012) 1.
- [8] K. Guillois, S. Mangematin, A. Tuel, V. Caps, *Catal. Today* 203 (2013) 111.
- [9] ANR-funded PICATA project (ANR-14-OHRI-0005-01).
- [10] M. Carosso, A. Lazzarini, A. Piovano, R. Pellegrini, S. Morandi, M. Manzoli, J. G. Vitillo, M. Jimenez Ruiz, C. Lamberti, E. Groppo, *Faraday Discuss.* 208 (2018) 227.



# Low-temperature steam reforming of flare gases to methane-rich mixtures under extremely low steam to carbon ratios

S.I. Uskov<sup>a,b</sup>, D.I. Potemkin<sup>a,b,\*</sup>, A.B. Shigarov<sup>b</sup>,

P.V.Snytnikov<sup>a,b</sup>, V.A. Kirillov<sup>a,b</sup>, V.A. Sobyenin<sup>a</sup>

<sup>a</sup>Novosibirsk State University, Novosibirsk, Russia

<sup>b</sup>Boreskov Institute of Catalysis, Novosibirsk, Russia

Nowadays, there is an urgent problem of gas flaring all over the world. Billions of cubic meters of gas are wasted in flare installations due to the lack of required transportation or refinery infrastructure or economical inefficiency. This includes associated petroleum gas (APG), separation gas from gas conditioning units at off-shore fields, shale gas and plant gas. These multi-component gas mixtures predominantly consist of methane and its homologues with some inert components such as CO<sub>2</sub>, N<sub>2</sub> and can neither be pumped to pipelines due to high dew point temperature, nor directly used as a fuel for internal combustion engines (ICE) due to high calorific effect (NCV) and detonation risk. Thus, an alternative way of APG utilization is necessary.

Low temperature steam reforming (LTSR) of flare gases (FG) represents a promising method of FG utilization. The process occurs at 250-350 °C and low steam to carbon molar ratio H<sub>2</sub>O/C<sub>C<sub>2</sub>+</sub> 0.5-1 (Fig. 1a) and therefore differs from conventional pre-reforming. Overall process convert C<sub>2</sub>+hydrocarbons into CH<sub>4</sub>, CO<sub>2</sub> and H<sub>2</sub>, which results in lowering net calorific value, Wobbe index and dew point temperature of the gas obtained.

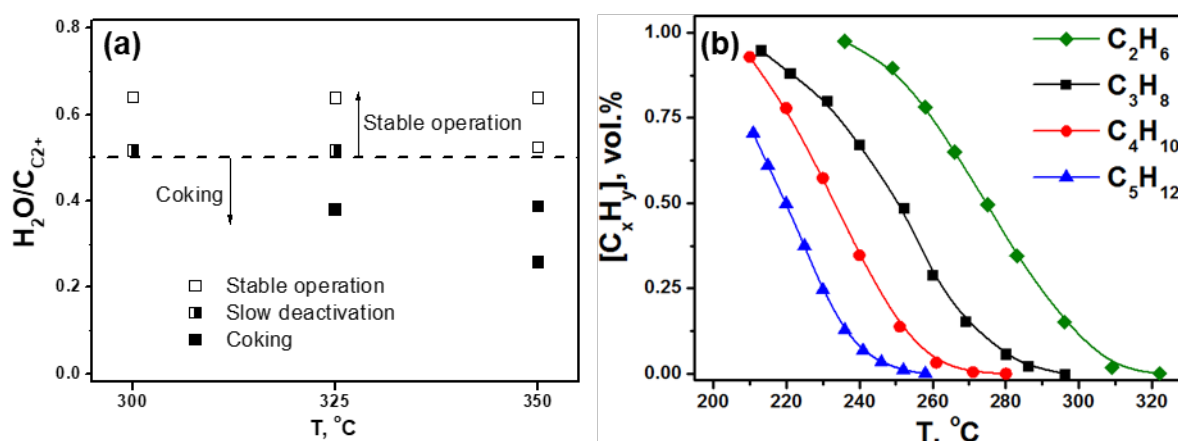


**Fig. 1.** (a) Critical conditions for carbon formation during LTSR of model propane (33 vol.%) – methane (67 vol.%) mixture. (b) Temperature dependencies of outlet concentrations (on dry basis) for steam reforming of C<sub>2</sub>H<sub>6</sub>, C<sub>3</sub>H<sub>8</sub>, C<sub>4</sub>H<sub>10</sub> and C<sub>5</sub>H<sub>12</sub>.

Inlet gas mixture (vol.%): 58.4 CH<sub>4</sub>, 0.6 C<sub>n</sub>H<sub>2n+2</sub>, 41 H<sub>2</sub>O. P = 1 bar, GHSV = 3000 h<sup>-1</sup>.

However, complete conversion of C<sub>2+</sub>-hydrocarbons leads to excessive dilution of methane by CO<sub>2</sub> and H<sub>2</sub> according to equilibrium product distribution and to insufficient energy content of gas for fuel applications. In this case, kinetically controlled partial conversion of ethane and propane provides a way to obtain methane-rich mixtures with desired calorific properties for various applications. This idea was verified experimentally. The reactivity of hydrocarbons under low-temperature steam conversion conditions was shown to increase in the order: C<sub>2</sub>H<sub>6</sub> < C<sub>3</sub>H<sub>8</sub> < n-C<sub>4</sub>H<sub>10</sub> < n-C<sub>5</sub>H<sub>12</sub> (Fig. 1b), making background for preferable conversion of butanes and pentanes and production of methane-rich mixtures with low dew point temperature and sufficient energy content.

Kinetic study of C<sub>2</sub>H<sub>6</sub>-C<sub>5</sub>H<sub>12</sub> low-temperature steam conversion was performed. A simple macrokinetic model, which included irreversible first-order kinetics for C<sub>2</sub>H<sub>6</sub>-C<sub>5</sub>H<sub>12</sub> steam conversion and quasi-equilibrium mode for CO<sub>2</sub> methanation, was suggested. The model adequately described the experimental data on the conversion of model flare gas mixtures at various temperatures and flow rates and was applied to predict reaction conditions which would allow obtaining methane-rich mixtures with the desired properties for various applications from APG of different fraction C<sub>2+</sub>-hydrocarbons. Fig. 2 represents an example of such calculation for "light APG".

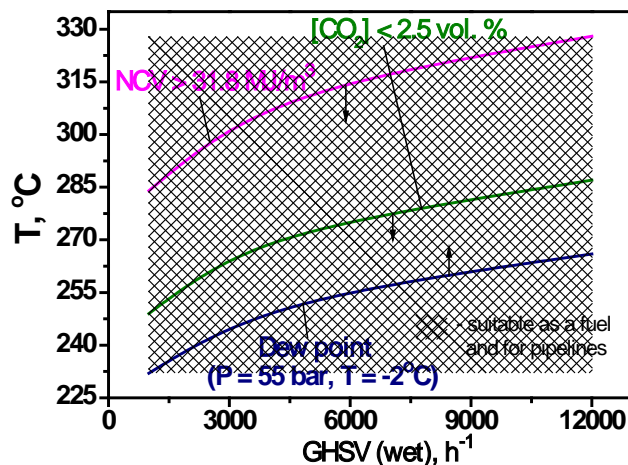


**Fig. 2.** Calculated area of reaction conditions that allow obtaining product gas mixtures which meet the requirements on natural gas according to the standard of "Gazprom" company (Russian Federation). Only dry gas is taken into account. H<sub>2</sub>O/C<sub>C2+</sub> = 0.7, P = 1 bar. Inlet gas mixture (vol.%): (vol.%): 86.5 CH<sub>4</sub>, 5.6 C<sub>2</sub>H<sub>6</sub>, 4.9 C<sub>3</sub>H<sub>8</sub>, 1.2 C<sub>4</sub>H<sub>10</sub>, 0.50 Σ-C<sub>5+</sub>, 0.6 CO<sub>2</sub>, 0.8 N<sub>2</sub>.

The work was supported by RFBR project 18-29-24015 mk.

# Synthesis Routes to Supported Bimetallic Ni-Fe Catalysts for the Understanding of Promoter Effects in the CO<sub>2</sub> Methanation

*Hannah M. S. Augenstein, Lisa Groll, Thomas Burger, Klaus Köhler, Olaf Hinrichsen  
Technical University of Munich, Department of Chemistry, Lichtenbergstr. 4, 85748  
Garching, Germany*

*Technical University of Munich, Catalysis Research Center, Ernst-Otto-Fischer-  
Straße 1, 85748 Garching, Germany*

## Introduction

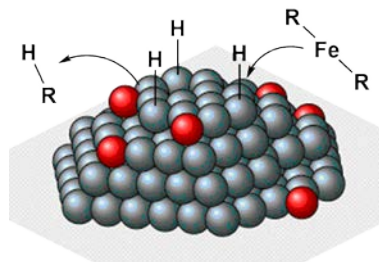
The CO<sub>2</sub> methanation reaction is of interest for its role in the power-to-gas concept.<sup>[1]</sup> Besides a decent catalyst activity, the high exothermicity of the reaction ( $\Delta H_R^0 = 165 \text{ kJ mol}^{-1}$ ) leads to a demand for highly thermostable catalysts for industrial fixed bed application to avoid excessive catalyst deactivation,<sup>[2]</sup> and to increase catalyst lifetime. Fe has been claimed to enhance the activity and stability of Ni-based catalyst systems,<sup>[3]</sup> but the promoting mechanisms in particular for the increase in catalyst life time are not yet clear.<sup>[4]</sup> When applying conventional catalyst preparation techniques like impregnation or (co-)precipitation, the promoter is distributed on the catalyst surface or within the catalyst structure, and the location of the promoter relative to the active metal centers and its oxidation degree are generally unknown. Therefore, this work addresses the investigation of the promoting effect of Fe on an oxide supported nickel methanation catalyst, where iron is selectively doped to pre-reduced Ni-nanoparticles in three different ways: (i) chemical reaction of organometallic precursors with metallic Ni surfaces (“Surface Organometallic Chemistry” approach), (ii) adsorption of Ni-Fe colloids onto the support, and (iii) by a surface redox reaction technique. The preparation and investigation of such model systems is shown to lead to a better understanding of the promoter effect.

## Experimental

Ni/Al<sub>2</sub>O<sub>3</sub> catalysts were prepared by impregnation, deposition precipitation or co-precipitation (pH 9, 30 °C) with varying nickel loadings (10 or 50 wt%). Bimetallic model catalysts are prepared by (i) reaction of an iron(II) amido complex with the H-covered surface of a nickel catalyst (Fig. 1) and by (ii) adsorption of colloidal bimetallic Ni-Fe nanoparticles on the oxide support. (iii) For the surface redox reaction, Fe<sup>3+</sup> ions dissolved in EtOH react with Ni atoms on the activated Ni/Al<sub>2</sub>O<sub>3</sub>

catalyst. The Fe species are deposited at the sites, where the electrons are supplied, or maintain in solution as  $\text{Fe}^{2+}$ , while the oxidized  $\text{Ni}^{2+}$  ions go into solution. The catalysts were structurally characterized and tested for activity under differential and integral conditions and for thermal stability (aging at 500 °C, 8 bar, 32 h) in the methanation reaction of  $\text{CO}_2$  (“inert” transfer to the micro-reactor).

Fig. 1: Targeted doping of a nickel catalyst with an organometallic iron complex.



## Results and Discussion

All three synthesis methods led to selectively Fe-doped metallic Ni centers on  $\text{Ni}/\text{Al}_2\text{O}_3$  catalysts. Material characterization studies comprising  $\text{H}_2$  and  $\text{CO}_2$  chemisorption, ICP-OES, XRD, Ferromagnetic Resonance (FMR) and BET show that Fe can be selectively deposited in the vicinity of Ni nanoparticles. Doping with Fe leads to an increase of the catalytic activity at low Fe loadings, attributed to electronic effects through the formation of Ni-Fe alloy particles, and to an enhancement in thermal stability at higher Fe loadings, which is assumed to be caused by a dynamic variation of the Ni and Fe metal interactions depending on the reaction conditions. This holds in particular for co-precipitated  $\text{NiAlO}_x$  ( $n_{\text{Ni}}/n_{\text{Al}} = 1$ ) catalysts modified with Fe by means of the surface redox reaction technique. Additional effects like a strong and unexpected influence of the solvent used for Fe doping by the surface organometallic chemistry route and adsorption characteristics of preformed Ni-Fe colloids make the situation more complex for the two other synthesis methods. Nevertheless, it can be demonstrated that the application of different synthesis routes to alloyed metal nanoparticles and careful interpretation can be a valuable tools for deeper understanding of promoter effects and structure-activity relationships in the hydrogenation of carbon dioxide.

## References

- [1] M. Sterner, Kassel University 2009.
- [2] C. H. Bartholomew, *Appl. Catal. A* 2001, **212**, 17-60.
- [3] B. Mutz, M. Belimov, W. Wang, P. Sprenger, M.-A. Serrer, D. Wang, P. Pfeifer, W. Kleist, J.-D. Grunwaldt, *ACS Catal.* 2017, 6802.
- [4] T. Burger, F. Koschany, O. Thomys, K. Köhler, O. Hinrichsen, *Appl. Catal. A*, 2018, **558**, 44.

# Synthesis and characterization of MIL-101 based catalysts: bulk MIL-101 and immobilized MIL-101 on $\gamma$ -Al<sub>2</sub>O<sub>3</sub> as catalytic supports

*Maria Mihet\**, Oana Grad, Gabriela Blanita, Mihaela D. Lazar

*National Institute for R&D of Isotopic and Molecular Technologies – INCDTIM, Cluj-Napoca, Donat Street, 67-103, 400293, Romania (maria.mihet@itim-cj.ro)*

## Introduction

Lately, metal-organic frameworks (MOFs) – a class of very versatile compounds due to their exceptionally high surface area and tunable porous structure, as well as their structural diversity [1,2] – have known a growing interest, especially in respect to their applications in adsorption processes, storage and separation of gases, molecular sensing, catalysis, etc. For catalytic applications, MOFs are of great interest due to the diversity of catalytic functionalities which can be introduced in precise locations during synthesis or post synthetically [3]. On the other hand, the gas sorption and storage capacity of the MOF scaffolds can be advantageous for catalytic applications, mostly for reactions involving gaseous reactants and/or products, leading thus to the gas sorbent role of a MOF based catalyst, besides the catalytic role. Considering the CO<sub>2</sub> methanation process, the sorbent role of the catalytic support might be crucial considering that the activation of CO<sub>2</sub> occurs on the support surface [4].

The aim of this work is to report the synthesis and characterization of MIL-101 based catalysts, considering two approaches for the catalytic support: (1) either use of bulk MIL-101 scaffold, or (2) immobilized MIL-101 on  $\gamma$ -Al<sub>2</sub>O<sub>3</sub> by macrostructural templating. For catalytic applications, immobilization of MOFs on porous supports (i.e. alumina) has several important advantages, such as: (a) enhanced mechanical stability; (b) effective use of catalytic active material; (c) enhanced diffusion and/or minimized pressure drop along the packed bed [2].

## Experimental

Both MIL-101 and MIL-101/ $\gamma$ -Al<sub>2</sub>O<sub>3</sub> were synthesized by a green synthetic path, using only water as solvent, and the precursors in equimolar ratio (CrCl<sub>3</sub> and terephthalic acid). In the case of immobilized MIL-101, a selected amount of  $\gamma$ -Al<sub>2</sub>O<sub>3</sub> was placed inside the autoclave, in order for the MOF structure to grow on the

alumina pellets. Ni nanoparticles (NiNPs) were subsequently deposited inside the pores of the MIL-101 based supports using the “double solvent” (DS) method (target concentration of 10 wt.%). Characterization of MIL-101 based materials (supports and catalysts) was performed by N<sub>2</sub> adsorption – desorption isotherms (BET method), X-ray powder diffraction (XRD), thermogravimetric analysis (TGA), infra-red spectroscopy (FTIR), scanning and transmission electronic microscopy (SEM, TEM), and temperature programmed desorption of CO<sub>2</sub> and H<sub>2</sub> (CO<sub>2</sub>-TPD, H<sub>2</sub>-TPD).

## Results and Discussions

MIL-101 was successfully deposited on  $\gamma$ -Al<sub>2</sub>O<sub>3</sub> due to the large number of weak basic sites on the alumina surface (FTIR, CO<sub>2</sub>-TPD), resulting in a composite with large surface area (1032 m<sup>2</sup>/g) and pore structure similar to the bulk MIL-101, but with larger pores due to the growth inside the alumina pores (Fig 1, Table 1). SEM images reveal the growth of octahedral MIL-101 crystallites on the alumina pellets (Fig. 2). Functional characterization by CO<sub>2</sub>-TPD of the MIL-101 based supports revealed a good CO<sub>2</sub> chemisorption capacity, both molecularly and dissociatively, indicating good premises for enhanced catalytic activity in the CO<sub>2</sub> methanation process. Deposition of Ni by the DS method resulted in very well dispersed ultrasmall NiNPs.

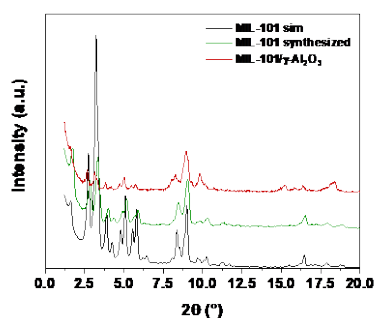


**Fig. 1.** XRD patterns of the MIL-101 based catalytic supports.

**Table 1.** Structural properties of the MIL-101 based catalytic supports.

Sample	S <sub>BET</sub> (m <sup>2</sup> /g)	V <sub>p</sub> (cm <sup>3</sup> /g)	D <sub>m</sub> (nm)
MIL-101	3275	2.25	0.4 – 1.0; 1.8 – 3.0
$\gamma$ -Al <sub>2</sub> O <sub>3</sub>	247	0.26	1.5 – 5.0
MIL-101/ $\gamma$ -Al <sub>2</sub> O <sub>3</sub>	1032	0.77	1.5 – 2.8; 3.2 – 5.0

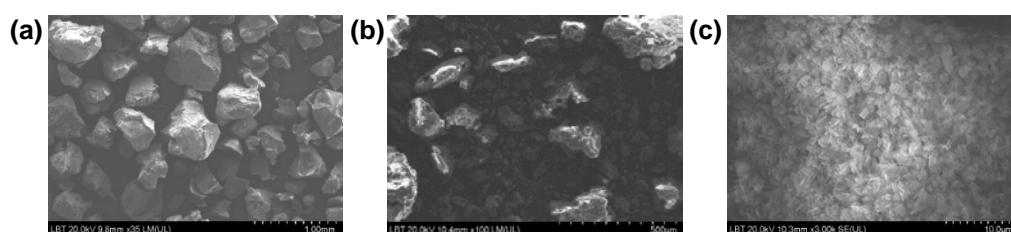


**Fig. 2.** SEM images for (a)  $\gamma$ -Al<sub>2</sub>O<sub>3</sub> pellets and (b) – (c) MIL-101/Al<sub>2</sub>O<sub>3</sub>.

## References

- [1] P. Falcaro, R. Ricco, A. Yazdi, I. Imaz, S. Furukawa, D. Maspooh, R. Ameloot, J.D. Evans, C.J. Doonan, *Coord. Chem. Rev.* 307 (2016) 237–254.
- [2] J. Gascon, A. Corma, F. Kapteijn, F.X. Llabres i Xamena, *ACS Catal.* 4 (2014) 361–378.
- [3] G. Prieto, H. Tuysuz, N. Duyckaerts, J. Knossalla, G. Wang, F. Schuth, *Chem. Rev.* 116 (22) (2016) 14056.
- [4] M. Mihet, M.D. Lazar, *Catal. Today.* 306 (2018) 294–299.

**Acknowledgement:** This work was supported by a grant of CNCS - UEFISCDI, Romania, project number PN-III-P1-1.1-PD-2016-1228, within PNCDI III.

# A dual-reactor concept for propanol synthesis from CO<sub>2</sub>, C<sub>2</sub>H<sub>4</sub> and H<sub>2</sub>

*Duc Truong Duc<sup>1,2)</sup>, MT Le<sup>2)</sup>, David Linke<sup>1)</sup>, Evgenii V. Kondratenko<sup>1)</sup>\**

<sup>1)</sup>*Leibniz-Institut für Katalyse e.V., Albert-Einstein-Str. 29a, 18059 Rostock, Germany*

<sup>2)</sup>*SCE, Hanoi University of Science and Technology, Vietnam*

## Introduction

The emissions of CO<sub>2</sub> contributing to global warming have strongly increased since the industrial revolution. Therefore, reducing CO<sub>2</sub> release into the atmosphere is of enormous environmental interest. This can be achieved by either its capture/storage or utilization as a reactant for producing fuels and useful chemicals in an environmentally friendly manner. Recently, we developed Au-containing supported catalysts for the conversion of CO<sub>2</sub> into propanol in the presence of C<sub>2</sub>H<sub>4</sub> and H<sub>2</sub> [1-2]. The major drawback of this sustainable and innovative route is the C<sub>2</sub>H<sub>4</sub> hydrogenation to C<sub>2</sub>H<sub>6</sub>. The present study was aimed to elucidate the potential of a dual-reactor concept for improving the selectivity. To this end, a first reactor is used to convert CO<sub>2</sub> to CO through the reverse water gas shift (RWGS) reaction, while the hydroformylation of ethylene takes place in a second reactor at a different temperature.

## Experimental

Catalysts were synthesized by deposition–precipitation of gold hydroxide from H<sub>2</sub>AuCl<sub>4</sub> (41.1 wt% Au, Chempur) on TiO<sub>2</sub> (BASF). Briefly, the support was impregnated with a H<sub>2</sub>AuCl<sub>4</sub> solution to yield the catalyst precursor with 2 wt% Au. Next step was the incipient wetness impregnation of dried Au/TiO<sub>2</sub> with a CsNO<sub>3</sub> solution (99.9%, Chempur). The Cs loading was varied between 1 and 13 wt%. All catalysts were calcined in air at 773 K for 4 h. Catalytic tests with consecutive ethylene hydroformylation were performed in a set-up equipped with two independently heated furnaces. Reaction temperature was varied from 443 to 873 K.

## Results and discussion

Figure 1 (a) shows the conversion of C<sub>2</sub>H<sub>4</sub> and the selectivity to oxo-products (propanal plus propanol) on the basis of C<sub>2</sub>H<sub>4</sub> as obtained when our dual-reactor concept or a single reactor were applied. Importantly, reaction temperature of the hydroformylation reactor in the former approach was the same as in the single reactor and the both reactors were filled with 4Cs-Au/TiO<sub>2</sub>. It is obvious that the

\*Corresponding author: [evgenii.kondratenko@catalysis.de](mailto:evgenii.kondratenko@catalysis.de)

selectivity to the desired oxo-products was very low in the single reactor as a consequence of high catalyst activity for the hydrogenation of ethylene to ethane. This undesired reaction could be partially suppressed when using the dual-reactor concept. This is due to the fact that significant amounts of CO were formed in the first reactor operated at 450°C. High CO partial pressures are favorable for the hydroformylation reaction. The oxo-products selectivity obtained at 250°C increases with rising temperature for the RWGS reaction (Figure 1(b)) as a consequence of increased CO<sub>2</sub> conversion into CO (Figure 1(c)). In addition to favoring the hydroformylation reaction, CO hinders ethylene hydrogenation as concluded from the fact that overall ethylene conversion decreased with a rise in CO<sub>2</sub> conversion in the first reactor used for the RWGS reaction at different temperatures.

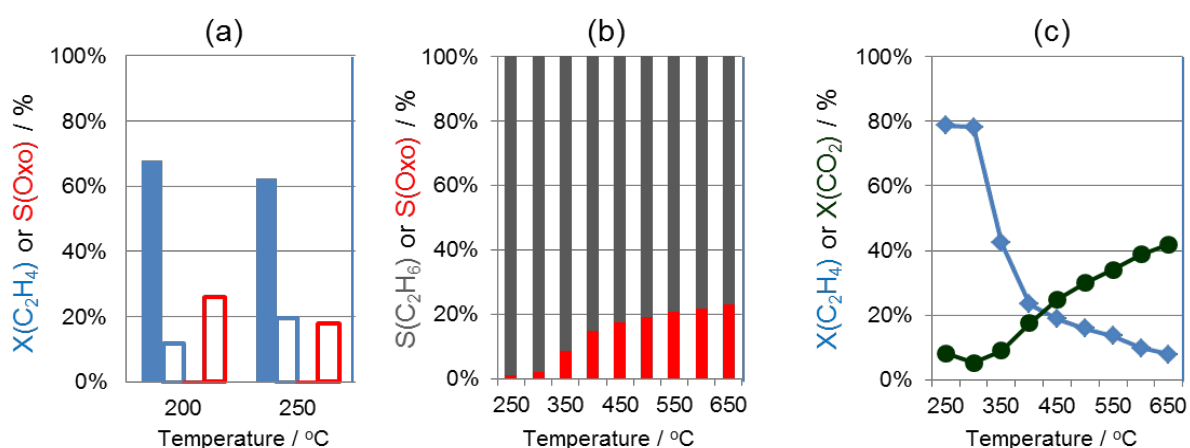


**Figure 1.** (a) Conversion of ethylene ( $X(\text{C}_2\text{H}_4)$ ) and oxo-products selectivity ( $S(\text{Oxo})$ ). Solid and open bars stand for the single and dual-reactor approaches respectively. The temperature of RWGS reactor was kept at 450°C. (b) The selectivity to ethane and oxo-products in the dual reactor concept. (c) The conversion of ethylene ( $X(\text{C}_2\text{H}_4)$ ) and CO<sub>2</sub> ( $X(\text{CO}_2)$ ) in the dual reactor concept; the RWGS reactor operated between 250 and 650°C, while the temperature of the hydroformylation reactor was 250°C. 4Cs-Au/TiO<sub>2</sub> was used as a catalyst for all tests at 2 MPa using a CO<sub>2</sub>/H<sub>2</sub>/C<sub>2</sub>H<sub>4</sub>/N<sub>2</sub> = 4:4:1:1.

## Conclusion

We have demonstrated for the first time the feasibility of a dual-reactor concept for conversion of CO<sub>2</sub> with C<sub>2</sub>H<sub>4</sub> in H<sub>2</sub> presence into propanal and propanol. This method helps to hinder the undesired hydrogenation of ethane to ethylene in favor of oxo-products formation through controlling CO partial pressure for the hydroformylation reactor. Further progress could be envisioned when more active and selective hydroformylation catalysts would be developed.

## Reference

- [1] S.J. Ahlers, U. Bentrup, D. Linke, E.V. Kondratenko, ChemSusChem 7 (2014) 2631-2639.
- [2] S.A. Mavlyankariev, S.J. Ahlers, V.A. Kondratenko, D. Linke, E.V. Kondratenko, ACS Catal. 6 (2016) 3317-3325.



## Electrocatalytic water oxidation by a water insoluble Cu(II) complex

*M.M. Móricz, Surface Chemistry and Catalysis Department, MTA Centre for Energy Research, Budapest, Hungary; T. Benkó, Surface Chemistry and Catalysis Department, MTA Centre for Energy Research, Budapest, Hungary; J.S. Pap, Surface Chemistry and Catalysis Department, MTA Centre for Energy Research, Budapest, Hungary*

Modification of (photo)anodes applied in the water oxidation half-cell reaction with catalyst units consisting of abundant elements is of crucial importance in order to construct advanced artificial photosynthetic systems. Our aim was to exploit second-order attractive forces between a model semiconducting surface and a putative molecular water oxidation catalyst (WOC) unit, governed by the intrinsic molecular properties of the latter. We envisioned a low-cost and gentle method to fabricate functional composites, in which the often fragile anisotropic morphology of the nanostructured semiconductor is preserved after functionalization by the WOC.

Therefore we explored the behavior as WOC of a known, water-insoluble Cu(II) complex made with a pincer ligand, 1,3-bis(2'-pyridyl-imino)isoindoline (indH) that was meant to facilitate the surface attachment of the complex  $[\text{Cu}(\text{indH})(\text{NCCH}_3)(\text{OCIO}_3)](\text{ClO}_4) \cdot \text{CH}_3\text{CN}$ , **Cu-indH** (Fig. 1) to an electrode by hydrophobic interactions.

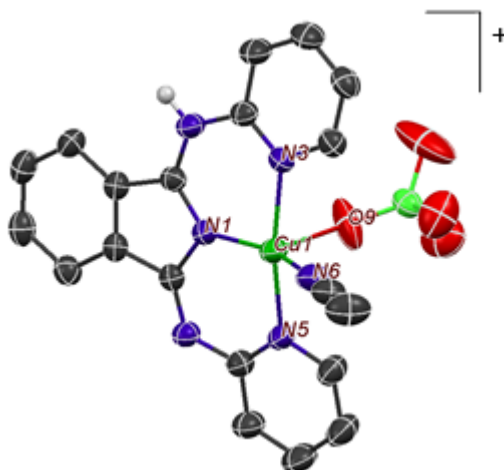


**Figure 1.** Structure of the **Cu-indH** complex [1]

**Cu-indH** was investigated both under homogeneous and heterogeneous electrocatalytic conditions. In the homogeneous system **Cu-indH** was dissolved in acetonitrile containing  $\text{Bu}_4\text{NClO}_4$  and investigated by cyclic voltammetry (CV) in the presence or absence of added water. The CV of **Cu-indH** (Fig.2) revealed increased irreversible anodic current after addition of water suggesting electrochemical  $\text{O}_2$

evolution. Importantly, the irreversible Cu(II/I) reduction and Cu(III/II) oxidation peaks separated by large potential gaps undergo changes upon addition of water. This observation is consistent with ligand exchange reactions between acetonitrile, perchlorate and water competing for the available sites at the copper center that eventually, through the formation of a ternary indH-Cu-water species is thought to lead to electrocatalytic water oxidation, most likely following a water nucleophilic attack (WNA) mechanism.

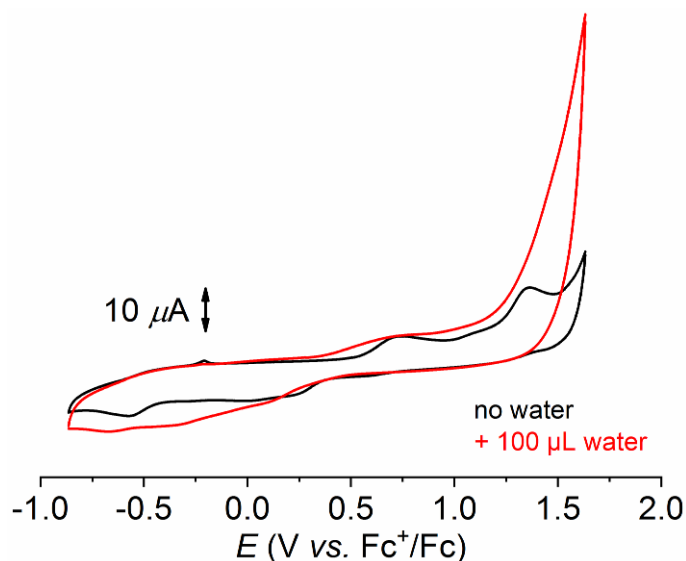


**Figure 2.** CVs of **Cu-indH** complex (1 mM) in acetonitrile ( $\text{Bu}_4\text{NClO}_4$  of 0.1M) at  $\nu = 100$  mV/s, GCE working electrode, Pt aux. electrode and Ag/AgCl ref. electrode.

Under heterogeneous conditions the complex was drop-casted onto a smooth indium tin oxide (ITO) surface and the thus functionalized **Cu-indH/ITO** was used as working electrode in borate, phosphate or carbonate buffer, at different pH values. The electrocatalytic performance of the **Cu-indH/ITO** electrodes was investigated by chronoamperometry at high anodic potentials, and revealed a stable and differently increased catalytic current depending on the applied buffer. We plan to extend our work to explore whether the molecular properties tuned by modifications in the ligand might be transferred to semiconducting surfaces?

**Acknowledgements.** This work was funded by the National Research, Innovation and Development Office of Hungary, grant number NKFI-128841, the VEKOP-2.3.2-16-2016-00011 grant supported by the European Structural and Investment Funds and the János Bolyai Research Scholarship by the Hungarian Academy of Sciences (J.S. Pap).

## References

[1] S Pap, B Kripli, V Bányai, M Giorgi, L Korecz, T Gajda, D Árus, J Kaizer, G. Speier; *Inorg. Chim. Acta* 376 (2011) 158-169.

## **The complex role of materials in plasma based CO<sub>2</sub> conversion**

*I. Michielsen, Department of Chemistry, LADCA and PLASMANT, University of Antwerp, Wilrijk, Belgium, Y. Uytendhouwen, Department of Chemistry, LADCA and PLASMANT, University of Antwerp, Wilrijk, Belgium, S. Rana, Department of Chemistry, LADCA and PLASMANT, University of Antwerp, Wilrijk, Belgium, P. Cool, Department of Chemistry, LADCA, University of Antwerp, Wilrijk, Belgium, A. Bogaerts, Department of Chemistry, PLASMANT, University of Antwerp, Wilrijk, Belgium, V. Meynen, Department of Chemistry, LADCA, University of Antwerp, Wilrijk, Belgium*

Plasma technology uses (renewable) electrical energy for gas ionization at non-equilibrium conditions, giving access to alternative reaction pathways compared to the current (thermal) chemical processes. This enables process intensification, new production methodologies and Power-to-X.

However, current bottlenecks of chemical plasma conversion are its low selectivity and energy efficiency in case of DBD (dielectric barrier discharge) reactors, requiring the addition of packing materials and/or catalysts. The efficiency of plasma conversion (time space yield, selectivity and energy efficiency) can be substantially improved through the implementation of structured (formulated) (catalytic) packing's. Implementing these materials in the plasma discharge, unlocks an interplay of different physical and chemical phenomena by interactions of the materials with the plasma and vice versa.

The key parameters to optimize these mutual interactions are however still largely unknown and not fully understood. Therefore, our research is focused on understanding the different interacting phenomena in the plasma and at the surface of the materials (packing and/or catalysts) to enable targeted development of materials, to maximally improve efficiency and induce tailor-made selectivity in plasma catalytic conversion reactions. In the presentation, the impact of different packing materials, reactor set-ups and operating conditions on the CO<sub>2</sub> splitting

reaction and dry reforming of methane with CO<sub>2</sub> will be discussed with respect to conversion enhancement and selectivity.

## References

1. I. Michielsen, Y. Uytendhouwen, A. Bogaerts, V. Meynen, accepted in Catalysts (2019)
2. Y. Uytendhouwen, S. Van Alphen, I. Michielsen, V. Meynen, P. Cool, A. Bogaerts, Chem. Eng. J. (2018) 557-568
3. I. Michielsen, Y. Uytendhouwen, J. Pype, B. Michielsen, M. Mertens, F. Reniers, V. Meynen, A. Bogaerts, Chem. Eng. J. (2017) 477-488

# Hydrodeoxygenation of bio-oil model compounds over unsupported *in situ* and *ex situ* generated nickel phosphide

Golubeva M.A.<sup>1</sup>, Maximov A.L.<sup>1,2</sup>

1 – A.V.Topchiev Institute of Petrochemical Synthesis RAS, Moscow, Russia

2 – Lomonosov Moscow State University, Moscow, Russia

Nowadays effective conversion of biomass into chemicals and fuels is a problem of current interest. Lignocellulosic biomass consists of polysaccharides such as cellulose, hemicellulose and a phenolic polymer – lignin. One of the biofuels is a bio-oil. It is produced from biomass by fast pyrolysis [1]. In contrast to fossil fuels, which include large amount of sulfur-containing compounds, bio-oil includes a lot of oxygen-containing compounds. High content of oxygen makes bio-oil unstable, corrosiveness and prone to polymerization in aerobic atmosphere. Upgrading of bio-oil improves its quality characteristics.

Conventional hydrotreating catalysts, which are utilized for fossil fuels, contain transition metal sulfides. Due to high sulfur content in this type of fuels, transition metal sulfides stay active for a long time. However, in feedstocks with low sulfur and high oxygen content these catalysts may be deactivated easily.

An interesting class of hydrotreating catalysts is a number of transition metal phosphides. These catalysts are explored insufficiently and interest towards them has increased in recent years. The most active phosphide is a nickel phosphide Ni<sub>2</sub>P. In most cases it is synthesized from nickel inorganic salts and phosphorous-containing acids and its salts or from oil-soluble nickel salts and organic derivatives of phosphorous [2, 3].

In present work, hydrogenation-hydrodeoxygenation processes of guaiacol and furfural over nickel phosphide catalysts generated *in situ* and *ex situ* were investigated. Guaiacol is a lignin-derived and furfural is a hemicellulose-derived compound. Both of them are components of bio-oil [4].

Unsupported nickel phosphide, obtained in two different pathways, was used in catalytic tests. The first was nickel phosphide, which was synthesized *ex situ* as in typical experiment [5] from nickel (II) acetate and hypophosphorous acid. The second was nickel phosphide which was generated *in situ* from nickel hypophosphite during the hydrogenation-hydrodeoxygenation processes of bio-oil model compounds.

Catalytic tests were carried out at 523-623 K and at initial pressure of hydrogen of 3-7 MPa in a stainless-steel autoclave. Different polar and non-polar solvents were used. Hydrodeoxygenation of guaiacol has occurred better in non-polar solvents. Cyclohexane, cyclohexanol and cyclohexanone have been obtained as main products. The main product from furfural in polar and non-polar solvents was tetrahydrofurfuryl alcohol. The qualitative composition was determined by GC-FID and GC-MS analyses and the quantitative composition was determined only by GC-FID. Generated *in situ* and *ex situ* nickel phosphide was analyzed by a set of physico-chemical methods (TEM, XPS, XRD).

### **Acknowledgements**

This work was supported by Russian Foundation for Basic Research, project no. 18-03-01186 A.

### **References**

1. Mohan D., Pittman Ch.U., Jr., Steele Ph.H. Pyrolysis of Wood/Biomass for Bio-oil: A Critical Review // *Energy Fuels*. 2006. V.20. PP.848-889.
2. Bussell M.E. New methods for the preparation of nanoscale nickel phosphide catalysts for heteroatom removal reactions // *React. Chem. Eng.* 2017. V.2. PP.628-635.
3. Oyama S.T., Gott T., Zhao H., Lee Y.-K. Transition metal phosphide hydroprocessing catalysts: A review // *Catal. Today*. 2009. V.143, PP.94-107.
4. Mullen Ch.A., Boateng A.A. Chemical Composition of Bio-oils Produced by Fast Pyrolysis of Two Energy Crops // *Energy Fuels*. 2008. V.22. PP.2104-2109.
5. Guan Q., Li W., Zhang M., Tao K. Alternative synthesis of bulk and supported nickel phosphide from the thermal decomposition of hypophosphites // *J. Catal.* 2009. V.263. PP.1-3.

# CO<sub>2</sub> hydrogenation to CH<sub>3</sub>OH on Cu/Zn catalysts promoted by Zr or Nb

Cássia S. Santana<sup>1</sup>; Domingos S. A. Silva<sup>1</sup>; Ernesto A. Urquieta-González<sup>1</sup>;

Elisabete M. Assaf<sup>2</sup>; Janaína F. Gomes<sup>1</sup>; José M. Assaf<sup>1\*</sup>

<sup>1</sup>Federal University of São Carlos, Department of Chemical Engineering, São Carlos-SP, Brazil

<sup>2</sup>University of São Paulo, São Carlos, Institute of Chemistry, São Carlos-SP, Brazil

\*+55 16 3351 8264, [mansur@ufscar.br](mailto:mansur@ufscar.br)

## Introduction

Strategies to reduce CO<sub>2</sub> emissions and control the increase in the atmospheric CO<sub>2</sub> levels are urgent. In this scenario, a promising strategy comprises the development of alternative routes to the fabrication of chemical products based on carbon in which CO<sub>2</sub> may be used as raw material. In particular, methanol is an interesting product that can be obtained from the CO<sub>2</sub> hydrogenation. Methanol is currently produced on Cu/Zn-based catalysts from syngas at 50 bar and 250°C [1]. One of the difficulties associated to the production of methanol from CO<sub>2</sub> and H<sub>2</sub> is that catalysts present low CO<sub>2</sub> conversion, low selectivity towards the formation of a specific product and low stability under the reaction conditions. To improve the catalytic performance of Cu-based catalysts, their stability and to enable the production of methanol from CO<sub>2</sub> and H<sub>2</sub>, promoters can be added. In the present work, we investigated the catalytic performance of Cu/Zn catalyst promoted by Zr or Nb towards the CO<sub>2</sub> hydrogenation to methanol.

## Experimental

Cu/Zn and Cu/Zn/X (X = Zr or Nb) catalysts were prepared by co-precipitation, as described in a previous work [2]. The nominal composition of the Cu/Zn and Cu/Zn/X was 50/50 and 50/45/5 (wt.%), respectively, and their properties were investigated by XRF, XRD, N<sub>2</sub>-physisorption, H<sub>2</sub>-TPR and CO<sub>2</sub>-TPD. The CO<sub>2</sub> hydrogenation reaction was carried out between 200 and 280 °C at 30 bar using a fixed bed flow reactor fed with a gas mixture of H<sub>2</sub> and CO<sub>2</sub> with a molar ratio of H<sub>2</sub>/CO<sub>2</sub> = 3/1. The stainless-steel reactor contained 0.2 g of catalyst diluted with 0.2 g of SiC. Before the reaction the precursor catalysts were reduced under H<sub>2</sub> flow (30 mL min<sup>-1</sup>) at 300 °C for 1 h. The reaction products were evaluated online by gas chromatography.

## Results

The chemical composition of the materials, as investigated by XRF, was close to the corresponding nominal value, indicating the accuracy of the applied synthesis method. XRD data revealed the presence of CuO and ZnO crystalline phases in the prepared Cu/Zn precursor catalysts. The H<sub>2</sub>-TPR profiles of the materials presented a peak between 270-300 °C, which is related to the reduction of Cu<sup>2+</sup> to Cu<sup>0</sup>. Based on these results, the reduction temperature before the reaction was set to 300 °C. The specific surface area of the promoted catalysts increased up to 2 and 5 times in comparison with that of the unpromoted one ( $S_{\text{BET}} = 17, 48$  and  $9 \text{ m}^2 \text{ g}^{-1}$  to Cu/Zn/Zr, Cu/Zn/Nb and Cu/Zn catalysts, respectively). This may be attributed to the role of the promoters as structural spacer, in accordance with previous studies [3]. By the CO<sub>2</sub>-TPD it was verified that the number of basic sites of the promoted materials was higher than that of the unpromoted one. As shown in Figure 1, the CO<sub>2</sub> hydrogenation on the investigated catalysts resulted in the formation of CH<sub>3</sub>OH (Figure 1B) and CO (Figure 1C) as the main products. With the increase of the temperature, the conversion of CO<sub>2</sub> increases (Figure 1A), but the formation of methanol decreases while that related to CO increases. Promoted Cu/Zn catalysts were more active and more selective to methanol than the unpromoted Cu/Zn one. Cu/Zn/Nb was the most active catalyst in the investigated temperature range. Furthermore, that material presented the highest selectivity to methanol. Its best catalytic performance may be associated with its higher specific surface area and its higher number of basic sites.

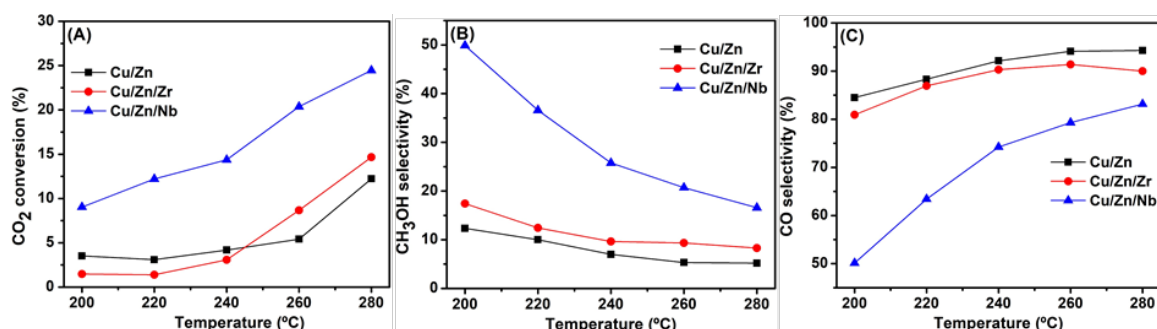


**Figure 1.** (A) Activity of the unpromoted and promoted Cu/Zn catalysts and the selectivity to: (B) CH<sub>3</sub>OH, (C) CO.

## Conclusion

Under the explored conditions, the investigated promoters of the studied Cu/Zn catalyst enhanced the activity and selectivity to methanol from CO<sub>2</sub> hydrogenation. Cu/Zn/Nb presented the best catalytic performance among the investigated materials.



## **Acknowledgments**

The authors thank to FAPESP (2015/06246-7, 2017/08420-0, 2017/05241-7) for the financial support.

## **References**

- [1] F. Studt, M. Behrens, E. L. Kunkes, N. Thomas, S. Zander, A. Tarasov, J. Schumann, E. Frei; J. B. Varley, F. Abild-Pedersen. *ChemCatChem* 7 (2015) 1105.
- [2] T. Witoon, N. Kachaban, W. Donphai, P. Kidkhunthod, K. Faungnawakij, M. Chareonpanich, J. Limtrakul, *Energy Convers. Manag.* 118 (2016) 21.
- [3] R. T. Figueiredo, A. Martínez-Arias, M. L. Granados, J. L. G.Fierro, *J. Catal.* 178 (1998) 146.

# Single-step and room temperature dry reforming of CH<sub>4</sub> and CO<sub>2</sub> to acetic acid and methanol via plasma-catalysis

Yaolin Wang, Li Wang, Michael Craven, Xin Tu\*

*Department of Electrical Engineering and Electronics, University of Liverpool,  
Liverpool, L69 3GJ, UK.*

\*corresponding author: [xin.tu@liv.ac.uk](mailto:xin.tu@liv.ac.uk)

## Introduction

Dry reforming of methane with carbon dioxide has attracted significant interest due to simultaneously utilisation and reduction of two major greenhouse gases whilst generating higher value chemicals and fuels. However, both CH<sub>4</sub> and CO<sub>2</sub> are highly stable, therefore high temperatures (> 700 °C) are usually required to achieve reasonable conversions of CH<sub>4</sub> and CO<sub>2</sub> and syngas yield due to the thermodynamic barrier of this reaction, resulted in high energy consumption. Catalyst deactivation due to carbon deposition on the catalyst surface remains another challenge for this process. Non-thermal plasma or cold plasma offers a promising and attractive alternative for the activation of CH<sub>4</sub> and CO<sub>2</sub> at low temperatures and ambient pressure, providing a unique way to enable thermodynamically unfavourable reactions to take place at ambient conditions [1-2].

In this study, we report a novel, room temperature (30 °C) and one-step process for the direct conversion of CH<sub>4</sub> and CO<sub>2</sub> to liquid fuels and chemicals (e.g. acetic acid, methanol, ethanol and formaldehyde) using a cold plasma coupled with catalysis at ambient pressure, to avoid conventional multiple-step high temperature and high pressure catalytic processes.

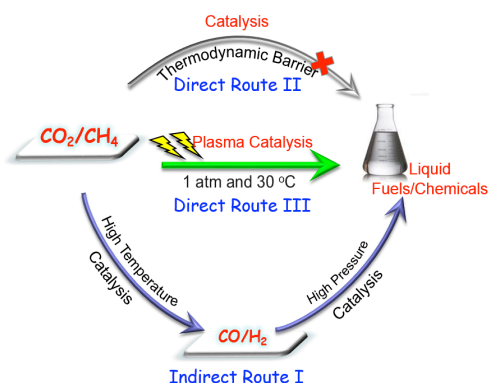
## Experimental

In this work, a novel and unique dielectric barrier discharge (DBD) reactor using water as a ground electrode has been developed for the conversion of CO<sub>2</sub> and CH<sub>4</sub> to oxygenates at room temperature (around 30 °C) and atmospheric pressure. The discharge length was 45 mm with a discharge gap of 3 mm. Three catalysts (Cu/Al<sub>2</sub>O<sub>3</sub>, Pt/Al<sub>2</sub>O<sub>3</sub> and Au/Al<sub>2</sub>O<sub>3</sub>) were tested in the plasma-catalytic reaction. The discharge power was kept at 10 W. The gaseous and liquid products were quantitatively analyzed by gas chromatography. The dry reforming of methane (DRM) reaction was carried out at the same temperature (~30 °C) under three different

operating modes: plasma only, catalysis only and plasma-catalysis. In the catalysis-only mode, no reaction occurred at a temperature of around 30 °C.

## Results and discussion

In the plasma process without a catalyst ('plasma-only'), a total liquid selectivity of 59.1% was achieved with 33.7%, 11.9%, 11.9% and 1.6% for acetic acid, ethanol, methanol and acetone, respectively. Coupling the plasma process with a catalyst shows great potential to manipulate the production of different oxygenates at ambient conditions. Packing the Cu/ $\gamma$ -Al<sub>2</sub>O<sub>3</sub> catalyst in the DBD plasma enhanced the selectivity of acetic acid to 40.2%, compared to the plasma-only mode. HCHO was formed only when the supported noble catalysts were used in the plasma reaction. The plausible reaction mechanism and pathways in the plasma-catalytic process has been proposed and discussed through a comprehensive analysis of the gaseous and liquid products, together with the plasma diagnostics and plasma chemical kinetic modelling.



## Significance

This work has successfully demonstrated that non-thermal plasma can be used to convert  $\text{CH}_4$  and  $\text{CO}_2$  into higher value liquid fuels and chemicals in a single step process at ambient conditions, bypassing the formation of syngas. The total selectivity of liquid chemicals was ca. 50-60%, with acetic acid being the major product.

## Reference

- [1]. L. Wang, Y. H. Yi, C. F. Wu, H. C. Guo, X. Tu, *Angewandte Chemie International Edition*, 2017, 56, 13679-13683.
- [2]. L. Wang, Y. H. Yi, H. C. Guo, X. Tu, *ACS Catalysis*, 2018, 8, 90-100.

## **Catalytic reforming of highly paraffinic naphtha feedstocks**

*Sinqobile V. L. Mahlaba; Sanele Moloji; Abdul S. Mahomed,; Holger B. Friedrich  
School of Chemistry and Physics, University of KwaZulu-Natal, University Road,  
Westville, Private Bag X54001, Durban, 4000, South Africa*

Catalytic naphtha reforming is an important process in oil refineries for upgrading low octane naphtha to high-octane gasoline required to meet current fuel specifications. This process has become even more important due to the banning of high octane fuel additives such as methyl-tert-butyl ether [1]. Catalytic naphtha reforming is achieved with the use of a bimetallic, bifunctional Pt-Sn/Al<sub>2</sub>O<sub>3</sub>-Cl catalysts, where Pt is the metallic function for dehydrogenation and hydrogenation processes, while Cl provides the acidic function for isomerization reactions. Sn is added as a structural promoter that enhances the Pt dispersion, whilst also providing stability of the catalyst against coking and sintering [2].

Although a lot of work has been published on catalytic reforming [3-6], most of it pertains to petroleum based naphtha. To that effect, there is limited knowledge regarding the reforming of highly paraffinic feedstocks, due to the difficulty of reforming of such feedstocks, and the requirement of harsh operating conditions, compared to crude oil derived naphtha [7]. Hence, the aim of this study was to synthesize a Pt-Sn/Al<sub>2</sub>O<sub>3</sub>-Cl reforming catalyst and to test its performance for the reforming of highly paraffinic naphtha feedstocks and C<sub>7</sub>-C<sub>9</sub> linear model feeds. The catalyst was characterized with SEM-EDX, HRTEM, H<sub>2</sub> chemisorption, n-propylamine TPD and BET surface area analysis. Catalytic tests were performed in a continuous flow, fixed bed micro-reactor. Preliminary testing results showed the catalyst to be highly active for the reforming of linear paraffins at temperatures around 520°C, although the catalyst underwent deactivation on stream.

In addition, a model for the estimation of the reformate Research Octane Number (RON) and Motor Octane Number (MON) was adapted from [8], and used to estimate the octane number of reformate samples obtained from the reforming of highly paraffinic naphtha. The RON and MON values estimated by the model were plotted against the values determined from engine analyses. Figure 1 shows the correlation between the estimated and actual octane numbers.

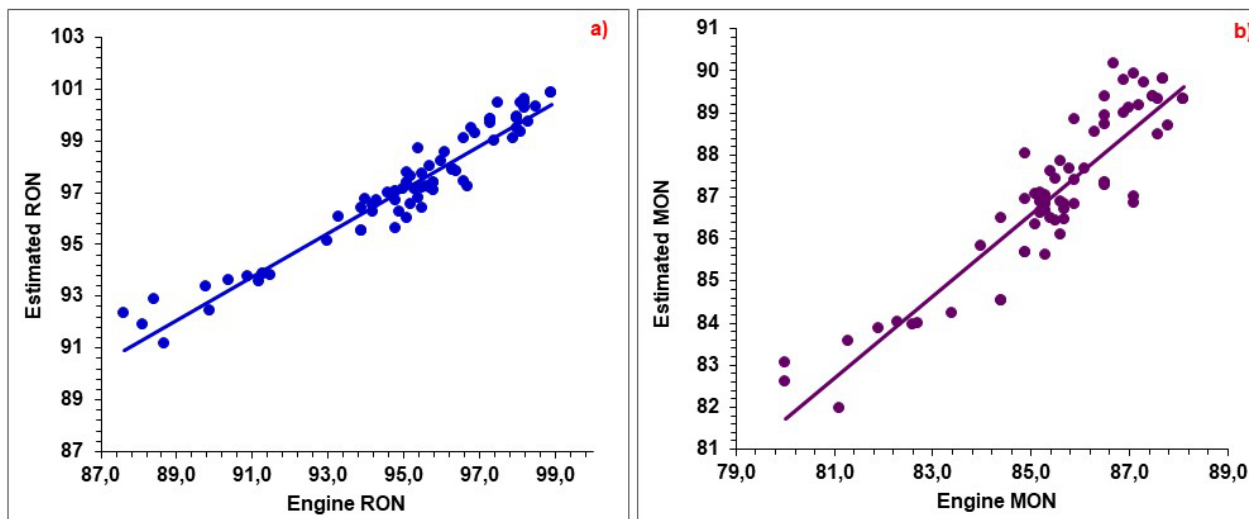


Figure 1: The correlation between the estimated RON and the engine RON (a), as well as the estimated MON and the engine MON (b)

### Acknowledgements

The authors would like to acknowledge N. M. Prinsloo and R. Kotze for helpful discussions.

### References

- [1] F. M. Elfghi, *Journal of Advanced Catalysis Science and Technology*, **2016**, 3, 27-42
- [2] A. Jahel *et al.*, *Journal of Catalysis* **2010**, 272, 275-286
- [3] F. G. Ciapetta and D. N. Wallace, *Catalysis Reviews: Science and Engineering* **1972**, 5:1, 67-158
- [4] G. J. Antos and A. Aitani (eds), *Catalytic Naphtha Reforming 2nd Edition*, Marcel Dekker Inc., New York, **2004**, 183-185
- [5] P. Avenier *et al.*, *Oil & Gas Science and Technology – Rev. IFP Energies nouvelles* **2016**, 71, 41
- [6] P. Raybaud *et al.*, *Journal of Catalysis* **2013**, 308, 328-340
- [7] E. Caricato *et al.*, *Industrial & Engineering Chemistry Research* **2017**, 56 (23), 6854–6863
- [8] P. Ghosh *et al.*, *Industrial & Engineering Chemistry Research* **2006**, 45, 337-345

## CO oxidation, CO-PROX and possible methanol synthesis over Pd-CeO<sub>2</sub> synthesised via solution combustion using tartaric acid as a fuel

Thabiso P. O. Mkhwanazi\*, Lingokuhle B. Ngema, Sbusiso Motha, Bongokuhle S. Xaba, Majid D. Farahani and Holger B. Friedrich  
School of Chemistry and Physics, University of KwaZulu-Natal, Private Bag X54001, Durban 4000, South Africa  
\* Email: 213570101@stu.ukzn.ac.za

*This study aims to investigate the activity of Pd/CeO<sub>2</sub> synthesised by solution combustion synthesis (SCS) using tartaric acid as a fuel for CO-oxidation, CO-PrOX and possible methanol synthesis.*

Preparing Pd/CeO<sub>2</sub> catalysts by solution combustion results in Ce<sup>4+</sup> being substituted by Pd<sup>2+</sup>, which results in the formation of lattice oxygen vacancies and a Ce-O-Pd supercell structure, which has high stability and activity for oxidation reactions [1]. The microstructure, surface area and palladium dispersion of the prepared catalyst were determined prior to catalytic activity testing for CO-oxidation and preferential oxidation of CO (CO-PrOX). Furthermore, this catalyst will be tested for methanol synthesis via CO<sub>2</sub> hydrogenation. The prepared catalyst was characterized by X-ray diffraction (XRD), transmission electron microscopy (TEM), energy dispersive X-ray spectrometer (EDX), laser raman spectroscopy (LRS), scanning electron microscopy (SEM), transmission electron microscopy (TEM) and Brunauer–Emmett–Teller (BET) nitrogen adsorption prior to all catalytic testing.

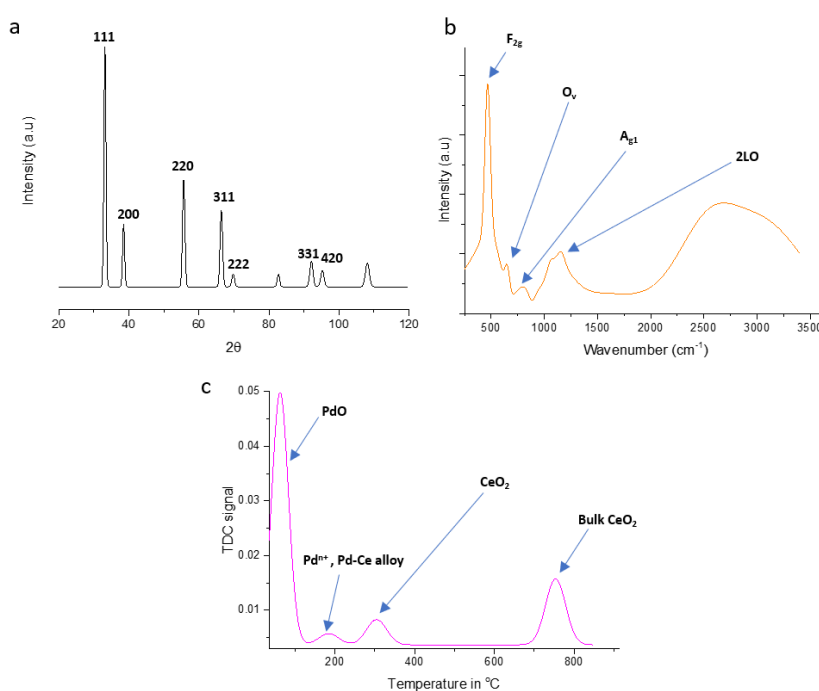


Figure 1: The a) XRD, b) Raman spectra and c) H<sub>2</sub>-TPR of the Pd<sub>0.03</sub>Ce<sub>0.97</sub>O<sub>2.5</sub>-tartaric acid

Table 1: The surface composition of the synthesized catalyst.

Catalyst	Surface area	Oxygen vacancies $\left[ \frac{I_{660\text{cm}^{-1}}}{I_{500\text{cm}^{-1}}} \right]$	Hydrogen Consumption at 250°C mmol	Type of Pd <sup>2+</sup> (%)	
				Pd <sup>2+</sup> in CeO <sub>2</sub>	PdO
Pd <sub>0.03</sub> Ce <sub>0.97</sub> O <sub>2-δ</sub> -tartaric acid	35	0.175	0.328	100	0

The prepared catalyst was observed to be highly active in the CO oxidation reaction with the T<sub>100</sub> achieved at a temperature below 200 °C at a GHSV of 24000 h<sup>-1</sup> and this catalytic activity was attributed to the presence of lattice oxygen (**Fig.1b**) and the high Pd dispersion (**Table 1**). In the PrOX reaction, this catalyst was observed to be highly active and selective for hydrogen oxidation (**Fig.2b and 2c**) which could be attributed to PdO reduction during the reaction. The Pd-based catalyst tends to adsorb hydrogen rather than CO in PrOX reactions which suggest that the CO active sites on the catalyst are blocked by the adsorbed hydrogen [2]. From these observations, the catalyst will be further tested for methanol synthesis due to the ease of Pd reduction.

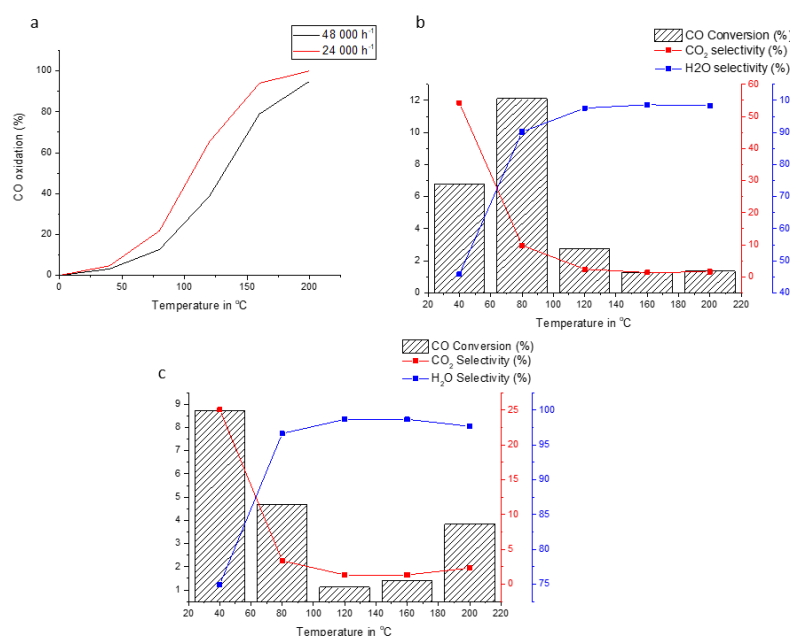


Figure 2: The catalytic activity of Pd<sub>0.03</sub>Ce<sub>0.97</sub>O<sub>2-δ</sub>-tartaric acid under a) CO oxidation, b) CO-PrOX at 48 000h<sup>-1</sup> and c) CO-PrOX at 24 000 h<sup>-1</sup>.

## References

- Colussi, Sara, et al. "Influence of Different Palladium Precursors on the Properties of Solution-Combustion-Synthesized Palladium/Ceria Catalysts for Methane Combustion." *ChemCatChem* 7.14 (2015): 2222-2229.
- Navlani-García, Miriam, et al. "Pd/zeolite-based catalysts for the preferential CO oxidation reaction: ion-exchange, Si/Al and structure effect." *Catalysis Science & Technology* 6.8 (2016): 2623-2632

# Gadolinium-promoted Ru/Ce<sub>0.5</sub>Zr<sub>0.5</sub>O<sub>2</sub> nanorods for the efficient methane reforming with CO<sub>2</sub>

*Subhasis Das,<sup>1,2</sup> Ankur Bordoloi,<sup>1</sup> Martin Muhler<sup>2</sup>*

*1. Conversions & Catalysis Division, CSIR-Indian Institute of Petroleum, Uttarakhand, India*

*2. Laboratory of Industrial Chemistry, Ruhr-University Bochum, D-44780 Bochum, Germany*

## **Introduction:**

Rapid growth of civilization and industrialization enhances the energy demand sharply. According to Exxon's 2040 Energy Outlook projects an 85% increase in global electricity demand over the period of 2010–2040 has been detected<sup>1</sup>. To fulfill the energy demand either we have to build the same number of thermal/nuclear power plants or to enhance the use of other alternative energy resources. Among the alternative energies, increasing methane reserves in terms of natural gas, bio gas, shale gas attracts researcher's attention to use them as future fuel option. In addition, enhanced concentration of CO<sub>2</sub> in the earth atmosphere also causes global warming. In this perspective methane reforming with CO<sub>2</sub> possesses a significant potential to mitigate the greenhouse effect. In addition, the generated syngas is also suitable for production of higher oxygenates<sup>2-4</sup>. Although this process has significant potential, however till date this process is not commercialized owing to unavoidable coke deposition and metal sintering under the harsh reaction conditions. In the present study, we explore ceria, zirconia and a ceria-zirconia mixed oxide supported Ru catalysts towards long-term coke-free methane reforming. In addition, we also explore the effect of Gd towards long-term catalytic activity.

## **Experimental:**

The catalysts have been prepared by a single step hydrothermal approach using CTAB as structure-directing agent and hydrazine as capping agent. The catalytic activity of the prepared catalysts has been examined in methane reforming with CO<sub>2</sub> at atmospheric pressure for 200 h at a GHSV of 10000 mL h<sup>-1</sup> g<sup>-1</sup> in a fixed-bed downflow microreactor at 700 °C.



## Result and Discussion:

The XRD patterns of the fresh catalysts confirm the presence of RuO<sub>2</sub> as an active metal in the catalysts, which decreases marginally due to coke deposition after 200 h activity analysis over ceria and zirconia supported catalysts. However, the RuO<sub>2</sub> reflections do not change in intensity during 200 h analysis over the mixed ceria-zirconia supported catalysts, confirming the superiority of ceria-zirconia supported Ru catalysts. The higher activity of the prepared catalysts has been assigned to the high exposed Ru surface area. A homogeneous distribution of these particles was further confirmed by elemental mapping analysis. Introduction of a small amount of (0.5 wt.%) Gd into the supported Ru catalysts further enhances the catalytic activity and improves the H<sub>2</sub>/CO ratio of the generated syngas.

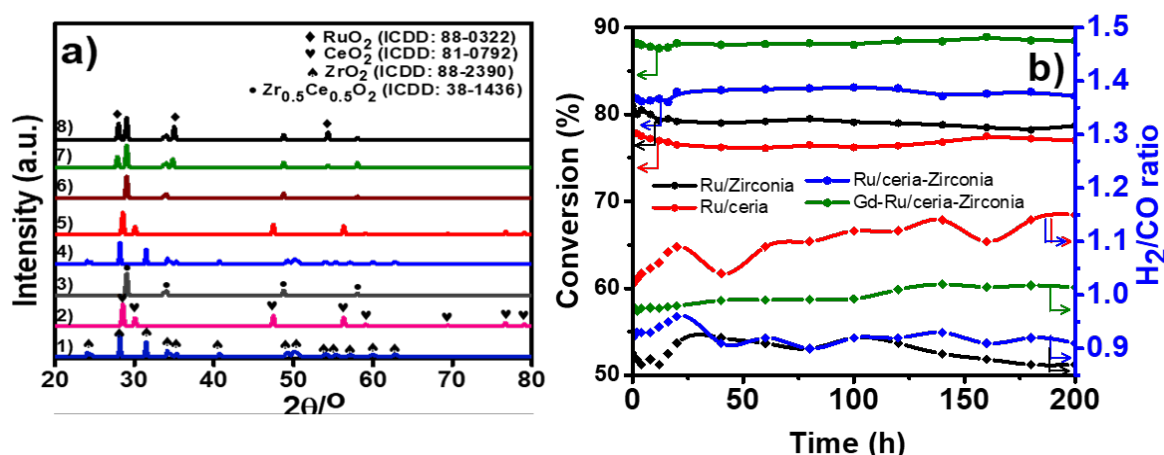


Fig.1: a) XRD patterns of the prepared catalysts b) activity analysis of the prepared catalysts 1) ZrO<sub>2</sub> 2) CeO<sub>2</sub> 3) Zr<sub>0.5</sub>Ce<sub>0.5</sub>O<sub>2</sub> 4) Ru/ZrO<sub>2</sub> 5) Ru/CeO<sub>2</sub> 6) Ru/Zr<sub>0.5</sub>Ce<sub>0.5</sub>O<sub>2</sub> 7) 0.5%Gd Ru/Zr<sub>0.5</sub>Ce<sub>0.5</sub>O<sub>2</sub> 8) 1%Gd-Ru/Zr<sub>0.5</sub>Ce<sub>0.5</sub>O<sub>2</sub>

## Conclusion:

Gd-modified Ru supported on ceria-zirconia has been prepared by a single step hydrothermal approach using hydrazine as a capping agent and CTAB as a structure-directing agent. The catalyst shows a constant activity of 90% conversion with a H<sub>2</sub>/CO ratio in the generated syngas very close to one during entire 200 h time on stream.

## References

1. E. Mobile, The Outlook for Energy: A view to 2040 *Exxon Mobile*, 2012.
2. S. Das, S. Thakur, A. Bag, M. S. Gupta, P. Mondal and A. Bordoloi, *Journal of Catalysis*, 2015, **330**, 46-60.
3. S. Das, M. Sengupta, A. Bag, M. Shah and A. Bordoloi, *Nanoscale*, 2018, **10**, 6409-6425.
4. S. Das, M. Sengupta and A. Bordoloi, *ChemCatChem*, 2017, **9**, 1845-1853.

# Ex-solution catalysts for H<sub>2</sub> production through hydrocarbon fuel reforming processes

*E.V. Matus<sup>1</sup>, I.Z. Ismagilov<sup>1</sup>, O.B. Sukhova<sup>1</sup>, M.A. Kerzhentsev<sup>1</sup>, Z.R. Ismagilov<sup>1,2</sup>*

*<sup>1</sup>Boriskov Institute of Catalysis SB RAS, Novosibirsk, 630090, Russia*

*<sup>2</sup>Institute of Coal Chemistry and Material Science FRC CCC SB RAS, Kemerovo, 650000, Russia*

## 1. Introduction

Small metal nanoparticles stabilized in oxide matrix are widely used as an active component of catalysts and characterized by high surface area, developed metal-support interface, elevated intrinsic activity and a low rate of coking [1]. Tailoring metal-support interaction is an effective way to create appropriate supported metal species for catalytic applications [2, 3]. The extreme case of strong metal-support interaction is the formation of joint surface or bulk phases, for example, solid solutions with a fluorite or perovskite structure, mixed oxides of the spinel structure. Ex-solution of metal from the structure of mixed oxides in a reducing atmosphere at high temperatures provides formation of nanoparticles or clusters in close contact with the support and benefits catalytic properties. In this work, we used the ex-solution concept for the development of Ni catalysts for hydrocarbon fuel reforming processes stable against deactivation. The effect of the composition of oxide matrix ((Ce<sub>1-x</sub>La<sub>x</sub>)<sub>0.8</sub>Ni<sub>0.2</sub>O<sub>y</sub> and (Ce<sub>1-x</sub>Mg<sub>x</sub>)<sub>0.8</sub>Ni<sub>0.2</sub>O<sub>y</sub>) and calcination temperature (300-900°C) on the physicochemical properties and functional characteristics of materials in the hydrocarbon fuel reforming processes were studied.

## 2. Experimental

The (Ce<sub>1-x</sub>La<sub>x</sub>)<sub>0.8</sub>Ni<sub>0.2</sub>O<sub>y</sub> and (Ce<sub>1-x</sub>Mg<sub>x</sub>)<sub>0.8</sub>Ni<sub>0.2</sub>O<sub>y</sub> (x = 0, 0.2, 0.5, 0.8, 1; y = 1-1.5) were used as precursors of Ni catalysts. Materials were synthesized by polymerizable complex method with following thermal treatments at appropriate temperatures, characterized by TA, BET, XRD, HRTEM-EDX, HAADF-STEM, SEM, DRS UV-Vis, Raman spectroscopy and H<sub>2</sub>-TPR and tested in autothermal reforming of ethanol (200-600°C, molar ratio C<sub>2</sub>H<sub>5</sub>OH:H<sub>2</sub>O:O<sub>2</sub>:He = 1/3/0.4/0.7) and steam/CO<sub>2</sub> reforming of methane (600-800°C, molar ratio CH<sub>4</sub>:CO<sub>2</sub>:H<sub>2</sub>O:He = 1.0/0.81/0.38/2.8).

### 3. Results and discussion

The systematic study of  $(\text{Ce}_{1-x}\text{La}_x)_{0.8}\text{Ni}_{0.2}\text{O}_y$  and  $(\text{Ce}_{1-x}\text{Mg}_x)_{0.8}\text{Ni}_{0.2}\text{O}_y$  by a group of methods indicates that the genesis, physicochemical and functional properties of Ni ex-solution catalysts are determined by their composition. In a wide range of the La/Ce molar ratio (0-4), the materials after calcination at 300–500°C are  $\text{CeO}_2$ -based solid solution (4-6 nm in size) with sparsely supported nickel oxide particles (less 3 nm in size). Nickel cations are preferentially stabilized in the structure of Ce-La-Ni-O solid solution. The particularity of  $(\text{Ce}_{1-x}\text{Mg}_x)_{0.8}\text{Ni}_{0.2}\text{O}_y$  materials is a formation two-phase system containing  $\text{CeO}_2$ -based and MgO-NiO solid solutions. The introduction of La or Mg in the composition of  $\text{Ce}_{0.8}\text{Ni}_{0.2}\text{O}_{1.8}$  increases structure defectiveness, improves texture properties and stability against sintering but makes worse the reducibility of Ni cations. Treatment in reducing conditions causes the release of the Ni cations and formation of  $\text{Ni}^0$  on the surface of the oxide. The effects of the composition and conditions of thermal treatment of Ni ex-solution catalysts on their coking resistance and functional properties in reforming reactions were elucidated. The catalysts of optimal composition provide hydrogen yields (55% at 600°C in autothermal reforming of ethanol and 85% at 750°C in steam/ $\text{CO}_2$  reforming of methane) which are close to thermodynamic equilibrium values.

### 4. Conclusions

The genesis and properties of ex-solution Ni catalysts obtained from the  $(\text{Ce}_{1-x}\text{La}_x)_{0.8}\text{Ni}_{0.2}\text{O}_y$  and  $(\text{Ce}_{1-x}\text{Mg}_x)_{0.8}\text{Ni}_{0.2}\text{O}_y$  materials were studied. The composition-structure-properties correlation was established and stable against deactivation Ni catalysts for hydrocarbon fuel reforming processes were developed.

### Acknowledgements

The authors are thankful to Dr. V.A. Ushakov, Dr. S.A. Yashnik, Dr. O.A. Stonkus, Dr. E.Y. Gerasimov and Dr. A.P. Nikitin for their help with catalyst characterization. This work was conducted within the framework of the budget project No. AAAA-A17-117041710090-3 for Boreskov Institute of Catalysis.

### References

1. K. An, G.A. Somorjai, *Catal Lett* 145 (2015) 233-248.
2. Z.R. Ismagilov, E.V. Matus, I.Z. Ismagilov, O.B. Sukhova, S.A. Yashnik, V.A. Ushakov, M.A. Kerzhentsev, *Catal. Today*. 323 (2019) 166-182.
3. M. Cargnello, P. Fornasiero, R.J. Gorte, *Catal Lett* 1452 (2012) 1043–1048.

# Improvement of conductivity of carbon material using direct methane reforming

*Fumitaka Kondo, Naruka Tamai, Noriyasu Okazaki,  
Kitami institute of technology, Kitami, Hokkaido, Japan*

## Introduction

The methane direct reforming reaction (DMR:  $\text{CH}_4 \rightarrow \text{C} + 2\text{H}_2$ ) is a reaction that directly decomposes methane to hydrogen and nano-carbon (NC) using a catalyst, and the NC generated can be applied as a conductive material. We succeed in producing it in quantities by a short time in use of DMR[1]. NC can be applied as a functional carbon material because it has electrical and heat conduction property. On the other hand, carbon is used as a conductive material, but its conductivity greatly differs depending on the manufacturing method. In particular, charcoal has poor conductivity. Therefore, in this study, attempts were made to improve conductivity by forming DMC in charcoal form to produce NC.

## Experimental

Was prepared by an impregnation method using an aqueous solution of Fe (NO<sub>3</sub>)<sub>3</sub>·9H<sub>2</sub>O adjusted to make Fe 10 wt% with respect to activated carbon. Also, after impregnating biomass raw materials (mint, oka, sawtooth oak) so that Fe was 3, 15 wt%, carbonization treatment was carried out and pulverization was carried out to prepare. And, the biomass material was impregnated so as to be 8, 20 wt% after carbonizing treatment, and prepared.

The reaction device used a fixed bed flow type reactor. The catalyst was put in the center of quartz tube (an inner diameter and length 2.5 and 100 cm, respectively). DMR was carried out using methane as a reaction gas. The reaction temperature was 750 °C, reaction time was 180 min, and catalyst weight was set to 0.1 g.

The composition of the outflow gas from the reactor was determined by GC (TCD). The activity was evaluated by the conversion rate of the reaction gas to hydrogen. The catalysts of before and after reaction were analyzed with XRD and raman spectrometer.

## Results and discussion

When each catalyst was subjected to DMR at a reaction temperature of 750 °C, Fe(3wt%)/C(mint) showed the maximum activity 20 minutes after the start of the reaction and gently deactivated therefrom. On the other hand, at Fe(3wt%)/C(sawtooth oak, oak), the maximum activity was shown immediately after the start of the reaction, and then it was rapidly inactivated. Different activities are considered to be due to the fact that mint of raw material is perennial, while sawtooth oak and oak are wood. Further, when Fe(15wt%)/C(mint) was reacted at a reaction temperature of 750 °C by increasing the impregnation amount of Fe, the maximum activity was exhibited after 60 minutes, and the activity remained without being inactivated therefrom. Therefore, in the case of Fe(15wt%)/C(mint), the reaction was carried out by changing the reaction temperature to 760 °C, 800 °C and 850 °C, the order of activity was 850 °C > 800 °C > 760 °C > 750 °C became. On the other hand, the activity when using activated carbon as a carrier was markedly lower than when using biomass carbon as a carrier.

Comparing each catalyst of after reaction from the crystallite diameter of Fe calculated from Scherrer's equation of X-ray diffraction, the crystallite diameter of Fe at Fe (8%)/C(mint) or Fe(10%)/AC was about 3 times higher than the one of Fe (3%)/C (mint). Therefore, it is considered that the former reaction is more inactive than the latter reaction due to sintering of the active species Fe, after the reaction.

Next, the conductivity of the carbon formed after the reaction was evaluated by comparison before and after the reaction. When the DMR progressed and the product carbon was confirmed, the volume resistivity decreased and the conductivity improved (Table 1) when compared with the catalyst before and after the reaction, regardless of which catalyst was used. Among them, in C (peppermint) 15%, the conductivity improved as the reaction temperature increased (Table 2). Therefore, it can be said that DMR is an effective means for imparting conductivity to a carbon-based material.

Table 1 Volume resistivity of produced carbon.

Catalysts	Before reac. ( $\Omega \cdot \text{cm}$ )	After reac. ( $\Omega \cdot \text{cm}$ )
Fe(3wt%)/C(mint)	12.4	3.1
Fe(3wt%)/C(oak)	Over Range	1.1
Fe(3wt%)/C(sawtooth oak)	0.9	0.7

Table 2 Volume resistivity of carbon produced at Fe (15 wt%) / C (mint)

Reac. temp.	Before reac. ( $\Omega \cdot \text{cm}$ )	After reac. ( $\Omega \cdot \text{cm}$ )
750 °C	13.9	2.3
760 °C	13.9	0.7
800 °C	13.9	0.6
750 °C	13.9	0.5

## References

[1] A. Tada, T. Matsunaga, N. Okazaki, *Trans. of the MRS-J*, **33**[4] 1059 (2008).

# Malachite-based catalyst precursors for methanol synthesis from CO<sub>2</sub>-rich synthesis gas

*G. Behrendt, A. Hüttner, M. Behrens,  
Inorganic Chemistry, University of Duisburg-Essen, Essen, Germany*

## Introduction

Methanol synthesis over Cu-based catalysts is promoted by Zn [1], which in industrial catalysts is provided by strong metal support interaction (SMSI) between Cu and ZnO [2]. This catalyst is active in the hydrogenation of CO<sub>2</sub> which is a cheap and well available resource. In conventional methanol synthesis, additional CO is needed to increase the methanol yield and to prevent the inhibition of the catalyst by the co-product water. We study the role of Zn and different promoters on the Cu catalyst's performance and selectivity in CO<sub>2</sub> hydrogenation. Transition metal promoters like Co or Fe may also favour the synthesis of higher alcohols like ethanol. For this purpose, we partially substitute copper in the malachite precursor structure (Cu<sub>2</sub>CO<sub>3</sub>(OH)<sub>2</sub>) by iron or cobalt. As non-reducible component we use magnesium, which also can substituted for Cu in a wide range of ratios. In this sense, we use a Cu/Mg-malachite (mcguinnessite) as precursor for a structurally promoted copper catalyst Cu/MgO in methanol synthesis, without any electronical promotion. The effect of different synthesis parameters of precursor co-precipitation was systematically investigated. In a subsequent step, the different promoter species can be added for example by impregnation [3]. In this work, we focus on the catalyst synthesis of Cu/MgO and our first results of methanol synthesis with differently promoted catalysts.

## Experimental

Mg-containing malachite (mcguinnessite), pokrovskite, kolwezite, and chukanovite with different Cu:Mg, Cu:Co:Mg and Cu:Fe:Mg ratios were synthesized in an automated laboratory reactor system by co-precipitation with sodium carbonate as precipitation agent. For selected samples, a hydrothermal post-treatment step was carried out at 102 °C for 20 hrs. Promoters like zinc were added by impregnation or by adding several metal salts during co-precipitation. A subsequent calcination step was carried out at 330–420 °C in air depending on the precursor. Before catalysis, all samples were reduced for one hour under 1 bar H<sub>2</sub> at 260 °C.

## Results

N<sub>2</sub> physisorption analysis shows specific surface areas > 70 m<sup>2</sup> g<sup>-1</sup> for all precursors. PXRD patterns confirm crystallization of the malachite-like structure after the wet-chemical synthesis. Calcination leads to the formation of poorly crystalline mixed oxides and reduction in hydrogen yields metallic copper nanoparticles and partially or fully reduced iron or cobalt, depending on the sample, reduction temperature and time. Methanol synthesis was performed over Cu/MgO with different amounts of Zn promoter in H<sub>2</sub>/CO<sub>2</sub> = 3:1 at 4.9 MPa, with 200 mg catalyst diluted with 400 mg SiC and temperatures between 200 and 260 °C (Fig. 1). The samples were less active than the highly optimized industrial-like sample “FHI standard” [4]. However, at low temperature, an increased selectivity towards methanol was observed, which seems to increase with increasing amount of Zn.

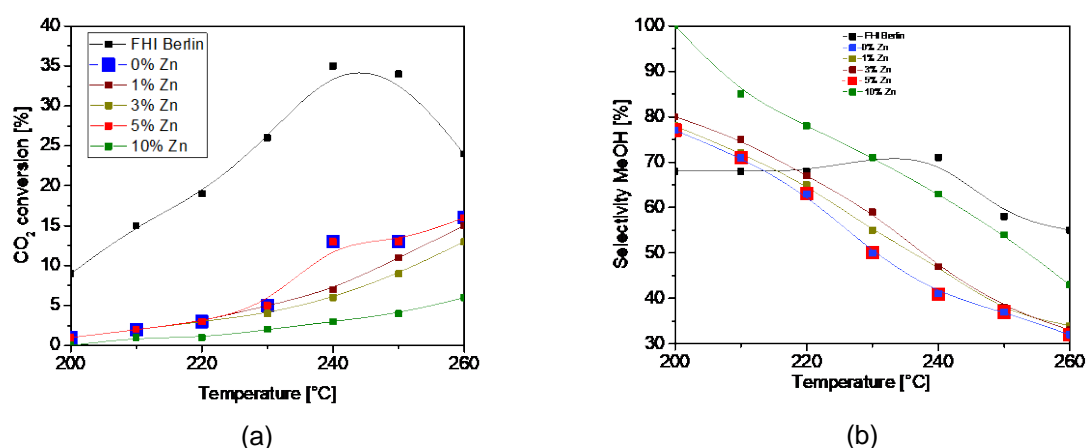


**Fig. 1:** (a) CO<sub>2</sub> conversion of different Zn containing Cu/MgO catalysts synthesized from mcguinnessite compared to a commercial-type Cu/ZnO:Al catalyst (FHI standard), (b) selectivity toward methanol as a function of temperature.

We acknowledge the collaboration with Surface Chemistry Laboratory at the University of Tsukuba, Japan (X. Zhang and J. Nakamura) for help with the catalytic measurements, and the DFG-SPP 2080 as well as the DAAD for financial support.

## References

- [1] J. Nakamura, Y. Choi, T. Fujitani, *Top. Catal.* **2003**, *22*, 277–285.
- [2] S. Zander, E. L. Kunkes, M. E. Schuster, J. Schumann, G. Weinberg, D. Teschner, N. Jacobsen, R. Schlögl, M. Behrens, *Angew. Chem. Int. Ed.* **2013**, *52*, 6536–6540.
- [3] H. Arakawa, *Stud. Surf. Sci. Catal.* **1998**, *114*, 19–30.
- [4] J. Schumann, T. Lunkenbein, A. Tarasov, N. Thomas, R. Schlögl, M. Behrens, *ChemCatChem* **2014**, *6*, 2889–2897.

## Design of active sites in Ni/CeO<sub>2</sub> catalysts for the methanation of CO<sub>2</sub>: tailoring the Ni-CeO<sub>2</sub> contact

A. Cárdenas-Arenas<sup>a</sup>; E. Bailón García<sup>a</sup>; A. Davó-Quiñonero<sup>a</sup>; D. Lozano-Castelló<sup>a</sup>; A. Quindimil<sup>b</sup>, B. Pereda-Ayo<sup>b</sup>, J. A. González-Marcos<sup>b</sup>, J. R. González-Velasco<sup>b</sup>, Agustín Bueno-López<sup>a</sup>, <sup>a</sup>Univ. of Alicante, <sup>b</sup>Univ. of the Basque Country, Spain

The burning of fossil fuels has caused an increase in the atmospheric CO<sub>2</sub> levels, increasing the greenhouse effect and contributing to the global warming. This has led to an increase in interest in the search for alternative clean and sustainable energy sources or CO<sub>2</sub> transformation methods. Methanation of CO<sub>2</sub> is a sustainable solution since the methane produced can be directly injected into the existing network of natural gas pipelines and be used as fuel. Nevertheless, the main problem in the transformation of CO<sub>2</sub> is the great stability of the C=O bonds, making necessary the use of a suitable catalyst to reach acceptable reaction rates.

The reduction of CO<sub>2</sub> requires the presence of two active sites: a catalyst component that can activate the molecule (i.e. Ni<sup>2+</sup>-ceria interface) and a reduced metal sites that are capable of dissociating H<sub>2</sub> [1].

Herein, the proportion of each required active sites was varied by the modification of the Ni interaction with the CeO<sub>2</sub> support and the influence of this proportion in the CO<sub>2</sub> methanation was deeply analyzed. This interaction was modified by the Ni incorporation method and by controlling the surface of the ceria support. In this sense, three dimensionally ordered macroporous (3DOM) structures were synthesized in which the Ni was introduced in situ during the 3DOM synthesis by coimpregnation (Ni-Ce catalysts) or successive impregnation (CeO<sub>2</sub>/Ni catalysts) of Ni and Ce precursors or after the CeO<sub>2</sub> synthesis by Ni impregnation (Ni/CeO<sub>2</sub> catalysts). Materials with uncontrolled structures (Ref) were also prepared.

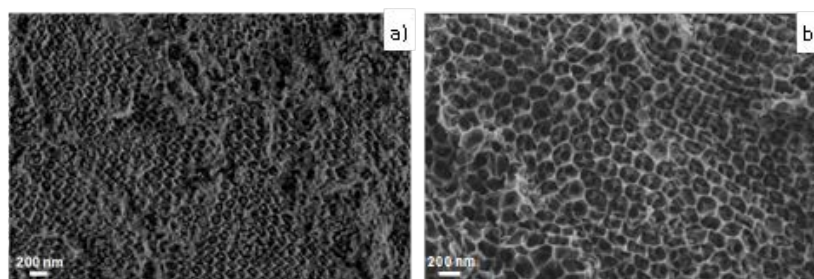


**Figure 1.** SEM images of a) Ni/CeO<sub>2</sub> and b) CeO<sub>2</sub>/Ni 3DOM-catalysts.



Well-defined 3DOM structures were obtained in all cases. The presence of Ni during 3DOM structure formation improves the definition of the structure (Figure 1) and affects the crystallinity and reducibility of the CeO<sub>2</sub> phase.

As it was pointed out by XPS and H<sub>2</sub>-TPR, the proportion of surface Ni and Ni in intimate contact with ceria depends on the Ni-incorporation method and the reducibility of ceria surface. The addition of Ni prior to the synthesis of CeO<sub>2</sub> structure generates a high proportion of Ni in intimate contact with ceria, which improves the reducibility of the ceria surface (Ce<sup>3+</sup> sites), whereas less contact is obtained for impregnated samples. Consequently, the former presents a high number of active sites for the dissociation of CO<sub>2</sub>, but not enough for the dissociation H<sub>2</sub> whereas the latter have a high number of sites for the dissociation and transfer of H<sub>2</sub>, but not enough for the dissociation of CO<sub>2</sub>. At this sense, an optimal proportion of both sites is obtained for maximum CO<sub>2</sub> conversion with 30 % surface Ni for the H<sub>2</sub> dissociation and 70 % of Ni in intimate contact with ceria for CO<sub>2</sub> dissociation (Figure 2a). Increasing the Ni in intimate contact to higher levels, the CO<sub>2</sub> dissociation is improved, but the dissociation and transfer of H<sub>2</sub> is avoided and, as consequence, CO is the main product (Figure 2b), i.e. 3DOM CeO<sub>2</sub>/Ni catalyst. The activity also decreases, because chemisorbed CO desorption is the limiting step, and CO blocks the active sites. If surface Ni increase, the transfer of dissociated H atoms to the chemisorbed CO is favored, increasing the activity and selectivity to methane.

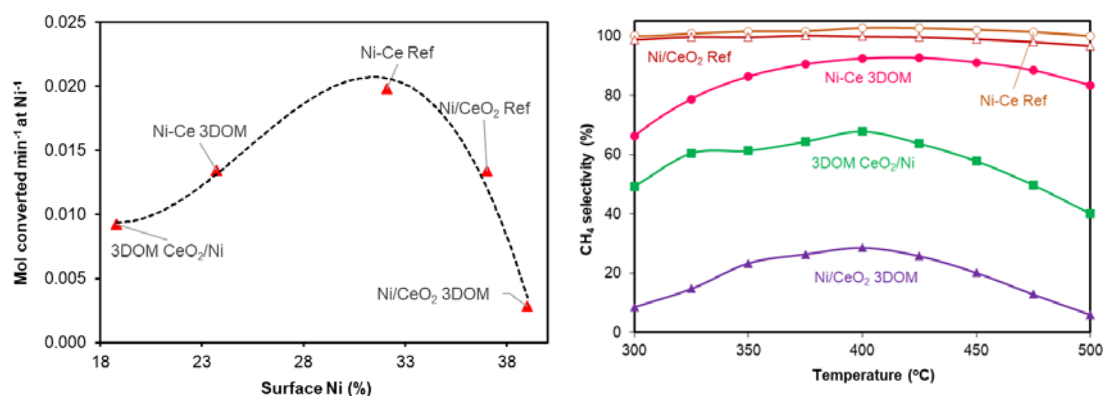


**Figure 2.** (Left) Relationship between activity per surface active sites and the proportion of surface Ni species and (right) CH<sub>4</sub> selectivity.

#### Acknowledgements

Projects PROMETEO/2018/076, CTQ2015-67597-C2-1-R and CTQ2015-67597-C2-2-R, grant FJCI-2015-23769 and FPU14/01178 and the UE (FEDER funding).

#### References

- [1] V. Alcalde-Santiago et al. Ni/LnO<sub>x</sub> Catalysts (Ln=La, Ce or Pr) for CO<sub>2</sub> Methanation. ChemCatChem 10 (2018) 1–11.

# Production of syngas from biogas on Ni-rich smectite based catalyst

Salma Baraka<sup>1, 2</sup>, Rachid Brahm<sup>2</sup>, Laurent Caner<sup>1</sup>, Claude Fontaine<sup>1</sup>, Florence Epron<sup>1</sup>, Sabine Petit<sup>1</sup>, Nicolas Bion<sup>1</sup>

<sup>1</sup> Institut de Chimie des Milieux et Matériaux de Poitiers (IC2MP) - University of Poitiers, CNRS, 86073 Poitiers Cedex 9, France

<sup>2</sup> Laboratory of Coordination and Analytical Chemistry (LCCA) - Chouaib Doukkali University, BP.20, 24000 El Jadida, Morocco.

The valorization of biogas requires innovation & development to look for efficient processes. Dry reforming of methane (DRM) reaction  $\text{CH}_4 + \text{CO}_2 \rightarrow 2\text{CO} + 2\text{H}_2$  is particularly appropriate for the valorization of biogas inasmuch as the two reactants are the two main compounds of the biogas (after purification to remove impurities like  $\text{H}_2\text{S}$ ). In addition, DRM has attracted much attention during the last two decades, since it is considered as a greenhouse gas consuming reaction [1]

The catalytic dry reforming over noble metal-based catalysts exhibit high catalytic activity and selectivity toward syngas production. However, the cost and the sensitivity to sulfur poisoning are the major drawbacks for noble metal (Pt, Rh...) Catalysts. Therefore, the development a new low-cost catalyst with promising activity is still a challenge. The aim of this work is to compare two catalysts consisting in an Rh/NiO- $\text{Al}_2\text{O}_3$  sample developed in our laboratory and Ni-rich clay material (originated from Niquelândia in Brazil). In the latter sample, Ni is associated to smectite-type clay minerals which may contain up to 25 wt% Ni located inside the

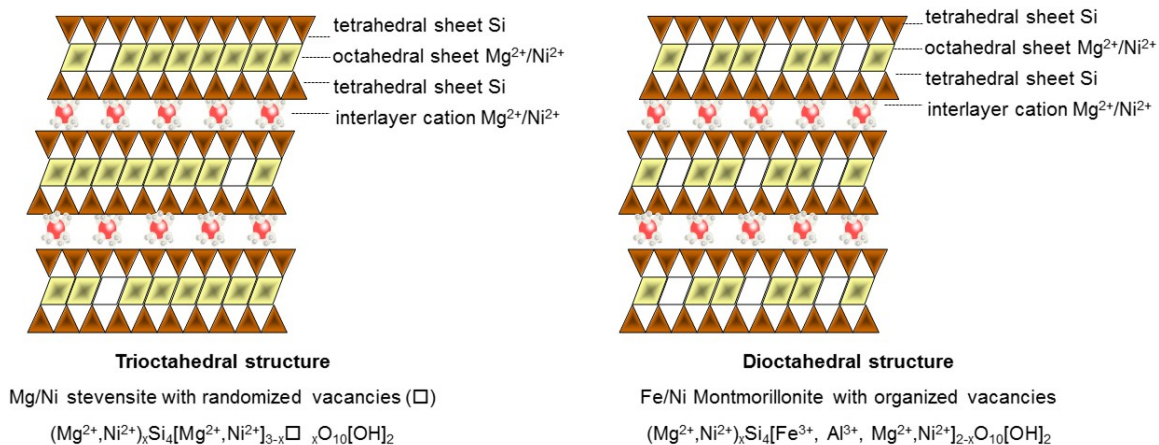


**Figure 1** : Structure of smectite-type clay minerals

structure (octahedral layer) or as exchangeable cation in the interlayer space (Figure 1) [2]. The materials were fully characterized by several characterization techniques (textural; structural and elemental analysis). Both catalysts were tested in catalytic dry reforming under different experimental conditions in order to study their performances in terms of catalytic activity, selectivity, and durability.

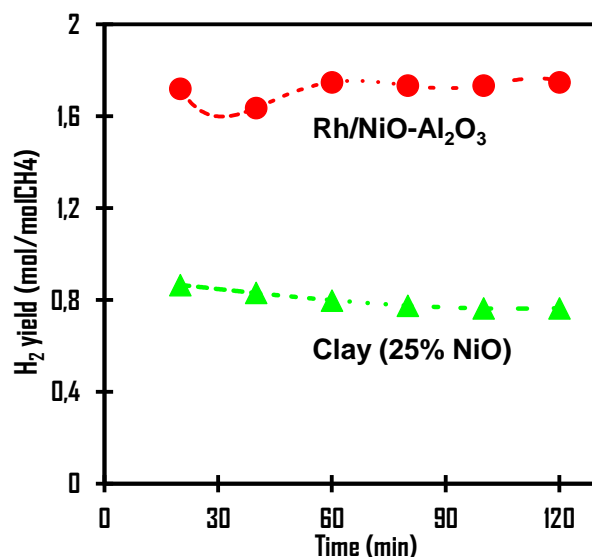


**Figure 2.** Evolution of the H<sub>2</sub> yield as a function of time during DRM reaction at 800°C

In the Figure 2 are presented the hydrogen yield obtained for Rh supported on NiO-Al<sub>2</sub>O<sub>3</sub> containing 0.36 wt-% Rh and 18.07 wt-% Ni and Ni-rich clay samples. For a ratio CH<sub>4</sub>:CO<sub>2</sub>=1, Rh/NiO-Al<sub>2</sub>O<sub>3</sub> gives 86% of CH<sub>4</sub> converted, 91 % of CO<sub>2</sub> converted for 1.74 mol H<sub>2</sub> and 1.77 mol CO produced per mol of CH<sub>4</sub> introduced which is close to the values expected at the thermodynamic equilibrium. In comparison the conversions and yields obtained for the clay material are lower but remain significant despite the absence of any purification of the bare material. Deep characterization of the different phases that constitute the clay mineral enabled the establishment of relationships between the material composition, the location of Ni and the catalytic performances.

The results reveals that a catalyst based on bare clay mineral without any modification is a promising and low-cost catalyst which still deserve some optimizations to limit the deactivation phenomenon. It could then be an alternative of noble metal-containing catalyst.

## References

- [1] Fischer, F., Tropsch, H., *Brennst. Chem.* 3 (1928) 39–46.
- [2] Mano, E.S., Caner, L., Petit, S., Chaves, A.P., Mexias, A.S. *Clays Clay Min.* 62 (2014) 324–335.

# Thermodynamic insights into the hydrotreatment of used vegetable oils using ASPEN PLUS simulations

*Uttaran Basak, Department of Chemical Engineering, IIT Delhi, New Delhi-110016, India; Rajarshi Bandyopadhyay, Haldor Topsoe India Pvt. Ltd., Faridabad-121003, Haryana, India; Sreedevi Upadhyayula, Department of Chemical Engineering, IIT Delhi, New Delhi-110016, India*

## Introduction

The dwindling fossil fuel reserves and environmental issues associated with its extraction and processing have forced the society to look for alternatives to meet its ever-increasing energy demand[1]. One such alternative is hydroprocessing of 'used cooking oil' to produce renewable diesel. This work is aimed at recovering diesel range hydrocarbons from the used oils which have been used in households and outside eateries. This helps in disposal of these oils and also to cater to the industries using diesel as a fuel thereby reducing the load on diesel obtained from fossil sources. Cooking oil is rich in triglycerides and fatty acids and has long aliphatic chains. These long aliphatic chains can be converted to straight chain hydrocarbons (paraffins) using hydrogen; giving a product that is commonly known as Hydrotreated Vegetable Oil (HVO)[2]. There are two main pathways for this process - hydrodeoxygenation (HDO) and decarboxylation (DCO). The HDO pathway gives us paraffins having the same number of carbons as in the fatty acid. In the DCO pathway,  $\text{CO}_2$  is released and hence the resultant hydrocarbon has one carbon lesser than the fatty acid. For industrial application, the HDO pathway is favored over the DCO pathway. This is because the  $\text{CO}_2$  produced in DCO pathway reacts with the excess  $\text{H}_2$  present in the system to form water and CO (Reverse Water Gas Shift reaction), which in turn undergoes methanation reaction to produce  $\text{CH}_4$ .  $\text{CH}_4$  is an undesired product as it reduces hydrogen partial pressure in the reactor system and hence needs to be purged out – a process that also results in loss of hydrogen. Our work aims at performing a thermodynamic equilibrium analysis between these two reaction pathways to understand their dependence on the different operating parameters from a thermodynamic perspective. The equilibrium reactor module RGIBBS (minimizes Gibbs free energy change) of ASPEN PLUS (v9) was used for the study. Sensitivity analysis of the effect of the following process parameters: temperature, pressure and amount of  $\text{H}_2$  in the feed on the product distribution was

analysed by simulations. This analysis will help in optimizing the process parameters for maximising the selective yields of diesel range hydrocarbons from these used oils.

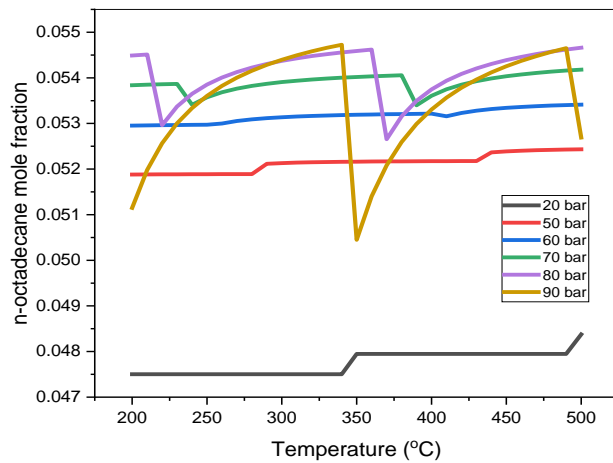


Figure 1: Mole fraction of n-octadecane with change in temperature

It was varied with pressure at intervals of 5 bars (few simulations are shown here for clarity). The operating temperature was 200°C-500°C as this is the temperature range followed in industries.

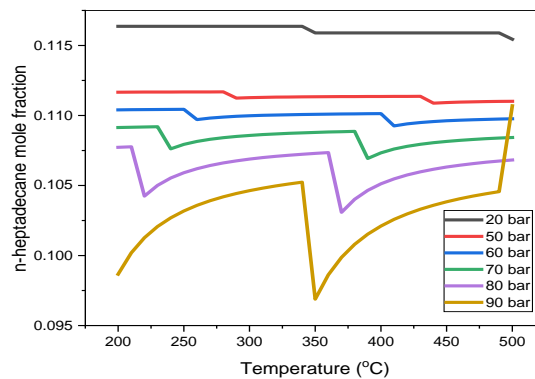


Figure 2: Mole fraction of n-heptadecane with change in temperature

## Conclusion

Using the RGIBBS reactor in ASPEN Plus, the sensitivity analysis was done in which the DCO pathway was favorable at lower pressures whereas the HDO pathway was favorable at higher pressures. Similar to this pressure sensitivity, hydrogen to oil ratio was also varied to check its sensitivity.

## References

- [1] M. Hook, X. Tang, Depletion of fossil fuels and anthropogenic climate change-A review, Energy Policy 52 (2013), 797-809. doi:10.1016/j.enpol.2012.10.046
- [2] R. Arvidsson, S. Persson, M. Froling, M. Svanstrom, Life cycle assessment of hydrotreated vegetable oil from rape, oil palm and Jatropha, Journal of Cleaner Production 19 (2011), 129-137
- [3] A.B. Chhetri, K.C. Watts, M.R. Islam, Waste Cooking Oil as an alternate feedstock for Biodiesel Production, Energies 1 (2008), 3-18. doi:10.3390/en1010003

Oleic acid ( $C_{18}H_{34}O_2$ ) was chosen as the model compound as it is the major component in waste cooking oils[3] and it was hydrotreated so as to see the equilibrium mole fractions of n-octadecane (Figure 1) and n-heptadecane (Figure 2).

# Hydrothermal conversion of dihydroxyacetone (DHA) using Al, Pb or Nb doped TiO<sub>2</sub> catalysts obtained by sol-gel synthesis

*Antonio de Brito Santiago Neto, IRCELYon, France, Universidade Federal do Ceara, Brazil; Alcineia C. Oliveira, Universidade Federal do Ceara, Brazil; M. Gabriely Alves da Cruz, IRCELYon, France, Universidade Federal do Ceara, Brazil; Nadine Essayem, IRCELYon, France; Shashank Mishra, IRCELYon, France.*

## Scope

In the frame of catalysts design for biorefineries, TiO<sub>2</sub> based materials are addressing increasing interest due to its hydrothermal stability which makes it a support of choice for catalytic transformation in hot water. TiO<sub>2</sub> was largely applied as support for noble metals for reduction or oxidation reactions, but also as well as water tolerant acid-base [1,2]. The available commercial TiO<sub>2</sub> contain additives such as Si, Fe or S, together with usual low specific surface areas. Pure TiO<sub>2</sub>, with enhanced textural features, can be obtained via sol-gel methods to design water tolerant Lewis solids solid acids catalysts [2]. Besides, catalysts with Lewis acid properties have found increasing applications for carbohydrates transformations such as zeolites with variable Si/Al ratio, Sn-Beta zeolite... However, these materials, which present well defined active sites in terms of dispersion and coordination, present as main drawback, their poor stability in hot water. It might be a real breakthrough to design materials with a controlled dispersion of active metallic centers in controlled coordination, strongly anchored in a water tolerant support such as TiO<sub>2</sub>. This is the objective of this study.

## Results and discussion

New modified alkoxides of aluminium (III), titanium (IV), niobium (V) and lead (II) namely [Al<sub>4</sub>(mdea)<sub>6</sub>], [Ti<sub>2</sub>(OEt)<sub>4</sub>(mdea)<sub>2</sub>(EtOH)<sub>2</sub>], [Nb(OEt)<sub>3</sub>(mdea)], [Pb<sub>2</sub>(mdea)<sub>2</sub>].mdeaH<sub>2</sub>, (where mdeaH<sub>2</sub> = N-methyldiethanolamine) were prepared and used as sol-gel precursors to obtain Al, Nb and Pb doped TiO<sub>2</sub> nanoparticles. The purity of the as-synthesized precursors was demonstrated by XRD and NMR. The calcined samples were characterized XRD, N<sub>2</sub> isotherms, HRTEM-HAADF, calorimetry and FTIR of CO<sub>2</sub> or pyridine adsorption. Their catalytic performances were evaluated in a model reaction, DHA conversion in hot water. The doped TiO<sub>2</sub>,

after calcination at 500°C, present exclusively the anatase TiO<sub>2</sub> phase with high S<sub>BET</sub> for TiO<sub>2</sub> doped with 10% Nb or Pb, respectively 253 and 355 m<sup>2</sup>.g<sup>-1</sup>. TiO<sub>2</sub> doped with 10% Al presents a lower S<sub>BET</sub>, of 60 m<sup>2</sup>.g<sup>-1</sup>.

The evaluation of their catalytic performances in the model reaction were compared to the benchmark P25 catalyst and to an un-doped sol-gel TiO<sub>2</sub> (S<sub>BET</sub> = 155 m<sup>2</sup>.g<sup>-1</sup>). Our data revealed that the presence of the Nb, Pb or Al dopant accelerates significantly the reaction rate, irrespective of the S<sub>BET</sub>. Moreover, in agreement with our expectations, the materials exhibit excellent hydrothermal stability: the chemical analysis of the reaction media at the end of the reaction show the absence of significant leaching of the catalyst elements (Table1).

## Conclusion

Kinetic investigations revealed unexpected yield for new products which cannot be simply explained by the well accepted acid catalyzed chain mechanism, where Lewis and Brønsted acid sites promote the DHA dehydration into the pyruvaldehyde intermediate formation, which can be further converted into lactic acid over Lewis acid sites.

Table 1: DHA transformation, Ti, Pb, Al, Nb analysis in the liquid reaction media.

Samples	Initial rate of DHA transformation (mol.h <sup>-1</sup> .g <sup>-1</sup> )	Leaching of elements in the reaction media after 4h
P25	0.13	Ti ~ 0 %
Sol-gel TiO <sub>2</sub>	0.01	Ti ~ 0%
Nb/TiO <sub>2</sub>	0.34	Nb < 0.1 %, Ti ~ 0.6%
Pb/TiO <sub>2</sub>	0.33	Pb < 0.1%, Ti ~ 0.6%
Al/TiO <sub>2</sub>	0.27	Al ~ 0.5%, Ti ~ 0%

Conditions:  $m_{DHA} = 0.18 \text{ g}$ ,  $m_{cata} = 0.05 \text{ g}$ ,  $m_{H_2O} = 20 \text{ g}$ ,  $T = 90 \text{ }^\circ\text{C}$ .

## References

- [1] M.Watanabe, Y.Aizawa, T.Iida, R.Nishimura, H.Inomata App.Catal.A:General 295 (2005) 150-156.  
 [2] M.Hattori, K.Kamata, M.Hara Phys.Chem.Chem.Phys.19 (2017) 3688.

# Mesoporous materials for efficient utilization of CO<sub>2</sub> in Fischer Tropsch process

*Shashank Bahri, Department of Chemical Engineering, IIT Delhi, New Delhi-110016, India; India; Uttaran Basak, Department of Chemical Engineering, IIT Delhi, New Delhi-110016, India; India; Sreedevi Upadhyayula, Department of Chemical Engineering, IIT Delhi, New Delhi-110016, India*

## Introduction

The objective of our work is to convert CO<sub>2</sub> containing syngas into diesel range hydrocarbons to alleviate CO<sub>2</sub> levels in the atmosphere and also to meet the ever-increasing demands for diesel fuel. Fischer Tropsch (FT) [1] is a well-known commercial process for producing liquid fuel from syngas since 1936 and it is followed in conversion of CO<sub>2</sub> containing syngas to synthetic diesel. Water Gas Shift (WGS) reaction over Fe-based catalyst [2] helps us to overcome the H<sub>2</sub> deficient nature of syngas obtained with 0.37 Ribblet Ratio but it also increases the CO<sub>2</sub> content which may lead to lower catalytic efficiency and fast catalyst deactivation.

The support (zeolite) was pre-treated so as to get some mesopores. Fe-Co bimetallic[3] metals supported on commercial zeolites is used for production of synthetic diesel from CO<sub>2</sub> containing syngas. The reported FT catalyst with bifunctional sites are capable of selective production of diesel range hydrocarbons in one catalytic step with stable time on stream for 120 h.

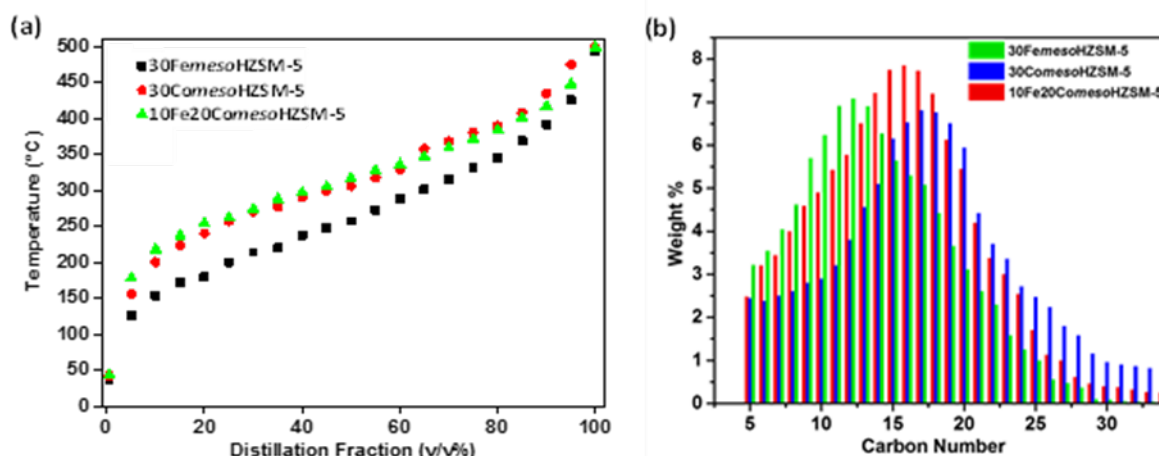


Figure 1 Quantification of liquid products obtained after the 120 h time-on-stream run (a) Simulated Distillation analysis and (b) Weight % v/s carbon number.



As shown in Figure 1(a), simulated distillation so as to quantitatively acquire the amount of hydrocarbons present in the product. Design of Experiment (DOE) a statistical tool, was used to optimize process parameters.

The collegial effect of the uneven distribution of weaker acidic sites in conjugation with hierarchical porous structure showed 50.6% selectivity towards linear chain C<sub>13</sub>-C<sub>23</sub> range hydrocarbons which had high cetane number and CO<sub>2</sub> utilization as a carbon feedstock makes conventional FT a sustainable and economical process.

The hydrocarbons present in the product was determined qualitatively using Gas Chromatography with Mass Spectroscopy (GC-MS) as shown in Figure 1 (b).

## Conclusion

The remarkable impact of combining developed post synthesis mesoporosity on the catalyst with preserved micropore structure and medium acidic strength along with Fe-Co bimetallic active metal resulted in positive conversion of CO<sub>2</sub> despite WGS reaction and also it resulted in production of cleaner diesel range fuels in H<sub>2</sub> deficient conditions. Thus, it has an impact on the commercial biomass-to-liquid fuel technology for economical and greener conversion of CO<sub>2</sub> containing syngas.

## References

- [1] M.E. Dry. High quality diesel via the Fischer-Tropsch process- a review, *J Chem Technol Biotechnol* 77 (2001), 46-50. doi:10.1002/jctb.527
- [2] P. Sirikulbodee, T. Ratana, T. Sornchamni, M. Phongaksorn, S. Tungkamani, Catalytic performance of Iron-based catalyst in Fischer-Tropsch synthesis using CO<sub>2</sub> containing syngas, *Energy Procedia* 138 (2017), 998-1003. doi: 10.1016/j.egypro.2017.10.112
- [3] M.K.Gnanamani, G. Jacobs, H.H. Hamdeh, W.D. Shafer, F. Liu, S.D. Hopps, G.A. Thomas, B.H. Davis, Hydrogenation of Carbon Dioxide over Co-Fe Bimetallic Catalysts, *ACS Catal.* 6 (2016), 913-927. doi: 10.021/acscatal.5b01346

# **Description of (La,Sm)(Mn,Co)O<sub>3</sub> Perovskite Surfaces using XPS, XAS, STEM and EELS and the Effect on Oxidative Dehydrogenation of Propane**

*Gregor Koch, BasCat, UniCat BASF Jointlab, TU Berlin, Berlin, Germany; Michael Hävecker, Fritz Haber Institute, Berlin, Germany; Walid Hetaba, Max Planck Institute for Chemical Energy Conversion, Mülheim an der Ruhr, Germany; Pierre Kube, Fritz Haber Institute, Berlin, Germany; Frank Rosowski, BASF SE, Ludwigshafen, Germany; Robert Schlögl, Fritz Haber Institute, Berlin, Germany; Annette Trunschke, Fritz Haber Institute, Berlin Germany*

## **Introduction**

The ABO<sub>3</sub> perovskites exhibit a wide range of combinations of A and B metal atoms as well as partial substitution of A with A' or B with B'. Therefore, perovskites are employed in many applications, for instance as total combustion catalysts.[1] With respect to formation of propene a set of four ternary (La,Sm)(Mn,Co)O<sub>3</sub> perovskites was tested in oxidative dehydrogenation of propane to reveal the effect of A and B [2] on the performance of these catalysts employing different feeds for oxidative dehydrogenation of propane.

## **Experimental**

The perovskites were synthesized via Pechini route.[3] Sieve fractions of catalysts ranging from 100 to 200 μm were deposited in parallel tubular fixed bed reactors. The ODH of propane was tested in different feeds under steady state conditions varying O<sub>2</sub> content and adding H<sub>2</sub>O. The propane/O<sub>2</sub>/N<sub>2</sub>/H<sub>2</sub>O feeds were 5/10/85/0, and 5/10/45/40. Catalytic performance was tested in the temperature range between 250 °C and 310 °C.

XPS spectra were conducted at the ISSS beamline at the BESSY II synchrotron facility. Catalysts were pressed to pellets and measured in a stream of reaction feed at 270 °C, and a pressure of 0.25 mbar was adjusted.

## **Results**

XRD analysis showed phase purity of synthesized catalysts. The catalysts showed already at low temperatures of 250 °C activity in ODH of propane. Only propene and CO<sub>2</sub> were observed as products at every condition employed. In general, increasing

temperature resulted in increasing activity while only minor decrease in selectivity was observed. The conversion of propane was also enhanced by increasing the O<sub>2</sub> content in the feed indicating distinctly O<sub>2</sub> activation. After adding H<sub>2</sub>O to the O<sub>2</sub> rich feed, the selectivity to propene was increased from 18% to 39% and from 20% to even 50% using LaMnO<sub>3</sub> and SmMnO<sub>3</sub> catalyst, respectively (Figure 1, left). Contrarily, the corresponding ACoO<sub>3</sub> catalysts exhibited decreased selectivity to propene if H<sub>2</sub>O was added to the feed. In general, an increased ratio between  $B/A \geq 1$  in the bulk was beneficial pointing at excess of *B* atoms. Indeed, the abundance of the *B* atom, *i. e.* Mn or Co, in the near surface region was observed using STEM, EELS and *in situ* XPS. The abundance of the *B* atom was constant when applying various reaction feeds (Figure 1, right). Furthermore, the abundance of *B* correlated with the selectivity to propene if wet feed was applied. *In situ* XPS spectra of the O1s core level showed less contribution of lattice oxygen compared to those of fresh catalysts indicating creation of defective sites at the surface which is also accompanied by small amounts of hydroxyl and carbonate species. Hence, sites for total oxidation of hydrocarbons might be blocked by H<sub>2</sub>O, hydroxyl and carbonates leading to increased selectivity to the valuable product propene.

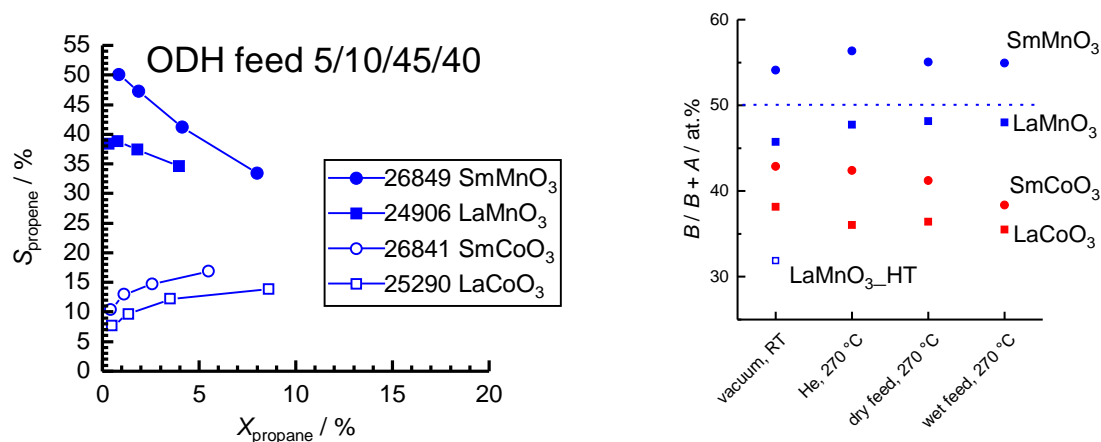


**Figure 1** Relationship of propane conversion and selectivity to propene of (La,Sm)(Mn,Co)O<sub>3</sub> catalysts in ODH employing wet feed (left). Calculated *B* element fraction referring to *A* and *B* in the surface region on basis of XPS measurements employing different conditions given below. LaMnO<sub>3</sub>-HT sample was obtained via hydrothermal intermediate step.

## References

- [1] S. Royer, D. Duprez, F. Can, X. Courtois, C. Batiot-Dupeyrat, S. Laassiri, H. Alamdari, *Chem. Rev.* **2014**, *114*, 10292-10368.
- [2] H. Najjar, H. Batis, *Catal. Rev.* **2016**, *58*, 371-438.
- [3] P. W. Cooper, S. R. Kurowski, *Technology of Explosives*, Wiley, New York, NY, **1996**.

# **Cu- and/or Zn-modified CrO<sub>x</sub>/Al<sub>2</sub>O<sub>3</sub> catalysts for a fixed-bed isobutane dehydrogenation**

*Salaeva A.A.; Salaev M.A.; Mamontov G.V., Tomsk State University, Tomsk, Russia*

## **Introduction**

The dehydrogenation of light paraffins is of high importance for petrochemical industry, and CrO<sub>x</sub>/Al<sub>2</sub>O<sub>3</sub> catalysts are widely used in both fixed-bed (Catofin, Catadiene) and fluidized bed processes [1]. Commercial operation of alumina-chromia catalysts proceeds under harsh conditions: high process temperature (500-650 °C), repeated rotational cycles of oxidative regeneration and reduction, local overheating, etc. Therefore, the catalyst must have high thermal stability, high activity and selectivity towards corresponding olefins and high stability up to a year. To improve the efficiency and increase the producibility, the catalysts with improved performance characteristics are required. Various modifiers based on Ca [2], K [3], group VIII metals (Fe, Co, Ni) [4] and other compounds are actively used to enhance the performance of CrO<sub>x</sub>/Al<sub>2</sub>O<sub>3</sub> catalysts. The interest to Cu and Zn is connected with their wide use in a number of catalytic processes of dehydrogenation of organic compounds [5]. The present work is focused on the study of the effect of copper and zinc addition on the textural and redox properties as well as catalytic activity in isobutane dehydrogenation of chromia-alumina catalysts.

## **Experimental**

The pseudoboehmite was used as a precursor of the support ( $\gamma$ -Al<sub>2</sub>O<sub>3</sub>). The series of modified alumina supports (loading of Cu and/or Zn was 0-3.2 %wt.) were synthesized by the incipient wetness impregnation of boehmite by an aqueous solution of copper and zinc nitrate followed by drying at 170 °C for 12 h and calcination at 500 °C for 6 h. After the calcination, the modified supports were impregnated by the aqueous solution of chromium oxide (VI) followed by drying at 120 °C for 12 h and calcination at 700 °C for 5 h. The nominal loading of Cr<sub>2</sub>O<sub>3</sub> in the catalysts was 4.5 %wt. The prepared supports and catalysts were characterized by the low-temperature N<sub>2</sub> adsorption, TPR-H<sub>2</sub>, XRD, UV-vis and Raman spectroscopy. The activity of the catalysts in isobutane dehydrogenation was studied using the quartz tubular reactor with a fixed bed of catalyst at 540 °C.

## Results

The introduction of Cu and Zn modifiers results in a shift of pore size distribution in the range of smaller pore sizes and increases the specific surface in comparison with the unmodified  $\text{Al}_2\text{O}_3$ . The XRD and UV-vis data show that Zn and Cu are distributed on the surface of  $\text{Al}_2\text{O}_3$  support to yield the surface aluminates. The Raman data show that chromium on the surface of catalysts is distributed predominantly as mono- and/or dimeric Cr (VI) species. The introduction of Cu and Zn modifiers led to higher amount of monochromia species. TPR- $\text{H}_2$  data show that the introduction of Cu modifier facilitated the enhanced reducibility and stability of the redox chromia species. As opposed, Zn decreased the reducibility of chromia species.

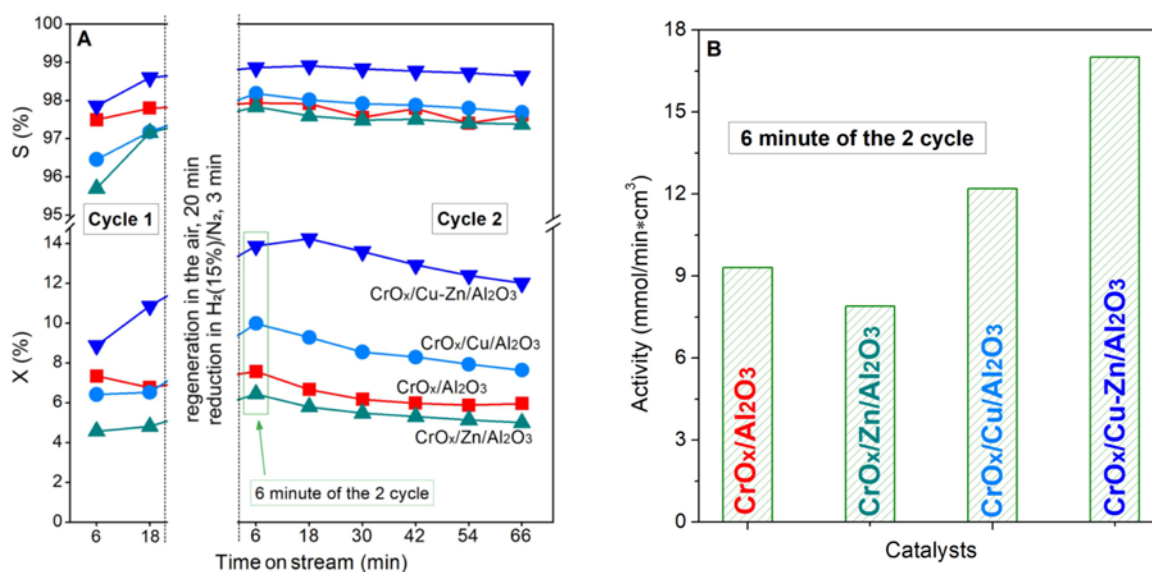


Fig. 1 Dependence of conversion (X, %) and selectivity (S, %) on the time on stream (A), Activity of the catalysts for isobutane dehydrogenation into isobutylene (B).

The introduction of Zn into the  $\text{CrO}_x/\text{Al}_2\text{O}_3$  catalyst decreases the activity and selectivity in isobutane dehydrogenation (Fig. 1a). The introduction of Cu modifier leads to growth of activity, selectivity and stability of the catalyst. The highest activity was achieved over  $\text{CrO}_x/\text{Al}_2\text{O}_3$  catalyst modified with both Cu and Zn. Thus, the synergetic effect of Cu and Zn modifier may be used to improve the properties of the  $\text{CrO}_x/\text{Al}_2\text{O}_3$  catalysts for dehydrogenation of light paraffins.

## References

- [1] J. J. H. B. Sattler, J. Ruiz-Martinez, et al., Chem. Rev. 114 (2014) 10613.
- [2] E. Rombi, M.G. Cutrufello, V. Solinas, S. De Rossi, et al., Appl. Catal. A: General. 251 (2003) 255.
- [3] G. Neri, A. Pistone, S. De Rossi, E. Rombi, et al., App. Catal. A: General. 260 (2004) 75–86.
- [4] M. Beccari, U. Romano, Encyclopaedia of Hydrocarbons. 2 (2006) 687-700.
- [5] M. Bahmani, B.V. Farahani, S Sahebdehfar, Appl. Catal. A: General. 520 (2016) 178-187.

# Effect of Swelling and Selective Adsorption on the Catalytic Behavior of Acid Exchange Ionic Resins

*E. Santacesaria, CEO Eurochem Engineering srl, Milano, Italy,*

*R. Tesser, M. Di Serio, Department of Chemical Science, University of Naples, Italy*

## Introduction

Polymeric ion-exchange resins can be used for promoting many different reactions such as, for example, fatty acid esterification with methanol to produce biodiesel. Due to their particular cross-linked structure, these materials are subjected to a remarkable swelling phenomena when are contacted with polar solvents such as methanol or water. This aspect is often neglected when the kinetic behavior of the reactions promoted by acid exchange resins are studied. Moreover, the high liquid volume retained and the selectivity towards the adsorption of one particular reagent can result in a significant alteration of the liquid reactive mixture composition inside the catalyst particles. In this situation, the bulk liquid phase and the adsorbed phase are different in composition and the kinetics could be strongly affected as the chemical reaction occurs mainly on the internal surface of the resin particles. Therefore, the correct description of the kinetics for such systems requires additional information regarding the phase partitioning of the various components between the liquid and the absorbed phase. Experimental absorption data, concerning the binary system methanol-water partitioned in the presence of Amberlyst 15 and Relite CFS, two sulphonic ion-exchange resins, typically used as esterification catalysts, will be presented. The data collected on binary systems water-methanol, at different temperatures, have been successfully correlated by a multicomponent competitive absorption model that could be useful in a wider kinetic study.

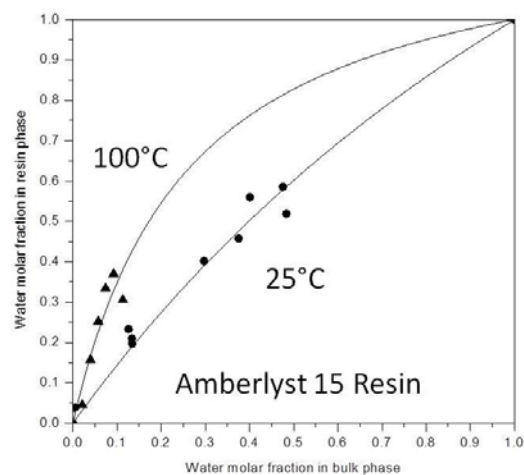
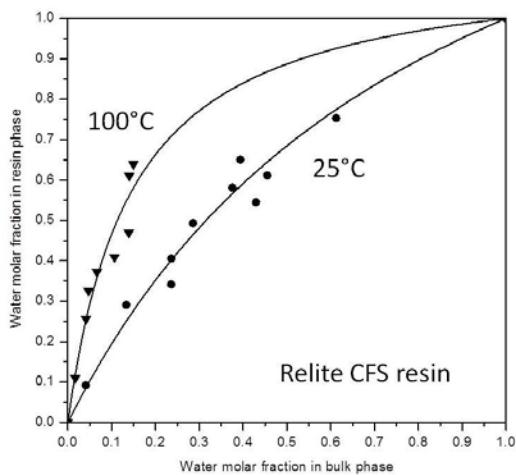
Starting from experimental data, related to the fatty acid esterification with methanol, the phase partitioning of the various components between the liquid phase and the adsorbed phase, a kinetic approach based on a new partition model was developed and related parameters were determined. Using this new kinetic model the esterification of fatty acid with methanol in batch reactors has been described more accurately. The same model has also been used to describe the behavior of loop and continuous packed bed reactors, obtaining in any case a good agreement between experimental and calculated values.

### Swelling tests and development of a predictive model

Some independent swelling tests have been performed with the scope to evaluate the swelling factors of both Amberlyst 15 and Relite CFS resins, at temperature of 25°C, and in contact with methanol and water, pure or in mixtures with different composition. Some swelling tests have also been made with pure water, at 95°C, in order to appreciate the effect of temperature on swelling. A model predicting the swelling behavior has been developed and verified.

### Partition test runs and development of the corresponding interpretation model

Solutions at different concentration of water in methanol were prepared and put into contact with a weighed amount of dry resin in vials that was then rapidly capped. Residual water concentration in the solution was analyzed by gas-chromatography evaluating the weight fraction of water not absorbed and by difference with respect to the loaded amount, the absorbed quantity. Runs have been made at two different temperatures and a partition model, based on the competition between water and methanol in filling the void volume of the resin has been developed. An example of fitting the partition experimental data can be appreciated in the following figures reporting the phase diagram for the adsorption of the binary system water-methanol at 25 and 100°C with respectively Relite CFR and Amberlyst 15 resins.



At last, the developed partition model, with the related determined parameters has been inserted with very satisfactory results in a kinetic model interpreting the data of esterification of fatty acids with methanol.

# **An Experimental Study Aiming to Enhance the Performance of OSR of a Fuel Processor**

*Cihat Öztepe, Boğaziçi University, Department of Chemical Engineering, İstanbul, Turkey; B. Selen Çağlayan, Boğaziçi University, Advanced Technologies R&D Center, İstanbul, Turkey; A. Erhan Aksoylu\*, Boğaziçi University, Department of Chemical Engineering, İstanbul, Turkey*

The aim of this study was to analyze the performance of methane OSR unit of the Fuel Processor Prototype-FPP and to determine the optimum operating parameters. A Box-Behnken experimental design was used with the experimental parameters temperature, S/C (steam-to-carbon) and O/C (oxygen-to-carbon) ratios of the feed, and the catalyst weight (or residence time, W/F). Methane conversion was found to be increased with increasing temperature, S/C and O/C ratios whereas it was mostly decreased with increasing W/F. A thermodynamic analysis was also performed to form a reference basis for comparing with the trends observed in experimental results.

## **Experimental**

A Box-Behnken experimental design consisting of operating parameters - temperature, S/C and O/C ratios of the feed, and W/F- was constructed to perform experiments and to make a further statistical modelling possible. 350-450 °C, 3-5, 0.74-1.33 and 1.50-2.00 mg.min/ml were the ranges that were used in the design for temperature, S/C ratio, O/C ratio and W/F, respectively [1,2,3].

## **Results and Discussion**

Due to the nature of a Box-Behnken experimental design, effects of all parameters were observed and compared at their maximum and minimum values only. The effects of operating parameters on methane conversion, H<sub>2</sub> product concentration and H<sub>2</sub>/CO ratio in the product were examined. Temperature, S/C and O/C ratios in the feed were found to increase methane conversion, with certain exceptions, whereas they had various effects on H<sub>2</sub> product concentration and H<sub>2</sub>/CO ratio in the product at different conditions. When temperature was increased from 350 °C to 450 °C, methane conversion increased significantly with increasing H<sub>2</sub> product concentration while H<sub>2</sub>/CO ratio in the product decreased tremendously. These variations are presented in Figure 1 as an example of parametric effect comparison.



A thermodynamic study was also performed to compare the trends, and results obtained by thermodynamic calculations were presented as if an infinity value of W/F ratio was used, as presented in Figure 2. Decreasing methane conversion with increasing W/F and higher methane conversions than thermodynamic calculations were remarkable conclusions. These situations were caused by the existence of simultaneous multiple, serial and/or competitive, reactions running at different speeds in the reactor .

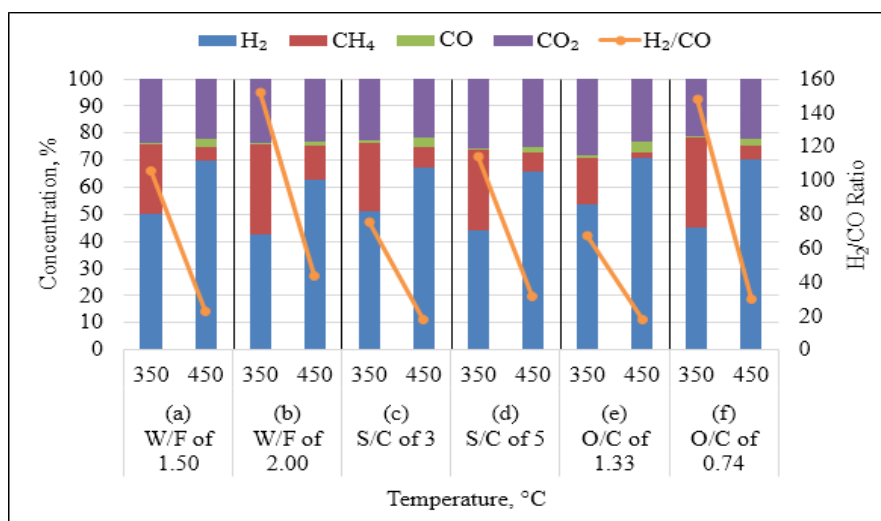


Figure 1. Steady state performance results comparison at different conditions

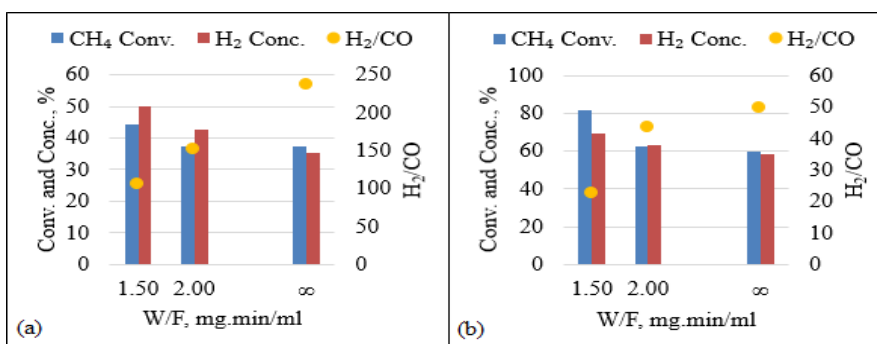


Figure 2. Experimental and thermodynamic CH<sub>4</sub> conversion and H<sub>2</sub> concentration percentages, and H<sub>2</sub>/CO ratio comparison with respect to W/F

### Acknowledgements

The financial support was provided by TÜBİTAK through project 215M312 and Turkish Ministry of Development through project 2016K121160.

### References

- [1] Gökaliler, F., B. A. Göçmen and A. E. Aksoylu, 2008, "The Effect of Ni:Pt Ratio on Oxidative Steam Reforming Performance of Pt-Ni/Al<sub>2</sub>O<sub>3</sub> Catalyst", *International Journal of Hydrogen Energy*, Vol. 33, pp. 4358-4366.

- [2] Başar, M. S., B. S. Çağlayan and A. E. Aksoylu, 2016, "Steady state performance analysis of OSR and serial OSR-WGS reactors", *Fuel Processing Technology*, Vol. 152, pp. 240-249.
- [3] Erdinç, E., B. S. Çağlayan and A. E. Aksoylu, 2017, "Methane OSR over Pt-Ni/ $\delta$ -Al<sub>2</sub>O<sub>3</sub>: Performance and power law type kinetics", *International Journal of Hydrogen Energy*, Vol. 42, pp. 20568-20578.

# The Influence of Extraframework Aluminium on NiMo/H-REY Catalyzed Hydrocracking of Vacuum Gas Oil

*I.G. Danilova, A.A. Gabrienko, P.P. Dik, E.A. Paukshtis, M.O. Kazakov, O.V. Klimov, A.S. Noskov, Boreskov Institute of Catalysis, Novosibirsk, Russia; T.P. Sorokina, V.P. Doronin, Institute of Hydrocarbon Processing Problems, Omsk, Russia*

## Introduction

Hydrocracking catalysts are bifunctional systems, where sulfided Ni-Mo(W)-S component performs hydrogenating and hydrodesulfurisation reactions while acidic supports, usually based on ultrastable zeolite Y, performs cracking and isomerization reactions. It is generally accepted that strong Brønsted acid sites, the framework bridging SiOHAl groups of zeolites, are the active sites for these reactions. The role of the extraframework aluminium species in the catalytic transformation of hydrocarbons has been vividly debated [1-2]. The aim of this study was to find relationships between the acidity of zeolites (including variety of extralattice species) and performance of the Ni-Mo catalysts in vacuum gas oil (VGO) hydrocracking.

## Scope of the work

A series of ultrastable zeolite Y ( $\text{SiO}_2/\text{Al}_2\text{O}_3 \sim 25$ ) in the H-form (CBV-720, Zeolyst) and cation-decationated form denoted as REY-(%Ln) ( $\text{Na}_2\text{O} = 0.5 \text{ wt\%}$ ,  $\text{Ln}_2\text{O}_3 = 0.35\text{-}3.3 \text{ wt\%}$ , where Ln is a lanthanide) were used to catalysts preparation. Zeolite powders were characterized by XRD, SEM and nitrogen adsorption. The concentration of different O-H groups of zeolites has been reliably established with  $^1\text{H}$  MAS NMR, using methane and benzene as internal standards and compared with IR spectroscopy data. The acidity of zeolites were studied in detail by TPD- $\text{NH}_3$  and IR spectroscopy of adsorbed CO, quinoline and *in situ* desorption of pyridine.

Several types of LAS and BAS were found on the zeolite surface, the concentration and strength of which depended on the Ln content. The concentration of strongest BAS (the value of the low frequency shift of OH vibrations with adsorbed CO ( $\Delta\nu_{\text{OH/CO}}$ ) was  $340\text{-}380 \text{ cm}^{-1}$ ), the framework SiOHAl groups, declined with increasing Ln content. Three types of medium strength BAS ( $\Delta\nu_{\text{OH/CO}} = 190\text{-}280 \text{ cm}^{-1}$ ), the bridging AlOHAl groups with  $\nu_{\text{OH}} 3670$  and  $3690\text{-}3695 \text{ cm}^{-1}$  (2.7-3.1 and 3.7-3.5 ppm) and defect silanol groups with  $\nu_{\text{OH}} 3735 \text{ cm}^{-1}$  (2.1 ppm), were found on the REY

surface. The concentration of the AlOHAl groups on the REY surface was unusually high and close to the concentration of lattice BAS (Tabl.) in contrast to CBV-720 zeolite [3]. It was found that washing the zeolites from extraframework ions by tartaric acid (TA), accompanied by a sharp decrease in the content of 6- and 5-coordinated Al atoms according to  $^{27}\text{Al}$  NMR, led to a predominant removal from the surface of two types of OH groups - with  $\nu_{\text{OH}}$  3690 and 3735  $\text{cm}^{-1}$  (Fig., Table).

NiMo catalysts (3 wt% Ni and 10 wt% Mo) were prepared by co-impregnation of 30%HY+70%Al<sub>2</sub>O<sub>3</sub> supports with solutions containing precursors of active metal and citric acid. The Brønsted acidity of the catalysts was formed by properties of the initial zeolites. Testing of stacked beds in the one-through hydrocracking of VGO was carried out in a fixed-bed flow reactor under 16.0 MPa at 390-410°C [3-4]. The VGO conversion and diesel fraction (130-360°C) yield did not correlated with the concentration of strongest BAS. The effect of the different extraframework Al species have been discussed. It was found that washing the zeolites from extraframework species drastically reduced the diesel fraction selectivity and yield (Table).

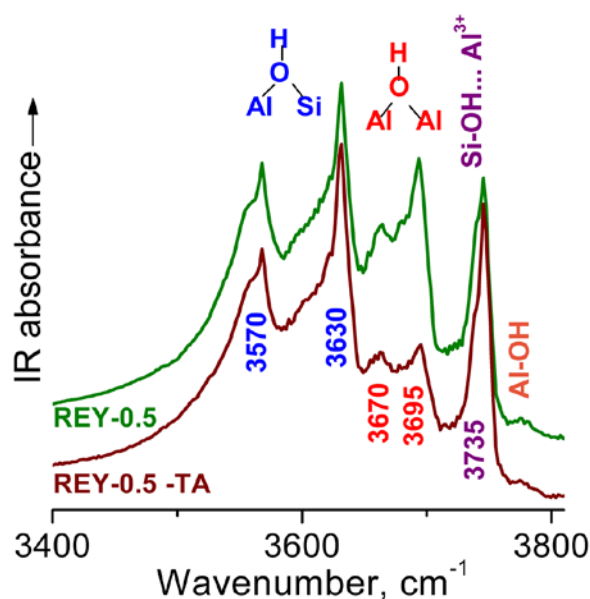


**Fig.** IR spectra of REY-0.5 zeolites after activation in vacuum at 500°C.

Zeolites		REY-0.5	REY-0.5 TA
Properties			
$^1\text{H}$ NMR $\mu\text{mol/g}$	Si-O(H)-Al	610	630
	Al-O(H)-Al	480	350
$^{27}\text{Al}$ NMR	AlO <sub>4</sub> / AlO <sub>6</sub> +AlO <sub>5</sub>	0.92	1.5
IR CO, $\mu\text{mol/g}$	LAS	60	16
Diesel fraction yield	S (at X=50%)	76.3	70.6
	Y (410°C)	46.9	44.3

**Table.** The effect of REY-0.5 zeolite (0.5 wt % Ln) washing by tartaric acid.

## References

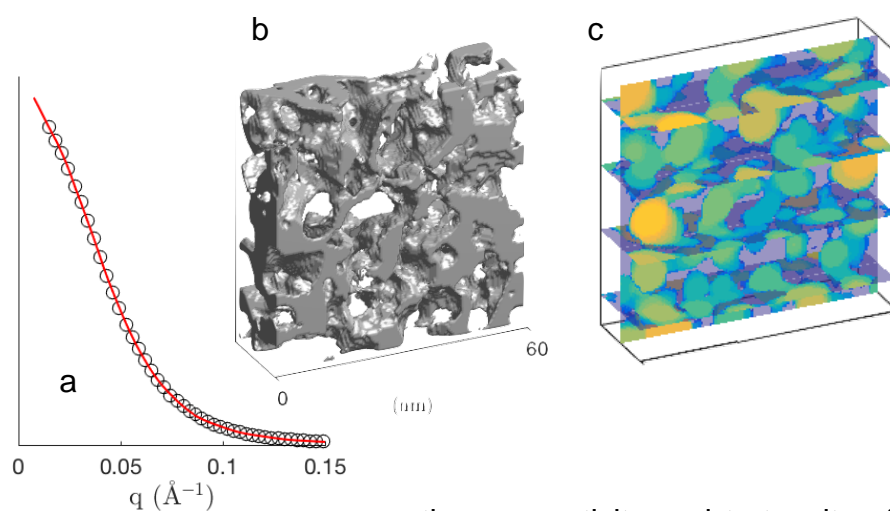
- S. Schallmoser, T. Ikuno, M.F. Wagenhofer, R. Kolvenbach, G.L. Haller, M. Sanchez-Sanchez, J.A. Lercher, *J. Catal.* 316 (2014) 93–102.
- T.F. Narbeshuber, A. Brait, K. Seshan, J.A. Lercher, *Appl. Catal. A: General* 146 (1996) 119-129
- M.O. Kazakov, K.A. Nadeina, I.G. Danilova, P.P. Dik, O.V. Klimov, V.Yu. Pereyma, E.Yu. Gerasimov, I.V. Dobryakova, E.E. Knyazeva, I.I. Ivanova, A.S. Noskov, *Catal. Tod.*, 305 (2018) 117–125.
- P.P. Dik, I.G. Danilova; I.S. Golubev; M.O. Kazakov; K.A. Nadeina; S. V Budukva; V.Y. Pereyma; O.V. Klimov; I.P. Prosvirin; E.Y. Gerasimov; T.O. Bok; I.V. Dobryakova; E. E Knyazeva; I.I. Ivanova; A.S. Noskov, *Fuel*. 237 (2019) 178-190.

## 3D Reconstruction of Porous Materials with Small-Angle Scattering and Stochastic Models

*Cedric J. Gommès, Department of Chemical Engineering, University of Liège, Belgium, and Fonds for Scientific Research, F.R.S.-FNRS, Belgium*

Small-angle scattering of either x-rays (SAXS) or neutrons (SANS) is one of the few experimental techniques that can be used to study the structure of porous materials on the entire range from 1 to 100 nm, which makes it particularly suited to characterize microporous and mesoporous materials. Because the information in scattering patterns is a correlation function, however, models are generally needed to convert scattering data into structurally meaningful information. This is particularly challenging for many porous materials of practical interest in catalysis, which have disordered structure. We discuss five stochastic models that capture qualitatively different disordered structures, notably in what concerns the connectivity and the tortuosity of the solid and the pore spaces [1].

The procedure is illustrated in Figure 1, with the SAXS pattern of mesoporous alumina, the structure of which is reconstructed with a clipped Gaussian random field model. The reconstruction can then be used to derive non-trivial structural information, such



as the connectivity and tortuosity of the phases  
Figure 1. Example of a SAXS pattern of mesoporous alumina (a), the reconstructed 3D structure using a Gaussian random field model (b), and the measurement of the largest spheres inscribed in the pores (c).

We illustrate the methodology with the SAXS analysis of a carbon xerogel, of a fumed silica and of mesoporous alumina. The reconstructions obtained from the SAXS are compared with pore size distributions derived from nitrogen physisorption. In the case of the xerogel and silica it is possible to pinpoint a single model that describes the structure best. In the case of the alumina, however, the scattering cannot discriminate the models. Even so, the models are useful because they enable one to quantitate the structural ambiguity of the SAXS data. Having a realistic structural model of the porous material is also necessary for in situ SAXS studies [2], as well as to analyze the influence of geometrical disorder on the physicochemical phenomena happening inside the pores [3].

### References

- [1] Cedric J. Gommes, *Stochastic models of disordered mesoporous materials for small-angle scattering analysis and more*, Microporous and Mesoporous Materials 257 (2018) 62-78;
- [2] Cedric J. Gommes, *Three-dimensional reconstruction of liquid phases in disordered mesopores using in situ small-angle scattering*, Journal of Applied Crystallography 46 (2013) 493-504;
- [3] Cedric J. Gommes and Anthony P. Roberts, *Stochastic analysis of capillary condensation in disordered mesopores*, Physical Chemistry Chemical Physics 20 (2018) 13646-13659.

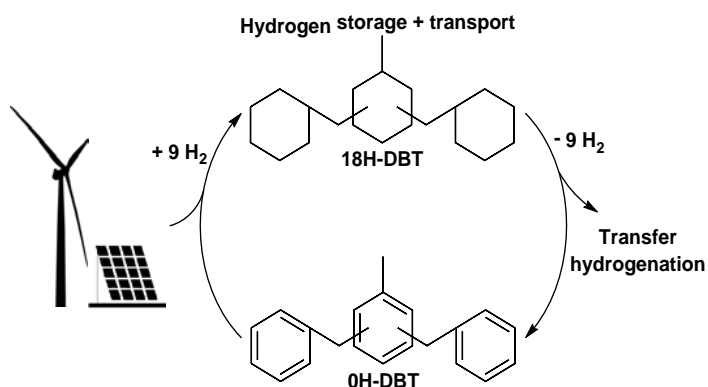
# Homogeneous Transfer Hydrogenations with Liquid Organic Hydrogen Carriers at Moderate Reaction Conditions

*Meria Ronge, Institute for Technical and Macromolecular Chemistry, RWTH Aachen University, Germany, Markus Hölscher, Institute for Technical and Macromolecular Chemistry, RWTH Aachen University, Germany, Walter Leitner\*, Max Planck Institute for Chemical Energy Conversion, Mülheim an der Ruhr, Germany; Institute for Technical and Macromolecular Chemistry, RWTH Aachen University, Germany*

## Abstract

Hydrogenation reactions play a key role in a variety of applications in the chemical industry. In terms of process engineering, some of the most crucial challenges are the long-term storage of hydrogen gas and the requirement of severe safety measures and extremely high pressures when using gaseous reactants. Thus, finding a replacement for gaseous hydrogen as a reactant for industrial hydrogenation is a fundamental step towards a safer working environment and saving resources. Potential methods for the implementation of other hydrogen sources are physisorption by porous materials,[1a] metal hydrides,[1b] complex hydrides,[1c] chemical hydrides,[1d] and Liquid Organic Hydrogen Carriers (LOHCs).[1e] Considering reversibility, gravimetric and volumetric hydrogen capacity, thermodynamics and the challenge of implementing the new technology into the existing infrastructure, LOHCs are widely discussed as the most competitive and promising solution.[2] Finding LOHCs with suitable properties for efficient the long-term use is as much a challenge as designing the respective catalysts to perform the hydrogenation and dehydrogenation in the energy cycle. Prof. Wasserscheid and his group succeeded at designing the LOHC system DBT (dibenzyltoluene), that meets all requirements and has already been commercialized as a hydrogen storage system in the energy and fuel sector.[3] Beside the grand advantages of being non-hazardous, non-flammable, relatively cheap (< 5 €/kg) and widely commercially available as a heat transfer medium, it offers a very high boiling point and similar flow properties to gasoline and can thus easily be implemented into the existing infrastructure. Both the energy and the chemical industry are highly interested in hydrogen carriers such as DBT. In the chemical industry, hydrogen is used in large

quantities in hydrogenation reactions. With hydrogen as a gaseous compound, these reactions can be technically demanding due to the requirements to the high pressure equipment. An appealing solution is the direct transfer of hydrogen from a carrier molecule such as DBT to the respective acceptor molecules.



In this work, we present the optimization of transfer hydrogenation reactions using this LOHC, hydrogenated dibenzyltoluene (18H-DBT) as hydrogen donor. In a pre-screening of late metal-pincer complexes, ruthenium-acriphos[4] proved to be the most efficient system. Substrate and catalyst screening are presented as well as the influence of the electronic and steric properties of the catalyst.

## References

- [1] a) I. Krkljus,; M. Hirscher, *Microporous Mesoporous Mat.*, **2011**, 142, 725-729; b) B. Sakintuna, F. Lamari-Darkrim, M. Hirscher, *Int. J. Hydrog. Energy*, **2007**, 1121–1140.; c) S.-I. Orimo, Y. Nakamori, J. R. Eliseo, A. Züttel, C. M. Jensen, *Chem. Rev.*, **2007**, 4111–4132.; d) F. H. Stephens, V. Pons, R. T. Baker, *Dalton Trans.*, **2007**, 25, 2613–2626. (e) H. Jorschick, P. Preuster, S. Durr, A. Seidel, K. Müller, A. Bosmann, P. Wasserscheid, *Energy Environ. Sci.*, **2017**, 1652–1659.
- [2] P. T. Aakko-Saksa, C. Cook, J. Kiviaho, T. Repo, *J. Power Sources*, **2018**, 396, 803.
- [3] D. Geburtig, P. Preuster, A. Bösmann, K. Müller, P. Wasserscheid, *Int. J. Hydrogen Energy*, **2016**, 1010-1017
- [4] K. Rohmann, M. Hölscher, W. Leitner, *Angew. Chem. Int. Ed.*, **2016**, 55, 8966-8969



# On the effect of the stoichiometry of hydroxyapatite on the catalytic properties of the Ni/HAP system in dry reforming of methane

Zouhair Boukha<sup>a</sup>, María Pilar Yeste<sup>b</sup>, Miguel Ángel Cauqui<sup>b</sup>,

Juan R. González-Velasco<sup>a</sup>

(a)Chemical Technologies for Environmental Sustainability Group, Department of Chemical Engineering, Faculty of Science and Technology, University of the Basque Country UPV/EHU, P.O. Box 644, E-48080 Bilbao, Spain

(b)Departamento de Ciencia de los Materiales e Ingeniería Metalúrgica y Química Inorgánica, Campus Río San Pedro s/n, 11510, Puerto Real, Cádiz, Spain

[zouhair.boukha@ehu.es](mailto:zouhair.boukha@ehu.es)

## Introduction

Nickel-based catalysts are widely used for the methane dry reforming reaction (DRM) owing to their activity and competitive cost compared to noble metals [1-2]. Despite their high activity they suffer from a rapid deactivation, due to carbon deposition, which is considered a major drawback. The catalysts for DRM should exhibit adequate properties to endure the severe conditions of the reaction which is generally carried out at high operating temperatures (> 600 °C). The nature of the used support seems to play a crucial role in controlling the distribution and then the stability of the Ni active phases. In this sense, it would be essential to design Ni catalysts that exhibit suitable metal-support interaction in order to provide highly dispersed and resistant active phases.

The present study is dealing with the investigation on the influence of the Ca/P molar ratio on the textural, structural, surface chemistry (acid/base) and catalytic behaviour in DRM of a series of hydroxyapatite supported nickel samples (Ni/HAP). For this purpose, hydroxyapatite supports with different Ca/P molar ratios have been synthesised.

## Experimental

Table 1 reports characterization and catalytic data for the pre-reduced Ni/HAP catalysts. The analysis of these data sheds light on the crucial role that plays the composition of the hydroxyapatite materials when used as support for Ni catalysts in their catalytic properties in the DRM reaction. It seems that a preparation starting

from a sub-stoichiometric composition ( $\text{Ca/P} < 1.67$ ) results in suitable properties which give the highest catalytic performance compared with stoichiometric ( $\text{Ca/P} = 1.67$ ) and over-stoichiometric ( $\text{Ca/P} = 1.73$ ) compositions, respectively (Table 1 and Fig. 1). Interesting conclusions will be presented by correlating the very rich information provided by a wide battery of techniques (including BET, XRD, TEM, FTIR,  $\text{NH}_3$ -TPD,  $\text{CO}_2$ -TPD and TPO) and the catalytic performance of the investigated samples.

Table 1. Characterisation and catalytic activity data for the Ni/HAP catalysts

Sample	ICP		BET <sup>(a)</sup>			TEM	DRM at 750 °C ( $\text{CH}_4/\text{CO}_2$ : 1/1)		
	Ca/P	Ni, wt.%	$S_{\text{BET}}$ , $\text{m}^2 \text{g}^{-1}$	$V_p$ , $\text{cm}^3 \text{g}^{-1}$	$d_p$ , nm	$\text{Ni}^0$ , nm	$X_{\text{CH}_4}$	$X_{\text{CO}_2}$	$\text{H}_2/\text{CO}$
Ni/HAP-D1	1.57	3.41	24	0.28	44	18	75	83	0.78
Ni/HAP-D2	1.62	3.41	26	0.25	36	17	78	86	0.79
Ni/HAP-S	1.67	3.41	17	0.16	32	22	70	80	0.75
Ni/HAP-E	1.73	3.41	9	0.08	32	34	67	78	0.72

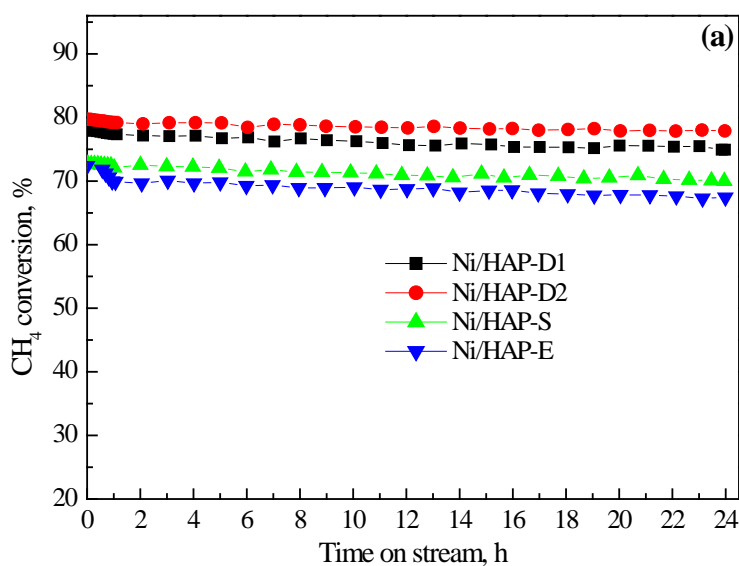


Fig. 1. DRM activity over Ni/HAP catalysts at 750 °C ( $\text{GHSV} = 60,000 \text{ cm}^3 \text{ h}^{-1} \text{ g}^{-1}$ )

## References

- [1] Z. Boukha, M. Kacimi, M.F.R. Pereira, J.L. Faria, J.L. Figueiredo, M. Ziyad, *Appl. Catal. A-Gen.* 317 (2007) 299-309.
- [2] C. Papadopoulou, H. Matralis, X. Verykios, Springer Science+Business Media, New York (2012), pp. 57-129.

## Acknowledgements

The financial support for this work provided by Ministerio de Economía y Competitividad (CTQ2015-73219-JIN (AEI/FEDER/UE) and Gobierno Vasco (GIC IT-657-13) is gratefully acknowledged.

# Structure-dependent microkinetic modelling of heterogeneous catalytic reactions: an application to the CPO on Rh

*Raffaele Cheula<sup>1</sup>; Alice Stucchi<sup>1</sup>; Matteo Maestri<sup>1</sup>*

*<sup>1</sup> Laboratory of Catalysis and Catalytic Processes, Dipartimento di Energia, Politecnico di Milano, via La Masa 34, Milano, Italy*

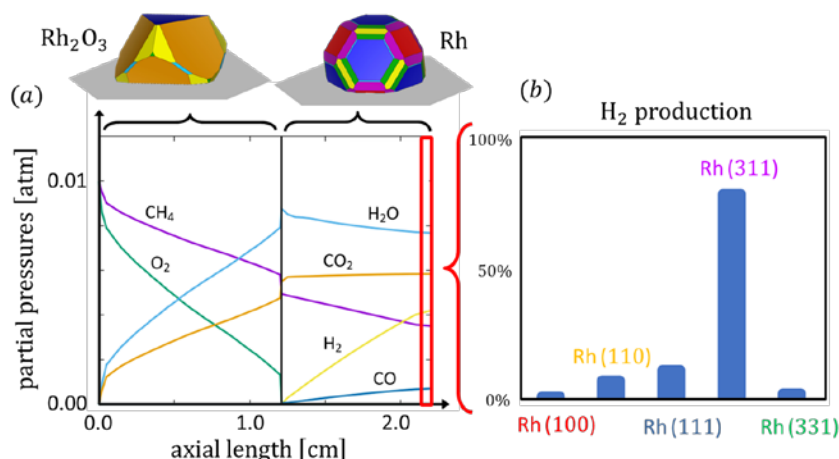
## Introduction

Catalyst nanoparticles in reaction conditions expose different crystal facets, making available different active sites for adsorption and reaction of chemical species. Depending on the geometrical arrangements of the atoms at the surface, the active sites interact differently with reaction intermediates and transition states, yielding specific observed catalytic activity. Besides, due to the dynamic nature of catalyst materials, the amount of the active sites changes according to the variation of the local operative conditions in the reactor. As a result, the actual contribution of each type of active site to the overall reaction rate results determined by both its catalytic activity and its abundance, and by how they are influenced by the variations in chemical environment inside the reactor [1].

In this contribution, following our previously proposed methodology for the modelling of the catalyst morphology in reaction conditions [2], we proceed by performing a detailed analysis of the reaction mechanisms on the different crystal facets that the catalyst shows in reacting conditions. We adopt a hierarchical structure-dependent microkinetic model for the calculation of the reaction rates, which accounts for the activity and abundance of the different active sites.

## Methods

A semi-empirical structureless microkinetic model [3] is adopted to simulate the macroscopic behavior of the catalytic system. The morphology of heterogeneous catalyst nanoparticles in dependence of the gas chemical potential is determined by *ab initio* thermodynamics and Wulff-Kaisew construction methods [4]. Density Functional Theory (DFT) calculations are performed with GGA-PBE ultrasoft pseudopotentials and the Quantum Espresso code. Nudged-elastic band and finite-differences vibrational analysis are employed to calculate the Gibbs free energies of reaction intermediates and transition states on the facets exposed by the catalyst.



Partial pressures axial profiles at the catalyst interface in an annular reactor for the CPO reaction.  $T = 500^{\circ}\text{C}$ ;  $P = 1 \text{ atm}$ . On top: 3D shape of  $\text{Rh}_2\text{O}_3$  and Rh catalyst particles, obtained by *ab initio* thermodynamics and Wulff-Kaishew construction. (b): Percentage net reaction rates of  $\text{H}_2$  production on different facets of Rh.

## Results and Discussion

The methodology is applied in the context of catalytic partial oxidation (CPO) of  $\text{CH}_4$ , water-gas shift (WGS) and reverse WGS reacting systems on a  $\text{Rh}/\text{Al}_2\text{O}_3$  catalyst. Twenty reversible elementary steps on five crystal facets of Rh are investigated to calculate the activity of the catalyst active sites at different operative conditions. At a certain reaction coordinate, we determine which are the facets of the catalyst that give predominant contribution to the overall reaction rate and unravel the reaction mechanism on each of them, by accounting for both their activity and their abundance. During CPO, after a bulk phase transition from  $\text{Rh}_2\text{O}_3$  to Rh [4], syngas starts producing. Rh(111) is the most abundant crystal facet, but due to its higher activity, Rh(311) is found to be the crystal facet which gives the predominant contribution to the overall reaction rate (Fig.1).

As whole, the proposed procedure has a great potential since it allows us to locally analyze a reacting system at the molecular level, explicitly accounting for the catalyst structure. Hence, this contribution introduces an important innovation in microkinetic modelling, making it possible to gaining fundamental insight in the structure-activity relations of heterogeneous catalysis.

## References

- [1] R. Schlögl, *Angew. Chem., Int. Ed.*, 54, 3465–3520 (2015).
- [2] R. Cheula, A. Soon and M. Maestri, *Catal. Sci. Technol.*, 8, 3493-3503 (2018).
- [3] M. Maestri, D. G. Vlachos, A. Beretta, G. Groppi and E. Tronconi, *AIChE J*, 55, 993–1008 (2009).
- [4] J. Rogal and K. Reuter, *Exp. Model. Simul. Gas-Surface Interact. React. Flows Hypersonic Flights*, 1–18 (2007).

# **Biomass derived fuel additives: Selective Hydrogenation of 5-Hydroxymethylfurfural to 2,5-bis(hydroxy)methylfuran using Octahedral Molecular Sieve supported Catalyst**

*Jennifer Dicks<sup>1</sup>, Vivek V. Ranade<sup>1</sup>, Haresh Manyar<sup>\*1</sup>*

<sup>1</sup> *School of Chemistry and Chemical Engineering, Queen's University Belfast, David-Kier Building, Stranmillis Road, Belfast BT9 5AG, UK*

*\*Corresponding author: h.manyar@qub.ac.uk*

## **Introduction:**

An increasing energy demand, growing population and depleting crude oil resources have led to the need for development of alternative renewable energy and chemical processes. Functionalised furans are an attractive biomass derived feedstock that can be sustainably produced at large scale from abundant waste biomass. 5-Hydroxymethyl furan (HMF) is a key platform chemical, which can be converted into several value-added products including; 2,5-dimethylfuran (DMF)(biofuel-additive) and 2,5-Bis(hydroxymethyl)furan (BHMF)(Polymers)[1]. In this study, we have developed a catalytic process for the selective hydrogenation of HMF to BHMF, under mild reaction conditions using water as the reaction medium. Although there are reports in literature for selective hydrogenation of HMF, the reported processes are mainly performed using dilute feedstocks in organic solvents, expensive designer catalysts and stringent reaction conditions, which limit the scope for scale up and potential commercialization. We have developed a facile and scalable hydrogenation process for selective hydrogenation of HMF under mild reaction conditions, using water as reaction medium and manganese oxide octahedral molecular sieves (OMS-2) and Pt/OMS-2 catalysts, which makes our process industrially attractive and economically viable for scale up studies. We have reported the first complete study of selective hydrogenation of HMF to BHMF using manganese oxide materials including kinetic analysis and insights on the role of lattice oxygen vacancies and alkali metal ions on the plausible reaction mechanism.

## **Materials and methods:**

All catalysts were synthesized at QUB and thoroughly characterized using XRD, XPS, BET, TPR, Raman, SEM and HRTEM analyses. Hydrogenations were carried

out in a 100 cm<sup>3</sup> Autoclave Engineers autoclave. In a typical experiment, the reactor was charged with HMF (0.004 mol) and catalyst (0.15 g) suspended in water (30 cm<sup>3</sup>). The reactor was heated to 110 °C, pressurized to 20 bar H<sub>2</sub> and agitated at 1500 rpm. The reaction was sampled at regular intervals, with analysis by GC-FID using a capillary column.

## Results and Discussion:

The hydrogenation of HMF to BHMF using 4%Pt/OMS-2 catalyst, at 110 °C, and hydrogen pressure of 20 bar, was completed in less than 1 hour, with 92% selectivity to BHMF. A typical HRTEM image of the 4%Pt/OMS-2 catalyst is shown in Figure 1a and the reaction composition-time profile is shown in Figure 1b. The activity of different metals such as Pt and Pd supported on TiO<sub>2</sub> and OMS-2 were compared and 4%Pt/OMS-2 showed the highest selectivity to BHMF (Figure 1c). To further optimize the process, reactions were carried out between 5 to 20 bar H<sub>2</sub>, 60 to 110 °C temperature and 0.05 to 0.3 mol dm<sup>-3</sup> HMF feed concentration, 0.5 to 4% Pt loading and 0.001 to 0.005 gm/cm<sup>3</sup> catalyst loading.

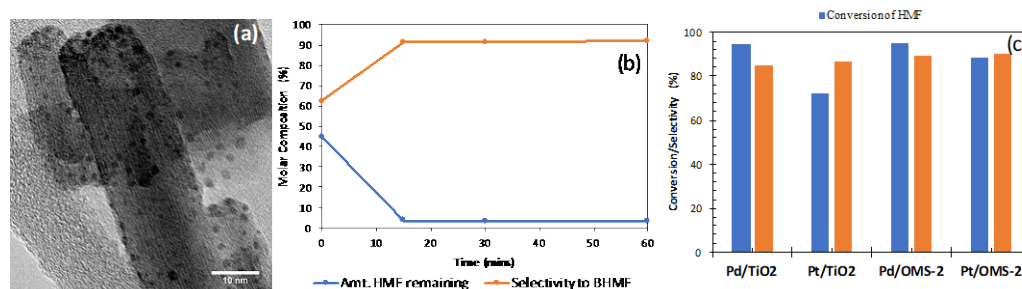


Figure 1 (a) HR-TEM image of 4 wt% Pt/OMS-2, (b) Reaction composition-time profile for hydrogenation of HMF using 4%Pt/OMS-2, and (c) Efficacy of various catalysts.

In this study, we have developed a selective hydrogenation process for conversion of HMF to BHMF under mild reaction conditions using water as the reaction medium. The catalyst is stable, active, and selective and shows good reusability. Effects of different process parameters were studied, and reaction mechanism and kinetic model developed. The process is green and novel for synthesis of BHMF from HMF.

## References

[1] Chen, J. *et al.* (2017) 'Selective hydrogenation of biomass-derived 5-hydroxymethylfurfural using palladium catalyst supported on mesoporous graphitic carbon nitride', *Journal of Energy Chemistry*. Elsevier B.V., 0, pp. 1–7. doi: 10.1016/j.jechem.2017.04.017.

# **Microemulsion vs. Precipitation: Selecting the support synthesis of nickel-ceria based catalysts for ethanol steam reforming**

*Cristina Pizzolitto<sup>1,2</sup>, Federica Menegazzo<sup>1</sup>, Michela Signoreto<sup>1</sup>,*

*<sup>1</sup> Dipartimento di Scienze Molecolari e Nanosistemi, Università Ca' Foscari  
Venezia, 30172 Venezia Mestre, Italy*

*V. Cortés Corberán<sup>2</sup>,*

*<sup>2</sup> Inst. of Catalysis and Petroleumchemistry (ICP), CSIC, Madrid, Spain*

Hydrogen is considered the energy carrier of the future thanks to its high potentiality in fuel cell application, and the possibility to obtain it from renewable resources. Ethanol steam reforming (ESR) is one of the most practical ways to produce it from biomass, and to investigate robust, selective and active catalysts for this reaction is the goal of this research. Nickel, one of the most economic and active non-noble metal, has been chosen as active phase for its high activity to break carbon-carbon bond. However, due to its low thermal stability toward sintering and low coke resistance, the role of support is essential. Therefore, the focus of this work is the stabilization of the active phase by careful study of the support preparation, looking for suppressing side reactions and reducing formation of by-products such as acetone and ethylene, which are coke precursors. Ceria is an attractive support because of its redox ability, which can positively influence the reaction. In fact, it favors the oxidative removal of carbonaceous species on the surface, limiting coke deposition. Moreover, ceria redox ability can be modulated by a careful control of structural defects: the highest is the number of defective sites, the most effective is the redox pump. For this reason, lanthanum oxide has been introduced as promoter, due to its possible substitution as  $\text{La}^{3+}$  in the  $\text{Ce}^{4+}$  support lattice [1].

In this work, two synthetic approaches have been evaluated to modulate the intrinsic features of support: precipitation (with urea) and microemulsion. Precipitation is the conventional method while microemulsion approach is an innovative technique involving the use of thermodynamic stable colloidal solution. In fact, microemulsion can guarantee a good atom distribution of support particles, through the formation of micelles that work as small precipitating reactors [2]. Support materials based on ceria and lanthana were prepared using both methods (samples are denoted P for Precipitated or M for Microemulsion). After the calcination process, the nickel active

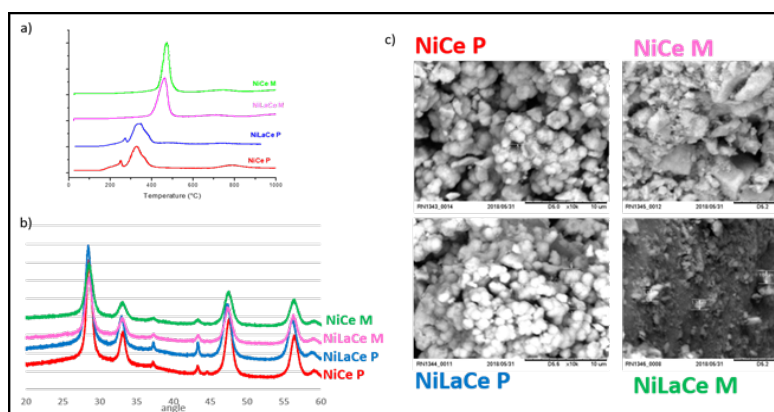


**Fig. 1. Catalysts characterization: a) TPR, b) XRD and c) SEM** structural features and how these relate to catalytic properties. The two methods gave strong differences in features (Fig.1): P catalysts showed higher reducibility (which involves higher oxygen mobility) with more homogeneous Ni particle size distribution.

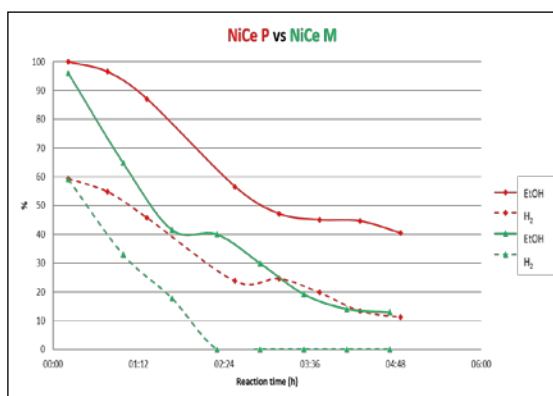


**Fig. 2. Evolution of ethanol conversion and H<sub>2</sub> yield with run time on NiCe P (red) and NiCe M (green) catalysts**

Catalytic tests (at 500 °C for 5 h using strong GHSV conditions) revealed also different behaviour for each catalyst type (Fig. 2). Though initial conversion (near total) and H<sub>2</sub> yield (60%, i.e., 3.6 mol H<sub>2</sub>/mol ethanol) were equal for both, deactivation of catalyst M was much faster and its H<sub>2</sub> production was fully deactivated after just 2 h. Similar trends were found for La-promoted supports. Catalysts deactivation was related to coke deposition as shown by TPO and TEM of the

used samples. One may conclude that precipitation method allows preparing more stable catalysts regardless the support composition. This is due to the higher oxygen mobility (and higher reducibility) of P catalysts that reduces the coke deposition rate by removing the coke precursors more easily. In addition, M method did not provide a good dispersion of the active phase, leading to bigger active phase particles.

Funding by PRIN 2015 project 20153T4REF\_006 HERCULES (Italy) and MINECO project CTQ2015-71823-R (Spain) is gratefully acknowledged

## References

- [1] C. Pizzolitto, F. Menegazzo, E. Ghedini, G. Innocenti, A. Di Michele, G. Cruciani, F. Cavani and M. Signoretto; ACS Sustain. Chem. & Eng., 6 (2018) 13867-13876.
- [2] F. Basile, R. Mafessanti, A. Fasolini, G. Fornasari, E. Lombardi and A. Vaccari; J. Eur. Ceram. Soc., 39 (2019) 41-52.



# Effect of a promoter (Ce or Mg) on the catalytic performance of nickel aluminate catalysts in the Aqueous Phase Reforming (APR) of glycerol.

*A. Morales-Marín, A.J. Reynoso, U. Iriarte-Velasco, M.A. Gutiérrez-Ortiz, J.L. Ayastuy, Department of Chemical Engineering, University of the Basque Country UPV/EHU, Bilbao, Spain*

The present work is focused on the development of an active catalyst for hydrogen production from the aqueous phase reforming (APR) of glycerol. Global biodiesel production has increased by 700% from 2005 to 2015, producing a large surplus of low value-added glycerol [1]. During the last years, hydrogen has gained a relevant place as an environmental friendly energy carrier, and has promoted the development of new fuel-cell technologies [2]. Among the catalysts developed for glycerol APR, nickel aluminate spinels ( $\text{NiAl}_2\text{O}_4$ ) have demonstrated promising results for hydrogen production [3]; however, selectivity to hydrogen is still compromised because of the undesired reactions related to the surface acidity. In this work we prepared stoichiometric  $\text{NiAl}_2\text{O}_4$  (NiAl) catalysts impregnated (with nominal metal loading 5 wt.%) by either Ce and Mg promoters (5CeNiAl and 5MgNiAl) and studied the effect of doping metal on the catalytic performance. The physico-chemical properties of the freshly reduced and spent catalysts were evaluated by a sort of techniques. The catalytic performance of the synthesized materials, in situ pre-reduced at 700 °C, were tested at 235 °C/35 bar in a bench-scale fixed-bed reactor using as feedstock 10 wt.% glycerol aqueous solution.

## Results

The characterization of the prepared solids was carried out after reduction at the reaction temperature (700 °C), and some of the obtained results are shown in Table 1. All the samples presented high specific surface area (around 80 m<sup>2</sup>/g), in spite of the high reduction temperature. On the other hand, the addition of promoters (and especially cerium) increased reducibility and density of surface basic sites (Ce: 71% and 70%; Mg: 48 and 26%, respectively). Consequently, the amount of metallic nickel increased in the doped assays. It is noteworthy to note that cerium doping notably decreased the Ni<sup>0</sup> crystallite size and thus, boosted the accessible nickel

species ( $H_{2,chem}$ ); however, magnesium showed a detrimental effect on Ni dispersion causing a three-fold decrease in the accessible nickel amount.

Table 1. Properties of the reduced catalysts and selectivity to hydrogen.

Catalyst	$S_{BET}$ ( $m^2/g$ )	$H_{2,chem}$ ( $\mu mol \cdot g^{-1}$ )	$Ni^0$ (%)	Basic sites density ( $\mu mol_{CO_2}/m^2$ )	$S_{H_2}$ (%)
NiAl	83	21	51	1.10	30
5MgNiAl	79	8	75	1.39	29
5CeNiAl	85	174	87	1.88	40

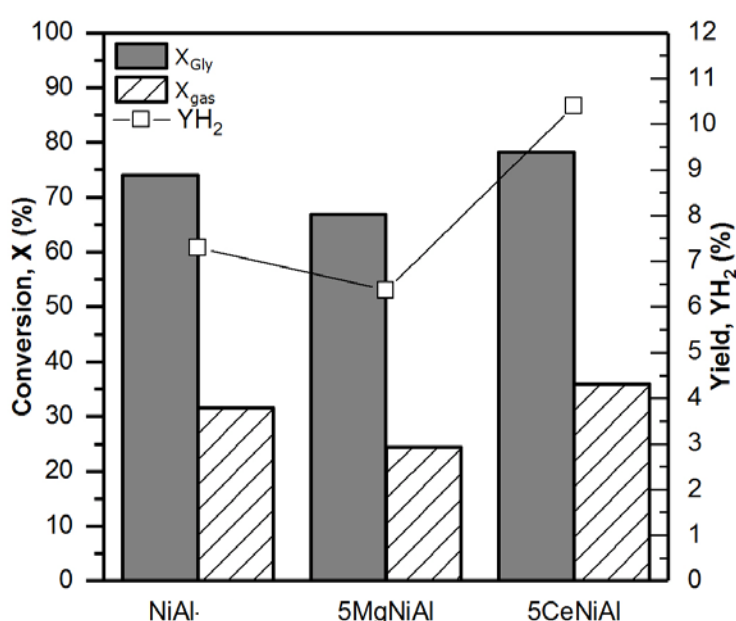


Figure 1. Activity in APR at 1 h.

Before the activity test, all the samples were reduced at 700 °C. For all the catalysts, the main gaseous product was hydrogen (>50%), followed by methane (<26%). As illustrated in Figure 1, base catalyst (NiAl) showed 74%  $X_{Gly}$ , 60%  $Y_{H_2}$  and 32%  $X_{gas}$ . Ce doping improved catalytic performance, with 43% and 33% increase in  $Y_{H_2}$  and

selectivity to  $H_2$  ( $S_{H_2}$ , Table 1), respectively. Contrarily, Mg addition reduced APR activity. According to characterization data, the promotion by Ce could be assigned to the increment of both, surface basicity and accessible metallic Ni atoms; the remarkable decrease of the later upon Mg addition restricted the activity of 5MgNiAl.

#### Acknowledgements

This work was supported by ENE2016-74850-R.

#### References

- [1] R.L. Naylor et al. *Glob. Food Sec.* 16 (2018) 75-84.
- [2] A.C. Olesen et al. *Electrochim. Acta* 293 (2019) 476-495.
- [3] A. Morales-Marín et al. *Appl. Catal., B* 244 (2019) 931-945.

# Critical Impact of Transition Metal Promoters in the MOF-Mediated Synthesis of Co@C Solid Catalysts

*Miguel Rivera-Torrente, Carlos Hernández Mejía, Thomas Hartman, Krijn P. de Jong, Bert M. Weckhuysen, Inorganic Chemistry and Catalysis, Debye Institute for Nanomaterials Science, Utrecht University*

Metal-Organic Frameworks (MOFs) have been extensively studied as template materials for preparing metal@C composites with different properties in what has been named as MOF-mediated synthesis (MOF-MS).<sup>[1]</sup> However, a common issue has been structuring the carbon matrix, which may limit accessibility to the embedded metal atoms or metal particles. Some routes to enhance porosity or modify the particle size distribution have been described, but they are often complex and include numerous steps.

In our work, we describe a simple method to increase the available Co surface, consisting of dry impregnation of two transition metal (Nb, Pt) molecular precursor into the pores of an archetypal Co-MOF topology prior to its pyrolysis. Formation of large ~25 nm mesopores and an increase of the accessible metallic surface area were demonstrated by N<sub>2</sub> physisorption and H<sub>2</sub> chemisorption. Moreover, in-situ X-ray diffraction (XRD) and transmission electron microscopy (TEM) revealed a critical effect on particle size growth of Co when the promoter is present.

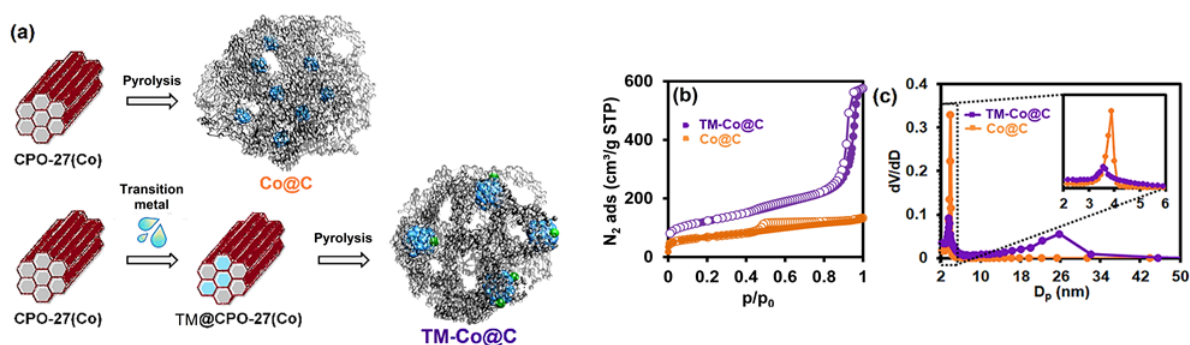


**Figure 1.** (a) Impregnation of transition metal precursors leads to different pore structures of the metal@C materials, as revealed in the (b) N<sub>2</sub> adsorption isotherms at 77 K and the (c) pore size distributions.

Testing of the prepared materials in the conversion of syngas into hydrocarbons (fixed-bed, 220 °C, H<sub>2</sub>:CO = 2, 1 bar, 100 h TOS) showed that, for instance, while Co@C was practically inactive, Nb-Co@C showed nearly two orders of magnitude higher activities, comparable to other Co-supported catalysts, as well as improved selectivity ( $8.9 \cdot 10^{-6}$  mol CO·gCo<sup>-1</sup>·s<sup>-1</sup> and S<sub>C<sub>5+</sub></sub> = 56%). These results show that metal@C materials obtained by MOF-MS can be upgraded in terms of porosity, thus, its performance improved by a simple incipient wetness impregnation strategy, paving the way for the design of new metal@C materials.

#### References

- [1] Oar-Arteta, L.; Wezendonk, T.; Sun, X.; Kapteijn, F.; Gascon, J. Metal–Organic Framework-Mediated Synthesis in Catalysis. *Nanotechnology in Catalysis 2017*, WILEY-VCH

# Liquid-phase synthesis of butyl levulinate with simultaneous water removal catalyzed by acid ion-exchange resins

Montserrat Iborra, Javier Tejero, Carles Fité, Eliana Ramírez, Fidel Cunill

Department of Chemical Engineering and Analytical Chemistry,

University of Barcelona, Martí i Franquès, 1, 08028 Barcelona, Spain

## Introduction

Levulinic acid (LA), a useful platform chemical, can be obtained from lignocellulosic biomass, the most abundant and bio-renewable carbon source on earth. Alkyl levulinates are probably the most remarkable LA-derived compounds to be used as biofuels, because of their favourable properties and relatively inexpensive feedstock. Most of studies in the literature are focused on ethyl levulinates (EL) from ethanol. Butyl levulinate (BL) from butanol is a promising alternative as additive for diesel. Biobutanol can be produced from biomass through the acetone-butanol-ethanol fermentation technology (ABE process). Heterogenous catalysis with Brønsted acid centers, including acidic resins, is preferred to homogeneous catalysis with mineral acids to avoid environmental effects (toxicity) and operational drawbacks (separation and corrosion). The esterification of levulinic acid with 1-butanol is a reversible reaction limited by a low equilibrium constant. LA conversion is favoured by an stoichiometric excess of 1-butanol and removal of formed water. Additionally, removing water minimizes its inhibitor effect on the catalytic activity of the resin.

The aim of present work is to identify the best acidic resin that maximizes butyl levulinate production by reaction of 1-butanol with levulinic acid with water removal.

## Experimental section

The experimental set-up was a Pyrex round-bottom distilling flask submerged in a thermostatic bath at 498 K, a Dean-Stark device and a Dimroth reflux condenser, which allows to separate continuously the formed water. Operating conditions were atmospheric pressure and the boiling point of the reaction mixture. Initially, the flask was loaded with 400 mL of BuOH/LA mixture (molar ration 3:1) and about 2.8 g of dry catalyst. Experimental runs differed in the used catalyst (Table 1). Removed water volume and boiling temperature of the reaction medium were monitored from the instant when the first drop of the condensed water was collected. An experimental run finished when the stoichiometric amount of water was obtained (18 cm<sup>3</sup>). Low amounts (max. 5%-wt) of dibutyl ether and dibutenes were detected.

## Results and discussion

A typical evolution of an experimental run is shown in Figure 1 (Amberlyst-15). At the beginning, temperature increases until a maximum, due to the BL formation, the formed water being uptaken by the resin. Then, further formed water is released to the medium and the trend of the boiling point changes, also due to the BL formation and reactants consumption: temperature decreases until a minimum and, afterwards, it increases progressively until the reaction end (total LA consumption). Experimental results are summarized in Table 1. For all resins, LA conversion was practically complete. Butanol conversion and selectivity to BL was similar in all cases, within the experimental error. Completion reaction time was found to be correlated with the

volume of gel phase of the resin,  $V_{sp}$  (Figure 2), which can be used as a criterium for resin screening. Gel-type resins (lower crosslinking, larger  $V_{sp}$ ) required the shortest time. A larger volume of the gel phase, due to the resin

Table 1: Used catalysts and results summary

	Resin	Contact time (min)	$X_{LA}$ (%)	$X_{BuOH}$ (%)	$S_{BuOH}^{BL}$ (%)	$V_{sp}$ ( $cm^3/g$ )
Macroreticular	Amberlyst-15	618	99.8	32.3	93.6	0.62
	Amberlyst-16	643	99.8	33.0	90.1	1.14
	Amberlyst-35	643	99.8	34.5	91.2	0.50
	Amberlyst-36	554	99.5	34.6	91.2	1.26
	Amberlyst-39	586	100	33.7	93.7	1.64
	Amberlyst-46	780	100	31.0	95.6	0.19
Gel-type	Amberlyst-121	406	100	33.7	94.9	3.15
	Dowex50Wx2	356	100	32.1	93.6	2.68
	Dowex50Wx4	446	100	31.7	94.3	1.92
	Dowex50Wx8	656	99.5	29.0	91.1	1.40

swelling induced by the uptake of formed water during the initial period, would explain a better accessibility to acid sites and higher catalytic activity. Finally, homogeneous catalysis by LA also takes place, as evidenced by a run carried out in the absence of resin: after 4h of reaction time, LA conversion was 51%.

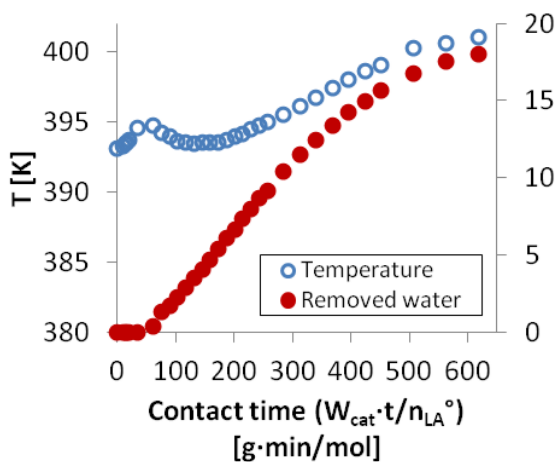


Figure 1: Typical evolution of a experimental run

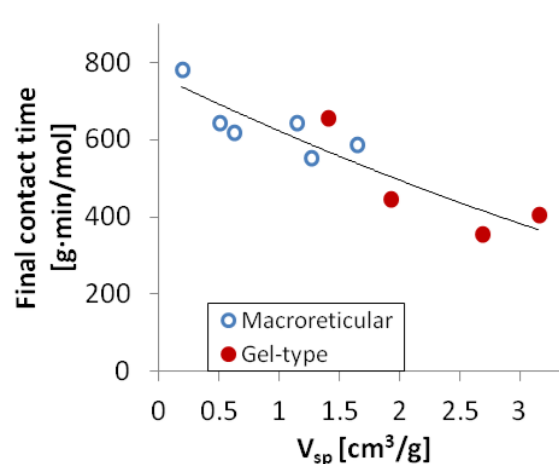


Figure 2: Effect of the volume of gel phase,  $V_{sp}$ , of each resin on the time to reaction completion

# Selective Electrochemical Reduction of CO<sub>2</sub> to C<sub>2</sub> products

Zongdeng Wu<sup>1</sup>; Qingli Hao<sup>\*1</sup>; Bin Zhang<sup>1</sup>; Jiawei Fan<sup>1</sup>; Wu Lei<sup>1</sup>

School of Chemical Engineering, Nanjing University of Science and Technology,  
Nanjing, China

With the rapid development of economy, the increasing consumption of energy brings plenty of environmental problems, such as global warming, greenhouse effect and soil erosion, which are mainly attributed to the large amount of CO<sub>2</sub> emission. So recent studies have focused on how to improve the utilization of renewable energy and transform the existing energy storage mode, where reducing CO<sub>2</sub> to prepare clean and available energy is becoming one of the most promising research directions. Electrochemical reduction of CO<sub>2</sub> has been one of the most important approaches to cyclically utilize carbon resources. Especially, selective conversion of CO<sub>2</sub> to C<sub>2</sub> compounds still remains a greater challenge compared to C<sub>1</sub> products due to the more electrons needed during the reduction process[1,2]. Here, a novel electrocatalyst of CuO-based hollow composite was successfully prepared via hydrothermal synthesis followed by annealing. It was used for catalyzing the reduction of CO<sub>2</sub> in aqueous 0.1 M NaHCO<sub>3</sub> electrolyte. This catalyst exhibited the best selectivity for the only liquid product of ethanol, with faradic efficiencies (FE) over 70%. And it showed strong reduction ability and stability in the controlled potential electrolysis experiment. The possible reaction mechanism was proposed in this report. Such high performance will be useful in the future practical application.

## Acknowledgements

The work was supported by the National Natural Science Foundation of China (Nos. 21576138, 51572127, 51872140), China-Israel Cooperative Program (2016YFE0129900), and the program for Science and Technology Innovative Research Team in Universities of Jiangsu Province, China.

## References

- [1] Gao, S.; Lin, Y.; Jiao, X.; Sun, Y.; Luo, Q.; Zhang, W.; Li, D.; Yang, J.; Xie, Y. Partially oxidized atomic cobalt layers for carbon dioxide electroreduction to liquid fuel. *Nature* **2016**, 529, 68.
- [2] Zhang, C.; Yang, S.; Wu, J.; Liu, M.; Yazdi, S.; Ren, M.; Sha, J.; Zhong, J.; Nie, K.; Jalilov, A. S., Electrochemical CO<sub>2</sub> Reduction with Atomic Iron - Dispersed on Nitrogen - Doped Graphene. *Advanced Energy Materials* **2018**, 1703487.

# Cobalt Ferrite on porous Algae-derived Nitrogen-doped Carbon for Electrocatalytic ORR

*Bin Zhang<sup>1</sup>; Huaping Bai<sup>1</sup>; Lei Lu<sup>1</sup>; Wu Lei<sup>1</sup>; Qingli Hao<sup>\*1</sup>*

*School of Chemical Engineering, Nanjing University of Science and Technology,  
Nanjing, China*

Wide applications of nitrogen-doped porous carbon (NPC) materials have been intensively investigated in various energy conversion and storage devices, such as the cathodic oxygen reduction reaction (ORR) in fuel cells [1], benefiting from their stable skeleton, doping effects, large surface area and porous structure. The introduction of nitrogen atoms can influence the spin density and charge distribution of the adjacent C atoms to induce more active sites for ORR. Moreover, porous nanostructure of NPCs can afford more pores and higher specific surface area, where these pores can act as additional reaction sites. Here, we report a porous nitrogen-doped carbon derived from enteromorpha algae (N-EA), using a one-step pyrolysis process at only 600°C to simultaneously achieve doping, carbonization and activation. After anchoring CoFe<sub>2</sub>O<sub>4</sub> on N-EA, CoFe<sub>2</sub>O<sub>4</sub>/N-EA, not only inherits the high surface area, porous structure, active nitrogen species from N-EA, but also benefits from the active sites from CoFe<sub>2</sub>O<sub>4</sub>. The synergistic effect makes CoFe<sub>2</sub>O<sub>4</sub>/N-EA an alternative catalyst to commercial Pt/C for ORR with superior activity and stability. Green preparation, waste utilization and good ORR performance of CoFe<sub>2</sub>O<sub>4</sub>/N-EA could make it a promising candidate for fuel cells.

## **Acknowledgements**

The work was supported by the National Natural Science Foundation of China (Nos. 21576138, 51572127, 51872140), China-Israel Cooperative Program (2016YFE0129900), and the program for Science and Technology Innovative Research Team in Universities of Jiangsu Province, China.

## **References**

1. Zhou, M.; Wang, H.; Guo, S., Towards high-efficiency nanoelectrocatalysts for oxygen reduction through engineering advanced carbon nanomaterials, *Chem. Soc. Rev.* 2016, 45, 1273-1307.



# The structurally distinct model Au/ $\alpha$ -Fe<sub>2</sub>O<sub>3</sub> interfaces: How to determine catalytic behaviors in low temperature water-gas shift

Lingli Gu,<sup>1</sup> Yiqiang Zeng,<sup>1</sup> Yina Feng,<sup>1</sup> Wu Jiang,<sup>1</sup> Weijie Ji,<sup>1,\*</sup> Chak-Tong Au<sup>2</sup>

<sup>1</sup> Key Laboratory of Mesoscopic Chemistry, MOE, School of Chemistry and Chemical Engineering, Nanjing University, Nanjing 210023, China; <sup>2</sup> Department of Chemistry, Hong Kong Baptist University, Hong Kong.

## Introduction

Transition metal oxide supported Au catalysts have been widely studied due to their high potentials in a few reactions <sup>[1]</sup> including the water gas shift (WGS). Although lots of factors were investigated, establishing a clear structure-activity correlation is ambiguous due to the complexity of catalyst surfaces, which asks for mechanistic study on the structurally clear model catalysts. Herein, we present the findings about the evolution of various surface intermediates in the 100–260 °C range via *in situ* FTIR, CO-TPSR, and XPS studies. The significance of surface OH/H<sub>2</sub>O reactivity and interfacial structure in tailoring intermediate species and controlling H<sub>2</sub> production has been demonstrated.

## Experimental

The truncated hexagonal bipyramid (THB), hexagonal plate (HS), and quasi cubic (QC)  $\alpha$ -Fe<sub>2</sub>O<sub>3</sub> were prepared following the procedures previously reported by us <sup>28</sup>, and denoted as  $\alpha$ -Fe<sub>2</sub>O<sub>3</sub>-THB,  $\alpha$ -Fe<sub>2</sub>O<sub>3</sub>-HS, and  $\alpha$ -Fe<sub>2</sub>O<sub>3</sub>-QC, respectively. The fresh Au-loaded samples were prepared by the controlled deposition-precipitation approach <sup>28</sup>, further subjected to air-calcination at 200 °C for 2 h; and denoted as Au/ $\alpha$ -Fe<sub>2</sub>O<sub>3</sub>-THB-Air, Au/ $\alpha$ -Fe<sub>2</sub>O<sub>3</sub>-HS-Air, and Au/ $\alpha$ -Fe<sub>2</sub>O<sub>3</sub>-QC-Air, respectively. The catalysts were characterized by means of XRD, SEM, N<sub>2</sub> sorption, (HR)TEM, CO-TPSR, XPS, and *in situ* FTIR, and evaluated for the WGS reaction at 120-260 °C.

## Results and Discussion

Three structurally distinct interfaces, *i.e.* Au/ $\alpha$ -Fe<sub>2</sub>O<sub>3</sub>-THB-Air, Au/ $\alpha$ -Fe<sub>2</sub>O<sub>3</sub>-HS-Air, and Au/ $\alpha$ -Fe<sub>2</sub>O<sub>3</sub>-QC-Air, with the major substrate facet being {113}, {012}, and {001} respectively, were prepared in a controllable manner. The low temperature WGS reaction (100-260 °C) was applied to these unique interfacial structures to reveal how these structurally distinct interfaces can impact on the reaction behaviour. With the detailed performance evaluation together with the characterizations of CO-TPSR, XPS, and *in situ* FTIR, the correlations between the evolution of intermediates and the distinct catalytic behaviours have been established. The substrate facet structure plus the Au entity largely determine the form and reactivity of surface OH/H<sub>2</sub>O species which in turn determine the formation of different intermediates and eventually the product selectivity. The Au/ $\alpha$ -Fe<sub>2</sub>O<sub>3</sub>-THB-Air interface is enriched with the oxygen vacant sites, favourable for dissociative adsorption of H<sub>2</sub>O, carboxyl intermediate (COOH) formation and H<sub>2</sub>

production. The Au/ $\alpha$ -Fe<sub>2</sub>O<sub>3</sub>-HS-Air is enriched with surface lattice oxygen, favourable for molecular adsorption of H<sub>2</sub>O, formate intermediate (HCOO) formation, and CO<sub>2</sub> production only. The Au/ $\alpha$ -Fe<sub>2</sub>O<sub>3</sub>-QC-Air interface is enriched with surface Fe sites, favourable for dissociative adsorption of H<sub>2</sub>O and evolution of stable carboxyl intermediate as well as isolated OH species at low reaction temperatures. The findings are informative to control the interfacial structure for the desired product formation in the WGS and other reactions.

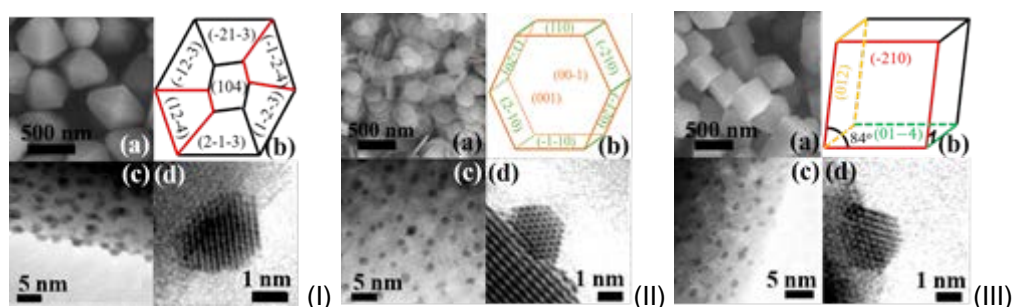


**Fig. 1** SEM image and schematic diagram of  $\alpha$ -Fe<sub>2</sub>O<sub>3</sub>-HS (a and b); HRTEM images (c and d) of (I) Au/ $\alpha$ -Fe<sub>2</sub>O<sub>3</sub>-HS-Air, (II) Au/ $\alpha$ -Fe<sub>2</sub>O<sub>3</sub>-HS-Air, and (III) Au/ $\alpha$ -Fe<sub>2</sub>O<sub>3</sub>-HS-Air.

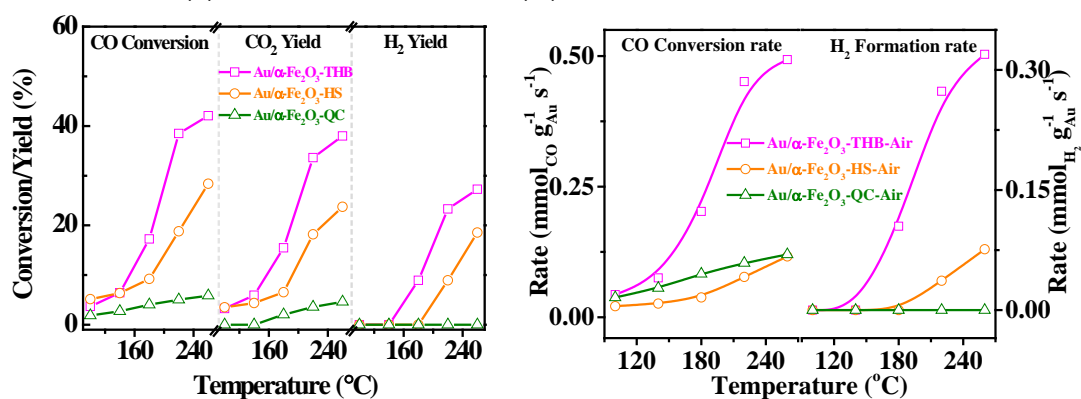


**Fig. 2** The WGS reaction performances over the three model catalysts.

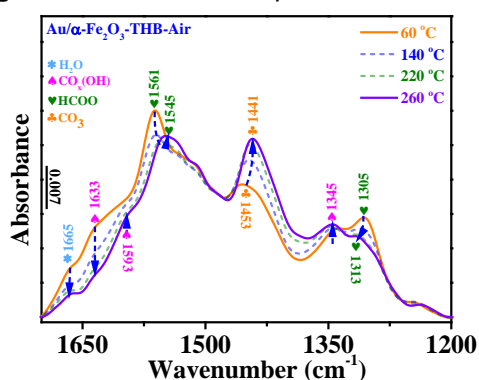


**Fig. 3** FTIR spectra of surface carbonates developed over Au/ $\alpha$ -Fe<sub>2</sub>O<sub>3</sub>-THB-Air.

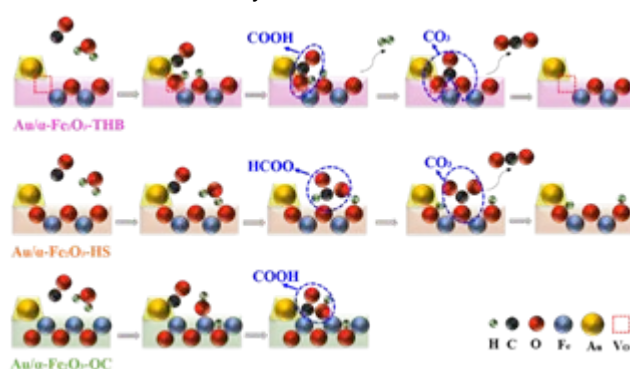


**Fig. 4** The possible evolution of intermediate species on the three model catalysts in the 140-260 °C range.

## References

- [1] Flytzani-Stephanopoulos, M. *Accounts Chem. Res.*, 2014, 47, 783-792.
- [2] Gu, L. L.; Su, Q.; Jiang, W.; Yao, Y.; Pang, Y. J.; Ji, W. J.; Au, C.-T. *Catal. Sci. Technol.*, 2018, 8, 5782-5793.

# A cascade reaction to produce sustainable bio-diesel from a cellulose-derived platform molecule

*Lisa Mullins and James A Sullivan,*

*UCD School of Chemistry, Belfield, Dublin 4, Ireland*

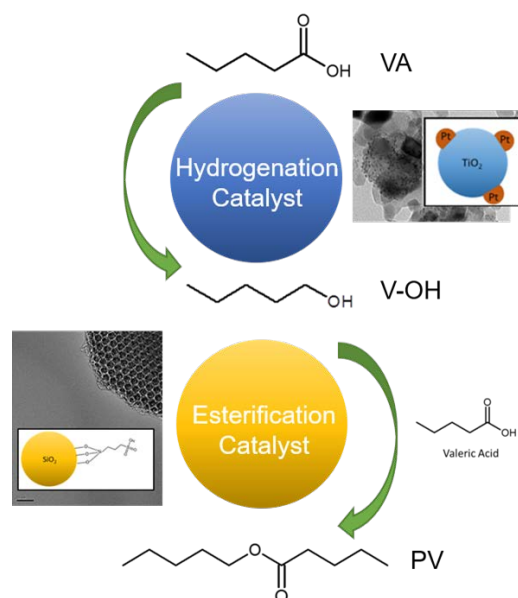
Two equivalents of valeric acid are converted into pentyl valerate in a one pot cascade reaction containing valeric acid and H<sub>2</sub> over a reduction catalyst (to catalyse the selective reduction to pentanol) and an acidic catalyst (to catalyse the esterification of the pentanol with valeric acid). The effects of catalyst loading within the reactor and reaction temperature are considered the contribution concludes with a discussion of the problems associated with cascade reactions.

## Introduction

While carbon-neutral combustion of biomass-derived diesel seems an attractive solution to the CO<sub>2</sub> and resource depletion problems associated with the use of fossil fuels, currently available Fatty Acid Methyl Ester biodiesel suffers from a range of social (food vs fuel), environmental (N<sub>2</sub>O generation, alkaline waste, significant biomass waste) and sustainability. Life cycle analyses suggest that in certain cases their combustion is very far from carbon-neutral [1].

Generating diesel from easily grown cellulose offers the possibility of ameliorating the majority of these problems and there has been significant interest in the hydrolysis of cellulose to platform molecules and the potential use of these to generate sustainable fuels and chemicals.

One of these platform molecules that can be sustainably generated from cellulose is valeric (or pentanoic) acid. This can be esterified with pentanol to form pentyl valerate which has the same flow and combustion properties as petroleum derived diesel [2]. In this work we present a 1-pot cascade reaction which converts valeric acid to pentyl valerate (PV) through a sequential selective reduction and esterification reaction (see figure).



## Experimental

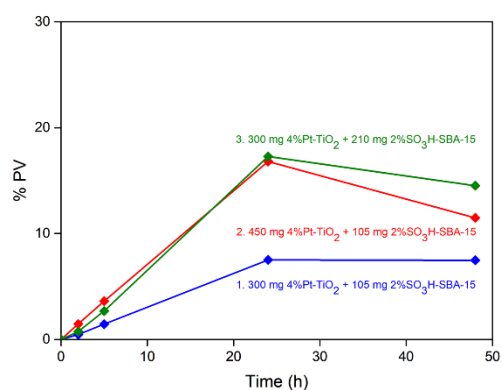
Selective reduction catalysts were 4% Pt/TiO<sub>2</sub> prepared by wet impregnation, while the esterification catalysts were sulfonic acid-modified SBA-15 catalysts prepared by condensation of the relevant tri-ethoxysilane to the surface of previously-prepared SBA-15.

The reactions are carried out in a stirred stainless-steel autoclave at 130 °C and at 20 bar H<sub>2</sub> for 48 h.

## Results and Discussion

Prior to the cascade reaction the activities and selectivities of several selective hydrogenation and esterification catalysts were measured at 130 °C. In the single step reactions it was found that sulfonic acid tethered to SBA-15 were the most active catalysts while in the selective hydrogenation 4% Pt/TiO<sub>2</sub> were the most active and selective.

The figure shows the formation of PV as a function of time over various different admixtures of the two catalysts. It is clear that



changing the loadings of the different catalysts affects reaction outcomes (with PV formation being related to both the levels of the hydrogenation catalyst and the esterification catalyst). Higher levels of the hydrogenation catalyst have led to a greater decrease with time in the levels of PV and this is ascribed to hydrogenation to pentane rather than hydrolysis to pentanol (as levels of pentanol also drop with time after peaking at 20h).

## Conclusions

A reactor containing valeric acid and hydrogen in combination with a selective hydrogenation catalyst and an esterification catalyst held at produced pentyl valerate biodiesel. Over time the formed ester hydrolyzed in the reactor and evidence of a side reaction generating pentane was also observed.

## Acknowledgements

The UCD School of Chemistry is thanked for providing a studentship for LM.

## References

- 1 <https://ec.europa.eu/energy/sites/ener/files/documents/Technical%20report.pdf> (Jan 21 2019)
- 2 J.P. Lange, R. Proce, P.M. Ayoub, J. Louis, L.Petrus, L.Clarke, H.Gosselink, *Angewandte Chemie, International Edition*, (2010), 49, 4479 – 4483

# Study of new methodologies for the monitoring of the conversion of wheat straw, poplar and pine chips into valuable chemicals in a biorefinery scheme

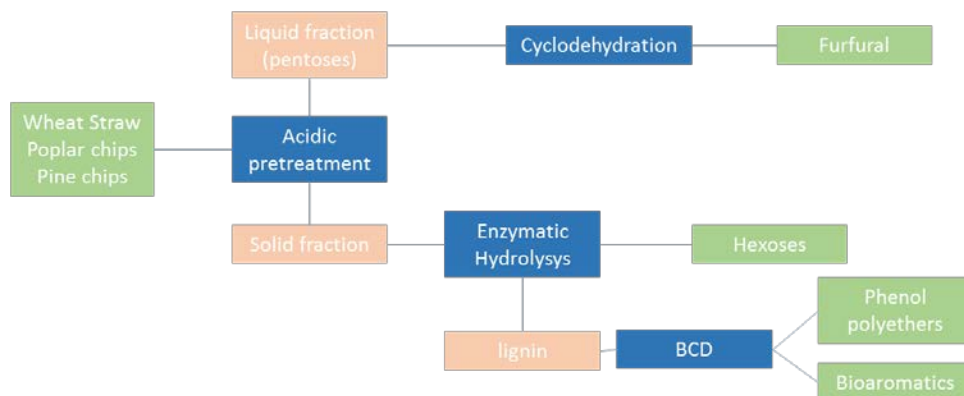
*Alfonso Cornejo<sup>a</sup>, María J. Gil<sup>a</sup>, Íñigo Sarobe<sup>a</sup>, Íñigo García-Yoldi<sup>a</sup>, David Sánchez<sup>b</sup>, Eduardo Otazu<sup>b</sup>, Ibai Funcia<sup>b</sup>, Irantzu Alegría<sup>b</sup>, Víctor Martínez-Merino*

*a) Dpt. of Sciences, Public University of Navarre, E31006 Pamplona, Spain*

*b) Dpt. of Biomass, National Renewable Energy Centre, E31261 Sarriguren, Spain*

In recent years, an increasing effort has been devoted to replace fossil fuels and fossil-fuel derived chemicals. Wheat straw, poplar and pine chips are abundant biomass sources in Navarre and can be used as raw materials in the production of 2G bioethanol in a hypothetical biorefinery.

Thermochemical pretreatment of the raw materials under acid conditions provides, besides the cellulose fraction, residual hemicellulosic and lignin fractions whose valorisation is essential in order to achieve sustainability of the process.



Scheme. Diagram of the biomass valorisation process

The hemicellulosic fractions is rich in xylose and the xylose contents were determined using a new methodology based on  $^{13}\text{C}$  NMR. Xylose was qualitatively transformed in excellent yields to furfural by heating under biphasic conditions in acidic media allowing valorization of these typically underused fraction. Furfural yields were also determined using  $^1\text{H}$  NMR.

The lignocellulosic solid fraction was hydrolyzed using an enzymatic cocktail that afforded a liquid fraction rich in fermentable carbohydrates and a solid fraction rich in

lignin. Lignin was converted in good yields (8-9 %) in bioaromatics under base catalysed depolymerisation (BCD). The molecular weight of the polyhydroxyethers could be approximated using DOSY-NMR spectroscopy.<sup>1</sup>

In this work, we show the optimization of the cyclodehydration reaction of xylose to furfural using microwave irradiation depending on the reaction time and temperature as well as the biphasic medium composition and the biomass source. Similarly, enzymatic hydrolysis optimization was optimized depending each biomass source. Finally, base catalyzed depolymerization optimization of the lignin fraction depending on temperature, base concentration and reaction time will be shown.

#### References

1. W. Ge *et al.*, *ACS Sustain. Chem. Eng.* **2016**, *4*, 1193-1200

# **Lanthanum and Copper-promoted hematite catalysts for WGSR**

*Veronica Silveira de Andrade, María do Carmo Rangel, Laboratório de Reatividade e Catálise. Universidade Federal do Rio Grande do Sul. Porto Alegre, Brazil; Caio Luis Santos Silva, Grupo de Estudos em Cinética e Catálise. Universidade Federal da Bahia, Salvador, Brazil; João Victor Alves Loiola, Escola de Arquitetura e Engenharia. Universidade Salvador, Bahia, Brazil*

## **Introduction**

The water gas shift reaction (WGSR) is a well-known reaction commercially used to purify hydrogen-rich streams, produced during the industrial production of hydrogen. The reaction is performed in two steps at high (High Temperature Shift, HTS) and low temperatures (Low Temperature Shift, LTS). Spite of several advantages, there a demand to find new catalysts for carrying out the process in one step, decreasing the production costs. An attractive approach is to modify hematite (commercial catalyst), by adding new promoters. In a previous work [1], we have found that lanthanum was an efficient promoter for hematite. In the present work, we have studied the effect of lanthanum and copper on the properties of hematite-based catalysts by using an industrial stream, aiming to find efficient and no toxic catalysts for WGSR in one step.

## **Experimental**

Catalysts were prepared by simultaneous hydrolysis of iron nitrate and lanthanum nitrate using ammonium hydroxide. Copper was impregnated in the iron and lanthanum mix gel with an aqueous or an alcoholic solution of copper nitrate. Pure hematite and hematite with lanthanum, copper and with both promoters were also prepared. Samples were characterized by thermogravimetry, Fourier transform infrared spectroscopy, X-ray diffraction, specific surface area measurements, temperature programmed reduction and X-ray photoelectronic spectroscopy. The catalysts were evaluated at 370 °C, under a gas mixture close to the industrial one. Samples were characterized before and after reaction.

## **Results and Discussion**

It was noted that lanthanum made hematite production easier and copper did the same, this effect being stronger for the sample obtained with the aqueous copper

solution. By combining lanthanum and copper, hematite can be obtained at temperatures as low as 127 °C, instead at 179 °C for pure hematite ( $\alpha$ -FeO<sub>3</sub>). Therefore, lanthanum and copper-promoted hematite prepared using alcoholic copper solution demands less energy consumption. X-ray diffractograms confirmed hematite formation pure sample. Lanthanum largely decreased the crystals size, regardless copper. For copper-containing solids, copper oxide (CuO) was also observed, except for the sample prepared with the aqueous solution. In accordance with these results, both lanthanum and copper increased the specific surface areas, this effect being stronger for the sample containing only lanthanum; however, the influence was decreased when both promoters were used. For spent catalysts, magnetite (Fe<sub>3</sub>O<sub>4</sub>) was detected for all samples, indicating the phase transition from hematite to magnetite (active phase). During the transition, the specific surface areas sharply decreased, mainly for lanthanum-free samples, which reached values of 7.0 m<sup>2</sup> g<sup>-1</sup>. However, lanthanum-containing catalysts kept the values higher than 27 m<sup>2</sup> g<sup>-1</sup>, which is much higher than pure hematite (13 m<sup>2</sup> g<sup>-1</sup>). Lanthanum and copper favored hematite reduction but made magnetite reduction more difficult, indicating that both promoters improved the catalysts by making the active phase formation easier and delaying its destruction. At the end of reaction, both promoters increased the activity, their combination increasing even more. The promoters also increased the activity per specific surface area, indicating an electronic action on magnetite. Lanthanum acted as textural promoter. The most active catalyst was that containing lanthanum and impregnated with an alcoholic copper solution.

## Conclusion

Both lanthanum and copper are efficient promoters for hematite-based catalysts. During reaction, hematite goes on phase transition to produce magnetite (active phase). Both metals act as electronic promoters increasing the activity per specific surface area, while lanthanum acts also as textural promoter. The lanthanum-containing catalyst and impregnated with an alcoholic copper solution was the most promising for performing the reaction in one step.

## References

M. C. Rangel, P. S. Querino; S. M. S. Borges, S. G. Marchetti, J. M. Assaf, D. Ruiz, C. B. Rodella, T. de Freitas; A. H. M. da Silva, A. P. Ramon. *Catal. Today* 296 (2017) 262–271.



## **Self-assembly mesoporous silica on clay nanotubes as a component of sulfur removal additives to cracking catalysts**

*A. Glotov, N. Levshakov, E. Smirnova, A. Stavitskaya, E. Ivanov, Gubkin Russian State University of Oil and Gas, Moscow, Russia; Y. Lvov, Louisiana Tech University, Ruston, USA*

Production of ultra-low sulfur content gasoline and diesel is a major trend of refinery nowadays. Up to 40 % sulfur of total gasoline pool volume can be traced from FCC (Fluid Catalytic Cracking) unit. To decrease sulfur content in gasoline fraction, sulfur removal additives to FCC catalysts can be used [1]. Commercial additives consist of alumina based support with Zn-Mg and form spinels. The main disadvantages of these additives are decrease of FCC gasoline fraction yields and high coke formation [1, 2].

Earlier we reported highly efficient sulfur removal additives based on ordered mesoporous silica oxides [2, 3]. But commercial application of these materials is limited due to their low steaming and mechanical stabilities. To improve these properties we suggested reinforcing mesoporous structure by halloysite nanotubes – natural aluminosilicate clay with silica outside and alumina inside surfaces which can be selectively modified for different core-shell structures formation [4].

Material MCM-41/halloysite (50/50 wt %) was synthesized using sol-gel method resulted in self-assembly of ordered mesoporous silica MCM-41 type on halloysite nanotubes. Dried and calcined carrier was impregnated by aqueous solutions of  $\text{La}(\text{NO}_3)_3$ ,  $\text{Mg}(\text{NO}_3)_3$  and  $\text{Zn}(\text{NO}_3)_3$  to deposit 5 % wt of metals on MCM-41/halloysite. According to low-temperature nitrogen adsorption/desorption data resulted samples are mesoporous materials with pore diameter of 2.5 nm and BET surface area about 616  $\text{m}^2/\text{g}$ . It is also confirmed by TEM (pore diameter around 2.4 nm). TEM microphotographs confirm mesoporous structure of the samples with pore diameter around 2.4 nm. XRD reveals peaks at small angles (2-6 °) indicating mesoporous silica oxide phase MCM-41 type formation. Additives were blended with commercial equilibrium zeolite-containing FCC catalyst (e-cat) with mass ratio of 1/10 and tested on MAT-unit with a fixed bed reactor at 500 °C and VHSV of 15.6  $\text{h}^{-1}$ . Vacuum gas oil with sulfur content of 1.93 wt % was used as a feed. Liquid products were analyzed on a gas chromatograph “Chromos GC-1000”. The concentration of sulfur in liquid products was determined by XRF analysis.

Synthesized MCM-41/halloysite composite is thermally stable up to 1100 °C and has a good steaming resistance. All additives with e-cat are active in sulfur removal from liquid products of vacuum gas oil cracking (sulfur decreasing – 15-25 %) compared to e-cat without additives. It should be noted that highly active La/MCM-41/halloysite provides the best sulfur removal (25 %) with only 1 wt % gasoline loss with light cycle oil increasing. In the case of magnesium and zinc based additives sulfur removal was lower with gasoline yield increasing by 1-2 wt % compared to e-cat.

### **Acknowledgements**

This work was supported by the Ministry of Education and Science of the Russian Federation (Grant No 14.Z50.31.0035).

### **References**

- [1] T. Myrstad, H. Engan, B. Seljestokken, E. Rytter, *Appl. Catal. A: Gen.* 187, 1999, 207-212.
- [2] A. Glotov, N. Levshakov, A. Vutolkina, S. Lysenko, E. Karakhanov, V. Vinokurov. *Catal. Today*. 2019, *in press*, [doi.org/10.1016/j.cattod.2018.10.009](https://doi.org/10.1016/j.cattod.2018.10.009).
- [3] E.A. Karakhanov, A.P. Glotov, A.G. Nikiforova, A.V. Vutolkina, A.O. Ivanov, S.V. Kardashev, A.L. Maksimov, S.V. Lysenko, *Fuel Process. Technol.* 153, 2016, 50-57.
- [4] Y.M. Lvov, D.G. Shchukin, H. Mohwald, R.R. Price. *ACS Nano*, 2 (5), 2008, 814-820.

# Highly selective catalytic hydroprocessing of algal-oil to biodiesel over Ni hierarchical zeolites

*G. Papanikolaou, P. Lanzafame, G. Giorgianni, S. Abate, S. Perathoner\*, G. Centi  
Departments of ChiBioFarAm and MIFT- Section of Industrial Chemistry, University  
of Messina, ERIC aisbl and CASPE-INSTM, V.le F. Stagno d'Alcontres 31, 98166  
Messina, Italy. E-mail: perathon@unime.it*

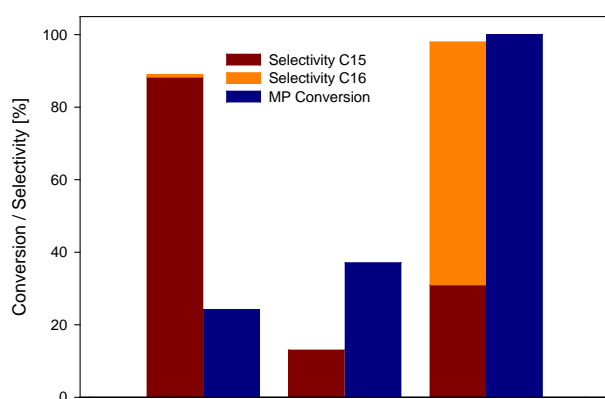
## Introduction

Catalytic hydroprocessing (HPR) of microalgal bio-resources to renewable fuels has attracted great attention in recent years [1-2]. In particular selective catalytic hydrodeoxygenation (HDO) of microalgal oil to alkane-type biodiesel is considered a key process to overcome the main drawbacks (high freezing point, low stability and caloric value) of the biodiesel produced currently by transesterification, due to the presence of oxygen atoms and unsaturated C-C bond. Aside the HDO, also the parallel pathway of the acid catalyzed decarbonylation and decarboxylation increase the production of biodiesel fraction. The development of bifunctional catalysts with hydrogenation and acid functions, not containing noble metals or sulphur (as promoter) is a general current requirement to increase the yields of HDO process. However, an aspect that deserves a more depth analysis is related to the localization and accessibility of the acid and hydrogenation sites, and the relationship with the catalytic behaviour. In this contribution, we investigate how the introduction of mesoporosity by controlled desilication and deallumination in zeolites catalysts, associated to the targeted localization of Ni NPs, affects the “proximity” effect between the acid and hydrogenation functions, leading to a highly active and selective catalytic system for the conversion of methyl palmitate (MP), an algal model compound, to alkane-type biodiesel.

## Results and discussion

Ni-based catalysts (around 8 wt%) were prepared by addressing the localization of Ni NPs inside the pores or on the external surface of silica based supports (Beta zeolite CP811E-75 and SBA15) using two different deposition methods (i.e. sol-immobilization and impregnation). In order to assess the role of structure, porosity and acidity of the catalysts in HDO, the commercial CP811E-75 was modified by desilication and desilication/deallumination treatments, while Al was introduced into SBA15 structure. The properties of the catalysts (textural, acidity, dimension and

dispersion of Ni NPs) were characterized by different analytic techniques and correlated to the results of catalytic testing in the HDO of MP (240°C, 40 barg H<sub>2</sub> and heptane as solvent), evidencing the role of the active sites in the above reaction. All catalytic systems showed activity in MP conversion, leading to the formation of pentadecane (C15), hexadecane (C16) and palmitic acid (PA), as main products. The best catalytic performances both in terms of conversion and selectivity to biodiesel fraction have been obtained with the zeolite based catalysts prepared by sol-immobilization, which presents the highest metal surface area value (MSA), due to the higher accessibility of Ni NPs located on the external surface. Furthermore, also acidity plays an essential role in governing the products distribution. In fact, in purely mesoporous Ni/SBA15 and Ni/Al-SBA15, despite the external location of Ni



NPs, the decarboxylation/decarbonation reactions to C15 were favored by the easier accessibility of acid sites. On the other hand, the introduction of mesoporosity in Beta zeolite by desilication, despite induces a significant increase of acidity, doesn't improve the catalytic activity, due to the low accessibility of the acid sites, induced by

the presence of Al extraframework. In fact the dealumination treatment of desilicated zeolite results beneficial to the catalytic performances (100% MP conversion) leading to a selective production of alkane-type biodiesel (98% selectivity) (Figure 1).

## Conclusions

Catalytic hydroprocessing of MP occurs with high selectivity (98%) to alkane-type biodiesel over Ni/D<sub>S</sub>D<sub>A</sub>Beta, obtained by addressing Ni NPs on the external surface of desilicated/dealuminated Beta zeolite, as result of a synergic role of the high MSA value and the improved acid sites accessibility, due to the removal of Al extraframework.

## References

- [1] C. Zhao, T. Brück, J. A. Lercher, *Green Chem.*, 2013, 15, 1720-1739.
- [2] P. Lanzafame, S. Perathoner, G. Centi, E. Heracleous, E.F. Iliopoulou, K.S. Triantafyllidis, A. A. Lappas, *ChemCatChem* 2017, 9, 1632-1640.

## **Nanostructured Pt-containing catalysts based on clay nanotubes for isomerization of aromatic compounds**

*M. Artemova, N. Demikhova, A. Glotov, A. Vutolkina, P. Gushchin, V. Vinokurov, Gubkin Russian State University of Oil and Gas, Moscow, Russia*

The reforming naphtha fraction is rich in C<sub>8</sub>H<sub>10</sub> aromatics, widely used in petrochemical industry for producing synthetic resins, fibers, and plasticizers. P-xylene is the most valuable isomer which usually used for terephthalic acid production [1]. The purpose of investigation was synthesis of new functional materials based on natural aluminosilicate halloysite nanotubes and testing them as components of catalysts for aromatics isomerization [2].

In this work new micro-mesoporous materials consist of natural halloysite nanotubes, zeolite ZSM-5 and aluminosilicate MCM-41 were obtained by using modified template synthesis. Tetrapropylammonium bromide and cetyltrimethylammonium bromide were applied as templates for micro- and mesopores materials formation respectively. Pt-containing catalysts based on resulting composites were obtained by wetness impregnation method. All resulting materials and catalysts were investigated by transmission electron microscopy (TEM), X-ray diffraction (XRD), nitrogen adsorption/desorption and ammonia temperature programmed desorption (NH<sub>3</sub>-TPD). Catalytic experiments were performed on a flow-type unit with a fixed bed under the following conditions: H<sub>2</sub>:feed molar ratio of 5, VHSV = 0,5-2 h<sup>-1</sup>, catalyst volume = 5 mL, hydrogen pressure = 1.0 MPa, and at the temperature range of 360–440°C. Liquid and gas products were analyzed by gas chromatography. The analysis of operating characteristics of the new catalysts was carried out in comparison with an industrial catalyst.

The formation of an ordered mesoporous structure of MCM-41 type and its retention after modification, and deposition of platinum was proved. The samples have high specific surface area (up to 800 m<sup>2</sup>/g) and a narrow pore size distribution (2-4 nm). The fully crystallized zeolite phase of ZSM-5 type with the average pore diameters of 0.5-0.6 nm was observed. Pt-containing catalysts based on micro-mesoporous materials ZSM-5/MCM-41 and ZSM-5/Halloysite demonstrated the highest selectivity with respect to p-xylene at 380°C. Compared with industrial catalyst, p-xylene yield increased more than 10% on Pt/ZSM-5/MCM-41 catalyst at 300°C and was 96 % of its theoretical value.

New functional micro-mesoporous materials were synthesized, characterized and tested as components of catalysts for isomerization of aromatic compounds. The operating characteristics of the developed catalysts exceeded the same of industrial analog. Obtained catalysts based on cheap and environmental friendly materials can be easily scaled up for industrial applications.

#### **Acknowledgements**

This work was supported by the Ministry of Science and Higher Education of the Russian Federation (Unique ID of the work RFMEFI57717X0239; agreement number 14.577.21.0239).

#### **References**

1. M. Guisnet, N.S. Gnep, S. Morin., *Microporous and Mesoporous Materials*. 2000. Vol. 35–36, P. 47.
2. H. Robson, *Verified Synthesis of Zeolitic Materials: Second Edition*, Amsterdam: Elsevier, 2001. – 198-199.

## **Bipyridine-based Covalent Triazine Framework as heterogeneous photosensitizer for photocatalytic CO<sub>2</sub> reduction**

*Marcelo Alves Fávaro, Regina Palkovits (ITMC, RWTH-Aachen University, Aachen - Germany); Elsje Alessandra Quadrelli (Université Claude Bernard Lyon 1, CPE Lyon, C2P2, Villeurbanne - France); Jérôme Canivet, Florian M. Wisser (Université Claude Bernard Lyon 1, CNRS, IRCELYON, Villeurbanne, France)*

Covalent Triazine Frameworks (or CTFs) are porous materials with interesting properties such as high surface area, high thermal and chemical stability. There are at least three different methods to synthesize CTFs, in which the most commonly used is the trimerization of nitriles in molten zinc chloride. This method leads to materials with a certain degree of crystallinity but as a drawback, partial carbonization caused by the harsh conditions of the synthesis. A recent strategy to synthesize CTFs, using very mild reaction conditions, is the condensation between an amidine and an aldehyde in presence of a strong base [1]. The material synthesized by this approach has some interesting features like layered structure, high surface area and more important, optical band gap. Taking advantage of the condensation method and thinking in a material that could be used as platform for many different reactions, bipyridine-based CTF was synthesized.

Bipyridine is one of the most used chelating ligands in chemistry of organometallic complexes, and a material based on binding units, such as bipyridine, can be used to support more active species. Bridging homogeneous and heterogeneous catalysis, the bipyridine-based CTF, when supporting a metal complex, has a well-defined structure (molecular catalyst) from the homogeneous catalyst, combined with porosity, visible light absorption (yellow to orange solids) and the advantages of working in heterogeneous conditions.

In this way, the material was used to heterogenize the photocatalytic reduction of carbon dioxide. So far, most of the photocatalytic systems use a photosensitizer. The photosensitizer is a homogeneous complex, usually Ru complexes based on bipyridine or phenanthroline ligands, which function is to absorb light and generate the electron-hole pair. The transfer of an electron to the active species starts the reduction. The use of a photosensitizer is actually the main drawback of such systems, because once the complex degrades, the electrons stops being generated

and the reduction stops. Looking for a long-term stability for this photocatalytic system, the bipyridine-based CTF was used as support for the active redox specie, a rhodium (III) complex (see Figure 1). Here, the well-defined active site of the organometallic complex provides selectivity and can drive the reaction to the desired pathway, while the porous material is responsible for the efficiency and activity, absorbing light, producing the electron-hole pairs, which is transferred to the metal complex to initiate the carbon dioxide reduction [3]. The fully conjugated structure of the CTF is very beneficial for electron transportation, additionally, the layered structure of this material represents a very interesting aspect for photocatalytic application since layered materials restrict the electron transportation to two dimensions, decreasing the recombination rate. The Bipyridine based CTF showed better performance than the state-of-art in the photocatalytic reduction of CO<sub>2</sub> to formate.

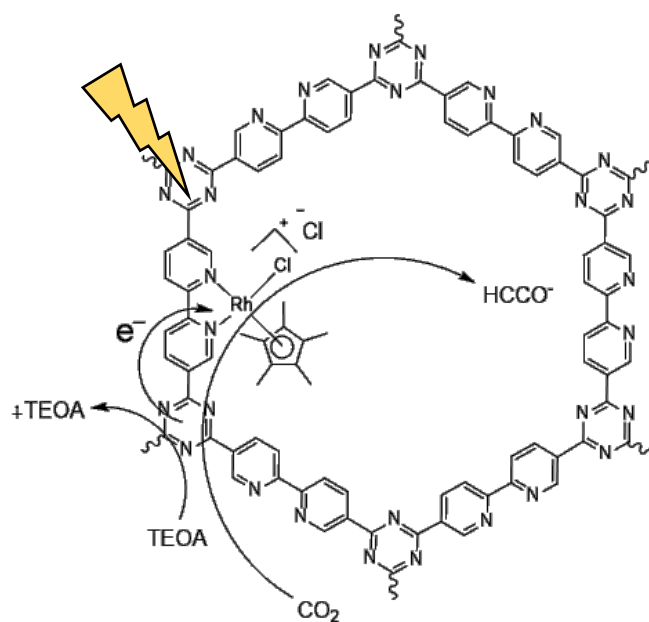


Figure 1. – Bipyridine based CTF as support for pentamethylcyclopentadienylrhodium(III) chloride as catalyst for photocatalytic CO<sub>2</sub> reduction.

#### References

- [1] K. Wang, L-M. Yang, X. Wang, L. Guo, G. Cheng, C. Zhang, S. Jin, B. Tan, A. Cooper, *Angew. Chem. Int. Ed.* 2017, 56, 14149 - 14153.
- [2] X. Wang, F. M. Wisser, J. Canivet, M. Fontecave, C. Mellot-Draznieks, *ChemSusChem* 2018, 11, 3315 - 3322.
- [3] C. S. Diercks, Y. Liu, K. E. Cordova, O. M. Yaghi, *Nature Materials*, 2018, 17, 301 - 307.



# Bioethanol steam reforming: Effect of bioethanol impurities at different steam-to-ethanol ratio

*Nestor Sanchez, Universidad de La Sabana, Chía, Colombia; Ruth Ruiz, Universidad de La Sabana, Chía, Colombia; Bernay Cifuentes, Universidad de Antioquia, Medellín, Colombia; July Paola Gomez, Universidad de LA Sabana, Chía, Colombia  
Martha Cobo, Universidad de La Sabana, Chía, Colombia*

## Introduction

The use of clean energy is a felt need to tackle climate change. Hydrogen (H<sub>2</sub>) is considered a promising energy source due to its high energy density and low emissions. Ethanol can react with water to produce synthesis-gas (syn-gas) through steam reforming (SR). RhPt/CeO<sub>2</sub>-SiO<sub>2</sub> is considered as a potential catalyst to produce H<sub>2</sub> from ethanol, as its yield is about 5.12 mol H<sub>2</sub>/mol ethanol [1]. Bioethanol impurities represent a challenge to produce H<sub>2</sub> through SR, as they ease carbon deposits formation over the catalytic surface [2]. To overcome this issue, a higher steam-to-ethanol (S/E) ratio might be used. The highest the water content, the lowest the carbon deposits ascribed to the coke gasification by water [3]. Hence, in this contribution we explore the effect of bioethanol impurities at different S/E ratio on the H<sub>2</sub> yield.

## Methodology

Raw bioethanol (RB) was obtained from the fermentation of 400 mL of synthetic glucose culture (160 gL<sup>-1</sup> glucose, 8.0 gL<sup>-1</sup> peptone, 11.5 gL<sup>-1</sup> yeast extract, 0.8 gL<sup>-1</sup> MgSO<sub>4</sub>·7H<sub>2</sub>O, 0.27 gL<sup>-1</sup> Ca<sub>3</sub>(PO<sub>4</sub>)<sub>2</sub>, and 0.64 gL<sup>-1</sup> NH<sub>4</sub>(SO<sub>4</sub>)<sub>2</sub>) at 30 °C, 200 rpm, 48 h. The resulting RB was distilled at 70 °C in a rotary evaporator (Heidolph®, Germany) to achieve three bioethanol samples with different S/E ratio (i.e., 3:1; 4:1; and 5:1). RhPt/CeO<sub>2</sub>-SiO<sub>2</sub> were prepared by incipient wetness impregnation method. Before reaction, 100 mg of catalyst diluted with 250 mg quartz was reduced in 8% H<sub>2</sub>/Argon (300 mL/min) at 700 °C and 1 h. Catalytic test was conducted at a gas hourly space velocity (GHSV) of 57,500 h<sup>-1</sup>, from 700 to 400 °C. Synthetic ethanol-water mixtures were also reformed to assess the effect of the impurities.

## Results

**Figure 1** shows product yield at different reaction temperature, S/E ratio, and bioethanol purity for both, synthetic ethanol:water mixtures (dashed lines) and raw bioethanol (continued lines). Regardless the S/E ratio, bioethanol impurities had a detrimental effect over H<sub>2</sub> yield at temperatures higher than 650 °C that could be ascribed to the adsorption competition between impurities and ethanol for the catalytic active sites, resulting in the thermal decomposition of ethanol into CO and CH<sub>4</sub> [2]. An increment of both CO (Figure 1b) and CH<sub>4</sub> (Figure 1d) were observed during SR of bioethanol at 700 °C.

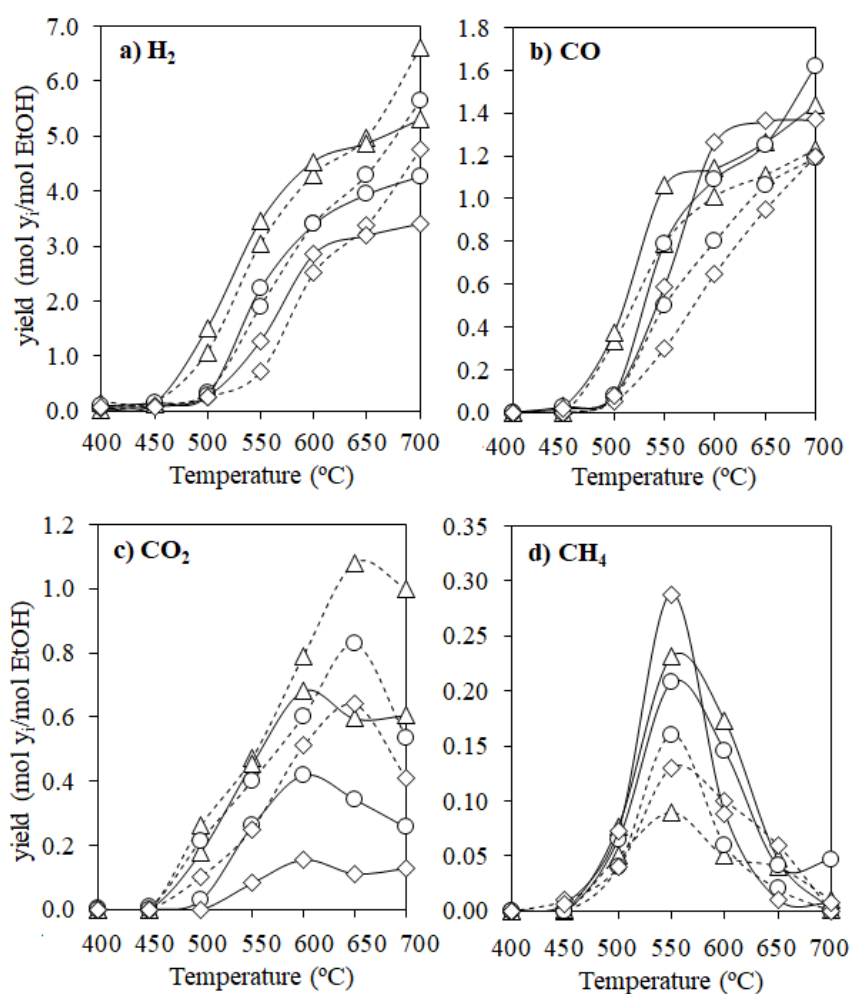


Figure 1. Yield of a) H<sub>2</sub>, b) CO, c) CO<sub>2</sub>, d) CH<sub>4</sub>. Continuous line: Bioethanol samples. non-continuous line: Synthetic samples.  $\Delta$  S/E=5:1;  $\circ$  S/E=4:1;  $\diamond$  S/E= 3:1.

## References

- [1] B. Cifuentes, M. Hernández, S. Monsalve, M. Cobo. *Appl Catal A-Gen.* 523 (2016) 282-293
- [2] A. Le Valant, A. Garron, N. Bion, D. Duprez, F. Epron. *Int J Hydrogen Energ.* 36 (2011) 311-318
- [3] V. Palma, C. Ruocco, A. Ricca. *Int J Hydrogen Energ.* 41 (2016) 11526 - 11536

# Characterization and CDRM performance of monolithic Ni<sub>0.5</sub>Co<sub>2.5</sub>O<sub>4</sub> nanoarray catalysts

*Aybüke Leba, Osmaniye Korkut Ata University, Osmaniye, Turkey; Ramazan Yıldırım, Boğaziçi University, İstanbul, Turkey*

Monolithic Ni<sub>0.5</sub>Co<sub>2.5</sub>O<sub>4</sub> nanoarray catalysts were investigated for CDRM activity at 600-900 °C with CH<sub>4</sub>/CO<sub>2</sub> ratio of 1. The catalyst showed high catalytic activity at all temperatures while the stability at 750°C was low. SEM and XRD tests showed some deterioration and high coke formation on nanoarray structures after reaction. To inhibit this coke, low amount of O<sub>2</sub> (%3) was added to the feed. Although CH<sub>4</sub> conversion and syngas ratio were increased in the presence of oxygen, the catalysts activity continued to decrease in 8 hours.

## 1. Introduction

Dry reforming of methane (CDRM) is a significant catalytic reaction since it is not only providing the utilization of main greenhouses at the same time in one process but also leading a hydrogen/carbon monoxide ratio close to one for the synthesis of valuable chemicals. Ni-Co based catalysts have been widely studied for this process due to their low cost and high catalytic activity; however, coke formation can be a major problem [1]. In this study, the catalytic performance of monolithic Ni<sub>0.5</sub>Co<sub>2.5</sub>O<sub>4</sub> nanoarray catalysts in CDRM has been investigated and the catalysts were characterized since this type of nano-structured catalyst can offer some advantages such as high surface area, easily scalable structure and low pressure drops.

## 2. Experimental study

Ni<sub>0.5</sub>Co<sub>2.5</sub>O<sub>4</sub> nanoarray synthesis over monoliths were prepared following the similar procedure of hierarchical nickel-cobalt nanoarray catalyst preparation method of Ren et al. [2]. Activity tests at a temperature range from 600°C to 900°C, TOS tests at 750°C for 8h were performed in a 10mm ID quartz reactor at 1 atm. Total flow rate was about 70 ml min<sup>-1</sup> (10 ml min<sup>-1</sup> of total flow was N<sub>2</sub> as internal standard while 60 ml min<sup>-1</sup> was reactant gases). Product stream was measured by gas chromatography. SEM and XRD analyses were performed over fresh and spent samples to understand the catalytic surface better.

### 3. Results and discussion

SEM test of the fresh  $\text{Ni}_{0.5}\text{Co}_{2.5}\text{O}_4$  showed that the catalysts were successfully synthesized as in the form of nanowires and well dispersed on the monolith surfaces (Figure 1a). In performance test, catalytic activity was considerably high; 84.5 %  $\text{CH}_4$  conversion and 91.3%  $\text{CO}_2$  conversion were obtained with a 0.93  $\text{H}_2/\text{CO}$  ratio 750°C (Figure 1.b). However, the catalyst lost its activity quite fast. Low amount of oxygen (3%) was added to the feed to see whether the coke formation can be prevented without altering product distribution. The conversions indeed increased, and a better product distribution was observed; however, the stability was not improved significantly.

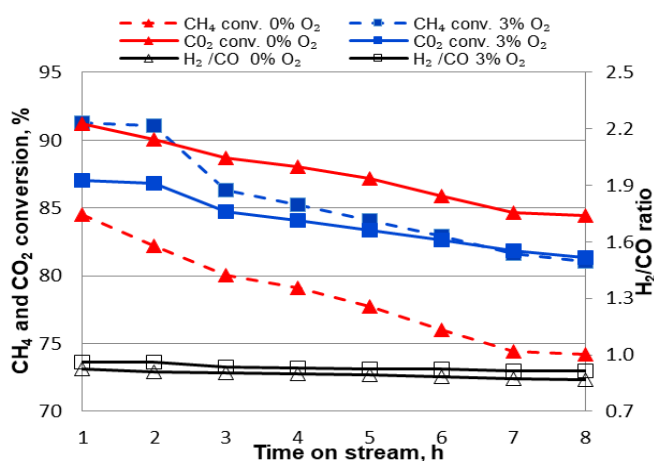
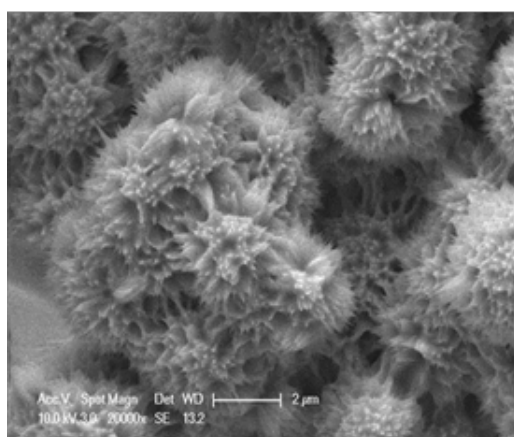


Figure 1. SEM image(a) and activity results(b) of  $\text{Ni}_{0.5}\text{Co}_{2.5}\text{O}_4$  nanoarray catalyst

### 4. Conclusion

$\text{Ni}_{0.5}\text{Co}_{2.5}\text{O}_4$  nanoarray catalyst is quite active in CDRM processes; however; its stability should be improved significantly for the consideration for practical applications.

**Acknowledgement:** This work was supported by Bogazici University Research Fund through Project No: 15A05D3.

### References

- [1] M Fan, AZ Abdullah, S Bhatia, ChemSusChem 2011, 4, 1643 – 1653.
- [2] Z Ren, V Botu, S Wang, Y Meng, W Song, Y Guo, R Ramprasad, SL Suib, PX Gao, Angew. Chem. Int. Ed, 2014, 53, 7223 –7227.

## **Bimetallic catalysts for CO<sub>2</sub> hydrogenation: Effect of Ru addition on alumina supported Ni dispersion**

*A. Quindimil, A. Bermejo-López, U. De-La-Torre, B. Pereda-Ayo, J. A. González-Marcos, J. R. González-Velasco, Department of Chemical Engineering, Faculty of Science and Technology, University of Basque Country UPV/EHU, 48940-Leioa, Spain; [juanra.gonzalez.velasco@ehu.es](mailto:juanra.gonzalez.velasco@ehu.es)*

The progressive substitution of fossil energies by renewable energies is presented as one of the best options in order to reduce CO<sub>2</sub> emissions. However, renewable energies still are not enough competitive and hence, various technological options are being developed in order to complement and promote renewables, among which, Power-to-CH<sub>4</sub> (P2G) is gaining interest. This consists of two-steps process: renewable H<sub>2</sub> generation by water-electrolysis and CO<sub>2</sub> hydrogenation into methane. P2G offers the possibility of storing renewable energy in form of CH<sub>4</sub> and simultaneously reducing CO<sub>2</sub> emissions through its recycling. With the aim of catalyzing CO<sub>2</sub> hydrogenation, recently, several formulations have been tested. Among them, Ni/Al<sub>2</sub>O<sub>3</sub> catalyst has been extensively studied and is also widely used in industry. However, it seems that it requires high metal loading (sometimes higher than 50%) and is easily deactivated [1]. Therefore, adding a promoter such as Ru could be the solution to those problems. Then, the main objective of this work is to study the effect of addition of low amounts of Ru (0.5, 1 and 1.5%) on the catalytic properties and performance of Ni/Al<sub>2</sub>O<sub>3</sub> formulation.

According to XRD results, the Ni crystallite size of bimetallic catalysts is lower than 10 nm and decreases with addition of Ru, as revealed by the wide XRD peak at 76.1 ° 2θ corresponding to elemental Ni. The presence of crystalline Ru was not detected in any case, suggesting that probably it is well dispersed. In line with XRD results, H<sub>2</sub>-TPD results revealed that addition of 1.5% of Ru increases the amount of adsorbed H<sub>2</sub> (from 73 to 148 μmol/g) and that leads to the formation of new H<sub>2</sub> adsorption sites associated with Ru<sup>0</sup>. Besides, the observed shift from 375 to 275 °C and the increase in intensity of the H<sub>2</sub>-TPD peak attributable to Ni<sup>0</sup> sites, also suggests that Ni dispersion is enhanced by Ru addition [2].

Figures 1a and 1b show TEM micrograph of Ni/Al<sub>2</sub>O<sub>3</sub> reference catalyst and STEM image combined with EDX mapping of Ni-1.5%Ru/Al<sub>2</sub>O<sub>3</sub>, respectively. Figure 1a shows the distribution of Ni oval/spherical particles for monometallic catalyst.

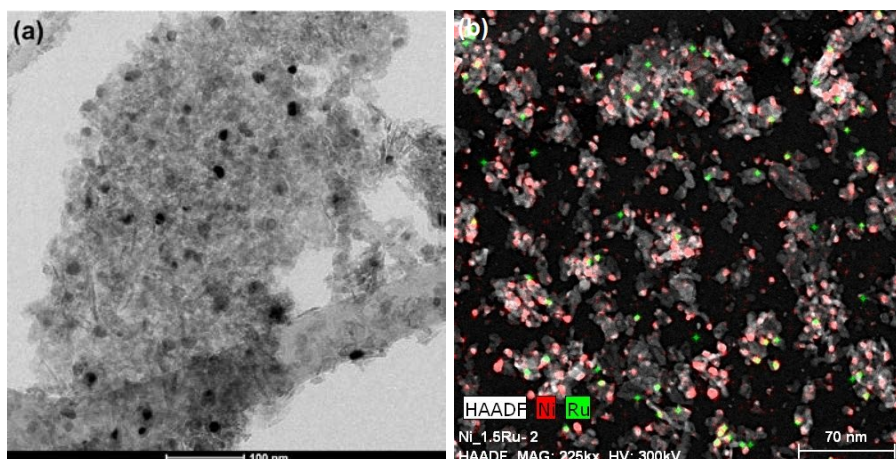


**Figure 1.** Micrographs of (a) Ni/Al<sub>2</sub>O<sub>3</sub> and (b) Ni-1.5%Ru/Al<sub>2</sub>O<sub>3</sub> catalysts.

This presents a particle size distribution ranging from 4 to 18 nm, with mode at 10 nm and an average particle size of 13 nm, corresponding to about 10% of metal dispersion.

On the other hand, Figure 1b shows the distribution of Ni (red colored) and Ru (green colored) particles. It can be noticed that both Ni and Ru are homogeneously dispersed in spherical nano-particles with sizes around 5 and 3 nm, respectively. According to these results, Ru addition leads to a considerable Ni dispersion increase (from 10 to 23%), due to ruthenium acting as a structural promoter.

Reference Ni/Al<sub>2</sub>O<sub>3</sub> and bimetallic catalysts were evaluated in a fixed bed reactor at  $W/F_{A0} = 4.7 \text{ g h mol}^{-1}$ . As a general trend, it was observed that Ru addition (from 0.5 to 1.5%) promotes CO<sub>2</sub> conversions ( $X_{CO_2}$ ) in the range of studied temperatures. In fact, Ni-1.5%Ru/Al<sub>2</sub>O<sub>3</sub> presents a  $T_{50}$  value (temperature at which  $X_{CO_2}$  is 50%) 40 °C lower than Ni/Al<sub>2</sub>O<sub>3</sub> catalyst (300 vs. 340 °C). The greatest differences in activity with the increase of Ru content occur at 300 °C: CO<sub>2</sub> conversion increases from 20 to 51%, whereas selectivity to CO decreases from 2.6 to 0.6%. The observed enhancement in catalytic performance is related to a major dispersion of Ni and to a higher ability of Ru to dissociate H<sub>2</sub> (rate determining step in reaction mechanism) [3].

In conclusion, the coimpregnated Ru not only increases Ni dispersion, but also participates in the reaction, improving notably the activity of Ni/Al<sub>2</sub>O<sub>3</sub> catalyst.

## References

- [1] S. Abate, C. Mebrahtu, E. Giglio, F. Deorsola, S. Bensaid, S. Perathoner, R. Pirone, G. Centi, *Ind. Eng. Chem. Res.* 55 (2016) 4451-4460.
- [2] S. Velu, S. K. Gangwal, *Solid State Ionics* 177 (2006) 803-811.
- [3] J. H. A. Dreyer, P. Li, L. Zhang, G. K. Beh, R. Zhang, P. H.-L. Sit, W. Y. Teoh., *Appl. Catal., B* 219 (2017) 715–726.

# Intensification of Biogas Steam Reforming at low Steam/CH<sub>4</sub> Ratios

P. Tarifa,<sup>1,2</sup> N. Schiaroli,<sup>1</sup> P. H. Ho,<sup>1</sup> F. Ospitali,<sup>1</sup> A. Monzon,<sup>2</sup> C. Lucarelli,<sup>3</sup> G.

Fornasari,<sup>1</sup> A. Vaccari,<sup>1</sup> P. Benito<sup>1,\*</sup>

<sup>1</sup> *Dip. Chimica Industriale "Toso Montanari", Università di Bologna, Bologna, Italy*

<sup>2</sup> *INA-ICMA (CSIC-UNIZAR), Zaragoza, Spain*

<sup>3</sup> *Dip. Scienza e Alta tecnologia, Università dell'Insubria, Como, Italy*

\*patricia.benito3@unibo.it

## Introduction

Clean biogas produced by anaerobic digestion can be valorized in delocalized small plants through reforming converting CH<sub>4</sub> and CO<sub>2</sub> into syngas. Different configurations have been proposed to deal with heat issues, carbon formation and exit composition of the syngas [1]. The addition of steam reduces carbon formation, but two highly endothermic reactions, steam (SR) and dry reforming (DR), are coupled, and large steam/CH<sub>4</sub> (S/C) ratios suppress CO<sub>2</sub> conversion. Structured catalysts made of metallic open-cell foams enhance mass and heat transfer rates and decrease pressure drop, thus being an optimal choice to decrease temperature gradients working at high GHSV under transient conditions [2]. Herein, we propose the intensification of the steam reforming of clean biogas process, at low S/C ratios, over Rh and Ru activated NiCrAl open-cell foams, also investigating the mechanism of carbon formation.

## Experimental

Disks of NiCrAl open-cell foam (10 x1.6 mm, 450 μm cell size) were pre-treated in HCl 1M for 15 min, and washed with distilled water. Then, Rh/Mg/Al hydrotalcite-like (HT) materials were electrodeposited in a 0.06M electrolyte containing Rh(Ru)/Mg/Al = 5/70/25, 2/70/28 (at. ratio) at -1.2 V vs SCE for 2000 s [3]. Coated foams were dried (40 °C, 24 h) and calcined (900 °C, 12 h). Structured catalysts (4 disks) were reduced at 900°C for 2 h. SR of biogas (60% CH<sub>4</sub>, 40% CO<sub>2</sub>) was carried out at 5 bar, 30,000 and 40,000 h<sup>-1</sup> (ca. 8x10<sup>5</sup> and 1x10<sup>6</sup> mLg<sup>-1</sup>h<sup>-1</sup>), 700-900 °C and S/C ratios= 0.5 or 1. Catalysts were characterized by XRD, N<sub>2</sub> adsorption/desorption, SEM/EDS, HRTEM, micro-Raman, H<sub>2</sub>-TPR, and XPS.

## Results and discussion

A thin (ca. 15μm) and homogeneous film of HT-derived catalysts coat the bumpy NiCrAl foam surface (Fig 1a). The coating layer of MgO and MgAl<sub>2</sub>O<sub>4</sub> contains well-



dispersed Rh and Ru species [3]. Metallic loadings are 0.46wt.% for Rh5, and 0.22wt.% for Rh2 and Ru2 (referred to the total structured catalyst weight). After reduction, it is observed the formation of metallic nanoparticles spread in the catalytic coating, even at high loadings, which are stable against sintering during tests.

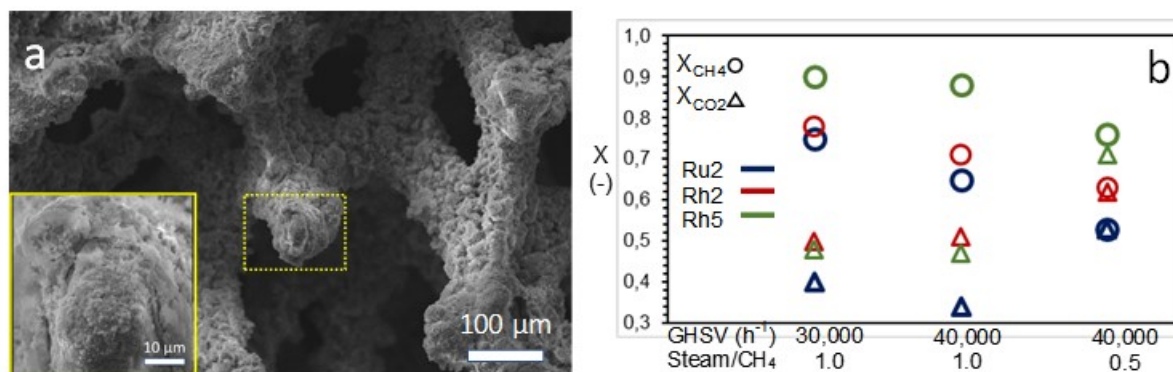


**Figure 1.** a) SEM image of a Rh5 catalyst b) CH<sub>4</sub> and CO<sub>2</sub> conversions at 900°C

CH<sub>4</sub> and CO<sub>2</sub> conversions are ca. 0.90 and 0.5, respectively, at S/C=1; 40,000 h<sup>-1</sup>, 900°C, using the Rh5 sample (Fig 1b). Over the Rh2 catalyst, with a lower Rh content, it was obtained a 0.7 of CH<sub>4</sub> conversion. The syngas composition obtained, H<sub>2</sub>/CO=1.9 and 1.8, made it suitable for CH<sub>3</sub>OH synthesis or Fischer Tropsch reaction. In order to promote the DR route a lower S/C=0.5 was used attaining 75% of CO<sub>2</sub> conversion, stable operation and producing a 1.5 H<sub>2</sub>/CO syngas. Rh catalysts are stable for more than 30 h of time-on-stream in the 900-700°C range. Ru catalyst is also active but deactivates. After reaction, characterization of the foams pieces placed at different bed positions allows knowing the amount and type of carbon deposits (amorphous and graphitic), gaining a valuable information of the reaction mechanism involved.

## Conclusions

Biogas reforming under flexible conditions, modulating CO<sub>2</sub> conversion and H<sub>2</sub>/CO ratio, is feasible over Rh structured catalysts. The open-cell NiCrAl foams reactors allow operations at high space velocities, attaining high mass and heat transfer rates, and therefore high effectiveness factors; and also low carbon formation.

## References

- [1] L. Yang, X. Ge, C. Wan, F. Yu, Y. Li, *Renew. Sust. Energ. Rev.* 2014, 40, 1133–1152.
- [2] A. Montebelli, C.G. Visconti, G. Groppi, E. Tronconi, C. Cristiani, C. Ferreira, S. Kohlerd, *Catal. Sci. Technol.* 2014, 4, 2846-2870.
- [3] P. H. Ho, W. de Nolf, F. Ospitali, A. Gondolini, G. Fornasari, E. Scavetta, D. Tonelli, A. Vaccari, P. Benito, *Appl. Catal. A: Gen.*, 2018, 560, 12–20.



# Deoxygenation mechanisms of propanoic acid over palladium: a theoretical DFT study

*Ravshan S. Shamsiev, MIREA – Russian Technological University, M.V. Lomonosov*

*Institute of Fine Chemical Technologies, Moscow, Russia;*

*Filipp O. Danilov, MIREA – Russian Technological University, M.V. Lomonosov*

*Institute of Fine Chemical Technologies, Moscow, Russia;*

*Vitaly R. Flid, MIREA – Russian Technological University, M.V. Lomonosov Institute*

*of Fine Chemical Technologies, Moscow, Russia*

Deoxygenation of fatty acids and their derivatives is a basis of industrial technologies for producing biodiesel from renewable feedstocks [1]. Theoretical modeling of the main deoxygenation pathways – decarboxylation (DCC) and decarbonylation (DCN) – for propanoic acid on small palladium clusters [1, 2] showed that the COOH\* particle is formed at the C-C bond cleavage stage. The transformations of the COOH\* particle determine the deoxygenation by the reactions: DCC (COOH\* → CO<sub>2</sub>+H\*) or DCN (COOH\* → CO+OH\*).

In this work the comparative calculations of the DCC and DCN reaction mechanisms of propanoic acid on the flat (111) and rough (edges and tops) palladium surfaces were carried out. The all-electron scalar-relativistic DFT-PBE approximation was used. According to the calculations, the mechanisms of the DCC reaction on rough and flat surfaces are identical and include elimination of two H atoms from carboxyl group and β-carbon atom before the C–C bond cleavage. The DCN reaction on a rough palladium surface is initiated by the C<sub>2</sub>H<sub>5</sub>CO–OH bond cleavage, but on the Pd (111) surface first C<sub>2</sub>H<sub>5</sub>COOH\* → C<sub>2</sub>H<sub>4</sub>COOH\* dehydrogenation occurs and then the CO–OH bond breaks.

The better coordination accessibility of palladium atoms on a rough surface leads to decrease of activation barriers by 8–13 kcal/mol comparing to Pd(111). Close values of activation barriers for DCC and DCN reactions explain the formation of observed products of both deoxygenation reactions of carboxylic acids.

Acknowledgments: this work was supported by the Russian Foundation for Basic Research (project № 18-03-00689).

## References

1. Berenblyum A.S., Danyushevsky V.Ya., Kuznetsov P.S., Katsman E.A., Shamsiev R.S. *Petroleum Chemistry* (2016), 56, 663-671.
2. Berenblyum A.S., Shamsiev R.S., Podoplelova T.A., Danyushevsky V.Ya. *Russ. J. Phys. Chem. A* (2012), 86, 1199-1203.

# **New insights the deactivation mechanism of Ni-based CO<sub>2</sub> methanation catalysts under industrial-relevant conditions**

*Chalachew Mebrahtu<sup>†,‡</sup>, Siglinda Perathoner<sup>‡</sup>, Gianfranco Giorgianni<sup>†</sup>, Gabriele Centi<sup>†</sup>, Florian Krebs<sup>‡</sup>, Regina Palkovits<sup>‡</sup>, Rosa Arrigo<sup>§</sup>, Salvatore Abate<sup>†</sup>*

<sup>†</sup> *Depts. MIFT and ChimBioFarAM (Industrial Chemistry), University of Messina, ERIC aisbl and INSTM/CASPE, V.le F. Stagno D'Alcontres 31, 98166 Messina, Italy.*

<sup>‡</sup> *Lehrstuhl für Heterogene Katalyse und Technische Chemie, Institut für Technische und Makromolekulare Chemie (ITMC) RWTH Aachen University, Worringerweg 2, 52074 Aachen, Germany.*

<sup>§</sup> *Diamond Light source Ltd., Harwell Science & Innovation Campus, Didcot, Oxfordshire OX 11 0DE, UK*

## **Introduction**

Significant reductions in CO<sub>2</sub> emissions and the development of no fossil fuel energy sources are critical to minimize the effects of CO<sub>2</sub> as a greenhouse gas in the atmosphere and reduce our dependence on nonrenewable energy sources. The use of synthetic fuels obtained from CO<sub>2</sub> and excess renewable electricity offer a solution to manage fluctuating output of renewable energy and mitigating CO<sub>2</sub> emissions at the same time. P2G “Power-to-gas” is an interesting route for using surplus and low-priced electricity to produce hydrogen via water/steam electrolysis, afterwards converted into methane by reacting with CO<sub>2</sub> through a catalytic methanation reaction.

Whilst, studies in literature focus on investigating reaction conditions above 400°C and with highly diluted feeds, the development of active catalyst under more industrially-relevant reaction conditions is auspicious to attain higher conversion. However, reaction conditions such as 300-320°C and stoichiometric mixture (H<sub>2</sub>/CO<sub>2</sub> = 4) impose challenges not only on finding suitable active materials but generates also materials stability issues. Typically, deactivation of Ni-based CO<sub>2</sub> methanation catalysts is attributed to the formation of carbon [1]. In this contribution, we will show that other deactivation mechanisms are present under our reaction conditions. We apply in situ ambient pressure X-ray photoelectron spectroscopy to provide insights into the structural dynamics responsible of catalyst deactivation.

## Results and discussion

In previous studies, we were able to prepare hydrotalcite (HT) derived Ni-based catalysts which showed higher activity with respect to commercial Ni/Al<sub>2</sub>O<sub>3</sub> catalysts. Fe content as second metal and its promotional effect on the hydrotalcite type catalysts was also optimized [2]. Herein, we synthesized a novel Ni-Fe bimetallic catalysts, with high amount of Ni (70% wt) derived from layered hydrotalcite (HT). A comparison between Ni-HT and Ni-Fe-HT (Fe 7.5 %wt) was performed for CO<sub>2</sub> methanation reaction under industrial relevant conditions (T=300 °C; GHSV=5000-20000 h<sup>-1</sup>; H<sub>2</sub>/CO<sub>2</sub>=4; P=5 bar). The as prepared catalysts and the spent one, were characterized by XRD, XPS, BET, H<sub>2</sub>-TPR and CO-chemisorption. Particularly the role of Fe on the stability of HT catalysts was investigated. Preliminary results on the Ni-Fe-HT catalyst showed both higher activity and stability. On the contrary, the Ni-HT catalyst suffered from deactivation related to the water which forms in-situ during CO<sub>2</sub> methanation. The deactivation was due to the formation of Ni-hydroxide, which at low temperatures, does not completely reduce to metallic Ni with a subsequent decrease of the active phase (Ni<sup>0</sup>), easier sintering, and formation of inactive species. But, the incorporation of Fe to the Ni/HT catalyst found to limit the presence of the Ni-hydroxide species (figure 1). These results were confirmed performing some tests feeding H<sub>2</sub>O but maintaining the same H<sub>2</sub>/CO<sub>2</sub>=4.

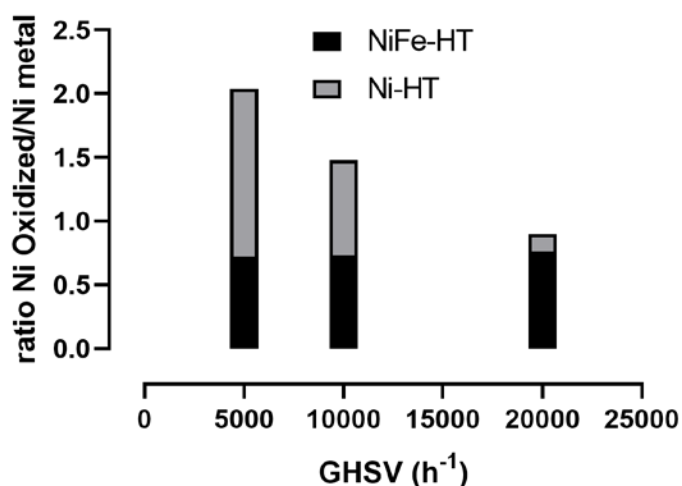


Figure 1 - Surface ratio of Ni oxidized to Ni<sup>0</sup> measured by XPS for the samples after the long-term reaction at different GSHVs.

## References

- [1] Mutz, B.; Sprenger, P.; Wang, W.; Wang, D.; Kleist, W.; Grunwaldt, J.-D; *Appl. Catal., A: General* 2018, 556, 160-171.
- [2] Mebrahtu, C.; Krebs, F.; Perathoner, S.; Abate, S.; Centi, G.; Palkovits, R. *Catal. Sci. Technol.* 2018, 8 (4), 1016–10

# Characterisation of cobalt nanoparticles at the metal-support interface

*Chengwu Qiu<sup>1,2</sup>, Yaroslav Odarchenko<sup>1,2</sup>, Andrew M. Beale<sup>\*1,2</sup>*

<sup>1</sup>*Department of Chemistry, University College London, London, WC1H 0AJ, UK;*

<sup>2</sup>*RCaH, Rutherford Appleton Laboratory, Didcot, OX11 0FA, UK*

## Introduction

The metal-support interface (MSI) plays an important role in supported metal catalysis since it defines the shape of the nanoparticles and also affects the catalyst's reactivity and stability.<sup>1,2</sup> Cobalt nanoparticles (CoNPs) immobilized on the oxide supports are catalysts of choice for the Fischer-Tropsch Synthesis (FTS), and the CoNPs' species, their structure, FTS reactivity and deactivation are affected through the interface.<sup>3,4</sup> The MSI is commonly formed during preparation and reduction of a catalyst.<sup>4</sup> Previous efforts to understand the evolution of the MSI were performed using the bulk samples (powders and pellets) where the signal was averaged over a large number of NPs of different size. Thus we performed a micro-spectroscopy study on a single Co nanoparticles during reduction-oxidation-reduction (ROR) process that is often used in FTS catalyst preparation. A series of model 2D catalysts with a monolayer of the CoNPs supported on the SiO<sub>2</sub>/Si(100) and TiO<sub>2</sub>(110) single crystal substrates were prepared using a combination of the reverse micelle synthesis and a dip coating deposition methods. This advanced fabrication approach allows to conveniently control particle size, size distribution and interparticle distance in the catalysts. Stability of the Co/SiO<sub>2</sub>/Si and Co/TiO<sub>2</sub> catalysts were compared by using quasi in situ X-ray Photoemission Electron Microscopy.

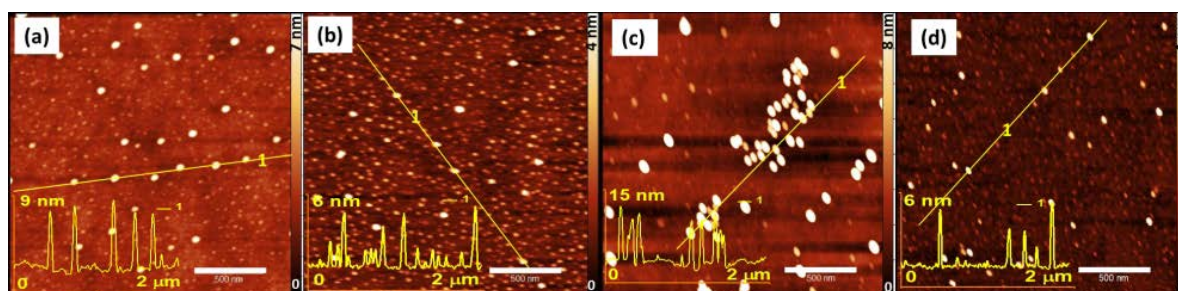


**Figure 1** AFM images of the Co/SiO<sub>2</sub>/Si(100) (a,c) and Co/TiO<sub>2</sub>(110) (b,d) catalysts before (a,b) and after (c,d) redox treatment. The inserts are the 1D profiles on line-labelled directions, showing the NPs height in the corresponding samples. The CoNPs sizes on SiO<sub>2</sub>/Si are much bigger than that on TiO<sub>2</sub>, meaning agglomeration of the NPs on SiO<sub>2</sub>/Si.

## Results and discussion

Atomic Force Microscope (AFM) data (Figure 1) after redox reaction show that CoNPs' size and shape are strongly dependent on the support type. The nanoparticles on SiO<sub>2</sub>/Si support were not stable and agglomerated into bigger NPs (particle size increased > x 2) while those on TiO<sub>2</sub> were partially embedded and/or spread into the substrate.

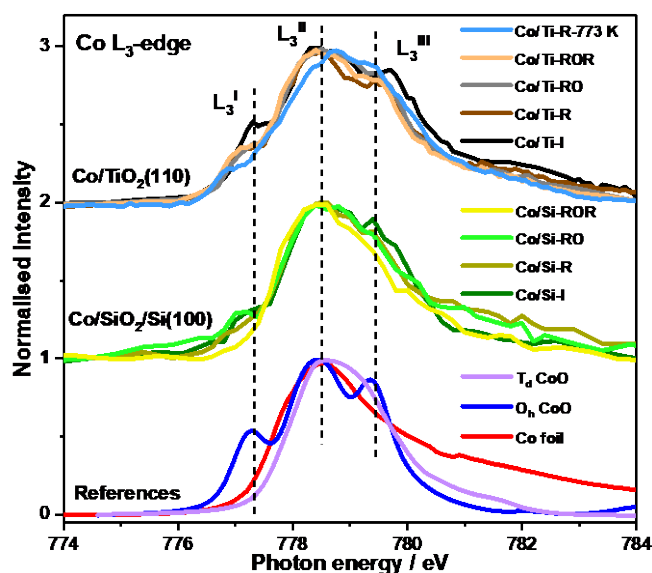


**Figure 2** XAS spectra of Co L<sub>3</sub>-edge of CoNPs supported on SiO<sub>2</sub>/Si(100) and TiO<sub>2</sub>(110) substrate during redox process. Where I is equal to initial state, R reduction (623 K/773 K) and O oxidation (573 K). Dosage of oxygen in was controlled at a pressure of 5×10<sup>-7</sup> mbar, while that of hydrogen was 1×10<sup>-6</sup> mbar. CoNPs on SiO<sub>2</sub>/Si can be fully reduced at 623 K (L<sub>3</sub><sup>I</sup> features lost) and re-oxidised at 573 K (L<sub>3</sub><sup>I</sup> feature regenerated), while that on TiO<sub>2</sub> only can be partly reduced under 773 K.

The soft X-ray Absorption Spectroscopy (XAS) spectra (Figure 2) during redox process show that CoNPs on SiO<sub>2</sub>/Si can be relatively easily reduced and oxidized, whereas in comparison, Co/TiO<sub>2</sub> catalysts form a strong metal-support interaction rendering the CoO resistive to reduction even at temperatures as high as 773 K.

### Summary and Conclusion

CoNPs on SiO<sub>2</sub>/Si are easily reduced but also become agglomerated due to weak metal-support interaction while the NPs are strongly interacted with TiO<sub>2</sub> creating poor reducibility. Therefore, we hope to design a catalyst with good reducibility and stability by using mixed support to modify such metal-support interaction.

### References

- [1] Liu, J. J. Advanced Electron Microscopy of Metal-Support Interactions in Supported Metal Catalysts. *ChemCatChem* **3**, 934–948 (2011).
- [2] Fu, Q., Yang, F. & Bao, X. Interface-confined oxide nanostructures for catalytic oxidation reactions. *Acc. Chem. Res.* **46**, 1692–1701 (2013).
- [3] Hernández Mejía, C., van Deelen, T. W. & de Jong, K. P. Activity enhancement of cobalt catalysts by tuning metal-support interactions. *Nat. Commun.* **9**, 1–8 (2018).
- [4] Tsakoumis, N. E., Rønning, M., Borg, Ø., Rytter, E. & Holmen, A. Deactivation of cobalt based Fischer-Tropsch catalysts: A review. *Catalysis Today* **154**, 162–182 (2010).

## **Catalytic Methane Decomposition over Nanostructured Fe-based Materials**

*Shih-Yuan Chen,\* Takehisa Mochizuki, Takagi Hideyuki*

*Research Institute of Energy Frontier (RIEF), Department of Energy and Environment, National Institute of Advanced Industrial Science and Technology (AIST), 16-1 Onogawa, Tsukuba, Ibaraki 305-8589, Japan.*

*E-mail: sy-chen@aist.go.jp*

Nanostructured  $\text{Fe}_2\text{O}_3/\gamma\text{-Al}_2\text{O}_3$  materials with a  $\text{Fe}_2\text{O}_3$  loading of 50 wt% (shortly termed 50wt% $\text{Fe}_2\text{O}_3/\gamma\text{-Al}_2\text{O}_3$ ) were prepared by wet impregnation method and utilized as solid catalysts for catalytic methane decomposition at 750-850 °C and ambient pressure, in comparison to a commercial production of Fe(II) oxide nanoparticles (shortly termed nano- $\text{FeO}_x$ ). The 50wt% $\text{Fe}_2\text{O}_3/\gamma\text{-Al}_2\text{O}_3$  catalyst was superior to nano- $\text{FeO}_x$  in catalyzing methane decomposition into  $\text{CO}_2$ -free hydrogen and nanostructured carbon materials with high surface area and porosity. Besides, the formation rate of  $\text{CO}_2$ -free hydrogen and structure of those carbon materials could be finely tuned by the reaction conditions, such as temperature and space velocity.

### **1. Scope**

Hydrogen has been considered as next-generation clean energy source because it only generates water by reacting with oxygen in the presence of heat and catalysts. However, hydrogen is most synthesized by the steam reforming process, which produces massive amounts of carbon dioxide. Hydrogen is also difficult to store, transport, and utilize due to its very low boiling point (−252.8 °C), high flammability, and price (particularly when hydrogen is produced by renewable energy). These technical problems have hindered the extensive use of hydrogen, especially renewable hydrogen, as a primary energy source. Catalytic decomposition of methane is a potential process to produce  $\text{CO}_2$ -free hydrogen and valuable carbon materials with tunable nanostructures. Transition metals, such as Fe, Co and Ni, have been studied in catalytic methane decomposition at high temperature (600-1000 °C) and ambient pressure. Among them, the Fe-based catalysts can give better thermodynamic conversion of methane decomposition at high temperature and they

are inexpensive and environmental-friendly. In this study, the  $\text{Fe}_2\text{O}_3$  species supported on the mesoporous alumina materials (namely  $50\text{wt}\%\text{Fe}_2\text{O}_3/\gamma\text{-Al}_2\text{O}_3$ ) were prepared by wet impregnation method, followed by calcining at  $500\text{ }^\circ\text{C}$  in air. Characterizations of  $50\text{wt}\%\text{Fe}_2\text{O}_3/\gamma\text{-Al}_2\text{O}_3$  were carried out by several techniques, such as X-ray diffraction pattern (XRD),  $\text{N}_2$  physisorption, thermogravimetry analysis (TGA) and temperature-programmed reduction (TPR) and electron microscopy (EM), and the results were correlated to its activity in catalytic decomposition of methane into  $\text{CO}_2$ -free hydrogen and nanostructured carbon materials, in comparison to that of commercial nano- $\text{FeO}_x$  sample (20-40 nm, FujiFilm Wako).

## 2. Results and discussion

The  $50\text{wt}\%\text{Fe}_2\text{O}_3/\gamma\text{-Al}_2\text{O}_3$  catalyst with amorphous  $\text{FeO}_x$  species showed high surface area ( $189\text{ m}^2\text{ g}^{-1}$ ), moderate pore volume ( $0.42\text{ cm}^3\text{ g}^{-1}$ ) and large mesopores (14.5 nm), indicating that the  $\text{FeO}_x$  species were uniformly incorporated in the mesoporous alumina framework. In contrast, the nano- $\text{FeO}_x$  sample was a mixture of  $\text{Fe}_2\text{O}_3$  and  $\text{Fe}_3\text{O}_4$  and its showed low surface area ( $39\text{ m}^2\text{ g}^{-1}$ ) and pore volume ( $0.33\text{ cm}^3\text{ g}^{-1}$ ) without mesopores. The activity of  $50\text{wt}\%\text{Fe}_2\text{O}_3/\gamma\text{-Al}_2\text{O}_3$  catalyst in methane decomposition was carried out in a tubular quartz reactor at  $750\text{-}850\text{ }^\circ\text{C}$  for 6 h using a flow of methane ( $50\text{ mL min}^{-1}$ ), in comparison to that of nano- $\text{FeO}_x$  samples. Fig. 1 shows that the formations of  $\text{CO}_2$ -free hydrogen and nanostructured carbon species over the  $50\text{wt}\%\text{Fe}_2\text{O}_3/\gamma\text{-Al}_2\text{O}_3$  catalyst were increased by increasing the reaction temperature, and its activity was higher than the nano- $\text{FeO}_x$  samples. The resulting carbon species also gave higher surface area and porosity. It indicated that the  $\text{FeO}_x$  species homogeneously impregnated on the mesoporous alumina materials were highly active in catalytic methane decomposition.

## 3. Conclusions

The  $50\text{wt}\%\text{Fe}_2\text{O}_3/\gamma\text{-Al}_2\text{O}_3$  catalyst with uniformly-impregnated  $\text{FeO}_x$  species and mesoporosity gave high activity in catalytic decomposition of methane into  $\text{CO}_2$ -free hydrogen and nanostructured carbon species under moderate conditions.

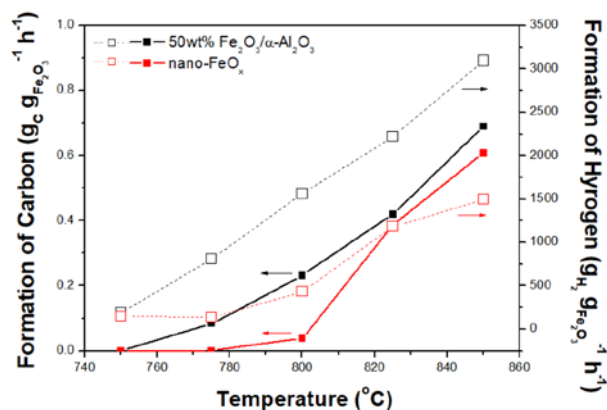


Fig. 1. Formation of  $\text{CO}_2$ -free hydrogen and carbon species as a function of reaction temperature over prepared  $50\text{wt}\%\text{Fe}_2\text{O}_3/\gamma\text{-Al}_2\text{O}_3$  catalyst, in comparison to commercial c- $\text{Fe}_2\text{O}_3$  catalyst.

# Regulation of the Catalytic Properties of Cu-substituted Zeolites in methane partial oxidation by hydrogen peroxide

*Yashnik S.A.<sup>1</sup>, Boltenkov V.<sup>1</sup>, Taran O.P.<sup>1</sup>, Parmon N.V.<sup>1</sup>*

*<sup>1</sup>Boreskov Institute of Catalysis, Novosibirsk, Russia*

## Introduction

The range of practical application of copper-substituted zeolites is not limited only to the processes of gas emissions control [1,2] and ecotoxics removal from wastewater [3]. More and more, they are being studied as catalysts for the synthesis of valuable organic compounds [4, 5]. The catalytic characteristics of Cu-containing zeolites in the deep and selective oxidation of organic compounds are controlled by the oxidizing properties of Cu-structures, which are determined by the copper electronic state, the presence of reactive oxygen within Cu-structures, their interaction with the zeolite lattice, and the process conditions. The present study was aimed at revealing the influence of Cu-ZSM-5 catalysts mentioned properties on the catalytic performance in H<sub>2</sub>O<sub>2</sub> decomposition and partial peroxide oxidation of the methane.

## Experimental

Two preparation modes were applied for postsynthetic modification of the zeolite with Cu(II) ions: 1) ion exchange with aqueous and ammonia solutions of copper acetate [1], and 2) polycondensation of hydrated copper ions with ammonia solution in zeolite pores [2]. The isolated Cu(II) ions, bi/polynuclear oxo/hydroxo clusters of Cu(II) ions in zeolite channels, and copper oxide/hydroxide nanoparticles on the external surface of zeolite crystallites were stabilized by targeted variation the preparation conditions (solution concentration, pH, temperature, etc.)

The catalysts were characterized by ESR, UV-Vis DR, FTIR, TPR-H<sub>2</sub> methods and tested in the peroxide oxidation of methane under the following conditions: 50 °C, pressure 30 bar, mixing speed 1500 rpm, catalyst weight 104 mg, volume 40 ml, 1M solution of H<sub>2</sub>O<sub>2</sub>.

## Results and discussion

Cu-ZSM-5 zeolites catalyze the oxidation of methane with hydrogen peroxide to methanol, formic acid, and other oxygenates (formaldehyde hydrate,



methylhydroperoxide),  $\text{CO}_2$  is formed as a by-product. The activity and selectivity of the methane oxidation are controlled by the catalyst composition, the structure of Cu-sites as well as pH of the reaction solution.

In an acidic medium,  $\text{H}_2\text{O}_2$  decomposes by a radical mechanism (with the formation of  $\text{OH}^\cdot$  и  $\text{HO}_2^\cdot$ ) catalyzed by  $\text{Cu}^{2+}$  ions; whereas in an alkaline medium, the decomposition rate of  $\text{H}_2\text{O}_2$  decreases 3-4 times and the activation energy increases from 60-62 to 71-75 kJ/mol due to the formation of Cu(II) peroxocomplexes. According to the UV-Vis DR spectroscopy, the isolated  $\text{Cu}^{2+}$  ions form the terminal peroxocomplexes Cu-OOH when  $\text{H}_2\text{O}_2$  is added (CTB L-M at  $36000\text{ cm}^{-1}$ ), and the structures of  $\text{Cu}^{2+}$  ions with extraframework oxygen and complexes  $[\text{Cu}(\text{NH}_3)_4]^{2+}$  form in the alkaline environment binuclear Cu(II) peroxocomplexes connected via a terminal OOH-group (CTB L-M at  $20700\text{ cm}^{-1}$ ) or a bridging OO-group (CTB L-M at  $26700\text{ cm}^{-1}$ ).

The route of decomposition of  $\text{H}_2\text{O}_2$  in the presence of Cu-ZSM-5 affects the pathway of the methane functionalization. On the other hand, in the presence of methane, the  $\text{H}_2\text{O}_2$  conversion increases. The  $\text{CH}_4$  conversion over Cu-ZSM-5 and the selectivity to the formation of formic acid are higher in acidic media than in alkaline. Alkalization of the medium during the methane peroxidation promotes the formation of methylhydroperoxide, further oxidized to formaldehyde. For isolated  $\text{Cu}^{2+}$  ions, there is a weak tendency for an increase in the selectivity of methanol formation.

## Conclusion

It is assumed that similar the reactions of deep oxidation of organic compounds, methane peroxidation in acidic media proceeds via a radical mechanism, and in alkaline one — through the formation of copper peroxocomplexes.

**Acknowledgements.** The study was carried out with the financial support of the Russian Science Foundation (project No. 17-73-30032).

## References

1. Yashnik SA, Ismagilov ZR. *Appl. Catal. B* 170-171 (2015) 241.
2. Yashnik SA, Salnikov AV, Vasenin NT, Anufrienko VF, Ismagilov ZR. *Catal. Today* 197 (2012) 214.
3. Taran OP, Yashnik SA, Ayusheev AB, Piskun AS, Prihod'ko RV, Ismagilov ZR, Goncharuk VV, Parmon VN. *Appl. Catal. B* 140– 141 (2013) 506.
4. Beznis N, Weckhuysen B, Bitter J. *Catal. Lett.* 138 (2010) 14.
5. Hammond C, Jenkins RL, Dimitratos N, Lopez-Sanchez JA, Rahim MH, Forde MM, Thetford A, Murphy DM, Hagen H, Stangland EE, Moulijn JM, Taylor SH, Willock DJ, Hutchings GJ. *Chem. – A Eur. J.* 18 (2012) 15735.

# Extracting kinetic information in the era of Open Data

*Pedro S. F. Mendes, Sébastien Siradze, Joris W. Thybaut*

*Laboratory for Chemical Technology, Ghent University, Ghent, Belgium*

## Introduction

The replacement of fossil resources by more sustainable (and ultimately circular) ones as the main source for carbon-based molecules is a major societal challenge which will imply the development of a significant number of new (catalytic) processes. Accordingly, a whole generation of catalysts suitable for novel chemistries has to be developed. Therefore, a breakthrough in catalyst design is of critical importance. Fundamental kinetic modelling has frequently been postulated as the ideal tool for catalyst design. Indeed, the use of fundamental relationships, particularly when based on micro-kinetic (e.g. SEMK) models, enables the identification of the optimal catalyst structures, set of operating conditions, and reactor configuration; ensuring as well extrapolative properties [1]. However, the burdens associated with the fastidious data collection and extraction of kinetic information for model development, have precluded a widespread utilization of kinetic modelling for catalyst design up to now. This work aims at **developing a methodology which will evaluate the kinetic information that can be retrieved in a set of experimental (open) data.**

## Open Data survey

Prior to any mathematical model development, a set of catalysts featuring a high diversity is firstly screened experimentally. A long period of experimental data acquisition is thus required. Concomitantly, current and forthcoming policies, mainly promoted by funding bodies (e.g. EU Commission), but also supported by scientific publishers, are spreading the storage of data in open access repositories. In this study, the current storage of data on catalysis was evaluated. To do so, well-known repositories and databases were surveyed using the keyword “hydrodeoxygenation”, as an example of catalysed reaction (Table 1).

**Table 1: Number of Open Access datasets on hydrodeoxygenation (October 2018).**

REPOSITORY	DATASETS	DATABASE	DATASETS
Mendeley Data	3	OpenAIRE	3
Zenodo	0	DataCite	5
Figshare	349	Google Search	11
ResearchGate	13	SHARE	3

The overall number of available datasets is modest as compared to the number of publications in the same field (ca. 2600). Particularly, if one excludes Figshare (mainly a repository of article's preprints). In the other cases, not all search results are relevant (e.g. data generated by molecular modelling calculations), and data is often unstructured and flawed. More data sharing, better curation and standardized formats, following the FAIR Data Principles [2], can improve Open Access data.

### **Kinetic information extraction**

The first step into the establishment of a kinetic model is the evaluation of the experimental data. As of today, this step relies solely on the researcher's prior knowledge and experience. The methodology under development aims at filling in this gap. In practice, this means that all kinetic features (e.g. variations in conversion) must be identified and, preferably, classified in terms of relevance. Likewise for the experimental variables (e.g. partial pressure) that might explain the variability in the outcome variable (e.g. conversion). This can be achieved via the recognition of patterns and fingerprints [3], e.g. abrupt variations in the performance indicators of interest (e.g. conversion, selectivity, reaction rate). The method herein applied splits the evolution of a variable (e.g. conversion) into intervals with high variability identifying then the location (with respect to the experimental variables), shape, and variability. Such method will be implemented in Python and applied to an *in-house* hydrodeoxygenation dataset, due to the lack of adequate open access ones.

### **Summary**

The lack of curated and standardized Open Access data on catalysis precludes its use at present, but the ongoing policies will overcome this obstacle. To efficiently make use of such data, a methodology for automated kinetic information extraction is under development. It relies on analytical pattern and fingerprint recognition. The corresponding tool will be constructed and evaluated.

### **Acknowledgments**

The authors thank L. Pirro for fruitful discussions. Funding was granted by the BOF of Ghent University (BOF18/PDO/093) and EU commission (ERC Grant No. 615456).

### **References**

- [1] K. Van der Borght, K. Toch, V. Galvita, J. Thybaut and G. Marin, *Catalysts*, 2015, **5**, 1948.
- [2] M. D. Wilkinson *et al.*, *Scientific Data*, 2016, **3**, 160018.
- [3] J. M. Caruthers, J. A. Lauterbach, K. T. Thomson, V. Venkatasubramanian, C. M. Snively, A. Bhan, S. Katare, G. Oskarsdottir, *J. Catal.*, 2003, **216**, 98-109.

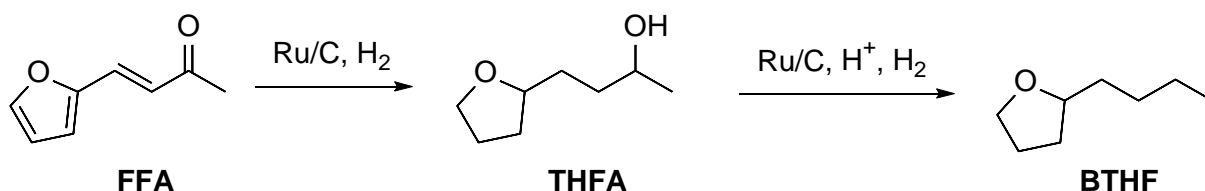
# Advanced Bio-Fuel Additive from the Continuous Flow

## Hydrodeoxygenation of Furfuralacetone

*Marc Strohmann, Andreas Vorholt and Walter Leitner, Max Planck Institute for Chemical Energy Conversion, Mülheim a. d. Ruhr, Germany*

The utilization of renewable biomass for the production of fuels and chemicals has been an ongoing field of research in the last decades. Lignocellulose is the most abundant source of biomass and considered the best alternative to oil as raw material for fuels. One potential route is the conversion of Hemicellulose into the intermediate product Furfuralacetone (FFA), which is deoxygenated into fuels or fuel additives afterwards. A lot of work focused on the complete deoxygenation of FFA to form hydrocarbons. However, fewer investigations dealt with the selective transformation of FFA towards oxygen containing products such as 1-Octanol or 2-Butyltetrahydrofuran (BTHF), which show to some extent even better combustion properties. Additionally, only discontinuous procedures towards 1-Octanol or BTHF have been reported so far.[1,2] In this study, the first example of a continuous flow production of BTHF from FFA is presented.

The transformation consist of two consecutive catalytic reactions for which commercial catalysts are applied. First, FFA is hydrogenated to 4-(tetrahydrofuran-2-yl)butan-2-ol (THFA) over Ru/C. The resulting THFA is hydrodeoxygenated to BTHF, in the second step, catalyzed by a combination of Ru/C and an acidic ion exchange resin (Scheme 1). The separation of the two reactions is necessary, in order to avoid polymerization of FFA under acidic conditions. A continuous flow process is finally realized in a custom-built miniplant, which is equipped with two consecutive tubular reactors.



Scheme 1: Conversion of Furfuralacetone into 2-Butyltetrahydrofuran

The first reaction step gives the fully hydrogenated product THFA with selectivity up to 97% and an open chain diol as main side product. In comparison to batch hydrogenations, the use of a continuous flow reactor leads to a higher productivity and provides an easy catalyst separation. The further conversion of THFA to BTHF in continuous flow is possible with a selectivity of up to 85%. However, batch experiments showed a selectivity towards BTHF of even up to 94%. Main side products are the BTHF isomer 2-Propyltetrahydrofuran and the linear 1-Octanol.

Long-term experiments of the FFA hydrogenation revealed that the Ru/C catalyst deactivates rapidly under certain conditions. Therefore, the catalyst was analyzed before and after the reaction with different microscopic and spectroscopic methods, in order to understand the nature of the deactivation.

#### References

- [1] J. Julis, W. Leitner, *Angew. Chem. Int. Ed.* **2012**, *51*, 8615-8619.
- [2] K. L. Luska, J. Julis, E. Stavitski, D. N. Zakharov, A. Adams, W. Leitner, *Chem. Sci.* **2014**, *5*, 4895-4905.

# Acid site effects on Ni-Cu catalyzed hydrodeoxygenation

Bo Haentjens<sup>a,b</sup>, Pedro S. F. Mendes<sup>a</sup>, Jeroen Lauwaert<sup>a,b</sup>, Jeriffa De Clercq<sup>b</sup>,

Joris W. Thybaut<sup>a</sup>

<sup>a</sup>Laboratory for Chemical Technology, Ghent University, Ghent, Belgium.

<sup>b</sup>Industrial Catalysis and Adsorption Technology, Ghent University, Ghent, Belgium.

## Introduction

As of today, the search for sustainable fuels is more urgent than ever. A promising route entails hemicellulose dehydration into furfural which is, subsequently, reacted in an aldol condensation to produce species with the desired carbon number [1]. Afterwards, the condensation products are hydrodeoxygenated at mild conditions in order to improve their thermal stability and energy density by selective oxygen removal. Up to now, the hydrodeoxygenation (HDO) of such compounds has been scarcely studied. Hence, this work aims at investigating the HDO of such products over Ni-Cu supported catalysts. As the presence of the furan ring will influence the product properties and acid sites are known to catalyse ring opening reactions [2], the focus is on catalyst featuring different acidic properties. As a benchmark, the catalysts were first evaluated in anisole hydrodeoxygenation and tests on furan-containing molecules are in progress at this moment.

## Catalyst synthesis and characterization

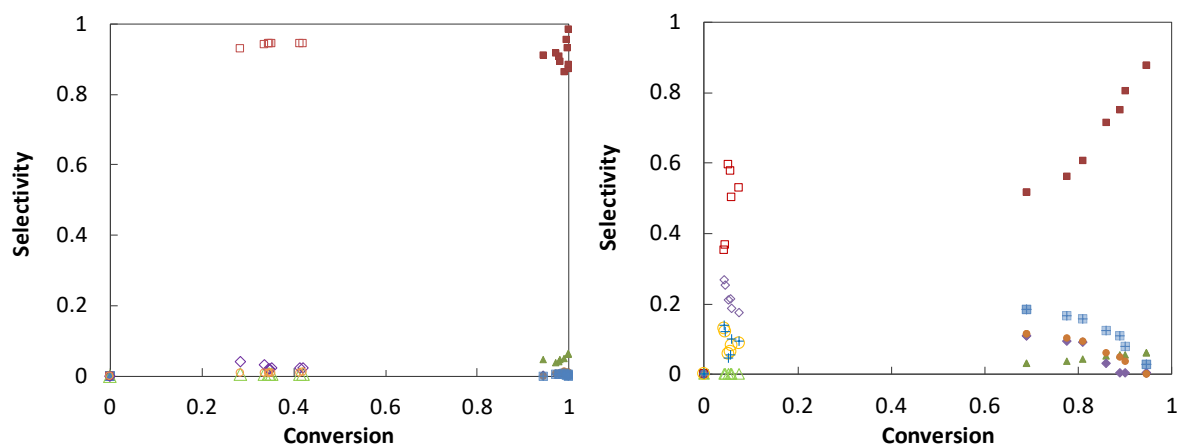
To study the effect of acid sites, a low acidity ( $\gamma$ -Al<sub>2</sub>O<sub>3</sub>) and a mainly amphoteric (SiO<sub>2</sub>) supports were selected. Those were loaded with 18 wt% of Ni and 2 wt% of Cu via wet impregnation [3]. The synthesized catalysts were characterized via N<sub>2</sub>-adsorption, XRD, and H<sub>2</sub>-TPR. In XRD, crystalline phases corresponding to NiO were clearly present, but no CuO phases nor mixed phases were visible. In H<sub>2</sub>-TPR (Table 1), a peak around 200 °C was attributed to the reduction of Cu<sup>2+</sup> species in both supports. Concerning Ni, two peaks were observed for both supports corresponding to weakly and strongly bounded species. In the  $\gamma$ -Al<sub>2</sub>O<sub>3</sub>-based material, the reduction temperatures were significantly higher than in the SiO<sub>2</sub>-based one. A stronger metal-support interaction is thus expected in the former case.

Table 1: H<sub>2</sub>-temperature programmed reduction results for Ni-Cu samples.

Reduction temperature (°C)	Cu <sup>2+</sup>	Ni <sup>2+</sup> (weak)	Ni <sup>2+</sup> (strong)
NiCu/Al <sub>2</sub> O <sub>3</sub>	178	234	302
NiCu/SiO <sub>2</sub>	217	366	518

## Anisole hydrodeoxygenation

After *in-situ* reduction at 400 °C under H<sub>2</sub> flow, the catalysts were evaluated in steady-state experiments under intrinsic kinetic conditions. The  $\gamma$ -Al<sub>2</sub>O<sub>3</sub>-based catalyst was observed to be four times more active than the SiO<sub>2</sub> one. The selectivity results are shown in Figure 1. Over NiCu/Al<sub>2</sub>O<sub>3</sub>, benzene was by far the main product, whereas this was only valid for very high conversions over NiCu/SiO<sub>2</sub>. Over the latter catalyst, significant amounts of phenol, o-cresol, and 2,6-dimethylphenol were also observed. Both the higher activity and selectivity in deoxygenated products over NiCu/Al<sub>2</sub>O<sub>3</sub> can be tentatively attributed to the additional reaction routes catalysed by the acid sites [4].



**Figure 1:** Molar selectivity as a function of conversion for anisole hydrodeoxygenation for NiCu/Al<sub>2</sub>O<sub>3</sub> (left) and NiCu/SiO<sub>2</sub> (right) at 225 °C (open symbols) and 275 °C (closed symbols): benzene (squares), toluene (triangles), phenol (diamonds), o-cresol (circles), and 2,6-dimethylphenol (crosses). Toluene and methyl-anisole not shown. Space-time: 100 kg s mol<sup>-1</sup>. H<sub>2</sub>/anisole: 50. Pressure: 6 bar.

## Conclusions

NiCu-based catalysts featuring different acidities were prepared, characterized, and evaluated. Higher activity and selectivity towards deoxygenation were observed over the  $\gamma$ -Al<sub>2</sub>O<sub>3</sub> catalyst as compared to the SiO<sub>2</sub> one.

## Acknowledgments

The authors thank H. Poelman, A. Bouriakova, A. de Reviere, and C. Ranga for their valuable help. Funding was granted by the Research Foundation - Flanders FWO (12Z2218N) and EU commission (ERC Grant No. 615456).

## References

- [1] J. Q. Bond et al., *Energy & Environmental Science*, 7 (2014) 1500-1523.
- [2] K. Gupta et al., *ChemCatChem* 10 (2018) 2326-2349.
- [3] C. Boscaglia et al., *Biomass and Bioenergy*, 83 (2015) 525-538.
- [4] Y. Shi et al., *Catalysis Science & Technology* 7 (2017) 2385-2415.

## New applications of quadrupole mass spectrometry for catalytic research

Adolf Goetz, Inprocess instruments Bremen

Mass spectrometry is used since many decades in catalytic research. In the last years, many new and advanced techniques were developed to follow the different steps in catalysis research. In this presentation a review and a wide range of applications will be presented with examples from different research work.

Inlet systems will be presented for working with the mass spectrometer under vacuum and ultra high vacuum conditions. Examples will be given also for high pressure application with inlet systems working from normal pressure (ambient pressure) up to 40 bar.

Beside standard analysis there are also new techniques available to analyse corrosive gas mixtures with different compositions and also gas mixtures with very high level of humidity or other condensing components.

For very high precision a sample reference technique can be used. The different concepts of calibrations will be shown and explained for gas mixture, solid samples, generation of gas mixtures and very high accuracy methods by mixing of gases with mechanical pumps.

Beside laboratory application also industrial processes will be presented to follow the kinetic of the process by analysing many components on line with update of the data in the range of few seconds to less than 1 second / data set.

Beside mass spectrometric measurements other analytical techniques can be included. Also different parameters like pressure, flow, temperature, humidity can be measured with the PLC system in the mass spectrometer and included in the data file.

A new robotic system will be shown for full automatic analysis of up to 100 samples including wet chemistry processes with corrosive components. The processes run under different conditions including inert gas and heating up to 120°C.



# **Unsupported versus supported metal nanoparticles: ethanol steam reforming and CO<sub>2</sub> methanation over nickel or cobalt.**

*E. Finocchio, G. Garbarino, T. Cavattoni, P. Riani, G. Busca, DICCA, DCCI, and DIFAR, University of Genova, Genova, Italy*

## **Introduction.**

Metals represent a main family of heterogeneous catalysts, largely applied for hydrogenation, oxidation and steam reforming processes. Most of industrial metallic catalysts are constituted by nanoparticles (NPs) supported on carriers such as alumina, silica, zirconia, titania, alkali earth aluminates, zeolites, carbon materials. However, the real effect of the support on catalytic activity and stability is still under debate. Bio-ethanol Steam Reforming (ESR) is a potentially useful process for producing renewable hydrogen and syngas. Ni and Co catalysts are active for this process and we have recently investigated a number of these catalytic systems. In the case of ESR over Cobalt catalysts we found that unsupported NPs [1,2] and NPs mechanically supported on low area support ( $\alpha$ -alumina) [3] display high activity and stability, comparable or even higher than that of alumina supported samples. As for Nickel catalysts, unsupported and alumina-supported catalysts have comparable activity [4]. Addition of lanthana and silica to Ni/ $\gamma$ -Al<sub>2</sub>O<sub>3</sub> increases remarkably the activity [5,6]. We present here data on the role of silica and lanthana over Ni/Al<sub>2</sub>O<sub>3</sub> catalysts for both ESR and CO<sub>2</sub> methanation. Results on the behavior of unsupported vs. silica-supported Co catalysts in the same reactions are also reported.

## **Experimental**

The experimental conditions and methods are detailed in references [1-8].

## **Results and discussion.**

The nature of the catalytic support and its modifications have already shown a relevant effect in SR of ethanol and phenol, where the addition of La enhances Ni/Al<sub>2</sub>O<sub>3</sub> activity, likely due to Ni-La interactions and to the tuning of surface acidity of the catalysts [6]. Also in the case of CO<sub>2</sub> methanation catalysts, La<sub>2</sub>O<sub>3</sub> doping increases the activity of Ni/ $\gamma$ -Al<sub>2</sub>O<sub>3</sub> [7]. IR spectra show that alumina support is able to adsorb CO<sub>2</sub> in the form of hydrogencarbonates. The adsorption strength increases by addition of lanthana, producing carbonates (fig.1,A). On the other side, the addition of silica decreases the amount of hydrogencarbonates, which are not formed over pure silica. Clearly, the increased support basicity has a positive effect because

it acts as a reservoir for CO<sub>2</sub>. Both silica and lanthana modify also the nature and dispersion of the metal species in alumina supported catalysts. Conversely, silica-supported samples are active, but their stability significantly depends on precursor salt [8]. Two 20 wt.%Co/SiO<sub>2</sub> catalysts have been tested in CO<sub>2</sub> methanation at atmospheric pressure. They show good activity but deactivate fast at 623-673 K, due to formation of encapsulating carbon. However, they retain more stable activity in the reverse Water Gas Shift reaction, producing CO. Also unsupported Cobalt nanoparticles can be active in the methanation of CO<sub>2</sub> but their activity is influenced by the preparation procedure. The Co/SiO<sub>2</sub> catalyst produced from cobalt acetate precursor, shows also stable activity in ESR at 873-973 K, producing Carbon nanotubes that, however, do not cause catalyst deactivation at the laboratory conditions and timescale. The catalyst produced starting with cobalt nitrate is even more active in ESR but it deactivates fast. At lower temperature or when deactivated with respect to ESR, both catalysts shift to high activity in ethanol dehydrogenation to acetaldehyde, showing that ability to activate water is mostly lost. During reaction, cobalt species react with the silica support producing cobalt silicates (fig.1,B) and metallic Cobalt nanoparticles embedded in silica.

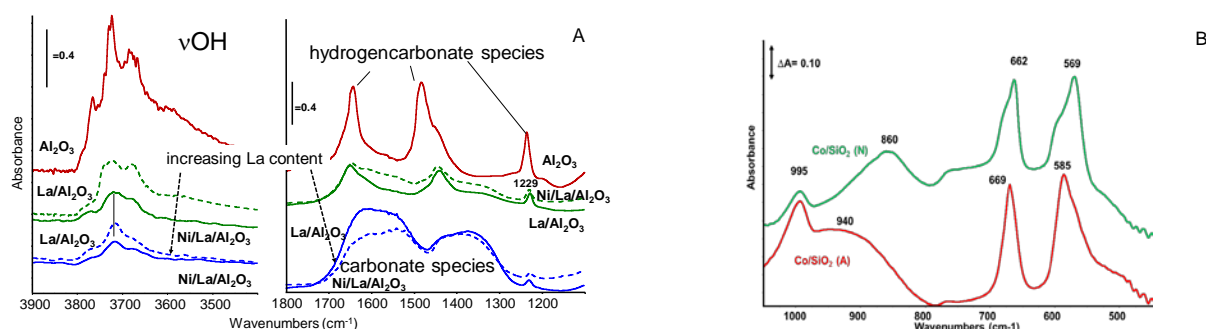


Fig. 1. FTIR spectra of 13.6%Ni/La<sub>2</sub>O<sub>3</sub>/Al<sub>2</sub>O<sub>3</sub> (A) and FTIR subtraction spectra of Co/SiO<sub>2</sub> samples (B)

In sum, the support plays an important role, affecting nature, stability and dispersion of active metal species but also acting as reservoir of reactants thus contributing to the increased activity of metal particles.

## References

1. G. Garbarino, P. Riani, M. Lucchini, F. Canepa, S. Kawale, G. Busca, *Int. J. Hydr. En.*, 38 (2013) 82-91
2. P. Riani, G. Garbarino, A. Infantes-Molina, E. Rodríguez-Castellón, F. Canepa, G. Busca, *Appl. Catal. A: Gen.*, 518 (2016) 67-77.
3. P. Riani, G. Garbarino, F. Canepa, G. Busca, *J. Chem. Tech. Biotech.* 94 (2019) 538-546
4. P. Riani, G. Garbarino, M. Lucchini, F. Canepa, G. Busca, *J. Mol. Catal. A Chem.* 383 (2014) 10-16
5. G. Garbarino, S. Chitsazan, T.K. Phung, P. Riani, G. Busca, *Appl. Catal. A: Gen.*, 505 (2015) 86-97
6. G. Garbarino, C. Wang, I. Valsamakis, S. Chitsazan, P. Riani, E. Finocchio, M. Flytzani-Stephanopoulos, G. Busca, *Appl. Catal. B: Envir.* 174-175 (2015) 21-34
7. G. Garbarino, C. Wang, T. Cavattoni, E. Finocchio, P. Riani, M. Flytzani-Stephanopoulos, G. Busca *Appl. Catal. B: Envir.* (2019), in press
8. T. Cavattoni, G. Garbarino, P. Riani, G. Busca, submitted paper

# **Kinetic modelling of the aqueous-phase reforming of Fischer-Tropsch water over nickel-copper on ceria-zirconia catalyst**

*Aitor Arandia, Aalto University, Finland; Irene Coronado, VTT Technical Research Centre of Finland Ltd, Finland; Reetta Karinen, Aalto University, Finland; Riikka Puurunen, Aalto University, Finland; Matti Reinikainen, VTT, Finland; Juha Lehtonen, VTT, Finland*

## **Introduction and scope**

The production of biofuels in the Fischer-Tropsch (FT) synthesis is accompanied by the production of a significant amount of water with 1 % to 10 % mass fraction of oxygenated hydrocarbons including alcohols [1]. The organic hydrocarbons in the FT water fraction can be converted into hydrogen through aqueous-phase reforming (APR). Kinetic studies have been conducted to identify the rate-limiting steps in the APR of methanol and ethylene glycol [2] and to evaluate the reaction selectivity of ethylene glycol over different catalysts [3]. Later kinetic studies involved the development of models for the APR of ethylene glycol [4] and sorbitol [5]. A great challenge in the development of kinetic models is to define a reaction scheme that represents the actual APR process where several parallel and in series reaction-pathways along with the formation of intermediates. For this work, APR of FT water, which included organic compounds such as C<sub>1</sub>-C<sub>7</sub> alcohols, aldehydes or acids was conducted over a copper-doped nickel supported on ceria-zirconia catalyst (Ni(10%)-Cu(5%)/25% CeO<sub>2</sub>-ZrO<sub>2</sub> (NiCu/25CeZr) [6]) at different operating conditions (pressure, temperature and space velocity). The results of the APR experiments were utilized to develop a kinetic model in Matlab for describing the APR of FT water. The results of this work are meaningful for the development of APR and its potential to be integrated in the biofuel production process through FT synthesis.

## **Experimental**

The experiments were conducted for 6 h in a down-flow, continuous, fixed-bed reactor at two different pressures (3.2 MPa and 4.5 MPa), at three different temperatures at each pressure (210, 220 and 230 °C; and 220, 230 and 240 °C respectively), and with three weight hour space velocities (WHSV) (40, 80 and 200 h<sup>-1</sup>), calculated as mass flow rate of FT water fed into the reactor per mass of catalyst, at each temperature-pressure combination. The reaction model was built considering the most relevant reactions in APR according to the composition of the

feedstock and the product distribution. Empirical power law model was selected to describe the rates of those reactions. Furthermore, the concentrations of non-condensable compounds dissolved in the liquid phase was evaluated using Henry's law constants, whereas the mass transfer limitations at gas-liquid-solid interphases was assessed applying the Weisz-Prater criterion. The system of differential equations was solved by 'ode15s' function, whereas 'fminsearch' and 'lsqnonlin' functions were applied to minimize the experimental and calculated concentrations.

## Results and conclusions

Individual conversions between 5-40 % were common for C<sub>1</sub>-C<sub>5</sub> alcohols (major compounds), whereas the conversion of C<sub>6</sub>-C<sub>7</sub> alcohols was above 50 %. The gaseous products obtained experimentally were H<sub>2</sub>, CO, CO<sub>2</sub>, CH<sub>4</sub>, C<sub>2</sub>H<sub>6</sub> and C<sub>3</sub>H<sub>6</sub>, with H<sub>2</sub> as the main compound and yields between 3-22 %, the highest achieved at 4.5 MPa, 240 °C and a WHSV of 40 h<sup>-1</sup>. The only liquid product considered in the model was acetic acid (formed through ethanol hydration). Accordingly, the reaction model proposed for the APR of FT water comprises full reforming of the major alcohols, i.e. MeOH, EtOH, PrOH and BuOH, to form CO and H<sub>2</sub>; CO conversion via WGS reaction to form CO<sub>2</sub> and H<sub>2</sub>; decarbonylation of alcohols to form alkanes and additional CO and H<sub>2</sub>. According to the calculations, there are no internal diffusion limitations due to a Weisz-Prater parameter much lower than 1 (experimental values in the 10<sup>-7</sup>-10<sup>-6</sup> range). Therefore, a pseudo-homogeneous model that considers the catalyst as a part of the liquid phase was applied. The kinetic model suitably fitted the experimental results of C-containing gases (CO, CO<sub>2</sub>, CH<sub>4</sub> and hydrocarbons) as well as the liquid phase composition in a wide variety of operating conditions. In contrast, the model was not able to describe the H<sub>2</sub> composition, which was notably lower than the experimental values. Based on the analysis of the products and the proposed kinetic parameters, a more complete understanding about the reaction network for the APR of real and complex aqueous fractions was achieved.

## References

- [1] R.J.J. Nel, A. De Klerk, *Ind. Eng. Chem. Res.* 46 (2007) 3558-3565.
- [2] J.W. Shabaker, R.R. Davda, G.W. Huber, R.D. Cortright, J.A. Dumesic, *J. Catal.* 215 (2003) 344-352.
- [3] J.W. Shabaker, J.A. Dumesic, *Ind. Eng. Chem.* 43 (2004) 3105-3112.
- [4] S. Kandoi, J. Greeley, D. Simonetti, J. Shabaker, J. A. Dumesic, M. Mavrikakis, *J. Phys. Chem. C* 115 (2011) 961-971.
- [5] A. Kirilin, J. Wärnå, A. Tokarev, D.Y. Murzin, *Ind. Eng. Chem. Res.* 53 (2014) 4580-4588.
- [6] I. Coronado, M. Pitínová, R. Karinen, M. Reinikainen, R.L. Puurunen, J. Lehtonen, *Appl. Catal. A Gen.* 567 (2018) 112-121.

# Microwave assisted synthesis of zirconia: catalyst for biomass valorisation

*Alessia Giordana<sup>1</sup>, Eliano Diana<sup>1</sup>, Giuseppina Cerrato<sup>1</sup>, Lorenza Operti<sup>1</sup>, Cristina Pizzolitto<sup>2</sup>, Elena Ghedin<sup>2</sup>, Michela Signoretto<sup>2</sup>*

<sup>1</sup> *Department of Chemistry, Università degli Studi di Torino, Torino, Italy*

<sup>2</sup> *Department of Molecular Sciences and Nanosystems, Università Ca' Foscari Venezia, Venezia, Italy*

One of the challenges of this century is the transition toward a sustainable development. Employment of renewable resource for energy and chemicals production is a key factor to be chased. Lignocellulosic biomass, agriculture and forestry residues, non-edible crops are employed as feedstock in second generation bio-fuels and platform chemicals [1].

Zirconia (ZrO<sub>2</sub>) has found application in various technological fields, because of its interesting physical and chemical properties. In heterogeneous catalysis in particular, ZrO<sub>2</sub> has been used in many reactions as both metal catalysts' support and pure catalyst. For example, it has shown good activity and selectivity in alkene isomerization, esterification of fatty acids in biodiesel production and ethanol conversion, but its employment in lignocellulosic valorization is still limited [2].

We report a quick procedure to obtain zirconia based on a microwave-assisted sol-gel synthesis, followed by microwave-assisted calcination. Microwave-assisted processing can help to overcome disadvantages of common synthetic techniques by reducing reaction time, improving yield and leading the preparation of a nanoparticles with homogenous distribution of both shape and dimensions [3]. The product obtained is almost tetragonal ZrO<sub>2</sub>, as confirmed by different techniques (PXRD, HR-TEM, Raman and FT-IR spectroscopies). Using the same synthetic procedure, sulfated zirconia (SZ) and Nickel supported on SZ materials have been obtained.

SZ was tested as catalyst in hydrolysis of glucose for 5-(hydroxymethyl)furfural (HMF) production. Comparing our catalyst with SZ prepared by precipitation route, a better selectivity towards HMF is observed. Further tests are currently performed in order to (i) optimize reaction parameters and (ii) tune the balance of basic and Lewis/Brønsted acid sites required respectively to isomerize glucose to fructose and to dehydrate fructose to HMF.

## References

- [1] S. De, S. Dutta, B. Saha, *Catal. Sci. Technol.* 6 (2016) 7364–7385
- [2] J. Joo, T. Yu, Y.W. Kim, H.M. Park, F Wu, J.Z. Zhang, T.J. Hyeon, *J. Am. Chem. Soc.* 125 (2003) 6553–6557
- [3] H.J. Kitchen, S.R. Vallance, J.L. Kennedy, N. Tapia-Ruiz, L. Carassiti, A. Harrison, A.G. Whittaker, T.D. Drysdale, S.W. Kingman, D.H. Gregory, *Chem. Rev.* 114 (2014) 1170–1206

# Defect-engineered $\text{CoFe}_2\text{O}_4$ -particles by pulsed laser post processing for catalysis research

S. Zerebecki, F. Waag, S. Barcikowski, S. Reichenberger

Technical Chemistry I and Center for Nanointegration Duisburg-Essen (CENIDE),  
University of Duisburg-Essen, 47057 Duisburg, Germany

Identifying and understanding real structure-activity/selectivity correlations is a keystone in catalysis research for the development and improvement of tailored catalysts [1]. Pulsed Laser Post Processing (PLPP) has recently been applied as promising tool to tune nanomaterials regarding e.g. optical and electrochemical properties, phase composition (see Fig 1 B-C), particle size or defect density [2–5]. Therefore, applying PLPP allows to implement a correlational research agenda to individually study materials properties and catalytic performance and stability of well-defined catalyst materials before and after PLPP.

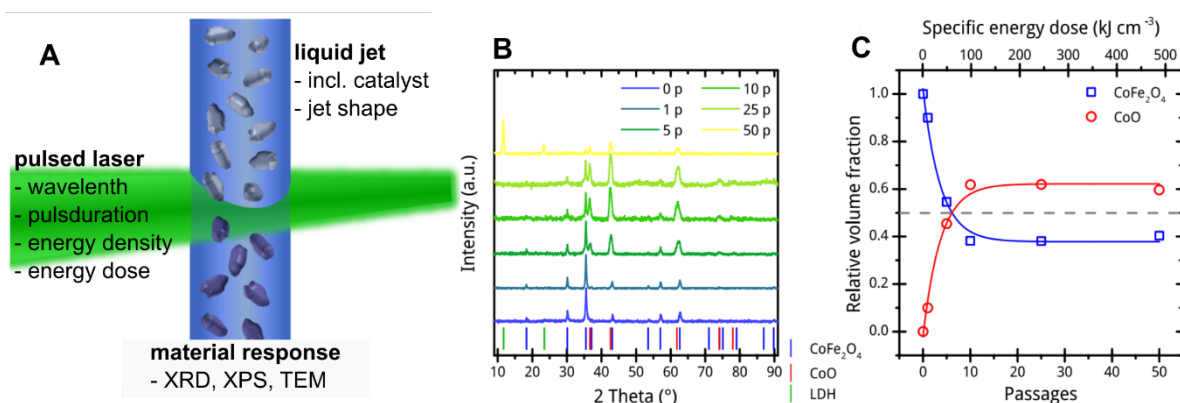


**Fig. 1: A : Schematic representation of PLPP in a liquid jet [3]. B : PXRD patterns of  $\text{CoFe}_2\text{O}_4$  at different numbers of passage-cycles through a PLPP setup [4]. C : Plot of the phase composition versus the number of PLPP passages representing different specific energy doses, respectively [4].**

The poster presents recent methodical advances of PLPP to systematically analyze how the local laser-beam profile and inhomogeneous energy distributions within the liquid jet (see Fig. 1 A) affects the final properties of laser-treated nanomaterials. Understanding the latter is a mandatory prerequisite to subsequently study and systematically understand the underlying mechanisms for laser-based defect-formation/annihilation [2] on applying different laser parameters (pulse duration, photon energy) and mass-specific energy doses (see Fig. 1 A). It will be shown, that the optical properties and surface chemistry as well as catalytic activity can be tuned during PLPP using a modified liquid-jet setup operating under constant flow

conditions. In this context, first results on the impact of inhomogeneous irradiation conditions during PLPP will be presented. Furthermore, the catalytic results will be discussed in terms of laser-based modifications of the morphology and the materials defect density.

#### **Acknowledgments:**

The authors gratefully acknowledge the German Research Foundation for funding the collaborative research centre / transregio CRC/TRR 247 « Heterogeneous Oxidation Catalysis in the Liquid Phase » project-number 388390466.

#### **References**

- [1] A.J. Medford, A. Vojvodic, J.S. Hummelshøj, J. Voss, F. Abild-Pedersen, F. Studt, T. Bligaard, A. Nilsson, J.K. Nørskov, *Journal of Catalysis* 328 2015 36–42.
- [2] M. Lau, S. Reichenberger, I. Haxhiaj, S. Barcikowski, A.M. Müller, *ACS Appl. Energy Mater.* 2018.
- [3] M. Lau, *Laser Fragmentation and Melting of Particles*, Springer, Wiesbaden, 2016.
- [4] F. Waag, B. Gökce, C. Kalapu, G. Bendt, S. Salamon, J. Landers, U. Hagemann, M. Heidelmann, S. Schulz, H. Wende, N. Hartmann, M. Behrens, S. Barcikowski, *Scientific reports* 7 (1) 2017 13161.
- [5] D. Zhang, J. Liu, P. Li, Z. Tian, C. Liang, *ChemNanoMat* 3 (8) 2017 512–533.

# Disposable Nappies to Fine Chemicals

*Rhodri Maunder<sup>a</sup>, Jennifer Edwards<sup>a</sup> Jonathan Bartley<sup>a</sup> Meenakshisundaram*

*Sankar<sup>a</sup>*

*<sup>a</sup> Cardiff Catalysis Institute, Cardiff, United Kingdom*

## Background

When given the choice between re-useable and single use disposable nappies, over 90% of parents opt to use the latter.[1] They are engineered to be effective, convenient and hygienic. Disposable nappies and sanitary products commonly end up in landfill where their component parts decompose over a timescale of hundreds of years, all the while releasing greenhouse gases into the atmosphere and leachates into the ground.

The purpose of this study is to investigate alternative uses for the materials present in recycled single-use nappies and sanitary products by their conversion into value-added products. The material used in this study undergoes a recycling process by NappiCycle, a nappy and absorbent hygiene product recycling service based in Ammanford, West Wales. The waste is converted into the dry and workable material pictured in figure 1 by a series of washing, pressing, bleaching and shredding steps.

The material is a homogenised mixture of a typical nappy's component parts, namely cotton, superabsorbent polymers and hydrocarbon polymers such as polyethylene and polypropylene. The most abundant component is cotton, making up approximately 40% by mass, as determined by thermogravimetry. Cotton is a highly pure form of cellulose.[2] The abundance of cellulose within the material and the extensive research that's already been conducted on its conversion made cellulose a natural focus for investigation as a conversion candidate.

## Current Research Direction

The hydrolysis of cellulose to glucose is a necessary first step in a typical conversion process.[3] The challenges of this reaction become apparent when the properties of cellulose are considered. The intra and intermolecular bonds that give it a highly ordered crystalline structure make it highly resistant to chemical attack.[4] The



**Figure 1: The material obtained from NappiCycle's recycling process.**



development of solid acid catalysts for the reaction aims to overcome the serious drawbacks associated with the use of concentrated mineral acids.[5]

Hydrolysis reactions with a commercially available solid acid catalyst (Amberlyst-15) were carried out in deionised water at autogenic pressure. Both this and sulphuric acid were used as benchmarks and to confirm the efficacy of analysis methods. Ball-milling was used as a pre-treatment step as a means to increase product yield. The products identified and quantified with HPLC were glucose and mannose. In all instances, the yield of glucose and mannose increased if the material was pre-treated with ball-milling. This is expected, as the pre-treatment results in a reduced degree of crystallinity within the cellulose, as calculated using X-Ray diffraction. Though the degree of crystallinity of the cellulose within the recycled nappy fibre material is lower than that of Avicel (69% versus 86%), the extent of Avicel's reduction was greater (54% versus 66%), which provides an explanation for the higher initial yield of products achieved without ball-milling, yet the marginal increase observed post ball-milling. The recalcitrance of the recycled nappy fibres towards this pre-treatment method has yet to be determined. Future work includes the synthesis, characterisation and testing of novel solid acid catalysts that are optimised for use with the recycled nappy fibre material, with significant progress expected in the next several months. An investigation into other cellulose pre-treatment methods will also be conducted, along with the feasibility of separating and re-generating the superabsorbent polymers that are deactivated during the recycling process.

Though the degree of crystallinity of the cellulose within the recycled nappy fibre material is lower than that of Avicel (69% versus 86%), the extent of Avicel's reduction was greater (54% versus 66%), which provides an explanation for the higher initial yield of products achieved without ball-milling, yet the marginal increase observed post ball-milling. The recalcitrance of the recycled nappy fibres towards this pre-treatment method has yet to be determined. Future work includes the synthesis, characterisation and testing of novel solid acid catalysts that are optimised for use with the recycled nappy fibre material, with significant progress expected in the next several months. An investigation into other cellulose pre-treatment methods will also be conducted, along with the feasibility of separating and re-generating the superabsorbent polymers that are deactivated during the recycling process.

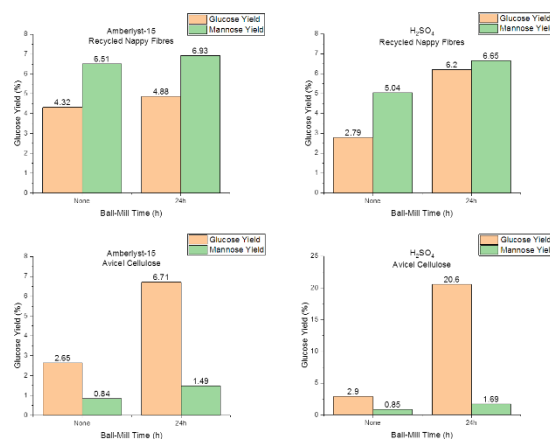


**Figure 2: The yield of glucose and mannose over Amberlyst-15 and sulphuric acid.**

**Reaction conditions: 1.2g Amberlyst-15/300µL H<sub>2</sub>SO<sub>4</sub>, 300mg cellulose/RNF 12mL water, 120°C, 24h**

## References

- [1]K. S. Kim and H. S. Cho, "Pilot trial on separation conditions for diaper recycling," *Waste Manag.*, vol. 67, pp. 11–19, Sep. 2017. [2] D. Klemm, B. Heublein, H. P. Fink, and A. Bohn, "Cellulose: Fascinating biopolymer and sustainable raw material," *Angewandte Chemie - International Edition*. 2005. [3] C. H. Zhou, X. Xia, C. X. Lin, D. S. Tong, and J. Beltrami, "Catalytic conversion of lignocellulosic biomass to fine chemicals and fuels," *Chemical Society Reviews*, vol. 40, no. 11. The Royal Society of Chemistry, pp. 5588–5617, 17-Oct-2011. [4] T. Komanoya, H. Kobayashi, K. Hara, W. J. Chun, and A. Fukuoka, "Catalysis and characterization of carbon-supported ruthenium for cellulose hydrolysis," *Appl. Catal. A Gen.*, vol. 407, no. 1–2, pp. 188–194, Nov. 2011. [5] L. Hu, L. Lin, Z. Wu, S. Zhou, and S. Liu, "Chemocatalytic hydrolysis of cellulose into glucose over solid acid catalysts," *Appl. Catal. B Environ.*, vol. 174–175, pp. 225–243, 2015.

# **Ni-based catalysts for one-pot hydrothermal upgrading of biomass with *in situ* hydrogen production**

*R.G. Kukushkin, Boreskov Institute of Catalysis SB RAS, Novosibirsk, Russia and Novosibirsk State University, Novosibirsk, Russia;*

*P.M. Yeletsky, Boreskov Institute of Catalysis SB RAS, Novosibirsk, Russia;*

*A.V. Fedorov, Boreskov Institute of Catalysis SB RAS, Novosibirsk, Russia and Novosibirsk State University, Novosibirsk, Russia;*

*O.A. Bulavchenko, Boreskov Institute of Catalysis SB RAS, Novosibirsk, Russia and Novosibirsk State University, Novosibirsk, Russia;*

## **Introduction**

Currently, biofuels production from lignocellulosic feedstocks through biomass liquefaction requires at least three stages: 1) fast pyrolysis of raw material to obtain fast pyrolysis oil; 2) hydrogen production; 3) catalytic hydrodeoxygenation / hydrocracking of the fast pyrolysis oil to reduce the oxygen content. The multistageness and the need for addition of hydrogen produced separately, give rise to the higher cost as well as the low quality of the upgraded fast pyrolysis oil.

Hydrothermal liquefaction (HTL) of biomass allows to obtain liquid products (bio-oil). The main difference between fast pyrolysis and HTL is the need to carry out the pre-drying stage of feedstocks in the first case. One of the most used type of plant raw materials processing by HTL is a wood raw material (lignocellulosic biomass) [1]. As the obtained bio-oil cannot be directly used as a fuel, a further processing of the bio-oil is required to increase its stability and quality, due to the high content of oxygen-containing and high-molecular compounds in its composition.

Glycerol aqueous-phase reforming for hydrogen production is a relatively new approach to obtain energy from plant biomass [2]. Currently, there is a steady increase in the production of biodiesel and, as a consequence, glycerol as the main by-product [3]. The aqueous-phase reforming is carried out at lower temperatures than steam reforming (470 – 535 K) and at elevated pressure (of 1.5 – 5.0 MPa) [4].

This work is aimed at the development of upgraded bio-oil production from plant biomass by its liquefaction in hydrothermal conditions in one stage. Glycerol being a multi-tonnage byproduct, formed in the production of biodiesel acts as a

hydrogen source. Thus, this process combines in one stage three catalytic processes in the same reactor, which are usually carried out sequentially in three stages: bio-oil production through biomass liquefaction, hydrogen production and bio-oil hydrotreatment. Such a merger would lead to improved process energy efficiency and lower capital and operating costs.

## Results

A series of nickel-based catalysts modified by various metals (Mo, Cu and P) was synthesized. The catalysts were investigated by a wide range of techniques (XRD, XPS, TEM etc.). The influence of the calcination temperature, an order of modification of the active component on properties of the catalysts as well as CO absorption were studied.

In this part of the project the attention was mainly given to studying of catalysts active component reduction. This reduction could take place as a preliminary catalyst activation stage (usually in a hydrogen flow) before, as well as directly during the process. Thus, the study of the kinetics of the reduction of bimetallic catalytic systems based on nickel is of interest both from a practical and fundamental point of view.

The effect of Cu and Mo modification of the nickel-based catalysts and the heating rate on the hydrogen uptake were studied by the H<sub>2</sub>-TPR method. The shift of hydrogen uptake peaks towards higher temperatures when heating rate increasing in the case of both monometallic - Ni, Cu and bimetallic Ni-Cu catalysts was shown. Phase composition of Ni and Ni-Cu samples during the reduction in hydrogen flow at different heating rates was studied by XRD *in situ*. Based on the data obtained, a model of Ni and Ni-Cu component reduction was proposed and the kinetic parameters of the reduction of the active component of Ni and Ni-Cu catalysts were calculated.

*This work was supported by RFBR Grant № 17-53-10005 "Multifunctional catalysts for one-stage hydrothermal upgrading of biomass with in-situ hydrogen production"*

## References

1. Dimitriadis A. *Renew. Sustain. Energy Rev.* **2017**, *68*, 113-125.
2. Tuza P.V. *Renew. Energy*, **2013**, *50*, 408-414.
3. Silva J. M., *Renew. Sustain. Energy Rev.* **2015**, *42*, 1187-1213.
4. Shabaker J.W. *J. Catal.* **2004**, *222*, 180-191.

# Promoting the Activity of Ru/ $\gamma$ -Al<sub>2</sub>O<sub>3</sub> in the Selective CO Methanation by Distinct Metal-Support Interactions

*S. Chen,<sup>1</sup> A.M. Abdel-Mageed,<sup>1</sup> M. Parlinska-Wojtan,<sup>2</sup> J. Bansmann,<sup>1</sup> R.J. Behm,<sup>1</sup>  
<sup>1</sup>Institute of Surface Chemistry and Catalysis, Ulm University, 89069 Ulm, Germany  
<sup>2</sup> Institute of Nuclear Physics, Polish Academy of Sciences, Krakow 31-342, Poland*

## Introduction

The selective methanation of CO has attracted much attention due to its potential application for the removal of CO from H<sub>2</sub>-rich feed gases for low temperature fuel cells.<sup>[1]</sup> Oxide supported Ru catalysts are by far the most active and stable catalysts for this reaction.<sup>[2]</sup> Recently, it was demonstrated that metal-support interactions (MSIs) can play an important role for improving the activity of Ru catalysts based on reducible oxides such as Ru/TiO<sub>2</sub>.<sup>[3]</sup> Interestingly, very recent theoretical work by Yang et al. indicated a possible role of MSIs for CO<sub>2</sub> dissociation on Ru/Al<sub>2</sub>O<sub>3</sub>, with a non-reducible support.<sup>[4]</sup> Also, from oxygen-exchange with CO<sub>2</sub> measurements it was suggested that interfacial O species at the Ru-O-Al interface of Ru/Al<sub>2</sub>O<sub>3</sub> catalysts play a critical role in CO<sub>2</sub> methanation.<sup>[5]</sup> Among various parameters, the variation of the reaction temperature was found to strongly affect the MSIs.<sup>[6]</sup>

In order to better understand the role of MSIs in the reaction on Ru/ $\gamma$ -Al<sub>2</sub>O<sub>3</sub> we examined the impact of high reaction temperatures and strongly reducing reaction conditions on the interaction of Ru and  $\gamma$ -Al<sub>2</sub>O<sub>3</sub> during the selective CO methanation, and correlated this with their activity and CO adsorption properties.

## Experimental

The 2.2 wt% Ru/ $\gamma$ -Al<sub>2</sub>O<sub>3</sub> catalyst (SA: 120 m<sup>2</sup> g<sup>-1</sup>) was prepared by incipient wetness impregnation of commercial  $\gamma$ -Al<sub>2</sub>O<sub>3</sub> by RuCl<sub>3</sub> hydrate salt (Sigma Aldrich). Reaction kinetics and CO adsorption were evaluated after calcination (10% O<sub>2</sub>/N<sub>2</sub> at 150°C for 30 min) under a continuous flow of a semi-realistic gas mixture (0.6% CO, 15.5% CO<sub>2</sub>, 80.9% H<sub>2</sub> and N<sub>2</sub>) at 190°C for 1000 min, followed by temperature programmed reaction (TPR: from 190°C to 350°C, then back to 190°C).

## Results

Comparison of the Ru mass-normalized reaction rate and turn over frequency (TOF) for CO methanation at 190°C (Fig.1a), both after calcination (190°C-1) and after subsequent TPR (190°C-2), shows a distinctly higher activity after the TPR (5-fold increase). This results in a rate of  $35 \mu\text{mol}_{\text{CH}_4} \text{g}^{-1}_{\text{Ru}} \text{s}^{-1}$ , comparable to that on the most active supported Ru catalysts (Ru/zeolite and Ru/TiO<sub>2</sub>).<sup>[3,7]</sup> CO adsorption measurements further indicate that the CO<sub>ad</sub> coverage on the Ru NPs on Ru/ $\gamma$ -Al<sub>2</sub>O<sub>3</sub> at 30°C is 2-fold higher after the TPR (Fig.1b). Here, a characteristic band at  $\sim 2073 \text{ cm}^{-1}$ , assigned to multicarbonyl and on-top CO<sub>ad</sub> species on Ru monolayer particles, was found to increase significantly after TPR.<sup>[5]</sup> This holds true also for the band at  $2130 \text{ cm}^{-1}$ , which is assigned to Ru-multicarbonyls on undercoordinated sites at the perimeter. Hence, the fraction of flat monolayer Ru particles and interface Ru sites at the periphery increases significantly after TPR, while the relative intensity of the bands characteristic for hemispherical Ru particles ( $1974 - 2003 \text{ cm}^{-1}$ ) decreased. Apparently, reaction at high temperature ( $350^\circ\text{C}$ ) leads to the formation of planar monolayer Ru particles on the Al<sub>2</sub>O<sub>3</sub> surface. Such behavior is most likely at high temperatures, where water byproducts can be activated to form OH groups (detected by IR), which then lead to the oxidative disruption of Ru-Ru bonds.<sup>[7]</sup> Surprisingly, HAADF-STEM and EDS mapping micrographs indicate a partial overgrowth of the Ru NPs by Al<sub>2</sub>O<sub>3</sub> after TPR. Furthermore, XP spectra indicate that the Al 2p and O 1s are shifted to higher binding energies after TPR. These results will be discussed, together with findings from detailed structural characterization by *operando* EXAFS, pyrrole titration, and H<sub>2</sub>/D<sub>2</sub> adsorption / desorption measurements.

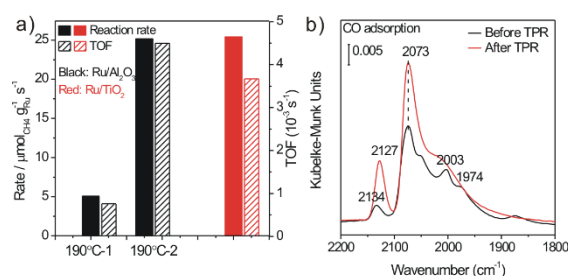


Fig. 1. a) Steady-state reaction rates and TOFs of Ru/Al<sub>2</sub>O<sub>3</sub> at 190°C before (190°C-1) and after TPR (190°C-2), b) DRIFT spectra after CO adsorption at 30°C on Ru/Al<sub>2</sub>O<sub>3</sub> before and after TPR.

## References

- [1] Chen A. et al., *Angew. Chem. Int. Ed.* **2010**, *49*, 9895-9898.
- [2] Takenaka S. et al., *Int. J. Hydrogen Energy*, **2004**, *29*, 1065-1073.
- [3] Abdel-Mageed A.M. et al., *ACS Catal.* **2015**, *5*, 6753-6763.
- [4] Yang J. et al., *J. Phys. Chem. C.* **2018**, *122*, 17287-17300.
- [5] Yan Y. et al., *J. Catal.* **2018**, *367*, 194-205.
- [6] Tauster S.J. et al., *Science* **1981**, *211*, 1121-1125.
- [7] Abdel-Mageed A. M. et al., *J. Am. Chem. Soc.* **2015**, *137*, 8672-8675.

# Hydrodeoxygenation of oleic acid catalyzed by $\text{Mo}_2\text{C}$ and $\text{NbMo}_{1,75}\text{C}$ supported on $\gamma$ -alumina

Thiago M. C. Pereira, PEQ/COPPE/UFRJ, Rio de Janeiro, Brazil; Cristiane A. Henriques, PPGEQ/IQ/UERJ, Rio de Janeiro, Brazil; Pedro A. Arroyo, DEQ/UEM, Maringá, Brazil; Victor Teixeira da Silva, PEQ/COPPE/UFRJ, Rio de Janeiro, Brazil.

## Introduction

Biofuels appear as renewable energy source able to provide a significant part of world fuel demand, reducing environmental depletion and the concern about the medium and long-term supply of fossil fuels [1]. An example of renewable fuel is the *green diesel* derived from oleaginous plantings, microalgae oil, waste cooking oils, and animal fats. In this work, the catalytic hydrodeoxygenation of a model fatty acid (oleic acid) was evaluated using  $\beta\text{-Mo}_2\text{C}/\gamma\text{-Al}_2\text{O}_3$  and  $\text{NbMo}_{1,75}\text{C}/\gamma\text{-Al}_2\text{O}_3$  as catalysts aiming at to put insights on the reaction route for the production of the *green diesel*.

## Experimental

The transition metal carbides were synthesized by temperature programmed carburization (TPC) of their precursors prepared by incipient wetness methodology for the  $\text{Mo}_2\text{C}/\gamma\text{-Al}_2\text{O}_3$  and wet impregnation for the  $\text{NbMo}_{1,75}\text{C}/\gamma\text{-Al}_2\text{O}_3$ . Determination of crystalline phases, specific area, and amount of the active sites was determined by XRD,  $\text{N}_2$  physisorption, and CO chemisorption, respectively. The catalytic tests were carried out in a Micro ActivityReference – PID Eng&Tech unit in a trickle-bed operation, under  $\text{H}_2$  (30 atm), varying the temperature (280 °C – 360 °C) and the weight hourly space velocity (WHSV) from 7 to 40  $\text{h}^{-1}$ .

## Results and discussion

X-ray diffractograms of the catalysts reveal that only the characteristic peaks of  $\gamma\text{-Al}_2\text{O}_3$  were observed, indicating that the carbide particles were well dispersed on the support. As to the textural characteristics, the support and both catalysts have similar BET specific areas (close to 175  $\text{m}^2/\text{g}$ ) indicating that no clogs or blockages of the pores of the support were observed upon the incorporation of the active phase. High CO chemisorption values, along with water and carbon monoxide release during synthesis, confirmed the formation of the carbide forms for each catalyst.  $\text{NbMo}_{1,75}\text{C}/\gamma\text{-Al}_2\text{O}_3$  (227  $\mu\text{mol CO/g}$ ) presented a higher chemisorption capacity than

Mo<sub>2</sub>C/γ-Al<sub>2</sub>O<sub>3</sub> (150 μmol CO/g), although both had the same metal loading, implying that the incorporation of niobium to the catalyst increased the number of active sites. However, TOF results show that Mo<sub>2</sub>C/γ-Al<sub>2</sub>O<sub>3</sub> was more active than NbMo<sub>1,75</sub>C/γ-Al<sub>2</sub>O<sub>3</sub>. Both transition metal carbide catalysts deactivated during the reaction due to the strong adsorption of unsaturated compounds, this effect being more significant for the bimetallic carbide. As to the reaction route, it was observed that the transition metal carbides favored the removal of the oxygen of the carboxylic group forming octadecenal as a primary product. Double bond hydrogenation of oleic acid competed with its hydrodeoxygenation since the formation of stearic acid as a primary product also occurred. Temperature and WHSV variations indicated that Mo<sub>2</sub>C/γ-Al<sub>2</sub>O<sub>3</sub> is a more promising catalyst since the selectivity to the formation of n-octadecane (desired product for the first stage of *green diesel* production) through the hydrogenation of the carboxyl group followed by dihydroxylation was higher over this catalyst.

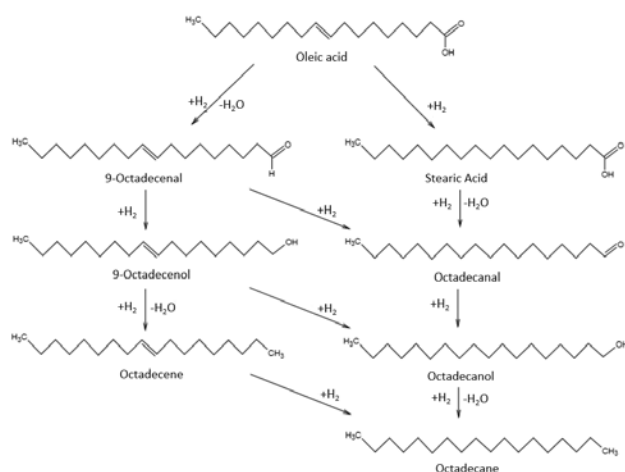


Figure 1 – Hydrodeoxygenation of oleic acid over β-Mo<sub>2</sub>C/γ-Al<sub>2</sub>O<sub>3</sub> and NbMo<sub>1,75</sub>C/γ-Al<sub>2</sub>O<sub>3</sub>

## Conclusion

Over the studied catalysts, the hydrodeoxygenation reaction occurred through two parallel reaction pathways having stearic acid and octadecenal as primary products. Both catalysts favored the hydrodeoxygenation pathway over decarboxylation and decarbonylation pathways, having low yields of heptadecane and heptadecene. Temperature and WHSV variation results showed that Mo<sub>2</sub>C/γ-Al<sub>2</sub>O<sub>3</sub> catalyst led to a higher diesel range product yield, 82 %, using less severe operating conditions than over NbMo<sub>1,75</sub>C/γ-Al<sub>2</sub>O<sub>3</sub>.

## References

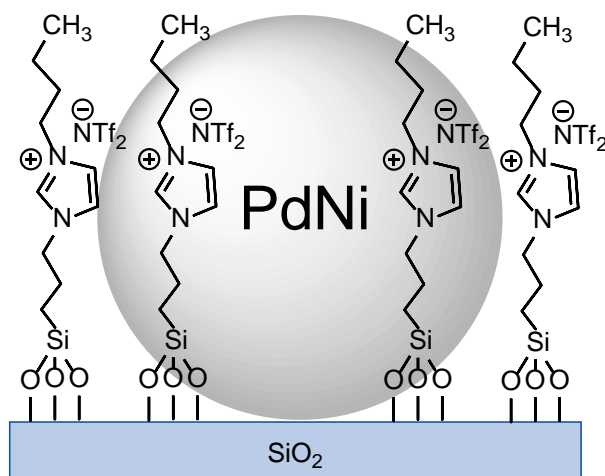
- [1] P. M. Veiga, A. S. Luna, M. F. Portilho, C. O. Veloso, C. A. Henriques; Energy, 75, 453, 2014.

## PdNi@SILP catalysts for selective hydrogenation

*Hannah T. Kreissl<sup>1</sup>, Alexis Bordet<sup>1</sup>, Walter Leitner<sup>1,2\*</sup>*

*1)Max-Planck-Institut für Chemische Energiekonversion, 45470 Mülheim a.d. Ruhr,  
Germany*

*2)Institut für Technische und Makromolekulare Chemie, RWTH Aachen University,  
Worringerweg 2, 52074 Aachen, Germany*



Palladium catalysts are widely used in selective hydrogenation reactions. Their application areas range from traditional industrial processes such as acetylene to ethylene conversion to newer research fields such as biomass hydrodeoxygenation [1-2]. The downside of palladium is its high price, asking for cost-efficient use. Here nanoparticle catalysis is advantageous due to the high surface-to-volume ratio achieved, and further cost improvements can be reached with the design of bimetallic nanoparticles. Substituting palladium partially with the cheaper but chemically related nickel is a common choice, but the synthesis of bimetallic systems is not straightforward, leading to a wide range of characteristics and catalytic behavior [3-5]. Factors such as particle size, composition and support effects influence electronic structure and particle geometry, which in turn affect substrate adsorption and catalytic conversion. In this work, we study palladium-nickel nanoparticles of different metal ratios, synthesized in solution from metal precursor reduction onto a silica supported ionic liquid phase (PdNi@SILP). SILPs are interesting as the ionic liquid



phase offers a tunable matrix for nanoparticle deposition and tends to enhance mass transfer, while at the same time limiting catalyst recovery problems due to linkage onto silica [6]. For the synthesis of bimetallic palladium-nickel nanoparticles, it is further of interest that the SILP structure appears to prevent the commonly occurring formation of a nickel oxide-silica layer decorated with palladium [7]. The synthesized PdNi@SILP catalysts are tested for example in the selective hydrogenation of benzylic ketones, in the conversion of biomass model substrates, and in phenylacetylene hydrogenation.

## References

- [1] Ravanchi, M. T.; Sahebdehfar, S.; Komeili, S.; Acetylene selective hydrogenation: a technical review on catalytic aspects. *Rev. Chem. Eng.* **2018**, 34(2), 215–237.
- [2] Xu, X.; Li, Y.; Gong, Y.; Zhang, P.; Li, H.; Wang, Y.; Synthesis of Palladium Nanoparticles Supported on Mesoporous N-Doped Carbon and Their Catalytic Ability for Biofuel Upgrade. *J. Am. Chem. Soc.* **2012**, 134, 16987–16990.
- [3] Yang Y.; Reber, A. C.; Gilliland, S. E.; Castano, C. E.; Gupton, B. F.; Khanna, S. N.; Donor/Acceptor Concepts for Developing Efficient Suzuki Cross-Coupling Catalysts Using Graphene-Supported Ni, Cu, Fe, Pd, and Bimetallic Pd/Ni Clusters. *J. Phys. Chem. C* **2018**, 122, 25396–25403.
- [4] Mauriello, F.; Paone, E.; Pietropaolo, R.; Balu, A. M.; Luque, R.; Catalytic Transfer Hydrogenolysis of Lignin-Derived Aromatic Ethers. *ACS Sustainable Chem. Eng.* **2018**, 6, 9269–9276.
- [5] Offner-Marko, L.; Bordet, A.; Moos, G.; Tricard, S.; Rengshausen, S.; Chaudret, B.; Luska, K. L.; Leitner, W.; Bimetallic Nanoparticles in Supported Ionic Liquid Phases as Multifunctional Catalysts for the Selective Hydrodeoxygenation of Aromatic Substrates. *Angew. Chem.* **2018**, 130, 12903 –12908.
- [6] Migowski, P.; Luska, K. L.; Leitner, W.; Nanoparticles on Supported Ionic Liquid Phases – Opportunities for Application in Catalysis. *Nanocatalysis in Ionic Liquids*, **2017**, Wiley-VCH Verlag GmbH & Co. KGaA, First Edition.
- [7] Zhang, P.; Yuan, Q.; Chen, L.; Xue, T.; Guan, Y.; Wu, P.; Low temperature hydrogenation of angelica lactone on silica supported Pd–NiO catalysts with synergistic effect. *RSC Adv.* **2016**, 6, 65377–65382.

## **Highly active OER catalysts with decreased noble metal oxide content achieved by solution combustion synthesis method**

*Sorin Bunea and Atsushi Urakawa, Institute of Chemical Research of Catalonia (ICIQ), Barcelona Institute of Science and Technology (BIST), Tarragona, Spain*

In the electrochemical water splitting, the main challenges lie at the anode side, where the oxygen evolution reaction (OER) takes place. The most efficient electrocatalysts reported to date for oxygen evolution are noble metal oxides such as IrO<sub>2</sub> and RuO<sub>2</sub> [1]. The scarcity of these elements in the Earth crust and their consequent high price have driven electrochemists and material scientists to investigate the possibility of decreasing the loading of noble metal oxides in PEM electrolyzers, improve the performance of the noble metal oxide catalysts by increasing their dispersion and surface area, or even replacing them by Earth-abundant metals or metal oxides.

The state-of-the-art method to synthesize IrO<sub>2</sub>-based catalysts for the electrochemical water oxidation is the so-called Adams fusion method, where an iridium salt, most often IrCl<sub>3</sub>, is oxidized in molten NaNO<sub>3</sub> to yield IrO<sub>2</sub> [2-4]. A washing step is employed after the synthesis, in order to remove Cl<sup>-</sup> ions. In a recent publication, our group has proposed an alternative synthesis method for IrO<sub>2</sub>-based electrocatalysts, namely the solution combustion method, which gives catalysts with superior features in terms of noble metal dispersion and loading [5]. Furthermore, the catalysts synthesized by the solution combustion method do not require the tedious washing step. This is a clear advantage of the method, allowing to synthesize pure noble metal oxide catalysts or supported noble metal electrocatalysts in one single step (Fig. 1).

Herein we report next-generation IrO<sub>2</sub>-based anode catalysts prepared by the solution combustion method but mixed with another promoting metal oxide in the structure. By employing a mixture of the IrCl<sub>3</sub> precursor and Sn- and Ti-containing precursors, we prepared IrO<sub>2</sub>/SnO<sub>2</sub> and IrO<sub>2</sub>/TiO<sub>2</sub> catalysts at 25 wt% IrO<sub>2</sub> loading. We tested these electrocatalysts in a PEM water electrolyser and we obtained 1 A/cm<sup>2</sup> current density by applying only a 3% higher potential than to a membrane electrode assembly (MEA) containing pure IrO<sub>2</sub> as anode electrocatalyst (1.83 V vs 1.78 V) (Fig. 2). We proved that TiO<sub>2</sub> can also be used as a support in the solution

combustion synthesis of IrO<sub>2</sub>-based catalysts, and although the performance is slightly lower than of the SnO<sub>2</sub> supported IrO<sub>2</sub> catalyst, it proves the versatility of the method and the ability to use the desired support material for IrO<sub>2</sub>. The highly dispersed nature of IrO<sub>2</sub> within the matrix of SnO<sub>2</sub> and TiO<sub>2</sub> was verified by microscopic studies. The amount of IrO<sub>2</sub> in the MEA was decreased from 2 mg/cm<sup>2</sup> to 0.5 mg/cm<sup>2</sup>, which represents a significant step forward in decreasing the amount of noble metal oxide loading in PEM electrolyzers and increasing the attractiveness of these electrochemical cells for commercial hydrogen production in the future.

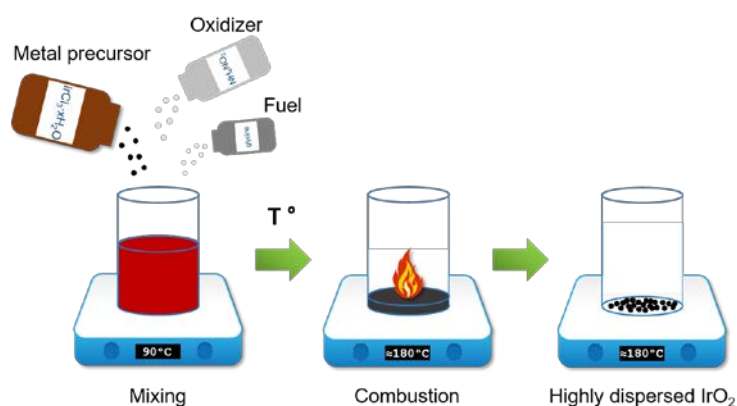


Fig. 1: Schematic representation of solution combustion synthesis of highly dispersed IrO<sub>2</sub> OER catalyst.

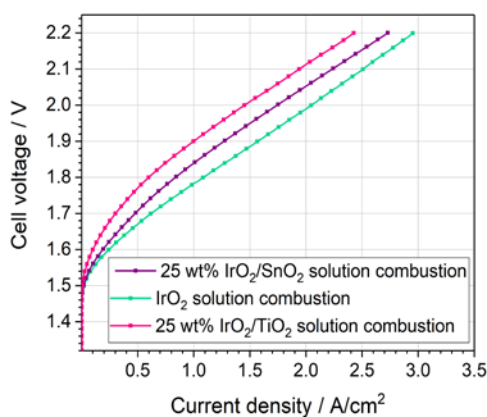


Fig. 2: Polarization curve for IrO<sub>2</sub>-based OER catalyst in a PEM water electrolyzer at 80°C, Nafion 115 membrane.

## References

- [1] M. Carmo et al. *Int. J. Hydrogen Energy* **2013**, *38*, 4901-4904.
- [2] S. Siracusano et al. *Applied Catalysis B: Environmental* **2015**, *164*, 488-495.
- [3] J. Lim et al. *Adv. Funct. Mater.* **2018**, *28*, 1704796.
- [4] D. Lebedev et al. *Chem. Mater.* **2017**, *29*, 5182-5191.
- [5] M. Chourashiya, A. Urakawa. *J. Mater. Chem. A* **2017**, *5*, 4774-4778.

# SYNTHESIS, CHARACTERIZATION & CATALYTIC PROPERTIES OF NANOSTRUCTURED NiW CATALYSTS

Cesar Huerta<sup>1</sup>, Posgrado de la Facultad de Ingeniería Química, UMSNH, Morelia, Michoacán, México; Rafael Huirache<sup>2</sup>, Posgrado de la Facultad de Ingeniería Química, UMSNH, Morelia, Michoacán, México; Ramesh Kumar Chowdari<sup>3</sup>, Gabriel Alonso Núñez<sup>3</sup>, Sergio Fuentes Moyado<sup>3</sup>, Jorge Noé Díaz de León<sup>3</sup>, UNAM, Centro de Nanociencias y Nanotecnología, Ensenada, Baja California, México.

## 1. Introduction

Ultra low sulfur fuels can be produced by deep removal of sulfur compounds from fossil fuels that requires a hydrodesulfurization (HDS) process which is generally carried out over Ni promoted Mo(W)S catalytic systems [1]. Due to the stringent environmental legislations the unsupported catalysts attracts much attention due to high activity (2-3 fold) than supported catalysts [2]. In this work we report synthesis of self-supported NiW catalysts, characterization and activity evaluation for the HDS of 3-methyl thiophene (3MT).

## 2. Experimental

A series of NiW catalysts was prepared in two steps. Initially, WO<sub>3</sub> precipitated by hydrothermal method from ammonium metatungstate. In the next step aq. NiCl<sub>2</sub> solution impregnated on WO<sub>3</sub> obtained in the previous step followed by calcination. Catalysts denoted as NiW-3, NiW-4, NiW-5, NiW-6 synthesized using HCl, HCl+NaNO<sub>3</sub>, HNO<sub>3</sub>-24 h, HNO<sub>3</sub>-48 h, respectively. The materials were widely characterized. Catalytic activity tests were performed in continuous flow micro reactor at 1 atm, 280-320 °C with ultra pure 3-methyl-Thiophene.

## 3. Results and discussion

Figure 1 shows the SEM images of the WO<sub>3</sub> obtained for different precursors. The WO<sub>3</sub> synthesized using HCl exhibited a sphere-like shape morphology with rough surface (A,B) and was made by self assembly of nano flakes. Where as in the case of HNO<sub>3</sub>, the catalyst particles are random in shape and larger in size (C,D).

The XRD analysis of the WO<sub>3</sub> samples indicated presence of monoclinic phase in all the samples. UV-Vis spectroscopic results showed that presence of WO<sub>3</sub> octahedral species for the samples prepared using HCl and tetrahedral species observed for the samples synthesized using HNO<sub>3</sub>. Low BET surface areas observed

for all the  $\text{WO}_3$  samples ( $11\text{-}16 \text{ m}^2/\text{g}$ ). The nano flakes are clearly seen in the TEM images of  $\text{WO}_3$  sample synthesized using HCl.

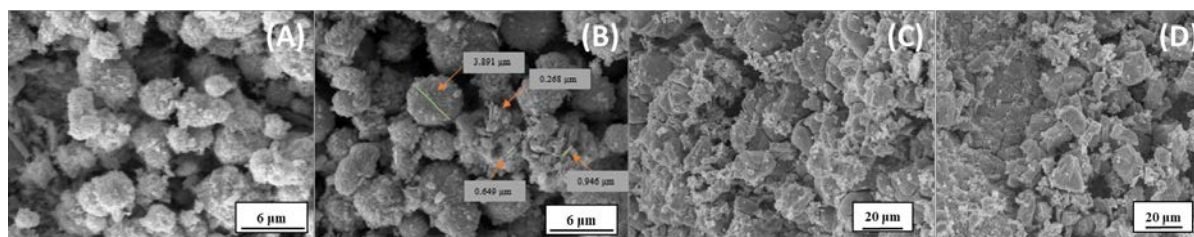


**Figure 1** SEM images of  $\text{WO}_3$  prepared using (A) HCl-24 h, (B) HCl+ $\text{NaNO}_3$ -24 h, (C)  $\text{HNO}_3$ -24 h and (D)  $\text{HNO}_3$ -48 h

Figure 2 shows the HDS of 3-methylthiophene over various synthesized catalysts. Irrespective of the reaction temperature, activity of the catalysts resulted as follows: NiW-4  $\approx$  NiW-6 < NiW-3 < NiW-5. Highest reaction rate ( $341 \times 10^8 \text{ mol}_{3\text{MT}} \cdot \text{g}_{\text{Cat}}^{-1} \cdot \text{s}^{-1}$ ) achieved for the NiW-5 catalyst compared to other synthesized catalysts. High selectivity towards isoprene for all the catalysts indicating the HDS mechanism proceeds mainly through direct desulfurization (DDS) route.

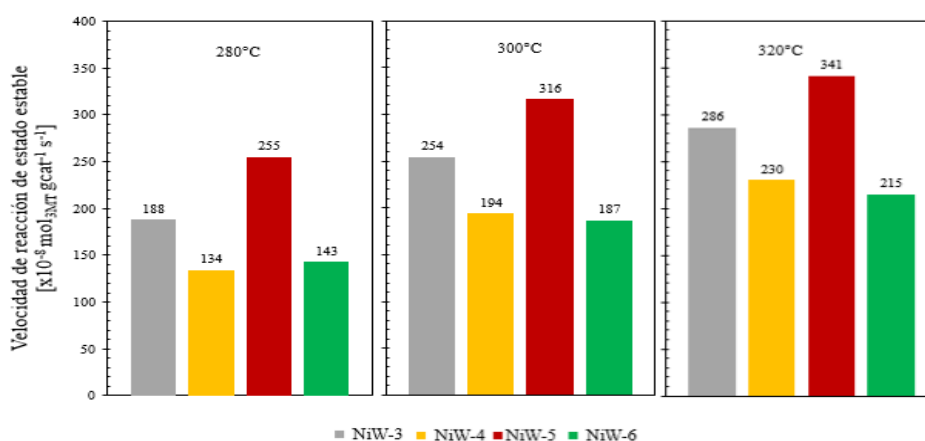


**Figure 2** HDS of 3-MT reaction rate over various synthesized NiW catalysts.

#### 4. Conclusion

High active and selective (DDS route) catalyst developed for the HDS of 3-methylthiophene. Compared to all synthesized catalysts the NiW-5 presented a greater catalytic activity which can be used for refractive compounds like dibenzothiophene and its derivatives.

#### References

1. J.N. Díaz de León, Ch. Ramesh Kumar, J.A. García, S.F. Moyado, *Catalysts* **2019**, 9(1), 87.
2. T.C. Ho, J.M. McConnachie, *J. Catal.* **2011**, 277, 117.

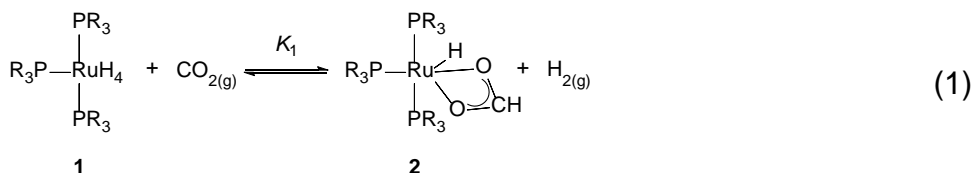
# The Effect of Ligand Electronics on the Catalytic Hydrogenation of CO<sub>2</sub> using Ru Triphosphine Complexes

*Deven P. Estes,<sup>a</sup> Alexis Bordet,<sup>a</sup> Markus Hölscher,<sup>b</sup> Lukas Schubert,<sup>a</sup> Walter Leitner,<sup>ab</sup> a)Max Planck Institute for Chemical Energy Conversion, Mülheim (Ruhr), Germany, b)RWTH Aachen, Aachen, Germany.*

## Abstract

Ruthenium triphosphine complexes catalyze the hydrogenation of CO<sub>2</sub> to not only formate derivatives, but also to the formaldehyde and methanol levels.<sup>1</sup> However, it is not clear as to why these catalysts work better than many others of the same basic structure type. In order to understand these catalysts better, we need to understand the effects that changing ligand structure (sterically and electronically) have on the reactivity of these complexes with CO<sub>2</sub>, i.e. develop a structure activity relationship. Of particular interest is how the ligand structure affects the catalyst performance and stability.

To this end, we have synthesized and fully characterized (IR, NMR, EA) a series of compounds of the type H<sub>4</sub>Ru(P(C<sub>6</sub>H<sub>4</sub>R)<sub>3</sub>)<sub>3</sub>, where R = H, Me, OMe, and CF<sub>3</sub>. We then reacted these complexes with CO<sub>2</sub> to synthesize the corresponding HRu(OOCH)(P(C<sub>6</sub>H<sub>4</sub>R)<sub>3</sub>)<sub>3</sub> complexes having a κ<sup>2</sup>-formate ligand. In addition, since the steric repulsion of the groups in the para position is very small, changing the substituent in the para position allows us to change the electronics of the complex as a whole. This gives us the opportunity to learn about the electronic effect of the ligand on reactivity.



Thus, we measured the basic reactivity of these complexes. Measuring the equilibrium in eq 1 by NMR under an H<sub>2</sub>:CO<sub>2</sub> mixture showed that more electron rich complexes react more exergonically with CO<sub>2</sub>. In fact, the data is modeled very well by using the appropriate Hammett parameters (σ<sub>para</sub>). In addition the rates of reaction with CO<sub>2</sub> also showed a trend with Hammett parameters. Indeed, changing the

electronics of the group in the para position seems to have significant effects on both kinetics and thermodynamics. We also compared the catalytic performance of such catalysts in the hydrogenation of CO<sub>2</sub> in MeOH as solvent. Our results show that making the complexes more electron rich is not always beneficial to catalysis and that a balance must be struck between electron donating and withdrawing substituents. This helps us understand how the basic reactivity of these complexes is connected to catalysis and how to make better CO<sub>2</sub> hydrogenation catalysts in the future.

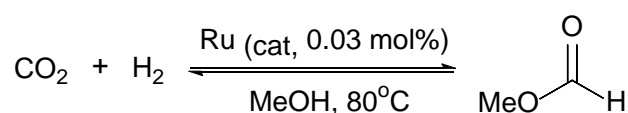


**Figure 1.** Conversion of CO<sub>2</sub> to methyl formate using Ruthenium complexes as catalyst

#### References

- [1] a) S. Wesselbaum; V. Moha; M. Meuresch; S. Brosinski; K. M. Thenert; J. Kothe; T. v. Stein; U. Englert; M. Holscher; J. Klankermayer; W. Leitner, *Chem. Sci.* 2015, 6 (1), 693-704; b) K. Thenert; K. Beydoun; J. Wiesenthal; W. Leitner; J. Klankermayer, *Angew. Chem. Int. Ed.* 2016, 55 (40), 12266-12269.

# **Pd Nanoparticles Supported on TiO<sub>2</sub>-Al<sub>2</sub>O<sub>3</sub> Catalysts for the Mild Hydrotreatment of Tars Type Compounds**

*Zaher Raad, ITQ (UPV-CSIC), Valencia, Spain, and MCEMA-CHAMSI, EDST, Beyrouth, Liban; Joumana Toufaily, MCEMA-CHAMSI, EDST, Beyrouth, Liban; Tayssir Hamieh, MCEMA-CHAMSI, EDST, Beyrouth, Liban; Marcelo E. Domine\*, ITQ (UPV-CSIC), Valencia, Spain*

Tars, which are liquid dense mixtures of refractory aromatic hydrocarbons produced during petroleum refining (and/or even during gasification of municipal solid wastes), are interesting alternative source for the production of chemicals and fuels. Catalytic hydrocracking (simultaneous cracking and hydrogenation) of these tars could be performed over bi-functional metal-zeolites (i.e. Pt-USY) and also other metal supported materials possessing both acid and redox functionalities capable to generate the corresponding aliphatic and/or cyclic saturated hydrocarbons[1]. Nevertheless, this hydrotreating process requires high temperatures (>350 °C) and H<sub>2</sub> pressures (>70 bar) with increasing energy and H<sub>2</sub> consumptions, while catalyst deactivation becomes problematic. New types of catalysts[2] have been studied for the transformation of tars but only working with unique model compounds (PAHs or even non-specific molecules) at high temperature and pressure, thus limiting their scope and use. In this study, Pd nanoparticles supported on TiO<sub>2</sub>-Al<sub>2</sub>O<sub>3</sub> catalysts are prepared and used to valorize a mixture of model compounds found in real tars operating at mild hydrotreatment conditions, thus making our study more valuable and closer to realistic conditions for further applications. The catalytic activity for tars hydrogenation of Pd/TiO<sub>2</sub>-Al<sub>2</sub>O<sub>3</sub> material is compared to other Pd supported on mono-metallic oxides (i.e TiO<sub>2</sub> and γ-Al<sub>2</sub>O<sub>3</sub>, among others). In addition, the application scope of this Pd-based catalyst is extended to the hydrogenation of other interesting molecules (i.e. fatty acids).

## **Experimental**

Pd supported on mono- and bi-metallic oxides catalysts were prepared by incipient wetness impregnation method by using Pd(NH<sub>3</sub>)<sub>4</sub>Cl<sub>2</sub>.H<sub>2</sub>O as precursor and analyzed by different techniques. Tars hydrogenations were carried out in an autoclave-type reactor by introducing a model mixture comprising naphthalene (0.125g), acenaphthylene (0.125g), phenanthrene (0.125g) and 1-methylnaphthalene (0.125g) diluted in 4g of n-hexadecane together with the catalyst (0.2g) at 200-300 °C and P<sub>H<sub>2</sub></sub> = 30 bar during 7 h. Liquid samples were withdrawn and analyzed by GC-FID and GC-MS.



## Results and discussion

Initially, different  $\approx 2\text{wt}\%$  Pd/catalysts (i.e. Pd/MgO, Pd/SiO<sub>2</sub>, Pd/ $\gamma$ -Al<sub>2</sub>O<sub>3</sub> and Pd/TiO<sub>2</sub>) were prepared and evaluated in the mild hydrotreatment of tars at 250 °C and P<sub>H<sub>2</sub></sub> = 30 bar. Best results were found with Pd/TiO<sub>2</sub> and Pd/ $\gamma$ -Al<sub>2</sub>O<sub>3</sub> catalysts (PAHs Conv. of 89% and 74%, respectively). After that, a Pd/TiO<sub>2</sub>-Al<sub>2</sub>O<sub>3</sub> material was prepared in which the Ti/Al molar ratio (1.2) and the Pd loading (1.3wt% of Pd), as well as its textural (S<sub>BET</sub> = 313 m<sup>2</sup>/g) and structural (Anatase TiO<sub>2</sub> in an amorphous alumina environment) were fully optimized. The effect of pH and aging during the synthesis procedure was also studied. This optimized material was evaluated in the hydrotreatment of tars and its catalytic activity compared to Pd/TiO<sub>2</sub> and Pd/ $\gamma$ -Al<sub>2</sub>O<sub>3</sub>, as well as other Pd/bi-metallic oxides (i.e. TiZr, SiAl, ZrAl, SiTi, etc.). Pd/TiO<sub>2</sub>-Al<sub>2</sub>O<sub>3</sub> showed higher catalytic activity than Pd/ $\gamma$ -Al<sub>2</sub>O<sub>3</sub> and Pd/TiO<sub>2</sub> (Figure 1). The proper interaction between the homogeneously dispersed Pd nanoparticles combined with the moderate acidity and the high resistance to deactivation of TiO<sub>2</sub>-Al<sub>2</sub>O<sub>3</sub> are responsible of this excellent catalytic behavior. Finally, and trying to extend the scope of the Pd/TiO<sub>2</sub>/ $\gamma$ -Al<sub>2</sub>O<sub>3</sub> material, its catalytic activity in the selective hydrogenation of fatty acids was also proven with promising and better results when comparing to the Pd-based catalysts listed before.

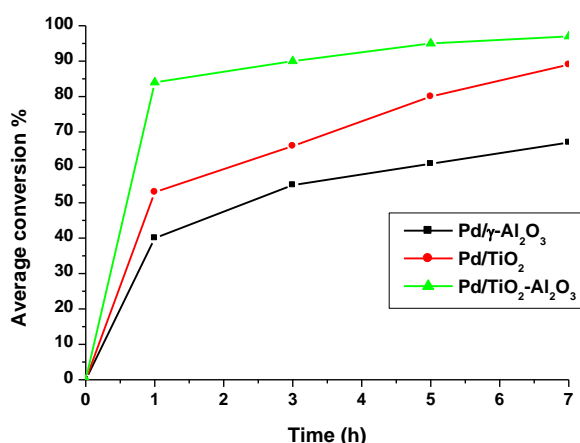


Figure 1. Average conversion in PAHs hydrotreatment for selected Pd-supported catalysts.

## Conclusions

Summarizing, Pd/TiO<sub>2</sub>-Al<sub>2</sub>O<sub>3</sub> has demonstrated to be an efficient catalyst for the mild hydrotreatment of tars, better than other Pd-based analogous systems. Its application scope was extended to other hydrogenations like selective hydrogenation of fatty acids with enhanced results compared to other Pd-catalysts. Further studies are now carrying out to establish the corresponding structure-reactivity correlations in this promising catalyst, and results will be shown and discussed during presentation.

## References

- [1] V. Calemma, R. Giardino, M. Ferrari, *Fuel Proc. Technol.* 91(7) (2010) 770-776.
- [2] K. Yong-Su, Y. Gwang-Nam, L. Yong-Kul, *Catal. Commun.* 45 (2014) 133-138.

# Nanostructured Ni/CN supported catalyst for electrocatalytic methanol oxidation

*I. S. Pieta<sup>1</sup>, A. Rath<sup>2</sup>, P. Pieta<sup>1</sup>, R. Nowakowski<sup>1</sup>, Manoj B. Gawande<sup>2</sup>, R. Zboril<sup>2</sup>*

<sup>1</sup> *Institute of Physical Chemistry PAS, 01-224 (Poland)*

<sup>2</sup> *Regional Centre of Advanced Technologies and Materials, Palacky University, 771 46 (Czech Republic)*

*\*[ipieta@ichf.edu.pl](mailto:ipieta@ichf.edu.pl)*

## Introduction

Direct methanol fuel cells (DMFC) is a promising energy source in a portable devices [1]. However, for an economical methanol use as DMFC fuel, catalysts that are sufficiently efficient, stable, durable and inexpensive are required. In this aspect, the challenging is the enhancement of the kinetics of methanol oxidation reaction (MOR) at the anode of DMFC to increase the overall efficiency of DMFC [1, 2]. The most commonly applied Pt-based anode catalyst is usually associated with several inherent drawbacks such as high cost, limited reserve and poor poison tolerance to the species such as CO or HCO [2,3]. Thus the performance of this catalyst does not meet the requirement for practical application due to slow kinetic of MOR and the oxygen reduction reaction (ORR) on the current noble-metal catalyst.

In this work, we are reporting the novel approach towards development of economic, stable and active anode material using Cu, Ni and Ni–Cu nanostructures on ultrathin support g-C<sub>3</sub>N<sub>4</sub> nanosheets (CN).

## Materials and Methods

One- and two-dimensional Ni, Cu nanostructures have been obtained by thermochemical method and unvaryingly distributed in ultrathin two dimensional (2D) abundant CN polymer. The surface morphology and composition of the hybrid nanostructures catalyst have been studied by various conventional physico-chemical techniques.

## Results and Discussion

The hierarchical hetero-structures of the nanometer-scale hybrid material showed stable catalytic performance during methanol catalytic electrooxidation. The use of ultrathin CN as a conductive nanoparticles support prevented Ni aggregation during material synthesis. The obtained Ni-2D nanocomposite facilitated reactants access and the quick release of product(s) from the catalyst surface.

It has been demonstrated, that nanosized Ni particles finely dispersed over carbon support are very active as an electrocatalyst with high MOR efficiency and outstanding stability, and its performance is among the best noble-metal-free MOR electrocatalysts that could be applied under basic conditions. Moreover, the results represent an important step towards light enhanced electro reactivity and sensors, where the formation of hetero-junctions can promote faster electron-hole separation and favor more efficient energy transfer (Fig.1).

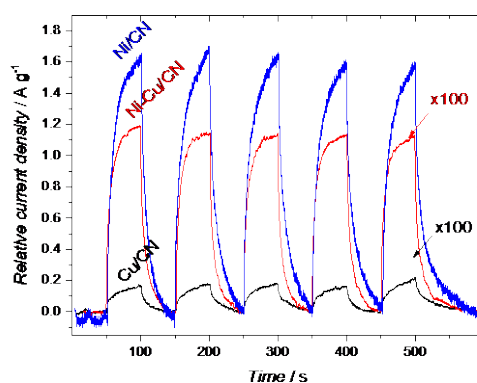


**Figure 1.** Photoactivities of different modified CN electrodes in darkness and under visible light illumination.

## Significance

The obtained results suggest that the hierarchical nanostructures can be of importance for DMFC, clean energy conversion and sensors. It has been shown that visible light irradiation can increase the performance of modified and bare CN electrodes in the MOR via synergistic electro- and photo-catalytic oxidation for Ni/CN ( $127 \text{ A g}^{-1}$ ) > Cu-Ni/CN ( $7.14 \text{ A g}^{-1}$ ) > Cu/CN ( $1.71 \text{ A g}^{-1}$ ) catalysts.

## References

- [1] I. S.Pieta, Anuj Rathi, P. Pieta, R. Nowakowski, M. Hołdyski, M. Pisarek, A. Kaminska, M. B. Gawande, R. Zboril, *Appl. Catal. B: Environmental* 244 (2019) 272-283
- [2] M.B. Gawande, A. Goswami, F.X. Felpin, T. Asefa, X. Huang, R. Silva, X. Zou, R. Zboril, R.S. Varma, *Chem. Rev.*, 116 (2016) 3722–3811
- [3] P.J. Kulesza, I.S. Pieta, I.A. Rutkowska, A. Wadas, D. Marks, K. Klak, L. Stobinski, J.A. Cox, *Electrochim Acta*, 110 (2013) 474-483.

# Effect of vanadium oxide content on the performance of Pd/V/SiO<sub>2</sub> catalysts for hydrogenoxygenation of phenol

Guilherme S. Garrido.<sup>1,2</sup>, Raimundo C. Rabelo-Neto.<sup>2</sup>, Alejandra Teran<sup>3</sup>, Gary Jacobs<sup>3</sup>, Fabio B. Noronha<sup>1,2</sup>

<sup>1</sup>Military Institute of Engineering, Chemical Engineering Department, Rio de Janeiro, Brazil

<sup>2</sup>National Institute of Technology, Catalysis Division, Rio de Janeiro, Brazil

<sup>3</sup>University of Texas at San Antonio, Chemical Engineering Program, Department of Biomedical Engineering, 1 UTSA Circle, San Antonio, TX 78249 USA.

## Introduction

The bio-oil produced from fast pyrolysis of biomass is a complex mixture of several organic compounds. Due to the large amount of oxygen, the bio-oil cannot be used as a transportation fuel unless it is upgraded. Hydrodeoxygenation (HDO) is a strategy of great potential for the reduction of oxygen content to improve the quality of bio-oil [1]. However, the development of a catalyst that can selectively remove the oxygenated functional group remains a challenge, and the design of an appropriate catalyst for HDO requires detailed knowledge of the reaction mechanism. Different model molecules, such as phenol, have been used to investigate the mechanism of HDO reactions. Recently, our group studied the role of the support on the mechanism of the HDO of phenol [2]. We reported that the selectivity to deoxygenated products depends on the oxophilicity of the support and the deoxygenation pathway occurring at the metal-oxophilic site interface. Among all the supports, vanadium oxide is a promising candidate that could exhibit the oxophilicity required for deoxygenation of phenol [3]. The goal of this work is to investigate the effect of vanadium oxide content on the HDO of phenol over Pd/V/SiO<sub>2</sub>.

## Experimental

V/SiO<sub>2</sub> samples were prepared by SiO<sub>2</sub> impregnation with an aqueous solution of ammonium metavanadate in order to obtain different vanadium contents (0.5; 1.0; 2.5; 5.0; 10.0; 20.0). The samples were calcined under airflow at 773 K (2 K/min) for 4 h. Pd/SiO<sub>2</sub> and Pd/V/SiO<sub>2</sub> samples were obtained by incipient wetness impregnation of the supports with a solution of palladium nitrate in nitric acid. Then, the samples were calcined under air flow at 673 K for 4 h. The samples were characterized by in situ X-ray absorption (XAS), in situ X-ray diffraction (XRD),

DRIFTS of adsorbed cyclohexanone, Raman spectroscopy, and the cyclohexanol dehydration probe reaction. Vapor-phase catalytic conversion of phenol was performed using a fixed- reactor at 573 K and 1 atm.

## Results and discussion

The Raman spectroscopy analysis revealed that the main vanadium oxide species were  $\text{VO}_4$  and  $\text{V}_2\text{O}_5$  NPs, which depended on vanadium content [4]. The diffractograms of the calcined samples revealed the presence of vanadium oxide ( $\text{V}_2\text{O}_5$ ) only for the samples containing 10 and 20% of vanadium. During reduction, it was observed that  $\text{V}^{5+}$  converted to  $\text{V}^{4+}$ . For the samples with lower vanadium content, the lines characteristic of vanadium oxide were not detected, which agrees with the Raman spectra that showed the presence of 2-dimensional surface  $\text{VO}_4$  species. The acidity of the catalysts increased as the vanadium oxide loading increased.

The product distribution over all catalysts at similar levels of conversion (around 10%) are listed in Table 1. For Pd/SiO<sub>2</sub> catalyst, cyclohexanone was the main product formed, but the addition of vanadium significantly changed the product distribution. For Pd/V/SiO<sub>2</sub> catalysts, benzene was mainly produced, whereas the formation of cyclohexanone was reduced. The highest selectivity to benzene for Pd/V/SiO<sub>2</sub> catalysts is due to the presence of oxophilic sites (i.e.,  $\text{V}^{5+}/\text{V}^{4+}$  cations) located in close proximity to the periphery of metal particles. Decreasing the V content increased the selectivity to benzene, indicating that the isolated V species favor deoxygenation.

**Table 1 - Product distribution at low conversion for HDO of phenol**

Catalyst	X (%)	Selectivity(%)				
		BZ	ANE	ENE	ONE	OL
Pd/SiO <sub>2</sub>	11.5	12.3	0.1	0	86.6	1.0
Pd/0.5V/SiO <sub>2</sub>	9.9	85.9	0.6	1.3	11.3	1.0
Pd/1.0V/SiO <sub>2</sub>	15.2	84.3	0.6	1.4	12.7	0.9
Pd/2.5V/SiO <sub>2</sub>	9.8	77.1	1.4	0.8	18.6	1.9
Pd/5.0V/SiO <sub>2</sub>	11.2	79.8	1.4	0.9	16.6	1.2
Pd/10.0V/SiO <sub>2</sub>	10.3	78.9	1.3	0.6	17.5	1.7
Pd/20.0V/SiO <sub>2</sub>	10.7	76.2	0.9	0.3	19.9	2.7

BZ: Benzene; ANE: Cyclohexane; ENE: cyclohexene; ONE: Cyclohexanone; OL: Cyclohexanol.

## References

- [1] G.W. Huber, S. Iborra, A. Corma, Chem Rev 106 (2006) 4049.
- [2] P.M. de Souza, R.C. Rabelo-Neto, L.E.P. Borges, G. Jacobs, B.H. Davis, D.E. Resasco, F.B. Noronha, ACS Catal. 7 (2017) 2058-2073.
- [3] K.P. Kepp, Inorg. Chem. 2016, 55, 9461–9470.
- [4] C. A. Carrero, R. Schloegl, I. E. Wachs and R. Schomaecker, ACS Catal., 2014, 4, 3357.

# Influence of chlorine on the activity of Ni/ $\gamma$ -Al<sub>2</sub>O<sub>3</sub> catalyst in $\gamma$ -valerolactone production by hydrogenation of levulinic acid using internal hydrogen source

*Emilia Soszka, Marcin Jędrzejczyk, Jacek Grams, Agnieszka M. Ruppert*

*Institute of General and Ecological Chemistry, Łódź University of Technology, ul.*

*Żeromskiego 116, 90-924 Łódź, Poland*

*Izabela Rzeźnicka, Shibaura Institute of Technology, Graduate School of Science and Engineering, 3-7-5 Toyosu, Tokyo 135-8548, Japan*

Lignocellulosic feedstock has recently undergone extensive research in the field of sustainable production of high-value chemicals and liquid fuels.  $\gamma$ -Valerolactone (GVL) is considered as one of the most important molecules which can be obtained from biomass feedstock, due to its various applications like biofuel additive or precursor for the production of valuable chemicals. GVL production with the formic acid (FA) used as hydrogen source catalyzed by the non-noble based catalysts still remains a challenge. Our recent study showed that Ni can constitute promising catalyst for C=O reduction reactions performed in protic solvent due to the decrease of effective energetic barrier of Ni in this process. In order to increase its catalytic

Table 1. Influence of the catalyst composition and chlorine addition in the hydrogenation of levulinic acid (LA) to  $\gamma$ -valerolactone (GVL) with formic acid (FA) used as hydrogen source.

Catalyst	Conversion [%]		Yield [%]
	FA	LA	GVL
4%Ni	26	0	0
4%Ni-1%Rh(Cl)	88	0	0
4%Ni-1%Ag(Cl)	95	0	0
4%Ni-1%Ru(Cl)	42	0	0
4%Ni-1%Pd(Cl)	100	56	51
4%Ni-1%Pd(N)	99	10	2
1%Ni-4%Pd(Cl)	100	43	37
2%Ni-3%Pd(Cl)	100	38	33
2.5%Ni-2.5%Pd(Cl)	100	31	26
3%Ni-2%Pd(Cl)	100	28	23

Reaction conditions: 190°C; 2h; 0.6 g catalyst; 1g LA, 0.4 ml FA and 30 ml water; (Cl)- catalysts prepared from chlorine containing precursor, (N)- catalysts prepared from nitrate containing precursor; all catalysts are supported on  $\gamma$ -Al<sub>2</sub>O<sub>3</sub>

performance, stability and resistance to poisoning several approaches were considered like addition of dopants to Ni catalysts, use of different synthesis routs and optimization of the catalyst composition [1].

Our studies showed that palladium addition to Ni/ $\gamma$ -Al<sub>2</sub>O<sub>3</sub> allowed to obtained the highest activity among all noble metals used as dopants (Pd, Pt, Ru, Rh) (table 1). The highest catalytic performance was reached when the 4:1 wt.% ratio of Ni:Pd was used. It was found that it is possible to tune the catalytic

activity to higher extend by the optimization of the preparation method. The use of chloride precursor during the catalyst preparation and high temperature were considered as a key factors stimulating the catalyst activity. It was found out that the presence of chlorine ions facilitates the Ni-Pd reduction (TPR) and improves the

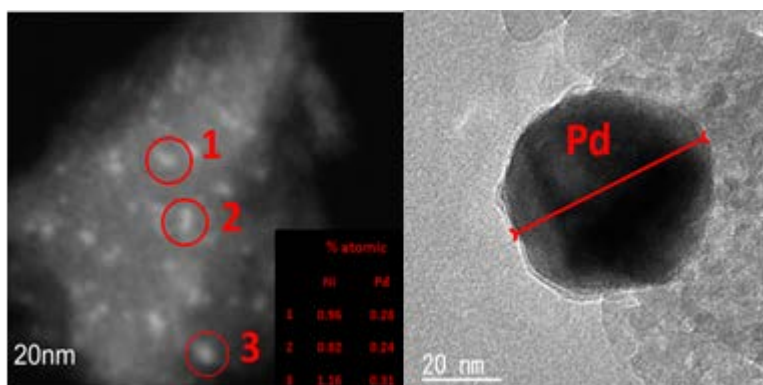


Figure 1. TEM images Ni-Pd(Cl)/ $\gamma$ -Al<sub>2</sub>O<sub>3</sub> and Ni-Pd(N)/ $\gamma$ -Al<sub>2</sub>O<sub>3</sub>

dispersion of metals on the catalyst surface (evidenced by the high intensity of Pd and Ni ions (ToF-SIMS study) and presence of small Ni particles (TEM-EDX)).

The chlorine presence during catalysts synthesis could also limit the formation of Pd-Ni alloy (as shown by ToF-SIMS study the presence of Ni<sub>2</sub>Pd species was only identified for catalysts prepared with non-chlorine containing precursors). This stays in contrast to catalysts prepared from nitrate precursor where the formation of Ni-spinels after high temperature treatment was identified (XRD), as well as the presence of large Pd aggregates was observed (TEM-EDX) [2]. The performed studies showed that the high activity of bimetallic catalysts prepared in the presence of chlorine can be attributed to the synergistic Ni-Pd interaction and weakening the metal interaction with support, as well as high metal dispersion, which was observed in the case of chlorine-containing catalysts.

### Acknowledgment

The authors gratefully acknowledge that this work was financially supported by a grant from the National Center of Science (NCN) in Krakow (Poland) (2016/22/E/ST4/00550).

### References

- [1] C. Michel et al., Chem. Commun., 2014, 50, 12450,
- [2] E. Soszka et al., ACS Sustainable Chem. Eng. 2018, 6, 14607-1461.

# **XAS and XRD *in situ* study on the microstructure of Cu particles of Cu/SBA-15 catalysts in methanol steam reforming**

*Gregor Koch, Thorsten Ressler, Department of Analytical and Inorganic Chemistry of TU Berlin, Berlin, Germany*

## **Introduction**

Cu based catalyst play a significant role in methanol chemistry.[1] Crucial for catalyst performance is the interplay between the used support and Cu nanoparticles having significant disorder. In particular, the important contribution of ZnO has been shown. Not only the covering of Cu nanoparticles with defect rich nano-structured ZnO<sub>x</sub> layers [2] but also the microstrain in the Cu nanoparticles was observed. For example, the Cu/ZnO interface was discussed as reason for the microstrain [3,4]. Aiming at exclusion of beneficial effects of ZnO we chose thus the Cu/SBA-15 model catalysts [5] to understand structure activity correlation and to elucidate changes in catalytic activity using methanol steam reforming as model reaction.

## **Experimental**

Oxidic precursors, CuO/SBA-15, were synthesized as described in [5]. CuO/SBA-15 catalysts were reduced in diluted H<sub>2</sub> to Cu/SBA-15 catalysts prior to subsequently tested activity in methanol steam reforming. The catalyst powders were diluted with BN and placed in a fixed bed reactor. MSR activity was measured in 2% H<sub>2</sub>O and 2% methanol atmosphere at 250 °C. Cu surface areas were determined using chemisorption of N<sub>2</sub>O. Furthermore, *in situ* measurements at the Cu K edge of activated Cu particles were performed at beamline X at HASYLAB at DESY, Hamburg. Catalysts were measured in laboratory *in situ* XRD. Quantification of reactants and products was achieved using a gas chromatograph.

## **Results**

The CuO/SBA-15 oxidic precursors consisted of well distributed CuO<sub>x</sub> structures and nanocrystalline CuO according to calcination conditions [5]. *In situ* XRD and XAS experiments revealed presence of only metallic Cu nanoparticles after reduction in diluted H<sub>2</sub>. XRD analysis showed significant differences in Cu particle size and strain due to synthesis. Accordingly, the TOF of H<sub>2</sub> increased rapidly when particle sizes fell below round about 3 nm (Fig. 1, left) which is accompanied by increased microstrain. Moreover, EXAFS refinement showed also various Cu particles sizes



agreeing well with XRD analysis. Furthermore, EXAFS refinement showed different degrees of disorder given by Debye-Waller-Factor. This can be attributed to microstrain in the Cu nanoparticles and correlated with H<sub>2</sub> TOF (Fig. 1, right). The microstructure of Cu nanoparticles is not only determined by ZnO support but also by synthesis [5] and correspondingly by Cu particle size and interaction with the silica support. Following the principle of chemical memory effect, differently structured oxidic precursors can be transformed into differently structured Cu nanoparticles having different activity in methanol steam reforming.

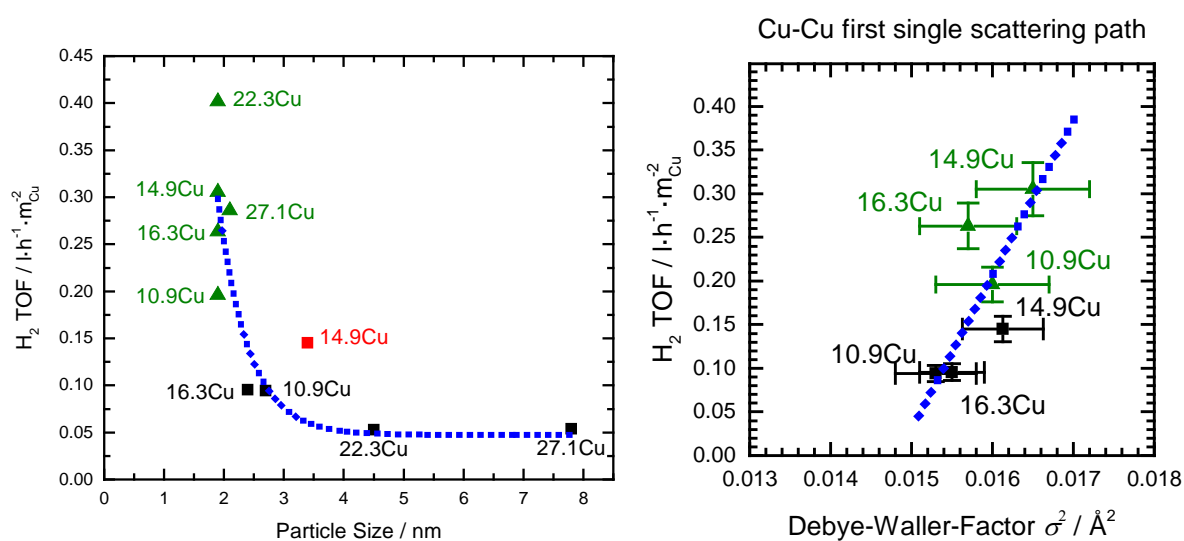


Fig. 1 Activity in methanol steam reforming given as H<sub>2</sub> TOF at 250 °C for Cu/SBA-15 catalysts with different loadings as a function of particle size (left) and as a function of the Debye-Waller-Factors extracted from EXAFS fits of *in situ* conducted spectra (right). Number before Cu represents weight % of Cu in oxidic precursors.

## Acknowledgement

HASYLAB at DESY in Hamburg is acknowledged for providing beamtime.

## References

- [1] M. Behrens *et al.*, *Science* **2012**, 336, 893.
- [2] Lunkenbein *et al.*, *Angew. Chem. Int. Ed.* **2016**, 55, 12708.
- [3] M. M. Günther *et al.*, *J. Catal.* **2001**, 203, 133–149.
- [3] P. Kurr *et al.*, *Appl. Catal. A: General* **2008**, 348, 153.
- [5] G. Koch, L. Schmack, T. Ressler *ChemistrySelect* **2016**, 1, 2040.

# Effect of Fe/Co wt ratio on TiO<sub>2</sub> supported catalysts for Fischer-Tropsch synthesis using syngas with H<sub>2</sub>/CO ratio < 2

M. Russo<sup>1</sup>, M.L. Testa<sup>1</sup>, V. La Parola<sup>1</sup>, G. Pantaleo<sup>1</sup>, R. Bal<sup>2</sup>, A. M. Venezia<sup>1</sup>  
<sup>1</sup>*Istituto per lo Studio dei Materiali Nanostrutturati, CNR-ISMN, Palermo, Italy*  
<sup>2</sup>*Institute of Petroleum, CSIR, Dehradun, India*

## Introduction

The continuous depletion of conventional fossil fuel reserves and the concern about climate changes, enhanced by CO<sub>2</sub> emission resulting from fossil fuel consumption, is driving nowadays a renewed interest in Fischer–Tropsch synthesis (FTS). Such gas-to liquid process is becoming particularly attractive when using *bio syngas*. This gas mixture, rich in CO and H<sub>2</sub>, derives indeed from biomass gasification and is characterized by a H<sub>2</sub>/CO ratio lower than the value of 2, appropriate for hydrocarbon syntheses [1]. In the present study, TiO<sub>2</sub> supported cobalt catalysts are combined with iron, active in the water gas shift reaction (WGS), aiming to increase H<sub>2</sub> in the synthesis reactor. To investigate the role of iron in different Fe/Co weight ratios, monometallic Co, Fe and bimetallic CoFe catalysts are prepared and tested in FTS. Structural and electronic properties of the obtained materials are investigated by XRD, TPR, XPS and TEM techniques.

## Results and Discussion

Mono metallic Co/TiO<sub>2</sub> and Fe/TiO<sub>2</sub> and two bimetallic catalysts (Co/Fe =1 and Co/Fe = 5) with a total metal loading of 12 wt% are synthesized by a microwave assisted co-precipitation procedure. The FTS tests are performed at 1atm in a fixed-bed flow reactor with reagent gas mixture of CO, H<sub>2</sub> and He (CO:H<sub>2</sub>:He volume ratio of 1:1.7:2.3) using GHSV = 1.9 L<sub>syngas</sub> g<sub>cat</sub><sup>-1</sup> h<sup>-1</sup> and a temperature range of 275-350 °C. Before test, the catalysts are reduced under H<sub>2</sub> flow for 16 h at 350 °C.

All the catalysts exhibit good CO conversion, due to the presence of highly dispersed Fe and Co nanoparticles favoured by the microwave assisted catalyst synthesis. In the bimetallic catalysts, as expected, the presence of iron enhances CO<sub>2</sub> production and, as compared to the monometallic cobalt catalyst, it increases the selectivity to higher hydrocarbons. According to the structural characterization and to XPS results shown in Fig. 1, the better activity of the mixed 10Co2Fe/TiO<sub>2</sub> catalyst can be related to the formation of metal carbides during reaction.

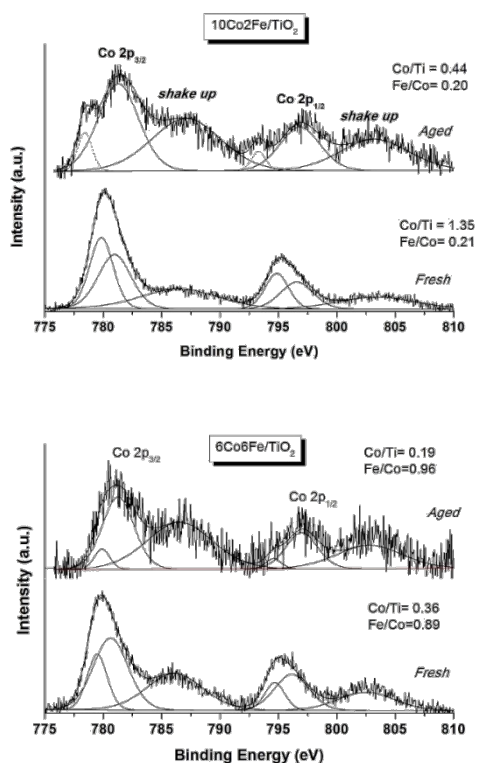


**Fig.1** Co 2p XP spectra of fresh and spent catalysts.

Moreover, a direct correlation between catalyst reducibility and activity is clearly indicated by the TPR profiles shown in

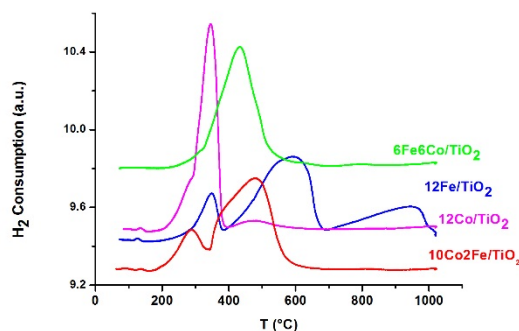


**Fig. 2.**

**Fig. 2** TPR profiles of different catalysts.

High resolution TEM images evidence a mixture of amorphous and graphitic carbon over the spent catalysts, explaining some deactivation occurring during reaction.

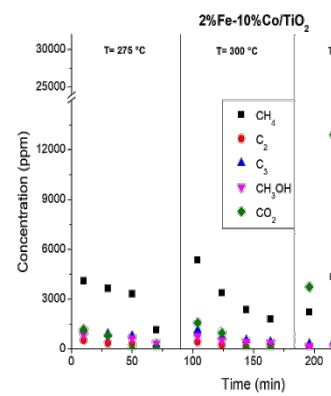
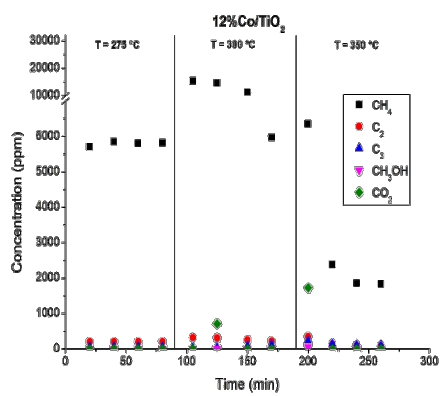
Overall, the results suggest that in order to have the desired FTS outcome, in terms of CO conversion and C<sub>5+</sub> selectivity, it is important to play with the Fe/Co weight ratio. Indeed, a limited amount of Fe is beneficial because it provides an additional supply of H<sub>2</sub> by the WGS reaction and at the same time it does not overwhelms the FTS reaction activated by cobalt. In virtue of this compromise the 10Co2Fe/TiO<sub>2</sub> catalyst exhibits the best catalytic behavior.

### Acknowledgements

M.R. thanks the Italian Government for post-doc fellowship within the project P.O. FSE 2014/2020. Financial support by MATTM / MAECI in the frame of Strategic Relevance Project between Italy and India (Prot. No. MAE01054762017) is kindly acknowledged.

## References

[1] Hu, J.; Yu, F.; Lu, Y. *Catalyst* **2012**, 2, 303-326.



## **Active site structures of Me-N-C catalysts for the ORR and OER**

*Lingmei Ni; Stephan Wagner; Ali Shahraei, Markus Kübler; Natascha Weidler;  
Charlotte Gallenkamp; W. David Z. Wallace; Stephen Paul; Ulrike I. Kramm\**

*all authors: Catalysis and Electrocatalysis, Department of Chemistry and Department  
of Materials- and Earth Sciences, Technische Universität Darmstadt, Otto-Berndt-  
Str. 3, 64287 Darmstadt, Germany*

Me-N-C catalysts (specifically Me = Fe) are the most promising substituent to Pt/C catalysts for the oxygen reduction reaction (ORR) in Proton Exchange Fuel cells (PEFCs). There are several ex-situ results that indicate a participation of FeN<sub>4</sub> sites embedded in graphene layers as ORR active sites (see . There are also different reports on hydrogen evolution reaction (HER) and oxygen evolution reaction (OER) on these catalysts, whereas then Co gave highest activity in comparison to other 3d transition metals [ref].

The composition of these catalysts is often rather heterogeneous. This hinders structure-activity relations. Furthermore, for some reaction conditions the composition might change during operation. Based on this, in-situ, operando and post-mortem characterization play a crucial role towards a better understanding of the contribution of different structure units in the catalyst.

The talk will discuss two types of catalysts: Fe-N-C catalysts were characterized by in-situ Mössbauer spectroscopy to get new insights into the active site structure and reduction mechanism on Fe-N-C catalysts. Our results show that indeed specific FeN<sub>4</sub> sites correlate in-situ with the ORR activity.

Beside this, sulfur-doped Co-N-C catalysts – as of interest for HER and OER were investigated by a step-by step approach combining X-ray induced photoelectron spectroscopy and identic location transmission electron microscopy.

In case of HER, strong evidence is given for the contribution of CoN<sub>4</sub>-sites to the HER. The best performing catalyst reached 10 mA cm<sup>-2</sup> with only 200 mV overpotential and gave promising results in terms of stability. In case of OER, also the performance was good (370 mV overvoltage for 10 mA cm<sup>-2</sup>). Nevertheless, the results clearly demonstrate that CoN<sub>4</sub> sites did not remain stable under these reaction conditions. In contrast, a structural transformation towards cobalt hydroxide species is found.

Thus our results indicate that caution need to be taken to transfer directly conclusions made for the one operation condition to another one. More important, the structural composition should in best case be checked in-situ or by a stepwise approach.

## **References**

List and number all bibliographical references at the end of the paper. When referenced within the text, enclose the citation number in square brackets, i.e. [1]

# Catalytic Hydrogenation of CO<sub>2</sub> to MeOH

*Anisa Tariq., Cardiff University, Cardiff, Wales.*

## Introduction

The annual global CO<sub>2</sub> emission in 2014 was recorded to be 39, 250 Mt, of which fossil fuel emissions accounted for about 91% of the emissions from human sources. Consequently, the atmospheric CO<sub>2</sub> concentration increased from ~270 ppm in the pre-industrialization era to ~410 ppm in 2017 and this has prompted a number of international actions from governments and industries established over the past decades, including: The Intergovernmental Panel on Climate Change (IPCC) and the United Nations Framework Commission on Climate Change. [1] It is therefore not surprising that current research is focused on the valorization of CO<sub>2</sub>, specifically as an alternative carbon feedstock, for the production of useful chemicals and energy carriers as opposed to CO<sub>2</sub> capture and storage alone. One example is the direct catalytic transformation of CO<sub>2</sub> into methanol. Olah et al. introduced the anthropogenic carbon cycle concept for utilising carbon dioxide for synthetic hydrocarbon products. In this concept methanol is used as a green starting chemical for the synthesis of fuels and various other synthetic hydrocarbon products, and therefore CO<sub>2</sub> conversion to methanol is a crucial initial step. [2] However, the thermodynamic stability of CO<sub>2</sub> means that significant amounts of energy are required for activation and conversion into value-added products. The choice of catalysts is important to provide active sites for C-O bond dissociation and H-insertion in order to ensure high yields of methanol. [3]

## Project Summary

The current project explores the key issues mentioned above and looks at developing active and selective Cu-based catalysts for the hydrogenation of CO<sub>2</sub> to MeOH, primarily for low temperature operation (150-250°C), in addition to optimising catalyst composition and nanoparticle morphology thus improving on the existing conditions utilised in industry. Data so far has shown Cu/ZrO<sub>2</sub> prepared via oxalate gel to be a promising catalyst, with activity directly comparable to that of an industrial

standard (Alfa Aesar 45776) despite having lower Cu loadings and lower Cu surface area. Catalysts are tested in a custom fixed-bed (6-bed) reactor using a reaction mixture of CO<sub>2</sub>:H<sub>2</sub>:N<sub>2</sub> (1:3:1), with a flow of 30 ml min<sup>-1</sup> (STP) at P(total) of 20 bar. An investigation into the phase composition and development of an accelerated aging protocol is currently under investigation and will provide a greater insight into the structure and stability of the catalysts supported by advanced characterisation techniques.

## References

- [1] S. Roy, A. Cherevotan and S. C. Peter, *ACS. Energy. Lett.*, 2018, **3**, 1938.
- [2] G. A. Olah, G. K. S. Prakash and A. Goepfert, *J. Am. Chem. Soc.*, 2011, **133**, 12881.
- [3] A. Álvarez, A. Bansode, A. Urakawa, A. V. Bavykina, T. A. Wezendonk, M. Makkee, J. Gascon and F. Kapteijn, *Chem. Rev.*, 2017, **117**, 9804.



# Plasma-catalytic ammonia synthesis for decentralized power-to-ammonia applications: a kinetic analysis for Ru-based catalysts

*Kevin Rouwenhorst, University of Twente, Enschede, The Netherlands; Leon Lefferts, University of Twente, Enschede, The Netherlands*

Ammonia may also be one of the energy carriers of the future, functioning as a hydrogen carrier [1, 2]. Ammonia can be produced from surplus electricity from intermittent renewables, thereby facilitating energy storage over seasons [3]. In decentralized systems, this requires on-demand technologies rather than high temperature, high pressure technologies such as the Haber-Bosch process. While the H<sub>2</sub> production and N<sub>2</sub> production can be scaled-down easily, the ammonia synthesis loop cannot be scaled-down easily to the sub-MW scale due to the severe operating conditions (400-500°C and 100-300 bar). Plasma-catalysis is a potential on-demand technology [4], which may replace the Haber-Bosch process for decentralized applications.

However, plasma-catalytic ammonia synthesis is not fully understood. The highest energy efficiencies reported so far for plasma-catalysis (20-35 g kWh<sup>-1</sup> [5, 6]) are two orders of magnitude lower than the required energy efficiencies of 100-200 g kWh<sup>-1</sup> for small-scale applications [7]. A major challenge is maintaining the energy efficiency of at least 100-200 g kWh<sup>-1</sup> at high ammonia yields (>1 mol.%), such that ammonia can be separated by absorbents or adsorbents.

The status quo of plasma-catalytic ammonia synthesis is discussed, after which a kinetic analysis is presented for plasma-catalysis over Ru catalysts. Through a kinetic analysis it is determined that the apparent activation barrier decreases from about 60-115 kJ mol<sup>-1</sup> for thermal catalysis to about 20-40 kJ mol<sup>-1</sup> for plasma-catalysis [8]. Mehta et al. [9] postulated that the dissociation of N<sub>2</sub> can be enhanced through plasma-induced vibrational excitation of N<sub>2</sub>, while the subsequent hydrogenation steps on the catalyst surface and ammonia desorption are not influenced by the plasma (see **Figure 1**). Furthermore, it is found that activity trends for Ru catalysts in thermal catalysis and plasma-catalysis are similar, and the electronegativity of the support and promoter determine the activity [8].

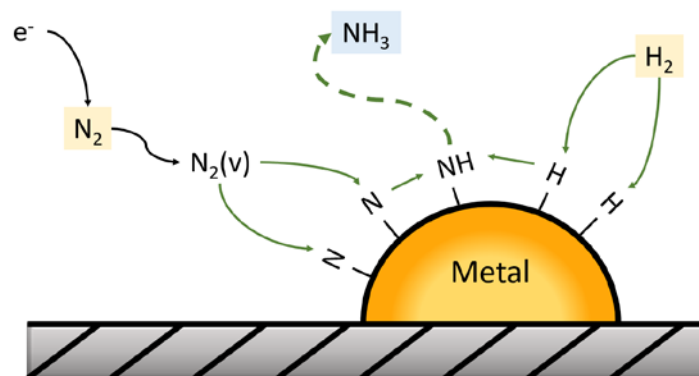


**Figure 1:** Proposed mechanism for plasma-enhanced catalytic ammonia synthesis.

## References

1. Christensen, C. H., Johannessen, T., Sørensen, R. Z., & Nørskov, J. K. (2006). Towards an ammonia-mediated hydrogen economy? *Catalysis Today*, 111(1–2), 140–144. doi:10.1016/j.cattod.2005.10.011
2. Guo, J., & Chen, P. (2017). Catalyst: NH<sub>3</sub> as an Energy Carrier. *Chem*, 3(5), 709–712. doi:10.1016/j.chempr.2017.10.004
3. Nayak-Luke, R., & Bañares-Alcántara, R. (2018). Long-Term Energy Storage: What is the Need and is Ammonia a Solution? *Computer Aided Chemical Engineering*, 44, 1843–1848. doi:10.1016/B978-0-444-64241-7.50302-5
4. Brandenburg, R., Bogaerts, A., Bongers, W., Fridman, A., Fridman, G., Locke, B. R., ... Ostrikov, K. K. (2018). White paper on the future of plasma science in environment, for gas conversion and agriculture. *Plasma Processes and Polymers*, (April 2018), 1–18. doi:10.1002/ppap.201700238
5. Kim, H.-H., Teramoto, Y., Ogata, A., Takagi, H., & Nanba, T. (2017). Atmospheric-pressure nonthermal plasma synthesis of ammonia over ruthenium catalysts. *Plasma Processes and Polymers*, 14(6), 1–9. doi:10.1002/ppap.201600157
6. Peng, P., Chen, P., Addy, M., Cheng, Y., Anderson, E., Zhou, N., ... Liu, Y. (2019). Atmospheric Plasma-Assisted Ammonia Synthesis Enhanced via Synergistic Catalytic Absorption. *ACS Sustainable Chemistry & Engineering*, 7, 100–104. rapid-communication. doi:10.1021/acssuschemeng.8b03887
7. Kim, H.-H., Teramoto, Y., Ogata, A., Takagi, H., & Nanba, T. (2016). Plasma Catalysis for Environmental Treatment and Energy Applications. *Plasma Chemistry and Plasma Processing*, 36(1), 45–72. doi:10.1007/s11090-015-9652-7
8. Rouwenhorst, K. H. R., Kim, H.-H., & Lefferts, L. (2019). Vibrationally excited activation of N<sub>2</sub> in plasma-enhanced catalytic ammonia synthesis: a kinetic analysis. *ACS Sustainable Chemistry & Engineering*, Submitted.
9. Mehta, P., Barboun, P., Herrera, F. A., Kim, J., Rumbach, P., Go, D. B., ... Schneider, W. F. (2018). Overcoming ammonia synthesis scaling relations with plasma-enabled catalysis. *Nature Catalysis*, 1(4), 269–275. doi:10.1038/s41929-018-0045-1

# Iron Nanoparticles Dispersed on Self-Standing Graphene Papers as Oxygen Reduction Reaction Electrocatalysts

*M. Oguzhan Bicer, Department of Chemistry, Koç University, Istanbul, Turkey; Tugce Beyazay, Material Science and Engineering, Koç University, Istanbul, Turkey; Tolga Kocer, Department of Chemical and Biological Engineering, Koç University, Istanbul, Turkey; F. Eylul Sarac Oztuna, Department of Chemistry, Koç University, Istanbul, Turkey; Ugur Unal, Department of Chemistry, Koç University, Istanbul, Turkey*

Oxygen electrochemistry is at the center of clean and renewable energy storage and conversion technology. While oxygen evolution reaction provides molecular oxygen to a simple hydrogen-oxygen fuel cell, oxygen reduction reaction (ORR) transforms the produced O<sub>2</sub> into water. [1] Due to the sluggish kinetics of the afore-mentioned reactions, an electrocatalyst is required to drive the reactions at low overpotentials. The choice of catalyst for ORR is generally Pt, albeit rare and expensive. [2] As an alternative to Pt, transition metal electrocatalysts are generally utilized to reduce the cost without compromising catalytic activity. [3] Typically, a nano-sized electrocatalyst is dispersed on a high surface area support material to exploit the catalytic activity of the metal and enhance reaction rates. In this regard, graphene, a honeycomb network composed of sp<sup>2</sup>-hybridized carbon atoms, is a promising support material with its excellent electrical conductivity, high theoretical surface area, and enhanced mechanical strength. [4] Herein, we report facile production of free-standing iron nanoparticle/reduced graphene oxide (rGO) composite papers as possible ORR electrocatalysts. The composite papers were fabricated via vacuum-assisted filtration system and thermally reduced in flowing NH<sub>3</sub> gas to enable N-doping in the graphitic support. Incorporation of Fe nanoparticles into the rGO support not only provided mechanical integrity to the system, but also shifted the half-wave potential for ORR to 0.77 V vs RHE.

In order to enhance the electrocatalytic activity of rGO paper in the absence of metallic nanoparticles, a graphene oxide (GO) paper was thermally reduced at 700 °C in flowing Ar:NH<sub>3</sub> (50:50). Thus, it was anticipated that rGO structure was doped with N atoms with NH<sub>3</sub> treatment [5], which is utilized as a general route to promote electrocatalytic activity towards ORR. Figure 1a shows the corresponding cyclic voltammogram of bare rGO paper. While the voltammogram measured in N<sub>2</sub>-

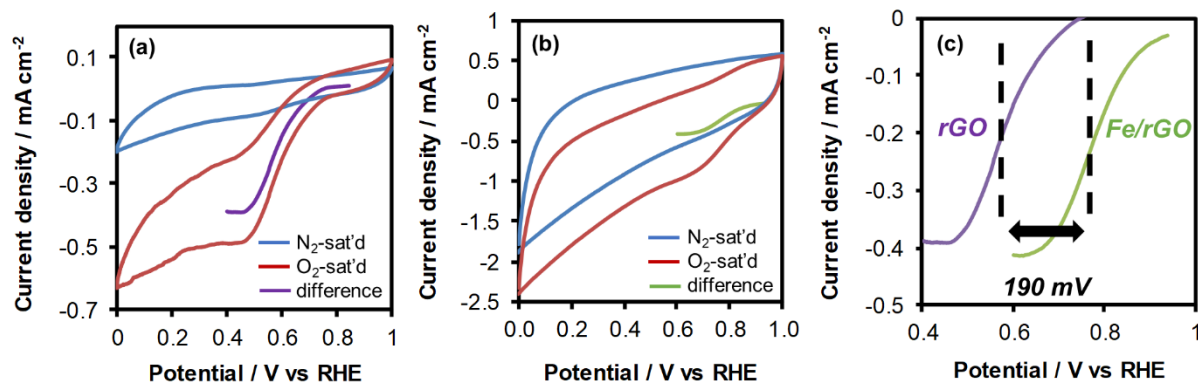


**Figure 1.** Cyclic voltammograms of (a) bare rGO paper, (b) Fe/rGO composite paper, and (c) rGO and Fe/rGO overlapped. Vertical dashed lines in (c) correspond to the half-wave potentials of ORR for rGO and Fe/rGO. Electrolyte solution: 0.1 M KOH. Scan rate: 20 mV s<sup>-1</sup>. Bare rGO paper was obtained by chemical reduction of GO paper with hydrazine vapor at 90 °C for 10 h followed by thermal reduction at 700 °C for 1 h in flowing Ar:NH<sub>3</sub> (50:50). Fe/rGO was produced by filtrating a Fe<sup>3+</sup> and GO mixture followed by thermal reduction at 700 °C for 1 h in flowing Ar:NH<sub>3</sub> (50:50).

saturated solution exhibited solely a capacitive current, switching the purging gas to O<sub>2</sub> resulted in formation of a new cathodic peak around 0.5 V, which is the reduction peak of O<sub>2</sub>. Note that, this GO paper was reduced chemically with hydrazine vapor prior to NH<sub>3</sub> treatment to obtain a flexible paper. [6] Without hydrazine reduction step, rGO paper had no mechanical integrity. On the other hand, a flexible paper was obtained after NH<sub>3</sub> treatment in the presence of Fe nanoparticles without the need for a chemical reduction. Moreover, incorporation of Fe into the structure shifted the potential of the cathodic peak to more positive values, indicating higher activity towards ORR (around 0.7 V, Figure 1b). From the difference curves between the voltammograms measured in O<sub>2</sub> and N<sub>2</sub>-saturated solutions, the half-wave potentials for ORR were calculated for bare rGO and Fe/rGO and they were respectively 0.58 and 0.77 V vs RHE (Figure 1c).

In conclusion, bare self-standing rGO paper without any metal nanoparticles had a considerable activity for ORR thanks to the N-doping provided by NH<sub>3</sub> treatment. Addition of Fe nanoparticles in the structure enhanced the mechanical properties of rGO paper, promoted the activity towards ORR, and the half-wave potential for the reaction was improved by 190 mV.

## References

1. Katsounaros I, Cherevko S, Zeradjanin AR, Mayrhofer KJJ (2014) *Angew Chemie Int Ed* 53:102–121.
2. Sarac Oztuna FE, Barim SB, Bozbag SE, et al (2017) *Electrochim Acta* 250:174–184.
3. Ge X, Sumboja A, Wu D, et al (2015) *ACS Catal* 5:4643–4667.
4. Allen MJ, Tung VC, Kaner RB (2010) *Chem Rev* 110:132–145.
5. Li X, Wang H, Robinson JT, et al (2009) *J Am Chem Soc* 131:15939–15944.
6. Beyazay T, Sarac Oztuna FE, Unal U (2019) *Electrochim Acta* 296:916–924.

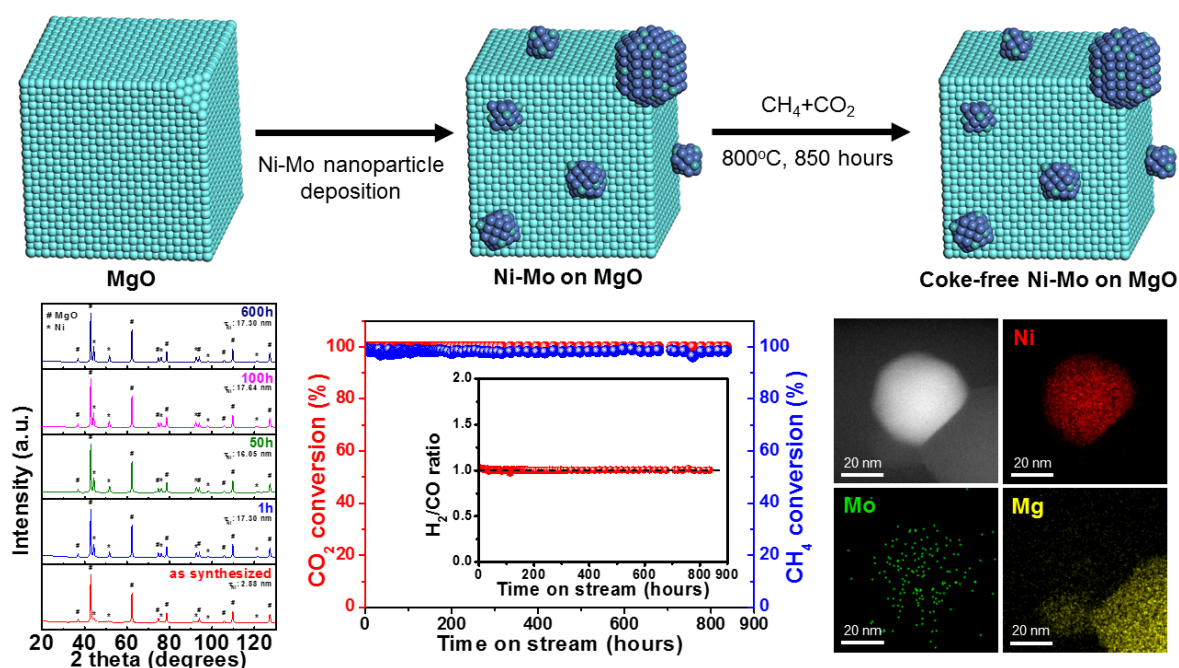
# **Coking-free MgO Supported Ni-Mo Catalyst for Dry Reforming of Methane**

*Youngdong Song, Korea Advanced Institute of Science and Technology (KAIST), Daejeon, South Korea; Ercan Ozdemir, Gebze Technical University, Kocaeli, Turkey; Sreerangappa Ramesh, Korea Advanced Institute of Science and Technology (KAIST), Daejeon, South Korea; Aldiar Adishev, Korea Advanced Institute of Science and Technology (KAIST), Daejeon, South Korea; Saravanan Subramanian, Korea Advanced Institute of Science and Technology (KAIST), Daejeon, South Korea; Aadesh Harale, Saudi Aramco, Dhahran, Saudi Arabia; Aqil Jamal, Saudi Aramco, Dhahran, Saudi Arabia; Dohyun Moon, Pohang Accelerator Laboratory, Pohang, South Korea; Sun Hee Choi, Pohang Accelerator Laboratory, Pohang, South Korea; Cafer T. Yavuz, Korea Advanced Institute of Science and Technology (KAIST), Daejeon, South Korea*

Dry reforming of methane (DRM) has gained tremendous attention since the two of the major greenhouse gases, carbon dioxide and methane, are used to produce industrially valuable syn-gas [1]. Catalysts play the most crucial role in DRM, so research has been focused on developing noble metal catalysts such as palladium, platinum, and rhodium due to their excellent activity and stability [2]. However, the use of noble metal catalysts in industry is unattractive because of the cost and the scale required for DRM. Nickel has been considered as a sustainable alternative, since it shows great activity but vulnerable to coke formation. Here, we synthesized Ni-Mo bimetallic nanoparticle catalysts on MgO as a support and studied for dry reforming of methane. The catalyst showed quantitative conversion in DRM for 850 hours (35 days) at 800°C without any evidence of coking.

Bimetallic Ni-Mo nanoparticle is synthesized through a polyol reduction method and loaded on the MgO support. The synchrotron powder X-ray diffraction patterns show 2.8 nm of Ni-Mo particles in as-prepared catalysts, and they further agglomerate up to 17 nm during activation process and does not change throughout the reaction. Spent catalyst was analysed by TEM, TPO, and Raman spectroscopy in order to investigate possible coke formation. No graphitic carbon was detected after 850 hours of continuous reaction. XANES and EXAFS revealed that molybdenum alloys with nickel, and this is in accordance with synchrotron PXRD result since

neither Mo oxide nor metallic Mo were observed. The activity of the catalyst was investigated extensively by changing the reaction parameters such as temperature, pressure, and gas hourly space velocity. Hollow cylindrical pellets were formed for the high-pressure tests and exhibited high activity up to 15 bar without deactivation. In comparison, we prepared control catalysts that are made through conventional wet impregnation and tested under the same conditions. The results show that the catalysts prepared through wet impregnation suffer from severe coke formation. We believe our findings will contribute to the heterogeneous catalysis field and ultimately to the petrochemical industries.



## References

- [1] Fan, M. S.; Abdullah, A. Z.; Bhatia, S., Catalytic Technology for Carbon Dioxide Reforming of Methane to Synthesis Gas. *Chemcatchem* **2009**, 1 (2), 192-208.
- [2] Pakhare, D.; Spivey, J., A review of dry ( $\text{CO}_2$ ) reforming of methane over noble metal catalysts. *Chem Soc Rev* **2014**, 43 (22), 7813-7837.

## **Alumina/boron nitride as a filler of thermally conductive materials**

*G. Jeon, Jeonnam State University, Jeonnam, South Korea ; H. Han, Jeonnam State University, Jeonnam, South Korea ; K. Hong, Komax Co., Jeonnam, South Korea ; D. Choi, Komax Co., Jeonnam, South Korea*

*\* Corresponding author(gjeon@dorip.ac.kr)*

### **INTRODUCTION**

Thermally conductive polymer composites have attracted tremendous attention recently due to their heat dissipation performance in highly integrated electronic devices such as high power laser, high brightness light-emitting diode, and solar cells [1]. The increasing miniaturization of electronic device components poses higher requirements for heat dissipation, fire safety and electrical insulating, it is thus imperative to develop polymer composites with high thermal conductivity [2]. The high loading of more than 50 wt% of thermal filler into polymer matrix is usually required to endow polymers with satisfactory thermal conductivities, which makes resultant polymer composites difficult to be processed. Incorporating thermally conductive fillers [3] into the polymer matrix has been proved to be one of the most efficient methods to enhance the thermal conductivity of the polymer [4,5]. Such high filler loading favors the formation of completely thermally conductive pathways in the polymer matrix. Boron nitride, with a very high thermal conductivity, has great advantage in thermally conductive composites compared with other fillers. Because the price of boron nitride is expensive, the expensive boron nitride in thermal filler was partly replaced to cheap alumina. Therefore, the highly effective thermal filler was needed to show high thermal conductivity at low loading into polymer matrix. In this study, hybrid filler composed of alumina and boron nitride was developed and the characteristics of hybrid filler were measured.

### **EXPERIMENTAL**

Spherical alumina particles with mean sizes of 50  $\mu$  were provided by CIS Co. Ltd (South Korea) and boron nitride were purchased from 3M Co. Ltd. (South Korea). Characteristic properties of hybrid thermal filler were measured by surface area, pore size distribution, XRD, XRF, SEM and particle size analysis. Hybrid thermal filler was observed with a JEM-7401F field emission scanning electron microscope (JEOL,

Japan). The thermal conductivities of the hybrid filler with a diameter of 13 μm and a thickness of 2 μm were measured with LFA 467 thermal meter (Netzsch Co. Germany).

## **SUMMARY**

The surface area, particle size, XRD, XRF, SEM, density, thermal diffusivity, and a thermal conductivity of hybrid filler were studied. The synergistic effect of alumina/boron nitride hybrid thermal filler on the thermal conductivity was shown. This synergistic effect is so remarkable that it is really necessary to understand why the thermal conductivity of hybrid filler is enhanced simply by replacing boron nitride with alumina.

## **ACKNOWLEDGEMENT**

This work (Grants No. S2647981) was supported by Business for Cooperative R&D between Industry, Academy, and Research Institute funded Korea Small, Medium and Venture Business Administration in 2018.

## **REFERENCES**

- [1] G. Lee, M. Park, J. Kim, J. Lee and H. Yoon, "Enhanced thermal conductivity of polymer composites filled with hybrid filler", *Compos. Part A-Appl.* Vol.37, pp727–734 (2006).
- [2] M. Harada, N. Hamaura, M. Ochi and Y. Agari, "Thermal conductivity of liquidcrystalline epoxy/BN filler composites having ordered network structure", *Compos. Part B-Eng.* Vol. 55, pp306–313 (2013).
- [3] H. Ishida and S. Rimdusit, "Very high thermal conductivity obtained by boronnitride-filled polybenzoxazine", *Thermochim. Acta* Vol.320, pp177–186 (1998).
- [4] X. Cui, P. Ding, N. Zhuang, L. Shi, N. Song, S. Tang, "Thermal conductive and mechanical properties of polymeric composites based on solution-exfoliated boron nitride and graphene nanosheets: a morphology-promoted synergistic effect", *ACS. Appl. Mater. Interfaces* Vol.7, pp19068–19075 (2015).
- [5] C. Choy, E. Ong, F. Chen, "Thermal diffusivity and conductivity of crystalline polymers", *J. Appl. Polym. Sci.* Vol.26, pp2325–2336 (1981).



# Enhancement of natural zeolite as acidic catalyst for glycerol etherification process

Hieu Do Trung<sup>1\*</sup>, Hendrik Kosslick<sup>1,2\*</sup>, Son Le Thanh<sup>3</sup>, Axel Schulz<sup>1</sup>

<sup>1\*</sup> Institute of Chemistry, University of Rostock, Germany

<sup>2</sup> Leibniz-Institute for Catalysis, Rostock, Germany

<sup>3</sup> Faculty of Chemistry, VNU – Hanoi University of Science, Vietnam

**Email:** [trung.do@uni-rostock.de](mailto:trung.do@uni-rostock.de)

Nowadays, the energy and environmental situation is a big problem especially for developing countries, which are faced with limited fossil resources. Additionally, the CO<sub>2</sub> emission from fuel consumption for heating and transportation is a main source of air pollution and climate change due to global warming. Therefore, the green synthesis of materials and the use of sustainable feedstock are very important issues. Catalysis plays a key role for the environmental protection and development of green processes. Heterogeneous catalysts allow improving the process efficiency and the environmental protection. This study deals with the preparation, characterization and testing of a hierarchical porous clinoptilolite-based natural zeolite as a potential acid catalyst for the conversion of renewable glycerol feedstock to valuable fuel additives [1]. So far the use of resin and Zeolite-based catalysts like amberlyst A-15 and zeolite mordenite, beta, and ZSM5 was reported [2, 3], the modified zeolite [4] could be a promising catalyst for this reaction, But there are no report for this type of catalysts. The natural zeolite clinoptilolite was ion exchanged with ammonium and activated at different temperatures in order to obtain the acid form of the zeolite. The catalysts were characterized by XRD, FTIR, TG-DSC, TPD of ammonia, and nitrogen adsorption and desorption (BET). The catalytic performance of prepared materials was investigated in the acid catalyzed etherification of glycerol with tert-butanol. The acid catalysts were highly acidic and showed high activity in the etherification of glycerol with tert-butanol to the corresponding mono and diethers. The catalysts showed high stability in the liquid phase reaction under reflux conditions and elevated temperature. The conversion and the selectivity were strongly influenced by the reaction temperature.

## References

- [1] C. Cannilla, G. Bonura, L. Frusteri, and F. Frusteri, "Glycerol etherification with TBA: High yield to poly-ethers using a membrane assisted batch reactor," *Environ. Sci. Technol.*, 48, (2014), 6019–6026.
- [2] C. Miranda *et al.*, "Exploring the impact of zeolite porous voids in liquid phase reactions: The case of glycerol etherification by tert-butyl alcohol," *J. Catal.*, 365, (2018), 249–260.
- [3] S. Magar, S. Kamble, G. T. Mohanraj, S. K. Jana, and C. Rode, "Solid-Acid-Catalyzed Etherification of Glycerol to Potential Fuel Additives," *Energy and Fuels*, (2017), 12272-12277.
- [4] P. Lanzafame *et al.*, "Comparison of H<sup>+</sup> and NH<sub>4</sub><sup>+</sup> forms of zeolites as acid catalysts for HMF etherification," *Catal. Today*, 304, (2018), 97–102.

## Author details

\*Full name: Do Trung Hieu

\*Contact number: +49 15232163492

\*Category: Oral presentation

\*Session Number: Catalysis in Oil and Gas \*Session Name: Catalysis in Oil and Gas

## Biography

MSc. Do has completed his Master degree from Rennes 1 University, Rennes, France and continued his PhD in the field of advanced catalyst and sustainable development in University of Rostock, Germany. He is a lecturer in Department of Chemistry, Hanoi University of Science, Vietnam. He has published more than 15 papers in scientific journals

## **A Fully Reversible Water Electrolyzer Cell made up from FeCoNi (Oxy)hydroxide Atomic Layers**

**Qingran Zhang<sup>1</sup>, Xunyu Lu<sup>1,\*</sup>, Rose Amal<sup>1,\*</sup>**

<sup>1</sup> Particles and Catalysis Research Group, School of Chemical Engineering, The University of New South Wales, Sydney, NSW 2052, Australia

\*Email address: xunyu.lu@unsw.edu.au, r.amal@unsw.edu.au

Photovoltaic (PV) cells powered water electrolysis systems provide a facile and viable way to convert the abundant but intermittent solar energy into hydrogen (H<sub>2</sub>) fuel<sup>1</sup>. The large-scale deployment of such systems requires the development of efficient and cost-effective catalysts for overcoming the sluggish reaction kinetics associated with the anodic oxygen evolution reaction (OER) and cathodic hydrogen evolution reaction (HER) in water splitting<sup>2</sup>. Further, the integration of water electrolyzer cells with PV cells also calls for the exceptional robustness of the catalyst materials that can effectively withstand the frequent power interruptions caused by cell shutdowns and/or weather changes<sup>3</sup>. To date, these requirements have posed a grand challenge in material development. In this work, atomically thin FeCoNi (oxy)hydroxide nanosheets (FeCoNi-ATNs) were prepared via a facile and scalable one-step bottom-up method. The obtained FeCoNi-ATNs exhibited extremely high mass activities for both OER and HER (1931 A g<sup>-1</sup> at 330 mV for OER; 1819 A g<sup>-1</sup> at 200 mV for HER) in alkaline solutions, which were among the highest of all catalyst materials reported so far. More excitingly, by employing FeCoNi-ATNs as the catalyst material for both anode and cathode, a fully reversible water electrolyzer cell (WEC) was assembled, which exhibited a robust reversibility between two half reactions in water electrolysis under a high current density (100 mA cm<sup>-2</sup>). The as-fabricated WEC can effectively overcome the stability issues caused by electrode depolarization during frequent power interruptions, an inevitable phenomenon which is commonly brought about by the usage of intermittent renewable energy supplies.

Reference:

1. Z. W. Seh, J. Kibsgaard, C. F. Dickens, I. Chorkendorff, J. K. Nørskov and T. F. Jaramillo, *Science.*, 2017, **355**.
2. Y. Gorlin and T. F. Jaramillo, *J. Am. Chem. Soc.*, 2010, **132**, 13612–13614.
3. W. Hug, H. Bussmann and A. Brinner, *Int. J. Hydrogen Energy*, 1993, **18**, 973–977.

# Development and assessment of a criterion for the application of Brønsted-Evans-Polanyi relationships for dissociation catalytic reactions at surfaces

*Zhao-Bin Ding<sup>1</sup> and Matteo Maestri<sup>1</sup>*

*<sup>1</sup>Laboratory of Catalysis and Catalytic Processes, Dipartimento di Energia, Politecnico di Milano, Via Lambruschini, 4, 20156 Milano (Italy)*

## Introduction

First-principles-based microkinetic modeling of catalytic processes stands at the basis of the mechanistic understanding of the catalysis phenomenon at different operating conditions. The construction of a predictive microkinetic model, however, requires accounting for all the possible reaction pathways of the process, which is not feasible through a full-first-principles calculation. One way to circulate such complexity is to calculate the kinetic parameters using an empirical or a semi-empirical method. One of the most widely used empirical correlations for estimating the reaction barriers is the Brønsted-Evans-Polanyi (BEP) relation, which linearly correlates the activation barrier,  $E_a$  and the reaction energy,  $\Delta E$ . However, the BEP is not applicable to some reactions such as trans-COOH dissociation reactions[1]. Therefore, a first-principles assessment of the accuracy of BEP is therefore required for clarifying the extent of the applicability of the BEP relationships for different reactions, metals, and surface structures. In this work, we propose and assess a criterion based on the thermochemistry of the reactions for qualitatively assessing the applicability of BEP relations. Such finding paves the way towards its quantitative use for the exploration of complex reaction networks for different metals and surfaces.

## Methods

Periodic DFT calculations with PBE functional are performed with Quantum ESPRESSO code. the activation barriers of CH, CO and trans-COOH dissociation reactions on (100), (110), (111) and (211) surfaces of Ni, Cu, Rh, Pd, Ag, Pt are considered. Grimme-D2 van der Waals corrections are considered for all the trans-COOH dissociation reactions.

## Results and Discussion

We decompose both  $E_a$  and  $\Delta E$  to the components that describe the different processes involved in the dissociation reactions in the range of conditions to be

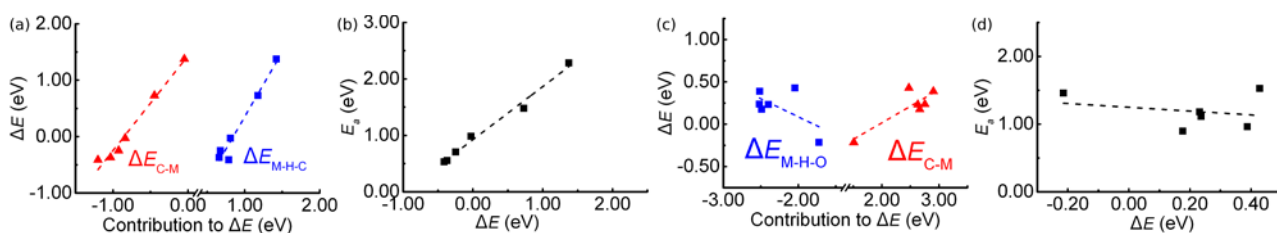


Figure 1. Correlation between  $\Delta E$  and both of its contributions for (a) CH dissociation and (c) for trans-COOH dissociation reactions. The BEP correlations of both reactions are shown in (b) and (d), respectively. Figures are adapted from [2].

described by the BEP relation. For example, for CH dissociation reactions, they can be decomposed to the variation of the interaction within the  $[M\text{--}H\text{--}C]^{\ddagger}$  complex ( $\Delta E_{M\text{--}H\text{--}C}$ ) and the variation of carbon-hydrogen interactions ( $\Delta E_{C\text{--}H}$ ). For both CH and trans-COOH dissociation reactions, we find that both contributions of the activation energy are linearly correlated to the corresponding contributions of the reaction energies[2]. Therefore the TS nature can be represented by the nature of the reaction path. Figure 1(a) shows that for CH dissociation reaction, both contributions are linearly correlated to  $\Delta E$ . It thus indicates a consistent TS nature on all the surfaces involved, therefore suggests that the  $E_a$  and  $\Delta E$  are linearly correlated, which agrees to the accurate BEP shown in Figure 1(b). In contrast, Figure 1(c) shows that for trans-COOH dissociation reactions on (100) surfaces, both contributions are anti-correlated, which suggests that the TS nature varies from one metal to the other. It matches the absence of the BEP as shown in Figure 1(d).

## Conclusions

Our work reveals that BEP is applicable for the reactions at different conditions when they satisfy two conditions: (i)  $\Delta E$  correlates to both of its components that describe different processes involved in the dissociation reactions, and (ii) the variation of these components is consistent. Such criterion allows for an estimation of the applicability of BEP only on the basis of thermodynamics of the reaction, thus facilitates the development of structure-dependent microkinetic models in heterogeneous catalysis.

## References

1. Yoo, J. S.; Abild-Pedersen, F.; Norskov, J. K.; Studt, F. ACS Catal., 2014, 4, 1226-1233
2. Ding, Z. -B.; Maestri, M. Ind. Eng. Chem. Res., accepted

## Advances to operando methods for characterization of heterogeneous catalysts.

*Donato Decarolis*<sup>1,2</sup>, *P. Wells*<sup>2,3</sup>, *A. Goguet*<sup>2,4</sup>, *E. Gibson*<sup>2,5</sup>, *C. Stewart*<sup>4</sup>, *E. Dann*<sup>2,6</sup>, *K. Morgan*<sup>4</sup>, *G. Cibir*<sup>7</sup>, *A. Dent*<sup>7</sup>, *C. Hardacre*<sup>8</sup>, *E. Kondratenko*<sup>9</sup>, *V. Kondratenko*<sup>9</sup>, *C. McManus*<sup>4</sup>, *S. Rogers*<sup>2,6</sup>, *C. Stere*<sup>2,8</sup>, *S. Chansa*<sup>8</sup>, *Y. Wang*<sup>10</sup>, *S. Haigh*<sup>10</sup>, *R. Catlow*<sup>2,5,11</sup>, *V. Cellorio*<sup>6</sup>, *P. Collier*<sup>12</sup>, *T. Eralp*<sup>12</sup>, *M. Amboage*<sup>6</sup>, *A. Kroner*<sup>6</sup>, *A. Raj*<sup>12</sup>

1. School of Chemistry, Cardiff University, Cardiff, CF10 3AT, UK 2. UK Catalysis Hub, Research Complex at Harwell, Rutherford Appleton Laboratory, Harwell Oxon, Didcot OX11 0FA, United Kingdom 3. University of Southampton, School of Chemistry, University Road, Southampton SO17 1BJ, United Kingdom 4. Queen's University Belfast, School of Chemistry, David Keir Building, Stranmillis Rd, Belfast BT9 5AG, United Kingdom 5. School of Chemistry, Joseph Black Building, University of Glasgow, Glasgow G12 8QQ, United Kingdom 6. Department of Chemistry, University College London, 20 Gordon Street, London WC1H 0AJ, United Kingdom 7. Diamond Light Source Ltd., Harwell Science and Innovation Campus, Chilton, Didcot OX11 0DE, United Kingdom 8. School of Chemistry, The University of Manchester, Oxford Road, Manchester M13 9PL, United Kingdom 9. Leibniz-Institut für Katalyse e.V, Universität Rostock, Albert-Einstein-Straße 29a, Rostock D-18059, Germany 10. Cardiff Catalysis Institute, School of Chemistry, Cardiff University, Main Building, Park Place, Cardiff CF10 3AT, United Kingdom 11. School of Materials, University of Manchester, Manchester M13 9PL, U.K. 12. Johnson Matthey Technology Centre, Blounts Court Road, Sonning Common, Reading RG4 9NH, United Kingdom

In order to optimize the performance of heterogeneous catalysts, the structure-activity relationship must be fully understood. A common approach to unravel this relationship is through the use of operando methods, where spectroscopic techniques are paired with a simultaneous analysis of the effluent gases [1].

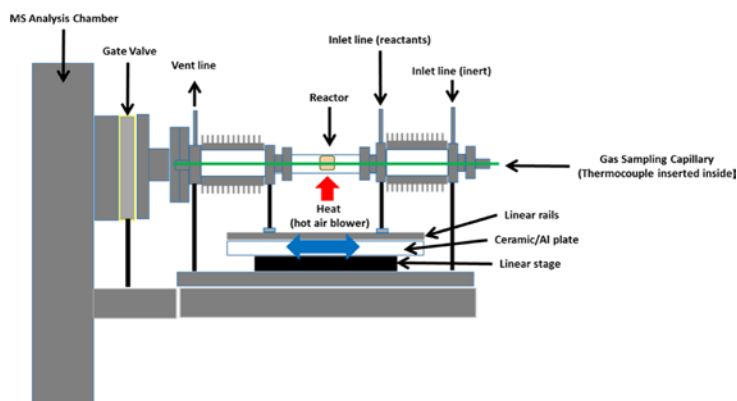


Figure 1. Schematic of the SPACI-FB [5]

However, as there could be a concentration and a temperature gradient along the axial length of a plug-flow reactor, simple analysis of end-pipe gases might not be able to provide a clear picture of the behavior of the catalyst [2]–[4]. Operando techniques must therefore have a similar spatial resolution, in order to obtain both spectroscopic and catalytic information at different point along the bed. In order to solve this problem, our group has developed the SPACI-FB [5], [6], a technique, shown in figure 1, which provides profiles of gas concentration and temperature within the catalyst while allowing simultaneous collection of spectroscopic data. This technique has been successfully used to understand the role of H<sub>2</sub> in the oxidation of CO over Pd catalysts [5]. The active catalyst is consistent of Pd nanoparticles with absorbed

surface O, of which a specific concentration is required before light-off is observed, as shown in figure 2a. The presence of hydrogen causes an activation of the catalyst much closer to the

front end of the bed (figure 2b), most likely via the reaction of  $H_2 + O_2$  to form adsorbed OHs, therefore promoting the catalytic activity.

Another successful approach developed in our group is a

reaction cell which allows for synchronous, spatially resolved XAFS/DRIFTS measurements, shown in figure 3 [2]. This would allow to obtain information about the gas composition at different point using IR and collect relevant structural information. This set-up was used to obtain insights into the kinetic oscillations,

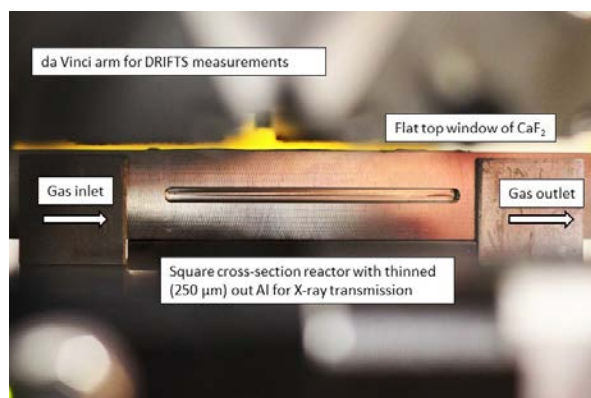


Figure 3. Schematic photograph of the new XAFS/DRIFTS reaction cell [2].

between periods of high and low activity, which happens during CO oxidation on  $Pd/\gamma-Al_2O_3$ . Initially, the CO ignition occurs at the end of the catalyst bed, and the reaction front propagates upstream with increasing temperature. This oscillating behaviour only appears at the front of the catalyst bed, after light-off temperature and is caused by the competition between CO storage and

surface oxide formation at the nanoparticle surface[2]. These results show how spatially resolved measurement are essential to obtain a full understand of the structure-activity relationship and obtain further insights in the reaction process.

[1] A. Gurlo et al., *Angew. Chemie Int. Ed.*, vol. 46, no. 21, pp. 3826–3848, May 2007. [2] E. K. Dann et al., *J. Catal.*, vol. 373, pp. 201–208, 2019. [3] A. M. Gänzler et al., *J. Catal.*, vol. 328, pp. 216–224, 2015. [4] M. A. Newton, A. J. Dent, S. Diaz-Moreno, S. G. Fiddy, B. Jyoti, and J. Evans, *Chem. – A Eur. J.*, vol. 12, no. 7, pp. 1975–1985, Feb. 2006. [5] C. Stewart et al., *ACS Catal.*, vol. 8, no. 9, pp. 8255–8262, Sep. 2018. [6] J. Touitou et al., *Catal. Sci. Technol.*, vol. 2, no. 9, pp. 1811–1813, 2012.

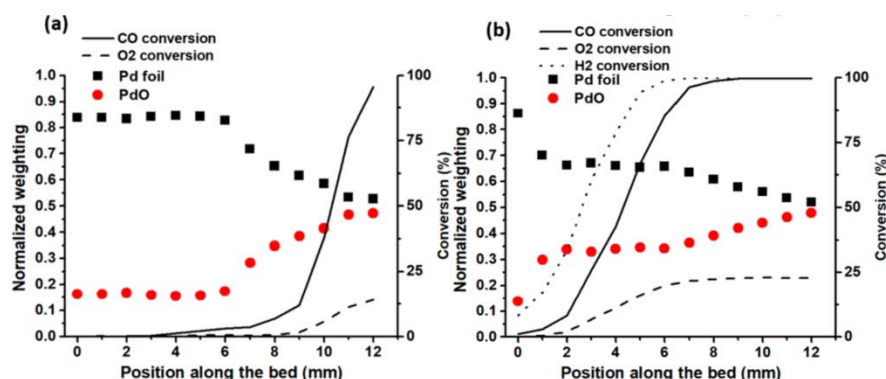


Figure 2. Relative contributions of a Pd metal standard and PdO as a function of position in the catalyst bed during (a) CO oxidation and (b) CO oxidation with  $H_2$ . [5]

# Effects of Interfacial Properties and Charges of Reactive Hydrogen Species during Guaiacol Hydrodeoxygenation on Ru Clusters

*Haoyu Nie,<sup>1</sup> Junnan Shangguan,<sup>1</sup> Alyssa J. R. Hensley,<sup>1</sup> Zhishan Li,<sup>1</sup> Jacob Bray,<sup>2</sup> Jean-Sabin McEwen,<sup>2</sup> and Ya-Huei (Cathy) Chin\**

<sup>1</sup> *Department of Chemical Engineering and Applied Chemistry, University of Toronto, Toronto, Ontario M5S 3E5, Canada \*cathy.chin@utoronto.ca*

<sup>2</sup> *The Gene & Linda Voiland School of Chemical Engineering and Bioengineering, Washington State University, Pullman, Washington 99164, United States*

The catalytic hydrodeoxygenation (HDO) of lignin-derived phenolic monomers is a promising route for producing sustainable bio-fuels and value-added chemicals. Among the phenolic reactants, guaiacol is a representative model compound, because it contains all characteristic chemical functional groups of C-O bonds [1]. Rates and selectivities of HDO on transition metal clusters depend strongly on the interfacial properties of the catalyst surfaces, where the identity of solvent matters [2]. At protic solvent-metal interfaces, a portion of the H atoms ( $H^*$ ) may undergo ionization assisted by solvent molecules and acquire proton ( $H^+$ ) characters. Both  $H^*$  and  $H^+$  may participate in H addition events during HDO and their relative abundance could lead to different catalytic performances, but the respective roles of these H species and reaction mechanisms have not been rigorously identified at the molecular level. Here, we describe the mechanistic differences during guaiacol HDO on different interfaces, each with their unique interfacial properties, of: (1) water (protic solvent)-Ru, (2) cyclohexane (aprotic solvent)-Ru, and (3) vapor-Ru.

At water-Ru interfaces, guaiacol- $H_2$  reactions (30 bar  $H_2$ , 423 K) proceed through the desired C-OCH<sub>3</sub> cleavage route ( $r_{C-O}$ ), which produces predominantly cyclohexanol (23% selectivity), and undesired H addition route ( $r_{H-A}$ ), which forms 2-methoxycyclohexanol (72% selectivity) [1]. The  $r_{C-O}$  is near zero-order dependence to guaiacol, suggesting that guaiacol derived species saturate Ru cluster surfaces. DFT calculations indicate a preferential dehydrogenation of guaiacol that forms guaioxy [ $C_6H_4(OCH_3)(O)^*$ ] as the most abundant surface intermediate (MASI). The  $r_{C-O}$  acquires a first reaction order to  $H_2$ , indicating the requirement of two H addition events to the guaioxy before the kinetically relevant step. The selective H-D isotopic exchange during guaiacol- $D_2$  reactions detected by GC-MS and  $H^1$ -NMR reveals successive  $H^*$  additions to the oxygen atom and then to the meta carbon (relevant to the hydroxyl group) of guaioxy. The resulted  $C_6H_5(OCH_3)(OH)^*$  undergoes C-OCH<sub>3</sub>



cleavage via an intramolecular proton transfer, during which the H in its hydroxyl group is ionized, transport to the methoxy group via an adjacent water molecule, and form a  $C_6H_5(O)^*$  and a methanol molecule. DFT calculations show that this process is stabilized in protic environment and its activation free energy is more than  $40 \text{ kJ mol}^{-1}$  smaller than the direct  $C-OCH_3$  cleavage via metal insertion. At aprotic cyclohexane-Ru interfaces (30 bar  $H_2$ , 473 K), guaiacol- $H_2$  reactions exhibit comparable selectivities but the rate of  $r_{C-O}$  is still 40% lower than that in water solvent at a lower temperature of 423 K. Guaiacol- $D_2$  reactions in cyclohexane do not lead to H-D exchange, in agreement with DFT results that the exchange requires water-assisted H ionization on the meta carbon to decrease the barrier for H abstraction after D addition. The lack of protic solvent makes the intramolecular proton transfer infeasible, thereby leading to the observed decrease of  $C-OCH_3$  cleavage rate.

In the contrasting case of vapor-Ru interface, guaiacol- $H_2$  reactions show  $> 97\%$  selectivity towards  $r_{C-O}$ , forming predominantly phenol (0.1-0.9 kPa guaiacol, 10-90 kPa  $H_2$ ). The  $r_{C-O}$  rate is seven times larger than that in cyclohexane under similar conditions, despite the lack of surface reactive proton species ( $H^+$ ) at both vapor-Ru and cyclohexane-Ru interfaces. At vapor-Ru interfaces, 91% guaiacol molecules undergo unselective H-D exchange in guaiacol- $D_2$  reactions. This result, at first glance, contradicts to the required water assistance in H abstractions on phenolic rings. The difference between exchange results in liquid and vapor reveals that direct H abstraction occurs preferentially at vapor-Ru interfaces, when the solvent effect is eliminated. The  $r_{C-O}$  is zero-order to guaiacol, consistent with DFT results that guaioxy is the MASI in vapor, and first-order to  $H_2$ . These orders are identical to those in water, but in vapor a H abstraction instead of H additions occurs on the MASI and the formed  $C_6H_3(OCH_3)(O)^*$  then undergoes direct  $C-OCH_3$  cleavage via metal insertion.

In summary, Ru clusters catalyze guaiacol HDO via different reaction mechanisms, depending on the interfacial property and the charge of the reactive H species. Protic water solvent enables the catalytically favorable intramolecular proton transfer that ruptures the  $C-OCH_3$  bond after  $H^+$  additions, which does not occur in aprotic cyclohexane solvent deprived of  $H^+$ . The vapor phase  $C-OCH_3$  cleavage proceeds via H abstraction from the phenolic ring followed by direct metal insertion.

## References

- [1] J. Shangguan, N. Pfriem, Y.-H. Chin, *J. Catal.* **2019**, *370*, 186-199.
- [2] J. Shangguan, Y.-H. C. Chin, *ACS Catal.* **2019**, *9*, 1763-1778.

# Selective adsorption of water on Pt-Fe model catalyst exposed to O<sub>2</sub> and trace water

*Teng Ma<sup>1\*</sup>, Rui Cao<sup>1</sup>, Xue Bao<sup>1</sup>, Er'bing Hua<sup>1</sup>, Mu Yang<sup>1</sup>, Yaqin Wang<sup>1,2</sup>*

*1. Institute of Science, Shenyang Agricultural University, Shenyang, China;*

*2. Shenyang Ligong University, Shenyang, China*

## **Introduction:**

The coadsorption studies of molecular O<sub>2</sub> and H<sub>2</sub>O on Pt surfaces are basic but important for understanding CO oxidation at low temperatures or in H<sub>2</sub> stream. However, for a long time, they are omitted and not well explored. By using high resolution electron energy loss spectroscopy (HREELS), we took coadsorption experiments of O<sub>2</sub> and a trace amount of H<sub>2</sub>O molecules at cryogenic temperatures (105 K) and observed that the selective adsorption of trace water over O<sub>2</sub> on Pt/Fe/Pt(111) surface of Pt-Fe model catalysts. The results could provide a hint that the well-tuned electronic structure of bimetallic catalysts could reverse the relative amount of surface species, and might influence the CO reaction route significantly.

## **Experiment and Results:**

The work was taken in one vacuum system at the base pressure of 1.0-3.0×10<sup>-10</sup> mbar. The HREELS spectra were taken at 60 degree angle of emission with respect to the surface normal in the specular direction. The electron beam energy of HREELS was 7.287 eV. The Pt/Fe/Pt(111) surface has a sandwich structure of the topmost Pt atomic layer, subsurface Fe layer and underlying Pt(111) bulk, and presents the lower density of states (DOS) at 0-2.0 eV below the Fermi level with reference to Pt(111), as is shown in Fig.1. On the Pt/Fe/Pt(111) surface the

chemisorption of both O<sub>2</sub> and H<sub>2</sub>O would be weakened with different extents, which would change the relative order of their adsorption strength. At 105 K and exposure to O<sub>2</sub> with 0.1% v/v water, chemisorbed water species are dominated on the Pt/Fe/Pt(111) surface, while chemisorbed O<sub>2</sub> species are dominated on Pt(111) surface, as is shown in Fig.2. The O<sub>2</sub> adsorption has become weaker than H<sub>2</sub>O on Pt/Fe/Pt(111), which is consistent with the features of electronic structure on Pt/Fe/Pt(111) surface because Pt 5d states for O<sub>2</sub> adsorption reside mainly within 0-2 eV, while them for H<sub>2</sub>O adsorption reside locally around 4 to 5 eV .

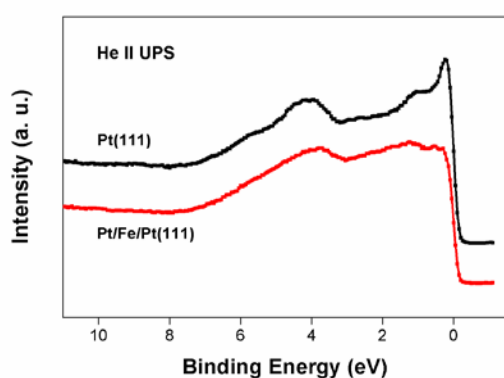


Fig. 1 The He II UPS spectra ( $h\nu=40.8$  eV) of Pt/Fe/Pt(111) and Pt(111) surfaces

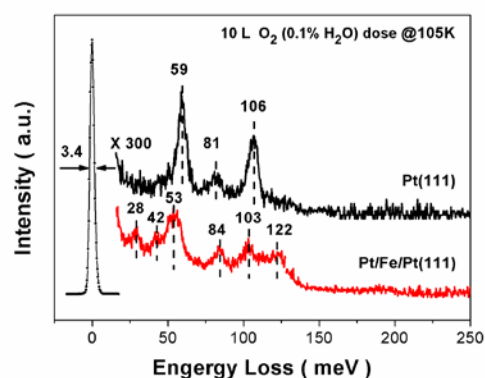


Fig. 2. HREELS spectra of Pt/Fe/Pt(111) and Pt(111) exposed to O<sub>2</sub> with 0.1 % water at 105 K

## References

- [1] Sun, G.; Jin, Y.; Zhang, Z.; Wang, Z.; Chai, P.; Xiong, F.; Huang, W., The Double-Edged Sword Effect of Water in the Low-Temperature CO Oxidation on Pt(111) Surface. *J. Phys. Chem. C* **2018**, *122*, 22530-22537.
- [2] Fujitani, T.; Nakamura, I., Mechanism and Active Sites of the Oxidation of CO over Au/TiO<sub>2</sub>. *Angew. Chem. Int. Ed.* 2011, *50*, 10144-10147.
- [3] Li, R.; Li, H.; Xu, S.; Liu, J., Theoretical investigation on coadsorption effect of O<sub>2</sub> and H<sub>2</sub>O on Pt(111) surface. *Comput. Mater. Sci.* **2015**, *102*, 174-182.
- [4] Cui, Y.; Harada, Y.; Ikenaga, E.; Li, R.; Nakamura, N.; Hatanaka, T.; Ando, M.; Yoshida, T.; Li, G.-L.; Oshima, M., In Situ Hard X-ray Photoelectron Study of O<sub>2</sub> and H<sub>2</sub>O Adsorption on Pt Nanoparticles. *J. Phys. Chem. C* **2016**, *120*, 10936-10940.
- [5] Hyman, M. P.; Medlin, J. W., Effects of Electronic Structure Modifications on the Adsorption of Oxygen Reduction Reaction Intermediates on Model Pt(111)-Alloy Surfaces. *J. Phys. Chem. C* **2007**, *111*, 17052-17060.

# Aqueous Grafting Ionic Liquid on Graphene Oxide for CO<sub>2</sub> Cycloaddition

*Jie Zhu, School of Petrochemical Engineering, Changzhou University, Changzhou, China; Mohong Lu, School of Petrochemical Engineering, Changzhou University, Changzhou, China; Yongxin Li, School of Petrochemical Engineering, Changzhou University, Changzhou, China; Mingshi Li, School of Petrochemical Engineering, Changzhou University, Changzhou, China;*

## **Abstract:**

In this study, a facile and environment-friendly approach was developed to immobilize water-soluble imidazolium- and pyridinium-based ionic liquids (ILs), i.e. [Smlm]X (X=Cl and I) and [SPy]I, on graphene oxide (GO) sheets in aqueous medium by controlling the grafting temperature. Several characterizations including OEA, FT-IR and XPS techniques have been applied to investigate the effects of the grafting temperature on the preparation for GO-ILs in aqueous medium. As-prepared composites were employed as heterogeneous catalysts for CO<sub>2</sub> cycloaddition. Results showed that the amount of [Smlm]I on GO sheets reached a high level (about 1.7 mmol/g GO) under the mild temperature (i.e. 40-60 °C), owing to the inhibition of the self-condensations among ILs molecules in water under the mild temperature. The resulting composites exhibited excellent catalytic activity to CO<sub>2</sub> cycloaddition, affording the maximum conversion of propylene oxide (PO) as about 93% in 4 h, much higher than that on [Smlm]I. It could be explained that the abundant hydrogen bonding donor (hydroxyl groups) on GO sheets assisted in the ring opening of PO, which promoted the reaction. These heterogeneous catalysts could be reused for at least five runs without significant loss in activity, implying the stable and reusable capability of as-prepared catalysts. The aqueous grafting mechanism was proposed here, which went through a two-step reaction. ILs with silane coupling agent are firstly hydrolyzed to silanol in water, and grafting reaction then happens by removing H<sub>2</sub>O molecules under the mild temperature due to the low activation energy for dehydration. It differs greatly from the traditional grafting mechanism in organic solvents, which involves the direct dealcoholization under the high temperature because of the high activation energy for the reaction.

**Keywords:** graphene oxide; ionic liquid; aqueous grafting; CO<sub>2</sub> cycloaddition

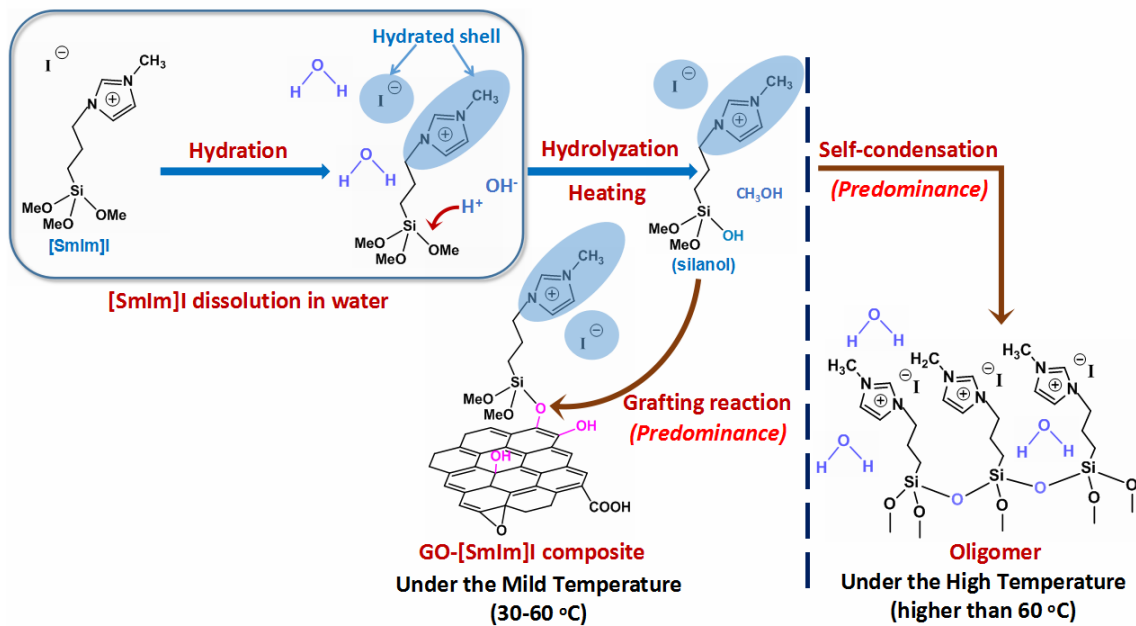


**Figure:** The grafting mechanism of water-soluble [Smlm]I on GO in water under the mild temperature (30-60 °C) and the high temperature (beyond 60 °C).

## References

List and number all bibliographical references at the end of the paper. When referenced within the text, enclose the citation number in square brackets, i.e. [1]

# Supported Precious Group Metal Catalysts for Various Hydrogenation Reactions and as Sustainable Resource

*Hendrik Spod\*, Gisa Meißner,*

*Heraeus Deutschland GmbH & Co. KG, Heraeusstraße 12-14, 63450 Hanau,  
Germany*

Catalysis has an enormous importance and economical relevance for the global chemical industry. More than 80 % of present industrial processes use different types of catalysts for the synthesis of a variety chemical, petrochemical and biochemical products as well as for the production of polymers. [1] Based on the twelve principles of green chemistry, selectivity, efficiency and sustainability are playing an important key role. [2]

Here, we present the lifecycle of industrially scalable palladium-based catalysts and discuss strategies for tailoring these catalysts for specific applications.

## Experimental

All experiments were performed in a 100 mL batch reactor (Mettler-Toledo) equipped with a sampling tool. Typical reaction conditions were 25 – 50 °C, 1 – 3 bar H<sub>2</sub>, 500 mg substrate and 25 mg of catalyst.

## Results

The lifecycle of a heterogeneous catalyst can be structured into five main steps: Precious metal winning, production of a precious metal solution, catalyst synthesis, performance as active catalyst and finally serving again as precious metal source through recycling.

Generally, different parameters such as precious metal precursors, loadings, supporting materials, synthesis method significantly impact the activity, selectivity and yield of a target product. Furthermore, these parameters can be used to customize catalysts for a specific application. We investigated a standardized synthesis method for a Pd-catalyst with a 5 wt.-% load and various supporting materials (Fig. 1, left). We studied the influence on activity with respect to two

hydrogenation reactions using these catalysts. The observed activity differences are based on different precious metal surfaces and intrinsic characteristics of the support. Further, we have tested the influence of different Pd-loadings between 1 and 10 wt.-% and obtained a linear increase of the activity in the hydrogenation of a double bond or nitro group (Fig. 1, right). This shows a successful catalyst preparation with the same particle size for Pd-loadings up to 10 wt.-% onto inert supports. In fact, we are able to modify the Pd-content onto the catalyst and finally this allows an increase of the Pd-content inside a reaction system, resulting in a higher activity without increasing mass of catalyst.

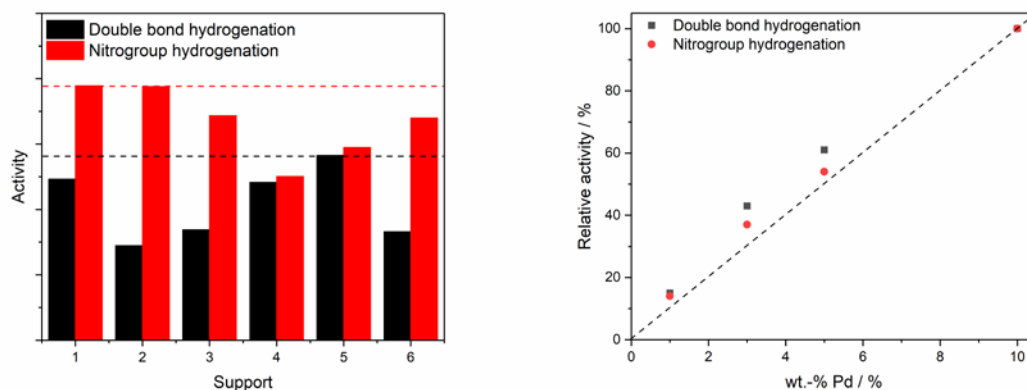


**Fig. 1:** Influence on the activity in the hydrogenation of a double bond or nitro group: Using different supports with 5%Pd/support (left) and using different Pd-loadings (right).

Finally, if the catalyst is deactivated and separated from the reaction mixture, we close the loop and recover the precious metal.

## References

- [1] O. Deutschmann, H. Knözinger, K. Kochloefl, T. Turek, in *Ullmann's Encyclopedia of Industrial Chemistry*, Wiley-VCH Verlag GmbH & Co. KgaA, **2000**.
- [2] M. Poliakoff, P. Licence, *Nat.* **2007**, *450*, 810-812.

\*Hendrik.Spod@heraeus.com

# Synthesis of perovskites-like PbBiO<sub>2</sub>I/GO composites enhanced visible-light-driven photocatalytic activity

*Fu-Yu Liu, Yong-Ming Dai, Chiing-Chang Chen\*, Department of Science Education and Application, National Taichung University of Education, Taichung 403, Taiwan, ROC*

A novel PbBiO<sub>2</sub>I/Graphene oxide (GO) heterostructure photocatalyst was synthesized successfully by hydrothermal technique using PbBiO<sub>2</sub>I as the starting material for the first time. The composition and morphologies of the composites were controlled by adjusting the experimental conditions: the reaction pH value, temperature, and molar ratio. The samples were characterized using XRD, FE-SEM-EDS, HR-TEM, XPS, DR-UV-vis, BET, PL, EPR, and UPS. These as-prepared samples were subjected to the photocatalytic degradation of Crystal Violet (CV) under visible light irradiation. Under the optimal synthesized conditions, PbBiO<sub>2</sub>I/GO composites showed greatly enhanced photocatalytic performance in PbBiO<sub>2</sub>I composites. Additionally, the rate constant values of PbBiO<sub>2</sub>I/GO composites are obtained as the maximum degradation rates of 0.1807 h<sup>-1</sup> by using the first-order linear fit of the data, which are much higher than the PbBiO<sub>2</sub>I. The enhanced photocatalytic activity can be attributed to the effective separation of photo-generated carriers driven by the photoinduced potential difference generated at these heterostructures interface, transfer of photo-generated electrons through the GO skeleton and favorable well-aligned straddling band-structure from the PbBiO<sub>2</sub>I/GO. The possible photodegradation mechanisms was proposed and discussed in this study. Overall, this work may provide a facile way to synthesize the highly efficient PbBiO<sub>2</sub>I/GO composites photocatalysts with promising applications in environmental pollution and control.

**Figure 1** shows the XRD patterns of the as-prepared samples; the patterns clearly show the existence of the composites, PbBiO<sub>2</sub>I/GO. All the samples as-prepared contain PbBiO<sub>2</sub>I phase (JCPDS 38-1007) and GO. **Figure 2** displays that PbBiO<sub>2</sub>I/GO are composed of different-size layers, consistent with the TEM observations. In addition, the EDS spectrum shows that the sample contains the elements of Bi, Pb, I, O, and C. In **Figure 2(d)**, the HRTEM image demonstrates that two sets of lattice images are obtained with d-spacings of 0.3013 nm, corresponding



to the (103) plane of  $\text{PbBiO}_2\text{I}$ , which is in strong agreement with the XRD results. The results suggest that the  $\text{PbBiO}_2\text{I}/\text{GO}$  phases have been formed in the composites, which are favorable for the separation of photoinduced carriers, yielding high photocatalytic activities.

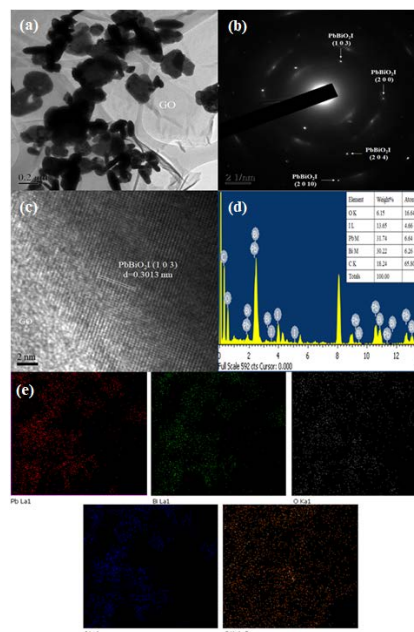
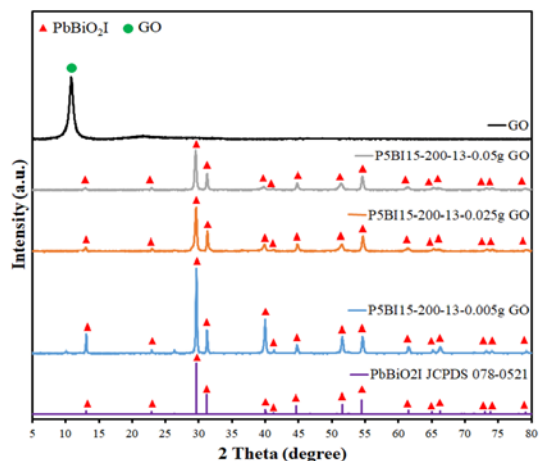


**Figure 1.** XRD patterns of as-prepared samples under  $\text{PbBiO}_2\text{I}$  with different GO grams, pH = 13 values at reaction temperature 200 °C and reaction times 12 h.

**Figure 2.** (a) FE-TEM images, (b) SAD, (c) HR-TEM, (d) EDS of  $\text{PbBiO}_2\text{I}/\text{GO}$  (P5BI15-200-13-12-0.05g GO), and (e) mapping sample by the hydrothermal autoclave method.

The durability of  $\text{PbBiO}_2\text{I}/\text{GO}$  is evaluated by recycling the used catalyst. After each cycle, the catalyst is collected by centrifugation. No apparent loss is observed in the photocatalytic activity when CV is removed in the 3rd cycle; even during the sixth run, the decline in the photocatalytic activity is 7.0%. The used  $\text{PbBiO}_2\text{I}/\text{GO}$  is also examined by XRD, and no detectable difference is observed between the as-prepared and the used samples; hence,  $\text{PbBiO}_2\text{I}/\text{GO}$  has good photostability.

## References

- [1] Wang, B.; Di, J.; Liu, G.; Yin, S.; Xia, J.; Zhang, Q.; Li, H. *J. Colloid & Interface Sci.* **2017**, *507*, 310-322.
- [2] Wang, B.; Di, J.; Zhang, P. F.; Xia, J. X.; Dai, S.; Li, H. M. *Appl. Catal. B: Environ.* **2017**, *206*, 127-135.
- [3] Liu, F. Y.; Jiang, Y. R.; Chen, C. C.; Lee, W. W. *Catal. Today*, **2018**, *300*, 112-123.
- [4] Liu, F. Y.; Lin, J. H.; Dai, Y. M.; Chen, C. C. *Catal. Today*, **2018**, *314*, 28-41.

# Preparation of g-C<sub>3</sub>N<sub>4</sub>/Bi<sub>2</sub>MoO<sub>6</sub> and Their Photocatalytic Degradation for RhB

Mingzhu xia\*, Hongjing Zhen

School of Chemical Engineering, Nanjing University of Science and Technology  
Nanjing 210094, Jiangsu (China)

\*863271491@qq.com

**Introduction** In recent years, bismuth-based semiconductors have caused a wave in the field of photocatalysis due to their special electronic structure. Among them, Bi<sub>2</sub>MoO<sub>6</sub> has potential values in photocatalysis due to its special electronic layer structure and appropriate band gap. However, there are still some problems such as low utilization of visible light and high recombination rate of photogenerated electron-hole pairs. G-C<sub>3</sub>N<sub>4</sub> polymer semiconductors have excellent catalytic properties due to their good stability, appropriate bandgap energy and very negative conductive bands. And they are widely used in building heterojunction structures [1]. In this paper, flexible cotton flocculent g-C<sub>3</sub>N<sub>4</sub>/Bi<sub>2</sub>MoO<sub>6</sub> (GBM) composites were prepared for the first time. The results show that the composites have strong visible light absorption and high light-induced carrier migration rate.

**Materials and Methods** GBM materials were obtained by solvothermal method. Nanosheet of g-C<sub>3</sub>N<sub>4</sub> colloidal solution was prepared by ultrasonic based on bulk g-C<sub>3</sub>N<sub>4</sub>, which was synthesized with urea as precursor. G-C<sub>3</sub>N<sub>4</sub> colloidal solution was reacted with Bi<sub>2</sub>MoO<sub>6</sub> precursor solution via solvothermal method.

## Results and Discussion

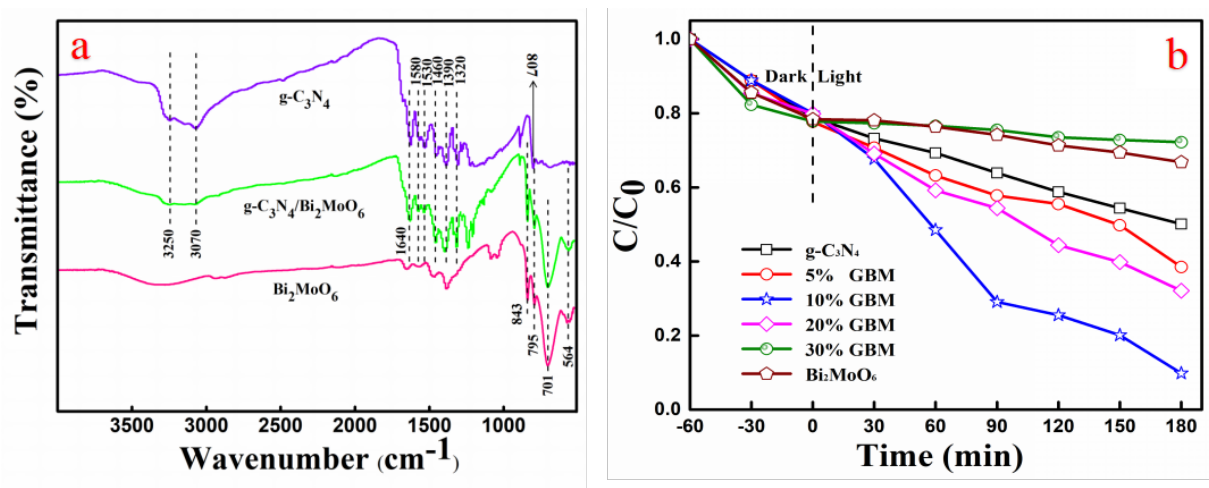


**Figure 1.** The FT-IR patterns of the g-C<sub>3</sub>N<sub>4</sub>, Bi<sub>2</sub>MoO<sub>6</sub>, 10%-GBM composites (a) and the effect of photocatalytic degradation for RhB under visible light radiation (b)

Figure 1(a) shows the Fourier transform infrared (FT-IR) patterns of the g-C<sub>3</sub>N<sub>4</sub>, Bi<sub>2</sub>MoO<sub>6</sub>, 10%-GBM composites. The pure Bi<sub>2</sub>MoO<sub>6</sub> shows Bi-O bond vibration at

564  $\text{cm}^{-1}$ , Mo-O-Mo bond vibration at 701  $\text{cm}^{-1}$  and Mo-O bond stretching vibration at 795 and 843  $\text{cm}^{-1}$ . The absorption peaks at 1320, 1390, 1460, 1530 and 1580  $\text{cm}^{-1}$  can be attributed to the stretching vibration mode of aromatic C-N, 1640  $\text{cm}^{-1}$  is C=N stretching vibration and 3070 and 3250  $\text{cm}^{-1}$  are coincide with the stretching vibration of NH or  $\text{NH}_2$  at the end of the aromatic defect [2]. Through hydrothermal recombination, we found that the compound of 10%-GBM has not only Bi-O, Mo-O-Mo and Mo-O bond stretching vibration in  $\text{Bi}_2\text{MoO}_6$ , but also absorption peaks in the range of 800-3500  $\text{cm}^{-1}$  in  $\text{g-C}_3\text{N}_4$ . The effect of photocatalytic degradation for RhB under visible light radiation ( $\lambda \geq 420 \text{ nm}$ ) is shown in Figure 1(b). It shows that RhB is almost completely degraded by 10%-GBM composite after 180 min. It proves that the as-prepared 10%-GBM composite is more efficiently than pure catalysts.

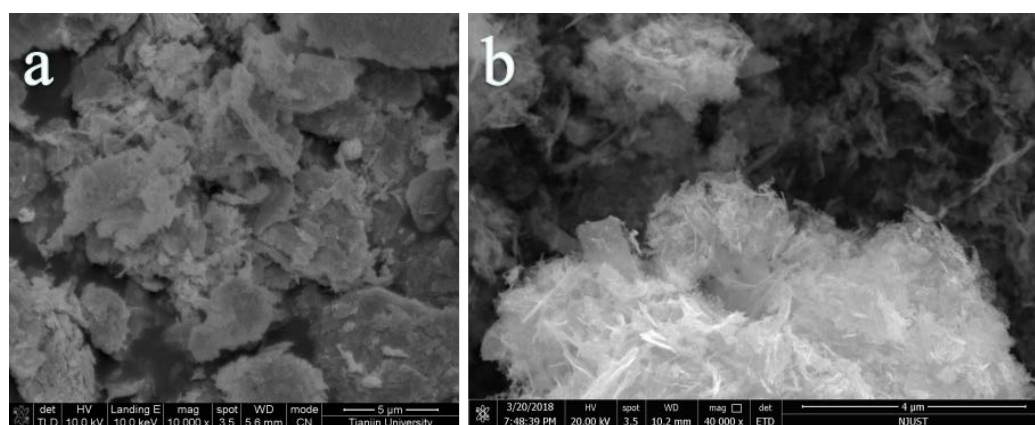


**Figure 2.** The SEM images of the as-prepared  $\text{Bi}_2\text{MoO}_6$  (a) and 10%-GBM composites (b)

The SEM images of catalysts are shown in Figure 3. It is obvious that  $\text{Bi}_2\text{MoO}_6$  has irregular lamellar aggregation morphology with hard texture and large particle size (Fig.2a). When 10%  $\text{g-C}_3\text{N}_4$  was doped, the morphology of the material changed dramatically, and a flexible cotton-like heterojunction semiconductor material was presented (Fig.2b). Compared with pure  $\text{Bi}_2\text{MoO}_6$ , the particle size of the composites is smaller, and the flexible cotton flocculent heterojunction provides more active sites and larger specific surface area for photocatalytic RhB dye wastewater, which helps to improve the photocatalytic activity.

## References

- [1] J. E. Lowther, Physical Review B 1999, 59, 11683-11686.
- [2] B. Hu, F. Cai, T. Chen, M. Fan, C. Song, X. Yan and W. Shi, Acs Appl Mater Interfaces 2015, 7, 18247-18256.

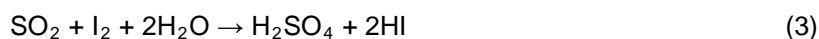
# Enhanced Lifetime of Supported Pt Catalysts in SO<sub>3</sub> Decomposition for Solar Thermochemical Water Splitting Cycles

*Alam S.M. Nur, Satoshi Hinokuma, Hiroshi Yoshida, Masato Machida*

*Kumamoto University, Kumamoto, Japan*

## Introduction

Thermochemical water-splitting cycles using concentrated solar radiation as a heat source are promising large-scale and cost-effective solar hydrogen production from water. A representative candidate is the sulfur–iodine process, which is a cycle system consisting of the following three reactions:



The final step of (1) involves the decomposition of SO<sub>3</sub> into SO<sub>2</sub> + 1/2O<sub>2</sub>, which requires very high temperatures (≥800 °C). In order to drive this reaction using a heat fluid (~600 °C) supplied from solar collectors, the development of active and stable SO<sub>3</sub> decomposition catalysts that work at moderate temperatures is urgently required. Conventionally, Pt-based catalysts are known as promising candidates, although their catalytic property and stability in such a moderate temperature range have not been studied in detail. Herein, we report that a Pt catalyst supported on Ta<sub>2</sub>O<sub>5</sub> is much more stable than conventional Pt catalysts for the SO<sub>3</sub> decomposition reaction at 600 °C. Among possible SO<sub>3</sub>-resistant metal oxides (TiO<sub>2</sub>, Nb<sub>2</sub>O<sub>5</sub>, Ta<sub>2</sub>O<sub>5</sub>, and WO<sub>3</sub>), which were studied comparatively as support materials for Pt catalysts, the long-term stability of Pt/Ta<sub>2</sub>O<sub>5</sub> for the SO<sub>3</sub> decomposition reaction at 600 °C was demonstrated over a total of 1,800 h.

## Results and Discussion

The long-term stability of Pt catalysts under harsh reaction environments is very important for practical applications. The catalyst-stability tests were performed at  $T = 600$  °C and  $\text{WHSV} = 11$  g-H<sub>2</sub>SO<sub>4</sub> g-cat<sup>-1</sup> h<sup>-1</sup>. Fig. 1 plots the relative activity as a function of time-on-stream. Because the initial SO<sub>3</sub> conversions of these catalysts are similar, the relative activities of the different catalysts can be compared directly. Clearly, the extent of deactivation is strongly dependent on the support material and decreases in the sequence WO<sub>3</sub> > Nb<sub>2</sub>O<sub>5</sub> > TiO<sub>2</sub> > Ta<sub>2</sub>O<sub>5</sub> [1]. Among the materials tested, Pt/Ta<sub>2</sub>O<sub>5</sub> shows no noticeable deactivation over 1,800 h of continuous use,

and the overall deactivation after 1,000 h is only 1.5% of the initial SO<sub>3</sub> conversion. This is lower than the activity loss of Pt/TiO<sub>2</sub> (approximately 4% per 1,000 h). The deactivation observed for Pt/Ta<sub>2</sub>O<sub>5</sub> is less than 3% after 1,800 h of the reaction.

The deactivation kinetics of SO<sub>3</sub> decomposition over Pt/Ta<sub>2</sub>O<sub>5</sub> was studied using a simple power-law equation,

$$-r_d = -\frac{da}{dt} = -k_d a^d$$

where  $r_d$  and  $k_d$  are the rate of deactivation and rate constant for deactivation, respectively, and  $d$  is the order of deactivation. The relative catalyst activity ( $a$ ) is expressed as the rate of reaction over the deactivated catalyst with time ( $r_t$ ) divided by that over the fresh catalyst ( $r_0$ ). Assuming  $d = 2$  with initial limits of  $t = 0$  and  $a = 1$ ,

simulated deactivation curves with different  $k_d$  values were obtained (Fig.2). Comparison with the observed activity data suggests that  $k_d$  would be approximately  $1.5 \times 10^{-5} \text{ h}^{-1}$  and the estimated deactivation after 1 year (~8,000 h) is nearly 10%.

This is superior to the estimated deactivation for Pt/TiO<sub>2</sub> (> ~25%) in our previous study [2].

The higher stability of is due to the abundance of metallic Pt, which favors the dissociative adsorption of SO<sub>3</sub> and the smooth desorption of the products (SO<sub>2</sub> and O<sub>2</sub>). This feature is in accordance with a lower activation energy and a less negative partial order with respect to O<sub>2</sub>. Pt sintering under the harsh reaction environment was suppressed compared to that observed with the use of other support materials.

The higher stability of is due to the abundance of metallic Pt, which favors the dissociative adsorption of SO<sub>3</sub> and the smooth desorption of the products (SO<sub>2</sub> and O<sub>2</sub>). This feature is in accordance with a lower activation energy and a less negative partial order with respect to O<sub>2</sub>. Pt sintering under the harsh reaction environment was suppressed compared to that observed with the use of other support materials.

This feature is in accordance with a lower activation energy and a less negative partial order with respect to O<sub>2</sub>. Pt sintering under the harsh reaction environment was suppressed compared to that observed with the use of other support materials.

## References

- [1] A. S. M. Nur, T. Matsukawa, E. Funada, S. Hinokuma, M. Machida, ACS Appl. Energy Mater. 1 (2018) 744.
- [2] A. S.M. Nur, T. Matsukawa, S. Hinokuma, M. Machida, ACS Omega 2 (2017) 7057.

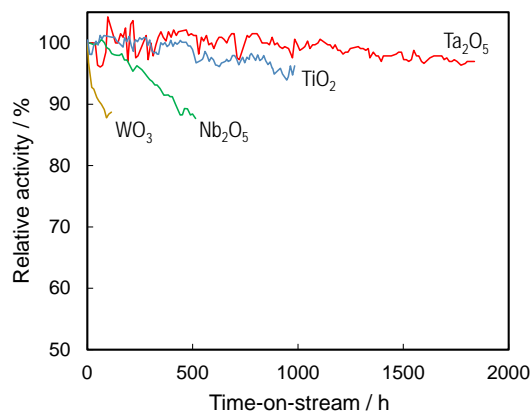


Fig.1 Catalyst stability tests at 600 °C for supported Pt catalysts [1]. WHSV = 11 g-H<sub>2</sub>SO<sub>4</sub> g-cat<sup>-1</sup> h<sup>-1</sup>.

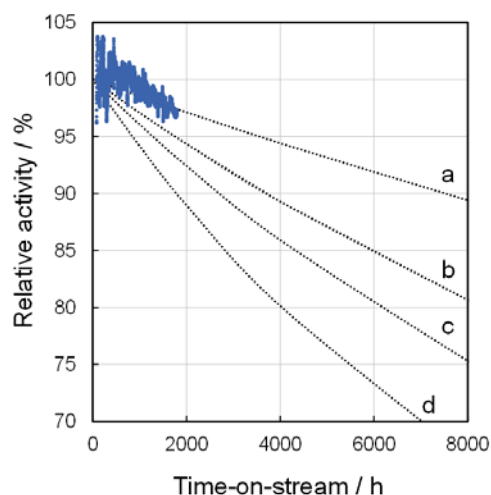


Fig.2 Deactivation rate analysis for Pt/Ta<sub>2</sub>O<sub>5</sub> at 600 °C [1]. The dotted lines are drawn using the kinetic expression with the deactivation rate constants,  $k_d =$  (a)  $1.5 \times 10^{-5}$ , (b)  $3.0 \times 10^{-5}$ , (c)  $4.1 \times 10^{-5}$ , and (d)  $6.2 \times 10^{-5} \text{ h}^{-1}$ .

## Can Iron Oxides Keep Up with Noble Metals in Carbon Monoxide Oxidation?

*Steffen Schlicher, Roland Schoch, Matthias Bauer, University of Paderborn, Faculty of Science, Paderborn, Germany; Christian Singer, Sven Kureti, Technical University of Freiberg, Institute of Energy Process Engineering and Chemical Engineering, Freiberg, Germany; Jürgen Gieshoff, Umicore AG & Co. KG, Hanau, Germany.*

As a consequence of ongoing industrial growth air pollution and the search for new ways of counteraction have never been a more relevant and yet challenging topic in scientific research. By the use of petrol and diesel engines in vehicles as well as raw materials processing

industry, especially in the combustion of fossil and biological materials, every year large amounts of nitric oxides ( $\text{NO}_x$ ), incompletely burnt hydrocarbons, carbon monoxide and carbon dioxide are emitted into the air. Because of its toxic effect, binding irreversibly onto haemoglobin and hence decreasing the amount of oxygen

transported through blood<sup>[1]</sup>, carbon monoxide and its conversion<sup>[1]</sup> to carbon dioxide play a primary role in this project. By using catalysts based on palladium, platinum or rhodium it is possible to remove CO in exhaust gases by oxidation to carbon dioxide using residuary oxygen and thus to reduce its emission into the atmosphere. Unfortunately use of noble metals is limited to low resources leading to extraordinary high and continuously increasing prices. Additionally, the harmful effect of these noble metal catalysts on the environment is still unknown and discussed controversially.

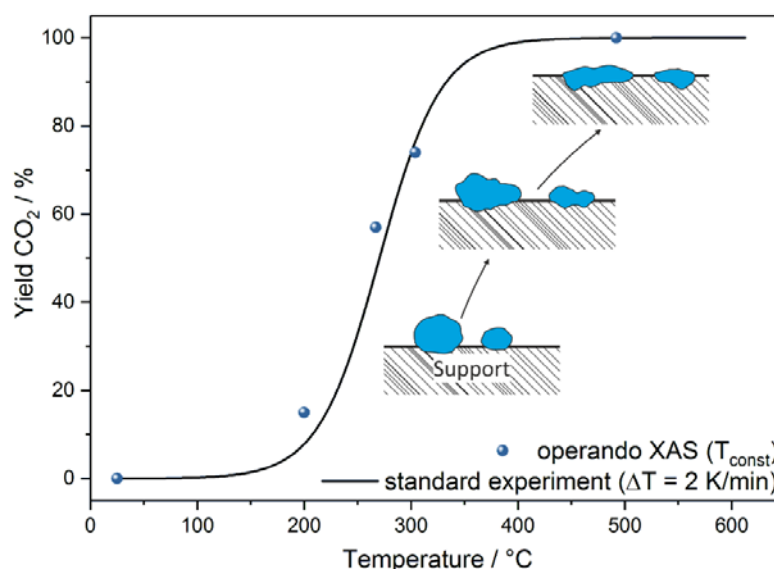


*Fig. 1: standard carbon monoxide oxidation experiment (black line) compared to static measurements during operando X-ray absorption spectroscopy (dots) and the behaviour of the isolated iron species on the support surface concluded from EXAFS analysis.*



Because of this we want to strike new paths searching for cheap and biocompatible alternatives as catalysts for carbon monoxide oxidation. In previous work it could be shown, that with the use of iron as catalytic centre it is possible to oxidise a certain amount of CO in a defined gas stream completely at moderate temperatures<sup>[2]</sup>. To compensate lower activity in comparison to noble metal catalysts, the systems based on iron have to be optimised. Such an optimisation is based on the elucidation of structure-activity correlations for a broad range of catalysts, which are tested under model conditions, as well as the determination of the reaction mechanism of carbon monoxide oxidation on iron catalysts.

The diversity of the tested catalysts presented in this contribution derives mainly from choice of support material and the metal precursor as well as the parameters applied within impregnation and calcination step. Typically  $\gamma$ -alumina is used as support and loaded with pure or pre-reduced iron(III) acetylacetonate by incipient wetness



Fig. 2: experimental setup of the self-designed XAS reactor for *in-situ* measurements at beamline P65, DESY, Hamburg.

impregnation and afterwards calcinated<sup>[3]</sup> to yield in iron oxide more or less incorporated into the support lattice. Differences in activity of the catalysts can be related to parameters like particle size of the iron species, the amount and distribution of active sites at the support surface and their accessibility as well as coordination geometry of the present iron species. To correlate

these parameters with catalytic activity in carbon monoxide oxidation and to gain more insights into the mechanism of this reaction, analytics like Brunauer-Emmett-Teller adsorption isotherme (BET), X-ray diffraction (XRD), transmission electron microscopy (TEM), diffuse reflectance UV-Vis and *in-situ* diffuse reflectance infrared Fourier transformed spectroscopy (DRUVS & DRIFTS) are carried out as well as *ex-situ* and especially *in-situ* X-ray absorption spectroscopy (XAS, fig. 1), latter performed in a self-designed XAS reactor (fig. 2).

## References

- [1] J. A. Raub, M. Mathieu-Nolf, N. B. Hampson, S. R. Thom, *Toxicology* **2000**, 145, 1-14.
- [2] R. Schoch, H. Huang, V. Schünemann, M. Bauer, *ChemPhysChem* **2014**, 15, 3768-3775.
- [3] R. Schoch, M. Bauer, *ChemSusChem* **2016**, 9, 1996-2004.

# Application of ATR-FTIR Measurements in Ceria-Based Catalytic Systems

*E. Iwanek (nee Wilczkowska)<sup>1)</sup>, Sheridan College, Brampton, Canada; L.F. Liotta<sup>2)</sup>, ISMN-CNR, Palermo, Italy; G. Pantaleo<sup>2)</sup>; P. Kaur<sup>1)</sup>; W. Raróg-Pilecka<sup>3)</sup>, Warsaw University of Technology, Warsaw, Poland; D.W.Kirk<sup>4)</sup>, University of Toronto, Toronto, Canada; J. Petryk<sup>3)</sup>; M. Gliński<sup>3)</sup>*

## Introduction

The adsorption of CO<sub>2</sub> and water vapour upon exposure of metal oxide catalysts to air can be used to probe the basic and acidic sites on their surfaces. The method of aging of magnesium oxide catalysts prior to ATR-FTIR measurements has been described by us [1]. The aim of this research is to demonstrate that the spectra obtained during ATR-FTIR measurements can be a valuable tool in the investigation of the properties of ceria-based catalytic systems.

## Experimental

The ATR-FTIR spectra were performed on a Perkin Elmer Spectrum Two instrument. For each sample four scans were collected with a resolution of 4 cm<sup>-1</sup> within the range 450 to 4000 cm<sup>-1</sup>. All measurements were repeated at least twice.

Four series of samples were studied. The first series are pure ceria supports: commercial (AnalaR, 99.9%) and those obtained from ammonium ceric nitrate (BDH, ACS reagent) via an aqueous route and thermal decomposition. The second series are catalysts comprising cobalt oxide and ceria with a different Ce:Co ratio. The third series is a set of cobalt oxide and ceria catalysts which differs in the barium content: CeCo+yBa (where y is 0 to 0.2445g per gram of catalyst). The fourth series were catalysts with gold deposited onto ceria obtained from via the aqueous route.

## Results and Discussion

The surfaces of over 20 samples of ceria-based supports and catalysts were studied using ATR-FTIR spectroscopy. The influence of the method of ceria preparation on the obtained spectra showed that the two different commercial ceria samples have spectra which are practically the same (e.g. Fig. 1a) though substantially different than the ceria obtained using other methods. The impact of ceria content in cobalt-oxide catalysts on the spectra is shown in Figure 1. Our



previous studies on Co-Ce oxide systems have shown that there is an optimal Co-Ce ratio in the catalysts for its activity in  $N_2O$  decomposition [2] and  $C_3H_8$  oxidation [3]. In the case of the former reaction, two distinct groups of catalysts were distinguished: those which did not benefit from the addition of oxygen to the inlet stream ( $x$  up to 64) and those whose activity increased upon the addition of  $O_2$ . The results of ATR-FTIR measurements also divided this set of catalysts into two groups: one type of spectra was obtained for catalysts for  $Ce_xCo$  where  $x \leq 64$  and another for higher Co loadings (Fig. 1 top and bottom panels, respectively). Similarly, the spectra of Au- $CeO_2$  catalysts whose activity was different in CO oxidation exhibited differences in some bands, whereas those with similar activity had similar spectra. The division of the fourth set of catalysts into two groups on the basis of the spectrum corresponds to the subsets in which barium cerate forms under  $NH_3$  synthesis conditions and the other in which it doesn't form.

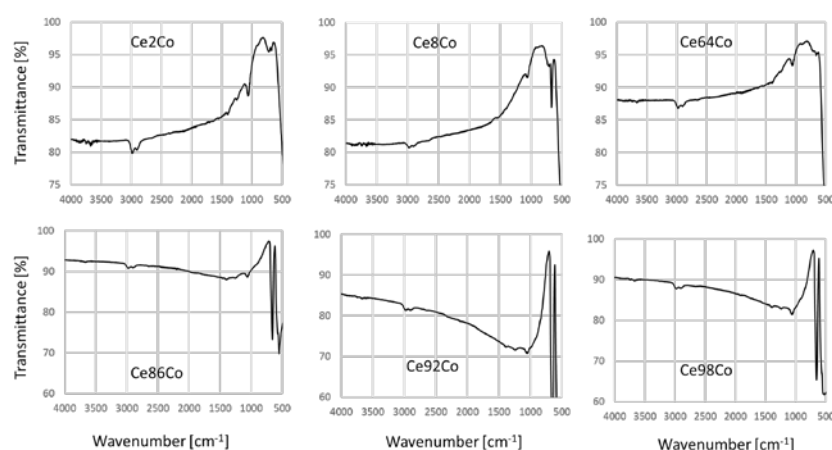


Figure 1. ATR-FTIR spectra of  $CoO_x-CeO_2$  catalysts

## Conclusions

ATR-FTIR spectra of various ceria-based systems were measured and the analysis of the data has shown that it is a technique which, in the case of ceria supports, can be useful for predicting and explaining trends in activity of the catalytic systems.

## Acknowledgements

The authors are grateful to the NSERC of Canada for grant number 523834-18.

## References

- [1] Iwanek E., Ulkowska U., Glinski M., *Surf Interface Anal.* 49 (2017) 945
- [2] Iwanek E., Krawczyk K., Petryk J., Sobczak J.W., Kaszkur Z., *Appl. Catal. B* 106 (2011) 416
- [3] Liotta L., Ousmane M., Di Carlo G., Pantaleo G., Deganello G., Marci G., Retailleau L., Giroir-Fendler A., *Appl. Catal. A* 347 (2008) 81

# Selective catalytic reduction of nitric oxide with propylene over Fe/Beta catalysts under lean-burn conditions

Hao Zhou<sup>1, \*</sup>, Meng Yao Ge<sup>1</sup>, Huishuang Zhao<sup>1</sup>, Shiguo Wu<sup>1</sup>, Meng Yu Li<sup>1</sup>, Yaxin Su<sup>2</sup>

<sup>1</sup> Changzhou Institute of Engineering Technology, Changzhou 213164, PR China

<sup>2</sup> School of Environmental Science and Engineering, Donghua University, Shanghai 201620, PR China

## Introduction

Up to now, the removal of NO<sub>x</sub> in the exhaust of diesel engine under lean-burn conditions is still a significant challenge. Selective catalytic reduction of NO<sub>x</sub> by hydrocarbons (HC-SCR) is a promising technology for reducing NO<sub>x</sub> [1, 2]. Fe-based zeolites are more attractive for HC-SCR because of their moderate activity at high temperature and better hydrothermal stability [3]. In this work, Fe/Beta catalysts were prepared by different methods used for SCR of NO by C<sub>3</sub>H<sub>6</sub>. Furthermore, a combination of characterization techniques was applied to identify active Fe species.

## Experimental

Fe/Beta catalysts were prepared by liquid ion-exchange (LIE), solid-state ion-exchange (SIE) and incipient wet-impregnation (IWI) methods. H-Beta (Si/Al<sub>2</sub>=25) and Fe(NO<sub>3</sub>)<sub>3</sub>·9H<sub>2</sub>O were used as the parent zeolite and Fe precursor, respectively. The resulting catalysts with the Fe loading of about 1.5 wt.% were denoted as Fe/Beta(LIE), Fe/Beta(SIE), Fe/Beta(IWI), respectively.

## Results and Discussion

C<sub>3</sub>H<sub>6</sub>-SCR activity tests (Fig.1) showed that the catalytic activity decreased in the following order as Fe/Beta(LIE) > Fe/Beta(IWI) > Fe/Beta(SIE). Fe/Beta(LIE) sample exhibited NO conversion >90% and N<sub>2</sub> selectivity >95% at temperature 300-450 °C. Hydrothermal durability tests showed hydrothermal aged had a slight inhibition effect at high temperatures on C<sub>3</sub>H<sub>6</sub>-SCR. At nearly the same iron content, Fe/Beta(LIE) catalyst exhibited superior catalytic activity than other catalysts, indicating that the preparation method might lead to the different distribution of iron species, which was an important factor affecting C<sub>3</sub>H<sub>6</sub>-SCR activity.

According to the percentage of Fe species and NO conversion over Fe/Beta catalysts, we correlated the content of isolated Fe<sup>3+</sup> and Fe<sub>2</sub>O<sub>3</sub> nanoparticles with the NO conversion rate at 200 °C respectively (Fig.2). It can see that NO conversion rate increased monotonically with increasing the content of isolated Fe<sup>3+</sup> species, while

the NO conversion rate decreased linearly with an increase in Fe<sub>2</sub>O<sub>3</sub> nanoparticles on Fe/Beta. In situ DRIFTS showed that more isolated Fe<sup>3+</sup> sites on Fe/Beta(LIE) would enhance the formation of the key intermediates, i.e., NO<sub>2</sub> adspecies and formate species, then led to the superior C<sub>3</sub>H<sub>6</sub>-SCR activity.

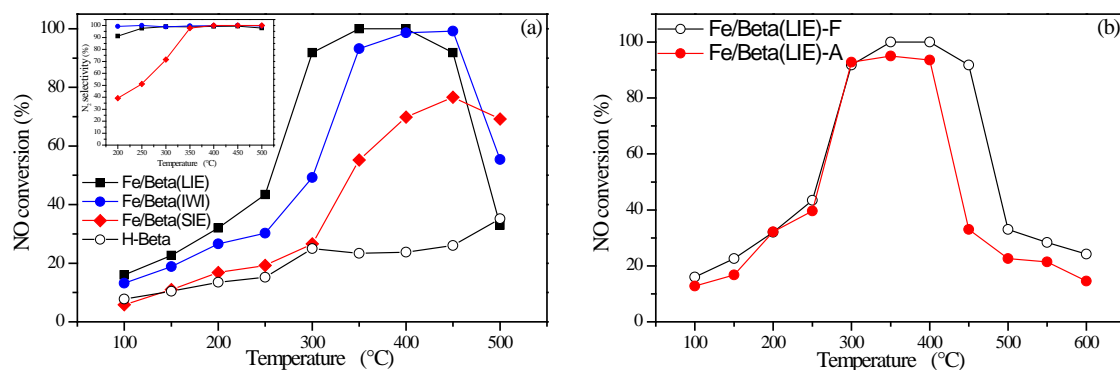


**Fig. 1.** NO conversion and N<sub>2</sub> selectivity over Fe/Beta catalysts (a) and NO conversion over the fresh and aged Fe/Beta(LIE) catalysts (b). The inlet gas mixture consisting of 0.05% NO, 0.05% C<sub>3</sub>H<sub>6</sub>, 2% O<sub>2</sub> and balance N<sub>2</sub>. GHSV=15,000 mLg<sup>-1</sup>h<sup>-1</sup>.

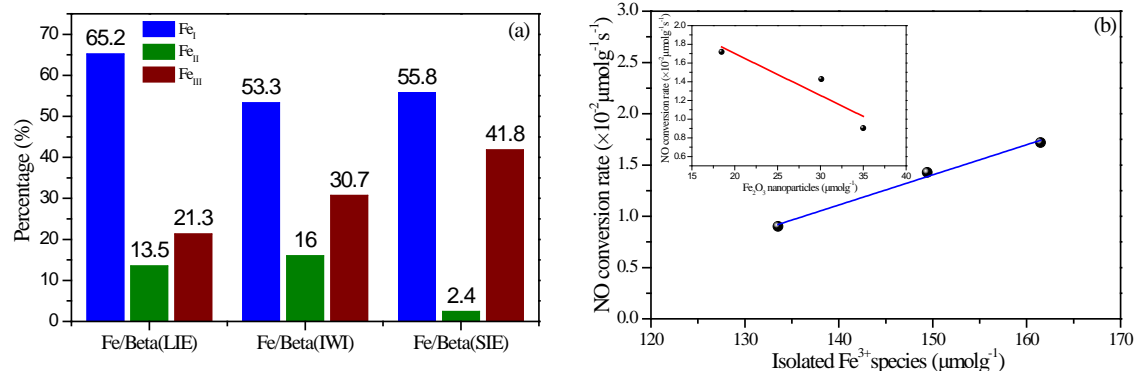


**Fig. 2.** Percentage of various Fe species over Fe/Beta catalysts prepared by different methods (I) Isolated Fe<sup>3+</sup> in tetrahedral and octahedral coordination, (II) Oligomeric Fe<sub>x</sub>O<sub>y</sub> clusters, and (III) Fe<sub>2</sub>O<sub>3</sub> nanoparticles (a), the correlations of the NO conversion rate at 200 °C with the isolated Fe<sup>3+</sup> and Fe<sub>2</sub>O<sub>3</sub> nanoparticles content (inset) on Fe/Beta catalysts (b).

## Conclusion

The selective catalytic reduction of NO with C<sub>3</sub>H<sub>6</sub> over Fe/Beta catalysts prepared by LIE, SIE and IWI methods. C<sub>3</sub>H<sub>6</sub>-SCR activity showed Fe/Beta(LIE) sample exhibited the highest catalytic activity with NO conversion >90% and N<sub>2</sub> selectivity >95% at temperature 300-450 °C. Reaction kinetics studies suggested that isolated Fe<sup>3+</sup> species were more active for NO reduction, whereas Fe<sub>2</sub>O<sub>3</sub> nanoparticles enhanced the hydrocarbon combustion in excess of oxygen. According the results of in situ DRIFTS, more isolated Fe<sup>3+</sup> sites on Fe/Beta(LIE) would enhance the formation of NO<sub>2</sub> adspecies and formate species, then led to the superior C<sub>3</sub>H<sub>6</sub>-SCR activity.

## References

- [1] H. Zhou, M. Ge, S. Wu, B. Ye, Y. Su, Fuel, 220 (2018) 330.
- [2] H. Zhou, K. Li, B. Zhao, W. Deng, Y. Su, F. Zhong, Chem. Eng. J., 326 (2017) 737.
- [3] P.S. Metkar, N. Salazar, R. Muncrief, V. Balakotaiah, M.P. Harold, Appl. Catal. B, 104 (2011) 110.

# Analysis of charge handling in g-C<sub>3</sub>N<sub>4</sub>/TiO<sub>2</sub> photocatalytic composites

U. Caudillo-Flores,<sup>1</sup> M. J. Muñoz-Batista,<sup>2</sup> R. Luque,<sup>2</sup> A. Kubacka,<sup>1</sup> M. Fernández-García,<sup>1</sup>

1) Instituto de Catálisis y Petroleoquímica, CSIC.C/Marie Curie 2, 28049-Madrid, Spain. [mfg@icp.csic.es](mailto:mfg@icp.csic.es); 2) Dpto Química Orgánica, Universidad de Córdoba, Campus de Rabanales, Edificio Marie Curie (C-3), Ctra Nnal IV-A, Km 396, E14014, Cordoba, Spain

The study of charge handling in composite systems is rather complex and, more importantly, does not usually offer a link of charge events with specific reaction steps taking place under illumination [1]. Here we study the contact between (previously prepared) Mn-promoted g-C<sub>3</sub>N<sub>4</sub> (2 wt.% Mn; ca. 15 m<sup>2</sup>g<sup>-1</sup> [2]) and TiO<sub>2</sub> (pure anatase; ca. 12 nm and 47 m<sup>2</sup>g<sup>-1</sup> [2]) prepared by impregnation followed by calcination (350 °C). Composites with 1, 2 and 4 wt. % of g-C<sub>3</sub>N<sub>4</sub> were synthesized and used in the gas-phase photo-oxidation of toluene.

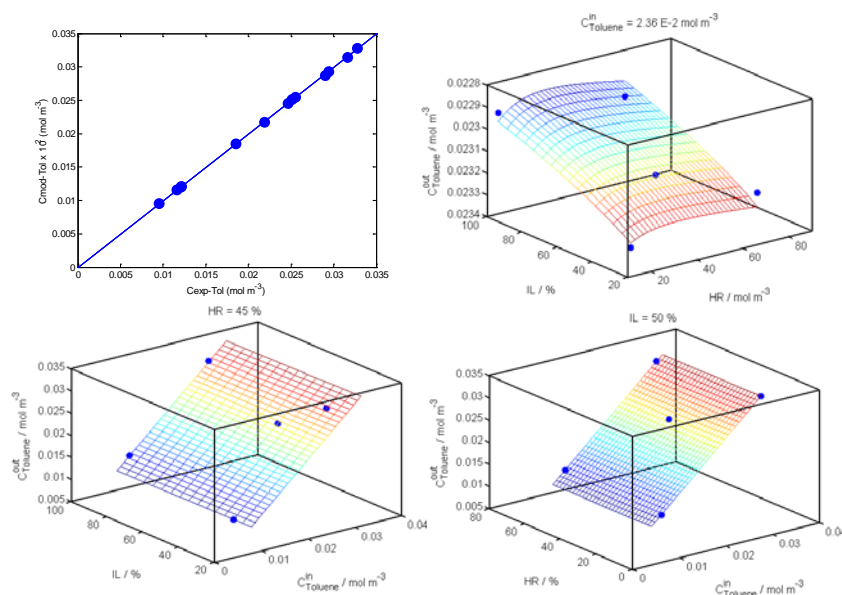


Figure 1. Parity plot between experimental and model Toluene concentrations. .3D (projection) plots of experimental (circles) and model prediction (net) of Toluene.

The overall handling of charge has been previously studied with photoluminescence (PL) and EPR [2]. To measure the effect of the charge handling in critical steps of the reaction we developed a kinetic model under a Box-Behnken experimental design using 3 factors (toluene concentration, light intensity and water content) [1]. The model considers i) that the reaction is hydroxyl-radical mediated as previously

demonstrated for titania [2]; and ii) solve toluene and products (Benzaldehyde and CO<sub>2</sub>) mass balance (set of 2 independent) differential equations at the reactor, using a kinetic model with intrinsic treatment of light (though the calculation of the superficial rate of photon absorption) [1,2]. It uses only 5 independent parameters. The fitting renders outstanding results as illustrated in Figure 1 for the toluene case. The combined fitting of the reactant and the products allows to obtaining information of the kinetic constants of hydroxyl generation and recombination. This thus measured the availability of the hydroxyl species at the surface of the materials to generate chemistry. The ratio between the kinetic rates of these two processes is included in Table 1 for a 2 wt. % material (the material presenting optimum photocatalytic performance) and reference systems. The model also yields the ratio between the kinetic constant of the hydroxyl attack to the toluene (Tol) and the initial product, benzaldehyde (Bz). This parameter can dictate the selectivity of the reaction and allows to differentiate between adsorption and kinetic effects between the main molecules (toluene and benzaldehyde) present at the catalyst surface.

Table 1. Reaction rate and Kinetic-derived information for toluene photo-oxidation.

Sample	Rate / mol m <sup>-2</sup> s <sup>-1</sup>	Ratio (OH generation / recombination)	Ratio (OH attack Tol/Bz)
Mn-2g/TiO <sub>2</sub>	3.40x10 <sup>-9</sup>	5.02x10 <sup>-7</sup>	2.01x10 <sup>-2</sup>
2g/TiO <sub>2</sub>	1.85x10 <sup>-9</sup>	2.77x10 <sup>-7</sup>	1.67 x10 <sup>-2</sup>
TiO <sub>2</sub>	0.75x10 <sup>-9</sup>	1.04x10 <sup>-7</sup>	0.87 x10 <sup>-2</sup>

A linear relationship (correlation coefficient > 0.99) is presented between the reaction rate and the first ratio of Table 1 demonstrating that OH radicals are involved in the limiting steps of the reaction and, at the same time, validating the model. They show that the Mn-g / TiO<sub>2</sub> interface boosts activity by 4.5 times with respect to the components by direct effect in OH formation. The second ratio of Table 1 interprets the selectivity (Bz vs. CO<sub>2</sub>) and quantify the importance of competitive adsorption and kinetic hole attack under reaction conditions. Comparison with adsorption measurements, PL and EPR results indicated the OH radical attack to Bz is two order of magnitude less prone and controls selectivity in the titania-based composites.

## References

- [1] M.J. Muñoz-Batista, et al., *Chem. Soc. Rev.* (2018) DOI: 10.1039/c8cs00108a.  
 [2] M.J. Muñoz-Batista, et al., *Catal. Sci. Technol.* 4 (2014) 2006; *Appl. Catal. B* 203 (2017) 663.

## **Building-up of a UV-Vis-NIR Broadband g-C<sub>3</sub>N<sub>4</sub>/W-TiO<sub>2</sub> Material**

A. Kubacka,<sup>1</sup> M.J. Muñoz-Batista,<sup>1</sup> M. Ferrer,<sup>1</sup> M. Fernández-García,<sup>1</sup>

1) Instituto de Catálisis y Petroleoquímica, CSIC.C/Marie Curie 2, 28049-Madrid,  
Spain. mfg@icp.csic.es

Titania materials have been used for purification and disinfection of water but one main limitation is the electromagnetic range that can be used to excite such (titania-based) materials. Here we dope titania with tungsten and introduce carbon nitride at the surface of the materials to overcome such limitation [1]. Using this approach, here we provide evidence that the joint use of both tungsten and carbon nitride renders a strong synergistic effect in the disinfection capability of the titania-based materials, covering a UV-Visible-nearIR range of useful photons of the sun. The titania (sample TiO<sub>2</sub>) precursor was prepared by microemulsion, doped with a 15 at. % W (cationic basis; sample WTiO<sub>2</sub>), and calcined at 450 °C for 2h [1]. The g-C<sub>3</sub>N<sub>4</sub> material was obtained by calcination (550 °C, 2h) of melamine followed by physical separation of the more exfoliated part by ultrasonication for 4 h [1]. The g-C<sub>3</sub>N<sub>4</sub> was deposited (2 wt. %) onto TiO<sub>2</sub> and WTiO<sub>2</sub> by wetness impregnation and dried (100 °C, 12 h). Titania displays a surface area of 77 m<sup>2</sup> g<sup>-1</sup>, with an anatase particle size of ca. 13 nm and a band gap energy of 3.04 eV. Tungsten increases area (115 m<sup>2</sup> g<sup>-1</sup>) and decrease anatase particle size (8.8 nm) with no effect on band gap, although extend light absorption up to the nearIR range due to presence of W-surface species. g-C<sub>3</sub>N<sub>4</sub> incorporation does not affect all these physico-chemical parameters.

The activity of the catalysts (0.6 g L<sup>-1</sup>) was essayed using a Gram-positive (*S. Aureus*) and a Gram-negative (*E. coli*) bacterium. Figure 1 shows data for *E. coli* inactivation. Blank experiments without catalysts demonstrate the little effect produced by light itself irrespective of the excitation wavelength. Dark experiments (not shown) render a maximum decrease of ca. 0.2 log units in the time frame of Figure 1. The three panels of Figure1 correspond to illumination with pure UV, visible and nearIR illumination. The latter is representative for results obtained with excitation above ca. 500 nm. Catalysts show a strong dependence of the wavelength. Under UV radiation we observe that TiO<sub>2</sub>, g-C<sub>3</sub>N<sub>4</sub>, and WTiO<sub>2</sub> do not display marked differences among them. However, the presence of carbon nitride boots activity significantly in composites. The two composite samples display ca. 4 log units reduction in ca. 50 min. For visible excitation (up to ca. 500 nm) we observe

differences among the three reference samples, being titania the most active. Our titania is active in the visible (nearUV) region due to its nanostructure and corresponding defects states [2]. Importantly, both composite materials are more active (as under UV) than the references but in this case they do show differences. The g-WTiO<sub>2</sub> is significantly more active than g-TiO<sub>2</sub>, by 3 log units (in ca. 50 min). Finally, above 500 nm only the g-WTiO<sub>2</sub> sample shows disinfection capability. The doping of the anatase reference renders a system displaying photoluminescence (PL) intensity below the reference anatase, irrespective of the illumination wavelength. This clearly shows that W presence decrease charge carrier recombination for all excitation wavelengths. The combination of g-C<sub>3</sub>N<sub>4</sub> and bare or W-doped anatase drives to a more complex behavior in terms of charge de-excitation. Under UV the PL intensity of composite systems is in between the two reference materials, a fact interpreted as if the holes of the carbon nitride and the electrons of anatase annihilates. This drives to an efficient Z-scheme charge separation under UV. Under visible light it appears that electrons are transferred from the g-C<sub>3</sub>N<sub>4</sub> component to anatase, again facilitating the separation of charge. Both processes favor photo-killing activity in the g-TiO<sub>2</sub> and g-WTiO<sub>2</sub> materials for excitation wavelengths below 500 nm. Above ca. 500 nm however the g-TiO<sub>2</sub> (and corresponding reference systems) does/do not show significant photo-killing activity. Nevertheless, the g-WTiO<sub>2</sub> does show important activity (Figure 1). The broad plasmon resonance associated with W allows electrons (produced directly in a surface WO<sub>3-x</sub> phase –detected and characterized with Raman) to have increasing energy with respect to the excitation energy, facilitating the photo-killing process.

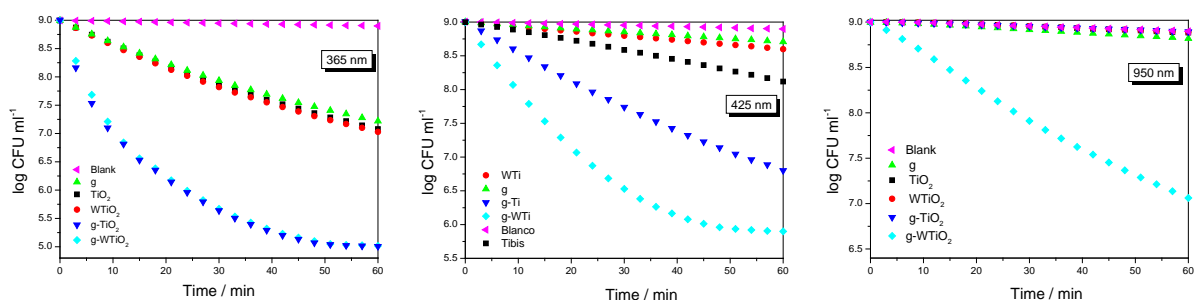


Figure 1. Time of course of the *E. coli* inactivation in presence of the samples.

## References

- [1] (a) A. Kubacka, M.J. Muñoz-Batista M. Fernández-García, Catal. Sci. Technol. 4 (2014) 2006-2015; (b) ibid Appl. Catal. B 128 (2018) 113-129.  
 [2] (a) Z. Zhang, B. Dong, Adv. Mater. 29, (2017) 1606688; (b) A. Kubacka, M. Muñoz-Batista, M. Ferrer, M. Fernández-García, Appl. Catal. B 140–141 (2013) 680– 690.

# Reaction mechanism of nitrite hydrogenation on Pd catalyst:

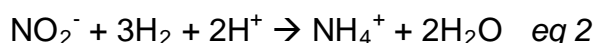
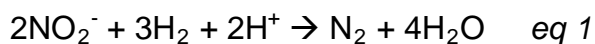
## Extreme variation in reaction orders

*Pengyu Xu; Shilpa Agarwal; Leon Lefferts*

*Catalytic Processes and Materials group, Faculty of Science and Technology,  
MESA+ Institute for Nanotechnology, University of Twente, PO Box 217, 7500 AE  
Enschede, The Netherlands*

### Abstract:

Nitrate and nitrite in drinking water are potential human health hazards that decrease the oxygen-carrying capacity of blood. Catalytic denitrification, converting nitrite selectively to nitrogen (eq 1), is a promising solution if the yield of ammonia (eq 2) can be minimized. Thorough knowledge on the kinetics is therefore clearly required. Previous work in our lab suggested competitive adsorption of  $\text{NO}_2^-$  and  $\text{H}_2$  [1,2] whereas no kinetic data are available in literature supporting this.



Palladium on  $\gamma\text{-Al}_2\text{O}_3$  catalyst was synthesized via wet impregnation method. The kinetic experiments were performed in a very wide window of nitrite (0.3 – 10 mM) and hydrogen (0.01 – 0.8 bar) concentrations in an isothermal semi-batch slurry reactor operating at atmospheric pressure. Reduction of nitrite proceeds rapidly with high selectivity to  $\text{N}_2$  using continuous hydrogen gas flow in the presence of  $\text{CO}_2$  (10 % v/v) acting as a pH buffer to prevent pH variation. Despite the very high intrinsic activity, mass transfer limitation was prevented by using extremely small catalyst support particles (below 20  $\mu\text{m}$ ).

Based on the kinetic study, hydrogen and nitrite orders are obtained in a wide hydrogen and nitrite concentration range. Figure 1 shows an overview of the orders in hydrogen and nitrite in different concentration regimes. Clearly, the orders in hydrogen and nitrite are strongly influenced when varying hydrogen concentrations whereas nitrite concentration has a much weaker effect. Surprisingly, at low hydrogen pressure (0.01 – 0.2 bar), we observe significantly high order of 2 in hydrogen and a negative order (around -0.5) in nitrite, independent of the nitrite concentration. This confirms that nitrite and hydrogen adsorb competitively on Pd.



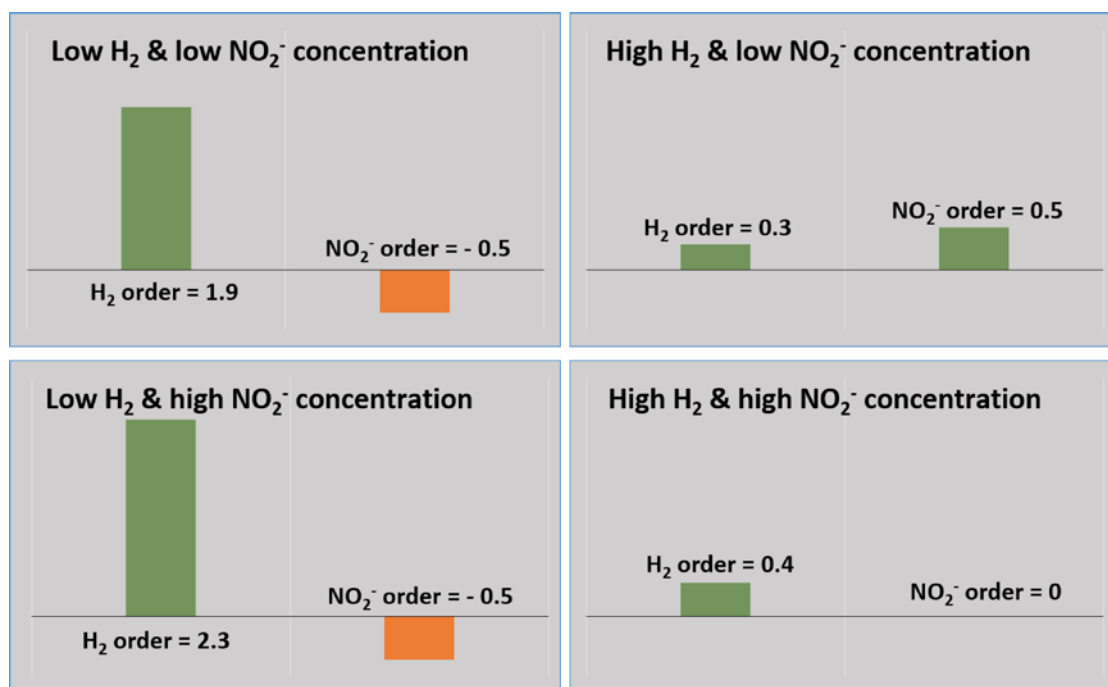


Figure 1. Orders in hydrogen and nitrite in different hydrogen (0.01 – 0.8 bar; 0.01 – 0.6 mM) and nitrite (0.3 – 10 mM) concentration regimes

Based on the results and literature reports, we propose the reaction mechanism for nitrite hydrogenation in Figure 2. Furthermore, this mechanism is used to obtain a Langmuir-Hinshelwood rate equation resulting in reaction orders in good agreement with our experimental findings. The high order in H<sub>2</sub> suggests that adsorbed H is not only involved in the rate determining step (R.D.S.), but is also involved in three pre-equilibria elementary steps that determine the concentration of N<sub>ads</sub> in the R.D.S.

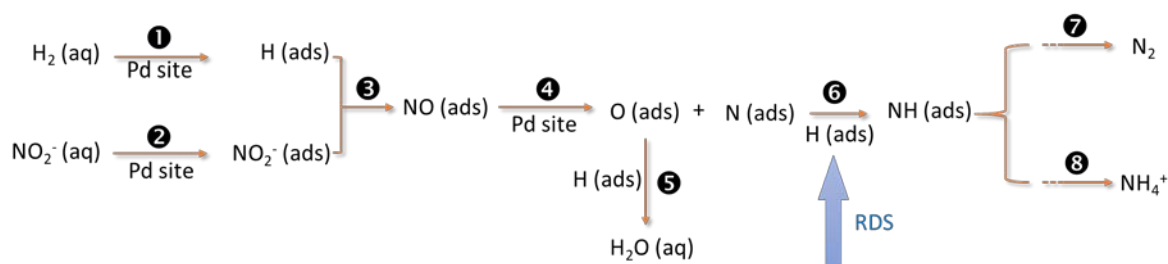


Figure 2. Reaction mechanism of nitrite hydrogenation over Pd/γ-Al<sub>2</sub>O<sub>3</sub> catalyst

## References

- [1] R.S. Postma, R. Brunet Espinosa, L. Lefferts, Competitive Adsorption of Nitrite and Hydrogen on Palladium during Nitrite Hydrogenation, (2018). doi:10.1002/cctc.201800523.
- [2] R. Brunet Espinosa, D. Rafieian, R.G.H. Lammertink, L. Lefferts, Carbon nano-fiber based membrane reactor for selective nitrite hydrogenation, Catal. Today. 273 (2016) 50–61. doi:http://dx.doi.org/10.1016/j.cattod.2016.02.057.

# Oscillating CO over Ni: Experiment and Modelling

*V. Yu. Bychkov, M.M. Slinko, V.N. Korchak Institute of Chemical Physics, Moscow, Russia; A.G. Makeev, N.V. Peskov Faculty of Computational Mathematics and Cybernetics, Lomonosov Moscow State University, Moscow, Russia*

## Introduction

CO oxidation is one of the most studied reactions due to its importance to both automotive catalysis and removal of trace CO in hydrogen streams. The well known oscillations during CO oxidation over Pt, Pd, Rh, Ir and Ru catalysts were observed in the oxygen excess. No oscillations during CO oxidation over Ni has been observed yet. In this work we discovered the oscillations during CO oxidation on Ni in the CO excess, while all other catalysts produced kinetic oscillations in the oxygen excess. The goal of the present work is to reveal the origin of CO oscillating behavior over Ni and to create a first mathematical model, generating oscillations under reducing conditions.

## Experimental

Catalytic experiments were carried out in a tubular quartz flow-through reactor (i.d. 6 mm), operated at atmospheric pressure. The reactor was inserted into a furnace which allowed observation and recording of the state of the Ni foil surface by a photo-video camera Canon EOS 70D. Simultaneously the reactants and products concentrations were measured by mass spectrometer Pfeiffer, OmniStar GSD 301.

## Results

Regular periodic oscillations during CO oxidation over the Ni foil were observed in the temperature range 570-630 °C for the reactant mixture containing 40% CO and 10% O<sub>2</sub> in He. The region of oscillations was not large and was bounded with the lower and upper explosions limits of CO in oxygen. Fig.1 demonstrates the oscillations of the gas phase concentrations and temperature variation at furnace temperature of 590 °C. The reaction rate oscillations were accompanied by synchronous variations of color changes of the Ni foil. The video films will be presented, showing that the CO oxidation rate and the oscillation waveform were strongly affected by the spatiotemporal dynamics and the movement of the waves corresponding to the surface reduction (light color) and the surface oxidation (dark color).

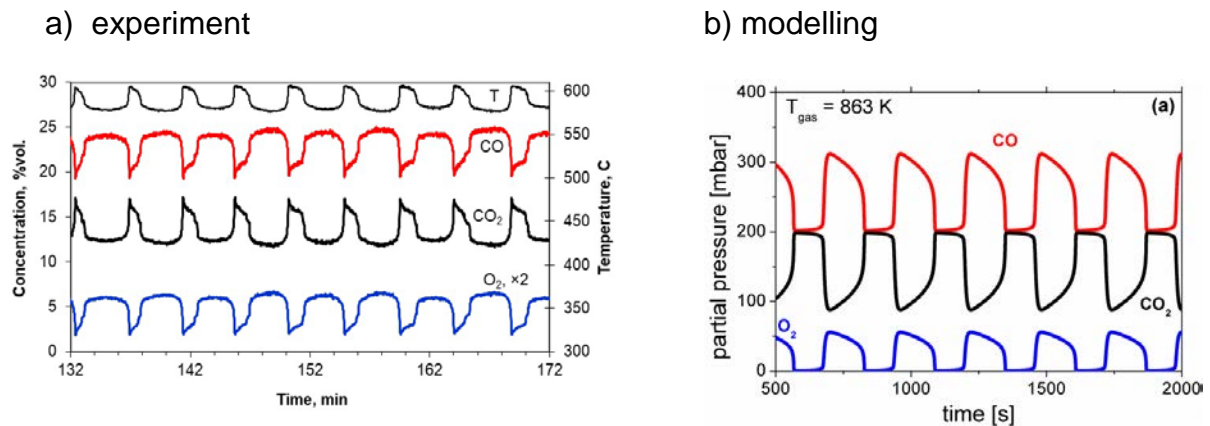


Fig.1. Experimental and simulated variations of gas concentrations at 863 K.

### Discussion and modelling

The periodic variation of oxygen imbalance and synchronous variation of the colour changes during the oscillations indicated that the origin of the observed oscillations was closely connected with the reversible oxidation of Ni to NiO. The well-known Sales-Turner- Maple (STM) model, describing oscillations during CO oxidation over Pt group metals can simulate oscillations only in O<sub>2</sub> excess [1]. Therefore, the new model was developed for the oscillatory behaviour of CO oxidation in CO excess. The main feature of the model is the CO adsorption into the precursor state over filled surface sites with a small value of Kisliuk parameter. Similar to STM model oscillations originate due to the Ni oxidation in the high activity state and the Ni reduction in the low activity state. In contrast with the STM-model the oscillations under reducing conditions in the new model proceed on a surface with a very low adsorbed oxygen coverage. The model successfully simulates the dependence of the oscillations waveform and period upon the temperature.

### Conclusions

For the first time the oscillatory behaviour during CO oxidation over Ni has been discovered. The waveform and period of oscillations were determined by the fronts of propagation of the reduced and oxidised states of Ni. The first mathematical model, producing the oscillatory behaviour due to the periodic oxidation-reduction processes in the CO excess has been developed.

### Acknowledgments

This work was supported by the Russian Science Foundation (grant N 17-13-01057).

### References

[1] B.C. Sales, J.E. Turner, M.B. Maple, Surf. Sci. 114 (1982) 381–394.

# Support effects in $K_2CO_3$ on carbon– towards efficient materials for $CO_2$ capture from air

*Nazila Masoud, Guillermo Bordanaba Florit, Tomas van Haasterecht, and Harry Bitter*

*Wageningen University, Biobased Chemistry and Technology, Wageningen, Netherlands*

It is well-known that in heterogeneous catalysis the support of a catalyst can affect the catalysts' performance via different mechanisms.[1] The support can direct the adsorption of reactants, products or intermediates; it can indirectly tune the structural properties of the catalyst like dispersion of the active site over the support upon catalyst preparation or it can modify the electronic properties of the active phase. However, little is known about the influence of the support on performance of a similar category of materials, solid sorbents, where an active sorbent material is also dispersed over a support.

Here we studied the use of supported potassium carbonate as solid sorbent for the capture of  $CO_2$  from air. Development of  $CO_2$  capture technologies that directly capture from air is of prime importance to mitigate negative effects of global warming. A first step is to develop suitable sorbents that are able to capture  $CO_2$  efficiently, to release it with little energy input, and to sustain its performance for a long time. Supported  $K_2CO_3$  is a promising candidate for this. This type of sorbent can match the energy efficiency of the commercially applied liquid phase amines for  $CO_2$  capture from flue gas.[2] The use of a solid sorbent (instead of e.g., the liquid amines) is beneficial for practical reasons. Notably, amines are expensive, corrosive, and have toxicity issues.  $K_2CO_3$  reversibly reacts with  $CO_2$  in the presence of water, in an endothermic reaction at room temperature to produce potassium bicarbonate. The enthalpy of the reverse reaction is only 38 kJ/mol, and full decomposition of the bicarbonate product could be achieved below 150 °C.

To make efficient use of  $K_2CO_3$  it must be dispersed on a support. Carbon based supports were chosen because of their high hydrothermal stability. However the carbons have different structural and chemical properties like different surface area, porosity and surface functionalities. These properties can be tuned, upon production of carbon as support for any specific application.[3] However the relation between the support properties and their performance, after  $K_2CO_3$  deposition, is still unknown.

Here we focused on three different commercial carbon supports: CA1, SX ultra, and Ketjen Black. These carbons are different in their porosity and surface functionalities. CA1 and SX ultra are mainly microporous while Ketjen black is mesoporous. CA1 has polar surface functions with point of zero charge of 2 while SX ultra and Ketjen Black show more apolar surface properties with point of zero charge of 7. Figure (left) shows evolution of H<sub>2</sub>O, CO and CO<sub>2</sub> from CA1 support upon heat treatment up to 800°C indicating presence of acidic groups while such groups are not present on SX ultra and Ketjen Black supports. The figure (right) shows a breakthrough curve of CO<sub>2</sub> using K<sub>2</sub>CO<sub>3</sub> supported on these supports. Only Ketjen Black induced fast sorption kinetics and displayed a high CO<sub>2</sub> uptake capacity of the sorbent. Hence, the support affected the performance of K<sub>2</sub>CO<sub>3</sub> via different mechanisms. These will be discussed in more detail in conference contribution.

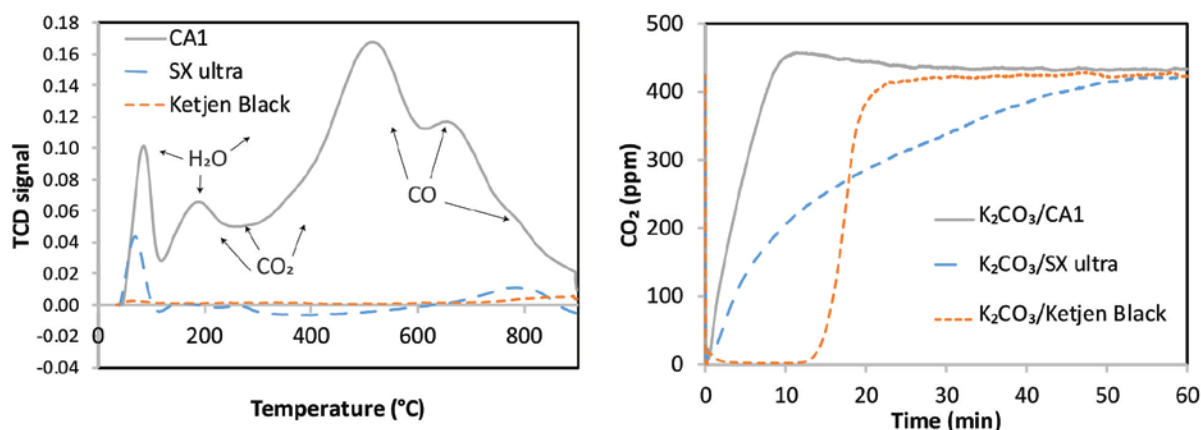


Figure. Left) Functional groups evolved from different supports (50 mg) upon high temperature treatment (10°C/min) under flow of He (20 mL/min). Evolved gases were detected by online mass spectrometer, Right) CO<sub>2</sub> breakthrough curves during CO<sub>2</sub> capture from air. The air passed down-flow through different sorbents (16 wt% K<sub>2</sub>CO<sub>3</sub> on CA1 and 10 wt% K<sub>2</sub>CO<sub>3</sub> on SX ultra and Ketjen Black, 50 mg), at 60°C, air flow 50 mL/min, water content: 3 wt% (vapor generated at 25°C).

## References

1. Masoud, N.; Delannoy, L.; Schaik, H.; van der Eerden, A.; de Rijk, J. W.; Silva, T. A. G.; Banerjee, D.; Meeldijk, J. D.; de Jong, K. P.; Louis, C.; de Jongh, P. E. Superior stability of Au/SiO<sub>2</sub> compared to Au/TiO<sub>2</sub> catalysts for the selective hydrogenation of butadiene. *ACS Catalysis*. 2017, 7 (9), 5594.
2. Meis, N. N. A. H.; Frey, A. M.; Bitter, J. H.; de Jong, K. P. Carbon nanofiber-supported K<sub>2</sub>CO<sub>3</sub> as an efficient low-temperature regenerable CO<sub>2</sub> sorbent for post-combustion capture. *Industrial & Engineering Chemistry Research* 2013, 52 (36), 12812.
3. Donoeva, B.; Masoud, N.; de Jongh, P. E. Carbon support surface effects in the Gold-Catalyzed oxidation of 5-Hydroxymethylfurfural. *ACS Catalysis* 2017, 7 (7), 4581.

# Adsorption and photocatalytic properties of titanium pyrophosphate catalysts.

*E. Mokrane*<sup>1,2\*</sup>, UHBC, Chlef, Algeria; *S. Barama*<sup>2</sup>, USTHB, Algiers, Algeria; *N. Fodil Cherif*<sup>3</sup>, CRAPC, Algiers, Algeria ; *A. Barama*<sup>2</sup>, USTHB, Algiers, Algeria ; *Y.H. Taufiq-Yap*<sup>4</sup>, University Putra, Malaysia

<sup>1</sup> Département de SANH, Faculté SNV, UHBC, BP151 Hay Es-salem, Chlef, 02000, Chlef, Algérie.

<sup>2</sup> LMCCCO, Faculté de Chimie, USTHB, BP32 EL Alia 16111 Bab Ezzouar, Alger, Algérie.

<sup>3</sup> Centre de recherche en analyse physico-chimique, CRAPC, Bousmail, Algérie.

<sup>4</sup> CSTRC, Faculty of Science, Universiti Putra Malaysia, UPM 43400, Serdang, Selangor, Malaysia

(\*) corresponding author: [zinamokrane@gmail.com](mailto:zinamokrane@gmail.com)

## Introduction

In this work we study titanium pyrophosphate catalysts characterization, and "methylene orange" (MO) elimination in water. MO is an organic mono azoic textile dye, his adsorption max Wavelength is 465 nm. Phosphates have a good capacity for photocatalytic degradation of organic molecules. In this study, titanium pyrophosphate catalysts (TiPO), synthesized by dry route (solid phase method "S") are tested in water depollution by two techniques, adsorption and photocatalysis, in order to determine the effectiveness of the catalysts in comparison with titanium dioxide and charcoal as references [1-4].

Before catalytic tests, the samples are characterized by TGA analysis (before calcinations); Powder X-ray diffraction (XRD); Fourier transform infrared (FTIR); Sample contents are quantitatively determined by atomic adsorption (ICP). The specific surface areas are measured by Brunauer-Emmett-Teller (BET) method. Finely acidity and acidic strength distribution of catalysts are studied by thermo programmed desorption of ammonia (TPD-NH<sub>3</sub>) analysis. The microstructure images of nano and microstructures of TiPO catalysts are acquired by using a field emission scanning electron microscopy (FESEM) and scanning electron microscopy (SEM).

## Results and discussion

Characterizations results explain the physico-chemical properties of TiPO-S solids. The elemental analysis results are very closely with the theoretical P/Ti ratio of catalysts. The superficial analysis of the TiPO-S catalysts gives expected results, all catalysts have low specific surfaces, from 1.7 to 6.05 m<sup>2</sup>/g. The BET isotherm is type -IV, forming a hysteresis loop [1].

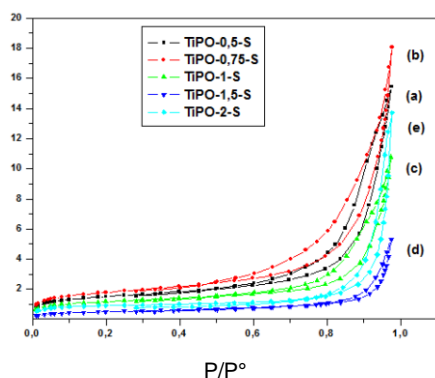


**Fig. 1.** Nitrogen adsorption isotherms

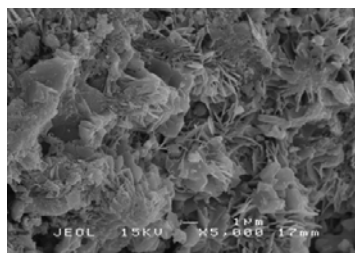


**Fig. 2.** FE-SEM images of TiPO-2-S

**Tableau.1.** Elemental chemical analysis (ICP-AES)

TiPO-S catalysts	Experimental atomic ratio P/Ti
TiPO-0,5-S	0,43
TiPO-0,75-S	0,69
TiPO-1-S	0,98
TiPO-1,5-S	1,47
TiPO-2-S	1,97

These catalysts are mesoporous despite their low specific surfaces and porous volumes. The average pore diameter is from 132 to 238 Å. DRX analysis identifies the presence of two phases of mixed oxides: titanium oxide and titanium pyrophosphate for the TiPO-S catalysts with a P/Ti ratio of 0.5; 0.75; 1 1.5; 2. Only the TiPO-2-S and TiPO-0 catalysts are made of a single pure phase. These results are predictable. The FTIR analysis confirms the results of the DRX by identifying the vibrations of elongation and deformation bond of the PO<sub>3</sub> Terminal Group and O-Ti-O combination. The FTIR spectra confirm the presence of the Pyrophosphates group and titanium oxide. The DSC/ATG analysis gives the phosphate and pyrophosphate phases temperatures of formation.

The heterogeneous photocatalytic degradation of OM on titanium pyrophosphate catalysts prepared by solid phase: TiPO-0.5, TiPO-0.75, TiPO-1, TiPO-1.5, TiPO-2, gives results reaching 70% degradation. The average photocatalytic degradation varies according to the P/Ti ratio of TiPO-S catalysts.

The results of adsorption and photocatalytic degradation of OM dyes are an interesting application of these titanium pyrophosphates materials on the depollution towards new perspectives.

## References

- [1] E. Mokrane; S. Barama; A. Barama; F.H. Alhassan; Y.H. Taufiq-Yap; H. Messaoudi; S. Slyemi; L. Pinard. Solid-phase and precipitation synthesis of Ti-pyrophosphate for the catalytic oxydehydrogenation of n-butane. *CRC. Vol: 20, Issue: 11, 1631-0748, 1037-1046* (2017).
- [2] Masui, T., Hirai, H., Imanaka, N. & Adachi, G. Y. New sunscreen materials based on amorphous cerium and titanium phosphate. *J. Alloys Compd.* 408–412, 1141–1144 (2006).
- [3] Cao, J., Xu, B., Lin, H. & Chen, S. Highly improved visible light photocatalytic activity of BiPO<sub>4</sub> through fabricating a novel p-n heterojunction BiOI/BiPO<sub>4</sub> nanocomposite. *Chem. Eng. J.* 228, 482–488 (2013).
- [4] Pan, C., Xu, J., Chen, Y. & Zhu, Y. Influence of OH-related defects on the performances of BiPO<sub>4</sub> photocatalyst for the degradation of rhodamine B. *Appl. Catal. B Environ.* 115–116, 314–319 (2012).

# Copper-zirconium-titanium oxide mesoporous nanocomposites for sustainable environmental protection

*Tanya Tsoncheva<sup>1</sup>, Alexandra Mileva<sup>1</sup>, Gloria Issa<sup>1</sup>, Momtchil Dimitrov<sup>1</sup>, Daniela Kovacheva<sup>2</sup>, Genoveva Atanasova<sup>2</sup>, Jiří Henych<sup>3</sup>*

<sup>1</sup>*Institute of Organic Chemistry with Centre of Phytochemistry, Bulgarian Academy of Sciences, Sofia, Bulgaria*

<sup>2</sup>*Institute of General and Inorganic Chemistry, Bulgarian Academy of Sciences, Sofia, Bulgaria*

<sup>3</sup>*Institute of Inorganic Chemistry, Czech Academy of Sciences, Řež, Czech Republic*

## Introduction

Recently, there is a permanently increasing interest to the nanoscale transition metal oxide composites as alternative of the expensive and highly sensitive to various pollutants precious metal based catalysts. In our previous study we demonstrated the potential of mesoporous zirconia-titania binary systems as catalysts for sustainable environmental protection [1]. This investigation is focussed on the catalytic behaviour of these materials after their modification with copper oxide nanoparticles. The effect of the preparation procedure and the variation in the Zr/Ti ratio on the state of the catalytic active sites was studied in methanol decomposition as a source of hydrogen and total oxidation of ethyl acetate (EA) as representative VOCs.

## Experimental

Mesoporous ZrO<sub>2</sub>-TiO<sub>2</sub> (xZryTi) oxides with different x/y mol ratio were prepared by hydrothermal procedure using CTAB as a template [1]. Their copper modifications (Cu=8 wt.%) were obtained by incipient wetness impregnation (WI) with aqueous solution of Cu(NO<sub>3</sub>)<sub>2</sub>·2H<sub>2</sub>O. Alternatively, step-wise “chemisorption” and “hydrolysis” of copper ammonia complex (CH) was performed, as described in [2].

## Results and discussion

The Nitrogen physisorption and XRD study demonstrated preservation of the porous structure of ZrO<sub>2</sub>-TiO<sub>2</sub> supports after the modification with copper. The ternary systems exhibited improved dispersion and higher BET surface area as compared to dual Cu/ZrO<sub>2</sub> and Cu/TiO<sub>2</sub> composites. For the latter, segregation of relatively large tenorite particles was observed and it was in higher extent for the WI modifications.



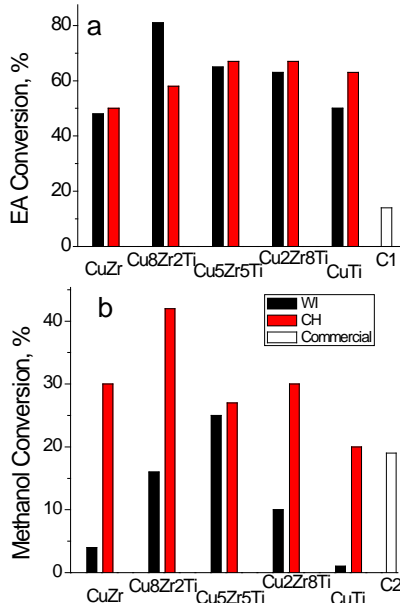


Figure 1. Ethyl acetate (575 K) and methanol (500 K) conversion. For comparison: Pt/Al<sub>2</sub>O<sub>3</sub>(C1) and Cu/Al<sub>2</sub>O<sub>3</sub>(C2) commercial catalysts.

The UV-Vis spectra revealed co-existence of CuO<sub>x</sub> entities and well crystallized CuO phase which proportion depended on the support composition. The Raman spectra showed incorporation of copper ions into the TiO<sub>2</sub>, ZrO<sub>2</sub> or mixed oxide lattice. According to XPS measurements this process was accompanied with the formation of oxygen defects and stabilization of Cu<sup>1+</sup> and Ti<sup>3+</sup> ions. This effect was more pronounced for the ternary systems and it was facilitated when the WI technique was used for modification. The TPR and HRTEM data evidenced that the xZr<sub>y</sub>Ti binary oxides and CH modification procedure provoked the formation of more homogeneous and finely dispersed copper oxide phase. The ternary composites exhibited improved catalytic activity in EA oxidation and methanol

decomposition as compared to their dual analogues (Fig. 1). Generally, the CH procedure facilitated the catalytic activity but this effect depended in a complex way on the Zr/Ti ratio of the support and the peculiarities of the catalytic process. The physicochemical study suggested superposition of effects related to the improved dispersion, changes in the BET surface area and formation of structure defects.

## Conclusion

Due to the different mechanism of interaction of the precursors with the ZrO<sub>2</sub>-TiO<sub>2</sub> binary supports, the CH modification procedure facilitates deposition of more homogeneous and finely dispersed CuO nanoparticles, while the WI method provokes the formation of Cu<sup>1+</sup> and Ti<sup>3+</sup> defects and segregation of larger CuO crystallites. This influences in a complex way the catalytic behavior of the composites in EA oxidation and methanol decomposition. The variations in the Ti/Zr ratio and the modification procedure used ensure synthesis of catalysts with improved catalytic activity as compared to the reference commercial catalysts.

**Acknowledgements.** Financial support project KΠ-06-H27/9 is acknowledged.

## References

- [1] T. Tsoncheva et al. J. Env. Chem. Eng. 6 (2018) 2540–2550.
- [2] T. Tsoncheva et al. Applied Catalysis A: General 406 (2011) 13– 21.

# Ti-doped SBA-15 catalysts for aqueous phenol oxidation: Influence of catalyst preparation methods and light, heat or plasma promotion

*Ghadeer Almohammadi, Sean Kelly, Colin O'Modhrain and James A Sullivan, UCD School of Chemistry, Belfield, Dublin 4, Ireland*

## Introduction

The oxidation of phenol in aqueous solutions using atmospheric O<sub>2</sub> over a catalyst is a useful probe reaction for depollution technologies [1]. Such technologies will become more important with time as access to potable water becomes problematic.

Wet air oxidation, photo oxidation and the use of plasma technologies in the presence of catalysts have all been suggested as realizable methods of phenol oxidation. In this work we look at families of Ti-doped mesoporous silicas as catalysts to promote phenol oxidation using the methods mentioned.

Ti-containing SBA-15 catalysts have been synthesized using (a) co-condensation of Ti during condensation of the SBA-15 material [2] and (b) grafting of Ti-containing species on the surface of pure SBA-15 [3] using a condensation reaction with the surface silanols of SBA-15. The former material should have Ti dispersed throughout the SBA-15 solid phase (both at its surface and in its bulk) while the latter can only have Ti atoms at the surface.

The materials have been characterized using a range of techniques including elemental analysis, UV Visible, FTIR and Raman spectroscopies, BET surface area measurements and TEM and SEM (including EDX).

Following preparation, their activities in promoting the total oxidation of a model aqueous pollutant (phenol) under wet air oxidation (in an autoclave held at 150 °C), solar irradiation (in an Atlas Suntest TM CPS+ instrument using a 300 W Xe lamp) and within a plasma (in a gas phase discharge setup where the liquid surface acted as a ground electrode for a corona type plasma discharge powered by a resonant HV power supply (PVM500 Information Unlimited)) were analyzed.

## Characterisations

Figure 1 shows typical TEM images and BET profiles collected from both families of catalyst (co condensed and grafted). These show that the porous SBA-15 structure is maintained following incorporation of Ti prepared using both techniques.

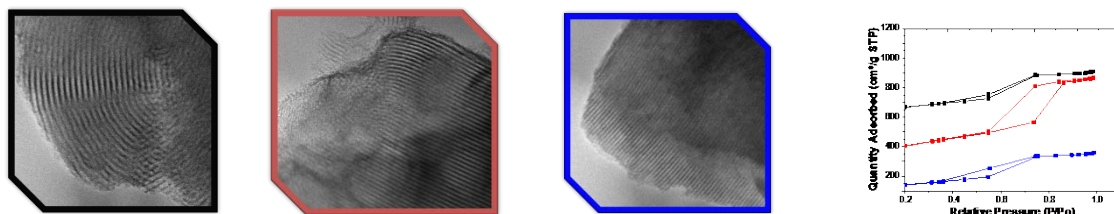


Figure 1. TEM images and BET profiles of SBA-15 (black) and Ti-SBA-15 prepared using (a) co-condensation (red) and (b) grafting (blue).

## Reactivity measurements

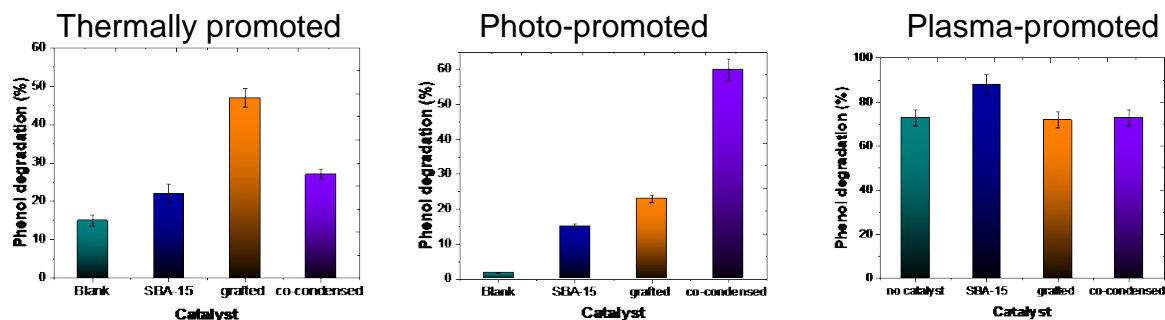


Figure 2 Reactivity under (a) wet air oxidation, (b) photo-promotion and (c) plasma-promotion in the presence of no catalyst, SBA-15, and Ti SBA-15 prepared by (a) co-condensation and (b) grafting.

For the first two modes of promotion both the type of catalyst as well as the type of reaction influence phenol conversion. For plasma-promotion phenol conversion is significantly higher but the presence of Ti-containing catalysts is not beneficial.

## Conclusions

Two families of Ti-doped SBA-15 catalysts have been prepared, characterized and applied in the oxidation of phenol using three different modes of oxidation. The location of Ti within the SBA-15 sample affects the reactivity of the catalysts when heat or light are used to promote oxidation. Furthermore, the routes of oxidation (and the generation of by-products) differ under each type of reaction condition. The effect of a catalyst is less clearcut in the cases where plasmas are used (where in some instances the catalysts presence decreases reactivity).

## Acknowledgements

The Saudi Cultural Bureau are thanked for providing a studentship for GA, the Irish Research Council are thanked for funding under GOIPD/2017/1000.

## References

- [1] L. F. Velasco, J. B. Parra and C. O. Ania, *Adsorpt. Sci. Technol.*, 2010, 28, 727–738.
- [2] H. Zhang, C. Tang, Y. Lv, F. Gao and L. Dong, *J. Porous Mater.*, 2014, 21, 63–70.
- [3] J. Zhao, Q. Huo, N. Melosh, G. H. Fredrickson, B. F. Chmelka, G. D. Stucky and F. Dongyuan, *Science* (80-), 1998, 279, 548–552.

# Addressing stability issues in gold/silver plasmonic photocatalysis

Sammy W. Verbruggen,

*Sustainable Energy, Air & Water Technology, University of Antwerp, Belgium*

## Background

Semiconductor photocatalysis has become an established technology to mitigate indoor and outdoor air pollution.[1] The last decade the combination with plasmonic noble metal nanoparticles has been investigated extensively with the aim of increasing the photocatalytic efficiency and/or to shift the activity toward the visible light region of the solar spectrum.[2,3] One of the main drawbacks of these metallic nanostructures, especially when based on silver, is their tendency for oxidation and/or clustering, which will again lower performance over time due to loss of the plasmonic effect.

## Scientific solution

To circumvent the limitations mentioned above, silver-polymer and gold-polymer core-shell nanoparticles with ultra-thin polymer shells are prepared using the layer-by-layer (LbL) technique (Figure 1a).[4,5] Encapsulation of the metal nanoparticle with this thin protective shell is shown to prevent oxidation and clustering, without compromising the plasmonic properties. Using finite element numerical simulations, it is demonstrated that application of this well-controlled shell does not disrupt the plasmonic near field enhancement effect, as long as the shell is kept sufficiently thin (< 3 nm).

Next, plasmonic Ag-TiO<sub>2</sub> and Au-TiO<sub>2</sub> photocatalysts are prepared by depositing the developed core-shell nanoparticles on the TiO<sub>2</sub> surface. The long-term stability of this photocatalytic system is evaluated by means of the gas phase photocatalytic degradation of acetaldehyde in air, monitored over a prolonged period of four months (Figure 1b). The results show that our protected plasmonic photocatalyst outperforms pristine TiO<sub>2</sub> and retains its plasmonic enhancement in contrast to TiO<sub>2</sub> modified with bare (i.e. unprotected) metal nanoparticles. With this an important step is made toward the development of long-term stable plasmonic applications for efficient (solar) light energy conversion. In addition, it is also shown that the particles can

serve as substrates for Surface Enhanced Raman Spectroscopy. By controlling the thickness of the polymer shell, the plasmonic near-field enhancement in the hot spot region between adjacent nanoparticles can be tuned.

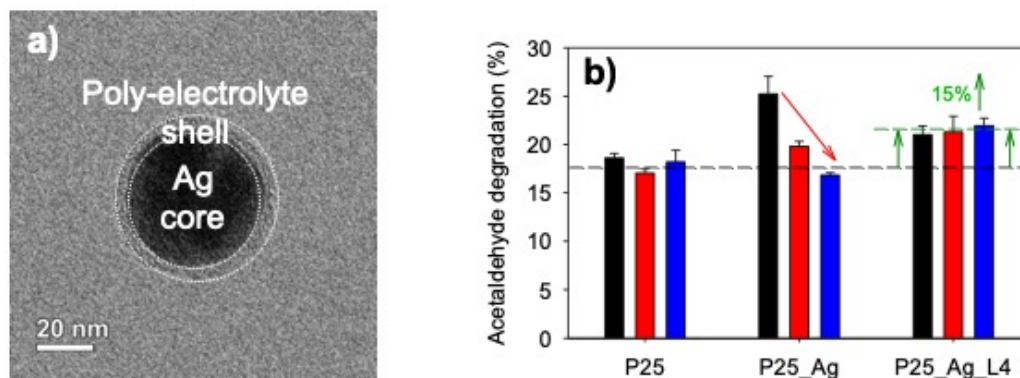


**Figure 1. a)** TEM image of a silver-polymer core-shell nanoparticle in which the homogeneous shell can be well observed. **b)** photocatalytic activity test of acetaldehyde degradation in air directly after catalyst synthesis (black), 4 weeks of ageing (red) and 4 months of ageing (blue). For unmodified TiO<sub>2</sub> P25 the activity does not change, while for P25 modified with bare Ag nanoparticles, the activity drops significantly. For P25 modified with core-shell nanoparticles, the 15% increased activity is retained over the entire ageing period.

#### References

- [1] S.W. Verbruggen, J. Photochem. Photobiol. C 24 (2015) 64.
- [2] S.W. Verbruggen et al., Appl. Catal. B 188 (2016) 147.
- [3] S.W. Verbruggen et al. Appl. Catal. B 156 (2014) 116.
- [4] R. Asapu et al., Appl. Catal. B 200 (2017) 31.
- [5] R. Asapu et al., ACS Appl. Mater. Interface. 9 (2017) 41577.

# Aerosol-assisted preparation of nanostructured Ru/TiO<sub>2</sub> catalysts for CO<sub>2</sub> methanation

*Paulina Melo Bravo<sup>a</sup>, Damien P. Debecker<sup>a,\*</sup>*

<sup>a</sup> *Institute of Condensed Matter and Nanosciences. UCLouvain, Louvain-la-Neuve, Belgium. [\\*damien.debecker@uclouvain.be](mailto:*damien.debecker@uclouvain.be)*

## Introduction

Global warming, caused by the increasing CO<sub>2</sub> level in the atmosphere, is a major contemporary concern. Catalytic approaches to transform CO<sub>2</sub> into useful chemicals is one of the topical research strategy to tackle this issue. For example, the so-called methanation allows for the conversion of CO<sub>2</sub> into methane which can then be used as a fuel or further transformed [1]. The conventional catalysts used for methanation processes are generally based on Fe, Co, Ru, Rh, Pd or Ni [2]. Particularly Ru is known as the most active metal, showing good activity even at low temperature (~200°C) [3]. In terms of catalyst support, it has been shown that using TiO<sub>2</sub> instead of SiO<sub>2</sub> or Al<sub>2</sub>O<sub>3</sub> produces a greater catalytic activity for the methanation of CO<sub>2</sub> by one order of magnitude. The latter being attributed to the creation of new active sites in the metal-support interface [4]. Consistently, we showed that the crystalline TiO<sub>2</sub> structure plays a major role in the formation of active sites [5]. Thus, one current challenge is to optimize this interaction between the Ru nanoparticles and the TiO<sub>2</sub> support.

In this work we present the preparation, characterization and catalytic testing of a new type of Ru/TiO<sub>2</sub> methanation catalysts obtained by an aerosol process.

## Experimental

Ru/TiO<sub>2</sub> catalysts were prepared by spray-drying [6] an aqueous suspension containing a Ru precursor (preformed RuO<sub>2</sub> nanoparticles or RuCl<sub>3</sub>) together with TiO<sub>2</sub> (P25, rutile or anatase) in a "Mini Spray Dryer B-290" (Büchi). The dried catalysts were annealed at 350°C or 450°C and the Ru loading was screened in the 1.1-3.3 wt.% range (verified by ICP-AES). Benchmark catalysts were prepared by simple impregnation on the P25 support. Catalysts were characterized by N<sub>2</sub>-physisorption, H<sub>2</sub>-chemisorption, XRD and H<sub>2</sub>-TPR. Before reaction the catalysts were reduced in situ in H<sub>2</sub> at 200 °C. CO<sub>2</sub> methanation tests were conducted in the

50 – 225 °C range in a fixed bed reactor, using a feed of CO<sub>2</sub>:H<sub>2</sub>:He=1:4:5, and adapting the contact time to remain in the initial activity regime.

## Results and discussion

Under these reaction conditions, all catalysts were 100% selective to CH<sub>4</sub>. All samples also had similar activation energy. Consistent with previous results [7], the catalyst prepared with TiO<sub>2</sub> rutile as the support were more active than the P25 equivalent (Fig. 1).

Strikingly, the catalyst based on TiO<sub>2</sub> anatase was totally inactive.

This correlates with a poor dispersion, as evidenced by the detection of large RuO<sub>2</sub> particles by XRD after annealing. The annealing temperature and the nature of the Ru precursor had little effect only on the final performance. The Ru loading seemed to be optimal at 2.2 wt.%. The highest specific activity was obtained with the

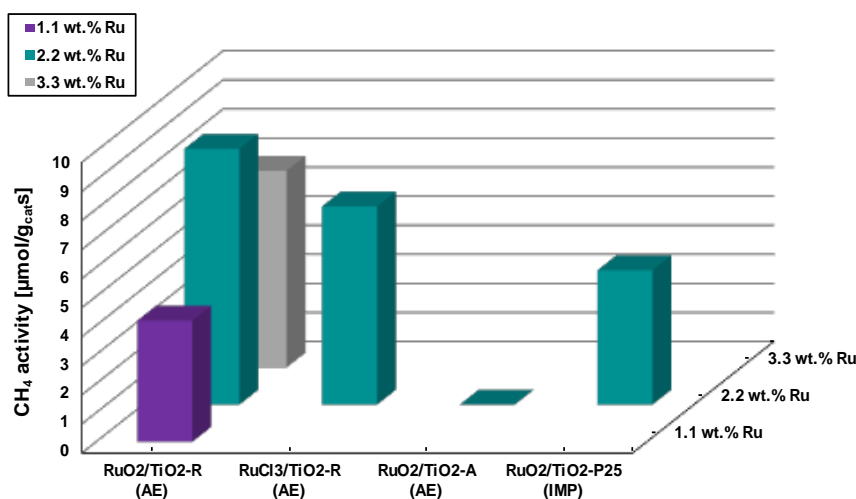


**Figure 1: CH<sub>4</sub> activity in CO<sub>2</sub> methanation at 200°C over Ru/TiO<sub>2</sub> catalysts.**

2.2%Ru/TiO<sub>2</sub>-rutile catalyst calcined at 350 °C: 8.7 μmolCH<sub>4</sub>/g<sub>cat</sub>·s. This outcompetes the equivalent catalyst prepared by wet impregnation instead of aerosol (4.6 μmolCH<sub>4</sub>/g<sub>cat</sub>·s). This result is rationalized by the fact that the spray drying technique allows for a better dispersion of the Ru nanoparticles (H<sub>2</sub>-chemisorption), resulting in a higher reducibility of the catalyst (TPR), indicative of the formation of more abundant active sites.

## Conclusions

The aerosol method is an attractive method for the preparation of Ru/TiO<sub>2</sub> methanation catalysts with higher catalytic performance in CO<sub>2</sub> hydrogenation to CH<sub>4</sub> as compared to the classical impregnation routes. We confirm that TiO<sub>2</sub>-rutile is the best support to maintain a high Ru dispersion and obtain high activity.

## References

- [1] Centi, G., E.A. Quadrelli, and S. Perathoner. *Energ. Environ. Sci.*, 2013. 6(6): p. 1711-1731.
- [2] Aziz, M. A. A, et al. *Green Energy*. 2015, 17(5): p. 2647-2663.
- [3] Powell, J.B. and S.H. Langer. *J. Catal.*, 1985. 94(2): p. 566-569.
- [4] Li, D., et al. *Appl. Catal A-Gen.*, 1999. 180(1): p. 227-235.
- [5] Kim, A., et al. *Catal. Sci. & Technol.*, 2016. 6(22) : p. 8117-8128.
- [6] Debecker, D. P., et al. *Chem. Soc. Rev.*, 2018. 47(11) : p. 4112-4155.
- [7] Kim, A., et al. *Appl. Catal. B-Environ.*, 2018. 220 : p. 615-625.



# The better performances of Fe-Fer catalyst compared to Fe-ZSM5 in industrial relevant conditions for NO<sub>x</sub> and N<sub>2</sub>O abatements from Nitric acid plants

*Alberto Garbujo<sup>1\*</sup>, Roberto Lanza<sup>2</sup>, Emmanuel Rohart<sup>3</sup>, Arnaud Lahougue<sup>3</sup>, Raffaele Ostuni<sup>1</sup>, Pierdomenico Biasi<sup>1</sup>.*

<sup>1</sup>Casale SA, Lugano, Switzerland;

<sup>2</sup>Verdant, Stockholm, Sweden;

<sup>3</sup>Alsys, Ploemeur, France.

*\*Corresponding author: [a.garbujo@casale.ch](mailto:a.garbujo@casale.ch)*

## Introduction

Nitric acid is one of the most produced commodity worldwide. It is mainly used as a strategical chemical for the fertilizer synthesis and in 2013 the production reached 78 million tons [1] [2]. In recent years, the higher awareness in the greenhouse effect and in the environmental pollution, have highlighted the importance of a new development in the nitric acid tail gas treatment, especially concerning the N<sub>2</sub>O and NO<sub>x</sub> species [1]. Many metal oxide and zeolite catalysts have been developed for the selective reduction of N<sub>2</sub>O and NO<sub>x</sub>, each one with benefits and drawbacks. The state of art materials are based on Fe-zeolites which could achieve both NO<sub>x</sub> and N<sub>2</sub>O abatement with the same catalyst. Many Fe zeolites have been explored, such as Ferrierite (Fer), ZSM5 and BEA [3].

In this paper, the comparison of fresh and aged Fe-Fer and Fe-ZSM5 industrial catalysts, both supplied by ALSYS, has been carried out. Fe-Fer catalyst is a proprietary catalyst of CASALE and ALSYS and to be used in nitric acid plants [4]. The results from field and laboratory showed that Fe-Fer (Casale – Alsys proprietary catalyst [4]) will allow customer to benefit from a higher catalytic activity and greater stability compare to the current commercial solution with Fe-ZSM5.

## Results and discussion

Fe-Fer and Fe-ZSM5 extruded catalysts have been subjected to a simulated aging procedure to investigate the catalytic behaviour under stressed condition. The catalysts tested were a blend of zeolite exchanged with Fe and alumina binder, extruded in a cylindrical shape (in the typical composition and shape of industrial catalyst). The catalytic tests were performed under relevant industrial deN<sub>2</sub>O and

deNO<sub>x</sub> reaction conditions. The aging treatment was kept for 150h at two temperatures (600 and 700°C) with 12% of O<sub>2</sub> and 6% of H<sub>2</sub>O.

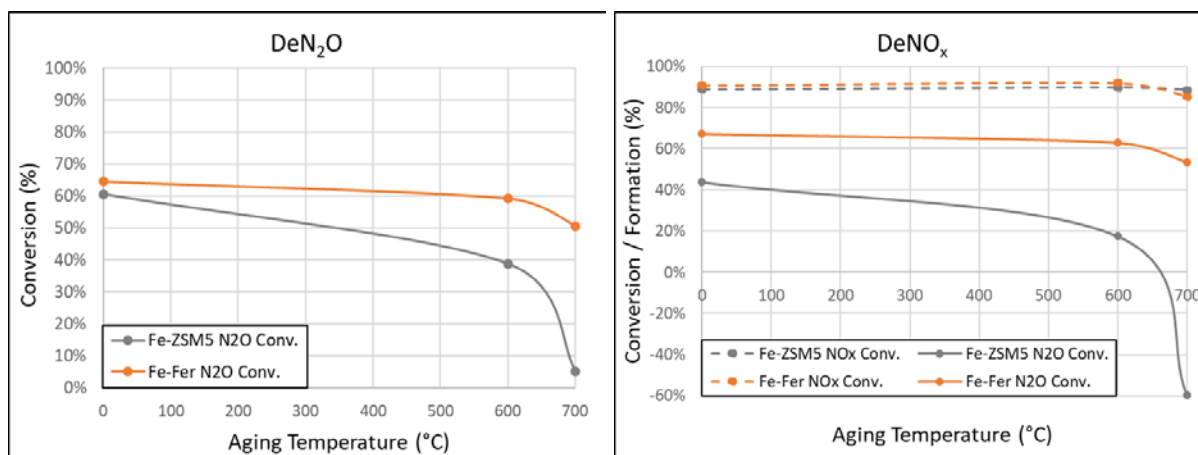


Figure 1: deN<sub>2</sub>O condition: NO 70 ppm, NO<sub>2</sub> 30 ppm, N<sub>2</sub>O 900 ppm, O<sub>2</sub> 3.0%, H<sub>2</sub>O 0.3% and N<sub>2</sub> balance;  
deNO<sub>x</sub> condition: NO 325 ppm, NO<sub>2</sub> 325 ppm N<sub>2</sub>O 40 ppm NH<sub>3</sub> 650 ppm, O<sub>2</sub> 3.0%, H<sub>2</sub>O 0.3% and N<sub>2</sub> balance.

The results (figure 1) display the higher catalytic activity of Fe-Fer compared to Fe-ZSM5. The superior Fe-Fer catalytic activity becomes particularly significant after the aging procedure where a different catalytic behaviour is observed. Fe-Fer, slightly decreased its activity, after the aging treatment, while the Fe-ZSM5 dramatically dropped its performances. In addition, N<sub>2</sub>O formation is detected under deNO<sub>x</sub> condition for Fe-ZSM5, while the Fe-Fer does not exhibit any N<sub>2</sub>O formation.

The characterizations performed revealed that the reduced activity of Fe-ZSM5 compared to the Fe-Fer is due to the Fe species present in the catalyst.

## Conclusions

In this work, we have investigated two industrial catalysts under plant conditions before and after severe aging treatments. Results showed that Fe-Fer is the most stable catalyst and high performance that can be used for tail gas treatment in nitric acid plants. Moreover Fe-Fer did not show N<sub>2</sub>O formation even after severe aging while the Fe-ZSM5 exhibited a larger undesired N<sub>2</sub>O formation. The Fe-Fer catalyst for DeN<sub>2</sub>O and DeNO<sub>x</sub> applications with superior performances compared to the Fe-ZSM5.

## References

- [1] M. Thiemann, E. Scheibler, and K. W. Wiegand, "Nitric Acid , Nitrous Acid , and Nitrogen Oxides," *Ullmann's Encycl. Ind. Chem. Vol. 24*, vol. 2003, Vol 24. 177-223.
- [2] C. A. Grande *et al.*, *Ind. Eng. Chem. Res.*, vol. 57, no. 31, pp. 10180–10186, 2018.
- [3] K. Skalska, J. S. Miller, and S. Ledakowicz, *Sci. Total Environ.*, vol. 408, no. 19, pp. 3976–3989, 2010.
- [4] C. Hamon, D. Le Guern, O. Le Lamer, and L. Navascues, EP1918016B1, 2006.

# Characterization of reduced graphene oxide obtained by mild reducing agents

*D. Kichukova<sup>1</sup>, D. Kovacheva<sup>1</sup>, I. Spassova<sup>1</sup>, A. Staneva<sup>2</sup>*

*<sup>1</sup>Institute of General and Inorganic Chemistry, Bulgarian Academy of Sciences, Sofia, Bulgaria;*

*<sup>2</sup>University of Chemical Technology and Metallurgy, Sofia, Bulgaria*

## Introduction

Graphene is two-dimensional carbon material with interesting properties such as tunable surface area, high electrical and thermal conductivity, light weight, strong mechanical strength and chemical stability. Graphene and graphene-based materials find applications in electronics, energy generation and storage devices, as well as for environmental protection. The use of highly ordered graphene is essential in some applications (electronic devices), but for other the defects and imperfections of graphene are important or desirable. The most common way for the synthesis of bulk graphene is based on exfoliation of graphite. This method involves oxidation of graphite using highly oxidizing agents and subsequently reducing graphene oxide (GO) to graphene. Reduced graphene oxide (RGO) is prepared from reduction of GO by thermal, chemical or electrical treatments. Different reducing agents are widely used for the chemical reduction. However, many of the reducing agents are very hazardous, therefore to decrease the level of toxicity, "green" materials recently were applied. In the present study a new approach for preparation of RGO is implemented, which involves the use of mild and nontoxic reducing agents, namely ascorbic acid and glycine combined with hydrogen peroxide as an additional reducing component.

## Experimental

GO was synthesized through a modified Hummers method. For this purpose graphite powder was mixed with H<sub>2</sub>SO<sub>4</sub> in an ice bath and KMnO<sub>4</sub> and NaNO<sub>3</sub> were added. After 3 h a mixture of H<sub>2</sub>O<sub>2</sub> and water was added. Exfoliation of graphite oxide to GO sheets was performed by sonication of the graphite oxide suspension for 1h using ultrasonic processor (20KHz, 750W). The obtained product was filtered, washed with distilled water and dried at 80°C. RGO was obtained from the GO suspension mixed with L-ascorbic acid or glycine without or with addition of H<sub>2</sub>O<sub>2</sub>. The produced RGO was washed with distilled water and dried under vacuum at 80°C. The obtained GO

and RGO were characterized by XRD, N<sub>2</sub> adsorption, Raman and FTIR, as well as by SEM and TEM.

## Results and discussion

Powder XRD shows complete reduction with the both applied reducing agents. FTIR spectra of GO and RGO obtained with different reducers show that the peaks characteristic for C-O vibrations at GO disappear in the reduced samples and the peaks responsible for the C-C aromatic groups increase (especially with the addition of H<sub>2</sub>O<sub>2</sub>). When combining H<sub>2</sub>O<sub>2</sub> and reducing agents, a displacement of the G-band in the Raman spectra is observed (Fig. 1), indicating the presence of deformations and three new bands pointing the presence of C-H bonds and defect carbon rings appear. Such deformations are not observed in the spectra of the samples obtained with pure acids.

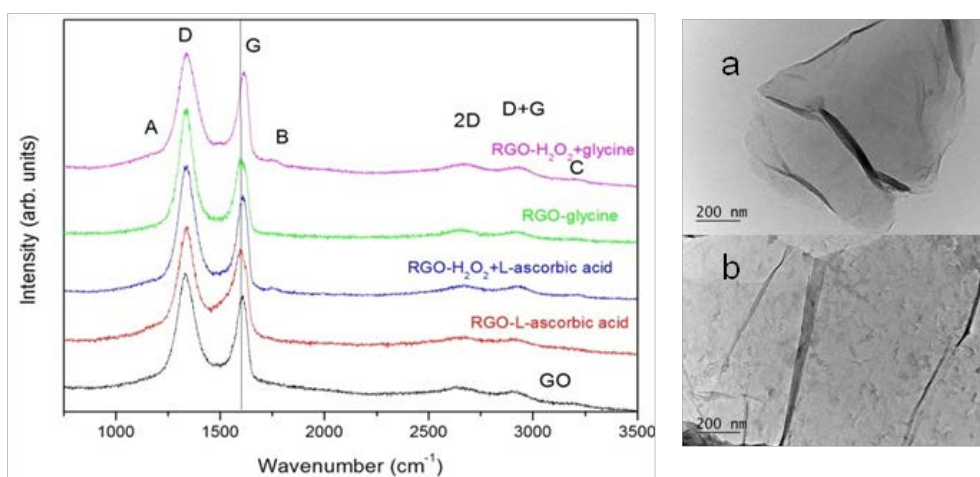


**Fig.1.** Raman spectra of GO and RGO samples and TEM images of RGO obtained by glycine without (a) and with (b) H<sub>2</sub>O<sub>2</sub>.

TEM images revealed that the samples reduced with pure acids show bare and smooth graphene sheets, while the materials obtained with H<sub>2</sub>O<sub>2</sub> addition show large graphene sheets along with much smaller pieces of sheets obviously produced by tearing of the sheets.

## Conclusion

In summary, RGO is successfully synthesized using ascorbic acid and glycine as green reducing agents. The use of the H<sub>2</sub>O<sub>2</sub> addition resulted in change of the morphology of the RGO obtained.

**Acknowledgements:** The work was financed by the National Science Fund of Bulgaria, Project KP-06-H27/9.

## Facile synthesis of Ag-modified manganese oxide for effective catalytic ozone decomposition

*Jinzhu Ma, State Key Joint Laboratory of Environment Simulation and Pollution Control, Research Center for Eco-Environmental Sciences, Chinese Academy of Sciences, Beijing, China; Hong He, State Key Joint Laboratory of Environment Simulation and Pollution Control, Research Center for Eco-Environmental Sciences, Chinese Academy of Sciences, Beijing, China*

Ozone is a double-edged sword: ozone in the stratosphere can protect the creatures of the earth from ultraviolet radiation; however, ozone near the ground is a threat to human health and ecosystem. Outdoor ozone pollution is mainly derived from photochemical reactions involving nitrogen oxides ( $\text{NO}_x$ ) and volatile organic compounds (VOCs) [1]. Electrostatic equipment, ultraviolet disinfection devices and related ozone air purifiers make a great contribution to indoor ozone pollution [2]. Therefore, the study of ozone removal is of great significance to human health and environmental protection. In this study, Ag-modified manganese oxides ( $\text{AgMnO}_x$ ) were synthesized by a simple co-precipitation method. The effect of calcination temperature on the activity of  $\text{MnO}_x$  and  $\text{AgMnO}_x$  catalysts was investigated. The effect of the amount of Ag addition on the activity and structure of the catalysts was further studied by activity testing and characterization by a variety of techniques. The calcination temperature of  $600^\circ\text{C}$  was demonstrated to be the most appropriate for  $\text{AgMnO}_x$ . The activity of the 8% $\text{AgMnO}_x$  catalyst was the best among all the catalysts. The activity of 8% $\text{AgMnO}_x$  for ozone decomposition was significantly enhanced due to the formation of the  $\text{Ag}_{1.8}\text{Mn}_8\text{O}_{16}$  structure, indicating that this phase has excellent performance for ozone decomposition. The weight content of  $\text{Ag}_{1.8}\text{Mn}_8\text{O}_{16}$  in the 8% $\text{AgMnO}_x$  catalyst was only about 33.76%, which further indicates the excellent performance of the  $\text{Ag}_{1.8}\text{Mn}_8\text{O}_{16}$  phase for ozone decomposition. The  $\text{H}_2$  temperature programmed reduction ( $\text{H}_2$ -TPR) results indicated that the reducibility of the catalysts increased due to the formation of the  $\text{Ag}_{1.8}\text{Mn}_8\text{O}_{16}$  structure. This study provides guidance for a follow-up study on Ag-modified manganese oxide catalysts for ozone decomposition.

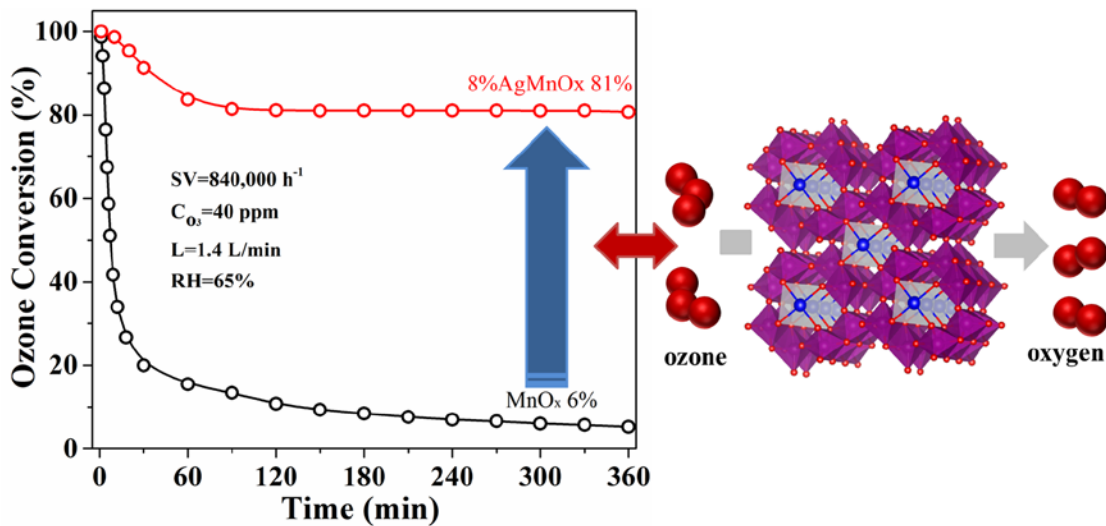


Figure 1 Conversion of ozone on the MnO<sub>x</sub> and 8%AgMnO<sub>x</sub> catalysts. Conditions: ozone inlet concentration 40 ppmV, temperature 30°C, relative humidity 65%, space velocity 840,000 hr<sup>-1</sup>

## References

- [1] Cooper, O.R., Parrish, D.D., Stohl, A., Trainer, M., Nedelec, P., Thouret, V., et al., 2010. Increasing springtime ozone mixing ratios in the free troposphere over western North America. *Nature*. 463 (7279): 344-348.
- [2] Fadeyi, M.O., 2015. Ozone in indoor environments: Research progress in the past 15 years. *Sustain. Cities. Soc.* 18: 78-94.

# Catalytic oxidation of light hydrocarbons on nanosized manganese ferrites prepared by solution-combustion method with various fuel mixtures

Ts. Lazarova<sup>1</sup>, D. Kovacheva<sup>1</sup>, G. Tyuliev<sup>2</sup>, I. Spassova<sup>1</sup>, A. Naydenov<sup>1</sup>

<sup>1</sup>*Institute of General and Inorganic Chemistry, Bulgarian Academy of Sciences, Sofia, Bulgaria;*

<sup>2</sup>*Institute of Catalysis, Bulgarian Academy of Sciences, Sofia, Bulgaria*

## Introduction

Transition metal ferrites with spinel type structure ( $M^{2+}Fe_2O_4$ ,  $M^{2+} = Mn, Fe, Co, Ni, Cu, Zn$ ) are nanosized materials with interesting for practical applications catalytic properties and offer possibilities for increasing the productivity of solid catalysts due to their high specific surface area and small particle sizes. Catalytic properties of the spinel ferrites depend on the redox properties of cations and on their distribution among the octahedral and tetrahedral sublattices. Manganese ferrite is one of the most attractive due to the relatively low redox potential of manganese and the partial inverse cation distribution. Various methods have been developed to obtain materials with desirable physical and chemical properties and among them the combustion method [1] is found to be suitable for preparation of materials with tunable properties. The aim of the study is to investigate the influence of the glycerol-glycine fuel mixing ratio on the structure, morphology and catalytic properties in hydrocarbon oxidation of nanosized  $MnFe_2O_4$  prepared by solution-combustion method.

## Experimental

$Mn(NO_3)_2$  and  $Fe(NO_3)_3$  were taken in a molar ratio 1:2 and as fuel in the solution-combustion reaction, mixtures of glycerol (Gl) and glycine (Gn) in reducing power ratios [1]: 1:0, 0.75:0.25; 0.5:0.5; 0.25:0.75 were used. The final products were treated at 400°C for 2 h in Ar. The materials were characterized by XRD,  $N_2$  adsorption, DTA-TG, SEM, XPS, TPR. The catalytic tests in C1-C4 n-alkanes oxidation were carried out with GHSV 60 000  $h^{-1}$  and inlet hydrocarbon concentration 0.10 vol. %, 20.0 vol.%  $O_2$ , the balance is  $N_2(4.0)$ .

## Results and discussion

The materials are nanosized single phase with cubic spinel-type structure (SG Fd-3m) and depending on the fuel mixture ratio different particle sizes and unit cell parameter are observed. The results are in correlation with the adsorption data

where a change of the specific surface area and pore volume by varying the fuel mixing ratio is registered. XPS analyses reveal enrichment on the surface of the spinels with manganese, as well as the concomitant presence of manganese and iron in 2<sup>+</sup> and 3<sup>+</sup> oxidation states.

The complete oxidation of C1-C4 n-alkanes proceeds at relatively low temperatures depending on the type of the catalyst and the n-alkane used. For example, the ethane oxidation degree at 400°C is 99.7% for MnFe-0, 99.6 % for MnFe-25, 99.7 % for MnFe-50 and 91.5 for MnFe-75.

The results from the catalytic experiments as pre-exponential factors ( $k_0$ ) and the apparent activation energies ( $E_{app}$ ) are presented in Table 1. For the calculations the data from the conversion– temperature dependencies for conversions below 45% were utilized and the first order kinetics has been applied.

**Table 1.** Reaction parameters for the complete oxidation of hydrocarbons on manganese ferrites.

Sample	MnFe-0 (Gl:Gn=1:0)		MnFe-25 (Gl:Gn=0.75:0.25)		MnFe-50 (Gl:Gn=0.5:0.5)		MnFe-75 (Gl:Gn=0.25:0.75)	
	$k_0 \cdot 10^{-7}, s^{-1}$	$E_{app.}, kJ/mol$	$k_0 \cdot 10^{-7}, s^{-1}$	$E_{app.}, kJ/mol$	$k_0 \cdot 10^{-7}, s^{-1}$	$E_{app.}, kJ/mol$	$k_0 \cdot 10^{-7}, s^{-1}$	$E_{app.}, kJ/mol$
Methane	6,5	88,2	2,2	87,7	2,5	88,2	1,3	89,9
Ethane	28,6	82,6	67,1	86,9	34,5	84,1	14,4	85,9
Propane	76,5	77,5	365,0	84,3	186,0	81,5	57,4	83,0
n-Butane	24,7	78,3	276,0	79,2	280,0	79,3	80,9	80,8

As expected, the highest temperature for conversion is measured for methane combustion and the observed decrease of the reaction temperature from methane to n-butane can be correlated with the strength of the weakest H-C bond of the corresponding n-alkane.

## Conclusion

The results from characterization of MnFe<sub>2</sub>O<sub>4</sub> materials prepared in this study reveal that structural and morphological characteristics of the prepared spinels could be finely tuned by varying the ratios in the fuel mixtures. The nanoparticles obtained with glycerol and with a mixture fuel with glycine up to 50 % show better oxidation properties than the sample obtained with a fuel containing 75 % glycine.

**Acknowledgements:** The work was financed by the National Science Fund of Bulgaria, Project KP-06-H29/2.

## References

[1] S. Jain, K. Adiga, V Pai Vernekar, *Combustion and Flame*, 40, 71 (1981).



# Development of structured catalyst for N<sub>2</sub>O decomposition based on functional correlation: composition-morphology-performance

*S. Wójcik<sup>1</sup>, C. M. Quintero<sup>2</sup>, G. Grzybek<sup>1</sup>, P. Indyka<sup>1</sup>,*

*S. Specchia<sup>2</sup>, Z. Sojka<sup>1</sup>, A. Kotarba<sup>1</sup>*

*<sup>1</sup>Faculty of Chemistry, Jagiellonian University, Krakow, Poland*

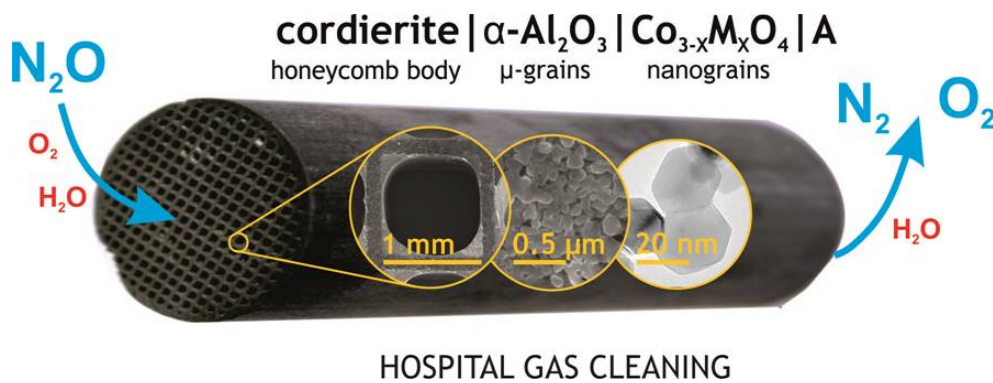
*<sup>2</sup>Department of Applied Science and Technology, Politecnico di Torino, Turin, Italy*

Nitrous oxide (N<sub>2</sub>O) is recognized as a dangerous greenhouse gas. In spite of the negative impact of N<sub>2</sub>O on the ozone layer, this gas is still widely used for anesthesia in several countries (e.g. Sweden, Finland, Norway, England, Australia, Canada, and New Zealand) because of its high effectiveness, low price and easy application for the patient themselves. Currently, the process of N<sub>2</sub>O abatement from hospital ventilation systems is catalyzed by noble metal-based systems. There are no well-documented investigations reported for such catalyst based on transition metal oxides for this application. Cobalt spinel (Co<sub>3</sub>O<sub>4</sub>) was found as one of the most active and stable active phases in deN<sub>2</sub>O reaction. However, the spinel activity substantially depends on its morphology and promotion (bulk and surface) [1].

With regard to the mentioned facts, the aim of presented studies was to develop a structured, Co<sub>3</sub>O<sub>4</sub>-based catalyst for N<sub>2</sub>O decomposition emitted from hospital ventilation systems. The particular emphasis was placed on optimal composition, morphology, preparation method of catalyst and practical aspects such as simplicity and low cost of the catalyst fabrication, possibility of its regeneration, and scaling-up. The requirements for the catalyst is to exhibit high activity (N<sub>2</sub>O conversion > 95% at a temperature of 450°C in the flow of air containing 0-2% N<sub>2</sub>O, 40-60% humidity), and stability in the working temperature window 400-600°C. Designed catalyst dedicated for conditions present in hospital ventilation systems consists of the structured monolithic honeycomb body (cordierite) covered by an interfacial micrometric washcoat (Al<sub>2</sub>O<sub>3</sub>) with dispersed nanoparticles of promoted spinel active phase. Whereas the monolithic body provides the stable 3D structure of the catalyst, the role of inert  $\alpha$ -alumina washcoat is to ensure high dispersion of the active phase and block the undesired cordierite ions (Mg<sup>2+</sup>, Al<sup>3+</sup>) migration to spinel crystals.

Two strategies of active phase deposition were applied and evaluated: wetness impregnation from aqueous solution as well as Solution Combustion Synthesis (SCS)

with the glycine as a fuel. It was found out that the optimal spinel content in the structured catalyst is in the range 7-8 wt.%. The particular attention was paid to the concentration and localization of bulk (selective substitution of  $\text{Co}^{2+}$  in  $T_d$  position) and surface (ensure the contact of  $\text{K}^+$  with spinel active phase) promoters. The overview of the morphology of the catalyst is schematically presented in the figure below. It is worth to underline that for high efficacy of the catalyst, the morphology control has to be provided for the washcoat ( $0.1\text{-}0.3\ \mu\text{m}$ ) and active phase ( $20\text{-}50\ \text{nm}$  with the preferentially exposed 100 spinel plane).



The performed catalytic tests in the flow of model (5%  $\text{N}_2\text{O}/\text{He}$ ) and hospital gas mixture (containing  $\text{H}_2\text{O}$ ,  $\text{O}_2$  contaminants) revealed that the developed catalyst meets the requirements of the de $\text{N}_2\text{O}$  removal. The effectiveness factor evaluated, based on catalyst morphological features and de $\text{N}_2\text{O}$  catalytic results, was found to be  $\approx 1$  [2]. The determined mass transfer coefficients and type of the catalyst working regime (purely kinetic in the whole temperature range) provide the useful platform for the rational design of a real de $\text{N}_2\text{O}$  catalyst.

### Acknowledgement

Authors would like to acknowledge National Science Centre in Poland funding awarded by the decision number 2016/23/N/ST8/01512. S.W. acknowledges the Erasmus+ Programme for her Visiting Scholarship at Politecnico di Torino.

### References

- [1] G. Grzybek, S. Wójcik, P. Legutko, J. Gryboś, P. Indyka, B. Leszczyński, A. Kotarba, Z. Sojka, Thermal stability and repartition of potassium promoter between the support and active phase in the  $\text{K-Co}_{2.6}\text{Zn}_{0.4}\text{O}_4|\alpha\text{-Al}_2\text{O}_3$  catalyst for  $\text{N}_2\text{O}$  decomposition: Crucial role of activation temperature on catalytic performance, *Appl. Catal. B Environ.* 205 (2017).
- [2] S. Wójcik, G. Ercolino, M. Gajewska, C.W.M. Quintero, S. Specchia, A. Kotarba, Robust  $\text{Co}_3\text{O}_4|\alpha\text{-Al}_2\text{O}_3|\text{cordierite}$  structured catalyst for  $\text{N}_2\text{O}$  abatement – Validation of the SCS method for active phase synthesis and deposition, *Chem. Eng. J.* (2018).

# Modification of silicalite-1 with ammonium compounds to prepare an acidic support for iridium hydrogenation catalyst

*Ewa Janiszewska<sup>1</sup>; Michał Zieliński<sup>1</sup>; Monika Kot<sup>1</sup>; Mariusz Pietrowski<sup>1</sup>*

*<sup>1</sup>Adam Mickiewicz University in Poznań, Faculty of Chemistry,  
Umultowska 89b, 61-614 Poznań, Poland*

The catalytic activity in hydrogenation reactions depends on both metallic active phase and catalyst support, particularly its porosity, surface chemical properties and crystalline structure. Silicalite-1, the alumina free MFI structure, known of its rather negligible acidity, arouses interest in a possibility of the catalytic use. It is possible to modify the acidity of its surface by its synthesis in different conditions as well as post-synthesis treatment.

In this paper the inert silicalite-1 was modified by means of post-synthesis treatment with solutions of different ammonium agents - (NH<sub>4</sub>Cl, NH<sub>4</sub>F, NH<sub>4</sub>OH) followed by further thermal treatment in order to generate the acidic sites in starting material. The obtained silica samples were used as supports for iridium catalysts. The influence of the support acidity on the activity of iridium catalyst for toluene hydrogenation was examined.

**Table 1.** Characterization of supports calcined at 550°C (air, 8h).

Sample code	Physical characterization of supports <sup>a)</sup>		
	Surface area, m <sup>2</sup> ·g <sup>-1</sup>	Total pore volume, cm <sup>3</sup> ·g <sup>-1</sup>	Average pore diameter, nm
Sil-1	311.1	0.18	2.3
Sil-1_OH	357.9	0.29	3.2
Sil-1_Cl	352.0	0.19	2.2
Sil-1_F	349.6	0.24	2.7

<sup>a)</sup> The Brunauer-Emmet-Teller surface areas determined by N<sub>2</sub> adsorption. Total pore volume and average pore size determined by the Barrett-Joyner-Halenda (BJH) method.

The modification of silicalite-1 leads to increase of the BET surface area for all supports regardless of the type of ammonium agents – Table 1. The increase of the total pore volume and average pore diameter was observed after the use of NH<sub>4</sub>OH as ammonium

agent. The acidity of modified MFI was estimated by means of temperature-programmed desorption of ammonia (NH<sub>3</sub>-TPD) and FT-IR spectra of adsorbed pyridine. The acidity of the support depends on the type of ammonium agents and increases in order Sil-1\_OH < Sil-1\_Cl < Sil-1\_F.

The catalysts with Ir loading of 1 wt.% supported on modified silicalite-1 materials were prepared by conventional impregnation of supports with the aqueous solution of

H<sub>2</sub>IrCl<sub>6</sub>. The prepared catalysts were characterized by N<sub>2</sub> adsorption/desorption measurements, H<sub>2</sub>-TPR. The mean size of metal particles was determined by hydrogen chemisorption measurements – Table 2.

**Table 2.** Characterization of iridium catalysts reduced at 400°C (H<sub>2</sub>, 2h).

Sample code	Physical characterization of iridium catalysts <sup>a)</sup>			Hydrogen chemisorption data for Ir/support catalysts <sup>b)</sup>		
	Surface area, m <sup>2</sup> ·g <sup>-1</sup>	Total pore volume, cm <sup>3</sup> ·g <sup>-1</sup>	Average pore diameter, nm	Total H <sub>2</sub> volume adsorbed, cm <sup>3</sup> ·g <sup>-1</sup>	Dispersion of Ir, %	Mean size of Ir, nm
Ir/Sil-1	319.3	0.17	2.2	0.128	21.7	5.1
Ir/Sil-1_OH	359.0	0.26	2.9	0.195	33.5	3.3
Ir/Sil-1_Cl	344.4	0.18	2.1	0.187	32.0	3.5
Ir/Sil-1_F	354.9	0.23	2.6	0.171	29.4	3.8

<sup>a)</sup> The Brunauer-Emmet-Teller surface areas determined by N<sub>2</sub> adsorption. Total pore volume and average pore size determined by the Barrett-Joyner-Halenda (BJH) method.

<sup>b)</sup> Dispersion and mean size of Ir particles (in nm) determined by H<sub>2</sub> chemisorption. Prior to hydrogen chemisorption, fresh samples were reduced with H<sub>2</sub> at 400°C for 2 h. Chemisorption of hydrogen was carried out at 35°C, and the isotherms were determined using five different pressures in the range of 12-40 kPa (H<sub>t</sub> - total adsorbed hydrogen). Dispersion calculated from total adsorbed hydrogen. Mean size of metal particles calculated from the amount of total chemisorbed hydrogen.

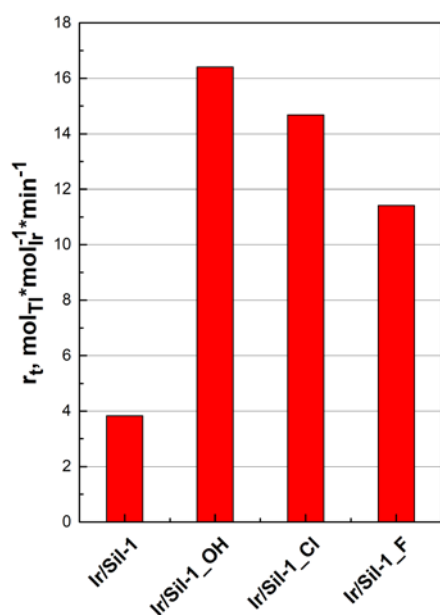


**Figure 1.** The effect of support on apparent rate of hydrogenation of toluene at 125°C.

The acidity of the support has affected the dispersion and particle size of metallic phase – Table 2. It was observed decrease of iridium dispersion and increase of Ir particle size with the raise of supports acidity (strength of acid sites).

The combination of iridium active phase and chemically modified silicalite-1 material as a support allowed to obtain new catalysts with high activities for toluene hydrogenation, greater than that of iridium supported on unmodified silicalite-1 – Figure 1. The activity of the catalysts is higher for Ir dispersed on supports with moderate acid sites.

### Acknowledgements

Monika Kot acknowledges the financial support from the National Science Center (Poland), grant PRELUDIUM UMO-2017/27/N/ST5/02042.

# Improving mayenite (C12A7) textural properties via an assisted solution combustion toward an enhancement of its catalytic performance in soot combustion

*Isaac Meza-Trujillo<sup>a</sup>, François Devred<sup>b</sup>, Eric M. Gaigneaux<sup>a\*</sup>*

*<sup>a</sup>Institute of Condensed Matter and Nanosciences, Université catholique de Louvain, Louvain-la-Neuve, Belgium*

Mayenite ( $12\text{CaO}\cdot 7\text{Al}_2\text{O}_3$ : C12A7) is an attractive material that is studied in diverse fields because of its interesting features such as ionic conduction, anion exchangeability, and oxidative catalytic properties, which are mostly attributed to the presence of clathrated extra-framework oxygen species [1,2]. C12A7 is conventionally prepared via a solid-state reaction at temperatures over 1300 °C for extended calcination periods. Because of such synthesis procedure, C12A7 obtained so far shows a negligible porosity and a very low specific surface area ( $\sim 1 \text{ m}^2 \text{ g}^{-1}$ ), which could lead to poor catalytic performances (e.g. low conversion), and limit its use as potential support for other catalytic species [2,3]. Even when a recent alternative via a hydrothermal method made possible the synthesis of mayenite at lower temperatures ( $\sim 400 \text{ °C}$ ) [3], it still requires a planetary ball-milling step to achieve an acceptable specific surface area ( $20 \text{ m}^2 \text{ g}^{-1}$ ), which is a costly, energy-consuming process that involves specialized equipment. Thus, it is desirable to search other strategies to produce porous mayenite at mild conditions and in an efficient way.

Here, we report a new, efficient, and simple way to produce mesoporous mayenite at temperatures lower than the ones reported in the literature so far. Our preparation method stands on the solution combustion synthesis (SCS) technique via a reaction between calcium and aluminum nitrates with urea and  $\beta$ -alanine as fuels. In a first stage, the influence of several variables was evaluated and exploited, such as furnace temperature and fuel-to-oxidizer ratio ( $\Phi$ ). Furthermore, a modification in our former protocol, by adding oxalic acid (OA) as pore generator was attempted to improve the textural properties of C12A7. The as-synthesized powder, obtained from the modified protocol, was then hydrated with hot distilled water (80 °C), filtered and dried. Finally, the solid was crushed and calcined in the range of 300-800 °C for 4 hours. The samples were characterized by XRD, *in situ* thermo-XRD, TGA-MS,

N<sub>2</sub> physisorption, SEM and Raman spectroscopy. The catalytic activity was tested in the soot oxidation using a commercial carbon black (printex-U) as diesel soot model.

**Table 1.** Textural properties of non-porous and porous mayenite samples

Sample	Calcination temperature (°C)	S <sub>BET</sub> (m <sup>2</sup> g <sup>-1</sup> )	BJH cumulative pore volume (cm <sup>3</sup> g <sup>-1</sup> )	Average pore diameter (nm)
SCS-C12A7-50	500*	1	-	-
@SCS-C12A7-30	300	55	0.22	29.3
@SCS-C12A7-40	400	74	0.29	24.3
@SCS-C12A7-60	600	52	0.31	21.8
@SCS-C12A7-80	800	30	0.26	33.1

\*Directly obtained after the combustion reaction at 500°C without the addition of oxalic acid

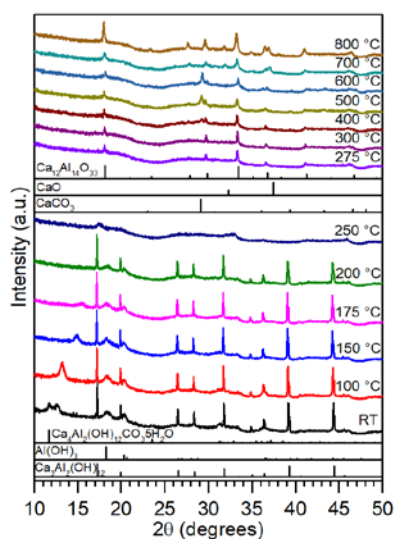


**Fig. 1.** *In situ* XRD of preformed precursor from room temperature (RT) to 800 °C

XRD results confirm the presence of a highly-crystalline C12A7 phase in the samples obtained directly after the combustion reaction at temperatures as low as 250 °C, while an increase in the furnace temperature to 500 °C promotes the disappearance of side phases. However, a non-porous C12A7 was always obtained, regardless of the temperature or  $\Phi$ -ratio tested. In contrast, our method involving the addition of OA produced porous mayenite from 275 °C after calcination of a preformed precursor, displaying a remarkable S<sub>BET</sub> of 74 m<sup>2</sup> g<sup>-1</sup> at 400 °C, as confirmed by *in situ* XRD and N<sub>2</sub> physisorption (Fig. 1 and Table

1). Thus, at 800 °C, a highly pure crystalline mesoporous C12A7 is obtained revealing a S<sub>BET</sub> 30-fold higher than those obtained through the conventional ceramic route.

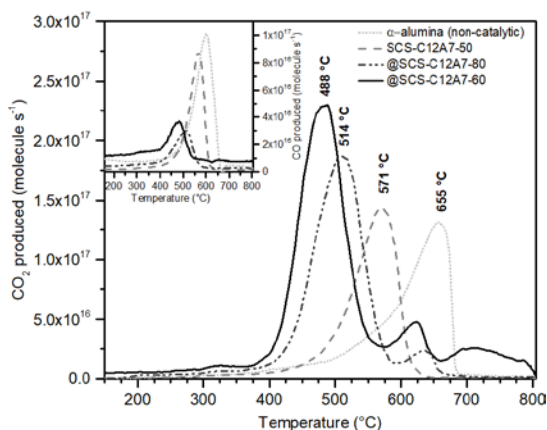


**Fig. 2.** CO<sub>2</sub> and CO (inset) produced during the catalytic oxidation of soot (Printex U)

Thanks to such enhancement of the textural properties of our SCS-derived porous mayenite, a remarkable increase in its catalytic activity for the soot combustion was recorded, shifting the complete soot oxidation to lower temperatures (Fig. 2). Furthermore, the improvement in the textural properties also seems to have a

beneficial influence in the selectivity towards CO<sub>2</sub>, drastically reducing the CO formation.

#### References

1. Hayashi, K. ... Hosono, H. *J. Am. Chem. Soc.* **124**, 738–739 (2002).
2. Ruszak, M. ... Sojka, Z. *Catal. Letters* **126**, 72–77 (2008).
3. Li, C. ... Suzuki, K. *Mater. Res. Bull.* **46**, 1307–1310 (2011).

# MnOx modified MgAl<sub>2</sub>O<sub>4</sub>/CeO<sub>2</sub> compositions with improved NOx-storage/release properties

*Marcos Schöneborn, Thomas Harmening*

*Sasol Germany GmbH, Anckelmannsplatz 1, 20537 Hamburg (Germany)*

*Javier Giménez-Mañogil, Juan Carlos Martínez-Munuera, Avelina García-García  
MCMA Group, Department of Inorganic Chemistry and Institute of Materials,  
University of Alicante, Carretera Sant Vicent del Raspeig s/n, 03690, Sant Vicent del  
Raspeig, Alacant, (Spain)*

## Introduction

Most common lean NOx trap catalysts (LNT) contain mixtures of BaO, CeO<sub>2</sub> and  $\gamma$ -Al<sub>2</sub>O<sub>3</sub> in order to store NOx over a wide-temperature range [1]. Significant improvements in NOx-storage, SOx tolerance and thermostability can be achieved by the replacement of alumina with spinel (MgAl<sub>2</sub>O<sub>4</sub>) [2]. Nonetheless, deactivation of LNTs at elevated temperatures and decreasing NOx storage performance due to incomplete regeneration during rich-cycles are perpetual challenges.

The present work focuses on improved thermal stability and NOx-storage/release behavior of MnOx-modified MgAl<sub>2</sub>O<sub>4</sub>/CeO<sub>2</sub> compositions with and without BaO [3].

## Materials and Methods

Compositions of MgAl<sub>2</sub>O<sub>4</sub> and 20% CeO<sub>2</sub> (Sasol, PURALOX MG20 Ce20) were modified subsequently with 9 wt% MnOx and 15 wt% BaO via impregnation with the acetate salts. The resulting materials were then thermally aged at 850°C in order to study the stabilizing effect of MnOx-addition. The phase compositions of the as-prepared samples were analyzed with powder X-ray diffraction. NOx adsorption experiments were conducted in a quartz tubular reactor connected to specific NDIR-UV gas analyzers for NO, NO<sub>2</sub>, CO, CO<sub>2</sub>, and O<sub>2</sub>, and the measurement data were recorded every 10 seconds. The NOx adsorption (500ppm NO/5%O<sub>2</sub>/balance N<sub>2</sub>) was performed at 300°C in a dual bed with a 1%Pt/Al<sub>2</sub>O<sub>3</sub> catalyst placed upstream of the samples. The TPD experiments were carried out under N<sub>2</sub> up to 700°C (5°C/min).

## Results and Discussion

The addition of MnOx significantly improves the thermal stability of MgAl<sub>2</sub>O<sub>4</sub>/CeO<sub>2</sub>/BaO resulting in improved NOx storage capacities (Table 1). High temperatures lead to the deactivation of barium by the formation of BaAl<sub>2</sub>O<sub>4</sub> which



can be suppressed to by a surface modification with MnOx resulting in the formation of BaMnO<sub>3</sub> which is known to be active for NOx storage [4,5].

The presence of MnOx also shows a remarkable effect on the strength of adsorbed species and the resulting NOx desorption behaviour (figure 1).

**Table 1.** NOx storage performance (300°C) and maximum desorption Temperatures.

Composite	MgAl/Ce	MgAl/Ce/Mn	MgAl/Ce/Ba	MgAl/Ce/Ba/Mn
mmol NOx/g	0.31	0.27	0.30	0.37
T <sub>des.max.</sub>	530°C	430°C	635°C	550°C
Ba-phase (XRD)	/	/	BaAl <sub>2</sub> O <sub>4</sub>	BaMnO <sub>3</sub> (main) BaAl <sub>2</sub> O <sub>4</sub> (minor)

The Mn-modified materials and with and without barium fully desorb NOx at approximately 80 – 100°C lower temperatures than the unmodified samples. The high-temperature peak present in these materials completely disappears upon Mn-addition leading to a very narrow temperature window for the NOx desorption process, especially in the Ba-free material. Both, the improved thermostability and the exceptional low temperatures required for NOx desorption make the MnOx-modified versions appealing candidates for LNT-catalysts. The Ba-free composition desorbs the majority of stored NOx species already below 350°C, which points to a good suitability of this version for passive NOx adsorbers (PNA).

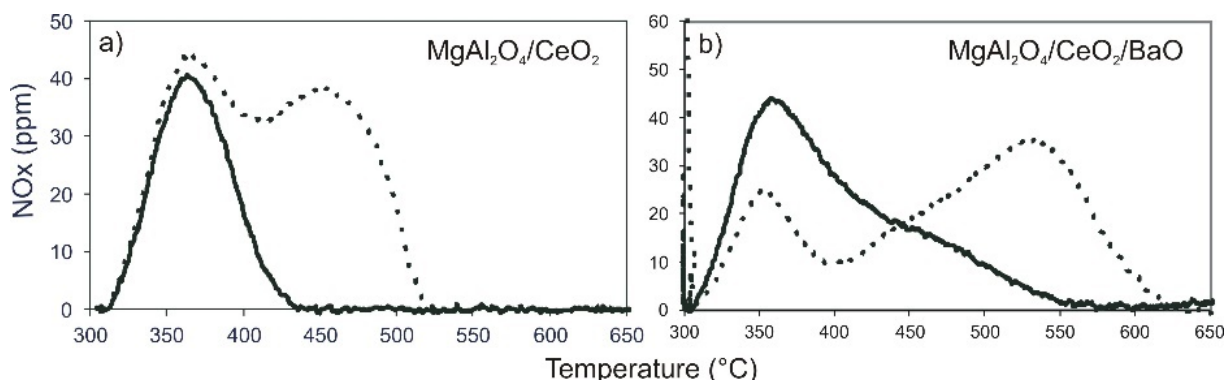


**Figure 1.** NOx TPD profiles of samples with (solid lines) and without (dotted lines) MnOx addition. a) MgAl<sub>2</sub>O<sub>4</sub>/CeO<sub>2</sub> b) MgAl<sub>2</sub>O<sub>4</sub>/CeO<sub>2</sub> with 15% BaO.

## References

1. Chan, D., Gremminger, A., and Deutschmann, O. *Top. Catal.* 56, 293 (2013).
2. Kwak, J.H., Kim, D.H., Szanyi, J., Cho, S.J., and Peden, C.H.F. *Top. Catal.* 55, 70 (2012).
3. Schöneborn, M., Harmening, T., Giménez-Mañogil, J., Martínez-Munuera, J.C., García-García, A. *Materials* 12, 13 (2019).
4. Gao, Y., Wu, X., Liu, S., Wenig, D., Zhang, H., Ran, R. *Catal. Today* 253, 83 (2015).
5. Xiao, J.H., Li, X-H., Denk, S., Xu, J.C., Wang, L.F., *Acta Phys. Chim. Sin.* 22, 815 (2006).

# Gliding arc plasma: a multifunctional tool for Mn based nanomaterials synthesis and plasmacatalytic device.

**F.W. Boyom Tatchemo<sup>a,b\*</sup>, S. Laminsi<sup>a</sup>, E. M. Gaigneaux<sup>b\*</sup>**

<sup>a</sup>*Department of Inorganic Chemistry, University of Yaounde I, P.O. Box 812, Yaounde, Cameroon*

<sup>b</sup>*Institute of Condensed Matter and Nanosciences (ICMN), Université catholique de Louvain, Place Louis Pasteur 1, L4.01.09, Louvain-la-Neuve 1348, Belgium.*

*[\\*franck.boyom@uclouvain.be](mailto:franck.boyom@uclouvain.be), [eric.gaigneaux@uclouvain.be](mailto:eric.gaigneaux@uclouvain.be)*

## 1. Scope

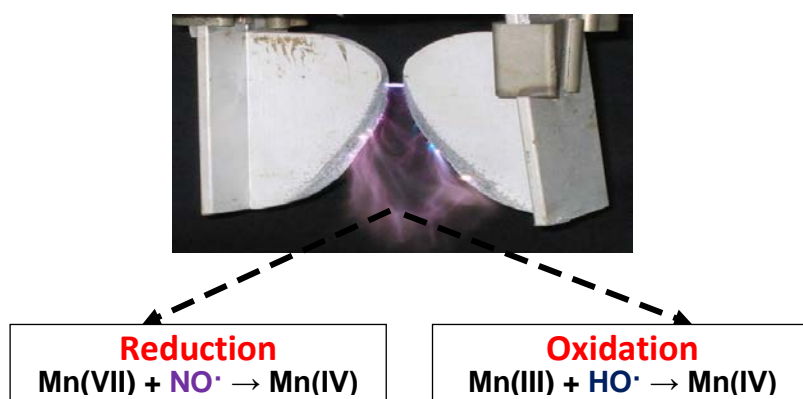
Synthesis of nanomaterials with a control of their size, shape, crystallinity, and porosity has become a major challenge, in order to ensure their performance in various applications such as magnetism, electronic, and catalysis [1]. So, nanostructured MnO<sub>2</sub> has received a great attention due firstly to its low cost and environmental friendliness, secondly to its large applicability as catalyst, biosensor and energy storage [2]. We report here the synthesis of different polymorphs of MnO<sub>2</sub> nanomaterials, by the plasmachemical reduction or oxidation of Mn(VII) and Mn(III) salts through respectively NO· and HO· radicals generated by a gliding arc plasma discharge at ambient temperature and under humid air. The influence of plasma parameters such as voltage and air flow has been studied. Plasmacatalytic activities of the synthesized materials were measured during bleaching and degradation of the organic pollutant Acid Yellow 23 (Tartrazin Yellow, TY).

## 2. Results and discussion

Mesoporous  $\alpha$ -MnO<sub>2</sub> nanorods named cryptomelane and  $\delta$ -MnO<sub>2</sub> nanosheets with specific area of 98 and 186 m<sup>2</sup>/g respectively were obtained after plasmachemical reduction of KMnO<sub>4</sub> at high (600V) and low (480V) voltages respectively. While mesoporous  $\gamma$ -MnO<sub>2</sub> nanospheres named nsutite and  $\delta$ -MnO<sub>2</sub> nanoflakes named birnessite with specific area of 48 and 289 m<sup>2</sup>/g respectively were obtained after plasmachemical oxidation of Mn(CH<sub>3</sub>COO)<sub>3</sub>·2H<sub>2</sub>O at high and low voltages respectively. The change of crystalline structure (polymorph), morphology and the increase of specific area with the decrease of the voltage are ascribed to the decrease of the energy transferred from the electrical source to the molecules of the plasma gas, thus to a decrease in the amount of reactive species (NO·, HO·)

produced therein. Otherwise, a decrease of the airflow under which the plasma plume is formed from 800 to 600 L/h at high voltage during the plasmachemical reduction of  $\text{KMnO}_4$  also led to changes of crystalline structure and morphology, and to an increase of specific area. These changes are ascribed to the decrease of the volume of plasma produced, thus provoking a smaller formation of reducing species ( $\text{NO}\cdot$ ) within the plume.

Plasmacatalytic activity measurement consisted in associating  $\text{MnO}_2$  plasmasynthesized to plasma as light source. So,  $\alpha\text{-MnO}_2$  and  $\gamma\text{-MnO}_2$  obtained respectively after plasmachemical reduction and oxidation at high voltage (600V) have been used as catalysts. Bleaching degrees of 11, 26 and 48% were obtained after 60 min of plasma alone,  $\alpha\text{-MnO}_2$  alone, and plasma/ $\alpha\text{-MnO}_2$  respectively. Correspondingly, bleaching degrees of 11 and 42% were recorded with  $\gamma\text{-MnO}_2$  alone and plasma/ $\gamma\text{-MnO}_2$ . So, bleaching degree of plasmacatalytic system is superior to the sum of those obtained after plasma alone, and catalyst alone treatments, revealing a synergy between both.



### 3. Conclusion

Gliding arc discharge allowed preparing mesoporous  $\text{MnO}_2$  nanomaterials through plasmachemical reduction and oxidation routes. The  $\text{MnO}_2$  polymorph can change with the precursor, and with plasma parameters such as voltage and airflow applied during synthesis. This work presents plasma gliding arc on the one hand, as a promising simple and versatile synthesis process of nanomaterials based on  $\text{MnO}_2$  allowing controlling their structure, texture and morphology, on the other hand, as plasmacatalytic device for oxidative bleaching of organic pollutants in wastewaters.

### 4. References

1. M. Zheng, H. Zhiang, X. Gong, R. Xu, Y. Xiao, H. Dong, X. Liu, Y. Liu, *Nano.Res.Let.* **2013**, 8:166.
2. W.H. Ry, D.W. Han, W.K. Kim, H.S. Kwon, *J.Nanopart.Res.* **2011**, 13:10, 4777-4784.

# Temporal post-discharge reaction effect on the catalytic, photocatalytic, and plasmacatalytic activities of plasma-synthesized $\alpha$ -MnO<sub>2</sub> nanorods.

**F.W.Boyom Tatchemo<sup>a,b\*</sup>, S.Laminsia, E.M.Gaigneaux<sup>b\*</sup>**

<sup>a</sup>*Department of Inorganic Chemistry, University of Yaounde I, P.O. Box 812, Yaounde, Cameroon*

<sup>b</sup>*Institut de la Matière Condensée et des Nanosciences (IMCN), Université catholique de Louvain, Place Louis Pasteur 1, L4.01.09, Louvain-la-Neuve 1348, Belgium*

\*[eric.gaigneaux@uclouvain.be](mailto:eric.gaigneaux@uclouvain.be), [franck.boyom@uclouvain.be](mailto:franck.boyom@uclouvain.be)

## 1 Scope

For decades, manganese oxides (MnO, MnO<sub>2</sub>, Mn<sub>2</sub>O<sub>3</sub>, and Mn<sub>3</sub>O<sub>4</sub>) have attracted considerable attention from researchers, because of their distinctive physicochemical properties, and their potential applications [1]. Among them, MnO<sub>2</sub> received a great attention because of its low cost, environmental friendliness, various polymorphs ( $\alpha$ -,  $\beta$ -,  $\gamma$ -,  $\delta$ -,  $\epsilon$ -, and  $\lambda$ -MnO<sub>2</sub>), and has large application as catalyst, biosensor, and energy storage material [2]. The controlled synthesis of MnO<sub>2</sub> nanoparticles is of major importance in these contexts. Therefore, Gliding Arc Plasma (GAP) appears as an innovative process, based on the production of highly reactive primary species such as HO·, and NO· radicals on the one hand, and on the other hand of secondary species such as H<sub>2</sub>O<sub>2</sub>, HOONO, and HNO<sub>2</sub> likely to participate in temporal post-discharge reactions [3].

## 2 Results and discussion

We report here the influence of ageing time and temperature under temporal post-discharge conditions on the physicochemical properties of  $\alpha$ -MnO<sub>2</sub> nanorods (reference material) obtained after reduction of KMnO<sub>4</sub> solution via gliding arc plasma process. This consisted to recover the precipitate obtained after extinction of the gliding arc discharge, age it at ambient temperature (~25°C) for 24, 48 and 72 hours, or at 100°C using a boiling water bath for 1, 2 and 3 hours. Physicochemical characterization of materials obtained at 25°C revealed obtaining a mix of phases, precisely of  $\alpha$ -MnO<sub>2</sub> and  $\gamma$ -MnO<sub>2</sub> polymorphs named cryptomelane and nsutite respectively. A partial transformation of  $\alpha$ -MnO<sub>2</sub> (cryptomelane) to  $\gamma$ -MnO<sub>2</sub> (nsutite), which could be ascribed to a maturation process of the reference material, occurred

during the ageing at plasma temporal post-discharge at 25°C. We also recorded (i) an increase of the specific surface area from 98 to 141 m<sup>2</sup>/g, and (ii) the conversion of nanorods to nanoneedles after 24 and 48 hours of ageing, then to nanosheets after 72 hours of ageing. Moreover, ageing at 100°C revealed after characterization, that a mixture of the phases  $\alpha$ -MnO<sub>2</sub> and  $\gamma$ -MnO<sub>2</sub> was obtained, but a more marked transformation of  $\alpha$ -MnO<sub>2</sub> to  $\gamma$ -MnO<sub>2</sub> than along the ageing at 25°C. Nevertheless, we obtained a decrease of specific surface area from 98 to 35 m<sup>2</sup>/g due to the shrinkage of the pores, and conversion of nanorods to bulkier agglomerates after 3 hours of ageing. Catalytic, photocatalytic, and plasmacatalytic activities of the different materials obtained were performed on Tartrazin Yellow as organic pollutant. We recorded an increase of the bleaching activities when the material is aged at 25°C, which is ascribed to the increase of the specific area observed. Contrarily, ageing at 100°C led to a decrease of the activity, due to the decrease of the specific area.

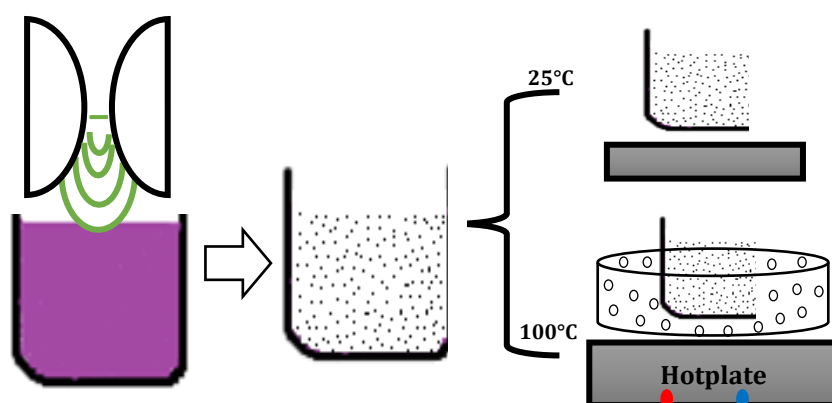


**Figure 1.** Temporal post-discharge reaction/Ageing process.

### 3 Conclusion

Ageing at 25°C affects positively the physicochemical properties of plasma-synthesized  $\alpha$ -MnO<sub>2</sub>, and is more beneficial in the sense that it requires no energy input compared to the ageing at 100°C. This work shows the plasma glidarc as an innovative synthesis process, which is capable to generate useful *in situ* reactive species useful for temporal post-discharge reactions.

### 4 References:

1. M. Zheng, H. Zhiang, X. Gong, R. Xu, Y. Xiao, H. Dong, X. Liu, Y. Liu, *Nano.Res.Let.* **2013**, 8:166.
2. W.H. Ry, D.W. Han, W.K. Kim, H.S. Kwon, *J.Nanopart.Res.* **2011**, 13:10, 4777-478.
3. S.A. Djepang, S. Laminsi, E.N. Tamungang, C. Ngnintedem, J.-L. Brisset, *Chem.Mater.Eng.* **2014**, 2, 1, 14-23.

# In situ characterization of fresh and sulfur contaminated Cu-zeolite SCR catalysts using XAFS

*Susanna Liljegren Bergman, Yale-NUS College, Singapore; Sandra Dahlin, KTH, Stockholm, Sweden; Du Yonghua, A\*STAR, Singapore; Xi Shibo, A\*STAR, Singapore, Lars Pettersson, KTH, Stockholm, Sweden, Steven L. Bernasek, Yale-NUS College, Singapore.*

## Introduction

In systems for the after-treatment of exhaust from heavy-duty diesel vehicles, both diesel oxidation catalysts (DOC) for the removal of unburned hydrocarbons and carbon monoxide, and ammonia driven selective catalytic reduction (NH<sub>3</sub>-SCR) catalysts to remove nitrogen oxides are used. We report here an *in-situ* study of the Cu-zeolite Cu-SSZ-13 SCR catalyst using synchrotron based X-ray absorption spectroscopy for characterization of the catalyst under oxidizing and reducing conditions. Both the freshly prepared Cu-SSZ-13 catalyst, and the sample contaminated by exposure to SO<sub>2</sub> are examined. Near edge spectra (XANES) are considered.

## Experimental

Cu-SSZ-13 samples, with 2.5% Cu loading by weight, were provided by collaborators at Scania. The fresh sample was used as supplied, the sulfur contaminated sample was exposed to a flow of SO<sub>2</sub> for 8 hours while being held at 250°C. Samples were examined while heating under oxidizing (flow of pure air) or reducing (flow of 5% H<sub>2</sub> in N<sub>2</sub>) atmospheres in the catalysis end-station XAFCA at the Singapore Synchrotron Light Source [1]. X-ray absorption spectra of the Cu K edge in the energy range of 8800 to 9100 eV were collected. Near edge (XANES) spectra and extended fine structure (EXAFS) spectra were analyzed.

## Results and discussion

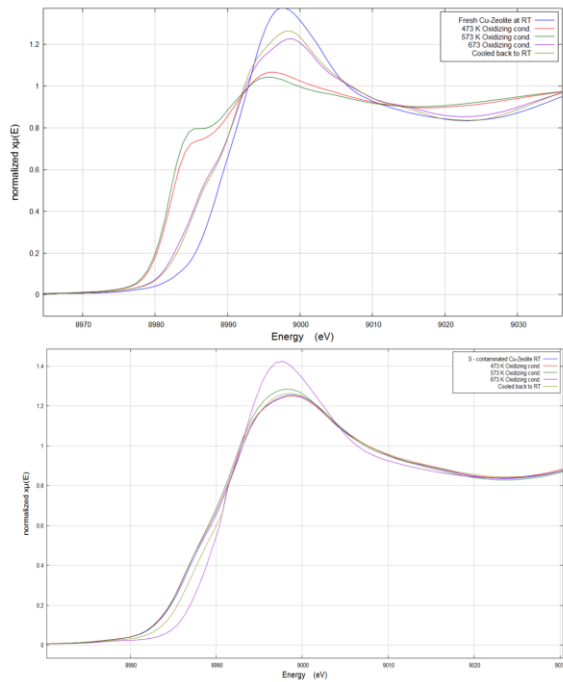
Figure 1 (upper) shows the XANES spectra of the fresh sample for the Cu K edge as it is heated from room temperature to 400°C in an oxidizing atmosphere. Figure 1 (lower) shows the spectra for the sulfur contaminated sample during this oxidation process. The spectra for the fresh sample show two peaks in the edge region, one at around 8985 eV (Cu<sup>+</sup>) and the other just below 9000 eV (Cu<sup>+2</sup>). The relative intensities of these peaks change as the sample is heated in air, indicating a change in oxidation state of the active Cu in the zeolite. For the sulfur exposed sample, only

the peak just below 9000 eV is clearly visible, and the relative intensities of the two regions do not change significantly during heating in air. This suggests that the  $\text{Cu}^{+2}$  state is locked in for the sulfur exposed sample, perhaps by formation of sulfate during the poisoning. Figure 2(upper) and (lower) shows the fresh and S

contaminated sample following exposure to a reducing flow of  $\text{H}_2$  in  $\text{N}_2$ . The spectra indicate reduction of the Cu site in both cases, suggesting that the sulfur poisoned sample can be regenerated by heating in hydrogen.

### Conclusions

XANES spectra of the K edge of Cu for Cu-SSZ13 ammonia selective catalytic reduction catalysts have been obtained for freshly prepared and sulfur poisoned samples under oxidizing and reducing conditions.



The relative concentrations of  $\text{Cu}^+$  and  $\text{Cu}^{+2}$  present in the catalysts under oxidizing and reducing conditions are determined for both samples, with clear differences observed for the processes. The S poisoned sample appears to have a preponderance of  $\text{Cu}^{+2}$  under oxidation, perhaps due to the formation of stable copper sulfate during the poisoning process. Reduction in hydrogen results in a return to the initial pre-oxidation state for both samples under reducing conditions indicating that hydrogen

treatment may be used to regenerate the S poisoned catalyst.

### References

[1] XAFCA beamline, built and maintained by ICES, A\*STAR, Singapore

Figure 1. Oxidizing conditions

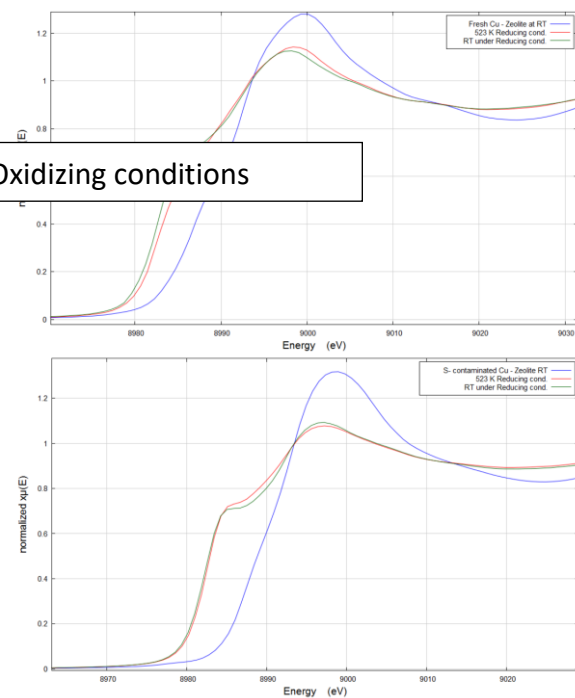


Figure 2. Reducing conditions

# Kinetic study on reaction mechanism of hydrogenolysis over Pt/WO<sub>3</sub>/Al<sub>2</sub>O<sub>3</sub> catalyst

*Takeshi Aihara<sup>1</sup>, Hiroki Miura<sup>1,2,4</sup>, Tetsuya Shishido<sup>1,2,3,4</sup>*

<sup>1</sup>*Graduate School of Urban Environmental Sciences, Tokyo Metropolitan University, 1-1  
Minami-Osawa, Hachioji, Tokyo 192-0397, Japan*

<sup>2</sup>*Research Center for Hydrogen Energy-Based Society, Tokyo Metropolitan  
University, 1-1 Minami-Osawa, Hachioji, Tokyo 192-0397, Japan*

<sup>3</sup>*Research Center for Gold Chemistry, Tokyo Metropolitan University, 1-1 Minami-  
Osawa, Hachioji, Tokyo 192-0397, Japan*

<sup>4</sup>*Elements Strategy Initiative for Catalysts & Batteries, Kyoto University, Goryo-Ohara,  
Nishikyo-ku, Kyoto 615-8520, Japan*

## Introduction

Selective conversion of biomass compounds to value-added chemicals has attracted a great deal of attention. The hydrogenolysis is one of the useful reactions to produce diols which are used as a monomer for resin. Recently we have reported that the perimeter interface between 2D-monolayer WO<sub>3</sub> domains and  $\gamma$ -Al<sub>2</sub>O<sub>3</sub> has an important role in selective hydrogenolysis of glycerol to 1,3-propanediol (PDO) [1]. 1,3-PDO was formed with high selectivity, however, 1,2-PDO and 1-PrOH were also produced as by-products. The mechanism of hydrogenolysis is still unclear. In this study, to get the fundamental knowledge about controlling the dissociation position of C-O bond in polyols, the mechanisms of diols (with/without vicinal OHs) hydrogenolysis were investigated.

## Experimental

WO<sub>3</sub>/Al<sub>2</sub>O<sub>3</sub> catalysts were prepared by impregnation of  $\gamma$ -Al<sub>2</sub>O<sub>3</sub> with (NH<sub>4</sub>)<sub>10</sub>W<sub>12</sub>O<sub>42</sub> · 5H<sub>2</sub>O and calcined at 1123 K for 3h in dry air [2]. Pt/WO<sub>3</sub>/Al<sub>2</sub>O<sub>3</sub> catalysts were prepared by impregnating WO<sub>3</sub>/Al<sub>2</sub>O<sub>3</sub> with an aqueous solution of H<sub>2</sub>PtCl<sub>6</sub> and calcined in a flow of dry air at 573K for 3 h. The hydrogenolysis was carried out in a Teflon vessel placed in a stainless steel autoclave. The products were analyzed by FID- and TCD-GC.

## Results and discussion



The hydrogenolysis of PDOs over Pt/WO<sub>3</sub>/Al<sub>2</sub>O<sub>3</sub> catalyst was investigated. The reaction rate of 1,2-PDO was faster than that of 1,3-PDO. The reaction orders with respect to substrate concentration and H<sub>2</sub> pressure were also estimated (Table

**Table 1.** Reaction order in the hydrogenolysis of various substrate over Pt/WO<sub>3</sub>/Al<sub>2</sub>O<sub>3</sub>.

Substrate	Order	
	[Substrate]	P <sub>H<sub>2</sub></sub>
1,2-PDO	1.0	1.0
1,3-PDO	0.97	-0.20

Conditions: Catalyst (100 mg), Substrate (1–4 mmol), H<sub>2</sub>O (9 mL), P<sub>H<sub>2</sub></sub>= 2–5 MPa, T= 453 K.

1). The reaction orders with respect to the both 1,2- and 1,3-PDO concentration were estimated to be almost one. This result indicates that the strength of substrate adsorption on catalyst is same. However, the reaction orders of H<sub>2</sub> pressure were different each other. The orders of 1,2- and 1,3-PDO hydrogenolysis were positive and almost zero, respectively. These results imply that the hydrogenolysis of 1,2- and 1,3-PDO proceeds through different mechanism.

From these results, we propose the plausible hydrogenolysis mechanisms of diols hydrogenolysis (Figure 1). In the case of secondary OH dissociation (hydrogenolysis of 1,2-PDO) the substrate initially adsorbs onto the Al<sub>2</sub>O<sub>3</sub> surface, following by the protonation of secondary OH by the Al-(OH)-W site. Then, dehydration proceeds to form secondary carbocation. Third, the intermediate is attacked by hydride. Finally, alkoxide species desorbed to form 1-PrOH. On the other hand, in the case of primary OH dissociation (hydrogenolysis of 1,3-PDO) the substrate adsorbed and dehydration is proceeded by Lewis acid site on Al<sub>2</sub>O<sub>3</sub>. And then, hydrogenation and desorption proceed. Finally product is formed. In this mechanism, rate-determining step may be dehydration step.

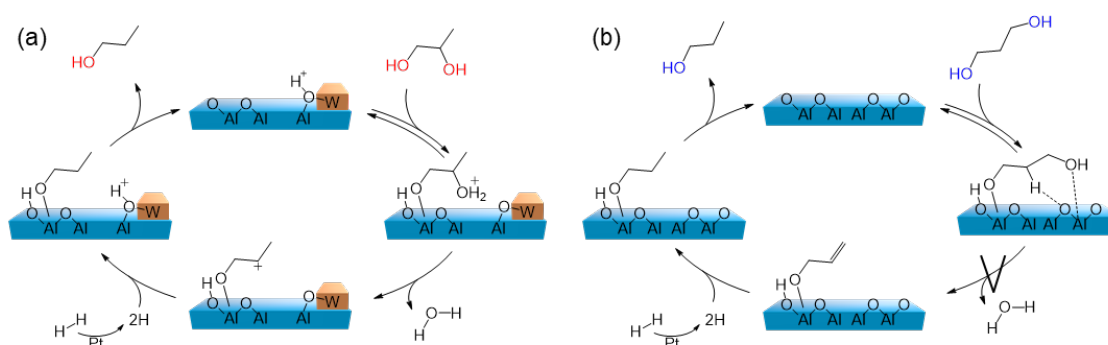


**Figure 1.** Reaction mechanism of (a) 1,2-PDO and (b) 1,3-PDO hydrogenolysis over Pt/WO<sub>3</sub>/Al<sub>2</sub>O<sub>3</sub> catalyst.

## References

- [1] T. Aihara, H. Kobayashi, S. Feng, H. Miura and T. Shishido, *Chem. Lett.* **2017**, *46*, 1497.
- [2] T. Kitano, T. Hayashi, T. Uesaka, T. Shishido, K. Teramura and T. Tanaka, *ChemCatChem* **2014**, *6*, 2011.

# Complete oxidation of CH<sub>4</sub> over Co-Ce catalysts:

## Effect of preparation method

Darda S.<sup>1,2</sup>, Pachatouridou E.<sup>1</sup>, Lappas A.A.<sup>1</sup>, Lemonidou A.<sup>2</sup>, Iliopoulou E.F.<sup>1,\*</sup>

<sup>1</sup>Chemical Process & Energy Resources Institute (CPERI), Centre for Research & Technology Hellas (CERTH), Thessaloniki, Greece; \*eh@cperi.certh.gr

<sup>2</sup>Department of Chemical Engineering, Aristotle University of Thessaloniki (AUTH), Thessaloniki, Greece;

### Introduction

Today, CH<sub>4</sub>, N<sub>2</sub>O, and CO<sub>2</sub> emissions represent 98% of the total greenhouse gas (GHG) inventory worldwide, while their share is expected to increase in the near future. Methane, the main compound of natural gas (NG) in oil fields, is used in various industrial processes and also as energy source in gas turbines or NG fueled vehicles, which are predicted to soon represent a much larger percentage of the total fleet. As methane is in addition a substantially more potent greenhouse gas (GHG) than CO<sub>2</sub>, catalytic oxidation converters are needed for its abatement [1, 2].

The current study aims to novel Co-Ce catalytic materials for CH<sub>4</sub> oxidation. The effect of both the synthesis method of the CeO<sub>2</sub> support (either hydrothermal or precipitation technique) and the metal loading (0, 2, 5 and 15 wt.% Co) are investigated on the catalytic performance and durability for complete CH<sub>4</sub> oxidation.

### Synthesis, characterization and evaluation of catalysts

The CeO<sub>2</sub> carrier and bare Co<sub>3</sub>O<sub>4</sub> (synthesized for comparison reasons) were prepared following either the precipitation (labeled as CeO<sub>2</sub>-P, Co<sub>3</sub>O<sub>4</sub>-P) or the hydrothermal (labeled as CeO<sub>2</sub>-H, Co<sub>3</sub>O<sub>4</sub>-H) technique. Ce(NO<sub>3</sub>)<sub>3</sub>·6H<sub>2</sub>O and Co(NO<sub>3</sub>)<sub>2</sub>·6H<sub>2</sub>O were used as precursor salts for both synthesis methods. The as-obtained materials were dried overnight at 110°C and then calcined at 500°C for 5h under air flow. The incorporation of cobalt over the CeO<sub>2</sub> supports was conducted by incipient wetness impregnation method, using aqueous solutions of Co(NO<sub>3</sub>)<sub>2</sub>·6H<sub>2</sub>O. The physicochemical characteristics of all materials were investigated by various complementary techniques (N<sub>2</sub> Physisorption, XRD, H<sub>2</sub>-TPR, O<sub>2</sub>-TPD and TEM). The catalytic combustion of CH<sub>4</sub> was performed in a fixed-bed reactor (feed: 0.5% vol. CH<sub>4</sub>, 10% vol. O<sub>2</sub>, balanced with He, flow rate: 900cm<sup>3</sup>/min, corresponding to a Gas Hourly Space Velocity (GHSV): ~40,000 h<sup>-1</sup>). Catalysts' efficiency on CH<sub>4</sub> conversion was explored in the 300-600°C temperature range.

## Results

Use of hydrothermal synthesis for the preparation of ceria support results in the most efficient Co-Ce catalysts, as compared with the materials prepared over precipitated ceria. In particular, a  $\text{CeO}_2$  support of smaller crystallite size (11.8nm), larger surface area ( $110.9\text{m}^2/\text{g}$ ) and enhanced reducibility leads to more efficient Co-Ce catalysts. A shift of all corresponding reduction peaks to lower temperatures, observed in  $\text{H}_2$ -TPR profiles of Co-Ce materials, also implies synergetic effects between the deposited  $\text{Co}_3\text{O}_4$  and the  $\text{CeO}_2$  carrier. Enhanced oxygen mobility of both oxides ( $\text{CeO}_2$  and  $\text{Co}_3\text{O}_4$ ) is also evidenced by  $\text{O}_2$ -TPD studies (not shown here), when using the hydrothermal synthesis method and when incorporating Co on the ceria support.

Catalytic performances of all materials are presented in Figure 1. The limited  $\text{CH}_4$  oxidation activity over pure  $\text{CeO}_2$  samples is significantly enhanced by Co incorporation and further improved by higher Co loadings, especially in the case of Co incorporation on the  $\text{CeO}_2$ -H (ceria nanorods). The optimum catalyst 15wt. % Co/ $\text{CeO}_2$ -H achieved 90%  $\text{CH}_4$  conversion at  $600^\circ\text{C}$ . Moreover, a significantly improved performance ( $T_{50\%}=440^\circ\text{C}$ ) was observed at lower GHSV $\sim 10,000\text{h}^{-1}$  (as compared to  $T_{50\%}=520^\circ\text{C}$  with standard GHSV $\sim 40,000\text{h}^{-1}$ .)

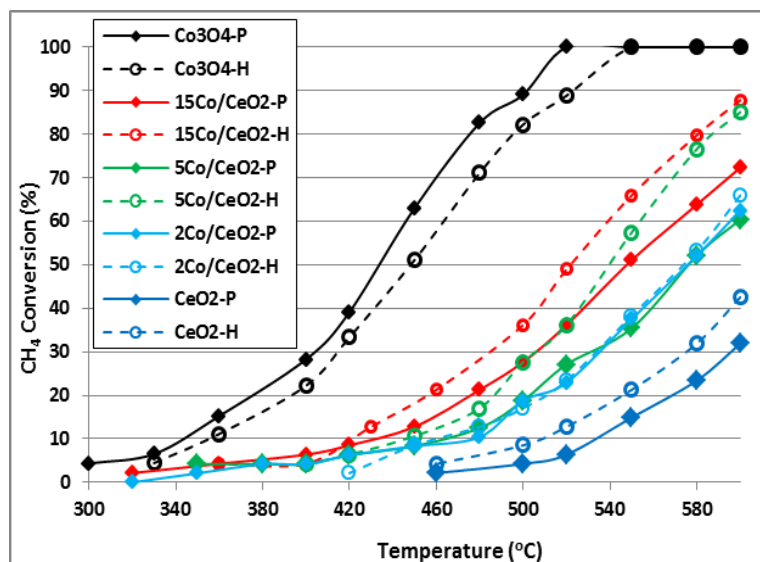


Figure 1. Catalytic performance in complete  $\text{CH}_4$  oxidation.

## Conclusions

The superior performance of 15wt. % Co/ $\text{CeO}_2$ -H is probably related with the optimized physicochemical properties of  $\text{CeO}_2$ -H support: smaller  $\text{CeO}_2$  crystallites, higher surface area and enhanced reducibility, additionally combined with induced synergetic effects between the deposited  $\text{Co}_3\text{O}_4$  and the  $\text{CeO}_2$  carrier.

## References

- [1] N.N. Clark, D.R. Johnson, D.L. McKain, W.S. Wayne, H. Li, J. Rudek, R.A. Mongold, C. Sandoval, A.N. Covington, J.T. Hailer, Journal of the air & waste management association 67(12) (2017) 1328–1341.
- [2] R.J. Farrauto, Science 337 (2012) 659–660.

# ***Novel SCR catalysts prepared by surface organometallic chemistry with enhanced activity : mechanistic study***

*Hai P Nguyen*<sup>1\*</sup>, *Sandra Palma*<sup>2</sup>, *Nicolas Merle*<sup>3</sup>, *Marc-Olivier Charlin*<sup>3</sup>, *Cherif Larabi*<sup>3</sup>,  
*Szeto Kai Chung*<sup>3</sup>, *Mostafa Taoufik*<sup>3</sup>, *Olivier Marie*<sup>2</sup>

<sup>1</sup>*Toyota Motor Europe, 1930 Zaventem, Belgium*

<sup>2</sup>*LCS – UMR6506 – UNICAEN- ENSICAEN, France*

<sup>3</sup>*UMR 5265 C2P2-LCOMS CNRS, France*

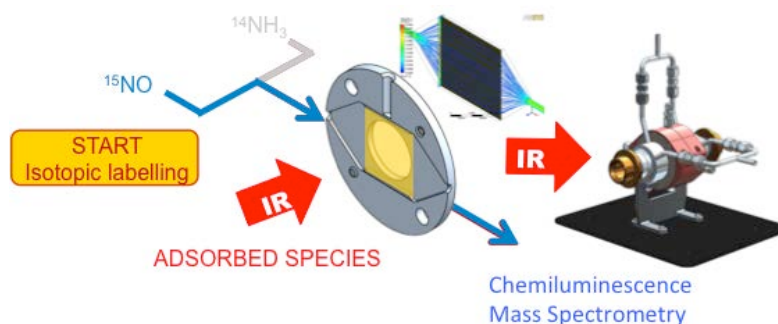
*\* hai.p.nguyen@toyota-europe.com*

## **Introduction**

Selective catalytic reduction (SCR) with ammonia as reducing agent is one of the key technology that catalytically converse NO<sub>x</sub> gases into harmless nitrogen. Some metals in Groups V or VI such as V, W are known to be good catalysts for NO<sub>x</sub> conversion, mostly in the form of oxides or supported particles prepared by classical methods [1,2]. In order to access well-defined active sites, we recently developed selective catalytic reduction (SCR) catalysts using surface organometallic chemistry (SOMC) methodology.[3] These catalysts comprising of a metal selected from Group V or Group VI elements grafted on metal oxides possess high NO<sub>x</sub> conversion compared to those catalysts prepared by conventional methods such as impregnation. Characterization (EXAFS, FTIR, UV-Vis) of the catalysts suggest that a high portion of the grafted metal stays at atomic dispersion, which may be related with the excellent performance of the reported catalysts. We report here the mechanistic study by FTIR in combination with isotopic labelling.

## **Materials and Methods**

The catalysts are synthesized by grafting of suitable commercially available Niobium organometallic precursors on CeO<sub>2</sub> catalysts support.



NMR, EPR, FTIR, and Raman spectroscopies are used to monitor changes during grafting processes. The products are characterised by TEM, XPS, ToF-SIMS after calcination at 500 °C in air.

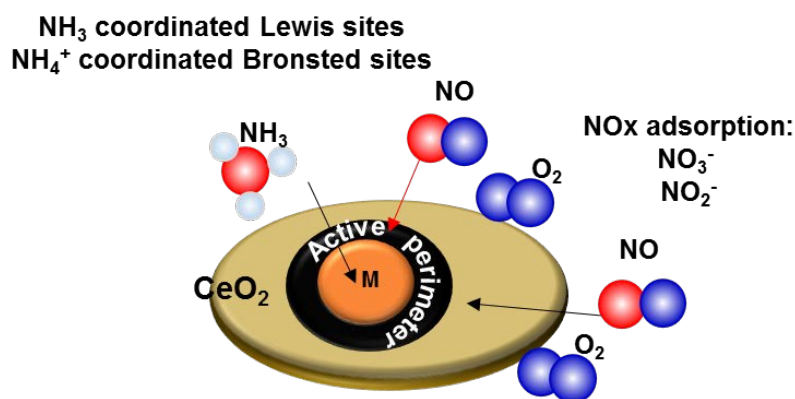
An isotopic labelling methodology was applied during the *operando* experiments.  $^{15}\text{NO}$  isotope was used to interact with  $^{14}\text{NH}_3$  in presence or not of 10%  $\text{O}_2$  balanced with Ar at 300°C while surface species and gas phase were simultaneously monitored through FTIR and complementary FTIR, MS and chemiluminescence respectively. These experiments allowed distinguishing various nitrogen containing species on the surface and in the gas phase, and the dynamics of interaction between them.

## Results and Discussion

The applied methodology showed that reaction of  $\text{NH}_3$  with pre-adsorbed  $\text{NO}_x$ -species (in a rather high amount) leads to a long SCR period but with poor instantaneous efficiency. On the contrary, the reaction of NO with pre-adsorbed  $\text{NH}_3$  (in a rather low amount) leads to a short SCR period but with high instantaneous efficiency suggesting the presence of highly favoured specific adsorption sites for NO in close vicinity of adsorption sites for ammonia, the subsequent interaction between neighbouring adsorbed reactants being very fast.

## Conclusions

Based on the above analysis, the scheme below proposes that most of the SCR reactions take place on the active perimeter around each metal site, where  $\text{NH}_3$



adsorbed on metal are in contact and react with NO adsorbed on the support oxide or at the interface between the support and the metal according to a Langmuir-Inschelwood mechanism.

## References

1. Appl. Catal. B 144 (2014) 538–546
2. Catal. Today 258 (2015) 11–16.
3. Chem. Soc. Rev., 2013, 42, 9035-9054

## LaCoO<sub>3</sub> perovskite as selective PROX catalyst:

### *operando* XAS, XRD and DRIFTS

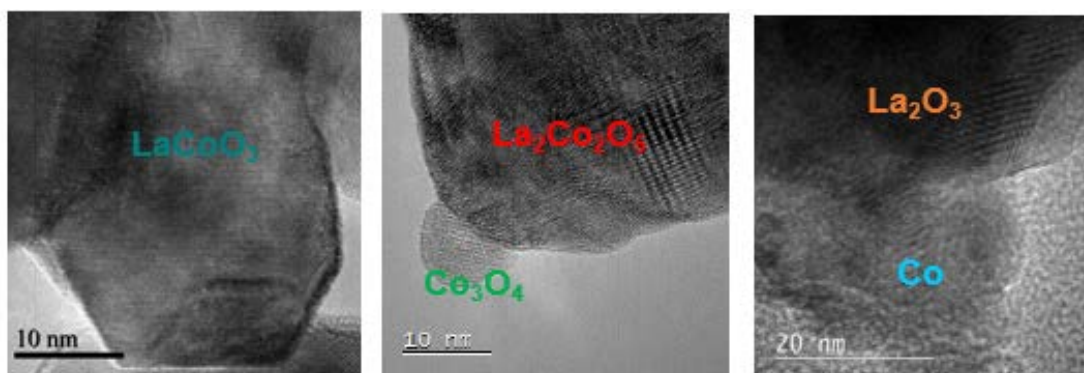
Nevzat Yigit<sup>1</sup>, Liliana Lukashuk<sup>1,2</sup>, Johannes Bernardi<sup>3</sup>, Karin Föttinger<sup>1</sup>,  
Günther Rupprechter<sup>1</sup>

<sup>1</sup> Institute of Materials Chemistry, TU Wien, Vienna, 1060, Austria

<sup>2</sup> Current address: Johnson Matthey, PO Box 1, Belasis Avenue, Billingham,  
Cleveland, TS23 1LB, UK

<sup>3</sup> USTEM, TU Wien, Wiedner Hauptstrasse 8-10, 1040 Vienna, Austria

The potential of the LaCoO<sub>3</sub> (LCO) perovskite for preferential CO oxidation (PROX) was explored. LCO was synthesized via the modified Pechini method and characterized by X-ray diffraction (XRD), high resolution transmission electron microscopy (HRTEM), CO- and H<sub>2</sub>- temperature programmed reduction (TPR), temperature programmed desorption (TPD) and tested as a catalyst for PROX, focusing on the effect of different pretreatment conditions on the catalytic performance. Different pretreatments of LCO led to formation of La<sub>2</sub>Co<sub>2</sub>O<sub>5</sub>, Co/La<sub>2</sub>O<sub>3</sub> and Co<sub>3</sub>O<sub>4</sub>/La<sub>2</sub>O<sub>3</sub> structures. In contrary to La<sub>2</sub>Co<sub>2</sub>O<sub>5</sub>, Co/La<sub>2</sub>O<sub>3</sub> and Co<sub>3</sub>O<sub>4</sub>/La<sub>2</sub>O<sub>3</sub>, Co<sup>3+</sup> incorporated into the LaCoO<sub>3</sub> perovskite structure was more resilient towards overreduction, as long as CO oxidation was dominant.



Hydrogen production and purification are industrially important processes. Hydrogen is used for ammonia synthesis<sup>1</sup>, in fuel cell technology, and for the manufacturing of numerous chemicals<sup>2</sup>. Particularly for ammonia synthesis, CO-free hydrogen is of importance, because even ppm concentrations of CO deactivate the iron-based ammonia synthesis catalyst by strong CO adsorption to metallic iron. The same applies to fuel cells, when even ppm concentrations of CO poison the Pt electrodes<sup>3</sup>. Catalytic preferential CO oxidation (PROX) is a key reaction for removing traces of CO from the H<sub>2</sub>-rich stream for fuel cells. Transition metal oxides, especially cobalt-based materials, are perspective catalysts for PROX.

Among the most attractive materials in the modern chemical industry (e.g., catalysis, chemical sensors, electrode materials, and fuel cells), the perovskite oxides have been recently emerged as very promising and alternative catalytic material to transition metal oxides. The interest in perovskite materials of  $ABO_3$  structure type, where A is a rare earth/alkaline earth and B a transition metal cation, is explained by the perovskite unique properties such as high thermal and structure stability of the B cations, making these materials resistance towards sintering and reduction, especial for high-temperature applications. It is also reported that the cobalt based perovskite catalysts more active for the oxidation reaction than manganese, nickel or iron based perovskites <sup>4</sup>.

The main objective of this work was to investigate the correlation between the structure and oxidation state and the active sites/phases of Co-based perovskites. To obtain a better understanding of the catalytic system, *operando* DRIFTS, XAS and XRD were performed during PROX, revealing the adsorption properties, structural changes and oxidation state of the catalyst. The  $LaCoO_3$  bulk structure remained intact during PROX and cobalt was preserved in a high oxidation state. When compared to simple oxide like  $Co_3O_4$  or  $CoO$ ,  $Co^{3+}$  was more stable, resulting in a wider PROX temperature window, highlighting the usefulness of cobalt-based perovskites for preferential CO oxidation <sup>5-6-7</sup>.

**Acknowledgments:** Supported by the Austrian Science Fund (FWF) via Doctorate School Solids4Fun (W1243) and SFB FOXSI (F4502-N16).

## References

- [1] Erisman, J. W.; Sutton, M. A.; Galloway, J.; Klimont, Z.; Winiwarter, W., How a century of ammonia synthesis changed the world. *Nature Geoscience* **2008**, *1* (10), 636-639.
- [2] Ramachandran, R.; Menon, R. K., An overview of industrial uses of hydrogen. *Int. J. Hydrogen Energy* **1998**, *23* (7), 593-598.
- [3] Baschuk, J. J.; Li, X., Carbon monoxide poisoning of proton exchange membrane fuel cells. *International Journal of Energy Research* **2001**, *25* (8), 695-713.
- [4] Tanaka, H., An intelligent catalyst: the self-regenerative palladium-perovskite catalyst for automotive emissions control. *Catalysis Surveys from Asia* **2005**, *9* (2), 63-74.
- [5] Lukashuk, L.; Föttinger, K.; Kolar, E.; Rameshan, C.; Teschner, D.; Havecker, M.; Knop-Gericke, A.; Yigit, N.; Li, H.; McDermott, E.; Stöger-Pollach, M.; Rupprechter, G., Operando XAS and NAP-XPS studies of preferential CO oxidation on  $Co_3O_4$  and  $CeO_2-Co_3O_4$  catalysts. *J. Catal.* **2016**, *344*, 1-15.
- [6] Lukashuk, L.; Yigit, N.; Rameshan, R.; Kolar, E.; Teschner, D.; Hävecker, M.; Knop-Gericke, A.; Schlögl, R.; Föttinger, K.; Rupprechter, G., Operando Insights into CO Oxidation on Cobalt Oxide Catalysts by NAP-XPS, FTIR, and XRD. *ACS Catal* **2018**, *8* (9), 8630-8641.
- [7] Lukashuk, L.; Yigit, N.; Li, H.; Bernardi, J.; Föttinger, K.; Rupprechter, G., Operando XAS and NAP-XPS investigation of CO oxidation on meso- and nanoscale  $CoO$  catalysts. *Catal. Today* **2018**, doi.org/10.1016/j.cattod.2018.12.052.



## Surface science studies of modified $\text{Co}_3\text{O}_4(111)$ thin films

*Thomas Haunold, Christoph Rameshan, Günther Rupprechter*

*Institute of Materials Chemistry, TU Wien, Getreidemarkt 9, 1060 Vienna, Austria*

Over the past decades, cobalt oxides have served as inexpensive key materials for many applications. These range from heterogeneous catalysis of important oxidizing reactions (e.g. low-temperature CO-oxidation [1, 2], preferential oxidation of CO (PROX) [3-5], Ostwald synthesis of nitric acid by oxidation of ammonia [6], and oxidation of hydrocarbons [1, 7]), to the Fischer-Tropsch synthesis of hydrocarbons and liquid fuels [8], and the conversion of volatile organic compounds (VCOs) [9].

Recently,  $\text{Co}_3\text{O}_4$  has also been investigated as potential anode material for Li ion batteries (LIBs) [10, 11], featuring high theoretical discharge capacities. However, the formation of a solid electrolyte interface (SEI) competes with reversible  $\text{Li}^+$  ion intercalation and thus reduces the capacity of LIBs [12]. A similar behavior is observed in solid-state batteries where metallic Li anodes are used.

The most effective approach to explain and improve the functionality of cobalt oxides is to conduct experiments at a microscopic or even atomic level. This can be achieved by preparation and study of model-systems. Therefore,  $\text{Co}_3\text{O}_4$  and Li thin films were prepared by physical vapor deposition (PVD) under ultrahigh vacuum (UHV) conditions. Film growth was monitored visually in real-time using low energy electron microscopy (LEEM). Afterwards, thin film characterization was carried out by X-ray photoelectron spectroscopy (XPS), low energy electron diffraction (LEED) and temperature-programmed desorption (TPD).

Reactivity testing of  $\text{Co}_3\text{O}_4$  demonstrated that CO oxidation in the mbar range occurs already at room temperature in case of powders. For  $\text{Co}_3\text{O}_4(111)$  thin films an onset temperature of 200 °C was observed which agrees well with previous results reported in the literature [13]. However, the presence of moisture led to a decrease of CO conversion due to water dissociation (formation of hydroxyl groups) and blocking of active sites.



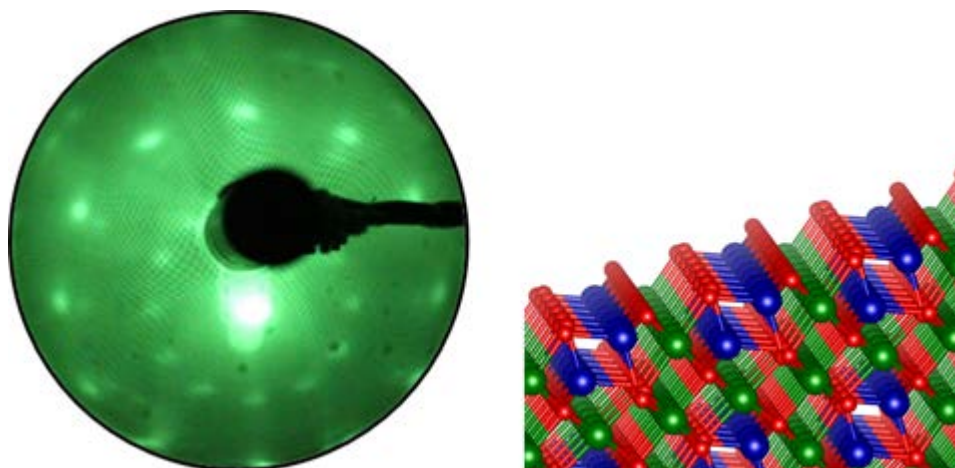


**Figure 1:** LEED pattern of  $\text{Co}_3\text{O}_4(111)$  (left) and surface structure (right; red:  $\text{O}^{2-}$ , blue:  $\text{Co}^{2+}$  and green:  $\text{Co}^{3+}$ )

*Acknowledgments:* This work was supported by the Austrian Science Fund (FWF) through the international DACH program I 1041-N28 (COMCAT) and through Doctorate School Solids4Fun (W1243).

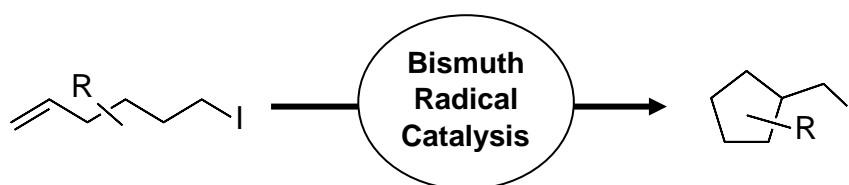
## References

- [1] Y. F. Y. Yao, *Journal of Catalysis* 33.1, (1974) 108-122
- [2] X. Xie, Y. Li, Z.-Q. Liu, M. Haruta, W. Shen, W., *Nature*: 458, (2009) 746-749
- [3] G. Marbán, I. López, T. Valdés-Solís, A. B. Fuertes, *International Journal of Hydrogen Energy* 33(22), (2008) 6687-6695
- [4] L. Lukashuk, K. Föttinger, E. Kolar, C. Rameshan, D. Teschner, M. Hävecker, A. Knop-Gericke, N. Yigit, H. Li, E. McDermott, M. Stöger-Pollach, G. Rupprechter, *Journal of Catalysis* 344, (2016) 1-15
- [5] L. Lukashuk, N. Yigit, R. Rameshan, E. Kolar, D. Teschner, M. Hävecker, A. Knop-Gericke, R. Schlögl, K. Föttinger, G. Rupprechter, *ACS Catal* 8(9), (2018), 8630-8641
- [6] K. Shojaee, B. S. Haynes, A. Montoya, *Applied Surface Science* 316, (2014) 355-365
- [7] Z. Tian, N. Bahlawane, F. Qi, K. Kohse-Höinghaus, *Catalysis Communications* 11(2), (2009) 118
- [8] H. Oosterbeek, *Physical Chemistry Chemical Physics* 9(27), (2007) 3570-3576.
- [9] T. Garcia, S. Agouram, J. F. Sanchez-Royo, R. Murillo, A. M. Mastral, A. Aranda, I. Vazquez, A. Dejoz, B. Solsona, *Applied Catalysis a-General* 386 (1-2), (2010) 16-27
- [10] H. C: Liu, S. K. Yen, *Journal of Power Sources* 166(2), (2007) 478-484
- [11] Y. Dou, J. Xu, B. Ruan, Q. Liu, Y. Pan, Z. Sun, S. X. Dou, *Advanced Energy Materials* 6(8), (2016) 1501835
- [12] M. B. Pinson, M. Z. Bazant, *Journal of the Electrochemical Society* 160(2), (2013) A243-A250
- [13] Jansson, J.; Palmqvist, A. E. C.; Fridell, E.; Skoglundh, M.; Osterlund, L.; Thormahlen, P.; Langer, V., On the catalytic activity of  $\text{Co}_3\text{O}_4$  in low-temperature CO oxidation. *Journal of Catalysis*, 211(2), (2002), 387-397

# Transition Metal Bismuthanes: Radical Catalysts in Cyclo-Isomerizations

Jacqueline Ramler, Ivo Krummenacher, Crispin Lichtenberg\*

*Department of Inorganic Chemistry, Julius-Maximilians Universität Würzburg, Am Hubland, 97074 Würzburg, Germany*



**Scheme 1.** Bismuth-mediated radical catalysis.

Bismuth salts,  $\text{BiX}_3$ , are used as Lewis acid catalysts in organic transformations such as Friedel-Crafts- or Mannich-reactions ( $\text{X} = \text{Cl}, \text{Br}, \text{I}, \text{O}_3\text{SCF}_3$ ), but other catalytic applications of bismuth species in organic synthesis are rare.<sup>[1]</sup> We became interested in transition metal bismuthanes, i. e. complexes featuring a Bi–TM bond (TM = transition metal). Here we demonstrate for the first time that these species can undergo controlled radical reactions with a high functional group tolerance, leading to the first catalytic application for this class of compounds.<sup>[2]</sup>

The atom transfer cyclo-isomerization of simple hexenyl iodides was chosen as model reaction (see Scheme 1). For the parent compound, 6-iodo-1-hexene, catalyzed radical cyclo-isomerizations have so far only been realized under photochemical conditions.<sup>[3]</sup> With the new bismuth species as catalysts, cyclo-isomerizations of iodoalkenes such as 6-iodo-1-hexene are now possible under thermal conditions. Radical reaction pathways were identified based on EPR spectroscopic experiments. An important role of the bismuth component was confirmed by test reactions.<sup>[2]</sup>

In the context of these studies, the bismuth transition metal complexes **1–3** with Bi–Mn, Bi–Fe and Bi–Co bond have been synthesized, isolated and fully characterized (see Figure 1).

These complexes show a non- / weakly-polar covalent Bi–TM bond, as determined by structural and spectroscopic analysis as well as reactivity studies.<sup>[2]</sup>

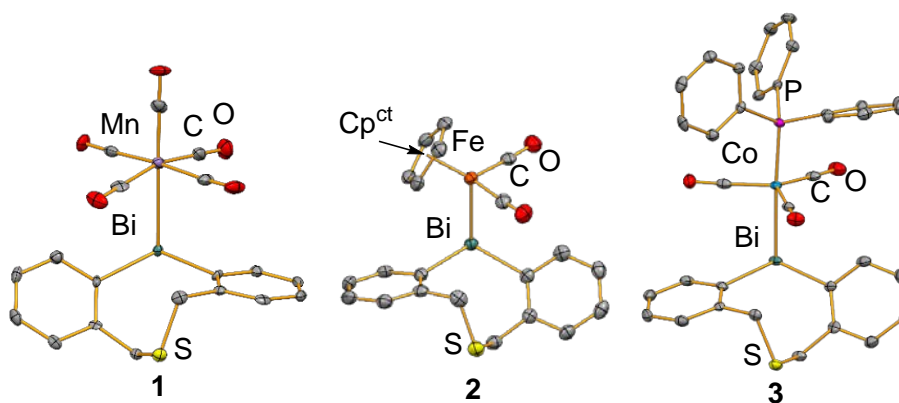


**Figure 1.** Molecular structure of transition metal bismuthanes **1–3**.

## References

- [1] T. Ollevier, E. Nadeau, *J. Org. Chem.* **2004**, *69*, 9292-9295; H. Sun, R. Hua, S. Chen, Y. Yin, *Adv. Synth. Catal.* **2006**, *348*, 1919-1925.
- [2] J. Ramler, I. Krummenacher, C. Lichtenberg, *manuscript submitted*.
- [3] a) D. P. Curran, D. Kim, *Tetrahedron Lett.* **1986**, *27*, 5821-5824; b) T. Cohen, H. Gibney, R. Ivanov, E. A.-H. Yeh, I. Marek, D. P. Curran, *J. Am. Chem. Soc.* **2007**, *129*, 15405-15409.

## **Open cellular structures for NO<sub>x</sub> abatement intensification**

*Tommaso Selleri<sup>1</sup>, Matteo Ambrosetti<sup>1</sup>, Mauro Bracconi<sup>1</sup>, Riccardo Balzarotti<sup>1</sup>, Gianpiero Groppi<sup>1</sup>, Isabella Nova<sup>1</sup> and Enrico Tronconi<sup>1</sup>; <sup>1</sup> Laboratory of Catalysis and Catalytic Processes, Energy Department, Politecnico di Milano, via La Masa 34, 20156, Milano (Italy)*

NH<sub>3</sub>-SCR is the leading technology for NO<sub>x</sub> abatement from lean burn and Diesel engines and is traditionally operated in catalytic converters made of washcoated honeycomb monoliths. A paradigm shift is now required to tackle the stringent limits imposed by new emission regulations worldwide. In this work, we provide a preliminary analysis of the potential of open random or regular cellular microstructures [1], like open-cell foams or periodic open cellular structures (POCS), as innovative catalyst substrates to improve the exhaust aftertreatment performances. A new modeling tool, based on state-of-the-art correlations, is developed and used to: i) gain insight in the general behavior of these supports; ii) select interesting structures for experimental testing; iii) develop new ideas for system configurations.

### **Materials and Methods**

A transient 1D+1D heterogeneous model of SCR converters, embedded with a complete SCR kinetic scheme and with recently developed and already extensively validated correlations for heat and mass transfer as well as pressure drops [2], is herein developed. Open cellular structures geometry and morphological properties are described by a state-of-the-art analytical model [3]. The resulting tool is used to simulate both steady state and fast transient SCR operation of foam and POCS catalysts, as shown with some examples in the next section.

### **Results and Discussion**

Simulations in Figure 1A compare a reference monolith substrate with 400 CPSI and a 5 mils wall thickness to foams with 60 PPI and different void fractions (0.83-0.96) in steady-state Standard SCR runs. All samples are loaded with the same amount of catalyst and are tested at the same GHSV. Overall, increasing the void fraction and adopting a sufficiently high PPI, foams can grant a relevant increase in the NO overall conversion at medium-high temperatures, due to a significant reduction in external mass transfer resistances. Unfortunately, this improvement in DeNO<sub>x</sub>

performances corresponds to a notable increase in pressure drops, which is related to the flow pattern inside these structures.

Figure 2 shows the beneficial effect on the heat-up dynamics of the SCR converter when an open-cell foam is used as catalyst support. In this example, the catalyst is firstly exposed to 500 ppm of NO and NH<sub>3</sub> at 100 °C (not shown) and then the temperature is rapidly increased from 100°C to 300°C (100°C/min) in NO and NH<sub>3</sub> flow. Due to its lower thermal mass and enhanced volumetric heat transfer coefficient, the foam substrate can better follow the imposed heating ramp (dashed lines), leading to a faster onset of the SCR reactions, so important in cold-start transients but also during rapid changes of operating conditions, eventually achieving better performances in terms of overall deNO<sub>x</sub> efficiency.

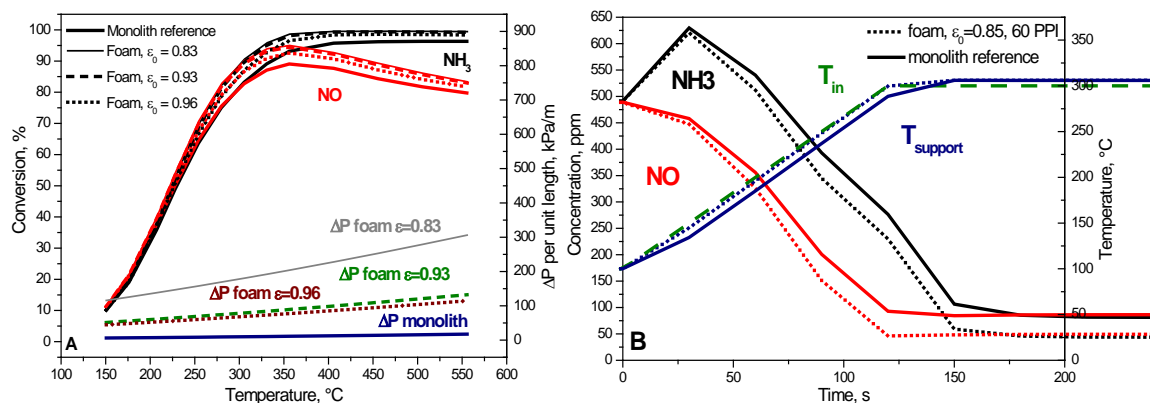


**Fig. 1.** Std. SCR simulation. NO=NH<sub>3</sub>=500 ppm, O<sub>2</sub>=H<sub>2</sub>O=10%v/v, GHSV=175000 h<sup>-1</sup>. A) Steady-state conversion and pressure drop; B) Transient heat-up (100 °C/min)

Based on these simulations, cordierite foams with different ranges of  $\epsilon$  (0.8-0.9) and PPI (20-60), are currently under testing in a dedicated synthetic gas rig.

Using the same approach, we are investigating also regular cellular structures (POCS). Preliminary results show that the adoption of POCS, combined with different flow configurations impossible in conventional monoliths, can provide additional degrees of freedom, to be exploited for EAT system design and optimization, and might result in more flexible, compact and lightweight converters.

### Acknowledgments

MIUR – FARE RICERCA IN ITALIA – progetto BEATRICES – R16R7NLWPW

### References

1. Giani, L., Groppi, G., Tronconi, E., *Ind. Eng. Chem. Res.*, 44, (2005).
2. Bracconi, M., Ambrosetti, M., Maestri, M., Groppi, G., Tronconi, E. *Chem. Eng. J.*, 352, (2018).
3. Ambrosetti, M., Bracconi, M., Groppi, G., Tronconi, E., *Chem. Ing. Tech.*, 89, (2017).

# Probing the mobility of Cu-active sites in zeolite NH<sub>3</sub>-SCR catalysts by *in situ* impedance spectroscopy

*V. Rizzotto, RWTH Aachen University, Aachen, Germany;*

*P. Chen, South China University of Technology, Guangzhou, China;*

*U. Simon, RWTH Aachen University, Aachen, Germany*

Copper-exchanged SSZ-13 (Cu-SSZ-13) is one of the technically most relevant catalysts for the selective catalytic reduction of NO<sub>x</sub> with NH<sub>3</sub> (NH<sub>3</sub>-SCR) in exhaust after-treatment systems. Together with other small-pore chabazite (CHA) zeolites (e.g. Cu-SAPO-34), Cu-SSZ-13 demonstrates not only higher stability under SCR conditions, but also higher efficiency in the reduction of NO<sub>x</sub>, as compared to other large- or medium-pore Cu-exchanged zeolite catalysts (e.g. Cu-ZSM-5) [1]. In order to explain such superior performances, the catalytic mechanism taking place in CHA zeolite has been the object of extensive studies. Recently, it was documented that the mobility of NH<sub>3</sub>-solvated Cu species in the CHA framework plays a determinant role in the SCR cycles by forming [Cu<sup>I</sup>(NH<sub>3</sub>)<sub>2</sub>]<sup>+</sup>-O<sub>2</sub>-[Cu<sup>I</sup>(NH<sub>3</sub>)<sub>2</sub>]<sup>+</sup> intermediates [2,3]. Subsequently, our research group has shown how impedance spectroscopy (IS) combined with density-functional theory calculations allows to directly monitor the [Cu<sup>I</sup>(NH<sub>3</sub>)<sub>2</sub>]<sup>+</sup> local movement under SCR-related conditions [4,5].

Here we present a comparative study between Cu-SSZ-13 and Cu-ZSM-5 with defined Si/Al ratio and variable Cu-loading (Cu/Al). We applied *in situ* IS to analyse the frequency-dependent ion conduction processes in these zeolites, to which mobile solvated Cu<sup>2+</sup> species may contribute, in order to probe the mobility of [Cu<sup>II</sup>(NH<sub>3</sub>)<sub>n</sub>]<sup>2+</sup> species and their interaction with the zeolite framework [6]. Fig. 1a illustrates the so-called modulus plot ( $M''$  vs.  $\nu$ ) obtained by *in situ* IS over SSZ-13 in NH<sub>3</sub> atmosphere (100 ppm in N<sub>2</sub>) [7]. At high frequencies (i.e. 10<sup>4</sup>-10<sup>6</sup> Hz), each modulus spectrum presents a resonance peak that is attributed to the local ion movement and is supposed to result from a combination of the short-range movement of H<sup>+</sup> and Cu<sup>2+</sup> ions after NH<sub>3</sub> solvation [7]. Under similar conditions, the Cu-SSZ-13 catalysts show different behaviours from those of Cu-ZSM-5 (Fig. 1b): an increasing Cu-loading results in a significant shift of the resonance maximum to higher frequencies, which indicates an increased ion mobility, while Cu-ZSM-5 presents an opposite trend. Our assumption is that this difference results from the different crystal structures (i.e. CHA

and MFI for SSZ-13 and ZSM-5, respectively): the electrostatic interactions with the small-pore CHA framework seem to enable the motion of the  $\text{NH}_3$ -solvated  $\text{Cu}^{2+}$  species, so that they can significantly contribute to the overall ion conductivity. This hypothesis is corroborated by temperature-dependent IS measurements, from which the activation energy ( $E_a$ ) for local ion conduction in presence of  $\text{NH}_3$  was derived (Fig. 1c). Again, exactly opposite trends are shown for the two zeolites: while Cu-ZSM-5 shows an increase of  $E_a$  with increasing Cu/Al (similarly to the observed trend for pristine zeolites in  $\text{NH}_3$ -free state), the  $E_a$  of Cu-SSZ-13 progressively decreases with the increase of Cu loading, suggesting a favored short-range motion of  $\text{Cu}^{\text{II}}(\text{NH}_3)_n$  at a higher Cu loading.

These and further experiments have proven how *in situ* IS can be a relevant technique to understand the molecular mechanisms of  $\text{NH}_3$ -SCR cycle in Cu-zeolites and to guide the development of new zeolite catalysts.

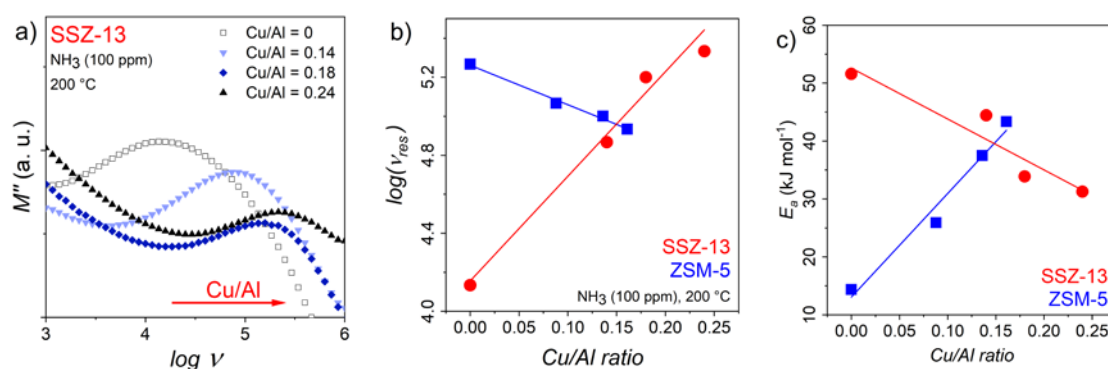


**Figure 1.** a) Modulus plots of *in situ* IS results on H- and Cu-SSZ-13 in  $\text{NH}_3$  (100 ppm in  $\text{N}_2$ ) at 200 °C; b) resonance frequencies ( $\nu_{res}$ ) for the local ion motion within Cu-SSZ-13 (red) and Cu-ZSM-5 (blue) catalysts with varying Cu/Al ratios;  $\nu_{res}$  was determined by the corresponding modulus plot as exemplified in a); c) activation energy ( $E_a$ ) for the local ion motion in  $\text{NH}_3$ -loaded Cu-SSZ-13 (red) and Cu-ZSM-5 (blue) catalysts with varying Cu/Al ratios;  $E_a$  was calculated based on *in situ* IS measurements between 180 and 240 °C.

## References

- [1] A. M. Beale, F. Gao, I. Lezcano-Gonzalez, et al. *Che. Soc. Rev.*, **2015**, *44*, 7371-7405.
- [2] C. Paolucci, I. Khurana, A.A. Parekh, et al. *Science*, **2017**, *357*, 898-903.
- [3] F. Gao, D. Mei, Y. Wang, et al. *J. Am. Chem. Soc.* **2017**, *139*, 4935-4942.
- [4] P. Chen, A. Khetan, M. Jabłońska, et al. *Appl. Catal. B: Environ.*, **2018**, *237*, 263-272.
- [5] P. Chen, V. Rizzotto, K. Xie, U. Simon, *React. Chem. Eng.*, **2019**, DOI:10.1039/C8RE00283E.
- [6] V. Rizzotto, P. Chen, U. Simon, *Catalysts*, **2018**, *8*, 162-175.
- [7] U. Simon, U. Flesch, *J. Porous Mater.* **1999**, *6*, 33-40.

# Toluene hydrogenation over iridium supported on MCM-41 materials

*Monika Kot<sup>1</sup>; Michał Zieliński<sup>1</sup>; Ewa Janiszewska<sup>1</sup>*

*<sup>1</sup>Adam Mickiewicz University in Poznań, Faculty of Chemistry,  
Umultowska 89b, 61-614 Poznań, Poland*

Recently catalytic hydrogenation of aromatic compounds has attracted great attention. This class of reactions is very important due to environmental issues as well as industrial applications [1]. The hydrogenation reactions are often catalyzed by supported noble metals, particularly platinum. However, due to the fact that platinum is sensitive to poisoning with impurities, especially sulphur compounds, other metallic active phases are investigated. An interesting alternative could be iridium, other platinum group metal, which is distinguished by high corrosion resistance.

The catalytic activity in hydrogenation reaction depends on active phase as well as support of the catalyst. Ordered mesoporous silicas, especially MCM-41 materials seem to be promising supports because of their unique properties like high surface area and uniform pore system. It was shown that activity for hydrogenation of monoaromatics enhanced over noble metal catalysts supported on acidic supports. Pure siliceous MCM-41 materials show no acidity. Incorporation of aluminum atoms into the amorphous walls of ordered mesoporous silicas generates acidic properties of these materials and is crucial for their catalytic activity [2].

The presented study investigates the catalytic behaviour of iridium catalysts supported on silica and aluminosilicate MCM-41 in toluene hydrogenation. The influence of acidity of the support and iridium precursor on the activity was studied. The MCM-41 and AIMCM-41 supports were prepared by hydrothermal synthesis. The catalysts containing 1 wt.% of iridium supported on mesoporous materials were prepared by conventional impregnation (two different iridium precursors:  $\text{H}_2\text{IrCl}_6$ , and  $\text{Ir}(\text{acac})_3$  were investigated). The prepared catalysts and supports were characterized by XRD,  $\text{N}_2$  adsorption/desorption measurements, and  $\text{H}_2$ -TPR. The mean size of metal particles was estimated by hydrogen chemisorption measurements. The supports show ordered mesopore systems and the structure is maintained after the impregnation and reduction procedures. The obtained supports and catalysts have high surface areas (from 328 to 960  $\text{m}^2/\text{g}$ ). After  $\text{H}_2$  reduction the iridium catalysts



contain small iridium nanoparticles (below 5 nm, dispersion from 27% to 49%). The catalysts were tested in toluene hydrogenation and their activity was compared with catalysts supported on commercially used silica and alumina.

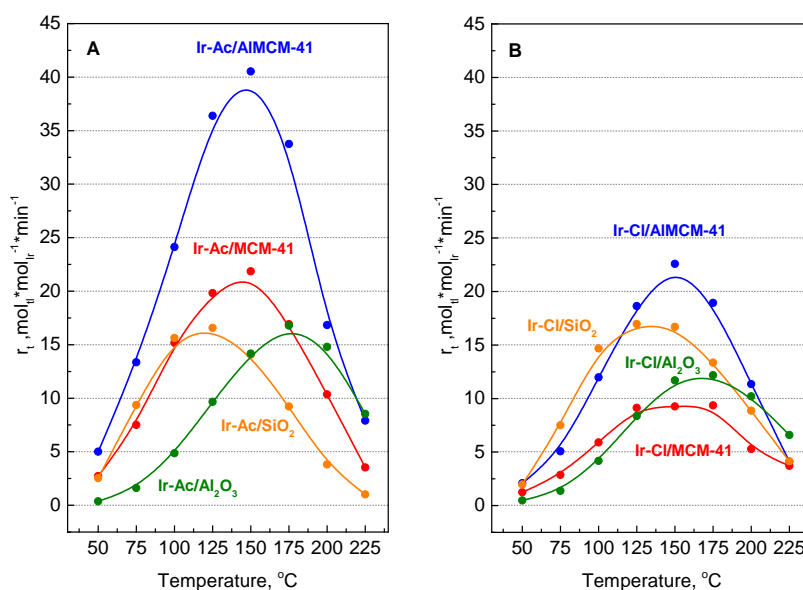


**Figure 1.** The effect of support and iridium precursor (iridium acetylacetonate – **A**, hydrogen hexachloroiridate – **B**) on apparent rate of hydrogenation of toluene as a function of temperature.

The catalysts supported on AIMCM-41 are more active in toluene hydrogenation than the catalysts supported on silica MCM-41. The catalytic activity depends also on the type of iridium precursor. The catalysts obtained from iridium acetylacetonate indicate higher activity than those prepared using hydrogen hexachloroiridate.

## Acknowledgements

The work was supported by grant no. POWR.03.02.00-00-I023/17 co-financed by the European Union through the European Social Fund under the Operational Program Knowledge Education Development.

## References

- [1] A. Stanislaus, B. Cooper, Aromatic Hydrogenation Catalysis: A Review, *Catal. Rev.* 36 (1994) 75–123.
- [2] R.M. Martín-Aranda, J. Čejka, Recent advances in catalysis over mesoporous molecular sieves, *Top. Catal.* 53 (2010) 141–153.

# Structure and Chemistry of Cu–Fe–Al Nanocomposite Catalysts for CO Oxidation

*V.V. Kaichev, A.V. Fedorov, O.A. Bulavchenko, A.M. Tsapina, A.A. Saraev, V.A. Yakovlev, Boreskov Institute of Catalysis, Novosibirsk, Russia*

High-active Fe–Al and Cu–Fe–Al nanocomposite catalysts were synthesized by fusion of aluminium, iron, and copper salts and then tested in the oxidation of CO. It was found that the activity of Fe–Al catalysts depends on the Fe concentration and the maximum is achieved when the Fe<sub>2</sub>O<sub>3</sub> content is approximately 82 wt%. The XRD and FTIR data indicate that the catalysts contain the α-Fe<sub>2</sub>O<sub>3</sub> and γ-Al<sub>2</sub>O<sub>3</sub> phases and Al<sup>3+</sup> cations dissolve in the Fe<sub>2</sub>O<sub>3</sub> lattice. The iron oxide is protohematite (metastable modification of iron (III) oxide) characterized by a high concentration of structure defects. The catalyst calcinated at 400 °C is more active than the catalyst calcinated at 700 °C in the low-temperature CO oxidation. According to the FTIR study, the enhanced activity is due to a high concentration of crystal water that provides a high concentration of different defects inside Fe<sub>2</sub>O<sub>3</sub>-Al<sub>2</sub>O<sub>3</sub> nanoparticles. The addition of Cu leads to a significant increase in activity at high temperatures. XANES spectroscopy indicated that the Cu–Fe–Al catalysts in addition contain CuO and CuFe<sub>2</sub>O<sub>4</sub> oxides in an amorphous state [1]. The Raman spectroscopy study indicates that the addition of Cu hinders the dissolution of Al<sup>3+</sup> cations in the Fe<sub>2</sub>O<sub>3</sub> lattice. These Cu-containing phases and the structure defects may be responsible for the enhanced catalytic activity of the Cu–Fe–Al nanocomposite catalysts. According to the kinetic measurements, the activation energy is 104 and 88 kJ/mol for Fe-Al and Cu-Fe-Al nanocomposite catalysts, respectively. It should be noted that the values are comparable with the activation energy for the oxidation of CO over high-tech Cu-based catalysts. As shown by Feng and Zheng As shown by Feng and Zheng [2], the activation energy for the oxidation of CO over CuO nanowires is in the range 79–115 kJ/mol.

**Acknowledgement.** This work was supported by the Russian Science Foundation, grant 17-73-20157.

## References

- [1] A.A. Saraev, A.M. Tsapina, A.V. Fedorov, A.L. Trigub, O.A. Bulavchenko, Z.S. Vinokurov, Y.V. Zubavichus, V.V. Kaichev, *Rad. Phys. Chem.* In press. DOI: 10.1016/j.radphyschem.2018.11.025.
- [2] Y. Feng, X. Zheng, *Nano Lett.* 10 (2010) 4762.

# DFT study on oxidative activation of Cu(I) species in NH<sub>3</sub>-SCR over Cu-CHA zeolite

*Chong Liu, Takashi Toyao, Ken-ichi Shimizu\**

*Institute for Catalysis, Hokkaido University, Sapporo, Japan*

*\*kshimizu@cat.hokudai.ac.jp*

## Introduction

The control of harmful nitrogen oxides (NO<sub>x</sub>) from diesel combustion represents a crucial challenge in automotive emission [1]. One important process to convert such NO<sub>x</sub> into harmless N<sub>2</sub> is the selective catalytic reduction (SCR) with NH<sub>3</sub> as reducing agent. Cu-exchanged chabazite (Cu-CHA) zeolite as an efficient catalyst for the NH<sub>3</sub>-SCR reaction has been extensively studied [1-3]. However, the reaction mechanism for the oxidative activation of Cu(I) into Cu(II) species is still not well understood [4,5]. In this study, the elementary steps of Cu(I) activation were thoroughly investigated by periodic DFT calculations, and the importance of NH<sub>3</sub> and H<sub>2</sub>O assisted conversions during the activation cycle was highlighted.

## Methodology

Spin-polarized DFT calculations were performed using VASP. The PBE functional and dispersion-corrected DFT-D3 was used. The electron-ion interactions were described with projected augmented waves method. The Brillouin zone sampling was restricted to the  $\Gamma$  point. The energy cut-off was set to 500 eV. The CHA zeolite model was represented by periodic 36 T unit cell (Figure 1a). The convergence was assumed to be reached when the forces on each atom were below 0.05 eV Å<sup>-1</sup>.

## Results and discussion

The activation of Cu(I) ion by O<sub>2</sub> as exclusive oxidant was firstly studied. Figure 1b shows a stoichiometric representation for the proposed mechanism, in which four Cu(I) ions react with one O<sub>2</sub> molecule to yield four Cu(II) species. Under typical SCR conditions, the Cu(I) ions in CHA zeolite mainly exist as mobilized [Cu(NH<sub>3</sub>)<sub>2</sub>]<sup>+</sup> [3,5]. Here we considered such a species as the starting point for oxidative activation. The O<sub>2</sub> adsorption and dissociation with a pair of [Cu(NH<sub>3</sub>)<sub>2</sub>]<sup>+</sup> generate a dimeric species of [(NH<sub>3</sub>)<sub>2</sub>Cu(μ-O)<sub>2</sub>Cu(NH<sub>3</sub>)<sub>2</sub>]<sup>2+</sup>, and this process is strongly exothermic by -76 kJ/mol with an activation barrier of only 20 kJ/mol. The further activation was proposed to occur via a tetranuclear intermediate, which can be formed from the

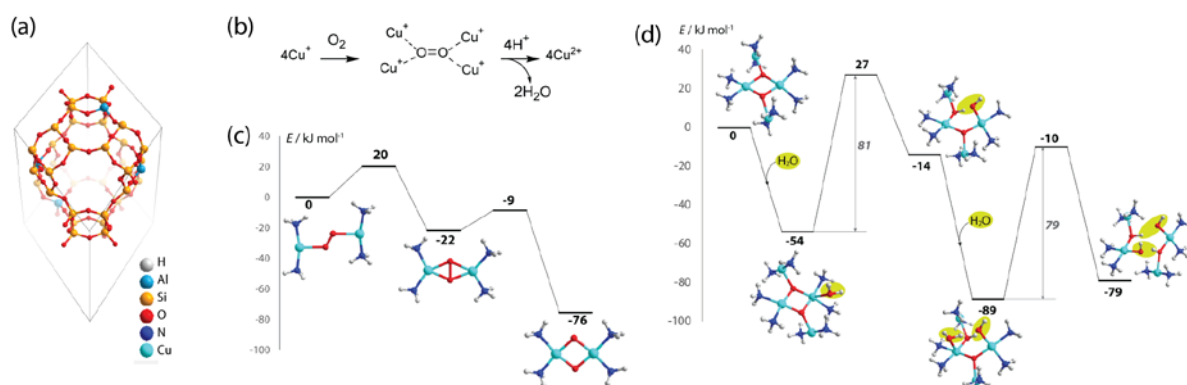


**Figure 1.** (a) Computational model of CHA unit cell; (b) Proposed mechanism for the oxidative activation of Cu(I) into Cu(II) species; Energy profiles for (c)  $O_2$  dissociation and oxidation of two mononuclear  $[Cu(NH_3)_2]^+$  and (d) water-assisted decomposition of Cu tetramer.

adsorption of another pair of  $[Cu(NH_3)_2]^+$  coordinating to the bridging oxygens in the Cu dimer (Figure 1d). The decomposition of the tetramer occurs via the consecutive hydrolysis of Cu-O bonds with the assistance of water molecules, and the activation barriers are ca. 80 kJ/mol to form two hydroxylated Cu dimers. Such dimeric Cu clusters can further decompose into Cu monomers such as  $[Cu(OH)(NH_3)_3]^+$  and  $[Cu(NH_3)_4]^{2+}$  with calculated barriers of ca. 50 kJ/mol. The presence of  $NH_3$  and  $H_2O$  as ligands can sufficiently decrease the reaction barriers of the activation process.

The activation of Cu(I) species with both  $O_2$  and NO as oxidants was also considered. The presence of NO can promote the oxidation activation with moderate barriers, but the regeneration of  $NO_x$ -ligand-free Cu(II) species is strongly unfavored. Those Cu(II) species with ligands like  $NO_2$  or  $NO_3^-$  may act as resting states and play minor effect on the catalyst performance.

## Conclusions

The oxidative activation mechanism of Cu(I) species in CHA zeolite during  $NH_3$ -SCR reaction was investigated by periodic DFT calculations. The results show that the activation of Cu(I) with assistance of  $H_2O$  can efficiently occur with only  $O_2$  as oxidant, and the presence of NO is less important during the oxidation part of the activation cycle. It is proposed that the oxidative activation of Cu(I) species by exclusive  $O_2$  plays a key role during the  $NH_3$ -SCR reaction.

## References

- [1] Zhang, R., et al., *Chem. Rev.* **2016**, *116*, 3658-3721.
- [2] Paolucci, C., et al., *J. Am. Chem. Soc.* **2016**, *138*, 6028-6048.
- [3] Paolucci, C., et al., *Science* **2017**, *357*, 898.
- [4] Gao, F., et al., *J. Am. Chem. Soc.* **2017**, *139*, 4935-4942.
- [5] Chen, L., et al., *J. Catal.* **2018**, *358*, 179-186.

# **The tunable effects of boron and nitrogen dopants on the nanostructured carbon support on the catalytic property of the supported single Au revealed from first principle simulation**

*Bo Li*

*boli@imr.ac.cn*

*Institute of Metal Research, Chinese Academy of Science, ShenYang 110016 China*

The nanostructured carbon material is one of the most important supports for the metal catalysts due to their unique properties such as chemical stability, easiness to recover metal etc<sup>[1]</sup>. The boron and nitrogen atoms have the similar radius with the carbon atom which can enter carbon matrix and they are the most often observed dopants on the nanostructured carbon materials. As boron or nitrogen has one less or more valence electron compared with carbon, it is expected that the different effects induced by the boron or nitrogen doping. In this work, the tunable effects from boron and nitrogen dopants on the carbon nanotube and graphene on the catalytic property of supported single Au in CO oxidation and acetylene hydrochlorination are revealed from the first principle calculations<sup>[2,3]</sup>

For CO oxidation on the single Au, the results reveal that boron and nitrogen doped SWCNTs can enhance the binding strength and catalytic activity of Au catalysts compared with the pristine SWCNTs. Moreover, the boron and nitrogen doping donate or withdraw charges to and from the Au atom. The excess positive or negative charges on Au can significantly modify its interactions with CO and O<sub>2</sub> molecules. We have found that O<sub>2</sub> binds stronger than CO on Au/B-SWCNTs, but weaker than CO on Au/SWCNTs and Au/N-SWCNTs. The adsorption preference of CO and O<sub>2</sub> molecules on the doped SWCNTs gives a distinct coadsorption pattern of the reactants which is closely related to the dopant configurations. Furthermore, the calculations reveal that the reactions proceed via either the bi-molecular Langmuir–Hinshelwood (BLH) mechanism or the bi-molecular Eley–Rideal (BER) mechanism with a relatively low energy barrier of 0.22 and 0.28 eV. The peroxide-like (OOCO) complex is a key intermediate in the reaction pathway in both BER and BLH mechanisms. Besides the traditional BLH and BER mechanisms, a tri-molecular Eley–Rideal (TER) mechanism is also observed, which is almost a barrierless process on Au/B-SWCNTs.

The similar tunable effects is also found for supported single Au in acetylene hydrochlorination reaction by nitrogen and boron doping. The nitrogen and boron dopants on the carbon nanotube not only behave as stable anchoring positions for the single Au but also render the distinct charge state and reactivity in the reaction. It is found that the supported single Au on nitrogen doped SWCNT become positively charged while it becomes negatively charged on boron doped case. The different charge state of Au directly influences the interactions with reactant, C<sub>2</sub>H<sub>2</sub>. The calculations indicate that the adsorption energy of C<sub>2</sub>H<sub>2</sub> is bigger on single Au supported on boron doped SWCNT than the counterpart of nitrogen doped case. From the reaction pathway analysis, it is interesting to observe that both positive and negative charged single Au can be an effective catalyst with the comparable reaction barrier. It is first time observed that negative Au is able to catalyze the acetylene hydrochlorination. Furthermore, the single Au undertook a redox cycle during reaction which charges are decreased firstly and then restored to the original state. It is suggested the too strong adsorption of C<sub>2</sub>H<sub>2</sub> is detrimental to activity as it hinders the HCl addition to form product. Therefore, a balanced activity between C<sub>2</sub>H<sub>2</sub> adsorption and HCl activation is required for the optimal catalytic performance.

#### References

- [1] Su, D. S.; Perathoner, S.; Centi, G.: *Chemical Reviews* **2013**, 113, 5782-5816.
- [2] Ali, S.; Liu, T.; Lian, Z.; Li, B.; Su, D. S. *J. Mater. Chem. A* **2017**, 5, 16653-16662.
- [3] Sun, X.; Han, P.; Li, B.; Zhao, Z, *Journal of Physical Chemistry C* **2018**, 3, 1570-1576

# **Fe<sub>3</sub>O<sub>4</sub> Modified Mesoporous Graphitic Nitride (*mpg*-C<sub>3</sub>N<sub>4</sub>) Photocatalysts for Selective Photocatalytic NO Oxidation and Storage under Visible Light Irradiation**

*Muhammad Irfan*<sup>1</sup>, *Melike Sevim*<sup>2</sup>, *Merve Balci*<sup>1</sup>, *Yusuf Koçak*<sup>1</sup>, *Önder Metin*<sup>3</sup>,  
*Emrah Ozensoy*<sup>1,4</sup>

<sup>1</sup>*Chemistry Department, Bilkent University, 06800 Bilkent, Ankara, Turkey*

<sup>2</sup>*Chemistry Department, Atatürk University, 25030, Yakutiye, Erzurum, Turkey*

<sup>3</sup>*Chemistry Department, Koç University, 34450 Sariyer, Istanbul, Turkey*

<sup>4</sup>*UNAM-National Nanotechnology Center, Bilkent University, 06800, Ankara, Turkey*

[ozensoy@fen.bilkent.edu.tr](mailto:ozensoy@fen.bilkent.edu.tr)

## **Abstract**

Atmospheric pollution has been recognized as one of the major threats for modern society. Among the various manmade air pollutants, nitrogen oxides (NO<sub>x</sub>) induce the ozone production in troposphere and cause acid rains. In addition, NO<sub>x</sub>, especially nitric oxide (NO) and nitrogen dioxide (NO<sub>2</sub>) severely affect respiratory and immune systems<sup>[1]</sup>. Despite its favourable properties like chemical inertness, long-term stability and low cost, TiO<sub>2</sub> photocatalyst has a band gap of 3.2 eV. This large band gap enables the harvesting of UV light only, which accounts for 4-5% of incoming solar energy<sup>[2]</sup>. Among alternative photocatalytic systems, two-dimensional graphitic carbon nitride is one of the strong candidates owing to its metal-free nature, thermal stability, non-toxicity, cost efficiency with a low electronic band gap (2.7 eV, 454 nm) falling in the visible range of the solar spectrum<sup>[3]</sup>.

In this study, highly organized mesoporous graphitic carbon nitride (*mpg*-C<sub>3</sub>N<sub>4</sub>) photocatalysts were synthesized by the thermal polycondensation of guanidine hydrochloride using hard template-assisted synthesis approach. The polycondensation process was performed at different temperatures, accompanied by comprehensive structural analysis of the *mpg*-C<sub>3</sub>N<sub>4</sub> materials using different characterization techniques. These porous structures were then tested in NO photo-oxidation under visible light, showing a remarkable activity in NO<sub>x</sub> abatement and a high selectivity for nitrate species. The activity of best *mpg*-C<sub>3</sub>N<sub>4</sub> photocatalyst (*mpg*-C<sub>3</sub>N<sub>4</sub>500) was further improved by the addition of magnetite nanoparticles which were synthesized by the surfactant assisted high-temperature decomposition of iron(III) acetylacetonate. Fe<sub>3</sub>O<sub>4</sub>/*mpg*-CN500 photocatalyst revealed significantly

superior photocatalytic NO<sub>x</sub> abatement performance under visible light as compared to the commercial P25 titania benchmark photocatalyst. Fe species in the Fe<sub>3</sub>O<sub>4</sub>/mpg-CN500 photocatalyst structure were determined to be in Fe<sup>2+</sup> and Fe<sup>3+</sup> oxidation states. These iron species both existed as FeO<sub>x</sub> nanoparticles with an average diameter of ca. 10 nm on mpg-C<sub>3</sub>N<sub>4</sub> surface and were also directly incorporated into the 2D mpg-C<sub>3</sub>N<sub>4</sub> layers as cations.

Incorporation of the Fe species to the photocatalyst formulation enhanced the total light absorption in the visible region, decreased the electronic band gap of mpg-C<sub>3</sub>N<sub>4</sub> and also generated structural defects resulting in crystallographic disorder. Introduction of Fe<sup>2+</sup>/Fe<sup>3+</sup> species significantly increased the oxygen reduction capacity of mpg-CN500 resulting in lower NO<sub>2</sub> production which ultimately resulted in enhanced selectivity in photocatalytic NO<sub>x</sub> abatement. Fe<sub>3</sub>O<sub>4</sub>/mpg-CN500 photocatalyst showed high activity, selectivity and stability even after five successive experimental runs without any regeneration step. Enhanced photocatalytic efficiency could be mainly attributed to the unique mesoporous structure, high surface area, high charge separation efficiency and prolonged life time of charge carriers.

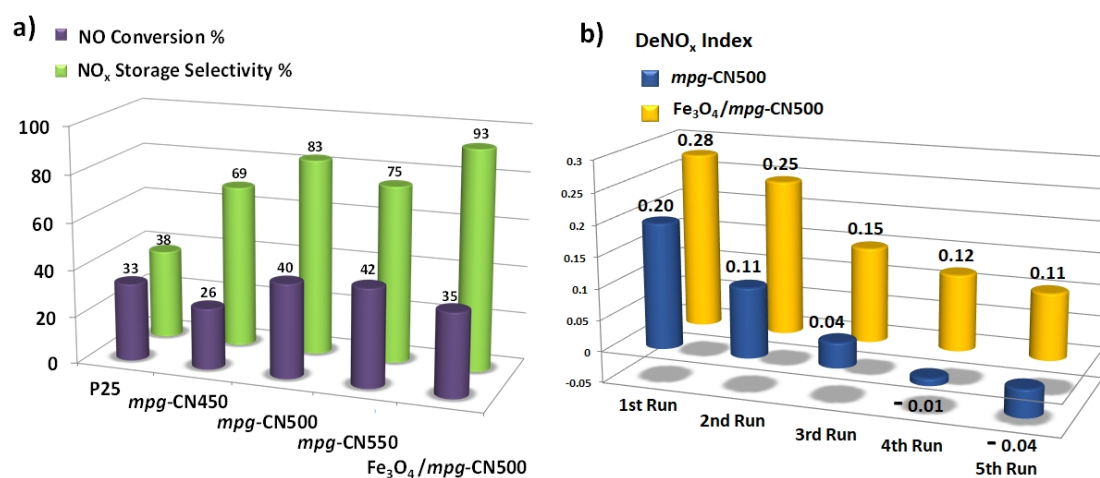


**Fig. 1.** NO(g) conversion % (purple bars) and NO<sub>2</sub> storage selectivity % (green bars) values for mpg-CN450, mpg-CN500, mpg-CN550 and Fe<sub>3</sub>O<sub>4</sub>/mpg-CN500 photocatalysts obtained via Vis-light irradiation; (b) corresponding DeNO<sub>x</sub> index values for mpg-CN500 and Fe<sub>3</sub>O<sub>4</sub>/mpg-CN500 photocatalysts calculated for each run of the reusability tests.<sup>[4]</sup>

## References

- [1] K. Skalska, J. S. Miller and S. Ledakowicz, *Science of The Total Environment* **2010**, *408*, 3976-3989.
- [2] M. Pelaez, N. T. Nolan, S. C. Pillai, M. K. Seery, P. Falaras, A. G. Kontos, P. S. M. Dunlop, J. W. J. Hamilton, J. A. Byrne, K. O'Shea, M. H. Entezari and D. D. Dionysiou, *Applied Catalysis B: Environmental* **2012**, *125*, 331-349.
- [3] Z. Zhao, Y. Sun and F. Dong, *Nanoscale* **2015**, *7*, 15-37.
- [4] M. Irfan, M. Sevim, M. Balci, Y. Kocak, O. Metin and E. Ozensoy, *Applied Catalysis B: Environmental* **2019**, submitted.



# Spongy graphitic carbon nitride (sg-C<sub>3</sub>N<sub>4</sub>) as a new high surface area material

*Emilia Alwin<sup>1</sup>, Mariusz Pietrowski<sup>1</sup>*

*<sup>1</sup>Adam Mickiewicz University in Poznań, Faculty of Chemistry, Poznań, Poland*

Graphitic carbon nitride (g-C<sub>3</sub>N<sub>4</sub>) is a layered polymer the structure of which is analogous to graphite. Its layers are formed of heptazine units connected together. As a typical semiconductor with a smaller energy gap than popular photocatalysts, it can be used in photodegradation of organic pollutants or photoreduction of water to hydrogen under the visible light irradiation [1]. In order to improve the catalytic and photocatalytic properties of carbon nitride, its surface is subjected to doping with metals due to which its catalytic activity increases several times. Carbon nitride, in addition to its many advantages, has several shortcomings. One of them is a small specific surface area of 10-30 m<sup>2</sup>/g. However, it can be increased either by using hard template methods during the preparation or by exfoliation of carbon nitride into

nanosheets. Unfortunately, all these methods are not very effective.

We have established that the exposition of highly dispersed metals supported on carbon nitride to hydrogen at elevated temperatures results in a tremendous development of carbon nitride porous structure and a release of large amounts of gases (NH<sub>3</sub>, CH<sub>4</sub>, HCN). The carbon nitride structure was “nibbled” due to hydrogenation of C-N bonds catalyzed by active metals which resulted in a significant increase in the surface area and formation of a sponge-like structure (Fig. 1). This is why we have called it “spongy graphitic carbon nitride” (sg-C<sub>3</sub>N<sub>4</sub>).

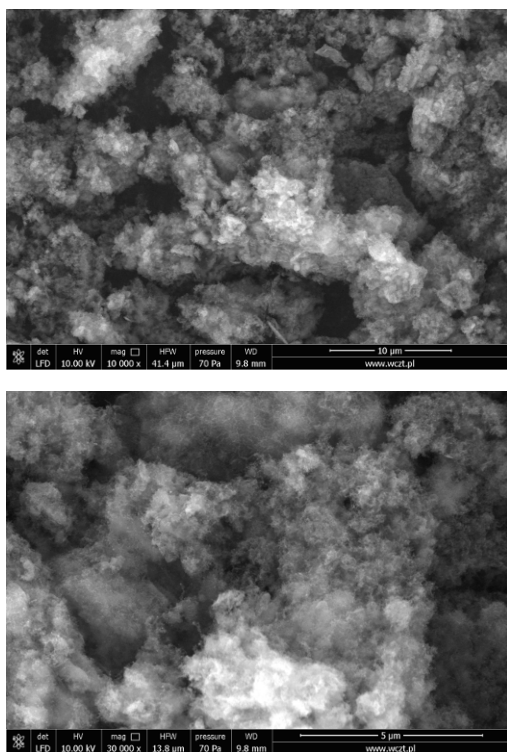


**Figure 1.** SEM image of 1%Ni/sg-C<sub>3</sub>N<sub>4</sub>.

By subjecting a metal/carbon nitride system to reduction with hydrogen in the appropriate temperature range (500-550°C), we have obtained the surface of about 380 m<sup>2</sup>/g, whereas the surface area of the pristine carbon nitride was only 24 m<sup>2</sup>/g.

An interesting feature of the mechanism of the reduction process of metal/carbon nitride system is a different course for various metals. We observed this process using temperature programmed reduction (TPR) coupled with on-line mass spectrometry (TPR-MS).

Depending on the catalytic properties of a metal, the process of “nibbling” the carbon nitride occurs differently and proceeds at different temperature ranges (Fig.2). Ruthenium, known for its high hydrogenation activity (eg. in the methanation reaction), catalyzes the rupture of carbon-nitrogen bonds already at 350°C and this is accompanied by a release of methane and ammonia. On the other hand, nickel is active at 500°C.

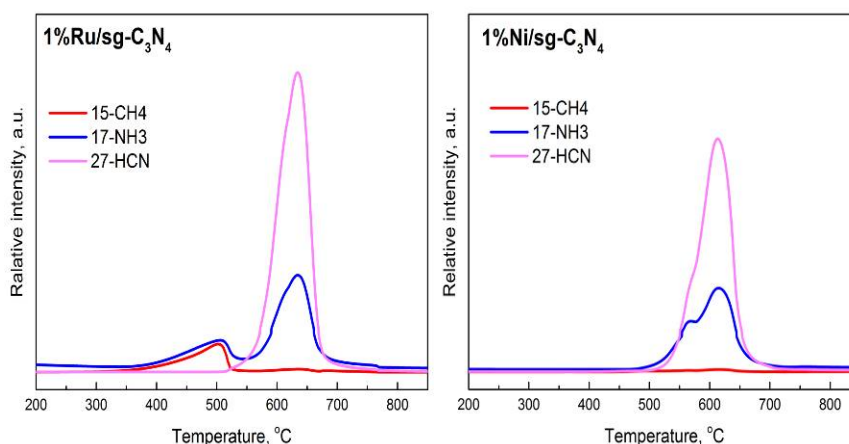


**Figure 2.** TPR-MS profiles of 1%Ru/sg-C<sub>3</sub>N<sub>4</sub> and 1%Ni/sg-C<sub>3</sub>N<sub>4</sub>.

## Acknowledgements

The work was supported by grant No. POWR.03.02.00-00-I023/17 co-financed by the European Union through the European Social Fund under the Operational Program Knowledge Education Development.

## References

- [1] X. Wang, K. Maeda, A. Thomas, K. Takanabe, G. Xin, J. M. Carlsson, K. Domen, and M. Antonietti, *Nat. Mater.*, vol. 8, no. 1, pp. 76–80, 2009.

# Preparation of different metal oxides supported on ceria-titania for the selective catalytic reduction of NO<sub>x</sub> with NH<sub>3</sub>

*J. Mosrati<sup>1,2</sup>, H. Atia<sup>2</sup>, R. Eckel<sup>2</sup>, U. Armbruster<sup>2</sup>, M. Mhamdi<sup>1,3</sup>, S. Wohlrab<sup>2</sup>*

*<sup>1</sup>Faculty of Sciences, Tunis - El Manar, Tunisia; <sup>2</sup>Leibniz-Institut für Katalyse, Rostock, Germany;*

*<sup>3</sup>Institute Superior of Medical Technologies, Tunis, Tunisia*

## Introduction

The reduction of NO<sub>x</sub> emissions has become a great challenge in environmental protection, and selective catalytic reduction (SCR) is considered as the most efficient technology to reduce it [1]. It is of high interest to develop a highly active catalyst for NH<sub>3</sub>-SCR in low-temperature range (100-300 °C) for NO<sub>x</sub> removal from both flue gases of stationary plants and mobile sources such as diesel vehicles [1].

Ceria-based catalysts are promising candidates due to their remarkable oxygen storage capacity, redox cycle (Ce<sup>4+</sup> → Ce<sup>3+</sup>) and low price [2]. Addition of titania to ceria increases ceria dispersion, fraction of active surface oxygen and acidity which enhance the SCR performance. Doping with oxides of other metals such as Nb, Mo, Ta, Sn, Mn, Cu and Fe further improves the catalyst performance due to their excellent redox behaviour. Therefore, in the present work different metal oxides were supported on Ce-Ti oxide by wet impregnation in order to improve SCR activity at low temperature.

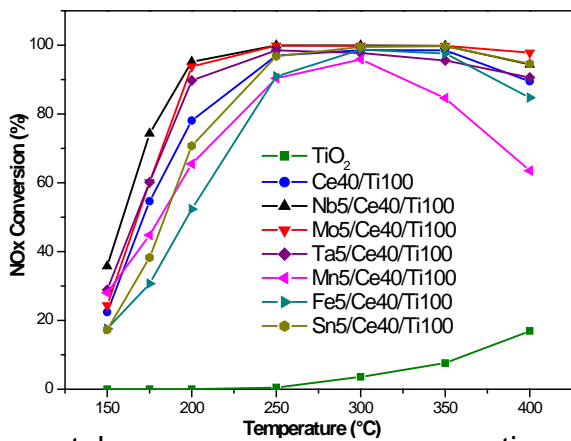
## Experimental

Ce<sub>40</sub>/Ti<sub>100</sub> mixed oxide (molar ratio 0.4:1) was prepared by sol-gel method. 5 wt% M (Nb, Mo, Ta, Sn, Mn, Cu and Fe) was impregnated, and samples are named as M<sub>5</sub>/Ce<sub>40</sub>/Ti<sub>100</sub>. All precursors were calcined at 500 °C for 3 h. The fresh catalysts were characterized by ICP-OES, N<sub>2</sub>-physisorption, XRD, Raman spectroscopy, NH<sub>3</sub>-TPD, DRIFTS, XPS, and H<sub>2</sub>-TPR. Activity tests were run from 150 to 500 °C (1000 ppm NO<sub>x</sub>, 1000 ppm NH<sub>3</sub>, 5% O<sub>2</sub>, 8% H<sub>2</sub>O (if used), 100 ppm SO<sub>2</sub> (if used), rest He).

## Results and discussion

Among all the catalysts tested, Nb<sub>5</sub>/Ce<sub>40</sub>/Ti<sub>100</sub> and Mo<sub>5</sub>/Ce<sub>40</sub>/Ti<sub>100</sub> exhibited highest activity with 95% conversion at 200 °C (Fig. 1). Furthermore, both catalysts showed 99% N<sub>2</sub> selectivity in the temperature range of 150-500 °C (Fig. 2). Otherwise, with Cu<sub>5</sub>/Ce<sub>40</sub>/Ti<sub>100</sub> and Mn<sub>5</sub>/Ce<sub>40</sub>/Ti<sub>100</sub> the N<sub>2</sub> selectivity decreased

with raising temperature. This might be due to the high oxidation potential of related



metals, converting  $\text{NH}_3$  preferably to  $\text{N}_2\text{O}$  at high temperature [3].

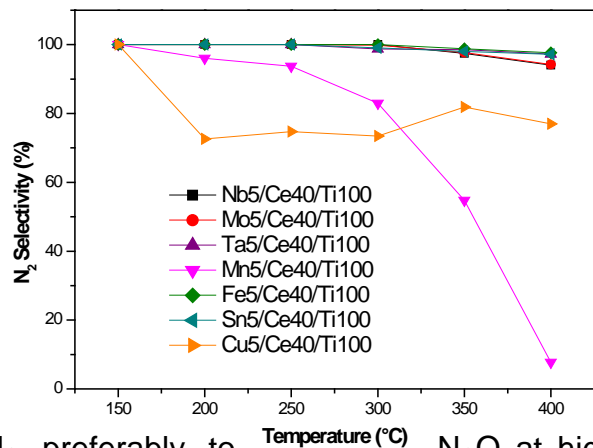


Fig. 1:  $\text{NO}_x$  conversion for different catalysts

Fig. 2:  $\text{N}_2$  selectivity for different catalysts

Nb and Mo modified Ce40/Ti100 showed the highest surface areas of 112.5 and 101.1  $\text{m}^2\cdot\text{g}^{-1}$ , respectively. There is a clear correlation between catalytic activity and surface area. XRD showed no reflexes for  $\text{Nb}_2\text{O}_5$  or  $\text{MoO}_3$ , suggesting high dispersion or amorphous state in the catalysts (Fig. 3). On the other hand, Mn, Fe, Sn and Cu catalysts showed reflexes of corresponding oxide domains, indicating lower dispersion which might explain their poor catalytic activity and selectivity. Additionally, the activity was measured in the presence of  $\text{H}_2\text{O}$  and  $\text{SO}_2$  for the most efficient Nb and Mo catalysts (Fig. 4).

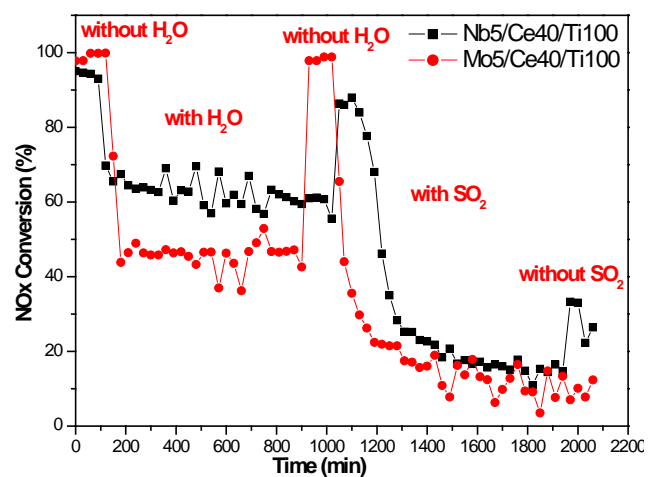
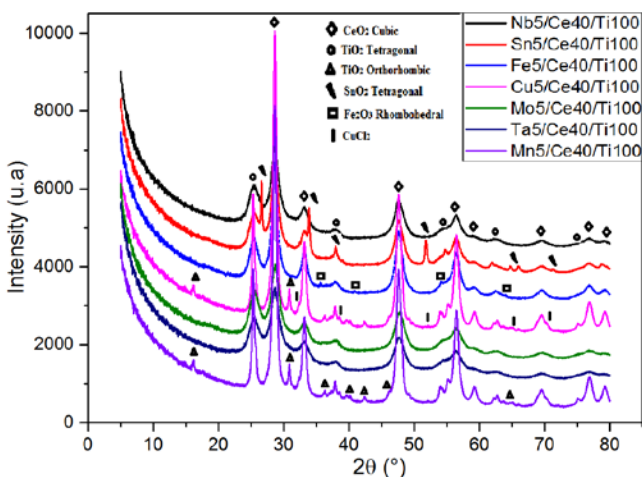


Fig.3: XRD patterns of the fresh catalysts.

Fig.4: Long-term activity and influence of H<sub>2</sub>O and SO<sub>2</sub> on the SCR activity at 200 °C.

The effect of H<sub>2</sub>O was reversible, although both catalysts deactivated, but less pronounced for Nb sample. In presence of SO<sub>2</sub> both catalysts deactivated which could be ascribed to the formation of sulphate and blocking of the active sites.

### References

- [1] G. Busca, L. Lietti, G. Ramis, F. Berti, Appl. Catal. B: Environ.18 (1998) 1-36.
- [2] W. Shan, F. Liu, Y. Yu, H. He, Chin. J. Catal. 35 (2014) 1251-9.
- [3] X. N. Lu, C. Y. Song; S. H. Jia ; Z. S. Tang, Y. X. Teng, Chem. Eng. J. 260 (2015) 776-784.

# Does Bulk Matter ? : Controlling Bulk Oxygen Vacancies Enhances Catalytic Reactivity of Perovskite Surfaces

Kerem Emre Ercan Department of Chemistry, Bilkent University, 06800, Ankara, Turkey, Zafer Say, Department of Physics, Chalmers University of Technology, Göteborg, 41296, Sweden, Merve Kurt, Department of Chemistry, Bilkent University, 06800, Ankara, Mustafa Karatok, <sup>3</sup>Department of Chemistry and Chemical Biology, Harvard University, MA 02138, USA, Zehra Aybegüm Ok, The Scientific and Technological Council of Turkey (TUBITAK), Ankara, 06100, Turkey, Emrah Ozensoy, <sup>1</sup> Department of Chemistry, Bilkent University, 06800, Ankara, Turkey, UNAM-National Nanotechnology Center, Bilkent University, 06800, Ankara, Turkey, Corresponding Author: Emrah Ozensoy; e-mail: [ozensoy@fen.bilkent.edu.tr](mailto:ozensoy@fen.bilkent.edu.tr); Website: <http://web3.bilkent.edu.tr/ozensoy/>

## Introduction

Due to their high costs and dynamic raw material prices, platinum group metals (PGM: Pt, Pd, Ir, Rh etc.) containing catalytic systems are typically unfavorably expensive [1]. Cost of these globally important and mass-produced catalytic systems can be lowered by decreasing the PGM loadings, which may result in a decrease in catalytic performance. Co and Mn containing perovskite systems offer promising catalytic opportunities in a variety of catalytic oxidation, reduction [2-5] and coupling [6,7] processes thanks to their dynamic redox properties and fine-tunable chemical/surface/electronic structures offering a wide playground for catalyst optimization.

In this study, we demonstrate that bulk-oxygen vacancies can have a strong influence on the redox activity of the hybrid perovskites allowing them to efficiently switch between high and low B-site oxidation states in a reversible fashion under relatively moderate redox conditions without requiring elevated temperatures for regeneration, unlike  $\text{LaCoO}_3$  and  $\text{LaMnO}_3$  benchmark systems. In hybrid perovskite systems such as  $\text{La}_{1.01}\text{Co}_{0.75}\text{Mn}_{0.24}\text{O}_{2.97}$  and  $\text{La}_{1.04}\text{Co}_{0.65}\text{Mn}_{0.31}\text{O}_{2.97}$ , we illustrate that perovskites with a particular bulk-oxygen vacancy population and electronically-modified hybrid B-site cations with specific oxidation states can reveal superior reactivity in transforming  $\text{NO}_2$  (g) into surface nitrates/nitrites that can surpass single B-site benchmark perovskites such as  $\text{LaCoO}_3$  and  $\text{LaMnO}_3$ . This may be accomplished by the diffusion of bulk oxygen vacancies to the surface which eventually governs the surface catalytic reactivity.

## Materials and Methods

**Catalyst Preparation.** Citrate method developed by General Motors Company was used to synthesize  $\text{LaCoO}_3$  and  $\text{LaMnO}_3$  benchmark perovskites, while a slightly modified version of this protocol was utilized for the synthesis of  $\text{LaCo}_x\text{Mn}_{1-x}\text{O}_3$  hybrid perovskites. **Ex-situ Characterization measurements (XRD, BET, TEM, ICP-MS, XPS)** were performed to reveal structure and functionality relationships of hybrid perovskites. **In-situ and Ex-situ X-Ray Absorption Near Edge Spectroscopy (XANES) measurements** were conducted to obtain full catalyst stoichiometry and demonstrate redox reversibility of corresponding perovskites. **In-situ Fourier Transform Infrared (FTIR) and Temperature Programmed Desorption experiments** were also carried out to establish link between oxygen vacancy population and  $\text{NO}_x$  oxidation capability of hybrid perovskite systems.

## Results and Discussion

In the current work, bulk-oxygen vacancies were found to have a strong effect on the redox activity of the hybrid perovskites allowing them to efficiently switch between high and low B-site oxidation states in a reversible fashion under relatively moderate redox conditions

without requiring elevated temperatures for regeneration, unlike  $\text{LaCoO}_3$  and  $\text{LaMnO}_3$  benchmark systems (see Figure 1). Hybrid perovskites with a particular bulk-oxygen vacancy population and electronically-modified hybrid B-site ions with specific oxidation states can yield greater  $\text{NO}_2$  conversion into surface nitrates/nitrites which may outperform single B-site benchmark perovskites such as  $\text{LaCoO}_3$  and  $\text{LaMnO}_3$ . Presumably, this is realized by the diffusion of bulk oxygen vacancies to the surface which dictate the surface redox reactivity. To estimate entire bulk stoichiometry and the bulk oxygen deficiency of the hybrid perovskites, we combined average bulk-oxidation state information provided by XANES and bulk A-site and B-site atomic ratios obtained via ICP-MS. (see Table 1).

**Table 1.** Estimation of the oxygen stoichiometry of the investigated perovskites by combining the current *ex-situ* XANES and ICP-MS results.

Sample Name	Relative # of La atoms per formula unit	Relative # of Co (or Mn) atoms per formula unit	Total # of A & B Cations per formula unit	Average Oxidation State of A-site cation: La	Average Oxidation States of B-site cations: Co (Mn)	Total positive charge per formula unit	Relative # of $\text{O}^{2-}$ anions per formula unit required for electrical neutrality	Oxygen deficiency/surplus coefficient « $\alpha$ »
$\text{ABO}_{3+\alpha}$	1.00	1.00	2.00	+3	+3.00	+6	3.00	0.00
$\text{LaCoO}_{3+\alpha}$	0.97	1.03 (N/A)	2.00	+3	+2.83 (N/A)	+5.82	2.91	-0.09
$\text{LaCo}_{0.8}\text{Mn}_{0.2}\text{O}_{3+\alpha}$	1.01	0.75 (0.24)	2.00	+3	+2.71 (+3.65)	+5.94	2.97	-0.03
$\text{LaCo}_{0.7}\text{Mn}_{0.3}\text{O}_{3+\alpha}$	1.04	0.65 (0.31)	2.00	+3	+2.59 (+3.63)	+5.93	2.97	-0.03
$\text{LaMnO}_{3+\alpha}$	0.97	N/A (1.03)	2.00	+3	N/A (+3.33)	+6.34	3.17	+0.17

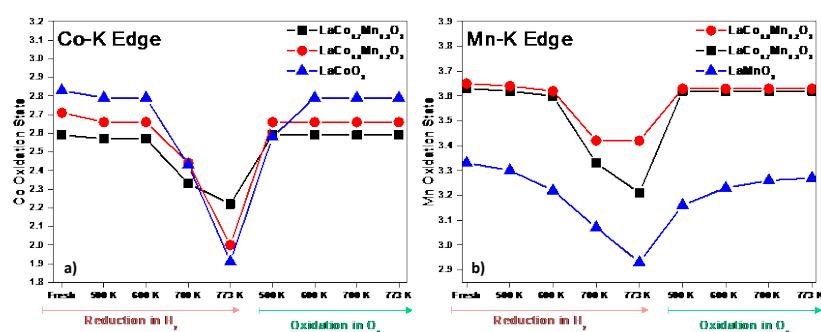


**Figure 1.** Numerical representation of Co (a) and Mn (b) K-edges (*in-situ*-XANES) for the variable temperature reduction and successive oxidation/regeneration of  $\text{LaCoO}_3$ ,  $\text{LaCo}_{0.8}\text{Mn}_{0.2}\text{O}_3$  and  $\text{LaCo}_{0.7}\text{Mn}_{0.3}\text{O}_3$

## References

- [1] Qi, G., Li, W. Pt-free, *Catal. Today* 184,72–77 (2012).
- [2] Heqing, J., Haihui, W., Fangyi, L., Steffen, W., Thomas, S., Jürgen, C. *Angew. Chem. Int. Ed.* 48, 2983–2986 (2009).
- [3] Zhang, J.; Haribal, V.; Li, F. *Sci. Adv.*, 3, e1701184 (2017).
- [4] Say, Z.; Dogac, M.; Vovk, E. I.; Kalay, Y. E.; Kim, C. H.; Li, W.; Ozensoy, E. *Applied Catalysis B: Environmental*, 2014 (154-155) 51-61
- [5]. Kurt, M.; Say, Z.; Ercan, K. E.; Vovk, E. I.; Kim, C. H.; Ozensoy, E. *Topics in Catal.*, 2017 (60) 40
- [6] Smith, M. D.; Stepan, A. F.; Ramarao, C.; Brennan, P. E.; Ley, S. V. *Chem. Commun.* 21, 2652–2653 (2003).
- [7] Andrews, S. P., Stepan, A. F., Tanaka, H., Ley, S. V., Smith, M. D. *Adv. Synth. Catal.* 2005, 347, 647–654.

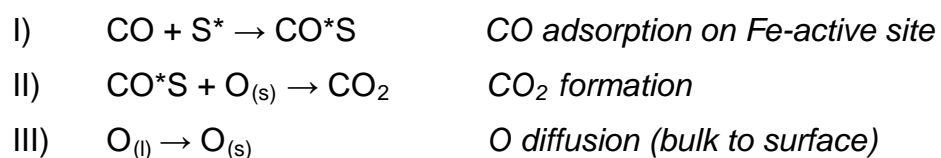
# Role of oxygen diffusion in LaFeO<sub>3</sub> catalyst on CO oxidation

*Benedetta Oliani, Paolo Canu*

*Industrial Engineering Dept., University of Padova - via Marzolo 9, Padova 35131, Italy  
[benedetta.oliani@phd.unipd.it](mailto:benedetta.oliani@phd.unipd.it), [paolo.canu@unipd.it](mailto:paolo.canu@unipd.it)*

Three-Way Catalysts (TWCs) are efficient exhaust after-treatment, but also the main consumers of Platinum Group Metals (PGMs) and subject to increasingly strict emission standards. Perovskite-based catalysts are interesting candidates in the development of alternative, PGM-free converters for automotive, thanks to their stability and tailorable properties. Their catalytic activity takes advantage of the oxygen storage capacity and mobility in the lattice, with the formation of structural vacancies [1]. The rational exploitation of perovskite catalysis requires a quantitative description of the lattice and bulk oxygen formation, involvement in the reaction and migration, through vacancies, by means of a chemically-based, quantitative reaction mechanism that accounts for these features.

The intrinsic redox potential of Fe-cation makes LaFeO<sub>3</sub> (LFO) a promising model perovskite to study simultaneous NO<sub>x</sub> reduction and CO oxidation. The LFO contribution in supplying oxygen is essential for TWC oxidation function. We specifically addressed the integration of the oxygen diffusion in the lattice into a Mars-Van Krevelen reaction mechanism of CO oxidation over LFO:



In our investigation, LFO is exposed to an oscillating oxygen and CO concentrations; CO conversion is expected also in O-lean conditions. The low-temperature CO oxidation is a surface reaction requiring O vacancies next to metal atoms that activate CO by adsorption and cause O<sub>(l)</sub> transport to the surface [1]. Oxygen diffusion, driven by vacancies formation, becomes an activated process [2] ruled by an Arrhenius-type diffusion coefficient. Temperature plays a key role in all the reaction steps. Accordingly, we studied the process through isothermal experiments (250, 300, 400, 500°C), where the total O available from the LFO was determined by feeding CO without any O<sub>2</sub>. First, experiments in a packed-bed flow reactor were carried out. LFO was first oxidized at fixed conditions (20%O<sub>2</sub>, 10°C/min, 400°C for 1h) and then a diluted (0.7%) CO/inert mixtures were fed to the reactor, once the set



temperature was stabilized, to prevent any activation at lower temperatures. The outlet gas mixture was continuously monitored (by FTIR). The loss of oxygen from LFO was calculated from the total CO<sub>2</sub> produced. The CO<sub>2</sub> by other reactions (e.g. carbonates decomposition) was quantified and subtracted through experiments at high temperature under inert flow.

The amount of CO<sub>2</sub> produced, reflecting the O made available by LFO for CO oxidation, increases with temperature (Fig.1). It suggests either a progressive involvement of different layers in LFO (grouped into surface or  $\alpha$ -O, and bulk or  $\beta$ -O) [1], at increasing temperature, or the increase of O diffusion from the bulk to the surface of LFO, where O is actually consumed. The O consumption at 250°C is correlated to the surface area, evidencing an artificial boundary between the two macro-layers. However, we rather emphasize the relevance of O migration to the surface, by diffusion at a fixed temperature. Lattice diffusion is expected to increase exponentially with temperature, still being a function of time because of the corresponding, gradual smoothing of the O gradients in the lattice. In these conditions, small extents of O lattice diffusion make the CO<sub>2</sub> concentration greater than zero for long time, since the O concentration gradient along the layers becomes crucial.

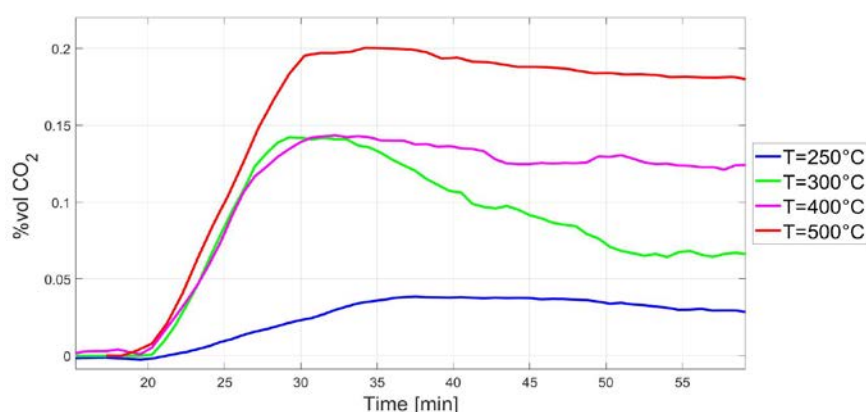


Fig.1: CO<sub>2</sub> initial concentration profiles at different temperatures.

A second set of tests, to validate the results above, is under completion. They are based on the double check of lattice O consumption by means of weight reduction, together with CO<sub>2</sub> production, in a precision microbalance.

## References

1. Royer, S. *et al.* Perovskites as substitutes of noble metals for heterogeneous catalysis: Dream or reality. *Chem. Rev.* **114**, 10292–10368 (2014).
2. Berenov, A. *et al.* Structure and transport in rare-earth ferrates. *Solid State Ionics* **179**, 1090–1093 (2008).

# Upscaling Perovskite Production: Effect of Synthesis on Catalytic Activity

*E. Brusamarello, University of Padua, Padua, Italy; C. Salazar Castro, Centro Tecnológico Lurederra, Los Arcos, Spain; A. Glisenti, University of Padua, Padua, Italy*

## Introduction

The development of innovative catalysts for exhaust control has been oriented towards perovskite as versatile materials, which allow the incorporation of different cations in their structure. Thus, adding inexpensive and largely available, catalytically active transition metal cations can represent a novel approach for TWC [1] that allows minimizing noble metals. The aliovalent doping in the perovskite A and B sites induces the formation of structural defects and of different oxidation states, together with the presence of cations redox couples. [1] A very relevant problem, however is in the synthesis of the catalysts both in terms of reproducibility, and upscale. In this contribution a comparison between different synthetic industrial approaches in terms of properties and reactivity is carried out. Catalysts obtained by Flame Spray Pyrolysis (FSP) and by Co-precipitation (COP) have been compared. Doped manganates and ferrites have been considered because of their high activity in TWC, low cost and absence of noble metals. Moreover, catalysts obtained at different phases of the FSP process have been considered.

## Experimental section

FSP-obtained perovskites were produced with a prototype reactor owned by Lurederra. The methodology consists of a one-step process where a mixture of metal precursors in an appropriate solvent is sprayed with an oxidizing gas ( $O_2$ ) into a flame. Thus, the droplets are individually combusted, obtaining nano-sized perovskite particles. Operational parameters such as precursor feed flow, amount of dispersant gas, nozzle pressure, etc allow to control properties such as high purity, low aggregation and small particle size, which are typically resulting from this process. Several processes occur simultaneously in the flame in microseconds, such as fine atomization, aerosol droplet evaporation, combustion, agglomeration, sintering and surface growth and the resulting powder is immediately collected. The corresponding catalysts prepared by traditional co-precipitation from nitrates solution are also reported for comparison.

## Results

A first set of samples, consisting in 4 batches of  $\text{La}_{0.6}\text{Ca}_{0.2}\text{Fe}_{0.8}\text{Cu}_{0.2}\text{O}_3$  (LCFC A, B, C and D respectively) collected at successive stages of the FSP, showed significant changes in morphology, composition and structural features. SEM images underline the formation of highly dispersed particles on a porous structure and, with the process advancement, of globular particles (diameter of about 100 nm), most likely combustion remains. LCFC A diffraction pattern, unlike B to D, suggests incomplete formation of perovskite phase, in favor of a mixture of oxides ( $\text{La}_2\text{O}_3$ ,  $\text{Fe}_2\text{O}_3$ ), as confirmed by XP spectra. EDX/XPS compositional analysis point out the surface segregation of La and Cu on

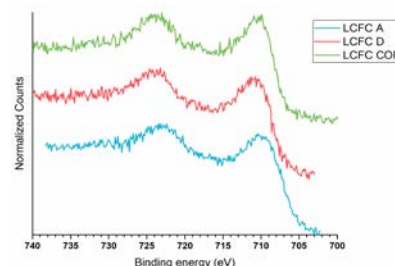


Figure 2. XP Fe2p spectrum of LCFC A, D and LCFC COP.

the surface, whereas Fe segregates only in LCFC D. Significant differences are evident focusing on  $\text{La}_{0.7}\text{Fe}_{0.8}\text{Cu}_{0.2}\text{O}_3$  obtained by FSP (LFCFSP) and  $\text{La}_{0.6}\text{Ca}_{0.2}\text{Fe}_{0.8}\text{Cu}_{0.2}\text{O}_3$  obtained by FSP (LCFCFSP) and coprecipitation (LCFCCOP), As instance, coprecipitation method does not prove to efficiently form perovskite phase, as confirmed by XPS [2] (see Figures 1 and 2).

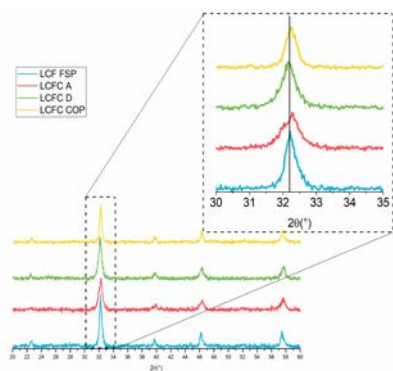


Figure 3. XRD pattern for LCF FSP, LCFC A, D and LCFC COP.

A last group of samples,  $\text{La}_{0.9}\text{K}_{0.1}\text{Mn}_{0.9}\text{Co}_{0.1}\text{O}_3$ , were obtained by FSP (LKMCFSP) and coprecipitation (LKMCCOP): once again coprecipitation seems less effective in originating pure perovskite phase (Figure 3). Interestingly the preparation procedure also affects the presence of active oxygen species, of the reducibility and of the reactivity in pollutants' abatement reactions.

Figure 1. XRD pattern inset for LKMC FSP, COP.

## References

- [1] A. Glisenti, M. Pacella, M. Guiotto, M.M. Natile, P. Canu, Largely Cu-doped  $\text{LaCo}_{1-x}\text{Cu}_x\text{O}_3$  perovskites for TWC: Toward new PGM-free Catalysts, *Applied Catalysis B: Environmental* 180, 2016, 94
- [2] M. Guiotto, M. Pacella, G. Perin, A. Iovino, N. Michelon, M.M. Natile, A. Glisenti, P. Canu, Washcoating vs. Direct Synthesis of  $\text{LaCoO}_3$  on Monoliths for Environmental Applications, *Applied Catalysis A: General* 499, 2015, 146

# Innovative approach in synthesis of the MOR zeolite

*Kinga Mlekodaj, Veronika Pashkova, Agnieszka Kornas, Milan Bernauer, Petr Klein, Jirí Dedecek, J. Heyrovský Institute of Physical Chemistry, Academy of Sciences of the Czech Republic, Prague, Czech Republic*

## Introduction

Synthetic mordenite is used as a catalyst in the petrochemical industry for the acid-catalyzed isomerisation of alkanes and aromatics. This structure features small micropores and Si/Al ratio in a wide range (5-25).

The environmental and economical restrictions put high demand on the zeolite synthesis and its sustainability in terms of materials, energy and generation of liquid waste. Present work explores possibilities of mechanochemical pre-treatment [1] and ultrasonic pre-treatment [2] for the facilitation of zeolite MOR synthesis.

## Experimental

- 1) Milling by planetary mill was applied for the preliminary treatment of the synthesis mixture, consisting of precipitated silica, sodium aluminate and sodium hydroxide (cheap, available reagents). Small amount of water was added to keep mixture visually dry. Synthesis was performed without organic SDA (green approach). Such obtained dry gels underwent heating for crystallization.
- 2) Ultrasonic pre-treatment was applied as a modification of the existing synthesis procedure [3].

All obtained samples were calcined and ion-exchanged for further characterization. Samples and milled “dry gels” were characterized by the XRD, XRF (chemical analysis), SEM,  $^{27}\text{Al}$  and  $^{29}\text{Si}$  MAS NMR, nitrogen sorption. Authors aimed in the estimation of Influence of treatments and possibilities to use them as a way to MOR synthesis facilitation (improvement of product/gel ratio, shortening synthesis time, better textural characteristics).

## References

- [1] Morris, R. E.; James, S. L. *Angew. Chem., Int. Ed.* (2013), 52, 2163
- [2] Askari S.; Alipour S.M.; Halladj, S.M.R.; Hossein, M. et al., *J Porous Mater* (2013) 20, 285
- [3] <http://www.iza-online.org/synthesis/Recipes/Mordenite.html>

Authors acknowledge support of the Grant Agency of the Czech Republic under projects 17-09188Y

# **NaAlO<sub>2</sub>-based mesoporous materials obtained by sol-gel chemistry and used as basic catalysts for the room temperature Knoevenagel condensation reaction**

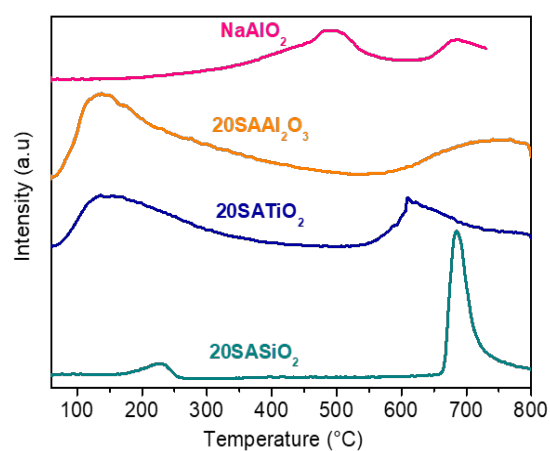
Sreerangappa Ramesh, Francois Devred and **Damien P. Debecker\***

Institute of Condensed Matter and Nano sciences (IMCN), UCLouvain, Place Louis Pasteur, 1, box L4.01.09, 1348 Louvain la-Neuve, Belgium. Email: [damien.debecker@uclouvain.be](mailto:damien.debecker@uclouvain.be)

For the demand of sustainable development and green chemistry implementation, increasing attention has been given to the substitution of conventional homogeneous base catalysts (KOH, NaOH and alkali carbonates) with heterogeneous ones. Among heterogeneous catalysts, mesoporous solids having strong basic sites are extremely intriguing for applications in environmentally friendly catalytic processes.[1,2] In this work, novel mesoporous solid base catalysts were synthesized by promoting sodium aluminate (NaAlO<sub>2</sub>) within mesoporous supports. These latter were fully characterized using a wide variety of molecular and solid-state techniques to determine their structural and textural properties. Silica in its pure form showed high surface area of 471 m<sup>2</sup>/g, whereas after incorporation of sodium aluminate gradually decreases with increase in NaAlO<sub>2</sub> amount. The catalyst promoted with 20% NaAlO<sub>2</sub> showed 80-90 m<sup>2</sup>/g, (Similar results are observed with titania and alumina.) which is much higher when compared to pure sodium aluminate (2 m<sup>2</sup>/g). The basicity of the prepared catalysts was evaluated by using CO<sub>2</sub>-TPD and CO<sub>2</sub> DRIFTS measurements. The basicity of the catalysts are in the following order 20SASiO<sub>2</sub>, 20SATiO<sub>2</sub>, 20SA Al<sub>2</sub>O<sub>3</sub>. Sodium aluminate belongs to a class of super base, possessing strong basic sites in much higher quantity compared to the SA promoted mesoporous materials.

The activities of the prepared catalysts tested in the Knoevenagel condensation of benzaldehyde (BA) with ethyl cyanoacetate (ECA) under solvent free green reaction conditions. The reaction is usually considered as a probe reaction for evaluating basic strength of the catalysts. The target product, ethyl-2-cyano-3-phenyl acrylate, detected exclusively with all the catalysts studied for the screenings verified by GC and <sup>1</sup>HNMR analysis. Initially, prepared catalysts along with benchmark catalysts - screened for the condensation reaction at room temperature and the results are represented in the table 1. The pure NaAlO<sub>2</sub> showed much higher activity

in short reaction time, almost reaching equilibrium (~95% BA conversion in 2 h) - actually, 58% BA conversion reached within 30 min of reaction.



Catalyst	Conversion
Blank	04.0
NaAlO <sub>2</sub>	95.0
SiO <sub>2</sub>	08.0
5SA SiO <sub>2</sub>	38.0
10SA SiO <sub>2</sub>	51.0
20SA SiO <sub>2</sub>	60.0
20SA Al <sub>2</sub> O <sub>3</sub>	93.0
20SA TiO <sub>2</sub>	71.0
Hydrotalcite	15.0
MgO	54.0

Figure 1 CO<sub>2</sub>-TPD of the SA promoted mesoporous catalysts Table 1 Catalytic activity of solid base catalysts

Yet, NaAlO<sub>2</sub> in its pure solid form is highly hygroscopic and corrosive, and thereby difficult to handle. Hence supporting NaAlO<sub>2</sub> on a suitable support was inspected.[3,4] The basicity measurement from CO<sub>2</sub>-TPD also showed that, 20SASiO<sub>2</sub> total basicity is very low as a result; it showed low activity in the condensation reaction studied. Whereas, SA supported on alumina possess high surface basic strength and showed higher BA conversion. From the results, it is clear that, alumina is the best support to generate basicity in mesoporous materials; hence, further optimization and reusability studies conducted with 20 SAAI<sub>2</sub>O<sub>3</sub> only. In order to investigate the heterogeneous nature of the catalysts, a hot filtration test and reusability was conducted, from the results it was confirmed that the catalysts are truly heterogeneous.

## References

1. G. Busca, *Chem. Rev.*, 2010, **110**, 2217-2249.
2. L.-B. Sun, X.-Q. Liu and H.-C. Zhou, *Chem. Soc. Rev.*, 2015, **44**, 5092-5147.
3. S. Ramesh and D. P. Debecker, *Catal. Commun.*, 2017, **97**, 102-105.
4. S. Ramesh, D. François, v. d. B. Ludivine and D. P. Debecker, *ChemCatChem*, 2018, **10**, 1398-1405.

# Composite materials based on bismuth silicates for photocatalytic application

*Yulia Belik, Andrei Vodyankin, Tamara Kharlamova, Olga Vodyankina, National Research Tomsk State University, Russia*

## Introduction

Bismuth silicates exist in three modifications: bismuth metasilicate  $\text{Bi}_2\text{SiO}_5$  with perovskite-type structure, sillenite  $\text{Bi}_{12}\text{SiO}_{20}$ , the framework structure of which is similar to  $\gamma\text{-Bi}_2\text{O}_3$ , and bismuth orthosilicate  $\text{Bi}_4\text{Si}_3\text{O}_{12}$  with a structure close to the framework type. While being applied as scintillators [1] etc., bismuth silicates are also used as photocatalysts [2].

In this work, two opposite approaches were employed. Environmentally friendly mechanochemical activation was applied as the “top-down” approach. Conventional hydrothermal treatment was also used to prepare materials, but as the “bottom-up” approach. With these methods of synthesis, the influence of preparation methods as well as molar ratio of initial reagents on phase composition and properties of prepared samples were investigated.

## Experiment

For the first time, bismuth silicates were obtained via mechanochemical activation followed by calcination (BSM samples). Bismuth oxide  $\text{Bi}_2\text{O}_3$  and hydrous silica  $\text{SiO}_2 \cdot n\text{H}_2\text{O}$  were used as precursors. The stoichiometric mixtures with different composition (ratios of  $\text{Bi}_2\text{O}_3:\text{SiO}_2$  were 1:1, 2:3, 6:1) were activated in a high-power planetary ball mill AGO-2 for 10 min [3]. For hydrothermal treatment,  $\text{Bi}(\text{NO}_3)_3 \cdot 5\text{H}_2\text{O}$  and  $\text{Si}(\text{C}_2\text{H}_5\text{O})_4$  were used as starting materials (ratios of Bi:Si were 2:1, 4:3, 12:1), ethylene glycol as solvent and  $\text{HNO}_3$  as catalyst (BSO samples). Synthesis was carried out in steel autoclave at 180 °C for 12 h, and then samples were dried at 60° for 24 h. Ratios of initial substances were chosen in order to prepare model phases  $\text{Bi}_2\text{SiO}_5$ ,  $\text{Bi}_{12}\text{SiO}_{20}$ ,  $\text{Bi}_4\text{Si}_3\text{O}_{12}$  in both approaches.

Physical and chemical processes occurring in the mixtures during following temperature treatment were studied by TG-DSC. In both cases, materials were calcined at different temperatures for 2 h, with calcination temperatures being chosen according to the data of TG-DSC. The phase composition of the samples was investigated by X-Ray diffraction and FTIR spectroscopy. On the basis of aforementioned methods a scheme of solid-state reactions was proposed for “top-

down” approach. To study optical properties, UV-VIS diffuse reflectance spectroscopy, and photoluminescence measurement were employed. A photocatalytic study of all prepared materials in the reaction of Rhodamine B decolorization was carried out.

## **Discussion**

According to XRD data, both preparation methods led to the multiphase composition, despite the stoichiometric ratios at start. Only  $\text{Bi}_{12}\text{SiO}_{20}$  sillenite phase was available to be synthesized. FTIR data was in a good agreement with XRD analysis. It was also established that the small amount of amorphous  $\text{SiO}_2$  was present in the materials with calcination temperatures below 600 °C.

Results of photocatalytic tests showed that the BSM samples did not demonstrate activity; rate constant values were even below than those for a blank experiment. The highest photocatalytic activity was detected for the BSO sample calcined at 700 °C with ratio of Bi:Si=1:1, which contained three phases and possessed the highest surface area.

For both series, photoluminescence (PL) effect was detected for all samples containing  $\text{Bi}_4\text{Si}_3\text{O}_{12}$  phase, with the excitation peak at 250 nm and the broad emission peak at visible area. UV-VIS DRS data showed that prepared bismuth silicates absorbed visible light and according to XRD data possessed different phase composition. Moreover, the step-like curve shapes for the BSM samples may be explained by the fact that phases did not contact with each other.

## **Conclusions**

The “top-down” and “bottom-up” methods led to notably different results in terms of phase composition, optical properties, and photocatalytic properties. The “top-down” approach did not lead to the creation of photocatalytically active samples, with them possessing strong luminescent properties. The differences in the results obtained by two preparation methods will be discussed.

This research was supported by “The Tomsk State University competitiveness improvement programme”.

## **References**

1. J. Kaewkhao, N. Udomkan, W. Chewpraditkul and P. Limsuwan, *IJMPB*, 2009, 23, 2093-2099.
2. Sh. Ding, X. Xiong, X. Liu, Y. Shi, Q. Jiang and J. Hu, *Catal. Sci. Technol.*, 2017, 7, 3791–3801.
3. T. Kharlamova, S. Pavlova, V. Sadykov, M. Chaikina, T. Krieger, O. Lapina, D. Khabibulin, A. Ishchenko, V. Zaikovskii, *Chr. Argirusis, J. Frade, Eur. J. Inorg. Chem.* 2008, 939–947.



# **3D-printing of Hydrotalcite for Increased Productivity in Productivity in Sorption-Enhanced Water-Gas Shift Reaction**

*S. N. Sluijter, P. D. Cobden, R. de Boer ECN part of TNO, Petten, the Netherlands;  
A. M. Cormos, A. Imre-Lucaci; Babes-Bolyai University, Cluj-Napoca, Romania*

Developing energy efficient carbon capture technologies is of great importance to combat climate change. Sorption-enhanced water-gas shift (SEWGS) is a combination of the water-gas shift (WGS) reaction and on-site adsorption of CO<sub>2</sub> catalyzed by potassium-promoted hydrotalcite (K-HTC) [1]. The process is very attractive for an energy efficient pre-combustion CO<sub>2</sub> capture, as it enables direct conversion of syngas into separate streams of H<sub>2</sub> and CO<sub>2</sub> at high temperatures and pressures. Currently, the commercialization of this technology is hampered by both the size of equipment and the energy associated with the carbon abatement. This project will solve these challenges by significantly increasing the productivity (kg CO<sub>2</sub>/m<sup>3</sup>hr) by structuring K-HTC through 3D-printing.

Structured adsorbents and catalysts have recently gained significant interest owing to the advantages of lower pressure drop and faster mass transfer over conventional shaped materials [2,3]. The required porous ceramic materials for these technologies are prepared using the latest innovations in additive manufacturing (3D-printing). This technology allows to prepare bespoke materials, with tailored channel sizes and wall thickness, having improved heat and mass-transfer characteristics, that are not available through traditional material preparation routes.

## **Development of 3D-printed microporous ceramic materials**

The 3D-technology used to develop the structured K-HTC is Digital Light Processing (DLP; Figure 1). This technology consists of an indirect slurry-based process that uses a photo-active material to initiate binding. After printing the structure layer by layer by illuminating cross-sections of the design, a delamination and sintering step is required to obtain the final structured adsorbents.

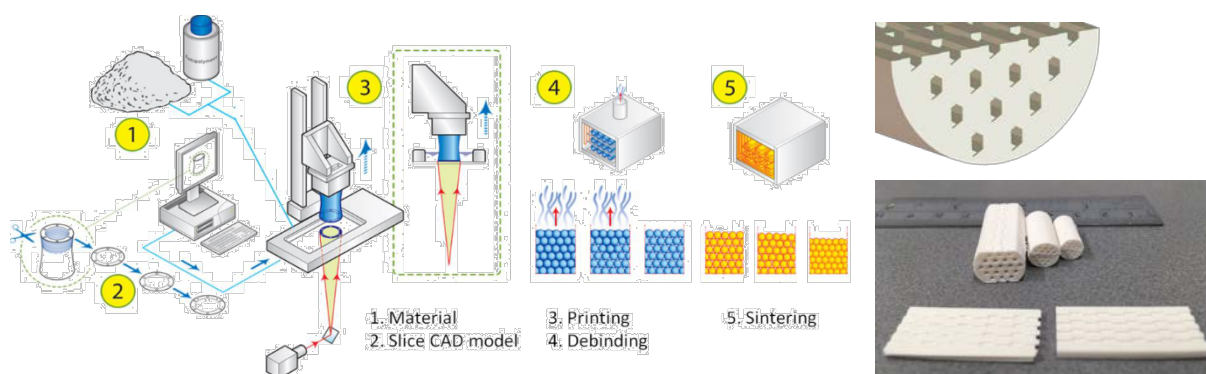


Figure 1. Left: Schematic representation of DLP technology. The printer (3) illuminates the paste (1) layer-by-layer as a projected cross-section (2). After each layer, the structure is moved up, and the layer of paste is restored. After printing, delamination (4) and sintering (5) lead to the final structured catalyst. Right: Design and 3D-printed monoliths with zig-zag channels.

The slurries for 3D-printing have been developed and used to prepare various advanced monolithic structures, that have been determined and investigated by mathematical modelling. The adsorption characteristics (equilibrium isotherms and kinetic parameters) of the resulting 3D printed adsorbents are measured for the relevant gaseous components ( $\text{CO}_2$ ,  $\text{N}_2$ ,  $\text{H}_2\text{O}$ ). The properties of the 3D structured materials have been studied and evaluated against traditional pellets and the results will be presented in this contribution.

**Acknowledgements:** The ACT 3D-CAPS project # 271503 has received funding from RVO (NL), RCN (NO), UEFISCDI (RO), and is co-funded by the  $\text{CO}_2$  Capture Project (CCP) and the European Commission under the Horizon 2020 programme ACT, Grant Agreement No 691712.

### References

- [1] J. Boon; P. D. Cobden, H.A.J. van Dijk, C. Hoogland, E. R. van Selow, M. van Sint Annaland, M.; Chem. Eng. J. 248 (2014) 406–414.
- [2] M. Sireesha; J. Lee; A.S. Kranthi Kiran; V. J. Babu; B. B. T.; S. A Ramakrishna; RSC Adv. 40 (2018) 22460–22468.
- [3] C. Parra-Cabrera; C. Achille; S. Kuhn; R. Ameloot; Chem. Soc. Rev. 47 (2018) 209–230.

# **Hydrocarbon tolerant Copper Zeolites for Combination of NH<sub>3</sub>/ and HC/SCR**

**Iljeong Heo, Korea Research Institute of Chemical Technology  
(KRICT), Daejeon, Korea**

**In-Sik Nam, Pohang University of Science and Technology  
(POSTECH), Pohang, Korea**

## **Introduction**

Urea/SCR has emerged as the best deNO<sub>x</sub> technology for lean-burn engine exhaust due to its outstanding performance. However, it has inherent drawbacks, i.e. periodical refill of urea solution to a reservoir tank, and supplying systems such as a urea solution injector and pump [1,2]. Thus, another SCR technology using fuel hydrocarbons (HCs), HC/SCR, has extensively studied as a potential deNO<sub>x</sub> system, although NO<sub>x</sub> reduction performance by HC/SCR is insufficient for real application to date. One way to improve the deNO<sub>x</sub> performance in HC/SCR system is to employ NH<sub>3</sub> as additional reductant which is produced during the course of HC/SCR. However, NH<sub>3</sub>/SCR catalysts, particularly zeolite based catalysts, are prone to be inactivated by HCs present in the exhaust. Therefore, the effect of HCs on NH<sub>3</sub>/SCR over five type of Cu zeolites has been systematically examined in this study, to apply the zeolite based catalysts to combined SCR system by HC and NH<sub>3</sub>.

## **Results and Discussion**

CuSSZ-13 and CuFER revealed a strong tolerance to the catalyst poisoning by heavy HCs, due to their smaller pore size than the kinetic diameters of the HCs including C<sub>8</sub>H<sub>10</sub> and C<sub>12</sub>H<sub>26</sub>. C<sub>3</sub>H<sub>6</sub>, as a short-chain HC, was a dominant poisoning precursor for the deactivation of the CuSSZ-13. CuFER exhibited a much narrower temperature window and much severe HC poisoning by C<sub>3</sub>H<sub>6</sub>, which is most likely due to the lower dimensionality (2D) of its pore network compared with the 3D of CuSSZ-13. On the other hand, CuZSM-5 and CuBEA having the 3D medium- and large-pore channels revealed significant decreases in their NH<sub>3</sub>/SCR performances by all HCs. Among HCs, the long chain linear C<sub>12</sub>H<sub>26</sub> was the primary precursor for HC poisoning over both catalysts, although the CuBEA was further

poisoned by C<sub>8</sub>H<sub>10</sub> due to its larger pore size than the kinetic diameter of C<sub>8</sub>H<sub>10</sub>. The CuMOR having 1D large pore channels showed a milder HC poisoning behavior, regardless of the types of HCs.

The pore size and interconnectivity of channel networks of zeolite catalysts are the key factors for their HC adsorption and diffusion, resulting in the unique HC poisoning behavior depending on HCs included in the feed. The more interconnected channel system, the severer HC poisoning of the Cu zeolite catalysts. Although the states of Cu on the catalyst surface were hardly changed by the adsorption of HC onto the catalyst surface, the decrease of their surface areas depends on the amounts of HCs adsorbed.

Both NH<sub>3</sub> adsorption and surface NO oxidation were inhibited by the strong adsorption of HCs: the effect of HC on of the NO oxidation reaction rate was closely related to its effect on the rate of the NO reduction by the NH<sub>3</sub>/SCR in the low temperature region. In the medium temperature region, the consumption of NH<sub>3</sub> via the ammoxidation reaction further decreased the deNO<sub>x</sub> activities of NH<sub>3</sub>/SCR over the Cu zeolite catalysts except CuMOR. The complete conversion of NO at 330 °C over the CuMOR is ascribable to the negligible ammoxidation reaction during the NH<sub>3</sub>/SCR in the presence HCs at this temperature. On the other hand, the HC/SCR reaction induced by HCs increased the high-temperature deNO<sub>x</sub> performance of the catalysts poisoned by HCs in the high reaction temperature region.

## References

[1] J.H. Baik, S.D. Yim, I.-S. Nam, *Ind. Eng. Chem. Res.*, 45 (2006) 5258.

[2] S.D. Yim, S.J. Kim, J.H. Baik, I.-S. Nam, *Ind. Eng. Chem. Res.*, 43 (2004) 4856.

## **V<sub>2</sub>O<sub>5</sub> nanosheets for selective catalytic reduction of NO with NH<sub>3</sub>**

*Yang Yang, Research Center for Eco-Environmental Sciences, Chinese Academy of Sciences, Beijing, China; Hong He, Research Center for Eco-Environmental Sciences, Chinese Academy of Sciences, Beijing, China*

### **Introduction**

V<sub>2</sub>O<sub>5</sub>-WO<sub>3</sub>/TiO<sub>2</sub> has been used as a commercial catalyst for NH<sub>3</sub>-selective catalytic reduction(SCR) of NO<sub>x</sub>. Despite of numerous investigations, questions about the mechanism of this reaction still remain. V<sub>2</sub>O<sub>5</sub> is recognized as the active component and three forms of V<sub>2</sub>O<sub>5</sub> exist on TiO<sub>2</sub>, including monomeric vanadyls, polymeric vanadates, and crystallites of V<sub>2</sub>O<sub>5</sub>[1]. Among them polymeric vanadates are the most active species[2]. Inspired by this understanding, a catalyst with exclusive polymeric vanadates species should be advantageous to the clarification of the reaction mechanism. Coincidentally, V<sub>2</sub>O<sub>5</sub> is a natural layered material and all V<sub>2</sub>O<sub>5</sub> are in the form of polymeric vanadates in every single layer[3].

### **Experiments and Discussions**

Here V<sub>2</sub>O<sub>5</sub> nanosheets were prepared via a hydrothermal process and tested for NH<sub>3</sub>-SCR of NO<sub>x</sub>[4]. As shown in Figure 1, V<sub>2</sub>O<sub>5</sub> nanosheets are indeed active and its activity is clearly much higher than its bulk counterpart. Thus these nanosheets can be used as model catalyst to investigate the reaction mechanism.

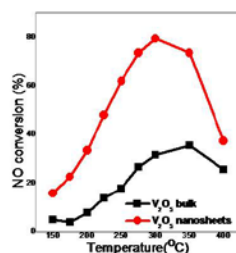


Figure 1 NH<sub>3</sub>-SCR of NO reactions over V<sub>2</sub>O<sub>5</sub> bulk and nanosheets. conditions: space velocity(SV)=300,000 mL (g<sub>cat</sub> h)<sup>-1</sup>; [NH<sub>3</sub>]=[NO]=500 ppm, 5%O<sub>2</sub>, balance N<sub>2</sub>.

A series of in situ diffuse reflectance Fourier transform infrared spectroscopy (DFRIST) under different conditions at 150 °C were collected. In Figure 2a , NO+O<sub>2</sub> was exposed after NH<sub>3</sub> was pre-adsorbed and purged. Peaks at 1233, 1252, 1604 and 3253 were attributed to NH<sub>3</sub> adsorbed on Lewis acidic sites, while peaks at 1418, 2700-3500 to NH<sub>3</sub> adsorbed on Bronsted acidic sites. All NH<sub>3</sub> except those adsorbed at 1604 and 3253 were cleared off with the exposure of NO+O<sub>2</sub>. Bronsted acidic sites are the main active sites considering the peak area of NH<sub>3</sub> adsorbed on these two kinds of sites. Spectra in Figure 2b can be interpreted in a similar way, where NO showed almost no adsorption on V<sub>2</sub>O<sub>5</sub> nanosheets.

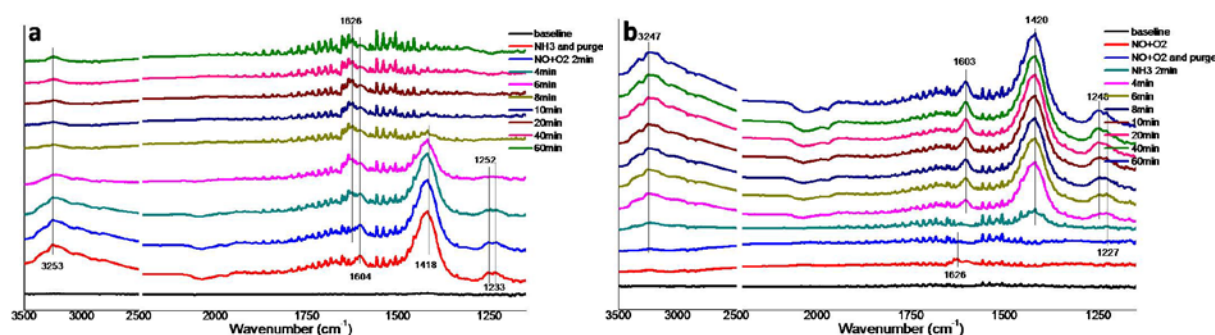


Figure 2 *In situ* DFRIST spectra over V<sub>2</sub>O<sub>5</sub> nanosheets.

## Conclusions

Based on a V<sub>2</sub>O<sub>5</sub> nanosheets model catalyst research, an Eley– Rideal (E-R) mechanism is more reasonable, where NH<sub>3</sub> is adsorbed on several kinds of acidic sites and then reacted with NO from gas. Our data highlight the significance of Bronsted acidic sites on V<sub>2</sub>O<sub>5</sub> surface in V<sub>2</sub>O<sub>5</sub> based NH<sub>3</sub>-SCR reactions.

## References

- [1] Went G T , Leu L J , Bell A T. *J. Catal.* 1992, 134, 479.
- [2] Went G T , Leu L J , Rosin R R et al. *J. Catal.* 1992, 134, 492.
- [3] Nicolosi V, Coleman N et al. *Science* 2013, 340, 1226419.
- [4] Liang S, Cao G et al. *Nano Energy* 2015, 13, 58.

# Structure-activity relationships of Pt/TiO<sub>2</sub> catalysts for ammonia low-temperature oxidation

*Andrey Stadnichenko, Elena Slavinskaya, Dmitry Svintsitskiy, Anatoly Romanenko, Elizaveta Derevyannykova, Olga Stonkus, Andrei Boronin, Boreskov Institute of Catalysis, SB RAS, Novosibirsk, Russia; Valery Svetlichnyi, Tomsk State University, Tomsk, Russia; Vasyl Marchuk, Dmitry Doronkin, Maria Casapu, Anna Zimina, Jan-Dierk Grunwaldt, Karlsruhe Institute of Technology, Karlsruhe, Germany*

## Scope

Ammonia and its derivatives are considered excellent energy storage materials, as alternative to elementary hydrogen and thus as energy carriers for mobile applications. To provide fuel cell grade hydrogen ammonia is catalytically cracked. Since NH<sub>3</sub> decomposition is an equilibrium process, NH<sub>3</sub> slip inevitably occurs during H<sub>2</sub> generation. Further sources of ammonia are exhaust gas aftertreatment systems of power plants and automobiles. In these cases the exhaust contains NO<sub>x</sub> which is removed by reacting with ammonia. For higher NO<sub>x</sub> removal efficiency excess of NH<sub>3</sub> is dosed, resulting in its slip in the exhaust. Because of its toxicity, NH<sub>3</sub> needs to be removed before it reaches the environment. Selective oxidation of NH<sub>3</sub> to N<sub>2</sub> over so-called ammonia slip catalysts (ASC) is currently the only way to prevent unreacted ammonia reaching the environment.

Due to their high activity and stability under realistic working conditions (e.g. with H<sub>2</sub>O vapour), Pt-based catalysts are predominantly used as ASCs. Current efforts on improving the ASCs are on a trial and error basis. In order to efficiently improve low-temperature activity of Pt catalysts and to increase their selectivity to N<sub>2</sub> it is essential to understand structure activity relationships of Pt based catalysts in selective NH<sub>3</sub> oxidation.

## Experimental

In order to highlight the role of platinum interaction with support two different types of 2%Pt/TiO<sub>2</sub> catalysts were used. The first series of catalysts was synthesized by coprecipitation/incipient wetness impregnation technique based on commercial TiO<sub>2</sub> P-25 aeroxide (Evonik). The second one was synthesized by annealing mixture of TiO<sub>x</sub> and Pt NPs produced by pulsed laser ablation (PLA). Catalytic properties were studied in an automated installation with a flow quartz reactor using the

temperature-programmed reaction method (TPR-NH<sub>3</sub>+O<sub>2</sub>). Used reaction mixture was 0.1 vol% NH<sub>3</sub> and 4 vol% O<sub>2</sub> in helium, a flow rate of 500 cm<sup>3</sup>/min (GHSV 120 000 h<sup>-1</sup>). The samples were tested twice up to 400°C at the rate of 10°C/min. Concentrations of NH<sub>3</sub>, N<sub>2</sub>O, NO, NO<sub>2</sub> were recorded using IR spectroscopy. Concentrations of O<sub>2</sub> and N<sub>2</sub> were recorded using gas chromatography. Catalysts were characterised using XRD, XPS, HR TEM, XANES analysis. To understand the possible changes of platinum oxidation state and interaction with TiO<sub>2</sub> under reaction conditions operando XAS measurements were performed at PETRA III P65.

## Results

Pt/TiO<sub>2</sub> catalyst based on P-25 is characterized by rutile and anatase phases mixture, the platinum is presented by NP size ≤ 1nm. According to the XPS results, platinum is present in oxidised states Pt<sup>2+</sup> and Pt<sup>4+</sup>. Pt<sup>0</sup> appears after calcination at 600-800°C. In case of PLA produced samples consists of amorphous TiO<sub>x</sub> particles, anatase phase appears after annealing at 400°C. Platinum is presented by 1-3 nm metallic particles. Both catalysts series are active in NH<sub>3</sub> oxidation starting from approx. 140°C. Calcination leads to a slight increase of activity of PLA samples and activity loss of impregnated samples. In situ XAS investigations allow correlating changes in catalytic activity with transformations of Pt oxidation states.

## Acknowledgements

The work was supported by Helmholtz – Russian Science Foundation Joint Research Groups grant #18-43-06201 from 03.09.2018 (RSF) / #HRSF-0046 from 01.09.2018 (HGF).



# **Redox treatment as an efficient approach to improve the catalytic activity of Rh-doped CeO<sub>2</sub> catalysts in CO+NO reaction**

*Lidiya Kibis, Dmitry Svintsitskiy, Tatyana Kardash, Elena Slavinskaya, Olga Stonkus, Andrei Boronin, Boreskov Institute of Catalysis, Novosibirsk State University, Novosibirsk, Russia; Elizaveta Derevyannikova, Boreskov Institute of Catalysis, Novosibirsk, Russia; Valery Svetlichnyi, Tomsk State University, Tomsk, Russia*

## **Scope**

Lately, the reduction/oxidation treatments have been discussed in the literature as an efficient way to improve the catalytic characteristics of CeO<sub>2</sub>-based systems [1,2]. We recently showed that pretreatment of Rh-doped CeO<sub>2</sub> systems with CO or H<sub>2</sub> resulted in a significant improvement of their activity in CO oxidation reaction at low temperature [3]. Rhodium-based systems are known to be active in the reactions of nitrogen oxides neutralization. Therefore, it is of interest to study the influence of the redox treatment on the activity of Rh-CeO<sub>2</sub> catalysts in the reaction of NO reduction by CO.

## **Results and discussion**

The Rh-doped CeO<sub>2</sub> systems were prepared by coprecipitation of rhodium and cerium (III) nitrates with further calcination at 450, 800 and 1000<sup>0</sup>C. The obtained catalysts were analyzed by a complex of methods: XRD, TEM, Raman, XPS, TPR CO, TPR CO+NO. For samples calcined at T<800<sup>0</sup>C rhodium was present in a highly dispersed Rh<sup>3+</sup> state without the formation of metallic or oxide phases of rhodium [3,4]. An increase of the calcination temperature resulted in the formation of Rh<sub>2</sub>O<sub>3</sub> oxides [4].

The TPR CO+NO experiments showed that the conversion curves of CO and NO were close regardless of the calcination temperature of the samples (Fig. 1a). With an increase of the calcination temperature the activity of the samples at low temperature decreased. Analysis of the selectivity revealed that initially N<sub>2</sub>O oxide was formed with the appearance of molecular nitrogen after a 100% conversion of NO was reached.

Pretreatment with CO led to a slight decrease of the CO conversion at low temperature for Rh-CeO<sub>2</sub> samples calcined at 450 and 800<sup>0</sup>C (Fig.1b). At the same time, for the sample calcined at 1000<sup>0</sup>C, a significant decrease of the temperatures of

a 50% conversion of CO and NO was observed. The samples pretreatment with CO also increased the selectivity in the NO reduction reaction towards  $N_2$  formation.

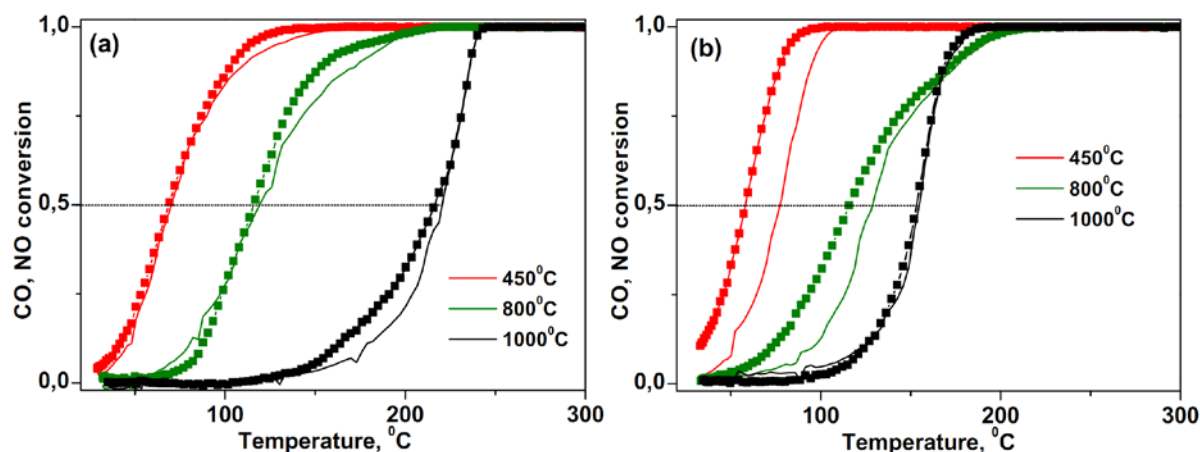


Fig.1. TPR-CO+NO data for (a) the initial Rh-CeO<sub>2</sub> catalysts, (b) the Rh-CeO<sub>2</sub> catalysts pretreated with CO at 300<sup>0</sup>C (solid lines - CO conversion, symbol lines- NO conversion).

The data of structural and spectroscopic methods showed that the preliminary treatment of the samples with CO led to the formation of the rhodium clusters on the surface of the samples while CeO<sub>2</sub> structure was characterized by a large number of defects.

## Conclusions

The reduction treatment of Rh-CeO<sub>2</sub> catalysts can be used to increase their activity in the reaction of the NO reduction by CO as well as selectivity towards  $N_2$  formation. Rh-CeO<sub>2</sub> samples calcined at 1000<sup>0</sup>C showed the most pronounced improvement of the catalytic characteristics with reduction pretreatment that can be used as a tool for preparation of the thermally stable and active catalysts.

## Acknowledgments

This work was partially supported by Russian Foundation for Basic Research and the government of the Novosibirsk region of the Russian Federation, grant №18-43-543009.

## References

- [1] A.M. Gänzler *et al.* *Angew. Chemie Int. Ed.* 56 (2017) 13078–13082.
- [2] S. Gatla *et al.* *Catalysis Today* (2018) doi: 10.1016/j.cattod.2018.06.032
- [3] L.S. Kibis *et al.* *J. Phys.Chem.C* 121 (2017) 26925-26938
- [4] E.A. Derevyannikova *et al.* *PhysChemChemPhys* 19 (2017) 31883-31897

# **Operando XAS - UV-Vis of NH<sub>3</sub>-SCR over highly dispersed Cu catalysts on mesoporous alumina**

*Samuel K. Regli, Ole H. Bjørkedal and Magnus Rønning*

*Department of Chemical Engineering, Norwegian University of Science and Technology (NTNU),  
Trondheim, Norway*

## **Introduction**

Heavy duty engine exhaust from the marine sector constitutes approximately 15% of the total global nitric oxide (NO<sub>x</sub>) emissions [1]. State-of-the-art NO<sub>x</sub> removal from heavy engine exhaust includes selective catalytic reduction (SCR) where NO<sub>x</sub> is reduced by ammonia (NH<sub>3</sub>), usually generated in situ from urea. Modern engines operate with high fuel efficiencies, and high catalytic activity at low temperatures is therefore necessary. SCR catalysts usually contain an active component (transition metal or noble metal) dispersed on a porous support. For low-temperature NH<sub>3</sub>-SCR, Cu-ion exchanged zeolites are highly promising catalysts [2], but lack stability in hydrothermal conditions and resistance to impurities present in the exhaust of marine applications leading to rapid deactivation [3].

As a support material for catalysts,  $\gamma$ -Al<sub>2</sub>O<sub>3</sub> offers high thermal stability (< 850 °C), slight acidity and the capacity to store NO<sub>x</sub> at low temperatures. An approach to prepare mesoporous alumina is using triblock copolymers as pore forming agents [4]. This evaporation-induced self-assembly (EISA) synthesis opens up new possibilities to tailor the interaction between the metal and the support [5]. Previous experiments with Cu/mesoporous alumina prepared by impregnation have shown low SCR activity, possibly due to low dispersion of the active metal. The catalyst synthesis has therefore been modified to drastically increase the metal dispersion by using a one-pot synthesis [6]. This synthesis method has now been adapted for Cu and applied to the NH<sub>3</sub>-SCR reaction.

## **Materials and Methods**

Cu supported mesoporous alumina has been prepared by impregnation and one-pot synthesis. The samples have been characterized by BET, TEM and operando powder X-ray diffraction (PXRD), UV-Vis spectroscopy and X-ray Absorption Spectroscopy (XAS) as well as operando Fourier-Transform Infrared (FTIR) Spectroscopy combined with UV-Vis spectroscopy during NH<sub>3</sub>-SCR reaction. The synchrotron experiments were carried out in a quartz capillary reactor at atmospheric

pressure in the range of 200 – 400 °C and a mass spectrometer was used to analyze gaseous products. The feed was between 200 - 500 ppm NO and 200 - 500 ppm NH<sub>3</sub> in 6% O<sub>2</sub> and He as inert gas.

## Results and Discussion

The high dispersion of the Cu in the one-pot synthesis is confirmed by *ex situ* TEM as well as extended X-ray absorption fine structure (EXAFS) and PXRD. NH<sub>3</sub>-SCR activity was measured for different temperatures and the speciation of Cu was followed with XANES and UV-Vis and the adsorbed reactants by FTIR.

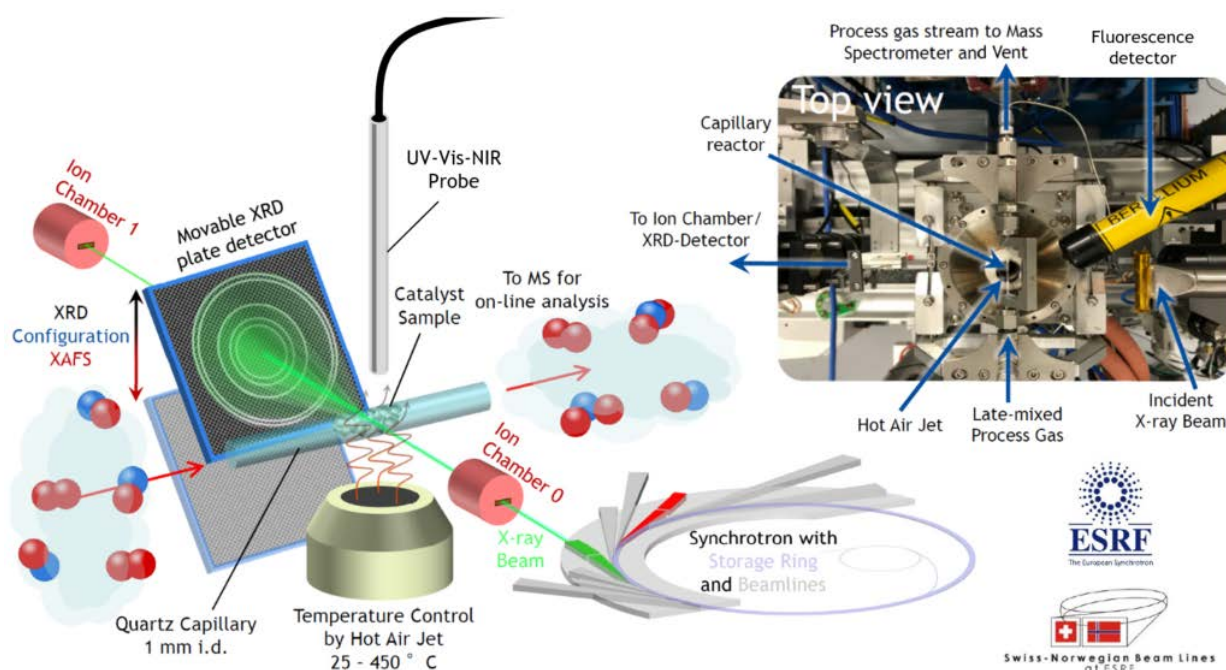


**Figure 1.** Experimental setup at the Swiss-Norwegian beamline BM31 at the European Synchrotron Radiation Facility allowing for simultaneous UV-Vis spectroscopy and X-ray absorption spectroscopy, powder X-ray diffraction and on-line mass spectrometry of the reaction products during operando NH<sub>3</sub>-SCR reaction.

## References

1. Eyring V, Isaksen ISA, Berntsen T, Collins WJ, Corbett JJ, Endresen Ø, Grainger RG, Moldanova J, Schlager H, Stevenson DS. *Atmos Environ.* **2010**,44:4735-4771.
2. Nedyalkova R, Shwan S, Skoglundh M, Olsson L. *Appl Catal B.* **2013**,138-139:373-380.
3. Nova I, Tronconi E. **2014**. *Urea-SCR technology for deNOx after treatment of diesel exhausts* (p. 123-148). New York: Springer.
4. Yuan Q, Yin AX, Luo C, Sun LD, Zhang YW, Duan WT, Liu HC, Yan CH. *J Am Chem Soc.* **2008**,130:3465-3472.
5. Li ZX, Shi FB, Li LL, Zhang T, Yan CH. *Phys. Chem. Chem. Phys.* **2001**,13:2488-2491.
6. Voss G, Chavez E, Fløystad JB, Middtveit A, Gibaud A, Breiby DB, Rønning M. *J Mater Chem A.* **2014**,2:9727-9735.

# Structural Insight into Strong Pt–CeO<sub>2</sub> Interaction: From Single Pt Atoms to PtO<sub>x</sub> Clusters

*Derevyannikova E.A., Boreskov Institute of Catalysis SB RAS, Novosibirsk, Russia;*

*Kardash T. Yu., Stadnichenko A.I., Stonkus O.A., Slavinskaya E.M., Boronin A.I.,*

*Boreskov Institute of Catalysis SB RAS,*

*Novosibirsk State University, Novosibirsk, Russia;*

*Svetlichnyi V.A., Tomsk State University, Tomsk, Russia;*

## Introduction

In Pt–CeO<sub>2</sub> systems strong metal-support interaction enhances catalytic activity and thermostability substantially [1, 2]. Many researchers point out that the effect of strong metal-support interaction is due to the formation of an ionic forms of Pt [3]. However, how the ionic forms of Pt interact with ceria has not been known yet. The aim of this work was to determine the structural features of the Pt–CeO<sub>2</sub> interactions.

## Experimental/ methods

Pt–CeO<sub>2</sub> catalysts with different Pt loading (1-30 wt.%) were prepared by coprecipitation method, followed by calcination in air at 600°C. All the catalysts were studied using set of structural (XRD, EXAFS, PDF and HRTEM) and spectroscopic (XPS and Raman spectroscopy) methods. The Pair Distribution function (PDF) method were obtained at ID22 station of the ESRF. XANES and EXAFS spectra at Pt LIII-edge were collected at XAFS beamline of the ELETTRA Synchrotron. The temperature-programmed reduction by H<sub>2</sub> (TPR-H<sub>2</sub>) was performed in the reaction mixture containing 10 vol.% H<sub>2</sub> and He in balance. Before TPR-H<sub>2</sub> experiments, the samples were heated in 20 vol.% O<sub>2</sub> in He at 450°C to remove surface admixtures.

## Results and discussion

According to the XRD and HRTEM data, all samples are single fluorite nanosized phase. The XPS data indicate Pt<sup>2+</sup> and Pt<sup>4+</sup> states in the catalysts, but no Pt oxide phases were formed. In the samples with high Pt loading Pt-Pt interactions are presented in distorted phase.

PDF analysis shows the generation of new distances in the local structure of Pt–CeO<sub>2</sub> catalyst. Using these distances, the models of Pt local structure were proposed (Fig. 1a). The EXAFS modeling of the samples with different Pt loading was made (Fig. 1b). It was shown the formation of Pt single-atom forms on CeO<sub>2</sub> surface in the

1wt.% Pt–CeO<sub>2</sub> catalyst. The increase of Pt loading leads to the formation of additional PtO<sub>x</sub> clusters in CeO<sub>2</sub> distorted interphase.

All Pt–CeO<sub>2</sub> catalysts showed hydrogen consumption at temperatures lower than 150°C. The 1 wt.% Pt–CeO<sub>2</sub> samples showed a broad reduction peak at 125°C, which is attributed to Pt single-atom ionic forms reduction. The increase of Pt loading is accompanied by a shift of the reduction peak to lower temperatures [4].

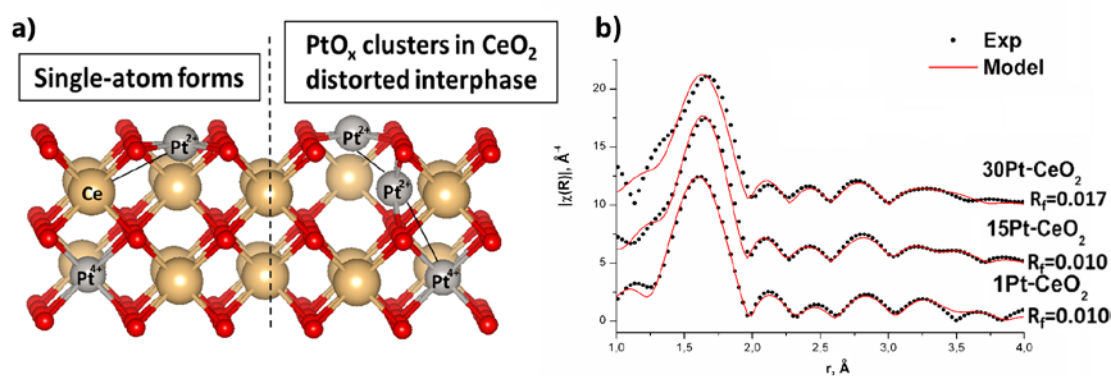


**Fig. 1.** The atomic model of Pt–CeO<sub>2</sub> local structure (a) and EXAFS modeling (b).

## Conclusions

In this work it is shown that coprecipitation method allowed obtaining Pt single-atom state or/and PtO<sub>x</sub> clusters on ceria surface depending on Pt loading. It is assumed that the close arrangement of platinum ions is responsible for the effective redox properties of the catalysts.

## Acknowledgement

The reported study was funded by RFBR according to the research project № 17-03-00754.

## References

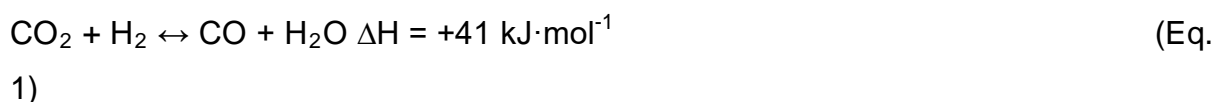
- [1] Gatla S., Aubert D., Agostini G., Mathon O., Pascarelli S., et al. *Catal.* 2016, 6, 6151–6155.
- [2] Nagai Y., Hirabayashi T., Dohmae K., Takagi N., Minami T., et al. *S. J. Catal.* 2006, 242, 103–109.
- [3] Bruix A., Lykhach Y., Matolínova I., Neitzel A., Skala, T., et al. *Angew. Chem.* 2014, 53, 10525–10530.
- [4] Derevyannikova E.A., Kardash T.Y., Stadnichenko A.I., Stonkus O.A., Slavinskaya E.M., Svetlichnyi V.A., Boronin A.I. *J. Phys. Chem. C.* 2019. doi: 10.1021/acs.jpcc.8b11009.

# Highly efficient Ni/CeO<sub>2</sub>-Al<sub>2</sub>O<sub>3</sub> catalysts for CO<sub>2</sub> upgrading via Reverse Water-Gas Shift: Effect of selected transition metal promoters

*L. Yang, University of Surrey, Guildford, UK; L. Pastor-Pérez, University of Surrey, Guildford, UK; S. Gu, University of Surrey, Guildford, UK; T.R. Reina, University of Surrey, Guildford, UK.*

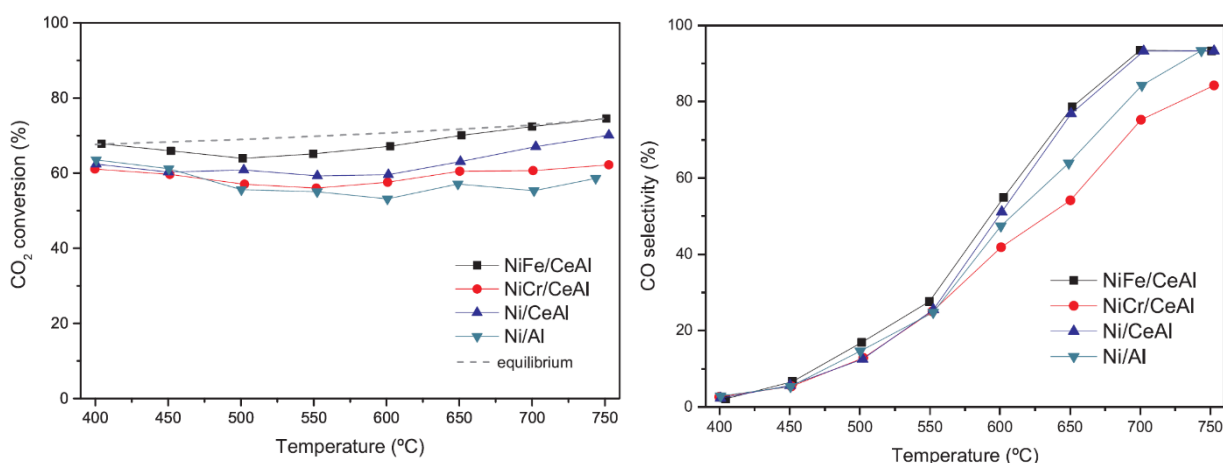
## Introduction

Excess atmospheric Carbon dioxide (CO<sub>2</sub>) concentration leads to strong impact on the equilibrium condition of weather and global climate. The reverse water-gas shift (RWGS) reaction (Eq. 1) has been regarded as a key intermediate step for CO<sub>2</sub> utilization to produce value-added chemicals and fuels through processes like Fischer-Tropsch (FT) synthesis [1].



Due to its endothermic nature, RWGS is thermodynamically favourable at high temperatures to obtain satisfactory level of CO<sub>2</sub> conversion and reaction rate. Traditionally, Ni based catalysts are efficient systems for this reaction. However, this catalytic system suffers from carbonaceous deposition and thermal sintering under high reaction temperature. To overcome this drawback, we adopted Fe- and Cr- as metal promoters [2], and prepared a new family of multicomponent catalysts (NiFe/CeAl and NiCr/CeAl) through wet-impregnation method for the RWGS reaction in this study.

## Results and Discussion





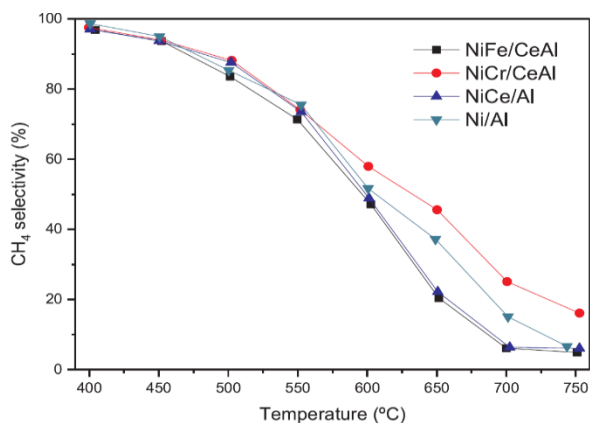


Fig.1 CO<sub>2</sub> conversion and CO & CH<sub>4</sub> activity/selectivity balance reached by electronic density due to the FeO<sub>x</sub>-Ni interaction, facilitating CO<sub>2</sub> adsorption.

Besides, FeO<sub>x</sub> greatly enhances Ni dispersion on the surface which also helps to deliver higher activity in RWGS.

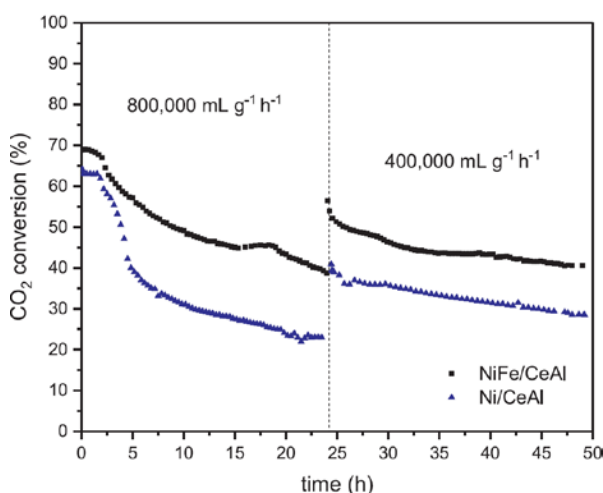


Fig.2 CO<sub>2</sub> conversion for NiFe/CeAl & NiCe/Al samples at hard conditions.

NiFe/CeAl and Ni/CeAl presented higher CO<sub>2</sub> conversion over the studied catalysts (Fig. 1). Furthermore, the presence of FeO<sub>x</sub> as dopant promoted RWGS in terms of CO<sub>2</sub> conversion and CO selectivity. While CrO<sub>2</sub> helped Ni for CO<sub>2</sub> methanation instead. From catalyst characterisation, the outstanding

NiFe/CeAl is attributed to the higher

To compare the two best materials, NiFe/CeAl and Ni/CeAl were tested at high demanding conditions. From Fig.2, the deactivation phenomenon is more prominent for Ni/CeAl sample during the first 24 h at 800,000 ml·g<sup>-1</sup>·h<sup>-1</sup>. Besides, when the space velocity is released to 400,000 ml·g<sup>-1</sup>·h<sup>-1</sup>, the CO<sub>2</sub> conversion was restored immediately and improved for Fe-doped sample, but not recovered at all for Ni/CeAl.

## Conclusion

Ni/Al<sub>2</sub>O<sub>3</sub> can be highly promoted by adding different dopants such as CeO<sub>2</sub> and FeO<sub>x</sub>. Al<sub>2</sub>O<sub>3</sub>-CeO<sub>2</sub> with high thermal stability provides a large surface for active phase dispersion and allows for oxygen vacancies generation to improve catalytic performance. But CrO<sub>x</sub> as dopant favours the CO<sub>2</sub> methanation. NiFe/CeAl reveals an outstanding catalytic performance with respect to activity, selectivity and stability.

## References

1. P. Kaiser, et al., *Production of Liquid Hydrocarbons with CO<sub>2</sub> as Carbon Source based on Reverse Water-GasShift and Fischer-Tropsch Synthesis*. Chem. Eng. Technol., 2013. **85**: p. 489-499
2. Yang, L., et al., *Highly efficient Ni/CeO<sub>2</sub>-Al<sub>2</sub>O<sub>3</sub> catalysts for CO<sub>2</sub> upgrading via reverse water-gas shift: Effect of selected transition metal promoters*. Appl. Catal. B, 2018. **232**: p. 464-471.



# **Rh/ZSM-5 as a Sulfur Tolerant Catalyst for Methane Oxidation**

*Yu Zhang, Jakob Munkholt Christensen, Anker Degn Jensen, Peter Glarborg,  
DTU Chemical engineering, Technical University of Denmark (DTU), Kgs. Lyngby,  
DK-2800, Denmark;*

*Keld Johansen, Haldor Topsoe A/S, Kgs. Lyngby, DK-2800, Denmark*

## **Introduction**

Natural gas can be an alternative fuel for ships in coastal zones to minimize the emissions of CO<sub>2</sub>, NO<sub>x</sub>, and particulates from diesel engines. However, unburnt methane can slip from the engine, causing another emission problem. CH<sub>4</sub> is a green-house gas with an atmospheric potential of 26-28 times that of CO<sub>2</sub> [1] and it need to be mitigated from the exhaust gas. Converting CH<sub>4</sub> to CO<sub>2</sub> and H<sub>2</sub>O catalytically in the after treatment system can be promising. However, an efficient catalyst that remains sufficiently active under real exhaust gas conditions (350-550 °C, 5-10 vol.% H<sub>2</sub>O and 1-2 ppm SO<sub>2</sub>) is still being sought. Pd based catalysts are the most active in the absence of H<sub>2</sub>O and SO<sub>2</sub>[2], but they deactivate severely by SO<sub>2</sub> even at low ppm levels. In this contribution, it is investigated if Rh catalysts on a suitable carrier material can be developed to tolerate the exhaust gas conditions above. Here Rh/ZSM-5 was prepared and tested under simulated engine exhaust gas conditions with both H<sub>2</sub>O and SO<sub>2</sub> present. The influence of operating temperature and SO<sub>2</sub> concentration were studied.

## **Materials and Methods**

The 2 wt.% Rh/ZSM-5 (Zeolyst, Si:Al = 280) catalyst was prepared by the Incipient Wetness Impregnation (IWI) method followed by calcination in air at 600 °C for 6 h. A fixed-bed quartz reactor was used to test the performance of the catalyst under different conditions. In each experiment, 0.12 g catalyst was diluted with 1.08 g sand. The gas hourly space velocity (GHSV) was kept at 150,000 ml/(g<sub>cat</sub>·h). The reaction gas consisted of 2500 ppm CH<sub>4</sub>, 10 vol. % O<sub>2</sub>, 5 vol. % H<sub>2</sub>O and 1-20 ppm SO<sub>2</sub> when present, balancing with N<sub>2</sub>. The exit gas was analyzed with an online IR gas analyzer to monitor CO<sub>2</sub>, CO, O<sub>2</sub>, and SO<sub>2</sub> concentrations, and a Micro GC for CH<sub>4</sub> concentration. The measured CH<sub>4</sub> concentration was used to calculate CH<sub>4</sub> conversion. The fresh and spent catalysts were characterized by TEM and CO-DRIFTS.

The fresh catalyst was tested at 450, 475 and 500 °C. Initially, a 15 h test was done in the absence of SO<sub>2</sub>, and then 1 ppm SO<sub>2</sub> was introduced to the reaction stream until the conversion of CH<sub>4</sub> became stable. Then the SO<sub>2</sub> concentration was raised in steps to 2, 5, 10, and 20 ppm SO<sub>2</sub> awaiting steady state at each SO<sub>2</sub> concentration level. Based on these data, a Temkin isotherm was used to find the adsorption heat of SO<sub>2</sub> on the 2 wt.% Rh/ZSM-5 catalyst with the assumption that the fraction of remaining activity correspond to the fraction of sites not covered by SO<sub>2</sub>.

## Results and Discussions

The conversion of CH<sub>4</sub> was stable at 450, 475, and 500 °C in the absence of SO<sub>2</sub> (Figure 1). By addition of 1 ppm SO<sub>2</sub>, the conversion of CH<sub>4</sub> decreased significantly at the three operating temperatures. The stabilized conversion after around 50 h in the presence of 1 ppm SO<sub>2</sub> could be improved significantly (from 27 % to 79%) by elevating the operating temperature from 450 to 500 °C. As the SO<sub>2</sub> concentration was increased to 2, 5, 10, and 20 ppm SO<sub>2</sub>, the conversion of CH<sub>4</sub> further decreased. It indicates that it is possible to get stable conversion in the presence of H<sub>2</sub>O and SO<sub>2</sub> on the 2 wt.% Rh/ZSM-5 catalyst. The CH<sub>4</sub> removal efficiency can be significantly improved by elevating the operating temperature and lowering the SO<sub>2</sub> concentration to a low level. The SO<sub>2</sub> concentration in the real natural gas engine condition is 1-2 ppm, thus a high CH<sub>4</sub> removal efficiency can be achieved around 500 °C, which is achievable in a real engine system.

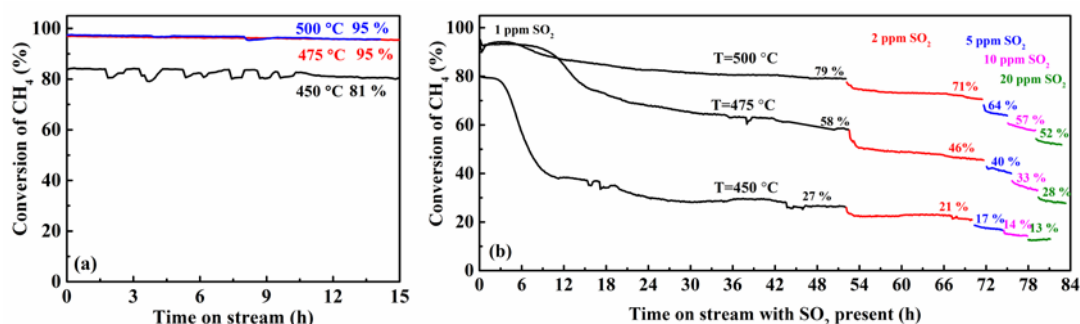


Figure 1. Conversion of CH<sub>4</sub> on 2 wt.% Rh/ZSM-5 catalyst in long-term stability test in the absence of SO<sub>2</sub> (a) and presence (b) of 1-20 ppm SO<sub>2</sub> at 450, 475, and 500 °C. 2500 ppm CH<sub>4</sub>, 10 vol.% O<sub>2</sub>, 5 vol.% H<sub>2</sub>O, 1-20 ppm SO<sub>2</sub> when present, balanced with N<sub>2</sub>, GHSV= 150,000 ml/(g<sub>cat</sub>·h)

## References

- [1] Chai, X., David, J.T., and Devinder, M. Prog. Energy Combust. Sci. 33, 56 (2016).
- [2] Yang, L., Jian, M., and Wende, H. ACS Catal. 8127 6 (2016).

# Hydrogenation of toluene over Ni particles supported on binary $\text{MgF}_2\text{-AlF}_3$ system

*Angelika Kiderys<sup>1</sup>, Michał Zieliński<sup>1</sup>, Maria Wojciechowska<sup>1</sup>*

*<sup>1</sup>Adam Mickiewicz University in Poznań, Faculty of Chemistry,  
Umultowska 89b, 61-614 Poznań, Poland*

More than 90% of chemical industry processes are carried out with catalysts. The metal oxides are commonly used supports or catalysts in heterogeneous catalysis due to their good thermal and mechanical stability and low price. Thanks to the oxygen which is the second strongest electronegative element, the metal oxides are characterized by wide ranging acidic and basic properties. The metal fluorides are also chemically and thermally as stable as oxides. Taking into account that the fluorine is more electronegative element than oxygen, metal fluorides should expect higher acidity in comparison with their oxides counterparts. Recently, a growing interest of researchers in fluoride support, including magnesium and aluminum fluoride is observed. The most important was the application of metal fluorides in organofluorine chemistry as catalysts for chlorine elimination from harmful chlorofluorocarbons (CFCs) [1]. Fluoride-containing systems are also promising catalysts for ethylbenzene oxidation [2] or Friedel-Crafts reactions (alkylation and acetylation) [3]. Moreover, the application of metal fluorides in the synthesis of vitamins E and K1 is very important [4].

It seems to be very interesting to combine two metal fluorides which are characterized by different acid-base properties as a binary support  $\text{MgF}_2\text{-AlF}_3$ . It is known from literature that the surface of  $\text{AlF}_3$  is dominated by strong Lewis and Brønsted acidic centers, and magnesium fluoride - by weak acidic-basic centers. Differences in the surface properties affect the catalytic activity in the hydrogenation reactions. The hydrogenation of aromatic compounds is important for industry. It finds applications in such fields of technology as e.g. quality improvements of motor fuels, production of nylon fibers, solvents and hardening of fats.

The aim of the presented work was the preparation of nickel catalysts (5wt.% Ni) supported on binary  $\text{MgF}_2\text{-AlF}_3$  systems and investigation their catalytic activity in the hydrogenation of toluene. The catalytic activity was compared with catalysts supported on  $\text{AlF}_3$  and  $\text{MgF}_2$  supports. The binary support were obtained by

suspension method in the reaction of ammonium aluminum carbonate hydroxide (AACH) and magnesium carbonate (cMg) with aqueous solution of HF or  $\text{NH}_4\text{F}$  (NF). The influence of the fluorine precursor on the physicochemical properties of supports was studied. The prepared supports and catalysts were characterized by XRD,  $\text{N}_2$  adsorption/desorption measurements, TPR- $\text{H}_2$ . The mean size of metal particles was determined by  $\text{H}_2$  chemisorption measurements. The obtained 50wt.% $\text{MgF}_2$ -50wt.% $\text{AlF}_3$ -NF ( $73 \text{ m}^2\cdot\text{g}^{-1}$ ) system shows higher surface area than  $\text{MgF}_2$ -NF ( $24 \text{ m}^2\cdot\text{g}^{-1}$ ) and  $\text{AlF}_3$ -NF ( $20 \text{ m}^2\cdot\text{g}^{-1}$ ) alone. The nickel catalysts supported on  $\text{MgF}_2$ - $\text{AlF}_3$  were evaluated in toluene hydrogenation and their catalytic activity was compared with single-component systems  $\text{MgF}_2$  and  $\text{AlF}_3$ . Generally, the catalytic activity depends on the type of supports and the type of fluorine precursor using during synthesis. The catalyst supported on  $\text{MgF}_2$ - $\text{AlF}_3$  (prepared from HF) shows greater activity in hydrogenation of toluene than the catalysts supported on  $\text{MgF}_2$  and  $\text{AlF}_3$  (Figure 1).

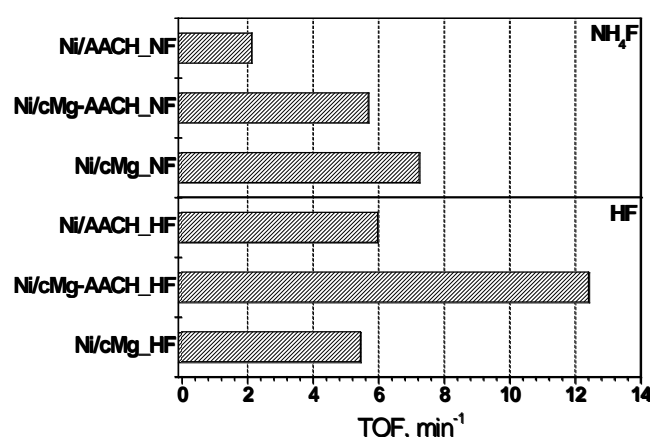


**Figure 1.** The effect of the fluorine precursor on toluene hydrogenation for nickel catalysts reduced at  $500^\circ\text{C}$  for 2h,  $\text{H}_2=100 \text{ cm}^3\cdot\text{min}^{-1}$ . Reaction:  $\text{H}_2=50 \text{ cm}^3\cdot\text{min}^{-1}$ ,  $C_{\text{Tl}}=0,75 \mu\text{mol}\cdot\text{cm}^{-3}$ ,  $175^\circ\text{C}$ .

### Acknowledgements

The work was supported by grant no. POWR.03.02.00-00-I023/17 co-financed by the European Union through the European Social Fund under the Operational Program Knowledge Education Development.

### References

- [1] L.E. Manzer, V.N.M. Rao, *Adv. Catal.*, 39 (1993) 329.
- [2] I.K. Murwani, K. Scheurell, E. Kemnitz, *Catal. Commun.*, 10 (2008) 227.
- [3] J.K. Murthy, U. Groß, S. Rüdiger, E. Unveren, E. Kemnitz, *J. Fluor. Chem.*, 125 (2004) 937.
- [4] N. Candu, S. Wuttke, E. Kemnitz, S.M. Coman, V.I. Parvulescu, *Appl. Catal. A*, 391 (2011) 169.

## **Non-Platinum Group Metal Catalysts for Benzene Oxidation**

*Jin Hee Lee, Hyeyeon Jang, Iljeong Heo, Center for Environment and Sustainable Resources, Korea Research Institute of Chemical Technology, 34141 Daejeon, South Korea.*

The removal of aromatic hydrocarbon is of great interests due to their harmful effects on environment and human body. Thermal/catalytic oxidation, adsorption, absorption and bio-filtration have been developed to reduce air pollutants. The state-of-the-art catalysts on hydrocarbon oxidation are based on the platinum group transition metals. The developments of low price catalyst that can substitute platinum group catalysts are highly desirable for cost reduction and practical applications.

We developed the non-platinum group catalyst for benzene oxidation, which composed of copper and silver as the active species. The catalyst exhibited high benzene oxidation activity comparable to platinum group catalysts. The studies of the catalyst surface by infrared spectroscopy provided the insights into the active sites and the roles of the each metals on benzene oxidation. The detailed experimental design and the results will be presented.

# Effect of calcination temperature on activity of K-modified Co-Mn-Al mixed oxide catalyst for N<sub>2</sub>O decomposition

*K. Karásková, K. Pacultová, L. Obalová, VŠB – Technical University of Ostrava, Institute of Environmental Technology, Ostrava, Czech Republic; K. Jirátová, Institute of Chemical Process Fundamentals CAS v.v.i., Prague, Czech Republic*

## Introduction

Potassium promoted Co-Mn-Al mixed oxide catalysts belong to active catalysts for catalytic N<sub>2</sub>O decomposition [1]. Many factors can influence catalytic activity of prepared catalyst. Therefore, in this study the effect of calcination temperature on physico-chemical properties and catalytic activity of K/Co<sub>4</sub>MnAlO<sub>x</sub> mixed oxide was investigated.

## Experimental

The Co-Mn-Al layered double hydroxide with Co:Mn:Al molar ratio of 4:1:1 was prepared by coprecipitation of corresponding nitrates and resulting product was re-suspended in a solution of KNO<sub>3</sub>, which concentration was adjusted to obtain a desired concentration of 3 wt% K in the mixed oxide. Product was dried and calcined for 4 hours at 500 °C in air. Then the prepared sample was calcined again for 4 hours at 600 and 700 °C in air. Prepared catalysts were denoted as “K/Co<sub>4</sub>MnAlO<sub>x</sub> - *calcination temperature*”. Samples were characterized by different methods (BET, AAS, TPR-H<sub>2</sub>, XRD) and tested for N<sub>2</sub>O decomposition in helium or simulated waste gas from nitric acid plant in temperature range of 300 – 450 °C, space velocity 20 - 60 l g<sup>-1</sup>h<sup>-1</sup> was applied.

## Results/Discussion

As expected, Co and Mn contents were the same for all catalysts. The decrease of specific surface area was observed with increasing calcination temperature from 500 to 700 °C. From XRD patterns, the presence of spinel phase was confirmed for all samples and increase of crystallite size with increasing calcination temperature was observed. TPR-H<sub>2</sub> showed that all catalysts were reduced in two main temperature regions. The low-temperature reduction peak represents the reduction of Co<sup>III</sup> → Co<sup>II</sup> → Co<sup>0</sup> in Co<sub>3</sub>O<sub>4</sub> and the reduction of Mn<sup>IV</sup> to Mn<sup>III</sup> oxides [2]. The high temperature

peak was attributed to the reduction of Co and Mn ions surrounded by Al ions in spinel-like phase.  $\text{Mn}^{\text{III}} \rightarrow \text{Mn}^{\text{II}}$  can take place in both temperature regions [2].

$\text{N}_2\text{O}$  conversions in inert atmosphere over catalysts calcined at 500 and 600 °C were nearly the same, while for sample calcined at 700 °C, a slight decrease of  $\text{N}_2\text{O}$  conversion was observed (Fig. 1). The influence of inhibiting components ( $\text{O}_2$ ,  $\text{H}_2\text{O}$ ,  $\text{NO}_x$ ) led to shift of conversion curves to higher temperatures (Fig. 2), nevertheless observed inhibition was reversible. The effect of calcination temperature on conversion was more significant, especially when  $\text{NO}$  was present in the feed gas. This can be connected with catalyst basicity, which depends on the K residual content.

It can be concluded that calcination temperature of 500 °C is optimal temperature for preparation of K-modified Co-Mn-Al mixed oxide catalysts in terms of catalytic activity for  $\text{N}_2\text{O}$  decomposition.

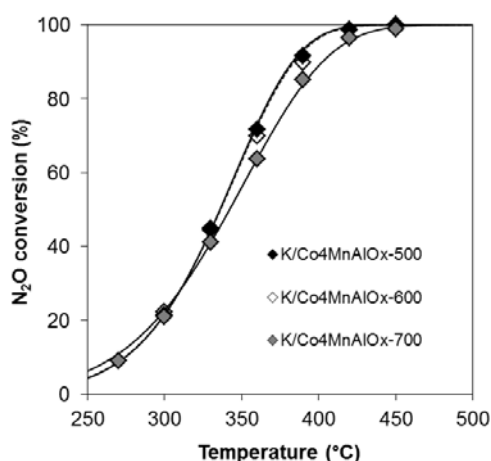


Fig. 1: Temperature dependence of  $\text{N}_2\text{O}$  conversion over potassium promoted Co-Mn-Al mixed oxide calcined at different temperatures. Points: experimental data, lines: 1<sup>st</sup> order kinetic equation model. Conditions: 0.1 mol. %  $\text{N}_2\text{O}$  in He,  $\text{WHSV} = 60 \text{ l g}^{-1} \text{ h}^{-1}$

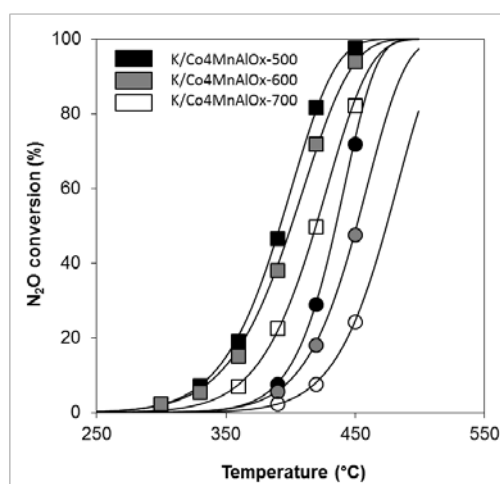


Fig. 2: Temperature dependence of  $\text{N}_2\text{O}$  conversion in simulated waste gas over potassium promoted Co-Mn-Al mixed oxide calcined at different temperatures. Points: experimental data, lines: 1<sup>st</sup> order kinetic equation model. Conditions: **square**: 0.1 mol. %  $\text{N}_2\text{O}$ , 5 mol. %  $\text{O}_2$ , 0.9 mol. %  $\text{H}_2\text{O}$ , **circle**: 0.1 mol. %  $\text{N}_2\text{O}$ , 5 mol. %  $\text{O}_2$ , 3 mol. %  $\text{H}_2\text{O}$ , 0.01 mol. %  $\text{NO}$ , 0.01 mol. %  $\text{NO}_2$  in He,  $\text{WHSV} = 20 \text{ l g}^{-1} \text{ h}^{-1}$

### Acknowledgements

The work was supported from ERDF "Institute of Environmental Technology – Excellent Research" (No. CZ.02.1.01/0.0/0.0/15\_019/0000853).

### References

- [1] L. Obalová, K. Karásková, K. Jirátová, F. Kovanda, *Appl. Catal.*, B 90 (2009) 132-140.
- [2] A. Klyushina, K. Pacultová, K. Karásková, K. Jirátová, M. Ritz, D. Fridrichová, A. Volodarskaja, L. Obalová, *J. Mol. Catal. A: Chem.* 425 (2016) 237-247.

# Potassium promoted Co-Mn-Al mixed oxides for direct NO decomposition - effect of chemical composition

*K. Pacultová, K. Karásková, A. Klegová, D. Fridrichová, L. Obalová, Institute of Environmental Technology, VŠB-Technical University of Ostrava, Ostrava, Czech Republic;*

*K. Jiráťová, J. Balabánová, Institute of Chemical Process Fundamentals of the CAS, v.v.i., Prague, Czech Republic*

## Introduction

Many catalysts have been tested for direct NO catalytic decomposition up to now; however, none has been sufficiently stable, active and selective at economically feasible temperatures [1]. It was found out that (i) the catalytically less active oxides can be activated by the alkali promoters, (ii) further increase in the catalyst activity would be difficult to achieve with metals or alloys alone or simple metal oxides, (iii) a more active system might require a bifunctional surface presented e.g. on mixed oxides. Co-Mn-Al mixed oxide catalysts are active in N<sub>2</sub>O decomposition [2] and VOC oxidation [3]. In both cases, the existence of a cooperative effect between Co and Mn was published. Since potassium promoted Co-Mn-Al mixed oxides are also active for NO decomposition [4], the effect of Co and Mn substitution in K/Co-Mn-Al mixed oxide catalysts for direct NO decomposition was tested in this paper.

## Experimental/methodology

K/Co<sub>z</sub>Mn<sub>5-z</sub>AlO<sub>x</sub> mixed oxides (z was from 0 to 5) with different amount of Co and Mn were prepared by co-precipitation of corresponding nitrates while maintaining constant molar ratio of (Co+Mn)/Al = 5/1, calcination at 700 °C for 4 h and impregnated by KNO<sub>3</sub> to obtain K content of 2 wt. % with subsequent calcination at 700 °C for 4 h. Samples were characterized by different methods (BET, AAS, TPR-H<sub>2</sub>, TPD-CO<sub>2</sub>, XRD) and tested for NO decomposition in temperature range of 560 – 700 °C.

## Results and discussion

Spinel phase was confirmed in K/Co<sub>5</sub>AlO<sub>x</sub> sample, while in K/Mn<sub>5</sub>AlO<sub>x</sub> sample only Mn<sub>2</sub>O<sub>3</sub> was found out by XRD. Both phases were found out in samples where Co



and Mn were present simultaneously. Although all samples were impregnated with the same K amount, the K containing phase was visible by XRD only in the samples containing Mn in the form of potassium manganese oxide.

Dependence of NO conversion on Co molar amount in mixed oxide, while maintaining constant molar ratio of  $(\text{Co}+\text{Mn})/\text{Al} = 5/1$ , is shown on Fig. 1. The increase of NO conversion is visible up to molar ratio  $\text{Co}/\text{Mn} = 3/2$ . Since potassium non-modified samples were totally inactive, the active phase is probably formed by cobalt species located in specific sites interacting with potassium species in amorphous form.

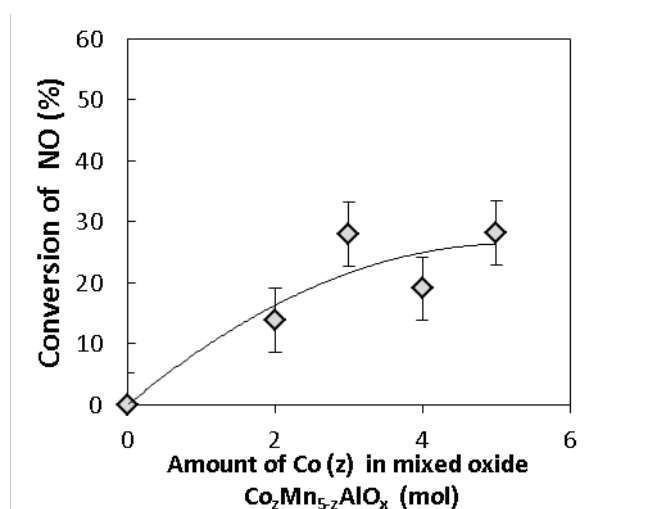


**Fig. 1:** Dependence of NO conversion (650 °C) on Co molar amount in mixed oxide. Conditions: 1000 ppm NO in  $\text{N}_2$ , GHSV =  $6 \text{ l g}^{-1} \text{ h}^{-1}$ .

## Acknowledgement

The work was supported from ERDF "Institute of Environmental Technology – Excellent Research" (No. CZ.02.1.01/0.0/0.0/15\_019/0000853), Czech Science Foundation - project No. 18-19519S and by VŠB-TU student project No. SP2019-91.

## References

- [1] M. Haneda, H. Hamada, Recent progress in catalytic NO decomposition, *Comptes Rendus Chimie*, 19 (2016) 1254-1265.
- [2] L. Obalová, K. Pacultová, J. Balabánová, K. Jirátová, Z. Bastl, M. Valášková, Z. Lacný, F. Kovanda, Effect of Mn/Al ratio in Co–Mn–Al mixed oxide catalysts prepared from hydrotalcite-like precursors on catalytic decomposition of  $\text{N}_2\text{O}$ , *Catal. Today*, 119 (2007) 233-238.
- [3] M.H. Castaño, R. Molina, S. Moreno, Cooperative effect of the Co–Mn mixed oxides for the catalytic oxidation of VOCs: Influence of the synthesis method, *Appl. Catal. A*, 492 (2015) 48-59.
- [4] K. Pacultová, V. Drašíková, Ž. Chromčáková, T. Bílková, K.M. Kutláková, A. Kotarba, L. Obalová, On the stability of alkali metal promoters in Co mixed oxides during direct NO catalytic decomposition, *Molecular Catalysis*, 428 (2017) 33-40.

# Potassium modified Co-Mn-Al mixed oxides for NO direct decomposition – effect of potassium precursor

*K. Pacultová, K. Karásková, A. Klegová, D. Fridrichová, J. Oprštný, T. Bílková, L. Obalová, Institute of Environmental Technology, VŠB-Technical University of Ostrava, Ostrava, Czech Republic*

## Introduction

The effect of potassium promoter precursor of mixed oxide based catalysts was published for N<sub>2</sub>O direct decomposition [1], soot oxidation [2] or selective catalytic oxidation of NO to NO<sub>2</sub> [3]. In this work, the effect of potassium precursor (type, amount) in Co-Mn-Al mixed oxide catalysts on their physicochemical properties as well as catalytic activity for direct NO decomposition was investigated.

## Experimental/methodology

Co<sub>4</sub>MnAlO<sub>x</sub> mixed oxide was prepared by co-precipitation of corresponding nitrates and calcination at 700 °C for 4 h. Potassium promoter (0.5 – 5.5 wt. %) was added by impregnation with different potassium salts (KNO<sub>3</sub>, K<sub>2</sub>CO<sub>3</sub>, CH<sub>3</sub>COOK, C<sub>2</sub>K<sub>2</sub>O<sub>4</sub>) by pore filling method with subsequent calcination at 700 °C for 4 h. Samples were characterized by different methods (BET, AAS, TPR-H<sub>2</sub>, TPD-CO<sub>2</sub>, XRD) and tested for NO decomposition in temperature range of 560 – 700 °C.

## Results and discussion

Temperature dependence of NO conversion over K-promoted samples prepared from KNO<sub>3</sub> promoter precursor containing different amount of promoter is shown on Fig. 1 and shows that for the best catalytic performance, the wide and flat maximum of K content exists. The effect of K precursor type is shown on Fig. 2. While KNO<sub>3</sub>, K<sub>2</sub>CO<sub>3</sub>, and CH<sub>3</sub>COOK had the same effect, the C<sub>2</sub>K<sub>2</sub>O<sub>4</sub> precursor caused increase in NO conversion, when the same amount of potassium was used for impregnation. Since the sample modified by 4 wt. % of K contained optimal amount of K, the visible precursor effect is not connected with residual K amount in the sample but with type of active sites, which were generated during catalyst calcination after C<sub>2</sub>K<sub>2</sub>O<sub>4</sub> impregnation.

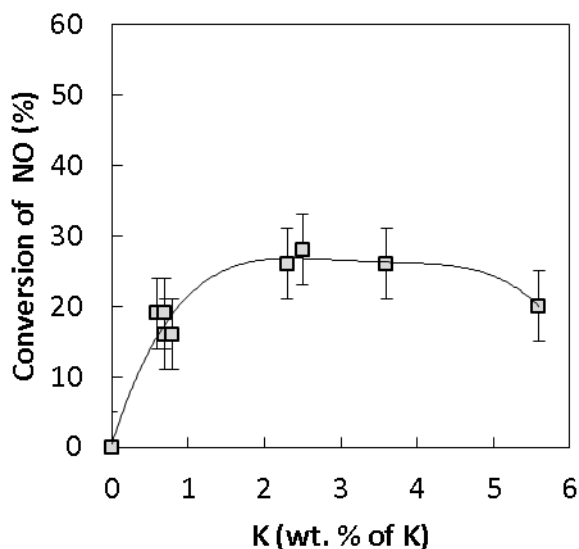


**Fig. 1:** Dependence of NO conversion on K amount in  $K/Co_4MnAlO_x$  impregnated by  $KNO_3$ . Conditions: 1000 ppm NO in  $N_2$ , GHSV =  $6\text{ l g}^{-1}\text{ h}^{-1}$ .

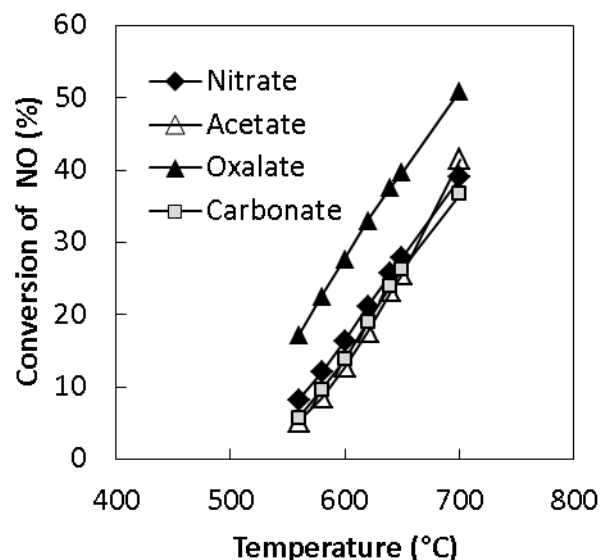


**Fig. 2:** Temperature dependence of NO conversion on  $K/Co_4MnAlO_x$  modified by 4 wt. % K from different K precursor. Conditions: 1000 ppm NO in  $N_2$ , GHSV =  $6\text{ l g}^{-1}\text{ h}^{-1}$ .

## Acknowledgement

The work was supported from ERDF "Institute of Environmental Technology – Excellent Research" (No. CZ.02.1.01/0.0/0.0/15\_019/0000853), by Czech Science Foundation - project No. 18-19519S and by VŠB-TU internal student project No. SP2019-91.

## References

- [1] G. Maniak, P. Stelmachowski, A. Kotarba, Z. Sojka, V. Rico-Pérez, A. Bueno-López, Rationales for the selection of the best precursor for potassium doping of cobalt spinel based de $N_2O$  catalyst, *Appl. Catal. B*, 136-137 (2013) 302-307.
- [2] P. Legutko, T. Jakubek, W. Kaspera, P. Stelmachowski, Z. Sojka, A. Kotarba, Soot oxidation over K-doped manganese and iron spinels — How potassium precursor nature and doping level change the catalyst activity, *Catal. Commun.*, 43 (2014) 34-37.
- [3] X. Tang, F. Gao, Y. Xiang, H. Yi, S. Zhao, X. Liu, Y. Li, Effect of Potassium-Precursor Promoters on Catalytic Oxidation Activity of Mn-Co $O_x$  Catalysts for NO Removal, *Industrial & Engineering Chemistry Research*, 54 (2015) 9116-9123.

# **Chlorophenols Oxidation by Oxidoreductases Immobilized on Biopolymeric Microspheres**

*Tikhonov B.B., Tver State Technical University, Tver, Russia; Stadolnikova P.Yu., Tver State Technical University, Tver, Russia; Sidorov A.I., Tver State Technical University, Tver, Russia; Sulman E.M., Tver State Technical University, Tver, Russia; Matveeva V.G., Tver State Technical University, Tver, Russia, Tver State University, Tver, Russia*

One of the most acute environmental problems of our time is the pollution of water resources with organochlorine compounds which are formed from untreated wastewater of chemical technology, paint, cellulose, paper, and pharmaceutical industries, as well as during water chlorination. These types of pollutants can have harmful effects on humans and animals due to the high toxicity and carcinogenicity. Chemical oxidation of organochlorine compounds to CO<sub>2</sub> and H<sub>2</sub>O or insoluble polymers is traditionally used to purify water from organochlorine pollutants, but none of the existing methods lead to their complete removal from water.

To increase the efficiency of removal of organochlorine contaminants a method of oxidation by hydrogen peroxide in the presence of horseradish peroxidase, obtained from vegetable raw materials (horseradish root ordinary *Armoracia rusticana*), and glucose oxidase from *Aspergillus niger*, immobilized on microspheres of natural polymer – sodium alginate was developed resulting in insoluble polymer compounds, separated by centrifugation. Alginate microspheres were obtained by successive emulsification with ultrasonic action of microcrystalline calcium carbonate in 1.5 % aqueous solution of sodium alginate and soybean oil, adding a small amount of glacial acetic acid to reduce the pH of the emulsion and release of calcium ions and washing the formed microspheres with distilled water to remove soybean oil residues. Immobilization of peroxidase and glucose oxidase on alginate microspheres was carried out by activation of sodium alginate carboxyl groups with N-hydroxysuccinimide and 1-ethyl-3-(3-dimethylaminopropyl)carbodiimide hydrochloride and formation of an amide bond between activated carboxyl groups and amino groups of enzyme molecules. For determining the activity of the immobilized enzyme, 4-chlorophenol was used as a substrate, forming colored products in the presence of 4-amino antipyrine and horseradish peroxidase, recorded

at a wavelength of 506 nm. The reaction of glucose oxidation by glucose oxidase was used as a source of hydrogen peroxide.

Experiments have shown that peroxidase and glucose oxidase covalently immobilized on alginate microspheres retain about 75% of the activity of the native enzyme, while the heterogenization of enzymes makes it possible to reuse the biocatalyst. Kinetic parameters of enzymes were determined as the following: limiting reaction rate ( $V_m$ , mmol/L·s) –  $2,3 \cdot 10^{-3}$  (native),  $1,8 \cdot 10^{-3}$  (immobilized); Michaelis constant ( $K_M$ , mmol/L) – 0,07 (native), 0,08 (immobilized). Immobilized biocatalyst retains more than 65% of the initial activity in 5 successive oxidation cycles of 4-chlorophenol. The obtained results indicate the high efficiency of the developed biocatalyst in the oxidation of organic contaminants in water resources.

### **Acknowledgment**

This work was supported by the Russian Foundation for Basic Research, grant 18-08-00424.

# Photocatalytic hydrogen production over La/TiO<sub>2</sub> photocatalysts from methanol solution

*Miroslava Edelmannová<sup>1</sup>, Vendula Meinhardová<sup>2</sup>, Rostislav Daňhel<sup>2</sup>, Lada Dubnová<sup>2</sup>, Helena Drobná<sup>2</sup>, Naghmeh Abouali Galedari<sup>1</sup>, Libor Čapek<sup>2</sup>, Kamila Kočí<sup>1</sup>*

*<sup>1</sup>VŠB-Technical University of Ostrava, Institute of Environmental Technology, Ostrava-Poruba, Czech Republic*

*<sup>2</sup>University of Pardubice, Faculty of Chemical Technology, Pardubice, Czech Republic*

Great attention is focusing on the formation of hydrogen by photocatalytic water splitting processes. Higher amounts of hydrogen were then published after the addition of alcohol, i.e. in a water-alcohol solution (mainly methanol). Methanol has lower splitting energy than water and it is added to the reaction as a sacrificial agent. The La/TiO<sub>2</sub> based photocatalysts with various La loading were prepared by (i) sol-gel method and (ii) impregnation. Firstly, we focused on the structural and textural properties affecting their optical and electron properties. Secondly, the key factors playing the role in the photocatalytic decomposition of methanol-water solution were described.

There were studied structural (XRD, XPS, Raman spectroscopy), textural (N<sub>2</sub> adsorption), optical (DRS) and electron (fluorescence and photoelectrochemical measurements) properties. The prepared photocatalysts were studied in the photocatalytic decomposition of methanol-water solution in batch reactor and in presence 8 W Hg lamp (with a peak light intensity at 365 nm wavelength).

Hydrogen production was positively affected by the low crystallite size, the high specific surface area of the materials, and the low-size of surface La-particles. Hydrogen production correlated with the photoelectrochemical response.

The optimal amount of La depended on the preparation method. The highest amount of hydrogen was produced on La-TiO<sub>2</sub> with 0.2 wt. % La (sol-gel method) and La-TiO<sub>2</sub> with 2.0 wt. % (impregnation of commercial TiO<sub>2</sub>) (Fig. 1).

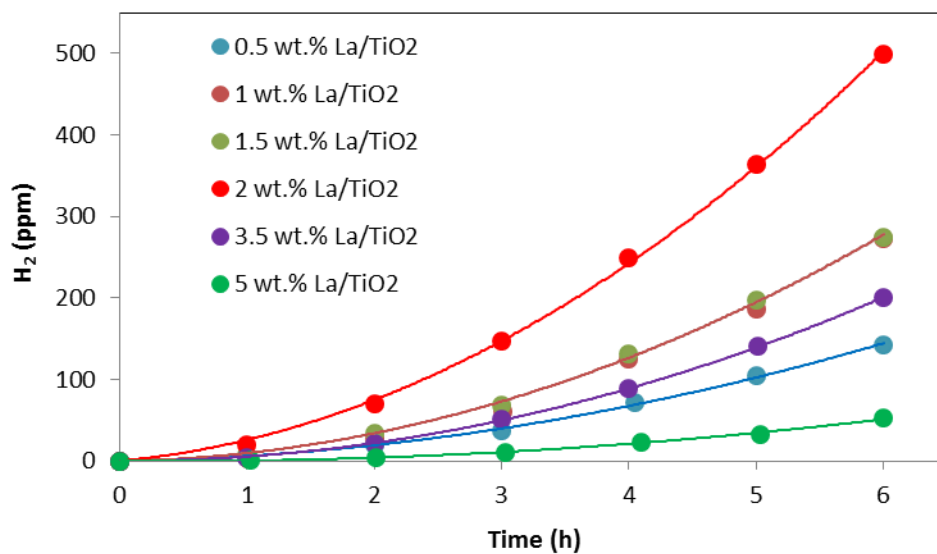


Fig. 1: Time dependence of yields of hydrogen over La doped TiO<sub>2</sub> photocatalysts prepared by impergnation.

### Acknowledgements

Authors thank to the financial support of the Grant Agency of the Czech Republic (project No. 17-20737S). All employees of VŠB-Technical University of Ostrava also thank to the support of ERDF "Institute of Environmental Technology – Excellent Research" (No. CZ.02.1.01/0.0/0.0/15\_019/0000853).

# **New copper-based materials as PGM-free three-way catalysts for automotive exhaust control**

Tim Van Everbroeck, Pegie Cool,

*Laboratory of Adsorption and Catalysis, University of Antwerp,*

*Universiteitsplein 1, 2610 Wilrijk, Belgium*

Ever since the 1970s catalytic converters in cars are using Platinum Group Metals (PGMs, Pt, Pd and Rh) in order to reduce the emission of hydrocarbons, carbon monoxide and NO<sub>x</sub>. [1] However despite their great catalytic performance, PGMs are very costly and their rising scarcity drives research towards more common and economically more beneficial alternatives. CuO is a promising candidate for selective catalytic reduction of NO<sub>x</sub> with hydrocarbons, as well as for the oxidation of CO. [2] However its activity is much lower compared to PGMs, so new methods have to be developed to improve the activity. Research has shown that small nanoparticles of CuO on the surface of materials provide an increased catalytic activity, while other literature reports highlight the role of copper in the bulk of a material working synergistically with other metals. [3]

In our research we used two approaches to achieve dispersed CuO nanoparticles. In a first approach we applied the ammonia driven deposition method (ADP) in order to deposit nanoparticles of CuO on the surface of mesoporous alumina, titania, ceria-zirconia and zirconia. The ammonia functions as a spacer and increases the pH, leading to a strong interaction between the Cu-ammonia complexes and the negatively charged support. [2] Copper loadings up to 15 wt% were used on different mesoporous support materials. The objective is to investigate how the support material influences the catalytic activity and the dispersion degree of the deposited copper oxide nanoparticles.

In a second research approach we concentrated on developing copper containing mixed metal oxides by calcination of Layered Double Hydroxides (LDHs). A special property of LDHs is that after calcination to mixed metal oxides the material is able to structurally reconstruct back to the LDH structure when exposed to aqueous solutions containing anions. Carja et al. [4] used this property to fabricate nanoparticles of metal oxides on the surface of the LDHs by reconstruction in a metal acetate solution. We have used this method to obtain different mixed metal oxides and to study their synergies in the catalytic performance tests. Different calcined LDHs were synthesized containing a mixture of metals such as Cu, Zn, Al, Ti, Fe and Mn. By this study we investigated the possible synergies between the different metals and Cu as mixed oxides.

The materials were catalytically tested in a temperature programmed reactor where a mixture of gases (CO, hydrocarbons, NO, H<sub>2</sub>O, O<sub>2</sub>, CO<sub>2</sub>, H<sub>2</sub> and N<sub>2</sub>) was used to simulate automobile exhaust gas at different temperatures. Different conditions were tested (ratio air/fuel : lean, rich, stoichiometric, CO/NO/O<sub>2</sub>, hydrocarbons/NO/O<sub>2</sub>).

It was found that the copper oxide based materials were indeed very effective in oxidation reactions (of CO and hydrocarbons). Moreover, some NO reduction capacity was also achieved depending on the different parameters such as particle size and type of support material. The results prove that the mixed oxide composition of Cu and Mn is very interesting for automobile exhaust gas conversion.



Figure 1 shows the conversion of CO and NO in function of temperature in an experiment with CO, NO and O<sub>2</sub> in a 3:1:1 ratio. It is notable how CuO and MnO<sub>2</sub> are separately unable to convert NO in this experiment but combined in a spinel structure (Spinel MnCu) and as LDH-derived material (Cu/MnAl LDO) they can.

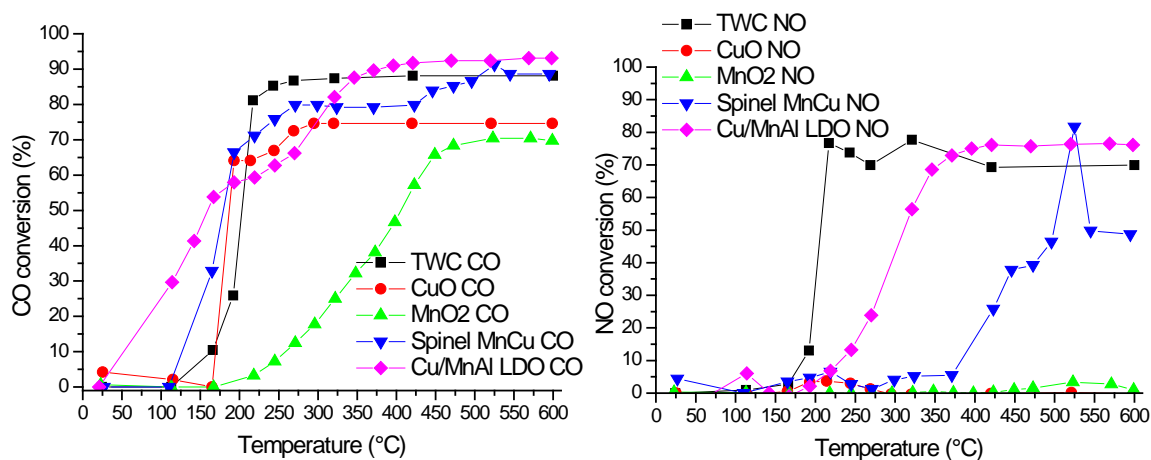


**Figure 1: Conversion of CO and NO in function of temperature in a CO/NO/O<sub>2</sub> experiment on different catalysts: TWC: commercial three-way catalyst sample, CuO: copper oxide powder, MnO<sub>2</sub>: manganese oxide powder, Spinel MnCu: a spinel material of Mn and Cu, Cu/MnAl LDO: a calcined LDH material containing Cu, Mn and Al.**

## References

- [1] M. V. Twigg, Catalytic control of emissions from cars, *Catal. Today*. (2011). doi:10.1016/j.cattod.2010.12.044.
- [2] Q. Xin, A. Glisenti, C. Philippopoulos, E. Poulakis, M. Mertens, J.L. Nyalosaso, V. Meynen, P. Cool, Comparison between a Water-Based and a Solvent-Based Impregnation Method towards Dispersed CuO/SBA-15 Catalysts: Texture, Structure and Catalytic Performance in Automotive Exhaust Gas Abatement, *Catalysts*. 6 (2016).
- [3] D. Yuan, X. Li, Q. Zhao, J. Zhao, M. Tadé, S. Liu, A novel CuTi-containing catalyst derived from hydrotalcite-like compounds for selective catalytic reduction of NO with C<sub>3</sub>H<sub>6</sub> under lean-burn conditions, *J. Catal.* 309 (2014) 268–279. doi:http://dx.doi.org/10.1016/j.jcat.2013.09.010.
- [4] G. Carja, L. Dartu, K. Okada, E. Fortunato, Nanoparticles of copper oxide on layered double hydroxides and the derived solid solutions as wide spectrum active nano-photocatalysts, *Chem. Eng. J.* 222 (2013) 60–66. doi:10.1016/j.cej.2013.02.039.

# Nanozymes for ROS generation – decomposition of H<sub>2</sub>O<sub>2</sub> over transition-metal oxides

*Piotr Pietrzyk, Kamila Sobańska, Bartosz Mozgawa, Weronika Śliwa, Zbigniew Sojka, Jagiellonian University, Faculty of Chemistry, Gronostajowa 2, 30-387 Krakow, Poland*

## Introduction

Nanozymes are the functional inorganic nanomaterials that mimic chemical reactivity of selected enzymes [1]. They are emerging as novel artificial enzymes due to their unique properties compared with natural enzymes and classic artificial enzymes, e.g. thermal stability and wide temperature windows, various structures and compositions, tailored properties. Although nanozymes are more cost-effective and robust than protein enzymes, they can suffer from lack of specificity. Until now, lots of nanomaterials have been studied to mimic various natural enzymes such as peroxidase or catalase activity for wide applications [2,3].

## Experimental

In this contribution we show unexpected activity of non-redox, amorphous oxides of the late transition metals (TM) of IV and V groups, in generation of reactive oxygen species (ROS) via H<sub>2</sub>O<sub>2</sub> decomposition. The activity was modified by introduction of the redox-active centres (isolated TM and nanocrystals of iron and cobalt oxides). Reactivity of amorphous ZrO<sub>2</sub>, HfO<sub>2</sub>, Nb<sub>2</sub>O<sub>5</sub>, Ta<sub>2</sub>O<sub>5</sub> oxides and their composites with redox TM oxides was investigated by means of EPR/HYSCORE and auxiliary spectroscopic (Raman, UV-Vis, XPS) techniques combined with zeta-potential and dissolved O<sub>2</sub> measurements. The catalysts were investigated with TG-MS, XPS, TEM/STEM and EDX/EELS techniques. As test reactions, activity in decolouration of water-soluble dyes was examined.

## Results

The redox active materials exhibit typical Fenton-like reactivity, while for the non-redox, amorphous oxides, formation of ROS is not trivial and involves interfacial electroprotic reactions [3]. We show that  $\cdot\text{OH}$  and  $\text{O}_2^{\cdot-}$  radicals can be formed simultaneously during reaction of H<sub>2</sub>O<sub>2</sub> with surface of amorphous oxides (ZrO<sub>2</sub>, Nb<sub>2</sub>O<sub>5</sub>) and their relative concentration could effectively be controlled by varying pH

of the reaction medium. The reaction follows the electroprotic mechanism  $\text{HO}_2^- + \text{H}_2\text{O}_2 = \text{O}_2^{\cdot-} + \cdot\text{OH} + \text{H}_2\text{O}$ . It is found that  $\text{O}_2^{\cdot-}$  species are stabilized on the surface of the amorphous supports, as indicated by a characteristic EPR and HYSCORE spectra. Generation of  $\cdot\text{OH}$  radicals has been confirmed by means of EPR using DMPO spin trap and additionally by a test reaction with OPD substrate by means of UV-Vis spectroscopy proving peroxidase-like activity. By increasing the pH of the system its reactivity changed into catalase-like activity featured by production of  $\text{O}_2$  which exceeded ROS formation. This pH-switchable reactivity is illustrated below for  $\text{HfO}_2$  and  $\text{Nb}_2\text{O}_5$  amorphous oxides as two examples.

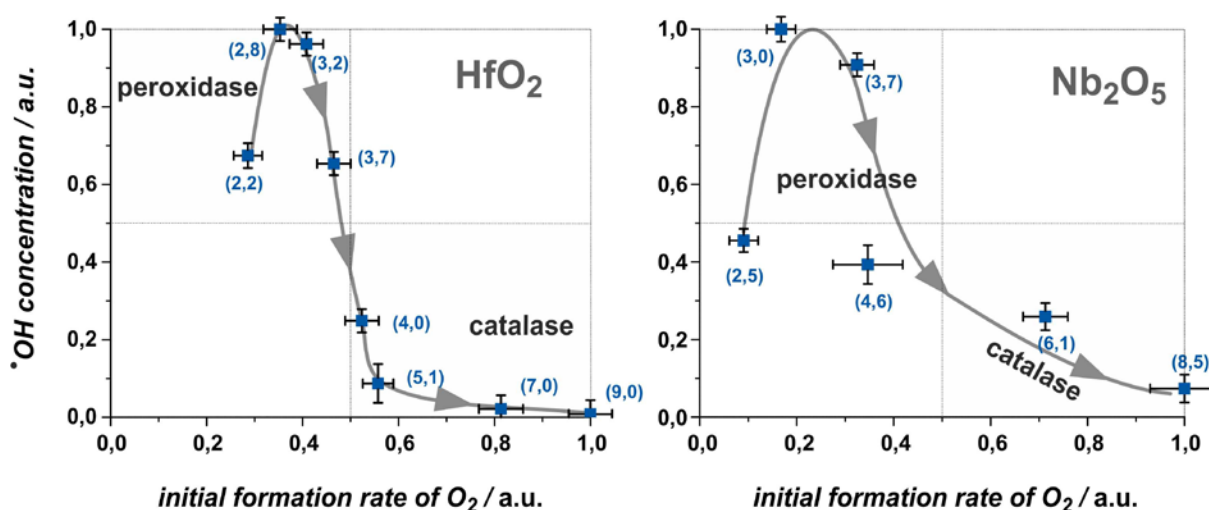


Fig. 1 Concentration of  $\cdot\text{OH}$  radicals vs. formation rate of  $\text{O}_2$  during decomposition of  $\text{H}_2\text{O}_2$  on amorphous oxides at various pH.

Further discussion is connected with enhancing peroxidase activity thanks to the formation of amorphous-crystalline composites based on the amorphous active supports and redox nanocrystals with Fenton-like reactivity ( $\text{Fe}_3\text{O}_4$ ,  $\text{Co}_3\text{O}_4$ ).

### Acknowledgment

This work was financially supported by the National Science Centre, Poland (NCN), grant no. 2017/26/E/ST4/00794.

### References

- [1] H. Wei, E. Wang, *Chem. Soc. Rev.*, **2013**, 42, 6060; J. Wu, X. Wang, Q. Wang, Z. Lou, S. Li, Y. Zhu, L. Qina, H. Wei, *Chem. Soc. Rev.*, DOI: 10.1039/c8cs00457a
- [2] M. Ziółek, I. Sobczak, P. Decyk, K. Sobańska, P. Pietrzyk, Z. Sojka, *Appl. Catal. B: Environ.*, **2015**, 164, 288.
- [3] K. Sobańska, P. Pietrzyk, Z. Sojka, *ACS Catal.*, **2017**, 7, 2935.

# Understanding the Mechanochemical Synthesis of Perovskite LaMnO<sub>3</sub> and its Catalytic Behavior

*Rachel Blackmore, University of Southampton, Southampton, UK; Maria Elena Rivas, Johnson Matthey, Sonning, UK; Paul Collier, Johnson Matthey, Sonning, UK; Peter Wells, University of Southampton, Southampton, UK*

## Background

The tightening of emission regulations and increasing prices of precious metals for existing commercial catalysts drives the need to develop cheaper, more sustainable catalysts. With the properties of catalysts highly dependent on the method of preparation changing the synthetic route results in different phase composition, surface area and particle size, all of which affects crystallinity, texture and morphology. [1] Mechanochemistry has gained attention as a viable way of producing catalysts for industrial processes; it offers a solvent free, low waste method of preparation, whilst also introducing additional active sites for catalysis, e.g. defects and oxygen vacancies. Perovskites are known to readily form via mechanochemical grinding from their single metal oxide precursors, however, the use of grinding media and the formation of amorphous materials presents significant challenges when analysing the reaction and its resulting materials. [2-4] Here we describe how XAFS offers significant advantages over conventional characterisation techniques (e.g. XRD) for understanding the underlying chemistry of the mechanochemical process and its influence on preparing LaMnO<sub>3</sub> for the decomposition of the environmental pollutant N<sub>2</sub>O.

## Results and Discussion

In this work we assessed 'time slices' of mechanochemically prepared LaMnO<sub>3</sub> after different durations of milling. All samples were prepared using a planetary ball mill, where Mn<sub>2</sub>O<sub>3(s)</sub> and La<sub>2</sub>O<sub>3(s)</sub> were added to ZrO<sub>2</sub> grinding jars and milling media, before subsequently milling at 400 rpm. Assessing these 'time-slices' with XRD indicated that the onset of crystalline perovskite formation occurred from 1 h of milling, with 100% crystalline LaMnO<sub>3</sub> at 3 h. However, characterisation by XAFS, which does not rely on periodic ordering, provided a different perspective. At the La L<sub>3</sub>-edge, XAFS shows structural alterations after 1 h of milling indicative of La-Mn scattering, with no further changes observed from 1 to 4 h (Figure 1A). However, at the Mn K-edge (Figure 1B) the model after 1 h of milling is consistent with Mn<sub>2</sub>O<sub>3</sub>.

The combined data supports a model of La initially being dispersed over the  $\text{Mn}_2\text{O}_3$  surface. As milling time increases there is disruption to  $\text{Mn}_2\text{O}_3$  resulting in an increased association between Mn and La. At the Mn K-edge after 2 h of milling a shift is observed within the second coordination shell corresponding to a Mn-La scattering path, indicating the formation of  $\text{LaMnO}_3$ . Performing EXAFS fitting of the final milled material shows the  $\text{LaMnO}_3$  catalyst to have a degree of oxygen deficiency, as well as two Mn-La scattering paths; associated with both the amorphous and crystalline content. Ultimately, the identification of 'phase pure'  $\text{LaMnO}_3$  through XRD does not adequately describe the final milled samples. During the decomposition of  $\text{N}_2\text{O}$  ( $\text{deN}_2\text{O}$ ) the milled  $\text{LaMnO}_3$  catalysts exhibit comparable behaviour to that of the sol-gel prepared sample, (Figure 2). The 3 h ball milled sample has a much earlier onset production of  $\text{N}_2$ , suggesting a high level of oxygen vacancies on the catalyst surface, consistent with our XAFS analysis.

## Conclusions

$\text{LaMnO}_3$  has been successfully synthesised via mechanical grinding in the absence of high temperature thermal annealing. Though XRD shows 100% crystalline perovskite formation, it is clear from XAFS analysis this is not a complete description of the materials prepared. Further analysis of the final ball milled  $\text{LaMnO}_3$  shows a degree of oxygen deficiency and a distorted Mn-La scattering path, which could contribute to the higher onset production of  $\text{N}_2$  during  $\text{deN}_2\text{O}$  compared to a sol-gel synthesis analogue.

## References

- [1] S. Keav, S. Matam, D. Ferri and A. Weidenkaff, *Catalysts*, 2014, **4**, 226-255 [2] S. Kaliaguine, A. Van Neste, V. Szabo, J. E. Gallot, M. Bassir and R. Muzychuk, *Appl. Catal. A Gen.*, 2001, **209**, 345-358 [3] Q. Zhang and F. Saito, *J. Alloys Compd.*, 2000, **297**, 99-103 [4] B.D. Stojanovic, *J. Mater. Process. Technol.*, 2003, **143-144**, 78-81

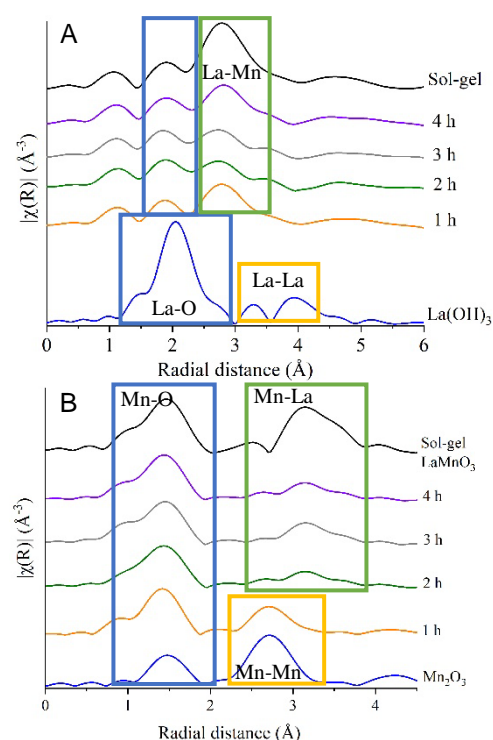


**Figure 1:** Non phase-corrected Fourier transform at the (A) Mn K-edge and (B) La L<sub>3</sub>-edge for  $\text{LaMnO}_3$  synthesised by sol-gel and by ball milling from 1 h to 4 h compared to the precursor

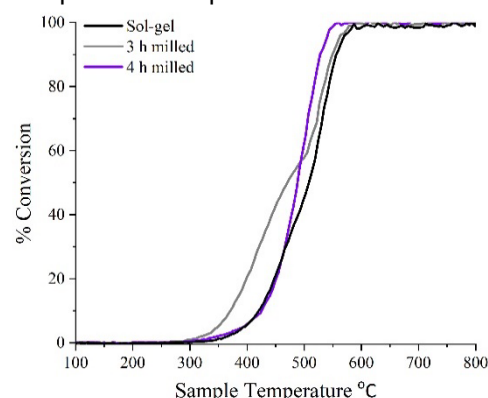


**Figure 2:** Light-off curve showing the  $\text{deN}_2\text{O}$  over ball milled and sol-gel synthesised  $\text{LaMnO}_3$

# **Catalytic reduction of NO<sub>x</sub> under pre-turbine exhaust conditions: Influence of varying pressures and hydrocarbon poisoning on the performance of NH<sub>3</sub> assisted selective catalytic reduction**

*Deniz Zengel<sup>1</sup>, Maria Casapu<sup>1</sup>, Jan-Dierk Grunwaldt<sup>1\*</sup>*

<sup>1</sup>*Institute for Chemical Technology and Polymer Chemistry, Karlsruhe Institute of Technology (KIT), Engesserstrasse 20, Karlsruhe, 76131, Germany*

\*grunwaldt@kit.edu

## **Introduction**

Considering the decrease of the exhaust gas temperature due to a more efficient engine management, positioning of the exhaust gas aftertreatment system closer to the engine represents an attractive solution [1]. Particularly, the location upstream of the turbocharger is interesting. Apart from higher temperatures of up to 180 °C also an increased pressure and, thus, a higher residence time of the reactants is achieved [2-3]. Recent studies report strong benefits of implementing a diesel oxidation catalyst (DOC) or a catalyst for selective catalytic reduction (SCR) of NO<sub>x</sub> with NH<sub>3</sub> at the pre-turbine position [3-5]. Nevertheless, several challenges of a pre-turbine application remain, such as higher concentration of hydrocarbons, especially if a DOC is not positioned in front of the turbocharger. In this study, we investigate different state-of-the-art SCR catalysts, with the focus on the impact of varying pressures and the presence of hydrocarbons (such as C<sub>3</sub>H<sub>6</sub> and C<sub>12</sub>H<sub>26</sub>) on catalyst performance.

## **Materials and methods**

A vanadium based catalyst was prepared by incipient wetness impregnation with a composition of 2 wt% V<sub>2</sub>O<sub>5</sub> and 9 wt% WO<sub>3</sub>. The differently tested zeolites were prepared by ion exchange of commercially available zeolites and resulted in 1,7 wt% Cu-SSZ-13 (Si/Al=14) and 1,5 wt% Fe-ZSM-5 (Si/Al=13). Catalytic tests were performed with coated cordierite honeycombs in a stainless-steel reactor from 150 - 550 °C using typical gas mixtures for standard and fast SCR with a GHSV of 100,000 h<sup>-1</sup>. While the pressure was varied from 1-5 bar, the total mass flow was kept constant. The gas composition was monitored by a MKS FTIR instrument.

## Results and Discussion

With increasing pressure, a significant improvement of the catalytic activity was observed over the whole temperature range for all tested catalytic systems. This increase is most probably due to the longer residence time at higher pressures. The addition of  $C_3H_6$  to the SCR gas mixture decreased the activity of the ion exchanged zeolites while the vanadium catalyst maintained its original activity Fig. 1. In the presence of longer chain hydrocarbons like dodecane a pronounced negative influence on all catalysts was visible especially at high temperatures. Besides poisoning the catalyst, hydrocarbons caused side reactions in the gas phase under increased pressure (e.g.  $NH_3$  oxidation), which resulted in a drop of the catalytic activity. All catalysts converted hydrocarbons mainly to CO and  $CO_2$ , with small amounts of side products like HCHO at temperatures above 250 °C. Like for the  $NO_x$  conversion, the increased pressure resulted in an improved hydrocarbon conversion.

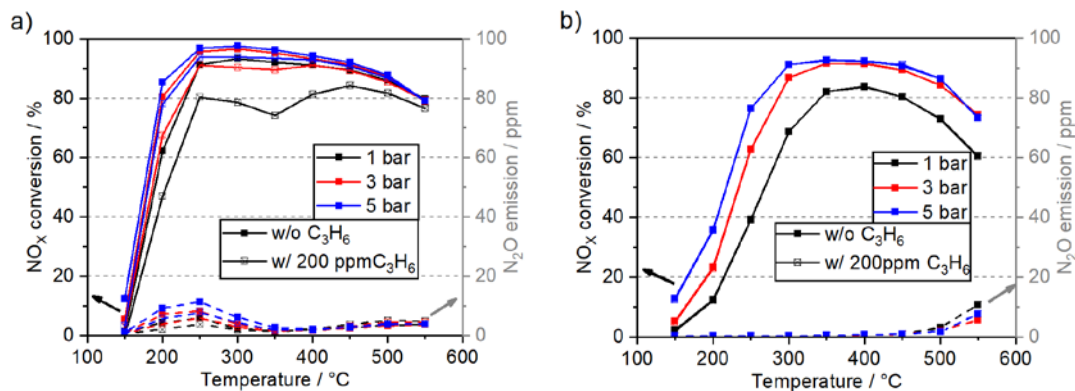


**Fig. 1**  $NO_x$  conversion (continuously line) and  $N_2O$  emissions (dashed line) during Standard-SCR of a) Cu-SSZ-13 and b)  $V_2O_5$ - $WO_3$ /TiO<sub>2</sub> at 1 - 5 bar with and without  $C_3H_6$ .

## Conclusions

The results of this study show the improvement of  $NO_x$  removal with increasing pressure. At the same time, limitations due to interaction with further exhaust gas components or the formation of high CO emissions were identified. Hence, further investigations are necessary to evaluate the true potential of the overall catalyst system under pre-turbine conditions, also including the presence of a DOC catalyst.

## References

1. M. Presti, A. Scheeder, O. Holz, R. Brück, *Motornahe Abgasnachbehandlung im Nutzfahrzeug: Eine Lösung für CARB 2020 NOx?*, Lohmar Germany, (2016).
2. F. Jayat, L. Pace, R. Konieczny, *Aufladetechnische Konferenz Emitec GmbH* (2007).
3. V. Joergl, P. Keller, O. Weber, K. Müller-Haas, R. Konieczny, *SAE Int. J. Fuels Lubr.* 1 (2008) 82.
4. O. Kröcher, M. Elsener, M. Bothien, W. Doelling, *MTZ* 75 (2014) 68-73.
5. T. Günter, J. Pesek, K. Schäfer, A. B. Abai, M. Casapu, O. Deutschmann, J.-D. Grunwaldt, *Appl. Catal. B* 198 (2016) 548.

# **n-Butane isomerization over iron promoted MELCat sulfated zirconia**

*Iryna Chepurna, Dave Scapens, Hazel Stephenson;  
Luxfer MEL Technologies, Elektron Technology Centre, Lumns Lane, Swinton,  
Manchester, M27 8LN, UK  
iryna.chepurna@luxfer.com*

## **Introduction**

There is a significant regulatory driving force to push for isomerization and alkylation technologies to be implemented on the less efficient refineries around the world due to constant push for gasoline with high RON. Higher octane fuels lead to less knocking in automotive vehicles, which inspire automakers to increasingly adopt turbocharging and other engine technologies in order to improve power and fuel efficiency (e.g. to meet CO<sub>2</sub> regulations).

*Doped metal oxides* combine the advantages of zeolites and chlorinated alumina. They are resistant to poisoning, offer the relatively low operation temperature, high isomerisation yields and high octane number of isomerizate. Also mentioned materials have been shown to be “super” acid catalysts [1]. By varying the synthesis route, it is possible to modify mentioned materials properties that affect the performance in the number of various organic reactions [2].

## **Experimental**

The sulphated (SZ) zirconia catalysts were prepared by calcining the corresponding hydroxides (Luxfer MEL Technologies, Manchester, UK) at 600°C for 2h. Porous structure of the sample was measured using low temperature N<sub>2</sub> adsorption on the Micromeritics TriStar 3020 analyser. Crystallinity was characterised by X-ray diffraction via Bruker D8 Advance instrument. Butane isomerisation testing was carried out on iron impregnated samples (2.5 wt.% Fe<sub>2</sub>O<sub>3</sub>) after activation at 550 °C/2hr in 20%O<sub>2</sub>/He; [25%n-C<sub>4</sub>H<sub>10</sub>/75%He, 110 °C, ambient pressure], using a mass spec detector (specifically m/z=28).

## **Results and discussion**

The fast deactivation of SZ has limited its use in commercial processes. Incorporation of transition metal oxides, particularly iron, has been reported to enhance the thermal stability and the stability of the surface sulphate species [1-3]. The detailed investigation of the physico-chemical characterisation of iron promoted SZ prepared via a novel precipitation method (sample 3) was attempted. Suggested



synthetic approach allows to prepare materials, beneficial in porosity, acidity, thermostability compare to well-known commercial analogues.

The surface area values for pure and SZ samples are presented in Table 1.

	Fe-SZ	Oxide 600/2					
		Fe <sub>2</sub> O <sub>3</sub> , %	SO <sub>3</sub> , %	SA, m <sup>2</sup> /g	TPV, cm <sup>3</sup> /g	APD, nm	% Butane conversion after 20 min on stream
1	Undoped, reference	2.5	-	59	0.23	15.5	5.1
2	SZ commercial	2.4	8.5	124	0.14	4.5	6.4
3	SZ development	2.5	6.5	168	0.47	11.2	10.9

Table 1. Characterisation of 2.5% Fe<sub>2</sub>O<sub>3</sub> loaded samples

The enhancement in the surface area of the sulphated samples can be explained on the basis of the higher resistance to sintering acquired via sulphation [4]. The dispersion of Fe<sub>2</sub>O<sub>3</sub> particles causes a further rise in the surface area values.

XRD data supports the stabilisation of the catalytically active tetragonal phase after incorporation of sulphate and iron species. In comparison with pure zirconia, the XRD patterns of sulphated and iron-incorporated zirconia samples showed an enrichment of the tetragonal phase.

Also usage of suggested method allowed to obtain samples with Lewis Acidity, which look promising in n-butane conversion (conversion 10.9% (sample 3) vs 6.4 % (sample 2)). According to [5], isomerization process is occurring based on typical induction/deactivation mechanism, where n-butane gives a significant m/z=28 peak in the mass spec, whereas i-butane has low intensity (Fig.1).

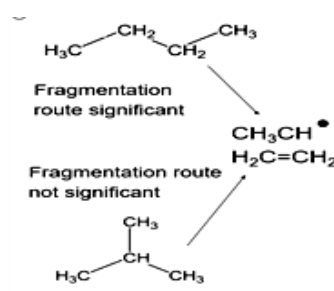


Fig. 1 Products of the decay in the mass-spec.

#### Reference

- [1] M. Miao, W. Hua, J. Chen, Z. Gao, Catal. Lett. 37 (1996) 187.
- [2] M. Scheithauer, E. Bosch, U.A. Schubert, H. Knozinger, T.K. Cheung, F.C. Jentoft, B.C. Gates, B. Tesche, J. Catal. 177 (1998) 137.
- [3] M. Hino, Catal. Lett. 34 (1996) 125.
- [4] X. Song, A. Sayari, Catal. Rev. Sci. Eng. 38 (3) (1996) 329.
- [5] Risch, M.A., Wolf, E., Studies in surface science and catalysis 139 (2001) 237.

# Reaction Pathway Analysis of CO<sub>2</sub> Capture over Amine-Functionalized Mesoporous Silica using DFT

*Umay Topcubasi, Department of Chemical Engineering, Yeditepe University, 34755, Istanbul, Turkey; Tugba Davran-Candan, Department of Chemical Engineering, Yeditepe University, 34755, Istanbul, Turkey*

## 1. Scope

The dramatic increase observed in the level of atmospheric CO<sub>2</sub> since the industrial revolution has been accused of being the primary cause of global warming and post-combustion capture followed by the sequestration of the emitted CO<sub>2</sub> is regarded as a potential near-term solution for the mitigation of the adverse effects of this warming. Among the capture technologies considered, CO<sub>2</sub> adsorption by amine-functionalized mesoporous silica substances has come out as one of the most promising approaches benefitting from both the high affinity of amines towards CO<sub>2</sub> and the lower regeneration heats of dry methods. Despite of the extensive research executed in the field, adsorption capacities are still far below the numbers required to fulfill the 2100 emission targets established by the fifth assessment report of the IPCC [1] indicating that there is still a lot to achieve in the field.

For the development of a successful adsorbent that would possess high capacity, stability and selectivity, it is critical to clarify the interaction mechanism of CO<sub>2</sub> with the adsorbents. Based on the IR findings, early studies assumed that CO<sub>2</sub> was captured either in the form of carbamates or bicarbonates as it was in the case of wet (amine stripping) methods [2-3]. However, strong overlaps observed in the infrared bands resulted in disagreements in the assignment of these bands leading to speculation about the reaction mechanism of CO<sub>2</sub> capture over amine-modified silica sorbents [4]. Although the formation of other products like carbamic acid has been verified through experimental and theoretical studies [5], the details of the reaction pathways are still unknown.

This study aims to provide an atomic-level understanding of the interaction mechanism of CO<sub>2</sub> with APTMS ((3-aminopropyl)-trimethoxy-silane)-modified mesoporous silica using DFT method.

## 2. Results

For the construction of the APTMS-functionalized mesoporous silica adsorbents, two APTMS molecules were grafted onto two different locations of a cluster of 8 SiO<sub>2</sub> units. Our geometry optimizations demonstrated that the amine groups should not be in direct interactions with the surface silanol groups in order to be available for the adsorption of CO<sub>2</sub>.

Chemisorption of CO<sub>2</sub> was shown to take place in the form of either carbamic acid or carbamate and a strong interaction between the surface silanol groups and products (and intermediates) is required for the stabilization of these end products. Although these silanol groups played a critical role on the stabilization of the products, there was no evidence that they actively participated in the capture process.

Finally, in addition to the end products, all the intermediates and transition states involved in the carbamate and carbamic acid pathways were identified and the energetics of both pathways was obtained.

## 3. Conclusion

Our reaction pathway analysis of CO<sub>2</sub> adsorption over APTMS-modified mesoporous silica sorbent demonstrated that the capture mechanism was quite different than the one reported for aqueous systems and the surface silanol groups played a critical role on the mechanism.

## References

- [1] Synthesis Report. Contribution of Working Groups I, II and III to the Fifth Assessment Report of the Intergovernmental Panel on Climate Change, in: R.K. Pachauri, C.W. Team, L.A. Meyer (Eds.) Climate Change 2014, IPCC, Geneva, Switzerland, 2014, p. 151.
- [2] Khatri, R. A.; Chuang, S. S. C.; Soong, Y.; Gray, M. *Ind. Eng. Chem. Res.* 2005, 44 (10), 3702-3708.
- [3] Wang, X.; Schwarz, V.; Clark, J. C.; Ma, X.; Overbury, S.; Xu, X.; Song, C. *J. Phys. Chem. C* 2009, 113 (17), 7260-7268.
- [4] Pinto, M. L.; Mafra, L.; Guil, J. M.; Pires, J.; Rocha, J. *Chem. Mater.* 2011, 23, 1387-1395
- [5] Mafra, L.; Cendak, T.; Schneider, S.; Wiper, P. V.; Pires, J.; Gomes, J. R. B.; Pinto, M.L. *J. Am. Chem. Soc.* 2017, 139, 389-408.

# **Catalyst libraries with discrete composition spreads: preparation via inkjet printing and characterization by micro-spectroscopy in a parallel milli/micro-reactor testing device**

*Patrick Fleischer, Chemnitz University of Technology, Chemnitz, Germany; Klaus Stöwe, Chemnitz University of Technology, Chemnitz, Germany.*

Heterogeneously catalyzed reactions are essential attribute of the most important processes in modern chemical industry. To reduce the amount of expensive catalytically active metals needed supported catalysts with high catalyst utilization ratio are of special interest. Therefore, the search for supported catalysts of higher efficiency is constantly pushed on, which can be significantly accelerated by High-Throughput Technologies (HTT). Here, we present a newly designed reactor system suitable for HT screening of catalyst activity.

## **Catalyst preparation**

Even the application of High-Throughput methods to supported catalysts is often associated with their sequential and tedious preparation via sol-gel methods, wet or incipient wetness impregnation. We use inkjet printing as an alternative and comparatively simple method to prepare supported catalyst libraries.[1] We employed it to create discrete quasi-binary libraries consisting of metal oxides supported on alumina or titania, but with the setup used even ternary and quaternary systems are accessible. The principle is demonstrated by the example of the well-understood copper manganese mixed metal oxide system. Two suitable metal salt solutions of the desired metals are dispensed onto a porous substrate via a drop-on-demand technique as micro-droplets with volumes in the pico-liter range. Dispensing both solutions onto the same spot of the substrate surface leads to mixing of the metal salt solution. After thermal treatment, the mixed drop forms the catalyst. With known micro-droplet volumes, the composition ratio of both metals on a given spot can be adjusted. Thus, only the volume of the dispensed micro-droplets limits the compositional step size of the discrete composition spread samples. As the sequential droplet deposition is associated with problems regarding capillary and chromatographic effects (see Runge images), special techniques to ensure sufficient mixing are crucial.

## Catalytic testing

To determine catalyst activity, we employ a newly designed parallel gas phase reactor where the reaction gas simultaneously flows over 16 inkjet printed catalyst spots of a library. Each catalyst spot is confined to an individual reaction space. Educat or product concentrations and adsorbates are accessible via *in situ* IR micro-spectroscopy. The library is mapped with regard to signals corresponding to desired components. We use conventional preparation and activity testing for comparative validation of results. In the same parallel setup *in situ* Raman micro-spectroscopy is used to gather complimenting information like identification of active catalyst species. Thus, structure-activity relationships can potentially be explored.

Testing of complex catalytic gas phase reactions is feasible in the presented reactor system as long as relevant components are accessible via spectroscopy. In the initial stages of our investigations, CO oxidation was chosen as a well-known model reaction.

## References

- [1] K. Stöwe, W. F. Maier, B. Weidenhof, Inkjet-Printing of Composition Spread Libraries, MRS Symposium Proceedings 1425 (2012) DOI:10.1557/opl.2012.203.

# Electrochemically assisted catalytic methane oxidation on SOFC system

*NAU Alexandre, COMMINGES Clément, BION Nicolas*

*Institut de Chimie des Milieux et Matériaux de Poitiers (IC2MP), University of Poitiers, CNRS, UMR 7285, 4 Rue Michel Brunet, TSA 51106, F-86073 Poitiers 9, France*

Alternatives to fossil resources are highly needed to drive the energetic transition. Among the different possibilities currently investigated, the methane molecule is expected to be a potential candidate as a pure energy source as well as a building block for the synthesis of various chemicals, taking the benefit of its eco-friendly production from wastes and biomass degradation.

Several studies have been carried out on Pd/Al<sub>2</sub>O<sub>3</sub> to convert methane in CO<sub>2</sub> [1]. Pd is known as one of the most efficient metal to activate the C-H bond of methane [2]. Catalytic methane oxidation may also occur implying a Mars Van Krevelen (MvK) mechanism in which lattice oxygen atoms are involved [3]. In the present work, Pd was supported over 8 mol% yttria stabilized zirconia (YSZ) which is well known in the electrocatalysis field for its use as an electrolyte in solid oxide fuel cell (SOFC) system because of its high ionic conductivity for oxygen ions above 600°C. YSZ was also recently reported to be able to activate CH<sub>4</sub> [4] and to have highly labile oxygen network even below 600°C [5].

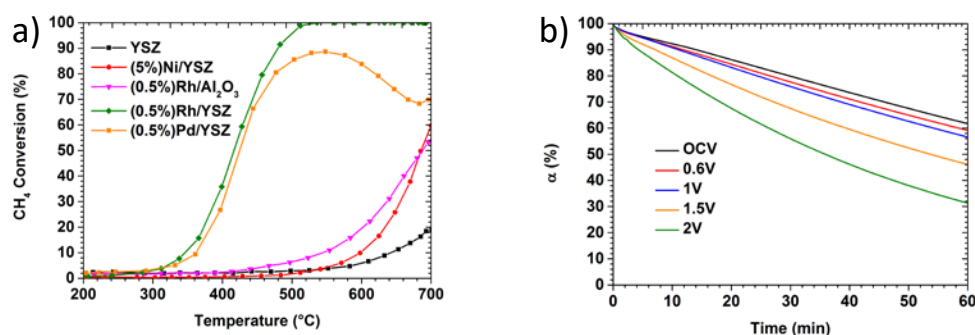


**Figure 1: a) light-off curves for the combustion of methane (1 % CH<sub>4</sub>, 2 % O<sub>2</sub>, He balance); b) Evolution of the atomic fraction of <sup>18</sup>O in the gas phase (α) during the isotopic exchange on Pt/YSZ/Pt cell at 600°C under different potential bias values.**

In a first set of experiments, the catalytic performances of YSZ-supported Pd was compared to Rh (known for its use in the dry reforming of methane [6]), and Ni catalyst (known for its use in combination with YSZ as anode in SOFC system [7]). The catalysts 0.5 wt % Rh/YSZ, 0.5 wt Pd/YSZ and 5 wt% Ni/YSZ were prepared by

wet impregnation of  $\text{Rh}(\text{NO}_3)_2$ ,  $\text{Pd}(\text{NH}_3)_2(\text{NO}_3)_2$  and  $\text{Ni}(\text{NO}_3)_2$  respectively over commercial YSZ (Tosoh, TZ-8Y, 8 mol%  $\text{Y}_2\text{O}_3$ ).

Figure 1a shows that Pd/YSZ and Rh/YSZ are very active below 500°C contrarily to Ni/YSZ. At high temperature (>500°C), a deactivation effect can be noticed on the Pd/YSZ while  $\text{CH}_4$  conversion remains complete for Rh/YSZ. This behaviour was already reported for Pd supported over several oxides like  $\text{Al}_2\text{O}_3$  or  $\text{ZrO}_2$  by Farrauto *et coll.* [8] who demonstrated that at high temperature the catalytically active PdO sites are decomposed in not active Pd. Interestingly when supported on  $\text{Al}_2\text{O}_3$ , Rh loses completely its high performance at low temperature indicating a significant synergetic effect between Rh and YSZ for the methane combustion that will be discussed in the presentation.

The electrochemical promotion of the catalytic reaction was then investigated in these systems with particular attention to the influence of the electrical bias applied on the oxygen mobility. To study such a phenomenon the oxygen isotopic exchange technique (using  $^{18}\text{O}_2$ ) was combined to a SOFC test bench and the isotopic distribution was continuously monitored by mass spectrometry. By using a model Pt/YSZ/Pt symmetrical system, we very recently demonstrated that a polarization of the cell clearly improves the exchange of the oxygen atoms of the YSZ electrolyte as it can be seen in the Figure 1b. This methodology was applied to the different catalytic systems and a comparison is proposed in terms of surface exchange rate and oxygen diffusion coefficients.

## Conclusions

Finally, the catalyst Rh/YSZ is a promising catalyst due to its high and stable catalytic performances in methane combustion. The utilization of oxygen isotopic exchange in a SOFC cell is a powerful tool to investigate the effect of a polarization on the MvK mechanism by observing the influence of the bias on the lattice oxygen mobility.

## References

- [1] D. Gao, C. Zhang, S. Wang, Z. Yuan, S. Wang, *Catal. Commun.* 9 (2008) 2583–2587.
- [2] Y.-H. Chin, C. Buda, M. Neurock, E. Iglesia, *J. Am. Chem. Soc.* 135 (2013) 15425–15442.
- [3] D. Ciuparu, M.-R. Lyubovsky, E. Altman, L.-D. Pfefferle, A. Datye, *Catal. Rev.* 44 (2002) 593–649.
- [4] M. Richard, *et al.* *ChemCatChem*. 8 (2016) 1921–1928.
- [5] C. S. Cooper, R. J. Oldman, C. R. A. Catlow, *Chem. Commun.* 51 (2015) 5856.
- [6] A. Drif, *et al.*, *Appl. Catal. A: Gen.* 504 (2015) 576–584.
- [7] T. Takeguchi, *et al.*, *J. Power Sources*. 112 (2002) 588–595.
- [8] R. J. Farrauto, J. K. Lampert, M. C. Hobson, E. M. Waterman, *Appl. Catal. B: Env.* 6 (1995) 263–270.

# Copper and Platinum Doped Titania for Photocatalytic Reduction of Carbon Dioxide

*Nela Ambrožová<sup>a</sup>, Martin Relř<sup>a</sup>, Marcel Šihor<sup>a</sup>, Miroslava Edelmannová<sup>a</sup>, Ivana Troppová<sup>a</sup>, Jaroslav Lang<sup>a</sup>, Anna Rokicińska<sup>c</sup>, Piotr Kuřtrowski<sup>c</sup>, Jeffrey C.S. Wu<sup>d</sup>, Kamila Koč<sup>ab\*</sup>*

*Address: <sup>a</sup>Institute for Environmental Technology, <sup>b</sup>Energy Units for Utilization of non Traditional Energy Sources, VŠB-Technical University of Ostrava, 17. listopadu 15, Ostrava-Poruba, Czech Republic; <sup>c</sup>Faculty of Chemistry, Jagiellonian University, Ingardena 3, 30-060 Kraków, Poland; <sup>d</sup>Department of Chemical Engineering, National Taiwan University, Taipei 10617, Taiwan;*

*\*kamila.koci@vsb.cz*

Fossil fuels are one of the major sources of energy. Combustion of fossil fuels leads to emission of large amounts of CO<sub>2</sub> into the atmosphere, thereby causing global climate change and many environmental problems. Heterogeneous photocatalysis is one of potential modern approaches for the mitigation of carbon dioxide emission resulting from human activities [1]. TiO<sub>2</sub> is the most frequently applied semiconductor photocatalyst due to its availability, low cost, high photocatalytic activity and resistance to corrosion [2]. Especially, photocatalytic reduction of CO<sub>2</sub> with H<sub>2</sub>O is important in the development of solar energy based on the carbon neutral cycle. There are several aspects, which influence the photocatalytic performance of nanoparticles such as the absorption edge energy, specific surface area and other structural properties and the most importantly electrons and holes energies.

All these aspects can be significantly positively affected by modifying the TiO<sub>2</sub> by Pt and/or Cu. Appropriate modification of the optical and electronic properties of TiO<sub>2</sub> can reduce the absorption edge energy it can also increase the lifetime of the photogenerated electrons and holes by effective charge carrier separation and decrease the electron–hole recombination rate. The correlation between the textural, optical and photo-electrochemical properties and the photocatalysts activity was a subject of this research. The parent TiO<sub>2</sub>, platinum and copper doped TiO<sub>2</sub> photocatalysts with 0.5–2 wt. % Pt, 0.5–2 wt. % Cu and 1 wt. % Pt combined with 1 wt. % Cu were prepared by using the sol-gel method followed by calcination



at 500 °C for 5 hours in an atmosphere of technical air. All the prepared photocatalysts were tested for the CO<sub>2</sub> photocatalytic reduction in a stirred batch reactor irradiated by 8W Hg lamp with maximum peak intensity at 254 nm. The main reaction product was methane; however, hydrogen and carbon monoxide were also detected. Products were analyzed in a highly sensitive gas chromatograph with a barrier discharge detector (BID). The textural, (micro)-structural, optical and electronic properties of photocatalysts were characterized in detail by low-temperature nitrogen physisorption, X-ray powder diffraction, EDX, HRTEM, X-ray fluorescence, X-ray photon spectroscopy, scanning electron microscope, transmission electron microscope and diffuse reflectance UV–vis spectroscopy. The photoelectrochemical characteristics of the photocatalysts were determined using a photoelectric spectrometer. The experimental results indicated that three of the prepared photocatalysts (2 wt. % Cu/TiO<sub>2</sub>, 0.5 wt. % Cu/TiO<sub>2</sub> and pure TiO<sub>2</sub>) showed significantly higher photoactivity than Evonik P25. These three photocatalysts were characterized by entirely amorphous character. It was suggested based on the conducted experiments that both the amount of chemisorbed oxygen or/and hydroxyl species on the TiO<sub>2</sub> surface and specific surface area of photocatalyst highly influence the photocatalytic activity.

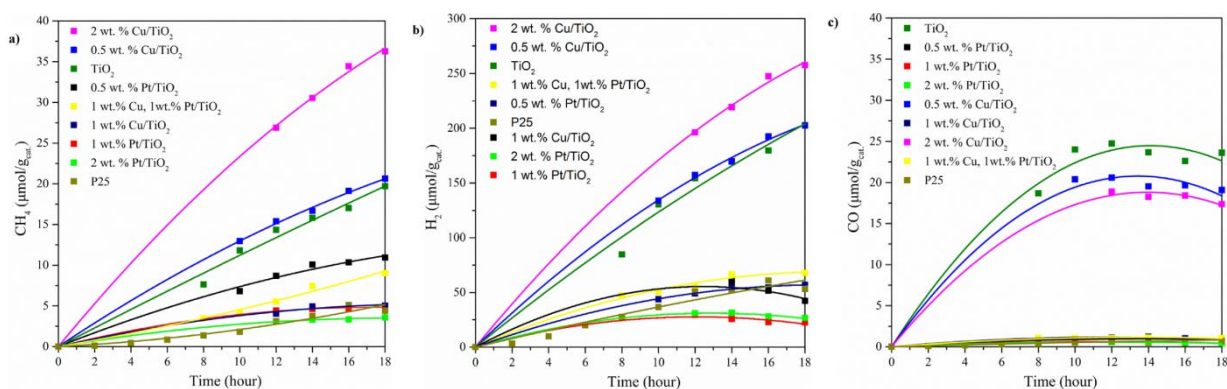


Fig. 1: Time dependence of yields of methane (a), hydrogen (b) and carbon monoxide (c) over TiO<sub>2</sub> and Cu, Pt doped TiO<sub>2</sub> photocatalysts.

## References

- [1] K. Kočí, L. Obalová, Z. Lacný. Photocatalytic reduction of CO<sub>2</sub> over TiO<sub>2</sub> based catalysts. *Chemical Papers- Slovak Academy of Sciences* 62(2015)1-9.
- [2] M.A. Fox, M.T. Dulay. Heterogeneous photocatalysis. *Chemical Reviews* 93(1993) 341–357.

## Acknowledgements

The work was supported from ERDF "Institute of Environmental Technology – Excellent Research " (No. CZ.02.1.01/0.0/0.0/15\_019/0000853).

## **Cu-containing mesoporous alumina as catalysts for NH<sub>3</sub>-SCR**

*Ole H. Bjørkedal, Dept. of Chemical Engineering, Norwegian University of Science and Technology (NTNU), Trondheim, Norway; Samuel K. Regli, Dept. of Chemical Engineering, NTNU, Trondheim, Norway; Magnus Rønning, Dept. of Chemical Engineering, NTNU, Trondheim, Norway;*

Reducing emissions of nitrogen oxides (NO<sub>x</sub>) is an important task in both industry and transportation. The transportation sector has recently struggled to meet increasingly stricter regulations for NO<sub>x</sub>-emissions, displaying a need for more efficient NO<sub>x</sub>-reduction catalysts. Efficiency at low temperature and dynamic conditions, stability, and low cost are important characteristics for NO<sub>x</sub>-reduction catalysts, such as catalysts for selective catalytic reduction by ammonia (NH<sub>3</sub>-SCR).

Inspired by Cu/zeolite catalysts, Cu/mesoporous Al<sub>2</sub>O<sub>3</sub> could be a potential catalyst for NH<sub>3</sub>-SCR. Mesoporous alumina may be synthesized by a sol-gel process, using micellular polymers as a template for pore structure [1, 2]. The resulting amorphous alumina has narrow pore size distribution and high surface area compared to  $\gamma$ -Al<sub>2</sub>O<sub>3</sub>, and is well suited for use as a catalytic support material [3].

A common way to introduce the active metal is to impregnate the mesoporous Al<sub>2</sub>O<sub>3</sub> support. An alternative method (illustrated in Figure 1) is to introduce the metal precursor during the sol-gel process where the support structure is formed, thus synthesizing the catalyst in one step [4, 5]. One advantage with this method is that it surpasses transportation limitations related to other two-steps synthesis methods. Furthermore the synthesis sol is well mixed and homogeneous, which facilitates a high dispersion of the metal on the support, even for high metal loading.

Here, samples of Cu/mesoporous Al<sub>2</sub>O<sub>3</sub> with varying degree of Cu-loading were synthesized by impregnation and one-step synthesis and characterized by N<sub>2</sub> physisorption, transmission electron microscopy (TEM), powder X-ray diffraction (PXRD) and temperature programmed reduction (TPR). Preliminary NH<sub>3</sub>-SCR performance tests have been performed. *In situ* X-ray absorption spectroscopy studies have also been conducted to investigate the state of copper under SCR-conditions.

Surface area measurements (BET) indicate no significant loss of surface area due to Cu loading in the one-step synthesized samples, indicating that there is no

formation of Cu particles blocking the pores of the mesoporous alumina. BJH pore size distribution, together with TEM-imaging (Figure 2), showed that the material is mesoporous with a narrow pore size distribution. PXRD shows a largely amorphous alumina structure, and extended X-ray absorption fine structure indicates near atomic dispersion of Cu.

The synthesized materials have some of the characteristics of ion-exchanged zeolites, such as a specific pore structure, high surface area and highly dispersed active centers. Further investigation and optimization of reaction kinetics and stability is required, but preliminary results indicate that this system may be a viable option for selective catalytic reduction of nitrogen oxides.

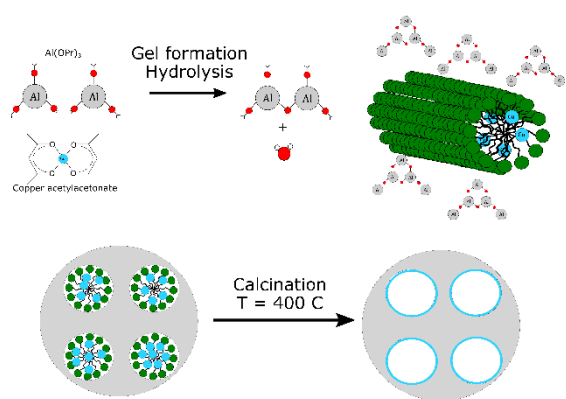


Fig. 1: Illustration of the sol-gel synthesis of one-pot Cu/MA. The hydrophobic Cu-precursor orients itself towards the inner, non-polar part of the micelles.

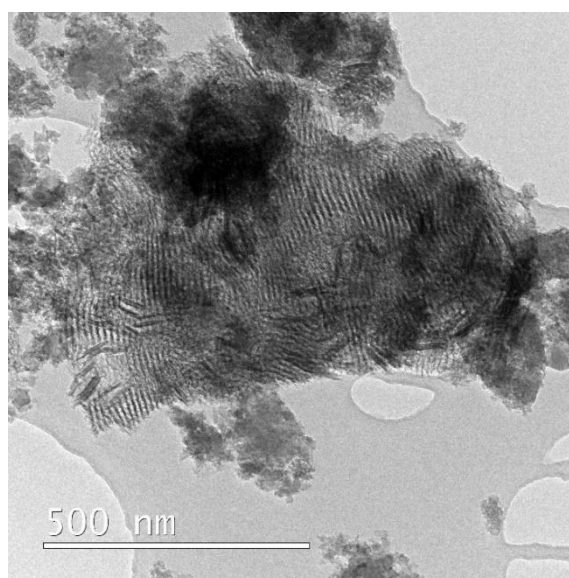


Fig. 2: TEM image of mesoporous  $\text{Al}_2\text{O}_3$

## References

1. Yuan, Q., et al., *Facile synthesis for ordered mesoporous gamma-aluminas with high thermal stability*. J. Am. Chem. Soc., 2008. **130**(11): p. 3465-3472.
2. Armatas, G.S., et al., *Synthesis and acidic catalytic properties of ordered mesoporous alumina-tungstophosphoric acid composites*. Journal of Materials Chemistry, 2010. **20**(39): p. 8631-8638.
3. Čejka, J., *Organized mesoporous alumina: synthesis, structure and potential in catalysis*. Applied Catalysis A: General, 2003. **254**(2): p. 327-338.
4. Li, Z.-X., et al., *A facile route to ordered mesoporous-alumina-supported catalysts, and their catalytic activities for CO oxidation*. Physical Chemistry Chemical Physics, 2011. **13**(7): p. 2488.
5. Voss, G.J.B., et al., *Mesostructured alumina as powders and thin films*. J. Mater. Chem. A, 2014. **2**(25): p. 9727-9735.

# Promoters for Enhanced Performance of Pd/BEA for Passive NO<sub>x</sub> Adsorption

Rojin Feizie Ilmasani<sup>1</sup> (Presenting Author), Derek Creaser<sup>1</sup>, Louise Olsson<sup>1</sup>

<sup>1</sup>Chemical Engineering; Competence Centre for Catalysis, Chalmers University of Technology, 412 96, Göteborg, Sweden.

## Introduction

NO<sub>x</sub> reduction from diesel engines is a challenging process and many advanced techniques are proposed and being investigated. For high NO<sub>x</sub> reduction efficiency, urea-SCR (Selective catalytic reduction) has been implemented commercially. However, this method has limitations for low temperature conditions like low engine loads because urea cannot be effectively decomposed to ammonia at temperatures less than about 200°C. As a solution, PNA (passive NO<sub>x</sub> adsorber) has been introduced. In this method NO<sub>x</sub> should be stored at low temperature and later released at higher temperature when it can be effectively reduced by a downstream urea-SCR catalyst [1, 2].

## Objective

The objective of this work is to find an appropriate promoter for Pd/zeolite based catalysts to enhance their performance in a PNA process. The investigated promoters included Zirconium, Lanthanum and Ceria (10wt%) in which Lanthanum showed the most interesting behavior with a wide temperature range of NO<sub>x</sub> release, largely above 200°C. Moreover, the influence of Lanthanum loading was investigated.

## Method

In this study, samples are saturated with NO<sub>x</sub> at 80°C and it is released during a temperature ramp to 650°C under constant flow with the same gas conditions used for saturation. Furthermore, different characterizations were performed such as, XPS, BET, ICP-SFMS, STEM, TPO and *in-situ* DRIFT in order to understand the influence of the promoters on the properties and adsorption behaviors of the catalysts. Pd-based BEA zeolite with a SAR (Si-to-Al ratio) of 38 was used as a PNA catalyst base on which different promoters for improving NO<sub>x</sub> trap performance were evaluated.

## Results

The results for different promoters are shown in Figure 1 during TPD with 200 ppm NO, 8% oxygen and 5% water in argon carrier. All promoters were able to reduce the NO<sub>x</sub> release below minimum urea dosing temperature, however only La could effectively shift most of the NO<sub>x</sub> release to temperatures above 200°C.

Moreover, influence of the loading of La ranging from 2.7 to 10 wt% is summarized in Figure 2. The results showed that with 5.4 wt% La, there was largely no release of NO<sub>x</sub> at low temperatures followed by a high release of NO<sub>x</sub> at higher temperatures peaking at about 350°C.

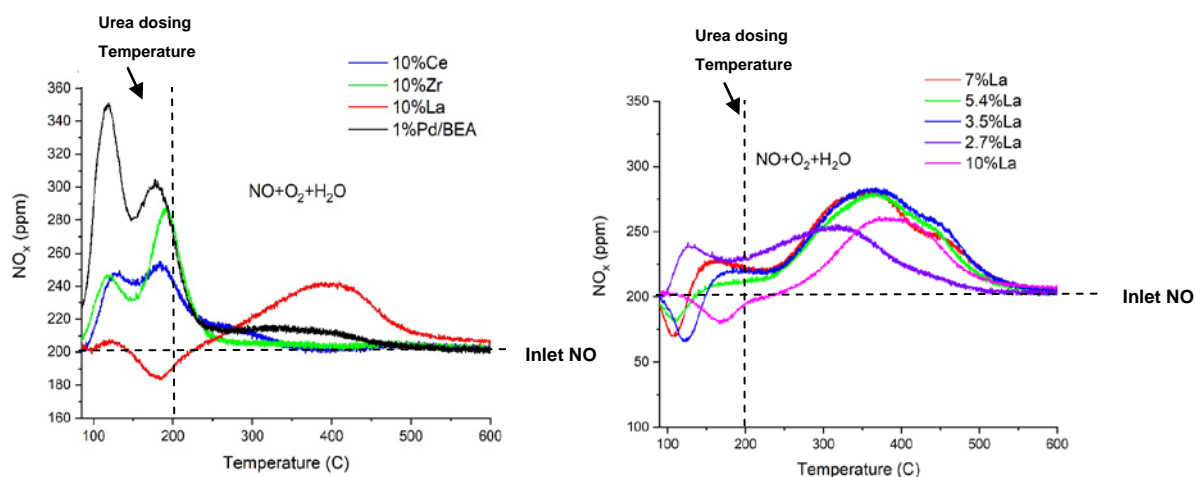


**Figure 1** TPD results for constant flow with 200ppm NO, 8% O<sub>2</sub>, 5%H<sub>2</sub>O in Ar, for different promoters on 1%Pd/BEA base (bare 1%Pd/BEA Included for reference).

**Figure 1** TPD results for constant flow with 200ppm NO, 8% O<sub>2</sub>, 5%H<sub>2</sub>O in Ar, for different loading of La on 1%Pd/BEA base.

## Conclusion

To sum up, La loading is remarkably effective for tuning the NO<sub>x</sub> desorption temperature window of a PNA based on Pd/BEA. In addition, the optimal La lading appeared to be 5.4 wt% for this purpose.

## References

1. Mihai, O., et al., *The Effect of Si/Al Ratio for Pd/BEA and Pd/SSZ-13 Used as Passive NO<sub>x</sub> Adsorbers*. Topics in Catalysis, 2018. **61**(18): p. 2007-2020.
2. Vu, A., et al., *Effects of CO on Pd/BEA Passive NO<sub>x</sub> Adsorbers*. Catalysis Letters, 2017. **147**(3): p. 745-750.

## Activity of large gold agglomerates in total oxidation of VOCs

*Pavel Topka, Luděk Kaluža, Jana Gaálová, Institute of Chemical Process*

*Fundamentals of the CAS, v. v. i., Prague, Czech Republic*

Catalytic oxidation is efficient, cost-effective and environmentally friendly way to treat the emissions of volatile organic compounds (VOCs). We recently reported the positive effect of gold on catalytic performance and/or selectivity of ceria-zirconia in total oxidation of chlorobenzene [1] and dichloromethane [2]. The aim of this work was to study the effect of gold loading on ceria-zirconia support, and to investigate the influence of VOC type on the catalytic performance. A key part of the work reveals a less known role of the large gold agglomerates in the oxidation process.

$\text{Ce}_{0.5}\text{Zr}_{0.5}\text{O}_2$  was impregnated with a constant volume of aqueous solution of gold(III) acetate. The concentration of the solution varied in order to obtain different gold loadings. The samples were calcined 5 h at 500 °C to obtain highly stable and robust catalysts.  $\text{H}_2$ -TPR and OSC measurements confirmed the positive effect of gold loading on reducibility and oxygen mobility.

The contribution of low and high gold loading to the catalytic performance of  $\text{Au}/\text{Ce}_{0.5}\text{Zr}_{0.5}\text{O}_2$  catalysts (Fig. 1) is depicted as  $\Delta T_{50}$ , i.e. as the difference between  $T_{50}$  of pristine  $\text{Ce}_{0.5}\text{Zr}_{0.5}\text{O}_2$  and  $T_{50}$  of a gold catalyst. Thus, the positive value of  $\Delta T_{50}$  indicates the improvement of catalytic performance that can be attributed to gold particles. The data for low gold loading (~ 0.3 wt.%) illustrate the effect of gold nanoparticles (mean particle size 20 nm) and small agglomerates (mean particle size 39 nm) on the catalytic performance of the  $\text{Ce}_{0.5}\text{Zr}_{0.5}\text{O}_2$  support. On the other hand, the data for high gold loading (~ 3 wt.%) reveal the effect of both gold nanoparticles (mean particle size 29 nm) and large agglomerates (mean particle size 114 nm). Therefore, the difference between the catalytic performances of the catalysts with high and low gold loading (Fig. 1) can be assigned to the effect of large agglomerates of gold particles.

In dichloromethane oxidation, neither gold nanoparticles nor the agglomerates contributed to the catalytic performance in terms of  $T_{50}$  (Fig. 1). The same slight improvement in  $T_{50}$  that was observed for both low and high gold loading in toluene oxidation can be ascribed to gold nanoparticles and small agglomerates. This result also shows that the activity of gold nanoparticles is similar for both Au loadings.

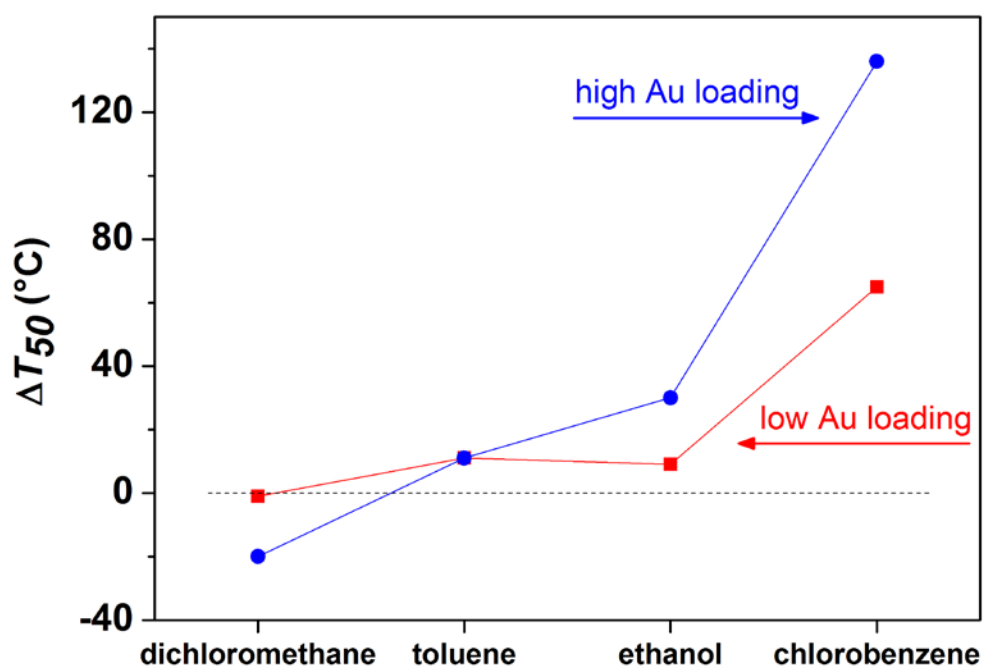


Fig. 1. Contribution of low (0.3 wt.%) and high (3 wt.%) gold loading to the catalytic performance of the  $\text{Ce}_{0.5}\text{Zr}_{0.5}\text{O}_2$  support in the oxidation of different types of VOCs.

In ethanol oxidation, the improvement in catalytic performance at high gold loading indicates the positive effect of large gold agglomerates. Finally in chlorobenzene oxidation, highly positive contribution of low gold loading and even more pronounced improvement at increased gold loading can be seen, showing that large gold agglomerates significantly contributed to the catalytic performance in this reaction. We have shown earlier by XPS analysis that some part of gold atoms in the  $\text{Au}/\text{Ce}_{0.5}\text{Zr}_{0.5}\text{O}_2$  catalysts is positively charged [3]. The beneficial effect of large gold agglomerates can be thus tentatively ascribed to the positive role of partially positively charged gold particles, which may serve as adsorption sites for nucleophilic chlorobenzene molecules.

#### Acknowledgement

The authors thank the TACR for the financial support (project TN01000048).

#### References

- [1] P. Topka, R. Delaigle, L. Kaluža, E.M. Gaigneaux, *Catal. Today*, 253 (2015) 172-177.
- [2] L. Matějová, P. Topka, L. Kaluža, S. Pitkäaho, S. Ojala, J. Gaálová, R.L. Keiski, *Appl. Catal. B*, 142-143 (2013) 54-64.
- [3] P. Topka, M. Klementová, *Appl. Catal. A*, 522 (2016) 130-137.

# Copper ammonia species studied by EPR in Cu-CHA for Selective Catalytic Reduction of NO<sub>x</sub>

*David Nielsen, Susanne Mossin, Centre for Catalysis and Sustainable Chemistry, Technical University of Denmark, 2800 Kgs. Lyngby, Denmark*

## Copper zeolite as catalyst for NO removal

Nitrogen oxides are formed in combustion processes where nitrogen from the atmosphere or from the fuel is oxidized, primarily into NO and NO<sub>2</sub> (NO<sub>x</sub>). NO<sub>x</sub> is harmful to the environment and for human health and NO<sub>x</sub> emission is limited by legislation. One technique for removal of NO<sub>x</sub> is Selective Catalytic Reduction (SCR) by ammonia [1]. Copper exchanged zeolites can be applied as a catalyst for the SCR process and is used in diesel exhaust gas treatment, due to the stability and low-temperature activity [2]. Cu<sup>2+</sup>-ions can be exchanged into the structure of the zeolite when Al atoms substitute Si atoms. The particular distribution of the aluminium in the zeolite will influence the distribution of copper in the structure, determining the active sites of the catalyst.

## Cu atoms as probe for Electron Paramagnetic Resonance

Electron paramagnetic resonance spectroscopy (EPR) is very sensitive towards paramagnetic Cu<sup>2+</sup> and offers the possibility for both quantification and speciation of Cu<sup>2+</sup> sites with unrivalled sensitivity [3]. Recent results obtained on Cu-CHA show that the elucidation of the different copper species is possible using EPR by exposing the Cu-CHA to different gas mixtures [4,5]. In this way, the Cu sites are probes to investigate the local microenvironment of the zeolite framework.

CHA zeolites prepared by different methods were investigated in-situ by exposing the samples to varying concentrations of gaseous NH<sub>3</sub>, NO, O<sub>2</sub> and H<sub>2</sub>O or mixtures thereof in balance He. The parallel region of the blue EPR spectrum in Figure 1 reveal at least two different Cu<sup>2+</sup> sites (site A and site B) with different local aluminium configuration, i.e 2Z Al-sites located in para- and meta-positions in a 6-membered ring. Exposure to ammonia at low temperature gives the red spectrum in Figure 1 identified as [Cu(NH<sub>3</sub>)<sub>4</sub>]<sup>2+</sup>, which is loosely contained within the CHA cage. The development in the EPR spectrum during changes in temperature and gas composition reveal the reduction of Cu(II) to Cu(I), the gradual loss of coordinated ammonia and the formation of Cu nitrate species.



Determining the area under EPR absorption curves allow quantification of different  $\text{Cu}^{2+}$  sites and show the transformation of EPR inactive Z-CuOH species to EPR active  $[\text{Cu}(\text{NH}_3)_4]^{2+}$  and  $[\text{Cu}(\text{NH}_3)_3(\text{OH})]^+$  species in  $\text{NH}_3$  containing gas streams.

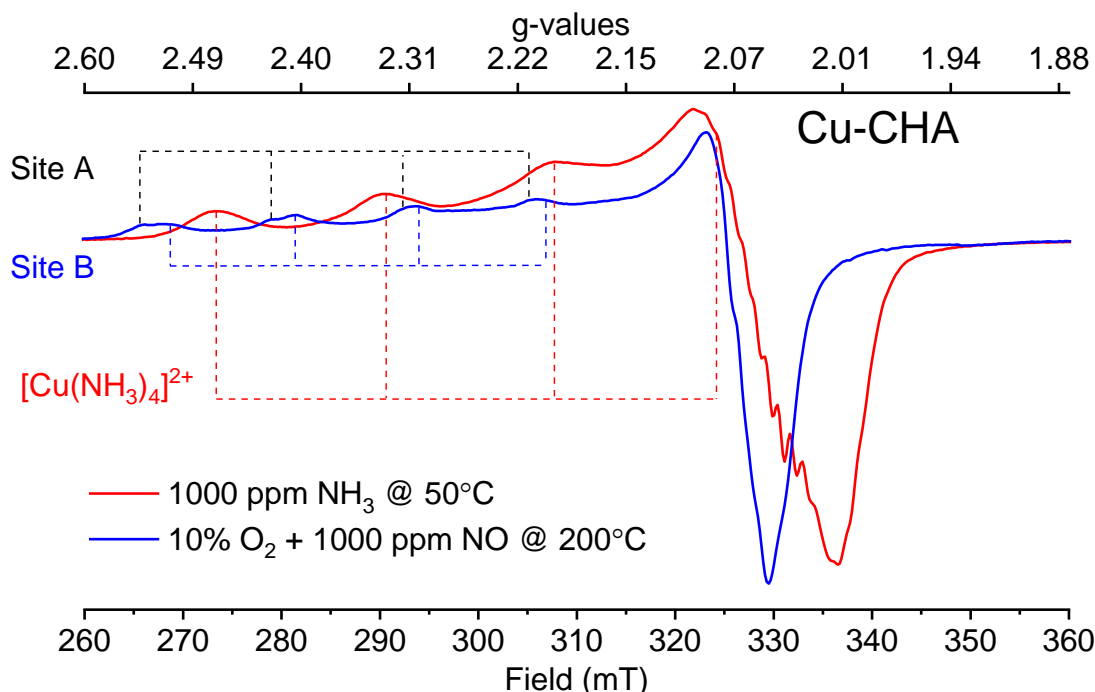


Figure 1: EPR spectra of a Cu-CHA catalyst recorded at 50°C after exposure to ammonia (red) and at 200°C after exposure to NO and oxygen (blue).

## Conclusions

The use of in-situ and operando EPR to probe the Cu-sites in small pore zeolites open the possibility for a deeper understanding of the species present in the SCR reaction in the temperature interval 100-250°C. This may allow the design of catalyst with specific metal sites that are highly active for catalytic processes. Electron Paramagnetic Resonance (EPR) spectroscopy provides a sensitive method to distinguish different Cu-sites in the framework of the zeolite.

## References

- [1] U. Deka et. al. ACS Catal. 3, (2013), 413.
- [2] M. Moliner et.al. Chem. Commun. 48, (2012), 4264.
- [3] A. Godiksen et. al J. Phys. Chem. C 118, (2014), 23126.
- [4] A. Godiksen et. al. Top. Catal. 2017, 10, (2018), 366.
- [5] T. V. W. Janssens et. al. ACS Catal. 5, (2015), 2832.

# Estimating the Effect of Reaction Conditions in Catalytic Homogeneous Hydrogenations with QM and ML Approaches

*Anton A. Bondarenko, Anton V. Domnin, Pavel O. Kulyaev, Mikhail V. Polynski,*

*TheoMAT group, ITMO University, Saint Petersburg, Russia;*

*Evgeny A. Pidko, ISE group, TU Delft, Delft, the Netherlands*

[polynskimikhail@gmail.com](mailto:polynskimikhail@gmail.com); [e.a.pidko@tudelft.nl](mailto:e.a.pidko@tudelft.nl)

Catalytic homogeneous hydrogenation is an efficient tool for the sustainable reduction of multiple C-heteroatom bonds and a promising tool for CO<sub>2</sub> fixation and/or H<sub>2</sub> storage. The efficiency of these reactions depends not only on the choice of a metal-complex catalyst (including ligand choice) but on the reaction conditions (concentrations of reactants, H<sub>2</sub> and CO<sub>2</sub> pressure, temperature, solvent) as well [1]. Predicting the effect of reaction conditions on reaction rates and yields with conventional computational chemistry methods is a challenge [2]. Machine learning (ML) approaches gain popularity in this regard by straightforward inclusion of reaction conditions in ML models [3]. In this report, we describe two computational approaches for the prediction of the effect of reaction conditions in homogeneous hydrogenations.

First, we used a dataset of 1117 distinct catalytic hydrogenation reactions obtained from in-house laboratory journals and published articles to train an ML model. The model was trained using a decision tree algorithm implemented in the LightGBM framework [4]. Descriptors of catalytic systems in the dataset included reaction conditions, as well as transition metal (e.g., number of d-electrons) and ligand parameters (by using Mordred program [5]). To interpret the results, we used the Shapley value explanation (SHAP) approach (Figure 1). The trained ML model showed that TOF and TON numbers can be considered adequate metrics for catalytic hydrogenation efficiency. The statistical importance of reaction conditions was on par with catalyst properties. This stresses the importance of the design of hydrogenation catalytic systems as an essential catalyst-optimal reaction conditions duo instead of optimization of the metal and ligand alone.

At the second stage we aimed at developing a framework to account for these parameters in computational catalysts. We developed an interface allowing to combine gas-phase/ideal solution DFT computations and computations of liquid phase thermodynamics in real solvents. The program allows to compute in an

automated fashion concentration-dependent free energy surfaces covering large fractions of condition space and to analyze the obtained results to extract the optimal conditions for a target catalytic reaction. The approach was validated by considering the concentration-dependencies of the kinetics and thermodynamics of the catalytic and deactivation paths for homogeneous CO<sub>2</sub> reduction to formates with homogenous Ru PNP- and CNC-catalysts [6]. The results obtained reveal substantially non-linear concentration dependencies of the energetics of the reactions on the process conditions such as concentration of base promotor, composition of the reaction mixtures, reactant pressures. The presented methodology provides a practical tool enabling operando computational studies of liquid phase catalytic transformations.

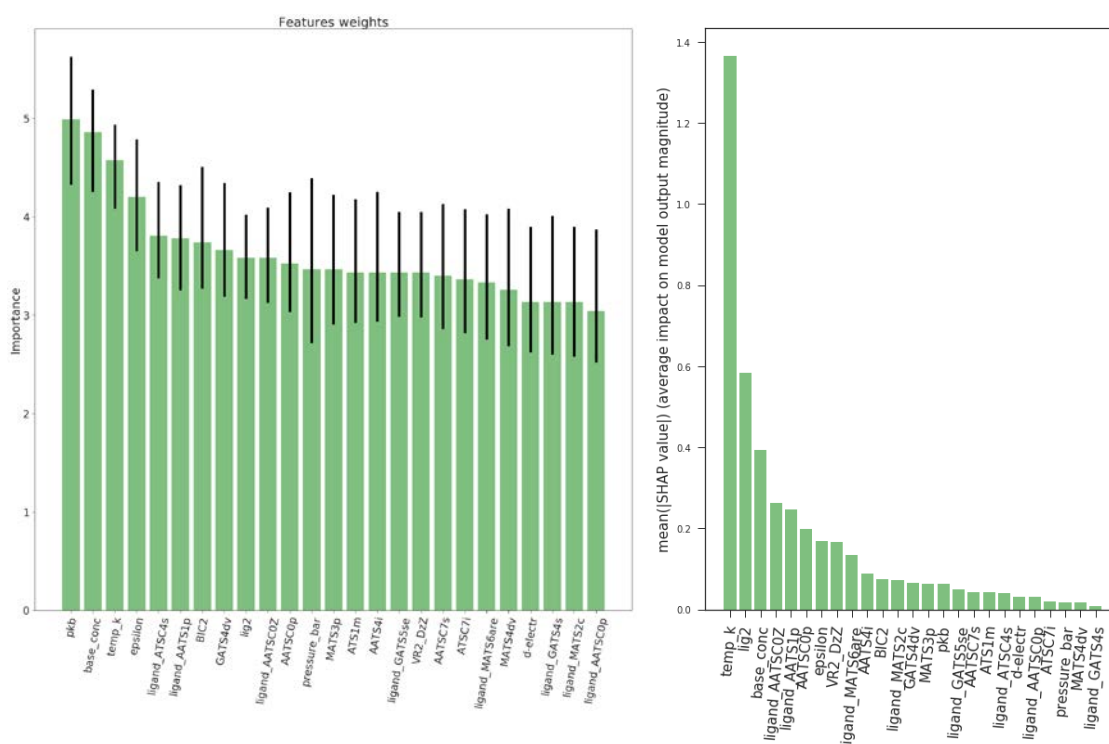


**Figure 1.** Left: logarithmic importance (decision tree weights) of the descriptors in the model using TOF as a reaction efficiency metric; right: mean SHAP value impact.

## References

- [1] Filonenko, Pidko et al. *Chem. Soc. Rev.*, 2018, **47**, 1459.
- [2] Vogiatzis, Pidko et al. *Chem. Rev.*, Article ASAP, DOI: 10.1021/acs.chemrev.8b00361.
- [3] Pidko, Nachtigall et al. *Chem. Soc. Rev.*, 2018, **47**, 8307.
- [4] <https://github.com/Microsoft/LightGBM>.
- [5] Moriwaki et al. *J. Cheminform.*, 2018, **10:4**.
- [6] Pidko et al. *ChemCatChem*, 2014, **6**, 1526; Pidko et al. *ACS Catal.*, 2015, **5**, 1145.

## Promotional effect of ceria on the activity of $\text{Co}_3\text{O}_4/\gamma\text{-Al}_2\text{O}_3$ catalyst in $\text{deN}_2\text{O}$ reaction

*K. Ciura<sup>1</sup>, G. Grzybek<sup>1</sup>, A. Davó-Quiñonero<sup>2</sup>, A. Bueno-Lopez<sup>2</sup>, A. Kotarba<sup>1</sup>*

*<sup>1</sup>Faculty of Chemistry, Jagiellonian University, Krakow, Poland*

*<sup>2</sup>Department of Inorganic Chemistry, University of Alicante, Alicante, Spain*

$\text{N}_2\text{O}$  is one of the most harmful greenhouse gases with a temperature of thermal decomposition above  $650^\circ\text{C}$  and global warming potential 310 times higher than for  $\text{CO}_2$ . [1] Hence, the important challenge in environmental catalysis is to design a catalytic system for  $\text{N}_2\text{O}$  removal from the nitric acid plants, where low temperature, low  $\text{N}_2\text{O}$  concentration and presence of inhibitors limit the catalyst efficiency. So far, various materials (noble metals, metal oxides, zeolites) have been investigated as active phases in  $\text{deN}_2\text{O}$  reaction, whereas cobalt spinel was found to be the most active. However, due to the high cost of cobalt as well as difficulty in spinel formation into the form of extrudes practical application of bare  $\text{Co}_3\text{O}_4$  is highly limited. In order to reduce the catalyst cost, the active phase can be spread over supports [2]. In our previous papers [2] we have presented that the cobalt spinel nanocrystallites can be successfully supported over  $\text{Al}_2\text{O}_3$ , assuring catalyst durability in terms of thermal and mechanical properties. On the other hand, a positive impact of ceria (as a support or additive) on catalytic activity of  $\text{Co}_3\text{O}_4$  in  $\text{deN}_2\text{O}$  reaction has been shown [1]. The aim of this study was to check the possibility of improving the catalytic performance by promotion the alumina support with ceria.

The active phase (10% wt. $\text{Co}_3\text{O}_4$ ) was dispersed on ceria,  $\gamma$ -alumina (Puralox SCFa-230, Sasol Germany GmbH) and the ceria-alumina mixed phase ( $\text{CeAlO}_3$ ) using an incipient wetness impregnation with a  $\text{Co}(\text{NO}_3)_2 \cdot \text{H}_2\text{O}$  aqueous solution, next the samples were dried and calcined. The new support  $\text{CeAlO}_3$  was prepared by impregnation of  $\gamma$ -alumina (Puralox) with an aqueous cerium nitrate solution. Then dried and heated at temperature  $1100^\circ\text{C}$  in a hydrogen flow [3]. The synthesized samples were characterized with respect to chemical composition (XRF), structure (XRD, Raman Spectroscopy). The impact of the applied support on the catalytic performance was examined in  $\text{deN}_2\text{O}$  reaction (model gas mixture - 5%  $\text{N}_2\text{O}/\text{He}$ ) in TPSR mode. The results are shown in Figure 1, where the experimental data are

expressed as N<sub>2</sub>O conversion versus temperature. The catalyst supported on ceria carrier exhibits higher activity in comparison to that supported over alumina. However, the positive effect of Ce-promotion can be also easily noticed: the Co<sub>3</sub>O<sub>4</sub> over CeAlO<sub>3</sub> support exhibits higher activity than the one over bare Al<sub>2</sub>O<sub>3</sub>.

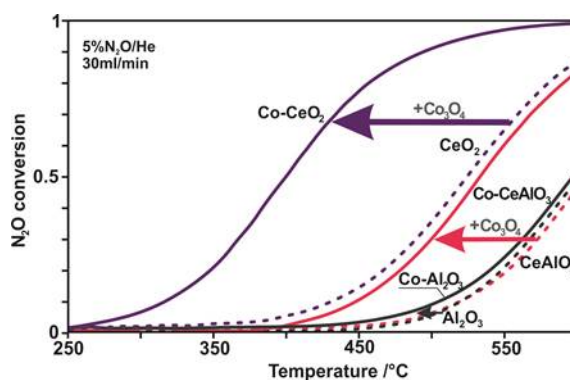


Figure 1. The effect of support on the deN<sub>2</sub>O catalytic activity of cobalt spinel (bare supports (- -) and Co<sub>3</sub>O<sub>4</sub>|support catalysts (-)).

As explained in our previous work [1], the N<sub>2</sub>O decomposition over Co<sub>3</sub>O<sub>4</sub>|CeO<sub>2</sub> goes with a two-step mechanism, where the redox properties of the Co<sub>3</sub>O<sub>4</sub> is responsible for the dissociation of N<sub>2</sub>O molecules and formation of surface oxygen intermediates, whereas the ceria periphery is responsible for the enhanced diffusion and recombination of oxygen adspecies, closing the catalytic cycle. The modification of alumina by ceria improves the catalytic activity of Co<sub>3</sub>O<sub>4</sub>|Al<sub>2</sub>O<sub>3</sub> catalyst probably by promoting the second mechanistic step (oxygen recombination).

Further optimization of the proposed catalytic system is in progress (e.g. catalytic test with a presence of NO and H<sub>2</sub>O inhibitors). However, the obtained results clearly show that the introduction of Ce into alumina can stimulate its redox character while preserving the mechanical stability, which can enhance the application of the developed catalyst in N<sub>2</sub>O removal.

#### Acknowledgement

Klaudia Ciura would like to acknowledge the Erasmus+ for internship at University of Alicante.

#### References

- [1] G. Grzybek et. al., Appl. Catal. B Environ., 180 (2016), 622-629.
- [2] G. Grzybek et. al., Catal. Sci. Technol., 7 (2017), 5723-5732.
- [3] M.A. Malecka et. al., Cryst. Eng. Comm., 17 (2015), 2273-2278.

# **Silver-Zirconia Catalyst for Diesel Soot Oxidation: from the Lab Study to Engine Test**

*L. Nossova<sup>1</sup>, G. Caravaggio<sup>1</sup>, B. Rubel<sup>2</sup>, D. Young<sup>2</sup>*

*<sup>1</sup>Natural Resources Canada, CanmetENERGY-Ottawa, Ottawa, Canada*

*<sup>2</sup>Natural Resources Canada, CanmetMINING-Ottawa, Ottawa, Canada*

A major concern with diesel vehicles is the emission of particulate matter (PM) into the atmosphere, which affects human health and contributes to climate change [1]. Diesel particulate filters (DPF) are currently the most effective aftertreatment devices for controlling PM/soot emissions from diesel engines. Catalyzed DPFs combine filtering with continuous catalytic oxidation of soot particles. In commercial systems, Pt is the most widely applied catalyst. Due to its high cost and high sensitivity to sulfur, its replacement by a cheaper active phase is very desirable.

In this study, the catalyst formulation comprising silver supported on tetragonal zirconia was developed, thoroughly characterized and optimized. The catalyst performance for soot oxidation was initially evaluated by temperature-programmed oxidation in a flow reactor using simulated diesel exhaust conditions and carbon black as a model soot. These reactor studies revealed a high activity of the developed catalyst for elimination of soot particles in the temperature range typical of diesel exhaust (200-500°C) and in the presence of oxygen, water and nitrogen oxide [2]. However, due to reactor testing limitations, engine evaluation was required to further assess the catalyst activity under real engine exhaust conditions.

The next step of this work involved scaling up of the silver-zirconia catalyst and coating of a commercial 12.5 L wall-flow ceramic filter with the catalytic phase to produce a prototype catalyzed diesel particulate filter (CanmetENERGY p-CDPF). The performance of the manufactured p-CDPF was evaluated using a Detroit Diesel heavy-duty mining engine (6063-WK32, 11.1 L, Series 60) with ultra-low S mining diesel fuel. The Balance Point Temperature (BPT) was determined in order to assess the catalyst ability to regenerate the filter passively. The BPT represents the temperature at which the soot accumulation rate is approximately equal to the oxidation rate. Thus, a lower BPT exhibits better regeneration function of the catalyst during engine operation.

A test procedure to determine the BPT was developed based on a progressive load test in accordance with the program [3]. The procedure involved pre-loading the filter with soot to a predetermined level. Then a stepwise increase of the filter's inlet temperature was undertaken by increasing the engine load that was accompanied by recording the filter pressure drop. The temperature at which the pressure drop decreased was determined as the filter BPT. For comparison, an engine test of a commercial reference CDPF (Cattrap, CDTi Advanced Materials Inc.) was carried out under the same testing conditions.

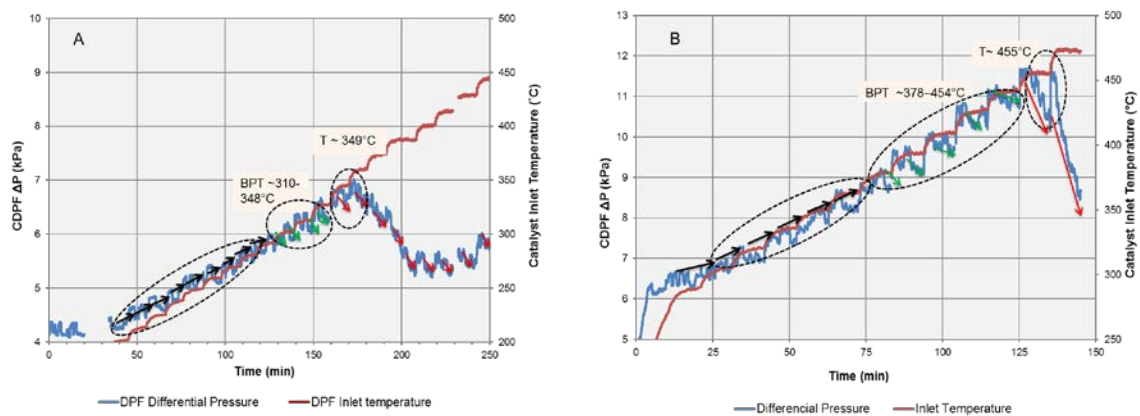


Figure 1. Engine test results: A - CanmetENERGY p-CDPF, B - "Cattrap" CDPF

Both CDPFs showed a capacity to regenerate diesel particulate matter under the chosen engine operation conditions. The BPT of the CanmetENERGY p-CDPF was in the range from 310 to 348°C (Figure 1A). In comparison, the BPT of the commercial CDPF "Cattrap" was in the range from 378 to 454°C (Figure 1B). The significantly lower BPT of the CanmetENERGY p-CDPF shows its higher passive soot oxidation ability than that of the commercial one.

Overall, the engine test results agreed with the reactor test results confirming that the CanmetENERGY p-CDPF coated with a new less expensive silver-based catalyst offers low temperature oxidation of collected particulate matter. Thus providing continuous passive regeneration of the filter at normal engine operating conditions. A lowering of the BPT allows avoiding active regeneration or decreasing the number of such cycles that reduce the use of fuel as well as CO<sub>2</sub> emissions.

## References

1. U.S. Environmental Protection Agency. Report to Congress on Black Carbon (2010).
2. L. Nossova, G. Caravaggio, M. Couillard, S. Ntais, Appl. Catal. B 225 (2018) 538-549.
3. Diesel Emissions Control Sulfur Effects (DECSE) Program, Phase 1, Interim Report 1, US Department of Energy, Washington DC, August 1999.

# Catalytic performance of Ni-CeO<sub>2</sub>/Ca-ZrO<sub>2</sub> catalysts in the aqueous-phase reforming of methanol

D. Goma<sup>1,2</sup>, J.J. Delgado<sup>1,2</sup>, M.A. Cauqui<sup>1,2</sup>, J. Faria<sup>3</sup>, L. Lefferts<sup>3</sup>

<sup>1</sup> Departamento de Ciencia de los Materiales e Ingeniería Metalúrgica y Química Inorgánica. Universidad de Cádiz, Puerto Real (Cádiz). España.

<sup>2</sup> IMEYMAT, Instituto de Microscopía Electrónica y Materiales. Universidad de Cádiz.

<sup>3</sup> Catalytic Processes and Materials. Mesa + Institute for Nanotechnology. University of Twente. Enschede. The Netherlands.

## Introduction

The aqueous phase reforming (APR) constitutes a promising technology for obtaining hydrogen from oxygenated hydrocarbons present in wastewaters derived from biorefineries. Nobel metals, mainly Pt, have been used as efficient catalysts for this reaction. Also nickel catalysts have been proposed as a less expensive alternative, although some improvements are still necessary to make them competitive with Pt-based systems. The addition of promoters and/or the correct choice of the support are interesting strategies to achieve this goal [1,2]. In this work we investigate a Ni-CeO<sub>2</sub>/Ca-ZrO<sub>2</sub> catalyst for the aqueous-phase reforming of methanol. The effect of the well-known redox properties of ceria in combination with the basicity of calcium and the occurrence of metal-support interactions on the catalyst performance have been specially addressed.

## Experimental

A series of Ca<sub>n</sub>ZrO<sub>2-n</sub> (n=0, 4, 14%-mol, named as Zr, 4CSZ and 14CSZ) oxides were prepared by hydrothermal method (200°C, 24 hours) starting from the corresponding Zr and Ca nitrate precursors. After calcination at 600°C, Ce (12% wt) and (6% wt) Ni were incorporated sequentially by impregnation with nitrate solutions. Finally, the samples were dried, crushed, sieved and calcined in a muffle oven at 500°C. Prior to catalytic activity measurements, they were reduced in inert diluted H<sub>2</sub> at 750°C. A set of techniques such as N<sub>2</sub> and H<sub>2</sub> volumetric adsorption, ICP-AES, DRX, TPR-H<sub>2</sub>, TPD-CO<sub>2</sub>, XPS, HR-TEM, HAADF, EDX were used for the characterization of the catalysts. Aqueous-phase reforming tests were performed in continuous-flow fixed reactor using 5%-wt. methanol in water as a feed. Reactions

Kommentar [jfa1]: Is this TPD?



were carried out at 230°C and 32 bar with a total flow of 0.338 ml/min (without inert gas dilution) and using 250 mg of catalyst (WSHV=4h<sup>-1</sup>). Gaseous and liquids products were separated and analysed by means of a micro-gas chromatograph (GC, Varian CP4900, equipped with MS5 and PPQ columns) and by performing HPLC (RID-10A detector, Aminex HPX-87H column 300x7.8mm), respectively.

## Results and discussion

X-Ray Diffraction results revealed the stabilization of the cubic/tetragonal structure of ZrO<sub>2</sub> in the case of Ca-containing supports. Small peaks corresponding to cubic NiO and CeO<sub>2</sub> fluorite were also observed. Table 1 gathers the properties and catalytic behavior of the catalysts. Only unreacted methanol was detected in the analysis of the liquid at the reactor outlet. H<sub>2</sub>, CO<sub>2</sub> and traces of CO and CH<sub>4</sub> were the only products detected in the gas phase. As it can be seen, the incorporation of Ce does not improve the Ni/Zr (or Ni/xCSZ) activity in terms of methanol conversion. However, a slight increase in H<sub>2</sub> selectivity is observed in Ce-promoted catalysts. The addition of Ca (4%) has a significant effect on the conversion values. Increasing the Ca content from 4% to 14% does not have a beneficial consequence regarding conversion or H<sub>2</sub> selectivity results. A correlation between the characteristics and properties of the samples (metal dispersion, support structure, basicity and redox properties) and the catalysts behavior will be discussed.

Sample	BET (m <sup>2</sup> g <sup>-1</sup> )	Metal surface (m <sup>2</sup> g <sup>-1</sup> )	Methanol conv. (%)*	Selectivity (%)			
				H <sub>2</sub>	CO <sub>2</sub>	CO	CH <sub>4</sub>
Ni/Zr	30	1.75	48	72.9	20.2	4.6	2.2
NiCe/Zr	30	1.63	40	76.8	20.5	1.8	0.9
Ni/4CSZ	48	2.10	75	73.9	23.9	0.2	2.1
NiCe/4CSZ	47	2.06	67	73.8	23.4	0.6	2.2
Ni/14CSZ	54	1.23	63	73.8	23.7	0.5	2.1
NiCe/14CSZ	67	1.41	44	75.7	21.6	1.9	0.9

**Table 1:** Characteristics of the samples and catalytic behavior in APR of methanol (methanol conversion was measured after 5-hours reforming\*).

## References

- [1] R.R. Davda, J.W. Shabaker, G.W. Huber, R.D. Cortright, J.A. Dumesic, *Appl. Catal. B Environ.* 56 (2005) 171–186.
- [2] M. Stekrova, A. Rinta-Paavola, R. Karinen, *Catal. Today* (2017) 0–1.

## Acknowledgements

Financial support obtained from Ministerio de Economía y Competitividad (Project Reference MAT2013-40823-R) is gratefully acknowledged.

**Kommentar [jfa2]:** This is in terms of conversion, but in terms of selectivity this catalyst makes more CH<sub>4</sub>.

Also, this catalyst has a higher surface area of metallic Nickel, so it might be actually equally or less active, and less selective. (For example, Ni/4CSZ 0.75/2.1=0.35 and for Ni/14CSZ 0.63/1.23=0.51). I know that these levels of conversion are rather high to make TOF calculations, but the statement that you are posting in regard to the performance could be misleading in its present form.

# **BaMn<sub>0.7</sub>Cu<sub>0.3</sub>O<sub>3</sub> catalysts for NO<sub>x</sub>-assisted diesel soot oxidation: effect of using a hard template during the sol-gel synthesis method**

*Verónica Torregrosa-Rivero, Vicente Albaladejo-Fuentes, María-Salvadora Sánchez-Adsuar, María-José Illán-Gómez, Carbon Materials and Environment Research Group, University of Alicante, Alicante, Spain*

In a previous study the BaMnO<sub>3</sub> mixed oxide and the corresponding materials doped with copper (BaMn<sub>0.7</sub>Cu<sub>0.3</sub>O<sub>3</sub>) were tested for the NO<sub>2</sub>-assisted diesel soot oxidation. The results showed that the best catalytic performance was featured by the copper content catalyst due to the high amount of oxygen vacancies generated by the presence of Mn (III) and Cu (II) in the perovskite structure [1]. Other option to improve the catalytic performance is using hard or soft templates during the sol-gel synthesis method [2]. Thus, in a previous work [3], the BaMnO<sub>3</sub> was synthesized by adding a mesoporous silica (SBA-15) or a carbon black (VULCAN XC72-R) as hard templates to the sol obtained during the sol-gel synthesis [1]. The strong interaction between barium and silica hinders the formation of the perovskite as major phase, but the carbon black allows reducing the calcination temperature to get the perovskite structure and, consequently, increases the oxygen mobility, enhances the reducibility and improves the catalytic activity [3].

## **Results and discussion**

A series of BaMn<sub>0.7</sub>Cu<sub>0.3</sub>O<sub>3</sub> (BMC3) catalysts have been synthesized through a modified sol-gel method in which carbon black (C) has been added as hard template and different calcination temperatures have been employed. The catalysts have been designated as BMC3-CX, where X indicates the calcination temperature. The reference catalysts (BMC3 for BaMn<sub>0.7</sub>Cu<sub>0.3</sub>O<sub>3</sub> and BMC0 for BaMnO<sub>3</sub>) were synthesized using the sol-gel method but without the addition of the hard template. The catalysts characterization was performed by ICP-OES, N<sub>2</sub> adsorption, XRD, XPS, O<sub>2</sub>-TPD and H<sub>2</sub>-TPR. The activity for NO oxidation to NO<sub>2</sub> and for NO<sub>2</sub>-assisted diesel soot oxidation has been tested by Temperature Programmed Reaction (TPR).

Figure 1 shows the XRD profiles for the synthesized BMC3-CX catalysts and for the corresponding reference catalysts (BMC0 and BMC3). The presence of carbon black hinders the formation of the new perovskite-like structure (politype) showed for BMC3

[1]. At 700°C the new structure begins to form, so, the catalysts obtained using a higher calcination temperature show both phases ( $\text{BaMnO}_3$  2H-hexagonal and the polytype). The Mn(IV)/Mn(III) XPS ratio decreases with the calcination temperature, therefore the electroneutrality after the copper incorporation seems to be achieved by the generation of oxygen vacancies.

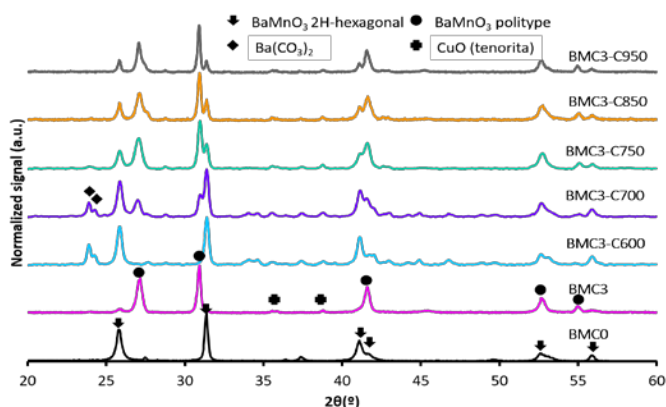


Figure 1. XRD patterns of the BMC3-CX catalysts and the references BMC3 and BMC0

The  $O_{\text{lattice}}/(\text{Ba}+\text{Mn}+\text{Cu})$  XPS ratio, which is lower than the nominal one, and lower than that observed for BMC3, confirms this hypothesis.

The TPR soot conversion profiles reveal that all the catalysts are active since the

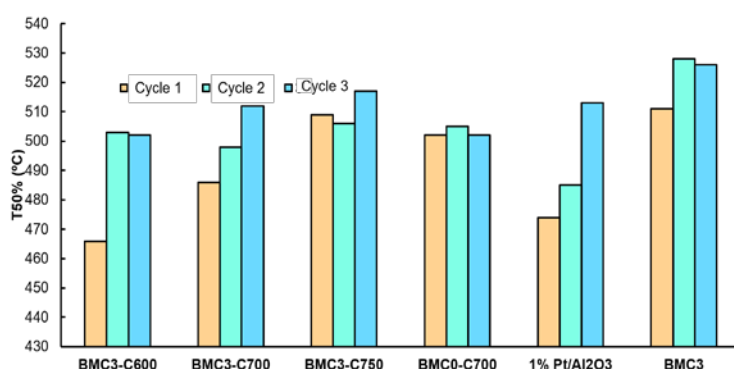


Figure 2. T50% values for cyclic TPR experiments

temperature required to reach the 50% of soot conversion (T50%) is lower than the corresponding to a blank experiment (without catalyst). Figure 2 shows the T50% values for successive TPR cycles for: BMC3-CX catalysts,

BMC3, BMC0-C700 (which is the best catalyst from the series BMC0-CX [3]) and for standard 1%Pt/Al<sub>2</sub>O<sub>3</sub> catalyst. Based on the 2<sup>nd</sup> and 3<sup>rd</sup> TPR cycles (where stability seems to be achieved) BMC3-C600 shows the lowest T50% among the BMC3-CX catalysts, which is similar to that of BMC0-C700. Note that the former catalyst presents  $\text{BaMnO}_3$  2H-hexagonal structure as unique perovskite phase (Figure 1), so, it seems that the mixture of perovskite phases decreases the catalysts activity.

**Acknowledgements.** The authors thank Spanish Government, UE and Generalitat Valenciana (MINECO project CTQ2015-64801-R, FEDER Funding and Prometeo 2018/076) for the financial support. Verónica Torregrosa-Rivero thanks the Generalitat Valenciana for her Ph.D. grant (ACIF 2017/221)

#### References

- [1] V. Torregrosa-Rivero, V. Albaladejo-Fuentes, M.S. Sánchez-Adsuar, M.J. Ilán-Gómez, RSC Adv. 56 (2017) 35228-35238
- [2] M. Bonne, D. Sellam, J.P. Dacquin, A.F. Lee, K. Wilson, L. Olivi, A. Cognigni, P. Marécot, S. Royer, D. Duprez, Chem. Commun. 47 (2011) 1509–1511
- [3] V. Torregrosa-Rivero, V. Albaladejo-Fuentes, M.S. Sánchez-Adsuar, M.J. Ilán-Gómez, Optimización de catalizadores DPF basados en  $\text{BaMnO}_3$  mediante el uso de plantillas sólidas, XXVI CICAT LIVRO DE ATAS (2018), 169-174, ISBN: 978-989-8124-23-4

# Reaction mechanism of direct NO decomposition over K-promoted Co-Mn-Al mixed oxides

*Bílková, T., Pacultová, K., Fridrichová, D., Obalová, L., Institute of Environmental Technology, VŠB-Technical University of Ostrava, 17. listopadu 15, 708 33 Ostrava, Czech Republic; Haneda, M., Advanced Ceramics Research Center, Nagoya Institute of Technology, 10-6-29 Asahagioka, Tajimi, Gifu 507-0071, Japan.*

## Introduction

Nitric oxide (NO) belongs to a group of oxides known as NO<sub>x</sub> (NO, NO<sub>2</sub>). Direct NO decomposition was tested using many types of catalysts (noble metals, oxides, zeolites) and different reaction mechanisms have been described by several authors [1].

During our previous studies was found out that K-promoted Co-Mn-Al mixed oxides are suitable for direct NO decomposition unlike non-promoted mixed oxides are inactive [2]. In the present article, the aim was to evaluate a possible reaction mechanism through transient state experiments of NO catalytic decomposition in inert gas over K-promoted Co-Mn-Al mixed oxide.

## Experimental/ methodology

K/Co<sub>4</sub>MnAlO<sub>x</sub> mixed oxides were prepared by co-precipitation of corresponding nitrates. Bulk promotion method was used for 0.5-3.1 wt. % potassium incorporation. Samples were calcined in two steps (i) at 500 °C for 12 h and (ii) at 650 °C in-situ at the beginning of the reaction.

Isotopic transient kinetic analysis was performed by switching the flowing gas from 1000 ppm <sup>14</sup>NO to 1000 ppm <sup>15</sup>NO diluted in He at 650 °C. The effluent gas was continuously monitored by a quadrupole mass spectrometer for all the isotopic molecules of NO, N<sub>2</sub> and N<sub>2</sub>O.

The diffuse reflectance FT-IR spectra were recorded during catalytic reaction. The reaction gas contained 1000 ppm NO in He; the flow of 30 ml/min for 20 min followed by purging in He (30 min) and cooling to lower temperature was applied to the 80 mg of catalyst.

The TPD-NO and step response experiments were performed on Autochem II 2920 and the effluent gas was continuously monitored by a quadrupole mass spectrometer for NO, N<sub>2</sub>, O<sub>2</sub> and Ar.

## Results and discussion

The adsorbed surface ionic nitrogen species ( $\text{NO}_2^-$ ,  $\text{NO}_3^-$ ,  $1288\text{-}1482\text{ cm}^{-1}$ ) formed during NO decomposition over K-promoted  $\text{Co}_4\text{MnAlO}_x$  especially at lower temperatures indicating low thermal stability of  $\text{NO}_x$  adspecies at  $> 600^\circ\text{C}$  (Fig. 1).

TPD-NO measurements showed that the amount of NO adsorbed on the catalyst surface differs according to the potassium amount (Fig. 2) and confirmed the presence of several  $\text{NO}_x$  and/or oxygen species on the surface after reaction.

The results from transient kinetic analysis (Fig. 3.) suggested that the surface adsorbed species can act as intermediates in NO decomposition (Langmuir-Hinshelwood mechanism). However, formation of mixed labeled  $\text{N}_2$  ( $^{14}\text{N}^{15}\text{N}$ ) proceeded in only very small amount and for that reason the possibility of Eley-Rideal mechanism should be also taken into account.

## References

- [1] Haneda, M., Hamada, H.: *C. R. Chim.* 19 (10), 2016, 1254-1265.
- [2] Pacultová, K. and col.: *Mol. Catal.* 428, 2017, 33-40.

## Acknowledgement

The work was supported from ERDF "Institute of Environmental Technology – Excellent Research" (No. CZ.02.1.01/0.0/0.0/15\_019/0000853), Czech Science Foundation (project No. 18-19519S) and by VŠB-TU student project No. SP2019-91.

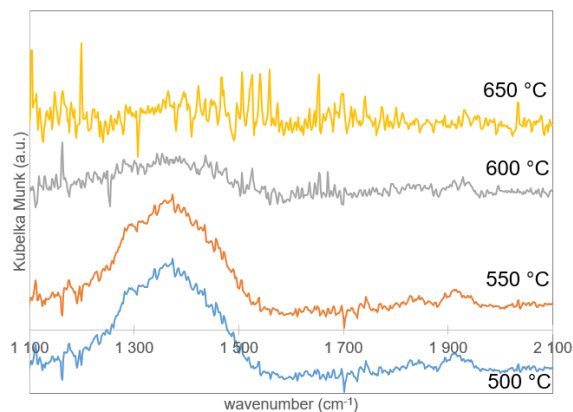


**Fig. 1:** Diffuse reflectance FT-IR spectra recorded for 2 wt.%K/ $\text{Co}_4\text{MnAlO}_x$  at 500-650 °C.

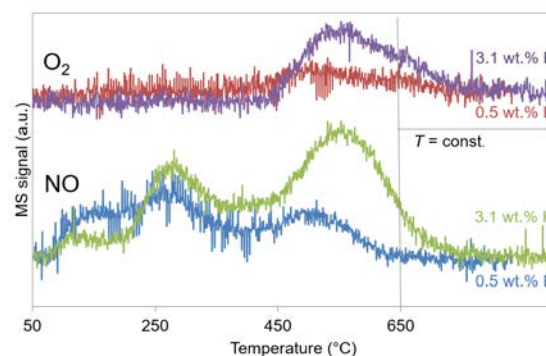


**Fig. 2:** TPD profiles of NO and  $\text{O}_2$  followed NO adsorption on 0.5 wt.% K/ $\text{Co}_4\text{MnAlO}_x$  and 3.1 wt.% K/ $\text{Co}_4\text{MnAlO}_x$ .

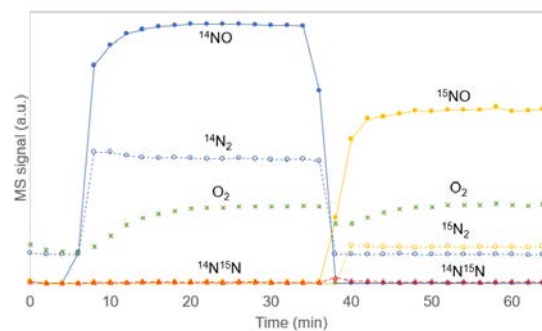


**Fig. 3:** Product responses following the replacement of  $^{14}\text{NO}/\text{He}$  with  $^{15}\text{NO}/\text{He}$  in the reaction stream at  $650^\circ\text{C}$ .

# Pd and Pd-Ce metallozeolites for environmental reactions of removal of CH<sub>4</sub>/NO

*Aneta Krasowska, Janusz Janas, Kinga Góra-Marek, Zbigniew Sojka, Piotr Pietrzyk, Jagiellonian University, Faculty of Chemistry, Gronostajowa 2, 30-387 Krakow, Poland*

## Introduction

Palladium-containing zeolites or bimetallic palladium zeolites are known to activate methane molecules and other diatomic gas-phase molecules of environmental importance (CO, NO). In this study we examined redox properties of Pd and Ce sites inside ZSM-5 and Y matrices and their interaction with NO/CH<sub>4</sub> in the context of selective catalytic reduction of NO.

## Experimental

Metal-exchanged zeolites (Y, SiO<sub>2</sub>/Al<sub>2</sub>O<sub>3</sub> = 5.1; ZSM-5, SiO<sub>2</sub>/Al<sub>2</sub>O<sub>3</sub> = 20) were obtained via subsequent ionic exchange in aqueous solutions. Initially obtained Pd-zeolites were reduced in H<sub>2</sub> in order to recover sorption capacity of the zeolite matrices, and then ionic exchange with Ce(NO<sub>3</sub>)<sub>3</sub> was carried out. XRF analysis was used for determination of chemical composition of the materials. Formation and identification of Pd nanocrystals in the activated/reduced materials was followed with TEM measurements. In situ adsorption experiment were carried out by means of EPR and FTIR measurements. Temperature-programmed reactions (TPSR) with of NO, O<sub>2</sub>, CH<sub>4</sub> mixtures in He as a gas carrier were monitored with QMS spectrometer.

## Results

Owing to its electronic properties, NO molecule ( $\pi^{*1}$ ) can be studied by means of EPR spectroscopy. In fact, EPR is sensitive both to the gas-phase reactant as well as to the palladium active sites (Pd(III), 4d<sup>7</sup> and Pd(I), 4d<sup>9</sup>), whose valence state is decisive for the spectral parameters or lack of X-band EPR signal (4d<sup>8</sup> electron configuration, Pd(II)). It was found that palladium in Y and ZSM-5 zeolites exhibited versatile redox chemistry depending on the treatment of the samples. All possible valence states were identified (Pd(III), Pd(II), Pd(I), Pd(0)). When activated in O<sub>2</sub>, isotropic EPR signal showed formation of Pd(III) cations ( $g_{iso} = 2.23$ ), while reduction in H<sub>2</sub> led to a more complicated, multicomponent signal ( $g_{||} \approx 2.90 - 2.74$  and  $g_{\perp} \approx$

2.13 – 2.11), characteristic of Pd(I) [1]. Apart from Pd(I), reduction in H<sub>2</sub> led to the formation of metallic Pd species of nanometer size (average size of 5 nm) detected and identified with TEM and EELS analysis.

The presence of all implicated valence states of Pd were confirmed with FTIR of adsorbed CO. The characteristic bands for CO interacting with Pd<sup>3+</sup> in Y zeolite (2210 cm<sup>-1</sup>) and Pd<sup>2+</sup> in Y and ZSM-5 (2192 cm<sup>-1</sup>), Pd<sup>+</sup> in Y and ZSM-5 (2160, 2140, 2134, 2120 cm<sup>-1</sup>), metallic Pd (below 2000 cm<sup>-1</sup>) were observed.

Formation of surface adducts with NO was investigated with EPR and IR techniques. For oxidized and reduced samples characteristic EPR signal with hyperfine structure was observed. It originated from the coupling with magnetic moment of nucleus <sup>105</sup>Pd (22.3%, *I* = 5/2). In addition, in the case of interaction with Pd(I), the superhyperfine structure could be observed, which was assigned to two nuclei of nitrogen (<sup>14</sup>N, *I* = 1) coming from dinitrosyl species Pd<sup>+</sup>(NO)<sub>2</sub>. While in the case of Pd(I) they were formed by simple addition reaction 2Pd + 2NO = 2{Pd<sup>+</sup>(NO)<sub>2</sub>}, for the oxidized centers reactive adsorption was observed, which led first to a reduction of Pd<sup>3+</sup> to Pd<sup>2+</sup> and Pd<sup>+</sup>, and subsequent formation of the paramagnetic mono- Pd<sup>2+</sup>NO and dinitrosyls Pd<sup>+</sup>(NO)<sub>2</sub>. The conclusions obtained from magnetic resonance was supported by corresponding FTIR measurements. Both diamagnetic and paramagnetic forms were detected, including mononitrosyls Pd<sup>2+</sup>NO at 1874 (Y) and 1800 cm<sup>-1</sup> (ZSM-5) as well as dinitrosyls at 1830 and 1815 cm<sup>-1</sup> (asymmetric and symmetric bands, respectively) in both, Y and ZSM-5, matrices [2].

TPSR profiles recorded for H<sub>2</sub>-reduced catalysts PdY (Pd nanoparticles as major active phase) showed that onset of CH<sub>4</sub> oxidation in O<sub>2</sub> was already located below 300°C, while decomposition of NO alone produced N<sub>2</sub> and N<sub>2</sub>O only above 300°C. Reactions with NO+CH<sub>4</sub> and NO+CH<sub>4</sub>+O<sub>2</sub> showed that NO reduction competed with CH<sub>4</sub> oxidation and the temperature windows for both these processes diverge. This apparent misfit of the temperature windows could be diminished by introducing cerium components which helped in binding nitrogen oxide forming surface nitrates.

## References

[1] L.S. Stokes, D.M. Murphy, R.D. Farley, C.C. Rowlands, S. Bailey, *Phys. Chem. Chem. Phys.*, **1999**, *1*, 621.

[2] C. Descorme, P. Gelin, M. Primet, Ch. Lecuyer, *Catal. Lett.*, **1996**, *41*, 133.

# ***How to study the influence of support oxygen for oxidation reactions?***

*Helena Kaper, Pierre-Alexis Répécaud, Daniel Aubert, Ceramic Synthesis and Functionalization Laboratory, Cavaillon, France;*

*Werner Paulus, Bartosz Penkala, Monica Ceretti, Institut Charles Gerhardt, University of Montpellier, Place Eugène Bataillon, 34095 Montpellier, France*

## **Introduction**

Perovskites and related materials represent a promising class of catalysts and catalyst supports for oxidation reactions.[1] In the case of a Mars-van Krevelen (MvK) mechanism, lattice oxygen from the support participates to the reaction. Detailed studies on the role of the support usually include the work with  $^{18}\text{O}$  or  $\text{C}^{18}\text{O}$ , as in a Steady-State Isotopic Transient Kinetic Analysis (SSITKA) experiment. Here, we present an alternative way to known isotopic studies, combining an  $^{18}\text{O}$  exchange in the materials followed by a catalytic reaction using pulses of  $\text{O}_2$  onto a continuous flow of CO (see figure 1a), recently named isotope labeling pulse temperature programmed oxidation reaction (ILPOR).[2]

## **Experimental**

All experiments were carried out in an automated catalyst characterization system (AutoChem II 2920) coupled with a quadrupole mass spectrometer (QMS) (ThermoStar TM GSD301T, Pfeiffer Vacuum). 100 mg of an  $^{18}\text{O}$ -enriched sample was loaded into a U-shaped Quartz reactor. The sample was heated (2K/min) under 1%  $\text{C}^{16}\text{O}$  to 500°C. Onto this, pulses of  $^{16}\text{O}_2$  were injected every 60 s.

## **Results and Discussion**

We study three catalyst supports, ceria as well-known catalyst support (results not shown here) and two Brownmillerites ( $\text{CaFeO}_{2.5}$  and  $\text{SrFeO}_x$ ), recently studied for their oxygen mobility[3] and CO oxidation capability.[2] Indeed,  $\text{CaFeO}_{2.5}$  is known as stable line phase, showing oxygen mobility at higher temperature than  $\text{SrFeO}_x$ , known as support with facilitated oxygen mobility. Looking at the ILPOR results, in the case of  $\text{CaFeO}_{2.5}$ , only  $\text{C}^{16}\text{O}^{16}\text{O}$  is produced at low temperature (figure 1b).



Therefore, lattice oxygen does not participate in the reaction at low temperature. At elevated temperature, also  $C^{18}O^{16}O$  and  $C^{18}O^{18}O$  are found as products, demonstrating the participation of lattice oxygen. In contrast, using  $SrFeO_x$  as support (figure 1C),  $C^{16}O^{18}O$  and to a minor extent also  $C^{18}O^{18}O$  are produced next to  $C^{16}O^{16}O$  as soon as the reaction takes place. In this case, lattice oxygen participates in the reaction from the beginning.

In order to exclude side reactions such as surface exchange of CO or the produced  $CO_2$  with  $^{18}O$ , additional studies on the surface exchange of CO and  $CO_2$  were done. The results confirm that ILPOR can be used as powerful technique to study the role of lattice oxygen in oxidation reactions.

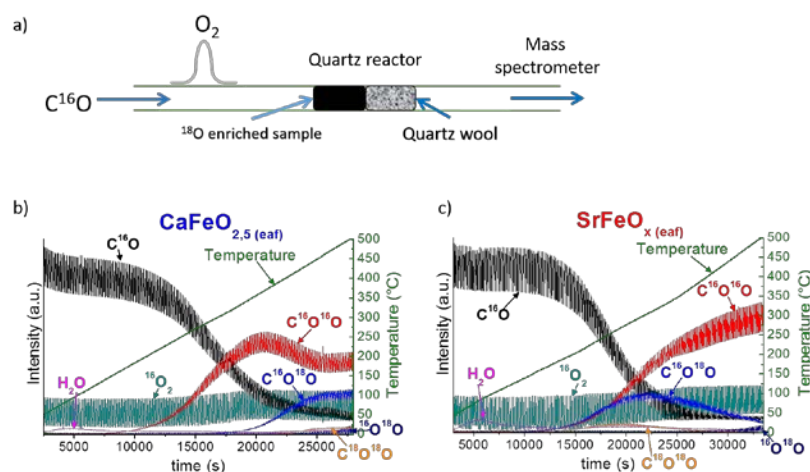


**Fig. 1.** Figure 1: a) experimental setup of the ILPOR experiment. b) ILPOR results for  $CaFeO_{2.5}$  and b)  $SrFeO_{2.5}$ .

## Conclusion

We present a novel analytical method to determine lattice oxygen

participation in oxidation reactions, based on  $^{18}O$ -enriched samples that are used for CO oxidation under dynamic conditions. The results correlate to the oxygen mobility of the pure support material. This approach allows distinguishing between bulk lattice participation and surface implication.

## References

- [1] S. Royer, D. Duprez, F. Can, X. Courtois, C. Batiot-Dupeyrat, S. Laassiri, H. Alamdari, Perovskites as Substitutes of Noble Metals for Heterogeneous Catalysis : Dream or Reality, *Chem. Rev.* 114 (2014) 10292–10368. doi:10.1021/cr500032a.
- [2] B. Penkala, D. Aubert, H. Kaper, C. Tardivat, K. Conder, W. Paulus, The role of lattice oxygen in CO oxidation over  $Ce^{18}O_2$ -based catalysts revealed under operando conditions, *Catal. Sci. Technol.* 5 (2015) 4839–4848. doi:10.1039/C5CY00842E.
- [3] W. Paulus, H. Schober, S. Eibl, M. Johnson, T. Berthier, O. Hernandez, M. Ceretti, M. Plazenet, K. Conder, C. Lamberti, Lattice dynamics to trigger low temperature oxygen mobility in solid oxide ion conductors, *J. Am. Chem. Soc.* 130 (2008) 16080–16085. doi:10.1021/ja806144a.

# DFT study of Pt on CeO<sub>2</sub> under oxidizing and reducing conditions

J. Jelic<sup>1</sup>, A. M. Gänzler<sup>2</sup>, F. Maurer<sup>2</sup>, J.-D. Grunwaldt<sup>1,2</sup>, F. Studt<sup>1,2</sup>

<sup>1</sup>*Karlsruhe Institute of Technology, Institute of Catalysis Research and Technology,  
Karlsruhe, Germany*

<sup>2</sup>*Karlsruhe Institute of Technology, Institute for Chemical Technology and Polymer  
Chemistry, Karlsruhe, Germany*

## Introduction

Pt on CeO<sub>2</sub> has been used as catalyst for oxidation reactions like low-temperature CO oxidation, the water-gas shift reaction, steam reforming and so on. However, identification of an active site remains an issue, in particular under dynamic oxidizing to reducing conditions. In their experimental work many groups have shown [1-5] that at small Pt loading, full dispersion over CeO<sub>2</sub> can be achieved. Oxidizing conditions enhance Pt dispersion while in the reducing conditions Pt sintering takes place. The size of the Pt particles is correlated to the Pt oxidation state and this, in return, dictates the rate of oxidation process. This has furthermore led to redispersion protocols that allow to reactivate Pt/CeO<sub>2</sub> catalysts [3]. A more fundamental understanding is required which is the scope of this work.

## Methods

In this work, we have systematically performed set of periodic DFT calculations (VASP code [6] with GGA+U correction [7], a plane-wave basis set with a cutoff energy of 450 eV, the projector augmented wave method (PAW)[8, 9] and the Bayesian Error Estimation Functional with van der Waals correlations (BEEF-vdW [10] exchange correlation functional) in order to investigate process of Pt adsorption on different CeO<sub>2</sub> facets under different oxidation-reduction conditions as well as its effect on the process of CO oxidation.

## Results

Presence of a specific, open adsorption site at (002) and (211) facets of CeO<sub>2</sub> will make a huge impact on Pt dispersion process, allowing spontaneous, single Pt atom adsorption. This process is enhanced at slightly to fully oxidizing conditions. In CO rich regime PtOx species will be reduced and at some point, sintering of Pt will take

place. Fully dispersed and oxidized PtOx species are not very active toward CO oxidation. In addition, during reduction, the Pt particles may sinter too strongly leading to a loss of the active surface Pt and interfacial Pt-O-Ce entities.

At the same time, process of Pt adsorption over more compact facets of CeO<sub>2</sub>, like (111) and (221), is much more dependent on the oxidation state of Pt. Possible PtOx – CeO<sub>2</sub> substitution at these facets was taken in to account.

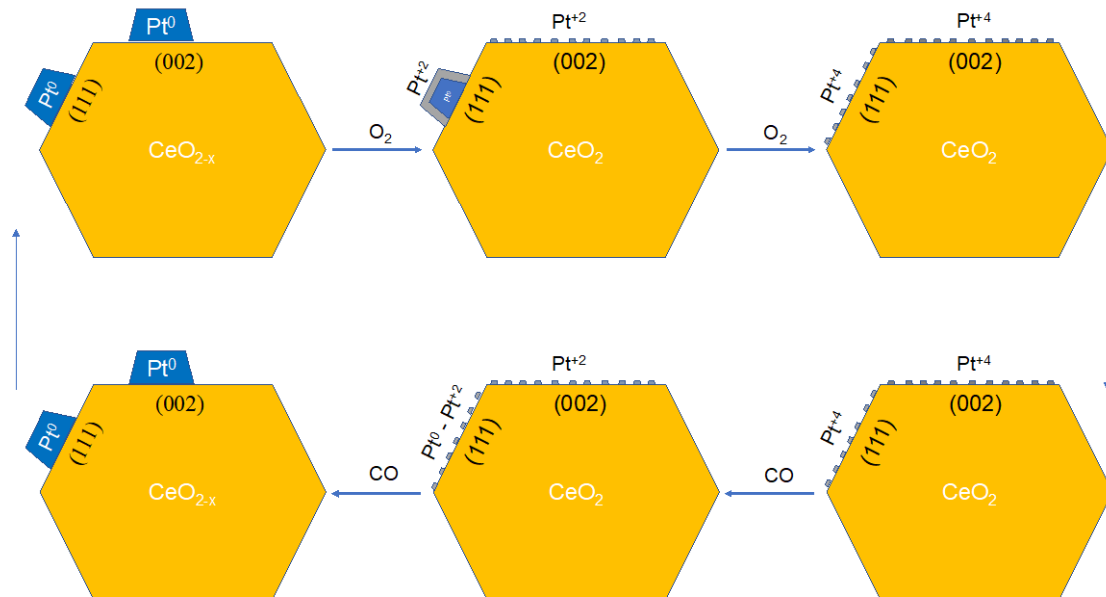


Figure 1: Schematic representation of the Pt over CeO<sub>2</sub>(002) & CeO<sub>2</sub>(111) under oxidizing – reducing conditions

## References

- [1] Andreas M. Gañizler et al., *ACS Catal.* **2018**, 8, 4800–4811
- [2] Jaeha Lee et al., *J. Phys. Chem. C* **2018**, 122, 4972–4983
- [3] Andreas M. Gañizler et al., *Angew. Chem. Int. Ed.* **2017**, 56, 13078 –13082
- [4] Filip Dvorak et al., *Nat. Commun.* **2016** | 7:10801 | DOI: 10.1038
- [5] Qi Fu et al., *Science* **2003**, 301, 935-938
- [6] G. Kresse et al., *Physical Review B* **1996**, 54, 11169-11186
- [7] G. Kresse et al., *Phys. Rev. B: Condens. Matter Mater. Phys.* **1998**, 57, 1505–1509
- [8] P.E. Blochl et al., *Phys. Rev. B* **1994**, 50, 17953
- [9] G. Kresse et al., *Phys. Rev. B* **1999**, 59, 1758
- [10] J. Wellendorff et al., *Phys. Rev. B – Condens. Matter Mater. Phys.* **2012**, 85, 32–34

# Development of heterojunctions Cu-TiO<sub>2</sub> for clean H<sub>2</sub> production by the visible light photo-electrochemical dissociation of water.

Wissame Chettah<sup>1</sup>; Siham Barama<sup>2</sup>; Anne Davidson<sup>3</sup>; Samira Sleymi<sup>2</sup>; Akila Barama<sup>2</sup>; Amel Boudjemaa<sup>4</sup> and Mohamed-Salah Medjram<sup>1</sup>. LGCES-universit -20-aout-1955<sup>1</sup>, Skikda<sup>1</sup>, Algeria<sup>1</sup>; LMCCCO-USTHB<sup>2</sup>, Algiers<sup>2</sup>, Algeria<sup>2</sup>; LRS-UPMC<sup>3</sup>, Paris<sup>3</sup>, France<sup>3</sup>; CRAPC<sup>4</sup>, Tipaza<sup>4</sup>, Algeria<sup>4</sup>

## Abstract.

Given that a great hope is placed on hydrogen fuel cells for the environmental impact, in this present study, a particular interest is focused on the production of hydrogen. Currently, gaseous hydrogen is synthesized up to 90% from industrial processes of transformation of organic compounds such as natural gas, coal or biomass, but these not-clean processes needed a CO<sub>2</sub> capture [1]. A transition is therefore to be made to more "clean" modes of H<sub>2</sub> production. It's known that there are several technological sectors produce H<sub>2</sub> from different sources such as natural-gas reforming, charcoal gasification, bio-resources fermentation, electrolysis of water, photo-synthesis by micro-organisms or algae. The electrolysis of water is one of promising way for clean production of hydrogen (with zero emissions); however, it's known that this process (at 25°C, 1 atm) is characterized by voltage -1.23V, which means this reaction needs high energy in large-scale [2]. To remedy this inconvenient, the photo-electrolysis of water under the visible light or sunlight, where electrodes is replaced by an efficient photocatalyst, could be a promising alternative to classical decomposition of water by electrolysis [3].

For catalysts preparation, commercial material Millennium-PC500 (Degussa, TiO<sub>2</sub> anatase) has chosen as starting reagent. Support, noted "a-TiO<sub>2</sub>" (a: anatase), is elaborated from a mixture of 80% of non-calcined Millennium-PC500 and 20% of calcined Millennium-PC500 followed by thermal activation at 400°C under air. The fabrication of the heterojunction photocatalysts has been realized by three methods: (1) wet-impregnation, (2) copolymer emulsion (using Triblock Pluronic-P123) and (3) surfactant emulsion (using Triton-X100). After calcination step or treatment under argon (at 500°C), the obtained solids, noted XCu/a-TiO<sub>2</sub> (X=3.5 %weight), 3Cu-P123/a-TiO<sub>2</sub>, 3Cu-TX100/a-TiO<sub>2</sub>, are characterized by X-rays diffraction, X-rays fluorescence, UV-visible spectroscopy (band gap (BG) calculation) and HR-

SEM/EDX. As shown in Fig.1, all diffraction peaks can be indexed to TiO<sub>2</sub> anatase phase (ICDD#021-1272) with body-centered tetragonal lattice and *I41/amd* space-group. For all samples, crystallographic study by Rietveld refinement showed some lines attributed to the presence of CuO oxide in nanoparticles form (ICDD#003-1018). Similar results were observed by fluorescence-X and EDX compositions. Photo-catalytic performances of our samples were evaluated through the reduction of water to hydrogen under visible light. The reaction was conducted at room temperature ( $50 \pm 1^\circ\text{C}$ ) with 200mL of NaOH electrolyte in water (concentration=0.5 M), using 50 mg of sample. Visible-lamp (200 W) was used as light source. Whole was stirred for 35 min in dark room (to establish equilibrium). Amounts of hydrogen were determined volumetrically by TCD detector and water manometer. After 60 min of photo-electrochemical dissociation of water, the largest gaseous amount of hydrogen is obtained with 5Cu/a-TiO<sub>2</sub> (20.9mL) followed by 3Cu/a-TiO<sub>2</sub> (18.3mL), both prepared with impregnation method. In contrast, copolymer-emulsion and surfactant-emulsion methods (treated under air and Ar) have revealed smaller hydrogen quantities (not exceeding 6mL) related to the lowest values of their BG. In conclusion, method of preparation strongly influences catalysts optical properties and consequently plays a very important role in hydrogen production via the photo-electrochemical dissociation of water under visible light.

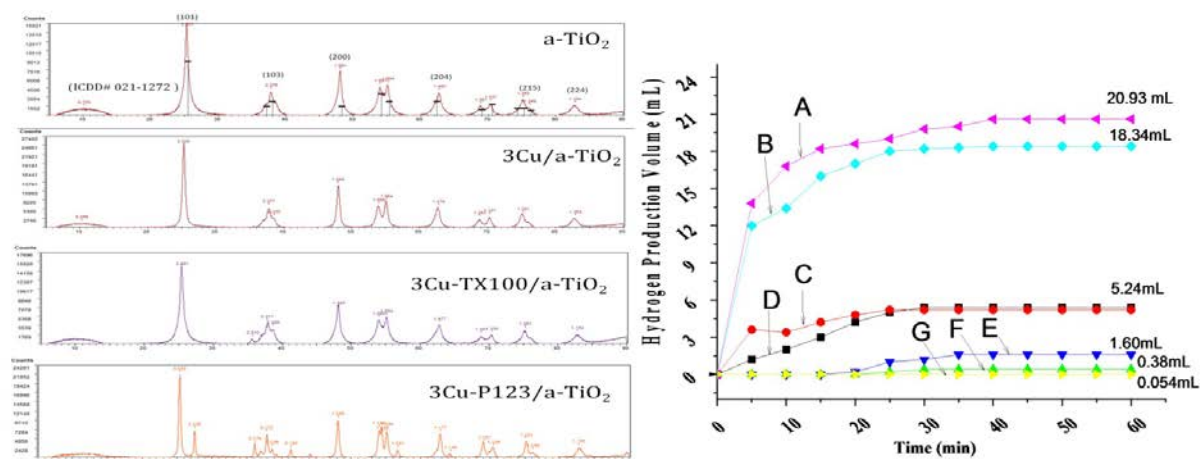


**Figure1. (Right)** Photo-electrochemical dissociation of water for hydrogen production (in mL) with: (A) 5Cu/a-TiO<sub>2</sub> (B) 3Cu/a-TiO<sub>2</sub> (C) 3Cu-P123/a-TiO<sub>2</sub>/air (D) 3Cu-P123/a-TiO<sub>2</sub>/Ar (E) 3Cu-TX100/a-TiO<sub>2</sub>/Ar (F) 3Cu-TX100/a-TiO<sub>2</sub>/air (G) a-TiO<sub>2</sub> support **(Left)** XRD patterns of catalysts calcined under air.

**References.** [1] Dennis Y.C. Leung, Giorgio Caramanna, M. Mercedes Maroto-Valer, "An overview of current status of carbon dioxide capture and storage technologies", *Renewable* 39 (2014) 426-443. [2] Hauch, A.; Ebbesen, S. D.; Jensen, S. H.; Mogensen, M., "Highly Efficient high temperature electrolysis", *J. Mater. Chem.* 18 (2008) 2331–2340. [3] H. Hentit, A. Boudjema, A. Bouchama, J.C Jumas, K. Bachari, M.S Ouali, "Cobalt containing microporous aluminophosphates as new photocatalyst for hydrogen generation under visible irradiation", *Materials Research Bulletin* 106 (2018) 418-427.

# **Influence of different intra-layer alkali cations on the catalytic activity of birnessite in soot oxidation**

*Tomasz Jakubek, Camillo Hudy, Andrzej Kotarba,*

*Department of Chemistry, Jagiellonian University, ul. Gronostajowa 2, Krakow,  
30-387, Poland*

The main purpose of the presented work was a punctilious study of the catalytic properties of birnessite ( $\text{AMn}_4\text{O}_8$ ) and the tuning of its properties by the insertion of different alkali cations ( $A = \text{H}^+, \text{Li}^+, \text{Na}^+, \text{K}^+, \text{Rb}^+, \text{Cs}^+$ ) into the interlayer space (see the structure in Fig. 1a). Mainly, the studies were directed at the modification of structure and the resulting increase of catalytic activity in a model soot combustion reaction. This research will help to produce a catalyst that allows the lowering of the temperature of soot combustion while following the 3E rule (effective, ecological, economic). In order to achieve the objective, the series of the catalyst based on the birnessite-type ( $\text{AMn}_4\text{O}_8$ , hereafter ABir) phases with various alkali cations intercalated into the interlayer space between the  $\text{MnO}_6$  octahedral layers were obtained during  $\text{Mn}^{2+}$  oxidation in an alkali environment. The chemical composition, purity, structure, morphology, electrodonor properties and thermal stability of the obtained products were thoroughly studied by means of several physicochemical methods (ED-XRF, XRD, RS, TEM, work function, TGA-QMS ex-situ). The catalysts were tested in a temperature-programmed surface reaction of soot oxidation as well as NO oxidation.

The diffractograms present a series of peaks which are common for birnessite. Of note is a slight altering of the position of the first reflex (001) – its position determines the distance between layers. The introduction of ions with a larger ionic radius causes an increase in the separation between layers. With the decreasing ionic radius, the thermal stability decreases—samples with smaller intercalated cations have greater weight loss in the temperature range of 260-840°C. The QMS measurements conducted ex-situ revealed this weight loss is connected with the release of oxygen. The measurements of the work function show an expected tendency: birnessite phases containing cations with greater electronegativity are characterized by a lower WF. The catalytic activity was determined during temperature-programmed soot combustion experiments in different modes of contact between soot and catalyst particles: loose (LC) and tight

(TC) contact and with several mixtures of gases flow through the reactor: O<sub>2</sub>/He, O<sub>2</sub>+NO/He and NO/He. The most active phase in each reaction is HBir, lowering the temperature of 50% soot conversion by 200°C (TC in O<sub>2</sub>/He and LC in O<sub>2</sub>+NO/He) when compare to an uncatalyzed reaction. The order of the remaining active phases in each reaction is as follow: TC in O<sub>2</sub>/He (LiBir~NaBir<<CsBir~KBir<RbBir), LC in O<sub>2</sub>/He (RbBir<KBir<CsBir<LiBir<NaBir) and LC in O<sub>2</sub>+NO/He (NaBir<LiBir<KBir<CsBir<RbBir). The sequence of the NO conversion curves in the reaction of its oxidation confirms the higher efficiency of the catalyst for transformation of NO into more reactive NO<sub>2</sub> indicating the release of oxygen in lower temperatures.

The obtained results show the two main consequences of different alkali cation insertion. Firstly, the catalytic activity in soot oxidation can be tuned. All of the examined phases present high catalytic activity. Moreover, on the contrary to the hypothesis, the insertion of cations with the lower ionization potential results in higher catalytic activity in soot oxidation (in both loose and tight contact modes). Thus the activity is no longer related to the formation of ROS via electron transfer, which mainly occurred in similar studies [1,2]. Secondly, with the different inserted cation, the ease of oxygen release changes. In general, based on the obtained results, the catalytic activity in the reaction of soot oxidation is highly linked with the capability of the material to release oxygen from the birnessite surface (see Figure 1b). It is concluded, that soot combustion over the synthesized catalysts operates mainly via the Mars-van Krevelen mechanism.

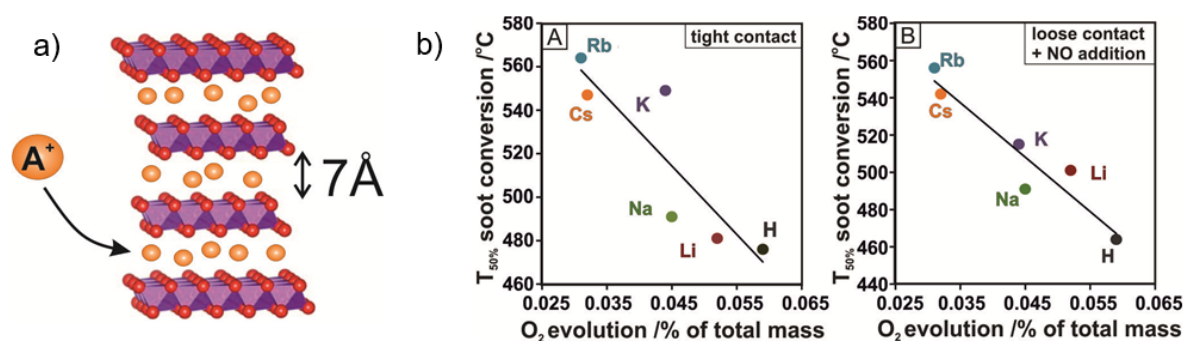


Figure 1. a) Structure of birnessite-type phases, b) Correlation between catalytic activity and release O<sub>2</sub> from the surface of catalyst

## References

- 1 Jakubek, T., Kaspera, W., Legutko, P. et al. *Top Catal* (2016) 59: 1083.
- 2 Legutko, P., Stelmachowski, P., Trębala, M. et al. *Top Catal* (2013) 56: 489.

# Cogent Tuning of Intrinsic and Extrinsic Redox Processes Involved in N<sub>2</sub>O Decomposition over Cobalt Spinel Nanocubes

Camillo Hudy, Janusz Janas, Filip Zasada, Andrzej Kotarba, Zbigniew Sojka

*Department of Chemistry, Jagiellonian University, ul. Gronostajowa 2,*

*Krakow, 30-387, Poland*

Fundamental understanding and mastering of various interfacial redox processes involved in N<sub>2</sub>O and O<sub>3</sub> decomposition, oxidation of CO, CH<sub>4</sub>, VOC and soot combustion or NO<sub>x</sub> reduction, belong to the key challenges in environmental catalysis. However, despite a large progress that has been made recently, this problem still remains not fully resolved.

The aim of this work is to provide an insight into the role of redox events associated with interfacial electron transfer and back electron transfer that trigger decomposition of nitrous oxide on the surface of model cobalt spinel catalysts of the nano-cube morphology. They are associated with the reductive N<sub>2</sub>O dissociation ( $\text{N}_2\text{O} + \text{e}^- \rightarrow \text{N}_{2(\text{g})} + \text{O}^-_{\text{surf}}$ ) and the oxidative oxygen evolution ( $\text{O}^-_{\text{surf}} + \text{h}^\bullet \rightarrow \frac{1}{2}\text{O}_{2(\text{g})}$ ) steps, induced by an electron or hole transfer, respectively. The iono-sorbed O<sup>-</sup> intermediates lead to development of a charge layer on the (100) surface exposed by the Co<sub>3</sub>O<sub>4</sub> nanocubes, which hinders the interfacial electron transfer via surface potential enhancement. Furthermore, since the electron holes h<sup>•</sup> take part in the second step of the reaction, regulation of their concentration by hypovalent doping of the Co<sub>3</sub>O<sub>4</sub> nanocrystals with Li<sup>+</sup> ions allows for facile promotion of the oxygen evolution via oxidative O<sup>-</sup> recombination.

In order to verify these conjectures experimentally, a series of bare and lithium doped cobalt spinel model catalysts of the nanocube shape were obtained by hydrothermal method without use of any template molecules. Lithium doping was achieved by impregnation of the bare Co<sub>3</sub>O<sub>4</sub> nanocrystals with an aqueous solution of LiNO<sub>3</sub>, followed by calcination at 700°C. The samples were thoroughly characterized by XRD, ED-XRF, FTIR, RS, SEM methods, along with the work function and the electric conductivity measurements (panel a). The catalytic active performance of Co<sub>3</sub>O<sub>4</sub> and Li-Co<sub>3</sub>O<sub>4</sub> nano-cubes in the N<sub>2</sub>O decomposition was studied in the TPSR and isothermal modes, as a function of contact time and N<sub>2</sub>O



pressure (panel b), also with addition of  $^{16}\text{O}_2$  or  $^{18}\text{O}_2$  to examine the role of the surface charge layer formation on the reaction progress.

Results obtained from the catalytic  $\text{N}_2\text{O}$  decomposition were interpreted by means of a kinetic equation,  $\frac{X}{1-X} = \frac{k^{obs} m}{F_v^0 \rho} \left( \frac{1}{1 + K_o (0.5 \cdot X p_{\text{N}_2\text{O}})^{0.5}} \right)$ , with an auto-genic retardation term due to the presence of the surface  $\text{O}^-$  intermediates. The latter produce a Helmholtz charge layer, which leads to enhancement of the activation energy from  $\Delta E_{\text{intr}} = 70$  to  $\Delta E_{\text{app}} = \Delta E_{\text{intr}} + \chi = 100$  kJ/mol, where  $\chi$  indicates the build-up surface potential ( $\chi = ne\mu/\epsilon\epsilon_0$ ), gauged independently by the work function measurements, and  $\mu$  is the surface dipole produced by an  $\text{O}^-$  adatom (panel c).

The influence of tuning the redox properties of  $\text{Co}_3\text{O}_4$  nano-cubes by incorporation of  $\text{Li}^+$  cations on the  $\text{N}_2\text{O}$  decomposition is shown in panel d. A systematic shift of the TPSR profiles toward lower temperatures, documents the beneficial role of the generated electron holes in the recombination of the  $\text{O}^-$  intermediates, which apparently is slower than the first  $\text{N}_2\text{O}$  dissociation step. The concentration of holes was assessed by a noncontact electron conductivity and work function measurements. The result can be explained in terms of an adjustment of the active redox couple  $\text{Co}^{3+}/\text{Co}^{4+}$  to the investigated reaction.

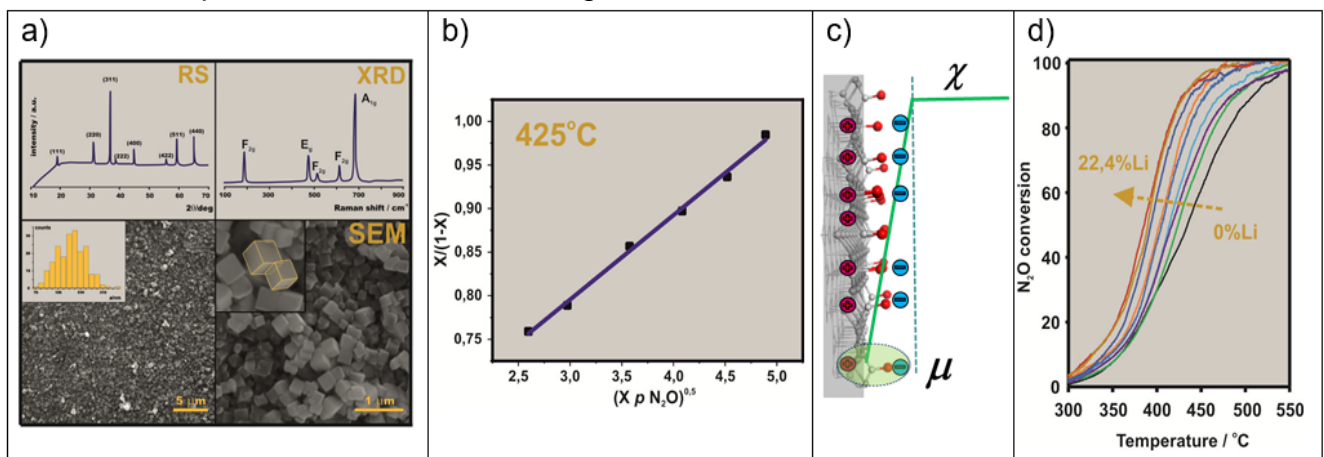


Figure. a) Characterization of the  $\text{Co}_3\text{O}_4$  nanocubes by RS, XRD and SEM methods, b) kinetic results of the  $\text{N}_2\text{O}$  decomposition at various  $p_{\text{N}_2\text{O}}$  pressure at  $T = 425^\circ\text{C}$ , c) model of the surface Helmholtz layer produced by the  $\text{O}^-$  intermediates, d) influence of Li-doping of  $\text{Co}_3\text{O}_4$  nanocubes on  $\text{N}_2\text{O}$  decomposition TPSR profiles.

### Acknowledgments

This work was supported by the Project OPUS No 2017/27/B/ST4/01155 financed by the Polish National Science Center.

Camillo Hudy has been partly supported by the EU Project POWR.03.02.00-00-I004/16.

# **Different activation of CuO nanoparticles on $\text{La}_{0.8}\text{K}_{0.2}\text{MO}_3$ (M=Cr,Mn) perovskites: oxygen exchange interaction between metal and support material**

*G. Peron, Dept. of Chemical Sciences, University of Padua, Italy; G. Carollo, Dept. of Chemical Sciences, University of Padua, Italy; A. Glisenti, Dept. of Chemical Sciences, University of Padua, Italy*

## **Introduction**

Our group has long studied CuO@perovskites nanocomposite materials as a possible alternative to noble metals in automotive exhaust abatement device [1,2]. The different surface and bulk properties of oxygen in citrate route-prepared  $\text{LaCrO}_3$  and  $\text{LaMnO}_3$  perovskites lead to very different results in soot oxidation and CO reduction by NO, after doping with potassium [3]. The higher mobility of oxygen in the bulk and the relative weakness of Mn-O bond give to Mn-based perovskites a high oxidation activity. The lower mobility of oxygen in  $\text{LaCrO}_3$  however, seems to stabilize superficial oxygen vacancies, avoiding the replenishment via migration from the bulk. The higher concentration of  $\text{O}^{2-}$  defects greatly enhances NO reduction activity with respect to the  $\text{LaMnO}_3$  perovskite.

The present study aims to further investigate the oxygen exchange capabilities of these two perovskites in CuO nanocomposites material. Good redox activity of dispersed copper nanoparticles can modify and enhance the reactivity of the perovskite. The preparation of the catalyst follows a combustion method of deposition that allows to improve the dispersion of copper with respect to the traditional wet impregnation method [4]. Due to the good dispersion obtained, it was possible to establish an oxygen exchange interaction between copper and the support perovskite, ruled by oxygen mobility and M-O bonding strength. Mixed Cr-Mn perovskites have been synthesized to investigate the possibility of a synergetic effect.

## **Synthesis and Characterization**

The doped perovskites have been prepared by wet chemistry procedure and characterized by means of X-Ray Diffraction (XRD), X-Ray Photoelectron Spectroscopy (XPS), Scanning Electron Microscopy (SEM), Energy Dispersive X-Ray Analysis (EDX), Temperature Programmed Reduction (TPR), and BET. Catalytic activity was evaluated with model reaction such as soot oxidation by  $\text{O}_2$  and NO and

NO reduction by CO, as well as in more complex mixtures, containing also soot, oxygen and hydrocarbons.

## Results and discussion

XRD analysis confirms that copper did not enter in the perovskite cell, but is dispersed on the surface as Cu(II) oxide. The Temperature Programmed Reduction shows that in Mn-containing samples the reducibility of the support is increased by the combustion deposition of copper.

The catalytic properties of the perovskitic support influence the catalytic activity of copper, as it is clearly shown by the results of NO reduction by CO. Cr-perovskite supported nanocomposites perform better than manganite-supported (figure 1 left). This was interpreted on the base of more effective oxygen activation. Obtained results suggest more oxygen can be supplied to copper from the bulk, deactivating it towards NO reduction. This is confirmed by soot oxidation tests (figure 1 right) in tight contact mode, where copper on Mn-perovskite is much more effective than the chromite supported. This interaction is observed to strongly depend on the deposition procedure and so on the intimate contact between the supported specie and the perovskite.

Interesting synergetic effects have been observed in Cr+Mn-containing supports.

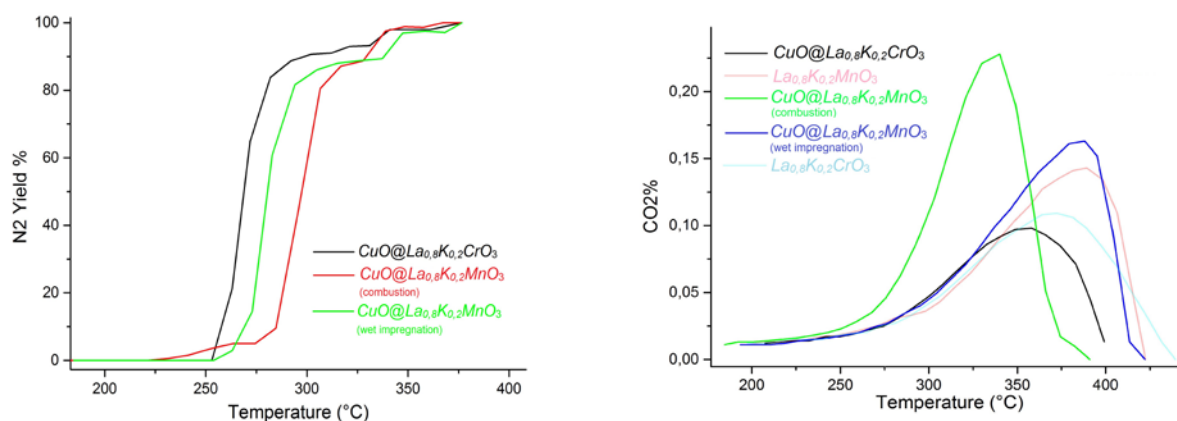


**Fig.1** Left: N<sub>2</sub> yield for some nanocomposite materials in NO reduction by stoichiometric CO. Right: soot oxidation by O<sub>2</sub> and NO results, in comparison with results without copper deposition.

## References

- [1] - M. Pacella, A. Garbujo, J. Fabro, M. Guiotto, Q. Xin, M.M. Natile, P. Canu, P. Cool, A. Glisenti, Applied Catalysis B: Environmental, Volume 227, 2018, Pages 446-458
- [2] - G. Perin, J. Fabro, M. Guiotto, Q. Xin, M.M. Natile, P. Cool, P. Canu, A. Glisenti, Applied Catalysis B: Environmental, Volume 209, 2017, Pages 214-227
- [3] - G. Peron, A. Glisenti, Topics in Catalysis, 2018 (in press)
- [4] - G. Carollo, A. Garbujo, A. Bedon, D. Ferri, M.M. Natile, A. Glisenti, International Journal of Hydrogen Energy, 2018 (in press)

# Improved asymmetrical honeycomb monolith catalyst prepared by 3D printing

Arantxa Davó-Quiñonero, Débora Sorolla-Rosario, Esther Bailón-García, Dolores Lozano-Castelló and Agustín Bueno-López.

*Inorganic Chemistry Department, University of Alicante, Alicante, Spain;*

## Introduction

Three dimensions (3D) printing is doing successful advances in topics like chemistry or medicine, among others, since it opens new options for fabrication of substrates with total freedom in the design [1,2].

In this study, a honeycomb-like monolith has been prepared using 3D printing machines with enhanced catalytic activity. This improved support consists of a honeycomb-like structure with asymmetrical channels (see Figure 1). Conventional and improved monoliths were prepared by 3D printing and were coated with the same active phase (5 wt. % Cu/Ceria). The catalysts were characterized and tested in two chemical reactions with practical relevance: CO oxidation in excess oxygen, which is relevant for gas pollution control, and preferential oxidation of CO in the presence of H<sub>2</sub> (CO-PROX), which is a topic of ongoing research for H<sub>2</sub> purification in fuel cells.

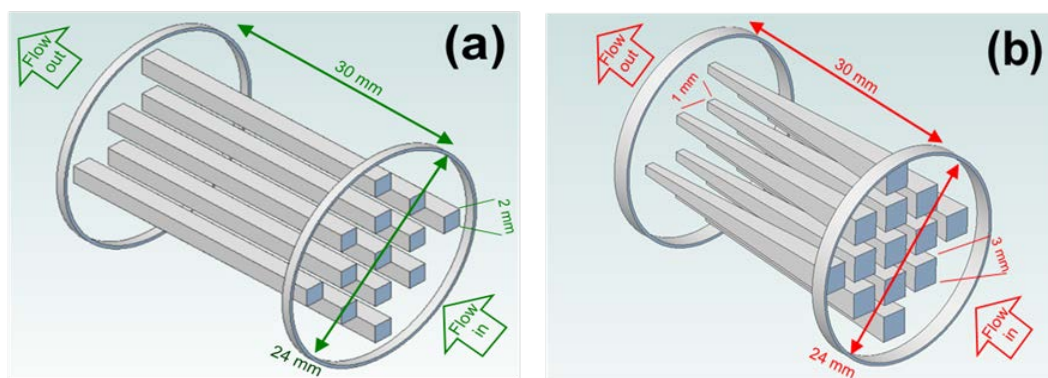


**Figure 1.** Scheme of channels for the (a) symmetrical and (b) asymmetrical monoliths designed and fabricated in this study.

## Results and discussion

Physical-chemical characterization by means of XRD, SEM and Raman studies show that for both conventional and asymmetrical monoliths there are not crystalline differences in the Cu/Ceria active phase, nor the washcoated thicknesses or catalyst

distribution along the channel length either. Therefore, variation in catalytic activity must be attributed to the particularities in the shape of the channels, considering constant the surface area per unit bed volume.

Figures 2 and 3 present catalytic behaviour of the prepared active monoliths, demonstrating a better performance in both CO oxidation and CO-PROX conditions a beneficial effect in the unconventional design. For the asymmetrical monolith, channel section is larger at the reactants entrance side than in the exit side, improving with regard to conventional monoliths both the reaction rate, when reaction behaves under kinetic rate control, and the radial diffusion of reactants, when reaction behaves under external gas diffusion rate control

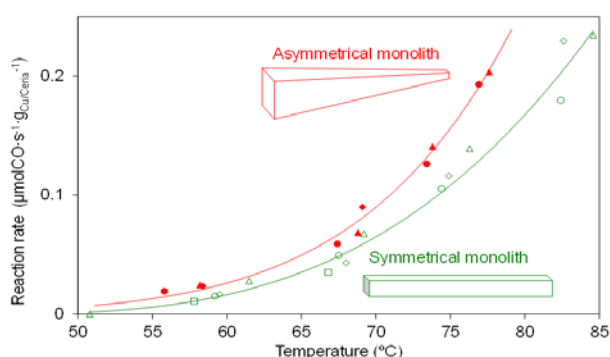


**Figure 2.** Reaction rate as a function of temperature for CO oxidation experiments performed with excess oxygen (1% CO + 17% O<sub>2</sub> in He) under different total gas flows (ml/min): ■ 400, ● 500, ▲ 600, ◆ 700.

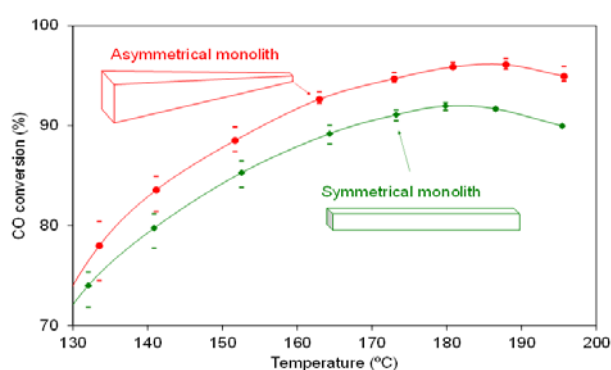


**Figure 3.** CO conversion as a function of temperature in CO-PROX experiments. (1% CO + 1% O<sub>2</sub> + 30% H<sub>2</sub>; total gas flow: 700 ml/min).

## Conclusions

The improved supported catalyst with asymmetrical channels has two benefits with regard to a counterpart catalyst with conventional symmetrical channels. The novel supported catalyst improves the reaction rate with regard to the conventional one because it fits better to the equation rate, and the asymmetrical channels favor the turbulent regime of gases with regard to the laminar flow that prevails in symmetrical channels.

## Acknowledgments

Generalitat Valenciana (PROMETEO/2018/076); Spanish Ministry of Economy and Competitiveness (CTQ2015-67597-C2-2-R); Spanish Ministry of Education (grant FPU14/01178).

## References

- [1] Eckel et al., *Science* **351** (2016) 58-62.
- [2] Li et al., *J. Mater. Chem. A* **6** (2018) 5695-5702.

# CO oxidation on bimetallic AuTi nanoparticles

*Alexander Krabbe<sup>1</sup>, Niklas Mørch Secher<sup>1</sup>, Jens Fuglsang Ringsholm<sup>2</sup>, Jakob Kibsgaard<sup>1</sup>, Ib Chorkendorff<sup>1</sup>*

<sup>1</sup>Section for Surface Physics and Catalysis, DTU Physics, Technical University of Denmark, DK-2800 Lyngby, Denmark

<sup>2</sup>Nano-Science Center & Department of Chemistry, University of Copenhagen, DK-2100, Copenhagen, Denmark

## Introduction

Gold nanoparticles on TiO<sub>2</sub> supports are good CO oxidation catalysts and the reaction mechanism has been discussed[1]. Gold is often hindered by rapid sintering effects that ruin the size effect of gold-based catalysts in heterogeneous catalysis. Ti has previously been shown to reduce these sintering effects and stabilize the gold nanoparticles[2]. Mass-selected Au/Ti clusters deposited on TiO<sub>2</sub> support appear to be a promising candidate for sustainable gold-based nanocatalysts. In this study small bi-metallic mass-selected Au/Ti nanoparticles are deposited on TiO<sub>2</sub> and SiO<sub>2</sub> support and experimentally tested using CO oxidation as a model reaction for the catalytic efficiency and stability.

## Setup and Sample Preparation

The microreactor setup developed at DTU to specifically test and investigate catalytic phenomena on nanoparticles is exceptionally good in combining high pressure reactions and still enable Quadrupole Mass Spectrometry (QMS) in Ultra High Vacuum (UHV) through a capillary to analyse the entire gas composition and all products formed by the reaction[3]. See figure 1.

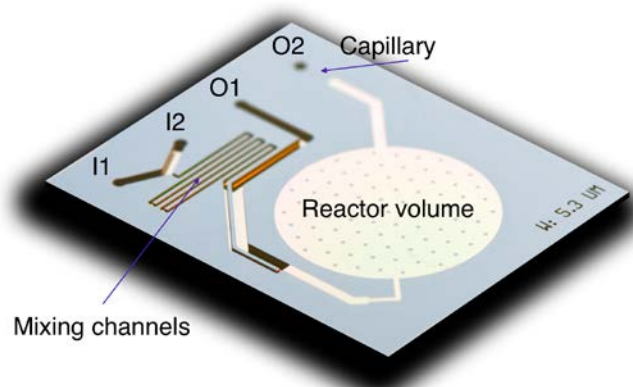


Figure 1. Schematics of the microreactor. Photo by Thomas Andersen, DTU.

The samples are produced by sputtering a TiO<sub>2</sub> thinfilm on the microreactor. The microreactor is then inserted into the cluster source at SurfCat to prepare the mass-selected bi-metallic Au/Ti by magnetron sputtering and mass separated by a time-of-flight before impregnated onto the microreactor. See figure 2. The samples are then analysed and characterised using ISS, XPS and SEM.

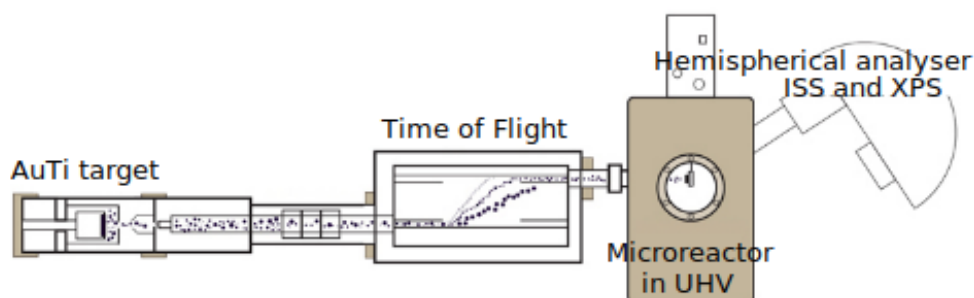


Figure 2. Schematics of the cluster source and AuTi target. Schematics by Ifan Stephens

Catalytic testing is done at various pressures and temperatures of up to 1 bar and 140 degrees. The gas composition has been varied from 0.25:1:1.75 to 1:1:1 (O<sub>2</sub>:CO:Ar).

### Acknowledgement

This research is funded by Villum fonden as part of the Villum Center for Science of Sustainable Fuels and Chemicals

### References

- [1] Widmann, D., Krautsieder, A., Walter, P., Brückner, A., and Behm, R. J., "How Temperature Affects the Mechanism of CO Oxidation on Au/TiO<sub>2</sub>: A Combined EPR and TAP Reactor Study of the Reactive Removal of TiO<sub>2</sub> Surface Lattice Oxygen in Au/TiO<sub>2</sub> by CO" *ACS Catalysis* 2016 6 (8), 5005-5011 DOI: 10.1021/acscatal.6b01219
- [2] Niu, Y., Schlexer, P., Sebok, B., Chorkendorff, I., Pacchioni, G., and Palmer, R. E., "Reduced sintering of mass-selected Au clusters on SiO<sub>2</sub> by alloying with Ti: an aberration-corrected STEM and computational study", *Nanoscale*, 2018,10, 2363-2370, 10.1039/C7NR06323G
- [3] Henriksen, T. R., Olsen, J. L., Vesborg, P. C. K., Chorkendorff, I., & Hansen, O. (2009). "Highly sensitive silicon microreactor for catalyst testing". *Review of Scientific Instruments*, 80(12), 124101. 10.1063/1.3270191



## Platinum states and structural features of Pt/Al<sub>2</sub>O<sub>3</sub> catalysts in the NH<sub>3</sub> oxidation reaction

*Andrei Boronin, Andrey Stadnichenko, Elena Slavinskaya, Dmitry Svintsitskiy, Anatoly Romanenko, Olga Stonkus, Elizaveta Derevyannykova, Boreskov Institute of Catalysis, SB RAS, Novosibirsk, Russia; Valery Svetlichnyi, Tomsk State University, Tomsk, Russia; Vasyly Marchuk, Dmitry Doronkin, Maria Casapu, Anna Zimina, Jan-Dierk Grunwaldt, Karlsruhe Institute of Technology, Karlsruhe, Germany*

We report a fundamental study of catalytic oxidative neutralization of ammonia in excess oxygen on Pt/Al<sub>2</sub>O<sub>3</sub> catalysts. A series of Pt/Al<sub>2</sub>O<sub>3</sub> catalysts with high Pt dispersion were synthesized and systematically studied. The catalysts were supported on  $\gamma$ -Al<sub>2</sub>O<sub>3</sub> prepared by calcining pseudoboehmite Pural SCF-55 in air at 550 or 750°C (catalysts 1 and 2, respectively). Platinum was deposited from a solution of commercial platinum nitrate. Structural (XRD, TEM), spectroscopic (XPS, XAS), and kinetic (TPR-NH<sub>3</sub>+O<sub>2</sub>) methods were used to characterize the morphology, dispersion, structure and electronic state of the active component in the as-prepared, reduced in hydrogen and tested catalysts. The catalysts are characterized by a high dispersion of the active component with particles of supported platinum in the range from 0.5 to 2 nm and with a varying ratio of Pt<sup>0</sup>, Pt<sup>δ+</sup>/Pt<sup>2+</sup> and Pt<sup>4+</sup> species, as uncovered by XPS and XAS investigations. Despite the identical content of platinum in the catalysts, the activity and selectivity for different products (N<sub>2</sub>, N<sub>2</sub>O, NO and NO<sub>2</sub>) differ. From the initial activity data, the rate of catalytic reaction, TOFs value and activation energy for all catalysts were determined.

It was found that the activity of catalysts and selectivity to N<sub>2</sub> and N<sub>2</sub>O products, depending on the reaction temperature (Figure 1), are determined by a combination of factors: dispersion and oxidation state of platinum species, and also, probably, by their interaction with the support. The effective oxidation of ammonia was observed at temperatures above 150°C. In the range from 150 to 250°C, the main oxidation products were N<sub>2</sub> and N<sub>2</sub>O (Fig.1b and 1c). Note that the appearance of N<sub>2</sub>O in the reaction mixture coincided in temperature with the start of ammonia conversion for all tested samples. At temperatures above 250°C, NO and NO<sub>2</sub> appear as reaction products. With increasing temperature, the concentration of nitrogen oxides in the



mixture increased, while the content of  $N_2$  and  $N_2O$  decreased. Note that the tested catalysts differed significantly among themselves in their activity, which was manifested in the shift of the  $NH_3$  conversion curve on a temperature scale. Thus, the reduction in hydrogen contributed to an increase in the activity of catalysts 2%Pt/ $Al_2O_3$  in the reaction of ammonia oxidation in an excess of oxygen.

One can conclude that at temperatures up to 250° C, a high activity in the oxidation of ammonia with the formation of both,  $N_2$  and  $N_2O$ , is observed over metallic platinum. At the same time, higher selectivity to  $N_2$  was recorded for the catalysts containing predominantly oxidic Pt. Above 250°C, these factors cease to be decisive due to the oxidation of platinum, which is accompanied by the appearance of NO and  $NO_2$  as main ammonia oxidation products.

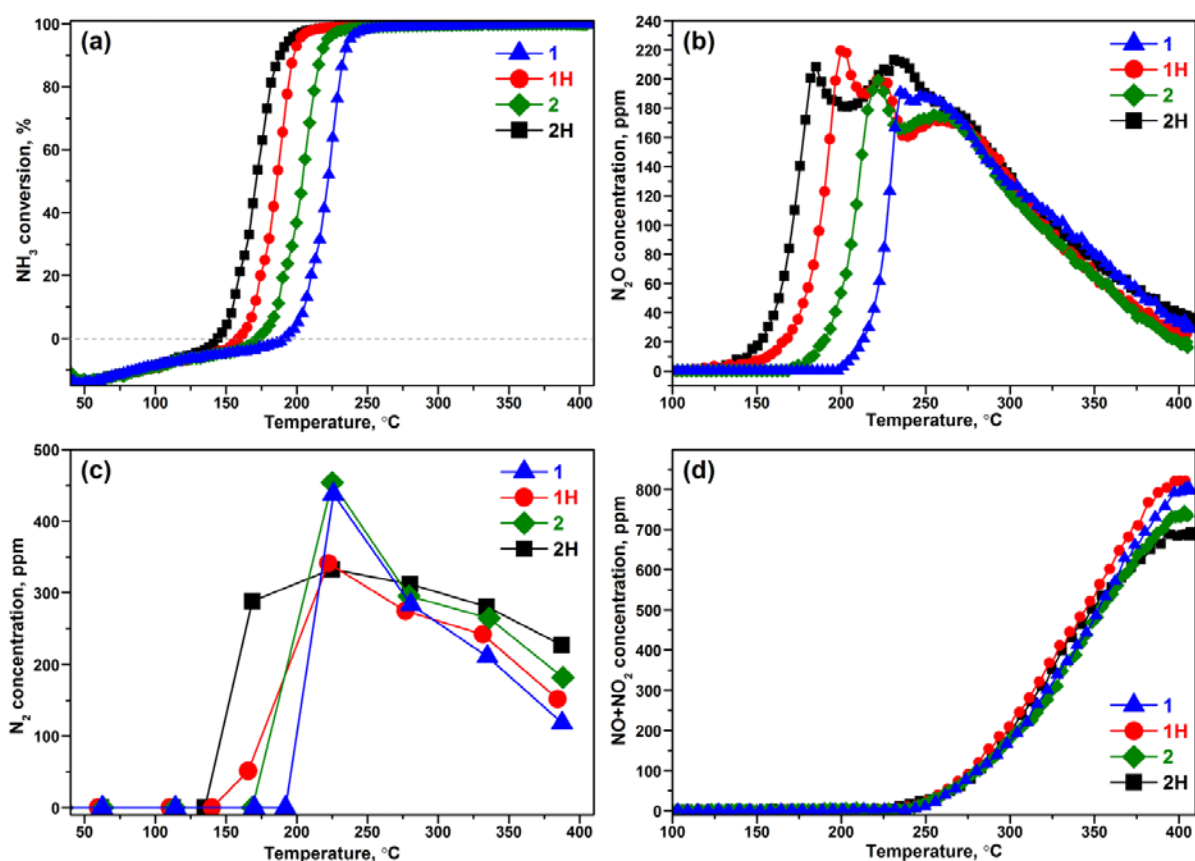


Figure 1. Temperature dependences of  $NH_3$  conversion and concentration of reaction products during the second heating in the reaction mixture for 2%Pt/ $Al_2O_3$  catalysts before and after their reduction in hydrogen at 250°C (marked as H): (a)  $NH_3$  conversion, concentration (b)  $N_2O$ , (c)  $N_2$  and (d)  $NO + NO_2$ .

## Acknowledgements

The work was supported by Helmholtz – Russian Science Foundation Joint Research Groups grant #18-43-06201 (RSF) / HRSF-0046 (HGF).

# Bottom Up Design of a Novel CuRu Nanoparticulate Catalyst for Low Temperature Slip Ammonia Catalyst

*Christian Danvad Damsgaard<sup>1,2</sup>, Debasish Chakraborty<sup>1</sup>, Nicolai Hagen<sup>3</sup>, Ib Chorkendorff<sup>1</sup>*

<sup>1</sup>*Section for Surface Physics and Catalysis, DTU Physics, Technical University of Denmark, DK-2800 Lyngby, Denmark*

<sup>2</sup>*DTU Nanolab, Technical University of Denmark, DK-2800 Lyngby, Denmark*

<sup>3</sup>*RenCat ApS, Fysikvej 309, DK-2800 Lyngby, Denmark*

## Introduction

The removal of NO<sub>x</sub> in exhaust gases as a bi-product of chemical reactions is important because of the harmful effect of NO<sub>x</sub> on the environment and the human health. The level of NO<sub>x</sub> emission limits e.g. for diesel engines and other sectors have become more stringent over the past years. The selective catalytic reduction (SCR) of NO<sub>x</sub> by ammonia is an effective and well-developed method for the NO<sub>x</sub>-removal. However, this leads to unconverted ammonia emission from tail pipes, which for industrial applications is limited to below 10 ppm. To decrease the ammonia slip, most processes are carried out under the condition of NH<sub>3</sub>/NO<sub>x</sub><1, which, however, is sub-stoichiometric resulting in a tradeoff in NO<sub>x</sub> reduction efficiencies.

In view of the present discussions in exhaust gas after treatment, the focus is stronger on more efficient NO<sub>x</sub> removal. For increasing the NO<sub>x</sub> reduction efficiency an increase in the inlet NH<sub>3</sub> feed to the SCR catalyst to stoichiometric or even higher and in a subsequent stage selectively oxidizing the unreacted ammonia over a downstream catalyst called the Ammonia Slip Catalyst (ASC) is more plausible.

We recently reported in *Angewandte Chemie* a novel nanoparticulate catalyst of copper and ruthenium designed for low temperature ammonia oxidation at near stoichiometric mixtures using a bottom up approach<sup>1</sup>. A synergistic effect of the two metals is found: an optimum CuRu catalyst shows reaction rate three-fold higher than Ru and forty-fold higher than Cu. X-ray Absorption Spectroscopy (XAS) suggests that in the most active catalyst Cu forms one or two monolayer thick patches on Ru and the catalysts are less active once 3D Cu-islands form. In this paper, we extend the idea of ammonia oxidation on Cu/Ru catalyst to ammonia slip catalyst (ASC) application. We will show the result of ammonia oxidation in simulated exhaust gas

composition with huge excess of oxygen (10%) present in the stream. We are also going to investigate the effect of water in the reaction stream.

## Methods

The high surface powder catalyst was prepared by first synthesizing Ru/Al<sub>2</sub>O<sub>3</sub> catalyst and then by electroless Cu deposition on Ru nanoparticles. The supported nanoparticles were then tested for ammonia oxidation. The

characterization was performed by in-situ X-ray diffraction, Transmission Electron Microscopy and in-situ X-ray absorption spectroscopy.

## Results and discussion

The catalytic conversion of NH<sub>3</sub> and O<sub>2</sub> to N<sub>2</sub> and H<sub>2</sub>O at 170°C for a series of CuRu catalyst of varying nominal copper overlayer thickness. The CuRu nanoparticulate catalyst, similar to the thin film, has a better performance than both copper and ruthenium separately. The highest conversion is observed for a nominal Cu overlayer thickness of 0.8ML exhibiting over a factor 3 higher conversion than pure ruthenium and performing 40 times better than pure copper<sup>1</sup>. When the catalyst has been tested for a huge excess of oxygen (10%) to simulate the ammonia slip catalyst atmosphere, a very high low temperature activity and selectivity of towards N<sub>2</sub> are observed (Figure 1). The complete conversion has been reached at 200°C with N<sub>2</sub> selectivity of over 90%. The other very interesting feature of the catalyst is the very low N<sub>2</sub>O selectivity for the temperature range tested (180-350°C).

## Conclusions

The Cu-Ru/ Al<sub>2</sub>O<sub>3</sub> catalysts showed very promising activity and selectivity as ASC. With it's potential to lower cost and higher performance, the catalyst can be an effective replacement for Pt based catalysts for the ammonia oxidation reaction.

## References

[1] D. Chakraborty, C.D. Damsgaard et al., *Angewandte Chemie*. 56 (2017) 8711–8715.

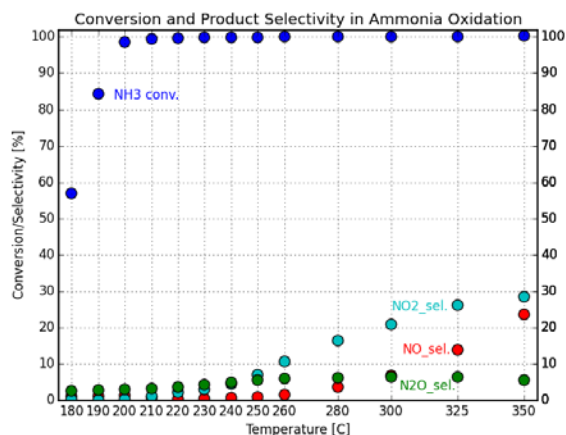


**Figure 1.** Activity and selectivity of selective ammonia oxidation on Al<sub>2</sub>O<sub>3</sub> supported Cu/Ru catalyst. Reaction gas mixture: 1000 ppm ammonia in 10% O<sub>2</sub> and rest Ar. Catalyst : CuRu/Al<sub>2</sub>O<sub>3</sub> ( 2wt% Ru).

# Co-Mn mixed oxides prepared by magnetron sputtering on meshes as catalysts for oxidation of organic compounds

*K. Jiráková, J. Balabánová, M. Koštejn, P. Topka, Institute of Chemical Process  
Fundamentals of the CAS, Prague, Czech Republic;*

*R. Perekrestov, P. Kšířová, M. Čada, Z. Hubička, Institute of Physics of the CAS,  
Prague, Czech Republic;*

*M. Dvořáková, F. Kovanda, Department of Solid State Chemistry, University of  
Chemistry and Technology, Prague, Czech Republic*

Catalysts in the form of meshes possess a lot of advantages in their using in catalytic reactors: a low pressure drop and good heat transfer [1]. Oxides of Co and Mn show high catalytic activity in various oxidation reactions. Catalysts in the present study were prepared as follows: Stainless steel meshes used as supports were coated with thin  $\text{Co}_3\text{O}_4$  film by RF magnetron sputtering and further  $\text{Co}_3\text{O}_4$  layer by subsequent electrochemical deposition followed by heating. The meshes with deposited  $\text{Co}_3\text{O}_4$  were then coated with additional MnO (samples A-C) or Co-Mn mixed oxide (Co:Mn molar ratio of 1:3, samples D-F) thin films of various thickness (approximately 100, 200, and 300 nm) by RF magnetron sputtering and heated at 500 °C in air. The structured Co-Mn oxide catalysts with various Mn content were examined by XRD, SEM, FTIR, XPS, and  $\text{H}_2$ -TPR, tested in the gas-phase oxidation of model organic compound (ethanol) and compared with pelletized commercial Co-Mn-Al mixed oxide catalyst (Astin 2-100, Czech Republic, Co:Mn:Al molar ratio of 4:1:1).

## Results and discussion

Besides the stainless steel support, XRD measurements revealed only  $\text{Co}_3\text{O}_4$  and no discrete Mn-containing phase was detected in the deposited Co-Mn oxide layers. XPS analysis showed that Mn occurs mainly as MnO on the catalysts surface. Catalytic properties of the prepared catalysts are summarized in Table 1. According to  $T_{50}$ , ethanol oxidation proceeded slightly faster over the catalysts with thicker additional MnO coating. Additional coating of the deposited  $\text{Co}_3\text{O}_4$  layer with Co-Mn mixed oxide was not so effective in improvement of the catalysts activity. More precise evaluation of catalyst activity according to  $r_{200}$  values (mmol of EtOH reacted over gram of active oxides per hour) slightly changed the order of reactivity: The

catalyst with 100 nm MnO coating over the Co<sub>3</sub>O<sub>4</sub> was more active than the others, very likely, because of intimate contact of Co<sub>3</sub>O<sub>4</sub> and MnO. The Co/(Co+Mn) molar ratio around 0.25 provided the most active Co-Mn mixed oxide catalysts for ethanol oxidation. Simple MnO<sub>x</sub> catalyst showed lower temperature of T<sub>50</sub>, however, concentration of undesirable reaction byproduct, CO, was nearly two times higher than those observed at the structured catalysts (Table 1). It follows from the finding that MnO catalyzes oxidation of alcohols with high reaction rate but the rate of CO to CO<sub>2</sub> oxidation is substantially lower than those observed at structured catalysts. As compared with the pelletized Astin 2-100 catalyst, the temperatures required for 95 % conversion of ethanol to CO<sub>2</sub> over the catalysts on stainless steel meshes were by 100 °C lower. The Astin 2-100 catalyst did not exhibit the formation of CO, very likely, due to longer contact of reaction component with active sites in the catalyst pellets.

The activity of all supported catalysts in the total oxidation of ethanol to CO<sub>2</sub> was higher than that of the commercial Astin 2-100 catalyst, though the content of active components in the bed of structured catalysts was more than 50 times lower.

Table 1 Characteristics of the catalysts and their activity (GHSV=21±1 l g<sub>cat</sub><sup>-1</sup> h<sup>-1</sup>, 760 ppm EtOH in air).

Catalyst	(Co)-Mn layer thickness <sup>1</sup> nm	Co/(Co+Mn) mol/mol	Oxides wt. %	T <sub>50</sub> EtOH °C	CO <sub>max</sub> °C/ppm	T <sub>95</sub> CO <sub>2</sub> °C	R <sub>200</sub> <sup>2</sup> mmol EtOH g <sub>oxides</sub> <sup>-1</sup> h <sup>-1</sup>
A	100	0.88	0.57	236	285/119	300	34.8
B	200	0.82	0.55	224	279/119	289	26.3
C	300	0.74	0.64	224	280/113	287	23.4
F	100	0.86	0.44	241	265/115	313	24.1
D	200	0.85	0.72	234	283/125	274	21.1
E	300	0.67	0.41	235	185/89	298	24.2
MnO <sub>x</sub> <sup>3</sup>	2000	0.00	0.47	221	324/211	289	43.0
Pellets <sup>4</sup>	-	0.80	55.0	195	0/0	371 <sup>4</sup>	1.0

<sup>1</sup> additional coating by magnetron sputtering, <sup>2</sup> per g of active phase, <sup>3</sup> coating of the meshes with MnO<sub>x</sub> only, <sup>4</sup> Astin 2-100 at 90 % conversion

### Acknowledgement

The authors thank the Czech Science Foundation for the financial support (project 17-08389S).

### References

[1] S.L. Suib (Ed.), New and Future Developments in Catalysis, Elsevier, 2013.

## Comparative Study of Photo-induced Formation of Peroxide Ions over Cubic and Monoclinic lanthanide Sesquioxides\*

*W. Z. Weng\**, C. L. Liu, Y. H. Zheng, Y. G. Zhang, Y. P. Zheng, Z. H. Zhou

*State Key Laboratory of Physical Chemistry of Solid Surfaces, National Engineering Laboratory for Green Chemical Productions of Alcohols, Ethers and Esters, Department of Chemistry, College of Chemistry and Chemical Engineering, Xiamen University, Xiamen 361005, China*

Photo-induced activation of molecular oxygen ( $O_2$ ) to generate reactive oxygen species (ROS) such as singlet oxygen ( $^1O_2$ ), superoxide radical ( $\bullet O_2^-$ ), hydrogen peroxide ( $H_2O_2$ ) et al. is an important process in the photocatalytic reaction. During a study on the lanthanide sesquioxides ( $Ln_2O_3$ ) under  $O_2$  by microprobe laser Raman spectroscopy, we found that laser excitation of the Raman spectrometer can induce the formation of lanthanide peroxide ions ( $Ln^{3+}-O_2^{2-}$ ) on the  $Ln_2O_3$  surface <sup>[1]</sup>. The results of mechanistic study of the process have confirmed that the  $O_2^{2-}$  are generated through a photo-induced reaction between  $O_2$  and the lattice oxygen ( $O^{2-}$ ) species in lanthanide sesquioxides, in which photoexcitation provides the energy for the transformation of triplet  $O_2$  to the singlet state to satisfy the requirement of the spin conservation rule <sup>[2]</sup>. It therefore provides us with a new pathway of activating  $O_2$  under mild conditions and may potentially be applied in photocatalytic reactions. As a continuation of the previous research, here we examine the photo-induced formation of  $O_2^{2-}$  over cubic (c-) and monoclinic (m-)  $Sm_2O_3$  and  $Gd_2O_3$ , with attention focused on the effect of crystal structure of  $Ln_2O_3$  on the photo-induced oxygenation reaction. Fig. 1 shows the Raman spectra of the cubic and monoclinic  $Sm_2O_3$  and  $Gd_2O_3$  after the samples under  $O_2$  were continuously irradiated with a focused 325 nm laser beam of the Raman spectrometer at indicated powers and temperatures for 30 min. For the samples irradiated with laser beam of a fixed power (e.g. 5 mW) at a temperature between 30 and 400 °C, intensities of the  $O_2^{2-}$  bands (840~852  $cm^{-1}$ ) over c- $Ln_2O_3$  were found to peak at temperature below 200 °C. Comparatively, maximum intensity of the  $O_2^{2-}$  band over m- $Ln_2O_3$  can only be observed at temperature above 300 °C. For the experiments carried out at a fixed temperature (e.g. 100 °C), higher photo irradiation power is also beneficial to the  $O_2^{2-}$  formation on m- $Ln_2O_3$  samples. These results indicate that, compared with c- $Ln_2O_3$ , higher energy input is required to generate  $O_2^{2-}$  over m- $Ln_2O_3$ .

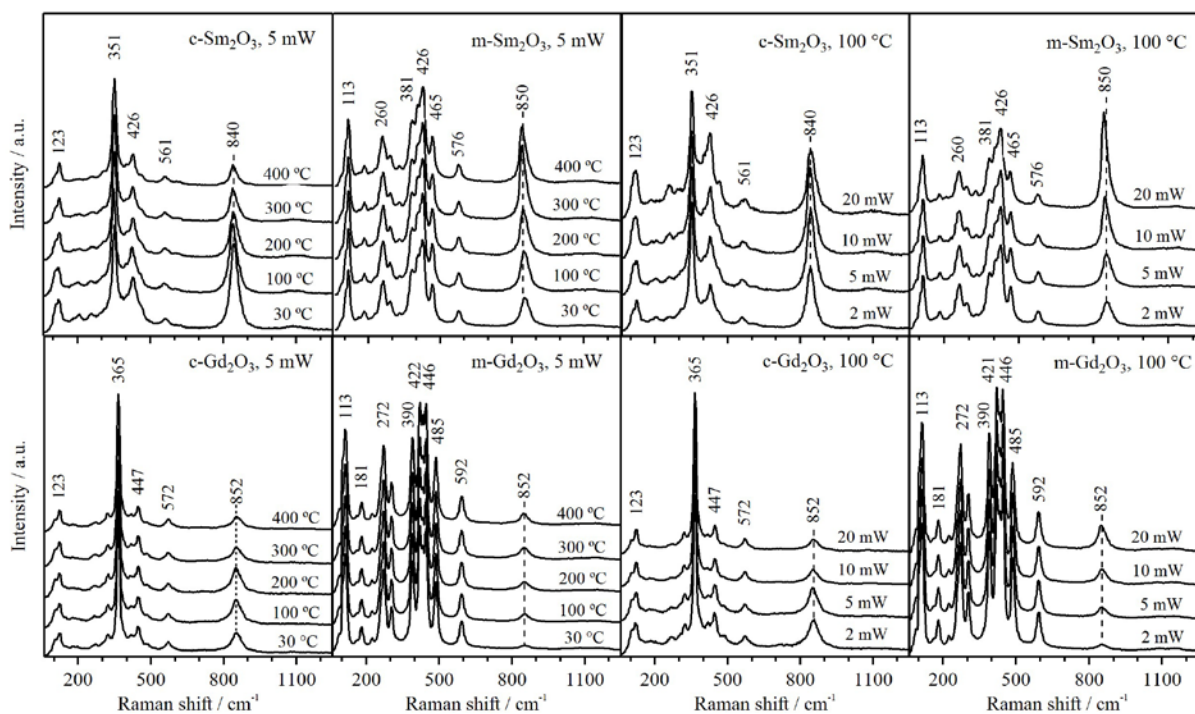


Fig. 1 Effect of temperature and photo irradiation power on the intensity of the Raman band for the  $O_2^{2-}$  species formed by photo-induced reaction of molecular oxygen with the lattice oxygen of cubic and monoclinic  $Ln_2O_3$ .

Based on the results of  $O_2$ -TPD,  $CO_2$ -TPD and  $^{18}O$  isotope exchange experiments shown in Fig. 2, it can be concluded that the significant difference in the behavior of  $O_2^{2-}$  formation over the  $Ln_2O_3$  of two structures can be related to the difference in the capacity of the samples to adsorb molecular oxygen as well as to the difference in basicity and mobility of the lattice oxygen species of cubic and monoclinic  $Ln_2O_3$ .

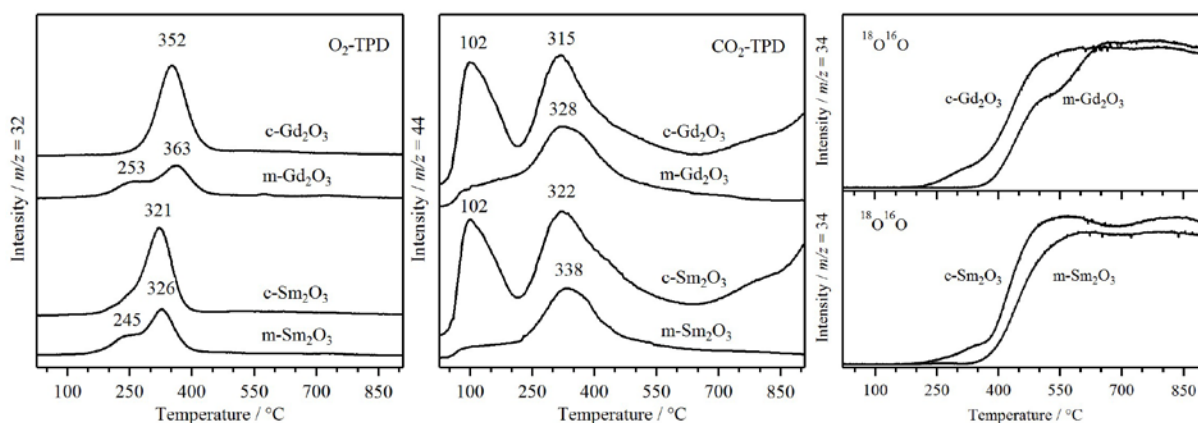


Fig. 2  $O_2$ -TPD (left),  $CO_2$ -TPD (middle) and  $^{18}O$  isotope exchange (right) profiles of the cubic and monoclinic  $Ln_2O_3$  ( $Ln = Sm, Gd$ ) samples.

\* This work is supported by the National Natural Science Foundation of China (No. 21872111)

## References

- [1] W. Z. Weng, H. L. Wan, J. M. Li, Z. X. Cao, *Angew. Chem. Int. Ed.*, 2004, 43, 975-977
- [2] X. L. Jing, Q. C. Chen, C. He, X. Q. Zhu, W. Z. Weng, W. S. Xia, H. L. Wan, *Phys. Chem. Chem. Phys.*, 2012, 14(19), 6898-6904

# **Co-Mn mixed oxide catalysts prepared by hydrothermal deposition on stainless steel wire meshes**

*F. Kovanda, M. Dvořáková, Department of Solid State Chemistry, University of Chemistry and Technology, Prague, Czech Republic;*

*K. Jirátová, J. Balabánová, P. Topka, Institute of Chemical Process Fundamentals of the CAS, Prague, Czech Republic*

The present work was focused on preparation of supported Co-Mn mixed oxide catalysts as both Co and Mn oxides show high catalytic activity in various oxidation reactions and catalysts supported on metal meshes can be applied in any kind of reactor especially that designated for fast reactions [1]. Thin layer of active oxides enables their high utilization due to low internal diffusion effects. The stainless steel meshes used as support were treated under hydrothermal conditions in Co and Mn nitrates aqueous solutions containing urea and then heated at 500 °C in air to obtain supported Co-Mn mixed oxides with various Co:Mn molar ratios. The other set of non-supported catalysts was prepared by coprecipitation of Co and Mn nitrates and subsequent heating at 500 °C in air. The XRD, SEM, TPR, and XPS were used for the catalysts characterization and their activity was examined in deep oxidation of ethanol.

## **Results and discussion**

Large crystals of Co and Mn carbonates were formed on supports during hydrothermal reaction and morphology of the precursors remained preserved after heating. Powder XRD showed  $\text{CoMnO}_3$  as a main crystalline phase in the resulting Co-Mn mixed oxides whereas  $\text{Co}_3\text{O}_4$  and  $\text{Mn}_2\text{O}_3$  were identified in the samples containing only single active component (Co and Mn, respectively). The supported catalysts contained from 1.1 to 5 wt. % of active oxides deposited on the meshes. The grained catalysts (particle size of 0.160-0.315 mm) obtained by heating of coprecipitated hydroxide precursors contained analogous Co and Mn oxides like the supported catalysts. The  $T_{50\text{EtOH}}$  and  $T_{90\text{CO}_2}$  temperatures, at which 50% ethanol conversion and 90% conversion of all organic compounds to  $\text{CO}_2$  were achieved, were used for comparison of the catalysts activity in ethanol total oxidation (Table 1). As expected, the oxide catalysts deposited on stainless steel meshes were less active than the grained ones due to much lower content of active Co and Mn



components:  $T_{50}\text{EtOH}$  and  $T_{90}\text{CO}_2$  temperatures of about 50 – 80 °C higher were found for the supported Co-Mn mixed oxide catalysts. The Co/(Co+Mn) molar ratio of 0.2 was found as the best to obtain Co-Mn mixed oxide catalysts with high efficiency in the ethanol oxidation. Acetaldehyde was produced in low concentrations as byproduct during ethanol oxidation over the examined catalysts. Carbon monoxide was also detected in the reaction off-gas; its concentration decreased with increased Mn content in the catalysts.

Table 1: Activity of the examined catalysts in total oxidation of ethanol (GHSW of  $21\pm 1 \text{ l g}_{\text{cat}}^{-1} \text{ h}^{-1}$ , 760 ppm of ethanol in air)

Co/(Co+Mn) molar ratio	Supported catalysts			Grained catalysts		
	Oxides content / wt. %	$T_{50}\text{EtOH}$ / °C	$T_{90}\text{CO}_2$ / °C	Oxides content / wt. %	$T_{50}\text{EtOH}$ / °C	$T_{90}\text{CO}_2$ / °C
0	4.97	200	248	100	159	200
0.2	1.14	195	253	100	113	190
0.4	2.55	195	251	100	113	181
0.5	3.28	185	244	100	116	188
0.6	2.95	194	264	100	113	186
0.8	1.91	189	254	100	112	179
1	1.95	224	269	100	103	188

## References

[1] M.V. Twigg, D.E. Webster, Structured Catalysts and Reactors, 2nd Edition, A. Cybulski and J.A. Moulijn editors, Taylor and Francis, Chemical Industries Series, 110 (2006) 7.

## Acknowledgements

Authors thank the Czech Science Foundation for the financial support (project 17-08389S).

## **Synthesis and catalytic properties of Cu-Fe-Al oxide nanocomposites - a catalyst for CO oxidation**

*A.V. Fedorov, O.A. Bulavchenko, A.A. Saraev, A.M. Tsapina, Z.S. Vinokurov, V.A. Yakovlev, V.V. Kaichev, Boreskov Institute of Catalysis SB RAS, Novosibirsk*

Catalytic combustion of fuels in fluidized bed has many advantages in comparison with the traditional ways of burning. One of the most important are the low combustion temperature (650-750°C), high fuel utilization factor (~93%), low emission of harmful substances into the atmosphere, a small size of installations and etc. [1]. Also, the process allows us to combust of municipal wastewater sediments from sludge fields [2]. Currently, Cr-containing catalyst ( $\text{CuCr}_2\text{O}_4/\text{Al}_2\text{O}_3$ ) is using for processes of fuel combustion in the fluidized catalyst bed. The main disadvantages of this catalyst are a presence of chromium and the high cost of this catalyst. The Cu-Fe-Al oxide nanocomposites are perspective alternative to existing catalyst due to its high catalytic activities [3]. The aim of this work is to investigate Fe-Al and Cu-Fe-Al oxide composites in deep CO oxidation using recirculating plug flow reactor. The Fe-Al and Cu-Fe-Al oxide nanocomposite catalysts were synthesized by fusion of aluminum, iron, and copper salts, followed by calcination at 700°C. A weight ratio of  $\text{Fe}_2\text{O}_3$  to  $\text{Al}_2\text{O}_3$  was 82 to 18 in all catalysts. The CuO loading was ranged from 0-10 wt.%. The obtained catalysts were investigated by various methods: XRD, XPS, TEM. The kinetic measurements were performed in a differential reactor with a flow-circulating configuration. The reactor was equipped with an external circulation pump. The constant space velocity of the reactants through the catalyst bed was more than 15 recirculations per minute. This provided the total mixing mode and the absence of a gradient. The feed consisted of 2 vol.% CO, 1-4 vol.%  $\text{O}_2$ , and  $\text{N}_2$  in balance. The sample was heated from 100 to 300 °C with 5°/min rate. In the work, an alternative method was used to calculate CO oxidation rates based on light-off curves data. It was shown nonlinear dependence of catalytic activity on copper oxide loading in the samples. The increase in copper oxide content up to 5% leads to the increase in catalytic activity in CO oxidation. With further increase of CuO content up to 10%, the decrease in catalytic activity was observed. The activation energy for the samples with 0, 5 and 10% CuO content was 104, 88 and 74 kJ/mole, respectively. However, the value of the deep oxidation rate has a maximum with 5% copper oxide loading in the sample. This results could be explained by the different phase of the CuO active

component. According to XPS, XRD, and TEM, the samples with 5% CuO loading represent a high-dispersive CuO nanoparticles, meanwhile the samples with higher CuO loading are bulk Fe-containing  $\text{CuAl}_2\text{O}_4$  phase. In this work it is shown that obtained catalysts have high catalytic activities in CO oxidation. Sample containing 5% CuO has the highest steady-state oxidation rate due to the fact that the active component is represented as a high-dispersive CuO nanoparticles.

**Acknowledgement.** This work was supported by the Russian Science Foundation, grant 17-73-20157.

### References

- [1] Z.R. Ismagilov, M.A. Kerzhentsev, *Cat.Today*. 1999, 47, 339-346.
- [2] A.D. Simonov, O.V. Chub, N.A. Yazykov, *Chemistry for Sustainable Development*, 2010, 18, 657-661.
- [3] A.V. Fedorov, A.M. Tsapina, O.A. Bulavchenko, A.A. Saraev, G.V. Odegova, D.Y. Ermakov, Y.V. Zubavichus, V.A. Yakovlev, V.V. Kaichev, *Catal. Let.* 2018. V. 148 . N 12. P. 3715-3722.

# Directed functionalization of oxide nanomaterials for the creation of Ni catalysts for combined steam/CO<sub>2</sub> reforming of methane

*E.V. Matus<sup>1</sup>, L.B. Okhlopkova<sup>1</sup>, I.Z. Ismagilov<sup>1</sup>, O.B. Sukhova<sup>1</sup>,*

*M.A. Kerzhentsev<sup>1</sup>, P. Bharal<sup>2</sup>, Z.R. Ismagilov<sup>1,3</sup>*

*<sup>1</sup>Boreshkov Institute of Catalysis SB RAS, Novosibirsk, 630090, Russia*

*<sup>2</sup>Tezpur University, Napaam, Tezpur - 784 028 Assam, India*

*<sup>3</sup>Institute of Coal Chemistry and Material Science FRC CCC SB RAS, Kemerovo, 650000, Russia*

## 1. Introduction

The use of CO<sub>2</sub> as an initial raw material for chemical processes is a rather urgent task directed to solve the problems of environmental safety and rational management of natural resources. The combined steam/CO<sub>2</sub> reforming of methane allows utilization of greenhouse gases and generation of the synthesis gas that serves as an initial raw material for the production of synthetic liquid fuels and basic chemical products [1]. To create efficient nanosized catalysts with specified physicochemical and catalytic properties, the Ni/MO<sub>y</sub> catalysts were synthesized and systematically studied at the variation of the composition of oxide matrix (M = Ce, La, Mg, Ce-La, Ce-Mg). For the development of methods for control of catalysts activity and their resistance to coking, the strength of metal-support interaction was regulated by means of variation of oxides functionalization method (decomposition of metal salts precursors, polymerizable complex method, sol-gel method).

## 2. Experimental

The Ni/MO<sub>y</sub> samples with different M/Ce molar ratio (M = Ce, La, Mg, Ce-La, Ce-Mg; La/Ce = Mg/Ce = 0-4; y = 1-1.5) were prepared by the incipient wetness impregnation (I-series), polymerizable complex (P-series) and sol-gel (S-series) methods. The catalysts were calcined at 500°C and activated in a reductive atmosphere at 800°C. To determine the “synthesis parameters – structure – properties” relationships, the materials were characterized by TA, BET, XRD, HRTEM-EDX, HAADF-STEM, SEM, DRS UV-Vis, Raman spectroscopy and H<sub>2</sub>-TPR methods and tested in steam/CO<sub>2</sub> reforming of methane at 600-800°C and molar ratio CH<sub>4</sub>:CO<sub>2</sub>:H<sub>2</sub>O:He = 1.0/0.81/0.38/2.8.

### 3. Results and discussion

It was shown that the preparation method and M/Ce molar ratio affected the textural and structural properties of catalysts, as well as their reducibility. Ni catalysts of P-series in comparison of those of I-series were different by thermal genesis, specific surface area (100 vs. 60 m<sup>2</sup>/g), defectiveness and dispersion of CeO<sub>2</sub> (3 vs. 11 nm), type of Ni species (solid solution Ce-M-Ni-O vs. NiO), and their reducibility. The activation of catalysts in reductive atmosphere leads to the formation of Ni<sup>0</sup> active species whose dispersion grows with an increase of the M/Ce molar ratio. The characteristics of catalysts correlate with their functional properties in steam/CO<sub>2</sub> reforming of methane. It was demonstrated that the realization of strong nickel-support interaction promoted the stability against carbonaceous deposits under reaction conditions similar to Ni catalysts in autothermal reforming of methane or ethanol [2, 3]. The developed catalysts provide H<sub>2</sub> yield up to 85% and the conversion of reagents ~ 80% at 750°C in steam/CO<sub>2</sub> reforming of methane

### 4. Conclusions

With the aim to create Ni catalysts with superior anti-sintering and anti-coking behaviour for combined steam/CO<sub>2</sub> reforming of methane directed functionalization of oxide nanomaterials MO<sub>y</sub> (M = Ce, La, Mg, Ce-La, Ce-Mg; La/Ce = Mg/Ce = 0-4; y = 1-1.5) were performed by means of the decomposition of metal salts precursors, polymerizable complex method or sol-gel method. The relationships between the preparation mode and catalyst properties were established. Highly active and stable catalysts for combined steam/CO<sub>2</sub> reforming of methane to synthesis gas were developed.

### Acknowledgements

This work was conducted within the framework of RFBR project No. 18-53-45012. The authors are thankful to Dr. V.A. Ushakov, Dr. S.A. Yashnik, Dr. O.A. Stonkus, Dr. E.Y. Gerasimov, Dr. A.P. Nikitin, Ms. T.Ya. Efimenko and Ms. G.S. Litvak for their help with catalyst characterization.

### References

1. S. Sengupta, G. Deo, J. CO<sub>2</sub> Util. 10 (2015) 67-77.
2. Z.R. Ismagilov, E.V. Matus, I.Z. Ismagilov, O.B. Sukhova, S.A. Yashnik, V.A. Ushakov, M.A. Kerzhentsev, Catal. Today. 323 (2019) 166-182.
3. E.V. Matus, L.B. Okhlopkova, O.B. Sukhova, I.Z. Ismagilov, M.A. Kerzhentsev, Z.R. Ismagilov, J. Nanoparticle Research. 21 (2019) 11.

# Study on Red-Ox properties and CO oxidation activity of nanocrystalline $\text{Ce}_{0.9}\text{Pd}_{0.1}\text{O}_{1.9}$ and $\text{Ce}_{0.7}\text{Yb}_{0.2}\text{Pd}_{0.1}\text{O}_{1.8}$ mixed oxides

*Piotr Kraszkiewicz, Michalina Kurnatowska*

*Institute of Low Temperature and Structure Research, Polish Academy of Sciences,  
Wrocław, Poland*

## Introduction

Cerium oxide continues to arouse much interest due to its unique structural properties [1–2]. One of the most important features is the formation of solid solutions with many metals resulting in mixed oxides with unique properties [3]. New technology is looking for materials that will act as efficient catalysts, that reduce the environment pollution. It seems the nanocrystalline cerium mixed oxides catalyst are promising materials for this purpose [4].

## Methods

Cerium mixed oxides were obtained with hydrothermal and reverse microemulsion methods [5]. Chemical composition of the samples was analyzed by EDS. Samples were characterized using methods: TEM, XRD, EDS. The reducing and oxidizing treatments were carried out by heating of the mixed oxides in gas flow ( $\text{H}_2$  or  $\text{O}_2$ ) at 500–800 °C for 2h. Samples after different thermal treatments were characterized by XRD and TEM. Oxygen storage capacity of samples was measured by  $\text{H}_2$ -TPR (5%  $\text{H}_2/\text{Ar}$ , 10 °C/min up to 900 °C) and catalytic activity was tested in low-temperature CO oxidation.

## Results

The obtained nanocrystalline  $\text{Ce}_{0.9}\text{Pd}_{0.1}\text{O}_{1.9}$  and  $\text{Ce}_{0.7}\text{Yb}_{0.2}\text{Pd}_{0.1}\text{O}_{1.8}$  oxides were homogeneous fluorite-type nanocrystallites with very small size (4–5 nm). The structure studies of the samples annealed in pure  $\text{H}_2$  showed no structure and morphology changes up to 400 and 500 °C for  $\text{Ce}_{0.9}\text{Pd}_{0.1}\text{O}_{1.9}$  and  $\text{Ce}_{0.7}\text{Yb}_{0.2}\text{Pd}_{0.1}\text{O}_{1.8}$ , respectively. Reduction at a temperature higher by 100 °C caused the phase separation and small (2 nm) palladium particles were observed on the oxides surface. The  $\text{H}_2$ -TPR studies revealed strong reduction peak below 50 °C for both samples. The amount of consumed hydrogen indicated that at this

temperature along with Pd<sup>2+</sup>, a certain amount of Ce<sup>4+</sup> was reduced. The reduced palladium was stabilized in the ceria matrix and the addition of ytterbium further stabilized the entire system. The obtained materials were active in low-temperature CO oxidation. The higher activity of the pre-reduced catalysts was attributed to the partially reduced Pd species or metallic Pd clusters at the catalyst surface, undetectable for TEM and XRD.

### **Acknowledgements**

This work was financially supported by the National Science Center in Poland (grant 2015/19/D/ST5/00722).

### **References**

- [1] T. Montini, M. Melchionna, M. Monai and P. Fornasiero, *Chem. Rev.* 116 (2016) 5987.
- [2] M. S. Hegde, G. Madras, K. C. Patil, *Acc. Chem. Res.* 42 (2009) 704.
- [3] *Catalysis by Ceria and Related Materials*, ed. A. Trovarelli and P. Fornasiero, Imperial College Press, London UK, 2002
- [4] Gupta A., Waghmare U. V., Hegde M. S., *Chem. Mater.* 2010; 22: 5184–5198
- [5] M. Kurnatowska, L. Kepinski and W. Mista, *Appl. Catal. B*, 117-118 (2012) 135.

# Sintering-resistant sub-2 nm gold clusters on SBA-15 support, highly active in room temperature CO oxidation

*Piotr Kraszkiewicz, Małgorzata Małecka, Włodzimierz Miśta*

*Institute of Low Temperature and Structure Research, Polish Academy of Sciences,  
Wrocław, Poland*

Gold, in the bulk form is chemically inert, but few-nanometer-sized gold particles are very active catalysts in many reactions, like total and selective oxidation or hydrogenation reactions. It is generally accepted that the size of gold nanoparticles should not exceed 5 nm [1]. Many works devoted to gold catalysts are focused on the preparation of small gold nanoparticles, however the preparation of stable gold catalysts is still challenging. Gold has a relatively low melting temperature (1064 °C for Au vs. 1768 °C for Pt). Moreover, it has been shown that few-nm gold particles can melt in the 300–500 °C temperature range [2]. A low thermal stability of gold catalysts is one of the obstacles to commercial applications, and the achievement of long-term durability is more important than improving their activity [3].

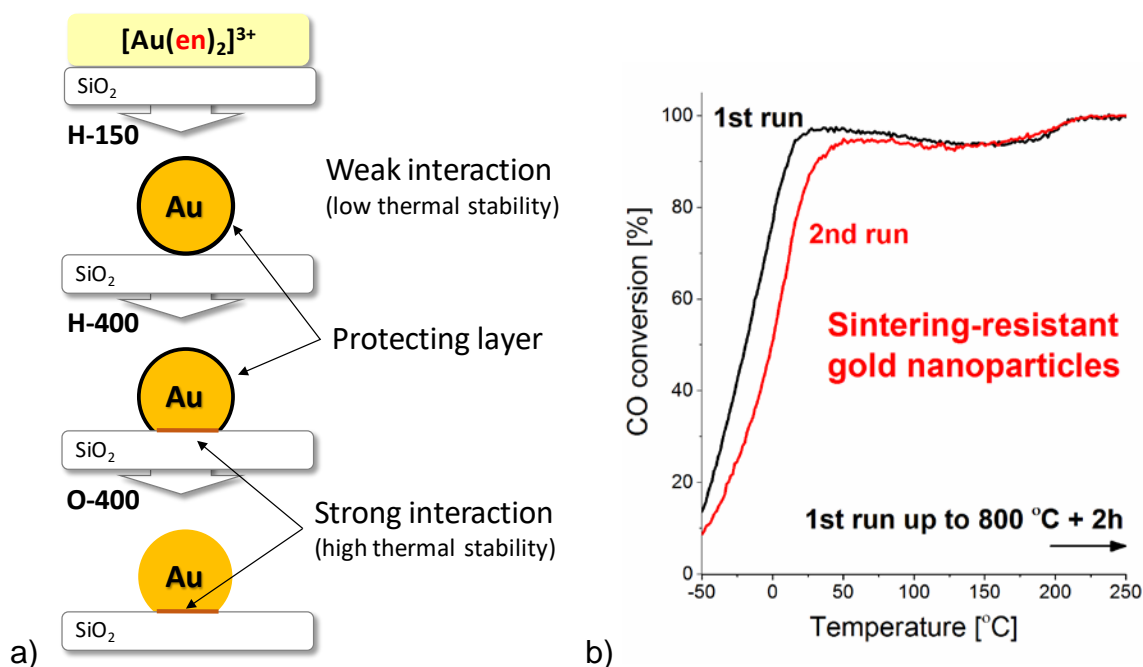


Fig. 1 Proposed mechanism of gold nanoparticles stabilization on the support surface a), results of CO oxidation tests (catalyst: 4.8%Au/SBA-15, 30 mg; 1% CO, 5% O<sub>2</sub> and He, 50 cm<sup>3</sup>/min) b)



In this work, we present the results of our research on the stabilization of gold nanoparticles on the SBA-15 mesoporous silica support. The catalyst was prepared by electrostatic adsorption of  $[\text{Au}(\text{en})_2]\text{Cl}_3$  (en = ethylenediamine) complex on the SBA-15 mesoporous silica surface in aqueous solution. We demonstrated that pre-treatment in hydrogen at 400–600 °C allows stabilizing sub 2-nm gold clusters on the SBA-15 support [4]. Moreover, the obtained gold catalysts are highly active in room-temperature CO oxidation and show unusual resistance to sintering, even at 800 °C (Fig. 1b).

The obtained results suggest that during decomposition of catalyst precursor in hydrogen at high temperature (400 °C) some carbonaceous layer is formed on the surface of gold [4]. This layer may serve as a temporary structure, protecting gold against sintering until strong interaction between gold and silica support is created (Fig. 1a). The existence of strong interaction between gold and silica support explains the high stability of gold nanoparticles after removal of the carbonaceous material during calcination in oxygen.

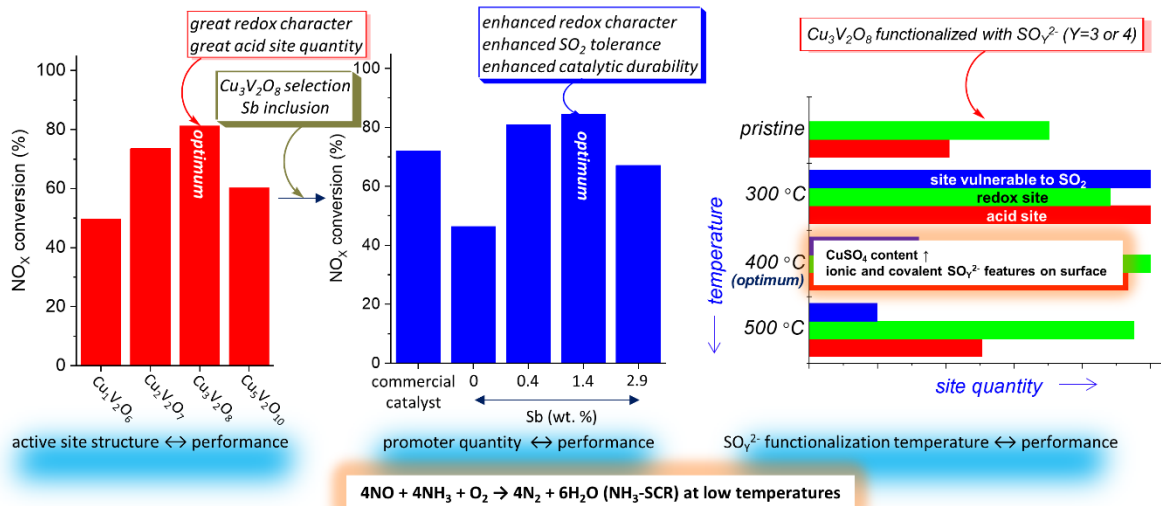
## References

- [1] M. Haruta, *Angew. Chem. Int. Ed.* 53 (2014) 52–56.
- [2] P. Buffat, J.-P. Borel, *Phys. Rev. A.* 13 (1976) 2287–2298.
- [3] C.W. Corti, R.J. Holliday, D.T. Thompson, *Top. Catal.* 44 (2007) 331–343.
- [4] P. Kraszkiewicz, W. Mista, *Catal. Commun.* 110 (2018) 14–17.

# Cu/V Stoichiometry-Variable Copper Vanadate Catalytic Phases for Selective NO<sub>x</sub> Reduction

*Jongsik Km, Korea Institute of Science and Technology, Seoul, South Korea;*  
*Dong Wook Kwon, Korea Institute of Science and Technology, Seoul, South Korea;*  
*Heon Phil Ha, Korea Institute of Science and Technology, Seoul, Republic of Korea*

Abating NO<sub>x</sub> emitted from stationery/mobile sources via NH<sub>3</sub>-assisted selective catalytic NO<sub>x</sub> reduction (NH<sub>3</sub>-SCR) is vital to release global environmental concerns associated with atmospheric fine particulate matters (PM<sub>2.5</sub>) [1,2]. One of feasible ways to promote NH<sub>3</sub>-SCR consequence is to structurally amend V oxides (V<sub>2</sub>O<sub>5</sub> and VO<sub>2</sub>), which are conventionally employed as active sites for NH<sub>3</sub>-SCR. In this presentation, we detail our efforts for creating a series of novel vanadate phases with the use of cheap, ubiquitous Cu as a structural modifier of V oxides (*i.e.*, Cu<sub>1</sub>V<sub>2</sub>O<sub>6</sub> (Cu<sub>1</sub>), Cu<sub>2</sub>V<sub>4</sub>O<sub>7</sub> (Cu<sub>2</sub>), Cu<sub>3</sub>V<sub>2</sub>O<sub>8</sub> (Cu<sub>3</sub>), and Cu<sub>5</sub>V<sub>2</sub>O<sub>10</sub> (Cu<sub>5</sub>)) [1]. The resulting copper vanadate phases are demonstrated to be active in and selective to NH<sub>3</sub>-SCR, while providing surface properties distinct one another [1]. This allows for locating the optimum vanadate phase for NH<sub>3</sub>-SCR (Cu<sub>3</sub>), which exhibits the greatest Brönsted/Lewis acidity coupled with the best redox trait among all vanadate phases [1]. We also engineer Cu<sub>3</sub> phase via its functionalization with SO<sub>Y</sub><sup>2-</sup> species (Y= 3 or 4) to further tune the catalytic property of Cu<sub>3</sub> adequate to proceed NH<sub>3</sub>-SCR at low temperatures (*i.e.*, ≤300 °C) [2]. The SO<sub>Y</sub><sup>2-</sup>-functionalized Cu<sub>3</sub> phase is verified to 1) better catalyze NH<sub>3</sub>-SCR than a control simulating a commercial catalyst and 2) to be of significant tolerance against H<sub>2</sub>O, SO<sub>2</sub>, and poisons including alkali-metals and ammonium (bi) sulfates during NH<sub>3</sub>-SCR at low temperatures [1,2]. Our study remarks the SO<sub>Y</sub><sup>2-</sup>-modified, optimum Cu<sub>3</sub> can be greatly preferred as an active site and be of appreciable efficiency to accelerate NH<sub>3</sub>-SCR at low temperatures.



## References

- [1] J. Kim,<sup>1</sup> D. W. Kwon, S. Lee, H. P. Ha\* *Appl. Catal. B* 236 (2018) 314-325.
- [2] J. Kim,<sup>1,\*</sup> S. Lee,<sup>1</sup> D. W. Kwon, K. Y. Lee, H. P. Ha\* *Appl. Catal. A* 570 (2019) 355-366.

# Practical Applications of CeO<sub>2</sub>-Added Sb-V<sub>2</sub>O<sub>5</sub>/TiO<sub>2</sub> Catalyst to Stationery and Mobile NO<sub>x</sub> Reduction Units

*Heon Phil Ha, Korea Institute of Science and Technology, Seoul, South Korea;*  
*Dong Wook Kwon, Korea Institute of Science and Technology, Seoul, South Korea;*  
*Jongsik Kim, Korea Institute of Science and Technology, Seoul, Republic of Korea*

Inventing a catalytic solid with high activity and selectivity to reduce NO<sub>x</sub> by NH<sub>3</sub> to form N<sub>2</sub> and H<sub>2</sub>O (NH<sub>3</sub>-SCR) is recently sought after to attenuate the atmospheric concentration of NO<sub>x</sub>, leading to mitigate severe air pollution [1-3]. We discover a catalytic nano-composite (denoted as 'SVCT') for low-temperature NH<sub>3</sub>-SCR, where V oxides (acting as active sites) and Ce/Sb oxides (acting as promoters) are highly dispersed throughout anatase (TiO<sub>2</sub>) support [1-3]. Unique combination of V, Ce, and Sb ingredients inherent to the SVCT provides such acidity and redox feature as to significantly accelerate NH<sub>3</sub>-SCR at low temperatures ( $\leq 250$  °C), readily recover its NH<sub>3</sub>-SCR performance post the regeneration under mild conditions, and substantially tolerate alkali-metal poison [1-3]. In this presentation, we highlight our recent pilot studies on the SVCT to diagnose its practical applicability as a catalyst for NH<sub>3</sub>-SCR unit built in private or public sector located in South Korea. The SVCT is mass-produced, engineered to be the part of a monolith or a corrugate-typed catalyst bed, and installed in the NH<sub>3</sub>-SCR unit used for the mobile (marine diesel engine of HSD ENGINE) or the stationery NO<sub>x</sub>-emitting sources (sintering furnace of POSCO). Our pilot studies corroborate that in comparison with a commercial catalyst (V<sub>2</sub>O<sub>5</sub>-WO<sub>3</sub> on TiO<sub>2</sub>), the SVCT reveals greater NO<sub>x</sub> conversions and superior resistance to poisons including SO<sub>2</sub> and ammonium (bi) sulfate. The SVCT, therefore, can provide outstanding long-term stability to catalyze NH<sub>3</sub>-SCR at low temperatures. This is evidenced by time-on stream studies of the SVCT in the presence of H<sub>2</sub>O/SO<sub>2</sub>-included flue gas stream at 240 °C and 250 °C, where NO<sub>x</sub> conversions are  $\geq \sim 80$  % up to  $\sim 700$  hours and  $\geq \sim 95$  % up to  $\sim 1,300$  hours, respectively.

## References

- [1] K. J. Lee,<sup>1</sup> A. K. Pullur, M. S. Maqbool, K. N. Rao, K. H. Song, H. P. Ha\* *Appl. Catal. B* 142-143 (2013) 705-717.
- [2] M. S. Maqbool,<sup>1</sup> A. K. Pullur, H. P. Ha\* *Appl. Catal. B* 152-153 (2014) 28-37.
- [3] D.W. Kwon,<sup>1</sup> K. B. Nam, S. C. Hong\* *Appl. Catal. B* 166-167 (2015) 37-44.

## **Three-dimensionally ordered macroporous PrO<sub>x</sub>: an improved alternative to soot combustion ceria catalysts**

*Virginia Alcalde-Santiago; Esther Bailón García; Arantxa Davó-Quñonero; Dolores Lozano-Castelló; Agustín Bueno-López, University of Alicante, Alicante, Spain*

In recent years, significant efforts have been made in order to develop new systems to eliminate the carbon particles (soot) emitted by diesel engines, since these particles are responsible for severe environmental and health problems. These systems usually consist of a filter placed in the exhaust pipe, where the particles are retained and burned. Nevertheless, the temperature of the exhaust gases of modern diesel engines is relatively low (150–500 °C) and consequently, is not enough for the spontaneous combustion of soot (550-700 °C) [1]. Thus, a catalyst is required to decrease the combustion temperature of retained particles. Cerium oxide is one of the most promising catalysts, since ceria can generate highly reactive oxygen species, named “active oxygen”, which are highly oxidizing and very efficient for soot combustion. Praseodymium oxide could be presented as an improved alternative to ceria catalysts because of, akin ceria, can adopt oxygen-deficient stoichiometries, and even, the Pr<sup>4+</sup>/Pr<sup>3+</sup> pair has a greater reduction potential than the Ce<sup>4+</sup>/Ce<sup>3+</sup> pair, and moreover, presents higher ability for the NO<sub>2</sub> production.

Nevertheless, one of the main problems of this solid-solid reaction is the poor contact between the solid particles of carbon and the solid particles of catalyst. It has been demonstrated by several authors that the use of ceria with a three-dimensional ordered macroporous structure (3DOM) greatly improves the soot combustion due to the improvement the active oxygen transfer from the catalysts to the soot [2].

Herein we describe the synthesis of PrO<sub>x</sub>-3DOM and its use, for the first time, in the soot combustion. Its behavior has been compared with that of CeO<sub>2</sub>-3DOM, and non-structured CeO<sub>2</sub> and PrO<sub>x</sub> catalysts (which are referred to as “Ref”) have been also prepared and tested for comparison.

This novel PrO<sub>x</sub>-3DOM catalyst is presented as an improved noble-metal-free alternative to CeO<sub>2</sub> as soot combustion catalyst. The PrO<sub>x</sub>-3DOM catalyst presents a well-defined 3DOM structure with high macropores volume (Figure 1a), which significantly enhances the solid-solid soot-catalyst contact. This enhanced contact, together with the improved reducibility of PrO<sub>x</sub> regarding CeO<sub>2</sub> (Figure 1c),

ameliorate the active oxygen production and its transfer to soot particles, improving the soot combustion with  $O_2$ .

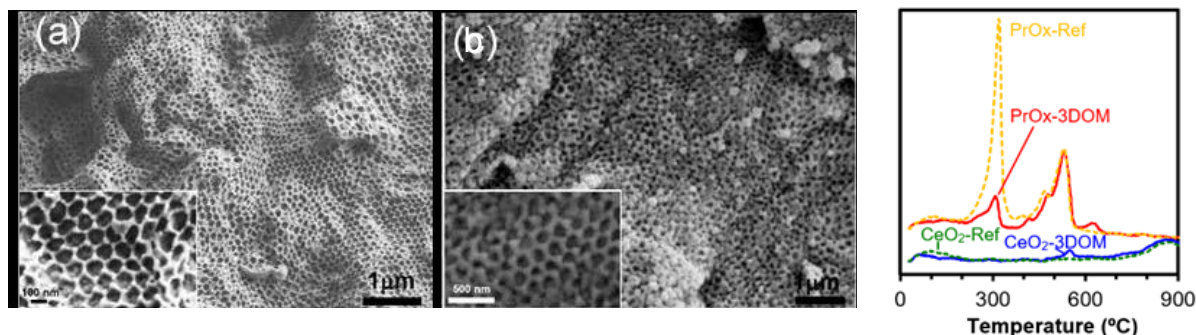


**Figure 1.** SEM images of a) PrOx-3DOM and b) CeO<sub>2</sub>-3DOM and c) H<sub>2</sub>-TPR characterization of catalysts.

In addition, PrO<sub>x</sub> presents higher ability to oxidize NO to NO<sub>2</sub> than CeO<sub>2</sub> (Figure 2a), which participates in the generation of active oxygen favoring the soot combustion in higher extend in presence of NO<sub>x</sub> (Figure 2b). The catalytic activity of PrO<sub>x</sub>-3DOM after several soot combustion cycles is also confirmed.

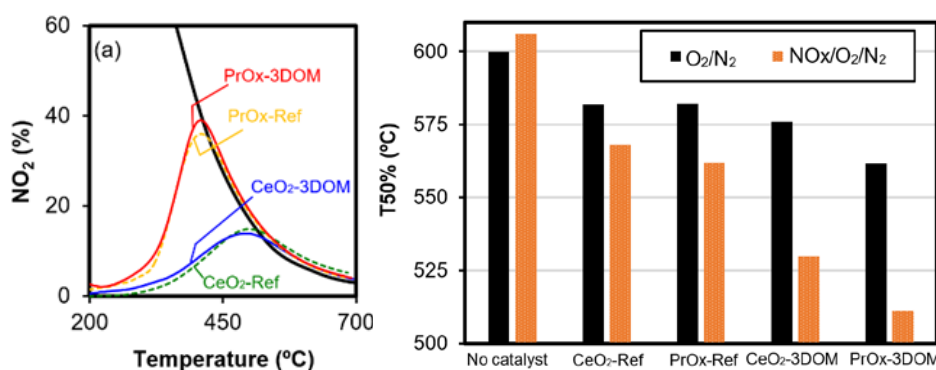


**Figure 2.** a) NO oxidation to NO<sub>2</sub> in catalytic experiments performed without soot and b) Comparison of soot combustion in the absence and presence of NO<sub>x</sub>. (T50% is the temperature where 50% of soot is oxidized).

Consequently, three-dimensionally ordered macroporous PrO<sub>x</sub> presents an improved behaviour to generate active oxygen and to transfer it to soot, which provide an improved performance for the soot combustion with regard to ceria.

### Acknowledgements

The authors thank the financial support of the Spanish Ministry of Economy and Competitiveness (Project CTQ2015-67597-C2-2-R and grant FJCI-2015-23769), the Generalitat Valenciana (PROMETEO/2018/076) the Spanish Ministry of Education, Culture and Sports (grant FPU14/01178) and the UE (FEDER funding).

### References

- [1] R. Ramdas, E. Nowicka, R. Jenkins, D. Sellick, C. Davies, S. Golunski. *Appl. Catal. B Environ.* 176–177 (2015) 436–443.
- [2] V. Alcalde-Santiago, A. Davó-Quñonero, D. Lozano-Castelló, A. Bueno-López. *Appl. Catal. B Environ.* 234 (2018) 187–197

# Development, synthesis and investigation of titania-zirconia nanomaterials for selective hydrogenation of 2-methyl-3-butyn-2-ol in microcapillary reactor

L.B. Okhlopkova<sup>1</sup>, M.A. Kerzhentsev<sup>1</sup>, Z.R. Ismagilov<sup>1,2</sup>

<sup>1</sup>*Boriskov Institute of Catalysis SB RAS, Novosibirsk, 630090, Russia*

<sup>2</sup>*Institute of Coal Chemistry and Material Science FRC CCC SB RAS, Kemerovo, 650000, Russia*

## Introduction

The use of microreactor technology for fine organic synthesis is an urgent task directed to solve the problems of environmental safety and control of selectivity in sequential reactions. Multicrystalline oxide coatings nanoparticles have increased mechanical strength and thermal stability as compared to titanium dioxide coatings [1]. In this paper, by changing the Ti/Zr molar ratio, TiO<sub>2</sub>-ZrO<sub>2</sub> composites and coatings were fabricated through EISA process. The effect of the composition of oxide matrix on porous and crystalline structures and catalytic properties of materials in selective hydrogenation of 2-methyl-3-butyn-2-ol (MBY) in microcapillary reactor was studied.

## Experimental

Ordered mesoporous titania-zirconia Ti<sub>x</sub>Zr<sub>1-x</sub>O<sub>2</sub> composites were synthesized by varying Ti/Zr molar ratio (Ti/Zr = 0.18, 0.25, 0.43, 1, 2.3) via self-assembly using titanium isopropoxide and zirconium oxychloride as titania and zirconia sources and triblock copolymer F127 as a template [2]. The structure of pore walls and their thermal stability are systematically studied by XRD, TEM and low-temperature adsorption of nitrogen. Mesoporous coatings doped with nanoparticles were obtained by one-step synthesis using a PdZn colloid. The catalytic coatings of 1 wt.% PdZn/Ti<sub>x</sub>Zr<sub>1-x</sub>O<sub>2</sub> (x = 1, 0.8, 0.5) were synthesized on the inner surface of a 0.53-mm-long capillary reactor with a length of 10 m. Coatings were tested in the selective hydrogenation of MBY at 333 K and 1 atm. H<sub>2</sub>.

## Results and discussion

In most cases, the process of EISA in the synthesis of mesoporous oxide materials requires the addition of acid to slow the hydrolysis-condensation reaction of metal precursors. In this case, no acid is added to regulate the rate of hydrolysis, which is

important in the synthesis of catalytic coatings for microreactors. A series of titanium-zirconium nanocomposites with controlled properties was prepared by varying the Ti/Zr ratio. Composites have an ordered mesostructure of pores, a high specific surface area (up to 157 m<sup>2</sup>/g), a large volume of pores (0.13–0.21 cm<sup>3</sup>/g) and a uniform pore size distribution (3.6–3.7 nm).

The productivity of the microcapillary reactor after 32 hours of continuous stream increases in the series PdZn/TiO<sub>2</sub> < PdZn/Ti<sub>0.8</sub>Zr<sub>0.2</sub>O<sub>2</sub> < PdZn/Ti<sub>0.5</sub>Zr<sub>0.5</sub>O<sub>2</sub> at constant selectivity (more than 96%) and productivity of the catalysts (1.2, 1.5 and 1.3 gMBE/s/gPd) due to thickening of the coating. The high selectivity for PdZn nanoparticles embedded to titania-zirconia matrix is due to the decrease in the constant of direct hydrogenation and the ratio of the alkene and alkyne adsorption constants derived by kinetic modelling.

### **Conclusions**

With the aim to create of PdZn coatings with high stability, activity and selectivity for hydrogenation of 2-methyl-3-butyn-2-ol ordered mesoporous titanium-zirconium composites were synthesized via an EISA process. A catalytic coating based on TiO<sub>2</sub>-ZrO<sub>2</sub> composites with PdZn-embedded nanoparticles showed high activity and selectivity in the hydrogenation of 2-methyl-3-butyn-2-ol.

### **Acknowledgements**

This work was conducted within the framework of the budget project No. AAAA-A17-117041710090-3 for Boreskov Institute of Catalysis. The authors are thankful to Dr. V.A. Ushakov, Dr. E.Y. Gerasimov, Ms. T.Ya. Efimenko and Ms. G.S. Litvak for their help with catalyst characterization.

### **References**

1. L. B. Okhlopko, M. A. Kerzhentsev, Z. R. Ismagilov, Surf. Eng. 31 (2015) 78 -83.
2. Yuan, Q., Liu, Y., Li, L., Li, Z.-X., Fang, C.-J., Duan, W.-T., Li, X.-G., Yan, C.-H., Micropor. Mesopor. Mater. 124 (2009) 169–178.



## **Dual function materials for the storage and methanation of CO<sub>2</sub>.**

### **Selection of nickel loading, adsorbent and impregnation sequence.**

A. Bermejo-López, A. Quindimil, B. Pereda-Ayo, J. A. González-Marcos, J. R. González-Velasco\* Department of Chemical Engineering, Faculty of Science and Technology, University of the Basque Country UPV/EHU, 48940-Leioa, Bizkaia, España. \*juanra.gonzalezvelasco@ehu.eus

#### **Introduction**

It has been very recently published for the first time in the scientific literature the use of dual function materials (DFM) for the methanation of CO<sub>2</sub> from diluted streams through the Sabatier equation, without the need for the previous stage of sequestration and concentration [1-3]. The DFMs contain an alkaline or alkaline earth product that acts as an adsorbent allowing the storage of CO<sub>2</sub> and a noble metal that assists the direct conversion to methane without the need for intensive energy consumption intermediate thermal processes. In this way, the energy requirement of the process is limited to obtaining H<sub>2</sub> and, therefore, the CO<sub>2</sub> capture process, conversion to CH<sub>4</sub> and subsequent use of the fuel approximates to a CO<sub>2</sub> neutral cycle, with no net emissions of this gas to the atmosphere. This requires obtaining hydrogen from a renewable energy source. In this context, the objective of this study is to analyse different contents of nickel (5, 10 and 15%) over 15% CaO/ $\gamma$ -Al<sub>2</sub>O<sub>3</sub> or 10% Na<sub>2</sub>CO<sub>3</sub>/ $\gamma$ -Al<sub>2</sub>O<sub>3</sub> and the impregnation sequence.

#### **Results and discussion**

The addition of nickel causes a progressive decrease of the specific surface area and pore volume. The dispersion of Ni markedly decreased with increasing the loading in the CaO contain catalysts, whereas Ni dispersion was hardly affected in the Na<sub>2</sub>CO<sub>3</sub> contain catalyst. The dispersion values were corroborated by the Ni particle size observed by TEM.

The presence of 15% CaO provides the catalyst with weak, medium and strong basicity sites, while the presence of 10% Na<sub>2</sub>CO<sub>3</sub>, only provides weak and medium basicity. The addition of Ni, irrespective of the impregnation sequence, barely varies the CO<sub>2</sub> desorption profiles during basicity measurements. Regarding the reducibility, three H<sub>2</sub> consumption peaks belonging to three nickel species ( $\alpha$ ,  $\beta$  and  $\gamma$ ) were detected during H<sub>2</sub>-TPR experiments. Besides, an additional H<sub>2</sub> consumption peak was observed due to methane production with preadsorbed CO<sub>2</sub>. Samples

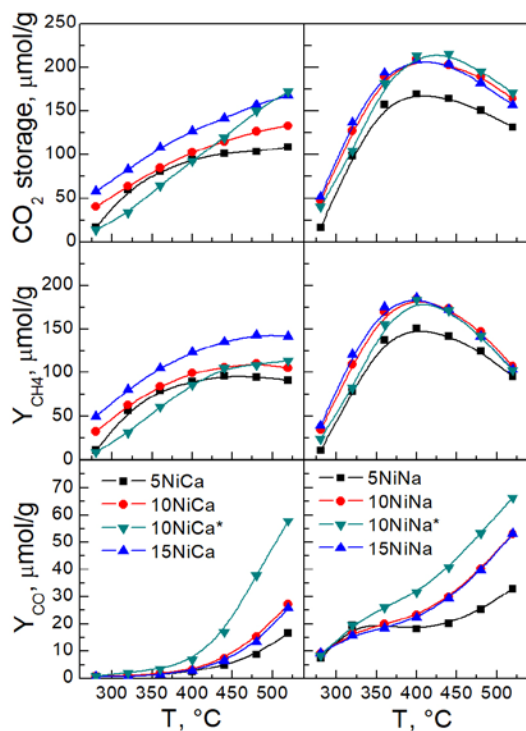


**Figure 1.** Evolution of the storage capacity of CO<sub>2</sub>, production per cycle of CH<sub>4</sub> and CO with temperature.

govern the process.

Figure 1 shows the evolution of the storage capacity of CO<sub>2</sub> and the production per cycle of CH<sub>4</sub> and CO with temperature. It is observed that the amount of CO<sub>2</sub> stored and the CH<sub>4</sub> production per cycle follow a similar trend. CH<sub>4</sub> production increases with temperature irrespective the nickel loading for CaO containing catalysts, whereas maximum CH<sub>4</sub> production is observed around 400 °C for Na<sub>2</sub>CO<sub>3</sub> containing catalysts. On the other hand, the higher the nickel loading the higher the CH<sub>4</sub> production is. The CO production increases as the temperature and nickel loading increase, being significantly higher for coimpregnated samples.

In summary, the catalyst with 10% nickel and 10% Na<sub>2</sub>CO<sub>3</sub> sequentially impregnated presents the highest production of methane with a selectivity of 89% at a lower temperature than CaO based catalysts, requiring less energetic operating conditions to carry out the capture and methanation of CO<sub>2</sub>.

#### References

- [1] M. S. Duyar, M. A. A. Treviño, R. J. Farrauto, A. Catalysis B: Environmental, 168-169 (2015) 370.
- [2] Duyar MS, Wang S, Arellano-Treviño MA, Farrauto RJ. J CO<sub>2</sub> Util. 65-71 (2016) 15.
- [3] Wang S, Farrauto RJ, Karp S, Jeon JH, Schruck ET. J CO<sub>2</sub> Util. 390-7 (2018) 27.

#### Acknowledgements

This work has been financed by the Ministry of Economy and Competitiveness for the project (CTQ2015-67597-C2-1-R-MINECO/FEDER,EU) and the predoctoral grant (BES-2016-077855).

containing Na<sub>2</sub>CO<sub>3</sub> as adsorbent present a larger amount of  $\gamma$ -NiO species due to the higher interaction of nickel with the support. The coimpregnation of nickel and the adsorbent also results in a greater interaction of Ni with the support. This results have been also corroborated by XPS.

The process of storage or capture of CO<sub>2</sub> (1200 ml/min (45000 h<sup>-1</sup>), 11% CO<sub>2</sub>/Ar during 1 min) followed by its hydrogenation or methanation to CH<sub>4</sub> (1200 ml/min, 10% H<sub>2</sub>/Ar, during 2 min), with an intermediate Ar purge, has been monitored. The temporal evolution of the concentration of reactants and products has been described in both cycles, determining the basic chemical reactions that

# Effect of Cu-state in Cu-ZSM-5 on their SCR NO-NH<sub>3</sub> behavior

*S.A. Yashnik<sup>1</sup>, Z.R. Ismagilov<sup>1,2</sup>*

<sup>1</sup>*Borekov Institute of Catalysis, Novosibirsk, Russia*

<sup>2</sup>*Institute of Coal Chemistry and Material Science, Kemerovo, Russia*

## Introduction

At present, the increasingly stringent requirements, which are limiting NO<sub>x</sub> and soot emissions from light and heavy duty diesel engines in EU countries [1], motivate the search for new ways to improve the behavior and stability of Cu-zeolites in ammonia-based selective catalytic reduction of NO<sub>x</sub> (SCR NO-NH<sub>3</sub>). The relationships between the copper loading, types of Cu active species, and activity for SCR NO-NH<sub>3</sub>, that were revealed through a comparative study of Cu-ZSM-5 by physicochemical (ESR, DR UV-Vis, DRIFT, H<sub>2</sub>-TPR, NH<sub>3</sub>-TPD, etc.) and kinetic (TPD and steady-state modes, sorption/desorption dynamics) methods, will be discussed.

## Experimental

Cu-ZSM-5(Si/Al 17) samples were prepared according to the ion exchange procedure described elsewhere [2]. The preferential stabilization of Cu<sup>2+</sup> ions in Cu-ZSM-5 as isolated ions, Cu-structures with extra-lattice oxygen or CuO-like clusters were controlled by NH<sub>4</sub>OH/Cu<sup>2+</sup> ( $\alpha$ ) ratio in the ion-exchanged copper-acetate solution, and their number ( $n$ , %) was controlled by the concentration of copper in solution. Copper concentration and NH<sub>4</sub>OH/Cu<sup>2+</sup> molar ratio (in ammonia solutions of copper acetate) were varied in the range 0.007 – 0.15 M and 0 – 30, respectively.

The SCR NO-NH<sub>3</sub> and NH<sub>3</sub> sorption-desorption dynamics over Cu-ZSM-5 were measured at 200-550 °C with the gas flow rate 42000 h<sup>-1</sup> and the feed composed of 300-600 ppm NO, 300-600 ppm NH<sub>3</sub>, 3.1-3.2 vol% O<sub>2</sub> and Ar balance; the latter was analyzed on-line using analyzer TEST-1 equipped with electrochemical sensors.

## Results and discussion

The ammonia sorption-desorption dynamics over n%Cu( $\alpha$ )-ZSM-5 as well as the genesis of the copper(II) structures were studied by varying the temperature (25-300 °C) and the feed composition (NH<sub>3</sub>; NH<sub>3</sub>+O<sub>2</sub>; NH<sub>3</sub>+NO+O<sub>2</sub>). The ammonia sorption capacity and the amount of strongly adsorbed ammonia rapidly decreased with increasing temperature and at oxygen addition to feed. Parameters of ESR

( $g_{\parallel} = 2.24$ ,  $g_{\perp} = 2.06$ ,  $A_{\parallel} = 180$  G) and DR UV-Vis ( $14700\text{ cm}^{-1}$ ) spectra of the n%Cu( $\alpha$ )-ZSM-5 with adsorbed ammonia illustrated a transformation of Cu(II)-complexes with oxygen-containing ligands to ammonia complexes. NH<sub>3</sub>-TPD of n%Cu( $\alpha$ )-ZSM-5 showed 3-4 peaks corresponding to: the weakly-bound NH<sub>3</sub> adsorbed on the CuO-like species (175-200 °C), the physisorbed NH<sub>3</sub> and NH<sub>3</sub> adsorbed on weak Bronsted acid sites of the surface silanol groups (220-240 °C), the coordinated NH<sub>3</sub> in the [Cu(NH<sub>3</sub>)<sub>n</sub>]<sup>2+</sup> complex (280-375°C), the strongly bound NH<sub>3</sub> on Bronsted acid sites (425-450 °C). The first type of the adsorbed ammonia is characteristic only of 3.5%Cu(3)-ZSM-5 with CuO-like nanoparticles, its adsorption heat was near 50-60 kJ/mol. The [Cu(NH<sub>3</sub>)<sub>n</sub>]<sup>2+</sup> complex ( $\Delta H = 95 \pm 5$  kJ/mol) and the strongly bound NH<sub>3</sub> ( $\Delta H = 110 \pm 10$  kJ/mol) dominated in 0.5-2%Cu(0)-ZSM-5 with the isolated Cu<sup>2+</sup> ions. The samples 0.5-2.5%Cu(6,10,15)-ZSM-5 with isolated Cu<sup>2+</sup> ions and Cu(II)-structures with extra-lattice oxygen showed the coordinated ( $\Delta H = 75-80$  kJ/mol) and the strongly bound ( $\Delta H = 95 \pm 5$  kJ/mol) ammonia, but the heat of NH<sub>3</sub> adsorption over them were lower compared to catalysts with the isolated ions. At 300 °C, NH<sub>3</sub> was adsorbed only over strong sites of 2.5%Cu(6,10,15)-ZSM-5, apparently as NH<sub>4</sub><sup>+</sup>, but its adsorption by 0.5-2%Cu(0)-ZSM-5 and 0.5-2%Cu(30)-ZSM-5 was insignificant.

When NH<sub>3</sub> was adsorbed on the catalyst 2.5%Cu(15)-ZSM-5 from the mixture NH<sub>3</sub>+NO+O<sub>2</sub>, the NH<sub>3</sub> and NO conversion at 200°C were equal to 42% and 100%, respectively. After NH<sub>3</sub> removal from the catalyst by NO+O<sub>2</sub>+Ar, NO<sub>2</sub> and NO were registered in the gas mixture. These facts indicate the "fast route" of SCR NO-NH<sub>3</sub>[4].

## Conclusion

The nature of the copper species and their loading affect the SCR NO-NH<sub>3</sub> behavior of the Cu-ZSM-5. Ammonia storage as well as NO-to-NO<sub>2</sub> oxidation on the Cu active sites are crucial for the low-temperature SCR NO-NH<sub>3</sub>. NO oxidation is catalyzed by Cu-structures with extra-lattice oxygen, which are formed using the ion-exchange mode at NH<sub>4</sub>OH/Cu<sup>2+</sup> = 6-15 and thermal treatment of the high-copper-loaded Cu-ZSM-5. The isolated Cu<sup>2+</sup> ions of the ion-exchanged Cu-ZSM-5 ensure high NO conversion at high temperatures due to their low NH<sub>3</sub> oxidation activity.

**Acknowledgements.** This work was conducted within the framework of the budget project #AAAA-A17-117041710086-6 for Boreskov Institute of Catalysis.

## References

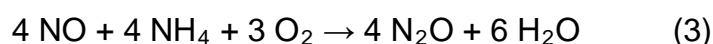
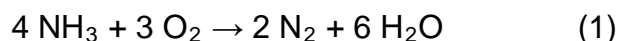
1. Regulation (EC) No 715/2007, 20 June 2007; Regulation (EC) No 595/2009, 18 June 2009.
2. Yashnik SA, Ismagilov ZR. *Appl. Catal. B.* 170-171 (2015) 241.
3. Yashnik SA, Ismagilov ZR. *Top. Catal.* (2019).
4. Komatsu T, Nunokawa M, Moon S, Takahara T, Namba S, Yashima T. *J. Catal.* 148 (1994) 427.

# Hydrotalcite derived Cu-Mg-Al and Ce/Cu-Mg-Al mixed metal oxides as effective catalysts for selective oxidation of ammonia to dinitrogen

*Sylvia Górecka, Institute of Environmental Technology, VŠB – Technical University of Ostrava, 17. listopadu 15, 708 33, Ostrava, Czech Republic; Bogdan Samojeden, AGH University of Science and Technology, Faculty of Energy and Fuels, Al. Mickiewicza 30, 30-059, Kraków, Poland, Lucjan Chmielarz, Jagiellonian University, Faculty of Chemistry, Gronostajowa 2, 30-387, Kraków, Poland*

## Introduction

Atmospheric pollutants such as nitrogen oxides and ammonia are one of the major environmental problems, especially in the industrial sector. Increasing amount of these compounds resulted in stricter regulations on their emission and intensification of studies focused on optimization of existing technologies and development of new solutions for emission abatement from different sources. Presented work is focused on the selective oxidation of ammonia by the oxygen to dinitrogen and water vapour (NH<sub>3</sub>-SCO) which is one of most promising methods for the removal of NH<sub>3</sub> from oxygen containing waste gases. According to the equations, given below, main products of NH<sub>3</sub>-SCO are dinitrogen and water vapour (equation 1), and main side products are NO and N<sub>2</sub>O (equations 2 and 3).



Effective catalysts of NH<sub>3</sub>-SCO should be active at a relatively low temperature range and should be selective directly to the main products: N<sub>2</sub> and H<sub>2</sub>O. Mixed metal oxides obtained by calcination of hydrotalcite like precursors have been found as an effective catalysts of NH<sub>3</sub>-SCO reaction [1,2]. In presented studies series of Cu-Mg-Al and Ce/Cu-Mg-Al metal oxides with a various Mg/Al ratios and different temperatures of calcination have been examined as catalysts for the NH<sub>3</sub>-SCO process.

## Experimental

The hydrotalcite-like precursors with intended Cu/Mg/Al molar ratios of 5/77/18, 5/72/23, 5/67/28 and 5/62/33 were synthesized by co-precipitation method from aqueous solutions of metal nitrates and Na<sub>2</sub>CO<sub>3</sub> as precipitating agent. The pH was

controlled by NaOH dropwise addition. After synthesis, dried samples were calcinated in an air atmosphere at 600, 700 and 800 °C for 9 h.

Additionally, samples obtained by calcination of 5/62/33 precursor at 600 °C were impregnated by various content of Ce (0.5 mol.% or 3 mol.%). After modification samples were dried and calcinated again at 600 °C.

The mechanism of thermal decomposition of precursors to mixed metal oxides was studied by thermogravimetric method combined with residual gas analysis and *in situ* high temperature XRD measurements.

Physicochemical analyses of calcinated samples included: determination of textural parameters (BET), structure (XRD) and form of aggregation of transition metal species (UV-vis-DRS, H<sub>2</sub>-TPR).

Calcinated samples were tested as catalysts of NH<sub>3</sub>-SCO process in a plug flow microreactor system combined with quadrupole mass spectrometer.

## Results

Metal oxides obtained by calcination of hydrotalcite-like precursor have been found as effective catalysts of NH<sub>3</sub>-SCO process. Both the Mg/Al ratio and temperature of calcination strongly influence the activity and selectivity. In general, an increase of calcination temperature and decrease of Mg/Al ratio increased selectivity to dinitrogen, what is related to formation of spinel phases (e.g. CuAl<sub>2</sub>O<sub>4</sub>) in the Al-rich samples calcined at 800 °C. Addition of Ce also improves the activity of mixed metal oxides, which is related to formation of easily reducible cerium oxide species.

## Acknowledgments

This work was supported by EU structural funding in Operational Programme Research, Development and Education, project No. CZ.02.1.01./0.0/0.0/17\_049/0008419 „COOPERATION“.

## References

- [1] S. Basąg, Z. Piwowarska, A. Kowalczyk, A. Węgrzyn, R. Baran, B. Gil, M. Michalik, L. Chmielarz, *Appl. Clay Sci.* 129 (2016) 122–130.
- [2] S. Basąg, K. Kocoł, Z. Piwowarska, M. Rutkowska, R. Baran, L. Chmielarz, *React. Kinet. Mech. Catal.* 121 (2017) 225–240.

# **MnO<sub>x</sub>-CeO<sub>2</sub> catalysts for the simultaneous abatement of NO<sub>x</sub> and dioxins in MSWI plants**

*J.A. Martín-Martín, M.P. González Marcos, A. Aranzabal, J.R. González-Velasco  
Department of Chemical Engineering, Faculty of Science and Technology, University of  
Basque Country (UPV/EHU), P.O. Box 644, E-48080 Bilbao (Spain)*

## **1. Scope**

dDiNO<sub>x</sub> is a process that implies the simultaneous abatement of NO<sub>x</sub> and dioxins in the exhaust gases of Municipal Solid waste Incineration plants (MSWI) in order to operate in a more environmentally-efficient way. Previous work [1] demonstrated that the traditional, commercial catalyst (VO<sub>x</sub>/TiO<sub>2</sub>) used for SCR of NO<sub>x</sub> with NH<sub>3</sub> is suitable for o-dichlorobenzene (o-DCB, dioxins model) oxidation and, consequently, for dDiNO<sub>x</sub>. However, the temperature range in which high conversion of both pollutants is achieved with this catalyst is narrow and located at relatively high temperature (260-360°C). MnO<sub>x</sub>-CeO<sub>2</sub>-based catalysts have shown high efficiency in low temperature SCR because of the multivalence states of Mn and the high mobility of oxygen species provided by Ce [2]. Thus, the main goal of the present work is to study the MnO<sub>x</sub>-CeO<sub>2</sub> formulation as an alternative catalyst for dDiNO<sub>x</sub>, capable of working at lower temperatures than VO<sub>x</sub>/TiO<sub>2</sub> catalysts. For this purpose, MnO<sub>x</sub>-CeO<sub>2</sub> catalysts, prepared with different Mn/(Ce+Mn) ratios by co-precipitation, were characterized and tested in simulated conditions close to those employed in MSWI.

## **2. Results and discussion**

Fig 1 shows the light-off curves of MnO<sub>x</sub>-CeO<sub>2</sub> catalysts for NO and o-DCB. Regarding SCR, Mn content favour NO conversion at low temperature. Hence, below 300°C, total removal of NO is achieved with Mn/(Mn+Ce) ratio above 0.5. However, higher temperatures produce a drastical decrease of NO conversion due to side reactions such as NH<sub>3</sub> oxidation. In the same way, Mn content has a positive effect in oxidation, shifting the o-DCB oxidation light-off curves to lower temperatures. As a result, o-DCB conversions above 80% are obtained at 180°C with Mn/(Mn+Ce) ratio above 0.8, which reduces the working temperature by 80°C with respect to commercial VO<sub>x</sub>/TiO<sub>2</sub> catalysts.

Regarding selectivity, N<sub>2</sub>O and CO were detected as reaction by-products, with two peaks at low and high temperature. In the case of N<sub>2</sub>O, the peak at low temperature

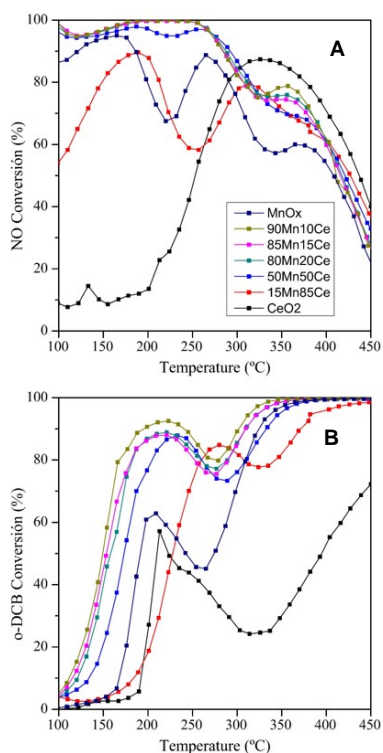


**Fig 1.** Catalytic activity of MnO<sub>x</sub>-CeO<sub>2</sub>. A: NO reduction; B: o-DCB oxidation.

is proposed to be associated to non-selective catalytic reduction, whereas the high temperature peak is due to NH<sub>3</sub> oxidation.

Additionally, catalysts were characterized in order to associate their catalytic behaviour with their physical and chemical properties. The main diffraction peaks of MnO<sub>x</sub>-CeO<sub>2</sub> in XRD are associated to cubic fluorite structure. Mn content produces a decrease in lattice parameter, which suggests Mn incorporation to CeO<sub>2</sub> lattice to form the solid solution. The solid solution was also confirmed by Raman, due to a slight shift of the F<sub>2g</sub> band to lower wavenumber. Moreover, the increase of Raman band at 597 cm<sup>-1</sup> with Mn content denotes an increase in oxygen vacancies, which is in accordance with the decrease of fluorite crystal size and the

increase of BET surface area and pore volume, caused by the structural defect created by the incorporation of Mn to CeO<sub>2</sub> lattice. H<sub>2</sub>-TPR was used to corroborate the improvement of redox properties due to the higher oxygen mobility. In addition, the average oxidation state of Mn in the bulk was estimated to be between +4 and +3, which is in accordance with the different MnO<sub>x</sub> crystal aggregates observed at higher Mn contents in XRD. Acidity also increases with Mn content, which indicates that MnO<sub>x</sub> aggregates may be the species more contributing to this property.

### 3. Conclusions

Conversion of NO and o-DCB above 80% has been achieved with catalysts whose Mn/(Mn+Ce) ratio is above 0.8, at lower temperatures than commercial catalyst. Characterization corroborates that Mn incorporates into CeO<sub>2</sub> lattice, and the excess is segregated in MnO<sub>x</sub> crystals, which provides for different Mn oxidation states and high oxygen mobility, thus improving redox and acidic properties.

### References

- [1] Gallastegi-Villa, M. et al., *Catalysis Today* 254, 2-11 (2015)
- [2] Wang Xingyi. et al., *Applied Catalysis B* 86, 166-175 (2009)

### Acknowledgements

The authors thank MINECO/EU (CTQ2015-64616 MINECO/FEDER BES-2016-077849), Basque Government (GIC-07/67-JT450-07) and UPV/EHU (UFI 11/39, INF 12/37) for their economic support.



# **New insight on the red-ox kinetic nature of Hg<sup>0</sup> oxidation: an investigation on O<sub>2</sub>, NO and NH<sub>3</sub> effects over a SCR V/Mo/Ti catalyst**

*A. Lanza<sup>1</sup>, S. Alcove Clave<sup>2</sup>, J. Collier<sup>2</sup>, L. Lietti<sup>1</sup>, R. Matarrese<sup>1</sup>, A. Beretta<sup>1\*</sup>*

*<sup>1</sup>Laboratory of Catalysis and Catalytic Processes, Politecnico di Milano, Milan, Italy;*

*<sup>2</sup>Johnson Matthey Technology Centre, Sonning Common, United Kingdom;*

*\*alessandra.beretta@polimi.it*

This study addresses an investigation on Hg<sup>0</sup>-oxychlorination over commercial V<sub>2</sub>O<sub>5</sub>/MoO<sub>3</sub>/TiO<sub>2</sub> SCR catalysts and complete previous studies over the same catalyst [1,2]. Hg<sup>0</sup> oxidation is recognized to be a red-ox reaction catalyzed by V-sites as NH<sub>3</sub>-SCR reaction is. The study focused on the identification and comprehension of the common kinetic features of the two processes. In a previous work, Beretta et al. [1] developed a global DeNO<sub>x</sub> redox rate equation (1) which accounts for: (i) the importance of both reduction and re-oxidation steps, (ii) the promoting effect of NO on re-oxidation and (iii) the NH<sub>3</sub> inhibition due to spillover from acidic to redox sites.

**(1)**

Interestingly, SO<sub>2</sub>-oxidation over the commercial SCR catalysts has been also reported to be weakly promoted by NO and strongly inhibited by NH<sub>3</sub> [3]. Besides, similar effects were found for Hg<sup>0</sup>-oxidation over V-based catalysts [4].

We herein report the results of an extensive experimental campaign on Hg<sup>0</sup>-oxidation in a pilot scale reactor which were performed over a commercial V/Mo/Ti catalyst in the form of slabs, aimed at a quantitative analysis of the effects of O<sub>2</sub>, NO and NH<sub>3</sub> and a comparison with same effects on NH<sub>3</sub>-SCR. The feed composition was: 22 µg/Nm<sup>3</sup> Hg, 10 ppm HCl, 0.025-6% O<sub>2</sub>, 10.5% H<sub>2</sub>O, 0-300 ppm NO cofeed, 0-300 ppm NH<sub>3</sub> cofeed, N<sub>2</sub> as carrier. Data were quantitatively analyzed by a heterogeneous 1D model of the reactor cell accounting for interphase and intraporous mass transfer [2]. Furthermore, an insight of the NO+O<sub>2</sub>-surface and NH<sub>3</sub>-surface interaction was pursued by operando FT-IR experiments.

To investigate the redox nature of Hg<sup>0</sup>-oxychlorination reaction, activity tests were performed at largely varying O<sub>2</sub> concentration (fig.1a). Hg<sup>0</sup> conversion was progressive almost unaffected by a decrease of O<sub>2</sub> content for the range of very low concentrations (<0.5%). This suggests a more important kinetic role of the reduction

step over the oxidation step than in NH<sub>3</sub>-SCR. A dual step reaction rate (eq. 2) was proposed, incorporating the reduction rate expression developed in [2] and the formalism of re-oxidation as in Eq. 1. Data in fig. 1a).

$$(2) \quad R_{Hg-ox} = \frac{1}{1+K^*_{Hg-NH_3} \frac{\theta_{NH_3}}{1-\theta_{NH_3}}} \left( \frac{1}{k_{Hg-ox} P_{Hg} (\theta_{HCl})^2} + \frac{1}{k_{ox} (1+\alpha C_{NO}) (P_{O_2})^{1/4}} \right)^{-1}$$

Hg-oxidation experiments with NO-cofeed and with NH<sub>3</sub>-cofeed were also performed. As in the case of NH<sub>3</sub>-SCR, it was found that Hg conversion increased upon cofeed of NO (fig. 1b) up to medium temperatures, while at temperatures above 350°C a negative trend of conversion was measured. The low-temperature promoting effect could be entirely explained by the same kinetic effect of NO in the re-oxidation step, while the high-temperature data can be well explained by assuming that the NO-cofeed produces a surface effects affecting the heat of adsorption of the HCl on V-sites. Experiments with NH<sub>3</sub> co-feed showed significant inhibiting effect on Hg<sup>0</sup>-oxidation (not reported for brevity).

The operando FT-IR tests allowed to deepen the comprehension of the redox chemistry of the V-based catalyst surface. In fig. 1c) is shown as an example the adsorption of NO+O<sub>2</sub> on dried and wetted samples, both surfaces were pre-reduced: the storage of NO<sub>x</sub> was larger than on wetted sample, thus suggesting the strong H<sub>2</sub>O inhibiting effect.

In conclusion common features are clearly evident on the DeNO<sub>x</sub> and Hg<sup>0</sup>-ox, which suggest that NO promoting and NH<sub>3</sub> inhibiting effects are intrinsic features of V-redox.

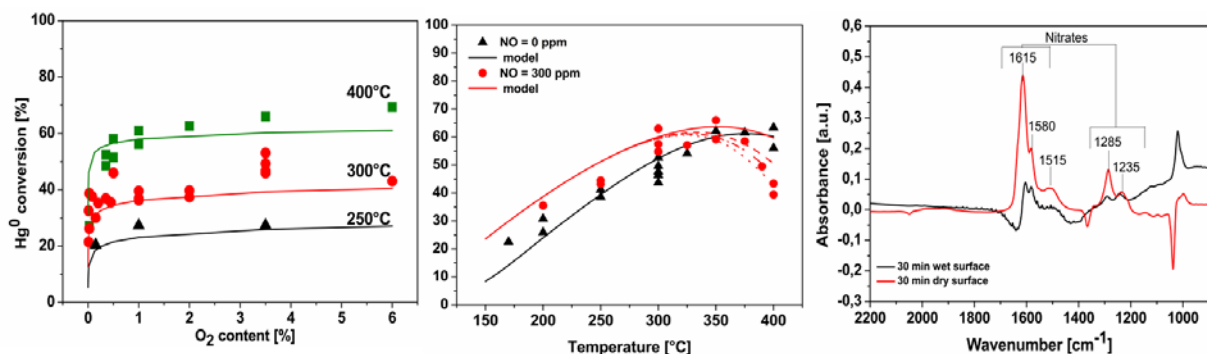


**Fig.1 a)** O<sub>2</sub> effect on Hg<sup>0</sup> conversion; **b)** NO effect on Hg<sup>0</sup> conversion; **c)** IR spectra in NO+O<sub>2</sub>, comparison of stored nitrates at 50°C after 30 minutes in a pre-reduced sample.

## References

1. Beretta, A., Lanza, A., Lietti, L. Alcove Clave, S., Collier, J., Chem. Eng. J., 359 (2019), 88-98.
2. Usberti, N., Beretta, A., Alcove Clave, S., Nash, M., Appl. Catal. B: Environ., 193(2016), 121-132.
3. Forzatti et al., "Structured catalysts and reactors", 171-214. CRC Press, Boca Raton, 2006.
4. Stolle, R., Koeser, H., Gutberlet, H., Appl. Catal. B: Environ., 144 (2014), 486-497.

# **Control of distribution of Ag and CeO<sub>2</sub> in SBA-15 structure and catalytic properties of Ag-CeO<sub>2</sub>/SBA-15 catalysts**

*A. Taratayko<sup>1</sup>, N. Mikheeva<sup>1</sup>, Yu. Larichev<sup>2</sup>, V. Zaikovskii<sup>2</sup> and G. Mamontov<sup>1</sup>*

*<sup>1</sup>Tomsk State University, Tomsk, Russia*

*<sup>2</sup>Boreskov Institute of Catalysis, Novosibirsk, Russia*

The stabilization of small nanoparticles of active component on the support surface is of high importance in designing of heterogeneous catalysts. Mesoporous ordered silicas SBA-15 and MCM-41 are promising supports for the catalysts due to high specific surface area and ordered structure of the cylindrical mesopores. The small diameter of these pores (3-10 nm) may be used to synthesize the small nanoparticles (NPs), since the wall of the pores prevents the agglomeration of the NPs during the calcination. The interest toward silver catalysts is connected with a relatively low cost in comparison with other noble metals and high activity in the oxidative processes. The main disadvantage of silver catalysts consists in the difficulties of synthesis and stabilization of small silver NPs. Two types of silver NPs were shown to form on the surface of MCM-41 and SBA-15. The particles with the sizes of 3-8 nm were formed on the external surface, while small NPs with the sizes below 2 nm were formed inside the pores of MCM-41 [1] and SBA-15 [2] (Fig. 1). Thus, the pores of MCM-41 and SBA-15 may be used as nanoreactors for the synthesis of small silver NPs.

The interest to CeO<sub>2</sub>-based catalysts is attributed to their redox and semiconducting properties as well as the phenomena of strong metal-support interaction (SMSI) and electronic metal-support interaction (EMSI). All these properties are favorable for the oxidative catalysis, electro- and photocatalysis. It was shown that a combination of citric method and a unique porous structure allows synthesizing the CeO<sub>2</sub>/SBA-15 composites with the uniformly distributed small ceria particles (~3 nm) on the SBA-15 surface with a ceria loading up to 20 wt.% [3]. The prepared CeO<sub>2</sub>/SBA-15 composites were characterized by the increased reducibility due to the small size and high value of the surface oxygen and a red shift of light adsorption (band gap of 3.0 eV) that is favorable for their application in photocatalysis under visible light.

The present work is focused on the preparation of Ag-CeO<sub>2</sub>/SBA-15 composites. The combination of silver and ceria in the SBA-15 structure is of interest due to a synergetic effect in the oxidative catalysis and photocatalysis. The special attention is

given to the interaction of small silver and ceria NPs, because the cooperation of their active sites is attributed to the formation of the Ag-CeO<sub>2</sub> interface.

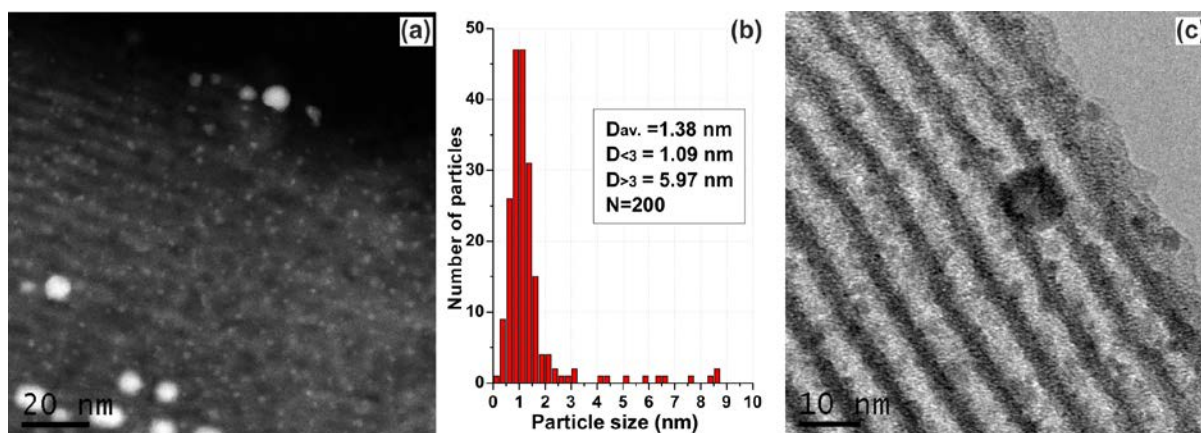


Fig. 1. The HAADF-STEM image of Ag/SBA-15 catalyst (a), corresponding particles size distribution (b) and TEM image (c) of Ag/SBA-15 catalyst.

The series of Ag-CeO<sub>2</sub>/SBA-15 catalysts were synthesized using the impregnation techniques and characterized by N<sub>2</sub> adsorption-desorption, XRD, SAXS, HR TEM and HAADF-STEM, UV-vis spectroscopy, TG-DSC-MS, TPR H<sub>2</sub>, TPO, TPD, etc. The synthesis was carried out varying the sequence of the introduction of silver and ceria precursors, the presence and absence of citric acid, etc. The impregnation of the Pluronic P123@SBA-15 hybrid material by ceria and/or silver precursors was also carried out. It was established that the Pluronic P123 copolymer positively influenced on the distribution of the precursor and provided the formation of ultrasmall ceria particles (~1.8 nm according to SAXS) inside the SBA-15 pores.

It was shown that the formation of both small silver and ceria NPs and their interaction led to enhanced activity in CO oxidation, total oxidation of methanol and toluene. The interaction of Ag and CeO<sub>2</sub> particles led to the cooperation of oxidative species that provide the growth of oxidation activity. It was shown that the EMSI took place for these catalysts, and a shift from 400 nm to 550 nm of plasmonic adsorption of silver NPs interacting with ceria was detected that has high importance for photocatalysis.

#### Acknowledgements

This work was supported by Russian Science Foundation (Grant № 18-73-10109)

#### References

- [1] Mamontov G.V., Gorbunova A.S., Vyshegorodtseva E.V., Zaikovskii V.I., Vodyankina O.V. Catal. Tod. 2019 (in press) DOI: 10.1016/j.cattod.2018.05.015
- [2] Mikheeva N.N., Zaikovskii V.I., Mamontov G.V. J. Sol-Gel Sci. Tech. 2019 (in press).
- [3] Mikheeva N.N., Zaikovskii V.I., Mamontov G.V. Microporous Mesoporous Mater. 277 (2019) 10-16.

# Preferential oxidation (PROX) of CO with spray-flame made $\text{LaMnO}_3$ perovskite nanoparticles

*Steven Angel<sup>1,3</sup>, Juan David Tapia<sup>2</sup>, Jaime Gallego<sup>2</sup>, Christof Schulz<sup>1</sup>,  
Hartmut Wiggers<sup>1</sup>*

<sup>1</sup> IVG, Institute for Combustion and Gas Dynamics – Reactive Fluids and CENIDE, Center for Nanointegration, University of Duisburg-Essen, Duisburg, Germany

<sup>2</sup> Química de Recursos Energéticos y Medio Ambiente-QUIREMA. Instituto de Química, Universidad de Antioquia, Medellín, Colombia.

<sup>3</sup> Max-Planck-Institute CEC, Mülheim an der Ruhr, Germany

$\text{LaMnO}_3$  perovskite is currently being investigated as a potential and inexpensive alternative to noble metals (eg., Pd or Pt) for catalytic reactions [1]. A specific focus is on decontamination and purification reactions such as the preferential oxidation (PROX) of CO in excess hydrogen. In order to synthesize suitable, high-surface-area  $\text{LaMnO}_3$  nanomaterials, spray-flame synthesis (SFS) was used as it provides a continuous, single-step and cost-efficient production pathway [2]. Concerning the formation of a functional and active catalyst, the main challenges of SFS includes avoiding multimodal and broad particle-size distributions and the formation of secondary non-active phases.

Metal nitrates ( $\text{La}(\text{NO}_3)_3 \cdot x\text{H}_2\text{O}$  and  $\text{Mn}(\text{NO}_3)_2 \cdot 4\text{H}_2\text{O}$ ) as cost-effective precursors were dissolved in ethanol or mixtures of ethanol and 2-ethylhexanoic acid (2-EHA), whereas the latter combination is known to support the formation of extremely fine-grained materials [3]. A specific interest was in the thermal and chemical stability of the as-prepared solutions. Therefore, liquid phase temperature-dependent ATR-FTIR and UV-VIS studies of the solutions were performed. While the ethanol solutions did not show any changes in chemical composition, esterification between ethanol and 2-EHA was observed and most likely catalyzed by manganese ions. Moreover, an oxidation of  $\text{Mn}^{2+}$  to  $\text{Mn}^{3+}$  and  $\text{Mn}^{4+}$  was found above  $40^\circ\text{C}$ . However, these solutions showed excellent stability and enabled the formation of small particles with a unimodal and narrow size distribution in the SFS process ( $d_p = 7.3$  nm) while synthesis from pure ethanol-based solutions resulted in a multimodal particle-size

distribution with sizes ranging from 6 to 140 nm. Traces of an oxygen-rich  $\text{LaMnO}_{3+\delta}$  phase were identified on the particles' surface containing a  $\text{Mn}^{4+}/\text{Mn}^{3+}$  ratio of 0.5 (as determined by XPS).

In order to understand the surface reducibility, the samples synthesized from 2-EHA-containing solutions, presented an important surface reduction step at  $164^\circ\text{C}$  as identified in  $\text{H}_2$ -Temperature Programmed Reduction (TPR) (Figure 1a) in contrast with the sample from the ethanol-based solution, which reduction step started only after  $196^\circ\text{C}$ . Other analytical techniques were used to further characterize the materials: BET, SEM, EDX-TEM and  $\text{O}_2$ -Temperature Programmed Desorption (TPD).

The samples were evaluated for CO-PROX with the best performing sample being the one made from a solution containing 50/50 volume proportion of ethanol and 2-EHA (Figure 1b), obtaining at  $220^\circ\text{C}$  a conversion of CO of 85% (and a 50% CO conversion at  $198^\circ\text{C}$ ) while keeping the conversion of hydrogen below 10%.

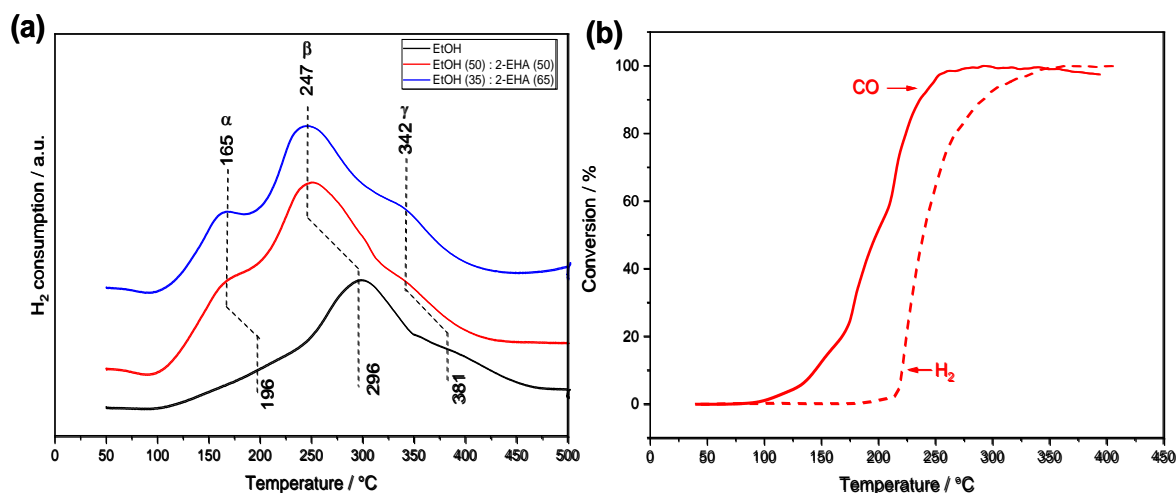


**Figure 1. (a)**  $\text{H}_2$ -TPR of the  $\text{LaMnO}_3$  perovskites made metal nitrates solutions in ethanol (EtOH), 50%V/50%V EtOH/2-EHA and 35%V/65%V EtOH/2-EHA. **(b)** CO-PROX of the perovskite sample made from the 50%V/50%V EtOH/2-EHA solution.

## References

- [1] P. Granger and V. I. Parvulescu, *Perovskites and Related Mixed Oxides*. Weinheim, Germany: Wiley-VCH Verlag GmbH & Co. KGaA, 2016.
- [2] C. Schulz, T. Dreier, M. Fikri, and H. Wiggers, "Gas-phase synthesis of functional nanomaterials: Challenges to kinetics, diagnostics, and process development," *Proc. Combust. Inst.*, vol. 0, pp. 1–26, 2018.
- [3] C. Rosebrock, T. Wriedt, and L. Mädler, "The Role of Microexplosions in Flame Spray Synthesis for Homogeneous Nanopowders from Low-Cost Metal Precursors," *Am. Inst. Chem. Eng.*, vol. 62, no. 2, pp. 381–391, 2016.

## Recyclable Amination Catalysts in Reactive Ionic Liquids

*Thiemo A. Faßbach, Andreas J. Vorholt, Max-Planck-Institute for Chemical Energy Conversion, Mülheim a.d.R., Germany / TU Dortmund University.*

Highly substituted amines are of great interest for the chemical industry since they are used as building blocks, e.g. for surfactants. Homogeneously catalyzed aminations can be conducted under milder conditions and with high selectivity towards the often-desired linear amines. The most important disadvantage of homogeneously catalyzed reactions is the often-challenging catalyst recycling, making it too expensive for industrial means. An elegant solution to this problem in the synthesis of dimethyl amine derivatives is the use of dimethyl ammonium dimethyl carbamate (dimcarb, Figure 1), which is obtained by the reaction of dimethylamine and CO<sub>2</sub>.<sup>[1]</sup>

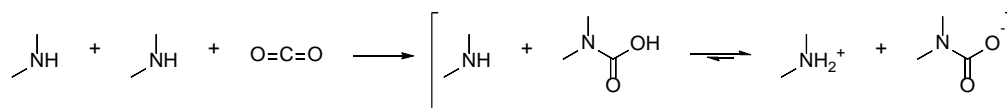


Figure 1: Structure and reactivity of dimcarb.

It has very promising properties, because it is predominantly present in the ionic form, yet serves as an amine source. Consequently, it can be considered a reactive ionic liquid.

### Hydroamination of 1,3-Dienes

The catalytic conversion of 1,3-dienes with amines to linear allylic amines is well-known.<sup>[2]</sup> A palladium-based catalyst and the DPPB ligand is used for converting the renewable terpene  $\beta$ -farnesene to dimethyl amine derivatives (Figure 2). These farnesyl amines are interesting building blocks for nitrogen-based surfactants.<sup>[3]</sup>

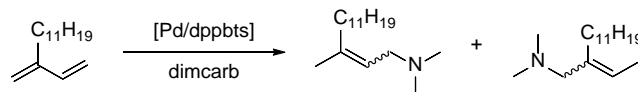


Figure 2: Hydroamination of  $\beta$ -farnesene with dimcarb.

The solvent-free hydroamination leads to a yield of 89% of the desired products. Furthermore, spontaneous phase separation takes place, which allows removing the non-polar product phase and reusing the polar catalyst phase. The sulfonated DPPB analogue can efficiently be immobilized in the dimcarb phase and be reused several times (Figure 3), increasing the total turnover number by the factor of ten. This concept also works for other 1,3-dienes, like  $\beta$ -myrcene and isoprene.

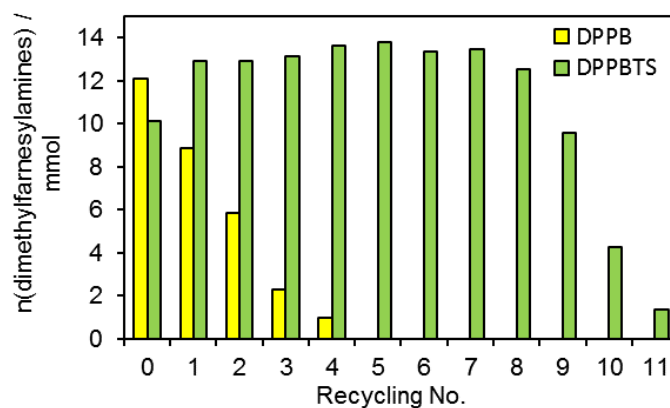


Figure 3: Catalyst recycling in the hydroamination of  $\beta$ -farnesene with dimcarb.

### Telomerization of 1,3-Butadiene

The telomerization is dimerization of 1,3-dienes with an addition of a nucleophile.<sup>[4]</sup> Applying dimcarb and 1,3-butadiene without any solvent leads to dimethyl octadienyl amines (Figure 4).

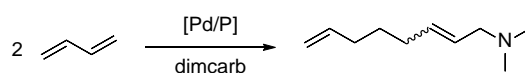


Figure 4: Telomerization of 1,3-butadiene with dimcarb

Since the product is soluble in dimcarb, it must be extracted with cyclohexane. The catalyst is immobilized in dimcarb by using a tri-sulfonated  $\text{PPh}_3$  ligand (TPPTS). In this way, the catalyst can be recycled more than 30 times in a row (Figure 5) without any loss in activity or selectivity at all.<sup>[5]</sup>

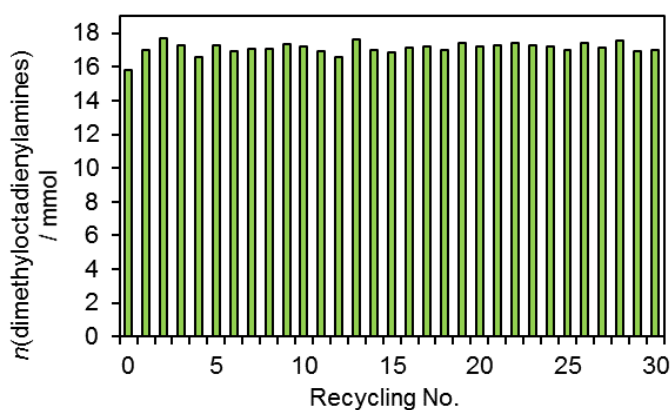


Figure 5: Catalyst recycling in the telomerization of 1,3-butadiene with dimcarb.

### References

- [1] R. Radeaglia, J. Andersch, W. Schroth, *Zeitschrift für Naturforsch. B* **1989**, *44*, 181–186.
- [2] A. Behr, L. Johnen, N. Rentmeister, *Adv. Synth. Catal.* **2010**, *352*, 2062–2072.
- [3] T. A. Faßbach, N. Gösser, F. O. Sommer, A. Behr, X. Guo, S. Romanski, D. Leinweber, A. J. Vorholt, *Appl. Catal., A* **2017**, *543*, 173–179.
- [4] A. Behr, M. Becker, T. Beckmann, L. Johnen, J. Leschinski, S. Reyer, *Angew. Chem., Int. Ed.* **2009**, *48*, 3598–3614.
- [5] T. A. Faßbach, R. Kirchmann, A. Behr, A. J. Vorholt, *Green Chem.* **2017**, *19*, 5243–5249.



# Using Ion-beam Sputtering to modify Heterogeneous Nanodispersed Catalysts

Ruairi O'Donnell<sup>1\*</sup>, Salvatore Scaglione<sup>2</sup>, Rosa Chierchia<sup>3</sup>, Veronica Celorrio<sup>4</sup>, Nancy Artioli<sup>1\*</sup>

<sup>1</sup>Queen's University Belfast, Belfast, BT9 5AG, U.K.

<sup>2</sup>ENEA CR Casaccia, Rome, 00123, Italy

<sup>3</sup> Diamond Light Source Ltd., Harwell Science and Innovation Campus, Didcot, Oxfordshire  
OX11 0DE, UK

## Introduction

Ion beam sputtering [1] is an advanced technique for the controlled modification of the surface of nanomaterials to enhance their catalytic performance and resistance to aging, and eventually assess the noble metal substitution [2]. This technique has been investigated using a conventional Pt/Ce<sub>0.5</sub>Zr<sub>0.5</sub>O<sub>2</sub> catalyst used on emission control mobile application [3][4]. Different ion beam parameters (energy, type of ion, doses) have been investigated to understand the effect on the resulting catalytic activity. Modeling of the treatment has also been introduced to describe erosion of the surface through ion sputtering, and explain the significant enhancement in catalytic activity.

## Materials and Methods

A sample of Pt (1% w/w) Ce<sub>0.5</sub>Zr<sub>0.5</sub>O<sub>2</sub> was commercially sourced. Three samples were then bombarded with N<sup>+</sup> ion beams with an energy of 1.5KeV, a current of 20mA and an incident angle of 28° to the catalyst surface. The samples are denoted as Pt1.5(**X**), where **X** represents the number of times the sample was treated for 15 min each (doses). The treated samples were compared with an untreated sample, denoted as 'Fresh'. Catalytic testing was carried by using a reaction mixture composed of 10% O<sub>2</sub>, 4.5% H<sub>2</sub>O, 2000ppm of each CO, CH<sub>4</sub>, C<sub>3</sub>H<sub>6</sub>, and 200ppm NO with a total flow of 100ml/min. Light-off tests were performed from 303K to 773K at a rate of 5K/min. The outlet from the reactor was analysed using an online Pfeiffer Vacuum quadrupole mass spectrometer. Extended X-ray Absorption Fine Structure (EXAFS) tests were carried out and spectra were collected at the Pt L<sub>3</sub>-edge on each of the samples to investigate the size and distribution of the Pt nanoparticles on the catalyst surface.

## Results and Discussion

The catalytic activity was assessed and the results are reported in terms of CO and C<sub>3</sub>H<sub>6</sub> conversion in Fig. 1. The results show that the catalyst showed improved activity for oxidation of both CO and C<sub>3</sub>H<sub>6</sub> after ion bombardment. T<sub>50</sub> values for CO oxidation were 503K, 503K and 511K for Pt1.5(32), Pt1.5(16) and Pt1.5(8) respectively, lower temperatures compared to the untreated sample Pt Fresh, which had a T<sub>50</sub> values of 513K. The T<sub>50</sub> values for C<sub>3</sub>H<sub>6</sub> oxidation over Pt1.5(32), Pt1.5(16) and Pt1.5(8) were 528K, 533K and 538K respectively; a more relevant reduction compared to the fresh sample (546K). The results are in line with EXAFS Fourier transform analysis, which revealed that the sample, after ion bombardment, is characterized by a distribution of Pt nanoparticles which is decreasing with the intensity of the bombardment, as well as by the formation of atom vacancies and incomplete terraces (HRTEM and H<sub>2</sub> reduction FTIR studies).

## Conclusions

The results show that Ion beam irradiation can be used as a method for the manipulation of the surface properties of the material, and thus the enhancement of its catalytic properties, lowering the temperature at which they are active in oxidation. This opens up the idea of using ion bombardment as a useful tool for the controlled processing of nanodispersed heterogeneous catalytic materials.

## References

- [1] L. Hanley and S. B. Sinnott, "The growth and modification of materials via ion – surface processing," *Surf. Sci.*, vol. 500, pp. 500–522, 2002.
- [2] N. Artioli *et al.*, "Highly active nanocatalysts by ion beam surface modification," vol. 77, pp. 2–3, 2000.
- [3] M. Ozawa, "Role of cerium–zirconium mixed oxides as catalysts for car pollution: 1 A short review," *J. Alloys Compd.*, vol. 275277, pp. 886–890, 1998.
- [4] R. M. Heck and R. J. Farrauto, "Automobile exhaust catalysts," *Appl. Catal. A Gen.*, vol. 221, no. 1–2, pp. 443–457, 2001.

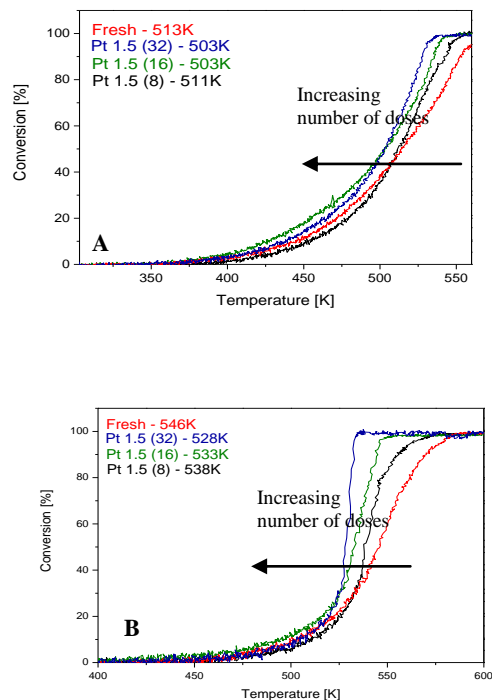


Fig 1. CO conversion (A) and C<sub>3</sub>H<sub>6</sub> conversion (B) as a function of temperature for the Pt (1% w/w) Ce<sub>0.5</sub>Zr<sub>0.5</sub>O<sub>2</sub> fresh and treated with different ion doses (8-16-32).

## **Multiscale imaging and in situ analysis of industrially relevant materials for emission control.**

*Monik Panchal, UCL Department of Chemistry, London, UK Catalysis Hub, Harwell, UK; Dr Emma Gibson, UK Catalysis Hub, Harwell, University of Glasgow, Glasgow, UK; Prof Richard Catlow, UCL Department of Chemistry London, Cardiff Catalysis Institute, Cardiff, UK Catalysis Hub, Harwell, UK; Prof Andrew M. Beale, UCL Department of Chemistry, London, UK Catalysis Hub, Harwell, UK; Dr Timothy Hyde, Johnson Matthey Technology Centre, Reading, UK; Dr Manfred Erwin Schuster, Johnson Matthey Technology Centre, Reading, UK; Prof. Andrew York, Johnson Matthey Technology Centre, Reading, UK.*

### **Introduction**

Sustainable fuel sources such as pure-electric and fuel cell powered systems have the potential to produce transport that emits near-zero tailpipe gases and particles. However, these technologies are still an infancy-stage thus can be considered only a long-term solution. Emission standards and emission limits to specific air pollutants were established as a measure to control pollution levels in the short-term, leading to novel solutions to meet the ever-tightening standards. [1], [2]

Particulate matter (PM) are a known pollutant and carcinogen, which are comprised of carbon-based soot and incombustible material deposited as ash residues. The particle mass and the number of particles emitted from vehicle exhaust has been regulated by standards. Though PM constraints have been the main concern for Diesel engines, they have been managed using an after-treatment solution such as Particulate Filter (PF) [3], [4]. Recent emission standards by the European Union (EU6c), have focused on reducing the gasoline particulate emissions to levels comparable to diesel engines ( $6 \times 10^{11} \text{ km}^{-1}$ ). Gasoline Particle Filter (GPF) technologies which involve incorporating the Three-way catalyst (TWC) washcoat onto the particulate filter in one unit, are expected to be implemented to comply with regulatory limits.

The challenge with the system involves understanding the role of the PM deposition on the catalyst washcoat and how it affects the catalyst performance and filtration efficiency. [5] Thus by observing how the PM interacts within particulate filters, the distribution of metal catalyst and how the regeneration of the catalyst affects performance are keys towards improving after-treatment technology. With this

in mind, this project is focused on the analysis of GPF containing a relevant PdRh catalyst with varying amounts of PM deposition, understanding the effect of ageing and PM deposition on the system using synchrotron-based techniques and imaging. Ultimately, correlating *in-situ* TEM imaging with tomographic studies to analyse the catalytic activity over a broad range scale.

## Results and Discussion

The initial sample analysed had varying amounts of ash deposition and aged under 'rich-lean' conditions to simulate >100 000 km of use. XANES analysis of Pd K-edge (fig. 1a) suggests a reduction of the Pd species upon ageing. EDS-STEM analysis (fig. 1b) of the coatings on the walls of the monolith suggests the active species is well distributed on the oxide support on the fresh samples. However, ageing of the samples seems to cause movement of the PM species onto the binding material and cordierite (fig. 1c). This may support the proposed sintering seen from the XANES analysis. Nanoprobe XRF mapping also showed the spatial distribution of PM and the washcoat, observing ash components interacting with different regions of the washcoat with complementary results seen from EDS-STEM analysis.

## Significance and Outlook

Initial work of this system suggests that the ageing process may have a key role in the catalytic activity of the GPF. With supporting information from XANES studies, XRF and EDS mapping support the sintering of Pd upon ageing. Further characterisation is in progress including atomic resolution microscopy and *in situ* studies to understand the role PM deposition plays on catalytic activity.

## References

- [1] P. Zelenka, W. Cartellieri and P. Herzog, *Appl. Catal. B Environ.*, 1996, **10**, 3–28.
- [2] D. Gerard and L. B. Lave, *Technol. Forecast. Soc. Change*, 2005, **72**, 761–778.
- [3] Emission Reduction with Diesel Particle Filter with SCR Coating (SDPF) | SpringerLink, <https://link.springer.com/article/10.1007/s40825-015-0018-7>, (accessed 7 November 2017).
- [4] D. Fino, S. Bensaid, M. Piumetti and N. Russo, *Appl. Catal. Gen.*, 2016, **509**, 75–96.
- [5] M. Václavík, M. Plachá, P. Kočí, M. Svoboda, T. Hotchkiss, V. Novák and D. Thompsett, *Mater. Charact.*, 2017, **134**, 311–318.

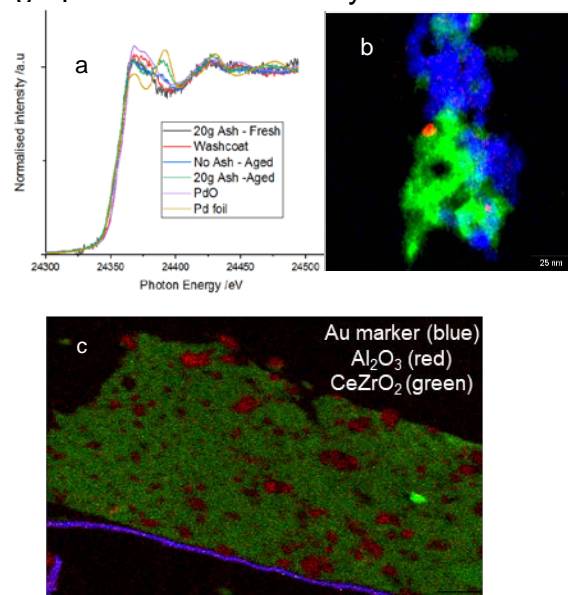


Fig. 1: (a). Normalised XANES of a fresh catalyst, ash loaded and aged sample ; (b). EDS-STEM image of washcoat showing Pd(red), Al(green), Ce/Zr(blue); (c). 25  $\mu\text{m}^2$  XRF map of washcoat surface.

# The effect of using a biogas powered Euro VI engine on the Pd/Pt oxidation catalyst and the V<sub>2</sub>O<sub>5</sub>-WO<sub>3</sub>/TiO<sub>2</sub> SCR catalyst

Johanna Englund<sup>1\*</sup>, Kunpeng Xie<sup>2</sup>, Sandra Dahlin<sup>3</sup>, Soran Shwan<sup>2</sup>, Lennart Andersson<sup>2</sup> and Magnus Skoglundh<sup>1</sup>

<sup>1</sup>Competence Centre for Catalysis, Chalmers University of Technology, Gothenburg, Sweden

<sup>2</sup>Volvo Group Trucks Technology, Gothenburg, Sweden

<sup>3</sup>Department of Chemical Engineering, KTH Royal Institute of Technology, Stockholm, Sweden

\*johanna.englund@chalmers.se

## Introduction

Biogas is in many aspects very similar to natural gas since the main constituent is CH<sub>4</sub>. The source of the raw material used for the production of biogas will impact the presence of catalyst poisons in the fuel. Many studies have investigated the impact from various catalyst poisons like S and P though many of these studies are investigating single poisons or single component of the emission control system in the vehicle [1]. The presence of an oxidation catalyst in front of the SCR catalyst is known to oxidize the catalyst poison SO<sub>2</sub> to SO<sub>3</sub> which could affect the SCR catalyst differently and this shows the importance to take all the parts of the system in consideration when studying the deactivation of the catalytic converters in heavy duty vehicles. In this study we have used an engine bench to simulate conditions as similar to the vehicle conditions as possible. The emission control system that we have used is a Euro VI compliant system with oxidation catalyst, particulate filter, SCR catalyst (three consecutive) and ammonia slip catalyst in the specified order. Pure biogas has been used to be able to see as much effect as possible from the fuel.

## Materials and Methods

Fresh samples of full size DOC (Pt-Pd/Al<sub>2</sub>O<sub>3</sub>) and SCR catalyst V<sub>2</sub>O<sub>5</sub>-WO<sub>3</sub>/TiO<sub>2</sub>: 260 cpsi, 2.3 wt% V, 8 wt% W) were aged using an engine bench operated on biogas. The engine was run for 900 h by repeating a predefined engine cycle. After these 900 hours samples were taken from the inlet and outlet of the oxidation catalyst as well as the inlet and outlet of the first and last of the three SCR catalysts. These samples were then evaluated using a synthetic gas bench reactor. The activity of the oxidation catalyst samples was evaluated in terms of CH<sub>4</sub>, NO, CO and SO<sub>2</sub> oxidation activity when compared to a fresh sample. The impact on CH<sub>4</sub> oxidation in the presence of NO and CO, compared to only O<sub>2</sub> was also investigated (8 % O<sub>2</sub> and 5 % water was present in all experiments apart from the SO<sub>2</sub> oxidation where only O<sub>2</sub>

was present, argon was used for balance). A regeneration in two steps were also performed for these samples at 600°C. The SCR catalyst samples were evaluated in terms of standard, fast and NO<sub>2</sub>-rich SCR activity with a gas composition of 1000:500:250 ppm NO respectively and 0:500:750 ppm NO<sub>2</sub> respectively, all experiments contained 1100 ppm NH<sub>3</sub>, 8 % O<sub>2</sub> and 5 % H<sub>2</sub>O with argon as balance. NH<sub>3</sub>-oxidation and TPD were also preformed to evaluate the catalysts. The GHSV used in all gas bench reactor experiments was 48,000 h<sup>-1</sup>. To characterize all catalyst samples XRF was used as well as SEM-EDX. TEM was also used to measure the particle size of the Pd and Pt on the oxidation catalyst samples.

## Results and Discussion

From the oxidation experiments we could see a very significant decrease in activity for all types of oxidation and especially for CH<sub>4</sub> oxidation as seen in Figure 1. What we could also see was that the presence of NO and CO increased the CH<sub>4</sub> oxidation activity. It was also a clear difference between the inlet sample compared to the outlet sample from the oxidation catalyst where the inlet was more deactivated then the outlet.

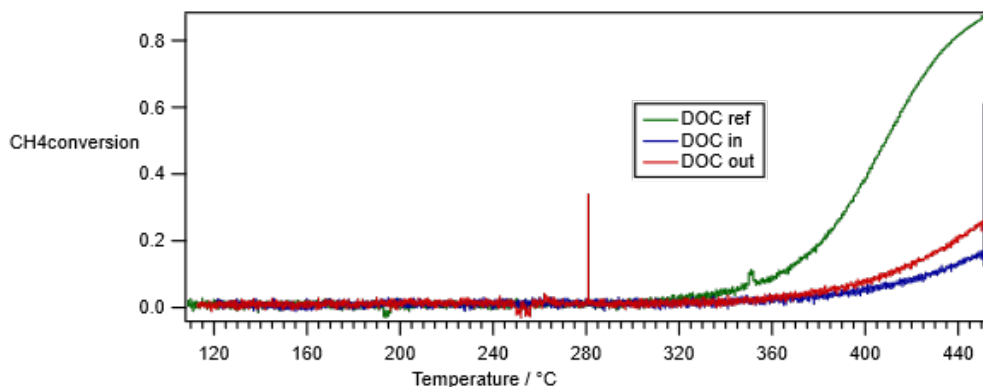


**Figure 1.** Methane conversion of the inlet and outlet sample from the oxidation catalyst as well as a reference sample. Test conditions: 1000 ppm CH<sub>4</sub>, 8 % O<sub>2</sub>, 5 % H<sub>2</sub>O and argon as balance, temperature ramp 5°C/min

For the SCR catalyst the deactivation was not as significant as for the oxidation catalyst. When evaluating the standard SCR activity of the first and third SCR catalyst no significant deactivation was detected, only a slightly higher degree of deactivation was seen for the sample taken from the outlet of the third SCR catalyst.

## References

1. S. Dahlin, C. Lantto, J. Englund, B. Westerberg, F. Regali, M. Skoglundh, and L.J.Pettersson, *Catalysis Today*, Vol. 320 p. 72-83. (2018).

# Transformation synthesis of aluminosilicate SSZ-39 zeolite from ZSM-5 and Beta zeolite

Hao Xu,<sup>1</sup> Qinming Wu,<sup>1</sup> Xiangju Meng,<sup>1</sup> Feng-Shou Xiao,<sup>1</sup> Andrei-Nicolae Parvulescu,<sup>2</sup> Ulrich Müller,<sup>2</sup> Weiping Zhang,<sup>3</sup> Toshiyuki Yokoi,<sup>4</sup> Xinhe Bao,<sup>5</sup> Bernd Marler,<sup>6</sup> Dirk E. De Vos,<sup>7</sup> Ute Kolb,<sup>8</sup>

<sup>1</sup> Zhejiang University, Hangzhou 310028, China;

<sup>2</sup> BASF SE, GCC/PZ-M311, Ludwigshafen 67056, Germany;

<sup>3</sup> Dalian Institute of Technology, Dalian 116012, China;

<sup>4</sup> Tokyo Institute of Technology, Yokohama 226-8503, Japan;

<sup>5</sup> Dalian Institute of Chemical Physics, Dalian 116023, China;

<sup>6</sup> Ruhr University Bochum, Bochum 44780, Germany;

<sup>7</sup> KU Leuven, Kasteelpark Arenberg 23, Leuven 3001, Belgium;

<sup>8</sup> Johannes Gutenberg University Mainz, Mainz 555128, Germany

Recently, small pore zeolites have been received great attention due to their excellent performances in catalysis and separation. One of the practical applications for these small pore zeolites is selective catalytic reduction of NO<sub>x</sub> with NH<sub>3</sub> (NH<sub>3</sub>-SCR). As a crucial small pore zeolite, aluminosilicate SSZ-13 zeolite with CHA structure shows outstanding performance in the NH<sub>3</sub>-SCR, and nowadays has been industrialized.

More recently, it is reported that aluminosilicate SSZ-39 zeolite with AEI structure is also a promising candidate for the above application because of its unique 3D micropores with the size of 3.8×3.8 Å. Generally, the synthesis of aluminosilicate SSZ-39 zeolite is prepared from interzeolite transformation using high silica Y zeolite as a starting source in the presence of alkyl-substituted cyclic quaternary ammonium or tetraethylphosphonium cations as organic templates.

It is worth noting that the previous literature suggests that the interzeolite transformations mainly occur for the zeolites from low framework density to high framework density. Of course, the interzeolite transformation from high silica Y to SSZ-39 follows this assumption. However, the preparation of high silica Y normally requires complex post-treatments, which is environmentally unfriendly and costly. Therefore, it is strongly desirable to use low-cost and widely used ZSM-5 and Beta

zeolites for the replace of high silica Y zeolite in the synthesis of SSZ-39 zeolite, but the interzeolite transformations from ZSM-5 and Beta zeolites into SSZ-39 strongly challenge the rule from low framework density to high framework density. Notably, there are very successful examples for the interzeolite transformation from high framework density to low framework density, but it is not successful for the synthesis of SSZ-39 yet.

It is observed that the organic templates are necessary in the interzeolite transformation. Therefore, the interzeolite transformation should consider the contribution of organic templates. According to this idea, the stability energy between DMP and zeolite frameworks (MFI, \*BEA, FAU, AEI) is theoretically calculated. Very interestingly, the stability energy between DMP and zeolite frameworks associated with MFI, \*BEA, and FAU is obviously higher than that between DMP and AEI zeolite framework, suggesting a possibility for the interzeolite transformations from ZSM-5 and Beta zeolite to SSZ-39 zeolite. As expected, it is successful for these transformations, as reported in this work. Very importantly, the copper-exchanged newly prepared SSZ-39 zeolites exhibited comparable catalytic performances in NH<sub>3</sub>-SCR with those of SSZ-39 zeolite synthesized with conventional Y zeolite synthesis (Fig. 1).

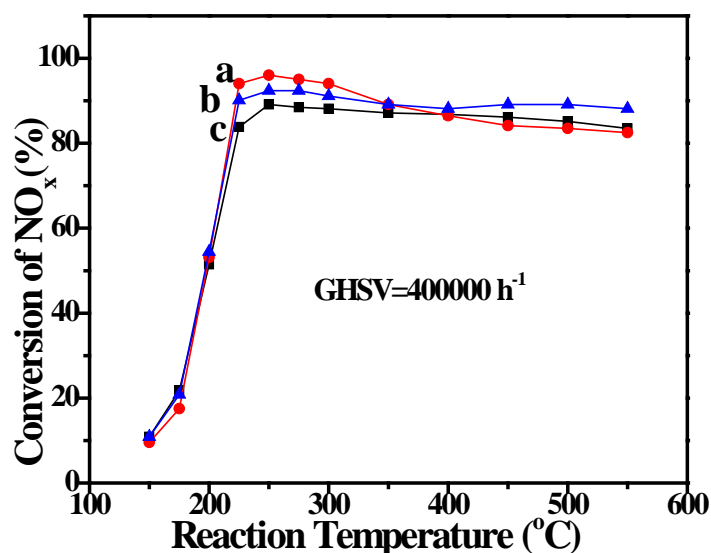


**Fig.1** NO<sub>x</sub> conversion as a function of temperature in NH<sub>3</sub>-SCR over the Cu-SSZ-39 catalysts synthesized from (a) ZSM-5, (b) Beta, and (c) high silica Y zeolite as a starting silicon source, respectively.



## Progresses Concerning the Catalyse of Hydrogen - Water Isotopic Exchange Process

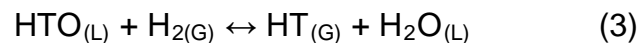
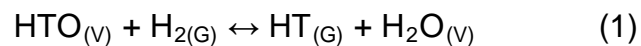
Gheorghe Ionita, Ciprian Bucur and Ionut Spiridon.

National Institute for Research and Development for Cryogenics and Isotopic Technologies,

Uzinei Street; No. 4; PO Box 7, Raureni, 240050 - Rm Valcea;Romania

One of the most suitable processes for removal and recovery of tritium from tritiated water produced in nuclear reactors, it is water- hydrogen isotopic exchange (LPCE process). The LPCE processes take place in two consecutive steps.

The first step (1), it is an isotopic exchange reaction, consisting of tritium transfer from water vapors in hydrogen gas and becomes effective only in presence of *hydrophobic catalysts*. The second one (2), it's a conventional water distillation process which needs a *hydrophilic packing* as an efficient contact element. The mixture consisting of hydrophobic catalyst and hydrophilic packing it's called "*catalytic mixed packing*" and this play the key role in increasing of LPCE process' efficiency.



After long research years, several countries, have developed many types of contact elements which differ by composition, structure, shape, physic-textural parameters and operating conditions. Based on the authors' experiments and results and on the literature' review, the present paper it is focused on the recent progresses concerning the LPCE technology and especially on the mixed catalytic packing.

Each component (catalyst and hydrophilic packing) it is analyzed and evaluated as well their ensemble as catalytic mixed packing. Two main categories of hydrophobic catalysts which proved high catalytic activity and stability are evaluated:

- 1) Platinum on Carbon and Teflon (Pt/C/ PTFE), developed and applied in various types in Romania, Belgium, Canada and Germany;
- 2) Platinum on styrene-divinyl-benzene (Pt/SDC) copolymer, developed and applied in Korea, Japan and Russia

The comparison between the two categories of catalysts it's focused on preparation ways, physico-structural parameters, catalytic activity and lifetime.

The hydrophilic packing it's similarly discussed relating to its nature, composition wettability and pressure drop. The ensemble "mixed catalytic packing" are also analyzed and evaluated relating to: inner geometry and structure; mixing ratio; hydrodynamic characteristics and separation performances.

An improved mixed catalytic packing based on Platinum on Carbon and polytetrafluorethylene (Pt/C/PTFE) and stainless steel hydrophilic packing developed by the authors is presented and discussed in comparison with previous mixed catalytic packing. The main improvements are discussed related to the increasing of the wettability of hydrophilic packing , increasing of hydrophobicity and activity of the catalyst as well as the new ratio between them and a new internal structure.

This improved mixed catalytic packing has been proposed to equip the LPCE columns within the future Pilot Plant for Tritium Removal Facility at Cernavoda NPP (Romania).

# CO<sub>2</sub> hydrogenation to methanol over CuO/ZnO/M<sub>x</sub>O<sub>y</sub>/Al<sub>2</sub>O<sub>3</sub> catalysts.

M. Kourtelesis, K. Kousi, D.I. Kondarides,

Department of Chemical Engineering, University of Patras, Patras, Greece

## Introduction

The catalytic conversion of CO<sub>2</sub> to methanol with the use of renewable hydrogen is an environmentally friendly process for the elimination of CO<sub>2</sub> emissions into the atmosphere [1]. Methanol is an important product of the modern chemical industry as it can be used directly as a fuel, as an energy carrier in fuel cells, or as primary raw material for the production of value added products such as formaldehyde, acetic acid and olefins. Methanol is industrially produced by synthesis gas (mixture of CO and H<sub>2</sub>), containing small amounts of CO<sub>2</sub>. The catalysts used for the CO<sub>2</sub> hydrogenation, usually contain Cu and Zn oxides as major components and various modifiers [2, 3]. In the present study, the catalytic performance of CuO/ZnO/M<sub>x</sub>O<sub>y</sub>/Al<sub>2</sub>O<sub>3</sub> catalysts has been investigated for the title reaction, where M<sub>x</sub>O<sub>y</sub> is one of the oxides La<sub>2</sub>O<sub>3</sub>, Ga<sub>2</sub>O<sub>3</sub> or CeO<sub>2</sub> (denoted below as CuZnLaAl, CuZnGaAl and CuZnCeAl respectively).

## Results and Discussion

The catalysts were synthesized by a coprecipitation method, using nitrate salts of the metals as precursors, followed by calcination at 300 °C for 3h. In all cases, the composition (% mol) of the materials was 61.7% CuO, 30.1% ZnO 4.1% Al<sub>2</sub>O<sub>3</sub> and 4.1% M<sub>x</sub>O<sub>y</sub>. The samples were characterized both after preparation and after the catalytic tests using several techniques including BET, XRD and TPD-CO<sub>2</sub>, in order to study their physicochemical properties. The catalytic performance was examined in the temperature range of 160-260 °C, at atmospheric pressure using a feed composition consisting of 90% H<sub>2</sub> and 10% CO<sub>2</sub>. Results obtained are shown in Fig. 1 where methanol

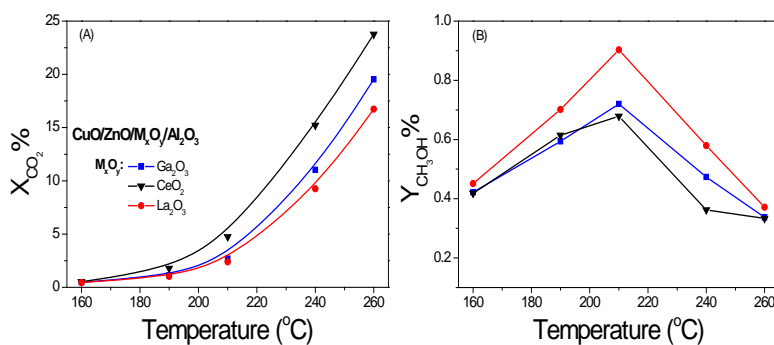


Figure 1. (A) CO<sub>2</sub> conversion and (B) methanol yield, as a function of temperature over CuO/ZnO/M<sub>x</sub>O<sub>y</sub>/Al<sub>2</sub>O<sub>3</sub> catalysts.

conversion ( $X_{CO_2}$ ) (Fig.1A) and yield of methanol (Fig.1B) are plotted as a function of reaction temperature. CuZnCeAl catalyst presented the highest values of CO<sub>2</sub> conversion for the entire temperature range studied, with  $X_{CO_2}$  reaching 24% at 260 °C, followed by CuZnGaAl and CuZnLaAl catalysts. For all catalysts studied, the main reaction products were methanol and CO. Methanol yield was found to increase with increasing temperature, reaching a maximum at 210 °C, and then decreased at higher reaction temperatures. The highest yield of methanol (0.9% at 210 °C) was obtained over the CuZnLaAl catalyst (Fig. 1B).

Since the most promising results concerning methanol production were acquired for the CuO/ZnO/La<sub>2</sub>O<sub>3</sub>/Al<sub>2</sub>O<sub>3</sub> catalyst, the effect of La<sub>2</sub>O<sub>3</sub>:Al<sub>2</sub>O<sub>3</sub> molar ratio on the performance of CuZnLaAl catalysts was investigated. Two more samples were prepared as previously described, with compositions (%mol): 1.9% La<sub>2</sub>O<sub>3</sub> + 6.3% Al<sub>2</sub>O<sub>3</sub> (denoted as CuZnLaAl\_b) and 6.3% La<sub>2</sub>O<sub>3</sub> + 1.9% Al<sub>2</sub>O<sub>3</sub> (denoted as CuZnLaAl\_c). Results obtained (not shown for brevity) showed that the CuZnLaAl\_b and CuZnLaAl\_c catalysts gave similar values of CO<sub>2</sub> conversion, which were higher than that of CuZnLaAl for the entire temperature range examined. Concerning product variation, while CO yield was found to increase monotonically with increasing temperature, methanol yield acquired a maximum value at 210 °C. Best results concerning methanol production were obtained for the CuZnLaAl catalyst with La<sub>2</sub>O<sub>3</sub>:Al<sub>2</sub>O<sub>3</sub> ratio of 1:1.

## Conclusions

The catalytic performance of CuO/ZnO/M<sub>x</sub>O<sub>y</sub>/Al<sub>2</sub>O<sub>3</sub> mixed oxides was investigated for the production of methanol via CO<sub>2</sub> hydrogenation. Addition of La<sub>2</sub>O<sub>3</sub> resulted in higher methanol yields compared to Ga<sub>2</sub>O<sub>3</sub> or CeO<sub>2</sub>. The optimum composition of CuZnLaAl catalyst was found to be CuO:ZnO:La<sub>2</sub>O<sub>3</sub>:Al<sub>2</sub>O<sub>3</sub> = 1.000:0.490:0.065:0.065 (molar ratio).

## Acknowledgement

This research is implemented through the Operational Program "Human Resources Development, Education and Lifelong Learning" and is co-financed by the European Union (European Social Fund) and Greek national funds.

## References

- [1] A. Álvarez, A. Bansode, A. Urakawa, A.V. Bavykina, T.A. Wezendonk, M. Makkee, J. Gascon, F. Kapteijn, Chem. Rev. 117 (2017) 9804-9838.
- [2] G. Jadhav, P.D. Vaidya, B.M. Bhanage, J.B. Joshi, Chem. Eng. Res. Des. 92 (2014) 2557-2567.
- [3] M. Kulawska, M.M. Lachowska, Chem. Process Eng. 34 (2013) 479-496.

# Unprecedented chlorine-free hydrothermal synthesis of Pt/Pd colloidal alloys for catalytic applications

*Federico Spolaore, UNIPD, Padova, Italy; Michele Mariz, UNIPD, Padova, Italy; Franz Dornhaus, UMICORE, Hanau, Germany, Bernd Wittek, UMICORE, Hanau, Germany, Silvia Gross, UNIPD, Padova, Italy*

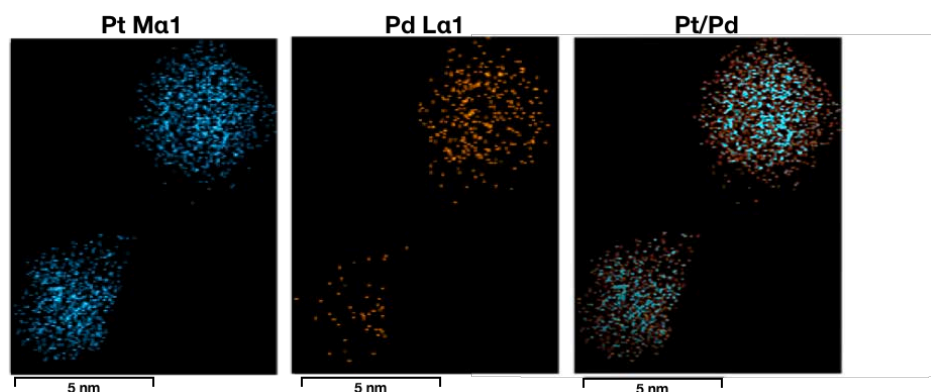
A water based colloidal synthesis for the preparation of chlorine-free Pt/Pd alloyed nanoparticles was successfully optimized under hydrothermal conditions.

Metal alloys are deeply investigated nowadays since the synergic effect that two metals has been demonstrated beneficial toward harsh temperature conditioning, where the Ostwald Ripening (OR) mechanism is the dominant process leading to particle growth.[1]

In particular, recent ageing studies demonstrated that, under high temperature conditions, the presence of Pd could prevent the oxidation of Pt, thus reducing the degree of deactivation of bimetallic supported nanoparticles such as the sintering caused by OR.[2]

Halides-free syntheses are of particular interest for catalytic applications, as these elements tend to preferentially adsorb on precious group metal (PGM) based particles, thus hindering catalytic activity and enhancing surface mobility thus leading to fast sintering at elevated temperatures.[3]

In this study, different platinum and palladium ratios were explored for the preparation of the targeted alloys, as well as different synthetic conditions to optimize average particle size and dispersion. The successful formation of alloyed nanoparticles was revealed by means of Energy Dispersive X-ray (EDX) spectroscopy coupled with High Resolution Transmission Electron Microscopy (HRTEM), X-Ray Diffraction (XRD) and X-ray Photoelectron Spectroscopy (XPS).



## References

- [1] A. D. Benavidez, L. Kovarik, A. Genc, N. Agrawal, E. M. Larsson, T. W. Hansen, A. M. Karim, A. K. Datye; *ACS Catal.* 2012, 2, 2349-2356.
- [2] H. Xiong, E. Peterson, G. Qi, A. K. Datye; *Catal. Today*, 2016, 272, 80-86.
- [3] M. Paulis, H. Peyrard, M. Montes; *J. Catal.*, 2001, 199, 1, 30-40.

# The Contribution of Metal Loaded Mesoporous Catalysts to Recycling of Polylactic Acid

*Seda Sivri; Cerag Dilek; Naime Aslı Sezgi\**

*Chemical Engineering Dept., Middle East Technical University, Ankara, Turkey*

*\*sezgi@metu.edu.tr*

## Introduction

The global plastic waste issue has promoted the usage of the biodegradable polymers, which are taking the place of conventional plastic materials. In this regard, polylactic acid (PLA) is a commonly known renewable biodegradable polymer, which serves a wide range of aims in terms of environmental impact, bioavailability and material performance. The favorable properties has led to a dramatic increase in the production rate of PLA during the last decade. However, with the high demand for the polymer, a waste problem is expected to arise in a short period of time. The biodegradability of the material would not offer a key solution to the rising waste issue since PLA is mainly decomposed very slowly under certain conditions via specific types of bacteria in a limited number of industrial compost plants. Recycling of PLA waste will become a significant environmental concern in the near future unless new techniques emerge. Yet, a limited number of work concentrated on recycling of PLA has been presented in the literature. Focusing on this waste problem, in this work; catalytic degradation of PLA was studied to reduce the waste accumulation and convert the waste into value-added chemicals. For this aim, metal loaded silica aerogel catalysts were synthesized for the pyrolysis of PLA. The performances of the silica aerogel catalysts were evaluated in thermal degradation of PLA using thermogravimetric analyzer.

## Experimental

The sol-gel method was followed using tetraethyl orthosilicate as the silica precursor to synthesize the silica aerogels. Metal loading of SA was carried out using the wet impregnation method. Silica aerogels catalysts were calcined at 500 °C with a heating rate of 1 °C/min for at least 12 hours under helium atmosphere with a flow rate of 50 mL/min. The same procedure was applied for the different metal loadings (2.5, 5 and 15 wt. %) [1]. The synthesized silica aerogel based catalysts were characterized using BET, SEM-EDX, and NH<sub>3</sub>-TPD techniques. Degradation

experiments were performed under nitrogen atmosphere with a flow rate of 50 mL/min from ambient temperature to 500 °C with a heating ramp of 5 °C/min. The weight ratio (PLA/Catalyst) was 2.

## **Results and Discussion**

Type IV isotherm and H1 hysteresis, an indication of mesoporosity, were detected for aluminum loaded silica aerogel based catalysts. With aluminum loading, a reduction in the surface area, pore volume and pore diameter of the catalysts was observed, which is attributed to the blockage of the pores with the loaded metal. The presence Si-O stretching vibration, Si-C stretching and Si-O-Si stretching in the FTIR spectrum pointed out that the synthesized material was silica aerogel. Pore size distribution and SEM analysis of the SA demonstrated the presence of microporous, mesoporous and macroporous sites. Pore sizes of the aluminum loaded silica aerogel catalysts decreased with an increase in metal loading amount, which was also verified with SEM analyses. TPD analyses revealed that an increase in metal loading induced an increase in their total acidic capacity of the catalysts.

Thermogravimetric analyses demonstrated that aluminum loaded silica aerogel catalyst had a positive impact on the degradation profile of PLA due to the presence of acidic sides in the structure of the catalyst. The decrease in the activation energy of degradation was provided with an increase in the metal content of the catalysts based on acidity. 15 wt. % aluminum loading resulted in approximately 28 % reduction in the activation energy of the PLA degradation.

## **Conclusion**

The findings of the work revealed that aluminum loaded silica aerogel catalysts can be used for the thermal recycling process of PLA with their favorable pore characteristics and their acidity affecting the degradation performance.

## **References**

[1] Sivri, S., Dilek, C., Sezgi, N.A. (2018). Synthesis and Characterization of Aluminum Containing Silica Aerogel Catalysts for Degradation of PLA. *International Journal of Chemical Reactor Engineering*. <https://doi.org/10.1515/ijcre-2018-0163>.

## **A novel route towards iron doped rice husk silica support materials**

*Alexander Grimm, Dirk Enke, University of Leipzig, Germany, Andreas Roppertz, Michael Frieß, Emission Partner GmbH & Co. KG, Ramsloh, Germany*

In recent years, environmental responsibility has become a major and global concern. With the limited amount of fossil fuels as well as the impact of global warming becoming more and more evident, a reconsideration in the sector of energy production is inevitable and has already commenced on a political but also scientific level. There is a general consensus about the necessity of a transition from fossil fuels in energy production towards sustainable resources, amongst which wind and solar energy are already being utilized on a large scale. Anyhow, due to their dependence on the local weather more reliable alternatives are of great interest. Biogas combined heat and power (CHP) plants represent a good combination of both the usage of renewables and reliability. In a typical biogas power plant methane is combusted generating both heat and electricity. The incomplete conversion of methane, however, leads to toxic side products like carbon monoxide and formaldehyde. This circumstance makes a catalytic post-treatment of the exhaust gas indispensable.

It has been shown that platinum based catalysts possess superior catalytic activity in the combustion of carbon monoxide (CO) and formaldehyde [1,2]. The high costs of platinum group metals represents the drawback of these catalysts. Thus, it is necessary to find ways for reducing the amount of noble metals used for these catalysts while maintaining their catalytic activity. It is known that the choice of support material can have a major impact on the catalytic performance [3]. Hence, the preparation and investigation of innovative catalyst supports is of high relevance. This work focuses on the synthesis of biogenic silica produced by the combustion of rice husk (RH), an agricultural waste product, for use as a catalyst support. By introducing iron salts into the rice husk via a liquid phase grafting method we were able to lower the required combustion temperature (Fig. 1) from about 600 °C to 450 °C reducing the overall energy consumption for the production of rice husk silica (RHS).



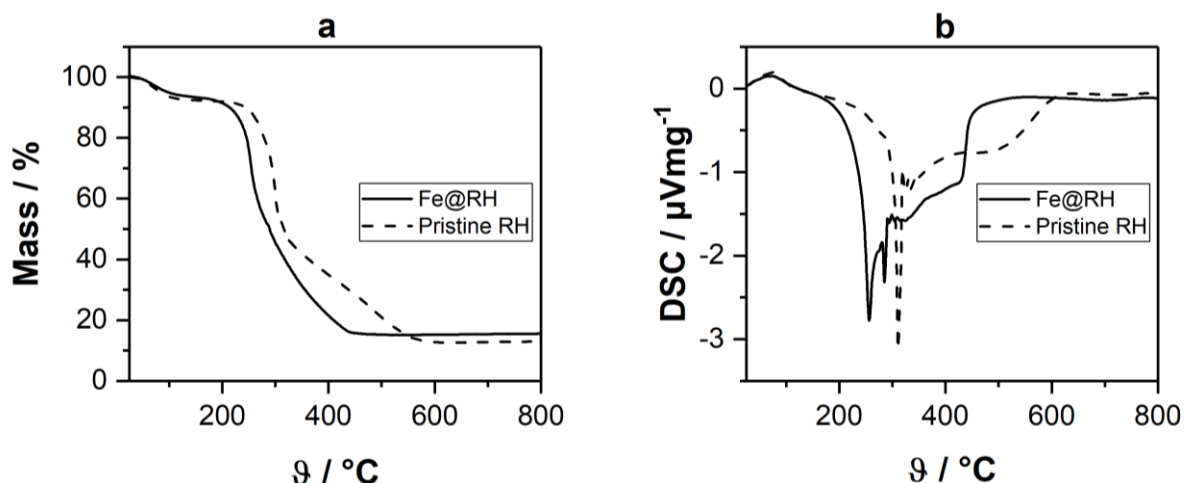
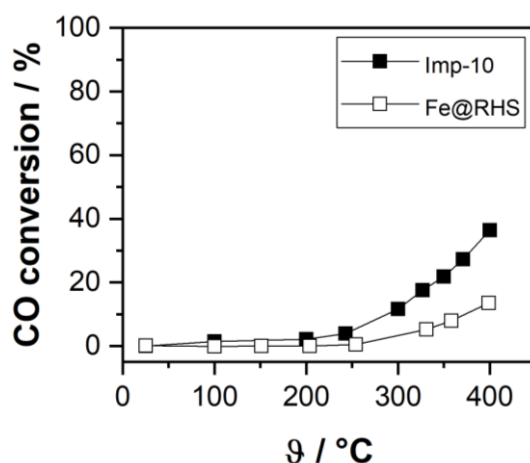


Fig. 1: Thermogravimetric analysis (a) and differential scanning calorimetry (b) of pristine and iron doped rice husk.

In addition, the resulting iron doped (1 wt%) RHS has a higher BET surface area (SSA) as well as a higher pore volume ( $352 \text{ m}^2\text{g}^{-1}$ ,  $0.53 \text{ cm}^3\text{g}^{-1}$ ) compared to silica from pristine RH ( $302 \text{ m}^2\text{g}^{-1}$ ,  $0.41 \text{ cm}^3\text{g}^{-1}$ ) and could thus contribute to a greater dispersion of active compounds during the following impregnation. Despite no noble metal is being involved the as prepared material shows slight activity towards CO oxidation that is even comparable to a reference system with a loading of 10 wt% iron



(Imp-10) prepared via a classical impregnation route of RHS (Fig. 2).

Fig. 2: CO oxidation performance of Fe@RHS and Imp-10. (GHSV =  $20000 \text{ h}^{-1}$ , 1000 ppm CO in air.)

This base activity alongside with the high SSA makes the prepared Fe@RHS a promising material for supported noble metal catalysts in exhaust gas treatment.

## References

- [1] ... C. Zhang *et al.*, *Catalysis Communications* 6 (2005) 211–214.
- [2] ... L. Zhang *et al.*, *Applied Catalysis B: Environmental* 219 (2017) 200–208.
- [3] ... M. Kim *et al.*, *Catalysts* 3 (2013) 88–103.

# CO<sub>x</sub>-free Hydrogen Production from Ammonia over Modified Red Mud-Supported Ruthenium

*Samira Fatma Kurtoğlu, Department of Chemical Engineering, Koç University, Istanbul, Turkey; Sezen Soyer-Uzun, Department of Chemical Engineering, Boğaziçi University, Istanbul, Turkey; Alper Uzun, Department of Chemical Engineering, Koç University, Istanbul, Turkey; Koç University TÜPRAŞ Energy Center (KUTEM), Koç University, Istanbul (Turkey); Koç University Surface Science and Technology Center (KUYTAM), Koç University, Istanbul (Turkey)*

## Introduction

Utilization of industrial wastes as catalysts is a highly promising and environmentally-friendly approach mainly because they are cost-effective and high in metal and metal oxide content [1]. Recently, we showed that RM, the by-product of the aluminum industry and one of the mostly produced industrial wastes globally rich in Fe<sub>2</sub>O<sub>3</sub>, can be converted into a highly efficient Fe-based catalyst to produce H<sub>2</sub> from NH<sub>3</sub> [2]. Results showed that upon modifying RM by simple acid treatments, a record high hydrogen production rate among all non-noble metal catalysts at 700 °C can be obtained [2]. Here, we showed that this exceptional performance can be even enhanced by using modified red mud (MRM) as a support for Ru which is known to be the most active metal for NH<sub>3</sub> decomposition. Findings show that MRM supported Ru provides high and stable performance for more than 7 days.

## Materials and Methods

RM was kindly provided by ETI Seydişehir Aluminum, Konya (Turkey). To enhance the properties of RM, simple acid treatments were performed to obtain MRM as described previously [2,3]. Ru was loaded at 1, 2, and 5 wt.% on freshly calcined MRM (at 900 °C for 3h in air) by incipient wetness impregnation using RuCl<sub>3</sub>·H<sub>2</sub>O. For the performance measurements, 25 mg of catalyst was mixed with fumed silica at a ratio of 1:20 (g:g) and loaded into a quartz ½” tube reactor placed into a Carbolite split furnace. Catalysts were reduced under pure H<sub>2</sub> at 700 °C (at a ramp rate of 5 °C/min) for 2 h. After reduction, catalysts were left under pure NH<sub>3</sub> flow over-night resulting in the formation of nitrated iron species from the iron content of reduced MRM was [4]. Conversion was measured by a Hidden QGA mass spectrometer calibrated for H<sub>2</sub>, N<sub>2</sub>, and NH<sub>3</sub>.

## Results and Discussion

Modification of RM resulted in an increase in surface area (from 17.9 m<sup>2</sup>/g to 50.0 m<sup>2</sup>/g) and an increase in Fe<sub>2</sub>O<sub>3</sub> content (from 46.5 to 54.7 wt.%). Temperature programmed reduction patterns of all catalysts showed that both Ru and Fe species can be completely reduced at the selected reduction procedure. X-ray diffraction patterns of reduced catalysts represented intense Fe peaks in all samples emerging due to the reduction of Fe<sub>2</sub>O<sub>3</sub> content of MRM to Fe. No Ru contribution could be detected in XRD proving high dispersion of Ru species. SEM images of reduced catalysts provided bulk Fe species together with smaller Ru particles dispersed on MRM. Results illustrated that the 5 wt.% Ru loaded sample (MRM-5Ru-R) provided superior performance. MRM-5Ru-R provides an almost complete NH<sub>3</sub> conversion at a very high space velocity of 240 000 cm<sup>3</sup> NH<sub>3</sub> h<sup>-1</sup> g<sub>cat</sub><sup>-1</sup> and 700 °C (Figure 1 a). Used catalyst characterization by XRD showed the nitrated iron formation upon NH<sub>3</sub> activation and reaction. The performance of MRM-5Ru-R can be maintained for more than 7 days which indicates the absence of structural deformation (Figure 1 b).

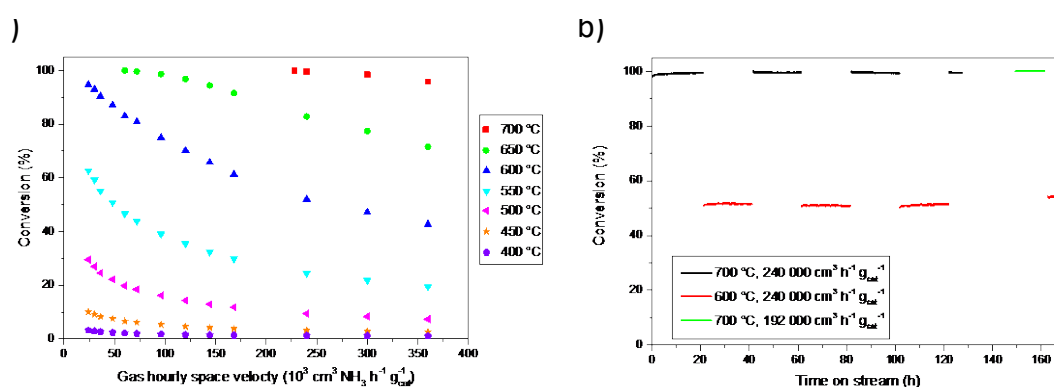


**Figure 1.** a) Catalytic performance of MRM-5Ru-R at different space velocities and temperatures, b) Catalytic stability test of MRM-5Ru-R at several conditions.

## Conclusions

Results show that the performance of MRM can be enhanced significantly upon Ru addition providing on-par, if not superior, activity with several Ru-based catalysts. We showed an effective approach for the remediation of RM in an environmentally-friendly and cost-effective way to produce CO<sub>x</sub>-free hydrogen.

## References

- [1] Sushil et al., *Chem. Eng. J.*, 166, 568 (2011).
- [2] Kurtoğlu, S.F. et al., *Int. J. Hydrogen Energy* 43, 20525 (2018).
- [3] Kurtoğlu, S.F. et al., *Ceram Int.* 42 17581 (2016).
- [4] Kurtoğlu, S.F. & Uzun, A. *Sci. Rep.* 6, 32279 (2016).

# Operando study of CO oxidation over Au-Pd/alumina catalysts

Yanyue Feng<sup>1</sup>, Peter Velin<sup>1</sup>, Felix Hemmingsson<sup>1</sup>, Andreas Schaefer<sup>1</sup>, Hanna Härelind<sup>1</sup>, Kirill Lomachenko<sup>2</sup> and Per-Anders Carlsson<sup>1</sup>

<sup>1</sup>Department of Chemistry and Chemical Engineering, Chalmers University of Technology, Gothenburg, Sweden

<sup>2</sup>European Synchrotron Radiation Facility, Grenoble, France

## Introduction

The oxidation of CO over bimetallic catalysts has been studied widely in the past decades. Among those studies, catalysts with alloyed gold and palladium nanoparticles supported on metal oxide materials are of great interest thanks to their high catalytic activity [1, 2]. Still, however, the understanding of the active phase is not complete, especially the structure and chemical state of the Au-Pd particles under operating conditions.

In this work, a catalyst with alloyed Au-Pd particles supported on alumina was synthesized by wet chemical impregnation and characterized with standard *ex situ* methods (BET, CO chemisorption and XRD). The main part of the study was then to study the catalyst with various operando techniques during transient CO oxidation, i.e., oxygen pulse response experiments, as to correlate physicochemical properties of the catalyst with the CO oxidation activity.

## Operando Characterization

Time-resolved energy-dispersive XAFS measurements were carried out at the ID24 beamline at the European Synchrotron Radiation Facility in Grenoble, France. About 40 mg of Au-Pd powder catalyst was loaded in a 5 mm diameter stainless steel sample cup placed in a flow-through reaction cell. The direction of the gas flow was downwards and the powder was held in place by a stainless-steel gauze. Air-actuated high-speed four-way valves (Valco, VICI) were used to switch the feed gas compositions as make modulation excitation spectroscopy. The X-ray absorption spectra were obtained by monitoring the Pd K-edge at 23.45 keV. The energy calibration was performed by using Pd foil (Goodfellow, 99.99% purity). Simultaneously with the XAFS measurements, infrared spectroscopic

characterization in diffuse reflectance mode was used to monitor adsorbate changes during the pulsed-oxygen experiment. Moreover, complementary high-energy X-ray diffraction measurements have been carried out at beamline ID15, ESRF.

### **Concluding remarks**

With the employed methods we will present how the CO oxidation activity of Au-Pd/alumina catalysts depend on both, oxidation state/local structure and long-range order of the Pd phase, as well as the adsorbate composition. Thereby, we will establish a so-called structure-function relationship.

### **References**

- [1] Liu, J.-X.; Su, Y.; Filot, I. A. W., et al., *Journal of the American Chemical Society* **2018**, *140* (13), 4580-4587.
- [2] Saavedra, J.; Pursell, C. J.; Chandler, B. D., *Journal of the American Chemical Society* **2018**, *140* (10), 3712-3723.

# Mechanism of N<sub>2</sub>O formation over Pt-Ba/ $\gamma$ -Al<sub>2</sub>O<sub>3</sub> catalysts

I. S. Pieta<sup>1</sup>, M. Cortes-Reyes<sup>2</sup>, M.A. Larrubia<sup>2</sup>, L. J. Alemany<sup>2</sup>, W. S. Epling<sup>3</sup>

<sup>1</sup> Institute of Physical Chemistry PAS, 01-224 (Poland)

<sup>2</sup> University of Malaga, Malaga E-29071 (Spain)

<sup>3</sup> University of Virginia, VA 22904-4741 (U.S.A.)

\*[ipieta@ichf.edu.pl](mailto:ipieta@ichf.edu.pl)

## Introduction

The removal of NO<sub>x</sub> under lean conditions can lead to by-product N<sub>2</sub>O or NH<sub>3</sub> formation [1-2]. NH<sub>3</sub> formation during the regeneration phase is the basis for the in series NSR-SCR aftertreatment technology [3], while N<sub>2</sub>O formation is a more complex problem with its global warming potential being nearly 300 times higher than CO<sub>2</sub>.

In the current work possible N<sub>2</sub>O formation pathways over a model Pt-Ba/ $\gamma$ -Al<sub>2</sub>O<sub>3</sub> (1/20/100, w/w) NO<sub>x</sub> storage/reduction (NSR) catalyst were studied using NH<sub>3</sub> as a reducing agent. NH<sub>3</sub> reactivity with catalyst surface nitrite and nitrate species was investigated using temperature programmed surface reaction. The study aims also to quantify ammonia consumption under different stoichiometric conditions and gas-phase NO presence, and show reacted ammonia selectivity toward N<sub>2</sub> as well as toward undesired N<sub>2</sub>O.

## Materials and Methods

The powder Pt-Ba/ $\gamma$ -Al<sub>2</sub>O<sub>3</sub> catalyst was prepared by a two-step impregnation of  $\gamma$ -Al<sub>2</sub>O<sub>3</sub> (Puralox, Sasol, surface area 200 m<sup>2</sup>/g, pore volume 0.7 m<sup>3</sup>/g) using Pt(NH<sub>3</sub>)<sub>2</sub>(NO<sub>2</sub>)<sub>2</sub> (Aldrich Chemical) and Ba(CH<sub>3</sub>COO)<sub>2</sub> (Merck, 99%).

The reaction studies were performed in a quartz fixed-bed reactor connected to a QMS 200 mass spectrometer (Pfeiffer Vacuum PrismaTM) for outlet gas analysis. Diffuse reflectance infrared Fourier transform spectroscopy (DRIFTS) studies were performed in a continuous flow Harrick Praying Mantis reaction chamber. A FTIR Nicolet Nexus 470 spectrometer was used to characterize the interactions between the gas species and the catalyst surface during the TPSR experiments in a

temperature range RT-723 K. Spectra were recorded in diffuse reflectance mode, and 45 scans were collected at a resolution of  $1\text{ cm}^{-1}$ .

## Results and Discussion

The results show that the highest amount of  $\text{N}_2\text{O}$  was formed when using lower  $\text{NH}_3$  concentrations and for higher ammonia concentration  $\text{N}_2\text{O}$  was formed below 438 K (Fig.1). Above 423 K, for  $\text{NH}_3$  concentrations higher than stoichiometric, only  $\text{N}_2$  was detected. Moreover, comparing the results with and without nitrites/nitrates pre-formed it can be concluded that ammonia first reacts with gas-phase NO and then with pre-formed nitrites/nitrates. The slopes of the  $\text{N}_2\text{O}$  and  $\text{N}_2$  production rates and the amounts of  $\text{N}_2\text{O}$  and  $\text{N}_2$  produced up to 423 K indicate that the reaction rates are similar and most likely are not controlled by  $\text{NH}_3$  concentration (Fig 1 a vs b).

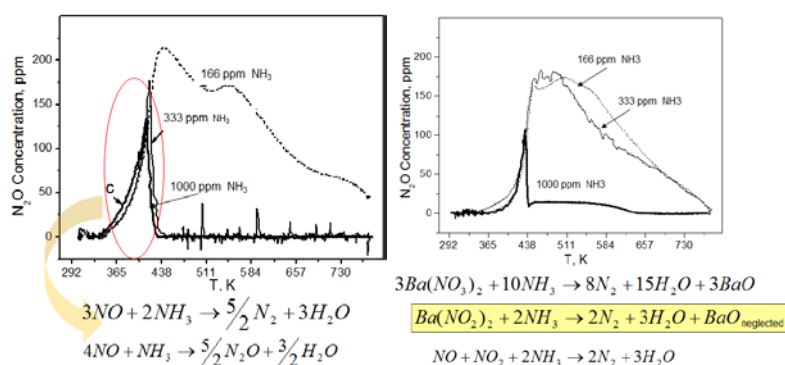


**Figure 1.**  $\text{N}_2\text{O}$  production over the Pt Ba/AlPox catalyst without (A) and with (B) preformed nitrites/nitrates upon admission of 500 ppm of NO and (a) 166 ppm, (b) 333 ppm and (c) 1000 ppm of  $\text{NH}_3$ . Flow  $100\text{ ml min}^{-1}$ , He as a carrier. T ramp  $10\text{ K min}^{-1}$ .

## Significance

$\text{N}_2\text{O}$  was mainly formed at low temperatures, and correlates with low NO and  $\text{NH}_3$  conversions. Increasing temperature and thus NO and  $\text{NH}_3$  conversions,  $\text{N}_2$  selectivity increases. The experiments with nitrites/nitrates pre-formed showed that the reduction of surface N-species is complete only for high  $\text{NH}_3/\text{NO}$  ratios and when  $\text{NH}_3$  is the limiting reactant, they remain on the catalyst surface unreacted until temperatures higher than 623 K, where they decompose giving  $\text{NO}_2$  and  $\text{O}_2$ .

## References

- [1] S.A. Malamis, M. Li, W.S. Epling, M.P. Harold, Appl. Catal. B: Environmental, 237 (2018) 588-602
- [2] I. S.Pieta, M. Cortes, M.A. Larrubia, L. J. Alemany, W. S. Epling, Topics Catal. (2018) in press.
- [3] P. Forzatti, L. Lietti, I. Nova, E. Tronconi, Cat. Today 151 (2010) 202

# **NH<sub>3</sub>-SCR of NO using highly active, supported H<sub>(3+x)</sub>PV<sub>x</sub>Mo<sub>(12-x)</sub>O<sub>40</sub> heteropolyacid catalysts**

*Anna Bukowski<sup>a</sup>, Leonhard Schilf<sup>b</sup>, Anders Riisager<sup>b</sup>, Rasmus Fehrmann<sup>b</sup>, Jakob Albert<sup>a</sup>*

<sup>a</sup> *Lehrstuhl für Chemische Reaktionstechnik, Friedrich-Alexander-Universität Erlangen-Nürnberg, Egerlandstraße 3, 91058 Erlangen, Germany*

<sup>b</sup> *Centre for Catalysis and Sustainable Chemistry, Department of Chemistry, Technical University of Denmark, Kemitorvet 206, 2800 Kgs. Lyngby, Denmark*

## **Introduction**

Keggin type heteropoly acids (HPA) based on the combination of P,V and Mo atoms (H<sub>(3+x)</sub>PV<sub>x</sub>Mo<sub>(12-x)</sub>O<sub>40</sub>) are inexpensive, easy to synthesize and have been successfully used for catalytic reactions such as: extractive oxidative desulphurization [1], biomass conversion to formic acid in the so-called OxFA process [2] and selective oxidation of humins to low-chain carboxylic acids [3]. NH<sub>3</sub>-SCR of NO is another reaction which might be catalyzed by this kind of HPA because some of the commercially used catalysts contain both MoO<sub>3</sub> and V<sub>2</sub>O<sub>5</sub> supported on TiO<sub>2</sub>. Several studies have shown that using H<sub>3</sub>PMo<sub>12</sub>O<sub>40</sub> instead of MoO<sub>3</sub> can lead to both higher activity and resistance towards potassium [4-6], one of the major catalyst poisons, especially in biomass fueled power plants.

## **Experimental**

H<sub>(3+x)</sub>PV<sub>x</sub>Mo<sub>(12-x)</sub>O<sub>40</sub> compounds with x of 1 to 5 were synthesized as described in [7]. The HPAs were supported on TiO<sub>2</sub> (anatase), SiO<sub>2</sub>, ZrO<sub>2</sub> and activated carbon using the incipient wetness impregnation method and thoroughly characterized by NH<sub>3</sub>-TPD, N<sub>2</sub>-physisorption, XRD, XPS and FTIR. Activity measurements were conducted in a fixed bed quartz reactor using a simulated flue gas at temperatures between 200 and 350 °C. NO, NO<sub>2</sub> and NH<sub>3</sub> concentrations were monitored with a chemiluminescent analyzer. N<sub>2</sub>O was in some cases monitor using gas chromatography. The most promising catalyst underwent a long term (12 h) test at 350 °C.



## Results

Anatase was by far the most promising support for vanadium containing HPAs. Both the loading of HPA and the degree of substitution of Mo by V were optimized. The best performing catalyst showed stable activity at 350 °C during the long term exposure (12h) and neither generated N<sub>2</sub>O nor oxidized NH<sub>3</sub> to a significant extent. A (V<sub>2</sub>O<sub>5</sub>-MoO<sub>3</sub>)/TiO<sub>2</sub> catalyst having the same V/Ti and Mo/Ti molar ratios as the optimum HPA/TiO<sub>2</sub> one was prepared and showed lower activity, suggesting that the Keggin structure has a promotional effect. The extensive characterization will help to understand this effect and potassium tolerance studies might be conducted in the near future to test the catalysts' applicability to biomass fueled power plants.

## References

- [1]: Energy Fuels 2018, 32, 8683-8688
- [2]: Energy and Environmental Science 2015, 8, 2985-2990
- [3]: Chemistry Select 2017, 24, 7296-7302
- [4]: Catalysis Letters 2018, 148, 1228-1235
- [5]: Catal. Sci. Technol. 2011, 1, 631
- [6]: Applied Catalysis B: Environmental 2016, 183, 282-290
- [7]: React.Kinet.Catal.Lett 2008, 95, 21-28

# Magnetic Cu-Mn Composites as a Photo-Fenton Catalysts for Wastewater Treatment at Neutral pH

*Ivalina Trendafilova, National institute of Chemistry, Ljubljana, Slovenia and Institute of Organic Chemistry with Center of Phytochemistry, Bulgarian Academy of Sciences, Sofia, Bulgaria; Andraž Šuligoj, National institute of Chemistry and Faculty of Chemistry and Chemical Technology, University of Ljubljana, Slovenia; Alenka Ristić, National institute of Chemistry, Ljubljana, Slovenia; Albin Pintar, National institute of Chemistry, Ljubljana, Slovenia; Nataša Novak Tušar, National institute of Chemistry, Ljubljana and University of Nova Gorica, Slovenia*

## Introduction

One of the most important classes of water pollutants are organic compounds. Promising alternative for solving the problem associated with total degradation of organic pollutants is given from advanced oxidation processes (AOPs). The interest towards AOPs is associated with their capability to generate highly reactive free hydroxyl radicals, which decompose organic compounds (dyes, antibiotics, pesticides, etc.) to non-harmful H<sub>2</sub>O, CO<sub>2</sub> and inorganic species. Iron based Fenton AOP is one of the most effective and inexpensive AOPs in wastewater treatment. However, Fenton AOP application as a homogeneous catalytic process is limited because of its disadvantages such as i) optimum efficiency typically achieved under acidic pH (pH=3), ii) formation of large amounts of ferrous iron sludge and iii) the presence of iron ions after the reaction in the effluents.

In the present study we upgraded previously obtained Mn porous silica supported catalyst for Fenton AOP working at neutral pH [1] to magnetic Cu-Mn composite catalyst. The magnetic properties of the catalyst are premise to its easy separation and recovery from the treated water after the reaction. The combination of Mn and Cu also enabled to obtain Fenton AOP catalyst working under UV and/or visible light (photo-Fenton AOP).

## Experimental

Magnetic nanoparticles were synthesized via coprecipitation of iron salts in inert atmosphere. The magnetic mesoporous silica support was synthesized by incorporation of ironoxide nanoparticles into the silica framework. For this purpose, freshly prepared magnetic nanocrystals were added directly into the solution

containing silica source and structure-directing agents (templates). The template free materials were obtained by extraction in ethanol. For the incorporation of the active catalytic components (Mn and Cu) different techniques were used (incipient wetness impregnation, template ion exchange and direct synthesis) in order to investigate the influence of the incorporation procedure to catalytic activity and structural properties of the catalysts.

Materials are characterized by XRD, elemental analysis, SEM, atomic resolution transmission electron microscopy (AR TEM), surface techniques (N<sub>2</sub> physisorption, Zeta potential etc.) and spectroscopies (UV-VIS, XPS).

Photocatalytic tests are performed with different dyes (e.g. methylene blue) as model organic pollutants at neutral pH under UV and/or visible light.

### **Results and Discussion**

Cu-Mn composites with magnetic properties have been successfully synthesised. The magnetic support was obtained by coating of iron magnetic nanoparticles with mesoporous silica in template assisted procedure. The bimetal catalyst was prepared by incorporation of Mn and Cu into the silica framework. Cu was determined as CuO on the silica surface and Mn as incorporated Mn into the silica surface. No synergistic effects between Cu and Mn were recorded, meaning Cu and Mn sites were acting as separate active sites, which was confirmed with AR TEM imaging as well as UV spectroscopy studies. The combination of Cu-Mn active sites on the surface of amorphous porous silica has proven successful for dye decomposition for two reasons: 1) Cu addition significantly reduces Mn leaching and 2) Cu functions also as a photocatalyst.

### **Conclusions**

Evaluation of prepared magnetic Cu-Mn composite materials showed that they are promising catalysts for photo-Fenton AOP heterogeneous catalytic process for wastewater purification: 1) they can be easily removed from the effluent after the reaction, 2) lower Mn leaching from the catalyst was obtained if compared with previously obtained Mn porous silica supported catalyst, 3) they work under neutral pH, 4) they work also as photocatalyst.

### **References**

[1] Tušar, N.N., Maučec, D., Rangus, M., Arčon, I., Mazaj, M., Cotman, M., Pintar, A., Kaučič, V., Manganese functionalized silicate nanoparticles as a Fenton-type catalyst for water purification by Advanced Oxidation Processes (AOP), *Advanced Functional Materials* 22 (4), 2012, 820-826.

# Low-cost alumina supported bimetal Cu-Fe catalyst for catalytic oxidation of VOCs

*Tadej Žumbar, National institute of Chemistry, Ljubljana, Slovenia; Margarita Popova, Institute of Organic Chemistry, Bulgarian Academy of Sciences, Sofia, Bulgaria; Alenka Ristić, National institute of Chemistry, Ljubljana, Slovenia; Nataša Zabukovec Logar, University of Nova Gorica and National institute of Chemistry, Nova Gorica and Ljubljana, Slovenia; Nataša Novak Tušar, University of Nova Gorica, Nova Gorica, Slovenia and National institute of Chemistry, Ljubljana, Slovenia*

## Introduction

Volatile organic compounds (VOCs) are a growing environmental issue and are one of the most complex air pollutants that have to be treated in industry. Most common abatement of industrially produced VOCs is done with thermal (incineration) or catalytic oxidation. Both are expensive methods from the point of view of energy input or catalysts cost, where the noble metals like palladium and platinum show the best efficiencies. Catalytic oxidation offers many opportunities in cost reduction when non-noble metals are used. Our group studied non-noble metal porous silica supported catalysts. [1-3] Bimetal Cu-Fe porous silica supported catalyst showed high efficiency. [3]

Due to the high costs of porous silica support for production on industrial scale, we have studied bimetal Cu-Fe alumina supported catalyst with low-cost alumina support. In this work we evaluate different alumina supports and structure-performance relationship of the catalysts.

## Experimental

Different alumina supports were prepared, with varying characteristics and properties. Cu-Fe functionalized alumina samples (Cu-Fe/Al<sub>2</sub>O<sub>3</sub>) with different Fe/Al molar ratios and constant Cu loading (6 wt. %) were prepared using a two-step synthesis approach. In the first step Fe/Al<sub>2</sub>O<sub>3</sub> samples were prepared with co-precipitation and in the second step, copper species was added via impregnation following solid-state thermal conversion (Cu-Fe/Al<sub>2</sub>O<sub>3</sub>).

Characterization was performed using elemental analysis, XRD, SEM, atomic resolution transmission electron microscopy (AR TEM) as well as surface characterization techniques ( $N_2$  physisorption, TPR, TPD, etc.).

Catalytic tests were performed using toluene as a model VOC.

## **Results and discussion**

Characterization results showed that 1) Cu impregnation and calcination leads to the formation of CuO and Cu-Fe-oxo surface species covering the alumina supports and 2) the characteristics of alumina supports and the presence of iron within the alumina matrixes have a significant impact on the formation of copper oxide phases.

Catalytic tests showed that 1) the catalytic performance of the catalysts depends on the metal loading in the alumina matrixes and 2) the molar ratio of CuO and Cu-Fe-oxo species leads to the different catalytic performance of the catalysts.

## **Conclusion**

Structure-performance relationship of the evaluated catalysts was determined. Prepared catalysts are promising low-cost catalysts for catalytic oxidation of VOCs.

## **References**

- [1] M. Popova, A. Ristić, K. Lazar, D. Maučec, M. Vassileva, in N. Novak Tušar, *ChemCatChem*, 2013, 5, 986–993.
- [2] M. Rangus, M. Mazaj, G. Dražič, M. Popova, N. Novak Tušar, *Materials* 2014, 7, 4243-4257.
- [3] Popova, M.; Ristić, A.; Mazaj, M.; Maučec, D.; Dimitrov, M.; Novak Tušar, N. *ChemCatChem* 2014, 6, 271-277.

# **Titania-Silica Photocatalytic Films for Air Treatment: New Findings on Stability of the Films**

*Andraž Šuligoj, National institute of Chemistry, Ljubljana and Faculty of Chemistry and Chemical Technology, University of Ljubljana, Slovenia; Mohamed El-Roz, Laboratoire Catalyse et Spectrochimie, Université de Caen Basse-Normandie, ENSICAEN CNRS, Caen, France; Goran Dražić, National institute of Chemistry, Ljubljana Slovenia; Urška Lavrenčič Štangar, Faculty of Chemistry and Chemical Technology, University of Ljubljana, Slovenia; Nataša Zabukovec Logar, National institute of Chemistry, Ljubljana and University of Nova Gorica, Slovenia; Nataša Novak Tušar, National institute of Chemistry, Ljubljana and University of Nova Gorica, Slovenia*

## **Introduction**

Volatile organic compounds (VOC) are the main class of pollutants. Photocatalysis is one of the most efficient advanced oxidation processes (AOP) for removal of VOCs from indoor-air. Titanium dioxide ( $\text{TiO}_2$ ) is the most used semiconductor for photocatalytic removal of VOCs from indoor air. A common approach to enhance the photocatalytic activity of  $\text{TiO}_2$  is also to increase its surface area ( $100\text{--}200 \text{ m}^2 \text{ g}^{-1}$  to  $400\text{--}1000 \text{ m}^2 \text{ g}^{-1}$ ) and to introduce the mixed oxide synergetic effect. This can be achieved by immobilization of  $\text{TiO}_2$  on the porous supports such are for example porous silica and the preparation of such a catalyst in the form of film using appropriate carrier. However, such as composites possess often low stability.

We have shown before, that the use of colloidal titania acts beneficial as a step in the sol-gel synthesis, facilitating the mixing of reactants, resulting in high homogeneity of the nanoparticles in the final sol. [1] However, stability of the films is another factor which hinders the implementation of such materials. Hence, the use of binders in form of colloidal silica were studied for this research.

## **Results and discussion**

Colloidal  $\text{SiO}_2$  was chosen because: (1) of its mesoporosity, which would increase the surface area of the catalysts, (2) disordered  $\text{SiO}_2$  materials have higher degree of hydroxylation, (3) they are more stable towards dehydroxylation/rehydroxylation procedures and (4) they are more stable towards water and acid treatment than their

ordered analogues. Usually, high temperature or high pressures are used for the binding process, which is burdensome in the view of energy use and environmental impact. Moreover, at high temperatures, colloidal silica particles sinter and bind components together or form a hard glassy surface coating, while at lower temperatures, colloidal SiO<sub>2</sub> can form an inorganic matrix based on covalent bonds. The latter principle was exploited in this research.

We found out that to achieve excellent stability of TiO<sub>2</sub>/SiO<sub>2</sub> photocatalytic films, special care must be put to the sizes of nanoparticles involved in the system, the particle sizes of active (TiO<sub>2</sub>) and inactive phase (SiO<sub>2</sub>) should match each other. Also the exact match of the surface –OH density between these two phases was found to have profound influence on the stability of the films.

The efficiency of TiO<sub>2</sub>/SiO<sub>2</sub> photocatalytic films on the glass surface was tested by oxidation of toluene and formaldehyde, which are being considered as surrogates for two of the six major classes (aromatics, aldehydes, alkanes, ketones, alcohols, and chlorocarbons) of indoor air contaminants. We found out that TiO<sub>2</sub>/SiO<sub>2</sub> photocatalytic films with the highest stability showed also the highest photocatalytic efficiency.

## Conclusion

Here, we present new insights on the stability of TiO<sub>2</sub>/SiO<sub>2</sub> films applied on glass surface. We found out that to achieve excellent stability of TiO<sub>2</sub>/SiO<sub>2</sub> photocatalytic films, special care must be put to the sizes of TiO<sub>2</sub> and SiO<sub>2</sub> nanoparticles involved in the system and –OH density between both phases.

Colloidal TiO<sub>2</sub> was used as active phase while different mesoporous SiO<sub>2</sub> were added to increase the surface area and/or to improve stability of films.

The highest photocatalytic efficiency was observed for TiO<sub>2</sub>/SiO<sub>2</sub> films with the highest stability for decomposition of formaldehyde and toluene as two of the most common indoor air pollutants.

## References

- [1] A. Šuligoj, U. Lavrenčič Štangar, A. Ristić, M. Mazaj, D. Verhovšek, N. Novak Tušar, *Appl. Catal. B Environ.* 184, (2016), 119–131.
- [2] A. Šuligoj, M. El-Roz, G. Dražič, U. Lavrenčič Štangar, N. Zabukovec Logar, N. Novak Tušar, sent for publication (2019).

# Graphene-ZnO composites to enhance antimicrobial activity of photocatalytic coatings

Laura Valenzuela, University of Alcalá, Alcalá de Henares, Spain; Ana Iglesias Juez Instituto de Catálisis y Petroleoquímica, Madrid, Spain; Belén Bachiller Baeza, Instituto de Catálisis y Petroleoquímica, Madrid, Spain; Roberto Rosal, University of Alcalá, Alcalá de Henares, Spain

## Introduction

Photocatalytic antimicrobial coatings involving metal oxide nanoparticles have shown promising potential for inactivating a wide range of microorganisms preventing transmission and infection problems [1]. ZnO attracts considerable technological interest due to its large variety of nanometric architectures with peculiar optical and electronic properties [2]. On the other hand, the unique two-dimensional structure of graphene related materials have distinctive electronic, thermal and mechanical properties [3]. The aim of this work was to combine the remarkable electrical properties offered by reduced graphene oxide (rGO) with the high antibacterial performance of ZnO nanoparticles [4] to prepare improved photoactive bactericidal surfaces. The bioactivity of ZnO and ZnO-rGO coatings was assayed by means of cultures of the gram-positive bacterium *Staphylococcus aureus* and the reusability was evaluated by repeating cell viability tests under identical conditions for several consecutive cycles. The structural, electronic and morphological properties were characterized by XRD, Raman, UV-Visible, Photoluminescence, TEM and SEM. The wettability and hydrophobicity were also determined and adhesion tests were performed.

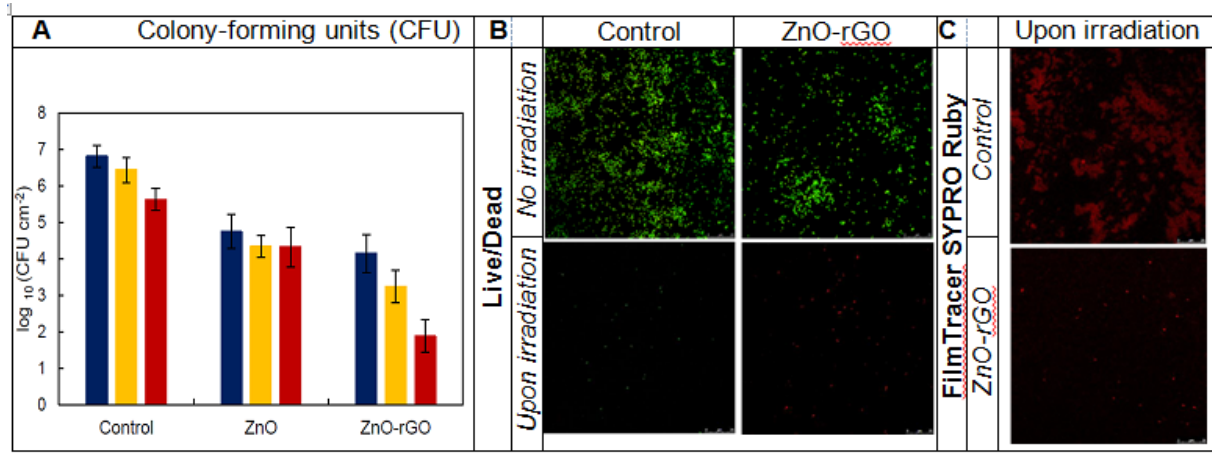
## Results and discussion

Figure A shows the antimicrobial behaviour of ZnO and ZnO-rGO-functionalized surfaces against *S. aureus* incubated for 20 hours at 37 °C in aerosol exposure mode. The application of bacteria-containing aerosol either using ZnO and ZnO-rGO, or winter and summer irradiation, led to > 99.5% (> 2-log) reduction in CFU compared to non-irradiated controls.

Non-functionalized surfaces showed extensive colonization by viable bacteria and a clear biofilm formation revealed by the Live/Dead (Figure B) and SYPRO Ruby stains (Figure C), respectively. However, the presence of a photocatalytic material on the surface reduces the amount of attached bacteria to the surface and, upon UV



irradiation, drastically decreased the number of viable bacteria (becoming red-marked and therefore membrane-damaged, and inhibited biofilm formation Figure B). rGO presence enhanced the antimicrobial activity and also confers improved surface mechanical resistance as the coatings were reusable several times without losing efficiency significantly.



**Figure A.** Colony-forming units (CFU) of *S. aureus* measured from the surface after bacteria-containing aerosol spraying. Uncoated (control), ZnO and ZnO-rGO coated specimens, in absence of irradiation (■) and upon winter (■) and summer (■) irradiation. **Figure B.** Live/Dead BacLight Bacterial Viability Test results from uncoated and ZnO-rGO specimens in absence of irradiation and upon summer irradiation. **Figure C.** FilmTracer SYPRO Ruby Test results from uncoated (control) and ZnO-rGO specimens upon summer irradiation.

## Conclusions

ZnO-based photocatalytic coatings greatly inhibited bacterial colonization keeping the surface essentially free of viable cells and biofilm matrix. The presence of rGO allowed to obtain more efficient photoactive systems as the new interactions between the surfaces and the high electrical conductivity of graphene hinders recombination of photogenerated hole-electron pairs. The incorporation of rGO enhanced both antimicrobial activity and mechanical properties of the surface.

*Acknowledgements: This work has been funded by the Ramón Areces Foundation (Project Ref: OTR02666). L.V. thanks the Spanish Ministry of Education for the FPU grant FPU17/03096.*

## References

- [1] V. K. Yemireddy, Y.-C. Hung, *Compr. Rev. Food Sci. F.* 16 (2017) 617-631.
- [2] J.-S. Na, B. Gong, G. Scarel, G. N. Parsons, *ACS Nano* 3 (2009) 3191-3199.
- [3] S. Stankovich, D. A. Dikin, G. H. B. Dommett, K. M. Kohlhaas, E. J. Zimney, E. A. Stach, R. D. Piner, S. T. Nguyen, R. S. Ruoff, *Nature* 442 (2006) 282.
- [4] L. Valenzuela, A. Iglesias-Juez, M. Faraldos, A. Bahamonde, R. Rosal, *J. Hazard. Mater.* (2019) (Accepted).

# **Frustrated carbocation Lewis acid/pyridine Lewis base cocatalyzed cyclic ester ring -opening polymerization**

*Zhenjiang Li, Corresponding authors, Nanjing, China; Zhiwei Yao, Nanjing, China;  
Kai Guo, Corresponding authors, Nanjing, China*

## **Background**

The study of ring-opening polymerization (ROP) reactions has made significant achievements over the past two decades. Olefin polymerization for the production of commodities and specialty polymers has once attracted extensive research and attention from industry and academia, but the non-renewability of fossil resources, price instability and growing environmental problems have made people realize The development of renewable and biodegradable polymer materials is of great significance. At present, polymer materials mainly include fibers, plastics, rubber, etc., which have been widely used in packaging, textile, construction, transportation, biomedicine and microelectronics<sup>[1-3]</sup>.

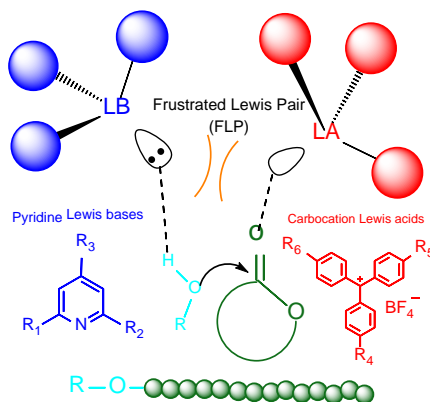
Among many synthetic polymer materials, aliphatic polyesters occupy an important position due to their excellent biodegradability, bioabsorbability and biocompatibility, and have become a research hotspot in recent years<sup>[4-5]</sup>. The main chain of the aliphatic polyester is formed by linking aliphatic structural units through easily hydrolyzable ester bonds, and is easily degraded into non-toxic water-soluble oligomers or monomers by a large number of microorganisms in the natural world or enzymes in animals and plants. It is then oxidized to carbon dioxide, water and energy. Aliphatic polyesters are mainly used in medical surgical sutures, drug carriers, and biological tissue engineering. The most widely studied and commercially valuable polyesters are poly- $\epsilon$ -caprolactone, polylactide, polyglycolide, poly- $\beta$ -butyrolactone and polytrimethylene carbonate. Among them, polylactide and polytrimethylene carbonate have received extensive attention due to their good biocompatibility, biodegradability and unique physical and mechanical properties.

## **This study**

In the past two decades, the use of acid-base cocatalysts to catalyze the ring-opening polymerization of cyclic esters has achieved considerable success. The preparation of biodegradable polymers by Lewis acid/base to the catalytic system has attracted great interest in the academic community. Different types of Lewis acid/base pairs have been shown to be effective in catalyzing ring-opening

polymerization. From the traditional organometallic Lewis acid/base to the new non-metallic boron Lewis acid/base catalyst system, there are related reports in the literature, and organic carbocations as a strong Lewis acid have not been applied in the field of ring-opening polymerization. Organic carbocations are widely used in the field of small molecule catalysis, including Diels–Alder reaction, conjugate addition reaction, halogenation reaction and epoxy rearrangement reaction. In particular, trityl carbocation has certain stability and strong Lewis acidity due to its unique structure. Among the many carbocations, trityl carbocations are valued by more and more chemists. The stability and Lewis acidity of the trityl carbocation can be adjusted by changing the electron cloud density of the aromatic ring.

In this study, a well-structured organic carbocation is used as the Lewis acid, and a Lewis acid-base cocatalyst system with an appropriate structure and properties is selected to catalyze the ring-opening polymerization of the cyclic monomer, and is expected to be It is carried out in an living-controlled manner and has a wide range of monomer suitability. The development of the frustrated carbocation Lewis acid/base catalyst system can provide a new path for the preparation of new aliphatic polyesters, and has played an active role in the synthesis of aliphatic polyesters.



## References

- [1] Grossand R A, Kalra B .Science, 2002, 297 (5582), 803-807.
- [2] Coat es G W, Hillmyer M A. Macromolecules, 2009, 42 (21), 7987-7989.
- [3] Gandini A. Macromolecu les , 2008, 41 (24), 9491-9504.
- [4]van de Weert M, Hennink WE, Jiskoot W. Pharmaceutical research, 2000, 17 (10): 1159-1167.
- [5]Fu K, Pack DW, Klivanov AM, et al. Pharmaceutical research, 2000, 17 (1): 100-106.